2011

ANNUAL PROGRESS REPORT

DOE Hydrogen and Fuel Cells Program



U.S. DEPARTMENT OF ENERGY

DOE/GO-102011-3422
November 2011

U.S. Department of Energy
1000 Independence Avenue, S.W.
Washington, D.C. 20585-0121

FY 2011
PROGRESS REPORT FOR THE DOE HYDROGEN AND FUEL CELLS PROGRAM

November 2011
DOE/GO-102011-3422

Approved by Sunita Satyapal, Hydrogen and Fuel Cells Program Manager

NOTICE

This report was prepared as an account of work sponsored by an agency of the United States government. Neither the United States government nor any agency thereof, nor any of their employees, makes any warranty, express or implied, or assumes any legal liability or responsibility for the accuracy, completeness, or usefulness of any information, apparatus, product, or process disclosed, or represents that its use would not infringe privately owned rights. Reference herein to any specific commercial product, process, or service by trade name, trademark, manufacturer, or otherwise does not necessarily constitute or imply its endorsement, recommendation, or favoring by the United States government or any agency thereof. The views and opinions of authors expressed herein do not necessarily state or reflect those of the United States government or any agency thereof.

Available electronically at http://www.osti.gov/bridge

Available for a processing fee to U.S. Department of Energy
and its contractors, in paper, from:

U.S. Department of Energy
Office of Scientific and Technical Information
P.O. Box 62
Oak Ridge, TN 37831-0062
Phone: (865) 576-8401
Fax: (865) 576-5728
E-mail: mailto:reports@adonis.osti.gov

Available for sale to the public, in paper, from:

U.S. Department of Commerce
National Technical Information Service
5285 Port Royal Road
Springfield, VA 22161
Phone: (800) 553-6847
Fax: (703) 605-6900
E-mail: orders@ntis.fedworld.gov
Online ordering: http://www.ntis.gov/ordering.htm



Printed on paper containing at least 50% wastepaper, including 20% postconsumer waste

Table of Contents

I. Introduction . . . 1

II. Hydrogen Production . . . 15

II.0 Hydrogen Production Sub-Program Overview . . . 17

II.A Distributed BDL Production . . . 25

II.A.1 Pacific Northwest National Laboratory: Biomass-Derived Liquids Distributed (Aqueous Phase) Reforming . . . 25

II.A.2 National Renewable Energy Laboratory: Distributed Bio-Oil Reforming . . . 29

II.A.3 Argonne National Laboratory: Distributed Reforming of Renewable Liquids Using Oxygen Transport Membranes (OTMs) . . . 33

II.B Biomass Gasification . . . 37

II.B.1 United Technologies Research Center: A Novel Slurry-Based Biomass Reforming Process . . . 37

II.B.2 Gas Technology Institute: One Step Biomass Gas Reforming-Shift Separation Membrane Reactor . . . 42

II.C Separations . . . 46

II.C.1 Arizona State University: Zeolite Membrane Reactor for Water-Gas Shift Reaction for Hydrogen Production . . . 46

II.C.2 Media and Process Technology Inc.: Development of Hydrogen Selective Membranes/Modules as Reactors/Separators for Distributed Hydrogen Production . . . 53

II.C.3 Pall Corporation: High Performance Palladium-Based Membrane for Hydrogen Separation and Purification . . . 58

II.D Hydrogen From Coal . . . 62

II.D.1 Praxair, Inc.: Advanced Hydrogen Transport Membranes for Coal Gasification . . . 62

II.D.2 Eltron Research & Development Inc.: Scale Up of Hydrogen Transport Membranes for IGCC and FutureGen Plants . . . 66

II.D.3 United Technologies Research Center: Advanced Palladium Membrane Scale Up for Hydrogen Separation . . . 69

II.D.4 Worcester Polytechnic Institute: Composite Pd and Alloy Porous Stainless Steel Membranes for Hydrogen Production and Process Intensification . . . 73

II.E Electrolysis . . . 79

II.E.1 Giner Electrochemical Systems, LLC: PEM Electrolyzer Incorporating an Advanced Low-Cost Membrane . . . 79

II.E.2 Proton Energy Systems: High Performance, Low Cost Hydrogen Generation from Renewable Energy . . . 83

II.E.3 Avalence, LLC: High-Capacity, High Pressure Electrolysis System with Renewable Power Sources . . . 87

II.E.4 National Renewable Energy Laboratory: Renewable Electrolysis Integrated System Development and Testing . . . 92

II.E.5 H2Pump, LLC: Process Intensification of Hydrogen Unit Operations Using an Electrochemical Device . . . 95

II.E.6 National Renewable Energy Laboratory: Hour-by-Hour Cost Modeling of Optimized Central Wind-Based Water Electrolysis Production . . . 98

II.F Hi-Temp Thermochemical . . . 102

II.F.1 Science Applications International Corporation: Solar High-Temperature Water Splitting Cycle with Quantum Boost . . . 102

II.F.2 Argonne National Laboratory: Membrane/Electrolyzer Development in the Cu-Cl Thermochemical Cycle . . . 108

II.F.3 Sandia National Laboratories: Solar Hydrogen Production with a Metal Oxide-Based Thermochemical Cycle . . . 112

II. Hydrogen Production (Continued)

II.F Hi-Temp Thermochemical (Continued)

II.F.4 University of Colorado: Solar-Thermal ALD Ferrite-Based Water Splitting Cycle . . . 118

II.G Photoelectrochemical . . . 123

II.G.1 Stanford University: Nano-Architectures for 3rd Generation PEC Devices: A Study of MoS_2, Fundamental Investigations and Applied Research . . . 123

II.G.2 National Renewable Energy Laboratory: Semiconductor Materials for Photoelectrolysis . . . 129

II.G.3 Lawrence Livermore National Laboratory: Characterization and Optimization of Photoelectrode Surfaces for Solar-to-Chemical Fuel Conversion . . . 134

II.G.4 University of Nevada, Las Vegas: Characterization of Materials for Photoelectrochemical (PEC) Hydrogen Production . . . 140

II.G.5 MVSystems, Incorporated: Photoelectrochemical Hydrogen Production . . . 146

II.G.6 Midwest Optoelectronics, LLC: Critical Research for Cost-Effective Photoelectrochemical Production of Hydrogen . . . 150

II.G.7 University of Arkansas, Little Rock: PEC-Based Hydrogen Production with Self-Cleaning Solar Concentrator . . . 154

II.G.8 University of Nevada, Reno: Photoelectrochemical Hydrogen Generation from Water Using $TiSi_2$–TiO_2 Nanotube Core-Shell Structure . . . 160

II.G.9 University of South Dakota: USD Catalysis Group for Alternative Energy . . . 164

II.G.10 University of Nebraska, Omaha: Novel Photocatalytic Metal Oxides . . . 170

II.G.11 University of Nevada, Reno: Solar Thermal Hydrogen Production . . . 173

II.G.12 National Renewable Energy Laboratory: Photoelectrochemical Materials: Theory and Modeling . . . 176

II.G.13 Synkera Technologies Inc.: Nanotube Array Photoelectrochemical Hydrogen Production . . . 181

II.H Biological . . . 185

II.H.1 National Renewable Energy Laboratory: Biological Systems for Hydrogen Photoproduction . . . 185

II.H.2 National Renewable Energy Laboratory: Fermentation and Electrohydrogenic Approaches to Hydrogen Production . . . 190

II.H.3 J. Craig Venter Institute: Hydrogen from Water in a Novel Recombinant Oxygen-Tolerant Cyanobacterial System . . . 195

II.H.4 University of California, Berkeley: Maximizing Light Utilization Efficiency and Hydrogen Production in Microalgal Cultures . . . 200

II.H.5 Purdue University: Purdue Hydrogen Systems Laboratory: Hydrogen Production . . . 203

II.I Production Analysis . . . 207

II.I.1 National Renewable Energy Laboratory: H2A Production Model Updates . . . 207

II.J Production . . . 211

II.J.1 Giner Electrochemical Systems, LLC: Unitized Design for Home Refueling Appliance for Hydrogen Generation to 5,000 psi . . . 211

II.J.2 Proton Energy Systems: Hydrogen by Wire - Home Fueling System . . . 215

II.J.3 University of Texas, Arlington: Value-Added Hydrogen Generation with CO_2 Conversion . . . 218

II.J.4 Physical Optics Corporation: Photochemical System for Hydrogen Generation . . . 225

II.K Basic Energy Sciences . . . 228

II.K.1 Stanford University: SISGR: Using *In vitro* Maturation and Cell-free Evolution to Understand [Fe-Fe]hydrogenase Activation and Active Site Constraints . . . 228

II.K.2 University of Washington: Phototrophic metabolism of organic compounds generates excess reducing power that can be redirected to produce H_2 as a biofuel . . . 232

II.K.3 University of Georgia: Fundamental Studies of Recombinant Hydrogenases . . . 234

II.K.4 University of Washington: Prospects for Hydrogen Production from Formate by *Methanococcus maripaludis* . . . 237

II.K.5 National Renewable Energy Laboratory: Structural, Functional, and Integration Studies of Solar-Driven, Bio-Hybrid, H_2-Producing Systems . . . 240

II.K.6 University of Oklahoma: Genes Needed For H_2 Production by Sulfate Reducing Bacteria . . . 242

II. Hydrogen Production (Continued)

II.K Basic Energy Sciences (Continued)

II.K.7 University of Missouri: Genetics and Molecular Biology of Hydrogen Metabolism in Sulfate-reducing Bacteria . . . 245

II.K.8 National Renewable Energy Laboratory: Regulation of H_2 and CO_2 Metabolism: Factors Involved in Partitioning of Photosynthetic Reductant in Green Algae . . . 248

II.K.9 University of Rochester: Excited State Dynamics in Semiconductor Quantum Dots . . . 250

II.K.10 Princeton University: Theoretical Research Program on Bio-inspired Inorganic Hydrogen Generating Catalysts and Electrodes . . . 253

II.K.11 Virginia Polytechnic Institute and State University: Photoinitiated Electron Collection in Mixed-Metal Supramolecular Complexes: Development of Photocatalysts for Hydrogen Production . . . 257

II.K.12 University of California, Santa Cruz: Hydrogen Generation Using Integrated Photovoltaic and Photoelectrochemical Cells . . . 260

II.K.13 University of Pennsylvania: Modular Designed Protein Constructions for Solar Generated H_2 from Water . . . 264

II.K.14 University of Alabama, Tuscaloosa: Protein-Templated Synthesis and Assembly of Nanostructuctures for Hydrogen Production . . . 267

II.K.15 Brookhaven National Laboratory: Catalyzed Water Oxidation by Solar Irradiation of Band-Gap-Narrowed Semiconductors . . . 270

II.K.16 Stony Brook University: Quantum theory of Semiconductor-Photo-Catalysis and Solar Water Splitting . . . 273

II.K.17 University of Arizona: Formation and Characterization of Semiconductor Nanorod/Oxide Nanoparticle Hybrid Materials: Toward Vectoral Electron Transport in Hybrid Materials . . . 275

II.K.18 University of Wyoming: Combinatorial methods for the Improvement of Semiconductor Metal Oxide Photoelectrodes . . . 279

II.K.19 Pennsylvania State University: A Hybrid Biological-Organic Half-Cell for Generating Dihydrogen . . . 281

II.K.20 California Institute of Technology: Fundamental Optical, Electrical, and Photoelectrochemical Properties of Catalyst-Bound Silicon Microwire Array Photocathodes for Sunlight-Driven Hydrogen Production . . . 283

II.K.21 National Renewable Energy Laboratory: New Directions for Efficient Solar Water Splitting Based on Two Photosystems and Singlet Fission Chromophores . . . 286

III. Hydrogen Delivery . . . 291

III.0 Hydrogen Delivery Sub-Program Overview . . . 293

III.1 Sandia National Laboratories: Hydrogen Embrittlement of Structural Steels . . . 299

III.2 Argonne National Laboratory: Hydrogen Delivery Infrastructure Analysis . . . 303

III.3 Oak Ridge National Laboratory: Vessel Design and Fabrication Technology for Stationary High-Pressure Hydrogen Storage . . . 307

III.4 National Renewable Energy Laboratory: Hydrogen Delivery Analysis . . . 312

III.5 Lawrence Livermore National Laboratory: Demonstration of Full-Scale Glass Fiber Composite Pressure Vessels for Inexpensive Delivery of Cold Hydrogen . . . 316

III.6 Savannah River National Laboratory: Fiber Reinforced Composite Pipeline . . . 322

III.7 Lincoln Composites, Inc.: Development of High Pressure Hydrogen Storage Tank for Storage and Gaseous Truck Delivery . . . 326

III.8 Concepts NREC: Development of a Centrifugal Hydrogen Pipeline Gas Compressor . . . 331

III.9 Mohawk Innovative Technologies, Inc.: Oil-Free Centrifugal Hydrogen Compression Technology Demonstration . . . 338

III.10 FuelCell Energy, Inc.: Electrochemical Hydrogen Compressor . . . 342

III.11 Praxair, Inc.: Advanced Hydrogen Liquefaction Process . . . 345

III.12 University of Illinois at Urbana-Champaign: A Combined Materials Science/Mechanics Approach to the Study of Hydrogen Embrittlement of Pipeline Steels . . . 349

III.13 Oak Ridge National Laboratory: Composite Technology for Hydrogen Pipelines . . . 354

III.0 Hydrogen Delivery (Continued)

III.14 Lawrence Livermore National Laboratory: Thermodynamic Modeling of Rapid Low Loss Cryogenic Hydrogen Refueling . . . 358
III.15 Oak Ridge National Laboratory: Integrity of Steel Welds in High-Pressure Hydrogen Environment . . . 362
III.16 Argonne National Laboratory: Hydrogen Pipeline Compressors . . . 367
III.17 Prometheus Energy: Active Magnetic Regenerative Liquefier . . . 371

IV. Hydrogen Storage . . . 375

IV.0 Hydrogen Storage Sub-Program Overview . . . 377

IV.A Metal Hydride . . . 383
IV.A.1 Savannah River National Laboratory: Amide and Combined Amide/Borohydride Investigations . . . 383
IV.A.2 Northwestern University: Efficient Discovery of Novel Multicomponent Mixtures for Hydrogen Storage: A Combined Computational/Experimental Approach . . . 388
IV.A.3 University of Hawaii: Fundamental Studies of Advanced High-Capacity, Reversible Metal Hydrides . . . 393
IV.A.4 Ohio State University: Lightweight Metal Hydrides for Hydrogen Storage . . . 398
IV.A.5 University of Illinois at Urbana-Champaign: Reversible Hydrogen Storage Materials - Structure, Chemistry, and Electronic Structure . . . 403
IV.A.6 Brookhaven National Laboratory: Aluminum Hydride . . . 409
IV.A.7 Savannah River National Laboratory: Electrochemical Reversible Formation of Alane . . . 413
IV.A.8 Sandia National Laboratories: Tunable Thermodynamics and Kinetics for Hydrogen Storage: Nanoparticle Synthesis Using Ordered Polymer Templates . . . 416
IV.A.9 National Institute of Standards and Technology: Neutron Characterization in Support of the DOE Hydrogen Storage Sub-Program . . . 420

IV.B Chemical Hydrogen Storage . . . 425
IV.B.1 University of Oregon: Hydrogen Storage by Novel CBN Heterocycle Materials . . . 425
IV.B.2 Los Alamos National Laboratory: Fluid Phase Chemical Hydrogen Storage Materials . . . 429

IV.C Hydrogen Sorption . . . 432
IV.C.1 Texas A&M University: A Biomimetic Approach to Metal-Organic Frameworks with High H_2 Uptake . . . 432
IV.C.2 University of California, Los Angeles: A Joint Theory and Experimental Project in the Synthesis and Testing of Porous COFs/ZIFs for On-Board Vehicular Hydrogen Storage . . . 439
IV.C.3 University of Missouri: Multiply Surface-Functionalized Nanoporous Carbon for Vehicular Hydrogen Storage . . . 444
IV.C.4 Northwestern University: New Carbon-Based Porous Materials with Increased Heats of Adsorption for Hydrogen Storage . . . 450
IV.C.5 Argonne National Laboratory: Hydrogen Storage through Nanostructured Porous Organic Polymers (POPs) . . . 455
IV.C.6 Pennsylvania State University: Hydrogen Trapping through Designer Hydrogen Spillover Molecules with Reversible Temperature and Pressure-Induced Switching . . . 459
IV.C.7 National Renewable Energy Laboratory: Weak Chemisorption Validation . . . 464
IV.C.8 State University of New York, Syracuse: Nanostructured Activated Carbon for Hydrogen Storage . . . 470
IV.C.9 University of California, Los Angeles: Hydrogen Storage in Metal-Organic Frameworks . . . 474

IV.D H2 Storage Engineering Center of Excellence . . . 479
IV.D.1 Savannah River National Laboratory: Hydrogen Storage Engineering Center of Excellence . . . 479
IV.D.2 National Renewable Energy Laboratory: System Design, Analysis, Modeling, and Media Engineering Properties for Hydrogen Energy Storage . . . 486
IV.D.3 Los Alamos National Laboratory: Chemical Hydride Rate Modeling, Validation, and System Demonstration . . . 491

IV. Hydrogen Storage (Continued)

IV.D H2 Storage Engineering Center of Excellence (Continued)

IV.D.4 Jet Propulsion Laboratory: Key Technologies, Thermal Management, and Prototype Testing for Advanced Solid-State Hydrogen Storage Systems . . . 494

IV.D.5 Savannah River National Laboratory: SRNL Technical Work Scope for the Hydrogen Storage Engineering Center of Excellence: Design and Testing of Metal Hydride and Adsorbent Systems . . . 498

IV.D.6 Pacific Northwest National Laboratory: Systems Engineering of Chemical Hydride, Pressure Vessel, and Balance of Plant for On-Board Hydrogen Storage . . . 503

IV.D.7 United Technologies Research Center: Advancement of Systems Designs and Key Engineering Technologies for Materials-Based Hydrogen Storage . . . 511

IV.D.8 General Motors Company: Optimization of Heat Exchangers and System Simulation of On-Board Storage Systems Designs . . . 517

IV.D.9 Ford Motor Company: Ford/BASF-SE/UM Activities in Support of the Hydrogen Storage Engineering Center of Excellence . . . 522

IV.D.10 Oregon State University: Microscale Enhancement of Heat and Mass Transfer for Hydrogen Energy Storage . . . 530

IV.D.11 Lincoln Composites, Inc.: Development of Improved Composite Pressure Vessels for Hydrogen Storage . . . 534

IV.E Storage Testing, Safety and Analysis . . . 538

IV.E.1 United Technologies Research Center: Quantifying and Addressing the DOE Material Reactivity Requirements with Analysis and Testing of Hydrogen Storage Materials and Systems . . . 538

IV.E.2 Argonne National Laboratory: System Level Analysis of Hydrogen Storage Options . . . 544

IV.E.3 TIAX, LLC: Cost Analyses of Hydrogen Storage Materials and On-Board Systems . . . 550

IV.E.4 Sandia National Laboratories: Analysis of H_2 Storage Needs for Early Market Non-Motive Fuel Cell Applications . . . 554

IV.E.5 National Renewable Energy Laboratory: Analysis of Storage Needs for Early Motive Fuel Cell Markets . . . 558

IV.E.6 Southwest Research Institute®: Standardized Testing Program for Solid-State Hydrogen Storage Technologies . . . 562

IV.E.7 H2 Technology Consulting LLC: Best Practices for Characterizing Engineering Properties of Hydrogen Storage Materials . . . 567

IV.E.8 Hydrogen Education Foundation: Administration of H-Prize for Hydrogen Storage . . . 571

IV.F Tanks . . . 576

IV.F.1 Oak Ridge National Laboratory: High Strength Carbon Fibers . . . 576

IV.F.2 Oak Ridge National Laboratory: Lifecycle Verification of Polymeric Storage Liners . . . 581

IV.G Cross-Cutting . . . 585

IV.G.1 Purdue University: Purdue Hydrogen Systems Laboratory: Hydrogen Storage . . . 585

IV.G.2 University of Nevada, Las Vegas: HGMS: Glasses and Nanocomposites for Hydrogen Storage . . . 590

IV.G.3 Delaware State University: Hydrogen Storage Materials for Fuel Cell-Powered Vehicles . . . 593

V. Fuel Cells . . . 597

V.0 Fuel Cells Sub-Program Overview . . . 599

V.A Analysis/Characterization . . . 605

V.A.1 National Renewable Energy Laboratory: Analysis of Laboratory Fuel Cell Technology Status – Voltage Degradation . . . 605

V.A.2 Directed Technologies, Inc.: Mass-Production Cost Estimation for Automotive Fuel Cell Systems . . . 609

V.A.3 Argonne National Laboratory: Drive-Cycle Performance of Automotive Fuel Cell Systems . . . 614

V.A.4 Oak Ridge National Laboratory: Characterization of Fuel Cell Materials . . . 621

V. Fuel Cells (Continued)

V.A Analysis/Characterization (Continued)

V.A.5 National Institute of Standards and Technology: Neutron Imaging Study of the Water Transport in Operating Fuel Cells . . . 626
V.A.6 Los Alamos National Laboratory: Technical Assistance to Developers . . . 631
V.A.7 National Renewable Energy Laboratory: Enlarging the Potential Market for Stationary Fuel Cells Through System Design Optimization . . . 634
V.A.8 Argonne National Laboratory: Fuel Cell Testing at the Argonne Fuel Cell Test Facility: A Comparison of U.S. and EU Test Protocols . . . 637

V.B Impurities . . . 640
V.B.1 National Renewable Energy Laboratory: Effect of System Contaminants on PEMFC Performance and Durability . . . 640
V.B.2 University of Connecticut: The Effects of Impurities on Fuel Cell Performance and Durability . . . 644
V.B.3 Hawaii Natural Energy Institute: The Effect of Airborne Contaminants on Fuel Cell Performance and Durability . . . 649
V.B.4 Clemson University: Effects of Impurities on Fuel Cell Performance and Durability . . . 654
V.B.5 Los Alamos National Laboratory: Effects of Fuel and Air Impurities on PEM Fuel Cell Performance . . . 659

V.C Membranes . . . 662
V.C.1 3M Company: Membranes and MEAs for Dry, Hot Operating Conditions . . . 662
V.C.2 Giner Electrochemical Systems, LLC: Dimensionally Stable Membranes (DSMs) . . . 667
V.C.3 Giner Electrochemical Systems, LLC: Dimensionally Stable High Performance Membrane (SBIR Phase III) . . . 671
V.C.4 Case Western Reserve University: Poly(p-Phenylene Sulfonic Acids): PEMs with Frozen-In Free Volume . . . 675
V.C.5 Vanderbilt University: NanoCapillary Network Proton Conducting Membranes for High Temperature Hydrogen/Air Fuel Cells . . . 680
V.C.6 Colorado School of Mines: Novel Approaches to Immobilized Heteropoly Acid (HPA) Systems for High Temperature, Low Relative Humidity Polymer-Type Membranes . . . 685
V.C.7 FuelCell Energy, Inc.: High-Temperature Membrane with Humidification-Independent Cluster Structure . . . 690
V.C.8 Ion Power Inc.: Corrugated Membrane Fuel Cell Structures . . . 694
V.C.9 University of Central Florida: Lead Research and Development Activity for DOE's High Temperature, Low Relative Humidity Membrane Program . . . 696

V.D Catalysts . . . 699
V.D.1 3M Company: Advanced Cathode Catalysts and Supports for PEM Fuel Cells . . . 699
V.D.2 UTC Power: Highly Dispersed Alloy Catalyst for Durability . . . 708
V.D.3 3M Company: Durable Catalysts for Fuel Cell Protection During Transient Conditions . . . 714
V.D.4 National Renewable Energy Laboratory: Extended, Continuous Pt Nanostructures in Thick, Dispersed Electrodes . . . 719
V.D.5 Argonne National Laboratory: Nanosegregated Cathode Catalysts with Ultra-Low Platinum Loading . . . 723
V.D.6 Brookhaven National Laboratory: Contiguous Platinum Monolayer Oxygen Reduction Electrocatalysts on High-Stability Low-Cost Supports . . . 729
V.D.7 Los Alamos National Laboratory: The Science and Engineering of Durable Ultralow PGM Catalysts . . . 734
V.D.8 Lawrence Berkeley National Laboratory: Molecular-Scale, Three-Dimensional Non-Platinum Group Metal Electrodes for Catalysis of Fuel Cell Reactions . . . 738
V.D.9 National Renewable Energy Laboratory: Tungsten Oxide and Heteropoly Acid Based System for Ultra-High Activity and Stability of Pt Catalysts in PEM Fuel Cell Cathodes . . . 745
V.D.10 Illinois Institute of Technology: Synthesis and Characterization of Mixed-Conducting Corrosion Resistant Oxide Supports . . . 752

V. Fuel Cells (Continued)

V.D Catalysts (Continued)

V.D.11 Northeastern University: Development of Novel Non-PGM Electrocatalysts for Proton Exchange Membrane Fuel Cell Applications . . . 756
V.D.12 General Motors Company: High-Activity Dealloyed Catalysts . . . 760
V.D.13 University of South Carolina: Development of Ultra-Low Platinum Alloy Cathode Catalyst for PEM Fuel Cells . . . 764
V.D.14 Los Alamos National Laboratory: Engineered Nano-Scale Ceramic Supports for PEM Fuel Cells . . . 770
V.D.15 Pacific Northwest National Laboratory: Development of Alternative and Durable High Performance Cathode Supports for PEM Fuel Cells . . . 777

V.E Degradation Studies . . . 783
V.E.1 Argonne National Laboratory: Polymer Electrolyte Fuel Cell Lifetime Limitations: The Role of Electrocatalyst Degradation . . . 783
V.E.2 Los Alamos National Laboratory: Durability Improvements Through Degradation Mechanism Studies . . . 788
V.E.3 E. I. du Pont de Nemours and Company: Analysis of Durability of MEAs in Automotive PEMFC Applications . . . 794
V.E.4 Ballard Power Systems: Development of Micro-Structural Mitigation Strategies for PEM Fuel Cells: Morphological Simulations and Experimental Approaches . . . 797
V.E.5 Nuvera Fuel Cells, Inc.: Durability of Low Platinum Fuel Cells Operating at High Power Density . . . 802
V.E.6 UTC Power: Improved Accelerated Stress Tests Based on FCV Data . . . 806
V.E.7 Los Alamos National Laboratory: Accelerated Testing Validation . . . 810

V.F Transport Studies . . . 814
V.F.1 CFD Research Corporation: Water Transport in PEM Fuel Cells: Advanced Modeling, Material Selection, Testing, and Design Optimization . . . 814
V.F.2 Sandia National Laboratories: Development and Validation of a Two-Phase, Three-Dimensional Model for PEM Fuel Cells . . . 818
V.F.3 Giner Electrochemical Systems, LLC: Transport in PEMFC Stacks . . . 822
V.F.4 General Motors Company: Investigation of Micro- and Macro-Scale Transport Processes for Improved Fuel Cell Performance . . . 827
V.F.5 Plug Power Inc.: Air-Cooled Stack Freeze Tolerance . . . 833
V.F.6 Nuvera Fuel Cells, Inc.: Transport Studies Enabling Efficiency Optimization of Cost-Competitive Fuel Cell Stacks . . . 837
V.F.7 Lawrence Berkeley National Laboratory: Fuel Cell Fundamentals at Low and Subzero Temperatures . . . 841

V.G Portable Power . . . 846
V.G.1 National Renewable Energy Laboratory: Novel Approach to Advanced Direct Methanol Fuel Cell (DMFC) Anode Catalysts . . . 846
V.G.2 Arkema Inc.: Novel Materials for High Efficiency Direct Methanol Fuel Cells . . . 850
V.G.3 University of North Florida: New MEA Materials for Improved Direct Methanol Fuel Cell (DMFC) Performance, Durability, and Cost . . . 854
V.G.4 Los Alamos National Laboratory: Advanced Materials and Concepts for Portable Power Fuel Cells . . . 858

V.H Hardware . . . 863
V.H.1 TreadStone Technologies, Inc.: Low-Cost PEM Fuel Cell Metal Bipolar Plates . . . 863
V.H.2 Argonne National Laboratory: Metallic Bipolar Plates with Composite Coatings . . . 867

V.I Innovative Concepts . . . 872
V.I.1 Los Alamos National Laboratory: Resonance-Stabilized Anion Exchange Polymer Electrolytes . . . 872

V. Fuel Cells (Continued)

V.I Innovative Concepts (Continued)

V.I.2 Versa Power Systems: Advanced Materials for RSOFC Dual Mode Operation with Low Degradation . . . 876

V.J Balance of Plant . . . 879

V.J.1 W.L. Gore & Associates, Inc.: Materials and Modules for Low-Cost, High-Performance Fuel Cell Humidifiers . . . 879

V.J.2 Honeywell Aerospace: Development of Thermal and Water Management System for PEM Fuel Cell . . . 883

V.J.3 Dynalene Inc.: Large Scale Testing, Demonstration and Commercialization of the Nanoparticle-Based Fuel Cell Coolant . . . 886

V.K Distributed Energy . . . 890

V.K.1 Acumentrics Corporation: Development of a Low-Cost 3-10 kW Tubular SOFC Power System . . . 890

V.K.2 Intelligent Energy: Development and Demonstration of a New Generation High Efficiency 10 kW Stationary PEM Fuel Cell System . . . 894

V.K.3 IdaTech, LLC: Research & Development for Off-Road Fuel Cell Applications . . . 899

V.K.4 InnovaTek, Inc.: Power Generation from an Integrated Biomass Reformer and Solid Oxide Fuel Cell . . . 901

V.L Cross-Cutting . . . 905

V.L.1 University of Akron: Development of Kilowatt-Scale Coal Fuel Cell Technology . . . 905

V.L.2 University of Southern Mississippi: Alternative Fuel Cell Membranes for Energy Independence . . . 909

V.L.3 Rolls Royce Fuel Cell Systems Inc.: Extended Durability Testing of an External Fuel Processor for SOFCs . . . 914

V.L.4 University of South Carolina: Hydrogen Fuel Cell Development in Columbia (SC) . . . 918

V.L.5 Stark State College of Technology: Fuel Cell Balance of Plant Reliability Testbed . . . 923

V.L.6 Colorado School of Mines: Biomass Fuel Cell Systems . . . 927

V.L.7 Dynalene Inc.: Fuel Cell Coolant Optimization and Scale Up . . . 933

V.L.8 Kettering University: 21st Century Renewable Fuels, Energy, and Materials Initiative . . . 937

V.L.9 University of Connecticut Global Fuel Cell Center: Improving Reliability and Durability of Effi cient and Clean Energy Systems . . . 943

V.L.10 Stark State College of Technology: Solid Oxide Fuel Cell Systems Print Verification Line (PVL) Pilot Line . . . 950

VI. Manufacturing R&D . . . 953

VI.0 Manufacturing R&D Sub-Program Overview . . . 955

VI.1 National Renewable Energy Laboratory: Fuel Cell Membrane Electrode Assembly Manufacturing R&D . . . 959

VI.2 Ballard Material Products, Inc.: Reduction in Fabrication Costs of Gas Diffusion Layers . . . 963

VI.3 UltraCell Corporation: Modular, High-Volume Fuel Cell Leak-Test Suite and Process . . . 968

VI.4 W.L. Gore & Associates, Inc.: Manufacturing of Low-Cost, Durable Membrane Electrode Assemblies Engineered for Rapid Conditioning . . . 971

VI.5 Rensselaer Polytechnic Institute: Adaptive Process Controls and Ultrasonics for High-Temperature PEM MEA Manufacture . . . 977

VI.6 National Institute of Standards and Technology: Cause-and-Effect: Flow Field Plate Manufacturing Variability and its Impact on Performance . . . 983

VI.7 BASF Fuel Cell, Inc.: High Speed, Low Cost Fabrication of Gas Diffusion Electrodes for Membrane Electrode Assemblies . . . 987

VI.8 Pacific Northwest National Laboratory: MEA Manufacturing R&D Using Drop-On-Demand Technology . . . 991

VI.9 Quantum Fuel Systems Technologies Worldwide, Inc.: Development of Advanced Manufacturing Technologies for Low Cost Hydrogen Storage Vessels . . . 995

VI. Manufacturing R&D (Continued)

VI.10 National Institute of Standards and Technology: Non-Contact Sensor Evaluation for Bipolar Plate Manufacturing Process Control and Smart Assembly of Fuel Cell Stacks 999
VI.11 National Institute of Standards and Technology: Optical Scatterfield Metrology for Online Catalyst Coating Inspection of PEM (Fuel Cell) Soft Goods. 1003

VII. Technology Validation 1009
VII.0 Technology Validation Sub-Program Overview 1011
VII.1 National Renewable Energy Laboratory: Controlled Hydrogen Fleet and Infrastructure Analysis 1017
VII.2 General Motors Company: Hydrogen Vehicle and Infrastructure Demonstration and Validation 1023
VII.3 Mercedes-Benz Research & Development North America, Inc.: Hydrogen to the Highways – Controlled Hydrogen Fleet and Infrastructure Demonstration and Validation Project 1027
VII.4 Air Products and Chemicals, Inc.: Validation of an Integrated Hydrogen Energy Station 1032
VII.5 National Renewable Energy Laboratory: Technology Validation: Fuel Cell Bus Evaluations . . . 1036
VII.6 Air Products and Chemicals, Inc.: California Hydrogen Infrastructure Project. 1040
VII.7 Hawaii Natural Energy Institute: Hawaii Hydrogen Power Park 1043
VII.8 University of Central Florida: Florida Hydrogen Initiative (FHI). 1046
VII.9 California State University, Los Angeles: Sustainable Hydrogen Fueling Station, California State University, Los Angeles. 1050

VIII. Safety, Codes & Standards 1053
VIII.0 Safety, Codes & Standards Sub-Program Overview 1055
VIII.1 Sandia National Laboratories: Hydrogen Safety, Codes and Standards R&D – Release Behavior 1061
VIII.2 Sandia National Laboratories: Risk-Informed Safety Requirements for H2 Codes and Standards Development 1067
VIII.3 National Renewable Energy Laboratory: Component Standard Research and Development. . . . 1072
VIII.4 Sandia National Laboratories: Hydrogen Materials and Components Compatibility 1075
VIII.5 Sandia National Laboratories: Component Testing for Industrial Trucks and Early Market Applications 1079
VIII.6 National Renewable Energy Laboratory: National Codes and Standards Coordination. 1083
VIII.7 National Renewable Energy Laboratory: Codes and Standards Outreach for Emerging Fuel Cell Technologies. 1087
VIII.8 Los Alamos National Laboratory: Leak Detection and H_2 Sensor Development for Hydrogen Applications 1090
VIII.9 Los Alamos National Laboratory: Hydrogen Fuel Quality Research and Development 1096
VIII.10 Pacific Northwest National Laboratory: Hydrogen Safety Panel 1100
VIII.11 Pacific Northwest National Laboratory: Hydrogen Safety Knowledge Tools 1104
VIII.12 Pacific Northwest National Laboratory: Hydrogen Emergency Response Training for First Responders. 1107
VIII.13 Lawrence Livermore National Laboratory: Hydrogen Safety Training for Researchers and Technical Personnel 1110
VIII.14 Intelligent Optical Systems, Inc.: Hydrogen Leak Detection System Development 1114
VIII.15 Sandia National Laboratories: International Energy Agency Hydrogen Implementing Agreement Task 19 Hydrogen Safety. 1118
VIII.16 Oak Ridge National Laboratory: MEMS Hydrogen Sensor for Leak Detection. 1122

IX. Education. 1125
IX.0 Education Sub-Program Overview 1127
IX.1 Argonne National Laboratory: Employment Impacts of Early Markets for Hydrogen and Fuel Cell Technologies 1131

IX. Education (Continued)

IX.2 Connecticut Center for Advanced Technology, Inc.: State and Local Government Partnership . . . 1135
IX.3 Clean Energy States Alliance: Hydrogen Education State Partnership Program . . . 1139
IX.4 South Carolina Hydrogen and Fuel Cell Alliance: Development of Hydrogen Education Programs for Government Officials . . . 1142
IX.5 Commonwealth of Virginia: VA-MD-DC Hydrogen Education for Decision Makers . . . 1144
IX.6 Technology Transition Corporation: H2L3: Hydrogen Learning for Local Leaders . . . 1148
IX.7 Ohio Fuel Cell Coalition: Raising H_2 and Fuel Cell Awareness in Ohio . . . 1153
IX.8 Carolina Tractor & Equipment Co. Inc.: Dedicated to The Continued Education, Training and Demonstration of PEM Fuel Cell-Powered Lift Trucks In Real-World Applications . . . 1155
IX.9 California State University, Los Angeles: Hydrogen and Fuel Cell Education at California State University, Los Angeles. . . . 1158
IX.10 Humboldt State University Sponsored Programs Foundation: Hydrogen Energy in Engineering Education (H_2E^3) . . . 1161
IX.11 Michigan Technological University: Hydrogen Education Curriculum Path at Michigan Technological University . . . 1166
IX.12 University of Central Florida: Hydrogen and Fuel Cell Technology Education Program (HFCT) . . . 1170
IX.13 University of North Dakota: Development of a Renewable Hydrogen Production and Fuel Cell Education Program . . . 1173
IX.14 National Energy Education Development Project: H_2 Educate! Hydrogen Education for Middle Schools . . . 1177
IX.15 University of California, Berkeley: Hydrogen Technology and Energy Curriculum (HyTEC) . . . 1180

X. Market Transformation . . . 1185
X.0 Market Transformation Activities . . . 1187
X.1 Sandia National Laboratories: Fuel Cell Mobile Lighting . . . 1191
X.2 Longitude 122 West, Inc.: Economic Analysis of Bulk Hydrogen Storage for Renewable Utility Applications . . . 1196
X.3 Hawaii Natural Energy Institute: Hydrogen Energy Systems as a Grid Management Tool. . . . 1200
X.4 Pacific Northwest National Laboratory: Fuel Cell Combined Heat and Power Industrial Demonstration . . . 1202
X.5 National Renewable Energy Laboratory: Green Communities . . . 1205
X.6 National Renewable Energy Laboratory: Direct Methanol Fuel Cell Material Handling Equipment Demonstration . . . 1209
X.7 South Carolina Hydrogen and Fuel Cell Alliance: Landfill Gas-to-Hydrogen . . . 1212
X.8 Lawrence Livermore National Laboratory: Incorporation of Two Ford H_2 ICE Buses into the Shuttle Bus Fleet . . . 1214
X.9 Sandia National Laboratories: PEM Fuel Cell Systems for Commercial Airplane Systems Power . . . 1217
X.10 Pacific Northwest National Laboratory: Assessment of Solid Oxide Fuel Cell Power System for Greener Commercial Aircraft . . . 1220

XI. Systems Analysis. . . . 1223
XI.0 Systems Analysis Sub-Program Overview . . . 1225
XI.1 Oak Ridge National Laboratory: Non-Automotive Fuel Cells: Market Assessment and Analysis of Impacts of Policies . . . 1231
XI.2 National Renewable Energy Laboratory: Hydrogen Infrastructure Market Readiness Analysis . . . 1236
XI.3 National Renewable Energy Laboratory: Infrastructure Analysis of Early Market Transition of Fuel Cell Vehicles . . . 1240

XI. Systems Analysis (Continued)

XI.4 Sandia National Laboratories: Analysis of the Effects of Developing New Energy Infrastructures . . . 1244
XI.5 National Renewable Energy Laboratory: Cost and GHG Implications of Hydrogen for Energy Storage . . . 1248
XI.6 Argonne National Laboratory: Emissions Analysis of Electricity Storage with Hydrogen . . . 1251
XI.7 National Renewable Energy Laboratory: NEMS-H2: Hydrogen's Role in Climate Mitigation and Oil Dependence Reduction. . . . 1254
XI.8 Argonne National Laboratory: GREET Model Development and Life-Cycle Analysis Applications . . . 1257
XI.9 National Renewable Energy Laboratory: Macro-System Model . . . 1261
XI.10 National Renewable Energy Laboratory: HyDRA: Hydrogen Demand and Resource Analysis Tool . . . 1265
XI.11 Lawrence Livermore National Laboratory: Energy Informatics: Support for Decision Makers through Energy, Carbon and Water Analysis . . . 1270
XI.12 Argonne National Laboratory: Fuel Quality Effects on Stationary Fuel Cell Systems. . . . 1275

XII. American Recovery and Reinvestment Act Activities . . . 1279
XII.0 American Recovery and Reinvestment Act Activities . . . 1281
XII.1 MTI Micro Fuel Cells Inc.: Commercialization of 1 Watt Consumer Electronics Power Pack . . . 1287
XII.2 Jadoo Power, Inc.: Jadoo Power Fuel Cell Demonstration . . . 1291
XII.3 University of North Florida: Advanced Direct Methanol Fuel Cell for Mobile Computing. . . . 1294
XII.4 Delphi Automotive Systems, LLC: Solid Oxide Fuel Cell Diesel Auxiliary Power Unit Demonstration . . . 1297
XII.5 Sprint Nextel: Demonstrating Economic and Operational Viability of 72-Hour Hydrogen PEM Fuel Cell Systems to Support Emergency Communications on the Sprint Nextel Network . . . 1300
XII.6 ReliOn Inc.: PEM Fuel Cell Systems Providing Backup Power to Commercial Cellular Towers and an Electric Utility Communications Network . . . 1304
XII.7 National Renewable Energy Laboratory: Analysis Results for ARRA Projects: Enabling Fuel Cell Market Transformation . . . 1308
XII.8 Nuvera Fuel Cells, Inc.: H-E-B Grocery Total Power Solution for Fuel Cell-Powered Material Handling Equipment . . . 1312
XII.9 FedEx Freight: Fuel Cell-Powered Lift Truck FedEx Freight Fleet Deployment. . . . 1316
XII.10 Sysco of Houston: Fuel Cell-Powered Lift Truck Sysco Houston Fleet Deployment . . . 1319
XII.11 GENCO Infrastructure Solutions: GENCO Fuel Cell-Powered Lift Truck Fleet Deployment. . . . 1322
XII.12 Plug Power Inc.: Highly Efficient, 5 kW CHP Fuel Cells Demonstrating Durability and Economic Value in Residential and Light Commercial Applications . . . 1325
XII.13 Plug Power Inc.: Accelerating Acceptance of Fuel Cell Backup Power Systems. . . . 1328

XIII. Small Business Innovation Research . . . 1331
XIII.0 Small Business Innovation Research (SBIR) Hydrogen Program New Projects Awarded in FY 2011. . . . 1333

Phase I Projects . . . 1333
XIII.1 Ultra-Lightweight High Pressure Hydrogen Fuel Tanks Reinforced with Carbon Nanotubes. . . . 1333
XIII.2 Alternative Fiber Evaluation and Optimization of Filament Winding Processing. . . . 1334
XIII.3 New High Performance Water Vapor Membranes to Improve Fuel Cell Balance of Plant Efficiency and Lower Costs . . . 1334
XIII.4 Fuel Cell Range Extender for Battery-Powered Airport Ground Support Equipment . . . 1334

XIV. Acronyms, Abbreviations and Definitions. . . . 1335

XV. Primary Contacts Index. . . . 1353

XVI. Hydrogen Program Contacts 1357

XVII. Project Listings by State 1361

XVIII. Project Listings by Organization 1385

I. INTRODUCTION

I.0 Introduction

The Department of Energy Hydrogen and Fuel Cells Program (the Program) conducts comprehensive efforts to enable the widespread commercialization of hydrogen and fuel cell technologies in diverse sectors of the economy. The Program is coordinated across the Department of Energy (DOE or the Department), including activities in the offices of Energy Efficiency and Renewable Energy (EERE), Science (SC), Nuclear Energy (NE), and Fossil Energy (FE), and it is aligned with DOE's strategic vision and goals–its efforts will help to secure U.S. leadership in clean energy technologies and advance U.S. economic competitiveness and scientific innovation.

With emphasis on applications that will most effectively strengthen our nation's energy security and improve our stewardship of the environment, the Program engages in research, development, and demonstration (RD&D) of critical improvements in the technologies, as well as diverse activities to overcome economic and institutional obstacles to commercialization. The Program addresses the full range of challenges facing the development and deployment of hydrogen and fuel cell technologies by integrating basic and applied research, technology development and demonstration, and other supporting activities.

In Fiscal Year (FY) 2011, Congress appropriated approximately $150 million for the DOE Hydrogen and Fuel Cells Program.[1] The Program is organized into distinct sub-programs focused on specific areas of RD&D, as well as other activities to address non-technical challenges. More detailed discussions of Program activities and plans can be found in EERE's *Fuel Cell Technologies Program Multi-Year RD&D Plan*; FE's *Hydrogen from Coal RD&D Plan*; and SC's *Basic Research Needs for the Hydrogen Economy*. All of these documents are available at www.hydrogen.energy.gov/program_plans.html.

In the past year, the Program made substantial progress toward its goals and objectives. Highlights of the Program's accomplishments are summarized below. More detail can be found in the sub-program chapters of this report.

PROGRAM PROGRESS AND ACCOMPLISHMENTS

Fuel Cells

The Fuel Cells sub-program continued to make progress toward meeting targets through advancements achieved in both catalysis and membrane R&D. Technological advances in several component areas led to significant improvements in performance and durability, with reduced cost. In FY 2011, the catalyst utilization in polymer electrolyte membrane (PEM) automotive fuel cell systems improved from 2.8 kW/g in 2008 to 5.6 kW/g in 2011 (as measured in units of kW per gram of platinum group metal).[2] This exceeds the Program's 5.5 kW/g target set for FY 2011and has contributed to reducing the high-volume manufacturing cost of fuel cells. This cost is currently projected to be $49/kW (assuming manufacturing volumes of 500,000 units/year), which represents a more than 30% cost reduction since FY 2008.[3]

[1] This includes $98 million for the Fuel Cell Technologies Program within the Office of Energy Efficiency and Renewable Energy, $38 million for hydrogen and fuel cell–related research in the Basic Energy Sciences program within the Office of Science, $12 million for hydrogen production R&D in the Office of Fossil Energy and $2.8 million for hydrogen production R&D in the Office of Nuclear Energy.

[2] See Report V.D.1., "Advanced Cathode Catalysts and Supports for PEM Fuel Cells," in the Fuel Cells chapter of this volume.

[3] DOE Hydrogen and Fuel Cells Program Record #11012, http://hydrogen.energy.gov/pdfs/11012_fuel_cell_system_cost.pdf.

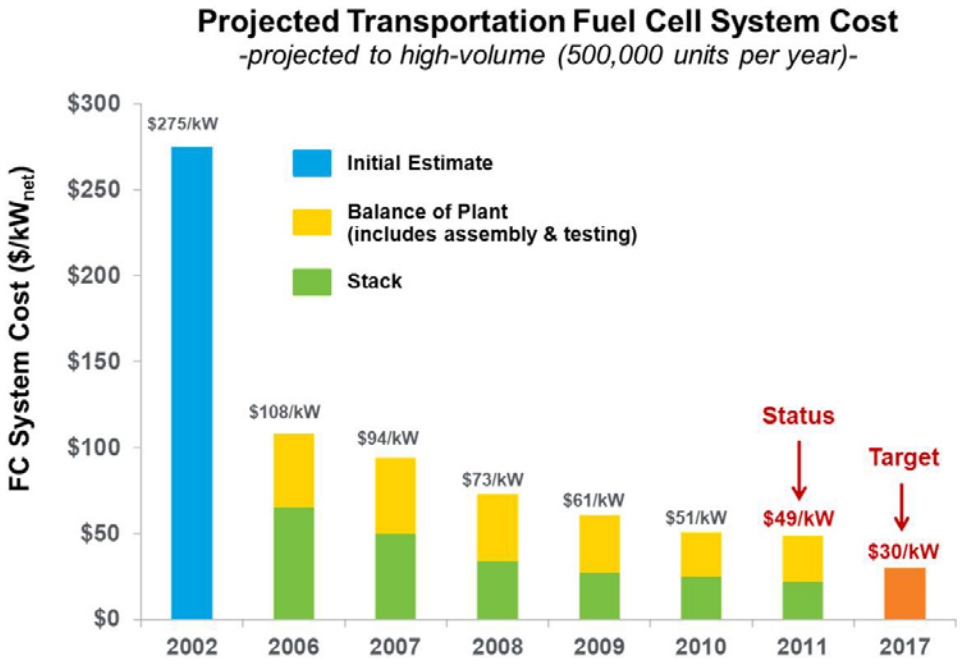


FIGURE 1. Current Modeled Cost of an 80-kW Automotive Fuel Cell System Based on Projection to High-Volume Manufacturing (500,000 Units/Year)[4]

FY 2011 also saw the development of a perfluoroimide acid membrane, for higher-temperature operation (120°C) that meets most DOE targets, including most membrane resistance targets. Progress over the last year enabled a 40% reduction in membrane resistance at 120°C and 40 kPa water vapor, with an additional 13% reduction still required to meet the 2017 DOE target of 0.02 ohm cm^2.[5] Efforts in FY 2011 also led to the development of solid-oxide fuel cell (SOFC) systems for remote power and micro-combined heat and power applications with increased durability, enabling more than 12,000 hours of operation of an SOFC system.[6] This advance represents a significant step toward production of an SOFC system for widespread commercialization and builds on the performance improvements demonstrated in FY 2010.

Hydrogen Production

The FY 2011 Hydrogen Production sub-program continued to focus on developing technologies that enable the long-term viability of hydrogen as an energy carrier for a diverse range of end-use applications, including stationary power, backup power, specialty vehicles, transportation, and portable power. In FY 2011, the sub-program continued to make progress in several key areas, including autothermal reforming of bio-derived liquids, electrolysis, photoelectrochemical (PEC) hydrogen production, and biological hydrogen production.

In the area of bio-derived liquids, increases in process efficiency from 47% to 62% and increases in yield from 7.4 g to 10.1 g hydrogen per 100 g bio-oil were achieved for bench-scale tests of catalytic steam reforming of pyrolysis oil as a result of improvements in catalyst performance through the use of a 0.5% Pt/Al_2O_3 BASF catalyst.[7] Progress in the area of electrolysis included demonstration of a PEM electrolyzer incorporating advanced low-cost membrane electrode assemblies (MEAs) with chemically etched supports.[8] Due to improvements in MEAs and flow fields and reductions in catalyst loading, the projected capital cost of electrolyzer stacks was reduced to less than $400/kW, representing a cost reduction of more than 10% relative

[4] DOE Hydrogen and Fuel Cells Program Record #11012, http://hydrogen.energy.gov/pdfs/11012_fuel_cell_system_cost.pdf.

[5] See Report V.C.1, "Membranes and MEAs for Dry, Hot Operating Conditions," in the Fuel Cells chapter of this volume.

[6] "V.L.1. Development of a Low Cost 3-10kW Tubular SOFC Power System," in the Fuel Cells chapter of this volume.

[7] See Report II.A.2, "Distributed Bio-Oil Reforming," in the Hydrogen Production chapter of this volume.

[8] See Report II.E.1, "PEM Electrolyzer Incorporating an Advanced Low-Cost Membrane," in the Hydrogen Production chapter of this volume.

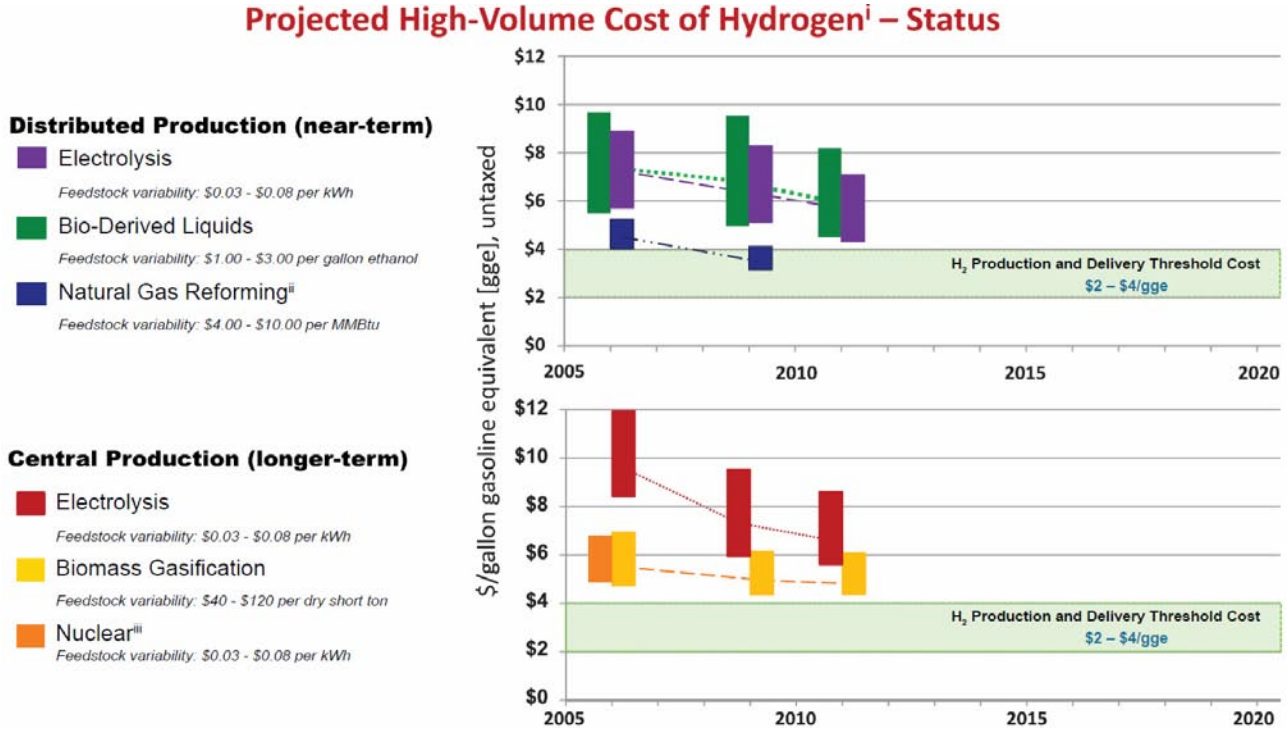


FIGURE 2. Hydrogen Production and Delivery Cost Status. Significant progress has already been made in several hydrogen production pathways. The Hydrogen Threshold Cost represents the cost at which hydrogen fuel cell electric vehicles are projected to become competitive on a cost-per-mile basis with competing vehicles (gasoline hybrid-electric vehicles) in 2020. Notes: (i) Costs shown include all delivery and dispensing costs, but do not include taxes. A cost of $1.80 for forecourt compression, storage, and dispensing is included for distributed technologies, and $2.60 is included as the total cost of delivery (including transportation, compression, storage, and dispensing) for centralized technologies. All delivery costs are based on the Hydrogen Pathways Technical Report (NREL, 2009). Projections of distributed costs assume station capacities of 1,500 kg/day, with 500 stations built per year. Projections of centralized production costs assume capacities of ≥50,000 kg/day. Cost ranges for each pathway are shown in 2007 dollars, based on high-volume projections from H2A analyses, reflecting variability in major feedstock pricing and a bounded range for capital cost estimates. (ii) DOE funding of natural gas reforming projects was completed in 2009 due to achievement of the threshold cost. Incremental improvements will continue to be made by industry. (iii) High-temperature electrolysis activities are ongoing under the Next Generation Nuclear Plant Program.

to 2010 projections.[9] In the area of PEC hydrogen production, the Program demonstrated exceptional stability in quantum-confined MoS_2 nanoparticle photocatalysts with bandgaps optimized at 1.8 eV, showing stable operation over 10,000 voltage cycles of accelerated lifetime testing. In complementary work, novel macroporous scaffolds, which are transparent and conductive, were developed as electrode substrates to support PEC photocatalyst materials, such as MoS_2, in high-efficiency devices.[10] Finally, in the area of biological hydrogen production, the gene mutation responsible for the decrease in chlorophyll antenna size, previously observed to increase light utilization efficiency to 15% from 3% in wild-type organisms, was identified and characterized. Efforts to identify the mutation responsible for light utilization of up to 25% are ongoing, along with R&D to optimize hydrogen production in microalgal cultures.[11]

[9] See Report II.E.1, "PEM Electrolyzer Incorporating an Advanced Low-Cost Membrane," and Report II.E.2, "High Performance, Low Cost Hydrogen Generation from Renewable Energy," in the Hydrogen Production chapter of this volume.

[10] See Report II.G.1, "Nano-Architectures for 3rd Generation PEC Devices: A Study of MoS2, Fundamental Investigations and Applied Research," in the Hydrogen Production chapter of this volume.

[11] See Report II.H.4, "Maximizing Light Utilization Efficiency and Hydrogen Production in Microalgal Cultures," in the Hydrogen Production chapter of this volume.

Hydrogen Delivery

Hydrogen Delivery sub-program activities continued to focus on reducing the cost and increasing the energy efficiency of hydrogen delivery, to enable the widespread use of hydrogen as an energy carrier. In FY 2011, the sub-program continued to make progress in all major areas, including the following examples. A design trade study for a 5,000 pounds per square inch (psi) vessel was completed; this showed a projected 33% increase in capacity at 15°C and ~10% reduction in capital cost (on a per kilogram of transported hydrogen basis).[12] In addition, burst testing on fiber reinforced polymer pipe with 40% through-wall flaws was also completed and demonstrated a 3x margin above the rated pressure for the pipe. Researchers also showed that industry-standard compression fittings will meet Department of Transportation requirements for joint leakage between pipe segments.[13] FY 2011 also saw the development of a two-stage electrochemical hydrogen compressor that achieved 420 bar of compression.[14]

Hydrogen Storage

In FY 2011, the Hydrogen Storage sub-program's materials-discovery projects developed a number of new materials and improved the performance of other materials. Key accomplishments in FY 2011 include: characterization of high surface area sorbents with specific surface areas greater than 6,000 m^2 per gram and excess hydrogen sorption capacities exceeding 8% by weight at 77 K;[15] demonstration of cycling of $Mg(BH_4)_2$ at hydrogen capacities greater than 12% by weight under high-temperature and high-pressure conditions;[16] demonstration of alane slurry with 60% capacity by weight and with kinetics exceeding non-slurried alane;[17] and determination that thermal stability of ionic liquids is dominated by choice of cation. The Hydrogen Storage Engineering Center of Excellence (HSECoE) completed a baseline assessment of storage system models for reversible metal hydrides, cryo-sorbents, and both solid- and liquid-phase off-board regenerable chemical hydrogen storage material systems. The HSECoE assessed these models against the full set of DOE onboard storage targets. Also in FY 2011, the sub-program increased its emphasis on reducing the cost of compressed hydrogen gas storage tanks by initiating new efforts on low-cost, high-strength carbon fiber. Inexpensive storage vessels for compressed hydrogen gas are considered the most likely near-term hydrogen storage solution for the initial commercialization of fuel cell electric vehicles (FCEVs), as well as for other early market applications.

Manufacturing R&D

FY 2011 saw a number of advances in manufacturing of fuel cells and storage systems. Ballard made several improvements that resulted in significant improvement in quality yields and a gas diffusion layer cost reduction of over 60%, while increasing manufacturing capacity nearly four-fold.[18] For example, they improved thickness and basis weight uniformity of gas diffusion layers by adding mass flow meters to the "Many-at-a-Time" coating equipment. W.L. Gore reduced membrane thickness, eliminated membrane backers, reduced scrap with better coating process, and eliminated finishing operations such as electrode and membrane edge trim (Gore previously demonstrated, using their cost model, that a new three-layer membrane electrode assembly process has the potential to reduce membrane electrode assembly cost by 25%).[19] And Quantum saved 17.4 kg of composite from the baseline (all fiber wound) high-pressure hydrogen storage vessel (a 23% savings).[20]

[12] See Report III.7, "Development of High Pressure Hydrogen Storage Tank for Storage and Gaseous Truck Delivery," in the Hydrogen Delivery chapter of this volume.

[13] See Report III.6, "Fiber Reinforced Composite Pipeline," in the Hydrogen Delivery chapter of this volume.

[14] See Report III.10, "Electrochemical Hydrogen Compressor," in the Hydrogen Delivery chapter of this volume.

[15] See Report IV.C.4, "New Carbon-Based Porous Materials with Increased Heats of Adsorption for Hydrogen Storage," and Report IV.C.1, "A Biomimetic Approach to Metal-Organic Frameworks with High H2 Uptake," in the Hydrogen Storage chapter of this volume.

[16] See Report IV.A.3, "Fundamental Studies of Advanced High-Capacity, Reversible Metal Hydrides," in the Hydrogen Storage chapter of this volume.

[17] See Report IV.A.6, "Aluminum Hydride," in the Hydrogen Storage chapter of this volume.

[18] See Report VI.2, "Reduction in Fabrication Costs of Gas Diffusion Layers," in the Manufacturing R&D chapter of this volume.

[19] See Report VI.4, "Manufacturing of Low-Cost, Durable Membrane Electrode Assemblies Engineered for Rapid Conditioning," in the Manufacturing R&D chapter of this volume.

[20] See Report VI.9, "Development of Advanced Manufacturing Technologies for Low Cost Hydrogen Storage Vessels," in the Manufacturing R&D chapter of this volume.

In conjunction with the National Renewable Energy Laboratory, the Manufacturing R&D sub-program also held a workshop to prioritize challenges and barriers to manufacturing hydrogen and fuel cell systems and components and to identify R&D activities that government can support to overcome barriers.

Basic Research

The Basic Energy Sciences program within the DOE Office of Science supports fundamental scientific research addressing critical challenges related to hydrogen storage, hydrogen production, and fuel cells. This basic research complements the applied R&D projects supported by other offices in the Program.

Progress in any one area of basic science is likely to spill over to other areas and bring advances on more than one front. The subjects of basic research most relevant to the Program's key technologies are:

- *Hydrogen Storage:* Nanostructured materials; theory, modeling, and simulation to predict behavior and design new materials; and novel analytical and characterization tools.
- *Fuel Cells:* Nanostructured catalysts and materials; integrated nanoscale architectures; novel fuel cell membranes; innovative synthetic techniques; theory, modeling, and simulation of catalytic pathways, membranes, and fuel cells; and novel characterization techniques.
- *Hydrogen Production:* Longer-term approaches such as photobiological and direct photochemical production of hydrogen.

By maintaining close coordination between basic science research and applied R&D, the Program ensures that discoveries and related conceptual breakthroughs achieved in basic research programs will provide a foundation for the innovative design of materials and processes that will lead to improvements in the performance, cost, and reliability of fuel cell technologies and technologies for hydrogen production and storage. This is accomplished in various ways–for example, through monthly coordination meetings between the participating offices within DOE, and at the researcher level by having joint meetings with participation from principal investigators who are funded by the participating offices.

Technology Validation

The Technology Validation sub-program demonstrates, tests, and validates hydrogen and fuel cell technologies and uses the results to provide feedback to the Program's R&D activities. The Technology Validation sub-program has been focused on conducting learning demonstrations that emphasize co-development and integration of hydrogen infrastructure with FCEVs to permit industry to assess progress toward technology readiness. As the vehicle and infrastructure demonstrations in are coming to a close, the sub-program is increasing its focus on other areas, such as combined hydrogen, heat, and power (tri-generation or CHHP) as well as stationary power applications.

The Program's vehicle and infrastructure demonstrations in the National Hydrogen Learning Demonstration have deployed 155 FCEVs and 24 hydrogen fueling stations to date. Over the course of the demonstration, the vehicles have traveled more than 3 million miles. Vehicles and infrastructure in these demonstrations have validated the status of several key technologies in integrated systems under real-world operating conditions, including vehicular fuel cell efficiency of up to 59%, projected durability of 2,500 hours (nearly 75,000 miles) with less than 10% degradation, a range of more than 250 miles between refueling (the Program has validated one vehicle–not in the Learning Demonstration–that is capable of traveling more than 430 miles on a single fill), and refueling times of approximately five minutes for 4 kg of hydrogen. The Technology Validation sub-program also collected and analyzed data from over 45,000 fuel cell fork truck lift refuelings at Defense Logistics Agency sites.

A major accomplishment in FY 2011 was demonstrating the world's first fuel cell energy station that produces electric power and hydrogen from wastewater treatment gas.[21] The energy station provides hydrogen as a transportation fuel to the public and electric power to the wastewater treatment facility; it also has the potential to operate in "trigeneration" (or combined-heat-hydrogen-and-power) mode, if waste heat from the fuel cell is captured and provided to the facility. The energy station began operation at the Orange County Sanitation District's facility in Fountain Valley, California, sending hydrogen to a fueling station for FCEVs

[21] See Report VII.4, "Validation of an Integrated Hydrogen Energy Station," in the Technology Validation chapter of this volume.

first in February 2011. The combined co-production efficiency of hydrogen and power was 54% at the energy station, exceeding DOE's target of 50% for FY 2011.

Safety, Codes and Standards

The Safety, Codes and Standards sub-program continued to support critical R&D to establish key requirements and address knowledge gaps in safety, codes and standards. Building on work from previous years, the sub-program continued to facilitate collaborative activities among relevant stakeholders in an effort to harmonize domestic and international regulations, codes, and standards. Significant accomplishments include the development of *National Fire Protection Association (NFPA) 2: Hydrogen Technologies Code*, which consolidates all building codes and requirements for hydrogen installations in the United States into a single document. NFPA 2 also includes a qualitative risk assessment introduced by DOE for separation distances for hydrogen bulk storage. Another achievement was the development of an international hydrogen fuel specification standard (ISO TC 197 WG 12), which was led by the United States and ensures performance and durability of PEM fuel cells. In addition, a final draft of a Global Technical Regulation for hydrogen-fueled vehicles has been submitted to the United Nations Economic Commission for Europe. The sub-program also took a leadership role in international coordination by co-organizing the International Conference on Hydrogen Safety in California with Sandia National Laboratories.

Education

The Education sub-program facilitates hydrogen and fuel cell demonstrations and supports commercialization by providing technically accurate and objective information to key target audiences both directly and indirectly involved in the use of hydrogen and fuel cells. FY 2010 appropriations supported these activities.

To support early market outreach, the Education sub-program implemented several end-user, state and local government, and safety and code official education activities. Accomplishments include the development of a model to analyze the economic impacts on early market deployment of fuel cells in primary power, backup power, and material-handling applications through a user-friendly spreadsheet tool used to calculate impacts on production, installation, and utilization at a regional or national level. The tool will be available for beta testing at the end of 2011. Videos were also developed to be aired on TV and posted online to YouTube and other sites, including the development of two segments for MotorWeek entitled "Hydrogen and Fuel Cells Emerging Markets" and "Vehicles and Infrastructure Update." In FY 2011, the sub-program also organized, publicized, and facilitated 10 webinars on hydrogen and fuel cell topics of interest to state policymakers, local leaders, and end users, including: "The Top 5 Fuel Cell States: Why Local Policies Mean Green Growth," "Hydrogen and First Responders," "Financing Fuel Cell Installations," and others.

Systems Analysis and Integration

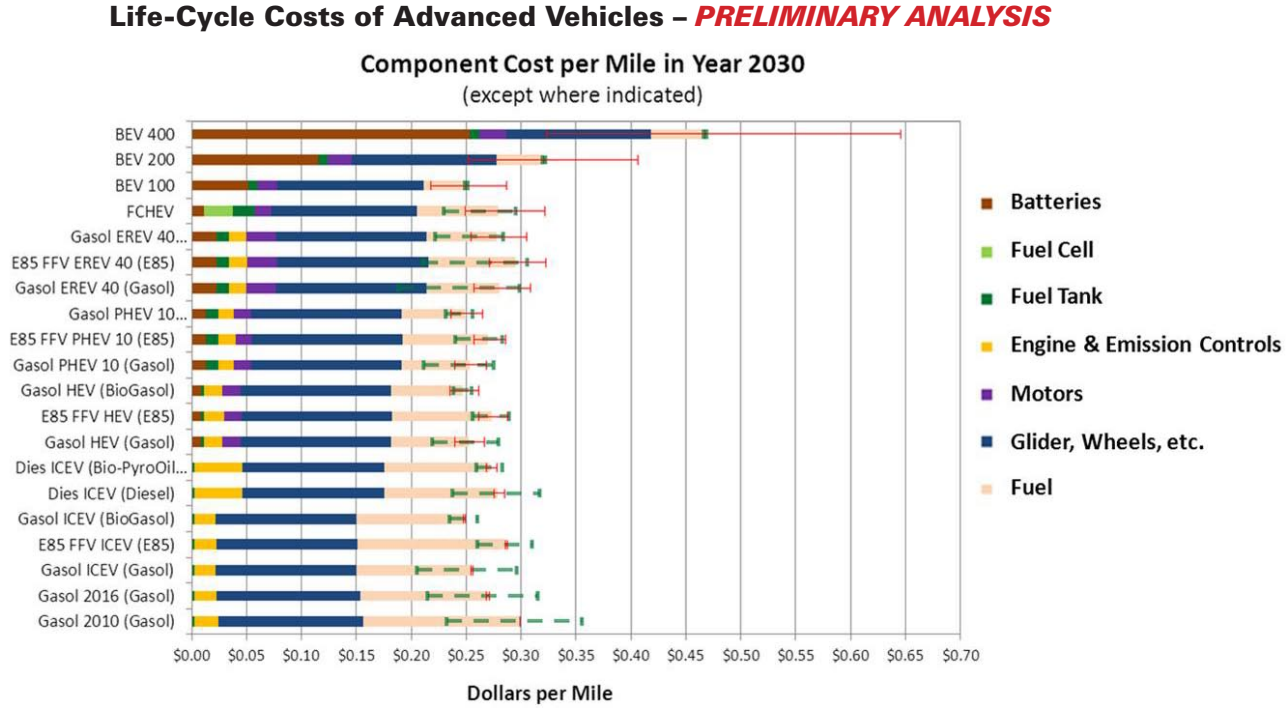
Systems Analysis supports decision-making by providing a greater understanding of technology gaps, options, and risks. Analysis is also conducted to assess cross-cutting issues, such as integration with the electrical sector and use of renewable fuels. Particular emphasis is given to assessing stationary fuel cell applications, fuel quality impacts on fuel cell performance, resource needs, and potential infrastructure options.

Accomplishments in FY 2011 include the development of a hydrogen cost threshold in the range of $2-$4/gasoline gallon equivalent (in 2007 dollars) to assist DOE in focusing and prioritizing R&D options. The cost threshold represents the cost at which hydrogen FCEVs are projected to become competitive on a cost-per-mile basis with the competing fuel/vehicle combination–gasoline in hybrid-electric vehicles. A graphical representation of the hydrogen threshold, relative to current projected production and delivery costs is shown in Figure 2 in the "Hydrogen Production" section of this Introduction. Also in FY 2011, a comparison of cost estimates for non-automotive fuel cells showed a 50% or greater reduction in costs between 2008 and 2010.[22] Despite these large cost reductions, the analysis concluded that the continuation or enhancement of current policies such as the investment tax credit and government procurement combined with progress by industry will be necessary to establish a viable domestic fuel cell industry. In addition,

[22] Greene, David et al. "Status and Outlook for the U.S. Non-Automotive Fuel Cell Industry: Impacts of Government Policies and Assessment of Future Opportunities" Oak Ridge National Laboratory, May 2011.

infrastructure analysis revealed that synergies between fuel cells for stationary power generation and transportation could be realized in the early phases of market adoption of hydrogen for light-duty fuel cell vehicles. Model results that indicate hydrogen produced from combined hydrogen, heat, and power systems could result in smaller stations with higher capital utilization and lower hydrogen cost; this hydrogen could supplement hydrogen supplied from distributed natural gas–based steam methane reforming, particularly for the early years of FCEV penetration scenarios where hydrogen demand and station sizes are initially small.

In FY 2011, the Systems Analysis sub-program collaborated with counterparts in the DOE Vehicle Technologies Program and the DOE Biomass Program to prepare and release an EERE-wide request for information (RFI) on the total cost of operation of future light-duty vehicles, including petroleum fuels and alternative fuels pathways, based on three levels of technology success. Comments from the public were requested on the projected cost reductions and the financial analysis approach used in estimating the cost per mile for each pathway. Responses to the RFI are due on December 16, 2011. Figure 3 shows the preliminary EERE estimates of costs per mile that were released for comments under the RFI.



BEV – battery electric vehicle; FCHEV – fuel cell hybrid electric vehicle; Gasol – gasoline; EREV – extended range electric vehicle; FFV – flexible fuel vehicle; PHEV – plug-in hybrid electric vehicle; HEV – hybrid electric vehicle; ICEV – internal combustion engine vehicle

FIGURE 3. Preliminary EERE Estimates of the Life-Cycle Costs of Several Advanced Vehicle Pathways. Error bars illustrate the sensitivity of costs per mile to fuel prices (green) and vehicle technology success (red).

Market Transformation

To ensure that the benefits of its efforts are realized in the marketplace, the Program continued to facilitate the growth of early markets for fuel cells used in portable, stationary, and specialty-vehicle applications. Market transformation activities are helping to reduce the cost of fuel cells by enabling economies of scale through early market deployments and by overcoming a number of barriers, including the lack of operating performance data, the need for applicable codes and standards, and the need for user acceptance. FY 2011 activities primarily involved project startup and kickoff from FY 2010 appropriations. The Market Transformation sub-program is currently focused on building on past successes in material handling equipment (e.g., lift trucks) and emergency backup power applications, which received support from Recovery Act

funding. These Recovery Act projects are highly leveraged with an average of over half the funds or cost share provided by partner resources, and they are providing valuable data on the status of the technologies in real-world operation that will be used to validate the benefits and potential needs for further R&D. (For more information on Recovery Act projects, see "American Recovery and Reinvestment Act Projects" under the "Other Program Activities" section of this Introduction.) The Market Transformation sub-program is seeking to expand on the success of these activities by exploring other potential and emerging applications for market viability.

Specific accomplishments in FY 2011 include a joint effort by the Department of Defense's (DOD's) U.S. Army Corps of Engineers and the Program, which was conducted under the Memorandum of Understanding (MOU) signed between DOE and DOD in July 2010. The project consists of installation of emergency backup power fuel cells at eight DOD locations across the country. Additionally, demonstration and testing of fuel cell-powered mobile lighting prototypes were conducted at the National Aeronautic and Space Administration Kennedy Space Center and the San Francisco International Airport, among others. Activities conducted at entertainment industry events such as the 2011 Golden Globe Awards and 2011 Grammy Awards ceremonies had the added value of exposing fuel cell technology to the public.[23] Also in FY 2011, a total of 22 hydrogen-powered buses were deployed at federal facilities and national labs across the country to demonstrate hydrogen buses and infrastructure with widespread public visibility. The 12-passenger buses are used for special events, campus tours, new employee orientations, and as part of shuttle bus fleets. The buses were shown to thousands of attendees at special events throughout the year. During FY 2011, the technical viability of using landfill gas (LFG) as a cost-effective source of hydrogen production was demonstrated at BMW's assembly plant in South Carolina. Once fully implemented, this project will represent a "first-of-its-kind" LFG-to-hydrogen production project in the nation, and serve as a model for future adoption of renewable biogas as a feedstock for hydrogen production.[24] Finally, in FY 2011, the substantial effects of market transformation became apparent in the material-handling equipment sector when successful DOE projects led industry to plan deployments of more than 3,000 fuel cell forklifts with no additional DOE funding.[25]

OTHER PROGRAM ACTIVITIES

American Recovery and Reinvestment Act Projects

The American Recovery and Reinvestment Act (Recovery Act or ARRA) has been a critical component of the Program's efforts to accelerate the commercialization and deployment of fuel cells in the market. With approximately $41.9 million from the Recovery Act and $54 million in cost-share funding from industry participants–for a total of nearly $96 million–this funding is supporting the deployment of up to 1,000 fuel cell systems in emergency backup power, material handling, and combined heat and power applications. Twelve projects were competitively selected to develop and deploy a variety of fuel cell technologies including polymer electrolyte, solid oxide, and direct-methanol fuel cells in stationary, portable, and specialty vehicle applications. In FY 2011, ARRA investments led to 610 additional fuel cell deployments into the market. As of the end of September 2011, more than 460 fuel cell lift trucks and more than 370 fuel cell backup-power systems for cellular communications towers and stationary backup-power systems had been deployed, and over 80% of the ARRA project funds had been spent by the projects. A total of 46 direct jobs have been created or retained as a result of the Fuel Cell Technologies ARRA projects (if supply chain and other indirect jobs are included, the total jobs created or retained is estimated to be more than 180 from these ARRA projects alone). These projects are helping to build a competitive domestic supply base, reduce costs, and demonstrate the economic and performance benefits of fuel cells as a competitive option for stationary, portable, and specialty vehicle applications.

Tracking the Commercialization of Technologies

One indicator of the robustness and innovative vitality of an R&D program is the number of patents applied for and granted, and the number of technologies commercialized. The Program continued to assess the commercial benefits of Program funding by tracking the commercial products and technologies developed with the support of the EERE Fuel Cell Technologies Program. DOE-funded R&D has resulted in more

[23] See Report X.1, "Fuel Cell Mobile Lighting," in the Market Transformation chapter of this volume.
[24] See Report X.7, "Landfill Gas-to-Hydrogen," in the Market Transformation chapter of this volume.
[25] DOE Hydrogen and Fuel Cells Program Record #11017, http://hydrogen.energy.gov/program_records.html.

than 310 patents and more than 60 emerging technologies while 30 hydrogen and fuel cell technologies have entered the market.[26] DOE also tracks the impact of its funding in terms of industry revenues and investment–for example, $70 million in funding for specific projects that were tracked was found to have led to more than $200 million in industry revenues and investment.

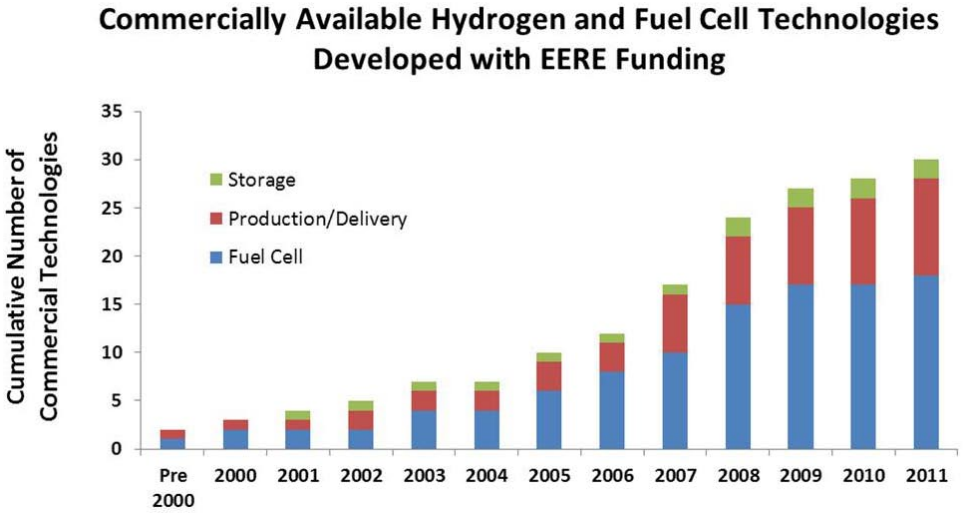


FIGURE 4. Cumulative Number of Commercially Available Technologies Developed with Funding from the Fuel Cell Technologies Program

INTERNATIONAL ACTIVITIES

International Partnership for Hydrogen and Fuel Cells in the Economy

The United States is a founding member of the International Partnership for Hydrogen and Fuel Cells in the Economy[27] (IPHE), which includes 17 member countries (Australia, Brazil, Canada, China, France, Germany, Iceland, India, Italy, Japan, New Zealand, Norway, the Republic of Korea, the Russian Federation, South Africa, the United Kingdom, and the United States) and the European Commission. The IPHE is a forum for governments to work together to advance worldwide progress in hydrogen and fuel cell technologies. IPHE also offers a mechanism for international R&D managers, researchers, and policymakers to share program strategies. In FY 2011, the 15th Steering Committee Meeting was held in Vancouver, Canada, on May 13 and 14. An IPHE Roundtable with Stakeholders is planned for November 17 in Berlin, along with the 16th Steering Committee Meeting also in Berlin on November 18th.

International Energy Agency

The United States is also involved in international collaboration on hydrogen and fuel cell R&D through the International Energy Agency (IEA) implementing agreements; the United States is a member of both the Advanced Fuel Cells Implementing Agreement[28] (AFCIA) and the Hydrogen Implementing Agreement[29] (HIA). These agreements provide a mechanism for member countries to share the results of research, development, and analysis activities. The AFCIA currently includes six annexes: Molten Carbonate Fuel Cells, Polymer Electrolyte Fuel Cells, Solid Oxide Fuel Cells, Fuel Cells for Stationary Applications, Fuel Cells for Transportation, and Fuel Cells for Portable Power. The participating countries are Australia, Austria, Belgium, Canada, Denmark,

[26] *Pathways to Commercial Success: Technologies and Products Supported by The Fuel Cell Technologies Program*, Pacific Northwest National Laboratory, September 2011, http://www1.eere.energy.gov/hydrogenandfuelcells/pdfs/pathways_2011.pdf.
[27] http://www.iphe.net/
[28] www.ieafuelcell.com
[29] www.ieahia.org

Finland, France, Germany, Italy, Japan, South Korea, the Netherlands, Mexico, Sweden, Switzerland, Turkey, and the United States. The IEA HIA is focused on RD&D and analysis of hydrogen technologies. It includes 11 tasks: Hydrogen Safety, Biohydrogen, Fundamental and Applied Hydrogen Storage Materials Development, Small-Scale Reformers for On-site Hydrogen Supply, Wind Energy and Hydrogen Integration, High-Temperature Production of Hydrogen, Advanced Materials for Hydrogen from Water Photolysis, Near-Market Routes to Hydrogen by Co-Gasification with Biomass, Large Scale Hydrogen Delivery Infrastructure, Distributed and Community Hydrogen for Remote Communities, and Global Hydrogen Systems Analysis. The United States participates in all of these tasks. Members of the HIA are Australia, Canada, Denmark, the European Commission, Finland, France, Germany, Greece, Iceland, Italy, Japan, South Korea, Lithuania, the Netherlands, New Zealand, Norway, Spain, Sweden, Switzerland, Turkey, United Nations Industrial Development Organization-International Center for Hydrogen Energy Technologies, and the United States.

EXTERNAL COORDINATION, INPUT, AND ASSESSMENT

Hydrogen and Fuel Cell Technical Advisory Committee (HTAC)

As required by the Energy Policy Act of 2005, HTAC was created in 2006 to advise the Secretary of Energy on issues related to the development of hydrogen and fuel cell technologies and to provide recommendations regarding DOE's programs, plans, and activities, as well as on the safety, economic, and environmental issues related to hydrogen and fuel cells. HTAC members include representatives of domestic industry, academia, professional societies, government agencies, financial organizations, and environmental groups, as well as experts in the area of hydrogen safety.

HTAC met three times in FY 2011. In March 2011, HTAC released its third annual report, which summarizes hydrogen and fuel cell technology domestic and international progress in RD&D projects; commercialization activities; and policy initiatives. More information about HTAC, including its annual reports, is available at: http://www.hydrogen.energy.gov/advisory_htac.html

Federal Agency Coordination—the Interagency Task Force and the Interagency Working Group

The Hydrogen and Fuel Cell Interagency Task Force (ITF), mandated by the Energy Policy Act of 2005, includes senior representatives from federal agencies supporting hydrogen and fuel cell activities, with the DOE/EERE serving as chair. Recently efforts by the ITF focus on facilitating federal deployment of hydrogen and fuel cells in emerging technology applications such as stationary power and specialty vehicles. In June 2011, DOE hosted the first ITF meeting of this administration. During this meeting, Deputy Secretary of Energy Daniel Poneman announced a DOE and DOD collaboration with the Army Corps of Engineers to deploy emergency backup power units for critical loads at eight DOD locations across the nation. In addition, ITF members provided feedback on the recently drafted *Interagency Action Plan*.

The Hydrogen and Fuel Cell Interagency Working Group (IWG), co-chaired by DOE and the White House Office of Science and Technology Policy, continues to meet monthly to share expertise and information about ongoing programs and results, to coordinate the activities of federal entities involved in hydrogen and fuel cell RD&D, and to ensure efficient use of taxpayer resources.

DOD-DOE MOU Workshops

DOD and DOE entered into an MOU for the purpose of coordinating efforts to enhance national energy security and demonstrate federal government leadership in transitioning to a low-carbon economy. A key focus area of the MOU is DOD-DOE collaboration on a broad range of innovative, technology-driven solutions to reduce petroleum use, among other objectives.[30] As a large developer and end user of technology, DOD will aim to speed the movement of innovative energy technologies and technical expertise from DOE's research laboratories to military end users, using military installations as test beds and early markets. Activities undertaken through this collaboration can also help DOD installations meet the requirements of additional regulations that affect their strategies for energy use.

[30] *Memorandum of Understanding between U.S. Department of Energy and U.S. Department of Defense,* DOE and DOD, July 22, 2010, www.energy.gov/news/documents/Enhance-Energy-Security-MOU.pdf.

In support of this MOU, the Program held a series of workshops with DOD and other stakeholders focusing on hydrogen and fuel cell activities. The "Waste-to-Energy Using Fuel Cells" workshop was held on January 13, 2011, the "Shipboard Auxiliary Power Unit" workshop was held on March 29, 2011, and the "Aircraft Petroleum Use Reduction" workshop was held on September 30, 2010. Presentations and outcomes can be found in the Market Transformation section of the Program's workshops Web page, which is located at http://www1.eere.energy.gov/hydrogenandfuelcells/wkshp_proceedings.html.

The National Academies

The National Research Council (NRC) of the National Academies provides ongoing technical and programmatic reviews and input to the Hydrogen and Fuel Cells Program. The NRC has conducted independent reviews of both the Program[31] and the R&D activities of the U.S. DRIVE Partnership.[32] On May 19, 2011, Secretary Chu announced U.S. DRIVE, a cooperative partnership with industry to accelerate the development of clean, advanced, energy-efficient technologies for cars and light trucks and the infrastructure needed to support their widespread use. Formerly known as the FreedomCAR and Fuel Partnership, U.S. DRIVE (Driving Research and Innovation for Vehicle efficiency and Energy sustainability) works together on an extensive portfolio of advanced automotive and energy infrastructure technologies, including batteries and electric-drive components, advanced combustion engines, lightweight materials, and hydrogen and fuel cell technologies.

FY 2011 Annual Merit Review and Peer Evaluation

The Program's Annual Merit Review (AMR) took place May 9-13, 2011, providing an opportunity for the Program to obtain an expert peer review of the projects it supports and to report its accomplishments and progress. For the third time, this meeting was held in conjunction with the annual review of DOE's Vehicle Technologies Program. During the AMR, reviewers evaluate the Program's projects and make recommendations; DOE uses these evaluations, along with other review processes, to make project funding decisions for the upcoming fiscal year. The review also provides a forum for promoting collaborations, the exchange of ideas, and technology transfer. This year, more than 1,700 participants attended, and the Hydrogen and Fuel Cells Program had 207 oral presentations and 87 poster presentations. More than 200 of the Program's projects were peer-reviewed, and there were 210 contributing reviewers. The report summarizing the results and comments from these reviews is available at http://www.hydrogen.energy.gov/annual_review11_report.html. In 2012, the AMR will be held May 14-18 in Arlington, Virginia.

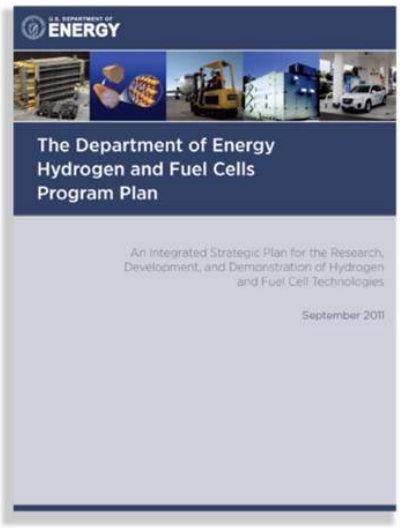
IN CLOSING...

The Program will continue to pursue a broad portfolio of RD&D activities for fuel cell applications across multiple sectors. Efforts will span the full spectrum of technology readiness, including: early market applications that are already viable or are expected to become viable in the next few years, such as forklifts, backup power, and portable power applications; mid-term markets that are expected to emerge in the 2012-2015 timeframe, such as residential combined heat and power systems, auxiliary power units, fleet vehicles, and buses; and longer-term markets that are expected to emerge in the 2015-2020 timeframe, including light-duty passenger vehicles and other transportation applications. The Program will also continue to pursue activities to enable commercialization and stimulate the markets for hydrogen and fuel cells as they achieve technology readiness. Supporting these markets will not only help to achieve the economic, environmental, and energy security benefits that fuel cells provide in those specific applications, but it will complement the Program's longer-term R&D efforts by helping to increase current sales and manufacturing volumes, providing essential cost reductions–through economies of scale–for many of the same technologies that will be used in longer-term applications. Supporting earlier markets can also reduce many non-technological barriers to the deployment of hydrogen and fuel cell technologies and lay the groundwork for the larger infrastructure and

[31] *The Hydrogen Economy: Opportunities, Costs, Barriers and R&D Needs*, National Research Council and National Academy of Engineering, National Academies Press, 2004.

[32] Review of the Research Program of the FreedomCAR and Fuel Partnership: First Report, National Research Council, National Academies Press, 2005, http://www.nap.edu/catalog.php?record_id=11406; Review of the Research Program of the FreedomCAR and Fuel Partnership: Second Report, National Research Council, National Academies Press, 2008, http://www.nap.edu/catalog.php?record_id=12113; Review of the Research Program of the FreedomCAR and Fuel Partnership: Third Report, National Research Council, National Academies Press, 2010, www.nap.edu/catalog.php?record_id=12939.

supply base that will be needed for fuel cell vehicles. Communication and outreach remain critical to all these efforts, and the Program actively pursues opportunities to publicize its activities and progress, releasing more than 70 news items in FY 2011, including DOE press releases, progress alerts, success stories, and blogs.



Finally, a major undertaking in FY 2011 was the complete revision of the Program's strategic plan (the *Hydrogen and Fuel Cells Program Plan*),[33] which outlines the strategy, activities, and plans of the DOE Hydrogen and Fuel Cells Program, covering hydrogen and fuel cell activities within the EERE Fuel Cell Technologies Program and the DOE offices of Nuclear Energy, Fossil Energy, and Science. It describes the Program's activities, the specific obstacles addressed by each sub-program, the strategies employed, key milestones, and future plans for each sub-program and the Program as a whole. The last time the *Plan* had been updated was in 2006 (then it was known as the *Hydrogen Posture Plan*). The new version reflects extensive input from stakeholders, the Hydrogen and Fuel Cell Technical Advisory Committee, and public feedback on the draft version that was posted online for public comment.

We are pleased to present the U.S. Department of Energy's *2011 Hydrogen and Fuel Cells Program Annual Progress Report*. The report is divided into chapters and is organized by technology area (e.g., fuel cells, hydrogen storage, etc.). Each chapter opens with an overview written by a DOE technology development manager that summarizes the progress and accomplishments of the previous fiscal year. The projects outlined in this document represent the work of the many innovative scientists and engineers supported by DOE. They are the ones responsible for the progress and technical accomplishments reported in this year's *Annual Progress Report*. We would like to recognize them for their hard work, commitment, and continued progress.



Sunita Satyapal
Program Manager
Hydrogen and Fuel Cells Program
Fuel Cell Technologies Program
Office of Energy Efficiency and Renewable Energy
U.S. Department of Energy

[33] *The DOE Hydrogen and Fuel Cells Program Plan*, U.S. Department of Energy, September 2011, http://www1.eere.energy.gov/hydrogenandfuelcells/program_plans.html.

II. HYDROGEN PRODUCTION

II.0 Hydrogen Production Sub-Program Overview

The Hydrogen Production sub-program supports research and development (R&D) of technologies that will enable the long-term viability of hydrogen as an energy carrier for a diverse range of end-use applications including stationary power (e.g., backup power and combined-heat-and-power systems), transportation (e.g., specialty vehicles, cars, trucks, and buses), and portable power. A variety of feedstocks and technologies are being pursued.

Three DOE offices are engaged in R&D relevant to hydrogen production:

- The Fuel Cell Technologies Program, within the Office of Energy Efficiency and Renewable Energy (EERE), is developing technologies for distributed and centralized renewable production of hydrogen. Distributed production options under development include reforming of bio-derived renewable liquids and electrolysis of water. Centralized renewable production options include water electrolysis integrated with renewable power generation (e.g., wind, solar, hydroelectric, and geothermal power), biomass gasification, solar-driven high-temperature thermochemical water splitting, direct photoelectrochemical water splitting, and biological processes.
- The Office of Fossil Energy (FE) is advancing the technologies needed to produce hydrogen from coal-derived synthesis gas, including co-production of hydrogen and electricity. Separate from the Hydrogen and Fuel Cells Program, FE is also developing technologies for carbon capture and sequestration, which will ultimately enable hydrogen production from coal to be a near-zero-emissions pathway.
- The Office of Science's Basic Energy Sciences (BES) program conducts research to expand the fundamental understanding of biological and biomimetic hydrogen production, photoelectrochemical water splitting, catalysis, and membranes for gas separation.
- The Office of Nuclear Energy (NE) is conducting efforts in development of high-temperature electrolysis, under the Next Generation Nuclear Plant (NGNP) project, which also includes evaluations of other end-user applications and energy transport systems. The Nuclear Hydrogen Initiative was discontinued as a separate program in Fiscal Year (FY) 2009 after the selection of steam electrolysis as the hydrogen production pathway most compatible with the NGNP.

Goal

The goal of the Hydrogen Production sub-program's portfolio is to develop low-cost, highly efficient hydrogen production technologies that utilize diverse domestic sources of energy, including renewable resources (EERE), coal with sequestration (FE), and nuclear power (NE).

Objectives[1]

The objective of the EERE hydrogen production portfolio is to reduce the cost of hydrogen dispensed at the pump to a cost that is competitive with gasoline, on a cents-per-mile basis (based on current analysis, this translates to a hydrogen threshold cost of $2-4 per gallon gasoline equivalent [gge]). Technologies are being researched to achieve this goal in timeframes appropriate to their current stages of development.

The objectives of FE's efforts in hydrogen production are documented in the *Hydrogen from Coal Program Research, Development and Demonstration Plan* (September 2009). They include proving the feasibility of a near-zero emissions, high-efficiency plant that will produce both hydrogen and electricity from coal and reduce the cost of hydrogen from coal by 25 percent compared with current technology, by 2016.

FY 2011 Technology Status

The current projected cost of hydrogen from several production pathways is shown in Figure 1. The current status of cost and performance for several other hydrogen production pathways, as determined by independent reviews, are shown in Table 1. These reviews, along with cost projections from the Hydrogen

[1] Note: Targets and milestones are under revision; therefore, individual progress reports may reference prior targets.

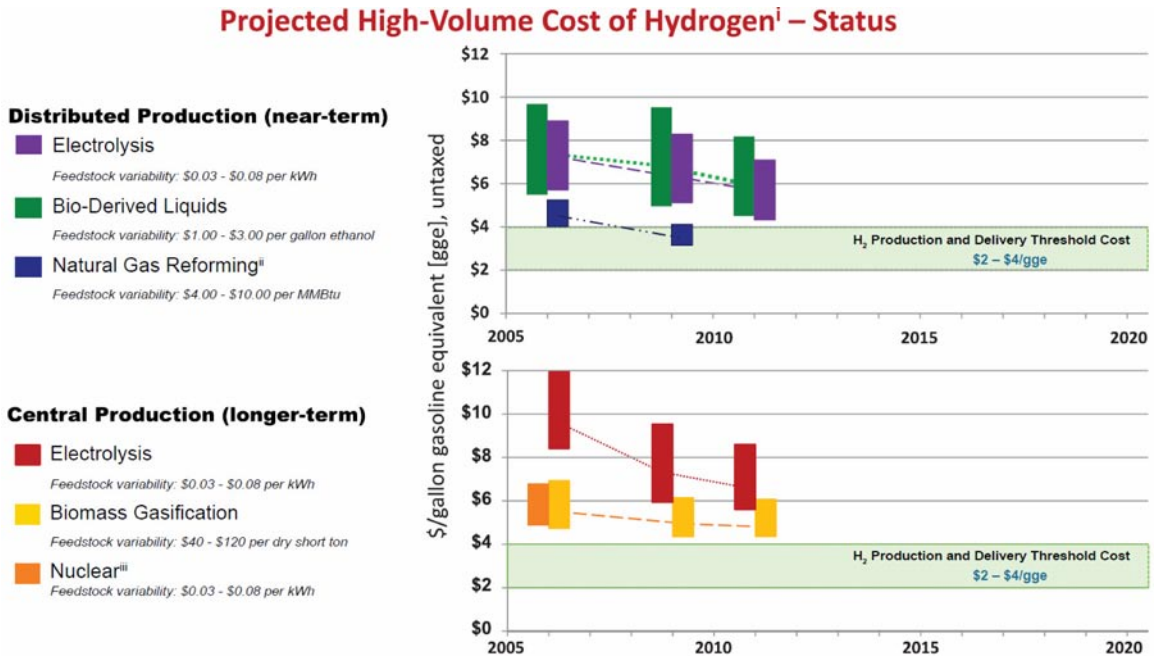


FIGURE 1. Hydrogen Production and Delivery Cost Status. Significant progress has already been made in several hydrogen production pathways. The Hydrogen Threshold Cost represents the cost at which hydrogen fuel cell electric vehicles are projected to become competitive on a cost-per-mile basis with competing vehicles (gasoline hybrid-electric vehicles) in 2020. Notes: (i) Costs shown include all delivery and dispensing costs, but do not include taxes. A cost of $1.80 for forecourt compression, storage, and dispensing is included for distributed technologies, and $2.60 is included as the total cost of delivery (including transportation, compression, storage, and dispensing) for centralized technologies. All delivery costs are based on the Hydrogen Pathways Technical Report (NREL, 2009). Projections of distributed costs assume station capacities of 1,500 kg/day, with 500 stations built per year. Projections of centralized production costs assume capacities of ≥50,000 kg/day. Cost ranges for each pathway are shown in 2007 dollars, based on high-volume projections from H2A analyses, reflecting variability in major feedstock pricing and a bounded range for capital cost estimates. (ii) DOE funding of natural gas reforming projects was completed in 2009 due to achievement of the threshold cost. Incremental improvements will continue to be made by industry. (iii) High-temperature electrolysis activities are ongoing under the Next Generation Nuclear Plant Program.

Analysis (H2A) model, were also used in the development of the Hydrogen Production sub-program's chapter of the *Multi-Year Research, Development and Demonstration Plan (MYRD&D Plan)*, where they were used as the basis for establishing the status of the different technologies and for determining appropriate pathway-independent targets. The 2006 report *Distributed Hydrogen Production from Natural Gas*[2] provided the basis for DOE to discontinue R&D of steam methane reforming for hydrogen production–verifying that the use of existing steam methane reforming technologies in distributed hydrogen production could meet the cost target at high-volume production. Targets for hydrogen production efforts in FE, along with information on the status of the technologies, are documented separately in the *Hydrogen from Coal Program Research Development and Demonstration Plan* (2009).

[2] Distributed Hydrogen Production from Natural Gas, National Renewable Energy Laboratory, October 2006, http://www.hydrogen.energy.gov/pdfs/40382.pdf.

TABLE 1. Recent Independent Reviews of Production Pathway Costs

Pathway	Report	Status[1]
Steam Methane Reforming[2]	*Distributed Hydrogen Production from Natural Gas,* NREL, October 2006	$2.75–$3.05/gge
Electrolysis[3]	*Current (2009) State-of-the-Art Hydrogen Production Cost Estimate Using Water Electrolysis*, NREL, September 2009	**Distributed:** $4.90–$5.70/gge ~75% membrane efficiency (proton exchange membrane [PEM]) **Central (Wind):** $2.70–$3.50/gge ~75% membrane efficiency (PEM)
Photoelectro-chemical (PEC) Production[4]	*Technoeconomic Analysis of Photoelectrochemical (PEC) Hydrogen Production,* Directed Technologies Inc., December 2009	$4–$10/gge (projected cost assuming technology reaches technology readiness); promising PEC materials identified, but durability issues remain
Biological Production[5]	*Technoeconomic Boundary Analysis of Biological Pathways to Hydrogen Production,* Directed Technologies Inc., September 2009	$3–$12/gge (projected cost assuming technology readiness) 15% solar-to-chemical energy efficiency by microalgae
Biomass Gasification	*Hydrogen Production Cost Estimate Using Biomass Gasification,* Independent Panel Review [DRAFT], NREL, April 2011	Preliminary results: feedstock costs, capital costs, and financing structure are primary influences on overall cost.
Solar Thermochemical Production[6]	*Cost Analyses on Solar-Driven High Temperature Thermochemical Water-Splitting Cycles*, TIAX, February 2011	**Hybrid Cycles:** $3.90–$5.40 (in 2025) **Hi-Temp Cycles:** $2.40–$4.70 (in 2025)

[1] Based on H2A V.2.1 using 2005$ inputs for costs, with the exception of the 2011 Solar Thermochemical Production study which used 2007$ inputs.
[2] *Distributed Hydrogen Production from Natural Gas,* National Renewable Energy Laboratory, October 2006, http://www.hydrogen.energy.gov/pdfs/40382.pdf.
[3] *Current (2009) State-of-the-Art Hydrogen Production Cost Estimate Using Water Electrolysis,* National Renewable Energy Laboratory, September 2009, HYPERLINK "http://www.hydrogen.energy.gov/pdfs/46676.pdf" www.hydrogen.energy.gov/pdfs/46676.pdf.
[4] *Technoeconomic Analysis of Photoelectrochemical (PEC) Hydrogen Production,* Directed Technologies Inc., December 2009, http://www1.eere.energy.gov/hydrogenandfuelcells/pdfs/pec_technoeconomic_analysis.pdf.
[5] *Technoeconomic Boundary Analysis of Biological Pathways to Hydrogen Production,* Directed Technologies Inc., September 2009, http://www1.eere.energy.gov/hydrogenandfuelcells/pdfs/46674.pdf.
[6] *Cost Analyses on Solar-Driven High Temperature Thermochemical Water-Splitting Cycles,* TIAX, February 2011, http://www1.eere.energy.gov/hydrogenandfuelcells/pdfs/solar_thermo_h2_cost.pdf.

This year an updated version of H2A (H2A version 3) was published with updated economic data and assumptions; this version also converts all costs to 2007 dollars. Updated economic and cost-sensitivity analyses are currently being performed using H2A version 3, incorporating the most up-to-date information on pathway technologies and technology-readiness projections. These analyses will serve as the basis for updating the status information in Table 1 and will be used to revise pathway-specific targets in an updated version of the *MYRD&D Plan*.

FY 2011 Accomplishments

Biomass Gasification

- The National Renewable Energy Laboratory (NREL) completed the initial draft of an independent panel review of costs for hydrogen production from biomass gasification and performed an analysis of near-term markets for hydrogen from biomass gasification.
- The United Technologies Research Center (UTRC) demonstrated a novel slurry-based fuel-flexible and carbon-neutral biomass reforming process that exceeded 2012 targets in both projected cost and plant efficiency (current status: $1.54/gge and 51.1% efficiency, respectively).
- The Gas Technology Institute completed a membrane design for a one-step, shift-separation membrane reactor for close-coupling with a biomass gasifier. The module demonstrated a flux rate of 80+ standard cubic feet per hour (SCFH)/ft^2 and is capable of 125 SCFH/ft^2. Economic analysis indicates that the technology can meet the production threshold cost target of <$2.00/gge.

Bio-Derived Liquid Pathways

- In the area of autothermal reforming of bio-derived liquids, NREL replaced their catalyst with a better-performing commercial catalyst and reduced the amount of hydrogen oxidized to H_2O during reforming, resulting in increased yield from 7.4 g hydrogen to 10.1 g hydrogen per 100 g bio-oil during short-term, bench-scale tests of catalytic steam reforming at ~650°C, and increased process efficiency from 47% to 62%.
- Pacific Northwest National Laboratory (PNNL) evaluated the feasibility of aqueous phase reforming (APR) of pyrolysis oil and demonstrated successful reforming of most oil components, but also identified key challenges in reforming the acetic acid component. H2A analysis indicated APR of bio-oil is economically feasible only with complete reforming of all oil components.
- Argonne National Laboratory (ANL) demonstrated a more-than-threefold increase in hydrogen production rate by using a Rh-based catalyst coating on an $BaFe_{0.9}Zr_{0.1}O_x$ (BFZ1) oxygen transport membrane (OTM) compared to that of a lanthanum strontium cobalt iron oxide (LSCF) OTM tube with a $BaFe_{0.9}Zr_{0.1}O_x$ (BFZ1).

Separation Processes

- Pall Corporation demonstrated durable, high-performance palladium alloy membranes for hydrogen separation and purification, achieving 270 SCFH/ft^2 flux in pure H_2/N_2, 400 pounds per square inch operation, 88% hydrogen recovery, 99.99% hydrogen permeate quality, and a projected cost of <$1,000/ft^2, meeting or exceeding the 2012 targets for dense metallic membranes.
- Media and Process Technologies developed hydrogen-selective membranes/modules based on thin-film palladium for use as reactors/separators for distributed hydrogen production, with field tests demonstrating >99% CO conversion, >99.9% hydrogen purity and >83% hydrogen recovery, meeting or exceeding the 2012 targets for dense metallic membranes.
- The University of Cincinnati developed methods and techniques to prepare zeolite membranes for water gas-shift reactions for hydrogen production. High hydrogen permeance (1.26 x 10^{-7} mol m^{-2} s^{-1} Pa^{-1}) and H_2/CO_2 separation factor improvements from 4.95 to 25.3 were observed for bilayer membranes modified to include a yttria-stablized zirconia intermediate diffusion barrier layer.

Electrolysis Hydrogen Production

- Giner Electrochemical Systems (GES) demonstrated a proton exchange membrane (PEM) electrolyzer incorporating advanced low-cost membrane electrode assemblies using dimensionally stable membranes with chemically etched supports, which exhibited lifetimes over 1,000 hours operating at 80°C. GES additionally demonstrated significantly reduced hydrogen embrittlement in C/Ti cell separators, indicating expected lifetimes of more than 60,000 hours. Projected stack capital costs of <$0.70/gge based on these improvements meets a critical Program milestone.
- Proton Onsite (formerly Proton Energy Systems) demonstrated new catalyst application techniques for lower-cost hydrogen production, with 55% reduction of catalyst loading on the anode and >90% reduction of catalyst loading on the cathode, with negligible effect on stack performance. Projected stack capital costs of <$0.70/gge based on these improvements meets a critical Program milestone.
- NREL completed more than 2,000 hours of testing on a PEM electrolysis system. The system generated 13 kg of hydrogen per day, running continuously, with full stack-monitoring capabilities and with stacks operating on wind power for stack-decay analysis.

Photoelectrochemical (PEC) Hydrogen Production

- Stanford University demonstrated exceptional stability in their quantum-confined 1.8 eV MoS_2 nanoparticle photocatalyts for PEC hydrogen production, showing stable operations over 10,000 voltage cycles of accelerated lifetime testing. Stanford also developed a high-surface-area macroporous scaffold, which is transparent and conducting, as an efficient electrode substrate for the MoS_2 photocatalysts and other PEC materials.

- NREL validated new benchmark levels of solar-to-hydrogen (STH) conversion efficiency in the 16%–18% range in optimized photoelectrode systems using high-quality III-V semiconductor materials in multi-junction configurations.
- Lawrence Livermore National Laboratory (LLNL), Los Alamos National Laboratory (LANL), the University of Nevada, Las Vegas (UNLV), and NREL worked collaboratively to complete the initial phase of a "III-V Surface Validation Study" to optimize STH performance and enhance lifetime of III-V semiconductor PEC interfaces in aqueous solutions. Ab initio quantum molecular dynamic models of the interface were created by LLNL, and the initial phase of model validation was completed using materials synthesized by NREL/LANL and characterized by UNLV using state-of-the-art spectroscopic facilities.
- MV Systems with the University of Hawaii at Manoa demonstrated 4.3% STH efficiency and device lifetimes exceeding 250 hours in multi-junction devices based on thin-film copper-gallium-diselenide semiconductors, representing a new benchmark in this low-cost class of PEC photoelectrode devices, and representing progress toward the 2010 Program target of stabilized 10% STH.
- The Midwest Optoelectronic Company accelerated development of efficient low-cost substrate-type PEC systems based on multi-junction thin film Si photoelectrodes; they also supplied multi-junction thin-film silicon devices for integration with novel Suncatalytix thin-film catalysts into solar water-splitting demonstration systems. This project demonstrates effective coordination between EERE and Advanced Research Projects Agency-Energy activities.

Biological Hydrogen Production

- University of California, Berkeley successfully characterized the function of a gene that regulates antenna size in chlorophyll (*Tla2*), and cloned another for further analysis (*Tla3*). These findings will be applied to reducing chlorophyll antenna size to increase the utilization efficiency of incident solar light energy.
- NREL—through their collaboration with the University of Manitoba, Canada—used a custom-designed plasmid, along with improved transformation protocols, to obtain two mutant lines of *C. thermocellum*. These lines will serve as the foundation for future genetic engineering efforts with *C. thermocellum* for fermentative hydrogen production.
- The J. Craig Venter Institute, in collaboration with NREL, successfully expressed and purified a stable recombinant hydrogenase. This is a significant step in transferring a more oxygen-tolerant hydrogenase from photosynthetic bacteria into hydrogen producing cyanobacteria.
- NREL used computational methods to understand the geometries and energies of the gas diffusion barrier protecting the hydrogen cluster in two hydrogenases. This information guided mutagenesis techniques to randomize the amino acid residues around the diffusion barriers with the aim of reducing the oxygen sensitivity of hydrogenase.

Solar-Thermochemical Hydrogen Production

- The University of Colorado demonstrated atomic layer deposition thin-film ferrite-based materials with a peak production rate 100 times faster than that in the bulk material, with the thin-film materials remaining active for up to 30 water splitting cycles, with no signs of deactivation.
- Sandia National Laboratories developed a reactor system concept capable of annual average STH production efficiency in excess of 20% with a heat-to-hydrogen conversion efficiency of 40%, predicting through system models that annual average STH efficiency could reach 23%.
- ANL identified two membranes for the electrolysis step of the hybrid Cu-Cl cycle that are chemically and thermally stable at 80°C for over 36 hours, addressing the key barrier to this cycle.
- SAIC reduced the voltage of their electrolysis cell at 80°C to levels similar to those previously demonstrated at 130°C in order to optimize the electrolysis step in their hybrid sulfur-ammonia cycle; they also demonstrated the feasibility of molten salt storage for continuous operation.
- TIAX LLC completed a report analyzing the costs of solar-driven high temperature thermochemical water-splitting cycles and identifying the key cost drivers for the reaction cycles.

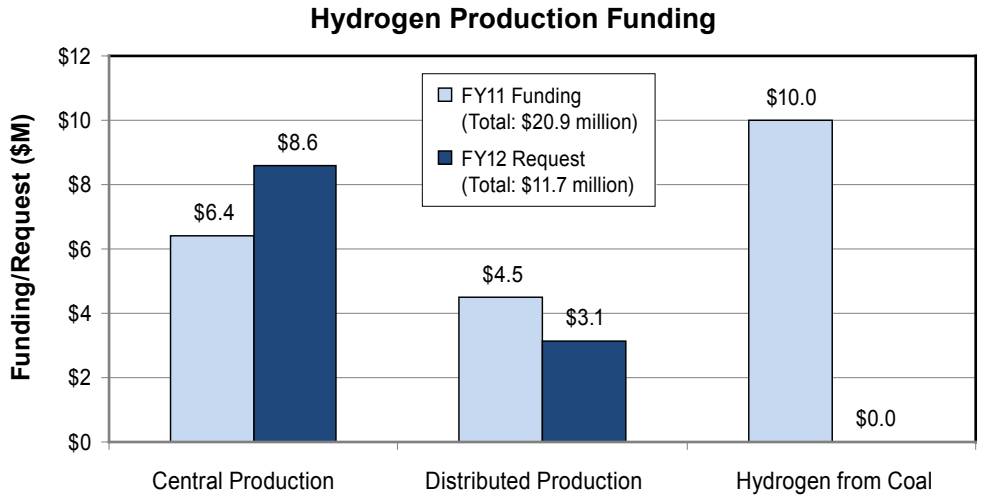
Fossil Energy—Hydrogen from Coal

In FY 2011, the first H_2/CO_2 separation membranes were exposed to coal derived syngas under gasification conditions.

- The National Energy Technology Laboratory's Office of Research and Development in collaboration with Worcester Polytechnic Institute (WPI) and UTRC have obtained over 1800 hours of membrane coupon exposures at the National Carbon Capture Center (NCCC.) Preliminary analysis indicates a stable body-centered-cubic Pd-alloy phase under gasification conditions.
- WPI has completed over 750 hours of membrane tests at the NCCC. Tests have demonstrated stable hydrogen flux levels and hydrogen purity in excess of 99.9%.
- UTRC has completed over 500 hours of membrane tests on the TRIG (transport gasifier) at the Energy & Environmental Research Center. Tests have demonstrated stable hydrogen flux levels and hydrogen purity in excess of 99.9%.
- The Colorado School of Mines has demonstrated reasonable flux and moderate selectivity using a non-precious metal membrane under laboratory conditions.

Budget

The FY 2011 DOE appropriation provided $20.9 million for continued R&D efforts in hydrogen production. EERE received $10.9 million, providing $6.4 million for R&D of centralized renewable hydrogen production and $4.5 million for R&D of distributed renewable hydrogen production; FE received $10.0 million for R&D of hydrogen production from coal.



The President's FY 2012 budget request for EERE provides $11.7 million for hydrogen production, with an emphasis on materials and processes for hydrogen from renewable resources.

FY 2012 Plans

- Continue emphasis on addressing major challenges in hydrogen production. Performance and durability enhancements in materials and systems will remain a priority, and cost reductions will be achieved through process optimization for all production pathways and technologies. Additional efforts will also address reducing the cost of materials and capital equipment.
- Continue EERE coordination with the Office of Science, which plans approximately $50 million in basic research related to hydrogen and fuel cell technologies. Through Basic Science activities, a fundamental understanding of issues related to hydrogen production–particularly in the longer-term R&D areas of PEC

and biological processes–can help address the challenges of hydrogen production. Coordination of the PEC-related fundamental research activities in the Office of Science's Solar Fuels Innovation Hub with the hydrogen production systems-oriented PEC R&D in EERE will be a high priority.

- Complete fabrication of a prototype alkaline electrolyzer unit capable of providing 30 kg of hydrogen per day at 6,500 psi; complete field testing of a prototype PEM electrolyzer capable of providing 12 kg of hydrogen per day at 300-400 psi; and initiate transition of electrolysis production pathways to the "technology validation" stage.
- Complete lifetime measurements of $GaInP_2$/GaAs devices for PEC production of hydrogen and determine the durability benchmarked against the target of a 100-hour operational lifetime at 10% efficiency.
- Demonstrate 100 hours of total catalyst operation in an integrated bench-scale system for production of pure hydrogen from steam reforming of pyrolysis oil at a rate of 100 liters per hour and with a yield of 10 g of hydrogen from 100 g of bio-oil.
- Operate a microalgae system continuously for two months, with the culture being induced to anaerobiosis with prolonged hydrogen production through use of a physiological switch activated by sulfur deprivation.
- Demonstrate–on-sun, using the NREL High Flux Solar Furnace–the cobalt ferrite/alumina "hercycnite" thermochemical reaction cycle with 1,300°C reduction/1,000°C oxidation thermochemical redox cycling to split water, with hydrogen production of >100 micromoles per gram of active material.
- Continue coordination with deployment projects funded by American Recovery and Reinvestment Act to gain lessons learned related to hydrogen production technologies.

Sara Dillich
Hydrogen Production & Delivery Team Lead (Acting)
Fuel Cell Technologies Program
Department of Energy
1000 Independence Ave., SW
Washington, D.C. 20585-0121
Phone: (202) 586-7925
E-mail: Sara.Dillich@ee.doe.gov

II.A.1 Biomass-Derived Liquids Distributed (Aqueous Phase) Reforming

David King (Primary Contact), Yong Wang, Liang Zhang, Ayman Karim, David Heldebrant, Daryl Brown, Sarah Widder
Pacific Northwest National Laboratory (PNNL)
P. O. Box 999
Richland, WA 99352
Phone: (509) 375-3908
E-mail: david.king@pnl.gov

DOE Manager
HQ: Sara Dillich
Phone: (202) 586-7925
E-mail: Sara.Dillich@ee.doe.gov

Subcontractor:
The Gene and Linda Voiland School of Chemical Engineering and Bioengineering
Washington State University, Pullman, WA

Project Start Date: October 1, 2004
Project End Date: Project continuation and direction determined annually by DOE

Fiscal Year (FY) 2011 Objectives

- Evaluate and develop bio-derived liquids aqueous phase reforming (APR) technology for hydrogen production, with a specific focus on aqueous-soluble bio-oil, that can meet the DOE 2017 cost target of <$3.00/gasoline gallon equivalent (gge).
- Identify and control the catalyst composition, reaction pathways, and catalyst preparation methods to enhance hydrogen selectivity, productivity, and catalyst life.

Technical Barriers

This project addresses the following technical barriers from the Production section of the Fuel Cell Technologies Program Multi-Year Research, Development and Demonstration Plan:

(A) Reformer Capital Cost
(C) Operation & Maintenance
(D) Feedstock Issues
(E) Greenhouse Gas Emissions

Technical Targets

For production of hydrogen from bio-derived liquids, we have been focusing on identifying the specific role of the different catalyst components, delineating the mechanistic pathways leading to desired and undesired products, and understanding the causes of catalyst deactivation. This improved understanding is aimed at reducing operating costs, which will lower cost of hydrogen production. The following are our technical targets:

- Cost: $3.80/gge in 2012 and $3.00 in 2017 ($3.00/kg H_2)
- Catalyst life: 100 h without loss of selectivity

FY 2011 Accomplishments

- Completed a series of acidity characterization studies with Pt-Re catalysts. Verified that the amount of acid sites as measured by ammonia temperature programmed desorption (NH_3 TPD) correlated with the amount of Re added to the catalyst, making clear the role of Re in the generation of acid sites on the catalyst surface.
- Showed the presence of Bronsted acid sites on Pt-Re/SiO_2 catalysts after exposure to water vapor by infrared studies and pyridine adsorption. This sheds more light on the character of the acidity with this particular metal combination.
- A cell was constructed to allow measurements of the Pt-Re/C catalyst under operating conditions in X-ray absorption experiments, to be carried out at the Brookhaven National Laboratory Synchrotron source. Preliminary experiments (not in situ) were carried out, demonstrating operability of the system and indicating areas for upgrading the hardware.
- APR studies of aqueous-soluble bio-oil components were carried out with the Pt-Re/C catalyst. We showed successful reforming of most oxygenated species, but also identified difficulty in reforming acetic acid, which is a component present in significant concentration.
- H2A analysis indicates that the DOE H_2 production target of $3.00/kg H_2 can be achieved, but only with virtually complete reforming of all the components present in the bio-oil to H_2 and CO_2.



Introduction

The conversion of biomass-derived liquids to hydrogen is attractive because of the near carbon-neutral footprint it provides, and availability of such feedstocks in many regions of the U.S. We have previously targeted sugars and sugar alcohols, along with other polyols such as glycerol, as feedstocks. In FY 2011, we made a transition to bio-oil as a feedstock, specifically water-soluble bio-oil which contains a large fraction of oxygen-containing functionality, but is overall a more complex mixture that can be expected to raise some new challenges. Much of our catalyst development

work in the APR area has focused on understanding the correlation between catalyst function and performance. Our primary catalyst system has comprised Pt-Re/C, which is a highly active catalyst. We continued work with this same catalyst as we changed feedstock.

Approach

For the APR of bio-oil, we used our standard testing conditions of relatively low temperatures (225-265°C) and sufficient pressure (about 30 bar) to maintain the system in the liquid phase. We started by first identifying and assembling a slate of representative components known to be present in the aqueous-soluble bio-oil, and testing them individually for performance. We then combined these individual components into a single feed, and again compared performance, giving us insight into whether there might be interactions between components that could not be predicted from the individual component studies. This would provide us with guidance regarding what kind of modifications might be required for our catalyst.

For catalyst characterization, we focused primarily on identifying and quantifying the acidity that is developed with the Pt-Re/C catalyst, a result of Pt-Re interactions under both reduced and aqueous phase conditions. This provided insights into the nature of the acidity and how to develop approaches to mitigate the effects of this acidity, including the possibility of complete catalyst modification/substitution.

Results

Our original list of representative compounds was selected based on a literature report from the Huber group [1]. This list is provided in Figure 1. Subsequently, we found that furfural and guiacol, two of the identified components, were insoluble in water at ambient temperature at the concentrations necessary for APR studies. We later made substitutions for these compounds: furfuryl alcohol for furfural, and p-methoxyphenol for guiacos, but these two components were not present in our first pass screening studies.

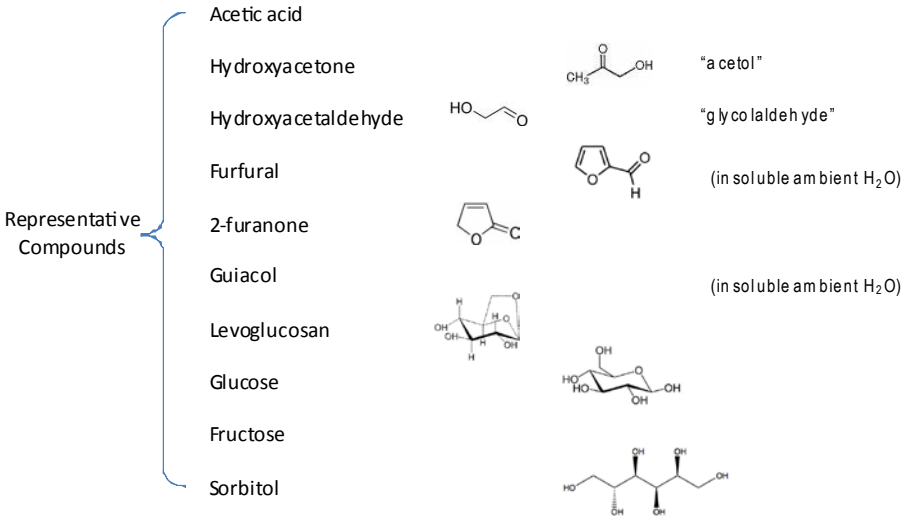


FIGURE 1. Initial List of Representative Compounds for Study of Bio-Oil APR

Figure 2 provides a graphical comparison of the performance of the other components under APR testing conditions. Glycerol is added for comparison. Two feedstocks show poor H_2 selectivity (levoglucosan and fructose), and two showed virtually no selectivity (acetic acid and furanone). The poor selectivity of the first two we believe can be improved significantly through an adjustment in reaction conditions to lower flow rates and possibly carrying out the reaction at higher temperature. The performance of the latter two compounds is more problematic. Acetic acid is present in significant concentration, and we must find a way to increase the reactivity of the catalyst system or find an alternate catalyst system to handle acetic acid. Furanone is structurally more difficult in principle since both unsaturation and ring-opening must be contended with, and hydrogen is not initially present to remove the unsaturation. This may be alleviated by co-feeding hydrogen, and we expect furanone and similar molecules may only be tackled effectively by focusing on hydrogenolysis to form methane, rather than relying on catalytic conversions for hydrogen production. Furanone is present at significantly lower concentration than is acetic acid, thus it is only a very minor constituent. However, acetic acid is present at much higher concentrations, pointing to the primary importance in focusing on effective APR of acetic acid.

In Figure 3 we see the effect of acetic acid on the APR of glycerol. Both components were present at 10 wt% in the feed. It can be seen that the addition of acetic acid reduces the conversion of glycerol. Thus, it is not only that acetic acid is unreactive, but that it also inhibits the conversion of other feed molecules, presumably by strongly adsorbing on the catalyst surface and thereby making fewer active catalyst sites available. It can be seen that this is an effect specifically of the acetic acid and is not an effect of general acidity– addition of nitric acid has virtually no apparent effect on either activity or selectivity in the APR of glycerol.

In Figure 4 we show the results of characterization of the Pt-Re/C catalyst for surface acidity by ammonia TPD. This acidity has been responsible for generation of a significant byproduct alcohol and alkane production from glycerol to the detriment of H_2 production. It is clear that the acidity correlates with Re loading, although there is also some acidity present just with Pt/C. However, this acid strength

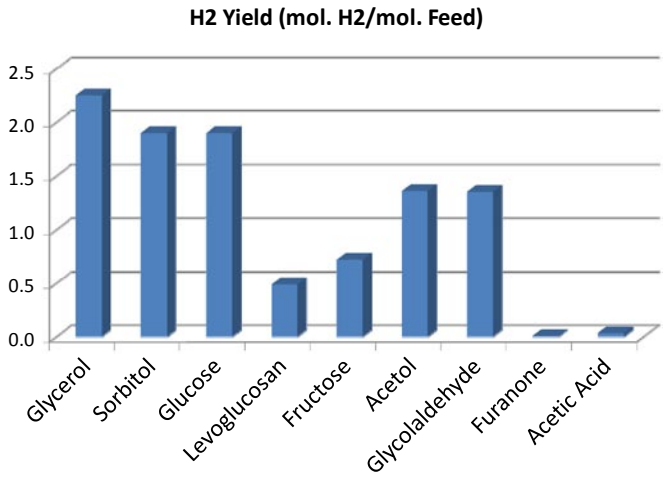


FIGURE 2. H_2 selectivity from the APR of representative bio-oil compounds with Pt-Re/C catalyst. Conditions: 225°C, 420 psig, 0.1 mL/min flow rate, all feeds present at the same molar concentration.

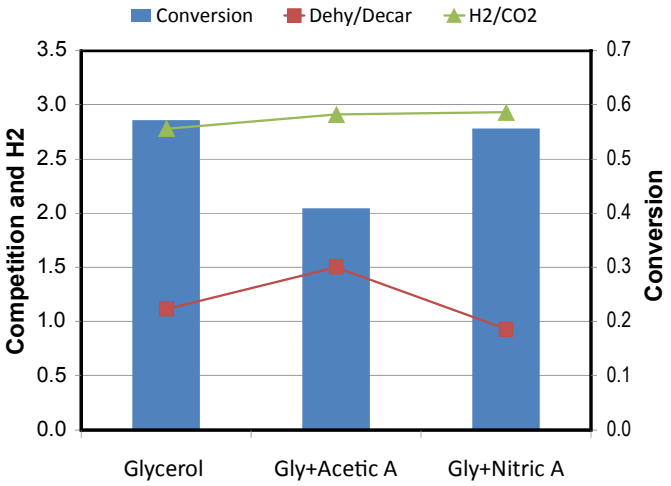


FIGURE 3. Effect of Acetic Acid and Dilute Nitric Acid on the APR of Glycerol with Pt-Re/C

(evidenced by a lower temperature peak) is significantly less than that obtained with the Pt-Re system. Finding methods to decrease or obviate this acidity is important to improve H_2 selectivity in APR. It is interesting to note that despite the surface acidity generated on the catalyst surface by Re, this is not sufficient to repel acetic acid, so that the acetic acid maintains an inhibitory effect on catalyst performance. This points to the possibility of the acid sites being distinct and different from the metal sites present on the catalyst.

Conclusions and Future Directions

We have shifted feedstocks this FY from glycerol and sorbitol to aqueous fraction bio-oil. This shift was necessitated in order to work with cheaper biomass-derived

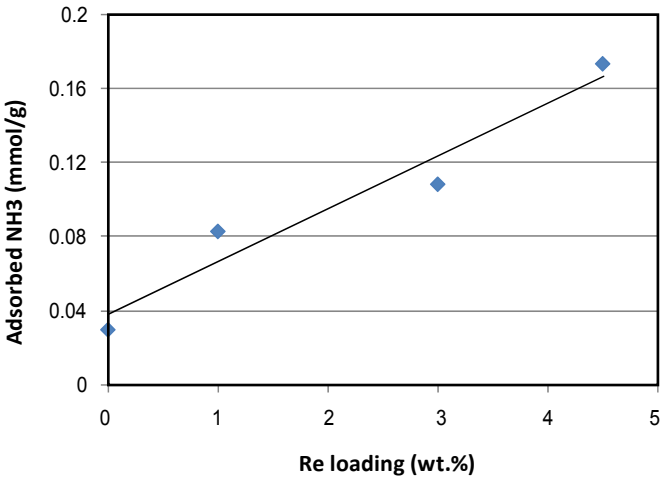


FIGURE 4. Correlation between Re Loading and Total Catalyst Surface Acidity as Measured by TPD of Ammonia

feedstocks that had a greater probability to meet the DOE target of $3.00/gge in 2017. We developed a slate of representative bio-oil components and found that there are some significant challenges with this new feedstock, notably the low activity and apparent poisoning effect of acetic acid. In FY 2012, we will focus especially on catalyst development in order to improve the reactivity of bio-oil, especially dealing with the presence of acetic acid. One strategy that we intend to investigate is to increase the C-C bond breaking activity of our catalyst, for example by adding Ru to Pt/C, as well as evaluating alternate supports. One possibility is that in order to increase C-C cleavage activity we may also increase hydrogenolysis, leading to greater methane co-production. This might require co-feeding hydrogen. We believe that this may not be a negative outcome, since it will be possible to steam reform by-product methane (at higher temperature) using known technology. Such an approach would of course have to still meet the H_2 production cost targets, which will require H2A analysis and verification.

FY 2011 Publications/Presentations

Publications

1. Ayman M. Karim, Yu Su, Mark H. Engelhard, David L. King, and Yong Wang. Catalytic Roles of Co0 and Co2+ during Steam Reforming of Ethanol on Co/MgO Catalysts. ACS Catal., 2011, 1, 279–286.

2. King, David L., Liang Zhang, Gordon Xia, Ayman M. Karim, David J. Heldebrant, Xianqin Wang, Tom Peterson, Yong Wang. Aqueous phase reforming of glycerol for hydrogen production over Pt-Re supported on carbon. Applied Catalysis B: Environmental (2010), 99, 206-213.

3. Ayman M. Karim, Yu Su, Junming sun, Cheng Yang, James J. Strohm, David L. King, Yong Wang. A Comparative Study between Co and Rh for Steam Reforming of Ethanol. Applied Catalysis B: Environmental (2010), 96, 441-448.

Presentations

1. David L. King, Liang Zhang, Ayman Karim, Yong Wang, Acidity of Bimetallic Catalyst under Hydrothermal Environment in Aqueous Phase Reforming of Bioliquids, presented at the 241st meeting of the American Chemical Society, Anaheim, CA March 2011.

2. Zhang L, AM Karim, G Xia, Y Yang, DJ Heldebrant, DL King, and Y Wang. Roles of Re in Pt-Re/C Catalysts for Production of Hydrogen through Aqueous Phase Reforming, presented at the Pacifichem, Honolulu, Dec. 2010.

3. Zhang L, AM Karim, G Xia, Y Yang, DJ Heldebrant, DL King, and Y Wang. .Pt-Re Interaction in Pt-Re/C Catalysts under Hydrothermal Environment for Production of Hydrogen and Biofuels through Aqueous Phase Reforming, presented at the 240th ACS Meeting in Boston, MA, August 2010.

4. Karim AM, J Sun, VMC Lebarbier, Y Su, MH Engelhard, DL King, and Y Wang. Effect of Cobalt Oxidation State on Ethanol Steam Reforming. Oral presentation at the Annual Meeting of the Pacific Coast Catalysis Society, Seattle, WA, March 2010.

5. Ayman Karim, Yu Su, Junming Sun, Vanessa Lebarbier, James Strohm, David King and Yong Wang. On the Role of Co0 and Co2+ in Steam Reforming of Ethanol. Presented orally at the 239th meeting of the American Chemical Society, San Francisco, CA, March 2010.

6. Liang Zhang, Yong Yang, Gordon Xia, David Heldebrant, David L. King, Yong Wang. Pt-Re Interaction in PtRe/C Catalyst under Hydrothermal Environment for Production of Hydrogen and Biofuels through Aqueous Phase Reforming. Oral presentation at the Annual Meeting of the Pacific Coast Catalysis Society, Seattle, WA, March 2010.

7. Liang Zhang, Ayman Karim, Yong Yang, Gordon Xia, David Heldebrant, David L. King, Yong Wang. Pt-Re Interaction under Hydrothermal Conditions and Its Effect on Aqueous Phase Reforming Reaction Pathways. Poster presentation at the Gordon Conference on Catalysis, New London, NH, June 26 – July 2, 2010.

8. Liang Zhang, David L. King, Yong Wang, Lawrence F. Allard. Morphological and Electronic Structure of Pt-Re Nanoparticles Supported on Carbon for Aqueous Phase Reforming of Bioliquids. Oral presentation at the Microscopy & Microanalysis Annual Meeting, Portland, OR, Aug 2010.

9. Liang Zhang, Ayman Karim, David L. King, Yong Wang. Pt-Re Interaction under Hydrothermal Environment in Aqueous Phase Reforming of Bioliquids for Hydrogen Production. Oral presentation at the AICHE Annual Meeting, Salt Lake City, UT, Nov.10, 2010.

10. Karim AM, Y Su, MH Engelhard, DL King, and Y Wang. In-situ XPS Analysis of Co and Co2+ During Steam Reforming of Ethanol on Supported Cobalt Catalysts, poster, 57th AVS National Symposium & Exhibition, Albuquerque, NM, October 2010.

References

1. T.P. Vispute and G. W. Huber, Green Chem., 2009, 11, 1433–1445.

II.A.2 Distributed Bio-Oil Reforming

Stefan Czernik (Primary Contact), Richard French, Michael Penev
National Renewable Energy Laboratory (NREL)
1617 Cole Blvd.
Golden, CO 80401
Phone: (303) 384-7703
E-mail: Stefan.Czernik@nrel.gov

DOE Manager
HQ: Sara Dillich
Phone: (202) 586-1623
E-mail: Sara.Dillich@ee.doe.gov

Subcontractor:
University of Minnesota, Minneapolis, MN

Project Start Date: October 1, 2004
Projected End Date: Project continuation and direction determined annually by DOE

Fiscal Year (FY) 2011 Objectives

- By 2012, develop and demonstrate distributed reforming technology for producing hydrogen from bio-oil at $3.80/kilogram (kg) purified hydrogen.
- By 2011, develop a prototype that incorporates the key operations: bio-oil injection, catalytic auto-thermal reforming, water-gas shift, and hydrogen isolation.
- By 2010, demonstrate the process of auto-thermal reforming of bio-oil including a long-term catalyst performance, yields of hydrogen, and mass balances.
- Develop the necessary understanding of process chemistry, bio-oil compositional effects, catalyst chemistry, and deactivation and regeneration strategy to form a process definition basis for automated distributed reforming to meet the DOE targets.

Technical Barriers

This project addresses the following technical barriers from the Production section of the Fuel Cell Technologies Program's Multi-Year Research, Development and Demonstration Plan:

(A) Fuel Processor Capital
(C) Operation & Maintenance
(D) Feedstock Issues

Technical Targets

TABLE 1. Progress toward Meeting DOE Distributed Hydrogen Production Targets

Distributed Production of Hydrogen from Bio-Derived Renewable Liquids			
Process Characteristics	**Units**	**2012/2017 Targets**	**2011 NREL Status**
Production Unit Energy Efficiency	%	72/65-75	62
Total Hydrogen Cost	$/gge	3.80/<3.00	4.63
Hydrogen Production Cost	$/gge		2.75

gge – gasoline gallon equivalent

FY 2011 Accomplishments

- Demonstrated 60 hours of hydrogen production by auto-thermal reforming of bio-oil using a commercial (BASF) 0.5 Pt/Al_2O_3 catalyst in the bench-scale reactor system.
- Demonstrated catalyst regenerability in several reforming/regeneration cycles.
- Optimized process conditions and achieved the hydrogen production of 10.1 g/100 g bio-oil with 90% bio-oil to gas conversion.
- Based on those results, the total production cost in a 1,500 kg/day hydrogen plant, was estimated at $2.75/gge and the total delivered cost at $4.63/gge.
- Constructed an integrated bench-scale system for producing 100 L/h of pure hydrogen by reforming bio-oil.



Introduction

Renewable biomass is an attractive near-term alternative to fossil resources because it has near zero life-cycle carbon dioxide (CO_2) impact. Recent assessments have shown that more than one billion tons of biomass could be available in the United States each year at less than $50/ton [1]. This biomass could be converted to 100 million tons of hydrogen, enough to supply the light-duty transportation needs of the United States. This work addresses the challenge of distributed hydrogen production with the target of hydrogen cost of $3.80/kg by 2012 [2]. Pyrolysis is used to convert biomass to a liquid that can be transported more efficiently and has the potential for automated operation of the conversion system [3,4]. "Bio-oil" can then be converted to hydrogen and CO_2 in a distributed manner at fueling stations.

The objective of this project is to develop a system that will provide distributed production of hydrogen from bio-oil at filling stations. To accomplish this we are developing a simple fixed-bed reactor suitable for unsupervised automated operation.

Approach

Research is focused on developing a compact, low-capital-cost, low/no maintenance reforming system to enable achievement of the cost and energy efficiency targets for distributed reforming of renewable liquids. In this project, we are evaluating the following steps in the process:

- Bio-oil volatilization using ultrasonic atomization. We need to control physical and chemical properties of the liquid (e.g., viscosity), so blending with alcohol may be necessary.
- Heterogeneous auto-thermal reforming of bio-oil derived gas and vapor. Precious metal catalysts appear to be the most effective in the application to bio-oil and its partial oxidation products.

Early in the project, experiments were carried out using a micro-scale, continuous flow, tubular reactor coupled with a molecular beam mass spectrometer (MBMS) for analyzing the product gas composition. In the last two years, we conducted a series of tests using a bench-scale reactor system that allowed for a longer-duration steady-state operation and provided more reliable data for mass balance calculations. In the bench-scale auto-thermal reforming tests carried out in 2011 we used two types of commercial (BASF) platinum catalyst: alumina-supported pellets and a monolith, both with 0.5% Pt. The experiments were carried out in the systems shown in Figure 1. Poplar pyrolysis bio-oil diluted with 10 wt% methanol was fed at 60 g/h using a membrane pump to the top of the 34 mm internal diameter, 45 cm long tubular quartz reactor. The bottom section of the reactor contained a fixed bed comprising 100 g of pelletized catalyst or 55 g of the monolith. In the freeboard, the liquid in the form of a very fine mist produced by a 60 kHz ultrasonic nozzle (Sono-Tek) contacted air and steam; steam was produced by a home-made micro-generator. The excess steam and some liquid organics were collected in two condensers. The outlet gas flow rate was measured by a dry test meter. The concentrations of CO_2, CO, and CH_4 in the product gas were monitored by a non-dispersive infrared analyzer (NDIR Model 300 from California Analytical Instruments); the hydrogen concentration was tracked by a thermal conductivity detector (TCD) TCM4. In addition, the gas was analyzed every four minutes by an on-line Varian (Model 4900) micro

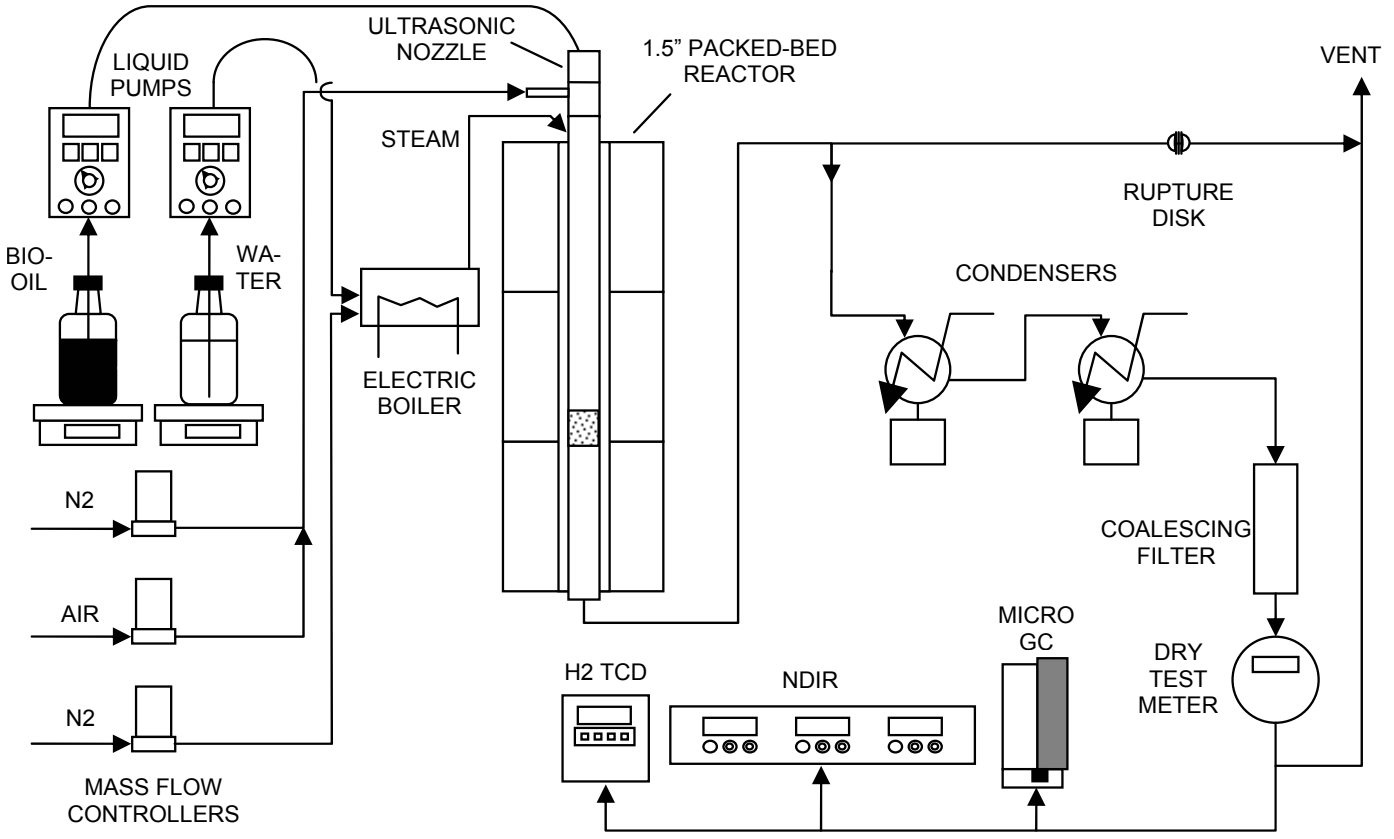


FIGURE 1. Schematic of the Bench-Scale Auto-Thermal Reforming System

gas chromatograph (GC), which provided concentrations of H_2, CO, CO_2, CH_4, C_2H_4, O_2, and N_2. The temperatures in the system, as well as the flows, were recorded and controlled by an OPTO 22 data acquisition and control system. Based on the flows and compositions of the process streams, mass balances as well as the yields of hydrogen generated from the feed were calculated.

Last year, we applied the conditions that assured the optimal system operation in the micro-scale tests: process temperature of 800-850°C, oxygen-to-carbon ratio (O/C)=1.5, molar steam-to-carbon ratio S/C=1.6, and methane-equivalent space velocity equal to 5,200 h^{-1}. This year, using the 0.5% Pt/Al_2O_3 catalyst from BASF, we varied O/C and steam to carbon ratio (S/C) to find the optimal conditions for maximizing the hydrogen yield while still operating in the auto-thermal range.

Results

A series of auto-thermal reforming tests included production and regeneration cycles. After each hydrogen production test, the catalyst was regenerated by air oxidation and reused in the subsequent tests carried out at the same process conditions. Figure 2 shows the product gas composition as a function of time for one of the experiments. The results of the tests are summarized in Table 2.

Despite a lower carbon-to-gas conversion, the increase in S/C and the decrease in O/C resulted in higher hydrogen yields because a larger part of bio-oil reacted by steam reforming that forms more hydrogen than partial oxidation. The increase in space velocity had a negative impact on both carbon-to-gas conversion and hydrogen yield. Based on those tests, the optimum process conditions that will assure an autothermal operation and high hydrogen yields are temperature 850°C, O/C of 0.9-1, S/C=3, and weight hourly space velocity (WHSV)=0.6. Assuming those reactor conditions and performances, the hydrogen production cost estimated using H2A for a 1,500 kg H_2/day plant is $2.75/gge and the cost of delivered hydrogen is $4.63/gge.

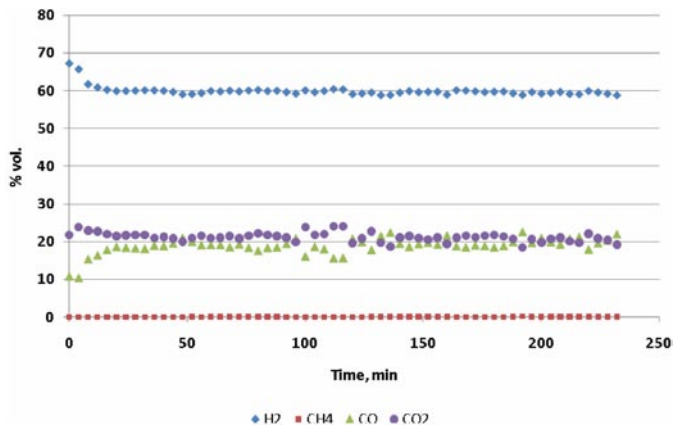


FIGURE 2. Product Gas Composition from Auto-Thermal Reforming of Poplar Bio-Oil Using BASF 0.5% Pt/Al_2O_3 Pelletized Catalyst

TABLE 2. Hydrogen Yields Produced at Different Process Conditions Using 0.5 Pt/Al_2O_3 at 850°C

WHSV (g/h bio-oil/ g cat)	O/C (mol/mol)	S/C (mol/mol)	Hydrogen yield (g H/100 g bio-oil)	C-to-gas Conversion, %
0.6	0.5	3	10.3	72
	0.89	3	10.1	86
	1.6	1.6	7.0	90
1.2	0.85	2.8	5.9	76
2.4	1.5	3	5.6	80
	0.9	3	4.1	60
4.8	1.3	2.8	4.7	80

The monolith platinum catalyst of nominally the same composition as the pellets did not perform as well as the packed bed. During all the tests, the product gas composition as a function of time (Figure 3) changed more than in the packed bed experiments. Especially, the water-gas shift activity decreased with time that was observed as the increase in the concentration of CO and the decrease of CO_2. As before, the highest yields of hydrogen were obtained for lower values of WHSV, lower O/C, and higher S/C. However, these yields as well as carbon to gas conversion were lower than those achieved in the packed bed reactor at the same conditions. In the best case, for O/C=1, S/C=5, and G_{C1}HSV=2,000 h^{-1} the hydrogen yield was 8.5 g/100 g bio-oil and the carbon to gas conversion was 80% compared to respectively 10.1 g/100 g bio-oil and 90% carbon conversion for the packed bed reactor. The reason might be shorter residence time of the bio-oil vapors and especially of the carbon solids in the channels of the monolith than in the packed bed.

The construction of an integrated system for producing 100 L/h of hydrogen by auto-thermal reforming of bio-oil was completed. The main components of the system include

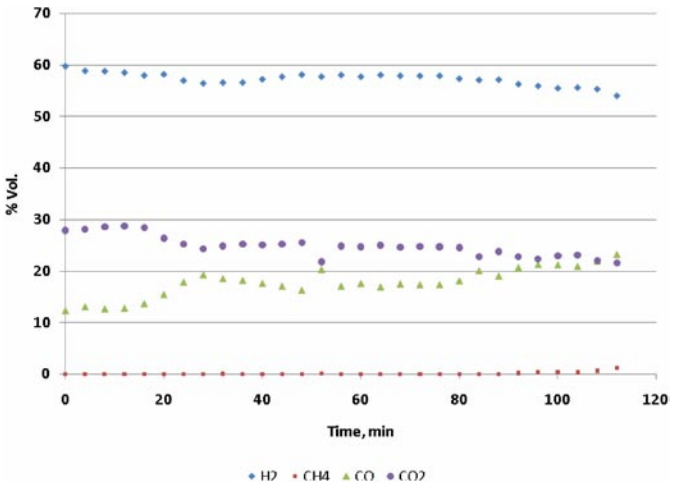


FIGURE 3. Product Gas Composition from Auto-Thermal Reforming of Poplar Bio-Oil Using BASF 0.5% Pt/Al_2O_3 Monolith Catalyst

a bio-oil evaporator, reforming reactor, water-gas shift convertor, and hydrogen separator.

Conclusions and Future Direction

- Bench-scale reactor tests of catalytic auto-thermal reforming of bio-oil performed using 90 wt% bio-oil/10 wt% methanol mixtures produced hydrogen yields of 10 g/100 g bio-oil with 90% of carbon-to-gas conversion.
- The optimal process conditions for the bench-scale system are: temperature 850°C, O/C of 0.9-1, S/C=3, and WHSV=0.6 (BASF 0.5%Pt/Al_2O_3 catalyst).
- The construction of a prototype system including bio-oil evaporator/filter, catalytic reformer, water-gas shift reactor, and electrochemical hydrogen separator was completed. The system will produce 100 L/h of pure hydrogen. The performance of that prototype will be tested in FY 2012 and will help to make a go/no go decision on further process development.

FY 2011 Publications/Presentations

1. Czernik, S., French, R., Penev, M., *2011 DOE Hydrogen, Fuel Cells & Infrastructure Technologies Program Review*, May 2011.

References

1. Perlack, R., Wright, L., Turhollow, A., Graham, R., Stokes, B., Erbach, D. "Biomass as Feedstock for a Bioenergy and Bioproducts Industry: The Technical Feasibility of a Billion-Ton Annual Supply," A Joint U.S. Department of Energy and U.S. Department of Agriculture Report DOE-GO-102995-2135 and ORNL/TM 2005-66, April 2005.

2. U.S. Department of Energy. *Hydrogen, Fuel Cells and Infrastructure Technologies Program, Multi-Year Research, Development and Demonstration Plan*, Section 3.1 Hydrogen Production, 2006. U.S. Department of Energy, Office of Energy Efficiency and Renewable Energy: Washington, D.C.

3. Czernik, S., Elam, C., Evans, R., Milne, T. "Thermochemical Routes to Hydrogen from Biomass–A Review." In *Science in Thermal and Chemical Biomass Conversion*, Bridgwater AV, Boocock DGB, eds., CPL Press: Newbury, UK, 2006, pp.1752–1761.

4. Evans, R.J., Czernik, S., French, R., Marda, J. "Distributed Bio-Oil Reforming," *DOE Hydrogen Program FY2007 Annual Progress Report,* 2007.

II.A.3 Distributed Reforming of Renewable Liquids Using Oxygen Transport Membranes (OTMs)

U. (Balu) Balachandran (Primary Contact), C.Y. Park, T.H. Lee, Y. Lu, J.J. Picciolo, J.E. Emerson, and S.E. Dorris
Argonne National Laboratory
9700 S. Cass Ave.
Argonne, IL 60439-4838
Phone: (630) 252-4250
E-mail: balu@anl.gov

DOE Manager
HQ: Sara Dillich
Phone: (202) 586-7925
E-mail: Sara.Dillich@ee.doe.gov

Subcontractor:
Directed Technologies, Inc. (DTI), Arlington, VA

Project Start Date: May, 2005
Project End Date: Project continuation and direction determined annually by DOE

Fiscal Year (FY) 2011 Objectives

Develop a compact ceramic membrane reactor that meets the DOE 2017 cost target of <$3.00/gasoline gallon equivalent (gge) for producing hydrogen by reforming renewable liquids. Specific objectives for FY 2011 were:

- Use oxygen transport membrane (OTM) to reform ethanol (EtOH) at ≤700°C in presence of catalyst.
- Perform detailed Design for Manufacturing and Assembly and H2A analyses to assess benefits of approach.

Technical Barriers

This project addresses the following technical barriers from the Production section (3.1.4) of the Fuel Cell Technologies Program Multi-Year Research, Development and Demonstration Plan:

(A) Reformer Capital Costs
(B) Reformer Manufacturing
(C) Operation and Maintenance
(N) Hydrogen Selectivity
(P) Flux
(R) Cost

Technical Targets

This project is developing compact dense ceramic membranes that transport pure oxygen to efficiently and cost-effectively produce hydrogen by reforming renewable liquid fuels such as EtOH and bio-oil. Cost-effective small-scale reformer technology will be developed to integrate process steps, thereby minimizing unit size, capital cost, energy use, and operating cost and helping to meet DOE technical targets:

Production Unit Energy Efficiency:	72% (lower heating value, LHV) by 2012 65-75% (LHV) by 2017
Production Unit Capital Cost (un-installed):	$1.0M by 2012 $600K by 2017
Total Hydrogen Cost:	$3.80/gge (delivered) at the pump by 2012 < $3.00/gge (delivered) at the pump by 2017

A preliminary techno-economic analysis in FY 2010 estimated a cost of ≈$3.40/gge for producing hydrogen by reforming EtOH with an OTM.

FY 2011 Accomplishments

- Significantly increased EtOH conversion using $BaFe_{0.9}Zr_{0.1}O_x$ (BFZ1), an OTM that gives significantly higher oxygen flux at low temperature (≈500°C), but analysis of the products indicated the need for a suitable catalyst to increase hydrogen production.
- Used Rh-based catalyst on a small (1.3 cm^2) BFZ1 disk to nearly quadruple the hydrogen production rate compared to that of a much larger (15.3 cm^2) lanthanum strontium cobalt iron oxide (LSCF) tube.
- Estimated a hydrogen production cost of $3.40/kg H_2 for a station with a 1,500 kg H_2/day capacity, (analysis by DTI).



Introduction

Others have shown that supplying oxygen with an OTM reduced the costs of methane reforming by ≈30-40% and energy consumption by ≈30%. Supplying oxygen during EtOH reforming increases EtOH conversion and enhances catalyst performance by preventing coke formation [1]. An OTM can supply high-purity oxygen for EtOH reforming by separating it from air without using a separate gas separation unit. Because the OTM is a mixed conductor, the oxygen transport requires neither electrodes nor external power circuitry, i.e., the process is non-galvanic. The oxygen flux

through the membrane depends on the membrane's electron and oxygen-ion conductivities, its surface oxygen exchange kinetics, and the oxygen partial pressure (pO_2) gradient across the membrane.

The goal of this subtask is to develop a dense OTM that provides oxygen for efficiently and economically producing hydrogen through the reforming of renewable liquid fuels such as EtOH and bio-oil. To assess the potential for reducing the cost and energy consumption associated with EtOH reforming. DTI performed a detailed system analysis to determine the cost and energy benefits of using an OTM to supply high-purity oxygen from air. While generating the necessary data for DTI's system analysis, we continued developing OTMs that transport oxygen at an industrially significant rate at low temperature (≈500°C) and possess sufficient mechanical and chemical stability under the large stresses that develop from having air on one side of the OTM and carbonaceous fuels on the other side.

Approach

In order to be cost-effective during the reforming of renewable liquids, an OTM must efficiently transport oxygen. For efficient oxygen transport, an OTM must have an appropriate combination of electronic and ionic conductivity; therefore, we use conductivity measurements to identify promising membrane materials. If a material has sufficient conductivity ($>10^{-1}$ ohm^{-1}-cm^{-1}), we measure its hydrogen production rate, which is directly related to its oxygen transport rate. In order to increase the oxygen transport rate, we adjust the OTM's composition, decrease its thickness, coat it with porous layers to increase its active area, and modify its microstructure to overcome limitations from surface reaction kinetics. With promising OTMs, catalysts are used to promote reforming reactions. We measure the hydrogen production rate under various reaction conditions for periods up to ≈1,000 h to evaluate the chemical stability of OTMs, because OTMs must be stable for extended periods to cost-effectively produce hydrogen. Because OTMs must be available in a shape with a large surface area, e.g. tubes, we fabricate small tubular OTMs and test their performance. In order to assess the expected cost- and energy-benefits of reforming renewable liquids with an OTM, we shared our oxygen flux data to an independent party, DTI, who conducted a detailed system analysis.

Results

BFZ1 powder was prepared by conventional solid-state synthesis using $BaCO_3$, Fe_2O_3, and ZrO_2 as starting materials. Stoichiometric amounts of starting materials were ball-milled for 1-3 days with zirconia media in isopropyl alcohol (IPA). After drying the mixture, it was heated in ambient air at 800-850°C for 10-20 h and then ball-milled as before for one day. The dried powder was heated again in ambient air at 880-900°C for 10-20 h, and then was ball-milled again.

Although the microstructure of BFZ1 thin films is acceptable, they have shown a tendency to crack during EtOH reforming conditions; therefore, an EtOH reforming experiment was done using a relatively thick (0.67 mm) BFZ1 disk. A disk (1 inch diameter) was uniaxially pressed from BFZ1 powder and was then sintered at 1,340°C for 10 h in 100 ppm H_2/balance N_2. To deposit Rh-catalyst on one face of the disk, rhodium nitrate ($Rh(NO_3)_3 \cdot 2H_2O$, Alfa Aesar, 99.9%) was dissolved in deionized water, and then a binder and BFZ1 powder was added to the solution. Heating the solution with binder and powder at <80°C while stirring gave a viscous paste that was painted onto the surface of the BFZ1 disk. The painted disk was dried in air and installed for an EtOH reforming test at 600°C.

A glass ring was used to seal the Rh-coated BFZ1 disk to the test fixture by heating overnight at 650°C while flowing He on the Rh-catalyst side and air on the other side. After obtaining a seal at 650°C, the tube was cooled to 600°C for the EtOH reforming test. The EtOH partial pressure (p_{EtOH}) was fixed on the Rh-coated side of the disk by bubbling ultrahigh purity He or N_2 through absolute EtOH at 23°C (p_{EtOH} ≈0.067 atm), while air was flowed on the other side of the disk. During the measurements, both gases flowed at a rate of 200 ml/min. The concentrations of products from EtOH reforming were measured with an Agilent gas chromatograph.

Figure 1 shows cross-sectional and plan views of a BFZ1 disk coated with catalyst. An EtOH reforming test with the sample shown in Figure 1 was unsuccessful, because a gas-tight seal was not made. EtOH reforming results were obtained with a second sample. The sample shown in Figure 1 was heated overnight at 930°C, because a gold ring was used to make a gas seal rather than a glass ring. Other than being heated to higher temperature in order to make a seal, the unsuccessful sample (Figure 1) was identical to the sample used in the successful reforming test. The porous catalyst-containing layer on top of the BFZ1 disk had a thickness of ≈10 μm. The BFZ1 disk itself had several isolated pores but the pores did not appear to be interconnected.

An EtOH reforming test was conducted at 600°C with a Rh catalyst-coated BFZ1 disk. Table 1 summarizes the results for the BFZ1 disk coated with catalyst along with data that was the reported previously [2] for an LSCF thin-film tube not coated with catalyst. Figure 2 compares the total production rates for the products of EtOH reforming with the BFZ1 disk and the LSCF thin-film tube. Figure 3 plots the relative hydrogen production rates, i.e., the ratios of the hydrogen production rate to the production rates for the other products of reforming.

The carbon balance and EtOH conversion of BFZ1 were 90.9% and 28.0%, respectively. The EtOH conversion for the BFZ1 disk was lower than that of the LSCF thin-film tube due to the disk's smaller active area (≈1.3 vs. 15.3 cm^2). Despite its lower EtOH conversion and its smaller active area, the total hydrogen production rate of BFZ1 was

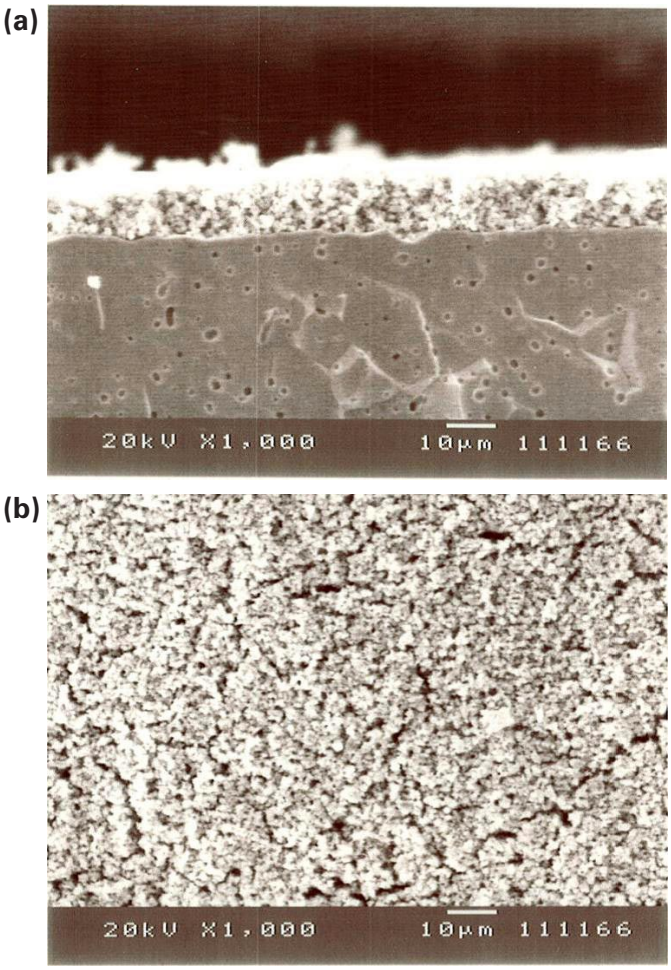


FIGURE 1. Secondary electron images of a) fracture-surface and b) plan view of Rh catalyst-coated BFZ1 disk.

TABLE 1. Results of EtOH Reforming Experiments at 600°C

OTM	EtOH Reforming Results				
	OTM Thickness	HPR* (cm^3/min)	H_2/Total	C Balance (%)	EtOH conversion (%)
LSCF thin-film tube	~30 μm	0.27	0.031	75.8	61.8
BFZ1 disk + Rh	0.67 mm	0.96	0.360	90.9	28.0

* HPR = hydrogen production rate

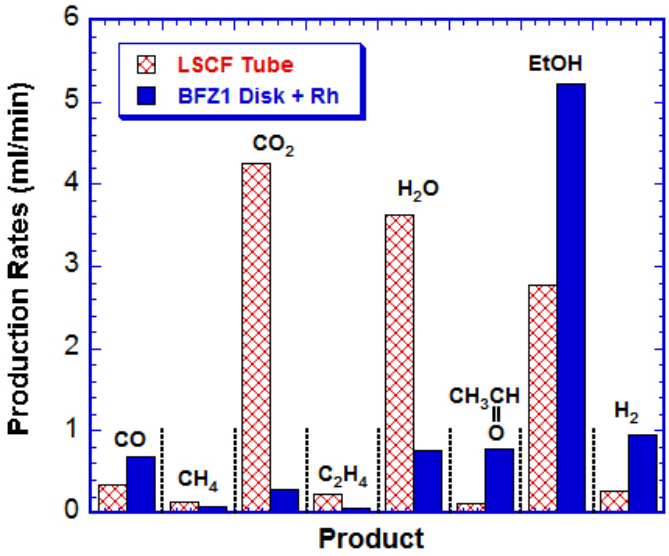


FIGURE 2. Total production rates for products of EtOH reforming at 600°C with Rh catalyst-coated BFZ1 disk (thickness=0.67 mm, active area=1.3 cm^2) and LSCF tubular thin-film (thickness=0.03 mm, active area=15.3 cm^2) not coated with catalyst.

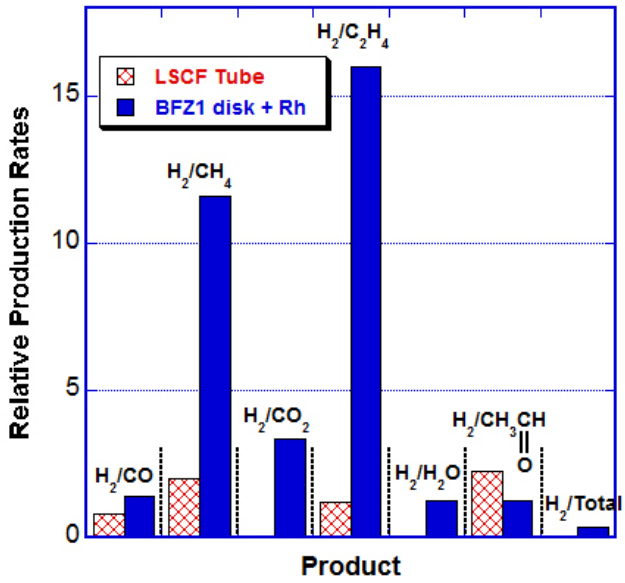


FIGURE 3. Relative production rates for products of EtOH reforming at 600°C with Rh catalyst-coated BFZ1 disk (thickness=0.67 mm, active area=1.3 cm^2) and LSCF tubular thin-film (thickness=0.03 mm, active area=15.3 cm^2) not coated with catalyst.

0.96 cm^3/min, which is 3.6 times higher than that of the LSCF tube. Only a small amount of coke was found after the experiment with the BFZ1 disk, an observation that is consistent with the improved carbon balance for the BFZ1 disk, compared to that for the LSCF thin-film tube.

Figure 2 shows that, in addition to its higher production rate, the BFZ1 disk gave lower production rates for the major products (CO_2 and H_2O) from EtOH reforming with the LSCF thin-film tube. The shift toward hydrogen production is seen more clearly in Figure 3, which plots the relative hydrogen production rates for the BFZ1 disk and LSCF tube. The catalyst-coated BFZ1 disk gave considerably higher relative hydrogen production rates for all products except acetaldehyde (CH_3CHO). The ratio of the hydrogen production rate to the sum of production rates

for all other products, given by H_2/Total in Figure 3 and Table 1, was more than an order of magnitude higher for the BFZ1 disk with catalyst than for the LSCF tube without catalyst (0.360 for Rh+BFZ1 vs. 0.031 for LSCF). The results indicate that the addition of the Rh catalyst played an important role for increasing the hydrogen selectivity and decreasing coke formation.

DTI completed a detailed techno-economic analysis of EtOH reforming with an OTM to evaluate its cost- and energy-benefits. For the analysis, Argonne provided oxygen flux and EtOH conversion data for promising OTMs. The analysis shows that the cost of the EtOH feedstock comprises a major fraction (≈70%) the cost of producing hydrogen by EtOH reforming with an OTM. The cost of producing hydrogen by EtOH reforming with an OTM was estimated to be ≈$3.10-$3.60/kg H_2, depending on the EtOH fuel efficiency.

Conclusions and Future Directions

Significant progress was made in demonstrating that a dense OTM can enhance the reforming of renewable liquids. In order to further evaluate the benefits of this approach, if funding becomes available to continue this work, we will:

- Continue testing the performance of OTMs during EtOH reforming at lower temperatures (≈500°C).
- Study effect of EtOH concentration, gas flow rates, and OTM thickness.
- Evaluate effect of Rh-catalyst during EtOH reforming using tubular OTM with larger active area (≈15 cm^2).
- Evaluate performance of other catalysts during EtOH reforming with OTM.
- Evaluate chemical stability of OTM during reforming of EtOH.
- Provide DTI with data on improved performance of OTMs to refine the cost and energy analysis and better evaluate the merits of using OTM to enhance H_2 production by EtOH reforming.

FY 2011 Publications/Presentations

1. Distributed Reforming of Renewable Liquids using an OTM, DOE Hydrogen Program FY 2011 1st Quarter report, January 2011.

2. Distributed Reforming of Renewable Liquids using an OTM, DOE Hydrogen Program FY 2011 2nd Quarter report, April 2011.

References

1. F. Frusteri et al., *Intl. J. Hyd. Energy*, 31, 2193-2199 (2006).

2. U. Balachandran, Distributed Reforming of Renewable Liquids using an OTM--Quarterly Report for Apr. – Jun. 2010, Argonne National Laboratory.

II.B.1 A Novel Slurry-Based Biomass Reforming Process

Sean C. Emerson
United Technologies Research Center (UTRC)
411 Silver Lane
East Hartford, CT 06108
Phone: (860) 610-7524
E-mail: emersosc@utrc.utc.com

DOE Managers
HQ: Sara Dillich
Phone: (202) 586-7925
E-mail: Sara.Dillich@ee.doe.gov
GO: Katie Randolph
Phone: (720) 356-1759
E-mail: Katie.Randolph@go.doe.gov

Contract Number: DE-FG36-05GO15042

Subcontractor:
Energy & Environmental Research Center (EERC), University of North Dakota, Grand Forks, ND

Project Start Date: May 2, 2005
Project End Date: June 3, 2011

Fiscal Year (FY) 2011 Objectives

- Develop an initial reactor and system design, with cost projections, for a biomass slurry hydrolysis and reforming process for hydrogen (H_2) production from woody biomass.
- Develop a cost-effective catalyst for liquid phase reforming of biomass hydrolysis-derived oxygenates.
- Perform a proof-of-concept demonstration of a micro-scale pilot system based on liquid-phase reforming of biomass.
- Demonstrate that the proposed H_2 production system will meet the 2012 efficiency and cost targets of 43% lower heating value (LHV) and \$1.60/kg H_2 for a 2,000 ton/day (dry wood) plant.

Technical Barriers

This project addresses the following technical barriers from the Production section of the Fuel Cell Technologies Program Multi-Year Research, Development and Demonstration Plan [1]:

(T) Capital Costs and Efficiency of Biomass Gasification/ Pyrolysis Technology

Technical Targets

This project consists of three key elements: plant and system design, catalyst research, and a proof-of-concept demonstration. The information obtained from all three efforts will be used to demonstrate that the proposed H_2 production system will meet the DOE's 2012 Biomass Gasification/Pyrolysis Hydrogen Production energy efficiency and total H_2 cost targets of 43% (based on feedstock LHV) and \$1.60/kg H_2, respectively. The current progress toward achieving the DOE's technical targets based on the preliminary plant and system design is shown in Table 1.

TABLE 1. Technical Progress for the Project as Measured Against the DOE's Technical Targets for Biomass Gasification/Pyrolysis Hydrogen Production

Characteristics	Units	2012 Target	Current Status
Hydrogen Cost (Plant Gate)	\$/gge	1.60	1.54 (1.31–2.11)
Total Capital Investment	\$M	150	170 (117–304)
Energy Efficiency	%	43	51.1

FY 2011 Accomplishments

- Demonstrated 100% conversion of wood using an inexpensive base metal catalyst.
- Examined the effect of base concentration on liquid phase reforming H_2 selectivity and yield.
- Developed a promoted Ni catalyst that maintains a high selectivity to H_2 with minimal base.
- Elucidated the liquid phase reforming reaction pathways for ethylene glycol over Ni and Pt via atomistic modeling.
- Demonstrated a continuous flow H_2 production system for 1 wt% wood at 50 g min^{-1}.



Introduction

This project is focused on developing a catalytic means of producing H_2 from raw, ground biomass, such as fast growing poplar trees, willow trees, or switch grass. The use of a renewable, biomass feedstock with minimal processing can enable a carbon neutral means of producing H_2 in that the carbon dioxide produced from the process can be used in the environment to produce additional biomass. For economically viable production of H_2, the biomass is hydrolyzed and then reformed without any additional purification steps. Any unreacted biomass and other byproduct streams are burned to provide process energy. Thus, the development of a catalyst that can operate in the demanding corrosive environment and presence of potential poisons is vital to this approach.

Approach

The concept for this project is shown in Figure 1. The initial feed is assumed to be a >5 wt% slurry of ground poplar wood in dilute base. Potassium carbonate (K_2CO_3), derived from wood ash, is an effective base. Base hydrolysis of the wood is carried out at high but sub-critical pressures and temperatures in the presence of a solid catalyst. A Pd alloy membrane allows the continuous removal of pure H_2, while the retentate, including methane is used as fuel in the proposed plant.

Results

The economics of the alkali hydrolysis-based plant design using Ni-based catalysts were updated using the latest version of the H2A tool from the DOE with input from HYSYS plant models. For all cases, a Pd membrane-based separator was used to produce >99.9999% H_2 from the process for fuel cell use. For the baseline economics, the H_2 was then compressed from atmospheric pressure up to a pipeline delivery pressure of 300 psia. The use of a H_2 compression system was a more economical investment compared to using a larger Pd membrane separator operating with a 300 psia back pressure. However, the electrical demands of the plant increase significantly due to the compression system.

There were several assumptions common to the HYSYS/H2A model analyses. The wood feedstock price was set at $41/ton to keep with the DOE's cost target basis, although realistic feedstock prices will be higher. The cost of K_2CO_3 feed for the plant was set at $900/ton and the design assumed that 95% of the K_2CO_3 will be recycled within the system. The reforming catalyst was assumed to be equivalent to Raney Ni at a cost of $20/lb with catalyst replacement occurring every three years. The reformer liquid residence time was fixed at 16 minutes with a catalyst to wood mass ratio set at a very conservative 20.

In general, the hypothetical 2,000 dry ton per day biomass plant can be run in three different modes. Table 2 shows the summary of the technoeconomic modeling results compared to the DOE targets. The first of these modes would use an inexpensive fuel source, such as natural gas, to provide the heat required to operate the endothermic hydrolysis, reforming, and H_2 separation processes. The second mode of operation assumes that the plant is operated to achieve "carbon neutrality" in terms of CO_2 emissions, not counting the secondary emissions that come from electricity provided from the grid for H_2 compression. Instead of using inexpensive fossil fuels to provide the heat required for the plant, the retentate stream from the membrane separator, which contains H_2, is burned to produce heat. This carbon neutrality comes at a cost both in terms of the H_2 cost, but the efficiency as well, as H_2 that could be delivered from the plant is diverted to heat production instead. The final mode of operation assumes that the plant is operated in a "carbon neutral; electric grid independent" mode. To achieve electric grid independence, the electrical demand from the H_2 compression system was reduced to the point that electricity generated from expanders in the plant could provide all the power needed. As a result, the delivery pressure of the H_2 was also reduced to 44.09 psia. The cost of H_2 in this scenario does not change relative to the "carbon neutral" mode, but the capital costs are lowered and the plant efficiency is reduced.

First principles atomistic modeling was previously used to gain an insight into the factors that control the activity and selectivity toward H_2 production by ethylene glycol reforming on Ni catalysts. Ethylene glycol was chosen as a model compound due to its oxygen bonding to adjacent carbons

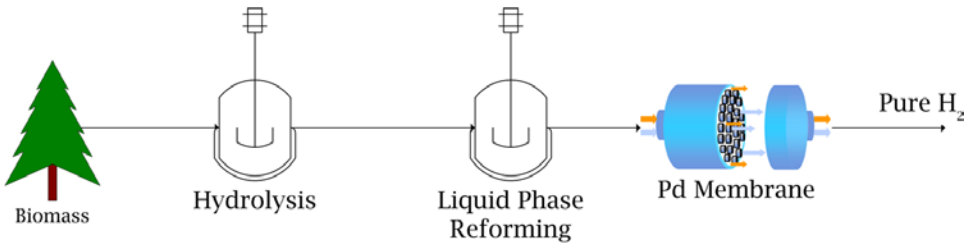


FIGURE 1. The UTRC Approach to Biomass Slurry Reforming

TABLE 2. Technoeconomic Modeling Results for Different Modes of Operation for a 2,000 Dry Tons of Wood per day Plant Compared to the DOE's Technical Targets for Biomass Gasification/Pyrolysis Hydrogen Production

Characteristics	Units	2012 Target	Natural gas fuel mode	Carbon neutral mode	Carbon neutral, electric grid independent mode
Hydrogen Cost (Plant Gate)	$/gge	1.60	1.27 (1.05–1.84)	1.54 (1.31–2.11)	1.54 (1.31–2.11)
Total Capital Investment	$M	150	188 (116–370)	170 (117–304)	164 (117–283)
Energy Efficiency	%	43	56.3	51.1	46.1

which represents some fragments of biomass. The schematic diagram of reforming pathways for ethylene glycol on Ni is depicted in Figure 2. For ethylene glycol on a Ni surface, the first step after adsorption is hydroxyl bond breaking to form an ethylenedioxy intermediate. At the surface coverage considered, the activation of C-O bond in ethylenedioxy and rearrangement to form the acetaldehyde intermediate and adsorbed oxygen are thermodynamically favorable. Subsequent dehydrogenation and C-C bond scission of acetaldehyde yields the CO and CH_3 as final decomposition intermediates. CO is shifted in water to CO_2 and H_2 while the methyl is hydrogenated into methane. In a basic environment, CO can also be converted to a formate ion in solution through hydrophilic attack, consistent with the experimental observation of formic acid in the spent liquor.

To further investigate the impact of base to wood ratio on H_2 yield and selectivity, batch, single-step hydrolysis and reforming experiments were performed at EERC. The experiments were performed using a standard, unmodified Raney nickel catalyst and potassium hydroxide base in EERC's 7.6-L autoclave system with a constant wood concentration of 8 wt%. The H_2 yield and H_2 selectivity results for the experiments are summarized in Figures 3 and 4, respectively. Consistent with previous predictions from atomistic and thermodynamic modeling for ethylene glycol, as well as batch wood reforming experiments performed at UTRC, increasing the base to wood ratio increased the selectivity of the process toward hydrogen production versus methane. However, the higher base levels decreased the H_2 yield, most likely favoring organic acid formation over gas production.

Earlier testing work used Pt-based catalysts before switching to less expensive Ni-based catalysts, and there is current interest for liquid phase reactions using precious metals. Thus, first principles atomistic modeling was used to understand the differences in reaction mechanisms. A schematic diagram of the reforming pathways for ethylene glycol on Pt is depicted in Figure 5. For ethylene glycol on the Pt surface, the first steps after adsorption are

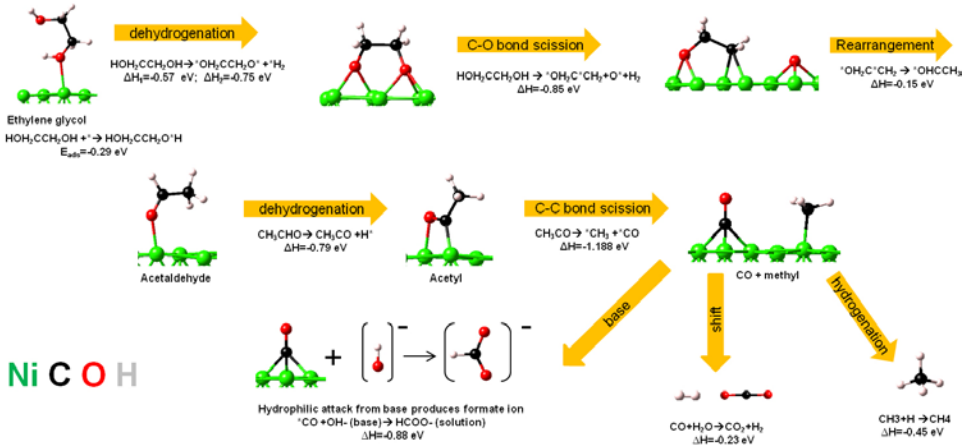


FIGURE 2. Atomistic modeling analysis of the reforming of ethylene glycol over Ni showing the intermediate reaction steps and the reaction enthalpies of their formation.

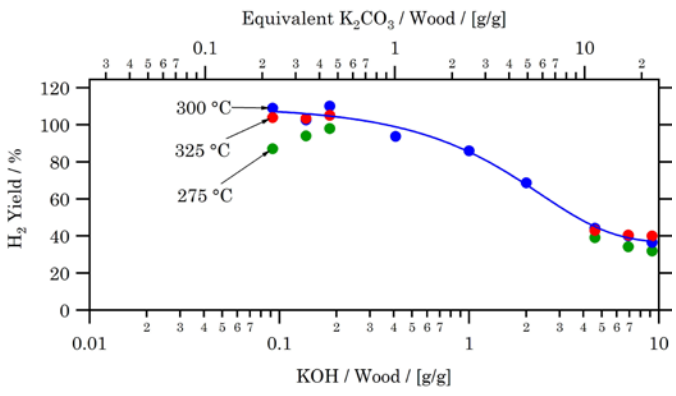


FIGURE 3. Impact of KOH to wood ratio on the H_2 yield with Raney Ni of 8 wt% hybrid poplar in a batch reactor. Also shown on the chart is the equivalent K_2CO_3 to wood ratio.

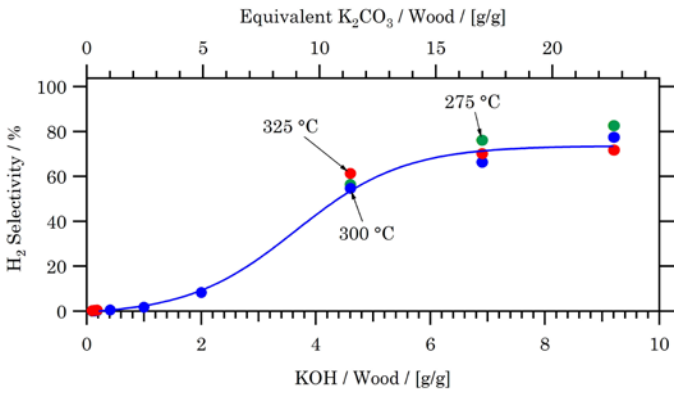


FIGURE 4. Impact of KOH to wood ratio on the H_2 selectivity with Raney Ni of 8 wt% hybrid poplar in a batch reactor. Also shown on the chart is the equivalent K_2CO_3 to wood ratio.

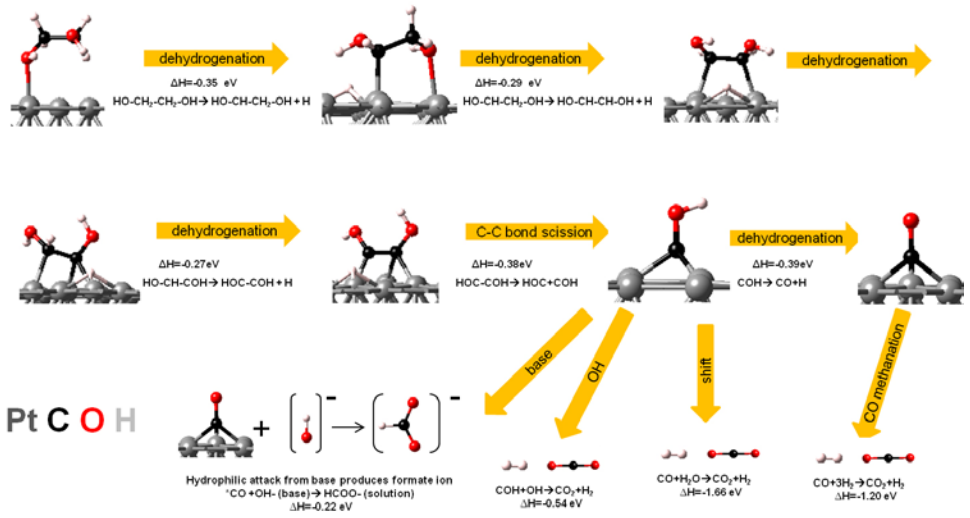


FIGURE 5. Atomistic modeling analysis of the reforming of ethylene glycol over Pt showing the intermediate reaction steps and the reaction enthalpies of their formation.

dehydrogenations. Unlike Ni catalysts, Pt appears to prefer C-C breaking rather than C-O breaking as the first step. As a result, the dehydrogenated species does not go through an ethylenedioxy intermediate as is the case with Ni, but rather undergoes a direct C-C bond scission which results in two COH species. The resulting COH groups can undergo a direct reaction with OH- from the base to form CO_2 and H_2. Alternatively, the COH group can dehydrogenate further to a CO surface species which can react with hydrogen to form methane or be shifted in water to CO_2 and H_2 as happens with Ni. Also similar to the Ni case, the CO can be converted to a formate ion in solution through hydrophilic attack in a basic environment.

These modeling results offer an explanation as to why Pt-based catalysts favor reforming to H_2 while Ni prefers to form methane. Ni-based catalysts prefer to break C-O bonds, which result in both the formation of a methyl group and a CO. Pt-based catalysts prefer to break C-C bonds, resulting in only CO species. The increased preference toward CO species most likely leads to an increase in hydrogen production over methane.

Based on the successful work with base metal catalysts, the final step of the project was the construction and testing of a demonstration unit for H_2 production. This continuous flow demonstration unit consisted of wood slurry and potassium carbonate feed pump systems, two reactors for hydrolysis and reforming, and a gas-liquid separation system. The technical challenges associated with unreacted wood fines and Raney Ni catalyst retention limited the demonstration unit to using a fixed bed Raney Ni catalyst form. The lower activity of the larger particle Raney Ni in turn limited the residence time and thus the wood mass flow feed rate to 50 g min^{-1} for a 1 wt% wood slurry. The project demonstrated continuous flow H_2 yields with unmodified, fixed bed Raney Ni, from 63% to 100% with corresponding H_2 selectivities of 6% to 21%, for periods of several hours. The fixed bed form of the Raney Ni exhibited signs of deactivation which requires further study.

Conclusions and Future Directions

The project showed that it is possible to economically produce H_2 from woody biomass in a carbon neutral manner. However, further development work is required before this process can be commercialized. Some of the key technical areas for future projects are listed in the following.

- Further investigate catalyst kinetics for better reactor sizing.
- Demonstrate >90% base recycle in an integrated system.
- Investigate catalyst durability and higher activity base metal catalysts.
- Wood slurry pump development.
- Integration of a burner unit with the reformer.
- Demonstration of the system on a larger scale.
- Demonstration of the system with power generation (e.g., fuel cell, turbine, or internal combustion engine).

Acknowledgments

This research used resources of the National Center for Computational Sciences at Oak Ridge National Laboratory, which is supported by the Office of Science of the Department of Energy under Contract DE-AC05-00OR22725.

FY 2011 Publications/Presentations

1. Emerson, S.C.; Vanderspurt, T.H. Quarterly Progress Report: A Novel Slurry-Based Biomass Reforming Process, DOE Award

Number DE-FG36-05GO15042, United Technologies Research Center: East Hartford, CT, July 2010.

2. Emerson, S.C.; Vanderspurt, T.H. Quarterly Progress Report: A Novel Slurry-Based Biomass Reforming Process, DOE Award Number DE-FG36-05GO15042, United Technologies Research Center: East Hartford, CT, October 2010.

3. Emerson, S.C. Quarterly Progress Report: A Novel Slurry-Based Biomass Reforming Process, DOE Award Number DE-FG36-05GO15042, United Technologies Research Center: East Hartford, CT, January 2011.

4. Emerson, S.C. Quarterly Progress Report: A Novel Slurry-Based Biomass Reforming Process, DOE Award Number DE-FG36-05GO15042, United Technologies Research Center: East Hartford, CT, April 2011.

5. Davis, T.D.; Emerson, S.C.; Zhu, T.; Willigan, R.R.; Peles, A.; She, Y.; Vanderspurt, T.H. Liquid Phase Reforming of Wood Flour to Hydrogen, Presented at the 2010 AIChE Annual Meeting, Salt Lake City, UT November 7–12, 2010.

References

1. DOE Office of Energy Efficiency and Renewable Energy. Hydrogen, Fuel Cells & Infrastructure Technologies Program Multi-Year Research, Development and Demonstration Plan, U.S. Department of Energy: Washington, D.C., 27 April 2007.

II.B.2 One Step Biomass Gas Reforming-Shift Separation Membrane Reactor

Michael Roberts (Primary Contact),
Razima Souleimanova
Gas Technology Institute (GTI)
1700 South Mount Prospect Rd.
Des Plaines, IL 60018
Phone: (847) 768-0518
E-mail: mike.roberts@gastechnology.org

DOE Managers
HQ: Sara Dillich
Phone: (202) 586-7925
E-mail: Sara.Dillich@ee.doe.gov
GO: Katie Randolph
Phone: (720) 356-1759
E-mail: Katie.Randolph@go.doe.gov

Contract Number: DE-FG36-07GO17001

Subcontractors:
- National Energy Technology Laboratory (NETL), Pittsburgh, PA
- Schott North America, Duryea, PA
- ATI Wah Chang, Albany, OR

Project Start Date: February 1, 2007
Project End Date: June 30, 2013

Fiscal Year (FY) 2011 Objectives

GTI together with its partners, NETL, Schott North America and ATI Wah Chang are working to determine the technical and economic feasibility of using the membrane gasifier to produce hydrogen from biomass. Specifically, the team plans to:

- Reduce the cost of hydrogen from biomass to $2-4/gasoline gallon equivalent (gge) H_2[1] (excluding delivery).
- Develop an efficient membrane reactor that combines biomass gasification, reforming, shift reaction and H_2 separation in one step.
- Develop hydrogen–selective membrane materials compatible with the biomass gasification conditions.
- Demonstrate the feasibility of the concept in a bench-scale biomass gasifier.

Technical Barriers

This project addresses the following technical barriers from the Hydrogen Production section of the Hydrogen, Fuel Cells and Infrastructure Technologies Program Multi-Year Research, Development and Demonstration Plan:

(L) Impurities
(N) Hydrogen Selectivity
(O) Operating Temperature
(P) Flux

Technical Targets

This project is directed at developing a membrane reactor that can be closely-coupled with a gasification reactor while having a sufficiently high hydrogen flux to achieve a hydrogen production cost of $2-4/gge (without delivery) per the DOE 2012 technical target.

FY 2011 Accomplishments

- Development of metallic, glass-ceramic membranes is in progress.
- Preliminary process development and economic analysis with initial candidate membrane proves economic feasibility of the process.
- Membrane module design with initial candidate membrane is finished.
- Fabrication of membrane module is in progress.

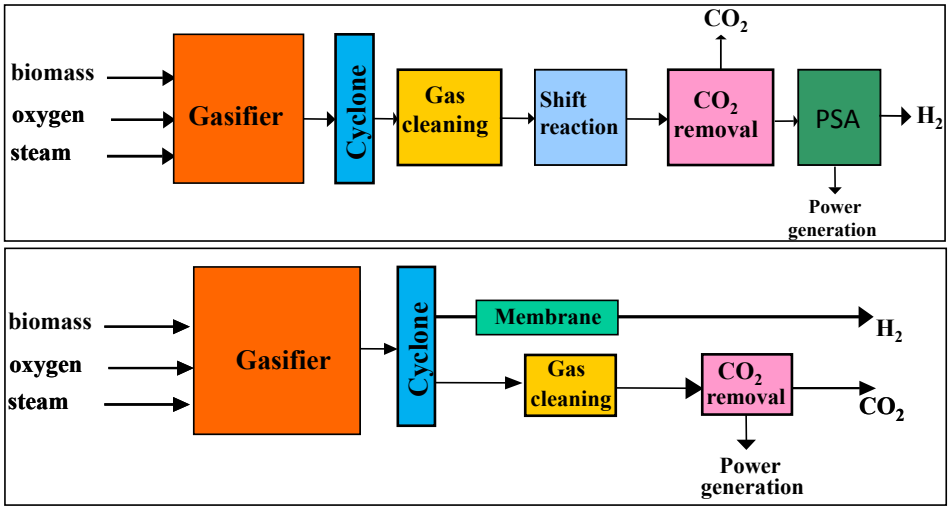


Introduction

GTI has developed a novel concept of membrane reactor for clean, efficient, and low cost production of hydrogen from biomass-derived syngas. Our approach is presented in Figure 1 and shows conventional hydrogen production from biomass gasification and a hydrogen-selective membrane closely coupled with a reforming or gasification reactor for direct extraction of hydrogen from the syngas.

The specific objective of the project is to develop high temperature metallic or glass membranes that can be used closely-coupled with a biomass gasifier. The technical feasibility of using the membrane reactor to produce hydrogen from a biomass gasifier will be evaluated. GTI with its project team (Schott Glass, NETL, and Wah Chang) has been evaluating potential membranes (metal, ceramic and glass) suitable for high temperature, high pressure, and the harsh environment of a biomass gasifier. The project team has been screening and testing each type of material, investigating its thermal and chemical stability, and conducting durability tests.

[1] From presentation on 2011 Annual Merit Review by DOE.



PSA - pressure swing adsorption

FIGURE 1. Conventional Hydrogen Production from Biomass Gasification and Biomass Gasifier with Close-Coupled Membrane

Approach

To conduct commercially successful research, GTI has developed a plan where efforts are concentrated in four major areas: membrane material development, membrane module development, membrane process development and membrane gasifier scale up. The initial focus of the project has been concentrated on membrane material development. Metallic and glass-based membranes have been identified as hydrogen selective membranes under the conditions of the biomass gasification, temperatures above 700°C and pressures up to 30 atmospheres. Membranes are synthesized by arc-rolling for metallic type membranes and incorporating Pd into a glass matrix for glass membranes. Testing for hydrogen permeability properties has been completed and the effects of hydrogen sulfide and carbon monoxide were investigated for perspective membranes. The initial candidate membrane chosen in 2008 was selected for preliminary reactor design and cost estimates. The overall economics of hydrogen production from this new process will be assessed and compared with traditional hydrogen production technologies from biomass. The final deliverable of the project will be a gasification membrane reactor system that is expected to meet or exceed the DOE's cost target for hydrogen production from biomass. This will be demonstrated by a bench-scale gasification membrane reactor that can process approximately 2~10 kg/hr of woody biomass for hydrogen production.

Results

GTI and partners from NETL and Schott continued researching new candidates for hydrogen-selective membranes.

NETL is pursuing a new approach for hydrogen permselective Pd alloys for high temperature use. Superpermeable alloys have desirable characteristics for hydrogen membrane applications including high permeability, high temperature strength and cost, but are very susceptible to poisoning of surface catalytic sites and surface corrosion. A good method to counter these effects is by coating the alloy with a second alloy such as one containing Pd to provide catalytic activity and corrosion protection. Unfortunately, such coatings are likely to be unstable at the temperatures of interest. Therefore, alternative methods of protecting these materials are needed. One possibility being investigated is an inorganic, nonmetallic coating that can protect these alloys at the conditions of interest. Potential inorganic coating systems are being investigated in the literature and synthesis of new tertiary alloy formulations based on Pd metal is in progress.

Two new Pd-based ternary alloys are being fabricated. The alloying components were selected to attempt to improve high temperature strength and alter surface chemistry to improve impurity resistance. A new niobium/tantalum alloy has been identified that may offer high temperature stability under the conditions of interest. These alloys offer good resistance to the corrosive conditions of the post-gasifier environment, however, their hydrogen permeability is not known. More information on the characteristics of these alloys is currently being sought. If they continue to look promising, samples will be acquired or synthesized for testing. Also, 55 wt% Ni-Pt and PdPtAl synthesized earlier in the presence of H_2S is being tested. Due to membrane testing relocations, very restricted membrane testing facilities have been available for several months.

Schott continued development of glass ceramic membranes based on results of membranes synthesized by them and tested by GTI. A new melting protocol was completed to produce larger quantities of material with

greater homogeneous properties for permeability testing. Total conductivity was measured. Electrical conductivity results indicated Schott has fabricated highly-conducting samples; however, this is likely a necessary condition, though not sufficient, to ensure H permeation. Only direct permeation measurements can address this point.

Glass membranes were obtained from Schott and tested for hydrogen permeation. Unfortunately, these new samples, processed using similar means as in 2008, did not yield measurable H permeation at 800°C during testing at GTI. Schott plans to focus on other Pd-containing glass-ceramics, including Pd-Cu and Pd-Ag alloys, and subsequent submittal of these materials for testing by GTI.

GTI continued to test membranes fabricated by GTI and other team members as they become available. The initial candidate membrane Pd-Cu was tested for long-term stability at 800°C in syngas (20% hydrogen, 20% carbon monoxide, 10% carbon dioxide, 10% water and 0.03 % of hydrogen sulfide with balance of helium) atmosphere. The membrane has 83% of initial hydrogen permeation flux after 22 hours. The test was stopped due to a sealing failure. New sealing techniques that can withstand a sour atmosphere were researched.

$Pd_{90}Ta_{10}$ and $Pd_{60}Cu_{20}Ni_{20}$ foils were tested for hydrogen permeation. The results show lower hydrogen permeability as compared with initial candidate membrane ($Pd_{80}Cu_{20}$). Also, $Pd_{80}Cu_{20}$ with thickness 5 microns was purchased. Based on reverse dependence of hydrogen permeation with thickness, we expect to increase hydrogen flux four times. GTI continues to search for a new more promising alloy.

The design of a membrane module that is compatible with the biomass gasifier was completed. The module must be reliable, durable and cost-effective. The membrane module is of planar design for the initial candidate membrane ($Pd_{80}Cu_{20}$). Calculations were made to ensure no diffusion limitation for hydrogen permeation process and uniform gas distribution. Sealing was developed to withstand high temperatures and high pressures of operation. A support was designed to ensure high mechanical stability. Wah Chang assisted in review of membrane module design and their suggestions were incorporated to the membrane module design. Figure 2 shows membrane module inside the pressure vessel.

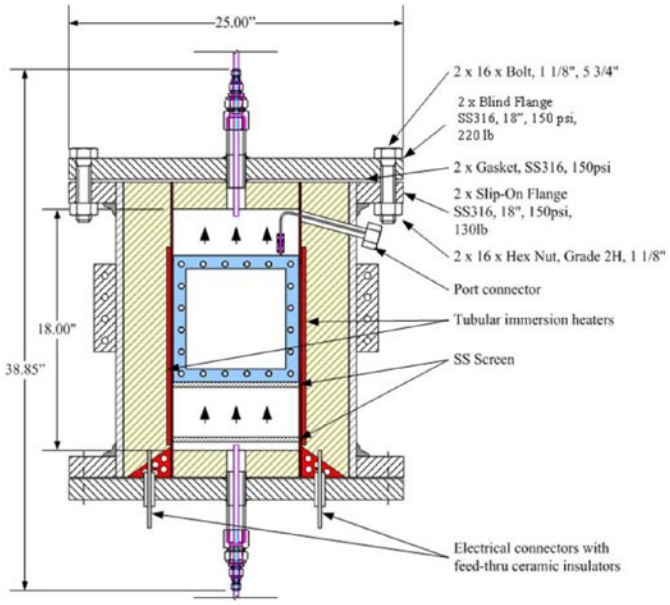


FIGURE 2. Membrane Module Unit in Pressure Vessel

A preliminary techno-economic analysis was performed to determine the potential economic viability of hydrogen production from biomass gasification using an initial candidate membrane-$Pd_{80}Cu_{20}$ foil. Estimating the costs of the process compared to the conventional technology can determine the economic feasibility of a project. Also the analysis is useful in directing research toward areas in which improvements will result in the greatest cost reductions. As the economics of a process are evaluated throughout the life of the project, advancement toward the final goal of commercialization can be measured.

Figure 3 shows the modeling software sequence for process development and costing. RENUGAS® modeling software output such as syngas composition, temperature, pressure, etc was used as input data for the HYSYS® software. The HYSYS model of the process was used to determine the membrane area needed at the specified process conditions for a given level of hydrogen recovery. The Aspen model of the process was then used to determine the stream flow rates and/or process heat duties for all the process steps so that equipment sizes could be estimated.

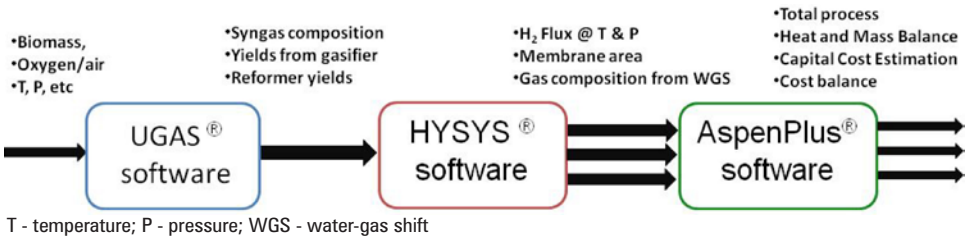
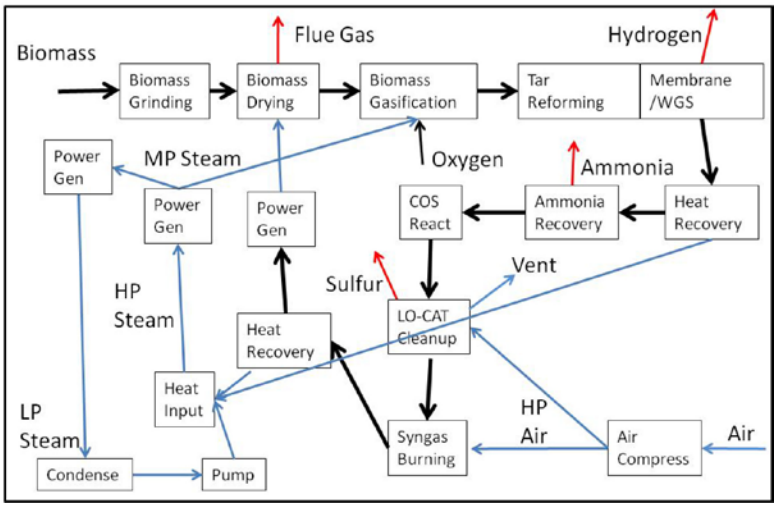


FIGURE 3. Process Modeling Scheme



HP - high pressure; LP - low pressure

FIGURE 4. Process Steps in Gasification with Hydrogen Selective Membrane

The capital cost basis was taken from the pressure swing adsorption (PSA) advanced case [1], and capital cost requirements were scaled from that for the membrane cases. In all the cases, hydrogen compressors were included to raise the pressure of the permeate hydrogen to 300 psi for consistency with the PSA cases. Figure 4 shows that the scope of the membrane process includes feed drying, gasification, reforming with hydrogen recovery, heat recovery, gas clean-up, combustion, and power generation. The main conclusions for Task 2 "Process Development and Techno-Economic Analysis" are:

- Identified process variables affecting process economics.
- Economic optimization was conducted for the variables of reforming (membrane) temperature, permeate pressure, and hydrogen recovery level for membranes 5 microns in thickness. Optimum permeate pressure is about 0.2 bar. Optimum membrane/water-gas shift temperature is at 1,382 °F (750°C) or less. Optimum hydrogen recovery is at 100% of reformer product H_2.
- Economic cost of hydrogen production is comparable with PSA.

Conclusions and Future Directions

- GTI and partners will continue to pursue development of membranes with greater flux and higher resistance to contaminants for the best candidate membrane.
- GTI will continue development of the membrane gasifier process and full economic analysis will be conducted.
- Membrane module design was completed. The module demonstrated a flux rate of 80+ SCFH/ft^2 and is capable of 125 SCFH/ft^2.
- Fabrication of membrane module with initial candidate membrane is in progress.
- GTI will test feasibility of membrane module closely-coupled with a biomass gasifier.

FY 2011 Publications/Presentations

1. Oral presentation (PD070) Roberts, 2011 Annual Merit Review, Washington, D.C., May 9-13, 2011.

References

1. P. Spath, A. Aden, T. Eggeman, M. Ringer, B. Wallace, and J. Jechura, "Biomass to Hydrogen Production Detailed Design and Economics Utilizing the Battelle Columbus Laboratory Indirectly-Heated Gasifier," NREL/TP-510-37408, May 2005.

II.C.1 Zeolite Membrane Reactor for Water-Gas Shift Reaction for Hydrogen Production

Jerry Y.S. Lin
Chemical Engineering
School for Engineering of Matter, Transport and Energy
Arizona State University
Tempe, AZ 85287
Phone: (480) 965-7769
E-mail: Jerry.Lin@asu.edu

DOE Managers
HQ: Amy Manheim
Phone: (202) 586-1507
E-mail: Amy.Manheim@ee.doe.gov
GO: Katie Randolph
Phone: (720) 356-1759
E-mail: Katie.Randolph@go.doe.gov

Contract Number: DE-PS36-05GO15043

Subcontractors:
- University of Cincinnati, Cincinnati, OH
- Arizona State University, Tempe, AZ
- Ohio State University, Columbus, OH

Start Date: July 1, 2005
Projected End Date: October 30, 2011

Fiscal (FY) 2011 Objectives

- To synthesize chemically and thermally stable silicalite membranes with hydrogen permeance >5 x 10^{-7} mol/m^2·s·Pa and H_2/CO_2 selectivity >50.
- To fabricate tubular silicalite membranes and membrane reactor module suitable for membrane reactor applications.
- To identify experimental conditions for the water-gas shift (WGS) reaction in the zeolite membrane reactor that will produce a hydrogen stream with at least 94% purity and a CO_2 stream with 97% purity.

Technical Barriers

This project addresses the following technical barriers from the Production section (3.1) Hydrogen Production of the Fuel Cell Technologies Program Multi-Year Research, Development and Demonstration Plan:

(A) Reformer Capital Costs
(C) Operation and Maintenance (O&M)
(K) Durability
(N) Hydrogen Selectivity
(P) Flux

Technical Targets

This project is focused on fundamental studies of zeolite membrane reactor for WGS reaction for hydrogen production. Insights gained from these studies will be applied towards the development of low-cost, high-efficiency technology for distributed and central hydrogen production that meets the following DOE 2010 hydrogen storage targets:

- Cost: $0.4/kg
- Flux rate: 200 scfh/ft^2
- Hydrogen recovery: >80%
- Hydrogen quality: 99.5%
- Operating capability: 400 psi
- Durability: 26,280 hr

FY 2011 Accomplishments

- Modified silicalite/Zeolite Socony Mobil (ZSM)-5 bilayer membrane synthesized on the yttria-stablized zirconia (YSZ)-coated alumina porous supports for H_2/CO_2 separation factor improvement.
- MFI (zeolite structure code) membranes have negligible water vapor permeance with H_2/H_2O selectivity of about 100, and the presence of water vapor has minimum effect on H_2 permeance and H_2/CO_2 selectivity.
- High H_2/CO_2 separation factor (25) and considerable H_2 permeance (1.26×10^{-7} mol m^{-2} s^{-1} Pa^{-1}) were obtained on the modified silicalite/ZSM-5 bilayer membrane.
- Developed alumina tubular porous supports coated with YSZ barrier layer for stability improvement of tubular MFI zeolite membranes.
- Conducted WGS reactions in the modified disk MFI zeolite membrane reactor at pressures up to 6 atm to enhance the CO-conversion and hydrogen recovery.
- Developed and characterized the most effective catalysts for high-temperature (HT) WGS in the presence of 400 ppm H_2S.



Introduction

Gasification of biomass or heavy feedstock to produce hydrogen fuel gas using current technology includes partial oxidation to produce syngas, the WGS reaction to convert carbon monoxide with water to hydrogen, separation of hydrogen from the product stream, and removal of water vapor and other impurities (such as H_2S)

from the CO_2 containing stream. Commercially, WGS is normally conducted in two or more reactor stages with inter-cooling to maximize conversion for a given catalyst volume. Complete conversion of WGS is possible in a single membrane reactor at high temperatures (~400°C). The membrane removes product hydrogen from the reactor, facilitating higher conversion at a given temperature.

This project is focused on experimental and theoretical studies of the synthesis of a new hydrogen permselective and thermally/chemically stable zeolite membrane and its use in the membrane reactor for the WGS reaction to produce hydrogen and CO_2 rich streams. The membrane reactor system is designed for operation with feeds containing sulfur or other biomass residual contaminants. The zeolite membrane consists of a continuous thin (1-3 μm), aluminum-free silicalite film without intercrystalline micropores on a support with macroporous zirconia and mesoporous silicalite intermediate layers. These composite silicalite membranes in disk and tubular geometries were prepared by a unique technique that combines several synthesis methods including a template-free secondary growth step. Research efforts were also directed towards development of the cost-effective microwave method to synthesize the MFI (a zeolite structure code) zeolite (silicalite and high Si/Al ratio ZSM-5) membranes in disk and tubular geometries.

A new catalyst was developed for the WGS reaction under membrane reactor conditions. The final research task is to perform experimental and modeling studies on the performance of the WGS reaction in the membrane reactors with the silicalite membranes and the catalyst developed in this project. The results obtained in this project will enable development of a large-scale one step membrane reactor process for the WGS reaction for cost-effective production of hydrogen to below $0.40/kg.

Approach

The approach used in this project is to study fundamental issues related to synthesis of high quality, stable zeolite membranes and a membrane reactor for WGS reaction and hydrogen separation. The details of project are to: (1) synthesize disk-shaped and tubular supports with desired intermediate layers and silicalite membranes with a template-free hydrothermal synthesis method; (2) optimize the hydrothermal synthesis condition and perform thorough permeation and separation characterization of silicalite and ZSM-5 membranes; (3) perform chemical vapor deposition for improvement of H_2 permselectivity; (4) develop a microwave synthesis approach to more efficiently and cost-effectively synthesize high quality silicalite membranes; (5) obtain a new WGS catalyst with activity and selectivity comparable to the best available commercial catalyst with improved chemical stability for SO_2 and H_2S containing WGS reaction stream; and (6) develop methods to fabricate a tubular membrane support with desired intermediate layers and a membrane module and sealing system for a tubular membrane reactor that can be operated in WGS conditions.

Results

In order to obtain modified MFI zeolite membrane with high H_2/CO_2 separation factor, considerable H_2 permeance and high chemical and thermal stability, a silicalite/ZSM-5 bilayer membrane consisting of a ZSM-5 top thin layer and a silicalite bottom thick layer was synthesized on an alumina support coated with a YSZ intermediate barrier layer. The YSZ barrier layer was used to prevent the diffusion of Al^{3+} from the alumina porous support into zeolite membrane to improve the stability of the zeolite membrane. The synthesized silicalite/ZSM-5 membrane was modified through catalytic cracking deposition of methyl-diethoxy silane (MDES) carried by equimolar H_2/CO_2 mixture gas at 450°C to improve the H_2/CO_2 separation factor of the membrane.

Figure 1 shows the variations of H_2, CO_2 permeance and H_2/CO_2 separation factor during the on-stream catalytic cracking deposition (CCD) modification of the silicalite/ZSM-5 bilayer membrane at 450°C under H_2/CO_2 reducing environment. The H_2/CO_2 separation factor of the membrane was improved from 4.95 to 25.3 after CCD modification for one hour and got stabilized, indicating that the CCD modification process was fast which is consistent with the previous observation on modification of MFI zeolite disk membranes. The H_2 permeance decreased from 1.85×10^{-7} mol·m^{-2}·s^{-1}·Pa to 1.26×10^{-7} mol·m^{-2}·s^{-1}·Pa with only a reduction rate of 31.9%. The significant improvement of H_2/CO_2 factor with only modest reduction in H_2 permeance is ascribed to the unique structure of the silicalite/ZSM-5 bilayer membrane. Because CCD of MDES precursor only occurred in the ZSM-5 top thin layer instead of the entire

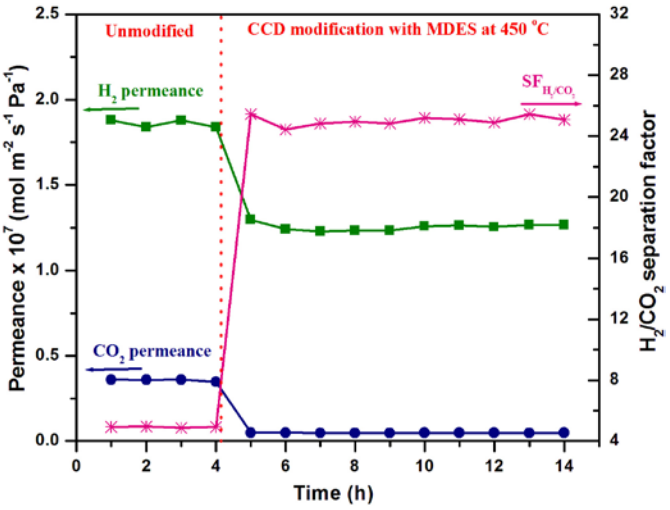


FIGURE 1. On-stream CCD modification of the stability improved silicalite/ZSM-5 bilayer membrane on YSZ coated alumina porous support.

diffusion channel along the membrane thickness direction, the resistance for the gas diffusion through the modified silicalite/ZSM-5 bilayer membrane is much smaller when compared to the membrane with the entire diffusion channel modified with MDES precursor. As a result, the H_2/CO_2 separation factor of the modified bilayer membrane was improved significantly with only modest reduction in H_2 permeance. The silicalite/ZSM-5 bilayer membrane is being shifted to the tubular porous supports with a YSZ intermediate barrier layer for stability improvement.

Understanding the effects of water vapor on gas permeation and separation properties of MFI zeolite membranes was important to the use of the zeolite membranes in WGS. The effects of water vapor on H_2 and CO_2 permeation and separation properties of ZSM-5 (Si/Al~80) zeolite and aluminum-free silicalite membranes were studied by comparing permeation properties of H_2 and CO_2 with the feed of equimolar H_2/CO_2 binary and $H_2/CO_2/H_2O$ ternary mixtures in 300°C-550°C. For both membranes, water vapor permeance was very low, with H_2/H_2O selectivity about 100. The presence of water vapor lowers H_2 and CO_2 permeance to the same extent, resulting in negligible effect on the H_2/CO_2 separation factor. The suppression effect of water vapor on H_2 and CO_2 permeation is larger for the less hydrophobic ZSM-5 zeolite membrane than for the hydrophobic silicalite membrane, and, for both membranes, is stronger at lower temperatures and higher water vapor partial pressures.

The modified silicalite/ZSM-5 bilayer membrane with improved H_2/CO_2 separation property was packed with a catalyst under WGS reaction conditions to examine the long-term stability of the membrane. Figure 2 presents the variations of CO-conversion and H_2 recovery of the modified disk membrane reactor during the long-term stability testing under WGS reaction conditions. The stability testing was conducted at 500°C, gas hourly space velocity (GHSV)=60,000, and H_2O/CO=3. As can be seen from this figure, the CO-conversion increased from 81% to 85% for the first a few days because the catalyst was not fully activated initially. After that, the CO-conversion kept constant at a value of 85% over the entire long-term stability testing period, indicating that the activity of the catalyst was very stable at high temperature under WGS reaction conditions. The H_2 recovery increased from 22.6% to 23.5% with an increase rate of only 3.9% over the stability testing for 28 days. These results also reveal that the modified silicalite/ZSM-5 bilayer membrane reactor with an YSZ intermediate barrier layer was very stable under WGS reaction conditions.

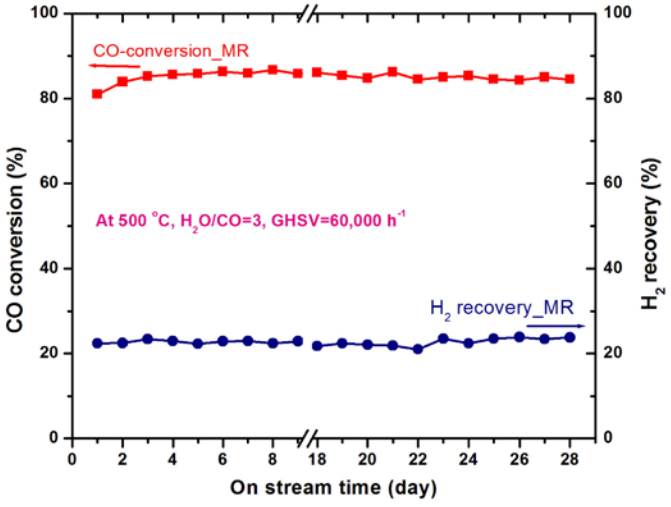


FIGURE 2. Results of stability tests (CO-conversion and H_2 recovery) of the modified silicalite/ZSM-5 bilayer/YSZ membrane disk under water gas shift reaction conditions, (at 500°C, $H_2O/CO=3$, GHSV=60,000 h^{-1}).

To make good quality α-Al_2O_3 tubular supports with YSZ barrier layer for stability improvement of tubular MFI zeolite membranes, the deposition of YSZ support layers was investigated with commercial tubular α-Al_2O_3 carriers from Pall Corporation. The carrier tubes have inner and outer diameters of 7 and 10 mm, respectively, and a specified nominal pore size of 800 nm. A 10 wt% YSZ dispersion was first prepared by dispersing 8 mol% yttria YSZ (TZ-8Y, Tosoh Co.) in an aqueous suspension adjusted to pH 2 with HNO_3. The dispersion was then ultrasonically mixed with a Branson Digital sonifier (Branson Ultrasonics Corp.) for approximately 20 min and screened with 20 µm nylon mesh to remove any agglomerates and external contaminants. A polyvinyl alcohol (PVA) solution was prepared by mixing 3 wt% PVA (Celvol® 125, Celanese Chemicals) with pH 2 HNO_3. The YSZ dispersion was then mixed with the PVA solution in a 3:2 volume ratio and flow coated onto the tubular carriers with an actuator speed of 10 mm/s and residence time of 30 s. The coating procedure was repeated a second time after waiting 30 s. The coated tubes were allowed to dry overnight at room temperature and calcined at 1,000°C for 3 hr with heating and cooling rates of 1.67°C/min.

Scanning electron microscopy (SEM) cross-sections of the YSZ-coated Pall carriers are shown in Figure 3. Figure 3 (a) illustrates the multilayer structure of the modified Pall carriers. A single continuous YSZ coating is observed on top of the two layer α-Al_2O_3 substrate (with an 18 µm thick top layer). From the high magnification SEM cross-section in Figure 3(b), the thickness of the YSZ coating is estimated to be approximately 3 µm. After performing a surface analysis of the coated Pall carrier (Figure 3(c)), the YSZ coating was found to have a much smoother surface than the uncoated carrier (Figure 3(d)). The YSZ-coated tubular alumina porous supports have good quality for MFI zeolite membrane synthesis.

During the reporting period, the work on catalysts was focused on screening the best catalysts for HTWGS reactions in the presence of 400 ppm H_2S. Several different kinds of ferrite-based HTWGS catalysts were synthesized according to the procedure reported in the previous annual report. The best HTWGS catalysts that can be used at

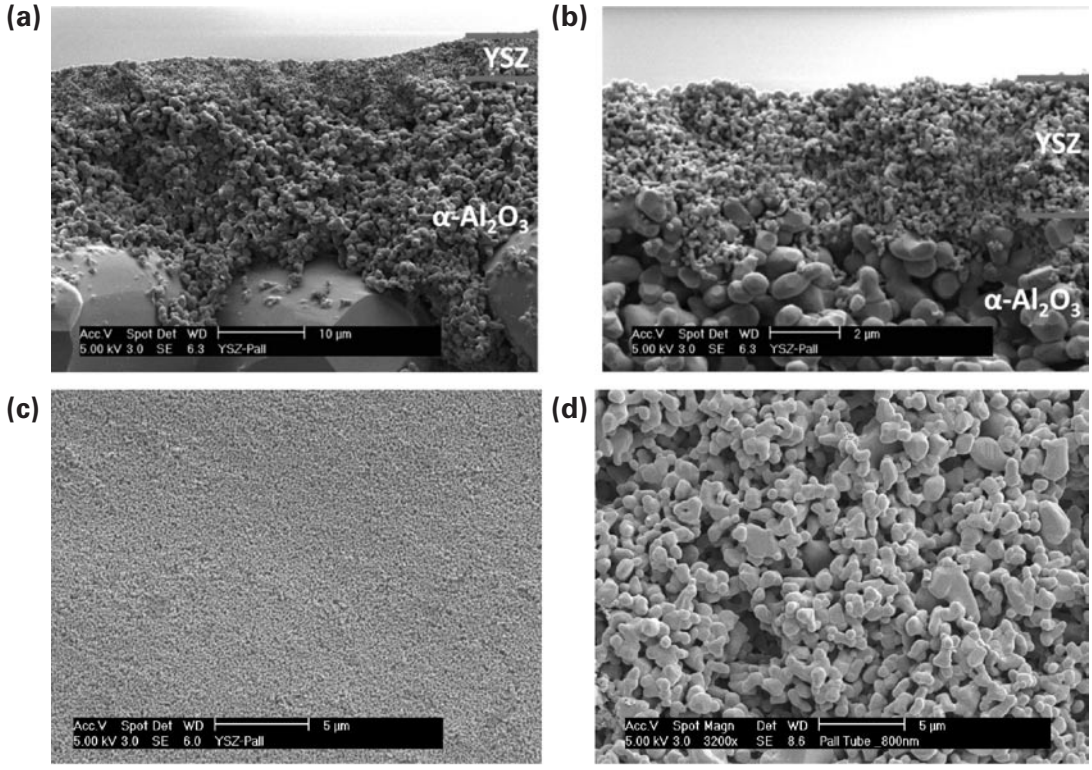


FIGURE 3. Microstructure of the YSZ coated and uncoated alumina tubular support. (a) SEM cross-section of an YSZ coating on a Pall tubular α-Al_2O_3 carrier, (b) High magnification SEM cross-section of YSZ coating on a Pall tubular carrier, (c) SEM surface image of an YSZ coating on a Pall tubular carrier, and (d) SEM surface image of an uncoated Pall tubular carrier.

relatively low and high H_2O/CO ratios in the presence of H_2S were selected and tested, respectively.

HTWGS reaction has been carried out over the catalysts at temperature 500°C and compared with commercial catalyst. WGS reaction was performed at low steam to CO ratio (H_2O/CO=1.5) in the presence of 400 ppm of sulfur. A relatively high space velocity of 60,000 h^{-1} was maintained in all the experiments. On the whole, the WGS operating conditions were chosen to mimic conditions found in a membrane reactor. Before the reaction, all the ferrite catalysts are activated in the presence of process gas at 400°C for 4 h. The activation process was described in our previous reports. WGS activity profile of Fe/Ce/Cr and commercial catalysts for 30 days time on stream experiment is presented in Figure 4(a) at steam to CO ratio of 1.5 and 400 ppm of H_2S. Remarkably, Fe/Ce/Cr catalyst exhibited excellent stability for 30 days. There is no decrease in CO conversion within the permissible error during the 30 days of reaction. On the other hand commercial catalyst started to deactivate from the 4th day onwards. The deactivation continued up to the 13th day and the catalyst became stable. Hence, our shift activity results show that our Fe/Ce/Cr catalyst exhibits better stability compared to the commercial catalyst at specific activation and reaction conditions. The excellent stability of Fe/Ce/Cr is due to the promotional effect of ceria and stabilization effect of chromium.

However, at high steam to CO ratio (H_2O/CO=3.5), the Fe/Ce catalyst exhibited the best long-term stability with/without the presence of 400 ppm H_2S in the gas stream. WGS activity profile of the Fe/Ce catalyst for 30 days time on stream experiment is presented in Figure 4(b) at a steam to CO ratio 3.5. Remarkably, the Fe/Ce catalyst exhibited excellent stability for 30 days. The CO conversion is decreased only from 84 to 80% during the 30 days of reaction. The excellent stability of Fe/Ce is because both iron and ceria undergo a facile charge transfer reaction between $Fe^{III} \leftrightarrow Fe^{II}$ and $Ce^{IV} \leftrightarrow Ce^{III}$ redox couples, respectively; the synergism between the two couples could be responsible for the improved WGS activity. Additionally, at higher temperatures, the rapid transformation of oxygen exchange between Ce^{3+}/Ce^{4+} redox couple, as well as the improvement in the oxygen storage capacity of ceria will help the magnetite to keep its shift stability from CO poisoning. The experiments were also carried out in the presence of 400 ppm of sulfur to check the resistance of Fe/Ce towards sulfur. Interestingly, Fe/Ce catalyst exhibited excellent stability towards sulfur for 30 days as shown in Figure 4(c). The Fe/Ce catalysts in the presence of sulfur exhibited same activity as Fe/Ce catalyst in the absence of sulfur. Here also, the CO conversion is decreased only from 83 to 79% during 30 days of reaction. These results reveal that sulfur has no effect on the structure of Fe/Ce catalyst for the WGS reaction.

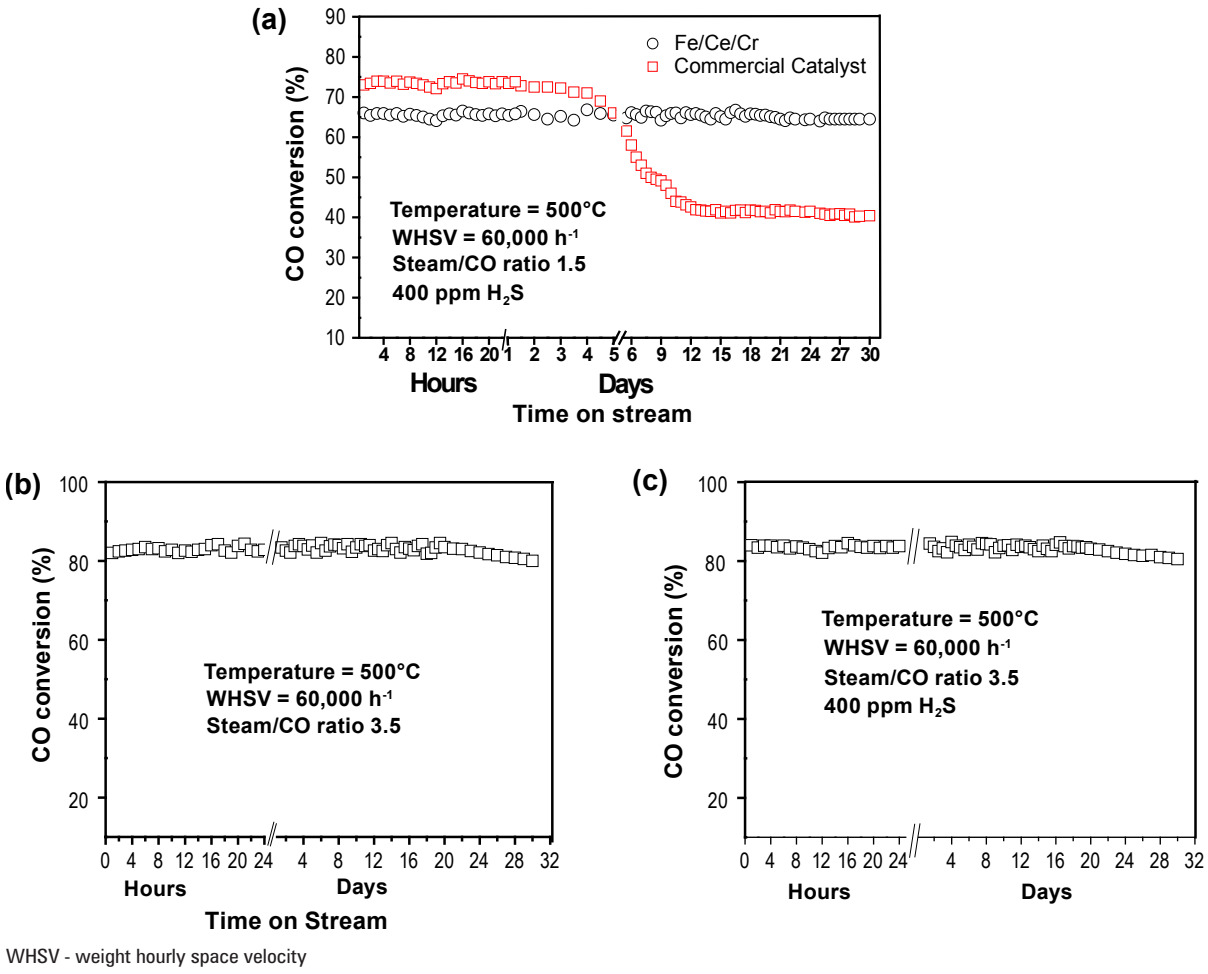


FIGURE 4. (a) Long-term stability of Fe/Ce/Cr and commercial catalysts at steam to CO ratio of 1.5 and 400 ppm of H_2S, (b) long term stability of the Fe/Ce catalyst at steam to CO ratio of 3.5 in the absence of H_2S, and (c) long term stability of the Fe/Ce catalyst for at steam to CO of 3.5 in the presence of 400 ppm of H_2S.

The work conducted on zeolite membrane reactor during the reporting period was focused on WGS reactions in the modified zeolite disk membrane reactor at different pressures (2~6 atm) with fixed GHSV and H_2O/CO ratios. MFI zeolite membranes were synthesized on the alumina porous supports with a YSZ barrier layer for stability improvement. The synthesized membranes were modified through catalytic cracking deposition of MDES precursor for H_2/CO_2 separation factor improvement. HTWGS reaction catalysts that can be used at relatively high and low H_2O/CO ratios were synthesized, respectively. The long-term stability of the catalysts was tested with/without the presence of 400 ppm H_2S in a fixed bed reactor.

The WGS reaction was performed at various feed pressures (2~6 atm) and different temperatures (400-550°C) in a modified disk MFI zeolite membrane. The permeate side pressure was kept at 1 atm. Figure 5 presents the CO conversion in the disk zeolite membrane reactor (MR) at a fixed GHSV of 7,500 h^{-1} as a function of pressure in comparison with the traditional reactor (TR) and the previous results obtained from a tube MR (H_2/CO_2 separation factor ~40). At all temperatures, the CO conversion in the disk MR was increased when feed pressure increased from 2 to 6 atm (constant permeate pressure of 1 atm) because high feed pressure increases ΔP_{H2}, the driving force for H_2 permeation that in turn increases H_2 removal from the catalyst bed. In the TR, the dependence of the CO conversion on the reaction pressure was not significant, with a slight increase in CO conversion of <2%. The CO conversion in disk zeolite MR was higher than that in TR and also higher than the equilibrium CO conversions at 500°C and 550°C, indicating that faster reaction rate and higher H_2 permeance under higher temperature facilitated the WGS reaction to overcome the equilibrium CO conversion. As temperature increased, the CO conversion in disk MR increased gradually to the level of CO conversion in tube MR which has better quality than disk membrane. This suggests that the membrane quality becomes less influential on the MR performance when temperature is sufficiently high.

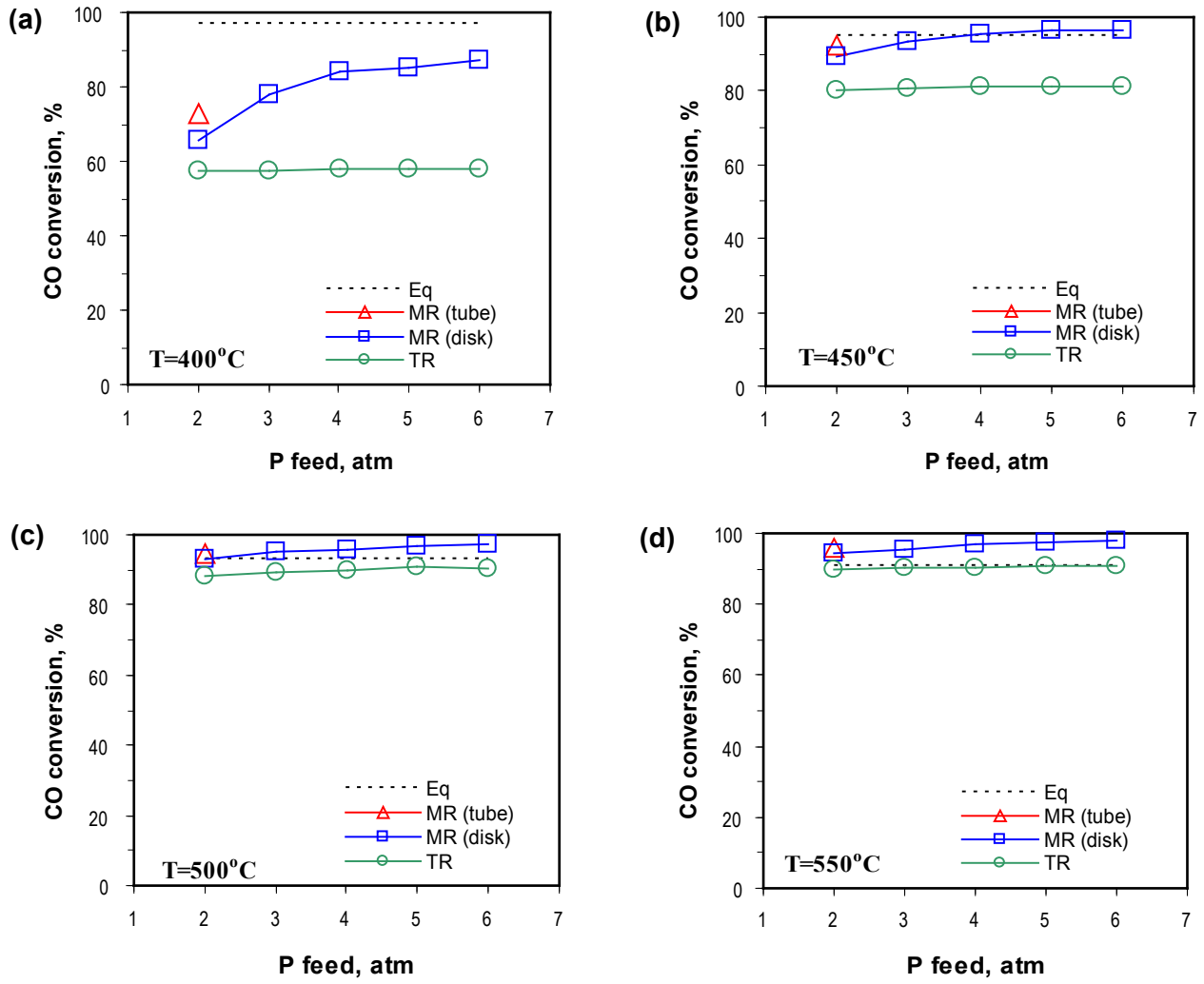


FIGURE 5. CO conversion for a fixed GHSV=7,500 h^{-1} and various temperature of (a) 400°C, (b) 450°C, (c) 500°C and (d) 550°C: (---) equilibrium CO conversion; (Δ) CO conversion under feed pressure 1.5atm in tube MR of previous work; (□) CO conversion in disk MR; (o) CO conversion in TR.

Conclusions and Future Directions

Conclusions

- Silicalite/ZSM-5 bilayer membrane consisting of a silicalite bottom thick layer and a ZSM-5 top thin layer was synthesized on the alumina porous supports coated with YSZ barrier layer for stability improvement.
- The modified silicalite/ZSM-5 bilayer membrane exhibited high H_2/CO_2 separation factor and considerable H_2 permeance.
- Alumina tubular porous supports with YSZ barrier layer for stability improvement were obtained through optimization of a flow coating procedure.
- Several different kinds of ferrite-based catalysts were synthesized and tested in a fixed-bed reactor. The long-term stability of the best sulfur-tolerant HTWGS catalyst was tested in the presence of 400 ppm H_2S.
- WGS reactions were conducted in a modified disk membrane at pressures up to 6 atm to obtain higher CO-conversion and hydrogen recovery.

Future Work

- Test the long-term stability of the modified silicalite/ZSM-5 bilayer membrane under WGS reaction conditions in the presence of 400 H_2S.
- Synthesize and modify the silicalite/ZSM-5 bilayer membrane on the alumina tubular porous supports coated with YSZ barrier layer.
- Conduct WGS reactions in the modified MFI zeolite membrane reactor at pressures up to 20 atm.
- Perform the atmospheric kinetics by using the best catalytic system Fe/Ce/Cr for HTWGS and determine kinetic parameters for that catalyst.
- Economic evaluation of the project results to validate the scale up and operation in an industrial scale.

FY 2011 Publications/Presentations

Journal Papers

1. M.C. Schillo, I.S. Park, W.V. Chiu and H. Verweij, "Rapid Thermal Processing of Inorganic Membranes," *J. Membrane Sci.*, **362,** 127–133 (2010).

2. X.F. Zhu, H.B. Wang, and Y.S. Lin, "Effect of the Membrane Quality on Gas Permeation and Chemical Vapor Deposition Modification of MFI-Type Zeolite Membranes", *Ind. Eng. Chem. Res.* **49**, 10026–10033 (2010).

3. G.K. Reddy, K. Gunasekara, P. Boolchand, and P.G. Smirniotis, "Cr - and Ce – Doped Ferrite Catalysts for the High Temperature Water-Gas Shift Reaction – TPR and Mossbauer Spectroscopic Study", *J. Phys. Chem. C,* **115**, 920–930 (2010).

4. Z. Tang, S.J. Kim, G.K. Reddy, J.H. Dong and P. Smirniotis, "Modified zeolite membrane reactor for high temperature water gas shift reaction", J. Membr. Sci., **354**, 114-122 (2010).

5. H.B. Wang and Y.S. Lin, "Effects of Synthesis Conditions on MFI Zeolite Membrane Quality and Catalytic Cracking Deposition Results", *Microporous and Mesoporous Materials*, **142**, 481-488 (2010).

6. G.K. Reddy, and P.G. Smirniotis, "High Temperature WGS Reaction over Copper Doped Fe/Ce and Fe/Cr Catalysts", *Catalysis Letters* **141**, 27 (2011).

7. G.K. Reddy, K. Gunasekara, P. Boolchand, J. Dong and P.G. Smirniotis, "High temperature water gas shift reaction over nano crystalline copper co-doped modified ferrites". *J. Phys. Chem. C*, **115**, 7586–7595 (2011).

8. H.B. Wang and Y.S. Lin, "Effects of water vapor on gas permeation and separation properties of MFI zeolite membranes at high temperatures", *AIChE Journal*, 2011, DOI: 10.1002/aic.12622.

Conference Presentations

1. Y.S. Lin, "Zeoltie membranes for high temperature gas separations", Plenary Lecture, 2010 Chemical Engineering Conference, Amman, Jordan, Oct.10–13, 2010.

2. H.B. Wang and Y.S. Lin, "Improving H_2/CO_2 separation factor of MFI zeolite membranes through catalytic cracking deposition of silane", Gordon Research Conference: Membrane Materials and Processes, (Poster) New London, NH, July 25, 30, 2010.

3. Y.S. Lin and H. B. Wang, "Effects of water vapor on gas separation properties of zeolite membranes," ACS National Meeting, Anaheim, CA, March 26-30, 2011.

4. H.B. Wang, Y.S. Lin, "Synthesis and catalytic cracking modification of silicalite/ZSM-5 bilayer membrane", NAMS Meeting, Las Vegas, NV, June 4–8, 2011.

5. S. Kim, J. Provenzano, Z. Xu, G. Reddy, P. Smirniotis, J. Dong, "High temperature water gas shift reaction in a modified zeolite membrane reactor: effect of operation pressure and long term stability", NAMS Meeting, Las Vegas, NV, June 4–8, 2011.

6. S. Kim, J. Provenzano, Z. Xu, G. Reddy, P. Smirniotis, J. Dong, "Water gas shift reaction of simulated syngas in a zeolite membrane reactor", NAMS Meeting, Las Vegas, NV, June 4–8, 2011.

II.C.2 Development of Hydrogen Selective Membranes/Modules as Reactors/ Separators for Distributed Hydrogen Production

Paul KT Liu
Media and Process Technology Inc. (M&P)
1155 William Pitt Way
Pittsburgh, PA 15238
Phone: (412) 826-3711
E-mail: pliu@mediaandprocess.com

DOE Managers
HQ: Amy Manheim
Phone: (202) 586-1507
E-mail: Amy.Manheim@ee.doe.gov
GO: Katie Rudolph
Phone: (720) 356-1759
E-mail: Katie.Randolph@go.doe.gov

Contract Number: DE-FG36-05GO15092

Subcontractor:
University of Southern California, Los Angeles, CA

Project Start Date: July 1, 2005
Projected Ended Date: December 31, 2011

Fiscal Year (FY) 2011 Objectives

- Develop a highly efficient, low-temperature membrane-based bench-scale water-gas shift (WGS) reaction process, test it at pilot scale, and demonstrate the process in a field test unit.
- Screen existing membranes and modify the membranes for the proposed process and reactor.
- Determine hydrogen production costs and define system integration requirements for commercialization.
- Reduce capital and operating costs for distributed hydrogen production applications.

Technical Barriers

This project addresses the following technical barriers as presented in Section 3.1 Hydrogen Production Technical Plan, Fuel Cell Technologies Program, Multi-Year Research, Development and Demonstration Plan for 2005 to 2015 (updated October 2007):

(K) Durability
(L) Impurities (Hydrogen Quality)
(M) Membrane Defects
(N) Hydrogen Selectivity
(P) Flux
(R) Cost

Technical Targets

The WGS reaction is considered one of the least efficient unit operations for hydrogen production via steam reforming. This project focuses on developing a highly efficient, low-temperature, low-cost membrane-based WGS reaction process. 2010 Technical Target values for dense metallic membranes include:

- Flux Rate - 250 scfh/ft^2 at 20 psig pressure
- Membrane Material and All Module Costs - $1,000/$ft^2$ of membrane
- Durability – 2,680 hours
- Operating Capability - 400 psi
- Hydrogen Recovery - >80% (of total gas)
- Hydrogen Quality - 99.99%

FY 2011 Accomplishments

- Verified palladium (Pd) membrane bundle performance and separation properties at pilot plant and end-user site.
- Confirmed Pd membrane bundles long term thermal cycling stability in nitrogen are similar to results for single membrane tubes (~20°C to 350°C).
- Developed a post treatment hydrogen product purity strategy that reduced 300, 70 and 10 ppm CO in hydrogen to 16, 1.2 and 0.3 ppm respectively.
- Identified a potential alloy for upgrading our Pd membrane product that will support improved stability during cooling in the presence of hydrogen.



Introduction

Membrane separation traditionally has been considered a simple, low-cost and compact process. At the same time, the WGS reaction is one of the least efficient unit operations for hydrogen production via steam reforming. This project will focus on the development of technology components associated with a WGS reactor/separator membrane process to enhance the hydrogen production efficiency for distributed hydrogen production.

Pd membranes, one set of dense metallic membranes, are capable of delivering high purity hydrogen product with a high recovery ratio. Specifically, this project will fabricate tubular Pd membranes by depositing Pd thin film over a ceramic substrate and bundling the tubes into a reactor. During 2010-2011, a test quantity of Pd membrane bundles suitable for packaging into the membrane reactor were field tested. The project target of producing a hydrogen

product stream with <<10 ppm CO was achieved. Also, an evaluation of a series of Pd-alloy foils established the fundamental basis for the development of a Pd-based membrane with cooling stability in the presence of hydrogen. Further confirmation through field testing will be pursued in FY 2011-2012.

Approach

Our overall technical approach includes three steps as follows:

1. Bench-Scale Verification
   - Evaluate membrane reactor: use existing membrane and catalyst via math simulation.
   - Experimental verification: use upgraded membrane and existing catalyst via bench unit.
   - Validate membrane and membrane reactor performance and economics.
2. Pilot Scale Testing
   - Prepare membranes, module, and housing for pilot testing.
   - Perform pilot-scale testing.
   - Perform economic analysis and technical evaluation.
   - Prepare field testing.
3. Field Demonstration
   - Fabricate membranes and membrane reactors and prepare catalysts.
   - Prepare site and install reactor.
   - Perform field test.
   - Conduct system integration study.
   - Finalize economic analysis and refine performance simulation.

Results

1. Produced an 11-tube 24-Inch Length Second Generation Pd Membrane Bundle

Ceramic-based Pd membrane tubes were successfully developed and tested previously. In addition, a membrane bundling technique was developed for potting these tubes into a bundle for packaging into a membrane housing for commercial use. Over the last year, several Pd membrane tube bundles have been produced and evaluated, and these bundles will be packaged into the membrane reactor for field testing to demonstrate the proposed WGS membrane reactor in FY 2012. Table 1 shows the performance of the four bundles produced. One of these bundles (Pd-B-4) was evaluated for its mixed gas performance. Mixed gas testing was conducted at ca. 380˚C using an 80/20 vol% H_2/Ar blend. The H_2 permeance and H_2/Ar selectivity in the mixture were 7.1 and 1,220 $m^3/m^2/hr/bar$, respectively, and are consistent with the pure component result. Furthermore, the performance of these Pd membranes has been confirmed in field testing at our end-user facility using both synthetic and actual reformate.

2. Tested Thermal and Thermal Cycling Stability of Our Pd Membrane Tube Bundles

This year membrane tube bundles were subjected to thermal and thermal cycling stability testing similar to testing performed last year on Pd membrane tubes for >2,500 hours (see Figure 1). About 140 thermal cycles between 25 and 350°C have been performed. The Pd membrane bundle maintains its excellent H_2/N_2 selectivity of ~4,000. Separately the thermal stability of the membrane bundle was tested for ~400 hours. The bundle maintains its hydrogen permeance of ~15 $m^3/m^2/hr/bar$ and selectivity of 10,000 – 15,000 at 350°C. This thermal stability test will be continuing into the next year. In summary, the thermal and thermal cycling stability of the Pd membrane tube bundles are excellent, similar to the tubes tested previously, and the improved performance is, in part, the result of the potting technique developed for the proposed applications.

3. Demonstrated H_2 Post-Treatment CO Reduction in the WGS-Membrane Reactor

Our previous bench-top WGS membrane reactor experimental study demonstrated the ability of our membrane to reduce CO contamination of hydrogen to 50 ppm or below, depending in part upon the degree of hydrogen recovery, and the transmembrane pressure drop. During this year, we have developed a post-treatment technique that is to be integrated into our membrane reactor to further reduce the CO level. Our experimental study demonstrated the reduction of CO from 50-300 ppm to ~0.3 to 16 ppm respectively, as illustrated in Figure 2. In

TABLE 1. Pure Component Permeance and Selectivity of the Pd Bundles Prepared and Tested during 2010-2011

Bundle ID (-)	Tube Count (#)	Temperature (°C)	Pressure (psig)	H_2 ($m^3/m^2/hr/bar$)	H_2/N_2 (-)	Comments
#1	11	336	2.6	6.1	1,100	Broken
#2	14	337	2	9.8	1,600	
#3	14	338	2	7.9	780	
#4	14	337	2	6.2	1,800	

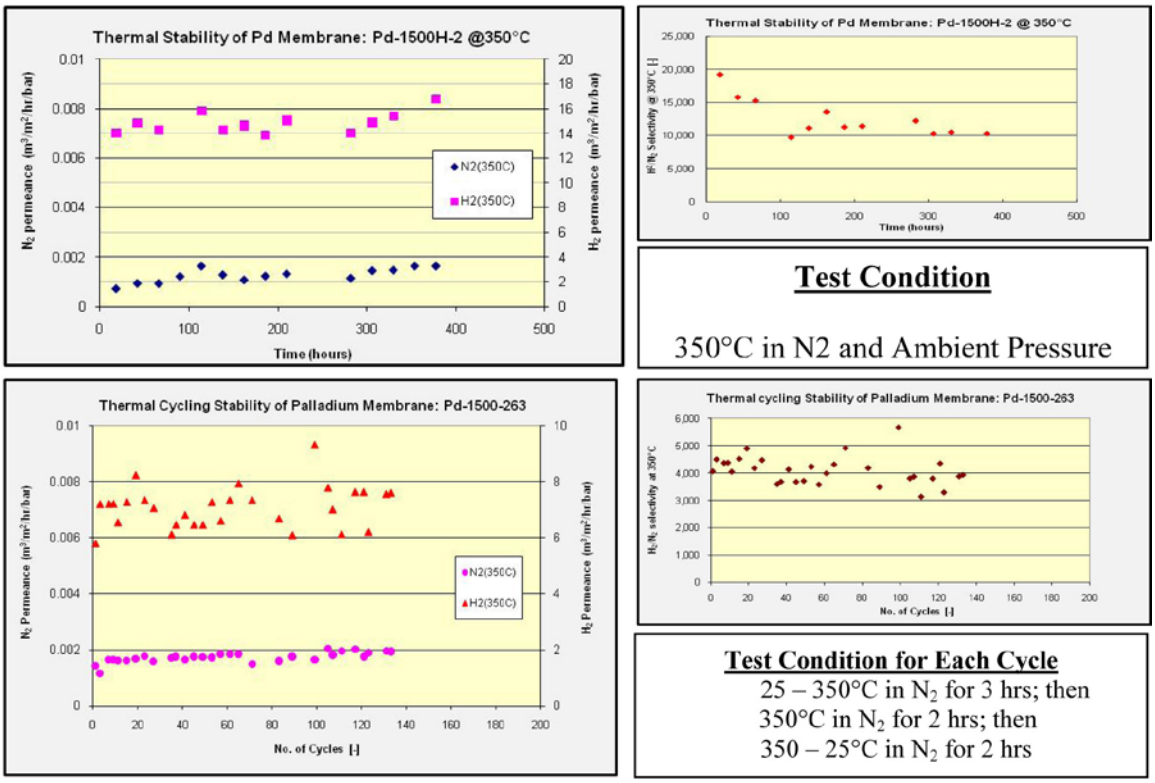


FIGURE 1. Evaluation of Thermal and Thermal Cycling Stability of the Pd Membrane Tube Bundles

the upcoming year, we will perform WGS membrane reactor runs integrated with this post treatment to demonstrate the reduction of CO in the final product to <<10 ppm.

4. Cooled Pd Membranes in the Presence of Hydrogen

The application selected by our end-user requires the ability to cool the membrane in the presence of residual

CO Contaminant in the Hydrogen Stream Produced from WGS-MR

As shown in our previous membrane reactor study, our palladium membrane has been able to deliver a hydrogen product stream with ~50 ppm CO using our standard Pd membrane as a reactor.

Our Proposed Solution to Reduce CO Contaminant Level

A post treatment strategy has been developed and experimentally demonstrated on the technical feasibility in reducing CO contaminant to an extremely low level, such as <10-1 ppm as shown below

Concentration of CO in Feed [ppm]	Residual CO in Product [ppm]	W/F [g catalyst/(mol CO/hr)]
300	16	4,148
70	1.1	17,778
50	0.3	24,889

Activities Planned in 2011

- demonstrate this post treatment strategy in conjunction with our WGS-MR.
- further incorporate this post treatment into our WGS-MR as an integrated membrane reactor.

FIGURE 2. Post-Treatment for Reduction of CO Contaminant Level in Hydrogen Produced from our WGS-Membrane Reactor

hydrogen following shut-down of the hydrogen generator. Although this is a very desirable feature for the commercial use of the Pd membrane, very few literature studies have addressed this issue. The pure Pd membrane such as those we have produced thus far failed to maintain their membrane materials stability through cooling from 350 to 25°C in the presence of hydrogen. This year we conducted a laboratory evaluation study using commercially available Pd alloy flat discs to determine the alloy formula required to sustain the cooling cycle. The results of our evaluation for the Pd-Ag (23%) and Pd-Cu (40%) alloys are presented in Figures 3 and 4. No damage through the cooling test for both alloys was observed under visual and scanning electron microscope examination. However, the H_2/N_2 selectivity

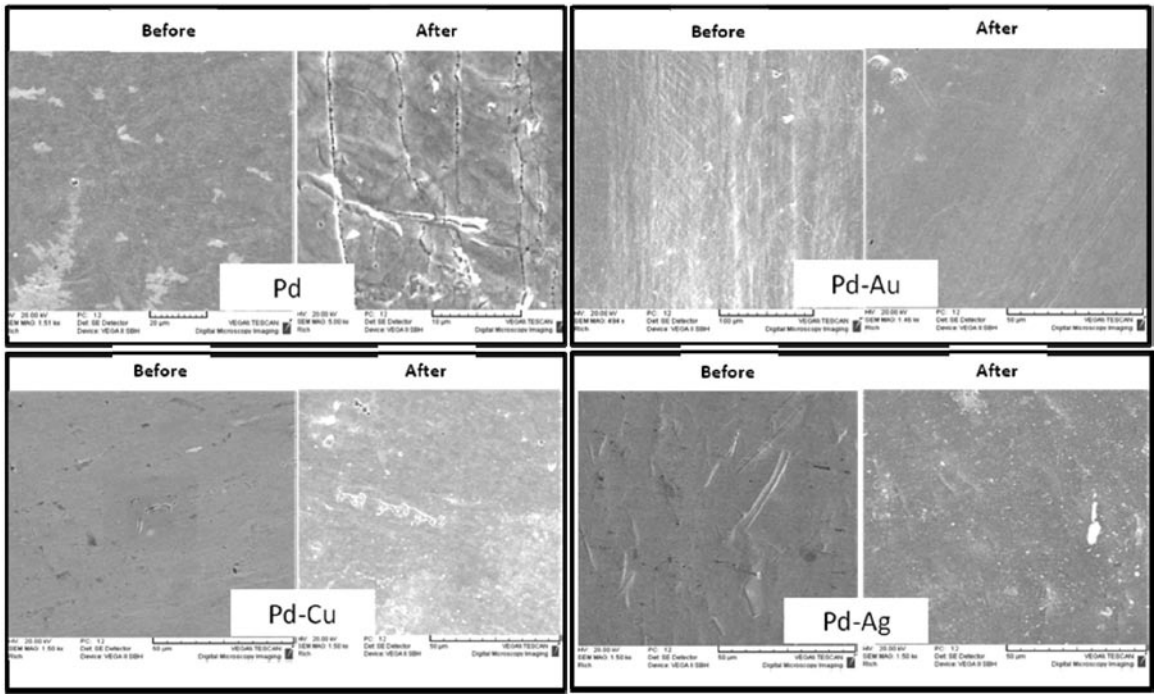


FIGURE 3. Evaluation of Pd Alloy Flat Discs for their Cooling Stability in the Presence of Hydrogen Required by Our Target Applications

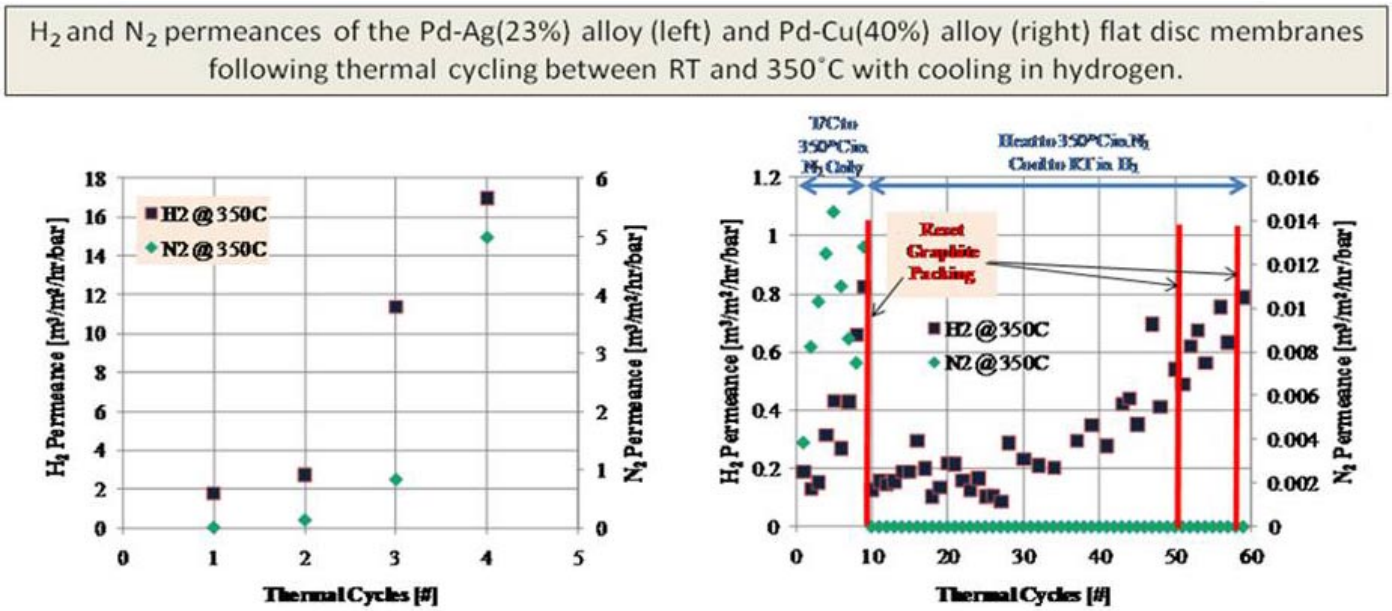


FIGURE 4. Evaluation of Pd-Ag vs. Pd-Cu for the Cooling Stability in the Presence of Hydrogen

for the Pd-Ag alloy deteriorates severely after 3-4 cycles while the Pd-Cu remains intact (i.e., N_2 permeance ≤0.01 $m^3/m^2/hr/bar$) for up to 60 cycles. In addition when the Pd-Au alloy was used in the Pd membrane considerable damage was exhibited throughout the test. In summary, we believe the Pd-Cu (40%) offers a fundamental basis for us to prepare a supported Pd membrane which can sustain the cooling in the presence of hydrogen. We will pursue fabrication of the Pd-Cu alloy membrane on our ceramic support in FY 2012.

Conclusions and Future Direction

- A newly developed potting technique has enabled packaging low-cost Pd membrane tubes into commercially viable bundles.
- Both pilot and field tests confirmed the separation efficiency of the Pd membrane bundles is similar to the performance of single membrane tubes.
- Bench-top feasibility tests indicate that the new post treatment strategy should reduce CO contamination to well below 10 ppm.
- A full-scale membrane reactor packed with our Pd membrane bundles and equipped with internal cooling coils has been designed and is currently under fabrication for the field test to be conducted in 2011.
- Commercially available Pd alloy foils of Pd-Ag (23%) and Pd-Cu (40%) remain intact through multiple cooling cycles, suggesting that Pd-Cu alloy could produce cooling stability for the reactor in the presence of hydrogen. This cooling stability is a desirable feature for our target application.

Our FY 2012 activities will be focused on the following areas:

- Complete fabrication and field test the full-scale membrane reactor packed with the Pd membrane bundles and equipped with cooling coils.
- Integrate the post-treatment strategy into the membrane reactor to deliver hydrogen product with <<10 ppm CO.
- Conduct a field test with the use of the membrane reactor at the participating end-user site.
- Develop the third generation Pd membrane with the cooling stability in the presence of hydrogen.

FY 2011 Publications and Presentations

1. Abdollahi, M., Yu, J., Liu, P.K.T., Ciora, R., Sahimi, M., and Tsotsis, T.T., "Process Intensification in Hydrogen Production from Syngas," *Ind. Eng. Chem. Res*., 49, 10986, 2010.

2. Tsotsis, T.T., Sahimi, M., Fayyaz-Najafi, B., Harale, A., Park, B.G., Liu, P.K.T., "Hybrid Adsorptive Membrane Reactor," *U.S. Patent* 7,897,122, March 1, 2011.

3. Abdollahi, M., Yu, J., Liu, P.K.T., Ciora, R., Sahimi, M., and Tsotsis, T.T., "Ultra Pure Hydrogen Production from Reformate Mixtures using a Palladium Membrane Reactor System," submitted to *J. Membrane Sci.*

II.C.3 High Performance Palladium-Based Membrane for Hydrogen Separation and Purification

Ashok Damle
Pall Corporation
25 Harbor Park Drive
Port Washington, NY 11050
Phone: (516) 801-9581
E-mail: Ashok_Damle@Pall.com

DOE Managers
HQ: Amy Manheim
Phone: (202) 586-1507
E-mail: Amy.Manheim@ee.doe.gov
GO: Katie Randolph
Phone: (720) 356-1759
E-mail: Katie.Randolph@go.doe.gov

Contract Number: DE-FG36-05GO15093

Subcontractors:
- Colorado School of Mines, Golden, CO
- Oak Ridge National Laboratory, Oak Ridge, TN

Project Start Date: July 1, 2005
Project End Date: September 30, 2011

Fiscal Year (FY) 2011 Objectives

The overall project objective is the development, demonstration and economic analysis of a Pd-alloy membrane that enables the production of 99.99% pure H_2 from reformed natural gas as well as reformed bio-derived liquid fuels such as ethanol at a cost of $2-3/gasoline gallon equivalent by 2011. The specific objectives for the past year were:

- Conduct long-term durability testing of Pd-alloy membranes in syngas/water-gas shift (WGS) reaction environments meeting Phase III performance goals.
- Determine the optimal Pd-alloy membrane composition and thickness to assure stable performance with respect to product hydrogen flux and purity in WGS reaction environments.
- Scale up the substrate and membrane synthesis processes to 12" elements.
- Design and fabricate multi-tube modules minimizing concentration polarization effects at high hydrogen recoveries.
- Work with an end user to compare cost/performance of a membrane-based system to pressure swing adsorption (PSA) and solvent-based systems for large-scale hydrogen production with CO_2 capture.

Technical Barriers

This project addresses the following technical barriers from the Hydrogen Production section of the Fuel Cell Technologies Program Multi-Year Research, Development and Demonstration Plan and the technical targets indicated in Table 1:

(K) Durability
(L) Impurities (Hydrogen Quality)
(M) Membrane Defects
(N) Hydrogen Selectivity
(O) Operating Temperature
(P) Flux
(Q) Testing and Analysis
(R) Cost

TABLE 1. Applicable Technical Targets for Dense Metallic Membranes and Current Project Status

Performance Criteria	2010 Target	2015 Target	Pall Status 2011
Flux SCFH/ft^2 @20 psi ΔP H_2 partial pressure and 15 psig permeate side pressure	250	300	270*
Membrane Cost, $/ft^2 (including all module costs)	$1,000	<$500	<$1,000
ΔP Operating Capability, system pressure, psi	400	400-600	>600 PSI
Hydrogen Recovery (% of total gas)	>80	>90	>80**
Hydrogen Permeate Quality	99.99%	>99.99%	99.999%***
Stability/Durability	2 years	>5 years	To be determined

*Maximum observed. Averaged over more than 20 samples ~190 scfh/ft^2.
** Measured on a 50%H_2/21%H_2O/up to 3.5% CO/balance CO_2 mixed gas stream. Hydrogen flux and recovery measurements are planned with other impurities starting in mid-2009. The experimentally observed recovery is determined by chosen operating conditions and is not necessarily a limit of the membrane performance.
*** Projected purity based on H_2/N_2 ideal selectivity.

FY 2011 Accomplishments To Date with Specific Barriers Addressed

- Determined optimal Pd-alloy membrane composition as $Pd_{90}Au_{10}$ to assure stable performance with respect to product hydrogen flux and purity in WGS reaction environments (K, L, N, P, Q).
- Increased membrane operating capabilities to 400 psi at 550°C through use of 310SC stainless steel tubular substrate.

- Optimized and scaled up the membrane and diffusion barrier coating process to 12-inch lengths. The substrate tube manufacturing capability is up to 1 m length (N, R).
- Developed a commercial welding process for non-porous fittings to porous tubes (N, R).
- Met Phase III performance goal demonstrating up to 500 hours of durability testing on Pd-alloy membranes in syngas/WGS reaction environments meeting Phase III performance goals (K, L, N, P, Q).
- Observed high mixed gas hydrogen flux rate (145 scfh/ft^2-atm$^{0.5}$) and high hydrogen purity (<99.95%) for up to 120 hours at an operating feed side pressure of >200 psig (K, L, N, P, Q).
- Observed a reversible H_2 flux decline with H_2S exposure during testing with low concentration H_2S exposure (K, L, N, P, Q).
- Demonstrated membrane performance stability with thermal cycling (50–400°C) (K, Q).
- Showed an achievable end-user cost of less than $1,000 per ft^2 of area for a stand-alone membrane separator device (R).
- Minimized concentration polarization effects while maintaining high hydrogen recoveries for a 12-tube, 12-inch long, multi-tube module (P, R).
- Directed Technologies, Inc. calculated that a membrane-based process can enable cost reduction through process intensification and that the hydrogen production cost target of $3/kg is achievable. The capital equipment cost estimate is based on sale price to the end user for membrane in a module (R).



Introduction

This project is focused on optimizing the overall composition of the Pd alloy, intermediate layers and tubular support, as well as on the manufacturing methods required to produce a very thin, high-flux, cost-effective membrane for H_2 separation and purification on a robust, porous, inorganic substrate. The substrate[1] is readily scalable to high volume production as it is manufactured in long lengths. Robust high area modules can be made by welding multiple tubes into a pressure vessel, eliminating low temperature seal materials.

Approach

The approach is to further develop and optimize the performance of Pd alloy membranes that have been shown to have both high flux rate and high separation factor for H_2 from reformate. This is being accomplished by design of a composite membrane based on robust, tubular, porous metal media as a substrate. The substrate is modified by the addition of a uniform, fine pore size diffusion barrier layer. The deposition methods are modified to produce a thin, uniform, functional gas separation Pd-alloy membrane layer. The project plan includes commercial scale up of the high quality porous metal substrate and diffusion barrier layer that enables the development of a technically and economically viable composite membrane. Membrane alloy composition and thickness is optimized for assuring high hydrogen flux and selectivity as well as long-term durability with tolerance to contaminants. The membrane performance is determined under typical operating conditions for a reformed natural gas or bio-derived liquid fuels stream. The H2A model, modified to incorporate a membrane reactor design, is used to verify economic viability. Our plan is to confirm an increase in the overall energy efficiency of a H_2 reforming system through the use of membrane technology for process intensification. Economic modeling is conducted to determine the cost benefit of an integrated membrane reactor that results from fewer pressure vessels and reduced catalyst volumes. An end user is conducting system economic and energy analyses and comparing the results to PSA and amine-based systems.

[1] Pall's AccuSep® inorganic media

Results

Membrane Development

The process for depositing ceramic on the porous metal tubes was modified to increase the diffusion barrier substrate surface roughness and eliminate potential film stresses and membrane film delaminations observed in some of the earlier composite Pd-alloy membrane samples. Synthesis of membrane with varying thickness in 3 to 9 micron range and Pd-Au alloy composition in 0-30% Au range were prepared for determining optimal membrane composition and thickness for long-term stable membrane performance.

The substrate as well as Pd-alloy composite membrane synthesis processes were successfully scaled up to prepare elements of 12" overall length with 10" active membrane length. The scaled up membranes were tested to confirm their hydrogen separation performance as observed in shorter (2" active length) membranes. Several 12" overall length ceramic porous metal AccuSep® substrates were prepared and composite Pd-alloy membranes are being prepared for assembling them in a multi-tube module and testing in WGS environment. For the 12-tube module assembly, eight Pd-alloy membranes are complete while five more are currently being fabricated.

Membrane Durability Testing in WGS Streams and Membrane Optimization

Extensive testing of Pd-alloy membranes in pure gas streams and in methanol/natural gas reformate environments was conducted for parametric evaluation of their performance. For example, effect of concentration polarization and CO concentration was observed in another test with a $Pd_{95}Au_5$ membrane of 8 µm thickness with three

different feed gas mixtures consisting of H_2/Ar, H_2/Ar/steam and WGS mixture (50% H_2, 25%CO_2, 20% H_2O, 5%CO – WGS-5) at 400°C and 132 psi feed pressure with a feed flow rate of 2,000 mL/min. The permeate pressure was 17 psia. The results shown in Figure 1 indicated a H_2 flux reduction due to the concentration polarization effect of ~20%, with an additional flux reduction of 20% due to CO.

The standard WGS composition was determined to be insufficient to cause a decline in flux or H_2 purity of most of the membranes for determination of the optimum alloy composition or thickness. For example, a 2.2 micron thick $Pd_{87}Au_{13}$ alloy membrane on Pall Accusep® support was tested in WGS with high CO content and steam to CO ratio of 1:1 (50% H_2 10% CO_2, 20% CO and 20% steam – WGS-20). Temperature was varied between 400°C and 450°C. This composition also was determined to be insufficient to cause a decline in flux or purity and stable permeance and purity performance over ~400 hours is shown in Figure 2.

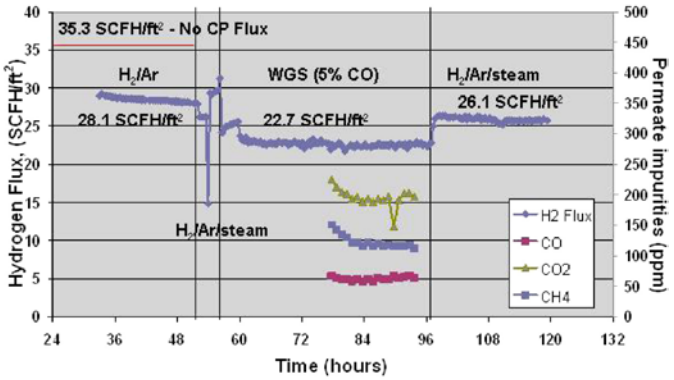


FIGURE 1. Hydrogen Flux Reduction due to Concentration Polarization and CO

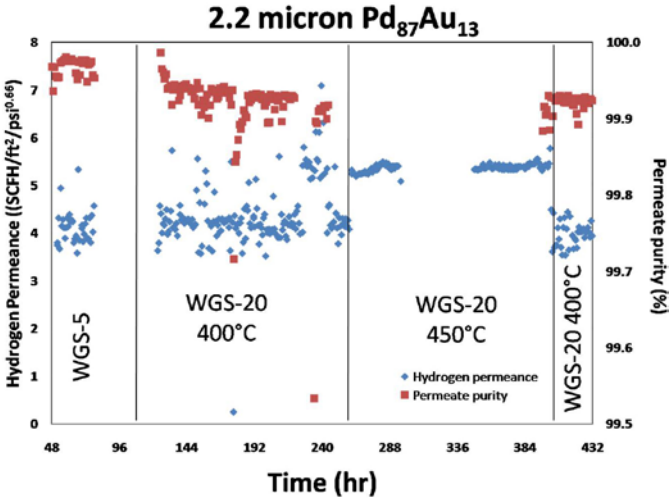


FIGURE 2. Stable Membrane Performance in WGS-5 and WGS-20 Syngas Conditions

To facilitate rapid durability evaluation of several alloy compositions an accelerated life test based on an aggressive variant of the WGS composition was tested and determined to be sufficient to cause a decline in the H_2 purity and H_2 recovery in the 100 hour range. The accelerated test conditions use a WGS gas mixture without any steam (50% H_2, 30% Ar, 20% CO – WGS-20D). As shown in Figure 3, a linear decrease in permeate purity was obtained in approx 100 hours for the same membrane referenced in Figure 2. Evaluation of two sets of three membranes with varying alloy composition were tested with results given in Table 2. One membrane of each composition was tested at each location. From the performance in WGS20D the $Pd_{90}Au_{10}$ alloy was selected for next durability tests.

TABLE 2. Performance evaluation of membranes of varying alloy compositions in accelerated test conditions for a minimum of 100 hours.

Thickness (micron)	Au content (wt%)	Purity Decline (ppm/day)
3.0	0	42
4.1	0	74
4.0	9	0
3.9	11	6
3.6	20	356
3.6	24	652

Module Development

A major advantage of using the porous metal AccuSep® is the ability to weld individual membrane elements in a metal tube sheet similar to the conventional shell and tube architecture. However, a multi-tube module must be designed to minimize the concentration polarization effect typically observed at high hydrogen recoveries. Different concepts of multi-tube membrane module design were

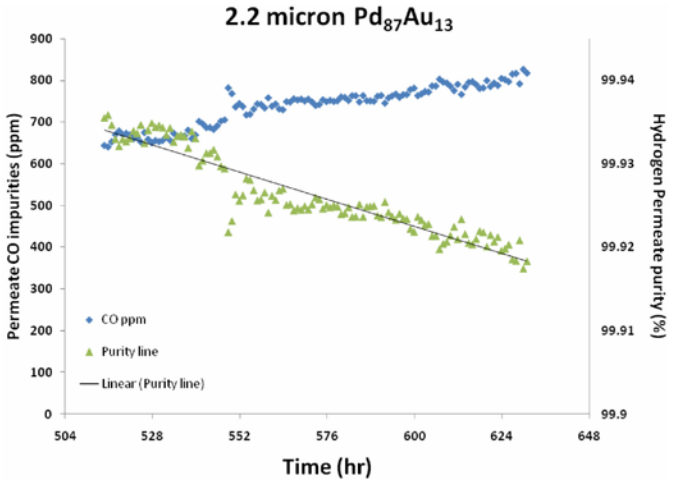


FIGURE 3. Membrane Degradation in WGS-20D Syngas Conditions

evaluated to overcome concentration polarization effects[2]. Multi-tube modules were fabricated and tested to confirm hydrogen flux and recovery as predicted by the model shown in Figure 4. A test facility with a feed gas flow capacity of 200 liters/minutes needed for testing the performance of the 12-tube module is being assembled.

System Economic and Energy Analysis

The end user conducted a techno-economic study to compare Pd-membrane-based process to competing PSA and solvent scrubbing-based processes for large-scale hydrogen production (~36,000 kg/hr) from natural gas with CO_2 capture. This analysis assumed an autothermal oxygen-blown reforming of natural gas to provide hydrogen-rich reformate gas for further processing by the three option processes considered. A two-stage cascade of WGS reactor/membrane separator was found to be able to provide the desired 90% H_2 recovery with 90% H_2 purity. Utilization of an inert nitrogen sweep gas stream in the second stage was necessary to achieve the target 90% recovery from the reformate gas mixture generated by autothermal reforming of natural gas. The amount of sweep gas that could be used was dictated by the requirement of achieving the 90% target hydrogen purity. Pall Corporation provided estimates of total membrane area needed to produce 36,000 kg/hr of hydrogen. The total costs of the membrane system were estimated assuming utilization of 2,000-tube modules. This analysis included the costs of sequestration-ready CO_2 capture in addition to that would be needed for just the hydrogen production. As a result additional equipment was needed to be incorporated increasing the costs of processes based on hydrogen separation, i.e. PSA and membrane-based processes, significantly increasing the costs of those processes when compared to the amine scrubbing option. This report is being reviewed to modify the analysis to conform to the goals of hydrogen production in our DOE contract. A separate report is being prepared for DOE's review.

[2] The resultant module designed to reduce concentration polarization was developed using Pall Corporation's internal funds in a separate project.

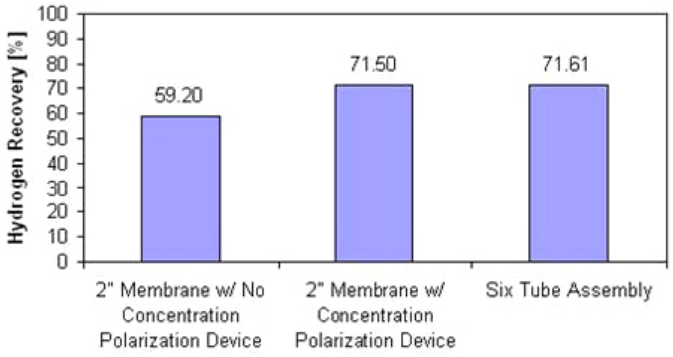


FIGURE 4. Multi-Tube Module Design with Minimization of Concentration Polarization

Conclusions

- Eliminated delaminations and improved membrane quality by optimizing the substrate/diffusion barrier substrate process.
- The PdAu alloy membranes were stable in a standard WGS stream environment.
- Developed more aggressive gas stream compositions to accelerate a decline in membrane performance in a reasonable time.
- Verified long-term durability of the optimal $Pd_{90}Au_{10}$alloy composition.

Future Plans

- Complete membrane optimization tests to determine both the optimum membrane composition and thickness to assure long-term durability in WGS reaction environments.
- Demonstrate additional long-term durability to meet Phase III goals using membranes with optimum composition and thickness.
- Complete fabrication of 12-inch overall length PdAu membranes for the multi-tube module assembly and test a module with at least six tubes.
- Demonstrate multi-tube module performance is close to single-tube performance.
- Complete the techno-economic analysis of the membrane-based hydrogen production process.

FY 2011 Publications/Presentations

1. Ø. Hatlevik, M.K. Keeling, K. Rekczis, J.D. Way, " High carbon monoxide test conditions for accelerated qualitative evaluation of palladium gold alloy membranes for use in CO_2 capture from water-gas-shift mixtures ," presented at the North American Membrane Society annual meeting, Las Vegas, NV, June 2011.

2. Hatlevik, Ø., Gade, S.K., Keeling, M.K., Thoen, P.M. and J.D. Way, " Palladium and Palladium Alloy Membranes for Hydrogen Separation and Production: History, Fabrication Strategies, and Current Performance," *Separation and Purification Technology*, 73, 59-64(2010).

3. A. Damle, "Commercialization of Pd Membrane for H_2 Production," presented at the Fuel Cell Seminar, San Antonio, TX, October, 2010.

II.D.1 Advanced Hydrogen Transport Membrane for Coal Gasification

Joseph Schwartz
Praxair, Inc.
175 East Park Drive
Tonawanda, NY 14150
Phone: (716) 879-7455
E-mail: Joseph_Schwartz@Praxair.com

DOE Manager
Elaine Everitt
Phone: (304) 285-4491
E-mail: Elaine.Everitt@netl.doe.gov

Contract Number: DE-FE0004908

Subcontractors:
- Colorado School of Mines (CSM), Golden, CO
- T3 Scientific, Blaine, MN

Project Start Date: October 1, 2010
Project End Date: Project continuation and direction determined annually by DOE

Fiscal Year (FY) 2011 Objectives

- Demonstrate hydrogen transport membrane performance in syngas derived from coal or coal-biomass.
- Separate 800 scfh of hydrogen from syngas.
- Design a membrane reactor to separate at least 4 tons/day of hydrogen from a large-scale gasifier.

Technical Barriers

This project addresses the following technical barriers from the Production section of the Fuel Cell Technologies Program Multi-Year Research, Development and Demonstration Plan:

(K) Durability
(L) Impurities
(M) Membrane Defects
(P) Flux
(R) Cost

Technical Targets

TABLE 1. Progress towards Meeting Technical Targets for Dense Metallic Membranes for Hydrogen Separation and Purification[a]

Performance Criteria	Units	Status	2010 Target	2015 Target
Flux Rate[b]	scfh/ft^2	>200	250	300
Module Cost (including membrane material)[c]	$/ft^2 of membrane	1,000	1,000	<500
Durability[d]	hr	<8,760	26,280	>43,800
Operating Capability[e]	psi	300	400	400-600
Hydrogen Recovery	%	88	>80	>90
Hydrogen Qualityf	% of total (dry) gas	> 99.98	99.99	>99.99

[a]Based on membrane water-gas shift reactor with syngas.
[b]Flux at 20 psi hydrogen partial pressure differential with a minimum permeate side total pressure of 15 psig, preferably >50 psi and 400°C.
[c]Although the cost of Pd does not present a significant cost barrier due to the small amount used, the equipment and labor associated with depositing the material (Pd), welding the Pd support, rolling foils or drawing tubes account for the majority of membrane module costs. The $1,500 cost status is based on emerging membrane manufacturing techniques achieved by our partners and is approximately $500 below commercially available units used in the microelectronics industry.
[d]Intervals between membrane replacements.
[e]Delta P operating capability is application dependent. There are many applications that may only require 400 psi or less. For coal gasification 1,000 psi is the target.
[f]It is understood that the resultant hydrogen quality must meet the rigorous hydrogen quality requirements. These membranes are under development to achieve that quality. Membranes must also be tolerant to impurities. This will be application specific. Common impurities include sulfur and carbon monoxide.

Most tests have been conducted at higher pressure than 20 psi, but our current test unit is limited to 200 psi. A new reactor is under construction that will allow testing at 450 psi.

FY 2011 Accomplishments

- Demonstrated 90+% of original flux from membranes coated with MembraGuard® in pure gas and mixtures with no sulfur.
- Demonstrated high flux from Pd alloy membranes.
- Determined impact of ethylenediaminetetraacetic acid (EDTA) on membrane performance.
- Improved membrane seal.
- Designed and began construction of new test reactors to test larger membranes with H_2S and at higher pressure and flow rate.
- Coated membranes up to two feet in length.

Introduction

Hydrogen membranes can be used to separate hydrogen from syngas produced by coal gasification and facilitate CO_2 capture and sequestration. Currently, these membranes have not had widespread commercial success because of durability and performance issues, including susceptibility to sulfur contamination.

Approach

The project will examine different membrane alloys and determine the most appropriate alloys for different syngas compositions produced by gasification. The alloy(s) will be selected based on the expected contaminants in the syngas and their resistance to those contaminants. Other methods, such as sorption, will be used to remove contaminants, but employing a contaminant-resistant alloy will help ensure the success of the project. The alloy must be incorporated into a manufactured membrane. The project will examine different membrane architectures and manufacturing techniques to select the optimum membrane based on performance and manufacturing cost. The project will examine different manufacturing methods to select the most reliable low-cost production method that can produce large membranes on a commercial scale.

The membranes must be incorporated into a membrane unit that separates hydrogen from syngas. The project will examine different membrane reactor designs, including use of catalysts and sweep streams, to select the optimum membrane reactor configuration. Reactor modeling will evaluate different configurations and estimate the impact of reactor design on performance. In Phase I, a small proof-of-concept reactor will be built to separate at least 2 lbs/day (about 15 scfh) of hydrogen from coal-derived syngas. In Phase II, a pilot-scale reactor will be built and integrated with an operating gasifier to produce at least 100 lbs/day (about 800 scfh) of hydrogen. The reactors must be incorporated into a membrane process that produces hydrogen and power at a lower cost than competing processes. The project will examine different integrated process designs to select the most economical process based on the total cost of power and hydrogen produced. In Phase III, this process will be used as the basis for designing a commercial-scale hydrogen transport membrane unit capable of producing at least 4 tons per day of hydrogen.

Results

A Pd-Au membrane was tested for H_2 flux over a temperature range of 300-400°C and a pressure range of 20-200 psid as shown in Figure 1. The membrane showed H_2 fluxes of 96 and 511 scfh/ft^2 at 400°C and 20 and 200 psid, respectively. This is a very encouraging result because a high H_2 flux with a high Au content is expected to provide acceptable performance and resistance to contamination due to impurities including sulfur. The best fit for the H_2 flux showed a pressure dependence of 0.56, indicating that the Pd-Au film is responsible for most of the resistance to hydrogen permeation.

The membrane was then tested in a mixed gas stream with CO (1%), CO_2 (30%), H_2 (50%), and H_2O (19%) and a feed flow rate of 6.2 slpm. As shown in Figure 2, the hydrogen recovery increased with pressure and reached 82% at a feed pressure of 200 psi. The composition of H_2 in the retentate decreased from 57 to 33% while the composition of CO_2 increased from 41 to 64% as the feed pressure increased from 50 to 200 psia.

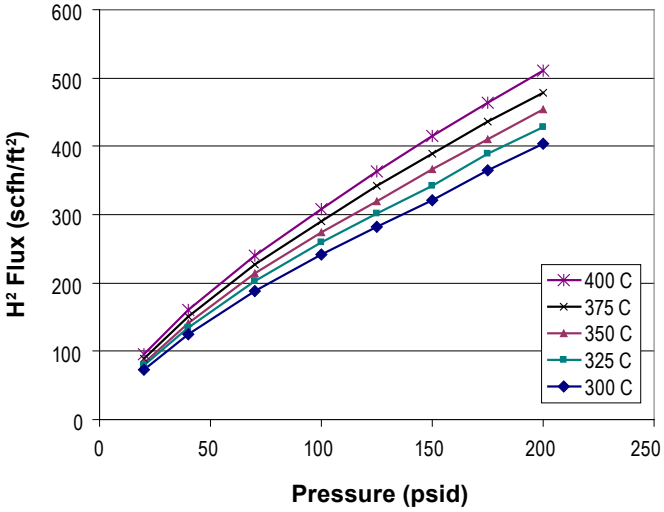


FIGURE 1. Flux Test Results for a Binary Pd-Au Membrane at 300-400°C

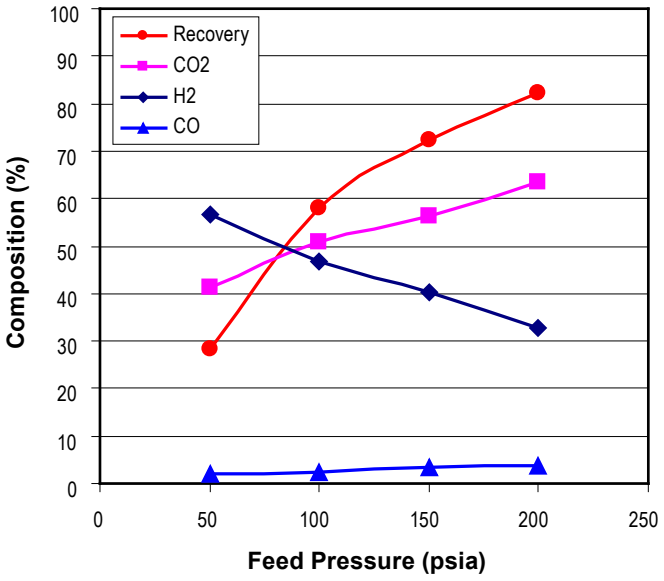


FIGURE 2. H_2 Recovery and Dry Gas Composition on the Retentate Side for a Pd-Au Membrane in a Mixed Gas Test

Other experimental work focused on understanding the effect of EDTA on hydrogen permeation in pure Pd films. EDTA is a bath stabilizer utilized to keep Pd ions in solution and to prevent formation of Pd particles during electroless plating of Pd. EDTA is added to the standard Pd electroless plating solution in amounts that bracket literature values. The plating temperature, hydrazine amount, and length of time in the plating bath were all held constant to understand the effect of EDTA on plating kinetics, which were shown to decrease as the amount of EDTA increased. Pure gas hydrogen permeation tests were completed and are discussed in detail in the following.

Effects of EDTA

The amount of EDTA added to the Pd electroless plating solution for the study was 0–80 g/l, spanning the amount used in the literature. The average amount of EDTA currently being used in the membrane literature is about 40 g/L EDTA. The single-gas permeation results are compared with Pd membranes made without EDTA as seen in Figure 3.

As the amount of EDTA used in the plating bath increases, the hydrogen permeability decreases. The percent differences from the estimated value of 0 g/L EDTA (linear fit trend line) are 2.6%, 5.7%, 14.3%, and 31.7% for the 20, 40, 60, and 80 g/L EDTA films, respectively. All of the films were exposed to air at 300°C for a minimum of five hours at 5 psi. Exposure to air provides a boost in hydrogen flux, more for membranes containing EDTA than for those that do not. As a result of air exposure, the flux for 0 g/L EDTA increased by a factor of 1.5, while it increased by factors of 1.8, 2.0, 2.42, and 3.1 for 20, 40, 60, and 80 g/L EDTA, respectively. This increase in flux did not allow EDTA membranes to be equivalent to those made without EDTA. A possible explanation is that although the carbon on the surface may have been cleared off with the air, there is still carbon left in the bulk and/or grain boundaries that is inhibiting the hydrogen transport.

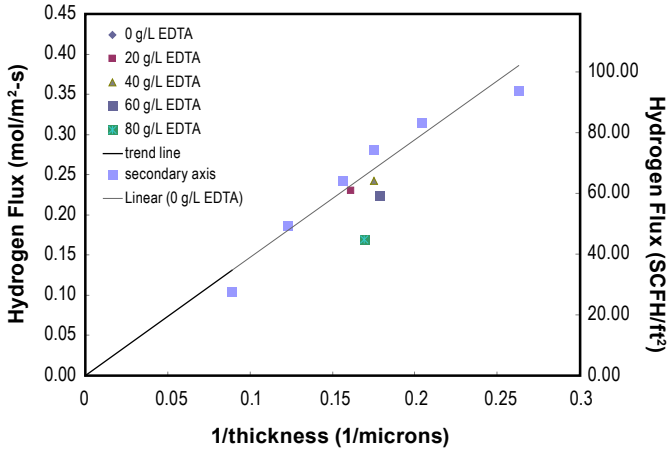


FIGURE 3. Hydrogen Flux of Pd Membranes Made With and Without EDTA at 400°C and 20 psi

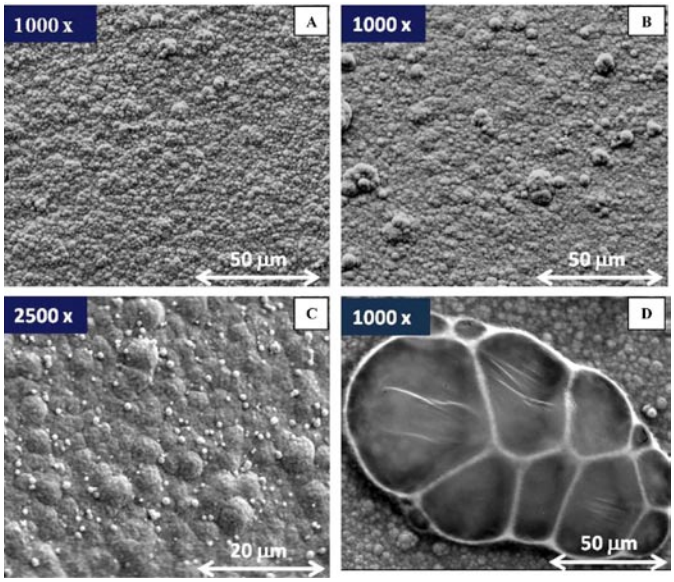


FIGURE 4. SEM micrographs of films made with EDTA. 20 g/L EDTA (A), 40 g/L EDTA (B), 60 g/L EDTA (C), and 80 g/L EDTA (D)

All of the membranes were examined with scanning electron microscopy (SEM)/energy dispersive X-ray spectroscopy (EDS) after testing. Interestingly, as the amount of EDTA decreases, the films begin to resemble ones made without EDTA in that the surface is connected, bubbly, and "cauliflower" like. SEM micrographs of these films can be seen in Figure 4.

The 60 and 80 g/L EDTA films had noticeable carbon enrichment on the surface. In the case of 60 g/L, this can be seen in the small, white spheres (Figure 4C), which were identified by EDS in the peak magnitude of the carbon as compared to the larger, darker bubbles. In the case of 80 g/L EDTA, contamination could be seen with the naked eye and looked like black tar on the membrane surface. The micrograph in Figure 4D is a close up of one of the spots.

Future work with the EDTA membranes will have the objective to try to understand why the hydrogen permeation is suppressed. As hydrogen is transported through a palladium membrane using a solution-diffusion mechanism, permeability, P, is a function of solubility, S, and diffusivity, D, as seen in equation 1:

$$P = D \cdot S \quad (1)$$

Conclusions and Future Directions

- High flux has been demonstrated using Pd and Pd alloy membranes that are expected to have good resistance to contaminants, including H_2S.
- Future research will focus on demonstrating performance with H_2S contamination.

- Small-scale gasifier testing has begun at Colorado School of Mines.
- Future research will focus on integrating a membrane test unit with the gasifier to demonstrate performance in coal-derived syngas.

FY 2011 Publications/Presentations

1. DOE Annual Hydrogen Review Meeting.

Copyright © 2011 Praxair Technology, Inc.

The Recipient grants to the Government, and others acting on its behalf, a paid-up, nonexclusive, irrevocable worldwide license in such copyrighted data to reproduce, prepare derivative works, distribute copies to the public, and perform publicly and display publicly, by or on behalf of the Government.

II.D.2 Scale Up of Hydrogen Transport Membranes for IGCC and FutureGen Plants

Carl Evenson (Primary Contact), Doug Jack
Eltron Research & Development Inc.
4600 Nautilus Ct. S.
Boulder, CO 80301
Phone: (303) 530-0263
E-mail: cevenson@eltronresearch.com

DOE Manager
Arun Bose
Phone: (412) 386-4467
E-mail: Arun.Bose@NETL.DOE.GOV

Contract Number: DE-FC26-05NT42469

Subcontractor:
Eastman Chemical Co., Kingsport, TN

Project Start Date: October 1, 2005
Project End Date: June 2012; American Recovery and Reinvestment Act (ARRA) funded extension through September 2015

Fiscal Year (FY) 2011 Objectives

- Demonstrate a cost-effective H_2/CO_2 membrane separation system.
- Scale up membrane manufacturing.
- Construct, install, and operate subscale engineering prototype.
- Down-select engineering, procurement, and construction firm and conduct pre-front end engineering design for a 4-10 ton per day pre-commercial scale up.

Technical Barriers

This project addresses the following technical barriers from the Hydrogen Production section of the Fuel Cell Technologies Program Multi-Year Research, Development and Demonstration Plan:

(K) Durability
(Q) Testing and Analysis
(R) Cost

Technical Targets

Eltron's hydrogen membrane system has demonstrated high flux rates of >99.99% pure hydrogen at expected temperatures and differential operating pressures. This project is currently focused on scaling up these membranes while meeting the following 2015 DOE technical targets for dense metallic membranes:

- Module Cost: $500/ft^2 of membrane
- Durability: >43,800 hours
- Hydrogen Recovery: 90%

FY 2011 Accomplishments

- Membrane manufacturing was scaled up to produce 5 ft-long tubular membranes. These tubular membranes are ½ inch outside diameter and have a wall thickness of 500 microns.
- Two foot-long membranes were tested at Eltron Research & Development and demonstrated 70% hydrogen recovery.
- A subscale engineering prototype pilot reactor was designed, constructed, and installed at Eastman Chemical Co.



Introduction

The overall objective of this project is to scale up the hydrogen transport membrane technology system for energy efficient carbon capture and hydrogen separation from industrial sources thereby enabling early technology commercialization by reducing time, technology risk, and cost. The goal of the project is to scale up Eltron's dense hydrogen transport membranes which can extract and purify hydrogen to very high levels from coal-derived water-gas shift mixtures, while minimizing the pressure drop of CO_2 in order to lower capital and compression costs for CO_2 sequestration. Dense hydrogen separation membranes are being developed to be compatible with high-temperature water-gas shift reactor conditions for water-gas shift reactors placed downstream from coal gasifiers in integrated gasification combined cycle (IGCC) type systems. Hydrogen separation membranes must be compatible with high-temperature water-gas shift reactor temperatures (approximately 320-440°C) and with mixtures of water-gas shift components containing hydrogen, steam, CO_2 and CO as well as residual impurities which escape upstream warm-gas clean up systems and the beds of water-gas shift catalyst. The hydrogen separation membranes must also function at pressures near that of the coal gasifiers, 450-1,000 psi.

Approach

Eltron is addressing all key issues to successfully scale up this technology. Bench scale testing is being conducted to demonstrate flux, hydrogen recovery, and durability. In addition, process modeling and techno-economic analyses are being developed. Eltron is scaling up this technology in three steps. Reactors nominally sized for 12 lbs/day

and 250 lbs/day hydrogen separation will be designed, constructed, and operated. Eltron was awarded an ARRA project to further scale up this technology to a 4-10 ton per day pre-commercial module scale. The approach for the ARRA portion of the project is to continue membrane development, conduct pre-front end engineering design and front end engineering design engineering packages for the selected pre-commercial module site; and to design, construct, and operate the pre-commercial module and conduct appropriate engineering analyses.

Results

Figure 1 shows a general schematic of Eltron's membrane system. The membrane is composed of three dense metal alloy layers. The center layer is 500 microns thick and is a low-cost metal alloy with high hydrogen permeability. A thin catalyst layer (<1 micron) is deposited on both the inside and outside surface of the membrane. High pressure shifted syngas is fed to the outside surface of the membrane. Pure hydrogen is collected on the inside of the tube. This membrane was designed to operate at water-gas shift conditions and retain CO_2 at high pressures to minimize compression costs for CO_2 capture and sequestration.

In FY 2011, Eltron scaled up the manufacturing of these tubular membranes to 5 ft-long tubes. These tubes are ½ inch outside diameter tubes with a wall thickness of 500 microns. Eltron deposits metal alloy catalysts on the inside and outside surface of the tubes. A scanning electron microscope image of a deposited catalyst layer is shown in Figure 2. The deposited catalyst is uniform, dense, and well-adhered to the bulk metal surface.

Two foot pieces of membrane were tested at Eltron at 340°C and a differential pressure of 400 psig in a simulated water-gas shift feed stream. Figure 3 shows the observed hydrogen flux as a function of time. A stable flux rate of 28 scfh/ft^2 was observed for 16 hours. This flux rate was lower than expected due to the effect of concentration polarization inherent in low-flow rate bench-scale reactors. In this particular test the membrane was able to recovery 70% of the hydrogen in the feed stream.

Finally, Eltron designed and constructed the first reactor in our three step scale up plan. Figure 4 shows the constructed sub-scale engineering prototype. This reactor was designed to separate up to 12 lbs/day of hydrogen from a gasified coal feed stream at Eastman Chemical Co. site in Kingsport, TN.

On the ARRA portion of the project Eltron has down-selected URS as the engineering, procurement, and construction firm for the pre-commercial module. URS and Eltron are evaluating three potential sites for operating the pre-commercial module.

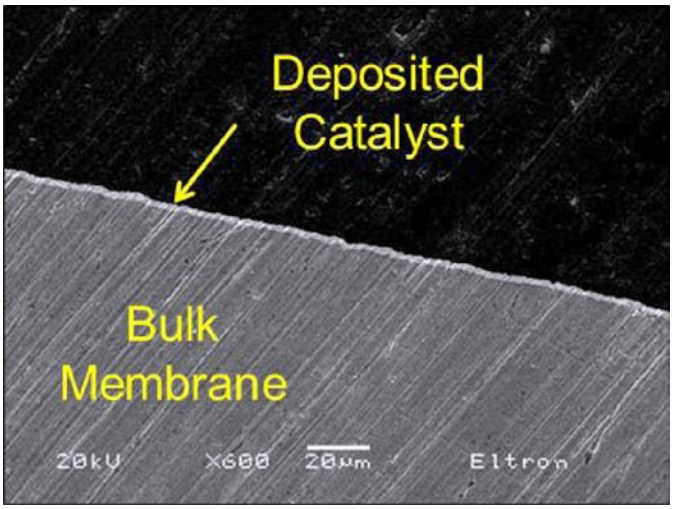


FIGURE 2. Scanning Electron Microscope Image of Deposited Catalyst

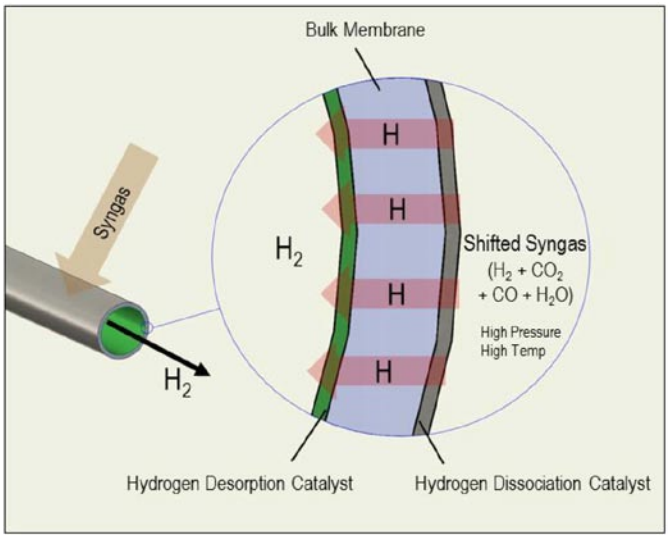


FIGURE 1. Schematic of Eltron's Dense Metal Tubular Membrane System

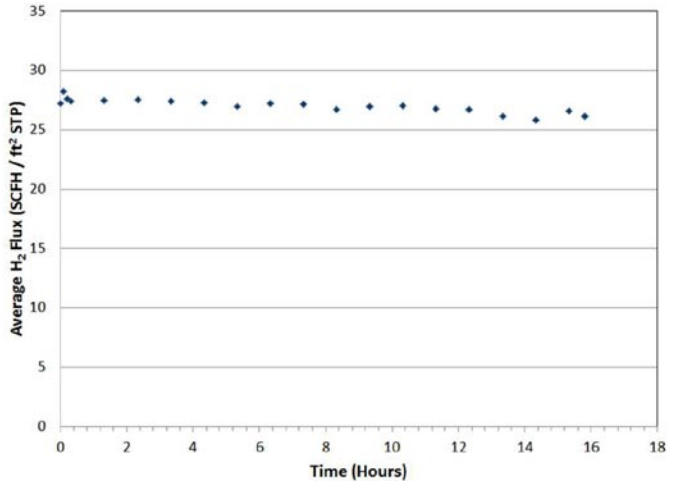


FIGURE 3. Hydrogen Flux vs. Time Recorded for a Two Foot-Long Membrane Tested at 340°C and 400 psig Differential Pressure

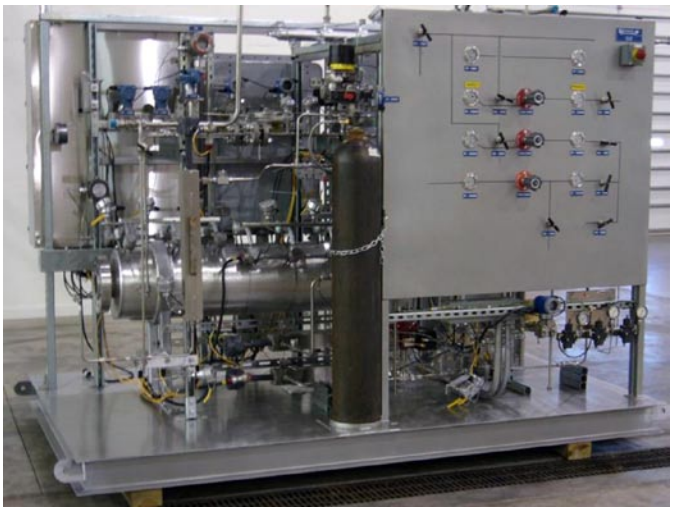


FIGURE 4. Completed Sub-Scale Engineering Prototype

Conclusions and Future Directions

In FY 2011 Eltron scaled up manufacturing of our tubular membrane and successfully tested membranes up to two feet long under expected operating conditions. In addition, Eltron designed, constructed, and installed the first scale-up reactor. During the next FY Eltron will operate the sub-scale engineering prototype, update our economic models with the results, and begin the design process for the next scale up step. Front end engineering design will be conducted on the down-selected site for the pre-commercial module.

Patents Issued

1. Mundschau, M.; Xie, X.; Evenson, C.; Grimmer, P.; Wright, H. Hydrogen Separation Process. US Patent 7,947,116. May 24, 2011.

FY 2011 Publications/Presentations

1. David Anderson. Carl Evenson. John Faull. Doug Jack. Scale-up of Membranes for Separation of Hydrogen from Syngas for Carbon Capture. 2010 AIChE Annual Meeting. November 9, 2010.

2. Michelle Livingston. *et. al.* Advanced Membrane System for Hydrogen Separation and Carbon Dioxide (CO_2) Capture. 2011 North American Membrane Society Meeting. June 8, 2011.

II.D.3 Advanced Palladium Membrane Scale Up for Hydrogen Separation

Sean C. Emerson
United Technologies Research Center
411 Silver Lane
East Hartford, CT 06108
Phone: (860) 610-7524
E-mail: emersosc@utrc.utc.com

DOE Manager
Daniel Driscoll
Phone: (304) 285–4717
E-mail: Daniel.Driscoll@netl.doe.gov

Contract Number: DE–FE0004967

Subcontractors:
- Power & Energy, Inc., Ivyland, PA
- Energy & Environmental Research Center, University of North Dakota, Grand Forks, ND

Project Start Date: October 1, 2010
Project End Date: December 31, 2011

Fiscal Year (FY) 2011 Objectives

- Construct, test, and demonstrate a PdCu metallic tubular membrane micro-channel separator capable of producing 2 lb/day of H_2 at ≥95% recovery when operating downstream of an actual coal gasifier.
- Quantify the impact of simulated gas composition and temperature on separator performance.
- Compare the performance and durability of a surface-modified, higher H_2 flux PdCu membrane with the baseline PdCu tubular membrane.
- Evaluate various materials of construction for the separator's non-Pd structural parts to ensure durability under harsh gasifier conditions.
- Perform an engineering analysis using National Energy Technology Laboratory (NETL) guidelines of the separator design based on gasifier test performance for the co-production of electric power and clean fuels.

Technical Barriers

This project addresses the following technical barriers from the Hydrogen Separations section of the Fuel Cell Technologies Program Multi-Year Research, Development and Demonstration Plan [1]:

(K) Durability

(L) Impurities

Technical Targets

The focus of this project is to construct, test, and demonstrate a PdCu separator capable of producing 2 lb/day H_2 operating downstream of a coal gasifier. As such, the emphasis is on achieving progress against the DOE technical targets pertaining to impurities (sulfur and CO tolerance) and durability. The current progress toward the DOE's 2015 technical targets for hydrogen separation is given in Table 1.

TABLE 1. Technical Progress for the Project as Measured Against the DOE's Technical Targets for Hydrogen Separation

Performance Criteria	Units	DOE 2015 Target	Current Status
H_2 Flux	$ft^3h^{-1}ft^{-2}$	300	125 (500°C, enhanced PdCu) (200 psia feed pressure, 185.3 psid)
Temperature	°C	250–500	250–600
Sulfur tolerance	ppmv	>100	618 h at 5–39 ppmv S (0.008 psia S) >24 h at 236–963 ppmv S (0.0104–0.0425 psia S) [8 h at 236 ppmv S (0.0104 psia S)] [5 h at 472 ppmv S (0.0208 psia S)] [4 h at 708 ppmv S (0.0312 psia S)] [7.5 h at 963 ppmv S (0.0425 psia S)] With reversible, low impact on permeability
Cost	$/ft^2	<100	400–500 (metal cost, without recycle & leasing strategy)
ΔP operating capability	psi	800–1,000	400
CO tolerance	–	Yes	13.3% CO at 90 psia >9% CO at 204.7 psia
H_2 purity	%	99.99	99.9999
Stability/ Durability	Years	5	1,031 h

FY 2011 Accomplishments

- Demonstrated negligible impact of gas species for temperatures ≥400°C and pressures ≤200 psia. Sulfur partial pressures up to 0.008 psia and CO partial pressures up to 2 psia do not affect H_2 flux for temperatures ≥400°C.
- Identified potential non-membrane materials of construction superior to SS-316.
- Constructed four laboratory-scale separators and two pilot-scale separators capable of separating >2 lb/day H_2.
- Compared the performance and durability of a surface-modified, higher H_2 flux PdCu membrane with the baseline PdCu tubular membrane.

Introduction

Advancements in hydrogen (H_2) membrane separation are critical to allow the development of a viable H_2 economy based on coal/biomass processing with CO_2 capture. United Technologies Research Center (UTRC), in collaboration with Power+Energy, Inc. (P+E) and the Energy & Environmental Research Center at the University of North Dakota (EERC), therefore proposed to demonstrate palladium (Pd)-based membrane separation of H_2 from coal-derived syngas at the pre-engineering/pilot scale.

In Phase I, the objectives are to: (1) construct, test, and demonstrate a PdCu metallic tubular membrane micro-channel separator capable of producing 2 lb/day of H_2 at ≥95% recovery when operating downstream of an actual coal gasifier; (2) quantify the impact of simulated gas composition and temperature on separator performance; (3) compare the performance and durability of a surface modified, higher H_2 flux PdCu membrane with the baseline PdCu tubular membrane; (4) evaluate various materials of construction for the non-Pd separator structural parts to ensure durability under harsh gasifier conditions; (5) perform an engineering analysis using NETL guidelines of the separator design based on gasifier test performance for the co-production of electric power and clean fuels; and (6) select a gasification facility partner for Phase III.

Approach

This project is a continuation of the UTRC-led team's approach to increase the technology readiness level of Pd-based metallic membranes for H_2 separation from coal-biomass gasifier exhaust or similar H_2-containing gas streams. The current project is aimed at demonstrating at the pre-engineering/pilot scale the separation of H_2 from coal-derived syngas using a proprietary, surface-modified, palladium-copper (PdCu) tubular membrane separator. It will include testing of separators capable of producing 2 lb/day of H_2 and, in follow-on phases, separators capable of producing 100 lb/day of H_2.

UTRC's subcontractor, P+E will manufacture the separators and EERC will test the separators downstream of a coal gasifier. The main objective of the first phase (Phase I) of the project is to construct, test, and demonstrate a PdCu dense metallic tubular membrane separator capable of producing 2 lb/day of H_2 at a minimum 95% recovery when operating downstream of an actual coal gasifier. The project will also acquire engineering data to reliably scale up PdCu membrane separators to a size of 4 tons per day (tpd) of H_2 and assess the combined effects of coal gas constituents and trace contaminants on membrane performance and durability. The data will be evaluated against the DOE's 2015 targets for H_2 membrane separation and used in an engineering analysis of the separation and production method using NETL guidelines.

Results

By the end of June 2011, P+E had delivered four out of six laboratory-scale (≈0.1 ft^2) separators as well as two out of six pilot-scale (≈1.5 ft^2) separators. Based on the information from preliminary corrosion tests, as well as the availability of alloys in the forms needed for fabrication, it was decided that all remaining separators to be delivered in Phase I of the project would be made out of C-22 and/or C-276. As a result, two of the laboratory-scale separators and both pilot-scale separators were made using these alloys. Due to manufacturing delays, the first two pilot-scale separators were made with non-surface enhanced PdCu alloys. All future pilot-scale separators will be made with the enhanced PdCu membranes.

Seven separators (identified as 5265, 5266, 5276, 5277, 5290, 5291, and 5297) have been evaluated for their hydrogen separation capability. An Arrhenius plot of the pure hydrogen permeability for each of the separators versus temperature is given in Figure 1. All but two separators (5266 & 5297) demonstrated similar performance, which was greater than that of conventional PdCu, although not as high as the original target for the enhanced PdCu.

Separator 5266 was a single-tube membrane separator from a previous DOE contract (DEFC2607NT43055) that was sent to EERC for gasifier testing and returned to UTRC. The data obtained at UTRC for separator 5266 indicated that the separator was leak tight and that performance of the membrane was equivalent to conventional PdCu after gasifier testing. Separator 5266 was used to establish reproducibility between EERC's and UTRC's testing hardware and will be characterized to determine the impact of gas contaminants on its materials of construction.

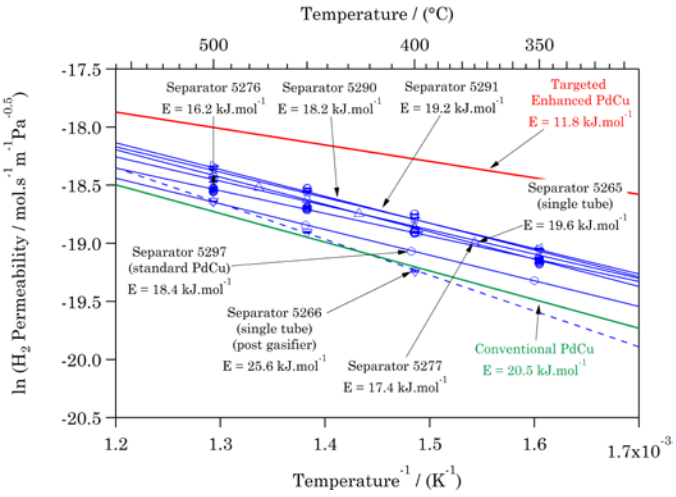


FIGURE 1. Arrhenius plot of the pure hydrogen permeability versus temperature for the PdCu separators tested so far on this project. Shown for reference are the hydrogen permeability curves for conventional PdCu membranes as well as the target performance for the surface modified, enhanced PdCu membranes.

Separator 5276 was tested for 1,031 hours, including 618 hours of hydrogen sulfide (H_2S) exposure with no signs of performance degradation. The impact of non-sulfur gas contaminants on hydrogen permeability for temperatures greater than or equal to 400°C appeared to be negligible when compared to pure hydrogen experiments as shown in Figure 2. Furthermore, the addition of H_2S to the same gas mixtures also had a negligible effect on the hydrogen permeability as shown in Figure 3. One objective of the sulfur tests was to determine the length of time required for the membrane performance to come to a steady state upon exposure to H_2S. Preliminary durability data suggested that the separator needed to be equilibrated for at least 100 hours before stable gas contaminant testing could be measured.

Separator 5297 is a pilot-scale separator that was tested with pure H_2 and H_2/N_2 mixtures at feed pressures of 44.1 psia and 88.2 psia, respectively, to verify separator performance with UTRC's separator model. The separator was also tested with H_2S in H_2 to verify its ability to withstand gasifier poisons. The maximum H_2S concentration used was 963 ppmv at 44.1 psia, approximately five times the maximum sulfur partial pressure used for testing separator 5276. At 500°C, the reduction in H_2 permeation from the 0.043 psia H_2S was approximately 50% but the H_2 performance fully recovered after exposure to pure H_2. Separator 5297 was also pressure checked at 400 psia and found to be leak free. The separator was exposed to four thermal cycles in H_2/N_2 from 200°C to 500°C with no performance degradation and no leaks. Separator 5297 was shipped to EERC after a total of 356 hours of testing at UTRC to serve as the test article for a coal gasifier test before the end of September.

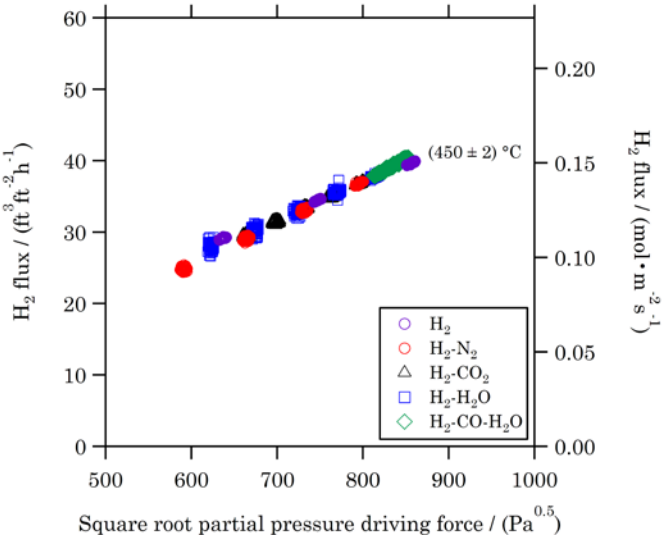


FIGURE 2. Hydrogen flux at (450 ± 2)°C versus the square root hydrogen partial pressure driving force for separator 5276 for different gas mixtures, not including H_2S. The separator was tested at feed pressures varying from 29.4 psia to 200 psia with different binary and ternary gas mixtures.

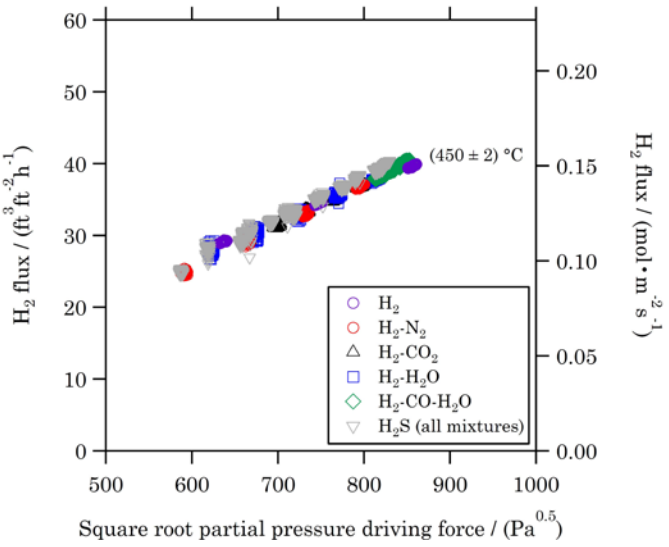


FIGURE 3. Hydrogen flux at (450 ± 2)°C versus the square root hydrogen partial pressure driving force for separator 5276 for different gas mixtures, including H_2S. The separator was tested at feed pressures varying from 29.4 psia to 200 psia with different binary and ternary gas mixtures. The H_2S gas concentration was varied from 5 ppmv to 39 ppmv.

UTRC began preliminary corrosion testing under a slightly modified DOE test 2A condition at 500°C in February. Initial Round 1 coupon tests were performed for 474 hours with samples of SS-316, SS-309, C-22 and C-276. After 474 hours of testing, it was observed that SS-309, C-22, and C-276 had weight gain constants that were two orders of magnitude lower than SS-316. This was likely due to their improved resistance to H_2S compared to SS-316. Some coupons exhibited crevice corrosion where the metal samples sat in a ceramic "dee-tube." Thus, a new fixture was designed for Round 2 testing in which samples hang from an alumina rod to minimize this effect.

The Round 2 corrosion test included two Oak Ridge National Laboratory alloys (OC-10 and OC-11) as well as HR-120 and SS-310. Corrosion testing of these alloys is currently in progress, with more than 1,500 hours of accumulated run time. Round 2 corrosion testing will continue until approximately 2,000 hours of total run time has been achieved, after which the Round 1 coupon tests will be repeated for approximately 2,000 hours.

In addition to lab-scale tests performed at UTRC, a total of 24 samples were prepared for exposure testing under actual gasifier conditions at the National Carbon Capture Center (NCCC) in Alabama. The coupons were made of eight different alloys (SS-316, SS-309, SS-310, HR-120, C-22, C-276, OC-10, and OC-11) and were sent to NCCC in late March.

Conclusions and Future Directions

- Dense metallic, PdCu membranes can fully tolerate the DOE test protocol conditions for pressures up to 200 psia and temperatures between 400°C and 500°C.
- The impact of H_2S for partial pressures <0.008 psia on H_2 permeability was insignificant for temperatures between 400°C and 500°C, although exposure to partial pressures as high as 0.043 psia H_2S showed a reduction in permeability up to 50% which was completely reversible.
- The surface enhanced PdCu membranes show higher hydrogen permeability than the conventional PdCu, particularly at lower temperatures (<450°C).
- Several non-membrane materials of construction have been identified that have superior corrosion resistance to the DOE protocol conditions compared to SS-316.
- Samples of the non-membrane materials of construction were sent to the NCCC in Alabama for exposure testing under real gasifier conditions.
- A single-tube separator was exposed to coal gasifier exhaust and will be characterized to determine the impact of gas contaminants on the materials of construction.
- A pilot-scale separator will be tested at 400 psia downstream of a coal gasifier at EERC by September to evaluate the impact of real gasifier exhaust on membrane performance.

FY 2011 Publications/Presentations

1. Emerson, S.C. Advanced Palladium Membrane Scale-up for Hydrogen Separation, invited presentation at Advancing the Hydrogen Economy Action Summit III, University of North Dakota EERC's National Center for Hydrogen Technology, Grand Forks, ND, September 13–15, 2010.

2. Emerson, S.C. Quarterly Progress Report: Advanced Palladium Membrane Scale-up for Hydrogen Separation, DOE Award Number DE–FE0004967, United Technologies Research Center: East Hartford, CT, January 2011.

3. Emerson, S.C. Quarterly Progress Report: Advanced Palladium Membrane Scale-up for Hydrogen Separation, DOE Award Number DE–FE0004967, United Technologies Research Center: East Hartford, CT, April 2011.

References

1. DOE Office of Energy Efficiency and Renewable Energy. Fuel Cell Technologies Program Multi-Year Research, Development and Demonstration Plan, U.S. Department of Energy: Washington, D.C., 27 April 2007.

II.D.4 Composite Pd and Alloy Porous Stainless Steel Membranes for Hydrogen Production and Process Intensification

Yi Hua Ma
Worcester Polytechnic Institute (WPI)
Center for Inorganic Membrane Studies
100 Institute Road
Worcester, MA 01609
Phone: (508) 831-5398
E-mail: yhma@wpi.edu

DOE Manager
Daniel Driscoll
Phone: (304) 285-4717
E-mail: Daniel.Driscoll@netl.doe.gov

DOE Project Officer
Jason Hissam
Phone: (304) 285-0286
E-mail: Jason.Hissam@netl.doe.gov

Contract Number: DE-FC26-07NT43058

Subcontractor:
Adsorption Research, Inc. (ARI), Dublin, OH

Project Start Date: May 7, 2007
Project End Date: November 6, 2011

Fiscal Year (FY) 2011 Objectives

- Synthesis of composite Pd and Pd/alloy porous metal (316L, Inconel, Hastelloy) membranes for water-gas shift (WGS) reactors with long-term thermal, chemical, and mechanical stability with special emphasis on the stability of H_2 flux and selectivity.
- Demonstration of the effectiveness and long-term stability of the WGS membrane shift reactor for the production of fuel cell quality H_2.
- Research and development of advanced gas clean-up technologies for sulfur removal to reduce the sulfur compounds to <2 ppm (ARI).
- Development of a systematic framework towards process intensification to achieve higher efficiencies and enhanced performance at a lower cost.
- Rigorous analysis and characterization of the behavior of the resulting overall process system, as well as the design of reliable control and supervision/monitoring systems.
- Assessment of the economic viability of the Pd-based membrane reactors integrated into integrated gasification combined cycle (IGCC) plants through a comprehensive calculation of the cost of energy output and its determinants (capital cost, operation cost, fuel cost, etc.), followed by comparative studies against existing pertinent energy technologies.

Technical Barriers

This project addresses the following technical barriers from the Production section of the Fuel Cell Technologies Program Multi-Year Research, Development and Demonstration Plan:

(K) Durability associated with the determination of optimum temperature for the WGS reaction.

(L) Impurities associated with adsorbent selection and pressure swing adsorption (PSA) system build-up, testing completed with syngas + H_2O, H_2S and carbon oxysulfide (COS).

(M) Membrane defects associated with the study of membrane surface upon WGS reaction.

(N) Hydrogen selectivity, leak growth will be mitigated by working at 400-450°C.

(P) Flux and reproducibility of high H_2 flux targets already achieved. Setting of Pd thickness and support characteristics to meet 2015 DOE targets.

(R) Cost, two-dimensional (2D) model for catalytic membrane reactor (CMR) simulations, safety and economic analysis.

Technical Targets

A number of composite Pd and Pd/alloy porous metal (316L, Inconel, Hastelloy) membranes for WGS reactors have been synthesized and long-term thermal, chemical, and mechanical stability and hydrogen flux and selectivity have been determined. Technical targets and current membranes operational data are listed in Table 1. The typical microstructure of composite Pd membranes listed in Table 1 is shown in Figure 1.

This project is conducting fundamental studies on composite Pd membranes permeance and selectivity stability in WGS reaction conditions. Insights gained from these studies will be applied toward the design and synthesis of hydrogen storage materials that meet the following DOE 2011 hydrogen storage targets:

- Durability (K): we are targeting a 1,000 hour WGS reaction long-term experiment with a stable H_2 permeance and H_2/He selectivity.
- Impurities (L): membranes were tested up to 20 ppm H_2S in pure H_2.
- Membrane defects (M): All membrane surfaces were studied after testing to investigate surface changes in syngas atmospheres.
- Hydrogen selectivity (N): a selectivity (H_2/N_2) of 10,000 at 180 psig was targeted.

TABLE 1. Characteristics and Results of Tested Pd Membranes at WPI

	DOE Targets		Current WPI membranes					
	2010	2015	#029	#031	#33	#038	#039	#RK04
Thickness (μm)	n/a	n/a	7.6	7	8.7	6	7.3	13
Flux (scfh/ft^2)	200	300	166	26.6	72.5	196	171	114
ΔP (psi) H_2 Partial Pressure (P_{low} = 14.7 psi)	100	100	100	15	100	100	100	100
Temp. (°C)	300-600	250-500	450	450	450	450	450	450
H_2/He Ideal Selectivity	n/a	n/a	∞	4,500	9,725	330	335	1,000
Test duration (hrs.)	n/a	n/a	4,500	2,200	800	170	165	1,250
WGS activity	Yes	Yes	Not tested	Not tested	Not tested	Not tested	Not tested	Not tested
CO Tolerance	Yes	Yes	Yes	Not tested	Not tested	Not tested	Not tested	Not tested
S Tolerance	20	>100	Not tested	Not tested	Not tested	Not tested	Not tested	Not tested
H_2 Purity At 180 psig	99.5	99.99	>99.999	>99.98	>99.99	>99	>99	>99.9
ΔP Operating Capability (Max System Pressure, psi)	400	800-1,000	225	15	100	30	100	100

n/a – not applicable

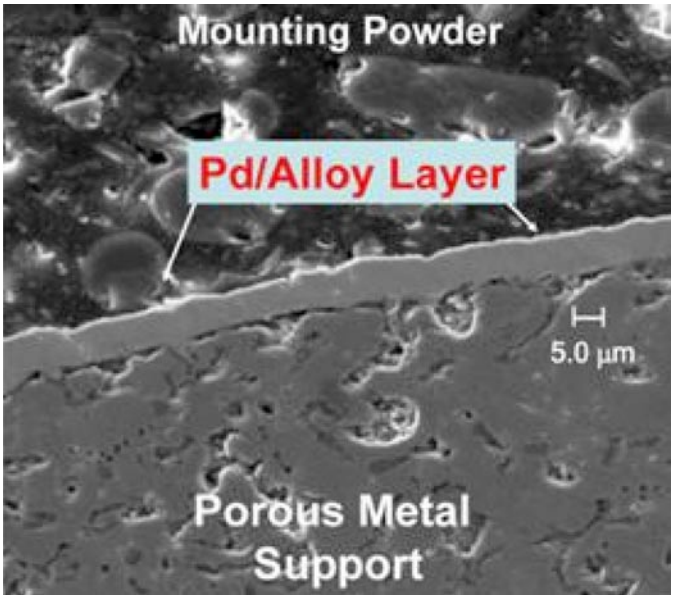


FIGURE 1. Composite Pd/Porous Metal Support Microstructure

- Flux (P): H_2 permeances ranging from 29.2 to 43.8 scfh/ft^2 psi$^{0.5}$ were targeted to achieve DOE 2010-2015 targets.
- Cost (R): 1,000 $/ft^2 to meet DOE's target.

FY 2011 Accomplishments

- Shown and re-produced selectivity H_2/He stability at 400-450°C over thousands of hours.
- Consistently achieved composite Pd membranes with thicknesses ranging between 4-12 μm porous metal supports indicating the reproducibility of our fabrication method.
- Pd/316L-PSS membranes have been synthesized and tested under WGS and H_2/H_2O mixed gas conditions at 400°C for 65 and 225 hours, respectively. The membrane leak growth was less than 11% over those testing periods.
- An integration option of the WGS-composite membrane reactor into IGCC plants was proposed and the performance of the industrial-scale WGS-composite membrane reactor's performance was assessed via a more accurate 2D model to achieve 98% CO conversion and 95% H_2 recovery.
- In the net present value (NPV)-based comparative assessment analysis, the positive NPV of $40M for IGCC-membrane reactor (MR) with carbon capture with a net power output of 550 MW showed the advantage of the membrane reactor technology over more traditional options such as supercritical pulverized coal (SC-PC), IGCC baseline, IGCC-PBR (IGCC with traditional packed bed reactor) with CO_2 capture in the presence of CO_2 taxes.
- The uncertainty analysis performed with the Monte-Carlo techniques to access the risk associated with the Pd-based membrane reactor technology indicated that regulatory action on CO_2 emissions would induce an appealing NPV profile for the IGCC-MR technology option.
- Accomplished PSA studies in collaboration with ARI.



Introduction

Combining the coal-derived syngas WGS reaction in a Pd-based membrane reactor leads to high purity hydrogen (>99.999%), high pressure CO_2 ready to be sequestered and energy and capital costs savings. The integration of the membrane technology into coal-fired power plants is an attractive option particularly due to benefits associated with both H_2 and CO_2 separation. MR technology should be economically competitive with the SC-PC, IGCC baseline and IGCC-PBR. Thus, the NPV-based economical analysis was performed on the basis of co-production of hydrogen and power from coal using Pd-based composite membrane reactors with sequestration. Moreover, the inherent uncertainty of the inputs of the NPV model has to be recognized and explicitly taken into account in investment decision-making.

However, coal gasification feedstocks raised challenges such as hydrogen permeance stability under H_2S, COS and heavy metal pollutants [1,2]. Selectivity stability was the second largest challenge since thin electrolessly deposited membranes developed leaks at temperatures ranging from 400 to 450°C [3]. The objective of this project was to develop a membrane module for the production of hydrogen using WGS reaction working at temperatures close to 450°C and under real gasification conditions.

Approach

Composite Pd membrane preparation consisted of the pretreatment of the porous stainless steel support i.e. deposition of an intermetallic diffusion barrier and a grading layer, surface activation and Pd deposition by the electroless plating method [4-5]. Pd thicknesses of 4-12 microns were targeted in order to reach DOE's flux target without compromising H_2/He leak stability at 450-500°C. WPI worked in collaboration with ARI to develop a PSA process to decrease contaminants level in syngas feed. In a parallel fashion Pd-Au alloy membranes and special protective coatings are being developed at WPI to mitigate H_2S and other coal contaminants. A complete WGS-CMR, seen in Figure 2, was also built at WPI to test 1-inch outer diameter, 10-inch long composite Pd membranes with synthetic syngas shown in Figure 3.

A comprehensive economic analysis was performed to identify the industrial-scale membrane reactor module cost, capital and operating and maintenance costs of the whole IGCC plant with the Pd-based membrane reactor technology. The NPV model was included into the economical analysis to compare the profitability of power plants with a net power output of 550 MWe both with and without future CO_2 taxes. In addition, the consequences and impact on project value of uncertain futures was calculated with the Monte Carlo simulation effectively. Detailed Monte Carlo simulations integrated into the detailed NPV model were performed in order to explicitly take into account the main uncertainty drivers associated with the NPV of the whole IGCC-MR, namely, the plant capacity factor, initial CO_2 tax, CO_2 tax growth rate, nominal discount rate, inflation rate, electricity selling price, Pd price, support price and membrane life.

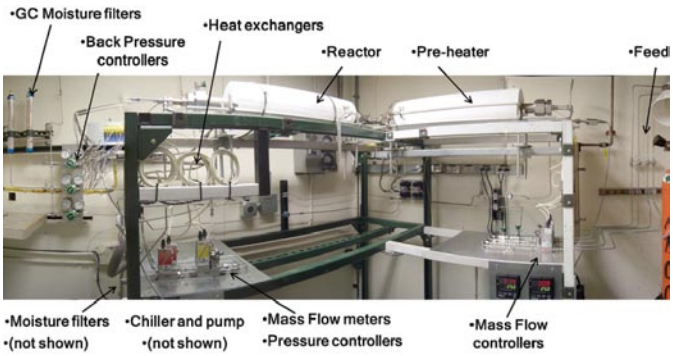


FIGURE 2. WGS-CMR for the Test of 1-Inch Outer Diameter, 10-Inch Long Composite Pd-Alloy/Porous Metal Membranes

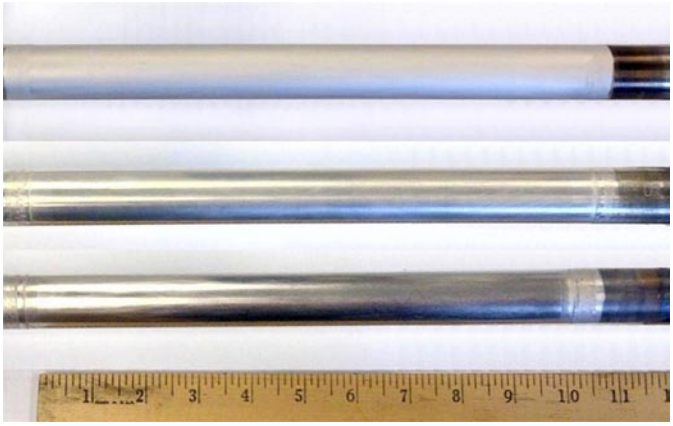


FIGURE 3. 1-Inch Outer Diameter, 10-Inch Long Pd/Porous 316L Composite Membranes

Results

- Achieved excellent long-term H_2/He selectivity stability, of essentially infinite value, over over a total testing period of ~3,550 hours (>147 days) at 300-450°C and at a ΔP of 15-100 psi (P_{Low}=15 psia).
- At 450°C, achieved re-producible, long-term H_2/He selectivity stability with several membranes with H_2 purity ≥99.99% over a testing period of 30 to 90 days.
- Achieved flux of ~359 scfh/ft^2, which exceeded DOE's 2010 and 2015 H_2 flux targets (T=442°C and ΔP of 100 psi [with P_{Low}=15 psia]). Such high fluxes were also achieved on high surface area composite Pd membranes 1-inch outer diameter, 10-inch long shown in Figure 3.
- Conducted an additional ~3,000 hours of mixed gas permeation experiments (61.7% H_2, 37.1% CO_2 & 1.2% carbon monoxide [CO] w/ and w/o 19% steam).

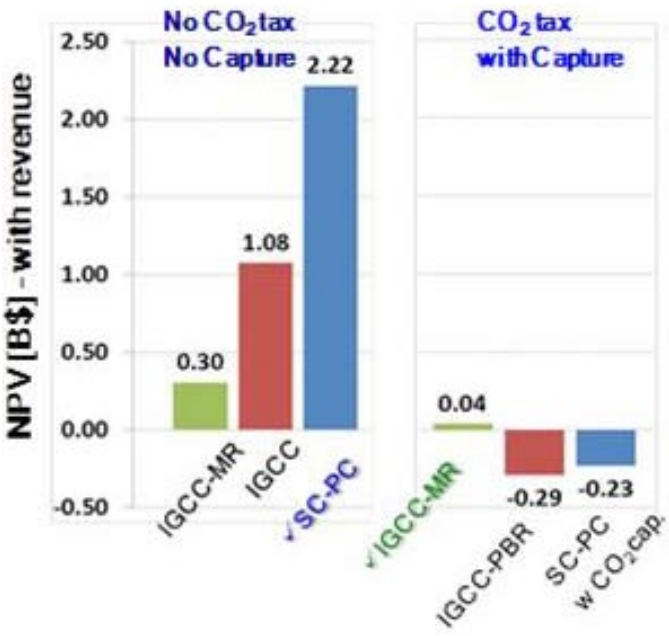


FIGURE 4. Single-Point NPV with Revenue Results of the Power Plants in Case of no CO_2 Tax (Without Capture) and with CO_2 Tax (With Capture)

- Reduced the number of synthesis steps for the large-scale membrane preparation for potential commercialization of WPI's composite Pd-based membrane production technologies.
- Achieved 99% total CO conversion and 89.9% H_2 recovery in a 12.5 µm-thick Pd-based CMR operated at ~350°C, ΔP=200 psi (P_{Low}=15 psia) H_2O/CO=1.44 and gas hourly space velocity ($GHSV_{stp}$)=150 h^{-1}, exceeding equilibrium conversion of 93.4% and traditional packed bed conversion of 92.7% [5].
- Successfully completed steady-state methane steam reforming (MSR) and WGS reaction modeling studies and process intensification analysis.
- Successfully completed unsteady-state WGS reaction modeling studies and implemented process control strategies.
- Successfully completed a 2D model for WGS tube and shell membrane reactors.
- Successfully used the 2D model to calculate CO conversion and H_2 recovery for different configurations of MR integration into IGCC plants.
- Completed capital, operating and maintenance costs of a IGCC-MR plant.
- Completed NPV analysis of IGCC, IGCC-PBR, IGCC-MR and SC-PC plants.
- Completed isotherm measurements for the selected adsorbents (ARI).
- Completed the PSA system construction and PSA testing at 200°C and a feed pressure of 200 psia (with P_{low}=1 atm.), (ARI).
- A WGS experiment was conducted with a 10.3 µm Pd/316L-PSS membrane over 65 hours at 400°C, 200 psig, and with a feed rate of 2,100 h^{-1} syngas feed (23% CO, 45% H_2O, 22% H_2, 10% CO_2). A stable CO conversion of 96% was achieved with an H_2 recovery in excess of 80%. The H_2 recovery declined by 10% over the course of the reaction due to coke formation on the membrane surface.
- The single estimate/projection NPV results showed that the IGCC-MR was an economically attractive technology option generating a positive NPV in a scenario with a $25/ton CO_2 tax starting in 2015 as shown in Figure 4. The negative NPV values of IGCC-PBR and SC-PC with CO_2 capture plants would possibly preclude these options from investment consideration in the presence of regulatory action on carbon emissions.
- The expected total capital investment (average) for membrane reactor module consisting of 10 micron thick Pd-based membrane tubes was estimated at 1,285 $/ft^2 which was slightly higher than the 2015 DOE target of 1,000 $/ft^2 with a maximum and minimum of 2,267 and 310 $/ft^2 (lower than the 2015 target), respectively.
- A comparatively more attractive NPV/cost distribution profile obtained in the IGCC-MR case assessed against the ones in the IGCC-PBR and SC-PC cases in the presence of regulatory action on CO_2 emissions made the Pd-based membrane reactor technology option integrated into an IGCC power plant a promising investment choice.

Conclusions and Future Directions

- Membrane preparation led consistently to thin 4-12 µm membranes. Some membranes experienced relatively low flux when considering their thicknesses indicating the presence of mass transfer resistance in the porous metal support.
- Consistent H_2/He selectivities over thousands of hours were obtained at 400-450°C.
- The membrane stability during long-term WGS reaction and H_2/H_2O mixed gas conditions has been demonstrated, and the synthesis methodology necessary for producing those membranes has been developed.
- Total capital investment for the membrane reactor module was calculated to be around 1,285 $/ft^2 very close to the DOE target (1,000 $/ft^2).
- NPV analysis suggested that if CO_2 taxes were implemented, IGCC-MR with carbon capture would be a quite attractive technology option. The most significant risk source was technological (reflected on lower capacity factor values) due to the lack of IGCC-membrane reactor operating experience, adversely impacting project value.
- Monte-Carlo techniques were used to study the effect of uncertainties namely, capacity factor, initial CO_2 tax, CO_2 tax growth rate on project economic value,

suggesting that regulatory action on CO_2 emissions, would induce an appealing NPV-profile for the IGCC-MR technology option.

Future Work (to be conducted under new award #FE0004895)

- A long-term WGS experiment will be conducted with a Pd-316L/PSS membrane for up to 1,000 hours at 400°C, 200 psig, and with a feed rate of 2,700 h^{-1} syngas feed (19% CO, 55% H_2O, 18% H_2, 8% CO_2).
- Pd-Au and Pd-Ru membranes will be synthesized for testing under WGS conditions for up to 200 hours with up to 20 ppm H_2S present in the feed.
- Flexibility analysis will be included into the NPV-based economical model for the integration of the membrane reactor technology into IGCC plants to increase the value of the project (increased NPV) and also to decrease the risk associated with the membrane reactor technology.
- Prepare thin and stable composite pure Pd membranes on 1-inch outer diameter PSS 316 and test them under real gasification conditions at National Center for Carbon Capture, Wilsonville, Alabama.
- Conduct DOE Test 2A (simulated effluent of WGS reactor) on MembraGuard®-coated Pd membrane to further confirm the stability of MembraGuard®-coated membrane under WGS reaction conditions.
- Composite Pd membranes will be prepared on new supports with higher initial He permeability in order to decrease mass transfer resistance within the support.

FY 2011 Publications/Presentations

1. Koc R,; Kazantzis N.K. and Ma, Y.H. "Membrane Reactor Technology Integrated Into IGCC Power Plants: An Economic Evaluation in the Presence of Uncertainty", Presented at the 2011 North American Membrane Society Annual Meeting. Las Vegas, NV, June 4–8, 2011

2. Augustine A.; Mardilovich I.; Ma Y.H. and Kazantzis N.K. "Long-term testing of H_2 permeable, PSS supported Pd-membranes under mixed gas and water-gas shift reaction conditions". Presented at the 2011 North American Membrane Society Annual Meeting. Las Vegas, NV, June 4–8, 2011.

3. Augustine, A.S., Ma, Y.H., Kazantzis, N.K. "*High pressure palladium membrane reactor for the high temperature water-gas shift reaction.*" International Journal of Hydrogen Energy. 36(2011), 5350-5360.

4. Pomerantz, N. and Ma, Y.H., "Isothermal Solid-State Transformation Kinetics Applied to Pd/Cu Alloy Membrane Fabrication", AIChE J, 56, 3062 – 3073 (2010).

5. Chen, Chao-Huang and Ma, Yi Hua, "The Effect of H2S on the Performance of Pd and Pd/Au Composite Membrane", 362(1-2), 535-544(2010).

6. Pomerantz, N., Ma, Y.H., "Novel Method for Producing High H2 Permeability Pd Membranes with a Thin Layer of the Sulfur Tolerant Pd/Cu fcc Phase", J Memb Sci., 370, 97-108 (2011).

7. Koc, Reyyan, .Kazantzis, Nikolaos K and Ma, Yi Hua, "A Process Dynamic Modeling and Control Framework for Performance Characterization and Enhancement of Pd-Based Membrane Reactors Used in Hydrogen Production", International J of Hydrogen Energy", Vol. 36, Issue 8, 4934-4951, (2011).

8. Ma, Yi Hua, "Composite Pd and Pd Alloy Porous Stainless Steel Membranes for Hydrogen Production and Process Intensification", US DOE FY11 Advanced Fuels Peer Review", October 18–22, 2010, Morgantown, WV.

9. Koc, Reyyan, Kazantzis, Nikolaos K. and Ma, Yi H., "A Process Dynamic Modeling Framework for Performance Assessment of Pd-Based Membrane Reactors", Oral presentation, Session: Process Modeling, NAMS/ICIM, July 17–22 2010, Washington, D.C., USA.

10. Koc, Reyyan, Kazantzis, Nikolaos K, and Ma, Yi H., "Theoretical study for the integration of the Pd-based water gas shift membrane reactors into the IGCC plants", Poster presentation, 240th ACS National Meeting, Division of Environmental Chemistry, August 22–26, 2010, Boston, MA, USA.

11. Koc, Reyyan, Kazantzis, Nikolaos K. and Ma, Yi H., "Process Safety Aspects in Water-Gas-Shift (WGS) Catalytic Membrane Reactors Used for Pure Hydrogen Production", Mary Kay O'Connor Process Safety Center International Symposium, October 26–28, 2010, College Station, TX, USA.

12. Koc, Reyyan, Kazantzis, Nikolaos K and Ma, Yi Hua, "Process safety aspects in water-gas-shift (WGS) membrane reactors used for pure hydrogen production"

13. Koc, Reyyan, Kazantzis, Nikolaos K and Ma, Yi Hua, "The Integration of Pd/alloy-Based Water-Gas Shift Membrane Reactors into Coal Gasification Plants: A Performance Assessment Study", Presented at the 2011 International Congress on Membranes and Membrane Processes, Amsterdam, Holland, July 23–29, 2011.

14. Koc, Reyyan, Kazantzis, Nikolaos K and Ma, Yi Hua, "A Dusty Gas-Based Modeling Framework to Characterize the Selectivity of Pd/Alloy-Based Membrane Reactors Under Water-Gas Shift Conditions in the Presence of Defects", Presented at the 2011 International Congress on Membranes and Membrane Processes, Amsterdam, Holland, July 23–29, 2011.

References

1. Chen, C.H. and Ma, Y.H. "the effect of H2S on the performance of Pd and Pd/Au composite membranes". Journal of membrane science, 362(1-2), 535-544 (2010).

2. Pomerantz, N. and Ma, Y.H. "Effect of H_2S on the Performance and Long-Term Stability of Pd/Cu Membranes". Ind. Eng. Chem. Res., 2009, 48 (8), pp 4030–4039.

3. Guazzone, F.; Ma, Y.H. "Leak Growth Mechanisms in Composite Pd Membranes Prepared by the Electroless Deposition Method." AIChE Journal, 54(2), 2008, 487-494.

4. Guazzone, F. "Engineering of substrate surface for the synthesis of ultra-thin composite Pd and Pd-Cu membranes for H_2 Separation", PhD Thesis (2005).

5. Ma et al. US patent 7 727 596 (2010), US patent 7 255 726 (2007), US patent 7 175 694 (2007), US patent 6 152 987 (2007), US patent 6 152 987 (2000).

6. Augustine, A.S.; Ma, Y.H.; Kazantzis, N.K. "High pressure palladium membrane reactor for the high temperature water-gas shift reaction." International Journal of Hydrogen Energy, 36(2011), 5350-5360.

II.E.1 PEM Electrolyzer Incorporating an Advanced Low-Cost Membrane

Monjid Hamdan (Primary Contact), Tim Norman
Giner Electrochemical Systems (GES), LLC
89 Rumford Ave.
Newton, MA 02466
Phone: (781) 529-0526
E-mail: mhamdan@ginerinc.com

DOE Managers
HQ: Eric Miller
Phone: (202) 287-5829
E-mail: Eric.Miller@ee.doe.gov
GO: Paul Bakke
Phone: (720) 356-1436
E-mail: Paul.Bakke@go.doe.gov

Contract Number: DE-FG36-08GO18065

Subcontractors:
- Virginia Polytechnic Institute and State University, Blacksburg, VA
- Parker Hannifin Ltd domnick hunter Division, Hemel Hempstead, United Kingdom

Project Start Date: May 1, 2008
Project End Date: April 30, 2012

Fiscal Year (FY) 2011 Objectives

Develop and demonstrate advanced low-cost, moderate-pressure proton exchange membrane (PEM)-based water electrolyzer system to meet DOE targets for distributed electrolysis:

- Develop high-efficiency, low-cost membrane
- Develop long-life cell-separator
- Develop lower-cost prototype electrolyzer stack and system
- Demonstrate prototype at the National Renewable Energy Laboratory (NREL)

Technical Barriers

This project addresses the following technical barriers from the Hydrogen Production section of the Fuel Cell Technologies Program Multi-Year Research, Development and Demonstration Plan:

(G) Cost - Capital Cost

(H) System Efficiency

Technical Targets

TABLE 1. GES Progress toward Meeting DOE Targets for Distributed Electrolysis Hydrogen Production

Characteristics	Units	2012/2017 Target	GES Status
Hydrogen Cost	$/kg H_2	3.70/<3.00	4.66*
Electrolyzer Capital Cost	$/kg H_2	0.70/0.30	0.60
Electrolyzer Energy Efficiency	% (LHV)	69/74	75**

*Using H2A model rev 2.1.1. A cost of $1.80 is included for H_2 compression, storage, and delivery
** Stack efficiency; System efficiency ~68%
LHV – lower heating value

FY 2011 Accomplishments

Membrane

- Demonstrated enhanced dimensionally stable membrane (DSM™) performance (>Nafion® 1135 membrane).
- Completed 5,000-hour life-test with DSM™ (@80°C).
- DSM™ operating lifetime estimated at 55,000 hours.
- Reduced membrane support costs by one order of magnitude in the past year.

Cell-Separator

- Demonstrated reduced hydrogen embrittlement in titanium/carbon cell-separator.
- Projected longevity of the carbon/titanium cell-separators (>60,000 hours).

Electrolyzer Stack and System Design

- Completed fabrication of electrolyzer stack utilizing low-cost components.
- Reduced electrolyzer stack costs by 60% over a four year period.
- Completed fabrication of electrolyzer system incorporating a high-efficiency hydrogen dryer.
- Completed extensive safety review of electrolyzer system.
- Completed modeling of electrolyzer capital and operating costs; performed economic analysis using the DOE H2A model illustrating cost-reductions.



Introduction

The DOE has identified hydrogen production by electrolysis of water at forecourt stations as a critical technology for transition to the hydrogen economy, and as the hydrogen economy matures, for hydrogen production at centralized locations using renewable energy sources. However, state-of-the-art electrolyzers are not economically competitive for forecourt hydrogen production due to their high capital and operating costs. The cost of hydrogen produced by present commercially available electrolysis systems is estimated to be \$5.20/kg-H_2, considerably higher than the DOE target of \$3.70/kg-H_2 by 2012 [1]. Analysis of electrolyzer systems performed by GES and others using the DOE H2A model indicate that the major cost elements are the cost of electricity, the capital costs of electrolyzer stacks and systems, and the high cost of hydrogen compression, storage, and delivery.

GES has developed PEM-based electrolyzer technology that operates at differential pressure for producing hydrogen at moderate to high pressure directly in the electrolyzer stack, while oxygen is evolved at near-atmospheric pressure. In this system, liquid water, which is a reactant as well as coolant, is introduced into the oxygen side at near-atmospheric pressure. The goals of the project are to reduce the cost of the stack and system, improve electrolyzer efficiency, and to demonstrate electrolyzer operation at moderate pressure.

Approach

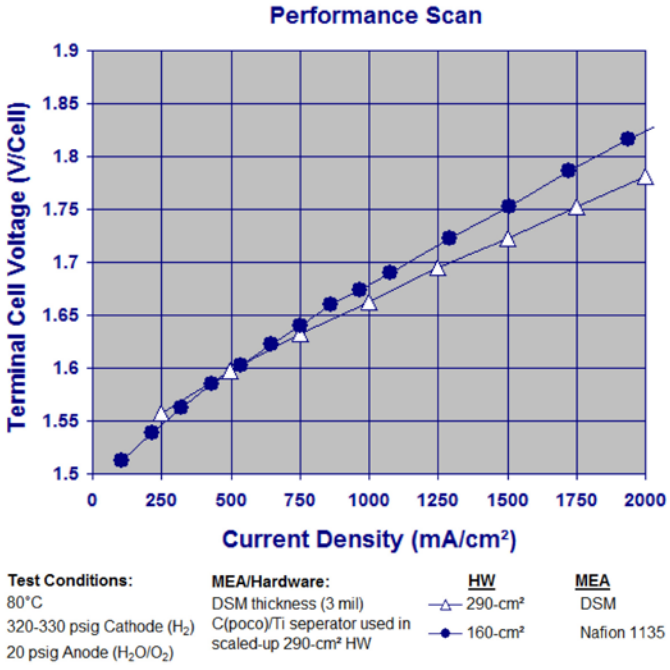
To reduce the cost of PEM-based electrolyzers, GES is improving electrolyzer stack efficiency and reducing stack cost through development of an advanced low-cost, high-strength, membrane using a perforated polyimide support imbibed with perfluorosulfonic acid (PFSA) ionomer. GES is also reducing stack capital cost and increasing stack life through development of a long-life bipolar stack cell-separator, decreasing stack costs by initiating scale-up to a larger active area, and reducing the system capital cost by applying commercial production methods to PEM-based electrolyzer systems. In each of the key development areas, GES and its team members are conducting focused development of advanced components in laboratory-scale hardware, followed by life-testing of the most promising candidate materials. The project will culminate in fabrication and testing of an electrolyzer system for production of 0.5 kg-H_2/hr and validation of the electrolyzer stack and system in testing at NREL.

Successful development of the advanced electrolyzer stack and system will result in a high-efficiency; low-capital-cost electrolyzer that will meet the DOE cost targets for hydrogen production, assuming high-volume production. This will provide competitively priced hydrogen for delivery at forecourt stations to enable transition to the hydrogen economy.

Results

DSM™ Membrane Performance: To improve electrolyzer efficiency, GES has developed an advanced supported membrane having an ionic resistance comparable to that of a 0.0020- to 0.0035-inch-thick Nafion® membrane, but having significantly improved mechanical properties. This advanced membrane is referred to as a dimensionally stable membrane (DSM™) due to the membrane support that minimizes changes in dimensions (swelling/contraction) under high-pressure operation and with changes in water content. The support structure utilized in the development of the DSM™ consists of a polyimide (Kapton®) base film with a definable open pattern. The support structure is then imbibed with 1100-equivalent-weight (EW) PFSA ionomer to a thickness of 2 to 3 mil (0.002-0.003”). Initially the membrane support structures were fabricated using a laser-drilling procedure. A more cost-effective technique of fabricating the support structures via chemical-etching has recently been implemented by GES, reducing the cost of the membrane by one order of magnitude.

Polarization scans of the DSM™ were conducted in scaled-up, full-size electrolyzer hardware through a current density range of 0-2,000 mA/cm², a differential pressure of 300 psid, and temperature of 80°C. Results are compared to Nafion® 1135 membrane with similar cathode and anode electrode structures, Figure 1. During testing, the DSM™ exceeded the criterion for performance: exhibiting lower cell voltages and thus higher cell efficiencies than that of a Nafion® 1135 membrane.



HW - hardware; MEA - membrane electrode assembly

FIGURE 1. Performance Scans: DSM™ vs. Nafion® 1135

Durability of the DSM™ was also demonstrated in the scaled-up, hardware via fluoride release rate (FRR) measurements at constant-current operation. Since PFSA ionomer is used as the membrane material and in the binder for the catalyst layer, the loss of fluoride is used as a measurement of membrane degradation. An FRR rate of 3.7 µg F^- ion/hr or less than 10 micrograms F^- ion/liter (<10 ppb) was present in the cathode effluent (electro-osmotically transported water) at the end of the 1,000-hour life test. Based on electrolysis FRR results, the lifetime of the DSM™ is projected to be between 45,000 and 55,000 hours, which exceeds the durability requirements of the electrolyzer system. In addition to its durability, the DSM™ exhibits high cell efficiencies in the range of 75% LHV (88.8% higher heating value) at an operating current density of 1,500 mA/cm².

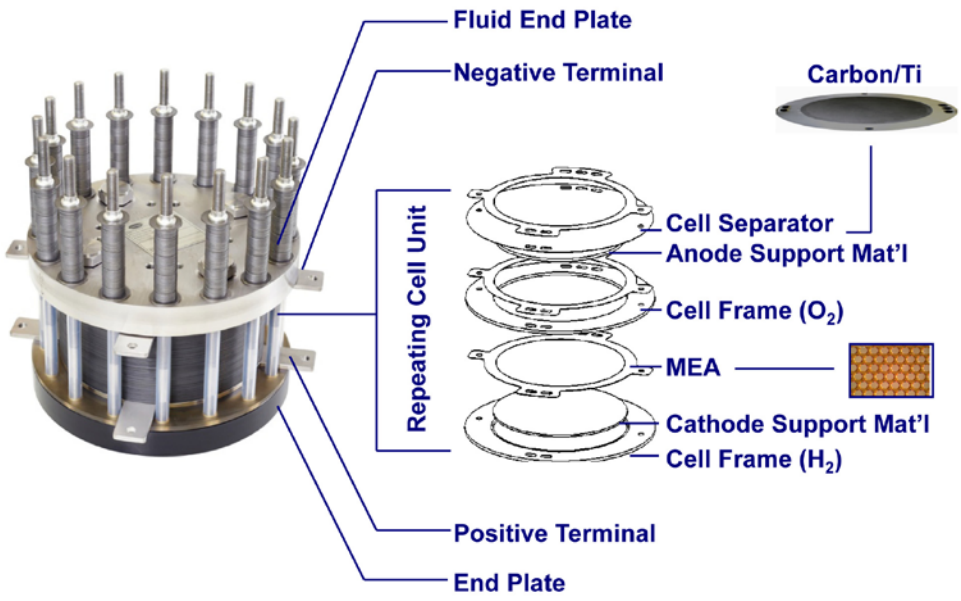


FIGURE 2. Low-Cost Electrolyzer Stack

Cell-Separator Development: The cell separator is a gas-impermeable conductive sheet that separates the hydrogen and oxygen compartments in the bipolar stack. The separator must be highly conductive, as well as resistant to hydrogen embrittlement and to corrosion in an oxidizing environment. GES's legacy high-pressure naval electrolyzers use a complex multi-layer cell-separator incorporating a conductive compliant member and sheets of niobium and zirconium metal. Zirconium is used due to its high resistance to hydrogen embrittlement. GES has previously evaluated a low-cost, dual-layer titanium cell-separator. Although performance was comparable to that of niobium/zirconium cell-separators, lifetimes were limited to 5,000 hours due to hydrogen embrittlement.

The most promising approach for long-term implementation has been achieved by coating titanium with a low-cost electrically conductive, embrittlement-resistant carbon coating. The challenge was the development of a pinhole-free, highly adherent coating with the required characteristics. Under the cell-separator development task, GES demonstrated performance of a carbon/titanium cell separator in scaled-up 290-cm² electrolyzer stack hardware. Performance is comparable to that of the niobium-zirconium separator. In addition, life expectancy of the carbon/titanium separator, determined via hydrogen-uptake analysis over a 1,000-hour period, indicates lifetimes exceeding the 50,000-hour system requirement.

Electrolyzer Stack and System Fabrication: The full-size (27-cell, 290-cm² active area) electrolyzer stack developed during this project is shown in Figure 2. The electrolyzer stack, capable of producing 0.5 kg-H_2/hr at an operating current density of 1,500 mA/cm², is designed with low-cost components. In addition to the use of chemically etched DSM™ and carbon/titanium cell-separators, the electrolyzer stack includes several modifications to GES's legacy hardware; (1) an increase in cell active area from 160 to 290 cm², effectively reducing the number of cells required to produce a given amount of hydrogen, thus reducing the stack manufacturing labor, (2) an overall decrease in the parts count per cell (from 41 to 10), (3) a 75% reduction in anode and cathode catalyst loadings, (4) molded thermoplastic cell frames, resulting in a cost reduction of 95% as compared to machining this component, (5) a 33% reduction in cell frame thickness, thus reducing the anode and cathode support materials and costs by 33%, and (6) a low-cost carbon-steel end plate. As a result of the component and membrane development during this project, the overall projected capital cost of the electrolyzer stack has decreased from greater than $1,000/kW in 2007 to <$400/kW in 2011 (Figure 3).

As shown in Figure 4, the system build, undertaken at the Parker facility, is in its advanced stages. The electrolyzer system required detailed planning with respect to system layout and fabrication sequence. Several factors, including specific codes and standards that are pertinent to hydrogen electrolyzer systems, were considered during the system layout. To meet these requirements, the system was designed with three separate compartments; the oxygen (O_2), the hydrogen (H_2), and the electrical (controller and power supply) compartments. The O_2 compartment contains the oxygen gas-phase separator, a circulating liquid pump, and the de-ionized water feed tank. The H_2 compartment encloses a novel high-efficiency (97%) hydrogen dryer assembly, high- and low-pressure hydrogen gas-phase separators, a

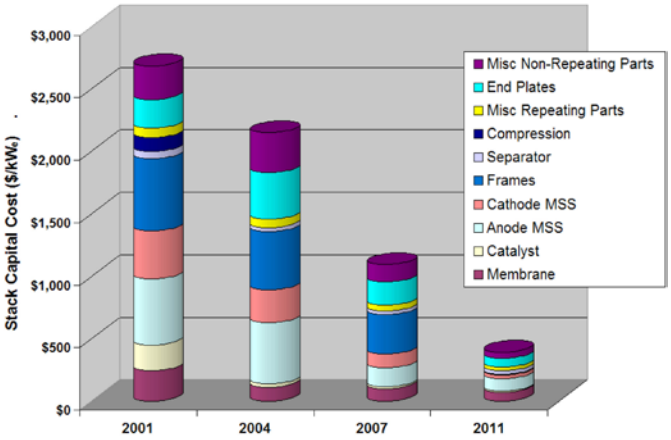


FIGURE 3. Electrolyzer Stack Capital Costs



FIGURE 4. Electrolyzer System

heat exchanger, cooling fans, and various flow valves. The electrolyzer stack is powered via a high-efficiency power supply rated at 94% located in the electrical compartment. The outside platform is also used as the staging area for the nitrogen (N_2) tanks that will provide N_2 gas for purging the electrolyzer stack during start-up and shutdown.

Conclusions and Future Directions

Significant progress has been made in DSM™ membrane development. GES has demonstrated membrane reproducibility and durability as well as a significant improvement in electrolyzer cell efficiency that exceeds the DOE's 2017 efficiency targets. In addition, development efforts conducted under this project have resulted in significant cost reductions in the PEM-based electrolyzer stacks and systems, an increase in the life of the low-cost cell-separators, and improved balance-of-plant components efficiency. The future objectives are to:

- Complete critical design review.
- Install electrolyzer stack into system.
- Assist in system start-up at Parker facilities and evaluate overall performance.
- Deliver and demonstrate the prototype electrolyzer system at NREL for validation.

FY 2011 Publications/Presentations

1. M. Hamdan, *PEM Electrolyzer Incorporating an Advanced Low-Cost Membrane.* 2011 Hydrogen Annual Program Merit Review Meeting. Presentation #pd_030_hamdan, May 11, 2011.

2. M. Hamdan, *Hydrogen Production by PEM Electrolysis.* Fuel Cell Technologies Program webinar. http://www1.eere.energy.gov/hydrogenandfuelcells/webinar_archives.html, May 23, 2011.

References

1. The Department of Energy Fuel Cell Technologies Program Multi-Year Research, Development and Demonstration Plan, http://www1.eere.energy.gov/hydrogenandfuelcells/pdfs/program_plan2010.pdf

Nafion® and Kapton® are registered trademarks of E.I. du Pont de Nemours and Company

II.E.2 High Performance, Low Cost Hydrogen Generation from Renewable Energy

Dr. Katherine Ayers (Primary Contact), Andy Roemer
Proton Energy Systems dba Proton OnSite
10 Technology Drive
Wallingford, CT 06492
Phone: (203) 678-2190
E-mail: kayers@protononsite.com

DOE Managers
HQ: Eric Miller
Phone: (202) 287-5829
E-mail: Eric.Miller@hq.doe.gov
GO: Paul Bakke
Phone: (720) 356-1436
E-mail: Paul.Bakke@go.doe.gov

Contract Number: DE-EE000276

Subcontractors:
- Entegris, Inc., Chaska, MN
- The Electrochemical Engine Center at Penn State, University Park, PA
- Oak Ridge National Laboratory, Oak Ridge, TN

Project Start Date: September 1, 2009
Project End Date: September 30, 2013

Fiscal Year (FY) 2011 Project Objectives

- Improve electrolyzer cell stack manufacturability through:
  - Consolidation of components.
  - Incorporation of alternative materials and manufacturing methods.
  - Improved electrical efficiency.
- Reduce cost in electrode fabrication through:
  - Reduction in precious metal content.
  - Alternative catalyst application methods.
- Design scale up for economy of scale including:
  - Scale up of the design to a large active area cell stack platform.
  - Development and demonstration of a robust manufacturing process for high volume plate production.
- Quantification of the impact of these design changes through utilization of the H2A model.

Technical Barriers

This project addresses the following technical barriers from the Production section of the Fuel Cell Technologies Program Multi-Year Research, Development and Demonstration Plan:

(G) Capital Cost
(H) System Efficiency
(J) Renewable Electricity Generation Integration

Technical Targets

TABLE 1. Proton Energy Systems Progress towards Meeting Technical Targets for Distributed Water Electrolysis Hydrogen Production

Characteristics	Units	2012 Target	2017 Target	Proton Status
Hydrogen Cost	$/gge	<3.70	<3.00	3.46
Electrolyzer Capital Cost	$/gge	0.70	0.30	0.64
Electrolyzer Energy Efficiency	% (LHV)	69	74	67

gge - gasoline gallon equivalent; LHV - lower heating value
Note: Estimates are based on H2A v2.1, for electrolysis only (compression-storage-delivery not included). Model assumes $0.05/kWh.
Electrolyzer cost based on 1,500 kg/day capacity, 500 units/year. Efficiency based on system projections and demonstrated stack efficiency of 74% LHV efficiency.

FY 2011 Accomplishments

- Alternate electrode structures enabled 55% less precious metal on the anode (Proton process) and >90% less on the cathode (3M nano-structured thin-film [NSTF] structures).
- A new flow field design resulting in >20% part cost savings (12% stack cost savings) passed production validation and was commercially released.
- Composite bipolar plates from Entegris exhibited stability over >3,000 hours of operation.
- Alternative flow field manufacturing methods were surveyed and a path to additional 50% cost reduction in the subassembly was defined.
- Penn State comprehensive electrolyzer cell model was validated against physical test data and is being leveraged for cell characterization.
- Nitride coatings on flow fields and separators from Entegris, Proton, and Oak Ridge were characterized before and after cell operation and found to remain intact on surface after >500 hours.



Introduction

This project addresses the DOE Hydrogen Program objective for distributed production of hydrogen from proton exchange membrane (PEM) water electrolysis. The DOE Technical Targets for hydrogen cost as well as electrolyzer efficiency and capital cost will be directly addressed through the advancement of key components and design parameters.

Currently, a significant portion of the electrolyzer system capital cost comes from the cell stack(s). When added together, the flow fields and membrane electrode assemblies (MEAs) constitute over half of the total cell stack cost (Figure 1). Significant cost reductions of these components as demonstrated with this research are required in order to reach the targets. Further optimization of cell stack components results in efficiency gains at the system level and ultimately a reduction in the cost to produce hydrogen.

Approach

The scope of work for this project allowed for research and development in several key areas relating to cell stack cost reduction. Topics included: 1) catalyst formulation, 2) flow field design, 3) computational performance modeling, and 4) flow field coating development. Higher efficiency oxygen evolution catalysts are of interest because the oxygen evolution reaction is inefficient and therefore requires high catalyst loadings to achieve reasonable operational voltages at the desired current densities. Improving catalyst utilization can substantially reduce the cost of the MEA by reducing the noble metal content in the catalyst layers. Novel electrode structures have been constructed using alternate synthesis and processing techniques and are being characterized for performance and durability.

Advancements in flow field design are intended to be advantageous for low-cost, high-volume manufacturing. Alternatives to the current flow field design included either 1) composite bipolar plates or 2) unitized flow fields, which consolidate parts and reduce the amount of required precious metal plating. A parallel path is being followed, utilizing the top candidate from each category. Material testing samples for the composite materials are under test for compatibility with the corrosive environment known to exist within operating electrolyzer cells. Prototype flow fields will be fabricated and tested to determine dimensional capability. Computational modeling of an electrolyzer cell will allow for optimization studies to be performed around flow field material and architecture. Cell performance can be quantified in ways not typically possible with standard physical test experiments. Alternate coating strategies are also being investigated which eliminate metal plating entirely. Validation of all of the previously mentioned design changes will be achieved through cost analysis based on the H2A model V2.1.

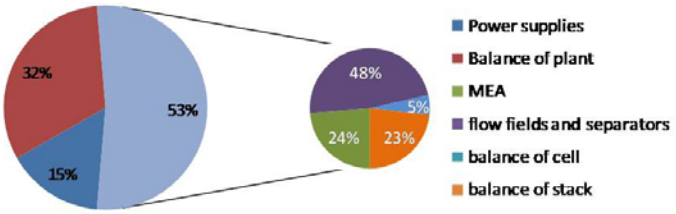


FIGURE 1. Relative Cost of Electrolyzer System Components

Results

Significant advancements have been made in the development of an optimized catalyst formulation and application technique. This work has demonstrated a 55% reduction in the amount of precious metal used in the anode catalyst layers of the MEA vs. current commercial production. Durability testing showed no degradation over the duration of the test. The application technique represents an improvement over existing production techniques in that it allows for improved accuracy and uniformity while also enabling higher speed throughput. Work with 3M has also shown feasibility of greater than 90% reduction in catalyst loading vs. current commercial production on the cathode side of the cell utilizing 3M's NSTF electrodes. Even with 15% higher membrane thickness, the reduced loading cathodes demonstrated roughly equivalent performance to a Proton baseline (Figure 2), and durability was demonstrated to over 3,500 hours. A non-proprietary test cell was also qualified and shared with collaborators for increased throughput and cost sharing.

Near-term electrolyzer stack cost reductions of 12% vs. Proton's 2010 commercial product were identified through the testing and validation of non-metal cathode flow field components. The new part was implemented in Proton's commercial product, with thousands of cells manufactured to date.

Composite bipolar plates which enable substantial further reduction in metal content were procured and have been on test for over 3,000 hours without significant voltage decay (Figure 3). Samples were nitrided to protect the part from oxidative corrosion and hydrogen embrittlement. Selected samples will be examined after longer operating times to predict overall life based on any signs of corrosion

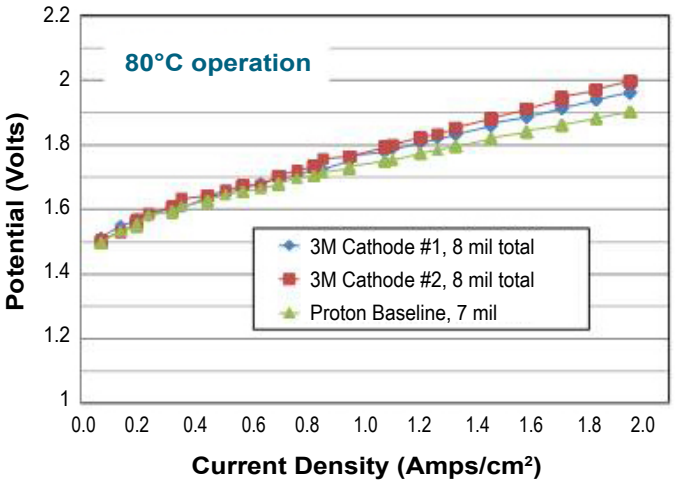


FIGURE 2. Performance of NSTF Electrodes as Electrolysis Cathodes

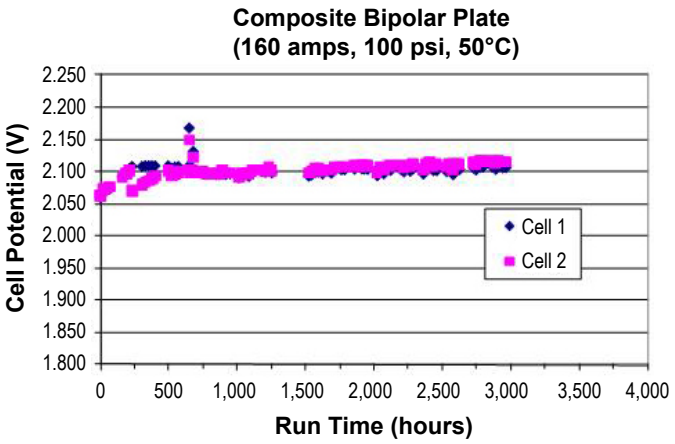


FIGURE 3. Voltage Trend for Composite Bipolar Assembly

or material degradation. A survey was also completed of over 30 bipolar assembly concepts, which showed opportunity for 50% cost savings in the subassembly over the production change already implemented. In addition to the composite plate, an alternate unitized part was selected for prototyping to verify cost and dimensional tolerancing.

The comprehensive computational model of an electrolyzer cell developed at Penn State was shown to be capable of predicting performance parameters based on the geometry of the flow fields and specified operating conditions. Calculated parameters included overall cell potential, distribution of potential and current density distribution, as well as volume fractions of water, oxygen and hydrogen in various regions of the cell. Predicted polarization curves were shown to be consistent with actual data. A parametric study was performed to flex the model variables. Learnings from this model will be used for refinement of cell component architecture for improved water distribution within the cell and better thermal management.

Nitriding was studied on both the composite parts as discussed above as well as metal parts. Characterization at Oak Ridge National Laboratory showed that both samples maintained similar thicknesses of the nitrided layer after electrolysis operation (Figure 4). Thermal nitriding was also explored at Oak Ridge and samples were tested for 500 hours in the electrolysis environment without evidence of corrosion. These results validate the potential for multiple options for plate fabrication and coating while eliminating noble metal coatings or plating.

Conclusions and Future Directions

- Cost reductions can be made by controlling the catalyst formulation process and through advanced application techniques. Further work is needed to integrate the anode and cathode benefits realized in this project into a single MEA configuration.
- Initial cost reductions on the cathode flow field were successfully implemented in production.
- Tests have shown that alternative conductive materials can remain stable in the corrosive environment of operational electrolyzer cells for tests over 3,000 hours. Further analysis is required to determine durability projections and progress towards the 30,000 hour minimum operational life of Proton cell stacks, but no obvious degradation has been observed.
- A unitized flow field plus frame assembly has been selected as the parallel path to the composite bipolar plate, with initial predictions of over 50% part cost reduction.
- Electrolyzer cell performance can be predicted with the use of a comprehensive computational model and flow distribution across the bipolar assembly can be modeled to provide valuable insights on design and flow requirements.

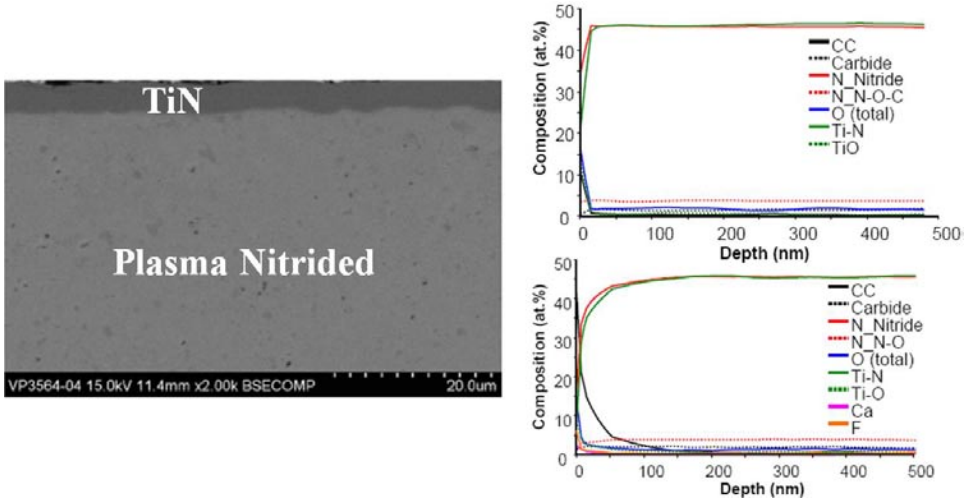


FIGURE 4. Image of Nitrided Part and Analysis of Composition vs. Layer Depth and Operation

- Nitride coatings fabricated by different methods appear to be very stable in electrolysis conditions and may enable reduction in metal coatings. Further process development will be performed to determine the best approach for manufacturability.

II.E.3 High-Capacity, High Pressure Electrolysis System with Renewable Power Sources

Paul M. Dunn
Avãlence, LLC
1240 Oronoque Road
Milford, CT 06460
Phone: (203) 874-6786
E-mail: pmd@avalence.com

DOE Manager
HQ: Eric Miller
Phone: (202) 287-5829
E-mail: Eric.Miller@hq.doe.gov
GO: Paul Bakke
Phone: (720) 356-1426
E-mail: Paul.Bakke@go.doe.gov

Contract Number: DE-FG36-08GO18066

Subcontractor:
HyPerComp Engineering, Inc., Brigham City, UT

Start Date: June 1, 2008
Estimated Project End Date: September 30, 2012

Fiscal Year (FY) 2011 Objectives

- Achieve at least a 15X increase in the gas production rate of a single high-pressure production cell.
- Demonstrate the high pressure cell composite wrap which enables significant weight reduction.
- Build and test a $1/10^{th}$-scale pilot plant.
- Have fabrication ready drawings for full-scale plant (300 kg/day, 750 kW).

Technical Barriers

This project addresses the following technical barriers from the Production section of the Fuel Cell Technologies Program Multi-Year Research, Development and Demonstration Plan:

(G) Capital Costs of Hydrogen Generation by Electrolysis Systems
(H) System Efficiency
(J) Renewable Electricity Generation Integration

Technical Targets

TABLE 1. DOE Technical Targets: Distributed Water Electrolysis Hydrogen Production

Characteristics	Units	2012 Target	2017 Target
Hydrogen Cost	$/gasoline gallon equivalent (gge)	3.70	<3.00
Electrolyzer Capital Cost	$/gge $/kW	0.70 400	0.30 125
Electrolyzer Energy Efficiency	% (lower heating value)	69	74

Distributed Water Electrolysis Hydrogen Production

In this project Avãlence is developing an enlarged version of its present electrolyzer design that will have 15X the capacity of the current single tubular cell. To achieve this, the diameter of the current Avãlence design individual tubular cell is being enlarged to enable an innovative cell core design: multiple coaxially arranged cylindrical electrodes, nested in a uni-polar configuration. This design is the core of a distributed water electrolysis hydrogen production system that will meet the following DOE 2017 targets:

- Hydrogen cost: $3.00 gge
- Electrolyzer energy efficiency: 74 kWh/kg

FY 2011 Accomplishments

Detailed engineering and design and construction of the test cell continued during 2011. Significant engineering focus was directed toward a detailed design to seal the inner electrodes and membranes and the pressure flange and provide inlet and exit ports for the water and H_2 and O_2 gases. The cell prototype will be tested at 1,000 psi on an existing test stand at Avãlence that will provide electrical and pressure control and electrolyte level balancing. 2011 accomplishments include:

- Detailed design drawings for the prototype cell (Figure 1) to include the following elements:
  - A top gas exit manifold made of polyvinyl chloride (PVC) that will have gas collection channels machined into the manifold. Oxygen will be collected and sent to a center outlet port. The hydrogen manifold will be split into four quadrants with outlet ports in each of the four quadrants. The manifold, which will have an electrode sealing mechanism or clamp, is at the top end of the cell.

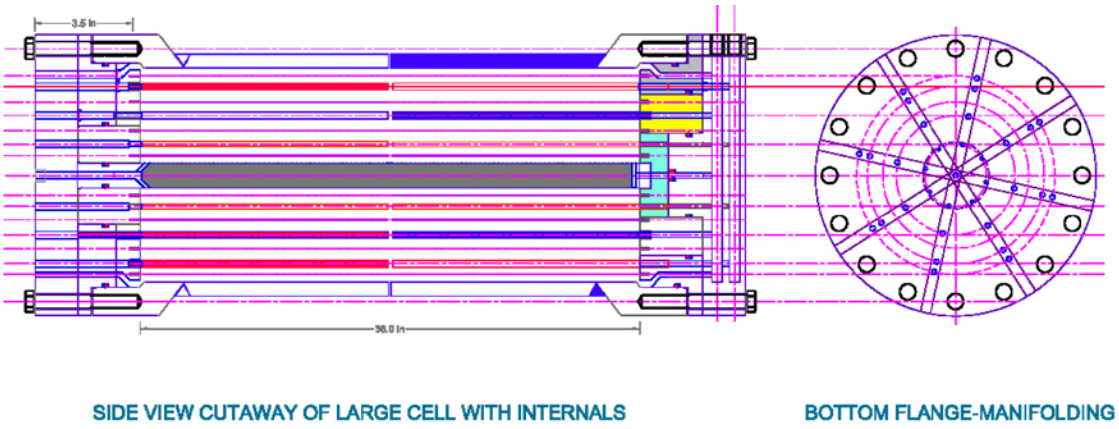


FIGURE 1. Cutaway View of Cell Nested Components

- An innovative method of joining and securing the electrode and membrane ends to the top and bottom of the cell via a mounting collar made of PVC.

- Detailed design of the exact geometry of the internal nested cylindrical components which consist of two inner anodes, two cathodes, and the four membranes that form the boundaries between the anolyte and catholyte chambers. The design utilizes 8-inch, 6-inch, 4-inch and 2-inch 316 stainless steel.
- Detailed engineering design of the inner and outer pressure flanges that will allow the assembly of inner electrodes and membranes in two modules:
  - One outermost piece of the outer flange assembly that holds an anode, inner cathode, and two membranes.
  - A second assembly that includes a flange which is sandwiched underneath the outermost flange. This assembly holds the second anode and the center cathode, plus two membranes in place.
  - Design of plastic mounting disks which are placed inside and are locked into position by the outer flange pieces to seal the electrodes and membranes in place.
  - The outermost piece of the outer flange is bolted through the second assembly (sandwich) flange into the inner flange of the cathode/pressure cylinder, pressure sealing the entire cell.
  - The design calls for a top outer flange/mounting disk assembly with gas exit paths, and a bottom outer flange/disk assembly with liquid distribution and recirculation.
  - In a departure from the current smaller scale Avãlence product design [1], the cell membranes are sealed at both ends of the cell to prevent anolyte and catholyte from mixing. This will ensure high purity by preventing H_2 and O_2 gases dissolved in the electrolyte from crossing the cell boundaries formed by the membranes by eliminating an open circulation path below the membrane. Anolyte and catholyte entrained in the exiting gas bubbles (through gas paths in the top of the cell) will return to the appropriate cell chambers via external circulation and reinjection through the bottom outer flange/disk assembly.
  - The design makes extensive use of O-rings to seal leak paths through liquid inlets and gas outlets, as well as to seal the flanges at both ends of the cell.
- The outer cathode/pressure cylinder was cut from an 8-inch pipe and the inner flanges machined from a stainless steel solid bar stock at Avãlence and welded together and dye penetrant-checked, see Figures 2 and 3.
- The cylinder was shipped to HyperComp in Brigham City, Utah, for wrapping with carbon fiber, see Figure 4.



Introduction

Avãlence has existing technology that is globally unique in its ability to deliver hydrogen directly at storage-ready pressures of 2,500 and 6,500 psi without a separate compressor. Using an alkaline electrolyte process, the Avãlence Hydrofiller systems integrate the production and compression processes by operating the electrolytic cells at the desired delivery pressure. The systems can interface directly with renewable electricity supplies and have been shown in previous work (DOE Small Business Innovation Research project completed in April 2005) that the electrolyzer operates through the full range of voltages output from the connected photovoltaic (PV) array without using any power conditioning equipment. These characteristics result in a renewable hydrogen production and delivery system that is significantly more efficient and reliable, and substantially less expensive than existing commercially available electrolyzer and compressor system sets. The smaller scale Hydrofillers are based on a single cathode/anode tubular cell design with production

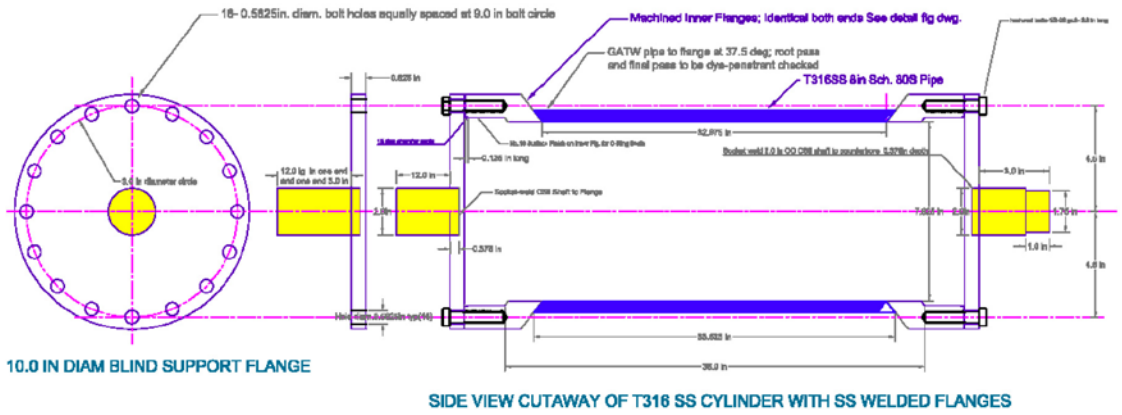


FIGURE 2. Cell with Flange Ends for Carbon Fiber Wrapping



FIGURE 3. Photograph of Cell Prior to Carbon Fiber Wrapping

capability of about 0.1 kg/day per cell. A revolutionary design approach to this high-pressure cell core is needed for an order-of-magnitude capacity scale up of the individual electrolyzer modules.

Approach

In this project, Avãlence is developing an enlarged version of the current Avãlence design that will have at least 15X the capacity of our present single tubular cell. The diameter of the large individual cell will be substantially increased in order to enable an innovative cell core design – multiple coaxially arranged cylindrical electrodes, nested in a uni-polar configuration – enabling up to 1½ kg/day of production per individual cell. In order to accomplish this cell diameter increase with a practical pressure boundary while operating at either 2,500 or 6,500 psi, Avãlence has partnered with a composite cylinder manufacturer, HyPerComp Engineering Inc. They will develop a custom designed containment vessel/cathode using their composite technology expertise that will allow an increase in the diameter of the individual electrolysis cell, enable operation at 2,500 psi and above, and reduce the cell weight and cost relative to conventional metal containment (similar to what is seen today with composite storage tanks used on vehicles). Ninety-six of these high-capacity cells will now produce a single unit (module) with a production capacity of 150 kg/day.

To complete this development process, Avãlence is proposing to build a quarter-scale pilot plant to be composed of 20 cells that will replicate the full plant design and operation, but minimize the cost to DOE for this technology demonstration. The pilot plant will be sent to the National Renewable Energy Laboratory for verification testing. The final result of the project will be a commercially operating 30 kg/day pilot plant integrated with a wind turbine and/or PV array, and delivering H_2 gas at pressure directly to storage cylinders. Operation of this plant and extensive testing of this and earlier development versions throughout the course of the project will thoroughly document the performance and operation of the technology. This combination of an operating pilot plant and substantial performance and operating data will position the technology for commercialization.

Results

Initial test work on nested components, with passive circulation, was conducted during the first quarter of FY 2011. The test results from one nested set did demonstrate substantial recirculation (driven only passively at this point). The recirculation had a very positive effect in that purity of hydrogen (before the catalyst) increased from 98.5% typical at 2,200 psig to >99.5% at 2,200 psig. The recirculation resulted in less dwell time inside the cells for the gas bubbles and therefore less opportunity to diffuse or leak by whatever minute paths exist. This is an indication that Avãlence should be able to return to high pressure operation (6,000 psig) with no compressor, and stay below the required safety limit of 2% impurity before the catalysts. The test cell, with five nested electrodes, will use active circulation, which should further reduce dwell time, so even better results



FIGURE 4. HyperComp Wrapping Sequence and Finished Cylinder

are anticipated. In support of the multi electrode testing, Avãlence has selected circulation pumps for testing of the five nested electrodes.

Based on the tests conducted during the first quarter of FY 2011 and additional analysis, there is a problem of excessive voltage drop associated with axial electrical conductivity in the nested set of 316 stainless steel electrodes. As a result, additional design work was undertaken to decrease electrical resistance within the cells and associated with pass through (sealed) conductors. This is focusing on the selection and construction of the anodes and cathodes that provide the axial conductivity and electrical pass through, and which are also of acceptable cost. The test cell design is limited to 3' height due to concern over voltage loss axially. This means that the pilot plant cells at 6' will require that electrical connections are made at both ends of the electrodes or another solution is devised in order to improve the conductivity. For example, it is possible to solve this problem with a change in material (to nickel for example), but this is costly. Avãlence is working on other concepts such as layering (cladding) the electrodes to deliver both the conductivity required and to manage the cost.

Lastly, design work focused on how to align the plurality of electrodes and membranes top and bottom for better manufacturability. This is being addressed by securing the membranes and inner electrodes to a top alignment mount made of PVC that will be glued to the upper gas manifold (also made of PVC). The relatively thin membranes will be reinforced at the bottom with a PVC guide ring glued to the membranes. The membranes and electrodes are attached to a PVC bottom alignment guide, and the entire assembly can then be inserted into an outer anode and flange assembly. Avãlence is researching the manufacture and supply of stiff tubular membranes made by casting a membrane material onto a rigid ceramic, extruded PVC, or other support.

Conclusions and Future Directions

Conclusions

Through changes in conceptual design and detailed engineering design currently underway, Avãlence is addressing the design challenges of this unique high pressure concentric ringed electrolysis cell, all of which impact manufacturability, gas purity, and high pressure operation:

- Electrode and membrane sealing to cell ends
- Gas collection
- Axial conductivity
- Electrolyte balancing
- Cell cooling
- Etc.

Future Directions

- Demonstrate large diameter cell operation at 1,000 psi:
  - The cell will be tested on a test stand that Avãlence has adapted from the balance of plant of a Hydrofiller 15.
  - Will circulate electrolyte on both sides using cat pumps.
  - No gas recirculation will be required until the design pressure goes above 2,500 psig.
- Test long-term 6,500 psi operation approaches:
  - Using existing small cell apparatus.
  - Purified gas "recirculation/dilution" approach as required to achieve lower explosive level requirements.
  - Neutral electrolyte chamber approach – membrane related effort.

FY 2011 Publications/Presentations

1. *High Pressure, High Capacity Electrolysis System*, presented at the 2011 Fuel Cell and Hydrogen Association Conference, February 15, 2011.

II.E.4 Renewable Electrolysis Integrated System Development and Testing

Kevin Harrison (Primary Contact), Todd Ramsden, Genevieve Saur, Chris Ainscough
National Renewable Energy Laboratory (NREL)
1617 Cole Blvd.
Golden, CO 80401
Phone: (303) 384-7091
E-mail: Kevin.Harrison@nrel.gov

DOE Manager
HQ: Eric Miller
Phone: (202) 287-5829
E-mail: Eric.Miller@ee.doe.gov

Subcontractor:
Spectrum Automation Controls, Arvada, CO

Project Start Date: October 1, 2003
Project End Date: Project continuation and direction determined annually by DOE

Fiscal Year (FY) 2011 Objective

- Optimize the coupling between wind and solar electric resources and the hydrogen-producing stacks of commercially available electrolyzer systems.
- Quantify performance differences between variable and constant current operation of electrolyzer stacks and systems.
- Collaborate with industry and utilities to advance the commercialization of integrated renewable electrolysis systems.
- Demonstrate the technical readiness of DOE-awarded advanced electrolysis systems.

Technical Barriers

This project addresses the following technical barriers from the Production section (3.1) of the Fuel Cell Technologies Program Multi-Year Research, Development and Demonstration Plan:

(G) Capital Cost
(H) System Efficiency
(J) Renewable Electricity Generation Integration

Technical Targets

Results from the project demonstrate improved system efficiency and offer opportunities to reduce capital costs by reducing redundant components in a renewable-coupled system. Previously, testing conducted under this project of a DOE-awarded system, from Giner Electrochemical Systems, demonstrated small-scale (16-kW) electrolyzer system energy efficiency of 55% (lower heating value, LHV). The current (2009) state-of-the-art cost for delivered hydrogen from electrolysis for a forecourt refueling station ranges from \$4.90/kg-H_2 to \$5.70/kg-H_2 dispensed at the pump, with a base-case estimate of \$5.20/kg-H_2. This base-case estimate of \$5.20/kg-H_2 includes an electrolysis production cost of \$3.32/kg-H_2 and compression, storage and dispensing costs of \$1.88/kg-H_2. These costs are evaluated using Energy Information Administration Annual Energy Outlook 2005 High A Case industrial electricity costs (\$0.053/kWh on average) [1]. In the coming year, this project will test the performance of two DOE-awarded systems to demonstrate their technical readiness for improved stack efficiency and higher pressure (>2,500 psig) hydrogen product directly from the electrolyzer stack. Based on information provided by electrolyzer suppliers for their state-of-the-art technologies, both alkaline and polymer electrolyte membrane (PEM) electrolyzers are now capable of producing hydrogen using less than 50 kWh/kg, representing a lower heating value efficiency of greater than 67% [1].

TABLE 1. Progress toward Meeting DOE Technical Targets for Distributed Water Electrolysis Hydrogen Production

Characteristics	Units	2012 Target	Status
Hydrogen Cost	\$/gge	3.70	4.90-5.70
Electrolyzer Energy Efficiency	% (LHV)	69	67-75

gge – gasoline gallon equivalent

FY 2011 Accomplishments

- Completed Fuel Cell Technologies Program milestone for Hydrogen Fuel R&D for Quarter 1: "Complete testing (300 hours) of multiple commercial electrolysis stacks into a wind-to-hydrogen system to characterize the impacts of the power electronics interface and varying wind power input on electrolyzer performance and cost of renewable-based hydrogen production."
  - Conducted varying current stack testing continuously for more than 3,800 hours by the end of July 2011.
  - The testing revealed that the duration of full-current steady-state operation embedded between long-duration, varying-current wind profile operation influences the anode catalyst oxidation state and may have a role in transient voltage behavior.
- Demonstrated 10% efficiency improvement by combining direct-coupled photovoltaic (PV) and power converter-to-stack operation based on solar irradiance.
- Installed new test facility and power switch gear at the Wind-to-Hydrogen (Wind2H2) project to support testing of DOE-awarded electrolyzer systems in FY 2012.

- Installed refurbished alkaline stack and balance-of-plant components enabling side-by-side comparison testing of similarly sized competing electrolyzer technologies.
- Completed initial hourly analysis of central wind electrolysis production facility (50,000 kg/day). See project II.E.6, "Hour-by-Hour Cost Modeling of Optimized Central Wind-Based Water Electrolysis Production".



Introduction

Renewable electrolysis is inherently distributed, but large-scale wind and solar installations are becoming more common and will take advantage of economies of scale. Life cycle assessments of large-scale wind turbines, for example, show payback for the greenhouse gas emissions required to manufacture the equipment in about nine months [2]. Renewable electricity sources, such as wind and solar, can be closely (and in some cases directly) coupled to the hydrogen-producing stacks of electrolyzers to improve system efficiency and lower the capital costs of this near-zero carbon pathway.

Approach

The Xcel Energy/NREL Wind2H2 project is advancing the integration of renewable electricity sources with state-of-the-art electrolyzer technology. Real-world data from daily system operation are revealing opportunities for improved system design and unique hardware configurations to advance the commercialization of this technology. Lessons learned and data-driven results provide feedback to the analytical and modeling components of this project [3].

In hydrogen production facilities even small increases in system efficiency result in significant reductions in hydrogen cost. DOE is funding electrolyzer manufacturers to design and build improved stacks and system balance of plant to reduce the cost of electrolytically produced hydrogen. This project provides independent testing and verification of the technical readiness of these advanced electrolyzer systems by operating them from the grid and renewable electricity sources.

Results

We conducted side-by-side testing and comparison of stack voltage decay rates between constant and variable current operation. Two, 34-cell stacks of an H-Series PEM electrolyzer, from Proton On Site, were operated with a highly variable wind profile for more than 3,800 hours between November and July 2011. The third stack was operated over the same time with a constant stack current while having the same average current as the two variable stacks. Varying wind current profile was normally operated for hundreds of hours continuously and only interrupted to operate all three stacks at their full-current steady-state point for a few days at a time.

Table 2 summarizes these results, which are based on over 3,800 hours of combined varying wind and full-current steady-state operation through July 2011. Before delivery to NREL, the stacks under test faced severe abuse with no hydration for about a year in a warehouse without operation or attention. Furthermore, this testing is intended only to reveal relative stack decay rates between a variable wind profile and constant current operation if there is any difference. Stack decay rates of today's PEM stacks are in the range of 2–5 µV/cell-h.

TABLE 2. Summary of Full-Current Steady-State Scans and Resulting Decay Rate

Mode	Stack Voltage (104°F)					Average Decay µV/cell-hr
	1/7/2011	2/9/2011	4/12/2011	6/10/2011	7/22/2011	
Variable	76.5	77.6	78.6	79.1	78.3	13.9
Variable	74.5	75.5	76.9	77.2	76.3	13.7
Constant	75.1	75.9	77.1	77.3	76.7	12.4
Cumulative Hours		594	1,853	3,143	3,803	

The cell membrane resistance supports the linear fitting and extrapolation to 104°F (40°C) to establish a common temperature to compare the full-current scans. The data indicate a narrow band of operation during the colder winter months and the wider temperature operating range from the April 12 full-current scan (Figure 1). We expect that hotter summer months will shift stack operating temperature to even higher temperatures, which is the reason 104°F was selected as the comparison temperature.

Original plans to operate the three stacks in full-current steady-state mode for tens of hours between the varying wind profile were quickly replaced when longer duration full-current scans revealed a change in the voltage behavior. The longer duration full-current scans suggested that the anode catalyst layer has a role in this transient voltage behavior. As a result, all future full-current steady-

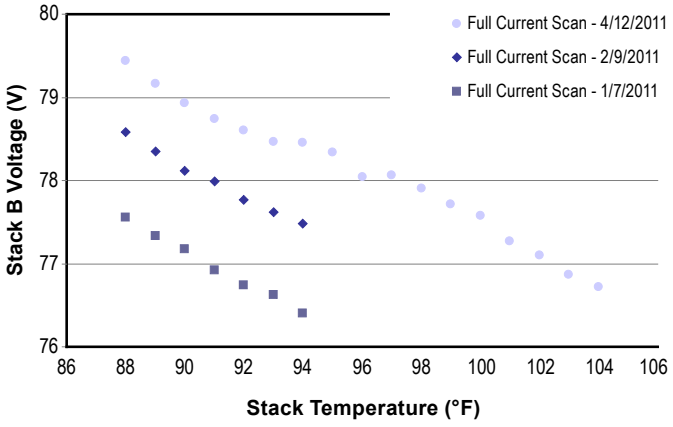


FIGURE 1. Stack B (Varying Stack) Voltage Responses During Full-Current Steady-State Operation

state scans will be run for several days. Proton On Site has suggested a brief electrolyzer shutdown between varying stack and full-current steady-state mode may provide further insight to stack voltage behavior.

The three stacks are periodically brought to their full-current steady-state operating point to enable comparison of their stack voltages at stable conditions. Input and output deionized (DI) water temperature, stack current, and voltage are monitored. DI input and output water temperatures are averaged and binned for every 1°F and the corresponding stack voltages are averaged for each bin. Stack B (varying stack) voltage responses are shown in Figure 1 for three of the full-current steady-state periods and are representative of each stack. Each stack responded similarly during these full-current steady-state operation periods.

In FY 2010, NREL conducted testing comparing the performance of direct coupling a PV array to a PEM electrolyzer stack with that of a power converter using maximum power point tracking. The electrolyzer stack operating point was intentionally aligned with that of PV array. In FY 2011, the power converter switching losses and diode reverse recovery were investigated. The direct coupling and power converter data were further analyzed to show a 10% system efficiency improvement if direct coupling were used in solar irradiances less than 500 W/m^2 and the power converter was used when higher irradiances were present (Figure 2).

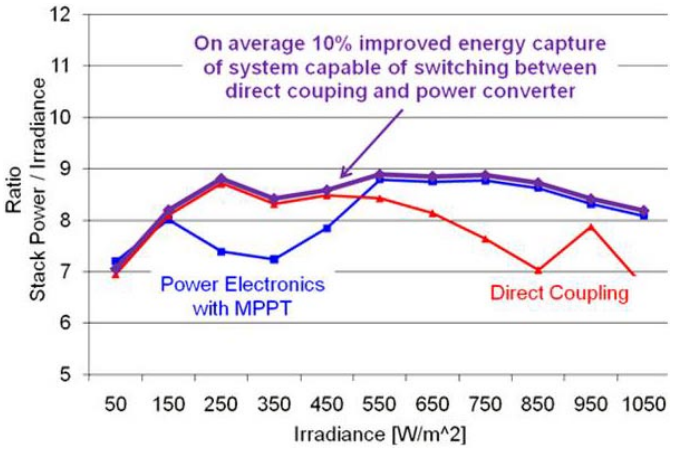


FIGURE 2. 10% Improved Energy Capture by Taking Advantage of Direct Coupling at Solar Irradiances Less Than 500 W/m^2 and Power Conversion when Irradiances are Greater

Conclusions and Future Direction

Through the end of July 2011, NREL conducted more than 3,800 hours of varying wind profile stack current testing with two PEM electrolyzer stack while holding a third stack at constant current. As these results are preliminary, the testing continues.

NREL's comparison testing between direct coupling a PV array to a PEM electrolyzer stack versus a power converter using maximum power point tracking provides an opportunity to improve system efficiency. System efficiency can improve by 10% if direct coupling is used in solar irradiances less than 500 W/m^2 and the power converter is used when higher irradiances are present.

- To support the opportunity to use electrolyzers as dispatchable loads for grid support services, NREL plans to induce frequency disturbances on its 80 kW and 125 kW diesel generators using resistive step loads. Both the PEM and alkaline electrolyzers will be triggered to shed or add load to the microgrid to mitigate these frequency changes.
- Similarly, the 5 kW PEM fuel cell will be direct current coupled with the PV array to quantify its response time as clouds passing by the PV array induce load changes.
- NREL plans to test the performance of two DOE-awarded electrolyzer systems in the coming year. These advanced systems were designed and built to improve stack efficiency and high-pressure electrochemical operation of the stack.
- Equipment downtime, reliability, and maintenance data will be tracked to help quantify the performance of this integrated renewable hydrogen production system.
- Multiple stack electrical isolation tests will highlight the challenges of electrical floating and bipolar stack operation. If successful, multiple stacks could be configured to take advantage of the direct current bus of large-scale variable-speed wind turbines.

FY 2011 Publications/Presentations

1. Harrison, K.; Novachek, F.; Ramsden, T.; Ainscough, C., NREL and Xcel Energy Collaboration on Wind-to-Hydrogen (Presentation); Fuel Cell and Hydrogen Energy Association Conference, February 14–16, 2011, Washington, D.C.

2. Harrison, K.W.; Remick, R.; Hoskin, A.; Martin, G.D., Hydrogen Production: Fundamentals and Case Study Summaries; NREL Report No. CP-550-47302.

References

1. Independent Panel Review, Current (2009) State-of-the-Art Hydrogen Production Costs Estimate Using Water Electrolysis, Report No.: NREL/BK-6A1-46676, September 2009.

2. Life Cycle Assessment of electricity produced from onshore sited wind power plants based on Vestas V82-1.65MW turbines, retrieved June 1, 2011 from www.vestas.com/en/about-vestas/sustainability/wind-turbines-and-the-environment/life-cycle-assessment-%28lca%29.aspx.

3. Harrison, K.; Ainscough, C.; Ramsden, T.; Saur, G. 2011. Hour-by-Hour Cost Modeling of Optimized Central Wind-Based Water Electrolysis Production. Presentation given at the DOE Annual Merit Review, May 10, 2011. www.hydrogen.energy.gov/pdfs/review11/pd085_saur_2011_p.pdf.

II.E.5 Process Intensification of Hydrogen Unit Operations Using an Electrochemical Device

Glenn Eisman (Primary Contact), Daryl Ludlow, Dylan Share
H2Pump, LLC
11 Northway Lane North
Latham, NY 12110
Phone: (518) 783-2241
E-mail: glenn.eisman@h2pumpllc.com

DOE Manager
HQ: Richard Farmer
Phone: (202) 586-1623
E-mail: Richard.Farmer@ee.doe.gov

Contract Number: DE-SC0002185

Subcontractors:
- PBI Performance Products, Inc., Rock Hill, SC
- Plug Power, Inc., Latham, NY

Project Start Date: Phase II: August 15, 2010
Project End Date: August 15, 2012

Fiscal Year (FY) 2011 Objective

Develop and demonstrate a multi-functional hydrogen production technology based on a polybenzimidazole (PBI) membrane which exhibits:

- High efficiency (70%)
- 100 scfh pumping capability
- CO_2 and CO tolerance
- 300 psig (differential) pressurization capability
- $3/kg operating costs

Technical Barriers

This project addresses the following technical barriers addressed in the Production section of the Fuel Cell Technologies Program Multi-Year Research, Development and Demonstration Plan.

(K) Durability
(L) Impurities
(N) Hydrogen selectivity
(O) Operating temperature
(P) Flux
(R) Cost

Technical Target

This project is focused on fundamental chemical and mechanical engineering studies on PBI proton exchange membranes and electrochemical cell hardware, respectively. Learnings gained from these studies will be applied to the membrane fabrication process as well as toward the electrochemical cell architecture to meet the following key targets:

- 300 psid differential pressure operation at 160°C
- CO_2 tolerance
- High efficiency

FY 2011 Accomplishments

- 300 psig compression demonstrated at 160°C for over 600 hours on a PBI-based electrochemical pump.
- A process to increase the membrane durability and performance was developed.
- Advancements in the pump support and seal design (50 cm^2 format).
- Characterization of the gas diffusion layer (mechanical properties), enhanced pump architecture, and a 1st generation large format pump design completed to achieve the program target of 100 scfh.

✧ ✧ ✧ ✧ ✧

Introduction

One of the barriers to fuel cell acceptance is the lack of a simple, reliable, cost-effective and robust process to purify, pump, and pressurize hydrogen. This challenge is magnified by impurities and hydrogen generation occurring at near ambient pressure. Technical means of pressurizing the hydrogen is especially daunting for low to moderate flow rates. If the pressurization, purification, and recovery of the hydrogen can be developed into a single unit operation, the key goals relating to cost and reliability via process simplification could be an attractive and enabling option. Application of electrochemical methods is a potential solution. H2Pump has leveraged its extensive experience in electrochemical separation and pressurization systems to meet the project objectives with a high temperature membrane-based electrochemical hydrogen pump. The solutions have been based on developing a chemically and mechanically robust membrane in conjunction with advancements in cell hardware.

The significance of the success of the project to date is that multiple unit operations have been combined into a

single device and demonstrated to be capable of generating the targeted pressures and impurity tolerances.

Approach

H2Pump has shown that electrochemical methods to recover, purify, and pressurize hydrogen is a viable option for low to moderate volumes of hydrogen containing gases. The main challenge for this specific application is the lack of a proton conducting membrane which exhibits carbon dioxide and carbon monoxide tolerance and at the same time pressurize the hydrogen from atmospheric pressure to 300 psig. The approach has been to work closely with its partner, PBI Performance Products, to enhance the membrane properties relevant to this application while at the same time address cell hardware architecture so as to support the high temperature, CO_2 and CO tolerant membrane. The results (properties) of the membrane modifications were then used to guide the cell hardware program in which cell components have been assessed and characterized for the desired operating conditions. The combined efforts have led to the successful operation of 50 cm^2 cells which meet or exceed the program targets. Design guidelines developed with lab-scale pumps are then applied to a larger format to meet the volume requirements of the effort.

Results

The most significant result during this period is having achieved the targeted 300 psig compression using the high-temperature CO_2, CO tolerant membrane. Other accomplishments include membrane enhancement and characterization, gas diffusion layer characterization and selection, enhanced pump architecture, and completion of a 1st generation large format pump design. High pressure electrochemical hydrogen compression was achieved through rigorous material characterization and selection processes in conjunction with advancements in the pump support and seal design. Presented in Figure 1 are the data for a 300 psig 50 cm^2 pump operated at 160°C on humidified hydrogen for 300 hours. Membrane enhancement was accomplished via various treatments with the intent to improve material durability and performance over long lifetimes. Acid absorption, mechanical strength and electrochemical performance were studied after membrane treatments were performed. Polarization data for the pump operating with a 300 psig differential pressure are presented in Figure 2. Hardware design and material preparation methods were studied and improved to boost the maximum differential pressures within the hydrogen pump. This work was essential to address the failure modes which are unique to the high temperature and high pressure operation.

Tests are currently underway to assess lifetime of the multi-functional device at the targeted operating conditions. Additional cells have been tested with various sealing designs at pressures between ambient and 300 psig to assess the impact of the sealing method on high differential

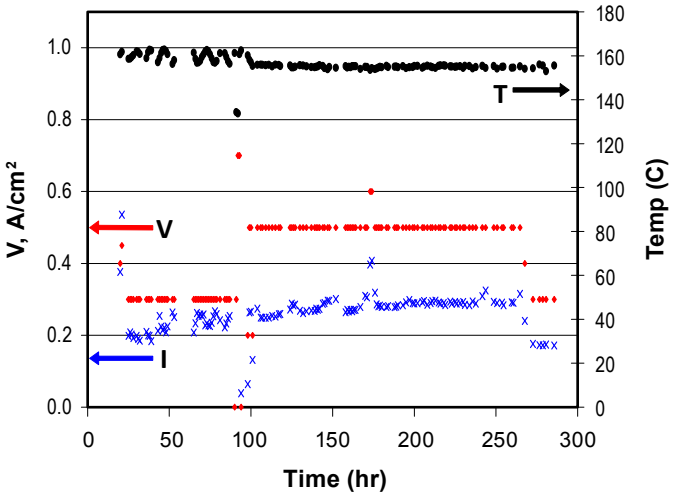


FIGURE 1. Cumulative Run Time: voltage, current, and temperature vs. time. 50 cm^2 PBI Performance Products enhanced membrane operating at 300 psi differential pressure in the H2Pump advanced cell hardware.

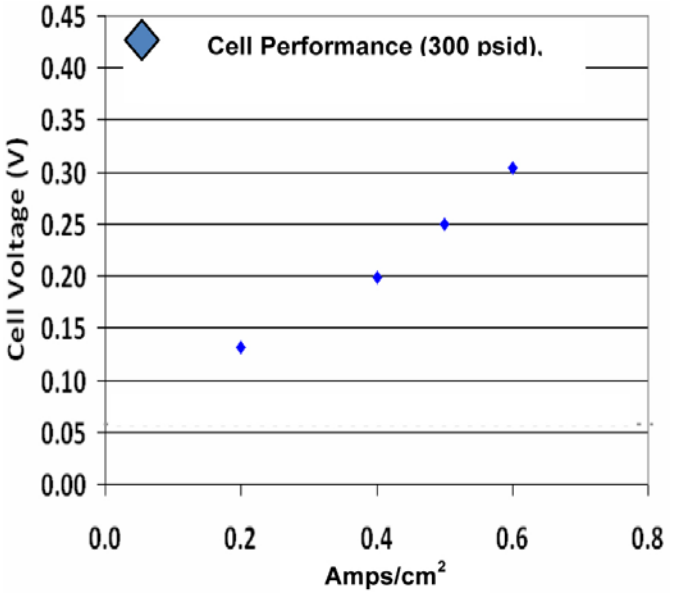


FIGURE 2. Voltage vs. current density: 50 cm^2 cell operating at 300 psi differential pressure with the PBI Performance Products enhanced membrane.

pressure operation. There are currently two approaches which have proven viable for the 300 psig pressurized operation, both relating a novel sealing and support design. In future activities one will be down-selected. Single cells operating at 300 psid have now exceeded 600 hours and remain on test.

Additional work is being carried out on enhancing the membrane properties via two approaches, thermal and chemical cross-linking of the polymer in the PBI membranes. Results of both methods (impact on stability and mechanical properties) have guided the effort to date.

Conclusions and Future Directions

- In collaboration with our partner, PBI Performance Products, PBI membrane has been successfully modified and is now stable in the targeted operating environment.
- Enhancement of the membrane – electrode interface successfully completed.
- Cell hardware has been modified and sub-components evaluated and down-selected.
- 300 psig differential pressure operation has been demonstrated for hundreds of hours.
- Life testing, impact of operating conditions, and durability will continue to be evaluated.
- Scale up of the membrane and electrode assemblies as well as the hardware is underway so as to achieve the 100 scfh target.
- Gas quality and analytical tests will be performed to further assess the performance of the 300 psig pump cells.
- Plans and preparation for an on-site demonstration of the technology will commence in the forthcoming months.

FY 2011 Publications/Presentations

1. Eisman, G., Ludlow, D., "Process Intensification of Hydrogen Unit Operations Using an Electrochemical Device, Proceedings of the DOE Hydrogen and Fuel Cell Annual Merit Review Meeting, Crystal City, VA., May, 2011.

II.E.6 Hour-by-Hour Cost Modeling of Optimized Central Wind-Based Water Electrolysis Production

Genevieve Saur (Primary Contact), Todd Ramsden, Kevin Harrison, Chris Ainscough
National Renewable Energy Laboratory (NREL)
1617 Cole Blvd.
Golden, CO 80401
Phone: (303) 275-3783
E-mail: genevieve.saur@nrel.gov

DOE Manager
HQ: Eric Miller
Phone: (202) 287-5829
E-mail: Eric.Miller.ee.doe.gov

Project Start Date: October 1, 2010
Project End Date: Project continuation and direction determined annually by DOE

Fiscal Year (FY) 2011 Objectives

- Corroborate recent wind electrolysis cost studies using a more detailed hour-by-hour analysis.
- Examine consequences of different system configuration and operation for four scenarios.
- Initiate understanding of sizing implications between electrolyzers and wind farms.
- Identify areas for further analysis and cost reduction.
- Determine the sensitivity of the cost of hydrogen to various inputs, such as turbine cost, electrolyzer efficiency, electrolyzer capital cost, capacity factors, and availability.

Technical Barriers

This project addresses the following technical barriers from the Production section (3.1) of the Hydrogen, Fuel Cells and Infrastructure Technologies Program's Multi-Year Research, Development and Demonstration Plan:

(G) Capital Cost
(H) System Efficiency
(J) Renewable Electricity Generation Integration

Technical Targets

This analysis shows that using current prices for electricity from Class 4-6 wind resources, the hydrogen cost can approach the DOE 2012 cost per gallon of gasoline equivalent ($/gge) target. (See Table 1 for more details.) Using wind electricity prices collected in the 2000 to 2002 time frame, which are lower than now (2011), a Class 6 wind resource could produce hydrogen at the production plant gate for $3.06/gge. This analysis focused on the production components of hydrogen cost, including, electrolyzer capital, electricity cost, depreciation, and operation and maintenance. Table 1 includes an additional $1.88/kg for compression, storage, and dispensing, the value assumed by an independent review panel on low-temperature electrolysis from which the electrolyzer performance and costs were derived for this analysis [1].

TABLE 1. Progress towards Meeting Technical Targets for Distributed Water Electrolysis Production

Characteristics	Units	2012 Target[1]	2017 Target[1]	Status	Analysis
Hydrogen Cost at Production Gate	$/gge	3.70	<3.00	4.90-5.70[2]	5.70-7.49[3]

[1] 2012 and 2017 target for forecourt hydrogen station includes production and CSD (compression, storage, and delivery)
[2] The current (2009) state-of-the-art cost for delivered hydrogen from electrolysis for a forecourt refueling station ranges from $4.90/kg-H2 to $5.70/kg-H2 dispensed at the pump, with a base-case estimate of $5.20/kg-H2. This base-case estimate of $5.20/kg-H2 includes an electrolysis production cost of $3.32/kg-H2 and compression, storage and dispensing costs of $1.88/kg-H2. These costs are evaluated using Energy Information Administration Annual Energy Outlook (AEO) 2005 High A Case industrial electricity costs ($0.053/kWh on average)[1].
[3] The analysis found production gate values between $3.82-5.61/kg. Additional CSD of $1.88 CSD is included in agreement with the independent review panel [1].

FY 2011 Accomplishments

- Completed initial hourly analysis of central wind electrolysis production facility (50,000 kg/day).
- Determined that Class 4-6 wind sites can produce green hydrogen for between $3.82-$5.61/gge at the production plant gate without additional compression, storage, or dispensing.
- Presented results at the Fuel Cell Hydrogen Energy Association (FCHEA) conference, Feb. 14–16, 2011, Washington, D.C.
- Technical paper.
- Saur, G. and T. Ramsden, *Wind Electrolysis–Hydrogen Cost Optimization*. NREL/TP-5600-50408. Golden, CO: NREL 2011.

Introduction

This project is a analytical component of the "Renewable Electrolysis Integrated System Development and Testing" and is aimed at understanding the barriers and costs associated with large-scale (50,000 kg/day) wind-based hydrogen generation plants. Such plants can

take electrical energy from the wind or from the grid and use it to split water molecules into hydrogen and oxygen molecules. The hydrogen can then be used for a variety of purposes, including vehicle fuel, fertilizer feedstocks, petroleum upgrading, metal processing, and other industrial processes. The hydrogen can also be stored, converted back to electricity, and sold to an electric utility for the grid.

Approach

The approach used in this analysis was to review a range of wind sites from Class 1 to 6 for their ability to produce hydrogen economically by electrolysis. An hourly model was created by modifying the DOE H2A Production model version 2.1 to work in conjunction with an hourly analysis. The wind sites were modeled using 8,760 hr/yr data calculated from profiles in Western Wind Data Sets [2] and 3 MW turbine performance profiles adapted from the WindPACT Turbine Rotor Design Study [3]. Wind farms were created as a number of 3 MW wind turbines. Wind turbine costs came from the 2008 Wind Market Report [4]. The electrolyzer performance and cost was modeled consistently with an independent review panel on high volume production costs of the current state-of-the-art low-temperature electrolyzers [1]. Further, each site was analyzed under four different scenarios run hourly over a year.

A. Cost balanced: $ grid purchased electricity = $ wind electricity sold.
B. Power balanced: kilowatt-hour (kWh) grid purchased electricity = kWh wind electricity sold.
C. Same as A, but no purchase of summer peak electricity.
D. Same as B, but no purchase of summer peak electricity.

In addition to these scenarios, sensitivities to various inputs were analyzed, including wind turbine capital cost, wind electricity costs, electrolyzer efficiency, electrolyzer capital cost, capacity factor, and availability.

Results

This analysis found that in power balanced scenarios, the cost of hydrogen at the production plant gate can range from nearly $12/gge down to $3/gge, depending on the class of the wind site. It is only in wind sites of Class 4 or better that such a plant begins to approach DOE technical targets. This analysis looked at electricity prices in the California market. Electricity process will have an influence on the quality of the wind resource required.

An example of the range of costs for all the wind sites analyzed can be seen in Figure 1 which shows a power-balanced scenario where no summer peak electricity was bought from the grid. In this scenario the wind electricity sold to the grid was balanced with the grid electricity bought on a per megawatt basis per year. The electrolyzer was run at peak capacity except during summer peak hours in which it was run separate from any wind electricity

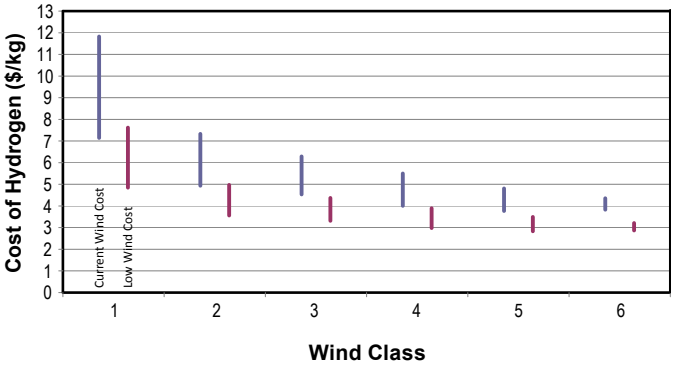


FIGURE 1. Power Balanced Scenario – Range of Costs at the Production Plant Gate

available. A ramification of this scenario was that slightly less than 50,000 kg/day of hydrogen was produced during the summer, but the cost of hydrogen at the production plant gate was also slightly less (~$0.10/kg) than it would be if expensive summer peak grid electricity was purchased. Figure 1 shows the range of costs for the power-balanced, no-summer-peak scenario across the different wind class sites analyzed.

In places with low-cost electricity (no production tax credit included), <$0.10/kWh, hydrogen can be produced for approximately $3.79-$5.90/gge at the production plant gate with no additional compression, storage, or dispensing. This was true of both power and cost-balanced scenarios. Scenarios with no-summer-peak electricity buy resulted in lower hydrogen costs but could also result in unmet hydrogen demand. The difference in the cost of hydrogen at the production plant gate between buying summer peak electricity and not buying was more pronounced in the cost-balanced scenarios, but resulted in <$0.10/kg for all of the power-balanced and between about $0.50-$0.10/kg for the cost-balanced scenarios depending on the quality of the wind profile. See Figure 2 for more details.

In order to produce 50,000 kg of hydrogen per day, the required installed wind capacity varies greatly with the wind class, and thus with the cost of wind electricity. It can be as low as 200 megawatt (MW) (Class 6), and as much as 850 MW (Class 1) (see Figure 3).

In the sensitivity analysis, the largest component changes in hydrogen cost were caused by wind turbine capital cost, followed by electrolyzer efficiency (see Figure 4).

In summary, at the production plant gate the largest hurdles to hydrogen cost from water electrolysis remain wind turbine capital cost and electrolyzer efficiency. Figure 4 shows the sensitivity of costs for a particular Class 5 wind site using the power-balanced, no-summer-peak scenario described previously. Table 2 shows the base case assumptions for the different variables with the high and low values used to calculate the cost of hydrogen at the production plant gate. As seen in Figure 4, a 20% reduction in wind turbine capital will reduce hydrogen costs by

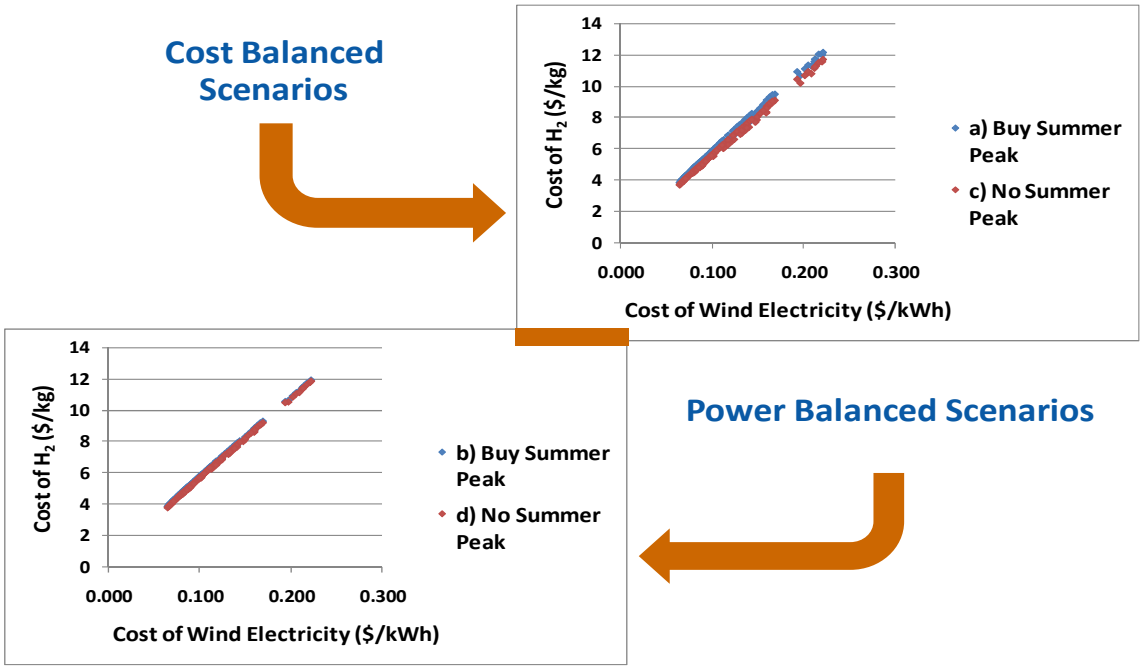


FIGURE 2. The Effect of Wind Electricity on the Cost of Hydrogen at the Production Plant Gate for Two Scenarios

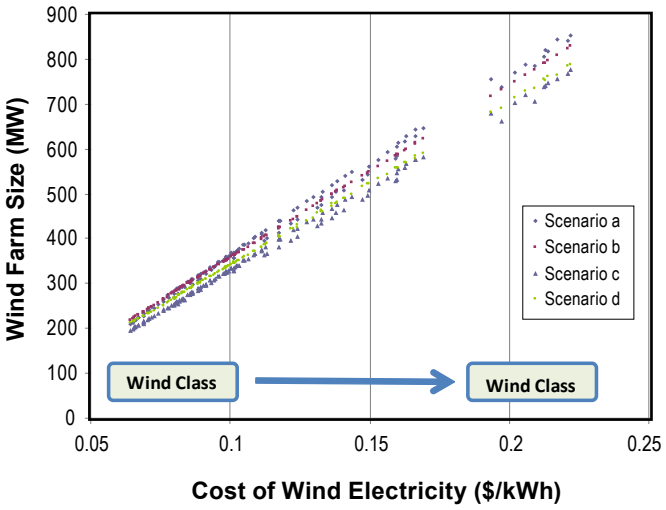


FIGURE 3. The Effect of Wind Electricity on the Installed Capacity of a Wind Farm Capable of Producing 50,000 kg/day of Hydrogen

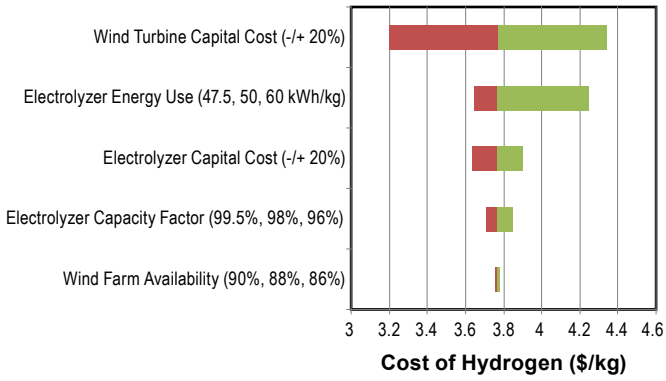


FIGURE 4. EHydrogen Cost at the Production Plant Gate - Example Sensitivity for a Power-Balanced Case, No-Summer-Peak Scenario, Wind Class 5

$0.58/gge, or 15%. Similarly, dropping electrolyzer-specific energy use from 50 to 47.5 kWh/kg can remove another $0.13/gge from the hydrogen cost. Other sites and scenarios exhibited very similar ranges in the cost of hydrogen at the production plant gate for these sensitivity values.

TABLE 2. Base Case and Sensitivities for a Power-Balanced, No-Summer-Peak Class 5 Wind Site, Cost of Hydrogen at the Production Plant Gate

Variable Name	Base Case Value	Low Value	High Value
Wind Turbine Capital Cost ($/kW)	1,964	1,571	2,356
Electrolyzer Energy Use (kWh/kg)	50	47.5	60
Electrolyzer Capital Cost ($/kW)	384	307	461
Wind Farm Availability (%)	88	90	86
Electrolyzer Capacity Factor (%)	98	99.5	96

Conclusions and Future Direction

Given the large influence of electricity pricing on this type of system, future work will analyze areas of the country with high electricity prices and good wind resources (Hawai'i and New England, for instance).

In addition to different geographical regions, the analysis will be deepened to look at solar integration and possibly smaller generation stations supporting the emerging vehicle and material handling fleet vehicle markets. Future analysis will include:

- More sensitivities to various inputs possibly including grid pricing, wind farm size, and production tax credit.
- Use of curtailed wind.
- Regionally expanded grid pricing structures.
- Examination of solar integration.
- Other optimal electricity/hydrogen production balance scenarios.

FY 2011 Publications/Presentations

1. Saur, G. and T. Ramsden, *Wind Electrolysis – Hydrogen Cost Optimization*, presented at FCHEA conference, Feb. 14–16, 2011, Washington, D.C.

2. Saur, G., Ramsden, T., Harrison, K., and Ainscough, C., *Hour-by-Hour Cost Modeling of Optimized Central Wind-Based Water Electrolysis Production*, presented at DOE Annual Merit Review, May 9–13, 2011, Washington, D.C.

3. Saur, G. and T. Ramsden, *Wind Electrolysis–Hydrogen Cost Optimization*. NREL/TP-5600-50408. Golden, CO: National Renewable Energy Laboratory, 2011.

References

1. Genovese, J., et al. Current (2009) State-of-the-Art Hydrogen Production Cost Estimate Using Water Electrolysis: Independent Review. NREL/BK-6A1-46676. Golden, CO: NREL, 2009.

2. NREL: Wind Integration Datasets - Western Wind Dataset. [cited 2010 July 15]; Available from: http://www.nrel.gov/wind/integrationdatasets/western/methodology.html.

3. Malcolm, D.J.; Hansen, A.C. WindPACT Turbine Rotor Design Study, June 2000–June 2002 (Revised). NREL/SR-500-32495. Golden, CO: NREL, 2006.

4. Wiser, R.H., et al. 2008 Wind Technologies Report. LBNL-2261E. Berkeley, CA:LBNL, 2009.

II.F.1 Solar High-Temperature Water Splitting Cycle with Quantum Boost

Robin Taylor (Primary Contact), Roger Davenport, David Genders[1], Peter Symons[1], Lloyd Brown[2], JanTalbot[3], Richard Herz[3]

Science Applications International, Corp. (SAIC)
10210 Campus Point Drive
San Diego, CA 92121
Phone: (858) 826-9124
E-mail: taylorro@saic.com

DOE Managers

HQ: Sara Dillich
Phone: (202) 586-7925
E-mail: Sara.Dillich@ee.doe.gov

GO: Paul Bakke
Phone: (720) 356-1436
E-mail: Paul.Bakke@go.doe.gov

Contract Number: DE-FG36-07GO17002

Subcontractors:

1 Electrosynthesis Co. (ESC), Inc., Lancaster, NY
2 Thermochemical Engineering Solutions (TCHEME), San Diego, CA
3 University of California, San Diego (UCSD), CA

Project Start Date: September 1, 2007
Project End Date: August 31, 2014

Fiscal Year (FY) 2011 Objectives

- Demonstrate a cost-effective high-temperature water splitting cycle for hydrogen production using concentrated solar energy.
- Evaluate photocatalytic and electrolytic options for generating hydrogen that meet DOE's solar high temperature H_2 production efficiency and cost goals.
- Confirm the feasibility of the selected cycle via bench-scale experiments.
- Determine the economic prospects of the selected cycle using the Aspen Plus chemical process model and H2A economic analysis program.
- Demonstrate a fully-integrated pilot-scale solar H_2 production unit.

Technical Barriers

This project addresses the following technical barriers from the Production section (3.1.4) of the Fuel Cell Technologies Program Multi-Year Research, Development and Demonstration Plan:

(U) High-Temperature Thermochemical Technology
(V) High-Temperature Robust Materials
(W) Concentrated Solar Energy Capital Cost
(X) Coupling Concentrated Solar Energy and Thermochemical Cycles

Technical Targets

Table 1 presents the progress made, to date, in achieving the DOE technical targets as outlined in the §3.1.4 Multi-Year Research, Development and Demonstration Plan – Planned Program Activities for 2005-2017 (updated Oct. 2007 version), Table 3.1.9: Solar-Driven, Thermo-chemical High-Temperature Thermochemical Hydrogen Production.

TABLE 1. Progress towards Meeting Technical Targets for Solar-Driven High-Temperature Thermo-chemical Hydrogen Productiona

Characteristics	Units	U.S. DOE Targets			Project Status
		2008	2012	2017	
Solar-Driven High-Temperature Thermo-chemical Water Splitting Cycle Hydrogen Production Cost	$/gasoline gallon equivalent H_2	10.00	6.00	3.00	$7.74 (2015) $4.65 (2025)
Heliostat Capital Cost (installed cost)	$/m^2	180	140	80	97[b]
Process Energy Efficiency[c]	%	25	30	>35	19.3

[a] Electrolytic system projected costs based on latest H2A analysis.
[b] Based on SAIC glass-reinforced concrete structure with 10 sq.m. area and low production quantity.
[c] Plant energy efficiency is defined as the energy of the hydrogen produced (lower heating value) divided by the sum of the energy delivered by the solar concentrator system plus any other net energy imports (electricity or heat) required for the process.

FY 2011 Accomplishments

- An independent thermodynamic and chemical plant analysis reaffirmed that the cycle can be closed and indicated cycle viability.
- A high pressure reactor was developed to allow high temperature operation of the electrolytic cell. Various catalysts, cell configurations and membranes were tested.
- Steady progress was made and a total cell voltage of 0.8 V @ 160 mA/cm^2 and 1.02 V @ 300 mA/cm^2 (in short term runs) was attained while achieving near quantitative hydrogen production and sulfite conversion.
- Initial lab results prove the feasibility of the all-(liquid/gas) $K_2SO_4/K_2S_2O_7$ chemistry for the high-temperature oxygen evolution sub-cycle using potassium sulfate. Residual gas analysis equipment was added to the thermogravimetric analysis (TGA) unit at UCSD and the combined system is producing results.

- An improved Aspen Plus model of the sulfur-ammonia system was developed by UCSD and is being refined based on lab results and additional data.
- H2A economic model results were updated and aligned with DOE program assumptions showing the 2015 estimated hydrogen cost of $7.74/kg and the 2025 cost of $4.65/kg. The results assume no credit for excess electrical production. The process is being optimized to eliminate excess electrical production, improve efficiency and thus reduce cost.



Introduction

Thermo-chemical production of hydrogen by splitting water with solar energy is a sustainable and renewable method of producing hydrogen. However, the process must be proven to be efficient and cost effective if it is to compete with conventional energy sources.

Approach

To achieve the project objectives, the Bowman-Westinghouse "sulfur-family" hybrid thermo-chemical water splitting cycle (aka "Hybrid Sulfur, HyS" cycle) was modified by introducing ammonia as the working reagent, thus producing the sulfur-ammonia, or "SA," cycle. The purpose of the modification is to attain a more efficient solar interface and less problematic chemical separation steps. Several versions of the SA cycle were developed and evaluated experimentally as well as analytically using the Aspen Plus chemical process simulator.

Two approaches were considered for the hydrogen production step of the SA cycle, namely: photocatalytic and electrolytic oxidation of ammonium sulfite to ammonium sulfate in an aqueous solution. Also, two sub-cycles have been considered for the oxygen evolution side of the SA cycle, namely: zinc sulfate/zinc oxide and potassium sulfate/potassium pyrosulfate sub-cycles. The laboratory testing and optimization of all the process steps for each version of the SA cycle were then carried out. Once the optimum configuration of the SA cycle has been identified and the cycle has been validated in closed loop operation in the lab, it will be scaled up and tested on-sun.

Results

Cycle Evaluation and Analysis

In previous years, significant work was performed on the photo-catalytic SA cycle. During the past year, work focused on the electrolytic SA cycle, which is summarized in the following equations:

$SO_{2(g)} + 2NH_{3(g)} + H_2O_{(l)} \rightarrow (NH_4)_2SO_{3(aq)}$	(1 – chem. absorption)	25°C
$(NH_4)_2SO_{3(aq)} + H_2O_{(l)} \rightarrow (NH_4)_2SO_{4(aq)} + H_2$	(2 - electrolytic)	80-150°C
$(NH_4)_2SO_{4(aq)} + K_2SO_{4(l)} \rightarrow K_2S_2O_{7(l)} + 2NH_{3(g)} + H_2O_{(g)}$	(3 – solar thermal)	400°C
$K_2S_2O_{7(l)} \rightarrow K_2SO_{4(l)} + SO_{3(g)}$	(4 – solar thermal)	550°C
$SO_{3(g)} \rightarrow SO_{2(g)} + ½\ O_{2(g)}$	(5 – solar thermal)	850°C

The electrolytic oxidation of the ammonium sulfite solution occurs more efficiently at higher temperatures requiring the development of a system capable of running at higher pressures. Reactions (3) and (4) form a sub-cycle by which potassium sulfate is reacted with ammonium sulfate in the low temperature reactor, to form potassium pyrosulfate. That substance is then fed to the medium temperature reactor where it is decomposed to SO_3 and K_2SO_4 again, closing the sub-cycle. The potassium sulfate and pyrosulfate form a miscible liquid melt that facilitates the separations and the movement of the chemicals in reactions (3) and (4). The oxygen production step (5) occurs at high temperature over a catalyst. Separation of the oxygen from SO_2 occurs when they are mixed with water in reaction (1). The net cycle reaction represented by reactions 1-5 is decomposition of water to form hydrogen and oxygen. All of the reaction steps described above have been demonstrated in the laboratory and shown to occur without undesirable side reactions. Figure 1 shows a schematic of the electrolytic SA cycle.

Independent Thermodynamic and Chemical Plant Analyses

An independent thermodynamic analysis of the feasibility of the SA Cycle was performed. The first step was to perform a preliminary thermodynamic analysis of the SA cycle. Subsequently a detailed analysis of the potassium pyrosulfate/electrolytic version of the SA cycle was performed. The analysis reaffirmed that the cycle can be closed and indicated cycle viability. The thermodynamic analysis was based on ideal solutions using HSC Chemistry 7.0 (Outotec Oyj, Espoo, Finland) augmented with SO_3 vapor pressure over $K_2SO_4/K_2S_2O_7$ solutions from reference [1]. The analysis was performed with Excel using add-in links to the HSC database enthalpy, and Gibbs energy functions. Vapor pressure data was fit using non-linear least squares analysis to generate functions for use in an Excel spreadsheet.

The major concerns to be addressed were in the oxygenation subsystem: the decomposition of ammonium sulfate, the formation of potassium pyrosulfate and the liberation of SO_3 from potassium pyrosulfate. Figure 2 shows details of the high temperature portions of the oxygen generation subsystem. The analysis assumed that the oxygen generation system would be operated at one bar and that the

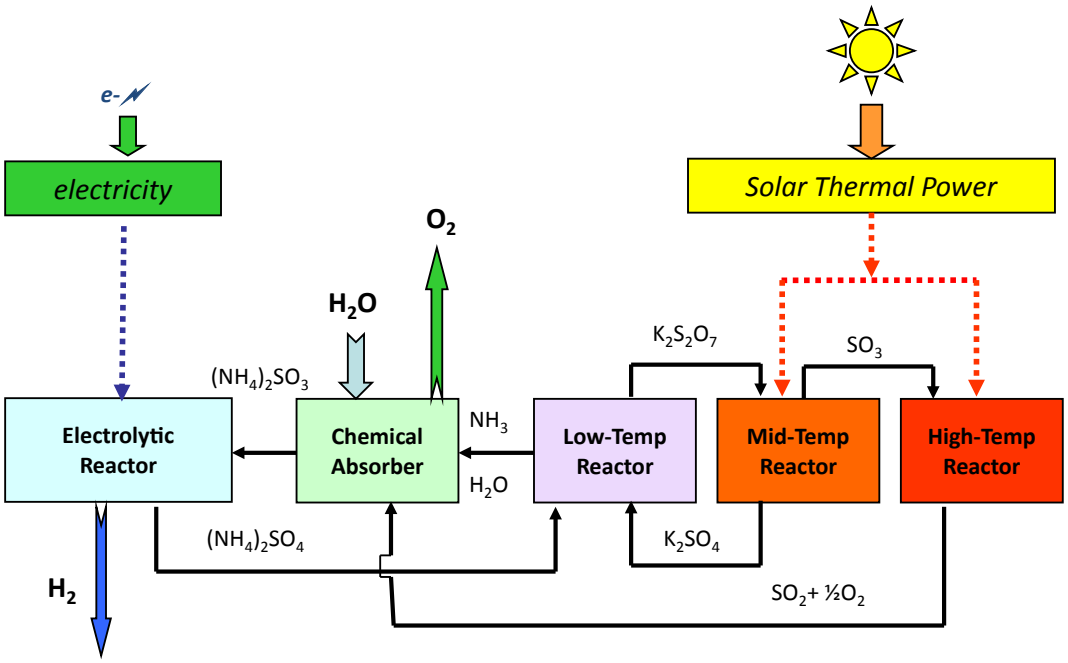


FIGURE 1. Schematic of the Electrolytic SA Cycle

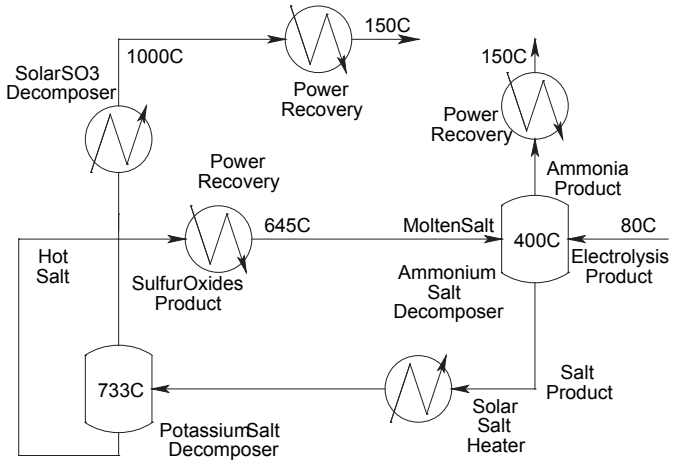


FIGURE 2. High-Temperature Portion of the SA Oxygen Generation Subsystem

ammonium sulfate decomposition step (low-temp reactor of Figure 1) would be accomplished at 400°C. For this analysis, the SO_3 decomposition temperature (high-temp reactor of Figure 1) was assumed to be 1,000°C. The composition of the electrolyte fed to the oxygen generation, obtained from ESC was H_2O: $(NH_4)_2SO_4$:$(NH_4)_2SO_3$ = 7.2:1:0.05. The minimum melting point of a $K_2SO_4/K_2S_2O_7$ mixture occurs at about 8.3 mole percent K_2SO_4 at about 400°C. The ratio K_2SO_4:$K_2S_2O_7$ = 2:10 in the molten salt fed to the ammonium salt decomposer was chosen such that, after absorbing one mole of SO_3 from the $(NH_4)_2SO_4$, the composition would be K_2SO_4:$K_2S_2O_7$ = 1:11, or 8.33 mole percent K_2SO_4.

The exact temperature of the NH_3/SO_3 separation is not of major importance, but it must be at least 400°C so that the $K_2SO_4/K_2S_2O_7$ product is molten. If slightly higher temperatures are required, there may be some recycle of SO_3 back to the electrolysis section with the NH_3 but this will have a minimal effect on the efficiency. What must be minimized is ammonium species accompanying the potassium salts into the high temperature section where the NH_3 will react in the catalytic SO_3 decomposer according to the reaction $2NH_3 + 3SO_3 \rightarrow 3SO_2 + 3H_2O + N_2$. If this occurs, not only will ammonia reduce the oxygen yield, and thus indirectly the amount of hydrogen generated, ammonia will have to be purchased continually or manufactured on site to make up the lost material.

The temperature of the potassium salt decomposer (the mid-temp reactor of Figure 1), 733°C is the temperature required to vaporize one mole of SO_3 from the salt product to return it to the required composition for feed to the ammonium salt decomposer. The stream must be cooled to 645°C such that when mixed with the electrolysis feed the resultant temperature of the ammonium salt decomposer is the specified 400°C. The only use of the heat from 733°C to 645°C is the production of electricity. This amount of heat is sufficient to power the electrolysis system at a voltage of 1.5 volts if the electricity is generated at 25% efficiency. If the hydrogen is produced at a reasonable voltage (0.5 to 0.8 volts) and the electricity is generated at normal efficiencies (30-40%) there will be a large excess production of electricity available for export. Since we intend to operate the hydrogen production system on a continuous 24/7 basis and the SO_3 decomposition system only during insolation, the hot molten salt will be available to generate electricity continuously.

Electro-Oxidation of Aqueous Ammonium Sulfite Solutions

Optimization of the electrolytic process continued at ESC. New catalysts and electrode materials have been screened at 80°C, with the most promising materials including spinels ($M_xN_{3-x}O_4$ where M,N=Fe/Ni/Co), platinum/cobalt mixtures and alternate felts. These materials were further screened in a new high pressure reactor which was built for this project and is shown in Figure 3. The high pressure reactor is capable of operation at 150 psi and 260°C. Cell performance with the Pt/Co catalyst at 130°C gave 0.8 V @ 160 mA/cm^2 and 1.02 V @ 300 mA/cm^2 as shown in Figure 4 with further improvements at higher temperature. Work also showed that the use of an undivided cell is most likely not possible at temperatures above 60°C, as the present cathode structure becomes inefficient with reduction of sulfite competing with hydrogen production.

High-Temperature Cycle Step Evaluation

Evaluation of the all-liquid/gas high-temperature cycle steps continued. As shown in Figure 5, TGA experiments were conducted to show the evolution of ammonia and water vapor at ~365°C, followed by evolution of sulfur trioxide at 496°C. A residual gas analyzer was used to detect the gases from the reaction. However, as tiny amounts (~10 mg) of reactants are used for the TGA with an argon purge stream, the product concentrations are very diluted, and often not detectable. A large reactor system is being built to use ~10 g of reactants to study the reaction kinetics and evolution of gases products under more realistic operating conditions. The reactant ratios will be optimized to increase the temperature difference between the evolution of ammonia and SO_3.

Aspen Plus Process Analysis

The Florida Solar Energy Center (FSEC) supplied a copy of their model of the SA plant in Aspen Plus. Unfortunately, the data supplied was not sufficient to run the



FIGURE 3. Pressure Vessels Required for Electrochemical Cell Operation at High Temperature

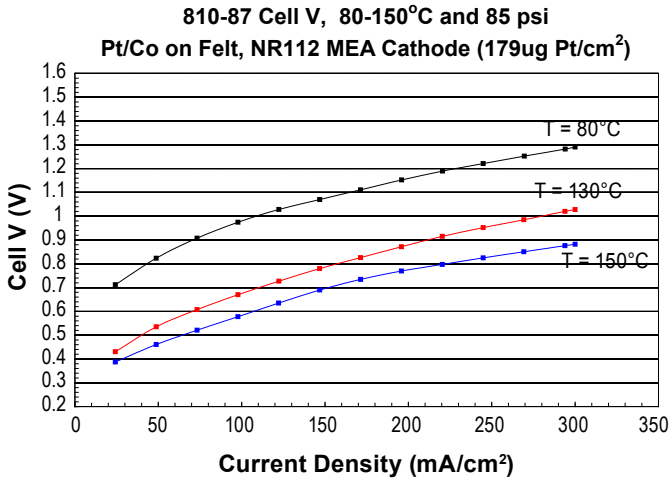
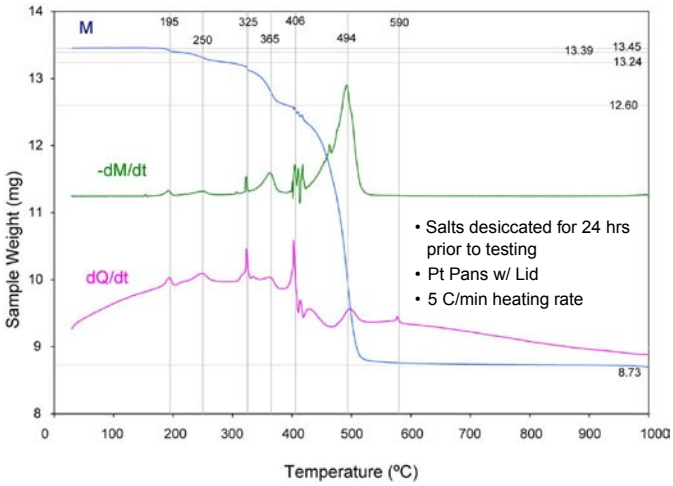


FIGURE 4. Cell Performance as a Function of Current Density and Temperature



- 195°C desorbed water
- 250°C desorbed water
- 325°C $K_2S_2O_7$ solid phase change
- 365°C NH_3+H_2O gas production
- 406°C $K_2S_2O_7$ melting
- 460°C K_2SO_4 solidification
- 494°C SO_3 gas production
- 590°C K_2SO_4 solid phase change

FIGURE 5. TGA/Differential Thermal Analysis of:
$(NH_4)_2SO_4 + 2\ K_2SO_4 + 8\ K_2S_2O_7 \rightarrow 2\ NH_3 + H_2O + 9\ SO_3 + 10\ K_2SO_4$

model with revised input values. UCSD supplied additional specifications for recycle streams within the plant so that the model could be run with new input values.

Using the FSEC model as a guide, UCSD is developing its own Aspen Plus model of the plant. This is being performed for several reasons. The first is to better understand all the characteristics of the plant model. Another reason is to include better thermodynamic data for some of the less common materials in the plant such as the molten sulfate/pyrosulfate mix in the oxygen section of the plant. To date, all units have been incorporated into the UCSD model and the material balance has been closed. Current work involves performing a process heat integration analysis, or pinch analysis, of the plant in order to place heat exchangers and optimize the thermal energy efficiency of the plant. UCSD is also developing rate/kinetic models of the individual unit operations in the plant.

Solar Field Optimization

The solar field configuration has continued to be updated as the thermo-chemical system evolves.

Evaluations were performed to determine the optimum way that the system could operate continuously on a 24/7 basis. The all-liquid $K_2SO_4/K_2S_2O_7$ system provides the opportunity to absorb and store heat directly in the reactants of the system. The molten salt solubility curves are such that a large excess of $K_2S_2O_7$ is needed to keep the mixture liquid, so much more heat capacity is present than is needed to operate the reactions. The sensible energy contained in the salts in the medium-temperature reactor is therefore also sufficient to provide the heat needed for the low-temperature reactor, and the excess energy is used to produce electricity that runs the electrolysis process. The highest-temperature oxygen evolution process can be operated in a solar-only mode using a separate high-temperature receiver, or electricity produced from the excess heat of the molten salt mixture can be used to operate that reaction 24/7 as well.

Economic Analysis

The H2A economic model for the electrolytic SA process was updated. Discrepancies between the inputs for the SA model and those of other groups were removed by using scaled values from the Sandia heliostat field analysis to update the solar field model. Updated results for the electrolytic process efficiency were also included in the calculation. The resulting estimated production costs for hydrogen were found to be $7.74/kg in 2015, and $4.65 in 2025.

The H2A cost analysis program was also used to examine the optimization of the electrolytic portion of the system. The electrolytic system design is a balance between capital costs for electrolytic cells and operating costs for electricity. Recent test data for the polarization curve of the electrolytic cell (i.e., voltage vs. current density) were combined with estimated costs from H2A for the electrolysis

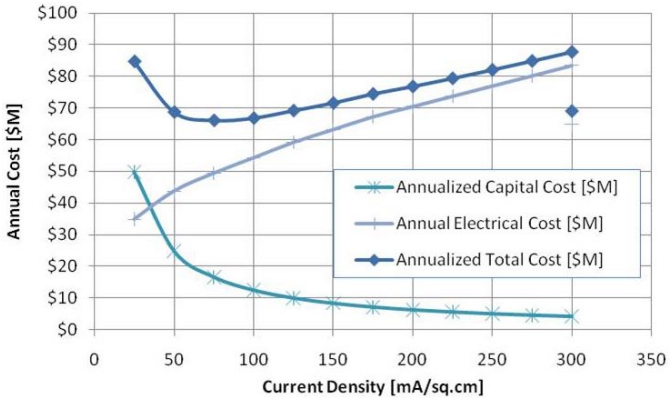


FIGURE 6. Economic Optimization Study Results

cells ($/m^2) and for electricity. The capital costs were annualized using the capital recovery factor from H2A and combined with the annual electricity costs to obtain a levelized annual cost for the electrolytic system, and the calculation was repeated over a range of current densities from 25 mA/cm^2 to 300 mA/cm^2. The results are shown in Figure 6. At low current densities, the cost is high because of the large area of electrolysis cells needed to pass the required electrolysis current. At very high current density, the increase in cell overpotential leads to high electricity so the cost again increases. The lowest cost point is at 75 mA/cm^2. This is a much lower value than had been expected. For comparison, the target value of 0.8 V at 300 mA/cm^2 is plotted on the figure as the separate point to the far right – note that the minimum cost point predicted using our current data is actually lower than the cost for that set of conditions.

The conclusion from this study is that it is more important to focus our efforts on reducing cell voltage to reduce electrical costs rather than focusing on increasing current density to reduce capital costs. Sensitivity studies of the results confirm this conclusion. Increasing electricity costs drive the minimum cost to lower current densities, but not strongly. Doubling the cost of electricity reduces the minimum cost point from 75 to about 50 mA/cm^2. Likewise, doubling the capital cost of the electrolysis system components only moves the minimum cost point to about 100 mA/cm^2.

Conclusions and Future Directions

In summary:

- An independent thermodynamic and chemical plant analyses reaffirmed that the cycle can be closed and indicated cycle viability.
- Significant progress was made in reducing the cell voltage and increasing the current density of the electrolytic cell by operating at higher temperatures and with improved cell design. Improvements made over

the last year have enabled us to increase the current density by a factor of 2.5 times to 160 mA/cm^2 at a total cell voltage of 0.8 V.
- Additional evaluations of the all-liquid/gas high-temperature oxygen generation cycle steps continued to prove the subcycle feasibility.
- A new Aspen Plus chemical plant model has been developed that is more robust and more accurately models the thermodynamic characteristics of the model.
- Evaluations were performed that show the SA system with solar energy storage can operate continuously on a 24/7 basis.
- The H2A economic model for the electrolytic SA process was updated and aligned with the assumptions for other hydrogen production cycles. H2A analyses show that the lowest total annualized cost of hydrogen achieved to date at 0.6 V and 75 mA/cm^2 is actually lower than our target performance of 0.8 V and 300 mA/cm^2.

Activities planned for the upcoming year include:

- Further optimization of the electrolytic process and cell. This will include identification of catalysts that will reduce the over-potential at the anode and allow operation at high current densities. The best catalyst will be evaluated in longer term operation by performing a 500 hour durability test.
- Complete evaluation of the K_2SO_4 oxygen subcycle reactions. A large reactor system will be constructed to use ~10 g of reactants to study the reaction kinetics and evolution of gases products under more realistic operating conditions.
- Using Aspen Plus, optimize the thermal energy efficiency of the plant.
- Development of the thermal reactor/receiver designs including materials specification and testing.
- Development of the solar field configuration and design to match the final chemical plant requirements.
- Continue to update H2A economic analyses to document the potential cost of hydrogen from the SA cycle.

After completion of phase 1, the next phase of the project will involve laboratory validation of the closed-loop SA cycle leading to on-sun hydrogen production demonstration.

FY 2011 Publications/Presentations

1. Davenport, R., Taylor, R., Genders, D., Brown, L., Talbot, J., Presentation at the 2011 U.S. DOE Hydrogen and Fuel Cell Program and Vehicle Technologies Program Annual Merit Review and Peer Evaluation Meeting, Washington, D.C., May 9–13, 2011. (PowerPoint presentation).

2. Wang, M., Ramzi, S., Talbot J., Thermogravimetric Study of a Solar Sulfur-Ammonia Thermochemical Water Splitting Cycle, Poster Presentation at the Jacobs School of Engineering Research Expo, University of California, San Diego, April 14, 2011.

3. Taylor, R., Genders, D., Davenport, R., Brown, L., Presentations at the STCH Technical Progress Meeting, University of Colorado, Boulder, October 27, 2010 (PowerPoint presentations).

4. Davenport, R., Taylor, R., T-Raissi, A., Genders, D., Muradov, N., Presentation at the DOE Annual Merit Review and Peer Evaluation Meeting – DOE Hydrogen Program and Vehicle Technologies Program, Washington D.C., June 8–11, 2010. (PowerPoint presentation).

References

1. Lindberg, D., Backman, R., & Chartrand, P. (2006). Thermodynamic evaluation and optimization of the (Na_2SO_4+K_2SO_4+$Na_2S_2O_7$+$K_2S_2O_7$) system. The Journal of Chemical Thermodynamics, 38(12), 1568-1583.

II.F.2 Membrane/Electrolyzer Development in the Cu-Cl Thermochemical Cycle

M.A. Lewis (Primary Contact), M. Ferrandon, S. Lvov, C. Fan, S. Ahmed (Principal Investigator)
Argonne National Laboratory
9700 S. Cass Avenue
Argonne, IL 60439
Phone: (630) 881-5973
E-mail: lewism@cmt.anl.gov

DOE Manager
HQ: Sara Dillich
Phone: (202) 586-7925
E-mail: Sara.Dillich@ee.doe.gov

Start Date: October 2010
Projected End Date: September 2012

Fiscal Year (FY) 2011 Objectives

The strategic objective is to develop a robust process for producing hydrogen that meets DOE's targets for cost and energy usage; the tactical objectives are the following:

- Identify methods that prevent copper deposition at the cathode of the electrolyzer while meeting targets for cell potential (0.7 V) and current density (500 mA/cm^2 to be met in three years).
  - Identify membranes with low copper permeability and sufficient proton conductivity.
  - Optimize operating conditions and electrolyzer design to further minimize copper crossover.
- Continue collaborative work on the themal reactions with Canada.

Technical Barriers

This project addresses the following technical barriers from the Hydrogen Production section of the Fuel Cell Technologies Program Multi-Year Research, Development and Demonstration Plan:

(U) High-temperature Thermochemical Technology
(V) High-Temperature Robust Materials
(W) Concentrated Solar Energy Capital Cost

Technical Targets

The technical targets are the cost of hydrogen production and the process energy efficiency.

- For 2017, these are $3.00 per gasoline gallon equivalent (gge) H_2 and >35% (lower heating value, LHV), respectively.

FY 2011 Accomplishments

- Identified several membranes with low copper permeability at 80°C.
- Conducted electrolysis tests that showed no visible copper crossover with two membranes–double layer Nafion® and CG2, a porous separator. The hydrogen production efficiency exceeded >80-90% when the cell potential was 0.7 V and the current density was 100-150 mA/cm^2.
- Scaled up the electrolyzer from 5 to 31 cm^2 and obtained a stable current for almost 800 hours with CG2 and a cell potential of 0.7 V and a current density exceeding 100 mA/cm^2.
- Developed a speciation model of the electrolyzer's anolyte to calculate any thermodynamic property such as decomposition potential, solubility of CuCl(s) in HCl(aq) anolyte, concentration of HCl(aq) to dissolve Cu(s) in catholyte, etc. over a wide temperature range from 25 to 100°C.
- Continued collaborations with Atomic Energy of Canada Limited and a group of Canadian universities.



Introduction

The U.S. Department of Energy's Office of Energy Efficiency and Renewable Energy (DOE-EERE) is supporting the development of H_2 production technologies that use solar heat. One approach involves thermochemical cycles whose heat source is the solar power tower, which is near commercialization and provides heat near 550°C now and up to 650°C in the future. The CuCl cycle is unique because its maximum temperature is 550°C.

The three major reactions in the Cu-Cl cycle are shown in Table 1. All reactions have been verified at the temperatures shown. Note that the maximum temperature is less than 550°C.

TABLE 1. Three Major Reactions in the Cu-CL Cycle

$CuCl_2 + H_2O \Leftrightarrow Cu_2OCl_2 + 2HCl(g)$	Hydrolysis, ~375°C
$Cu_2OCl_2 \Leftrightarrow 2CuCl + ½O_2$	Decomposition, 450-525°C
$2CuCl + 2HCl \Leftrightarrow CuCl_2 + H_2$	Electrolysis, ~80 -100°C

No separations or phase changes are specified in this high level representation. There is a significant challenge in the electrolysis reaction because of copper crossover, which has been observed at the Atomic Energy of Canada Limited and at laboratories in the U.S. Copper crossover can lead to catastrophic failure of the cell. Work in the past year has therefore been focused on reducing copper crossover.

Approach

A collaboration involving several laboratories with expertise in different types of membranes was established. Pennsylvania State University investigated s-Radel (polysulfone-type) membranes, some of which were crosslinked, as well as double layered Nafion®. Argonne National Laboratory modified Nafion® by copolymerizing it with intertwining various aliphatic and aromatic polymers to reduce the pore size and also developed a cross-linked polybenzimidazole. Seven commercial separator-type membranes, which were available to Gas Technology Institute (GTI) for use in another study and were characterized by their manufacturers as having low metal ion transport and good chemical and thermal stability, were also examined. Screening evaluations were conducted with permeability and conductivity measurements. Electrolysis tests were conducted with the most promising membranes at 80°C.

Results

Permeability Measurements: The various membranes were screened by measuring copper permeability at 80°C and through-plane conductivity at room temperature. An initial target permeability of 10% of Nafion®'s was used. The permeability was measured in a diffusion cell, which consisted of two compartments, clamped together but separated by a membrane. The solute side contained a solution of $CuCl_2$ in10.2 M HCl. The solvent side contained 10.2 M HCl. The permeability was calculated from the equation,

$$k = \left(\frac{lV_{sample}}{At_{\exp}}\right)\ln\left(\frac{C_1}{C_1 - C_2}\right)$$

where l is the thickness of the wet membrane (cm), V_{sample} is the volume of the sample solution in our cell (cm^3), A is the surface area of membrane (cm^2), t_{exp} is the time of the exposure (sec), C_1 is initial concentration of Cu^{2+} in the first compartment (1 M), and C_2 is concentration of Cu^{2+} measured in the sample in the second compartment at $t = t_{exp}$. Ideally k values should not be dependent on time as long as the properties of the membrane are stable and osmotic pressure does not result in significant solvent diffusion. The test period was 24 hours in most cases. However, large volume changes in the solute side due to osmotic pressure caused some permeability tests to be terminated after only several hours.

The membranes with the lowest copper(II) permeabilities are shown in Figure 1. Only one of the seven separator-type membranes examined, CG2, had very low copper permeability and further work, e.g., supports and pretreatments, was justified on this basis. The CG2 membrane is significantly thinner than Nafion® as shown in Table 2. Mechanical supports are therefore being developed to facilitate fabrication of membrane electrode assemblies (MEAs). CG2's proton conductivity is also relatively small (see Table 2) and various pretreatments are being investigated to increase this property. In addition, this membrane has the highest osmotic pressure and the diffusion tests can be run for very limited time periods. The membrane consisting of a double layer of Nafion® exceeded the permeability target by almost a factor of 6

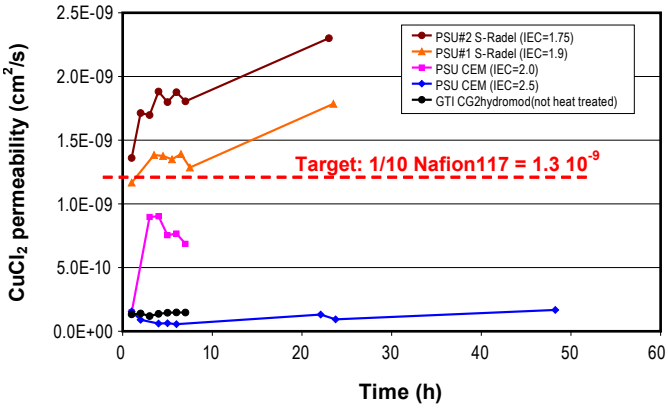


FIGURE 1. Permeability measurements at 80°C vs. time. HCl concentrations are 10.2 M in both compartments of the diffusion cell.

TABLE 2. Properties of Membranes for Possible Use in the Cu-Cl Electrolyzer

Membrane	Pretreatment	Thickness, / (mm)	Conductivity, σ (S/cm)	Permeability k * 10^{-9} (cm^2/s)	Selectivity σ / k x 10^5
Nafion® 117	20 h in 2 M HCl, 25°C	0.180	0.086	0.18	48
Double-layer Nafion	20 h in 2 M HCl, 25°C	0.350	0.083	5.80	143
Mit-1 (from GTI)	None	0.003	Inconclusive		
CG2 (from GTI)	None	0.030	0.0054	94	57
s-Radel, IEC 2.0	None	0.054	0.038	3.68	102
s-Radel, IEC 2.0, crosslinked	None	0.107	0.053	4.77	111
s-Radel, IEC 2.5, crosslinked	None	0.100	0.045	83.5	535
s-Radel, IEC 2.5, crosslinked	66 h in 3.3 M HCl + 1 M $CuCl_2$, 25°C	0.109	0.045	1.48	300
s-Radel, IEC 2.5, crosslinked	2 h in 10 M HCl, 80°C	0.107	0.072	0.112	64

but this membrane had the highest proton conductivity and therefore the highest selectivity see Table 2. Two of the s-Radel membranes were very close to the target. After cross-linking, their permeabilities were below the target. Co-polymerized Nafion®-type membranes had low permeability at room temperature but exceeded the target at 80°C and further effort on this type of membrane was terminated. Studies are still ongoing with the crosslinked polybenzimidazole.

Conductivity Measurements: Conductivity was measured using the two-electrode through -plane method in 2 mol/L HCl(aq) solution at ambient temperature and pressure. Conductivity values were calculated using measured membrane resistance (R), thickness of wet membrane (δ), and exposed membrane surface area (A=0.74 cm^2), as follows: $k = \delta / (R \times A)$. The equipment and method are described in detail elsewhere [1]. No target was set for proton conductivity except that it had to be measurable. Those membranes which met the targets were tested in electrolyzers at GTI and Pennsylvania State University for a more realistic evaluation.

The results of the through-plane conductivity measurements are given in Table 2. Nafion® 117 membrane was used as a bench mark. Table 2 also summarizes permeability and selectivity data. The latter are calculated by dividing the conductivity by the permeability. Some of the samples were pretreated. The data in Table 2 for the cross-linked s-Radel membranes show that pretreatment affects selectivity. Pretreatment processes are still under development for CG2.

Electrolyzer Results: Electrolyzers were built at both Pennsylvania State University and GTI. Details of the electrolyzer at Pennsylvania State University are published elsewhere [1]. The performance of the electrolysis process was monitored by taking polarization data and comparing experimental and theoretical hydrogen production. Targets for the cell potential and the current density in the model are 0.7 V and 500 mA/cm^2, respectively. However, short term targets specify lower current densities for cell potentials of 0.7 V.

Several MEAs were tested in the electrolyzers. The MEA fabricated from the double-layer Nafion® gave promising results in a 24-hour test at 80°C with 10.2 M HCl as the catholyte and 1 M CuCl in 10.2 M HCl as the anolyte. Hydrogen production followed Faraday's Law, as shown in Figure 2. There was, however, some degradation with time as shown by the polarization curve in Figure 3, which may be due to the consumption of CuCl. At the conclusion of the test, no copper deposition was observed on the cathode, membrane or gas diffusion layers. Photographs of the latter are shown in Figure 4. Similar results were obtained with CG2 using the same conditions but with deionized water as the catholyte. Lifetime tests at GTI were run intermittently for almost 800 hours with the intermittent addition of CuCl.. The cell voltage was 0.7 V and the current density was stable near 150 mA/cm^2. Hydrogen production followed Faraday's

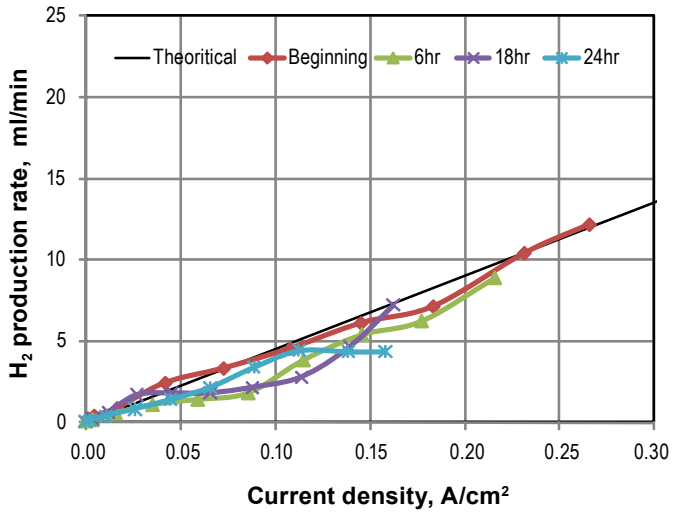


FIGURE 2. Hydrogen production as a function of cell voltage over 24 hours with the double layer Nafion® membrane.

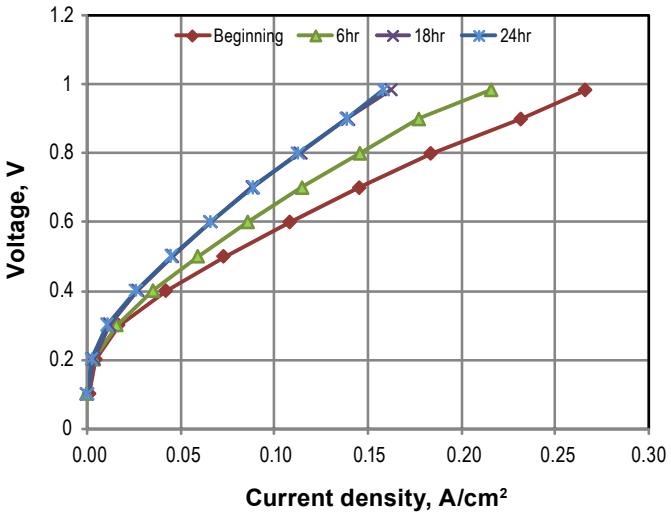


FIGURE 3. Current vs. voltage as a function of time with the double layer Nafion® membrane.

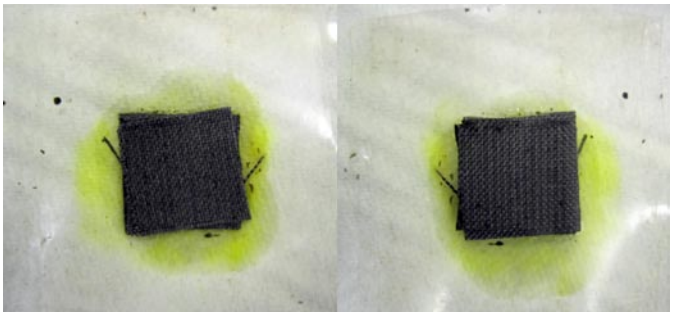


FIGURE 4. Photographs of the MEA diffusion layers facing the cathode (left) and anode (right) of the electrolysis cell used in the 24-hour electrolysis test with double layer Nafion® that show no visible copper deposits.

Law. No copper deposition was visible on the components of the cell after the test was terminated. Comparison of peak hydrogen production in the two electrolyzers showed essentially identical results. Electrolyzer tests with the cross-linked s-Radel membranes are planned.

Collaborations: Collaborations between the U.S. team members and their Canadian colleagues are focused on the study of the hydrolysis and oxychloride decomposition reactions using X-ray absorption near edge structure at the Advanced Photon Source. It is hoped that these measurements will result in kinetic measurements and mechanistic understanding of these two thermal reactions. Information is exchanged periodically, e.g., Ontario Workshop Foundation workshops (see presentation #2) and in discussions between the researchers, especially in modeling activities.

Conclusions

- Identified two membranes that had low copper diffusion in permeability tests and had sufficient proton conductivity.
- Conducted electrolyzer tests that showed no visible copper deposition in/on the cell components.

Future Directions

- Develop methods to improve the mechanical stability of CG2.
- Optimize the electrolyzer's performance by investigating other compositions for the anolyte and catholyte, flow rates, flow field design, electrode surface, mass transport media, etc. to obtain higher current densities at 0.7 V.
- Investigate the degradation mechanisms in the electrolyzer and develop methods to mitigate these.
- Continue collaboration with staff at Atomic Energy of Canada Limited and six Canadian universities.

FY 2011 Publications/Presentations

Presentations

1. CuCl Electrolyzer for Hydrogen Production via Cu-Cl Thermochemical Cycle, Oral presentations (R. Sharna, M. Fedkin, and S. Lvov, Penn State University) 219th ECS Meeting, Montreal, Canada May 1–6, 2011.

2. Current R&D Status for the Cu-Cl Thermochemical Cycle (2-2011), M. Lewis, C. Fan, R. Sharna, M. Fedkin, S. Lvov, M. Ferrandon, S. Ahmed and S. Niyogi, Ontario Research Foundation Workshop, Oshawa, Ontario, Canada, February 23, 2011.

Publications

1. Balashov, V.N., Schatz, R.S., Chalkova, E., Akinfiev, N.N., Fedkin, M.V., and Lvov, S.N., CuCl Electrolysis for Hydrogen Production in the Cu-Cl Thermochemical Cycle, *J. Electrochemical Soc.*, 2011, **158**, B266-B275.

2. Naterer, G.F. et al., Canada's Nuclear Hydrogen Program on the Thermochemical Copper-Chlorine Cycle, submitted to International Journal of Hydrogen Energy.

References

1. Balashov, V.N., Schatz, R.S., Chalkova, E., Akinfiev, N.N., Fedkin, M.V., and Lvov, S.N., CuCl Electrolysis for Hydrogen Production in the Cu-Cl Thermochemical Cycle, *J. Electrochemical Soc.*, 2011, 158, B266-B275.

II.F.3 Solar Hydrogen Production with a Metal Oxide-Based Thermochemical Cycle

Nathan Siegel (Primary Contact), Ivan Ermanoski, Tony McDaniel
Sandia National Laboratories (SNL)
PO Box 5800
Albuquerque, NM 87185-1127
Phone: (505) 284-2033
E-mail: npsiege@sandia.gov

DOE Manager
HQ: Sara Dillich
Phone: (202) 586-7925
E-mail: Sara.Dillich@ee.doe.gov

Subcontractors:
- Jenike and Johanson, San Luis Obispo, CA
- University of Colorado, Boulder, CO

Project Start Date: June 2004
Project End Date: Project continuation and direction determined annually by DOE

Fiscal Year (FY) 2011 Objectives

- Characterize reactive materials suitable for thermochemical hydrogen production under realistic operating conditions (e.g. temperature, atmosphere, heating rate).
- Develop a particle-based thermochemical reactor suitable for deployment on a central receiver platform and embodying several key design features.
- Evaluate the likely system level performance of the reactor concept and identify energy losses and opportunities for performance improvement.

Technical Barriers

This project addresses the following technical barriers from the production section of the Fuel Cell Technologies Program Multi-Year Research, Development and Demonstration Plan:

(U) High-Temperature Thermochemical Technology

(V) High-Temperature Robust Materials

(X) Coupling Concentrated Solar Energy and Thermochemical Cycles

Progress toward the technical targets is shown in Table 1. Hydrogen cost from the particle reactor system has not yet been evaluated because the system level design is not complete and this is needed as the basis for an economic analysis. Heliostat cost reduction is not actively funded by this project, but is an element of the DOE Solar Program. The thermochemical efficiency for the particle reactor has been estimated to be 37% using commercially available cerium oxide reactant powder. This material is not the ideal from a thermodynamic perspective and will likely be improved upon as the project progresses. The reactor itself can be configured for any particulate reactant.

TABLE 1. Progress towards Meeting Technical Targets for Solar Drive High Temperature Thermochemical Hydrogen Production

Characteristic	Units	2012 Target	2017 Target	SNL 2011 Status
Hydrogen Cost	$/gasoline gallon equivalent H_2	6	3	N/A
Heliostat Cost	$/m^2	140	80	N/A
Process Efficiency	%	30	>35	30% estimated[1]

[1] This number is the product of receiver efficiency (solar in to heat available, ~82%) and thermochemical efficiency (heat available to lower heating value H_2 ~37%).
N/A - not available

Additional project targets outside of those listed in Table 1 are given as follows:

- Thermochemical Cycle (reactive materials): Oxidation and reduction reactions must reach 90% completion within two minutes.
- Reactor: Demonstrated conversion efficiency for the prototype reactor (5 kW_{th}) must be in excess of 20% at a pressure greater than 10 Pa.
- System: Estimated system level efficiency including collection and conversion losses must be in excess of 19% annual average for a dish system and 14% for a tower system.

Accomplishments

- Reactor
  - A detailed reactor performance model was developed and indicates that heat to hydrogen conversion efficiency in excess of 37% is possible using a cerium oxide-based thermochemical cycle.
  - Evaluated the compatibility of cerium oxide reactant with reactor construction materials including Al_2O_3, SiC, and Haynes 214 at nearoperational temperatures. SiC and Haynes 214 showed minimal or no interaction to 1,400°C, Al_2O_3 showed no interaction to 1,450°C.
  - Designed a particle conveyor system (subcontract with Jenike and Johanson) suitable for moving a powder reactant vertically in a packed bed arrangement. This configuration is required to achieve the best-case efficiency in the particle reactor. Prototype construction of the conveyor is currently in progress.

- Materials
  - A laser-based heating method was incorporated into our stagnation flow reactor that enables rapid thermal processing of sample materials. Heating rates in excess of 100°C/s are achievable at 500 W/cm^2 (5,000 suns).
  - The thermal reduction of various CeO_2 reactive structures, comprised of powders, felts, and fully dense forms, was characterized at operating pressures and heating rates relevant to solar thermochemical applications. It was determined that for CeO_2 reactive structures with characteristic dimensions less than 1 mm, oxygen evolution kinetics would likely not limit use of this material in the proposed reactor configurations.
  - Experiments to characterize the thermal reduction and water splitting kinetics for the following material structures and chemistries have been conducted: CeO_2 felt, CeO_2 and Mn-doped CeO_2 powder, atomic layer deposition (ALD) thin film Fe_2O_3/CeO_2, ALD thin film Fe_2O_3/m-ZrO_2, ALD thin film Fe_2O_3/Al_2O_3 (hercynite). We are in the process of analyzing the complete data set.
- System
  - A general system level model was developed to estimate the annual average hydrogen production efficiency of the particle reactor system. Results show that an annual average solar-to-hydrogen conversion efficiency of 24% is possible in a dish based system with a cerium oxide reactant.
  - A separate system model that includes a more detailed description of the reactor (temperature dependent properties, rigorous treatment of chemical reactions) was developed in ASPEN.



Introduction

Solar-powered thermochemical water splitting produces hydrogen using only water, heat from the sun, and chemicals that are completely re-cycled so that only hydrogen and oxygen are produced and only water and solar thermal energy are consumed in the cycle. All known thermochemical cycles face obstacles that could include extremely high temperature, highly corrosive chemicals, difficult separations of chemicals during sequential cycle steps, multiple reaction steps necessary to close the cycle, or side reactions with stable products that poison the process upon recycling, Many of these barriers can be overcome, but generally at the expense of energy efficiency, consumption of feedstocks other than water, and possibly much higher temperature to drive reactions to completion. All of these measures add cost to the product, inhibit acceptable production rates, or prevent the realization of plant designs with acceptable lifetimes. Overcoming these barriers is made even more difficult by turning to solar radiation for the driving energy source, primarily because of its transient nature and relatively low power density. The low power density characteristic of solar power requires large collector areas and efficient concentrators to drive energy-intensive processes like water splitting.

The ultimate success of solar thermochemical hydrogen production is contingent on developing suitable reactive materials and on incorporating these materials into an efficient solar thermochemical reactor. Currently, SNL and the University of Colorado are working together to identify and characterize prospective thermochemical cycles and associated reactive materials. Recent efforts have focused on ferrites, cerium oxide, and hercynite as potential candidate material "families". Additional research and development efforts are directed at reactor and system level challenges related to collecting and applying solar thermal energy to the water splitting function within each of these cycles. Solar thermochemical reactors for ultra-high temperature processes (T >1,300°C) are being developed and tested by SNL.

Approach

Metal oxide-based materials, such as those containing cerium oxide or iron oxide (ferrites), have demonstrated the capability of splitting water in a two-step cycle consisting of a high temperature, oxygen-liberating thermal reduction reaction (up to 1,500°C) and a lower temperature, hydrogen-producing water oxidation reaction (<1,000°C). In order to achieve large hydrogen production volumes in a practical device these two reactions should be run in a continuous manner. In addition, in order to achieve high efficiency it is desirable to maximize the extent of reaction and essential to recover sensible heat between the high and low temperature reactions (recuperation). Also, any practical solar-driven reactor will operate continuously for thousands of hours without requiring service. Any reactive materials used in such a reactor must demonstrate an acceptable level of chemical and mechanical durability.

We are developing a particle-based reactor concept suitable for continuous hydrogen production on-sun in either a central receiver or parabolic dish configuration. Our technical efforts are organized into three tasks:

- **Reactor Development:** This task focuses on the reactor design, performance estimation and eventual validation at the prototype level (5-10 kW_{th}). Specific areas of effort include the design of high temperature solar reactor components along with material compatibility studies to evaluate interactions between the thermochemical reactant and products and materials used in reactor construction.
- **Materials Characterization:** Although materials are available today that can achieve performance levels near the DOE targets, there is considerable room for improvement. In this task we use a unique experimental capability to evaluate the performance of prospective

materials under controlled conditions similar to what might be found during on-sun operation. This system, based on a laser heated reaction chamber, allows for the evaluation of reaction thermodynamics and kinetics of prospective thermochemical cycles.

- **System Level Analysis:** The ultimate goal of this project is to produce hydrogen efficiently from solar energy. In this task we estimate the performance of thermochemical technologies at the system level, identifying energy losses and calculating annual average hydrogen production efficiency based on the collection platform and facility location.

Results

The results from FY 2011 show that the combination of our particle reactor concept and cerium oxide-based reactive materials has the potential to achieve performance near the 2012 and 2017 DOE targets. Meeting these targets with actual hardware during on-sun operation will require additional effort in FY 2012 and beyond.

Reactor Development – The particle reactor being developed in this project uses cerium oxide powder in a two-step redox cycle to continuously produce hydrogen from solar energy and water. A schematic of the reactor concept is shown in Figure 1. Key attributes of the reactor are recuperation of sensible heat between the reaction steps, continuous flow, direct absorption of solar energy by the reactant, and the spatial separation of pressure, temperature, and reaction products within the device.

Our preliminary work in FY 2011 focused on estimating the likely level of reactor performance achievable in a mature technology. For this study we assumed that the reactant would be CeO_2, which has been shown to be suitable for two-step thermochemical hydrogen production, but is not considered to be ideal due to the relatively small amount of oxygen exchanged per mole of reactant. Even so, with recuperation the performance of the reactor in terms of the conversion of thermal energy to chemical energy in the form of a hydrogen product can exceed 40% at a thermal reduction pressure in excess of 100 Pa (Figure 2). With improved materials this level of performance can be even higher.

Efforts to design a reactor prototype at the 5-10 kW_{th} level have focused on identifying a suitable means of conveying a packed powder vertically within the reactor. To this end a contract was placed with Jenike and Johanson, specialists in the field of powder conveyance. They identified a conveyor based on the "Old's Elevator" approach in which particles are moved by friction up a stationary central screw by contact with a rotating cylindrical housing. A conceptual design of the conveyor system, included rotary airlocks and cyclone separators, is shown in Figure 3. This system will be modified during the final solar prototype design stage.

Our reactor design efforts also included a study of the compatibility of various construction materials with cerium oxide powder. We have shown that several materials including Haynes 214 and Al_2O_3, are compatible with cerium oxide up to 1,400°C. Our hope is that it will eventually be possible to use a metal like Haynes 214 for the main components of the screw conveyor as this would minimize difficulties with fabrication. This may not be possible at a temperature much in excess of 1,200°C due to material strength issues. We are therefore continuing to investigate options for fabricating the conveyor components from suitable ceramic materials.

Materials Characterization – A number of experiments were conducted that focused on the characterization of pure cerium oxide reactive materials. In this work, a

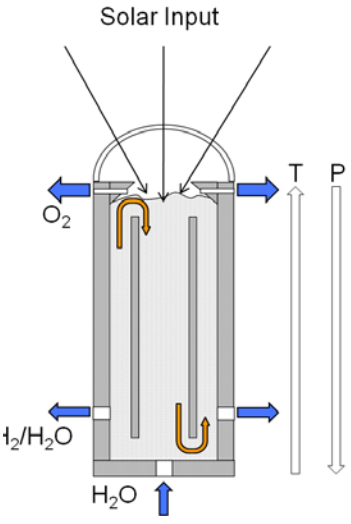


FIGURE 1. A schematic of the particle reactor concept. Particles must be conveyed vertically as a packed bed within the reactor. Concentrated solar energy enters from the top.

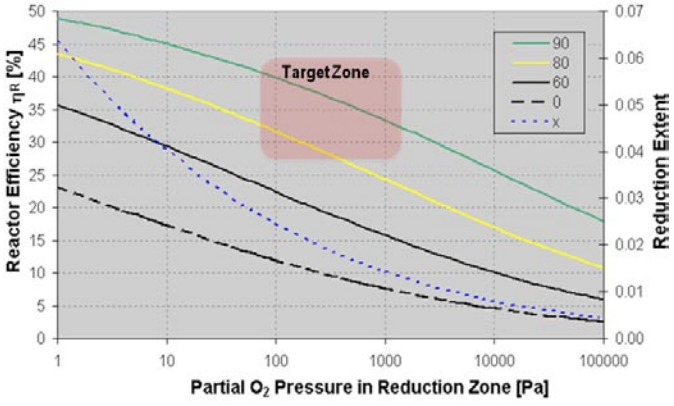


FIGURE 2. Predicted performance of the particle reactor using pure CeO_2 reactant. Reactor efficiency is analogous to the DOE "process efficiency" number.

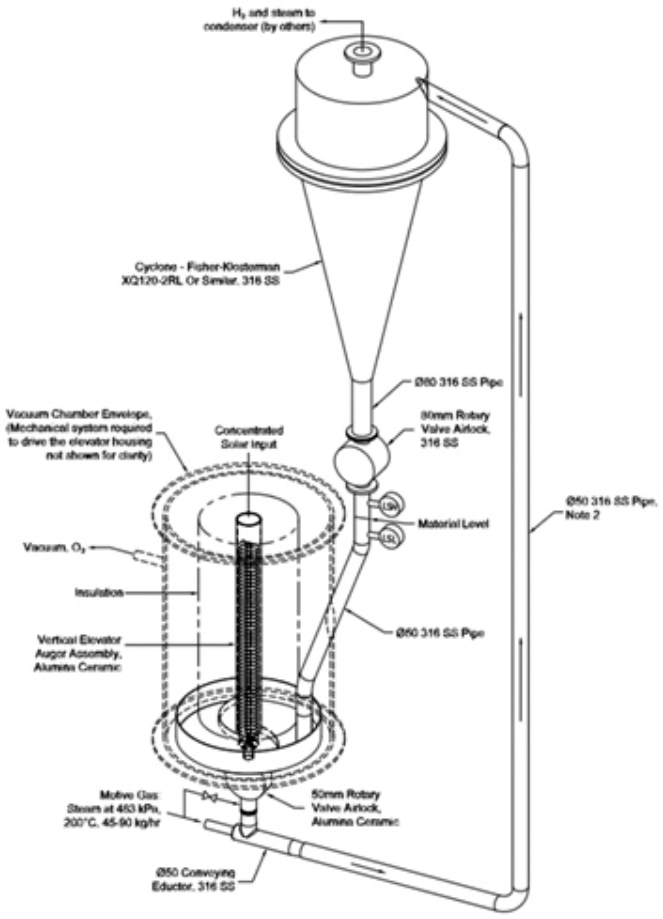
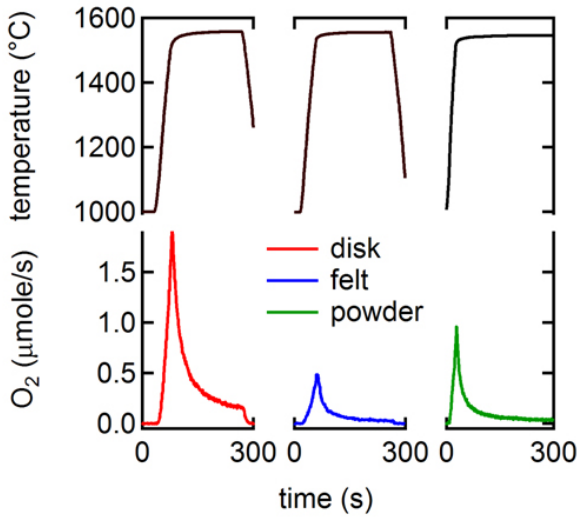


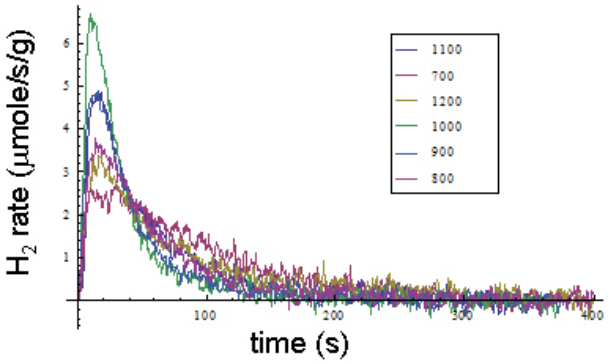
FIGURE 3. Conveyor system preliminary design.

laser-based heating method was used in conjunction with a stagnation flow reactor equipped with a mass spectrometer to investigate both the thermal reduction and oxidation reactions for cerium oxide powders, dense pellets, and felts. The rate of oxygen evolution during thermal reduction was measured for: (1) a powder having a ~5 µm particle diameter, (2) a 1,000 µm thick fully dense pellet, and (3) a felt with ~10 µm fiber diameter. Tests were conducted at a peak temperature slightly above 1,500°C and a heating rate in excess of 100°C/s. The results are illustrated in Figure 4 and show that the reaction rate and ultimate extent of thermal reduction was independent of the length scale over the range evaluated. The rate of the hydrogen-producing water splitting reaction using cerium oxide felt was measured over a range of temperatures in an attempt to characterize the optimal operating point for this type of reactive structure. These tests showed that the peak hydrogen production reaction rate varies with temperature, reaching a maximum near 1,000°C, but the overall amount of hydrogen production per unit mass of reactant was independent of reaction temperature (Figure 5). In the case of reaction at 1,000°C, the amount of time required for 90% completion is less than 90 seconds, which is consistent with



form	mass (mg)	mole O ($\times 10^{-6}$)	δ
disk	960	220	0.0394
felt	207	48	0.0398
powder	454	91	0.0350

FIGURE 4. Thermal reduction behavior observed for various forms of CeO_2.



temperature (°C)	total H_2 (µmole/g)	peak H_2 (µmole/s/g)
1200	274	3.27
1100	273	4.76
1000	249	6.51
900	229	4.75
800	235	3.60
700	285	2.64

FIGURE 5. Rate of H_2 production for thermally reduced CeO_2 felt.

the operational requirements of a solar thermochemical reactor. Thirty cycles were run over which the production characteristics remained constant, which indicates that there was no degradation of the reactive material or its physical structure. A number of other chemistries for solar thermochemical water splitting were also evaluated this FY, including modified cerium oxide and ALD-ferrite-coated reactive structures. Analysis of the data is ongoing and will be completed before the end of FY 2011.

System Level Analysis – The focus of the system level analysis was to identify all energy losses within the solar collection and reactor sub-systems and then estimate the annual average conversion efficiency of sunlight to hydrogen. The analysis was based on hourly meteorological data for a design location in Daggett, CA. System performance was calculated for each hour of an entire year and the energy inputs and hydrogen outputs summed over the year to determine the efficiency. Figure 6 is a summarized output showing principal energy losses within the system. It is important to note that 42% of the solar energy available to the parabolic dish collector is lost during collection and not available to power the thermochemical reaction. Although this may be improved slightly, the parabolic dish is a very efficient optical platform and large gains in collection efficiency are not likely. This fact is a compelling argument in support of dedicating significant effort to reactor design in order to maximize its efficiency.

The current system model, which was constructed in Excel, was provided to researchers at Pacific Northwest National Laboratory for inclusion in their ASPEN-based studies. We have also begun developing our own reactor models in ASPEN with the intent of eventually simulating the entire system (annual performance) with this code.

Conclusions and Future Directions

The progress made in FY 2011 will provide a strong foundation for continued work in FY 2012 that will hopefully culminate in the on-sun demonstration of a particle reactor prototype. Specific conclusions and future directions for each of the three main project elements are given as follows:

Reactor Development – In FY 2011 we have shown that the particle reactor concept can meet the DOE performance targets and are well on our way to completing the design of a 5-10 kW_{th} prototype system. In FY 2012 and beyond we will focus our efforts on completing the design and performing on-sun testing of the reactor. Past experience has shown that when dealing with thermochemical fuel production hardware it is essential to test systems under realistic condition to identify technical challenges that are not apparent when performing more idealized preliminary analysis and simulation activities.

Materials Characterization – In FY 2011 we experimentally characterized several promising reactive materials under operating conditions similar to what would be expected in a solar thermochemical reactor. In FY 2012 and beyond we will define a standard performance evaluation process and metrics that can be used to more easily compare various candidate materials. We will also continue to characterize promising new redox chemistries for non-volatile metal oxide cycles using the laser-based heating method incorporated into the stagnation flow reactor, subject to the material characterization protocols developed in FY 2012.

System Level Analysis – In FY 2011 we developed an annual system performance model that shows all major

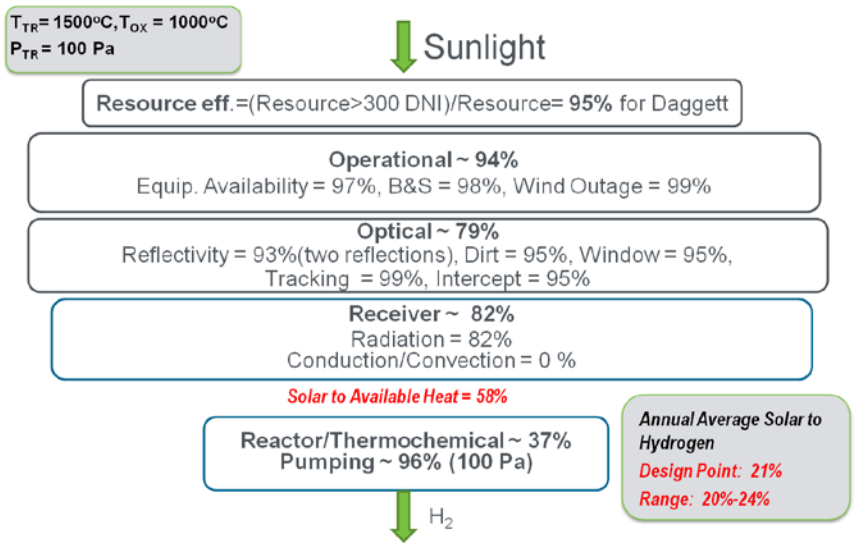


FIGURE 6. System level energy flow and annual average efficiency calculation.

energy losses in the system and enables the calculation of an annual average hydrogen production efficiency, a much more valuable number than a design point efficiency. In FY 2012 and beyond we will extend this model to a central receiver-based system configuration that will show the potential, and challenges, associated with scaling the particle reactor concept to larger sizes.

Definition of Terms

- Thermochemical Efficiency: This is the efficiency of the conversion of heat within the reactor to chemical fuel based on the lower heating value (LHV) of hydrogen. It does not include solar losses or energy losses from the receiver that are accounted for separately.
- Receiver Efficiency: The fraction of solar energy entering the reactor that is converted into useable heat available to the reactor. This term essentially accounts for radiation and convection losses from the receiver.
- Process Efficiency: The fraction of solar energy entering the reactor that is converted into chemical energy in the form of hydrogen on an LHV basis. This number is the product of receiver efficiency and thermochemical efficiency.
- Annual Average Efficiency: The total energy contained in hydrogen (LHV basis) produced over an entire year divided by the solar energy striking the collection system (mirrors) over the same period of time.
- Resource Efficiency: This quantity is the total solar energy that could be collected divided by the amount available over a year. Accounts for periods when the system is not operated by design.
- Operational Efficiency: The fraction of the total energy actually collected divided by the amount that could be collected over a year. This accounts for "wasted" energy when the collectors are not operating during the daytime due to weather outages or system maintenance.
- Optical Efficiency: The fraction of energy reaching the aperture of the reactor divided by the amount actually collected by the concentrator. Accounts for all reflection and transmission losses.

FY 2011 Publications/Presentations

1. Two abstracts submitted and accepted for presentation at SolarPaces 2011. Full papers are to be completed by July 31st, 2011.

2. A project summary was presented at the Annual Merit Review in Washington, D.C.

3. An invited talk entitled "*High temperature splitting of water and carbon dioxide using complex oxides as a route to solar fuels*" will be presented at the 242nd ACS National Meeting, Division of Fuel Chemistry, in August of 2011.

4. An abstract has been accepted for presentation at the 5th International Conference on Energy Sustainability hosted by the ASME in August of 2011.

5. "*Hydrogen Production via Chemical Looping Redox Cycles Using Atomic Layer Deposition-Synthesized Iron Oxide and Cobalt Ferrites*", Jonathan R. Scheffe, Mark D. Allendorf, Eric N. Coker, Benjamin W. Jacobs, Anthony H. McDaniel, Alan W. Weimer in Chemistry of Materials 2011 23 (8), 2030-2038.

II.F.4 Solar-Thermal ALD Ferrite-Based Water Splitting Cycle

Alan W. Weimer (Primary Contact) and
Melinda M. Channel
University of Colorado
Department of Chemical & Biological Engineering
424 UCB
Boulder, CO 80309
Phone: (303) 492-3759
E-mail: alan.weimer@colorado.edu

DOE Manager
HQ: Sara Dillich
Phone: (202) 586-7925
E-mail: Sarah.Dillich@ee.doe.gov

Project Start Date: March 31, 2005
Project End Date: This R&D is performed under subcontract to Sandia National Laboratories. Project continuation and direction determined annually by DOE.

Fiscal Year (FY) 2011 Objectives

- Finalize the ferrite process flow diagram and H2A economic analysis.
- Determine the most cost effect design and construction materials for the FY 2010 conceptualized scalable central solar reactor/receiver per H2A guidance on economics.
- Demonstrate suitable materials for robust redox/thermochemical cycling.

Technical Barriers

This project addresses the following technical barriers from page 3.1-26 of the Hydrogen Production section of the Fuel Cell Technologies Program Multi-Year Research, Development and Demonstration Plan:

(U) High-Temperature Thermochemical Technology

(V) High-Temperature Robust Materials

(W) Concentrated Solar Energy Capital Cost

(X) Coupling Concentrated Solar Energy and Thermochemical Cycles

Technical Targets

The technical targets are the cost of hydrogen and the process energy efficiency.

- For 2017, these are $3.00 per gasoline gallon equivalent (gge) H_2 and >35% (lower heating value, LHV), respectively.

A recent report on H2A cost analyses for solar-driven thermochemical conversion [1] included an analysis of the developed ferrite cycle. The key figures of merit used for this study are summarized in Table 1. The projected thermal efficiency for the developed process is 55.5% LHV, thus exceeding the >35% figure of merit for the 2025 case. For a solar-to-receiver annual average efficiency of 40.2%, the overall solar to H_2 efficiency is estimated at 22.3% (LHV). Furthermore, the $6/kg H_2 plant gate cost for the central 100,000 kg H_2/day facility 2015 case should be easily achieved for the $126.50/$m^2$ installed heliostat cost. The $3/kg H_2 plant gate cost for 2025 for a $90/$m^2$ installed heliostat field may be achievable.

TABLE 1. Key Figures of Merit Used for Cost Analyses for 2015 and 2025 for Solar-Driven High-Temperature Thermochemical Hydrogen Production [1]

Characteristics	Units	2015	2025
Plant Gate H_2 Cost Projections	$/kg H_2	$6	$3
Installed Heliostat Capital Cost	$/$m^2$	$126.50	$90
Process Energy Efficiency (thermal)	%	30	>35

FY 2011 Accomplishments

- Previously demonstrated that <5 nm thin ferrite films can be synthesized by atomic layer deposition (ALD) and provide for significant opportunities to reduce diffusional resistances and promote radiation-driven heat transfer; both potentially providing for rapid redox cycling. Since this material is not currently commercially available, determine the most reasonable market value (i.e. suggested retail price per kilogram of material) in order to finalize the H2A process economic analysis.
- Improved the design and materials of construction of a multi-tube absorbing fixed-bed cavity reactor/receiver that provides for efficient internal heat recuperation and the potential for rapid cycling; mitigates erosion and complications associated with transporting solids.
- Finalized the process design/H2A economic evaluation indicating that ALD of ferrite materials on 100 m^2/g supports cycling every 5 to 1 minutes will have H2A projected costs of less than $6/kg and $3/kg in 2015 and 2025, respectively [1].
- Cycling studies in a themogravimetric analyzer as well as on-sun cycling studies are currently in progress to demonstrate the thin film's robustness and lack of deactivation over time.



Introduction

The direct thermolysis to split water by reaction 1 requires materials operating at T >3,500°C as well as methods to separate the H_2 and O_2 gases at high temperature [2]. This seemingly impossible task can be overcome by implementing a two-step thermochemical water splitting cycle in which a ferrite spinel material (MFe_2O_4; M=Co, Ni) can be thermally reduced using concentrated sunlight to release O_2 as shown in reaction 2. The reduced ferrite is then subsequently oxidized (reaction 3) with steam producing H_2 [3-5] recovering the original spinel structure in the process. Reactions 2 and 3 combine to form a complete redox cycle with reactants and products equal to reaction 1.

1. $H_2O \rightarrow H_2 + ½\ O_2$
2. $MFe_2O_4 \rightarrow MeO\ (Fe^{2+} + Fe^{3+} + M^{2+}) + ½\ O_2$
3. $MeO\ (Fe^{2+} + Fe^{3+} + M^{2+}) + H_2O \rightarrow MFe_2O_4 + H_2$

The reduction step of this cycle occurs at 1,450°C while the oxidation step occurs at 1,000°C; with significantly lower operating temperatures this cycle is much more efficient and desirable than direct thermolysis.

Approach

The primary scientific barrier to successful implementation of a solar-thermal water splitting process is access to a robust active material for efficiently and rapidly carrying out redox cycles producing H_2. Further, the key engineering barrier to successful implementation is demonstration of a large scale solar reactor concept that allows for rapid redox cycling taking advantage of highly active thin film materials while providing for highly efficient usage of delivered solar energy. The key scientific challenges to successfully overcoming the primary scientific barrier are:

- Identify/synthesize high surface area active materials with favorable transport properties.
- Identify/demonstrate suitable interfacial substrate materials to facilitate rapid redox cycling.
- Combine the active/substrate materials into a characteristic volume sample and demonstrate robust cycling to split water, particularly if able to operate the reduction in air.

High surface area active ferrite materials ($M_xFe_{3-x}O_4$; M=Co, Ni) were synthesized using ALD to deposit nanometer thick films onto nanosized particles [6-9]. Nanoparticle substrates were placed in fluidized bed reactors and coated (Figure 1) with Fe_2O_3, CoO, and NiO thin films using self-limiting surface chemistry via metallocene [$(C_5H_5)_2M$; M =Fe, Co, Ni] and O_2 precursors. The approach recommended is to design the nanometer thick ferrite films and to deposit them on high surface area support materials.

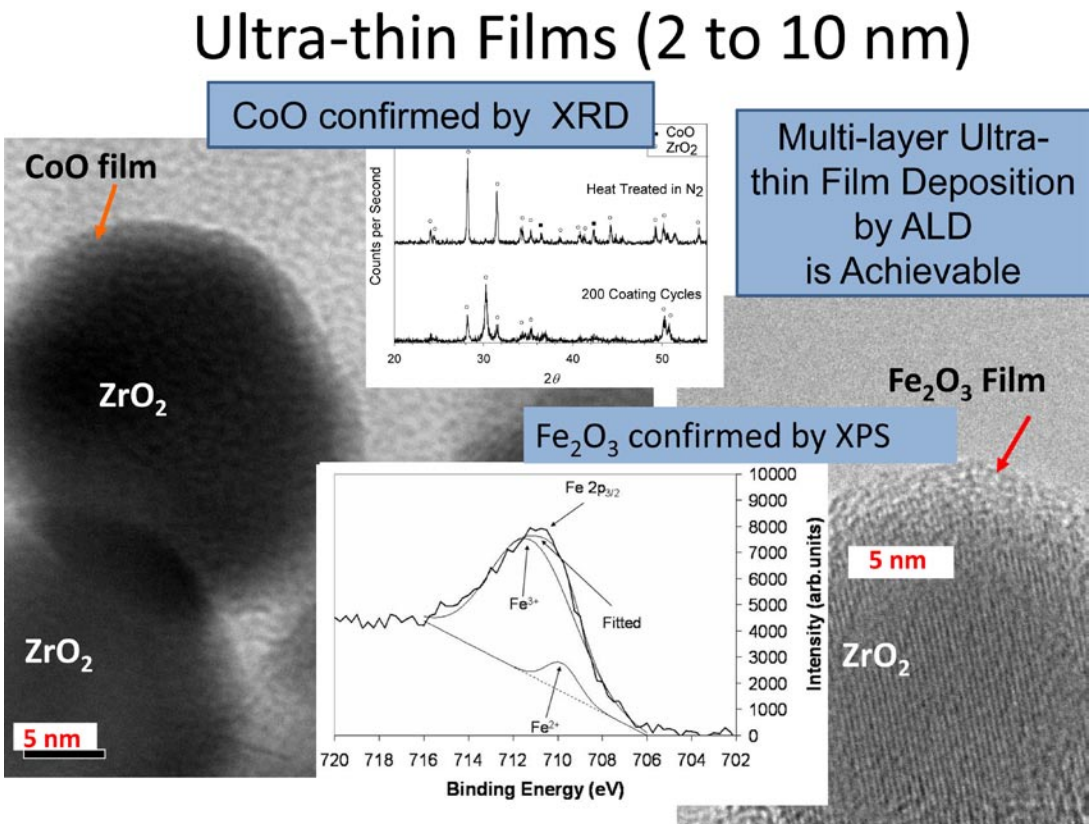


FIGURE 1. Thin Film Deposition of Ferrite Materials

Results

For this study, a 5-nm thick nickel ferrite film coated onto a 100 m^2/g high surface area ZrO_2 support was considered; resulting in 0.67 moles ZrO_2 for every mole of $NiFe_2O_4$. Using the FACTSage™ thermodynamic database, it was determined that the amount of solar heat input required for this process is minimized when the solar reduction reaction occurs at 1,450°C and the oxidation reaction occurs at 1,000°C.

The conceptualized thermochemical redox receiver/solar reactor is shown in Figure 2. The reactor consists of a cavity-receiver, i.e. a well-insulated enclosure with a small opening – the aperture – for the access of concentrated solar radiation. The receiver will contain an even number of closed-end SiC tubes. Each tube will contain a 2nd open end SiC tube with a porous SiC plug at the base. Active high surface area and porous nickel ferrite material will be packed in the annular region between the two tubes allowing for efficient heat and mass transfer and, consequently, fast overall kinetics. The inner tube will be packed with media providing surface area for improved heat transfer to drive the vaporization of water to steam. At a given instant, half of the tubes will be operated in the reduction mode at T_R while the remaining half will be operated in the oxidation mode at T_O. When the reactions reach completion, the operational modes will be switched.

The process flow diagram is shown in Figure 3; 32°C water is pumped into the reduction tubes of the solar reactor at 12 psig. The water pumps are centrifugal cast iron and require a total of 135 kWhr/day electricity. The reduction tubes operate at a reduced pressure of 380 torr reached via vacuum pumps. The vacuum pumps remove oxygen being produced to prevent recombination with reduced ferrites. The flowrate of oxygen through each of three single-stage large cast iron pumps is 52,160 ft^3/min requiring a total of 55,310 kWhr/yr electricity. The oxidation tubes of the solar reactor operate near atmospheric pressure producing hydrogen that must be compressed to 300 psig before entering the plant gate. The three stage compression system with intercoolers has a compression factor of 2.85 and the intercoolers have a 2 psig pressure drop. This system requires a total of 52,848 kWhr/yr electricity and is designed for four compressors with only three operating at any time. Six 223 meter tall towers are required to produce 100,000 kg H_2/day. With one solar reactor per tower the total solar input is 2,332 GWhr/yr. Each receiver has three heliostat fields with 65 acres of land per field and 2.09E6 m^2 of heliostats. The heliostat field requires 1.22 GWhr/yr of parasitic electricity. This field and process design results in a thermal efficiency of 55.5% and a solar to thermal efficiency of 22.3%.

An H2A analysis was completed using varying redox cycle times of 1, 5, and 15 minutes [1]. Reducing cycle times reduces the amount of ferrite required to produce 100,000 kg H_2/day, which also reduces the number of SiC reaction tubes required thus decreasing the size and cost of each solar reactor. Ferrites can be produced for the cost of materials plus a reasonable retail markup. The cost of $NiFe_2O_4$ precursors are approximately $225/kg of ferrite produced. Three retail markups were considered in this study: 20, 35, and 50%. The capital cost breakdown can be seen in Figure 4 and the resulting H_2 selling prices in Figure 5. With projected costs of $6/kg in 2015 and $3/kg in 2025, Figure 5 shows that with 10 minute cycles or less in 2015 the projection is achievable. However, in 2025 the projection is only achievable with cycles times of 1 minute or less. To date we have achieved cycles less than 15 minutes experimentally. With process improvements to not only the ferrite materials, but also the reactor and solar field 1 minute cycles can be reached by 2025. Lastly, Figure 5 shows that the resulting H_2 selling price is not sensitive to the purchase price of nickel ferrites.

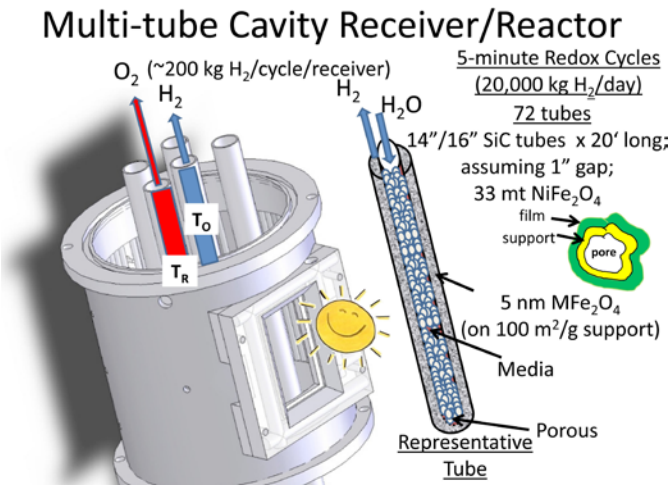


FIGURE 2. Schematic of Solar Reactor/Receiver

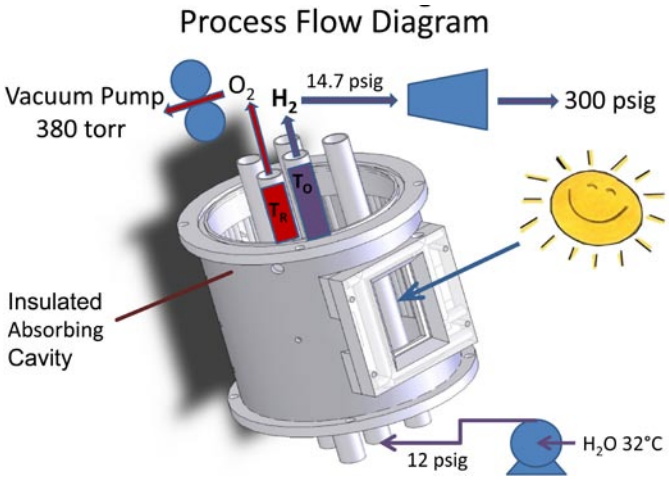


FIGURE 3. Process Flow Diagram

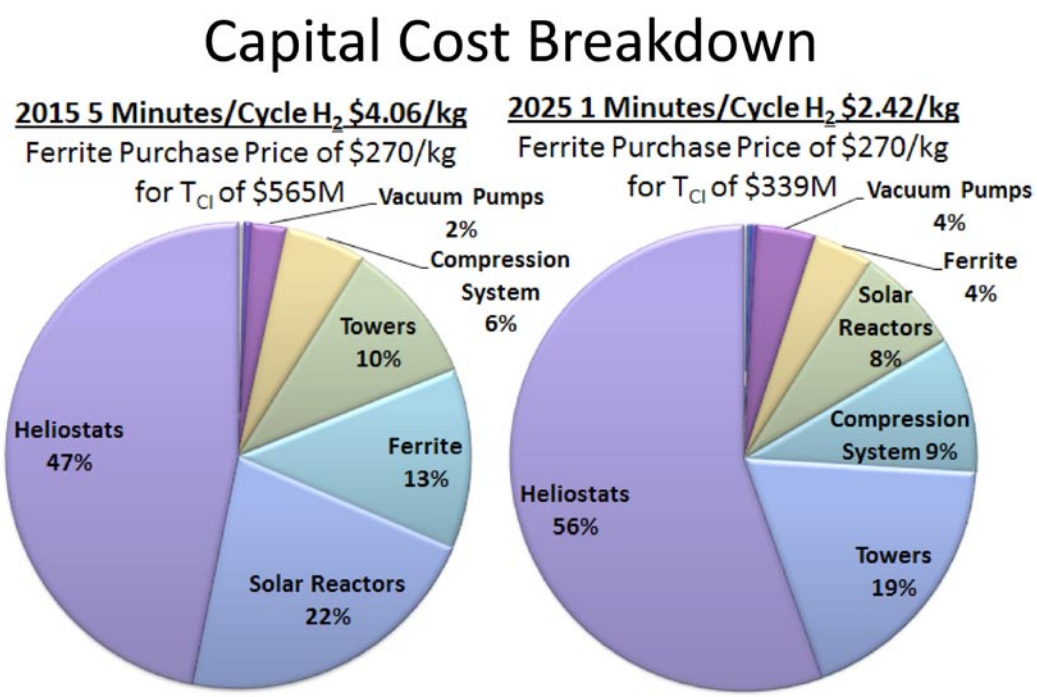


FIGURE 4. Capital Cost Breakdown

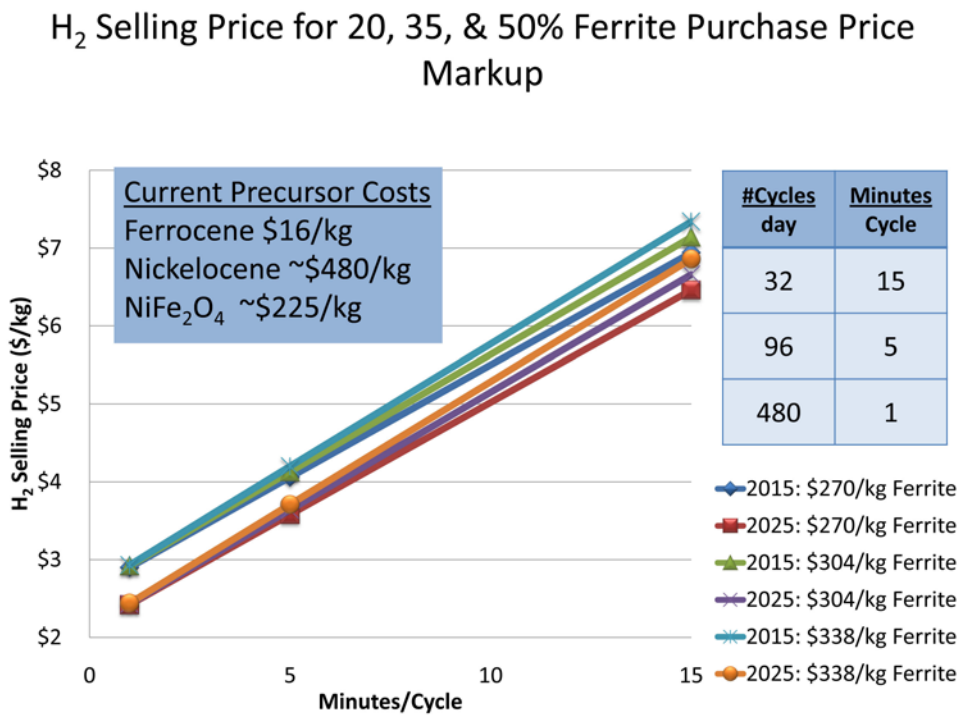


FIGURE 5. H2A Results of H_2 Selling Prices

Conclusions and Future Directions

- ALD materials remain active for up to 30 water spitting cycles with no sign of deactivation after initial aggregation.
- ALD thin films are ~100X more active than conventionally produced bulk ferrites; the challenge is holding them together.
- Ferrite process is anticipated to meet H2A cost projections of less than 6/kg and $3/kg for 2015 and 2025, respectively, if performance metrics are met [1].
- Future work will focus exclusively on the "hercynite" cycle which has been shown to be more stable than conventional ferrites and to operate over a lower temperature range (upper temperature limit ~1,300°C).

Special Recognitions & Awards

1. 2010 AIChE Excellence in Process Development Research Award.

2. 2010 Dean's Award for Outstanding Research (College of Engineering and Applied Science).

FY 2011 Peer-Reviewed Publications

1. Kreider, P.B., H.H. Funke, K. Cuche, M. Schmidt, A. Steinfeld and A.W. Weimer, "Manganese Oxide Based Thermochemical Hydrogen Production Cycle," International Journal of Hydrogen Energy," 36, 7028-7037 (2011).

2. Scheffe, J.R., M.D. Allendorf, E.N. Coker, B.W. Jacobs, A.H. McDaniel and A.W. Weimer, "Hydrogen Production via Chemical Looping Redox Cycles Using Atomic Layer Deposition-Synthesized Iron Oxide and Cobalt Ferrites," Chemistry of Materials," 23 (8), 2030-2038 (2011).

3. Martinek, J, M. Channel, A. Lewandowski and A.W. Weimer, "Considerations for the Design of Solar-thermal Chemical Processes," Journal of Solar Energy Engineering, 132, 031013 (2010).

4. Scheffe, J.R., J. Li, and A.W. Weimer, "A Spinel Ferrite/ Hercynite Water-Splitting Redox Cycle," International Journal of Hydrogen Energy, 35, 3333-3340 (2010).

5. Francis, T.M., P.R. Lichty, and A.W. Weimer, "Manganese Oxide Dissociation Kinetics for the Mn_2O_3 Thermochemical Water-splitting Cycle. Part I: Experimental," Chemical Engineering Science, 65, 3709-3717 (2010).

6. Francis, T.M., P.R. Lichty, and A.W. Weimer, "Manganese Oxide Dissociation Kinetics for the Mn_2O_3 Thermochemical Water-splitting Cycle. Part II: CFD Model," Chemical Engineering Science, 65, 4397-4410 (2010).

7. Francis, T.M., P.B. Kreider, P.R. Lichty, and A.W. Weimer, "An Investigation of a Fluidized Bed Solid Feeder for an Aerosol Flow Reactor," Powder Technology, 199, 70-76 (2010).

References

1. Kromer, M., K. Roth, R. Takata, and P. Chin, "Support for Cost Analyses on Solar-Driven High –Temperature Thermochemical Water-Splitting Cycles," Order DE-DT0000951, report by TIAX, LLC (February 22, 2011).

2. Perkins, C., and A.W. Weimer," Solar-Thermal Production of Renewable Hydrogen", *AIChE Journal* Vol. 55, No. 2, 2009, pp. 286-293.

3. Kodama, T., N. Gokon, and R. Yamamoto," Thermochemical two-step water splitting by ZrO2-supported NixFe3-xO4 for solar hydrogen production", *Solar Energy* Vol. 82, No. 1, 2008, pp. 73-79.

4. Kodama, T., Y. Kondoh, R. Yamamoto, H. Andou, and N. Satou," Thermochemical hydrogen production by a redox system of ZrO2-supported Co(II)-ferrite", *Solar Energy* Vol. 78, No. 5, 2005, pp. 623-631.

5. Kodama, T., Y. Nakamuro, and T. Mizuno," A two-step thermochemical water splitting by iron-oxide on stabilized zirconia", *Journal of Solar Energy Engineering-Transactions of the Asme* Vol. 128, No. 1, 2006, pp. 3-7.

6. Ferguson, J.D., A.W. Weimer, and S.M. George," Atomic layer deposition of ultrathin and conformal Al2O3 films on BN particles", *Thin Solid Films* Vol. 371, No. 1-2, 2000, pp. 95-104.

7. George, S.M.," Atomic Layer Deposition: An Overview", *Chemical Reviews* Vol. 110, No. 1, 2010, pp. 111-131.

8. Hakim, L.F., J.H. Blackson, and A.W. Weimer," Modification of interparticle forces for nanoparticles using atomic layer deposition", *Chemical Engineering Science* Vol. 62, No. 22, 2007, pp. 6199-6211.

9. King, D.M., J.A. Spencer, X. Liang, L.F. Hakim, and A.W. Weimer," Atomic layer deposition on particles using a fluidized bed reactor with in situ mass spectrometry", *Surface & Coatings Technology* Vol. 201, No. 22-23, 2007, pp. 9163-9171.

II.G.1 Nano-Architectures for 3rd Generation PEC Devices: A Study of MoS_2, Fundamental Investigations and Applied Research

Thomas F. Jaramillo (Primary Contact), Arnold J. Forman, Zhebo Chen
Dept. of Chemical Engineering, 381 N-S Axis
Stanford University
Stanford, CA 94305
Phone: (650) 498-6879
E-mail: jaramillo@stanford.edu

DOE Manager
HQ: Eric Miller
Phone: (202) 287-5829
E-mail: Eric.Miller@hq.doe.gov

Contract Number: DE-AC36-08GO28308

Subcontractor:
Board of Trustees of the Leland Stanford Junior University, Stanford, CA

Project Start Date: December 18, 2008
Projected End Date: September 30, 2011

Fiscal Year (FY) 2011 Objectives

- Develop a high surface area, transparent conducting (TC) scaffold as a broadly applicable substrate for photoelectrochemical (PEC) devices, as well as a scalable route to fabricate them.
- Plan, develop, and perform synthesis and characterization, both physical and PEC, of nanoscale transition metal dichalcogenides.
- Correlate atomic scale characterization of dichalcogenides with performance to iteratively optimize materials for water splitting efficiency and stability.
- Merge TC and dichalcogenide materials to yield enhanced performance high surface area catalyst systems and demonstrate their efficacy under standard operating conditions.
- Correlate physical characterization results of complete device with its PEC performance to tune subsequent syntheses in an effort to optimize water splitting efficiency and photoelectrode stability.

Technical Barriers

This project addresses the following technical barriers from the Production section of the Fuel Cell Technologies Program Multi-Year Research, Development and Demonstration Plan:

(Y) Materials Efficiency

(Z) Materials Durability

(AA) PEC Device and System Auxiliary Materials

(AB) Bulk Materials Synthesis

Technical Targets

The focus of this project is the development of a PEC device that incorporates a 3rd generation nanostructured absorber with a high aspect architecture support that enables efficient solar absorption and charge transport. If successful, this project will address the following DOE technical targets as outlined in the Multi-Year RD&D Plan.

TABLE 1. Progress towards Meeting Technical Targets for PEC Hydrogen Production

Characteristics	Units	2013 Target	2018 Target	2011 Status
Usable semiconductor bandgap	eV	2.3	2.0	1.8
Chemical conversion process efficiency	%	10	12	TBD
Plant solar-to-hydrogen efficiency	%	8	10	TBD
Plant durability	hr	1,000	5,000	TBD

TBD – to be determined

FY 2011 Accomplishments

- Developed a facile, scalable synthetic route to fabricate high surface area electrodes (HSEs) of transparent conducting oxide (TCO) materials.
- Electrochemically quantified relative enhancement of HSE surface area. Synthetic control garners 20-600 times surface area increase.
- Patent application pending for novel HSE fabrication method.
- Developed a facile, scalable, room temperature synthesis of quantum confined MoS_2 nanoparticles with bandgaps of 1.8 eV.
- Demonstrated accelerated stability of MoS_2 catalysts over 10,000 voltage cycles to simulate diurnal conditions.



Introduction

PEC water splitting is a promising route to produce high purity hydrogen (H_2) from a renewable resource [1].

Hydrogen produced in this manner represents a means of chemical storage of solar energy; the H_2 can potentially be used as a fuel. Current costs of H_2 production by photoelectrochemistry are not competitive with H_2 produced by the reformation of fossil fuels. However, a recent techno-economic analysis has shown that if high performance, stable, low-cost materials can be developed, the DOE target of $2-$4/gasoline gallon equivalent for dispensed hydrogen could be reached using solar photoelectrochemistry [2].

Development of high purity electrochemical H_2 generation systems requiring lower capital costs with sunlight as the sole energy input is the end goal of PEC water splitting research. Steps toward this goal include discovery and optimization of efficient, inexpensive, stable electrocatalysts, (photo)electrode materials, and high surface area electrode substrates on which to coat them. Integration of these components could result in a complete system capable of efficient, cost-effective, and sustainable production of solar-derived hydrogen.

Approach

Development of transparent HSEs to act as supports for both electrocatalyst and photoelectrode materials is an enabling technology at both the fundamental and applied research levels. In electrocatalysis, HSEs allow more electrocatalyst to be packed into a given area which increases the rate per projected area at which product is generated. For photoelectrochemistry, HSEs coated with ultra-thin layers of light absorbing material allow for more complete absorption of incoming light as compared to flat electrodes – a major challenge in thin-film solar technologies (see Figure 1) [3]. Enabling ultra-thin layers to completely absorb solar photons is particularly advantageous as only a short distance needs to be traversed by photo-excited charges in order for them to reach the solid-liquid interface (for minority carriers) or the back contact (for majority carriers). This should yield much improved charge collection efficiency, translating to improved external quantum efficiency (QE). The end result is an enhanced overall performance due to greatly increased interfacial area.

Such HSE structures require integration of materials that effectively absorb light to produce electronic charges that can efficiently drive the catalytic turnover of hydrogen and oxygen via water splitting. While high efficiency devices have been developed in this field [4], the costly processes and rare materials used in their production limit large scale deployment. Thus, it is imperative that new materials are discovered based on earth-abundant elements and produced using low cost methods. The approach used herein focuses on the development of MoS_2, a material which decades ago was studied and not considered a promising candidate for solar PEC water splitting as it is limited by an inadequate electronic band structure as well as poor hydrogen evolution kinetics at its surface [5]. The approach herein is to use nanostructuring to improve the relevant bulk and surface properties of MoS_2 for (photo)electrochemical applications [6]. By synthesizing nanoparticles of MoS_2, one can engineer the electronic band structure and light absorption properties through a quantum confinement effect [7], and expose edge sites for the improved catalytic turnover of hydrogen [8].

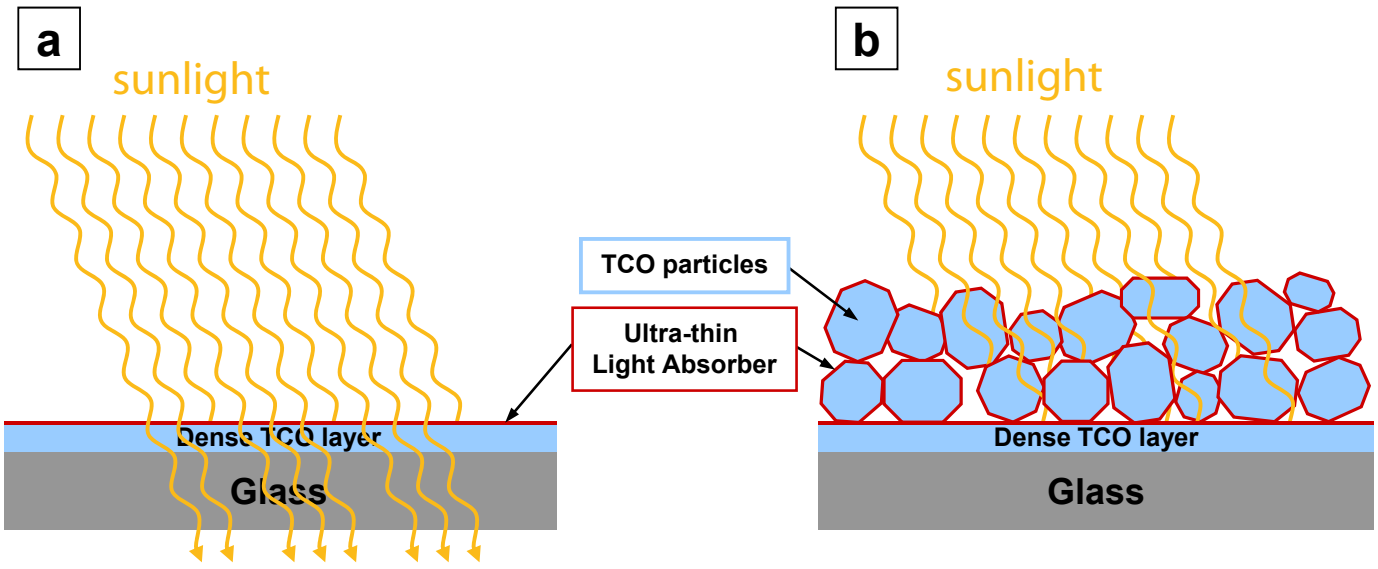


FIGURE 1. Quantum efficiency for photon-to-product conversion in PEC devices made from semiconductor absorber materials with poor electronic charge transport is maximized with ultra-thin semiconductor layers (a). However, the overall photon absorption (optical density) of these electrodes is typically very low (a), which limits the overall solar conversion efficiency. By conformally coating HSEs with ultra-thin absorber layers (b), the optical density is maximized while simultaneously maintaining high QE.

Results

One of the primary results of this project has been the development of an extremely high surface area TCO substrate that can be used with a wide variety of devices–namely those employed for PEC water splitting. In demonstrating this new development for the very first time, we have concurrently developed a synthetic route applicable to large-scale fabrication of HSE TCO electrodes. These TCOs include indium tin oxide (ITO), fluorine doped tin oxide (FTO), aluminum zinc oxide and many other well utilized electrode materials in the PEC, photovoltaic and electrochemical fields. The synthetic route involves spray deposition of a two part mixture containing solid TCO powder (~1-100 µm diameter particles) and TCO sol-gel precursors in an acidified ethanolic solvent, followed by heat treatment. Figure 2a exhibits a schematic representation of the resulting film morphology. The amount of mixture sprayed onto the appropriate conductive substrate controls the final surface area of the HSE. These TCO HSEs are capable of enabling PEC materials to simultaneously address three of the DOE technical barriers for Production (Y, AA, AB). Compared to more classical HSE fabrication techniques such as lithographic patterning, spray deposition offers significant cost savings and scalability – absolute necessities for an emerging solar energy technology seeking to generate copious domestic fuel.

The key performance criteria for TCO HSEs are three fold: surface area, electrical conductivity and transparency to visible light. Our proof-of-principle HSEs spray fabricated from ITO have demonstrated excellent performance in all three categories. Figure 2b reveals their optical transparency and Figures 2c and 2d show the general morphology as viewed by a scanning electron microscope (SEM). The faceted geometric shapes seen by SEM indicate good crystallinity of the ITO which translates into superior electrical conductivity while the porous, open network results in high surface area. This surface area is quantified by performing electrochemical capacitance (EC) measurements in 1.0 M NaOH (Figure 3). Here we see the EC of a planar, commercial ITO film compared to spray deposited HSEs of controllably higher surface area. The capacitance current, which is proportional to surface area, is read as the oxidative current at 0.3 V vs. saturated

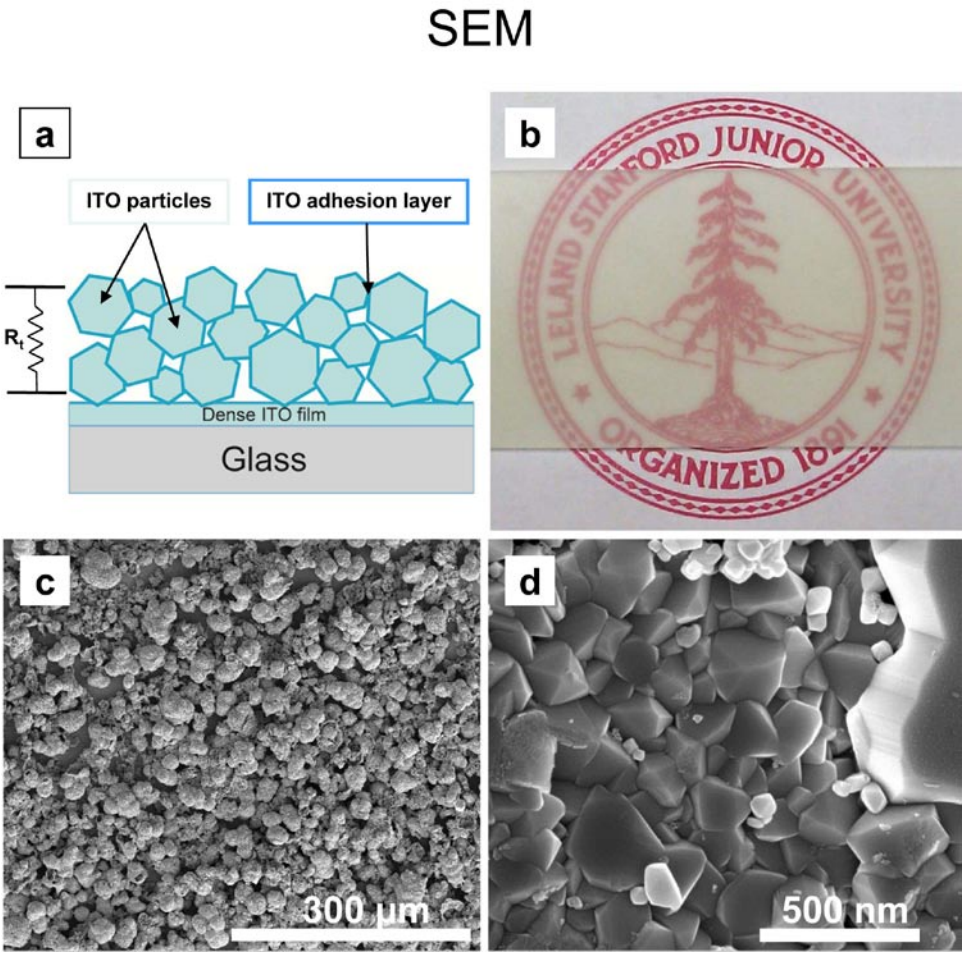


FIGURE 2. A schematic cross section (a) and optical photograph showing transparency (b) of the ITO HSE. SEM images show the textured particulate HSE surface (c) and the crystallinity of the ITO adhesion layer (d).

calomel electrode (SCE) (linear region) on Figure 3a. The relative ratio of capacitances or surface areas (roughened vs. planar) is termed roughness factor (RF) and is plotted against square root of scan rate for several typical spray films in Figure 3b. For the HSEs, capacitance charging is limited by solute diffusion at higher scan rates and the RF appears smaller. Therefore, extrapolation of the data to zero scan rate yields the true RF values. The EC data presented here shows HSEs that have RFs ranging from 250 to 800 relative to the planar ITO film. We have succeeded in fabricating films with RFs from ~20-800 via spray deposition, the right order of magnitude for roughness needed to maximize performance according to our calculations.

Electronic resistance measurements of these spray films indicate that resistance in the transverse direction, R_t, (see Figure 2a) is ~1 Ω/10 μm, or only about 10 Ω for the average film thickness. This resistance is superb given the low cost, low quality fabrication method employed.

We have just begun to coat these HSEs with ultra-thin layers of semiconductor material including manganese oxide and iron oxide, two excellent absorbers of visible light. The challenge here is that these absorber materials are performance limited by electronic charge transport. Therefore, ultra-thin layers will help facilitate extraction of photogenerated charge carriers to the back contact (the TCO) with a high QE. By conformally coating the HSEs with that same ultra-thin layer of absorber material we can combine the high QE carrier extraction of an ultra-thin layer with full absorption of incoming light because of the many layers coated across the high surface area. This device design has an optical density equivalent to an absorber layer X times thicker where X is proportional to the RF of the HSE.

Using an entirely room temperature synthetic procedure, we have produced nanoparticles of MoS_2 only several nanometers in size that exhibit a visible shift in light absorption towards lower wavelengths (Figure 4a) with an estimated bandgap of ~1.8 eV for the smallest nanoparticles as a result of quantum confinement. Transmission electron microscopy (TEM) reveals a range in nanoparticle size from 2.4 to 8.3 nm. In addition, PEC measurements of these nanoparticles have shown that they possess proper conduction and valence band alignments relative to the hydrogen and oxygen evolution potentials to enable unassisted water splitting.

We have also studied the long-term performance of highly nanostructured MoS_2 as an electrocatalyst for hydrogen evolution at current densities relevant to efficient solar conversion (~10 mA/cm^2). By carefully controlling the extent of thermal sulfidization treatments, we can optimize the growth of ultra-thin MoS_2 shell structures that are only a few nm thick at temperatures as low as 200°C on a high aspect ratio MoO_3 nanowire core support. These catalysts remain stable over ten thousand voltage cycles that simulate the diurnal conditions of solar irradiation (Figure 4b). Furthermore, they exhibit this stability in strongly acidic environments, a feature not possessed by other Earth-abundant hydrogen evolution catalysts such as nickel.

Conclusions and Future Directions

In order to reach our goal of developing a fully operational PEC water splitting device, we have been developing a 3rd generation light absorber material (MoS_2) while also producing a TC scaffold onto which it can be incorporated. We have achieved the following:

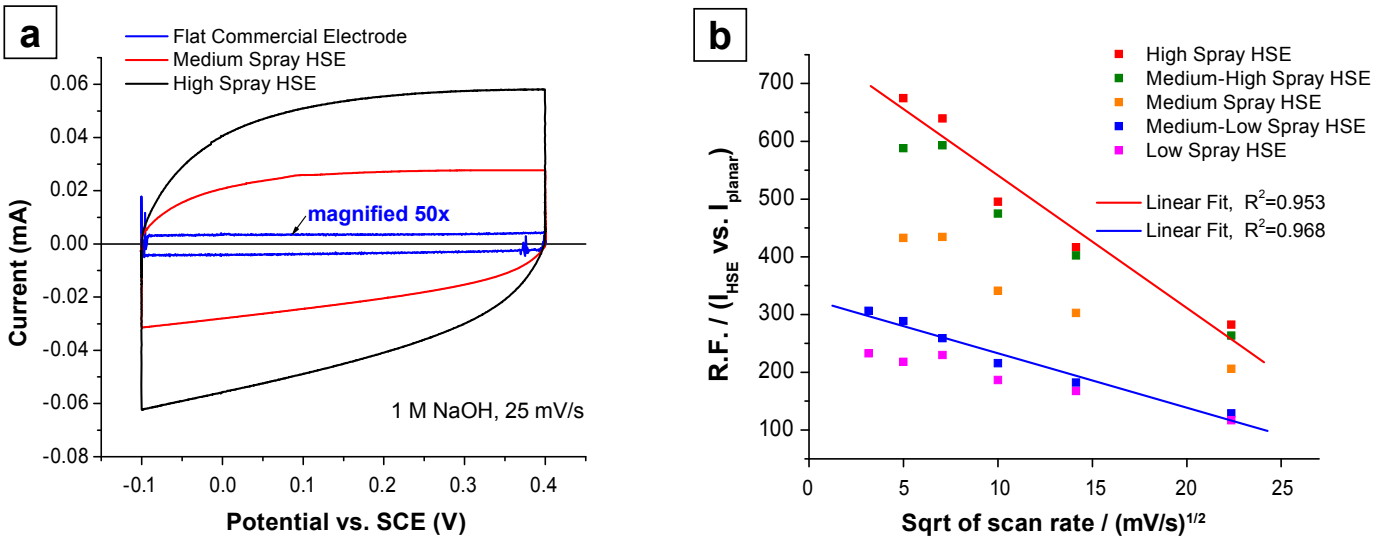


FIGURE 3. Advanced cyclic voltammograms (a) swept from -0.1 to 0.4 V vs. SCE where the scan is held at each vertex potential for 30 seconds. The third in a series of scans for each electrode is shown. Roughness factor as a function of square root of scan rate (b). Linear fits of two sample data sets are shown.

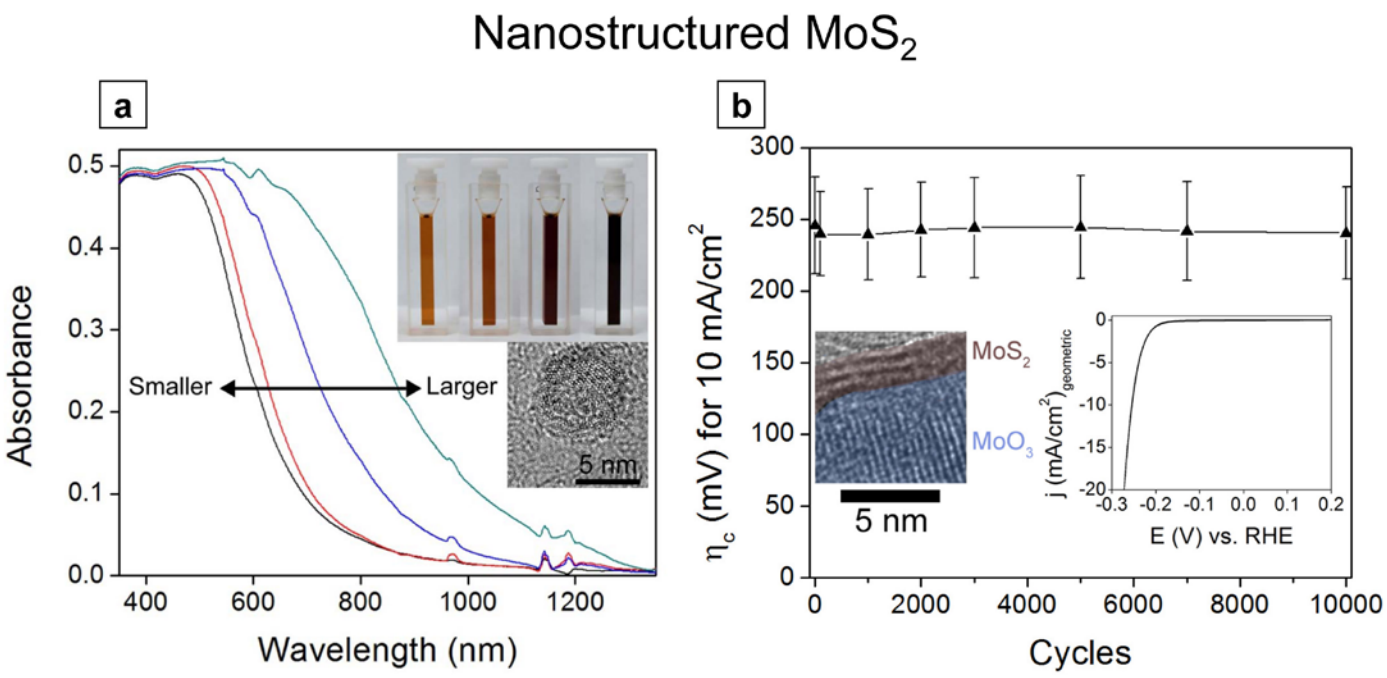


FIGURE 4. Spectroscopy, microscopy, and electrochemical performance of nanostructured MoS_2. Ultra-violet visual absorbance (a) of quantum confined MoS_2 nanoparticles with an inset photograph of solutions containing nanoparticles of increasing size towards the right, and an example TEM image of the nanoparticles. Electrochemical stability (b) of ultra-thin MoS_2 shell structures surrounding a MoO_3 core, assessed as a function of overpotential required to drive 10 mA/cm^2 of current density over the course of 10,000 potential cycles from -0.3 to 0.2 V vs. the reference hydrogen electrode. The inset shows a TEM image of the core-shell structures along with a cyclic voltammogram detailing their electrochemical performance for the hydrogen evolution reaction.

- A low-cost, scalable, facile route to fabrication of high surface area transparent conducting electrodes has been developed and a patent application is pending.
- Physical and electronic characterization of these electrodes indicates roughness factors of ~20-800 and electrical conductivity commensurate with requirements for PEC and many other electronic applications.
- Developed bandgap engineered nanoparticles of MoS_2 which possess the correct energetic for water splitting.
- Demonstrated long-term stability of highly nanostructured MoS_2 hydrogen evolution catalysts.

The next step in our work is the incorporation of nanostructured materials and thin films into our HSE platforms. We will accomplish this task through various objectives:

- Incorporate MoS_2 nanoparticles into the HSE and characterize their water splitting properties with respect to light absorption, charge transport, and stability.
- Demonstrate the broad applicability of the HSE platform for various other PEC materials.

Special Recognitions & Awards

1. DOE Hydrogen and Fuel Cells Program R&D Award to Prof. Thomas F. Jaramillo (PI).

Patents Issued

1. Arnold J. Forman, Zhebo Chen, and Thomas F. Jaramillo, "Synthesis of High Roughness Factor Transparent Conducting Oxide Thin Films" (patent application pending).

FY 2011 Publications/Presentations

1. J. Forman, Zhebo Chen, and Thomas F. Jaramillo, "Synthesis of High Roughness Factor Transparent Conducting Oxide Thin Films" (manuscript in preparation).

2. Zhebo Chen, Dustin Cummins, Benjamin N. Reinecke, Ezra Clark, Mahendra K. Sunkara, and Thomas F. Jaramillo, "MoS_2 Coated MoO_3 Nanowires: Active, Stable, and Earth-abundant Catalysts for Hydrogen Evolution in Acid" (submitted March 2011).

3. Zhebo Chen, Jakob Kibsgaard, and Thomas F. Jaramillo, "Nanostructuring MoS_2 for Photoelectrochemical Water Splitting," *Proc. SPIE*, Vol. 7770, 77700K-6 (2010).

4. Zhebo Chen, Shin-Jung Choi, Jakob Kibsgaard, and Thomas F. Jaramillo, "Nanostructured MoS_2 for Solar Hydrogen Production," *Proc. American Chemical Society*, San Francisco, CA. March 24, 2010.

5. Thomas F. Jaramillo, Zhebo Chen, Shin-Jung Choi, Jesse Benck, and Jakob Kibsgaard, Nano-architectures for 3rd generation PEC devices: A study of MoS2, fundamental investigations and applied research, DOE EERE Annual Merit Review, Crystal City, VA. May 12, 2011.

6. Zhebo Chen, Jakob Kibsgaard, Jesse Benck and Thomas F. Jaramillo, "Nanostructured MoS_2 for Solar Hydrogen Production," 2011 Spring Meeting of the Materials Research Society, San Francisco, CA. April 29, 2011.

7. Zhebo Chen, Jakob Kibsgaard, and Thomas F. Jaramillo, "Nanostructured MoS_2 for Solar Hydrogen Production," 2010 Annual Meeting of the American Institute of Chemical Engineers, Salt Lake City, UT. November 9, 2010.

8. T.F. Jaramillo, "Nano-structured materials for the synthesis of fuels from sunlight" Technical University of Denmark, Dept. of Physics, Lyngby, Denmark, August 2010.

9. Zhebo Chen, Jakob Kibsgaard, and Thomas F. Jaramillo, Nanostructuring MoS_2 for Photoelectrochemical Water Splitting, SPIE, San Diego, CA. August 4, 2010

10. Zhebo Chen, Jakob Kibsgaard, and Thomas F. Jaramillo, Nanostructured MoS_2 for Solar Hydrogen Production, 217th meeting of The Electrochemical Society, Vancouver, BC, Canada. April 25-30 (2010).

11. Zhebo Chen, Shin-Jung Choi, Jakob Kibsgaard, and Thomas F. Jaramillo, Nanostructured MoS_2 for Solar Hydrogen Production, National Meeting of the American Chemical Society, San Francisco, CA. March 24, 2010.

References

1. M.G. Walter, E.L. Warren, J.R. McKone, S.W. Boettcher, Q. Mi, E.A. Santori, N.S. Lewis, "Solar Water Splitting Cells" *Chem. Rev.* **2010**, 110, 6446–6473.

2. B.D. James, G.N. Baum, J. Perez, K.N. Baum, DTI Technologies, Inc. "Technoeconomic Analysis of Photoelectrochemical (PEC) Hydrogen Production," DOE Report (2009) Contract # GS-10F-009J.

3. F. Le Formal, M. Gratzel, and K. Sivula, "Controlling Photoactivity in Ultrathin Hematite Films for Solar Water-Splitting" *Adv. Funct. Mater.* **2010**, 20, 1099-1107.

4. O. Khaselev, J.A. Turner, "A Monolithic Photovoltaic-Photoelectrochemical Device for Hydrogen Production via Water Splitting" *Science **1998**, 28***0,*** 4***25-427.

5. H. Tributsch and J.C. Bennett, "Electrochemistry and Photoelectrochemistry of MoS_2 Layer Crystals. I" *J. Electroanal. Chem.* **1977**, 81, 97-111.

6. Our applied research on the photoelectrochemistry of MoS_2 is funded through this program; our more fundamental research on MoS_2 is currently supported by Center on Nanostructuring for Efficient Energy Conversion (CNEEC) at Stanford University, an Energy Frontier Research Center funded by the U.S. Department of Energy, Office of Science, Office of Basic Energy Sciences under Award Number DE-SC0001060.

7. J.P. Wilcoxon, P.P. Newcomer, and G.A. Samara. "Synthesis and optical properties of MoS_2 and isomorphous nanoclusters in the quantum confinement regime," *J. Appl. Phys*. **2007**, 81, 7934.

8. T.F. Jaramillo, K.P. Jørgensen, J. Bonde, J.H. Nielsen, S. Horch, I. Chorkendorff, "Identification of Active Edge Sites for Electrochemical H_2 Evolution from MoS2 Nanocatalysts," *Science* **2007,** 317, 100-103.

II.G.2 Semiconductor Materials for Photoelectrolysis

John Turner (Primary Contact), Todd Deutsch, Heli Wang, Adam Welch, Yanfa Yan, Wanjian Yin, Su-Huai Wei, Mowafak Al-Jassim
National Renewable Energy Laboratory (NREL)
1617 Cole Blvd.
Golden, CO 80401
Phone: (303) 275-4270
E-mail: John.Turner@nrel.gov

DOE Manager
HQ: Eric Miller
Phone: (202) 287-5829
E-mail: Eric.Miller@hq.doe.gov

Subcontractors:
- Stanford University, Palo Alto, CA
- University of Nevada, Las Vegas, Las Vegas, NV

Project Start Date: 2005
Project End Date: Project continuation and direction determined annually by DOE

Fiscal Year (FY) 2011 Objectives

Identify, synthesize, and characterize new semiconductor materials that have the capability of meeting the criteria for a viable photoelectrochemical (PEC) hydrogen-producing device, either as a single absorber or as part of a high-efficiency multi-junction device.

Technical Barriers

This project addresses the following technical barriers from the Production section of the Fuel Cells Technologies Program Multi-Year Research, Development and Demonstration Plan (MYP):

(Y) Materials Efficiency
(Z) Materials Durability
(AB) Bulk Materials Synthesis
(AC) Device Configuration

Technical Targets

This project is a materials discovery investigation to identify a single semiconductor material that meets the technical targets for efficiency and stability. The 2013 technical targets from the MYP PEC hydrogen production goals are as follows:

- Bandgap of 2.3 eV
- 10% conversion efficiency
- 1,000-hour lifetime

FY 2011 Accomplishments

- Improved the world-record water splitting efficiency of $GaInP_2$/GaAs tandem cells by using a more active RuO_2 counter electrode. Confirmed a maximum solar-to-hydrogen efficiency of 16.3% under real solar (outdoor) conditions, a significant improvement over the 12.4% previous record and greatly exceeding the MYP 2013 10% technical target.
- Identified potential surface nitride passivation of $GaInP_2$ by nitrogen ion bombardment and electrochemical routes. Nitrided surfaces exhibited less corrosion than untreated samples.
- Validated stability of low-cost amorphous Si/SiC hybrid photoelectrodes synthesized by our corporate partner MVSystems, Inc. The electrode was still able to generate photocurrent after 500 hours of testing at an applied current density of -1 mA/cm^2, and is half way to the MYP 2013 technical target of 1,000 hours of durability.
- Synthesized CuO, Cu_2O, and Ti alloyed Cu-Ti oxides with various structures and band gaps by reactive radio frequency (RF) magnetron sputtering. PEC characterizations of the Ti-Cu mixed oxide revealed improved performance and greater stability than Cu oxides alone.
- Characterized corrosion resistant p-$In_xGa_{1-x}N$ alloys synthesized by our collaborator at Los Alamos National Laboratory.



Introduction

Photoelectrochemistry combines a light harvesting system and a water splitting system into a single monolithic device. A semiconductor immersed in aqueous solution comprises the light-harvesting system. The catalyzed surface of the semiconductor is one part of the water splitting system, and the other part is another electrode in a separate compartment. The key is to find a semiconductor system that can efficiently and sustainably collect solar energy and direct it towards the water splitting reaction.

The goal of this work is to develop a semiconductor material set or device configuration that (i) splits water into hydrogen and oxygen spontaneously upon illumination, (ii) has a solar-to-hydrogen efficiency of at least 5% with a clear pathway to a 10% water splitting system, (iii) exhibits the possibility of 10 years stability under solar conditions, and (iv) can be adapted to volume-manufacturing techniques.

Approach

Our approach has two thrusts, i) the study of current material sets used in commercial solar cells as well as related materials, and ii) the discovery of new semiconducting materials using advanced theoretical calculations to identify promising candidates, closely coupled with synthesis and state-of-the art characterization. A major component of (i) focuses on III-V semiconductor materials that meet the efficiency target and engineering the surface to meet the durability target. Area (ii) has focused on chalcogenide and Cu-, W-, Ti-, and Bi-based multinary oxides.

Results

The $GaInP_2$/GaAs tandem cell has held the world-record efficiency (12.4%) for unbiased PEC water splitting for several years [1]. This benchmark for efficiency was established using platinum as a counter electrode anode material. We were able to improve upon this efficiency by using a counter electrode that is more active for oxygen evolution. Ruthenium dioxide (RuO_2) has a lower overpotential than platinum for the water oxidation reaction at the current densities relevant to PEC water splitting. The reduction in overpotential results in enhanced efficiencies. We electrodeposited RuO_2 from $RuCl_3$ solution on to a platinum electrode and gathered solar-to-hydrogen efficiency data under real-solar conditions at NREL's Solar Radiation Research Laboratory. Using a portable potentiostat in a two-terminal configuration we measured the current and applied circuit bias between the $GaInP_2$/GaAs working electrode and RuO_2 counter electrode. The current was due to water reduction (to hydrogen) at the photocathode and oxidation (to oxygen) at the counter electrode. The efficiency was calculated from the photocurrent density, circuit bias, and corresponding real-time measurement of solar irradiance. Two wafers were synthesized by metal organic chemical vapor deposition at different growth temperatures and each was subdivided into about twelve electrodes. The averaged two-electrode photocurrent-voltage measurements were used to calculate ensemble efficiencies for each wafer (Figure 1). The champion electrode, from the wafer that was grown at a lower temperature, had a peak solar-to-hydrogen efficiency of 16.3%. This efficiency greatly exceeds the MYP 2013 technical target of 10% and demonstrates very high solar-to-hydrogen efficiencies are possible through PEC conversion.

Although the $GaInP_2$ system is capable of high-efficiency conversion, it is prone to corrosion under operating conditions and does not meet the MYP technical target for durability (1,000 hours). We have previously observed that incorporating nitride into III-V semiconductor epilayers can provide enhanced stability [2] to water splitting photocathodes. However, this nitride incorporation through the bulk of the light absorber causes a reduction in conversion efficiency [3]. We hypothesize that surface nitridation might protect the interface with the electrolyte while not compromising the material's

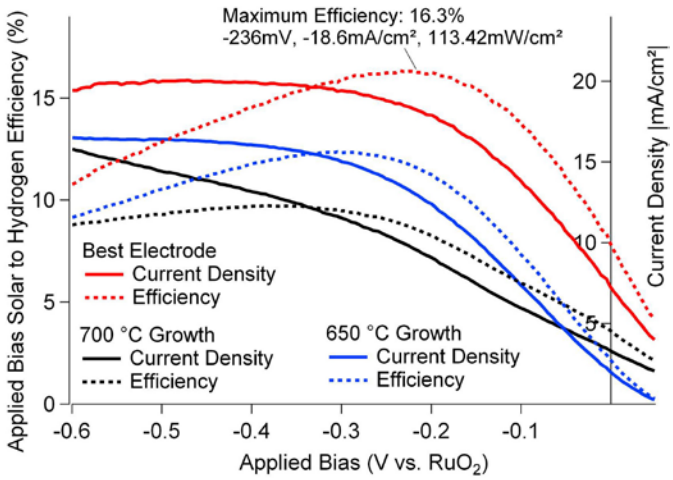


FIGURE 1. Two-electrode outdoor photocurrent-voltage testing of p-$GaInP_2$/GaAs tandem cells coupled with a RuO_2 counter electrode. Dashed lines are calculated efficiencies as a function of circuit bias. Data presented are the average of twelve electrodes from each wafer and the champion electrode plotted independently. The champion electrode was from the wafer grown at a lower temperature. The electrolyte used for testing was 3M H_2SO_4 with the fluorosurfactant Zonyl FSN-100.

high-efficiency bulk absorption properties. We achieved promising preliminary results from surface nitridation of $GaInP_2$ by two distinct routes; electrochemical and ion bombardment. The semiconductor surface appeared to be protected when $(NH_4)_2SO_4$ was used as the electrolyte for a 24-hour durability analysis. Afterwards, X-ray photoelectron spectroscopy (XPS) detected ammonia (NH_3) on the surface. Depth profiles, made by alternating sputtering with XPS analysis, found the control (unprotected) sample was gallium deficient and indium rich while the sample tested in $(NH_4)_2SO_4$ had a composition identical to as-grown material. Bombarding $GaInP_2$ surfaces with low-energy N_2^+ ions also appeared to provide some protection from corrosion. We performed ion surface treatments for 20, 45, and 60 seconds and all prevented a decline in photocurrent after operation for 24-hours in pH 0 sulfuric acid where untreated samples had a notable loss in performance. We also analyzed the durability solutions for trace levels of semiconductor components by inductively coupled plasma mass spectrometry (ICP-MS). In two of the three electrodes tested, the 45-second treatment was effective in reducing the amount of corrosion detected by ICP-MS (Figure 2). We are continuing to investigate surface nitridation as a potential route to achieve both the efficiency and durability targets in the MYP.

We continued to work with our private industry collaborator, MVSystems, Inc. to develop a potentially low-cost, high-volume water splitting material system with good durability. These amorphous (a-Si/SiC) semiconductors are synthesized by plasma enhanced chemical vapor deposition on transparent conductive substrates. The p-SiC is the capping layer and forms a PEC contact with the electrolyte.

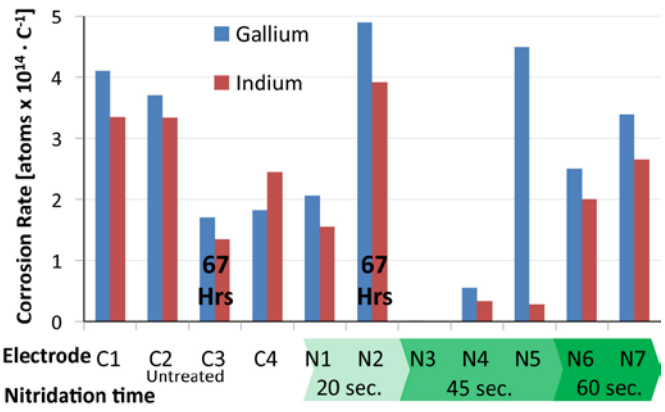


FIGURE 2. ICP-MS detected gallium and indium from control and ion bombardment nitrided p-GaInP$_2$ electrode corrosion solutions. The durability testing consisted of galvanostatic testing at -10 mA/cm^2 in 0.5M H_2SO_4 under AM1.5G illumination for 24 hours (except in the two noted durations of 67 hours). The analytes were detected in parts per million (mass) units and converted to atoms/Coulomb to normalize for variation in electrode surface area, charge passed, and solution volume.

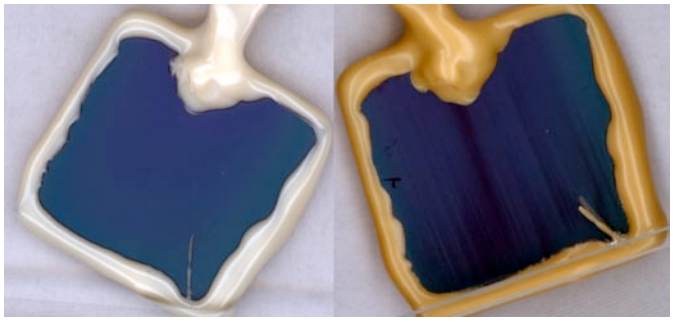


FIGURE 3. Photographs of an a-Si/a-SiC hybrid photoelectrode before (left) and after (right) 310 hours of durability testing showing a relatively unaltered surface. The semiconductor is about 4 cm^2 and encased in insulating epoxy.

It has a wider band gap and better stability than amorphous Si. There are two amorphous p-i-n buried photovoltaic (PV) junctions that provide the necessary potential difference needed for water electrolysis. The PV/PEC layers, known together as a hybrid photoelectrode, are stacked vertically in an integrated monolithic device. This device configuration is able to split water at 1.6% efficiency without an external bias. Recently, we were able to demonstrate this system is capable of extended durability. In one test we applied -1 mA/cm^2 in pH 2 buffer under AM1.5G (from a tungsten lamp) for 310 hours and the surface appeared almost completely unaltered by the testing, except for some streaking likely caused by hydrogen bubble evolution (Figure 3). The electrode did suffer a moderate (~30%) reduction in photocurrent magnitude after 310 hours of testing, but there was no dark current under high reverse bias, a common feature of damaged electrodes. We also performed a 500-hour test on a different electrode under the same conditions described above. After 500-hours of durability analysis, three-electrode current-potential curves exhibited both a decreased magnitude of photocurrent and dark current onset at a low potential. The electrode surface also appeared degraded afterwards. Even though the durability electrodes suffered a performance loss, the results demonstrate that the 2013 MYP technical target of 1,000-hours of operation could be achieved with this material. However, the testing conditions are relatively mild, compared to what a real-world electrode might see under operation. The goal for this material is 5% solar-to-hydrogen efficiency, which correlates to -4 mA/cm^2, a current density four times higher than these electrodes were subjected to.

We also synthesized and characterized several oxide and chalcopyrite semiconductors that theoretical calculations had identified as good candidates for photoelectrolysis. We synthesized CuO, Cu_2O, and Ti alloyed Cu-Ti and found that the band gaps of CuO and Cu_2O could be engineered by incorporating Ti. We found that Ti incorporation improved the film quality and as a result, Ti incorporated CuO films exhibited much lower dark current than the pure CuO, indicating enhanced stability. Despite band gaps in the visible portion of the electromagnetic spectrum, the overall magnitude of photocurrent for these films is well below what is necessary to be considered viable for solar photoconversion.

We also synthesized $BiVO_4$ thin films by co-evaporation of Bi_2O_3 and V_2O_5 and evaluated their PEC performance. We observed that a Bi:V ratio of roughly 1:1 leads to n-type conductivity behavior and very low dark current. When the Bi:V ratio was increased to 1.1:1 the result was a compensated film. A compensated semiconductor exhibits both n-type and p-type behavior, depending on the bias. It is known that cation vacancies can form easily in $BiVO_4$ and the act as acceptors. It is possible that under certain vapor pressures, Bi or V vacancies may form and lead to p-type conductivity. This effect might be exploited for developing a solid-state, oxide p/n homojunction photovoltaic cell.

Ternary I-III-VI_2 chalcopyrite materials have drawn great interest in recent years due to their potential application for solar cells. In general, I-III-VI_2 chalcopyrite materials have a variety of direct band gaps and have excellent optical absorption coefficients, good carrier transport properties, and stability. We synthesized and characterized chalcopyrite $CuAlTe_2$ thin films by both co-evaporation and sequential deposition methods. Several films were synthesized that had ideal band gaps for photoelectrolysis, in the range of 1.64 - 2.25 eV. Energy dispersive X-ray spectroscopy detected oxygen in all $CuAlTe_2$ samples. The oxygen contamination during the evaporation seems to deteriorate the film quality and lead to serious carrier recombination resulting in poor photoconversion efficiencies. In addition to low photocurrents, the $CuAlTe_2$ films were unstable during PEC characterizations and are, therefore, not viable for photoelectrolysis using these synthesis conditions.

Pure nitride semiconductors (instead of mixed group V) are also an area of interest as they have high stability and potentially high efficiency. We characterized p-doped $In_xGa_{1-x}N$ synthesized by our collaborator at Los Alamos National Laboratory. The p-doping allows the semiconductor to operate as a photocathode, a generally more stable operating configuration that pushes highly corrosive, oxidizing holes towards the bulk of the material and away from the interface. The photocurrents achieved by these materials were very low due to growth on an insulating sapphire substrate. We are currently characterizing a set of $In_xGa_{1-x}N$ that was synthesized on conductive substrates and are evaluating the stability under current densities in the 10 mA/cm^2 range, a magnitude equivalent to what a deployed device would see.

Conclusions

- p-$GaInP_2$/GaAs is capable of over 16% solar-to-hydrogen conversion efficiency and could meet the MYP efficiency and durability technical targets with an appropriate corrosion mitigation treatment, even if the treatment results in a loss of efficiency.
- Surface nitridation of $GaInP_2$ has demonstrated the ability to offer protection to the semiconductor surface after 24-hours of simulated operational conditions.
- Thin film a-Si-based carbides have the potential to be inexpensive water splitting electrodes and have demonstrated good durability over several hundred hours of low current density water splitting.
- The Cu-Ti alloyed oxides that we synthesized have variable band gaps, but have poor photoconversion properties and inadequate stability.

Future Direction

- We plan to continue to investigate stabilization of the $GaInP_2$ interface through nitridation. We will work in collaboration with theory and advanced characterization groups to identify the corrosion mechanism and develop a passivation strategy.
- Because of their stability, we plan to investigate other III-V nitride semiconductor configurations and evaluate efficiencies.
- We plan to continue to work with MVSystems, Inc. on improving efficiency and stability of a-Si/a-SiC hybrid photoelectrodes through targeted surface modification techniques.
- We plan to synthesize and photoelectrochemically characterize new oxide and chalcopyrite semiconductors and evaluate their potential for water splitting photoelectrodes.

FY 2011 Publications/Presentations

Publications

1. W.-J. Yin, H.W. Tang, S.-H. Wei, J. Turner, M.M. Al-Jassim, Yanfa Yan, "Band structure engineering of semiconductors for enhanced PEC water splitting" *Phys. Rev. B* ***82****, 045106 (2010)*.

2. W.-J. Yin, S.-H. Wei, M.M. Al-Jassim, J. Turner, and Yanfa Yan, "Doping properties of monoclinic $BiVO_4$ studied by the first-principle density-functional theory" *Phys. Rev. B* ***83****, 155102 (2010)*.

3. L. Chen, S. Shet, H.W. Tang, H.L. Wang, T. Deutsch, Yanfa Yan, J. Turner, M. Al-Jassim, "Electrochemical deposition of copper oxide nanowires for photoelectrochemical applications" *J. Mater. Chem.* **20**, 6962 (2010).

4. L. Chen, S. Shet, H. Tang, K.-S. Ahn, H. Wang, Yanfa Yan, J. Turner, and M. Al-Jassim, "Amorphous copper tungsten oxide with tunable band gaps" *J. Appl. Phys.* **108**, 043502 (2010).

5. S. Shet, K.-S. Ahn, H. Wang, R. Nuggehalli, Y. Yan, J. Turner, and M. Al-Jassim, "Effect of substrate temperature on the photoelectrochemical responses of Ga and N co-doped ZnO films" *J. Mater. Sci.* **45**, 5218-5222 (2010).

6. M. Huda, A. Walsh, Yanfa Yan, S.-H. Wei, and M.M. Al-Jassim, "Electronic, structural, and magnetic effects of 3d transition metals in hematite," *J. App. Phys.* **107**, 123712 (2010).

7. W.-J. Yin, S. Chen, J.-H. Yang, X.-G. Gong, Yanfa Yan, S.-H. Wei, "Effective band gap narrowing of anatase TiO_2 by strain along a soft crystal direction" *Appl. Phys. Lett.* **96**, 221901 (2010).

8. Heli Wang and John A. Turner, "Characterization of hematite thin films for photoelectrochemical water splitting in a dual photoelectrode device" *J. Electrochem. Soc.* **157**, F173 (2010).

Presentations

1. "Photoelectrochemical Production of Hydrogen: Issues and Possibilities", SPIE – Solar Hydrogen and Nanotechnology V, San Diego, CA, August 5, 2010. J. Turner, *Invited.*

2. "Material issues for photoelectrochemical water splitting", ORCAS 2010, International Conference on Energy Conversion, University of Washington, Friday Harbor, WA, September 22, 2010. J. Turner, *Invited.*

3. "Material Issues for Photoelectrochemical Water Splitting", Lawrence Livermore National Lab Colloquium, Livermore, CA, September 30, 2010. J. Turner, *Invited.*

4. "Semiconducting Materials for Photoelectrochemical Water Splitting", at the Solar Fuels: Catalysis and Photoconversion meeting, University of North Carolina at Chapel Hill, January 13, 2011. J. Turner, *Invited.*

5. "Materials Issues for Photoelectrochemical Water Splitting", at the official opening of the Solar Fuels Laboratory, Nanyang Technological University, Singapore, February 8, 2011. J. Turner, *Invited.*

6. "Semiconducting Materials for Photoelectrochemical Water Splitting", Third Annual Workshop on Electrochemistry at the Center for Electrochemistry at the University of Texas at Austin, February 20, 2011. J. Turner, *Invited.*

7. "Impact of oxygen evolution catalysts on the efficiency of photoelectrochemical water splitting", session: Chemical Carbon Mitigation: A Physiochemical Approach, American Chemical Society Meeting, March 30, 2011, Jeff Lou presenting, *Invited.*

8. "Semiconductor Photoelectrodes for Direct Water Splitting" Pacifichem 2010 Congress, Honolulu, HI. December 15–20, 2010. T. Deutsch, *Contributed.*

9. "Bandgap engineering of metal oxides for PEC water splitting" SPIE's Solar Hydrogen and Nanotechnology V, San Diego, CA, August 1–5, 2010. Y. Yan, *Invited.*

10. "The durability of p-$GaInP_2$ for photoelectrochemical water splitting" SPIE's Solar Hydrogen and Nanotechnology V, San Diego, CA, August 1–5, 2010. H. Wang, *Invited.*

11. "Durability of p-$GaInP_2$ for photoelectrochemical water splitting" Pacifichem 2010 Congress, Honolulu, HI. December 15–20, 2010. H. Wang, *Contributed.*

12. "Direct Water Splitting Using Visible Light" GE Global Research Solar Fuels Symposium, Niskayuna, New York. November 1, 2010. T. Deutsch, *Invited.*

13. "Passivation of III-V Photoelectrochemical Water Splitting Electrodes via Surface Nitridation" Gordon Research Conference, Renewable Energy: Solar Fuels, Ventura, California. January 16–21, 2011. T. Deutsch, *Poster.*

References

1. O. Khaselev and J.A. Turner, *Science* **280**, 425 (1998).

2. T.G. Deutsch, K.A. Koval, J.A. Turner, *J. Phys. Chem. B* **110**, 25297 (2006).

3. T.G. Deutsch, J. Head, J.A. Turner, *J. Electrochem. Soc.* **155**(9), B903 (2008).

II.G.3 Characterization and Optimization of Photoelectrode Surfaces for Solar-to-Chemical Fuel Conversion

Tadashi Ogitsu (Primary Contact), Brandon Wood
Lawrence Livermore National Laboratory (LLNL)
7000 East Ave., L-413
Livermore, CA 94550
Phone: (925) 422-8511
E-mail: ogitsu@llnl.gov

DOE Manager
HQ: Eric Miller
Phone: (202) 586-5000
E-mail: Eric.Miller@ee.doe.gov

Project Start Date: March 1, 2010
Project End Date: Project continuation and direction determined annually by DOE

Fiscal Year (FY) 2011 Objectives

- Develop theoretical tool chest for modeling photoelectrochemical (PEC) systems, including experimental validation using model III-V systems.
- Compile publications database of research on relevant photoelectrode materials.
- Uncover key mechanisms of surface corrosion of semiconductor photoelectrodes.
- Understand dynamics of water dissociation and hydrogen evolution at the water-photoelectrode interface.
- Evaluate electronic properties of the surface and water-electrode interface.
- Elucidate relationship between corrosion and catalysis.
- Provide simulated X-ray spectra to the University of Nevada, Las Vegas (UNLV) for interpretation of experimental results and validation of theoretical models.
- Share research insights with the PEC Working Group members

Technical Barriers

This project addresses the following technical barriers from the Hydrogen Production section (3.1) of the Fuel Cell Technologies Program Multi-Year Research, Development and Demonstration Plan:

(Z) Materials Durability

(Y) Materials Efficiency

Technical Targets

This project is conducting fundamental theoretical studies of mechanisms of corrosion and catalysis in III-V semiconductor-based photoelectrode materials for PEC hydrogen production. Insights gained from these studies will be applied toward the optimization and design of semiconductor materials that meet the following DOE 2013 PEC hydrogen production targets:

- Usable semiconductor bandgap: 1.8-2.3 eV
- Chemical conversion process efficiency: 10%
- Plant solar-to-hydrogen efficiency: 8%
- Plant durability: 1,000 hrs.

FY 2011 Accomplishments

- Compiled, reviewed, and shared available information on III-V electrode materials (ongoing).
- Performed quantum molecular dynamics of water-electrode interfaces:
  - Evaluated importance of surface oxygen in determining reactivity. In FY 2010, we discovered that bonding topology of oxygen at InP(001) surface dictates the catalytic activity for water splitting. In FY 2011, we expanded this study to include different III-V (GaP), and on wider variety of surface morphology. Quantitative reaction energetics were provided.
  - Established validity of local topological model and used it to extract model surfaces for further study (FY 2011).
- Group discussion of results led to formulation of three possible corrosion mechanisms (FY 2011).
- Recruited four external collaborators to develop theory/computational tool chest for PEC hydrogen research.
- Began joint theoretical/experimental study on III-V electrode surface (continue through FY11).



Introduction

Development of efficient processes for the carbon-free production of hydrogen is key to sustainable realization of a future hydrogen economy. One particularly promising approach is to use sunlight to catalyze direct evolution of hydrogen from water in a PEC cell. Semiconductor-based PEC devices are particularly attractive, thanks to a relatively simple device design and a wealth of data available for engineering efficient photon harvesting [1]. Results have demonstrated that one can achieve solar-to-fuel conversion efficiency in excess of the 2013 DOE targets (>12% using a tandem GaAs/$GaInP_2$ cell); however, this has come at the expense of short device lifetime due to fast degradation

of the electrode [2]. Further progress has been hindered by a poor understanding of the fundamental chemical processes operating at the electrode-water interface. Our research addresses this need from a theoretical perspective, leveraging realistic *ab-initio* simulations to determine the key mechanisms governing corrosion and catalysis at the water-semiconductor interface.

Approach

Further progress in semiconductor-based PEC photoelectrodes requires in-depth understanding of the complex relationship between surface stability and catalytic activity. This in turn relies on knowledge of the fundamental nature of the electrode-water interface, and of the chemical pathways explored during surface-active hydrogen evolution. As such, we are carrying out finite-temperature *ab-initio* molecular dynamics simulations and energetics calculations based on density-functional theory to understand the chemical, structural, and electronic properties of water/electrode interfaces under equilibrium conditions, as well as to understand the competing chemical reaction pathways visited during photocatalysis. Our approach uses (001) surfaces of InP, GaP and $GaInP_2$, which have known water-splitting activity, as model semiconductor electrodes. We are investigating on effect of the foreign chemical species on the stability and reactivity of the electrode surfaces, as suggested by our collaborators in J. Turner's group at the National Renewable Energy Laboratory (NREL) [3] and reports in the literature that surface oxygen may play a key role in motivating both the surface photocorrosion and the catalytic water splitting reaction [4,5]. Accordingly, we are evaluating the stability, structure and reactivity of the III-V(001)/water interfaces in the presence of surface oxygen, hydroxyl, and nitrogen, in order to correlate the results to experimentally observed surface compositions and morphologies. We also provide *ab-initio* derived X-ray spectroscopic data to enable direct comparison with experimental results from Prof. Heske's group at UNLV. This information is intended to suggest a strategy for device improvement.

Results

Over 700 papers related to PEC hydrogen research have been collected, indexed, and stored. Those deemed especially relevant to III-V semiconductor-based approaches have been summarized and shared with members of the III-V Surface Validation Team (LLNL/NREL/UNLV) of the DOE Photoelectrochemical Hydrogen Production Working Group using a limited-access community web forum and traditional email communication. Particularly detailed reviews were completed on $GaInP_2$, In_2O_3, and the growth interface between the two. We have discovered literature that points to competition between ordered and disordered surface phases, which can rationalize inconsistencies in device performance observed in NREL experiments. We have also reviewed literature suggesting the relevance of surface oxide growth for realizing both device performance and corrosion resistance. However, we also found reports that thin native oxide formation on III-V semiconductors can give rise to undesirable electrical properties if the oxide/III-V interface is rough [6]. Based on this review, it was suggested that careful, controlled growth of a high quality oxide layer on III-V semiconductor might improve the durability without compromising the hydrogen production efficiency.

In FY 2010, we studied (meta)stable surface structures of oxide and hydroxide on InP(001). We found that there are two categories of oxygen bonding configurations, In-O-In and In-O-P, consistent with experimental observations [7]. We then studied the reactivity of a water molecule on these surfaces and found that spontaneous dissociative absorption is observed only at the In-O-In site. In FY 2011, we significantly expanded this study in order to have a more complete understanding, accounting for a wider variety of possible surface structures and looking at other III-V semiconductors, including GaP. Despite minor differences, we were able to definitively conclude that the strong correlation between the chemical activity and the local bonding topology is universal, and that III-O-III is chemically active against H_2O absorption, while III-O-V is not (Figures 1 and 2).

When immersed in electrolyte, the electrode surface adopts a very complex morphology containing combinations of surface oxide and hydroxide. As such, efficient computational modeling using *ab-initio* techniques becomes very challenging due to exponential growth of the number of possible configurations. To address this issue, we have employed the Cluster Expansion method [8], in which the surface adsorption energetics is modeled by an Ising-type Hamiltonian, with interaction parameters fitted to total energies obtained using density functional theory. Using this method, we calculated the total energies of hydroxylated InP(001) surface as a function of OH coverage. We found that the ground-state energy varies little over a wide range of OH coverage, meaning varying concentrations of surface OH can be expected under realistic operating conditions (Figure 3). In contrast, the oxidized surface carries significant coverage dependence.

In addition, several *ab-initio* molecular dynamics simulations of III-V/water interfaces have been performed during FY 2010/FY 2011. These have led to the following findings: (1) On oxidized or hydroxylated cation (III group)-rich (001) surfaces, the hydrogen bonding network formed by the electrolyte in contact with surface O or OH is strengthened and becomes considerably less dynamic compared to the same network in bulk water; (2) Water molecules nearby oxygen atoms in a In-O-In bonding configuration show a high probability of dissociative adsorption, whereas the reactivity is negligible near oxygen sites in a In-O-P bonding topology, confirming our previous findings; and (3) Dissociative adsorption of H_2O is accompanied by collective motion of surrounding water molecules, which acquire enhanced hydrogen-bond strength.

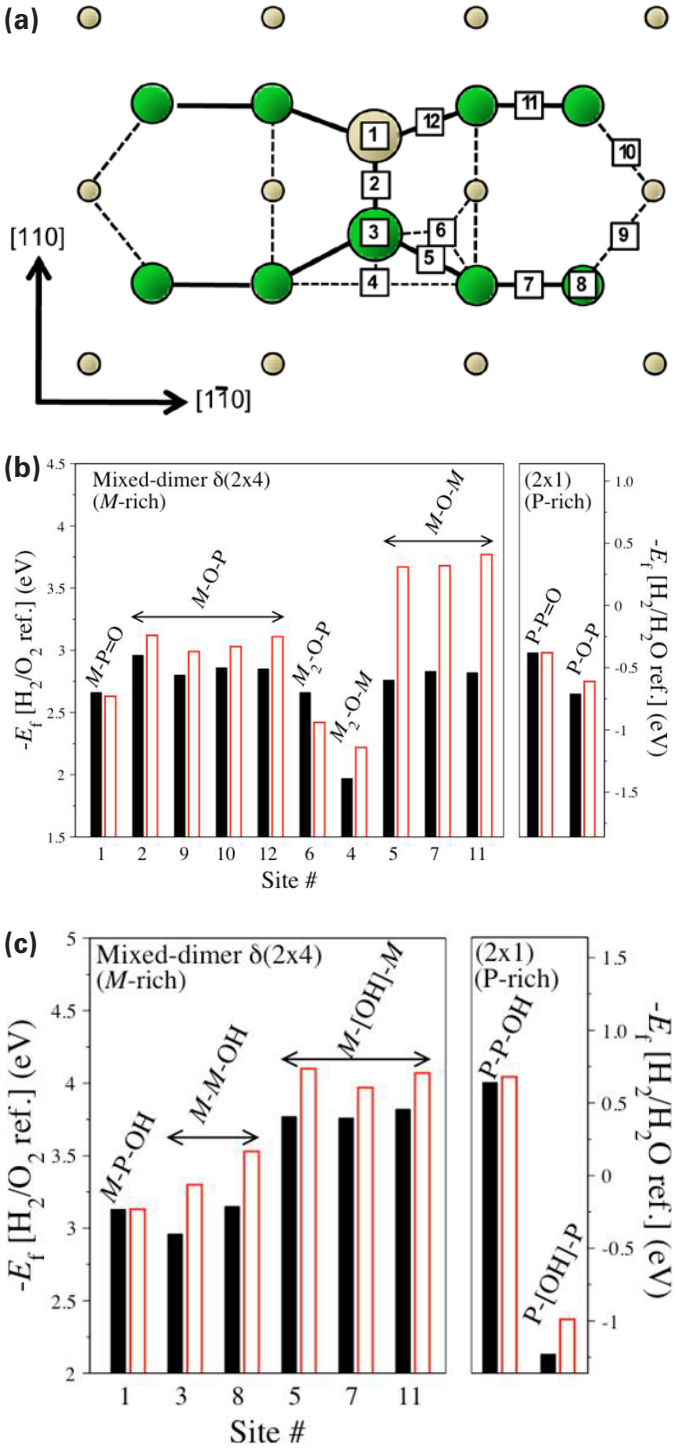


FIGURE 1. Oxygen and hydroxyl adsorption energies on δ-(4x2) type InP and GaP (001) surfaces. a) Schematic diagram of δ-(4x2) reconstructed surface. Green spheres correspond to cation atoms (In or Ga), and grey spheres correspond to phosphorus atoms. b) Oxygen adsorption energies and c) hydroxyl adsorption energies for the sites defined in a). In b) and c), filled bars are for InP and open bars are for GaP.

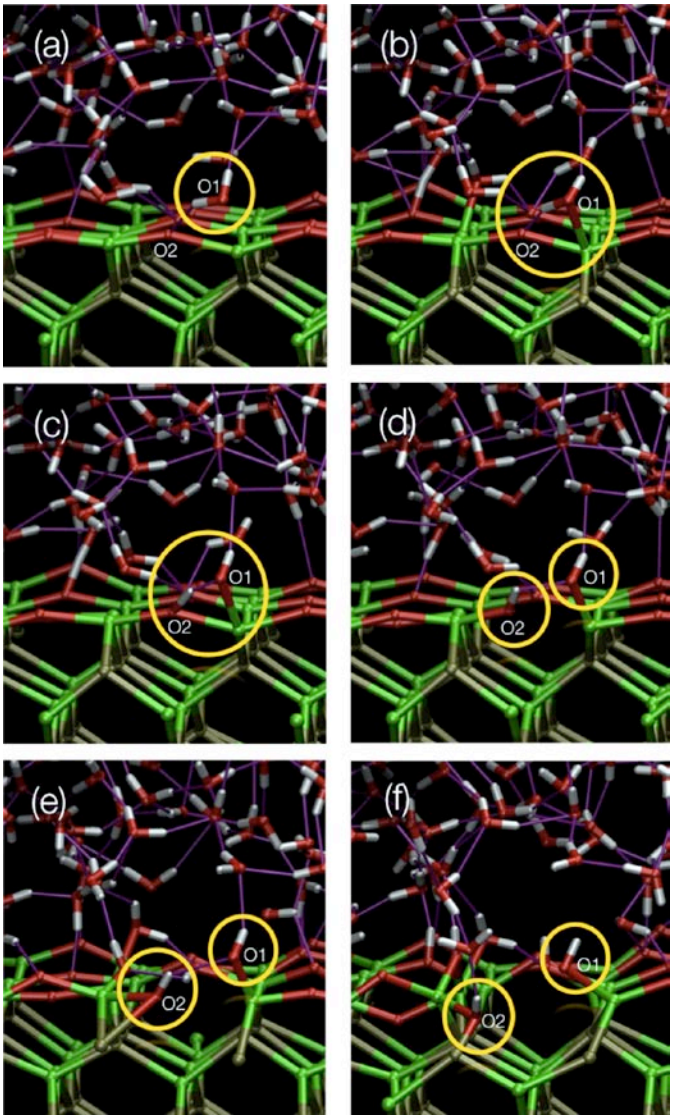


FIGURE 2. Snapshots of dissociative adsorption of a water molecule observed during our *ab-initio* dynamics simulation of the water-InP(001) interface. The yellow circles highlight the water molecule of interest (O1) and the oxygen atom that induces the dissociative adsorption (O2). (a) The water molecule (O1) is pulled toward an oxygen bound to two In atoms (O2). (b) O1 is bound to an In atom, with a hydrogen bond between its attached proton and O2. (c) The proton is transferred from O1 to O2. (d) One of the In-O bonds of O2 is breaks. (e), (f) Two OH species are formed.

At the III-V Surface Validation Team meetings and teleconferences, we have discussed three possible corrosion mechanisms based on combined results from our theoretical study, available information in literature, and experiments performed by other members of the Team. (1) The presence of hole-trap states introduced by defects and impurities are a known cause of semiconductor device degradation. We found two possible scenarios that could contribute to hole trapping in our III-V models: first, formation of specific atomic configurations that lead to the spatially and energetically localized surface states near the Fermi level, which we found could be induced either by chemically or mechanically; and second, an accumulation of anions at

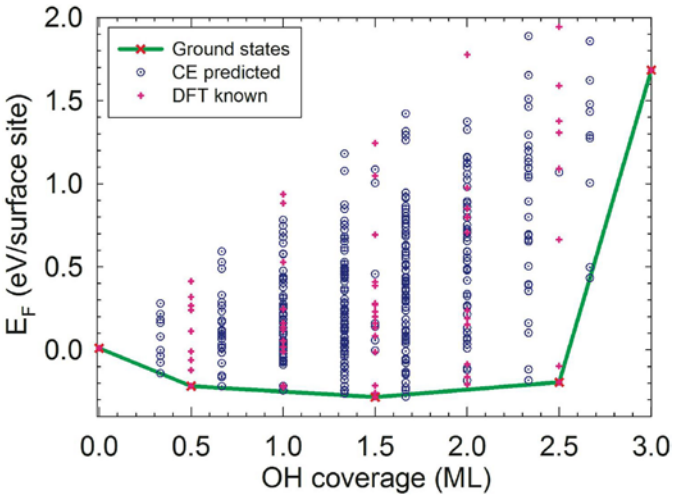


FIGURE 3. The OH adsorption energies as a function of OH concentration calculated by the Cluster Expansion (CE) method and Density Functional Theory (DFT).

the oxide/III-V interface, which is known to take place during natural oxide growth of III-V semiconductors [7]. (2) The formation of locally anodic regions can cause dissolution within the cathode due to loss of cathodic protection from a short-circuit current. Such regions can be formed by intrinsic inhomogeneity in the composition of the cathode material itself, or else by concentration gradients of adsorbed chemical species, such as OH. The former could be particularly relevant for $GaInP_2$ since this material is known to exhibit incomplete ordering, with ordered and disordered regions displaying distinct electronic properties (e.g., different bandgaps). (3) Undercoordinated cation atoms, which are often observed in our *ab-initio* molecular dynamics simulations as a consequence of local finite-temperature fluctuations in surface composition, can facilitate rapid direct dissolution of surface metal atoms.

In order to formulate an effective corrosion mitigation strategy, it is necessary to assess the likelihood of each of the aforementioned proposed corrosion mechanisms with appropriate experimental methods. Accordingly, the III-V Surface Validation Team plans to perform in situ X-ray spectroscopy studies of the photoelectrode-electrolyte system under illumination. Our contribution to this effort will be provide *ab-initio* derived theoretical spectra for interpretation of experimental results. In preparation, we have performed an initial assessment on accuracy of theoretical X-ray emission spectra using three reference bulk systems: InP, GaP and $GaInP_2$. We have confirmed that the calculated spectra show satisfactory agreement with the experimental data obtained by our III-V Surface Validation Team collaborators at UNLV, (Figure 4).

In order to develop a complete theoretical/computational tool chest for PEC hydrogen production research, we have established collaborations with the following four external researchers with specialized expertise: (1) Dr. David Prendergast at The Molecular Foundry (TMF), LBNL–First-principles X-ray Absorption/Emission Spectrum calculations of water-electrode interfaces (with whom we have a peer-reviewed TMF user project); (2) Prof. Chris Wolverton, Northwestern University–Cluster Expansion [8] for realistic modeling of III-V surfaces; (3) Dr. Minoru Otani, National Institute of Advanced Industrial Science and Technology, Japan–First-principles Effective Screening Medium method [9] to simulate interfaces under a bias voltage (part of the Japan-U.S. Ministry of Economy, Trade and Industry-DOE Clean Energy Technology Action Plan [10]). (4) Dr. Yoshitaka Tateyama, National Institute for Materials Science, Japan–First-principles methodology for simulation of redox potentials for charge transfer reactions at liquid/solid interfaces [11]. All collaborators have external research funding and do not require any additional cost to DOE.

Conclusions and Future Directions

- We have conducted extensive first-principles studies on native oxide formation on III-V (001) surfaces (III: In, Ga; V: P), and identified similarities and differences in the local bonding arrangement around the oxygen atom.
- Gas-phase water molecule adsorption simulations as well as *ab-initio* molecular dynamics simulations of water/III-V interfaces consistently show that III-O-III type local bonding arrangement induces dissociative adsorption of bound water, while III-O-V does not.
- We will investigate the link between the local chemical activity and the known macroscopic chemical behaviors, namely, corrosion and hydrogen evolution. The key technique will be to compare simulated spectral data to experiments by UNLV/NREL, with the specific goal of validating our proposed corrosion mechanisms. We will also work to ascertain the effect of surface nitridation on the relevant chemical reactions, motivated by its proven corrosion protection in recent experimental studies by NREL.
- We will design additional theoretical studies to refine our models of interfacial charge transfer reactions, leveraging the expertise of our separately-funded external collaborators. This will focus on the impact of photo-illumination, since the studies conducted to date considered only the properties of the interface precursory to illumination.

Special Recognitions & Awards

1. Best Poster Award, "Materials for Energy Applications: Experiment, Modeling, and Simulation" Conference, Los Angeles, CA, (2011).

2. Best Poster Award, LLNL Postdoctoral Poster Symposium (2010).

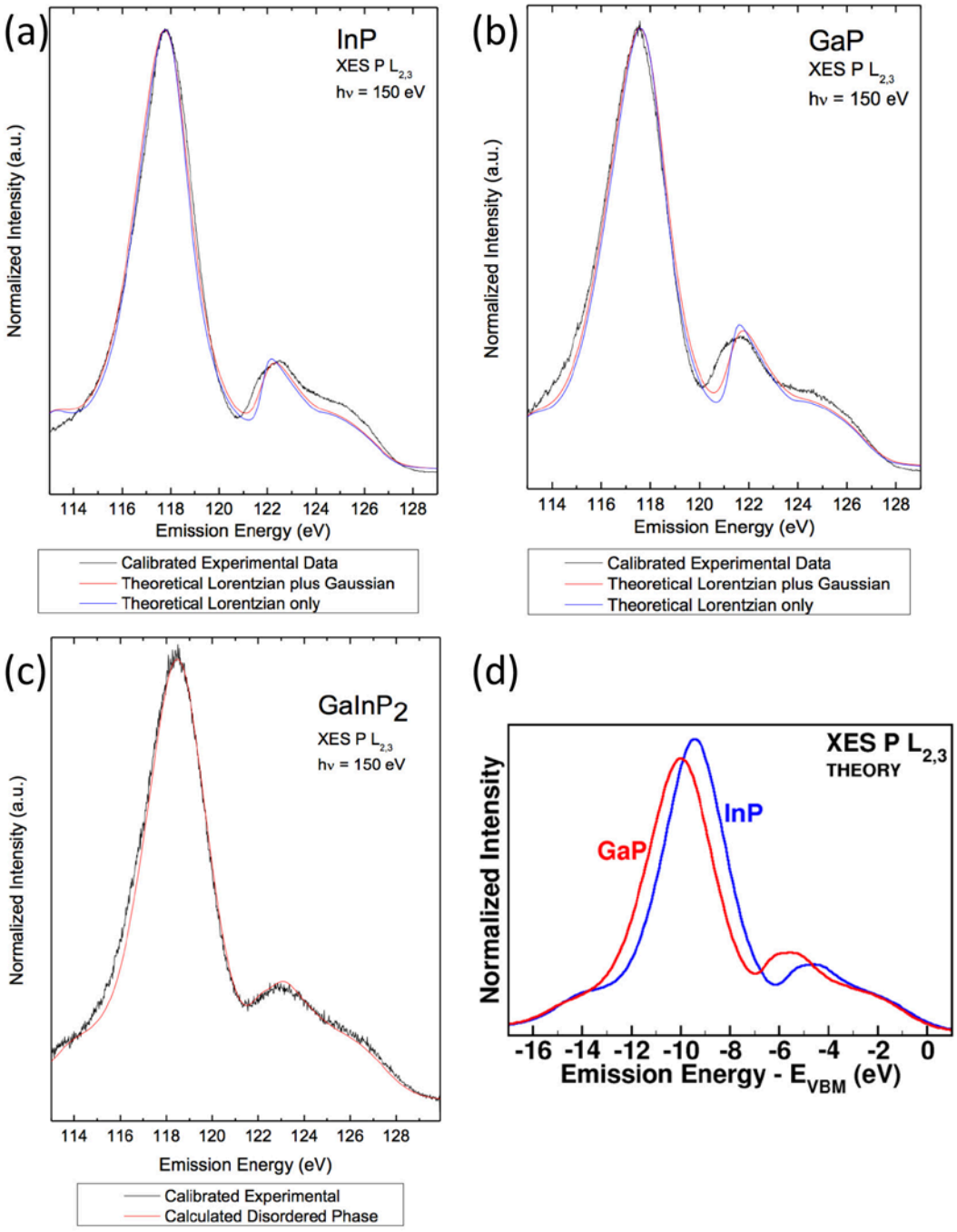


FIGURE 4. Calculated and measured phosphorus $L_{2,3}$ edge X-ray emission spectroscopy (XES) of bulk (a) InP, (b) GaP, and (c) $GaInP_2$. The experimental data is from Prof. Heske, UNLV. (d) The XES spectra of InP and GaP show clear differences. This indicates that a phase segregation of $GaInP_2$ into GaP and InP is detectable using XES measurements.

FY 2011 Publications/Presentations

Publications

1. B.C. Wood, T. Ogitsu, and E. Schwegler, "Ab-initio modeling of water-semiconductor interfaces for photocatalytic water splitting: The role of surface oxygen and hydroxyl," *Journal of Photonics for Energy* (in press).

2. B.C. Wood, T. Ogitsu, and E. Schwegler, "Ab-initio modeling of water-semiconductor interfaces for direct solar-to-chemical energy conversion," *Solar Hydrogen and Nanotechnology V, SPIE Proceedings* **7770**, 77700E (2010).

3. B.C. Wood, T. Ogitsu, and E. Schwegler, "Characterization and optimization of photoelectrode surfaces for solar-to-chemical fuel conversion," *Proceedings of the 2011 DOE Hydrogen Program Annual Merit Review* (2011).

Presentations

1. "Progress in *ab-initio* modeling of III-V semiconductor-water interfaces for photoelectrochemical hydrogen production," Hu'a Iki DOE Photoelectrochemical-IEA/HIA Joint Meeting, Honolulu, HI, December 2010.

2. "*Ab-initio* modeling of water-semiconductor interfaces for photoelectrochemical hydrogen production," AIST, Japan, November 2010.

3. "A first-principles investigation of III-V semiconductor-water interfaces for solar hydrogen production," 2011 Materials Research Society Spring Meeting, San Francisco, CA, April 2011.

4. "A first-principles investigation of III-V semiconductor-water interfaces for solar hydrogen production," 2011 American Physical Society March Meeting, Dallas, TX, March 2011.

5. "Structure and reactivity of III-V semiconductors for photoelectrochemical hydrogen production," 241st American Chemical Society National Meeting, Anaheim, CA, March 2011.

6. "Structure and reactivity of III-V electrode materials for photoelectrochemical H_2 production," 2011 Materials for Energy Applications: Experiment, Modeling, and Simulations, Los Angeles, CA, April 2011.

7. "Characterization and optimization of photoelectrode surfaces for solar-to-chemical fuel conversion," 2011 DOE Hydrogen Program Annual Merit Review, Washington, D.C., May 2011.

References

1. A. Fujishima and K. Honda, *Nature* **238**, 37 (1972).

2. O. Khaselev and J.A. Turner, *Science* **280**, 425 (1998).

3. T.G. Deutsch, C.A. Koval, and J.A. Turner, *J. Phys. Chem. B* **110**, 25297 (2006).

4. A. Heller, *Science* **223**, 1141 (1984).

5. J. Vigneron, M. Herlem, E.M. Khoumri, and A. Etcheberry, *Appl. Surf. Sci.* **201**, 51 (2002).

6. M. Milojevic, C.L. Hinkle, E.M. Vogel, R.M. Wallace, In "Fundamentals of III-V Semiconductor MOSFETs", Chapter VI "Interfacial Chemistry of Oxides on III-V Compound Semiconductors", Springer US (2010).

7. G. Chen, S.B. Visbeck, D.C. Law, and R.F. Hicks, *J. Appl. Phys.* **91**, 9362 (2002).

8. C. Wolverton and A. Zunger, *Phys. Rev. Lett.* **81**, 606 (1998).

9. M. Otani et al. *Phys. Chem. Chem. Phys.* **10**, 3609 (2008).

10. http://www.meti.go.jp/english/policy/energy_environment/global_warming/ e20091113a02.html.

11. Y. Tateyama, J. Blumberger, M. Sprik, and I. Tavernelli, *J. Chem. Phys.* **122**, 234505 (2005).

II.G.4 Characterization of Materials for Photoelectrochemical (PEC) Hydrogen Production

Clemens Heske
Department of Chemistry, University of Nevada,
Las Vegas (UNLV)
4505 S. Maryland Parkway
Las Vegas, NV 89154-4003
Phone: (702) 895-2694
E-mail: heske@unlv.nevada.edu

DOE Manager
HQ: Eric Miller
Phone: (202) 287-5829
E-mail: Eric.Miller@hq.doe.gov

Contract Number: NFH-8-88502-01 under prime contract DE-AC36-99GO10337

Project Start Date: May 6, 2008
Project End Date: September 30, 2011

Fiscal Year (FY) 2011 Objectives

Enhance the understanding of PEC materials and interfaces and promote break-through discoveries by:

- Utilizing and developing cutting-edge soft X-ray and electron spectroscopy characterization.
- Determining electronic and chemical structures of PEC candidate materials.
- Addressing materials performance, materials lifetime, and capital costs through close collaboration with partners from the PEC working group.

Technical Barriers

This project addresses the following technical barriers from the Production section of the Fuel Cell Technologies Program Multi-Year Research, Development and Demonstration Plan:

(H) System Efficiency

(K) Durability

(G) Capital Cost

Technical Targets

- Collaborate closely with partners within the DOE PEC Working Group to determine the electronic and chemical structure of candidate materials for solar water splitting.
- Aid the collaboration partners in the development and modification of novel candidate materials.
- Monitor deliberately introduced modifications of PEC candidate materials in view of the electronic and chemical structure.

FY 2011 Accomplishments

- Investigation of the chemical and electronic surface properties of $GaInP_2$ thin films and their variation after PEC testing (with the National Renewable Energy Laboratory, NREL, and Lawrence Livermore National Laboratory, LLNL, in the joint NREL/LLNL/UNLV surface validation group).
- Development of the benchmark electronic surface structure of a Fe_2O_3 thin film (with University of California, Santa Barbara).
- First exploratory experiments for the $(Mo,W)(S,Se)_2$ materials class (with Stanford University).
- First steps towards developing in situ PEC capabilities in soft X-ray spectroscopy (XPS).

✧ ✧ ✧ ✧ ✧

Introduction

This project is embedded into the Department of Energy's efforts to develop materials for PEC water splitting. If successful, PEC will provide an important route to convert the energy supplied by solar irradiation into a transportable fuel. In order to achieve this goal, suitable materials need to be developed that simultaneously fulfill several requirements, among them chemical stability and optimized electronic structure, both for absorption of the solar spectrum and for electrochemical water splitting at a solid/electrolyte interface. This project experimentally derives the chemical and electronic structure information to (a) judge the suitability of a candidate material, (b) show pathways towards a deliberate optimization of a specific material, and (c) monitor whether deliberate modifications of the material indeed lead to the desired changes in electronic and chemical structure.

Approach

A unique "tool chest" of experimental techniques is utilized that allows us to address all technical barriers related to electronic and chemical properties of various candidate materials. With these techniques it is possible to measure surface and bulk band gaps, the energy level alignment at interfaces, the chemical stability of the materials, and the impact of alloying and doping.

The tool chest includes photoelectron spectroscopy (PES) with XPS [1] and ultraviolet (UPS) excitation to

determine the occupied electronic states (core levels and valence electrons) and inverse photoemission (IPES) to determine the unoccupied electronic states. These techniques, performed in the lab at UNLV, are surface-sensitive and allow a complete determination of the electronic and chemical *surface* structure. They are complemented by X-ray emission (XES) and X-ray absorption spectroscopy (XAS), performed at Beamline 8.0 of the Advanced Light Source, Lawrence Berkeley National Laboratory. XES and XAS also probe the occupied and unoccupied electronic states, but with a larger information depth. Furthermore, they also give insight into the chemical structure, again complementary to the electron-based techniques performed in the lab at UNLV.

Results

In collaboration with our partners within the DOE PEC Working Group, we have investigated a variety of PEC candidate materials. Results were immediately shared with the collaboration partners and discussed in detail through powerpoint presentations, at phone conferences, and working group meetings. In this report, we will focus on the chemical surface properties of $GaInP_2$ samples obtained from NREL (T. Deutsch and J. Turner) and the electronic structure of Fe_2O_3 samples obtained from University of California, Santa Barbara (A. Forman, A. Kleiman-Shwarsctein, and E. McFarland). Further results, also for other material classes, are shown in the annual review presentation.

For the $GaInP_2$ experiments, two lines of work were pursued. First, we analyzed a series of samples that were deliberately exposed to PEC-relevant conditions, as listed in Table 1.

TABLE 1. Experimental Details of the $GaInP_2$ Samples Tested at NREL

Sample	Treatment	Electrolyte
MJ247-4	30 sec etch in concentrated sulfuric acid	none
MJ247-3	-8 mA/cm^2, 22 hrs, AM1.5G	0.1M HNO_3 + 0.5M NH_4NO_3 with Zonyl FSN-100
MJ247-2	-8 mA/cm^2, 22 hrs, AM1.5G	1M KOH with Zonyl FSN-100
MJ247-1	-8 mA/cm^2, 22 hrs, AM1.5G (+8 mA/cm^2 applied for ~1 sec prior to run)	0.5M H_2SO_4 with Zonyl FSN-100
MJ200	as-grown	none

An XPS surface chemical characterization of the samples is presented in Figure 1. The survey spectra in Figure 1 are normalized to the same height and offset for presentation. In addition to the expected Ga, In, and P peaks, the spectra also show O 1s and C 1s peaks of varying intensities. Samples MJ247-1 and MJ247-3 also show F 1s peaks, with this peak being the dominant feature in Sample MJ247-3. This is likely due to the Zonyl FSN-100

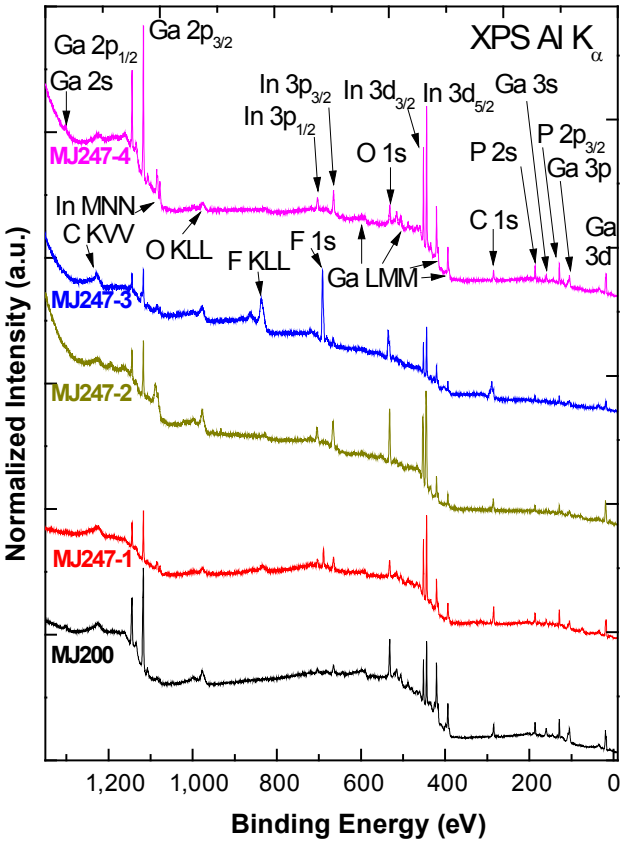


FIGURE 1. XPS survey spectra of selected $GaInP_2$ thin film samples after deliberate exposure to PEC-relevant environments, as listed in Table 1.

fluorosurfactant applied to the sample surfaces to facilitate movement of evolved H_2 from the electrode, but could also stem from the Teflon®-based environment of the sample surface during the tests.

As an example for the analysis of detail XPS spectra, we note that the Ga 2p region (not shown) clearly indicates the presence of multiple Ga species in the fluorine-rich sample MJ247-3 and, furthermore, exhibits variations in the lineshape of all samples, suggesting the presence of multiple chemical environments in those cases as well. For example, the MJ200 sample exhibits a shoulder at higher binding energy, most likely due to the native oxide- and carbon-containing surface contamination layer. Future experimental steps (currently being conducted in our lab at UNLV) thus focus on a removal of this surface contamination layer, such that "benchmark" spectra, e.g., of the Ga 2p core levels, but also of the valence and conduction band region of clean $GaInP_2$, can be obtained.

The second line of work on $GaInP_2$ focuses on a derivation of the electronic surface structure, as will be demonstrated below for the Fe_2O_3 system. In particular for the band gap determination, our experimental tool chest allows three different approaches, namely ultraviolet/visible light absorption (the "optical bulk band gap"), combining XES and XAS (the "electronic surface-near

band gap"), and combining UPS and IPES (the "electronic surface band gap", see discussion of Fe_2O_3). In fact, a combination of all three approaches can be used to follow band gap gradients [2]. Here, we show first experiments to combine XES and XAS studies on the same samples. For this purpose, we have studied the P $L_{2,3}$ edge of (air-exposed) GaP and InP reference powders, as well as one (untreated) $GaInP_2$ thin film. Figure 2 shows the associated spectra, demonstrating that it will be possible to determine both valence-band maxima (VBM) and conduction band minima (CBM) with this method. Note that, due to the above-mentioned surface contamination, the derived band gaps are not yet representative of functioning PEC devices (in which electrolyte exposure is expected to "clean" the surfaces), and hence no band gaps are given here. In future steps (currently being performed at UNLV), samples will be cleaned with an ion-stimulated desorption approach, which will allow us to determine depth-dependent band gaps of representative $GaInP_2$ surfaces. These can then be compared with theoretical results from our project partners at Lawrence Livermore National Laboratory (T. Ogitsu and B. Wood).

Having elucidated the impact of calcination (as shown in Figure 3) on the chemical surface properties of the University of California, Santa Barbara thin films in the previous FY, in particular uncovering significant Ti and Pt segregation processes, we focused on the analysis of the *electronic structure* of a Fe_2O_3 sample that demonstrated particularly high solar water splitting performance.

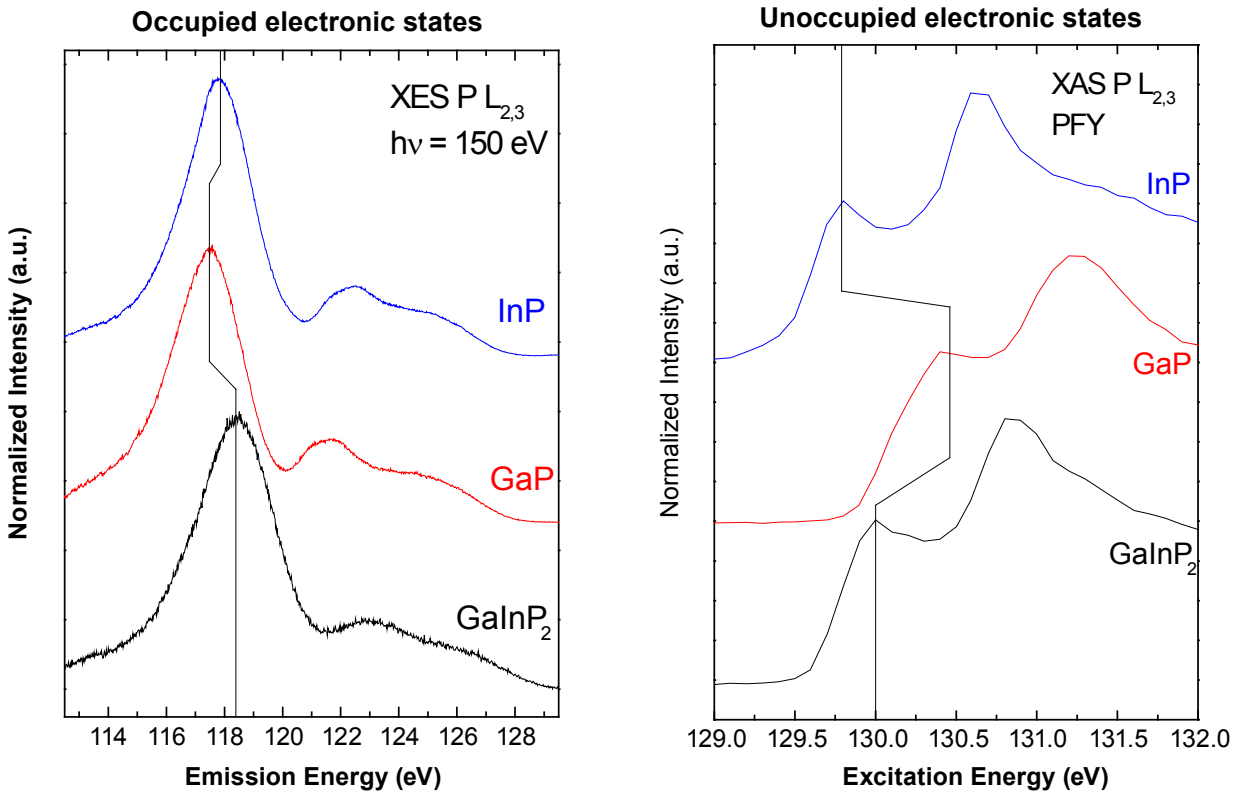


FIGURE 2. P $L_{2,3}$ XES (left) and XAS (right) of InP and GaP reference powders, as well as a $GaInP_2$ thin film (after air exposure, but without additional PEC testing). XES spectra probe the occupied states of the valence band, while XAS spectra give insights into the unoccupied conduction band states.

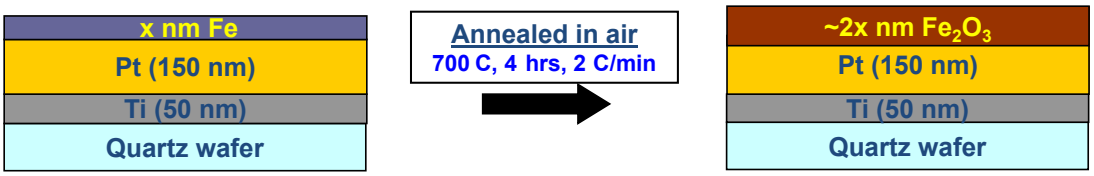


FIGURE 3. Schematic Calcination Process to Prepare Fe_2O_3 Thin Films at the University of California, Santa Barbara

The occupied and unoccupied electronic states were probed with UPS and IPES, respectively, as shown in Figure 4, left. The binding energies (abscissa) were adjusted relative to the Fermi Energy and plotted within the same graph. The leading edges of each spectrum were then extrapolated to the baseline. The positions of the intercepts with the baseline determine the positions of the VBM, in the UPS spectrum, (left) and CBM in the IPES spectrum, (right). The combination of both band edges allows a determination of the electronic surface band gap (2.0 ± 0.2 eV). Combining the band edge positions with the work function (4.23 ± 0.05 eV) of the sample, the band edge positions can be given with respect to the vacuum level. Furthermore, by applying an International Union of Pure and Applied Chemistry recommendation [3] and as done earlier for the case of WO_3 [4] and Mo:WO_3 [5], the vacuum level scale can be related to the normal hydrogen electrode (NHE) scale. By plotting the position of the VBM and CBM relative to the Fermi energy, vacuum level, and NHE on one plot, a comprehensive picture of the electronic picture can be painted, as shown in Figure 4 on the right.

Note that the plot in Figure 4 is derived from vacuum-based measurements and thus includes a potential surface band bending at the solid/vacuum interface. It does not, however, include potential variations of this band bending upon formation of the liquid-solid interface in an electrolyte environment. As is well known, a Helmholtz layer is formed in this case, and experimental and theoretical approaches to assess the impact of this layer on the electronic structure will need to be performed in subsequent experiments. In the current state, the plot in Figure 4 shows that the Fe_2O_3 sample surface simultaneously satisfies two conditions necessary for solar water splitting: the CBM and VBM straddle the H^+/H_2 reduction and H_2O/O_2 oxidation potentials, and the surface band gap lies in the optimal range for PEC hydrogen production with a single-gap material. However, a bias will clearly be needed to drive significant currents during PEC water splitting using this surface, since the CBM lies only slightly above the H^+/H_2 reduction level.

Conclusions and Future Directions

Conclusions:

- Successfully maintained operations of our multi-chamber ultra-high vacuum spectroscopy system despite limited funding.

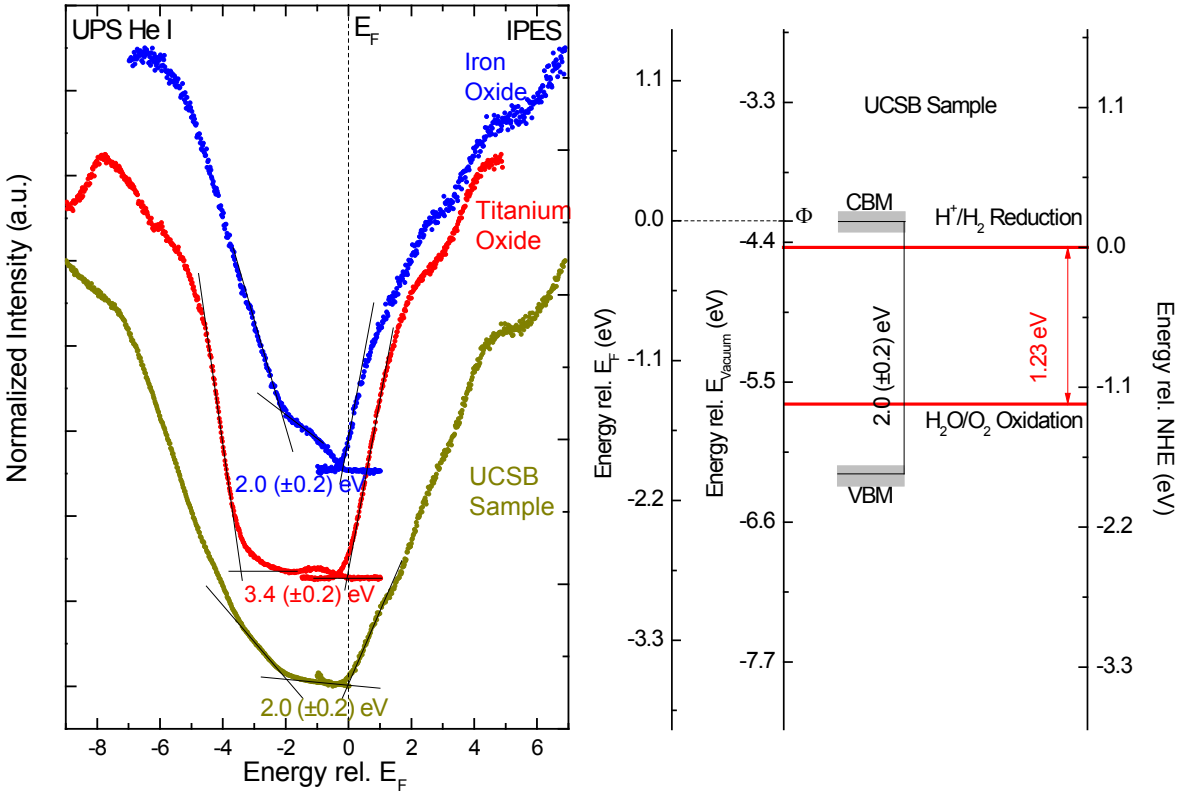


FIGURE 4. Left panel: UPS (left) and IPES (right) spectra of an Fe_2O_3 thin film grown at University of California, Santa Barbara (UCSB), and two *in-vacuo* grown reference systems (iron oxide and titanium oxide). Right panel: tentative electronic surface structure of the University of California, Santa Barbara Fe_2O_3 thin film.

- Continued experiments with select partners of the DOE PEC Working Group, primarily focusing on $GaInP_2$ and Fe_2O_3 thin films.
- Evaluated PEC candidate materials in view of their electronic and chemical properties, with primary focus on band gaps and level alignment.

Future Directions:

- Future directions will depend on availability of funding.
- If possible, we will continue the collaborations with our existing partners and bring new partners "on board".
- We will continue to determine electronic and chemical properties of various PEC candidate materials manufactured by the collaboration partners within the DOE PEC Working Group.
- For $GaInP_2$, we will focus on establishing a benchmark electronic structure of optimally cleaned thin film surfaces, which will allow us to monitor deliberate modifications of the $GaInP_2$ material and to correlate our results with theoretical calculations and predictions.

FY 2011 Publications/Presentations

1. "Using soft x-rays and electrons to characterize (understand?) materials for solar energy conversion", C. Heske, Heraeus-Seminar: "Energy Materials Research by Neutrons and Synchrotron Radiation", Bad Honnef, Germany, May 10, 2011 (invited).

2. "An International Effort to Develop Photoelectrochemical (PEC) Hydrogen Production Research Standards and Methods", H.N. Dinh* (NREL), Z. Chen, T.G. Deutsch, A. Kleiman-Shwarsctein, A.J. Forman, N. Gaillard, R. Garland, K. Takanabe, C. Heske, M. Sunkara, E.W. McFarland, K. Domen, E.L. Miller, J.A. Turner, and T.F. Jaramillo, MRS 2011 Spring Meeting, San Francisco, April 2011 (invited).

3. "So, when will there finally be a breakthrough for these solar thingies?", C. Heske, High School Day, American Chemical Society National Meeting, Anaheim, CA, March 27, 2011 (invited).

4. "Soft x-ray spectroscopy of materials for photoelectrochemical devices", C. Heske, M. Bär, and L. Weinhardt, Pacifichem 2010 conference, Waikiki, December 18, 2010 (contributed oral).

5. "Using soft x-rays to understand and optimize materials for energy conversion", C. Heske, Department of Physics, Hanoi University of Technology, Hanoi, Vietnam, Nov. 1, 2010 (invited).

6. "Using soft x-rays to look into (buried) interfaces of energy conversion devices based on compound semiconductors", C. Heske, 218th Electrochemical Society Meeting, Las Vegas, Oct. 12, 2010 (invited).

7. "Using soft x-rays to optimize materials for energy conversion devices", C. Heske, Department of Physics, Renmin University, Beijing, China, Oct. 10, 2010 (invited).

8. "Using soft x-rays to study the electronic and chemical properties of thin film solar devices", C. Heske, 15th International Conference on Solid Films and Surfaces (ICSFS-15), Beijing, China, Oct. 9, 2010 (invited).

9. "Using soft x-rays to understand and improve materials for energy conversion devices", C. Heske, Department of Chemistry, University of California Santa Cruz, September 29, 2010 (invited).

10. "SALSA – a soft x-ray spectroscopy endstation for the investigation of solids, liquids, and gases", M. Blum*, L. Weinhardt, O. Fuchs, M. Bär, Y. Zhang, M. Weigand, S. Krause, S. Pookpanratana, T. Hofmann, W. Yang, J.D. Denlinger, Z. Hussain, E. Umbach, and C. Heske, SRI2010 conference, Chicago, IL, September 2010 (contributed oral).

11. Invited, but symposium was canceled: "Soft x-ray spectroscopy of the electronic structure of water and materials for photoelectrochemical water splitting", C. Heske, Symposium on "In Situ Microscopy and Spectroscopy of Large Surfaces and Interfaces", XIX International Materials Research Congress 2010, Cancun, August 15–20, 2010 (invited).

12. "Soft x-ray and electron spectroscopies to study the electronic and chemical structure of surfaces and interfaces in photoelectrochemical devices", C. Heske, Solar Hydrogen and Nanotechnology V, SPIE International Symposium on Optics & Photonics, San Diego, August 1–5, 2010 (invited).

13. "Photoelectrochemical (PEC) hydrogen production research standards and methods development", H.N. Dinh* (NREL), Z. Chen, T.G. Deutsch, A. Kleiman-Shwarsctein, A.J. Forman, N.M. Gaillard, R. Garland, K. Takanabe, C. Heske, M.K. Sunkara, E.W. McFarland, K. Domen, E.L. Miller, J.A. Turner, and T.F. Jaramillo, "Solar Hydrogen and Nanotechnology V" Symposium, SPIE Optics and Photonics Conference, San Diego, CA, August 2010 (invited oral).

14. "Characterization of Fe_2O_3 thin films for photoelectrochemical hydrogen production", K. George*, C. Heske, S. Krause, Y. Zhang, E.W. McFarland, A.J. Forman, A. Kleiman-Shwarsctein, M. Bär, L. Weinhardt, W. Yang, and J.D. Denlinger, "Solar Hydrogen and Nanotechnology V" Symposium, SPIE Optics and Photonics Conference, San Diego, CA, August 1–5, 2010 (contributed oral).

15. "Using soft x-rays to look at surfaces and interfaces of photoelectrochemical devices", C. Heske, New Science with Resonant Elastic and Inelastic X-ray Scattering Satellite Meeting of the VUVX conference, University of Saskatchewan, Saskatoon, SK, Canada, July 8, 2010 (invited).

16. "Wie man mit Röntgenspektroskopie energierelevante Materialien und Systeme verstehen und verbessern kann", C. Heske, Organisch-Chemisches Kolloquium im Sommersemester 2010, Karlsruhe Institute of Technology, July 2, 2010 (invited).

17. "Using soft x-rays to look at surfaces and interfaces for energy conversion and storage", C. Heske, National Renewable Energy Lab (NREL), June 21, 2010 (invited).

18. "Using soft x-rays to look into interfaces of photoelectrochemical devices", C. Heske, Symposium on

Synchrotron and Neutron Techniques for Energy Materials Research, Materials Research Society Spring Meeting, San Francisco, April 5–9, 2010 (invited).

References

1. D. Briggs and M.P. Seah, *Practical Surface Analysis*, John Wiley and Sons, Chichester, 1990.

2. M. Bär, L. Weinhardt, S. Pookpanratana, C. Heske, S. Nishiwaki, W. Shafarman, O. Fuchs, M. Blum, W. Yang, and J.D. Denlinger, Appl. Phys. Lett. 93, 244103 (2008).

3. S. Trasatti, Pure Appl. Chem. **58**, 955 (1986).

4. L. Weinhardt, M. Blum, M. Bär, C. Heske, B. Cole, B. Marsen, and E.L. Miller, J. Phys. Chem. C 112, 3078-3082 (2008).

5. M. Bär, L. Weinhardt, B. Cole, B. Marsen, N. Gaillard, E.L. Miller, and C. Heske, Appl. Phys. Lett. 96, 032107 (2010).

II.G.5 Photoelectrochemical Hydrogen Production

Arun Madan
MVSystems, Incorporated (MVS)
372 Lamb Lane
Golden, CO 80401
Phone: (303) 271-9907
E-mail:ArunMadan@aol.com or amadan@mvsystemsinc.com

DOE Managers
HQ: Roxanne Garland
Phone: (202) 586-7260
E-mail: Roxanne.Garland@ee.doe.gov
GO: David Peterson
Phone: (720) 356-1747
E-mail: David.Peterson@go.doe.gov

Contract Number: DE-FC36-07GO17105, A00

Subcontractor:
University of Hawaii at Manoa (UH), Honolulu, HI

Project Start Date: September 1, 2007
Project End Date: December 31, 2012

Fiscal Year (FY) 2011 Objectives

- Work closely with the DOE Working Group on Photoelectrochemical (PEC) Hydrogen Production for optimizing PEC materials and devices.
- Develop new PEC film materials compatible with high-efficiency, low-cost hydrogen production devices.
- Demonstrate functional multi-junction device incorporating materials developed.
- Explore avenues toward manufacture-scaled devices and systems.

Technical Barriers

This project addresses the following technical barriers from the Photoelectrochemical Hydrogen Production section of the Fuel Cell Technologies Program Multi-Year Research, Development and Demonstration Plan:

(Y) Materials Efficiency
(Z) Materials Durability
(AA) PEC Device and System Auxiliary Material
(AB) Bulk Materials Synthesis
(AC) Device Configuration Designs

Technical Targets

Table 1 lists the technical targets for PEC hydrogen production using amorphous silicon carbide-compound (a-SiC), tungsten-compound (WO_3) and copper-chalcopyrite compound (CGSe) films.

FY 2011 Accomplishments

1. Improvement in performance of the hybrid photovoltaic (PV)/a-SiC device:
   – Good durability in pH2 buffered electrolyte for up to 310 hr.

TABLE 1. Technical Targets

Task #	Milestone	a-SiC	WO_3	CGSe
Year 1	Material photocurrent ≥3 mA/cm^2	Achieved	Achieved	Achieved
	Durability ≥100 hr	Achieved	Achieved	10% Achieved
Year 2	Material photocurrent ≥4 mA/cm^2	Achieved	90% Achieved	Achieved
	Durability ≥ 200 hr	Achieved	Achieved	Achieved
	Device STH efficiency ≥5%	32% Achieved	60% Achieved	62% Achieved
Passed Go/No-Go decision evaluation in November, 2010				
Year 3*	Device STH efficiency ≥5%	32% Achieved	60% Achieved	85% Achieved
	Durability ≥300 hr	100% Achieved	83% Achieved	66% Achieved
Year 4	Device STH efficiency ≥5%			
	Durability ≥500 hr			
	Completion of Final Energy/ Economics report on scale up and commercialization toward a $22/kg-$H_2$ plant production cost			

* As of writing this report.

  - Surface treatment by methylation (CH_3) termination and titanium (Ti) nano-particles increases photocurrent of the hybrid PV/a-SiC device by nearly two order of magnitude.
2. Improvement in performance of the WO_3 photoelectrode, including:
  - Synthesis of WO_3-based material with near to optimum band gap ($CuWO_4$).
  - Identification of an innovative monolithic integration scheme for WO_3-based PEC devices.
3. Improvement in performance of the I-III-VI_2 photoelectrode, including:
  - Highly durable down to pH0 sulfuric acid (200 hr resulting in improved performance).
  - Successful integration into a novel coplanar device approaching 5% solar-to-hydrogen (STH) efficiency.
  - Identification of possible surface modifications to decrease required voltage bias.



Introduction

Based on its potential to meet long-term goals, research and development (R&D) centering on multi-junction hybrid photoelectrode technology defines the scope of this collaborative project. Within this scope, particular emphasis is the development of low-cost photoactive materials integrated with a-Si-based solar cells as a driving force with photocurrents greater than 4 mA/cm^2, and with sufficient durability to meet lifetime requirement, i.e., ≥500 hours. In addition to the materials R&D activities, development of laboratory-scale demonstration devices and generation of preliminary energy/economic analysis for hydrogen production cost based on the developed PEC technology is included in the project scope as second-level priorities. To support the device-demonstration activities, appropriate auxiliary components are being developed for incorporation in PEC photoelectrode designs, including attention to the necessary process integration techniques.

Approach

The general approach of this collaborative effort focuses on the DOE PEC Working Group's "feedback" philosophy of integrating state-of-the-art theoretical, synthesis and analytical techniques to identify and develop the most promising materials classes to meet the PEC challenges in efficiency, stability and cost. Materials modeling, bulk-film optimization, film-surface enhancement, along with comprehensive material and device characterization is being employed to facilitate the R&D process. Specifically, the feedback approach is being applied to our focus material classes, including the tungsten-, copper-chalcopyrite- and silicon-based compounds, to enhance understanding of fundamental performance parameters, and expedite development of process-compatible forms of these materials. The most promising candidate materials are being identified, with the short-term goal of demonstrating laboratory-scale water-splitting devices, and with a long-term goal of transferring the fabrication processes toward the commercial scale.

Results

During this reporting period (June 2010–June 2011), extensive studies of the three material classes under investigation have focused on understanding and improving PEC behavior, specifically by applying our theoretical, synthesis and analytical techniques in identifying relevant aspects of structural, optoelectronic and electrochemical properties.

1. Amorphous Silicon Carbide-Based Compound Films

Surface methylation of the hybrid PV/a-SiC devices was accomplished by first eliminating SiOx from the a-SiC surface via HF (hydrofluoric acid) etching followed by immersion in NH_4F (ammonium fluorine) to produce hydrogen (H)-termination. Next, the H-terminated a-SiC surface was treated with a CH_3-containing species and then coated with Titanium (Ti) nanoparticles sputtered at 60 W direct current for 60 s. The treatment resulted in an anodic shift of ~0.3 V in flatband potential, as measured by the National Renewable Energy Laboratory (NREL). Figure 1 shows current-voltage (J-V) characteristics of the hybrid devices for various surface treatment conditions measured under AM1.5G illumination. Compared to the non-treated sample, the fill factor of the J-V curves in the surface-treated sample is improved greatly. At zero potential, the photocurrent density changes by as much as two orders of magnitude, from ~11 µA/cm^2 to ~1 mA/cm^2. This clearly shows that surface methylation reduces the a-SiC/electrolyte barrier allowing more photocurrent. More work to optimize this process is underway.

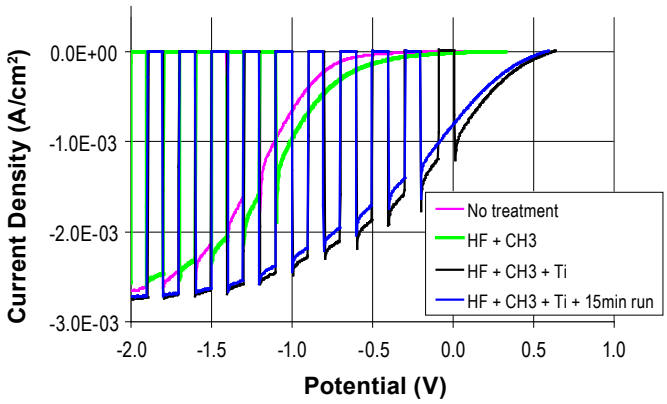


FIGURE 1. Two electrode PEC J-V curves of untreated, CH_3-terminated, and CH_3-terminated + Ti coated hybrid devices. The blue J-V curve was measured after 15 min of the first scan (black curve) in order to confirm the reproducibility.

In addition, the hybrid PV/a-SiC device exhibits good durability for up to 310 hr in pH2 electrolyte and under AM1.5G at 1 mA/cm^2, as confirmed by NREL.

2. Tungsten Oxide-Based Compound Films

During this reporting period, efforts were focused on copper tungstate ($CuWO_4$), known to have a bandgap (2.1 eV) ideal for PEC applications. $CuWO_4$ synthesized at 275°C using conventional reactive co-sputtering were p-type and amorphous with a bandgap of 2.1 eV, but exhibited poor PEC performances as shown in the inset in Figure 2. However, an 8 hr anneal at 500°C in argon led to a polycrystalline $CuWO_4$ structure with n-type conductivity, while optical bandgap remained unchanged. Finally, PEC performance improved with photocurrent density achieving ~0.5 mA/cm^2 (see Figure 2). It is noted that the flat-band potential (which determines photocurrent onset potential) is much lower than that expected for metal oxides (-0.3 V vs. saturated calomel electrode (SCE) for $CuWO_4$ versus +0.15 V vs. SCE for WO_3). Thus, it is expected that $CuWO_4$ could be integrated into a hybrid PEC device design comparable to what is currently used for a-SiC and WO_3 hybrid devices. Future doping studies with foreign elements to improve charge carrier separation and extraction are on going with the help of NREL's theory group.

Durability tests were also performed on WO_3 photoelectrode, under AM1.5G at 1.8 V, in pH2.5 H_3PO_4 electrolyte. High corrosion resistance of WO_3 in acidic solution for up to 250 hr has been observed.

3. I-III-VI$_2$ (Copper Chalcopyrite-Based) Films

It was observed in a successful 200 hr durability test that this material is highly stable in very acidic (pH0) sulfuric acid. In addition, such an extended operation

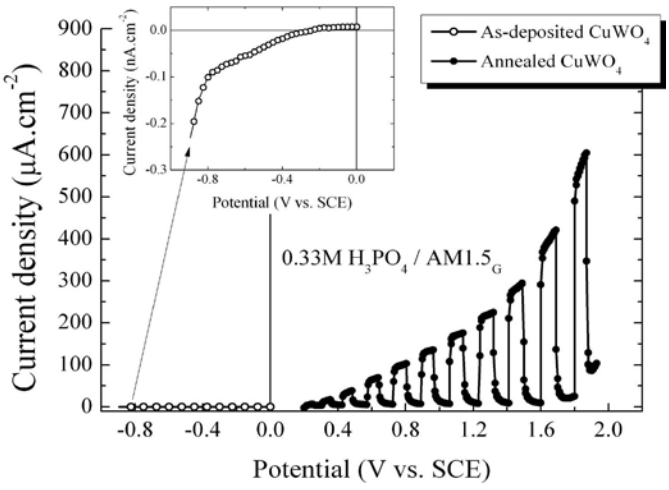


FIGURE 2. Three electrode PEC J-V curves of as-deposited and annealed $CuWO_4$ thin films. Test was done in 0.33M H_3PO_4 under AM1.5G simulated illumination.

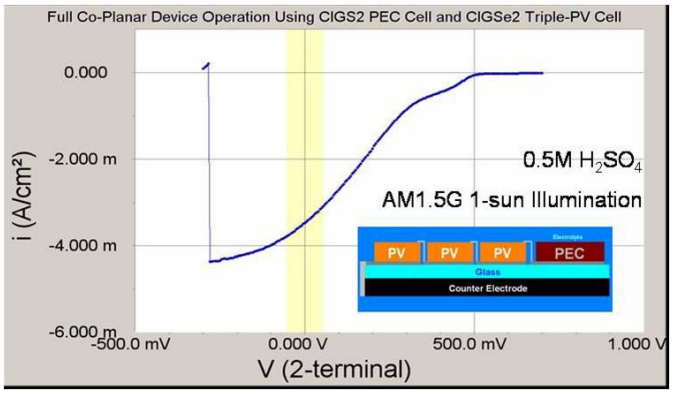


FIGURE 3. J-V characteristics of a coplanar device integrating three $CIGSe_2$ PV cells with a $CIGS_2$ PEC cell (as shown in schematic). Device indicated a 3.46 mA/cm^2 operating point at 0 V, equivalent to 4.3% STH efficiency.

improves the performance of $CGSe_2$ (i.e., photocurrent increased by 22%), possibly due to light-soaking or a surface sulfurization, detected by X-ray emission spectroscopy soft X-ray spectroscopy at the University of Las Vegas. Collaboration with Stanford University aims to perform a more controllable surface sulfurization (by annealing in an H_2S atmosphere). Figure 3 shows the J-V characteristics of a coplanar device integrating three $CIGSe_2$ PV cells with a $CIGS_2$ PEC cell (as shown in schematic). The device was tested in 0.5M H_2SO_4 and under AM1.5G 1-sun illumination, and produced a new material class record photocurrent of 3.46 mA/cm^2 at 0 V, equivalent to 4.3% STH efficiency.

Conclusions and Future Directions

Surface treatment of the hybrid PV/a-SiC device using CH_3 termination was found to reduce the photocurrent onset and enhance photocurrent by as much as two orders of magnitude at zero potential. In WO_3-based compound such as $CuWO_4$, the post-deposition annealing improves its conductivity and photo-response while the bandgap remains unchanged (2.1 eV). Finally, a STH efficiency of ~4.3% is achieved in the co-planar integrated PV/$CGSe_2$ device. The hybrid PV/a-SiC device, and other two photoelectrode thin film materials (WO_3 and copper chalcopyrite) show good durability in electrolyte for ≥200 hr.

In order to improve the STH efficiency, three main tasks will be performed: (1) improve interface energetics and kinetics with appropriate surface treatment for a-SiC photoelectrodes. Our goal for this year is to achieve 2.5-3% STH efficiency with 400-hour durability in the hybrid PV/a-SiC device; 2) identify a suitable foreign element for $CuWO_4$ doping and increase photocurrent density beyond 3.5 mA/cm^2 while passing the 400 hours durability mark; and (3) further lower valence band edge via Cu and Se (partial) substitution in I-III-VI2 photoelectrode materials to surpass 5% STH efficiency while maintaining material

durability for 400 hours this year. Surface treatment will be evaluated for all three material classes to prevent possible degradation beyond 250 hours. Such treatment may include CoMo for photocathodes (a-SiC and I-III-IV2) and RuO_2 for photoanode (WO_3 and $CuWO_4$).

FY 2011 Publications/Presentations

1. I. Matulionis, J. Hu, F. Zhu, J. Gallon, N. Gaillard, T. Deutsch, E. Miller, and A. Madan, "Surface modification of a-SiC:H photoelectrodes for photocurrent enhancement", presented at SPIE San Diego, August 2010.

2. N. Gaillard; Y. Chang; J. Kaneshiro; A. Deangelis; E.L. Miller , "Status of research on tungsten oxide-based photoelectrochemical devices at the University of Hawai'i", Solar Hydrogen and Nanotechnology V, SPIE proc. 7770, DOI: 10.1117/12.860970 (2010).

3. J. Kaneshiro, A. Deangelis, N. Gaillard, Y. Chang, J. Kowalczyk, E.L. Miller, "Copper-silver chalcporyites as top cell absorbers in tandem photovoltaic and hybrid photovoltaic/photoelectrochemical devices," *Photovoltaic Specialists Conference (PVSC), 2010 35th IEEE*, (2010) 002448 doi:10.1109/PVSC.2010.5614163.

4. J. Kaneshiro, A. Deangelis, X. Song, N. Gaillard, E.L. Miller, "I-III-VI2 (Copper Chalcopyrite-based) Thin Films for a Photoelectrochemical Water-splitting Tandem-hybrid Photocathode.," *Materials Research Society (MRS) Spring Meeting 2011*, Accepted for Publication.

II.G.6 Critical Research for Cost-Effective Photoelectrochemical Production of Hydrogen

Liwei Xu[1], Anke E. Abken[2], William B. Ingler[3], John Turner[4]
[1]Midwest Optoelectronics LLC (MWOE), Toledo, OH
[2]Xunlight Corporation
3145 Nebraska Ave.
Toledo, OH 43607
Phone: (419) 469-8610
E-mail: lxu@xunlight.com
[3]University of Toledo, Toledo, OH
[4]National Renewable Energy Laboratory, Golden, CO

DOE Managers
HQ: Eric Miller
Phone: (202) 287-5829
E-mail: Eric.Miller@hq.doe.gov
GO: David Peterson
Phone: (720) 356-1747
E-mail: David.Peterson@go.doe.gov

Contract Number: DE-FG36-05GO15028

Subcontractors:
- Xunlight Corporation, Toledo, OH
- University of Toledo, Toledo, OH
- National Renewable Energy Laboratory, Golden, CO

Project Start Date: April 1, 2005
Project End Date: December 31, 2012

Fiscal Year (FY) 2011 Objectives

- To develop critical technologies required for cost-effective production of hydrogen from sunlight and water using thin film (tf)-Si-based photoelectrodes.
- Two approaches are taken for the development of efficient and durable photoelectrochemical (PEC) cells:
  - An immersion-type PEC cell in which the photoelectrode is immersed in electrolyte.
  - A substrate-type PEC cell in which the photoelectrode is not in direct contact with electrolyte.

Technical Barriers

This project addresses the following technical barriers from the Production section (3.1.4) of the Hydrogen, Fuel Cells and Infrastructure Technologies Program Multi-Year Research, Development and Demonstration Plan:

(Y) Materials Efficiency

(Z) Materials Durability

(AB) Bulk Materials Synthesis

(AC) Device Configuration Designs

(AD) Systems Design and Evaluation

Technical Targets

This project focuses on the development of photoelectrode materials and tf-Si-based PEC cells required to achieve or exceed DOE's technical targets. The status of the MWOE project towards the DOE technical targets for PEC production of hydrogen for 2013 is:

TABLE 1. Progress towards Meeting Technical Targets for Immersion- and Substrate-type PEC Cells and Systems

Characteristic	Units	DOE 2013 Targets	MWOE 2011 Status
Solar-to-Hydrogen Efficiency	% Efficiency	8	5 (4"×12" module) (Substrate-type)
Durability	Hours	>1,000	1,000 (Cobalt Oxide)
Cost	$/gasoline gallon equivalent	2-4	To Be Determined
Photocurrent of TCCR	mA/cm^2	>8 (MWOE Target)	37.8 (Cobalt Oxide)
Photocurrent of PAS	mA/cm^2	>8 (MWOE Target)	0.0334 (Indium Iron Oxide) (Down-selected)
Deposition Temperature	°C	<250 (MWOE Target)	180-200 (Cobalt Oxide)
Transparency of TCCR	% Transmission	>90 (MWOE Target)	90 (Cobalt Oxide)
Voltage drop across TCCR/PV-cell layer stack	Volts	≤0.15	0.07 (Cobalt Oxide)

TCCR - transparent, conducting and corrosion resistant; PAS - photoactive semiconductor; PV - photovoltaic

FY 2011 Accomplishments

- A 12"×12" substrate-type PEC cell prototype was fabricated and has been tested.
- TCCR were developed (Task 1):
  - From a Go/No-Go meeting Co_3O_4 and In_2O_3-Fe_2O_3 were identified as the major material classes of study moving into the final grant period.
- Facilities and procedures for large-area deposition of Co_3O_4 for use in immersion-type PEC cells have been established and some runs have been carried out with very promising results (Task 1).

- Large-area electroplating of porous Ni as H_2 evolution catalyst has been developed using precursor salts in order to optimize the porous structure of the catalyst films (Task 4):
  - Many new precursors were studied for Ni electroplating and it was found that using $(NH_4)_2SO_4$ yielded the best results due to the increased porosity of the Ni layer.



Introduction

In this project, MWOE and its subcontractors are jointly developing the critical technologies required for cost-effective production of hydrogen from sunlight and water using tf-Si-based photoelectrodes. These triple-junction tf-Si-based electrodes include triple cells with either amorphous silicon germanium alloy (a-SiGe) or microcrystalline silicon (µc-Si) as the narrow band gap absorber material.

In this project two separate approaches have been pursued for the development of immersion- and substrate-type PEC photoelectrodes:

- In one approach, triple-junction tf-Si-based photoelectrodes (a-Si/a-SiGe/a-SiGe or a-Si/a-SiGe/µc-Si) are used to generate the voltage bias necessary for hydrogen generation. A TCCR coating is deposited on top of the photoelectrode for protecting the semiconductor layers from corrosion while forming an ohmic contact with the electrolyte.
- The second approach uses a hybrid structure, in which two tf-Si based junctions (middle and bottom junctions of the present triple-junction tf-Si cell) provide a voltage bias of about 1.1 V, and a third junction (the top junction) forms a rectifying junction between a PAS and the electrolyte. This approach was down-selected during a Go/No-Go review in December 2010.

State-of-the-art a-Si/a-SiGe/a-SiGe and/or a-Si/a-SiGe/µc-Si devices are used as photoelectrodes. The corrosion resistance and PEC mechanisms for a range of oxide-, nitride- and carbide-materials, and II-VI compounds are under investigation. High-performance, durable PEC cells and systems will be developed, optimized and demonstrated in this project.

Approach

Five technical tasks are being performed under this grant in order to accomplish the project objectives:

- Task 1: Transparent, conducting and corrosion resistant coating for a triple-junction tf-Si-based photoelectrode.
- Task 2: Hybrid multi-junction PEC electrode having semiconductor-electrolyte junction.
- Task 3: Understanding and characterization of photo-electrochemistry.
- Task 4: Development of device designs for low-cost, durable and efficient immersion-type PEC cells and systems.
- Task 5: Development of device designs for large area, substrate-type PEC cells.

During the Go/No-Go review in December 2010, it was decided that the immersion-type PEC work (Task 4) will proceed into the second phase and the substrate-type PEC work (Task 5) would come to an end. It was also determined the TCCR work (Task 1) will proceed and the PAS work (Task 2) will be halted.

Results

Tasks 1 focuses on the preparation of TCCR coatings deposited onto the top of the tf-Si photoelectrode. Many different material classes have been studied, including Fe_2O_3, TiO_2 and WO_3. Co_3O_4 has been identified as a promising candidate for use as a TCCR material: it can be sputtered at temperatures <250°C and provides sufficient transparency if the layer thickness is kept below ~30nm; Co_3O_4 layers are corrosion resistant in alkaline electrolytes which are used in immersion type PEC cells, and these layers provide good electrical conductivity. Co_3O_4 layer (sputtered onto Tec 15 glass) provides a current density of 37.8 mA/cm^2 at 1.8 V, which is the voltage of the PEC cell under operating conditions. The voltage drop across the TCCR layer for the TCCR/PV cell stack is ~0.07 V. For small-area studies, the TCCR films were deposited using radio frequency magnetron sputter deposition in argon and oxygen using multiple sputter guns simultaneously. From the completed work, the results indicate that samples made at 250°C with 100 W and a sputter deposition time of 30 minutes produced optimal results. These Co_3O_4 layers have demonstrated 1,000 hours of stability in ~30% KOH as electrolyte at the time of this report. During this reporting period emphasis was focused on fabricating and characterizing Co_3O_4 films and on developing a large-area deposition process for Co_3O_4 using Xunlight's roll-to-roll deposition system (Figure 1, Figure 2). Xunlight's roll-to-roll deposition system allows large-area fabrication of PEC electrodes including the deposition of TCCR layer without breaking the vacuum: the equipment simulates processing conditions which are comparable to a manufacturing environment. Process parameters such as sputtering power, line speed and oxygen content in the sputtering gas were optimized in order to achieve the best performing Co_3O_4 TCCR layer and PEC electrodes. Transmission measurements performed on the Co_3O_4 layer deposited onto glass slides showed that reducing the layer thickness by increasing the line-speed to 6"/min improved the transparency of the Co_3O_4 layer significantly. Reducing the sputtering power to 1.5 kW lead to transmission values of 80-100% in a wavelength range between 300-900 nm. The average thickness of these Co_3O_4 layers were ~135 nm.



FIGURE 1. Xunlight's Roll-To-Roll Deposition System For Large-Area Fabrication of PEC Electrodes

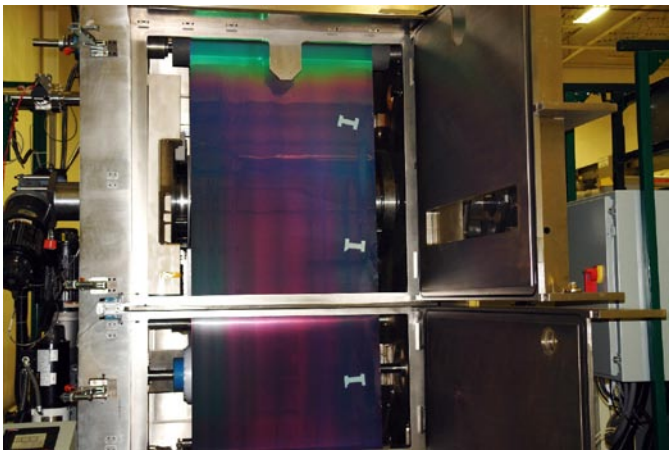


FIGURE 2. Opened Pay-Out Chamber of Xunlight's Roll-To-Roll Machine with Inserted Stainless Steel Web after Co_3O_4 Sputtering

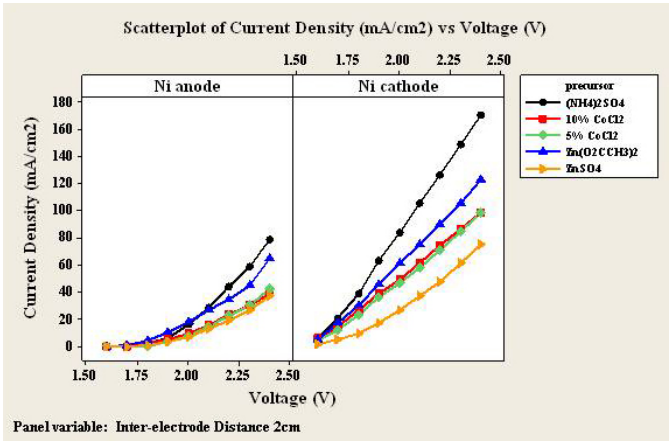


FIGURE 3. Current-voltage curves for porous Ni-electrodes used as anode or cathode with an electrode distance of 2 cm (counter electrode: Pt-mesh); precursor salts: $(NH_4)_2SO_4$, $CoCl_2$ (5% and 10%), $Zn(O_2CCH_3)_2$, $ZnSO_4$.

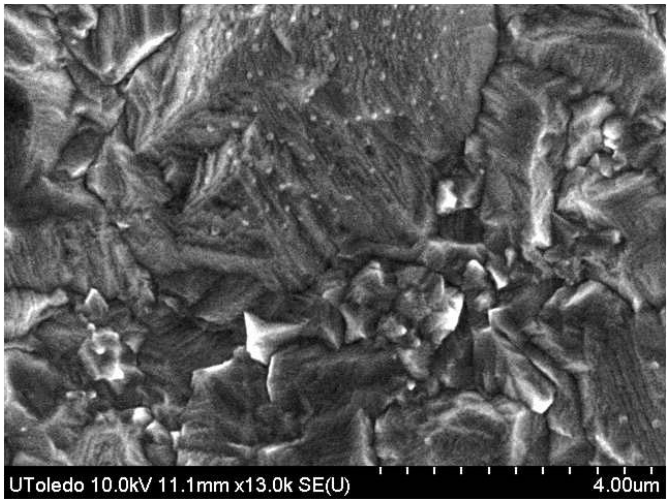


FIGURE 4. Scanning Electron Micrograph of Ni-Catalyst Prepared with $(NH_4)_2SO_4$ (10%)

Noteworthy is that the transmission of the Co_3O_4 layer does not change with the oxygen flow in the sputtering gas.

Under Task 4, a method for large-area electroplating of porous Ni used as H_2-evolution catalyst has been developed. Over the past year work has focused on the continued study of the addition of precursor salts such as ammonium sulfate, cobalt chloride, zinc acetate, and zinc sulfate to the Ni plating solution in order to improve micro- and macro-structures of the porous nickel films. The method uses the co-deposition of Ni and a precursor metal (Zn, Co) onto the back-side of tf-Si photoelectrodes; after Ni/Zn or Ni/Co electrodeposition the precursor metal is leached out leaving a porous Ni-structure behind. At this stage of research, using ammonium sulfate as a precursor material shows the best result, which is illustrated in Figure 3. The porosity of the nickel catalyst is shown in Figure 4.

Task 5 focuses on the development of large-area substrate-type PEC systems. Under this task several prototypes for 12"×12" PEC cell assemblies were fabricated. The porous Ni layer used as a hydrogen evolution catalyst was electroplated onto the backside of a tf a-Si device. The surface of the PEC electrode was encapsulated using a light-weight ethylene vinyl acetate-based encapsulation material, which protects the electrode from environmental impact under outdoor operating conditions. The generation of hydrogen and oxygen was confirmed under illumination. At this point of research solar-to-hydrogen efficiency data are not available for 12"×12" PEC systems. However, earlier experiments showed that a solar-to-hydrogen efficiency of 5% has been obtained for a 12"×4" substrate-type PEC system.

Conclusions and Future Directions

The proposed future work will include:

- Continue optimization of oxide materials suitable for TCCR coatings:
  - Material class studies will be focusing on In_2O_3-Co_2O_3.
  - Optimization work on Co_3O_4 TCCR will continue.
- Optimize large-area deposition of Co_3O_4 TCCR layer in the roll-to-roll system and fabricate large-area tf Si PEC electrodes with a Co_3O_4 TCCR coating:
  - Improve performance of large-area photoelectrodes.
- Demonstrate 4"×4" and 12"×12" immersion-type PEC systems:
  - Design of immersion-type PEC systems using triple-junction a-Si photoelectrodes with a TCCR layer.
  - The PEC system will employ porous Ni as H_2 evolution catalyst electroplated onto the backside of the triple-junction a-Si device.
  - Long-term reliability studies and solar-to-H_2 efficiency measurements will be performed.
- Complete techno-economic analysis and energy analysis for the PEC systems for hydrogen production.

FY 2011 Publications/Presentations

1. Ingler Jr., W.B., Bidurukontham, A. "Development of Porous Nickel Electrocatalyst for Hydrogen Production" 2010 International Chemical Congress of the Pacific Basin Societies (Pacifichem 2010), Hawaii Convention Center, Honolulu, HI. Dec. 18, 2010. (Poster)

2. Xu, L., Ingler Jr., W.B., Abken, A. and Turner, J. "Critical research for cost-effective photoelectrochemical production of hydrogen", DOE Hydrogen Program Annual Review Meeting, Washington, D.C., May 10, 2011. (Poster)

II.G.7 PEC-Based Hydrogen Production with Self-Cleaning Solar Concentrator*

M.K. Mazumder (Primary Contact), A.S. Biris, R. Sharma, H. Ishihara, G. Kannarpady, and P. Girouard
Department of Applied Science
University of Arkansas at Little Rock
2801 S. University Ave.
Little Rock, AR 72211
Phone: (617) 997-7049
E-mail: mkmazumder@ualr.edu

DOE Managers
HQ: Eric Miller
Phone: (202) 287-5829
E-mail: Eric.Miller@hq.doe.gov
GO: Katie Randolph
Phone: (720) 356-1759
E-mail: Katie.Randolph@go.doe.gov

Contract Number: DE-FG36-06GO86054

Project Start Date: July 1, 2006
Project End Date: June 30, 2011

*Congressionally directed project

Fiscal Year (FY) 2011 Objectives

- Synthesize nanostructured $TiO_{2-x}N_x$ photoanodes and tandem heterostructured photoanodes with WO_3 and $TiSi_2$ to improve absorption of light in the visible spectrum in conjunction with TiO_2 film at the outer surface forming interface between the solid electrode and the liquid electrolyte.
- Improve photocatalytic properties of photoanodes by plasma treatments for (a) removing contaminants and unwanted surface states, (b) doping the photoanode surface with nitrogen to create oxygen vacancies and vacant acceptor states to enhance oxidation of water, and (c) optimizing surface structure of nanotubular electrodes for increasing photocurrent density.
- Design optical system with self-cleaning Fresnel-lens based solar concentrator to operate the photoelectrochemical (PEC) electrode at 10 sun irradiance.
- Optimize surface structure of the layered electrodes for minimizing the charge carrier traps.

Technical Barriers

- Metal oxide semiconductor photoanodes, such as TiO_2, extensively studied for hydrogen production, cannot provide both the needed light absorption in the visible spectrum and yet provide resistance to photocorrosion.
- Hybrid tandem heterostructed PEC suffer from inefficient charge carrier transfer process across the semiconducting electrode/electrolyte junction due to the presence of interfacial energy traps, and lattice constant mismatch between layered semiconductors.
- Other nanostructured devices involving oxynitrides, such as $(Ga_{0.88}\ Zn_{0.12})(N_{0.88}\ O_{0.12})$ with co-catalysts, such as $Rh_{2-x}Cr_xO_3$ shows considerable promise for hydrogen production but the cost of the materials and toxicity involved in some cases show further studies are needed to synthesize electrodes for commercial hydrogen production.

Technical Targets

Solar-to-hydrogen efficiency: 10% by 2015 by developing photoanodes having efficient light absorption in the visible range by reaching quantum yield of 30% at 600 nm and long-term corrosion resistance for commercial-scale H_2 production.

FY 2011 Accomplishments

- Synthesized nanotubular TiO_2 photoanodes with stepped voltage anodization and surface modification of TiO_2 photoanodes with He plasma which minimized charge carrier traps and contaminants.
- Surface cleaning and doping of the photoanode with helium plasma treatment followed by nitrogen plasma followed by He plasma treatment, to form $TiO_{2-x}N_x$ at the surface thus leaving the bulk semiconductor for high electron conductivity and created oxygen vacancies at the surface for improved photocurrent density.
- Increased photocurrent density by more than 80% by plasma treatments and enhanced light absorption by 55% with modified nanotubular structure by step-voltage anodization compared to the untreated TiO_2 photoanodes.
- Synthesis of tandem heterostructured layered electrodes with lower bandgap layer (e.g. WO_3, $TiSi_2$,) behind a wide bandgap semiconductor (e.g. TiO_2) facing the electrolyte.
- Development of self-cleaning solar concentrator for operating the PEC devices at irradiance level of 10 sun for enhancing hydrogen generation rate.



Introduction

Hydrogen is an ideal renewable chemical fuel yet its production by splitting water using sunlight has been

one of the most formidable challenges for the last several decades [1–6]. While the potential advantages of PEC-based production of hydrogen have not yet been realized recent developments show emergence of new nanostructural designs of photoanodes and choices of materials with significant gains in photoconversion efficiency [7-16]. Significant efforts are being made for reaching the quantum yield of 30% and long-term durability needed for commercial production.

$TiO_{2-x}N_x$ meets nearly all the requirements for PEC-based hydrogen production with respect to its abundance, environmental safety, and durability [7], except for its wide bandgap and consequent poor absorption of sunlight in the visible spectrum. Until now, no single compound semiconductor photoanode has been found which satisfy both the critical needs of light absorption and the long-term durability against photocorrosion. For example, tantalum oxide and gallium nitrides have demonstrated better results for hydrogen production but their cost would be more than 50 times the cost of TiO_2 based catalyst [7]. Other nanostructured devices have surpassed the performance of TiO_2 for water splitting, but these materials involve, for example, La-doped $NaTaO_3$ and oxynitrides, such as $(Ga_{0.88}\ Zn_{0.12})(N_{0.88}\ O_{0.12})$ with co-catalysts, $Rh_{2-x}Cr_xO_3$ showing considerable promise for hydrogen production [15, 16] but the cost of the materials and toxicity involved in some cases are of concern.

Common to most of current investigations, are the studies on: (1) effects of nanostructural surface morphology (nanorods, nanotubes), (2) reduction of interfacial charge carrier traps, (3) increase in the effective surface area for enhancing light absorption at semiconductor-electrolyte interface, and (4) optimum level of sunlight irradiance for operation of the PEC devices at their maximum efficiency. The studies reported here are focused on the interfacial aspects of the PEC-based hydrogen production and optimization of solar irradiance at the photoanode surface.

Approach

To address the problem related to the wide bandgap of TiO_2, one approach is to develop a hybrid nanostructured photoanode (Figure 1) comprised of thin-film layers of semiconductors with lower bandgap (e.g. WO_3, $TiSi_2$,) behind a wide bandgap semiconductor (e.g. TiO_2) facing the electrolyte [15]. Similar photoanodes can be synthesized with nanotubular structures with outer layer of titanium dioxide (TiO_2) covering nanotubes of WO_3, CdS or $TiSi_2$. The low bandgap semiconductors have high efficiency in light absorption covering the visible solar spectrum while TiO_2 provides corrosion protection. The layered nanotubular electrodes can be arranged in a patterned array for trapping sunlight more effectively compared to the densely packed nanotubular structures, providing large illuminated area effective for electrolysis. While the nanostructure greatly improves the interfacial surface area and light absorption, the efficiency of the charge carrier transport across the interfaces and removal of charge carrier traps at the semiconductor-electrolyte interface need to be investigated for different heterostructures including layered films, nanotubes and nanoparticles.

Interfacial charge carrier transfer phenomena govern the PEC-based hydrogen generation process. Studies on the role of surface and interface states in the charge carrier transport and the necessity for matched lattice structure in using heterostructured semiconductors (such as TiO_2 and $TiSi_2$) have been reported in the literature [7], however, the chemical and physical control mechanisms for mitigating the losses due to the presence of charge carrier traps and for minimizing photocorrosion of the electrodes are yet to be established.

Optimization of the optical system for illuminating photoanode at the desired irradiance level with solar concentrator is needed for obtaining maximum efficiency at a low cost. For collecting sunlight at the maximum level it is necessary to use a solar concentrator with self-cleaning properties to avoid loss of light transmission efficiency due to the deposition of dust. It is expected that large-scale PEC-based hydrogen production facility will take place in semi-arid and desert locations where irradiance level is high but these places are often the dustiest locations.

Experimental Studies and Results

Our experimental studies consisted of: (1) synthesis nanotubular TiO_2 photoanodes by anodization of Ti foil followed by annealing under oxygen atmosphere; (2) surface modification of TiO_2 photoanodes with He plasma for removing organic contaminants and charge carrier traps; (3) surface doping of the photoanode surface with nitrogen plasma to form $TiO_{2-x}N_x$ (Figure 2a) and creating oxygen vacancies at the surface thus leaving the bulk semiconductor pristine in its crystalline TiO_2 structure for high electron conductivity for improved photocurrent density [17]; (4) optimization of the structure of the nanotubes by varying anodization voltage for increasing light absorption; (5) development of layered electrodes of WO_3, $TiSi_2$ and TiO_2; (6) analysis of the photoanode structures (Figure 2b) using X-ray photoelectron spectroscopy (XPS); and (7) evaluation of surface-modified nanostructured photoanodes for PEC generation of hydrogen.

The test photoanodes prepared for evaluating the photoelectrolytic properties were annealed under both oxygen and nitrogen atmospheres achieve crystallization of TiO_2 in its anatase form. The PEC apparatus used for measuring photocurrent density of the test photoanodes under dark and illuminated conditions consisted of: (1) a potentiostat/galvanostat electrochemical instrument Model 283, (2) a Xenon lamp (30 mW/cm^2), (3) a 60 mm-diameter quarts optical window, and (4) a reference electrode (Ag/AgCl) placed close to the photoanode. The electrolyte used was 1M KOH (pH ~ 14) + de-ionized water solution. The experimental arrangements are shown in Figure 1.

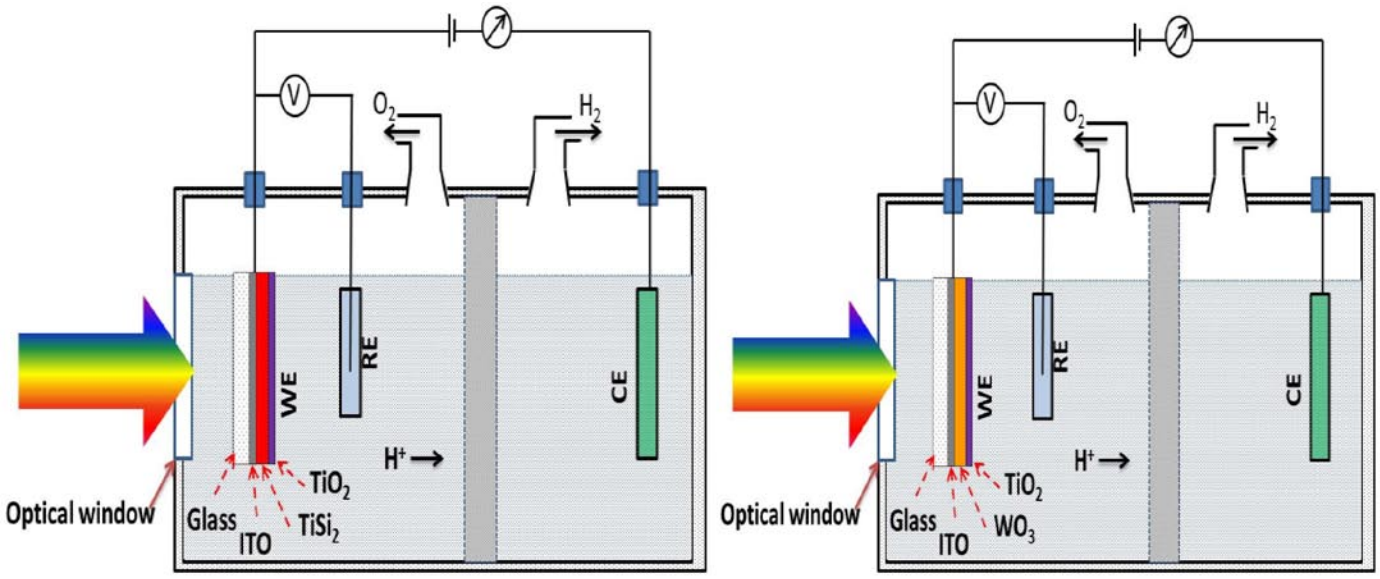


FIGURE 1. Experimental arrangement for PEC generation of hydrogen using different photoanodes (a) hybrid $TiSi_2$ and TiO_2 electrode (left) and (b) hybrid WO_3 and $TiSi_2$ electrode (right). A Pt counter electrode was used in both cases. WE, RE, and CE denote working electrode, reference electrode, and counter electrode respectively. The glass plate is coated with indium tin oxide (ITO) to form a transparent conductive substrate for depositing photoanodes.

An electrodynamic screen was developed for operating solar concentrators using Fresnel lens with self-cleaning properties against deposition of dust on the sunlight collector surface [8]. A transparent electrodynamic screen can remove the dust layer in less than two minutes without any need for water or mechanical method for cleaning.

Results

XPS analysis indicated the incorporation of N in titania lattice structure of the photoanode surface. As shown in Figures 2a and 2b, the narrow scan N 1s spectrum is demonstrated at 400 and 396 eV, which has been ascribed to the presence of nitrogen in the lattice structure either as substitutional dopants for O, or as interstitial dopants in the TiO_2 crystal structure.

Stepped-voltage anodization was used to synthesize titania nanotubes of variable diameters. Photocurrent density vs bias voltage plotted for samples anodized at different voltages. Annealing of the photoanodes was optimized. Most significant improvement came from the nitrogen plasma treatment of titania photoanodes which resulted in 80% increase in photocurrent density. Plasma surface cleaning with helium plasma and surface doping by nitrogen plasma increased photocurrent density of titania nanotubular

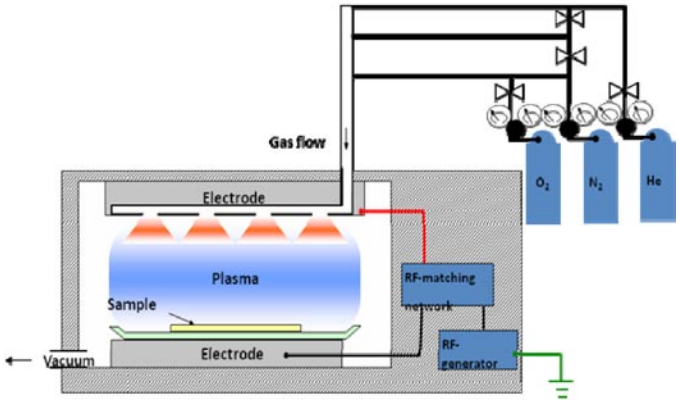


FIGURE 2a. Schematic of low-pressure plasma reactor used for surface modification including He–plasma for surface cleaning and minimizing surface charge carrier traps followed by surface doping of with N-plasma to form $TiO_{2-x}N_x$ at the photoanode surface.

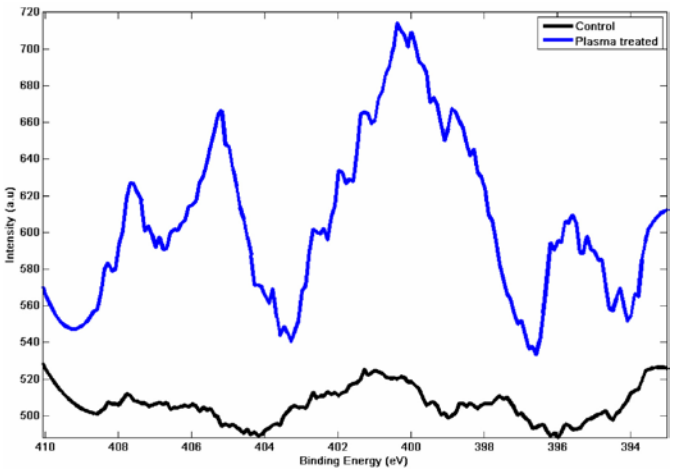


FIGURE 2b. XPS Spectrum (a) Control and (b) Nitrogen-Plasma treated $TiO_{2-x}N_x$ Photoanodes

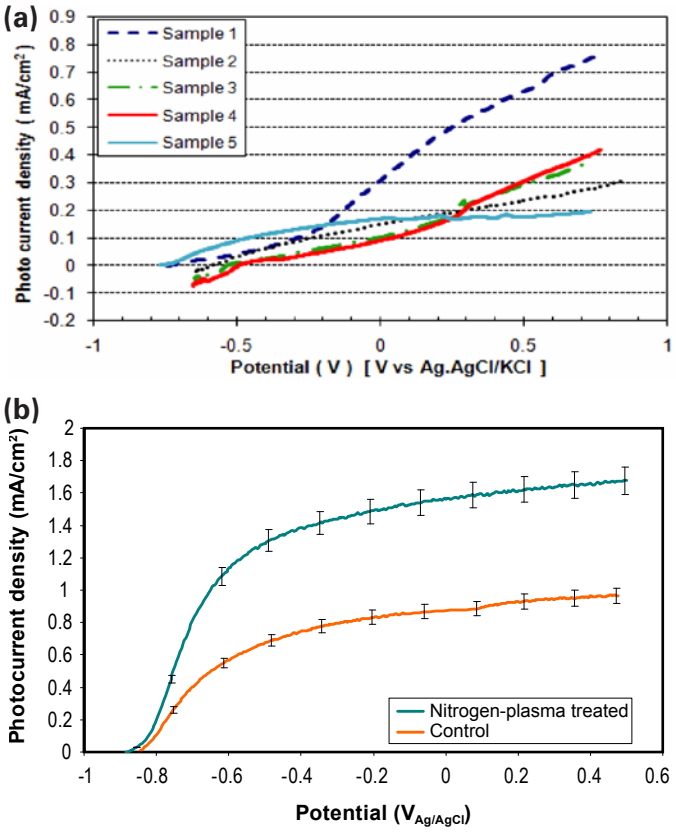


FIGURE 3. Photocurrent density measurements for evaluating photoanodes synthesized under different conditions. The electrolyte used was 1M KOH (pH~14) + de-ionized water solution. A Xe lamp was used to illuminate photoanodes at an irradiance level of 30 mW/cm^2. (a) Photocurrent density vs. stepped voltage anodization of TiO_2 nantubular electrodes; sample #1 was anodized at three steps: at 20 V for 40 min, next 40 V for 10 min, and finally 60 V for 10 min, Sample #2 was anodized in one step, 60 V for 60 min, sample #3 was anodized at 40 V for 60 min, and samples 4 and 5 were both anodized in one step at 20 V for 60 minutes. (b) Photocurrent density measurements for control and nitrogen plasma treated titania photoanodes before and after N plasma treatment to form followed by He plasma cleaning. $TiO_{2-x}N_x$ was formed at the surface of TiO_2 nanotubes. Photocurrent density increased from 0.93 mA/cm^2 to 1.68 mA/cm^2 at a bias voltage of 0.2 V.

electrodes [17]. The results showed enhanced light absorption and increased photocurrent density by 55% (Figure 3).

Several deposition processes for developing heterojunction $TiO_2/TiSi_2$ photoanodes have been studied; an e-beam deposition system has been used for depositing thin films of different photoanode materials. An electrospray system has been designed for electrostatic coating of $TiSi_2$ particles with nanoparticles of TiO_2.

Our experimental data show that deposition of fine atmospheric dust on solar collector with surface mass density of 4 g/m^2 can obscure sunlight by more than 40%. Design of a self-cleaning solar concentrator has been completed with mirrors and fiber optics for illuminating the photoanode surface at 10-sun level of irradiance is shown in Figures 4a and 4b.

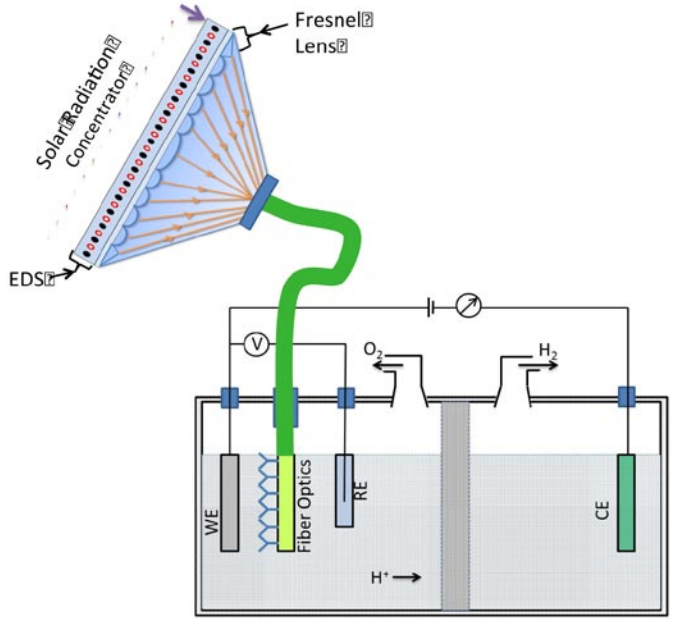


FIGURE 4a. Illumination of photoanode with self-cleaning solar concentrator at an irradiance level of 10 sun. A fiber optics-based light coupling is used to allow illumination of the photoanode at the front surface of the electrode to minimize reflection loss at the outer glass optical window and at the back surface of the inner indium tin oxide-coated glass substrate. An electrodynamic screen is used to remove dust deposited on the front surface of the Fresnel lens.

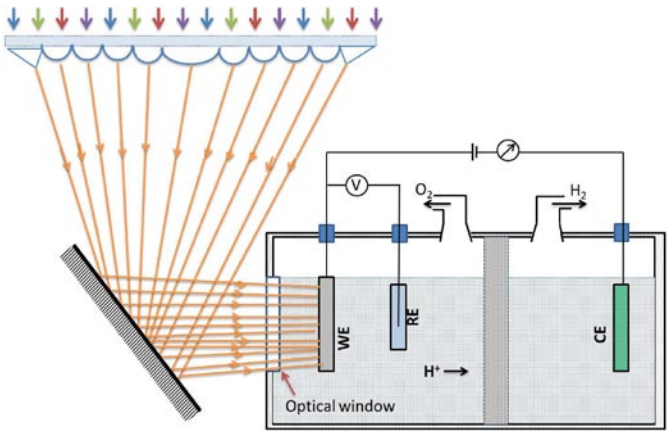


FIGURE 4b. Illumination of photoanode with self-cleaning solar concentrator at an irradiance level of 10 sun. A mirror is used is used to allow illumination of the photoanode at the back surface. This arrangement suffers from reflection losses at the outer glass window and the back surface of the inner indium tin oxide-coated coated glass substrate. There is no fiber optic coupling loss in this arrangement.

Conclusions

Our experimental studies with plasma surface treatments with helium and nitrogen gas show a significant

increase of $TiO_{2-x}N_x$ photoanode current density compared with the untreated surface of the electrodes. The nitrogen plasma treatment increased acceptor surface states and increased oxygen vacancies. Surface cleaning of the photoanode by low-temperature helium plasma treatment removed a major fraction of the contaminants (adsorbates) from the surface.

The present work reports the importance of systematic investigations of: (1) the morphological structure of the nanotube arrays, (2) the plasma treatment process for surface doping of TiO_2 nanotubular photoanode with N for increasing oxygen vacancies, and (3) optimization of the annealing process for crystallization of TiO_2 for improving photocatalytic generation of hydrogen from water. The test results show promising aspects of tuning several parameters involved in developing heterostructured photoanodes for PEC-based hydrogen production. Development and design of self-cleaning solar concentrator for increasing solar irradiance at the photoanode surface is reported.

Plan for Future Studies

Develop: (1) hybrid nanostructured photoanode comprised of thin-film layers of semiconductors with lower bandgap (e.g. WO_3, $TiSi_2$, CdS) behind a wide bandgap semiconductor (e.g. TiO_2) facing the electrolyte, (2) patterned array of nanotubular electrodes for trapping sunlight more effectively compared to the densely packed nanotubular structures, providing large illuminated surface area effective for electrolysis, and (3) encapsulated nanoparticles of core-shell design using narrow and wide bandgap materials.

We plan to investigate the charge carrier transport process across the interfaces and removal of charge carrier traps at the semiconductor-electrolyte interface by passivation of the dangling bonds for different heterostructures, including layered films, nanotubes and nanoparticles.

Study methods for: (1) optimizing the film thickness (in the nanometer to micrometer range, to improve tunneling and charge carrier transport); (2) matching the crystalline structures of the layered semiconductors; and (3) measuring the photocurrent conversion efficiency (incident photon conversion efficiency vs λ), corrosion resistance, and photo-generated carrier concentration decay rate (by using a radio frequency-conductivity probe); and (4) investigate the use of self-cleaning solar concentrator for operating the PEC at an optimum irradiance level.

FY 2011 Publications/Presentations

Publications

1. Rajesh Sharma, Hidetaka Ishihara, Alexandru S. Biris, Malay K. Mazumder, "Development of surface engineered nanostructured photoanodes for enhanced photo electrochemical processes," *IEEE Industry Applications Society 43rd Annual Meeting*, Houston, 2010.

2. Hidetaka Ishihara, Jacob P Bock, Rajesh Sharma, Franklin Hardcastle, Ganesh K Kannarpady, Malay K Mazumder, "Electrochemical Synthesis of Titania Nanostructural Arrays and their Surface Modification for Enhanced Photoelectrochemical Hydrogen Production," *Chemical Physics Letters*, Volume 489, Issues 1-3, 1 April 2010, Pages 81-85, 2010.

3. M.K. Mazumder, A.S. Biris, R. Sharma, H. Ishihara, G. Kannarpady, and P. Girouard "PEC Based Hydrogen Production with Self-Cleaning Solar Concentrator" Poster presentation at the DOE AMR meeting at Washington D.C., May 10, 2011.

Patent Application

1. "Plasma Treated Nanostructured Titania Photo-anode for Hydrogen Generation" Rajesh Sharma, Alexandru Biris, Malay Mazumder, US Provisional patent application, 2010.

References

1. Yamashita H, Honda M, Harada M, Ichihashi Y, Anpo M, Hirao T, Itoh N., and Iwamoto N 1998 *J. Phys. Chem.* B**102** 10707.

2. Park J H, Kim S and Bard A J 2006 *Nano Lett.* **6** 24

3. Umebayashi T., Yamaki T., and Itoh H., 2002 *Appl. Phys. Lett.* **81** 454.

4. Sakai N, Wang R, Fujishima A, Watanabe T and Hashimoto K 1998 *Langmuir* **14** 5918.

5. Negishi N, Takeuchi K and Ibusuki T 1998 *J. Mater. Sci.* **33** 5789.

6. Grimes C A 2007 *J. Mater, Chem.* **17** 1451.

7. Hernandez-Alonso, M. D., Fresno, F., Surez, S.,and Coronado, J. M., *Energy Environ. Sci, The Royal Soc. of Chemistry,* 2009, 2, 1231 – 1257.

8. Yu J C, Lin J, Lo D and Lam S K 2000 *Langmuir* **16** 7304.

9. Chiba Y, Kashiwagi K and Kokai H 2004 *Vacuum* **74** 643.

10. Jun J, Shin J H and Dhayal M 2006 *Appl. Surf. Sci.* **252** 3871.

11. Nakamura I, Negishi N, Kutsuna S, Ihara T, Sugihara S and Takeuchi K 2000 *J. Mol. Catal.* A **161** 205.

12. Garbassi F, Morra M and Occhielo E 1996 *Polymer Surfaces: From Physics to Technology* (New York: Wiley) p 223.

13. Chan C M 1994 *Polymer Surface Modification and Characterization* (Munich: Hanser Publications) p 225.

14. Changsheng L, Zhibin M A, Li J and Weihong W 2006 *Plasma Sci. Technol.*

15. Zhang, J.Z., *MRS Bulletin, Material Research Society, vol. **36**, Jan 2011, 48 – 55.*

16. Maeda, K., and Domen, K., *MRS Bulletin, Material Research Society, **36**, Jan 2011,25 –31.*

17. R. Sharma, P.P. Das, V. Mahajan, J. Bock, S. Trigwell, A.S. Biris, M.K. Mazumder, M. Misra, "Enhancement of Photoelectrochemical Conversion Efficiency of Nanotubular TiO_2 Photoanodes using Nitrogen Plasma Assisted Surface Modification," *Nanotechnology*, Vol. 20, 2009, 075704.

18. Mazumder, M.K., Biris, A.S., Johnson, C.E., Yurteri, C.Y., Sims, R.A., Sharma, K. Pruessner, S. Trigwell and. Clements, *Particles on Surfaces 9: Detection, Adhesion and Removal, Brill Publisher,, 2006, pp.1-29. ISBN 90 6764 435 8.*

II.G.8 Photoelectrochemical Hydrogen Generation from Water Using $TiSi_2$ –TiO_2 Nanotube Core-Shell Structure*

Dr. Mano Misra
University of Nevada, Reno
1664 N. Virginia, MS 388
Reno, NV 89505
Phone: (775) 784-1603
E-mail: misra@unr.edu

DOE Managers
HQ: Eric Miller
Phone: (202) 287-5829
E-mail: Eric.Miller@hq.doe.gov
GO: David Peterson
Phone: (720) 356-1747
E-mail: David.Peterson@go.doe.gov

Contract Number: DE-FC36-06GO 86066

Subcontractor:
Dr. John A. Turner
National Renewable Energy Laboratory (NREL), Golden, CO

Start Date: June 1, 2006
Projected End Date: September 30, 2012

*Congressionally directed project

Fiscal Year (FY) 2011 Objectives

- Develop high efficiency metal oxide nanotubular array photo-anodes for generating hydrogen by water splitting.
- Develop density functional theory to understand the effect of morphology of the nanotubes on the photo-electrochemical properties of the photo-anodes.
- Develop kinetics and formation mechanism of the metal oxide nanotubes under different synthesis conditions.
- Develop combinatorial approach to prepare hybrid photo-anodes having multiple hetero-atoms incorporated in a single photo anode.
- Improve the durability of the material.
- Scale-up the laboratory demonstration to production unit.

Technical Barriers

This project addresses the following technical barriers from the Production section (3.1.4) of the Fuel Cell Technologies Program Multi-Year Research, Development and Demonstration Plan:

(Y) Materials Efficiency

(Z) Materials Durability

Technical Targets

This project is investigating potential application of hybrid metal oxide nanotubes (NTs) for hydrogen generation by water photoelectrolysis. Insights gained from these studies will be applied toward the design and synthesis of high efficiency materials for hydrogen generation from water splitting that meet the following DOE targets:

- Usable semiconductor bandgap: 2.0eV by 2018.
- Chemical conversion process efficiency: 10% by 2013.
- Plant durability: 1,000 hr by 2013.

✧ ✧ ✧ ✧ ✧

Approach

In this current project, utilization of hybrid metal (Ti, Fe, Ta) oxide nanotubular arrays for generation of hydrogen from water using sunlight is studied. The metal oxide nanotubular arrays are found to be robust, photo-corrosion resistant, and can be used efficiently to generate hydrogen and most importantly active in the visible light portion of the solar spectrum. It is envisioned that the process can be efficient and economical in the production of solar hydrogen. The nanotubular arrays are prepared by electrochemical anodization of solid metal in different inorganic and organic electrolytes in the presence of fluoride ions. The effect of voltage, time, and solution chemistry on the size, uniformity, and self-assembly of nanotube formation is studied. It is found from preliminary work that materials prepared in organic solvents such as ethylene glycol by an ultrasonic assisted process are very stable and form an efficient pattern of nanotubes that have excellent photo-efficiency. We have already developed processes to synthesize metal oxide nanotubes in inorganic, organic and ionic liquids as electrolytes. This process is also found suitable to prepare mixed metal oxide nanotubes e.g. TiFe, TiMn and TiW. In addition to the preparation of metal oxide based photoanodes, we have also shown that these nanotubes can work efficiently as a cathode by nanoparticle modification. In addition to the anodization process, we have also developed new mixed metal oxide compounds by sol-gel method. This project is integrating a highly efficient photoanode, a cathode, and a modified electrolyte to design a photoelectrochemical (PEC) cell to generate hydrogen with at least 10% efficiency by 2013. The scale up process looks highly promising for large scale hydrogen generation.

The hydrogen generation work is conducted using a hybrid metal oxide nanotubular or mixed metal oxide photoanode in alkaline solutions in the presence of simulated solar light. The material stability and

photo-efficiency is determined as a function of time, electrochemical and analytical measurements. The photo-efficiency is determined by measuring current as well as volume of the hydrogen generated by gas chromatograph. The material stability and photo-efficiency is determined as a function of time, electrochemical and analytical measurements.

In the future our main focus for the research will be to understand:

- Synthesize photoanodes that can harvest the full spectrum of sunlight.
- Theoretical investigation on the materials synthesized.
- On-field testing under real solar irradiation.

On the basis of fundamental and applied research, a scale up experiment in the laboratory will be performed to elucidate the viability of the new catalysts for photo-electrochemical generation of hydrogen using sunlight.

FY 2011 Accomplishments

- The UNR team has developed a composite photocatalyst comprising of self-assembled titania (TiO_2) NTs coupled with titanium disilicide ($TiSi_2$) nanoparticles (NPs) for PEC hydrogen generation (Figure 1).
- A new approach is taken to synthesize TiO_2 NTs with bigger pore size and length so that more $TiSi_2$ particles can be loaded. Anodization of Ti to form TiO_2 NTs in the presence of a chelating agent disodium ethylenediamine tetraacetate ($Na_2[H_2EDTA]$) under high voltage (80 V_{DC}) makes the diameter of the NTs bigger than the conventional process (Figure 2). The back side of the TiO_2 NTs is etched with 5% hydrofluorhydric acid to form a TiO_2 nanotubular membrane.
- $TiSi_2$ NPs are produced from commercial bulk particles by a multiple ball milling followed by ultrasonicatation process (Figure 3). The $TiSi_2$ nanoparticles are sintered into the TiO_2 nanotube array to prepare the $TiSi_2/TiO_2$ NTs. This catalyst is then annealed under a nitrogen atmosphere to form a composite of $TiSi_2$ nanorods inside TiO_2 NTs at 500°C for 6 h. The prepared $TiSi_2$-TiO_2 material is then coated on Ti foil using a titanium tetrachloride solution followed by annealing at 500°C for 3 h under nitrogen. This also helped in sintering the $TiSi_2$ nanoparticles inside the TiO_2 nanotubes to form a nanorod array. The TiO_2 nanotubular array is found to be stable after the synthesis of $TiSi_2$ nanorods inside them (Figure 4). The $TiSi_2$ nanostructure is found to be homogeneously distributed throughout the TiO_2

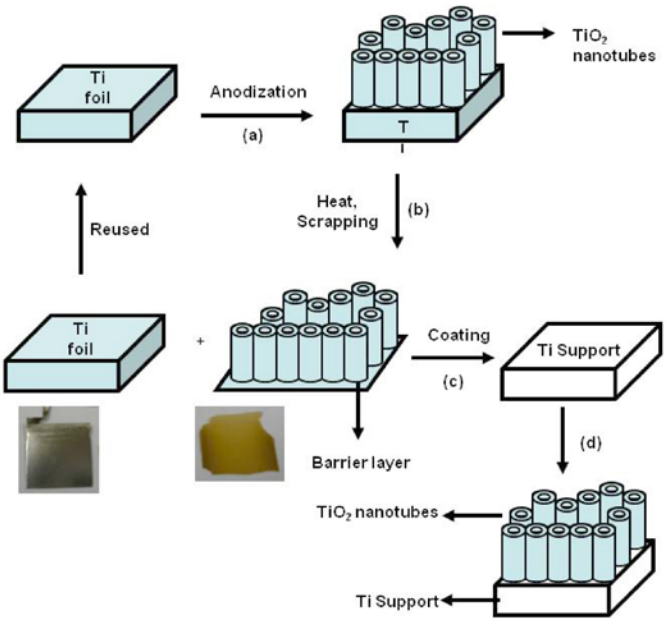


FIGURE 1. Schematic Showing the Formation of $TiSi_2/TiO_2$ NT Composite Structure

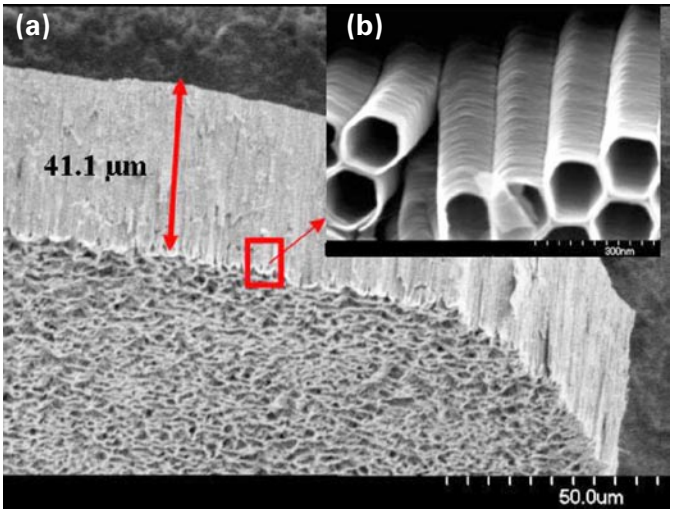


FIGURE 2. Field emission scanning electron microscope images of TiO_2 NTs prepared in organic medium at 80 V_{DC} for 30 min. (a) top view and (b) cross sectional view (close-up) view of the NTs.

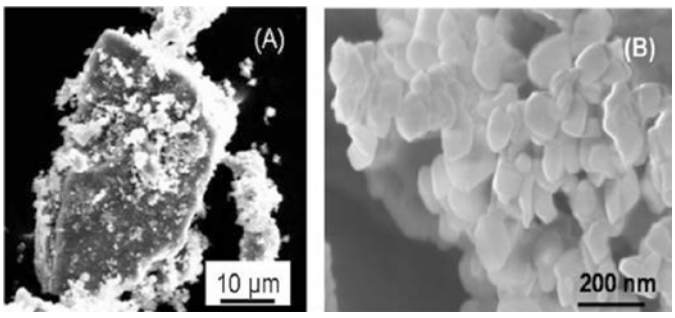


FIGURE 3. Field emission scanning electron microscope images of (A) as-received $TiSi_2$ particles (<44 µm), (B) ball-milled $TiSi_2$ particles (~50-60 nm).

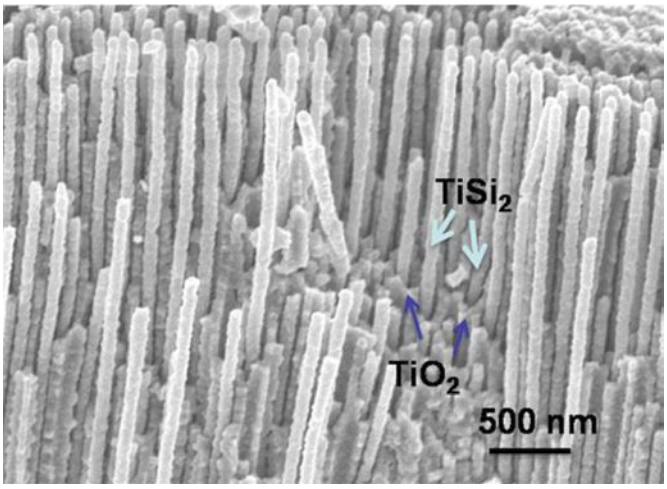


FIGURE 4. Field emission scanning electron microscope images of $TiSi_2$ particles sintered into the TiO_2 NT array.

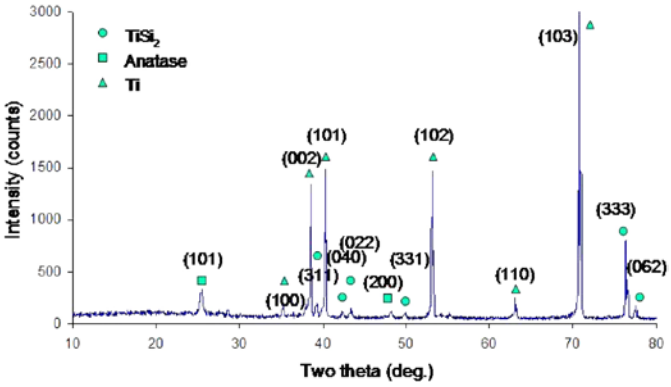


FIGURE 5. Glancing angle X-ray diffraction pattern of $TiSi_2$ NP/TiO_2NT. Orthorhombic $TiSi_2$ and anatase TiO_2 are observed in the heterostructure. A peak for the Ti base is also noticed.

nanotubular array. Energy dispersive spectroscopy analysis showed ~25 wt% $TiSi_2$ in the $TiSi_2/TiO_2$ NTs photocatalyst. Glancing angle X-ray diffraction pattern shows peaks corresponding to both $TiSi_2$ and TiO_2 (anatase) (Figure 5).

- The diffuse reflectance ultraviolet and visible spectrum of $TiSi_2/TiO_2$ NTs catalyst shows a sharp edge ~550 nm (band gap, $E_g = 2.25$ eV). The strong absorption peaks in both the ultraviolet and visible regions suggest that the $TiSi_2/TiO_2$ NT photocatalyst is prepared by combining the absorption properties of the TiO_2 NTs in the ultraviolet region and $TiSi_2$ in the visible region (Figure 6).
- The heterostructural composite photoanode exhibited an enhanced photocurrent density of 3.49 mA/cm^2 at 0.2 $V_{Ag/Ag/Cl}$ compared to TiO_2 nanotubes alone (0.9 mA/cm^2) and can be considered as a potential possible candidate for water splitting reaction using visible light (Figure 7).

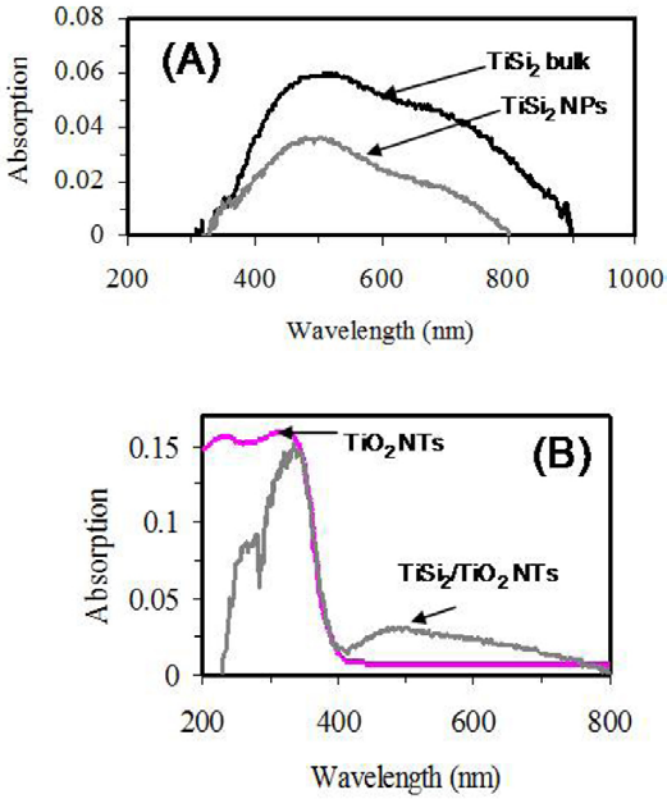


FIGURE 6. Diffuse reflectance ultraviolet and visible spectra of (A) $TiSi_2$ bulk and nanoparticles and (B) TiO_2 NTs and $TiSi_2/TiO_2$ NTs catalyst. $TiSi_2$ particles showed absorption in the visible light region and $TiSi_2/TiO_2$ NTs absorb light in both ultraviolet and visible region. Band gap = 2.25 eV.

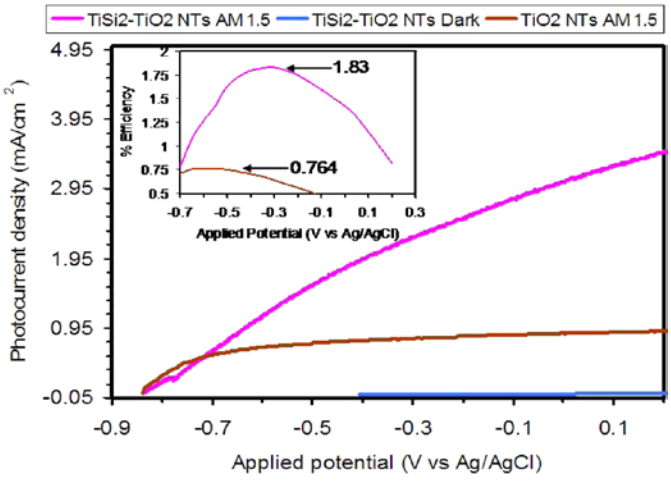


FIGURE 7. Potentiodynamic plot of annealed $TiSi_2/TiO_2$ NTs and TiO_2 NTs. Inset shows the solar-to-hydrogen conversion efficiency of $TiSi_2$-TiO_2 NTs and TiO_2 NTs under AM 1.5 illumination.

Conclusions and Future Actions

In the last year, we have developed a new type of coupled semiconductor photo-catalyst by coupling $TiSi_2$

nanoparticles and TiO_2 NTs by simple sintering method. A unique architecture, $TiSi_2$ nanorods inside $TiSi_2$ nanotubes, is prepared by this process. It showed four-fold enhancement in the amount of hydrogen generated compared to only TiO_2 NTs and ten times compared to P25 TiO_2 nanoparticles. The following bulleted list is indicative of the areas we will pursue in the coming year of the project:

- Synthesize visible light sensitive photoanodes.
- Kinetics studies of nanotube formation by titration using spectrophotometric analysis.
- Theoretical investigation of $BiFeO_3$ by density functional theory.
- To understand the ordering of oxygen vacancies and their role on charge transport properties and recombination losses in oxide and oxynitride semiconductors.
- Scale up the system.
- Design PEC system for on-field testing under real solar irradiation.
- Synthesize quantum dots incorporated inside TiO_2 NTs for PEC.

FY 2011 Publications/Presentations

Publications (2010-2011)

1. "Bismuth Iron Oxide Nanoparticles as Photocatalyst for Solar Hydrogen Generation from Water" *Journal of Fundamentals of Renewable Energy and Applications (JFREA)* (**2011**, *1*, Article ID R101204, 10 pages). **(INVITED)**

2. "Water Photooxidation by $TiSi_2$-TiO_2 Nanotubes" **S. Banerjee**, S.K. Mohapatra, M. Misra *J. Phys. Chem. C* **2011**, *115*,12643-12649.

3. "Morphology-Controlled ZnO Nanomaterials for Enhanced Photoelectrochemical Performance" *Mater. Express* **2011**, *1*, 59-67.

4. "Easy synthesis of bismuth iron oxide nanoparticles as photocatalyst for solar hydrogen generation from water" Master's Thesis by Deng, Jinyi, **2010**, 85 pages; AAT 1484020.

5. Quantum Dot Sensitized Nanotubes for Full Solar Spectrum Photovoltaic Cell Master's Thesis by *Khanal, Sohana*, **2010**, 104 pages; AAT 1484059.

II.G.9 USD Catalysis Group for Alternative Energy*

James D. Hoefelmeyer (Primary Contact),
Ranjit Koodali, Grigoriy Sereda, Dan Engebretson,
Jan Puszynski, Jacek Swiatkiewicz, Hao Fong,
Phil Ahrenkiel, Rajesh Shende
The University of South Dakota (USD)
414 E. Clark St.
Vermillion, SD 57069
Phone: (605) 677-6186
E-mail: jhoefelm@usd.edu

DOE Managers
HQ: Eric Miller
Phone: (202) 287-5829
E-mail: Eric.Miller@hq.doe.gov
GO: David Peterson
Phone: (720) 356-1747
E-mail: David.Peterson@go.doe.gov

Contract Number: DE-EE0000270

Subcontractor:
South Dakota School of Mines and Technology,
Rapid City, SD

Project Start Date: December 1, 2009
Project End Date: November 30, 2011

*Congressionally directed project

Fiscal Year (FY) 2011 Objectives

- Synthesize dye-sensitized TiO_2 nanorods with catalyst particles attached to the tips.
- Use Langmuir-Blodgett methods to incorporate nanorods as membrane-spanning units in lipid bilayers.
- Develop and test a prototype capillary reactor for photocatalysis of water-splitting.
- Synthesize high-surface area carbon nanofelt.
- Develop and test a prototype hydrogen fuel cell with carbon nanofelt incorporated as catalyst support material.

Technical Barriers

This project addresses the following technical barriers from the Photoelectrochemical Hydrogen Production and Fuel Cells sections of the Fuel Cell Technologies Program Multi-Year Research, Development and Demonstration Plan:

3.1.4 Photoelectrochemical Hydrogen Production

(Y) Materials Efficiency
(Z) Materials Durability
(AA) PEC Device and System Auxiliary Material
(AB) Bulk Materials Synthesis
(AC) Device Configuration Designs
(AD) Systems Design and Evaluation

3.4 Fuel Cells

(A) Durability
(B) Cost
(C) Performance

Technical Targets

TABLE 1. Technical Targets: Photoelectrochemical Hydrogen Production (from Table 3.1.10)

Characteristics	Units	2006 status	2013 target
Usable semiconductor bandgap	eV	2.8	2.3
Chemical conversion process efficiency	%	4	10
Plant solar-to-hydrogen efficiency	%	Not available	8
Plant durability	hr	Not available	1,000

Our strategy is to utilize TiO_2 as semiconductor (bandgap ~3.0 eV) that is dye-sensitized with visible light chromophore such as N719 dye (~1.7 eV). Ideally, the chromophore would be a broad-spectrum absorber to allow utilization of near infra-red (NIR) and visible light. Our project does not focus specifically on dye improvement, only utilization of established sensitization protocols. Dye-sensitization has the advantage that band-edge potentials can match requirements for component half-reactions of water-splitting while utilizing the solar spectrum (visible/NIR photons).

TABLE 2. Technical Targets: H_2 Fuel Cell (Transportation)

Characteristics	Units	2010 target	2015 target
Durability with cycling[a,b]	Hr	5,000	5,000
Cost[a]	$/kW$_e$	45	30
Cost[b]	$/kW$_e$	25	15

[a] Integrated transportation fuel cell power systems operating on direct hydrogen.
[b] Transportation fuel stacks operating on direct hydrogen.

FY 2011 Accomplishments

- Synthesis of anisotropic TiO_2 anatase nanocrystal with growth in <100>, <101>, or <001> direction with organo-carboxylate or organo-amine surface agent.

- Synthesis of mesoporous silica doped with Ti or W ions and demonstration of photocatalytic proton reduction in aqueous solution with methanol. Hydrogen turnover frequency was 0.0002 H_2•tungsten site^{-1}•s^{-1} ($220 < \lambda < 380$ nm transmitted).
- Synthesis of TiO_2 nanotube array double-layer. Pt nanoparticles were deposited on the TiO_2 surface. Demonstration of photocatalytic proton reduction in aqueous solution with methanol or iodide. Hydrogen evolution was 0.37 mL•s^{-1}•m^{-2} ($220 < \lambda < 400$ nm transmitted).
- Electrospinning of polymer nanofibers, ceramic nanofibers, and thermal treatment to yield graphitic carbon nanofibers.
- Acquisition of Langmuir-Blodgett trough, total organic carbon analyzer, graphitization furnace, gas chromatograph, and fuel cell test station as part of South Dakota research infrastructure improvement effort.



Introduction

There is demand for abundant energy without consequences of pollution that can be met with solar energy utilization. While there are many ways to use sunlight, we focus on the use of materials that allow fast conversion of light to hydrogen and fast conversion of hydrogen to electricity. These two processes can be accomplished with two types of devices, a photoelectrochemical cell and hydrogen fuel cell, respectively. Both processes are complex, and research into their optimization is a priority. Our research into photoelectrochemical cells is an effort to develop new materials that can produce hydrogen from sunlight and water at high efficiency and low cost; our research into hydrogen fuel cells will mostly focus on development of new materials to make a longer-lasting and lower cost device.

Approach

Photoelectrochemical cells include catalysts that rapidly capture sunlight and convert the energy to a chemical fuel and chemical oxidizer. This can be done by 'splitting' water to hydrogen and oxygen. More specifically, water undergoes autodissociation to give protons and hydroxide anions. If electrons are added to protons, then hydrogen is synthesized; while taking away electrons from hydroxide anions yields oxygen. The catalyst speeds up these two chemical processes. The catalyst must also be able to absorb sunlight. Upon doing so, the light energy causes the excitation of an electron. The electron is more reactive after excitation, and it leaves an electron 'hole'. The catalyst must be able to use the excited electron to synthesize hydrogen and to use the electron hole to synthesize oxygen. So far, no single material has been discovered that can accomplish all three tasks: light absorption, hydrogen synthesis, and oxygen synthesis. Combination of several materials, however, working together can enable the photoelectrochemical cell. This is somewhat similar to photosynthesis, wherein plants convert sunlight to fuel (sugars) and oxidizer (oxygen), in that several molecular pieces work together. For this reason, photocatalysis within a photoelectrochemical cell is sometimes referred to as artificial photosynthesis. The materials that we plan to use include nanocrystals of TiO_2, Pt, and RuO_2, dye molecules, and lipids. The materials will be organized in chemical reactions and self-assembly steps to produce a reactive free-standing membrane capable of solar photocatalysis in which water is converted to hydrogen and oxygen.

Hydrogen fuel cells catalyze the reverse reaction of photoelectrochemical cells that split water. Instead of giving back a photon; however, the fuel cell produces electricity. Thus hydrogen (fuel) and oxygen (oxidizer) combine in a membrane-electrode assembly to produce water and electric current. The membrane-electrode assembly includes cathode, anode, and proton exchange membrane. At the anode, hydrogen gives up electrons to form protons. At the cathode, electrons and protons that formed at the anode combine with oxygen to form water. The protons reach the cathode through the proton exchange membrane. The electrons reach the cathode through an external circuit. The reaction at the cathode is the driving force for the fuel cell, and force the flow of electrons through the external circuit thereby producing electric current. The hydrogen fuel cell has many material components, and these are susceptible to degradation that limits the utility, lifetime, and value of the fuel cell. Our work is focused making new materials for the electrodes that extend the lifetime. We plan to use carbon nanofelts composed of carbon nanofibers. The carbon nanofibers can be produced upon thermal graphitization of polymer or ceramic (metal carbide) electrospun nanofibers.

Results

TiO_2 nanorods were synthesized via solvothermal synthesis. The nanorods were characterized with electron microscopy, powder X-ray diffraction (XRD), ultraviolet (UV)-visible and luminescence spectroscopy (Figure 1). Powder X-ray diffraction data indicated presence of anatase crystallites with broadened peaks. The 004 reflection had less line broadening than other reflections in the powder pattern, which is evidence of the anisotropic nature of the crystal. The electron microscopy data show the presence of high aspect ratio nanorods. High resolution micrographs show presence of lattice fringes that indicate the highly crystalline nature of the nanorod. The TiO_2 nanorods disperse in non-polar solvents such as hexane. The dispersion, in hexane, was used for spectroscopic analysis. The nanorods absorb strongly in the UV spectrum, with the unusual feature that the absorbance is blue-shifted by 100 nm compared to bulk anatase. This effect is due to quantum confinement in the crystal in which the Bohr exciton radius is less than the diameter of the nanorod

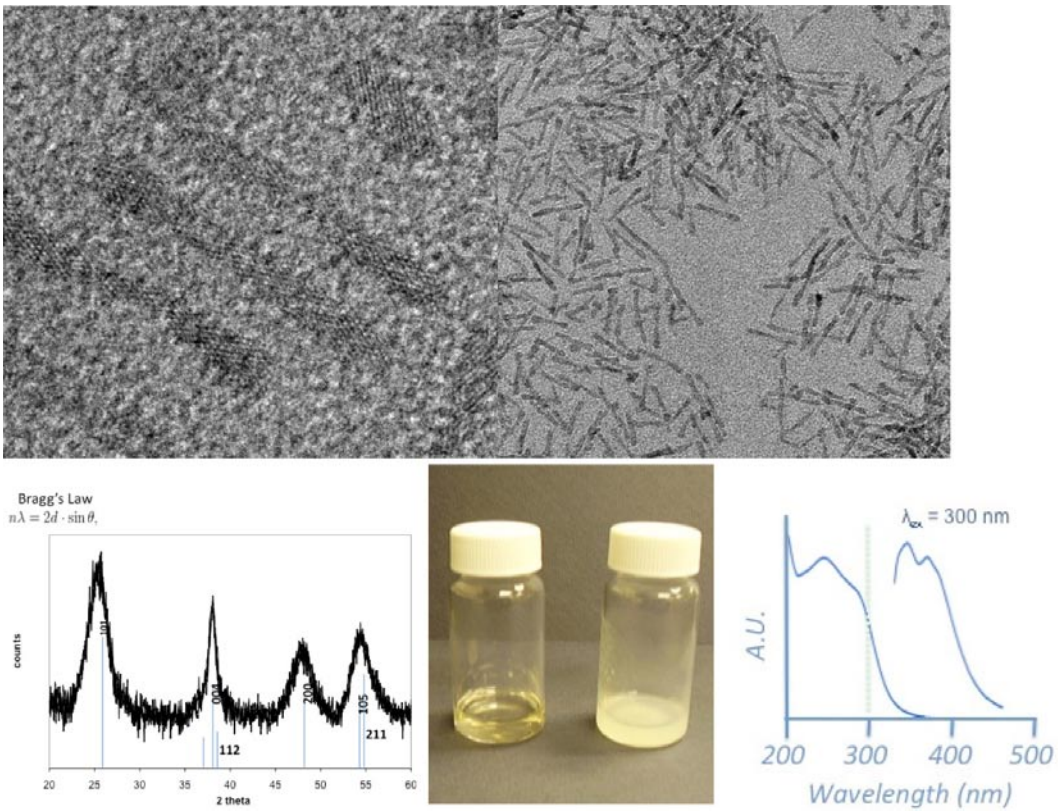


FIGURE 1. Characterization data of TiO_2 nanorods: (top) transmission electron micrographs, (bottom, from left to right) powder XRD, NR dispersion before and after exposure to visible light for 24 hrs, UV-visible and luminescence spectra.

(the effect was independent of nanorod length in the four fractions). The emission spectrum was recorded upon excitation at 300 nm. The TiO_2 nanorod dispersion is light sensitive. Over the course of several hours under visible light exposure, a white precipitate formed; whereas, dispersions protected from visible light exposure where stable for months. More recently, the growth of the anisotropic nanocrystal could be controlled to limit growth in <100>, <101>, or <001> directions dependent on conditions during synthesis.

We have attempted surface modification of the TiO_2 nanorods (NRs). One approach is selective nucleation of metal nanoparticles on the NR tips. The NRs were dispersed in high boiling solvent into which a metal precursor ($Pt(acac)_2$ or $Co_2(CO)_8$) was injected. The reactions led to formation of metal nanocrystals in solution; however, the nucleation did not occur on the NR tips (Figure 2). Another approach has been ligand exchange on the nanorods. TiO_2 NR were exposed to a solid support with dopamine chains. The NRs were attached to the surface of the support concomitant to displacement of linoleic acid. This may be due to two factors: 1) the chelating nature of the catecholate group may bind the TiO_2 surface more tightly, and 2) entropically, the reaction is favored due to the preorganization of ligands on the solid support. The solid support was washed to remove unbound TiO_2 NRs. The dopamine terminus of the solid support can be readily cleaved with trifluoroacetic acid, thereby liberating dopamine stabilized TiO_2 NRs. This was confirmed with transmission electron microscopy and nuclear magnetic resonance.

Synthesis of ordered mesoporous TiO_2 thin-film was performed using evaporation induced self assembly (EISA) and supercritical CO_2 assisted infusion methods. In EISA, a dilute solution containing Ti-butoxide, Pluronic123, HCl (38% in water), and butanol was spin coated on a glass substrate. The coated substrates were aged for 24 hr in a controlled humidity environment at 25°C. Films after aging were calcined at 350°C for 2 hr to remove the surfactant. In supercritical CO_2 infusion method, a glass substrate pre-coated with the Pluronic F108 surfactant film was loaded inside a PARR reactor, and it was heated to 60°C and pressurized to 3,000 psi with CO_2. At these processing conditions, a known amount of Ti-butoxide followed by water was injected into the reactor. As a result, solubilized portion of Ti-precursor in supercritical CO_2 was infused and hydrolyzed inside the solid surfactant film coated on a substrate. After 1 hr, the reactor was depressurized and cooled down to room temperature and the substrates were removed and calcined at 350°C. The films synthesized by both methods were characterized by scanning electron microscopy (SEM), atomic force microscopy (AFM), X-ray

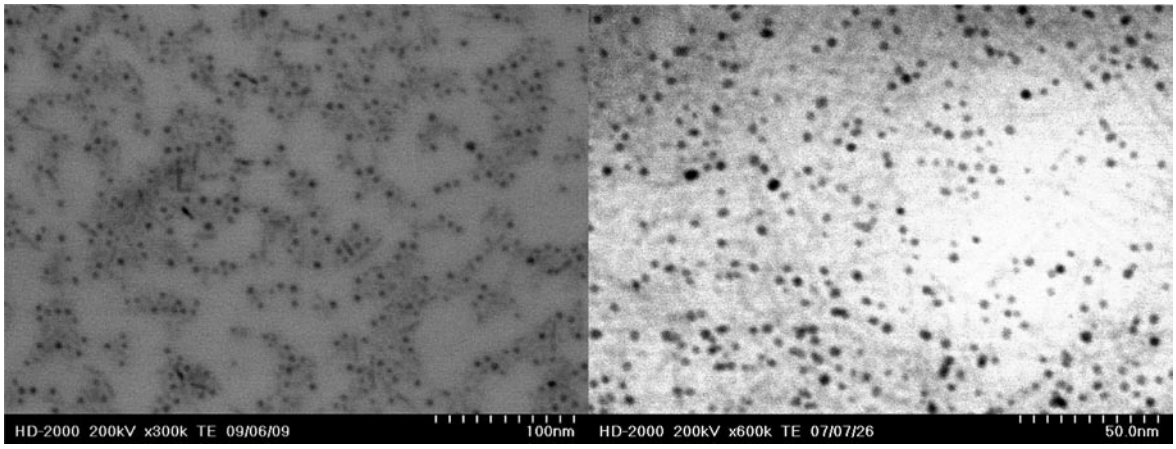


FIGURE 2. Nucleation of metals in the presence of TiO_2 NRs so far led to mixtures of metal nanocrystals and TiO_2 NRs with no evidence of metal-semiconductor interface: (left) Co nanoparticles and TiO_2 NRs (right) Pt nanoparticles and TiO_2 NRs.

diffraction, surface area, and ellipsometry. SEM images of TiO_2 film prepared by EISA reveal ordered mesoporous structure with three-dimensional cubic and two-dimensional hexagonal pore ordering with the d-spacing of 18.50 nm and 18 nm, respectively as determined by fast Fourier transform analysis. AFM images indicate highly ordered structure of the mesopores and partial pore ordering in the TiO_2 thin-films synthesized using supercritical CO_2-assisted infusion. The smaller size pores as evident in SEM and AFM images may provide mass transfer limitation for charge transport. Consequently, experiments were performed to increase pore size using pore swelling agent; for instance, 1,3,5 trimethyl benzene. Crack-free ordered mesoporous TiO_2 thin films with different thickness were prepared using EISA method. The film thickness ranges from 400 nm to 3,100 nm depending on number of layers coated and the average refractive index for these films was 1.5 as determined by ellipsometry.

We successfully demonstrated that Ti-MCM-48 mesoporous materials can be used for the photosplitting of water to generate hydrogen. Furthermore, the coordination state of Ti in the MCM-48 materials could be easily controlled by changing the order of addition of the Ti precursor. Ti-MCM-48 catalysts were tested for photocatalytic hydrogen. We extended this preparative method for the synthesis and characterization of WO_3 dispersed on MCM-48 materials and found that the photocatalytic evolution of hydrogen is dependent on the loading of WO_3. The long-range ordered mesoporous structure of MCM-48 was well preserved after tungsten incorporation. Tungsten oxide species were highly dispersed in MCM-48 matrix and no bulk crystalline WO_3 was formed. The as-prepared W-MCM-48 materials show notable photocatalytic activity for hydrogen evolution from methanol-water mixture under UV irradiation though commercial bulk WO_3 is not active for the reaction. The photocatalytic mechanism was studied by electron spin resonance spectroscopy. The tungsten oxide species that are highly dispersed in MCM-48 matrix possess a suitable band gap and sufficient reduction potential for the photocatalytic reduction of H_2O to generate H_2.

Efforts were made on the fabrication of double-sided TiO_2 nanotube membrane using electrochemical anodization method. Double sided TiO_2 nanotubes were grown using Ti foil (25 µm thick, 99.7% purity) purchased from Alfa Aesar. Ti sheet was degreased by sonicating sequentially in acetone, ethanol, and de-ionized water, followed by drying in a nitrogen stream. Electrochemical anodization of titanium was carried out at ambient conditions using a two-electrode system and a direct current power supply (Agilent Technologies, 0-60 V). Degree of anodization of Ti metal was controlled by limiting anodization voltage and H_2O content in the electrolyte. For anodization an organic electrolyte containing 0.3 wt% NH_4F and 2 vol% water in ethylene glycol was used. A platinum gauge electrode was used as a cathode in all the experiments. After anodization, the sample was washed in water to remove the impurities. The double sided TiO_2 nanotubes membrane was sensitized with 0.1 M dilute aqueous salt solution of hexachloroplatanic acid and sonicated for 5 minutes and finally annealed in argon environment containing 10 vol% H_2 at 400°C for 1 hr. The SEM image of annealed Pt/TiO_2 nanotubes is shown in Figure 3A whereas SEM image for the cross section of double sided TiO_2 nanotube membrane is depicted in Figure 3B. These images revealed tube length of about 17 µm on both side of etched Ti metal foil.

Hydrogen generation by photocatalysis using double-sided TiO_2 nanotubes membrane sensitized with Pt was investigated. This membrane was placed in a quartz cell containing aqueous solution with methanol or iodide, degassed with Ar, and irradiated with a 500 W high pressure Xe lamp equipped with AM 1.5G and IR filter ($220\ nm<\lambda<400\ nm$). Gas samples from the head space of the quartz cell were withdrawn periodically using a gas syringe and analyzed using a gas chromatograph equipped

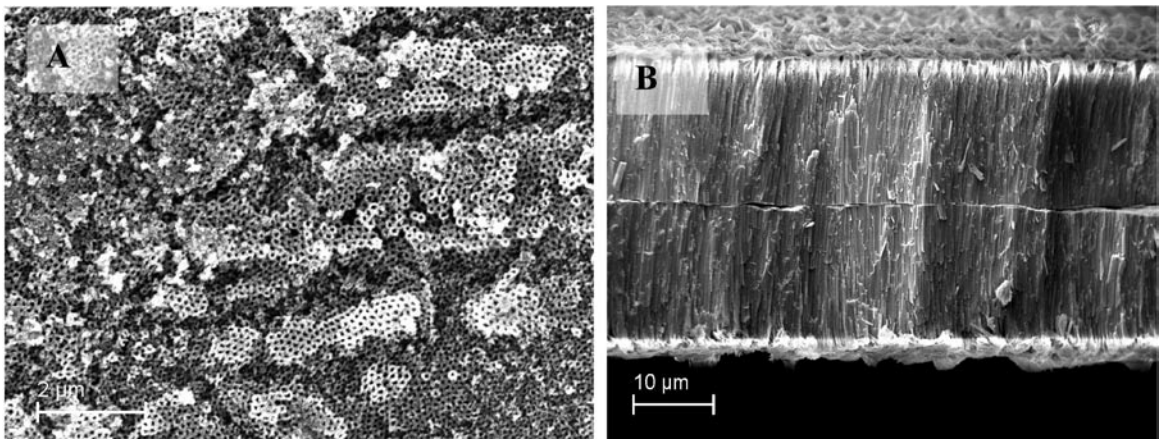


FIGURE 3. SEM images of A) TiO_2 nanotubes sensitized with Pt and B) cross section of double-sided TiO_2 nanotube membrane.

with a thermal conductivity detector. Hydrogen evolution rate was 0.37 $mL \cdot s^{-1} \cdot m^{-2}$.

Nonwoven fabrics made of electrospun polyacrylonitrile (PAN) polyvinyl alcohol, and titania carbide (TiC)-based carbon nanofibers, dubbed as Electrospun Carbon Nanofelt, with extremely high specific surface areas (up to 2,200 m^2/g) and other desired morphological and structural properties (e.g. high graphitic crystallinity), were synthesized. Conditions during electrospinning affect morphology of the polymer fibers such as diameter and porosity. Thermal treatment leads to carbon nanofibers (graphitization occurs at higher temperatures with retention of morphology). For example, electrospun PAN was graphitized thermally to yield carbon nanofibers (Figure 4). Owing to the unique morphology and structures, the electrospun carbon nanofelt is expected to out-perform carbon black as the catalyst support.

Conclusions and Future Directions

The work on photocatalyst materials for solar hydrogen involves use of high surface area TiO_2 to which functional materials on the surface enable photocatalytic water splitting. So far, several forms of high surface area TiO_2 were obtained: ordered mesoporous thin film, nanorod, nanotube arrays, or single site Ti (or W) on SiO_2-MCM-41. While doped MCM-41 was shown to catalyze proton reduction in aqueous solution, the materials still require catalyst sites and visible-light chromophore. Platinized TiO_2 nanotube arrays did show H_2 evolution under UV irradiation. So far, attempts toward selective nucleation of metals (Co or Pt) on the tips of TiO_2 NRs have proven unsuccessful despite reports in the literature. Thus one key challenge is the controlled organization of functional surface features on the TiO_2. Future work will include:

- Ligand exchange on the surface of TiO_2 nanostructures.
- Selective nucleation of metal (Co, Pt, Ru) on TiO_2 NR tips with new surface ligands.
- Sensitization of TiO_2 nanostructures with visible light chromophores.
- Photocatalyst evaluation (under simulated solar radiation) with attention to quantify turnover frequency.

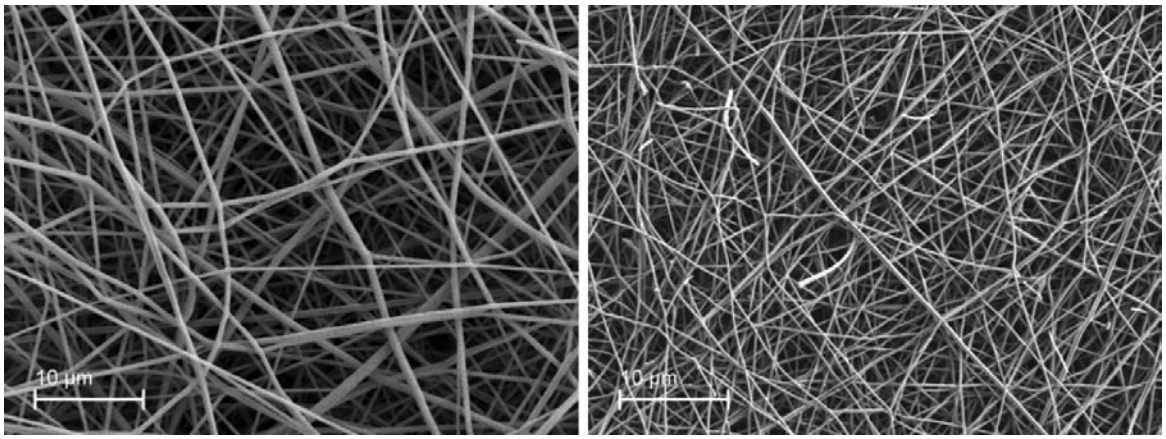


FIGURE 4. PAN-based electrospun nanofibers (left) and PAN-based carbon nanofibers (right).

The work toward carbon nanofelt for catalyst support in hydrogen fuel cell has been quite fruitful. Electrospinning of polymers is a viable technique to large-scale synthesis of nanofibers with tunable morphological properties. The polymer fibers could be graphitized to make carbon nanofibers with retention of morphology. Also, electrospun ceramic nanofibers could be produced, including TiC. Chemical oxidation of TiC led to extraction of the metal and formation of graphitic carbon nanofibers. The carbon nanofibers could show improved performance in working fuel cell environment. Future work will include:

- Construct a fuel cell that utilizes carbon nanofelt as electrode material (catalyst support).
- Test the prototype fuel cell.

Patents Issued

1. Qiquan Qiao, Hao Fong, Prakash Joshi, Lifeng Zhang, and David Galipeau. "TiO_2 Nanofiber/Nanoparticle Mixture Anode for Highly Efficient Dye Sensitized Solar Cells", patent in application.

FY 2011 Publications/Presentations

1. S. Budhi, H.S. Kibombo, D. Zhao, A. Gonshorowski, R.T. Koodali 'Synthesis of titania-silica xerogels by co-solvent induced gelation at ambient temperature' Mater. Lett. 2011 (published online Apr. 22, 2011) DOE: 10.1016/j.matlet.2011.04.054.

2. V. Presser, L. Zhang, J.J. Niu, J. McDonough, C. Perez, H. Fong, Y. Gogotsi 'Flexible Nano-felts of Carbide-Derived Carbon with Ultra-high Power Handling Capability' Adv. Ener. Mater. 2011 (published online Apr. 15, 2011) DOI: 10.1002/aenm.201100047.

3. S. Banerjee, A. Horn, H. Khatri, G. Sereda 'A green one-pot multicomponent synthesis of 4H-pyrans and polysubsituted aniline derivatives of biological, pharmacological, and optical applications using silica nanoparticles as reusable catalyst' Tetra. Lett. 2011, 52(16), 1878-1881.

4. H.S. Kibombo, D. Zhao, A. Gonshorowski, S. Budhi, M.D. Koppang, R.T. Koodali 'Cosolvent-Induced Gelation and the Hydrothermal Enhancement of the Crystallinity of Titania-Silica Mixed Oxides for the Photocatalytic Remediation of Organic Pollutants' J. Phys. Chem. C 2011, 115(13), 6126-6135. DOI: 10.1021/jp110988j.

5. C. Lai, G. Zhong, Z. Yue, G. Chen, L. Zhang, A. Vakili, Y. Wang, L. Zhu, J. Liu, H. Fong 'Investigation of post-spinning stretching process on morphological, structural, and mechanical properties of electrospun polyacrylonitrile copolymer nanofibers' Polymer 2011, 52(2), 519-528. DOI: 10.1016/j.polymer.2010.11.044.

6. S. Banerjee, V. Balasanthiran, R.T. Koodali, G. Sereda 'Pd-MCM-48: a novel recyclable heterogeneous catalyst for chemo- and regioselective hydrogenation of olefins and coupling reactions' Org. Biomol. Chem. 2010, 8, 4316-4321. DOI: 10.1039/C0OB00183J.

7. G. Sereda, V. Rajpara 'Photoactivated and photopassivated benzylic oxidation catalyzed by pristine and oxidized carbons' Catal. Comm. 2011, 12(7), 669-672. DOI: 10.1016/j.catcom.2010.12.027.

8. G. Sereda, V. Rajpara 'Exploration of Solid-Supported Reactions with Gold Nanoparticles' J. Chem. Ed. 2010, 87(9), 978-980.

9. D. Zhao, A. Rodriguez, N.M. Dimitrijevic, T. Rajh, R.T. Koodali 'Synthesis, Structural Characterization, and Photocatalytic Performance of Mesoporous W-MCM-48' J. Phys. Chem. C 2010, 114, 15278-15734.

10. L. Zhang, J. Hu, A.A. Voevodin, H. Fong 'Synthesis of Continuous TiC Nanofibers and/or Nanoribbons Through Electrospinning Followed by Carbothermal Reduction' Nanoscale 2010, 2, 1670-1673.

11. Z.C. Wu, Y. Zhang, T.X. Tao, L. Zhang, H. Fong 'Silver nanoparticles on amidoxime fibers for photo-catalytic degradation of organic dyes in waste water' Appl. Surf. Sci. 2010, 257, 1092-1097.

12. J. Liu, Y. Tian, Y. Chen, J. Liang, L. Zhang, H. Fong 'A surface treatment technique of electrochemical oxidation to simultaneously improve the interfacial bonding strength and the tensile strength of PAN-based carbon fibers' Mater. Chem. Phys. 2010, 122(2-3), 548-555.

13. D. Zhao, S. Budhi, A. Rodriguez, R.T. Koodali 'Rapid and facile synthesis of Ti-MCM-48 mesoporous material and the photocatalytic performance for hydrogen evolution' Int. J. Hydrogen Ener. 2010, 35(11), 5276-5283.

14. S. Wen, L. Liu, L. Zhang, Q. Chen, L. Zhang, H. Fong 'Hierarchical electrospun SiO2 nanofibers containing SiO2 nanoparticles with controllable surface-roughness and/or porosity' Mater. Lett. 2010, 64(13), 1517-1520.

15. Z. Zhou, K. Liu, C. Lai, L. Zhang, J. Li, H. Hou, D.H. Reneker, H. Fong 'Graphitic carbon nanofibers developed from bundles of aligned electrospun polyacrylonitrile nanofibers containing phosphoric acid' Polymer, 2010, 51(11), 2360-2367.

16. J.H. Son, M.A. Pudenz, J.D. Hoefelmeyer 'Reactivity of the Bifunctional Ambiphilic Molecule 8-(dimesitylboryl)quinoline: Hydrolysis and Coordination to CuI, AgI and PdII' Dalton Trans. 2010, DOI: 10.1039/C0DT00798F.

17. R.T. Koodali, D. Zhao 'Photocatalytic degradation of aqueous organic pollutants using titania supported periodic mesoporous silica' Energy Environ. Sci. 2010, 3, 608-614.

18. V. Rajpara, S. Banerjee, G. Sereda 'Iron Oxide Nanoparticles Grown on Carboxy-Functionalized Graphite: An Efficient Reusable Catalyst for Alkylation of Arenes' Synthesis, 2010, 16, 2835-2840. DOI: 10.1055/s-0029-1218851

19. P. Joshi, L. Zhang, D. Davoux, L. Liu, D. Galipeau, H. Fong, Q. Qiao 'Nanofiber/Nanoparticle Composites for Highly Efficient Dye Sensitized Solar Cells', Energy Environ. Sci. 2010, 3, 1507-1510.

II.G.10 Novel Photocatalytic Metal Oxides*

Robert W. Smith (Primary Contact), Wai-Ning Mei, Renat Sabirianov
University of Nebraska at Omaha
6001 Dodge Street
Omaha, NE 68182
Phone: (402) 554-3592
E-mail: robertsmith@unomaha.edu

DOE Managers
HQ: Eric Miller
Phone: (202) 287-5829
E-mail: Eric.Miller@hq.doe.gov
GO: David Peterson
Phone: (720) 356-1747
E-mail: David.Peterson@go.doe.gov

Contract Number: DE-EE0003174

Project Start Date: September 1, 2010
Project End Date: August 31, 2012

*Congressionally directed project

Fiscal Year (FY) 2011 Objectives

- Develop improved solid-state photocatalysts.
- Model candidate metal oxides through computer simulations.
- Synthesize and characterize materials identified by models.

Technical Barriers

This project addresses the following technical barriers from the Photoelectrochemical Hydrogen Production section of the Fuel Cell Technologies Program Multi-Year Research, Development and Demonstration Plan:

(Y) Materials Efficiency

(Z) Materials Durability

Technical Targets

Development of Semiconductor Materials for Photoelectrochemical Production of Hydrogen:
This project is conducting theoretical studies of cesium niobate ($Cs_2Nb_4O_{11}$) and its solid solution modifications to discover new, more efficient oxide catalysts for photoelectrochemical production of hydrogen from water. Compositions identified by computer modeling will then be fabricated and characterized. The materials should meet the following DOE targets:

- 2.3-eV useable bandgap
- 8% plant-to-hydrogen solar efficiency
- Projected durability of 1,000 hours

FY 2011 Accomplishments

- Calculated the band structure and bandgap for cesium niobate.
- Developed a sol-gel synthesis route to fabricate cesium niobate.
- Commenced computer doping study.



Introduction

This work seeks to develop new solid-state photocatalysts for the decomposition of water into hydrogen and oxygen gas. The catalyst should have band edges appropriate for the oxidation and reduction reactions that occur during the decomposition process. Appropriate band edges would result in a bandgap of about 2.3 eV, in accordance with DOE technical targets. This bandgap would place the catalyst's absorption edge into the visible portion of the spectrum and render the catalyst more efficient than current catalyst at utilizing the available solar spectrum. Cesium niobate is a newly discovered photocatalyst but has band edges that are not optimized for the oxidation and reduction reactions that occur during water decomposition. We are seeking to optimize the band edges by examining various solid solutions through computer modeling.

Approach

We are examining cesium niobate and solid solutions thereof through computer simulations to determine the composition with an electronic structure most conducive for the photocatalytic decomposition of water into hydrogen and oxygen gas. We conduct our calculations through the density functional theory (DFT) method, which is a commonly adopted approach utilized by the condensed matter community. The method treats many-particle systems, such as ionic solids, by approximating their wave functions from spatially dependent electron density. The method is effective in deducing electronic, optical, and mechanical properties of materials and facilitates explanation to and comparison with experimental results. In this project, we combine DFT with different boundary conditions and generate very large unit-cell structures, which is both laborious and time-consuming but essential for accurate prediction of materials properties.

We examine compositions with cesium niobate as the base but with judicious substitutions of other metals and

nonmetals in order to adjust the electronic band edges to the desired values. Compositions with the desired properties are then synthesized in the laboratory and characterized for structure, optical absorption, and catalytic activity.

Results

We have completed the band structure calculations of both the high and low-temperature phases of cesium niobate (CNO). Figure 1 shows the results for the low-temperature phase, which is the one that occurs at room temperature; the phase transition occurs at 165ºC. The calculated bandgap is about 3.1 eV. Understanding of the band structure allows us to calculate the optical absorption of CNO so as to monitor and modify the band edges as we engineer the CNO material to facilitate photocatalytic decomposition of water into its constituent gases.

The optical absorption spectra of CNO with polarized and unpolarized light are shown in Figures 2 and 3, respectively. In the range of 0-10 eV, two absorption peaks dominate all spectra: one around 4.8 eV and a second, higher one around 6.0 eV. The absorption intensity order is [100] > [001] > [010] for polarized light and [010] > [001] > [100] for unpolarized light, that is, in the opposite order. This is because, for unpolarized light, the spectrum of one incident direction (i.e., [100]) equals the spectrum average of polarized light in the vertical plane (i.e., [100]).

We have developed a sol-gel synthesis route to fabricate CNO at relatively short reaction times. In this procedure, niobium(V) chloride, cesium carbonate, anhydrous citric acid, and deionized water are used as starting materials. At room temperature, the niobium chloride is dissolved in methanol with constant stirring to get a clear, colorless solution. Citric acid is then added to the solution. Separately, stoichiometric cesium carbonate and additional citric acid are dissolved in deionized water and added to the niobium chloride methanolic solution. The final solution is heated with constant stirring at 80-110°C to evaporate the methanol and water and produce a clear gel. The gel is then heated at 400°C for one hour to produce a black amorphous material. Heating this material at 700°C for two hours or at 900°C for as little as 0.5 hours produces single-phase CNO. In contrast, fabrication through standard solid-state reaction from the metal oxides requires several days of heating at

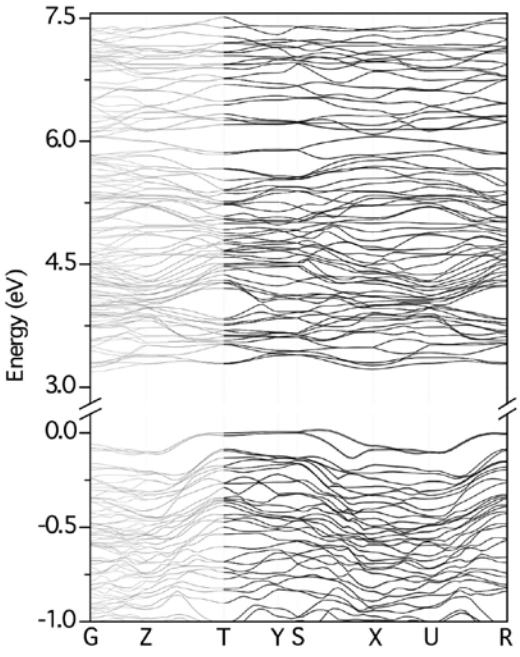


FIGURE 1. Band Structure for Low-Temperature CNO: G = (0,0,0), Z = (0,0,0.5), T = (–0.5,0,0.5), Y = (–0.5,0,0), S = (–0.5,0.5,0), X = (0,0.5,0), U = (0,0.5,0.5), and R = (–0.5,0.5,0.5).

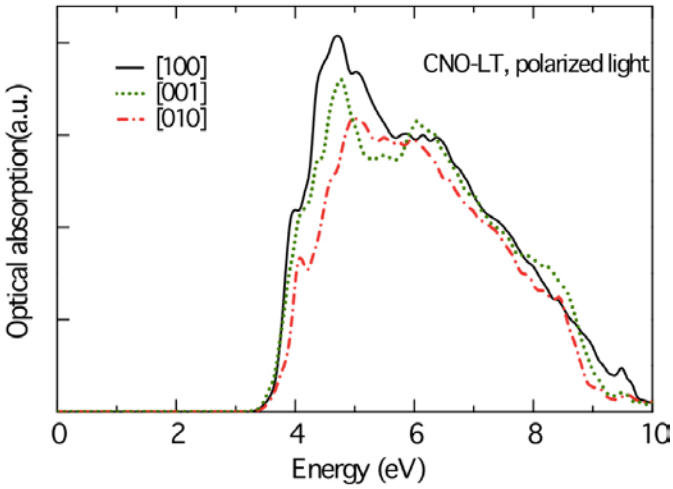


FIGURE 2. Optical Absorption Spectra of Low-Temperature (LT) CNO with Light Polarized along [100], [010], and [001]

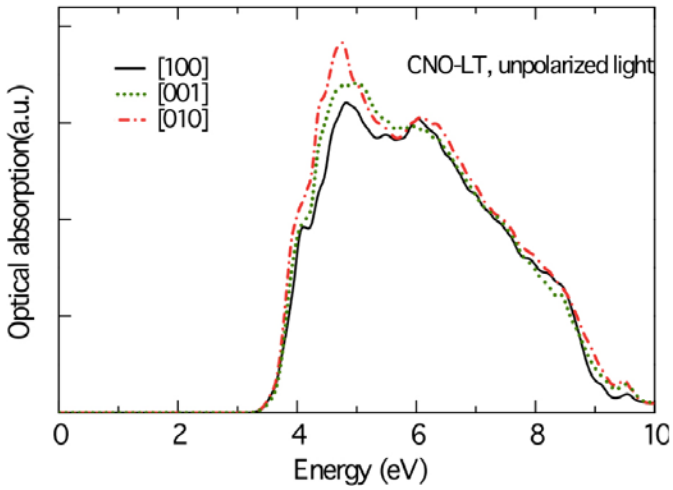


FIGURE 3. Optical Absorption Spectra of Low-Temperature CNO with Unpolarized Light along [100], [010], and [001]

high temperature and with several intermediate grinding. Figure 4 shows X-ray diffraction patterns of sol-gel samples heated for two hours at various temperatures.

Conclusions and Future Directions

The bandgap of CNO is approximately 3.1 eV and must be modified to a smaller value so that it absorbs into the visible portion of the solar spectrum. We have commenced a computer study to engineer a smaller bandgap material through elemental substitution in the CNO structure. We will fabricate and characterize any material deemed suitable that the computer study identifies.

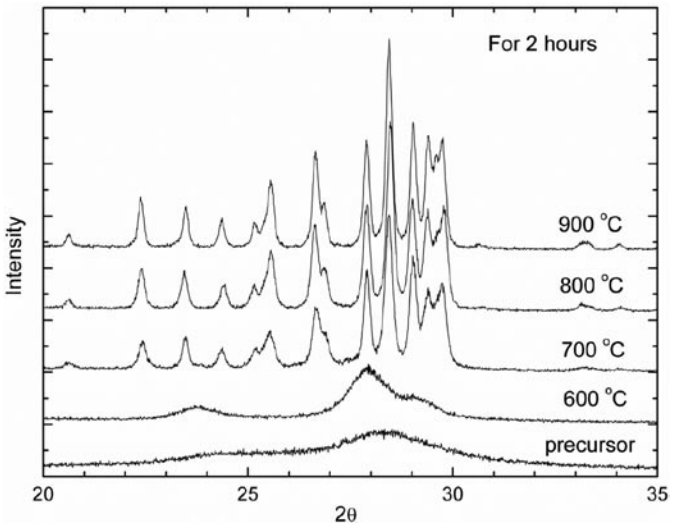


FIGURE 4. X-Ray Diffraction Patterns after Heat Treatment of the Precursor for Two Hours at Different Temperatures

II.G.11 Solar Thermal Hydrogen Production*

Vaidyanathan (Ravi) Subramanian
University of Nevada, Reno
1664 N. Virginia Street
Reno, NV 89557
Phone: (775) 784-4686
E-mail: ravisv@unr.edu

DOE Managers
HQ: Eric Miller
Phone: (202) 287-5829
E-mail: Eric.Miller@hq.doe.gov
GO: Katie Randolph
Phone: (720) 356-1759
E-mail: Katie.Randolph@go.doe.gov

Project Start Date: February 4, 2010
Project End Date: December 31, 2011

*Congressionally directed project

Fiscal Year (FY) 2011 Objectives

- Quantify hydrogen yield from catalytic cracking of methane in the presence of molten salts.
- Determine the effects of different catalysts.
- Demonstrate hydrogen production at possibly reduced temperature.

Technical Barriers

- Salt mixture-catalyst stability.
- Reduce temperature for hydrogen generation.

The main objective of the proposed work is to examine the effects of exposure of a slat mixture to different temperature levels for an extend period of time (up to 8 hr). The 8 hr limit was established since the peak sun intensity is expected to last only that long in one continuous cycle. The parameters for this study and anticipated goals for hydrogen production are summarized in Table 1.

TABLE 1. Project Goals

Performance Measure	Units	Qtr 1 and 2	Qtr 3 and 4
Salt-Catlyst Thermal Stability	Hours	3	8
Temperature Range	Celsius	400-700	400-800
Volume of Hydrogen	Milli-liter	<10	100

FY 2011 Accomplishments

- The dissociation of methane in the presence of a metal catalyst follows a sequence of dehydrogenation steps:
  - $CH_{4,s} \rightarrow CH_{3,s} + H_s$
  - $CH_{X,s} \rightarrow CH_{X-1,s} + H_s$ (X = 3,2, 1; s = surface)
- The presence of Fe, Ni, and Co show hydrogen generation (Table 2).

TABLE 2. Hydrogen Conversion Percentages

Catalyst System	% Conversion at:		
	500°C	600°C	700°C
LicI+KCl Eutectic	0	0	0
Fe Catalyst in LiCl+KCl	5	8	17.5
Ni Catalyst in LiCl+KCl	11.5	28.0	30
Co Catalyst in LiCl+KCl	7.2	11	16

Introduction

Conventional hydrogen generation process is often carried out at high temperature. This approach can be costly. The solar thermal approach seeks to use the high temperature obtained from solar energy with the help of concentrators. This process can, in principle, offset the need of fossil-based energy to produce high temperatures. A schematic of the approach to use solar energy in solar thermal process is given in Figure 1.

Approach

The approach is to use a simulated solar power condition using a box furnace. The furnace was customized to provide the necessary temperature ranges and the experimental conditions to perform catalytic cracking of methane. Summarily, the methane and carrier gas was delivered to a crucible containing the molten salt and the catalyst. The role of the catalyst and the temperature of the molten salt were monitored and its effects on methane cracking were monitored.

Figure 2 shows a schematic of the setup.

Results

The results (Figure 3) can be categorized into the following segments:

- Physical characterization of the eutectic.

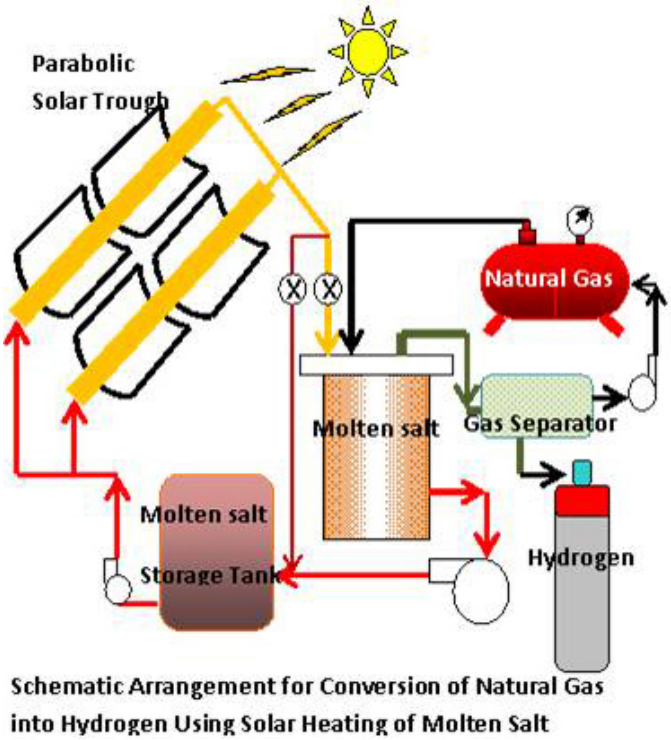


FIGURE 1. General Schematic of the Approach to Utilize Solar Thermal Energy

- Reaction products were noted to have varying color at different depths.
  - Therefore, while the reaction products were in liquid state, they were poured out and shock cooled (salt pour).
- Visual inspection shows the formation of black precipitates at the bottom.

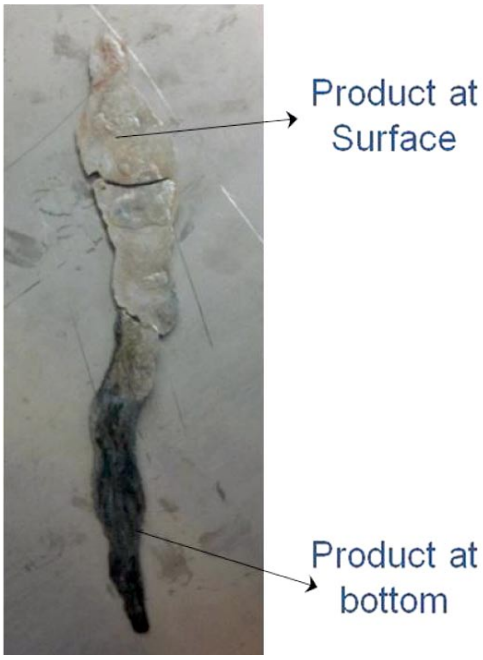


FIGURE 3. A representative photograph of the texture of the salt-catalyst mixture obtained after the catalytic cracking of methane.

  - The possible products could be carbon-based materials and may have value.
- Surface characterization of the salt mixture (Figure 4):
  - X-ray diffraction (XRD) analysis was performed to identify the residue after the reaction.
  - Solid–salt mixture was washed several times with water and dried before analysis.

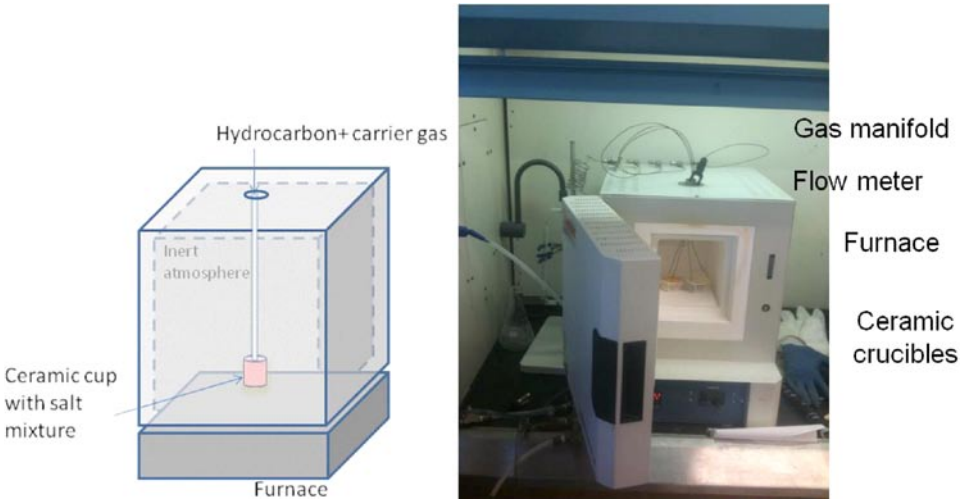


FIGURE 2. The setup that was developed to simulate a solar thermal process to produce hydrogen from methane using a catalyst.

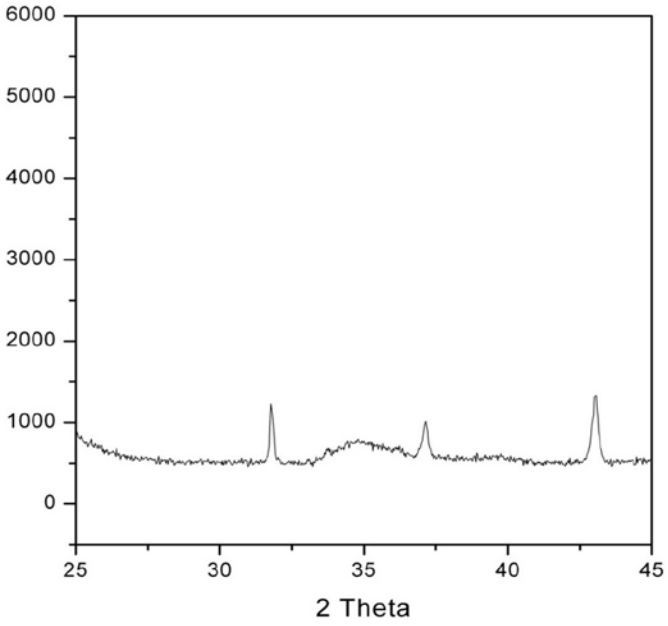


FIGURE 4. XRD of the products after the catalytic cracking indicates the formation of carbon-based residue.

  - XRD suggests the formation of carbonaceous species possibly ordered structures as noted from the XRD peaks.
- Product analysis (Figure 5):
  - Hydrogen and oxygen peaks are detected together. Oxygen peaks are attributable to the leaks in the oven.
  - In general:
    - Hydrogen is detected upwards of 600°C in the absence of catalyst in the salt mixture.
    - Hydrogen has been detected at lower temperatures with catalysts.

Conclusions and Future Directions

The preliminary work has shown that:

1. Including Fe as a catalyst with Li/K salt mixture will reduce the temperature at which hydrogen is produced from methane. Ni and Co may be promising as well.
2. The formation of carbonaceous residue indicates that the system does lead to cracking of methane.
3. The temperature from cracking appears to be reduced by at least a 100°C (possibly up to 200°C).

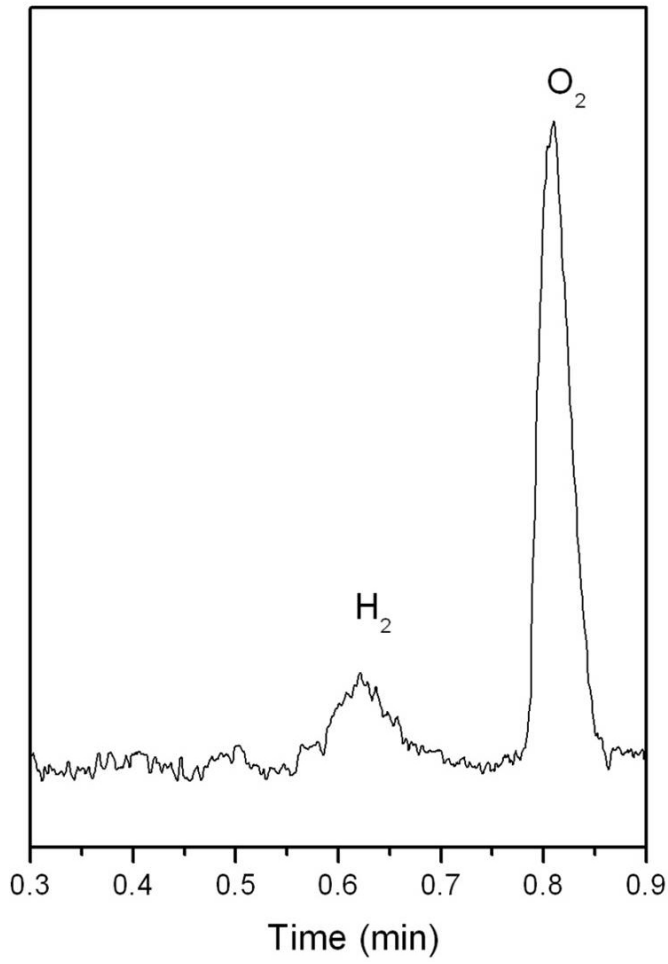


FIGURE 5. Representative gas chromatograph data indicating the products identified after the catalytic cracking of methane.

Future directions:

- To systematically interpret some of the compositional as well as the qualitative nature of the post cracking product(s).
- To finish an ongoing manuscript in this area based on this work.
- There are a few grant opportunities from state and federal agencies that will be explored for future funding.

FY 2011 Publications/Presentations

1. A poster titled "Solar thermal hydrogen production" was presented by Ravi Subramanian at the NVREC Project Meeting on August 20, 2010.

2. Ravi Subramanian also presented an update on this work at the annual DOE merit review meeting in Washington, D.C., May, 2011.

II.G.12 Photoelectrochemical Materials: Theory and Modeling

John Turner (Primary Contact), Wanjian Yin, Su-Huai Wei, Mowafak Al-Jassim, and Yanfa Yan
National Renewable Energy Laboratory
1617 Cole Blvd.
Golden, CO 80401
Phone: (303) 275-4270
E-mail: John.Turner@nrel.gov

DOE Manager
HQ: Eric Miller
Phone: (202) 287-5829
E-mail: Eric.Miller@hq.doe.gov

Project Start Date: 2007
Project End Date: Project continuation and direction determined annually by DOE

Fiscal Year (FY) 2011 Objectives

The main focus of the project is to:

- Understand the performance of current photoelectrochemical (PEC) materials.
- Provide guidance and suggest solution for performance improvement.
- Design and discover new materials.
- Provide theoretical basis for Go/No-Go decisions on PEC activities.

Technical Barriers

This project addresses the following technical barriers from the PEC water-splitting section of the Fuel Cell Technologies Program Multi-Year Research, Development and Demonstration Plan:

(Y) Materials Efficiency
(Z) Materials Durability
(AB) Bulk Materials Synthesis

Technical Targets

This project provides a theoretical understanding of the performance of current PEC materials and provides feedback and guidance for performance improvement.

FY 2011 Accomplishments

- Proposed the general strategies for the rational design of semiconductors to simultaneously meet all of the requirements for high-efficiency, solar-driven PEC water splitting materials.
- Studied the intrinsic and extrinsic doping properties of $BiVO_4$ and proposed good candidates for *p*-type dopants (Sr_{Bi}, Ca_{Bi}, Na_{Bi}, K_{Bi}) and *n*-type dopants (W_V and Mo_V).



Introduction

The electronic band structures of semiconductors are crucial for the performance of semiconductor-based PEC water-splitting. The requirements of those semiconductors include the following tightly coupled material property criteria: appropriate band gap (1.6-2.2 eV), efficient visible light absorption, high carrier mobility, and correct band-edge positions that straddle the water redox potentials. Trail-and-error synthesis approaches have proven ineffective in discovering a viable material, and the band structure engineering for existing materials is necessary [1,2]. So far, most of existing work on band structure engineering is to reduce the band gap without considering other tightly coupled properties described above [2-4]. As a result, the PEC efficiency sometimes became worse when impurities were introduced. It is critical to develop general strategies to address all the requirements simultaneously rather than only reducing band gap.

As an example, anatase TiO_2 is one of the most studied materials owing to its good photocatalytic activity, ease of synthesis, long-term chemical stability, and demonstrated PEC applications. However, its large band gap (~3.2 eV) fails to absorb a significant fraction of visible light, resulting in poor solar-to-hydrogen conversion efficiency. Great efforts have been devoted to chemically engineer TiO_2 to reduce its band gap but with only marginal success. For example, monodoping with impurities such as N or C in TiO_2 has been applied to reduce the band gap of TiO_2. However, the high concentration of these impurities needed for band gap reduction causes serious carrier recombination and produces inferior material quality, making efficient solar-to-hydrogen conversion impossible.

Our previous work demonstrated that donor-acceptor codoping can effectively enhance the PEC properties of ZnO due to the reduction of the recombination centers [5,6]. In the last year, we extended the donor-acceptor codoping concept to engineer the bandgap of TiO_2. We explored how the codoping would affect the other tightly coupled properties. We found that the properties are connected tightly with the concentration of dopants.

$BiVO_4$ has shown particular promise for water photodecomposition with the presence of both a low bandgap (2.4–2.5 eV) and reasonable band-edge alignment

with respect to the water redox potentials [7-9]. For implementation in the real device, both of the good *n*-type and *p*-type doping properties should be required to form Ohmic contacts with contact materials. However, to date, the intrinsic and extrinsic doping properties of $BiVO_4$ haven't been systematically explored.

Approach

We employ density functional theory (DFT) to study the electronic properties of the anatase TiO_2 and $BiVO_4$ and how doping would affect their electronic properties. Generalized gradient approximation (GGA) to DFT and the projected augmented wave basis as implemented in the Vienna *ab initio* simulation package (VASP) [10] are used. The plane-wave cut-off energy of 400 eV was used, and the ion positions were always relaxed until the force on each of them is 0.01 eV/Å or less. For TiO_2, the impurity co-incorporation was modeled using (2×2×1) supercells with a total of 48 atoms which randomly include the impurity pairs. The supercell sizes were allowed to relax. The k-point sampling was 7×7×3 for the conventional cell of anatase TiO_2 and equivalent k points for large supercells. The band offset was calculated by aligning the average potentials of host elements far away from impurities with that in pure bulk cell. The GGA band gap error was corrected using a scissor operator. For $BiVO_4$, the dopants were incorporated into a (2×1×2) supercell with 96 atoms. The k-point sampling was 2×3×3 for the supercell. For defect formation energy and transition energy calculation, the combined schemes of both Γ-point and special k-points were used which could predict the transition energy more precisely [11,12].

For rational band structure engineering of TiO_2, we have proposed four general strategies: (i) utilizing charge balanced donor-acceptor alloying to overcome solubility limit, reduce charged defects, and improve the quality of materials; (ii) using higher 4*d*, 5*d* transition metals substitution on Ti sites to lift up the conduction band; (iii) using C, N with higher 3*p* substitution in O site to raise the valence band and thus reduce the band gap; and (iv) using high concentration of the alloying elements to enhance optical absorption and improve the hole mobility.

Results

We first discuss the energetic favorability of donor-acceptor codoping. The incorporation of a single foreign element can often be limited by the solubility limit in host materials. In the case of high concentration, it may create other detrimental issues such as undesirable charged defects, inferior materials quality, and too high carrier concentration. Our previous work on ZnO showed that the donor-acceptor codoping could enhance doping concentration while keeping good carrier mobility. The charge transfer between the donor and acceptor and the interactions between these two neighbors play key roles. We investigated the interaction behavior of donor and acceptor in TiO_2. Table 1 shows the binding energies of various donor-acceptor pairs considered in our work.

TABLE 1. Binding Energies of Various Donor-Acceptor Pairs

Pairs	E_b(eV)	Pairs	E_b(eV)	Pairs	E_b(eV)	Pairs	E_b(eV)
(Cr,C)	3.02	(Nb,N)	1.97	(Zr,S)	-0.50	(2Ta,C)	1.82
(Mo,C)	3.24	(Ta,N)	1.92	(Hf,S)	-0.56	(2Nb,C)	2.11
(W,C)	2.86	(Ta,P)	0.40	(Zr,Se)	-0.37	(Mo,2N)	4.78
(V,N)	2.25	(Nb,P)	0.58	(Hf,Se)	-0.44	(W,2N)	4.80

Except for the Zr and Hf, the binding energies of donor-acceptor pairs are positive which means that the donor and acceptors favor to combine with each other, thus enhancing the solubility. The reason for negative values for Zr and Hf is that the Zr and Hf are isovalent to Ti and the substitutions don't have large charge transfer between cation and anion dopants.

Taking (Ta, N) as an example, Figure 1 shows that concentration of the incorporated donor and acceptor can affect significantly the electronic properties of TiO_2. Increasing the alloy concentration not only can further reduce the band gap, but can also simultaneously enhance the optical absorption in the long-wavelength regions and reduce the carrier effective mass. The results clearly show that as the concentration increases, the N 2*p* band broadens, the band gap decreases, and the dispersion of the N 2*p* band increases, leading to higher carrier mobility. The GGA calculated band gap reduction increased to 0.70 eV when 12.5% O is replaced by N. Figure 2 shows calculated optical absorption coefficient spectra for (Ta,N) co-incorporated TiO_2 with various concentrations. The results show clearly that as the concentration of (Ta,N) pairs increases, the absorption in the longer-wavelength region is dramatically enhanced. Most previous calculations have only focused in the low-concentration regime. Our results show, however, that there is a strong dependence of the band gap on the alloy concentration. The band-gap reduction predicted at the low-alloy concentration may not be applicable to the high-alloy concentration cases. Therefore, to provide a rational prediction of the band gap and band-edge positions, the calculations should be conducted at both low- and high-alloy concentrations.

Figure 3 shows the calculated band gaps and band-edge alignments in both of the low (Figure 3a) and high (Figure 3b) concentration regime. The results show that the incorporation of Ta, Nb, Zr, and Hf as donors can lead to desirable upshifts of the conduction band minimum (CBM) (marked by red positive values). The incorporation of Cr, Mo, W, and V lead to an unwanted downshift of the CBM. The calculated trends for the valence band maximum (VBM) are also consistent with these atomic trends. The (2Nb,C), (2Ta,C), (Mo,2N), and (W,2N) combinations give both better band gap reduction and band-edge positions. However, the (Mo,2N) and (W,2N) combinations are expected to produce

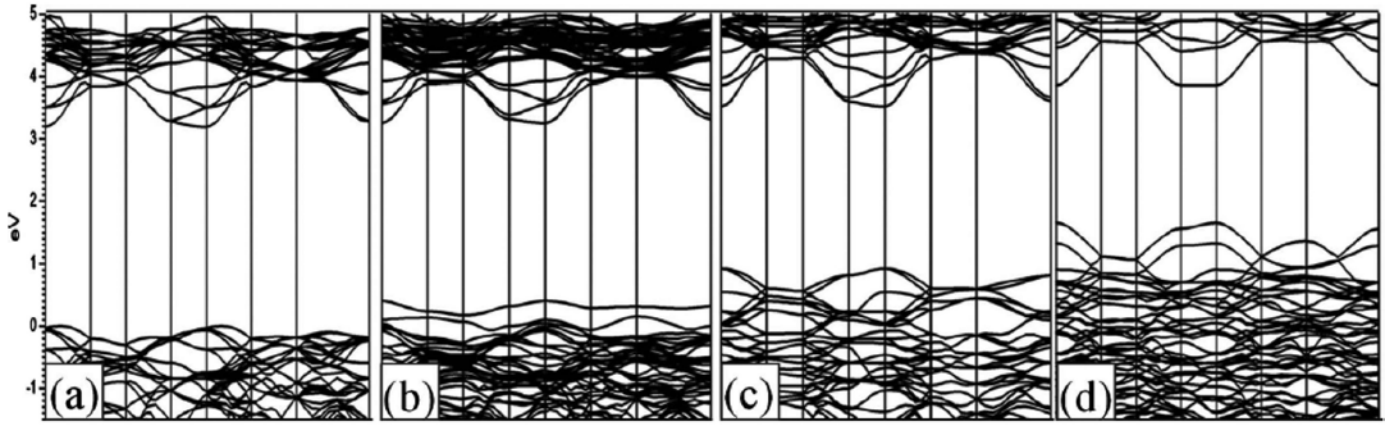


FIGURE 1. The band structures of (a) pure TiO_2, (b) 3.1% (Ta, N) co-incorporated TiO_2 with 3.1% O replaced by N, (c) (Ta, N) co–incorporated TiO_2 with 12.5% O replaced by N, (d) (Ta, N) co–incorporated TiO_2 with 25 % O replaced by N. The CBMs are aligned for guide of eyes as the conduction band structure characters near CBM are nearly unchanged.

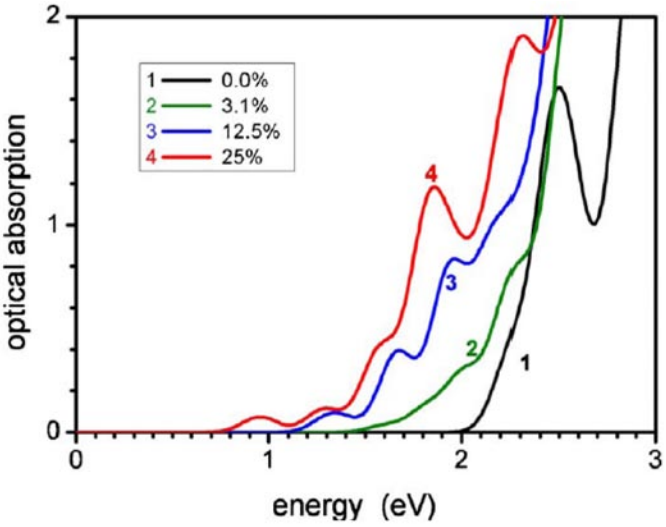


FIGURE 2. Optical absorption spectrum (the part near absorption edge) of pure TiO_2 and (Ta, N) co–incorporated TiO_2 with 3.1%, 12.5%, and 25% of O replaced by N, respectively.

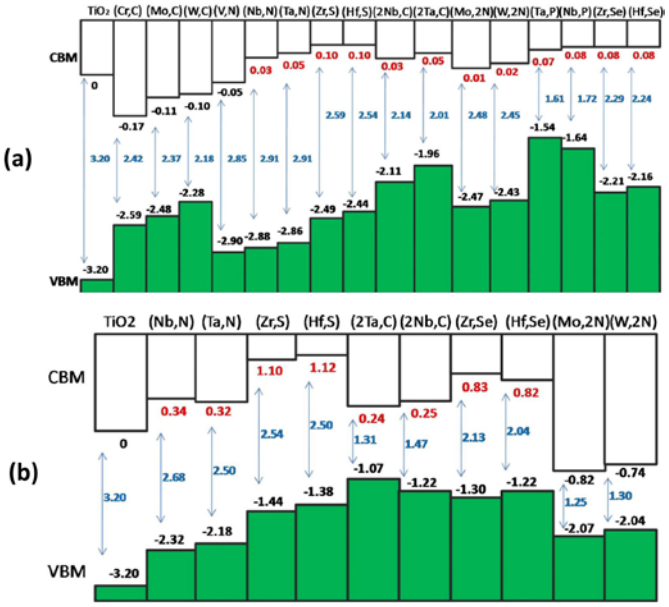


FIGURE 3. Calculated GGA band offset (at Γ point) for TiO_2 and TiO_2 alloyed with various donor-acceptor combinations in the (a) low-concentration regime and (b) high concentration regime. The CBM of pure TiO_2 is set to zero as the reference and the band gap is corrected by scissor operator.

more dispersive defect bands. At high concentration, TiO_2 co-incorporated with (Cr,C), (Mo,C), (W,C), and (V,N) becomes metallic due to too much band broadening of both unoccupied and occupied bands created by the donors and acceptors. The combinations used to give good band gaps in the low-concentration regime such as (2Nb,C), (2Ta,C), (Nb,P), and (Ta,P) now give band gaps that are too narrow due to their high VBM. While (Nb,N) and (Ta,N) combinations give the desirable band gaps estimated to be 2.68 eV and 2.50 eV, respectively, simultaneously with proper band-edge positions. Our results, therefore, suggest strongly that the band-edge positions and band gaps depend critically on the concentration of the incorporated donors and acceptors pairs. As a general guidance, one must consider carefully band gaps and concentration at the same time so that the appropriate donor-acceptor combinations can be chosen.

Simultaneously considering the band gap, band edge and binding energies, we predict that (Ta,N) and (Nb,N) pairs are the optimal donor-acceptor combinations in the high concentration regime, and (Mo,2N) and (W,2N) combinations are good candidates in the low-concentration regime for engineering TiO_2 for PEC water-splitting.

The properties of intrinsic defects in $BiVO_4$ were studied. Our results show that the Fermi level is always

pinned by Bi vacancy and O vacancy. Under O poor conditions, the Fermi level is pinned at ~0.35 eV below CBM and under O rich condition, the Fermi level is pinned at ~0.55 eV above VBM. As a result, without external doping, $BiVO_4$ should only exhibit moderate *n*-type or *p*-type conductivities, which is needed for good PEC absorbers.

We calculated the transition energies and formation energies for group-I, group-II, group-IV elements as dopants. We found that outstanding *p*-type conductivity can be achieved by Br, Ca, Na, or K doping at O-rich growth conditions because these impurities at Bi sites are shallow acceptors and have rather low formation energies. Excellent *n*-type conductivity can be realized by Mo or W doping at O-poor growth conditions, because they are very shallow donors at V sites and have very low formation energies. Figure 4a shows the formation energies of group-II (Zn, Mg, Ca, Sr) elements as p-type doping doping in O-rich conditions. The dashed lines are the curve of the lowest formation energy of the intrinsic defects. All the possible configurations of impurities, such as substitution and interstitials, are considered. It is seen that Ca and Sr exhibit excellent p-type doping properties, not only because their shallow transition energies (around 0.1 eV), but also because their formation energies are lower than that of intrinsic defects.

Figure 4 shows the formation energies of group-VI (Cr, Mo, W) elements doping in O-poor conditions. The Mo and W dopants exhibit good *n*-type properties. The (0/1+) ionization energies of Mo_V is as shallow as 0.04 eV. W_V is even shallower (0.01 eV), but its formation energy is a little higher than Mo_V, making the Fermi level pinning with Bi vacancy and thus the Fermi level is located at ~0.2 eV below CBM. Therefore, Mo and W are good candidates that could lead to excellent n-type conductivity in $BiVO_4$.

The impurities discussed in the above calculation are mostly on cation sites. On the other hand, *p*-type and *n*-type doping of metal oxides may also be realized by introducing impurities to O sites. In this case, C, N, and F are the most considered impurities. Because interstitials of these impurities usually have large formation energies, we will only consider substitutional defects, C_O, N_O, and F_O. However, these conventional dopants are not expected to lead to good p-type or n-type conductivities.

Conclusions and Future Direction

We have proposed general strategies for the rational design of semiconductors to simultaneously meet all of the requirements for a high-efficiency PEC water splitting material. As a case study, we applies our strategies for engineering anatase TiO_2. Previous attempts to modify known semiconductors often focused on a particular individual criterion. Our theoretical results show that with appropriate donor-acceptor coincorporation alloys with anatase TiO_2 hold great potential to satisfy all of the criteria for a viable PEC device. We predict that (Mo,2N) and (W, 2N) are the best donor-acceptor combinations in the low-alloy concentration regime whereas (Nb, N) and (Ta, N) are the best choice of donor-acceptor pairs in the high-alloy concentration regime.

Without external dopants, $BiVO_4$ exhibits moderate *p*-type in O-rich condition and moderate n-type in O-poor condition, which is just needed for good PEC absorber. On the other hand, for external dopants, Sr, Ca, Na, and K are proposed to be good p-type dopants and the Mo and W are proposed to be good *n*-type dopants for $BiVO_4$, which is needed for forming Ohmic contacts between absorber and

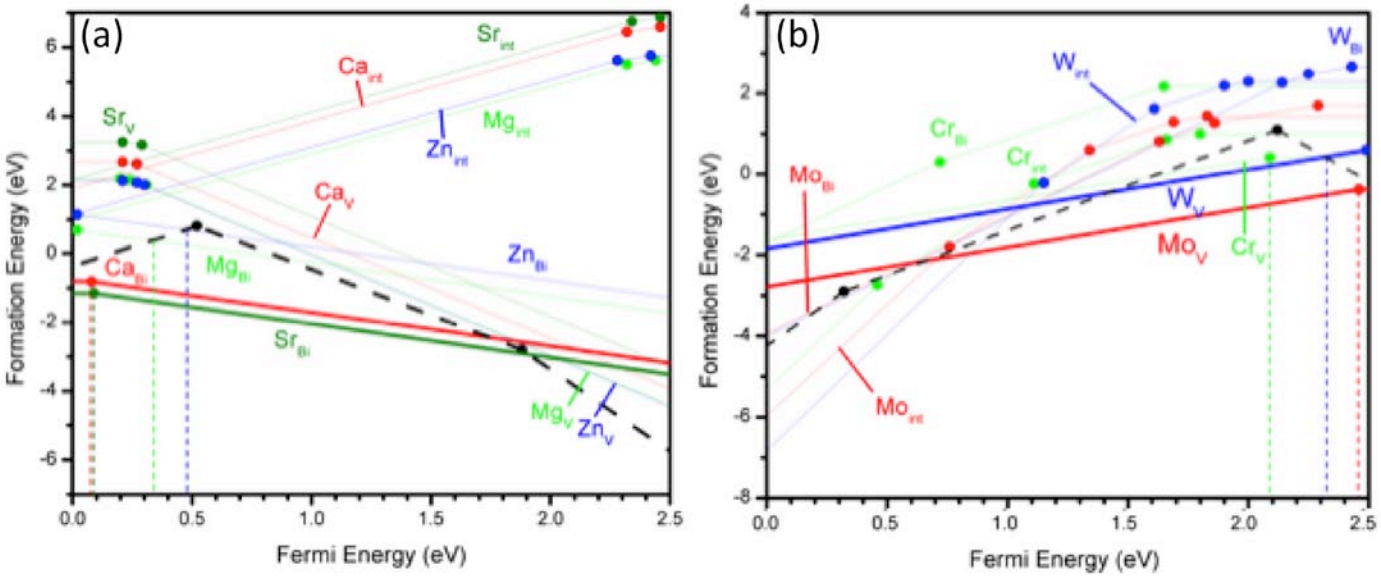


FIGURE 4. Calculated formation energies of (a) group-II (Zn, Mg, Ca, Sr) dopants in O-rich conditions and (b) group-VI (Cr, Mo, W) dopants in O-poor conditions.

contacts. C, N and F are found not to be good candidates for p-type or n-type doping of BVO_4.

Future direction includes the following:

- Apply the design strategies to engineer other metal oxides, such as Fe_2O_3.
- Understand the electronic properties of other metal oxides.
- Design new metal oxides for PEC applications.

FY 2011 Publications/Presentations

1. W.-J. Yin, H.W. Tang, S.-H. Wei, J. Turner, M.M. Al-Jassim, Yanfa Yan, "Band structure engineering of semiconductors for enhanced PEC water splitting" *Phys. Rev. B **82**, 045106 (2010)*.

2. W.-J. Yin, S.-H. Wei, M. M. Mowafak, J. Turner, and Yanfa Yan, "Doping properties of monoclinic BiVO4 studied by the first-principle density-functional theory" *Phys. Rev. B **83**, 155102 (2010)*.

3. L. Chen, S. Shet, H.W. Tang, H.L. Wang, T. Deutsch, Yanfa Yan, J. Turner, M. Al-Jassim, "Electrochemical deposition of copper oxide nanowires for photoelectrochemical applications," J. Mater. Chem., 20, 6962 (2010).

4. L. Chen, S. Shet, H. Tang, K.-S. Ahn, H. Wang, Yanfa Yan, J. Turner, and M. Al-Jassim, "Amorphous copper tungsten oxide with tunable band gaps, " J. Appl. Phys. 108, 043502 (2010).

5. S. Shet, K.S. Ahn, T. Deutsch, H. Wang, R. Nuggehalli, Yanfa Yan, J. Turner, M. Al-Jassim, "Influence of gas ambient on the synthesis of co-doped ZnO:(Al,N) films for photoelectrochemical water splitting," J. Power Source 195, 5801-5805 (2010).

6. S. Shet, K.-S. Ahn, H. Wang, R. Nuggehalli, Y. Yan, J. Turner, and M. Al-Jassim, "Effect of substrate temperature on the photoelectrochemical responses of Ga and N co-doped ZnO films," J. Mater. Sci. 45, 5218-5222 (2010).

7. M. Huda, A. Walsh, Yanfa Yan, S.-H. Wei, and M.M. Al-Jassim, "Electronic, structural, and magnetic effects of 3d transition metals in hematite," J. App. Phys. 107, 123712 (2010).

8. W.-J. Yin, S. Chen, J.-H. Yang, X.-G. Gong, Yanfa Yan, S.-H. Wei, "Effective band gap narrowing of anatase TiO_2 by strain along a soft crystal direction," Appl. Phys. Lett. 96, 221901 (2010).

9. S. Shet, K.S. Ahn. T. Deutsch, H.L. Wang, N. Ravindra, Yanfa Yan, J. Tuerner, M. Al-Jassim, "Synthesis and characterization of band gap reduced ZnO:N and ZnO:(Al, N) thin films for photoelectrochemical water splitting," J. Mater. Res. 25, 45 (2010).

References

1. X. Chen and S. S. Mao, *Chem. Rev.* **107**, 2891 (2007).

2. R. Asahi, T. Morikawa, T. Ohwaki, K. Aoki, and Y. Taga, *Science* **293**, 269 (2001).

3. K. Nishijima, B. Ohtani, X. Yan, T. Kamai. T. Chiyoya, T. Tsubota, N. Murakami, and T. Ohno, *Chem. Phys.* **339**, 64 (2007).

4. H. Irie, Y. Watanabe, and K. Hashimoto, *Chem. Lett.* **32**, 772 (2003).

5. K.-S. Ahn, Y. Yan. S. Shet, T. Deutsch, J. Turner, and M. Al-Jassim, *Appl. Phys. Lett.* **91,** 231909 (2007).

6. S. Shet, K.-S. Ahn, Y. Yan, T. Deutsch, K. M. Chrustowski, J. Turner, M. Al-Jassim, N. Ravindra, J. App. Phys. **103**, 073504 (2007).

7. A. Walsh, Y. Yan, M. N. Huda, M. M. Al-Jassim, and S.-H. Wei, *Chem. Mater.* **21**, 547 (2009).

8. H. Luo, A. H. Mueller, T. M. McCleskey, A. K. Burrel, E. Bauer, and Q. X. Jia, *J. Phys. Chem. C* **112**, 6099 (2008).

9. K. Sayama, A. Nomura, T. Arai, T. Sugita, R. Abe, M. Yanagida, T. Oi, Y. Iwasaki, Y. Abe, and H. Sigihara, *J. Phys. Chem. B* **110**, 11352 (2006).

10. G. Kresse and J. Furthmüller, *Comput. Mater. Sci.* **6**, 15 (1996).

11. S.-H. Wei, *Comp. Mater. Sci.* **30**, 337 (2004).

12. Y. Yan and S.-H. Wei, *phys. stat. sol. (b)* **4**, 641 (2008).

II.G.13 Nanotube Array Photoelectrochemical Hydrogen Production

Rikard Wind
Synkera Technologies Inc.
2605 Trade Centre Ave. Suite C
Longmont, CO 80534
Phone: (720) 494-8401 x111
E-mail: rwind@synkera.com

DOE Manager
HQ: Eric Miller
Phone: (202) 287-5829
E-mail: Eric.Miller@hq.doe.gov

Contract Number: DE-FG02-07ER84871

Consultant:
John Turner
National Renewable Energy Laboratory (NREL)
Golden, CO

Project Start Date: August 15, 2008
Project End Date: August 15, 2011

Fiscal Year (FY) 2011 Objectives

- Development of photoelectrochemical (PEC) material with required composition and architecture to achieve 5,000+ hour lifetime, 2.0 eV bandgap, and >10% conversion efficiency in the prototypes.
- Conformally deposit indium tin oxide (ITO) and Pt quantum dots inside nanoporous anodic aluminum oxide (AAO).
- Achieve bandgap ≤2.0 eV.
- Develop large area PEC samples.

Technical Barriers

This project addresses the following technical barriers from the Production section of the Hydrogen, Fuel Cells and Infrastructure Technologies Program Multi-Year Research, Development and Demonstration Plan:

(AA) PEC Device and System Auxiliary Material

(AC) Device Configuration Designs

Technical Targets

This project is conducting studies of PEC hydrogen production by creating a hybrid design that combines multiple layers of materials to simultaneously address issues of durability and efficiency. As part of this effort, techniques are being developed that can manufacture devices at commercial scales. The overall goal of this project is to create a PEC device that meets or exceeds the DOE 2018 PEC hydrogen production targets in Table 1.

TABLE 1. Progress towards Meeting Technical Targets for PEC Hydrogen Generation

Characteristic	Units	2013 Target	2018 Target	Synkera 2011 Status
Usable Bandgap	eV	2.3	2.0	2.06
Chemical Conversion Efficiency	%	10	12	Not available
Solar to Hydrogen Efficiency	%	8	10	1.1%
Plant Durability	hr	1,000	5,000	Not available

FY 2011 Accomplishments

- Produced conformal transparent conductive oxide (TCO) and TiO_2 nanotubes in a layered manner inside pores of AAO.
- Demonstrated deposition of platinum nanodots inside the TCO and TiO_2 nanotubes.
- Demonstrated direct bandgap of 2.06 eV in Pt coated TiO_2.
- Developed new process for depositing highly conductive ITO inside AAO.
- Demonstrate 4x current increase for ITO-based PCE versus previous results.
- Demonstrated conformal deposition of WO_3 inside AAO nanopores.

✧ ✧ ✧ ✧ ✧

Introduction

The cleanest method of hydrogen production is the use of sunlight to electrochemically split water into hydrogen and oxygen. Advances in photoelectrode materials are required to make PEC hydrogen production practical. Current materials representing the state of the art in this area suffer from significant lifetime limitation, bandgaps poorly matched with the solar spectrum, and low conversion-efficiency. The project aim is to develop and commercialize next-generation PEC materials that incorporate an innovative three-dimensional nanostructured architecture and a tailored bandgap.

Approach

The material architecture includes high-density, high-surface-area arrays of nanotubes formed inside the pores of the honeycomb-like, self-organized matrix of nanoporous AAO. The approach utilizes a synergistic combination of two technologies developed by the project team: (1) synthesis and integration of AAO with the required

porous structure; and (2) conformal atomic layer deposition (ALD) of materials inside the high-aspect-ratio pores to produce nanotubes with atomically controlled thickness of coaxial layers. The approach results in up to a 1,000-fold increase of the cross-section available for light absorption and the surface area available for electrochemical reactions, thus significantly increasing the hydrogen yield per area of the electrode.

The PEC materials developed in this project include a catalytic layer, surrounded by a layer of light absorbing material, surrounded by an outer shell of TCO (Figure 1). The architecture provides a long vertical path length for light absorption with a short lateral path length for efficient charge separation.

Results

Previously during this project we demonstrated that AAO membranes with larger pore periods and diameters were most effective as PEC scaffolds. All the development of PEC materials was conducted on free standing 13 mm diameter AAO coupons. In order to create functional PEC devices capable of meeting the cost targets for hydrogen, two issues must be addressed: 1) the area of AAO must be scaled up; and 2) the PEC device must be integrated into a system capable of capturing the generated hydrogen.

Synkera has addressed these two issues by creating 1"×5" AAO membranes that are integrated with an aluminum rim (Figure 1). The challenge in this effort was to create membranes with large pore diameters in this format and to anneal them to the required temperature prior to ALD. We have achieved both of these goals with 100% yield.

In earlier efforts we explored nitrogen and carbon doping of TiO_2 to reduce the bandgap of the material. We were able to reduce the bandgap from 3.1 eV to 2.5 eV using nitrogen doping. Additional efforts at nitrogen doping did not lead to further reduction in the bandgap. In order to overcome this limitation we explored Pt quantum dots as a means of decreasing the bandgap. Figure 2A shows a conceptual drawing of the AAO cross section. The nanoporous AAO is first conformally coated with a TCO (to form TCO nanotubes) and provide a path for the generated electrons to reach the cathode. Inside the TCO, nanotubes of TiO_2 are deposited to produce the catalytic surface. Finally platinum quantum dots are deposited on the TiO_2 surface. Figures 2B and 2C show scanning electron microscope side and top views of the AAO after 100 cycles of Pt ALD. Both views suggest that Pt ALD forms polycrystalline domains similar to the domains formed during metallic tungsten ALD on oxide surfaces [1]. Experience with tungsten ALD suggests that the Pt ALD proceeds via the formation of individual islands that coalesce as the number of cycles increases. By only depositing a few cycles of Pt on the TiO_2 surface, individual quantum dots of Pt can be obtained.



FIGURE 1. Annealed 1"×5" AAO Membranes Supported by Aluminum Rim

PEC samples consisting of aluminum doped zinc oxide (the TCO), TiO_2 , and a few ALD cycles of Pt were prepared (Figure 2A). These samples were sent to our consultant at NREL for analysis. NREL performed photocurrent spectroscopy by measuring the photocurrent while scanning the light wavelength from 550-900 nm. Direct electronic transitions are found by plotting the square of the normalized photocurrent (NPC) and extrapolating the linear regime to the abscissa (Figure 3). The figure shows that the PEC material had a direct bandgap of 2.06 eV. Additionally, plots of the square root of the NPC showed an indirect bandgap of 1.71 eV.

Additional tests at NREL using colored glass filters used to estimate wavelength dependent photoresponse. The Pt-coated PEC samples demonstrated the largest magnitude response to chopped illumination from photons with wavelengths longer than 695 nm ($h\nu$<1.78 eV) while bare TiO_2 had none. This result confirms photocurrent spectroscopy results that these configurations are visible-light active, and is responsive to photon energies below what would be expected from pure TiO_2.

In other recent efforts Synkera has developed a new ALD chemistry for deposition of highly conductive ITO conformally inside the pores of AAO. PEC samples were made using ITO and TiO_2 and compared to AZO/TiO_2 samples as well as AZO/TiO_2/Pt samples. Figure 4 shows the photocurrent for all three types of samples during chopped light experiments conducted at Synkera. The figure shows that the photocurrent is four times higher for the ITO samples compared to the AZO samples and two times higher than the samples modified by Pt. The reason for the much higher current is unclear, but will be further explored during the last two months of the project.

Synkera has also just completed samples that have WO_3 as the photocatalyst instead of TiO_2. These samples are undergoing evaluation.

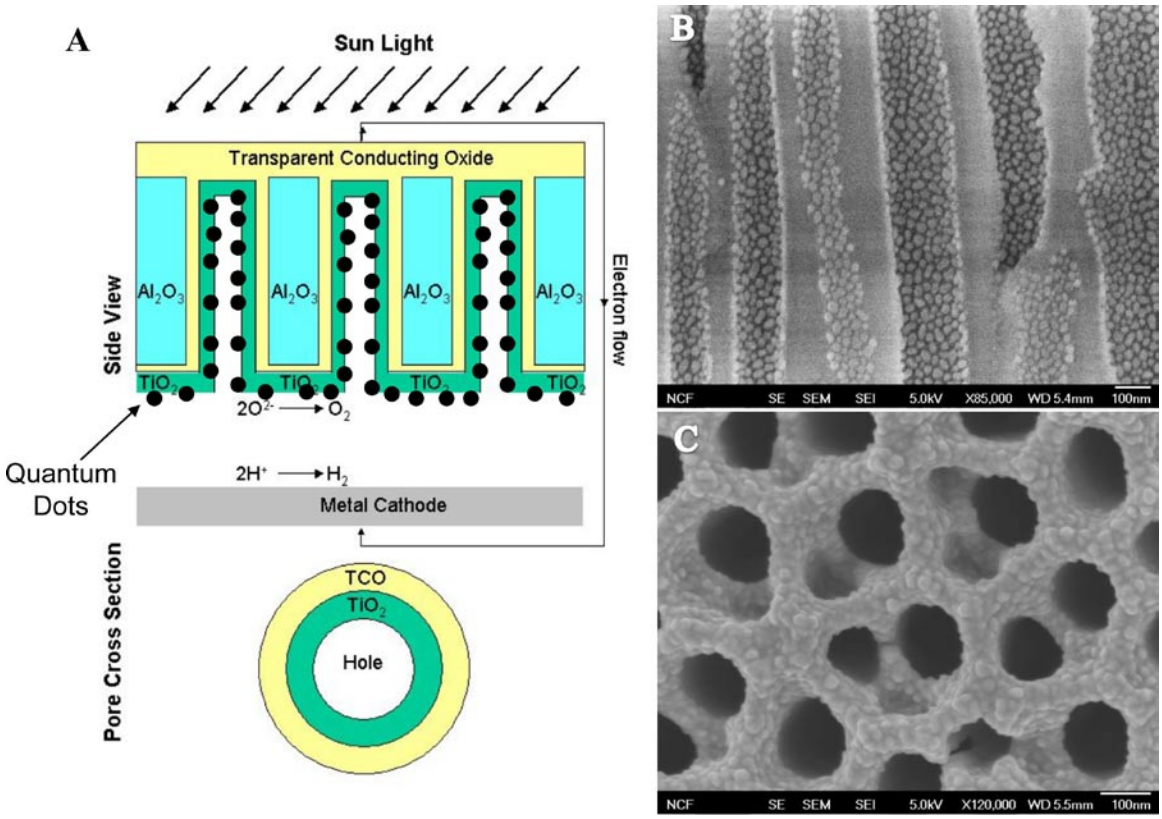


FIGURE 2. A: Conceptual drawing of PEC nanotube architecture with quantum dot catalyst. B: Side view of AAO after 100 cycles of Pt ALD. C: Top view of AAO after 100 cycles Pt ALD.

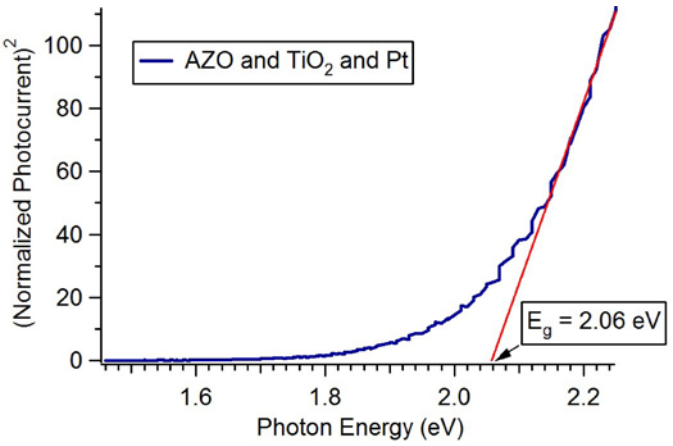


FIGURE 3. Photocurrent Spectroscopy Data Performed at NREL (Pt-coated PEC devices show a bandgap of 2.06 eV.)

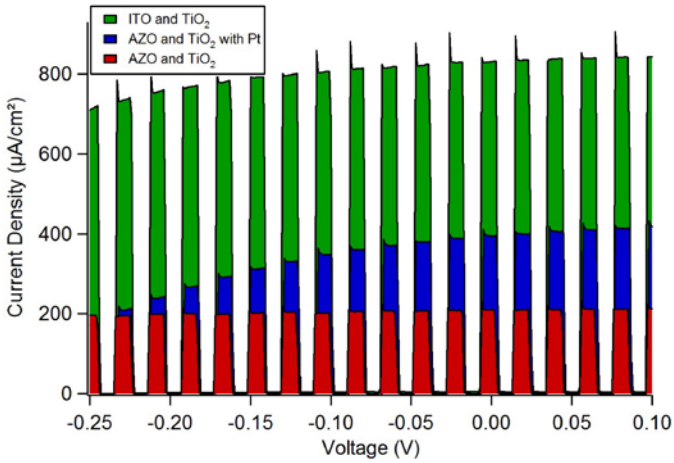


FIGURE 4. Photocurrent comparison in 0.1 M KOH (pH 13) on PEC samples with ITO/TiO_2, AZO/TiO_2/Pt, and AZO/TiO_2 as a function of applied potential (vs. Ag/AgCl electrode) under 1 sun illumination with chopped light.

Conclusions

We have developed a nanostructured PEC material that is manufactured using scalable techniques. We have successfully completed an intermediate scale up of the AAO scaffold for PEC applications. We have demonstrated a visible light photoresponse in our PEC samples. We have also demonstrated significantly enhanced photocurrent by using ITO to replace the AZO in the device.

Future Directions

- Complete testing of WO_3 PEC samples.
- Fabricate samples of ITO/TiO_2/Pt.
- Measure long-term stability of best performing PEC sample.
- Manufacture large area PEC sample.

Patents Issued

1. On August 30th 2010 we resubmitted a U.S. Provisional Patent Application No. 61/174,577 entitled "ENERGY CONVERSION DEVICES AND METHODS FOR MAKING SAME." This patent covers the architecture described in this project as well as related architectures for photovoltaics and other applications.

FY 2011 Publications/Presentations

1. We presented a poster on this work on May 10th 2011 at the DOE Hydrogen and Fuel Cells Program, and Vehicle Technologies Program Annual Merit Review and Peer Evaluation Meeting.

References

1. R.A. Wind, F.H. Fabreguette, Z.A. Sechrist and S.M. George, "Nucleation Period, Surface Roughness and Oscillations in Mass Gain per Cycle during W Atomic Layer Deposition on Al_2O_3", *J. Appl. Phys.* **105**, 074309 (2009).

II.H.1 Biological Systems for Hydrogen Photoproduction

Maria L. Ghirardi (Primary Contact), Paul W. King, Kathleen Ratcliff, David Mulder, Seth Noone and Lauren Magnusson.
National Renewable Energy Laboratory (NREL)
1617 Cole Blvd.
Golden, CO 80401
Phone: (303) 384-6312
E-mail: maria.ghirardi@nrel.gov

DOE Manager
HQ: Roxanne Garland
Phone: (202) 586-7260
E-mail: Roxanne.Garland@ee.doe.gov

Subcontractors:
- Drs. Anatoly Tsygangov and Sergey Kosourov, Institute of Basic Biological Problems, RAS, Pushchino, Russia
- Dr. Eric Johnson, Johns Hopkins University, Baltimore, MD
- Dr. Michael Flickinger, North Carolina State University, Raleigh, NC

Project Start Date: October 1, 2000
Project End Date: Project continuation and direction determined annually by DOE

Fiscal Year (FY) 2011 Objectives

Primary Objectives

- Develop and optimize aerobic, high solar-to-hydrogen (STH) photobiological systems for the production of H_2 from water by:
  - Engineering a H_2-producing catalyst ([FeFe]-hydrogenase) that has an extended half-life following exposure to O_2.
  - Introducing a more O_2-tolerant hydrogenase into the green alga, *Chlamydomonas reinhardtii.*
- Design a fusion between hydrogenase Ca1 and ferredoxin to re-direct a larger portion of photosynthetic electron transport to hydrogenase rather than to CO_2 fixation under aerobic conditions; advise Massachusetts Institute of Technology (MIT) regarding *in vitro* testing of the fusion.
- Further optimize and utilize an anaerobic, limited STH working platform to study biochemical and engineering factors that affect H_2 photoproduction by biological organisms; focus on the effect of a leaky chloroplast adenosine triphosphate (ATP) synthase on the rates of H_2 photoproduction.
- Integrate fermentative H_2 production using potato waste or sulfur-deprived, alginate-immobilized algal biomass as feedstock, with photosynthetic H_2 production by anaerobic, purple non-sulfur bacteria.

Technical Barriers

This project addresses the following technical barriers from the Production section of the Fuel Cell Technologies (FCT) Program Multi-Year Research, Development and Demonstration Plan.

(AH) Rate of H_2 Production
(AI) Continuity of H_2 Production
(AT) Feedstock Cost

Technical Targets

TABLE 1. Progress toward Meeting Technical Targets for Photobiological Hydrogen Production

Parameters	Current Status	2013 Targets	Maximum Potential
Duration of continuous photoproduction:			
• Aerobic, high STH (O_2-tolerant)	0	30 min.	12 hours daylight
• Anaerobic, low STH (S-deprivation)	90 days		Indefinite
• Aerobic, low STH (S-deprivation)	10 days		Indefinite
Cost[1] ($/kg H_2)			
• Aerobic, high STH			$2.99
• Anaerobic, low STH			$6.02
• Integrated (photobiological and fermentative)			$3.21

[1] Cost estimates based on B.D. James, G.N. Baum, J. Perez, K.N. Baum, 2009, http://nrel.gov/docs/fy09osti/46674.pdf

FY 2011 Accomplishments

- Used computational methods to identify differences in the geometries and energies of the gas diffusion barrier protecting the H-cluster in two [FeFe]-hydrogenases that display a 1,000-fold difference in the level of O_2 sensitivity.
- Used a previously-developed random mutagenesis technique to randomize the amino acid residues that comprise the areas identified above.
- Demonstrated the presence of double O_2-inactivation kinetics in green algal transformants expressing a clostridial hydrogenase, suggesting that the more O_2-tolerant clostridial enzyme Ca1 is active in wild-type green algae.

- Demonstrated an up to 2.6-fold increase in the H_2-photoproduction rates upon increases in the photobioreactor gas-to-liquid ratio, using either sulfur/phosphorus-deprived cell suspensions or alginate-immobilized, sulfur/phosphorus-deprived cultures. (The effect was shown to be due to inhibition of the reaction rates by H_2 that accumulated in the headspace.)
- Found that pre-treatment of alginate films with 0.1% polyethylenimine stabilized the films, resulting in a 14% increase in the H_2 yields but no significant increase in the period of performance.
- Showed a 40% improvement in the H_2 photoproduction rates by ATP synthase mutants due to dissipation of the proton gradient that limits photosynthetic electron transport in non-mutated cells.
- Demonstrated successful induction of a marker gene behind a chloroplast inducible promoter, a preliminary step for introduction of mutated ATP synthase subunits into *Chlamydomonas.*
- Obtained a 55% yield (based on 12 moles H_2/glucose) following fermentation of 2% starch (from potato waste), and subsequent utilization of the organic acid effluent using non-purple photosynthetic bacteria.



Introduction

Green algae can extract electrons from water and generate H_2 under illumination, using the concerted activities of the photosynthetic electron transport chain and the enzyme [FeFe]-hydrogenase. This pathway evolves O_2 as a by-product, which irreversibly inhibits the hydrogenase enzyme's catalytic center. The continuity of H_2 photoproduction is one of the major technical barriers to developing photobiological H_2-production systems that use water as the source of electrons (technical barrier AI).

A second major barrier to efficient algal H_2 photoproduction is the low rate of the reaction (technical barrier AH), which is dependent on many intracellular regulatory factors, including the competition for photosynthetic reductant between the H_2-production and the CO_2-fixation pathways; the down-regulation of photosynthetic electron transport from water under H_2-producing conditions; and the predominance of cyclic, unproductive electron transport over linear electron transfer under anaerobiosis.

Our current project addresses the O_2 sensitivity and low rates of algal H_2-production by using molecular engineering to alleviate these barriers and testing the results through the sulfur-deprivation platform. The latter allows us to measure the effects of molecular engineering on sustained hydrogen production, although at low STH conversion levels. Our project also addresses the performance of an integrated fermentative/photobiological H_2-producing system that holds the potential for lowering the costs and increasing the yields of photobiological H_2.

Approach

Task 1. Molecular Engineering Approaches to Increase the O_2 Tolerance and the Rates of H_2 Photoproduction

This task has three major objectives: (a) the engineering of increased O_2 tolerance in [FeFe]-hydrogenases through random mutagenesis, targeted to regions that control O_2 access to the catalytic site; (b) the expression of a functional, more O_2-tolerant clostridial [FeFe]-hydrogenase in *Chlamydomonas reinhardtii*; and (c) the design and testing of bacterial hydrogenase-ferredoxin fusions for activity and interaction with Photosystem I (NREL acted as a consultant for MIT).

The targeted mutagenesis approach is being guided by extensive computational study of gas diffusion in the clostridial *Clostridium pasteurianum* CpI hydrogenase (that has a solved crystal structure). These studies previously identified a cavity, present next to the H-cluster of [FeFe]-hydrogenases, as a high-energy barrier for O_2 diffusion to the cluster. However, site-directed mutagenesis of residues that comprise the barrier have not yielded mutants with higher O_2-tolerance. Alternative computational and mutagenesis approaches have been devised and are being pursued.

Our studies aimed at expressing a more O_2-tolerant hydrogenase from *Clostridium acetobutylicum* (Ca1) in *C. reinhardtii.* Linking it functionally to photosynthetic electron transport involved: (i) designing genetic constructs for expression, activation and translocation of the hydrogenase into the stromal compartment of algal chloroplast; (ii) testing transformants for the presence of recombinant hydrogenase enzyme and activity; (iii) testing for O_2-tolerance of H_2 photoproduction under different physiological conditions. The availability of an algal strain expressing a more O_2-tolerant enzyme will provide us with the opportunity to examine physiological effects of such an enzyme in algal metabolism.

Sustained H_2 photoproduction, which is currently achieved through sulfur deprivation (see task 2), requires that the algal cultures be anaerobic, which, in turn, inactivates CO_2 fixation. However, once an O_2-tolerant enzyme becomes available, H_2 photoproduction will compete with the CO_2 fixation pathway (at the level of the electron transport mediator, ferredoxin) for photosynthetic reductant. In order to direct the flux of reductant towards the hydrogenase, we worked with Prof. Shuguang Zhang's research group at MIT to design (NREL), construct and test (MIT) the performance of bacterial hydrogenase-ferredoxin fusions. The collaboration produced some computational models but experimental work was not done due to limited funding.

Task 2. Use of the Sulfur-Deprivation Platform to Test Biochemical and Engineering Factors

To induce sustained H_2 photoproduction, we collaborated with the University of California in the development of a physiological switch that is based on removing sulfate from the algal growth medium. This procedure has become a platform for testing the performance of a variety of algal mutants, growth conditions, immobilization surfaces and other engineering factors that may affect the overall H_2 yield.

Task 3. Integrated H_2 Production System

The FCT Hydrogen Biological Production working group identified a system for biological H_2 production that depends on the integrated activity of photosynthetic (oxygenic and non-oxygenic) and fermentative organisms. The potential advantages of this system are (a) the wider absorption spectrum or oxygenic and non-oxygenic phototrophs, (b) the utilization of spent algal and bacterial biomass as feedstocks by fermentative organisms for increased H_2 production, and (c) the utilization of the fermentative effluent for improved growth of algae and photosynthetic bacteria.

NREL has been testing two integrated system configurations. The first one is based on using potato waste as the feedstock for H_2-producing fermentative organisms, which co-generate organic acids that are used to support subsequent H_2-photoproduction by photosynthetic bacteria. The second configuration takes advantage of spent algal biomass (harvested at the end of a photobiological H_2-production process) as feedstock for fermentative H_2-producing microbes.

Results

Task 1. Molecular Engineering Approaches to Increase the O_2 Tolerance and the Rates of H_2 Photoproduction

Computational simulations identified differences in the geometries and energies of the gas diffusion barriers protecting the H-cluster in two [FeFe]-hydrogenases with a 1,000-fold difference in the level of O_2 sensitivity. We randomized the regions around the diffusion barriers (not the barrier residues *per se*) to test the information provided by the simulations. The resulting mutants will be expressed and screened in a new high-throughput technique previously developed at our laboratory.

Concomitantly, we have proceeded with the expression of the more O_2-tolerant, clostridial [FeFe]-hydrogenase in wild-type *C. reinhardtii*. Plasmids for constitutive or inducible expression of Ca1 hydrogenase were constructed and used to transform wild-type Chlamydomonas. The presence of the codon-optimized Ca1 gene was confirmed by polymerase chain reaction (PCR), and its transcription was detected by reverse-transcriptase-PCR. Measurement of hydrogenase activity was initially inconsistent, perhaps due to differences in gene expression from sample to sample. However, O_2-inhibition assays revealed double kinetics, suggesting that the more O_2-tolerant Ca1 gene was active. Optimization of the conditions for Ca1 expression will continue in order to unambiguously determine its contribution to overall hydrogenase activity in recombinant strains.

Our collaborative work with MIT helped to support the publication of a Proceedings of the National Academy of Sciences' manuscript, detailing the evidence for improved photosynthetic reductant flux to the hydrogenase *in vitro* using an algal hydrogenase-ferredoxin fusion. These results hold the promise to improve H_2 production rates *in vivo* as well.

Task 2. Use of the Sulfur-Deprivation Platform to Test Biochemical and Engineering Factors

Algal H_2-production is catalyzed by a reversible hydrogenase that is capable of H_2 production and H_2 oxidation, depending on the prevailing physiological conditions, such as the availability of photosynthetic reductant (favors H_2 production) and high headspace H_2 pressure (favors H_2 oxidation). We investigated the magnitude of the effect of different gas-to-liquid (or solid) ratios in the rates of H_2 production by suspension and immobilized algal cell reactors. The expectation is that, by diluting the H_2 produced by the cultures by increasing the headspace volume, it is possible to sustain high rates of H_2 production during the sulfur-deprivation process. Table 1 shows that increases in the gas-phase volume result in higher rates of H_2 photoproduction, with the highest reported rate of 12.5 μmoles mg Chl^{-1} h^{-1} being observed with a headspace volume of 925 mL. On the other hand, although the rates of H_2 photoproduction by cultures immobilized in alginate increase as the headspace volume is raised, they saturate at about 10 μmoles mg Chl^{-1} h^{-1}, perhaps due to limited diffusion of released H_2 within the alginate matrix. Also, the inhibitory effect of H_2 was quantified by measuring the yields of H_2 photoproduction by suspension cultures in the presence of different concentrations of added H_2, as shown in Figure 1. These combined results imply that the added cost of gas purging and gas separation must be balanced with the added benefit of increased H_2 productivities in order to achieve the most economical system.

TABLE 1. Rates of H_2 Photoproduction and Total Yield of H_2 as a Function of Headspace Volume

Gas space volume	Rate of H_2 production (mmoles x mg Chl^{-2} x h^{-1})	Total final yield of H_2
Suspension cultures		
165 mL	4.8	250 mL/L
545 mL	7.3	400 mL/L
925 mL	12.5	560 mL/L
Immobilized cultures		
9 mL	6.1	0.20 mol/m^3
20 mL	9.6	0.24 mol/m^3
35 mL	10	0.33 mol/m^3
54 mL	10	0.36 mol/m^3
119 mL	10	0.35 mol/m^3

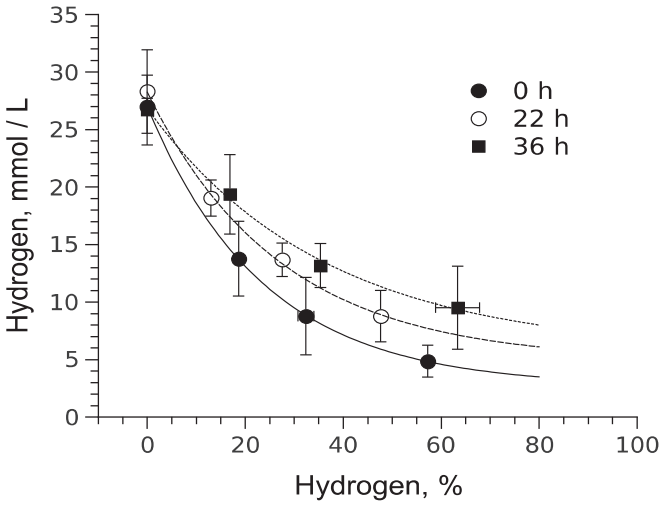


FIGURE 1. Final yield of H_2 as a function of the concentration of H_2 gas present in the bioreactor headspace at different time points (0, 22 and 36 hours) during the sulfur-deprivation process.

A second known limitation to the immobilized system is the low stability of alginate films over time. We examined the effect of treating the films with polyethyleneimine, a polymer that has been successfully used to increase the mechanical stability of a variety of films. We processed immobilized cultures through cycles of +S+P/-S-P and demonstrated that an increase in the polyetherimide (PEI) concentration up to 0.5% inhibits H_2 photoproduction but increases the mechanical stability of the film, allowing the cultures to undergo more cycles. The highest total H_2 yield was obtained in films pre-treated with 0.1% PEI, compared to untreated films. Our future studies will then be performed with cells immobilized in 0.1% PEI-treated films.

The sulfur-deprivation process was also used to test the performance of ATP synthase mutants designed to dissipate the proton gradient that is established during linear electron transfer (LEF) from H_2O to H_2 and that is known to down-regulate LEF (and thus H_2 production). Initial mutants, which were generated by Dr. Eric Johnson, Johns Hopkins University, had higher rates of H_2 photoproduction under high light but were affected in growth rates. New mutants were designed and are being tested to function under regulation of an inducible promoter, to allow the dissipation of the proton gradient to occur only under H_2-producing conditions.

Task 3. Integrated H_2 Production System

The integrated H_2-production system was tested, using a two-chamber reactor which separated the fermentative consortium from the photosynthetic bacteria. Unfortunately, many issues were found to affect the process, including (a) the low diffusion of volatile fatty acid feedstock; (b) the improper sealing of the membrane that did not prevent contamination; (c) inhibition of photosynthetic bacterial growth by factors present in the fermentative effluent; and (d) the nitrogen sources for photosynthetic bacteria need to be tightly controlled. This process was replaced by independent, successive cultivations with pH correction and addition of N_2 gas. The latter was tested with different amounts of feedstock, different dilutions of fermentative effluent before transfer to photobioreactor, and a new strain of *Rhodobacter capsulatus*. Yields of 55% (based on 12 moles H_2/glucose) were obtained with 2% starch (from potato waste), 75%–95% dilution of fermentative effluent before feeding the *R. capsulatus* strain N7. These yields are among the highest reported in the literature for an integrated system, and they serve as a baseline for our next step, where we will use spent algal biomass as the feedstock.

Conclusions and Future Direction

- **Task 1.** (a) continue the characterization of a wild-type *C. reinhardtii* transformant library harboring the Ca1 expression construct, and characterize new transformant library of Ca1 in a *C. reinhardtii* Hyd^- strain (developed under Basic Energy Sciences funding) that eliminates native hydrogenase activity; (b) express and screen a random mutant library of the bacterial hydrogenase Ca1 in *E. coli* to identify active mutants for O_2 tolerance characterization.
- **Task 2.** (a) design a more efficient immobilized H_2-production system, suitable for long-term H_2 photoproduction (two months compared to 10 days using the current configuration); (b) finish the development and test the function of an inducible promoter that will turn the mutated ATP synthase ON only under certain environmental conditions, to allow us to control the expression of the proton channel dissipation trait; (c) revisit the use of photoautotrophic cultivation conditions for sulfur-deprived cultures, aimed at increasing H_2 yields and decreasing cost by eliminating organic carbon substrate.
- **Task 3.** Will be discontinued due to budget restrictions.

Patents Issued

1. U.S. 7,732,174 B2 by Kosourov et al., "Multi-stage microbial system for continuous hydrogen production."

FY 2011 Publications/Presentations

Publications

1. Ghirardi, M.L.; Mohanty, P. 2010. "Oxygenic Hydrogen Photoproduction – Current Status Of The Technology." *Current Science Indi*a 98, 499-507.

2. Laurinavichene, T.V.; Belokopytov, B.F.; Laurinavichius, K.S.; Tekucheva, D.N.; Seibert, M.; Tsygankov, A.A. 2010. "Towards the Integration of Dark- and Photo-Fermentative Waste Treatment. 3. Potato as Substrate for Sequential Dark Fermentation and Light-Driven H_2 Production." *International Journal of Hydrogen Energy* 16, 8536-8543.

3. Eckert, C.; Dubini, A.; Yu, J.; King, P.; Ghirardi, M.; Seibert, M.; Maness, P.C. 2010. "Hydrogenase Genes and Enzymes Involved in Solar Hydrogen Production." In *State of the Art and Progress in Production of Biohydrogen.* N. Azbar and D. Levin, eds., Bentham Science Publishers, U.S., in press.

4. King, P.W.; Brown, K.A.; Ratcliff K.; Beer, L.L. 2010. "Photobiological and Photobiomimetic Production of Solar Fuels." In *Carbon Neutral Fuels and Energy Carriers*, N. Muridov, ed., Taylor and Francis, New York.

5. Kosourov, S.N., M.L. Ghirardi and M. Seibert. 2011. "A truncated antenna mutant of *Chlamydomonas reinhardtii* can produce more hydrogen than the parental strain." *Int. J. Hydrogen Energy* 36, 2044-2048.

6. Tekucheva, D.N., T.V. Laurinavichene, M.L. Ghirardi, M. Seibert, A.A. Tsygankov. 2010. "Immobilization of purple bacteria for light-driven H_2 production from starch and potato fermentation effluents." *J. Biotechnol*., in press.

Presentations

1. Visited our collaborator S. Zhang's research group at MIT (Apr. 2010, PK).

2. Departmental seminar at the North Carolina State University (May 2010, MS).

3. Invited to talk at the Christian-Albrechts University in Kiel, Germany (May 2010, MS).

4. Oral presentation at the Gordon Conference on Iron-Sulfur Enzymes, Colby-Sawyer College, NH (June 2010, PK).

5. Kendric C. Smith Lecture on Innovations in Photobiology at the American Society for Photobiology National Meeting (June 2010, MS).

6. Oral presentation at the CIMTEC 5th Forum on New Materials, Montecatini-Terme, Italy (June 2010, PK).

7. Poster and invited presentations at the International Conference on Hydrogenases and H_2 Production, Uppsala, Sweden (June 2010, MS and MLG).

8. Presentation to teams of visiting scientists from the Taiwan Academia Sinica and from the Australian National University (July and Aug. 2010, MLG).

9. Poster presentation at the 15th International Congress on Photosynthesis, Beijing, China (Aug. 2010, MS).

10. Invited talk at the Shanghai Normal University, China (Aug. 2010, MS).

11. Oral presentation at the American Chemical Society – Fall Annual Meeting, Boston (Aug. 2010, PK).

12. Invited talk at the ICCE Meeting, Cyprus, Turkey (Sept. 2010, MS).

13. Invited talk at the National Chung Hsing University, Taiwan (Nov. 2010, MS).

14. Attendance at DOE"s ARPA-E workshop on Solar Fuels (Dec. 2010, MLG).

15. Oral presentation at the Fuel Cell and Hydrogen Energy Meeting, Washington, D.C. (Feb. 2010, MLG).

II.H.2 Fermentation and Electrohydrogenic Approaches to Hydrogen Production

Pin-Ching Maness (Primary Contact), Katherine Chou, Lauren Magnusson, and Shiv Thammannagowda
National Renewable Energy Laboratory (NREL)
1617 Cole Blvd.
Golden, CO 80401
Phone: (303) 384-6114
E-mail: pinching.maness@nrel.gov

DOE Manager
HQ: Roxanne Garland
Phone: (202) 586-7260
E-mail: Roxanne.Garland@ee.doe.gov

Subcontractor:
Bruce Logan
Pennsylvania State University, University Park, PA

Start Date: October 1, 2004
Projected End Date: Project continuation and direction determined annually by DOE

Fiscal Year (FY) 2011 Objectives

- Perform hydrogen fermentation using cellulolytic bacteria and lignocellulosic biomass to lower feedstock cost.
- Perform metabolic pathway engineering to improve hydrogen molar yield via fermentation.
- Develop microbial electrolysis cell to improve hydrogen molar yield using waste from the fermentation of lignocellulosic biomass.

Technical Barriers

This project addresses the following technical barriers from the Hydrogen Production section (3.1.4) of the Hydrogen, Fuel Cells and Infrastructure Technologies Program's Multi-Year Research, Development and Demonstration Plan:

(AR) H_2 Molar Yield
(AS) Waste Acid Accumulation
(AT) Feedstock Cost

Technical Targets

TABLE 1. Progress toward Meeting DOE Technical Targets in Dark Fermentation

Characteristics	Units	2013 Target	2018 Target	2011 Status
Yield of H_2 from glucose	mole H_2/mole glucose	4	6	3.2
Feedstock cost	cents/lb glucose	10	--	12

Yield of H_2 from glucose: DOE has a 2013 target of an H_2 molar yield of 4 using glucose as the feedstock. In FY 2010 we achieved a molar yield of 3.2, accomplished by *Clostridium thermocellum* fermenting avicel (commercial cellulose) via fermentation only.

Feedstock cost: The DOE Biomass Program is conducting research to meet its 2013 target of 10 cents/lb biomass-derived glucose. NREL's approach is to use cellulolytic microbes to ferment cellulose and hemicellulose directly, which will result in lower feedstock costs.

FY 2011 Accomplishments

- Conducted sequencing fed-batch reactor experiments and determined hydraulic retention time and optimal amounts of solid feeding in bioreactor using the cellulose-degrading bacterium *C. thermocellum* fermenting avicel. We realized improved rates of H_2 production via retaining those microbes that were adapted to degrade cellulose.
- Using a custom-designed plasmid (University of Manitoba, Canada) and improved transformation protocols, we obtained two mutant lines of *C. thermocellum*, which serve as the foundation for future genetic engineering effort in this microbe.
- A prototype two-chamber microbial electrolysis cell (MEC) was designed, constructed, and tested to eliminate methane generation. The reactor was operated at three different hydraulic retention times (HRTs; 24 h, 16 h, and 10 h) and produced H_2 gas at a maximum rate of up to 191 ± 34 mL/d and a maximum volumetric current of 62 ± 1 A/m^3 at HRT 10 h. Using this new reactor design, nearly pure hydrogen was obtained.



Introduction

Biomass-derived glucose feedstock is a major operating cost driver for economic H_2 production via fermentation. The DOE Fuel Cell Technologies Program is taking advantage of the DOE Biomass Program's investment in

developing less expensive glucose from biomass to meet its cost target of 10 cents/lb by 2013. Meanwhile, one alternative and valid approach to addressing the glucose feedstock technical barrier (AT) is to use certain cellulose-degrading microbes that can ferment cellulose directly for H_2 production. One such example is the cellulose-degrading bacterium *Clostridium thermocellum* 27405 (*C. thermocellum*), which was reported to exhibit one of the highest growth rates using crystalline cellulose [1]. Another technical barrier to fermentation is the relatively low molar yield of H_2 from glucose (mol H_2/mol sugar; Technical Barrier AR), which results from the simultaneous production of waste organic acids and solvents. Biological pathways maximally yield 4 mole of H_2 per 1 mole of glucose (the biological maximum) [2]. However, most laboratories have reported a molar yield of 2 or less [3,4]. Molecular engineering to block competing pathways is a viable option toward improving H_2 molar yield. This strategy had resulted in improved H_2 molar yield in *Enterobacter aerogenes* [5].

A promising parallel approach to move past the biological fermentation limit has been developed by a team of scientists led by Bruce Logan at Pennsylvania State University (PSU). In the absence of O_2, and by adding a slight amount of negative potential (–250 mV) to the circuit, Logan's group has produced H_2 from acetate (a fermentation byproduct) at a molar yield of 2.9-3.8 (versus a theoretical maximum of 4) in a modified microbial fuel cell called an MEC [6]. It demonstrates for the first time a potential route for producing eight or more mole of H_2 per mole glucose when coupled to a dark fermentation process. Indeed, in FY 2009 the team reported a combined molar yield of 9.95 when fermentation was coupled to MEC in an integrated system [7]. Combining fermentation with MEC could therefore address technical barriers AR and AS (waste acid accumulation) and improve the techno-economic feasibility of H_2 production via fermentation.

Approach

NREL's approach to addressing feedstock cost is to optimize the performance of the cellulose-degrading bacterium *C. thermocellum*. To achieve this goal, we are optimizing the various parameters in a sequencing fed-batch reactor to improve longevity, yield, and rate of H_2 production. To improve H_2 molar yield, we are selectively blocking competing metabolic pathways in this organism via developing genetic methods. Via a subcontract, PSU is testing the performance of a MEC using both a synthetic effluent and the real waste stream from lignocellulosic fermentation generated at NREL.

Results

Lignocellulose Fermentation

Cellulose is a solid substrate and continuous feeding will eventually suffer from clogging of feed lines and over-exhaustion of the feed pump. A more feasible strategy for cellulose fermentation is via feeding the substrate at a predetermined interval in lieu of continuous feeding. This strategy can be realized via the development of a sequencing fed-batch bioreactor. This method also simultaneously retains the acclimated microbes to increase rate of H_2 production. We carried out the experiment in an Electrolab bioreactor with a working volume of 1 L. The medium was continuously sparged with N_2 at a flow rate of 16 ccm and agitated at 100 rpm. The HRT tested was 48 h with a daily carbon loading of 2.5 or 5.0 g/L of avicel. The reactor was initiated by running the fermentation using avicel at 2.5 g/L for 24 h, turning off the agitation for 1 h during which the unfermented substrate along with the attached microbes settled, followed by removing 500 ml of the clear supernatant, and adding back 500 ml fresh medium replenished with avicel (2.5 or 5.0 g/L). We completed a total of eight cycles, four cycles for each carbon loading condition (Table 2).

Initial results indicate that 5.0 g/L loading works better than 2.5 g/L, the residual avicel from the former caused retention of the acclimated *C. thermocellum*, which displayed an intense yellow color. Higher substrate also leads to faster rate of H_2 production. One of the benefits of sequencing batch fermentation is the decrease in the lag phase upon subsequent substrate feedings, once adapted. This is shown as a dramatic decrease in "time to peak H_2 production" (Table 2). The t_1 in batch one was almost 19 h, yet by the fourth cycle, it has dropped to mere 4 h, providing compelling evidence as to feasibility of the sequencing fed-batch process in fermenting solid substrates.

TABLE 2. Rate of Hydrogen and Metabolite Production in Sequencing Fed-batch Bioreactor with *Clostridium thermocellum* Fermenting Avicel Substrate

Batch	Avicel Concentration	Time to peak H_2 production	Amount of H_2 produced	Average H_2 Production Rate	Lactate	Formate	Acetate	Ethanol
	(g/L)	(t, h)	(mmoles)	(mmol L^{-1} h^{-1})	(mmol L^{-1})			
1	2.5	18:43	14.92	0.60	1.98	3.06	28.15	18.46
2-4		4:14	13.85					
5	5.0	8:09	17.57	0.92	13.07	5.02	40.79	32.12
6-8		5:27	22.11					

Metabolic Engineering

The ultimate goal of this approach is to develop tools to inactivate genes encoding competing metabolic pathways, thus redirecting more cellular flux to improve H_2 molar yield. Transformation in this organism has been challenging likely due to either an inefficiency of the plasmids used or an active restriction system in the host thus destroying the incoming plasmid. NREL established an active collaboration with the researchers from University of Manitoba, Canada. Using their proprietary plasmid along with optimized protocols, we successfully generated two mutant lines in *C. thermocellum* harboring the plasmid. The success is based on two lines of evidence: (a) growth in the antibiotic chloramphenicol (100 mg/L) (Figure 1A); and (b) polymerase chain reaction (PCR) of the chloramphenicol-encoding gene (cm^r) in the transformant (Figure 1B). For the latter, briefly, plasmid deoxyribonucleic acid (DNA) was isolated from *C. thermocellum* transformants using Qiagen mini prep kit protocol except 20 mg/ml lysozyme was added to the buffer for cells lysis. PCR was carried out using the primer for chloramphenicol-resistance gene. We obtained the anticipated 218 bp PCR product and confirmed the presence of plasmids in the two transformants tested (Figure 1B). Moreover, plasmid DNA was isolated from four *C. thermocellum* transformants and transformed to the *E. cloni* elite electro-competent cells (Lucigen, WI, USA). Plasmid DNA was then isolated from the *E. cloni* transformants and resulted in the restriction pattern with EcoRI (1.2 kb fragment) that is consistent with the presence of the correct proprietary plasmid in *C. thermocellum* (data not shown).

Microbial Electrolysis Cell

Previously, a 2.5 L-single chamber MEC equipped with eight electrode pairs was used to produce H_2 under continuous flow conditions. However, in this type of single-chamber MEC, all H_2 gas produced was converted to methane. In order to suppress methane production in single chamber MECs, anode potentials were set at different values (from –0.4 V to +0.2 V vs. Ag/AgCl) using a potentiostat. MEC performance with a potentiostat was compared to that obtained with an applied voltage of 0.6 V using a power supply. In batch tests the largest total gas production (46 ± 3 mL) and best overall energy recovery in terms of electrical energy used and substrate energy ($\eta_{E+S} = 58 \pm 6\%$) was achieved at a set anode potential of –0.2 V, and methane production was reduced at the higher set anode potentials (Figure 2). However, although the optimum set anode potential (–0.2 V) suppressed methane generation in batch tests, and stable H_2 was obtained at the beginning of the continuous flow operation, the gas composition became predominantly methane in continuous flow tests. Switching the anode to a new reactor immediately resulted in H_2 production and recovery with little methane production. This indicated that the methane originated primarily from non-anode associated microorganisms in the continuous flow tests.

A new type of tubular type MEC was designed and built for additional tests. In this new type of MEC the anode and the cathode chambers were separated by an anion exchange membrane. Although this increases costs, this greatly benefits gas purity and has minimal impact on production rates. The average volumetric current density (I_{vol}) was 59 ± 1 A/m^3 at an HRT of 24 h using acetic acid as a substrate.

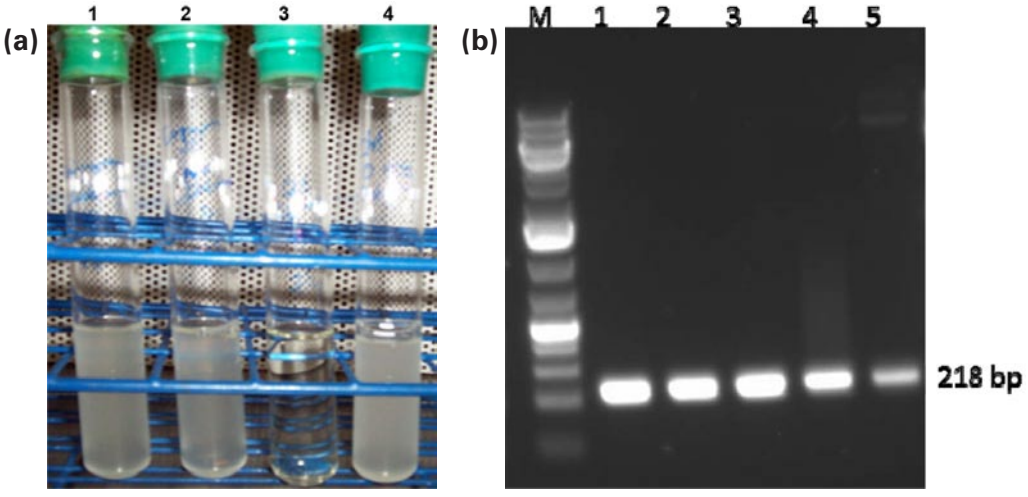


FIGURE 1. (A) Growth of *Clostridium thermocellum* transformants in liquid selection medium. 1. Transformants in 100 mg/L chloramphenicol, 2. Transformants without selection, 3. Control untransformed cells with 100mg/L chloramphenicol, 4. Control untransformed cells without antibiotic selection. (B) PCR amplification of chloramphenicl gene (cm^r) from plasmid DNA isolated directly from transformed *C. thermocellum.* Lanes 1, 2: colony # 1; lanes 3, 4: colony # 3, lane 5: plasmid positive control. M: molecular weight marker.

Shorter HRTs slightly increased the current, with average volumetric current densities of 60 ± 1 A/m^3 (HRT 16 h) and 62 ± 1 A/m^3 (HRT 10 h) (Figure 3). There were similar gas generation rates of 145 ± 34 mL/d at an HRT 16 h and 163 ± 51 mL/d at an HRT 24 h, but gas production increased to 191 ± 34 mL/d at HRT 10 h. This two-chamber MEC produced nearly pure H_2 in continuous mode as a result of the design that kept the cathode separated from the microorganisms on the anode and anode chamber.

Conclusions and Future Direction

- Using avicel cellulose as the substrate, we successfully conducted fermentation in the sequencing fed-batch mode. We determined that 5.0 g/L feeding was capable of retaining more acclimated *C. thermocellum* which attached to the residual unfermented cellulose. The outcomes lead to higher rates and yield of H_2. Retention of more acclimated microbes also significantly decreased lag time and led to a faster rate of H_2 production.
- We successfully developed genetic tools and produced two mutants in *C. thermocellum*. These tools will aid in the construction of targeted pathway mutants to improve yield of H_2.
- In single chamber MECs, methanogenesis was suppressed by using higher anode potentials set by a potentiostat. However, it was revealed that methanogen proliferation could not be eliminated in this reactor because the methanogens were not primarily anode-associated.
- By separating the cathode from biological conditions in a new reactor design, nearly pure H_2 production was successful in a two-chamber continuous flow MEC with reasonable H_2 gas flow rates.

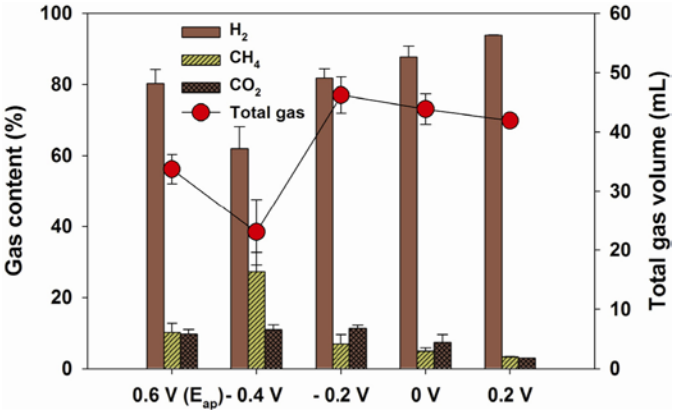


FIGURE 2. Hydrogen, methane, carbon dioxide contents and total gas volume at different set anode potentials and an added voltage of 0.6 V in batch tests.

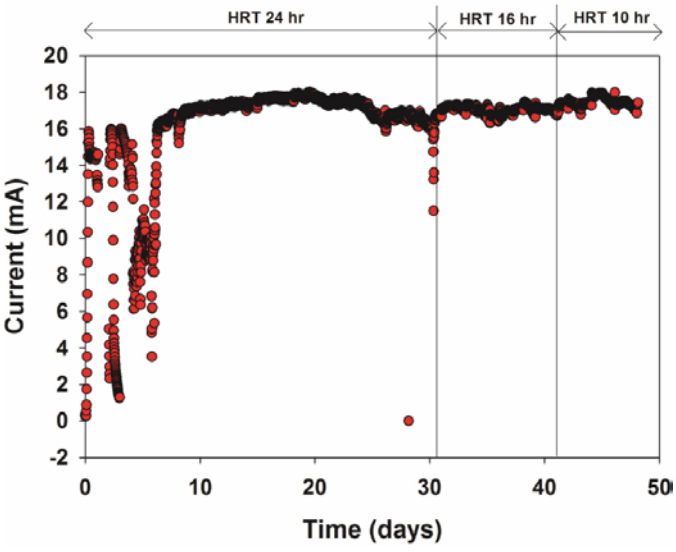


FIGURE 3. Current Generation at Different HRTs in a Two-Chamber MEC

In the future, we will conduct sequencing fed-batch fermentation to further optimize hydraulic retention time, carbon substrate loading, and the volume of liquid replacement to improve rate and yield of H_2 production. We will continue to develop genetic tools for molecular engineering in *C. thermocellum* to alter its metabolic pathway to improve H_2 molar yield. In future MEC tests, following complete analysis of fermentation effluent, fermentation wastewater will be supplied to a two-chamber MEC in order to examine H_2 production from an actual fermentation effluent.

FY 2011 Publications/Presentations

1. Thammannagowda, S; Magnusson, L; Jo, J.H.; Maness, P.C., Seibert, M. 2010. Renewable hydrogen production from biomass. *Enclyclo. Biol. Chem*. In press.

2. Levin, D.; Jo, J.; and Maness, P.C. 2011. Biohydrogen production from cellulosic biomass. Accepted for publication in "Integrated Forest BioRefineries" (ed. L. Christopher). Royal Society of Chemistry, Cambridge, UK.

3. Maness, P.C. "Hydrogen production in *Clostridium thermocellum* via dark fermentation of lignocellulose fermentation." Invited presentation at the 240th National ACS National Meeting & Expo. August 22–26, 2010, Boston, MA.

4. Maness, P.C.; Logan, B. DOE Fuel Cell Technology Program Review – Washington, DC – May 2011, Presentation PD#038.

5. Rader, Geoffrey K.; Logan, Bruce E. (2010). "Multi-electrode continuous flow microbial electrolysis cell for biogas production from acetate," *Intl. J. Hydrogen Energy*, **45**, 8848-8854.

6. Nam, Joo-Youn; Tokash, Justin C.; Logan, Bruce E. "Comparison of microbial electrolysis cells operated with added voltage or by setting the anode potential," *Intl. J. Hydrogen Energy*, In press.

References

1. Zhang, Y.P.; Lynd, L.R. (2005). Cellulose utilization by Clostridium thermocellum: bioenergetics and hydrolysis product assimilation. *Proc. Natl. Acad. Sci. USA* 102: 7321-7325.

2. Hawkes, F.R.; Dinsdale, R.; Hawkes, D.L.; Hussy, I. (2002). Sustainable fermentative hydrogen production: Challenges for process optimisation. *Intl. J. Hydrogen Energy* **27,** 1339–1347.

3. Logan, B.E.; Oh, S.E.; Kim, I.S.; Van Ginkel, S. (2002). Biological hydrogen production measured in batch anaerobic respirometers. *Environ. Sci. Technol*. **36,** 2530–2535.

4. Van Ginkel, S.; Sung, S. (2001). Biohydrogen production as a function of pH and substrate concentration. *Environ. Sci. Technol.* **35,** 4726–4730.

5. Rachman, M.A.; Furutani, Y.; Nakashimada, Y.; Kakizono, T.; Nishio, N. (1997). Enhanced hydrogen production in altered mixed acid fermentation of glucose by *Enterobacter aerogenes*. *J. Ferm. Eng.* **83,** 358–363.

6. Cheng, S.; Logan, B.E. (2007). Sustainable and efficient biohydrogen production via electrogenesis. *Proc. Natl. Acad. Sci. USA*. 104: 18871-18873.

7. Lalaurette, E., Thammannagowda, S., Mohagheghi, A., Maness, P.C., and Logan, B.E. 2009. Hydrogen production from cellulose in a two-stage process combining fermentation and electrohydrogenesis. *Intl. J. Hydrogen Energy* 34: 6201-6210.

II.H.3 Hydrogen from Water in a Novel Recombinant Oxygen-Tolerant Cyanobacterial System

Philip D. Weyman (Primary Contact),
Isaac T. Yonemoto, Hamilton O. Smith
J. Craig Venter Institute (JVCI)
10355 Science Center Dr.
San Diego, CA 92121
Phone: (858) 200-1815
E-mail: pweyman@jcvi.org

DOE Managers
HQ: Roxanne Garland
Phone: (202) 586-7260
E-mail: Roxanne.Garland@ee.doe.gov
GO: Katie Randolph
Phone: (720) 356-1759
E-mail: Katie.Randolph@go.doe.gov

Grant Number: DE-FC36-05GO15027

National Laboratory Collaborators:
Karen Wawrousek, Jianping Yu, and Pin-Ching Maness
National Renewable Energy Laboratory (NREL)
Golden, CO

Project Start Date: May 1, 2005
Project End Date: August 31, 2012

Fiscal Year (FY) 2011 Objectives

Develop an O_2-tolerant cyanobacterial system for sustained and continuous light-driven H_2-production from water.

Technical Barriers

This project addresses the following technical barriers from the Hydrogen Production section (3.1.4) of the Fuel Cell Technologies Program Multi-Year Research, Development and Demonstration Plan:

(AH) Rate of Hydrogen Production

(AI) Continuity of Photoproduction

Technical Targets

Characteristics	Current Status	2011 Target	2018 Target
Duration of continuous H_2 photoproduction in air	Zero to 30 seconds in air	Produce a cyanobacterial recombinant evolving H_2 through an O_2-tolerant hydrogenase	H_2 production in air for 30 min

FY 2011 Accomplishments

JCVI

- We achieved higher hydrogenase activity from the environmentally derived hydrogenase expressed in cyanobacteria by adding additional transcriptional regulation to the gene cluster.
- The cyanobacterial ferredoxin was found to serve as an electron mediator to the environmentally derived hydrogenase.

NREL

- We developed genetic tools to manipulate the genome of *Rubrivivax gelatinosus* CBS and generated an affinity-tagged hydrogenase active in hydrogen production. This development will simplify hydrogenase purification for characterization in the long run.
- The *Rubrivivax* hydrogenase was expressed and purified from a *Synechocystis* host. The recombinant hydrogenase was shown to contain all four subunits (CooLXUH) forming a stable complex during aerobic growth of *Synechocystis*, albeit with no activity.
- Four *Rubrivivax* NiFe-hydrogenase maturation genes (*hypFCDE*) were transferred to *Synechocystis*, and HypE protein expression was confirmed. Expression of the maturation genes is a prerequisite for assembly of an active *Rubrivivax* NiFe-hydrogenase in *Synechocystis*.

Introduction

Photobiological processes are attractive routes to renewable H_2 production. With the input of solar energy, photosynthetic microbes such as cyanobacteria and green algae carry out oxygenic photosynthesis, using sunlight energy to extract reducing equivalents from water. The resulting reducing equivalents can be fed to a hydrogenase system yielding H_2. However, one major difficulty is that most hydrogen-evolving hydrogenases are inhibited by O_2, which is an inherent byproduct of oxygenic photosynthesis. The rate of H_2 production is thus limited. Certain photosynthetic bacteria are reported to have an O_2-tolerant evolving hydrogenase, yet these microbes do not split water, and require other more expensive feedstocks.

To overcome these difficulties, we propose to construct novel microbial hybrids by genetically transferring O_2-tolerant hydrogenases from other bacteria into cyanobacteria. These hybrids will use the photosynthetic

machinery of the cyanobacterial hosts to perform the water-oxidation reaction with the input of solar energy, and couple the resulting reducing equivalents to the O_2-tolerant bacterial hydrogenase, all within the same microbe. By overcoming the sensitivity of the hydrogenase enzyme to O_2, we address one of the key technological hurdles to cost-effective photobiological H_2 production which currently limits the production of hydrogen in algal systems.

Approach

Our goal is to construct a novel microbial hybrid taking advantage of the most desirable properties of both cyanobacteria and other bacteria, to serve as the basis for technology to produce renewable H_2 from water. To achieve this goal, we use the following two approaches. The first approach is to transfer known O_2-tolerant hydrogenases from anoxygenic photosynthetic bacteria *Thiocapsa roseopersicina* and *Rubrivivax gelatinosus* to cyanobacteria. Since only a very limited number of O_2-tolerant hydrogenases are available, our second approach is to identify novel O_2-tolerant hydrogenases from environmental microbial communities and transfer them into cyanobacteria.

Results

JCVI

Previously, we reported the successful expression in cyanobacteria of active NiFe hydrogenases. These NiFe hydrogenases included the stable hydrogenase from *Thiocapsa roseopersicina* and a novel, environmentally-derived NiFe hydrogenase, HynSL, (previously named HyaAB). Although active hydrogenases were obtained indicating that all the required accessory proteins were expressed, the activity was low. We hypothesized that improved plasmid design may increase activity. The original expression plasmid, pRC41, expressed the environmentally-derived hydrogenase under the regulation of one promoter at the beginning of the 13 gene construct (Figure 1a). With such a long transcript (~13-kb), genes encoded at the end of the operon, such as the *hyp* genes, may not be expressed at sufficiently high levels to allow for maximal activity of the environmental hydrogenase in cyanobacteria. These genes at the end of the operon are required for maturation of the hydrogenase and must be transcribed at the optimal level.

In order to achieve higher expression throughout the gene cluster, we have re-engineered the expression plasmid to create pRC41-4 with an additional three promoters spaced throughout the operon (Figure 1a). The redesigned plasmid is also smaller after removing genes that we found did not contribute to hydrogenase maturation or function. Each new promoter sequence is preceded by a terminator sequence to create shorter transcripts that may be more stable.

When the plasmids were transferred to an *E. coli* strain lacking its native hydrogenases, strains containing the redesigned plasmid, pRC41-4, and the single promoter control, pIY003, produced hydrogenase activity at similar levels in *E. coli* (Figure 1b). These plasmids were then successfully transferred to the cyanobacterium *S. elongatus* PCC 7942, and hydrogenase activity was measured (Figure 1c). Strain RC41-4 had approximately three-fold higher hydrogenase activity than the RC41 strain. We are currently working to increase this expression through further transcriptional modification.

To test whether HynSL could accept electrons from the native cyanobacterial ferredoxin, PetF, we obtained purified PetF from our collaborator at NREL and used it in place of methyl viologen in our *in vitro* hydrogenase assays. We tested extracts from our HynSL-expressing cyanobacterial strains in assays with PetF, but because of low HynSL expression levels, no hydrogen was detected (data not shown). However, when we used extracts from an *E. coli* strain expressing HynSL at a much higher level than the cyanobacterial strains, we were able to detect hydrogen produced via the PetF electron mediator (Table 1). This result provides evidence that the cyanobacterial ferredoxin can serve as an electron mediator for hydrogen production in strains over-expressing HynSL.

TABLE 1. Cyanobacterial Ferredoxin (PetF) can act as an electron mediator for the novel environmental hydrogenase, HynSL, expressed in *E. coli.*

E. coli Strain	Treatment	nmole H_2/mg protein/ h
Empty Vector	Dithionite + PetF	0.00
pRC41	Dithionite	0.04
pRC41	Dithionite + PetF	0.16

NREL

The overarching goal for the NREL work is to construct a cyanobacterial recombinant harboring the O_2-tolerant hydrogenase from *Rubrivivax gelatinosus,* using *Synechocystis* sp. PCC 6803 as a model host. A prerequisite for success is to gain better understanding of the *Rubrivivax* hydrogenase and its underlying maturation machinery to ensure transfer of the correct genes into *Synechocystis*. As such, we successfully developed genetic tools to manipulate the genome of *Rubrivivax*. We generated an affinity-tagged *Rubrivivax* hydrogenase with hydrogen production activity similar to the wild type enzyme (Figure 2a), and protein immunoblot confirmed expression (Figure 2b). This outcome could simplify hydrogenase purification for characterization and for comparison to the heterologously expressed *Rubrivivax* hydrogenase in *Synechocystis*. Using these genetic tools, we also successfully generated a *Rubrivivax* mutant lacking the *hypE* gene, which is putatively involved in the assembly of the *Rubrivivax* hydrogenase. However, the mutant displayed a wild-type level of hydrogenase activity, suggesting the presence of

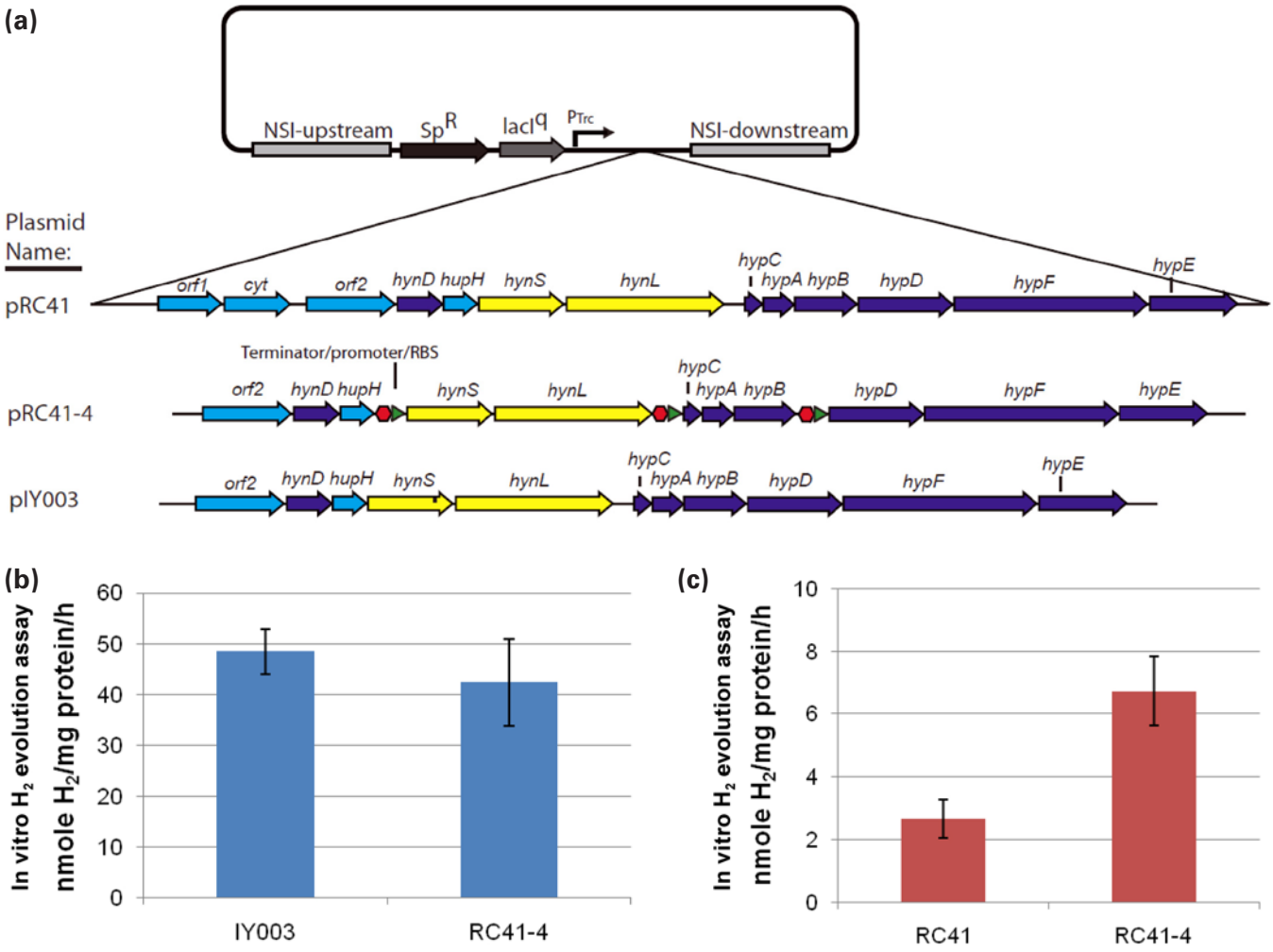


FIGURE 1. Re-engineered plasmids to express the environmentaly derived hydrogenase HynSL. (a) The map of the original expression plasmids, pRC41, and modified plasmids, pIY003 and pRC41-4. Colors depict hydrogenase structural genes, HynSL (yellow), genes encoding essential maturation factors (dark blue), non-essential factors (light blue). Plasmids pIY003 and pRC41-4 are similar to pRC41 but is shortened by two genes. Plasmid pRC41-4 also has three additional terminators (red octagons) and promoters (green arrows). (b) *In vitro* H_2 evolution assay from *E. coli* strains expressing the environmental hydrogenase from strains containing plasmid pIY003 and pRC41-4. (c) *In vitro* H_2 evolution assay from cyanobacterial strains expressing the environmental hydrogenase from strains RC41 and RC41-4.

multiple copies of the *hypE* gene (data not shown). Work is underway to sequence the genome of *Rubrivivax*, which will guide construction of the recombinant *Synechocystis*.

Working toward building the cyanobacterial recombinant, four genes (*cooLXUH*) encoding the multi-subunit *Rubrivivax* O_2-tolerant hydrogenase have been transformed in *Synechocystis*. The recombinant hydrogenase was purified, and protein immunoblot confirmed that all four subunits were expressed and formed a complex during aerobic growth of *Synechocystis*, albeit with no activity (Figure 3). This finding prompted us to additionally express the hydrogenase maturation genes, *hypABCDEF*, which are likely involved in the assembly and maturation of the *Rubrivivax* hydrogenase. We generated a construct containing the *Rubrivivax hypFCDE* genes and demonstrated integration of *hypFCDE* into the genome of *Synechocystis*. Protein immunoblot confirmed the expression of the HypE protein, suggesting the upstream HypFCD proteins are also expressed. However, no hydrogenase activity was detected in the *Synechocystis* recombinant line (already harboring the *cooLXUH*) lacking its native hydrogenase. The expression of *hypAB* is underway.

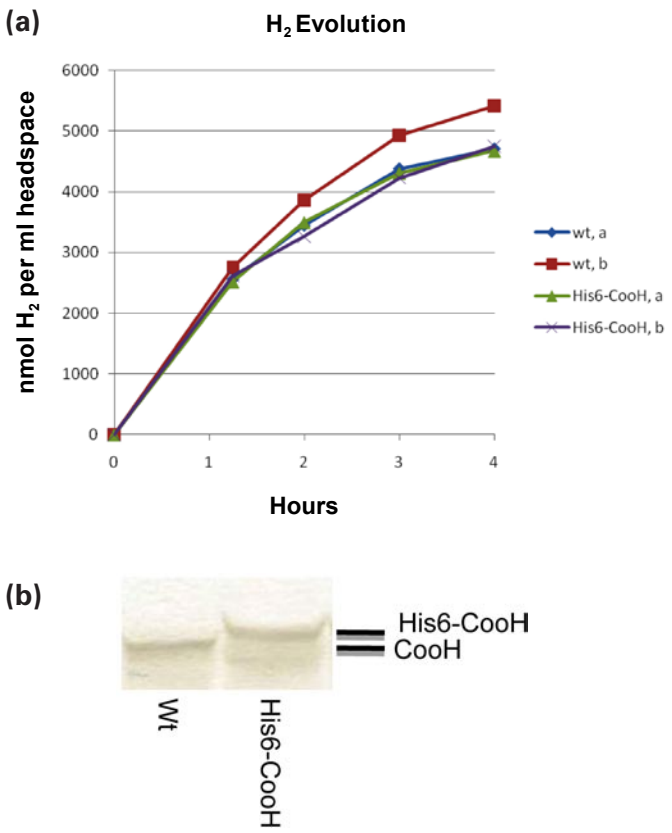


FIGURE 2. Hydrogen production in wild-type and affinity-tagged hydrogenase in *Rubrivivax gelatinosus* CBS. (a) wild-type and mutant *Rubrivivax* expressing His6-CooH were incubated with CO at time zero, and hydrogen evolution was monitored over time. (b) Protein immunoblot revealed that only the affinity-tagged version of the hydrogenase (His6-CooH) was expressed in the mutant cell line.

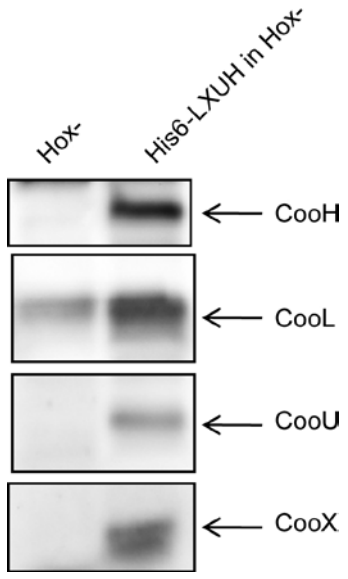


FIGURE 3. Protein immunoblot reveals expression of *Rubrivivax gelatinosus* CBS hydrogenase structural genes in a *Synechocystis* host.

Conclusions and Future Directions

Conclusions

JCVI

- Increased activity of the environmentally-derived hydrogenase can be achieved by modifying the transcriptional regulation of the gene operon.
- Cyanobacterial ferredoxin can act as an electron mediator to the environmentally derived hydrogenase.

NREL

- Using the genetic tools developed in *Rubrivivax*, we generated an active affinity-tagged hydrogenase to facilitate purification for characterization. Using these tools, we also successfully generated a *hypE* knock-out mutant in *Rubrivivax* to probe HypE function. However, the mutant displayed a wild-type level of hydrogenase activity, suggesting the presence of multiple copies of this maturation gene.
- Four *Rubrivivax* hydrogenase maturation genes (*hypFCDE*) were incorporated into the genome of a transgenic line of *Synechocystis* already harboring the *Rubrivivax* hydrogenase *cooLXUH* genes. We confirmed expression of HypE protein, albeit with no hydrogenase activity. Nevertheless, this *Synechocystis* strain will serve as the platform to express additional *Rubrivivax* hydrogenase maturation genes.

Future Directions

- We will continue to modify the environmentally-derived hydrogenase cluster to increase hydrogenase activity in cyanobacteria (JCVI).
- We will identify additional hydrogenase maturation genes using the sequenced genome of *Rubrivivax*. Once confirmed, these maturation genes of *Rubrivivax* will be transferred to express a functional O_2-tolerant hydrogenase in *Synechocystis* (NREL).
- We will optimize growth conditions to maximize the expression of the heterologous hydrogenase in *Synechocystis* (NREL).

FY 2011 Publications/Presentations

1. Carrieri, D., K. Wawrousek, C. Eckert, J. Yu, and P.C. Maness. 2011. The role of the bidirectional hydrogenase in cyanobacteria. Biores. Technol. In press.

2. Vanzin, G., J.P. Yu, S. Smolinski, V. Tek, G. Pennington, and P.C. Maness. (2010). Characterization of genes responsible for the CO-linked hydrogen production pathway in *Rubrivivax gelatinosus*. Appl. Environ. Microbiol. 76: 3715-3722.

3. Weyman, P.D., W.A. Vargas, R.Y. Chung, Y. Chang, H.O. Smith, and Q. Xu. 2011. Heterologous Expression of a Novel NiFe-Hydrogenase in E. coli. J. Bacteriol. 157: 1363-74.

4. Vargas, W.A., P.D. Weyman, Y. Tong, H.O. Smith, Q. Xu. 2011. A [NiFe]-hydrogenase from *Alteromonas macleodii* with unusual stability in the presence of oxygen and high temperature. Appl. Environ. Microbiol. 77: 1990-1998.

5. Weyman P.D., W.A. Vargas, Y. Tong, J. Yu, P.C. Maness, H.O. Smith, Q. Xu. 2011. Heterologous Expression of *Alteromonas macleodii* and *Thiocapsa roseopersicina* [NiFe] Hydrogenases in *Synechococcus elongatus*. PloS One. 6:e20126.

6. "The CO oxidation and H_2 production system in the photosynthetic bacterium *Rubrivivax gelatinosus* CBS." Gordon Research Conference, Molecular Basis of One-carbon Metabolism. August 1–6, 2010 (K. Wawrousek).

7. "The CO oxidation and H_2 production system in the photosynthetic bacterium *Rubrivivax gelatinosus* CBS." The 15th International Congress on Photosynthesis. August 22–27, 2010. Beijing, China (J. Yu).

8. "Hydrogen production by *Rubrivivax gelatinosus* CBS Coo hydrogenase." 20th Western Photosynthesis Conference, Pacific Grove, CA. January 9, 2011 (K. Wawrousek).

9. "Expression of oxygen-tolerant hydrogenases in *Synechococcus elongatus*". Molecular Bioenergetics of Cyanobacteria: From Cells to Community. April 10–15, 2011, San Feliu de Guixols, Spain. (P.D. Weyman).

10. 2011 DOE Hydrogen Program Annual Merit Review – Washington, DC, May 2011, Oral Presentation PD039 (P.D. Weyman and P.C. Maness).

II.H.4 Maximizing Light Utilization Efficiency and Hydrogen Production in Microalgal Cultures

Tasios Melis
University of California, Berkeley
Dept. of Plant & Microbial Biology
111 Koshland Hall
Berkeley, CA 94720-3102
Phone: (510) 642-8166
E-mail: melis@berkeley.edu

DOE Managers
HQ: Roxanne Garland
Phone: (202) 586-7260
E-mail: Roxanne.Garland@ee.doe.gov
GO: Katie Randolph
Phone: (720) 356-1759
E-mail: Katie.Randolph@go.doe.gov

Contract Number: DE-FG36-05GO15041

Start Date: December 1, 2004
End Date: November 30, 2011

Fiscal Year (FY) 2011 Objectives

- Minimize, or truncate, the chlorophyll antenna size in green algae to maximize photobiological solar conversion efficiency and H_2-production.
- Demonstrate that a truncated chlorophyll (Chl) antenna size would minimize absorption and wasteful dissipation of sunlight by individual cells, resulting in better light utilization efficiency and greater photosynthetic productivity by the green alga mass culture (Table 1).

Technical Barriers

This project addresses the following technical barriers from the Biological Hydrogen Production section of the Fuel Cell Technologies Program Multi-Year Research, Development and Demonstration Plan:

(AG) Light Utilization Efficiency: Low light utilization efficiency in photobiological hydrogen production due to a large photosystem chlorophyll antenna size.

Technical Targets

The Fuel Cell Technologies Program Multi-Year Plan technical target for 2005 for this project was to reach a 10% utilization efficiency of absorbed light energy (out of a theoretical maximum of 30% possible) in unicellular green. Progress has currently achieved a green alga utilization efficiency of absorbed light energy of about 25% (Table 2).

Approach

- Employ deoxyribonucleic acid (DNA) insertional mutagenesis, screening, biochemical and molecular genetic analyses for the isolation of "truncated Chl antenna size" mutants in the green alga *Chlamydomonas reinhardtii.*
- Clone and characterize the gene(s) that affect the "Chl antenna size" property in *Chlamydomonas reinhardtii*.
- Apply such genes to generate a "truncated Chl antenna size" in this and other green algae.

FY 2011 Accomplishments

1. Successfully cloned the *Tla2* gene and fully elucidated its function. Manuscript and disclosure in preparation.
2. Successfully cloned the *Tla3* gene. Currently, conducting biochemical analyses and are in the process of elucidating the *Tla3* gene function.

TABLE 1. *Chlamydomonas reinhardtii* cellular chlorophyll content (Chl/cell), chlorophyll antenna size for photosystem-II (Chl-PSII) and photosystem-I (Chl-PSI), and energy utilization efficiency in wild type, *tla1, tla2* and *tla3* mutant strains, as determined by spectrophotometric kinetic analysis (n = 5, ± standard deviation).

	wild type	*tla1*	*tla2*	*tla3*	Long-term goal
Chl/cell mol x10^{-15}	2.4 ±0.5	0.9 ±0.06	0.93 ±0.1	0.7 ±0.1	
Chl-PSII	222±26	115±36	80±30	50±30	37
Chl-PSI	240±4	160±12	115±10	105±10	95
Light Utilization Efficiency (Solar to Chemical)	~3%	~10%	~15%	~25%	~30%

TABLE 2. Progress Achieved *vs.* the DOE Targets: Utilization Efficiency of Incident Solar Light Energy, E_0xE_1

Year	2000	2003	2005	2008	2010	2015
Program Targets	3%	10%*			15%	20%
Actual Progress Achieved	3% Wild Type	10% tla1	15% tla2	25% tla3		

* Target adjusted upward to match ahead-of-schedule progress achieved.

Introduction

The goal of the research is to generate green algal strains with enhanced photosynthetic productivity and H_2-production under mass culture conditions. To achieve this goal, it is necessary to optimize the light absorption and utilization properties of the cells [1-4]. A cost-effective way to achieve this goal is to reduce the number of Chl molecules that function in the photosystems of photosynthesis. Thus, efforts are under way to isolate microalga mutants with a truncated chlorophyll antenna size.

The rationale for this work is that a truncated light-harvesting Chl antenna size in green algae will prevent individual cells at the surface of the culture from over-absorbing sunlight and wastefully dissipating most of it (Figure 1). A truncated Chl antenna size will permit sunlight to penetrate deeper into the culture, thus enabling many more cells to contribute to useful photosynthesis and H_2-production (Figure 2). It has been shown that a truncated Chl antenna size will enable about 3-4 times greater solar energy conversion efficiency and photosynthetic productivity than could be achieved with fully pigmented cells [5].

Approach

The focal objective of the research is to identify genes that control the Chl antenna size of photosynthesis and, further, to elucidate how such genes confer a truncated Chl antenna size in the model green alga *Chlamydomonas reinhardtii*. Identification of such genes in Chlamydomonas will permit a subsequent transfer of this property, i.e., "truncated Chl antenna size", to other microalgae of interest to the DOE Fuel Cell Technologies Program. This objective is currently being approached through DNA insertional mutagenesis/screening and biochemical/molecular/genetic analyses of *Chlamydomonas reinhardtii* cells.

Results

The *tla2* mutant plasmid insert site has been cloned and a gene of interest has been tentatively identified as causing the *tla2* mutation. This molecular and genetic analysis is currently in progress. Work further described the isolation and biochemical and physiological characterization of a new mutant of *Chlamydomonas reinhardtii*, termed *tla3*. Properties of the *tla* "truncated Chl antenna size" strains so far isolated are summarized in Tables 1 and 2, and Figure 3. The *tla3* mutant has the smallest yet Chl antenna size known in green algae.

Future efforts will be directed toward the cloning and characterizing the genes responsible for the ***tla*** phenotype in *tla2* and *tla3* mutants.

Conclusions

- Significant, ahead-of-schedule progress was achieved in terms of acquiring "truncated Chl antenna size" mutants. This demonstrates feasibility of the approach chosen and success of the methods employed.
- A truncated light-harvesting chlorophyll antenna size in the *tla-type* mutants enhanced solar conversion efficiencies and photosynthetic productivity under bright sunlight conditions.

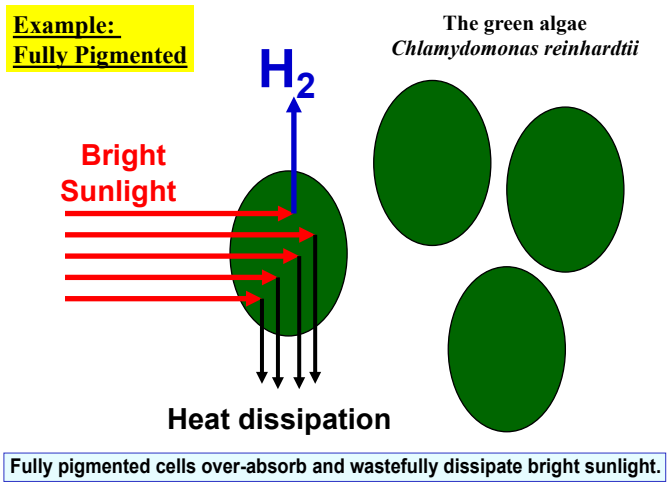


FIGURE 1. Schematic presentation of the fate of absorbed sunlight in fully pigmented (dark green) algae. Individual cells at the surface of the culture over-absorb incoming sunlight (i.e., they absorb more than can be utilized by photosynthesis), and 'heat dissipate' most of it. Note that a high probability of absorption by the first layer of cells would cause shading of cells deeper in the culture.

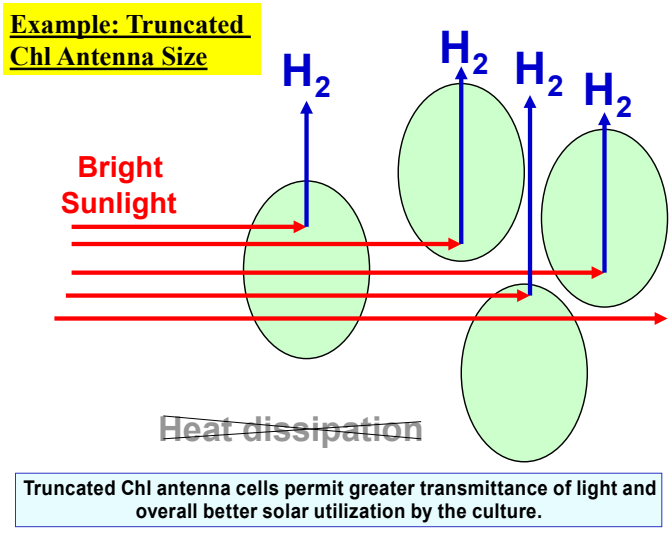


FIGURE 2. Schematic of sunlight penetration through cells with a truncated chlorophyll antenna size. Individual cells have a diminished probability of absorbing sunlight, thereby permitting penetration of irradiance and H_2-production by cells deeper in the culture.

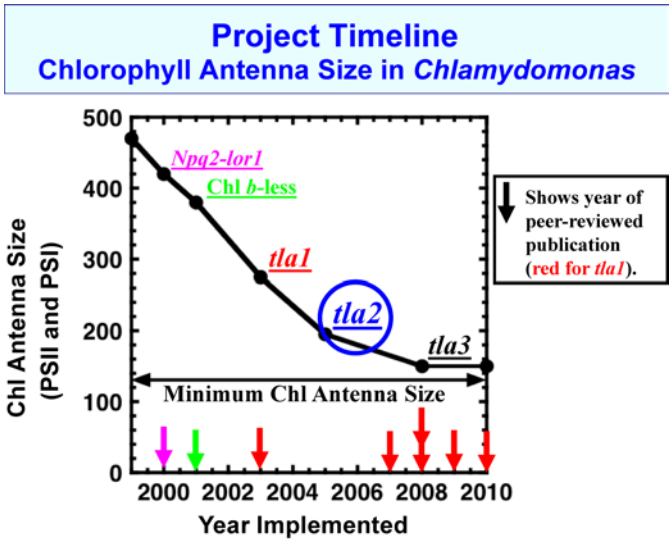


FIGURE 3. Project timeline and publications record on the truncated chlorophyll antenna size project. Arrows show publication year of peer-reviewed paper for each of the truncated Chl antenna size mutants. Note that work with the *tla2* and *tla3* strains is now reaching the stage of a peer-reviewed paper.

- Insights on the molecular mechanism for the regulation of the Chl antenna size by the *Tla1* gene were obtained (results not shown pending publication of these findings in a peer reviewed journal).

Future Directions

- Advance the biochemical and molecular characterization of the *tla2* and *tla3* strains.
- Publish results on the *tla2* and *tla3* phenotypes.
- Establish transformation (sense and antisense) protocols with *Tla*-type genes to enhance the down-regulation of the Chl antenna size in *Chlamydomonas reinhardtii.*

FY 2011 Publications/Presentations

1. Peer Reviewed Publication: Ort DR, Zhu X-G, Melis A (2011) Optimizing antenna size to maximize photosynthetic efficiency. Plant Physiology 155(1):79-85.

2. DOE Webinar: Melis A (2011) Photosynthesis for Hydrogen and Fuels Production. *January 24, 2011. <http://www1.eere.energy.gov/hydrogenandfuelcells/webinar_archives.html>*

Patents Issued

1. Melis A and Mitra M (2010) Suppression of *Tla1* gene expression for improved solar energy conversion efficiency and photosynthetic productivity in plants and algae. United States Patent 7,745,696 (issued 29-June-2010).

References

1. Kok B (1953) Experiments on photosynthesis by *Chlorella* in flashing light. In: Burlew JS (ed), Algal culture: from laboratory to pilot plant. Carnegie Institution of Washington, Washington D.C., pp 63-75.

2. Myers J (1957) Algal culture. In: Kirk RE, Othmer DE (eds), Encyclopedia of chemical technology. Interscience, New York, NY, pp 649-668.

3. Radmer R and Kok B (1977) Photosynthesis: Limited yields, unlimited dreams. Bioscience 29: 599-605.

4. Mitra M, Melis A (2008) Optical properties of microalgae for enhanced biofuels production. Optics Express 16: 21807-21820.

5. Melis A, Neidhardt J and Benemann JR (1999) *Dunaliella salina* (Chlorophyta) with small chlorophyll antenna sizes exhibit higher photosynthetic productivities and photon use efficiencies than normally pigmented cells. J. appl. Phycol. 10: 515-525.

II.H.5 Purdue Hydrogen Systems Laboratory: Hydrogen Production*

Jay Gore (Primary Contact), P. Ramachandran, A. Varma, T. Pourpoint, Y. Zheng, R. Kramer, D. Guildenbecher, R. Gejji, P. Gagare, K. Deshpande, S. Basu, T. Voskuilen, A. Al-Kukhun, D. Gao, H.T. Hwang, J. Mullings, E. Ting, L. Pelter
Purdue University
500 Central Drive
West Lafayette, IN 47907
Phone: (765) 496-2829
E-mail: gore@ecn.purdue.edu

DOE Managers
HQ: Grace Ordaz
Phone: (202) 586-8350
E-mail: Grace.Ordaz@ee.doe.gov
GO: Katie Randolph
Phone: (720) 356-1759
E-mail: Katie.Randolph@go.doe.gov

Contract Number: DE-FC36-06GO86050

Subcontractors:
- National Renewable Energy Laboratory, Golden, CO
- University of Wyoming, Laramie, WY

Project Start Date: September 16, 2006
Project End Date: September 30, 2011

*Congressionally directed project

Fiscal Year (FY) 2011 Objectives

- Investigate and evaluate initial processes for the production of hydrogen from various waste streams using microbial fermentation.
- Investigate paths for implementation of the research as a modular energy source initially for application in remote locations.

Technical Barriers

This project addresses the following technical barriers from the Biological Hydrogen Production section of the Fuel Cell Technologies Program Multi-Year Research, Development and Demonstration Plan:

(AR) H_2 Molar Yield

(AT) Feedstock Processing Cost

(AU) Systems Engineering

Technical Targets

Biological H_2 Production	Units	2013/2018	Purdue 2010
Hydrogen Yield Percentage	%	20/30	utilizing organic wastes

FY 2011 Accomplishments

- Currently completing the fourth generation of the experimental test matrix and continue to test various combinations of waste material and innocula under various operating conditions. The developed optimized process has significantly increased hydrogen production. For the test matrix, gas volume is being measure by a calculation employing head space pressure. These values are correlated with gas molecular composition values from the gas chromatograph to give hydrogen production levels. The optimized values are used in the energy model and initial design the modular energy system. Measurements of pH are recorded during a portion of data runs.
- Homogeneity of feed stock is assured through the use of statistical sampling techniques. The water content of the substrate was preliminarily reduced from 98% to 60% with minimal decrease in hydrogen production. Methods to further decrease water content and ways to support substrate were tested. Distiller's dried grains (DDGS) are being tested as a substrate for hydrogen production. A new process has been developed that has greatly increased hydrogen yields for DDGS. This could significantly increase the efficiency of ethanol production from corn. A continuous fermentor (New Brunswick, BioFlo®/CelliGen® 115, 3 L) is being used to consider larger batch sizes and the influence of continuous feed of substrate on the values of optimal operating parameters. Currently DDGS is being tested in the fermentor. We are also exploring existing catalytic methods including nano catalysts for capture of CO_2 from the fermentation process. The vacuum tube solar pre and post process apparatus is fully operational and being used for pre and post processing of waste material.

✧ ✧ ✧ ✧ ✧

Introduction

This project allows the creation of a Hydrogen Research Laboratory in a unique partnership between Purdue University's main campus in West Lafayette and the Calumet campus. This laboratory is engaged in basic research in hydrogen production and storage and has initiated

engineering systems research with goals established as per the DOE Fuel Cell Technologies Program.

Bio-production of hydrogen is potentially an important renewable source of energy. Using organic wastes for bio-production of hydrogen not only has the potential to generate cost-effective and renewable energy but also can reduce pollution in the environment and provide a source of fertilizer for growing crops. The purpose of the current research effort is to investigate, obtain data, and evaluate initial processes for the production of hydrogen from various waste streams using microbial fermentation and investigate possible paths for implementation of the technology as a local electric and thermal energy source. This effort is targeted to assure that the developed technology will be applicable for integration into various current and future energy supply options including the Department of Energy Road Map. This effort is investigating ways to develop a modular anaerobic biological hydrogen production and energy system for applications initially in remote locations. It is realized that hydrogen production levels from conventional anaerobic processes are not as great as is desired in the long-term perspective for bulk production systems. This research is focusing on a process that has multiple products and associated values. Value streams include hydrogen, waste disposal function, heat for buildings, drinking water, and possibly a marketable chemical product produced from process carbon dioxide. After it is proven, it is anticipated that the technology will be leveraged to larger applications in continuing research efforts. We have performed preliminary cost analysis studies, but factors such as the water content greatly influence the design and consequently the cost. It is also necessary to consider aspects such as the value of waste disposal, sanitized fertilizer, and ancillary energy. These aspects depend on the details of the process currently being developed. Preliminary estimates indicate that when all costs and benefits are considered, the technology has advantages over other alternatives for this application. The carbon dioxide capture portion of the process is intended principally for gas conditioning. Carbon dioxide is a co-product and H_2 purification is usually necessary. The potential for utilization of the captured CO_2 in the production of chemical products is under investigation as a part of maximizing the utility of the proposed self-contained system. Figure 1 shows an overview of major process inputs and products.

Approach

We have developed methods to optimize hydrogen production from waste through the use of a fermentation process. The optimization procedure forms the foundation for the subsequent development of a modular device that will use various waste streams, including garbage, animal or human waste, and DDGS for the production of hydrogen. This hydrogen will be separated from the bio-gas stream by use of nano catalyst or a membrane for use in a fuel cell or reciprocating engine to produce electricity locally. Methods

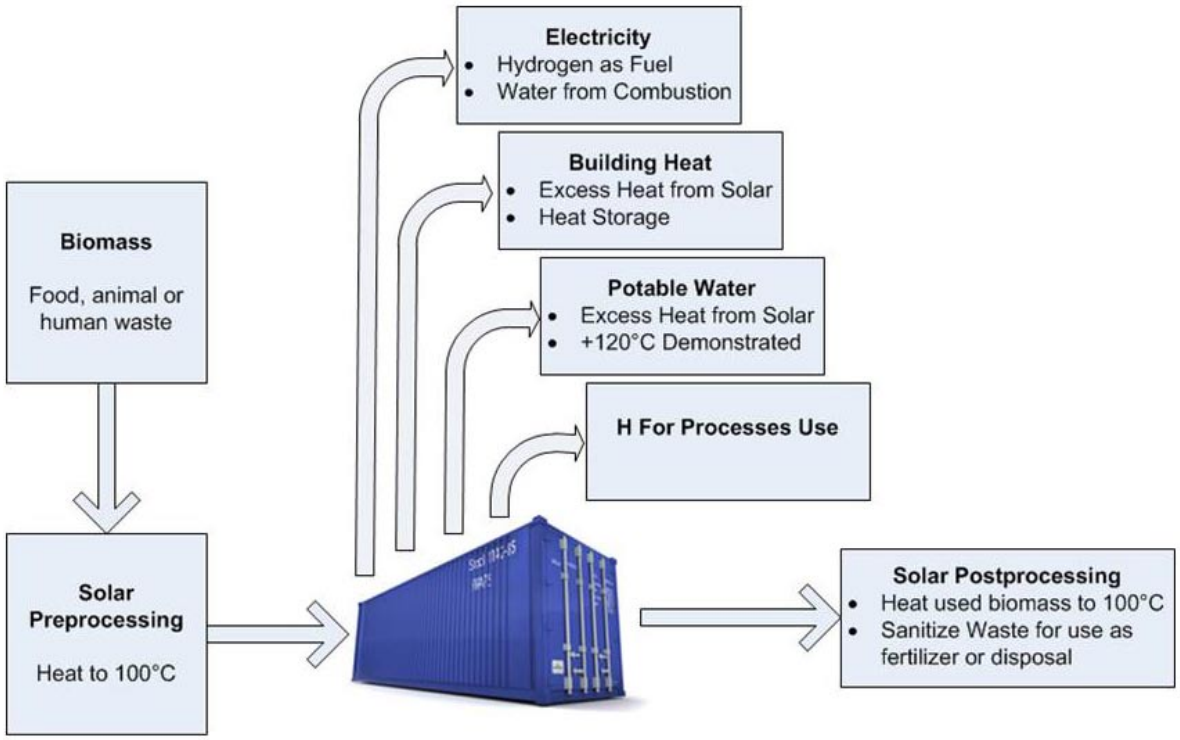


FIGURE 1. Modular System Major Inputs and Products

to sequester CO_2 as part of the process are also being considered. Energy for the pre- and post-processing of feed streams is being obtained from a solar collector system. A steam generator is attached to the solar system and is used to test production of potable water. Computer simulations of the process indicate that the system can be installed in a shipping container and used to provide local electric and thermal energy. Initial efforts have reduced the amount of water in the processed waste material from 98% to 75% with minimal decrease in hydrogen production. By reducing the fraction of water it will be possible to reduce the volume and weight of the bio reactor and increase the system efficiency and viability.

Results

Additional inoculua have been tested and the concentration of hydrogen in the produced gas has been correlated with the experimental variables: pH, temperature, and substrate concentration. We have developed a new procedure for producing hydrogen with DDGS that shows considerably higher hydrogen production levels than any observed to date. We continue to investigate this approach. If verified, this may provide a new alternative for increasing hydrogen production levels with DDGS and provide a potential enhancement to the energy balance for ethanol production. Considerable interest in these results has been shown by the Industrial Advisory Board for the project since it could be of value for multiple industrial processes.

Test samples and data are being exchanged between Purdue Calumet and Lafayette and trials to test repeatability continue. A micro gas chromatograph (GC, CP-4900 Dual Channel Micro-GC; Varian Inc., equipped with a thermal conductivity detector and a 10 M-5A molecular sieve column with argon as the carrier gas for hydrogen and a 10 M Poraplot® [Varian, Inc.] column with helium as the carrier gas for CO_2). The testing program is based upon a central composite experimental design. We are currently completing the fourth iteration for the optimization of the hydrogen production levels. This process identifies combinations of operating variables that maximizes hydrogen production. Figure 2 shows a comparison of hydrogen production from the initial and optimized procedure for hydrogen production from DDGS for the multiple testing device. The multiple testing device that was developed as part of this research effort is fully operational and is being used to generate data. This device provides the capability to conduct multiple simultaneous tests with automated data processing and monitoring. Continuous production testing is currently being conducted at Purdue Lafayette. Testing of dry substrate designs are being investigated at Purdue Calumet and Lafayette. The model for the modular energy system was updated based upon new experimental values. Efforts using a catalyst process for capture of carbon dioxide have been initiated. The solar system testing for sanitizing waste material and production of potable water is ongoing.

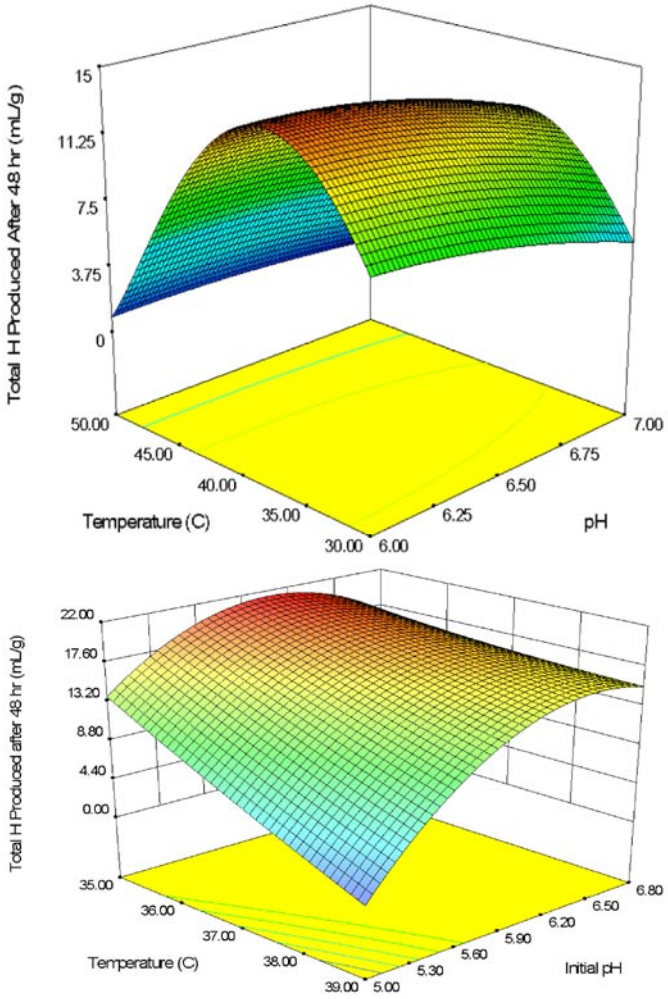


FIGURE 2. Comparison of H_2 Concentration for Previous (Top) and Optimized (Bottom) Method for DDGS

Conclusions and Future Directions

The biological hydrogen production work will include investigating optimal hydrogen production cultures for different substrates, reducing the water content in the substrate, and integrating results from the vacuum tube solar collector pre and post processing tests into an enhanced energy system model. The automated testing device will continue to be used to consider optimal hydrogen production conditions using statistical testing procedures. Testing with the continuous fermentor will be expanded to consider issues associated with continuous feed of substrate and scale up of the process. Gas flow from the fermentor is being measured with a mass flow meter. These flow values, combined with GC analysis data, are used to determine the concentration and volume of gas produced as a function of time. Values of pH are recorded continuously and are used to compare hydrogen, dissolved oxygen, and pH values as a function of time. We will also explore existing catalytic methods including nano catalysts for capture of CO_2 from

the fermentation process. The next phase of the research will involve the construction a bench top reactor based on the current test results and designs that will operate with dryer waste material and use solid material handling techniques. Funding is currently not available for the actual construction of the dry bench top test unit. This research considers hydrogen production, but also considers the leveraging of other value streams to overcome design issues that have arisen in the past. We consider this process to have significant value for waste processing and heat production as well as hydrogen production. The use of catalysis to condition the bio-gas stream also adds value to the process that has not been considered in the past for this application.

FY 2011 Publications/Presentations

1. Kramer, R., Pelter, L., Patterson, J., Kmiotek, K., " Modular Energy Production From Waste", accepted for publication World Energy Engineering Congress, 2011.

2. Kramer, R., Pelter, L., Patterson, J., Kmiotek, K., Ting, E., "Modular Waste/Renewable Energy System for Production of Electricity, Heat, and Potable Water in Remote Locations", submitted for publication, IEEE Global Humanitarian Technology Conference, 2011.

3. Kramer, R., Pelter, L., Liu, W., Branch, R., Martin, R., Kmiotek, K., "Utilization of Solar Heat for Processing Organic Wastes for Biological Hydrogen Production", Energy Engineering, 108, 3, 2011.

4. Kramer, R., Patterson, J., Pelter, L., Ting, E., "Modular Solar/Biological Waste Processing System for Local Production of Energy and Hydrogen," manuscript in preparation.

II.I.1 H2A Production Model Updates

Darlene Steward (Primary Contact), Olga Antonia
National Renewable Energy Laboratory (NREL)
1617 Cole Blvd.
Golden, CO 80401
Phone: (303) 275-3837
E-mail: Darlene.Steward@nrel.gov

DOE Manager
HQ: Sara Dillich
Phone: (202) 586-7925
E-mail: Sara.Dillich@ee.doe.gov

Subcontractor:
Directed Technologies, Inc., Arlington, VA

Project Start Date: 2010
Project End Date: Project continuation and direction determined annually by DOE

Fiscal Year (FY) 2011 Objectives

Update the H2A central and forecourt models to:

- Incorporate new knowledge.
- Incorporate new Annual Energy Outlook (AEO) fuel cost projections.
- Update baseline year.
- Re-evaluate assumptions.

Technical Barriers

This project addresses the following technical barriers from the Systems Analysis section (4.5) of the Fuel Cell Technologies Program Multi-Year Research, Development and Demonstration Plan:

(B) Stove-piped/Siloed Analytical Capability
(D) Suite of Models and Tools
(E) Unplanned Studies and Analysis

Technical Targets

The update of the H2A models directly supports the following milestones from the Systems Analysis function from FY 2004 through FY 2016.

Milestone 26	Annual model update and validation. (4Q, 2008; 4Q, 2009; 4Q, 2010; 4Q, 2011; 4Q, 2012; 4Q, 2013; 4Q, 2014; 4Q, 2015)
Milestone 39	Annual update of Analysis Portfolio. (4Q, 2007; 4Q, 2008; 4Q, 2009; 4Q, 2010; 4Q, 2011; 4Q, 2012; 4Q, 2013; 4Q, 2014; 4Q, 2015

FY 2011 Accomplishments

Three primary tasks were completed to update the H2A central and distributed case studies:

- Primary assumptions and values were reviewed and updated as needed.
  - Cost of land increased from $5,000 to $50,000 per acre.
  - Construction period increased from two to three years with little expenditure during the first year.
  - Compression, storage, and dispensing calculations were updated to reflect a new baseline of 10,000 psi onboard storage pressure.
- The reference year was updated to 2007.
  - Startup year changed from 2005 to 2010 current, 2020 future.
  - Feedstock prices were updated using the AEO 2009 reference case and program values.
  - Capital costs were updated to 2007 dollars using Chemical Engineering Progress Cost Indexes (CEPCI).
  - Operating and other material costs were updated using appropriate indexes (consumer price indexes, labor indexes, SRI chemical price indexes).
- Templates were developed for central and distributed case studies.



Introduction

In FY 2007 and FY 2008 the H2A hydrogen production discounted cash flow model was extensively revised and updated. The model was divided into separate forecourt and central versions and major new functionality including plant scaling, carbon sequestration, and new forecourt calculations were added. The model templates and 19 updated case studies were published in FY 2008. Version 2.1 of the H2A Hydrogen Production Model was uploaded to the H2A website on December 5, 2008. Version 2.1 incorporated minor fixes and improvements to the model. NREL, in consultation with researchers, is currently developing version 3 of the H2A hydrogen production models.

In Version 3, the reference year and costs have been updated to 2007 and major assumptions have been reviewed and updated as appropriate. Four new technologies have been added: solar thermo-chemical, photo-electrochemical and biological hydrogen production and reforming of bio-derived liquids.

Approach

Version 3 templates were developed for the H2A distributed and central hydrogen production models. The templates were reviewed for accuracy and completeness and the existing published H2A case studies were ported into the new templates. New case studies based on the templates, were developed for the four new technologies. All the completed case studies were reviewed for accuracy and completeness. The version 3 H2A case studies will be published on the DOE website (https://apps1.hydrogen.energy.gov/h2a_analysis.html). Case study reports outlining the changes to each technology case study were developed.

Results

The H2A production model central and forecourt primary assumptions were reviewed, and default values adjusted as necessary. New feedstock price tables were added to the model: AEO 2009 reference case, AEO 2009 high price case, and AEO 2010 reference case. CEPCI, consumer price index, labor index, and chemical price index tables were updated or added.

N^{th} plant assumptions were reviewed for the forecourt H2A models. The N^{th} plant assumption provides a context for estimating the effect of prior experience on capital and indirect costs for forecourt stations. At the technology readiness date, N^{th} plant assumptions apply; costs have decreased substantially because of learning, production economies, and modularization. Figure 1 presents a hypothetical hydrogen production cost reduction plot for a technology with a technology readiness date of 2015. N^{th} plant also applies to stations. Station design is assumed to be modular, but each site also has unique features that affect layout and design and increase costs for some aspects of the facility.

N^{th} plant assumptions include:

- Moderate annual system production rate: 50–150 systems per year.
- Substantial reduction in system cost but not full automation.
- Corresponding markups: could be ~50% gross margin.

Several new calculations were added to the forecourt model to provide more flexibility in specifying the facility's operating characteristics and to more accurately size equipment. New compression, storage, and dispensing calculations were added to model a new default refueling pressure of 700 bar (10,000 psi). The new calculations are based on the NREL H2A Delivery Components Model (NREL 2010, http://www.hydrogen.energy.gov/h2a_delivery.html). New calculations were also added to more accurately define the amount of onsite storage required to supply hydrogen during fluctuations in daily and weekly demand and during outages (see Figure 2) and to enable the user to define the weekly dispensing profile (Figure 3).

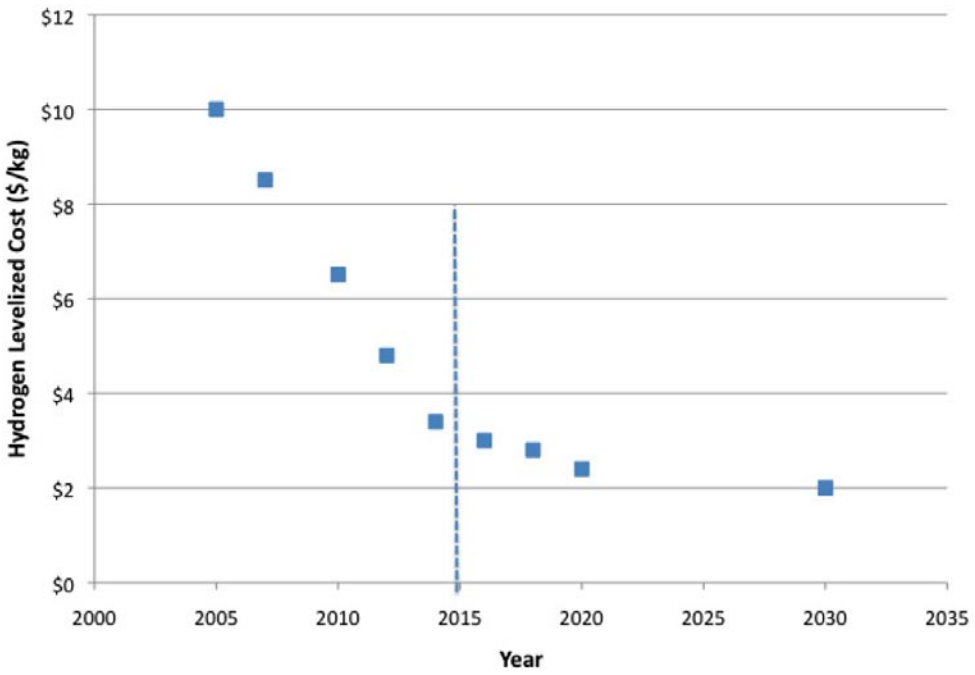


FIGURE 1. Hypothetical Hydrogen Cost Reduction Plot for a Technology with a Technology Readiness Date of 2015

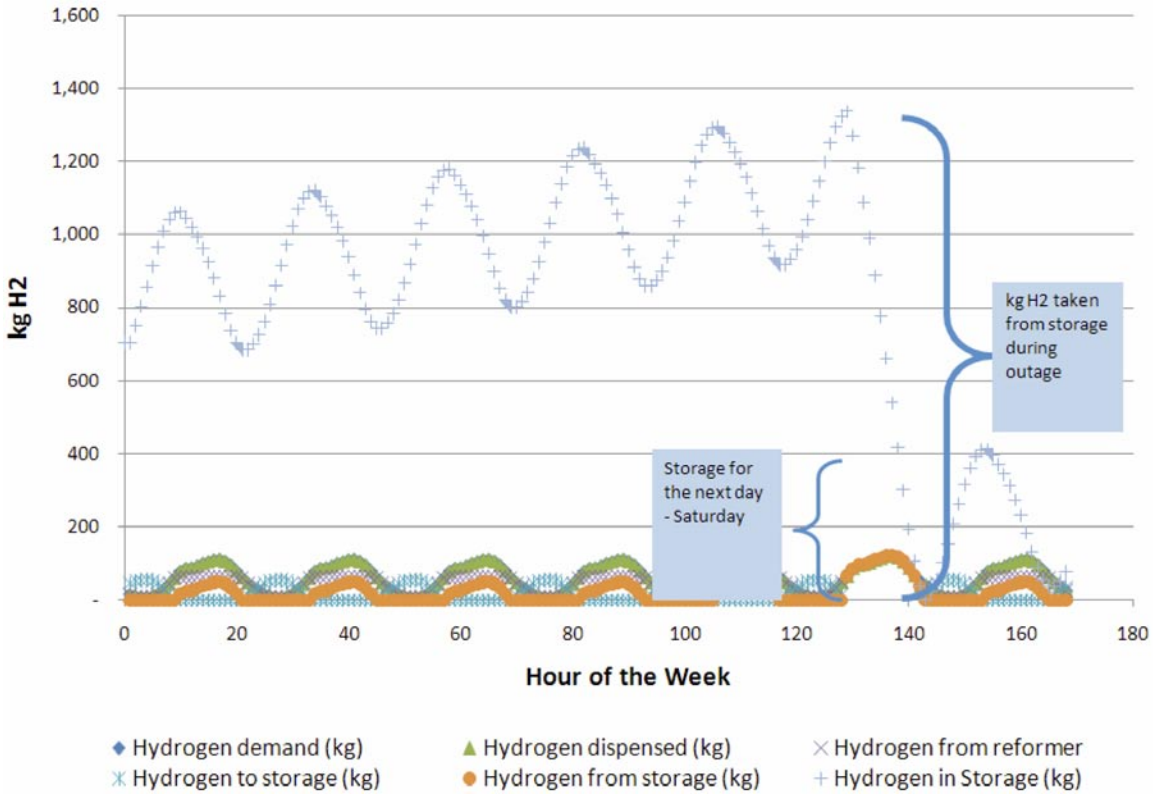


FIGURE 2. Hydrogen Dispensing and Storage Profile for a Week in the Summer – Worst Case Scenario Reformer Outage

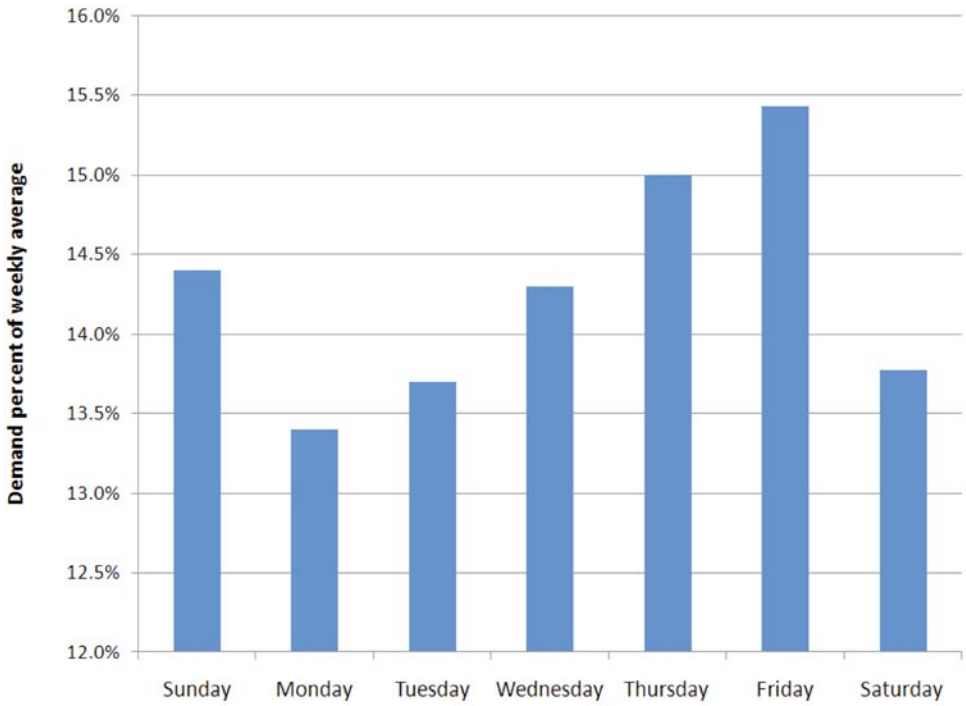


FIGURE 3. User-Defined Weekly Dispensing Profile

Conclusions and Future Directions

Development of Version 3 of the H2A hydrogen production models was necessary to maintain accuracy in the model and consistency with other DOE models. Updating to 2007 dollars and re-evaluation of N^{th} plant assumptions increased costs for all technologies. However, both top-down and bottom-up cost targets for all technologies are also being updated and will be using consistent assumptions.

FY 2011 Publications/Presentations

The following hydrogen production technology case studies will be published on the DOE website (https://apps1.hydrogen.energy.gov/h2a_analysis.html):

1. Current and Future Central Hydrogen Production via Biomass Gasification

2. Current and Future Central Hydrogen Production from Grid Electrolysis

3. Current and Future Central Hydrogen Production from Coal without CO_2 Sequestration

4. Current and Future Central Hydrogen Production from Coal with CO_2 Sequestration

5. Current and Future Central Hydrogen Production from Natural Gas without CO_2 Sequestration

6. Current and Future Central Hydrogen Production from Natural Gas with CO_2 Sequestration

7. Future Central Hydrogen Production from Nuclear Energy via High Temperature

8. Current and Future Forecourt Hydrogen Production from Grid Electrolysis (1,500 kg per day)

9. Current and Future Forecourt Hydrogen Production from Natural Gas (1,500 kg per day)

10. Current and Future Forecourt Hydrogen Production from Ethanol (1,500 kg per day)

II.J.1 Unitized Design for Home Refueling Appliance for Hydrogen Generation to 5,000 psi

Timothy Norman (Primary Contact),
Keith D. Patch, Monjid Hamdan
Giner Electrochemical Systems, LLC
89 Rumford Avenue
Newton, MA 02466
Phone: (781) 529-0556
E-mail: tnorman@ginerinc.com

DOE Manager
HQ: Eric L. Miller
Phone: (202) 287-5829
E-mail: Eric.Miller@hq.doe.gov

Contract Number: DE-SC0001486

Project Start Date: August 15, 2010
Project End Date: August 14, 2012

Fiscal Year (FY) 2011 Objectives

- Detail design and demonstrate subsystems for a unitized electrolyzer system for residential refueling at 5,000 psi to meet DOE targets for a home refueling appliance (HRA).
- Fabricate and demonstrate unitized 5,000 psi system (Year 2).
- Identify and team with commercialization partner(s).

Technical Barriers

This project addresses the following technical barriers from the Hydrogen Production section of the Fuel Cell Technologies Program Multi-Year Research, Development and Demonstration Plan [1]:

(G) Cost

(H) System Efficiency

Technical Targets

TABLE 1. Giner Electrochemical Systems, LLC (GES) Progress toward Meeting DOE Targets for Distributed Electrolysis Hydrogen Production [1]

Characteristics	Units	2017–2020 Targets	GES Status
Hydrogen Cost	$/kg H_2	2.00–4.00	2.99*
Electrolyzer Capital Cost	$/kg H_2	0.30	0.99
Electrolyzer Energy Efficiency	% (LHV)	74	73.6**

*Using H2A model rev 2.1.1; **5,000 psi operation; LHV = lower heating value

FY 2011 Accomplishments

- Determined performance and operational limits of a cathode-feed electrolyzer that circulated water using a thermosiphon, rather than a circulating pump.
- Updated electrolyzer and compressed hydrogen safety codes and standards.
- Performed 50 cm^2 2,000 psig (pumped cathode feed) electrolysis tests in a pressure dome.
- Tested Dimensionally Stable Membrane (DSM™) in balanced-pressure 17-cell 50 cm^2 2,000 psig (pumped anode feed) stack in pressure dome.
- Completed first round of tests on protective coatings for pressure containment dome internals.
- Assembled pressure swing absorber dryer for sorbent testing.
- Began preliminary system layouts of proton exchange membrane (PEM) electrolyzer HRA breadboard system.



Introduction

U.S. automakers have invested significant resources in the research and development of hydrogen fuel cell vehicles. However, to enable the widespread use of fuel cell vehicles, an additional major investment will be required to construct an infrastructure for hydrogen production and delivery to fueling stations. In order to facilitate this transition, it has been recommended that high-pressure hydrogen, generated at 5,000 psig for home refueling of fuel cell vehicles, be implemented as an intermediary approach.

GES has matured a PEM-based electrolyzer technology for producing hydrogen at moderate to high pressure directly in the electrolyzer stack, while oxygen is evolved at near-atmospheric pressure. In this system, liquid water, which is a reactant as well as coolant, is introduced into the oxygen side at near atmospheric pressure; high-pressure hydrogen is removed from the product side. An improved, low-cost process for producing high-pressure hydrogen from water by electrolysis will significantly advance the development of the hydrogen economy, providing hydrogen for fuel cell vehicles at a price competitive with that of gasoline on a per-mile basis. The ability to produce hydrogen economically, the relatively low capital cost of the electrolyzer unit, and the low maintenance cost of the unit will allow widespread distribution of hydrogen home fueling appliances deemed necessary for the introduction of fuel cell vehicles.

Approach

GES is currently conducting a multi-year development project for DOE (Contract DE-FC36-08GO18065) that aims to reduce commercial electrolyzer costs while simultaneously raising the efficiencies of the PEM-based water electrolyzer units operating in the range of 400 psi. Future extension of this technology to pressures of 5,000 psig is feasible with modifications to the electrolyzer stack, providing the ability to safely operate in a balanced hydrogen/oxygen pressure mode. Based on an innovative electrolyzer stack concept and recent developments in high strength membrane, GES has designed a PEM-based water electrolyzer system for home refueling applications that will be able to deliver hydrogen at pressures of 5,000 psi. The design concept generates high-pressure hydrogen by means of "unitizing" the electrolyzer stack with a high-pressure hydrogen/water phase-separator and other subsystems. The combination of components eliminates the need for bulky and costly stack parts and facilitates a method for fabricating an electrolyzer system that can safely operate at a balanced hydrogen pressure of 5,000 psi. In addition, a reduction of major system components and system cost is realized.

Results

Electrolyzer Stack Design: The HRA has been designed for on-demand operation. The system is designed with a small 6-cell 2 kWe electrolyzer stack, providing a vehicle tank fill of 0.5 kg of hydrogen over a 12-hour period. This will provide 30 miles of driving range based on current fuel cell vehicle fuel economy estimates of 60 miles/kg-H_2. The electrolyzer stack is totally enclosed in a pressure containment dome; the pressure in the pressure dome is matched to that of the electrolyzer's hydrogen and oxygen product streams. This pressure dome-based design markedly simplifies many of the stack design requirements. Operating in the dome at pressures up to 5,000 psig, the 6-cell stack has a design pressure of 100 psid, and a proof pressure of 150 psid, meeting the requirements of the draft International Organization for Standardization (ISO) Standard ISO_DIS_22734-2 [2].

Preliminary Design of a 5,000 psi "Unitized" Electrolyzer System for Home Refueling: A block diagram outlining the process configuration for the 5,000 psi (34.6 MPa) PEM HRA is shown in Figure 1. The direct production of high-pressure hydrogen in the electrolyzer is shown via combining the water storage tank, electrolyzer stack and hydrogen/water phase-separators inside a pressure-containment dome, eliminating the need for a high-pressure mechanical hydrogen compressor, along with its ancillary equipments. The simplified major subsystems of the high-pressure electrolyzer system include the electrolyzer; the electricity feed sub-system; a user-accessible de-ionized (DI) water feed and DI water handling system. Note that the oxygen/water phase-separator is eliminated in this cathode-fed design; product oxygen that is free of liquid water will be promptly reduced from its high pressure and vented safely from the system.

Electrolyzer Operation Without a Circulation Pump: The most important project task involved verifying the catholyte circulation rate that can be supported in a thermosiphon-based cathode-feed electrolyzer. If insufficient water is circulated to meet the stoichiometric reaction needs of the electrolyzer, the membrane electrode

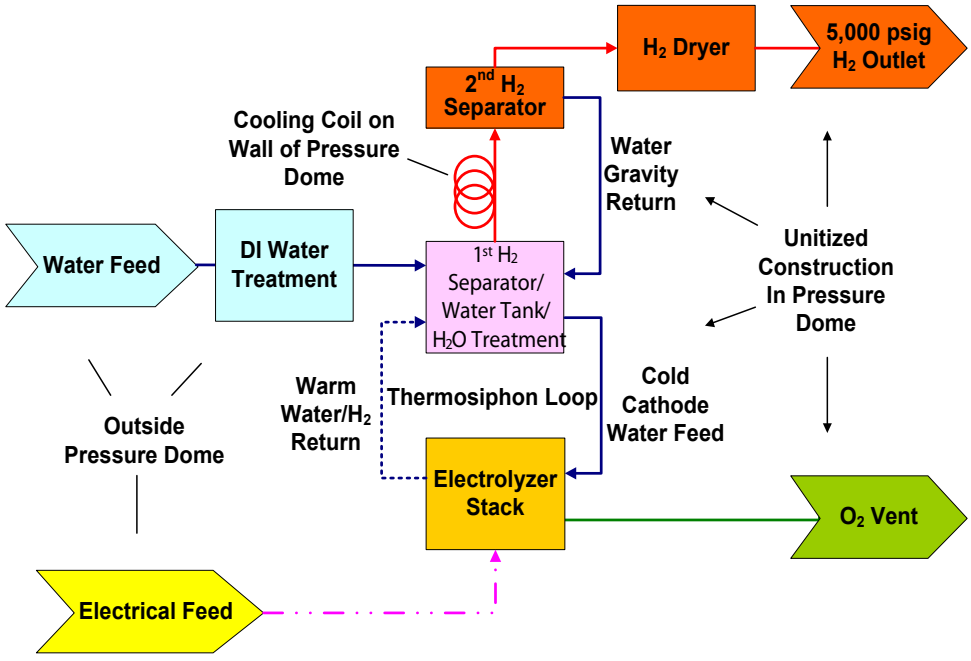


FIGURE 1. Cathode Feed Process Flow Diagram

assembly (MEA) can become water-starved, leading to membrane dry-out and inefficient electrolyzer operation, with eventual safety shutdown due to high voltage operation. Sufficient water circulation is also required for a second critical operational need: heat removal from the electrolysis reaction. As the electrolytic production of hydrogen and oxygen from water is not 100% efficient, byproduct waste heat is produced. The resultant waste heat must be removed from the electrolyzer. The standard GES electrolyzer design uses water circulation rates well in excess of the stoichiometric reaction requirements to remove the heat of reaction; the heat is then released to the surroundings through a separate heat exchange process.

Calculations during Phase I of this effort resulted in a thermosiphon water circulation rate prediction of 5.75 cc/min for a single 60-mil-thick, 160-cm^2 cathode-feed electrolyzer cell. Figure 2 illustrates the typical thermosiphon catholyte flow through a 90-mil cathode compartment. Flow measurements were quite consistent from ambient temperature up to 90°C. Thermosiphon flow ranged from a minimum of 36 cc/min. at 100 mA/cm^2, to a limit of 58 cc/min., reached over a range of 600–900 mA/cm^2. These flows are well in excess of the predicted flows: a factor of 6.3–10.1 times higher than the water circulation rate predicted in the project's earlier Phase I effort. Consequently, one of the most important HRA operational requirements, adequate thermosiphon flow, was validated for the 90-mil cathode compartment thickness.

Thermosiphon Electrolyzer Voltage Performance: After verifying the superior water circulation rates possible with the initial 90-mil thick, low-resistance cathode design, voltage performance data was collected at ambient pressure and operating temperatures up to 90°C. Figure 3 illustrates the resultant polarization scans at 80 and 90°C. As expected, the higher temperature, 90°C operating data provides better performance (lower voltage), relative to operation at 80°C. The performance benefit of 90°C operation ranges from a 21 mV improvement at 100 mA/cm^2, up to an 82-mV improvement at 850 mA/cm^2. Obviously, if electrolyzer performance can be proven to be reliable and stable at 90°C, the energy efficiency of hydrogen production will be increased.

Cathode Feed (Pumped) Operation in Pressure Dome: On a separate National Aeronautics and Space Administration-funded project developing high-pressure oxygen electrolysis for life support, successful differential-pressure operation of a 50-cm^2 1cell cathode-feed stack was conducted in a 2,000-psig pressure dome. Although not exactly in line with the goals of the HRA development project, this work demonstrated an advancement of state-of-the-art operations of high-pressure electrolyzers contained in pressure domes. Operation of both the 50-cm^2 1cell cathode-feed and a 50-cm^2 17cell anode-feed electrolyzer stacks was successful over a wide range of operating conditions. Figure 4 illustrates the resultant polarization scan from pumped anode-feed operation, for both 1,000- and 2,000-psig oxygen production pressures. (Cathode feed data is not shown.)

Data in Figure 4 illustrate the slight voltage penalty for producing oxygen gas at higher pressure, which occurs for all operating temperatures. At a constant 300 mA/cm^2, with

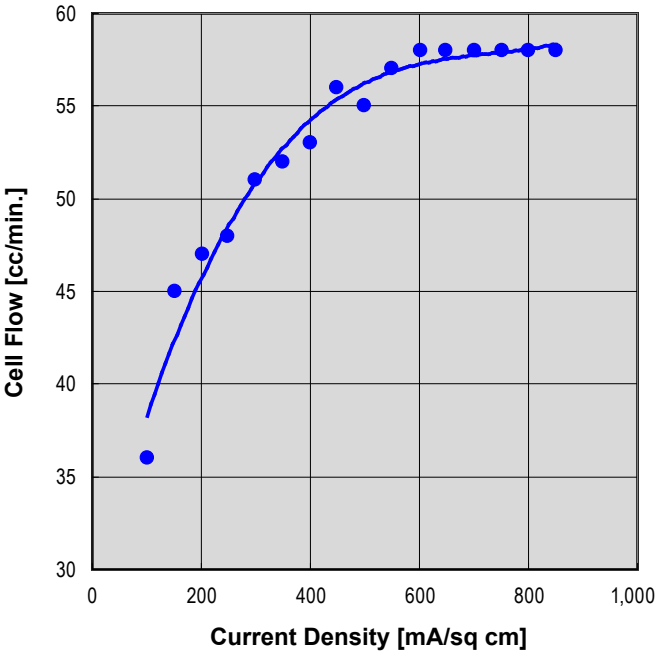


FIGURE 2. Cathode-Feed (Non-Pumped) 160 cm^2 Single-Cell Water Circulation Rate

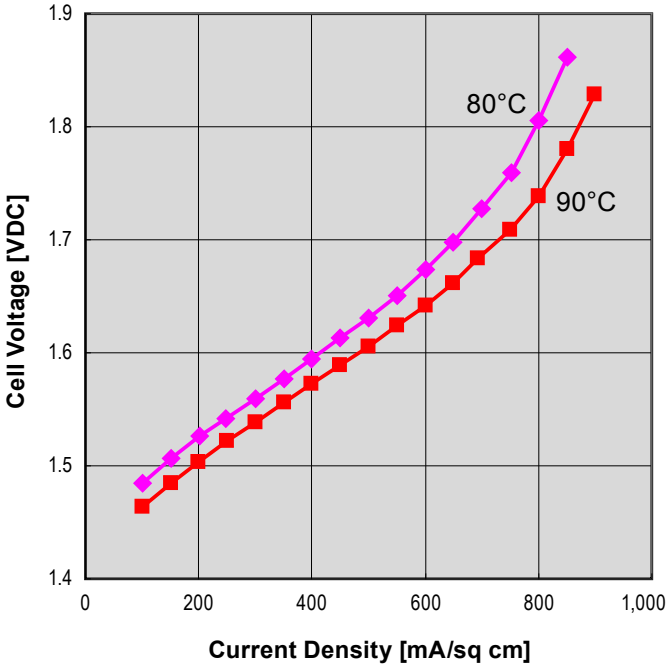


FIGURE 3. Cathode-Feed (Non-Pumped) 160 cm^2 Single-Cell Polarization Testing

40°C operation, raising the oxygen's production pressure from 1,000 to 2,000 psig requires an additional 42 mV. With 60°C operation, raising the oxygen pressure from 1,000 to 2,000 psig requires an additional 28 mV; at 80°C it requires an additional 20 mV.

Figure 4 also shows the advantages of raising the operating temperature from 40°C to 80°C. The primary advantage is to reduce the cell operating voltage, resulting in more efficient electrolyzer operation. For instance, at a constant 300 mA/cm^2 operation at 2,000 psig oxygen generation pressure, raising the cell temperature from 40 to 60°C reduces the voltage by 99 mV. In addition, further raising the cell temperature from 60 to 80°C reduces the voltage by an additional 57 mV. To summarize the cathode feed (pumped) tests in a pressure dome, the most efficient electrolyzer operation occurred at the highest temperature of 80°C.

Conclusions and Future Directions

The Phase II project is completing component tests that will lead to a practical design for a 5,000 psi "Unitized" breadboard system to be built and tested next year. The technology will be able to provide on-site residential hydrogen refueling at a cost that meets the DOE target of \$2.00–\$4.00/kg-H_2 in 2017–2020. In addition to unitizing the major components, the design incorporates numerous cost-saving (and reliability enhancing) simplifications, such as eliminating the need for any mechanical pumps, and utilizing passive cooling for low-cost, maintenance-free heat transfer. These design features eliminate the need for bulky and costly stack and system parts, and facilitate a method for producing a low-cost electrolyzer system that can safely operate at a hydrogen pressure of 5,000 psi in a residential setting. Future objectives are:

- Complete HRA component tests.
- Conduct a hazards and operational safety analysis/ failure modes and effects analysis of the breadboard HRA system.
- Detail design and fabrication of a full-scale electrolyzer stack sized for a hydrogen production rate of 0.5 kg H_2 per 12-hour operational period.
- Detail design, component fabrication, and assembly of a "unitized" breadboard HRA electrolyzer system for 5,000 psi delivery pressure.
- Performance and durability testing of unitized breadboard system prototype.
- Complete a preliminary design and economic analysis of a future commercial HRA system.
- Develop marketing strategy and partnerships for wide scale adoption of technology.

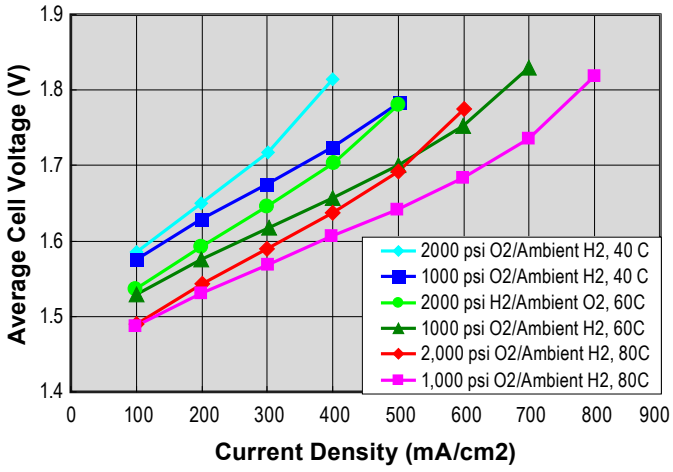


FIGURE 4. Cathode Feed (Pumped) Nafion® 117 Operation

FY 2011 Publications/Presentations

1. T. Norman, M. Hamdan and K. Patch, SBIR Phase II, *Unitized Design for Home Refueling Appliance for Hydrogen Generation to 5,000 psi*, DOE HPTT Presentation, November 2, 2010.

2. T. Norman, K. Patch and M. Hamdan, *Unitized Design for Home Refueling Appliance for Hydrogen Generation to 5,000 psi.* 2011 Hydrogen Annual Program Merit Review Meeting, Presentation #pd_065_norman, June 10, 2011.

References

1. Multi-Year Research, Development and Demonstration Plan, Hydrogen Production, Pg 3.1-14. http://www1.eere.energy.gov/hydrogenandfuelcells/mypp/pdfs/production.pdf.

2. ISO Draft International Standard ISO/DIS 22734-2, Hydrogen generators using water electrolysis process – Part 2: Residential applications, 2009.

Nafion® and Kapton® are registered trademarks of E.I. du Pont de Nemours and Company.

II.J.2 Hydrogen by Wire - Home Fueling System

Luke T. Dalton
Proton Energy Systems
10 Technology Drive
Wallingford, CT 06492
Phone: (203) 678-2128
E-mail: ldalton@protonenergy.com

DOE Manager
HQ: Eric L. Miller
Phone: (202) 287-5829
E-mail: Eric.Miller@hq.doe.gov

Contract Number: DE-SC0001149

Project Start Date: August 15, 2010
Project End Date: August 14, 2012

Fiscal Year (FY) 2011 Objectives

- Develop enabling technologies for 350-bar hydrogen home fueling.
- Design key electrolysis cell stack and system components.
- Fabricate, inspect and assemble prototype components.
- Demonstrate prototype 350-bar hydrogen generation.
- Demonstrate prototype 350-bar home fueling technologies.

Technical Barriers

This project addresses the following technical barriers from the Production section of the Fuel Cell Technologies Program Multi-Year Research, Development and Demonstration Plan:

(G) Capital Cost

(H) System Efficiency

Technical Targets

TABLE 1. Progress towards Meeting Technical Targets for Hydrogen Production via Distributed Water Electrolysis

Characteristics	Units	2012 Target	2011 Status
Hydrogen Cost	$/gge	3.70	5.99*
Electrolyzer Capital Cost	$/gge	0.70	2.62*
Electrolyzer Energy Efficiency	% (LHV)	69	57**

*Based on H2A model modified for residential (non-commercial) application
**Includes generation and compression to 350 bar with stack efficiency of 66% lower heating value (LHV)

FY 2011 Accomplishments

- Defined requirements for cell stack size.
- Completed cell stack concept designs.
- Initiated cell prototype component orders.
- Completed system plumbing and instrumentation diagram (P&ID).
- Drafted system electrical schematic and safety analysis.
- Specified and selected key system components (valves, etc.).
- Designed upgrades to pressure test apparatus.



Introduction

Based upon the results of the Phase 1 study, the fundamental requirements for a hydrogen home fueling appliance have been defined. The conclusion of the Phase 1 study indicated that an overnight-fill proton exchange membrane (PEM) electrolysis device that fills the vehicle directly to a maximum of 350 bar with no mechanical compressor or secondary hydrogen storage can cost effectively supply the daily hydrogen for a typical commuter operating a fuel cell vehicle. The case for including the hydrogen home fueling concept in the overall mix of fueling infrastructure is strong. The home fueler can grow in production volume and geographic distribution with individual vehicles as they are placed in the market with more flexibility than centralized fueling stations. Existing utility infrastructure (water, electricity) can be utilized within their existing capacities to cover the distribution aspect of the fueling infrastructure.

The goal of this Phase 2 project is to design and demonstrate the key hardware for 350-bar hydrogen home fueling based on PEM electrolysis. Proton Energy Systems has previously demonstrated durable PEM electrolysis equipment generating hydrogen at 165 bar. In addition, Proton has also demonstrated the ability of sub-scale prototypes to seal at the required proof pressure for 350-bar operation. Building upon this past work, designs have been initiated to utilize Proton's reliable PEM electrolysis cell stack and system technologies for hydrogen generation and vehicle fueling at 350-bar.

Approach

The approach to the Phase 2 project is threefold. First, utilize the data and modeling results from the Phase 1 project to provide approximate sizing for the hydrogen generation rate. Second, build upon Proton's proven cell stack design and development experience to undertake

the designs required for 350-bar operation. Third, utilize Proton's strong engineering processes that rely on a phased approach, with stage reviews, key written guidelines, and design output documentation to guide the successive levels of design refinement and demonstration. To that end, the project was organized into four main tasks: (1) Prototype System Design and Fabrication, (2) Prototype Stack Design, (3) Prototype Component Verification, and (4) Prototype System Testing. Task 1 utilizes engineering best practices to design and fabricate the prototype fueling system. This includes producing the P&ID, electrical schematics, bills of materials, control schemes and component specifications for the prototype system. In addition, Task 1 includes the procurement, fabrication, and acceptance testing of the prototype system. Task 2 includes producing the component designs and assembly models for the cell stack in three-dimensional (3-D) computer-aided design (CAD) format. Moreover, it includes completing design feasibility pressure testing using both sub-scale and full-scale active area components. Task 3 incorporates work on verifying the functionality of key components within the cell stack design and one or two custom components within the system design. Task 4 includes assembling and checking the first electrolysis-ready version of the new prototype stack design. Furthermore, it includes integrating the prototype stack into the prototype system and operating in electrolysis to generate hydrogen at 350 bar.

Results

During this first year, the team has made excellent progress toward the overall goals of the project. At the time of writing, the team has completed more than 40% of Task 1 and more than 70% of Task 2. At the end of year 1, we expect to be 50% complete with Task 1 and 100% complete with Task 2, which is on schedule to meet the deliverables at the end of Year 2.

Within Task 1, Prototype System Design and Fabrication, the initial conceptual designs of the major system components and system architecture were completed. This concept design effort culminated in an internal concept design review in December 2010. The design team then refined the concept design further through a prototype design stage. In this stage, the P&ID was modified to include more detail and finalize the piping architecture. The electrical schematic was completed, including the electrical safety circuit devices. The packaging of the mechanical components was completed in a 3-D CAD model (Figure 1). The actuated valves, piping, and fittings available for operation at 350 bar were evaluated and selections were made. The primary cell stack power supply was selected and a quote was requested. One key component, the hydrogen-water phase separator, required a higher level of detailed analysis because of the increases in system pressure, since the original phase separator had been designed for 165 bar operation. This part was re-designed and analyzed using finite element analysis (FEA) techniques to ensure that the stresses in the part would be acceptable at the 350 bar operating pressures (Figure 2). The approach for controlling the system as a laboratory prototype was selected to utilize the flexible programmable logic controller (PLC) type of hardware. The key inputs to and outputs from the PLC were identified and listed to facilitate the selection of the PLC in-out cards. Finally, the system-level hazard analysis was initiated by defining the subsystem nodes within the overall system, identifying the hazards, and identifying hazard mitigation strategies. This prototype design stage culminated in a second internal design review. At the time of writing, the specification of the remaining components necessary to have a complete bill of materials (BOM) is underway. The system BOM will be completed allowing orders for all the major components to be placed by the conclusion of year 1.

Within Task 2, Prototype Stack Design, the design process started with a continuation of the feasibility testing previously started by Proton under internal research and development funding to demonstrate overboard sealing of a sub-scale test article. The previous testing was extended by doing short duration elevated temperature soaks to more closely simulate the operating temperature of a cell stack. Finally, an optimization of the sealing features

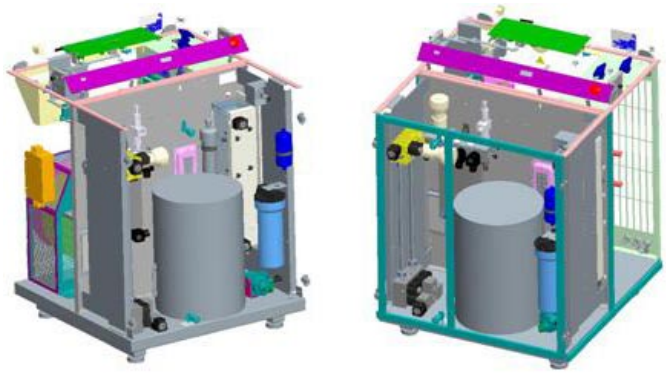


FIGURE 1. Prototype Test System 3-D Package Design

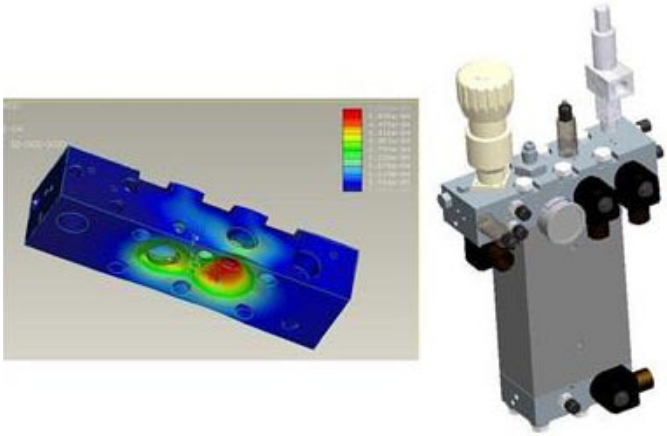


FIGURE 2. Phase Separator Design and Finite Element Analysis

was undertaken to permit more efficient sealing to the same proof pressure. The design of the full-scale stack started with rough sizing of the endplates and bolts for the required strength and stiffness of a 350-bar electrolysis cell stack (Figure 3). The design process continued with conceptual designs of the cell frames and the internal flow field components. As the design of the cell components firmed up, the initial rough designs of the endplate, fluid manifold, electrical bus plates, and tie rods were revised and refined (Figure 4). This iterative design effort included two intermediate design reviews and culminated with a concept stage design review. Based upon the approved designs, quotes were requested on the key components necessary for the first rounds of Task 3, Prototype Component Verification. Orders were placed for the key components to permit full-scale active area pressure testing. At this time, we anticipate that Task 2 will be 100% complete at the end of year 1.

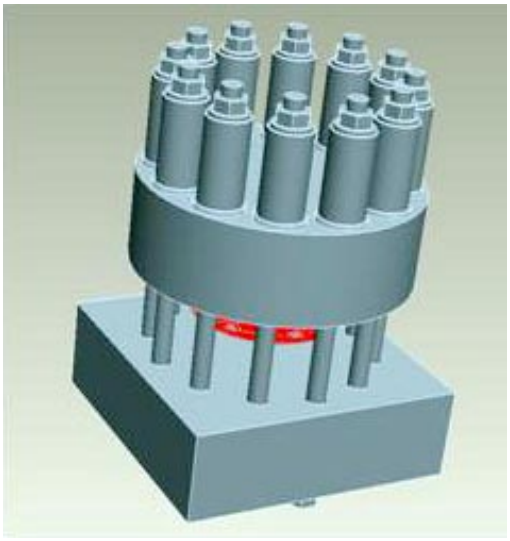


FIGURE 3. Initial Endplate and Tie Rod Sizing

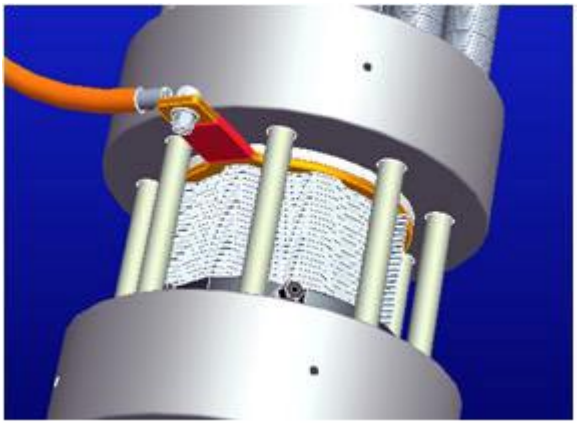


FIGURE 4. Initial Cell Component Design

Conclusions and Future Directions

The project team is making excellent progress toward the culminating demonstration of 350-bar capable electrolysis technology. Moving into year 2 of the project, Task 1 will heavily involve the fabrication and assembly of the prototype system. This task will culminate with the basic sensor calibrations and acceptance tests including leak, ground continuity, and hi-pot testing. As Task 2 reaches completion, Task 3 will pick up with the detailed design verification inspections and tests of the components. Non-operational stacks will be built to verify sealing to proof pressure and proper distribution of load through the components. Flow tests will be conducted on single- and multiple-cell stacks. All of the tasks will culminate in the Prototype System Testing (Task 4). In this task, an operational electrolysis cell stack will be fabricated, assembled, and checked through standard acceptance criteria. The stack will then be integrated with the system and operated for a significant demonstration of 350-bar electrolysis technology.

In summary, the following tasks have been completed and next steps planned for the 350-bar electrolysis fueling system development effort and the parallel 350-bar electrolysis cell stack development:

- The prototype system design is complete, including P&ID, electrical schematic, and 3-D CAD layout.
- The component BOM list is complete with all components quoted for prototype purchase.
- Key prototype system components have been ordered.
- Feasibility cell sealing tests were completed favorably, demonstrating overboard sealing at full proof pressure.
- Differential pressure cross-cell capability feasibility tests were completed at greater than operating pressure.
- Preliminary design calculations have been completed for a full-size cell stack.
- All cell components have been modeled in 3-D CAD and detailed engineering drawings have been drafted for the preliminary design.
- Key prototype cell stack components have been ordered.
- Initial rounds of component verification testing will begin at the end of year 1 and the start of year 2.

FY 2011 Publications/Presentations

1. E. Anderson, L. Dalton, and K. Ayers, “Small-Scale, High Pressure PEM Electrolysis for 350 and 700 bar Residential Fueling Applications,” Fuel Cell & Hydrogen Energy, Washington, D.C., 15 February 2011.

II.J.3 Value-Added Hydrogen Generation with CO_2 Conversion

Richard Billo (Primary Contact) and
Krishnan Rajeshwar
The University of Texas at Arlington
College of Engineering, Box 19019
Arlington, TX 76019
Phone: (817) 272-2708
E-mail: richard.billo@uta.edu

DOE Managers
HQ: Richard Farmer
Phone: (202) 586-1623
E-mail: Richard.Farmer@ee.doe.gov
GO: Paul Bakke
Phone: (720) 356-1436
E-mail: Paul.Bakke@go.doe.gov

Contract Number: DE-FG36-08GO88170

Project Start Date: August 15, 2008
Project End Date: August 30, 2011

Fiscal Year (FY) 2011 Objectives

TASK 1: Develop Homogeneous Ruthenium Photocatalysts for H_2 Production and CO_2 Reduction

- Synthesis of ruthenium-polypridyl complexes (RPCs) as photocatalysts.
- Screen RPCs for electroctalytic activity.
- Evaluate the photophysical properties of the RPCs.
- Demonstrate photocatalytic CO_2 reduction with RPCs.
- Optimize photocatalytic reaction.

TASK 2: Develop Hetergeneous Oxide Photocatalysts for H_2 Production and CO_2 Reduction

- Develop new oxide semiconductors for photocatalysis and photoelectrochemical catalysis.
- Demonstrate combustion synthesis of $BiVO_4$, Bi_2WO_6, and $AgBiW_2O_6$ nanoparticles.
- Demonstrate photoreduction of CO_2 using $BiVO_4$ nanoparticles.
- Develop method for photodeposition of Pt on $AgBiW_2O_6$.
- Optimizing Bi_2WO_6 and $AgBiW_2O_6$ for CO_2 photoreduction.

This project addresses the following technical barriers from the Production section (3.1) of the Fuel Cell Technologies Program Multi-Year Research, Development and Demonstration Plan:

Task 1: Technical Barriers Addressed

(D) Feedstock Issues
(E) Greenhouse Gas Emissions

Task 2: Technical Barriers Addressed

(Y) Materials Efficiency
(Z) Materials Durability
(AA) PEC Device and System Auxiliary Material
(AB) Bulk Material Synthesis

Technical Targets

Progress towards meeting Technical Targets for CO_2 Use as a Feedstock and Greenhouse Gas Remission

Task 1

- Synthesis of three ruthenium polypyridyl complexes.
- Proof-of-concept demonstration of CO_2 reduction to methanol using electrochemical and photochemical methods.

Task 2

- Combustion Synthesis of $BiVO_4$, Bi_2WO_6, and $AgBiW_2O_6$ nanoparticles.
- Photodeposition of Pt on $AgBiW_2O_6$ nanoparticles to enhance electron-hole separation under irradiation.
- Photocatalytic reduction of CO_2 using Pt-modified $AgBiW_2O_6$

FY 2011 Accomplishments

Task 1

- Prepared two photocatalysts containing a ruthenium chromophore linked to pyridyl moiety.
- Demonstrated that these photocatalysts are competent for CO_2 electroreduction to methanol with an optimum performance at pH of 2.0.
- Demonstrated that the two new photocatalysts are capable of CO_2 photoreduction to methanol but that they require a mixed MeCN-water solvent to function.

Task 2

- Prepared $BiVO_4$, Bi_2WO_6, and $AgBiW_2O_6$ nanoparticles by Combustion Synthesis.
- Demonstrated that the combustion synthesized nanoparticles possess higher photocatalytic performance

and larger surface area than those obtained by solid state reaction.

- Demonstrated the photocatalytic generation of H_2 and reduction of CO_2 using Pt-modified $AgBiW_2O_6$ nanoparticles.



Introduction

Given the current environmental concerns over CO_2 as a greenhouse gas and the need for fuels derived from renewable energy sources, the capture and reduction of CO_2 into fuels could help alleviate the environmental issue and turn this cheap and common feedstock into valuable fuels. The combustion of these fuels would regenerate CO_2 which could, in theory, be 'recycled' into fuel, leading to a closed carbon-cycle. Of course, there is a required energy input for this carbon-based fuel cycle, and ideally this would be based on solar-energy. Task 1 of this project describes the development of molecular photocatalysts, based on the discovery of Bocarsly and co-workers that pyridine is an excellent electrocatalyst for the reduction of CO_2 to methanol [1-3]. In this work, we covalently link a ruthenium chromophore to a pyridine co-catalyst to develop a homogeneous CO_2 reduction photocatalyst. The project involves the design, synthesis, characterization and testing of these photocatalysts for CO_2 reduction to methanol. Task 2 describes the preparation of $BiVO_4$, Bi_2WO_6 and $AgBiW_2O_6$ semiconductor nanoparticles by a "mild" (low-temperature) combustion synthesis. This method is both energy- and time-efficient because the exothermicity of the combustion reaction provides the energy for the synthesis and the reaction times are just few minutes. The resulting combustion synthesized nanoparticles are tested as photocatalyts for H_2 generation and CO_2 reduction. Sample characterization involves several techniques such as high resolution transmission electron microscopy, thermogravimetric analysis, Brunauer-Emmett-Teller (BET) surface area, diffuse reflectance spectroscopy, X-ray diffraction (XRD) and X-ray photoelectron spectroscopy (XPS).

Approach

Task 1

We designed and prepared complexes in which the well-established photochemistry of ruthenium-polypyridyl coordination complexes is used to generate a reduced pyridine functional group. These complexes are characterized electrochemically and photochemically to determine optimum reaction conditions. Excitation of each Ru(II) complex with visible light in the region of 400-500 nm forms an excited ^{1}MLCT (metal-to-ligand charge-transfer) state in which the pyridine-containing ligand is reduced by one electron. This excited state quickly relaxes to a second, long-lived, triplet excited state, ^{3}MLCT. Reductive quenching of the Ru^{3+} center traps the electron on the pyridyl ligand and thus has 'photogenerated' an analogue of the pyridine radical. Reaction of this radical anion with CO_2 at the proper pH leads to a sequence of photoreductions that ultimately produce methanol. We used electrochemistry to screen the photocatalysts for electrocatalytic CO_2 reduction activity under various pH conditions. Gas chromatography coupled with mass spectrometry was used to look for the reduced CO_2 products, specifically for methanol. The complexes ability function as photocatalysts was examined in a custom designed photoreactor with 470 nm ultrabright diode lamp. Reaction conditions included the presence of a sacrificial donor, triethanolamine (TEOA) to reductively quench the photoexcited complexes.

Task 2

We used solution combustion synthesis (SCS) to prepare $BiVO_4$, Bi_2WO_6 and $AgBiW_2O_6$ semiconductor nanoparticles. The selection of these three materials was based on their respective band gap energy overlapping the solar spectrum and thus making them able to perform heterogeneous photoreactions using solar light. Using SCS is very convenient as compared with the traditional solid-state reaction method for nanoparticles preparation. The combustion synthesis uses a fuel (i.e. urea) that in contact with the metal precursors promotes the combustion reaction in few minutes instead of the high energy consumption associated with the solid state reaction that normally takes several hours of heating at high temperatures. Furthermore, SCS generates much smaller nanoparticles because of the gases generated during the combustion reaction. The synthesized powders were characterized in their physical shape and size (high-resolution transmission electron microscopy [HRTEM], BET), composition, crystalline structure (XRD, energy dispersive X-ray spectroscopy, XPS), and light absorption (diffuse reflectance ultraviolet-visible spectroscopy [UV-Vis]). The ability of these nanoparticles as heterogeneous photocatalysts was examined in a 200 mL photoreactor containing 0.5 g of semiconductor nanoparticles in aqueous media irradiated from a light source (xenon or tungsten halogen lamp) placed in an inner Pyrex glass compartment.

Results

Task 1

We prepared the three photocatalysts shown in Figure 1 in 90% yield and have characterized them by nuclear magnetic resonance and elemental analysis. They are isolated as the hexafluorophosphate salt for solubility in acetonitrile or as chloride salt for solubility in water.

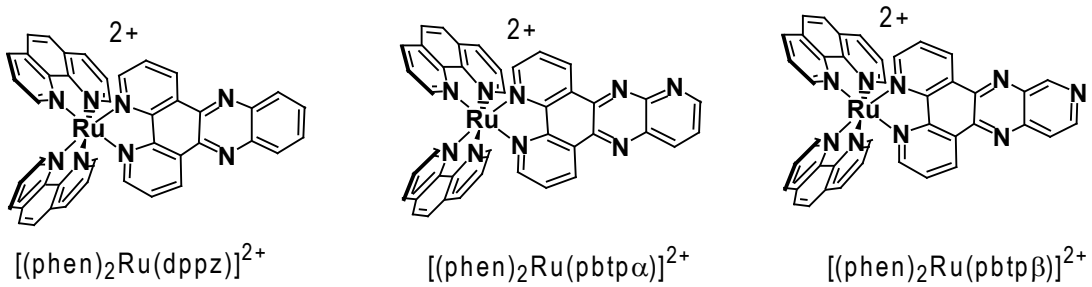


FIGURE 1. Structures of RPCs Described in Task 1

Electrochemistry

The voltammetric behavior of $[(bpy)_2Ru(ptpb\alpha)]^{2+}$ and $[(bpy)_2Ru(ptpb\beta)]^{2+}$ complexes in the presence of CO_2 is compared in Figure 2. It is worth noticing that both profiles are similar in shape although $[(bpy)_2Ru(ptpb\beta)]^{2+}$ is peaking at less negative potentials than its analog $[(bpy)_2Ru(ptpb\alpha)]^{2+}$ indicating a more facile interaction with CO_2 for the first complex. In both cases, the formation of a reactive nitrogen site in the pbpb (either α or β) ligand for CO_2 adduct formation in the form of a carbamate is expected. Figure 2 also shows that a neat increase of current is occurring at potentials more negative than -1.1 V for both complexes indicating that a next electron uptake is also a possible center for photocatalytic CO_2 reduction. This point is important in the view of the photochemical reduction of CO_2 as the ^{1}MLCT excitation of the Ru π→ ptpb dπ band in any of the complexes and reductive quenching of the ^{3}MLCT excited state by triethylamine could trap the electron on the ptpb ligand to form $[(bpy)_2Ru^{II}(ptp\beta^{-})]^{+}$ either in the bpy structure of the ptpb or at the farther N of the structure. The two different locations in the ptpb ligand might work properly in the photochemical reaction. In relation to the returning positive-going scan in Figure 2, it is clear that anodic currents are much smaller than those shown in the absence of CO_2 and pointing out to a chemical reaction of CO_2 with the reduced product of any of the complexes.

For the mechanistic aspects of the electrochemical reaction, the pH dependence of the electrocatalysis was examined. As shown in Figure 3, the reduction potential shifts positive as the pH is lowered as expected for a proton-coupled process. A 60 mV shift positive for every pH unit is in agreement with a one proton-one electron process. A separate measurement of the pK_a of the pyridine acid in $[(bpy)_2Ru(pbtp\beta)]^{2+}$ revealed a pK_a near 2.0 which corresponds nicely with the peak potential shift observed for the cathodic peak. Using this data and the findings by Bocarsly that pyridine electrocatalysis of CO_2 reduction works best at the pKa of the pyridine acid, we ran all subsequent photoreductions at pH 2 for complexes $[(bpy)_2Ru(ptpb\alpha)]^{2+}$ and $[(bpy)_2Ru(ptpb\beta)]^{2+}$ [3].

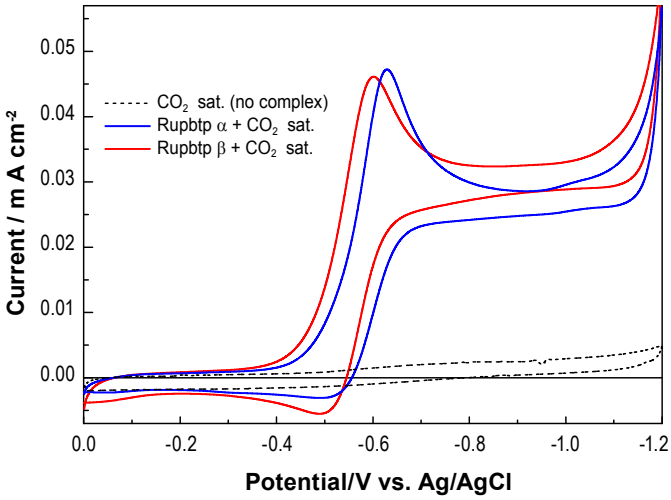


FIGURE 2. Comparison of the voltammetric behavior of $[(bpy)_2Ru(ptpb\alpha)]^{2+}$ and $[(bpy)_2Ru(ptpb\beta)]^{2+}$ in CO_2 saturated solution. Scan rate = 5 mV/s. The voltammogram of CO_2 in the absence of any complex is shown in black dot line.

Photochemistry and Photocatalysis

We examined the ability of $[(bpy)_2Ru(ptpb\alpha)]^{2+}$ and $[(bpy)_2Ru(ptpb\beta)]^{2+}$ to serve as photocatalysts for CO_2 reduction under a variety of conditions. As expected from the literature, pure water solutions were not practical as the excited state lifetime is too short for photoreactions [4]. Solvent mixtures of dimethylformamide (DMF)/water and acetonitrile (MeCN)/water resulted in suitable excited-state lifetimes for the photocatalysts. In a typical experiment, a water jacketed reaction vessel of 50 mL total volume was filled with ~25 mL MeCN that is 1.0 M H_2O, 0.20 M TEOA, and 100 μM Ru complex. The solutions are degassed and then placed in a homemade photochemical reactor in which blue light irradiation of wavelength 470 nm is provided by ultra bright diode array setup. Samples of both the headspace and solution are collected at various time periods and subjected to gas chromatographic (GC) analysis for product detection.

GC data was collected using a Haysep DB packed column with a length of 3 m and used N_2 as a carrier gas (starting at 110°C, a temperature ramp of 1°C/minute

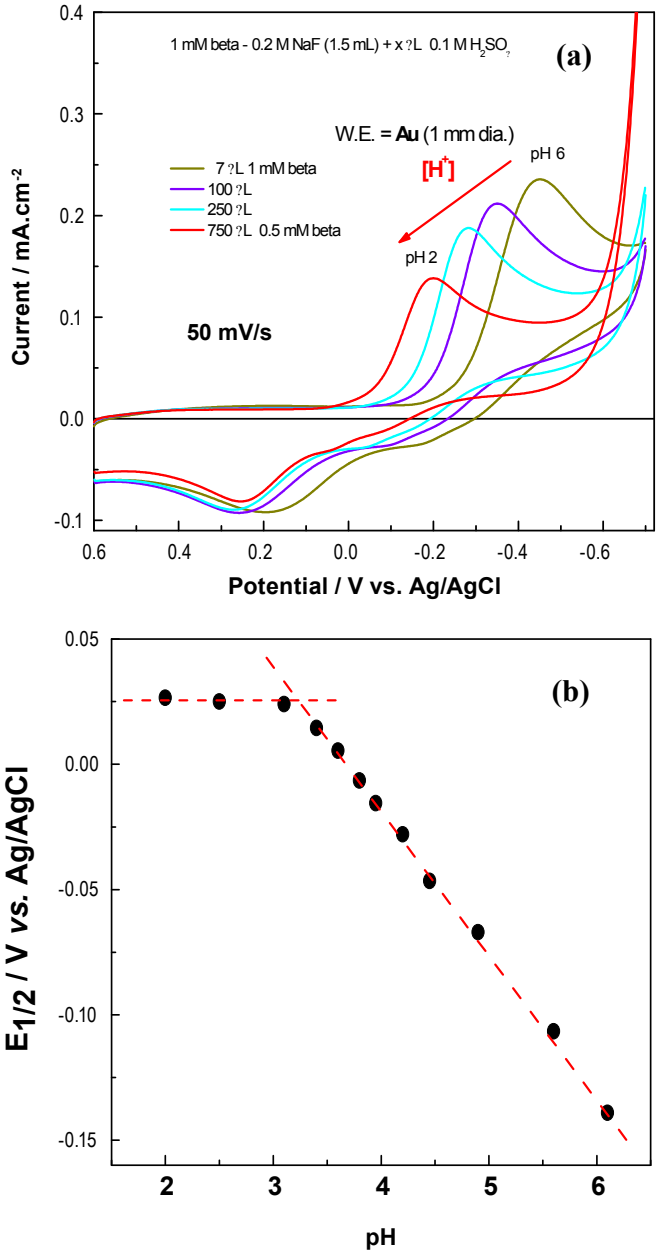


FIGURE 3. a) Selected voltammograms of $[(bpy)_2Ru(pbtp\beta)]^{2+}$ (1 mM) in aqueous media showing the effect of pH on the peak potential associated to the first electroreduction process. b) Linear shift of the half-wave potential ($E_{1/2}$) as a function of the solution pH.

temperature was done immediately after sample injection to a final temperature of 150°C). Retention times were as follows: carbon monoxide, 0.80 min.; methane, 0.88 min.; methanol, 5.8 min.; formaldehyde and formic acid, 8 min.

Methanol was detected under electrolytic and photolytic conditions. Methanol production increased with electrolysis time as expected. In the electrolysis experiment, conditions were 5 mM $[(bpy)_2Ru(pbtp\beta)]^{2+}$, 0.1 M KCl electrolyte, pH 2.0, constant CO_2 bubbling. Constant current at -0.45 mA was applied to a Pt working electrode using a Pt counter

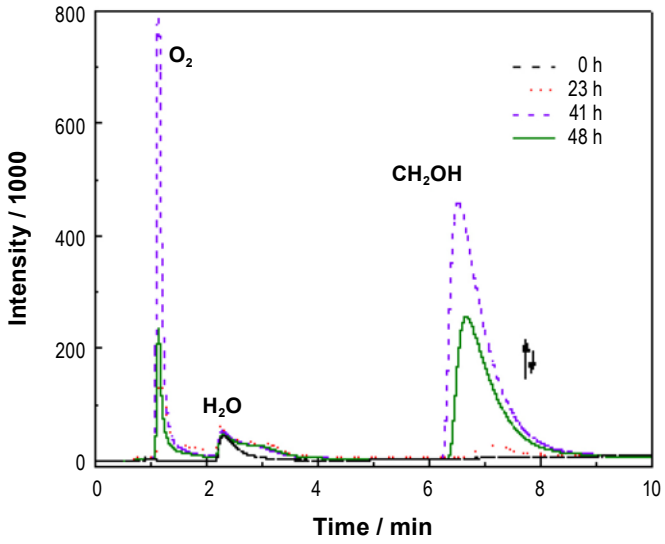


FIGURE 4. Selected GC runs of samples (liquid phase) taken during the $Ru(phen)_2pbtp\beta^{2+}$ + CO_2 electrolysis.

electrode in a separate compartment, and Ag/AgCl reference electrode in the working electrode compartment. These results are only semi-quantitative due to peak overlap in the gas chromatogram and need further refinement for yields and turnover numbers. Similarly, methanol was detected in a photochemical experiment. In a typical experiment, a water jacketed reaction vessel of 50 mL total volume was filled with ~25 mL MeCN or DMF that is 1.0 M H_2O (pH 2), 0.20 M ascorbic acid, and 100 mM Ru complex. The solutions are degassed, saturated with CO_2, and then placed in the photochemical reactor for irradiation at 470 nm. Samples of both the headspace and solution were collected at various time periods and subjected to GC analysis for product detection. Methanol was detected by GC of the solution phase (Figure 4) and its identity confirmed by mass spectrometry. As with the electrolysis result, the results are not quantitative as overlap of the MeOH peak with another species prevents accurate quantification. Work is in progress to find conditions for clear resolution of the MeOH peak by GC.

Task 2

$BiVO_4$, Bi_2WO_6 and $AgBiW_2O_6$ nanoparticles were prepared by SCS [5]. The band edges of these three semiconductor materials are shown in Figure 5 comparatively to other materials and also the redox potentials for CO_2 electroreduction and water splitting are shown there. The three selected materials have band gaps in the 2.4-2.7 eV range thus overlapping the solar spectrum and in contrast with TiO_2 which has served as a model workhorse for a stable and inert inorganic semiconductor although its 3.2 eV band gap is too high to be used as solar absorber.

All samples were fully characterized (by HRTEM, XPS, XRD, BET, UV-Vis and Raman spectroscopy) to ascertain

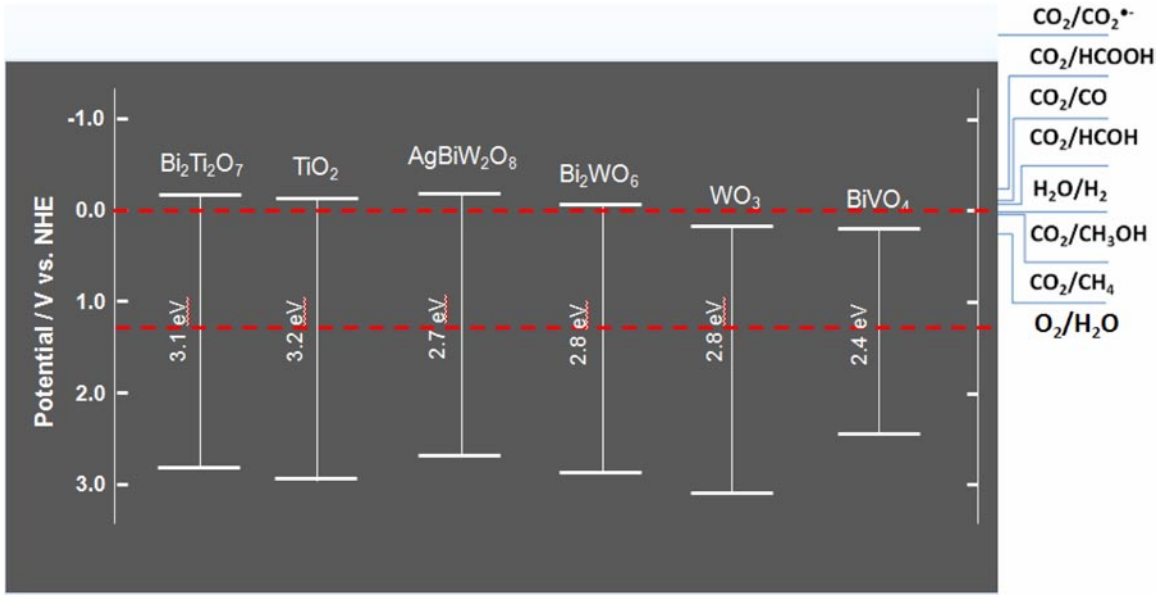


FIGURE 5. Comparison between the band edges of selected semiconductors (at pH 1) and the redox potentials for CO_2 reduction and water splitting.

particle size, composition, crystalline structure and absence of impurities [6]. Figure 6 shows the UV-visible diffuse reflectance data on a SCS-synthesized $AgBiW_2O_6$ sample processed in the form of Tauc plot of the square root of the Kubelka–Munk function vs. the photon energy. The band gap value estimated from this plot is 2.73 eV and in very good agreement with the value (2.75 eV) reported for this ternary oxide in a previous study on solid-state reaction (SSR) [7]. Much higher surface areas (as determined by BET isotherm, see Table 1) are found for the SCS samples than for those prepared by SSR, thus pointing out to a better quality product obtained in a time- and energy-efficient manner by SCS.

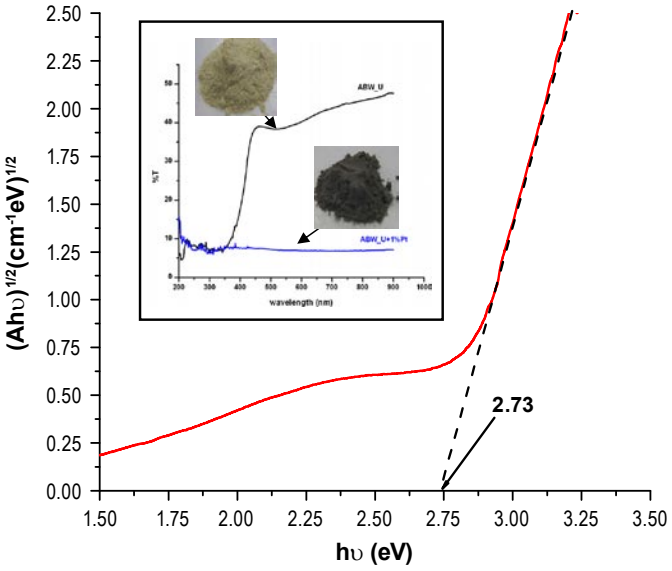


FIGURE 6. Tauc plot for combustion synthesized $AgBiW_2O_8$. The inset shows the percent transmittance data of the sample before (black line) and after photodeposition of 1wt% Pt (blue line), along with the corresponding sample photographs.

TABLE 1.

Photocatalyst	Micropore Area (cm^2)	External Surface Area (cm^2)	BET Surface Area ($m^2\ g^{-1}$)
SCS $AgBiW_2O_8$	5.488	28.938	34.44 (our work)
SSR $AgBiW_2O_8$	0.136	0.406	0.54 (our work)
SSR $AgBiW_2O_8$	-	-	0.29 (ref. 7)

A newly designed sealed photoreactor was then used to perform heterogeneous photocatalysis with the semiconductor particles suspended in CO_2 saturated water. The lamp (400 W medium-pressure Hg arc encased in Pyrex glass, photon flux: 235 mW/cm^2) was turned on and the gaseous products evolved were analyzed by gas chromatography (GC SRI 310) as a function of the illumination time using a Shin Carbon column and a thermal conductivity detector.

Best samples for photoreduction of CO_2 are the SCS-derived $AgBiW_2O_8$ powders which are able to perform the photocatalytic generation of syngas followed the principle outlined in Figure 7a. The rationale for using formate ions as the in situ precursor for CO_2 was two-fold. The direct electroreduction of CO_2 in aqueous media is beset both by the low partial pressure of CO_2 in the atmosphere (3.9×10^{-4} atm) and by its low solubility in water (1.5 g/L at

298 K) [8]. On the other hand, formate species have high solubility in water (945 g/L at 298 K) [9]; they have high proclivity for being adsorbed on oxide surfaces and are easily photoconverted to CO_2 (Figure 7a). The in situ generated CO_2 can be subsequently reduced by the photogenerated electrons in the oxide particle. For the simultaneous photogeneration of H_2, the photogenerated electrons must be stored on the oxide surface in noble metal catalyst (e.g., Pt) islands [10]. Thus, the $AgBiW_2O_8$ particles were loaded with 1 mass% Pt using a photocatalytic procedure described elsewhere [11]. After surface modification with Pt, the color of the oxide particles changed significantly from light yellow to a grayish hue as illustrated in Figure 6 (insert). The diffuse reflectance spectra also changed consequently as also shown in Figure 6 (insert). Thus, we envision that the portion of the photogenerated electrons channeled toward the Pt catalyst islands would reduce protons to hydrogen while those that diffuse to the (naked) oxide surface would be utilized for the reduction of CO_2 to CO (Figure 7a).

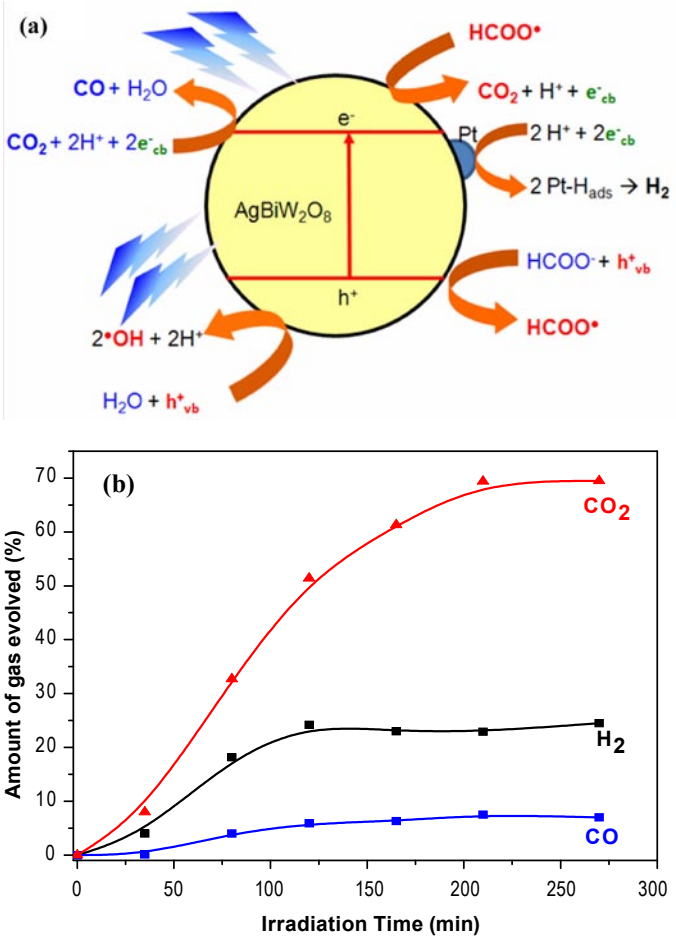


FIGURE 7. a) Diagram of heterogeneous photocatalytic formation of syngas on an illuminated AgBiW2O8-Pt nanoparticule. b) Amount of gas evolved (H2 and CO) as a function of irradiation time using in situ CO_2 generation from 0.1 M HCOOH.

The Pt-modified $AgBiW_2O_8$ particles were loaded into the photoreactor containing a de-aerated solution of 0.1 M HCOOH at a dose of 2 g/L. Figure 7b illustrates the temporal profiles of the three products of the overall photocatalytic reaction, namely, H_2, CO and CO_2. It is worth noting that the first products to be seen are the generation of CO_2 and H_2 from the oxidation of HCOOH using the photogenerated holes from the semiconductor valence band and the reduction of H^+ through photogenerated electrons in the conduction band of $AgBiW_2O_8$ respectively. The (subsequent) formation of CO tracks the in situ photogeneration of CO_2 at or near the particle surfaces. The run was terminated at 225 min at which time the gases accumulated were as follows: $H_2 = 1.0 \times 10^{-2}$ mol/gL, $CO = 3.0 \times 10^{-3}$ mol/gL and $CO_2 = 2.8 \times 10^{-2}$ mol/gL. These data are reported as the number of moles of product divided by the photocatalyst mass and liquid volume in the photoreactor. Quantum yields for the formation of syngas (H_2+CO) and CO_2 in the formic acid solution amount to $H_2 = 3.0$ %, $CO = 0.8$ % and $CO_2 = 4.5$ %.

Conclusions and Future Directions

Our findings in Task 1 show that properly designed RPCs can act as a homogeneous photocatalyst or electrocatalyst for CO_2 reduction to methanol. This proof of concept now needs to be refined and optimized to determine the efficiency of the process. Ultimately, we would need to couple the reductive process with a more practical oxidative process, for example water oxidation, to construct a practical system for solar fuel generation.

Our findings in Task 2 show that among the three heterogeneous photocatalysts, the Pt-modified $AgBiW_2O_8$ is capable of performing CO_2 photoreduction. The data described is a useful proof-of-concept for the following: (a) $AgBiW_2O_8$ can be simply and quickly prepared by SCS; (b) A mild photocatalytic procedure for syngas generation can be developed based on the use of formate ions as an in situ precursor for CO_2, and (c) The SCS-derived $AgBiW_2O_8$ powder, after Pt surface modification, can generate syngas via this procedure. Ultimately, better performances can be expected by optimizing the amount of Pt on the semiconductor nanoparticles and by using solvent mixtures of DMF/water and MeCN/water to enhance CO_2 solubility in the liquid phase.

References

1. Barton, C.E.; Lakkaraju, P.S.; Rampulla, D.M.; Morris, A.J.; Abelev, E.; Bocarsly, A.B. *J. Am. Chem. Soc.* **2010**, *132*, 11539-11551. 10.1021/ja1023496.

2. Barton, E.E.; Rampulla, D.M.; Bocarsly, A.B. *J. Am. Chem. Soc.* **2008**, *130*, 6342-6344. 10.1021/ja0776327.

3. Seshadri, G.; Lin, C.; Bocarsly, A.B. *J. Electroanal. Chem.* **1994**, *372*, 145-150.

4. Nair, R.B.; Cullum, B.M.; Murphy, C.J. Optical Properties of [Ru(phen)(2)dppz](2+) as a Function of Nonaqueous Environment. *Inorg Chem* **1997**, *36*, 962-965.

5. Rajeshwar, K.; de Tacconi, N.R. *Chem. Soc. Rev.* **2009**, *38*, 1984 - 1998.

6. Timmaji, H.K.; Chanmanee, W.; de Tacconi, N.R.; Rajeshwar, K. *J. Adv. Oxid. Technol.* **2011**, *14*, 1-13.

7. Tang, J.; Ye, J. *J. Mater. Chem.* **2005**, *15*, 4246 - 4251.

8. Palmer, D. A.; Van Eldik, R. *Chem. Rev*. **1983**, *83*, *651* - 731.

9. *CRC Handbook of Chemistry and Physics*, 82nd Edition, CRC Press: Boca Raton, FL, **2001-2002.**

10. Rajeshwar, K. *J. Appl. Electrochem.* **2007**, *37*, 765 - 787.

11. de Tacconi, N. R.; Chenthamarakshan, C. R.; Rajeshwar, K., Lin, W-Y.; Carlson, T.; Nikiel, L.; Wampler, W.A.; Sambandam, S.; Ramani, V. *J. Electrochem. Soc.* **2008**, *155*, B1102 – B1109.

II.J.4 Photoelectrochemical System for Hydrogen Generation

Alexander Parfenov (Primary Contact),
Juan F. Hodelin, Sunshine Holmberg, Jerry Shea,
Tin Win, Min-Yi Shih
Physical Optics Corporation
20600 Gramercy Place
Torrance, CA 90501
Phone: (310) 320-3088
E-mail: aparfenov@poc.com

DOE Manager
HQ: Eric Miller
Phone: (202) 287-5829
E-mail: Eric.Miller@hq.doe.gov

Contract Number: DE-FG02-07ER84869

Project Start Date: June 20, 2007
Project End Date: May 15, 2011

Fiscal Year (FY) 2011 Objectives

- Fabrication of components of scaled-up prototype photoelectrochemical (PEC) reactor cell.
- Integration of scaled-up prototype of a PEC reactor cell.
- Demonstration of the scaled-up prototype reactor cell with photoelectrodes and performance evaluation.

Technical Barriers

This project addresses the following technical barriers from the Production section of the Fuel Cell Technologies Program Multi-Year Research, Development and Demonstration Plan:

(Y) Materials Efficiency
(AC) Device Configuration Designs
(AD) Systems Design and Evaluation

Technical Targets

TABLE 1. Progress towards Meeting Technical Targets for PEC Hydrogen Production

Characteristic	Units	2013 Target	2011 Status
Usable Band Gap	eV	2.3	2.2
Chemical Efficiency	%	10	To be determined
Solar-to-Hydrogen Efficiency	%	8	~5% - to be verified
Durability	hr	1,000	0.5 - to be verified

FY 2011 Accomplishments

- Fabricated A2B6 photoelectrodes using solution deposition to produce CdS/ZnS bilayer (n-type) films.
- Designed, fabricated, and tested a third generation PEC reactor cell panel and mechanical framework (0.5 m x 0.5 m).
- Conducted techno-economic analysis for PEC reactor system.



Introduction

Sunlight is an abundant, renewable and domestically available energy source that can provide a significant proportion of carbon-free energy in the future, particularly if sunlight can be harnessed to generate hydrogen fuel for transportation. PEC hydrogen generation is an approach to generate hydrogen fuel directly from water by using sunlight to drive a water-splitting reaction on the surface of novel semiconductor materials. The primary technical barriers to the development of these semiconductor materials are that they absorb a sufficient amount of the incoming solar energy, efficiently transfer that energy to drive the water-splitting reaction, and remain durable and efficient for long operational times while remaining cost-competitive with other hydrogen generation approaches. In this project, Physical Optics Corporation is developing an approach for the low-cost fabrication of A2B6 semiconductor photoelectrode architectures and building a prototype PEC reactor cell for testing and demonstration.

Approach

The approach of this project is to increase the solar-to-hydrogen efficiency by using lower band gap A2B6 semiconductor materials (addressing the Materials Efficiency technical barrier). Using a lower band gap enables increased solar absorption due to capturing the abundant lower energy photons inaccessible to traditional high band gap PEC materials. Previously we selected a CdS/ZnS bilayer and also ZnTe as promising A2B6 material combinations with band gaps in the 2.2-2.4 eV range. Recently, we concentrated on the CdS/ZnS architecture and explored and evaluated different processes for producing the films. These processes included an electrodeposition approach for co-depositing CdS with the ZnS capping layer from a single solution and a sequential deposition of CdS followed by ZnS via chemical solution deposition. We concluded our investigation of the ZnTe film, based on additional testing which revealed that the durability of the electrodeposited ZnTe films was insufficient for system integration.

In addition to fabricating photoelectrode materials, we developed and assembled the third generation in a series of prototype reactor cell systems to house the photoelectrodes and capture the generated hydrogen. This PEC reactor housing is the final prototype for this project and will be used for testing and demonstration purposes. Technoeconomic evaluations of the hydrogen production cost have been made based on the prototype fabrication costs, the material costs, and the projected photoelectrode efficiency and lifetime of the mature system. This work directly addresses the Systems Design and Evaluation technical barrier.

Results

Our efforts on this project have focused on the development of the two major cell components: the semiconductor photoelectrode structure and the PEC reactor cell housing.

Electrodeposited A2B6 Photoelectrode Development

Previously we had developed a process for co-deposition of an *n-n* CdS/ZnS bilayer film using electrochemical deposition. Recently we have refined the deposition process to increase the thickness of the films as shown in Figure 1. The thicker films have higher overall durability, however the uniformity of the coating, particularly of the ZnS window layer requires further improvement. The co-deposition process utilizes both zinc and cadmium salts simultaneously in the reaction vessel along with a single organic sulfur source. Due to the electrodeposition of CdS proceeding more rapidly than the solution-deposited ZnS, as well as the lack of stirring during the electrodeposition, local concentration effects may be among those contributing to the poor uniformity.

To improve the ZnS coating uniformity, a solution deposition process was developed for coating previously electrodeposited CdS samples with a ZnS window layer. First, single layer ZnS films were developed and characterized. These samples bandgap around 3.5 eV which is consistent with zincblende ZnS. Next the coating process was applied to the electrodeposited CdS films immediately upon their removal from the CdS bath. These two fabrication step samples were tested and compared to the co-deposited samples, and test results indicated that while the two-step samples were more durable, the co-deposited films provided superior PEC performance. This is attributed to the continuous variation in stoichiometry that results from the co-deposited films allowing carriers to transfer between layers more efficiently, when compared to the abrupt interface present in the two-step samples. In the future, the next step would be to apply a hybrid procedure where the thickness of the ZnS layer of a co-deposited is incrementally increased through a second deposition in a fresh bath. This hybrid process may provide both a gradual stoichiometry change from CdS to ZnS along with an increased total ZnS coating thickness.

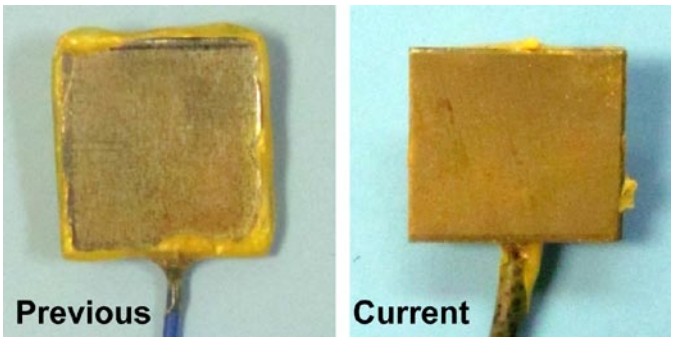


FIGURE 1. CdS/ZnS bilayer films showing increased thickness through two-step process as compared to previously deposited samples through the optimization of the coating process.

PEC Reactor Cell Development

After the successful testing of the second generation prototype for the PEC reactor cell which houses the photoelectrode, counterelectrode, water and evolved H_2 and O_2 gases, we scaled up the design and fabricated a third generation prototype as shown in Figure 2. The prototype takes advantage of the scalable and modular design to increase the total size of the system area to 65 cm x 50 cm with an available harvesting area of approximately 20 cm x 20 cm (due to excess area allocated to the counterelectrode and for gas capture). The system is designed to allow simple and flexible integration of photoelectrodes for loading and maintenance, as well as autonomous extraction of the hydrogen gas and refilling of the aqueous electrolyte. The prototype system has recently been evaluated for system cost and durability based on testing and projected performance parameters.

Conclusions and Future Directions

Physical Optics Corporation has explored a novel electrodeposition and chemical solution deposition approaches to fabricating CdS/ZnS bilayer films for PEC hydrogen generation. In addition, a third generation prototype of the reactor cell mechanical framework has been designed, assembled, and is being evaluated. Future work would work to improve the film uniformity and durability by optimizing the deposition process. We plan to continue to investigate opportunities for verification of PEC test results through collaboration with other members of the PEC workgroup. The results of the system development and economic analysis will provide a strong basis for further commercial development of PEC hydrogen production components or systems in the future while working to overcome DOE technical barriers.

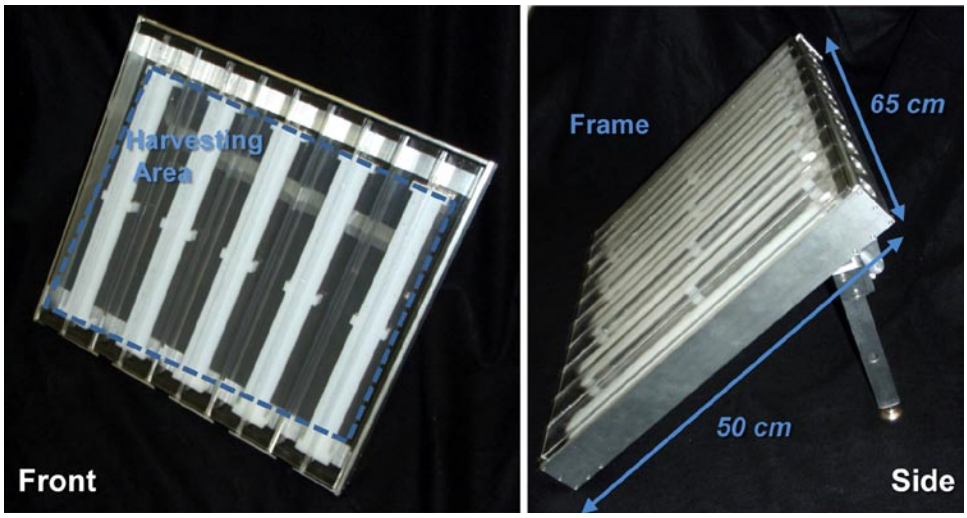


FIGURE 2. Third generation prototype PEC reactor photographed with electrodes removed. The prototype reactor was designed and built to be modular and scalable, and to have a low cost to fabricate and maintain.

II.K1 SISGR: Using *In vitro* Maturation and Cell-free Evolution to Understand [Fe-Fe]hydrogenase Activation and Active Site Constraints

James Swartz[1,2] * (PI), Jon M. Kuchenreuther[1], Alyssa Bingham[1], Phillip Smith[1], Celestine Grady-Smith[3,4], Simon J. George[3], and Stephen P. Cramer[3,4]

[1] Department of Chemical Engineering, Stanford University
[2] Department of Bioengineering, Stanford University
[3] Department of Applied Science, University of California, Davis, CA
[4] Physical Sciences Division, Lawrence Berkeley National Laboratory, Berkeley, CA
* Presenter's Address:
Stauffer III, Room 113
Stanford, CA 94305-5025
Phone: (650) 723-5398
E-mail: jswartz@stanford.edu

DOE Program Manager: Michael Markowitz
Phone: (301) 903-6779
E-mail: Mike.markowitz@science.doe.gov

Objectives

With this project, we seek increased understanding of the mechanisms for assembly and activation of [FeFe] hydrogenases as well as the structural role that the polypeptide scaffolding plays in forming and stabilizing this complex enzyme's active site. We are developing in vitro maturation methods to enable detailed study of the biochemical reactions required to provide precursors and to assemble the catalytic H-cluster as well as to install it into the apoenzyme. We are also searching for enzyme mutations that will reveal the role of the polypeptide structure. To accomplish these objectives and to help advance this important field of research, we are also developing improved methods for producing these complex enzymes and for evaluating various functional characteristics.

Technical Barriers

This project is designed to provide information relative to the maturation and structure function relationships of [FeFe] hydrogenases. Since these are nature's most prolific hydrogen producers, this information will facilitate the design, assembly and cost-effective production of improved biological and biomimetic catalysts for the production of hydrogen and for hydrogen based fuel cells. The project will also deliver improved methods for the evolution, evaluation, and production of improved hydrogen producing catalysts. Since the most plentiful proton source for producing hydrogen is water and oxygen is a side product, the project will also search for oxygen tolerant hydrogenase mutants and seek to understand the structure function relationships relative to oxygen tolerance.

Abstract

The first project objective is to elucidate the substrates and mechanisms for assembly and maturation of the 6Fe-6S active site of [FeFe] hydrogenases. An early *in vitro* maturation method was developed using an *E.coli* cell extract in which the three required maturases had been expressed and activated. The extract was also dialyzed to remove small molecules. We showed, for the first time, that activation of the purified apoenzyme was significantly enhanced by incubating this extract in the presence of S-adenosyl methionine, Fe(II), sulfide, and 20 amino acids. A design of experiment (DOE) investigation then showed that tyrosine was required and cysteine was beneficial for maturation. Further investigation showed that the para-hydroxyl substituent of tyrosine was required for efficient activation. An improved maturation procedure was then developed in which the three maturase proteins were expressed separately to avoid *in vivo* maturase interactions. Such interactions were thought to be important for function, and we sought to gain control over this portion of the maturation mechanism. In contrast to previous inferences, efficient apoenzyme activation was observed using the separately produced maturases. This new system enabled the production of much larger quantities of *in vitro* activated [FeFe] hydrogenase. This, in turn, enabled high resolution FTIR (Fourier transform infrared spectros-copy) analysis of the C-O and C-N stretches associated with the cyanide and carbon monoxide adducts in the 6Fe-6S active site. Isotopic labeling of tyrosine then conclusively showed that all three of the CO and both of the CN moieties in the active site are derived from tyrosine.

The second project objective is to gain better understanding of the impact of the polypeptide scaffolding on hydrogenase activity. The expression gene for the CpI [FeFe] hydrogenase from *Clostridium pasteurianum* was extensively mutated using nucleotide analogs, and isolates were identified that retained at least partial activity and also displayed increased stability during oxygen exposure. The most interesting isolate contained 13 mutations and was extensively analyzed. When two of the amino acid changes were reversed, full activity was restored. Three different mutations increased oxygen tolerance. Unexpectedly, none of these mutations are near the active site 6Fe-6S H-cluster, but four of the five mutations are close to the proximal 4Fe-4S center that either donates electrons to the active site H-cluster or receives them, depending on the direction of catalysis. These results suggest that the function of this ancillary iron-sulfur center has a stronger than expected

influence on enzyme function. During this work, we also observed that oxygen inactivation of [FeFe] hydrogenases can be substantially reversed in contrast to general belief. The reversibility also appears to be influenced by the ancillary Fe-S center. Future work will now seek to assess the function of the amino acids surrounding this ancillary center as well as those that support the active site.

During the course of these investigations, a number of methods were developed of general utility to this field of research. These include: the *in vitro* hydrogenase maturation protocols, a procedure for producing high levels of maturases and hydrogenases in *E.coli* cultures, improved methods for producing and screening hydrogenase mutants, and a new method for assessing sustained hydrogen production activity while using a reduced ferredoxin protein as the electron donor. In particular, the last method is very important as it will now allow us to screen for mutants with increased oxygen stability while they are actively making hydrogen. In addition, this method suggests the feasibility for cost-effectively producing hydrogen from biomass hydrolysates. A new research program has now been initiated to develop technology for the large scale production of hydrogen from biomass hydrolysates.

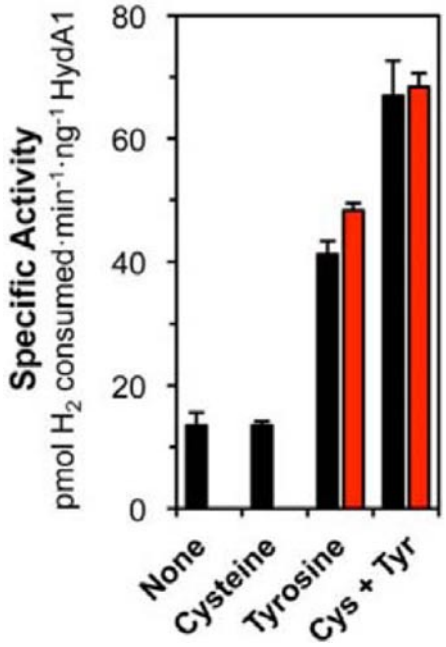


FIGURE 1.

Progress Report

Taking our lessons from the investigation of another important and complex enzyme, nitrogenase, we first sought to develop methods for the *in vitro* maturation of the [FeFe] hydrogenases. Although early work from the Peters lab at U. of Montana had achieved *in vitro* activation (although with very low yields), that system was not suitable for investigating the effects of small molecular weight substrates. Based on our success with cell-free protein synthesis of the hydrogenases (Boyer et al, 2008), we developed an *in vitro* maturation protocol that achieved substantial activation of the *C. rheinhardtii* HydA1 [FeFe] hydrogenase using cell extracts in which the three maturases, HydE, HydF, and HydG, had been expressed. These maturases were expressed from the relevant genes taken from *Shewanella oneidensis* and were produced under anaerobic conditions at 20°C to encourage proper folding. For convenience, the extracts were then prepared under aerobic conditions and were frozen for storage. The extracts were then dialyzed just before use to remove small molecules, and the maturases were reconstituted (reactivated) by anaerobic incubation with Fe(II) and S^{-2}. The apoenzyme was produced in *E.coli* cultures lacking the maturases and had no activity after purification. As expected, S-adenosyl methionine, Fe(II), and S^{-2} were necessary for activation. However, full activation was only achieved with the additional presence of a mixture of the 20 natural amino acids. A design of experiment (DOE) protocol then indicated that tyrosine was essential and cysteine was beneficial (see Figure 1) for hydrogenase activation.

A previous report had suggested that co-expression of the maturases was necessary for their activation. However, we reasoned that more information about hydrogenase maturation could be gained if the maturases could be expressed in separate *E.coli* cultures. This would then require that nearly all maturation related reactions take place during the *in vitro* activation. This protocol would also have a higher likelihood of enabling complete incorporation of isotopically labeled precursors into the H-cluster active site. Again, the apoenzyme was produced in cultures lacking the maturases and had no activity. At this point in the project, we had discovered that an *E. coli* strain with a Δ*iscR* deletion (Akhtar & Jones, 2008) produced more of the maturases as well as more apoenzyme. By mixing three extracts, each containing high levels of an individual maturase, effective apoenzyme activation was achieved. This protocol also efficiently matured the more complex CpI hydrogenase from *Clostridium pasteurianum*. After isotopically labeled tyrosine was added to the maturation reactions, the activated and purified hydrogenase samples were analyzed by FTIR. Distincitive shifts in the C-O and C-N stretches were observed as shown in Figure 2. These shifts indicated that all of the CN^- adducts in the active site H-cluster derived from the alpha carbon and amino nitrogen of tyrosine and all of the CO adducts derived from the carboxylate group of tyrosine. Recent work had shown that CO and CN could be extracted from the HydG maturase and that these species derived from tyrosine, but these recent publications had not shown that all of the adducts in the active enzyme derived from tyrosine.

The work to characterize the role of the polypeptide structure began with a mutant of the *C. pasteurianum* CpI hydrogenase that was isolated with 13 amino acid changes that conferred lower activity and improved oxygen tolerance. When the wild type amino acids were restored at positions 186 and 188, full activity was also restored. (See Figure 3)

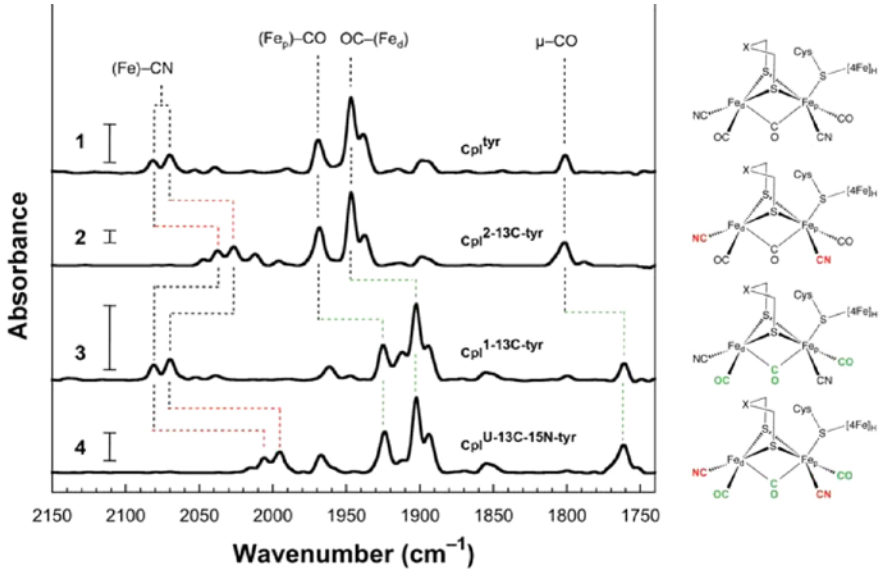


FIGURE 2.

Interestingly, these mutations were not near the active site, but rather adjacent to the electron conducting 4Fe-4S center proximal to the active site. It also turned out that the most influential mutation for conferring oxygen tolerance was at position 197, an amino acid that is adjacent to the same 4Fe-4S center. Amino acid position 160 was also influential for oxygen tolerance and was adjacent to the same cluster.

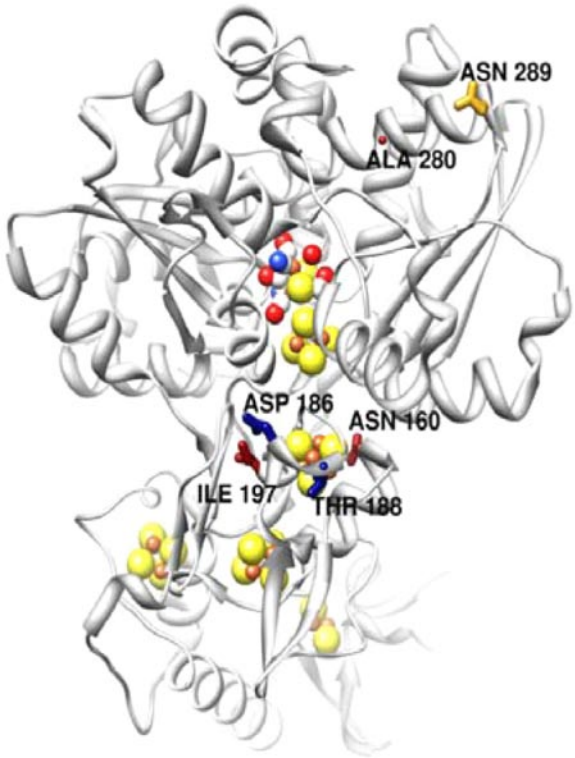


FIGURE 3.

It thus became clear that this 4Fe-4S cluster proximal to the catalytic center has strong influences on functional properties. The influences of the other amino acids surrounding this cluster will now be further characterized in addition to those surrounding the catalytic center.

Perhaps even more important than these specific discoveries is the collection of methods that have been developed. For example, paper no. 2 in our publication list describes a new production protocol that increases volumetric hydrogenase yields by 10 to 30 fold when produced by an rDNA *E.coli* culture. We have also established the ability to continually transfer electrons from NADPH to the hydrogenase to assess oxygen tolerance while the enzyme is making hydrogen. Unfortunately, this new technique showed that our oxygen tolerant mutant was only tolerant when in the resting state and not when it is producing hydrogen. This is a totally unexpected observation. It will be investigated further, but it also suggests that we need to adjust our screening assays. The new pathway from NADPH will form the basis for a high throughput screening assay that assesses oxygen tolerance for the active enzyme. This new method also forms the basis for a new pathway to convert biomass hydrolysates to hydrogen and this is now being pursued by a new project.

Future Directions

We now have accumulated a large variety of enzyme production and assessment methods and we can now enter a more active period to generate many new mutants that differ in functional characteristics. We will continue to work with our spectroscopy experts to gain a fuller understanding of the relationship between structural and functional changes and will most likely also begin a collaboration with X-ray structural experts to gain more detailed information about the impact of individual mutations. To better understand maturation, we will also work to establish catalytic maturation; i.e., the ability to catalyze multiple turnovers of the maturases when working to activate the hydrogenase.

References

1. Boyer ME …. Swartz JR. (2008) Cell-free synthesis and maturation of [FeFe] hydrogenases. Biotech. and Bioeng. **99**: 59-67.

2. Akhtar MK and Jones PR (2008) Deletion of iscR stimulates recombinant clostridial Fe-Fe hydrogenase activity and H2-accumulation in *Escherichia coli* BL21(DE3). Appl. Microbiol. and Biotechnol. **78**(5): 853-62.

Publication list (including patents) acknowledging the DOE grant or contract

1. Kuchenreuther JM, Stapleton JA, Swartz JR. (2009) Tyrosine, Cysteine and S-Adenosyl Methionine Stimulate *In Vitro* [FeFe] Hydrogenase Activation. PLoS ONE4(10): e7565.

2. Kuchenreuther JM, Grady-Smith CS, Bingham AS, George SJ, Cramer SP, Swartz JR. (2010) High-Yield Expression of Heterologous [FeFe] Hydrogenases in *E coli*. PLoS One 5(11): e15491.

3. Kuchenreuther JM, George SJ, Grady-Smith CS, Cramer SP, Swartz JR. (2011) Cell-free H-cluster synthesis and [FeFe] hydrogenase activation: all five CO and CN^- ligands derive from tyrosine. PLoS ONE (accepted, in revision)

4. Bingham AS, Smith PR, Swartz JR. (2011) Evolution of an [FeFe] hydrogenase with decreased oxygen sensitivity. International Journal of Hydrogen Energy; In Press.

5. Swartz JR, Smith PR (2010) A General Enzymatic Pathway for Hydrogen Production. Provisional Patent Application filed 9/3/2010.

II.K.2 Phototrophic metabolism of organic compounds generates excess reducing power that can be redirected to produce H_2 as a biofuel

Caroline S. Harwood and James B. McKinlay*
University of Washington
Box 357242
Seattle, WA 98195
Phone: (206) 221-2848; Fax: (206) 543-8297
E-mail: csh5@uw.edu

DOE Program Manager: Robert Stack
Phone: (301) 903-5652
E-mail: Robert.Stack@science.doe.gov

Objectives

The objectives of this project are (i) to use ^{13}C-metabolic flux analysis and other approaches to identify metabolic factors that influence the phototrophic production of H_2 from organic compounds by *Rhodopseudomonas palustris* and (ii) to use the resulting information to guide the engineering of *R. palustris* for improved H_2 production.

Technical Barriers

A technical barrier to engineering bacterial strains for enhanced H_2 production is a limited ability to follow electron flow through metabolism. Here we used ^{13}C-metabolic flux analysis, in combination with physiological and other 'omics' analyses, to overcome this barrier by tracking fluxes through redox reactions.

Abstract

Although most manufactured H_2 comes from fossil fuels, H_2 can also be produced biologically. The bacterium *Rhodopseudomonas palustris* uses energy from sunlight and electrons from organic waste to produce H_2 via nitrogenase. In order to understand and improve this process we used ^{13}C-substrates having various oxidation states to track and compare central metabolic fluxes in non-H_2 producing wild-type *R. palustris* and an H_2-producing mutant. The pathways by which substrates were oxidized generated excessive amounts of reducing power such that only 40-60% could be used for biosynthesis, depending on the growth substrate. Wild-type cells relied heavily on the CO_2-fixing Calvin cycle to oxidize the excess reduced electron carriers, using CO_2 produced from the organic substrates by other metabolic reactions. The H_2-producing mutant used a combination of CO_2 fixation and H_2 production to oxidize excess reduced electron carriers. The majority of electrons for H_2 production were diverted away from CO_2 fixation for all substrates. Microarray and qRT-PCR analyses indicated that this shift of electrons towards H_2 involved transcriptional control of Calvin cycle gene expression. These observations pointed to the Calvin cycle as a convenient single target to disrupt to force more electrons towards H_2 production. Blocking Calvin cycle flux by mutation in the H_2-producing strain resulted in higher H_2 yields for all substrates. The increase in H_2 yield was proportional to the Calvin cycle flux in the parent strain for most substrates. These results demonstrate how systems level approaches, such as ^{13}C-metabolic flux analysis, can lead to effective strategies to improve product yield. Furthermore, our results underscore that the Calvin cycle and nitrogenase have important electron-accepting roles separate from their better known roles in biomass generation and ammonia production.

Progress Report

We established ^{13}C-labeling techniques to determine metabolic fluxes in batch cultures of *R. palustris*. This information provided key insights into the physiology of *R. palustris*, some of which provide a better understanding of its genome sequence (e.g., an additional isoleucine pathway was identified by the labeling studies that was missed during genome annotation), or could not have been predicted from the genome sequence (e.g., 80-90% of the NADPH needed for biosynthesis comes from a transhydrogenase-like reaction and not from canonical sources such as the pentose phosphate pathway and isocitrate dehydrogenase). Our data also quantitatively answered a long-standing question of why an electron accepting process (e.g., CO_2 fixation or H_2 production) is needed during photoheterotrophic growth on relatively oxidized organic compounds. Additionally, we identified the Calvin cycle as the primary competing pathway for electrons against H_2 production during growth on multiple substrates. We show that the Calvin cycle is a convenient, non-essential, single target for disruption that leads to higher H_2 yields during growth on all substrates tested.

Future Directions

Even in our Calvin cycle mutants, the majority of substrate electrons are incorporated into cellular biomass. For example, 15% of the electrons in acetate are used for H_2 production while 85% are used for biosynthesis. Thus, using non-growing cells should result in much higher H_2 yields. Indeed, *R. palustris* produces H_2 from acetate at 60% of the theoretical maximum yield when completely starved of nitrogen. *R. palustris* is potentially well suited for use as a non-growing biocatalyst since it can remain metabolically active for months in a non-growing state using light energy and cyclic photophosphorylation to satisfy maintenance

energy demands. By the same token, *R. palustris* can serve as a model bacterium for studying the physiology of non-growing cells. We are now determining the fate consumed electrons in nitrogen-starved *R. palustris* by quantifying excreted products and changes to its biomass composition. Additionally, we are adapting our ^{13}C-labeling protocols to determine metabolic flux distributions in non-growing *R. palustris*. The resulting information will be used to engineer *R. palustris* to improve the H_2 yield under non-growing conditions.

Publication list (including patents) acknowledging the DOE grant or contract

1. McKinlay, JB and CS Harwood. 2011. Calvin cycle flux, pathway constraints and substrate redox state together determine the H_2 biofuel yield in photoheterotrophic bacteria. *mBio.* In press.

2. McKinlay, JB and CS Harwood. 2010. Carbon dioxide fixation as a central redox cofactor recycling mechanism in bacteria. *Proceedings of the National Academy of Sciences USA*. 107: 11669-11675.

3. McKinlay, JB and CS Harwood. 2010. Mini-review. Photobiological production of hydrogen gas as a biofuel. *Current Opinion in Biotechnology.* 21: 244-251.

II.K.3 Fundamental Studies of Recombinant Hydrogenases

Michael W.W. Adams
University of Georgia
Life Sciences Bldg., Green Street
Athens, GA 30602
Phone: (706) 542-2060; Fax: (706) 542-2009
E-mail: adams@bmb.uga.edu

DOE Program Officer: Robert Stack
E-mail: Robert.Stack@science.doe.gov

Subcontractors: n/a

Objectives

The Hydrogen Fuel Initiative Workshop report (www.science.doe.gov/bes/hydrogen.pdf) sponsored by DOE stated that a fundamental understanding is needed of the structure and chemical mechanism of the enzyme complexes, known as hydrogenases, that support hydrogen generation, and that we need to understand how these catalysts are assembled with their cofactors into integrated systems. The proposed research specifically addresses the issues of understanding the assembly and organization of hydrogenases. This is the first step to ultimately reducing their size and complexity and of determining structure/function relationships, including energy conservation via charge separation across membranes.

Technical Barriers

Remarkably, in spite of the large amount of research that has been carried out on hydrogenases, it is not possible to readily manipulate or engineer the enzyme using molecular biology approaches since a recombinant form produced in suitable amounts in a suitable host is not available. Such resources are essential if we are to understand what constitutes a "minimal" hydrogenase, and to design such catalysts with desired properties, such as resistance to oxygen, extreme stability and specificity for a given electron donor. However, this is very challenging from a technical perspective as numerous gene products are required to synthesize the catalytic nickel-iron (NiFe) catalytic site of the protein and to assemble the mature, active hydrogenase enzyme.

Abstract

As a model system we are using the NADP-dependent, cytoplasmic NiFe-hydrogenase I (SHI) of *Pyrococcus furiosus,* a hyperthermophile that grows optimally at 100°C. We made two breakthrough discoveries during the funding period. First, we have generated the catalytically-active form of the heterotetrameric SHI by heterologous gene expression in the mesophilic bacterium, *Escherichia coli.* Second, a genetic system is now available in *P. furiosus* and this allows us to generate modified forms of the SHI by homologous gene expression. Specifically, we have overexpressed SHI in *P. furiosus* such that the organism produces an order of magnitude more of the native enzyme, increasing the amount purified from native biomass by up to 50-fold. We have also taken the first step toward generating a 'minimal' hydrogenase by homologous expression of an affinity-tagged heterodimeric form of the heterotetrameric enzyme and by so doing we have also changed its electron carrier specificity. In contrast to the native form, the heterodimer does not use NADP/H as an electron carrier and directly interacts with the pyruvate-oxidizing enzyme, pyruvate ferredoxin oxidoreductase, thereby enabling direct hydrogen production from pyruvate by an as yet unknown mechanism.

Progress Report

1. Production of the Native Tetrameric Form of *P. furiosus* hydrogenase I (SHI) in *E. coli.*

Hydrogenases are extremely complex, air-sensitive enzymes that achieve catalysis using a binuclear nickel-iron cluster that contain cyanide and carbon monoxide ligands to the iron atom (see **Figure 1**). This cluster is covalently bound to the protein and receives electrons for proton reduction via multiple iron-sulfur (FeS) clusters. A very complicated maturation process is required to synthesize the [NiFe]-catalytic center and insert it into the apoenzyme (see **Figure 1**). We successfully produced in *Escherichia coli* the recombinant form of *P. furiosus* SHI using novel expression vectors for the co-expression of thirteen *P. furiosus* genes (four structural genes encoding the hydrogenase and nine encoding maturation proteins). Remarkably, the native *E. coli* maturation machinery will also generate a functional *P. furiosus* hydrogenase when provided with only the genes encoding the hydrogenase subunits and a single protease (frxA) from *P. furiosus*. Another novel feature is that its expression was induced by anaerobic conditions, whereby *E. coli* was grown aerobically and production of recombinant hydrogenase was achieved by simply changing the gas feed from air to an inert gas (N_2). The recombinant enzyme was purified and shown to be functionally similar to the native enzyme purified from *P. furiosus*, including its high stability towards oxygen ($t_{1/2} > 20$ hr in air) and the use of NADP(H) as an electron carrier. An enzyme that evolves hydrogen from NADPH holds promise for large-scale harvesting of molecular hydrogen from renewable biomass, and the methodology to produce the key hydrogen-producing enzyme has now been established.

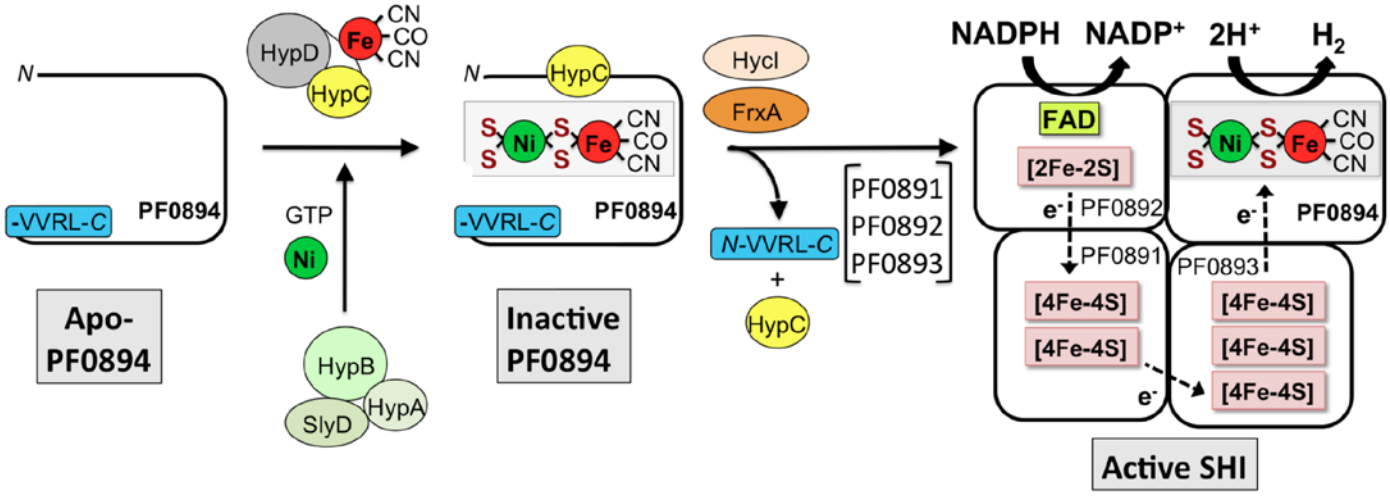


FIGURE 1. Biosynthesis of *P. furiosus* hydrogenase I (SHI) in *E. coli.*

2. Over-Production of the Native Tetrameric Form of *P. furiosus* Hydrogenase I (SHI) in *P. furiosus.*

A major breakthrough in the past year has been the development of a genetics system in *P. furiosus* in another on-going project in the PI's laboratory. We are utilizing this to develop expression systems for the hydrogenase I. This gives us the capability for both heterologous (in *E. coli*) and homologous (in *P. furiosus*) systems to engineer *P. furiosus* hydrogenases. Our first objective was to obtain a *P. furiosus* strain in which SHI was significantly over-expressed and where the protein contained an affinity tag for rapid purification. To achieve this we utilized a parental strain that had a deletion in a gene (*pyrF*) required for uracil biosynthesis in *P. furiosus.* This requires uracil for growth and is resistance to the uracil biosynthetic pathway inhibitor, 5-fluoroorotate (5-FOA). A 'knock-in' cassette was constructed containing the upstream (UFR) and downstream (DFR) flanking regions of the promoter region for SHI (P_{SHI}), together with *pyrF* (driven by the promoter for glutamate dehydrogenase, P_{GDH}), a terminator sequence (T1) and replacing P_{SHI} with P_{SLP}, the promoter for the S-layer protein (PF1399), and the strep-II tag (8 amino-acids) at the N-terminus of the PF0891 subunit of SHI. P_{SLP} is one of the most highly expressed genes in *P. furiosus* based on our DNA microarray data.

The specific hydrogenase activity of cytoplasmic extracts of wild type *P. furiosus* cells and the Δ*pyrF* strain were 0.77 ± 0.5 units/mg. The two strains in which SHI was over-expressed (OE-SHI) by P_{SLP} showed no obvious phenotype but their specific activities were 8.2 ± 0.2 units/mg, representing an increase of more than an order of magnitude in hydrogenase activity. The dramatic overexpression of SHI protein in the OE-SHI strains was confirmed by immuoanalysis using antibodies to PF0894 (the catalytic subunit of SHI). Given the extremely complex maturation process that is involved in synthesizing the hydrogenase, the results show that the wild-type level of the maturation machinery is able to process >10-fold more SHI than it usually does. This was somewhat surprising since no attempt was made to up-regulate these processing genes. Unfortunately, the Strep-II tag on PF0891 appeared to be partially buried as OE-SHI bound weakly to the strep-tactin column. Nevertheless, while five chromatography steps are normally needed to purify native SHI yielding 2-10 mg /500 g of cells, the OE-SHI strain yielded 11 mg/50 g of cells. The native and OE-forms had similar thermal stabilities and oxygen sensitivities.

3. Over-Production of a Heterodimeric form of *P. furiosus* Hydrogenase I (SHI) in *P. furiosus.*

As a first step towards making a 'minimal' hydrogenase, we produced the heterodimeric form of SHI containing only the large catalytic (LSU; PF0894) and the small FeS-cluster containing subunit (SSU, PF0894), as shown in **Figure 2**. The SSU contained an N-terminal His_9-tag and expression was driven by the P_{SLP} promoter. Recombinant Pf cells had no significant phenotype and a total of ~6 mg of the pure protein (148 U/mg) was obtained from the Ni-NTA column using 50 g of cells. The OE-dimer was less thermostable ($t_{1/2}$ 1 hr at 90°C) and more oxygen sensitive ($t_{1/2}$ 1 hr in air) than native heterotetrameric form of SHI. The dimer did not evolve H_2 from NADPH (since it lacked FAD-containing PF0892) nor did it evolve H_2 from reduced ferredoxin of *P. furiosus.* However, in contrast to the native form, the heterodimer directly interacted with the pyruvate-oxidizing enzyme, pyruvate ferredoxin oxidoreductase (POR) from *P. furiosus,* thereby enabling direct hydrogen production from pyruvate. It therefore appears that the novel heterodimeric hydrogenase is able to accept electrons by a direct enzyme-enzyme (hydrogenase-POR) interaction although the mechanism is unknown.

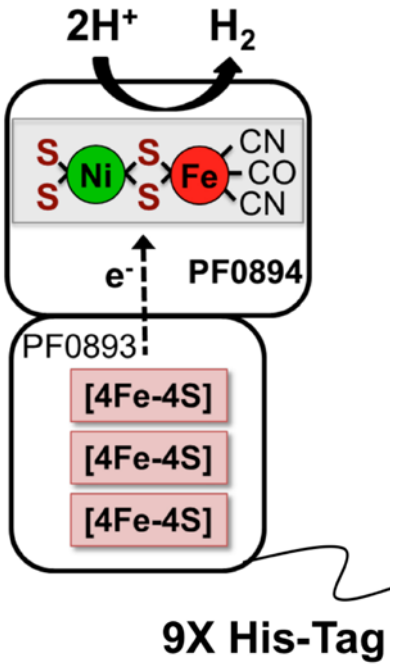


FIGURE 2. Structure of the heterodimeric form of SHI.

Future Directions

The longer term objectives of our research are to capitalize on the breakthroughs made in the current funding period and to a) optimize production of tagged recombinant forms of the cytoplasmic hydrogenase of *P. furiosus*, b) to obtain soluble and membrane-bound tagged recombinant forms of the ferredoxin-dependent, membrane-bound hydrogenase that is also present in *P. furiosus,* an enzyme that we have shown simultaneously evolves H_2 and pumps protons, c) to design 'minimal' hydrogenases with tailored catalytic activity, oxygen sensitivity and electron donor specificity, and d) to design membrane-bound hydrogenases in artificial membranes that generate ion gradients and evolve hydrogen. Such enzymes have potential utility in various biotechnological applications.

Publication list (including patents) acknowledging the DOE grant or contract

1. Sun, J., Hopkins, R.C., Jenney, F.E., Jr., McTernan, P. and Adams, M.W.W. (2010) Heterologous Expression and Maturation of an NADP-Dependent [NiFe]-Hydrogenase: A Key Enzyme in Biofuel Production. *PLoS ONE* 5:e10526, 1-11

2. Baker, S.E., Hopkins, R.C., Blanchette, C.D., Walsworth, V.L., Sumbad, R., Fischer, N.O., Kuhn, E.A., Coleman, M., Chromy, B.A., Létant, S.E., Hoeprich, P.D., Adams, M.W.W., and Henderson, P.T. (2009) "Hydrogen production by a hyperthermophilic membrane-bound hydrogenase in soluble nanolipoprotein particles" *J. Am. Chem. Soc.* 131, 7508-9

3. Ye, X., Wang, Y., Hopkins, R.C., Adams, M.W.W., Evans, B.R., Mielenz, J.R. and Zhang, Y.H. (2009) "Spontaneous high-yield production of hydrogen from cellulosic materials and water catalyzed by enzyme cocktails" *Chem. Sus. Chem.* 2, 149-152

4. Jenney, F.E., Jr. and Adams, M.W.W. (2008) "Hydrogenases of the model hyperthermophiles" *Ann. N.Y. Acad. Sci.* 1125, 252-266

5. Chou, C.-J, Jenney, F.E., Jr., Adams, M.W.W. and Kelly, R.M. (2008) "Hydrogenesis in hyperthermophilic microorganisms: implications for biofuels" *Metabolic Engineer.* 10, 394-404

6. Adams, M.W.W., Hopkins, R.C., Jenney, F.E., and Sun, J. (2007) Hydrogenase Polypeptides and Methods of Use, US Provisional Patent Application (#61/005,383; filed 12/05/07)

7. Schut, G., Bridger, S.L. and Adams, M.W.W. (2007) Insights into the metabolism of elemental sulfur by the hyperthermophilic archaeon *Pyrococcus furiosus*: characterization of a coenzyme A-dependent NAD(P)H sulfur oxidoreductase. *J. Bacteriol.* 189, 4431-4441

8. Zhang, Y.H.P., Evans, B.R., Mielenz, J.R., Hopkins, R.C. and Adams, M.W.W. (2007) High yield hydrogen production from starch and water by a synthetic enzyme pathway. *PLoS One* 5, e456 (1-6)

II.K.4 Prospects for Hydrogen Production from Formate by *Methanococcus maripaludis*

John A. Leigh[1]*, Murray Hackett[2], William B. Whitman[3], Boguslaw Lupa[3], Kyle C. Costa[1], and Thomas J. Lie[1]

Departments of Microbiology[1] and Chemical Engineering[2], University of Washington, Seattle, WA USA; and

[3]Department of Microbiology, University of Georgia Athens, GA USA

*University of Washington
Box 357242
Seattle, WA 98195-7242
Phone: (206) 685-1390; Fax: (206) 543-8297
E-mail: leighj@u.washington.edu

DOE Program Manager: Robert Stack
Phone: (301) 903-5652
E-mail: Robert.Stack@science.doe.gov

Objectives

We seek to understand the following features of hydrogenotrophic methanogenesis, all of which relate to strategies for the production of hydrogen from formate: First, for methanogens that use formate, how does formate feed electrons into the methanogenic pathway? Second, what is the basis for the uncoupling of methanogenesis from growth that is observed in hydrogenotrophic methanogens? Third, nitrogenase can be used to produce hydrogen; how is its activity regulated? Fourth, re-utilization of hydrogen must be prevented; what are the metabolic pathways be which hydrogen is utilized?

Technical Barriers

First, we must learn how to sustain growth, methanogenesis, and hydrogen production on formate in bioreactors. Second, we need to optimize the uncoupling of metabolism from growth. Third, we need to maintain maximum nitrogenase activity. Fourth, hydrogenotrophic methanogens use hydrogen; we need to figure out how to prevent re-utilization of hydrogen that is produced.

Abstract

Most methanogenic Archaea are hydrogenotrophic, specializing in the use of hydrogen to reduce CO_2 to methane. Even though these organisms have multiple hydrogenases that *use* hydrogen, there is good potential to use them for the net *production* of hydrogen. This is because some species can use alternative electron donors, most notably formate, and because some species have nitrogenases that can produce large amounts of hydrogen. *Methanococcus maripaludis* is one such species. In addition, *M. maripaludis* is the premiere model for hydrogenotrophic methanogens, grows well under laboratory conditions, and can be manipulated using an extensive set of genetic tools. In past work we studied the mechanisms for regulation of nitrogenase at the transcriptional and enzyme levels, in the process discovering and characterizing two novel regulators and generating mutants that had constitutive nitrogenase activity (1, 2). In recent work on methanogenesis, we have focused on mechanisms of energy conservation and pathways of hydrogen and formate utilization. R. Thauer proposed in 2008 that energy conservation depends on electron bifurcation (3). The pathways of methanogenesis and electron bifurcation are illustrated in Figure 1. Electrons from hydrogen reduce the flavin of heterodisulfide reductase (Hdr), where electron flow then bifurcates, reducing heterodisulfide (exergonic) and coupling this to reduction of a ferredoxin (endergonic). Since the reduced ferredoxin may be used for the endergonic first step on methanogenesis, chemiosmotic membrane potential may be saved for ATP production. Thauer's group subsequently showed that electron bifurcation occurs (4). However, whether electron bifurcation directly couples heterodisulfide reduction to the first step in methanogenesis has not been proven, nor has it been shown whether formate can replace hydrogen as the electron donor to Hdr. In addition, since growth yields vary markedly, the efficiency of energy conservation is also variable. Uncoupling of methanogenesis from growth could be useful in hydrogen production technologies.

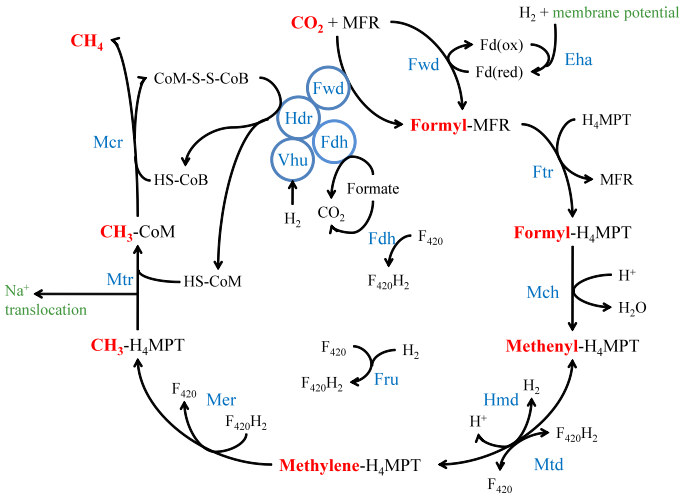


FIGURE 1. Methanogenic pathway showing the electron bifurcating Hdr complex and direct association of formate dehydrogenase.

Progress Report

Protein complexing suggests electron bifurcation and electron delivery from formate to heterodisulfide reductase. By purifying Hdr from *M. maripaludis*, we discovered a protein complex that contains not only Hdr but a hydrogenase (Vhu), a formate dehydrogenase (Fdh), and formylmethanofuran dehydrogenase (Fwd) (5). The existence of the complex supports a model of electron flow in which either hydrogen or formate directly reduce the flavin of Hdr, and electron bifurcation leads to the reduction of heterodisulfide and of CO_2 to formylmethanofuran (formyl-MFR). In addition, in a mutant deleted for Vhu, growth on hydrogen was poor but growth on formate was as good as wild type.

Genetic analysis reveals three pathways of hydrogen utilization for methanogenesis and an independent pathway of formate utilization. We have generated numerous deletion mutants in genes for hydrogenases. Only in a mutant deficient in three hydrogenases could we eliminate the ability of hydrogen to support methanogenesis. Thus, we eliminated F_{420}-reducing hydrogenase (Fru), Hdr-associated hydrogenase (Vhu), and the hydrogenase Hmd that can act in concert with Mtd to reduce F_{420} (6). This mutant required formate for growth even when hydrogen was present. It also required hydrogen, and evidence to be presented suggests that the hydrogen requirement is restricted to biosynthesis. This result alters the previous view in which methanogenesis from formate required production of hydrogen from formate. Instead, it now appears that formate can support methanogenesis directly (5, 7). In addition, the multiple-hydrogenase mutant should be unable to re-utilize for methanogenesis any hydrogen that is produced

Uncoupling of methanogenesis from growth does not depend on the energy-conserving hydrogenase Ehb. Growth yields (cell mass produced per methane produced) of *M. maripaludis* were three-fold higher under hydrogen limitation (in chemostats) compared to hydrogen excess. Thus, under hydrogen excess conditions metabolism partially uncouples from growth, enhancing prospects for growth-independent hydrogen production. Uncoupling could occur by several mechanisms, including depletion of chemiosmotic membrane potential by the energy-conserving hydrogenase Ehb (8). However, uncoupling still occurred in a *ehb* mutant.

Future Directions

Our strategy for hydrogen production from formate involves the derepression of nitrogenase in a mutant that is deficient in hydrogen re-uptake. Based on the above results, we are now ready to construct a strain that fulfills these criteria. In addition, using the purified Hdr complex we will test in vitro whether formate is indeed a direct electron donor and whether the complete pathway of electron bifurcation occurs. Finally, to maximize hydrogen production we seek to optimize the uncoupling of methanogenesis from growth, in order to direct maximal ATP to nitrogenase. To this end, we will test several hypotheses for the basis of uncoupling.

References

1. Dodsworth JA, Leigh JA. Regulation of nitrogenase by 2-oxoglutarate-reversible, direct binding of a PII-like nitrogen sensor protein to dinitrogenase. Proc Natl Acad Sci U S A. 2006;103(26):9779-84.

2. Lie TJ, Wood GE, Leigh JA. Regulation of *nif* expression in *Methanococcus maripaludis*: roles of the euryarchaeal repressor NrpR, 2-oxoglutarate, and two operators. J Biol Chem. 2005;280(7):5236-41.

3. Thauer RK, Kaster AK, Seedorf H, Buckel W, Hedderich R. Methanogenic archaea: ecologically relevant differences in energy conservation. Nat Rev Microbiol. 2008;6(8):579-91.

4. Kaster AK, Moll J, Parey K, Thauer RK. Coupling of ferredoxin and heterodisulfide reduction via electron bifurcation in hydrogenotrophic methanogenic archaea. Proc Natl Acad Sci U S A. 2011;108(7):2981-6.

5. Costa KC, Wong PM, Wang T, Lie TJ, Dodsworth JA, Swanson I, et al. Protein complexing in a methanogen suggests electron bifurcation and electron delivery from formate to heterodisulfide reductase. Proc Natl Acad Sci U S A. 2010;107(24):11050-5.

6. Hendrickson EL, Leigh JA. Roles of coenzyme F_{420}-reducing hydrogenases and hydrogen- and F_{420}-dependent methylenetetrahydromethanopterin dehydrogenases in reduction of F_{420} and production of hydrogen during methanogenesis. J Bacteriol. 2008;190(14):4818-21.

7. Lupa B, Hendrickson EL, Leigh JA, Whitman WB. Formate-dependent H_2 production by the mesophilic methanogen *Methanococcus maripaludis*. Appl Environ Microbiol. 2008;74(21):6584-90.

8. Major TA, Liu Y, Whitman WB. Characterization of energy-conserving hydrogenase B in *Methanococcus maripaludis*. J Bacteriol. 2010;192(15):4022-30.

Publication list (including patents) acknowledging the DOE grant or contract

1. Costa KC, Wong PM, Wang T, Lie TJ, Dodsworth JA, Swanson I, et al. Protein complexing in a methanogen suggests electron bifurcation and electron delivery from formate to heterodisulfide reductase. Proc Natl Acad Sci U S A. 2010;107(24):11050-5.

2. Lupa B, Hendrickson EL, Leigh JA, Whitman WB. Formate-dependent H_2 production by the mesophilic methanogen *Methanococcus maripaludis*. Appl Environ Microbiol. 2008;74(21):6584-90.

3. Hendrickson EL, Leigh JA. Roles of coenzyme F_{420}-reducing hydrogenases and hydrogen- and F_{420}-dependent methylenetetrahydromethanopterin dehydrogenases in reduction of F_{420} and production of hydrogen during methanogenesis. J Bacteriol. 2008;190(14):4818-21.

4. Major TA, Liu Y, Whitman WB. Characterization of energy-conserving hydrogenase B in *Methanococcus maripaludis*. J Bacteriol. 2010;192(15):4022-30.

II.K.5 Structural, Functional, and Integration Studies of Solar-Driven, Bio-Hybrid, H_2-Producing Systems

Maria L. Ghirardi (Principal Investigator),
P.W. King*, K. Kim, C. Chang, D. Gust, A.L. Moore, T.A. Moore, and M.J. Heben
National Renewable Energy Laboratory
1617 Cole Boulevard
Golden, CO 80401
Phone: (303) 384-6312; Fax: (303) 384-7836
E-mail: maria.ghirardi@nrel.gov

DOE Program Manager: Gail McLean
Phone: (301) 903-7807
E-mail: gail.mclean@science.doe.gov

Objectives

The overall goals of the project are to develop an understanding of [FeFe]-hydrogenases (H_2ase) as model hydrogen (H_2) activation catalysts, and to elucidate the parameters that control hydrogen production by H_2ases in photoelectrochemical cells and molecular photocatalytic complexes. The research objectives include: (i) developing theoretical models of H_2ase to understand electron/proton-transfer (ET and PT) and catalysis; (ii) characterizing redox-induced changes in H_2ase catalytic site structures using mutagenesis and infra-red (FTIR) spectroscopy; (iii) optical and electronic studies of H_2ase-carbon nanotube and nanoparticle complexes; and (iv) electrochemical characterization of native and structurally minimized H_2ases on Au-SAM electrodes using electrochemical STM. These efforts will provide fundamental knowledge how H_2, and how to functionally integrate them as components of artificial hydrogen production schemes.

Technical Barriers

Developing efficient solar hydrogen production requires robust and efficient catalysts, and the understanding of how to integrate them with photoactive materials into efficient artificial systems. The H_2ases possess many characteristics of an ideal catalyst, and elucidation their basic structure-function properties can help to guide efforts to develop synthetic catalysts. A fundamental challenge is to resolve how the metallo-clusters, essential ligands and the surrounding peptide function together to achieve an overall efficient catalytic process. Another is how to control molecular interactions between H_2ases and photoactive molecules to achieve self-assembly into bio-hybrid photocatalytic complexes for hydrogen production.

Abstract

We seek to advance the understanding of [FeFe]-hydrogenases (H_2ase) structure-function, and the parameters that control assembly, charge-transfer and catalytic efficiencies of H_2ases as model catalysts in bio-hybrid, solar H_2-production systems. The knowledge that is gained will help to elucidate the biochemistry of H_2 activation, and support design and development of more efficient solar-to-H_2 conversion by artificial photosynthetic schemes. H_2ases are expressed using a recombinant expression system, and purified enzymes are characterized using a combination of biochemical, electrochemical (electrochemical Scanning Tunneling Microscopy, STM) and spectroscopic (FTIR) techniques. The assembly and characterization of purified H_2ases in bio-hybrids is being studied using solution-phase, photoactive nanoparticles, and as an electrocatalyst in photoelectrochemical cells. Together with the experimental studies, theoretical models are being developed to investigate the H_2ase catalytic site, electron-transfer [FeS]-clusters, substrate transfer pathways, and bio-hybrid complexes. The latest progress in these respective research areas will be summarized.

Progress Report

(i) Computational chemistry studies of H-cluster models with perturbed diatomic ligands have revealed a potential role of the bridging ligand in buffering charge upon enzyme reduction during catalysis.

(ii) A quantum chemical H_2ase model encompassing the H-cluster, accessory [4Fe-4S]-clusters and surrounding protein was constructed. Custom computational methods allow for breaking the spin symmetry within accessory [4Fe-4S]-clusters, and integration of the initial gas-phase calculation into a QM/MM model of the complete H_2ase. The free energies along PT pathways were investigated using QM/MM and umbrella sampling techniques. Several important residues were identified and pK_a values estimated by thermodynamics integration method.

(iii) Brownian dynamics and molecular dynamics simulation techniques predicted the binding structures between H_2ase and SWNTs or bulk carbon surfaces, and ET rates. ET appears to be at least a 100-fold faster for SWNTs than for a bulk carbon surface, and independent of SWNT diameter.

(iv) The native H_2ase has been successfully adsorbed to Au electrodes bearing self-assembled thiol-based monolayers (SAMs) and retains activity. Binding is via interactions between positively charged patches on the enzyme and carboxylate groups on the SAM.

Single-molecule images have been obtained in an electrochemical STM and suggest tunneling currents increase under an applied bias. Removal of adsorbed H_2ase from the STM surface helped confirm that the features observed with the STM are H_2ase.

(v) Electrostatically guided assemblies of H_2ase with mercaptopropionic acid capped CdTe nanocrystals (NC) and CdS nanorods have been successfully formed in solution. Both types of complexes were isolated by gel electrophoresis and showed evidence of compositional heterogeneity. Photoluminescence and hydrogen evolution studies suggest that competition of electron transfer with internal relaxation pathways is favored for 1:1 molecular ratios. We have preliminary Transient Absorption kinetics for H_2ase:CdS complexes that shows the estimated electron-transfer step from CdS to H_2ase occurs at a timescale of ~10^2 nsec, whereas internal relaxation of CdS occurs at ~10 nsec.

Future Directions

- Tunneling currents will be examined between accessory [4Fe-4S]-clusters and the H-cluster in the H_2ase model. Dynamics trajectories will also be analyzed to determine protein conformational features correlating with large couplings, as approximated by empirical pathways analysis. The free energies along the PT pathways will be further refined based on the *pKa* calculation results.
- We will continue to investigate the binding free energies for H_2ase with SWNTs and bulk carbon surfaces using MD simulation techniques, and develop these models to predict binding modes, orientations and ET processes.
- We will continue to characterize redox-induced changes in catalytic site structures of H_2ases using FTIR spectroscopy to define ligand conformations of oxidized and reduced states, and use mutagenesis to characterize the role of the peptide environment.
- Single-molecule electrochemistry of immobilized H_2ase on Au-electrodes will continue to be developed to characterize the binding interaction, tunneling currents and the operating potentials of the enzyme. Mutated H_2ases lacking individual accessory iron-sulfur clusters functioning in electron-transfer will be studied in order to learn more about the conductive path through the protein.
- We will develop and apply FTIR spectroscopy to characterize the binding and charge-transfer reactions between H_2ases and SWNTs both in solution and in films, to identify how the SWNT intrinsic electronic properties affect redox active modes of H_2ase.
- Characterize redox-induced changes in H_2ase-NC complexes under photoexcitation using steady-state and time-resolved optical and FTIR techniques.

Publication list (including patents) acknowledging the DOE grant or contract

1. Cohen, J., and Schulten, K. **2007**. O_2 migration pathways are not conserved across proteins of a similar fold. *Biophys. J.* **93:**3591-600.

2. McDonald, T.J., Svedruzic, D., Kim, Y-H., Blackburn, J.L., Zhang, S.B., King P.W., and Heben, M.J. **2007**. Wiring up hydrogenase with single-walled carbon nanotubes. *NanoLetts.* **7**:3528-34.

3. Hambourger, M., Gervaldo, M., Svedruzic, D., King, P.W., Gust, D., Ghirardi, M., Moore, A.L. and Moore, T.A. **2008**. [FeFe]-hydrogenase-catalyzed H_2 production in a photoelectrochemical biofuel cell. *JACS*. **130**(6):2015-22.

4. Blackburn, J.L., Svedruzic, D., McDonald, T.J., Kim, Y-H., King P.W. and M.J. Heben. 2008. Raman spectroscopy of charge transfer interactions between single wall carbon nanotubes and [FeFe] hydrogenase. *Dalton Trans.* 5454-61.

5. Cohen, J., Olsen, K.W., and Schulten, K. **2008.** Finding gas migration pathways in proteins using implicit ligand sampling. *Meth. Enzymol.* **437**:439-57.

6. Gust, D., Kramer, D., Moore, A., Moore, T.A., and Vermaas, W. **2008**. Engineered and artificial photosynthesis: human ingenuity enters the game. *MRS Bull.* **33**:383-87.

7. Hambourger, M., Moore, G.F., Kramer, D.M., Gust, D., Moore, A.L., and Moore, T.A. **2009.** Biology and technology for photochemical fuel production. *Chem. Soc. Rev.* **38**:25-35.

8. Chang, C.H., and Kim, K. **2009.** Density functional theory calculation of bonding and charge parameters for molecular dynamics studies on [FeFe]-hydrogenases. *J. Chem. Theory Comput*. **5**(4):1137-45.

9. Hambourger, M., Kodis, G., Vaughn, M., Moore, G.F., Gust, D., Moore, A.L., and Moore., T.A. **2009**. Solar energy conversion in a photoelectrochemical biofuel cell. *Dalton Trans.* 9979-89.

10. Brown, K.A., Dayal, S., Ai, X., Rumbles, G. and King, P.W. **2010**. Controlled assembly of hydrogenase-CdTe nanocrystal hybrids for solar hydrogen production. *JACS*. **132**(28):9672-80.

II.K.6 Genes Needed For H_2 Production by Sulfate Reducing Bacteria

Lee R. Krumholz[1*] (Principal Investigator),
Xiangzhen Li[1], Peter Bradstock[1]
Michael McInerney[1], Jizhong Zhou[1], Judy Wall[2]
[1]The University of Oklahoma, Norman, OK and
[2]University of Missouri, Columbia, MO.
Email: krumholz@ou.edu

DOE Program Manager: Robert Stack
Phone: (301) 903-5652
E-mail: Robert.Stack@science.doe.gov

Objectives

Research objectives are to study genes and proteins within *Desulfovibrio* strain G20 that are involved in syntrophic interactions in coculture with a Syntrophic butyrate degrading bacterium and a during lactate oxidation in coculture with a hydrogenotrophic methanogen. Specifically, this has involved screening mutants for loss of ability to grow in coculture in order to identify genes in *Desulfovibrio* needed for syntrophic growth. Mutants, mutated genes and the proteins encoded by these genes are being characterized to determine their specific function during syntrophic growth. Characterization involves a determination of the effect of the mutation on growth characteristics as well as the properties of the protein encoded by that gene.

Technical Barriers

- Identify key enzymes involved in H_2 production by *Desulfovibrio*.
- Characterize these enzymes to determine their role in H_2 production.

Abstract

In order to identify proteins involved in H_2 metabolism in *Desulfovibrio desulfuricans G20,* transposon insertion mutants deficient in syntrophic growth were identified and are being characterized. A screening done with *G20* in a hydrogen uptake role in coculture with *Syntrophomonas wolfeii* found that mutants for the flhA flagellar biosynthesis gene, the fliF flagellar ring gene, and the pilA pilus assembly gene were unable to grow, suggesting a role for chemotaxis or other flagellar function in syntrophy. Microscopy showed the flhA mutant to lack flagella and both flagella mutants and the pilus mutant produced considerably less biofilm than the parent strain. Recent experiments suggest that the flagella mutants grow more slowly on H_2, perhaps indicating a need to motility during H_2 growth in laboratory cultures. We have also recently identified mutants in a membrane protein annotated as Rnf. This protein appears to be involved in H_2 uptake as G20 mutants will not grow on H_2 or formate. We are currently identifying the specific mechanisms by which the above proteins allow the cell to grow with H_2.

The membranes of several mutants of *Desulfovibrio vulgaris* including a qmo (quinone membrane oxidoreductase) mutant were extracted and separated on Blue Native gels to identify large protein complexes. The *qmo* mutant was found to be missing several bands compared to the parental strain. These bands were identified to be the qmo protein complex as well as a complex of the qmo and APS reductase, suggesting that these two proteins operate as a multiprotein complex during H_2 oxidation. Affinity tagged genes are being used to verify this phenomenon as well as to identify other proteins that may be involved in this electron transport complex.

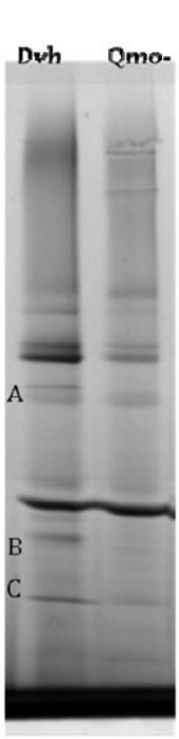
Progress Report

Genes involved in syntrophic growth. A number of genes have been identified which appear to be required for syntrophic growth of *Desulfovibrio* as the H_2 user with *Syntrophomonas wolfei*. Some characterization experiments have been done and results are presented below (table 1). Results show that both the presence of flagella as well as the Rnf protein play a role in H_2 uptake. Rnf has been characterized in *Rhodobacter capsulatus* and shown to be involved in nitrogen fixation (1). It is a large membrane spanning protein with homology to energy conserving oxidoreductases in many other bacteria. Although some species of *Desulfovibrio* contain genes for nitrogen fixation, strain G20 does not, suggesting that Rnf plays a different role. The mechanisms for disruption of H_2 metabolism will be investigated.

Membrane Protein Complexes in Desulfovibrio. Several mutants were grown in culture and their membranes were isolated and run on Blue Native gels to determine whether they formed large complexes. Gels run with a mutant in the QMO complex had three absent bands in comparison to the parental strain (Fig. 1). Bands were excised and proteins were identified by mass spectroscopy. One of the bands (C) appears to be the qmo complex while another band (B) appears to be a complex containing both QMO and APS reductase. This complex has been speculated to operate together for the reduction of sulfate (APS) to sulfite as both QMO genes and APS reductase genes are located adjacent to each other on the chromosome (2). As well, the QMO mutant will grow on sulfite but not on sulfate (3). This is the first evidence showing a physical interaction between these proteins. Affinity tagged strains have been produced and in

TABLE 1. Growth and biofilm formation by pure cultures of some syntrophy mutants. Results shown that mutations in flagellar function and pilus function affect both biofilm formation and growth on H_2. As well, rnf mutants do not grow on H_2. ND-not determined.

Gene number	Gene Name	Proposed Function	Growth			Biofilm Formation
			H2	Formate	Pyruvate	
Dde_0380	flhA	Flagella Biosynthesis	++	+++	++++	+
Dde_2933	qrc	Hydrogen metabolism	-	-	++	ND
Dde_0353	fliF	Flagellar Ring Protein	++	+++	++++	+
Dde2365	tadC	Pilus assembly prot.	++	+++	++++	++
Dde_0585	rnfA	Electron Flow	-	-	++++	ND
Dde_0582	rnfD	Electron Flow	-	-	++++	ND
Parent			+++	+++	++++	+++



	Label	Name	Unique Peptides	Spectral Count
A	DVU0847	ApsA	10	25
	DVU0694	QRC	12	13
	DVU3319	proline dehydrogenase	13	13
B	DVU0847	ApsA	9	22
	DVU0851	hypothetical protein (Qmo)	11	21
	DVU1820	preprotein translocase, YajC subunit	4	15
	DVU0849	QmoB	10	13
	DVU1067	Bmp family membrane protein	7	10
	DVU0848	QmoA	8	8
	DVU0846	ApsB	4	7
C	DVU0849	qmoB	21	52
	DVU0848	qmoA	14	28
	DVU0851	hypothetical protein (Qmo)	7	9
	DVU0850	qmoC	3	4
	DVU0847	ApsA	3	3

FIGURE 1. Blue native gel and peptide identification data for QMO mutant and WT.

the presence of detergent, both QMO and APS reductase have been purified to homogeneity from cell extracts of strain G20. These enzymes are expected to be present in complexes with each other as shown in figure 1. SDS gel banding patterns of each of the purified enzymes are identical suggesting that they all the contain the same set of proteins as a complex. However, to be certain we are in the process of identifying protein bands from SDS gels using mass spectroscopy. This will prove the association of QMO reductase and determine whether any other proteins are associated with this complex.

Future Directions

Determination of the role of syntrophy genes. RNF appears to play a role in the syntrophic interaction. The inability of G20 rnf mutants to grow in the presence of H_2 may be the reason for its inability to grow syntrophically. Rnf is a large membrane spanning protein complex that couples electron transfer to energy transduction (1). It is thought to also involve quinone reduction. The growth of rnf mutants will be further investigated to determine whether Rnf may interact with QMO or with DSR directly

of perhaps whether it plays a more indirect role in H_2 uptake. This is the first study that I am aware of that implicates Rnf in H_2 metabolism by *Desulfovibrio*. A group of three flagella and pilus genes have also been shown to be involved in syntrophy. The specific role that these genes play will be investigated. Through growth experiments, chemotaxis studies as well as experiments looking at the physical interaction between the two members of the syntrophic consortium

Membrane Protein Complexes in Desulfovibrio. This work will build on the above results showing the presence of respiratory membrane complexes in strain G20. Our recent work has demonstrated a role for a protein now referred to as Qrc (Mop) in the uptake of H_2 by *Desulfovibrio* G20. Qrc has recently also been purified and shown to interact with both tetraheme cytochrome C3 in the periplasm and menaquinone (most likely in the membrane) (4). It is therefore possible that Qrc interacts directly with QMO for the oxidation of H_2 coupled to the reduction of adenosine phosphosulfate (APS). We will test this hypothesis by reconstituting purified enzymes tetraheme cytochrome C3, Qrc, QMO, APS reductase available with affinity tags along with menaquinone to determine whether this process can occur in vitro.

Transcriptomic Analysis of Syntrophic Cocultures. A number of genes have been identified that are involved in syntrophic interactions, based on growth assays. In the original proposal, we described experiments using microarrays to validate the role of these genes in syntrophy. New and more powerful technologies are available and the most promising of these is RNA-seq. This technique involves extracting mRNA from active cultures and sequencing the RNA using Illumina technology. This technique is advantagious over microarrays in that there is no up front cost and effort and information is not only obtained on the amount of each transcript present, but the complete sequence of each transcript is also obtained providing information on operon structure, etc. Pure cultures and syntrophic co-cultures will be grown to log phase, cells will be harvested and transcript abundance will be determined. We will compare cocultures of *Syntrophomonas wolfei*, *Syntrophus aciditrophicus* and *Desulfovibrio* G20 grown with *Methanospirillum hungatei*. Pure cultures will also be tested. In this way, comparisons can be made and genes expressed only in co-cultures can be compared between cocultures to identify those with a direct role in coculture interaction.

References

1. Kumagai, H., T. Fujiwara, H. Matsubara, and K. Saeki. 1997. Membrane localization, topology, and mutual stabilization of the rnfABC gene products in *Rhodobacter capsulatus* and implications for a new family of energy-coupling NADH oxidoreductases. *Biochemistry 36* (18), 5509-5521

2. Pires, R.H., A.I. Lourenco, F. Morais, M. Teixeira, A.V. Xavier, L.M. Saraiva, I.A.C. Pereira. 2003. A novel membrane-bound respiratory complex from *Desulfovibrio desulfuricans* ATCC 27774, Biochim. Biophys. Acta. 1605: 67-82.

3. Zane, G.M., H. Yen, and J.D. Wall. 2010. Effect of the deletion of qmoABC and the promoter distal gene encoding a hypothetical protein on sulfate-reduction in *Desulfovibrio vulgaris* Hildenborough. Appl. Environ. Microbiol. 2010 0: AEM.00691-10

4. Venceslau, S.S., R.R. Lino and I.A.C. Pereira. The Qrc membrane complex, related to the alternative complex III, is a menaquinone reductase involved in sulfate respiration. J. Biol. Chem. jbc.M110.124305. First Published on May 24, 2010.

Publication list (including patents) acknowledging the DOE grant or contract

1. Li, X., Q. Luo, N.Q. Wofford, K.L. Keller, M.J. McInerney, J.D. Wall and L.R. Krumholz. 2009. A molybdopterin oxidoreductase is involved in H_2 oxidation in Desulfovibrio *desulfuricans* G20. J. Bacteriol. 191: 2675–2682.

2. Zane, G.M., Yen, H.B. and J.W. Wall. Effect of the Deletion of *qmoABC* and the Promoter-Distal Gene Encoding a Hypothetical Protein on Sulfate Reduction in *Desulfovibrio vulgaris* Hildenborough Appl. Environ. Microbiol., 76:5500-5509.

3. Castañeda-Carrión, I.N., M. Whiteley and L.R. Krumholz. 2009. Characterization of pNC1, a small and mobilizable plasmid for use in genetic manipulation of *Desulfovibrio africanus*. J. Microbiol. Methods. 79:23-31.

II.K.7 Genetics and Molecular Biology of Hydrogen Metabolism in Sulfate-reducing Bacteria

Judy D. Wall, PI; Barbara J. Rapp-Giles, Research Associate; Kimberly Keller, Postdoctoral Fellow
University of Missouri
117 Schweitzer Hall
Columbia, MO 65211
Phone: (573) 882-8726
E-mail: wallj@missouri.edu

DOE Program Manager: Robert Stack
Phone: (301) 903-5652
E-mail: Robert.Stack@science.doe.gov

Objectives

The energy transduction systems of the anaerobic sulfate-reducing bacteria of the genus *Desulfovibrio* are to be elucidated. The target strain is *D. alaskensis* G20 because of its robust fermentative growth on pyruvate that should allow mutant analysis of sulfate respiration. Mutations of various transmembrane complexes are to be analyzed to determine their role in the energy budget of the cell. The development of genetic transfer systems for manipulation of the G20 strain is necessary for this analysis.

Technical Barriers

The assumption that pyruvate fermentation generates ATP only through substrate-level phosphorylation may be inaccurate. Thus learning the pathway(s) of reoxidation of the reduced ferredoxin produced in pyruvate oxidation is likely to reveal electron transfer complexes pumping protons that contribute to a proton gradient used for ATP synthesis. The gene transfer capacity of the G20 strain through transformation has proven recalcitrant. Gene transfer by conjugation is more time consuming but it allows the generation of mutants to proceed.

Abstract

Energy generation by the strictly anaerobic sulfate-reducing bacteria has been a controversial topic because of the unique feature that sulfate is the only inorganic electron acceptor that requires an energy-consuming activation before reduction. During the initial stages of growth of batch cultures that are respiring sulfate with organic acids as electron donors, hydrogen is both produced and then consumed. This observation led to the interesting hydrogen-cycling hypothesis (Odom and Peck, 1981) as a mechanism for contributing to the energy budget of the cells. We seek to elucidate the role of hydrogen in the energy budget of these bacteria through genetic approaches. Exploration of electron flow in the *cycA* mutant of the G20 strain, I2, that lacks the type 1 tetraheme cytochrome c_3 (Tp1- c_3) has revealed an apparent minor role for fumarate as a terminal electron acceptor even during sulfate respiration. Further growth results with this mutant have shown that high pyruvate concentrations transiently inhibit sulfate respiration. In studies to determine the enzymes and compartments for hydrogen production during the hydrogen transient observed, it has been observed that putative cytoplasmic hydrogenases are not conserved among species of *Desulfovibrio*. Examination of our library of nearly 7000 random transposon mutants of the *D. vulgaris* Hildenborough strain constructed in cells grown on lactate/sulfate medium revealed that the cytoplasmic CO-associated hydrogenase complex was not interrupted by transposons. This result was interpreted to mean that this enzyme complex plays an important role in the metabolism of cells grown on these substrates. Interestingly this hydrogenase has been shown to be among a family of transmembrane hydrogenases that oxidize reduced ferredoxin generating hydrogen and pumping a proton. We will continue to generate mutations in genes encoding transmembrane complexes to elucidate their role(s) in energy generation in the sulfate-reducing bacteria.

Progress Report

1. Studies with the *Desulfovibrio* G20 tetraheme cytochrome c_3 (Tp1- c_3) mutant, CycA-, showed that sulfate respiration was transiently inhibited with electrons from pyruvate (Giles et al. under revision).
2. The alternative respiration of fumarate by G20 is robust (Fig. 1A) and analyses of excreted metabolites showed that some electrons are diverted to produce succinate even during sulfate reduction or pyruvate fermentation by the wild type G20 strain. CycA- mutant and a fumarate reductase transposon mutant are unable to respire fumarate (Fig. 1A).
3. Microarray and proteomics (Fig. 2) analysis of G20 and I2 revealed the surprising result that genes for fumarate respiration and, therefore, the enzymes were significantly decreased in the I2 mutant regardless of the growth mode. This suggests a redox control on transcription of these genes affected by the absence of the periplasmic cytochrome.
4. A putative two component regulatory operon was found upstream of the fumarate reductase operon (Fig. 3). A transposon mutation in the histidine kinase gene in that operon was tested for growth on fumarate and found to be unable to disproportionate fumarate

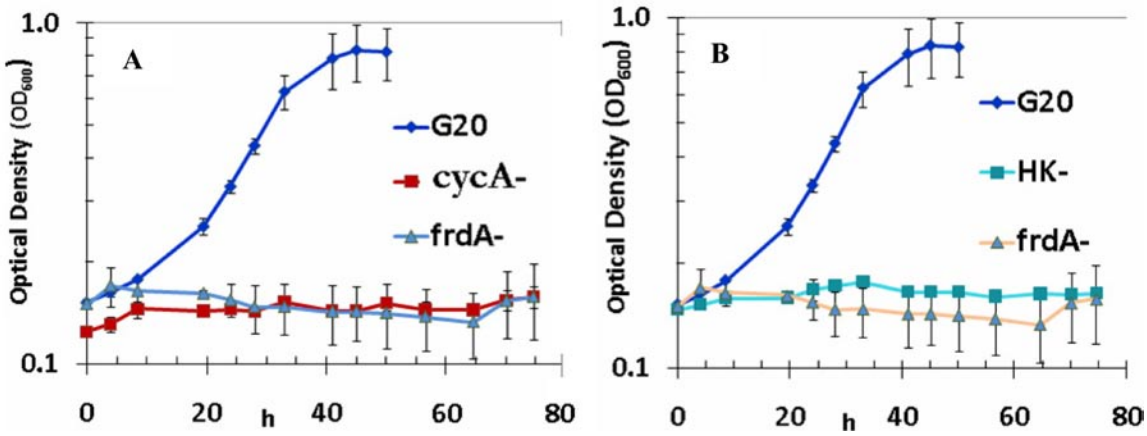


FIGURE 1. Growth by disproportionation of 60 mM Fumarate by *D. alaskensis* G20, a fumarate reductase (*frdA*) transposon mutant, the I2 mutant (*cycA*), and a transposon mutation in the histidine kinase (HK) upstream of the fumarate reductase operon.

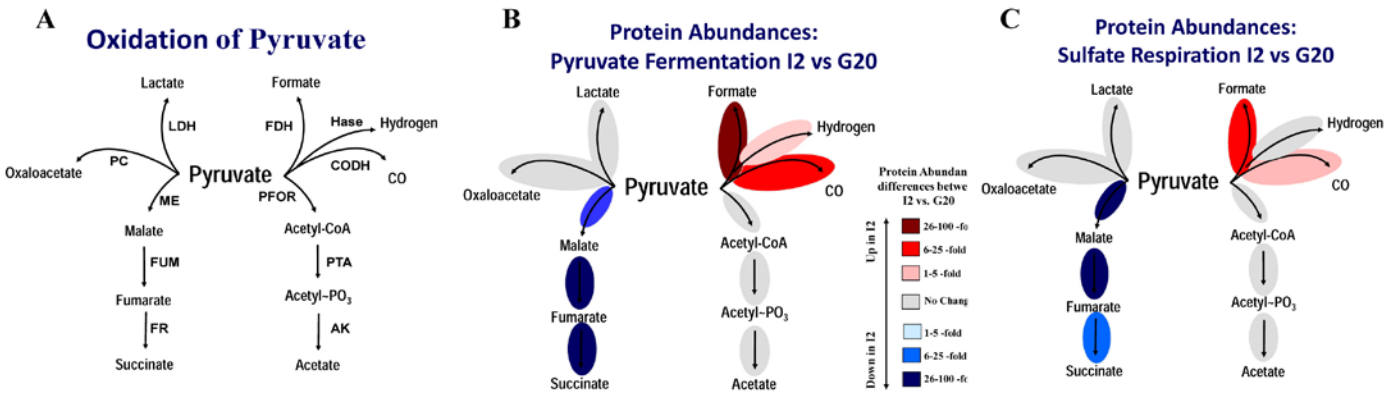


FIGURE 2. A) Metabolic fates of pyruvate in *Desulfovibrio.* LDH, lactate dehydrogenase; PC, pyruvate carboxylase; ME, malic enzyme; FUM, fumarate hydratase; FR, fumarate reductase; FDH, formate dehydrogenase; Hase, hydrogenases; CODH, CO dehydrogenase; PFOR, pyruvate formate oxidoreductase; PTA, phosphotransacetylase; AK, acetate kinase. B) Oval color represents the magnitude and direction of difference between protein abundances in I2 versus G20 for pyruvate fermentative cells. Grey is no difference. C) Colors as in B) for I2 versus G20 for lactate/sulfate grown cells.

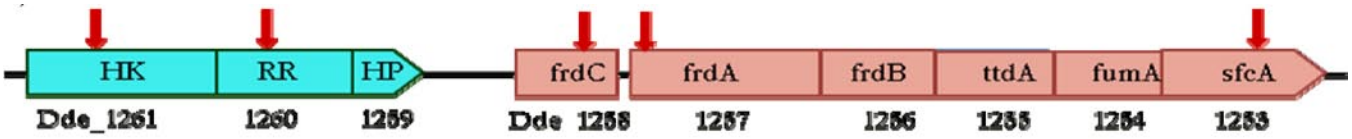


FIGURE 3. The fumarate reductase operon arrangement in *D. alaskensis* G20 in red and the upstream regulatory region (aqua). Red arrows are the relative positions of transposon insertion sites. HK, histidine kinase; RR, response regulator; HP, hypothetical protein. *frdCAB* encode a putative fumarate reductase, *ttdAfumA* encode the two subunits of a putative fumarase, and *sfcA*, a malic enzyme.

(Fig 1B). We will test to determine whether this is a redox sensing regulator affected by the redox changes occurring when the periplasmic tetraheme cytochrome is missing.

5. Over 7000 transposon mutations of *D. vulgaris* Hildenborough have been located through sequencing in collaboration with Adam Deutschbauer at LBNL. All selections have been performed with respiration of sulfur oxides and lactate as carbon source and electron donor. If randomly positioned, we would expect nearly two insertions per kb. When the insertion positions were examined, it was surprising that the genes encoding the CO-associated hydrogenase, covering about 7.5 kb, (but not the CO dehydrogenase enzyme) lacked transposons

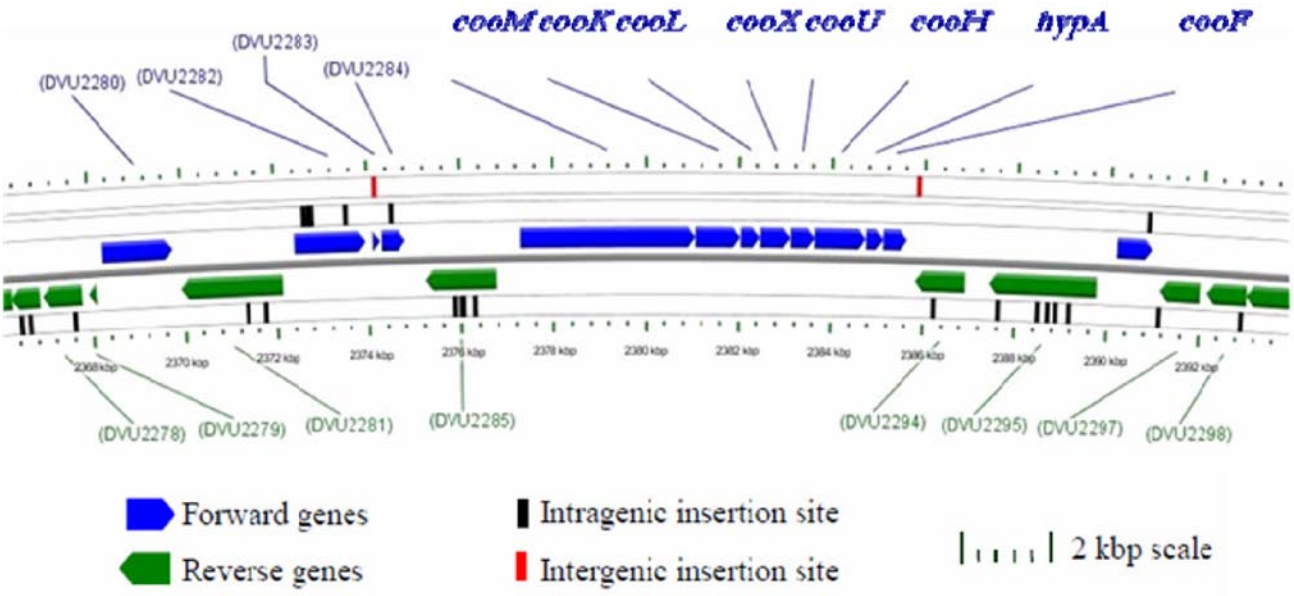


FIGURE 4. *D. vulgaris* chromosomal map in the region of the CO-associated cytoplasmic hydrogenase. Generated with CGView. CooMKLXUHhypAcooF had no transposon mutations.

(Fig. 4). We interpret this result as suggesting that strains with interruptions in these genes are not readily recovered in our procedures or that this enzyme complex is needed for growth under the conditions of selection. This hydrogenase has been predicted to be involved in energy conservation, acting as a primary proton pump in a ferredoxin-dependent electron transport system (Welte et al., 2010).

Future Directions

1. In *D. vulgaris*, we can construct multiple mutations in a single strain and propose to delete both the CO-associated as well as the Ech hydrogenase because these are the two candidates for cytoplasmic hydrogenases. The results of this experiment may allow us to resolve the debate about the hydrogen cycling contribution to the energy budget.
2. Candidates for energy conserving, ferredoxin-dependent complexes in G20 are not as obvious. There are now over 12,000 transposon mutants and no predicted cytoplasmic hydrogenase that lacks mutations. We will explore the heterodisulfide reductase complex mutants for growth rate comparisons with wild type cells to determine whether the mutants appear to be impaired because of an energy defect.

References

1. Odom, J.M., and H.D. Peck, Jr. 1984. Hydrogenase, electron-transfer proteins, and energy coupling in the sulfate-reducing bacteria *Desulfovibrio*. Annu. Rev. Microbiol. 38:551-592.

2. Welte, C., C. Krätzer, and U. Deppenmeier. 2010. Involvement of Ech hydrogenase in energy conservation of *Methanosarcina mazei*. FEBS J. 277:3396-3403.

Publication list (including patents) acknowledging the DOE grant or contract

1. Wall, J.D., A.P. Arkin, N.C. Balci, and B.J. Rapp-Giles, Genetics and genomics of sulfate respiration in *Desulfovibrio*. Springer-Verlag, Berlin, Heidelberg, Microbial Sulfur Metabolism (**1**):1-12 (2009)

2. Rapp-Giles, B.J., K.L. Keller, I. Porat, S.D. Brown and J.D. Wall. The role of cytochrome c_3 in electron flow for sulfate reduction and pyruvate metabolism in *Desulfovibrio* G20. In revision for, Appl. Environ. Microbiol.

II.K.8 Regulation of H_2 and CO_2 Metabolism: Factors Involved in Partitioning of Photosynthetic Reductant in Green Algae

Maria L. Ghirardi (Primary Contact) and
Narayana Murthy (Research Associate)
National Renewable Energy Laboratory
1617 Cole Blvd., Golden CO 80401
Phone: (303) 386-6312; Fax: (303) 384-6150
E-mail: maria_ghirardi@nrel.gov

DOE Program Manager: Gail McLean
Phone: (301) 903-7807
E-mail: gail.mclean@science.doe.gov

Objectives

The overall objective of this project is to develop fundamental understanding about the regulation of the partitioning of photosynthetic reductant between the H_2-production and the CO_2-fixation pathways. Specific objectives are to: (a) identify protein factors whose expression may be required for optimal hydrogenase expression; (b) identify active promoter regions and transcriptional elements for the two algal hydrogenases; and (c) determine whether the recently identified FIXL homologs in *C. reinhardtii* play a role in O_2-sensing mechanism and mediate components of the anoxic regulatory response that leads to hydrogenase expression.

Abstract

Photobiological H_2 production from water is a clean, non-polluting and renewable technology that could play a significant role in a future hydrogen economy. The potential light conversion efficiency to H_2 by biological organisms is theoretically about 10%. One of the limitations to meeting this efficiency is the low availability of reductant to the hydrogenase, due to the existence of competing metabolic pathways, such as CO_2 fixation. This project aims at understanding how photosynthetic reductant is partitioned between different metabolic pathways at the level of ferredoxin. In particular, the project continues to investigate the mechanism that underlies the anoxic regulation of hydrogenase in *C. reinhardtii* at the transcriptional and post-transcriptional levels. These goals are being pursued by (a) using high-quality sensors developed by Dr. Mathew Posewitz at Colorado School of Mines to identify and characterize candidate mutants displaying altered hydrogen production from insertional libraries; (b) fusing the truncated promoters of HYDA1 and HYDA2 to the SNAP reporter gene lacking its own promoter, to identify the DNA region required for anaerobic gene expression; (c) investigating the O_2 and CO-binding affinities of the truncated FXL1 and FXL5 homologues from *C. reinhardtii* expressed in *E.* col and further studying their role in hydrogenase signal transduction; (c) probing the physiological and metabolic differences between structurally different algal [FeFe]-hydrogenases.

Progress Report

- To define the role of individual hydrogenases in green algae, we screened a Chlamydomonas *hydA2* mutant background (generated under DOE's BER funding) for mutants lacking all hydrogenase activity. A double *hyda2hyda1* mutant has been identified; it is being further characterized and is being used as the background strain for expression of recombinant [FeFe]-hydrogenases in Chlamydomonas by DOE's FCT Program.
- To identify active promoter regions for the two algal hydrogenases, we fused the truncated promoters of HYDA1 and HYDA2 to the SNAP reporter gene. Transformants expressing the SNAP protein with truncated promoters were shown to be transcribed only under anaerobic condition. The results indicate that region between position -144 and -1 for HYDA1 and -149 to –1 for HYDA2 with respect to the transcription start site is required for anaerobic specific gene expression.
- To determine whether the recently identified FIXL homologs in *C. reinhardtii* play a role in O_2-sensing mechanism and mediate components of the anoxic regulatory response that leads to hydrogenase expression, we cloned the PAS domains of FXL1 and FXL5 from *C. reinhardtii*, overexpressed them in *Escherichia coli* and purified the ~13 kDa proteins. The recombinant FXL1 and FXL5 domain polypeptides both stained positively for heme, while ΔFXL1 and ΔFXL5, mutated in the conserved, ligand binding histidine residue resulted in loss of heme binding. Met-FXL1 and Met-FXL5 had their Soret absorption maximum around 415 nm followed by several weaker absorptions at longer wavelengths, 530/560 nm, which are characteristic of protein-bound heme, and are very similar to absorption spectra of Rhizobium FixL. Ligand binding measurements in varying partial pressures of O_2 and CO showed that FXL1 and FXL5 both bind O_2 and CO with high affinity. This indicates that the *Chlamydomonas* FXL proteins may use an O_2-sensing mechanism analogous to that reported in nitrogen-fixing bacteria, and thereby mediate components of the anoxic regulatory responses observed in this metabolically versatile alga. The present study unequivocally indicates the discovery of putative FXL-like proteins

in *Chlamydomonas reinhardtii* and demonstrates their heme and ligand binding properties.

- To probe the physiological and metabolic differences between two structurally different algal [FeFe]-hydrogenases, we assessed H_2 production in the trebouxiophyte *Chlorella* NC64A, which is the first alga known to encode both the H and F-clusters of hydogenases. We show for the first time that F-cluster-containing hydrogenases are coupled to both anoxic photosynthetic electron transport and dark fermentation in a green alga. Hydrogen photoproduction in *Chlorella* NC64A is as sensitive to O_2 inactivation as in *C. reinhardtii.* Phylogenetic analysis indicates that all known algal HYDA enzymes are monophyletic, suggesting that they emerged once within the algae. Furthermore, phylogenetic reconstruction indicates that the multiple *HYDA* copies in the algal taxa are the result of gene duplication events that occurred independently in each algal lineage, and that the ancestor of the Trebouxiophyceae and Chlorophyceae likely encoded a single, H and F-cluster-containing HYDA.

Future Directions

- Candidate transcription factor proteins for hydrogenase will be identified, over-expressed in *E. coli* and purified. We will perform direct interaction of transcription factor-hydrogenase promoter DNA binding assays. To understand the involvement of other downstream proteins with transcription factor, the latter will be tagged (strepatavidin or histidine tag) and used to search for interacting proteins.
- Selected *C. reinhardtii* mutants showing aberrant H_2 production will be further analyzed with respect to HYDA1 and HYDA2 transcript and protein levels. Complementation of the the phenotype with the transformed gene will be performed and physiological studies will be carried out to determine the role of the disrupted gene in algal metabolism.
- To understand the involvement (if any) of FIXL proteins in signal transduction in response to O_2, promising FIXL candidates will be tagged (streptavidin or histidine tag) and over-expressed in *C .reinhardtii*. Tagged FIXL proteins will be used to search for interacting proteins involved in the signal transduction pathway.
- To understand the mechanism that underlies the anoxic regulation of hydrogenase, we will express SNAP proteins under the regulation of the HYDA1 and HYDA2 promoters into *hydA1/hydA2* single or double mutants. Additionally, we will perform DNA binding assays to identify the transcription factors binding to the promoter regions of each hydrogenase.

References

1. Seibert, M., P. King, M.C. Posewitz, A. Melis, and M.L. Ghirardi. 2008. “Photosynthetic Water-Splitting for Hydrogen Production,” in Bioenergy (J. Wall, C. Harwood, and A. Demain, Eds.) ASM Press, Washington, DC, pp. 273-291.

2. Posewitz, M.C., A. Dubini, J.E. Meuser, M. Seibert and M.L. Ghirardi. 2008. “Hydrogenases, hydrogen production and anoxia” in The Chlamydomonas Sourcebook, Vol 2: Organellar and Metabolic Processes (D. Stern, ed.) Elsevier Scientific 217-255.

3. Ghirardi, M.L., A. Dubini, J. Yu and P.C. Maness. 2009. “Photobiological hydrogen-producing systems”. Chem. Soc. Rev. 38, 52-61.

4. Meuser, J.E., G. Ananyev, L.E. Wittig, S. Kosourov, M.L. Ghirardi, M. Seibert, G.C. Dismukes and M.C. Posewitz. 2009. “Phenotypic Diversity of Hydrogen Production in Chlorophycean Algae Reflects Distinct Anaerobic Metabolisms”. J. Biotechnol. 142, 21-30.

5. Maness, P.C., J. Yu, C. Eckert and M.L. Ghirardi. 2009. “Photobiological hydrogen production – prospects and challenges” Microbe 4, 275-280.

Research papers submitted

1. Narayana Murthy, U.M., Matt Wecker, Mathew C. Posewitz and Maria L. Ghirardi (2011). Cloning, expression and physical characterization of novel FixL-heme binding domains of oxygen sensing proteins in *Chlamydomonas reinhardtii* (submitted to Journal of Biological Chemistry in February 2011)

2. Narayana Murthy U.M. and Maria L. Ghirardi (2010). “Algal Hydrogen production” in Encyclopedia of Biological Chemistry, submitted.

3. Jonathan E. Meuser, Eric S. Boyd, Gennady Ananyev, Devin Karns Narayana Murthy U.M. Randor Radakovits G. Charles Dismukes, Maria L. Ghirardi, John W. Peters, and Matthew C. Posewitz (2011). Presence of accessory FeS clusters in the *Chlorella* NC64A [FeFe]-hydrogenases: new details into the evolution and diversity of algal hydrogen metabolism. (submitted to Planta in February 2011)

II.K.9 Excited States in Semiconductor Quantum Dots

Oleg Prezhdo, Heather Jaeger
Department of Chemistry, University of Rochester
120 Trustee Rd.
Rochester, NY 14627
(585) 275-4231; (585) 276-0205
E-mail: oleg.prezhdo@rochester.edu

Objectives

The research goal of the Prezhdo group is to obtain a theoretical understanding at the molecular level of chemical reactivity and energy transfer in complex condensed-phase chemical and biological environments. Motivated by recent experiments, we are modeling charge dynamics in semiconductor and metallic nanoparticles, carbon nanotubes and nanoribbons, and related nanoscale systems. Time-domain atomistic simulations of interactions between charges, spins and phonons in these materials create the theoretical basis for photovoltaic devices, optical and conductance switches, quantum wires, logic gates, miniature field-effect transitions and lasers.

Technical Barriers

While solar-to-electric energy conversion is an established technology, current solar cells are either too expensive or too inefficient for widespread application. Many alternative designs of photovoltaic (PV) systems have been proposed, yet the precise relationships between structure and spectral properties as well as the specific mechanisms of the energy transduction are still being unraveled. Our theoretical studies will address the fundamental aspects of solar energy transfer resulting in a predictive framework for the design of efficient, cost-saving PV devices for the production of hydrogen.

Abstract

The current perspective on the nature of photoexcited states in semiconductor quantum dots (QDs) is presented. The focus is on multiple excitons and photo-induced electron–phonon dynamics in PbSeand CdSe QDs, and the advocated view is rooted in the results of *ab initio* studies in both energy and time domains. As a new type of material, semiconductor QDs represent the borderline between chemistry and physics, exhibiting both molecular and bulk-like properties. Similar to atoms and molecules, the electronic spectra of QD show discrete bands and also exhibit conduction and valence bands as in bulk semiconductors. The electron–phonon coupling in QDs is weaker than in molecules, but stronger than in bulk semiconductors. Unlike either material, the QD properties can be tuned continuously by changing QD size and shape. The molecular and bulk points of view often lead to contradicting conclusions. For example, the molecular view suggests that the excitations in QDs should exhibit strong electron-correlation (excitonic) effects, and that the electron–phonon relaxation should be slow due to the discrete nature of the optical bands and the mismatch of the electronic energy gaps with vibrational frequencies. In contrast, a finite-size limit of bulk properties indicates that the kinetic energy of quantum confinement should be significantly greater than excitonic effects and that the electron–phonon relaxation inside the quasi-continuous bands should be efficient. Such qualitative differences have generated heated discussions in the literature. The great potential of QDs for a variety of applications, including photovoltaics, spintronics, lasers, light-emitting diodes, and field-effect transistors makes it critical to settle the debates. By synthesizing different viewpoints and presenting a unified atomistic picture of the excited state processes, our ab initio analysis clarifies the controversies regarding the phonon bottleneck and the generation of multiple excitons in semiconductor QDs. Both the electron–hole and charge-phonon interactions are strong and, therefore, optical excitations can directly generate multiple excitons, while the electron–phonon relaxation exhibits no bottlenecks, except at low excitation energies and in very small QDs.

Progress Report

The time-domain modeling [1] of the phonon-induced electronic relaxation performed with the novel approach [2] combining time-domain density functional theory and non-adiabatic molecular dynamics unifies the two, seemingly contradicting, experimental observations. In spite of the large line spacing in the CdSe and PbSe QD optical spectra, the phonon bottleneck to the electron–phonon relaxation does not exist. The simulation shows that the fast relaxation and the absence of the bottleneck are due to the high density of electron and hole states. Except for the lowest excitation energies and smallest QDs, the spacing between the state energies matches the phonon frequencies. The QD spectra are composed of multiple individual excitations that combine into distinct bands according to the optical selection rules. The selection rules are much more stringent for optical than for electron–phonon transitions. Even though relatively few excitations are strongly optically active, most of the excited states are available during the relaxation.

Sophisticated ab initio electronic structure calculations clarify the nature of the photoexcited states in the semiconductor QDs by explicitly including the high-order electron–hole interactions. Multi-excitons (ME) are found in the QD spectra above an energy threshold. PbSe in particular exhibits a unique electronic structure, creating

energy windows in which MEs completely dominate single excitons. Electronic structure calculations have also led to much progress on achieving a thorough understanding of the excitation properties of these materials when they are altered with charging, doping, or dangling bonds. The calculations show that the defects introduce new intra-band transitions, blue-shift the optical absorption spectra and increase the threshold for ME generation. Generally, doping and charging have similar effects on the excited state properties, while dangling bonds cause less severe changes.

The excited state properties determined in the ab initio calculations indicate that three mechanisms of the ME generation can take place in the semiconductor QDs. These include the incoherent II process, [3,4] the dephasing mechanism, [5] and the direct excitation mechanism. [6] Which mechanism is more important depends on the material under study. The direct mechanism should be particularly efficient in PbSe QDs, while in CdSe the other mechanisms will also play key roles.

Future Directions

A number of open questions remain in the investigations of the mechanisms and rates of the ME generation and the electron–phonon relaxation dynamics. Apart from the experimental controversies regarding the existence of MEs [8] and the phonon bottleneck, [9, 10, 11] several theoretical issues need to be solved. The mechanism of the dissociation of MEs into uncorrelated single excitons is not yet established, even though we argue here that the process can occur by the phonon-induced dephasing. This step is essential to completing the ME generation picture.

Recently, MEs were discovered in Si. [13] This discovery could lead to a major breakthrough in the solar cell industry, which is almost entirely Si-based, provided that MEs can dissociate into free charge carriers and that the free charge carriers can be extracted from Si QDs. In contrast to PbSe and CdSe, Si is an indirect bandgap semiconductor. Whether or not the mechanisms of ME generation and electron–phonon relaxation remain the same in this alternative type of semiconductor is not yet clear. Recent experiments show that small Si QDs with quantum confinement energies greater than 1 eV behave similarly to the direct gap QDs. [14] In this respect, Ge provides additional advantages, since the confinement-induced transformation to the pseudo-direct gap regime is less demanding in Ge than Si. [15]

Assemblies of QDs with other materials, such as molecular chromophores, [16] organic or inorganic semiconductors, and so on, present a new set of theoretical questions regarding the interface. The unique opportunities provided by the ab initio descriptions in time and energy domains motivate one to extend the current efforts to other related materials and problems.

References

1. S.V. Kilina, C.F. Craig, D.S. Kilin, O.V. Prezhdo, J. Phys. Chem. C 111 (2007) 4871.

2. C.F. Craig, W.R. Duncan, O.V. Prezhdo, Phys. Rev. Lett. 95 (2005) 163001.

3. A.J. Nozik, Annu. Rev. Phys. Chem. 52 (2001) 193.

4. A. Franceschetti, J.M. An, A. Zunger, Nano Lett. 6 (2006) 2191.

5. R.J. Ellingson et al., Nano Lett. 5 (2005) 865.

6. R.D. Schaller, V.M. Agranovich, V.I. Klimov, Nat. Phys. 1 (2005) 189

7. H. Kamisaka, S.V. Kilina, K. Yamashita, O.V. Prezhdo, Nano Lett. 6 (2006) 2295.

8. G. Nair, M.G. Bawendi, Phys. Rev. B 76 (2007) 08134.

9. R.D. Schaller, J.M. Pietryga, S.V. Goupalov, M.A. Petruska, S.A. Ivanov, V.I. Klimov, Phys. Rev. Lett. 95 (2005) 196401.

10. R.R. Cooney, S.L. Sewall, K.E.H. Anderson, E.A. Dias, P. Kambhampati, Phys. Rev. Lett. 98 (2007) 177403.

11. S.V. Kilina, C.F. Craig, D.S. Kilin, O.V. Prezhdo, J. Phys. Chem. C 111 (2007) 4871.

12. A.L. Efros, A.L. Efros, Sov. Phys. Semicond. 16 (1982) 772.

13. M.C. Beard et al., Nano Lett. 7 (2007) 2506.

14. M. Sykora, L. Mangolini, R. Schaller, U. Kortshagen, D. Jurbergs, V. Klimov, Phys. Rev. Lett. 100 (2008) 067401.

15. R.C. Jin, Y.W. Cao, C.A. Mirkin, K.L. Kelly, G.C. Schatz, J.G. Zheng, Nature 294 (2001) 1901.

16. D.S. Kilin, K. Tsemekhman, O.V. Prezhdo, E.I. Zenkevich, C. von Borczyskowski, J. Photochem. Photobio. A – Chem. 190 (2007) 342.

Publication list (including patents) acknowledging the DOE grant or contract

1. H. Bao, B.F. Habenicht, O.V. Prezhdo, and X. Ruan. Phys. Rev. B 79 (2009) 235306.

2. K. Hyeon-Deuk, A.B. Madrid, O.V. Prezhdo. Dalton T. 45 (2009) 10069.

3. B.F. Habenicht, O.V. Prezhdo. J. Phys. Chem. C 113 (2009) 14067.

4. C.M. Isborn, O.V. Prezhdo. J. Phys. Chem. C 113 (2009) 12617.

5. O.V. Prezhdo. Acc. Chem. Res. 42 (2009) 2005.

7. A.B. Madrid, K. Hyeon-Deuk, B. F. Habenicht, O.V. Prezhdo. ACS Nano 3 (2009) 2487.

7. D.S. Kilin, K.L. Tsemekhman, S.V. Kilina, A.V. Balatsky, O.V. Prezhdo. J. Phys. Chem. A 113 (2009) 4549.

8. D.A. Yarotski, S.V. Kilina, A.A. Talin, S. Tretiak, O.V. Prezhdo, A.V. Balatsky, and A.J. Taylor. Nano Lett. 9 (2009) 12.

9. H. Kamisaka, S.V. Kilina, K. Yamashita, and O.V. Prezhdo, J. Phys. Chem C 112 (2009) 7800.

10. O.V. Prezhdo, W.R. Duncan, V.V. Prezhdo, Prog. Surf. Sci., 84 (2009) 30.

11. O.V. Prezhdo, Chem. Phys. Lett., 460 (2008) 1.

12. O.V. Prezhdo, W.R. Duncan, and V.V. Prezhdo, Acc. Chem. Res. 41 (2008) 339.

13. A.V. Luzanov, O.V. Prezhdo Mol Phys. 105 (2007) 19.

14. D.S. Kilin, K. Tsemekhmana, O.V. Prezhdo, E.I. Zenkevich, C. von Borczyskowski, J. Photochem. Photobio. A: Chemistry 190 (2007) 342.

15. W.R. Duncan, C.F. Craig, O.V. Prezhdo. J. Am. Chem. Soc. 129 (2007) 8528.

16. S.V. Kilina, C.F. Craig, D.S. Kilin, O.V. Prezhdo, J. Phys. Chem. C 111 (2007) 4871.

17. O.V. Prezhdo J. Chem. Phys. 124 (2006) 201104.

18. Y.V. Pereverzev, O.V. Prezhdo, Phys. Rev. E, 75 (2007) 011905.

19. B.F. Habenicht, H. Kamisaka, K. Yamashita, and O.V. Prezhdo, Nano Lett. 7 (2007) 3260.

20. B.F. Habenicht, C.F. Craig, O.V. Prezhdo Phys. Rev. Lett. 96 (2006) 187401.

21. A.V. Luzanov, O.V. Prezhdo. J. Chem. Phys. 124 (2006) 224109.

22. Y.V. Pereverzev, O.V. Prezhdo Phys. Rev. E 73 (2006) 050902.

23. A.V. Luzanov, O.V. Prezhdo. J. Chem. Phys. 125 (2006) 154106.

24. H. Kamisaka, S.V. Kilina, K. Yamashita, O.V. Prezhdo. Nano Lett. 6 (2006) 2296.

II.K.10 Theoretical Research Program on Bio-inspired Inorganic Hydrogen Generating Catalysts and Electrodes

Annabella Selloni (Principal Investigator),
Patrick H.-L. Sit,* Morrel H. Cohen, Roberto Car
Department of Chemistry
Princeton University
Princeton, NJ 08544
Phone: (609) 258-3837; Fax: (609) 258-6746
E-mail: aselloni@princeton.edu

DOE Program Manager: Michael A. Markowitz
Phone: (301) 903-6779
E-mail: Mike.markowitz@science.doe.gov

Objectives

Our goal is the theoretical design of a model electrocatalytic or photo-electrocatalytic system for economical production of hydrogen from water and sunlight via the hydrogen evolution reaction. The system under investigation consists of an FeS_2 (100) surface decorated with a cluster derived by design from the active site of the di-iron hydrogenase enzyme. Immersed in acidified water with the FeS_2 the source of electrons and the water of protons, the system facilely produces H_2 in simulations. Our immediate goal is to design a protective structure which inhibits the attack of the clusters and the exposed FeS_2 sites by dissolved O_2.

Technical Barriers

For economic feasibility, a system for production from sunlight and water must be made of earth abundant materials and contain a catalyst active enough to utilize efficiently electrons generated from the solar flux. The active site of the hydrogenase enzyme would meet those requirements *if* (1) it could be redesigned to retain its activity when extracted from the enzyme while stably attached to a suitable electrode and exposed to acidified water *and if* (2) it could be protected from attack by the dissolved oxygen inevitably present. Our design of the unprotected decorated pyrite surface should help overcome barrier (1). Our current research on structured overlayers should help overcome barrier (2).

Abstract

We have designed a catalytic cluster, $[FeFe]_P$, derived from the active cluster of the di-iron hydrogenase and functionalized the pyrite (100) surface with it. Remaining stable throughout, it produces hydrogen from acidified water with a free-energy barrier of less than 8.2 kcal/mol in room temperature simulations. The rate-limiting step in the cycle is the first protonation, subsequent steps are barrier free and fast. A detailed mechanistic analysis of the bond switching, oxidation-state changes, and electron flow during that step was carried out. Oxygen binding studies suggested diminished O_2 sensitivity of $[FeFe]_P$ and a need to focus on the sensitivity of the exposed pyrite Fe sites.

Progress Report

The achievements to date are: 1. design of the $[FeFe]_P$ catalytic cluster; 2. demonstration of hydrogen production from acidified water; 3. demonstration of structural stability of the functionalized surface throughout the production cycle; 4. identification of the first protonation of the catalyst as the rate-limiting step in the cycle, with an upper bound of 8.2 kcal/mol for its free-energy barrier; 5. detailed mechanistic analysis of the bond switching, oxidation-state changes, and electron flow during the first protonation; 6. finding diminished O_2 sensitivity of $[FeFe]_P$.

Design of $[FeFe]_P$

We first studied the hydrogen production cycle by the unsupported $[FeFe]_H$ cluster in vacuo[1] and in acidified water.[2] In the di-iron $[FeFe]_H$ cluster, removed from the enzyme, two iron atoms are coordinated to CO and CN ligands and bridged by a chelating group, S-CH2-X- CH2-S where X can be a NH (DTMA) or CH2 (PDT) group, Figure 1. One iron atom, Fe_p, is 6-fold coordinated, the other, Fe_d, 5-fold with a vacant coordination site V at which the reaction occurs in the active isomer, Figure 1.

We made several critical modifications to $[FeFe]_H$ (with DTMA) to obtain a stable and functional pyrite-supported catalyst.[3] We obtained a stable link by stripping off the thiol from Fe_p and connecting it directly to a pyrite surface

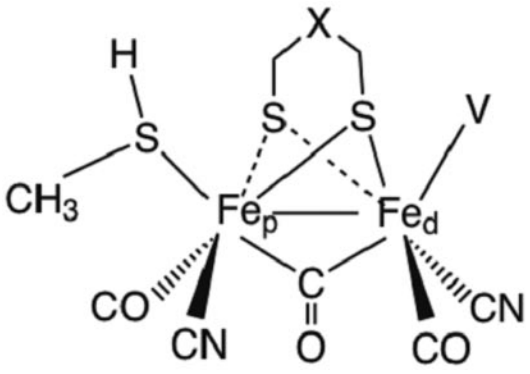


FIGURE 1. The active μ-CO isomer (after Ref. [1])

sulfur atom. Further stabilization was provided by linking a surface Fe atom to the N atom of the CN ligand of Fe_p. We interchanged the CO bridging group with the CN ligand of Fe_d to form a third stable link between the N atom and a surface Fe atom, locking the cluster into the bridging configuration. Lastly, the outer S in the chelating group was changed to an isoelectronic PH group to stabilize the Fe_d-chelating group bond to form $[FeFe]_P$, Figure 2.

Demonstration of structural stability and H_2 production

Both the cluster-electrode linkage and the cluster structure remain stable throughout the H_2 production cycle,[4] which is started with the functionalized electrode in the $[FeFe]_P^{-1}$ state. Both proton additions take place entirely at the vacant coordination site V on Fe_d. The structural and compositional modifications leading to $[FeFe]_P$ eliminate all other protonation sites and all structural lability and greatly simplify the reaction mechanism.

In water, the first proton moves towards Fe_d by a complex pathway along which there is a free-energy barrier. Because of the barrier, simulation of the reaction was carried out by constrained FPMD to prevent the proton from wandering away from the catalyst in the brief duration of the simulation. We obtained a strong upper bound of 8.2 kcal/mol (0.36 eV) for the barrier by thermodynamic integration.[4]

Electron flow and oxidation-state changes

First protonation is the rate-limiting step in hydrogen production from acidified water room-temperature simulations. Second protonation and desorption of the H_2 occur spontaneously during our picosecond-scale simulations.

We analyzed the mechanism of 1st protonation in Ref. [5] by computing densities of the maximally-localized Wannier functions (WD) and their centers of gravity (WC) for several states along the reaction pathway established in Ref. [5]. From the locations and forms of the WD and the locations and movements of the WC, we established that only the Fe_p, Fe_d, μ-C, and P atoms as well as the added H play significant roles in the reaction. We established the nature of their bonds, their oxidation states (OS), and the electron flow responsible for the OS changes and bond switching. The P atom acts as the initial proton attractor, the μC, Fe_d pair act as the redox center, and the Fe_p acts to facilitate bond switching from two 2-center μC-to-Fe bonds to one 3-center bond upon protonation. These features of the reaction mechanism are clearly displayed in Figure 3. This novel method of OS determination should be of broad use for the analysis of redox reactions; we illustrated it in [5] for the superoxide reductase enzyme as well.

O_2 sensitivity of pyrite and the catalyst

Undesirable oxidation of catalytic active centers is a common problem in catalyst design. The active center of hydrogenase is poisoned by O_2, as modelled in Ref. [6] and could be expected for $[FeFe]_P$ as well. Moreover, the pyrite electrode reacts readily with O_2 in the presence of water.[7,8] To address these issues, we first studied the binding of O_2 on the active center in vacuo. Table 1 shows O_2 binding energies, and Fe_d-O and O-O distances in the optimized binding structure at different charge states. As shown in the

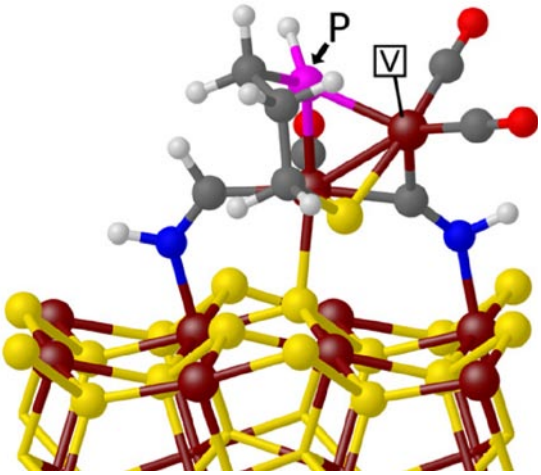


FIGURE 2. Side view of the $[FeFe]_P$ cluster linked to the FeS_2 (100) surface.

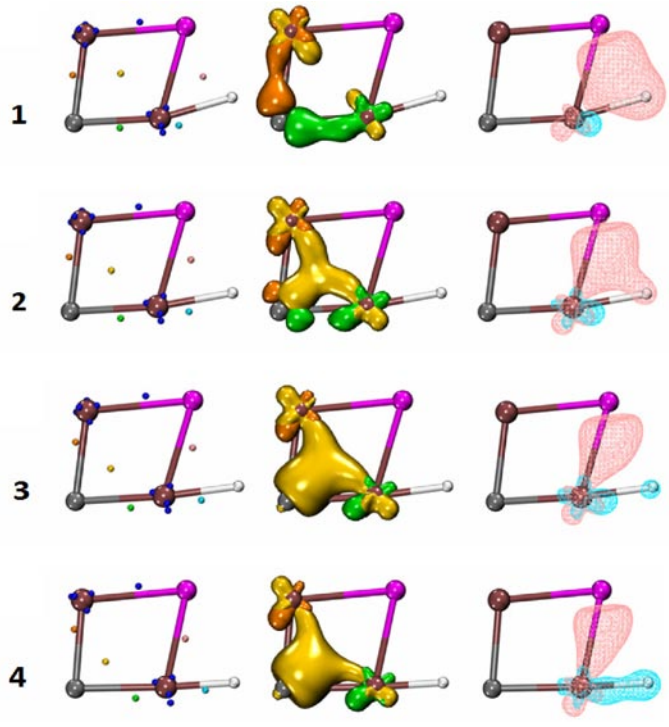


FIGURE 3. Four stages in the evolution of the relevant MLWF density and WC's as the first protonation proceeds. Fe atoms are brown; S atoms are yellow; the P atom is violet; C atoms are gray; N atoms are blue; O atoms are red; and H atoms are white. The isosurfaces are at 20% of their maximum values.

table, the neutral cluster has a small O_2 binding energy, -3.45 kcal/mol. On the other hand, the charge -1 cluster scarcely favors O_2 binding as indicated by the large Fe_d-O distance and negligible binding energy. Full-scale FPMD simulations in water are needed to confirm this weak or unfavorable binding of O_2, but these preliminary results imply that the active center could be inert to O_2 attack and focus could be placed on protecting the exposed pyrite surface.

TABLE 1. O_2 binding energies, and the Fe_d-O and O-O distances in the optimized binding structure at different charge states

	ΔE	d_{Fe-O}	d_{O-O}
$[FeFe]_p^{-1}$	-0.22 kcal/mol	3.64 Å	1.24 Å
$[FeFe]_p^{0}$	-3.45 kcal/mol	2.02 Å	1.29 Å

Accordingly, we studied O_2/H_2O co-absorption on the pyrite surface in vacuo We list several representative configurations in Figure 4. The corresponding absorption energies relative to an isolated O_2, an isolated H_2O, and a pristine surface are shown in Table 2. The most stable physisorption structure for O_2 is side-on where the two O atoms are linked two Fe atoms (configuration (a) and (b)). Compared to configuration (a), it is energetically less favorable for proton transfer from H_2O to the surface S, the surface Fe atoms, or O_2 in end-on binding conformation (configuration (c), (d) and (e)). A large gain in energy from configuration (a) is observed when the O-O bond breaks (configuration (f)) and the energy goes further downhill when one of the O atoms acquires a proton from H_2O (configuration (g)). This agrees with the experiments suggesting that pyrite oxidation occurs in the presence of only O_2 and that the oxidation rate is faster when water is present.

Future Directions

The calculations of O_2/H_2O absorption on pyrite in vacuo allow us to plan full-scale FPMD simulations to reveal the detailed reaction pathways and free-energy changes of pyrite oxidation. Although the active site of [FeFe]p exhibits weak or no affinity toward O_2 in vacuo, the presence of an aqueous environment could change O_2 sensitivity and initiate reactions with the water. Such detailed FPMD studies of O_2 and water interactions with both the active center and the exposed pyrite are necessary precursors to the design of structured protective overlayers. We therefore plan a systematic study of the reaction of the pristine pyrite surface and the decorated cluster with molecular oxygen in neutral water and in acidified water.

After the analysis of the sensitivity of the unprotected functionalized electrode, we plan to work on the individual design elements of a protective overlayer permitting nanochannel access of water and protons to the active sites and H_2 egress. We have already found that phosphonic acid forms a strong bidentate bond with the bare FeS_2 (100) surface after one OH is removed, making akylphosphonates promising candidates for the hydrophobic channel walls. The interaction of that end group with the decorated FeS_2 (100) surface will be studied in vacuo and in water with full quantum mechanical methods, but, when the alkyl chains are added, the increased complexity will require taking recourse to classical MD or QM/MM. The chain configuration in the protective overlayer will be studied with and without the cluster present and with and without water to build up the information needed for subsequent studies of the motion of H_2, and hydronium ions into and through the channels and the inhibition of oxygen penetration.

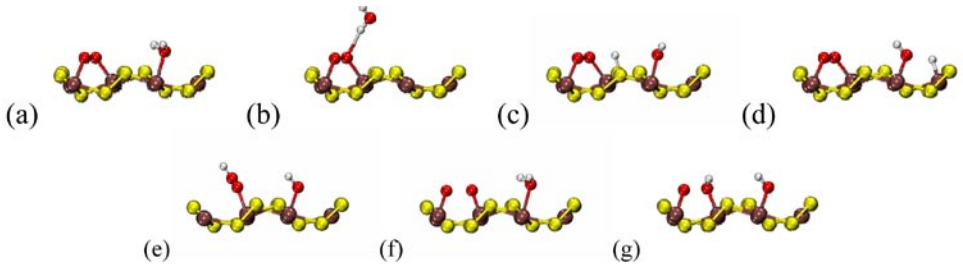


FIGURE 4. Seven representative O2/H2O co-absorption configurations. The corresponding binding energies are shown in Table 2.

TABLE 2. Binding energies of O2/H2O co-absorption configurations shown in Figure 4.

Configuration	a	b	c	d	e	f	g
Binding Energy (kcal/mol)	-29.59	-29.90	-2.32	-4.05	-20.45	-56.37	-60.65

References

1. C. Sbraccia, F. Zipoli, R. Car, M.H. Cohen, G.C. Dismukes, A. Selloni, J. Phys. Chem. B **2008,** *112* 13381-13390.

2. F. Zipoli, R. Car, M.H. Cohen, A. Selloni, J. Phys. Chem. B **2009,** *113* 13096-13106.

3. F. Zipoli, R. Car, M.H. Cohen, A. Selloni, J. Chem. Theo. Comput. **2010,** *6* 3490-3502.

4. F. Zipoli, R. Car, M.H. Cohen, A. Selloni, J. Am. Chem. Soc. **2010,** *132* 8593-8601.

5. P.H.L. Sit, F. Zipoli, J. Chen, R. Car, M.H. Cohen, A. Selloni, Angew. Chem. Int. Ed. Engl. **2011,** (Submitted).

6. M.T. Stiebritz, M. Reiher, Inorg. Chem. **2009,** *48* 7127-7140.

7. K.M. Rosso, U. Becker, M.F. Hochella, Am. Mineral. **1999,** *84* 1549-1561.

8. J.A. Rodriguez, I.A. Abreu, J. Phys. Chem. B **2005,** *109* 2754-2762.

Publication list (including patents) acknowledging the DOE grant or contract

1. *Simulation of Electrocatalytic Hydrogen Production by a Bio-inspired Catalyst Anchored to a Pyrite Electrode* **by F. Zipoli, R. Car, M.H. Cohen, A. Selloni,** Journal of the American Chemical Society, **2010**, 132 (25), 8593–8601

2. *Theoretical design by first principles molecular dynamics of a bio-inspired electrode-catalyst system for electrocatalytic hydrogen production from acidified water* **by F. Zipoli, R. Car, M.H. Cohen, and A. Selloni, 2010,** Journal of Chemical Theory and Computation, 2010, 6, 3490-3502

3. *Electrocatalyst design from first principles: a hydrogen-production catalyst inspired by Nature* **by F. Zipoli, R. Car, M.H. Cohen, and A. Selloni, 2010,** Catalysis Today (in press)

4. *Oxidation state changes, bond switching, and electron flow in enzymatic and electro-catalysis via Wannier function ananlysis* by **P. H.-L. Sit, F. Zipoli, J. Chen, R. Car, M.H. Cohen, and A. Selloni**, 2010, Angewandte Chemie International Edition (invited submission)

II.K.11 Photoinitiated Electron Collection in Mixed-Metal Supramolecular Complexes: Development of Photocatalysts for Hydrogen Production

Karen J. Brewer*, Travis White, Kevan Quinn, Jing Wang, Shamindri Arachchige, Jessica Knoll
Virginia Tech
Department of Chemistry
Blacksburg, VA 24061-0212
Phone: (540) 231-6579
E-mail: kbrewer@vt.edu

DOE Program Manager: Dr. Mark Spitler
E-mail: Mark.Spitler@science.doe.gov
Phone: (301) 903-4568

Objectives

- Design and study of new supramolecular complexes for the production of H_2 from H_2O using molecular devices for photoinitiated electron collection.
- Understand the mechanisms of complex, coupled reactions for the solar production of fuels as facilitated by supramolecular complexes.
- Probe the role of sub-unit variation on the functioning of supramolecular H_2 production photocatalysts to explore the impact of modulation of orbital energetics and excited state dynamics on this complicated photochemistry.
- Develop a fundamental understanding of the rates and mechanisms of multielectron photochemistry and photocatalysis in supramolecular complexes.

Technical Barriers

- Controlling the high purity assembly of multicomponent supramolecular complexes with reactive metal centers needed to photocatalyze H_2O reduction to H_2 in single component systems is a developing field that requires considerable synthetic expertise to prepare target systems.
- Few molecular systems are known that photochemically collect reducing equivalents and less are known that collect electrons at a reactive site.
- Understanding the factors that control multielectron photochemistry is still in its infancy and developing this understanding in supramolecular assemblies presents additional challenges.
- The process of collecting reducing equivalents on a molecular system followed by delivery to a H_2O substrate requires a series of carefully controlled and coordinated reactions, high overall efficiency reliant on the product of efficiency of individual steps.

Abstract

The growing energy needs of our Nation require that we explore and harness a variety of new energy sources within the coming decades. Fossil fuels are currently used to supply much of our Nation's energy needs, often derived from the sun's energy, as harnessed and converted by plants into biomaterials. The rate of our use of fossil fuels makes it necessary to explore alternative means to harvest this energy or alternative energy sources. One appealing alternative energy source is solar energy harnessed without the use of plants. In the Report of the Basic Energy Sciences Workshop on H_2 Production, Storage and Use in 2003, catalyst design for H_2 production was identified as an important goal with emphasis on nanoscale systems.[1] In the report of the Basic Energy Sciences Workshop on Solar Utilization, sunlight is identified as by far the largest of all carbon-neutral energy sources with 4.3×10^{20} J per hour reaching the earth's surface.[2] This represented more energy than that consumed on the planet in a year. The report from the Basic Energy Sciences committee in 2008 states "The ultimate transport solution would be solar fuels, made from using sunlight to split water and produce hydrogen…".[3] A major research need identified in the Workshop on H_2 Production was the development of systems that convert sunlight into chemical fuels for storage and distribution. This project addresses these fundamental issues within a molecular architecture that undergoes multielectron photochemistry and is capable of producing H_2 from water. Importantly the work aims to develop a deeper understanding of the fundamental nature of the multiple steps involved in the complex processes needed to use light energy to promote multielectron reactions as well as the catalysis of the multielectron reduction of substrates to produce transportable fuel. The basic structural motifs of interest focus on the use of Ru and Os MLCT light absorbers (LA) coupled through polyazine bridging ligands (BL) to reactive metal centers, typically Rh. These complexes contain the basic building blocks needed to prepare complexes that undergo photoinitiated electron collection (PEC) and catalyze the reduction of H_2O to produce H_2. Functioning single component systems have been developed with our understanding of their functioning allowing for substantial increases in photocatalytic turnover and quantum efficiency. Studies have focused on a development of a knowledge base concerning the role of device sub-units and excited state dynamics on functioning as well as elucidating the mechanism of functioning.

Progress Report

This project is aimed at developing and studying a class of mixed-metal supramolecular complexes with promising

redox and excited state properties. These systems couple charge transfer light absorbing metals to reactive metals such as rhodium(III) that will allow these systems to undergo PEC while possessing reactive metal sites capable of delivering collected electrons to a substrate such as H_2O to facilitate the production of H_2. The factors impacting multi-electron photochemistry and the reduction of water to produce H_2 have been explored aimed at providing a detailed understanding of the mechanism of action of these unique photocatalysts and the factors that impact functioning. The synthetic pathway to prepare these systems is illustrated in Figure 1 and represents a building block method that allows stepwise assembly and careful purification at each step.

The Rh centered supramolecular complexes must undergo a complex series of steps in order to undergo PEC and deliver collected electrons to a substrate to produce a fuel. This includes the absorption of a series of photons, excited state electron transfer reactions, and the delivery of multiple electrons to the water substrate including the bond breaking and making processes needed to produce hydrogen. The coupling of Ru polyazine light absorbers to Rh centers with low lying dσ* orbitals results in many low energy excited states providing for complicated excited state dynamics. Figure 2 shows the two lowest lying triplet states that are thought to be engaged in the excited state electron transfer leading to reduction of the photocatalysts. To explore the role of each state in the PEC process a series of complexes have been studied that vary the energy of the ^{3}MLCT and ^{3}MMCT states as a function of device components as well as a system able to undergo PEC but without a reactive Rh metal center. These studies illustrated that while the ^{3}MMCT seems to play a role in PEC, the ^{3}MLCT state when alone is able to undergo excited state reduction still leading to PEC and production of H_2 from water. The absence of a Rh metal center, using an Ir centered photoinitiated electron collector does not lead to H_2 production, pointing out the role of Rh in the photocatalysis. The addition of Hg(l) to our photocatalytic system does not impact H_2 production, indicative of the lack of colloidal metal functioning as a catalytic surface in our system.

We have investigated the photophysics and photocatalytic properties of a series of Ru,Rh,Ru trimetallic complexes (the $[\{(TL)_2Ru(dpp)\}_2RhX_2](PF_6)_5$ structural motif) as well as related bimetallic systems which couple one Ru light absorber to a cis-$Rh^{III}Cl_2$ moiety (the $[(TL)_2Ru(dpp)RhCl_2(TL')](PF_6)_3$ structural motif). The systems with X = Cl or Br and TL = bpy, phen and most recently Ph_2phen have been studied. We have found that these complexes emit from their Ru→dpp ^{3}MLCT excited state and this emission is quenched at RT due to electron transfer to generate a lower lying ^{3}MMCT excited state. The use of Br bound to the Rh center in place of Cl leads to systems with lower emission quantum yields and excited state lifetimes but larger quantum yields for H_2 production. The use of phen as the TL in place of bpy provides systems with shorter lifetimes and lower emission quantum yields in stark contrast to the typical extension of lifetimes in related $[\{(phen)_2Ru\}_2(dpp)]^{4+}$ and $[(phen)_2Ru(dpp)]^{2+}$ systems relative to the bpy analogs. The newly prepared and soon to be reported Ph_2phen systems provide for photocatalysts with higher H_2 production rates and yields. The newly prepared Ru,Rh bimetallic motif, $[(TL)_2Ru(dpp)RhCl_2(TL')](PF_6)_3$, has recently been established to have similar excited state dynamics with a low lying ^{3}MMCT excited state quenching the emission of the ^{3}MLCT excited state. We have recently shown this bimetallic motif undergoes photoinitiated electron collection generating Rh(I) systems. We have also demonstrated that despite this the Ru,Rh bimetallics are not photocatalysts for water reduction to produce H_2, as the Rh(I) form dimerizes. This is a very significant result that provides insight into the mechanism of the photocatalysis with our trimetallic systems and provides strong evidence that the supramolecular architecture remains intact and is critical to active photocatalysis.

We have explored the modification of our photocatalytic system showing our system can tolerate changes in solvent,

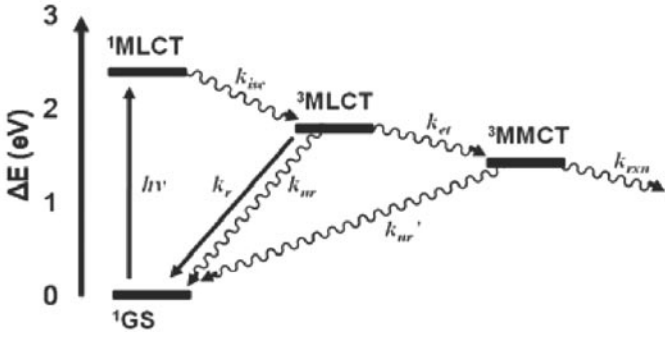


FIGURE 2. State diagram for $[\{(TL)_2Ru(dpp)\}_2RhX_2]^{5+}$ systems

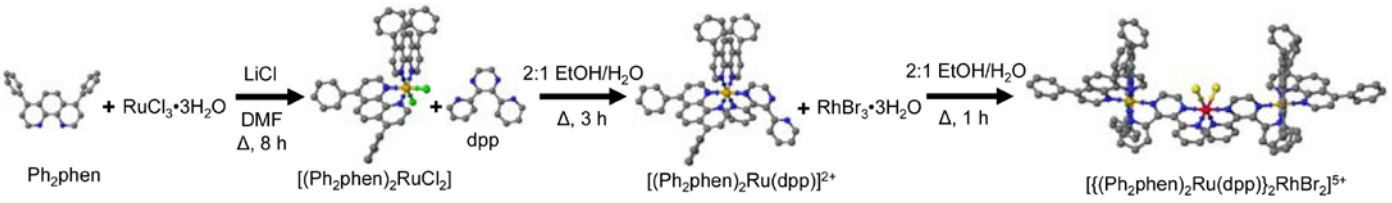


FIGURE 1. Building block method to prepare the TL-LA-BL-EC-BL-LA-TL assembly, $\{[(Ph_2phen)_2Ru(dpp)\}_2RhBr_2](PF_6)_5$, a photocatalyst for H_2O reduction to H_2.

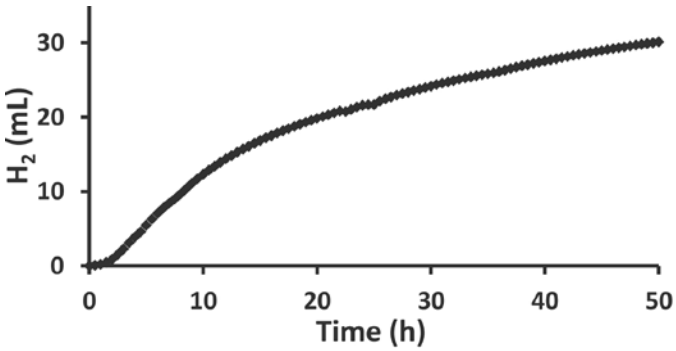


FIGURE 3. Real time H_2 production by supramolecular photocatalyst $\{(bpy)_2Ru(dpp)\}_2RhBr]^{5+}$ in DMF.

electron donor, light flux, etc.. Our system represents the first report of a PEC system that functions in water and our system also produces H_2. We have shown that DMF as a solvent impacts photocatalytic yield producing higher amounts of H_2, Figure 3.

Future Directions

The understanding of the mechanistic details of our photocatalytic system remains an overriding goal. We have made considerable progress on this goal. The use of varied sub-units in our Ru,Rh,Ru trimetallic motif has provided insight into the role of the various excited states and the driving force for excited state electron transfer on photocatalysis. We have investigated the role of the supramolecular architecture and shown through our studies with the new Ru,Rh bimetallics that simply producing a system in which Rh(I) is generated is not sufficient to produce active photocatalysts. The studies of the bimetallic systems have uncovered the possible role of Rh-Rh bond formation as a deactivating pathway in non-functioning Rh systems. We have moved to the direct synthesis of Rh(I) complexes. This work has progressed and preliminary results show with the proper design we can produce Ru(II),Rh(I) systems that can be active photocatalysts through the protection of the Rh site with a bulky ligand. Studies are ongoing to explore the mechanistic aspects of our important photocatalysis and photoreduction reactions.

References

1. "Basic Research Needs for the Hydrogen Economy," DOE Report by the Basic Energy Sciences Workshop on H_2 Production, Storage and Use, May 2003.

2. "Basic Research Needs for Solar Energy Utilization," DOE Report of the Basic Energy Sciences Workshop on Solar Utilization, Department of Energy, April 2005.

3. "New Science for a Secure and Sustainable Energy Future A Report from the Basic Energy Sciences Advisory Committee," Chair: John Hemminger University of California, Irvine U.S. Department of Energy, December 2008.

Publication list (selected) acknowledging the DOE grant or contract

1. "A New Structural Motif for Photoinitiated Electron Collection: Ru, Rh Bimetallic Providing Insight into H_2 Production via Photocatalysis of Water Reduction by Ru,Rh,Ru Supramolecular, J. Wang, T.A. White, S.M. Arachchige, K.J. Brewer, *Chem. Comm.* **2011**, in press.

2. "High Turnover in a Photocatalytic System for Water Reduction to Produce Hydrogen Using a Ru,Rh,Ru Photoinitiated Electron Collector," S.M. Arachchige, R. Shaw, T.A. White, V. Shenoy, H.-M. Tsui, and K.J. Brewer*, *ChemSusChem* **2011,** in press.

3. "Photocatalytic Hydrogen Production from Water," S.M. Arachchige, K.J. Brewer, *Energy Production and Storage-Inorganic Chemical Strategies for a Warming World, Encyclopedia of Inorganic Chemistry,* Robert Crabtree Editor, John Wiley and Sons, **2010**, in press.

4. "Solar Energy Conversion Using Photochemical Molecular Devices: Photocatalytic Hydrogen Production From Water Using Mixed-Metal Supramolecular Complexes," K. Rangan, S.M. Arachchige, J.R. Brown and K.J. Brewer, *J. Energy and Environ. Sci.* **2009**, 2(4), 410-19.

5. "Synthesis, Characterization, and Study of the Photophysics and Photocatalytic Properties of the Photoinitiated Electron Collector $[\{(phen)_2Ru(dpp)\}_2RhBr_2](PF_6)_5$," T.A. White, K. Rangan, K.J. Brewer, *J. Photochem. Photobiol. A: Chem.* **2010**, *209*, 203-209.

6. "Supramolecular Complexes as Photoinitiated Electron Collectors: Applications in Solar Hydrogen Production," S.M. Arachchige, K.J. Brewer, *On Solar Hydrogen and Nanotechnology*, Lionel Vayssieres Editor, John Wiley and Sons, **2010**, 589-617.

7. "Mixed-Metal Supramolecular Complexes Coupling Polyazine Light Absorbers and Reactive Metal Centers," S.M. Arachchige, K.J. Brewer, in *Macromolecules Containing Metal and Metal Like Elements: Supramolecular and Self-Assembled Metal-containing Materials,* Volume 9, John Wiley and Sons, Martel Zeldin, Editor, **2009**, 295-366.

8. "Design Considerations for a System for Photocatalytic Hydrogen Production from Water Employing Mixed-Metal Photochemical Molecular Devices for Photoinitiated Electron Collection," S.M. Arachchige, J.R. Brown, E. Chang, A. Jain, D.F. Zigler, K. Rangan, K.J. Brewer *Inorg. Chem.* **2009**, *48*, 1989-2000.

9. "Ruthenium(II) Polyazine Light Absorbers Bridged to cis-Dichlororhodium(II) Sites in a Bimetallic Molecular Architecture," D.F. Zigler, J. Wang, K.J. Brewer *Inorg. Chem.* **2008**, 47, 11342-11350.

10. "Photochemical Hydrogen Production from Water Using the New Photocatalyst $[\{(bpy)_2Ru(dpp)\}_2RhBr_2](PF_6)_5$," S.M. Arachchige, J. Brown, K.J. Brewer *J. Photochem. Photobiol. A. Chem.* **2008**, *197*, 13-17.

11. "Rhodium Centered Mixed-Metal Supramolecular Complex as a Photocatalyst for the Visible Light Induced Production of Hydrogen," M.C. Elvington, J. Brown, S.M. Arachchige, K.J. Brewer *J. Am. Chem. Soc.* **2007**, *129*, 10644-10645.

II.K.12 Hydrogen Generation Using Integrated Photovoltaic and Photoelectrochemical Cells

Jin Z. Zhang[1]* (Principal Investigator) and Yiping Zhao[2]

[1]Department of Chemistry and Biochemistry
University of California
1156 High Street
Santa Cruz, CA 95064
Phone: (831) 459-3776
E-mail: zhang@ucsc.edu

[2]Department of Physics and Astronomy
The University of Georgia
Athens, GA 30602
Phone: (706) 542-7792
E-mail: zhaoy@physast.uga.edu

DOE Program Manager: Jane Zhu
Phone: (301) 903-3811
E-mail: Jane.Zhu@science.doe.gov

Objectives

The primary objective of this project is to develop novel nanostructures with improved optical and electronic properties for photoelectrochemical (PEC) hydrogen generation from water splitting. Specifically, we seek to design and demonstrate new strategies based on combining quantum dot (QD)-sensitization and elemental doping to significantly enhance visible light absorption and thereby PEC properties of metal oxide (MO) nanostructures, e.g. TiO_2, WO_3, and ZnO. Interesting synergistic effect has been discovered from the combined use of QD sensitization and N-doping of TiO_2 nanoparticle (NP) and nanorods.[1] Similarly, combining Au NPs with CdSe QD sensitization of TiO_2 has shown strong synergistic effect as well in terms of PEC performance.[2] The fundamental mechanisms behind the observed synergistic effects have been proved using a combination of experimental techniques including spectroscopy, microscopy, and ultrafast laser.

Technical Barriers

Towards the development of efficient PEC cells for hydrogen generation based on nanomaterials, one of the technical barriers is to control the surface properties of all the components involved, e.g. the MO nanostructures, QDs, and metal NPs. The second technical barrier is to determine the local structures and exact energy levels of the dopant, e.g. N, since this is critical to develop appropriate models to explain the synergistic effects observed.[1] The third technical barrier is to probe and understand the exact role of metal NPs in the enhanced PEC performance, which has been tentatively attributed to increased light scattering of Au NPs, leading to enhanced light absorptions of the CdSe QDs.[2]

Abstract

Hydrogen is an extremely attractive fuel for clean alternative energy. New nanocomposite structures and advanced strategies have been developed to improve the performance of PEC cells for hydrogen generation from water splitting. Systematical studies have been carried out to probe the fundamentals behind, including charge carrier properties at interfaces. One of the most important discoveries we have made is strong synergistic effects in ternary nanocomposites that show significantly enhanced PEC properties compared to binary or single component systems. These strategies are promising for advancing energy conversion technologies in the future.

Progress Report

1. Generating hydrogen by PEC with CdSe QD sensitized and N-doped TiO_2 nanostructures

TiO_2 is the most researched material for PEC water splitting. Since the bandgap of the TiO_2 is large (E_g=3.2eV), it cannot absorb most of the sunlight. One effective way to increase the absorption of the sunlight is by using semiconductor QDs to sensitize the TiO_2 film. Another approach is elemental doping. PEC measurements carried out on TiO_2 NPs and nanorods demonstrated that there is a strong synergistic effect when QD sensitization is combined with N-doping.[1] The reason for the increase in photocurrent when CdSe sensitizes N-doped TiO_2 vs. TiO_2 alone is attributed to the increase in hole transport from the valence band of CdSe to the oxygen vacancies in N-doped TiO_2.

2. PEC Properties of CdSe/TiO_2 Mesoporous Hybrid Structures

In sensitizing metal oxides such as TiO_2 using QDs, small molecules are often used to link semiconductor quantum dots to TiO_2 films. Since these small molecules are mainly dielectric materials, they will block the transfer of the photoelectrons from the quantum dots to the TiO_2 film. In this project, we have developed a new method to link QDs and TiO_2 without using the small linking molecules by assembly the QDs and TiO_2 NPs together into colloid spheres.[2] The PEC characterization of CdSe/TiO_2 hybrid spheres shows an increase in the photocurrent when compared to TiO_2 alone and CdSe sensitized to TiO_2 using a linking molecule. The overall increase in photocurrent

from the CdSe/TiO_2 hybrid structure is believed to be due to better or stronger coupling between the CdSe and the TiO_2 when compared to the CdSe sensitized TiO_2 linked by short chain organic linker molecules.

3. Enhanced PEC Performance of CdSe QD-Sensitized Au/TiO_2 Hybrid Mesoporous Films

Metal NPs have also been considered for sensitizing of enhance PEC properties of metal oxides. We have demonstrated the first Au/TiO_2 hybrid structure (0-5%) that has also been sensitized with CdSe QDs for PEC water splitting. For the pristine TiO_2 film sample, the absorption onset is around 360 nm, with minimal visible light absorption. In contrast, the Au/TiO_2 film showed strong absorption in the visible region due to the surface plasmon resonance (SPR) of Au NPs, and the absorption increases with increasing amount of Au NPs loading. The strong enhancement for the photocurrent when Au is introduced with CdSe can be explained by an increase in scattering due to presence of the metal. The increase in scattering allows the CdSe to absorb more light and inject electrons into the conduction band of TiO_2. Since enhancement occurred over the entire visible spectral range and increased with decreasing wavelength, increased light scattering by Au NPs is suggested to be responsible for the enhanced PEC performance.

4. N-Doped ZnO Nanowire Arrays for PEC Water Splitting

N-doped zinc oxide (ZnO:N) nanowire arrays have also been studied as photoanodes in PEC hydrogen generation from water splitting. In comparison to ZnO nanowires without N-doping, ZnO:N nanowires show an order of magnitude increase in photocurrent density with photo-to-hydrogen conversion efficiency of 0.15% at an applied potential of +0.5 V (versus Ag/AgCl). These results suggest substantial potential of metal oxide nanowire arrays with controlled doping in PEC water splitting applications.

5. Photocatalytic Performance Improved in Nanorod Arrays

One way to effectively increase the photocatalytic performance of TiO_2 is to couple it with a metal, such as Ag, in order to create an effective charge-separation between the photogenerated electron-hole pairs. Ag NPs with different loadings were systematically coated onto uniformly aligned TiO_2 nanorod arrays, and their photocatalytic performance was found to be enhanced compared to bare TiO_2, and increased linearly with the Ag NP loading until a maximum photodecay rate was reached at 0.25 wt.% Ag loading, and then decreased linearly with further increasing Ag loading. A simple reaction model was developed to explain the experimental results. Using two consecutive glancing angle depositions (GLAD) at different deposition angles and with different material, a WO_3-core TiO_2-shell nanostructure has been fabricated. The core-shell nanostructures are much more efficient in the amount of photodegradation abilities that can be extracted per nm of TiO_2 deposited. For the core-shell nanostructures annealed at T_a =300°C, this ratio is 470 times, 90 times, and 18 times more efficient than the amorphous TiO_2, anatase TiO_2, and multi-layered TiO_2/WO_3 films. This huge improvement can be directly correlated to the larger interfacial area between TiO_2 and WO_3, which is optimized in this core-shell morphology.

Both WO_3/TiO_2 and TiO_2/WO_3 core/shell nanorod films were used to make electrodes for PEC water splitting. IPCE analysis showed that the WO_3/TiO_2 samples were more efficient at water splitting. The maximum efficiency for the TiO_2/WO_3 sample was under 5% at about 340 nm. The WO_3/TiO_2 achieved near 12% IPCE at 350 nm but the efficiency decreased sharply around 390 nm. These preliminary data show that the WO_3 is the better core material for these core/shell structures but improved efficiency in the visible region through sensitization or doping may allow these structures to achieve greater efficiency. Additional characterization will be needed to determine why the two structures showed such a marked difference in water splitting efficiency.

6. Double-Sided QD Co-Sensitized ZnO Nanowire Arrays for PEC Hydrogen Generation

An analogue of the typical tandem cell for PV devices has been produced by designing a photoanode which is coated on both sides with conductive substrate (FTO) and ZnO nanowires. To increase the visible light absorption, both sides have been coated in either CdS or CdSe. This unique structure integrates the motif of QD sensitization and tandem cell to provide a simple approach to enhance simultaneously the visible light absorption and carrier collection of nanostructured metal oxide photoelectrodes. The electrode with the highest photocurrent and efficiency was when the CdS/ZnO nanowire side was illuminated with light loading compared to the CdSe/ZnO on the opposite end. Controls were done on various double sided as well as single sided structures. Linear sweep measurements for the CdS/ZnO-ZnO/CdSe double sided nanowire electrodes showed enhanced photocurrent when compared to control structures. This is due to the elevation of the CdSe when the Fermi energies are aligned increasing electron and hole transport. Recombination of electrons and holes is also less in these devices which increases their overall performance.

Future Directions

Our plan for next year include optimization of composite structures in terms of ratio and morphology of constituent components, validation of the enhanced hole transport model proposed using ultrafast laser techniques using the new fs laser system acquired recently, and improvement of overall PEC performance by carefully considering, determining and controlling the key factors involved, including electrode, interfacial interaction, and optical absorption. A combination of microscopy, spectroscopy, dynamics, and electrochemistry techniques will be employed. Collaboration with appropriate groups will be

sought, including possible theoretical modeling in relation to the experimental work.

References

1. J. Hensel, G. Wang, Y. Li, and J.Z. Zhang, "Synergistic effect of CdSe quantum dot sensitization and nitrogen doping of TiO_2 nanostructures for photoelectrochemical hydrogen generation", Nano Letters, 10, 478-483, 2010.

2. L. Liu, G. Wang, Y. Li, Y. Li, and J. Z. Zhang, "Enhanced photoresponse of CdSe quantum dot sensitized TiO_2 nanoparticles by plasmonic gold nanoparticles", Nano Research, in press, 2010.

3. G. Wang, X. Yang, F. Qian, J.Z. Zhang and Y. Li, "Double-sided CdS and CdSe quantum dot co-sensitized ZnO nanowire arrays for photoelectrochemical hydrogen generation", Nano Letters, 10, 1088-1092, 2010.

Publication list (including patents) acknowledging the DOE grant or contract

1. K.L. Knappenberger, Jr., W. Xu, D.B. Wong, A.M. Schwartzberg, A. Wolcott, J.Z. Zhang, and S.R. Leone, "Excitation wavelength dependence of fluorescence intermittency in CdSe/TOPO nanorods", *ACS Nano*, 2, 10, 2143-2153, 2008.

2. A. Wolcott, W. A. Smith, T. R. Kuykendall, Y.P. Zhao, and J.Z. Zhang "Photoelectrochemical generation of hydrogen from water splitting based on dense and aligned TiO_2 nanorod arrays", *Small*, 5, 104-111, 2008.

3. G. Wang, D. Chen, H. Zhang, S. Nespurek , J.Z. Zhang and J. Li, "Tunable photocurrent spectrum and enhanced photocatalytic activity of well-oriented zinc oxide nanorod arrays", *J. Phys. Chem. C*, 112, 8850-8855, 2008.

4. J.Z. Zhang, C.D. Grant, "Optical and dynamic properties of semiconductor nanomaterials", *Ann. Rev. of Nano Research*, 2, 1, 2008 (invited review).

5. W. Smith and Y.-P. Zhao, "Enhanced photocatalytic activity by aligned WO_3/TiO_2 two-layer nanorod array," *J. Phys. Chem. C*, 112, 19635 -19641 (2008).

6. Y.-P. He, Z.-Y. Zhang, and Y.-P. Zhao, "Optical and photocatalytic properties of oblique angle deposited TiO_2 nanorod array," *J. Vac. Sci. Technol. B* 26, 1350 - 1358 (2008).

7. T. Lopez-Luke, A. Wolcott, L. Xu, S. Chen, Z. Wen, J. Li, Elder de La Rosa-Cruz, and J.Z. Zhang, "Nitrogen doped and CdSe quantum dot sensitized nanocrystalline TiO_2 films for solar energy conversion applications", *J. Phys. Chem. C*, 112, 1282-1292, 2008.

8. J. Li and J.Z. Zhang, "Optical properties and applications of hybrid semiconductor nanomaterials", Coord. Chem. Rev., 253, 3015-3041, 2009 (invited review).

9. Y. Li and J.Z. Zhang, "Hydrogen generation from photoelectrochemical water splitting based on nanomaterials", Lasers and Photonics Review, in press, 2009 (invited review).

10. Z. Wen, Y. Li, J. Li, J.Z. Zhang, "Metal oxide nanostructures for lithium-ion batteries" in book on "Metal Oxide Nanostructures and Their Applications", Chapter 3, 1-33, 2009.

11. A. Wolcott and J.Z. Zhang, "Multidimensional nanostructures for water splitting: synthesis, properties and applications", invited book chapter for "On Solar Hydrogen and Nanotechnology" edited by L. Vayssieres, Chapter 15, pp. 459-506, 2009.

12. X. Yang, A. Wolcott, G. Wang, A. Sobo, B. Fitzmorris, F. Qian, J.Z. Zhang, and Y. Li, "Nitrogen-doped ZnO nanowire arrays for photoelectrochemical water splitting", Nano Letters, 9, 2331-2336, 2009.

13. W. Smith, W. Ingram, and Y.-P. Zhao, "The scaling of the photocatalytic decay rate with the length of aligned TiO_2 nanorod arrays," Chem. Phys. Lett. **479**, 270–273, 2009.

14. W. Smith and Y.-P. Zhao, "Superior photocatalytic performance by vertically aligned core-shell TiO_2/WO_3 nanorod arrays," Catalysis Communications **10**, 1117-1121, 2009.

15. R. Sharma, J.P. Mondia, J. Schäfer, W. Smith, S.-H. Li, Y.-P. Zhao, Z.H. Lu, and L.J. Wang, "Measuring the optical properties of a trapped ZnO tetrapod," Microelectronics Journal **40**, 520-522, 2009.

16. J. Hensel and J.Z. Zhang, "Effect of ions on photoluminescence of semiconductor quantum dots", Science of Advanced Materials, 1, 4-12, 2009.

17. R.W. Meulenberg, J.R.I. Lee, A. Wolcott, J.Z. Zhang, L.J. Terminello, and T. van Buuren, "Determination of the exciton binding energy in CdSe quantum dots", ACS Nano, 3, 325-330, 2009.

18. G. Chornokur, S. Ostapenko, E. Oleynik, C. Phelan, N. Korsunska, T. Kryshtab, J.Z. Zhang, A. Wolcott, T. Sellers, "Scanning photoluminescent spectroscopy of bioconjugated quantum dots", Superlattices and Microstructures, 45, 240-248, 2009.

19. A. Wolcott, J.Z. Zhang, W.A. Smith, and Y.P. Zhao, "Photoelectrochemical Study of Nanostructured ZnO Thin Films for Hydrogen Generation from Water Splitting", Advanced Functional Materials, 19, 1849-1856 2009.

20. L. Liu, G. Wang, Y. Li, Y. Li, and J.Z. Zhang, "Enhanced photoresponse of CdSe quantum dot sensitized TiO_2 nanoparticles by plasmonic gold nanoparticles", Nano Research, in press, 2010.

21. A. Wolcott, R.K. Fitzmorris, O. Muzaffery, and J.Z. Zhang, "CdSe quantum rod formation aided By in situ TOPO oxidation" Chem. Mater., 22, 2814-2821, 2010.

22. G. Wang, X. Yang, F. Qian, J.Z. Zhang and Y. Li, "Double-sided CdS and CdSe quantum dot co-sensitized ZnO nanowire arrays for photoelectrochemical hydrogen generation", Nano Letters, 10, 1088-1092, 2010.

23. J. Hensel, G. Wang, Y. Li, and J.Z. Zhang, "Synergistic effect of CdSe quantum dot sensitization and nitrogen doping of TiO_2 nanostructures for photoelectrochemical hydrogen generation", Nano Letters, 10, 478-483, 2010.

24. L. Liu, J. Hensel, R.C. Fitzmorris, Y. Li, and J.Z. Zhang, "Preparation and photoelectrochemical properties of CdSe/TiO_2 hybrid mesoporous structures", J. Phys. Chem. Lett., 1, 155-160, 2010.

25. X.J. Lv, J.H. Li, Jennifer Hensel, Jin Z. Zhang, "Enhanced visible light photoelectrochemical performances with nitrogen doped TiO_2 nanowire arrays", Electrochemistry, 15, 432-440, 2009.

26. W. Smith, S. Mao, G. Lu, A. Catlett, J. Chen, and Y. Zhao, "The effect of Ag nanoparticle loading on the photocatalytic activity of TiO_2 nanorod arrays," Chem. Phys. Lett. **485**, 171–175, 2010.

27. C. Tansakul, E. Lilie, E.D. Walter, F. Rivera III, A. Wolcott, J.Z. Zhang, G.L. Millhauser and R. Braslau, "Distance-dependent fluorescence quenching and binding of CdSe quantum dots by functionalized nitroxide radicals", J. Phys. Chem. C, 114, 7793-7805, 2010.

28. J. Hensel, M. Canin, J.Z. Zhang, "QD co-sensitized and nitrogen doped TiO_2 nanocomposite for photoelectrochemical hydrogen generation", SPIE Proc., 7770, 121-128, 2010.

29. J. Hensel and J.Z. Zhang, "Photogenerated charge carriers in semiconductor nanomaterials for solar energy conversion" Int. Journal of Nanoparticles, (invited key review), in press, 2010.

30. J.Z. Zhang, "Metal oxide nanomaterials for solar hydrogen generation from photoelectrochemical

31. J.Z. Zhang, A. Wolcott, J. Hensel, T. Lopez-Luke, and Y. Li, "QD sensitized and N-doped TiO_2 solar cells", U.S. Provisional Patent Application disclosed on May 1st, 2008.

II.K.13 Modular Designed Protein Constructions for Solar Generated H_2 from Water

P. Leslie Dutton (Principal Investigator),
Christopher C. Moser (Co-PI)
University of Pennsylvania
Department of Biochemistry and Biophysics
Philadelphia, PA 19104-6059
Phone: (215) 573-3909; Fax: (215) 573-2235
E-mail: moserc@mail.med.upenn.edu

DOE Program Manager: Mike Markowitz
E-mail: Mike.Markowitz@science.doe.gov

Objectives

Our long-term objective is to harness the energy of the sun for the production of inexpensive chemicals and fuels useful to mankind. We aim to achieve this with simple, design-flexible artificial proteins called maquettes. Maquette protein designs are informed by engineering and structural principles we learn from impressive natural photosynthesis. Our aim is to turn these principles into guidelines for the practical assembly of maquettes equipped for tailored photochemistry.

Technical Barriers

Creation of very long-lived, light-activated charge-separated states will allow the accumulation of reductants and oxidants in the vicinity of catalytic centers within the protected environment of the artificial protein. With these lifetimes, even slow catalytic centers with significant activation energy barriers for making hydrogen or other fuels can operate, and then be iteratively redesigned to improved speed and function.

Abstract

There is an urgent need to meet global demands for clean, inexpensive and renewable sources of energy. Sunlight is an abundant energy source tapped by biological photosynthesis. Our project is inspired by the efficiency and speed of biological photosynthesis that draws on water as its source of electrons for reduction of CO_2 to produce its cellular materials and fuels. Our project is directed to the abstraction of key engineering and construction principles from natural photosynthetic proteins and their application to the creation of a family of artificial photosynthetic proteins tailored to harnessing solar energy to drive production of useful chemicals and fuels including hydrogen. It is also our intention that any artificial proteins proving valuable to mankind as planned, will be designed ready for expression in bacteria for minimized costs of scaled production and assembly.

Progress Report and Future Directions

Generic tunneling barriers in natural proteins: The theoretical basis for our electron tunneling expressions and their utility for calculating relevant tunneling parameters in natural and man-made photosynthetic systems is empirical. The generality of the expressions so far developed for analyzing parameters of electron tunneling in protein is therefore subject to reconsideration and refinement when new electron-transfer data from well-characterized proteins is received. The addition of over 20 new non-physiological electron tunneling reactions from semi-synthetic proteins continues to support our view that tunneling-barrier height has not been naturally selected to help or hinder electron transfer in natural photosynthesis. The barrier height does dictate the spatial essential required for light activated charge separating elements to generate high yield charge separated states stable into the millisecond times. Thus, natural reaction center proteins are scaled to approx 2.5 nm (25Å) while covalently bridged biomimetics require 5 nm (50 Å) and hence must be over twice as large to achieve the same performance.

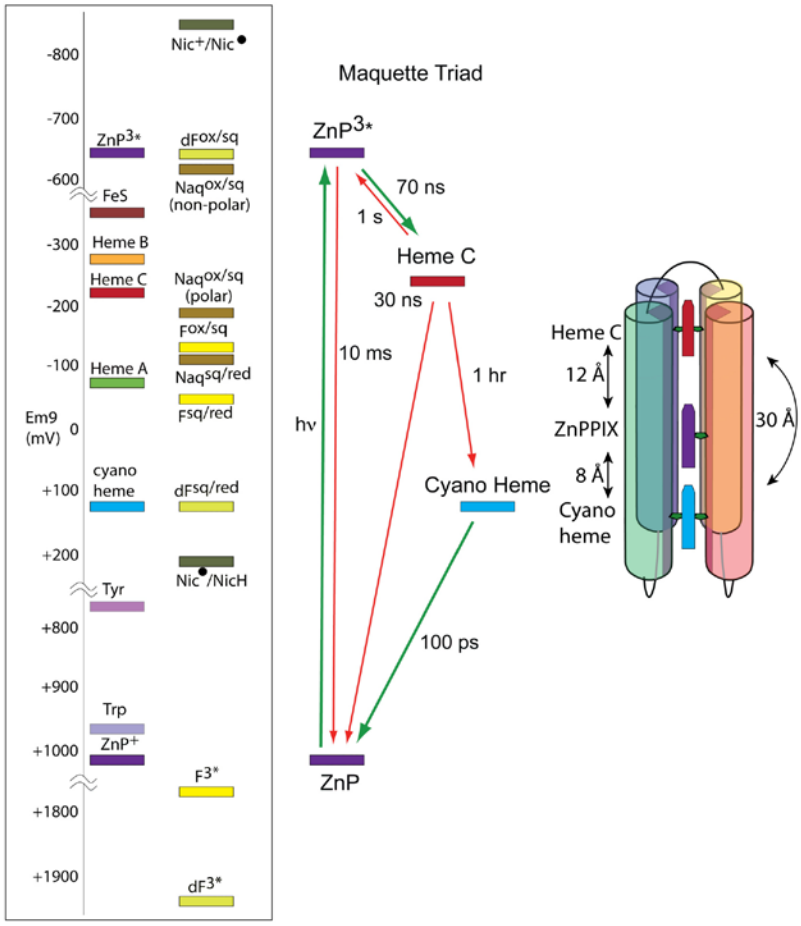
Coupling electron tunneling to redox catalysis: We have extended our expressions to guide the engineering and construction of maquettes that catalyze oxidative and reductive chemistries. We are moving from pure electron tunneling, now beginning to be well described, to simple catalysis involving two-electron hydride transfer that occurs in the large class of dehydrogenases and to two-or-more electron transfers linked to bond forming/breaking common in oxidative and reductive catalysis. There is an important interplay between distance and driving force in the design and engineering of natural oxidoreductases when an overall exergonic series of electron transfers includes one or more endergonic (uphill) steps. To some extent the increased height of an uphill step can be compensated for by shrinking the distance between donor and acceptor while still maintaining overall sequential electron-tunneling rates within the approximately millisecond working threshold. We find that the balance between tunneling distance and uphill driving force sketches an unexpectedly broad engineering choice in distances and driving forces to achieve acceptable nanosecond to milliseconds sequential electron-transfer rates. The distance/energetic boundaries where sequential electron-transfer mechanisms become unworkably slow are clear.

Synthetic protein backbone design: Our aims to reproduce photochemical energy conversion and chemical oxidation-reduction catalysis require the development

of maquette interiors that collect the characteristics fundamental to catalytic fitness in nature. Maquette interior design and the incorporation of cofactors go hand in hand. Despite the apparent low dielectric interior of the unlinked homodimeric maquettes, H/D exchange measurements indicate they offer comparatively little restriction for the entry of water. Regulation of water access is vital to the design of sites engaged in initial charge separation (low reorganization energies) and catalysis (chemical transformation sharply promoted or suppressed by water). We disulfide-linked maquette helices in a candelabra-like geometry, restricting helical motions, to dramatically slow H/D exchange and restrict water access to the interior of our simple maquettes well beyond the millisecond time scales of typical catalysis. We note that the interior of an analogous single-chain maquette excluded water despite substantial protein motion during rapid heme ligand exchange.

Tetrapyrrole designs: The lower symmetry of the single-chain maquette allows new design and assembly opportunities including covalent anchoring at specific positions of tetrapyrroles such as heme C as well as binding of single light activated centers such as Zn protoporphyrin IX and Zn-pheophorbide and bacteriochlorophilide in the presence of companion redox centers and tetrapyrroles. We have found the new single chain maquette family avidly binds tetrapyrroles with nanomolar dissociation constants provided they are polar on one side and nonpolar on one or other sides. We are finding that the maquettes that support the fastest and simplest binding time courses are those that in the apo form are known to have multi-structured interiors that become structured upon porphyrin/chlorin coordination as indicated by NMR. We can secure porphyrin cofactors at 9.4 and 15.9 Å edge-to-edge distances by constructing histidine ligation sites along a helix 3 or 4 turns apart. We avoid 1 or 2 turns because of steric collision between adjacent porphyrins. However, there is no such limit to histidine placement in an adjacent helix. Presently, we secure porphyrins in adjacent helices at the level of 0, 2 or 4 helical turns which leads to edge-to-edge distances between different tetrapyrroles of 3.4, 7.2 and 17.9 Å. The demonstrated flexibility in controlling which tetrapyrroles bind where (bis-histidine sites bind Fe tetrapyrroles, mono-histidine sites Zn, covalent sites Fe or Zn) and the spacing between tetrapyrroles provide a good palette for positioning these cofactors at optimal locations, orientations and distances apart in the design of reaction center maquettes and for catalysis.

Multi-electron redox cofactors: We have designed non-tetrapyrrole cofactors to serve as other candidates for light-activated-triad electron donors and acceptors, for cofactor relays to add stability to the initial charge-separated states and for multi electron function at catalytic sites. These include a naphthoquinone amino acid (Naq), which is functionally similar to the natural menaquinone or vitamin K family and structurally can substitute for tryptophan. We use an intein strategy to splice synthetic Naq peptides with expressed sequences. We have also developed a nicotinamide amino acid and secured various flavins to the maquette frameworks. Commonly, we react brominated flavins with Cys sulfur. We are increasing the flexibility of the approach by modifying flavins for attachment through the 8-a-methyl position, which tends to raise the flavin midpoint potential, in addition to our traditional 6-H position. We have also demonstrated the synthesis and characterization of a $(m\text{-}SR)_2Fe_2(CO)_6$ complex coordinated to a simple, α-helical peptide via two cysteine residues. Although this prototype showed no $H+/H_2$ exchange



Average energy levels of redox centers secured inside maquettes. The first column on the left lists one-electron donors/acceptors and the second column two-electron cofactors. The middle schematic shows energy levels and lifetime selected in a triad presently under construction depicted on the right.

catalysis, the peptide serves as a first generation [FeFe]-hydrogenase maquette and opens the chemical door through redesign for the creation of more sophisticated peptides containing second coordination sphere residues designed to modulate the properties of the di-iron site. We have also reengineered the four-helix bundles of a natural bacterioferritin to include light-activated chlorins that serve to photo-oxidize Mn, in a manner analogous to the photo-assembly of the Mn cluster of the oxygen evolving center in natural photosynthetic photosystem II.

Light-activated maquettes: We have explored the nanosecond to milliseconds spectral signatures of light activated electron transfer along the length of maquettes in chromophore dyads, using Zn PPIX or flavins as light-activated centers and various hemes as donors and acceptors. Longer charge separated lifetimes will be available in the light-activated triads we are currently constructing and testing in the single-chain four-helix bundle maquette designs (see figure). On the basis of our electron tunneling analysis, our current triad design should allow stable charge separation on the many minutes timescale, longer than any present chemical or biological construct, making it easier to achieve successful oxidative or reductive electron transfer at catalytic sites within the maquette. After successful construction of very long-lived charge-separated states, we will add a terminal cluster of redox centers to accumulate reductants within the maquette for catalysis at promising chemically constructed hydrogen producing centers secured within the maquettes.

Publication list (including patents) acknowledging the DOE grant or contract

1. Noy, D., Discher, B.M., Rubtsov, I.V., Hochstrasser, R.A., and Dutton, P.L. Design of amphiphilic protein maquettes: Enhancing maquette functionality through binding of extremely hydrophobic cofactors to lipophilic domains. **Biochemistry,** 44: 12344 -12354, 2005.

2. Koder, R.L., Valentine, K.G., Cerda, J.F., Noy, D., Wand, A.J., and Dutton, P.L. Native-like Structural Structure in Designed Four α-helix Bundles Driven by Buried Polar Interactions. **J. Am. Chem. Soc**., 128: 14450-14451, 2006.

3. Koder R.L and Dutton, P.L. Intelligent Design: The De novo Engineering of Proteins with specific functions**. Dalt. Trans**, 25: 3045-3051, 2006

4. Koder, R.L., Potyim, M., Walsh, J., Dutton, P.L., Wittebort, R.A., and Miller, A-F. N Solid-state NMR Provides a Sensitive Probe of Flavin Reactive Sites. **J. Am. Chem. Soc**., Vol 128, 45: 15200-15208, 2006.

5. Koder, R.L., Lichtenstein, B.R., Cerda, J.F., Miller, A-F. and Dutton, P.L. Flavin Analogue with Improved Solubility in Organic Solvents, **Tetrahedron Letters**, 48, 5517-5520, 2007.

6. Jones, A.K., Lichtenstein, B.R., Dutton, A., Gordon, G., and Dutton, P. L. Synthetic Hydrogenases: Incorporation of an Iron Carbonyl Thiolate into a Designed Peptide**, J. Am. Chem. Soc.** 129: 14844-14845, 2007.

7. Lichtenstein, B.R., Cerda, J.F., Koder, R.L., and Dutton, P.L. Reversible Proton Coupled Electron Transfer in a Peptide-incorporated Naphthoquinone Amino Acid. **The Royal Society of Chemistry. Chem. Comm,** 170, 168-170, 2008.

8. Cerda, J.F., Koder, R.L., Lichtenstein, R.R., Moser, C.C. Miller, A-F, and Dutton, P.L. Hydrogen Bond-Free Flavin Redox Properties: Managing Flavins in Extreme Aprotic Solvents. **Organic and Biomolecular Chemistry** 6**,** 2204-2212, 2008.

9. Moser, C.C., Chobot, S.E., Page, C.C. and Dutton, P.L. Distance Metrics for Heme Protein Electron Tunneling. **Biochim. Biophys. Acta, 1777**:1032-1037, 2008.

10. Koder, R.L., Anderson, J.L.R, Solomon, L.A. Reddy, K.S., Moser, C.C. and Dutton, P.L. Design and Engineering of an O_2 Transport Protein. **Nature**, 458**;** 305-309, 2009.

11. Conlan, B., Cox, N., Su, J., Hillier, W., Messinger, J., Lubitz, W., Dutton, P.L., and Wydrzynski, T. Photo-catalytic Oxidation of a Di-nuclear Manganese Centre **in an E**ngineered Bacterioferritin 'reaction centre'. **Biochim. Biophys. Acta,** 1787, 1112-1121, 2009.

12. Zheng, Z., Dutton, P.L., and Gunner, M. The Measured and Calculated Affinity of Methyl and Methoxy Substituted Benzoquinones for the QA Site of Bacterial Reaction Centers. **Proteins,** 78 (12) 2638-2654, 2010.

13. Moser, C.C., Anderson, J.L.R., and Dutton, P.L. Guidelines for Tunneling in Enzymes. **Biochim. Biophys. Acta,** 1797**,** 1573-1586, 2010.

II.K.14 Protein-Templated Synthesis and Assembly of Nanostructuctures for Hydrogen Production

Arunava Gupta[1]*, Peter E. Prevelige[2], Liming Shen[1], Ningzhong Bao[1], Rui Li[2], Anup Kale[1], Rajagopal Krishnan[2], and Tara Cartee[2]
[1] University of Alabama, Tuscaloosa, AL 35487
[2] University of Alabama, Birmingham, AL 35294
Phone: (205) 348-3822; Fax: (205) 348-2346
E-mail: agupta@mint.ua.edu; prevelig@uab.edu

DOE Program Manager: Dr. Michael Markowitz
E-mail: Mike.markowitz@science.doe.gov
Phone: (301) 903-6779

Objectives

Photocatalysis using solar radiation represents a significant opportunity for the development of renewable energy sources (H_2 production). In general, the visible-light-driven photocatalysis reactions that have been explored thus far exhibit low quantum efficiency for solar energy conversion, which limits their practical utility. The goal of the project is to develop protein-templated approaches for the synthesis and directed assembly of semiconductor nanomaterials that are efficient for H_2 production from water under visible light irradiation.

Technical Barriers

The low quantum efficiency for visible-light-driven photocatalysis is primarily because of materials-related issues and limitations, such as the control of the band gap, band structure, photochemical stability, and available reactive surface area of the photocatalyst. Synthesis of multicomponent hierarchical nano-architectures using biomimetic approaches, consisting of semiconductor nanoparticles with desired optical properties fabricated to maximize spatial proximity for optimum electron and energy transfer, represents an attractive route for addressing the problem.

Abstract

A variety of sulfide nanomaterials with controlled size, phase structure, and three-dimensional architectures have been synthesized using *E. Coli* bacteria and genetically engineered virus (P22) as affinity bio-templates. Photoelectrodes fabricated using the *E. Coli* templated synthesis of hollow CdS nanostructures exhibit excellent performance for photocatalytic hydrogen production with a photoconversion efficiency of 4.2 % under global AM 1.5 illumination in the presence of a sacrificial electron-donor of mixed S^{2-} and SO_3^{2-}. This is significantly better than the 1.34% efficiency obtained using CdS nanoparticles synthesized utilizing the same procedure in the absence of *E. Coli*. The potential of utilizing the P22 virus architecture to improve efficiency and durability of the IrO_2-Zn Porphyrin system for the water splitting reaction is also being explored. Moreover, the ability of the icosahedral P22 structures to act as scaffolds for energy harvesting via Förster resonance energy transfer (FRET) is being investigated.

Progress Report

(a) Bacterial syntheses of quantum dots, nanocrystals, and hollow nanostructures: Sulfide semiconductors have a wide variety of optical, electrical, and photoelectric applications. CdS has a narrow band gap and a valence band at relatively negative potentials, which offer them good visible-light-active photocatalysts. Nanoporous hollow nanostructures are one of the best architectures since they avoid agglomeration of the NCs and reduce bulk/interface electron/hole recombinations. However, it is challenging to assemble NCs into highly ordered hollow nanostructures. We have developed a general biotemplate synthesis approach to prepare hollow CdS nanostructrures by taking advantage of the natural morphology of the common bacteria *E. coli*. The CdS nanostructures are prepared with high yield under mild ambient conditions with the assistance of sonochemistry using cadmium acetate dehydrate and thioacetamide as reactants. The CdS coating on the *E.coli* can be controlled in the form of monodisperse quantum dots (1-2 nm), near monodisperse NCs (7-8 nm), discontinuous CdS NC agglomerates, and uniform porous coating of NCs. Both the band gap and crystal structure of these CdS NCs can be tuned by simply adjusting the synthetic conditions, such as reaction time and the concentration of precursors (Figure 1 a-c). The photoelectrodes fabricated using the synthesized hollow CdS nanostructures exhibit excellent performance for photocatalytic hydrogen production with a photoconversion efficiency of 4.2 % under global AM 1.5 illumination in the presence of a sacrificial electron-donor of mixed S^{2-} and SO_3^{2-} (Figure 1d). The method has been extended to the synthesis of other sulfides including ZnS, PbS, AgS, etc., with controlled size, structure, and optical adsorption properties.

(b) Virus protein-templated three-dimensional sulfide nanoarchitectures: We have successfully developed a facile bioinspired approach for the synthesis of ordered 3D nanostructures of sulfide NC assemblies over genetically engineered P22 viral capsids (Figure 2a-e). The assembly procedure consists of (1) the self-assembly of spherical protein templates from genetically engineered P22 coat protein, and (2) the nucleation and growth of NCs on the self-assembled protein templates (Figure 2c). We

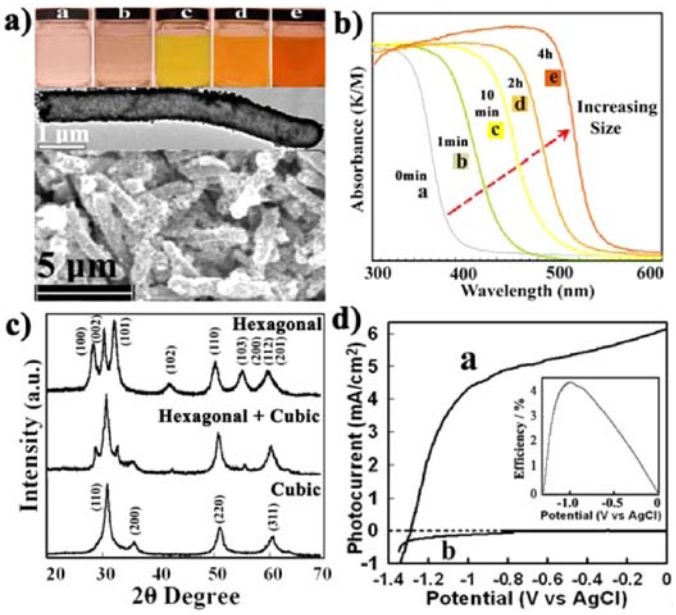


FIGURE 1. (a) SEM and optical images, (b) reaction time-dependent UV-vis spectra, (c) XRD patterns of *E. coli*-templated nanoporous hollow CdS microrods. (d) Photocurrent density (a) and dark current (b), and photoconversion efficiency (the inset) of a photoelectrode fabricated using nanoporous CdS hollow microrods.

have used ZnS and CdS grown on the engineered P22 coat protein assembly as a model system since binding peptides with strong affinity for these sulfides have been identified. Furthermore, the structure and assembly of the P22 coat proteins is reasonably well understood. By changing the reaction time and reactant concentration, the final protein-directed sulfide growth is expected to exhibit different structures, such as well ordered spherical NC assemblies (Figure 2d) during the early stage of growth that eventually develop into spherical hollow nanostructures for longer growth periods (Figure 2e). Both the diameter and configuration of the self-assembled P22 coat protein template can be controlled over a specific range by heating in solution at temperatures of up to 70 °C. This offers some degree of control over the size and shape of the synthesized inorganic nanostructures. Additionally, the crystallite size of the NCs can be varied by changing the reactant concentration and the reaction time. The synthetic strategy is quite general and can be extended to the fabrication of a variety of other nanostructures.

(c) Synthesis of IrO_2-Zn porphyrin labeled phage capsids: Filamentous viruses carrying Zn porphyrins which act as a photosensitizer and IrO_2 oxide hydrosol clusters which act as a catalyst have been demonstrated to effect photocatalytic water splitting, although immobilization of the viruses in a microgel was required to improve the structural durability. To evaluate the potential of spherical virus architecture to improve efficiency and durability we have inserted an IrO_2 binding peptide into the exterior surface of the bacteriophage P22 capsid and have taken advantage of a internal uniquely chemically reactive site (engineered in section 1.4 below) to conjugate a Zn porphyrin to the interior of the particle. A commercially available Zn porphyrin starting material was modified by the laboratory of Trevor Douglas by the introduction of a maleimide group which in turn is capable of efficient conjugation to the thiol group of the amino acid cysteine. Preliminary experiments suggest a modest level of conjugation of the porphyrin to the interior of the capsid at natural pH and optimization of the reaction is currently underway.

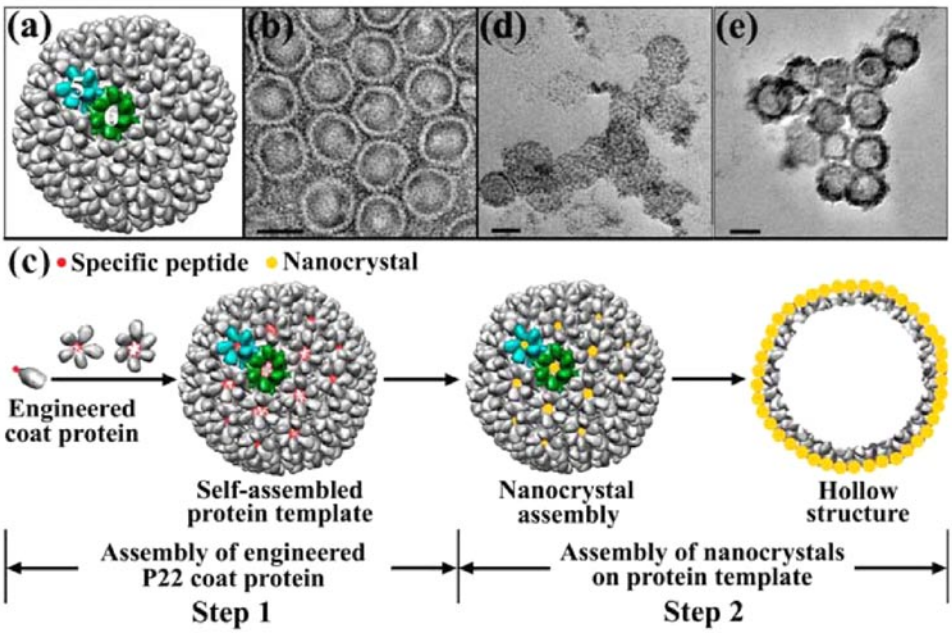


FIGURE 2. (a) Three-dimensional surface representation of P22 procapsid viewed along a 3-fold axis; (b) TEM image of stained protein assemblies of genetically engineered P22 coat protein; (c) Schematic illustration of the formation of ordered NC assemblies over self-assembled genetically engineered P22 coat proteins. Step 1: assembly of P22 coat proteins (gray) genetically engineered with specific peptide (red). Step 2: protein-directed nucleation and growth of NCs (yellow) on the protein assembly. (d and e) TEM images of sulfide NC assemblies grown on the self-assembled protein templates shown in Figure 1b. All scale bars represent 50 nm.

(d) Antenna effect studies using spherical P22 capsids: The antenna effect is the ability

of an ensemble of chromophores with similar absorbance bands to transfer energy to a common acceptor, hence to act as photon collecting antennas. We have analyzed the antenna effect displayed by chromophores on the exterior of the 60 nm spherical P22 capsid particle over a range of photon acceptor and donor densities. Our data indicated that the degree of donor emission increased with increasing fraction of labeled subunits up to a value of approximately 10% (~50 subunits) after which it decreased. The decrease was due to donor/donor collisional quenching. Under the most favorable conditions the antenna effect was limited to value of approximately 2 (meaning two donors could transfer to an acceptor). By mapping the site of the modification onto the capsid lattice it became evident that rather than being uniformly distributed on the capsid surface, as a result of the capsid architecture, the sites are locally clustered. It is the local clustering that result in the donor quenching and limited antenna effect. In collaboration with Reidun Twarock of the York Center for Complex Systems Analysis, an alternative site for modification which would result in a more uniform distribution of chromophores was identified.

(e) Construction of P22 phage capsids with internal chemically reactive sites: We have constructed a set of plasmids whose expression results in the production of P22 procapsids with chemically reactive amino acid residues located on the interior face of the capsid wall. Cysteine residues were inserted into a long a-helical region of the coat protein and the protein was tested for its ability to assemble into procapsids and the chemical reactivity of the cysteine residue in the various states of the procapsid was determined. Substitution of a cysteine at residue 110 of the capsid protein results in the formation of a properly dimensioned capsid in which the cysteine is reactive in the unexpanded procapsid form but unreactive in the expanded "wiffle ball" form. In contrast, substitution of residue 118 with cysteine results in a capsid in which the cysteine is reactive in the "wiffle ball" form but relatively unreactive in the procapsid form.

Future Directions

During the last phase of the current project, we are focusing on the fabrication of multicomponent inorganic nano-architectures over genetically engineered P22 capsids. The specific peptide sequences responsible for binding to different materials, including PbS, CdS, Fe_2O_3, and TiO_2, will be fused into the scaffolding protein of P22. The genetically engineered P22 capsids with the specific affinity for binding to PbS, CdS, Fe_2O_3, and TiO_2 will then be used to prepare porous hollow nanoballs, possibly consisting of multiple components. We will optimize synthetic conditions for control of the shell structure, the size of NC subunits, and the assembly of heterogeneous components. The physical and chemical properties of the products will be studied in detail. Photocatalytic activity and photoconversion efficiency of the obtained heterogeneous nanoarchitectures will be evaluated.

Publication list acknowledging the DOE grant

1. Kang, S., M. Uchida, A. O'Neil, R. Li, P.E. Prevelige, and T. Douglas; Implementation of P22 viral capsids as nanoplatforms. *Biomacromolecules.* 2010, 11, 2804-2809.

2. L. Shen, N. Bao, P.E. Prevelige, A. Gupta; Fabrication of Ordered Nanostructures of Sulfide Nanocrystal Assemblies over Self-Assembled Genetically Engineered P22 Coat Protein, *Journal of the American Chemical Society* 2010, 132, 17354-17357.

3. L. Shen, N. Bao, P.E. Prevelige; A. Gupta "Escherichia coli Bacteria-Templated Synthesis of Nanoporous Cadmium Sulfide Hollow Microrods for Efficient Photocatalytic Hydrogen Production, *J. Phys. Chem. C* 2010, 114, 2551-2559.

4. Y. Wang, N. Bao, A. Gupta; Shape-Controlled Synthesis of Semiconducting $CuFeS_2$ Nanocrystals, *Solid State Sciences* 2010, 12, 387-390.

5. Y. Wang, C. Pan, N. Bao, A. Gupta; Synthesis of Ternary and Quaternary $CuIn_xGa_{1-x}Se_2$ ($0<x<1$) Semiconductor Nanocrystals, *Solid State Sciences*, 2009, 11, 1961-1964.

II.K.15 Catalyzed Water Oxidation by Solar Irradiation of Band-Gap-Narrowed Semiconductors

Etsuko Fujita, Peter Khalifah, Sergei Lymar, James T. Muckerman,* Dmitry E. Polyansky, José Rodriguez
Chemistry Department, Brookhaven National Laboratory
Bldg 555
Upton, NY 11973
(631) 344-4356; (631) 344-5815
E-mail: fujita@bnl.gov

DOE Program Officer: Mark Spitler
Phone: (301) 903-4568
E-mail: mark.spitler@science.doe.gov

Objectives

- **Learn to design improved band-gap-narrowed semiconductors:** Design and characterize BGNSCs that are stable toward photo-oxidation, yet efficiently absorb a large fraction of solar radiation and with bands positioned to generate sufficiently energetic electrons and holes to drive H_2 and O_2 production reactions.
- **Elucidate homogeneous water oxidation catalysis pathways:** Understand and improve homogeneous water oxidation catalysis, where defined structure and mechanistic studies can give deep insight the $4e^-$ water-oxidation pathways
- **Understand interface-bound water oxidation catalysts:** Elucidate the factors controlling kinetics and efficiency of interface-bound catalysts through study of immobilized molecular catalysts and nanostructured inorganic catalysts.
- **Develop insight on water interactions and reactivity at band-gap-narrowed semiconductors:** Understand water interactions and reactivity at BGNSC interfaces and differences from wide band-gap semiconductors. Characterize photocatalysis of water at BGNSC interfaces with and without attached water oxidation catalysts.

Technical Barriers

- We need to design and characterize stable, low-cost and light absorbing materials as photoanodes for solar-driven water splitting
- There are no thermodynamically efficient and kinetically robust interface-bound oxidation catalysts that can facilitate charge transfer of holes from the semiconductor and catalyze water oxidation.
- The breakthroughs in overall device efficiency needed to support a hydrogen economy require integrated expertise in the co-dependent areas of semiconductor and catalyst development.

Abstract

We are attacking four major issues hindering progress in solar-driven water splitting using an integrated experimental and theoretical approach that offers fundamental insights into the underlying photoelectrolysis processes occurring in band-gap-narrowed semiconductor and catalyst components. First, we are tuning known photostable semiconductors to control their light-harvesting and charge-separation abilities in order to achieve a better understanding of their structural and electronic properties, and, in addition, design and characterize new classes of visible-light photoactive semiconductors. Second, we are developing viable catalysts for the difficult four-electron water oxidation process by exploring the catalytic activity and mechanisms of molecular transition-metal complexes. Third, we have begun immobilizing molecular catalysts and (non-precious) metal oxide catalysts on electrodes and/or metal-oxide nanoparticles in order to determine the kinetics of electrochemical water oxidation in the absence of mass transport limitations, and identify the intermediates by spectroscopic techniques. Finally, we plan to explore the interfacial water-decomposition reactions that occur at bare and catalyst-functionalized semiconductor surfaces using carriers generated by visible-light irradiation with the goal of understanding semiconductor–catalyst–water charge transport.

Progress Report

The combined experimental and theoretical research in our second funding period has resulted in a number of advances in the following areas. We investigated: (1) the properties of solid solutions of GaN/ZnO; (2) preparation and characterization of epitaxial $LaTiO_2N$ electrodes; (3) a number of new pyrochlore and pyrochlore-related semiconductors such as $AgBiNb_2O_7$ with strong visible light absorption (E_g ~ 2.7 eV) and band edges appropriately positioned for overall water splitting; (4) the detailed mechanism for water oxidation by the so-called "Tanaka catalyst," $[(Ru^{II})_2(OH)_2(Q)_2(btpyan)]^{2+}$ (Q = 3,6-di-*tert*-butyl-1,2-benzoquinone; btpyan = 1,8-bis(2,2′:6′,2″-terpyrid-4′-yl)anthracene) (Fig. 1, left) that stands apart from other dinuclear ruthenium catalysts not only in its stability and high turnover number but in the respect that it functions in an entirely different manner involving its redox-active quinonoid ligands; and (5) characterization of intermediates

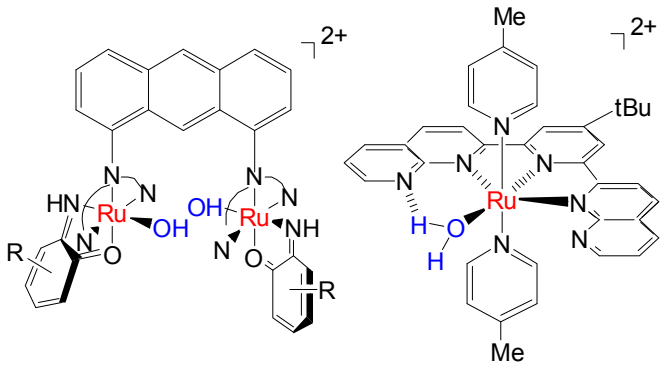


FIGURE 1. Structures of $[(Ru^{II})_2(OH)_2(Q)_2(btpyan)]^{2+}$ (left) and $[Ru(OH_2)(NPM)(pic)_2]^{2+}$ (right).

of Thummel's mononuclear water oxidation catalyst $[Ru(OH_2)(NPM)(pic)_2]^{2+}$ (NPM = 4-t-butyl-2,6-di-1′,8′-(naphthyrid-2′-yl)-pyridine, pic = 4-picoline) (Fig. 1, right). Furthermore, we demonstrated that the Co metal hydrous oxide can be immobilized on a suspension of TiO_2 or SiO_2 nanoparticles in basic aqueous solution, and that it is a very effective catalyst for water oxidation. Here we present some of our studies.

1. Photocatalytic Water Oxidation at the GaN (10$\bar{1}$0) – Water Interface. We constructed an atomistic model and proposed a sequence of intermediate steps for water oxidation at a pure GaN(10$\underline{1}$0)/water interface. Ab initio molecular dynamics simulations examined the fully solvated aqueous interface at ambient temperature. An appropriate cluster model, that includes a polarizable continuum in addition to explicit solvent water molecules, was cut out from snapshots of these AIMD simulations for additional DFT-based calculations of the water oxidation mechanism. The reaction intermediates follow a sequence of four proton-coupled electron transfers. Four UV photons are consumed to generate the four photo-holes which drive the oxidation, producing $4H^+ + O_2$ from $2H_2O$. Calculated standard free energies show that the photogenerated holes in GaN have sufficient energy to drive the overall water oxidation reaction. Implications for the operation of GaN/ZnO alloy photocatalysts, which absorb in the visible wavelength range, are presented. The calculated potentials show a remarkable parallelism to the known potentials for the sequential one-electron oxidation of water in homogeneous aqueous solution, suggesting that the proposed sequence may apply more generally than for the specific GaN (10$\underline{1}$0) surface catalyst.

2. Phase Diagram, Structure and Electronic Properties of $(Ga_{1-x}Znx)(N1-xOx)$ from DFT-Based Simulations. We constructed an accurate cluster expansion (CE) for the $(Ga_{1-x}Zn_x)(N_{1-x}O_x)$ solid solution based on density functional theory (DFT). A subsequent Monte Carlo simulation revealed a phase diagram which has a wide miscibility gap and an $x = 0.5$ ordered compound. The disordered phase displays strong short range order (SRO) at synthesis temperatures. To study the influences of SRO on the lattice and electronic properties, we conducted DFT calculations on snapshots from the MC simulation. Consistent with previous theoretical and experimental findings, lattice parameters were found to deviate from Vegard's law with small upward bowing. Bond lengths depend strongly on local environment, with a variation much larger than the difference of bond length between ZnO and GaN. The downward band gap bowing deviates from parabolic by having a more rapid onset of bowing at low and high concentrations. An overall bowing parameter of 3.3 eV is predicted from a quadratic fit to the compositional dependence of the calculated band gap. Our results indicate that SRO has significant influence over both structural and electronic properties.

3. Characterization of the Intermediates Involved in Water Oxidation: A detailed characterization of intermediates in water oxidation catalyzed by a mononuclear Ru polypyridyl complex $[\mathbf{Ru}\text{–}OH_2]^{2+}$ (**Ru** = Ru(NPM)(pic)$_2$) (Fig. 1, right) has been carried out using electrochemistry, UV-vis and resonance Raman spectroscopy, pulse radiolysis, stopped flow, and ESI-MS with $H_2{}^{18}O$ labeling experiments, and theoretical calculations. The results reveal a number of intriguing properties of intermediates such as $[\mathbf{Ru}{=}O]^{2+}$ and $[\mathbf{Ru}\text{–}OO]^{2+}$. Two consecutive one-electron steps take place at the potential of the $[\mathbf{Ru}\text{–}OH]^{2+}/[\mathbf{Ru}\text{–}OH_2]^{2+}$ couple, which is higher than the potential of the $[\mathbf{Ru}{=}O]^{2+}/[\mathbf{Ru}\text{–}OH]^{2+}$ couple. While pH-independent oxidation of $[\mathbf{Ru}{=}O]^{2+}$ takes place at 1410 mV vs NHE, bulk electrolysis of $[\mathbf{Ru}\text{–}OH_2]^{2+}$ at 1260 mV vs NHE at pH 1 (0.1 M triflic acid) and 1150 mV at pH 6 (10 mM sodium phosphate) yielded a red colored solution with a Coulomb count corresponding to the *net four-electron oxidation*. ESI-MS with labeling experiments clearly indicate that this species has an O–O bond. This species required an additional oxidation to liberate an oxygen molecule, and without any additional oxidant it slowly decomposed to form $[\mathbf{Ru}\text{–}OOH]^+$ in 2 weeks. We have assigned this species as $^1[\mathbf{Ru}\text{–}\eta^2\text{-}OO]^{2+}$ based on our electrochemical, spectroscopic, and theoretical data alongside a previously published conclusion by T.J. Meyer's group (*J. Am. Chem. Soc.* **2010**, *132*, 1545-1557).

Future Directions

Our ***four-part plan*** for developing functional photocatalytic systems builds upon the advances we have made in water oxidation catalysis and the elucidation of the properties of appropriate band-gap-narrowed semiconductors for use as photoanodes. First, we will work towards identifying new and promising semiconductors to serve as photoanodes in our mechanistic water oxidation studies. This will involve not only tuning their band gaps and absolute band edge energies, but also consideration of their suitability for use in well-defined interfacial mechanistic studies (*e.g.*, single crystals vs. films of powders). Second, we will develop improved transition-metal based

molecular catalysts for mechanistic investigation of water oxidation. Third, we will compare their electrochemical water-oxidation activity when immobilized on conducting electrodes with that in homogeneous aqueous solution. Fourth, we will pursue advances in these areas to uncover the core scientific challenges to the efficient coupling of the catalytic functions at the water interface under irradiation. This will be accomplished through the study of water oxidation at complex aqueous interfaces following the transfer of stored photo-produced electrical energy from a semiconductor through a catalyst into water.

We will also engage in related collaborative research to address the origin of two enhancement effects (*i.e.*, Cs ion pretreatment of semiconductors and the addition of carbonate ion) on efficient solar water splitting, originally discovered by K. Sayama's group (AIST). Using funds from METI, Japan *via* a program called U.S.-Japan Cooperation on Clean Energy Technologies, the AIST researchers will be able to stay at BNL for an extended period to carry out that related proposed work.

Publications (including patents) acknowledging the grant or contract (2008-2011)

1. Graciani, J.; Alvarez, L.J.; Rodriguez, J.A.; Fernandez-Sanz, J. "N Doping of Rutile TiO_2(110) Surface. A Theoretical DFT Study," *J. Phys. Chem. C* **2008**, *112,* 2624-2631.

2. Jensen, L.; Muckerman, J.T.; Newton, M.D. "First-Principles Studies of the Structural and Electronic Properties of the $(Ga_{1-x}Zn_x)(N_{1-x}O_x)$ Solid Solution Photocatalyst," *J. Phys. Chem. C* **2008**, *112*, 3439-3446.

3. Muckerman, J.T.; Polyansky, D.E.; Wada, T.; Tanaka, K.; Fujita, E. "Water Oxidation by a Ruthenium Complex with Non-Innocent Quinone Ligands: Possible Formation of an O–O Bond at a Low Oxidation State of the Metal. Forum 'on Making Oxygen'," *Inorg. Chem.* **2008**, *47*, 1787-1802.

4. Tseng, H.-W.; Zong, R.; Muckerman, J.T.; Thummel, R. "Mononuclear Ru(II) Complexes That Catalyze Water Oxidation," *Inorg. Chem.* **2008**, *47*, 11763-11773.

5. Chen, H.; Wen, W.; Wang, Q.; Hanson, J.C.; Muckerman, J.T.; Fujita, E.; Frenkel, A.; Rodriguez, J.A. "Preparation of $(Ga_{1-x}Zn_x)(N_{1-x}O_x)$ Photocatalysts from the Reaction of NH_3 with Ga_2O_3/ZnO and $ZnGa_2O_4$: In situ Time-Resolved XRD and XAFS Studies," *J. Phys. Chem. C* **2009**, *113*, 3650-3659.

6. Shen, X.; Allen, P.B.; Hybertsen, M.S.; Muckerman, J.T. "Water Adsorption on the GaN ($10\bar{1}0$) Non-polar Surface," (Letter) *J. Phys. Chem. C* **2009,** *113*, 3365–3368.

7. Graciani, J.; Alvarez, L.J.; Rodriguez, J.A.; Sanz, J.F. "N Doping of Rutile TiO_2(110) Surface. A Theoretical DFT Study," *J. Phys. Chem. C* **2009**, *113*, 17464-17470.

8. Tsai, M.-K.; Rochford, J.; Polyansky, D.E.; Wada, T.; Tanaka, K.; Fujita, E.; Muckerman, J.T. "Characterization of Redox States of $Ru(OH_2)(Q)(terpy)^{2+}$ (Q = 3,5-di-tert-butyl-1,2-benzoquinone, terpy = 2,2':6',2''-terpyridine) and Related Species through Experimental and Theoretical Studies," *Inorg. Chem.* **2009**, 48, 4372-4383.

9. Boyer, J.L.; Rochford, J.; Tsai, M.-K.; Muckerman, J.T.; Fujita, E., "Ruthenium Complexes with Non-innocent Ligands: Electron Distribution and Implications for Catalysis," *Coord. Chem. Rev.* **2010**, *254*, 309-330.

10. Rochford, J.; Tsai, M.-K.; Szalda, D.J.; Boyer, J.L.; Muckerman, J.T.; Fujita, E., "Oxidation State Characterization of Ruthenium 2-Iminoquinone Complexes through Experimental and Theoretical Studies," *Inorg. Chem*. **2010**, 49, 860-869.

11. Chen, H.; Wang, L.; Bai, J.; Hanson, J.C.; Warren, J.B.; Muckerman, J.T.; Fujita, E.; Rodriguez, J.A. "*In Situ* XRD Studies of ZnO/GaN Mixtures at High Pressure and High Temperature: Synthesis of Zn-rich $(Ga_{1-x}Zn_x)(N_{1-x}O_x)$ Solid Solutions," *J. Phys. Chem. C* **2010**, *114*, 1809-1814.

12. Concepcion, J.J.; Tsai, M.-K.; Muckerman, J.T.; Meyer, T.J. "Mechanism of Water Oxidation by Single-Site Ruthenium Complex Catalysts," *J. Am. Chem. Soc.* **2010**, *132*, 1545-1557.

13. Shen, X.; Small, Y,A. Wang, J.; Allen, P.B.; Fernandez-Serra, M.V.; Hybertsen, M.S.; Muckerman, J.T. "Photocatalytic Water Oxidation at the GaN (1010) – Water Interface," *J. Phys. Chem. C* **2010**, *114*, 13695-13704.

14. Wada, T.; Muckerman, J.T.; Fujita, E.; Tanaka, K. "Substituents Dependent Capability of Bis(ruthenium-dioxolene-terpyridine) Complexes Toward Water Oxidation," *Dalton Trans*. **2011**, *40*, 2225-2233.

15. Li, L.; Muckerman, J.T.; Hybertsen, M.S.; Allen, P.B. "Phase diagram, structure and electronic properties of $(Ga_{1-x}Zn_x)(N_{1-x}O_x)$ solid solution from DFT-based simulations," *Phys. Rev. B*, **2011**, in press.

16. Polyansky, D.E.; Muckerman, J.T.; Rochford, J.; Zong, R.; Thummel. R.P.; Fujita, E. "Water Oxidation by a Mononuclear Ruthenium Catalyst: Characterization of the Intermediates," *J. Am. Chem. Soc.,* submitted.

II.K.16 Quantum theory of Semiconductor-Photo-Catalysis and Solar Water Splitting

Philip B. Allen
Dept. of Physics and Astronomy
Stony Brook University
Stony Brook, NY 11794-3800
Phone: (631) 632-8179
E-mail: philip.allen@stonybrook.edu

DOE Program Manager: James Davenport
Phone: (301) 903-0035
E-mail: James.Davenport@science.doe.gov

Objectives

UV light, incident on a semiconductor-water interface, has been used to split water, but it is not known exactly how this happens or how to extend the wavelength range to the visible. The semiconductor alloy GaN/ZnO has been found promising by Domen's group in Japan. The objective of this research program is to use computational theory to help unravel how the oxidation process occurs, when photo-excitations in the semiconductor arrive at the semiconductor/water interface. What surface is most effective, how do photo-holes liberate protons from water molecules on the surface, what are the reaction sites and reaction intermediates, and what constraints must the semiconductor properties satisfy? How can we design materials to improve the efficiency and increase the wavelength range of the useful light?

Technical Barriers

Technical challenges to this kind of modeling are daunting. Density-functional theory makes band gap and self-interaction errors, and available computer power forces less-than-optimal system sizes to be modeled. Experiments are only slowly yielding microscopic details to guide theory. Water is a difficult molecule to model because of quantized nuclear motions and complicated polar properties causing bonding to be a mixture of electrostatic and covalent interactions. The relevant semiconductor surface is not yet firmly identified, and the degree of alloy disorder and surface alloy enrichment are poorly known, so that theory must attempt to answer a very large list of questions.

Abstract

Domen's group [1] found that GaN/ZnO alloys were particularly effective at absorbing sunlight and harvesting photo-holes, which then oxidize water to protons and O_2. A separate catalyst is needed to harvest the photo-electrons, which reduce the protons to H_2. The SWaSSiT* group (at Stony Brook University and Brookhaven National Lab) uses computational theory (mainly density-functional theory, DFT) to try to understand the process and how to optimize it. Most of our work, so far, has used the pure GaN (10-10) (non-polar) surface-to-water interface as a simplified model. We find this surface a particularly effective water oxidizer, since water has a strong tendency (according to theory) to dissociate into H^+ (attached to surface N atoms) and OH^- (attached to surface Ga atoms). The dissociated structure is found both for a monolayer of water at $T = 0$ (by static DFT), and for a thick water layer at room temperature (by DFT-driven Born-Oppenheimer molecular dynamics, AIMD). To analyze the photo-electro-chemical reaction, we make a cluster calculation, using B3LYP (partial exact exchange), explicit waters of hydration, and implicit waters represented by a polarizable medium. We propose a reaction path where the surface-bound OH^- interacts with photo-holes and water molecules. We find a sequence of four proton-coupled electron transfers (PCET). In each step, a photo-hole transfers to the surface-bound anion, releases a proton, and forms a new, bound, and hydrated, anion species: (1) O^-, (2) OOH^-, (3) OO^-, finally returning to (4) OH^-, releasing O_2 in this last step. This accomplishes the overall reaction $2H_2O \rightarrow 4H^+ + O_2$. Our attention is now turning in many new directions, some of which will be discussed. For example, the semi-polar (10-11) surface has recently been identified experimentally in powders of the alloy, and may play a role. We study its surface structures using a new DFT-based implementation of a genetic algorithm. We are starting to analyze the possible roles of semiconductor polarity in photocatalysis. We have studied the alloy thermodynamics of GaN/ZnO, and the concentration dependence of the band gap, using DFT with large supercells, supplemented by a cluster expansion and Monte-Carlo simulation. The resulting model has a stable binary compound $(GaN)_{0.5}(ZnO)_{0.5}$ which disorders above 850K, and wide miscibility gaps. Above 850K there is complete solid solubility, and materials formed above this temperature are likely to remain supercooled and completely miscible at lower T. There is significant short-range order at temperatures of 1400K and below, and a correlation between lower free-energy and larger band-gap configurations.

*Other members of SWaSSiT are Marivi Fernandez-Serra, Mark Hybertsen, Li Li, James Muckerman, Artem Oganov, Xiao Shen (emeritus), Yolanda Small, and Jue Wang.

Progress Report

As outlined in the abstract, three parts of the project were completed, another part was completed by colleagues funded by a separate DOE project, and a fifth

part is underway. These are (1) studies of a monolayer of water at T=0 on the GaN (10-10) surface; (2) ab initio molecular dynamics (AIMD) for the interface of bulk water at 300K with GaN (10-10); (3) quantum-chemical modeling of photo-hole-induced reactions which produce a likely pathway for oxidation of water into H^+ and O_2; (4) thermodynamics, local order, and band gap reduction in bulk GaN/ZnO alloys; and (5) studies of the semipolar (10-11) surface of GaN and its interaction with water.

Future Directions

We should soon be able to predict surfaces of GaN (10-11) without and with a water monolayer. We will give these to our colleague Fernandez-Serra for AIMD modeling. There are many important future directions, and we will pursue a number of them simultaneously. We expect to stimulate experiments that will help us choose the most promising directions for modeling studies. (1) Obvious future directions are studies of reaction routes on the GaN (10-11) semi-polar surface, and on surfaces of alloys, both (10-10) and (10-11). (2) A project in the advanced planning stages is the interaction of water with ferroelectric thin film surfaces with controllable polarity. (3) A project that will be initiated with a new graduate student is studies of the hole mobility, hole trapping, and hole transfer dynamics in GaN with various surface terminations, and in GaN/ZnO alloys. These projects cannot be done by the PI alone. Project (1) will probably be done in close collaboration with colleagues at BNL. Project (2) involves experimental collaborators at Stony Brook and BNL, and collaboration with SWaSSiT theorists, especially Fernandez-Serra and Oganov. Project (3) will involve collaborators at both BNL and Yale.

References

1. K. Maeda et al., J. Am. Chem. Soc. 127, 8286 (2005).

Publication list acknowledging the DOE grant or contract

1. X. Shen, P.B. Allen, M.S. Hybertsen, and J.T. Muckerman, "Water Adsorption on the GaN (1010) Nonpolar Surface," J. Phys. Chem. C Letters 113, 3365-3368 (2009).

2. X. Shen, Y.A. Small, J. Wang, P.B. Allen, M.V. Fernandez-Serra, M.S. Hybertsen and J.T. Muckerman, "Photocatalytic Water Oxidation at the GaN (1010)–Water Interface," J. Phys. Chem. C 114, 13695-13704 (2010).

3. Li Li, J.T. Muckerman, M.S. Hybertsen, and P.B. Allen, "Phase diagram, structure, and electronic properties of (Ga1-xZnx)(N1-xOx) solid solutions from DFT-based simulations," Phys. Rev. B (2011) in press, accepted Jan. 19.

II.K.17 Formation and Characterization of Semiconductor Nanorod/Oxide Nanoparticle Hybrid Materials: Toward Vectoral Electron Transport in Hybrid Materials

Neal R. Armstrong, S. Scott Saavedra,* Jeffry Pyun
Department of Chemistry
University of Arizona
Tucson, Arizona 85721
(520) 621-9761; (520) 621-8242
nra@email.arizona.edu, saavedra@email.arizona.edu,
jpyun@email.arizona.edu

DOE Program Manager: Dr. Mark Spitler
E-mail: Mark.Spitler@science.doe.gov

Objectives

We are developing new photoelectrocatalytic systems based on semiconductor nanocrystalline materials, ultimately intended to be the active layers in solar fuel forming systems. Photoactive nanocrystals are decorated with electron-rich ligands, and captured into asymmetric matrices that ensure efficient energy capture and vectorial photoelectrochemical energy conversion. New materials are being designed in parallel with unique spectroscopic and electrochemical characterization of their frontier orbital energies, to ensure highest possible rates of charge transfer in the critical energy conversion steps.

Technical Barriers

- There are significant challenges to the formation of stable low bandgap semiconductor nanocrystalline "dots" and "rods;"
- There are even greater challenges to the alignment of semiconductor nanorods into asymmetric arrays, which ensure electron transport in one direction (vectorial), and keep oxidation and reduction processes spatially separated;
- The frontier orbital energy levels of these nanocrystalline materials are difficult to characterize in photoelectrochemically-relevant environments; addition of protective ligands or polymer hosts can further alter these energies; nanocrystal-nanocrystal interactions also alter these energies, and need to be studied for isolated crystals, small aggregates and full assemblies.

Abstract

Our DOE Solar Photochemistry supported research (DE-FG03-02ER15753) has focused on the development and characterization of new semiconductor nanorod (SC-NR) materials coupled asymmetrically to conducting polymer hosts, or either metal or metal oxide supports, and the development of new nanocrystalline materials decorated with both metallic catalytic sites and metal oxide nanoparticles. The asymmetric structure of these nanomaterials is designed to ensure vectorial electron transfer in photoelectrochemical processes which may ultimately provide pathways for the formation of chemical fuels from sunlight. Recent activities have been centered on: (i) the formation of new nanomaterials and nanocrystals (NCs); (ii) the demonstration of photoelectrochemical processes with SC-NCs tethered to the surface of a conducting polymer; (iii) the characterization of the energetic of these materials by unique protocols involving photoemission spectroscopies of monolayer-tethered SC-NCs; and (iv) the spectroelectrochemical characterization of charge injection into surface-tethered SC-NCs on unique waveguide platforms.

Progress Report

Recent efforts (Fig. 1) have focused on the creation of functional nanocrystalline monolayers and ensemble materials, e.g. CdSe SC-NCs capped with ligands terminated with the monomer of CPs such as (poly(ethylenedioxythiophene) – PEDOT, and its ProDOT and di-ethylProDOT derivatives. New electrochemical protocols were developed to capture close packed monolayers of these NCs on the surface of the CP, following which we interrogated the relative rates of photoelectrochemical reduction of a solution electron acceptor by the CP, using the CdSe NC as the photosensitizer. Electron donation to the photoexcited NC by the CP ($r_{c,2}$) is the rate limiting step and is exponentially related to the excess free energy controlled by the quasi-Fermi level in the CP, and by the NC diameter, which controls E_{VB}. These results demonstrate an enabling method for the capture of SC-NCs in a functional format, which can be used to tailor the architecture of new materials where compositional and energetic asymmetry is required. For photoelectrochemical systems such as this both the electronic coupling and the excess free energy at each heterojunction (e.g. $E_{HOMO}^{MOx} - E_{LUMO}^{SC\text{-}NC}$; $E_{HOMO} \approx E_{VB}$; $E_{LUMO} \approx E_{CB}$) control the photovoltage of the complete system, and rates of ET for the redox reactions coupled to this structure.

We have recently developed new ways of characterizing frontier orbital energies of the NC in both high vacuum and solution environments. We demonstrated the successful capture of sub-monolayers of pyridine-capped CdSe NCs

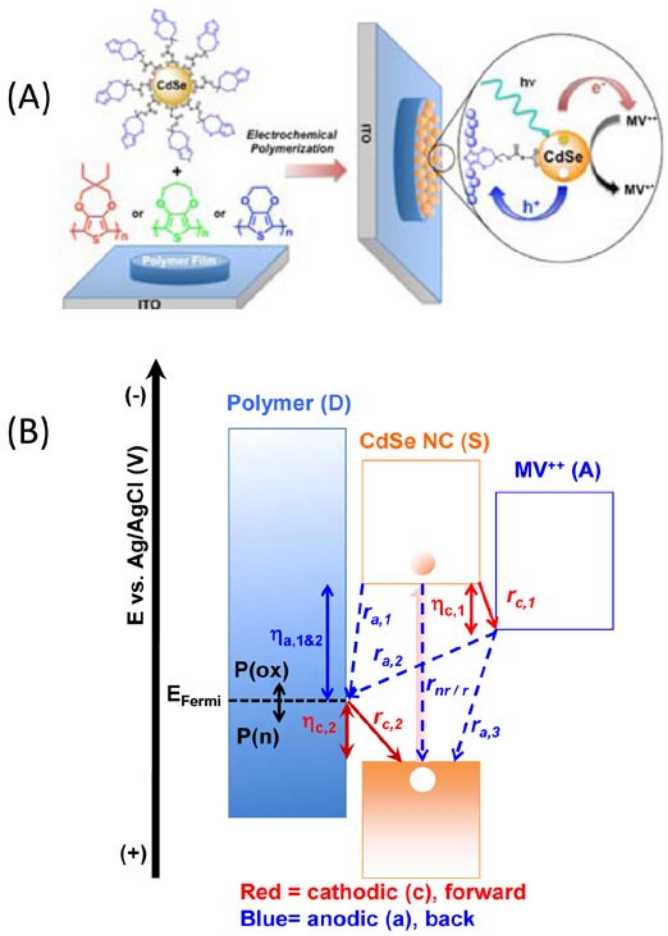


FIGURE 1. (A) Schematic view of the capping of CdSe NCs with ProDot-terminated ligands, followed by the electrochemical capture of the NCs at the surface of CPs based on PEDOT, ProDOT or di-ethylProDOT. A compositionally and energetically asymmetric material combination results, which can reduce a solution electron acceptor, with the CdSe NC acting as the photosensitizer; (B) The overall rate of MV++ reduction is determined by a complex series of ET events, and for this first generation of materials the slow step appears to be electron capture from the CP by the photoexcited NC. Excess free energy relationships summarized in Fig. 3 show that $r_{c,2}$ (for cathodic photocurrents) is determined by the free energy difference between the quasi-Fermi potential in the CP and E_{VB} of the NC.

(pyr-CdSe) on Au surfaces modified with a short dithiol modifier, and characterized their composition and frontier orbital energies (ionization potential (IP), E_{VB}) for the bare NC, and for NCs modified with short dipolar ligands that vary in their polarizability. We were able to account for the large (up to 1.0 eV) shift in vacuum level caused by even 15% of a monolayer of CdSe NCs adsorbed via dithiols to Au, and the additional increases or decreases in vacuum level caused by dipolar capping ligands.

We developed an alternative approach to characterization of frontier orbital energies of tethered NCs using spectroelectrochemical methods on waveguide substrates. Monolayers of thiol functional carboxylic acids

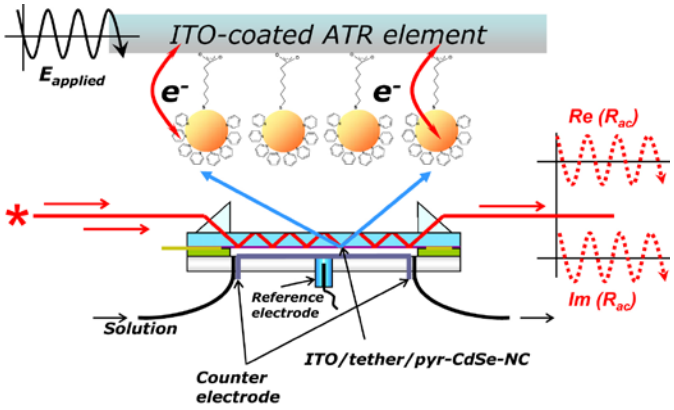


FIGURE 2. Schematic view of the spectroelectrochemical characterization of CdSe NCs, tethered at sub-monolayer coverages to ITO/ATR waveguide platforms. The potential (versus N.H.E. and vacuum) at which full bleaching of the lowest energy excitonic feature (at λ_{ex}) is used to estimate E_{CB} in solution environments. Modulation of the potential then provides in-phase and out-of-phase optical responses, which are used to estimate switching rates, related to k_{ET} to/from the NC.

are adsorbed to indium-tin oxide (ITO) substrates (the electroactive component of an ATR/waveguide element), which can then act as a capture surface for solution pyr-CdSe NCs. The lowest energy excitonic feature is reversibly bleached at a midpoint potential which leads to an estimate of $E_{CB} \approx$ -3.5 eV versus vacuum. Subsequent modulation of the electrode potential around this midpoint potential while measuring both in-phase and out-of-phase components of the ATR/reflectance signal allows for estimation of rates of bleaching/recovery of the monolayer tethered NC (k_s).

We have recently demonstrated the synthesis of p-type cobalt oxide nanowires and heterostructured Au-Co_3O_4 nanowires via *Colloidal Polymerization*. In these systems, metallic cobalt nanoparticles assemble into 1-D mesostructured "wires" in solution via magnetic dipolar interactions, and are subsequently converted into hollow oxide nanowires via oxidation reactions. Hollow Co_3O_4 nanowire networks were formed on ITO and were shown to be electrochemically active. UPS measurements provided an estimate of $E_{VB} \approx$ 5.3 +/- 0.2 eV for the as-deposited oxide nanowires, which appears to be close to the valence band energy required to drive OER in a photoelectrochemical energy conversion system, without external bias. As discussed further below, these band edge energies will provide large driving forces for photoelectrochemical processes when the oxide NP is married to semiconductor NCs or NRs, such as CdSe, forming true "Type II" heterojunctions. To enhance their catalytic properties these cobalt oxide nanowires were subsequently modified with noble metal inclusions. We demonstrated the ability to insert Au or Pt nanoparticles into the interior or exterior of the cobalt oxide nanowires. We saw a significant enhancement of the electrochemical activity associated with the change of redox states of the cobalt oxide as a consequence of noble metal inclusions.

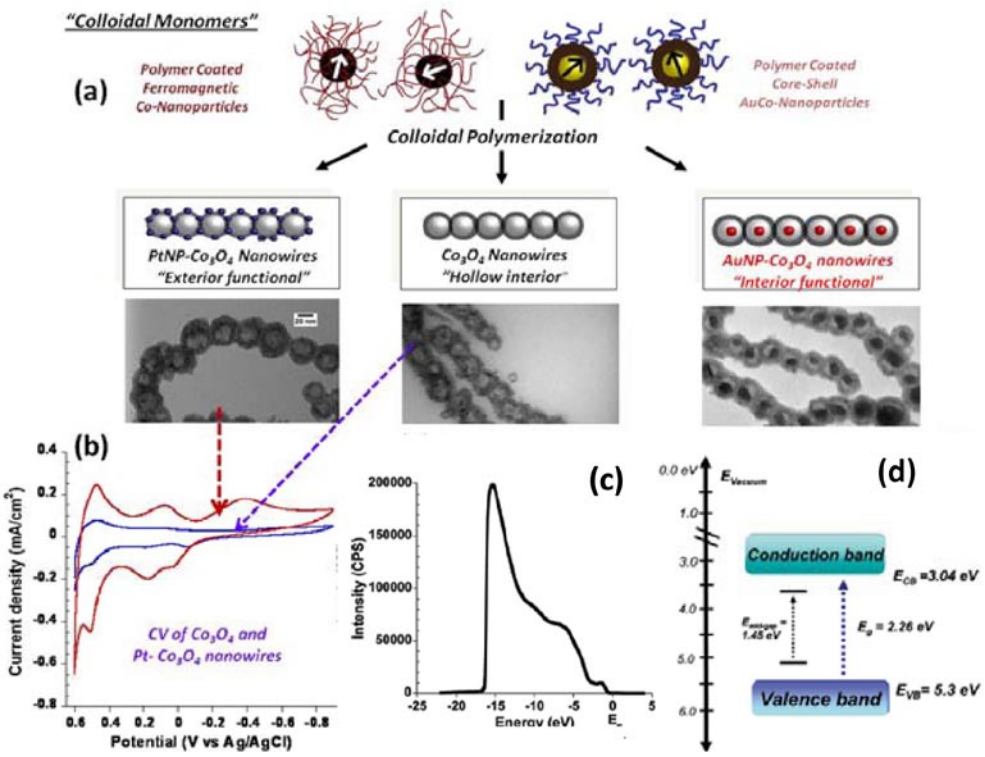


FIGURE 7. (a) Schematic for preparation of hollow Co_3O_4 nanowires, Au-Co_3O_4 nanowires with Au inclusions on the interior of nanowires and Pt-Co_3O_4 nanowires with Pt inclusions on exterior of nanowire. (b) CV of hollow Co_3O_4 vs. Pt-Co_3O_4 nanowires indicates a 7-fold enhancement of electroactivity as a consequence of Pt inclusions (c) UV-photoemission spectroscopy (He(I) UPS) of hollow Co_3O_4 nanowires and (d) estimated band edge energies of Co_3O_4 nanowires constructed from UPS and optical absorption data.

Future Directions

1. We will develop ligand-capped SC-NCs and SC-NRs providing for selective and asymmetric addition of metallic and oxide (e.g. cobalt oxide) catalytic sites, with control over their placement, electronic coupling, and catalytic activity.
2. We will explore directed self-assembly of rod-like molecular objects into vertically aligned arrays.
3. We will characterize band edge energies of monolayer-supported NCs and NRs using photoemission spectroscopies (UPS/XPS), characterizing E_{VB} and vacuum level changes as a function of NC coverage and capping ligand. We will probe NC-NC and NR-NR interactions and extend these studies to either randomly adsorbed or aligned NRs which have been modified with oxide or metallic catalytic sites.
4. We will extend our protocols for spectroelectrochemical study of SC-NCs on electroactive waveguides, to study NC-NC and NR-NR interactions which influence E_{CB} as a function of surface coverage, types of capping ligands, the introduction of asymmetric nanorods, and nanorods modified with catalytic sites.
5. We will develop the first prototypes of membrane encapsulated ensembles of these asymmetric, modified SC-NCs and the first demonstration of proton pumping in response to photoelectrochemical events on either side of the membrane.

Selected Recent Publications

1. Shallcross, R.C.; D'Ambruoso, G.D.; Pyun, J.; Armstrong, N.R., Photoelectrochemical Processes in Polymer-Tethered CdSe Nanocrystals. *Journal of the American Chemical Society* **2010,** *132* (8), 2622-2632.

2. Munro, A.M.; Zacher, B.; Graham, A.; Armstrong, N.R., Photoemission Spectroscopy of Tethered CdSe Nanocrystals: Shifts in Ionization Potential and Local Vacuum Level As a Function of Nanocrystal Capping Ligand. *Acs Applied Materials & Interfaces* **2010,** *2* (3), 863-869.

3. Araci, Z.O.; Shallcross, C.R.; Armstrong, N.R.; Saavedra, S.S., Potential-Modulated Attenuated Total Reflectance Characterization of Charge Injection Processes in Monolayer-Tethered CdSe Nanocrystals. *Journal of Physical Chemistry Letters* **2010,** *1* (12), 1900-1905.

4. Kim, B.Y.; Shim, I.B.; Araci, Z.O.; Saavedra, S.S.; Monti, O.L.A.; Armstrong, N.R.; Sahoo, R.; Srivastava, D.N.; Pyun, J., Synthesis and Colloidal Polymerization of Ferromagnetic Au-Co Nanoparticles into Au-Co3O4 Nanowires. *Journal of the American Chemical Society* **2010,** *132* (10), 3234-+.

5. Kim, B.; Keng, P.; Shim, I.-B.; Sahoo, R.; Oskan, Z.; Saavedra, S.S.; Armstrong, N.R.; Pyun, J., Synthesis and Colloidal Polymerization of Dipolar Au-Co Core-Shell Nanoparticles into Au-Co3O4 Nanowires *J. Am. Chem. Soc.* **2010,** *132*, 3234-3235.

II.K.18 Combinatorial methods for the Improvement of Semiconductor Metal Oxide Photoelectrodes

Bruce Parkinson (Principal Investigator),
Yongqi Liang*, Chunping Jiang, Jianghua He
University of Wyoming
Department of Chemistry and School of Energy Resources
1000 E. University Ave
Laramie, WY 82071
Phone: (307) 766-4844
E-mail: bparkin1@uwyo.edu, yliang1@uwyo.edu

DOE Program Manager: Richard Greene
Phone: (301) 903-4568
E-mail: Richard.Greene@science.doe.gov

Objectives

The main problem with photoelectrochemical water splitting is that no semiconducting materials are known that satisfy all the requirements necessary to construct and efficient and stable solar photoelectrolysis system. Metal oxide semiconductors can satisfy the stringent requirement that a photoelectrode will be stable in an electrolyte under full or concentrated sunlight for many years. However no stable metal oxide semiconductors with the proper band gap and band positions are known. Therefore we have developed a combinatorial search strategy to quickly and efficiently produce many thousands of metal oxides and screen them for photoelectrolysis activity.

Technical Barriers

- A metal oxide semiconductor that can meet stability and efficiency requirements will probably contain at least three different metals, greatly increasing the number of potential materials to be produced and screened.
- Once several promising materials are identified it will take considerable effort to optimize the electronic properties and nanostructured morphology to final have a few materials to construct a practical and efficient photoelectrode for a solar water splitting system.

Abstract

A combinatorial method to produce and screen for efficient photoelectrolysis activity was developed. The method employs high-throughput ink-jet printing of patterns of multiple oxide precursors onto conductive glass substrates. Subsequent pyrolysis yields a library of oxide electrodes that are screened for photoelectrolysis activity by immersing in an electrolyte and scanning a laser over the electrodes to map the photocurrent response.

Iron oxide is a d-band semiconductor that serves as a prototype for a future material that may be useful in a photoelectrolysis device. Therefore it is useful to explore how to optimize the photoactivity of this material. Since there are literature reports that "doping" small amounts of impurities could greatly influence the properties of α-Fe_2O_3, we investigated the effect of adding small amounts of Ti, Si, and Al on the photoelectrochemical activity of α-Fe_2O_3 was investigated using our combinatorial protocols. When Si and Al are individually added to iron oxide at the levels we studied, the photoelectrolysis activity decreased whereas low levels of Ti addition enhanced the photocurrents. Synergistic effects were observed resulting in enhanced photocurrents when multiple impurities were added to α-Fe_2O_3.

It was also found that the photoelectrolysis activity of the Bi-V oxides could be improved by the addition of various levels of W, Cu, Fe, Mg and Mn to Bi-V binary oxides. Some Bi-V-W ternary oxides had improved photoresponse of up to 18 times of that of the well-known $BiVO_4$ phase whereas Bi-V-Mo ternary oxides had very little photoresponse. However, when elements like Fe, Cr and Mg were introduced to the Bi-V-Mo oxides, their photoresponse could be increased.

Progress Report

With DOE Hydrogen Program support we have been pursuing a novel high throughput combinatorial search strategy for the identification of multicomponent metal oxide materials with suitable band gaps and band positions for water photoelectrolysis operating as either a photoanode or a photocathode. Our combinatorial search strategy uses ink jet printing of overlapping patterns of metal oxide precursors on to conductive glass substrates. Metal nitrates, one class of simple oxide precursors that we use, decompose to form metal oxides, oxygen and NO_2 by heating at relatively low temperatures (500 °C). Scanning a laser over the printed and fired electrodes while it is in an electrolyte produces a false color map of photocurrent response that can be related to the printed compositions. It is desirable for many groups to help with this search since it is easy to calculate the numbers of combinations that may have to produced and screened. If we prepare all possible ternary oxides, mixing N materials three at a time there are N!/3!(N-3)! combinations if we only consider 1:1:1 stoichiometries. Since there are ~60 possible candidate metals in the periodic table this results in >34,000 combinations to be produced and tested with only this simple stoichiometry. If a quaternary material is needed then there are N!/4!(N-4)! > 480,000 possible combinations. Again these numbers do not consider producing and screening the many possible stoichiometries. It is also possible that a ternary or quaternary material

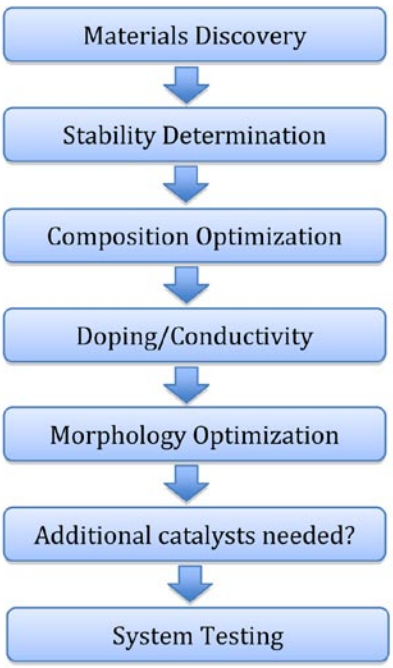


FIGURE 1. A flow chart illustrating the steps from a combinatorial discovery process through composition and conductivity optimization and progressing through configuring the materials for high device efficiencies.

will require small amounts of an additional element that acts as an electrical dopant to optimize its conductivity. These small amounts can often exist as impurities in the metal oxide precursors or may have to be discovered by additional combinatorial screening (discussed later in this chapter) greatly multiplying the number of experiments that must be done. However, some combinations could be excluded because it would not make sense to, for example, mix only large band gap oxide materials (i.e. Ti-Zr-Si-Y oxides) and expect visible light absorption. It is clear that given the large number of possible mixtures that need to be produced, a "high throughput" approach is needed as well as multidimensional experimental design to explore the parameter space more rapidly. And while it may not be reasonable to produce and test ALL of the possible combinations, it is certainly imperative that the throughput of materials screening be rapid relative to the serial approaches previously used.

Future Directions

New metal oxide semiconductors will be produced and screened for photoelectrolysis activity. Also we will be following up on "hits" obtained by the SHArK (Solar Hydrogen Activity research Kit), our outreach program that provides the tools to undergraduate and high school students to join the search for the "holy grail" of photoelectrochemistry. Currently we have over 40 sites participating. We will also support the efforts of DOE's newly funded Solar Hub at Caltech who have taken our idea and will expand it to an automated robotic high throughput screening.

Publication list (including patents) acknowledging the DOE grant or contract

1. Michael Woodhouse and B.A. Parkinson, "Combinatorial Approaches for the Identification and Optimization of Oxide Semiconductors for Efficient Solar Photoelectrolysis", Chemical Society Reviews, 38(1), 197-210, (2009)

2. Michael Woodhouse and B.A. Parkinson, "Combinatorial Discovery and Optimization of a Complex Oxide with Water Photoelectrolysis Activity", Chemisty of Materials, 20(7), 2495-2502, (2008)

3. B.A. Parkinson, "Distributed Research: A New Paradigm for Undergraduate Research and Global Problem Solving", Energy & Environmental Science, 3, 509-511, (2010)

4. Aron Walsh, Su-Huai Wei, Yanfa Yan, M.M. Al-Jassim, John A. Turner, Michael Woodhouse, and B.A. Parkinson, "Structural, magnetic, and electronic properties of the Co-Fe-Al oxide spinel system", Phys. Rev. B, 76, 165119, (2007)

5. B.A. Parkinson and M. Woodhouse, "A Digital Method for the Identification of Photoelectrolysis Catalysts for Water", Digital Fabrication, R. Mills, Ed., The Society for Imaging Science and Technology: Baltimore, MD, p190-193, (2005)

6. Michael Woodhouse, G.S. Herman and B.A. Parkinson, "A Combinatorial Approach to Identification of Catalysts for the Photoelectrolysis of Water", Chemistry of Materials, 17, 4318-4324, (2005)

7. Jianghua He and B. A. Parkinson, "A Combinatorial Investigation of the Effects of the Incorporation of Ti, Si, and Al on the Performance of α-Fe_2O_3 Photoanodes", ACS Combinatorial Science, in revision

8. Chunping Jiang, Ruilin Wang and B.A. Parkinson, "A Combinatorial Approach to Improve Photoelectrodes Based on $BiVO_4$", in preparation

9. In addition Frank Osterloh and B.A. Parkinson were guest editors for a special issue of the Materials Research Society Bulletin in January 2011 focused on Solar Hydrogen Production.

II.K.19 A Hybrid Biological/Organic Photochemical Half-Cell for Generating Dihydrogen

John H. Golbeck[1,2,*] (Principal Investigator),
Donald A. Bryant[1] (Co-Principal Investigator)
[1]Department of Biochemistry and Molecular Biology;
[2]Department of Chemistry
The Pennsylvania State University
University Park, PA 16802
Phone: (814) 865-1163; Fax: (814) 863-7024
E-mail: jhg5@psu.edu; dab14@psu.edu

DOE Program Manager: Dr. Michael Markowitz
Phone: (301) 903-6779
E-mail: Mike.Markowitz@science.doe.gov

Objectives

The objective of this work is to engineer a hybrid biological/organic half-cell that couples Photosystem I to [FeFe]-hydrogenase using molecular wire technology. The construct will carry out the light-driven half-cell reaction $2H^+ + 2e^- + 2\ h\nu \rightarrow H_2$. The methodology involves constructing a Photosystem I variant and a [FeFe]-hydrogenase variant so that a molecular wire can be attached directly to their surface-located iron-sulfur clusters. The objectives include optimizing the coupling chemistry between the two proteins; measuring the quantum yield and rate of dihydrogen production; and engineering long-term stability of the Photosystem I–molecular wire–[FeFe]-hydrogenase half-cell.

Technical Barriers

Three preconditions must be met for the proposed hybrid photochemical half-cell to function: (i) Photosystem I must be engineered so that a cysteine ligand to the terminal [4Fe-4S] cluster on the PsaC subunit is replaced with a glycine residue. (ii) An [FeFe]-hydrogenase variant must be engineered so that a cysteine ligand to one of the [4Fe-4S] clusters is similarly replaced with a glycine residue. These changes will expose iron atoms in Photosystem I and in [FeFe]-hydrogenase to the medium, allowing the -SH 'rescue ligand' from the molecular wire to form a strong coordination bond. (iii) A 'molecular wire' must be synthesized, which contains an electron transfer cofactor and a –SH group at each end so that the latter can serve as 'rescue' ligands to the modified [4Fe-4S] clusters on Photosystem I and on the hydrogenase. When all of these conditions are met, and in the presence of a sacrificial donor, Photosystem I will convert two photons into energetic electrons; these electrons will be transferred through the molecular wire to the tethered hydrogenase, which will reduce two protons to hydrogen.

Abstract

A molecular wire is used to connect two proteins through their physiologically relevant redox cofactors to facilitate direct electron transfer. Photosystem I (PS I) and an [FeFe]-hydrogenase serve as the test bed for this new technology. By tethering a photosensitizer module with a hydrogen-evolving catalyst, attached by Fe/S coordination bonds to the F_B iron-sulfur cluster of PS I and the distal iron-sulfur cluster of H_2ase, efficient electron transfer between the two components can be assayed via light-induced hydrogen evolution. These hydrogen producing nanoconstructs additionally self-assemble when the PS I variant, the hydrogenase variant and the molecular wire are combined.

Progress Report

We have recently reported the assembly of biological/organic hybrid nanoconstructs that generate hydrogen in the light. In these nanoconstructs, electrons are transferred directly from a photochemical module, Photosystem I (PS I), to a catalytic module, either a Pt nanoparticle (NP) or an [FeFe]-hydrogenase via a covalently attached molecular wire. In neither case are any spectroscopic changes visible that would allow electron transfer to be monitored between the photochemical and catalytic modules. In this

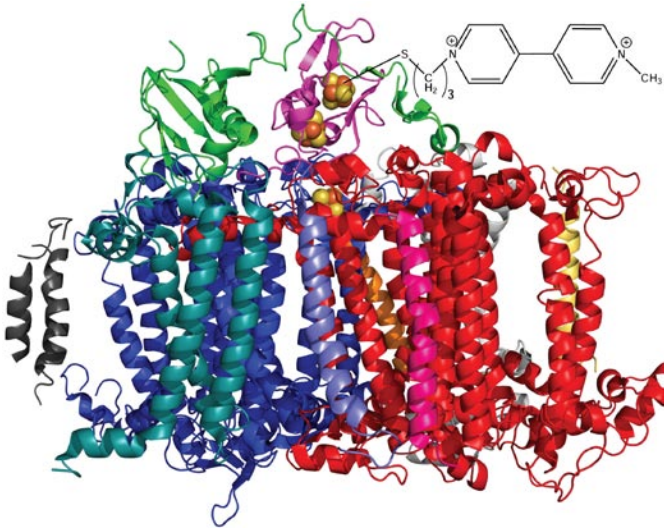


FIGURE 1. Depiction of the PS I—1-(3-thiopropyl)-1′-(methyl)-4,4′-bipyridinium construct. The electron transfer cofactors F_X, F_A, and F_B (from bottom to top) are shown as spheres within the protein scaffold. The molecular wire is attached at the F_B cluster, located inside the PsaC subunit (pink). The PsaD subunit (green) resides on top of the membrane spanning portion and adjacent PsaC. The TPMBP moiety is not drawn to scale.

study, the catalytic module was replaced with an organic cofactor consisting of 1-(3-thiopropyl)-1′-(methyl)-4,4′-bipyridinium chloride that allowed electron transfer to be measured to a spectroscopically observable marker. EPR and optical spectroscopy showed that the tethered redox cofactor was attached to PS I through the F_B cluster of PsaC. Under steady-state illumination, the rate of reduction of the 4,4′-bipyridinium cofactor was comparable to the rate of H_2 evolution observed for the PS I–molecular wire–Pt-NP and PS I–molecular wire–[FeFe]-hydrogenase nanoconstructs. These observations provide proof-of-concept for incorporating a redox cofactor in the molecular wire, thereby setting the stage for monitoring the rate and yield of electron transfer between PS I and the tethered [FeFe]-hydrogenase.

We have recently optimized our biohybrid biological/organic nanoconstruct that uses a covalently bonded molecular wire to connect the F_B cluster of the Photosystem I (PS I) from *Synechococcus* sp. PCC 7002 directly with the distal [4Fe-4S] cluster of the [FeFe]-hydrogenase I from *Clostridium acetobutylicum*. These studies show that in the presence of cross-linked Cyt c_6, with 1,8-octanedithiol as the molecular wire, in potassium phosphate buffer at pH 6.5, the PS I–molecular wire–[FeFe]- hydrogenase nanoconstruct evolves H_2 at a rate of 2850 µmoles mg Chl^{-1} h^{-1}, which is equivalent to an electron transfer throughput of 5700 µmoles mg Chl^{-1} h^{-1}, or 142 µmoles e^- PS I^{-1} s^{-1}.

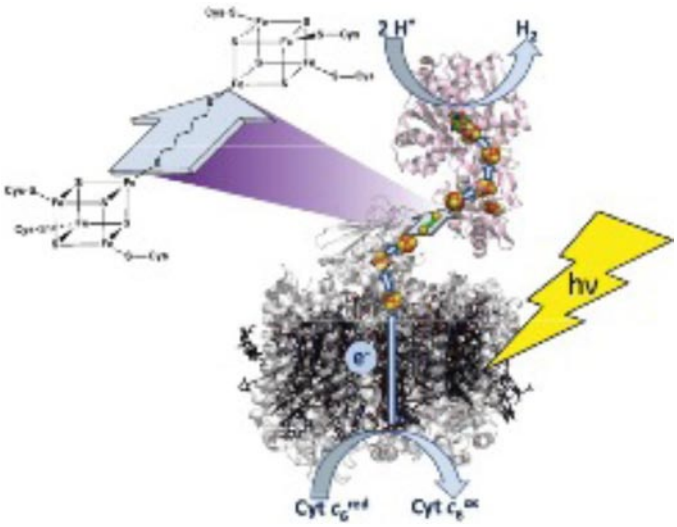


FIGURE 2. Schematic of the PS I-molecular wire-[FeFe]-hydrogenase nanoconstruct. Assembled photosynthetic nanoconstructs where the connecting wire is 1,6-hexanedithiol. Soluble electron donors include cytochrome c_6, ascorbate and PMS. Arrows indicate electron transfer through the system, including reduction of protons to H_2.

Putting this into perspective, cyanobacteria evolve O_2 at a rate of ~400 µmoles mg Chl^{-1} h^{-1}, which is equivalent to an electron transfer throughput of 1600 µmoles mg Chl^{-1} h^{-1}, or 46 e^- PS I^{-1} s^{-1}, assuming a PS I to PS II ratio of 1.8 as occurs in the cyanobacterium *Synechococcus* sp. PCC 7002. The significantly greater electron throughput by our hybrid biological/organic nanoconstruct over *in vivo* oxygenic photosynthesis validates our concept of tethering proteins through their physiologically relevant redox cofactors to overcome diffusion-based rate limitations on electron transfer.

Future Directions

Our plans for the future include (i) measuring the quantum yield of hydrogen evolution in the PS I–molecular wire–[FeFe]-hydrogenase nanoconstruct; (ii) docking the PS I–molecular wire–[FeFe]-hydrogenase nanoconstruct on either a graphene or gold electrode so that it functions as a cathode of an electrochemical cell; (iii) tethering a variant of an oxygen-tolerant [NiFe]-hydrogenase on the PS I–molecular wire module; (iv) investigating other entry portals for the molecular wire, including [2Fe-2S] clusters and cysteine residues placed near organic or inorganic cofactors of redox enzymes; (v) developing methods to produce these nanoconstructs biologically.

Publication list (including patents) acknowledging the DOE grant or contract

1. Grimme, R.A., Lubner, C.E., and Golbeck, J. (2009) Maximizing H_2 Production in Photosystem I/Dithiol Molecular Wire/Platinum Nanoparticle Bioconjugates, *Dalton Trans.*, 10106-10113.

2. Lubner, C.E., Grimme, R., Bryant, D.A., and Golbeck, J.H. (2010) Wiring photosystem I for direct solar hydrogen production, *Biochemistry 49*, 404-414.

3. Lubner, C.E., Knorzer, P., Silva, P.J.N., Vincent, K.A., Happe, T., Bryant, D.A., and Golbeck, J.H. (2010) Wiring an [FeFe]-Hydrogenase with Photosystem I for Light-Induced Hydrogen Production, *Biochemistry 49*, 10264-10266.

4. Lubner, C., Heinnickel, M., Bryant, D.A., and Golbeck, J.H. (2011) Wiring Photosystem I for Electron Transfer to a Tethered Redox Dye, *Energy Environ. Sci. (in press)*.

5. Lubner, C., Bryant, D.A., and Golbeck, J.H. (2011) Wired Reaction Centers, In *Molecular Solar Fuels* (Hillier, W., and Wydrzynski, T., Eds.), Royal Society of Chemistry, London.

6. Lubner, C., Applegate, A., Knörzer, P., Happe, T., Bryant, D.A., and Golbeck, J.H. (2011) Optimizing Light-Induced H_2 Evolution in Photosystem I-Molecular Wire-[FeFe]-H_2ase Constructs, *(in preparation)*.

II.K.20 Fundamental Optical, Electrical, and Photoelectrochemical Properties of Catalyst-Bound Silicon Microwire Array Photocathodes for Sunlight-Driven Hydrogen Production

Prof. Nathan S. Lewis (Principal Investigator), Prof. Harry A. Atwater, Dr. Bruce S. Brunschwig, Prof. Shannon W. Boettcher, Emily L. Warren, Dr. Morgan C. Putnam, Elizabeth A. Santori, Daniel Turner-Evans, Dr. Michael D. Kelzenberg, Dr. Michael G. Walter, James R. McKone, Dr. Joshua M. Spurgeon, Dr. Shane Ardo,* Dr. Chengxiang Xiang, Sang Hee Park, Dr. Qixi Mi, Dr. Karla R. Reyes-Gil

California Institute of Technology
Division of Chemistry and Chemical Engineering
Beckman Institute, Kavli Nanoscience Institute, and Joint Center for Artificial Photosynthesis
m/c 127-72, 210 Noyes Laboratory
1200 E. California Blvd.
Pasadena, CA 91125
Phone: (626) 395-6335; Fax: (626) 395-8867
E-mail: nslewis@its.caltech.edu

DOE Program Manager: Dr. Mark T. Spitler
Phone: (301) 903-4568
E-mail: Mark.Spitler@science.doe.gov

Objectives

The goal of this work is to develop a fundamental understanding of the properties and photoelectrochemical performance of Si wire-array based photocathodes for H2 evolution. This work has three general scientific objectives: to develop a fundamental understanding of Si microwire arrays, H2 evolving catalysts, and solution-based mass transport and bubble phenomena associated with H2 production. We will systematically vary the geometric, electronic, and compositional characteristics of the Si microwire arrays, to understand, and thus gain control over, the photoelectrochemical behavior of such systems. Experiments using the combined microwire array–catalyst material will be performed in order to determine active H2 catalysts based on alternatives to Pt, e.g. Ni–Mo alloy and MoS_2, and ideal catalyst loading, for optimization of the Si microwire array photoelectrochemical performance and catalytic turnover. Computational modeling, in conjunction with experimental measurements on Si microwire arrays under operating conditions, will be used to obtain a fundamental understanding of the energy penalty associated with mass-transport limitations, and complications due to production of H2 bubbles, for various photoelectrode geometries.

Technical Barriers

Current photovoltaic and photoelectrochemical technologies employ a planar-junction design, requiring the use of expensive, high-purity semiconducting materials for efficient and stable operation. Si microwire arrays afford rapid radial charge separation while using a fraction of the material and with relaxed purity requirements, while the micron-scale interwire spacing can present interesting, not-yet-elucidated issues involving mass transport of reactants and products under operating conditions. In addition, the formation of bubbles due to efficient H2 evolution at Si microwire array electrodes can reduce the overall photoelectrode performance. Realization of efficient technologies for photoelectrochemical H2 evolution using Si microwire arrays requires that the geometry and photophysical properties of the microwire arrays, light scattering elements, and electrocatalysts be optimized. Also, because noble metal materials, like Pt, are too expensive to serve as feasible components in a globally scalable H2-evolving photoelectrode, other potential catalysts must be identified.

Abstract

We have investigated and made significant progress on key components of a solar-driven water splitting scheme: Si microwire photocathodes, and metal oxide photoanodes. Radial $p–n^+$ (n^+p) junction Si microwire arrays functionalized with Pt or Ni nanoparticulate metallic electrocatalysts functioned as efficient photocathodes for H2 evolution. Further exploration of geometric parameters that influence the photoelectrochemical response of the Si microwire arrays is proposed. In addition, experimental measurements and computational modeling will be employed to investigate how catalysis is affected by mass-transport limitations, H_2 bubble formation, and the use of alternative electrocatalysts. The photoresponse of WO3 photoanodes was improved by implementation of a porous film geometry.

Progress Report

We have made very significant progress toward the goals listed under the DOE hydrogen fuel initiative project grant (DE-FG02-05ER15754) for p-Si microwire photocathodes and porous WO3 photoanodes. We have demonstrated a high level of control over the material and light absorption properties of p-Si microwire array photocathodes. We have tested the performance of p-Si microwire arrays embedded

in a flexible, processable set of polymeric membranes and have further demonstrated the ability to reuse the planar Si(111) growth substrate after the Si wire arrays were removed from the growth substrate. We have introduced a radial n^+p junction to improve the photoconversion efficiency of these electrodes in both regenerative and fuel-forming photoelectrochemical configurations. We have developed techniques to deposit Pt and Ni electrocatalyst particles onto the wire arrays, and have investigated their stability and performance for the hydrogen evolution reaction. Toward the development of a photoanode, we have synthesized a porous film morphology that improves the photoresponse of WO3 toward the oxygen evolution reaction. We have also developed a method to reduce the bandgap of WO3 from 2.6 eV to 1.8 eV by calcining ammonium para- or meta-tungstate in O2 at 420°C.

Future Directions

We are investigating the fundamental photoelectrochemical properties of Si wire-array based photocathodes for H2 evolution. The proposed research will focus on Si microwire arrays, H2 evolving catalysts, and solution-based mass transport and bubble phenomena associated with H2 production. Our recent demonstration of solar-driven H2 evolution from water at an n^+p-Si microwire array photocathode will be the starting point for the studies. The proposed work will elucidate the fundamental effects of interfacial structure on the chemistry and physics of such photocathodes. We will systematically vary structural variables, including the wire diameter, height, spacing, and pattern, as well as functional variables, including the doping density and junction area, of the Si microwire arrays, to comprehend, and thus gain control over, the photophysical and photoelectrochemical behavior of such systems. The fundamental properties of electrocatalysts on Si wire-array electrodes are also not yet understood. An effective catalyst, such as Pt, will be used to explore how the deposition and coverage affect the catalytic function on both planar Si and on Si microwire arrays. After gaining insight into those variables, other potential catalysts, such as Ni–Mo alloy and MoS2, will be investigated. The enhanced physical surface area of wire arrays affords increased rates of catalytic H2 evolution (per projected area) relative to planar Si. However, the aforementioned alternative microwire geometries, junction locations, and placement of electrocatalysts can result in issues involving mass transport of reactants and products and electrical and optical complications due to production of H2 bubbles. Computational modeling, in conjunction with experimental measurements on Si microwire arrays under operating conditions, will be used to obtain a fundamental understanding of these problems. The proposed fundamental science will aid in the development of systems not exclusively derived from Si microwire arrays. General guidelines for the design and implementation of successful systems that utilize interfacial reactions driven by light absorption at the photocathodes will be realized. Thus, the fields of photoelectrochemistry and photoinduced heterogeneous catalysis will both benefit from the results garnered by the proposed studies.

Publication list (including patents) acknowledging the DOE grant or contract

1. George W. Crabtree and **Nathan S. Lewis**, "Solar Energy Conversion" *AIP Conf. Proc. (Physics of Sustainable Energy)*, **2008**, *1044*, 309-321.

2. Brendan M. Kayes, Michael A. Filler, M. David Henry, James R. Maiolo III, Michael D. Kelzenberg, Morgan C. Putnam, Joshua M. Spurgeon, Katherine E. Plass, Axel Scherer, **Nathan S. Lewis**, and Harry A. Atwater, "Radial pn Junction, Wire Array Solar Cells", *Conference Record of the Thirty-third IEEE Photovoltaic Specialists Conference*, **2008**.

3. Michael D. Kelzenberg, Daniel B. Turner-Evans, Brendan M. Kayes, Michael A. Filler, Morgan C. Putnam, **Nathan S. Lewis**, and Harry A. Atwater, "Single-Nanowire Si Solar Cells", *Conference Record of the Thirty-third IEEE Photovoltaic Specialists Conference*, **2008**.

4. Michael D. Kelzenberg, Daniel B. Turner-Evans, Brendan M. Kayes, Michael A. Filler, Morgan C. Putnam, **Nathan S. Lewis**, and Harry A. Atwater, "Photovoltaic Measurements in Single-Nanowire Silicon Solar Cells", *Nano Lett.*, **2008**, *8(2),* 710-714.

5. Nathan S. Lewis, "Powering the Planet: Where in the World Will Our Energy Come From?", *Energeia*, **2008**, *19(4)*, 1.

6. James R. Maiolo III, Harry A. Atwater, and **Nathan S. Lewis**, "Macroporous Silicon as a Model for Silicon Wire Array Solar Cells", *J. Phys. Chem. C*, **2008,** *112(15)*, 6194-6201.

7. Stephen Maldonado, Anthony G. Fitch, and **Nathan S. Lewis**, "Semiconductor/Liquid Junction Photoelectric Chemical Solar Cells", in *Series on Photoconversion of Solar Energy Volume III - Nanostructured and Photoelectric Chemical Systems for Solar Photon Conversion*, Mary D. Archer and Arthur J. Nozik (Eds.), Imperial College Press: London, **2008**, 537.

8. Joshua M. Spurgeon, Harry A. Atwater, and **Nathan S. Lewis**, "A Comparison between the Behavior of Nanorod and Planar Cd(Se, Te) Photoelectrodes", *J. Phys. Chem. C*, **2008**, *112(15)*, 6186-6193.

9. Joshua M. Spurgeon, Katherine E. Plass, Brendan M. Kayes, Bruce S. Brunschwig, Harry A. Atwater, and **Nathan S. Lewis**, "Repeated Epitaxial Growth and Transfer of Arrays of Patterned, Vertically Aligned, Crystalline Si Wires from a Single Si(111) Substrate", *Appl. Phys. Lett.*, **2008**, *93*, 032112.

10. Nathan S. Lewis, "A Perspective on Forward Research and Development Paths for Cost-Effective Solar Energy Utilization", *ChemSusChem*, **2009**, *2(5)*, 383-386.

11. Katherine E. Plass, Michael A. Filler, Joshua M. Spurgeon, Brendan M. Kayes, Stephen Maldonado, Bruce S. Brunschwig, Harry A. Atwater, and **Nathan S. Lewis**, "Flexible Polymer-Embedded Si Wire Arrays", *Adv. Mater.*, **2009**, *21(3)*, 325-328.

12. Morgan C. Putnam, Daniel B. Turner-Evans, Michael D. Kelzenberg, Shannon W. Boettcher, **Nathan S. Lewis**, and Harry A. Atwater, "10 μm Minority-Carrier Diffusion Lengths in Si Wires Synthesized by Cu-Catalyzed Vapor-Liquid-Solid Growth", *App. Phys. Lett.*, **2009**, *95,* 163116.

13. Karla R. Reyes-Gil, Joshua M. Spurgeon, and **Nathan S. Lewis**, "Silicon and tungsten oxide nanostructures for water splitting", *Proc. SPIE*, **2009**, *7408*, 74080S.

14. Shannon W. Boettcher, Joshua M. Spurgeon, Morgan C. Putnam, Emily L. Warren, Daniel B. Turner-Evans, Michael D. Kelzenberg, James R. Maiolo, Harry A. Atwater, and **Nathan S. Lewis,** "Energy Conversion Properties of Silicon Wire-Array Photocathodes", *Science*, **2010**, *327(5962)*, 185-187.

15. Michael D. Kelzenberg, Shannon W. Boettcher, Jan A. Petykiewicz, Daniel B. Turner-Evans, Morgan C. Putnam, Emily L. Warren, Joshua M. Spurgeon, Ryan M. Briggs, **Nathan S. Lewis**, and Harry A. Atwater, "Enhanced absorption and carrier collection in Si wire arrays for photovoltaic applications", *Nature Mater.,* **2010**, 9(3), 239-244.

16. Joshua M. Spurgeon, Shannon W. Boettcher, Michael D. Kelzenberg, Bruce S. Brunschwig, Harry A. Atwater, and **Nathan S. Lewis,** "Flexible, polymer-supported, Si wire array photoelectrodes", *Adv. Mater.*, **2010**, *22(30)*, 3277-3281.

17. Emily L. Warren, Shannon W. Boettcher, James R. McKone, and **Nathan S. Lewis**, "Photoelectrochemical water splitting: silicon photocathodes for hydrogen evolution", *Proc. SPIE*, **2010**, *7770*, 77701F.

18. Shannon W. Boettcher, Emily L. Warren, Morgan C. Putnam, Elizabeth A. Santori, Daniel Turner-Evans, Michael D. Kelzenberg, Michael G. Walter, James R. McKone, Bruce S. Brunschwig, Harry A. Atwater, and **Nathan S. Lewis**, "Photoelectrochemical hydrogen evolution using Si microwire arrays", *J. Am. Chem. Soc.*, **2011**, *133(5)*, 1216–1219.

19. Michael D. Kelzenberg, Daniel B. Turner-Evans, Morgan C. Putnam, Shannon W. Boettcher, Ryan M. Briggs, Jae Yeon Baek, **Nathan S. Lewis**, and Harry A. Atwater, "High-performance Si microwire photovoltaics", *Energy Environ. Sci.*, **2011**, *4*, 866–871.

20. Emily L. Warren, Shannon W. Boettcher, Michael G. Walter, Harry A. Atwater, and **Nathan S. Lewis**, "pH-independent, 520 mV open-circuit voltages of Si/methyl viologen$^{2+/+}$ contacts through use of radial n^+p-Si junction microwire array photoelectrodes", *J. Phys. Chem. C*, **2011**, *115(2)*, 594–598.

II.K.21 New Directions for Efficient Solar Water Splitting Based on Two Photosystems and Singlet Fission Chromophores

Justin Johnson, Arthur J. Frank, Nathan R. Neale, Kai Zhu, Arthur J. Nozik*
National Renewable Energy Laboratory
1617 Cole Blvd
Golden, CO 80401
Phone: (303) 384-6603
E-mail: anozik@nrel.gov

Josef Michl
University of Colorado
Department of Chemistry and Biochemistry
Boulder, CO 80309

DOE Program Manager: Mark Spitler
Phone: (301) 903-4568
E-mail: mark.spitler@science.doe.gov

Objectives

The objective of this HFI project is to conduct the basic science that will lead to the discovery and ultimate development of photoconversion approaches that can produce hydrogen via H_2O splitting at costs competitive with or less than their present cost derived from steam reforming of natural gas. This will require a system with very high conversion efficiencies (>32%) coupled with very low capital costs (<$200/m^2). We focus on solar water splitting using two coupled photosystems (a photocathode and a photoanode), analogous to what occurs in biological photosynthesis, but where one of the photoelectrodes exhibits efficient photogenerated electron-hole pair multiplication via singlet fission (SF), a process that produces two triplet states from a singlet state. Thermodynamic calculations show that such coupled photosystems have the highest possible theoretical conversion efficiencies, exceeding those of single photoelectrode cells by ~50%, and that only one photoelectrode needs to undergo SF.

Technical Barriers

SF in the photoanode or photocathode must be very efficient, and for a tandem cell with both photoelectrodes in series optically and electrically, the SF chromophore should have its first excited singlet state at ~2 eV and its lowest triplet state at ~ 1 eV. The second photoelectrode should have a bandgap of ~1 eV and the energetic alignment of the two photoelectrodes must allow appropriate recombination of an electron and hole from the photoanode and photocathode, respectively, to maintain charge balance. In one optimum configuration the two chromophores at the photoanode and photocathode need to be electronically coupled to nanocrystalline electron-conducting and hole-conducting supports. The system must also be photostable and avoid photocorrosion of both photoelectrodes; one approach is to isolate the surfaces of the photoelectrodes from contact with water.

Abstract

The research objective of this HFI program is to conduct the basic science that will lead to the discovery and ultimate development of photoconversion approaches that can produce hydrogen via H_2O splitting at costs competitive with or less than their present cost derived from steam reforming of natural gas. This will require a system with very high conversion efficiencies (>32%), coupled with very low capital costs (< $200/m^2). We will focus on solar water splitting using two coupled photosystems (a photocathode and a photoanode), analogous to what occurs in biological photosynthesis, but where one of the photoelectrodes is based on a molecular chromophore that exhibits efficient singlet fission (SF), a photophysical process wherein two triplet states are created from the first excited singlet state produced by absorption of a single photon. We have demonstrated a 200% QY of triplet states formed from the first excited singlet state via SF in molecular crystals of diphenylisobenzofuran (DPIBF). Thermodynamic calculations show that such coupled photosystems have the highest possible theoretical conversion efficiencies, exceeding those of single photoelectrode water-splitting cells by 50%. The system is also expected to have significantly enhanced conversion efficiency (> 20% increase depending on overvoltage) when concentrated solar power is used; this effect will be experimentally investigated for the first time.

Progress Report

Thermodynamics

Our research shows clearly that the use of two photosystems produces much higher theoretical conversion efficiencies (by a factor of ~50%) for solar water splitting at all values of the total cell overpotential compared to cells with just one photoelectrode. These results are summarized in Figure 1. The lower lines show the maximum efficiency for a single photoelectrode cell as a function of the total cell overvoltage for H_2O splitting, and the upper lines show the efficiency dependence on overvoltage for a double-electrode tandem cell with different types of the two photoelectrodes. SF/M1 is the result when one photoelectrode produces SF and the second generates just 1 e^-/photon. SF/M2 has one electrode producing SF and the second producing 2 e^-/

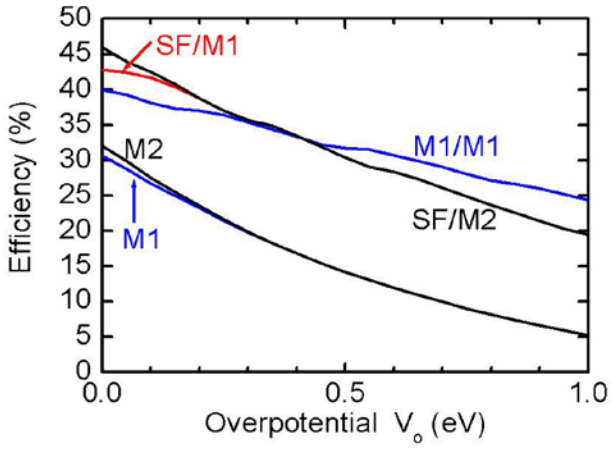


FIGURE 1. Maximum thermodynamic water-splitting conversion vs. total cell overvoltage for cells with single photoelectrodes (M1 and M2, bottom curves) and cells with two photoelectrodes (SF/M1, M1/M1, and SF/M2(SF), top curves). Definitions of the M1, M2, and SF characteristics are described in the text and shown in Fig. 2.

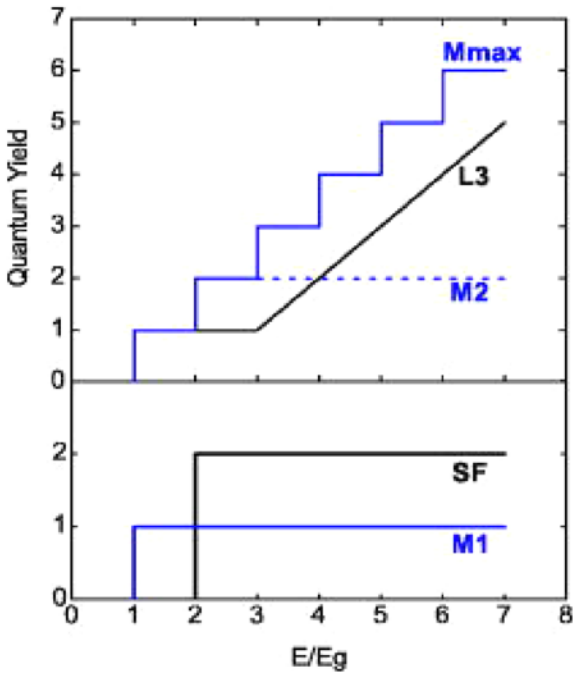


FIGURE 2. Characteristics of the QY vs. (photon energy/bandgap) that define M1, M2, Mmax, and SF. Characteristics labeled L(n) apply to the behavior of quantum dots and are not considered in this proposal.

photon after the photoexcitation equals twice the bandgap (E_g) energy; for our purposed here M2 is the same as SF. Finally, M1/M1 is a conventional electrode system in which both electrodes produce 1 e^-/photon. For SF, the molecular bandgap is defined as the triplet state energy, which is close to one-half the first excited singlet state energy, because it is the triplet energy at which the photogenerated electrons are emitted. Thus, SF is analogous to an indirect-bandgap semiconductor in which the lowest energy transition is forbidden. Figure 2 shows the QY characteristics as a function of photon energy normalized to the bandgap (E_{photon}/E_g) that defines M1, M2 (SF), Mmax, SF (L3 is a linear characteristic that is not considered here.)

Singlet Fission

We report the first designed molecular system that exhibits perfect SF efficiency, producing two triplet states from an excited singlet state of the molecule (1,3-diphenylisobenzofuran (DPIBF)–Figure 3). Our experiments indicated a quantum yield at 77K of 200% for the creation of the two triplets in DPIBF. Both molecular design principles and broader concepts of coupling chromophores into functional networks were key advances that produced 200% QYs via SF. The compound DPIBF was identified as a promising candidate by using theory to direct a search for chromophores likely to have a desirable ratio of singlet and triplet excitation energies, the latter being difficult to measure experimentally. Recent theory led to the discovery that the natural geometry that the molecules adopt while packing into crystals, a staggered stacked sandwich type orientation, was optimum for SF.

Thin polycrystalline films of DPIBF were made by subliming the compound in vacuum onto substrates. When done correctly, the films showed strong spectroscopic signatures indicating a high yield of triplets. In order to

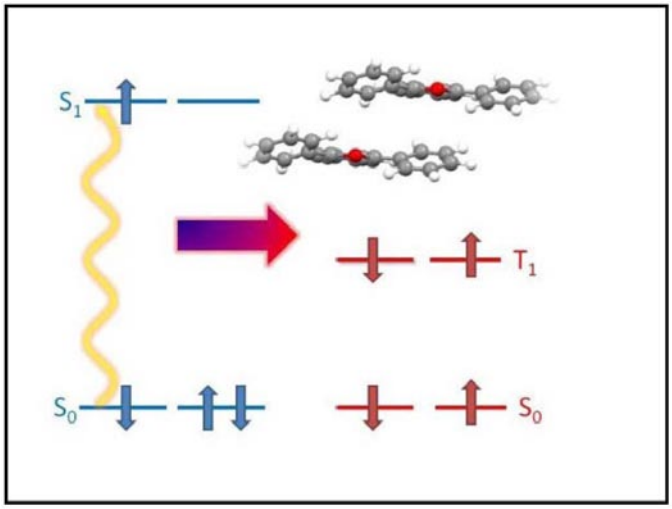


FIGURE 3. Depiction of the singlet fission process by which single absorbed photon creates an excited singlet state that evolves into two triplet states. Electron transfer can then occur from the two triplet states to produce two electrons per absorbed photon in a solar cell device. The molecules shown are DPIBF in a staggered stacking orientation known from its crystal structure.

quantify the yield, ultrafast laser experiments were performed to accurately measure the initial populations of photoexcited singlet states and their time evolution into triplets on a picosecond time scale. A careful analysis of the data led to yields approaching 200% and an increase in the triplet formation rate of more than ten thousand compared with

the isolated DPIBF molecule. Both observations support the notion that efficient singlet fission is occurring and that the design criteria set forth may be quite general.

Nanocrystalline Hole Conductors

One objective of the research was to develop porous hole-conducting nanocrystalline semiconductor supports to capture photogenerated holes from the ground state of optically excited chromophores (e.g., QDs and molecular dyes) and transport them to the hole-collecting substrate, which contacted a dark catalytic anode to drive water oxidation. Toward that end, we developed synthetic protocols for preparing inverse opal nanocrystalline films as hole conductors. Ordered polystyrene (PS) bead films were prepared as templates for directing the growth of ordered porous semiconducting materials. We developed a methodology to deposit 3–4-μm-thick films of 300-, 400-, and 500-nm PS beads arranged in a hexagonal close-packed array with periodic porosity. These PS templates were used to prepare CdSe inverse opals by electrochemical deposition. The resulting structures displayed significant light absorption over a wide portion of the near-infrared region. The unexpected enhanced light absorption in this spectral region was shown to result from a disordered pore structure and a high refractive index contrast present in the CdSe inverse opal architecture. Similar PS templates were used recently to prepare Cu–CuO core-shell inverse opals. Both of the copper oxides are intrinsically p-type with respective bandgaps of 1.4 eV for CuO and 2.1 eV for Cu_2O. An examination of the photonic bandgap of Cu_2O shows that it shifts from 680 to 895 nm when the pore size is increased from 300 to 400 nm. Transmission electron microscopy (TEM) and X-ray energy dispersive spectroscopy (EDS) measurements of the Cu-Cu_xO inverse opal electrodes showed a continuous Cu core surrounded by a 20-nm-thick oxide wall (Figure 4). We found that the Cu–CuO core-shell structures were about 15-fold more conductive than cupric oxide inverse opal electrode. The fact that adding a metal core to a poor conductor, such as the CuO, improved its electrical conductivity suggests that a similar approach might be useful for improving the conductivity of other poorly conducting p-type and n-type materials. We also prepared nanocrystalline films of ZnSe and ZnTe nanocrystals that were suitable for studying dye-sensitized hole injection and transport. Films comprising these nanocrystals with thicknesses of 2–3 μm were prepared by spin coating from concentrated solutions followed by thermal or amine-based chemical treatments to remove an initial surface layer of electrically insulating oleate ligands.

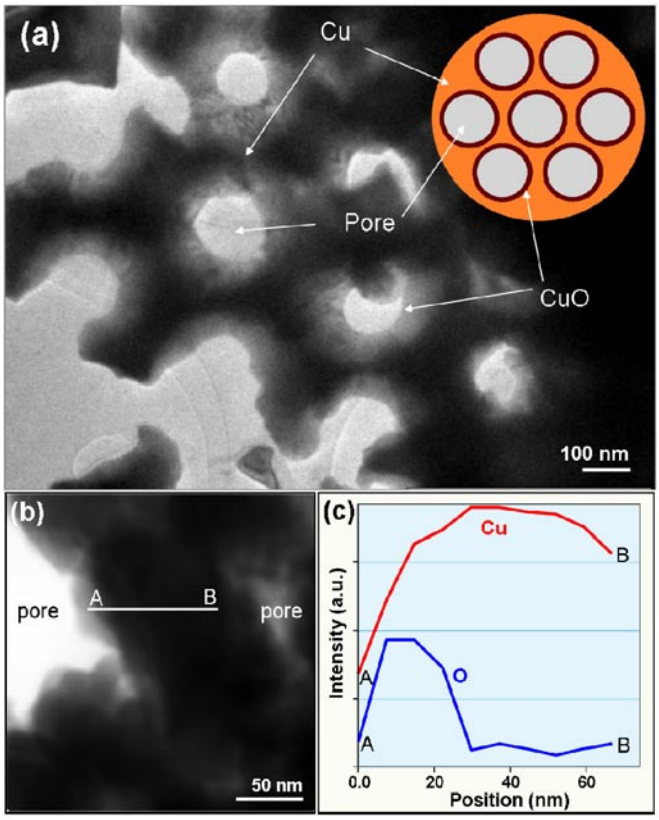


FIGURE 4. TEM images of Cu-CuO inverse opal nanowire mesh electrode with (a) low-magnification view, (b) higher-magnification view, and (c) the EDS cross-sectional line scan from point A to B in (b), highlighting the distribution profile of Cu and O across the core-shell nanowire mesh region.

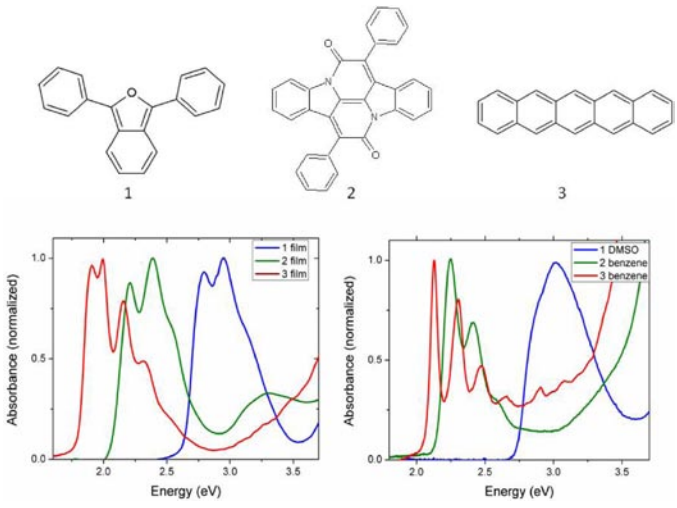


FIGURE 5. Molecular structures of monomeric SF compounds and their absorption spectra in film (lower left) and solution (lower right).

Future Directions

1,3-Diphenylisobenzofuran (**1**), cibalakrot (**2**), and pentacene (**3**) are all compounds that fulfill the important relations $E(S_1) \geq 2E(T_1)$ and $E(T_2) > E(S_1)$ for efficient SF (see Figure 5). We will expand our efforts from (**1**) to also investigate (**2**) and (**3**). We will study complete water splitting cells with two photoelectrodes, one of which exhibits efficient SF at the cathode. We will optimize new hole conducting nanocrystalline supports for the anodic

photoelectrode and investigate new hole-injecting dyes. We will study the effects of solar concentration on cell performance, which is predicted to greatly increase the water splitting efficiency based on initial thermodynamic calculations.

Publication list (including patents) acknowledging the DOE grant or contract

1. Hanna, M.C.; Nozik, A.J., Solar conversion efficiency of photovoltaic and photoelectrolysis cells with carrier multiplication absorbers. *Journal of Applied Physics* **2006,** *100* (7) .

2. Law, M.; Luther, J.; Song,).; Hughes, B.; Perkins, C.L.; Nozik, A.J.; Structural, optical, and electrical properties of PbSe nanocrystal solids treated thermally or with simple amines, **2008**, *Journal of the American Chemical Society* , 130, 5974.

3. Johnson, J.C.; Nozik, A.J.; Michl, J., High triplet yield from singlet fission in thin films of 1,3-diphenlyisobenzofuran. *Journal of the American Chemical Society* **2010,** *132*, 16302.

4. Johnson, J.C.; Nozik, A.J.; Michl, J., *manuscript in preparation*.

5. Schwerin, A.F.; Johnson, J.C.; Smith, M.B.; Sreearunothai, P.; Popovic, D.; Cerny, J.; Havlas, Z.; Paci, I.; Akdag, A.; MacLeod, M.K.; Chen, X.D.; David, D.E.; Ratner, M.A.; Miller, J.R.; Nozik, A.J.; Michl, J., Toward Designed Singlet Fission: Electronic States and Photophysics of 1,3-Diphenylisobenzofuran. *Journal of Physical Chemistry A* **2010,** *114* (3), 1457-1473.

6. Michl, J.; Nozik, A.J.; Chen, X.; Johnson, J.C.; Rana, G.; Akdag, A.; Schwerin, A.F., *Proceedings of the SPIE* **2007,** *6656*, 66560E1.

7. Johnson, J.C.; Akdag, A.; Chen, X.; Smith, M.; Michl, J.; Nozik, A.J., *manuscript in preparation* **2010**.

8. Greyson, E.C.; Stepp, B.R.; Chen, X.; Schwerin, A.F.; Paci, I.; Smith, M.B.; Akdag, A.; Johnson, J.C.; Nozik, A.J.; Michl, J.; Ratner, M., Singlet Exciton Fission for Solar Cell Applications: Energy Aspects of Interchromophore Coupling. *Journal of Physical Chemistry B* **2010**, *114,* 1423.

9. Neale, N.R.; Lee, B.G.; Kang, S.H.; Frank, A.J., *submitted to Phys. Chem. Chem. Phys*.

10. Kang, S.H.; Neale, N.R.; Zhu, K.; Halverson, A.F.; Kim, J.Y.; Yan, Y.; Frank, A.J., *in preparation*.

11. Patent Application: Ultra-High Solar Conversion Efficiency for Solar Fuels and Solar Electricity via Multiple Exciton Generation in Quantum Dots Coupled with Solar Concentration, Filed Feb 2011, Arthur J. Nozik and Mark Hanna.

III. HYDROGEN DELIVERY

III.0 Hydrogen Delivery Sub-Program Overview

The Hydrogen Delivery sub-program supports research and development (R&D) of technologies that enable low-cost, efficient, and safe delivery of hydrogen to the end-user. Activities include the development of technologies required for hydrogen transport, either as a liquid (in tanker trucks) or as a compressed gas (in pipelines or tube trailers). Cost-effective methods of transporting hydrogen from central production facilities are required to achieve sustainable, widespread commercialization of hydrogen fuel cells. In addition, there are several activities within the Delivery sub-program focused on developing innovative methods of compressing, storing, and dispensing hydrogen at the point of refueling. Advances in these technologies will facilitate reductions in the cost of hydrogen that is produced at both centralized and distributed facilities

Goal

The goal of this sub-program is to reduce the costs associated with delivering hydrogen to a point at which its use as an energy carrier in fuel cell applications is competitive with alternative transportation and power generation technologies.

Objectives[1]

The key objective of this sub-program is to develop low-cost, efficient, and safe technologies for delivering hydrogen from the point of production to the point of use–including stationary fuel cells and fuel cell electric vehicles (FCEVs). This objective applies to all of the possible delivery pathways. Interim and ultimate targets for various delivery components are being updated in the Fuel Cell Technologies Program's *Multi-Year Research, Development, and Demonstration Plan (MYRD&D Plan)*. Key objectives for specific delivery components include:

- **Tube Trailers:** Reduce the cost of compressed gas delivery via tube trailer by increasing vessel capacity and lowering trailer cost on a per-kilogram-of-hydrogen-transported basis.
- **Pipeline Technology:** Develop mitigation strategies for combined material fatigue and hydrogen-induced embrittlement in steel pipelines; advance the development and acceptance of alternative composite pipe materials that can reduce installed pipeline costs; and develop lower-cost, higher-reliability compression technology for hydrogen transmission by pipeline.
- **Liquefaction:** Reduce the capital and operating costs of hydrogen liquefiers and bulk liquid storage vessels.
- **Forecourt Technologies:**
  - **Compression:** Develop lower-cost, higher-reliability hydrogen compression technology for terminal and forecourt applications.
  - **Storage:** Develop lower capital cost off-board bulk storage technology and confirm the technical feasibility of geologic storage for hydrogen.
- **Analysis:** Conduct comprehensive analyses on potential near- and longer-term hydrogen delivery options, comparing the relative advantages of each and examining possible transition scenarios between the two timeframes.

Fiscal Year (FY) 2011 Technology Status

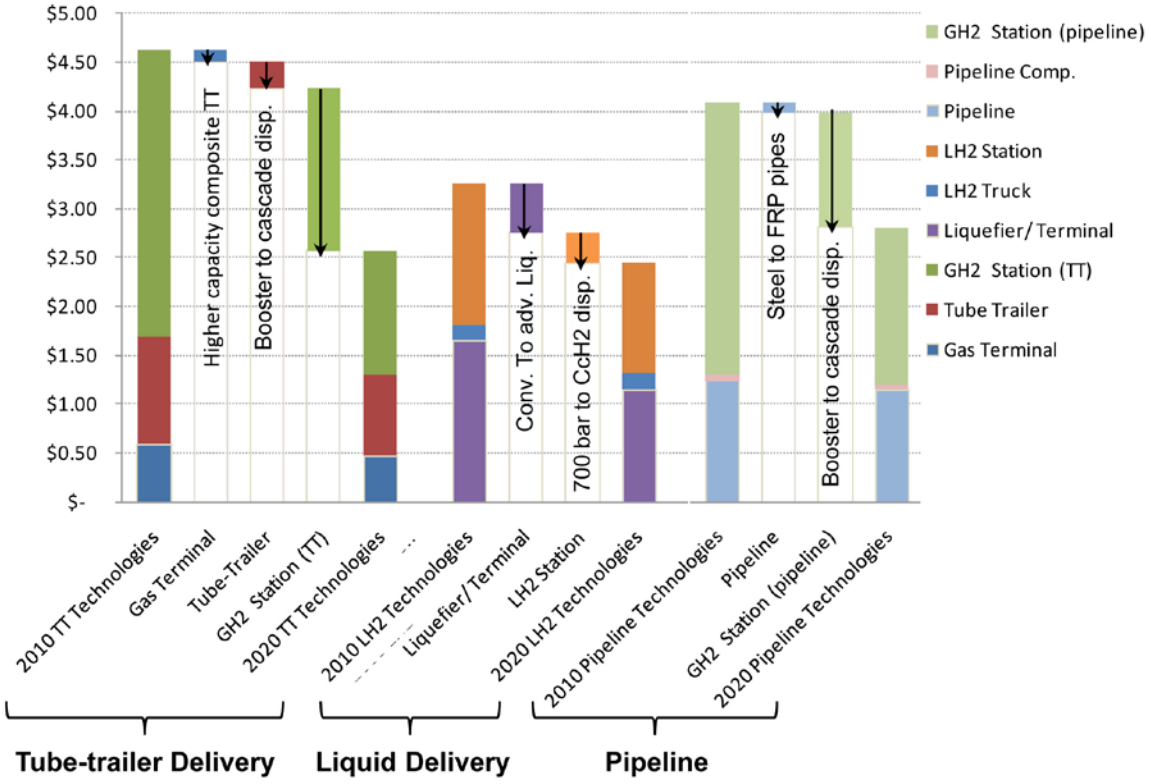
The projected costs for the delivery of hydrogen, based on current technologies, range from $3/gasoline gallon equivalent (gge) to $10/gge, depending on the quantity and distance transported. These projections include the costs of compression, storage, and dispensing at the refueling site. Progress towards current goals and targets is summarized in the following table.

[1] Note: Targets and milestones are under revision; therefore, individual progress reports may reference prior targets.

Delivery Element	Targets (2015/2017)[1]	Status[2]
Tube Trailers	• Reduce capital cost to <$200,000 • Increase capacity to 1,100 kg	• Capital cost: $470,000 (250 bar carbon fiber vessel) • Capacity: 550 kg • Cost contribution: $0.9/kg H_2
Pipeline Technology	• Reduce cost/mile (installed) to <$490K	• Installed steel pipeline cost: $3M/mile • Cost contribution: $1.7/kg H_2 • Compressor cost contribution: $0.1/kg H_2
Liquefaction	• Reduce installed capital cost to $100M • Increase energy efficiency to 87%	• Installed capital cost: $170M • System efficiency: 80% • Cost contribution: $1.6/kg H_2
Forecourt Compression (1,000 kg/day station)	• Reduce installed capital cost to $187.5K for 700 bar dispensing	• Capital cost: $1.5M for 700 bar dispensing (cost contribution of $2/kg H_2) • Capital cost $0.5M for 350 bar dispensing (cost contribution of $0.8/kg H_2)
Forecourt Storage (1,000 kg/day station)	• Reduce tank cost stored to $300 per kg of stored H_2	• Storage tank cost: $1,000 per kg of stored H_2 (cost contribution of $0.4/kg H_2)

[1] Based on current targets in the Fuel Cell Technologies Program's *MYRD&D Plan*. These are in the process of being updated.
[2] High-volume projections based on HDSAM version 2.3 (preliminary analysis; peer review underway).

Figure 1 shows the projected reduction in hydrogen delivery cost for various pathways due to technological advancement.



TT - tube trailer; GH2 - gaseous hydrogen; LH2 - liquefied hydrogen

FIGURE 1. Projected Reductions in Hydrogen Delivery Costs. Projections are based on Hydrogen Delivery Scenario Analysis Model (HDSAM) V2.3 for a well-established hydrogen market demand for transportation (15% market penetration). The specific scenarios examined assume central production of hydrogen that serves a city of moderately large size (population of about 1.2 million).

FY 2011 Accomplishments

Tube Trailers and Bulk Storage

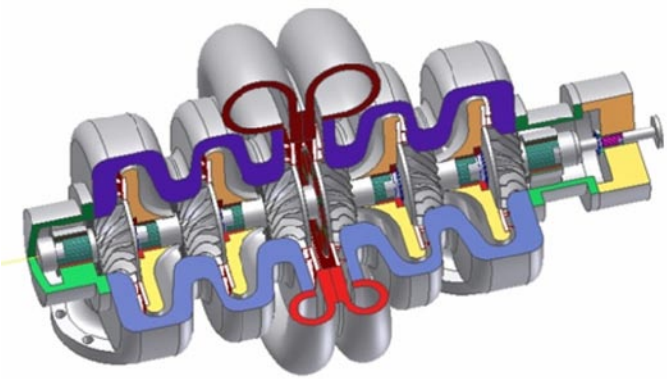
- Lincoln Composites completed a design trade study for a 5,000 pounds per square inch (psi) vessel, which includes a projected 33% increase in capacity at 15°C and ~10% reduction in capital cost on a per kilogram of transported hydrogen basis.
- Lawrence Livermore National Laboratory scaled up their design of a glass fiber pressure vessel to a full diameter of 23 inches and successfully hydroburst tested the vessel at strains above trailer design levels. The concept has the potential to reduce current tube trailer transport costs by up to 50% (Figure 2).



FIGURE 2. Carbon Fiber Composite Tube Trailer Pressure Vessel and International Standards Organization Container

Pipeline Technology

- Savannah River National Laboratory completed burst testing on fiber reinforced polymer pipe with 40% through-wall flaws, demonstrating a 3x margin above the rated pressure for the pipe. Researchers also demonstrated that industry-standard compression fittings will meet Department of Transportation requirements for joint leakage between pipe segments.
- Fatigue crack growth relationships determined by Sandia National Laboratories for X52 base metal and electric resistance welded seam specimens cut from actual pipeline were found to be quite similar, despite some variability in replicate data sets. The results indicate that the reliability and integrity of steel hydrogen pipeline likely will not be determined by the properties of the electric resistance welded seam.
- Concepts ETI completed the detailed design of a centrifugal compressor capable of providing 240,000 kg/day of hydrogen at 1,280 psi for pipeline-grade service and have initiated procurement of the major gearbox components for fabrication and testing. Mohawk Innovative Technology also completed the design of a centrifugal pipeline compressor that will employ advanced Ti-based rotors to achieve the tip speeds needed to meet the DOE's 2015 targets for this technology (Figure 3). They are currently fabricating components for initial laboratory testing.



Mohawk Innovative Technologies, Inc.

FIGURE 3. Double-Entry Centrifugal Compressor for Pipeline Compression

Liquefaction

- Praxair Inc. demonstrated a reduction in overall power consumption of ~2.5% by developing and employing a new ortho-para catalyst in the high-temperature heat exchanger of a traditional hydrogen liquefier design. Additionally, results from process modeling indicated that improved gas compression technology for these units can increase overall liquefier efficiency by 3%–6%.
- Prometheus Energy integrated all of the subsystems for their Phase-I linear active magnetic regenerative liquefier and demonstrated a sustainable magneto-thermal based reduction in temperature from 290 K to 120 K. Lessons learned are being applied to a Phase-II rotary design that will span 290 K to 20 K (Figure 4).

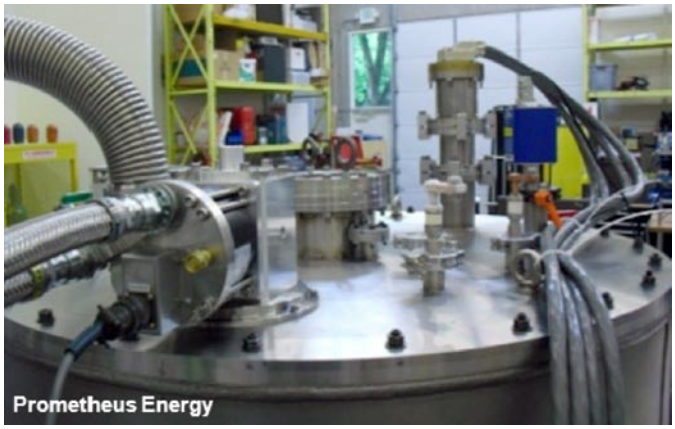


FIGURE 4. Active Magnetic Regenerative Refrigerator for Hydrogen Liquefaction

Forecourt Technology

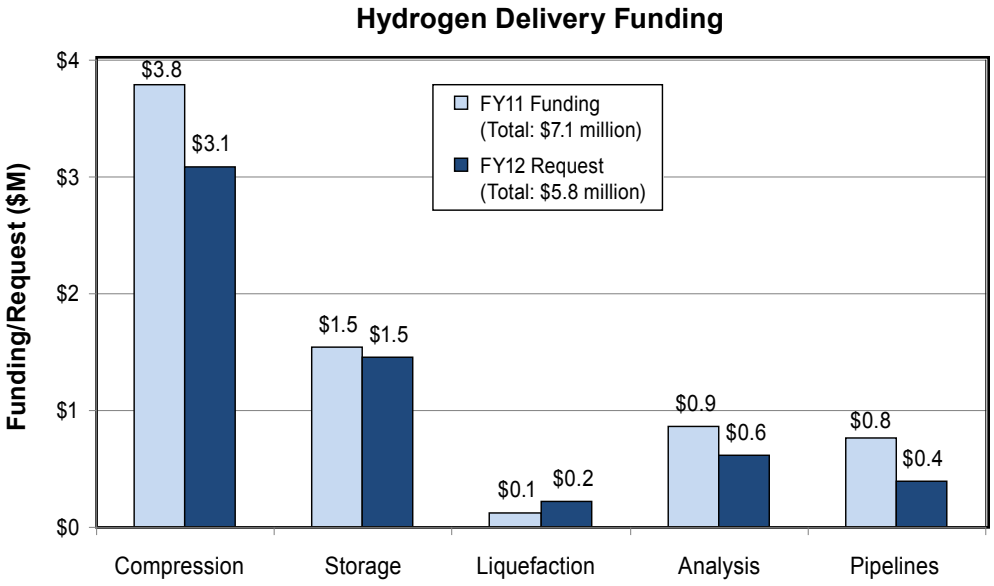
- FuelCell Energy developed a two-stage electrochemical hydrogen compressor that achieved 420 bar of compression, or a compression ratio of 300:1. To date, they have demonstrated 20 successful pressure cycles and 500 hours of durability with the device. They will be fabricating the support facilities to test this compressor to the ultimate pressure capability target of 840 bar.
- Conceptual designs for a steel-lined reinforced concrete hydrogen pressure vessel were completed at Oak Ridge National Laboratory. Preliminary cost estimates indicate that this concept has the potential to meet DOE's 2015 cost target for off-board bulk hydrogen storage.

Analysis

- Argonne National Laboratory completed cost and price index updates to HDSAM, evaluated factors affecting the capital and levelized cost of refueling stations, and carried out an analysis of key hydrogen infrastructure cost drivers in preparation for the sub-program's revised section of the *MYRD&D Plan*.
- Pacific Northwest National Laboratory completed a detailed analysis of pipeline costs, which was integrated into the updated HDSAM model.
- The National Renewable Energy Laboratory completed an analysis of hydrogen delivery by rail, finding this option to be the least costly means of transporting hydrogen over distances of more than 600 miles for early market scenarios–for example, when hydrogen is produced by renewable resources that are far from large demand centers. An analysis of hydrogen production and delivery costs from wind sources at remote, low-electricity-cost locations was also completed. It was found that under certain scenarios this option can provide dispensed hydrogen at a cost as low as $6/kg.

Budget

The FY 2011 budget provided $7.1 million for continued hydrogen delivery R&D. The President's FY 2012 budget request for the Office of Energy Efficiency and Renewable Energy provides $5.8 million for hydrogen delivery, with an emphasis on reducing pipeline and forecourt compression cost, increasing tube trailer capacity, and identifying viable low-cost early-market delivery pathways.



FY 2012 Plans

In FY 2012, the Delivery sub-program portfolio will be focused on two key areas:

1. **Long-term technologies expected to have market impact in 10–20 years.** In FY 2012 the Delivery sub-program portfolio will continue efforts on fiber reinforced polymer pipeline characterization for design code development; centrifugal compressor development and demonstration for pipeline transmission; hydrogen transmission as a cold, pressurized fluid; magnetic refrigeration; and electrochemical compression. Recognizing that hydrogen storage on-board future FCEVs may not be in the form of compressed gas (as is current practice) the Delivery and Storage sub-programs will collaborate to identify delivery challenges for future materials-based storage technologies. Analysis efforts will be initiated to evaluate options for the transition from compressed gas stations serving early vehicle markets to stations that could provide hydrogen for next generation FCEVs.
2. **Near-term technologies that reduce hydrogen delivery costs for emerging hydrogen and fuel cell applications (e.g., forklifts and backup power) and early adopter FCEV markets.** In FY 2012, the emphasis in these near-term areas will be on strategic analyses to: (a) determine delivery options that can reduce the cost of 700-bar compression at light-duty-vehicle refueling stations; (b) evaluate hydrogen delivery costs for sustainable non-automotive markets and establish possible "lessons learned" that can be applied to early localized FCEV markets; and (c) identify station costs not related to process operations (e.g., insurance and safety system requirements) and potential market incentives that can drive business decisions on station construction. Results from these analyses will be used to identify barriers for early market technologies and to help focus subsequent technology development efforts. A key FY 2012 Program milestone will be to identify delivery pathway(s) that can achieve a current, as-dispensed (350 bar) hydrogen cost of <$4/gge. Additional near-term R&D will include work to increase the hydrogen carrying capacity of current composite tube trailer designs by 15% or more and continued development of steel-lined reinforced concrete pressure vessels for station storage.

Sara Dillich
Hydrogen Production & Delivery Team Lead (Acting)
Fuel Cell Technologies Program
Department of Energy
1000 Independence Ave., SW
Washington, D.C. 20585-0121
Phone: (202) 586-7925
E-mail: Sara.Dillich@ee.doe.gov

K. Scott Weil
Hydrogen Delivery Team
Chief Scientist, Pacific Northwest National Laboratory
On assignment to the Fuel Cell Technologies Program
Department of Energy
1000 Independence Ave., SW
Washington, D.C. 20585-0121
Phone: (202) 586-1758
E-mail: Kenneth.Weil@ee.doe.gov

III.1 Hydrogen Embrittlement of Structural Steels

Jay Keller (Primary Contact), Brian Somerday, Chris San Marchi
Sandia National Laboratories
P.O. Box 969
Livermore, CA 94550
Phone: (925) 294-3316
E-mail: jokelle@sandia.gov

DOE Manager
HQ: Scott Weil
Phone: (202) 586-1758
E-mail: Kenneth.Weil@ee.doe.gov

Project Start Date: January 2007
Project End Date: Project continuation and direction determined annually by DOE

Fiscal Year (FY) 2011 Objectives

(1) Demonstrate reliability/integrity of steel hydrogen pipelines under cyclic pressure conditions:
- Measure fatigue crack growth rates and fracture thresholds of line pipe steels in high-pressure hydrogen gas, emphasizing welds.
- Evaluate performance of steel pipelines by applying code-based structural integrity model coupled with steel properties measured in hydrogen gas.
- Quantify effects of gas impurities (e.g., O_2) in mitigating hydrogen-accelerated fatigue crack growth.

(2) Enable development of micromechanics models of hydrogen embrittlement in pipeline steels:
- Establish physical models of hydrogen embrittlement in line pipe steels using evidence from analytical techniques such as electron microscopy.

Technical Barriers

This project addresses the following technical barriers from the Hydrogen Delivery section of the Fuel Cell Technologies Program Multi-Year Research, Development and Demonstration Plan:

(D) High Capital Cost and Hydrogen Embrittlement of Pipelines

(K) Safety, Codes and Standards, Permitting

Technical Targets

The principal target addressed by this project is the following (from Table 3.2.2):

- Pipeline Reliability/Integrity

The salient reliability/integrity issue for steel hydrogen pipelines is hydrogen embrittlement. One particular unresolved issue is the performance of steel hydrogen pipelines that are subjected to extensive pressure cycling. One of the objectives of this project is to enable safety assessments of steel hydrogen pipelines subjected to pressure cycling through the use of code-based structural integrity models. This structural integrity analysis can determine limits on design and operating parameters such as the allowable number of pressure cycles and pipeline wall thickness. Efficiently specifying pipeline dimensions such as wall thickness also affects pipeline cost through the quantity of material required in the design.

FY 2011 Accomplishments

Fracture properties for X52 line pipe steel were measured in high-pressure hydrogen gas to provide data for evaluating the reliability/integrity of steel hydrogen pipelines:

- Conducted replicate measurements of fatigue crack growth relationships for X52 base metal and seam weld in high-pressure hydrogen gas.
- Compared fatigue crack growth relationships for X52 base metal and seam weld, revealing that the reliability/integrity of steel hydrogen pipelines is not limited by the seam weld.



Introduction

Carbon-manganese steels are candidates for the structural materials in hydrogen gas pipelines, however it is well known that these steels are susceptible to hydrogen embrittlement. Decades of research and industrial experience have established that hydrogen embrittlement compromises the structural integrity of steel components. This experience has also helped identify the failure modes that can operate in hydrogen containment structures. As a result, there are tangible ideas for managing hydrogen embrittlement in steels and quantifying safety margins for steel hydrogen containment structures. For example, fatigue crack growth aided by hydrogen embrittlement is a well-established failure mode for steel hydrogen containment structures subjected to pressure cycling. This pressure cycling represents one of the key differences in

operating conditions between current hydrogen pipelines and those anticipated in a hydrogen delivery infrastructure. Applying code-based structural integrity models coupled with measurement of relevant material properties allows quantification of the reliability/integrity of steel hydrogen pipelines subjected to pressure cycling. Furthermore, application of these structural integrity models is aided by the development of micromechanics models, which provide important insights such as the hydrogen distribution near defects in steel structures.

Approach

The principal objective of this project is to enable the application of code-based structural integrity models for evaluating the reliability/integrity of steel hydrogen pipelines. The new American Society of Mechanical Engineers (ASME) B31.12 design code for hydrogen pipelines includes a fracture mechanics-based design option, which requires material property inputs such as the fracture threshold and fatigue crack growth rate under cyclic loading. Thus, one focus of this project is to measure the fracture thresholds and fatigue crack growth rates of technologically relevant line pipe steels in high-pressure hydrogen gas. These properties must be measured for the base materials but more importantly for the welds, which are likely to be most vulnerable to hydrogen embrittlement.

A second objective of this project is to enable development of micromechanics models of hydrogen embrittlement in pipeline steels. The focus of this effort is to establish physical models of hydrogen embrittlement in line pipe steels using evidence from analytical techniques such as electron microscopy. These physical models then serve as the framework for developing sophisticated finite-element models, which can provide quantitative insight into the micromechanical state near defects. Understanding the micromechanics of defects can ensure that structural integrity models are applied accurately and conservatively.

Results

The principal activity during FY 2011 was measuring the fatigue crack growth relationships for the base metal and electric resistance weld (ERW) from X52 line pipe steel in hydrogen gas. The fatigue crack growth rate (da/dN) vs. stress-intensity factor range (ΔK) relationship is a necessary material-property input into structural models that enable engineering analysis of the design life of steel hydrogen pipelines. One such design life methodology for steel hydrogen pipelines was recently published in the ASME B31.12 code. The measurements of subcritical cracking thresholds and fatigue crack growth relationships in this task thus support the objective of establishing the reliability/integrity of steel hydrogen pipelines.

The X52 line pipe steel was selected for this task because of its recognized technological relevance for hydrogen pipelines. The X52 steel from the round robin tensile property study (FY 2008) was tested for the following reasons: 1) some characterization of the material was already provided from the round robin study, 2) ample quantities of material were still available, and 3) the X52 steel was in the form of finished pipe, which is the most relevant product form and also allows samples to be extracted from the ERW seam.

The hydrogen-affected fatigue crack growth relationship (da/dN vs. ΔK) for the structural steel is the basic element in pipeline reliability/integrity models. The ASME B31.12 code requires measurement of the fatigue crack growth relationship for pipeline steels at the hydrogen gas operating pressure. Initial measurements of the fatigue crack growth relationship for X52 steel base metal were conducted in 21 MPa hydrogen gas (the upper limit specified for hydrogen pipelines in the ASME B31.12 code) at a load-cycle frequency of 1 Hz (Figure 1). This load-cycle frequency was selected to balance test effectiveness and test efficiency, since fatigue crack growth rates can be enhanced at lower test frequency but the test duration can become prohibitively protracted. Even at this relatively high load-cycle frequency, measurement of the fatigue crack growth relationship over the relevant range of ΔK could require several days. For example, the duration of the test conducted at a load ratio of 0.5 was 6 days. (Load ratio, R, is the ratio of minimum applied load to maximum applied load.)

Although the accepted trend is that increasing load-cycle frequency leads to lower (i.e., non-conservative) fatigue crack growth rates in hydrogen gas, this trend is predominantly based on fatigue crack growth rates measured for steels at relatively high ΔK, e.g., greater than 15 MPa $m^{1/2}$. The possibility of effectively measuring fatigue crack growth rates at high load-cycle frequency in the lower (and technologically relevant) range of ΔK was explored for the X52 steel in 21 MPa hydrogen gas. Fatigue crack growth rate relationships were measured at 10 Hz for two R ratios (0.1 and 0.5), and the results are compared to the fatigue crack growth relationships measured at 1 Hz in Figure 1. Although the fatigue crack growth relationships at 1 Hz and 10 Hz are not exactly coincident, there are only moderate differences in the fatigue crack growth rates over the ΔK range investigated. These preliminary results suggest that reliable fatigue crack growth relationships may be measured at high load-cycle frequency, which would allow the testing to be conducted more efficiently.

The fatigue crack growth relationship for the X52 ERW was also measured in 21 MPa hydrogen gas. Since steel microstructures in welds are not easily controlled, these weld microstructures can be inhomogeneous. Consequently, it is important to conduct replicate fatigue crack growth tests on welds to characterize potential variability in the data. Figure 2 shows the fatigue crack growth relationships measured for the X52 ERW from replicate tests. These tests were conducted at R=0.1 and 1 Hz so that the results could be directly compared to those for the X52 base metal. The following details are notable in Figure 2: 1) the da/dN vs. ΔK relationships for the X52 ERW exhibit significant variability,

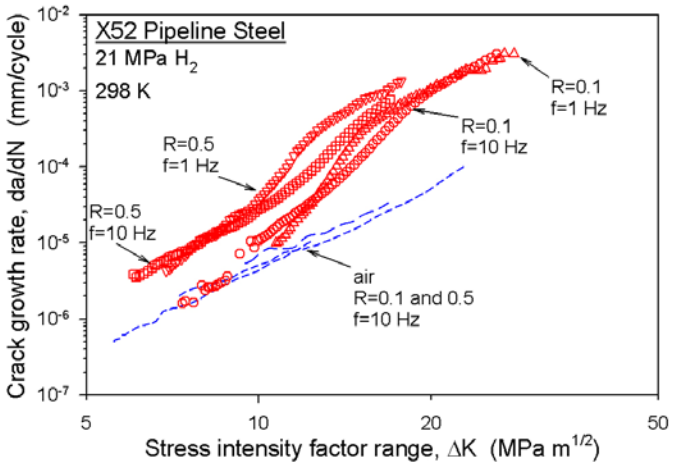


FIGURE 1. Fatigue crack growth rate (da/dN) vs. stress-intensity factor range (ΔK) plots for X52 steel base metal in hydrogen gas and air.

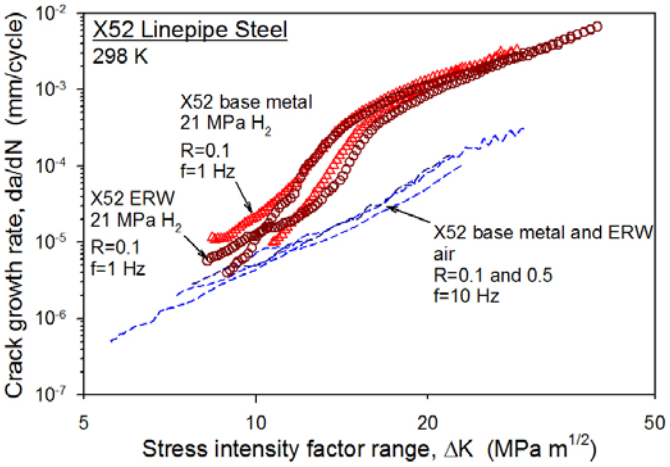


FIGURE 2. Fatigue crack growth rate (da/dN) vs. stress-intensity factor range (ΔK) plots for X52 steel base metal and ERW seam in hydrogen gas and air. Unstable cleavage fracture was observed for the ERW tested in air at K_{max} >40 MPa $m^{1/2}$.

2) the da/dN vs. ΔK relationships for the X52 base metal also exhibit variability, and 3) despite the variability in the da/dN vs. ΔK relationships, it is apparent that the fatigue crack growth rates are similar for the base metal and the weld in hydrogen gas.

While microstructure is one salient variable that can contribute to variability in the da/dN vs. ΔK relationships for X52, other variables must be considered as well. For example, the hydrogen test gas was sampled at the conclusion of both tests conducted on the X52 ERW. The leak rates from the pressure vessel were unusually high, and such an abnormal operating condition prompted sampling of the test gas. The hydrogen test gas contained relatively high concentrations of oxygen (>10 vppm) for both tests. Since oxygen is known to inhibit hydrogen uptake into steels, it is possible that the high levels of oxygen in the test gas affected the results. Additional tests are in progress on the ERW material to clarify whether variability in the da/dN vs. ΔK relationships can be attributed to oxygen in the test gas.

A fatigue crack growth test was also conducted on the X52 ERW in air. Such data serves as a baseline for comparison to measurements on the ERW in hydrogen gas as well as for comparison to measurements on the base metal in air. Test conditions for the ERW in air included R=0.5 and a load-cycle frequency of 10 Hz. Figure 2 shows that the da/dN vs. ΔK relationship for the ERW measured in air is similar to the relationship measured for the base metal in air. However, the test on the ERW was unexpectedly terminated at K_{max} ~40 MPa $m^{1/2}$ by unstable crack extension associated with cleavage fracture. This result suggests that some region of the ERW microstructure has extremely low fracture toughness. The consequence of this inherently low fracture resistance on hydrogen-assisted subcritical cracking must be explored.

Conclusions and Future Directions

Conclusions

- Fatigue crack growth relationships for X52 steel measured in hydrogen gas enable evaluation of reliability/integrity of steel pipelines under cyclic pressure conditions. Hydrogen embrittlement can be accommodated by coupling structural design models and measured fracture properties following the ASME B31.12 pipeline standard.
- The measured fatigue crack growth relationships for X52 base metal and ERW seam are similar. This trend was evident despite variability in replicate data sets. These results demonstrate that reliability/integrity of steel hydrogen pipelines is not limited by the ERW seam.

Future Directions

- Determine the threshold level of oxygen impurity concentration required to mitigate accelerated fatigue crack growth of X52 steel in hydrogen at gas pressures up to 21 MPa.
- Complete measurements of fatigue crack growth relationships for low-strength pipeline steel girth welds in hydrogen gas.

FY 2011 Publications/Presentations

1. "Microstructure and Mechanical Property Performance of Commercial Grade API Pipeline Steels in High Pressure Gaseous Hydrogen", D. Stalheim, T. Boggess, C. San Marchi, S. Jansto, B. Somerday, G. Muralidharan, and P. Sofronis, *Proceedings of IPC 2010 8th International Pipeline Conference*, Calgary, Alberta, 2010, Paper No. IPC2010-31301.

2. "Fracture Toughness and Fatigue Crack Growth of X80 Pipeline Steel in Gaseous Hydrogen", C. San Marchi, B. Somerday, K. Nibur, D. Stalheim, T. Boggess, and S. Jansto, *Proceedings of the ASME 2011 Pressure Vessels & Piping Division / K-PVP Conference (PVP11)*, Baltimore, MD, 2011, Paper No. PVP2011-57684.

3. "Improving the Fatigue Resistance of Ferritic Steels in Hydrogen Gas" (invited presentation), B. Somerday, I^2CNER Kick-off Symposium, Fukuoka, Japan, Feb. 2011.

Sandia National Laboratories is a multi-program laboratory managed and operated by Sandia Corporation, a wholly owned subsidiary of Lockheed Martin Corporation, for the U.S. Department of Energy's National Nuclear Security Administration under contract DE-AC04-94AL85000

III.2 Hydrogen Delivery Infrastructure Analysis

Marianne Mintz (Primary Contact) and
Amgad Elgowainy
Argonne National Laboratory
9700 S. Cass Ave.
Argonne, IL 60439
Phone: (630) 252-5627; 252-3074
E-mail: mmintz@anl.gov; aelgowainy@anl.gov

DOE Manager
HQ: Scott Weil
Phone: (202) 586-1758
E-mail: Kenneth.Weil@ee.doe.gov

Project Start Date: October, 2007
Project End Date: Project continuation and direction determined annually by DOE.

Partners:

- Pacific Northwest National Laboratory, Richland, WA
- National Renewable Energy Laboratory, Golden, CO

Fiscal Year (FY) 2011 Objectives

- Refine technical and cost data in the Hydrogen Delivery Scenario Analysis Model (HDSAM) to incorporate additional industry input and evolving technology improvements.
- Expand the model to include advanced technologies and other pathway options leading to new versions of the models.
- Improve methodologies for estimating key aspects of delivery system operation and optimizing cost and performance parameters.
- Explore options to reduce hydrogen delivery cost, including higher pressure and/or lower temperature gases, and operating strategies.
- Provide analyses to support recommended hydrogen delivery strategies for initial and long term use of hydrogen as a major energy carrier.

Technical Barriers

This project directly addresses technical barrier A (which implicitly includes barriers B, C, D, F, H and J) in the Delivery Technical Plan, as well as barriers B, C and E in the Systems Analysis Plan of the Fuel Cell Technologies Multi-Year Research, Development and Demonstration Plan. These are:

(A) Lack of Hydrogen/Carrier and Infrastructure Options Analysis

(B) Stove-Piped/Siloed Analytical Capability

(C) Inconsistent Data, Assumptions and Guidelines

(E) Unplanned Studies and Analysis

Technical Targets

The project is developing and using a computer model to evaluate alternative delivery infrastructure systems and components. Insights from the model are being used to help identify elements of an optimized delivery system which could meet DOE's long-term delivery cost target.

FY 2011 Accomplishments

- Completed a review and update of pipeline cost functions. Changes include:
  - Steel transmission and distribution pipelines:
    - Updated material, labor, right-of-way and miscellaneous cost estimates.
    - Developed revised equations for nine U.S. regions and total U.S.
  - Fiber-reinforced piping:
    - Review of current applications and technologies.
    - Evaluation of material, labor and total cost estimates and trends especially as compared to steel pipe.
  - Incorporation of revised equations into HDSAM pipeline model.
- Updated cost/price indexes in HDSAM.
- Analyzed factors affecting HDSAM fuel station capital investment and levelized cost, including:
  - Scale: station size
  - Station utilization
  - Investment and rate of return
  - Fuel cell vehicle (FCV) onboard storage option
  - Station design configuration
- Conducted delivery cost target analyses to:
  - Investigate impact of delivery technology options and economies of scale on hydrogen delivery cost.
  - Identify components for which research and development (R&D) offers greatest potential cost reduction.



Introduction

Initiated as part of the H2A project, the Hydrogen Delivery Scenario Analysis Model (HDSAM) is an Excel-based tool that uses a design calculation approach to

estimate the contribution of individual components of delivery infrastructure to hydrogen cost, energy use and greenhouse gas emissions. The model links the individual components in a systematic market setting to develop capacity/flow parameters for a complete hydrogen delivery infrastructure. Using that systems level perspective, HDSAM calculates the full, levelized cost (i.e., summed across all components) of hydrogen delivery, accounting for losses and tradeoffs among the various component costs. A graphical user interface (GUI) permits users to specify a scenario of interest. A detailed User's Guide and access to the DOE Energy Efficiency and Renewable Energy help desk also assist users in running HDSAM.

Results

Work continued on updating and expanding the HDSAM. Pipeline cost data were updated and equations were re-estimated. Factors affecting fuel station investment and levelized cost were examined. A delivery cost target analysis was conducted to investigate the impact of alternative technologies and scale on delivery cost and to identify those components for which R&D offers the greatest potential cost reduction.

Cost Updates

All cost estimates within HDSAM were updated to 2007 dollars using appropriate indices. Pipeline costs were re-estimated in a separate effort in which additional cost data were obtained, converted to 2007 dollars and analyzed. For transmission pipelines, a 30-yr time-series of steel pipeline cost data, compiled by the Oil and Gas Journal, was used to refine costs by element (material, labor, right-of-way, miscellaneous), diameter and census region (for the lower 48 states). A similar analysis of distribution pipelines was conducted using data compiled by the Pipeline and Gas Journal. Results of the two analyses were used to update transmission and distribution pipeline cost functions contained within HDSAM.

A separate analysis of fiber-reinforced piping was conducted to determine whether that technology might be cost competitive with steel piping. Although more costly than steel to purchase, reduced installation labor costs more than offset the difference. Fiber-reinforced pipe is commonly used in small-diameter natural gas gathering lines. Its inherent flexibility allows pipe diameters up to 6 inches to be wound onto a spool and then unwound during installation, significantly reducing pipe handling and joining costs. Because flexible fiber-reinforced pipe is relatively new, future cost reductions from installation learning and competition are expected. Such reductions could make multiple parallel fiber-reinforced pipes less costly than a single larger transmission line.

Refueling Station Analyses

Depending on delivery pathway, dispensing hydrogen at a refueling station can account for $800,000 to well over $2.5 million in capital investment and add $1-3/kg to the delivered cost of the fuel. In addition to station size or daily throughput (see Figure 1), a number of other factors – including learning, station utilization and the form in which hydrogen is used on board the vehicle – can affect both total investment and delivery cost.

Figure 2 shows the effect of station utilization on the station contribution to the levelized cost of hydrogen. For a 200 kg/day station, increased utilization brings hydrogen cost down from over $10/kg to under $4/kg at full utilization. Reductions occur proportionally in both installed capital and operations and maintenance (O&M).

Figure 3 shows how onboard storage affects station capital investment. For a 200 kg/day station with 700-bar onboard storage additional compression, storage and refrigeration equipment are needed at the station. Cryo-compressed (CcH2) onboard storage replaces some of the compression and refrigeration needs with cryo-pumping

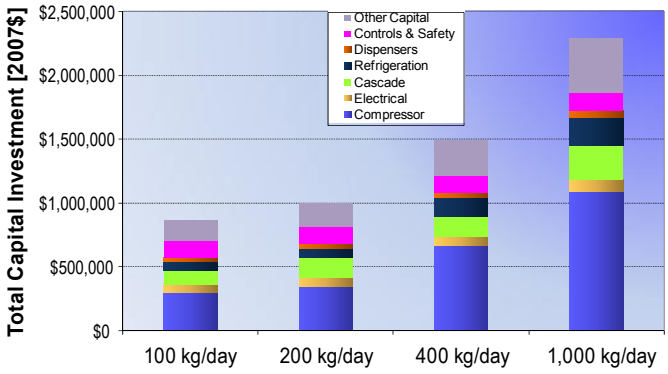


FIGURE 1. Effect of Size on Hydrogen Refueling Station Capital Investment

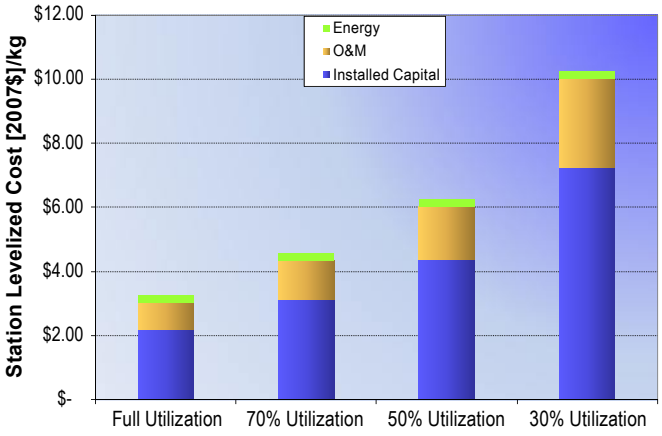


FIGURE 2. Effect of Station Utilization on Levelized Hydrogen Cost

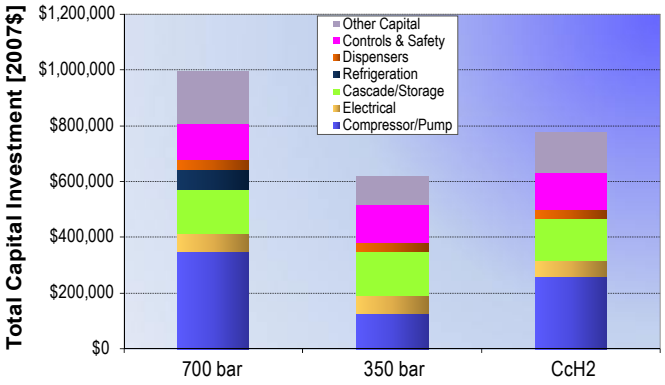


FIGURE 3. Effect of Onboard Storage Option on Station Capital Investment

which is less costly at the station (although some of the cost is shifted to the upstream component of liquefaction where it may be offset by economies of scale).

Delivery Cost Target Analyses

By combining delivery technologies into pathways and examining the cost of various combinations under different market assumptions, HDSAM permits the user to better understand the impact of a number of factors on hydrogen delivery cost. In addition to investigating the effect of delivery technology, scale, utilization, learning, and onboard storage, HDSAM provides insight into the individual components with the greatest impact on delivery cost. As shown in Figure 4, for pathways serving small, medium or large FCV markets with correspondingly small, medium or large fueling stations, preliminary analysis shows that hydrogen delivery costs drop from roughly $7 to $9/kg to below $3/kg. For liquid delivery pathways, liquefaction accounts for the largest share of delivery cost, followed closely by station costs; for gaseous pathways, the station represents the largest cost. Other costs (e.g., trucking or pipeline transportation, terminal and infrastructure storage) represent much smaller shares.

Conclusions and Future Directions

Hydrogen delivery infrastructure analysis seeks to identify aspects of hydrogen delivery that are likely to be especially costly (in capital and operating cost, energy and greenhouse gas emissions) and estimate the impact of alternative options on those costs. For the Fuel Cell Technologies Program this project has developed a model of hydrogen delivery systems to quantify those costs and permit analyses of alternative technologies and operating strategies. This work has been conducted collaboratively by staff of Argonne National Laboratory, Pacific Northwest National Laboratory and the National Renewable Energy Laboratory with the advice and assistance of several industrial partners. Regular interaction has also occurred with the Fuel Pathways and Delivery Tech Teams.

Through FY 2011, results affirm that hydrogen delivery could add $2.30 to over $9.00 to the levelized cost per kg of hydrogen “at the pump.” The most promising options for reducing delivery cost tend to level demand (thereby reducing the need for hydrogen storage) or increase the energy density of the delivered fuel (by maintaining low temperature or high pressure in the delivery pathway).

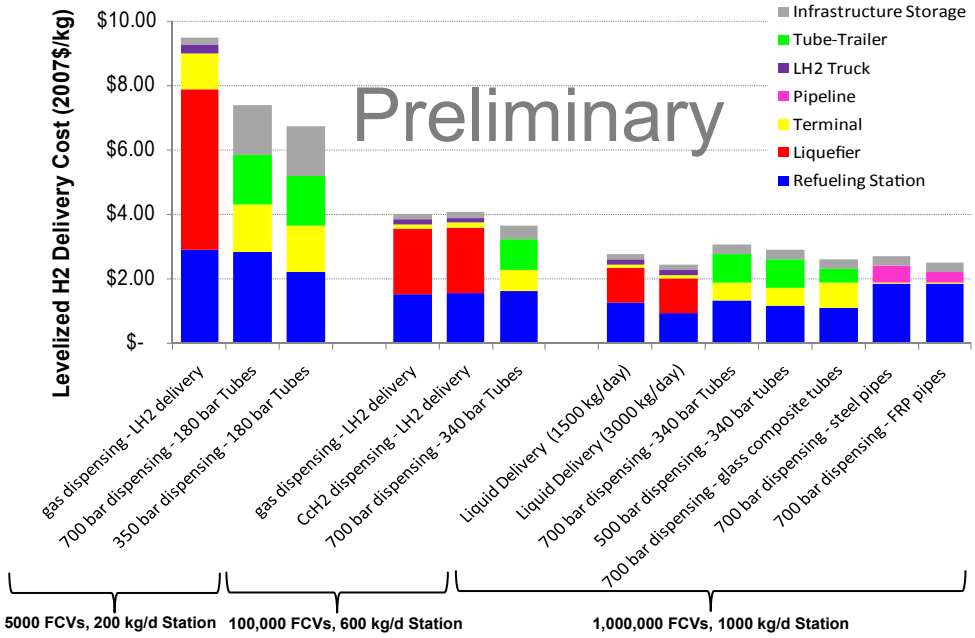


FIGURE 4. Levelized Hydrogen Delivery Cost for Select Pathways by Market Demand and Station Size

Improving the performance of individual, relatively costly delivery components is another promising option. Fueling station compressors are among the most costly of those components. In FY 2012 efforts will be directed to further study of advanced fueling compressor options, particularly as they relate to the HDSAM, and updating the model to reflect those options. In FY 2012, HDSAM will also be extended to model hydrogen delivery for early (non-automotive) fuel cell markets, especially forklift and cell tower backup power applications. Better understanding of delivery options for these early markets is critical to reducing hydrogen delivery cost for both automotive and non-automotive fuel cell applications.

Publications/Presentations

1. Elgowainy, A., M. Mintz, and D. Brown, *Hydrogen Delivery Modeling to Update Cost Targets and Identify Promising Deployment Options*, Fuel Cell and Hydrogen Energy Conference, Washington, DC, February 15, 2011.

2. Brown, D., J. Cabe, and T. Stout, *National Lab Uses OGJ Data to Develop Cost Equations*, Oil & Gas Journal, Jan. 3, 2011.

3. Elgowainy, A., M. Mintz, D. Steward, O. Sozinova, D. Brown and M. Gardiner, *Liquid Hydrogen Production and Delivery from a Dedicated Wind Power Plant*, draft report, Oct. 2010.

4. Elgowainy, A., M. Mintz and M. Gardiner, "Hydrogen Delivery Infrastructure: Analysis of Conventional Delivery Pathway Options" in *Handbook of Hydrogen Energy*, CRC Press, S.A. Sherif, D.Y. Goswami, E.K. Stefanakos and A. Steinfeld, eds., publication pending.

5. Gillette, J., M. Mintz and A. Elgowainy, *Land Requirements for Hydrogen Fuel Stations and Distribution Terminals*, draft report, May 2010.

III.3 Vessel Design and Fabrication Technology for Stationary High-Pressure Hydrogen Storage

Zhili Feng (Primary Contact), Jy-An Wang and Wei Zhang
Oak Ridge National Laboratory (ORNL)
1 Bethel Valley Rd, PO Box 2008, MS 6095
Oak Ridge, TN 37831
Phone: (865) 576-3797
E-mail: fengz@ornl.gov

DOE Manager
HQ: Scott Weil
Phone: (202) 586-1758
E-mail: Kenneth.Weil@ee.doe.gov

Subcontractors:
- Global Engineering and Technology, Camas, WA
- MegaStir Technologies, Provo, UT
- Victor Li Independent Consultant, Ann Arbor, MI

Project Start Date: October 1, 2010
Project End Date: Project continuation and direction determined annually by DOE

Fiscal Year (FY) 2011 Objectives

- Develop engineering designs and fabrication technology for cost-effective high-pressure hydrogen storage system for stationary applications. In particular, the stationary storage vessel will utilize:
  - Cost-effective commodity structural materials.
  - A systematic, integrated vessel design to mitigate hydrogen embrittlement associated with the use of high-strength steels for high-pressure hydrogen storage.
  - High-productivity and low-cost fabrication technology.
  - Application of embedded sensors to ensure the safe and reliable operation of the storage system.

Technical Barriers

This project addresses the following technical barriers from the Hydrogen Delivery section of the Fuel Cell Technologies Program Multi-Year Research, Development and Demonstration Plan:

(F) Gaseous Hydrogen Storage and Tube Trailer Delivery Cost

(G) Storage Tank Materials and Costs

Technical Targets

This project is to develop and demonstrate a cost-effective design of composite steel/concrete vessel for bulk high-pressure hydrogen storage and associated fabrication technology that can be adopted to meet different stationary storage needs such as those at refueling stations and renewable energy generation sites. Insights gained from this project will be applied toward the manufacturing of off-board gaseous hydrogen storage tanks that meet the following DOE 2015 hydrogen delivery targets:

- Storage Tank Purchased Capital Cost ($/kg of H_2 stored): $300 - Primary objective of this project.
- Volumetric Capacity (kg H_2/liter of storage volume): >0.035 - Secondary objective of this project.

FY 2011 Accomplishments

- Completed conceptual engineering design of the inner layered steel vessel for hydrogen storage capable of sustaining 5,000 psi design pressure based on industry standard American Society of Mechanical Engineers (ASME) Boiler and Pressure Vessel (BPV) Code - Section VIII. The conceptual designs for the outer reinforcement sleeve made of pre-stressed concrete and the interface between inner steel and outer concrete vessels will be completed by September/October 2011 timeframe.
- Preliminary cost estimate showed that the proposed design of composite steel/concrete vessel and fabrication technology have a sound basis for meeting the revised DOE cost target for off-board bulk storage. Improved cost modeling based on the conceptual engineering designs is expected to be completed by September/October 2011 timeframe.
- Efforts are ongoing for demonstrating technical proof-of-feasibility of key design concepts and construction technology including hydrogen embrittlement mitigation and friction stir welding of high-strength steels.



Introduction

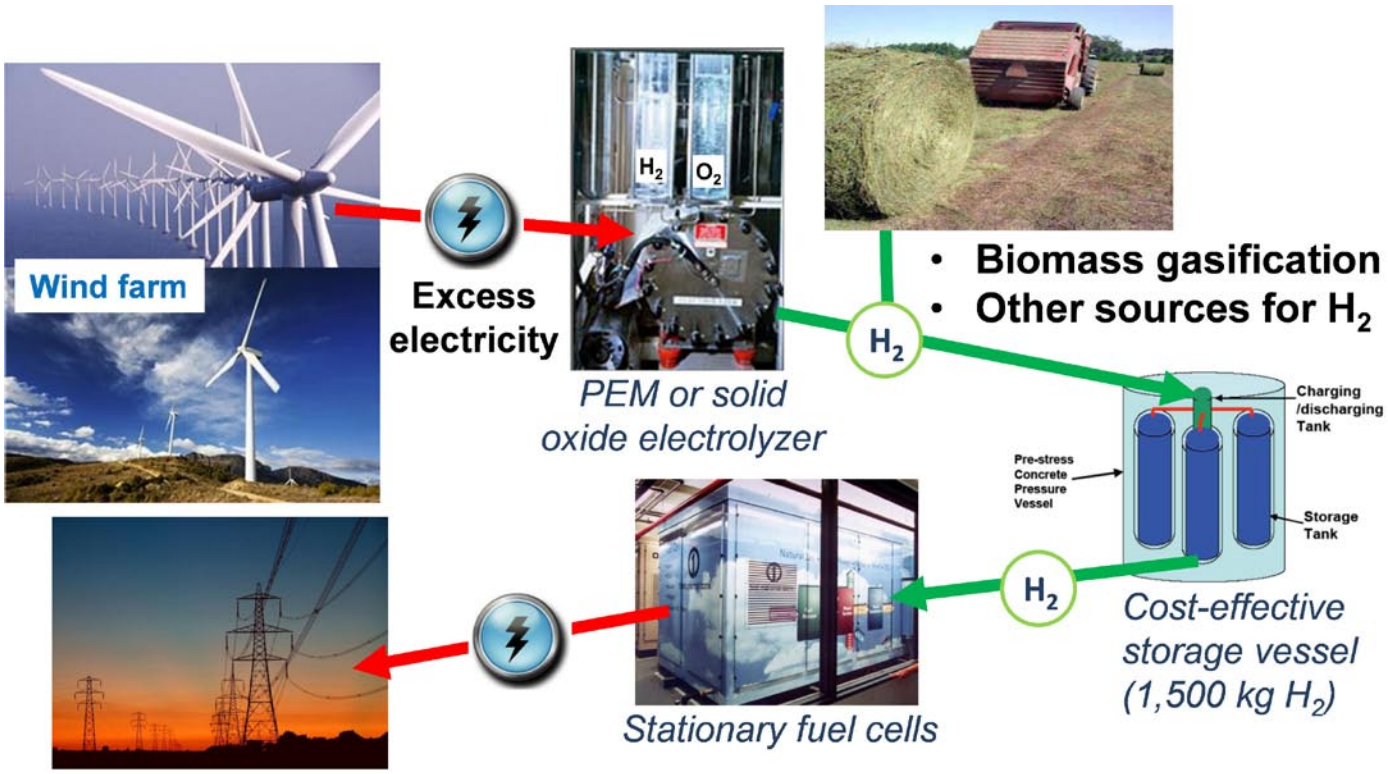
Low-cost off-board bulk stationary storage of hydrogen is a critical element in the overall hydrogen production and delivery infrastructure. Stationary storage is needed at central production plants, geologic storage sites, renewable energy generation sites, terminals, and refueling stations. Stationary storage also provides the surge capacity to handle hourly, daily, and seasonal demand variations. Figure 1



FIGURE 1. Application of Stationary Hydrogen Storage Vessel At Refueling Station

illustrates a potential application of the cost-effective hydrogen storage vessel for refueling of hydrogen. The vessel is designed to store 1,500 kg of gaseous H_2, which is sufficient to refill about 267 passenger cars (based on a 5.6 kg H_2 tank per car [1]). Another potential application of the hydrogen storage vessel at renewable energy generation sites is shown in Figure 2. The hydrogen, produced from water electrolysis using excess electricity from wind farms and/or biomass gasification, will be stored in the vessel. The 1,500 kg of H_2 can be used to generate about 24,200 kWh [2] (or 3 MW for peak-load daytime) back into electrical grid, sufficient electricity to power 780 U.S. homes per day [3].

The size and volume of the stationary hydrogen storage are expected to vary considerably depending on the intended usage, the location and other economic and logistic considerations. For instance, the storage vessel at a renewable energy generation site may have a lower hydrogen pressure but much larger storage volume compared to that at a refueling station. Therefore, it is important the storage vessel is "scalable" (i.e., it can be readily scaled for different



PEM - proton exchange membrane

FIGURE 2. Another application of stationary hydrogen storage vessel at renewable energy generation site for utility-scale load leveling and peak shaving (in conjunction with fuel cells).

sizes and pressures). In this project, ORNL leads a diverse multidisciplinary team consisting of industry and academia to develop and demonstrate a cost-effective integrated steel/concrete high-pressure hydrogen storage vessel design and fabrication technology that could be adopted to meet different stationary high-pressure hydrogen storage needs. Safety and economics are two prevailing drivers behind the integrated hydrogen storage technology.

Approach

Figure 3 is a schematic drawing of the overall engineering concept of the high-pressure hydrogen storage vessel. It has a modular design with scalability and flexibility for meeting different stationary storage needs. The particular design shown in Figure 3 is a composite structure with four inner steel tanks that are reinforced by an outer pre-stressed concrete sleeve. Commodity materials such as structural steels and concretes are used for cost-effectiveness. It is noted that the project team led by ORNL is working closely with the DOE Delivery Tech Team. Alternative designs may be studied based on the directions set forth by DOE.

A key enabler for the overall composite storage vessel is the use of a layered steel vessel for the inner steel tank. The layered steel vessel technology is proven and has shown significant cost and safety advantages over the conventional single solid section steel vessel. In this project, new designs and fabrication technology will be developed for the layered steel-based hydrogen storage including: (1) novel vessel design to avoid hydrogen embrittlement of high-strength structural steels, and (2) advanced fabrication technology based on friction stir welding (FSW) for layered steels. Sensors will be embedded into both inner steel tanks and outer concrete sleeve to ensure safe and reliable operation. Steel tanks are self-contained and can be shut down individually for improved reliability and safety. Finally, recently developed high-performance concretes will be evaluated for the interface material between the steel tank and the concrete sleeve to ensure the structural compatibility between the two.

Results

There are three major activities in this first year (FY 2011) of the project: (1) preliminary cost estimate of the composite storage vessel, (2) preliminary design and engineering of key vessel components including steel tank, concrete, and interface between the two, and (3) technical proof-of-feasibility study of key design concepts and construction technology. The results from the first year of substantial development are discussed as follows.

Preliminary Cost Estimate of Composite Storage Vessel

Table 1 shows the preliminary rough-order-of-magnitude (ROM) cost estimate for three different design concepts. As shown in this table, the steel tank, though much cheaper than other materials such as carbon fiber composite tank, still represents a major cost item in the composite vessel. By shifting more structural loads from the inner steel tank to the outer pre-stressed concrete vessel, the required thickness for the steel tank is reduced. Even though the concrete vessel cost increases, the decrease in the steel tank cost (due to thinner wall) is sufficient to reduce the total cost of composite vessel. It is noted that the preliminary ROM cost estimate does not include the expected additional cost reduction attainable by the use of new steel vessel fabrication technology, new vessel design/engineering concepts, and ultra-high strength steels that are being pursued in the project. The ROM cost estimate does not account for engineering challenges and costs in high-strength concrete materials and integration of the inner steel vessel and the outer concrete containment. An improved cost analysis model is being developed which will take into account the detailed engineering and designs of key vessel components.

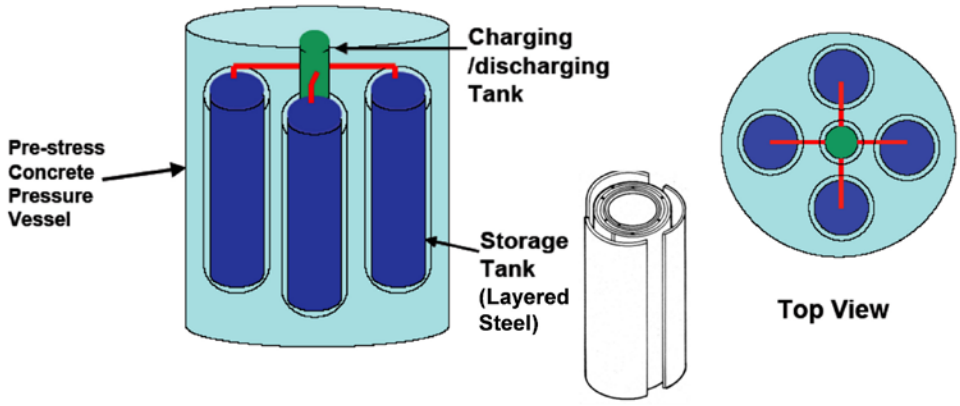


FIGURE 3. Schematic drawing of the overall engineering concept of the composite vessel for high-pressure hydrogen storage.

TABLE 1. Preliminary ROM Cost Estimate for Three Different Design Concepts of Stationary High-Pressure Hydrogen Storage Vessel *

	All Steel Layered Vessel				Composite Vessel with Concrete Carrying 50% Hoop Stress Only			Composite Vessel with Concrete Carrying 85% Hoop and Axial Stresses		
DOE Volumetric Capacity Target	2005 Status	2010 Target	2015 Target		2010 Target	2015 Target		2010 Target	2015 Target	
H_2 Pressure, psi	5000	7000	8700	10000	7000	8700	10000	7000	8700	10000
H_2 Weight, kg	1400	1820	2125	2340	1820	2125	2340	1820	2125	2340
Steel Vessel										
Wall thickness, in	7.7	11.0	14.0	16.4	5.3	6.6	7.7	1.5	1.9	2.2
Weight, lb	194,500	285,700	370,400	439,900	185,500	236,300	276,900	51,900	64,900	75,000
Steel Vessel Cost, $k	$933.7	$1,371.5	$1,777.7	$2,111.7	$895.7	$1,141.4	$1,337.4	$250.6	$313.7	$362.5
PCPV										
Wall thickness, in					24	24	24	48	48	48
Concrete, $k					$13.5	$13.7	$13.8	$48.5	$48.8	$49.0
Steel Tendon, $k					$109.8	$143.9	$171.5	$224.3	$284.2	$330.6
Rebar & Liner, $k					$61.0	$62.0	$62.8	$117.0	$117.7	$118.2
PCPV Cost, $k	$0	$0	$0	$0	$184.3	$219.6	$248.1	$389.8	$450.7	$497.8
Total Purchase Cost, $	$933.7	$1,371.5	$1,777.7	$2,111.7	$1,080.0	$1,361.0	$1,585.5	$640.4	$764.4	$860.3
Cost per kg H_2, $	***$667***	***$754***	***$837***	***$902***	***$593***	***$640***	***$678***	***$352***	***$360***	***$368***

* The basic premises in cost analysis include: (1) Reference vessel: a cylindrical vessel with semi-sphere heads, 12 ft. diameter and 21.7 ft. long (2,000 ft^3 storage volume), with piping attachment and maintenance access. (2) 50 ksi inner steel vessel design allowable stress (SA724 100 ksi grade high-strength steel) and 190 ksi steel tendon design stress (Grade 270 steel), per ASME Boiler and Pressure Vessel (BPV) Section VIII Division III design rules and material specification. (3) ASME BPV stress formulas to determine steel vessel wall thickness. (4) Layered steel vessel: steel plate cost at $2/lb, labor cost at $100/hr., and 6,000 hours to fabricate the reference vessel, estimated by a major steel vessel construction. (5) Pre-stressed concrete pressure vessel: material and construction cost for rebar, high-strength tendon, and high-strength concrete are $2.5/lb, $3.5/lb, and $400/cubic yard, respectively, based on 2007 steel and concrete market prices.

Design and Engineering of Key Vessel Components

The conceptual engineering design of the inner layered steel tank capable of sustaining 5,000 psi hydrogen pressure is developed based on industry standard ASME BPV Code - Section VIII. The layered steel tank consists of an inner thin liner with thin segmental cylinders wrapped around it to form the layered shells. The steel plate thickness is chosen to be 0.25 inch for ease of fabrication and to minimize the need for post-weld heat treatment. The concentric wrapped shells are welded to a single solid section steel head at each end. Special rules for welding, post-weld heat treatment and non-destructive examination required for layered steel tanks are included in the design. Such ASME code-based design is important for the industry acceptance and technology transfer and commercialization in a later stage of the project.

The conceptual designs for the outer reinforcement pre-stressed concrete pressure vessel and the interface between inner steel and outer concrete vessels are expected to be completed by the September/October 2011 timeframe. Structural analysis based on finite element modeling is being developed and used to aid the design of compatibility between steel and concrete vessels. Figure 4 shows preliminary results of stress distribution in a cross-section of the composite vessel at an internal hydrogen pressure of 5,000 psi. The predicted stress distribution is important to ensure the structure has enough capacity to sustain the design pressure.

Technical Proof-Of-Feasibility Study

The use of layered steels offers significant opportunities for further cost-reduction and safety and performance improvement. First, FSW has demonstrated to produce joint with superior mechanical strength when compared to conventional arc welding [4]. In the layered steel vessel construction, FSW can be used for the longitudinal seam weld of 0.25-in.-thick steel shells. Second, a novel design taking advantage of layered steel shells is being evaluated for mitigation of hydrogen embrittlement to high-strength structural steels. Finally, mechanical and chemical sensors can be embedded into both the steel and concrete vessels for monitoring structure health. In particular, state-of-the-art piezoelectric sensors are being studied for measuring strain/stress variations in the structure. These proof-of-concept studies are important to ensure the technical readiness of the proposed composite storage vessel.

Conclusions and Future Directions

From the above results gained in this first year of substantial development, it can be concluded: (1) the composite storage vessel utilizing commodity steel and concrete materials and advanced fabrication technology has a sound technical basis to meet the DOE revised cost target for off-board bulk storage, and (2) the preliminary engineering

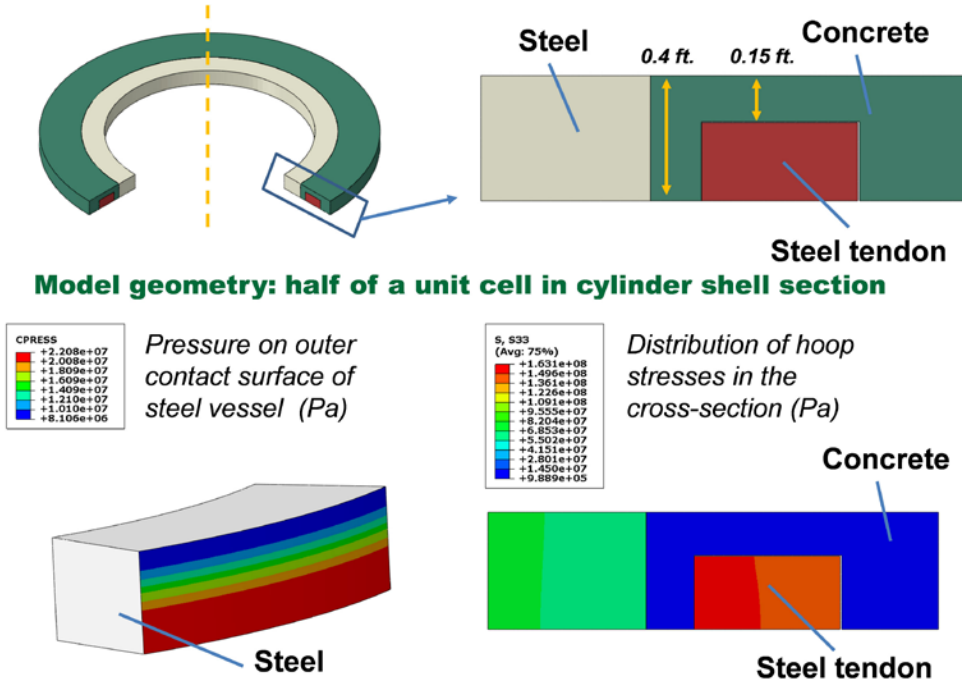


FIGURE 4. Preliminary results of finite element modeling for understanding stress distribution in the composite vessel.

design of inner layered steel vessel can sustain 5,000 psi hydrogen pressure based on relevant ASME BPV Code.

For the remainder of FY 2011, we plan to complete the preliminary designs of the outer pre-stressed concrete vessel and the steel/concrete interface. Detailed design and engineering analyses (including system cost), and mock-up vessel construction, testing and demonstration are planned in out-years.

Patents Issued

1. J. Wang, Z. Feng and W. Zhang: Conceptual Composite Tank Design for Stationary High-pressure Hydrogen Storage, ORNL Invention Disclosure No. 201102585, 2011.

FY 2011 Publications/Presentations

1. 2011 DOE Annual Merit Review, Fuel Cell Technologies Program, Washington, D.C., May 2011.

References

1. M. Kromer, et al.: Analyses of Hydrogen Storage Materials and On-Board Systems, DOE FCT Program FY 2010 Annual Progress Report.

2. M.L. Perry and S. Kotso: A Back-up Power Solution with No Batteries, INTELEC 2004 Proceedings, pp. 210-217 (2004).

3. U.S. Energy Information Administration: How much electricity does an American home use in 2009, http://www.eia.gov/tools/faqs/faq.cfm?id=97&t=3.

4. Feng, Z. Steel, R. Packer, S. and David, S.A. 2009. "Friction Stir Welding of API Grade 65 Steel Pipes," ASME PVP Conference, Prague, Czech Republic.

III.4 Hydrogen Delivery Analysis

Olga Sozinova
National Renewable Energy Laboratory (NREL)
1617 Cole Blvd.
Golden, CO 80401
Phone: (303) 275-3755
E-mail: Olga.Sozinova@nrel.gov

DOE Manager
HQ: Scott Weil
Phone: (202) 586-1758
E-mail: Kenneth.Weil@ee.doe.gov

Project Start Date: Fiscal Year (FY) 2004
Project End Date: Project continuation and direction determined annually by DOE

FY 2011 Objectives

- Provide hydrogen delivery cost analysis
- Update and maintain the H2A Delivery Components Model
- Design new delivery components and scenarios
- Support the other hydrogen models with delivery data

Technical Barriers

This project addresses the following technical barriers from the Hydrogen Delivery section of the Fuel Cell Technologies (FCT) Program Multi-Year Research, Development and Demonstration Plan:

(A) Lack of Hydrogen/Carrier and Infrastructure Option Analysis

(F) Gaseous Hydrogen Storage and Tube Trailer Delivery Costs

Technical Targets

This project aims to improve the efficiency of the hydrogen delivery process through analyzing various delivery pathways to understand the behavior and drivers of the fuel and vehicle markets and to meet Milestone 12 from the FCT Multi-Year Research, Development and Demonstration Plan: "By 2017, reduce the cost of hydrogen delivery from the point of production to the point of use at refueling sites to less than $1 per kg."

FY 2011 Accomplishments

- Completed analysis of hydrogen delivery by rail in comparison with the other delivery options and reviewed the congestion of U.S. railroad network.
- Introduced a pipeline branching algorithm and tested the delivery components for the multi-node delivery scenario model.
- Analyzed hydrogen delivery by composite tube-trailers with capacity of 550 kg of hydrogen, and reviewed highway regulations.
- Analyzed hydrogen delivery via existing natural gas pipelines, and reviewed U.S. natural gas networks.



Introduction

At NREL, for hydrogen delivery analysis, we use multiple models, such as the H2A Delivery Components Model, Scenario Evaluation, Regionalization and Analysis (SERA) Model, Fuel Cell Power Model and others. The H2A Delivery Components Model is an Excel-based, fully transparent model for the user, and publicly available. It can be used to calculate the cost of delivering hydrogen through multiple delivery pathways. SERA is an NREL dynamic optimization model. It is geographic information system (GIS)-based, java-coded software that determines the optimal production and delivery infrastructure build-outs and traces its evolution. The H2A Delivery Components Model also serves as a delivery cost data source for the NREL H2A Production Model, DTI HyPro Model, SERA Model, as well as for the NREL Biogas Model, Macro-System Model (through interconnection with HyPro), and HyDRA (through interconnection with SERA).

Approach

Since its start in 2004, the project has followed the general H2A approach and guidelines: closely collaborating with industry to update cost data and technical specifications, keeping consistency of the cost inputs across all H2A models, employing H2A standard assumptions, and maintaining publicly available models.

Results

Addressing barrier (A) - Lack of Hydrogen/Carrier and Infrastructure Option Analysis, we completed analysis of hydrogen delivery by rail in comparison with the other delivery options and performed a review on the U.S. railroad network congestion. Liquid hydrogen delivery by rail is the least expensive option for the large range of distances and demands (Figure 1). Therefore, it is well suited for delivering hydrogen produced from renewable sources for both early and mature markets. Analysis of the U.S. railroad networks [1] showed that 88% of the railroads are below capacity and could be potentially used to transport hydrogen.

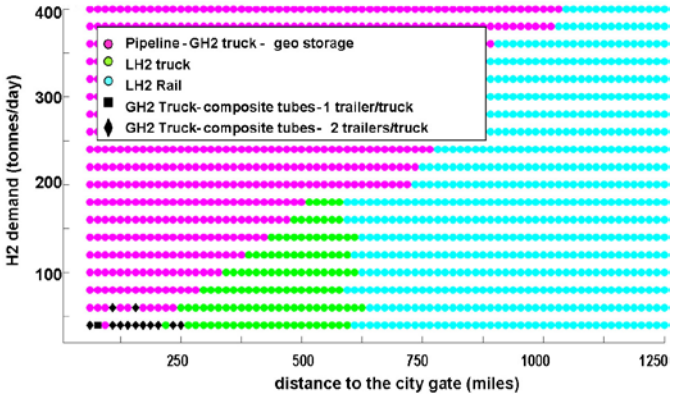


FIGURE 1. Lowest Delivery Cost Pathways

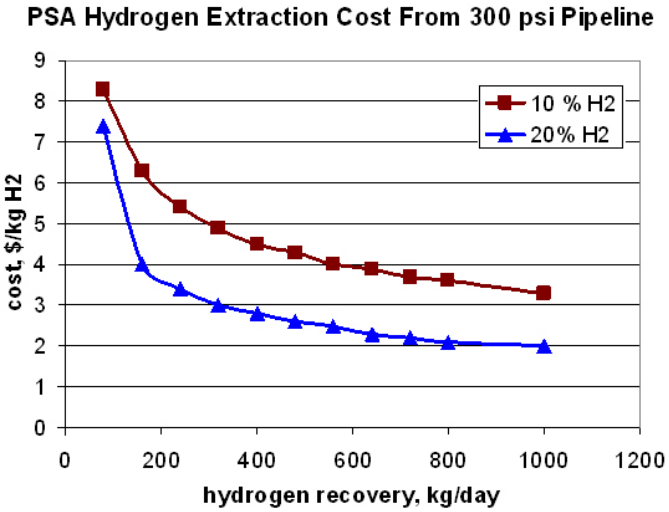


FIGURE 2. Estimated Cost of Hydrogen Extraction by PSA unit from 300 psi Distribution Pipeline (Assumed hydrogen recovery factor is 80%.)

Barrier (A) was also addressed though analyzing the delivery of hydrogen via existing natural gas infrastructure. This assessment [2] revealed that up to 20% hydrogen can be safely injected into the natural gas pipeline with no major concern for hydrogen induced failures and aging. Hydrogen addition to the distribution mains involves some modification for integrity management. Among the available gas separation technologies (membranes, electrochemical separation, and pressure-swing adsorption [PSA]), the PSA is the most commercially ready technology for today. We assessed the cost of hydrogen extraction by a PSA unit, assuming mass production and mature PSA technology. For 10% hydrogen concentration and 20% hydrogen recovery factor, the estimated cost of hydrogen extraction by PSA from a 300 psi distribution pipeline ranges from $3.3 to $8.3/kg of hydrogen extracted, depending on recovery rate. For 20% hydrogen concentration and 20% hydrogen recovery factor, the extraction cost ranges from $2.0 to $7.4/kg (see Figure 2). If hydrogen extraction can take place at a pressure reduction facility, (so the high recompression cost of natural gas can be avoided), the extraction cost would range from $0.3 to $1.3/kg of hydrogen extracted, depending on recovery rate.

We also addressed barrier (A) by assessing scenarios where hydrogen can play a role as an energy carrier. We designed and evaluated two wind-to-liquid hydrogen scenarios: grid-independent with seasonal storage, and grid-connected. Both scenarios assume hydrogen production in the amount of 40 tonnes daily near Albuquerque, New Mexico, and delivery by rail to Long Beach, California. We used NREL Wind Resource data [3], modified NREL's Fuel Cell Power Model [4] for wind farm optimization, and the H2A Delivery Components model for delivery cost. Also, we used NREL GIS data [5] for location and capacity of geologic storage, and for the nearest transmission line location and capacity. The cost of dispensed hydrogen in grid-independent case is $11.3/per kg, and $10.6 per kg in grid-connected case. As sensitivity analysis showed, there is a cost reduction possibility. Production cost is highly sensitive to the wind turbine cost. Recently, wind turbine market showed extensive volatility [6]. If wind turbines can be installed for $1,000/kW (instead of $1,500/kW – the number we used in the analysis), production cost can be dropped more than three times (to $2/kg instead of $6.6/kg) (see Figure 3). The grid-independent case is an attractive scenario in terms of energy sustainability. Nevertheless, it requires a significant amount of storage to accommodate seasonal wind variations. With the storage in geologic formation being the least expensive option for large hydrogen amounts, it is not currently feasible country-wide. Additional research and analysis has to be done to assess hydrogen storage in geologic formations.

Addressing barrier (F) - Gaseous Hydrogen Storage and Tube Trailer Delivery Costs, we analyzed the possibility of delivering gaseous hydrogen in a composite tube-trailer with a tube pressure of 250 bar and 550 kg of hydrogen capacity. Also, we reviewed Federal Highway Administration

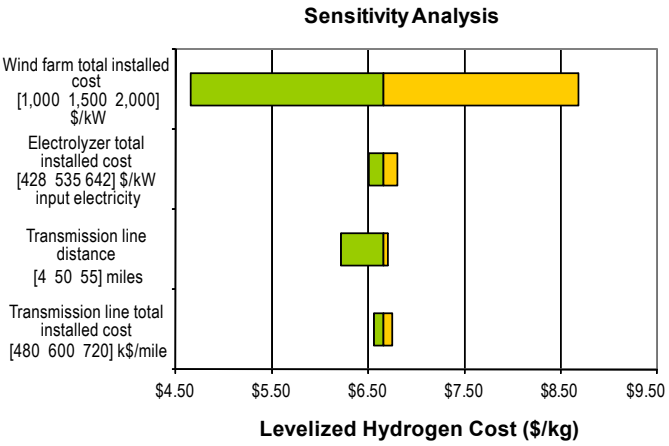


FIGURE 3. Sensitivity of Levelized Hydrogen Production Cost to Select Input Parameters

(FHWA) regulations regarding size and weight limitations on commercial motor vehicles [7]. For renewable (long-distance) hydrogen delivery, composite tube-trailers can compete with rail delivery only if a second trailer for a single truck can be allowed (Figure 4). As FHWA weight and size regulation review showed, this possibility potentially exists in the states of AK, AR, CO, ID, IN, IA, KS, MO, MT, NV, ND, OH, SD, UT, NM, NY, WY, and OR. Composite truck delivery also shows a potential for intra-city delivery, when a hydrogen production plant can be placed at the city border. The transportation cost in this case can be decreased twice with allowing for a second trailer, or increasing tube pressure up to 550 bar.

Barrier (F) was also addressed through developing a novel method of hydrogen delivery when a hydrogen plant not necessarily serves only one city, but can accommodate demand from multiple cities. By introducing these multi-node delivery scenarios, we can model pipeline and hydrogen storage systems shared between multiple cities that potentially can decrease the cost of storage designed for plant outage and demand surge. For designing multi-node delivery networks, we used the SERA Model. Considering that the SERA Model is not completely ready for multi-node delivery task, we enhanced the SERA delivery data block with coding delivery components directly into the SERA Model. The second phase of this process was completed this year. Fourteen delivery components were coded, and 10 of them were successfully tested against the H2A Delivery Components data.

Conclusions and Future Direction

In FY 2011, analyzing multiple delivery options, we reached the following conclusions:

- Hydrogen delivery by rail is the least expensive option for a large range of distances and volumes. Therefore, it is well suited for delivering renewable hydrogen; as in most cases, significant renewable sources are located far away from large demand centers.
- Delivering hydrogen in existing natural gas pipelines can be a safe and feasible option for up to 20% of hydrogen concentration. Although, the cost of this option seems to be prohibitively high except for limited cases when hydrogen extraction can be arranged at the pressure reduction facilities.
- Producing hydrogen from wind at the wind-abundant and low-electricity cost locations and delivering it to the centers of high energy demand over long distances can be a viable option to provide energy shortcomings for these areas. Such options can provide hydrogen (produced and dispensed) at the cost as low as $6/kg.
- Delivering hydrogen in composite tube-trailers has a potential of decreasing transportation cost by allowing for a second trailer per truck, or increasing tube pressure up to 550 bar.

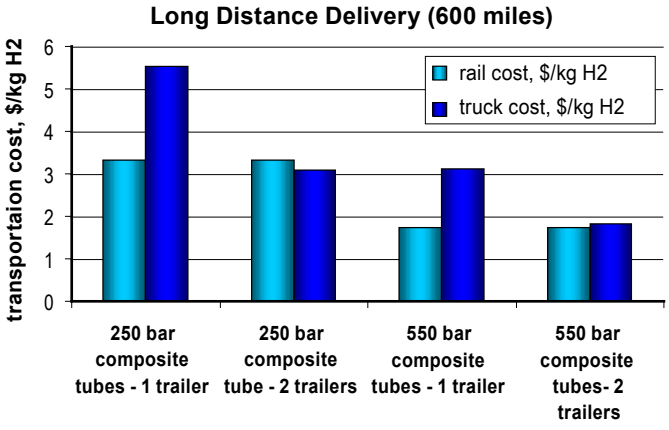


FIGURE 4. Total Cost of Gaseous Hydrogen Delivery by Rail or Truck over 600 Miles Distance

In the upcoming year, the major effort for the H2A Delivery Analysis and H2A Delivery Components Model will focus on:

- Maintaining and updating the H2A Delivery Components Model.
- Analyzing early- and mid-term delivery scenarios.

FY 2011 Publications/Presentations

1. Sozinova, O., "Hydrogen Delivery Analysis at NREL," Delivery Analysis Team Meeting, DOE Headquarters, Washington, DC, August 11, 2010.

2. Sozinova, O., "H2A Delivery Analysis at NREL," Delivery Analysis Team Meeting, DOE Headquarters, Washington, DC, February 18, 2011.

3. Bush, B.; Melaina, M.; Sozinova, O.; Steward, D. "Optimal Production, Transport, and Delivery Infrastructure for Hydrogen Production from Renewable Sources," Fuel Cell and Hydrogen Energy Conference and Expo, February 14, 2011.

4. Elgowainy, A; Mintz, M.; Steward, D.; Sozinova, O.; Brown, D.; Gardiner, M. "Liquid Hydrogen Production and Delivery From a Dedicated Wind Power Plant," October 2010 (in review).

5. Sozinova, O.; Melaina, M.; Penev, M. "Hydrogen Delivery in Natural Gas Networks," NREL Report (in review).

References

1. "Association of American Railroads, National Rail Infrastructure Capacity and Investment Study," prepared by Cambridge Systematics, Inc. (Washington, DC, September 2007).

2. Sozinova, O.; Melaina, M.; Penev, M. "Hydrogen Delivery in Natural Gas Networks," NREL Report (in review).

3. NREL Western Wind Resource Data: http://www.nrel.gov/wind/integrationdatasets/western/methodology.html.

4. NREL Fuel Cell and Power Model: http://www.hydrogen.energy.gov/fc_power_analysis.html.

5. NREL GIS: http://www.nrel.gov/gis/about.html.

6. Wiser, R. and Bolinger, M., "2009 Wind Technologies Market Report," Report No. LBNL-3716E. Berkeley, CA: Lawrence Berkeley National Laboratory. http://eetd.lbl.gov/ea/emp/re-pubs.html.

7. "Federal Size Regulations for Commercial Motor Vehicles," U.S. Department of Transportation Federal Highway Administration: http://ops.fhwa.dot.gov/freight/publications/size_regs_final_rpt/size_regs_final_rpt.pdf.

III.5 Demonstration of Full-Scale Glass Fiber Composite Pressure Vessels for Inexpensive Delivery of Cold Hydrogen

Andrew Weisberg (Primary Contact),
Salvador Aceves, Tim Ross, Blake Myers
Lawrence Livermore National Laboratory (LLNL)
P.O. Box 808, L-260
Livermore, CA 94551-0808
Phone: (925) 422-0864
E-mail: weisberg1@llnl.gov

DOE Manager
HQ: Scott Weil
Phone: (202) 586-1758
E-mail: Kenneth.Weil@ee.doe.gov

Subcontractor:
Spencer Composites Corporation (SCC), Sacramento, CA

Project Start Date: October 1, 2004
Project End Date: September 30, 2012

Fiscal Year (FY) 2011 Objectives

- Optimize hydrogen delivery by tube trailer.
- Demonstrate strength improvements of glass fiber pressure vessels at low temperature.
- Develop materials and manufacturing for low temperature hydrogen delivery.
- Quantify performance and economics of developed pressure vessels.

Technical Barriers

This project addresses the following technical barriers from the Hydrogen Delivery (3.2) section of the Fuel Cell Technologies Program Multi-Year Research, Development and Demonstration Plan:

(F) Gaseous Hydrogen Storage and Tube Trailer Delivery Cost

(G) Storage Tank Materials and Costs

Technical Targets

All capital cost projections are detailed to the component level for composite pressure vessels (CPVs) including manufacturing capital, labor, materials, and disposal. Costs of other trailer components, however, are much less detailed (plumbing, CPV mounting, and integration). These non-vessel costs have been estimated based on compressed natural gas trailers as 43% of the total 1,100 kg H_2 trailer cost and 33% of the 2,350 kg H_2 trailer cost.

TABLE 1. Progress towards Meeting Technical Targets for Hydrogen Delivery

Characteristic	2005 value (Table 3.2.2)	DOE Targets FY2012/2017	LLNL+SCC 2011 status
Delivery Capacity (kg of H_2)	280	700/1,100	1,100
Operating Pressure (psi)	2640	<10,000	<10,000
Purchased Capital Cost ($)	$165,000	<$300,000	<$291,000

Notes: LLNL has also designed a 2,350 kg delivery capacity cold glass CPV trailer option that uses the entire International Organization for Standardization (ISO) 20 ft. long container volume, with same operating pressures and temperatures, and a projected cost of under $477,000. This option cuts delivered cost estimates from $1.01/kg-delivered to $0.82/kg-delivered (not including forecourt storage, compression, or dispensing).

Delivery costs are based on H2A models for labor and cab, while operating pressure has been optimized (for minimum $/kg-delivered) at 7,500 psi. We calculated refrigeration costs assuming 33% exergetic efficiency to worst case 140 K. The estimated cost of refrigeration ($0.24/kg-delivered) is conservative based on refrigeration costs calculated by Argonne National Laboratory [1] at the gas terminal scale.

FY 2011 Accomplishments

- Designed and built multiple full-scale pressure vessels to implement trailer design capable of delivering hydrogen (over 100-mile round trip) for less than $1/kg-delivered.
- Qualified vessel design and manufacturing processes for pressures (0 to 22,500 psi) and temperature (ambient to -100°C) required to support cold delivery mission.
- Successfully burst tested first full-scale pressure vessel (with water at ambient temperature) as the first and most significant step in the technical proof of concept.



Introduction

This project has been funded to develop the key missing component necessary for LLNL's "cold glass" delivery approach: trailer-scale pressure vessels. Other technologies can build low-temperature-capable pressure vessels, but their vessels are either much too costly or too heavy for delivery trailers. Only CPVs are light enough to carry compressed hydrogen in sufficient quantity to achieve LLNL's optimized delivery costs within the volume and mass limitations of a trailer. Meeting the capital cost requirements of a trailer payload is not enough. Our target (below $1/kg-

delivered, not including forecourt storage, compression, or dispensing) must pay for the energy and capital required for refrigeration, plus the operating and capital costs of the trailer cab (including labor to drive and load/unload). The CPV technology LLNL is developing with partner Spencer Composites Corporation (SCC) has the potential to meet this economic target for hydrogen delivery.

When first proposed in 2007, the CPV development effort was expected to advance the manufacturing readiness level (MRL) for this technology from 4 to 8 [2]. This translates to moving the technology from proven manufacturing feasibility to manufacturing processes that operate at target cost, quality, and CPV performance. Over the course of development, it was realized that this characterization was incorrect and the development effort has been re-defined as progressing the technology from MRL 3 (manufacturing process identified) to MRL 7 (proven manufacturing processes). The change required significant pre-production materials testing, and the development process is currently on track with the first proof of CPV performance from a full-scale vessel.

Approach

The cold glass strength effect needed for the glass-fiber composite material to potentially meet cost, delivered mass, and trailer payload mass targets was demonstrated in 2007 and later through proprietary glass fiber characterization carried out by a major fiber producer. A requirement of 3,650 temperature cycles between ambient and 100 K can routinely be met by commercially available fiber, but not by economical composite matrix and CPV liner materials. A new system of plastic materials is being developed that can perform over these thermal cycles and enable the LLNL CPV design.

Full regulatory approval of CPVs sufficient to carry hydrogen on U.S. highways requires a sequence of 16 full-scale tests. Such a test project is clearly beyond the resources available for this development effort. Therefore all key technical risks of failing any of those tests are being addressed by an affordable plan of burst, cycling, and permeation tests. No regulatory approval process has yet been formulated by Department of Transportation (DOT), ISO, or American Society of Mechanical Engineers (ASME) standards organizations for low temperature CPV service, mobile or stationary, so low temperature operation risks are being addressed with subscale test articles. Testing of the articles and of small-scale tensile coupons also allows risk associated with materials process development to be reduced. However, the processes needed to manufacture composites and liners do not scale from one size to another without posing significant risk to vessel performance and cost, and therefore testing of full-scale diameter (23”) vessels is required once the technology has been shown to be acceptable prior to process scale up. However, to reduce materials process development risk, testing was first performed on small-scale tensile coupons and 3” diameter subscale vessels.

Results

The first successful burst test of a full-scale (23” diameter, length over 50” that can satisfy ASME Code X certification requirements for all greater lengths) is illustrated in Figure 1. This test was performed with pressurized water to meet permit requirements at SCC’s facility in Sacramento, CA. Testing CPVs filled with compressed hydrogen over a period of weeks is planned to prove that full-scale CPVs do not permeate at maximum operating pressure.

Before conducting this successful burst test in FY 2011, we had built three full-scale vessels from ‘proven’ components in early 2010 that failed ‘prematurely’ at varying pressures of several hundred psi. These failures were all slight leaks through cracks in their liners. The form and location of those cracks was similar to cracks found and overcome in 3” subscale CPV testing. Scale up from the 3” vessels to the first 23” vessels involved the costly construction of large tooling, and was only undertaken after 3” vessel manufacture had been adjusted to avoid those earliest CPV cracks at burst pressures above 22,500 psi (the maximum anticipated burst pressure required by LLNL’s proposed trailer delivery integration design). Therefore the premature failures encountered in the three full-scale 2010 burst tests came as a very unpleasant surprise.

The persistence of significant technical risks was not unexpected because of two previous kinds of failure experienced by this development project. Before the final of the three failed 2010 full-scale CPVs was built, the first attempt to cast its liner went awry in a very illuminating fashion. After succeeding in building a 51” long liner, the same materials, tooling, and process sequence was used to build a 114” long vessel, but the liner molding tool produced a horrid 200 pound lump of darkened plastic! This unexpected scale up failure came from tripling of resin mass put into the tool before it was employed for the fourth time to cast the longest liner. This problem was overcome with successive resin pours to prevent the thermoset plastic’s exothermic solidification reaction from thermal runaway. The catalysis reaction that solidifies our chosen, low-temperature-stable liner plastic was well known, but its dynamics in the molding tool was the first warning that thermal control during liner casting could be tricky.

The other development problem of 2009 was overcome entirely in the 3” subscale process development effort, and was apparently fixed by resin formulation changes. Since the liner cracks that caused problems in the 3” effort looked almost identical and appeared to originate in almost the same end dome location as the cracks that failed the 2010 full-scale test CPVs, it made sense to reopen the diagnosis of those cracks. Such debugging is simply not affordable at full-scale, so no more full-scale vessels were built until the



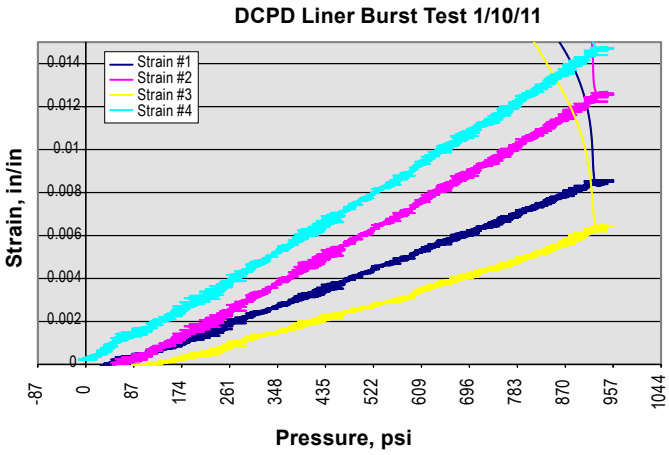


FIGURE 1. Successful Burst Test of Trailer-Scale CPV – Figure 1 shows a 23" diameter glass fiber composite pressure vessel that was burst tested with compressed water at ambient temperature. The photograph above shows the CPV after burst was declared, with its composite overwrap layer shredded. The vessel did not actually rupture, but lost most of its pressure and no fluid escaped. This is a very unusual outcome, due to the unprecedented toughness of SCC's liner material. The middle photograph shows the bulge that formed in the unruptured liner, which accounts for an internal volume increase of roughly 3%, and is enough to explain the depressurization due to the relative incompressibility of water. The bottom figure illustrates four strain gage traces during this test, which prove this CPV's manufacturing is adequate for designs that 'burst' at any pressure within the capabilities of plumbing seals.

problem was fixed in subscale articles without the earlier formulation changes. The same material that was cracking at low pressure in both early 3" and 2010 23" burst tests continues to stretch 18% in tensile tests, but something else had to be going on in particular end dome locations of liner castings for that material to crack at much lower strain. Figure 2 shows the variety of different hypotheses our team collected to explain these cracks, and the diagnosis we arrived at through skillful use of the scanning electron microscope (SEM) just in time to show dozens of SEM photographs at the 2010 annual merit review.

The internal features of our failing liners were responsible for the repeatable location of crack initiation. Defects had been built into the liner material during its casting process that were not built into the flat plaque tensile test specimens. Those defects were not visible to the naked eye, nor to an optical microscope, nor in unbroken liners – but they were visible in the SEM on the surfaces of cracks in the vicinity of crack initiation. When the liner cracking problem was first 'fixed' by resin reformulation, it appeared that the trouble was transient rather than built-in because almost all of the crack surface was shiny like the fracture surfaces on broken glass, indicating brittle failure. Resin additives that increased liner toughness and stretchiness (maximum elongation at tensile failure) appeared to fix it, until the problem returned at full scale.

The correct diagnosis was based on SEM imaging of the entire crack surface from the failed 23" liners. The cracks forked, with forks not left on the failure surface being those that didn't run faster than those that formed the surface. These 'diving' forks were later seen on examination with low power optical microscopy, saving considerable time in the SEM. The direction that the 'tines' of these forks pointed must be the crack propagation direction, so the crack initiation region was localized between a single pair of forks whose tines pointed away from each other. In that region, shiny surfaces gave way to slight localized frostiness; presumably before the crack propagation ramped up to high speed and could take advantage of orders of magnitude stress concentration at its crack tip. Those frosty regions are represented by the SEM sequence that appears in Figure 3, which focuses in on the "smoking gun" feature found on the complex surface of a diving fork.

That feature is a crater sticking up into a void, but not like craters seen in geology or astronomy. New materials have new failure modes, and this one occurred when the resin was a weak gel. Earlier SEM diagnosis had already determined that the forked cracks in the vicinity of crack initiation were not running in the maximum strain energy release direction (perpendicular to local tension), but went curling around with geometries that might be seen on the surface of puddings that had dried from neglect. The crater feature in question has sharp edges, but these could not have formed when ejecta blew into the void it sticks up in. Gas erupted through the surface of a weak gel into that void, then the gel shrank to form facets on the crater. Although density

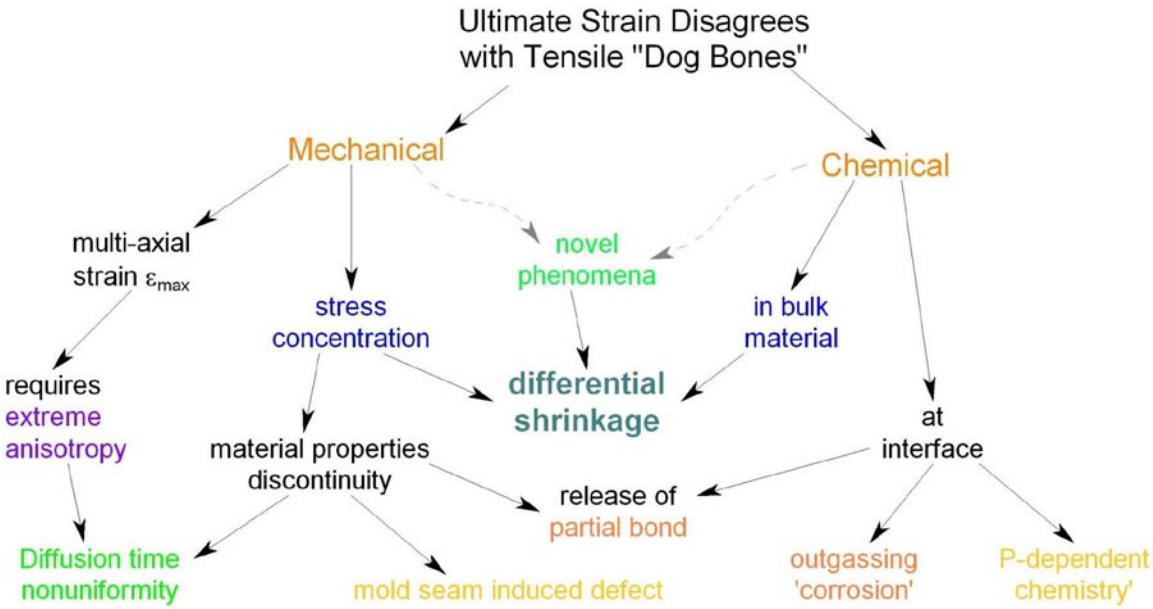


FIGURE 2. Tree Diagram of Hypotheses for Premature Liner Rupture - Figure 2 illustrates all the possibilities LLNL and SCC hypothesized to account for obscure failures observed in burst testing 3" and 21" diameter CPVs and unwrapped liners. For over two years experimental liner material formulations passed tensile testing at 8-9,000 psi ultimate stress and roughly 18% strain, yet failed when built into CPV liners at strains as low as 0.3%. These materials are not brittle, and most formulations were capable of toughness roughly 30-fold above epoxies. The materials failed as liners 'prematurely' despite passing every toughness test with an ASTM drop tower impact. Hypotheses in orange type were proven partially correct, yellow type were proven incorrect, and green type were verified. The odd conjecture shown in purple type was proven to be a result of the unprecedented solidification mechanisms of this material, while the hypothesis in teal type was found to be an unexpected part of that mechanism.

measurements have long shown a 6% densification of this resin upon solidification, how that shrinkage was distributed in space did not appear to matter. After LLNL's diagnosis, it was clear that the plastic was cracking itself just where it ran out of more liquid for a wave of catalysis to solidify.

Knowing what went wrong did not initially make it clear how to fix it. Another wave of dozens of 3" bottles became the front line for variations in the mold tool and resin pour sequence. Control was taken over where catalysis started, and care taken to never let the catalysis wave pass through liquid resin up against a solid wall, either of the mold or of previously solidified plastic. A technique was found to locate defective regions of castings without breaking them and to prepare the shards for SEM imaging, that is shown in Figure 4. But the next question was whether the project could afford to rebuild the 23" tool to incorporate these necessary improvements. The answer appeared to be no, before a real customer for such CPVs showed up in late summer of 2010. The customer could and did pay for a new tool which LLNL's liner mold fit into, but wanted CPVs built faster than SCC had any confidence they might pass ASME certification. This led to an extreme scramble to get LLNL development done on the tool the customer paid for, before the customer got its parts.

In January of 2011 the first good liner emerged from this tool to wind glass composite around, and then to burst test into the article shown in Figure 1. That burst test vindicated the improved liner molding process, because it ended in an unprecedented CPV failure mode, which might be called burst without rupture. Just because all the water remained inside after a loud noise and a big pressure drop does not mean this mode is really safer, since gaseous contents would not have dropped in pressure with just a little midriff bulge. But the survival of the liner in that bulge region does prove that the liner remained ductile under rapid straining to over 11% strain. Since design hydrogen delivery pressures only call for 3% liner strain, the liner component that has caused this project so much trouble has been proven to operate beyond its requirements at full scale.

Further surprises were in store when the happily undestroyed vessel in Figure 1 was cut into to see how well its liner's end dome was cast. If the vessel had burst in a more normal way, the region wherein more 'defects' were found might have been lost. Instead Figure 4 shows failure surfaces that have nothing to do with the performance of the CPVs LLNL and SCC are building, and everything to do with the nature of the new material we are developing. Composites built with this material as a matrix have all the right properties, including fiber 'translation' (material tensile strength divided by raw fiber strength) over 90% and no strength loss at 77 K. Castings built with it, however, can have localized frosty regions whereat catalysis ran out

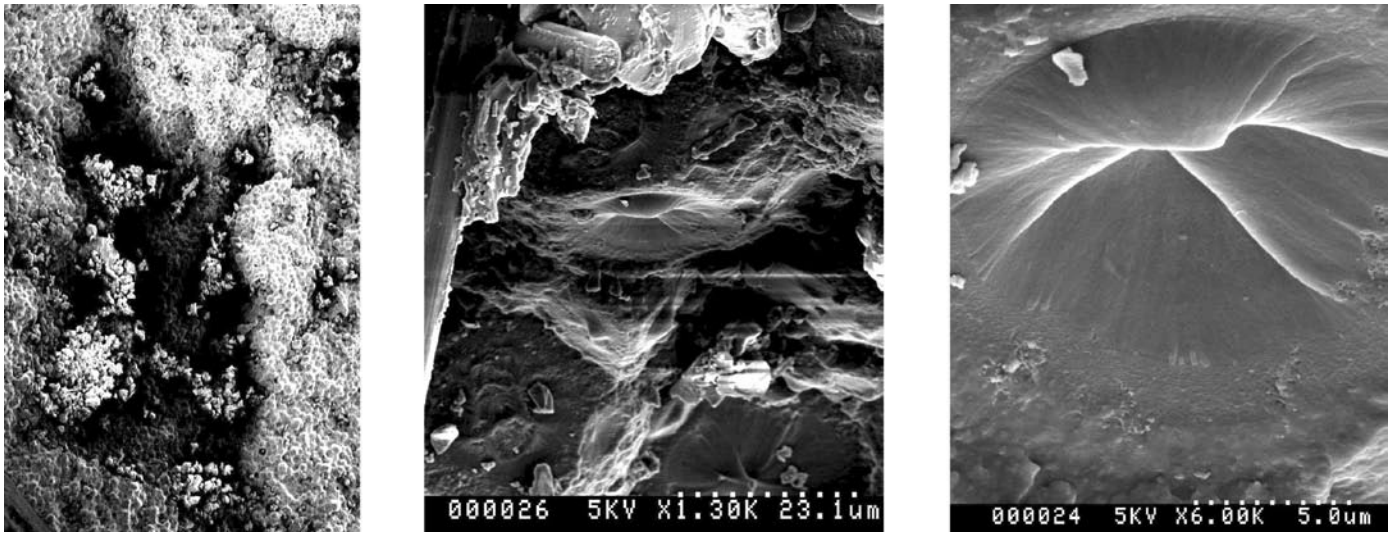


FIGURE 3. SEM Photographs of Liner Crack Surface – Figure 3 shows the "smoking gun" sequence of SEM photographs of a particular portion of the surface whereat a full scale (21" diameter) liner cracked inside of an early-2010 burst CPV. None of these features are visible in an optical microscope, and the sequence of photographs taken at the same point on the failed specimen increase in magnification from left to right. This particular spot was close to the origin of the crack that ruined this liner, causing the test CPV to leak below 800 psi and 0.7% nominal axial strain. The detective work that found the crack origin vicinity is based on forks in the cracked surface, whereat branches of the crack that did not succeed in forming part of the final separation surface dive beneath the surface on view. The origin of the crack must be somewhere between the two forks whose branches point away from that region. Looking into a fork of the crack, in the middle photograph shards of 2.7 micron glass fiber are visible which have been blown into a diving fork branch. On the wall inside that branch the odd "flying saucer" that appears centered in the micrograph at right initially resisted interpretation (since SEM views do not have darkness reflecting tilt angles as optical views do), but many attempts to view it at different angles convinced SEM operators this is a crater with sharp radial ridges.

of resin. This generation of 23' liners just happens to have one of those regions in a ring on its outer mold line (OML, casting terminology for exterior molded surface). The 3" liners that were cracking had several such regions on their inner mold line (IML, interior surface), and that surface goes into tension when the liner inflates, whereas the OML region on the 23" liners goes into compression.

The defective regions were actually visible to the naked eye, with the aid of a flashlight, when looked at through the polished edge of the burst success liner end dome cut out segment. They appear as a tenuous frostiness, which LLNL has come to term 'nanocracking', since any frosty region on a cast surface has the kind of frosty surface shown in Figure 3 when examined in the SEM. Once cast into the part, the penetrant dye that visualizes these regions in Figure 4 cannot get in to detect them, but when bar shaped specimens cut with this region in the middle were broken, the dye can be used to decorate the cracks. A forked crack is visible in the left micrograph of Figure 4, which was broken in tension at extreme elongation. A much more complex swirl appears in the right hand micrograph which failed at a few percent strain in torsion.

Although stress and strain have tensor rotation properties, it turns out that failure stress and strain do not rotate like a proper 2-tensor in these materials! Material so anisotropic that shear and longitudinal failure properties are decoupled is the consequence of its rapid solidification by Grubbs catalysis. It does not matter if shear stress is identical to tensile stresses exactly twice as large when the coordinate system is rotated by 45 degrees, because the molecular structure in nanocracked regions has almost no bonds to carry force in that direction. So an adequate solution for a 23" CPV liner is not the only fruit of these investigations: an informed strategy to design liners without bending stresses that put tension on the IML, and to design mold tooling that drives catalysis waves from IML to OML, enables progress (at customer expense) to be defect tolerant. The ability to detect defective regions before building CPVs around them, plus the advancing mass production of 3" CPVs with this technology improve the odds that reliable cold strength and inconsequential liner OML surface nanocracking can be proven before this project ends.

Conclusions and Future Directions

- First significant risk reduction test at full-scale passed with benign failure mode.
- More full-scale vessels under construction for cycling and permeation tests.
- Permeation test rig for dangerous compressed hydrogen filled, multi-week duration permeation tests under construction.
- Further quantitative proof of cold strength effect at various reduced temperatures anticipated with subscale (3") glass fiber pressure vessels tested in expendable dewar.

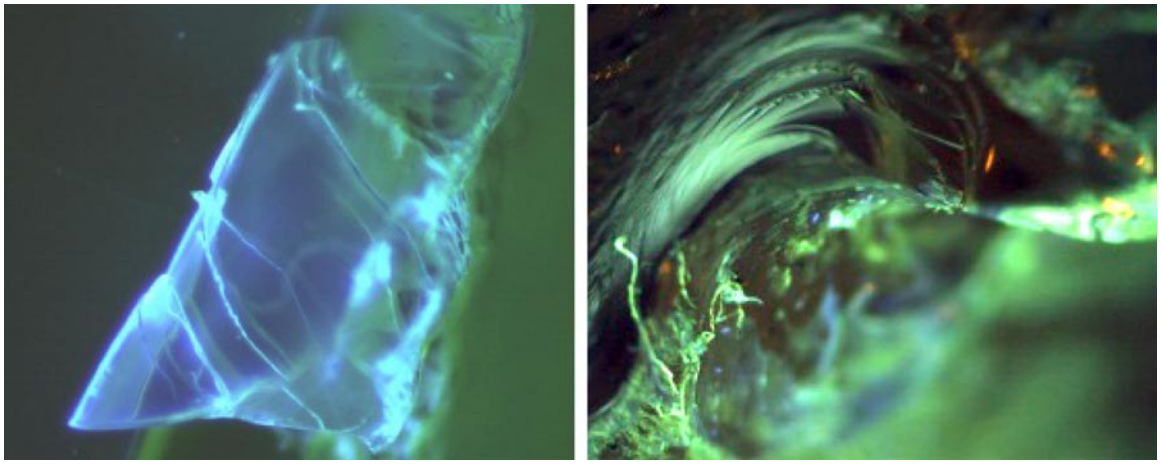


FIGURE 4. Observed Cracks in Specimens of Successful Liner – Figure 4 shows the splendid images resulting from two crude strength tests performed in a vise. These photographs are taken at low magnification with an optical microscope (commonly called a macroscope), in a combination of ultraviolet and visible illumination. SCC developed a diagnostic technique to make defective liner casting regions visible without a SEM, using a penetrating fluorescent dye. While the SEM cannot image regions likely to initiate cracks buried within cast parts, this technique cannot image defects directly on surfaces. Since the successful liner had not broken during burst testing, it made a fine vehicle to see whether defective regions could be found before they triggered cracks. This 'experiment' was conducted in January of 2011 by plunging an industrial vibratory cutter into the dome region of the unruptured yet burst CPV, then taking the wedge cut from the dome through a band saw to cut test specimens. The specimen at left was pulled with a vise grip pliers, and failed at over 100% strain, while the one at right was twisted and failed at several percent strain. They both failed in the millimeter-thick circumferential region where cloudy fuzziness is visible when polished edges of the wedge were illuminated by flashlight, on which the band saw cuts were centered to produce test specimens 3" long by roughly 0.3" square.

- ASME regulatory approval test program of nearly identical CPVs based on a batch of 20 full-scale (23" vessels) paid for by a private SCC customer anticipated in 2012.
- Joint DOE/DOT demonstration project possibility likely under discussion by early FY 2012 with hydrogen proponent DOT managers who currently have responsibility for certifying highway-rated pressurized containers.

FY 2011 Publications/Presentations

1. High-Density Automotive Hydrogen Storage with Cryogenic Capable Pressure Vessels, Salvador M. Aceves, Francisco Espinosa-Loza, Elias Ledesma-Orozco, Timothy O. Ross, Andrew H. Weisberg, Tobias C. Brunner, Oliver Kircher, International Journal of Hydrogen Energy, Vol. 35, pp. 1219-1226, 2010.

References

1. Mintz, M., and Elgowainy, A., "Hydrogen Delivery Infrastructure Analysis," Proceedings of the DOE Annual Merit Report, Washington, DC, 2010.

2. Manufacturing Readiness Level chart (and accompanying 72 page category descriptions) provided by DoD web site www.dtic.mil/whs/directives/corres/pdf/500002p.pdf.

III.6 Fiber Reinforced Composite Pipeline

Thad Adams
Savannah River National Laboratory (SRNL)
Materials Science & Technology
773-41A/151
Aiken, SC 29808
Phone: (803) 725-5510
E-mail: thad.adams@srnl.doe.gov

DOE Manager
HQ: Scott Weil
Phone: (202) 586-1758
E-mail: Kenneth.Weil@ee.doe.gov

Project Start Date: October 1, 2006
Project End Date: October 1, 2012

Fiscal Year (FY) 2011 Objectives

Fiber Reinforced Composite Pipeline (FRP)

- Focused evaluation of FRP for hydrogen service applications.
- Development of data needed for life management and codification FRP technical barriers.

This project addresses the following technical barriers from the Hydrogen Delivery section of the Fuel Cell Technologies Program Multi-Year Research, Development and Demonstration Plan:

(D) High Capital Cost and Hydrogen Embrittlement of Pipelines

(I) Hydrogen Leakage and Sensors

(K) Safety, Codes and Standards, Permitting

Technical Targets

This project is focused on the evaluation of FRP for hydrogen service applications. Assessment of the structural integrity of the fiber reinforced piping and joining components needed for hydrogen delivery are addressed. Insights gained will support qualifications of these materials for hydrogen service including the DOE 2012 delivery targets:

- Pipeline Transmission and Distribution Cost: $0.6 M/mile and 0.27 M/mile, respectively.
- Hydrogen Leakage: to be determined, <0.5% by 2017.

FY 2011 Accomplishments

- Multiple burst tests of FRP samples were completed to evaluate the design margins for flawed fiber piping to evaluate the consequence of third party damage to pipelines.
- Chemical exposure test of flaw samples were completed to evaluate address the influence of soil pH on FRP design margins.
- Completed initial literature review of flaw detection methodologies for FRP.



Introduction

The goal of the overall project is to successfully adapt spoolable FRP currently used in the oil industry for use in high-pressure hydrogen pipelines. The use of FRP materials for hydrogen service will rely on the demonstrated compatibility of these materials for pipeline service environments and operating conditions. The ability of the polymer piping to withstand degradation while in service, and development of the tools and data required for life management are imperative for successful implementation of these materials for hydrogen pipeline.

In FY 2009 a FRP life management plan was developed by SRNL and the American Society of Mechanical Engineers (ASME) to focus the direction for the research and testing needed to have FRP codified in the ASME B31.12 Hydrogen Piping Code. The plan also provided the tasks needed for the post construction management of FRP to insure structural integrity through end of life. The plan calls for detailed investigation of the following areas:

- System design and applicable codes and standards
- Service degradation of FRP
- Flaw tolerance and flaw detection
- Integrity management plan
- Leak detection and operational controls evaluation
- Repair evaluation

Approach

SRNL has completed the first areas of the Life Management Plan. Codes and standards for the high-pressure piping, process, and transport pressure vessels were reviewed and design margins and qualification techniques evaluated.

SRNL and Oak Ridge National Laboratory (ORNL) have collaborated on evaluating the service degradation of FRP in high-pressure hydrogen. Initial laboratory

testing indicated that there is not a degradation mechanism connected with the use of hydrogen in FRP. The codes and standard development organizations would like additional long-term data on this question to ensure the long-term life management of FRP.

SRNL has begun investigation to determine the flaw tolerance of FRP products. Creep data on glass fiber was also reviewed to evaluate the effect of creep life on the glass fiber. The results indicate that a deign margin of at least 3.5 is required to address long-term creep effects for a 20+ year design life. The use of the fiberglass creep data has been effective in evaluating the effect of flaw tolerance using a short-term burst test. Multiple tests have been completed to evaluate the effect of flaw tolerance on FRP samples for FRP designed to a recognized national consensus standard were used in the evaluation. Flaws for various depths were machined into the samples and burst tests have been performed.

Tests have also been performed to evaluate the effect of chemical environment on the FRP. The purpose of the chemical exposure tests are used to determine a measure of soil pH on the FRP materials. The first series of tests measured the chemical resistance of S- and E-type fiberglass strands that are typical of those that are used to fabricate the load-bearing overwrap used for the composite pipeline segments. Type S and E glass fiberglass strands were exposed to aggressive chemical environments in order to determine bounds on the base mechanical properties of tensile strength and chemical resistance. These bounds were comparable to technical literature on the subject [1] which have not been chemically exposed. These samples were subjected to solutions of pH 2.4, 7 and 10.6 for periods of either 24 hours or 120 hours (5 days) and then subjected to tensile strength testing using an Istron 4507 Electromechanical System with a strain rate of 200 µm/sec per ASTM 1557-03. Additionally, two flawed pipe sections were exposed to the same pH levels for 120 hours and burst tested.

Results

To address third party damage the sensitivity of FRP to flaws must be established. The flaw testing was performed over a range of flaw sizes to determine the flaw tolerance of the FRP. FRP with single layer reinforcement and multi-layer reinforcement were evaluated.

The results of the single layer FRP tests are shown in Figure 1. A reduction in burst pressure from unflawed condition to a 2-inch long flaw cutting the reinforcing layer of 75% was observed. With the 2-inch long flaw cutting the reinforcing layer the burst pressure drops below the rated pressure for the single-layer product The single layer reinforced piping does not provide sufficient redundancy to tolerate third party damage. Following a review of the results from the piping with the single layer reinforcement, it was determined that this type of fiber-reinforced piping was not an acceptable option for hydrogen piping.

The results of the multi-layer FRP tests are provided in Figure 2. Tests were conducted for increasing flaw depths up to 40% through wall. A 28% reduction in burst pressure from the unflawed condition to a 40% through wall flaw was observed. With the 40% through wall flaw there is still a margin of approximately 3x above the rated pressure of the FRP multi-layered product. The margin on burst of 3 provides an acceptable remaining product life to detect and repair flaws in FRP systems. Additional burst tests were conducted in on FRP samples with 40% through wall flaws to determine the variability between different samples. The results of the additional tests show that the variability between the tests is low and that all tests provide an acceptable design margin. The results for increasing the flaw length and width are also shown in Figure 1. The flaw with increased length showed no additional loss in design margin above the base flaw length. The flaw with increased width showed a small additional loss in design margin above the base flaw width. Two FRP samples were exposed to the high and low pH solutions and burst tested. The results are shown in Figure 2. The failure pressure for the chemically exposed samples fell within the variability of the unexposed data.

From the flawed samples, it was observed that as the flaw depth increased the failure mode changed from a local failure to a more global failure mode. The series of photos shown in Figure 3 illustrates these failure modes. The first photo from the left shows the failure of the unflawed sample indicating a global failure of the pipe. The next three photos illustrate how the failure mode changed as the flaw depth increased. The last photo on the right shows the 40% through wall flaw. In the 40% through wall photo, the failure encompasses most of the pipe circumference. Based on this data it was determined that the 40% through flaw was a reasonable upper limit to set for flaw detection.

The test results for glass fiber strands exposed to high and low pH solutions are shown in Figure 4. The red and blue curves in Figure 4 show the results for the untreated E- and S-type samples. As can be seen, mechanical failure typically occurred for the untreated samples below the 3% strain threshold, with the both samples showing

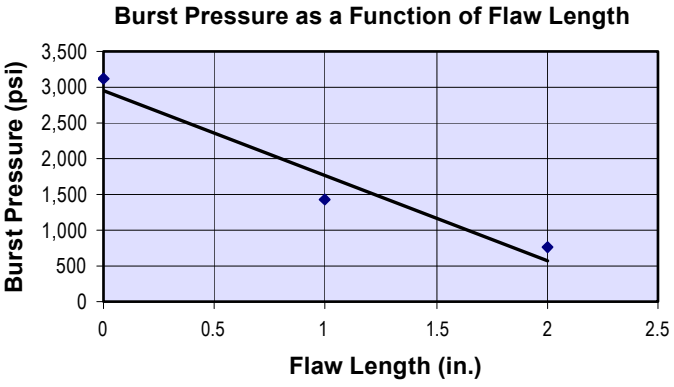


FIGURE 1. Single-Layer FRP Burst Test

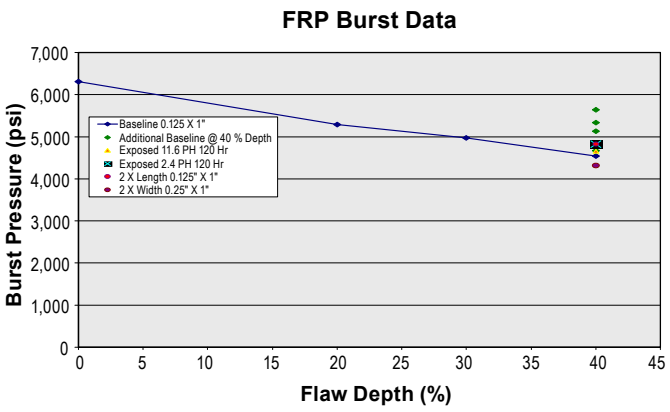


FIGURE 2. Multi-Layer FRP Flaw Tests

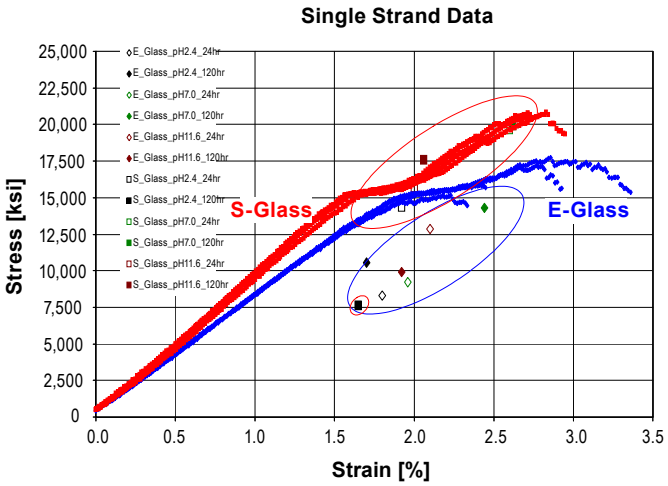


FIGURE 4. Test Results for Glass Fiber Strands



FIGURE 3. Photo Illustrating Failure Mode of FRP

reproducibility in the strain point of the initial point of failure. These tests were performed using thread grips and the samples were inspected after testing to ensure that failure occurred in a position not associated with applied stress or pinching at the grip surfaces.

Samples were taken from the same lot of fiberglass and were subjected to the chemical environments described above. The data in the blue circle provides the failure strain for the chemically exposed samples. It can be seen from a review of the chemically exposed data that the aggressive chemical environments can have a deleterious effect on their mechanical properties of the uncoated glass samples. Additional testing on chemically exposed uncoated glass sample indicated the effect of the chemical environment had resulted in corrosion of glass. Because the glass fibers are epoxy coated in the actual FRP product form, chemical exposure tests were conducted on flawed FRP samples. Two FRP samples were exposed to the high and low pH solutions and burst tested. The results are shown in Figure 2. The failure pressure for the chemically exposed samples fell within the variability of the unexposed data.

To establish a life management program the ability to detect external flaws in FRP by applying internal examination or smart pipe technology is needed for controlling failures and maintaining acceptable safety margins. The laser profilometry method is one technique to be investigated for inner diameter examination of FRP. In FY 2011 SRNL began work on flaw detection. A literature review was begun to investigate the potential for flaw detection using the laser profilometry method. In addition, to determine the effect of small flaws on FRP geometry, a flawed sample of FRP was pressurized to the rated design pressure and the sample was monitored for swelling. The initial result indicate that for the small flaw sizes the geometry changes for the sample will be negligible. The initial review for flaw detection data points to the need for smart pipe technology or an external flaw detection scheme.

Conclusions and Future Directions

Conclusions

- FRP is an attractive technology with potential to reduce overall pipeline installation cost.
- Field case studies indicate 20-60% reduced cost over steel pipeline.
- American Petroleum Institute standard 15HR is the most relevant standard reviewed to date for the fabrication of FRP line pipe for hydrogen service. This standard can be tailored to address the need for hydrogen pipelines.

- Flaw tolerance tests show that for flaws up 40% through reinforcement and up to 2 inch length and 0.25 inch width a factor of 3X margin is maintained on rated pressure.
- The current recommendation is to develop a performance-based design specification to be included in ASME B31.12.
- Workshop to discuss next steps toward ASME codification to be held in FY 2011.

Future Work

- Perform long-term stress rupture test for flawed FRP samples.
- Performed additional burst testing of flawed FRP samples on aged samples.
- Recommend performance qualification tests for FRP in hydrogen service to the ASME B31.12 committee.
- Evaluate B31.8S (Managing System Integrity of Gas Pipelines) for changes needed to address FRP in hydrogen service.
- Develop FRP hydrogen demonstration loop project among DOE, State of South Carolina, Aiken County, SRNL, ORNL, and ASME.

FY 2011 Presentations

1. SRNL FRP Piping Project, Presentation to Hydrogen Delivery Tech Team, Detroit MI, December, 2010.

2. SRNL FRP Piping Project, Presentation to Hydrogen Delivery Pipeline Working Group, Boulder, CO, April 2011.

III.7 Development of High Pressure Hydrogen Storage Tank for Storage and Gaseous Truck Delivery

Jon Knudsen (Primary Contact), Don Baldwin
Lincoln Composites
5117 N.W. 40th Street
Lincoln, NE 68524
Phone: (402) 470-5039
E-mail: jknudsen@lincolncomposites.com

DOE Managers
HQ: Scott Weil
Phone: (202) 586-1758
E-mail: Kenneth.Weil@ee.doe.gov
GO: Paul Bakke
Phone: (720) 356-1436
E-mail: Paul.Bakke@go.doe.gov

Contract Number: DE-FG36-08GO18062

Project Start Date: July 1, 2008
Project End Date: June 1, 2011 (request for extension to June 30, 2012)

Fiscal Year (FY) 2011 Objectives

The objective of this project is to design and develop the most effective bulk hauling and storage solution for hydrogen in terms of:

- Cost
- Safety
- Weight
- Volumetric Efficiency

Technical Barriers

This project addresses the following technical barriers from the Delivery section of the Hydrogen, Fuel Cells and Infrastructure Technologies Program Multi-Year Research, Development and Demonstration Plan:

(F) Gaseous Hydrogen Storage and Tube Trailer Delivery Costs

(G) Storage Tank Materials and Costs

Technical Targets

This project has focused primarily on the design and qualification of a 3,600 psi pressure vessel and International Organization for Standardization (ISO) frame system to yield a storage capacity solution of approximately 8,500 L of water. Second phase is to perform and qualify same size container at higher pressures.

TABLE 1. Progress towards Meeting Technical Targets for Hydrogen Storage

Characteristic	Units	2010 Target	2015 Target	Status	Comments
Storage Costs	$/kg	$500	$300	$675-$750	5,000 psi tank is expected to lower the cost
Volumetric Capacity	kg/liter	0.030	0.035	0.018	Estimated: 5,000 psi = >0 .024 kg/liter 8,300 psi = >0.035 kg/liter
Delivery Capacity, Trailer	kg	700	1,100	600	Estimated: 5,000 psi = >800 kg 8,300 psi = >1,150 kg

Accomplishments

- Successful completion of design and qualification of a 3,600 psi pressure vessel.
  - Qualification testing included:
    - Hydrostatic Burst
    - Ambient Pressure Cycle Test
    - Leak Before Burst Test
    - Penetration Test
    - Environmental Test
    - Flaw Tolerance Test
    - High Temperature Creep Test
    - Accelerated Stress Rupture Test
    - Extreme Temperature Cycle Test
    - Natural Gas Cycle Test with Blow-down
- Successful completion of design and qualification of an ISO frame capable of holding four 3,600 psi pressure vessels with a combined capacity of 600 kg of hydrogen. In addition to the structure, a system for loading, unloading, and pressure relief have been designed and implemented.
  - Qualification testing included:
    - Stress Analysis
    - Dimensional Analysis
    - Stacking
    - Lifting – Top and Bottom
    - Inertia Testing
    - Impact Testing
    - Bonfire Testing
- Successful completion of a trade study was achieved with respect to use and utilization of 5,000 psi pressure vessels.

- Factors used in the study:
  - Number of Pressure Vessels per Assembly
  - Working Pressure
  - Storage Temperature
  - Module/Cylinder Cost
  - Stress Ratio – reduce weight and cost by lower carbon fiber usage



Introduction

Hydrogen holds the long-term potential to solve two critical problems related to energy use: energy security and climate control. The United States transportation sector is almost completely reliant on petroleum, over half of which is currently imported, and tailpipe emissions remain one of the country's key air quality concerns. Fuel cell vehicles operating on hydrogen produced from domestically available resources would dramatically decrease greenhouse gases and other emissions, while also reducing our dependence on oil from politically volatile regions of the world.

Successful commercialization of hydrogen fuel cell vehicles will depend upon the creation of a hydrogen delivery infrastructure that provides the same level of safety, ease, and functionality as the existing gasoline delivery infrastructure. Today, compressed hydrogen is shipped in tube trailers at pressures up to 3,000 psi (about 200 bar). However, the low hydrogen-carrying capacity of these tube trailers results in high delivery costs.

Hydrogen rail delivery is currently economically feasible only for cryogenic liquid hydrogen; however, almost no hydrogen is transported by rail. Reasons include the lack of timely scheduling and transport to avoid excessive hydrogen boil-off and the lack of rail cars capable of handling cryogenic liquid hydrogen. Hydrogen transport by barge faces similar issues in that few vessels are designed to handle the transport of hydrogen over inland waterways. Lincoln Composites' ISO Tank Assembly will not only provide a technically feasible method to transport compressed hydrogen over rail and water, but a more cost and weight efficient means as well (Figure 1).



FIGURE 1. Assembled ISO Container Without Outer Panels

Approach

In Phase 1 of this project, Lincoln Composites will design and qualify a large composite pressure vessel and ISO frame that can be used for storage and transport of compressed hydrogen over road, rail or water.

The baseline composite vessel will have a 3,600 psi service pressure, an outer diameter of 42.8 inches and a length of 38.3 feet. The weight of this tank will be approximately 2,485 kg. The internal volume is equal to 8,500 liters water capacity and will contain 150 kg of compressed hydrogen gas. The contained hydrogen will be approximately 6.0% of the tank weight (5.7% of the combined weight).

Four of these tanks will be mounted in a custom-designed ISO frame, resulting in an assembly with a combined capacity of 600 kg of hydrogen. Installing the compressed hydrogen vessels into an ISO frame offers a benefit of having one solution for both transportable and stationary storage. This decreases research and development costs as well as the amount of infrastructure and equipment needed for both applications.

The large size of the vessel also offers benefits. A limited number of large tanks is easier to package into the container and requires fewer valves and fittings. This results in higher system reliability and lower system cost. The larger diameter also means thicker tank walls, which will make the vessel more robust and damage tolerant.

Phase 2 of the project will be to evaluate using the same approximate sized vessel(s) and ISO frame at elevated pressures. The pressures that are targeted for scope are 5,000 psi and 8,300 psi. Basic design of the individual vessels will remain approximately the same size at the 5,000 psi pressure and minor changes may be needed for the higher pressure. Higher pressures are needed to accommodate goals of the project.

Results

Design and Manufacture of a 3,600 Psi Pressure Vessel

The design of the 3,600 psi pressure vessel architecture has been completed using finite element analysis to find a composite solution that resolves the internal pressure requirements and expected external loads. This design was translated into a manufacturing process that addresses the feasibility of vessel production. Several development units were fabricated and pressurized until burst to validate the proposed manufacturing process and design.

With the completed design and working manufacturing process, several additional vessels were fabricated and tested to address optimizing manufacturing issues and minimize production expenses. One of the units was fabricated and tested to ensure the highest risk associated with material availability could be addressed. By ensuring multiple

sources of supplied materials, more leverage is available during procurement and lower production costs can be realized. Another vessel was fabricated to help establish confidence with migrating to a design having a higher margin of safety. Both of these vessels were subjected to a proof cycle and hydraulic burst test. The result of the testing met the expectations predicted by the design.

Qualification of 3,600 Psi Vessel

Due to the tanks geometry and construction, there are no published standards that can be used to directly qualify the product. There do exist, however, standards to qualify small pressure vessels of similar construction. These standards were reviewed for input to determine the appropriate requirements that would apply to a vessel of this geometry and construction and include:

- ISO 11439, gas cylinders – High Pressure Cylinders for the On-board Storage of Natural Gas as a Fuel for Automotive Vehicles
- ISO 11119-3, Gas Cylinders of Composite Construction (fully wrapped non-metallic liners)
- ANSI/CSA NGV2-2007, American National Standards for Natural Gas Vehicle Fuel Containers
- American Society of Mechanical Engineers (ASME) Code Case in Work/ASME BPV Project Team on Hydrogen Tanks and Section X

All qualification vessels have successfully been fabricated and completed through the following tests:

- Hydrostatic Burst
- Ambient Pressure Cycle Test
- Leak Before Burst Test
- Penetration Test
- Environmental Test
- Flaw Tolerance Test
- High Temperature Creep Test
- Accelerated Stress Rupture Test
- Extreme Temperature Cycle Test
- Natural Gas Cycle Test with Blow-down

Qualification of the ISO Frame

A complete assembly was constructed including ISO frame, four pressure vessels, and all relevant plumbing including pressure relief system. The following tests were performed on the entire assembly:

- Stress Analysis
- Dimensional Analysis
- Stacking
- Lifting – Top and Bottom
- Inertia Testing
- Impact Testing
- Bonfire Testing

American Bureau of Shipping has successfully approved the entire ISO assembly for production including, pressure vessels, ISO frame and subsequent valves, fittings and pressure relief system.

Trade Study for a 5,000 Psi Pressure Vessel

A trade study were undertaken to evaluate potential targets that would increase utilization storage design that best meet or exceed DOE targets. Lincoln Composites existing Titan Module was used as the baseline for the studies and a gap audit was conducted.

Design Baseline

- Intermodal ISO 668 1A Frame
- Four Type 4 Pressure Vessels
  - 250 bar Working Pressure
  - Carbon Fiber, 2.35 Stress Ratio

Gap Audit

- Increase Capacity (kg of hydrogen per liter)
  - Increase pressure and/or utilization
  - From 0.018 kg to 0.03 kg of hydrogen per liter
  - From 616 kg to 700 kg hydrogen capacity at 15°C
- Decrease Cost ($ per kg hydrogen)
  - From $500 per kg to $452 per kg hydrogen

Cylinder size was identified as a potential candidate for increase capacity through the increase of utilization of space. The study compared Lincoln Composites current four vessel configuration with a single large diameter vessel. Space utilization for the current Titan assembly is roughly 60% in volume while replacing it with a single, large tank would increase the utilization to 63%. However, when looking at the sheer size of a single tank, the thickness of a liner to manufacture this tank would not be very efficient and will have its limitations; i.e. pipe extrusion, and injection molding of the domes.

Lincoln Composites also looked at different scenarios of packing of pressure vessels within the current ISO frame. First scenario was to add an additional vessel down the center of the existing four vessels. This would increase the utilization of space to 68% from 60%, but the manufacturing of a small diameter tank that would fit in the available space would be difficult to achieve. This is due to the length/diameter (L/D) ratio. When this number becomes large, the tanks begin to bend due to the weight and decreased strength of the liner. Straightness is a key factor when trying to place the vessels next to each other within the frame.

This also increases the cost of the plumbing of the system. Second scenario is eight cylinders packed in a 3x2x3 matrix within the existing ISO frame. This arrangement would actually reduce the utilization from 60% to 56%. Lastly, Lincoln Composites performed a study to determine the potential to have many smaller cylinders packed within the frame assembly. Ninety-one smaller cylinders could be packed vertically with the frame. Again, the L/D ratio would increase and thus affect straightness and winding stability. If this were done, utilization would increase from 60% to 68%. However, the additional cost of plumbing this configuration would increase as well as the complexity of servicing the cylinders.

A third factor that was investigated through the study was to look at raising working pressure to increase compressed hydrogen density. By raising working pressure from 3,600 (250 bar) to 5,000 psi (350 bar) we could potentially see an increase of 33% in capacity at 15°C. Higher concentrations could be achieved at higher pressures, however cost increases need to be considered. As can be seen in Figures 2 and 3, the practical limit is 5,000 psi (350 bar). These costs are driven by several factors, i.e. higher pressures exacerbate thick-wall effects and reduced strength translation, the availability of high pressure plumbing hardware and the availability of hydrogen compressors.

Storage temperature was also investigated as a means to increase hydrogen density. As can be seen in Figure 4, with a decrease in storage temperature to -40°C, the current 3,600 psi tank could potentially see an increase of 33% in hydrogen density. With respect to a 5,000 psi tank, reducing the storage to the same temperature, -40°C, has the potential to increase hydrogen density by 61%. However, cold storage adds cost to the system.

Lincoln Composites also looked at full module costs as well as costs to manufacture pressure vessels for the Titan product line. The breakdown of costs associated with a full bulk hauling module and individual pressure vessels are as follows:

- Module
  - Pressure vessels make up approximately 72% of the total cost.
  - Frame and hardware make up approximately 28% of the total cost.
- Pressure vessel
  - End bosses make up approximately 3% of the total cost.
  - High-density polyethylene (HDPE) liner makes up approximately 11% of the total cost.
  - Composite material makes up approximately 86% of the total cost.

As part of the cost factor associated with this study, Lincoln Composites evaluated scenarios to reduce costs in

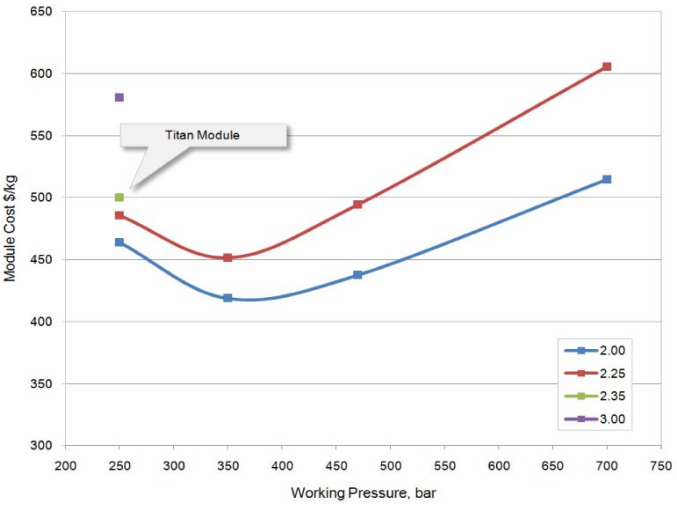


FIGURE 3. Working Pressure vs. Module Cost ($/kg)

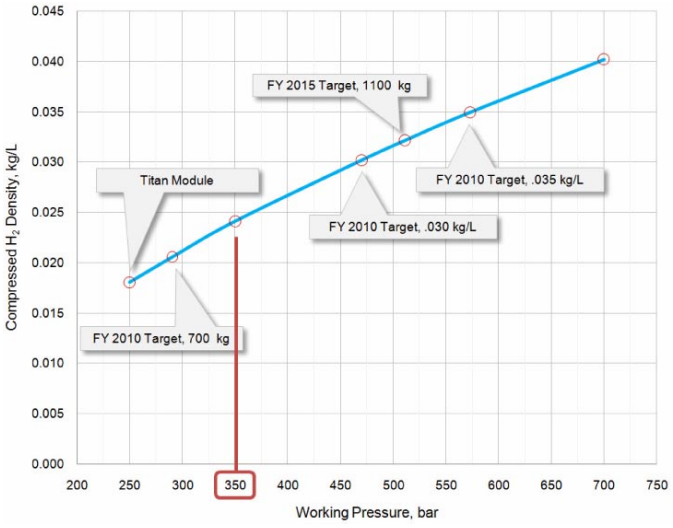


FIGURE 2. Working Pressure vs. Compressed Hydrogen (kg/L)

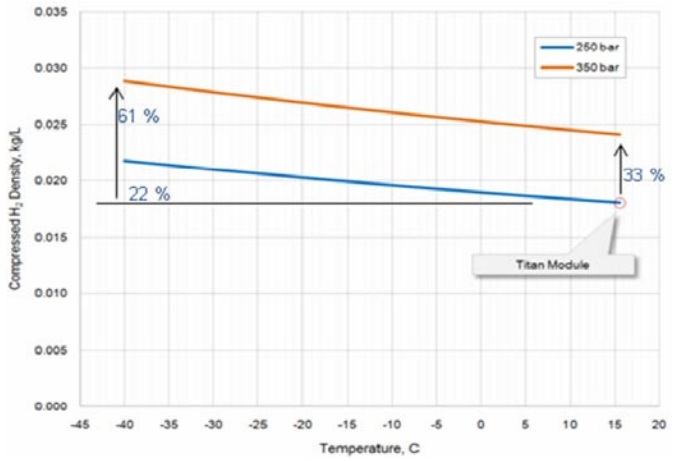


FIGURE 4. Temperature vs. Compressed Hydrogen Density (kg/L)

both the liners and the composite materials. Liner costs are associated with HDPE tubes/domes and the steel end bosses. Current construction and design of the liner shows that we are presently at minimum thickness/diameter ratio and any changes would result in difficulties in liner fabrication and filament winding of the vessel. The end bosses are constrained by the current mounting scheme and cost savings would be minimal if changes were made. As for the composite costs, the carbon fiber that is currently being used in the design contributes the lowest stress ratio of allowable fibers at 2.35. Current fiber possesses the greatest strength per unit cost. There are higher strength carbon fibers in existence but would have a 2-4 times increase in cost for a 15-40% increase in strength.

The last factor evaluated was that of reduction of stress ratio. By reducing the stress ratio, one could in turn lower the amount of carbon needed in the assembly of the pressure vessels and thus lower the cost of fiber used.

- Current Titan stress ratio is 2.35 based on compressed natural gas requirements
- ASME H2 allows for a 2.25 stress ratio
- 2.00 stress ratio is considered safe

Conclusions and Future Directions

Proposed objectives for Phase 1 of this project were completed in the fourth quarter of 2009. This includes successful completion of a large 3,600 psi pressure vessel able to contain 8,500 liter water capacity. The successful qualification of an entire assembly into an ISO container was also completed. Lincoln Composites will continue to evaluate cost reductions in design of the vessel as well as in the manufacturing processes. Pursuant of a higher pressure vessel is underway and will continue.

Trade studies have been completed for a increased service pressure of our current 3,600 psi Titan assembly. Based on the findings of this study, the logical next step is as follows:

- 5,000 psi pressure vessel design
- 2.25 stress ratio design will fit current Titan frame
- Will see an increase from 0.018 to 0.024 kg of hydrogen per liter
- Will see a hydrogen capacity increase from 616 to 822 kg of hydrogen
- Cost per kg of hydrogen would decrease from $500 to $452
- Cold storage would add cost
- Adding cylinders to the assembly adds cost

Future work will involve the fabrication and testing of a 5,000 psi pressure vessel. This will show results more closely to the targets for hydrogen storage.

FY 2011 Publications/Presentations

1. 2011 DOE Hydrogen Program Annual Merit Review, May 10, 2011.

III.8 Development of a Centrifugal Hydrogen Pipeline Gas Compressor

Francis A. Di Bella, P.E.
Concepts ETI, Inc., d.b.a. Concepts NREC
39 Olympia Avenue
Woburn, MA 01801
Phone: (781) 937-4718
E-mail: fdibella@conceptsnrec.com

DOE Managers
HQ: Scott Weil
Phone: (202) 586-1758
E-mail: Kenneth.Weil@ee.doe.gov
GO: Paul Bakke
Phone: (720) 356-1436
E-mail: Paul.Bakke@go.doe.gov

Contract Number: DE-FG36-08GO18059

Subcontractors:
- Praxair, Inc., Tonawanda, NY
- Texas A&M University, College Station, TX
- HyGen Industries, Eureka, CA

Project Start Date: June 1, 2008
Project End Date: September 1, 2012

Fiscal Year (FY) 2011 Objectives

Develop and demonstrate an advanced centrifugal compressor system for high-pressure hydrogen pipeline transport to support DOE's strategic hydrogen economy infrastructure plan.

- Delivering 100,000 to 1,000,000 kg/day of 99.99% hydrogen gas from generation site(s) to forecourt stations.
- Compressing from 350 psig to 1,000 psig or greater. Reduce initial installed system equipment cost to less than $9 M (compressor package of $5.4 M) for 240,000 kg/day system.
- Reduce package footprint and improve packaging design. Achieve transport delivery costs below $1/gasoline gallon equivalent (gge) ($2008 goal).
- Reduce maintenance cost to below 3% of total capital investment.
- Increase system reliability to avoid purchasing redundant systems.
- Maintain hydrogen efficiency (as defined by DOE) to 98% or greater.
- Reduce H_2 leakage to less than 0.5%.

Technical Barriers

This project addresses the following technical barriers from the Delivery (Section 3) of the Fuel Cell Technologies Program Multi-Year Research, Development, and Demonstration Plan [1]:

(B) Reliability and Costs of Hydrogen Compression

Technical Targets

The project has met the following DOE Targets as presented in DOE's 2007 Technical Plan for Hydrogen Delivery Projects [1] (Table 1).

Accomplishments for Phases I and II (completed from 2008 to 2010) and Phase III (in progress)

Developed computer models to aid in analysis of hydrogen compressor:

- System Cost and Performance Model
  - Suitable as a macro for DOE "HDSAM v2.0" economics model.

TABLE 1. Progress towards Meeting Technical Targets for Delivery of Hydrogen via Centrifugal Pipeline Compression

{Note: Letters correspond to DOE's 2007 Technical Plan-Delivery Sec. 3.2-page 16}				
Characteristic	Units	DOE Target	Project Accomplishment	STATUS
Hydrogen Efficiency (f)	[btu/btu]	98%	98%	Objective Met
Hyd. Capacity (g)	Kg/day	100,000 to 1,000,000	240,000	Objective Met
Hyd. Leakage (d)	%	< .5	0.2 (per FlowServe Shaft Seal Spec.)	Objective Met
Hyd. Purity (h)	%	99.99	99.99 (per FlowServe Shaft Seal Spec)	Objective Met
Discharge Pressure (g)	psig	>1000	1285	Objective Met
Comp. Package Cost (g)	$M	6.4	4.8	Objective Met
Main. Cost (Table 3.2.2)	$/kW hr	0.007	0.005 (per CN Analysis Model)	Objective Met
Package Size (g)	sq. ft.	360 (per HyGen Study)	260 (per CN Design)	Objective Met
Reliability (e)	# Sys.s Req.d	Eliminate redundent system	Modular sys.s with 240K kg/day with no redundency req.d	Objective Met

  - Identifies hydrogen compressor package performance and component cost with respect to a variety of compressor-gearbox configurations.
- System Reliability and Maintenance Cost Model
  - Estimates comparative reliabilities for piston and centrifugal compressors for pipeline compressors developed.
    - Failure Mode and Effects Analysis (FMEA) for component risk and reliability assessment.
  - Estimates operation and maintenance costs for compressor system.
    - Uses Federal Energy Regulatory Commission operation and maintenance database as the basis for determining the maintenance costs for a centrifugal compressor.
- Anti-surge algorithm developed to assist in controls analysis and component selection of preliminary design (completed) and detailed design of pipeline compressor module (in progress).
- Compressor design conditions confirmed by project collaborators.
  - P_{inlet}= 350 psig, P_{outlet}=1,250 psig; flow rate = 240,000 kg/day.
  - A six-stage, 60,000 revolutions per minute (rpm), 3.6 (max) pressure ratio compressor with a mechanical assembly of integrally geared, overhung compressor impellers.
  - Stress analysis completed.
  - Volute (compressor housing) design in progress for two-stage prototype.
  - Rotordynamics completed to verify shaft-seal-bearing integrity at operating speeds.
- Completed critical component development (compressor rotor, shaft seal, bearings, gearing, safety systems) and specifications for near-term manufacturing availability.
- Completed detailed design and cost analysis of a complete pipeline compressor and a laboratory-scale prototype for future performance lab verification testing.
- Completed a two-stage laboratory prototype compressor system to verify mechanical integrity of major components at full power ratings per stage.



Introduction

The DOE has prepared a Multi-Year Research, Development, and Demonstration Plan to provide hydrogen as a viable fuel for transportation after 2020, in order to reduce the consumption of limited fossil fuels in the transportation industry. Hydrogen fuel can be derived from a variety of renewable energy sources and has a very high Btu energy content per kg, equivalent to the Btu content in a gallon of gasoline. The switch to hydrogen-based fuel requires the development of an infrastructure to produce, deliver, store, and refuel vehicles. This technology development is the responsibility of the Production and Delivery sub-programs within the DOE. The least expensive delivery option for hydrogen involves the pipeline transport of the hydrogen from the production sites to the population centers, where the vehicles will see the highest demand, and thus, have the greatest impact on reducing the U.S. dependency on fossil fuel. The cost to deliver the hydrogen resource to the refueling stations will add to the ultimate cost per kg or per gallon equivalent that needs to be charged for the hydrogen fuel. Therefore, it is necessary that the cost to deliver the hydrogen be as kept as low as possible, which implies that the cost of the compressor stations, their installation costs, and their efficiency in pumping the hydrogen fuel to the refueling stations must be kept low. DOE has set a target of $1/gge ($2008 goal).

The delivery cost target can be met if the compressor system can be made more reliable (to reduce maintenance costs), more efficient (to reduce operation costs), and be a smaller, more complete modular package (to reduce the compressor system equipment, shipment, and its installation costs). To meet these goals, the DOE has commissioned Concepts NREC with the project entitled: The Development of a Centrifugal Hydrogen Pipeline Gas Compressor.

Approach

A three-phase approach has been programmed to implement the technical solutions required to complete a viable hydrogen compressor for pipeline delivery of hydrogen. This approach is summarized in Figure 1.

The technical approach used by Concepts NREC to accomplish these goals is to utilize state-of-the-art aerodynamic/structural analyses to develop a high-performance centrifugal compressor system for pipeline service. The centrifugal-type compressor is able to provide high pressure ratios under acceptable material stresses for relatively high capacities – flow rates that are higher than what a piston compressor can provide. Concepts NREC's technical approach also includes the decision to utilize commercially available, and thus, proven bearings and seal technology to reduce developmental risk and increase system reliability at a competitive cost. Using its expertise in turbomachinery analysis, design, machining, and testing, Concepts NREC is researching the use of a material that is compatible with hydrogen and that can enable the highest possible impeller tip speeds, reducing the number of required stages while meeting DOE's goals for overall pressure ratio and efficiency. In order to minimize the development time and ensure industrial acceptance of the design for the new pipeline compressor system, Concepts NREC has assembled a project team that will assist in the advanced engineering of the compressor while also preparing an implementation

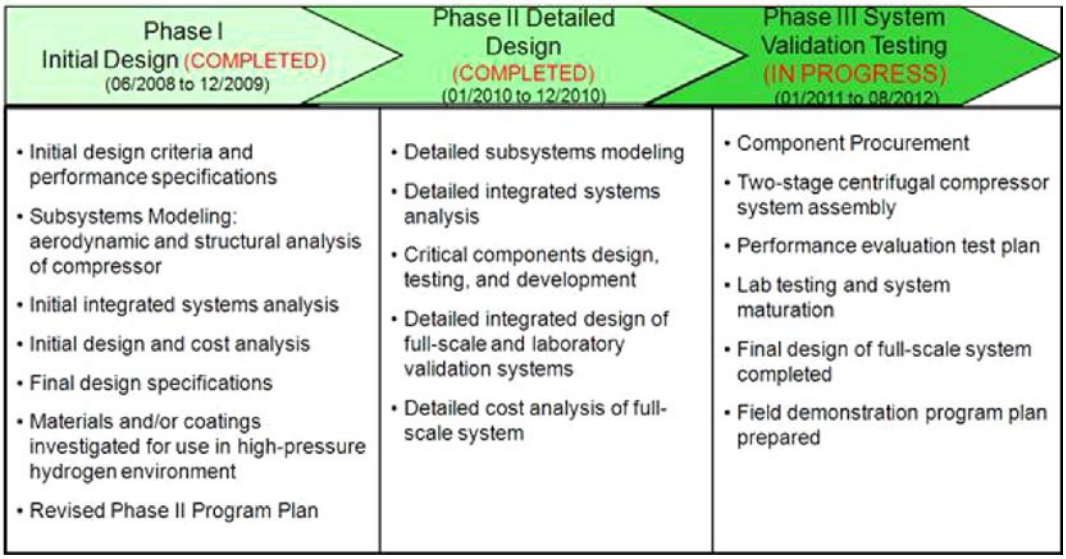


FIGURE 1. Three-Phase Project Approach

plan that can provide for near-term industrial pipeline applications.

The engineering challenge to implement this technical approach is to design a compressor stage that can achieve the highest acceptable pressure ratio and thermodynamic efficiency per stage, while also using as few stages as possible and employing the smallest diameter impeller. For centrifugal-type compressors, the pressure ratio is proportional to the square of the rotor speed (rpm^2) and the square of the radius ($radius^2$). Thus, even a small increase in tip speed or impeller radius results in significant increases in pressure. The aerodynamic design challenge in reducing the number of stages is to maximize tip speed of the centrifugal compressor impeller while staying within acceptable design safety levels of the strength limitations of the material, in addition to utilizing advanced diffuser systems to maximize recovery of dynamic head into static pressure. However, material stresses also increase proportionally to rpm^2 and $radius^2$, and also by material density. Ultimately, the major constraint is imposed by the limitations of the maximum stress capability of impeller material. This constraint is further aggravated by the need for the material selection to consider the effects of hydrogen embrittlement on the strength of the material. The selection of a rotor material that can enable the high tip speeds to be achieved while avoiding damage from hydrogen embrittlement was selected as the major technical challenge for the project. To eliminate other more conventional challenges when developing a new compressor, the engineering directive was also to select only commercially available components that are operated within the manufacturer's design guidelines for state-of-the-art materials, loads, stresses, operating speeds, and power ratings. Principal among these components is the choice of the bearings, shaft seals, gearing, and hydrogen controls and safety instrumentation.

Concepts NREC has met all of these engineering challenges in order to provide a pipeline compressor system that meets DOE's specifications for near-term deployment.

Results

Concepts NREC has developed several computer design models that have helped to optimize the design choice for the pipeline compressor module that complies with DOE requirements. These models include:

1. Compressor Package Performance and Cost Model using algorithms to determine the relative component cost and operational risks.
2. FMEA and Engineering Reliability and Maintenance Cost Model [2,3].
3. Completed detailed mechanical integration of compressor rotor-drive shaft with gearbox.
4. Detailed design of a six-stage centrifugal compressor module.
5. Detailed design of a 2-stage laboratory prototype compressor system for testing the mechanical integrity of the major compressor components: rotor, shaft seal, bearings, and gearing.
6. Successfully machined and spun compressor rotor (60,000 rpm to operating speed).

The engineering analysis conducted in Phase I and continuing in Phase II resulted in the design of the pipeline compressor package shown in Figure 2. The complete modular compressor package is 29 ft long x 10 ft tall x 6 ft wide at the base x 8 ft wide at the control panel, approximately one-half of the footprint of a piston-type, hydrogen compressor. The packaged module can be transported to the installation site as a pre-assembled

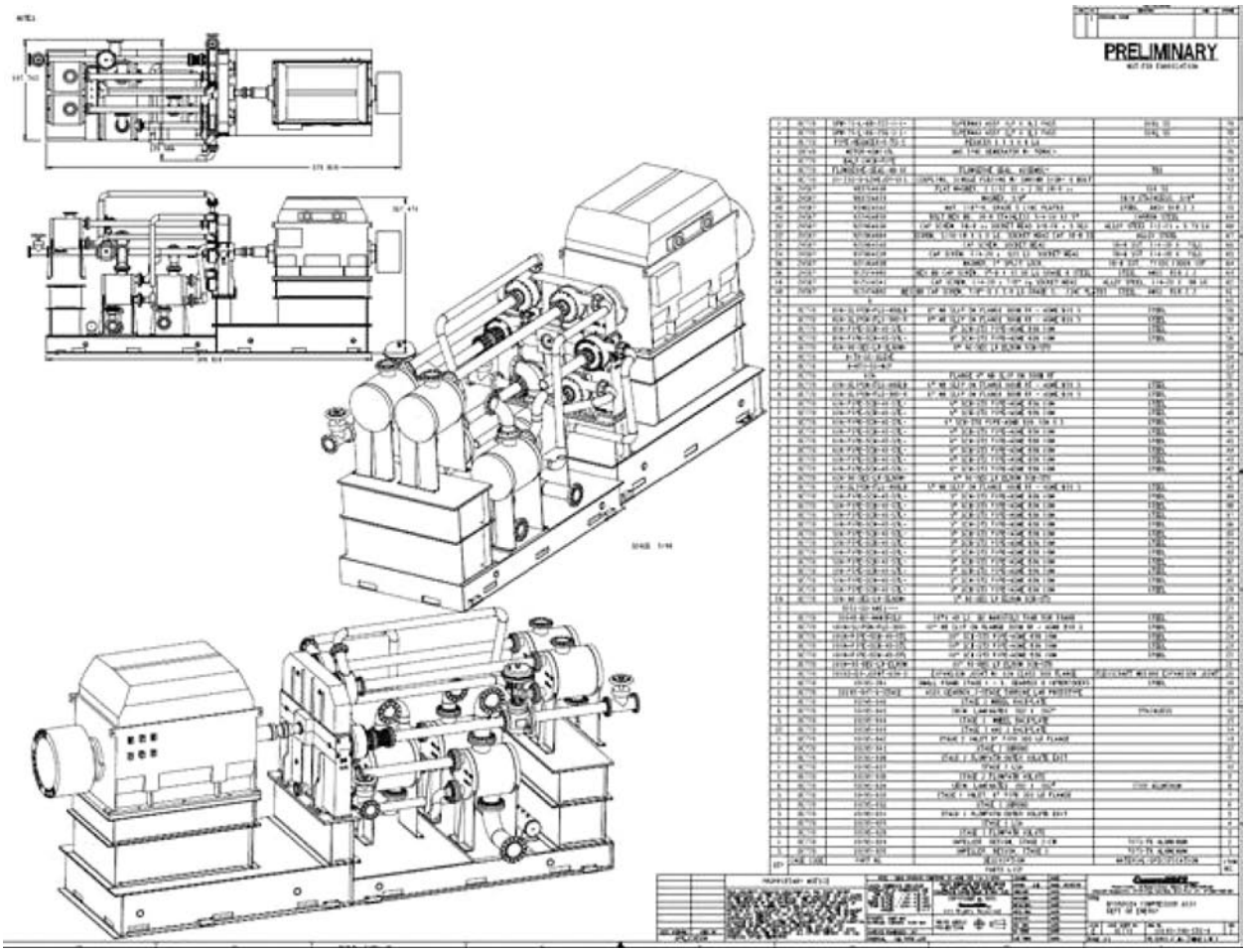


FIGURE 2. Engineering analysis and design results: pipeline hydrogen centrifugal compressor 240,000 kg/day; 350 to 1,285 psig; 6,300 kWe.

package with a minimum of final alignment, water piping and electrical power connections, and instrumentation and controls start-up.

The compressor selection uses six stages, each operating at 60,000 rpm with a tip speed of less than 2,100 ft/s. Each compressor rotor and drive shaft is 8 inches in diameter and has an overall stage efficiency of between 79.5 and 80.5%, for an overall compressor efficiency of 80.3%. The first and last stages have a slightly different length which helps to improve the rotordynamics for the last stages. Each compressor impeller is a single, overhung (cantilevered) impeller attached to a drive shaft that includes a shaft seal, bearing, and drive pinion (Figure 3) integrated with the gearbox drive. The impeller rotor is designed without a bored hub in order to reduce the hub "hoop" stresses. This requires the impeller to be mechanically attached to the high-strength steel alloy, a drive shaft with a patented design attachment system that enables the rotor to be removed from the gearbox without removing the drive shaft, and thus does not disturb the shaft seal and bearings. A gas face seal will provide the isolation of the hydrogen from the lubricating oil. The 1,400 hp per stage can be sustained by using two tilting-pad hydrodynamic bearings on either side of a 2.5-inch-long drive-pinion gear. The face seal and bearings are commercially available from Flowserve and KMC, respectively. The pinion and bull gear is part of a custom gearbox manufactured by Artec Machine Systems representing NOVAGEAR (Zurich, Switzerland) and utilizes commercially available gear materials that are subjected to stresses and pitch line speeds that meet acceptable engineering practice.

Also shown in Figure 3 is the encasement of each compressor rotor and (pressure recovery) volute. The encasement is made of nitronic-50 steel that is designed to sustain the highest compression pressure.

The material chosen for the compressor rotor and volute is an aluminum alloy. The choice is based on its mechanical strength-to-density ratio or (S_{yield}/ρ) which can be shown to be a characteristic of the material's ability to withstand centrifugal forces. Several grades of aluminum have a strength-to-density ratio that is similar to titanium and high-strength steels at the 140°F (max) operating temperatures that

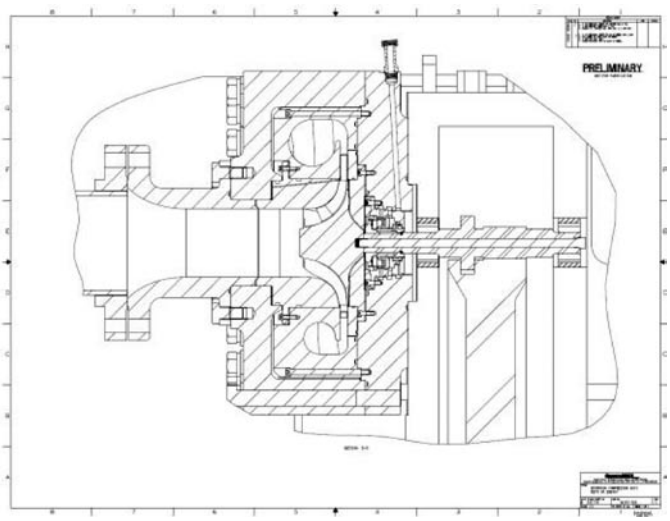




FIGURE 3. Mechanical Detailed Assembly of One of Six Stages of Pipeline Compressor

will be experienced by the hydrogen compressor. However, unlike titanium and most steels, aluminum is recognized by the industry as being very compatible with hydrogen.

Aluminum also helps to reduce the weight of the rotor, which leads to an improved rotordynamic stability at the 60,000 operating speed. A rotor stability and critical speed analysis has confirmed that the overhung design is viable. The 1st stage compressor rotor has been manufactured (Figure 3) and successfully spun to its 60,000 operating speed. A subsequent fluorescent penetrant inspection and strain measurements of the rotor after the spin test indicated no creep or micro-crack design flaws as a result of the test.

The project team includes researchers at Texas A&M, led by Dr. Hong Liang, who are collaborating with Concepts NREC to confirm the viability of aluminum alloys for this compressor application. Also assisting with a collegial collaboration of suggestions are several national laboratories, including: Sandia National Laboratories (fracture mechanics testing; Dr. Chris San Marchi), Savannah River National Laboratory (specimen "charging" with hydrogen plus tensile testing with H_2; Dr. Andrew Duncan and Dr. Thad Adams), and Argonne National Laboratory (Dr. George Fenske).

The Phase II work also completed the detailed design of a closed-loop one and two-stage prototype compressor modules. One of these modules will be selected for laboratory testing in Phase III of the project. The laboratory prototype is shown in Figure 4.

Conclusions and Future Directions

- An advanced pipeline compressor system has been designed that meets DOE's performance goals for:
  - High reliability with 350 to 1,200+ psig compression of 240,000 kg/day at 98% hydrogen efficiency.
  - Footprint 1/4 to 1/3 the size of existing industrial systems at projected cost of less than 80% of DOE's target.
- Utilize state-of-the-art and acceptable engineering practices to reduce developmental risk and provide a near-term solution for the design of a viable hydrogen pipeline compressor:
  - Aerodynamic/structural analyses for acceptable material (7075-T6 and Nitronic-50) stresses in hydrogen.
  - Industrially proven bearings, seal technology, gearing, heat exchangers, and lube system.
- Aerodynamic analysis and design of a cost-effective, 6-stage centrifugal compressor and a 2-stage full-power lab prototype have been completed. The 1-stage laboratory prototype will be tested at Praxair's facility.
- The collaborative team consists of Praxair, an industrial technical experienced user and host of lab prototype test; a materials researcher, Texas A&M; a hydrogen refueling industry consultant, HyGen; and the coordinated technical support of several national labs.
- Complete materials coating testing of specimens with Texas A&M: actual rotor forensics after high-speed testing as necessary.
- Start the procurement of major components for the laboratory testing of a prototype compressor-gearbox in Phase III; prepare test plan for lab test and coordination with Praxair.

The preliminary engineering and design of an advanced pipeline compressor system has been completed and meets DOE's performance goals for a reliable 98% hydrogen efficiency compressor system, with a footprint one-half the size of existing industrial systems and at a projected

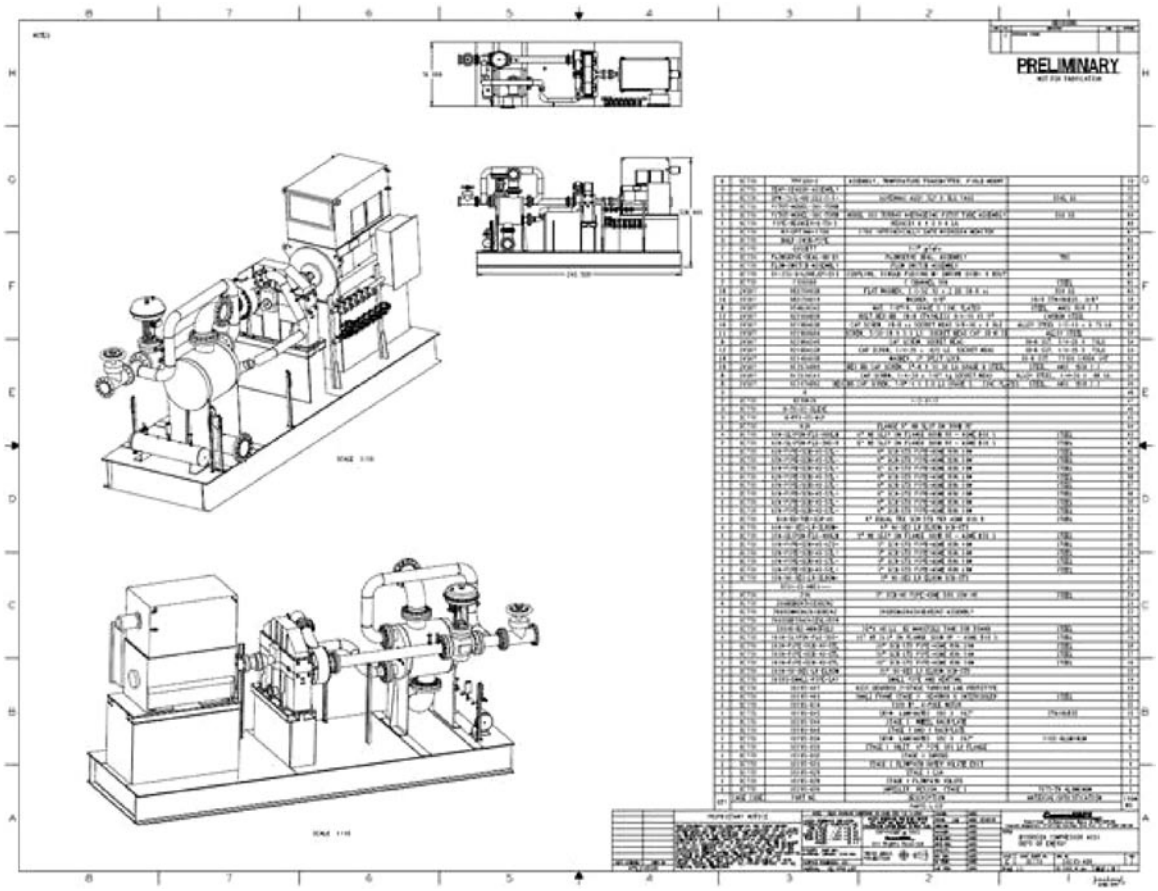


FIGURE 4. Detailed Design of a 1-Stage, Laboratory Prototype Compressor

system cost of approximately 75% of DOE's target, and a maintenance cost that is less than the $0.01/kWh. The detailed analysis of this pipeline compressor system is in progress in Phase II of the project. The advanced centrifugal compressor-based system can provide 240,000 kg/day of hydrogen from 350 to 1,280 psig high for pipeline-grade service. This has been accomplished by utilizing a state-of-the-art aerodynamic and structural analysis of the centrifugal compressor impeller to provide high pressure ratios under acceptable material stresses. The technical approach that has been successfully implemented includes using commercially available, and thus proven, bearings and shaft seal technology. This technical approach reduces the developmental risk and increases system reliability while maintaining a competitive cost.

The resultant design provides a compressor that not only meets DOE's hydrogen plan for using pipeline delivery, but also a compressor package that can be used by the industrial, hydrogen gas industry where there is presently 1,200 miles of pipeline providing 9 million tons per year of hydrogen gas for industrial process chemical applications. The collaborative team that has been assembled consists of an industrial user who has experience with hydrogen as a fuel source and as an industrial gas, a materials researcher (Texas A&M), and a consultant (HyGen Industries) with hands-on experience with the hydrogen refueling industry. This team is committed to producing the first commercially reliable hydrogen compressor for hydrogen pipeline delivery.

Future efforts include:

Phase III System Component Procurement, Construction, and Validation Testing (January 2011 to September 2012):

- Continue materials testing at Texas A&M University with hydrogen to determine effects of coatings that can be used with titanium.
- Component procurement for the 1- or 2-stage functional hydrogen compressor system.
- Assembly of the 1-stage centrifugal compressor system.
- Coordinating the integration of a laboratory prototype compressor module for testing with hydrogen.
- Conduct aerodynamic testing and assessment of mechanical integrity of the compressor system.

Patents Issued

1. Patent application filed on several innovations for centrifugal compressor design; filed March, 2010 (provision file March, 2009: SN 60/896985): "Centrifugal Compressor Design for Hydrogen Compression".

References

1. 2007 DOE Multi-Year Research, Development, and Demonstration Plan.

2. Smalley, A., *et al*., "Evaluation and Application of Data Sources for Assessing Operating Costs for Mechanical Drive Gas Turbines in Pipeline Service," Transactions of ASME, Vol. 122, July 2000.

3. Harrell Jr., J. and Smalley, A., "Benchmarking the Industry: Factors Affecting Compressor Station Maintenance Costs," A presentation at the GMRC Gas Machinery Conference, October 2000.

III.9 Oil-Free Centrifugal Hydrogen Compression Technology Demonstration

Hooshang Heshmat
Mohawk Innovative Technology, Inc. (MiTi®)
1037 Watervliet Shaker Road
Albany, NY 12205
Phone: (518) 862-4290
E-mail: HHeshmat@miti.cc

DOE Managers
HQ: Scott Weil
Phone: (202) 586-1758
E-mail: Kenneth.Weil@ee.doe.gov
GO: Paul Bakke
Phone: (720) 356-1436
E-mail: Paul.Bakke@go.doe.gov

Contract Number: DE-FG36-08GO18060

Subcontractor:
Mitsubishi Compressor Company (MHI), Hiroshima, Japan

Project Start Date: September 25, 2008
Project End Date: August 31, 2012

Fiscal Year (FY) 2011 Objectives

Demonstrate key technologies needed to develop reliable and cost-effective centrifugal compressors for hydrogen transport and delivery:

- Eliminate sources of oil/lubricant contamination.
- Increase efficiency by using high rotational speeds.
- Reduce system cost and increase reliability.

Technical Barriers

This project addresses the following technical barriers from the Hydrogen Delivery section of the Fuel Cell Technologies Program Multi-Year Research, Development and Demonstration Plan:

(B) Reliability and Costs of Hydrogen Compression
(I) Hydrogen Leakage and Sensors

Technical Targets

This project is directed towards the design, fabrication and demonstration of the oil-free centrifugal compression technology. It will identify the key technological challenges for development of a full-scale hydrogen/natural gas centrifugal compressor. The project addresses the following DOE technical targets from the Hydrogen Delivery section of the Fuel Cell Technologies Program Multi-Year Research, Development and Demonstration Plan (see Table 1).

TABLE 1. Technical Targets for Hydrogen Compression

Category	2005 Status	FY 2012	FY 2017
Reliability	Low	Improved	High
Energy Efficiency	98%	98%	>98%
Capital Investment ($M) (based on 200,000 kg of H2/day)	$15	$12	$9
Maintenance (% of Total Capital Investment)	10%	7%	3%
Contamination	Varies by Design		None

FY 2011 Accomplishments

- System cost analysis
- Off-design performance estimation
- Single-stage test rig design
- Manufacturing of the single-stage test rig



Introduction

One of the key elements in realizing the hydrogen economy is the deployment of a safe, efficient hydrogen production and delivery infrastructure on a scale that can compete economically with current fuels. The challenge, however, is that hydrogen, the lightest and smallest of gases with a lower viscosity than natural gas, readily migrates through small spaces. While efficient and cost effective compression technology is crucial to effective pipeline delivery of hydrogen, today's positive displacement hydrogen compression technology is very costly, and has poor reliability and durability, especially for components subjected to wear (e.g., valves, rider bands and piston rings). Even so called "oil-free" machines use oil lubricants that migrate into and contaminate the gas path. Due to the poor reliability of compressors, current hydrogen producers often install duplicate units in order to maintain on-line times of 98-99%. Such machine redundancy adds substantially to system capital costs. Additionally, current hydrogen compression often requires energy well in excess of the DOE 2% goal. As such, low capital cost, reliable, efficient and oil-free advanced compressor technologies are needed.

Approach

The MiTi® team will meet sub-program objectives by conducting compressor, bearing and seal design studies; selecting components for validation testing; fabricating the selected centrifugal compressor stage, and the corresponding oil-free bearings and seals; and conduct testing of the high-speed, full-scale centrifugal compressor stage, and oil-free

compliant foil bearings and seals under realistic pressures, and flows in a hydrogen gas environment. Specific tasks include: (1) preliminary oil-free, multi-stage, high-speed centrifugal compressor system design; (2) detailed design of a full-scale centrifugal compressor stage; (3) mechanical component detailed design of the oil-free bearings, seals and shaft system needed to test the compressor stage; (4) test hardware fabrication for the single-stage compressor; (5) dynamic test; (6) compressor performance test; (7) system design refinement; and (8) project management and reporting.

Results

The design analysis of MiTi®'s proposed multi-stage, oil-free, hydrogen compressor was continued and refined. The proposed hydrogen compressor is a direct drive, multi-stage, double-entry, centrifugal compressor. Two system design points have been analyzed:

- Design Point 1: P_{IN} = 500 psig, P_{OUT} = 1,200 psig, Flow= 500,000 kg/day
- Design Point 2: P_{IN} = 350 psig, P_{OUT} = 1,200 psig, Flow= 240,000 kg/kay

For design point 1, the proposed system consists of nine stages operating at 56,414 rpm at relatively conservative tip speeds, affording a reasonable safety margin. This approach is referred to as the "high-margin" design. To achieve design point 2, higher relative tip speeds were used to achieve the required pressure and flow in six stages operating at 65,000 rpm. This approach is referred to as the "high-performance" design. To validate the feasibility of the two approaches, further detailed design and cost analysis have been conducted. Experimental validation and proof of concept will be performed in FY 2012 with a single-stage compressor test rig that has been designed and is presently being developed. Based on the scope of this project and funding made available for this effort, the single-stage compressor is being based on design point 1.

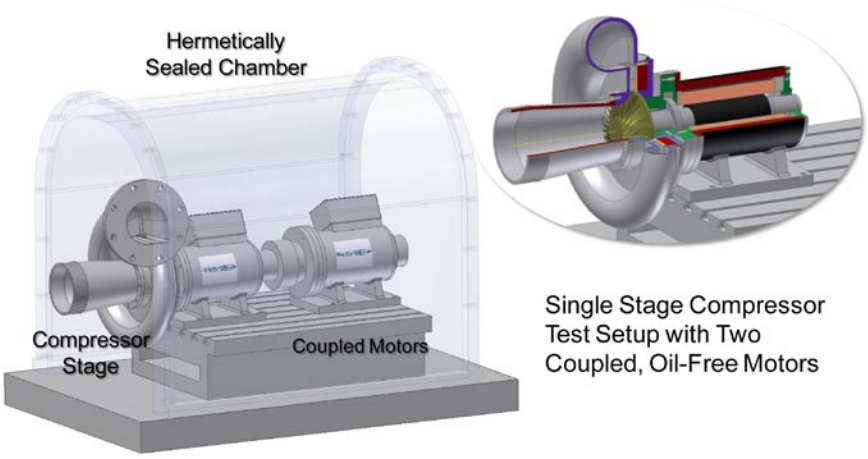


FIGURE 1. Detailed Model of the Single-Stage Compressor with Dual-Drive, Oil-Free Electric Motors

TABLE 2. Critical Nondimensional Parameters to Satisfy the Type 2 PTC-10 Test

Quantity	Symbol	Design Point Values	Type 2 Permissible Deviation
Specific Volume Ratio	vi/vd	1.072	1.018 – 1.126
Flow Coefficient	Φ	0.1253	0.120 - 0.130
Machine Mach No.	Mn	0.3266	0.141 - 0.532
Machine Reynolds No.	Rem	$1.55e^{6}$	$1.55e^{5}$ – $1.55e^{7}$

A detailed model of the proposed single-stage test rig is shown in Figure 1. The impeller and volute of the single-stage test rig are identical to that of a single stage within the first frame of the nine-stage system. The stage will be driven with two MiTi® oil-free electric motors, coupled together to produce up to 200 kW of shaft power. The test rig will be totally oil-free using MiTi® foil bearings and foil seals. The purpose of the single-stage testing is to validate the thermodynamic performance of the proposed centrifugal compressor design, as well as the rotor/bearing system performance under realistic speed and stress conditions expected in the nine-stage system. In order to validate the performance predictions, single stage testing will be conducted per American Society of Mechanical Engineers (ASME) performance test code 10 (PTC-10). This test code provides explicit test procedures to determine compressor thermodynamic performance with a high level of accuracy. There are two types of tests described within PTC-10; type 1 and type 2 tests. A type 1 test is one conducted with the design gas, at the design point. Under the scope of this project, testing with hydrogen is not feasible; therefore, a type 1 test will not be conducted. Since testing with all possible gases at all test conditions is often not feasible, ASME established the type 2 test based the standard design practice of compressor similitude. With this approach, key nondimensional parameters are maintained constant in testing so that thermodynamic performance of a compressor stage in one gas would apply to other gases and at other test conditions. The critical nondimensional parameters of the test stage to be held constant (within a permissible deviation) are listed in Table 2 along with the calculated values at the design point.

In the type 2 test, a similitude gas may be substituted for the design gas as long as nondimensional parameters are kept within specified limits. For this investigation, the best similitude gas is helium. Helium is an affordable and safe alternative to hydrogen with a similarly low molecular weight. It is critical that the first compressor stage performance testing not be complicated with the issues of hydrogen embrittlement. The issues of material compatibility and

embrittlement are being addressed in a parallel effort in this project, but these two issues are not integrated at this time. The use of helium in these first compressor performance tests allows us to focus on aerodynamic and thermodynamic characterization and to establish a performance baseline so that any performance effects, due to embrittlement, will be apparent at a later time.

Presently, no single, direct-drive 200 kW drive motor capable of operating at 56,000 rpm exists. MiTi® has developed (with internal funds) the 60,000 rpm 100 kW motor. Since the objective of this project is to demonstrate the thermodynamic performance of the compressor, MiTi® has opted to couple two high speed 100 kW motors together to provide the needed drive power rather than develop a single 200 kW, direct drive motor. To assure stable operation of the proposed dual motor drive system for the single stage compressor, detailed rotordynamic analysis was performed. The finite element model of the coupled shaft system is shown in Figure 2. The compressor is rigidly attached to the shaft on the left. The two rigid shafts are connected by a flexible coupling (a proprietary technology developed by MiTi®). Each individual shaft is supported on MiTi® compliant foil journal and thrust bearings.

Appropriate stiffness and damping values for bearings were selected and rotordynamic analysis was conducted with DyRoBes© software (Eigen Technology Inc.). The analysis indicates that each individual shaft will be operating safely below its bending critical speed (Figure 3). All bending within the system will occur within the flexible coupling, as designed, and as has been demonstrated by MiTi® in numerous other applications. With design and analysis of the single stage test rig complete, manufacturing of the parts was initiated and is currently in progress.

In a parallel effort MHI is designing a single entry centrifugal compressor and a single-stage compressor for performance validation with assistance of MiTi®. The primary difference between the two approaches is related to the inlet flow. The MiTi design uses a double-entry technique, which splits mass flow evenly between two inlets at either end of the shaft. The benefit of this approach is inherently balanced thrust forces. The MHI design uses a single-entry approach that requires a balance piston to resolve excessive thrust loads. The advantage of this approach is that it allows for easy manipulation of axial clearance at all compressor impellers.

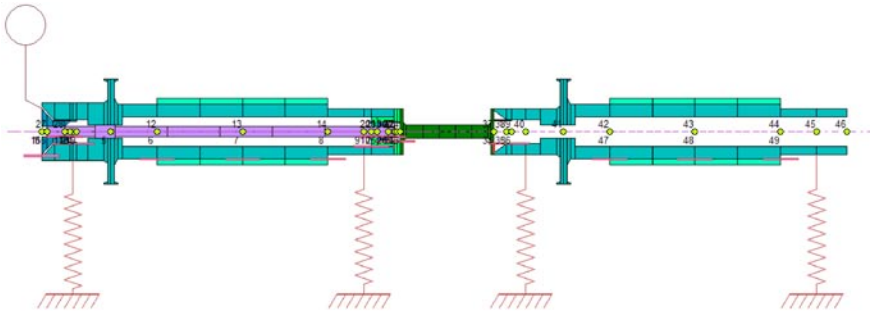


FIGURE 2. Finite Element Model of the Single-Stage Compressor And Dual-Drive System

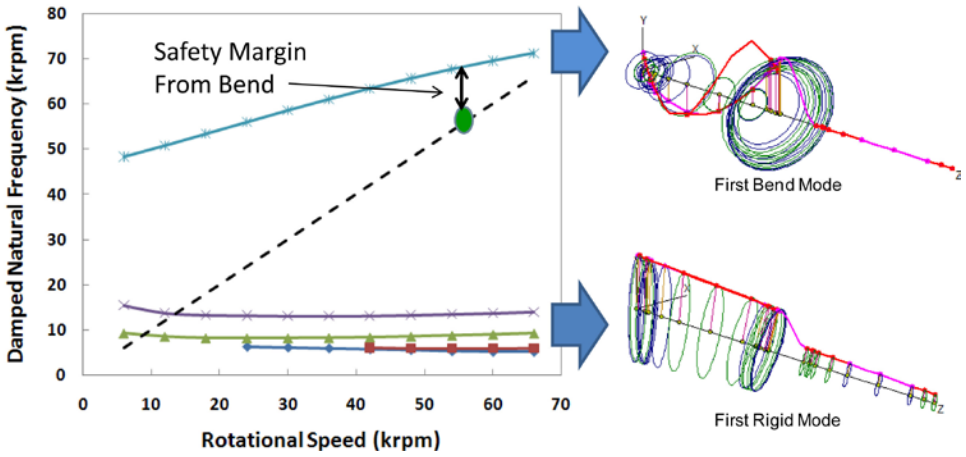


FIGURE 3. Rotordynamic Analysis of the Dual Drive Single-Stage Compressor

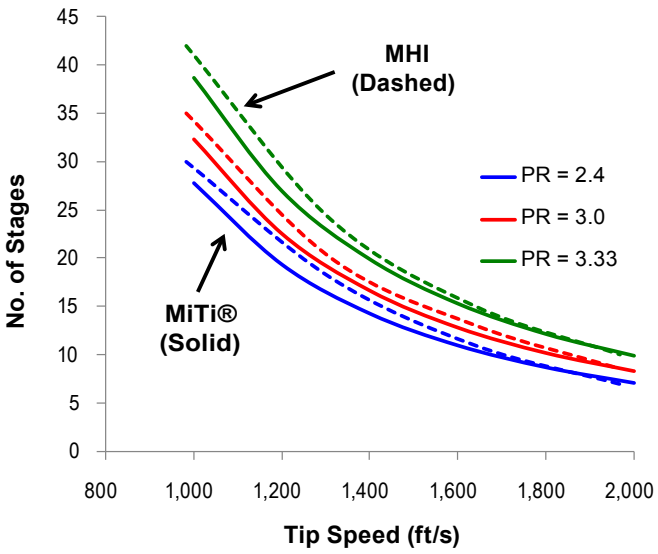


FIGURE 4. Estimation of Number of Stages Required as a Function of Tip Speed And Pressure Ratio (PR)

Despite the differences in design approaches, the overall performance of the two systems will be very similar. In Figure 4, independent results from MiTi® and MHI are presented. The number of stages required to reach a particular pressure ratio are presented as a function of tip speed. Despite the use of double- and single-entry compressor designs, the results from MiTi® and MHI correlate well, especially at higher tip speeds within the expected operating range. This is because the inlet conditions, fluid properties and design point used for each concept were identical. MiTi® and MHI both assumed similar conditions and both employ highly sophisticated, but different, software design tools.

Conclusions and Future Directions

During this reporting period, further design refinement was conducted. To demonstrate the feasibility of MiTi®'s design concept, a single-stage test rig was designed and fabrication of components was initiated. In parallel, a single-entry compressor concept is being developed with guidance from MiTi® by MHI. The following tasks are planned for the remainder of FY 2011 and FY 2012:

- Complete fabrication of single-stage compressor components for testing.
- Validate the proposed single-entry and double-entry compressor designs using performance data from the single-stage compressors.

FY 2011 Publications/Presentations

1. Heshmat H., Walton J.F., "Oil-Free Modular System Designs for Industrial Compressors and Renewable Energy Turbine Generator Systems," Clean Technology Conference and Expo, June 21, 2010, Anaheim, CA.

2. Heshmat H., Hunsberger A.Z., Ren Z., Jahanmir S., Walton J.F., "On the Design of a Multi-Megawatt Oil-Free Centrifugal Compressor for Hydrogen Gas Transportation and Delivery – Operation Beyond Supercritical Speeds", Proceedings of the ASME International Mechanical Engineering Congress and Expo, November 12-18, 2010, Vancouver, BC, Canada.

3. Heshmat H., *Invited Keynote*, "Tribological Requirements of High-Speed Oil-Free Rotating Machinery for Hydrogen Applications," 2011 Hydrogenous Tribology Symposium, February 3, 2011, Fukuoka, Japan.

4. Heshmat H., "Design of a Multi-Megawatt Oil-Free Centrifugal Compressor for Hydrogen Gas Transportation and Delivery," Fuel Cell and Hydrogen Energy Expo, February 15, 2011, National Harbor, Md.

III.10 Electrochemical Hydrogen Compressor

Ludwig Lipp (Primary Contact), Pinakin Patel
FuelCell Energy, Inc.
3 Great Pasture Road
Danbury, CT 06813
Phone: (203) 205-2492
E-mail: llipp@fce.com

DOE Managers
HQ: Kenneth S. Weil
Phone: (202) 586-1758
E-mail: Kenneth.Weil@ee.doe.gov
GO: Paul Bakke
Phone: (720) 356-1436
E-mail: Paul.Bakke@go.doe.gov

Contract Number: DE-EE0003727

Subcontractor:
Sustainable Innovations, LLC, Glastonbury, CT

Start Date: July 15, 2010
End Date: July 14, 2013

Fiscal Year (FY) 2011 Objectives

- Develop a solid-state electrochemical hydrogen compressor (EHC) building block capable of compressing hydrogen from near-atmospheric pressure to 2,000-3,000 psi.
- Study feasibility of an EHC multi-stage system capable of compressing hydrogen from near-atmospheric pressure to 6,000-12,000 psi.
- Increase compression efficiency to 95% (DOE 2015 target).

Technical Barriers

This project addresses the following technical barrier from the Hydrogen Delivery section (3.2) of the Fuel Cell Technologies Program Multi-Year Research, Development and Demonstration Plan:

(B) Reliability and Costs of Hydrogen Compression

Technical Targets

This project is directed at developing a solid-state EHC. The EHC is an enabling device for low-cost hydrogen delivery. Goals include the following:

- Single-stage compression of hydrogen from near-atmospheric pressure to 2,000-3,000 psi.
- Multi-stage compression of hydrogen from near-atmospheric pressure to 6,000-12,000 psi.
- Ensure no possibility of lubricant contamination of the hydrogen from compression (DOE 2015 target).
- Reduce EHC specific energy consumption.
- Scale up EHC to a capacity of 2-4 lb/day H_2.

The ultimate goal of the project is to meet the DOE targets for forecourt compressors [1].

FY 2011 Accomplishments

- Hydrogen Pressure: reached 6,000 psi hydrogen pressure in a two-stage EHC system (Figure 1).
- Compression Efficiency: reduced specific energy consumption to <5 kWh/kg H_2 when compressing from atmospheric pressure to 2,000 psi (Figure 2).
- Hydrogen Recovery: achieved 95% hydrogen recovery in a single cell.
- Capital Cost: increased hydrogen flux from 400 to 750 mA/cm^2.

✧ ✧ ✧ ✧ ✧

Introduction

With the depletion of fossil fuel reserves and a global requirement for the development of a sustainable economy, hydrogen-based energy is becoming increasingly important. Production, purification and compression of hydrogen represent key technical challenges for the implementation of a hydrogen economy, especially in the transportation sector where on-board storage of pure hydrogen may be required at

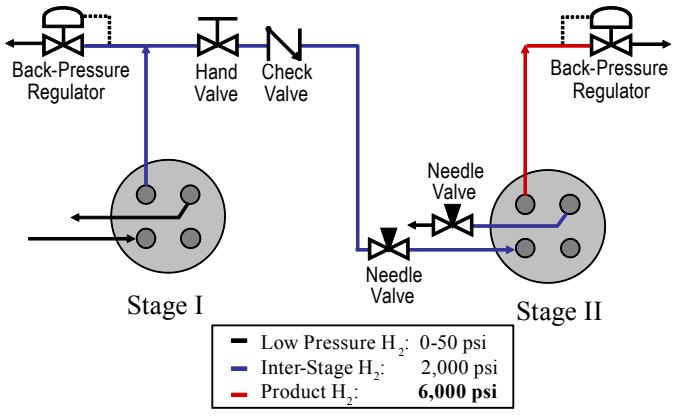


FIGURE 1. 2-Stage EHC System Concept

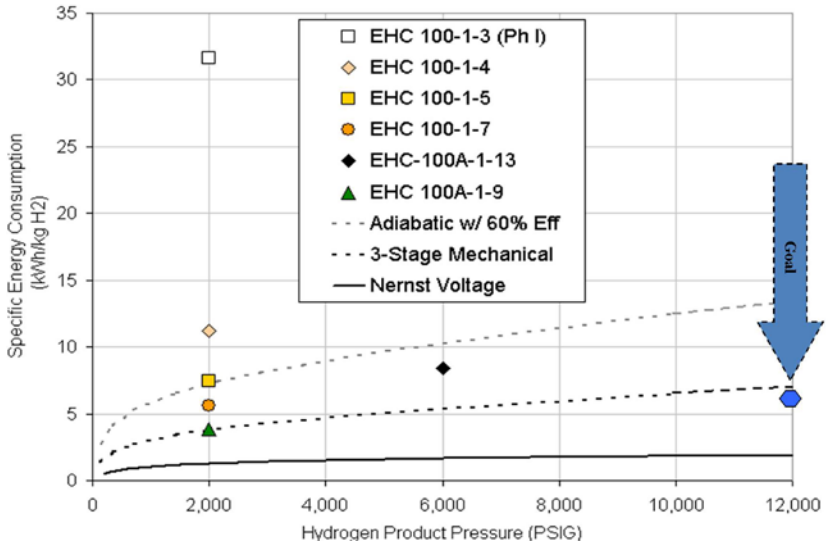


FIGURE 2. Reduction in the Specific Energy Consumption of the EHC

pressures up to 10,000 psi and compression of the hydrogen fuel up to 12,000 psi.

The level of maturity of current hydrogen compressor technology is not adequate to meet projected infrastructure demands. Existing compressors are inefficient and have many moving parts, resulting in significant component wear and therefore excessive maintenance. New technologies that achieve higher operational efficiencies, are low in cost, safe and easy to operate are therefore required. This project addresses high-pressure hydrogen needs by developing a solid-state EHC.

Approach

The approach to address the program goals consists of the following major elements:

- Increase hydrogen recovery efficiency by improving flow field design.
- Reduce capital cost by increasing the hydrogen flux.
- Reduce operating cost by improving membrane and electrode design.
- Develop a multi-stage system concept for compression to 6,000-12,000 psi.

To this end, the approach includes the design, fabrication and evaluation of improved cell architecture, and the development and demonstration of critical sealing technology to contain the high-pressure hydrogen within the EHC.

Results

A 2-stage EHC system concept was developed, in order to achieve higher hydrogen pressures using existing EHC designs. The challenge was to design a system that can automatically respond to changes in pressure, inlet flow and current density, while maintaining stable operation in both stages. The system also needs to safely operate without attendants, in order to demonstrate continuous operation. The high level system configuration and control strategy that was developed in FY 2011 is shown in Figure 1. Atmospheric pressure hydrogen is fed to the low-pressure side of stage I. The pressurized hydrogen (inter-stage pressure) is then fed to the low-pressure side of the stage II EHC. A check valve prevents hydrogen from flowing back from stage II to stage I. The product hydrogen exits the stage II EHC at the desired high pressure. For safe operation of the laboratory system, this pressure is controlled by a back-pressure regulator. The concept was validated in the laboratory by compressing from atmospheric pressure to about 2,000 psi in the first stage, followed by compression to 6,000 psi in the second stage. Then it was operated for several weeks at a variety of inter-stage and product pressures, and at different hydrogen flow rates. This experience will provide a solid basis for designing a multi-stage system capable of reaching 12,000 psi, as shown in Figure 3. A product pressure of 12,000 psi is desirable in order to efficiently refuel hydrogen vehicle tanks with a maximum fill pressure of 10,000 psi. This pressure is needed to enable a driving range similar to gasoline-fueled vehicles, while preserving the passenger and cargo capacity of the vehicles.

A major challenge in the commercialization of the EHC is capital cost. One way to address this challenge is to increase the hydrogen flux by increasing the operating current density. This, however, could lead to a higher operating cost, due to increased specific energy consumption. The latter is proportional to the cell resistance. To lower the cell resistance, efforts were



FIGURE 3. Multi-Stage System Capable of Reaching 12,000 PSI

focused on lowering the bulk and contact resistances of key cell components, such as membrane and bipolar plates. Improvements to the cell design and materials enabled a reduction in specific energy consumption to below 5 kWh/kg H_2. This performance was obtained when compressing hydrogen from atmospheric pressure to 2,000 psi, as shown in Figure 2. The hydrogen recovery was as high as 95%. The improvements in membrane and bipolar plate materials also enabled the desired increase in current density, which leads to a higher hydrogen flux and therefore reduced capital cost. Continuous operation at 750 mA/cm^2 was demonstrated in a 1,000 hour test.

Conclusions and Future Directions

The feasibility of a 2-stage EHC system to increase the pressure capability has been demonstrated. Improvements in materials have resulted in an 80% increase in hydrogen flux, which translates to a lower capital cost.

Future efforts will include further improvements in cell architecture, scale up and increase in pressure capability in a multi-stage system.

FY 2011 Publications/Presentations

1. L. Lipp, "Electrochemical Hydrogen Compressor", 2011 DOE Hydrogen Program Merit Review and Peer Evaluation Meeting, Arlington, VA, May 9–13, 2011.

References

1. Fuel Cell Technologies MYRDD Plan, Table 3.2.2 "Technical Targets for Hydrogen Delivery", section on Forecourt Compressors, page 3.2–14.

III.11 Advanced Hydrogen Liquefaction Process

Joseph Schwartz
Praxair, Inc.
175 East Park Drive
Tonawanda, NY 14150
Phone: (716) 879-7455
E-mail: Joseph_Schwartz@Praxair.com

DOE Managers
HQ: K. Scott Weil
Phone: (202) 586-1758
E-mail: Kenneth.Weil@ee.doe.gov
GO: Paul Bakke
Phone: (720) 356-1436
E-mail: Paul.Bakke@go.doe.gov

Contract Number: DE-FG36-08GO18063

Project Start Date: June 1, 2008
Project End Date: June 30, 2011

Fiscal Year (FY) 2011 Objectives

Develop low-cost hydrogen liquefaction systems to produce 30 and 300 tons/day:

- Improve liquefaction energy efficiency.
- Reduce liquefier capital cost.
- Integrate improved process equipment invented since last liquefier was designed.
- Continue ortho-para conversion process development.
- Integrate improved ortho-para conversion process.
- Develop optimized new liquefaction process based on new equipment and new ortho-para conversion process.

Technical Barriers

This project addresses the following technical barrier from the Delivery section (3.2.4) of the Hydrogen, Fuel Cells and Infrastructure Technologies Program Multi-Year Research, Development and Demonstration Plan:

(C) High Cost and Low Energy Efficiency of Hydrogen Liquefaction

Technical Targets

TABLE 1. Technical Targets for Liquid Hydrogen Delivery

Characteristic	Units	2012 Target	2017 Target
Small-Scale Liquefaction (30,000 kg/day)			
Installed Capital Cost	$	40M	30M
Energy Efficiency	%	75	85
Large-Scale Liquefaction (300,000 kg/day)			
Installed Capital Cost	$	130M	100M
Energy Efficiency	%	>80	87

We are addressing the capital cost and energy efficiency targets.

Capital Cost:

- Improved process design.
- Improved process equipment.

Energy Efficiency:

- Increased equipment efficiency.
- Improved process efficiency.
- Improved ortho-para conversion efficiency with a goal of reducing energy required for ortho-para conversion by at least 33%.

FY 2011 Accomplishments

- Constructed improved test unit capable of operating over a temperature range from 77 K to about 150 K.
- Developed spreadsheet model to calculate energy requirements for hydrogen liquefaction.
- Identified problems with commercial process simulation software for modeling ortho and para hydrogen and worked with project supplier to solve the problems.
- Prepared and tested new materials for improved ortho-para conversion using recipes and equipment that produce materials similar to those that could be produced in commercial quantities.
- Developed process models for existing and proposed liquefier designs.
- Showed that overall power consumption can be reduced by about 2.5% if catalyst is used in the high-temperature heat exchanger.
- Identified a process where the demonstrated performance of the improved ortho-para conversion process is sufficient to reduce total power consumption.

- Identified a process where the performance of the improved ortho-para conversion process, even when accounting for future improvement, is unlikely to be sufficient to reduce total power consumption.
- Evaluated different compressors for small and large-scale hydrogen liquefaction.
- Calculated potential overall efficiency improvement due to improved process equipment.
- Demonstrated that the combined improvements due to using more efficient compressors (4-7%), more efficient expansion turbines (2-3%), more efficient heat exchangers (<1%), an improved liquefaction process (2%), and an improved ortho-para conversion process (3-6%) can all contribute to significantly improve efficiency and reduce power requirements, but not enough to meet the DOE goal.



Introduction

Hydrogen liquefiers are highly capital intensive and have a high operating cost because they consume a significant amount of electrical power for refrigeration. There are only a few hydrogen liquefiers in the world and only six currently operating in the U.S. These plants are not built frequently, so they have not been thoroughly optimized for today's equipment. Furthermore, many of them were built when power was much less expensive than it is today, so those plants do not have optimized efficiency.

Approach

This project focused on improving liquefier efficiency and reducing overall liquefaction cost, including reducing capital cost. The project attempted to accomplish these goals using three different aspects of an integrated approach:

- Improved process design – Develop a more efficient refrigeration process including ortho-para conversion and refrigeration using available streams and equipment.
- Improved process equipment – Integrate improvements made in process equipment since the most recent liquefier design to take full advantage of the increased capabilities and improved efficiency. Project the impact of further improvements in process equipment, including novel devices currently being developed.
- Improved ortho-para conversion process – Ortho-para conversion consumes a significant amount of refrigeration energy because it requires cooling at low temperatures. Improvements in ortho-para conversion can lead to a significant reduction in power requirements.

This project built on previous work done at Praxair, some of which was part of a project funded through Edison Materials Technology Center (EMTEC). The previous project demonstrated that the improvements in ortho-para conversion were possible, but developing the complete optimized process design was beyond the scope of that project.

Results

The material screening test system used during the EMTEC project was recommissioned to perform additional material testing and test new materials. This system can test materials at the boiling point of the cooling fluid, such as liquid nitrogen. The system can test ortho-para conversion at pressures up to 400 psig and has the advantage of being a simple system that is excellent for preliminary screening of materials. Figure 1 shows this system. New materials work proceeded from the EMTEC project with new recipes and methods developed to provide samples with properties that more closely approximate those that would be obtained using commercial-scale materials manufacturing.

A pilot-scale system to conduct process testing on desired materials over a range of temperatures was built (Figure 2). This new test system is fully automated to allow for both remote control and material life testing. The system consists primarily of a series of pressure vessels, each of which houses a material bed. The annular space between the inside of the pressure vessel and the outside of the material bed contains a liquid coolant that can be pressurized. The ortho-para conversion process is conducted at very low temperatures (<150 K) and therefore a liquid coolant such as liquid nitrogen or liquid argon is required to achieve temperatures in this range. Each pressure vessel contains a vent line equipped with a back pressure control valve to allow for control of the liquid boiling pressure. By controlling the liquid boiling pressure, temperature can be controlled indirectly over a range of 77 K to 126 K using liquid nitrogen as the coolant and temperatures up to about 150 K using liquid argon.

This new test system was used to determine performance characteristics of the ortho-para conversion



FIGURE 1. Material Screening Test System



FIGURE 2. Pilot-Scale Test System

system. These results were used in the process model to determine the overall performance of a system using the improved ortho-para conversion process. These results are shown in Figures 3 and 4.

Modeling

Process simulations were developed for hydrogen liquefaction processes that used the improved ortho-para conversion process to compare those to processes that did not. Of the processes that did not use the improved ortho-para conversion process, it was found that adding ortho-para conversion catalyst to the high-temperature heat exchanger reduced overall energy consumption by about 2.5%.

Several different processes have been conceived that use the improved ortho-para conversion process. The modeling portion of the program compared these processes to hydrogen liquefaction processes with standard ortho-para conversion. Concept α and Concept β were evaluated. Figures 3 and 4 show the results.

The point in the center is the target based on ortho-para performance meeting the base case power target. The y-axis represents the power required for hydrogen liquefaction as a percentage of the base case power target. The x-axis shows ortho-para performance as a percentage of demonstrated performance in the laboratory. The target is based on demonstrated performance (100% of current ortho-para performance) meeting the base case power target. In this case, about 150% of the current demonstrated performance is required to meet the base case power target. Although there has been steady improvement in demonstrated performance throughout the project, marginal gains are lower than they were earlier in the project. It is unlikely that Concept α will meet the target required to be an economically viable process.

Figure 4 shows the same results for Concept β. In this case, 100% of the current demonstrated performance

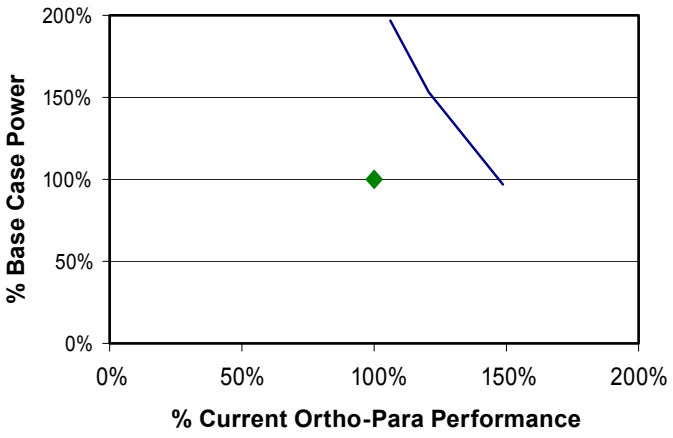


FIGURE 3. Ortho-Para Performance for Concept α

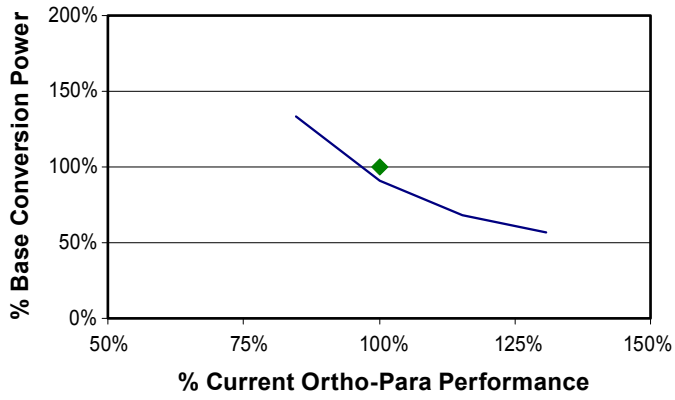


FIGURE 4. Ortho-Para Performance for Concept β

results in total power consumption below the base case power target. Concept β met the target required to be an economically viable process on an energy basis.

Process Equipment

Another way to improve the efficiency of hydrogen liquefaction is to improve the efficiency of the equipment used in the process. This includes compressors, turbines, and heat exchangers. Compression accounts for most of the power consumed by hydrogen liquefaction, so improvements in compressor efficiency can provide a significant benefit as discussed in the following. The impact of improving turbine or expander efficiency is small, but can reduce total power by about 2%. The impact of improving heat exchangers by reducing the pinch between hot and cold streams is even smaller than the impact of improving turbines.

Several different types of hydrogen compressor were evaluated. Reciprocating, screw, and centrifugal compressors were identified as being the most likely to apply to large-scale liquefaction. Metal hydride compressors were determined to be too small. Guided rotor and ionic liquid compressors were

determined to be in the developmental stage. Diaphragm compressors were unlikely to meet the capital cost target. Axial and shock wave compressors were determined to be a poor fit for a low molecular weight gas like hydrogen.

Table 2 shows some characteristics of the different types of compressor considered.

Screw compressors were expected to offer the lowest capital cost, but were also likely to have smaller capacity and lower efficiency. Reciprocating compressors offer larger size and higher efficiency, but at a higher initial cost and higher maintenance cost. Centrifugal compressors are expected to offer higher flow, lower maintenance cost, and similar efficiency compared to reciprocating machines.

Figure 5 shows the potential impact of improving compressor efficiency on the power consumption of the entire process assuming a base case with 80% adiabatic efficiency for all compressors. The main recycle compressor, which has three stages, consumes much more power than the low pressure recycle compressor, so improving its efficiency has a bigger impact on the total power. Improving the efficiency of each stage from 80 to 89%, the upper limit expected in Table 2, reduces total power by about 10%. Using an adiabatic efficiency value of 85%, closer to the middle of the range, reduces total power by about 6%.

Total Efficiency Improvement

The gains from each potential improvement discussed are additive; one does not reduce the ability to implement another. The total efficiency improvement is shown in the following:

TABLE 2. Hydrogen Compressor Options

Technology	Flow Range	First Cost	Relative Maintenance	Adiabatic Efficiency	Number of Units required	
	CFM				30 tpd	300 tpd
Screw	20,000	Low	Medium	70 to 75%	2	20
Reciprocating	40,000	High	High	83 to 89%	1	10
Centrifugal	80,000	Medium	Low	80 to 89%	1	5

tpd – tons per day

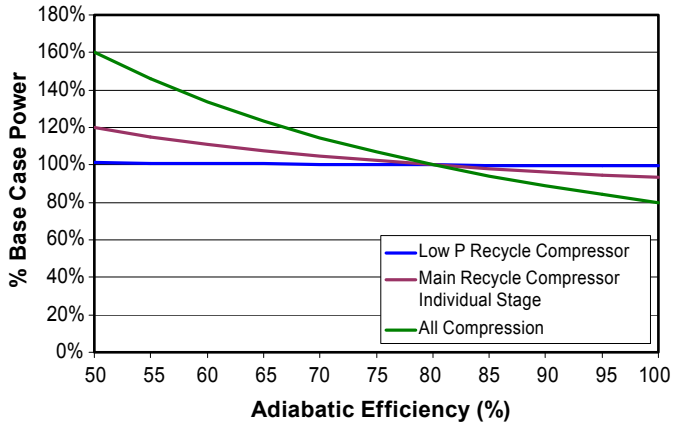


FIGURE 5. Effect of Compressor Efficiency on Total Power

Factor	Total Efficiency Improvement
Compressor Efficiency	6%
Turbine Efficiency	2%
Heat Exchanger Efficiency	<1%
Improved Liquefaction Process	2%
Improved Ortho-Para Conversion Process	5%
Total Efficiency Improvement	15%

The total efficiency improvement possible through using all of these methods is only 15%, less than the 20% goal of the project. Furthermore, each of these improvements potentially increases capital cost, making the goal of a 20% reduction in capital very unlikely to be possible for the highest efficiency process. Because of this result, the project was stopped after Phase II before completing the capital cost estimate.

Conclusions and Future Directions

- Improvements in overall process efficiency are possible through improved process equipment, improved process design, and an improved ortho-para conversion process.
- The total improvement is less than the project goal of 20%.
- Improvements are likely to add capital cost, making the other project goal of a 20% reduction in capital very unlikely.
- Ortho-para conversion performance was measured using laboratory and pilot reactors.
- The demonstrated performance is sufficient for at least one identified process concept to show reduced power cost when compared to hydrogen liquefaction processes using conventional ortho-para conversion.
- The impact of improved ortho-para conversion can be significant, but ortho-para conversion uses only about 20-25% of the total liquefaction power.
- Most of the energy used in liquefaction is for gas compression. Improvements in hydrogen compression will have a significant impact on overall liquefier efficiency.

FY 2011 Publications/Presentations

1. DOE Annual Hydrogen Review Meeting

Copyright © 2011 Praxair Technology, Inc.

This paper was written with support of the U.S. Department of Energy under Contract No. DE-FG36-08GO18063. The Government reserves for itself and others acting on its behalf a royalty-free, nonexclusive, irrevocable, worldwide license for Governmental purposes to publish, distribute, translate, duplicate, exhibit and perform this copyrighted report.

III.12 A Combined Materials Science/Mechanics Approach to the Study of Hydrogen Embrittlement of Pipeline Steels

P. Sofronis (Primary Contact), I. M. Robertson, D. D. Johnson
University of Illinois at Urbana-Champaign
1304 West Green Street
Urbana, IL 61801
Phone: (217) 333-2636
E-mail: sofronis@illinois.edu

DOE Managers
HQ: Scott Weil
Phone: (202) 586-1758
E-mail: Kenneth.Weil@ee.doe.gov
GO: Paul Bakke
Phone: (720) 356-1436
E-mail: Paul.Bakke@go.doe.gov

Contract Number: GO15045

Start Date: May 1, 2005
Projected End Date: December 31, 2011

Fiscal Year (FY) 2011 Objectives

- Mechanistic understanding of hydrogen embrittlement in pipeline steels in order to devise fracture criteria for safe and reliable pipeline operation under hydrogen pressures of at least 15 MPa and loading conditions both static and cyclic (due to in-line compressors).
- Explore suitable steel microstructures to provide safe and reliable hydrogen transport at reduced capital cost.
- Assess hydrogen compatibility of the existing natural gas pipeline system for transporting hydrogen.

Technical Barriers

This project addresses the following technical barriers from the Delivery section (3.2.4) of the Fuel Cell Technologies Program Multi-Year Research, Development and Demonstration Plan (Multi-Year RD&D Plan):

(D) High Capital Cost and Hydrogen Embrittlement of Pipelines

(G) Storage Tank Materials and Costs

(K) Safety, Codes and Standards, Permitting

Technical Targets

This project is conducting fundamental studies of hydrogen embrittlement of materials using both numerical simulations and experimental observations of the degradation mechanisms. Based on the understanding of the degradation mechanisms the project's goal is to assess the reliability of the existing natural gas pipeline infrastructure when used for hydrogen transport and suggest possible new hydrogen-compatible material microstructures for hydrogen delivery. These studies meet the following DOE technical targets for Hydrogen Delivery as mentioned in Table 3.2.2 of the Multi-Year RD&D Plan:

- Pipelines: Transmission–Total capital investment will be optimized through pipeline engineering design that avoids conservatism. This requires the development of failure criteria to address the hydrogen effect on material degradation (2012 target).
- Pipelines: Distribution–Same cost optimization as above (2012 target).
- Pipelines: Transmission and Distribution–Reliability relative to H_2 embrittlement concerns and integrity, third party damage, or other issues causing cracks or failures. The project's goal is to develop fracture criteria with predictive capabilities against hydrogen-induced degradation (2017 target). It is emphasized that hydrogen pipelines currently in service operate in the absence of design criteria against hydrogen-induced failure.
- Off-Board Gaseous Hydrogen Storage Tanks (tank cost and volumetric capacity)–Same cost optimization as in Pipelines: Transmission above. Current pressure vessel design criteria are overly conservative by applying conservative safety factors on the applied stress to address subcritical cracking. Design criteria addressing the hydrogen effect on material safety and reliability will allow for higher storage pressures to be considered (2015 target).

FY 2011 Accomplishments

- Discovered the nature and characteristics of the hydrogen degradation mechanisms of two promising microalloyed, low-carbon steel microstructures designated as B[1] and D[2] hereafter. The samples were provided by the DGS Metallurgical Solutions, Inc. The mechanisms of fracture were identified by using focused ion beam (FIB) machining to lift-out sections from fracture surfaces along with transmission electron microscopy (TEM) analysis of the extracted thin foils.

[1] Steel B is a typical low carbon (0.05% by wt.) Mn-Si-single microalloy API/Grade X70/X80 capable of producing a ferrite/acicular microstructure. The alloy was found to perform well in sour natural gas service.

[2] Steel D is a typical low carbon (0.03% by wt.) Mn-Si-single microalloy API/Grade X60, a predominantly ferrite microstructure with some pearlite. The alloy was found to perform very well in sour natural gas service.

- Identified the microstructure of pipelines steels through optical analysis, scanning electron microscopy (SEM), transmission electron microscopy (TEM), and identified particle composition through energy dispersive spectroscopy (EDS) for: a) laboratory specimens from Air-Liquide, Air Products, and Kinder-Morgan industrial pipelines; b) new microalloyed, low-carbon steels from Oregon Steel Mills provided by DGS Metallurgical Solutions, Inc.
- Developed a model for predicting hydrogen-induced fracture on the basis of the fracture mechanism acting at the microscale.
- Investigated the mechanism of fatigue fracture of 304 and 316 stainless steel in a hydrogen environment through FIB/TEM analysis. Unique localized martensitic lath bands were identified underneath the fracture surface.
- Augmented our modeling and simulation capabilities of transient hydrogen transport to account for the mechanical deformation and hydrogen-induced grain boundary decohesion in high strength steels. Predictions have been made of threshold stress intensities associated with subcritical crack growth.



Introduction

Hydrogen is a ubiquitous element that enters materials from many different sources. It almost always has a deleterious effect on material properties. The goal of the project is to develop and verify a lifetime prediction methodology for failure of materials used in pipeline systems and welds exposed to high-pressure gaseous environments. Development and validation of such predictive capability and strategies to avoid material degradation is of paramount importance to the rapid assessment of the suitability of using the current pipeline distribution system for hydrogen transport and of the susceptibility of new alloys tailored for use in hydrogen related applications.

We focused our effort on analyzing the fracture mechanisms of two promising steel microstructures (microalloy steels B and D) with large fracture resistance to hydrogen degradation. We also advanced our studies of the fracture mechanisms of 304 and 316 stainless steel samples fatigued in a hydrogen environment. Accounting for the identified hydrogen-induced fracture mechanisms, void growth at slip band intersection, we employ a tested model of the hydrogen-deformation interactions to develop a simulation tool for pipeline crack behavior with predictive capabilities.

Approach

Our approach integrates mechanical property testing at the microscale, microstructural analyses and TEM observations of the deformation processes of materials at the micro- and nano-scale, first principle calculations of interfacial cohesion at the atomic scale, and finite element modeling and simulation at the micro- and macro-level.

To understand the hydrogen-induced fracture processes, we use high resolution SEM with three-dimensional (3-D) visualization and TEM studies of samples taken from just below the fracture surface by the lift-out technique using FIB machining. We investigate the interaction of hydrogen transient transport kinetics with material elastoplastic deformation ahead of an axial crack either on the internal diameter (ID) or outer diameter (OD) surface of a pipeline. Using finite element simulations of the hydrogen transport in the neighborhood of the crack tip, we explore the transient and steady state hydrogen population profiles and how their development influences the fracture processes/events.

Results

Identification and Characterization of the Fracture Mechanisms

The study of the fractured surfaces of our compact tension specimens of B and D type steels revealed several distinct morphologies (such as feathery region, ductile ridges, and featureless flat areas) which were not observed in the overload fracture of compact tension specimens in the absence of hydrogen. The feathery region and ductile ridges were analyzed (see 2010 annual progress report) using high resolution SEM, 3-D visualization, and TEM studies of samples taken from just below the fracture surface by the lift-out technique using FIB machining. The analysis suggested that hydrogen-induced fracture mechanism is governed by dislocation slip activity [1].

In order to understand the fracture processes, we further studied the featureless flat regions of the fractured surfaces. The 3-D visualization demonstrated that the featureless surfaces are not really flat but are undulating. Figure 1a shows the high resolution SEM image of the flat surfaces. The micrograph reveals that those undulations are covered with very small rounded mounds. The roughness of the surfaces is confirmed by atomic force microscopy measurements. Our TEM analysis of the lift-out sections beneath the featureless flat regions shows enormously high dislocation densities (Figure 1b). These observations demonstrably confirm that severe plastic processes control the fracture of these pipeline steels in a hydrogen environment [2].

The identification of the precise mechanism of hydrogen-induced fracture in pipeline steel materials serves all objectives of the project.

Identification and Characterization of Fatigue Mechanisms

Along with the characterization of specimens fractured under monotonic or static loading, similar analysis was carried out for 304 and 316 stainless steel samples fatigued

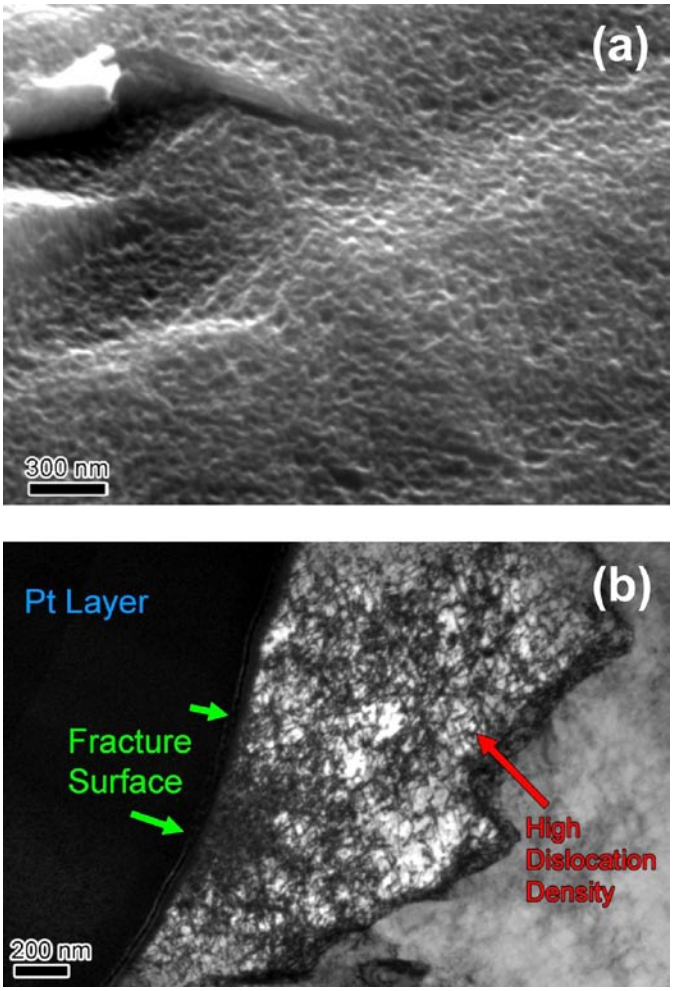


FIGURE 1. a) High-magnification SEM image of flat feature which shows that the flat surface in actuality is heavily dimpled. b) TEM micrograph showing the microstructure immediately beneath the flat features on the fracture surface. Image shows a high dislocation density suggesting that the fracture process is related to dislocation slip. The grains below the one shown have similar dislocation densities suggesting plasticity occurred not just immediately below the fracture surface.

in a hydrogen environment. Figure 2 shows the striations on the fractured surface which mark the progression of the fatigue crack with cycling. TEM analysis of sample extracted perpendicular to striations shows three sets of intersecting deformation bands (Figure 3). A large amount of plastic deformation, both in the bands and in the matrix, is visible. It appears that the bands intersect the surface at the striations, but further analysis is needed to confirm this. Diffraction analysis suggests that these bands are martensite laths which are localized closer to the crack tip with increasing hydrogen. This would suggest that with increasing hydrogen, martensite formation is localized closer to crack tip and produced in finer laths, which would be less visible to techniques such as electron backscatter diffraction. This is in agreement with the results of Mine et al. [3] who

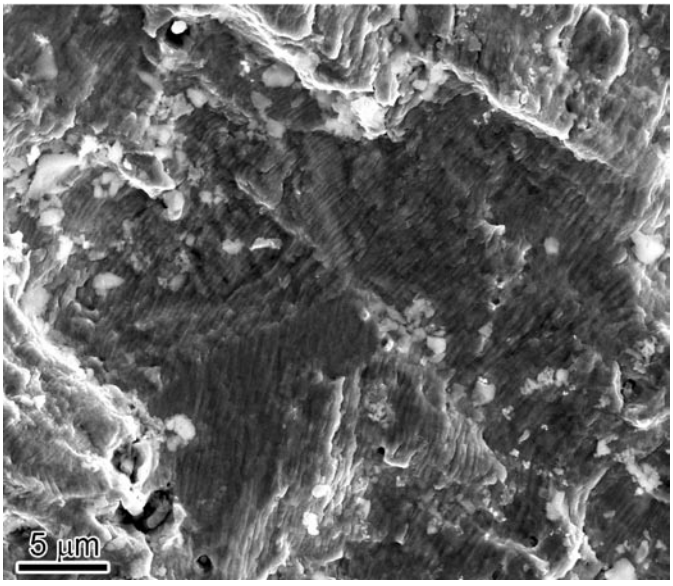


FIGURE 2. SEM image showing striations, a typical feature on fatigue surfaces, on the fracture surface of a 304 stainless steel sample fatigued under hydrogen atmosphere. A sample was extracted perpendicular to the marking and examined in the TEM.

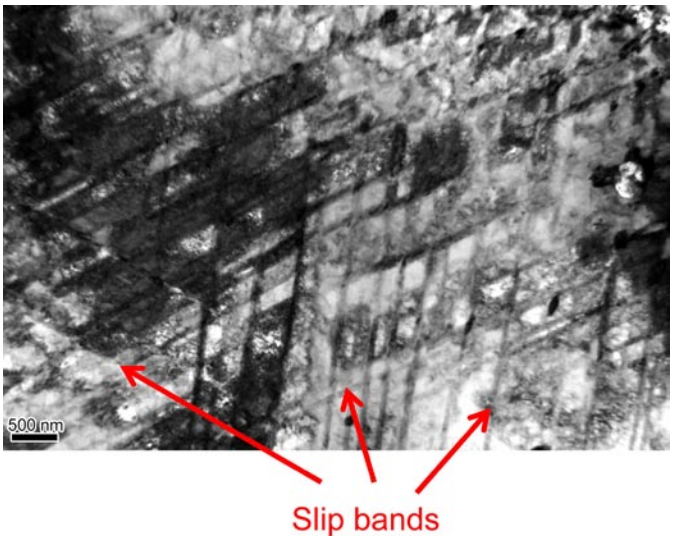


FIGURE 3. TEM micrograph showing the microstructure immediately beneath the fatigue fracture surface. The intersecting sets of deformation bands are visible. These features continue for several microns below the fracture surface.

observed the decrease in deformation induced martensite with increasing hydrogen saturation.

To further understand this phenomenon, we are investigating samples extracted by the FIB in a different way. From fatigued but unfractured specimens of the 304 and 316 steels, samples were extracted perpendicular to the polished surface and perpendicular to the crack in locations

identified to likely be similar to the striations observed on the fracture surface. This method will enable the observation of the microstructure directly ahead of the crack tip and possibly confirm that the microstructure is universal.

Micro- and Macro-Modeling and Simulation

The hydrogen-induced fracture mechanism of B and D type of steel pipelines under rising load has been identified as void nucleation and growth at slip band intersections [1]. We use a continuum mechanics description of the dislocation slip bands to investigate the conditions for a microcrack and then a void to be formed at slip band intersections in the hydrogen environment ahead of a crack tip.

We model the process by simulating the pile-up formation and interaction as shown in Figure 4. The simulation involves hydrogen-induced increased dislocation activity and interaction of dislocations with the applied load. We assume that fracture occurs when the energy of the system with a void forming at the intersection of the pile-ups is less than the energy in the absence of the void. The insertion of a void is considered energetically expensive due to the surface energy creation. We designate the stress intensity factor at which void formation occurs as a descriptor of the fracture resistance of the material to hydrogen embrittlement. This is one of the main project objectives, that is, to come up with a fracture criterion for these steels that is predicated on the underlying fracture mechanism acting at the microscale. The predictions will be compared with results obtained at Sandia Laboratories from rising load fracture toughness testing with B and D steels.

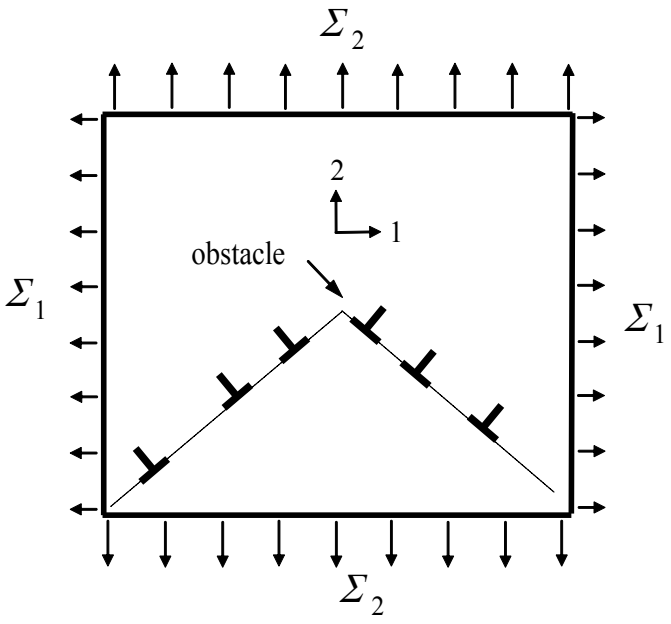


FIGURE 4. Schematic of the unit cell used for the modeling of the microcrack/void formation at the intersection of pile-ups. The cell is under applied macroscopic stress characteristic of the crack tip stress environment.

In order to understand the hydrogen/fatigue interactions, we developed a crystal plasticity constitutive model that accounts for the effect of hydrogen on the activation and operation of the slip systems. The face-centered cubic material version of the model has been implemented in the general purpose finite element code ABAQUS through a User Material subroutine. We are investigating the response of a crack whose tip is within a single grain to understand the material's response under cyclic loading. The development of a criterion for hydrogen-induced fatigue onset is also a central objective of our project.

The simulations described in this section are meeting all objectives of our project.

Conclusions and Future Directions

- In collaboration with Sandia National Laboratories, we carried out fracture testing of promising micro-alloyed, low-carbon steel microstructures. Our TEM analysis of lift-out sections beneath the fracture surface shows slip bands parallel to ridge edges, suggesting a fracture mechanism completely governed by dislocation slip. Such enhanced and confined slip activity is consistent with the hydrogen-induced localized plasticity mechanism for hydrogen embrittlement. This discovery of intense hydrogen-induced slip band formation also leads to the recognition that the coining of the term "quasi-cleavage" is misleading as it denotes cleavage events for a fracture that is controlled clearly by dislocation processes.
- In collaboration with the International Institute for Carbon Neutral Energy Research and the Institute for Hydrogen Industrial Use and Storage of Japan, we performed fatigue testing of stainless steel specimens in hydrogen environment. We analyzed the microstructure beneath the fracture surface and identified localized martensitic lath bands. This fatigue fracture testing is used for the damage tolerance assessment under cyclic pressure conditions.
- We model the discovered mechanism of failure, void nucleation and growth at slip band intersections, and implement the result in our finite element codes to simulate and predict onset of crack propagation under gaseous hydrogen transport at fixed pressure (static conditions). The results have been used to develop a fracture criterion for pipeline safe operation in terms of the hydrogen pressure, geometric, and material characteristics of the pipeline.
- We continue our collaboration with the International Institute for Carbon Neutral Energy Research and the Institute for Hydrogen Industrial Use and Storage of Japan. We participate in the annual meetings of the automobile Industry of Japan (Toyota, Honda, Nissan) on hydrogen technology standards.

Special Recognitions & Awards

1. P. Sofronis visited Japan from June 9 to June 25, 2006 as a fellow of the Japan Society for the Promotion of Science (JSPS) to collaborate on research related to hydrogen/material compatibility.

2. P. Sofronis and I. M. Robertson were invited speakers at the *International Hydrogen Energy Development Fora* organized by HYDROGENIUS at Fukuoka, Japan on January 31 – February 1, 2007, February 4-8, 2008, February 4-6, 2009, February 3–4, 2010, February 2-3, 2011.

3. P. Sofronis was elected to a fellow of the American Society of Mechanical Engineers (ASME) for his contributions to the field of hydrogen embrittlement.

4. P. Sofronis and I. M. Robertson received the 2011 Delivery Team Award from the Hydrogen and Fuel Cells Program of the U.S. Department of Energy.

FY 2011 Publications/Presentations

Publications

1. Robertson, I.M., Fenske, J., Martin, M., Bricena, M., Dadfarnia, M., Novak, P., Ahn, D.C., Sofronis, P., Liu, J.B., Johnson, D.D. (2010) "Understanding How Hydrogen Influences the Mechanical Properties of Iron and Steel." In Proceedings of the 2nd International Symposium on Steel Science.

2. Stalheim, D., Boggess, T., San Marci, C., Jansto, S., Somerday, B., Muralidharan, G., Sofronis, P. (2010) Microstructure and Mechanical Property Performance of Commercial Grade API Pipeline Steels in High Pressure Gaseous Hydrogen, Proceedings of IPC 2010 8th International Pipeline Conference, September 27 – October 1, 2010, Calgary, Alberta, Canada.

3. Martin, M., Fenske, J., Sofronis, P., Robertson, I.M. (2011), On the Formation and Nature of Quasi-Cleavage Fracture Surfaces in Hydrogen Embrittled Steels, Acta Materialia, 59 (4), 1601-1606.

4. Martin, M., Robertson, I.M., Sofronis, P. (2011) Interpreting Hydrogen-Induced Fracture Surfaces in Terms of Deformation Processes–A New Approach, Acta Materialia, 59 (9), 3680-3687.

5. Dadfarnia, M., Sofronis, P., Somerday, B.P., Balch, D.K., Schembri, P., and Melcher, R.J., (2011) On the Environmental Similitude for Fracture in the SENT Specimen and a Cracked Hydrogen Gas Pipeline, Engineering Fracture Mechanics, 78(12), 2429-2438.

6. Dadfarnia, M., Sofronis, P., Somerday, B.P., Balch, D.K., and Schembri, P. (2011) Degradation Models for Hydrogen Embrittlement. In: "Gaseous Hydrogen Embrittlement of High Performance Metals in Energy Systems." eds. R.P. Gangloff and B.P. Somerday.

Presentations

1. Martin, M.L., Robertson, I.M., Somerday, B., San Marchi, C., and Sofronis, P. (2010) Multi-scale Investigation of Hydrogen-Assisted Failure of X60 Pipeline Steel, Platform Talk, Microscopy and Microanalysis 2010 Meeting, August 1–5, 2010, Portland, OR.

2. Dadfarnia, M., Sofronis, P., Somerday, B.P., Balch, D.K., and Schembri, P. (2010) On Modeling Hydrogen-Induced Sustained-Load Intergranular Cracking, 47th Annual Technical Meeting, Society of Engineering Science, Ames, Iowa, October 4–6, 2010.

3. Martin, M.L., Robertson, I.M., Somerday, B., San Marchi, C., and Sofronis, P. (2010) Multi-scale Investigation of the Hydrogen-Assisted Failure of X60 Pipeline Steel, Platform Talk, Materials Science and Technology 2010 Conference and Exhibition, October 17–21, Houston, TX.

4. Dadfarnia, M. and Sofronis, P. (2011) Understanding Brittle Fracture in the Presence of Plasticity, ExxonMobil Research and Engineering Company, January 25, Clinton, NJ.

5. Dadfarnia, M., Martin, M., Sofronis, P., Robertson, I.M., Somerday, B.P., Balch, D.K., and Schembri, P. (2011) Mechanisms and Models of Hydrogen-Induced Cracking, HYDROGENIUS and I^{2}CNER Research Symposium, Fukuoka, Japan, February 3, 2011.

6. Sofronis, P., Dadfarnia, M., Martin, M.L., Robertson, I.M. (2011) Micromechanics of Hydrogen-induced Fracture: from Experiments and Modeling to Prognosis, Invited presentation in the 2011 Hydrogen Metal Systems Gordon Research Conference, Stonehill College, Easton, Massachusetts, July 17–22.

7. Martin, M.L., Robertson, I.M., Sofronis, P., and Murakami, Y. (2011) A Microstructural Based Understanding of Hydrogen-Enhanced Fatigue of Stainless Steels, Platform Talk, Materials Science and Technology 2011 Conference and Exhibition, Accepted for presentation in October 16, Columbus, OH.

References

1. Martin, M., Fenske, J., Sofronis, P., Robertson, I.M. (2011), On the Formation and Nature of Quasi-Cleavage Fracture Surfaces in Hydrogen Embrittled Steels, Acta Materialia, 59 (4), 1601-1606.

2. Martin, M., Robertson, I.M., Sofronis, P. (2011) Interpreting Hydrogen-Induced Fracture Surfaces in Terms of Deformation Processes–A New Approach, Acta Materialia, 59 (9), 3680-3687.

3. Mine, Y., Narazaki, C., Murakami, K., Matsuoka, S., Murakami, Y. (2009) Hydrogen Transport in Solution-Treated and Pre-strained Austenitic Stainless Steels and Its Role in Hydrogen-Enhanced Fatigue Crack Growth, International Journal of Hydrogen Energy, 34, 1097-1107.

III.13 Composite Technology for Hydrogen Pipelines

Barton Smith (Primary Contact), Barbara J. Frame and Lawrence M. Anovitz
Oak Ridge National Laboratory
P.O. Box 2008
Oak Ridge, TN 37831
Phone: (865) 574-2196
E-mail: smithdb@ornl.gov

DOE Manager
Scott Weil
Phone: (202) 586-1758
E-mail: Kenneth.Weil@ee.doe.gov

Start Date: January 2005
Project End Date: Project continuation and direction determined annually by DOE

Fiscal Year (FY) 2011 Objectives

- Investigate the use of composite pipeline technology (i.e., fiber-reinforced polymer [FRP] matrix composite pipelines) for transmission and distribution of hydrogen, to achieve reduced installation costs, improved reliability and safer operation of hydrogen pipelines.
- Evaluate current composite pipeline liner materials with respect to their performance as a hydrogen barrier; consider the hydrogen permeabilities of the materials to determine the degree of improvement (if any) that is necessary, and propose a path forward based on the available liner materials and modifications or treatments.
- Assess joining methods for composite pipelines.
- Determine integrated sensing and data transmission needs pipelines to provide health monitoring and operational parameters; report on state of the art in structurally integrated sensing and data transmission.

Technical Barriers

This project addresses the following technical barriers from the Hydrogen Delivery section (3.2.4.2) of the Fuel Cell Technologies Program (FCT) Multi-Year Research, Development and Demonstration Plan:

(D) High Capital Cost and Hydrogen Embrittlement of Pipelines

Technical Targets

The long-term project objective is to achieve commercialization and regulatory acceptance of FRP pipeline technology for hydrogen transmission and distribution. Accordingly, the project tasks address the challenges associated with meeting the DOE hydrogen delivery performance and cost targets for 2017 [1]:

- Transmission pipeline total capital cost: $490k per mile
- Distribution pipeline total capital cost: $190k per mile
- Hydrogen delivery cost: <$1.00/gasoline gallon equivalent (gge)
- Transmission and delivery reliability: acceptable for H_2 as a major energy carrier
- Hydrogen pipeline leakage: <0.5% (leakage target is currently under review by the Delivery Tech Team)

FY 2011 Accomplishments

- Completed tests on aging of glass reinforcement fibers in high-pressure hydrogen, and tensile tests indicate that long-term exposures to high-pressure hydrogen has a negligible effect on the strength of the fibers.
- Began cyclic fatigue testing on FRP pipeline specimen using cyclical hydrogen pressurization to pipeline maximum allowable working pressure. Measurements of the pressure-stress relationship and hydrogen leakage rate will provide information on liner collapse resistance and crack propagation, reinforcement layer resistance to micro-cracking, crazing, crack propagation, fiber-resin interface failure, and integrity of joint sealing.



Introduction

Pipelines could be a feasible long-term solution for delivering large quantities of gaseous hydrogen over long distances and distributing it in urban and rural settings. However, there are hydrogen compatibility issues in steel pipelines, and the capital costs for pipeline installation must be dramatically reduced. Composite pipeline technology is a promising alternative to low-alloy high-strength steel pipelines from both performance and cost considerations. For instance, FRP pipelines are engineered composite pipelines that are widely used in upstream oil and gas operations and in well interventions. FRP pipelines typically consist of an inner non-permeable liner that transports the fluid (pressurized gas or liquid), a protective layer applied to the liner, an interface layer between the protective layer and the reinforcement layers, multiple glass or carbon fiber reinforcement layers, an outer pressure barrier layer, and an outer protective layer. The pipeline has large burst and collapse pressure ratings, high tensile and compression strengths, and tolerates large longitudinal and hoop strains. Thousands of feet of continuous pipe can be unspooled and trenched as a seamless entity, and adjoining segments

of pipeline can be joined in the trench without welding using simple connection techniques. The emplacement requirements for FRP pipelines are dramatically less than those for metal pipe; installation can be done in a narrower trenches using light-duty, earth-moving equipment. This enables the pipe to be installed in areas where right-of-way restrictions are severe. In addition, FRP pipe can be manufactured with fiber optics, electrical signal wires, power cables or capillary tubes integrated within its layered construction. Sensors embedded in the pipeline can be powered from remote locations and real-time data from the sensors can be returned through fiber optics or wires. This allows the pipeline to be operated as a smart structure, providing the unique advantage of lifetime performance and health monitoring.

Approach

The challenges for adapting FRP pipeline technology to hydrogen service consist of evaluating the constituent materials and composite construction for hydrogen compatibility, identifying the advantages and challenges of the various manufacturing methods, identifying polymeric liners with acceptably low hydrogen permeability, critiquing options for pipeline joining technologies, ascertaining the necessary modifications to existing codes and standards to validate the safe and reliable implementation of the pipeline, and determining requirements for structural health monitoring and embedded real-time measurements of gas temperature, pressure, flow rate, and pipeline permeation.

These challenges are being addressed by performing bench-scale tests of FRP pipelines and constituent materials to determine their long-time compatibility with hydrogen, identifying pipeline liner materials that exhibit good performance in hydrogen environments, evaluating current methods for pipeline joining with consideration of the unique requirements for hydrogen service, and assessing the state of the art in integrated sensing technologies for composite structures.

Results

We used a straightforward accelerated aging process to evaluate the possibility that hydrogen could weaken the load-bearing capability of the glass fibers that are used as reinforcement in glass fiber-reinforced pipelines being considered for hydrogen delivery. Designing a test to screen for hydrogen-induced failures in glass fibers is difficult because potential chemical incompatibilities are largely unknown and because the permeation of hydrogen into glass is typically 3 to 7 orders of magnitude smaller than it is in most polymers and metals. Previous studies of the effects of hydrogen on glasses have focused on the ability of the glasses to store hydrogen or on the tendency of hydrogen to produce attenuation centers in the glasses (e.g., as in optical fibers).

To assess possible hydrogen-induced changes in mechanical strength of the glass fibers, we measured fiber tensile strengths in boron-free e-glass fibers (Advantex® SE 1200 Type 30) before, during and after accelerated aging in a pressurized hydrogen reactor. Our accelerated aging protocol was based on the Arrhenius model for an activated process where the aging rate is proportional to $e^{-\lambda/kT}$, where λ is the activation energy, T is the aging temperature, and k is the Boltzmann constant. We aged the fibers in a 70 bar pressure of hydrogen at a temperature of 60°C, which were the maximum allowable working pressure and temperature of the FRP pipeline. There were no stressors other than high-pressure hydrogen (i.e., no oxygen, water, chemicals, untraviolet light). From previous measurements done by others and us, we know that simply heating the fibers to 60°C for long periods of time does not degrade their tensile strength when it is subsequently measured at room temperature. We included tensile tests of untreated control specimens to compare with the specimens treated in hydrogen.

We removed fibers from the reactor at intervals of 1, 5, 11, 20, 39 and 62 weeks of exposure to perform tensile tests on fiber specimens with gauge lengths of 25 mm. We tested 30-100 fibers of both the hydrogen exposed and control groups at each interval. The distribution of tensile strength can be approximated by the two-parameter Weibull distribution

$$P(\sigma) = 1 - \exp(-L/L_0[\sigma/\beta]\alpha)$$

where α is the shape parameter, β is the scale parameter, and L and L_0 are the fiber gauge and reference lengths. Figure 1 shows representative test results in Weibull coordinates for the shortest and longest hydrogen exposures.

Using the Weibull parameters determined from the tensile strength measurements performed at each exposure interval, we calculated survival probabilities for the hydrogen-treated and control fibers. These survival probabilities are plotted versus exposure duration in Figure 2. The large error bars in the survival probabilities are likely due to the presence of both surface and bulk flaws in the fibers. Funding and time constraints did not allow us to censor the strength data by doing fractographic analysis to identify the type of flaw in each fiber tested, which would have allowed us to separate the data by flaw type and thereby obtain Weibull distributions with straight-line slopes. Nevertheless, the survival probabilities for the treated and untreated fibers do not change qualitatively with aging, implying that there was no hydrogen-induced degradation in the fibers during the 62-week exposure duration.

Fatigue testing using high-pressure hydrogen pressure cycling is the basis for verifying that combination of hydrogen environment and pressure-induced stress does not adversely affect composite pipeline integrity and service life. The results of high-pressure cyclic fatigue tests provide information on pipeline integrity after repeated hydrogen gas pressurization-depressurization cycles [2].

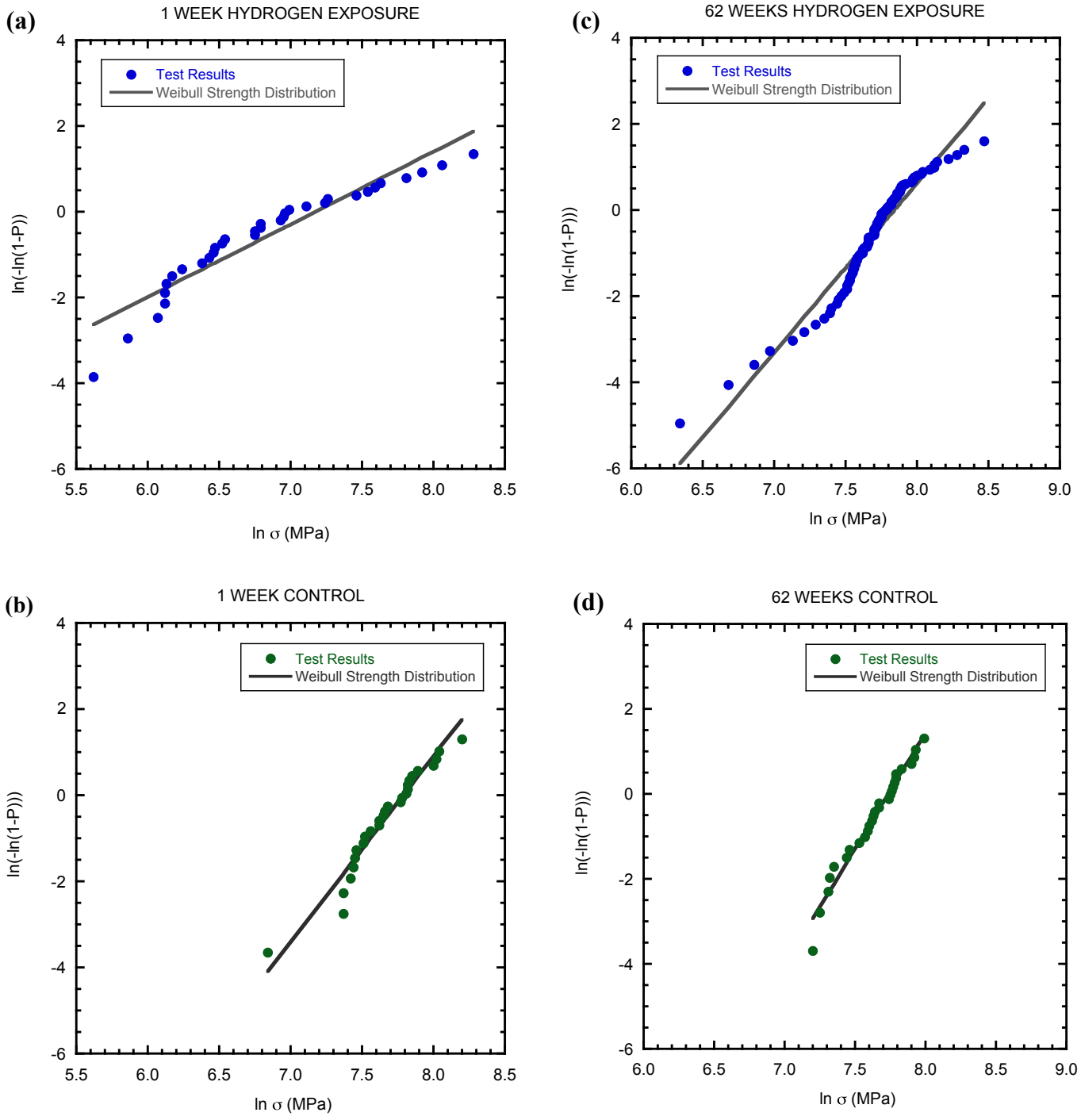


FIGURE 1. Representative test results in Weibull coordinates for fiber strengths measured following (a) 1-week and (c) 62-week hydrogen exposures. Circles are measured tensile strengths and the solid lines are the calculated Weibull distributions for the measured strengths. The corresponding tensile strength measurements for the control fibers are shown in (b) and (d).

Fatigue testing provides information that can't be derived from constant pressure testing, including liner collapse resistance (similar to blowdown testing), resistance to micro-cracking, crazing, crack propagation, fiber-resin interface failure, etc. of composite reinforcement layer, resistance to environmental stress-corrosion phenomena, and integrity of joint attachment/joint sealing under cyclic loading. We began cyclic fatigue testing of a Fiberspar glass-reinforced polymer pipeline in this project year and are on schedule to meet the milestone for this task, but the measurement results and analysis will not be completed until near the end of the

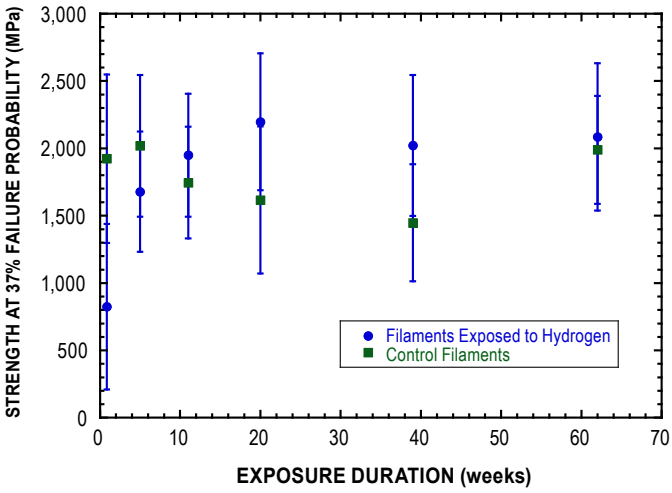


FIGURE 2. Survival probabilities of hydrogen-treated and untreated (control) fibers plotted versus accelerated aging duration. There was no statistically significant decrease in tensile strength during the 62-week exposure period.

fiscal year and will be reported in the last quarterly report of the year.

Conclusions and Future Directions

Conclusions from this year's work:

- E-glass fibers similar to those used as reinforcement in composite pipelines did not lose their tensile strength during a long-term exposure to high-pressure hydrogen gas. The intensity of the glass-fiber exposure was significantly higher than the actual exposure of fibers in the pipeline epoxy matrix and exceeded even a worst-case scenario. The conclusion reached is that e-glass should be durable in hydrogen service and the glass fibers should retain their mechanical function in a glass-fiber-reinforced pipeline during the anticipated hydrogen service lifetime.

During the remainder of this project year we expect to complete the first series of long-term stress rupture tests and report on the durability of the pipeline to further verify the expectation that composite pipelines can achieve the 2012 DOE H_2 transmission target of <$0.90/gge H_2:

- Our plans for the next project year are (1) to participate in the codification of fiber-reinforced (composite) pipelines in the American Society of Mechanical Engineers (ASME) B31.12 Hydrogen Piping Code by helping to identify and provide data needed to guide lifecycle management of composite pipelines, and (2) to monitor the performance of composite pipeline used to store hydrogen in a hydrogen and fuel cell market transformation project demonstration project at the Hawaii Natural Energy Institute. The opportunity to monitor the field demonstration of the pipeline is uncertain and is extremely contingent on funding and scheduling constraints. Nevertheless, the FCT program will have the chance to get initial real-world field data on the use of FRP pipe for hydrogen (e.g. pressure cycling, environmental exposure, and post-use microstructural analysis), which is particularly important as we begin to work with ASME on establishing a set of codes and standards for the commercialization of FRP (composite) pipelines.

FY 2011 Publications/Presentations

1. 2011 DOE Hydrogen Program Annual Merit Review – Arlington, Virginia – May 10, 2011, poster PD024.

References

1. HFCIT MYRDD Plan, Table 3.2.2, page 3.2–13, and footnote *b*, page 3.2-16.

2. *Qualification of Spoolable Reinforced Plastic Line Pipe*, API Recommended Practice 15S, First Edition, March 2006.

III.14 Thermodynamic Modeling of Rapid Low Loss Cryogenic Hydrogen Refueling

Salvador M. Aceves (Primary Contact), Gene Berry, Guillaume Petitpas, Tim Ross
Lawrence Livermore National Laboratory (LLNL)
7000 East Avenue, L-792
Livermore, CA 94551
Phone: (925) 422-0864
E-mail: saceves@llnl.gov

DOE Manager
HQ: Scott Weil
Phone: (202) 586-1758
E-mail: Kenneth.Weil@ee.doe.gov

Subcontractor:
Linde LLC, Hayward, CA

Start Date: October 1, 2009
Projected End Date: Project continuation and direction determined annually by DOE

Fiscal Year (FY) 2011 Objectives

- Demonstrate rapid refueling of cryogenic vessels.
- Refuel cryogenic vessels even when warm and/or pressurized.
- Refuel at high density (>80 kgH_2/m^3).

Technical Barriers

This project addresses the following technical barrier from the Delivery section of the Fuel Cell Technologies Program Multi-Year Research, Development and Demonstration Plan:

(J) Refueling Site Operations

TABLE 1. Progress toward Meeting DOE Hydrogen Delivery Technical Targets

Pressurized LH_2 pump				
DOE Targets for Forecourt Compressors	**Units**	**2010 Target**	**2015 Target**	**Pressurized LH_2 pump**
Reliability	-	Improved	High	High
Compression Energy Efficiency	%	94	95	95
Installed Capital Cost	k$/(kg/hr)	4	3	5
H_2 Fill Pressure	Peak psi	6,250	12,000	12,000

LH_2 – liquefied hydrogen

FY 2011 Accomplishments

- Developed model of vessel fill processes.
- Calculated final fill density as a function of initial vessel conditions (temperature, T, and pressure, p).
- Completed LH_2 pump contract negotiation with Linde LLC.



Introduction

Cryogenic pressure vessels have demonstrated highest performance for automotive hydrogen storage, with weight, volume, cost, and safety advantages [1,2]. One of the outstanding challenges for cryogenic pressure vessels is refueling. Today's hydrogen storage technologies (compressed and liquid hydrogen) operate at fixed temperature. Cryogenic pressure vessels, however, drift across the phase diagram depending on the level of use. The challenge is demonstrating rapid, inexpensive refueling that minimizes evaporative losses regardless of the initial thermodynamic state of the vessel.

Approach

We have identified a promising technology for cryogenic pressure vessel refueling: a liquid hydrogen pump. This pump takes LH_2 at low pressure (near atmospheric) and delivers it as high-pressure (200-880 bar) low temperature (30-50 K) high-density (>80 g/L) hydrogen that can be directly dispensed into a cryogenic pressure vessel, even when warm and/or pressurized. In this project we plan to install a LH_2 pump in the LLNL campus and demonstrate its virtues for rapid and efficient cryogenic vessel refueling.

Results

We have developed a model for vessel fill processes in an effort to evaluate the potential for future LH_2 pump high density refueling. Based on REFPROP [3], the model considers real gas hydrogen properties and enables quick calculation of relevant thermodynamic properties.

We start by considering a simplified case: a large forecourt vessel storing hydrogen at temperature T_i and pressure p_i. This vessel fills a (relatively small) vessel onboard a vehicle. The fill process is modeled with the first law of thermodynamics for open systems [4]:

$$Q + m_i h_i = U_f - U_o + m_e h_e + W \quad (1)$$

Mechanical work W is negligible for typical (rigid) pressure vessels, and we neglect heat transfer into the vessel Q as a first approximation. Mass flow out of the vehicle vessel m_e=0 during refueling, and the specific enthalpy h_i of the hydrogen flowing into the vessel is calculated at the conditions of the forecourt vessel (p_i, T_i), assumed constant due to its large relative size. The equation for the vehicle vessel therefore reduces to,

$$m_i h_i = U_f - U_o \quad (2)$$

Assuming an initially empty vessel with negligible thermal mass, the initial internal energy U_o=0. The final internal energy in the vehicle vessel $U_f = m_i u_f$, which leads to h_i=u_f, where u_f is the specific internal energy inside the vessel. From thermodynamics, $h_i \equiv u_i + p_i v_i = u_f$. The term $p_i v_i$, frequently named flow work, explains the heating that occurs when substances are forced into a vessel.

Figure 1 shows results for the fill process of an initially empty vessel with negligible thermal mass and heat transfer. The figure shows vessel temperature and density during the fill process as a function of pressure, for forecourt vessel conditions p_i=700 bar and T_i=100, 200, and 300 K. The figure shows that hydrogen flowing into the vehicle vessel heats substantially in the process, considerably reducing the vessel fill density. Temperature is nearly constant during the fill process, changing only slightly due to hydrogen's non-ideal behavior, especially at lower temperature. It is worth pointing out that hydrogen heats up as it flows into the vessel regardless of the value of the Joule-Thomson coefficient (negative at ambient temperature, near zero at 200 K, and positive at 100 K): vessel fill processes are not isenthalpic and therefore not controlled by the Joule-Thomson coefficient. Flow work plays the key role in understanding the process.

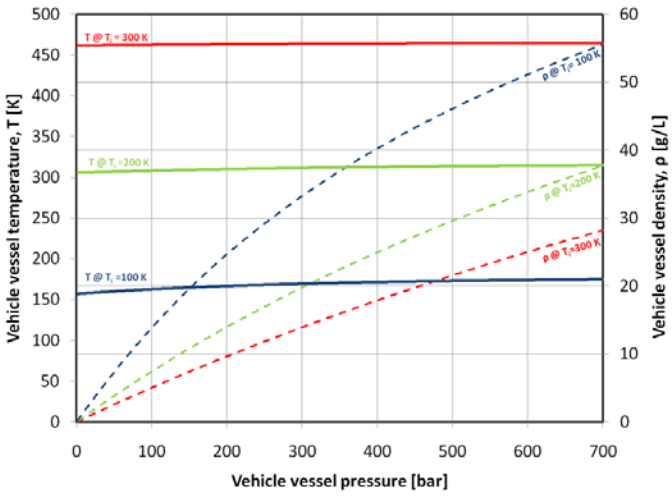


FIGURE 1. Automotive vessel temperature and density during the fill process as a function of pressure, for forecourt vessel conditions p_i=700 bar and T_i=100, 200, and 300 K, assuming an initially empty vessel with negligible thermal mass and heat transfer.

Results in Figure 1 can be generalized by varying p_i and T_i over broad ranges. Figure 2 shows vehicle vessel temperature (blue) and fill density (red), at the end of the refueling process, when pressure equilibrium is reached with the forecourt vessel (p=p_i), for an initially empty vessel with negligible thermal mass, for any combination of forecourt vessel pressure and temperature (p_i, T_i). As an example, assume that the forecourt vessel is filled with hydrogen at 100 K and 300 bar. From the figure, the vehicle vessel at the end of the fill process (when both vessels equilibrate at 300 bar) would be at 150 K and 40 g/L.

Figure 2 once again shows the considerable heating that occurs during the fill process. For an ideal gas with constant specific heat, heating is constant ($T = \gamma T_i$, where γ is the specific heat ratio c_p/c_v), and therefore temperature lines are fairly horizontal at low pressures and high temperatures. At higher pressures, deviations from ideality increase the heating. Minimum heating (minimum density losses) occurs at low temperature and pressure, where hydrogen's compressibility factor drops as hydrogen approaches liquid phase. This is observed by the 50 K blue line reaching a local maximum at ~50 bar.

Figure 2 also shows the exergy of the hydrogen inside the forecourt vessel (black lines). Exergy is defined as the minimum theoretical work necessary to compress and cool down hydrogen from the reference state (1 bar and 300 K) to any condition p_i, T_i in the diagram. Exergy is therefore an indication of the energy necessary for densifying hydrogen. Figure 2 shows that hydrogen compression is exergetically inexpensive compared to cooling: any level of densification from 10 to 60 g/L is achieved with minimum possible exergy by maximizing pressurization and minimizing cooling.

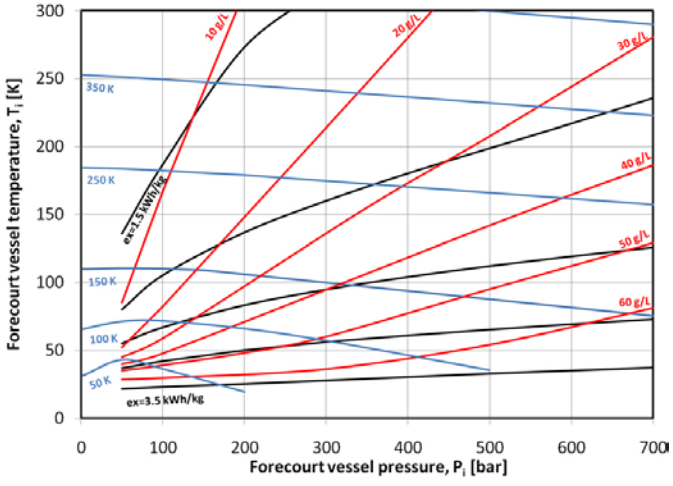


FIGURE 2. Vehicle vessel temperature (blue) and fill density (red), at the end of the refueling process, when pressure equilibrium is reached with the forecourt vessel (p=p_i), for an initially empty vessel with negligible thermal mass, for any combination of forecourt vessel pressure and temperature (p_i, T_i). The figure also shows the exergy of the hydrogen inside the forecourt vessel (black lines).

Hydrogen liquefaction is well known to be exergetically expensive (3.92-3.27 kWh/kg depending on whether para-ortho hydrogen conversion is included or not [5]). Investing energy in liquefaction, however, has the virtue of minimizing station energy consumption and capital cost, because liquid hydrogen can be pressurized with little exergy input as indicated by the nearly horizontal 3.5 kWh/kg exergy line (Figure 2).

The fact that pressurizing liquid hydrogen is exergetically inexpensive enables rapid compression and efficient densification with low evaporative losses. Demonstrating the potential for this technology is the purpose of this project. While LLNL moves forward issuing the pump contract and preparing for construction, we have applied our thermodynamic model to predict expected fueling performance.

Predicting pump refueling is similar to predicting vessel refueling, and Equation (2) still dominates the process. However, delivery temperature is a function of pump performance details, and it is therefore hard to predict. For this preliminary analysis, we estimate delivery temperature assuming *isentropic* compression from the forecourt Dewar with LH_2 saturated at 3 bar and 24.6 K. While real pumps will not reach this level of performance, final vessel density may be reasonably well approximated due to the low exergetic cost of LH_2 pumping.

Modeling results are shown in Figure 3, which shows hydrogen density after refueling (when the vehicle drives away from the fueling station) as a function of hydrogen density before refueling (when the vehicle drives into the refueling station), for multiple initial vessel temperatures (30 K, 50 K, 100 K, 200 K, and 300 K). Two sets of lines are shown: isentropic pump with negligible pressure vessel thermal mass (dashed); and isentropic pump including the vessel thermal mass, and assuming thermal equilibrium between vessel and hydrogen (solid lines).

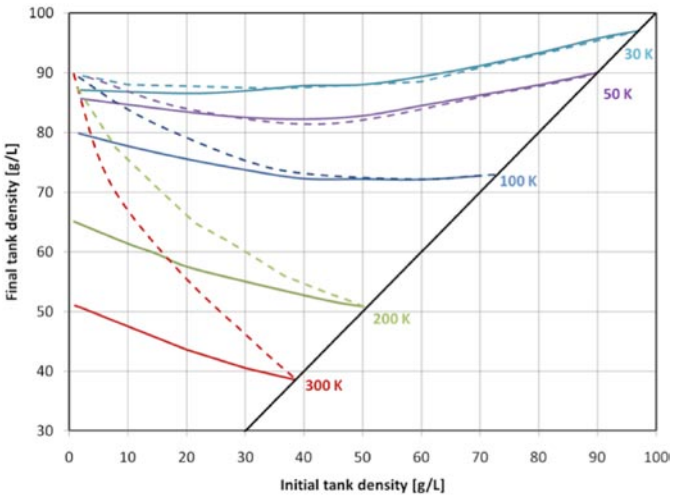


FIGURE 3. Hydrogen density after refueling (when the vehicle drives away from the fueling station) as a function of hydrogen density before refueling (when the vehicle drives into the refueling station), for multiple initial vessel temperatures (30 K, 50 K, 100 K, 200 K, and 300 K). Two sets of lines are shown: *isentropic* pump with negligible pressure vessel thermal mass (dashed); and *isentropic* pump including the vessel thermal mass, and assuming thermal equilibrium between vessel and hydrogen (solid lines).

Comparing dashed lines vs. solid lines in Figure 3 shows that vessel thermal mass plays a large role in fill density for warm, empty vessels. At very low temperatures (30-50 K), vessel thermal mass becomes very small, enabling high density refueling regardless of the initial fill level. An isentropic pump filling an initially cold and empty vessel may therefore enable ultimate densities beyond 85 g/L. Final densities beyond 90 g/L are obtained with very cold (30 K) nearly full vessels where the pump is essentially compressing low entropy H_2 already in the vessel.

The black diagonal line in the right of Figure 3 corresponds to a fully pressurized vessel at 700 bar. At this condition, no refueling is possible, and density after refueling equals density before refueling. Driving is necessary before refueling to reduce pressure and cool down the vessel.

In summary, the low exergetic cost of pumping LH_2 may lead to rapid and efficient refueling at high densities. Flow work is also lowest near the liquid phase (Figure 2) minimizing heating and density losses during vessel fill. Future experiments will reveal how closely real pump performance compares with the isentropic pump model.

Conclusions and Future Directions

- Rapid, low loss refueling of cryogenic vessels is possible through pressurized LH_2 dispensing.
- Modeling has revealed potential for high density refueling (85 g/L) for initially cold vessels.
- Model results need to be validated vs. future experimental results.

References

1. Aceves, S.M., Espinosa-Loza, F., Ledesma-Orozco, E., Ross, T.O., Weisberg, A.H., Brunner, T.C., Kircher, O., "High-density automotive hydrogen storage with cryogenic capable pressure vessels," International Journal of Hydrogen Energy, Vol. 35, pp. 1219-1226, 2010.

2. Ahluwalia, R.K. Hua, T.Q. Peng, J.-K. Lasher. S, McKenney. K. Sinha, J., Gardiner. M. "Technical assessment of cryo-compressed hydrogen storage tank systems for automotive applications," International journal of hydrogen energy, Vol. 35, pp. 4171–4184, 2010.

3. Lemmon, E.W., McLinden, M.O., Huber, M.L., "REFPROP: NIST reference fluid thermodynamic and transport properties," National Institute of Standards and Technology, 2004. NIST Standard reference database 23, version 7.1.

4. Van Wylen, G.J., Sonntag, R.E., "Fundamentals of Classical Thermodynamics," Wiley, New York, NY, 1978.

5. Peschka, W., "Liquid Hydrogen, Fuel of the Future," Springer-Verlag, Vienna, Austria, 1992.

FY 2011 Publications/Presentations

1. Hydrogen Storage in Cryogenic Capable Pressure Vessels, Salvador Aceves, Invited Presentation, University of Castilla la Mancha, Spain, March 2010.

2. Hydrogen Storage in Cryogenic Capable Pressure Vessels, Salvador Aceves, Invited Presentation, International Conference on Hydrogen Production and Storage, Istanbul, Turkey, June 2010.

3. High-density automotive hydrogen storage with cryogenic capable pressure vessels, Salvador M. Aceves, Francisco Espinosa-Loza, Elias Ledesma-Orozco, Timothy O. Ross, Andrew H. Weisberg, Tobias C. Brunner, Oliver Kircher, International Journal of Hydrogen Energy, Vol. 35, pp. 1219-1226, 2010.

4. Hydrogen Storage in Cryogenic Capable Pressure Vessels, Salvador Aceves, Invited Presentation, AICHE Topical Symposium on Hydrogen Production and Storage, Salt Lake City, October 2010.

5. Compact (L)H2 Storage with Extended Dormancy in Cryogenic Pressure Vessels, Salvador Aceves, Invited Presentation, International Conference on Sustainable Energy Storage, Belfast, Northern Ireland, UK, February 2011.

6. Cryogenic Hydrogen Storage, Delivery, and Safety, Salvador Aceves, Invited Presentation, Annual Congress of the Mexican Society of Mechanical Engineers, San Luis Potosi, Mexico, September 2011.

III.15 Integrity of Steel Welds in High-Pressure Hydrogen Environment

Zhili Feng (Primary Contact), Jy-An Wang, Fei Ren, Larry Anovitz and Wei Zhang
Oak Ridge National Laboratory (ORNL)
1 Bethel Valley Rd., PO Box 2008, MS 6095
Oak Ridge, TN 37831
Phone: (865) 576-3797
E-mail: fengz@ornl.gov

DOE Manager
HQ: Scott Weil
Phone: (509) 737-7346
E-mail: Kenneth.Weil@ee.doe.gov

Project Start Date: March 1, 2004
Project End Date: September 30, 2011

Fiscal Year (FY) 2011 Objectives

- Develop and demonstrate cost-effective welding technology that can mitigate hydrogen embrittlement (HE) concerns in constructing new pipelines and converting existing pipelines for high-pressure hydrogen delivery.
- Quantify the effects of welding and joining on the resistance to HE of high-strength pipeline and other structural steels under high-pressure hydrogen.
- Develop the technical basis and guidelines to manage the weld region to ensure structural integrity and safety of hydrogen delivery systems.
- Determine the hydrogen transport behavior (such as diffusion, trapping, etc.) in steels.

Technical Barriers

This project addresses the following technical barriers from the Hydrogen Delivery section of the Fuel Cell Technologies Program Multi-Year Research, Development and Demonstration Plan:

(D) High Capital Cost and Hydrogen Embrittlement of Pipelines

(K) Safety, Codes and Standards, Permitting

Technical Targets

This project aims at developing the scientific understanding, technical basis and cost-effective engineering solutions to control and mitigate hydrogen embrittlement in the weld region of steel pipelines and other high-pressure hydrogen delivery infrastructure systems. Insights gained from this project will be applied toward the hydrogen delivery infrastructure that meets the following DOE 2017 hydrogen pipeline delivery technical targets:

- Capital cost: $490K/mile for transmission, and $190K/mile for distribution pipeline.
- Reliability/Integrity: Acceptable for H_2 as a major energy carrier.
- Cost of delivery of hydrogen <$1.00/gasoline gallon equivalent (gge).

FY 2011 Accomplishments

- Baseline high-pressure hydrogen permeation measurements established the effects of weld microstructure, surface conditions, temperature and hydrogen pressure on hydrogen permeation, diffusion and trapping in selected pipeline steels.
- The in situ spiral notch torsion test (SNTT) and the associated finite element fracture mechanics modeling were applied to quantify the fracture toughness degradation of steel welds exposed to high-pressure hydrogen. For American Iron & Steel Institute (AISI) 4340 high-strength steel, a common material for hydrogen storage tank, preliminary testing results showed the fracture toughness of weld region in high-pressure hydrogen is as low as 25% of that in air (i.e., a degradation of 75%).
- Preliminary multi-notch tensile testing of American Petroleum Institute (API) 5L Grade X-65 pipeline steel in hydrogen showed encouraging results for the improved resistance to HE achieved by friction stir welding (FSW). Additional tests on X-65 FSW are ongoing and are expected to be completed by September-November 2011 timeframe.



Introduction

The hydrogen energy delivery infrastructure will require extensive use of steels and other cost-effective structural materials under high-pressure gaseous hydrogen exposure. For example, high-pressure (up to 3,000 psi) hydrogen pipelines are presently considered to be one of the most cost-effective and energy-efficient means to transport very large amounts of hydrogen to much of the market as is done for natural gas [1]. Under high hydrogen pressures, there are concerns about HE of steel pipelines and its potentially catastrophic consequences [2]. Concerns on HE are not limited to steel pipelines; according to a recent DOE Basic Energy Science report [3], HE needs to be addressed for a variety of hydrogen storage and delivery systems made of metallic materials that are exposed to hydrogen.

As in the case of natural gas and other energy carrier transmission pipelines, welding will be used to construct steel pipelines for high-pressure hydrogen delivery. Welding will also be widely used in fabrication of other system components for hydrogen production, storage, and delivery. However, welds in pipeline steels and other engineering materials are often the most susceptible regions to HE due to the formation of unfavorable microstructures and high tensile residual stresses. Furthermore, the weld region typically has substantially lower resistance to hydrogen crack initiation and higher crack growth rates, when compared to the baseline pipeline steel (base metal). In this regard, the weld region is oftentimes the weakest link for the structural integrity and safety of hydrogen pipelines and hydrogen delivery infrastructure. A systematic approach to deal with weld property degradation under high-pressure hydrogen exposure is critical to ensure the safe, cost-effective operation and long-term reliability of the hydrogen delivery infrastructure. Insights gained from this project will provide the scientific and technical basis for hydrogen pipelines that meet relevant DOE 2017 technical targets on total capital investment and reliability/integrity.

Approach

Currently, there exists only a limited amount of knowledge on the diffusion rate and amount of hydrogen in steels under high-pressure gaseous environment relevant to the hydrogen delivery infrastructure. Therefore, the first major effort of this project is directed toward the systematical study of (1) high-pressure H_2 permeation behavior in steels and their welds, and (2) the tolerance level to hydrogen of different steels before considerable mechanical property degradation would occur. A special hydrogen permeation testing system has been developed to test H_2 permeation and diffusion in coupon-size steel discs under high pressure (up to 5,000 psi). The effect of steel composition, microstructure, and sample surface conditions on H_2 transport behavior is studied.

As discussed earlier, the weld joint in steel pipeline is expected to be a critical region highly susceptible to HE due to the existence of unfavorable microstructure and high tensile residual stresses. Hence, the second major activity of this project focuses on generating weld property data for fracture-mechanics based pipeline design. To account for the highly inhomogeneous nature of the weld region, two special tests have been developed and validated. A tensile test is used for relative ranking of weld microstructure susceptibility to HE, while the spiral notch torsion test is used for quantifying fracture toughness degradation in steel welds.

The third major effort involves the development and validation of new welding technology for H_2 delivery steel pipelines. In particular, solid-state FSW is evaluated for improved mechanical property and reduced cost for pipeline construction and repair.

Results

The results achieved in this FY (2011) are highlighted as follows.

Quantitative Understanding of Hydrogen Embrittlement in Steel Weld Using In Situ SNTT

Although they may work for testing of base metal in hydrogen, current standard methods such as compact tension for testing hydrogen-induced mechanical property degradation have shown to be inadequate when applied to the weld due to the highly inhomogeneous microstructure and property gradients of the weld region [4]. Special, miniature and self-loading devices for in situ mechanical testing in high-pressure hydrogen were designed and fabricated previously. The FY 2011 activity is focused on fracture toughness measurement of welds exposed to a high-pressure gaseous hydrogen environment using in situ SNTT.

Figure 1 shows the in situ device for fracture toughness testing in high-pressure hydrogen. In the test, the specimen with a spiral notch is loaded in the load frame where a pure torsional load is applied to the specimen. The load frame containing the pre-stressed specimen is placed inside a high-pressure vessel. The strain gages attached to the load frame are connected to the data acquisition box via feedthroughs in the vessel cover/lid. After the assembly, the vessel is tightly sealed and is charged with hydrogen gas to the desired pressure (typically around 1,900 psi or 13.1 MPa). During the test, the strain gage readings are monitored for the variation of torsional load on the specimen, which is an indicator for hydrogen-induced cracking initiation. As the hydrogen permeation in steel can be slow at room temperature, the specimen is immersed in H_2 and tested for

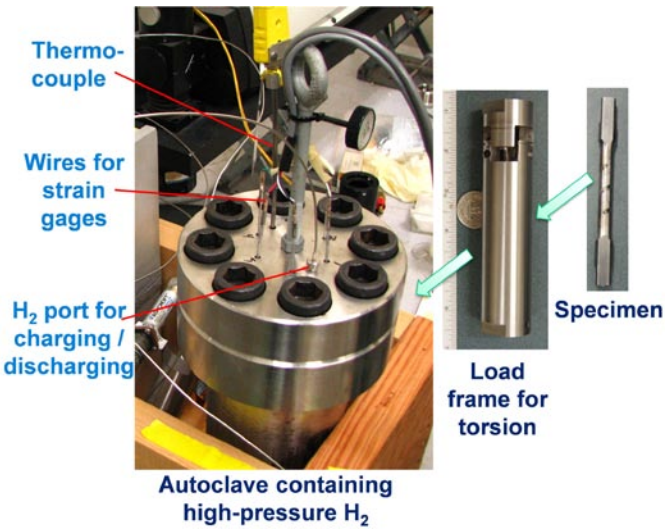


FIGURE 1. Special, in situ testing apparatus for measuring fracture toughness degradation of materials exposed to high-pressure hydrogen

one to three days to ensure sufficient time for hydrogen to diffuse to the crack tip.

As shown in Figure 1, the compact size and self-loading mechanism employed in the in situ SNTT device make it possible to accurately measure mechanical property degradation in high-pressure hydrogen without the use of a dedicated mechanical testing system. This minimizes the capital cost of the testing system and allows cost-effective study of the effect of weld microstructure and its inhomogeneity on HE resistance.

The steel studied using in situ SNTT is AISI 4340 high-strength steel, a material commonly used for hydrogen storage tank. Simulated weld heat-affected zone (HAZ), which is the most critical region to HE, is prepared using a Gleeble® thermal-mechanical system. Each specimen is subject to a heating and cooling cycle mimicking that encountered in practical welding condition. Using Gleeble to produce simulated weld specimens eliminates the need for fabricating a 4340 steel weld and machining specimens from the weld, which can be costly and time-consuming. After heat-treatment in Gleeble, the simulated weld specimens are cyclic-fatigued in air to induce sharp crack tips before testing in hydrogen.

Figure 2(a) shows the surface appearance of a fractured specimen after exposure to hydrogen at 1,900 psi. Figure 2(b) is the scanning electron microscope (SEM) image of fracture surface near the notch root, where primarily intergranular fractures (i.e., brittle) are observed. As it locates just underneath the surface directly exposed to hydrogen, the region near the notch root is likely saturated with hydrogen. The tensile stress field in front of the notch tip further enhances the hydrogen diffusion. The presence of hydrogen severally deteriorates the local microstructure resistance to HE, thus resulting in a brittle fracture. Figure 2(c) is the SEM image of fracture surface away from the notch root. Both dimples (ductile) and intergranular fractures (brittle) are observed, indicting a mixed ductile and brittle fracture behavior. Detailed microstructure analyses of this region is ongoing to understand the extent of hydrogen embrittlement there.

The preliminary testing results obtained on fatigue pre-crack specimens show that the fracture toughness of 4340 steel weld HAZ drops from 38.7 ksi·$\sqrt{in}$ in air to only 9.6 ksi·$\sqrt{in}$ in gaseous hydrogen at 1,900 psi. The measured fracture toughness values are consistent with those reported in the literature [5]. Exposure to high-pressure hydrogen results in significant reduction in fracture toughness for the 4340 steel weld HAZ. Such hydrogen embrittlement is indeed severe, though not unexpected. The 4340 steel relies on a martensitic microstructure for its high strength. The martensitic microstructure and associated high carbon content make 4340 steel prone to HE [5]. On the other hand, new generation pipeline steels often utilize micro-alloying for improved strength and favorable microstructure for HE resistance.

Cost-Effective FSW of Pipeline Steel for Improved HE Resistance

Figure 3(a) is a snapshot of FSW of X-65 steel pipe sections. The resulting pipe girth weld is shown in

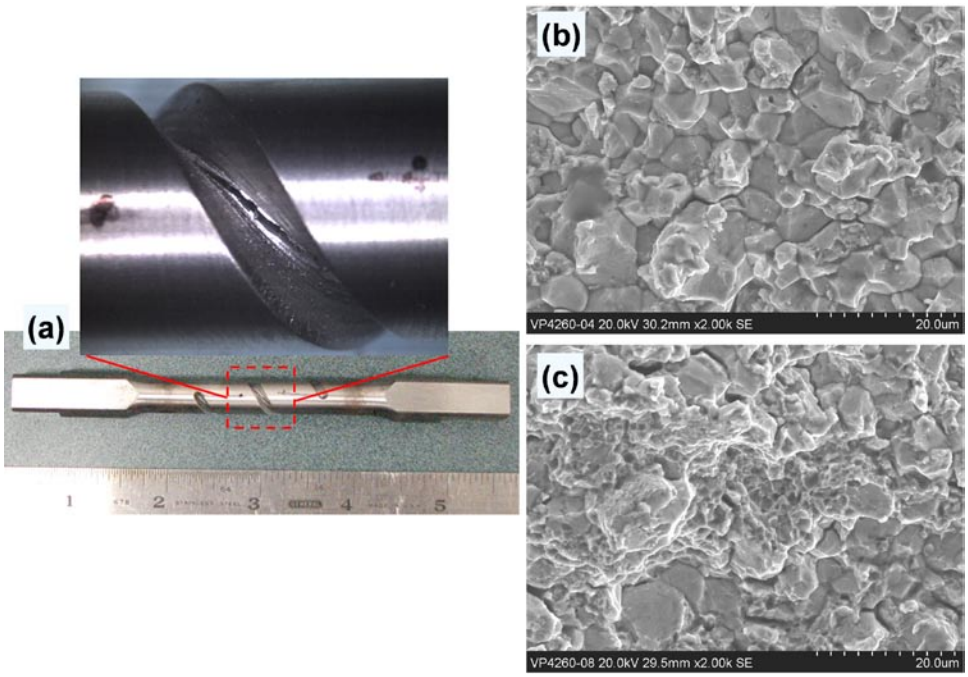


FIGURE 2. (a) Surface appearance of a fractured sample after hydrogen exposure, (b) SEM image of fracture surface near the notch root, and (c) SEM image of fracture surface away from the notch root

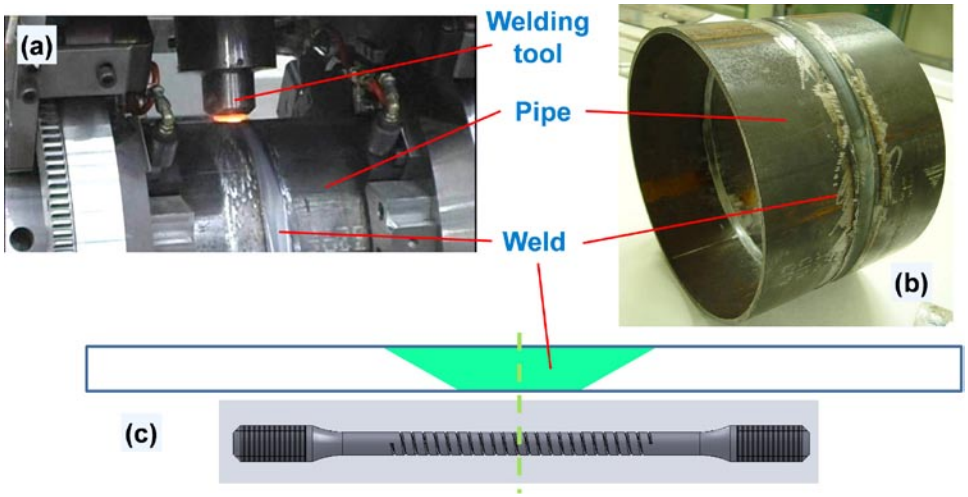


FIGURE 3. (a) Snapshot of FSW of X-65 steel pipe sections, (b) resulting pipe girth weld, and (c) schematic drawing of multi-notch tensile specimen

Figure 3(b). Previous studies on FSW of pipeline steel demonstrated considerable improvement of weld toughness and strength over the conventional arc weld in air [6]. In FY 2011, the in situ multi-notch tensile test is applied to study the resistance to HE of friction stir weld exposed to high-pressure hydrogen. Figure 3(c) is a schematic of the transverse cross-section of friction stir girth weld from which the multi-notch specimen is machined. The helical notch samples various weld regions including the stir zone, thermo-mechanically affected zone, HAZ and base metal. During testing, the notched sample is put into a load frame similar to that shown in Figure 1, where a tensile load rather than a torsional load is applied to the sample. The tensile load frame is placed inside the pressure vessel, charged to the desired hydrogen pressure, to measure the threshold tensile load for crack initiation in hydrogen.

It is noted that the multi-notch tensile test gives a qualitative ranking of microstructure sensitivity to HE. It is used because the notched samples can be readily machined from the relatively thin X-65 pipe (wall thickness = 0.24 in., or 6.1 mm). Nevertheless, such tests can provide insights into the relative performance of friction stir welds over conventional arc welds.

Preliminary tests have shown some encouraging results, as the friction stir weld sample exposed to hydrogen does not fracture at a load that is 70% of the fracture load in air. Additional tests on X-65 FSW are ongoing and are expected to be completed by September-November 2011 timeframe.

Improving Capability of Testing Apparatus

Since the current testing apparatus directly utilizes the regular hydrogen cylinder for pressuring, the maximum pressure is thus limited to about 1,900 psi. A new hydrogen charging system capable of maintaining or varying H_2 pressure up to 10,000 psi has been designed and assembled. The schematic drawing of the charging system is shown in Figure 4. The system will enable the study of the effect of hydrogen on material properties under very high pressures that are relevant to hydrogen production, delivery, and storage infrastructure.

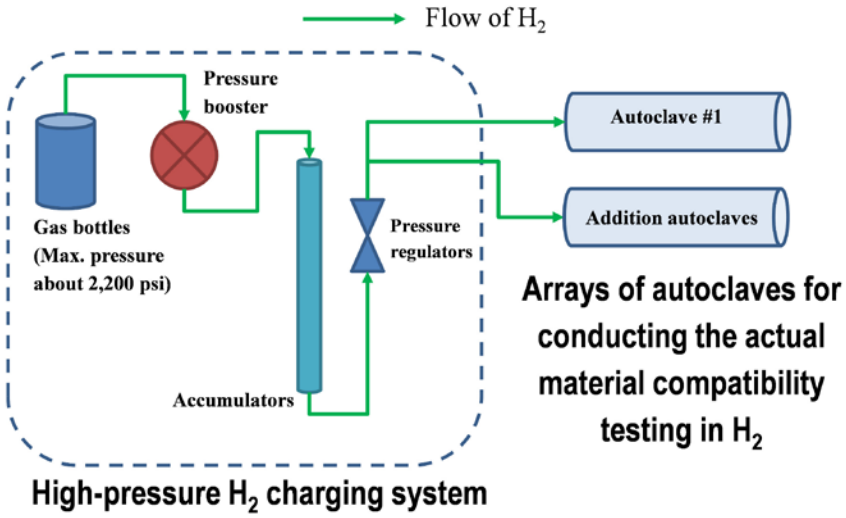


FIGURE 4. Schematic of a hydrogen charging system capable of maintaining or varying pressure up to 10,000 psi

Conclusions and Future Directions

- Demonstrated in situ SNTT for cost-effective and accurate measurement of the fracture toughness degradation in steel welds exposed to high-pressure hydrogen. The quantitative knowledge provides the technical basis for managing the weld region, i.e., the weakest link for the structural integrity and safety of hydrogen delivery infrastructure.
- Preliminary results showed FSW of pipeline steel could result in favorable microstructure with superior properties compared to the conventional arc welding.
- For the duration of FY 2011, we plan to complete (1) the study on HE resistance of X-65 steel pipe FSW, (2) the microstructure characterization of fracture surface of 4340 steel weld exposed to H_2, and (3) the assembly of high-pressure hydrogen testing system.
- At the discretion of DOE, future direction may include the application of special in situ testing methods and apparatus to study hydrogen-induced property degradation in other important materials and their welds relevant to hydrogen infrastructure.

FY 2011 Publications/Presentations

1. Wang, J., Ren, F., Zhang, W., Feng, Z., Anovitz, L.M., Chen Z. and Xu, H. 2011, "Development of in-situ Techniques for Torsion and Tension Testing in Hydrogen Environment," 2011 ASME PVP Conference, Baltimore, MD.

2. 2011 DOE Annual Merit Review, Fuel Cell Technologies Program, Washington, D.C., May 2011.

References

1. U.S. Department of Energy, "National Hydrogen Energy Roadmap," Nov. 2002, http://www.eere.energy.gov/hydrogenandfuelcells/pdfs/national_h2_roadmap.pdf.

2. U.S. Department of Energy, "Hydrogen, Fuel Cells & Infrastructure Technologies Program Multi-Year Research, Development and Demonstration Plan," Jan. 2005, pp. 3-40. http://www.eere.energy.gov/hydrogenandfuelcells/mypp/.

3. U.S. Department of Energy, "Basic Research Needs for the Hydrogen Economy," Basic Energy Sciences Workshop on Hydrogen Production, Storage, and Use, Feb. 2004, http://science.energy.gov/~/media/bes/pdf/reports/files/nhe_rpt.pdf.

4. Xu, K. "Evaluation of API 5L X80 in High Pressure Hydrogen Gas," ASTM G1.06 Hydrogen Embrittlement Workshop, Nov 8, 2005, Dallas, TX.

5. Bandyopadhyay et al, Metallurgical Transactions A, Vol. 14, pp. 881-888 (1983).

6. Feng, Z. Steel, R. Packer, S. and David, S.A. 2009. "Friction Stir Welding of API Grade 65 Steel Pipes," ASME PVP Conference, Prague, Czech Republic.

III.16 Hydrogen Pipeline Compressors

George Fenske (Primary Contact), Robert Erck
Argonne National Laboratory (ANL)
9700 S. Cass Ave.
Argonne, IL 60439
Phone: (630) 252-5910
E-mail: gfenske@anl.gov

DOE Manager
HQ: Scott Weil
Phone: (202) 586-1758
E-mail: Kenneth.Weil@ee.doe.gov

Project Start Date: October 1, 2006
Project End Date: September 30, 2011

Fiscal Year (FY) 2011 Objectives

- Develop advanced materials and coatings for hydrogen pipeline compressors.
- Achieve greater reliability, increased efficiency, and lower capital investment and maintenance costs in hydrogen pipeline compressors.
- Research existing and novel hydrogen compression technologies that can improve reliability, eliminate contamination, and reduce cost.

Technical Barriers

The project addresses the following technical barrier from the Hydrogen Delivery section (3.2.4.2) of the Fuel Cell Technologies Program Multi-Year Research, Development and Demonstration Plan:

(B) Reliability and Costs of Hydrogen Compression

Technical Targets

This project is directed toward the study of fundamental mechanisms associated with the tribology of hydrogen pipeline compressors (friction, wear, and degradation). The goal of the research is to identify materials and engineered surface treatments that provide low friction and wear resistance required to achieve the energy efficiency and reliability targets for pipeline compressors. Accordingly, the project tasks address the challenges associated with meeting the DOE hydrogen delivery performance and cost targets for 2017 in Table 1.

TABLE 1. Hydrogen Delivery Performance and Cost Targets for 2017

Technical Targets for Hydrogen Delivery		
Category	**FY 2012 Targets**	**2010 Status**
Reliability	Improved	Low
Energy Efficiency	98%	<98%
Total Capital Investment	$12M	>$15M
Maintenance	7%	>10%
Contamination	Varies	Unknown

FY 2011 Accomplishments

- Prior year accomplishments have been in the nature of finding a low-friction coating that can stand up to the conditions of unlubricated sliding in H_2. These tests were initially conducted with a modified in-house tribometer that could operate at room temperature.
- Candidate materials that were obtained in-house and from commercial companies were studied in detail and the general nature of each was characterized with the room-temperature tribometer.
- The design specifications and procurement of new high-temperature hydrogen tribometer was started in 2008, and the installed machine was accepted in 2010.
- The leading materials were found to be thin film carbon coatings, particularly hydrogenated carbon known as near-frictionless coating (NFC) 7, which shows very small wear in tests.
- Other counterface materials studies were MoS_2, carbon fiber, iron boride, sp^3 diamondlike carbon (DLC), Ni-poly-tetrafluoroethylene (PTFE), and carbon-carbon.
- Initial tests using the new elevated tribometer found the NFC7 carbon functioned to 300°C, but apparently has a temperature limit of 400°C in H_2 gas.



Introduction

Compressors are critical components used in the production and delivery of hydrogen. Current reciprocating compressors are costly, are subject to excessive wear, have poor reliability, and often require the use of lubricants that can contaminate the hydrogen (used in fuel cells).

The primary objective of this project is to identify – and develop as required – advanced materials and coatings that can achieve the friction, wear, and reliability requirements for dynamically loaded components (seal and bearings) in high-temperature, high-pressure hydrogen environments prototypical of pipeline and forecourt compressor systems.

The DOE Strategic Directions for Hydrogen Delivery Workshop identified critical needs in the development of advanced hydrogen compressors – notably, the need to minimize moving parts and to address wear through new designs (centrifugal, linear, guided rotor, and electrochemical) and improved compressor materials. The DOE is supporting several compressor design studies on hydrogen pipeline compression, specifically addressing oil-free designs that demonstrate compression in the 0-500 psig to 800-1,200 psig range with significant improvements in efficiency, contamination, and reliability/durability.

One of the designs by Mohawk Innovative Technology, Inc. (MiTi®) involves using oil-free foil bearings and seals in a centrifugal compressor, and MiTi® identified the development of bearings, seals, and oil-free tribological coatings as crucial to the successful development of an advanced compressor. MiTi® and Argonne have developed potential coatings for these rigorous applications; however, the performance of these coatings (as well as the nickel-alloy substrates) in high-temperature, high-speed hydrogen environments is unknown at this point.

Approach

The approach that is being undertaken is to evaluate the tribological performance of candidate seal and bearing materials under consideration by compressor manufacturers and provide data required to select the optimum seal and bearing material/coating configuration for a 300-kg/min centrifugal compressor and high-pressure, low-flow positive displacement compressor. This effort will include a) evaluating the effects of a hydrogen environment on the mechanical properties of Ni alloys, b) evaluating the feasibility of coating suitable substrates with Argonne's NFC and outside vendor coatings, c) establishing the requirements and testing needs for NFC and a series of foil seal coatings, and d) evaluating foil seal and bearings under conditions prototypic of the proposed MiTi® hydrogen compressor.

The research uses facilities and expertise at Argonne – notably the ability to deposit advanced high-performance coatings (e.g., NFC), to test and evaluate coatings under extreme conditions, and to characterize and understand friction, wear, and surface degradation phenomena that determine component lifetime and reliability.

Different contact stress/sliding speed regimes were identified, depending on compressor design:

- Positive displacement – high contact stress, low sliding speed
- Axial flow compressors – high speed, low contact stresses
- Centrifugal compressors – intermediate speeds and contact stresses

Based on the range of contact stresses and sliding speeds anticipated for these compressors, we will replicate lab conditions to encompass nominal contact stresses between 2 and 1,500 psi, with sliding speeds from 0.1 to 10 m/s. Operating temperatures up to 500°C due to working-gas adiabatic heating and flash/asperity heating can add an additional 500 to 750°C (depending on load, speed, thermal properties, and friction) to the temperature of near-surface asperities. The coating deposition is focused on NFC and commercial coatings based on conventional solid lubricants. The substrates chosen are stainless steels, nickel alloys, and Cr-Mo steels.

Results

New Test Machine

In the past year, the main focus was the acceptance and first tests using a new high-temperature test rig, which is shown in the photograph in Figure 1. The test machine exhibited deficiencies in operation which were repaired under warranty. Further deficiencies in the pressure control system were overcome in June 2011. Because the prescribed tests call for a low pressure sliding condition the machine needed to be modified from pin-on-disk to thrust washer configuration.

Continuing Tests to Evaluate Materials

In FY 2011, the FY 2011milestones were largely met. Milestone 1 required a satisfactory acceptance test demonstrating 2,000 rpm operation for 4 h in 0.9-bar H_2 gas at 500°C with continuous measurement of friction, wear,



FIGURE 1. Photograph of new high-temperature hydrogen test machine in open position for loading of test specimens.

temperature, and sliding distance. This milestone was met 100%. Figure 1 shows a photograph of the test machine installed and operational. Milestone 2 was to complete durability testing of a NFC7 compressor foil bearing material and demonstrate a coefficient of friction that meets the desired compressor design requirements of < 0.1 under 14 kPa load, over a temperature range of 100–500°C, and in 99.999% H_2 gas. This milestone was met 90% by obtaining room temperature, 100°C, 200°C, 300°C tests, on compressor foil-bearing material producing coefficients of friction <0.1, at 5.6 kPa load, in 99.999% hydrogen. Figure 2 shows that the coefficient of friction is below 0.1 at all test temperatures up to 300°C, meeting the target value. However, this was not the case at 400°C for which the coefficient of friction jumped to unacceptably high values. Figure 3 shows post-test images of the test coupons and reveals adequate durability for the NFC7 material at test temperatures up to 300°C, but failure at 400°C. Milestone 3 was to complete ball-on-disk tests on the test materials from inventory (N3FC, NFC6, MoS_2/graphite, X-750, boride, carbon composite) at temperatures up to 400°C for durations up to 12 hours or to point where materials fail. This was 10% completed by completed using the room temperature test rig in early part of FY 2011.

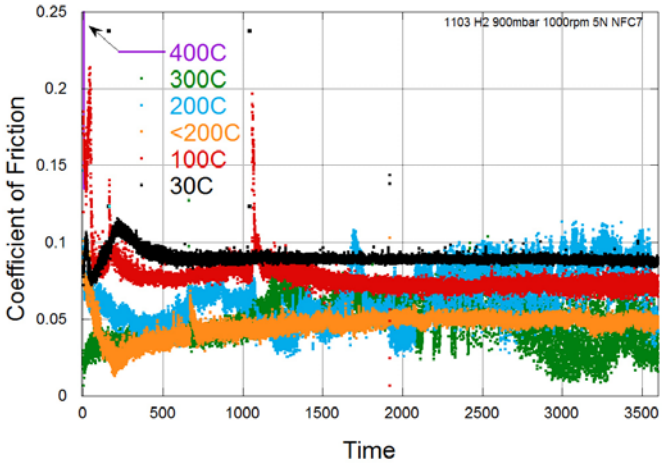


FIGURE 2. Graph showing coefficient of sliding friction as a function of test time for the NFC7 material sliding in H_2 gas against Hastelloy X at various indicated temperatures.

Most Recent Results

Table 2 shows the most recent tabular results for the most recent thrust washer tests, omitting those not run in H_2 gas. Most tests, except for those terminated early due to extreme wear, were for up to two hours duration with a 50% duty cycle, 50s on and 50s off at speeds up to 6,000 rpm. Typical results for a nickel-PTFE film are shown in Figure 4.

Conclusions and Future Directions

Longer-duration room-temperature testing was performed on existing (NFC6) and new (proprietary DLC and Argonne NFC7) materials, with excellent results for the latter. Final problems with the new elevated temperature tribometer were worked out, and initial tests showed the limitation of carbon-based materials may be 400°C. We will finish up testing of promising materials at typical in-service temperatures. The knowledge that is being gained will also be directly applicable to unlubricated forecourt compressors. The original goal of "Large Compressors: Transmission, Terminals, Geological Storage" is being broadened to include the section "Forecourt Compressors: Forecourt," and discussions have been started with two manufacturers of non-centrifugal hydrogen compressors who have products in the field that are exhibiting the need for frequent scheduled

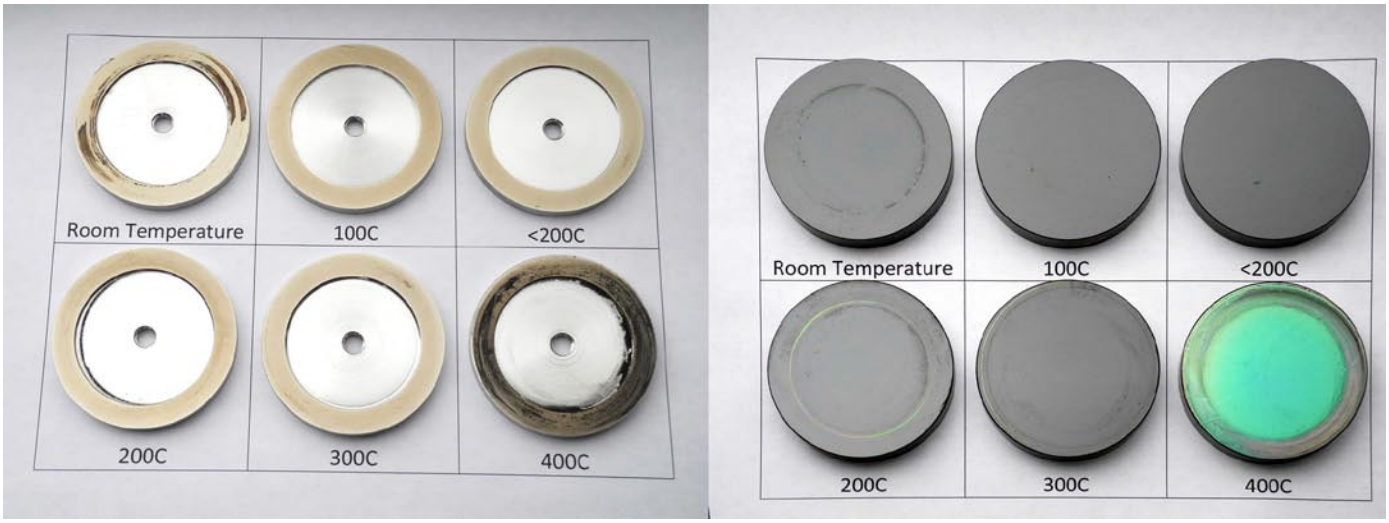


FIGURE 3. Photographs of worn thrust-washer test pairs (stationary bottom samples coated with NFC7-right, rotating Hastelloy X top samples-left) after 1 hr sliding at indicated test temperatures in H_2 gas.

TABLE 2. Most Recent Results From Thrust-Washer Tests

Rotating Face	Stationary Counterface	Environment	Friction	Wear Face	Wear Counterface
MK MoS_2	X750	Hydrogen	Medium 0.4	High abrasion	Low
Fe/Mo/Boride	316ss	Hydrogen	Med high 0.6	Low abrasion	Low
CF composite	X750	Hydrogen	Medium 0.4	Low	Low
N3FC	4118 steel	Hydrogen	Low 0.15	Low	Immeasurable
NFC6	Hastelloy X	Hydrogen	Low 0.1	None	Very low
Hastelloy X	Diamonex	Hydrogen	Medium 0.4	Low	Medium
NFC7	Hastelloy X	Hydrogen	Low 0.06	None	Immeasurable
SP3 DLC	4118 steel	Hydrogen	Low 0.05	Large	Large
Ni/PTFE	Ni/PTFE	Hydrogen	High 0.6	Large	Large
Hastelloy X	Im MoS2	Hydrogen	Medium 0.4	Low	Low

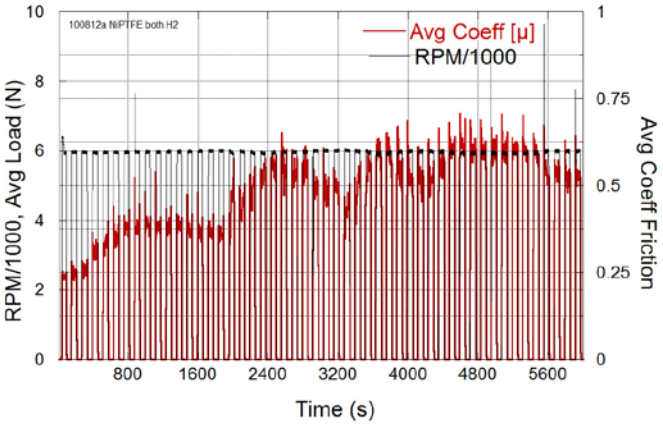


FIGURE 4. Graph showing coefficient of sliding friction as a function of test time for a Ni/PTFE composite sliding against itself in H_2 gas with 50% on/off duty cycle for 6,000s.

and unscheduled maintenance. This revised goal will involve conducting longer-term sliding tests on materials used in forecourt compressors for "bone dry" use (e.g., polyether ether ether ketone and carbon-tetrafluoroethylene instead of nickel alloys, as has been done so far). We will continue nanoindentation studies to elucidate the possible relationship of surface mechanical properties to tribology friction and wear. This research leverages facilities and expertise at Argonne used to develop advanced materials and coatings for dry sliding conditions – notably the ability to deposit advanced high-performance coatings, test and evaluate coatings under extreme conditions, and characterize and understand friction, wear, and surface degradation phenomena that determine component lifetime and reliability. Concurrently we will to initiate discussions with point-of-delivery compressor users and manufacturers to obtain and examine failed forecourt compressor parts from reciprocating compressor partner to identify failure mechanisms and possible remedies.

FY 2011 Publications/Presentations

1. Coatings for Centrifugal Compression, G. Fenske, R. Erck, and O. Eryilmaz, presented at 2010 DOE Hydrogen Program and Vehicle Technologies Program Annual Merit Review and Peer Evaluation Meeting, Washington, D.C., May 9–12, 2011.

III.17 Active Magnetic Regenerative Liquefier

John Barclay (Primary Contact), K. Oseen-Senda, L. Ferguson, J. Pouresfandiary, H. Ralph, A. Cousins, and T. Hampton,.
Heracles Energy Corporation d.b.a. Prometheus Energy
8511 154th Avenue NE, Building L
Redmond, WA 98052
Phone: (425) 830-2757
E-mail: jbarclay@prometheus-energy.com or jabarclay@comcast.net

DOE Managers
HQ: Scott Weil
Phone: (202) 586-1758
E-mail: Kenneth.Weil@ee.doe.gov
GO: Paul Bakke
Phone: (720) 356-1436
E-mail: Paul.Bakke@go.doe.gov

Contract Number: DE-FG36-08GO18064.A000

Project Start Date: June 1, 2008
Projected End Date: May 31, 2012

Fiscal Year (FY) 2011 Objectives

This project has several well defined objectives intended to experimentally demonstrate highly efficient hydrogen liquefiers. These include:

- Develop validated engineering design data for active magnetic regenerative liquefiers (AMRLs) for liquefied hydrogen (LH_2) (or liquefied natural gas) to meet or exceed DOE's liquefaction targets for both capital and energy efficiency.
- Analyze, design, fabricate, and test AMRL prototypes to experimentally demonstrate this technology and answer numerous questions such as how to design optimized layered magnetic regenerators with bypass flow of the heat transfer fluid.
- Validate the high figure of merit (FOM) predicted by our unique numerical simulation model used to analyze and design AMRL prototypes.
- From June 2009 through May 2011 our focus has been to analyze, design, fabricate, and test our first AMRL prototype with a target of spanning from ~290 K to ~120 K with a high FOM.

Technical Barriers

This project addresses the following technical delivery barrier from the Hydrogen Delivery section of the Fuel Cell Technologies Multi-Year Research, Development and Demonstration Plan, i.e.,

(C) High Cost and Low Energy Efficiency of Hydrogen Liquefaction

Technical Targets

Conventional hydrogen liquefiers at any scale have a maximum FOM of ~0.35 due primarily to the intrinsic difficulty of rapid, efficient compression of either hydrogen or helium working gases (depending on the liquefier design). The novel approach of this AMRL project uses solid magnetic working refrigerants cycled in and out of high magnetic fields to execute an efficient active regenerative magnetic liquefaction cycle that avoids the use of gas compressors. Numerical simulation modeling of high performance AMRL designs indicates certain achievable designs have promise to simultaneously lower installed capital costs/unit capacity and to increase thermodynamic efficiency from a FOM of ~0.35 toward ~0.5 to ~0.6. Results from experimental prototypes should support the design and deployment of hydrogen liquefier plants that meet the DOE 2011 hydrogen production and delivery targets:

- Delivery cost of LH_2 at <$1.00/kg.
- $40 MM capital cost for a turn-key plant with a capacity of 30 te/day.
- Operational efficiency of a complete liquefier plant of 75% as defined by DOE and commensurate with a liquefier FOM of ~0.6.

FY 2011 Accomplishments

- Successfully completed the design, fabrication, and test of the dual Gd magnetic regenerators, two pneumatic drives, and the heat transfer fluid subsystems of our reciprocating active magnetic regenerative refrigerator (AMRR) prototype.
- Mechanically and electrically integrated all eight subsystems of our first AMRR prototype into an operational system interfaced to the LabVIEW data acquisition and control program.
- Experimentally demonstrated the first cooling curves of our AMRR and begin to measure its performance under a variety of different operational parameters such as cycle frequency, magnetic field strength, heat transfer fluid flow rate, amount of bypass flow of the heat transfer fluid while measuring work input, temperature span, cooling capability as a function of cold temperature as a function of the amount of bypass flow of the heat transfer fluid for ~290 K to ~240 K temperature span.
- Began to analyze results to compare measured performance data against our numerical process

simulation calculations of this specific reciprocating dual regenerator AMRR prototype.

- Began to incorporate lessons learned from first prototype into the design of the second AMRL prototype with a rotary configuration with the objective to span from ~290 K to ~20 K and produce LH_2 with a FOM of ~0.5.



Introduction

AMRL technology promises cost-effective and efficient liquefaction of hydrogen because it eliminates the compressors, the largest source of inefficiency in Claude-cycle liquefiers. However, as with any innovative technique, many questions have to be investigated and understood before commercial applications happen. Since the mid-1970s, magnetic refrigeration technology for applications above 1 K beyond research laboratory use has been investigated with increasing understanding of magnetic cycles, magnetic refrigerants from ~4 K to ~300 K, and practical magnetic refrigeration prototype designs. The seminal patent on the 'active magnetic regenerator' was issued in 1982. The principle of operation this unique refrigeration cycle is illustrated as an AMRR in Figure 1. Only in the last ~15-20 years have there been significant engineering efforts on two commercial applications of magnetic refrigeration: those with small cooling power (~100 W), non-chlorofluorocarbon refrigeration near room temperature using permanent magnets and much larger capacity cryogenic liquefiers for hydrogen and natural gas (~100s of kW of refrigeration).

The AMRL project funded under this DOE award is an extensive engineering effort to analyze, design, fabricate, and test innovative natural gas and hydrogen liquefier prototypes. Successful demonstration of AMRL prototypes will answer a few key design questions and provide a proven knowledge base to enable use of advanced liquefiers for various hydrogen infrastructure projects that cost-effectively provide LH_2 energy storage/delivery for gaseous hydrogen produced by several sources including electrolysis at intermittent wind or solar energy plants. The AMRL technology readily scales up or down in capacity so it could be scaled to reach DOE's target of 30 te/day and down to a vehicular refueling station size of ~2-3 te/day where gaseous hydrogen continuously produced via steam methane reformation, or high temperature fuel cells, or electrolysis could be liquefied, stored and supplied as LH_2 and/or compressed hydrogen produced from liquid hydrogen (LCH_2).

Approach

During the past year our focus has been to complete the design, fabrication, integration and testing of our first AMRR prototype with the objective of spanning from ~290 K to ~120 K with multi-layer regenerators and bypass flow of the heat transfer fluid. We have demonstrated the initial results toward this objective. The experimental results will validate our numerical simulation mode and guide the design of the AMRL prototype spanning from ~290 K to ~20 K.

Results

The completed three-dimensional mechanical design of the first laboratory-scale AMRR prototype with dual regenerators reciprocating in and out of a 7 Tesla (T), large bore superconducting magnet is illustrated in Figure 2. It includes the various components of the eight subsystems required to execute the AMRR cycle. This prototype is designed to operate between ~290 K at the hot end and cold end temperatures down to as low as ~120 K. The design required numerous calculations of the thermodynamics, heat transfer, fluid dynamics, structural loads, and many related items. One of the more challenging design features was the support of the 4 K superconducting magnet that has to be structurally capable of withstanding large magnetic forces between the magnetic materials in the dual regenerators and the magnetic field of the magnet. The center access tube through the magnet is insulated from the magnet to enable the dual regenerators to operate between ~290 K and ~120 K.

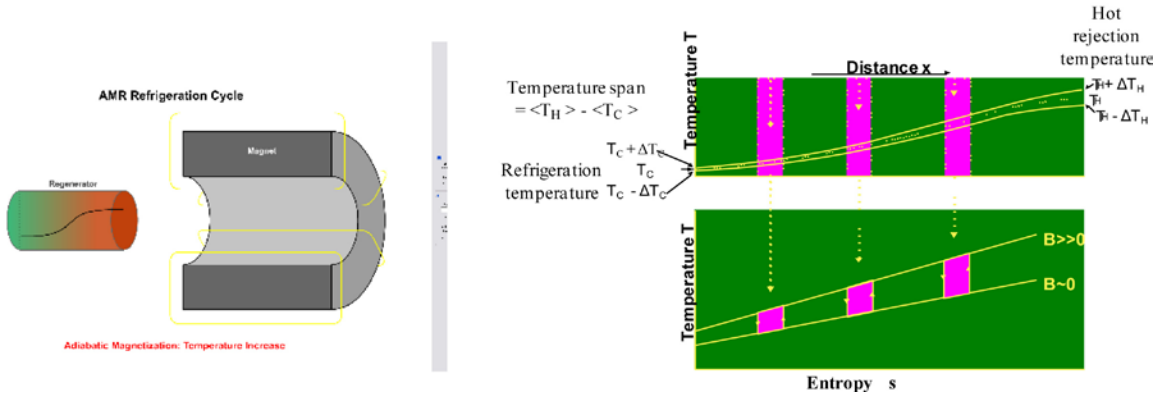


FIGURE 1. Active Magnetic Regenerative Liquefier

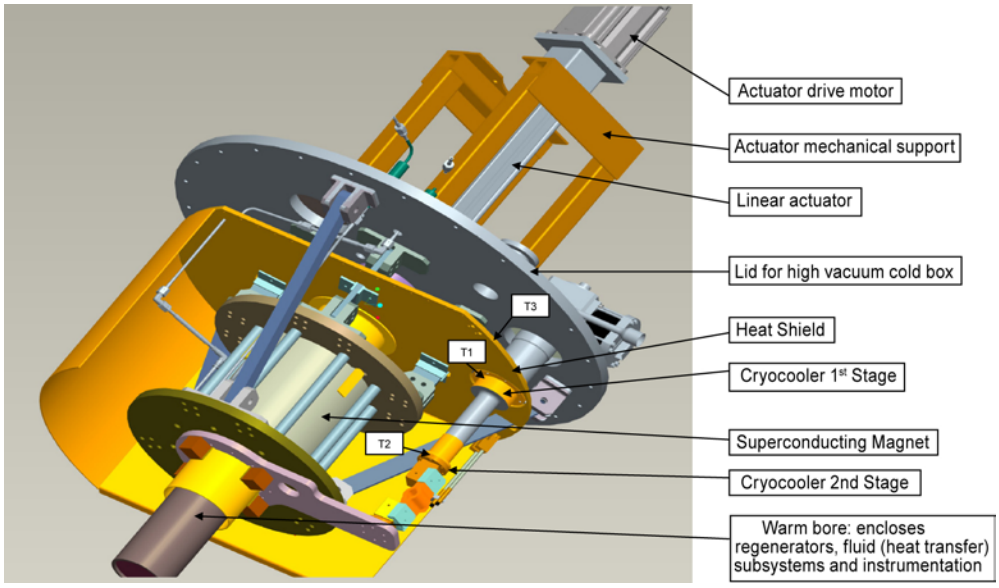


FIGURE 2. Reciprocating AMRR Prototype Design

The dual magnetic regenerators must be strong enough to react large magnetic forces and simultaneously be integrated with the pneumatically actuated mechanical drive mechanism and the helium heat transfer fluid subsystem pressurized to ~250 psia. The heat transfer fluid couples the heating and cooling of the magnetic regenerators to the hot heat sink and the cold heat exchanger between the dual regenerators. Figure 3 illustrates the resultant design of the two identical magnetic regenerators and the heat transfer fluid piping including the path for controlled bypass flow of the cold helium heat transfer fluid. Numerous sensors to measure temperature, helium flow rates, magnetic field strength, etc. are also integrated into these subsystems during the fabrication steps. All these sensors had to have vacuum-tight seals to insure that the high pressure helium did not leak into the high vacuum within the cold box during the AMRR operation. These sensors had to operate at high enough frequency to provide time resolution throughout the entire AMRR cycle. They were connected through high speed modules of a Compact-DAQ LabVIEW control and data acquisition computer.

Figure 4 presents the drive motions as a function of time from the pneumatically-actuated reciprocating drive of the dual magnetic regenerators and the drive motion of the pneumatically actuated positive displacement pump moving the heat transfer fluid as desired. Note that the two reciprocating motions are trapezoidal in time and out of phase with one another as required to properly execute the AMRR cycle.

Figure 5 illustrates a simplified piping and instrumentation diagram (P&ID) for the heat transfer fluid subsystem. It can be used to understand the relatively complex reciprocating flows of the heat transfer fluid during the AMRR operation. Figure 6 shows a photograph of the

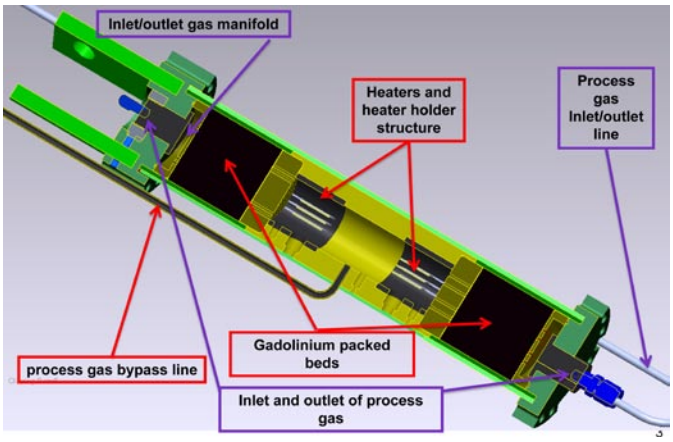


FIGURE 3. Dual Magnetic Regenerator Design Integrates Numerous Subsystems

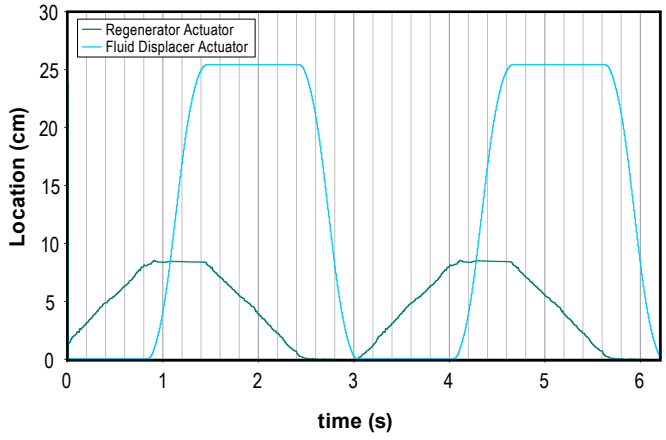


FIGURE 4. The Heat Transfer Fluid Flow and Regenerator Drive Motions for the AMRR Cycle

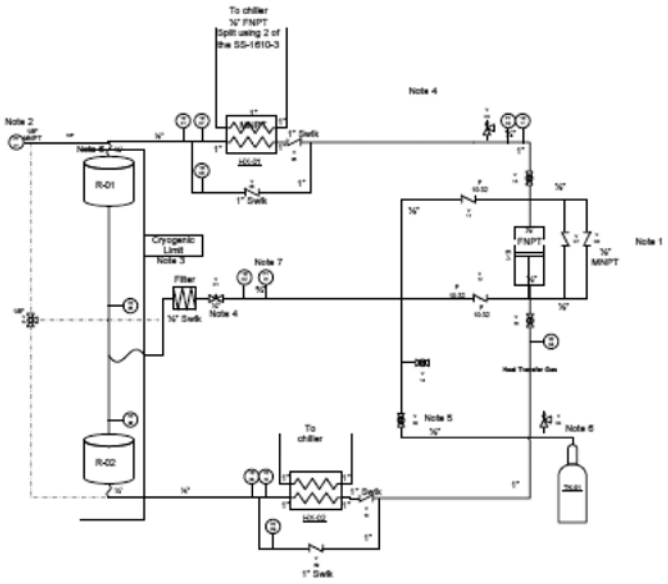


FIGURE 5. The Heat Transfer Fluid Subsystem is Illustrated on this Simplified P&ID

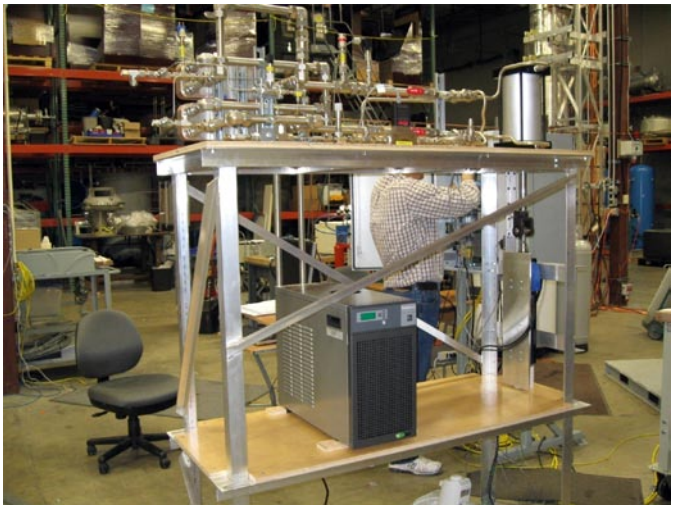


FIGURE 6. Heat Transfer Fluid Subsystem Components

heat transfer fluid subsystem components including the brazed plate frame, counter-flow heat exchangers to couple the hot helium heat transfer fluid to the cold refrigerant from the vapor compression cycle chiller used to ensure a stable hot temperature of the heat transfer fluid during an experimental run of the AMRR. The chiller is located in the center of this photograph.

The initial cooling results from our first AMRR prototype were obtained on May 10, 2011 shortly before the poster was presented at the Annual Merit Review. The test results were not available for this report.

Conclusions and Future Directions

Heracles/Prometheus has made excellent progress and completed the design, fabrication, assembly and initial demonstration of cooling in its first AMRR prototype. All subsystems of the first lab-scale prototype were designed, built, and successfully tested. The initial measurements with the LabVIEW data acquisition program include the temperature span, cold cooling power, hot heat rejection temperature, operating frequency, total heat transfer fluid flow rate, bypass flow, applied magnetic field, etc. The recently obtained initial results spanning from ~292 K to ~240 K are very encouraging but have yet to be analyzed. The operational AMRR prototype enables us to experimentally answer key questions such as the best recipe for multiple layers of different magnetic refrigerants in one or more integrated regenerators with varying amounts of bypass flow of the heat transfer fluid. Our performance simulation model predicts that ~10-15 % of bypass flow should significantly improve the thermodynamic performance but the proof is in the pudding, i.e., measured results from an operational AMRR prototype. To our knowledge, these results will be the first such results for cryogenic liquefiers. We expect to use new insights and knowledge from the experimental results from the first AMRR prototype to validate our performance simulation code, and use that model to guide the design a rotary-type multi-stage AMRL prototype. This larger AMRL prototype should be capable of spanning from ~290 K to ~20 K to make ~25 kg/day of LH_2. This will be the world's first AMRL to make LH_2. The technical and financial report obligations for this project are completed when due.

FY 2011 Publications/Presentations

1. Poster of the project for the AMR in May, 2011.
2. Several papers are being planned based on the impressive test results of our first AMRR prototype using Gd spheres.

IV. HYDROGEN STORAGE

IV.0 Hydrogen Storage Sub-Program Overview

The Hydrogen Storage sub-program supports research and development (R&D) of materials and technologies for compact, lightweight, and inexpensive storage of hydrogen. In Fiscal Year (FY) 2011, the sub-program continued to focus on R&D of low-pressure, materials-based technologies and engineered systems applicable to both stationary and transportation applications. Materials projects are focused in three main areas: metal hydrides, chemical hydrogen storage materials, and hydrogen sorbents. Additionally, increased efforts were directed at reducing the cost of compressed gas storage systems (i.e., physical storage) as a near-term commercialization pathway. The storage portfolio currently comprises projects involving 39 universities, 13 companies, and 14 federal laboratories and involves work in hydrogen storage materials discovery; materials-based system engineering; advanced high-pressure tank R&D; and system performance and costs analyses.

Goal

The sub-program's goal is to develop and demonstrate viable hydrogen storage technologies for transportation and early market fuel cell applications such as stationary power, backup power, and material handling equipment.

Objectives[1]

For light-duty vehicles, the key objective is to allow for a driving range of more than 300 miles (500 km), while meeting packaging, cost, safety, and performance requirements to be competitive with current vehicles. Although automakers have made progress in demonstrating some vehicles able to travel more than 300 miles on a single fill, using high-pressure tanks, this driving range must be achievable across different vehicle models without compromising space, performance, or cost. The sub-program's 2017 intermediate targets for transportation applications will allow some hydrogen-fueled vehicle platforms to meet customer performance expectations, while the ultimate targets are intended to facilitate the introduction of hydrogen-fueled propulsion systems across the majority of vehicle classes and models. Advanced storage materials and concepts will be needed to meet the 2017 and ultimate targets.

In pursuit of high level goals and targets for hydrogen storage, there are many requirements for achieving technical success, including improvements in volume, weight, cost, durability, cycle life, and transient performance. The full set of detailed hydrogen storage targets for light-duty vehicles can be found at: http://www1.eere.energy.gov/hydrogenandfuelcells/storage/pdfs/targets_on-board_hydro_storage.pdf. These targets are based on the requirements of the application–not the current status of the technologies–and they account for differences in vehicle architecture between conventional vehicles and fuel cell vehicles.

FY 2011 Technology Status

On-board hydrogen storage approaches under investigation include: high-capacity metal hydrides; high surface-area sorbents; chemical hydrogen storage carriers; low-cost and conformable tanks; compressed/cryogenic hydrogen tanks; and new materials or processes, such as conducting polymers, spillover materials, metal organic frameworks (MOFs), and other nanostructured materials (Figure 1). There are two principal classes of on-board storage systems: "on-board reversible" systems that can be refueled onboard the vehicle from a hydrogen supply at the fueling station and "regenerable off-board" systems involving materials that are not easily and quickly "refilled" or regenerated with hydrogen while onboard the vehicle. On-board reversible systems include physical storage systems, such as compressed/cryogenic tanks, as well as on-board reversible material systems such as metal hydrides and high-surface-area sorbents. Regenerable off-board systems include chemical hydrogen storage materials and certain metal hydrides where the temperature, pressure, kinetics, and/or energy requirements are such that the processes must be conducted off the vehicle.

The current projected storage system gravimetric and volumetric capacities are shown relative to the 2017 targets in Figures 2 and 3. On a routine basis the sub-program has system capacity projections made for the

[1] Note: Targets and milestones are under revision; therefore, individual progress reports may reference prior targets.

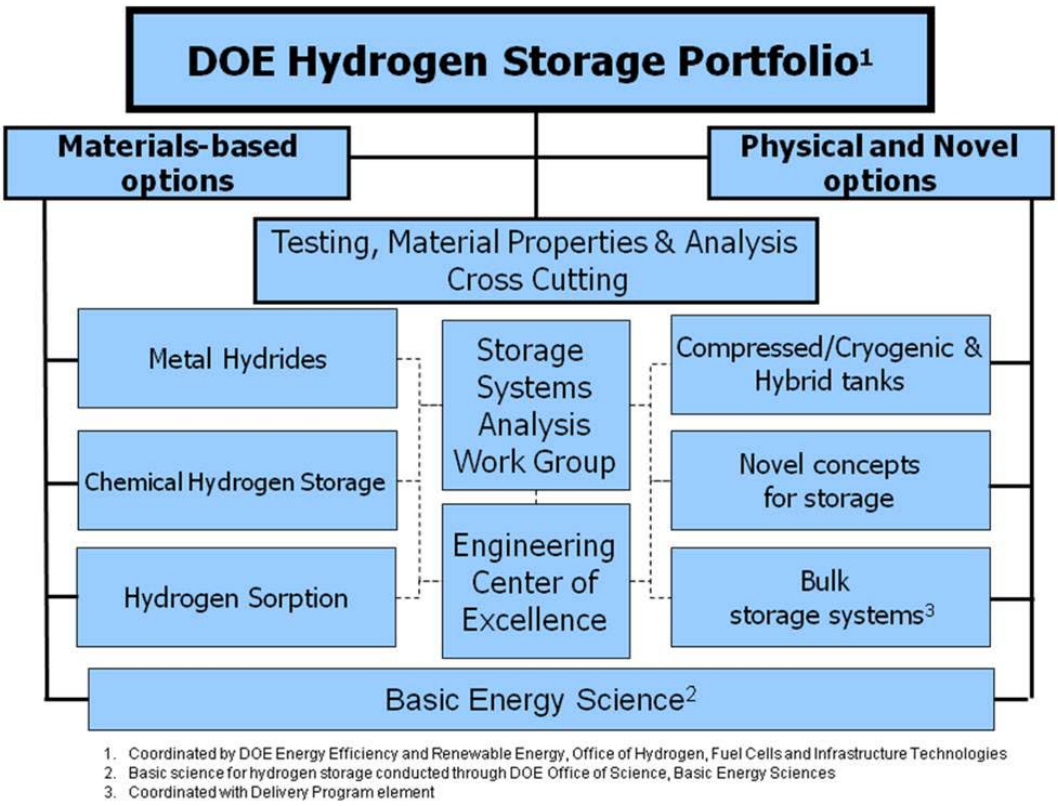
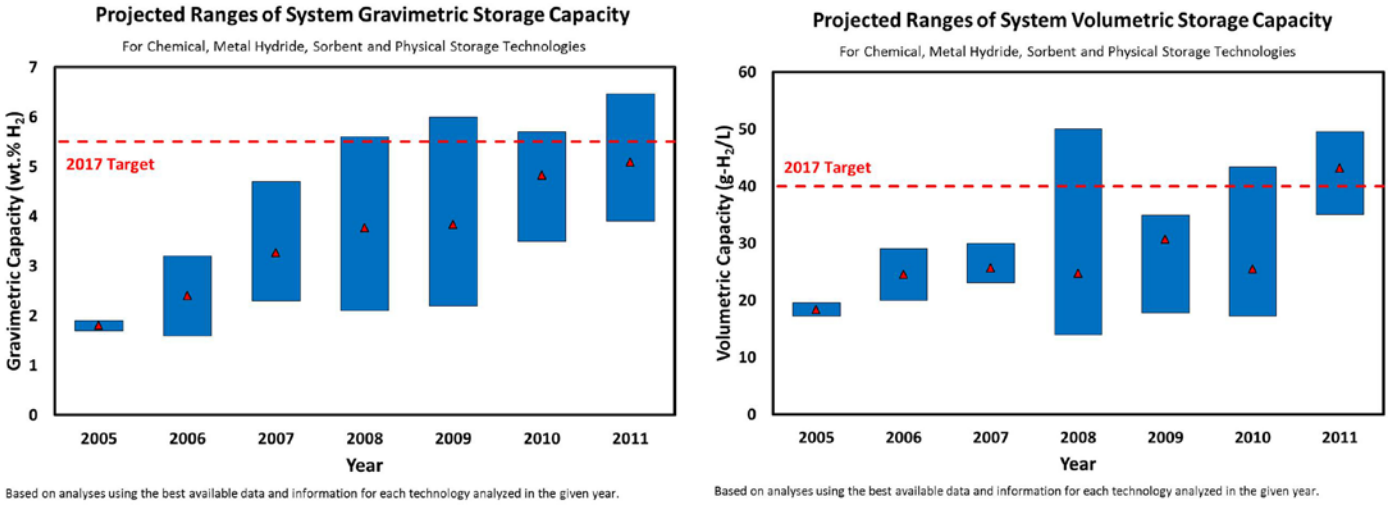


FIGURE 1. Structure of the DOE Hydrogen Storage Activities



FIGURES 2 AND 3. Status of projected hydrogen storage system gravimetric and volumetric capacities versus 2017 on-board system targets. Note that all systems were sized to provide 5.6 kg of useable hydrogen and that the plotted data points are the average value for all systems analyzed during each year while the bars correspond to the range of maximum and minimum values obtained for the year. Also note that systems with predicted capacities exceeding the gravimetric targets do not necessarily meet all other targets.

various on-board hydrogen storage technologies under development. Analytical models use the best available data for the technologies to project the gravimetric and volumetric capacities of complete storage systems that meet the required operational specifications. The capacity projections are periodically revised as new and more complete data become available and when improvements to system models are developed. Confidence

in the accuracy of the projection improves with the maturity of the technology; for instance, there is higher confidence in projections for relatively mature compressed gas systems than for much less mature complex hydride systems. The range bars shown in Figures 2 and 3 represent the ranges of volumetric and gravimetric capacity projections conducted for all the on-board storage technologies during the given year. The point within the bars is the average (mean) capacity for the technologies analyzed within the given year.

FY 2011 Accomplishments

Hydrogen Storage Materials

In FY 2011, the sub-program's materials-discovery projects developed a number of new materials and improved the performance of other materials. Key accomplishments in FY 2011 include: characterization of high surface area sorbents with specific surface areas greater than 6,000 m^2 per gram and excess hydrogen sorption capacities exceeding 8% by weight at 77 K; demonstration of cycling of $Mg(BH_4)_2$ at hydrogen capacities greater than 12% by weight under high temperature and pressure conditions; demonstration of alane slurry with 60% capacity by weight and with kinetics exceeding non-slurried alane; and determination that thermal stability of ionic liquids is dominated by choice of cation.

- Metal Hydrides
  - Brookhaven National Laboratory demonstrated 6 wt% hydrogen capacity from a slurry of alane, with desorption kinetics projected to meet the DOE targets at temperatures of ~100°C.
  - Demonstrated reversibility of greater than 12 wt% for $Mg(BH_4)_2$ under high pressure and temperature (950 bar and 400°C) conditions (University of Hawaii).
  - Demonstrated 2.5 wt% reversibility between $Mg(BH_4)_2$ and the triborane ($Mg(B_3H_8)_2$) under moderate pressure and temperature (100 bar and 200°C) conditions (University of Hawaii).
  - Demonstrated that nano-confined $NaAlH_4$ undergoes a single step desorption to NaH, Al, and H_2—i.e., it does not decompose through the Na_3AlH_6 phase as does bulk $NaAlH_4$, with a measured $\Delta H°$=47 kJ mol^{-1} and E_a = 47-53 kJ mol^{-1}(Sandia National Laboratories).
- Chemical Hydrogen Storage Materials
  - Partially identified cation/anion selection rules for ionic liquid performance (thermal degradation) resulting in desirable liquid fuel range, and identified ionic liquids with good thermal stability (Los Alamos National Laboratory/University of Pennsylvania).
  - Experimentally determined the energetic landscape of several favorable carbon-boron-nitrogen (CBN) materials and provided a direct comparison with results from the high-level computationally predicted values (University of Oregon).
  - Synthesized the parent six-membered fully charged fuel and partially charged parent BN-indole material system for the CBN materials (University of Oregon).
  - Formulated N-H, N-tBu, and N-Me materials as liquids at around 80°C (University of Oregon).
- Hydrogen Sorption Materials
  - A highly stable porous polymer network (PPN-4) was synthesized and independently validated at Southwest Research Institute® with a Brunauer-Emmett-Teller (BET) surface area of 6,460 m^2/g and 8.3 wt% excess hydrogen adsorption capacity at 77 K and 55 bar (Texas A&M University).
  - Demonstrated spectroscopic evidence that appears to support the spillover effect, through observation of C-H bonds via both diffuse reflectance infrared Fourier transform spectroscopy measurements where Pt-C showed a unique stretch that was tentatively assigned to spillover hydrogen atoms and neutron scattering that revealed apparent hydrogen wagging modes which correlated to those energies predicted by theory (National Renewable Energy Laboratory).
  - Manufactured boron-substituted carbon by deposition and thermolysis of B10H14, resulting in a high-surface-area (BET surface area greater than 2,100 m2/g), high-boron-containing (8.6 wt% boron) material that achieved a ~30% increase in hydrogen excess absorption relative to the carbon precursor (on a per-surface-area unit basis) due to the increase in the average binding energy provided by the substituted boron.

System Engineering

In FY 2011, the Hydrogen Storage Engineering Center of Excellence (HSECoE) completed a baseline assessment of storage system models for reversible metal hydrides, cryo-sorbents, and both solid- and liquid-phase off-board regenerable chemical hydrogen storage material systems. The HSECoE assessed these models against the full set of DOE on-board storage targets. The Hydrogen Storage Simulator, which couples the onboard storage system model with fuel cell power plant and vehicle performance models, was run through various drive cycles to vary the hydrogen demand required from the storage system. The comparison of storage system performance against the DOE storage targets was factored into the decision to continue cryo-sorbent and liquid-phase chemical hydrogen storage material systems into Phase II of the HSECoE. Work on solid-phase chemical hydrogen storage will not be continued, due to the difficulties involved in moving solid material onto and off the vehicle rapidly enough to meet the refueling-time target. In addition, the HSECoE will not continue work on reversible metal-hydride storage materials, because these materials require elevated temperatures for charging and discharging and/or have high sorption enthalpies. While there are complex hydride materials that could allow a system to meet the system gravimetric target, the additional hydrogen that is required to be consumed to provide the sorption temperatures and energy means that the systems cannot meet DOE performance targets for onboard vehicle use.

- Conducted a status assessment of complete, engineered, materials-based hydrogen storage systems to meet the DOE 2010 and 2017 on-board hydrogen storage targets. The assessments were used as a basis for go/no-go decisions for continuing or not continuing engineering development of systems into Phase II of the HSECoE for the material classes. A decision was made to continue development of sorbent and fluid-phase chemical hydrogen storage systems and not to continue development reversible metal hydride and solid-phase chemical hydrogen storage material systems in Phase II of the HSECoE.
- Completed a unified model utilizing the MATLAB®/SimuLink environment that incorporates the performance demands and requirements of a vehicle powered by a fuel cell and those of a fuel cell with the hydrogen storage system, including thermal management (HSECoE).
- Demonstrated that expanded natural graphite, when added at levels as low as 5% weight fraction, effectively improves the thermal conductivity of compacted metal hydrides and simplifies heat-exchanger design (United Technologies Research Center).
- Obtained a 4X improvement in excess volumetric capacity with only ~15% reduction in gravimetric capacity for compacted MOF-5 versus powder MOF-5 (Ford).
- Validated kinetic models for ammonia borane by pressure composition isotherm measurements and larger-scale testing (Pacific Northwest National Laboratory).
- Demonstrated ability to scrub borazine and diborane from hydrogen released from ammonia borane to meet fuel cell quality specifications (Los Alamos National Laboratory).

Compressed and Cryogenic Tanks

In FY 2011, the sub-program increased its efforts on reducing the cost of compressed hydrogen gas storage tanks by initiating new efforts on low-cost, high-strength carbon fiber. Inexpensive storage vessels for compressed hydrogen gas are considered the most likely near-term hydrogen storage solution for the initial commercialization of fuel cell electric vehicles, as well as for other early market applications. Carbon fiber composites can currently contribute as much as 75% or more to the overall cost of tanks. A topic on "reducing the cost of high-pressure hydrogen storage tanks" was included in the FY 2011 Small Business Innovation Research solicitation, and two projects were selected–a project by Quantum Fuel Systems Technologies Worldwide, Inc., addressing advanced high-pressure tank manufacturing techniques and a project by Applied Nanotech, Inc., addressing alternative glass fibers and lightweight, high-strength carbon nanotube reinforced composites for tanks. Additionally the Hydrogen Storage sub-program supported an effort (co-funded with the DOE Vehicles Technology Program) at Oak Ridge National Laboratory to investigate the use of low-cost textile-grade fibers made from polyacrylic nitrile with methyl acrylate comonomer as precursors for high-strength carbon fiber production.

In February 2011, DOE held two workshops to identify strategies and R&D needs for lowering the cost of high-pressure hydrogen storage systems and to identify R&D needs and technical pathways for continued development of cryogenic storage, including both cryo-sorbent and cryo-compressed systems. The input garnered from these activities will aid in identifying key challenges, priorities, and needs for both compressed and cryogenic hydrogen storage systems and in development of future solicitations for R&D in these areas.

- Demonstrated the ability to melt-spin PAN precursor fibers with the target denier (for fibers 10 to 20 microns in diameter) with a one-step spinning/drawing process (Oak Ridge National Laboratory).

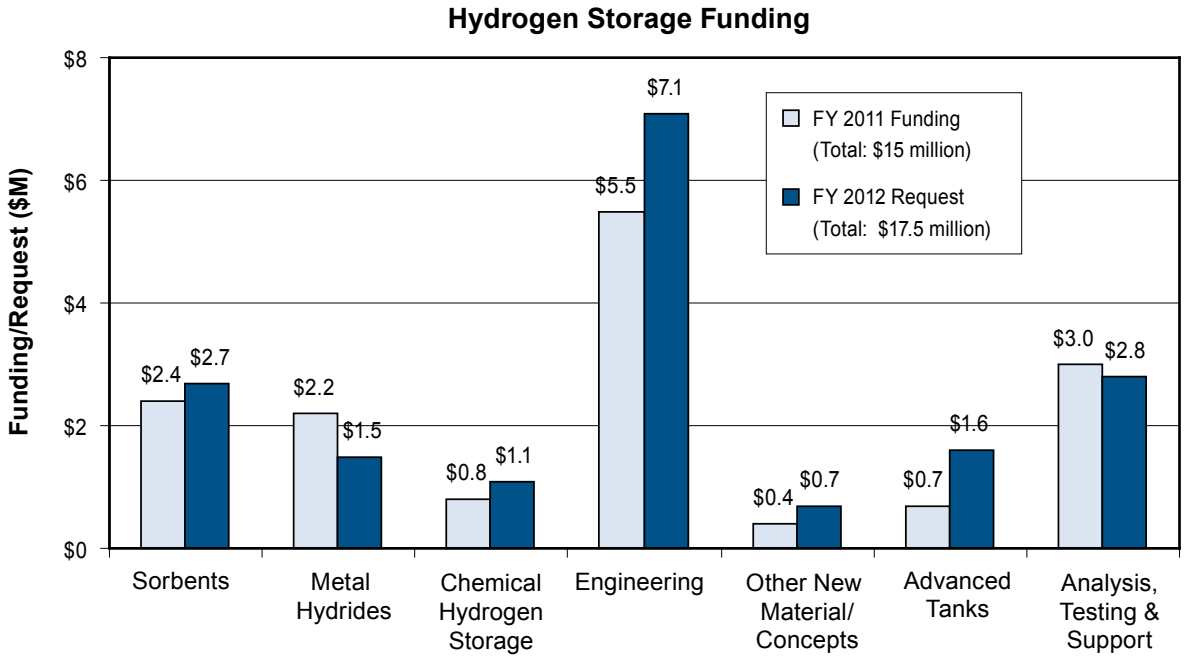
Testing, Materials Properties, and Analysis Cross-Cutting

In FY 2011, the Hydrogen Storage sub-program enlisted the National Renewable Energy Laboratory (NREL), Sandia National Laboratories (SNL), and the Pacific Northwest National Laboratory (PNNL) to carry out hydrogen storage needs assessments for non-automotive, early market applications. NREL and SNL were asked to identify the key early market applications for fuel cells where hydrogen storage presents a critical barrier for commercialization. They were also asked to determine the hydrogen storage needs for those applications and to perform gap analyses between the needs and current technologies. PNNL was asked to perform technology readiness level and manufacturing readiness level assessments of the applications and of hydrogen storage technologies these applications will require. These laboratories have gathered input (through workshops, interviews, and other activities) from stakeholders including end-users, integrators, and technology developers. The results from these assessments will be used by the sub-program to develop hydrogen storage targets, R&D plans, and future funding opportunity announcement topics for key early market applications.

- Performed system-level analysis of four hydrogen storage approaches (AX-21 and MOF-5 sorption, AB in ionic liquids, and alane), addressing capacity, charge/discharge rates, greenhouse gas emissions, safety, and cost, in addition to analysis of off-board regeneration (Argonne National Laboratory).
- Conducted and updated independent cost assessments of hydrogen storage systems using: MOF-177 sorption ($16/kWh), AX-21 sorption ($18/kWh), liquid hydrogen carriers ($16/kWh), and 350-bar ($15/kWh) and 700-bar ($19/kWh) high-pressure tanks. All of these analyses were conducted assuming systems with capacities of 5.6 kg of useable hydrogen. Also completed preliminary on-board cost assessments for 350 and 700 bar compressed single-tank systems at different manufacturing volumes—costs for the 350-bar system ranged from $15–$29 per kWh, and costs for the 700-bar system ranged from $19–$36 per kWh (TIAX, LLC).
- Three sections (Introduction, Capacity, and Kinetics) of the Best-Practices Document on the Characterization of Hydrogen Storage Materials were completed with two more sections (Thermodynamics and Cycle-Life Properties) 95% complete.
- Performed independent capacity validation of three storage materials:1) polyether ether ether ketone-derived carbon provided by State University of New York, 2) microporous carbon provided by the National Renewable Energy Laboratory, and 3) porous polymer network provided by Texas A&M University (Southwest Research Institute®).

Budget

The President's FY 2012 budget request includes $17.5 million for hydrogen storage–compared with the FY 2011 congressional appropriation of $15 million. In FY 2012, the Hydrogen Storage sub-program will continue to focus on materials discovery, system engineering for materials-based storage technologies, R&D to lower the cost of high-pressure storage systems, and systems analysis. The sub-program will also initiate activities focused on hydrogen storage for early market applications.



FY 2012 Plans

The technology portfolio for Hydrogen Storage emphasizes materials R&D to meet system targets for on-board and early market applications. While a focus on light-duty vehicle applications will continue, increased emphasis will be placed on new materials and novel concepts to meet performance requirements for early market applications. In FY 2012, goals and objectives for hydrogen storage for early market applications will be developed. The increased emphasis on developing lower-cost physical storage technologies will be strengthened. Specifically, the sub-program will use the Small Business Innovation Research program and coordinate with other efforts (e.g., DOE Vehicle Technologies Program, Defense Advanced Research Projects Agency, etc.) on development of approaches to produce low-cost carbon fiber for composite cylinders. System engineering and analysis will continue through the HSECoE and Argonne National Laboratory. Coordination with basic science efforts, including theory, characterization, and novel concepts, will continue during FY 2012. The sub-program will also coordinate with the National Science Foundation and Advanced Research Projects Agency–Energy through activities such as workshops and joint meetings.

Ned Stetson
Hydrogen Storage Team Lead
Fuel Cell Technologies Program
Department of Energy
1000 Independence Ave., SW
Washington, D.C. 20585-0121
Phone: (202) 586-9995
E-mail: Ned.Stetson@ee.doe.gov

IV.A.1 Amide and Combined Amide/Borohydride Investigations

Donald L. Anton (Primary Contact),
Christine Price, and Will James
Savannah River National Laboratory
Bldg 999-2W
Aiken, SC 29803
Phone: (803) 507-8551
E-mail: DONALD.ANTON@SRNL.DOE.GOV

DOE Manager
HQ: Ned Stetson
Phone: (202) 586-9995
E-mail: Ned.Stetson@ee.doe.gov

Project Start Date: October 1, 2011
Project End Date: Project continuation and direction determined annually by DOE

Fiscal Year (FY) 2011 Objectives

- Determine the sorption kinetics for the transition metal catalyzed $2LiH+Mg(NH_2)_2+MgH_2$ system under the full spectrum of temperatures and pressures required for hydrogen storage system design.
- Explore the effect of catalyst loading on both charge and discharge reaction pathways and kinetics as well as ammonia release.
- Identify reversible hydrogen storage compounds in the mixed metal/mix amide-borohydride system.

Technical Barriers

This project addresses the following technical barriers from the Hydrogen Storage section of the Fuel Cell Technologies Program Multi-Year Research, Development and Demonstration Plan in descending order of impact:

(A) System Weight and Volume
(E) Charging/Discharging Rates
(P) Understanding Chemisorption

Technical Targets

This project includes both fundamental studies of the sorption kinetics in the mixed metal amide, $LiH/Mg(NH_2)_2$ system, as well as new materials discovery in the mixed amide/borohydride system. Insights gained from these studies will be applied toward the design of storage systems that meet the following DOE 2010 and 2015 hydrogen storage targets (see Table 1 for values):

- System Gravimetric Capacity and Volumetric Density
- Charging/Discharging Rates
- Fuel Purity
- System Fill Time
- Minimum Hydrogen Delivery Rate

FY 2011 Accomplishments

- Majority of desorption products appear to be comprised of a mixture Mg_3N_2 and LiMgN while absorption products

TABLE 1. Technical Targets for Onboard Hydrogen Storage Systems for Light-Duty Vehicle Applications using LiMgN System[1]

Technical Target	Units	2010	2015	Ultimate	Spex milled	Fritsch milled	V_2O_5	Fe_2O_3	KH
Gravimetric Density	kg_{H2}/kg_{system}	0.045	0.055	0.075	4.2	4.6	3.8	3.5	3.9
Volumetric Density	kgH_2/L	0.028	0.04	0.07	0.023	0.025	0.021	0.019	0.023
Fill Time[2]	Min	4.2	3.3	2.5	30	30	30	30	30
Min. Full Flow Rate[3]	$(gH_2/s)/kW$	0.02	0.02	0.02	0.024	0.016	0.019	0.022	0.024
Min./Max Delivery Temp.	°C	-40/85	-40/85	-40/85	180/200	180/200	180/200	180/200	180/200
Min./Max Delivery Pressure	Bar	5/12	5/12	3/12	1/100	1/100	1/100	1/100	1/100
Fuel Purity	%	99.97	99.97	99.97	TBD	TBD	TBD	TBD	TBD

[1] Values were determined from the average between the 2nd, 3rd and 4th isothermal absorption cycles for each system with the 1st cycle was excluded.
[2] Long fill times account for 2-step reaction, which accounts for approximately 60–80% H_2 absorbed.
[3] Assumed 80 kW fuel cell for reported data,
TBD – to be determined

are comprised of MgH_2, LiH, $Mg(NH_2)_2$ (confirmed by Raman spectroscopy) and unreacted Mg_3N_2.
- All chemical dopants tested thus far, while significantly increasing desorption rate in the first cycle, have been shown to have no effect on sorption kinetics after the third cycle.
- A characteristic charging time (τ80) of 30 minutes, calculated for the isothermal charging results, is faster than those presented for this material elsewhere in the literature.
- Processing methods have been shown to greatly affect sorption kinetics and capacity with high energy processing leading to formation of NH_3 and loss of capacity (6.66 wt%) while lower energy processes minimizing NH_3 release and resulting in higher capacities (8.0 wt%) and sorption kinetics.



Introduction

In an effort to identify and synthesize a reversible metal hydride material capable of meeting the 2015 hydrogen storage technical targets, researchers are investigating various metal hydrides/catalyst combinations. To date, the most promising in situ reversible compound stemming from the Metal Hydride Center of Excellence is $2LiH/MgH_2/Mg(NH_2)_2$ [1,2]. This compound resides among a series of similar compound stoichiometries ranging from Li:Mg ratios of 1:1 through 4:1 [1-7]. It has been found that the greatest hydrogen absorbing material is $2LiH+Mg(NH_2)_2+MgH_2$ which decomposes to LiMgN plus 8.1 wt% H_2 [1] with a calculated enthalpy of desorption of 32 kJ/mole H_2. This composition has been reported to be reversible under fairly moderate conditions (160°C – 220°C for dehydriding, 160°C and 2,000 psi for rehydriding) [1]. This study of the LiMgN system used an autoclave-type high pressure charging apparatus and thermo-gravimetric analysis (TGA) measurements to confirm hydrogen storage capacities. The work reported in this investigation was designed to compliment the work of Lu *et al.* [1], by thoroughly measuring the isothermal kinetic hydrogen charge and discharge rates and further optimizing the kinetics through compositional adjustments.

Approach

$LiH/Mg(NH_2)_2$

The previously identified LiMgN material was studied by ball milling the precursor $LiNH_2$ and MgH_2 materials with the various modifiers to ensure a well-mixed and controlled initial state in terms of particle size. Material for this study was Frisch milled with a ball mass to material mass ratio of 30:1, following the work of Lu [1]. A Seivert's apparatus was used to measure the isothermal kinetics of hydrogen charge and discharge. The hydrogen uptake was monitored by the drop in the hydrogen pressure in the system while hydrogen release is monitored by the rise in hydrogen pressure. The present studies are intended to provide a detailed understanding of the isothermal kinetics of charging and discharging of the material, and the effects of materials synthesis and chemical modifications to these rates. The parameters that are explored in the current study are charge and discharge temperature, charge pressure, and the composition of the modifiers used to activate the material.

The gravimetric capacities were determined from the average of the lowest and highest weight percent of hydrogen absorbed into the 1:1 $LiNH_2$:MgH_2 mixtures. The desorption weight percents were not included due to the lack of composition data for the off-gas stream. The following equation shows the calculations used to convert weight percent to kg_{H2}/kg_{media}:

$$wt\% \rightarrow {gH_2}/{g_{media}} \rightarrow {kgH_2}/{kg_{media}}$$

where g_{H2} is the average weight of hydrogen absorbed during recharge and g_{media} is the weight of the loaded sample prior to discharge. The volumetric capacity of the metal hydrides was calculated from the gravimetric capacity and the powder packing density of the hydrogen storage materials. The following equation shows the series of calculation used to convert weight percent hydrogen to volumetric capacity in kWh/L.

$$wt\% \rightarrow {gH_2}/{g_{media}} \times \rho_{media} \rightarrow {gH_2}/{mL} \rightarrow {kgH_2}/{L}$$

where ρ_{media} is the packing density of the powder. The material used in the determination of the density for the $LiNH_2$:MgH_2 mixture was a three gram sample of 1:1 $LiNH_2$:MgH_2 milled for 2 hours using a planetary mill with a ball mill ball mass to sample mass ratio of 30:1 (for every one gram of sample, 30 grams of ball mill balls were added to the vial prior to milling). A 10 mL graduated cylinder was then gradually packed with small quantities of the milled powder with the mass and volume occupied of the powder recorded at each interval. The powder was packed via tapping the bottom of the cylinder and by inserting a plunger to pack the top of the powder. This reduced the number of layers within the powder. The average powder packing density was determined to be 0.554 g_{media}/mL.

Mixed Amide/Borohydrides

The synthesis of materials was accomplished by ball milling one component metal borohydride ($Ca(BH_4)_2$, $Mg(BH_4)_2$) with another metal amide ($LiNH_2$). This is also extended for metal amides ($Ca(NH_2)_2$, $Mg(NH_2)_2$) with lithium borohydride ($LiBH_4$). These precursors such as $LiNH_2$, $LiBH_4$, and $Mg(BH_4)_2$ are available commercially

through Aldrich, with others such as $Mg(NH_2)_2$ and $Ca(NH_2)_2$ prepared by the ammoniation of Mg and Ca inside a high pressure reactor. Once the desired metal hydrides are ball milled, powder X-ray diffraction (XRD) was used as the initial screening tool. Furthermore, thermo-gravimetric analysis, in conjunction with mass spectroscopy, was used to verify mass loss vs. temperature and identify the gas decomposition products as a function of temperature. Fourier transform infrared, Raman and nuclear magnetic resonance were used to verify investigate the characteristics of new formed compounds.

Results

$LiNH_2/MgH_2$ Kinetics

Previously, we reported the charge and discharge profiles for precursor materials $LiNH_2$ and MgH_2 in a 1:1 mole ratio with 1.5 mol% $TiCl_3$, VCl_3, $ScCl_3$, $NiCl_2$, or TiN added dopant. From TGA-residual gas analysis (RGA) data, the initial hydrogen desorption temperature began between 105°C and 120°C, depending on the dopant composition, which is lower than the 135°C release temperature for the unmodified material. Compositional additions also greatly affect ammonia release. Mixtures with $TiCl_3$, VCl_3, $ScCl_3$ and $NiCl_2$ released ammonia at temperatures lower or equal to the unmodified material, approximately 230°C. The sorption profiles were measured using a Sievert's apparatus under isothermal conditions. A standard discharge condition of 260°C into a nominal 1 bar back pressure for ~6 hours was selected, along with a standard charge condition of 180°C under a nominal 100 bar pressure for 6 hrs. These conditions were selected to reach maximum charge and discharge capacities in a single work day and were used to compare differing compositions, dopants etc.

Previous MHCoE work [1,2] on this material indicated the presence of a LiMgN phase which was not definitively confirmed in this study. Instead, a Mg_3N_2 or partially substituted $(Li,Mg)_3N_2$ phase was detected using powder XRD analysis. Other researchers have observed the presence of alternate discharge products in this system as well [3]. After cycling, no discernable kinetic affect remained from the additions. It is concluded that once the metathesis reaction between $LiNH_2$ and the halide modifiers is complete, the added metallic species are no longer active in the sorption cycle. This work has highlighted the requirement of cycling these materials to reach a steady-state operating chemistry to evaluate the effectiveness of potential additives as kinetic aids.

In order to investigate the effect of various modifiers, material was prepared to the stoichiometric composition of $LiNH_2$:MgH_2 (1:1) with 1.5 mol% vanadium oxide (V_2O_5) or iron oxide (Fe_2O_3) via Spex milling. A mixture containing 4 mol% potassium hydride (KH) was also investigated based on literature reporting an increase in kinetics of the 2:1 $LiNH_2$:MgH_2 system with the addition of KH [4]. To determine the onset of hydrogen and ammonia release, the samples were heated in the TGA at a rate of 5°C/min from 30°C to 400°C while the off-gas composition was determined from a connected RGA (Table 2).

TABLE 2. Summary of TGA/RGA Decomposition Data of the As-Milled Samples Without and Without and With Modifiers

No Modification	8.2	9.3	240	345	285°C
1.5 mol% Fe_2O_3	7.45	6.9	225	330	270°C
1.5 mol% V_2O_5	7.36	7.2	220	325	270°C
4 mol% KH	7.82	11.2	230	290	No ammonia detected

With the addition of oxide modifiers, the theoretical hydrogen capacity drops from 8.14 wt% to 7.45 wt% and 7.36 wt% for Fe_2O_3 and V_2O_5 respectively. The measured weight loss of the Fe_2O_3 modified sample was 6.9 wt% and 7.2 wt% for the V_2O_5 modified sample, which are both reasonably close to their respective theoretical capacities, indicating that the dehydrogenation process was complete without significant NH_3 release. The differences from theoretical weight capacity is attributed to the possible releasing hydrogen during the milling process. However, the KH-modified sample lost a total of 11.2 wt%, which is significantly more than the system's theoretical hydrogen content. Unlike the oxide modified samples, during the decomposition of the KH-modified sample there was no detectable release of ammonia. The addition weight loss can be attributed to the release of nitrogen gas. Desorption mechanisms for these systems are not well understood at this time.

The impact of the transition metal oxides and potassium hydride additions on average bed dis(re)charging rates were investigated with a discharge condition of 200°C into a nominal 1 bar back pressure for ~6 hours followed with a standard charge condition of 180°C under a nominal 100 bar pressure for 6 hrs. The bed recharge rates were calculated on a mass-specific basis, determining from data the quantity of hydride bed that would be required to store 5 kg of hydrogen. The bed discharge rates are not included in the values reported in Table 2 due to the lack of information on the off-gas composition, especially the concentration of ammonia and nitrogen.

As seen from Figure 1, the discharge rate was dependent on the dopant composition and cycle. Initially, the oxide modified samples showed a slight improvement over the unmodified system during the first two desorption cycles. However, after the third desorption, both samples demonstrated a continual decrease in desorption rate while the unmodified sample began to increase its rate. The reduction in discharge kinetics over four cycles can potentially be attributed to exposure to high temperatures which led to significant coarsening of the particles resulting in lowered kinetics [5]. The potassium hydride modified sample showed significantly worse discharge rates than the other samples. This indicates potential interference

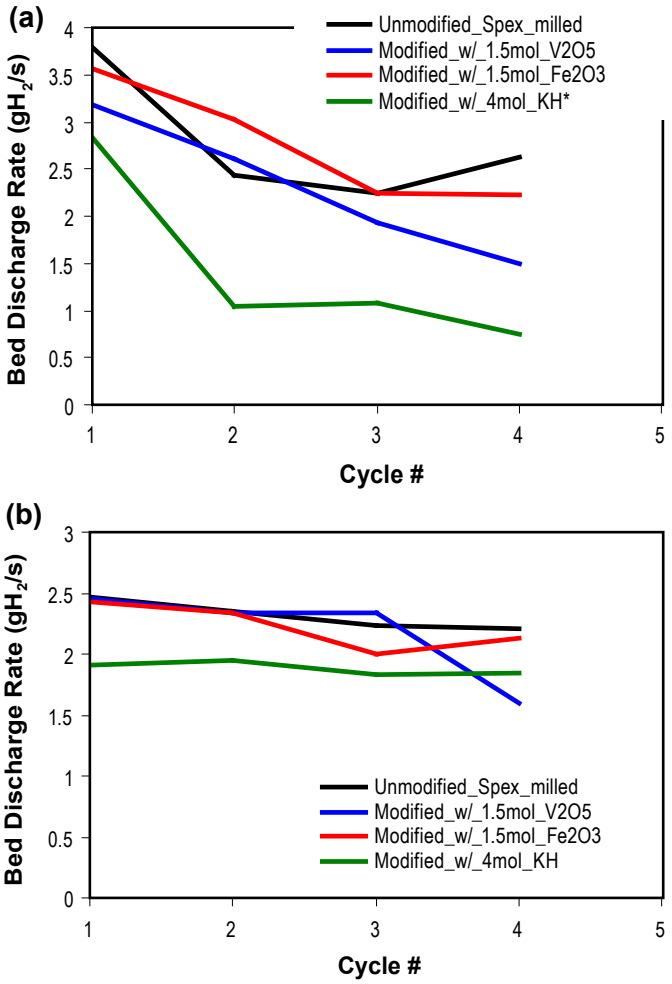


FIGURE 1. (a) Bed discharge (top) and (b) recharge (bottom) rate for unmodified (black), Fe_2O_3 (red), V_2O_5 (blue), and KH (green) modified samples. The cycling conditions are listed in the previous paragraph. (*Note: The KH sample was discharged into a smaller volume [1,030 mL] than the oxide and unmodified samples [1,190 mL] due to the use of a different pressure-concentration-temperature.)

of the modifier in the discharge reaction pathway, thus hindering the release of hydrogen from the system. An in situ diffraction study is needed to fully understand the interactions between the modifiers and the LiMgN system.

Unlike the discharge rates, the rate of recharging was not as dependent on composition of the modifier. However, the potassium hydride modified samples showed the slowest recharging rate, further indicating possible interference in the complex reaction pathway of the LiMgN system.

Mixed Amide/Borohydrides

Figure 2 shows the TGA results of $Mg(NH_2)_2$, $LiBH_4$, and various mixtures of $Mg(NH_2)_2/LiBH_4$. The unmodified samples show a much higher onset of decomposition with

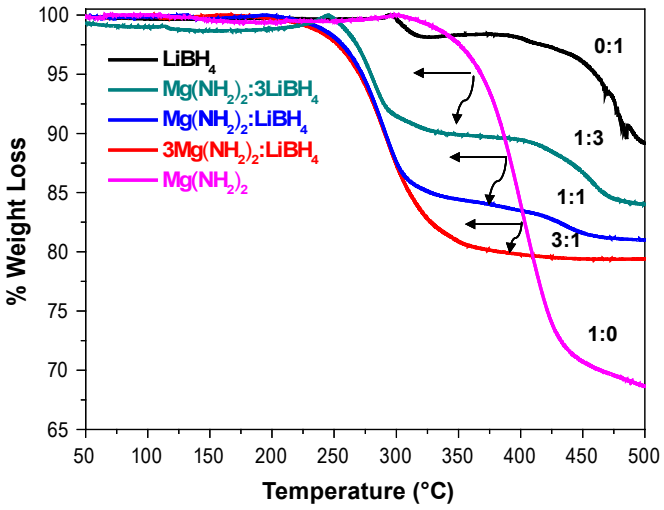


FIGURE 2. TGA Results for Mixed $Mg(NH_2)_2/LiBH_4$ Mixtures

respect to the mixtures. The addition of more $Mg(NH_2)_2$ resulted in a single decomposition similar to the starting amide material. This was also true for $3LiBH_4$:$Mg(NH_2)_2$, which had a 2-step decomposition reaction, but at a significantly lower temperature than pure $LiBH_4$. These samples were characterized using mass spectroscopy and XRD. From mass spectroscopy, the addition of $LiBH_4$ reduces the release of ammonia and increases the amount of hydrogen released. Similar results were found with the previously reported $Ca(NH_2)_2/LiBH_4$ systems, but the initial decomposition of the mixtures occur at a higher temperature. Isothermal Sievert's measurements were also conducted to evaluate the mixture's cyclic characteristics compared to their respective starting materials.

Conclusions and Future Directions

LiMgN

- Desorption at 260°C and above leads to the loss of essential nitrogen.
- The addition of Fe_2O_3 and V_2O_5 modifiers significantly reduced the amount of ammonia emission during the initial decomposition.
- V_2O_5 modified mixture showed faster sorption kinetics than the Fe_2O_3 mixture.
- Discharge rate of a hydride bed with transition metal oxide dopant at 200°C is a third of the 2010 DOE technical target of 3 g H_2/s.

Mixed Amide/Borohydrides

- Mixtures of $Mg(NH_2)_2$ with $LiBH_4$ have shown an decrease in the dehydrogenation temperature and an increase in the amount of hydrogen released.

The direction for future research is as follows:

- Couple experimental results with *ab-initio* calculations to identify kinetic enhancing mechanisms in complex metal hydride systems.
- Investigate the role of additional additives, which have been identified in other studies, on the kinetics.
- Study the role of ammonia release during cycling of modified $LiNH_2$: MgH_2.
- Determination of the transformation mechanism in $LiNH_2$:MgH_2 using Raman and infrared spectroscopy and neutron diffraction.
- Long-term cyclability studies to determine degradation in hydrogen capacity.
- Regeneration of $LiH/Mg(NH_2)_2$ using mix H_2/N_2 and H_2/NH_3 gas feeds for prolong cyclability.
- Further investigate the sorption characteristics of the $LiBH_4$ modified LiMgN system.

FY 2011 Publications/Presentations

Publications

1. Affects of mechanical milling and metal oxide additives on sorption kinetics of 1:1 $LiNH_2/MgH_2$ mixture, Donald L. Anton, Christine J. Price, and Joshua R. Gray, Energies, Accepted.

2. The Affects of Halide Modifiers on the Sorption Kinetics of the Li-Mg-N-H System, Christine Erdy-Price, Joshua Gray, Robert Lascola Jr, and Donald L. Anton, Special Edition AIChE in IJHE, Submitted.

Presentations

1. The Affects of Halide Modifiers on the Sorption Kinetics of the Li-Mg-N-H System, Christine Price, Joshua Gray, and Donald L. Anton, Fall AIChE Conference 2010, Salt Lake City, Utah.

References

1. Lu, J.; Fang, Z.Z.; Choi, Y.J.; and Sohn, H.Y. *J. Phys. Chem. C.*, **111**, pp. 12129. (2007)

2. Alapati, S.V.; Johnson, K.J.; Sholl, D.S. *J. Phys. Chem.* **110**, pp. 8769. (2006)

3. Yamane, H.; Okabe, T.H.; Ishiyama, O.; Waseda, Y., Shimada, M. *J. Alloys Compounds*, **319**, pp. 124. (2001)

4. Dehouche, Z.; Klassen, T.; Oelerich, W.; Goyette, J.; Bose, T.K.; Schulz, R. Cycling and thermal stability of nanostructured MgH_2–Cr_2O_3 composite for hydrogen storage. J. Alloys Compd. 2002, **347**, 319–323.

IV.A.2 Efficient Discovery of Novel Multicomponent Mixtures for Hydrogen Storage: A Combined Computational/Experimental Approach

Christopher Wolverton (Primary Contact), Vidvuds Ozolins, Harold H. Kung
Department of Materials Science & Engineering
Northwestern University
Evanston, IL 60208
Phone: (847) 467-0593
E-mail: c-wolverton@northwestern.edu

Cost-Sharing Partners:
Andrea Sudik and Jun Yang
Ford Motor Company, Dearborn, MI

DOE Managers
HQ: Ned Stetson
Phone: (202) 586-9995
E-mail: Ned.Stetson@ee.doe.gov
GO: Katie Randolph
Phone: (720) 356-1759
E-mail: Katie.Randolph@go.doe.gov

Contract Number: DE-FC36-08GO18136

Project Start Date: September 1, 2008
Project End Date: July 31, 2013

Fiscal Year (FY) 2011 Objectives

The objective of the project is to discover novel mixed hydrides for hydrogen storage, which enable the DOE 2010 system-level goals. Our goal is to find a material that desorbs 8.5 wt% H_2 or more at temperatures below 85°C. The research project will combine first-principles calculations of reaction thermodynamics and kinetics with material and catalyst synthesis, testing, and characterization. We will combine materials from distinct categories to form novel multicomponent reactions. Examples of systems to be studied include mixtures of complex hydrides and chemical hydrides and novel multicomponent complex hydride materials and reactions.

Technical Barriers

This project addresses the following technical barriers from the Storage section of the Fuel Cell Technologies Program Multi-Year Research, Development and Demonstration Plan:

(P) Lack of Understanding of Hydrogen Physisorption and Chemisorption

(A) System Weight and Volume

(E) Charging/Discharging Rates

Technical Targets

This study is aimed at fundamental insights into new materials and the thermodynamic and kinetic aspects of H_2 release and reabsorption from them. Insights gained from these studies will be applied toward the design and synthesis of hydrogen storage materials that meet the following DOE 2010 hydrogen storage targets:

- Specific energy: 1.5 kWh/kg
- Energy density: 0.9 kWh/L

FY 2011 Accomplishments

- Synthesis and characterization of two predicted promising hydride mixtures: $5LiBH_4 + 2Mg(BH_4)_2$ and $Mg(BH_4)_2 + Mg(NH_2)_2$.
- Prediction of new previously-unknown $MgBNH_6$ compound, stable with respect to $Mg(BH_4)_2 + Mg(NH_2)_2$.
- Proposed new metal-carbon catalyst: Tested on $NaAlH_4$, and applied to $Mg(BH_4)_2 + Mg(NH_2)_2$; Effective catalyst - lowers desorption temperature of both reactions, and reduces formation of NH_3 in the latter case.
- Predicted new CaB_2H_6 product in decomposition of $Ca(BH_4)_2$.
- Predicted structure of AlB_4H_{11} polymeric compound.
- Found new low-energy decomposition product of amidoborane reactions; found stability trends in ammonia-borane reactions to tailor ΔH to choice of metal cation.
- Extended prototype electrostatic ground state (PEGS) and grand-canonical linear programming (GCLP) to apply to nano-confined materials. Explored nano $NaAlH_4$ and $LiBH_4$ reactions.
- Developed predictive models of kinetics of mass transport. Application to $NaAlH_4$ and extension to borohydrides (in progress).



Introduction

The 2010 and 2015 FreedomCAR/DOE targets for hydrogen storage systems are very challenging, and cannot be met with existing materials. The vast majority of the work to date has delineated materials into various classes, e.g., complex and metal hydrides, chemical hydrides, and sorbents. However, very recent studies indicate that mixtures of storage materials, particularly mixtures between various classes, hold promise to achieve technological

attributes that materials within an individual class cannot reach. Our project involves a systematic, rational approach to designing novel multicomponent mixtures of materials with fast hydrogenation/dehydrogenation kinetics and favorable thermodynamics using a combination of state-of-the-art scientific computing and experimentation. Specifically, we focus on combinations of materials from distinct categories to form novel multicomponent reactions.

Approach

We use the accurate predictive power of first-principles modeling to understand the thermodynamic and microscopic kinetic processes involved in hydrogen release and uptake and to design new material/catalyst systems with improved properties. Detailed characterization and atomic-scale catalysis experiments elucidate the effect of dopants and nanoscale catalysts in achieving fast kinetics and reversibility. And, state-of-the-art storage experiments give key storage attributes of the investigated reactions, validate computational predictions, and help guide and improve computational methods. In sum, our approach involves a powerful blend of: 1) H_2 storage measurements and characterization, 2) state-of-the-art computational modeling, 3) detailed catalysis experiments, and 4) in-depth automotive perspective.

Results (Selected Examples)

Reaction Pathway Characterization for $Mg(NH)_2$-$Mg(BH_4)_2$

We have performed initial characterization experiments of the reaction pathway for the $Mg(NH)_2$-$Mg(BH_4)_2$ mixture. In particular, we have collected new in situ X-ray diffraction (XRD) and quenched Fourier transform infrared (FT-IR) data (Figure 1) toward characterization of the 2-step hydrogen desorption pathway which releases a total of ~11 wt% when heated to 550ºC. From these new data, we propose that the first hydrogen release step (room temperature to 300ºC and ~7 wt%) involves consumption of an amide reactant and formation of a product phase that involves boron-nitrogen bonding (infrared data). The second hydrogen release step (>300º and 4 wt%) involves decomposition of the B-N phase from step 1 and the formation of Mg and MgB_2 (infrared and XRD data). More experimental data and on-going computational studies are needed to determine the specific experimental and computational pathways from potential reactant hydride formation through complete dehydrogenation.

Facilitating Dehydrogenation of Complex Hydrides Using a Novel Metal-Carbon Catalyst

We have demonstrated that our metal-carbon catalysts are effective for facilitating dehydrogenation of solid-state hydrides, using $NaAlH_4$ as a model compound. The catalyst, comprised of metal nanoparticles and carbon support, serves multiple functions including nano-compartment of hydride, sites for nucleation, and hydrogen transport.

For low-melting point hydrides such as $NaAlH_4$, mixing the hydride with carbon materials such as activated carbon with high surface area and highly porous structure can significantly lower the dehydrogenation temperature (>100°C). The effect of carbon is mostly due to the nano-structuring of the hydride. As $NaAlH_4$ melts and diffuses into micropores of carbon, $NaAlH_4$ is confined into a

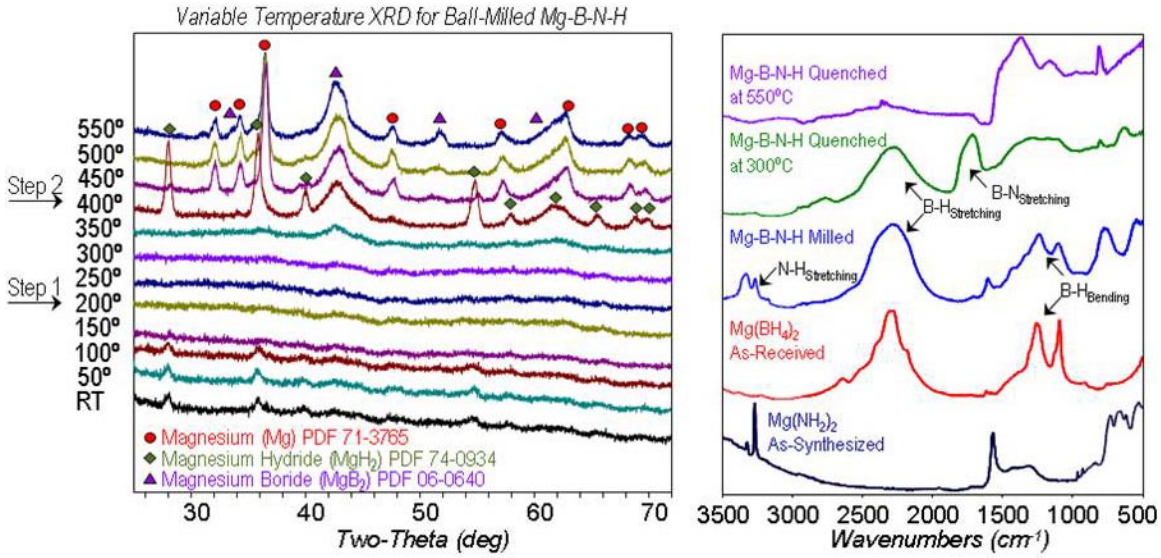


FIGURE 1. (a) In situ XRD data for ball-milled $Mg(NH)_2$-$Mg(BH_4)_2$ mixture (heating rate 1°C /min) (b) FT-IR data for ball-milled $Mg(NH)_2$-$Mg(BH_4)_2$ comparing reactants ($Mg(NH_2)_2$, (navy) and $Mg(BH_4)_2$, (red) with ball-milled mixture (blue) and quenched samples at 300°C (green) and 550ºC (purple).

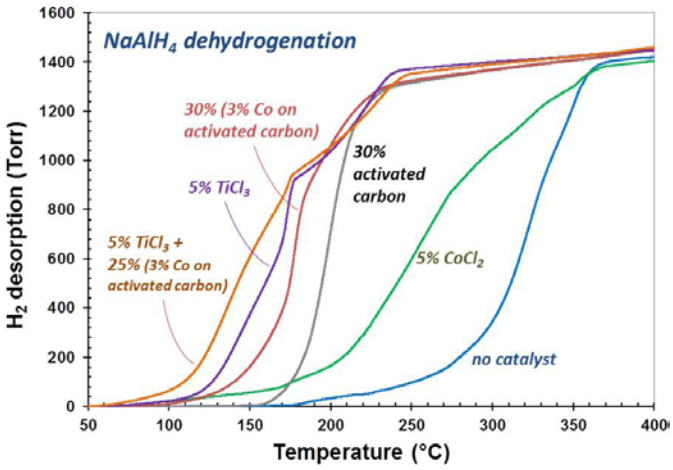


FIGURE 2. The Dehydrogenation of $NaAlH_4$ using Different Catalysts

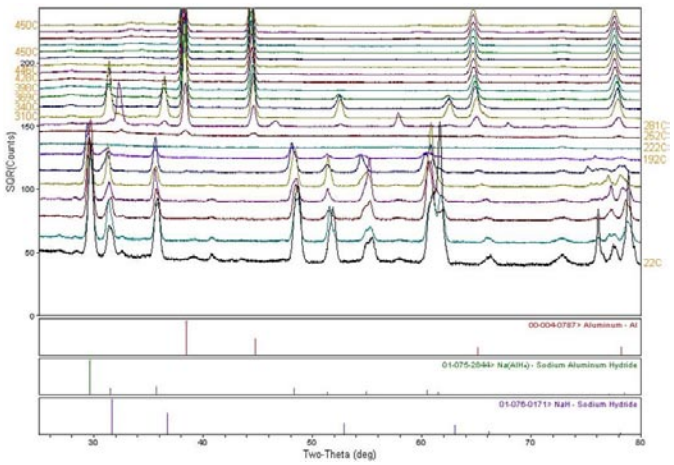


FIGURE 3. In Situ XRD of $NaAlH_4$ Dehydrogenation Without Catalyst

nano-size region and starts to dehydrogenate at a lower temperature as a result.

Adding a small amount of transition metal such as cobalt on the carbon can further enhance the catalytic effect. Mixing with such cobalt-carbon catalyst, $NaAlH_4$ starts to dehydrogenate below its melting point. This enhanced effect could be attributed to hydrogen spillover facilitated by metal nanoparticles–the hydrogen atoms dehydrogenated from hydride migrate to hydride-carbon surface and recombine on the metal surface to desorb into gas phase. The cobalt-carbon catalyst can catalyze $NaAlH_4$ dehydrogenation below 130°C. Typically it can only be done by using Ti-based catalysts, which catalyzed the reaction through forming Ti-Al intermediates to facilitate hydrogen transportation. However, unlike Ti-based catalysts deactivate due to $TiAl_3$ formation after several dehydrogenation–rehydrogenation cycles, cobalt-carbon catalysts do not interact with hydride to form intermediates and catalyze the dehydrogenation under a different working principle. As a result, we observed synergistic effect from combing cobalt-carbon and $TiCl_3$ catalysts for $NaAlH_4$–dehydrogenation starts even below 100°C (Figure 2).

As shown in Figure 3 and 4, the evidence of $NaAlH_4$ dehydrogenated below its melting point when catalyzed by a cobalt-carbon catalyst was provided by in situ XRD study of $NaAlH_4$ dehydrogenation from room temperature to 450°C. As can be seen in Figure 3, $NaAlH_4$ without catalyst melted at 222°C and no diffraction pattern can be detected (flat line). The subsequent diffraction patterns indicate the dehydrogenation began at a temperature above the melting point. In contrast, $NaAlH_4$ catalyzed by cobalt-carbon catalyst started to dehydrogenate at a temperature as low as 192°C and resulted in phase transformation of $NaAlH_4$ as can be seen in Figure 4.

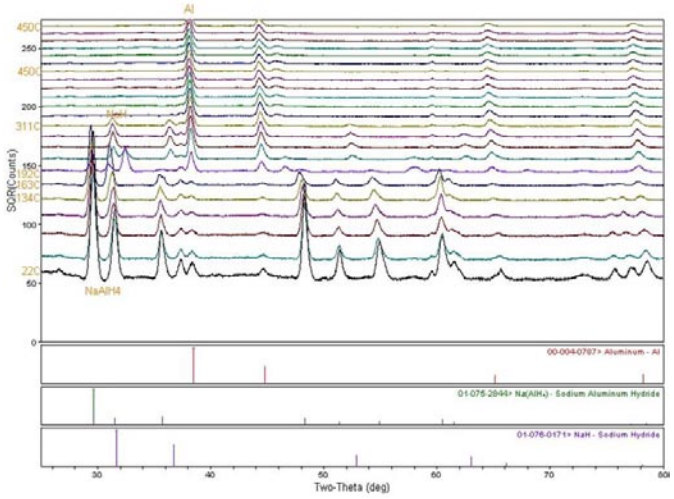


FIGURE 4. In Situ XRD of $NaAlH_4$ Dehydrogenation with 30% 3Co-AC-IWI-350°C

Using PEGS to Help Deduce Amorphous Hydride Structures: The Polymeric Structure of AlB_4H_{11} (collaboration with Ji-Cheng Zhao at Ohio State University)

The group of Prof. Zhao at Ohio State University synthesized the AlB_4H_{11} compound through the reaction $2Al(BH_4)_3+B_2H_6 \rightarrow 2AlB_4H_{11}+4H_2$. The H_2 reversibility of the new compound is observed at mild conditions: 200°C and 90 bar H_2, but its amorphous structure is unknown.

The PEGS method has been proved to be effective in the prediction of most "simple" complex hydrides with well-known anion geometries, like $Mg(BH_4)_2$. For the current AlB_4H_{11} stoichiometry, the structure of the $[B_4H_{11}]^{3-}$ anion geometry structure is presently unknown. Therefore, in the PEGS simulations, we split the AlB_4H_{11} into different small known fragments, $Al+[BH_4]+[BH_3]+2[BH_2]$ or

$[AlH_4]+3[BH_2]+[BH]$. Surprisingly, after the PEGS and density functional theory (DFT), the fragments of B except $[BH_4]$ bond together to form a larger B cluster. In the low-energy structure at one formula unit (fu), it contains Al, $[BH_4]$ and $[B_3H_7]$ clusters, and they forms a -Al$[BH_4]$-$[B_3H_7]$- polymer chain, which is consistent with the experimental evidence (e.g., nuclear magnetic resonance and other measurements performed at Ohio State). Comparing the theoretical phonon density of states (pDOS) calculations and experimental neutron vibration spectra, we find that our pDOS is in overall agreement with the experimental peaks.

Subsequently, experiments confirmed our PEGS predication that there are two kinds of B clusters, $[BH_4]$ and $[B_3H_7]$, but also suggest two kinds of Al environments that our initially predicted structure doesn't have, since we only performed calculations of one formula unit (and hence, only one Al atom). Therefore, we believe the two anion groups ($[BH_4]$ and $[B_3H_7]$) are correct and implement these into the PEGS code, and increased the cell size to two formula units. At 2 fu, a new low-energy AlB_4H_{11} structure is predicated, which is ~400 meV/fu lower than the previous one. In this new structure, it still shows the -Al$[BH_4]$-$[B_3H_7]$- polymer chain, and Al clearly has two kinds of surroundings. Its pDOS is excellent agreement with the experimental neutron vibration spectra. The PEGS predicted AlB_4H_{11} structure is therefore in excellent agreement with all the experimental data obtained. PEGS has previously been shown to provide accurate predictions of complex hydrides with well-known anion geometries. However, in this work, we extend the method and successfully apply it to cases where the anion geometry is unknown.

Computational Studies of Finite Size Effects in Lithium Borohydride Nanoclusters

Reducing the size of the bulk solids to the nanoscale regime is one approach that may allow for engineered equilibrium pressures and reaction kinetics that are more suitable for on-board hydrogen storage. First principles calculations on MgH_2 nanoparticles, for example, indicate that significant lowering of the desorption enthalpy is possible with decreasing cluster size [1]. Recent experimental work has demonstrated considerable changes in kinetics for hydrogen storage materials when incorporated in nanoporous frameworks. These frameworks include high surface area carbon aerogels [2,3], block-copolymer-templated highly ordered carbons [4], and metal-organic-frameworks (MOFs) [5].

In collaboration with Profs. Eric Majzoub from University of Missouri, St. Louis and Feng-Chuan Chuang from National Sun Yat-Sen University in Taiwan we are addressing the intrinsic reaction thermodynamics and decomposition pathways of gas-phase lithium borohydride clusters in the few nanometer size regime; such clusters can be synthesized in nanopores of high-surface-area carbons and MOFs, and are currently under investigation in the Northwestern group. We have recently generalized the GCLP method to determine thermodynamically preferred decomposition pathways in finite-size systems, which allows us to obtain the phase diagram of small, free clusters of complex hydrides [6]. In the case of $(NaAlH_4)_n$ clusters with $n\leq8$ we found that decomposition pathways of free-standing clusters are drastically different from those of bulk sodium alanate, favoring hydrogen release in a one-step reaction leading to the formation of mixed $(AlNa)_n$ nanoclusters. We also predicted nanocluster analogues of bulk destabilized reactions between simple hydride (NaH and AlH_3) and complex hydride ($NaAlH_4$) nanoclusters. It is considerable interest whether similar phenomena can be found in materials with higher hydrogen content than sodium alanate.

Using the recently developed PEGS method and genetic algorithm in conjunction with DFT calculations, we predict the structures of small clusters of $LiBH_4$ and its decomposition products (Li, B, Li_nB_n, LiH) with up to 12 Li and B atoms. A few representative structures are shown in Figures 5, 6 and 7. Just like the case for the bulk $LiBH_4$ compound, our preliminary results indicate that the decomposition pathway of $LiBH_4$ nanoclusters with $N\geq6$ involves the formation of closoboranes based on $(B_nH_n)^{2-}$ anions. The calculate decomposition enthalpies are shown in Figure 8 as functions of the cluster size. These results demonstrate that lithium borohydride nanoclusters higher enthalpies of hydrogen release than bulk materials, suggesting that any destabilization observed in recent experiments must come due to strong interaction effects with

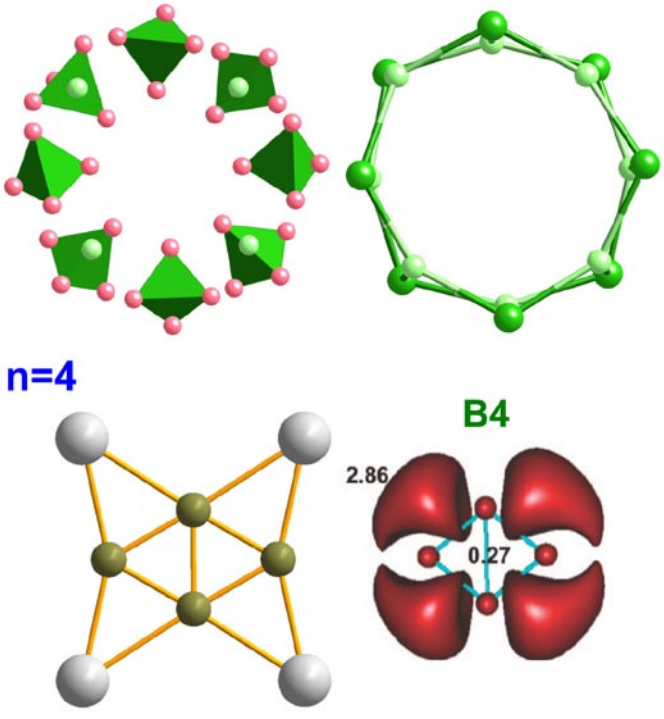


FIGURE 5. Top: Structure of $(LiBH_4)_8$ cluster found using PEGS and DFT. Bottom: structure of Li_4B_4 cluster found using genetic algorithm.

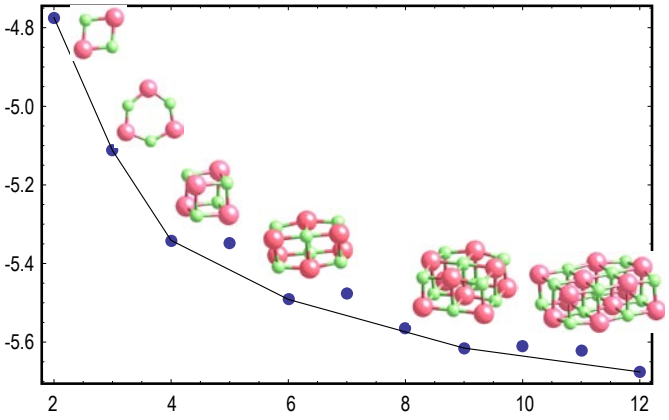


FIGURE 6. Energy of LiH clusters versus cluster size. Inset figures show the clusters that lie on the convex hull.

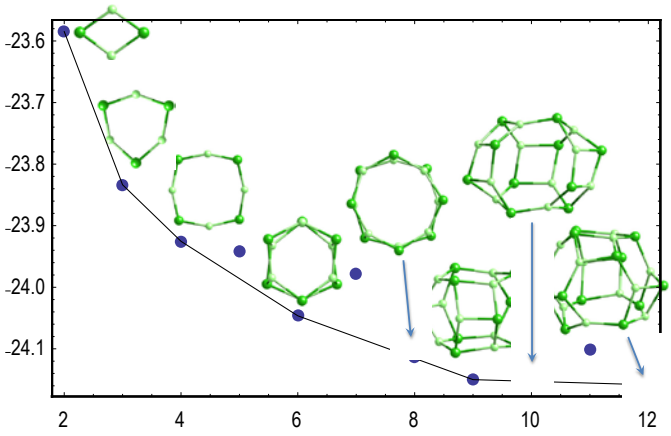


FIGURE 7. Energy of $LiBH_4$ clusters versus cluster size. Inset figures show the clusters that lie on the convex hull. Only Li and B atoms are shown.

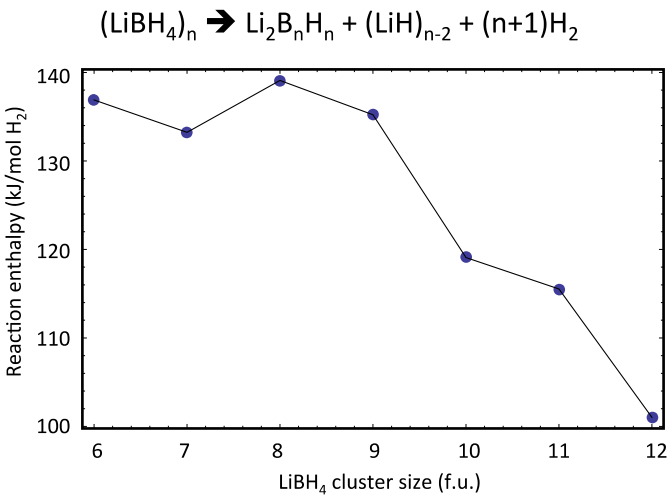


FIGURE 8. Calculated Decomposition Enthalpies of $LiBH_4$ Clusters as Functions of Cluster Size

the porous support. These results are in marked contrast to earlier DFT-based findings for metal nanoclusters, which suggested destabilization with decreasing size and the appearance of new decomposition pathways. We are currently in the process of refining the structures of B_nH_m nanoclusters using genetic algorithms. Inclusion of B_nH_m may yet change the preferred decomposition pathways and somewhat alter the preliminary conclusions reached so far.

Conclusions and Future Directions

- Experimentally characterize storage properties/reactions of $(NH_4)_2B_{12}H_{12}$ and other predicted reactions; elucidate decomposition pathway for $Mg(BH_4)_2$+$Mg(NH_2)_2$ mixture.
- Extend experimental catalyst studies to other predicted promising materials; explore optimal morphology of carbon/metal catalysts.
- Direct computational efforts to focus on kinetics, defects, diffusion/mass transport in promising predicted reactions.
- Continue some computational exploration for: novel BH_4/NH_2 compounds and reversible reactions, and mixed metal borohydrides.

References

1. Wagemans, R., van Lenthe, J., de Jongh, P., van Dillon, A., & de Jong, K. (2005). Hydrogen Storage in Magnesium Clusters: Quantum Chemical Study. *J. Am. Chem. Soc., 127*, 16675-16680.

2. Gross, A., Vajo, J., Van Atta, S., & Olson, G. (2008). Enhanced Hydrogen Storage Kinetics of LiBH4 in Nanoporous Carbon Scaffolds. *J. Phys. Chem. C, 112*, 5651.

3. Gross, A., Ahn, C., Van Atta, S., Liu, P., & Vajo, J. (2009). Fabrication and hydrogen sorption behaviour of nanoparticulate MgH2 incorporated in a porous carbon host. *Nanotechnology, 20*, 204005.

4. Liu, X., Peaslee, D., Jost, C., & Majzoub, E. (2010). Controlling the Decomposition Pathway of LiBH4 via Confinement in Highly Ordered Nanoporous Carbon. *J. Phys. Chem. C.*

5. Bhakta, R., Herberg, J., Jacobs, B., Highley, A., Behrens Jr., R., Ockwig, N., et al. (2009). Metal-Organic Frameworks As Templates for Nanoscale NaAlH4. *J. Am. Chem. Soc. Comm., 131*, 13198–13199.

6. Majzoub, E., Zhou, F. & Ozolins, V. (2011). "First-principles calculated phase diagram for nanoclusters in the Na-Al-H system: A single-step decomposition pathway for $NaAlH_4$. *To appear in Journal of Physical Chemistry C.*

IV.A.3 Fundamental Studies of Advanced High-Capacity, Reversible Metal Hydrides

Craig M. Jensen[1] (Primary Contact),
Derek Birkmire[1], Marina Chong[1], Paul Beaumont[1],
Henrietta Langmi[2], and G. Sean McGrady[2]
[1]University of Hawaii
Department of Chemistry
Honolulu, HI 96822
Phone: (808) 956-2769
E-mail: jensen@gold.chem.hawaii.edu
[2]University of New Brunswick, Fredericton, NB, Canada

DOE Managers
HQ: Ned Stetson
Phone: (202) 586-9995
E-mail: Ned.Stetson@ee.doe.gov
GO: Paul Bakke
Phone: (720) 356-1436
E-mail: Paul.Bakke@go.doe.gov

Contract Number: DE-FC36-05GO15063

Project Start Date: April 1, 2005
Project End Date: September 30, 2011

Fiscal Year (FY) 2011 Objectives

The objective of this project is to develop a new class of reversible materials that have the potential to meet the DOE kinetic and system gravimetric storage capacity targets. Current investigations include:

- The study of novel, high hydrogen capacity, borohydrides that can be reversibly dehydrogenated at low temperatures.
- The development of a method for the hydrogenation LiH/Al to $LiAlH_4$ at moderate pressures in non-conventional solvents.

Technical Barriers

This project addresses the following technical barriers from the Hydrogen Storage section of the Fuel Cell Technologies Program Multi-Year Research, Development and Demonstration Plan:

(A) System Weight and Volume
(E) Charging/Discharging Rates
(J) Thermal Management
(P) Lack of Understanding of Hydrogen Physisorption and Chemisorption

Technical Targets

The work on this project is currently exclusively devoted to materials that have demonstrated available hydrogen capacities of 7-17 wt% hydrogen. We have developed a system for the full reversible dehydrogenation of $Mg(BH_4)_2$ to MgB_2 that has shown a record, >12 wt% reversible hydrogen capacity but requires further development to meet kinetic performance targets within the target temperature. We have also developed a highly efficient method of the direct hydrogenation of LiH/Al to Ti-doped $LiAlH_4$ (7 wt% hydrogen capacity, rapid dehydrogenation at 120-150°C) at moderate pressure and room temperature that has been estimated to have a well-to-tank energy efficiency that approaches 60% and thus approaches DOE targets.

Accomplishments

We have provided the first example of the reversible, solid state dehydrogenation of a borohydride at temperatures below 350°C (200°C, 100 atm).



Introduction

The development of high capacity, hydrogen storage materials that can be recharged under moderate conditions is a key barrier to the utilization of hydrogen as an onboard energy carrier. Towards this end we have examined anionic borohydride complexes as hydrogen storage materials. Our initial focus was on anionic transition metal complexes. The anionic character of these compounds was found to result in an increased stability and a reduced volatility when compared to neutral transition metal borohydride complexes. Our efforts are currently focused on determining whether the thermodynamic parameters of these complexes will allow them to undergo reversible dehydrogenation. In the course of these investigations we have found that that ball-milled mixtures of MgB_2 and catalytic additives undergo full hydrogenation to $Mg(BH_4)_2$ at high pressures. In consideration of the >14 wt% hydrogen that is potentially cyclable with this system, it has become the focus of our efforts in the area of borohydride complexes.

In collaboration with the University of New Brunswick (UNB), we are also developing new approaches utilizing supercritical fluids and non-conventional solvents for the direct synthesis of AlH_3 and $LiAlH_4$. $LiAlH_4$ releases hydrogen according to the two reactions seen in equations 1 and 2. Although the second reaction is endothermic ($\Delta H = +25$ kJ/mol H_2), the first reaction is exothermic

$$3LiAlH_4 \rightarrow Li_3AlH_6 + 2Al + 3H_2 \quad (1)$$

$$Li_3AlH_6 \rightarrow 3LiH + Al + 1.5H_2 \quad (2)$$

($\Delta H = -10$ kJ/mol H_2). Since entropic change is strongly positive for hydrogen release, the first reaction is thermodynamically irreversible under all practical conditions and it has been widely accepted that $LiAlH_4$ cannot be recharged and there have been no reports of its use for reversible hydrogen storage. However, the unfavorable thermodynamics may be altered by carrying out the reaction in solution, with the solvation of $LiAlH_4$ contributing to an (ideally) endothermic ΔH value. As early as 1963, [1] reported that a mixture of LiH and activated Al in tetrahydrofuran (THF) or diglyme solvent reacted with 350 bar H_2 at 120°C to produce $LiAlH_4$. Improved syntheses of the THF adduct has recently been reported by [2] and researchers at Brookhaven National Laboratory by using Ti additives to significantly lower the required pressure and temperature. While the methods of both Ashby and Ritter result in the ultimate formation of $LiAlH_4$ from LiH, Al and H_2, they are impractical because of the requirements of high temperature, high pressure, and/or mechanical energy during the synthesis as well as subsequent heating removal the THF solvent (vacuum drying at 60°C for several hours). As Ashby noted, it is very difficult to remove the final vestiges of THF and the prolonged baking in vacuo required to remove THF results in the dehydrogenation of the majority of a Ti-activated product. We have discovered that by the this difficulty can be circumvented by utilizing liquefied dimethyl ether as the reaction solvent as it is sufficiently coordinating to support the nascent $LiAlH_4$ in the reaction environment, yet which is also volatile enough to be removed easily once it has served this purpose. Our highly efficient, room temperature direct synthesis of $LiAlH_4$ in liquefied Me_2O shows great promise as a practical method for the re-hydrogenation of LiH/Al to $LiAlH_4$.

Approach

Having demonstrated the reversible elimination of over 11 wt% hydrogen from $Mg(BH_4)_2$, we wish to develop methods for hydrogen cycling in this system under less forcing conditions. In order to accomplish this, we required a more detailed understanding of the dehydrogenation reaction pathway. Thus we have monitored both the dehydrogenation and re-hydrogenation reactions by X-ray diffraction and magic angle spinning boron-11 nuclear magnetic resonance spectroscopy (MAS ^{11}B NMR) and conducted quantitative thermal volumetric pressure-composition-temperature measurements.

We have found that nearly the entire 7.9 wt% theoretical cycling capacity can be restored in the first cycle of re-hydrogenation of Ti-doped LiH/Al in liquefied dimethyl ether at room temperature under 100 bar of Me_2O/H_2. Calculations show that this recharging process approaches 60% well-to-tank efficiency. Dimethyl ether performs well as the solvent for this reaction since it is more polar and volatile than diethyl ether, it forms a strong complex with Li^+, and it evaporates quickly at room temperature (boiling point = -24°C). However, the cycling capacity dramatically drops off over the first five cycles of dehyrogenation/re-hydrogenation. In order to overcome this limitation, we have explored the extension of the maximum cycling capacity of Ti-doped $LiAlH_4$ through variation of the dopant concentration, recharging conditions, and variation dopants.

Results

Task 1. Characterization of the Active Titanium Species in Ti Doped $NaAlH_4$

This task has been completed.

Task 2. Spectroscopic Studies of Complex Hydrides

This task has been completed.

Task 3. Thermodynamic Properties of Complex Hydrides

This task has been completed.

Task 4. Kinetic Enhancement of "Thermodynamically Tuned" Binary Hydrides

This task has been completed.

Task 5. Synthesis and Evaluation of Novel Borohydrides

Our earlier studies found that it was possible to fully hydrogenate MgB_2 to $Mg(BH_4)_2$ under high hydrogen pressures. It was not clear from the results of these study whether $Mg[B_{12}H_{12}]$ is an intermediate in the reaction pathway that operates under these conditions. To answer this question, we have studied the early stages of the solid state dehydrogenation Mg(BH4)2 in the solid state by ^{11}B NMR spectroscopy. The dehydrogenation of $Mg(BH_4)_2$, was followed by temperature programmed desorption/thermal gravimetric analysis over a set of isothermal temperatures (300, 350, 400°C) at various reaction times. The study was conducted with the concomitant analysis of the volatile gas species by temperature-programmed desorption/thermogravimetric analysis/mass spectroscopy (TPD/TGA/MS). Over this temperature range, a decrease of 6-10 mass% from the $Mg(BH_4)_2$ sample was observed with H_2 as the only volatile species detected by MS. At the end of each TPD experiment, the residual decomposition products were dissolved in aqueous media for analysis by solution phase NMR spectroscopy. Figure 1 shows representative $^{11}B[H]$ NMR spectra from samples heated to 300, 350 and 400°C. Four major resonances are observed in each spectra; boric acid at 5 ppm, $[B_{12}H_{12}]^{2-}$ at -15.6 ppm, $[B_{10}H_{10}]^{2-}$ at -29.2 ppm and $[B_3H_8]^-$ at -31 ppm. The results of these studies are summarized in Table 1. The major species observed in the ^{11}B NMR after hydrolysis of the thermal decomposition products is boric acid resulting from the hydrolysis of the unstable polyborane species

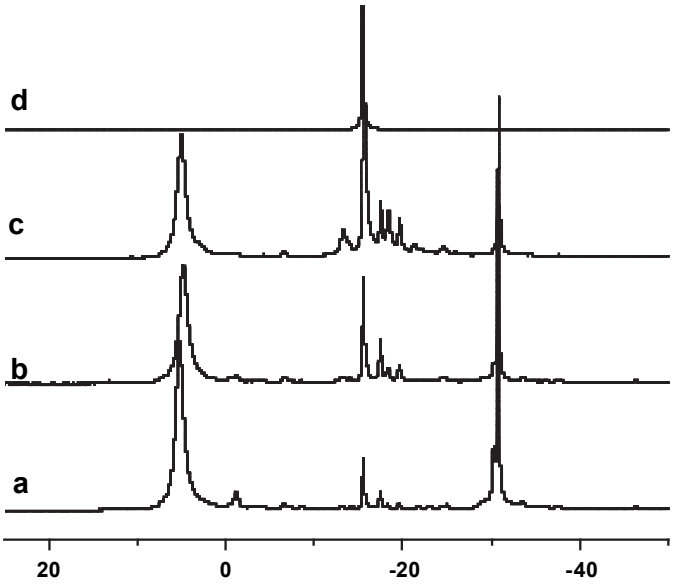


FIGURE 1. Solution $^{11}B\{H\}$ NMR of products resulting from dehydrogenated $Mg(BH_4)_2$ dissolved in aqueous solutions. a) $Mg(BH_4)_2$ heated to 300°C for 12 h, b) $Mg(BH_4)_2$ heated to 350°C for 6 h, c) $Mg(BH_4)_2$ heated to 400°C for 2 h, and d) $MgB_{12}H_{12}$.

TABLE 1. ^{11}B NMR analysis of the major products (mol%) formed in decomposition of $Mg(BH_4)_2$ followed by partial hydrolysis. Chemical shifts are reported relative to $BF_3{\cdot}OEt_2$ at 0 ppm.

(δ ppm)	Species	300°C	350°C	400°C
5	$B(OH)_4^-$	86	87	83
-15.2	$(B_{12}H_{12})^{2-}$	0.4	1.5	4.5
-29.2	$(B_{10}H_{10})^{2-}$	0.8	0.2	0.0
-30.3	$(B_3H_8)^-$	12.6	9.0	6.5

formed during the decomposition of $Mg(BH_4)_2$. In addition to the unstable polyborane species a small amount of the stable dodecaborane $[B_{12}H_{12}]^{2-}$ is observed. However, the yield, ranging from 0.4 to 4.5 mol% is significantly less than the theoretical yield assuming complete conversion of $Mg(BH_4)_2$ to magnesium dodecaborane, ca. 16.6 mol% $(B_{12}H_{12})^{2-}$ (8.0 wt% H_2). It is also notable that a signifcant concentration of the triborane is present, especially at lower temperatures. The results of these studies indicated that the first step in the decomposition of $Mg(BH_4)_2$ involves the formation of a meta-stable triborane species, $Mg(B_3H_8)_2$. In order to verify this conclusion, we investigated the slow dehydrogenation of $Mg(BH_4)_2$ en vacuo at 200°C over a five-week period. Solid state and solution ^{11}B NMR spectra (solution NMR seen in Figure 2a) of the dehydrogenated product showed that there is much higher selectivity for the production of $Mg(B_3H_8)_2$ at this lower temperature.

We next probed the reversibility of the dehydrogenation of the $Mg(BH_4)_2$ to $Mg(B_3H_8)_2$. Experiments were carried

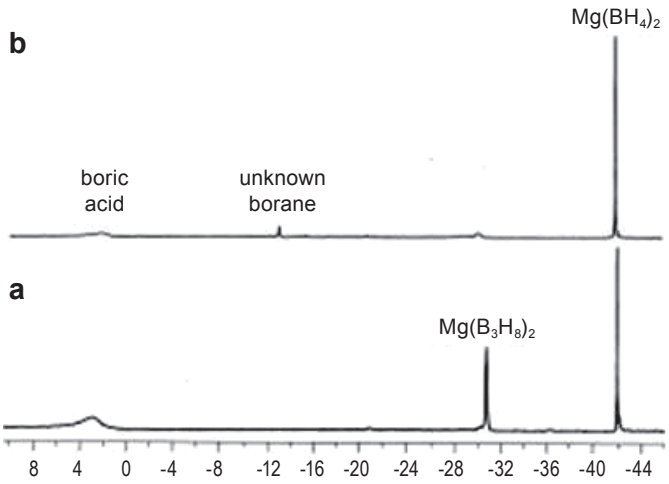


FIGURE 2. $^{11}B\{^1H\}$ spectra of: (a) $Mg(BH_4)_2$ following solid state dehydrogenation at 200°C for five weeks and (b) re-hydrogention of under 120 atm of H_2 at 250°C for 48 h.

at 250°C under 120 atm of H_2. As seen in Figure 2b, ^{11}B NMR analysis consistently indicated that $Mg(B_3H_8)_2$ undergoes nearly complete conversion of the triborane back to $Mg(BH_4)_2$ after 48 h. This is the first example of the **reversible**, solid-state dehydrogenation of a borohydride occuring at temperatures below 350°C. However, it is also noted that the hydrogen cycling capactity associated with the reaction seen in equation 3 is only 2.5 wt%.

$$3Mg(BH_4)_2 \Leftrightarrow Mg(B_3H_8)_2 + 2MgH_2 + 2H_2 \quad (3)$$

Our results suggests that the higher borane clusters form from the smaller clusters through a sequential borohydride insertions into growing polyboranes, in concert with the formation of hydrogen and the corresponding metal hydride. The stability of the corresponding metal hydride formed in the decomposition of borohydride may explain in part the observed reversibility for some borohydrides and the irreversibility of other borohydrides. The thermodynamics of the reaction, hydrogen desorption or hydrogen absorption, depends on the stability of the MH in addition to the stability of the polyborane intermediate. As such, formation of a more stable metal hydride, e.g., LiH compared to MgH_2, will make the thermodynamics for the reverse reaction less favorable. This mechanism provides an alternate explanation for incomplete reversibility in borohydrides as once $MgB_{12}H_{12}$ is formed, it is difficult to regenerate borohydride. Clearly hydrogen addition to arachnopolyborane species (observed as boric acid after hydrolysis of the decomposed borohydride) is kinetically accessible whereas hydrogen addition to the thermodynamically stable closoborane species is kinetically inaccessible.

As part of effort of this project, we have synthesized and fully characterized the novel anionic transition metal borobyhydride complexes, $LiSc(BH_4)_4$, $NaSc(BH_4)_4$, $KSc(BH_4)_4$ and $Na_2Mn(BH_4)_4$. As seen in Table 2, we have

found that these complexes all release a significant wt% of hydrogen upon to heating to moderate temperatures, <200°C. Thus it was of interest to probe whether, like $Mg(BH_4)_4$, re-hydrogenation could be achieved following dehydrogention to lower boranes at moderate temperatures. Promising initial results were obtained with $KSc(BH_4)_4$ as the ^{11}B NMR spectrum of samples of following dehydrogenation for 24 h at 200°C are predominated by a peak at -32 ppm, which clearly indicates that triborane, $[B_3H_8]^{2-}$ is the only major product of the dehydrogenation. Attempts were made to re-hydrogenate the material back to the starting borohydride by placing the dehydrogenation samples under 120 atm of H_2 at 250°C for five days. The MAS ^{11}B NMR spectrum showed that a hydrogenated product did arise. However, the -10 ppm chemical of the observed product peak clearly does not match the -38 ppm shift of $KSc(BH_4)_4$ but rather that of KBH_4. In a previous DOE collaborative project with UOP, we screened the hydrogen storage potential lithium salts of transition metal borohydride complexes of the first transition metal series using a high throughput apparatus. This study also indicated that several of these complexes were stable at room temperature and released hydrogen at temperatures relevant to on-broad hydrogen storage applications. However, lithium copper borohydride was the only compound to show reversibility under moderate conditions. This finding stands unique as no other transition metal borohydride complex has been found to be regenerate the parent borohydride complex upon direct hydrogenation or show a stable, non-diminishing hydrogen cycling capacity. We have attempted to confirm that $Li_2Cu(BH_4)_4$ will undergo reversible dehydrogenation. A sample of the complex hydride was prepared by ball milling a 4:1 molar mixture of $CuCl_2$ and $LiBH_4$. Similar to the findings of the earlier preliminary study, we found that heating our sample of $Li_2Cu(BH_4)_4$ to 230°C for five h resulted the in the release of 2.9 wt% hydrogen. However, the results of attempted re-hydrogenation under 120 atm of H_2 at 100°C for 24 h have been variable and no firm conclusions have been reached to date.

Task 6. Recharging of Light Metal Hydrides in Supercritical and Non-Conventional Fluids

In an attempt to stabilize the cycling hydrogen capacity, we investigated the effect of the substitution of $TiCl_3$ with other dopants (e.g. $ScCl_3$ and $CeCl_3$). Doping of LiH/Al with 0.05 mol% $ScCl_3$ resulted in only partial hydrogenation of the material (ca. 2 wt% H) while mixtures doped with same amount of $CeCl_3$ did not hydrogenation to any significant extend. When the level of dopant was increased to 1 mol%, the hydrogenated material was found to release approximately 6 wt% H upon dehydrogenation while the Ce-doped material did not show any signs of hydrogenation. These results indicate that for the $LiAlH_4$ system the catalytic performance of $ScCl_3$ supersedes that of $CeCl_3$, but does not reach that of $TiCl_3$.

TABLE 2. Temperatures and hydrogen wt% evolved during the first step in the dehydrogenation of novel anionic transition metal borohydride complexes.

Complex	T (°C)	wt% H (theoretical)
$LiSc(BH_4)_4$	175	3.5 (14.6)
$NaSc(BH_4)_4$	170	1.0 (12.8)
$KSc(BH_4)_4$	190	1.0 (11.3)
$Na_2Mn(BH_4)_4$	120	2.9 (6.9)

Conclusions

We have established that the initial borane species produced in the dehydrogenation of $Mg(BH_4)_2$ is $Mg(B_3H_8)_2$. This conversion has been shown to be reversible at moderate temperature and pressure thus provides the first example of direct hydrogen cycling of a borohydride under moderate conditions. Although the 2.5 wt% cycling capacity does not meet current on-board storage targets, our results provide key experimental evidence that practical hydrogen storage based on a boron hydride is plausible. Heating to higher temperatures results in a series of BH condesation reactions leading to a complex mixture of polyboranes. Given the nature of the reaction pathways discussed in this work it is recommended that the stability of the corresponding metal hydride (as well as the polyborane) be considered in the design and development of borohydrides for reversible hydrogen storage.

Future Directions

Adjustment of conditions to maximize trade off between cycling capacity and temperature/pressures required for reversible dehydrogenation of $Mg(BH_4)_2$ and perhaps other borohydrides under moderate conditions.

References

1. Ashby, E.C.; Brendel, G.J.; Redman, H.E. Inorg. Chem. 1963, 2, 499.

2. Wang, J.; Ebner, A.D.; Ritter, J.A. J. Am. Chem. Soc. 2006, 128, 5949.

FY 2011 Publications/Presentations

Publications

1. "Direct Hydrogenation of Magnesium Boride to Magnesium Borohydride: Demonstration of >11 Weight Percent Reversible Hydrogen Storage", Godwin Severa, Ewa Rönnebro, Craig M. Jensen; *Chemical Commun.* **2010**, *46*, 421.

2. "$NaSc(BH_4)_4$: A Novel Scandium Based Borohydride", Radovan Černy, Godwin Severa, Dorthe Ravnsbæk, Yaroslav Filinchuk, Vincenza d'Anna, Hans Hagemann, Yngve Cerenius, Craig M. Jensen, and Torben R. Jensen; *J. Phys. Chem. C.* **2010**, *114*, 1357.

3. "Reversible Vacancy Formation and Recovery During Dehydrogenation-Hydrogenation Cycling of Ti-doped $NaAlH_4$", Kouji Sakaki, Meredith T. Kuba, Yumiko Nakamura, Craig M. Jensen, Etsuo Akiba; *J. Chem. Phys. C* **2010** *114*, 6869.

4. "Modification of the H_2 Desorption Thermochemistry of $LiAlH_4$ through Ti Doping", Henrietta W. Langmi, G. Sean McGrady, Xiangfeng Liu, Craig M. Jensen; *J. Phys. Chem. C.* **2010**, *114,* 10666.

5. "Thermal Desorption,Vibrational Spectroscopic, and DFT Computational Studies of the Complex Manganese Borohydrides, $Mn(BH_4)_2$ and $[Mn(BH_4)_4]^{2-}$", Godwin Severa, Hans Hagemann, Moïse Longhini, Jakub W. Kaminski, Tomasz A. Wesolowski, Craig M. Jensen; *J. Phys. Chem. C.* **2010**, *114,* 15516.

6. "Discovery of a New ^{27}Al Species in Hydrogen Reactions of $NaAlH_4$", Timothy M. Ivancic, Son-Jong Hwang, Robert C. Bowman, Jr., Derek S. Birkmire, Craig M. Jensen, Terrence J. Udovic, Mark S. Conradi; *J. Phys. Chem. Lett.* **2010**, 1, 2412.

7. "Synthesis and characterization of $KSc(BH_4)_4$," Radovan Černý, Dorthe B. Ravnsbæk , Godwin Severa, Yaroslav Filinchuk, Vincenza d'Anna, Hans Hagemann, Dörthe Haase, Craig M. Jensen, Torben R. Jensen; *J. Phys. Chem. C.* **2010**, *114*, 19540.

8. "Reversible Dehydrogenation of Magnesium Borohydride to Magnesium Triborane in the Solid State Under Moderate Conditions", Marina Chong, Ahbi Kamkamkar, Tom Autrey, Shin-ichi Orimo, Satish Jalisatgi, and Craig M. Jensen; (invited contribution for themed issue on Hydrogen) *Chem. Commun*. **2011**, *47,* 1330.

Presentations

1. "Development of Processes for the Reversible Dehydrogenation of High Hydrogen Capacity Complex Hydrides"; Godwin Severa, Marina Chong, Zhouhui Wang, Xiangfeng Liu, G. Sean McGrady, Henrietta Langmi, Ewa Rönnebro, Tom Autrey, Ahbi Kamkamkar, and Craig M. Jensen; International Conference on Materials Science and Technology; Puspiptek Serpong Indonesia; October 19–23, 2010.

2. "Development of Processes for the Reversible Dehydrogenation of High Hydrogen Capacity Complex Hydrides"; Godwin Severa, Marina Chong, Zhouhui Wang, Xiangfeng Liu, G. Sean McGrady, Henrietta Langmi, Ewa Rönnebro, Tom Autrey, Ahbi Kamkamkar, and Craig M. Jensen; Marie Curie Actions Conference on Nano- and Surface Science Approches to Production and Storage of Hydrogen; Noordwijkerhout, The Netherlands, November 14–19, 2010.

3. "Development of Processes for the Reversible Dehydrogenation of High Hydrogen Capacity Complex Hydrides"; Godwin Severa, Marina Chong, Zhouhui Wang, Xiangfeng Liu, G. Sean McGrady, Henrietta Langmi, Ewa Rönnebro, Tom Autrey, Ahbi Kamkamkar, and Craig M. Jensen; 3rd International Symospium on Materials Chemistry; Bhabha Atomic Research Centre, Mumbai, India, December 7–11, 2010.

4. "Reversible Hydrogen Storage with Magnesium Borohydride"; Craig Jensen, Godwin Severa, and Marina Chong; 2010 Symposium on Advances in Chemistry and Materials for Hydrogen Storage, Alternative Energy Technology Division, International Chemical Congress of Pacific Basin Societies; Honolulu, Hawaii; December 15–20, 2010.

5. "Hydrogen Storage via Reversible Dehydrogenation of Magnesium Borohydride", Marina Chong, Ewa Ronnebro, Tom Autrey, Ahbi Kamkamkar, and Craig M. Jensen; Symposium on Hydrogen Storage at Study of Matter at Extreme Conditions 2011 Meeting, Western Caribbean, March 27 – April 2, 2011.

6. "Homogeneous Dehydrogenation of Liquid Organic Hydrogen Carriers Catalyzed by an Iridium PCP Pincer Complexs", Zhouhui Wang, Jack Belli, and Craig Jensen, Symposium Faraday Discussion 151: Hydrogen Storage Materials, Didcot, United Kingdom, April 18–20, 2011.

7. "Hydrogen Storage via Reversible Dehydrogenation of Magnesium Borohydride",Craig Jensen, Marina Chong, Tom Autrey, and Ahbi Kamkamkar, Symposium on Recent Developments in Hydrogen Storage at Materials Research Society Spring 2011 Meeting, San Francisco, April 26–28, 2011.

IV.A.4 Lightweight Metal Hydrides for Hydrogen Storage

J.-C. Zhao (Primary Contact), Xuenian Chen, Zhenguo Huang, Hima K. Lingam, Teshome Yisgedu, Beau Billet, Sheldon G. Shore
The Ohio State University (OSU)
286 Watts Hall, 2041 College Road
Columbus, OH 43210
Phone: (614) 292-9462
E-mail: zhao.199@osu.edu

DOE Managers
HQ: Ned Stetson
Phone: (202) 586-9995
E-mail: Ned.Stetson@ee.doe.gov
GO: Paul Bakke
Phone: (720) 356-1436
E-mail: Paul.Bakke@go.doe.gov

Contract Number: DE-FC3605GO15062

Project Start Date: January 1, 2005
Project End Date: August 31, 2011

Fiscal Year (FY) 2011 Objectives

- Develop a high-capacity lightweight hydride for reversible vehicular hydrogen storage, capable of meeting or exceeding the 2010 DOE/FreedomCAR targets.
- Synthesize and study aluminoborane compounds and other lightweight, high-capacity boron hydrides for hydrogen storage.
- Perform detailed characterization of the decomposition mechanisms, desorbed gaseous species and structures of the synthesized compounds.

Technical Barriers

This project addresses the following technical barriers from the Storage section of the Fuel Cell Technologies Multi-Year Research, Development and Demonstration Plan (MYPP):

(D) Durability/Operability

(P) Lack of Understanding of Hydrogen Physisorption and Chemisorption

(E) Charging/Discharging Rates

(J) Thermal Management

Technical Targets

This project is conducting synthesis and studies of the decomposition mechanism of aluminoborane compounds. Insights gained from these studies will be applied toward the design and synthesis of hydrogen storage materials that meet the following DOE 2010 hydrogen storage targets:

- Cost: $3-7/gasoline gallon equivalent at the pump
- Specific energy: 1.5 kWh/kg (4.5 wt% H)
- Energy density: 0.9 kWh/L (0.028 kg/L)

FY 2011 Accomplishments

- We modified the synthetic method of AlB_4H_{11}. Several grams of AlB_4H_{11} were synthesized using the modified method at OSU.
- Both infrared (IR) and pressure-composition-temperature (PCT) tests showed that AlB_4H_{11} is partially reversible at relatively mild condition such as 220°C and 100 bar of hydrogen. Differential scanning calorimetry (DSC) measurements also showed that AlB_4H_{11} dehydrogenates around 125°C with a broad endothermic peak.
- In collaboration with both Northwestern University and the National Institute of Standards and Testing (NIST), the structure units, a triangle of B_3 and a BH_4 group, were completely identified.
- We modified the synthetic method of AlB_6H_{13} (a sister compound to AlB_4H_{11}) and characterized its properties for potential hydrogen storage applications together with the Oak Ridge National Laboratory (ORNL).
- We recently developed simple and efficient methods for the preparation of both NaB_3H_8 and $NH_4B_3H_8$. They release more hydrogen during hydrolysis under mild condition than the most studied hydrogen storage materials such as $NaBH_4$ and NH_3BH_3.
- We developed a new method to prepare $[H_2B(NH_3)_2][B_3H_8]$ which has high hydrogen capacity of 18.4 wt%.



Introduction

The DOE defines on-board hydrogen storage for mobile vehicles as a “Grand Challenge”. It is one of the biggest hurdles to the implementation of hydrogen-powered vehicles. Metal hydrides have the advantages of the highest volumetric density, relatively low working pressure, and reasonable working temperature range. The disadvantage of current reversible hydrides is a significant weight penalty. Metal borohydrides have among the highest gravimetric hydrogen storage capacities with the potential to meet the DOE gravimetric density targets and to offset the system weight penalties. However, desorption temperature, reversibility and formation of gaseous borane compounds during desorption are challenging issues for these materials.

This project attempts to develop a high-capacity lightweight hydride for reversible vehicular hydrogen storage, capable of meeting or exceeding the 2010 DOE/FreedomCAR targets.

Approach

- Explore aluminoborane compounds such as AlB_4H_{11} and other high-capacity, lightweight boron hydrides.
- Study the structure and the decomposition mechanisms using multiple techniques such as interrupted PCT tests, nuclear magnetic resonance (NMR), IR, DSC, and residual gas analysis.
- Develop reversibility strategy from detailed mechanistic understanding of the complex desorption processes (such understanding is crucial for reversibility of all borohydrides).
- Synthesize new hydrides and complexes in collaboration with ORNL, Sandia National Laboratories, and NIST.

Results

A modified method for synthesizing aluminoborane, AlB_4H_{11}, was developed and applied to the preparation of AlB_4H_{11} in gram quantities at OSU. Careful measurements were performed on AlB_4H_{11} to investigate its properties as a potential hydrogen storage material. Both IR and PCT tests indicates that this compound is partially reversible at relatively mild conditions such as 220°C and 100 bar of hydrogen, which further supports our conclusion of reversibility based on previous NMR observations. Furthermore, DSC measurements show that AlB_4H_{11}, dehydrogenates around 125°C with a broad endothermic peak, thus it is thermodynamically reversible. Encouraged by these results which suggest that AlB_4H_{11} might be a good candidate for reversible vehicular hydrogen storage, we devoted considerable amount of effort to figure out the molecular structure of AlB_4H_{11}. Structural identification is crucial for understanding the desorption mechanisms and the partial reversibility.

The identification of the molecular structure of AlB_4H_{11} has been difficult because of its polymeric/amorphous nature and its insolubility in major solvents [1]. The former prevents us from determining the structure through X-ray diffraction or neutron diffraction. The latter prevents us from performing solution NMR and mass spectroscopy tests to obtain structural information. The available structural information from solid NMR and IR spectra is insufficient for structural identification. In collaboration with Northwestern University and NIST, we employ both experimental measurements (IR, NMR, and neutron vibration analysis) and theoretical calculations (prototype electrostatic ground state [PEGS] + density functional theory [DFT]) to define the structure of AlB_4H_{11}.

Even though AlB_4H_{11} was synthesized from a benzene solution, it is not soluble in benzene once it is formed. In order to gain more structural information from experiments, we examine the mother/residual solution by ^{11}B and $^{11}B\{^1H\}$ NMR after the precipitation of AlB_4H_{11} to determine if trace amount of the polymeric product is retained in the solution. Two boron signals at δ –36.7 and –53.3 ppm observed in solution NMR may be associated with the two signals at δ –37.4 and δ –50 ppm of product in its solid ^{11}B NMR [2]. The process of the reaction between $Al(BH_3)_4$ and B_2H_6 is also monitored by ^{11}B and $^{11}B\{^1H\}$ NMR with an attempt to find the transformation from staring materials to the product. Several small signals appeared at δ –33.5, –38.2, –44.7 –52.8 and –53.7 ppm as the reaction proceeds. The peaks at δ –38.2 and -44.7 ppm may be related to dimer or polymer of $HAl(BH_4)_n$ (δ –38.3 and δ –43.3 ppm) and the peaks at δ – 53.7 ppm may be associated to product (δ –50 ppm in its solid ^{11}B NMR) [3]. So the reaction probably starts with dimerization or polymerization of $Al(BH_4)_3$ and then transfers to the product. Though AlB_4H_{11} did not dissolve in major solvents, we found that it is soluble in (or reacted with) liquid ammonia without any bubble formation. The ^{11}B NMR spectra of AlB_4H_{11} in liquid ammonia clearly show a quintet and a nonet which are assigned to BH_4^- and $B_3H_8^-$ groups (Figure 1). This observation suggests that a B_1 unit and a B_3 unit groups exist in the structure of AlB_4H_{11}. The neutron vibration spectrum of AlB_4H_{11} is recorded in NIST (by Terry Udovic and his co-workers) for comparing with theoretical results.

Based on the available information, six possible structures were predicted through (PEGS + DFT) calculation by Northwestern University (Chris Wolverton, Yongli Wang, and Yongsheng Zhang). Three of these structures (#3, #5, and #6) are more stable than others based on the calculated ground-state energies. It is interesting that all these stable structures contain a B_1

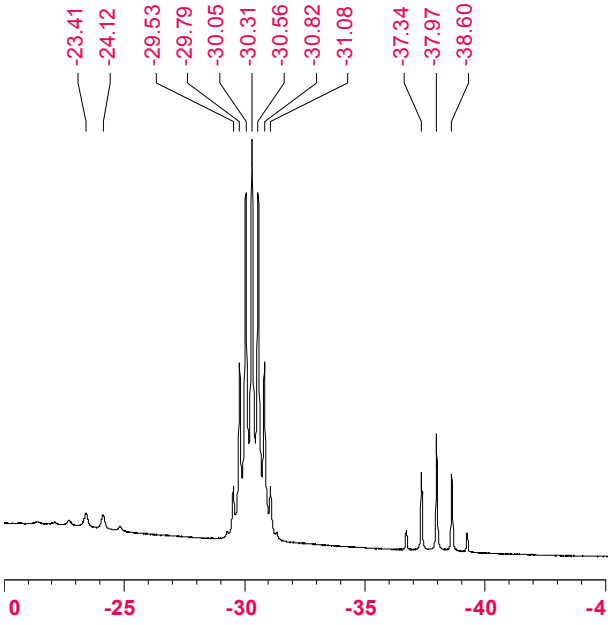


FIGURE 1. ^{11}B NMR Spectrum of AlB_4H_{11} in Liquid Ammonia

unit and a B_3 unit which either connected directly (as in structure #3) or separated by Al atom (as in structures #5 and #6). The presence of the B_1 unit and the B_3 unit in these structures is consistent with the experimental observations.

Simulation of the neutron vibration spectra for structures #5 and #6 has been performed by NIST for comparing with the experimental vibration spectra of AlB_4H_{11}. Figure 2 shows that even though some agreements are observable, the overall agreement is less than ideal, indicating that both structures #5 and #6 need further refinement to reflect the correct structure of AlB_4H_{11}. It is worthwhile mentioning that even for well-defined structures from single crystal data, the simulated and experimental neutron vibration spectra do not match perfectly for many compounds.

The ^{27}Al NMR of AlB_4H_{11} in liquid ammonia shows two Al signals which are inconsistent with structures #5 or #6 because that Al has an identical chemical environment in structure #5 or structure #6. With this new observation, the structure of AlB_4H_{11} is simulated again using PEGS+DFT by inputting only B_3H_7 and BH_4 units and Al atoms. It is surprising that the energy of the modified structure is at least 40 KJ/mol lower than that of structures #5 and #6.

After spending tremendous efforts by OSU, Northwestern University, and NIST on this collaborative research, the structure units are completely identified. The structure of AlB_4H_{11} consists of B_3H_7 units and BH_4 unit that are separated by Al atoms (Figure 3). Only a slight uncertainty still exists in terms of the exact arrangement of these structure units. The structural information will help us to understand the desorption mechanisms and partial reversibility of AlB_4H_{11}.

With the experience of preparing AlB_4H_{11}, we have successfully synthesized AlB_6H_{13}, another aluminoborane compound, through the reaction between $Al(BH_4)_3$ and B_4H_{10}. Since the starting materials are not commercially available, considerable efforts are devoted to the preparation of the precursors [4]. Overall, the process includes five reactions (reactions 1 to 5):

$$AlCl_3 + 3\ LiBH_4 \rightarrow Al(BH_4)_3 + 3\ LiCl \quad (1)$$

$$3\ THFBH_3 + K\text{-}Hg \rightarrow KB_3H_8 + \tfrac{1}{2}\ H_2 + 3\ THF + Hg \quad (2)$$

$$KB_3H_8 + [N(n\text{-}But)_4]Br \rightarrow [N(n\text{-}But)_4][B_3H_8] + KBr \quad (3)$$

$$[N(n\text{-}But)_4][B_3H_8] + BBr_3 \rightarrow B_4H_{10} + [N(n\text{-}But)_4]Br \quad (4)$$

$$Al(BH_4)_3 + 2\ B_4H_{10} \rightarrow AlB_6H_{13} + 3/2\ B_2H_6 + 2\ H_2 \quad (5)$$

However, preliminary characterization of its properties as a potential storage material, in collaboration with ORNL, shows a very discouraging result: a large amount of borane complexes were observed during desorption, which discourages further study of this compound for hydrogen storage.

To investigate more boron-containing lightweight hydrides for hydrogen storage, we focus on a type of boron compounds with a formula of $M_xB_3H_8$, which may be less stable than M_xBH_4 and thus may be easier for dehydrogenation and rehydrogenation. We first developed a simple and efficient route to unsolvated NaB_3H_8 [5], and investigated its hydrogen release properties. Pyrolysis test results are discouraging since large amount of gaseous species were observed, indicating that this compound is not suitable for on-board reversible hydrogen storage. It is

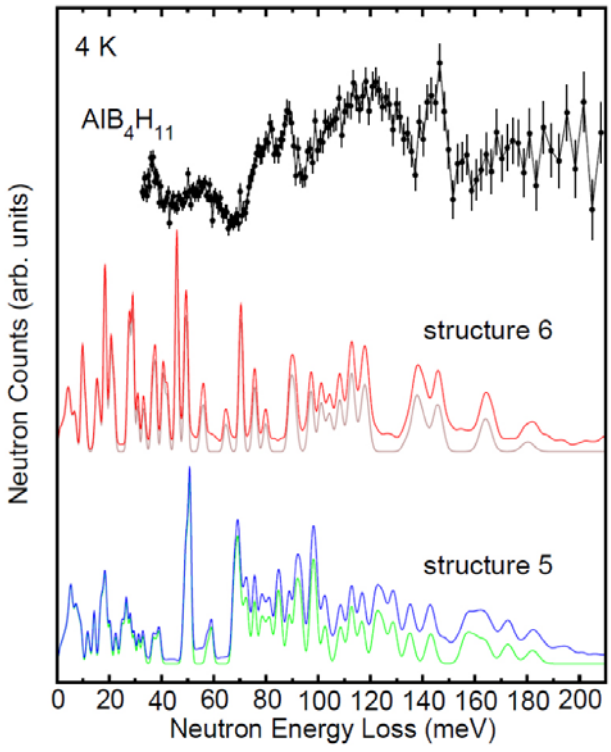


FIGURE 2. The Neutron Vibration Spectrum of AlB_4H_{11} and Simulated Vibration Spectra of Structures #5 and #6 predicted by the Northwestern University

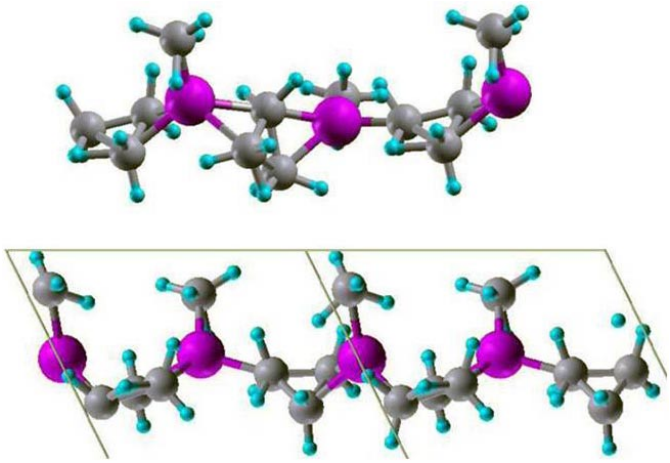


FIGURE 3. Two different lowest energy structures for AlB_4H_{11}. They have the same B_3H_7 and BH_4 structure units but slightly different arrangements.

found that NaB_3H_8 is highly soluble in water. Quantitative measurements of hydrogen released using a Toepler pump and gas buret showed that upon adding 14 mmol water to 1 mmol NaB_3H_8 with Pt/C (1 mol % Pt), a near theoretical value of 8.85 mol hydrogen is released in 20 mins via hydrolysis. Therefore, this system has a high theoretical hydrogen weight percent [wt% = $H_2/(NaB_3H_8 + H_2O)$] of 10.5 wt%. It is also observed that NaB_3H_8 is significantly more stable in water (distilled water is used in the study) than $NaBH_4$. The fairly stable aqueous NaB_3H_8 solution without additives can be a good candidate for certain applications where hydrogen is consumed continuously. In this regard, NaB_3H_8 has advantages over the most studied hydrogen storage materials such as $NaBH_4$ and NH_3BH_3 via hydrolysis [6].

We have also successfully developed a simple and high-yield synthesis of $NH_4B_3H_8$ through a metathesis reaction between unsolvated NaB_3H_8 and NH_4Cl [7]. The crystal structure shows weak $N–H^{\delta+}\cdots H^{\delta-}–B$ interaction in $NH_4B_3H_8$, which is different from the close $N–H^{\delta+}\cdots H^{\delta-}–B$ contacts observed in $NH_3B_3H_7$ and NH_3BH_3. $NH_4B_3H_8$ has a high hydrogen content of 20.5 wt%. Thermal decomposition analysis shows that 10 wt% hydrogen is released below 160°C, but with appreciable amounts of borane complexes. Therefore, $NH_4B_3H_8$ is unlikely a candidate for hydrogen storage through thermal decomposition.

Hydrolytic studies have shown that upon adding catalysts, $NH_4B_3H_8$ rapidly releases pure H_2 [7]. For an aqueous solution with a 1:18 molar ratio of $NH_4B_3H_8$ to H_2O, which represents a system density of 4.6 wt% H (water weight included), the commercially available 10 wt% Pt/C catalyst (1 mol% Pt) shows the best catalytic activity, with complete hydrolysis in less than 30 min (Figure 4). Lower-cost transition metal catalysts were also explored in our study and fairly good catalytic activity was observed for $CoCl_2$. With 4 mol% loading of $CoCl_2$, full hydrolysis was complete in about 100 min. A black powder appeared instantly when $CoCl_2$ was brought into contact with an aqueous $NH_4B_3H_8$ solution, suggesting the formation of cobalt boride as found during the hydrolysis of $NaBH_4$. The ^{11}B NMR spectrum of the catalyzed hydrolysis solution of $NH_4B_3H_8$ and H_2O (1: 18 ratio) reveals one broad peak centered at 16 ppm which is likely associated with $B_3O_3(OH)_4^-$ and $B_5O_6(OH)_4^-$, along with another sharp peak situated at around 0 ppm that is also due to $B_5O_6(OH)_4^-$. Similar products were also formed during the hydrolysis of $NH_3B_3H_7$.

Another amine borane compound, $(NH_3)_2BH_2B_3H_8$, with high hydrogen capacity of 18.4 wt%, has attracted little attention as a potential hydrogen storage material, probably because of its unavailability. The procedure reported before is through the reaction between ammonia and tetraborane, which is highly volatile and flammable [8,9]. Inspired by recent success in developing safe and efficient methods for synthesizing unsolvated NaB_3H_8 and $NH_4B_3H_8$, we developed a new method for synthesizing $(NH_3)_2BH_2B_3H_8$

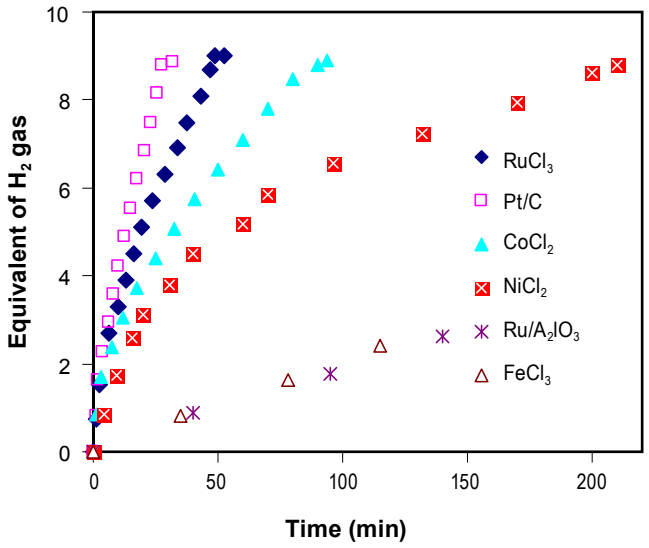


FIGURE 4. Hydrogen evolution at room temperature from an aqueous $NH_4B_3H_8$ solution (molar ratio of $NH_4B_3H_8$:H_2O being 1:18) containing 10 wt% Pt/C (1 mol% Pt); 5 wt% Ru/Al_2O_3 (1 mol% Ru), $RuCl_3$ (1 mol% Ru), $CoCl_2$ (4 mol% Co), $NiCl_2$ (4 mol% Ni) and $FeCl_3$ (4 mol% Fe). Molar ratios are referenced to $NH_4B_3H_8$.

via a metathesis reaction. The method includes three steps (reactions 6, 7, and 8):

$$3\ THF{\cdot}BH_3 + 3NH_3 \rightarrow (NH_3)_2BH_2BH_4 + NH_3BH_3 + 3\ THF \quad (6)$$

$$NH_4Cl + (NH_3)_2BH_2BH_4 \rightarrow (NH_3)_2BH_2Cl + NH_3BH_3 + H_2 \quad (7)$$

$$(NH_3)_2BH_2Cl + NaB_3H_8 \rightarrow (NH_3)_2BH_2B_3H_8 + NaCl \quad (8)$$

All three reactions are carried out in liquid ammonia. After the second step (reaction 7), $(NH_3)_2BH_2Cl$ is isolated from the tetrahydrofuran (THF) solution after removal of liquid ammonia. The desired $(NH_3)_2BH_2B_3H_8$ is extracted using THF. Overall, the new method is more efficient. The ^{11}B NMR spectrum of $(NH_3)_2BH_2B_3H_8$ in THF shows a triplet and a nonet corresponding to BH_2^+ and $B_3H_8^-$ group. Crystal structure of an adduct with crown ether, $(NH_3)_2BH_2B_3H_8{\cdot}$18-crown-6 has been determined in which one ammonia molecule orients toward the crown ether to form three $N–H\cdots O$ hydrogen bonds between the hydrogen atoms of the ammonia and the oxygen atoms of the ether. Further characterization of its desorption products and mechanism is in progress.

Conclusions and Future Directions

- In collaboration with Northwestern University and NIST, we have now identified the structure units in polymeric/amorphous AlB_4H_{11}. The structure consists of B_3H_7 and BH_4 groups linked to a polymer chain via Al atoms.
- AlB_6H_{13} (a sister compound to AlB_4H_{11}) was synthesized and characterized for potential hydrogen storage, and was found not a viable hydrogen storage material.

- Simple and efficient methods for the preparation of both NaB_3H_8 and $NH_4B_3H_8$ were developed. These compounds were found unsuitable for reversible hydrogen storage, but showed good properties via hydrolysis.
- We developed a new method to prepare $[H_2B(NH_3)_2][B_3H_8]$ which has high hydrogen capacity of 18.4 wt%.
- As the program/project is drawn to completion, we will do our best in completing the analysis and reporting.

FY 2011 Publications/Presentations

1. T.B. Yisgedu, X. Chen, H.K. Lingam, Z. Huang, S. Maharrey, R. Beherns, S.G. Shore, and J.-C. Zhao, "Synthesis, Structural Characterization, and Thermal Decomposition Study of $Mg(H_2O)_6B_{10}H_{10}•4H_2O$", *J. Phys. Chem. C.*, 115, 11793-11802 (2011).

2. Z. Huang, X. Chen, T. Yisgedu, J.-C. Zhao, and S.G. Shore, "High-Capacity Hydrogen Release through Hydrolysis of NaB_3H_8", *Inter. J. Hydrogen Energy*, 36, 7038-7042 (2011).

3. Z. Huang, X. Chen, T. Yisgedu, E.A. Meyer, S.G. Shore, and J.-C. Zhao, "Ammonium Octahydrotriborate ($NH_4B_3H_8$): New Synthesis, Structure and Hydrogen Storage Properties", *Inorg. Chem.*, 58, 3738-3742 (2011).

4. D.T. Shane, L.H. Rayhel, Z. Huang, J.-C. Zhao, X. Tang, V. Stavila, M.S. Conradi, "A Comprehensive NMR Study of Magnesium Borohydride", *J. Phys. Chem. C.*, 115, 3172-3177 (2011).

5. Z. Huang, G. King, X. Chen, J. Hoy, T. Yisgedu, H.K. Lingam, S.G. Shore, P.M. Woodward, and J.-C. Zhao, "A Simple and Efficient Way to Synthesize Unsolvated Sodium Octahydrotriborate", *Inorg. Chem. (Comm.)*, vol. 49, pp. 8185-8187 (2010).

6. X. Chen, J.-C. Zhao, and S.G. Shore, "Facile Synthesis of Aminodiborane and Inorganic Butane Analogue $NH_3BH_2NH_2BH_3$", *J. Am. Chem. Soc. (Comm.)*, 132, 10658-10659 (2010).

5. "Dihydrogen Bond Effects in Amine Borane Chemistry" (INOR-1001), X. Chen*, J.-C. Zhao, S.G. Shore, Abstracts of Papers, 241st ACS National Meeting & Exposition, Anaheim, CA, March 27–31, 2011.

6. "Aluminoboranes and Boron Compounds for Hydrogen Storage", J.-C. Zhao,* X. Chen. Z. Huang, T. Yisgedu, H.K. Lingman, B. Billet, S.G. Shore, (Oral presentation) TMS Annual Meeting, San Diego, California, February 27 to March 3, 2011.

7. "Lightweight Metal Hydrides for Hydrogen Storage", J.-C. Zhao*, X. Chen, Z. Huang, H. K. Lingam, T. Yisgedu, B. Billet, and S.G. Shore, (Oral presentation) International Energy Agency (IEA) Task 22 Hydrogen Storage Experts' Meeting, Fremantle/Perth, Australia, January 17–20, 2011.

8. "Lightweight Metal Hydrides for Hydrogen Storage", J.-C. Zhao*, X. Chen, Z. Huang, H.K. Lingam, T. Yisgedu, B. Billet, and S.G. Shore, (Oral presentation) US Department of Energy Hydrogen Storage Tech Team Meeting, USCAR, Southfield, MI, November 18th, 2010.

9. "Borohydrides, Aluminoboranes and Boron-Cage Compounds for Hydrogen Storage", J.-C. Zhao*, X. Chen, Z. Huang, H. K. Lingam, T. Yisgedu, B. Billet, and S.G. Shore, (Keynote lecture), First International Conference on Materials for Energy, Karlsruhe, Germany, July 4–8, 2010.

References

1. F.L. Himpsl, Jr., and A.C. Bond, ***J. Am. Chem. Soc.***, *103*, 1098 (1981).

2. J.-C. Zhao, D.A. Knight, G.M. Brown, C. Kim, and S.-J. Hwang, J.W. Reiter, R.C. Bowman Jr., J.A. Zan, J.G. Kulleck, **J. Phys. Chem. C**., 113, 2 (2009).

3. A.J. Downs, L.A. Jones, *Polyhedron* **1994**, *13*, 2401.

4. L.B. Leach, M.A. Toft, F.L. Himpsl, S.G. Shore, *J. Am. Chem. Soc.* **1981**, *103*, 988.

5. Z. Huang, G. King, X. Chen, J. Hoy, T. Yisgedu, H.K. Lingam, S.G. Shore, P.M. Woodward, J.-C. Zhao, *Inorg. Chem.* **2010**, *49,* 8185.

6. Z. Huang, X. Chen, T. Yisgedu, J.-C. Zhao, S.G. Shore, *Inter. J. Hydrogen Energy* **2011**, *36,* 7038.

7. Z. Huang, X. Chen, T. Yisgedu, E.A. Meyers, S.G. Shore, J.-C. Zhao, *Inorg. Chem.* **2011**, *50,* 3738.

8. G. Kodama, R.W. Parry, *J. Am. Chem. Soc.*, **1960**, *82*, 6250.

9. S.G. Shore, H.D. Johnson II, *J. Am. Chem. Soc.*, **1970**, *92*, 7586.

IV.A.5 Reversible Hydrogen Storage Materials – Structure, Chemistry, and Electronic Structure

Ian M. Robertson (Primary Contact) and
Duane D. Johnson
University of Illinois at Urbana-Champaign (UIUC)
Department of Materials Science and Engineering
1304 West Green Street
Urbana, IL 61801
Phone: (217) 333-6776
E-mail: ianr@illinois.edu

DOE Managers
HQ: Ned Stetson
Phone: (202) 586-9995
E-mail: Ned.Stetson@ee.doe.gov
GO: Paul Bakke
Phone: (720) 356-1436
E-mail: Paul.Bakke@go.doe.gov

Contract Number: DE FC36-05GO15064

Project Start Date: March 1, 2005
Project End Date: February 26, 2011

Objectives

The main focus of this research project is to:

- Advance the understanding of the microstructural and modeling characteristics of complex hydrides.
- Provide more reliable theoretical methods to assess hydrogen-storage materials, including key issues affecting materials under study.

Technical Barriers

This project addresses the following technical barriers from the Fuel Cell Technologies Program Multi-Year Research, Development and Demonstration Plan:

(A) System Weight and Volume
(E) Charging/Discharging Rates
(D) Durability/Operability

Technical Targets

This project is conducting fundamental experimental and theoretical studies of candidate light-weight systems for on-board regeneration. Insights gained from these studies will be applied toward the design and synthesis of hydrogen storage materials that meet the following DOE 2010 hydrogen storage targets:

- Cost: $4/kWh net
- Specific energy: 1.5 kWh/kg
- Energy density: 0.9 kWh/L



Introduction

The effort at the University of Illinois at Urbana-Champaign focuses on resolving issues within current hydrogen storage materials using a combination of electronic structure calculations and state-of-the-art compositional and structural characterization methods. We tie together theoretical understanding of electronic, enthalpic, thermodynamic, and surface effects affecting performance of storage materials with microcompositional and microstructural experimental analysis, coordinated with collaborative partnerships with other institutions; current partnerships are with Savannah River National Laboratory, Dr. Ragaiy Zidan, and University of Missouri, Professor Eric Majzoub. These efforts enable a more efficient approach to designing a new system with the required properties.

Approach

We employ state-of-the-art characterization tools to investigate the microstructural and microchemical changes that occur in candidate material systems during the uptake and release of hydrogen. The characterization is coupled with first-principles, electronic-structure and thermodynamic theoretical techniques to predict and assess meta-stable and stable phases, as well as surface effects that can poison or limit kinetics. Electronic-structure and thermodynamic calculations are used to enhance the understanding of experimental characterization results on candidate systems. This combined theoretical/characterization effort provides fundamental insight to the processes governing hydrogen uptake and release. In the following, a selection of the highlights from the work performed in Fiscal Year 2011 is described.

Experimental Project

Our experimental effort utilizes the advanced characterization capabilities of a state-of-the art transmission electron microscope (TEM). An environmental transfer TEM stage enables air-sensitive materials to be loaded into the stage in the environment of a glove box and transferred to the microscope without exposure to the environment. In addition, electron tomography is being applied to gain three-dimensional information as to the particle shape, the distribution of catalyst particles dispersed by ball-milling

and the infiltration of the storage medium in nano-confined scaffolds. These approaches are being used to characterize air-sensitive nano-confined hydrogen storage materials to gain a better understanding of the effect of processing conditions on the resulting specimen structure and the effect of the number of cycles. Finally, scanning tunneling microscopy (STM) experiments are being conducted to identify the roadblock to hydrogen uptake and release in Al. The progress made this fiscal year is described in the following sections.

Nano-Porous Frameworks for Supporting Hydrogen Storage Materials

In collaboration with Professor Eric Majzoub and coworkers from the University of Missouri, we are investigating $LiBH_4$-infiltrated nano-porous carbon scaffolds. Existing work suggests that reducing the particle size of complex metal hydride materials (to 10 nm or smaller) enhances the kinetics and thermodynamics of hydrogen uptake and release. Infiltrating these materials into nano-porous scaffolds holds potential as a means for constraining particle size to the scaffold pore size as well as preventing the storage medium from sintering or its constituents from diffusing too far away.

The scaffolds we are examining were reported to be nano-porous carbon composed of long cylindrical columns packed into a hexagonal arrangement that run the entire length of the powder grains. The bright-field electron micrographs presented as Figures 1a and 1d are of the carbon scaffold and were reported to be representative of a side view and a pore-down view of the columns, respectively [1]. In these images, the columns (light) appear to be 2.1-2.5 nm wide with wall thicknesses (dark) of 9.1-9.8 nm and a column spacing of 13 nm. Similarly, pore diameters are 3-4.25 nm and the pore spacing is 14 nm. In contrast, we have shown that in both bright-field and high-angle annular dark-field scanning transmission electron images, Figures 1b-c and 1e-f, the column widths and wall thicknesses are identical (4-5 nm with a spacing between 8-9.5 nm) irrespective of the viewing direction and imaging mode. A second size of column, roughly half the width and half the spacing, is also seen though is less common. Still, the column diameters and wall thicknesses match each other. These new findings conform to the expected values based off other measurement techniques.

Our investigation has also revealed a number of interesting features about the scaffold structure, which are providing insight into the connection between processing conditions and how the scaffold grows. The columns form a layered structure, the sheets of columns of which are not always oriented in the same direction. Figure 1f shows one such particle in which the column layers are offset at hexagonal angles, giving incorrectly the appearance of pores. Other particles possess not only different orientations of columns but different sizes and curvatures of columns all within the same powder grain. Many particles are also

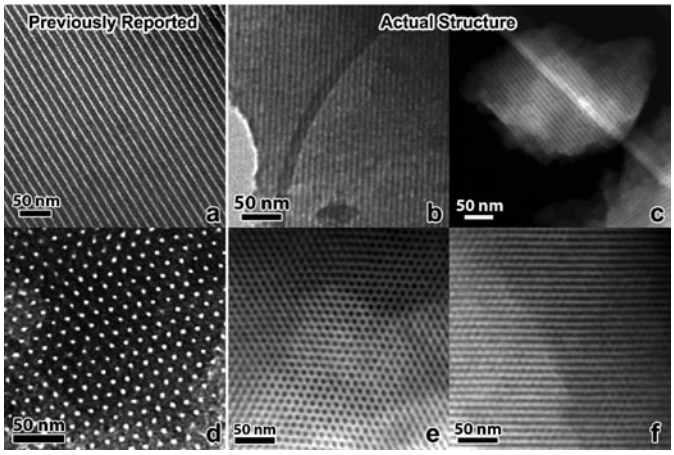


FIGURE 1. (a) Bright-field (BF) TEM micrograph from Mazjoub showing a large disparity between column width (light) and wall thickness (dark). (b) BF TEM micrograph taken at UIUC exhibiting no such disparity. (c) High-angle annular dark-field (HAADF) scanning transmission electron microscopy (STEM) micrograph taken at UIUC showing the same as (b). (d) BF TEM of pores again showing inaccurate structure. (e) HAADF STEM image from UIUC of pores and (f) layers of columns offset at hexagonal angles to give the appearance of pores.

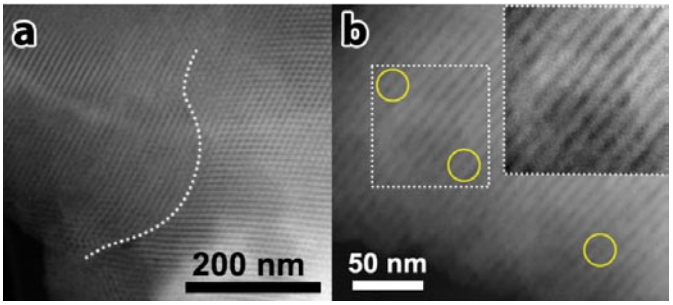


FIGURE 2. HAADF STEM micrographs showing (a) multiple domains of columns with different orientations within a scaffold particle (domain boundary shown by dotted line), and (b) column blockages (circled). The inset is a close-up of the boxed region, with the contrast adjusted for ease of viewing.

made of multiple domains of different column orientations, Figure 2a, the size and quantity of which may be a consequence of growth parameters. This domain structure might explain why the observed maximum practical loading capacity of these scaffolds is lower than would be expected according to scaffold volume. Any domains without pores directly open to the surface would be difficult or impossible to infiltrate fully. Similarly, column blockage has been observed, Figure 2b, and could also reduce the loading capacity. The extent of column blockage may be related to the concentration of oxygen flowed during synthesis. Further study of scaffold structures produced under a variety of processing conditions will elucidate their effect on the resulting microstructure, allowing optimal growth conditions to be determined.

In order to help understand and explain the gradual loss of total storage capacity observed with hydrogen cycling of

these systems [1], specimens that were desorbed at 500°C in a differential scanning calorimeter (DSC) were examined via electron microscopy. In these specimens, protruding material, in the form of bristles and nodules, were seen on the surfaces of the specimens. As shown in the images presented in Figure 3, the bristles were typically 16-24 nm wide with aspect ratios ranging from above 3:1 to over 6:1, though bristles down to around 13 nm and over 30 nm wide were observed. The nodules were usually many tens of nanometers in width and came in a variety of shapes. These bristles and nodules are not products of electron beam damage, as can sometimes be seen in bulk versions of these materials. Unlike the latter, these protrusions are present in their full form from the very beginning of observation and do not grow larger under continued exposure to the beam.

A possible explanation for these formations is that they are one or more components of the storage medium (Li and/or B) that migrates out from the carbon scaffold pores during hydrogen desorption, segregating to the scaffold particle surface where it grows into nodules and bristles. This reduces the amount of nano-scale infiltrated material available to participate in hydrogen uptake, lowering the total storage capacity of the system. Additionally, if the protrusions are composed of only either Li or B, this segregation of reaction components would also lead to a reduction in storage capacity, as would if the protrusions were a new stable, lower-reactivity compound. The low atomic mass of the storage medium (Li, B) makes chemical identification of the bristles and nodules quite difficult. In addition, the small size of the protrusions, as well as their composition, makes focused-probe methods impossible, as the bristles and nodules are immediately destroyed under such an intense electron beam. This behavior, though, strongly suggests that they are purely B and/or Li. We are currently investigating other techniques to find one that possesses the necessary resolution and chemical sensitivity, but will not destroy the protrusions.

The spatial density of surface bristles and nodules can vary dramatically across a single host scaffold particle. Some regions had densely packed patches of bristles while others were bare. It is possible that their distribution is related to where the column domains contact the surface.

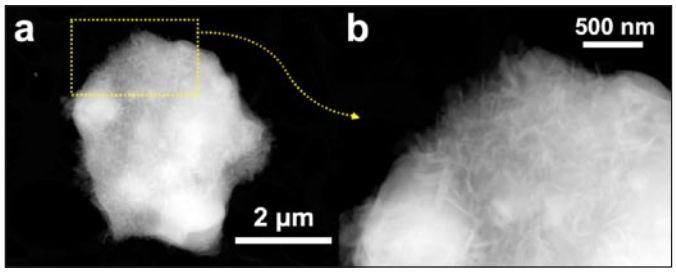


FIGURE 3. HAADF STEM images of a host scaffold particle covered in bristles and nodules. The area outlined in yellow in (a) is shown closer up in (b) to make the dense covering of bristles easier to see.

If the domain was oriented such that the column pores face the surface, it would be easier for the infiltrated storage material to migrate out of the pores and onto the surface to grow these protrusions.

The desorption temperature of these specimens (500°C) was higher than is used during standard cycling (300-350°C), so this behavior may be lessened or absent entirely under normal conditions. We are currently examining specimens of a variety of different filling ratios as they are heated from room temperature up to 500°C to determine the role of temperature in the formation of the bristles and nodules.

Preliminary studies, using a variable temperature scanning tunneling microscope, of clean Al surfaces and Al surfaces with sub-monolayer coverage of Ti, showed interesting results on the association of alane formation with the Ti atoms and with surface vacancies. Despite numerous attempts these results were difficult to reproduce. However, our recent first principle calculations, which are described in the following section, have provided insight as to the important role of surface defects. This insight suggests an alternate surface preparation strategy to the one used previously and another set of experiments has been initiated. New materials have been acquired, which we will use in our attempt to confirm our previous observations of Ti-catalyst activity on Al surfaces and the formation of alane with H_2 exposure.

Our latest experiments, using an STM with more sensitive spectroscopic capabilities to probe electronic structure, confirm that titanium catalyst deposited on an aluminum surface retains its metallic character; no energy gap is observed. Subsequent experiments will measure whether this changes with hydrogen exposure.

Theory

Transition-metal catalysts are used extensively in hydrogen storage materials to increase H absorption and desorption kinetics. Using density functional theory (DFT) calculations, we elucidated the catalytic effect of Ti substitution on H_2 desorption from a $MgH_2(110)$ surface. Kinetic energy barriers of different reaction pathways of H desorption are calculated via the nudged-elastic-band (NEB) method. We found that a single Ti dopant is effective in reducing the kinetic barrier by 0.41 eV due to a concerted motion of H_2 surface desorption and H bulk diffusion. We also find that magnetic degrees of freedom must be carefully included to describe the crossover of magnetic states during catalyzed H_2 surface desorption. As shown in Figure 4, there are two concerted activation steps. In the early stage of reaction, the diffusion of in-plane hydrogen from first and second tri-layers to the surface brings a high hydrogen coordination number (HCN) of 8 to Ti, and the system prefers to have a magnetic moment of 0 μ_B. The activation barrier is small. In the second activation step to desorb H_2, the barrier is large. And importantly, because of the decrease in HCN to 6, the system prefers to have a magnetic

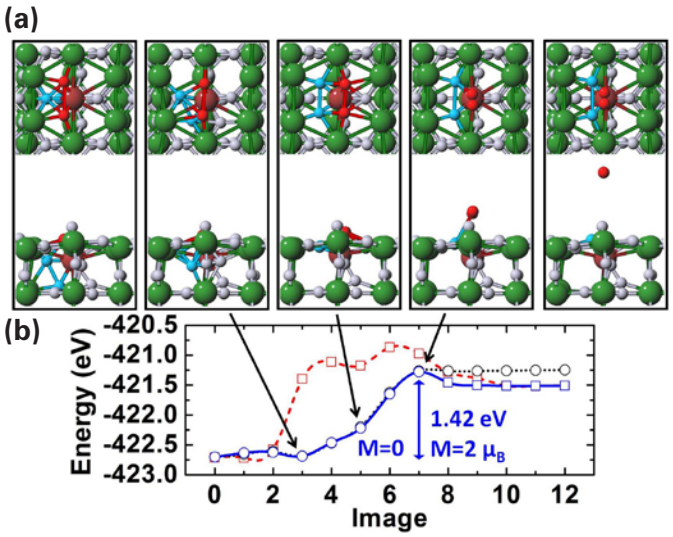


FIGURE 4. Minimum energy pathway (MEP) for H_2 desorption from Ti-doped MgH_2(110) surface, with large green spheres for Mg, large red for Ti and small gray for H. a) The leftmost (rightmost) sub-figure is the initial (final) state with a magnetic moment of 0 (2) μ_B. Three other intermediate states (Nudged elastic band images 3, 5 and 7 indicated by arrows) are also shown. Two bridge Hs that desorb from surface are highlighted in red. Two in-plane hydrogen atoms (one in the first tri-layer and the other in the second tri-layer) that diffuse to top of the surface are highlighted in blue. b) Total energy along reaction coordinates. MEP for the same initial state with moment of 0 μ_B and MEP for a degenerated initial state with a magnetic moment of 2 μ_B are included as red dashed line and black dotted lines for comparison. The activation barrier is 1.84 and 1.46 eV, respectively. The square (circle) stands for the state with a magnetic moment of 2 (0) μ_B.

moment of 2 μ_B. The overall kinetic barrier is 1.42 eV. In contrast, without such crossover of magnetic moment, the barrier is 1.46 eV for the same initial state with a magnetic moment of 2 μ_B and 1.84 eV for a degenerated state with a magnetic moment of 2 μ_B.

Our earlier report and also previous studies have shown that the overall desoprtion energy of H (or formation energy) from MgH_2 nanoparticles only decreases significantly when the size of the particle falls below 5 formula units. We have shown via DFT simulation that there is no size effect on the initial desorption of H from a MgH_2 surface and a MgH_2 amorphous nanoparticles. We have considered both singly- and doubly-bonded H. Figure 5(a) shows that a singly-bonded H is removed from an amorphous MgH_2 NP of 31 formula units. The desoprtion energy is 148 kJ/(mol-H_2) in reference to free H_2. Because a singly-bonded H cannot be found on MgH_2(110), where only doubly-bonded H exist, we constructued a stepped surface, see Figure 5(b). The desorption energy of singly-bonded H from this step surface is 140 kJ/(mol-H_2) and within 6% of that from a finite nanoparticle. For a doubly-bonded H, we found a similar result. All the data are shown in Figure 5(c). The lack of size effect in the initial H desorption can be understood by the fact that the Mg-H bond is ionic and local in nature.

Motivated by our earlier STM observations, we used DFT to study the atomic processes of alane formation on Ti-doped Al(111) surfaces and elucidate the role of Ti and vacancies. Figure 6 shows the reaction pathways of alane formation on Al(111) with and without Ti doping. Without Ti (see Figure 6(a)), the pristine Al(111) surface is known to react weakly with hydrogen. The dissociative adsorption

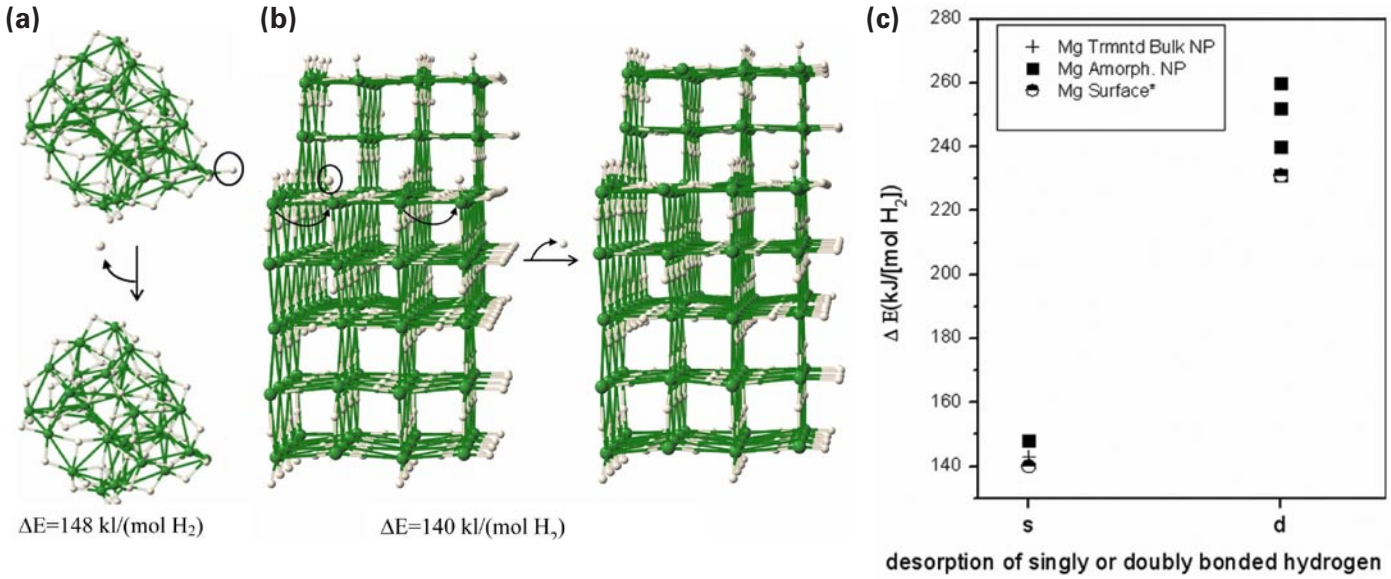


FIGURE 5. Desorption of H from MgH_2 nanoparticle and bulk surface. Singly-bonded H is desorbed from a) an amorphous MgH_2 nanoparticle and b) a stepped surface of MgH_2. c) Desorption energies for both singly- and doubly-bonded H in different structures. In the amorphous MgH_2 nanoparticle, several doubly-bonded H sites that are non-equivalent are shown together.

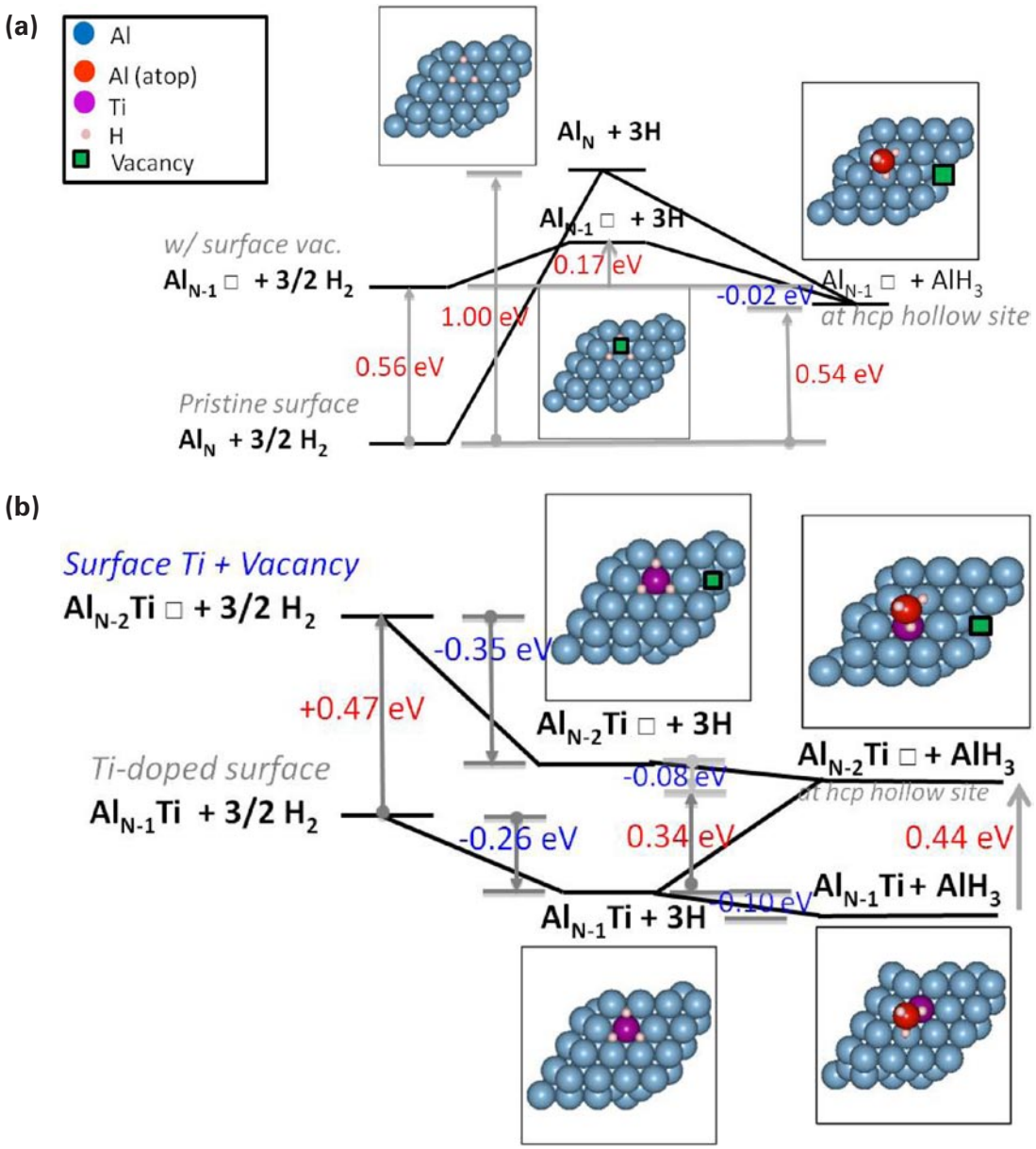


FIGURE 6. Reaction pathways for alane formation on Al(111) (a) without (b) with Ti dopant. In each case, both the absence and presence of Al vacancy are considered.

of H_2 on Al(111) surface costs energy. Using one and a half H_2 molecules and pristine Al(111) surface as the energy reference, the formation of three atomically adsorbed H on Al(111) is 1.00 eV higher. The system can lower energy by 0.46 eV with the formation of an alane molecule, which prefers to adsorb on a neighboring 3-fold hollow site, leaving behind a surface Al vacancy. Overall, the reaction to form alane on pristine Al(111) is endothermic with a reaction energy of 0.54 eV. In contrast, if Al(111) already has an Al vacancy, it only costs 0.17 eV to dissocate (3/2)H_2, which prefers to adsorb at the vacancy site. Then it gains 0.19 eV to form an alane molecule, such that the overall alane formation is slightly exothermic with a reaction energy of -0.02 eV. This is due to the fact that the initial reactant Al phase is destablized by creating one Al vacancy and moving the displaced Al atom to a bulk environment, which shifts the initial state to be 0.56 eV higher. More importantly, the presence of Al vacancy helps to lower the energy cost to dissociate H_2.

By introducing Ti on Al(111) (see Figure 6b), the Al vacancy formation energy is reduced to 0.47 eV, reflecting the tendence for Ti and Al to form an alloy. With Ti, the dissociation of H_2 becomes favored in both cases, with an energy drop of 0.26 and 0.35 eV without and with an Al vacancy, respectively. Atomic H prefers to stay with Ti and adsorbs on the 3-fold hollow site around Ti. Then

the formation of alane is favored by a small energy drop of 0.08 eV in the vacancy case. Without a vacancy, the formation of alane can also proceed with an energy drop of 0.10 eV provided an activated Al atom is available from the creation of a vacancy at another site. Otherwise, a direct conversion to alane by creating a local Al vacancy costs 0.34 eV. But the overall formation of alane in this case with Ti is slightly endothermic with a reaction energy of only 0.08 eV. With the avalability of an activated Al atom diffusing on the surface, the formation of alane molecule in both cases is endothermic. Further study of the kinetic energy barrier of each step is in progress.

Overall, however, these results explain and agree well with our STM studies performed on Al(111) dosed with Ti dopants and H_2; moreover, these results explain the observed formation of alane in ball-milling experiments, where vacancies occur as a inherent consequence of the processing, e.g., those at Ames Laboratory by V. Pacharsky.

Graduate Students and Post-Doctoral Fellows Supported

1. Stephen House, Aditi Herwadkar, Lin-Lin Wang, and Jason Reich

References

1. Majzoub, E.H., X.F. Liu, D. Peaslee, and C.Z. Jost, *Controlling the Decomposition Pathway of LiBH(4) via Confinement in Highly Ordered Nanoporous Carbon.* J Phys Chem C, 2010. 114(33): p. 14036-14041.

FY 2011 Publicatons

1. Location of Ti catalyst in the reversible AlH_3 adduct of triethylenediamine, D.D. Graham, J. Graetz, J. Reilly, J. Wegrzyn, and I.M. Robertson. Journal of Physical Chemistry C, 114, 15207-15211.2010.

2. Time-dependent, protein-directed growth of gold nanoparticles within a single crystal of lysozyme. W. Hui; W. Zidong; Z. Jiong: S. House; G. Yi-Gui; Y. Limin; H. Robinson; T. Li Huey; X. Hang; H. Changjun; I.M. Robertson; Z. Jian-Min; L. Yi. Nature Nanotechnology, 6, 93-97.2011.

3. Ordered metal nanostructure self-assembly using metal–organic frameworks as templates B.W. Jacobs; R.J.T. Houk; M.R. Anstey; S.D. House; I.M. Robertson; A.A. Talin; M.D. Allendorf, Chemical Science, 2, 411-416.2011.

4. Electron Tomographic Characterization of Nano-confined Hydrides for Hydrogen Storage S.D. House, E.H. Majzoub, R. Bhakta, M.D. Allendorf, and I.M. Robertson. Microscopy and Microanalysis conference, 2011.

5. Applications of Electron Microscopy to Complex Metal Hydrides (INVITED) S. House, I.M. Robertson and D. Graham, Microscopy and Microanalysis conference, 2011.

6. Hydrogen Desorption for MgH_2 Surfaces and Nanoparticles: Thermodynamics and Size Effects J. Reich, L.-L. Wang, and D.D. Johnson, in preparation (2011).

7. Kinetic Barriers and Ti-dopant Effects for Hydrogen Desorption on MgH_2(110): a DFT study J. Reich, L.-L. Wang, and D.D. Johnson, in preparation (2011).

8. Defect-mediated Alane Formation in Al(111): DFT comparison to Experiment Aditi Herwadkar, L.-L. Wang, S. House, P Martin, I.M. Robertson, D.D. Johnson, in preparation (2011).

FY 2011 Presentations

1. D.D. Johnson "Quantitative Prediction of Thermodynamic and Mechanical Properties of Real Materials," Invited, International Workshop on Ab-initio Description of Iron and Steel: Mechanical properties (ADIS2010), Ringberg Castle (Tegernsee, Germany) 24–29 October 2010.

2. D.D. Johnson and L-L. Wang, "Nanoparticle Structure and Properties: Universal Features, Structural Instabilities and the Effects of Size and Support", Dept. of Chemical Eng., U. of Pittsburg, 5 November 2010.

3. D.D. Johnson, "Transition-Metal Nanoparticle Structure and Properties: universal features for catalysis," Pennergy Colloquia Series, U. of Pennsylvania, 8 November 2010 (host Andrew Rappe).

4. D.D. Johnson, "Doping and Structural Defects – their import in determining critical materials behavior," Division of Materials Science and Engineering, Ames Laboratory, Iowa State U., 7 December 2010.

5. D.D. Johnson "Disorder-Mediated Quantum Criticality in Laves-phase NbFe2," Department of Physics, 22 February 2011.

6. Aditi Herwadkar and D.D. Johnson, "Defect-mediated Alane formation on Al(111)," 2011 APS March Meeting.

7. Jason Reich, LinLin Wang and D.D. Johnson, "Kinetic Barriers for Hydrogen Desorption for TM (un)doped MgH2(110), " 2011 APS March Meeting.

8. LinLin Wang and D.D. Johnson, "Thermodynamics of MgH2 H-storage materials: nanoparticle size and topological structural effects," 2011 APS March Meeting.

9. S.D. House, E.H. Majzoub, R. Bhakta, M.D. Allendorf, and I.M. Robertson. "Electron Tomographic Characterization of Nano-confined Hydrides for Hydrogen Storage," Microscopy and Microanalysis conference, 2011.

10. S. House, I.M. Robertson and D. Graham, Applications of Electron Microscopy to Complex Metal Hydrides (INVITED) Microscopy and Microanalysis conference, 2011.

11. S.D. House and I.M. Robertson "Microstructural characterization of nano-confined hydrogen storage systems" Gordon research conference, 2011 (INVITED).

IV.A.6 Aluminum Hydride

Jason Graetz (Primary Contact), James Wegrzyn, James Reilly
Brookhaven National Laboratory (BNL)
Building 815
Upton, NY 11973
Phone: (631) 344-3242
E-mail: graetz@bnl.gov

DOE Manager
HQ: Ned Stetson
Phone: (202) 586-9995
E-mail: Ned.Stetson@ee.doe.gov

Project Start Date: October 1, 2005
Project End Date: Project continuation and direction determined annually by DOE

Fiscal Year (FY) 2011 Objectives

Develop onboard vehicle storage systems using aluminum hydride that meets all of DOE's targets for the proton exchange membrane (PEM) fuel cell vehicle:

- Produce aluminum hydride material with a hydrogen storage capacity greater than 9.7% gravimetric (kg-H_2/kg) and 0.13 kg-H_2/L volumetric.
- Develop practical and economical processes for regenerating aluminum hydride.
- Assist in developing aluminum hydride slurry storage systems for better than 6% hydrogen gravimetric material density, 0.07 kg-H_2/L volumetric hydrogen storage capacity, and well-to-wheels efficiencies greater than 60%.

Technical Barriers

This project addresses the following technical barriers from the storage section of the Fuel Cell Technologies Program Multi-Year Research, Development and Demonstration Plan:

(A) System Weight and Volume
(B) System Cost
(E) Charging/Discharging Rates

Technical Targets

Listed in Table 1 are the 2015 Hydrogen Storage targets along with BNL's current 2011 aluminum hydride project status. The well-to-wheels efficiency listed in the table under the column for 2011 Status was taken from an independent analysis of an aluminum hydride storage system by Argonne National Laboratory. The Argonne analysis assumes 70-wt% aluminum hydride slurry, uses trimethylamine as the stabilizing agent for regenerating aluminum hydride and assumes the availability of low grade heat in determining the 55% efficiency. The tank's operating temperature of 80°C was the lowest temperature measured by BNL for AlH_3 slurries that meets the DOE fuel flow target of 0.02 (g/s)/kW. The criteria for meeting this flow target is 96% hydrogen release in 60 minutes or less from a 10 liter tank. The 0.0582 gravimetric storage parameter listed in Table 1 is a measured value from a 60-wt% slurry consisting of 9.7-wt% aluminum hydride particles and does not take into account the balance of plant weight.

TABLE 1. Progress in Meeting Technical Hydrogen Storage Targets

Aluminum Hydride Regeneration			
Storage Parameter	**Units**	**2015 Target**	**2011 Status**
Gravimetric	wt% H_2	0.055	0.0582
Volumetric	kg H_2/L	0.040	0.070
Full Flow Rate (temperature)	(g/s)/kW °C	0.02 80	0.02 80
Well-to-Wheels Efficiency	kW-H_2/kW	60%	55%
Refueling Time	min	3.3	To be determined

FY 2011 Accomplishments

- Demonstrated 6 wt% H_2 slurries using mineral oil and glycols as the liquid carrier.
- In the aluminum hydride synthesis process identified diphenyl methane as a safe solvent substitute for toluene.
- Demonstrated that aluminum hydride slurries can meet DOE's fuel flow targets at temperatures less than the fuel cell operating temperature of 100°C.



Introduction

The FY 2011 objective was to achieve DOE's 2015 system fill target of 5 kg of H_2 in 3.3 minutes. Since aluminum hydride exists only as a solid, this objective was redirected towards formulating a 'pumpable" 6% by H_2 wt AlH_3 slurry. In order to meet this 1.5 kg H_2 per minute target, the slurry had to be stable against phase separation and sedimentation with a viscosity less than 1,000 centipoise. This type of slurry could be made, however the condition of remaining "pumpable" after the

release of hydrogen at temperatures of 120°C was not met by using either mineral oil or glycol as the liquid carriers.

Approach

AlH_3 is classified as a kinetically stabilized material. In the past we have used a nucleation and growth chemistry model to describe the stability of AlH_3. This chemical model was useful in defining an induction period (nucleation) along with a kinetic decomposition period (growth). However recently, we found that a statistical approach (hyperbolic secant probability distribution function, Eqn. [1]) is very useful in describing the AlH_3 decomposition rate under isothermal conditions:

$$f(t) = (1/2t_k)\mathbf{sech}[(\pi/2)(t-t_m)/t_k)] \quad [1]$$

In Eqn. [1], t_m is the time when the decomposition rate reaches its peak value and $(1/2t_k)$ is the peak kinetic decomposition rate. The integration of the probability distribution function $f(t)$ over time yields the cumulative distribution function $F(t)$. This function is more convenient to work with than the probability density function, since it is the percent loss of hydrogen as a function of time. Integrating over time Eqn. [1] yields the following expression for the cumulative distribution function $F(t)$:

$$F(t) = (2/\pi)\mathbf{tan}^{-1}(\mathbf{exp}[(\pi/2)(t-t_m)/t_k]). \quad [2]$$

The induction period (IP) is now defined as the time when $F(t) = 0.02$. In other words, the time it takes for 2% decomposition. Setting $F(t) = 0.02$, replacing (t) with IP and solving for IP gives the following:

$$IP = t_m + (2t_k/\pi)\ \mathbf{ln}\{\mathbf{tan}(0.01\pi)\} = t_m - (2t_k/\pi)3.4601. \quad [3]$$

The time required for 96% release of hydrogen after the induction period is:

$$\Delta t(96\%) = (2t_k/\varpi)\ \mathbf{ln}\{\mathbf{tan}(0.49\varpi)\} - (2t_k/\varpi)\ \mathbf{ln}\{\mathbf{tan}(0.01\varpi)\} = (4t_k/\varpi)3.4601. \quad [4]$$

Note that $\ln\{\tan(0.49\pi)\}=3.4601$ and $\ln\{\tan(0.01\pi)\}= -3.4601$.

This model implies that surface coatings can increase the induction period by increasing t_m (see Eqn. [3]). Eqn. [4] shows that the time release of hydrogen $\Delta t(96\%)$ depends only on t_k and not t_m. Recall that $(1/2t_k)$ is the peak decomposition rate. Thus, the increase in IP, that results from increasing t_m, will essentially have no effect on the time it takes to release the remainder (96%) of the hydrogen. The results of this study support this model, since it shows that surface coatings can improve the stability of AlH_3 against decomposition; but once decomposition has started, the rate is then controlled by catalysts and the sample temperature.

Results

A 6% (or larger) by weight slurry is best achieved by using micron-sized particles. The preferred method for making micron-sized AlH_3 particles is by nucleating and growing these particles from an alane-etherate in an inert solvent solution. The inert solvent can be benzene or toluene; and just recently, we found that diphenyl methane is also a suitable medium. In simple terms, AlH_3 solubility decreases with increasing temperatures so by raising the temperature one would expect aluminum hydride to precipitate out of solution. The complication is that aluminum hydride decomposes at temperatures above 100°C. Thus far, only the alane etherate compounds have yielded aluminum hydride by this method. Attempts to recover aluminum hydride from alane-amine complexes have not yet been successful by this approach. We are, however, able to control particle size by controlling the rate at which the diethyl ether is removed from the reactor. Controlling the particle morphology is more challenging. Figure 1 shows individual particles and clusters of particles with aspect ratios close to 1, yet Figure 2 shows that under very similar conditions rod-shaped particles can also be produced. These particles are formed in batch and semi-continuous reactors. The batch reactor is 1 liter in size and makes 1.25 gram of product per batch. The recovered AlH_3 is then washed in either diethyl ether or hydrochloric acid. The semi-continuous method has a port connection for introducing the alane-etherate to a 1.5 liter reactor and we have used this method to produce up to 5 grams of AlH_3. After the wash, a milliliter of diethlylene dibutyl ether glycol (density 0.80 g/ml) is mixed with the 1.25 grams of AlH_3 to make a nominally 60% aluminum hydride-glycol slurry. A similar procedure was used to prepare a mineral oil slurry where 4 milliliters of mineral oil and 0.15 grams of dispersant (Triton x-100) was used along with the AlH_3.

A series of isothermal kinetic decomposition experiments were performed on these aluminum hydride glycol and minerial oil slurries. Figure 3 shows plots of

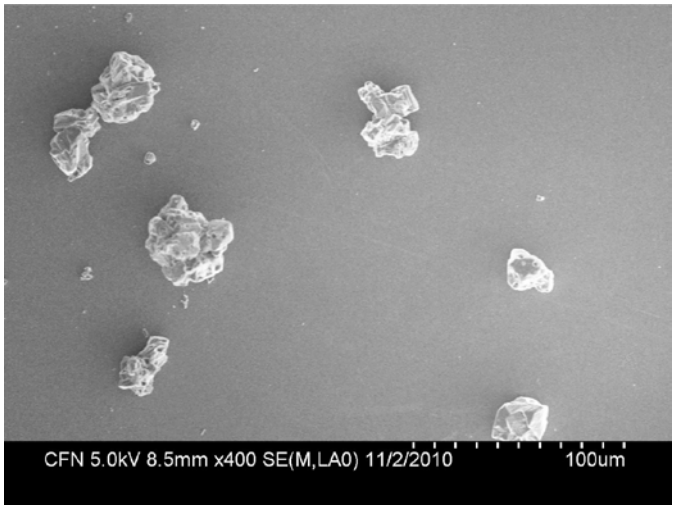


FIGURE 1. Electron micrograph of 97% pure alpha aluminum hydride particles in cluster shapes precipitated from an alane-etherate/toluene solution (sample AH-3390).

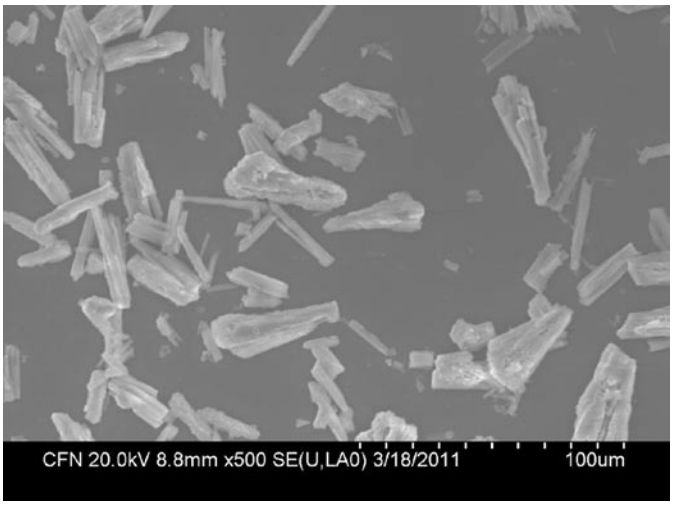


FIGURE 2. Electron micrograph of 97% pure rod shaped alpha aluminum hydride particles precipitated from an alane-etherate/toluene solution (Sample AH-3399).

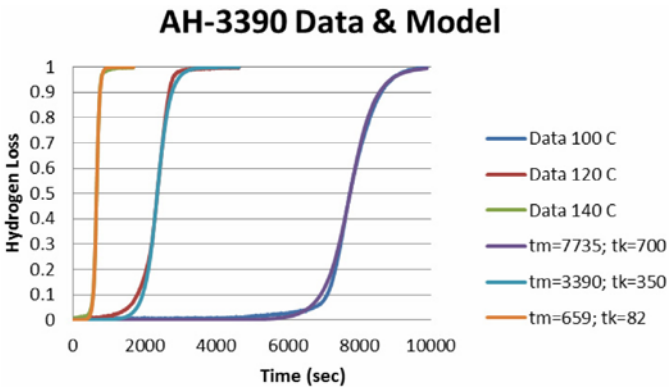


FIGURE 3. Fractional decomposition of AlH_3 at the three temperatures of 100, 120 and 140°C showing experimental data and fit using the statistical model.

the hydrogen loss as a function of time for the aluminum hydride-glycol slurry at three temperatures: 100, 120 and 140°C. Also plotted on this figure are the results from the statistic model with the corresponding two parameter fit (t_m, t_k). The good fit between the experimental data and model allows us to discuss the data in terms of t_m and t_k. For the catalyzed glycol slurries t_k ~250 (T = 120°C), while this parameter is much greater for the mineral oil slurries t_k ~700 (T = 120°C). At this point we can only speculate why the catalyzed glycol slurries have better decomposition kinetics than the mineral oil slurries. Figure 4 shows how the acid wash affects the IP. Incorporating a wash at the end of the synthesis increases the IP by applying an oxide/hydroxide coating on the surface of the AlH_3 particle. In this experiment one half the particles were acid washed and the other half were only washed in diethyl ether. Note that even though the IP increased after the acid wash, the peak

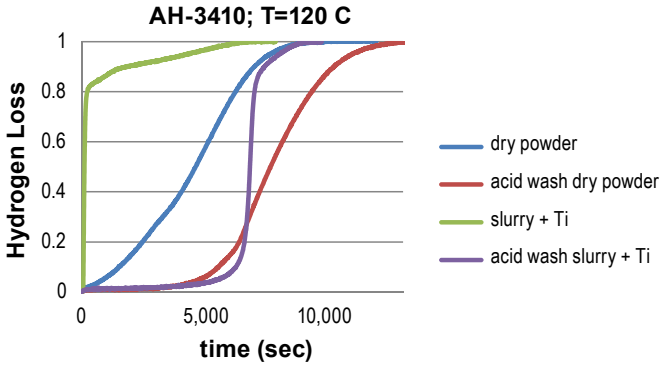


FIGURE 4. AlH_3 decomposition data for particles with and without acid wash as a function of time.

decomposition rate t_k remained essentially constant (t_k = 100 & 300 for the two Ti-catalyzed samples; t_k = 2,100 and 2,400 for the two samples without catalysts). The non-symmetric result (green line) for the catalyzed slurry in Figure 4 has been attributed to non-uniform mixing of the catalyst in the slurry.

Conclusions and Future Directions

- 6 wt% H_2 AlH_3 slurries were prepared and performed satisfactory at temperatures less than 100°C.
- Determined that surface coatings can stabilize AlH_3 against the start of decomposition. We also found that using a hydrochloric acid wash is an effective means of applying surface coatings on one micron or larger AlH_3 particles.
- The AlH_3 decomposition rates after the induction period are controlled mainly by temperature and catalyst loading. Morphology, particle size and the type of liquid carrier also affect decomposition kinetics, but to a lesser extent.
- The future direction is to develop the procedure and hardware to increase AlH_3 production from 5 grams/week to 50 grams/week.

FY 2011 Publications

1. B.M. Wong, D. Lacina, I.M.B. Nielsen, J. Graetz, and M.D. Allendorf, "Thermochemistry of Alane Complexes for Hydrogen Storage: A Theoretical and Experimental Investigation" *J. Phys. Chem. C*, **115** 7778 (2011).

2. D. Lacina, J. Wegrzyn, J. Reilly, J. Johnson, Y. Celebi and J. Graetz, Regeneration of Aluminum Hydride using Trimethylamine" *J. Phys. Chem. C*, **115** 3789 (2011).

3. J. Graetz, J.J. Reilly, V.A. Yartys, J.P. Maehlen, B.M. Bulychev, V.E. Antonov, B.P. Tarasov, I.E. Gabis, "Aluminum hydride as a hydrogen and energy storage material: past, present and future" *J. Alloys Compd*. doi:10.1016/j.jallcom.2010.11.115 (2010).

4. D. Lacina, J. Reilly, J. Johnson, J. Wegrzyn and J. Graetz "The Reversible Synthesis of Bis(Quinuclidine) Alane" *J. Alloys Compd*. DOI: 10.1016/j.jallcom.2010.10.010. (2010).

5. D.D. Graham, J. Graetz, J. Reilly, J. Wegrzyn, I.M. Robertson, "Location of Ti Catalyst in the Reversible AlH_3 Adduct of Triethylenediamine" *J. Phys. Chem. C*, **114** 15207–15211 (2010).

6. F.S. Manciua, L. Rezaa, W.G. Durrera, A. Bronsonb, D. Lacina and J. Graetz, "Spectroscopic and structural investigations of α-, β-, and γ-AlH_3 phases," *J. Raman Spectrosc.*, **42** 512-516 (2011).

7. D. Lacina, J. Wegrzyn, J. Reilly, Y. Celebi, J. Graetz "Regeneration of Aluminum Hydride using Dimethylethylamine" *Energy Env. Science*, *Energy Environ. Sci.*, **3** 1099 (2010).

FY 2011 Presentations

1. "Regeneration of Aluminum-Based Hydrides", *International Energy Agency (IEA) Task 22 Experts Meeting*, Fremantle, WA, Australia, January, 2011.

2. "Regeneration of aluminum-based hydrides" *The International Chemical Congress of Pacific Basin Societies*, Honolulu, HI, December, 2010.

3. "Aluminum hydride as an energy and hydrogen storage material: past present and future" Plenary Lecture, International Symposium on Metal-Hydrogen Systems (MH2010), Moscow, Russia, July, 2010.

4. "Regeneration of Aluminum Hydride", *International Energy Agency (IEA) Task 22 Experts Meeting*, Death Valley, CA, April, 2010.

5. "Regeneration of AlH_3 studied with Raman and Infrared Spectroscopy", *Materials Research Society Spring Meeting*, San Francisco, CA, April, 2010.

6. "Regeneration of Aluminum Hydride", *International Forum for Hydrogen Storage 2010*, Tokyo, Japan, March, 2010.

7. "Structural Properties of Aluminum Hydride", *Symposium on Synchrotron Radiation Research 2010 - Materials Science on Metal Hydrides*, Hyogo, Japan, February, 2010.

8. "New Approaches to Hydrogen Storage", *Materials Science Colloquium*, Stony Brook, New York, February, 2010.

IV.A.7 Electrochemical Reversible Formation of Alane

Ragaiy Zidan
Savannah River National Laboratory
999-2W Room 121
Savannah River Site
Aiken, SC 29808
Phone: (803) 646-8876
E-mail: ragaiy.zidan@srnl.doe.gov

DOE Manager
HQ: Ned Stetson
Phone: (202) 586-9995
E-mail: Ned.Stetson@ee.doe.gov

Contributors:
Michael Martinez-Rodriguez
Joe Teprovich
Scott Greenway

Project Start Date: October 1, 2006
Project End Date: October 1, 2011

Fiscal Year (FY) 2011 Objectives

- Identify energy efficiency improvements for the alane production process of over 50%.
- Characterize new electrochemical additives for alane production.
- Improve production process and properties of alane adducts.

Technical Barriers

This project addresses the following technical barriers from the Technical Plan - Storage section of the Fuel Cell Technologies Program Multi-Year Research, Development and Demonstration Plan:

(A) System Weight and Volume
(B) System Cost
(C) Efficiency
(R) Regeneration Processes

Technical Targets

In this project studies are being conducted to lower cost and improve efficiency of the electrochemical method to form AlH_3. This material has the potential to meet the 2015 technical target for on-board hydrogen storage as shown in Table 1.

TABLE 1. Alane Compared With 2015 Target

Storage Parameter	2015 Target	AlH_3
Gravimetric Capacity	0.055 kg H_2/kg System	0.1 kg H_2/kg AlH_3
Volumetric Capacity	0.04 kg H_2/L System	0.149 kg H_2/L AlH_3

FY 2011 Accomplishments

- Developed a pressurized dimethyl ether (DME)-based synthesis for alane that eliminates need for vacuum drying of alane and yield α-alane crystallites.
- Demonstrated electrochemically active compounds and used electrochemical impedance spectroscopy (EIS) to show that kinetic improvements were due to more than increased ionic conductivity.
- Continued production of gram quantities of alane with improving energy efficiency.

✧ ✧ ✧ ✧ ✧

Introduction

The DOE is supporting research to demonstrate viable materials for on-board hydrogen storage. Aluminum hydride (alane – AlH_3), having a gravimetric capacity of 10 wt% and volumetric capacity of 149 g H_2/L and a desorption temperature of ~60°C to 175°C (depending on particle size and the addition of catalysts) has the potential to meet the 2010 and 2015 DOE targets [1,2].

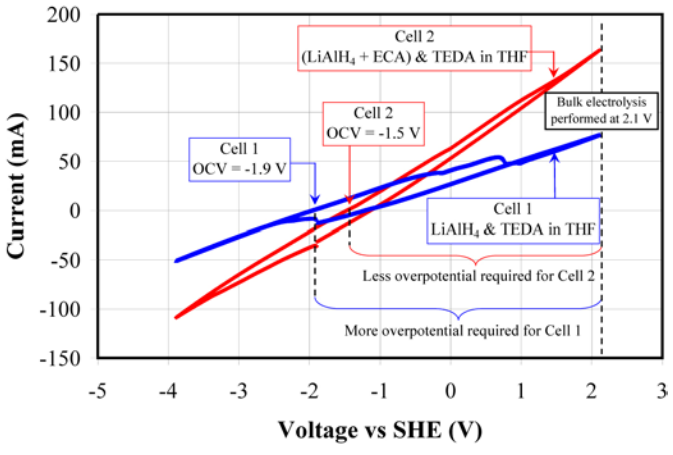
The main draw back for using alane as a hydrogen storage material is unfavorable thermodynamics towards hydrogenation. Past attempts to regenerate alane under mild conditions were reported, including attempts based on electrochemical methods [3, 4]. However, recent results on the regeneration of alane reported by Zidan et al. [5] were the first to show a reversible cycle utilizing electrochemistry and direct hydrogenation, where gram quantities of alane were produced, isolated and characterized. This regeneration method is based on a complete cycle that uses electrolysis and catalytic hydrogenation of spent Al(s). This cycle avoids the impractical high pressure needed to form AlH_3 and the chemical reaction route of AlH_3 that leads to the formation of alkali halide salts, such as LiCl or NaCl, which become a thermodynamic sink because of their stability. During FY 2011, the electrochemical synthesis of alane described in Zidan et al. [5] has been improved allowing higher cell efficiency while increasing the alane production rate. Improvements are achieved by the use of $LiAlH_4$ and the introduction of LiCl [6] which acts as an electro-catalytic additive (ECA) and greatly enhanced the electrochemical process. A pressurized solvent electrochemical method for alane production has also been developed and demonstrated that reduces the need for parasitic vacuum processing of the alane to remove solvents.

Approach

Experimentally, the electrolysis was carried out as described in the electronic supplementary information of Zidan et al [3]. However, $LiAlH_4$ was used instead of $NaAlH_4$. Both, tetrahydrofuran (THF) and diethyl ether (Et_2O) were used as aprotic solvents for the alane regeneration. Research on the electrochemical properties of $MAlH_4$ (M = Na, Li) in THF and Et_2O has been reported [7, 8] but these studies were not directed at the regeneration and characterization of alane. Also, the work of Senoh et al [7, 8] was performed with Ni electrodes different to this work in which Al is used as working electrode. The use of Al is essential to the alane regenerartive process and the reaction with the ECA as discussed later.

Results

To test the effect of the LiCl two cells were prepared using $LiAlH_4$ and triethylenediamine (TEDA) in THF and LiCl was added to one of the cells. TEDA was incorporated in the solution to easily detect and visualize the formation of alane as AlH_3-TEDA (white precipitate [3]) during the experimental test. Figure 1 shows 10 min of the bulk electrolysis at 2.1 V for the alane production using the two cells described above. The high potential used during the electrolysis was applied to produce enough alane in those 10 min for visualization purpose and comparison. Alane-TEDA is not expected to decompose during the conditions of these tests. Figure 2 shows an increase of 80% in the current when LiCl was used. The total charge for cell 2 was two times the total charge obtained with cell 1. Since the charge is proportional to the moles of product produced, the amount of AlH_3-TEDA was doubled when the ECA was used in cell 2. The precipitated alane-TEDA was separated from solution and weighted. Consistently, Cell 2 was found to produce twice as much AlH_3-TEDA.



OCV – open-circuit voltage; SHE – standard hydrogen electrode

FIGURE 1. Cyclic voltammograms at 50 mV/s for the formation of AlH_3-TEDA using identical electrochemical cells with 1 M of $LiAlH_4$ and TEDA in THF without LiCl (Cell 1) and with LiCl (Cell 2).

EIS was performed on the cells with and without the LiCl. Figure 3 shows that the high frequency value, which represents the resistance of the cells, is about 113 and 114 $\Omega \cdot cm^2$ for the cells without and with LiCl, respectively. This shows that LiCl does not have a significant effect in the resistance (or conductivity) of the solution. That is, the LiCl is not acting as an electrolyte. Consequently, the increase in current and efficiency discussed above are an electro-catalytic effect of the added species.

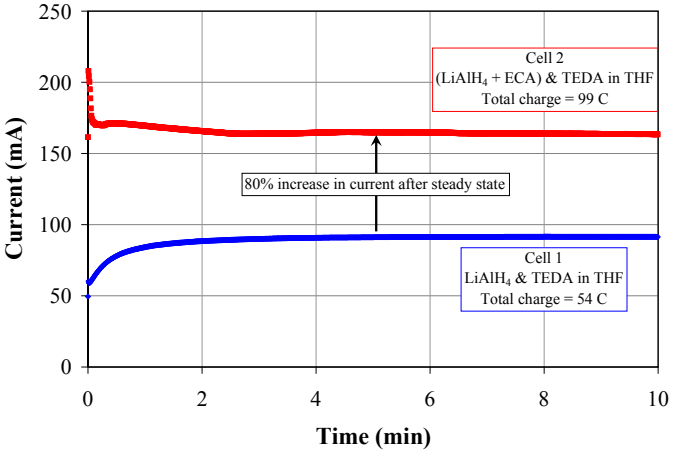


FIGURE 2. Bulk Electrolysis for the Production of AlH_3-TEDA using two Identical Electrochemical Cells with 1 M of $LiAlH_4$ in and THF without LiCl (Cell 1) and with LiCl (Cell 2)

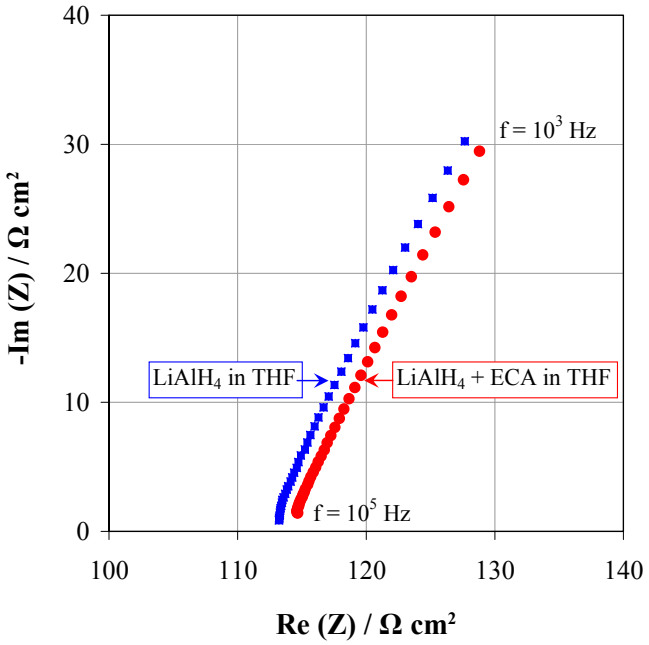


FIGURE 3. Nyquist Diagram for Identical Electrochemical Cells with 1 M of $LiAlH_4$ and TEDA in THF without LiCl (Cell 1) and with LiCl (Cell 2)

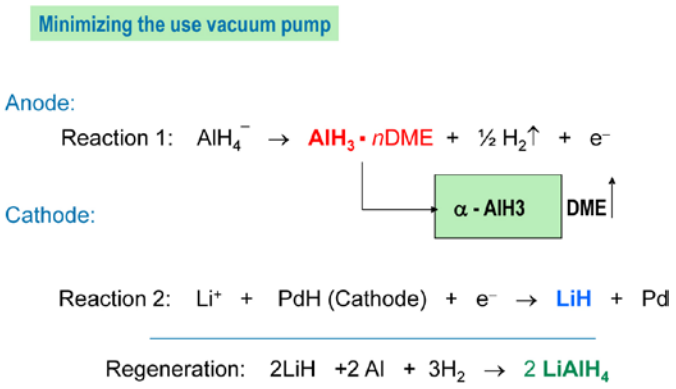


FIGURE 4. Pressurized Solvent System to Improve Overall Energy Efficiency of Alane Production

Therefore, the electrochemical synthesis of alane has been improved by adding LiCl to a solution of $LiAlH_4$-THF. We have shown that LiCl function as an electro-catalytic additive in a cyclic process that increases the current. This process lead to a higher cell efficiency and higher amount of alane produced.

Analysis from the DOE Hydrogen Storage Team and has shown that the main energy losses in the production of alane will be the energy required to run the vacuum pump during product separation. Therefore, a pressurized solvent system (similar to work reported earlier by Shane et al. on $LiAlH_4$ [9]) was developed to increase the energy efficiency of alane production and purification. Figure 4 outlines the concept for alane synthesis using a system with pressurized DME. The DME solvent is polar, aprotic and has good safety characteristics. Using this method, alane can be purified and crystallized just through the release of the DME solvent from the system. X-ray diffraction data from alane produce in DME shows a relatively pure crystalline alpha phase.

Conclusions and Future Directions

- Work with industrial partners to lower the cost of alane production for use as high energy density storage materials in near term portable power systems.
- Perform electrochemical production of alane and alane adducts in a pressurized solvent environment and demonstrate production of α-alane using these methods.

Patents Issued

1. Improving Electrochemical Methods for Producing and Regenerating Alane by the Addition of Halides to Electrolyte, Patent pending.

FY 2011 Publications/Presentations

1. "Progress in the Electrochemical Formation of Alane" MRS San Francisco, March 2011, *Invited Speaker.*

2. Ragaiy Zidan "Electrochemical Reversible Formation of Alane" 2011 Annual Merit Review Washington, D.C., May 2011.

3. Ragaiy Zidan "Electrochemical Reversible Formation of Alane" Hydrogen storage tech team meeting March 17, 2011 USCAR, Southfield, Michigan.

4. Ragaiy Zidan "Development and Characterization of Novel Hydrogen Storage Materials" IEA HIA Task 22 Meeting – Fundamental and Applied Hydrogen Storage Material Development January 16, 2011 Fremantle, Australia.

5. Ragaiy Zidan "Advances in Electrochemical Formation of Alane" Pacifichem December 15, 2010 - Honolulu, Hawaii Invited Speaker.

References

1. G. Sandrock, J. Reilly, J. Graetz, W.M. Zhou, J. Johnson and J. Wegrzyn, *J. Alloys Compd*., 2006, 421, 185-189.2.

2. J. Graetz and J.J. Reilly, Journal of Physical Chemistry B, 2005, 109, 22181-22185.

3. H. Clasen, Germany Pat., 1141 62315. H. Clasen, Germany Pat., 1141 623, 1962.2, 1962.

4. N.M. Alpatova, T.N. Dymova, Y.M. Kessler and O.R. Osipov, *Russ. Chem. Rev.*, 1968, 37, 99.

5. Ragaiy Zidan, Brenda L. Garcia-Diaz, Christopher S. Fewox, Ashley C. Stowe, Joshua R. Gray and Andrew G. Harter *Chem. Commun.*, 2009, 3717-3719, 114.

6. Improving Electrochemical Methods for Producing and Regenerating Alane by the Addition of Halides to Electrolyte, *Patent pending.*

7. H. Senoh, T. Kiyobayashi, N. Kuriyama, K. Tatsumi and K. Yasuda, *J. Power Sources,* 2007, 164, 94-99.

8. H. Senoh, T. Kiyobayashi and N. Kuriyama, *Int. J. Hydrogen Energy*, 2008, 33, 3178-3181..

9. Liu, Xiangfeng; McGrady, G. Sean; Langmi, Henrietta W.; Jensen, Craig M, J Am Chem Soc. 2009 Apr 15;131(14):5032-3.

IV.A.8 Tunable Thermodynamics and Kinetics for Hydrogen Storage: Nanoparticle Synthesis using Ordered Polymer Templates

Mark D. Allendorf (Primary Contact),
Eric Majzoub[1], Jeffery Grossman[2], Julie Herberg[3]
Mail Stop 9291
Sandia National Laboratories
Livermore, CA 94551-0969
Phone: (925) 294-2895
E-mail: mdallen@sandia.gov

DOE Manager
HQ: Ned Stetson
Phone: (202) 586-9995
E-mail: Ned.Stetson@ee.doe.gov

Subcontractors:
[1] University of Missouri, St. Louis, St. Louis, MO
[2] Massachusetts Institute of Technology, Cambridge, MA
[3] Lawrence Livermore National Laboratory, Livermore, CA

Start Date: September 30, 2008
Projected End Date: September 30, 2011

Fiscal Year (FY) 2011 Objectives

- Achieve tunable thermodynamics for high-gravimetric-capacity metal hydrides by creating and stabilizing nanoparticles with controlled size, composition, and properties.
- Develop synthetic routes for reactive metal nanoparticles within crystalline nanoporous materials and block copolymer templates.
- Systematically probe the effects of size and composition to determine the onset and extent of nanoscale effects on the thermodynamics and kinetics of hydrogen sorption.
- Benchmark theoretical approaches to modeling the thermodynamics of metal hydride nanoparticles, and develop computational tools to guide synthesis.

Technical Barriers

This project addresses the following technical barriers from the Storage section of the Fuel Cell Technologies Program Multi-Year Research, Development and Demonstration Plan:

(A) System Weight and Volume
(C) Efficiency
(P) Lack of Understanding of Hydrogen Physisorption and Chemisorption

Technical Targets

The objective of this project is to achieve tunable thermodynamics and/or kinetics by confining metal hydrides within the chemically and geometrically well-defined pores of templates such as metal-organic frameworks (MOFs) and porous carbons, thus allowing faster H_2 desorption at a lower temperature than bulk. The project addresses the following DOE technical target (Table 1), as outlined in the Fuel Cell Technologies Program Multi-Year Research, Development and Demonstration Plan:

TABLE 1. DOE Targets for Hydrogen Storage

Parameter	DOE 2010 Target	Project Status
Maximum Delivery Temperature	85°C	Tunable kinetics demonstrated for nano-confined $NaAlH_4$ and $LiBH_4$. Size-dependent desorption enthalpy observed for $NaAlH_4$.

FY 2011 Accomplishments

- Demonstrated size-dependent thermodynamics for $LiBH_4$ infiltrated into porous carbon templates: the bulk orthorhombic-to-hexagonal phase change is not observed, no melting transition occurs, and the material is amorphous.
- Showed that nano-confined $NaAlH_4$ thermodynamics are tunable: reaction to form the stable intermediate Na_3AlH_6 is not observed. The enthalpy of H_2 desorption for the one-step decomposition to form NaH, Al, and H_2 is size dependent, consistent with theoretical results.
- Nano-confined $NaAlH_4$ decomposes more than an order of magnitude faster than bulk hydride.
- Predicted that $(MgAlH_5)_n$ clusters are destabilized relative to MgH_2 and that compositional tuning of $\Delta H°$ is feasible.



Introduction

Some of the most attractive hydrogen storage materials, such as MgH_2, AlH_3, and $LiBH_4$, have unfavorable desorption thermodynamics and are either too stable (e.g. MgH_2 and $LiBH_4$) or too unstable (e.g. AlH_3) in bulk form to be of use for vehicular transport applications. However, recent theoretical and experimental results indicate that decreasing particle size can substantially reduce the stability of metal hydrides, leading to lower desorption temperatures. The key challenges that must be addressed

are to: 1) develop synthetic routes that provide controlled size and composition; 2) stabilize particles over time; and 3) develop computational tools to guide synthesis that can accurately address particle sizes spanning the micro-to-meso length scales. This project addresses all three challenges and, if successful, will create for the first time nanoscale hydrogen storage materials with tailorable composition and size compatible with fuel-cell materials over a wide range of operating temperatures.

Approach

We are using highly ordered, chemically tailorable nanoporous templates to create particles ranging in size from <1 nm to 20 nm, the critical size range at which nanoscale effects are anticipated. These templates are infiltrated with hydride precursors or hydrides themselves, using mild synthetic routes that eliminate template degradation. The resulting template-satabilized nanoparticles are characterized to determine particle size, composition, and desorption thermodynamics and kinetics. Validated computational modeling tools guide synthesis. This approach allows nanoparticle dimensions and hydride composition to be systematically varied, enabling the effects of nanoscale dimensions on hydride thermodynamics to be determined.

Results

Tunable Thermodynamics and Kinetics for Nano-Confined $NaAlH_4$

$NaAlH_4$ is perhaps the most thoroughly characterized hydride in terms of its thermodynamics and kinetics of H_2 desorption. As such, it is an excellent test case for determining the influence of size and confinement environment on hydride thermodynamics and kinetics. This year, we performed detailed measurements to determine both $\Delta H°$ and E_a, using an infiltrated MOF with 1.3-nm pores and a melt-infiltrated porous carbon with uniform 4-nm diameter pores. The results show that both thermodynamics and kinetics are modified and suggest that these properties can be tuned by adjusting pore size.

Our experiments show that confining $NaAlH_4$ to ≤4 nm pores has several effects on the reaction. The H_2 desorption data for particles in the 1.3-nm MOF template (Figure 1) display evidence of at least two distinct reaction zones: a thermodynamic vapor-solid equilibrium at low reaction extent (<110°C) and a kinetically limited regime at temperatures up to 170°C. We characterized the reactant-product mixture obtained from vapor-solid equilibrium regime, using the 1.3-nm templated hydride, and see no evidence of Na_3AlH_6. This shows that under these conditions the reaction proceeds by a one-step process, which is different from the bulk behavior.

We also measured the temperature dependence of the H_2 vapor pressure to determine the heat of desorption ($\Delta H°$).

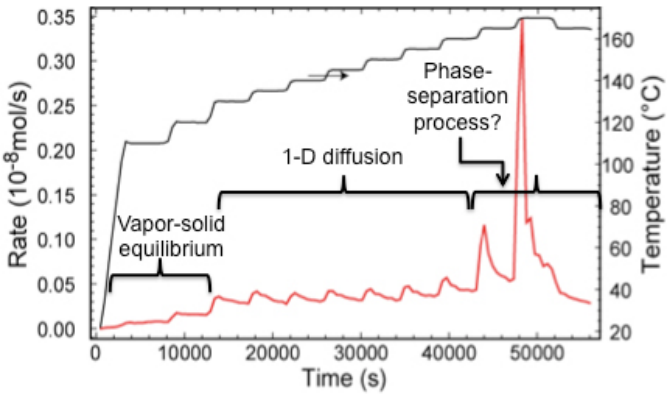


FIGURE 1. Hydrogen desorption from $NaAlH_4$ infiltrated into the 1.3-nm pores of the MOF Cu-BTC. Light-gray line indicates the temperature profile of the experiment, in which H_2 was detected using a molecular-beam mass spectrometer.

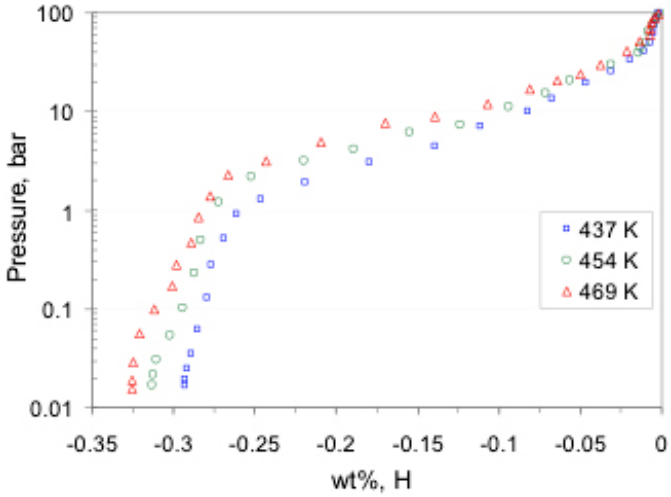


FIGURE 2. Pressure-Concentration-Temperature (PCT) Curves of $NaAlH_4$ Confined in 4-nm Nanoporous Carbon

The pressure-composition isotherms of $NaAlH_4$ confined in 4-nm nanoporous carbon (Figure 2) are not completely flat and exhibit only one plateau, whereas bulk Ti-catalyzed $NaAlH_4$ exhibits two flat plateaus corresponding to a two-step mechanism that forms first Na_3AlH_6 followed by NaH formation. Hydride confined to 4-nm pores has a lower $\Delta H°$ than bulk (Table 2), while hydride confined to the 1.3-nm pores of the MOF actually has a higher $\Delta H°$. The increased $\Delta H°$ for small particles agrees with the results of both our nano-prototype electrostatic ground state/density functional theory (DFT) calculations and with a report in the literature for $NaAlH_4$ within a porous (0.5–4 nm) carbon template [1]. This is the first quantitative evidence that hydrogen desorption thermodynamics can be tuned by controlling particle size. However, our results below concerning $LiBH_4$ show that this behavior is very specific to the particular hydride.

TABLE 2. Comparison of Measured $\Delta H°$ and E_a

Reaction	1.3 nm[a]		4 nm[b]		Bulk[c]	
	$\Delta H°$	E_a	$\Delta H°$	E_a	$\Delta H°$	E_a
$NaAlH_4 \rightarrow NaH + 0.33Al + 1.5H_2$	47	47–53	35±10	--	40	121
$NaAlH_4 \rightarrow 0.33Na_3AlH_6\ 0.67\ Al + 1.0H_2$	N/A	N/A	N/A	N/A	37	118

[a]Cu-BTC (MOF) template, solution infiltrated; [b]Porous carbon, melt-infiltrated; [c]Uncatalyzed; N/A – not applicable.

The behavior of the 1.3-nm $NaAlH_4$ (Figure 1) nanoparticles in the kinetic regime is consistent with a one-dimensional diffusion model. The measured activation energy (Table 2) is considerably smaller than the uncatalyzed bulk value and somewhat smaller than the value previously reported for 2–10 nm $NaAlH_4$ particles on carbon nanofiber [2]. This trend indicates that size has a stronger effect on the desorption kinetics than the chemical environment of the template. The activation energies obtained using the MOF template and the carbon nanofibers are rather similar, although the chemical environments are different; in fact, it is not clear that $NaAlH_4$ is actually "confined," but rather is "supported" on the surface of the carbon nanofibers, differentiating this template even further from the enclosed pores of the MOF.

Controlling the Decomposition Pathway of $LiBH_4$ via Confinement in Highly Ordered Nanoporous Carbon

We find that nanoscale $LiBH_4$ melt-infiltrating into 4-nm nanoporous carbon (NPC; 4-nm hexagonally packed cylindrical pores) is kinetically destabilized relative to bulk, but the thermodynamics are unchanged relative to bulk. The PCT for $LiBH_4$@NPC were measured at three different temperatures (Figure 3). The PCT has a clearly identified plateau region, from which we obtain $\Delta H°$ and entropy $\Delta S°$

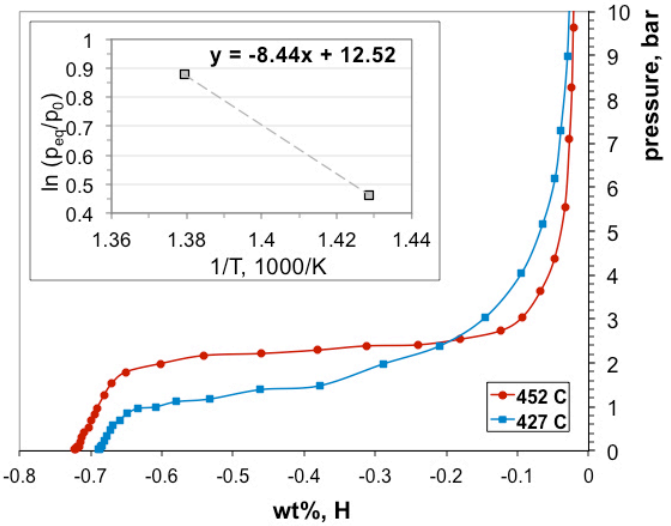


FIGURE 3. PCT Curves of $LiBH_4$@NPC Measured at Three Different Temperatures

of 70 kJ mol^{-1} H_2 and 104 J K^{-1} mol-H_2 $^{-1}$, respectively. This strongly suggests that in contrast to $NaAlH_4$, confinement, or particle size alone, has no effect on the thermodynamics of $LiBH_4$ decomposition. This result may be somewhat surprising in light of the many theoretical studies on nanoscale materials such as MgH_2 and other simple saline hydrides. It suggests, therefore, that decomposition of this hydride is thermodynamically limited by the strength of the B-H bonds in the BH_4 anion, which Fourier transform infrared data (not shown) indicate are similar to those of the bulk.

The benefits of incorporating $LiBH_4$ into ordered 4-nm pore frameworks are twofold. First, the desorption behavior up to six cycles is clearly reversible [3]. Second, the release of diborane per gram of infiltrated $LiBH_4$ can be dramatically reduced compared with both bulk hydride and hydride confined in 15 nm or 9 nm NPC. These observations clearly show that confining hydrides within a nanoporous material can change a material that is unusable in bulk form to one that could have practical utility in some applications. Importantly, the differences between the behavior of $NaAlH_4$ described above and $LiBH_4$ in these hard-carbon frameworks indicate that the interactions with the framework are hydride dependent, suggesting that a proper choice of hydride and framework chemistry can lead to a storage material having the desired properties.

Computational Modeling of Hydride Nanoparticles

The narrow range that $\Delta H°$ can assume for a successful vehicular hydrogen storage material (20–50 kJ mol^{-1}) lies roughly between two physical bounds: chemical bonds that are usually too strong, and hydrogen bonds that are usually too weak. One strategy for modulating $\Delta H°$ is to use compositional tuning in conjunction with nanoscale confinement. Our prior work demonstrated that MgH_2 nanoclusters are destabilized, but only at extremely small sizes (<5 formula units). Here, we describe high-accuracy fixed-node diffusion quantum Monte Carlo (DMC) calculations to evaluate the change in energy for the removal of H_2 from mixed Mg-Al clusters, which we hypothesized would have stability intermediate between MgH_2 and AlH_3. Our results show that this is indeed the case and show that $\Delta H°$ values between 20–50 kJ mol^{-1} can be obtained.

The DMC calculations confirm our hypothesis. First, they indicate that mixed Mg-Al nanoclusters are stable, i.e., ΔE is greater than zero (Figure 4). Second, the desorption

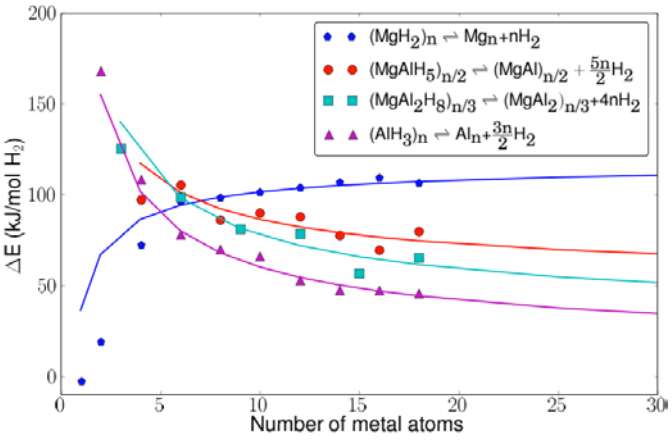


FIGURE 4. Alloying Mg and Al at the nanoscale results in particles with intermediate hydrogen desorption energy and enhanced stability over bulk. The hydrogen desorption energy is a function of size. All data are from DMC calculations.

energy of these clusters is intermediate between the pure materials. For example, the $MgAl_2/MgAl_2H_8$ stoichiometry in addition to the $MgAl/MgAlH_5$ stoichiometry, as is evident in Figure 4. This can be understood from the fact that the hydrides are ionic and the pure metallic clusters have metallic bonding. As a result, there are no bond networks to create nonlinear effects as a function of size. There are only magic numbers in the binding energy of the metals for small sizes, but this effect diminishes with increasing size and does not change the overall trend.

The size range at which ΔE is predicted to reach a value between 20 kJ mol^{-1} and 50 kJ mol^{-1} range is given in Table 3. From the DMC results, the estimated size range for the MgAl alloy is from ~74 metal atoms up to the bulk, whereas Al alone has only a very small range between 10 and 40 atoms. This confirms that alloying can significantly alter the size range in which nanoparticles have the desired desorption energies. However, the effects of errors in DFT predictions are very evident here. The estimated size ranges are dramatically different for the various functionals. It is thus clear that the accuracy of the method used to obtain ΔE is critical.

TABLE 3. Estimated Size Range with ΔE in the Range 20-50 kJ mol^{-1}

	DMC	B3LYP	LDA	M06	PBE
MgAl	74 – ∞	Never	44 – ∞	Never	16 – ∞
Al	10 – 40	17 – 2,000	13 – 100	15 – 80	7 – 20

Conclusions and Future Directions

- We demonstrated that size-dependent effects on both the thermodynamics and kinetics of hydrogen desorption from metal hydrides are possible as a result of nanoconfinement.
- Our results show that 1–4 nm $NaAlH_4$ nanoclusters undergo single-step decomposition with fast kinetics, effectively increasing the storage capacity by 50% under fuel cell conditions.
- We predict that MgH_2 H_2 desorption thermodynamics can be shifted to a more favorable thermodynamic regime by creating Mg-Al-H nanoclusters.
- During the remainder of the project, we will develop a synthetic method to make mixed Mg-Al-H nanoclusters, and will complete H_2 desorption measurements for $NaAlH_4$, MgH_2, $LiBH_4$, $LiNH_2$, and $Ca(BH_4)_2$ in MOFs and nanoporous carbons.

FY 2011 Publications/Presentations

1. Xiangfeng Liu, David Peaslee, Christopher Z. Jost, Eric H. Majzoub, Theodore F. Baumann "First-Principles Calculated Phase Diagram for Nanoclusters in the Na-Al-H System: A Single-Step Decomposition Pathway for $NaAlH_4$," *J. Phys. Chem. C.* 115 (2011), 2636.

2. Liu X.F., Peaslee D., Jost C.Z., E.H. Mazjoub et al. "Systematic Pore-Size Effects of Nanoconfinement of LiBH4: Elimination of Diborane Release and Tunable Behavior for Hydrogen Storage Applications," *Chem. Mater.* 23 (2011), 1331.

3. R.K. Bhakta, V. Stavila, A. Highley, B. Jacobs, S. Maharrey, T. Alam, R. Behrens, E.H. Mazjoub, M.D. Allendorf "Modified $NaAlH_4$ hydrogen desorption thermodynamics and kinetics by nanoconfinement in MOFs," submitted to *J. Phys. Chem. C.*

4. Lucas K. Wagner, Eric Mazjoub, Mark Allendorf, and Jeffrey C. Grossman "Using size and composition to tune the metal-hydride desorption energy: benchmark calculations," submitted to *J. Amer. Chem. Soc.*

5. Raghu Bhakta, Richard Behrens, Aaron Highley, Sean Maharrey, Deneille Wiese-Smith, Benjamin Jacobs, Mark Allendorf, Eric Majzoub, X. Liu, D. Peaslee, Lucas Wagner, Jeffrey Grossman "Investigation of metal hydride nanoparticles templated in metal-organic frameworks," presented at *Nano and Surface Science Approaches to Production and Storage of Hydrogen*," 14–19 November 2010, Noordwijkerhout, The Netherlands.

6. M.D. Allendorf, R. Bhakta, R. Behrens, Jr., E.H. Majzoub, X. Liu, D. Peaslee, J.L. Herberg, L.K. Wagner, J.C. Grossman "Effects of confinement on the thermodynamics and kinetics of metal hydrides templated in ordered nanoporous frameworks," 1st International Conference on Materials for Energy, Karlsruhe, Germany, July 5–8, 2010.

7. E.H. Majzoub "Thermodynamics of Nanocluster Complex Hydrides: Theory and Experiment", invited keynote lecture at MH2010, Moscow, Russia, July 2010.

References

1. Lohstroh et al., *ChemPhysChem* 2010, *11*, 789.

2. Baldé et al. J. Amer. Chem. Soc. 2008, 120, 6761.

3. X. Liu et al. *Chem. Mater.*, 23, 1331, 2011.

IV.A.9 Neutron Characterization in Support of the DOE Hydrogen Storage Sub-Program

Terrence J. Udovic (Primary Contact),
Craig M. Brown, Dan A. Neumann
NIST Center for Neutron Research
National Institute of Standards and Technology (NIST)
100 Bureau Dr., MS 6102
Gaithersburg, MD 20899-6102
Phone: (301) 975-6241
Email: udovic@nist.gov

DOE Manager
HQ: Ned Stetson
Phone: (202) 586-9995
E-mail: Ned.Stetson@ee.doe.gov

Project Start Date: June 2010
Project End Date: Project continuation and direction determined annually by DOE.

Fiscal Year (FY) 2011 Objectives

- Support the DOE-funded hydrogen storage projects by providing timely, comprehensive characterization of materials and storage systems using state-of-the-art neutron methods.
- Direct partner synthesis efforts based on the understanding gained through the use of these methods.
- Demonstrate the fundamental characteristics of useful hydrogen storage materials.

Technical Barriers

This project addresses the following technical barriers from the Storage section (3.3) of the Fuel Cell Technologies Program Multi-Year Research, Development and Demonstration Plan:

(A) System Weight and Volume

(P) Lack of Understanding of Hydrogen Physisorption and Chemisorption

Technical Targets

NIST provides important materials metrologies for Center partners using neutron-scattering measurements to understand and characterize hydrogen-substrate interactions of interest in a variety of materials ranging from H_2 adsorbed in nanoporous materials to H chemically bonded in complex-hydride materials. Insights gained from these studies will be applied toward the design and synthesis of hydrogen storage materials that meet the following DOE 2011 storage targets:

- Specific energy: 1.5 kWh/kg
- Energy density: 0.9 kWh/L
- Cost: $4/kWh net

FY 2011 Accomplishments

- Uptake, neutron powder diffraction (NPD), and neutron vibrational spectroscopy (NVS) measurements of H_2 in Fe-MOF-74 indicate even closer contacts between H_2 molecules compared to other MOF-74 variants.
- Robust yet low uptakes of H_2 in model zeolite compounds were characterized by NPD and NVS, marking the first time that H_2 adsorption sites were identified in a zeolite.
- Surfaces areas of synthesized amorphous metal-organic gels were found to be comparable to those of crystalline parent materials.
- NVS measurements of spillover hydrogen on activated carbons indicate excess-hydrogen modes at room temperature.
- The structure of the newly synthesized mixed-metal amidoborane $Na_2Mg(NH_2BH_3)_4$ was solved by X-ray diffraction (XRD), characterized by NVS, and found able to release 8.4 wt% hydrogen with significantly less toxic gases.
- NVS measurements of novel complex borohydrides NaB_3H_8, $NH_4B_3H_8$, and $NH_3B_3H_7$ indicated only limited agreement with density functional theory (DFT) phonon calculations, suggesting that the DFT descriptions of the bonding interactions need to be improved.
- Quasielastic neutron scattering (QENS) measurements of $Cs_2B_{12}H_{12}$ allowed us to characterize, in detail, the rotational dynamics of the $B_{12}H_{12}^{2-}$ anions, a by-product of borohydride dehydrogenation.
- QENS and NVS measurements of $LiBH_4$ sequestered in 2-nm-pore carbon scaffolds indicated that the $LiBH_4$ is disordered and exhibits significant non-bulk-like behavior with respect to BH_4^- rotational dynamics.



Introduction

To obtain the DOE levels of hydrogen storage in a timely manner, it is imperative that trial-and-error testing of materials be avoided. Thus, the focus must be upon the rational design of new systems. From a thorough understanding of the physics and chemistry that governs the hydrogen-substrate interactions, we will be able to make a more concerted effort to push the frontiers of new materials.

The key to improving materials is a detailed understanding of the atomic-scale locations of the hydrogen and determining how it gets there and how it gets out. Neutron scattering is perhaps the premier technique for studying hydrogen and the NIST Center for Neutron Research is currently the leading facility in the U.S. for studying these materials.

Approach

NIST provides important materials characterization for DOE-funded, hydrogen storage sub-program partners using neutron-scattering measurements to probe the amount, location, bonding states, dynamics, and morphological aspects of (i) molecular hydrogen in carbon-based materials such as polymers, metal organic frameworks (MOFs), and carbonaceous materials such as carbon nanohorns, and (ii) atomic hydrogen in a variety of complex hydride materials including those containing boron and nitrogen, as well as their intermediates and by-products. NIST works directly with DOE and other partners that produce novel hydrogen storage materials to analyze the most promising samples and to help determine and resolve the fundamental issues that need to be addressed.

Results

MOFs have recently come under intense investigation for gas storage and separation applications, owing to their high internal surface areas, convenient modular synthesis, and chemical tenability. Previously, we have reported a number of MOFs in which removal of a solvent molecule from the coordination sphere of the framework metal cations yielded strong adsorption sites for H_2. One possibility for improving the isosteric heat of adsorption within this structure type would be through constructing the structure with M^{2+} cations having a smaller radius. The greater charge density of the exposed metal cations on the framework surface should then be more effective at inducing a dipole in H_2, leading to stronger binding. In collaboration with University of California, Berkeley, the M^{2+}-MOF-74 (M^{2+}=Mg, Co, Ni, Zn) series of MOFs was extended to include Fe-MOF-74. With a high surface area measured at 1,300 m^2/g, and five-fold coordinated metal ions decorating the inside of the one-dimensional hexagonal pores, we have expanded the family as well as allowed ourselves to probe the extent of hydrogen interactions with the system incorporating magnetic ions. Neutron diffraction reveals three different adsorption sites as a function of increased loading (see Figure 1). The D_2-Fe^{2+} interaction is characterized by a relatively close 2.46 Å distance, with the higher loading sites interacting at a short van der Waals distance of 3.22 Å to 3.24 Å. This results in even closer contacts between hydrogen molecules, providing a very dense monolayer packing in the pore with inter-molecular distances from 2.86 Å to 3.07 Å. Further studies are ongoing.

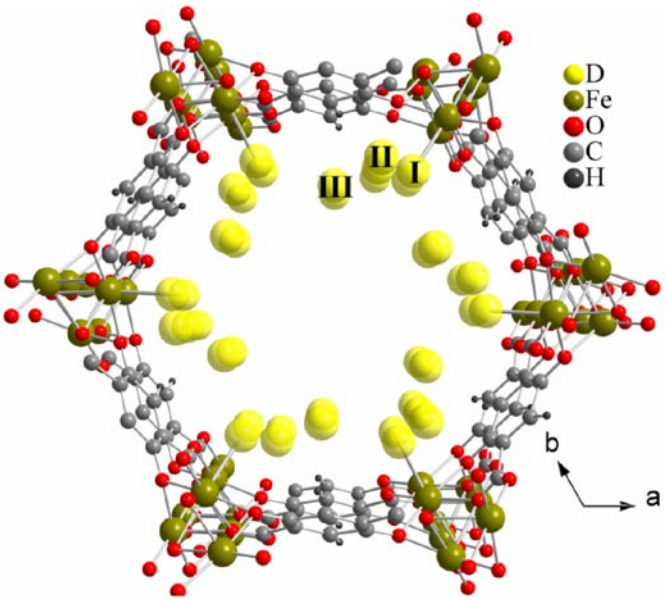


FIGURE 1. Neutron Diffraction Allows the Identification of Three Different D_2 Adsorption Sites in Fe-MOF-74

In collaboration with University of Maryland and University of Delaware, NPD and NVS measurements of hydrogen adsorption in Cu-SSZ-13 zeolite located two binding sites, one at the 8-member ring window and another near the Cu^{2+} cation. The Cu^{2+} site is not occupied at low hydrogen loadings but fully occupied at moderate pressures. The H_2 adsorption for the Cu^{2+}-exchanged zeolite is enhanced (by ≈4% at 1 bar) over H-SSZ-13 due to the extra Cu^{2+} binding sites. At 77 K and 1 bar, the mass ratios of adsorbed H_2/zeolite for H-SSZ-13 and Cu-SSZ-13 are relatively low, 1.38 g/kg and 1.48 g/kg, respectively.

In collaboration with Lawrence Livermore National Laboratory, we additionally attempted to synthesis amorphous MOF gels in an effort to further increase MOF surface areas and micropore volumes. Reaction of iron nitrate and benzenetricarboxalic acid in ethanol produced the desired short-range-ordered material, but with a low surface area of 280 m^2/g. The surface area increased to 510 m^2/g after annealing to 120°C, and was further improved to 1,300 m^2/g upon drying in supercritical CO_2. This is still a relative low surface area and would need to be improved upon. For this material, the increasing surface area is not reflected in the hydrogen uptake increases expected and speculate that the access for hydrogen is unhindered relative to nitrogen.

In collaboration with University of Maryland and General Motors, the first example of a mixed-metal amidoborane $Na_2Mg(NH_2BH_3)_4$ was successfully synthesized, and its structure (Figure 2) and bonding were characterized by XRD and NVS [1]. It forms an ordered arrangement in cation coordinations, i.e., Mg^{2+} bonds solely to N^- and Na^+ coordinates only with BH_3. Compared

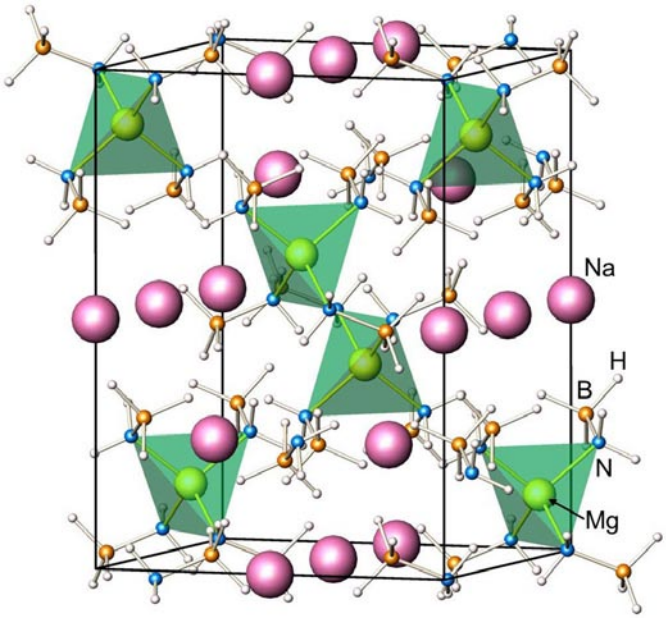


FIGURE 2. The Structure of $Na_2Mg(NH_2BH_3)_4$

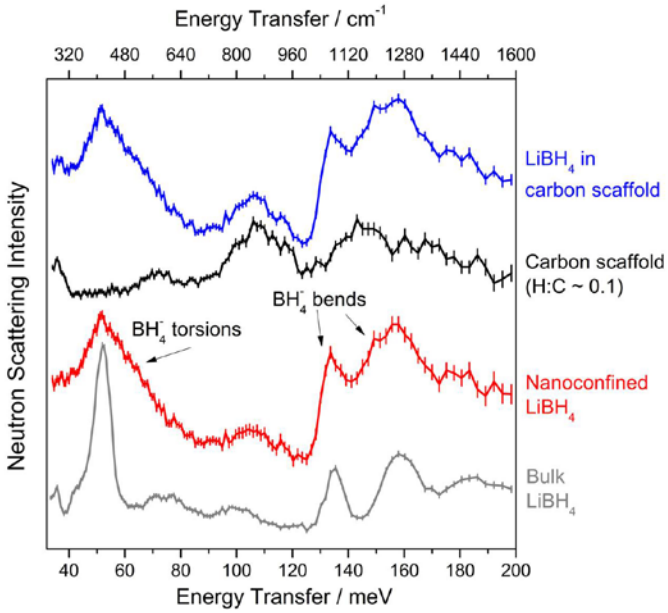


FIGURE 3. NV spectra of nanosequestered $LiBH_4$ + carbon scaffold (with 2 nm pores), the corresponding bare carbon scaffold, and bulk $LiBH_4$. The spectrum of the nanosequestered $LiBH_4$ with the carbon scaffold spectrum subtracted is also shown.

to ammonia borane and monometallic amidoboranes, $Na_2Mg(NH_2BH_3)_4$ can release 8.4 wt% hydrogen with significantly less toxic gases, such as ammonia and borazine, and no detectable diborane. This study suggests that hydrogen-release properties of amidoboranes can be rationally and significantly improved by tuning the atomic interactions and thus producing more desired structures through the formation of mixed-metal amidoboranes.

In collaboration with Ohio State University, we used NVS to characterize the bonding associated with the novel lightweight borohydride materials NaB_3H_8, $NH_4B_3H_8$, and $NH_3B_3H_7$. The limited agreement between the vibrational spectra and DFT phonon calculations suggested that the DFT descriptions of some weak bonding interactions present may be somewhat lacking. This reinforces the reality that there is a need to develop more accurate DFT descriptions of weak bonding potentials, such as associated with hydrogen-bonding interactions.

In collaboration with University Missouri-St. Louis, a comparison was made between $LiBH_4$ sequestered inside 2 nm ordered pores of a carbon scaffold [2] and bulk $LiBH_4$. Using QENS, the relative mean square displacement of H atoms determined from a neutron fixed-window scan shows that the onset of BH_4^- rotational motion occurs ~100 K lower for the nanoconfined material than for bulk $LiBH_4$. From NVS measurements (Figure 3), it is clear that the nanoconfined $LiBH_4$ exhibits a much broader BH_4^- torsion peak (at 52 meV or 419 cm^{-1}) compared with bulk $LiBH_4$. In contrast, the BH_4^- bending modes are little perturbed by nanoconfinement. Hence, although the bending modes are fairly insensitive to near-neighbor interactions, NVS indicates a large inhomogeneity in the rotational potentials experienced by the nanoconfined $LiBH_4$. Overall, compared

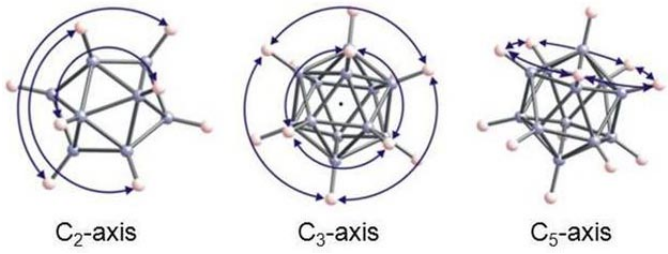


FIGURE 4. Possible Rotational Jumps of the $B_{12}H_{12}^{2-}$ Anion with Respect to its Local Axes of Symmetry

to prior results using carbon scaffolds with pores larger than 4 nm, nanoconfinement in the smaller 2 nm pores appears to more dramatically perturb the bulk thermodynamic properties of $LiBH_4$.

In collaboration with Sandia National Laboratories and University of Maryland, we used QENS to investigate the rotational dynamics of $B_{12}H_{12}^{2-}$ anions (Figure 4), which are by-products of borohydride dehydrogenation. Elastic incoherent structure factor data for the prototypical $Cs_2(^{11}B)_{12}H_{12}$ were measured from 430 K to 530 K [3], suggesting that the $B_{12}H_{12}^{2-}$ anion (encaged in a cube defined by eight Cs^+ cations) changes from uniaxial (C_3-axis or C_5-axis) rotational jumps near 430 K to a combined mechanism involving, on average, independent two-axis (C_3-axis and/or C_5-axis) rotational jumps between 480 K and 530 K. Alternatively, if one assumes that the anions are undergoing temperature-dependent rotational trapping, then

the elastic incoherent structure factor is also consistent with a jump model involving a temperature-dependent mobile fraction of anions statistically tumbling between discrete crystallographic sites.

Conclusions and Future Directions

- Neutron methods have provided crucial, non-destructive characterization tools for the DOE Hydrogen Storage sub-program.
- Fe-MOF-74 behaved similarly to other MOF-74 variants with respect to H_2 adsorption sites, with a relatively closer H_2-M^{2+} distance compared to other larger-cation variants.
- The observed H_2-Cu^{2+} interactions in Cu-SSZ-13 zeolite illustrate the need to better understand the relationship between accessible ions and hydrogen-storage characteristics in porous storage materials.
- The specific surface areas of synthesized amorphous metal-organic gels could not be enhanced relative to their crystalline parent materials.
- We synthesized the first mixed-metal amidoborane, one of a class of tailored compounds that may potentially have more favorable cycling behavior for hydrogen storage.
- The limited agreement between DFT phonon calculations and NV spectra for novel borohydride compounds reflects the need for better DFT descriptions of weak bonding interactions.
- We continued to characterize various aspects of nanoconfinement in an attempt to understand its effect on the hydrogen cycling of $LiBH_4$ and indeed observed more pronounced non-bulk-like effects as the pore size was decreased to 2 nm.
- We characterized the rotational dynamics of $B_{12}H_{12}^{2-}$ anions in the prototypical $Cs_2B_{12}H_{12}$ compound. Ongoing work will investigate the dynamics of this anion in the lighter alkali-metal variants, $Li_2B_{12}H_{12}$ and $Na_2B_{12}H_{12}$.
- We will continue to support the DOE Hydrogen Storage sub-program where needed.

FY 2011 Publications/Presentations

1. N. Verdal, W. Zhou, V. Stavila, J.-H. Her, M. Yousufuddin, T. Yildirim, and T.J. Udovic, "Alkali and Alkaline-Earth Metal Dodecahydro-*Closo*-Dodecaborates: Probing Structural Variations via Neutron Vibrational Spectroscopy," J. Alloys Compds. (in press 2011).

2. K. Sumida, C.M. Brown, Z.R. Herm, S. Chavan, S. Bordiga, and J.R. Long, "Hydrogen Storage Properties and Neutron Diffraction Studies of Mg_2(2,5-dioxido-1,4-benzenedicarboxylate)," Chem. Commun. 47, 1157 (2011).

3. V.K. Peterson, C.M. Brown, Y. Liu, and C. Kepert, "Structural Study of D_2 within the Trimodal Pore System of a Metal Organic Framework," J. Phys. Chem. C 115, 8851 (2011).

4. N. Verdal, T.J. Udovic, J.J. Rush, R. Cappelletti, and W. Zhou, "Reorientational Dynamics of the Dodecahydro-*Closo*-Dodecaborate Anion in $Cs_2B_{12}H_{12}$," J. Phys. Chem. A 115, 2933 (2011).

5. S. Gadipelli, J. Ford, W. Zhou, H. Wu, T.J. Udovic, and T. Yildirim, "Nanoconfinement and Catalytic Dehydrogenation of Ammonia Borane by Magnesium-Metal-Organic Framework-74," Chem. Eur. J. 17, 6043 (2011).

6. J.A. Dura, S.T. Kelly, P.A. Kienzle, J.-H. Her, T.J. Udovic, C.F. Majkrzak, C.-J. Chung, and B. Clemens, "Porous Mg Formation upon Dehydrogenation of MgH_2 Thin Films," J. Appl. Phys. 109, 093501 (2011).

7. K. Sumida, J-H. Her, M. Dinca, L.J. Murray, J.M. Schloss, C.J. Pierce, B.A. Thompson, S.A. FitzGerald, C.M. Brown, and J.R. Long, "Neutron Scattering and Spectroscopic Studies of Hydrogen Adsorption in $Cr_3(BTC)_2$ - A Metal-Organic Framework with Exposed Cr^{2+} Sites," J. Phys. Chem. C 115, 8414 (2011).

8. Y. Yang, C.M. Brown, C. Zhao, A.L. Chaffee, B. Nick, D. Zhao, P.A. Webley, J. Schalch, J.M. Simmons, Y. Liu, J.-H. Her, C.E. Buckley and D.A. Sheppard, "Micro-Channel Development and Hydrogen Adsorption Properties in Templated Microporous Carbons Containing Platinum Nanoparticles," Carbon 49, 1305 (2011).

9. H. Wu, W. Zhou, F.E. Pinkerton, M.S. Meyer, Q. Yao, S. Gadipelli, T.J. Udovic, T. Yildirim, and J.J. Rush, "Sodium Magnesium Amidoborane: The First Mixed-Metal Amidoborane," Chem. Commun. 47, 4102 (2011).

10. K. Sumida, S. Horike, S.S. Kaye, Z.R. Herm, W.L. Queen, C.M. Brown, F. Grandjean, G.J. Long, A. Dailly, and J.R. Long, "Hydrogen Storage and Carbon Dioxide Capture in an Iron-Based Sodalite-Type Metal-Organic Framework (Fe-BTT) Discovered via High-Throughput Methods," Chemical Science 1, 184 (2010).

11. D.L. Jacobson, D.S. Hussey, E. Baltic, T.J. Udovic, J.J. Rush, and R.C. Bowman, Jr., "Neutron Imaging Studies of Metal-Hydride Storage Beds," Intl. J. Hydrogen Energy 35, 12837 (2010).

12. N. Verdal, T.J. Udovic, J.J. Rush, R.L. Cappelletti, and W. Zhou, "Hydrogen Dynamics of the Dodecahydro-*Closo*-Dodecaborate Crystals," National Meeting of the American Chemical Society, Denver, CO (Aug. 2011).

13. C.M. Brown, "Determining Structures and Properties of Advanced Materials using Neutrons," U.C. Berkeley Chemistry Dept., Berkeley, CA (Apr. 2011).

14. C.M. Brown, "Applications of Neutron Scattering to Understanding Structure and Gas Storage Properties of Metal-Organic Frameworks and Related Materials," MRS Spring Meeting, San Francisco, CA (Apr. 2011).

15. W.L. Queen, C.M. Brown, M.R. Hudson, K. Sumida, E.D. Bloch, L.J. Murray, J.R. Long, D.K. Britt, and O.M. Yaghi, "Gas Adsorption Properties of Various Metal-Organic Frameworks with Coordinatively Unsaturated Metal Centers," 18th Annual Postdoctoral Poster Competition sponsored by the NIST chapter of Sigma Xi, Gaithersburg, MD (Feb. 2011).

16. M.R. Hudson, W.L. Queen, C.M. Brown, D.W. Fickel, and R.F. Lobo, "CO_2 Separation and Hydrogen Storage Properties of Zeolites for Clean Energy Applications," 18th Annual Postdoctoral Poster Competition sponsored by the NIST chapter of Sigma Xi, Gaithersburg, MD (Feb. 2011).

17. N. Verdal, T.J. Udovic, V. Stavila, and J.J. Rush, "Dynamics and Trends of Alkali Metal Dodecahydro-*Closo*-Dodecaborates," 18th Annual Postdoctoral Poster Competition sponsored by the NIST chapter of Sigma Xi, Gaithersburg, MD (Feb. 2011).

18. C.M. Brown, "Physical Aspects of Hydrogen Adsorption," Advances in Chemistry and Materials for Hydrogen Storage, Pacifichem Congress, Honolulu, HI (Dec. 2010).

19. C.M. Brown, "Understanding Hydrogen Storage in Microporous Materials using Neutrons," High Temperature Energy Materials Center Seminar, Korea Institute of Science and Technology, Seoul, South Korea (Nov. 2010).

20. C.M. Brown, "Understanding Hydrogen Storage in Microporous Materials using Neutrons," Department of Nuclear and Quantum Engineering Special Seminar, Korea Advanced Institute of Science and Technology, Daejong, South Korea (Nov. 2010).

21. C.M. Brown, "Studying Potential Hydrogen Storage Materials using Neutrons," Hanaro Symposium, Daejong, South Korea (Nov. 2010).

22. C.M. Brown, "Probing Adsorption in Microporous Materials using Neutrons," Spallation Neutron Source Seminar, ORNL, Oak Ridge, TN (Oct. 2010).

23. C.M. Brown, "Science as a Career," Mount St. Mary's College, Spinkhill, U.K. (Oct. 2010).

24. C.M. Brown, "Determining Structures and Properties of Advanced Materials," Bishop Justus C of E School, Bromley, U.K. (Sep. 2010).

25. C.M. Brown, "Application of Neutron Scattering to the Hydrogen Storage Problem," STAIR Graduate Student Seminar, U. Tennessee, Knoxville, TN (Sep. 2010).

26. N. Verdal, W. Zhou, V. Stavila, J.-H. Her, M. Yousufuddin, T. Yildirim, and T.J. Udovic, "Alkali and Alkaline-Earth Metal Dodecahydro-*Closo*-Dodecaborates: Probing Structural Variations *via* Neutron Vibrational Spectroscopy," MH2010 - International Symposium on Hydrogen-Metal Systems--Fundamentals and Applications, Moscow, Russia (Jul. 2010).

27. C.M. Brown, "Understanding how Hydrogen Interacts with Materials using Neutrons," Award Presentation, American Conference on Neutron Scattering, Ottawa, Canada (Jun. 2010).

29. N. Verdal, T.J. Udovic, J.J. Rush, R. Cappelletti, and W. Zhou, "Reorientation Dynamics of the Hydrogen Storage Intermediate Dodecahydro-*Closo*-Dodecaborate," American Conference on Neutron Scattering, Ottawa, Canada (Jun. 2010).

References

1. H. Wu, et al., Chem. Commun. **47,** 4102 (2011).

2. X. Liu, et al., J. Phys. Chem. C **114**, 14036 (2010).

3. N. Verdal, et al., J. Phys. Chem. A **115**, 2933 (2011).

IV.B.1 Hydrogen Storage by Novel CBN Heterocycle Materials

Shih-Yuan Liu
University of Oregon
Department of Chemistry
1253 University of Oregon
Eugene, OR 97403-1253
Phone: (541) 346-5573
E-mail: lsy@uoregon.edu

DOE Managers
HQ: Grace Ordaz
Phone: (202) 586-8350
E-mail: Grace.Ordaz@ee.doe.gov
GO: Jim Alkire
Phone: (720) 356-1426
E-mail: James.Alkire@go.doe.gov

Contract Number: DE-FG36-08GO18143

Project Start Date: September 1, 2008
Project End Date: March 31, 2012

Fiscal Year (FY) 2011 Objectives

The objective of this project is to develop novel boron-nitrogen heterocycles as liquid-phase hydrogen storage materials with storage capacities and thermodynamic properties that have the potential to lead to rechargeable systems capable of meeting DOE targets. We seek to:

- Develop new materials that:
  - are structurally well-defined along the desorption/absorption processes
  - exhibit appropriate enthalpy of H_2 desorption
  - are liquids at operating temperatures
  - possess high H_2 storage capacities
- Identify catalysts that will release hydrogen from these materials at temperatures <200°C.
- Develop conditions that will readily recharge the spent fuel.

Technical Barriers

This project addresses the following technical barriers from the Hydrogen Storage section of the Fuel Cell Technologies Program Multi-Year Research, Development and Demonstration Plan:

(A) System Weight and Volume
(C) Efficiency
(E) Charging/Discharging Rates
(R) Regeneration Process

Technical Targets

This project is developing new liquid phase materials for hydrogen storage that can be readily regenerated. Insights gained from these studies will be applied toward the design and synthesis of hydrogen storage materials that meet the following DOE 2015 hydrogen storage targets:

- Specific energy: 1.8 kWh/kg (5.5 wt%)
- Energy density: 1.3 kWh/L (4.0 vol%)

FY 2011 Accomplishments

- Synthesized the parent six-membered fully charged fuel of Material System (1) and partially charged parent BN-indole Material System (7).
- Formulated N-H (**1**), N-tBu (**1'**), and N-Me (**1"**) materials as liquids.
- Experimentally determined the energetic landscape of Material System (1) and provided a direct comparison with the computationally predicted values.
- Developed catalysts and conditions to optimize release of H_2 from Materials System (1).

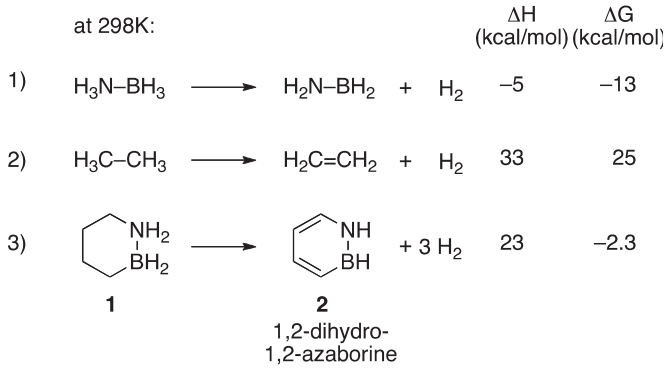
✧ ✧ ✧ ✧ ✧

Introduction

Hydrogen storage is a vital component in the development of a hydrogen-based energy infrastructure. Boron nitrogen containing compounds, e.g., ammonia borane ($H_3N–BH_3$ or AB), have attracted much attention as chemical H_2 storage materials because of their high gravimetric hydrogen densities and fast kinetics of H_2 release. This project is developing structurally well-defined liquid carbon-boron-nitrogen (CBN) hydrogen storage materials (i.e., heterocycles containing carbon, boron, and nitrogen) that have the potential to be reversibly regenerated using molecular hydrogen. A liquid phase, hydrogen storage system that can be regenerated using molecular hydrogen is highly desired for many reasons, including versatility, lower cost and improved efficiency, and durability. Such a storage material will allow on-board hydrogen storage. It can also be applied as an off-board energy carrier for vehicle and stationary applications that takes advantage of the existing liquid fuels infrastructure.

Approach

In order to accomplish reversibility, neutrality in free energy of the hydrogen release process (i.e., $\Delta G \sim 0$ kcal/mol) at the operating temperature is pivotal. The dehydrogenation of AB is exergonic by –13 kcal/mol at 298 K (eq 1). In contrast to AB, the dehydrogenation of



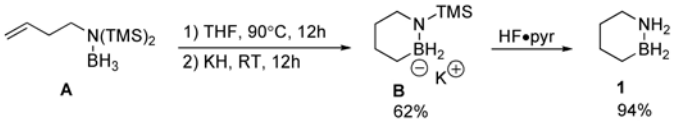
its isoelectronic organic counterpart, ethane (CH_3–CH_3), is endergonic by +25 kcal/mol (eq 2). The coupling of endothermic dehydrogenation from CC with exothermic dehydrogenation from BN in a cyclic six-membered framework could lead to a reversible H_2 storage system. Indeed, high-level computational analysis indicates that the release of H_2 from CBN heterocycles such as **1** has favorable overall thermodynamics conducive to reversibility, (e.g., see eq 3). The potential for reversible hydrogen release/uptake and the relatively high gravimetric hydrogen density of CBN heterocycle materials (e.g. 7.1 wt% for **1**) render their preparation and development an important goal. This project is investigating several CBN heterocycle materials for H_2 storage applications using a synergistic theoretical and experimental approach. Synthesis will be a crucial component of this project given the relatively unexplored nature of these CBN heterocycles. The structurally well-defined nature of these CBN heterocycle materials will facilitate their characterization and mechanistic investigation of the proposed desorption/absorption processes.

Results

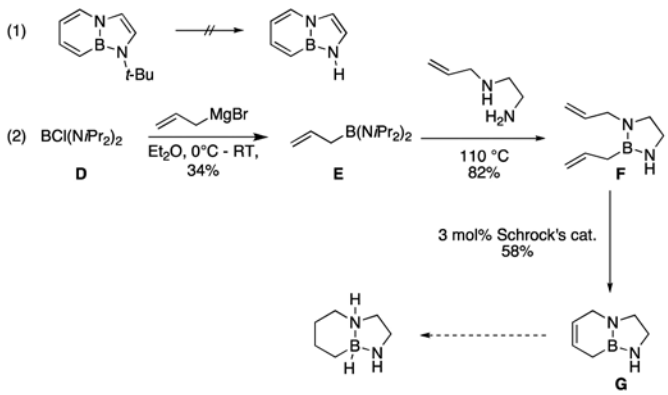
Synthesis of Parent CBN Heterocycle Materials

We have successfully synthesized the parent charged fuel, **1**, illustrated in Scheme 1. From the *N*-bis-protected homoallylic amine BH_3 adduct **A**, refluxing in tetrahydrofuran (THF) followed by treatment of the crude product with KH furnished the potassium salt **B** in 62% yield. Subsequent treatment with 2 equivalents of HF-pyridine afforded **1** in 94% yield.

In Phase I of this project we developed a synthesis of the *N*-*t*-Bu derivative of the spent fuel of Material (7). However, we found that it was challenging to remove



SCHEME 1. Synthesis of Parent Fuel Material System (1)



SCHEME 2. Progress toward the Synthesis of the Parent CBN Material System (7)

the *t*-Bu group from nitrogen to generate the parent unsubstituted fuel system (Scheme 2, eq 1). In Phase II, we developed a new synthetic route to (7) without the use of protecting group strategies (Scheme 2, eq 2). Treatment of chloroborane **D** with allyl magnesium bromide produced allylborane **E**. Condensation of **E** with *N*-allylethylene diamine furnished intermediate **F**, which upon ring closing metathesis produced the bicyclic material **G** without a protecting group on nitrogen. Intermediate **G** is a partially spent fuel intermediate of System (7), and we envision that it will serve as a very useful compound for the preparation of the fully charged fuel and other partially spent fuel of this system. Based on preliminary thermodynamic analysis, we believe that the challenges associated with System (7) are similar to those of System (1). Thus, we conclude that it would be most prudent to focus on System (1).

Formulation of CBN Heterocycles as Liquids

We formulated the parent fully charged fuel **1** and the *N*-substituted fuels **1'** and **1"** as liquids. Melting points and liquid densities were also determined for **1**, **1'** and **1"** (Table 1). Compounds **1** and **1"** are liquids at an

TABLE 1. Formulation of CBN Heterocycles as Liquids

entry	neat material	THF solution	Et_2O solution
1	mp: 63-63 °C d (kg/L): 0.99 ± 0.05 **vol (g H_2/L): 70** **wt (%): 7.1**	sol (g/L): 434 ± 20 d (kg/L): 0.8992 vol (g H_2/L): 30.7 wt (%): 3.4	sol (g/L): 346 ± 30 d (kg/L): 0.781 ± 0.02 vol (g H_2/L): 24.5 wt (%): 2.2
1'	mp: 96-98 °C d (kg/L): 0.61 ± 0.07 vol (g H_2/L): 25 wt (%): 4.3	sol (g/L): 284 ± 28 d (kg/L): 0.8892 vol (g H_2/L): 11.7 wt (%): 1.3	sol (g/L): 84.4± 4 d (kg/L): 0.7134 vol (g H_2/L): 3.47 wt (%): 0.4
1"	mp: 72-73°C d (kg/L): 0.87 ± 0.08 **vol (g H_2/L): 53** **wt (%): 6.1**	sol (g/L): 292 ± 5 d (kg/L): 0.8992 vol (g H_2/L): 17.8 wt (%): 2.0	sol (g/L): 106 ± 18 d (kg/L): 0.7134 vol (g H_2/L): 6.5 wt (%): 0.73

operating temperature of 80°C. Assuming the release of 3 equivalents of H_2, **1** and **1"** exhibit reasonable volumetric and gravimetric capacities (**1**: 7.1 wt%, 70 g H_2/L; **1"**: 6.1 wt%, 53 g H_2/L). At ambient temperatures **1** and **1"** are solids. When solubilizing additives are added to these materials at ambient temperature, the storage capacities are significantly reduced (e.g., see THF solution column). A slurry formulation will result in storage capacities that are between the limiting scenarios (i.e., values between the "neat material" and "THF solution" columns) at ambient temperatures.

Thermodynamics of Hydrogen Uptake and Release

We determined the enthalpy of hydrogenation uptake of the spent fuel material **2'** and the partially spent materials **3'**, **4'**, and **6'** ***experimentally*** via reaction calorimetry. As part of this process, we determined a lower resonance stabilization energy (RSE = 16.6 ± 1.3 kcal/mol) of our CBN heterocycle system vs. the corresponding non-BN-containing carbocyclic system (~32 kcal/mol). This is consistent with the observed improved H_2 adsorption ability of CBN materials compared to the carbocyclic system. We were also able to determine the enthalpy of the dehydrogenation from the *N*-*t*Bu model fuel **1'**, catalyzed by 10 mol% $Cl_2(PPh_3)_3Ru$. A representative heat flow trace is illustrated in Scheme 3 (left). Thus, we have completed the experimental thermodynamic analysis (values in parenthesis) of this material system shown in Scheme 3 (right), which agree reasonably with computationally predicted values (values in brackets).

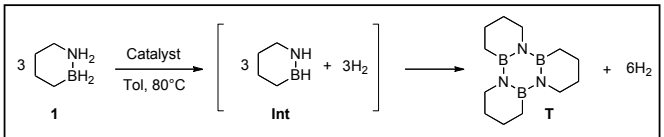
Development of Catalysts and Conditions to Optimize H_2 Release from **1**

During the course of our investigations of heterocycle **1**, we determined that it readily released two equivalents of H_2 to form trimer **T** in quantitative yield with virtually no formation of potential fuel cell poisons encountered in AB decomposition (e.g., no formation of ammonia or borazine).

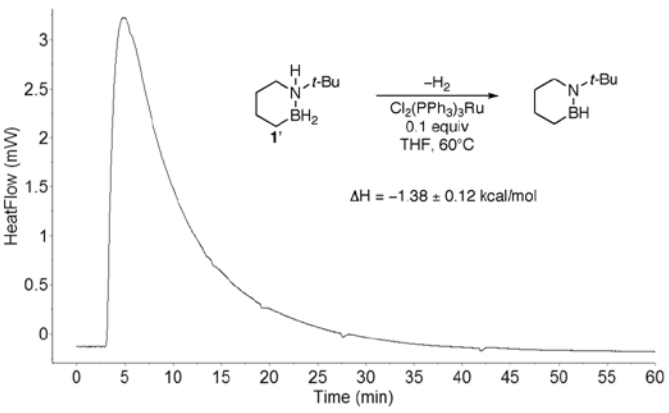
We screened a variety of hetero- and homogeneous catalysts and conditions to release up to two equivalents of H_2 from **1**. We focused on three main factors: 1) cost of catalyst; 2) catalyst loading; 3) reaction time. In a general procedure, we added a solution of **1** and the catalyst to a J-Young tube, which we sealed and immersed in an 80°C oil bath; reaction progress was monitored by ^{11}B nuclear magnetic resonance. Selected results are listed in Table 2. At 80°C in toluene, many catalysts enabled complete release of two equivalents of H_2 within 60 minutes. The most active catalysts were the rhodium dimers $[Cl(cod)Rh]_2$ and $[(nbd)ClRh]_2$ (entries 7 and 8, respectively) which achieved complete trimer formation in 15 minutes at 5 mol% catalyst loading. The low cost, heterogeneous catalyst $CoCl_2$ (entry 5) enabled the complete release of two equivalents H_2 in 30 minutes at 10 mol% catalyst loading. As a control, we heated a sample of **1** at 80°C in toluene with no catalyst; only starting material was observed after 3 hours.

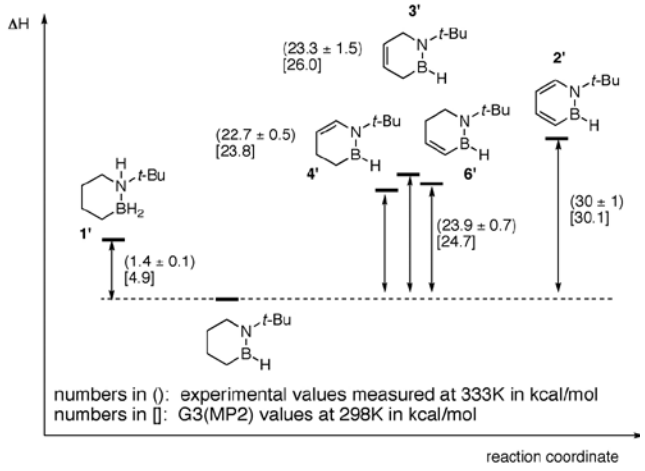
We measured the amount and rate of H_2 release from **1** with 5 mol% $CoCl_2$ in toluene using an automated gas burette system. As can be seen from Figure 1, release of

TABLE 2. Optimization Survey of Catalysts and Conditions to Release Two Equivalents of H_2 from the Parent of Material System (1)



Entry	Catalyst	Loading (mol%)	Time(min)	% Yield **T**
1	$(dppe)NiCl_2$	10	60	100
2	$[Cl(cod)Ir]_2$	10	60	100
3	$[(C_2H_2)_2ClRh]_2$	10	60	100
4	$(PPh_3)_2NiCl_2$	5	60	100
5	$CoCl_2$	10	30	100
6	Cp^*RuCl_2	5	30	100
7	$[Cl(cod)Rh]_2$	5	15	100
8	$[(nbd)ClRh]_2$	5	15	100





SCHEME 3. Thermodynamics of Hydrogen Release from CBN Material System (1)

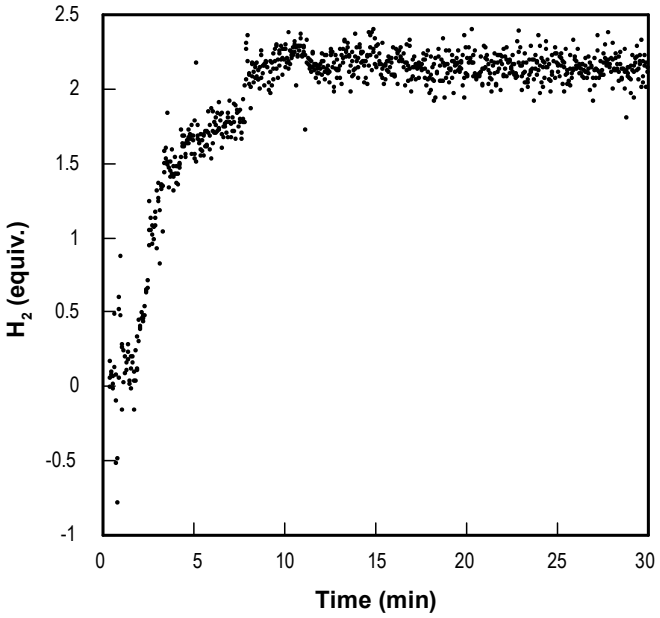


FIGURE 1. Automated Burette Measurement of H_2 Release from **1**

the first equivalent of H_2 from **1** takes place in less than 5 minutes from the instant the reaction flask is submerged in an 90°C oil bath. Trimer formation (coinciding with the release of an additional equivalent of H_2) is complete within 15 minutes of start of the reaction.

Conclusions and Future Directions

In summary, we expanded our synthetic toolbox for the preparation of CBN heterocycles to achieve the synthesis of the parent charged fuel **1**, and N-substituted derivatives **1'** and **1"**. The synthetic availability of CBN heterocycle materials enabled us to experimentally determine thermodynamic data for hydrogen uptake and release from these materials, and optimize conditions for release of H_2 from **1**. We determined that the parent charged fuel **1** readily releases two equivalents of H_2 in a clean and quantitative process to form a well-defined trimer product under mild conditions using a relatively cheap $CoCl_2$ catalyst. We also demonstrated that compound **1** is thermally stable up to its melting point, and that decomposition with concomitant H_2 release requires a catalyst.

In FY 2012, we will:

- Optimize our current synthesis with regard to scale up of Material System (1).
- Develop/optimize conditions/catalysts for H_2 desorption for Material System (1).
- Improve energy efficiency for recharging the spent fuel of Material System (1).

Selected FY 2011 Publications/Presentations

1. "Resonance Stabilization Energy of 1,2-Azaborines: A Quantitative Experimental Study by Reaction Calorimetry"; Patrick G. Campbell, Eric R. Abbey, Doinita Neiner, Daniel J. Grant, David A. Dixon, and Shih- Yuan Liu; *J. Am. Chem. Soc.* **2010**, *132*, 18048-18050.

2. "Hydrogen Storage by Carbon(C) Boron(B) Nitrogen(N) Heterocycles"; Patrick G. Campbell, Kshitij Parab, David A. Dixon, Shih-Yuan Liu; *24th International Conference on Organometallic Chemistry* (PS2-144), Taipei, Taiwan, July 2010.

3. "Developing the Basic Science and Applications of Boron(B)-Nitrogen(N)-Containing Heterocycles"; Shih-Yuan Liu; *Seminar*, National Taiwan University, Taipei, Taiwan, July 2010.

4. "Developing the Basic Science and Applications of Boron(B)-Nitrogen(N)-Containing Heterocycles"; Shih-Yuan Liu; *Seminar*, University of St. Andrews, St. Andrews, UK, September 2010.

5. "Developing the Basic Science and Applications of Boron(B)-Nitrogen(N)-Containing Heterocycles"; University of Calgary, Calgary, Alberta, Canada, *Seminar*, November 5, 2011.

6. "Developing the Basic Science and Applications of Boron(B)-Nitrogen(N)-Containing Heterocycles"; University of Pennsylvania, Philadelphia, PA, *Seminar*, November 9, 2011.

7. "Developing the Basic Science and Applications of Boron(B)-Nitrogen(N)-Containing Heterocycles"; University of California, Berkeley, Berkeley, CA, *Seminar*, December 2, 2010.

8. "Hydrogen Storage by Carbon(C) Boron(B) Nitrogen(N) Heterocycles"; Honolulu, Hawaii, *Pacifichem 2010 Symposium #69* "Advances in Chemistry and Materials for Hydrogen Storage"; *invited lecture*, December 17, 2010.

9. "Resonance Stabilization Energy of 1,2-Azaborines: A Quantitative Experimental Study by Reaction Calorimetry"; Patrick G. Campbell, Shih-Yuan Liu; *Materials Science Institute Conference*, Gleneden Beach, OR (2010), *Poster Presentation*, December 12, 2010.

10. "Hydrogen Storage by Novel CBN Heterocycle Materials"; USCAR, Detroit MI. *Department of Energy TechTeam Review*, March 17, 2011.

11. "Developing the Basic Science and Applications of Boron(B)-Nitrogen(N)-Containing Heterocycles"; Ohio State University, Columbus, OH, *Seminar*, April 8, 2011.

12. "Hydrogen Storage by Novel CBN Heterocycle Materials"; Washington DC, DOE Annual Merit Review, May 13, 2011.

13. "Developing the Basic Science and Applications of Boron(B)-Nitrogen(N)-Containing Heterocycles"; ETH Zürich, Zürich, Switzerland, *Seminar*, June 6, 2011.

14. "Developing the Basic Science and Applications of Boron(B)-Nitrogen(N)-Containing Heterocycles"; University of Würzburg, Würzburg, Germany, *Seminar*, June 8, 2011.

IV.B.2 Fluid Phase Chemical Hydrogen Storage Materials

Benjamin L. Davis (Primary Contact),
Tessui Nakagawa, Ruiqin Zhong,
Troy A. Semelsberger, and Gerie Purdy
Materials Physics and Applications, Materials Chemistry
Los Alamos National Laboratory (LANL), MS J514
P.O. Box 1663
Los Alamos, NM 87545
Phone: (505) 500-2463
E-mail: bldavis@lanl.gov

DOE Manager
HQ: Grace Ordaz
Phone: (202) 586-8350
E-mail: Grace.Ordaz@hq.doe.gov

Partner:
Professor Larry Sneddon, University of Pennsylvania,
Philadelphia, PA

Project Start Date: October 1, 2010
Project End Date: Project continuation and direction determined annually by DOE

Fiscal Year (FY) 2011 Objectives

- Develop liquid, pumpable ammonia-borane (AB) fuels with high H_2 content.
- Catalyst development for fluid phase storage materials that increases rate and extent of H_2 release while minimizing impurities.

Technical Barriers

This project addresses the following technical barriers from the Storage section of the Fuel Cell Technologies Program Multi-Year Research, Development and Demonstration Plan:

(A) System Weight and Volume
(B) System Cost
(C) Efficiency
(E) Charging/Discharging Rates
(R) Regeneration Processes

Technical Targets

A significant barrier to the application of off-board regenerable hydrogen storage materials is on- and off-boarding of the fuel and spent fuel, respectively. A fluid, pumpable liquid fuel that remains liquid through dehydrogenation to the spent fuel form is desired for more readily engineered fueling concepts. This project is exploring other compositions of AB/ionic liquid (IL) systems; the original concept was developed by the Center's partner, Professor Larry Sneddon of the University of Pennsylvania. This work showed great promise with gravimetric and volumetric capacities as well as charging/discharging rates. Subsequent work at LANL has shown that these IL-based fuels could also be regenerated off board without separating the spent fuel from the IL. Successful development of fluid systems should meet the following DOE 2015 targets:

- Gravimetric Capacity (3 kWh/kg)
- Volumetric Capacity (2.7 kWh/L)
- H_2 Discharge Rate (minimum full flow rate 0.02 H_2 g/s kW)
- H_2 Purity (99.99 % H_2)
- Start-Up Time to Full Flow (5 s @ 20°C, 15 s @ -20°C)
- Shelf life: Loss of Usable H_2 (0.05 g/hr-kg H_2 stored)

FY 2011 Accomplishments

- Thermal stability of the ILs is dominated by choice of the cations/anions that comprise the IL.
- Pt and Rh on alumina were screened for their ability to improve H_2 release and minimize impurities over the base AB/IL systems. No improvement was observed.
- Hydrazine regeneration method was determined compatible with a spent fuel/IL composition
- H_2 release in the presence of dipentylamine or trimethylborazine did not prevent a phase change in the spent fuel.



Introduction

Chemical hydrogen storage (CHS) involves storing hydrogen in molecular chemical bonds where an on-board chemical reaction is used to release hydrogen. Currently, the resulting spent fuel may be regenerated off-board using chemical processing. CHS provides a diversity of options to enable hydrogen for transportation as well as other niche and stationary applications. Especially attractive, CHS offers the potential for no direct hydrogen handling by the consumer, as well as low pressure storage concepts.

Researchers at LANL and the University of Pennsylvania are focused on the development of liquid AB fuels that integrate with the Hydrogen Storage Engineering Center of Excellence (HSECoE). We are currently studying the formation and stability of these liquid AB materials, as well as catalytic release of hydrogen. Candidate materials can be readily evaluated using resources developed by the HSECoE, including a validation test bed.

Approach

The large number of available ILs necessitates screening criteria. Using thermoanalytical methods (differential scanning calorimetry, thermogravimetric analysis [TGA]), properties of ILs were measured to gauge suitability for HSECoE's systems. To address the issue of H_2 release kinetics and impurity formation, commercially available heterogeneous catalysts were evaluated against the control (uncatalyzed) system. Research at the University of Pennsylvania addressed the phase change issue by dehydrocoupling AB in the presence of dipentylamine, a species known to make a form of spent AB fuel (polyborazylene) soluble in benzene.

Results

Thermal stability is an essential characteristic of any IL used to generate a liquid phase with AB. Using TGA, we have identified trends in cation/anionic choice which govern thermal stability (Figure 1). Further testing of ILs should yield greater confidence in compositional requirements.

To further reduce gaseous impurities and accelerate H_2 release, a selection of commercially available heterogenous catalysts (Pt, Rh) were evaluated. As can be observed (Figure 2), no substantial change in the rate or extent of H_2 release was observed with these catalysts (only Pt data shown). There was a qualitative reduction in borazine as seen in a flow-through experiment (results not shown), thus achieving one of our two stated goals. We are confident that further catalyst evaluation will result in accelerated H_2 release.

Lastly we endeavored to maintain the liquid phase of AB/IL throughout the dehydrogenation process by using additives. Work at the University of Pennsylvania

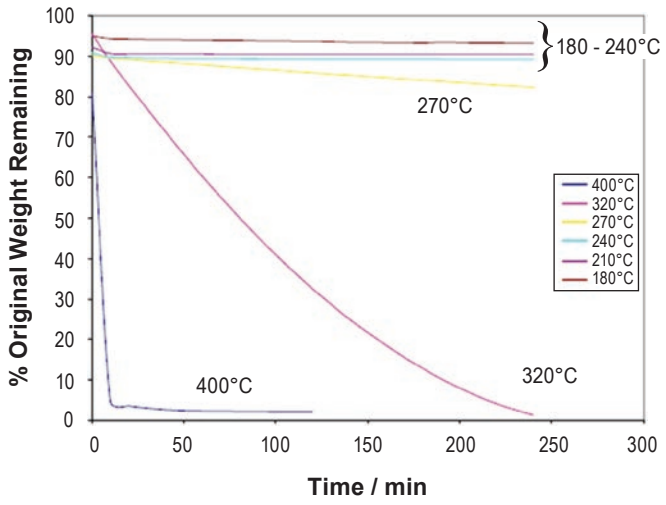


FIGURE 1. Decomposition of an IL assessed by isothermal TGA experiments. This IL shows a wide stability range (starts to decompose at 270°C) and will be used for the HSECoE validation test bed.

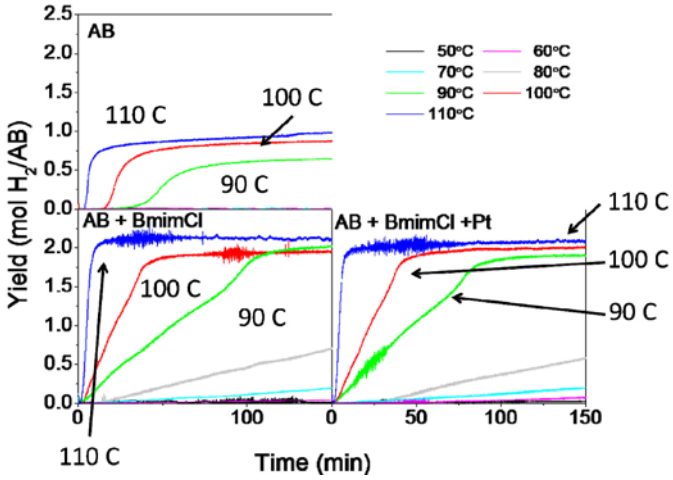


FIGURE 2. Dehydrogenation of AB, AB/IL (BmimCl), and AB/IL + Pt catalyst using an automated buret. The IL has a marked effect on H_2 release and extent relative to pure AB. The addition of the heterogenous catalyst, however, does not dramatically alter H_2 performance.

had previously identified a reagent, dipentylamine, which could transform polyborazlyene (a form of spent AB fuel) into a benzene soluble species [1]. With this knowledge, AB/IL dehydrocoupling was performed in the presence of dipentylamine and alkylated borazines with goal of making the spent fuel more soluble and preventing a phase change. As can be seen (Table 1), neither reagent prevented a phase change.

TABLE 1. Additives used with AB/IL Systems (Bmim – butyl, methylimidazolium, Bmmim – butyl, dimetylimidazolium, Pmim – propyl, methylimidazolium). Neither dipentylamine nor trimethylborazine at a 5% loading altered the state of the final spent fuel (solid in all cases).

IL	Temperature	Additives	Final Physical State
Bmim Cl	85°C	5% Dipentylamine	Solid
Bmmim Cl	85°C	5% Dipentylamine	Solid
Bmim Cl	85°C	5% trimethylborazine	Solid
Pmim I	85°C	5% trimethylborazine	Solid

Conclusions and Future Directions

- Cation/anion selection rules for IL performance (thermal degradation) have been partially identified. Further screening is required to be confident in these generalities. In the future, quantitative solubility of AB and spent fuel will be performed to further guide ionic liquid selection.
- A select group of commercially available noble metal catalysts were evaluated for their ability to accelerate H_2 release and reduce impurity formation. Qualitatively the impurity borazine was reduced in flow-through experiments using heterogenous platinum catalysts.

Continued catalyst evaluation is planned to meet the DOE targets.

- Regeneration of spent fuel/IL was performed and was generally a success. Characteristics of the IL to yield a more robust process were identified.
- A preliminary survey of additives that were postulated to maintain the liquid phase of AB/IL throughout H_2 release was completed. At the AB loading of 50 wt%, a solid product was obtained after >2 equivalent of H_2 was released indicating that more work is necessary on the spent fuel composition to maintain a fluid, pumpable state for off-boarding of spent fuel. Future work will focus on different alkylborazines and fuel blends which should impart additional solubility on the spent fuel.

References

1. Sneddon *et. al.*, *Chem. Mater.*, **1998**, *10*, 412-421.

IV.C.1 A Biomimetic Approach to Metal-Organic Frameworks with High H_2 Uptake

Hong-Cai (Joe) Zhou
Dept. of Chem., Texas A&M University
PO Box 30012
College Station, TX 77842-3012
Phone: (979) 845-4034
E-mail: zhou@mail.chem.tamu.edu

DOE Managers
HQ: Ned Stetson
Phone: (202) 586-9995
E-mail: Ned.Stetson@ee.doe.gov
GO: Jesse Adams
Phone: (720) 356-1421
E-mail: Jesse.Adams@go.doe.gov

Contract Number: DE-FC36-07GO17033

Project Start Date: August 2, 2007
Project End Date: August 1, 2012

Fiscal Year (FY) 2011 Objectives

- Design, synthesize, and characterize metal-organic frameworks (MOFs) with active metal centers aligned in porous channels and accessible by H_2 molecules.
- Through optimized, cooperative binding, the MOFs are expected to have enhanced affinity to H_2.
- These MOFs can help to reach the DOE 2010 and ultimately 2015 hydrogen storage goal.

Technical Barriers

This project addresses the following technical barriers from the Storage section (3.3.4) of the Fuel Cell Technologies Program Multi-Year Research, Development and Demonstration Plan:

(P) Lack of Understanding of Hydrogen Physisorption and Chemisorption

(Q) Reproducibility of Performance

Technical Targets

- The focus of the proposed research is the use of concepts evident in metalloproteins to guide the synthesis of MOFs with gas-adsorption affinity around 15 to 20 kJ/mol for hydrogen.
- The overall objective is to achieve the DOE 2010 and 2015 system goals, primarily the gravimetric and volumetric storage goals, at or near ambient temperatures and moderate pressure for on-board vehicular hydrogen storage (Table 1).

TABLE 1. Technical System Targets: On-Board Hydrogen Storage for Light-Duty Vehicles

Storage Parameter	Units	2010	2015	Ultimate
System Gravimetric Capacity Usable, specific-energy from H_2 (net useful energy/max system mass)	kWh/kg (kg H_2/kg system)	1.5 (0.045)	1.8 (0.055)	2.5 (0.075)
System Volumetric Capacity: Usable energy density from H_2 (net useful energy/max system volume)	kWh/L (kg H_2/L system)	0.9 (0.028)	1.3 (0.040)	2.3 (0.070)

FY 2011 Accomplishments

- A highly porous and robust 3,3,4-connected MOF (PCN-80) has been synthesized with a unique octa-topic ligand featuring 90°-angle-dicarboxylate moiety. PCN-80 has Brunauer-Emmett-Teller (BET) and Langmuir surface areas of 3,850 $m^2\ g^{-1}$ and 4,150 $m^2\ g^{-1}$, respectively. It exhibits high gas-uptake capacity for H_2 of 4.8 wt% (29 g L^{-1}) at 44 bar and 77 K.
- Porous polymer networks (PPNs) grafted with sulfonic acid (PPN-6-SO_3H) and its lithium salt (PPN-6-SO_3Li) exhibit dramatic increase in isosteric heats of hydrogen-adsorption.
- Highly stable PPNs are synthesized through Yamamoto homo-coupling reaction between tetrahedral monomers. Among those polymers, PPN-4 shows exceptionally high Langmuir surface area of 10,063 $m^2\ g^{-1}$ (SA_{BET}: 6,461 $m^2\ g^{-1}$). It also exhibits ultra-high hydrogen storage capacity (8.3 wt% at 55 bar and 77 K).



Introduction

In the past decade, there has been an escalation of interest in the study of MOFs due to their fascinating structures and intriguing application potential. Their exceptionally high surface areas, uniform yet tunable pore sizes, and well-defined adsorbate-MOF interaction sites make them suitable for hydrogen storage. Various strategies to increase the hydrogen capacity of MOFs, such as using pore size comparable to hydrogen molecules, increasing surface area and pore volume, utilizing catenation, and introducing coordinatively unsaturated metal centers (UMCs) have been widely explored to increase the hydrogen uptake of the MOFs. Recently, inelastic neutron scattering and neutron powder diffraction as well as computational studies suggest that the choice of both metal centers and ligands can play an important role in tailoring the gas-framework interactions.

Additionally, those ligands containing phenyl rings have been proved favorable for hydrogen adsorption. MOFs with hydrogen uptake approaching the DOE 2010 gravimetric storage goal under reasonable pressure but cryo-temperature (typically 77 K) were reported. However, the weak interaction between hydrogen molecules and MOFs has been the major hurdle limiting the hydrogen uptake of MOFs at ambient temperature.

Approach

Our strategy to enhance H_2 uptake was as follows: (1) prepared the catenation isomer pair to evaluate the contribution from catenation to the hydrogen uptake of a MOF material. Catenation can be utilized to reduce pore sizes in porous MOFs and has also been explored as an efficient method to improve the hydrogen uptake of MOFs. (2) Synthesized porous MOFs with high hydrogen adsorption capacities based on different coordinatively UMCs. The implementation of coordinatively UMCs into porous MOFs has been considered one of the most attractive ways to improve their affinities to hydrogen. (3) Hydrogen storage studies in MOFs containing nanoscopic cages based on double-bond-coupled di-isophthalate linkers. Those ligands containing phenyl rings in MOFs have been proved favorable for hydrogen adsorption. (4) Design and synthesize porous MOFs based on an anthracene derivative which can provide additional hydrogen binding sites to increase the hydrogen uptake. (5) Obtained stable MOFs with high surface areas by the incorporation of mesocavities and microwindows. (6) Constructed MOFs with "close-packing" alignment of open metal sites, which can increase the number of nearest neighboring open metal sites of each H_2-hosting void in a three-dimensional framework so that they can interact directly with the guests (H_2 molecules) inside the void. (7) Built up porous lanthanide MOFs and studied their potential application in gas adsorption. (8) Prepared an unprecedented linkage isomer pair of MOFs and studied the impact of pore size on H_2 storage capacity in MOFs. (9) Incorporated polyyne unit into MOFs, which has higher H_2 affinity. (10) Design and synthesize PPNs with high chemical stability suitable for further decoration. (11) Incorporated metal ions into PPNs, which can enhance the isosteric heats of hydrogen-adsorption.

Results

In the past year, we have prepared a series of MOFs and PPNs and explored their applications in hydrogen storage. Table 2 shows the comparison of hydrogen uptakes of selected MOFs and PPNs. Next we will discuss in detail the results of H_2 uptakes of these materials.

Functional MOFs Based on MOF-177

As we all know, MOF-177 is a porous material with high surface area ($SA_{Langmuir}$: 5,640 $m^2\ g^{-1}$) and high hydrogen storage (7.0 wt% at 60 bar and 77 K). Our tactics for preparing the functionalized MOF is to construct isostructural MOF-177 by designing a new functional organic ligand with the methyl, amino, hydroxyl and chiral group (Figure 1a). As expected, the four new ligands reacted with zinc salt to form four novel MOFs with isostructural MOF-177 (Figure 1b). Based on the N_2 sorption isotherm, PCN-103(N) has a BET surface area of 4,300 $m^2\ g^{-1}$ ($SA_{Langmuir}$: 5,500 $m^2\ g^{-1}$) and a total pore volume of 1.95 $cm^3\ g^{-1}$, which is similar to those results of MOF-177. PCN-103(O) has a BET surface area of 2,866 $m^2\ g^{-1}$ ($SA_{Langmuir}$: 4,587 $m^2\ g^{-1}$), while PCN-103(Ch) a BET surface area of 2,850 $m^2\ g^{-1}$ ($SA_{Langmuir}$: 4,144 $m^2\ g^{-1}$) (Figure 1c). The saturated excess gravimetric H_2 uptake of PCN-103(N) is 5.60 wt% at 40 bar, PCN-103(Ch) has a saturated excess gravimetric H_2 uptake of 5.10 wt% at 50 bar, while PCN-103(O) has a saturated excess gravimetric H_2 uptake of 5.40 wt% at 45 bar (Figure 1d).

TABLE 2. Comparison of Hydrogen Uptakes of Selected MOFs and PPNs

Material	ΔH_{ads} (kJ/mol)	H_2 Adsorption			
		Gravimetric H_2 Uptake (wt%)	Volumetric H_2 Uptake (g/L)	T (K)	P (bar)
PCN-26	6.81	2.86	24.7	77	32
PCN-69	8.14	5.20	19.5	77	50
PCN-103(N)	6.60	5.60	25.6	77	40
PCN-103(O)	-	5.40	24.6	77	45
PCN-103(Ch)	-	5.10	26.0	77	50
PCN-80	5.20	4.80	29.0	77	44
PCN-46	7.20	5.31	32.3	77	32
PPN-4	4.0	8.34	28.2	77	55

A Robust MOF with Flexible Octatopic Ligand

A newly designed flexible octatopic carboxylic acid ligand, tetrakis[(3,5-dicarboxyphenyl)-oxamethyl]methane acid (H_8TDM) has been used to react with $CuBr_2$ affording an MOF, $Cu_4(H_2O)_4$(TDM)·xS (PCN-26, S presents non-coordinated solvent molecules). PCN-26 was constructed by two different types of cages, octahedral and cuboctahedral, to form a polyhedron-stacked three-dimensional framework with open channels in three directions. In PCN-26, both $[Cu_2(O_2CR)_4]$ secondary building units (SBUs) and quaternary carbon atoms of TDM^{8-} act as four-connected nodes, while the CH_2O-isophthalate moieties act as three-connected nodes, the framework is a 3-nodal net and adopts a new network topology with the Schläfli symbol of $\{3^{11}.4^{10}.5^7\}_4\{3^2.6^2.7^2\}_2\{3^6\}$. Three-dimensional square channels are observed from the *a*, *b* and *c* axis with the sizes of 7.57 × 7.57 Å, 8.13 × 8.13 Å and 7.93 × 7.93 Å, respectively. N_2 sorption measurements were performed at 77 K, 1 bar, giving a Langmuir surface area of 2,545 $m^2\ g^{-1}$, a BET surface area of 1,854 $m^2\ g^{-1}$, and total pore volume of 0.84 $cm^3\ g^{-1}$.

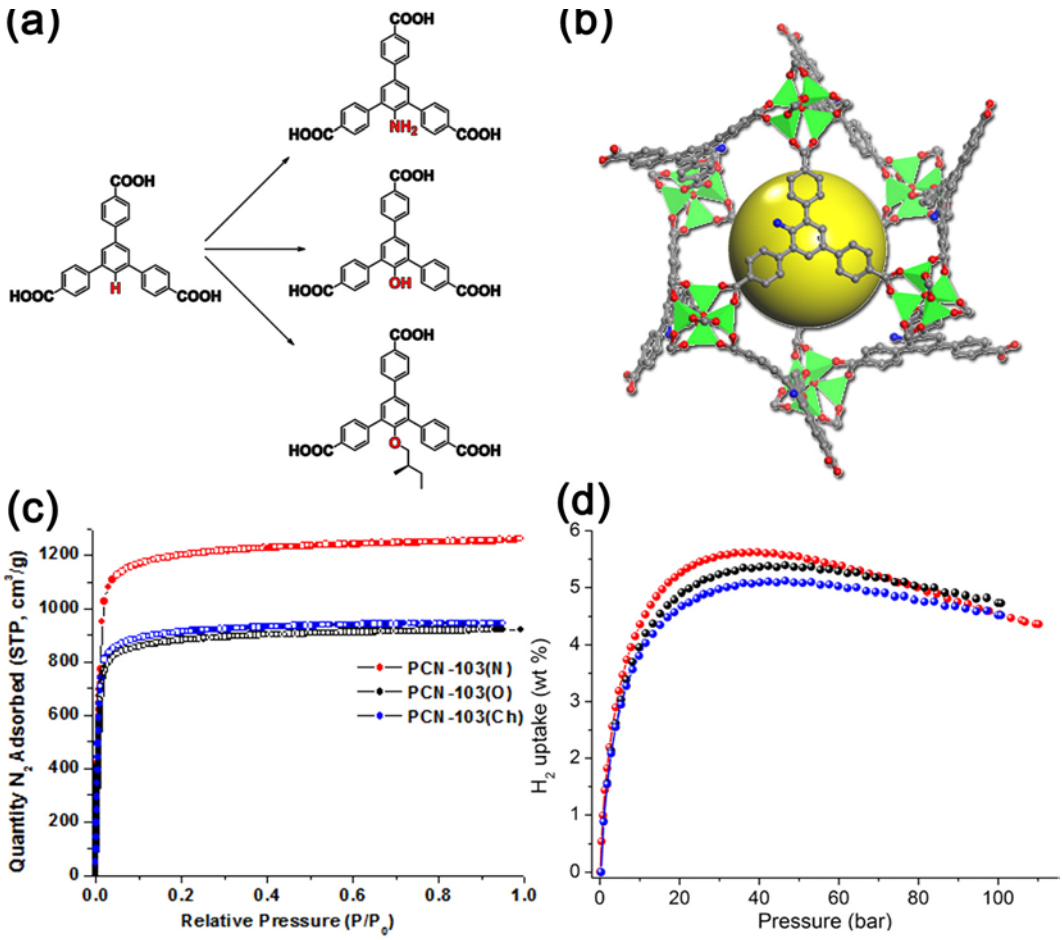


FIGURE 1. (a) The design of functional ligands; (b) the structure of PCN-103; (c) the N_2 isotherms of PCN-103(X) at 77 K; (d) the H_2 uptakes for PCN-103(X) at 77 K and high pressure range.

The PCN-26 has a saturated excess gravimetric hydrogen adsorption of 2.86 wt% at 77 K and 32 bar, with a hydrogen-adsorption enthalpy of 6.81 kJ mol^{-1}.

A Highly Porous and Robust 3,3,4-Connected MOF Assembled with a 90°-Angle-Embedded Octa-carboxylate Ligand

The octa-carboxylate ligand, BTTCD, with a 90°-angle-carbazole-3,6-dicarboxylate moiety as opposed to the widely used 120°-angle-isophthalate, was synthesized by a Cu(I)-catalyzed reaction between dimethyl 9H-carbazole-3,6-dicarboxylate and 3,3',5,5'-tetrabromo-1,1'-biphenyl followed by hydrolysis with potassium hydroxide in an overall yield of 30%. Solvothermal reaction of H_8BTTCD and $Cu(NO_3)_2$•2.5H_2O in N,N-dimethylformamide (DMF) in the presence of HBF_4 afforded tetragonal-shaped green crystals of PCN-80 with molecular formula $[Cu_2(BTTCD)]$•2DMF. PCN-80 crystallizes in tetragonal I4/mmm space group with a = b = 23.057(2), c = 30.762(3) Å. In the structure of PCN-80, the novel BTTCD ligand contains four 90°-angle subunits (Figure 2a) where the carbazole ring is perpendicular to the central benzene ring and the dihedral angle between adjacent carbazole rings is 47.4°. Every BTTCD ligand utilizes eight carboxylate groups to link eight 4-connected dicopper paddlewheel SBUs (Figure 2b) in a rectangular prismatic fashion to generate a porous (3,3,4)-connected network. There are three kinds of microporous cages with different sizes. L-cages (16.6 Å in diameter) are formed by eight $[Cu_2(O_2CR)_4]$ SBUs, and twelve BTTCD linkers (Figure 2c); M-cages (13.4 Å) from eight SBUs and four BTTCD linkers (Figure 2d); and S-cages (7.6 Å) through four SBUs and two BTTCD ligands (Figure 2e). The overall structure consists of these three types of cages packed in a 1:1:1 ratio (Figure 2f). From the viewpoints of topology, the SBUs serve as 4-connected nodes, whereas BTTCD ligands as 3,3-connected nodes. As a result, PCN-80 adopts the very rare 3,3,4-c 3-nodal net (Figure 2g) with topological point symbol of $\{7^2.8^2.11^2\}\{7^2.8\}\{7^3\}_2$, which is previously unreported.

The calculated free volume in fully desolvated PCN-80 is 72.1% by *PLATON* (1.8 Å probe radius), and pore volume is 1.25 cm^3 g^{-1}. To confirm the porosity of PCN-80, a fully desolvated sample was degassed under dynamic vacuum

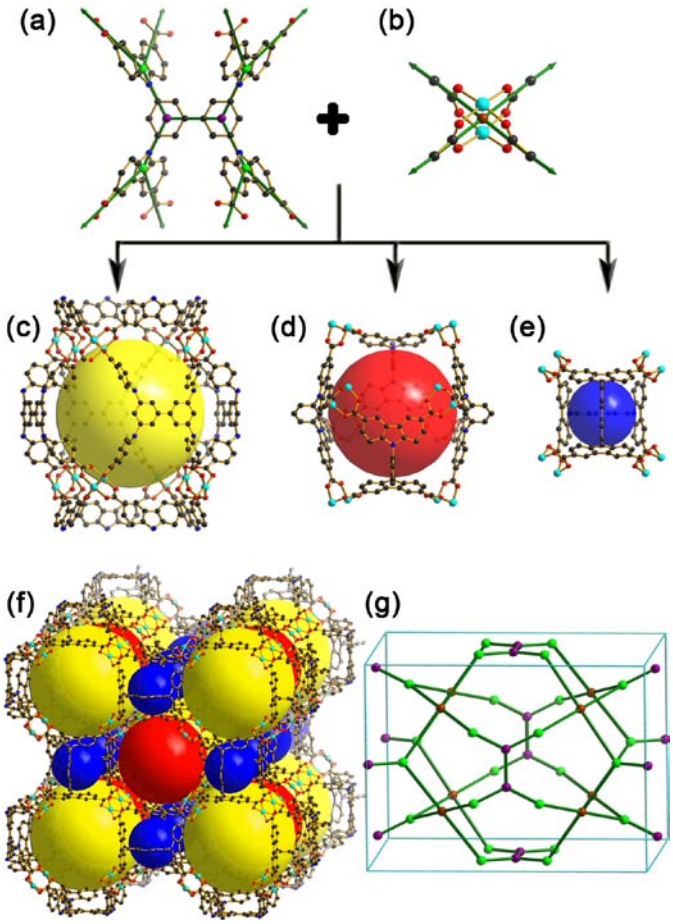


FIGURE 2. (a) 8-connected BTTCD ligand; (b) 4-connected dicopper paddlewheel SBU; (c) large size cage (L-cage); (d) middle size cage (M-cage); (e) small size cage (S-cage); (f) cages and their three-dimensional packing in PCN-80; (g) topology of PCN-80.

at 80°C for 10 h after solvent exchange with methanol and then dichloromethane. A color change from green to deep-purple-blue was observed, typical for dicopper-paddlewheel frameworks in which open copper sites are generated. The N_2 sorption for PCN-80 at 77 K exhibited a reversible *Type-I* isotherm, a characteristic of microporous materials. The estimated apparent BET surface area was ~3,850 $m^2 g^{-1}$ (calculated ~3,584 $m^2 g^{-1}$) and Langmuir surface area ~4,150 $m^2 g^{-1}$, which is similar to PCN-66 (BET ~4,000 $m^2 g^{-1}$), among the highest reported to date for porous MOFs or covalent organic frameworks. Notably, the experimental surface area of PCN-80 perfectly agrees with that calculated using Material Studio 5.5. On the basis of the N_2 sorption isotherm, PCN-80 has a calculated total pore volume of 1.47 $cm^3 g^{-1}$. Calculated with N_2 isotherm using DFT methods, the pore size distribution for PCN-80 indicates three different kinds of pores with diameters of 7.3, 11.8, and 14.5 Å, respectively, which is in good agreement with the crystal data.

In the low-pressure region, it is well known that the H_2-uptake capacity is mainly controlled by the hydrogen affinity towards the framework. PCN-80 exhibits H_2-uptake capacity as high as 2.3 wt% at 77 K and 1 bar, which is among the highest at low pressure. The excellent performance of PCN-80 can be largely attributed to its microporous nature as well as high open-metal-site density upon activation. High-pressure gas sorption was performed on PCN-80 using volumetric measurement method. **A**t 77 K, the excess H_2-uptake capacity of PCN-80 reached its maximum value of 4.8 wt% (29 g L^{-1}) at 44 bar. Based on a variant of the Clausium-Clapeyron equation, the H_2 isosteric adsorption enthalpy of PCN-80 reaches 5.2 kJ mol^{-1} at low coverage.

Highly Stable Porous Polymer Networks with Exceptionally High H_2-Uptake Capacities

Conventional Yamamoto homo-coupling reaction for polymerization was carried out at 80°C with DMF as the solvent. However, when the same reaction condition was applied to tetrakis(4-bromophenyl)silane or tetrakis(4-bromophenyl)admantane, the surface areas of the synthesized materials were much lower than the calculated data. With the assumption that reduced temperature would slow down the reaction to yield polymers with higher molecular weight and avoid any unwanted side reactions, we adopted an optimized Yamamoto homo-coupling procedure, in which the reactions were carried out at room temperature in a DMF/tetrahydrofuran mixed solvent. Using this procedure, we were able to synthesize PPN-3 (X: admantane), PPN-4 (X: silicon), and PPN-5 (X: germanium) with exceptionally high surface areas (Figure 3a and 3b). The surface area of PPN-3 synthesized through this procedure is much higher than the value previously reported, and the surface area of PPN-4 is close to the value predicted based on the molecular model, indicating the excellence of this optimized procedure. With the BET surface area of 6,461 $m^2 g^{-1}$ and Langmuir surface area of 10,063 $m^2 g^{-1}$, PPN-4 possesses, to the best of our knowledge, the highest surface area among all the reported porous materials so far. In addition, most of the pores in PPN-4 sit with the range of microporous or microporous/mesoporous range, which serves remarkably for gas storage purposes.

As the previously reported PPNs, PPN-3, PPN-4, and PPN-5 are off-white powders, not soluble in common organic solvents. There is no residual bromine from the elemental analysis result, indicating the completion of the reaction and the efficiency of Yamamoto homo-coupling. Surprisingly, a trace amount of nitrogen was detected in PPN-3 and PPN-5 (0.14 wt% and 0.11 wt%, respectively), which probably comes from the trapped 2,2'-bipyridine within the shrunken pores caused by network interpenetration. This network interpenetration may also account for the reduced experimental surface areas of PPN-3 and PPN-5 compared with the calculated data. Thermogravimetric analysis data show the three polymers possess good thermal stability and high decomposition temperatures of more than 450°C in a nitrogen atmosphere.

In addition, PPN-4 retains its structural integrity after being exposed to air for one month, as indicated by virtually no drop of N_2 uptake capacity at 77 K.

The exceptionally high surface area combined with excellent stability make PPN-4 a very attractive candidate for gas storage applications, particularly in H_2 for clean energy purposes. To evaluate its gas storage capacity, high-pressure excess adsorption of H_2 within PPN-4 were measured at 77 K (liquid nitrogen bath). As shown in Figure 3c, the excess H_2 uptake of PPN-4 at 77 K and 55 bar can reach 91 mg g^{-1} (8.34 wt%, total uptake: 158 mg g^{-1}, 13.6 wt%, 80 bar), which is by far the highest among all amorphous materials, and is also comparable to the best value reported in MOFs. The isosteric heat of adsorption for H_2 is around 4 kJ mol^{-1} (Figure 3d), which fits within the range of physisorption and indicates that the high surface area might be the sole factor in determining this high H_2 uptake capacity. Unlike MOFs, whose H_2 uptake capacity will decrease after several uptake-release cycles, the H_2 uptake capacity of PPN-4, even being exposed to air for several days, can be simply regenerated by heating under vacuum. The excellent physicochemical stability and impressively high delivery capacity (71 mg g^{-1}, 77 K, from 1.5 bar to 55 bar) make PPN-4 the currently unbeatable material for cryogenic H_2 storage application.

Post-Grafting Porous Polymer Networks for Hydrogen Storage

Theoretical studies on MOF and PPN materials have suggested that introduction of light, non-transition metal ions such as Li^+, Na^+ or Mg^{2+} might afford non-dissociative hydrogen binding, thus enhancing overall adsorption of H_2. In particular, Li-doped materials appear to be especially interesting in this regard. Here we report the post-grafting of PPN-6 with sulfonic acid and lithium sulfonate. PPN-6 (also known as porous aromatic framework [PAF]-1) was synthesized using an optimized Yamamoto homo-coupling reaction of tetrakis(4-bromophenyl)methane. The default diamondoid framework topology imposed by the tetrahedral monomers provides widely open and interconnected pores to efficiently prevent the formation of "dead space", more importantly, the extremely robust all-carbon scaffold of the network can stand harsh reaction conditions and makes it perfect to build up polar organic groups on the biphenyl units; indeed, by reacting with chlorosulfonic acid in dichloromethane, PPN-6 was modified into PPN-6-SO_3H,

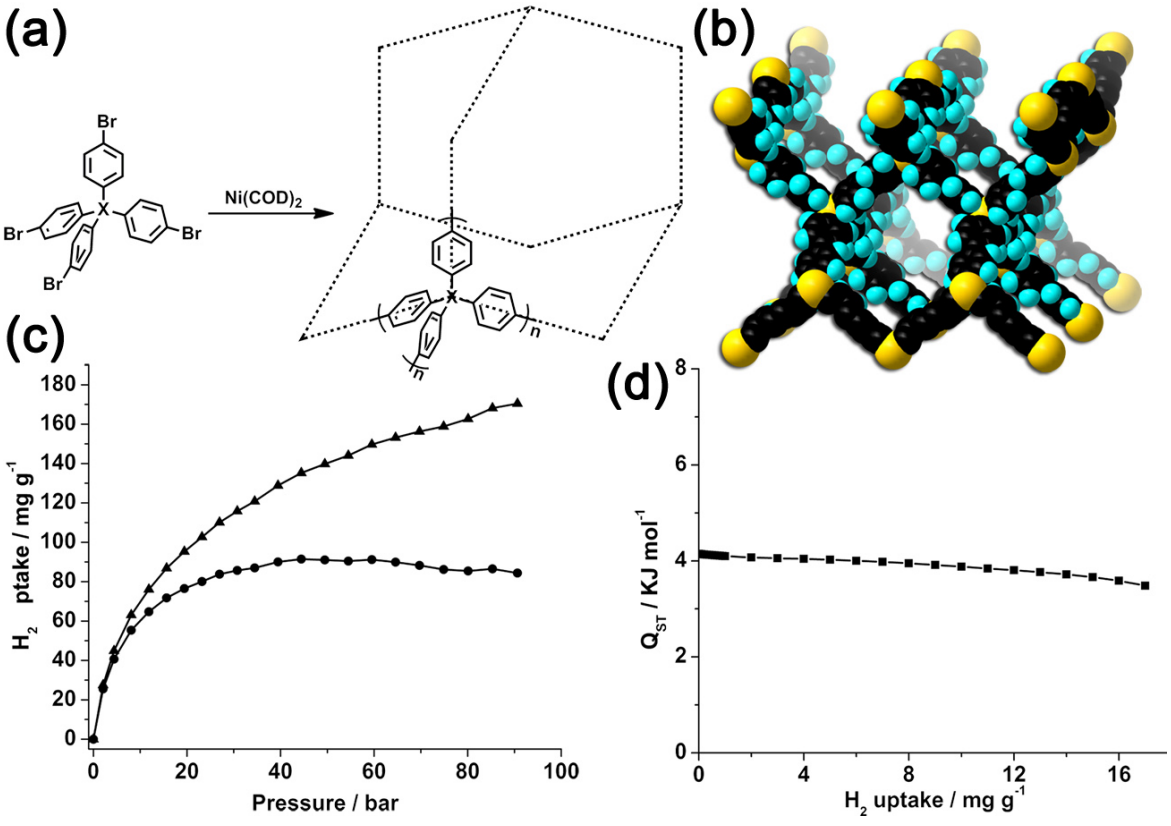


FIGURE 3. (a) Synthetic route for PPN-3 (X: Adamantane), PPN-4 (X: Si), PPN-5 (X: Ge), and PAF-1 (X: C); (b) The default noninterpenetrated diamondoid network of PPN-4 (black, C; cyan, H; yellow, Si); (c) Excess and total H_2 adsorption isotherms of PPN-4 at 77 K; (d) Isosteric heat of adsorption for H_2 in PPN-4.

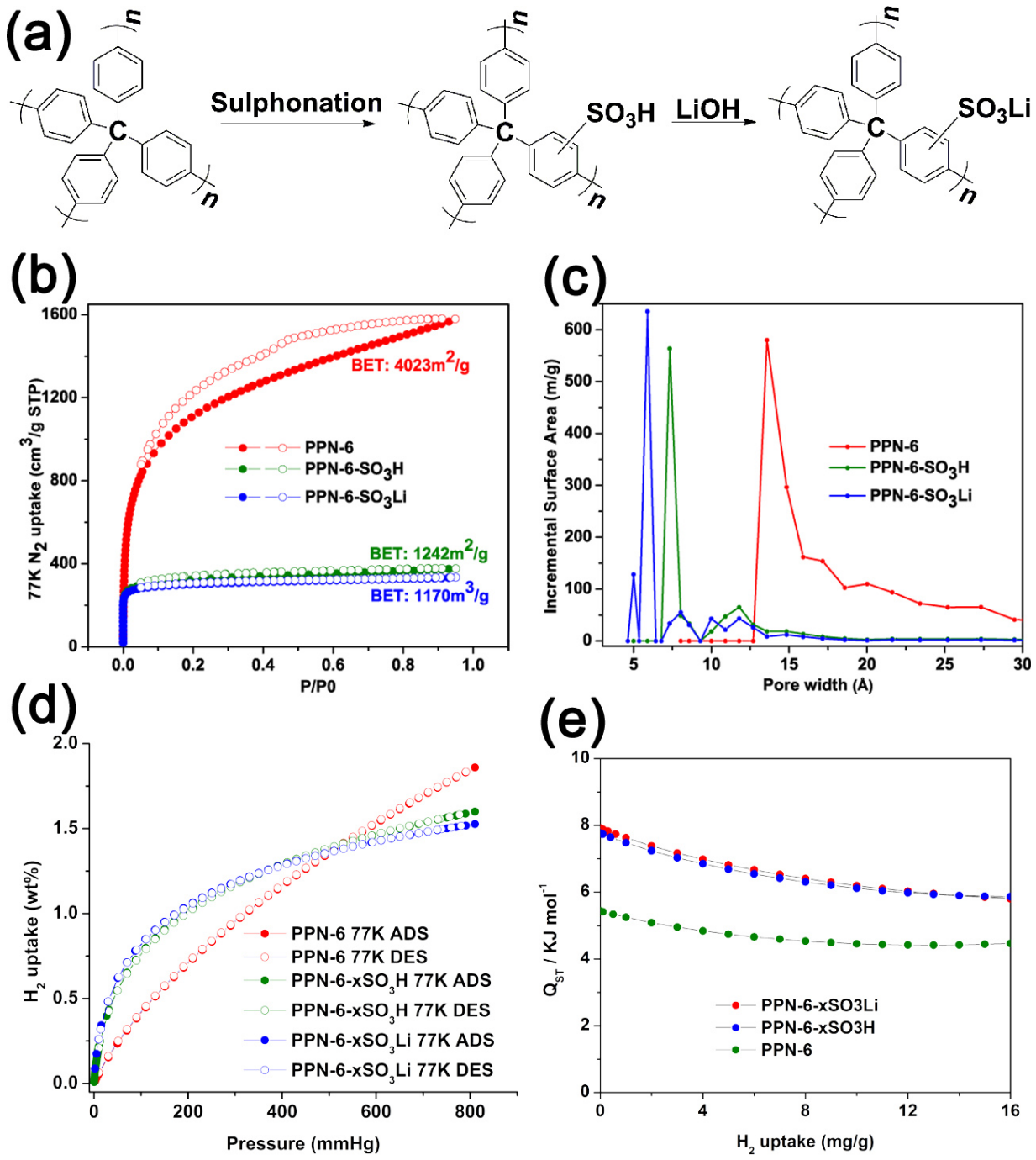


FIGURE 4. (a) Synthesis and post-synthetic grafting of PPN-6-X; (b) (a) N_2 adsorption (closed)/desorption (open) isotherms of PPN-6-X at 77 K; (c) Pore size distribution curves of PPN-6-X; (d) Excess adsorption isotherms of PPN-6-X at 77 K; (d) Isosteric heat of adsorption for H_2 in PPN-6-X.

which was further neutralized to produce PPN-6-SO_3Li (Figure 4a). Nitrogen gas adsorption/desorption isotherms of the three networks were collected at 77 K (Figure 4b). Notably, the huge hysteresis in PPN-6 adsorption/desorption isotherm disappeared into nearly type-I isotherms in functionalized PPN-6. The BET surface areas were calculated from the adsorption branch of the nitrogen isotherms over a BET-theory-satisfied pressure range and were found to be 4,023, 1,242, and 1,170 $m^2 g^{-1}$ for PPN-6, PPN-6-SO_3H and PPN-6-SO_3Li, respectively. The pore size distributions of the three networks have been calculated with their N_2 adsorption isotherms at 77 K (Figure 4c). Along with the decrease of surface area, the pore size becomes progressively reduced with aromatic sulfonation and lithiation. Recent studies have indicated several features that are desirable for enhancing storage capacity of small gas molecules. One such feature is the suitable pore size commensurate with the size of gas molecule. The relatively

small pore sizes of functionalized PPN-6 fall into the range of 5.0-10.0 Å. Though the experimental BET surface of PCN-6-SO_3Li area decreased, the H_2 isosteric heat increased 47% (Figure 4d and 4e), which is consistent with theoretical calculation. The introduction of other metal will also be studied, such as Mg, Ti, Ni, Co and so on.

Conclusions and Future Directions

Conclusions:

- Constructing new MOFs using 90°-angle-embedded octa-carboxylate ligand is proved as a general approach towards stable MOFs with high surface areas and high hydrogen uptake.
- PPNs with tunable pore size and surface area can be prepared with high chemical and thermal stability, which are good candidate for hydrogen storage.
- PPN postsynthetic modification and metal incorporation can remarkably enhance the heat of adsorption.

Future Directions:

- Further enhancement of H_2-MOF interaction by doping coordinatively unsaturated metal centers (heat of adsorption 15 kJ mol^{-1}). Based on theoretical calculations, main group metals such as Li, Mg and Ca will be tested.
- Working with partners, test H_2 uptake at temperatures higher than 77 K.
- Preparation of MOFs with high surface area and optimized cage size with newly designed ligands based on theoretical calculations.
- Incorporation of entatic-state metals based on theoretical guidance.
- Preparation of new PPNs containing active metals.

Special Recognitions & Awards

1. DOE Hydrogen Program Special Recognition Award as a member of the Hydrogen Sorption Center of Excellence (HSCoE), 2010.

FY 2011 Publications/Presentations

1. "The current status of hydrogen storage in metal–organic frameworks–updated", Sculley, J.; Yuan, D.; Zhou, H.-C., *Energy Environ. Sci.*, **2011**, *4*, 2721-2735.

2. "Construction of Two 3D Homochiral Frameworks with 1D Chiral Pores via Chiral Recognition", Li, H.-Y.; Jiang, L., Xiang, H.; Makal, T.; Zhou, H.-C.; Lu, T.-B., *Inorg. Chem*., **2011**, *50*, 3177-3179.

3. ''Surface functionalization of metal-organic polyhedron for homogeneous cyclopropanation catalysis", Lu, W.; Yuan, D.; Yakovenko, A.; Zhou, H.-C., *Chem. Comm*., **2011**, 47, 4968-4970.

4. "Metal-Organic Frameworks", Makal, T.A.; Yuan, D.; Zhao, D.; Zhou, H.-C., In *The Chemistry of Nanostructured Materials*, Vol. II Yang, P.; Ed. World Scientific: Singapore, **2011**, 37-64.

5. "Carbon Dioxide Capture-Related Gas Adsorption and Separation in Metal-Organic Frameworks", Li, J.-R.; Ma, Y.; McCarthy, M.C.; Sculley, J.; Yu, J.; Jeong, H.-K.; Balbuena, P.B.; Zhou, H.-C., *Coord. Chem. Rev*., **2011**, *255*, 1791-1823.

6. "Tune the Topology and Functionality of Metal-Organic Frameworks by Ligand Design", Zhao, D.; Timmons, D.J.; Yuan, D.Q.; Zhou, H.-C., *Accounts Chem. Res*., **2011**, *44*, 123-133.

7. "Surface Functionalization of Porous Coordination Nanocages Via Click Chemistry and Their Application in Drug Delivery", Zhao, D.; Tan, S.W.; Yuan, D.Q.; Lu, W.G.; Rezenom, Y.H.; Jiang, H.L.; Wang, L.Q.; Zhou, H.-C., *Adv. Mater*., **2011**, *23*, 90-93.

8. "A Stepwise Transition From Microporosity to Mesoporosity in Metal-Organic Frameworks by Thermal Treatment", Yuan, D.; Zhao, D.; Timmons, D.J.; Zhou, H.-C., *Chem. Sci.*, **2011**, *2*, 103-106.

9. "Functional Mesoporous Metal-Organic Frameworks for the Capture of Heavy Metal Ions and Size-Selective Catalysis", Fang, Q.-R.; Yuan, D.; Sculley, J.; Li, J.-R.; Han, Z.-B.; Zhou, H.-C., *Inorg. Chem*., **2010**, *49*, 11637-11642.

10. "Ligand Bridging-Angle-Driven Assembly of Molecular Architectures Based on Quadruply Bonded Mo–Mo Dimers", Li, J.-R.; Yakovenko, A.; Lu, W.; Timmons, D.J.; Zhuang, W.; Yuan, D.; Zhou, H.-C., *J. Am. Chem. Soc*., **2010**, *132*, 17599-17610.

11. "Recent Advances in the Study of Mesoporous Metal-Organic Frameworks", Fang, Q.-R.; Makal, T. A.; Young, M.D.; Zhou, H.-C., *Comments on Inorganic Chemistry*, **2010**, *31*, 165-195.

12. "Porous Polymer Networks: Synthesis, Porosity, and Applications in Gas Storage/Separation", Lu, W.; Yuan, D.; Zhao, D.; Schilling, C.I.; Plietzsch, O.; Muller, T.; Brase, S.; Guenther, J.; Blumel, J.; Krishna, R.; Li, Z.; Zhou, H.-C., *Chem. Mater*., **2010**, *22*, 5964-5972.

13. "Bridging-Ligand-Substitution Strategy for the Preparation of Metal–Organic Polyhedra", Li, J.-R.; Zhou, H.-C., *Nature Chem*., **2010**, *2*, 893-898.

14. "Two Robust Porous Metal–Organic Frameworks Sustained by Distinct Catenation: Selective Gas Sorption and Single-Crystal-to-Single-Crystal Guest Exchange", Yang, R.; Li, L.; Xiong, Y.; Li, J.-R.; Zhou, H.-C.; Su, C.-Y., *Chem.-Asian J*., **2010**, *5*, 2358-2368.

15. "Thermosensitive Gating Effect and Selective Gas Adsorption in a Porous Coordination Nanocage", Zhao, D.; Yuan, D.; Krishna, R.; Van Baten, J.M.; Zhou, H.-C., *Chem. Commun*., **2010**, *46*, 7352-7354.

16. "Control over Interpenetration in Lanthanide–Organic Frameworks: Synthetic Strategy and Gas-Adsorption Properties", He, H.Y.; Yuan, D.Q.; Ma, H.Q.; Sun, D.F.; Zhang, G.Q.; Zhou, H.-C., *Inorg. Chem*., **2010**, *49*, 7605-7607.

IV.C.2 A Joint Theory and Experimental Project in the Synthesis and Testing of Porous COFs and ZIFs for On-Board Vehicular Hydrogen Storage

Omar M. Yaghi
Department of Chemistry and Biochemistry
University of California, Los Angeles
607 Charles E. Young Drive East
Los Angeles, CA 90095
Phone: (310) 206-0398
E-mail: yaghi@chem.ucla.edu

DOE Managers
HQ: Ned Stetson
Phone: (202) 586-9995
E-mail: Ned.Stetson@ee.doe.gov
GO: Katie Randolph
Phone: (720) 356-1759
E-mail: Katie.Randolph@go.doe.gov

Contract Number: DE-FG36-08GO18141

Project Start Date: September 1, 2008 (funded from April 1, 2009)
Project End Date: January 31, 2013

Fiscal Year (FY) 2011 Objectives

- Design new covalent-organic frameworks (COFs) with strong H_2 binding sites.
- Predict H_2 uptake isotherm for designed frameworks employing a developed force field.
- Prepare stable frameworks with potential metal binding sites.
- Implement metalation experiments and evaluate their respective H_2 adsorption properties.
- Prepare a mixed-metal zeolitic imidazolate framework (ZIF).

Technical Barriers

This project addresses the following technical barriers from the Storage section (3.3.4.2) of the Fuel Cell Technologies Program Multi-Year Research, Development and Demonstration Plan:

(A) System Weight and Volume
(C) Efficiency
(E) Charging/Discharging Rates
(P) Lack of Understanding of Hydrogen Physisorption and Chemisorption

Technical Targets

This project consists of several fundamental studies on COFs and ZIFs. Insights gained from these studies will be applied toward the design and synthesis of hydrogen storage materials that meet the following DOE 2015 hydrogen storage targets:

- Volumetric density: 40 g L^{-1}
- Gravimetric density: 5.5 wt%

FY 2011 Accomplishments

- Synthesized new COFs via hydrazone and imine condensation.
- Initiated metalation experiments of COFs.
- Began synthesis of mixed-metal ZIFs for improved adsorption enthalpy.
- Found linkers with optimal binding energy for H_2 storage (20 kJ/mol).
- Designed new architectures with these linkers and began simulation calculations of H_2 uptake.



Introduction

Storage of hydrogen in porous materials is a promising approach to achieve the DOE system requirements for use of H_2 as a transportation fuel. After the first report of successful H_2 storage in metal-organic frameworks (MOFs), the Yaghi group has succeeded in incrementally increasing the gravimetric and volumetric capacities in order to to reach the highest H_2 uptake capacity, albeit at 77 K. However, for on-board vehicular H_2 storage it is necessary to improve the adsorption enthalpy of porous materials to achieve significant capacities at room temperature. Therefore, we are currently focusing our efforts on discovering highly porous materials with strong affinity for H_2.

Approach

To meet the DOE 2015 revised targets by physisorption, adsorbents must have high surface area (>3,500 m^2 g^{-1}) and relatively high density (>0.75 g cm^{-3}). We have previously demonstrated how to design high surface area MOFs and COFs; however, in many cases, these materials do not show steep H_2 uptake in the low-pressure region indicative of the weak interaction with H_2. It is predicted that the impregnation of COFs with metals will enhance the

adsorption enthalpy, which has led us to explore methods for the preparation of metalated COFs. In this FY, we developed a new class of COFs for metal impregnation. Moreover, we developed the force field from *ab initio* calculations, which are used to estimate the isotherm of COFs containing the hydrazone and imine moieties as well as the H_2 uptake for a full and partial Pd(II)-metalated COFs. In addition, a new mixed-metal ZIF was designed and synthesized to incorporate strong H_2 binding sites in the framework.

Results

Metal impregnation is one of the most promising strategies to improve the adsorption enthalpy of COFs. However, before the metal impregnation experiments are carried out, it is necessary to prepare stable COFs that are capable of introducing metal binding sites in the framework through the condensation reaction. To this end, we designed and prepared new COFs having hydrazone and imine moieties.

Preparation of Hydrazone COF. Despite the significant interest in developing COFs for industrially relevant applications, only a small number of organic functionalities, such as boronates, borosilicate, and imine condensations have been employed in their preparation [1-3]. The relatively few examples of COF architectures, with respect to the vast library of possible organic reactions, can be attributed to the significant challenge of synthesizing crystalline solids constructed solely from strong covalent bonds. We have previously shown that this challenge is overcome by using dynamic covalent systems coupled with precisely controlled reaction conditions. Thus, we employed these same principles in the selection of hydrazide and aldehyde moieties as novel building blocks for COF materials since the reversibility of hydrazone formation by modulating the pH is well documented.

COF-42 and COF-43 were synthesized by suspending 2,5-diethoxyterephthalohydrazide (**1**) and 1,3,5-triformylbenzene (**2**) or 1,3,5-tris(4-formylphenyl) benzene (**3**) in a flame-sealed Pyrex tube in a mixture of mesitylene, dioxane and acetic acid at 120°C (Figure 1). These materials were immersed in tetrahydrofuran to remove occluded guests for three days, and the solvent was subquently removed by heating at 85°C under dynamic vacuum.

Powder X-ray diffraction (PXRD) measurements were performed on samples of COF-42 and COF-43 to determine their crystallinity. The experimental PXRD patterns of both COFs were indexed based on a primitive hexagonal lattice. Next, the raw data was compared to models of possible crystal structures that can be obtained from linking the trigonal and the linear building blocks. It is anticipated that two-dimensional trigonal layers will be formed given that the hydrazone moiety is approximately coplanar with respect to the aromatic rings due to resonance effects and internal hydrogen bonding. These layers can pack in eclipsed **bnn** (*P*6/*mmm*), or staggered modes, **gra** ($P6_3/mmc$). However, at this resolution, the framework topologies, for both COFs, as either **bnn** or **gra** could not be assigned.

Gas adsorption isotherms were measured on fully activated samples in order to ensure the architectural stability and porosity of each COF. The Ar isotherm of COF-42 measured at 87 K showed a sharp uptake below $P/P_0 = 0.05$ with a step at $P/P_0 = 0.05$-0.20. This profile is best described as Type IV isotherm, which is characteristic of mesoporous materials. The Brunauer-Emmett-Teller (BET) surface area of COF-42 was calculated to be 710 $m^2 g^{-1}$. The 87 K Ar adsorption isotherm of COF-43 also possesses a type IV shape indicating that it is a mesoporous material. The BET surface area of COF-43 was calculated

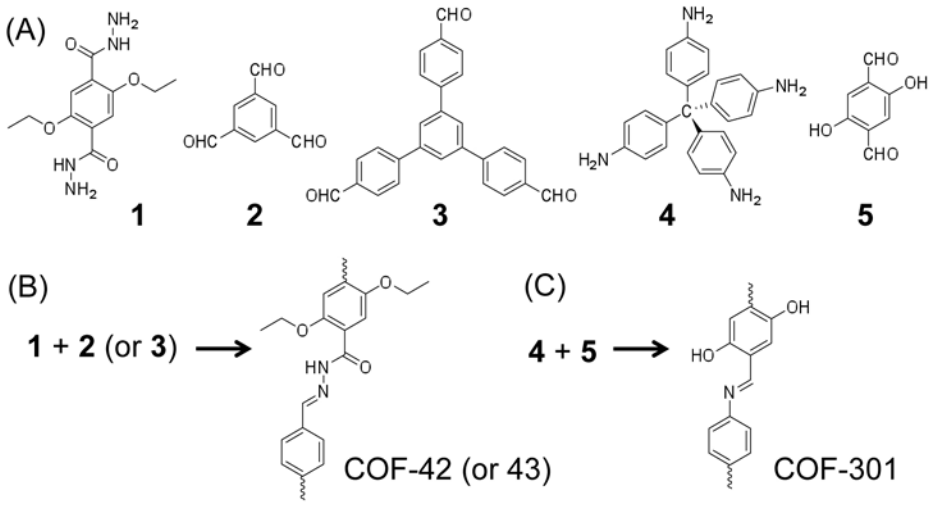


FIGURE 1. (A) Molecular structures of building units for COF synthesis. Reaction scheme of hydrazone (B) and imine COF (C) formation.

to be 620 $m^2 g^{-1}$. Notably, the surface area and pore volume values obtained for COF-42 and COF-43 are comparable to those of other two-dimensional COFs with hexagonal pore systems [4]. A non-local density functional theory model was fitted to the isotherms of COF-42 and COF-43 yielding average pore sizes of 23 and 38 Å, respectively, these values are in good agreement with the expected pore size observed in the crystal simulations based on a **bnn** topology. More importantly, this is large enough to accommodate metal ions (and possibly their counter anions) in the pore.

The H_2 isotherms for these COFs are illustrated in Figure 2. The H_2 uptake for COF-42 and 43 at 1 bar and 77 K is 0.60 and 0.51 wt%, respectively. Although COF-42 has a smaller BET surface area, the H_2 uptake for COF-42 under the present experimental conditions was larger than that of COF-43. We attribute these results to the smaller pore diameter of COF-42. Furthermore, this theory is supported by the isosteric heats of adsorption (Q_{st}) data for these COFs (Figure 2, inset). The initial Q_{st} values for both COFs are almost the same (6.6 kJ/mol), because of the similarity in the surface environment of COFs. Once a majority of strong binding sites are occupied by H_2, the adsorption potential in the pore should be more important (i.e. larger pore material has smaller adsorption potential). Consequently, it is likely that the values for COF-43 quickly dropped with an increase in the H_2 loading.

Preparation of Imine COF and its Metalation Reaction. We have demonstrated the condensation of the tetrahedral building block tetra-(4-anilyl)methane with the linear linking unit terephthaldehyde to produce a material with an extended three-dimensional framework structure (COF-300) [3]. COF-300 is an interpenetrated diamond net and has a one-dimensional channel with diameter of 7.8 Å. However, due to the lack of potential metal binding sites, it is not easy to metalate this material. To create metal binding sites in the COF frameworks, we believe salicylidene-aminophenyl and iminopyridine moieties are good candidates. This year, we synthesized a new imine COF (termed COF-301).

The synthesis of COF-301 was carried out by solvothermolysis of a suspension of tetra-(4-anilyl)methane (**4**) and 2,5-dihydroxyterephthalaldehyde (**5**) in a mixture of 1,4-dioxane and aqueous acetic acid (Figure 1). The material is insoluble in water and common organic solvents such as hexanes, methanol, acetone, tetrahydrofuran, and *N*,*N*-dimethylformamide. Therefore, it seems the resultant crystalline material is an extended structure. The formation of imine linkages in COF-301 was confirmed by Fourier transform infrared spectra. The crystallinity of COF-301 was confirmed by PXRD analysis. Although its atomistic connectivity is not determined yet, it is presumed that the connectivity (topology) of COF-301 is a diamond net due to the similarity of PXRD pattern. However, no information is available with regard to the degree of interpenetration.

The permanent porosity of COF-301 was demonstrated by measuring N_2 adsorption at 77 K. The isotherm shows a sharp uptake below $P/P_0 < 0.10$. The application of the BET model results in a surface area of 1,040 m^2/g. The N_2 isotherm was fit with non-local density functional theory models from which the pore size distribution was calculated, resulting in a value of 10.5 Å, which is close to the values observed in the proposed structure (ca. 9.5 Å).

Prior to the metalation reaction, we predicted the total H_2 isotherms of pristine and COF-301-Pd (using $PdCl_2$ as the source) with different metal loadings. As shown in Figure 3, metalated material shows steep H_2 uptake below 10 bar even at room temperature, which is in sharp contrast to the pristine COF-301. The total H_2 uptakes at 100 bar are calculated to be 4.5, 3.7, 2.7 wt% for 100%, 50%, and 25%

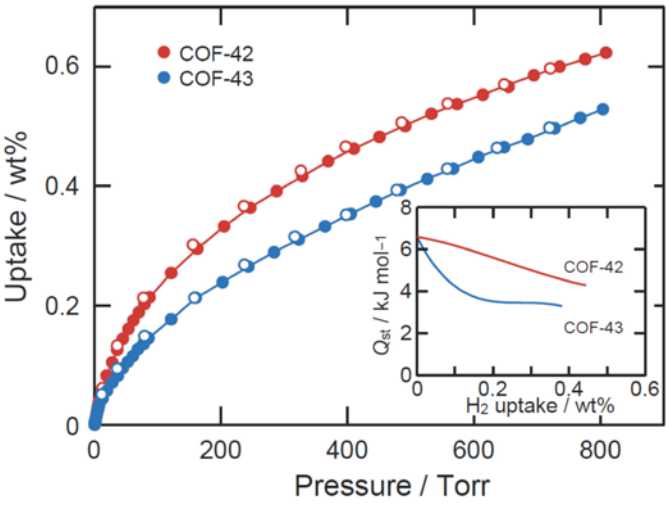


FIGURE 2. H_2 isotherms for COF-42 (red) and COF-43 (blue) at 77 K. Inset: coverage dependence of the isosteric heats of adsorption (Q_{st}) for H_2 in these COFs.

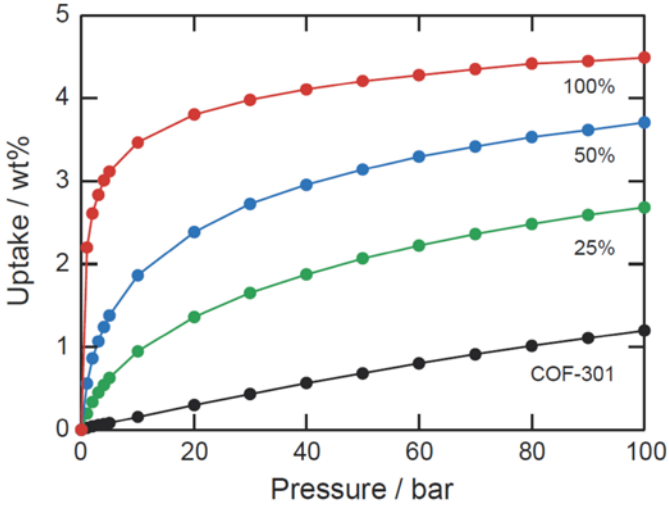


FIGURE 3. Predicted total gravimetric H_2 isotherms of pristine COF-301 and COF-301-$PdCl_2$ with different metal loadings (100%, 50%, and 25%).

Pd loading COF-301. These values are much greater than pristine COF-301 (1.2 wt%) under the same condition, so that it is presumed that the interaction between Pd and H_2 is strong enough to improve the H_2 uptake capacity. This is more obvious when we observe the average Q_{st} values which are 23.6, 17.8, 14.0 kJ/mol for 100%, 50%, and 25% Pd loading COF-301, while only 6.0 kJ/mol for pristine COF-301. Although the metalated compound would have a smaller pore volume and a larger bulk density, the simulated isotherms encourage us to implement the metalation. Therefore, we impregnated COF-301 with metal salts, and obtained materials are termed COF-301-M; M = Pd(II) and Pt(II).

The metalation of COF-301 was carried out by reflux reaction of a suspension of COF-301 and metal source ($PdCl_2$ or $PtCl_2$) in acetonitrile. The resulting yellow solid was filtered off, washed with ethanol, diethyl ether and dried under vacuum. After the metalation, the peak position of PXRD for metalated COF-301 is almost identical to that of COF-301. Therefore, we believe that the crystallinity of these metalated materials is retained, although the intensity of the pattern decreased. Currently, we do not have clear evidence to confirm whether the metal ion was bound to the framework. We plan to study the metal coordination environment using ^{15}N enriched material.

Before the H_2 tests, we measured N_2 isotherms of a series of materials. After the metalation, the BET surface areas of the samples were much smaller than that of the pristine material (60 m^2/g for COF-301-Pd, 20 m^2/g for COF-301-Pt). Although the metalated samples have a larger density than the original COF-301, this should not be the only reason for the significant surface area drop. Possible explanation of this drop is (i) the presence of leaving groups (perhaps two Cl^-) bound to the metal ion and/or unreacted metal salts (i.e. MCl_2), (ii) pore openings of the metalated samples could be partly blocked, which would reduce the accessible pore space, and/or (iii) crystallinity of the materials were partially lost. To mitigate the surface area drop, we will optimize metalation and sample activation conditions.

Preparation of Mixed-Metal ZIFs. To improve H_2 storage capacity, the number of metals per volume is a very important factor to keep in mind. In most cases, ZIFs have higher metal density because the length of the imidazolate is short [5]. However, these metal ions (i.e. Zn^{2+} and Co^{2+}) are fully coordinated to imidazolate linkers such that it is difficult to utilize these metals as strong H_2 binding sites. We believe it is possible to create open metal sites in ZIF structures, if we introduce another metal ion having different coordination geometry. To this end, we added another metal source (Cu^{2+}) to reaction mixtures.

The as-synthesized product (ZnCu(imidazolate)) was washed with methanol and evacuated at room temperature. The permanent porosity of the activated sample was confirmed by N_2 adsorption at 77 K. The profile of the N_2 isotherm for evacuated samples is classified typical Type I isotherm, whose BET surface area is calculated to be 1,460 m^2/g. This is one of the highest values in ZIF materials, although these are slightly smaller than ZIF-8 [6]. The H_2 isotherms for mixed metal ZIF are illustrated in Figure 4. The H_2 uptake at 1 bar and 77 K is 1.2 wt%. Considering that the isotherm is nearly straight in this region, the interaction between the framework and H_2 may not be strong. Indeed, the Q_{st} value did not change until 0.7 wt% of H_2 coverage (Figure 4, inset). Currently, we are studying the synthetic conditions for other mixed metal ZIFs with different metal ions with square planar geometry (e.g. Ni).

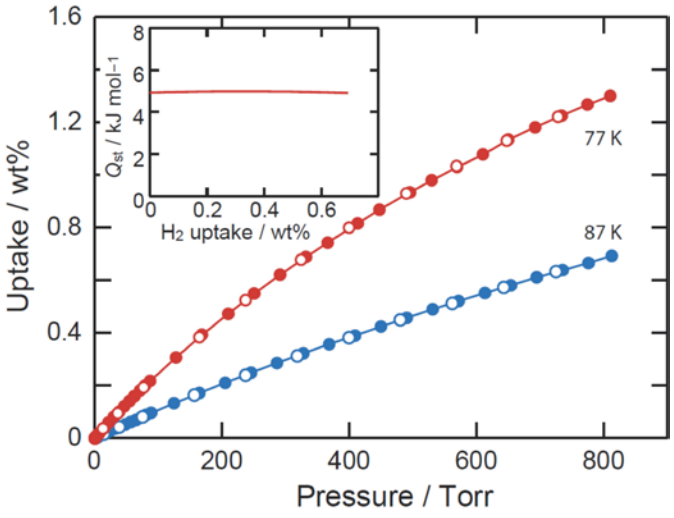


FIGURE 4. H_2 isotherms for the mixed metal ZIF at 77 K (red) and 87 K (blue). (Inset) Coverage dependence of the isosteric heat of adsorption (Q_{st}) for H_2 in the ZIF calculated from fits of its 77 and 87 K isotherms.

Conclusions and Future Directions

This year we experimentally demonstrated how to introduce potential metal binding moieties by connecting di-, tri-, and tetra-topic building units through condensation reactions (i.e. hydrazine and imine COFs). We started the metalation reactions using COF-301, although the metalation conditions are not optimized yet. We plan to screen candidates for metalation reactions of COFs through modeling studies, which will be experimentally evaluated. In addition, we will predict the binding energy between H_2 and metal unit.

- Material design assisted by the reticular synthesis.
- Calculate the H_2 isotherms for pristine and metalated COFs.
- Implement the metalation reaction based on the theoretical prediction.
- Calculate the free energy (ΔG) and entalphy (ΔH) for the metalation processes.
- Calculate the diffusion coefficient of H_2 in the frameworks to estimate the kinetic factor.

- Synthesize mixed metal ZIFs with different metal ions.
- Begin calculation of H_2 isotherms for mixed metals ZIFs.

Special Recognitions

1. The 2010 Centenary Prize from the Royal Society of Chemistry.

FY 2011 Publications

1. S.S. Han, S.H. Choi, W.A. Goddard, "Zeolitic Imidazolate Frameworks as H-2 Adsorbents: Ab Initio Based Grand Canonical Monte Carlo Simulation," *J. Phys. Chem. C,* **2010**, *114*, 12039-12047.

2. S. Wan, F. Gándara, A. Asano, H. Furukawa, A. Saeki, S.K. Dey, L. Liao, M.W. Ambrogio, Y.Y. Botros, X. Duan, S. Seki, J.F. Stoddart, O.M. Yaghi, "Covalent Organic Frameworks with High Charge Carrier Mobility," *Chem. Mater*., accepted.

3. F.J. Uribe-Romo, C.J. Doonan, H. Furukawa, K. Oisaki, O.M. Yaghi, "Reticular Synthesis of Mesoporous Covalent Hydrazone Frameworks," *J. Am. Chem. Soc.*, **2011**, *133*, 11478-11481.

4. J.L. Mendoza-Cortes, S.S. Han, W.A. Goddard, "High H_2 Uptake in pure, Li-, Na-, K-metalated Covalent Organic Frameworks and Metal Organic Frameworks at 298 K," submitted.

5. F.J. Uribe-Romo, "Design, synthesis and powder diffraction crystallography of porous framework materials", University of California - Los Angeles, 2010, Ph. D. thesis.

References

1. A.P. Côté, A.I. Benin, N.W. Ockwig, M. O'Keeffe, A.J. Matzger, O.M. Yaghi, *Science*, **2005**, *310*, 1166.

2. J.R. Hunt, C.J. Doonan, J.D. LeVangie, A.P. Côté, O.M. Yaghi, *J. Am. Chem. Soc.*, **2008**, *130*, 11872.

3. F.J. Uribe-Romo, J.R. Hunt, H. Furukawa, C. Klock, M. O'Keeffe, O.M. Yaghi, *J. Am. Chem. Soc.*, **2009**, *131*, 4570.

4. A.P. Côté, H.M. El-Kaderi, H. Furukawa, J.R. Hunt, O.M. Yaghi, *J. Am. Chem. Soc.*, **2007**, *129*, 12914.

5. A. Phan, C.J. Doonan, F.J. Uribe-Romo, C.B. Knobler, M. O'Keeffe, O.M. Yaghi, *Acc. Chem. Res.*, **2009**, *43*, 58.

6. K.S. Park, Z. Ni, A.P. Côté, J.Y. Choi, R.D. Huang, F.J. Uribe-Romo, H.K. Chae, M. O'Keeffe, O.M. Yaghi, *Proc. Natl. Acad. Sci. U.S.A.*, **2006**, *103*, 10186.

IV.C.3 Multiply Surface-Functionalized Nanoporous Carbon for Vehicular Hydrogen Storage

P. Pfeifer (Primary Contact), C. Wexler, P. Yu, G. Suppes, F. Hawthorne, S. Jalisatgi, M. Lee, D. Robertson
University of Missouri
223 Physics Building
Columbia, MO 65211
Phone: (573) 882-2335
E-mail: pfeiferp@missouri.edu

DOE Managers
HQ: Ned Stetson
Phone: (202) 586-9995
E-mail: Ned.Stetson@ee.doe.gov
GO: Jesse Adams
Phone: (720) 356-1421
E-mail: Jesse.Adams@go.doe.gov

Contract Number: DE-FG36-08GO18142

Subcontractor:
Midwest Research Institute, Kansas City, MO

Project Start Date: September 1, 2008
Project End Date: January 31, 2013

Fiscal Year (FY) 2011 Objectives

- Fabricate high-surface-area, multiply surface-functionalized carbon ("substituted materials") for reversible hydrogen storage with superior storage capacity (strong physisorption).
- Characterize materials and storage performance. Evaluate efficacy of surface functionalization, experimentally and computationally, for fabrication of materials with deep potential wells for hydrogen sorption (high binding energies).
- Optimize gravimetric and volumetric storage capacity by optimizing pore architecture and surface composition ("engineered nanospaces").

Technical Barriers

This project addresses the following technical barriers from the Hydrogen Storage section of the Fuel Cell Technologies Program Multi-Year Research, Development and Demonstration Plan:

(A) System Weight and Volume

(B) System Cost

(E) Charging/Discharging Rates

(J) Thermal Management

(P) Lack of Understanding of Hydrogen Physisorption and Chemisorption

Technical Targets

This project aims at the development of surface-engineered carbons, made from corncob or other low-cost raw materials, which simultaneously host high surface areas, created in a multi-step process, and a large fraction of surface sites with high binding energies for hydrogen, created by surface functionalization with boron, iron, and lithium. Targets are surface areas in excess of 4,500 m^2/g, average binding energies in excess of 12 kJ/mol, and porosities below 0.8, toward the design of materials that meet the following 2015 DOE hydrogen storage targets:

- Gravimetric storage capacity: 0.055 kg H_2/kg system
- Volumetric storage capacity: 0.040 kg H_2/liter system

FY 2011 Accomplishments

- Manufactured boron-substituted carbon by deposition and thermolysis of $B_{10}H_{14}$ on high-surface-area activated carbon, with B:C = 7-10 wt%, without compromising high surface areas (≥2,100 m^2/g). Developed plans for automated apparatus.
- Maintained an oxygen- and water-free environment for the manipulation, characterization, and analysis of boron-substituted carbon, which was fundamental for the observation of enhanced hydrogen sorption characteristics.
- Observed an increase of 30% in areal excess adsorption (excess adsorption per surface area) of hydrogen, at $T = 303$ K and $P = 200$ bar, on boron-substituted carbon (B:C = 8.6 wt%) compared to its boron-free precursor. The increase in excess adsorption at high temperature and pressure demonstrates an increase in average binding energy due to boron substitution.
- Optimized pore structure of undoped carbons by varying the KOH:C ratio and temperature during activation. High KOH:C and T lead to larger surface area, pore volume, and porosity, but a reduced fraction of narrow pores. Optimal conditions for hydrogen storage are observed for activation with a 3.5 KOH:C ratio at 800°C, which represents the best balance between increasing the pore volume and loss of high-binding-energy sites in narrow pores.
- At low KOH:C and T, the pore structure is consistent with large graphene sheets closely stacked, whereas for more aggressive activation conditions the pores are formed by small graphene sheets loosely stacked (surface areas larger than that of graphene, 2,600 m^2/g).

- Observed that carbon monoliths formed by activated carbon and polyvinylidine chloride (PVDC) binder outperforms powder samples at room temperature, consistent with findings that pyrolyzed PVDC is an attractive material for hydrogen storage (sample HS;0B) [1].
- Developed and applied a consistent method for the determination of isosteric heat of adsorption from the Clausius-Clapeyron equation. Validated by microcalorimetry measurements. The thermodynamic requirement that the isosteric heat cannot increase with increasing pressure and coverage gives a lower bound for the adsorbed film thickness (or volume).
- Established, via Fourier-transform infrared spectroscopy (FTIR), the presence of B-C bonds in boron-doped carbons (1,022 cm^{-1} line).



Introduction

High-surface-area carbons from corncob, as developed by our team, show considerable promise for reversible onboard storage of hydrogen at high gravimetric and volumetric storage capacity. An earlier carbon exhibited a gravimetric storage capacity of 0.11 kg H_2/kg carbon at 80 K and 50 bar. This project is a systematic effort to achieve comparable results at 300 K, by increasing surface areas from currently ~3,000 m^2/g to ~6,000 m^2/g, and substituting carbon with boron and other elements that increase the binding energy for hydrogen (electron donation from H_2 to electron-deficient B, and other charge-transfer mechanisms). Earlier high surface areas and high binding energies were hosted by sub-nm pores ("nanopores") in narrowly spaced "stacks of graphene sheets." New high-surface-area, boron-substituted materials are manufactured by thermolysis of volatile boron carriers in pores of stacks of graphene sheets. New surface area, created by fission tracks from boron neutron capture, in stacks of boron-substituted graphene sheets, or created in the form of stacks of small graphene sheets with large ratio of edge sites to in-plane sites, may add as much as another 3,000 m^2/g.

Approach

The approach is an integrated fabrication, characterization, and computational effort. Structural characterization includes determination of surface areas, pore-size distributions, and pore shapes. Storage characterization includes measurements of hydrogen sorption isotherms and isosteric heats. Computational work includes adsorption potentials and simulations of adsorbed films for thermodynamic analysis of experimental isotherms. Comparison of computed and experimental isotherms validates theoretical adsorption potentials and experimental structural data.

Results

Observation of Enhanced Hydrogen Sorption on Boron-Doped Samples

Upgrades to the laboratory during the current year allowed us to process for the first time all boron-doped samples in oxygen- and water-free conditions. Activated carbon samples were degassed and coated with a monolayer or less of decaborane, $B_{10}H_{14}$, by liquid/vapor deposition (Figure 1), followed by pyrolysis and high-temperature annealing. This process creates the necessary boron substitution (FTIR indicates B-C bonds consistent with B-substitution in the C matrix). Table 1 shows selected samples manufactured and their characteristics. Hydrogen sorption isotherms for selected samples are shown in Figure 2. For B:C = 8.6 wt%, the areal excess adsorption at 303 K and 200 bar is 30% higher than on undoped material. The fact that the increase is observed at high temperature and pressure demonstrates an increase in the average binding energy, not highest binding energy. This is consistent with that sample 3K-H60 (I,A) was doped by Method I (liquid deposition), which deposits significant amounts of boron only in large pores. An increase in H_2 sorption is not observed at 90 K because unblocked pores in undoped material support H_2 multilayers, not available in the doped material. O_2-free conditions were crucial for increased adsorption on B-doped samples (prior to the laboratory upgrade, no increase in H_2 sorption was observed in B-doped samples that had been exposed to air).

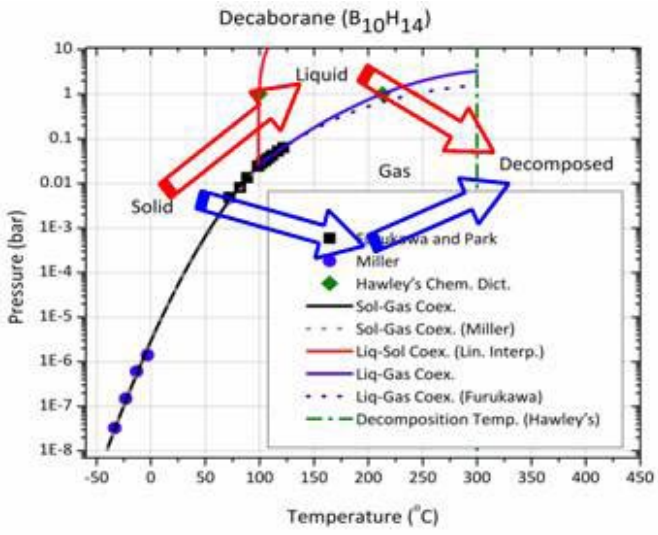


FIGURE 1. Schematic representation of deposition methods I (red, "liquid phase") and III (blue, "vapor phase"). Higher deposition rates are possible with Method I, but since the process involves liquid decaborane, pore blocking may occur, as indicated by the reduction in Brunauer-Emmett-Teller (BET) surface area (Table 1).

TABLE 1. Sample characteristics of boron-doped carbons. B:C concentration was determined by prompt gamma neutron activation analysis.

Sample	Precursor	B:C (wt%)	Σ_{N2} (m^2/g)	Φ_{N2}	Notes
3K 3/3/10-B	Self	0.0	2,700	0.77	
3K-H30 (I,A)	3K 3/3/10-B	8.4	2,300	0.75	B-H decomp., 600°C
3K-H31 (III,A)	3K 3/3/10-B	10.0	2,000	0.73	B-H decomp., 600°C
3K 3/3/10-B degassed @ 600°C	Self	0.0	2,600	0.76	
3K-H60 (I,A)	3K 3/3/10-B degassed @ 600°C	8.6	2,100	0.73	B-H decomp., 600°C
3K-H60 (I,B)	3K 3/3/10-B degassed @ 600°C	6.7	2,100	0.72	B-H decomp., 1,000°C

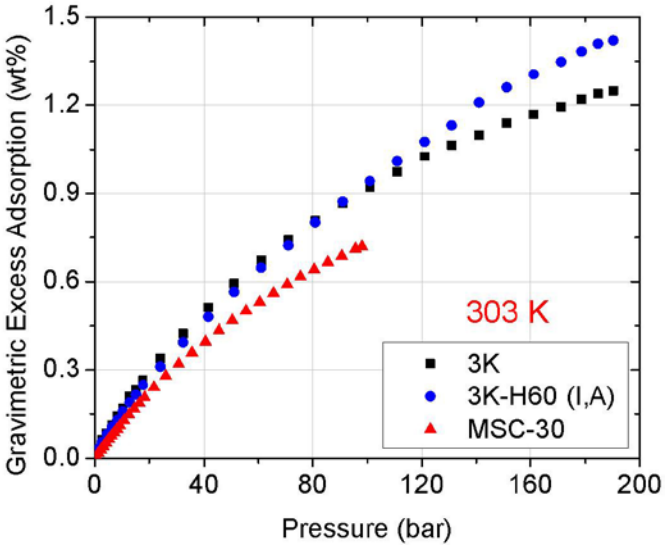


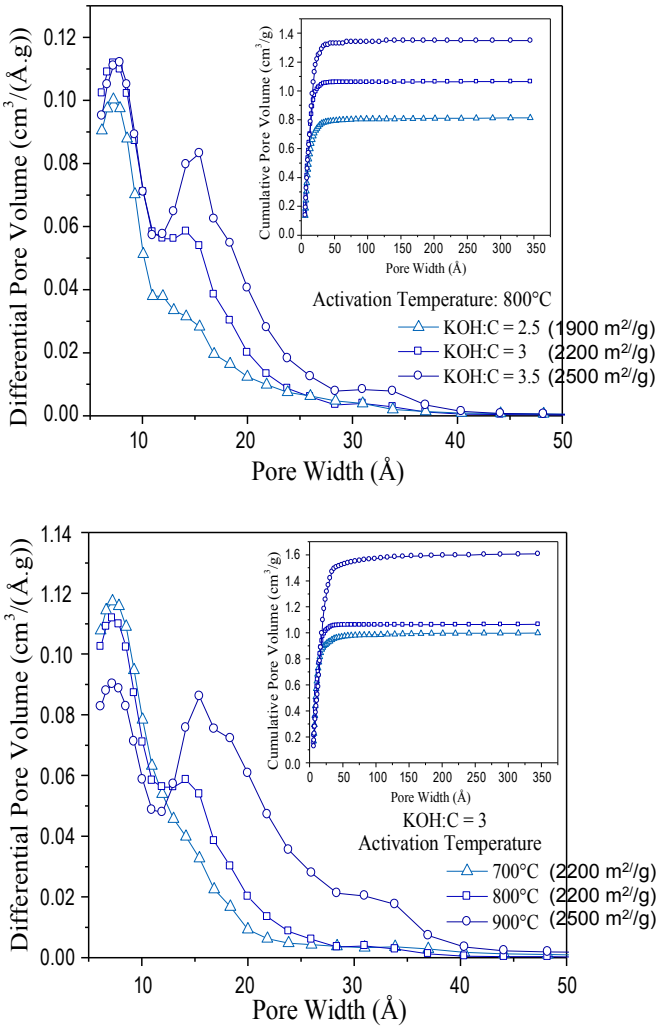
FIGURE 2. Hydrogen sorption on boron-doped sample 3K-H60 (I,A), its boron-free precursor (3K 3/3/10-B), and reference sample MSC-30 (Maxsorb, Kansai Coke and Chemicals, Ltd). Experimental results are from 4-9 adsorption/desorption isotherms and are highly reproducible. Areal excess adsorption on 3K-H60 (not shown) is 30% higher than on 3K.

Optimization of Pore Geometry

Efforts to optimize the pore geometries of carbon precursors for hydrogen sorption were undertaken as follows. Ground corncob is soaked with phosphoric acid and charred at 480°C under nitrogen. The carbon is then activated by KOH in an oven, resulting in oxidation of some carbon by oxygen, and penetration of metallic potassium into the graphitic lattice. The intercalated potassium separates the graphene sheets/flakes and results in the formation of a highly porous material upon removal of the alkali. The resulting structure can be controlled by the weight ratio of KOH:C and activation temperature. Table 2 shows sample characteristics and H_2 sorption for various samples activated under different KOH:C ratios and temperatures (Figures 3-4). High KOH:C and temperature lead to larger surface area, pore volume, and porosity, but at the cost of a reduction of fraction of narrow pores. Optimal conditions for hydrogen storage are observed for activation with a KOH:C of 3.5 ratio at 800°C, which represents the best balance between a large pore volume and a small loss of high-binding-energy sites in narrow pores. At low KOH:C and temperature, the pore structure is consistent with large graphene sheets closely stacked, whereas for more aggressive

TABLE 2. Sample characteristics of carbon precursors. Names indicate KOH:C weight ratio and temperature during activation (e.g., 3K 900°C was activated with KOH:C = 3 at 900°C). Specific surface areas, Σ_{N2}, from BET analysis of N_2 adsorption isotherms at 77 K and relative pressures 0.01-0.03, are rounded to nearest hundred. Porosities, Φ_{N2}, were determined from N_2 adsorption at 77 K at relative pressure 0.995. Values for gravimetric excess adsorption are presented for P = 100 bar at 80 K, 194 K, and 303 K. Best performances in each column are highlighted in bold face.

Sample	Σ_{N2} (m^2/g)	Φ_{N2}	Grav. Exc. Ads. 100 bar, 303 K (wt%)	Grav. Exc. Ads. 100 bar, 194 K (wt%)	Grav. Exc. Ads. 100 bar, 80 K (wt%)
2.5K 800°C	1,900	0.69	0.53	1.62	N/A
3K 700°C	2,200	0.65	0.67	2.01	N/A
3K 800°C	2,200	0.78	0.74	2.12	4.47
3K 900°C	2,500	0.78	**0.82**	**2.28**	4.68
3K 1000°C	2,000	0.78	0.60	1.80	4.05
3.5K 700°C	2,000	0.70	0.63	1.85	4.42
3.5K 800°C	2,500	0.75	**0.84**	**2.18**	**5.15**
3.5K 900°C	2,500	0.78	0.70	2.14	**5.18**
4K 800°C	2,600	0.81	0.56	N/A	5.02
5K 790°C	2,500	0.79	0.65	N/A	4.03



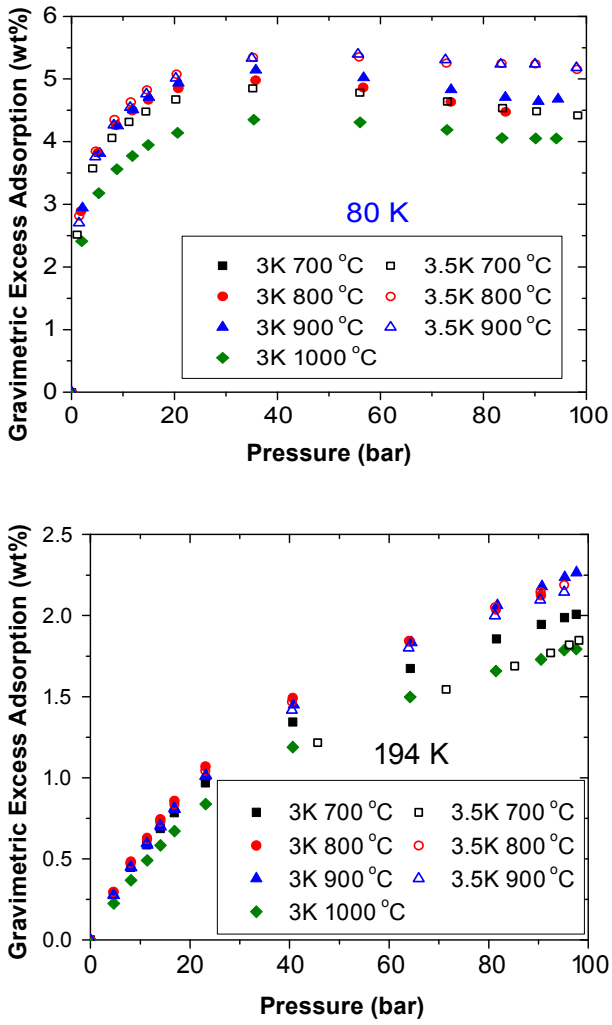


FIGURE 3. Differential and cumulative pore-size distribution from nitrogen adsorption for various activated carbons. Top: variation of KOH:C ratio at constant activation temperature. Bottom: variation of activation temperature at constant KOH:C ratio.

FIGURE 4. Gravimetric excess adsorption of H_2 on carbons produced with different KOH:C ratios and activation temperatures. Results are shown at T = 80 K, 194 K (dry-ice temperature), and 303 K.

activation conditions the pores are formed by small graphene sheets loosely stacked (edge sites generate surface areas larger than that of graphene, 2,600 m^2/g).

Comparison of Powders and Monoliths (Briquettes)

One method to enhance the volumetric storage capacity is to increase the density the activated carbon. We have investigated this densification by "briquetting," i.e., the production of monoliths. Powdered activated carbon was pressed into briquettes at 1,000 bar using PVDC as a binder (PVDC:carbon = 25-30 vol%), followed by pyrolysis of PVDC. The mass of a typical briquette was 70-100 g. Hydrogen sorption on briquettes was measured volumetrically for entire briquettes on a custom instrument with a 0.5-liter sample chamber ("Hydrogen Test Fixture,"

TABLE 3. Comparison of powdered activated carbon and three carbon monoliths (briquettes). All hydrogen adsorption data are at room temperature, 297 K, and 100 bar. Gravimetric and volumetric storage capacities were calculated based on intragranular porosity (from N_2 adsorption at 77 K) for powders, and on intergranular porosity (from bulk density) for briquettes, respectively [2]. All hydrogen measurements on briquettes were performed on the HTF. Best performances are highlighted in bold face.

Sample	Σ_{N2} (m^2/g)	Intragranular (intergranular) Density (g/cm^3)	Φ_{N2}	Grav. Exc. Ads. (wt%)	Grav. Storage Cap. (wt%)	Vol. Storage Cap. (g/L)
2.5K powder	1,900	0.62	0.69	0.53	1.3	8.2
3K powder	2,600	0.44	0.78	**0.93**	2.2	9.6
4K powder	2,600	0.38	0.81	0.56	2.1	7.8
MSC-30	2,600	0.42	0.79	0.72	2.3	8.8
2.5K Briquette (30% binder)	2,000	0.74 (0.70)	0.63 (0.65)	0.67	1.4	**9.7**
3K Briquette (25% binder)	1,900	0.56 (0.47)	0.72 (0.77)	0.75	2.0	9.5
4K Briquette (25% binder)	2,100	0.53 (0.37)	0.74 (0.81)	0.86	**2.6**	9.5

HTF). Measurements on the HTF were validated on the Hiden HTP-1 instrument. Table 3 shows a comparison of four activated carbon powders and three briquettes. We observe that: (a) briquetting raises the density of samples by 20-40%, relative to the powder; (b) carbon made from PVDC exhibits superior hydrogen uptake at room temperature (HS;0B; very high areal excess adsorption [1]); (c) briquettes outperform most powder samples in terms of volumetric storage capacity because low porosity gives high volumetric storage capacity; (d) all briquettes outperform MSC-30 at room temperature in terms of volumetric storage capacity and areal excess adsorption. 4K briquette outperforms MSC-30 also in terms of gravimetric storage capacity; (e) entire briquettes, measured on the HTF, lead to robust averages over possible sample inhomogeneities. A 10-liter tank, recently completed [3], will permit studies of flow rates, thermal management, and operation at dry-ice temperature (194 K).

Observation of B-C Bonds by Fourier-Transform Infrared Spectroscopy

FTIR spectroscopy was used in transmission mode to identify the presence of boron-carbon bonds in boron-doped activated carbon. An infrared spectrum represents a fingerprint of a sample with absorption peaks, which correspond to vibrational frequencies of structural units making up the material. The samples were prepared using KBr pellets with a sample/KBr ratio of 0.033 wt%. Each FTIR spectrum was collected as an average of 32 interferometric scans with a spectral resolution of 1 cm^{-1}. An aperture was used to limit the sampling size and select the sampling area (>10 µm). Figure 5 shows the microscopic FTIR spectra for boron-free and boron-containing carbons. The FTIR spectrum of boron-free sample 3K shows only carbon-related bands, including the C-OH stretch mode at 3,429 cm^{-1}, C-OH bend mode at 1,630 cm^{-1}, C=C double-bond stretch mode at 1,430 cm^{-1}, and C-O bond stretch mode at 1,050 cm^{-1}. B-C bonds in boron-doped samples, 3K-H30 (not shown) and 3K-H31 (Figure 5), were identified by comparing spectra with the spectrum of an activated boron carbide (not shown), a reference with the 1,022 cm^{-1} band characteristic of B-C bonds. The band at 1,022 cm^{-1} demonstrates the successful creation of boron-carbon bonds. Samples 3K-H30 and 3K-31, in addition to exhibiting C-OH and C-O modes seen in boron-free sample 3K, also exhibit a B-OH stretch mode at 3,220 cm^{-1} and B-O stretch mode 1,327 cm^{-1}, consistent with the fact that the samples were not kept in an oxygen- and water-free environment for the FTIR experiment. To the best of our knowledge, this is the first time that the existence of B-C bonds in boron-doped carbons (liquid/vapor deposition of $B_{10}H_{14}$) has been observed and, hence, the successful incorporation of boron in the carbon matrix has been demonstrated.

Conclusions and Future Directions

- Observed enhanced hydrogen physisorption in boron-doped samples, enabled by equipment upgrades, with operations in an inert atmosphere.
- Optimized pore structure of samples by control of KOH:C ratio and temperature during activation.
- Performed comparison of powders and monoliths: increase in room-temperature performance of monoliths attributed to presence of pyrolized PVDC [1].
- Established B-C bonds by means of Fourier-transform infrared spectroscopy.
- Future work: (a) Continue production and characterization of B-doped samples, using $B_{10}H_{14}$ as boron carrier; investigate chemical pathways during the pyrolysis of $B_{10}H_{14}$ and annealing (mass spectroscopy of decomposition products) and effects on H_2 storage; optimize pathway of vapor/liquid deposition of $B_{10}H_{14}$; raise surface area of doped samples by removal of B via high-temperature reaction with H_2; optimize annealing. (b) Measure FTIR spectra of B-doped samples systematically; find number of B-C bonds per surface area. (c) Characterize B-doped materials produced from BCl_3 and compare with B-doping from

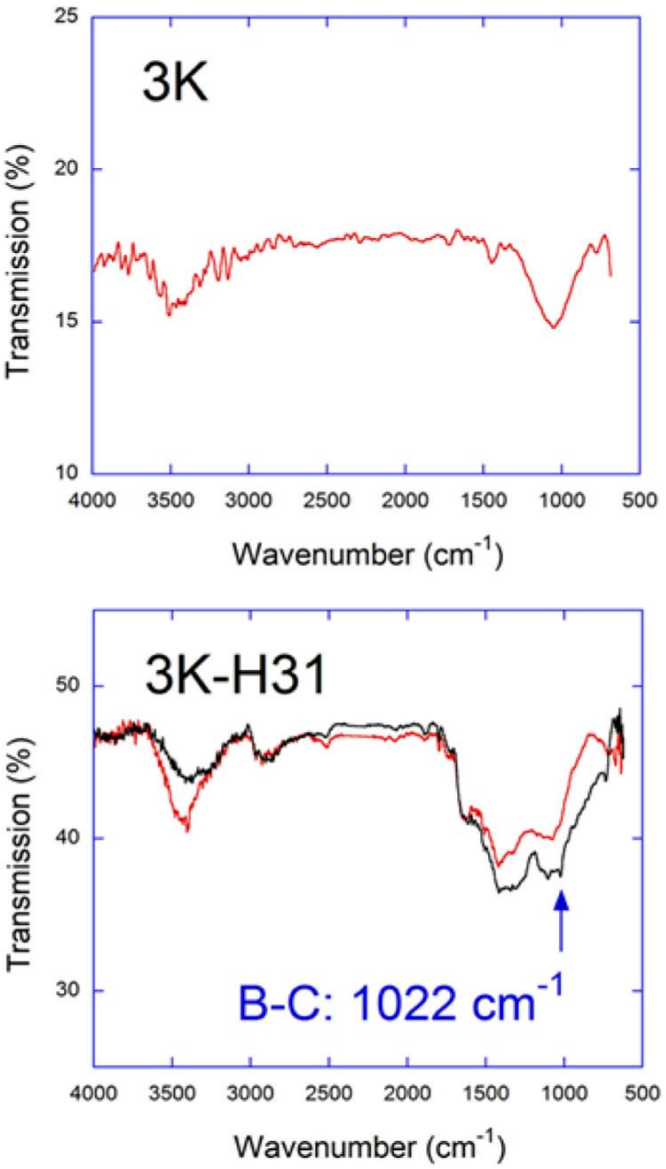


FIGURE 5. Microscopic FTIR spectra for samples 3K 3/3/10-B (boron-free) and 3K-H31 (III,A) (boron-doped). Each spectrum was obtained by limiting and selecting the sampling area through an aperture of an optical microscope (FTIR microscopy). The peak at 1,022 cm^{-1} is due to the B-C bond. The two spectra in 3K-H31 (III,A) correspond to different sampling locations.

$B_{10}H_{14}$. (d) Perform numerical simulations to investigate edge adsorption in finite pores, and compare results with experimental results on carbons activated at high KOH:C and high *T*. Determine pore structure and energetics from experimental H_2 isotherms. (e) Manufacture B-doped monoliths; test in 0.5-liter HTF and 10-liter tank; study flow rate and thermal management issues.

FY 2011 Publications/Presentations

1. R. Olsen, "Investigations of Novel Hydrogen Adsorption Phenomena." Ph.D. Dissertation, University of Missouri (2011).

2. C. Wexler, R. Olsen, P. Pfeifer, B. Kuctha, L. Firlej, Sz. Roszak, "Numerical Analysis of Hydrogen Storage in Carbon Nanopores." Int. J. Mod. Phys. B **24**, 5152-5162 (2010).

3. R.J. Olsen, L. Firlej, B. Kuchta, H. Taub, P. Pfeifer, and C. Wexler, "Sub-Nanometer Characterization of Activated Carbon by Inelastic Neutron Scattering." Carbon **49**, 1663-1671 (2011).

4. B. Kuchta, L. Firlej, S. Roszak, and P. Pfeifer, "A Review of Boron Enhanced Nanoporous Carbons for Hydrogen Adsorption: Numerical Perspective." Adsorption **16**, 413-21 (2010).

5. C. Wexler, P. Pfeifer, M. Kraus, M. Beckner, J. Romanos, D. Stalla, T. Rash, H. Taub, P. Yu, R. Olsen, and J. Ilavsky, "Characterization of Activated Carbon at the sub-nm Scale via Adsorption, TEM, FTIR, IINS and SAXS; and Application towards Optimization of H_2 Storage." *9th International Symposium on the Characterisation of Porous Solids (COPS 9)*, DECHEMA, Dresden, Germany, June 2011.

6. P. Pfeifer, C. Wexler, G. Suppes, F. Hawthorne, S. Jalisatgi, M. Lee, and D. Robertson, "Multiply Surface-Functionalized Nanoporous Carbon for Vehicular Hydrogen Storage." *2011 DOE Hydrogen Program Annual Merit Review*, Arlington, VA, May 9–13, 2011.

7. C. Wexler, "A Nanoporous Carbon 'Sponge' for Hydrogen Storage." Physics Colloquium, University of Buffalo, Buffalo, NY, April 2011.

8. Plus: 3 posters at various conferences and 7 contributed oral presentations at the APS March Meeting.

9. R. Olsen and C. Wexler, "Explaining the Hydrogen Adsorption of a Carbon Adsorbent Manufactured by the Pyrolosis of Saran." Physics Colloquium, University of Northern Iowa, Cedar Falls, IA, January 2011.

References

1. P. Pfeifer *et al.*, In: *DOE Hydrogen Program, FY 2010 Annual Progress Report*, ed. by S. Satyapal (U.S. Department of Energy, Washington, D.C., 2011), p. 474-480.

2. P. Pfeifer *et al.*, In: *DOE Hydrogen Program, FY 2009 Annual Progress Report*, ed. by S. Satyapal (U.S. Department of Energy, Washington, D.C., 2009), p. 646-651.

3. Work performed under a different project.

IV.C.4 New Carbon-Based Porous Materials with Increased Heats of Adsorption for Hydrogen Storage

Randall Snurr (Primary Contact), Joseph Hupp, Mercouri Kanatzidis, SonBinh Nguyen
Northwestern University (NU)
2145 Sheridan Road
Evanston, IL 60208
Phone: (847) 467-2977
E-mail: snurr@northwestern.edu

DOE Managers
HQ: Carole Read
Phone: (202) 586-3152
E-mail: Carole.Read@hq.doe.gov
GO: Katie Randolph
Phone: (720) 356-1759
E-mail: Katie.Randolph@go.doe.gov

Contract Number: DE-FG36-08GO18137/A001

Project Start Date: September 1, 2008
Project End Date: August 31, 2012

Fiscal Year (FY) 2011 Objectives

Develop new materials to meet DOE gravimetric and volumetric targets for hydrogen storage:

- Develop and optimize strategies for introducing cations into metal-organic frameworks (MOFs).
- Synthesize new polymeric-organic frameworks (POFs) that contain cations.
- Use computational modeling to understand existing materials and design new materials for hydrogen storage.

Technical Barriers

This project addresses the following technical barriers from the Hydrogen Storage section of the Fuel Cell Technologies Program Multi-Year Research, Development and Demonstration Plan:

(A) System Weight and Volume
(E) Charging/Discharging Rates
(P) Lack of Understanding of Hydrogen Physisorption and Chemisorption

Technical Targets

TABLE 1. Progress towards Meeting Technical Targets for Hydrogen Storage

Characteristic	2015 Targets	NU 2011 Status
System Gravimetric Capacity	0.055 kg H_2/kg system at ambient temperature and 100 bar	0.14 kg H_2/(kg sorbent + H_2) at 77 K and 70 bar
System Volumetric Capacity	0.040 kg H_2/L system at ambient temperature and 100 bar	0.045 kg H_2/L sorbent at 77 K and 70 bar

FY 2011 Accomplishments

- Computationally screened MOFs functionalized with Li, Mg, Mn, Ni, and Cu alkoxides for their deliverable hydrogen storage capacity and found that Mg-alkoxide is the most promising.
- Synthesized a MOF containing protected catechol groups and investigated methods for deprotection and introduction of Mg^{2+} to form the alkoxide.
- Developed a new class of POFs based on click chemistry, with surface areas up to 1,440 m^2/g.
- Developed POFs based on condensation of melamine and other building blocks and successfully incorporated up to 14 wt% Mg.



Introduction

One option for storing hydrogen on vehicles is to use tanks filled with porous materials that act as "sponges" to take up large quantities of hydrogen without the need for extremely high pressures. The materials must meet many requirements to make this possible. This project is developing two related classes of porous materials to meet these requirements. All materials are synthesized from molecular constituents in a building-block approach. This allows us to create a wide variety of materials in a tailorable fashion. The materials have extremely high surface areas, to provide many locations for hydrogen to adsorb. In addition, they are designed to contain cations that create large electric fields to bind hydrogen strongly but not too strongly.

Approach

The approach in this project is to introduce cations into MOFs and POFs to increase the hydrogen heats of adsorption, which will, in turn, increase the amount of

hydrogen that can be stored near room temperature. Many MOFs have enough surface area to meet the DOE hydrogen storage targets if the entire surface were covered with a monolayer of hydrogen. However, at room temperature, the energetic interactions between hydrogen and the surfaces are too weak to bind hydrogen. Thus, we are focused on increasing these energetic interactions. A variety of synthetic chemistries are being explored to increase the chances of success. In addition, molecular modeling is used to help explain experimental observations and provide guidance to the synthetic efforts.

Results

In FY 2010, we had developed a model for simulating hydrogen uptake in MOFs containing alkoxide groups. Briefly, second-order Moller-Plesset perturbation theory calculations with a large basis set (6-311+G**) were performed for a hydrogen molecule in ~200 different geometries near the alkoxide group, and these energies were fit with a combined Morse + Coulomb + Lennard-Jones potential. In FY 2011, we used this model in grand canonical Monte Carlo (GCMC) simulations to explore metal alkoxide functionalization for improving H_2 storage in isoreticular metal organic framework (IRMOF)-1, IRMOF-10, IRMOF-16, UiO-68, and UMCM-150, as some representative MOF structures [1]. We examined functionalization with lithium, magnesium, manganese, nickel, and copper alkoxides. We showed that lithium and magnesium alkoxides physically bind H_2 and manganese, nickel, and copper alkoxides chemically bind H_2. Hydrogen binding energies calculated with quantum mechanics are -10, -22, -20, -78, and -84 kJ mol^{-1}, respectively, for the first hydrogen molecule. Of these, lithium and manganese alkoxides bind H_2 too weakly to enhance adsorption at ambient temperature, even at 100 bar. Owing to the strong binding energies, Ni and Cu exhibit high uptake at low pressure, but metal alkoxide sites saturate at pressures as low as 1 bar. They thus exhibit poor deliverable capacities (calculated here as the wt% H_2 at 100 bar minus the wt% H_2 at 2 bar). The deliverable capacities from the simulations are shown in Figure 1 for MOFs with one functional group per linker. Magnesium alkoxide exhibits low uptake at low pressure and high uptake at high pressure and is a promising functional group for enhanced ambient-temperature hydrogen storage in all MOFs studied.

Additionally, we explored the effect of the number of alkoxide groups per MOF linker on hydrogen adsorption and the enthalpy of adsorption. We found that increasing the density of functional groups leads to an increase in hydrogen adsorption for a Mg-alkoxide-functionalized MOF but not for a Mn-alkoxide-functionalized MOF. The behavior can be explained by examining the enthalpies of adsorption in the different materials. These results show that increasing the number of alkoxide groups per linker significantly enhances the H_2 uptake and is thus a promising strategy for improving H_2 storage, but the strategy must be focused on the right metals.

Quantum mechanical results have also provided information on the nature of the hydrogen interactions

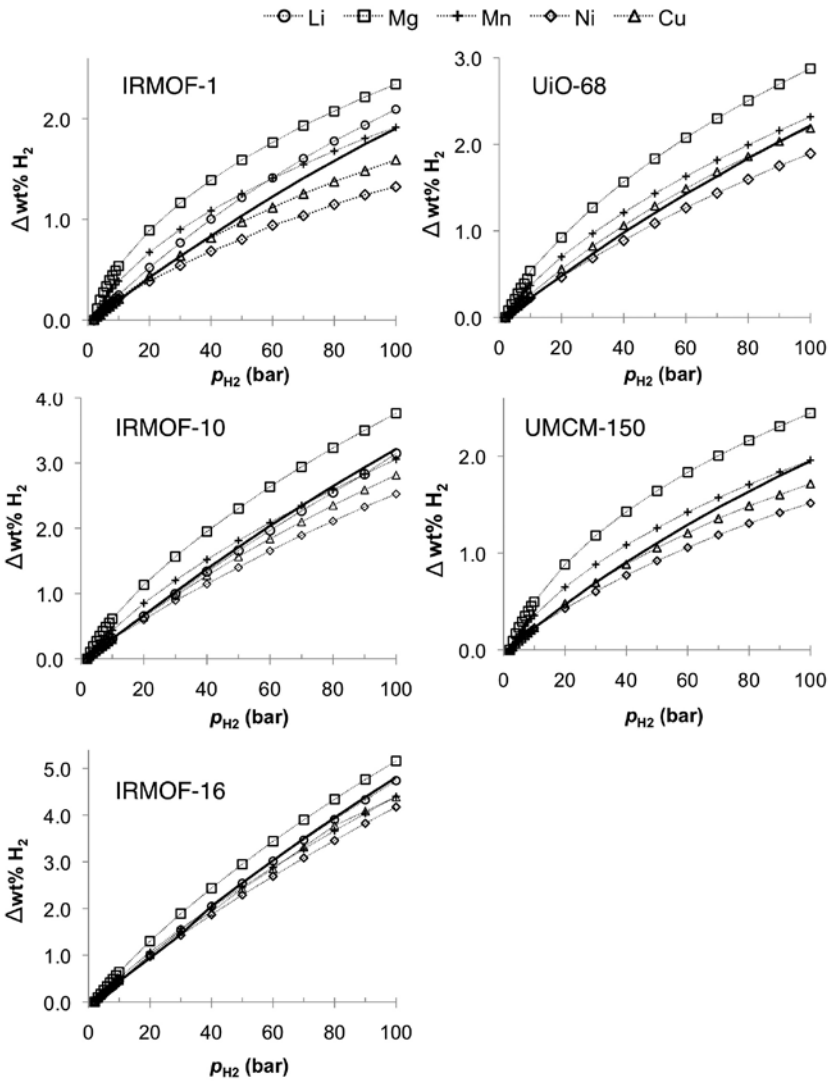


FIGURE 1. Deliverable hydrogen storage capacity [Δwt% = wt%(p_{H2}) – wt%(2 bar)] as predicted by GCMC simulations for metal alkoxide functionalized MOFs at 243 K. The MOFs are functionalized with one alkoxide site per linker. Deliverable capacities for unfunctionalized MOFs are depicted by thick solid lines without symbols.

with the exposed metal sites. (See Figure 2.) The average and differential hydrogen binding energies were also calculated for up to five H_2 molecules per metal atom. Results are shown in Figure 3. The binding energy on Li remains relatively constant for up to 3 H_2 molecules and then starts to weaken, whereas the binding energy on Mg weakens between $n = 1$ and $n = 2$ and then levels off before weakening again at $n = 4$. The binding energy to Mn alkoxide decreases between $n = 1$ and $n = 2$ and then remains relatively constant up to $n = 5$. (These trends are more easily seen in the differential binding energies of Figure 3.) In contrast, Ni and Cu bind H_2 very strongly initially, but the binding energies weaken dramatically as additional H_2 molecules adsorb.

Motivated by the modeling work, the experimental effort on MOFs this year has focused on synthesizing MOFs with divalent cations, especially Mg^{2+}, bound through a catecholate functionality. We synthesized a candidate MOF strut featuring a protected catechol group and successfully synthesized a MOF containing the strut in protected form. Suitable crystals for X-ray examination are in hand and awaiting analysis in our centralized X-ray characterization facility. Deprotecting the catechols once they are built into MOFs has proven challenging. We have tested several techniques. Preliminary studies (mainly with organic polymer analogues) indicate that high yields for deprotection are achievable with at least one of the techniques.

We have synthesized additional quantities of MOF NU-100, which will be sent to the National Renewable Energy Laboratory (NREL) for corroboration of our findings of high hydrogen uptake that were reported last year [2]. We also worked with NREL on validation and calibration of our own high-pressure sorption instrument.

In previous years of the project, we had developed microporous POFs using Schiff base and Bakelite chemistries. During FY 2011, we also reported a third class of highly stable, microporous POFs using "click chemistry." They are synthesized via copper-catalyzed alkyne-azide coupling between two rigid tetrahedral building blocks. We investigated the effect of the amount of the reducing agent (sodium azide) used on the pore properties of these "click-based" POFs. The highest surface area achieved for this type of POF was 1,440 m^2g^{-1} and the hydrogen uptake was also promising at low pressure (up to 1.6 wt% at 1 bar). Some effort this year was devoted to further optimizing the reaction conditions for the POF syntheses to enhance the microporosity and hydrogen uptake in these materials.

We have also attempted to attach metal cations in the phloroglucinol and "click-based" POFs to increase the hydrogen adsorption enthalpy. For example, phloroglucinol POFs have large numbers of OH groups that can react with alkyl metal compounds to produce metal functionalized POFs. We employed a variety of metal compounds and synthetic strategies to accomplish the metal introduction. In one case, we used POFs based on condensation reaction between melamine and different aromatic aldehyde

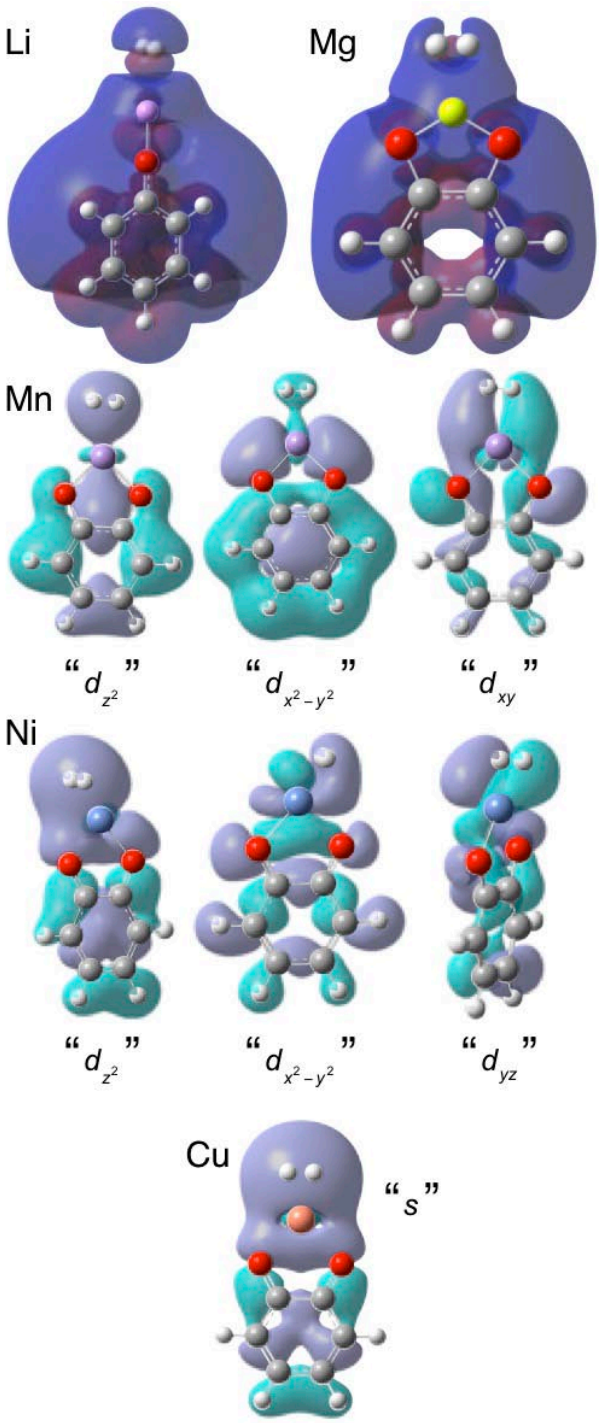


FIGURE 2. Binding properties for H_2 to metal alkoxide benzenes from quantum chemical calculations. (Top row) Charge density differences indicate Li and Mg polarize H_2, resulting in charge density accumulation between the metal cations and H_2. Regions of charge density accumulation and depletion are red and blue, respectively. (Second row) Molecular orbitals for H_2 adsorption to Mn alkoxide benzene indicate a variety of interactions between H_2 $1\sigma^*$ and Mn d orbitals. H_2 is strongly polarized and can interact with both spherical (d_{z2}) and nonspherical (d_{xy}) orbitals. (Third row) Nickel alkoxide benzene has a variety of d orbitals for interaction with H_2 $1\sigma^*$, and a representative subset is shown here. (Bottom row) Copper alkoxide benzene forms a strong σ bond with H_2.

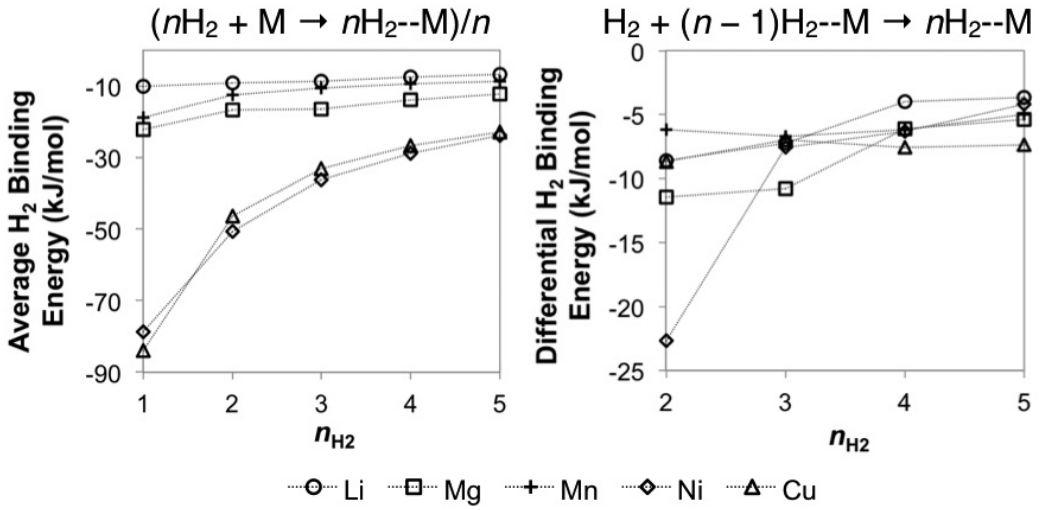


FIGURE 3. Average (left) and differential (right) binding energies for H_2 to metal alkoxide benzenes for 1–5 H_2 molecules, from quantum chemical calculations. Note that the average and differential energies are equal when $n = 1$.

building blocks with sites for metal binding. In our initial experiments we have successfully incorporated high amounts of metals like manganese (Mn) and magnesium (Mg) in our POFs (Table 2). Our next step is to study the effect of metal incorporation on the hydrogen uptake and the heats of adsorption in these POFs.

TABLE 2. Metal Loadings in POFs 2a and 2b

POF	Metal Source	wt% metal
POF 2a	$Mn(CH_3COO)_2$	30 wt% Mn
POF 2a	$Mg(CH_3)_2$	14 wt% Mg
POF 2b	$Mn(CH_3COO)_2$	23 wt% Mn

Conclusions and Future Directions

Conclusions

- We computationally screened Li, Mg, Mn, Ni, and Cu alkoxide-functionalized MOFs for their deliverable hydrogen storage capacity and found that Mg-alkoxide is the most promising of these metals.
- We synthesized a MOF containing protected catechol groups and found that the deprotection and introduction of Mg^{2+} is challenging. Preliminary studies with organic polymer analogs indicate that high yields for deprotection are achievable with at least one of the techniques investigated.
- We have developed a new class of POFs based on click chemistry, with surface areas up to 1,440 m^2/g.
- We have developed POFs based on condensation of melamine and other building blocks. Levels of Mg incorporation up to 14 wt% can be achieved.

Future Directions

- Finish validation (with NREL) of very high cryogenic hydrogen uptake in MOF NU-100.
- Finish optimization of deprotection strategies for introducing alkaline earth alkoxide functional groups into MOFs.
- Explore other chemistries for introducing alkaline earth alkoxide functional groups into MOFs and POFs.
- Test hydrogen uptake in recently synthesized POFs with high metal loading.
- Combine strategies for introducing cations into MOFs and POFs with strategies for producing MOFs and POFs with very large surface areas.
- Model new functionalities for introducing cations into MOFs and POFs.

FY 2011 Publications/Presentations

1. P. Pandey, A.P. Katsoulidis, I. Eryazici, Y. Wu, M.G. Kanatzidis, S.T. Nguyen, "Imine-linked microporous polymer organic frameworks," *Chem. Mater.* **22**, 4974-4979 (2010).

2. Y.-S. Bae, R.Q. Snurr, "Molecular simulations of very high pressure hydrogen storage using metal-organic frameworks," *Microporous and Mesoporous Materials* **135**, 178-186 (2010).

3. O.K. Farha, A.Ö. Yazaydin, I. Eryazici, C.D. Malliakas, B.G. Hauser, M.G. Kanatzidis, S.T. Nguyen, R.Q. Snurr, J.T. Hupp, "*De novo* synthesis of a metal-organic framework material featuring ultra-high surface area and gas storage capacities," *Nature Chem.* **2**, 944-948 (2010).

4. R.B. Getman, J.H. Miller, K. Wang, R.Q. Snurr, "Metal alkoxide functionalization in metal-organic frameworks for enhanced ambient temperature hydrogen storage," *J. Phys. Chem. C* **115**, 2066-2075 (2011).

5. P. Pandey, O.K. Farha, A.M. Spokoyny, C.A. Mirkin, M.G. Kanatzidis, J.T. Hupp, S.T. Nguyen, "A 'click-based' porous organic polymer from tetrahedral building blocks," *J. Mater. Chem.* **21**, 1700-1703 (2011).

6. A.P. Katsoulidis, M.G. Kanatzidis, "Phloroglucinol microporous polymeric organic frameworks with -OH functional groups and high CO_2 capture capacity," *Chem. Mater.*, in press.

References

1. R.B. Getman, J.H. Miller, K. Wang, R.Q. Snurr, "Metal alkoxide functionalization in metal-organic frameworks for enhanced ambient temperature hydrogen storage," *J. Phys. Chem. C* **115**, 2066-2075 (2011).

2. O.K. Farha, A.Ö. Yazaydin, I. Eryazici, C.D. Malliakas, B.G. Hauser, M.G. Kanatzidis, S.T. Nguyen, R.Q. Snurr, J.T. Hupp, "*De novo* synthesis of a metal-organic framework material featuring ultra-high surface area and gas storage capacities," *Nature Chem.* **2**, 944-948 (2010).

IV.C.5 Hydrogen Storage through Nanostructured Porous Organic Polymers (POPs)

Di-Jia Liu (Primary Contact), Shengwen Yuan, Desiree White, Alex Mason, and Briana Reprogle
Argonne National Laboratory
9700 S. Cass Ave.
Argonne, IL 60439
Phone: (630) 252-4511
E-mail: djliu@anl.gov

DOE Manager
HQ: Ned Stetson
Phone: (202) 586-9995
E-mail: Ned.Stetson@ee.doe.gov

Subcontractor:
Luping Yu and Zhuo Wang
Department of Chemistry and The James Franck Institute
The University of Chicago, Chicago, IL

Project Start Date: July 1, 2007
Project End Date: September 30, 2011

Fiscal Year (FY) 2011 Objectives

- To design, synthesize, and evaluate POPs as hydrogen storage adsorbents for transportation applications.
- To support POP development with in-depth understanding of hydrogen–adsorbent interactions through modeling/simulation and advanced characterization.

Technical Barriers

This project addresses the following technical barriers from the Hydrogen Storage section of the Fuel Cells Technologies Program Multi-Year Research, Development and Demonstration Plan:

(A) System Weight and Volume
(B) System Cost
(C) Efficiency
(D) Durability/Operability

Technical Targets

The focus of this project is to prepare new POPs as hydrogen adsorbents with improved storage capacity and heat of adsorption through rational design, guided by computational modeling and advanced characterization. It supports DOE's initiative in developing adsorption-based storage technology with high uptake capacity, reversibility, and stability. The successful outcome of the project will produce a new storage material that meets DOE 2015 targets:

- Gravimetric density: 1.8 kWh/kg
- Volumetric density: 1.3 kWh/L
- Cost: $2/kWh net

FY 2011 Accomplishments

- Successfully designed and synthesized a series of B-containing POPs with high specific surface areas (SSA) and narrow pore size distributions (PSD). Hydrogen uptake and isosteric heat of adsorption measurements found enhanced adsorption enthalpy for the POPs with higher boron-to-carbon ratio.
- Successfully designed and synthesized a series of metalloporphyrin POPs (PPOR) containing transition metals such as nickel, cobalt and iron. Excess H_2 storage capacities of 0.035 $kgH_2/(kg_{Adsorbent}+H_{2adsorbed})$ and 0.0026 $kgH_2/L_{Adsorbent}$ were achieved. Hydrogen adsorption enthalpy over PPOR was found to be dependent on the type of metal exchanged into macrocyclic ring with Ni having the highest value.
- Successfully designed and synthesized two POPs incorporated with high level transition metals through hydroxyquinoline ligation. Both Co and Ni were used for the synthesis and the adsorption enthalpy of 9.9 kJ/mol was achieved.
- Conducted measurement for hydrogen adsorption/desorption kinetics over a representative POP at both ambient and liquid nitrogen temperatures. The result indicated the surface equilibrium can generally be reached within 10 to 20 seconds.



Introduction

On-board hydrogen storage represents a critical technology for implementing H_2-powered fuel cell vehicles. To achieve a practical driving range, the storage system must meet the gravimetric and volumetric densities set by DOE. Our team addresses these challenges by exploring a new class of hydrogen adsorbent, POPs. Compared with other adsorbents, POPs have excellent thermal stability and tolerance to contaminants such as moisture. POPs also have low skeleton density and high intrinsic porosity generated by covalent bonds, capable of maintaining SSA during high pressure pelletizing for better volumetric density. Furthermore, they can be produced at a commercial scale with the existing industrial infrastructure. Significant progress has been made with the focus on improving hydrogen uptake capacity and the heat of adsorption by enhancing SSA, porosity, and surface-adsorbate interactions through rational design at the molecular level [1-5].

Approach

A key technology challenge for the physi-sorption based hydrogen storage media, in addition to capacity and cost, is the heat of adsorption which should be in the range of 15 to 20 kJ/mol for practical applications. Our design principles of improving POP's storage capacity at ambient temperature include: (a) high SSA to provide sufficient interface with H_2; (b) narrow pore diameter to enhance van der Waals interactions through confined space; and (c) "metallic" characters, either through π-conjugation or metal doping, to promote electronic orbital interactions with H_2. Since the inception of this project, we have prepared over 100 different POPs targeting to these properties, including aromatic, hetero-aromatic and transition metal (TM)-doped systems, and investigated the surface structural and chemical impacts to the adsorption enthalpy. In FY 2011, we remain focused on H_2 isosteric heat of adsorption improvement. Several new POPs were systematically designed and synthesized. One series is polycarborane POPs. We developed a synthetic strategy to successfully incorporate high level of boron in form of carborane in POPs with high SSA narrow PSD. We found clearly the adsorption enthalpy improvement through inclusion of boron. Another example is a series of TM-doped PPORs prepared via several parallel crosslinking chemistries. We successfully added three TM ions (Co^{+2}, Fe^{+3}, Ni^{+2}) into PPORs through chelation with porphyrin's N_4 macrocycle. We identified different impacts to the heat of adsorption depending on the type of TM. To increase the level of TM in POP therefore higher adsorption enthalpy, we also developed a new synthetic approach in preparing stable, porous framework through ligation between Co^{+2} or Ni^{+2} with hydroxyquinoline. We found indeed the enhanced hydrogen adsorption enthalpy over the new POP systems.

Results

From our cumulative experiences of over hundred synthesized POPs under three property categories, we conclude that the adsorbent pore size, within synthetically achievable sub-nanometer range, has relatively low influence to the hydrogen adsorption enthalpy [2]. Surface modification by introducing selected non-C main group elements or metals, on the other hand, does improve the interaction between hydrogen and POPs. Polycarborane POP represents an example of main-group elemental substitution. Boron-doped carbon cluster is known to promote non-dissociative hydrogen binding with adsorption energy of 19 kJ/mol was predicated [6]. Experimentally, improved adsorption energy was found in B-doped carbon produced by pyrolysis although the surface area was somewhat limited [7]. In our laboratory, we designed three different carborane-containing POPs, BPOP-1, 2 and 3 using trimerization and Friedel Crafts alkylation reactions. An example of the reaction scheme for BPOP-2 is shown in Figure 1. These

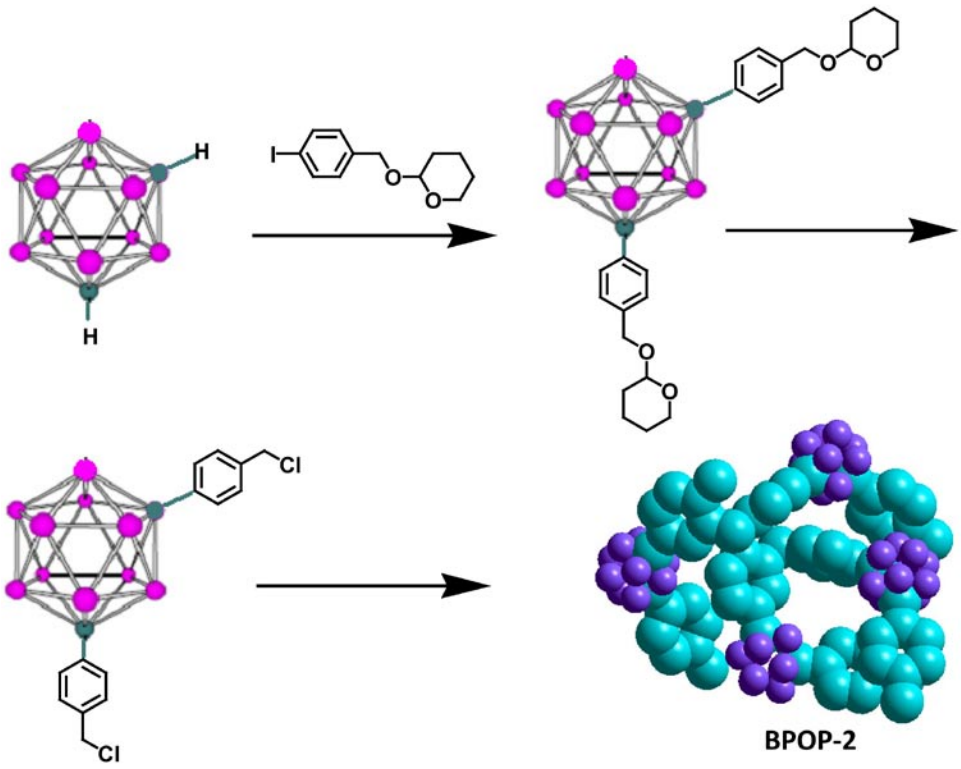


FIGURE 1. Synthetic Scheme for Preparing BPOP-2

cross-linking reactions yielded B-containing POPs with relatively high SSA from 400 to 1,100 m^2/g, narrow PSD, and perhaps most importantly, high B/C ratio in the composition. Table 1 lists the surface properties, hydrogen storage uptake and isosteric heat of adsorption obtained from N_2-Brunauer-Emmett-Teller (BET) and Sievert isotherm measurements. It demonstrates a positive correlation between B/C ratio and the adsorption enthalpy.

A second series we investigated is PPOR with different TMs exchanged into the macrocyclic ring. In such system, the TM ions are ligated by four nitrogens in a square-planar configuration, leaving the metals exposed to the interaction with hydrogen at both sides. We successfully prepared a variety of PPORs using several synthetic schemes, as are shown by the examples in Figure 2, and incorporated ionic Fe, Co and Ni into the POPs. We also measured surface property, excess hydrogen storage capacity and isosteric heat of adsorption. We found that while the impact to enthalpy by metal is limited with values in the range of 8 to 9 kJ/mol, their inclusion clearly enhances POPs interaction with hydrogen. The difference in adsorption enthalpy is relatively minor with respect to TM type used in this

TABLE 1. Surface Properties, Hydrogen Adsorption Capacities and Enthalpies of Different BPOPs

	BET SSA (m^2/g)	Langr. SSA (m^2/g)	Tot Pore Vol (cm^3/g)	μ-pore Volume (cm^3/g)	Pore Diameter (nm)	H_2 Gr. Uptake @ 77 K ($kgH_2/kgAds+H_2$)	B/C ratio	ΔH_{ads} (kJ/mol)
BPOP-1	422	592	0.14	0.04	0.68	0.014	1/1.8	10.2
BPOP-2	864	1,164	0.57	0.30	0.76	0.021	1/1.6	9.0
BPOP-3	1,037	1,497	1.12	0.33	0.77	0.028	1/3.0	8.2

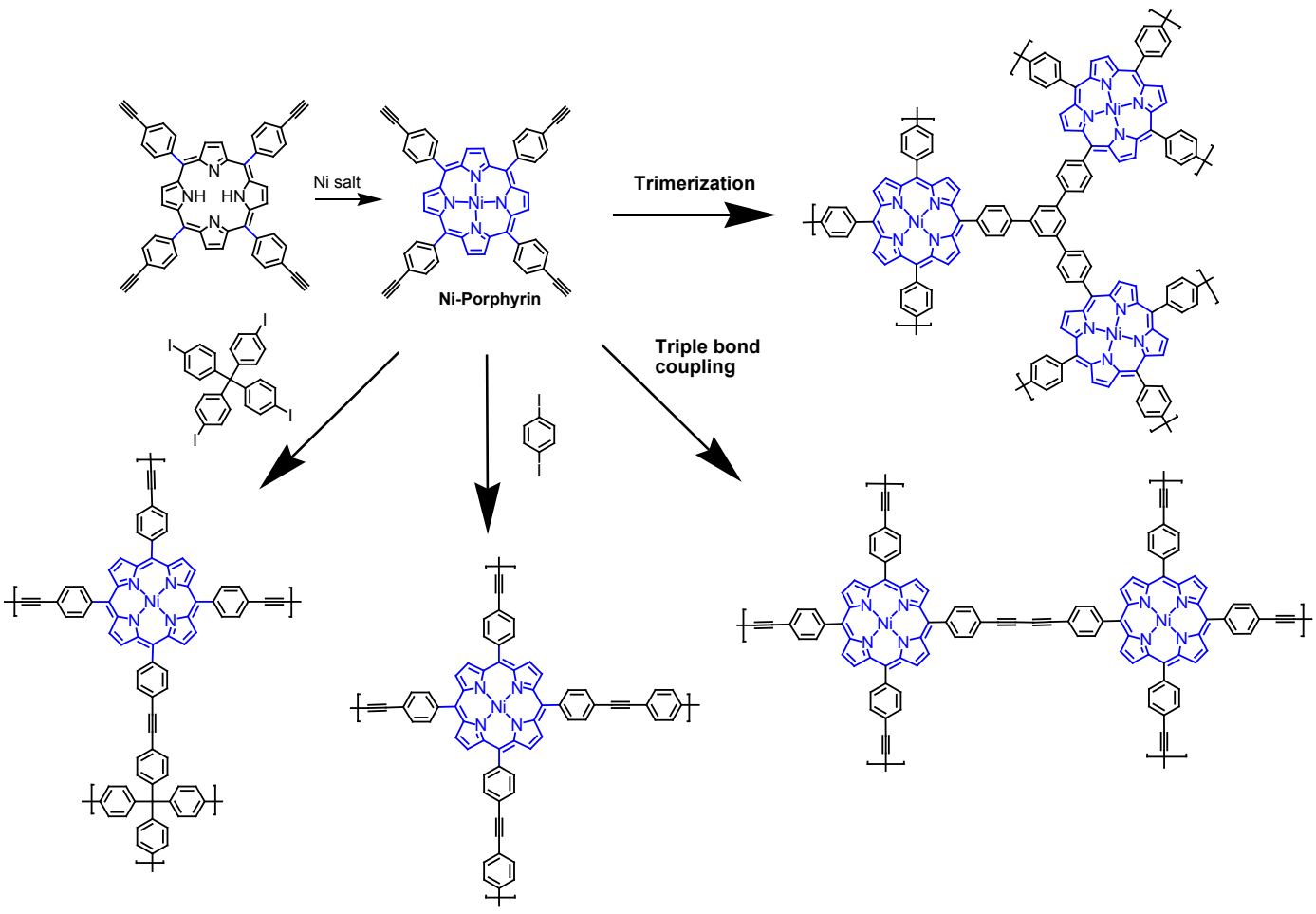


FIGURE 2. Four Parallel Synthetic Schemes for Preparing Different Ni-PPORs

study. The storage capacity is still mainly dominated by the SSA of the PPORs. To verify if the heat of adsorption behaves differently under different TM coordination, we also conducted a parallel study of two TM-containing POPs, prepared through chelation of Ni^{+2} or Co^{+2} with hydroxyquinoline. Both POPs have high metal contents (~14% by weight) and similar SSAs (~600 m^2/g). The key difference is that one is connected through square-planer (nickel) and the other through tetrahedral (cobalt) coordination. Our BET analysis showed that POP formed through the tetrahedral linkage has an average pore diameter of 0.8Å larger than that formed through the square-planer connection. Interestingly, the Co-based POP showed nearly 10 kJ/mol adsorption enthalpy, almost 2 kJ/mol higher that of Ni-based POP.

Conclusions and Future Directions

In summary, we produced a broad range of POP-based adsorbents with high SSA, narrow PSD, and excellent chemical stability. These POPs, particularly those with metal exchange capability or B-incorporated backbone, could serve as excellent platforms for further development of materials with better adsorption enthalpy for ambient temperature applications:

- New metal elements, from both transition and main groups, could be exchanged into POPs through chemical or physical means, to achieve sufficient adsorption enthalpy suitable for near-ambient temperature application as predicated by theory.
- New surface modification techniques, departing from the conventional synthetic approaches, could have the potential to produce high binding energy sites.
- New POP designs with tailored surface property and chemical composition could serve as the precursors for further chemical/physical processing to improve H_2 binding energy.

FY 2011 Publications/Presentations

1. "Porous Organic Polymers Containing Carborane for Hydrogen Storage", Shengwen Yuan, Desiree White, Alex Mason, and Di-Jia Liu, Accepted by *Int. J. of Energy. Research*.

2. "Exploring applications of nanomaterials for fuel cell & hydrogen storage", Di-Jia Liu, Shengwen Yuan, Gabriel Goenaga, Junbing Yang, Desiree White and Alex Mason, *Preprint Paper Am. Chem. Soc., Div. Fuel Chem*. 55 (1), xxxx (2010).

3. "Exploring applications of nanomaterials for fuel cell & hydrogen storage", Di-Jia Liu (invited) Presentation at American Chemical Society National Meeting, Anaheim, CA, March 26–31, 2011.

4. "Improving Hydrogen Adsorption Enthalpy through Coordinatively Unsaturated Cobalt in Porous Polymer", S. Yuan, D. White, A. Mason, B. Reprogle, L. Yu, and D-J Liu, to be submitted.

References

1. Yuan, S.; Kirklin, S.; Dorney, B.; Liu, D.-J.; Yu, L. *Macromolecules* 2009, 42, 1554-1559.

2. Yuan, S.; Dorney, B.; White, D.; Kirklin, S.; Zapol, P.; Yu, L.; Liu, D.-J. *Chem. Commun*. 2010, 46, 4547 – 4549.

3. Xia, J.; Yuan, S.; Wang, Z.; Kirklin, S.; Dorney, B.; Liu, D.-J.; Yu, L. *Macromolecules* 2010, 43, 3325–3330.

4. Cooper, A., *Adv. Mater*. 2009, 21, 1-5.

5. McKeown, N.B.; Ghanem, B.; Msayib, K.J.; Budd, P.M.; Tattershall, C.E.; Mahmood, K.; Tan, S.; Book, D.; Langmi, H.; Walton, A. *Angew. Chem. Int. Ed*. 2006, 45, 1804-1807.

6. Kim, Y.H.; Zhao, Y.; Williamson, A.; Heben, M.J.; Zhang, S.B. *Phys. Rev. Lett*. 2006, 96, 16102.

7. Chung, M.; Jeong, T.; Chen, Q., Kleinhammes, A.; Wu, Y. *J Am. Chem. Soc*. 2008, 130, 6668–6669

IV.C.6 Hydrogen Trapping through Designer Hydrogen Spillover Molecules with Reversible Temperature and Pressure-Induced Switching

Angela D. Lueking[1] (Primary Contact), Jing Li,[2] Sarmishtha Sircar,[1] Cheng-Yu Wang,[1] Qixiu Li,[1] Yonggang Zhao,[2] Haohan Wu,[2] Qihan Gong,[2] Milton W. Cole[1]

[1]The Pennsylvania State University
120 Hosler
University Park, PA 16802
Phone: (814) 863-6256
E-mail: adl11@psu.edu

DOE Managers
HQ: Ned Stetson
Phone: (202) 586-9995
E-mail: Ned.Stetson@ee.doe.gov
GO: Jesse Adams
Phone: (720) 356-1421
E-mail: jesse.adams@go.doe.gov

Subcontractor:
[2]Rutgers University, Piscataway, NJ

Contract Number: DE-FG36-08GO18139

Project Start Date: January 1, 2009
Project End Date: December 30, 2012

Fiscal Year (FY) 2011 Objectives

- Synthesize designer microporous metal-organic frameworks (MMOFs) mixed with catalysts to enable H-spillover for H_2 storage at 300 K-400 K and moderate pressures.
- Optimize volumetric analyzer to increase precision and accuracy at high-pressure.
- Improve better dispersion of nano-metal catalysts, and examine uptake of MMOFs mixed with catalysts. Vary catalyst mixing technique to ensure optimal interfacial contact for spillover.
- Demonstrate spectroscopic evidence for spilled over atomic hydrogen in a Pt/carbon system, to help resolve potential confusion regarding physisorption versus chemisorption in spillover materials.

Technical Barriers

This project addresses the following technical barriers from the Hydrogen Storage section of the Fuel Cell Technologies Program Multi-Year Research, Development and Demonstration Plan:

(A) System Weight and Volume

(D) Durability: Min/max temperature/maximum pressure

(E) Charging/Discharging Rates

(P) Lack of Understanding of Hydrogen Physisorption and Chemisorption

(Q) Reproducibility of Performance

Technical Targets

TABLE 1. System Gravimetric Capacity 2010/2015 Target (0.045/0.055) of Hydrogen Uptake via Spillover at 298 K

Sample	Pressure (bar)	Hydrogen in excess of He (kg H_2/kg)
PtC+IRMOF-8 (8 replicates; changes in mixing)	70-85	0.0028-0.0078
PtC+IRMOF-8 with bridging	70	0.0025-0.0030
Pt/M (Maxsorb Activated Carbon)	70	0.0079/0.0091[a]
Pt/MAr (950°C Ar anneal prior to doping)	70	0.0097[a]
Pt/MV (1,000 K vacuum anneal)	70	0.0101[a]
Pt/MKOH (KOH oxidation before doping)	70	0.0085[a]
Pt/$MHNO_3$ (oxidized in 70% HNO_3)	70	0.0093[a]
PtC/MMOF=O[c]	72	0.0017
PtC/MMOF-OH[c]	71	0.0069
Pt/AC-INER[b]	1	0.012

[a] Includes He adsorption correction for compatibility with literature.
[b] Provided by C.S. Tsao (INER, Institute of Nuclear Energy Research, Taiwan). Uptake is gravimetric. This sample used for subsequent in situ spectroscopy tests.
IRMOF – isoreticular metal organic framework

FY 2011 Accomplishments

- Improved accuracy of differential volumetric equipment 12-fold.
- Validated system against National Renewable Energy Laboratory blind sample.
- Explored mixing conditions on reproducibility of spillover of PtC/IRMOF. Demonstrated catalyst-MMOF contact needs improvement.
- Began new catalyst-MMOF mixing techniques.
- Demonstrated 22% increase in Maxsorb activated carbon after incorporating well-dispersed Pt catalyst.
- Demonstrated 1.2 wt% uptake on Pt/AC-INER at 1 bar and 298 K (supplied from collaborator INER, Taiwan).
- Synthesized new MMOFs with variations in surface chemistry for spillover studies.
- Developed MMOFs of high thermal and water stability by eliminating M-N bonds.

- Explored conditions to produce nanocrystals of MMOF samples for more efficient and uniform mixing with Pt/carbon catalyst.
- Raman in situ spectroscopy for the evidence of spilled over atomic hydrogen in Pt/carbon system and clarification of physisorption vs. chemisorption issue.
- Identified hydrogenation site for PtC/CuBTC via Fourier transform infrared and Raman spectroscopy.



Introduction

The term hydrogen spillover has been used to describe a synergistic effect between high-surface area adsorbents and associated catalysts. The associated catalyst may act to dissociate molecular H_2 into atomic H species. The atomic H is then free to migrate to surface sites on the high-surface area support; the net surface H concentration is a function of the relative rates of surface migration versus desorption from the surface. This process occurs at moderate temperature (i.e. 300 K) and generally leads to a much higher uptake than expected for the metal catalyst or high-surface area adsorbent alone. Spillover materials using MMOFs have been reported to have high uptake at ambient temperature: bridged ('br') PtC/IRMOF8 achieved 4 wt% excess adsorption at 100 bar and 298 K [1]. Independent groups have demonstrated up to 4.2 wt% at 6.9 MPa after extended equilibration for brPt/C/IRMOF-8 [2]. Subsequent reports on spillover materials at room temperature have varied from less than physisorption to almost 9 wt%, demonstrating difficulties in reproducibility and invoking controversy. These uptakes approach DOE goals; however, as the process is highly dependent upon synthesis, measurement, and catalytic particle size [3,4], the process remains poorly understood. It is anticipated that optimization of the MMOF structure, surface chemistry, and porosity will further increase uptake via spillover. Meeting DOE hydrogen storage targets at moderate temperature will have significant engineering advantages for mobile applications, as temperature of operation has implications for system weight.

Approach

The project relates to materials development and optimization of catalyst, surface chemistry, crystal and pore structure, and system parameters for the hydrogen spillover phenomenon. To optimize catalyst, platinum nanoparticle wet precipitation method [5] was used to get better metal dispersion. For surface chemistry, different MMOFs were mixed with catalyst to test hydrogen storage and the effect of functional groups. In addition, acid, base, and high temperature after-treatments were used in metal/carbon catalyst systems to have various surface functional groups and to test hydrogen uptake afterwards. We also scrutinized the effect of MMOF structural change on spillover hydrogen adsorption via different mixing strategy with Pt/C catalysts. The project is currently exploring materials without bridging, as bridging has unknown effects on the surface chemistry and structural parameters we hope to optimize.

As discrepancy and debates in spillover hydrogen storage arise, we have spent considerable effort improving our differential volumetric measurement method for better precision and accuracy. We have demonstrated that simple differences in data processing, volume calibration, pumping, and He blank treatment have a drastic effect on the precision of measurement. Validation against published data [6] for GX-31 superactivated carbon and multiple measurements for PtC/IRMOF8 demonstrates better reliability. Moreover, in situ high-pressure spectroscopy is currently being incorporated into the project to characterize spilled over atomic hydrogen.

Results

The measurement instrument employed for our sorption studies is a custom-built volumetric differential Sievert's apparatus with two high-accuracy pressure transducers; an absolute pressure transducer and a differential pressure transducer. Single-sided Sievert's apparatus are broadly used in hydrogen adsorption measurements [7], and a differential unit provides greater accuracy due to simultaneous collection of a blank, a measurement that is highly insensitive to temperature gradients, and generally a higher accuracy of the differential pressure reading relative to the absolute pressure reading. In all volumetric methods, the moles adsorbed are calculated via a mass balance, assuming mass loss from the gas phase is solely due to adsorption to the sample. The accuracy of the measurement relies on an accurate volume calibration, which in turn, relies on the accuracy of the pressure transducers. At 80 bar, 298 K, 100 mg sample measurement, the 'base' error in the measurement of our system (based on mathematical propagation of error using measured variations in volume calibration) is 1 ± 0.6 wt%, which would also be typical for a single-sided measurement. By using the more accurate differential pressure-transducer to calibrate the volume, the error is reduced 12-fold to 1 ± 0.05 wt% (obtained by error propagation with the same inputs, but different operating equation). Nonetheless, since high pressure He is used in this new improved method, it is expected to be prone to systematic error if He adsorbs or if trace residual H_2 is present in the system. The latter may lead to large error for spillover samples, so we are developing a new method that circumvents the high-pressure He calibration, but with a precision of the same level. Current data reported herein is subject to possible He adsorption and/or H_2/He cross-contamination and thus represents highly conservative values. All the methods were validated against published data for GX-31 [8].

Reports from Tsao et al. and Yang et al. [9] state that small catalyst size ($d<2$ nm) is essential for high uptakes via spillover. For a better platinum dispersion in Pt/C catalysts,

wet precipitation method was used as described in a recent publication [5]. Platinum on carbon Maxsorb (Pt/M) was synthesized with good metal dispersion and it confirms the spillover hydrogen uptake data (0.97 wt% at 71 bar, 300 K) published by Yang et al. [5].

With commercial Pt/C and custom synthesized Pt/M, we focused on reproducibility, preparation, and introduction of oxygen functional groups of MMOFs mixed with catalysts. In IRMOF-8 series, different ball milling ratios were used to alter structure. X-ray diffraction (XRD) of the resulting materials shows subtle difference, which can be attributed to damage induced from the mixing procedure [10]. The highest uptake was observed for a material with distorted–but still intact–XRD. Improved catalyst (Pt/M versus commercial Pt/C) did not consistently increase uptake of the mixed PtM/IRMOF8 (Table 1 and Figure 1), suggesting our current mixing procedure is insufficient for spillover to populate the IRMOF8. Thus, methods by which to directly incorporate catalysts into various MMOF structures are in progress. Also, frameworks made solely of strong M-O bonds are being developed which prove to have significantly enhanced thermal and water stability. We are currently exploring MMOFs with incorporated NH_2 groups, which serve as an anchoring site for direct metal-doping for H_2PtCl_6 [11]. Separately, carbonyl or hydroxyl groups functional groups were induced into MMOFs (MMOF=O and MMOF-OH) to test the role of these groups on spillover. After mixing, subtle changes are seen in XRD, but MMOFs remains largely intact. The adsorption amounts are still low (Table 1), but changes in MMOF surface chemistry is not likely to increase uptake until the catalyst MMOF interfacial contact issue can be addressed.

We also examined the effect of surface chemistry on carbon, when carbon serves as the receptor in primary spillover materials. Surface chemistry on Maxsorb was varied using different after-treatments, including high temperature anneal, acid oxidation, and basic oxidation. The removal or increase of surface oxygen groups affected the size of the supported metal: oxidation increased metal crystal size and reduced dispersion (Figure 2a), in certain cases, cations led to pre-precipitation of Pt particles and led to large metal particles. The best uptake achieved for this series of materials was 1.0 wt% for Pt/M_V (Table 1), which is a material that has been annealed to remove oxygen groups. The uptake represents a 22% increase over the undoped Maxsorb precursor.

A Pt-doped activated carbon (Pt/C-INER) provided by C.S. Tsao (INER, Institute of Nuclear Energy Research, Taiwan) showed high low-pressure gravimetric uptake of H_2 (i.e. 1.2 wt% at 298 K and 1 bar [measured at Penn State]; >5 wt% at 69 bar and 298 K [measured in Taiwan] [9]). It was used to probe the interactions between the carbon surface and dissociated hydrogen (H*) when the H* was

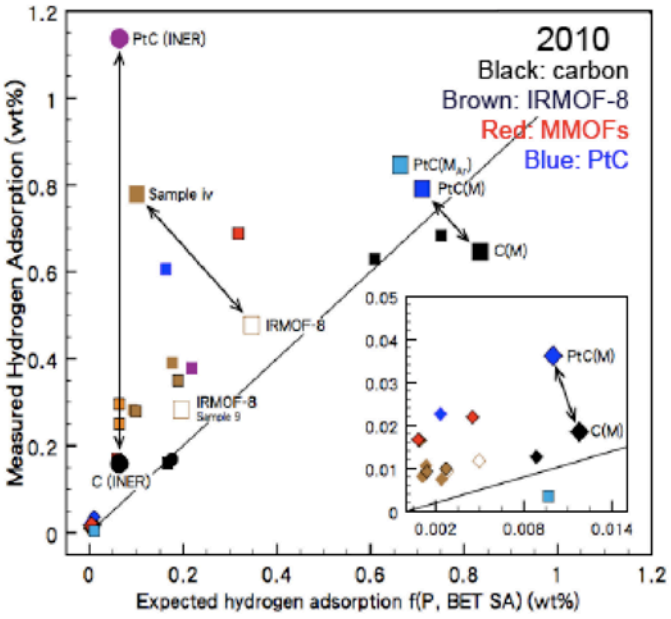


FIGURE 1. Summary of all 2010 H_2 uptake data (excess; relative to He blank at same conditions). H_2 uptake is plotted against uptake "Expected adsorption", which assumes uptake is linearly proportional to both surface area and pressure, i.e. an adapted Chahine Rule [12]. Data is plotted in this way to summarize multiple data at various adsorption pressures in one plot. MMOF samples (IRMOF8 in brown; modified surface chemistry in red) are physically mixed with PtC catalyst. Arrows are used to connect undoped precursor samples with those with catalyst, e.g. carbon (black) and Pt-doped carbon (blue).

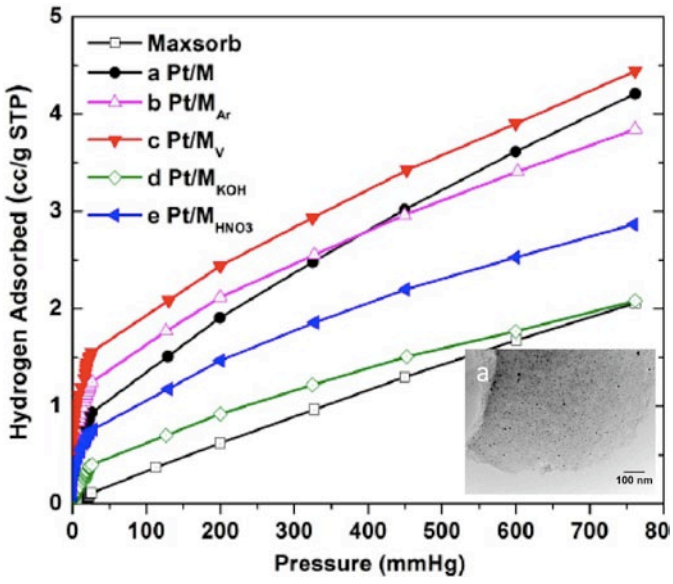


FIGURE 2. Effect of carbon surface chemistry on metal dispersion (low-pressure knee) and low-pressure H_2 isotherms at 1 bar for: (M) Maxsorb (M) activated carbon (a) Pt-doped M, following procedures of Yang et al.; (b) Pt/M_{Ar}: M is annealed at 950°C in Ar prior to Pt-doping; (c) Pt/M_V: M is anneled in vacuum at 1,000 K for 3 hours prior to Pt-doping; (d) Pt/M_{KOH}: M is oxidixed with KOH prior to Pt-doping; (e) Pt/M_{HNO3}: M is oxidized with concentrated (~70%) HNO_3 prior to Pt-doping. Inset (a): transmission electron microscope image of Pt/M shows high dispersion, which was not obtained prior to following the doping procedure of Yang et al.

provided by the adjacent Pt catalyst. In situ Raman (514 nm, 2 mW) measurements of Pt/C-INER were conducted within a silica fiber (wall thickness of 30 µm and center hole of 100 µm; see right, Figure 3) to allow for sequential He and H_2 gas exposures with intermittent degas). A series of sequential He and H_2 exposures were then performed, with a 72 hour vacuum degassing process at 300 K with the turbo pump between each gas introduction (Figure 3). Pt/C-INER in He shows features characteristic of a solid carbon, including a D-band (~1,350 cm^{-1}), G-band (~1,590 cm^{-1}). After He removal and pumping, Pt/C-INER in H_2 at the same spot shows additional bands at 1,180cm^{-1}. These new features vanish after H_2 gas is removed under vacuum and refilled with He gas at room temperature and reappear on a second H_2 exposure. The features were not found in Pt, activated carbon precursor, unactivated carbon, or fiber. Thus, the features at 1,180 cm^{-1} are consistent with a hydrogen spillover process, and given the frequency, can be assigned to a wagging mode coming from weakly bonded atomic hydrogen and the carbon substrate.

Conclusions and Future Directions

- Improvements are made in differential volumetric measurements. Current accuracy is at least 1 ± 0.05 wt% when a 100 mg sample is used.
- Pt-doped AC provided by INER had high uptake at low pressure (1.2 wt% at 1 bar), demonstrating continued promise of spillover mechanism.
- In situ spectroscopy for Pt/AC-INER shows a reversible Raman feature at 1,180 cm^{-1} in hydrogen only, associated with C-H chemical bond. The mode is reversible when H_2 is removed at 298 K. Reversibility is dependent upon carbon structure.
- Type and form of oxygen groups on carbon substrate affects Pt particle size and ultimate spillover.
- Current studies for spillover to MMOF are limited by interfacial contact. Future work will focus on methods to direct dope MMOFs with catalyst. MMOF structure is also an important parameter is obtaining uptake via spillover, and is dictated by mixing technique.
- Future work will explore new methods to facilitate catalyst-carbon-MMOF contact, including doping of MMOF-NH2; effect of particle size; addition of terminal ligand/solvent for surface amino modification for catalyst anchoring; addition of carbon aerogel for pre-formed bridge.
- Future work will alter MMOF structure to introduce high density hydrogenation sites, open metal sites and separately, introduce holes that may facilitate spillover.

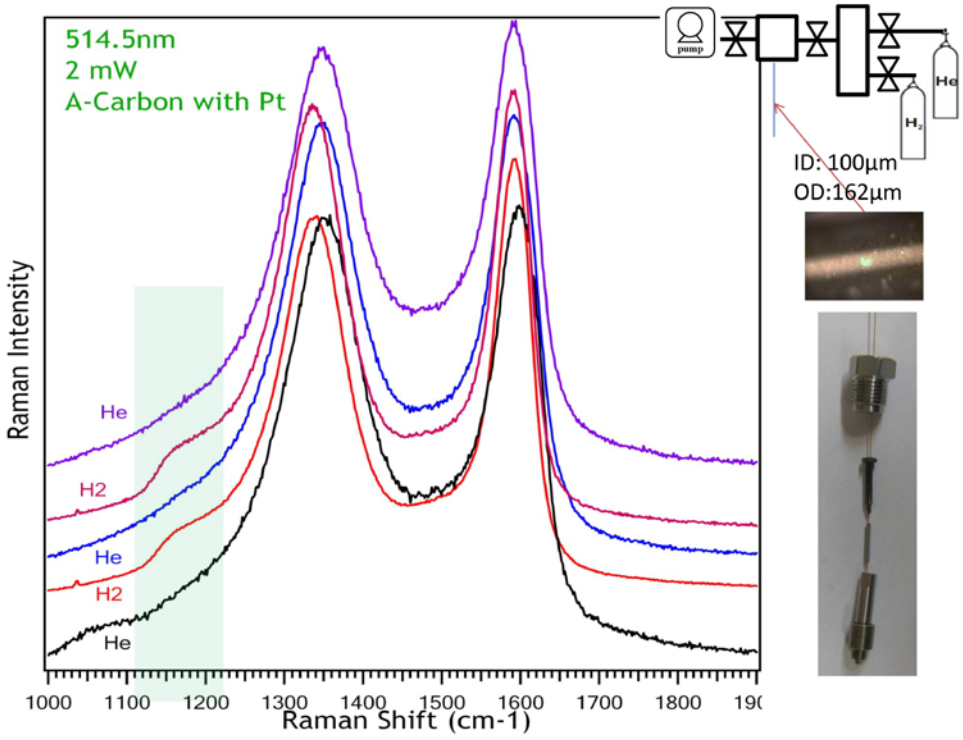


FIGURE 3. Raman spectra of Pt/C-INER at 298 K in a fiber (A) showing D-band (~1,350 cm^{-1}), G-band (~1,590 cm^{-1}), 2D-band (2,700 cm^{-1}) and a D+G band(~2,940 cm^{-1}), exposed sequentially (after intermittent degas at 298 K) to (a) He gas (b) H_2 (c) He (d) H_2, and (e) He. Reversible bands at 1,180 and 2,500 cm^{-1} are seen only in the presence of H_2 gas, and are removed after pressure reduction at 298 K (B).

- Future work will include a systematic study of introduced functional groups on MMOF-4,4'-bypyridine series with in situ spectroscopy.
- Write and submit papers on: (1) methods validation and reproducibility in differential volumetric analyzer; (2) hydrogen spillover on PtC/CuBTC; and (3) variation of MMOF structure/chemistry with secondary spillover studies.

FY 2011 Publications/Presentations

1. A. Lueking, J. Li, M.W. Cole, Four Quarterly Reports, FY2011; Annual Report, FY2011.

2. A. Lueking, Presentation at 2011 Hydrogen Program Annual Merit Review Meeting, May 12, 2011.

3. X.M. Liu, Y.J. Tang, E.S. Xu, T. Fitzgibbons, H.Y. Chuang, H.R. Gutierrez, M.S Yu, C.S. Tsao, J.V. Badding, V.H. Crespi, A.D. Lueking, In-Situ Micro Raman Detection of Reversible Basal Plane Hydrogenation in Pt-doped Activated Carbon, In Preparation.

4. C.-S.Tsao, Y. Liu, H.-Y.Chuang, H.-H. Tseng, T.-Y. Chen, C.-H. Chen, M.-S.Yu, Q.Li, A. Lueking, S.-H. Chen, Submitted to Journal of the American Chemical Society 2011.

5. Lee, J.Y.; Wu, H.H.; Li, J. "Enhancing Hydrogen Adsorption Properties of Microporous Metal Organic Frameworks (MMOFs) by Tuning Their Crystal and Pore Structures", *Intl. J. Hydro. Ener.*, Submitted.

References

1. Li, Y. and Yang, R.T. *J. Am. Chem. Soc.* 2006, *128*, 726-727.

2. Tsao, C.S.; Yu, M.S.; Wang, C.Y.; Liao, P.Y.; Chen, H.L.; Jeng, U.S.; Tzeng, Y.R.; Chung, T.Y.; and Wu, H.C. *J. Am. Chem. Soc.* 2009, *131*, 1404-1406.

3. Stadie, N.P.; Purewal, J.J.; Ahn, C.C.; and Fultz, B. *Langmuir.* 2010, *26*, 15481-15485.

4. Stuckert, N.R.; Wang, L.; and Yang, R.T. *Langmuir.* 2010, *26*, 11963-11971.

5. Chen, H. and Yang, R.T. *Langmuir.* 2010, *26*, 15394-15398.

6. Zielinski, J.M.; Coe, C.G.; Nickel, R.J.; Romeo, A.M.; Cooper, A.C.; and Pez, G.P. *Adsorption.* 2007, *13*, 1-7.

7. Blach, T.P. and Gray, E. *Journal of Alloys and Compounds.* 2007, *446*, 692-697.

8. Lachawiec Jr, A.J.; DiRaimondo, T.R.; and Yang, R.T. *Review of Scientific Instruments.* 2008, *79*, 063906.

9. Tsao, C.S.; Tzeng, Y.R.; Yu, M.S.; Wang, C.Y.; Tseng, H.H.; Chung, T.Y.; Wu, H.C.; Yamamoto, T.; Kaneko, K.; and Chen, S.H. *J. Phys. Chem. Lett.* 2010, *1*, 1060-1063.

10. Hafizovic, J.; Bjørgen, M.; Olsbye, U.; Dietzel, P.D.; Bordiga, S.; Prestipino, C.; Lamberti, C.; and Lillerud, K.P. *J. Am. Chem. Soc.* 2007, *129*, 3612-3620.

11. Hwang, Y.K.; Hong, D.Y.; Chang, J.S.; Jhung, S.H.; Seo, Y.K.; Kim, J.; Vimont, A.; Daturi, M.; Serre, C.; and Férey, G. *Angew Chem Int Ed Engl.* 2008, *47*, 4144-8.

12. Panella, B.; Hirscher, M.; and Roth, S. Carbon. 2005, 43, 2209-2214.

IV.C.7 Weak Chemisorption Validation

Thomas Gennett (Primary Contact), Lin Simpson, Jeffrey Blackburn, Katherine Hurst, Phillip Parilla, Chaiwait Engtrakul, Kevin O'Neill, Justin Bult
National Renewable Energy Laboratory (NREL)
1617 Cole Blvd.
Golden, CO 80401-3393
Phone: (303) 384-6628
E-mail: Ned.Stetson@ee.doe.gov

DOE Manager
HQ: Ned Stetson
Phone: (202) 586-9995
E-mail: Ned.Stetson@ee.doe.gov

Subcontractors:
- Craig M. Jensen, University of Hawaii, Honolulu, HI
- Plamen Atanassov, University of New Mexico, Albuquerque, NM
- Michael Hirscher, Max Planck Institute, Stuttgart, Germany
- Michel Latroche, Institut de Chimie et des Matériaux (ICPME), Paris, France
- Karl Gross, H2 Technology Consulting LLC, Newark, CA

Project Start Date: October 1, 2010
Project End Date: Project continuation and direction determined annually by DOE

Fiscal Year (FY) 2011 Objectives

- Evaluate the weak chemisorption/spillover process as a means to achieve DOE 2015 Hydrogen Storage goals.
  - Lead sample exchange and measurement validation efforts for weak chemisorption.
  - Perform round robin with "standard" high specific surface area sorbents to ensure all participating laboratories are measuring similar hydrogen storage capacities.
  - Evaluate universal reproducibility of enhanced adsorption weak chemisorption/spillover effects.
  - Determine type of interaction of the support with the spiltover hydrogen.
  - Establish if weak chemisorption/spillover is a viable process for hydrogen storage.
  - Communicate validated results to the community at large.
- Provide highly accurate hydrogen storage measurement support to the sorption community in order to validate exceptional results.
- Coordinate additional work for the Best Practices Document.

Technical Barriers

This project addresses the following technical barriers from the Storage section of the Fuel Cell Technologies Program Multi-Year Research, Development and Demonstration Plan:

(A) Cost
(B) Weight and Volume
(C) Efficiency
(E) Refueling Time
(M) Hydrogen Capacity and Reversibility
(N) Understanding of Hydrogen Physi- and Chemisorption
(O) Test Protocols and Evaluation Facilities

Technical Targets

This project is validating experimentally observed weak chemisorption. Insights gained from this work may be applied toward the future design and synthesis of hydrogen storage materials that meet the following DOE 2015 hydrogen storage targets:

- Cost: $4/kWh net
- Specific energy: 1.5 kWh/kg
- Energy density: 0.9 kWh/L

The specific technical objectives include:

- Verify at least 15% increase in hydrogen uptake over baseline sorbent material at room temperature conditions based on the effects of weak chemisorption/spillover.
- Via spectroscopic techniques, determine the type of hydrogen-substrate interactions from the enhanced spiltover hydrogen using diffuse reflectance infrared fourier transform spectroscopy (DRIFTS), nuclear magnetic resonance spectroscopy (NMR), RAMAN spectroscopy, and neutron scattering.

FY 2011 Accomplishments

- Completed round-robin analysis of standard samples:
  - Achieved <5% error on hydrogen capacity measurements on the same standard sorbents (two were distributed) at three different laboratories. Completing the standard measurements at three others.
- Completed synthesis of three different spillover samples and distributed the initial set to the different labs for evaluation.

  - Verified a >15% enhancement of hydrogen storage in Pd catalyst on template carbon (Pd/TC) materials via volumetric measurements (NREL and ICPME)
- Synthesized weak chemisorption/spillover materials at three different laboratories.
- Demonstrated spectroscopic evidence for spiltover C-H bonds.
  - DRIFTS measurements where both Pt-C and Pd/TC showed a unique stretch that was tentatively assigned to spiltover hydrogen.
  - Neutron scattering (Ru-BCx), revealed apparent hydrogen wagging modes which correlated to those energies predicted by theory.
  - Reported detailed findings and recommendations on hydrogen spillover results.
    - International Energy Agency Hydrogen Implementing Agreement (IEA-HIA) Task 22 meeting Freemantle, Australia.
    - DOE Fuel Cell Technologies Annual Merit Review, Washington, D.C.
    - Gordon Research Conference, Easton, MA (included a workshop meeting).
    - Pending: American Chemical Society (ACS) Meeting, (August 2011) and IEA-HIA Task 22 Hydrogen Storage Meeting (September 2011).
- Completed four out of five drafts for the Best Practices Document: 515 pgs, seven sections: Introduction, Capacity, Kinetics, Thermodynamics, Cycle-Life, Thermal Properties, Mechanical Properties Measurements.
- Evaluated the hydrogen sorption characteristics of two unique >5,000 M^2/g high surface area metal-organic frameworks from Northwestern and Texas A&M Universities.



Introduction

The ultimate goal of the Hydrogen Storage subprogram is the development of hydrogen storage systems that meet or exceed the DOE's goals for the onboard hydrogen storage in hydrogen powered vehicles. With the tremendous interest in weak chemisorption materials for hydrogen storage, NREL and DOE have dedicated considerable resources working with partner institutions to synthesize specific materials and to develop/perform the requisite measurements in order to establish the capacity, kinetics and overall performance of these materials. The key critical issues that must be resolved for these materials include reproducibility of material synthesis, understanding the kinetics of H transport on receptor surfaces, and which chemical reactions are desired and which are not. In addition, weak chemisorption properties are intricately linked to more standard H_2 storage mechanisms, so information gained on the hydrogen-substrate interactions should help accelerate viable sorbent development.

Approach

Organized and led an international group with IEA and International Partnership for the Hydrogen Economy members to validate weak chemisorption synthesis and measurement results. Participants include: Angela Lueking (Pennsylvania State University), Michael Hirscher (Germany), Michel Latroche (France), Thomas Gennett (NREL), Craig Brown (National Institute for Standards and Technology, NIST) Craig Jensen (University of Hawaii). Evan Gray (Griffith University), Craig Buckley (Curtin University), Mike Miller (Southwest Research Institute®), Channing Ahn (California Institute of Technology), and Tony Burrell (Argonne National Laboratory).

Our approach includes the synthesis and characterization of a series of materials with an unexplained enhancement of hydrogen sorption in the presence of catalysts, that is thought to be caused by hydrogen spillover. The materials selected are Pd/templated carbon, Pt/templated carbon, and Ru/BCx. These materials are being synthesized and validated across laboratories. As we move forward we will utilize volumetric measurements for verified capacity measurements. Then through spectroscopic evaluation of the materials with DRIFTS, neutron scattering and NMR we will determine correct peak assignments in order to determine if spiltover hydrogen spectroscopic modes are in regions expected for room temperature hydrogen desorption. There will then be a coordination of efforts for inter-laboratory comparison of characterization of results and eventually a reconciliation of spillover propagation mechanisms to thermodynamic parameters.

Results

- **Validation of volumetric analysis of standards across laboratories.** NREL was the lead and distributed a series of samples to various laboratories for testing, Figure 1. As is evident in the isotherms we were able to coordinate and establish an approximate 5% absolute variation in results across six laboratories. The variations in the data were found to be caused by calculation error, skeletal density assumptions and/or null volume assumptions.
- **Confirmation of hydrogen sorption enhancement in Pd-Templated carbon materials.** NREL and ICPME were able to achieve a similar enhancement in hydrogen sorption on Pd incorporated into a templated carbon matrix. This adsorption was beyond that expected for palladium hydride formation, Pd-H_2, possibly from the addition of the Pd. This was confirmed on two separate samples. A large batch synthesis by ICPME was completed, and those samples are under analysis by other laboratories. NREL is currently synthesizing

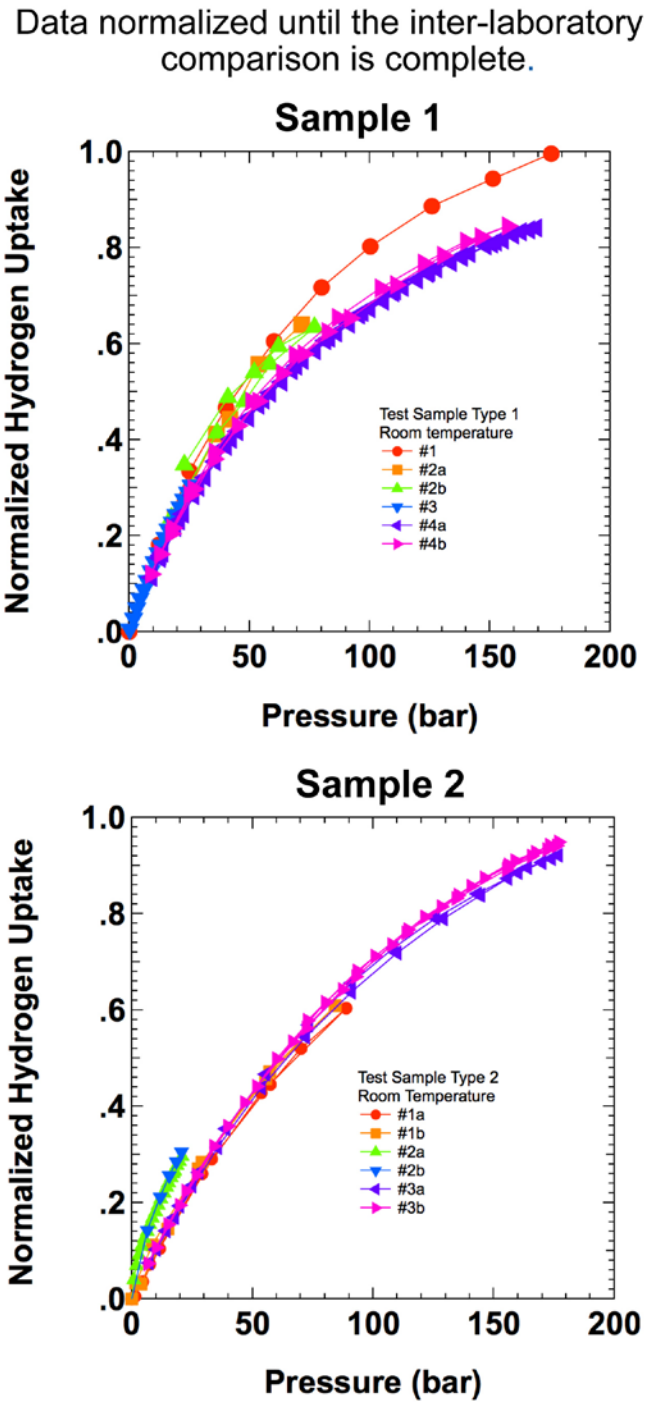


FIGURE 1. Inter-Laboratory Comparison of Volumetric Data for Two Distinct Samples

an independent batch of materials in order to confirm ability to synthesize in two distinct laboratories.

- **DRIFTS determination of new hydrogen-substrate interactions for an apparent spillover material.** Using infrared spectroscopy to identify distinct substrate-hydrogen interactions is an essential component of our work as we look to establish the energetics associated with the spiltover hydrogen. Figure 2 shows DRIFTS spectra for several samples charged with D_2 and treated at two different temperatures. In one experiment, labeled "D_2 activation", the sample is charged with ~200 psi (~14 bar) of D_2 at room temperature, and then heated up to 200°C in the D_2 atmosphere. The other experiment is simply a room temperature D_2 charge with no heat treatment. Three samples in Figure 2 were subjected to a D_2 activation: an amorphous platinum sample (Pt-amorph), an activated carbon sample with 40% platinum (40% Pt-Etek), and a carbon sample from one of our partners, loaded with 11% Pd (Latroche 11% Pd-C). Interestingly, the D_2 activation procedure yields the same four sharp peaks, labeled by the triangles, for all three of these samples. A group of three sharp peaks occur at 2,386, 2,254, and 2,135 cm^{-1}, along with an isolated peak at 1,068 cm^{-1}. The three higher energy peaks are in the range expected for surface hydroxyl (O-D) and/or alkane (C-D) vibrations. Because these higher energy peaks are also observed for the amorphous Pt sample, a sample that contains no carbon, the possibility that these peaks are related to the formation of C-D bonds is ruled out. Instead, we propose that these peaks correspond to the possible formation of isolated surface hydroxyl species on the metal nano- or microparticles. Additionally, the isolated and strongly bound nature of the surface hydroxyl species precludes the hydrogen bonding observed for loosely bound water (H_2O or D_2O) that typically results in a broad featureless peak. The narrow peak at 1,068 cm^{-1} would then most likely correspond to a bending motion of the surface-bound hydroxyls. We note that none of these peaks are observed for activation of a carbon sample that contains no metal catalyst.

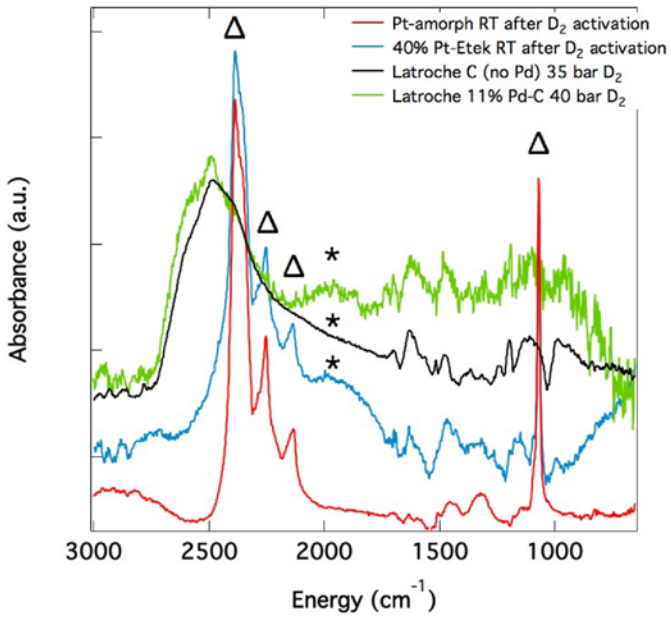


FIGURE 2. DRIFTS Spectra for Various Samples Charged with D_2 at Room Temperature

Finally, we also note that the energies observed for the grouping of peaks in the range of 2,100 to 2,400 cm^{-1} are significantly higher than what is expected for Pt-D bonds, which are expected to fall in the range of ~1,688 cm^{-1}.

For the samples treated with a room temperature D_2 charge, we evaluated the Pd-TC sample, along with a control carbon sample prepared by the same method, but without Pd incorporation (Latroche C, no Pd). This sample has shown reproducible adsorption capacity enhancement at room temperature, which is presumably due to spiltover hydrogen. The main feature observed for the control experiment (Latroche C, no Pd) is a broad absorption feature in the range of 2,000 to 2,800 cm^{-1}. This feature is assigned to loosely bound D_2O on the surface that most likely forms by the reaction of D_2 with surface-bound oxygen or hydroxyls. The same broad peak forms for the Pd-containing sample (Latroche 11% Pd-C), but a new broad feature also appears at ~1,900 cm^{-1}, which is noted with an asterisk (*). Interestingly, a similar peak is observed for all samples containing both a catalyst metal and carbon, and not observed for the activated Pt-amorph sample. Thus, we tentatively assign the broad peak in the range of 1,800–1,900 cm^{-1} to C-D peaks formed by spillover of deuterium from catalyst particles (Pt or Pd) to the carbon surface. Further experiments must be done to confirm this assignment. Finally, we note the presence of many small peaks in the range of 900 to 1,700 cm^{-1}. Several of these peaks are similar amongst the samples investigated, while some samples possess unique peaks within the range above. With the recent results from neutron scattering experiments, we are calculating the corresponding infrared energy peak and look for it in this region (900–1,400 cm^{-1}) to see if we can correlate the spectroscopic data.

- **Neutron scattering evidence for spiltover hydrogen on a ruthenium-BCx material.** NREL synthesized over 4 grams of ruthenium decorated BCx templated carbon materials for neutron scattering studies. The remarkable results are illustrated in Figure 3. This is by far the strongest hydrogen signal NIST has seen for a spillover type material. Interestingly the peaks in the spectrum appear to correspond directly with those predicted by Boris Yakospn at the University of Texas at Austin (private communication). This same sample is now undergoing a series of DRIFTS measurements to verify the peaks with a second spectroscopic method.

Conclusions and Future Direction

- Complete synthesis of the different spillover samples and distribute round-robin sets to the different labs for evaluation.
- Down select validated spillover materials and distribute samples to other labs for validation and additional spectroscopic characterization. This will include a synthesis of validated spillover materials by other labs.

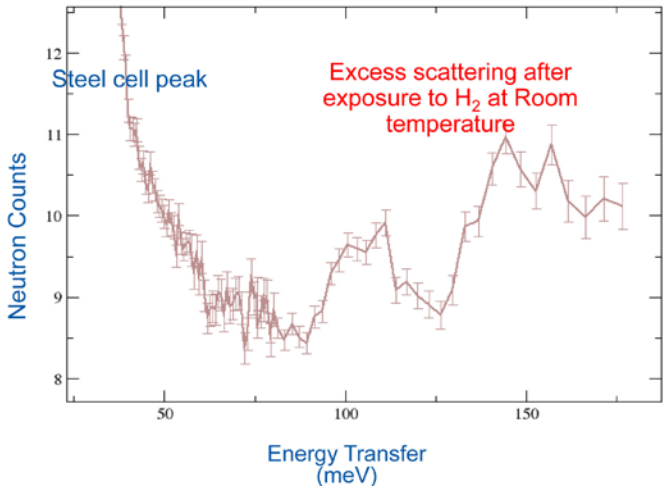


FIGURE 3. Neutron Scattering Data of BCx Material that Contains 6% w/w Ru

- Validate and assign specific types of interactions that have been observed from the spectroscopic evidence for spiltover C-H bonds in DRIFTS, and neutron scattering.
- Develop and utilize NMR and possibly near edge X-ray absorption fine structure absorption spectroscopy to further elucidate and confirm the presence of the spiltover hydrogen observed in DRIFTS and neutron scattering.
- Complete the remaining section, (Thermal Properties) and update the other sections within Best Practices.
- Report detailing findings and recommendations at ACS Meeting, (August 2011) and IEA-HIA Task 22 Hydrogen Storage Meeting (September 2011), final analysis will be presented at the 2012 Annual Merit Review meeting.

Validation and recommendations of weak chemisorption processes from this project will enable the hydrogen sorption community to accelerate development of room temperature hydrogen storage materials for light-duty vehicle and other early market applications.

Special Recognitions & Awards/Patents Issued

1. Jeffrey Blackburn: 2011 NREL Staff award for Scientific Excellence.

FY 2011 Publications/Presentations

Publications

1. Solution-Phase Synthesis of Heteroatom-Substituted Carbon Scaffolds for Hydrogen Storage, Zhong Jin, Zhengzong Sun, Lin J. Simpson, Kevin J. O'Neill, Philip A. Parilla, Yan Li, Nicholas P. Stadie, Channing C. Ahn, Carter Kittrell, and James M. Tour; J. Am Chem. Soc. 132, 15246 (2010).

2. Nano-Engineered Spacing in Graphene Sheets for Hydrogen Storage, Zhong Jin, Wei Lu, Kevin J. O'Neill, Philip A. Parilla, Lin J. Simpson, Carter Kittrell, and James M. Tour; Chemistry of Materials 23, 923 (2010).

3. "H2 Storage in Microporous Carbons from PEEK Precursors", Thomas P. McNicholas, Anmiao Wang, Kevin O'Neill, Robert J. Anderson, Nicholas P. Stadie, Alfred Kleinhammes, Philip Parilla, Lin Simpson, Channing C. Ahn, Yanqin Wang, Yue Wu, and Jie Liu, Journal of Physical Chemistry C, 2010, 114 (32), pp 13902–13908.

4. Spin crossover induced by molecular hydrogen adsorption in Fe(II)-exposed metal organic frameworks, Y. Y. Sun, Y-H Kim, K. Lee, D. West, and S. B. Zhang, J. Am. Chem. Soc., under review (2010).

5. Symmetry-assisted hydrogen adsorption and control on transition metal incorporated porphyrins, Y-H Kim, Y.Y. Sun, W. I. Choi, J. Kang, and S. B. Zhang, Phys. Rev. Lett. under review (2010).

6. Hole mediated diffusion of H on sp2 carbon networks, D. West, K. Lee, & S.B. Zhang, Phys. Rev. Lett. 104, 236101 (2010).

7. Theory of hydrogen Storage in nanoscale materials, Zhao, Kim, Zhang, Heben, in The Oxford Handbook of Nanoscience and Technology, Frontiers and Advances, Vol. 3, pp 700-736 (Oxford University Press, 2010)

8. Prediction of diamond-like, metallic boron structures, Yufeng Zhao, Qiang Xu, Lin J. Simpson, Anne C. Dillon; Chemical Physics Letters 496 (2010) 280–283.

9. "Hydrogen Sorption Center of Excellence Final Report," Department of Energy Office of Energy Efficiency and Renewable Energy, Fuel Cell Technologies Program, Lin Simpson, Director (2010).

10. Overview of the Hydrogen Storage Center of Excellence, as part of the DOE Annual Hydrogen Program Report (2010).

11. NREL Research as Part of the Hydrogen Sorption Center of Excellence, as part of the DOE Annual Hydrogen Program Report (2010).

12. Rich Chemistry and Structure Rule of sp2 and sp3 Boron," Y. Zhao, L.J. Simpson and A.C. Dillon, submitted.

13. An Electrical Study on Primary Hydrogen Spillover From Nanocatalyst to Amorphous Carbon Support, C. Lin, Z. Yang, T. Xu, and Yufeng Zhao, submitted.

14. Structural stability & hydrogen storage properties of Ti anchored on silica" Lee, K.; Lucking, M.; Sun, Y. Y.; Chen, Z.; Zhang, S., (to be submitted to Nano Lett.).

Invited talks

1. "Overview of Hydrogen Sorbents," Lin Simpson, Thomas Gennett, Philip A. Parilla, Kevin O'Neill, Katherine E. Hurst, Jeffery L. Blackburn, Chaiwat Engtrakul, Justin Bult, 242nd ACS National Meeting, Denver, Colorado, August 28 – September 1, 2011.

2. "Capacity, Reproducibility, and Kinetics of the Weak Chemisorptive (spillover) Hydrogen Sorption Process," Thomas Gennett, Philip A. Parilla, Kevin O'Neill, Katherine E. Hurst, Jeffery L. Blackburn, Chaiwat Engtrakul, Justin Bult, Lin J. Simpson, 2011 Hydrogen Metal Systems Gordon Research Conference, July 2011, MA.

3. "Weak Chemisorption Validation," Thomas Gennett, Philip A. Parilla, Kevin O'Neill, Katherine E. Hurst, Jeffery L. Blackburn, Chaiwat Engtrakul, Justin Bult, Lin J. Simpson, DOE Fuel Cell Technologies Annual Merit Review, May 2011.

4. "Inter-laboratory Comparison Results on Measuring High-Surface-Area Materials For Hydrogen Storage and Critical Calibration Issues", Philip A. Parilla, Kevin O'Neill, Katherine E. Hurst, Jeffery L. Blackburn, Chaiwat Engtrakul, Justin Bult, Lin J. Simpson, Thomas Gennett, Spring MRS 2011, San Francisco, CA.

5. "Sorbents for Hydrogen Storage," Lin Simpson, Thomas Gennett, Philip A. Parilla, Kevin O'Neill, Katherine E. Hurst, Jeffery L. Blackburn, Chaiwat Engtrakul, Justin Bult, Fuel Cell and Hydrogen Energy Association Conference, Washington DC, February 15, 2011.

6. Weak Chemisorption Validation, IEA HIA Task 22 Meeting, Freemantle, Australia Thomas Gennett, January 18th, 2011.

7. "NREL Weak Chemisorption Validation to DOE Hydrogen Storage Tech Team," Thomas Gennett, Philip A. Parilla, Kevin O'Neill, Katherine E. Hurst, Jeffery L. Blackburn, Chaiwat Engtrakul, Justin Bult, and Lin J. Simpson, November 18, 2010.

8. "Development of Heterogeneous Sorbents/Sorbent Isotherm Measurement Materials Exchange," L. J. Simpson, DOE LANL-AIST Hydrogen Workshop, August 17-20, 2010, San Francisco, CA.

9. "Fundamental Research Needed for H2 Storage by Sorbents," Lin Simpson, DOE-NSF Workshop, Alexandria VA, June 7, 2010.

10. "Research Needs for Hydrogen Storage," Lin Simpson, BES-EERE Workshop, Washington DC, June 3, 2010.

Presentations

1. "High Surface Area Boron Doped Carbon with Slow Hydrogen Desorption Kinetics," J. Bult, J. Blackburn, J. Lee, K. O'Neill, C. Engtrakul, P. Parilla, L. Simpson, T. Gennett, 2011 Annual Meeting of the Materials Research Society, San Francisco, CA.

2. "Sorbents for Hydrogen Storage," L. J. Simpson, Thomas Gennett, Philip A. Parilla, Kevin O'Neill, Katherine E. Hurst, Jeffery L. Blackburn, Chaiwat Engtrakul, Justin Bult, NHA, February 2011.

3. "Chemical Vapor Synthesis of Boron Doped Carbon for Hydrogen Storage," J. Bult, J. Blackburn, C. Engtrakul, T. Gennett, J. Barker, K. O'Neill, L. Simpson, 2010 Annual Meeting of the Materials Research Society, Boston, MA.

4. Justin Bult, Atomic Layer Deposition of Platinum onto Functionalized Aligned MWNTs, ECS-Oct. 2010, Las Vegas, NM.

5. "Room-temperature study of hydrogen adsorption on carbon-based nanomaterials using diffuse reflectance infrared spectroscopy," 240th American Chemical Society National Meeting, Boston, Massachusetts, August, 2010.

6. "Optical spectroscopy investigations of carbon-based nanomaterials for fundamental energy sciences research," 240th American Chemical Society National Meeting, Boston, Massachusetts, August, 2010.

IV.C.8 Nanostructured Activated Carbon for Hydrogen Storage

Professor Israel Cabasso (Primary Contact) and Dr. Youxin Yuan
State University of New York, Polymer Research Institute (esf), Syracuse Campus
1 Forestry Drive
Syracuse, NY 13210
Phone: (315) 470-6857
E-mail: icabasso@syr.edu

DOE Managers
HQ: Ned Stetson
Phone: (202) 586-9995
E-mail: Ned.Stetson@ee.doe.gov
GO: Jesse Adams
Phone: (720) 356-1421
E-mail: Jesse.Adams@go.doe.gov

Technical Advisor
Salvati Scott
Phone: (303) 275-4954; Fax: (303) 275-4753;
E-mail: scott.salvati@go.doe.gov

Contract Number: DE-FG36-05GO15009

Subcontractor:
PoroGen, LLC, Boston, MA

Start Date: May 2, 2005
Projected End Date: June 30, 2010 (no-cost extension to December 31, 2011)

Fiscal Year (FY) 2011 Objectives

Develop and demonstrate reversible nanostructured activated carbon hydrogen storage material which has at least a 5.5 wt% materials-based gravimetric capacity and a 40 gH_2/L material-based volumetric capacity at 235–358 K, and potential to meet the DOE 2015 system-level targets.

- Prepare and characterize nanostructured polymer derivatives as carbon precursors.
- Initiate the production of nanostructured activated carbon for hydrogen storage.
- Develop methods for sorbent-based doped polymer/carbon.

Technical Barriers

This project addresses the following On-Board Hydrogen Storage technical barriers (2007) section 3.3.4 outlined in the Fuel Cell Technologies Multi-Year Research, Development and Demonstration Plan:

(A) System Weight and Volume

(C) Efficiency

(E) Charging/Discharging Rate

(P) Lack of Understanding of Hydrogen Physisorption and Chemisorption

(Q) Reproducibility of Performance

Technical Targets

The research and development of novel high surface area nanostructured carbons for hydrogen storage has been conducted in this project. The project aims to address the critical need that has been recognized by DOE, which has established a national effort to develop new and advanced high-capacity hydrogen storage materials and technologies. This project is applied toward the synthesis of inexpensive carbon-based, high surface area sorbents that can be combined with chemical-interacting organic, and/or inorganic materials, to yield high storage materials. These new materials and concepts have been designed to meet the DOE 2015 goals concerning the production of low-cost, high specific hydrogen binding energy hydrogen storage materials.

TABLE 1. On-Board Hydrogen Storage System Targets

Storage Parameter	Units	2015 System Target	SUNY-Syracuse**
System Gravimetric Capacity	kWh/kg (wt% H_2)	1.8 (5.5 wt%)	2.4 (7.2 wt%)
System Volumetric Capacity	kWh/L(gH_2/L system)	1.3 (40)	1.2 (40)
Min/Max Delivery Temperature	K	233–358	77
Max Delivery Pressure	bar	100	60

** Data is based on material only, not system value

FY 2011 Accomplishments

- New type of polymer-based carbons that incorporate the metal (or metal ion) with high surface area and narrow pore size distribution has been developed with a hydrogen storage capacity of ~3.0 at 77K, 1 bar.
- Demonstrate the synthesis of modified polymer-based carbons with high surface area and low average pore width. Accomplished gravimetric storage capacity of ~6.7-7.0 wt% (77 K, 60 bar) and volumetric capacity 8 g H_2/L (237 K, 60 bar) with a high reproducibly on production in laboratory scale!
- Detail study on composition and morphology of new type of carbon nanotube with Fe and other metal into organocyclic-CNHn macromolecules rich with unsaturated bonds that should be available for room

temperature (RT) application at moderate pressures for H_2 storage systems.

- Products with an unlimited self-life! (Stable to extreme whether condition, including high humidity and temperature variation.)
- Products perform well at relatively low pressure (<20 bar).



Introduction

The State University of New York (esf) and PoroGen, LLC, have initiated a collaborative effort to develop superior high surface area nanostructured carbons for hydrogen storage. Synthesis of the carbon starts with the preparation of a nanoporous semicrystalline oriented polymer precursor having nanosize pores, with a uniform pore size distribution. This semicrystalline nanoporous polymer precursor is subsequently tailored to form high surface area activated carbons with slit-like microporous structure (pore width ~7-20 Å). The high surface area of the polymeric precursor aids in preparation of this unique carbon (Brunauer-Emmett-Teller surface area, S_{BET} >3,000 m^2/g) and enables doping initial material with chemical agents, which, upon carbonization, introduces specific interaction sites that significantly increase the hydrogen storage capacity of the nanostructured carbon material.

Approach

To achieve the project objectives, polymer-based nanostructured carbons have been synthesized by engineering the structure of the polymer precursors to produce carbon with the designed morphology for activation to high surface area and controlled micropores. Thus, polymer precursors (modified poly(phenylene oxide), MPEEK, poly(etherimide)) are spun at high melt shear rates further to controlled the morphology and orientation of crystalline regions. High orientation of polymer chains and alignment of crystalline lamellar regions leads to the formation of a porous material from oriented nano-size pores that upon carbonization, with specific activation agents, produce high surface area, high microporosity activated carbon. Consequently, procedures (including parameters such as heating rate, temperature and time) were developed to properly carbonize polymer precursors. In the activation (pore creation) step, the activation kinetics, including the reactivity size of activation agents, and the homogeneity of activation system, were addressed to control the carbons texture. Interaction of carbon with hydrogen is relatively low and may reach up to 6-7 kJ/mol. Since organocyclic-CNHn macromolecules with unsaturated bonds that exhibit rigid planar configuration and are abound in electronegative nitrogen atoms, can complex metal-salt and are enable for RT application for H_2 storage systems in moderate pressure. Thus the synthetic methods are expanded to incorporate reactive sites into the carbon nanostructures by doping polymerized unsaturated functionalized polycyclic complexes (Melem, Fe-Melem, and Nit-Melem). Alloying activated carbon with unsaturated functionalized polycyclic complex(ed) with Melem, the proper compositions, and the ratio of carbon/alloy and other components, is needed. Also, surface modifications of the nanostructures of polymer based carbons (by blending different polymer precursors) and control of hydrogen's binding energy with the carbon/alloys have been part of this study. Extensive physisorption and chemisorptions (of H_2 adsorption) characterizations have been performed to verify the synthetic effort.

Results

In FY 2010-2011, the main focus still remains the exploration of new polymer-based materials and synthetic routes by tailoring the morphology of polymer precursor to produce high surface area, higher microporosity and small pore size nanostructured carbons. Besides our laboratories, hydrogen storage measurement has been tested at other several industrial and government facilities. The porous textures and hydrogen storage capacity at 1 bar and 77 K are summarized in Table 2. These carbons gave S_{BET} from 1,000 to 3,200 m^2/g. All carbons (beside APKI-1 and APKI-4) have microporosity >90%, with average pore diameter d_{DR} ~10–20 Å. A hydrogen gravimetric storage capacity $W(H_2)$ ~2.98 wt% and $V(H_2)$ ~25 g/L was obtained at 77K and 1 bar.

TABLE 2. Porous Texture and Hydrogen Storage Capacity (77 K, 1 bar) of Polymer-Based Activated Carbon

Sample	S_{BET} m^2/g	V_{pore} mL/g	V_{mp} mL/g	d_{DR} Å	ρ_a g/mL	$W(H_2)$ wt%	$V(H_2)$ gH_2/L
NitCP-89	420	0.21	0.19	32.8	1.40	1.14	15.29
NitACP-119	1059	0.47	0.45	10.4	1.031	2.40	24.74
NitACP-121	2188	0.94	0.88	14.1	0.694	2.98	20.68
NitACP-109	2224	0.97	0.93	13.5	0.680	2.9	19.72
NitACP-127	2530	1.10	0.99	16.0	0.625	2.86	16.75
NitACP-133	2580	1.09	1.02	16.5	0.629	2.80	17.60
NitACP-136	2802	1.16	1.10	16.4	0.602	2.66	16.01
APKI-1	3255	1.71	1.24	20.0	0.444	2.93	13.02
APKI-4	3111	1.63	1.15	19.6	0.469	2.82	13.24
ACP-113	2315	0.97	0.93	15.3	0.680	2.97	20.16
ACP-125	3010	1.38	1.15	18.23	0.532	2.98	18.06
ACP-127	2530	1.10	0.99	16.0	0.625	2.86	17.88
ACP-136	2471	1.02	0.98	15.8	0.657	2.58	16.95

A new type of polymer-based carbons that incorporate metal ions with high surface area and narrow pore size distribution were developed. Figure 1 compares the 77

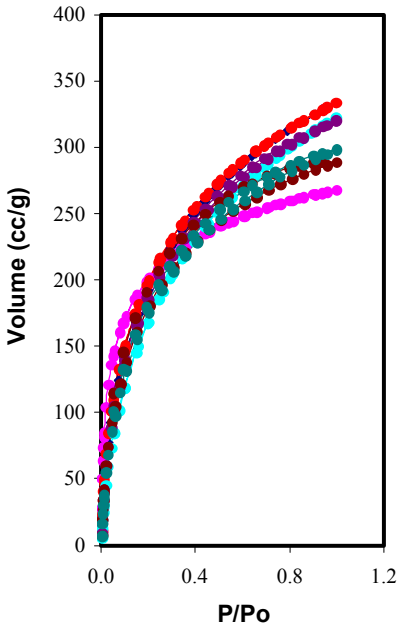


FIGURE 1. Hydrogen uptake (77 K, 1 bar) of polymer-based carbon (●) ACP-113; (●)NitACP-121;(●)ACP-127; (●)ACP-123; (●)NiACp-127; (●) ACP-136;(●) NitACP-136.

K hydrogen isotherms of nanostructured polymer-based (different polymer precursors) carbons synthesized under various conditions. Scanning electron microscope (SEM) images (Figure 2) of the carbon (NitCP-89) synthesis with metal gives nanotube structures (Figure 2a) with a diameter about 30 nm. Without metal ions, the carbon (APKI-1) shows a layer stack structure with small pours on the wall (Figure 2b). Although the BET surface area of NitCP-89 is lower at ~420 m^2/g compared with APKI-1 which is 3,225 m^2/g, the volumetric hydrogen uptake of NitCp-89 is 15.79 g/L (at 77K, 1 bar) higher than APKI-1 (~13.02 g/L).

Figure 3 shows a set of these carbons that were subjected to H_2 uptake at a pressure up to 20 bar at 77 K and 273 K up to 60 bar. At 273 K and 60 bar, the carbons made from phenyl phosphine oxide (NitACP-109 has S_{BET} ~2,224 m^2/g, V_{pore} ~0.97 cc/g and d_{DR} ~13.5 Å) shows the highest volumetric hydrogen capacity ~8g H_2/L. However, at 77 K and 20 bar, polyether ether ether ketone (APKI-1 has S_{BET} ~3,225 m^2/g, V_{pore} ~1.7 cc/g and d_{DR} ~20.0 Å) carbons have the same hydrogen storage capacity of ~5.8 wt% at 20 bar, and 77 K.

In the past year, we continued to focus on the synthesis of nanotube multicyclic ligand carbon. These carbons carbonized at 600°C with different pyrolysis times from 2 h to 60 hours giving a different morphology than were observed by transmission electron microscope images. The surface area and hydrogen storage capacity of melem-based carbon at 77 K, 1 bar are shown in the Table 2.

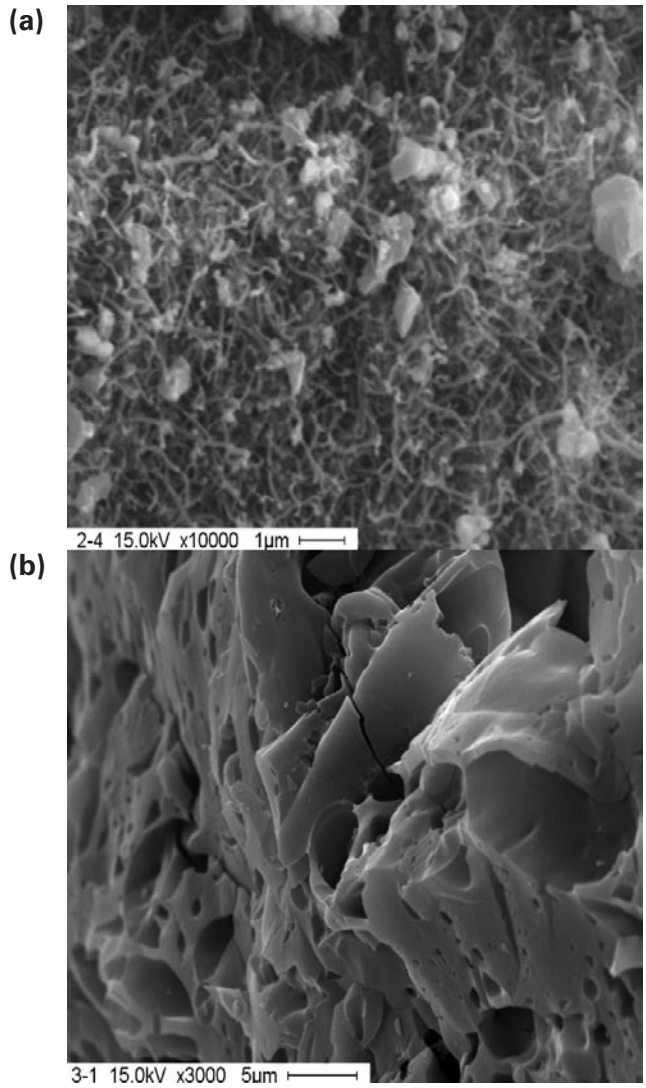


FIGURE 2. SEM image of (A) polymer-based carbon (NitCP-89) nanotube; B) activated polymer-based carbon.

TABLE 2. The Surface Area and Hydrogen Storage Capacity of Melem-Based Carbon at 1 bar, 77 K

Sample ID	S_{BET} (m^2/g)	H. C. (mL/g)
Ma015560-8	598.4	91.68
Ma015565-8	820.1	86.30
Ma015570-15	306.5	25.71
Ma015570-16	460.1	42.51
Ma015570-17	690.4	82.76
Nit70-2	189.0	23.50

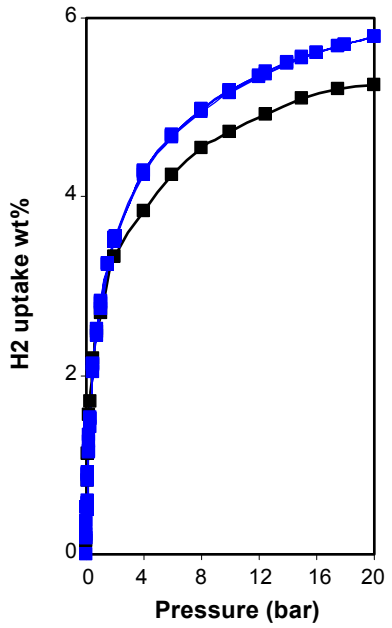


FIGURE 3. Gravimetric hydrogen uptake of APKI-1(■); PKOMe(●) at 77 K, up to 20 bar.

Conclusions

- A new type of polymer-based carbons with the incorporation of metal ions with high surface area and narrow pore size distribution were developed. The hydrogen storage capacity was ~3.0 at 77 K, 1 bar.
- Detailed study of composition and morphology of new type of carbon nanotube with Fe and other metal into organocyclic-CNHn macromolecules rich with unsaturated bonds that should be available for RT application at moderate pressures for H_2 storage systems.
- Demonstrated synthesis of modified polymer-based carbons with high surface area and low average pore width. Accomplished gravimetric storage capacity of ~6.7-7.0 wt% (77 K, 60 bar) and volumetric capacity 8 gH_2/L (237 K, 60 bar) with a high reproducibly on production in laboratory scale!

FY 2011 Presentations

1. I. Cabasso; and Youxin Yuan, "Polymer-based activated carbon for hydrogen storage", *DOE Annual Merit Review Highlights Hydrogen and Fuel Cell Projects*, port, June 9, 2011, Washington, D.C.

IV.C.9 Hydrogen Storage in Metal-Organic Frameworks

Omar M. Yaghi
Department of Chemistry and Biochemistry
University of California, Los Angeles
607 Charles E. Young Drive East
Los Angeles, CA 90095
Phone: (310) 206-0398
E-mail: yaghi@chem.ucla.edu

DOE Managers
HQ: Ned Stetson
Phone: (202) 586-9995
E-mail: Ned.Stetson@ee.doe.gov
GO: Katie Randolph
Phone: (720) 356-1759
E-mail: Katie.Randolph@go.doe.gov

Contract Number: DE-FG36-05GO15001

Project Start Date: May 1, 2005
Project End Date: April 30, 2011

Fiscal Year (FY) 2011 Objectives

- Expand the framework while keeping strong H_2 binding sites:
  - Design new porphyrin metal-organic frameworks (MOFs) to increase the storage space.
  - Expand Mg-MOF-74; high Q_{st} and Brunauer-Emmett-Teller (BET) surface area to achieve high H_2 density at room temperature.
- Preparation of high-surface area MOFs:
  - Large storage space, with minimization of dead space (*i.e.* high BET surface area).
  - Evaluate room temperature H_2 storage capacity by new high surface area MOFs.

Technical Barriers

This project addresses the following technical barriers from the Storage section (3.3.4.2) of the Fuel Cell Technologies Program Multi-Year Research, Development and Demonstration Plan:

(A) System Weight and Volume
(C) Efficiency
(E) Charging/Discharging Rates

Technical Targets

This project consists of conducting fundamental studies of MOFs. Insights gained from these investigations will be applied toward the design and synthesis of hydrogen storage materials that meet the following DOE 2015 revised hydrogen storage targets:

- Volumetric density: 40 g L^{-1}
- Gravimetric density: 4.5 wt%

FY 2011 Accomplishments

- Preparation of novel MOFs with metals.
- Highest BET surface area among porous solids.
- Fifteen and 2.7 wt% H_2 uptake by MOF-210 at 77 and 298 K.



Introduction

Conventional storage of large amounts of hydrogen in its molecular form is difficult and expensive because it requires employing either extremely high pressure as a gas or very low temperature as a liquid. Due to the described importance of hydrogen as a fuel, the DOE has set system targets for H_2 storage for the gravimetric (5.5 wt%) and volumetric (40 g L^{-1}) densities to be achieved by 2015. MOFs exhibit the highest hydrogen uptake of any porous materials and clearly demonstrate that the DOE targets are possible to achieve at 77 K. However, the implementation of room temperature hydrogen storage in MOF materials will require the design of new porous solids. Therefore, we are currently focusing our efforts on discovering novel highly porous materials with strong affinity for hydrogen.

Approach

To meet the DOE 2015 revised targets via physisorption, adsorbents must have high surface area (>3,500 m^2 g^{-1}) and relatively high density (>0.75 g cm^{-3}). We have already demonstrated how to design high surface area materials. However, in most cases these materials do not demonstrate steep H_2 uptake in the low pressure region, which is indicative of the weak interaction with H_2. Therefore, we aimed at increasing strong binding sites for maximum H_2 uptake capacity without losing pore volume. More specifically, we prepared and tested the H_2 storage capacity of three types MOFs: (i) metalated MOFs, (ii) MOFs with open metal sites and large pore, and (iii) ultrahigh surface area MOFs, which are materials having the highest BET surface area.

Results

Preparation of Porphyirin MOFs. To achieve strong H_2-MOF interaction, we believe that utilization of open metal sites is essential and the most effective method.

Several metal ions are known to form coordinatively unsaturated sites; however, it is fair to say that only a limited number of metal units, e.g. $Cu_2(CO_2)_4$ are available in MOF structure. In other words, it is important to design novel MOFs whose organic linker has potential metal binding site. We have prepared MOFs with porphyrin linkers that are connected by zinc paddle wheel units. However, H_2 uptake in these porphyrin MOFs is not high, likely due to moderate surface areas. To overcome this drawback, we prepared a new MOF with Zr ions.

Based on the reticular chemistry of these systems, it is expected that the $Zr_6O_4(OH)_4(CO_2)_{12}$ units (Figure 1A) are connected by tetratopic links to form new MOF structures, i.e. **ftw** net for square tetratopic link, **ith** net for tetrahedron. Therefore, we chose tetraphenylporphyrin as a square tetratopic link (Figure 1A) to synthesize a new free-base porphyrin MOF and its metalated versions (Cu and Pd ions). The porphyrin MOFs were prepared by a solvothermal reaction of a mixture of porphyrin link and zirconium chloride in *N,N*-dimethylformamide. Although, we did not finalize the structure, the powder X-ray diffraction pattern of this material is nearly identical to the simulated pattern of modeled material.

The permanent porosity was demonstrated by Ar adsorption isotherm for guest free samples. The compound shows typical type I isotherm, which indicates that the material has microporosity. The BET surface areas of activated MOFs are estimated to be 2,100, 1,850, and 1,700 m^2/g for free-base, Cu and Pd porphyrin MOFs, respectively. To evaluate the pore size distribution of porphyrin MOF, the Ar isotherm was analyzed using nonlocal density functional theory. The distribution calculated by fitting the adsorption data (17 Å) is close to the pore diameter from modeled structure of each MOF.

The H_2 isotherms of porphyrin MOFs were measured at 77 and 87 K. The H_2 uptake of free-base, Cu and Pd porphyrin MOFs at 1 bar and 77 K is 1.6, 1.7, and 1.6 wt%, respectively. These uptakes are larger than that of MOF-177. We also estimated the heat of adsorption (Q_{st}) and the initial Q_{st} value of the free-base porphyrin MOF was calculated to be 6.4 kJ/mol, which is similar to MOF-199 having open metal sites (6.8 kJ/mol) [1]. More importantly, the initial Q_{st} values of metalated porphyrin MOFs (7.0 and 6.8 kJ/mol for Cu and Pd version) were higher than that of free-base porphyrin MOF, indicating that the metal ions in the large aromatic (porphyrin) cycle can improve the H_2-MOF interaction. For the room temperature H_2 storage, further improvement of the Q_{st} is required; therefore, we plan to synthesize other metalloporphyrin MOFs.

Preparation of Expanded Version of Mg-MOF-74. To achieve room temperature H_2 adsorption, density of strong H_2 binding site per volume is one of the key factors. We have demonstrated that rod-type metal building units (Figure 1B) are sufficient systems for increasing the metal/

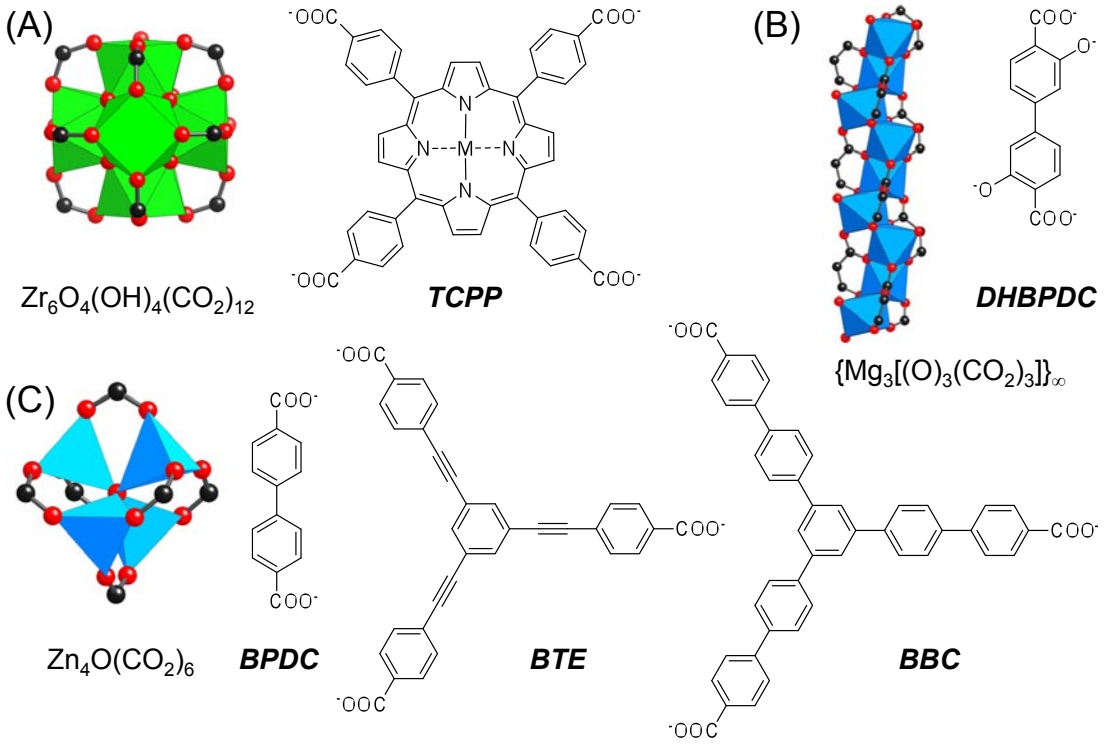


FIGURE 1. (A) $Zr_6O_4(OH)_4(CO_2)_{12}$-based MOFs with porphyrin linkers (TCPP, M = H_2, Cu, or Pd). (B) Expanded version of Mg-MOF-74 is prepared using 3,3′-dihydroxy-[1,1′-biphenyl]-4,4′-dicarboxylate (DHBPDC). (C) $Zn_4O(CO_2)_6$ unit is connected with organic linkers to form MOF-210 (BPDC and BTE) and MOF-200 (BBC).

ligand ratio (for example, MOF-74 shows excellent H_2 uptake behavior in the low pressure region at 77 K [1]). However, because of the moderate pore diameter of MOF-74, the surface area of MOF-74 is not high enough to meet the DOE targets of 5.5 wt%. We believe that expansion of the one-dimensional channel diameter would increase the total storage capacity. In this year, we prepared extended version of Mg-MOF-74 using 3,3′-dihydroxy-[1,1′-biphenyl]-4,4′-dicarboxylic acid (Figure 1B, this linker was provided by Prof. Stoddart group of Northwestern University) by a solvothermal reaction. Obtained micro crystals were analyzed by powder X-ray diffraction (PXRD) measurements.

To confirm the porosity and estimate the pore size distribution, we recorded Ar isotherm for the activated sample of expanded Mg-MOF-74 at 87 K. The compound shows a step at $P/P_0 = 0.05$, which indicates that the material has relatively large pore. The Langmuir and BET surface areas of activated MOF are estimated to be 3,200 and 2,740 $m^2\ g^{-1}$, respectively. The pore size distribution calculated by fitting the Ar adsorption data (19 Å) is close to the pore diameter from the crystal structure.

To calculate the Q_{st} for this MOF, low-pressure H_2 isotherms were recorded at 77 and 87 K. The initial Q_{st} value (10.1 kJ/mol) is almost the same as that of Mg-MOF-74 (10.1 kJ/mol [2]). The Q_{st} curves are sometimes influenced by the pore geometry with smaller pore materials tending to show better Q_{st} data. However in this case, it seems the initial Q_{st} value just reflects the Mg-H_2 interaction.

Figure 2 demonstrates a high-pressure excess H_2 isotherm of expanded MOF-74 at 77 K (red circles). The isotherm showed a steep raise below 10 bar, the excess uptake was saturated around 45 bar where the H_2 uptake was 4.5 wt%. As expected, the profile of high-pressure

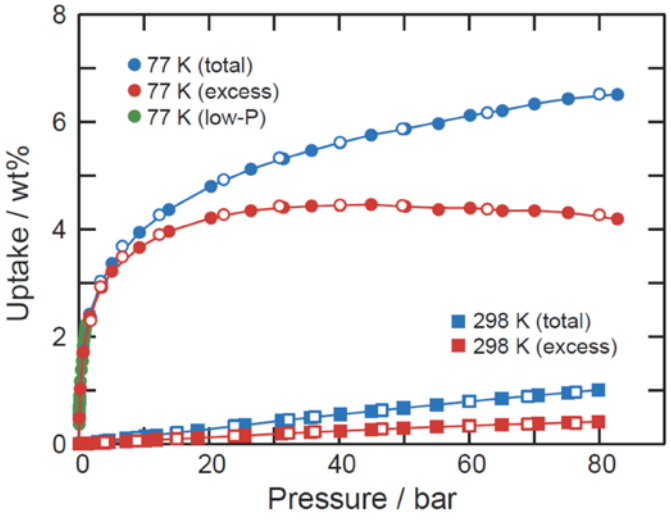


FIGURE 2. High-pressure H_2 isotherms of expanded Mg-MOF-74 at 77 K (red circles) and at 298 K (red squares). Calculated total uptake data were overlaid (blue symbols).

isotherm matches with the low-pressure data indicating that the measurements were properly carried out. Although the surface excess mass is a useful concept, the total amount that a material is able to store is more relevant to the practicality of using H_2 as a fuel. Therefore, we estimated this value by using a pore volume and bulk H_2 density ($N_{total} = N_{ex} + \rho_{bulk} V_p$). Estimated total H_2 uptake was plotted in Figure 2 (blue circles). Total uptake at 80 bar was calculated to be 6.5 wt%, which corresponds to 43 g/L. Due to the moderate BET surface area of expanded MOF-74, the total gravimetric uptake is not overwhelmingly exceptional. However, the volumetric uptake is well within the realm of the DOE system target albeit at 77 K.

We also measured H_2 isotherms of the same sample at 298 K (Figure 2). The excess uptake at 80 bar was 0.41 wt%, which was unfortunately smaller than the H_2 uptake at 87 K and 1 bar (1.5 wt%). This implies that a higher Q_{st} value is required to increase the H_2 density in MOFs even though the Q_{st} for expanded MOF-74 is ca. 10 kJ/mol. The estimated total H_2 uptake at 80 bar and 298 K was calculated to be 1.0 wt% (6.3 g/L). This volumetric uptake is slightly higher than the bulk density of H_2 at the same condition (6.2 g/L). In order to improve on these results, we plan to synthesize the isoreticular structures using Ni and Co ions instead, which are reported to have Q_{st} values greater than that of Mg-MOF [2].

Ultrahigh Porosity in MOF-200 and 210. One of the most important properties of MOFs is their high porosity and high specific surface area. An important consideration in maximizing the uptake of H_2 within MOFs is to increase the number of adsorptive sites within a given material. The simplest way to accomplish this is to use slim organic linkers in which the faces and edges of the constituent units are exposed for gas adsorption [3]. As shown in MOF-5 and MOF-177, the octahedral $Zn_4O(CO_2)_6$ (Figure 1C) has had a prominent role as a building unit in producing structures exhibiting exceptional porosity [1,3]. Therefore, we prepared the expanded forms of MOF-177 from 4,4′,4″-(benzene-1,3,5-triyl-tris(benzene-4,1-diyl))tribenzoate (BBC) to give MOF-200, and used mixed 4,4′,4″-(benzene-1,3,5-triyltris(ethyne-2,1-diyl))tribenzoate (BTE)/ biphenyl-4,4′-dicarboxylate (BPDC) links to obtain MOF-210 (Figure 1C).

MOF-200 and 210 were prepared from a solvothermal reaction of organic linkers and zinc nitrate, and obtained crystals were characterized single crystal X-ray diffraction. Considering the bulk density and void space calculated from the crystal structure analyses, MOF-200 and 210 are promising candidates to realize ultra-high surface area. However, preliminary trials revealed that the solvent exchange followed by pore evacuation under vacuum was not effective to activate MOF-200 and 210 without losing the porosity. Therefore, these crystals were fully exchanged with liquid CO_2, kept under supercritical CO_2 atmosphere, followed by their pores being bled of CO_2 to yield activated samples. Successful guest removal was confirmed by PXRD measurements and elemental analyses.

As shown in Figure 3, these MOF samples show distinctive steps ($P/P_0 = 0.14$ and 0.27 for MOF-200 and 210), and the profiles for MOF-200 and 210 are nearly the same as the predicted isotherms by grand canonical Monte Carlo simulations (Prof. Snurr group at Northwestern Univiversity). The maximum N_2 uptake capacities at 77 K in MOF-200 and 210 are 2,340 and 2,330 $cm^3\ g^{-1}$, respectively. More importantly, the measured values are near the values predicted based on the structure, indicating that these materials are well-activated. Because of the successful sample activation, extremely high BET (and Langmuir) surface areas were obtained: 4,530 (10,400) and 6,240 (10,400) $m^2\ g^{-1}$ for MOF-200 and 210. The BET surface area of MOF-210 is the highest reported for crystalline materials.

Given the exceptional properties of such materials, it is expected that these high surface area MOFs would exhibit exceptional H_2 storage capacity. These MOFs reach saturation uptakes, and the saturation pressure increases with an increase in the cavity size (Figure 4). The surface excess H_2 uptake in MOF-210 (7.9 wt%) was higher than MOF-177 and 200 (6.8 and 6.9 wt%) [4]. Given the pore volume and density of H_2 at 77 K, the total H_2 uptake in MOF-210 is calculated to be 15 wt%, which exceeds that of typical alternative fuels (methanol and ethanol) and hydrocarbons (pentane and hexane). MOF-200 also shows large total uptake (14 wt%); again, these values are higher than MOF-177 [4]. However, the volumetric total uptake (44 g/L for MOF-210; 36 g/L for MOF-200) was smaller than MOF-177 (50 g/L). The trend indicates that it is better to reduce the dead volume by introducing functionalities, which can interact positively with H_2.

Figure 4 displays the room temperature H_2 isotherms of MOF-210. The excess uptake at 80 bar was 0.53 wt%, which is similar to the room temperature H_2 uptake by MOF-177 (0.54 wt%). We believe that the excess H_2 uptake was not

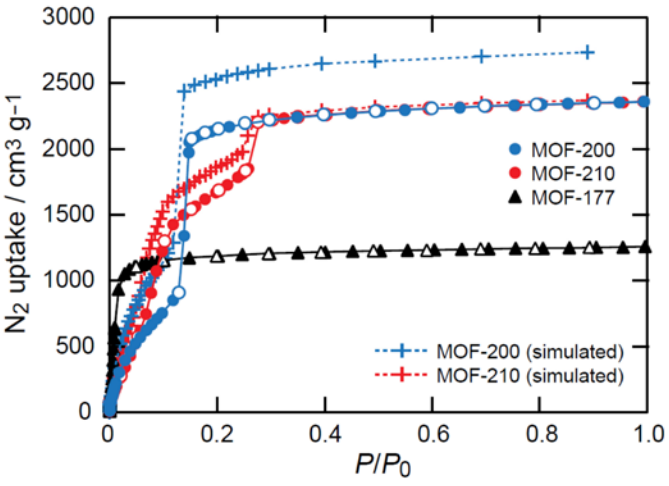


FIGURE 3. Low-pressure N_2 isotherms of MOF-177, -200, and -210 at 77 K. Simulated isotherms of MOF-200 and -210 were overlaid.

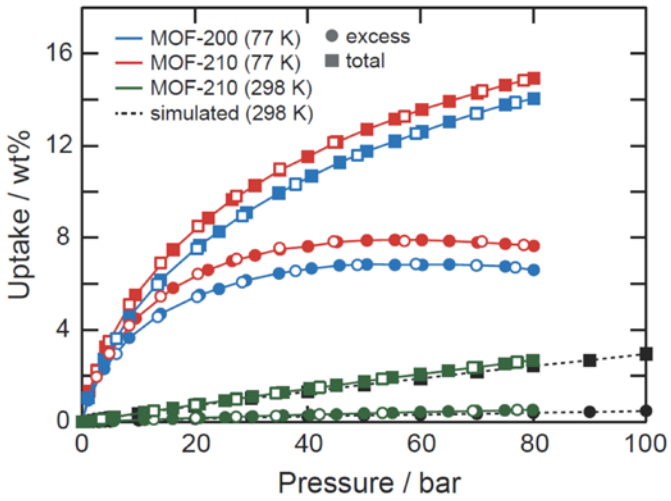


FIGURE 4. High-pressure H_2 isotherm of MOF-200 (blue circles) and 210 (red circles) measured at 77 K. Experimental (green) and simulated (black) H_2 isotherm of MOF-210 at room temperature are overlaid. Squares in the same color symbols represent calculated total uptake of H_2 under the same conditions.

improved because of the average pore diameter of MOF-210. The average pore diameter of MOF-210 is larger than the DOE recommendation for pore diameter size (0.7-1.2 nm to maximize the room temperature H_2 uptake capacity) with a significant storage space that still remains.

Calculated total H_2 isotherm is also shown in Figure 4. The total uptake at 80 bar was 2.7 wt%, which is the highest number reported for physisorptive materials. When the bulk density of MOF is applied, the volumetric H_2 uptake is calculated to be 6.9 g/L at 80 bar. Although the majority of the total uptake is attributed to the large pore volume (i.e. the contribution from $\rho_{bulk}V_p$), the volumetric H_2 uptake by MOF-210 remains higher than the bulk density of H_2 under the same conditions. Worth noting is that this finding is in sharp contrast to the fact that MOFs with larger density typically show even smaller volumetric uptakes than the bulk H_2 density.

Through the collaborative work with the Prof. Goddard group of Caltech, room temperature H_2 uptake by MOF-210 was predicted. As shown in Figure 4, these room temperature high-pressure H_2 data are in good agreement with predicted excess and total isotherms. However, H_2 isotherms recorded at room temperature sometimes contain significant errors due to their smaller uptake (compared to 77 K data). Therefore, it is fair to say that the simulation data provides reassuring support for the excellent experimental room temperature H_2 uptake capacity by MOF-210.

Conclusions and Future Directions

In this project, we aimed at developing the next generations of MOFs. It is presumed that the organic functionalities alone were not enough to show strong

binding energy, therefore, we prepared novel MOFs with metals. These MOFs showed improved adsorption enthalpy albeit a large pore volume is still a prerequisite feature. From the viewpoint of the storage space, we aimed at discovering high surface area MOFs. After many trials we optimized the synthesis and subsequent activation conditions of MOF-210, leading to 15 and 2.7 wt% of total H_2 uptake at 80 bar at 77 and 298 K, respectively. Although this project has finished, we will continue to pursue practical storage targets by the combination of the isoreticular metalation and the isoreticular expansion.

Special Recognitions

1. The 2010 Centenary Prize from the Royal Society of Chemistry.

FY 2011 Publications

1. H. Furukawa, N. Ko, Y.B. Go, N. Aratani, S.B. Choi, E. Choi, A.O. Yazaydin, R.Q. Snurr, M. O'Keeffe, J. Kim, O.M. Yaghi, "Ultra-High Porosity in Metal-Organic Frameworks," *Science*, **329**, 424-428 (2010).

2. D. Britt, C. Lee, F.J. Uribe-Romo, H. Furukawa, O.M. Yaghi, "Ring-Opening Reactions within Porous Metal-Organic Frameworks," *Inorg. Chem.*, **49**, 6387-6389 (2010).

3. S. Barman, H. Furukawa, O. Blacque, K. Venkatesan, O.M. Yaghi, and H. Berke, "Azulene Based Metal-Organic Frameworks for Polarized Binding of H_2," *Chem. Commun.*, **46**, 7981-7983 (2010).

4. D. Britt, "Metal-Organic Frameworks for Gas Separation," University of California - Los Angeles, 2010, Ph. D. thesis.

5. E. Choi, "The Construction of Metal-Organic Framework with Active Backbones by the Utilization of Reticular Chemistry," University of California - Los Angeles, 2011, Ph. D. thesis.

References

1. J.L.C. Roswell, O.M. Yaghi, *J. Am. Chem. Soc.*, **128**, 1304 (2006).

2. W. Zhou, H. Wu, T. Yildirim, *J. Am. Chem. Soc.*, **130**, 15268 (2008).

3. H.K. Chae, D.Y. Siberio-Perez, J. Kim, Y.-B. Go, M. Eddaoudi, A.J. Matzger, M. O'Keeffe, O.M. Yaghi, *Nature*, **427**, 523 (2004).

4. H. Furukawa, M.A. Miller, O.M. Yaghi, *J. Mater. Chem.*, **17**, 3197 (2007).

IV.D.1 Hydrogen Storage Engineering Center of Excellence

Donald L. Anton (Primary Contact) and Theodore Motyka
Savannah River National Laboratory
Bldg. 999-2W
Aiken, SC 29808
Phone: (803) 507-8551
E-mail: DONALD.ANTON@SRNL.DOE.GOV

DOE Manager
HQ: Ned Stetson
Phone: (202) 586-9995
E-mail: Ned.Stetson@ee.doe.gov

Technical Advisor
Robert Bowman
Phone: 818-354-7941
E-mail: rcbjr1967@gmail.com

Subcontractors:
- Pacific Northwest National Laboratory, Richland, WA
- United Technologies Research Center, E. Hartford, CT
- General Motors, Warren, MI
- Ford Motor Company, Dearborn, MI
- National Renewable Energy Laboratory, Golden, CO
- Los Alamos National Laboratory, Los Alamos, NM
- Jet Propulsion Laboratory, Pasadena, CA
- University of Michigan, Ann Arbor, MI
- California Institute of Technology, Pasadena, CA
- Oregon State University, Corvallis, OR
- Lincoln Composites LLC, Lincoln, NE
- BASF GmbH, Ludwigshafen, Germany
- Université du Québec à Trois-Rivières, Canada

Project Start Date: February 1, 2009
Project End Date: July 31, 2014

Fiscal Year (FY) 2011 Objectives

- Develop system models that will lend insight into overall fuel cycle efficiency.
- Compile all relevant materials data for candidate storage media and define future data requirements.
- Develop engineering and design models to further the understanding of on-board storage energy management requirements.
- Develop innovative on-board system concepts for metal hydride, chemical hydride, and adsorption hydride materials-based storage technologies.
- Design components and experimental test fixtures to evaluate the innovative storage devices and subsystem design concepts, validate model predictions, and improve both component design and predictive capability.
- Design, fabricate, test, and decommission the subscale prototype components and systems of each materials-based technology (adsorbents, metal hydrides, and chemical hydrogen storage materials).

Technical Barriers

This project addresses the following technical barriers from the Hydrogen Storage section of the Hydrogen, Fuel Cells and Infrastructure Technologies Program Multi-Year Research, Development and Demonstration Plan:

(A) System Weight and Volume
(B) System Cost
(C) Efficiency
(D) Durability/Operability
(E) Charging/Discharging Rates
(G) Materials of Construction
(H) Balance of Plant Components
(J) Thermal Management
(K) System Life Cycle Assessments
(L) High Pressure Conformality
(P) Lack of Understanding of Hydrogen Physisorption and Chemisorption
(S) By-Product/Spent Material Removal

Technical Targets

This project directs the modeling, design, build and demonstration of prototype hydrogen storage systems for each metal hydride, chemical hydride and hydrogen sorption material meeting as many of the DOE Technical Targets for light-duty vehicular hydrogen storage. The current status of these systems vs. the Onboard Hydrogen Storage System Technical Targets are given in Table 1.

FY 2011 Accomplishments

- Completed all requirements for moving the Center into Phase 2.
- Performed quality functional deployment analysis on Hydrogen Storage Technical Targets at both the 2010 and 2015 metrics and identified the relative trade offs incurred balancing targets with ordered list of technical targets given in Table 1.
- A unified model was completed utilizing the MATLAB®/SimuLink environment incorporating: (i) vehicle architecture and performance; (ii) fuel cell demands and requirements; and (iii) storage system demands and thermal management systems.

TABLE 1. System Status vs Technical Targets

	Technical Target	Units	2010	2015	Ultimate	Metal Hydride	Chemical Hydride	Adsorbent
Non-Quant-ified	Permeation & Leakage	*scc/hr*	#	#	#	s	s	s
	Toxicity		#	#	#	s	s	s
	Safety		#	#	#	s	s	s
	Gravimetric Density	*kgH$_2$/kgSystem*	0.045	0.055	0.075	**0.012**	**0.038**	**0.039**
Manditory	Min. Delivery Temp.	*°C*	-40	-40	-40	-40	-40	-40
	Max. Delivery Temp.	*°C*	85	85	85	85	85	85
	Min. Delivery Pressure (PEM)	*bar*	5	5	3	5	5	5
	Max. Delivery Pressure	*bar*	12	12	12	12	12	12
	Min. Operating Temperature	*°C*	-30	-40	-40	-30	-	-30
	Max. Operating Temperature	*°C*	50	60	60	50	50	50
Desirable	Min. Full Flow Rate	*[gH$_2$/s]/kW*	0.02	0.02	0.02	0.02	0.02	0.02
	System Cost*	*$/kWh net*	4	2	TBD	49.0	25.6	18.5
	On-Board Efficency	*%*	90	90	90	**78**	97	95
	Volumetric Density	*kgH$_2$/liter*	0.028	0.040	0.070	**0.012**	0.034	0.024
	Cycle Life	*N*	1000	1500	1500	1000	1000	1000
	Fuel Cost*	*$/gge*	3-7	2-6	2-3	7.3	-	4.89
	Loss of Useable Hydrogen	*[gH$_2$/hr]/kgH$_2$*	0.1	0.05	0.05	0.1	0.1	**0.44**
	WPP Efficency	*%*	60	60	60	**44.1**	**37.0**	**40.1**
	Fuel Purity	*%*	99.97	99.97	99.97	99.97	99.97	99.99
	Transient Response	*sec.*	0.75	0.75	0.75	0.75	0.49	0.75
	Start Time to Full Flow (-20°C)	*sec.*	15	15	15	15	1	15
	Fill Time	*min.*	4.2	3.3	2.5	**10.5**	**5.4**	**4.2**
	Start Time to Full Flow (20°C)	*sec.*	5	5	5	5	1	5

** Previous Values* # non-quantified s - satisfactory

gge - gasoline gallon equivalent; WPP - well to power plant

- Identified five drive cycles to be used in system analysis modeling.
- Systems analysis completed on metal hydride, chemical hydride and adsorbent systems resulting in:
  - Metal Hydride System
    - Completed system analysis on dual-bed $NaAlH_4$ system which was found to fully meet 10 targets, fall within 40% of six targets and below 40% of four targets (see Table 1).
    - Hydride compaction, enhanced hydride thermal conductivity and high temperature Type IV pressure vessels identified as critical technical barriers.
  - Chemical Hydride System
    - Completed system analysis on fluid ammonia borane (AB)/1-n-butyl-3-methylimidazolium chloride (BIMICl) system which was found to fully meet 13 targets, fall within 40% of four targets, below 40% of one target and two targets undefined (see Table 1).
    - Slurry identification/properties, flow through reactor control, low temperature fluid properties and reduced cost of balance-of-plant (BOP) components identified as critical technical barriers.
  - Adsorbent System
    - Completed system analysis on AX-21 system which was found to fully meet 14 targets, fall within 40% of gpit targets and below 40% of two targets (see Table 1).
    - Reduced cost of Type IV cryo-pressure vessel and BOP components; demonstration of peripheral sealing for flow through cooling, adsorbent compaction and enhanced adsorbent thermal conductivity identified as critical technical barriers.



Introduction

The Hydrogen Storage Engineering Center of Excellence (HSECoE) brings together all of the materials and hydrogen storage technology efforts to address onboard hydrogen storage in light-duty vehicle applications. The effort began with a heavy emphasis on modeling and data gathering to determine the state of the art in hydrogen storage systems. This effort spanned the design space of vehicle requirements, power plant and BOP requirements, storage system components, and materials engineering efforts. These data and models will then be used to design components and sub-scale prototypes of hydrogen storage systems which will be evaluated and tested to determine the status of potential system against the DOE 2010 and 2015 technical targets for hydrogen storage systems for light-duty vehicles.

Approach

A team of leading North American national laboratories, universities, and industrial laboratories, each with a high degree of hydrogen storage engineering expertise cultivated

through prior DOE, international, and privately sponsored programs has been assembled to study and analyze the engineering aspects of condensed phase hydrogen storage as applied to automotive applications. The technical activities of the Center are divided into three system architectures: adsorbent, chemical hydride and metal hydride matrixed with six technologies areas: Performance Analysis, Integrated Power Plant/Storage System Analysis, Materials Operating Requirements, Transport Phenomena, Enabling Technologies and Subscale Prototype Construction, Testing and Evaluation. The project is divided into three phases; Phase 1: System Requirements and Novel Concepts, Phase 2: Novel Concept Modeling Design and Evaluation and Phase 3: Subscale System Design, Testing and Evaluation.

Results

Materials

One prototypical material was selected for each storage materials type. These prototypical materials were selected due to their relatively high degree of data identified by the center and their relevance to other similar materials. These materials are not intended to be a selection of materials, but rather used to identify the current state of the art for storage system technologies.

Drive Cycles

A number of drive cycles were implemented to identify storage system performance. This is particularly relevant in the case of transient system performance, where the DOE targets have not identified the duration for which the targets need to be met. In many instances, engineering solutions have been implemented to meet the targets not directly related to the storage system media used. A summary of the drive cycles, and the targets which were determined by them are given in Table 2.

Systems

In order to determine the current state-of-the-art system performance, preliminary system architectures were designed and used in the unified modeling system run under MATLAB®-SimuLink and developed by the HSECoE. This SimuLink model included the hydrogen storage system, fuel cell system and vehicle system models.

Metal Hydride Systems

The baseline material used in this effort was sodium aluminum hydride ($NaAlH_4$), ball milled with 3 mole per cent $TiCl_3$ as a catalyst. The system used in this effort is given in Figure 1a and is composed of dual Type III $NaAlH_4$ tanks operational at 150 bar with an accompanying catalytic burner to supply the required enthalpy of dehydrogenation. A 150 bar buffer tank is included to facilitate cold-start and transient operations. The heat exchange system is a radial tube/fin design depicted in Figure 1a. The summary of these attributes is given in the spider diagram of Figure 1b where full realization of the target is denoted by filling in to the outer diameter.

Chemical Hydride Systems

The baseline material used in this effort was liquid AB composed of pure NH_3BH_3, dissolved in the ionic liquid BIMICl to a mass fraction of 50% AB. The chemical hydride system used in this effort is given in Figure 2a and is composed of bladder tank feeding a flow through reactor and a gas liquid separator which serves to separate the gaseous species from the spent fuel and as a high pressure

TABLE 2. Drive Cycles Utilized in System Target Status

Drive Cycle	Test Schedule	Cycle	Description	Target	Temp. (°C)
1	**Ambient Drive Cycle** - Repeat the EPA FE cycles from full to empty and adjust for 5 cycle post-2008	UDDS	Low speeds in stop-and-go urban traffic	System Size	24
		HWFET	Free-flow traffic at highway speeds		24
2	**Aggressive Drive Cycle** - Repeat from full to empty	US06	Higher speeds; harder acceleration & braking	Min. Flow Rate & Transient Response	24
3	**Cold Drive Cycle** - Repeat from full to empty	FTP-75 (cold)	FTP-75 at colder ambient temperature	Start time to Full Flow Rate (-20°C)	-20
4	**Hot Drive Cycle** - Repeat from full to empty	SC03	AC use under hot ambient conditions	Start time to Full Flow Rate (20°C)	35
5	**Dormancy Test**	n/a	Static test of the storage system-31 days	Dormancy	35

UDDS - Urban Dynamometer Driving Schedule; HWFET - Highway Federal Emissions Test; FTP75 - Federal Test Procedure; SC03 - supplementary cycle number 3; n/a - not applicable

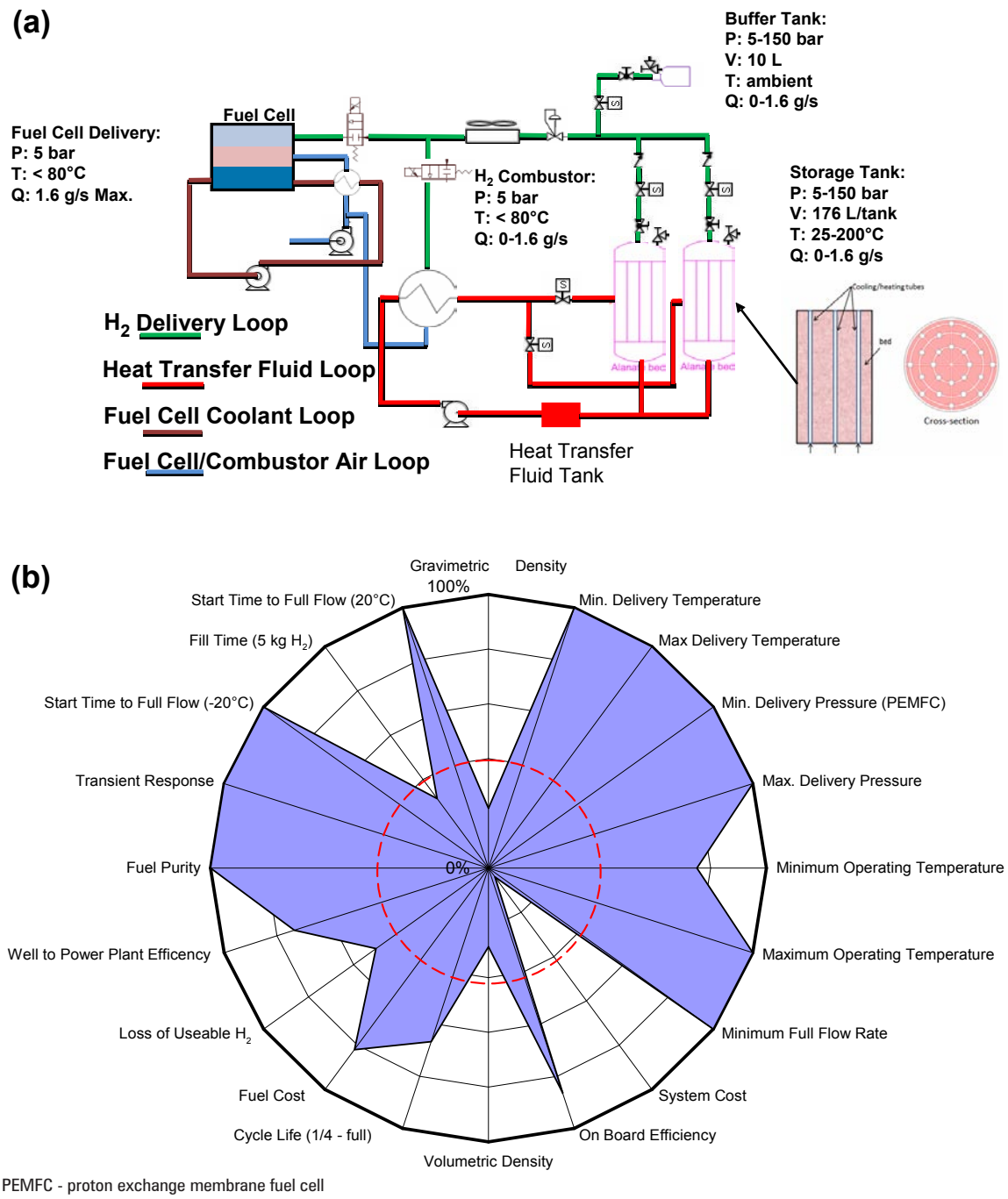


FIGURE 1. Metal Hydride System (a) configuration and (b) spider chart depicting metal hydride system performance characteristics against the 2015 technical targets.

ballast tank to feed hydrogen to the fuel cell in start-up and transient conditions. A pump is included to maintain both fresh and spent fuel flow with a portion of the spent fuel recirculate to absorb excess heat generated at the reactor. The summary of these attributes is given in the spider diagram of Figure 2b where full realization of the target is denoted by filling in to the outer diameter.

Adsorbent Systems

The baseline material used in this effort was a super activated carbon commercially available and designated as AX-21. The adsorbent system used for this effort is given in Figure 3a. It is composed of a 200 bar high pressure Type III pressure vessel enclosed in a multilayer vacuum insulated jacket with a 5 W heat leak at 80 K. Charging is achieved

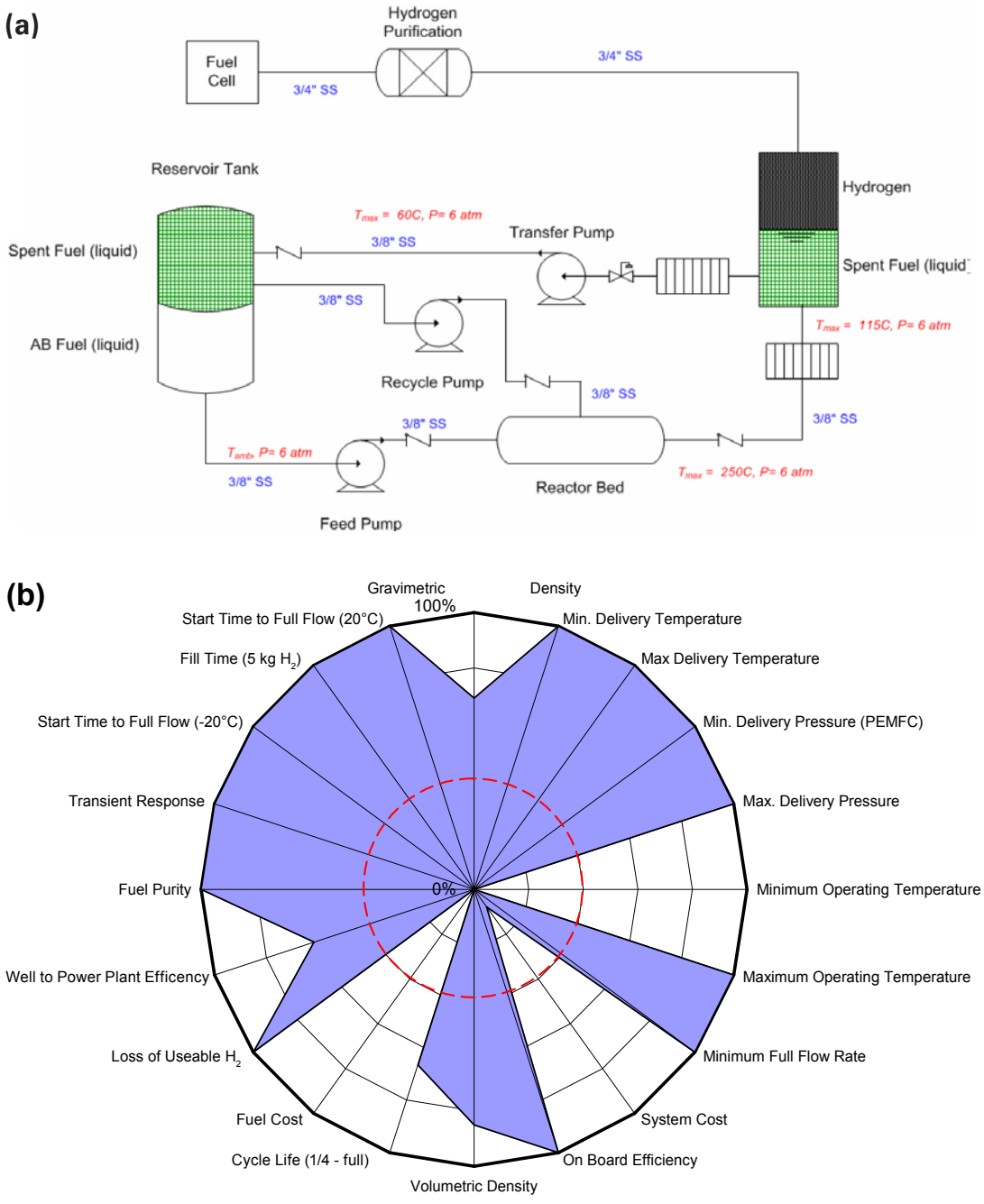


FIGURE 2. Chemical Hydride System (a) configuration and (b) spider chart depicting metal hydride system performance characteristics against the 2015 technical targets.

via flow-through cooling with an initial bed temperature 80 K. Desorption is achieved utilizing an in-tank electrical resistance heater. An external heat exchanger is utilized to heat the released hydrogen to ambient temperatures. The summary of these attributes is given in the spider diagram of Figure 3b where full realization of the target is denoted by filling in to the outer diameter.

Conclusions and Future Directions

The critical technical barriers identified to date and potential solutions being evaluated are given below for each of the storage system types.

- Metal Hydride System
  - Hydride compaction via mechanical constraint.

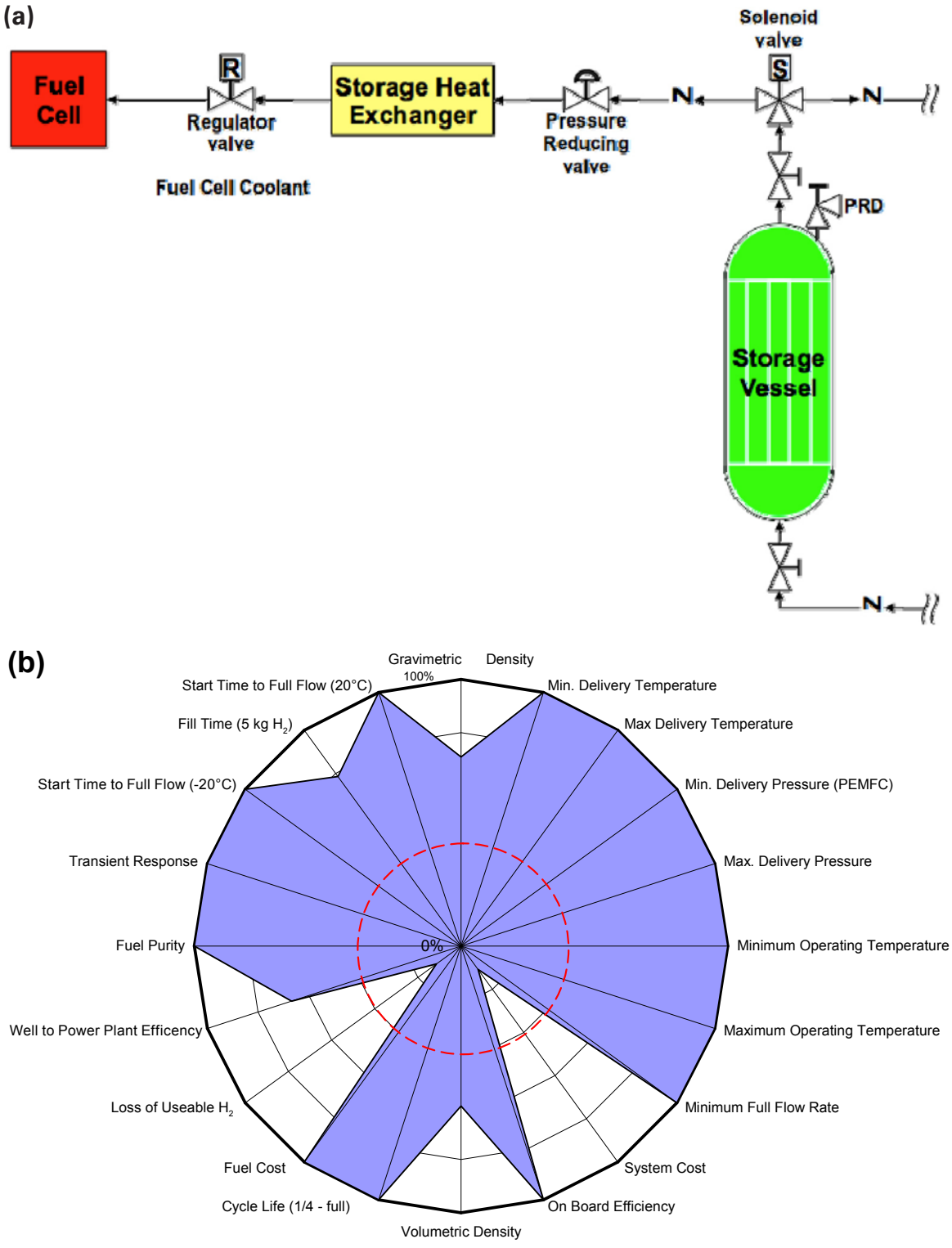


FIGURE 3. Adsorbent System (a) configuration and (b) spider chart depicting metal hydride system performance characteristics against the 2015 technical targets.

- Enhanced hydride thermal conductivity via additions of expanded natural graphite.
- High temperature Type IV pressure vessel development.

- Chemical Hydride System
  - Slurry/solvent identification/properties with nonreactive organic liquids/ionic, liquids.
  - Flow through reactor thermal control via spent fuel feedback.
  - Low temperature fluid properties.
- Adsorbent System
  - Type IV cryo-pressure vessel development.
  - Peripheral sealing for flow through cooling.
  - Adsorbent compaction via low temperature binderless techniques.
  - Enhanced adsorbent thermal conductivity via expanded natural graphite additions.

FY 2011 Publications

1. Systems Modeling, Simulation and Material Operating Requirements for Chemical Hydride Based Hydrogen Storage, Devarakonda, M., Brooks, K.P., Rassat, S., and Rönnebro, E., International Journal of Hydrogen Energy (Submitted).

2. Dynamic Modeling and Simulation Based Analysis of an Ammonia Borane (AB) Reactor System for Hydrogen Storage, Devarakonda, M., Holladay, J., Brooks, K.P., Rassat, S., and Herling, D., ECS Transactions, 33(1), pp. 1959-1972, 2010.

3. Systems Modeling of Ammonia Borane Bead Reactor for OnBoard Regenerable Hydrogen Storage in PEM Fuel Cell Applications, Brooks, K.P., Devarakonda, M., Rassat, S., King, D.A., and Herling, D., Proceedings of ASME 2010 Eighth Fuel Cell Science, Engineering and Technology Conference, Volume 1, ISBN: 978-0-7918-4404-5 pp. 729-734, 2010.

4. Increased volumetric hydrogen uptake of MOF-5 by powder densification, J. Purewal, D. Liu, J. Yang, A. Sudik, D.J. Siegel, S. Maurer, U. Mueller, Int. J. Hydrogen Energy, 2011, Accepted.

5. Engineering Improvement of NaAlH4 System, B.A. van Hassel, D. Mosher, J.M. Pasini, M. Gorbounov, J. Holowczak, X. Tang, R. Brown, B. Laube and L. Pryor, Int. J. Hydrogen Energy. (in press)

6. System modeling methodology and analyses for materials-based hydrogen storage, José Miguel Pasini, Bart A. van Hassel and Daniel A. Mosher, Int. J. Hydrogen Energy. (in press)

7. Sensitivity study of alanate hydride storage system, M. Bhouri, J. Goyette, B.J. Hardy, D.L. Anton., International Journal of Hydrogen Energy 36 (2011) 621-633.

8. Evaluation of Acceptability Envelope for Materials-Based H2 Storage Systems, C. Corgnale, B. Hardy, D. Tamburello, S. Garrison and D. Anton, Int. J. Hydrogen Energy. (in press)

9. Automatic Optimization of Metal Hydride Storage Tanks and Novel Designs, S. Garrison, M. Gorbounov, D. Tamburello, B. Hardy, C. Corgnale, D. Mosher and D. Anton, Int. J. Hydrogen Energy. (in press)

10. System Simulation Models for High-Pressure Metal Hydride Hydrogen Storage Systems, Raju M., Ortmann JP, Kumar S., Int J Hydrogen Energy 2010; 35: 8742- 54.

11. System Simulation Modeling and Heat Transfer in Sodium Alanate based Hydrogen Storage Systems, Raju M. and Kumar S., Int J Hydrogen Energy 2011; 1578-1591.

IV.D.2 System Design, Analysis, Modeling, and Media Engineering Properties for Hydrogen Energy Storage

Matthew Thornton (Primary Contact),
Lin Simpson, Aaron Brooker, and Laurie Ramroth
National Renewable Energy Laboratory (NREL)
1617 Cole Boulevard
Golden, CO 80401
Phone: (303) 275-4273
E-mail: Matthew.Thornton@nrel.gov

DOE Manager
HQ: Ned Stetson
Phone: (202) 586-9995
E-mail: Ned.Stetson@ee.doe.gov

Project Start Date: February 2, 2009
Project End Date: September 30, 2014

Fiscal Year (FY) 2011 Objectives

- Perform vehicle-level modeling and simulations of various storage systems configurations.
- Lead the storage system energy analysis and provide results.
- Compile and obtain media engineering properties for adsorbent materials.

Technical Barriers

This project addresses the following technical barriers from the Hydrogen Storage section of the Fuel Cell Technologies Program Multi-Year Research, Development and Demonstration Plan:

(A) System Weight and Volume
(B) System Cost
(C) Efficiency
(E) Charging/Discharging Rates
(I) Dispensing Technology
(K) Systems Life-Cycle Assessments

Technical Targets

This project is conducting simulation and modeling studies of advanced onboard solid-state hydrogen storage technologies. Insights gleaned from these studies are being applied toward the design and synthesis of hydrogen storage vessels that meet the following DOE 2015 hydrogen storage for light-duty vehicle targets:

- Cost: to be determined
- Specific energy: 0.055 kg H_2/kg system
- Energy density: 0.040 kg H_2/L system
- Charging/discharging rates: 3.3 min
- Well-to-power-plant (WTPP) efficiency: 60%

FY 2011 Accomplishments

- Developed a vehicle model framework and test cycle matrix to aid in the analysis and understanding of hydrogen storage system requirements for light-duty vehicles.
- Integrated the hydrogen storage simulator (HSSIM vehicle model) with the center fuel cell and hydrogen storage models to create a model framework that could be used across the center to evaluate all storage system designs on a common basis and with consistent assumptions.
- Used the vehicle model and the center modeling framework to evaluate the performance of specific storage system designs across all material classes and assess the impact on vehicle performance.
- Performed vehicle-level tradeoff analyses to better understand the impact of key engineering designs, for example, the tradeoff between mass, onboard hydrogen storage capacity, and vehicle range.
- Used the Hydrogen Delivery Scenario Analysis Model (HDSAM) to calculate preliminary greenhouse gas (GHG) emissions and WTPP efficiency figures for baseline physical storage systems and candidate solid-state storage systems for each material class.
- Identified potential materials for analysis and provided storage system design guidance to help meet DOE storage targets with adsorbent materials.



Introduction

Overcoming challenges associated with onboard hydrogen storage is critical to the widespread adoption of hydrogen-fueled vehicles. The overarching challenge is identifying a means to store enough hydrogen onboard to enable a driving range greater than 300 miles within vehicle-related packaging, cost, safety, and performance constraints. By means of systems analysis and modeling, hydrogen storage system requirements for light-duty vehicles can be assessed. With these findings and through collaboration with our Hydrogen Storage Engineering Center of Excellence (HSECoE) partners, optimal pathways for successful hydrogen storage system technology can be identified to enable future commercialization of hydrogen-fueled vehicles.

Approach

An array of tools and experience at NREL are being used to meet the objectives of the HSECoE. Specifically, extensive knowledge of multiple vehicle simulations, well-to-wheels (WTW) analysis, and optimization are being employed and integrated with fuel cell and material-based hydrogen storage system models developed by other HSECoE partners. This integrated model framework allows for the evaluation of various hydrogen storage options on a common basis. Engineering requirements are defined from these studies thus enabling the design of hydrogen storage vessels that could meet DOE performance and cost targets in a vehicle system context.

In the area of media engineering, attaining the objectives of the HSECoE relies on NREL's leadership in developing custom analytical instrumentation for hydrogen adsorbent analysis. These tools are used to thoroughly characterize hydrogen storage adsorbents so that an optimized storage vessel specific to the adsorbent material may be efficiently engineered. NREL will use these methods to analyze adsorbent materials identified by the HSECoE as holding promise for application in commercial on-vehicle refuelable hydrogen storage systems capable of meeting DOE targets.

Results

The following will provide results from work completed this year to support the HSECoE with a focus on five main tasks. In collaboration with our original equipment manufacturer (OEM) partners, NREL (1) worked on the development of a vehicle model (hydrogen storage simulator, HSSIM) and final structure of a test cycle matrix used to support the overall modeling effort; (2) worked on the integration of the vehicle model with the center fuel cell and hydrogen storage models to create a model framework; (3) worked with the systems architects to perform simulations and tradeoff studies to help with the high-level storage system design and engineering, including system sizing; (4) performed energy analysis on specific systems design being considered by the HSECoE; and (5) continued work in the area of adsorbent materials characterization and analysis.

A key result was working with the center OEMs on finalizing the test matrix that will be used to evaluate all the storage systems being considered across the center on a common basis. The test matrix was structured to evaluate the performance of the storage systems against the technical targets under standard and realistic transient driving condition. The matrix was also designed to exercise a given systems from full to empty to provide an understanding of its performance over the entire range of fill conditions. Therefore, the test cases were designed to repeat a drive cycle or set of drive cycles until the storage system being evaluated was empty. Standard drive cycles are typically not long enough to achieve this and would not even deplete a buffer tank in some systems. The important point here is that when evaluating the complex dynamics of hydrogen storage systems, this approach of repeating drive cycles to create test cases is critical to gaining the feedback necessary to refine and improve the systems.

As shown in Table 1, the center test matrix includes five test cases:

The first case combines repeats of the urban dynamometer driving schedule (UDDS) and the highway fuel economy test (HWFET) until the storage systems is depleted. This is used to determine the vehicle-level fuel economy and from that figure the vehicle range. The fuel economy is calculated using the current Environmental Protection Agency (EPA) five-cycle procedure of adjusting and weighting the UDDS and HWFET to provide one fuel economy figure that represents real-world use–it is not the raw figures that come directly from running the cycles. Similarly, the range is then calculated from the adjusted and weighted UDDS and HWFET figure and not simply the cycles miles achieved until the storage systems is empty. Again, this test matrix is key to providing a means to evaluate the fuel economy, range, and other vehicle level performance feature of the storage systems on a common and comparable basis.

Secondly, NREL worked with other center partners on the integration of the vehicle model with the fuel cell and storage systems models within a single modeling framework. Figure 1 shows a representation of the modeling framework that allows for a common and consistent evaluation of given storage systems. The key is the integration of the various storage system models with a common vehicle and fuel cell model in Simulink®. NREL played a critical role in the development and structure of this framework and helped with the coding in Simulink® to ensure reliable, accurate, and validated results.

A third activity was working the center system architects to provide high-level feedback on the performance and design of their given material systems. Figure 2 shows an example of a tradeoff study quantifying the relative range impacts resulting from changes to the storage system capacity and reductions to the vehicle glider mass. Table 2 shows the example results from the application of this type of study to a $NaAlH_4$ system.

Fourth, NREL continued to support the HSECoE by performing energy analyses on various storage system designs that have become available. These analyses provide the center system architects and other partners with high-level estimates about the overall energy inputs required by a given system, including WTPP efficiency (%), hydrogen cost ($/kg) and GHG emissions (carbon dioxide equivalent) on a gram per mile basis.

Fifth, the HDSAM I was used to estimate the above parameters for each system. To date the HDSAM model has been run for $NaAlH_2$ metal hydride system and the AX-21

TABLE 1. Test Matrix used Across the Center to Evaluate the Performance of all the Storage Systems

Case	Test Schedule	Cycles	Description	Test Temp (°F)	Distance per cycle (miles)	Duration per cycle (minutes)	Top Speed (mph)	Average Speed (mph)	Max. Acc. (mph /sec)	Stops	Idle	Avg. H2 Flow (g/s)*	Peak H2 Flow (g/s)*	Expected Usage
1	Ambient Drive Cycle - Repeat the EPA FE cycles from full to empty and adjust for 5 cycle post-2008	UDDS	Low speeds in stop-and-go urban traffic	75 (24 C)	7.5	22.8	56.7	19.6	3.3	17	19%	0.09	0.69	1. Establish baseline fuel economy (adjust for the 5 cycle based on the average from the cycles) 2. Establish vehicle attributes 3. Utilize for storage sizing
		HWFET	Free-flow traffic at highway speeds	75 (24 C)	10.26	12.75	60	48.3	3.2	0	0%	0.15	0.56	
2	Aggressive Drive Cycle - Repeat from full to empty	US06	Higher speeds; harder acceleration & braking	75 (24 C)	8	9.9	80	48.4	8.46	4	7%	0.20	1.60	Confirm fast transient response capability – adjust if system does not perform function
3	Cold Drive Cycle - Repeat from full to empty	FTP-75 (cold)	FTP-75 at colder ambient temperature	-4 (-20 C)	11.04	31.2	56	21.1	3.3	23	18%	0.07	0.66	1. Cold start criteria 2. Confirm cold ambient capability – adjust if system does not perform function
4	Hot Drive Cycle - Repeat from full to empty	SC03	AC use under hot ambient conditions	95 (35 C)	3.6	9.9	54.8	21.2	5.1	5	19%	0.09	0.97	Confirm hot ambient capability - adjust if system does not perform function
5	Dormancy Test	n/a	Static test to evaluate the stability of the storage system	95 (35 C)	0	31 days	0	0	0	100%	100%			Confirm loss of useable H2 target

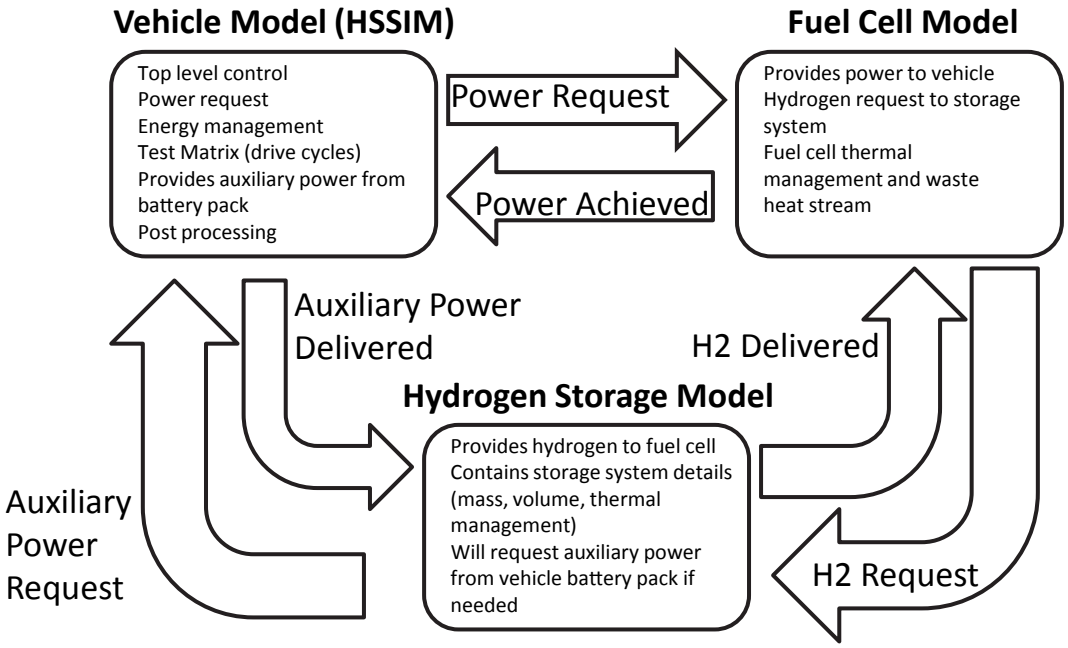


FIGURE 1. HSECoE Integrated Modeling Framework

and MOF-5 adsorbent systems to produce preliminary WTPP efficiency, GHG emissions, and hydrogen cost figures. NREL is currently working with the center adsorbent, metal hydride, and chemical hydride system architects to obtain these data and perform HDSAM runs for a liquid ammonia-borane and TiCr(Mn)H_2 systems.

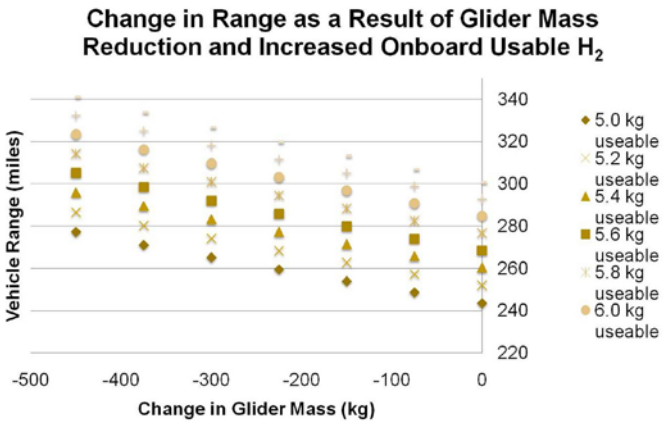


FIGURE 2. Example Storage System Design Tradeoff Study Results

TABLE 2. Example Storage System Design Trade-Off Study Results for a $NaAlH_4$ System

Vehicle Results	Units	$NaAlH_4$	$NaAlH_4$	$NaAlH_4$
Usable H_2	kg	5	6.4	5.6
Glider Mass	Kg	900	900	450
Vehicle Mass	kg	1791	1924	1398
UDDS Fuel Economy	mi/kg-H_2	46.6	44.9	52.6
HWFET Fuel Economy	mi/kg-H_2	51.5	49.8	57.0
Combined Fuel Economy	mi/kg-H_2	48.7	47.0	54.5
Range	miles	244	301	305
0 – 60 mph time	sec	10.8	11.3	9.3

For media engineering, NREL provided the HSECoE with specific engineering properties on adsorbent materials that were recommended as potential candidates for which to perform additional engineering analyses. These included high specific surface area (SSA) materials with high bulk densities, and searching for materials with higher than 10 kJ/mol hydrogen binding energies. Initially, this involved investigating representative materials that have more idealized and controlled pore sizes (in the range of 0.7 to 1.5 nm) such as pyrolized polyether-ether-ketone (PEEK) materials. As shown in Figures 3 and 4, these types of materials can be pressed to very high pressures (100,000 psi) with no significant loss of specific surface area or hydrogen storage capacities. At these pressures, bulk densities ranging from 0.7 to 1.5 g/mL can be achieved (Figure 3), resulting in substantial increases in Gibbs excess volumetric capacities (i.e., 40 to 80 g-H_2/L, see Figure 4). Thus, even though these materials may not have as high of Gibbs excess gravimetric capacities as metal-organic frameworks (Figure 3), due to their bulk densities being 2 to 5 times higher, their Gibbs excess volumetric capacities can be 2 to 4 times higher.

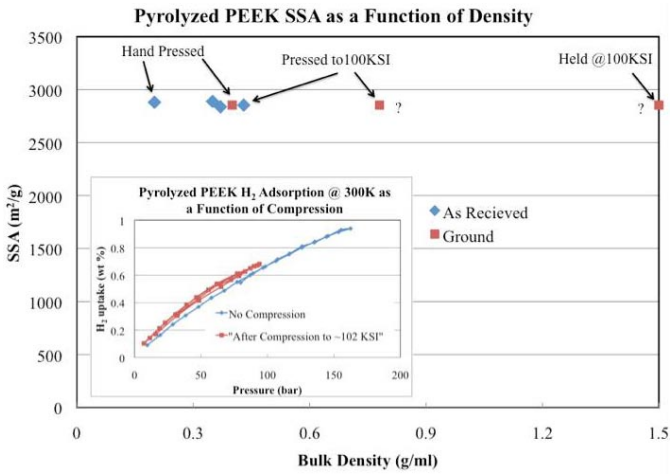


FIGURE 3. Engineering data of pyrolyzed PEEK materials demonstrating that very high bulk densities can be achieved with virtually no loss of SSA or hydrogen storage capacity.

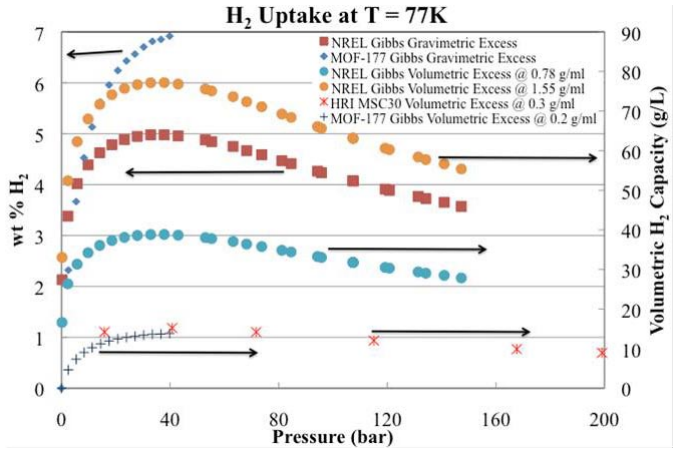


FIGURE 4. Engineering data for pyrolyzed PEEK that shows that volumetric capacity goals can be met with optimized pore size materials, much more easily than with lower bulk density materials such as MOFs.

Future Direction

- Continue to run vehicle simulations to support engineering design and support the center modeling framework refinements and enhancements:
  - Run vehicle simulations to support high-level storage system design and engineering tradeoffs.
  - Run vehicle simulations to support storage systems sizing analyses.
- Evaluate storage system impacts on vehicle performance (e.g., fuel economy, range).
- Evaluate storage system progress toward tech targets Run HDSAM to evaluate (liquid ammonia-borane and TiCr(Mn)H_2 systems:

  - WTPP efficiency
  - GHG emissions
  - H_2 cost
- Investigate adsorbent materials that enable high near-ambient temperature storage capacities including Pt/AC-IRMOF 8.

FY 2011 Publications/Presentations

1. Development of Heterogeneous Sorbents/ Sorbent Isotherm Measurement Materials Exchange, L.J. Simpson (invited talk), DOE LANL-AIST Hydrogen Workshop, September 17–20, 2010, San Francisco, CA.

2. Update of Sorbent Engineering Property Development Activities, L.J. Simpson (invited talk) DOE HSECoE Face-to-Face Architects Meeting, USCAR, September 17, 2010. Southfield MI.

3. Evaluation of Hydrogen Storage System Characteristics for Light-Duty Vehicle Applications (poster), M. Thornton, K. Day, and A. Brooker, National Hydrogen Association Conference & Expo, May 6, 2010, Long Beach, CA.

4. Evaluation of Hydrogen Storage System Characteristics for Light-Duty Vehicle Applications (poster), M. Thornton, K. Day and A. Brooker, World Hydrogen Energy Conference 2010, May 16, 2010, Essen, Germany.

5. Update of Sorbent Engineering Property Development Activities, L. J. Simpson (invited talk) DOE HSECoE Face-to-Face Meeting, PNNL, WA, October, 4–5, 2010.

6. A System Modeling Approach for Light-Duty Vehicle and On-Board Hydrogen Storage System, M. Thornton, K. Day, and A. Brooker, 2010 AIChE Annual Meeting, November 8, 2010, Salt Lake City, UT.

7. System Design, Analysis, Modeling, and Media Engineering Properties for Hydrogen Energy Storage, M. Thornton, DOE Annual Merit Review Meeting, May 11, 2011, Washington, D.C.

IV.D.3 Chemical Hydride Rate Modeling, Validation, and System Demonstration

Troy A. Semelsberger (Primary Contact),
Tommy Rockward, Eric L. Brosha, Gerie M. Purdy,
Tessui Nakagawa, Ben Davis, and Jose I. Tafoya
Los Alamos National Laboratory (LANL)
MS J579, P.O. Box 1663
Los Alamos, NM 87545
Phone: (505) 665-4766
E-mail: troy@lanl.gov

DOE Manager
HQ: Ned Stetson
Phone: (202) 586-9995
E-mail: Ned.Stetson@ee.doe.gov

Start Date: February 2009
Project End Date: February 2014

Fiscal Year (FY) 2011 Technical Objectives

- Develop fuel gauge sensors for solidstate hydrogen storage media.
- Mathematically model the aging characteristics (i.e., shelf-life) of candidate hydrogen storage materials.
- Develop rate models for hydrogen release on candidate chemical hydrides.
- Develop novel strategies for start-up and transient operation with candidate chemical hydrides.
- Identify hydrogen impurities and develop novel impurity mitigation strategies.
- Design, build, and demonstrate a subscale prototype reactor that releases hydrogen using chemical hydrides (technology area lead).
- Develop an on-board fluid-phase chemical hydrogen storage system; system designer.

FY 2011 Accomplishments

- Demonstrated novel acoustic fuel-gauge sensor is capable of tracking hydrogen states-of-charge for metal hydrides and metal hydride cycling.
- Performed preliminary fuel cell tolerance test with diborane impurity.
- Quantified borazine and diborane impurities generated from neat ammonia-borane (AB).
- Demonstrated that borazine and diborane can be scrubbed to produce fuel cell quality hydrogen.
- Developed base-case system designs for fluid-phase chemical hydrogen storage materials.
- Developed space filled model of base-case fluid-phase system design.



Introduction

Hydrogen storage systems based on chemical hydrides require a chemical reactor to release the hydrogen from the storage media, which is a fundamental difference from the other modes of hydrogen storage, adsorbents and metal hydrides. This hydrogen-release reactor is crucial to the performance of the overall storage system, especially in meeting the DOE targets for hydrogen generation rate, transient operation, and startup times. The reactor must be designed to achieve these targets while meeting the constraints of the overall system volume and weight targets.

LANL will also address the unique requirements of on-board automotive hydrogen storage systems. For example, these systems require fast startup, operation over a wide dynamic range (10:1 turndown or greater), and fast transient response to meet the demands of a drive cycle. The LANL team will develop novel reactor designs and operation strategies to meet these transient demands. In addition, the shelf life and stability of the hydrogen storage media is crucial for an automotive system, especially pertaining to safety and cost. Starting with the kinetics models, the LANL team will develop mathematical models for the aging characteristics of candidate hydrogen storage media (for example, complex metal hydrides or chemical hydrides) subjected to a range of environmental factors. These models can be incorporated into system-level models of performance and cost and also used for the development of accelerated aging protocols necessary for later testing.

Results

Fuel Gauge Sensor Development (Task 1)

Experiments were performed to determine the viability of employing acoustic sensor technology on metal hydrides as a fuel gauge sensor. Data were collected on commercial and noncommercial steel cylindrical pressure vessels containing metal hydride storage materials. In each case, the mass of metal hydride was small compared to the total mass of the system. However, large differences in the swept frequency response were observed, thus establishing a proof-of-principle that a hydrogen level sensor based on acoustic principles is feasible. Follow up experiments validated that the intermediate metal hydride state-of-charge can also be measured. Shown in Figure 1 are the resulting acoustic responses for various metal hydride states-of-charge. The acoustic response was observed to be inversely proportional to the metal hydride state-of-charge.

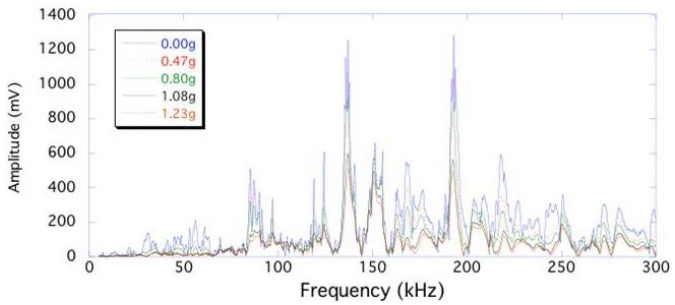


FIGURE 1. Acoustic Response as a Function of the Metal Hydride State-Of-Charge and Resonance Frequency

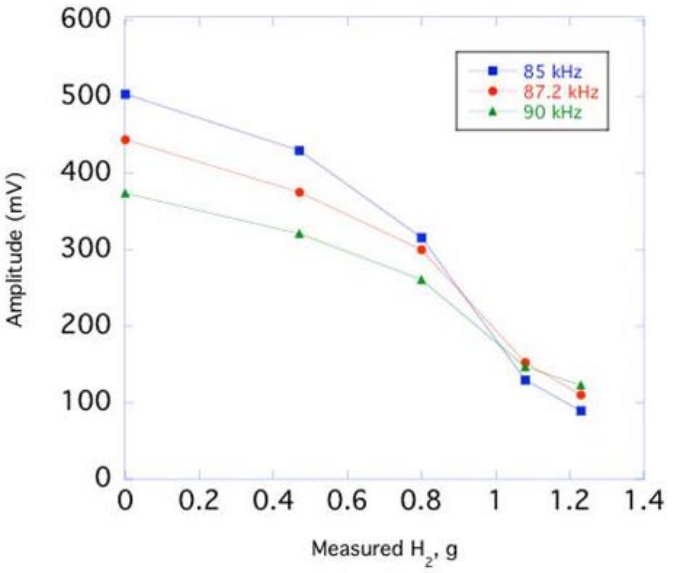


FIGURE 2. Acoustic Response for Three Resonance Frequencies as a Function of the Metal Hydride State-Of-Charge

The acoustic resonance frequencies were observed to be nonlinear with respect to the hydrogen state-of-charge. Figure 2 shows changes in three of the frequencies (85.0, 87.2, and 90.0 kHz) as a function of the metal hydride state-of-charge, with the lowest amplitudes occurring at the fully hydrided state-of-charge. The sensitivity in the acoustic amplitude was observed to be a function of not only the state-of-charge, but also the acoustic resonance frequency. The measured amplitude for a given resonance frequency exhibited monotonic behavior with respect to the state-of-charge, thus preventing multiple valued metal hydride states-of-charge.

Reproducibility of the state-of-charge is important if the sensor is to be commercialized. The sensor demonstrated reproducible results within 10%. The error is attributed to the fact that the metal hydride was in powder form. Performing acoustic measurements with engineered compacts will significantly lesson these errors.

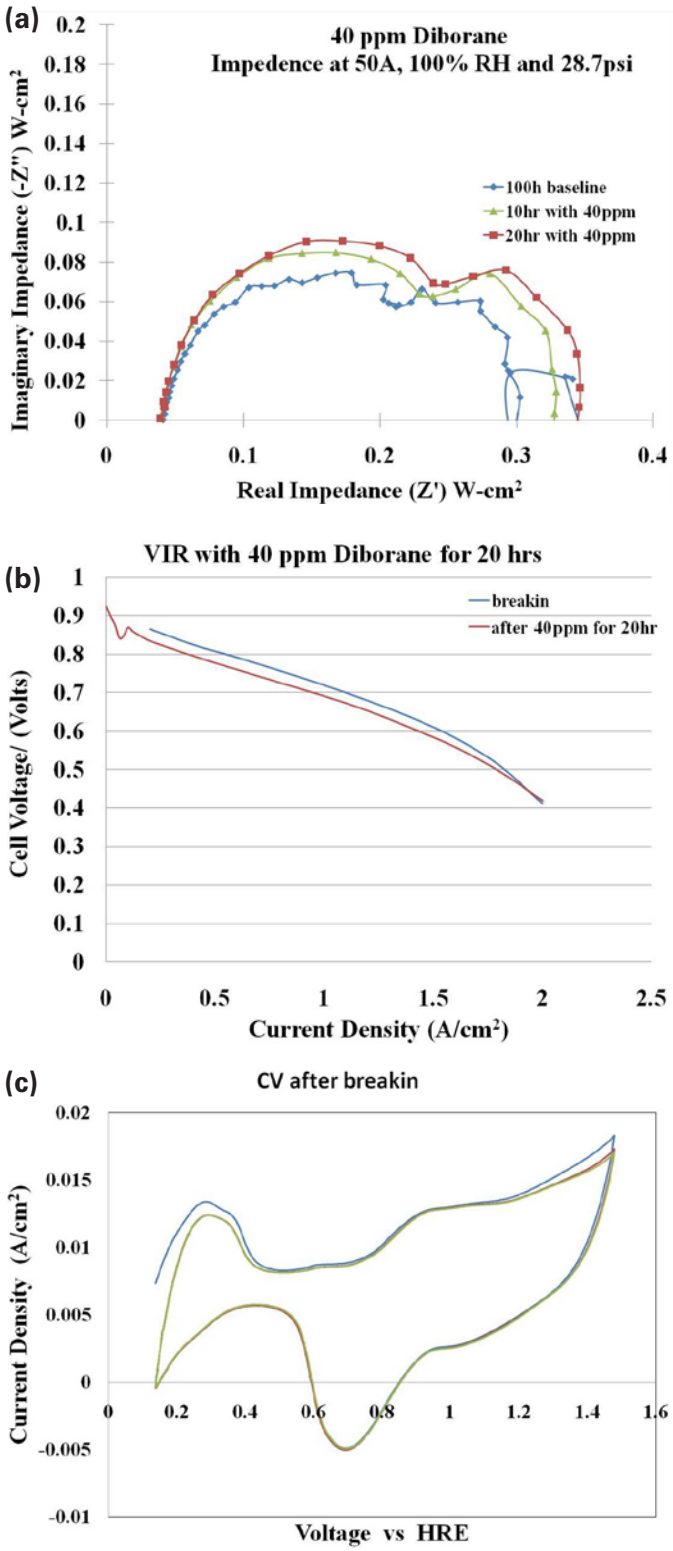


FIGURE 3. Fuel Cell Tolerance Test after 20 Hour Exposure with 40 ppm Diborane Impurity (a) Alternating Current Impendence, (b) Voltage-Current-Resistance Curve, and (c) Cyclic Voltammatry

Fuel Cell Tolerance Tests

In order accurately size an on-board hydrogen purification system for delivering fuel cell grade hydrogen, fuel cell tolerance levels for each of the impurities must be established. Diborane and borazine are known fuel cell impurities, but their levels for the safe and effective operation of a fuel cell are ill-defined. LANL performed preliminary fuel cell tolerance test with 2% diborane (balance ultra-high purity Ar) to investigate its effect on fuel cell performance. Shown in Figure 3 are the fuel cell tolerance test results after 20 hours of exposure with 40 ppm diborane. A decrease in fuel cell performance was observed after 20 hours of exposure to 40 ppm diborane, evidenced by a loss of 20 mV (Figure 3b). The electrochemical surface area remained constant throughout the preliminary 20 hour fuel cell tolerance test. The decrease in fuel cell performance can be attributed to an increase in the charge transfer resistance (Figure 3a). In addition, similar fuel cell tolerance tests are required for borazine.

Summary

- Successfully demonstrated that acoustic sensor technology can be used for tracking in real time the fully charged, fully discharged and the intermediate hydrogen state-of-charge of fixed metal hydride beds.
- Quantified impurities (diborane, ammonia, and borazine) generated from AB compositions.
- Performed preliminary fuel cell tolerance tests with diborane:
  - Fuel cell tolerance tests with 40 ppm diborane resulted in a 20 mV decrease in performance after 20 hours of exposure.
- Developed and designed automotive scale fluid-phase chemical hydrogen storage system.
- Developed and designed volume-based model of the automotive scale system design.
- Designed, built, and demonstrated a bench top fluid-phase chemical hydrogen validation test bed.

Future Directions

- Acoustic Fuel Gauge Sensor
  - Finish preliminary measurements on fluid-phase chemical hydrogen storage media
- Shelf-Life Modeling
  - Collect a complete set of shelf-life data on fluid-phase AB formulations.
  - Verify model accurately predicts shelf-life models for extended time periods.
- Reaction Rate Models for Hydrogen Release on Candidate Chemical Hydrides
  - Acquire complete set of kinetics data
    - Low temperature catalyst route
- Low Temperature Catalyst Development for Startup and Transient Operation
  - Continued efforts will focus on converting the room temperature homogeneous catalysts into heterogeneous form while maintaining room temperature activity.
- Hydrogen Impurities and Mitigation
  - In collaboration with LANL Chemical Hydrogen Storage Center of Excellence, quantify impurities from liquid AB formulations as a function of temperature.
- Subscale Component Design and Validation
  - Gas-liquid separator
  - Reactor
  - Hydrogen purification train

IV.D.4 Key Technologies, Thermal Management, and Prototype Testing for Advanced Solid-State Hydrogen Storage Systems

Joseph W. Reiter (Primary Contact),
Alexander Raymond, Channing C. Ahn (Caltech)
Jet Propulsion Laboratory (JPL)
4800 Oak Grove Drive, Mail Stop 79-24
Pasadena, CA 91109-8099
Phone: (818) 354-4224
E-mail: Joseph.W.Reiter@jpl.nasa.gov

DOE Manager
HQ: Ned Stetson
Phone: (202) 586-9995
E-mail: Ned.Stetson@ee.doe.gov

Subcontractor:
California Institute of Technology, Pasadena (Caltech), CA

Project Start Date: February 2009
Project End Date: September 2014

Fiscal Year (FY) 2011 Objectives

- Apply an understanding of storage system requirements for light-duty vehicles.
- Develop innovative on-board system concepts for materials-based storage technologies.
- Develop and test innovative concepts for storage subsystems and component designs.
- Identify technology gaps and identify trajectories to overcome technical barriers.
- Design, fabricate, and test subscale prototypes for each material-based technology.

Technical Barriers

This project addresses the following technical barriers from the Hydrogen Storage section of the Fuel Cell Technologies Program Multi-Year Research, Development and Demonstration Plan (referenced to 2015 targets, as revised 2009):

(A) System Weight and Volume: 5.5 %wt_{sys}, 55 gH_2/kg_{sys}, 40 gH_2/L_{sys}

(C) Efficiency: 90% on-board/60% off-board

(D) Durability/Operability: <1% degradation @ 1,500 cycles, etc.

(E) Charging/Discharging Rates: 3.3 min fill, 0.02 g/kW-s minimum full flow

(G) Materials of Construction

(H) Balance-of-Plant Components

(I) Dispensing Technology

(J) Thermal Management

Technical Targets

Regarding the technical barriers addressed by JPL's activities within the Hydrogen Storage Engineering Center of Excellence (HSECoE), the main areas that would be the focus of technical efforts would be the nature of loss of useable H_2, thermal management, balance-of-plant components, efficiency, and durability/operability; the last of these will be evaluated directly by a phased effort of analysis and follow-on testing at JPL.

FY 2011 Accomplishments

Technical efforts at JPL during the previous year have been focused on the development and testing of novel thermal architectures for hydrogen storage systems. In particular, JPL's expertise with low-temperature system design and analysis has proved a good match for the unique demands presented by the cryo-adsorption system, which needs to operate at temperatures below 160 K, and as low as 60 K. The JPL project is a mixed approach of analytical modeling and follow-on experimental validation aimed at the development of thermal components and their interaction at the system level. JPL has also continued in the role of System Architect for cryo-adsorbent system technology development. In this role, JPL provides oversight and coordination of the various technology areas within the HSECoE that have responsibility for developing credible paths toward satisfying the DOE Hydrogen Storage targets (2010/2015/ultimate). This role also has direct responsibility toward system engineering outcomes, providing guidance and oversight for conceptual system design. Finally, JPL serves within the Center as Technology Area Lead for the Enabling Technologies team, providing technology management and coordination for overcoming technical gaps and incorporating emergent technologies and approaches.

Specific accomplishments:

- High-Isolation Cryogenic Vessel Design: In 2010, JPL identified multi-layer vacuum insulation (MLI) as a key design requirement for the cryo-adsorption storage vessel due to its high level of thermal isolation. Using analytical models validated by preliminary experiment, JPL demonstrated in 2011 a new design for a thermal architecture using MLI that improves thermal isolation, reducing heat loads on the storage medium by up to

44% over current designs, increasing dormancy ("hold") times for the idle vehicle.

- Cryogenic Fuel Energy Management: Via analytical modeling, JPL designed a compact onboard heat exchanger ("downstream H_2 HX") for cryogenic hydrogen fuel conditioning. This crucial device will utilize fuel cell waste heat in a closed coolant loop to raise the temperature of fuel supplied to the fuel cell. The JPL model has been incorporated into the overall HSECoE model framework, and has been shown to operate as designed across the complete operating envelopes of both AX-21 and MOF-5-based storage system designs.
- Loop Desorption Heating: Developed a design criteria and initial analytical model for H_2-loop desorption heating, identifying additional onboard efficiency gains and promoting the H_2 circulator as a technology gap for further investigation in Phase II.
- Cryo-Adsorbent System Phase 1 Transition: In the role of System Architect, JPL assisted in guiding the cryo-adsorbent system design team through the Phase 1-2 transition, which involved standardizing performance metrics of defined baseline systems and identifying technology development opportunities and challenges.



Introduction

JPL is engaged in developing enabling technologies for vehicular hydrogen storage systems for meeting DOE/FreedomCAR technical targets. During this project year, the enabling technologies area has been primarily concerned with low-temperature thermal management for the cryo-adsorbent system with emphasis in three areas: 1) parasitic heat transfer reduction in pursuit of the 2015 loss of useable H_2 target of 0.05 g h^{-1} kg^{-1} useable H_2, 2) downstream hydrogen heating to achieve the -40°C target for hydrogen delivered by the storage system, and 3) controlled heating of the cryogenic vessel for desorption (i.e., desorption heating) to meet the required 1.6 g s^{-1} requirement full flow rate for anticipated drive cycles. In each of these areas, the current state of the art was either extended in relation to the technical targets, or it was shown that the technical targets could be fully satisfied.

Approach

First-order heat and mass transfer models were constructed to quickly evaluate various technologies in the areas of dormancy, downstream hydrogen heating, and desorption heating. In the case of dormancy, detailed higher-order models were used for thermo-mechanical evaluation of cryogenic standoffs. In the dormancy area, the challenge is designing standoffs capable of withstanding shock loads exceeding 8 g while providing high conduction resistance. JPL has sought to improve on the state of the art in vehicular cryogenic storage by adapting the baseline G10 system proposed by Lawrence Livermore National Laboratory and others for liquid H_2 storage to the cryo-adsorption system, and also by proposing a new method of insulation relying on fibrous suspension of the pressure vessel inside the vacuum jacket, which has led to significant reduction in H_2 loss rate. JPL has investigated various methods for accomplishing downstream H_2 heating with the objective of mitigating frost risks and minimizing heat exchanger volume. As of March 2011, JPL has begun construction on a cryogenic test facility capable of spanning the temperature range projected for cryo-adsorption storage. The first use of this facility is to validate the parasitic heat transfer model used for dormancy calculations. The cryogenic test facility will also be used in Phase II of the project for additional experiments.

Results

The primary benefits of cryogenic adsorption storage are increased gas phase density and increased adsorption mass fraction near 80 K. Unfortunately, this low temperature can yield large parasitic heat transfer rates; only a few watts of parasitic heat transfer are needed to induce H_2 venting after a few days of idle. Mechanical models of thermal standoffs were built to size supports for a rigid G10 design and a second Kevlar™ design such that the components did not yield when subjected to loads of 8 g perpendicular to the axis of the tank with a safety factor of 2. Kevlar™ cables were sized to support the same loading; because Kevlar™ rope is available in discrete sizes, only cables that met or exceeded the mechanical requirements were used for heat transfer calculations.

Heat transfer models were built to estimate conduction across standoffs, radiative exchange across MLI, and conduction through tubing. These models were parameterized as a function of cold-side temperature at a hot-side temperature of 26°C, representing a summertime diurnal average. The component-level heat transfer for the G10 architecture (Figure 1a) revealed that standoff heat transfer is the most significant constituent of the ~5 W total parasitic. By replacing the G10 standoff design with Kevlar™, it was estimated that the total parasitic heat transfer could be reduced by up to ~44% (Figure 1b).

The reduced parasitics of the Kevlar™ design lead to reduced H_2 losses by venting and longer dormancy. To quantify these improvements, a model was constructed to relate parasitic heat transfer to tank temperature and vent rate; para- to ortho- conversion during tank heating is accounted for. Figure 2 shows that the average vent rate over a 30-day period is about ~0.52 g h^{-1} kg^{-1} for the G10 design compared with ~0.35 g h^{-1} kg^{-1} for the Kevlar™ design, and that the dormancy for Kevlar™ is approximately 70% longer. Figures 1-2 document a 70 bar aluminum pressure vessel with AX-21 adsorbent. A 200 bar Type-III carbon fiber vessel with MOF-5 adsorbent has also been modeled. MOF-5 shows slightly lower vent losses and

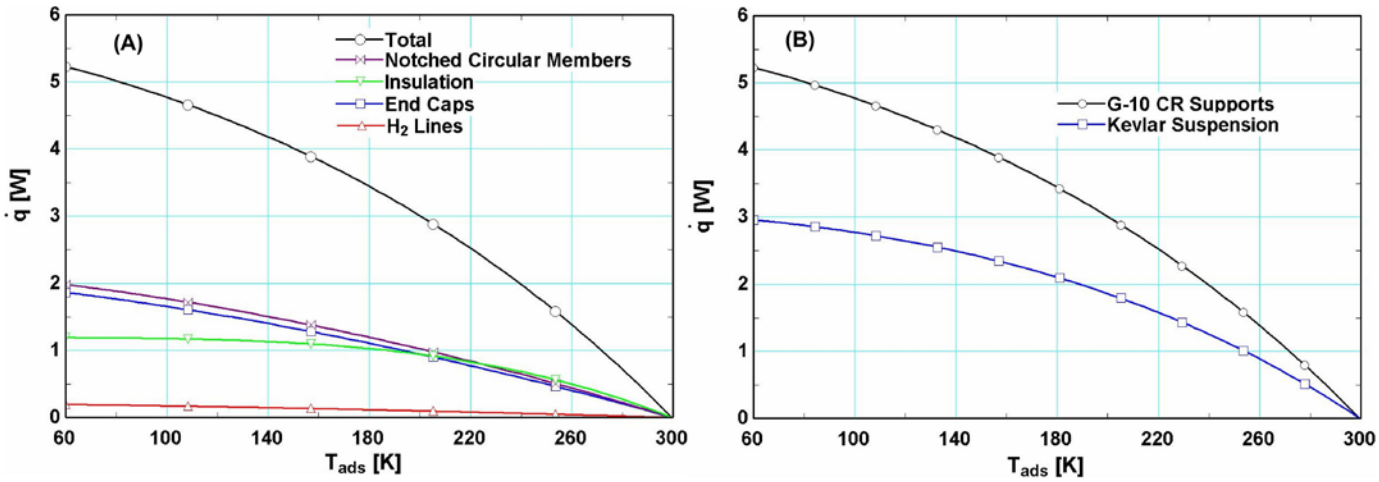


FIGURE 1. Breakout parasitic loads for G10 (state of art) and total parasitic loads for G10 and Kevlar™ (advanced) tank thermal isolation designs.

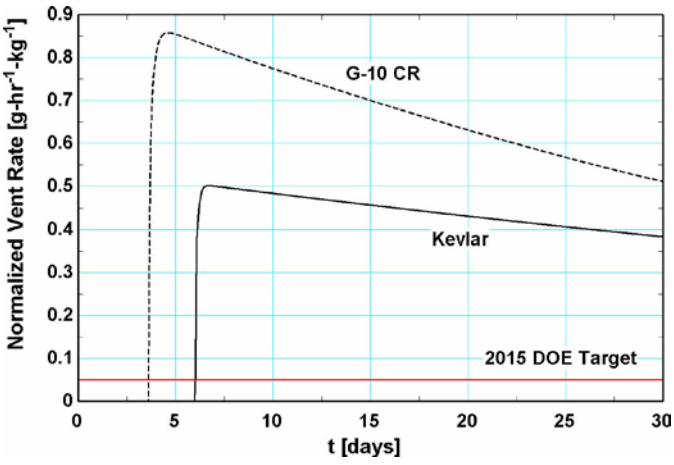


FIGURE 2. Vent rate histories for G10 (state of art) and Kevlar™ (advanced) thermal isolation designs.

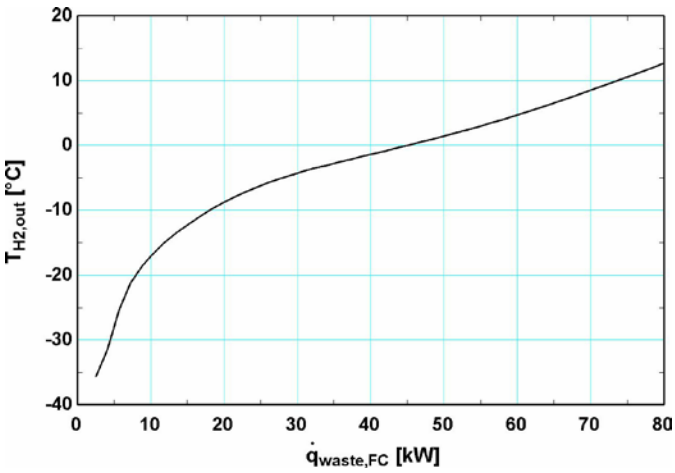


FIGURE 3. Delivered hydrogen temperature versus total fuel cell waste heat. Assumes 50% of waste heat is dissipated by coolant loop.

longer dormancy times, but the relative improvement of Kevlar™ over G10 is generally similar to the AX-21 case. Nevertheless, even the Kevlar™ design gives dormancy performance that falls short of the 2015 hydrogen loss target; the projected mass of hydrogen lost to venting is appreciable (~1 kg over 30 days) with the improved design. However, it should be noted that the scenario exercised in this model is a worst case and does not account for natural pressure relief through driving; a small amount of daily driving can extend dormancy indefinitely in this type of system.

In the downstream heat exchange area, three types of downstream heat exchange sub-systems were modeled with the common objective of heating stored low-temperature hydrogen to allowable temperatures en-route to the fuel cell or internal combustion engine. The modeled sub-systems included a direct air-coupled hydrogen heat exchanger with an air-side heater, a hydronic loop coupled to air, and a fuel cell coolant-coupled loop. The obstacles for each of these concepts were 1) the size and number of heat exchangers required, and 2) the potential for ice formation at various locations within the heat exchange equipment. The direct air-coupled heat exchanger model predicted frost build-up on the air side for most cases. The independent hydronic loop also showed the potential for icing at low temperatures in addition to requiring two dedicated heat exchangers. The fuel cell coolant-coupled loop is the leading design candidate. Waste heat from the fuel cell helps prevent icing on the coolant side, while the coolant loop axial flow fan and air-coupled heat exchanger are leveraged to reduce volume and parts count. At -30°C ambient and a hydrogen flow rate of 0.8 g s^{-1}, this system will deliver -40°C hydrogen with no waste heat input from the fuel cell. With a nominal amount of waste heat input, Figure 3 shows that this system exceeds the delivery target even in -40°C ambient conditions.

In desorption heating, a compressible flow network model was developed to model the flow-through heating

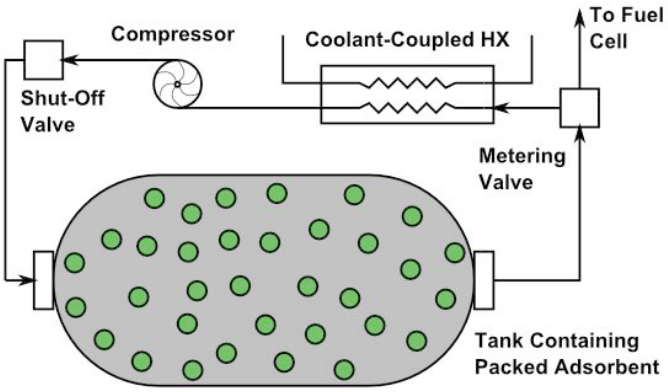


FIGURE 4. Flow-Through Desorption Loop Schematic

design shown in Figure 4. The most aggressive cases, delivering 1.6 g s^{-1} with a set point pressure of 20 bar, the H_2 circulation rate must be very large. For nominal quarter inch lines, pressure losses resulting from these flow rates can be significant; however, drive cycles incorporated into the framework model developed by Savannah River National Laboratory in conjunction with the United Technologies Research Center have suggested that such stringent cases do not exist in practice. Tank heating rates up to 1 kW should be realizable with this type of system. The model predicts that a circulator would need to provide 3 kPa of pressure rise in order to deliver ~1 kW of heating when transferring heat from fuel cell coolant at 52°C. The technology gap in this area, however, is procuring a circulator that is rated to operate at pressures exceeding 200 bar; investigations in this particular direction have already begun.

Conclusions and Future Directions

- Two thermal isolation architectures were studied in detail. A scaled parasitics experiment is being constructed to validate the predictive models, and in Phase II, a high-fidelity dormancy experiment based on the novel Kevlar™ architecture is planned. Pressure vessel outgassing experiments are also being developed, which will indicate the level of vacuum that is feasible.
- Various methods for downstream hydrogen heating were investigated, and it was determined that coupling to the fuel cell coolant loop offers the best protection against freezing while also meeting hydrogen conditioning requirements. JPL has started to develop higher-order models of this process and is in the planning stage of adapting an experimental facility to supplement those models.
- The HSECoE has identified flow-through heating as an alternative to Joule heating for desorption. A compressible flow network model was developed by JPL to model the flow-through design. Pressure-drops are reasonable current system configurations; however, the technology gap is the hydrogen circulator, which must operate at low temperature and high pressure. More work will be done to identify a path forward for desorption heating.
- During the next year, JPL plans to conduct a demonstration high-pressure burst test of a 200-350 bar composite pressure vessel at cryogenic (~77 K) temperatures. This proof-of-concept activity will begin a series of investigations that will include cryogenic pressure/temperature cycling as well as possible future burst tests. These investigations will be performed in conjunction with HSECoE partners Lincoln Composites, Pacific Northwest National Laboratory, and United Technologies Research Center, among others. The results will inform future investigations and safety/testing protocols during Phase II experimental work as well as eventual prototype storage system testing.

Patents Issued

1. Raymond A., Reiter J. (2011) Suspension for Thermal Isolation of Cryogenic Hydrogen Tanks for Terrestrial Applications. Provisional patent.

FY 2011 Publications/Presentations

1. Raymond, A. and Reiter, J. (2010) Parasitic heating and dormancy in cryo-adsorbent tanks for vehicular hydrogen storage. Poster Presentation. AIChE Annual Meeting. November 7–12. Salt Lake City, UT.

2. Raymond, A. and Reiter, J. (2011) Modeling and testing of cryo-adsorbent hydrogen storage tanks with improved thermal isolation. Cryogenic Engineering Conference. June 13–17, Spokane, WA.

IV.D.5 SRNL Technical Work Scope for the Hydrogen Storage Engineering Center of Excellence: Design and Testing of Metal Hydride and Adsorbent Systems

Theodore Motyka (Primary Contact),
Bruce J. Hardy
Savannah River National Laboratory
Bldg 999-2W
Aiken, SC 29808
Phone: (803) 507-8548
E-mail: ted.motyka@srnl.doe.gov
E-mail: bruce.hardy@srnl.doe.gov

DOE Manager
HQ: Ned Stetson
Phone: (202) 586-9995
E-mail: Ned.Stetson@ee.doe.gov

Subcontractor:
Université du Québec à Trois-Rivières, Quebec, Canada

Start Date: February 1, 2009
Projected End Date: July 31, 2014

Fiscal Year (FY) 2011 Objectives

The Savannah River National Laboratory (SRNL) and its sub-recipient the Université du Québec à Trois-Rivières (UQTR) will:

- Collect property data for select metal hydrides and adsorbents.
- Compile list of available analytical techniques to support materials property data requirements.
- Develop and evaluate the acceptability envelope for storage media and vessels.
- Develop numerical models to adequately predict storage system behavior for metal hydride and adsorbent based storage systems.
- Use the models to design optimized storage systems based on $NaAlH_4$, other metal hydrides, AX-21, and other potential absorbent materials.
- Direct metal hydride system testing and evaluations as the Metal Hydride System Architect for the Center.

Technical Barriers

This project addresses the following technical barriers from the Hydrogen Storage section (3.3) of the Hydrogen, Fuel Cells and Infrastructure Technologies Program Multi-Year Research, Development and Demonstration Plan:

(A) System Weight and Volume
(C) Efficiency
(E) Charging/Discharging Rate

Technical Targets

The goal of the entire Hydrogen Storage Engineering Center of Excellence (HSECoE) is to provide a system model for each material sub-class (metal hydrides, adsorption, chemical storage) which meets the "Technical System Targets: On-Board Hydrogen Storage for Light-Duty Vehicles", Table 3.3.2 in the DOE Multi-Year Research and Development Plan – April 2009. The end-of-Phase I, Go/No-Go milestone which is set for February 2011 for the entire HSECoE project is that:

1. Four of the DOE 2010 numerical system storage targets are fully met and that,
2. The status of the remaining numerical targets must be at least 40% of the target or higher.

For SRNL's specific technical portion of HSECoE, SRNL will:

- Direct the testing and evaluations necessary for the specific Go/No-Go milestones for metal hydride systems.
- Compile thermochemical data.
- Bound media operating characteristics for metal and adsorption hydride material.
- Develop and apply numerical models that couple mass, momentum and energy balances with chemical kinetics and/or isotherms to simulate hydrogen uptake and discharge.
- Develop and run system models for candidate adsorbent material systems.
- Identify technology gaps.
- Identify preliminary system designs to achieve DOE 2015 hydrogen storage goals.

FY 2011 Accomplishments

- Collected material operating data for LiMg-amide metal hydride materials including developing engineering kinetic expressions.
- Applied Acceptability Envelope to select metal hydride materials and systems.
- Studied 50 bar, 100 bar, and 150 bar sodium alanate optimal systems.
- Estimated isenthalpic (Joule-Thompson) temperature change for hydrogen flow through a throttling valve, which can be as large as an 18 K drop.
- Developed methodology and estimated pressure drop losses for flow in piping of cryo-adsorbent system for a range of conditions (mass flow rates, temperatures, and pressures) for use in system models.

- Developed improved methodology to estimate heat transfer coefficient for turbulent (radial) flow in micro-channel between cooling plates for analysis and COMSOL optimization of modular cryo-adsorbent designs.
- Studied in-line heat exchangers for hydrogen feed to fuel cell.
- Completed System Architect analysis of sodium alanate as a model material vs. DOE 2010 Go/No-Go Decision.

✧ ✧ ✧ ✧ ✧

Introduction

SRNL and its subrecipient, UQTR, are involved in several critical aspects of the HSECoE. SRNL is focused primarily on modeling, validating, and optimizing hydrogen storage designs for metal hydrides, adsorbents, and, to a lesser extent, chemical hydrides, and System Architect Analyses of metal hydride systems. SRNL is applying its expertise in modeling dynamic transport phenomena and chemical processes, materials testing, and system modeling to accomplish its objectives in the proposed effort– developing and applying models to identify viable subscale prototype designs, performing design calculations sufficiently accurate for engineering application, and defining the scope and required measurements for experiments with the selected prototypes.

UQTR is developing thermodynamic formulations for adsorbent isotherms that can be easily and efficiently implemented by SRNL into a numerical model that accurately predicts the behavior of an adsorption-based storage system over a range of operating conditions and system configurations. UQTR is extending its thermodynamic model, which currently applies to adsorption on activated carbons, to other adsorbents.

Relevance

The ultimate goals of the HSECoE are the design and testing of prototype hydrogen storage vessels, the interpretation of test data, and the implementation for full-scale vessels. Within the HSECoE, the Transport Phenomena Technology Area is responsible for the development and application of analyses for storage systems that are necessary to identify and design prototype media and vessel configurations having the best performance relative to the DOE Technical Targets. Storage vessel models developed by this Technology Area will be essential to interpret data obtained from prototype testing and to relate it to full scale systems.

Approach

In Phase I, SRNL and UQTR will:

- Evaluate, interpret, and assimilate data for media and vessel components.
- Develop and apply an "Acceptability Envelope" based on DOE targets.
- Develop, validate and test general models for scoping and detailed evaluation of storage system designs.
- Obtain material operating requirements for metal hydride and AX-21 materials.
- Perform System Architect analysis on candidate metal hydride systems for Phase I Go-No-Go decision.

Results

SRNL and its subrecipient UQTR to date have met and or exceeded their Phase I objectives for all of their major technical areas for the HSECoE. These major technical areas include: Transport Phenomena, Adsorbent Systems Modeling, Material Operating Requirements and System Architecture. Transport Phenomena and Adsorbent System Modeling results are shown below for adsorbents systems. Results for activities under Material Operating Requirements and System Architecture are shown for metal hydrides systems.

Transport Phenomena

- Developed Detailed and Thermodynamic Models for Adsorbent-Based Storage Vessels
  - Applied to MaxSorb™ (MSC-30™) and MOF-5™ (Basolite Z100-H)
  - Validated MaxSorb™ model against test data
- Applied Models for Charging and Discharging of Storage Vessel
  - Charging characteristics (see Figure 1)
    - Charging models were applied for DOE 2015 Technical Target time of 198 seconds (3.3 minutes)

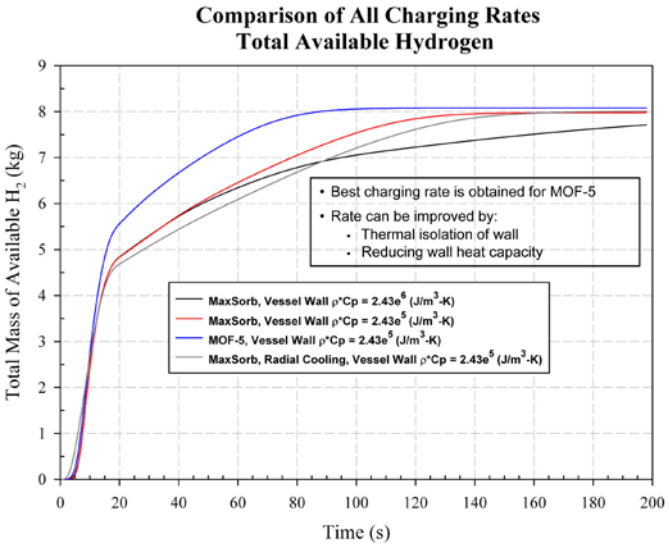


FIGURE 1. Comparison of system charging rate for different adsorbent materials and different wall thermal isolating conditions.

- Considered stored energy in vessel wall
- Heat removal by axial and radial convection via flow-through cooling
- Contributions of pressure work and heat of adsorption

– Discharging characteristics (see Figure 2)
- Resistance heater
- Flow-through cooling

Adsorbent System Modeling

- Developed and ran baseline system models for four adsorbent systems (AX-21 at 60 and 200 bar and MOF-5 at 60 and 200 bar) in support of the baseline Adsorbent System Go/No-Go decision (see Figure 3)
- Evaluated several tank heating input methods using the adsorbent system model
  – Hot hydrogen recirculation line
  – Heat switches
  – Internal resistance heater (currently the base case system option)
- Evaluated various heat exchanger options
  – None other than the exposed hydrogen piping
  – Air-to-hydrogen vessel heat exchanger
  – Air-to-fuel cell coolant heat exchanger (currently the base case system option)

Material Operating Requirements: Metal Hydrides

- Selected sodium aluminum hydride ($NaAlH_4$) material as initial baseline hydride candidate material for transport phenomena and system modeling development.
- Database updated for:
  – $NaAlH_4$ (with and without catalysts)
  – TiCrMn
  – Mg_2Ni
  – $8LiH:3Mg(NH_2)_2$
- Additional data added for:
  – 2:1 $LiNH_2:MgH_2$
  – 1:1 $LiNH_2:MgH_2$
  – MgH_2 (without catalysts)

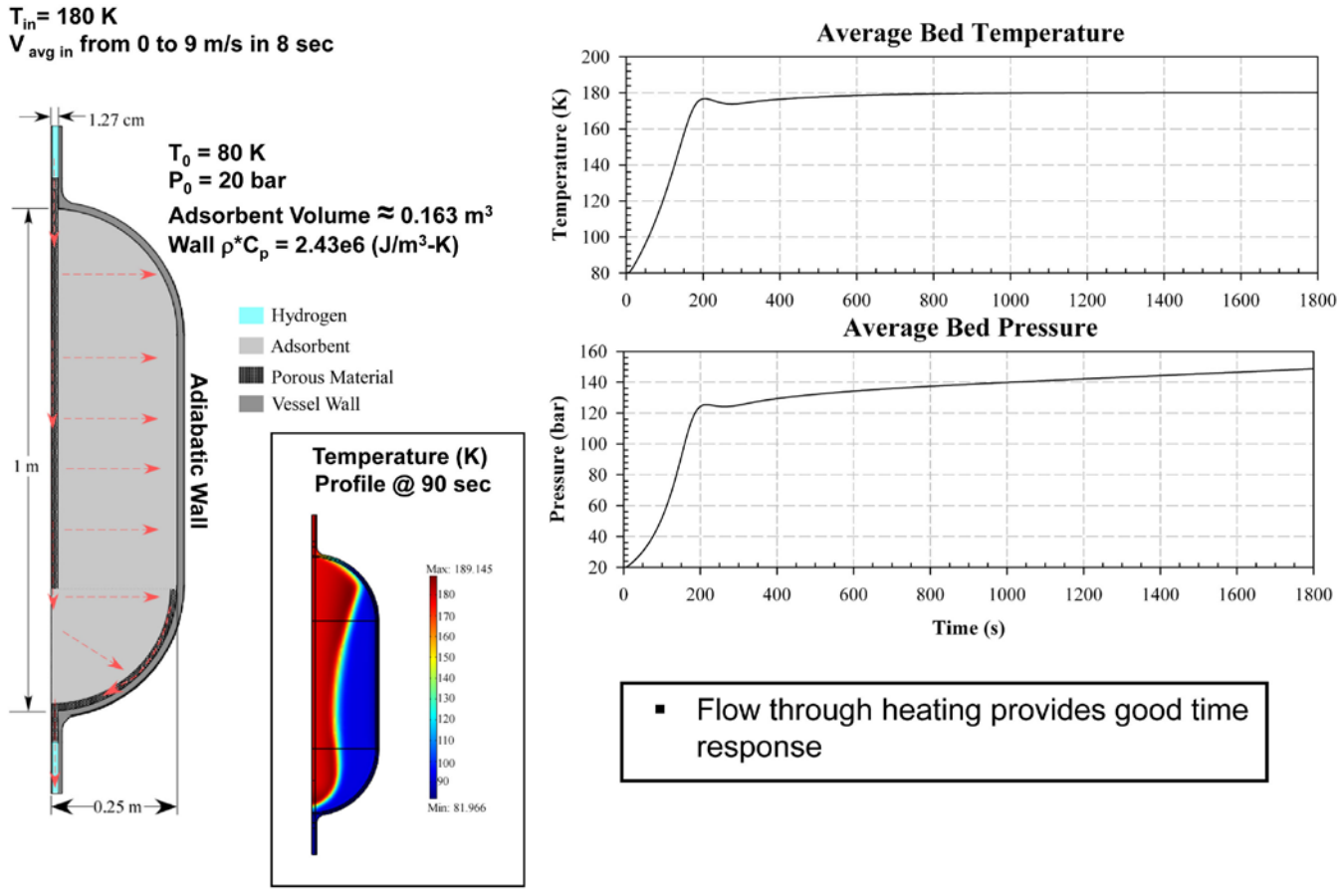


FIGURE 2. Average adsorbent bed temperature and pressure profiles with radial flow-through heating.

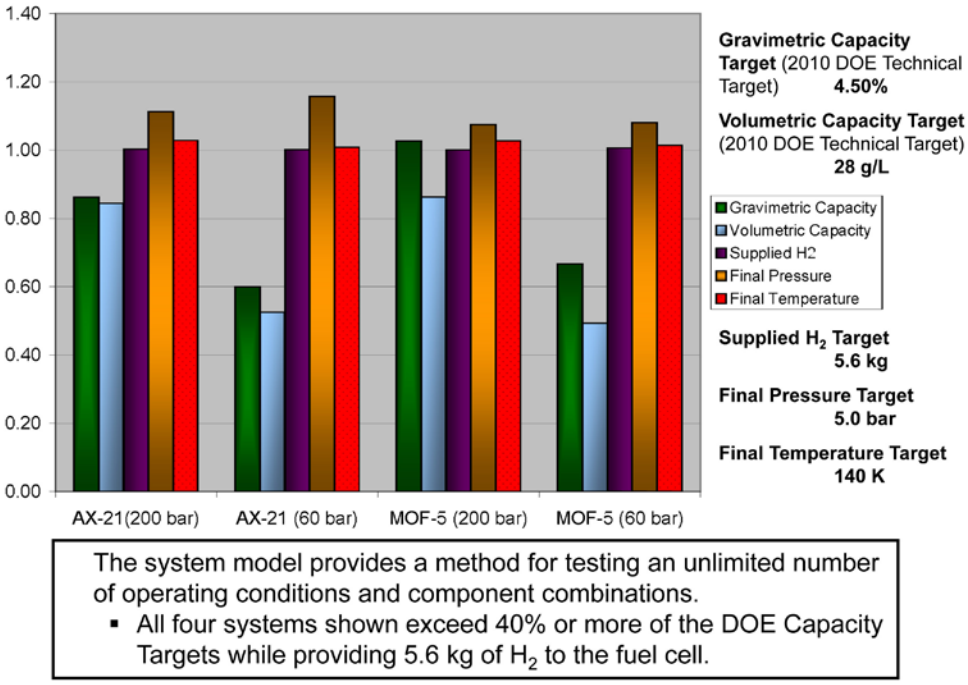


FIGURE 3. Adsorbent system modeling results compared to DOE 2010 system targets.

- Developed preliminary kinetic expressions for 2:1 $LiNH_2$:MgH_2 and 1:1 $LiNH_2$:MgH_2 to support system modeling analyses.
- Updated and improved the Acceptability Envelop to evaluate metal hydride materials for the Go/No-Go decision.

System Architect Analyses: Metal Hydride

- Selected Metal Hydride System for baseline Phase 1 Go/No-Go decision (see Figure 4).
- Documented selection criteria and assumptions for Metal Hydride Systems with respect to 2010 targets and Phase 1 Go/No-Go decision.
- Identified deficiencies and improvement areas for Metal Hydride Systems for Phase 2 development plan.

Conclusions and Future Directions

- Continue Metal Hydride System Architect analyses.
- Provide analyses for Phase 2 Go/No-Go decision.
- Investigate thermal and structural effects of bed expansion.
- Improve bed heat transfer for metal hydrides and adsorbents (expanded natural graphite addition and honeycomb lattice) - experiments will be guided by models.
- Investigate viability of flow-through concept for adsorbent systems.
- Optimize adsorbent system with respect to pressure work, enthalpy of hydrogen discharge flow, dormancy conditions and thermal interaction with container wall.

FY 2011 Publications/Presentations

1. M. Bhouri, J. Goyette, B.J. Hardy, D.L. Anton. "Sensitivity study of alanate hydride storage system." International Journal of Hydrogen Energy 36 (2011) 621-633.

2. C. Corgnale, B. Hardy, D. Anton. "Development of an acceptability envelope for metal hydrides: a system analysis", IEA HIA TASK 22 Meeting, January 2011, Australia.

3. S.L. Garrison; C. Corgnale; B.J. Hardy; D.A. Tamburello; T. Motyka; D.L. Anton. "Automatic optimization of metal hydride storage tanks and analysis of material property envelopes." Presented at the Pacifichem 2010 conference Dec.15–20, Honolulu, HI.

4. B. Hardy, C. Corgnale, R. Chahine, M-A Richard, D. Tamburello, S. Garrison, D. Anton. "Modeling of Adsorbent Based Hydrogen Storage Systems." Presented at the special session Hydrogen Storage System Engineering and Applications: Heat and Mass Transfer, of the AIChE 2010 Annual Meeting Nov 7–12 in Salt Lake City, Utah.

5. C. Corgnale, B. Hardy, D. Tamburello, S. Garrison and D. Anton. "Evaluation of Acceptability Envelope for Materials-Based H2 Storage Systems." Presented at the special session Hydrogen Storage System Engineering and Applications: Heat and Mass Transfer, of the AIChE 2010 Annual Meeting Nov 7–12 in Salt Lake City, Utah. Full paper submitted to the IJHE and currently in review.

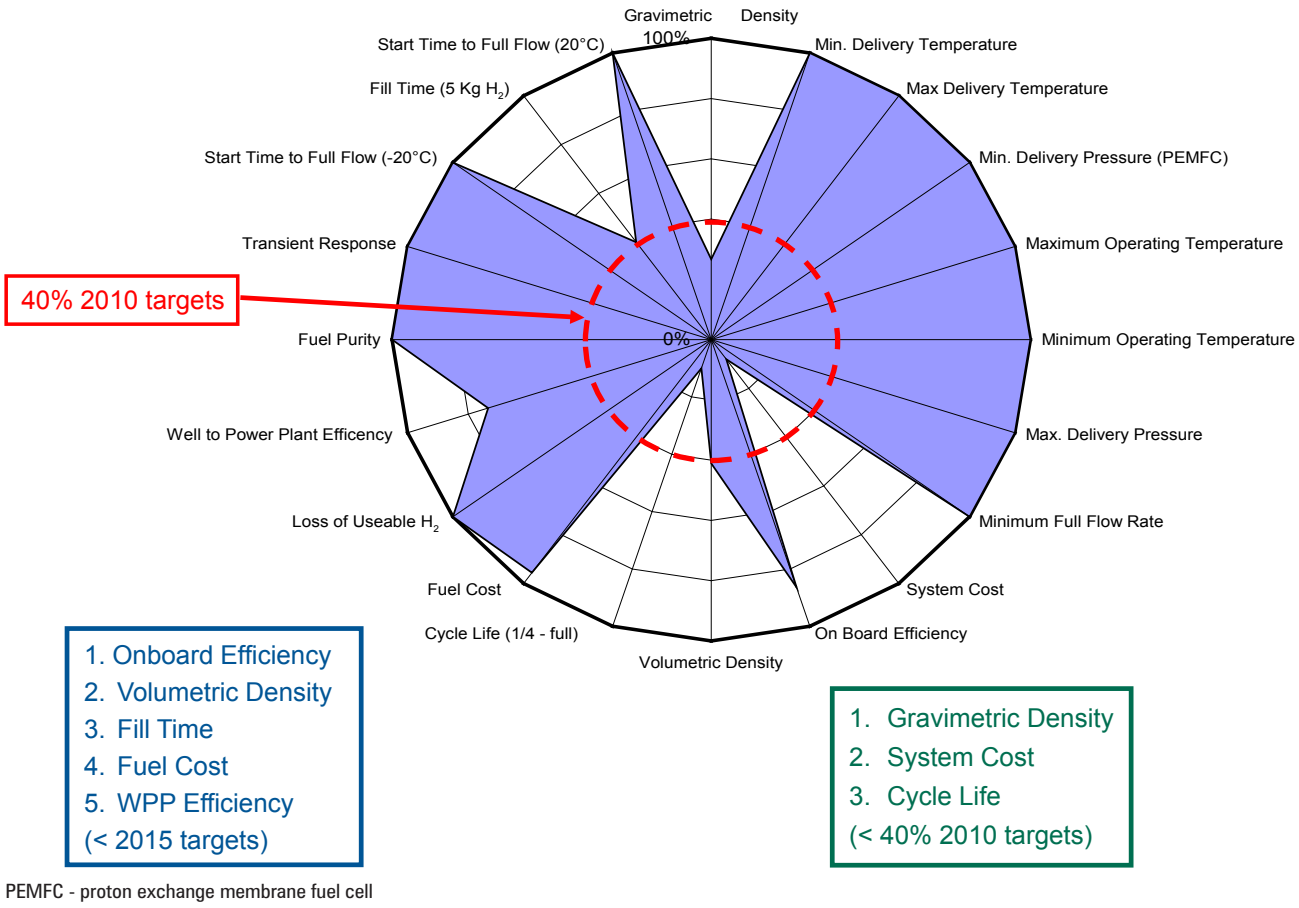


FIGURE 4. "Spider" chart showing baseline metal hydride case for the sodium alanate system versus DOE 2010 targets.

6. S. Garrison, M. Gorbounov, D. Tamburello, B. Hardy, C. Corgnale, D. Mosher and D. Anton. "Automatic Optimization of Metal Hydride Storage Tanks and Novel Designs." Presented at the special session Hydrogen Storage System Engineering and Applications: Heat and Mass Transfer, of the AIChE 2010 Annual Meeting Nov 7–12 in Salt Lake City, Utah. Full paper submitted to the IJHE and currently in review.

7. R. Chahine, "Evaluation of Sorption System for Hydrogen Storage" Presented at the special session Hydrogen Storage System Engineering and Applications: Heat and Mass Transfer, of the AIChE 2010 Annual Meeting Nov 7–12 in Salt Lake City, Utah. Full paper submitted to the IJHE and currently in review.

IV.D.6 Systems Engineering of Chemical Hydride, Pressure Vessel, and Balance of Plant for On-Board Hydrogen Storage

Jamie D. Holladay (Primary Contact),
Kriston P. Brooks, Ewa Rönnebro,
Kevin L. Simmons and Mark R. Weimar
Pacific Northwest National Laboratory (PNNL)
902 Battelle Blvd
Richland, WA 99352
Phone: (509) 371-6692
E-mail: Jamie.Holladay@pnnl.gov

DOE Manager
HQ: Ned Stetson
Phone: (202) 586-9995
E-mail: Ned.Stetson@ee.doe.gov

Project Start Date: February 1, 2009
Project End Date: January 31, 2014

Fiscal Year (FY) 2011 Objectives

The Pacific Northwest National Laboratory (PNNL) objectives address the critical engineering challenges currently limiting on-board hydrogen storage systems for light-duty fuel cell vehicles. Each of the project's objectives and tasks have been established to advance the state of the art in analysis, design and engineering for chemical hydride storage, pressure/containment vessel construction for metal hydride and cryogenic adsorbent systems, and component miniaturization for all systems to achieve PNNL, Hydrogen Storage Engineering Center of Excellence (HSECoE), and DOE goals.

- Demonstrate a high level of performance that meets DOE targets for key components (reactor, solids handling, and heat exchanger) of a solid chemical hydrogen storage system.
- Optimize the design of a chemical hydride storage bed and system performance through engineering including the establishment of bulk media and system kinetics data to aid in design activities.
- Reduce system volume and weight while optimizing system storage capability, fueling and dehydriding performance through application of microtechnology and associated architectures to the design of high-efficiency heat exchangers and balance-of-plant (BOP) components.
- Mitigate materials incompatibility issues associated with hydrogen embrittlement, corrosion, and permeability through suitable materials selection for vessel materials, heat exchangers, plumbing and BOP components.
- Demonstrate the performance of economical, compact lightweight vessels for a hybrid pressurized metal-hydride and adsorbent system, and containment vessel for a chemical hydride system.
- Guide design and technology down selection, Go/No-Go decision-making, and address vehicle and market impact through cost modeling and manufacturing tradeoff assessments of the three HSECoE prototype storage systems.

Achieving the objectives will enable PNNL, Savannah River National Laboratory (SRNL), and other HSECoE partners to demonstrate on-board hydrogen storage with the potential to meet 2015 DOE technical targets. This technology and design knowledge will be transferred to the participating automotive original equipment manufacturers and non-proprietary information and models will be made available to the fuel cell community, thus advancing the hydrogen market sector and production of future hydrogen-powered vehicles.

Technical Barriers

This project addresses the following technical barriers from the Fuel Cell Technologies Program Multi-Year Research, Development and Demonstration Plan:

General to All Storage Approaches

(A) System Weight and Volume
(B) System Cost
(C) Efficiency
(D) Durability/Operability
(E) Charging/Discharging Rates
(G) Materials of Construction
(H) Balance of Plant (BOP Components)
(I) Dispensing Technology
(J) Thermal Management
(K) System Life-Cycle Assessments
(O) Hydrogen Boil-Off

Off-Board Regenerable Specific

(S) By-Product/Spent Material Removal

Technical Targets

The HSECoE activities being conducted at PNNL range from process and reactor modeling and component design/engineering to technology application and prototype fabrication for demonstration. The final ultimate goal for the PNNL scope is to demonstrate, with Los Alamos National Laboratory (LANL) partners, a (100-g) scaled chemical hydrogen storage system that meets all the 2015 DOE storage performance targets. As a snapshot of progress to date,

the spider chart in Figure 1 represents the principal 2010 DOE performance targets and status toward achieving those targets as a percentage. The DOE has established an initial in-process review gate of 40% for each of the targets except system cost; the dashed line represents this 40% threshold.

FY 2011 Accomplishments

- Demonstrated refueling feasibility using a solid hydrogen storage material with both pellets and powders. The pellets where capable of achieving 75-100% of the DOE's refueling (fill and drain) 2010 targets and the powders were capable of achieving 27-50% of the 2010 targets. Low density polyethylene was used as a surrogate of an 80:20 ammonia-borane (AB)/methyl cellulose (MC) mixture by weight. Based upon the results of these tests, pellet form factors are recommended for solid chemical hydride fuels over powders.
- Validated AB kinetic models using pressure-concentration-temperature (PCT) and larger scale testing.
- Demonstrated self-sustaining hydrogen release of AB/MC pellets without foaming at atmospheric pressure and at 10 bar (system design pressure).
- Validated and modeled a new design which combines the fuel storage tank with the reactor and hydrogen ballast tank into a single fixed-bed design. The simple design consists of a single tank with multiple beds. Each bed is thermally isolated from the others. Therefore as hydrogen is needed, a single bed is heated to release the hydrogen. A single bed was used to validate the design. COMSOL and Simulink were used to predict and improve the reactor performance.
- Completed the Simulink modeling for eight system configurations including the fixed bed design, fluid system (AB dissolved in ionic liquids [IL] or a chemical hydride slurry), reactive transport systems such as an auger design, and a tape/roller system. The fixed bed system was modeled with AB/MC, the reactive transport and fluid systems were modeled with solid AB/MC, alane, AB slurries, alane slurries, and AB/ionic liquids.
- Predicted, using Simulink models integrated with the Vehicle Model that hydrogen storage technologies based upon solid and/or fluid chemical hydrides can meet the DOE delivery targets. Multiple cases were examined with the integrated models including: UDDS+HWFET, US06, and Cold FTP.
- Discontinued work on the reactive transport (or auger) concept based on concept validation tests. Hydrogen was successfully produced using an auger type reactor with AB/MC as the chemical hydride; however, the auger tended to clog. Based on the results, work on the reactive transport systems was discontinued.
- Down selected from greater than eight designs to one design for Phase II. Any design requiring replacement canisters or cassettes was discontinued due to safety concerns. Reactive transport concepts were

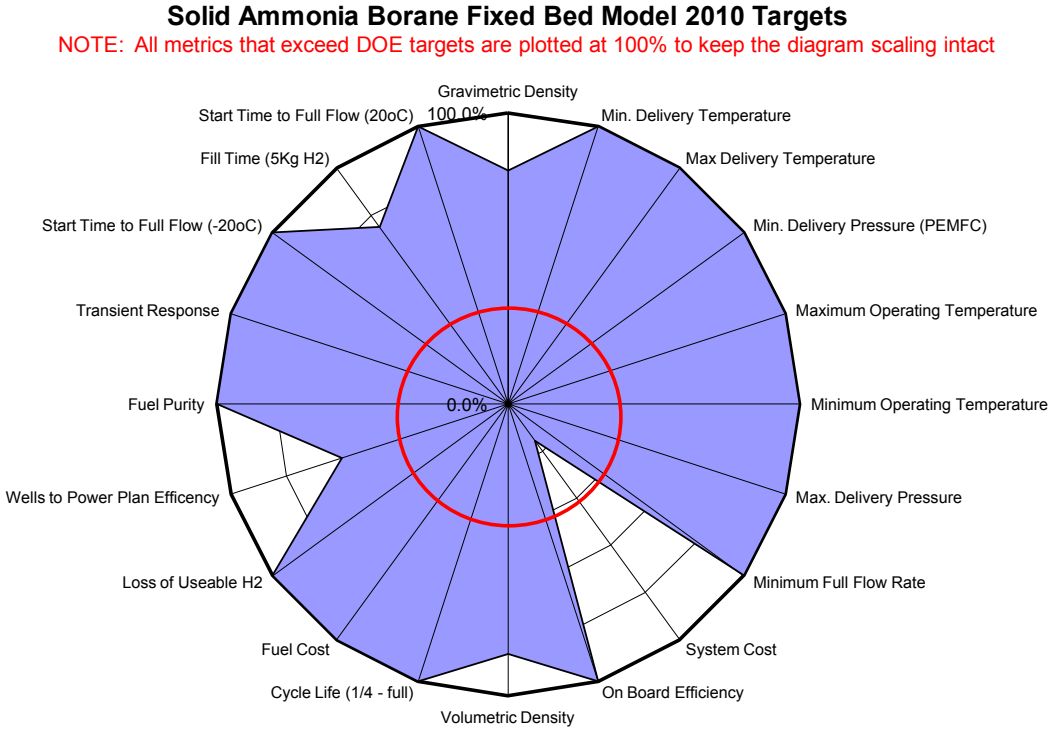


FIGURE 1. Progress toward achieving DOE performance targets for solid AB hydrogen storage. Fifteen targets are met at 100%, four targets met at >40% and system cost target at <40%.

discontinued based upon the results of the auger reactor testing. A fixed bed reactor concept was validated. The modeling and cost analysis revealed that a fixed bed reactor with a solid chemical hydride and fluid reactor (solid liquid slurry or AB in IL) would meet the DOE targets. Due to programmatic restraints, it was decided that only one design would go forward. After consultation with our HSECoE partners, including the manufacturers, it was decided to focus future efforts on the fluid system (slurries or AB in IL).

- Projected the mass and volume of four different systems including the metal hydride system, cryogenic adsorbent system, fixed bed reactor chemical hydride system and AB in IL system. As part of this work the heat exchangers and BOP components were sized, and vendors were identified. Care was taken to ensure that the materials were compatible with hydrogen, and the operational temperature and pressures. Value engineering to reduce the mass and volume of the BOP was begun.
- Completed the BOP catalogue which includes the vendor sources, materials of construction, mass, volume, operating temperatures, connection data (if applicable), and performance information (if applicable). This library will be made available to the public in FY 2012.
- Projected the storage system costs to be $9,200 and $4,800 for the metal hydride and chemical hydride systems when produced in high volumes (500,000 units/year). The cost of AX-21 material at high volumes was projected using models of the process as described in the literature. The projected cost was found to be ~$4/kg when made at high volumes. The complete system cost for the cryogenic adsorbent system is not complete since we have not received all the vender quotes. The single largest cost component for all the systems is the tank cost.
- Developed model to assess materials and design options for Tier 1-III pressure vessels.
- Assessed materials options and design options for Type IV liner materials.
- Developed experimental plan for burst testing Type IV pressure vessels under high and low temperature (cryogenic) thermal cycling.
- Optimized the vessel design in terms of cost and performance.
- Defined the geometry limitations for vessel size with manufacturers.



Introduction

To date there has been multiple on-board vehicle-scale hydrogen storage demonstrations, including several studies to examine phenomena and characteristics that impact the engineering of hydrogen storage systems. However, none of these demonstrations have simultaneously met all of the DOE hydrogen storage sub-program goals. Additionally, engineering of new chemical hydride approaches specifically is in its infancy, with ample opportunity to develop novel systems capable of reaching the DOE targets for storage capacity. Toward this goal, PNNL is leading efforts as part of the HSECoE led by Savannah River National Laboratory (SRNL), to design and fabricate a 100 g of hydrogen scaled system based on solid or slurry chemical hydride storage media. This system is intended to be demonstrated at LANL at the conclusion of the HSECoE effort.

Approach

The PNNL actively contributes to the five technology areas established as part of the HSECoE led by SRNL. The goal of this center, and PNNL's role, is to develop and demonstrate low-cost, high-performing, on-board solid-state hydrogen storage through a fully integrated systems design and engineering approach.

PNNL targets six key objectives to optimize performance characteristics and reduce the size, weight, and cost of a solid-state hydrogen storage system. This is being accomplished through carefully engineering and integrating design approach, including application of advanced materials (structural and hydrogen storage), and assessments of manufacturing and cost impact based on established models/approaches for technology tradeoff or "viability" studies.

PNNL also serves multiple leadership roles within the HSECoE technology area structure to help facilitate collaboration across the center partnership and to feed technical results back through and disseminate to other center partners. Achieving the objectives enables PNNL, SRNL, and other HSECoE partners to demonstrate on-board hydrogen storage with the potential to meet 2015 DOE technical targets. This technology and design knowledge will be transferred to the participating automotive original equipment manufacturers, thus advancing the hydrogen market sector and production of future hydrogen-powered vehicles. As appropriate, the models, catalogues, and lessons learned will be made available to the general fuel cell community to accelerate fuel cell technology penetration into commercial applications.

Results

Chemical Hydride Modeling, Concept Validation, and Down Selection

Three types of models were under development in FY 2010: kinetic models, COMSOL, and Simulink models. During FY 2011 the kinetic models were validated, the COMSOL and Simulink models were completed, and the Simulink model was integrated with the Vehicle System Model.

The kinetic models were validated using PCT and large-scale experiments using neat AB and AB mixed with

MC. The results of the PCT tests indicated the amount of H_2 released and the rate of release were consistent with the predicted values (Figure 2). In addition, no foaming was observed on the AB/MC mixture. Since the PCT tests were limited to mg amounts of material, larger tests using gram quantities were done using a quartz tube with thermal imaging and in a stainless steel tube under pressure. The quantity and rate of release was consistent with the models. For the quartz tube testing a heating element was placed at the bottom of the tube with 2.5 g AB powder or pellets placed on top. The experiments revealed that heat did not sufficiently propagate in the AB powder to release all of the H_2 even when the heating element was raised to 400°C. We believe the AB in direct contact with the heating element reacted quickly, but also foamed. The foaming moved the AB out of the heated area and there was not sufficient thermal propagation for all of the AB to react. However, the AB/MC mixture completed reacted and there were no heat propagation issues. Approximately 3-4 minutes were required for the reaction to complete. To investigate the impact of pressure, 2.5 g of AB/MC was tested in a stainless steel tube under 10 bar of Argon. The reactor was heated in a furnace. The H_2 released at a faster rate (2.5 equivalents released in ~15 seconds). The spent AB/MC fuel was stickier than fresh fuel.

During FY 2011 we completed the initial chemical hydride reactor models and construct was completed. Four configurations were considered: solids reactor vessel, auger reactor, recirculating fluid system, and a new fixed bed reactor. The auger and fluid reactors were modeled using Simulink with solid AB, alane, AB slurries, alane slurries, and AB dissolved in an IL. The auger and fixed bed reactor models were integrated with the Vehicle Level Model and run through three cases: UDDS-HWFET, US06, and Cold FTP. The models indicated the H_2 demand could be met throughout the entire drive cycles for each of the cases studied (Figure 3).

The fixed bed reactor concept was developed in FY 2011. The fixed bed reactor combined the hydrogen ballast tank, material storage tank and reactor into a single component. The fixed bed reactor consisted of eight thermally isolated sections in a single tank (Figure 4). The H_2 gas could flow freely between the sections to provide the ballast tank. When the H_2 pressure would decrease to a pre-specified level, a heat element would initiate the H_2 release reaction in one of the sections re-pressurizing the tank. At fueling the, AB beads could be pneumatically conveyed into and out of the bed and the tank re-pressurized. This reactor was modeled using COMSOL to predict pressure ranges, reaction rate, and reaction propagation to minimize the amount of heating required to initiate the reaction. The COMSOL model performance results were used in the Simulink models. The design concept was validated by the AB/MC experiments performed in a stainless steel tube at elevated pressure described previously.

In addition to the kinetic and fixed bed reactor experiments, auger reactor concept validation experiments

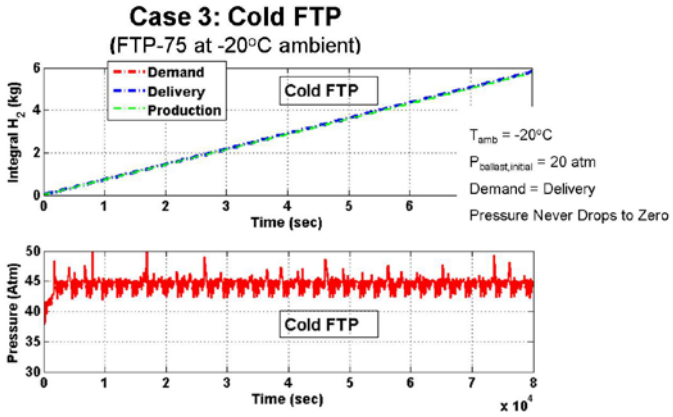


FIGURE 3. Results of AB in IL Chemical Hydride Simulink Model Integrated with the Vehicle Model Operating over the Cold FTP Case

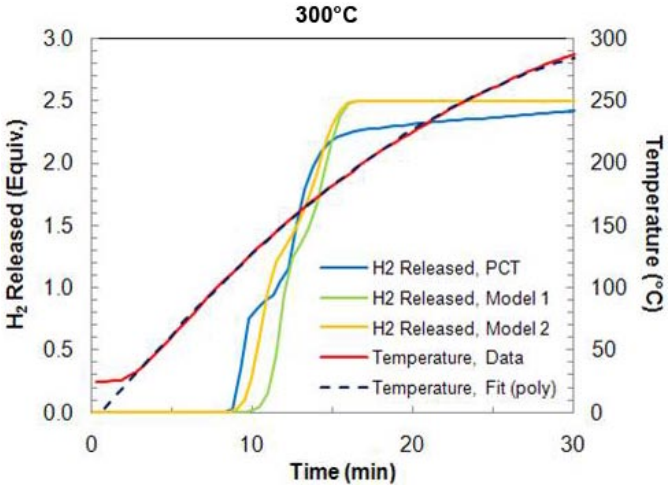


FIGURE 2. Kinetics of Solid AB/MC: Model Prediction vs. Experimental Results at 300°C

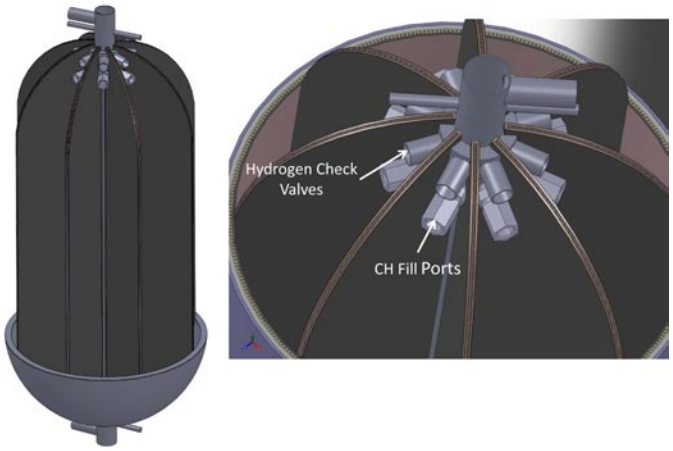


FIGURE 4. Conceptual Drawing of the Fixed Bed Reactor for Chemical Hydrides

were performed. An extruder for plastics was outfitted for hydrogen generation, by insulation, insertion of multiple thermocouples, and placed in a plastic case under an inert atmosphere to prevent any hydrogen generated from reacting with oxygen in the atmosphere. Hydrogen was successfully generated from the reactor with AB/MC as the chemical hydride simulant. However, the auger reactor consistently clogged. Due to the clogging issues, experimental and modeling work on this concept was discontinued early in FY 2011.

For a solid chemical hydride to be a viable solution for on-board hydrogen storage, material movement onto and off of the vehicle in a timely manner must be done. Movement of solid material onboard is being addressed by our partner United Technologies Research Center, or it can be avoided by using the fixed bed reactor. In FY 2010, we proposed using pneumatic conveyance for on/off boarding of the material. This concept was validated in FY 2011. The DOE target for fill time is 5.6 kg of H_2 in 4.7 minutes. Therefore, for AB/MC approximately 9.2 kg/minute must be transported to achieve the DOE target and >3.8 kg/min for the 40% requirement for the concept to be accepted to pass onto Phase II of the HSECoE project.[1] Since low density polyethylene (LDPE) has many of the same transport properties as AB and AB/MC, it was selected as a surrogate material for the tests. The pneumatic tests were done using a 2" heavy duty line vac (Exair) through 14–22 ft length of 2"plastic hose, either open ended or in/out of wedge shaped sections to simulate the fixed-bed tank. The tests were done with powder and beads of LDPE (Table1). For the open-ended tests, both the powder and pellets exceeded the DOE 2010 targets. However, when filling or draining from a vessel, the pellets exceeded the 40% minimum, but the powder did not. Based on the results of the test we recommend that a pellet form factor be used.

TABLE 1. Refueling Feasibility Test Results with LDPE

	Powder	Pellets
	kg/min (% target)	kg/min (% target)
Open-Ended (22')	14-15 (>100%)	14-15 (>100%)
Fill (14' hose)	2.5 (~27%)	5.4-6.9 (60-75%)
Drain (14' hose)	4.5 (~49%)	4.8-9.2 (50-100%)

Finally, during FY 2011, the HSECoE had a Phase I to Phase II transition where only the most likely design would be selected for continued development. Obviously the auger design was not selected since it failed in concept validation. After consultation with HSECoE manufacturer partners and the DOE, it was determined that any concept requiring an tank exchange would not be acceptable since, among other reasons, the interlocks could not be guaranteed to operate safely over the life of the tank. However, both the fixed-bed reactor with solid chemical hydrides and the fluid reactor[2] with either AB dissolved in IL or an AB liquid slurry would meet or surpass the 40% target threshold. Due to concerns over the slight increase in stickiness of the spent AB/MC fuel compared to fresh fuel, HSECoE manufacturer input, and using our engineering judgment on the most likely to succeed candidate, it was decided to focus Phase II efforts on the fluid chemical hydride system.

Vessels

During FY 2011 the main task was to design a series of carbon fiber and metal- and polymer-lined tanks for use in metal hydride and cryo-compressed storage applications, using an ANSYS finite element model. The center needed to determine a realistic range of weights and volumes for the tanks. The initial model was to develop tables comparing different liner materials and pressure combinations that would give the system architects an initial estimate of tank weight and volume. The model has continued to be refined by working with our center partner, Lincoln Composites, for a more detailed analysis as the center works to minimize the tank weight and volume. For example, the model needed to allow the carbon fiber to realistically slide relative to the liner. The temperature drop caused by the initial cryo-state cool down causes the liner to shrink faster than the carbon fiber, so the carbon fiber did not carry the intended load. A model refinement has the two dissimilar materials now working together in a load sharing mechanism which now allows for proper tank liner sizing that will help minimize the fatigue stresses in the type III metal lined tank.

BOP/Costing

Working with the other HSECoE partners, PNNL developed a baseline mass, volume, and cost estimates for the systems under consideration. During Phase II, work will be done to minimize the BOP components and reduce the mass, volume and cost. The system architects and modelers provided PNNL system schematics with predicted temperatures, pressures, and flow rates. PNNL then sized the appropriate components (valves, heat exchangers, etc) and identified specific components from vendors. Using this information, a BOP Catalogue was developed which lists the device, volume, mass, cost, operating parameters, model numbers, and links to vendors. Dimensions and materials of construction were used to estimate the mass or volume for components which did not have the information available. Based on comments from the manufacturers and the Storage Tech Team, the storage systems were designed to be stand alone, or in other words we did not assume that any components from the fuel cell (i.e. radiator) or other vehicle systems could be shared. This limitation made the mass and volume projections larger than if the fuel cell, storage systems, heating, ventilation, and air conditioning, etc. were integrated. Table 2 contains the

[1] This assumes simultaneous addition of fresh fuel and removal of spent fuel.

[2] See Annual Progress Report by HSECoE partner Troy Semelsberger of LANL.

mass and volume projections based on this bottoms-up approach (please note the 2010 targets were 0.045 kg H_2/kg and 0.028 kg H_2/L). In FY 2012 we plan on applying value engineering to minimize the largest, heaviest and most expensive components. For example, a pump for the coolant system for the metal hydride storage weighed 26 kg. We have identified an alternative which weighs only 2.3 kg, but requires an alternating current input and could not provide the needed flow. We are working with the vendor to project the size of a scaled up the system with a direct current input. This will need to be done with many of the BOP components, especially the storage vessels, in order to significantly reduce the mass of the system.

TABLE 2. Hydrogen Storage System Baseline Mass and Volume

	Calculated Mass/Volume	kg H_2/ System	Fraction of 2010 DOE Goal
Metal Hydride System			
Gravimetric Density	457.5 kg	0.0122	27%
Volumetric Density	488.7 L	0.0115	41%
ABMC Fixed Bed System			
Gravimetric Density	155.4	0.036	80%
Volumetric Density	236	0.0237	85%
AB IL Fluid System			
Gravimetric Density	147.85 kg	0.0378	82.6%
Volumetric Density	163.3 L	0.0344	122%
Cryogenic Adsorbent			
Gravimetric Density	145	0.0388	86%
Volumetric Density	238	0.0236	84%

Cost estimates were similarly done by a bottoms-up approach. Vendors identified in the BOP catalogue were contacted and provided estimates at production amounts of 10, 1,000, 10,000, 130,000 and 500,000 units per year (Table 3). Discounts were applied to the vendor estimates if the cost estimate was from a distributor and not the manufacturer. Progress ratios were applied to account for scaling, learning, and manufacturer requirements. These progress ratios were analogous to those used by the DOE in their fuel cell and Quantum tank cost estimates [1-2]. Oregon State University provided the cost estimate from their software for the combustor they are designing. Dynatek provided the tank price estimate. The AB cost, from the Dow presentation from the 2010 Annual Merit Review meeting, was $9/kg. For the metal hydride, sodium alanate plus a carbon additive to increase thermal conductivity was used as a surrogate with a cost range of $126 to $9/kg. For the cryogenic storage team directed us to use AX-21 for this cost estimate. Since there was no vendor source, we estimated the cost from the process described in the patent literature. The cost of AX-21 was estimated to be ~$4/kg. Unfortunately, we did not receive all of the vendor quotes for the cryogenic adsorbent system so the cost could not be calculated. For all the systems, the highest cost component was the storage vessel, with the hydrogen storage media a close second, and the BOP next. The HSECoE will be working on reducing the cost of the storage vessels in FY 2012.

TABLE 3. Estimated Storage System Baseline Costs

		Production Amount ($k)				
		10	1,000	10,000	130,000	500,000
Metal Hydride	Total Costs	$68.5k	$46.9k	$22.3k	$16.5k	$9.2k
	$/kWh					$49.3/kWh
Chem Hydride	Total Costs	$234k	$24.7k	$11.6k	$6.1k	$4.8k
	$/kWh					$25.6/kWh
Cryogenic Adsorbent	Total Costs	In Progress				
	$/kWh	In Progress				

Conclusions and Future Directions

- Solids and Materials Transport and System Design
  - Demonstrated on-off boarding of a solid material.
- Process Modeling and Engineering
  - Completed Simulink and COMSOL models:
    - Multiple designs
    - Multiple materials
  - Evaluated chemical hydride storage to predict that they can provide sufficient H_2 for the cold FTP drive cycle and the aggressive US06 drive cycles.
- Kinetics and Materials Property Measurements
  - Validated kinetic models with data.
  - Validated fixed bed reactor concept.
  - Discontinued Auger type reactor.
  - Completed reaction propagation tests.
  - Begun solid-liquid slurry work.
- BOP and Materials Reactivity and Compatibility
  - Completed BOP Library.
  - Detailed and sized BOP components for two chemical hydride systems, two metal hydride systems and cryogenic adsorbent systems.
  - Identified areas for decreasing mass and volume in BOP.
  - Identified technology gaps.
- Containment and Pressure Vessel Design
  - Developed cryogenic tank models:
    - Projected mass and volume of tanks.
    - Enables optimization of tank depending on pressure.

- Manufacturing and Cost Analysis
  - Completed cost analysis for metal hydride and chemical hydride systems.
  - Projected cost of AX-21 material $4/kg to $4.2/kg.
  - Initiated cost projection for cryo-sorbent system.

Future Work

For Phase II (FY 2012-FY 2013), the primary deliverable is detailed designs for a hydrogen storage system. To this end, we will:

Chemical Hydride System

- Detailed Design, Engineering and Analysis
  - Expand model to include additional physical properties.
  - Sensitivity analysis to determine the acceptable range of:
    - Viscosity
    - Settling/flocculation
    - Vapor pressure
    - Thermal stability
- Experimentally Validate Model Parameters
- Experimentally Validate Critical Components
- Solid-Liquid Slurry Development
  - Composition
  - Additives
- Work with HSECoE Partners in Detailed Design

BOP and Cost Analysis

- Value Engineering
  - Minimize mass and volume
  - Work with partners on BOP
  - Work with venders to push limits on components
- Pressure Vessel Engineering
  - Reduce cost, mass
  - Maintain safety
- Materials Compatibility/Reactivity
  - H_2 wetted material compatibility in components
- Cost Analysis
  - Complete cryo-sorbent
  - Work with partners, venders on reducing cost
  - Update analysis with detailed design

Patents Issued

1. Patent Application: Brooks, K., et.al. Variable Concentration Slurry Reactor System and Fixed Bed Reactor for Externally Regenerated Chemical Hydride System. Submitted. ID 16872-E

FY 2011 Publications/Presentations

Publications List

1. Devarakonda, M., Brooks, K.P., Rassat, S., and Rönnebro, E., "Systems Modeling, Simulation and Material Operating Requirements for Chemical Hydride Based Hydrogen Storage", International Journal of Hydrogen Energy (Submitted).

2. Rönnebro, E., Devarakonda, M., Brooks, K.P., Rassat, S., and Herling, D., "Dynamic Modeling and Simulation of Ammonia Borane Hydrogen Storage Systems", Proceedings of AIChE Annual Meeting, 2010.

3. Devarakonda, M., Holladay, J., Brooks, K.P., Rassat, S., and Herling, D., "Dynamic Modeling and Simulation Based Analysis of an Ammonia Borane (AB) Reactor System for Hydrogen Storage", ECS Transactions, 33(1), pp. 1959-1972, 2010.

4. Brooks, K.P., Devarakonda, M., Rassat, S., King, D.A., and Herling, D., "Systems Modeling of Ammonia Borane Bead Reactor for OnBoard Regenerable Hydrogen Storage in PEM Fuel Cell Applications", Proceedings of ASME 2010 Eighth Fuel Cell Science, Engineering and Technology Conference, Volume 1, ISBN: 978-0-7918-4404-5 pp. 729-734, 2010.

Presentations List

1. Brooks, K.P., Devarakonda, M.N., and Rassat, S.D., "Modeling of Chemical Hydrides in the HSECoE", SSAWG Annual Meeting, Denver, CO., Jan 11–12 2011.

2. Rönnebro, E., Devarakonda, M., Brooks, K.P., Rassat, S., and Herling, D., "Dynamic Modeling and Simulation of Ammonia Borane Hydrogen Storage Systems", AIChE Annual Meeting, Salt Lake City, UT., November 7–12, 2010.

3. Holladay, J., Brooks, K.P., Devarakonda, M., Rassat, S., King, D.A., and Herling, D., "Dynamic Modeling and Simulation Based Analysis of an Ammonia Borane (AB) Reactor System for Hydrogen Storage", 218th ECS Meeting, Las Vegas, NV., October 10–15, 2010.

4. Devarakonda, M., Brooks, K.P., Rassat, S., King, D.A., and Herling, D., "Systems Modeling of Ammonia Borane Bead Reactor for On Board Regenerable Hydrogen Storage in PEM Fuel Cell Applications", ASME 2010 Eighth International Fuel Cell Science, Engineering and Technology Conference, FuelCell2010-33272, Brooklyn, NY., June 14–16, 2010.

5. Rönnebro, E., Devarakonda, M., Brooks, K., Rassat, S., Simmons, K., Karkamkar, A., Herling, D., "Hydrogen Storage Materials Properties for Prototype System Concepts", Invited presentation, Hydrogen Technology Session at the Materials Challenges in Alternative & Renewable Energy Conference, Cocoa Beach, Florida, February 21–25, 2010.

6. Khalil, Y., Newhouse, N., Simmons, K., Dedrick, D., "Potential Diffusion-Based Failure Modes of Hydrogen Storage Vessels for On-Board Vehicular Use ," AIChE Annual Meeting, Salt Lake City, UT., November 7–12, 2010.

References

1. Leavitt, M. and BA Johnson. January 2010. "Development of Advance Manufacturing Technologies for Low Cost Hydrogen Storage Vessel." DOE Hydrogen Program 2009 Annual Summary.

2. James, BD, GD Ariff, RC Kuhn. June 2002. "DFMA Cost Estimates of Fuel-Cell Reformer Systems at Low/Medium/High Production Rates." Presented at Future Car Congress 2002. Directed Technologies, Inc., Arlington, VA.

IV.D.7 Advancement of Systems Designs and Key Engineering Technologies for Materials-Based Hydrogen Storage

Bart van Hassel (Primary Contact),
Jose Miguel Pasini, Mikhail Gorbounov,
John Holowczak, Igor Fedchenia, John Khalil,
Fanping Sun, Xia Tang, Ron Brown, Larry Pryor
and Bruce Laube
United Technologies Research Center (UTRC)
411 Silver Lane
East Hartford, CT 06108
Phone: (860) 610-7701
E-mail: vanhasba@utrc.utc.com

DOE Managers
HQ: Ned T. Stetson
Phone: (202) 586-9995
E-mail: Ned.Stetson@ee.doe.gov
GO: Jesse Adams
Phone: (720) 356-1421
E-mail: Jesse.Adams@go.doe.gov

Contract Number: DE-FC36-09GO19006

Project Start Date: February 1, 2009
Project End Date: July 31, 2014

Fiscal Year (FY) 2011 Objectives

- Collaborate closely with the Hydrogen Storage Engineering Center of Excellence (HSECoE) partners to advance materials-based hydrogen storage system technologies.
- Develop vehicle/power plant/storage system integrated system modeling elements to improve specification of storage system requirements and to predict performance for candidate designs.
- Establish detailed heat and mass transfer modeling and apply to design improved internal heat exchange configurations.
- Design and evaluate compacted/structured hydride powder beds including integration into the above heat exchange configurations.
- Assess the viability of on-board purification for various storage material classes and purification approaches.
- Conduct risk assessments during the progression of the phased HSECoE efforts to evaluate concepts regarding the "Environmental Health and Safety" target.

Technical Barriers

This project addresses the following technical barriers from the Storage section (3.3.4) of the Fuel Cell Technologies Program Multi-Year Research, Development and Demonstration Plan:

(A) System Weight and Volume
(C) Efficiency
(D) Durability/Operability
(E) Charging/Discharging Rates
(H) Balance of Plant (BOP) Components
(J) Thermal Management

Technical Targets

The goals of this project mirror those of the HSECoE which by the end of Phase I (March, 2011) seeks to define systems configurations which can fully meet four of the DOE 2010 numerical system storage targets as outlined in the Multi-Year Research, Development and Demonstration Plan (http://www.eere.energy.gov/hydrogenandfuelcells/mypp/) and partially meet the remaining numerical targets to at least 40% of the target or higher.

TABLE 1. Current Status of Four Key System Characteristics

Characteristic	Units	2010 Target	2015 Target	Compacted Material in System	UTRC 2011 Status
System Gravimetric Capacity	kg H_2/kg system	0.045	0.055	SAH	0.0142
				1:1 LAMH	0.0257
System Volumetric Capacity	kg H_2/L system	0.028	0.040	SAH	0.015
				1:1 LAMH	0.018
Efficiency	%	90	90	SAH	70
				1:1 LAMH	75
NH_3 Content	ppm	0.1	0.1	1:1 LAMH or/AB	0.1

SAH - sodium aluminium hydride; LAMH - lithium amide and magnesium hydride; AB - ammonia borane

FY 2011 Accomplishments

Accomplishments of the current project comprise:

- Developed Simulink framework to compare all H_2 storage systems on a common basis.
- Implemented two on-board reversible metal hydride systems in Simulink framework.
- Optimized volumetric capacity and thermal conductivity of two on-board reversible metal hydride materials through compaction and additives.
- Designed compact heat exchanger for SAH pellets that enables a 10.5 minutes refueling time.

- Developed H_2 purification cartridge that enables NH_3 removal down to 0.1 ppm, as required by the SAE J2719 APR2008 guideline.
- Completed qualitative risk assessment of all three H_2 storage system types.
- Demonstrated solid transport of AB surrogate material along a complex path with a flexible screw feeder.
- Evaluated vibration packing of AX-21/MaxSorb in order to increase density of cryo-adsorbent AX-21/MaxSorb but resulting density was only 0.3 g/cm^3 instead of the targeted 0.6 g/cm^3.



Introduction

Physical storage of hydrogen through compressed gas and cryogenic liquid approaches is well established, but has drawbacks regarding weight, volume, cost and efficiency which motivate the development of alternative, materials-based methods of hydrogen storage. Recent worldwide research efforts for improved storage materials have produced novel candidates and continue in the pursuit of materials with overall viability. While the characteristics of the storage materials are of primary importance, the additional system components required for the materials to function as desired can have a significant impact on the overall performance. Definition, analysis and improvement of such systems components and architectures, both for specific materials and for generalized material classes, are important technical elements to advance in the development of superior methods of hydrogen storage.

Approach

UTRC's approach is to leverage in-house expertise in various engineering disciplines and prior experience with metal hydride system prototyping to advance materials-based H_2 storage for automotive applications. UTRC focused in the second year of the HSECoE project on screening H_2 storage system improvement ideas resulting from compaction, thermal conductivity enhancement, H_2 purification, compact and low weight heat exchanger design and system integration. Results contributed to the selection of storage systems that were more likely to meet DOE targets when further developed in Phase 2 during the Phase 1 to Phase 2 go/no-go meeting.

Results

Complex metal hydrides like Ti-doped SAH and mixtures of LAMH offer a higher gravimetric hydrogen storage capacity (e.g. SAH: 3.2 wt% H_2; 1:1 LAMH: 8.2 wt%) than interstitial metal hydrides (e.g. $Ti_{1.1}CrMn$: 1.7 wt% H_2) but have a relative low density which affects their volumetric capacity. Applying these materials in powder form further reduces their volumetric capacity to levels below the 2015 volumetric capacity target (40 g H_2/L of system). It is therefore important to consider powder compaction.

The effect of powder compaction on the thermal conductivity of SAH was reported in the previous annual report and efforts in the second year focused on improving the thermal conductivity of SAH to 5-8 W/m/K by using additives. UTRC selected aluminum powder and expanded natural graphite (ENG). The results show that the effective thermal conductivity of the SAH/aluminum mixtures follows the series model for thermal conductivity which makes aluminum powder fairly ineffective in improving the thermal conductivity of SAH as a large aluminum volume fraction would be required [1]. It is better to apply aluminum in the form of fins in a fin and tube heat exchanger as an effective thermal conductivity of 4 W/m/K can be achieved with only 4 volume percent of aluminum and compacted SAH pellets. The effective thermal conductivity of SAH with expanded natural graphite followed the parallel model for thermal conductivity [1], which enabled high values of the thermal conductivity at a relatively low volume fraction of this additive. Best results were obtained when using ENG 'worms', kindly provided by SGL Carbon, that introduce thermal conductivity anisotropy upon uniaxial compaction with the highest value of the thermal conductivity perpendicular to the pressing direction and in the direction of the heat exchanger tube. A COMSOL model was developed in order to extract information about the thermal conductivity anisotropy from the thermal conductivity measurements. Heat exchanger tubes no longer require fins when using compacted SAH pellets with about 5 wt% ENG 'worms' to improve the thermal conductivity.

UTRC applied compaction know-how of SAH to the LAMH material in this second year of the HSECoE project. The LAMH material was much more difficult to compact than SAH and required the addition of expanded natural graphite binder in order to obtain samples with a sufficient strength. Thermal conductivity measurements showed that LAMH required a larger weight fraction of ENG 'worms' (e.g. 15 wt%) than SAH (e.g. 5 wt%) in order to obtain high thermal conductivity values in the direction of the heat exchanger tube that would allow a rapid refueling process when it would be possible to substantially improve the slow H_2 absorption kinetics and reversibility of the current LAMH material.

Kinetic measurements from Ti-doped SAH powders and pellets were analyzed in order to obtain values of the model parameters in the kinetic expressions that are used in the detailed COMSOL Multiphysics™ model [2,3], which was developed in the first year of the HSECoE project for obtaining a better understanding about the impact of thermal gradients during refueling upon the H_2 absorption rate. Results showed that one set of model parameters can be used for SAH in its powder and compacted form. The detailed COMSOL model was modified accordingly

and experimentally determined values of densities and thermal conductivities of SAH (without ENG 'worms') were implemented in order to optimize the heat exchanger configuration for a fast refueling time. The results are shown in Figure 1. Small diameter aluminum tubing with aluminum fins are projected to provide sufficient heat transfer in order to reach 90% of the materials H_2 storage gravimetric capacity in about 10.5 minutes, which was the maximum allowable refueling time for the Phase 1 to Phase 2 Go/No-Go decision. A faster refueling time will require materials development in order to improve the reaction kinetics and it will require an increase in the aluminum volume fraction of the heat exchanger in the metal hydride tank. Figure 1 clearly shows the benefit of compaction on the volumetric capacity of the SAH bed. Uncertainty about the heat transfer coefficient between the SAH pellet and the heat exchanger tube has driven the development of an experimental test apparatus which will be used to study H_2 absorption and heat transfer by SAH pellets stacked around a heat exchanger tube in Phase 2.

The H_2 storage system is expected to experience 1,500 cycles over its lifetime. A series of tests was performed in order to study the effect of H_2 absorption and desorption cycles on the strength of SAH pellets. SAH pellets with aluminum mesh reinforcement (Figure 2) have a higher strength than unreinforced SAH pellets but the strength of both types of pellets rapidly degrades upon cycling due to a substantial expansion of the SAH pellets.

UTRC leads the Integrated Power Plant Storage System Modeling technical area, which fostered a successful collaboration between the HSECoE partners. This resulted in a Simulink framework [4] that includes a vehicle level module (National Renewable Energy Laboratory), a fuel

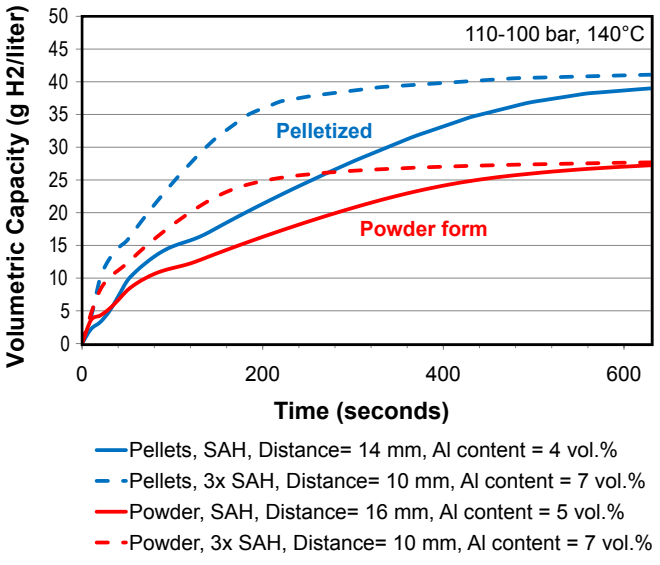


FIGURE 1. Volumetric capacity of the SAH bed, including the aluminum fin and tube heat exchanger, optimized for a 10.5-minute refueling time with SAH in powder or compacted form.

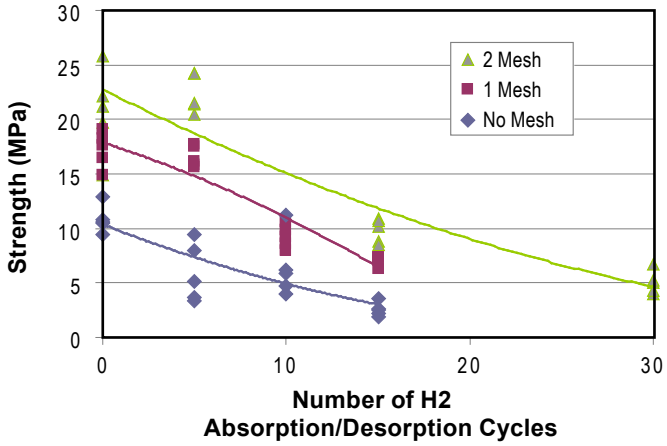


FIGURE 2. Effect of H_2 absorption and desorption cycles on the biaxial flexure strength of SAH pellets with and without internal mesh reinforcement.

cell module (Ford) and various representations of H_2 storage systems as formulated by General Motors (GM), UTRC, Jet Propulsion Laboratory, Savannah River National Laboratory, and the Pacific Northwest National Laboratory (PNNL), as shown in Figure 3. The framework is used within the HSECoE to compare all H_2 storage systems on a common basis. UTRC developed and implemented system models with SAH and LAMH in their powder or compacted form and 350 bar and 700 bar compressed H_2 gas benchmark systems in the Simulink framework. The LAMH system assumed similar heat transfer characteristics as the SAH system. Both systems operate at temperatures that are substantially higher than the temperature at which waste heat from the proton exchange membrane fuel cell can be made available and therefore require H_2 combustion in order to generate heat for hydrogen desorption during a drive cycle. H_2 combustion is also required to heat the storage systems to their operating temperature during a cold start. Such H_2 needs to be readily available and will hence need to be stored in the free volume of the tank or in a separate buffer volume. It was discovered from system simulations that the tank with compacted SAH pellets would no longer contain sufficient H_2 for a cold start and that therefore an additional buffer volume had to be made available to the system. This additional buffer volume reduces the benefits from powder compaction but the H_2 storage tank with the compacted material still occupies a smaller volume than a similar system with the material in its powder form. It is now being studied how the buffer volume can be reduced in order to improve the system volumetric capacity.

Balance of plant (BOP) components were selected by GM and PNNL and information about the weight of the carbon composite type IV pressure vessel were obtained from Lincoln Composites. This information was used to calculate the gravimetric and volumetric capacity of these two metal hydride H_2 storage systems and the results are shown in Figure 4, and also reported in Table 1. The

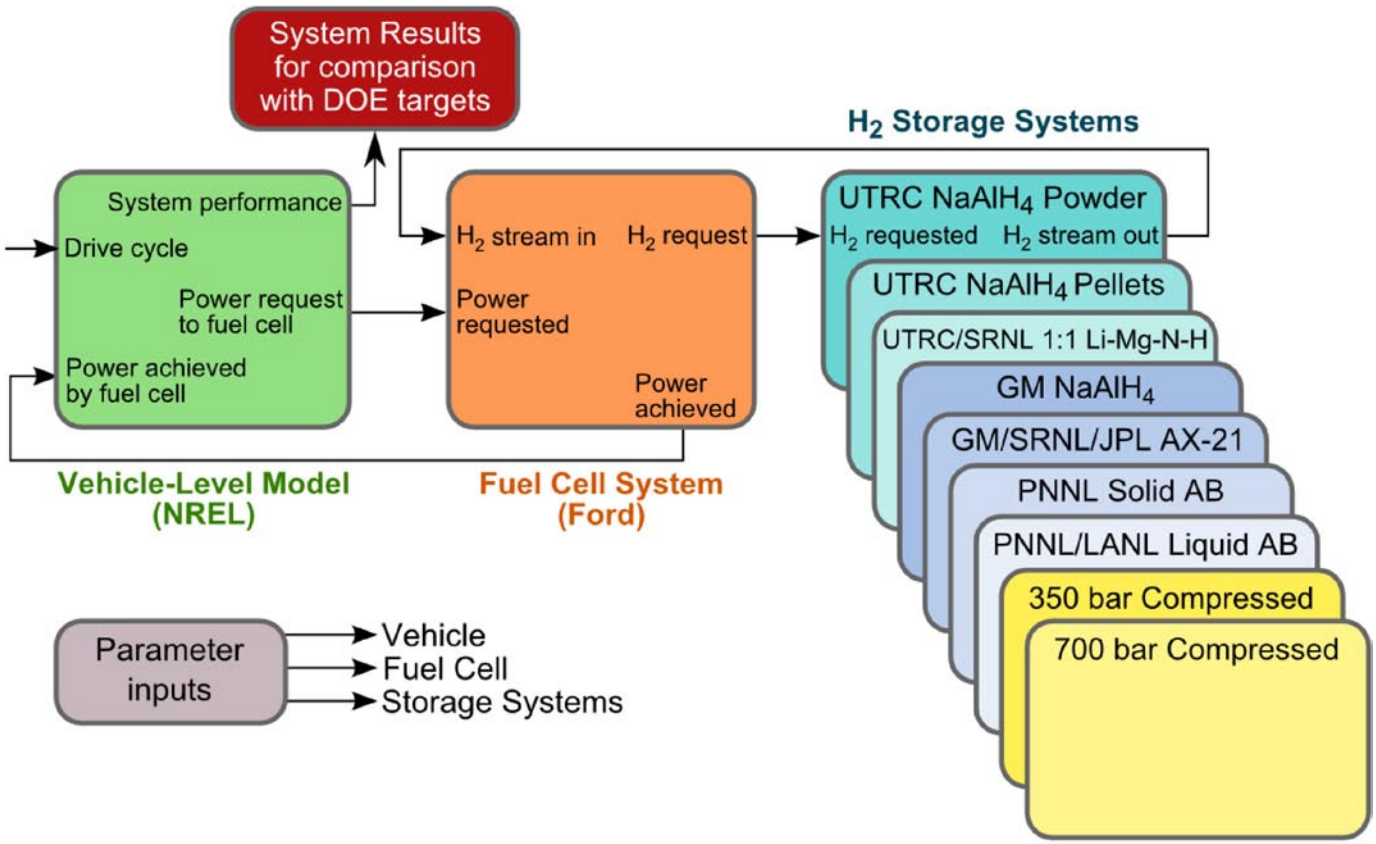


FIGURE 3. Simulink Framework for Comparing all H_2 Storage Systems on a Common Basis

gravimetric capacity of both systems is below the 2010 target and so is their volumetric capacity. It is therefore concluded that the on-board reversible metal hydride systems considered during Phase 1 of the HSECoE are heavy and occupy a much larger volume than the DOE targets allow. This is partly driven by the relative high weight and volume of the BOP components. This gets aggravated when using the heavy BOP components in combination with metal hydride materials like LAMH that have a higher materials gravimetric capacity. Reducing the BOP weight and volume is therefore critical when developing on-board reversible metal hydride H_2 storage systems that require supplementary heating by means of H_2 combustion.

All three H_2 storage systems in the HSECoE have issues related to H_2 quality [5] that need to be addressed. Particulate filters have been recommended by two suppliers in order to contain the cryo adsorbent and on-board reversible metal hydride materials within the pressure vessel while meeting the SAE J2719 APR2008 H_2 purity guideline (particulate size: <10 µm; particulate concentration: <1 µg/l). The standard test method ASTM D7650 standard was identified for assessing the presence of particulates in hydrogen released by the storage systems. UTRC characterized chemical and physical adsorbents for removing NH_3 from hydrogen that is released by the chemical hydride AB and the metal hydride LAMH. Most of the sorbents had a NH_3 dynamic sorption capacity of about 2 wt%. It was shown that the physical adsorbent Selexsorb CD™ (BASF) has the advantage that is can be regenerated without loss of capacity. Cu-BTC metal organic framework was shown to have a very high NH_3 dynamic sorption capacity (12 wt%) but unfortunately it was very expensive and experiments showed that it could not be regenerated after NH_3 exposure.

UTRC performed qualitative risk assessments of all three H_2 storage systems with the objective to identify the critical risks, failure modes and other technical challenges. One critical risk for a sodium alanate H_2 storage system is dust explosion in air caused by an accidental rupture of the storage vessel upon collision. An example of a critical risk for an AB-based chemical hydride system is a runaway chemical reaction resulting from a loss of the exothermic heat removal capability in the system. Loss of vacuum insulation is a critical risk for the cryo-adsorbent system. It has been suggested to develop a framework for safety categorization of H_2 storage materials for on-board vehicular applications as the risks associated with the various materials vary widely.

Brainstorming resulted in several concepts that could be used to transport chemical hydrides like AB in their solid form on board a vehicle. The flexible screw feeder concept was selected for an experimental evaluation. The system was designed and constructed from off the shelve components

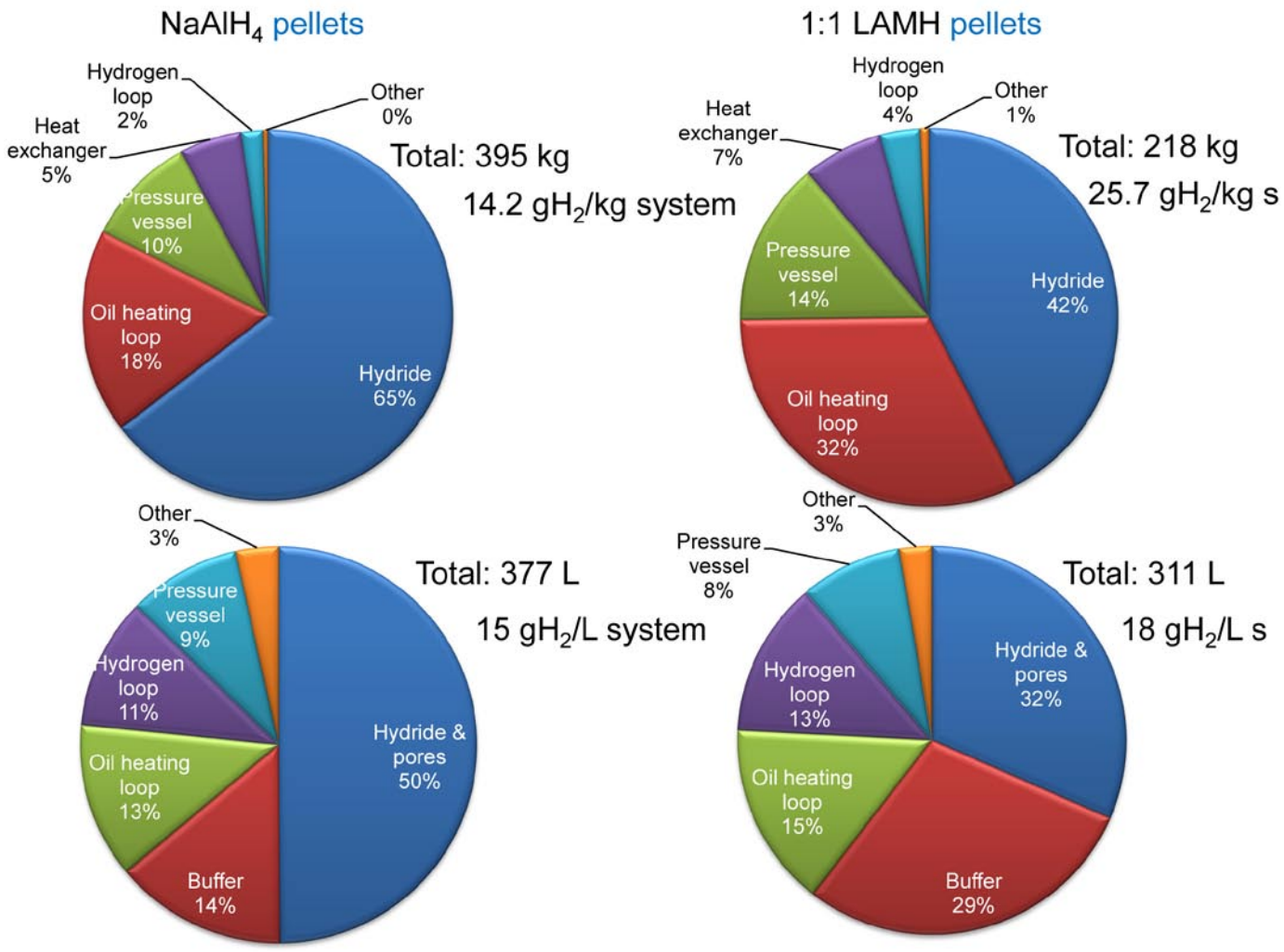


FIGURE 4. Effect of BOP Components on the Gravimetric and Volumetric Capacity of H_2 Storage Systems using SAH or LAMH

and is shown in Figure 5 with the flexible screw transporting an AB surrogate material in a powder form at high rate along a complex path with a 180 degrees bend. Tests were performed to quantify solid transport rate as a function of the flexible screw pitch, rotational speed and bend angle. Solid transport was rejected as a viable technology after PNNL experienced practical problems with transporting AB powder through a heated zone by means of an auger.

Conclusions and Future Directions

Conclusions derived from the work in FY 2011 are:

- ENG 'worms' are effective additives that increase the thermal conductivity of (complex) metal hydride materials and can serve as a binder for materials like LAMH mixtures.
- SAH pellets with and without internal mesh reinforcement show a rapid decline of their strength upon H_2 absorption and desorption cycles due to volumetric expansion of the SAH phase.
- The current generation of BOP components is heavy and occupies a large volume, which negatively impacts the gravimetric and volumetric capacity that can be achieved with the complex metal hydrides considered during Phase 1 of the HSECoE.
- Complex metal hydrides that require supplemental heating need a substantial H_2 buffer volume in order to enable a cold start during which the system is heated to its operating temperature.
- Several sorbents have been identified that can capture NH_3 emissions from materials based H_2 storage systems based on AB and LAMH in order to improve H_2 quality.

Future work will comprise:

- Explore binderless compaction of AX21/MaxSorb.

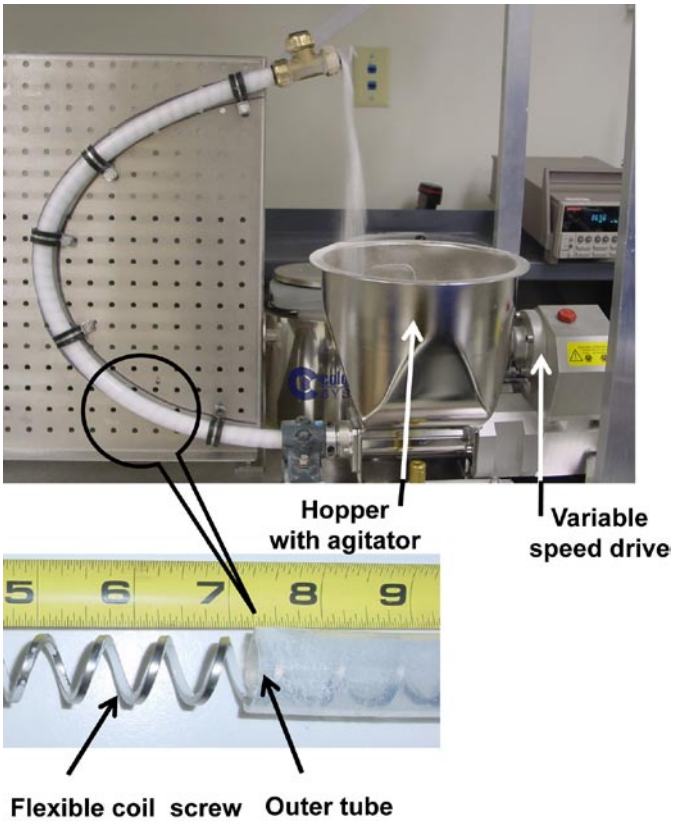


FIGURE 5. Solid Transport of a Surrogate Material with a Flexible Screw along a Complex Path

- Identify ideal material properties of on-board reversible metal hydride material that will enable H_2 storage systems that meet all DOE targets.
- Sensitivity studies with Simulink framework in order to optimize system design.
- Improve understanding of repeated cold starts on system performance.
- Engineering of specialty components for H_2 storage systems and their experimental evaluation.
- Experimental evaluation of purification cartridge connected to H_2 generated from the thermolysis of liquid AB.
- Particulate mitigation strategy evaluation.
- Design failure modes and effects analysis of H_2 storage systems.
- Improve understanding of Department of Transportation requirements for materials-based H_2 storage systems.

FY 2011 Publications/Presentations

1. B.A. van Hassel, D. Mosher, J.M. Pasini, M. Gorbounov, J. Holowczak, X. Tang, R. Brown, B. Laube and L. Pryor, Engineering Improvement of $NaAlH_4$ System, AIChE Topical Conference: Hydrogen Production and Storage: Hydrogen Storage System Engineering and Applications, November 7–12, 2010, Salt Lake City, UT, USA, to be published in the Int. J. Hydrogen Energy.

2. José Miguel Pasini, Bart A. van Hassel, Daniel A. Mosher and Michael J. Veenstra, System modeling methodology and analyses for materials-based hydrogen storage, AIChE Topical Conference: Hydrogen Production and Storage: Hydrogen Storage System Engineering and Applications, November 7–12, 2010, Salt Lake City, UT, USA, to be published in the Int. J. Hydrogen Energy.

3. Bart A. van Hassel, D. Mosher, J.M. Pasini, M. Gorbounov, J. Holowczak, X. Tang, R. Brown, B. Laube, L. Pryor, Fanping Sun, Igor Fedchenia and A.E. Kuczek, Engineering progress in materials based H_2 storage for light-duty vehicles, IEA HIA Task 22, Fremantle, WA, Australia, January 16–20, 2011.

4. Bart A. van Hassel, J.M. Pasini, D. Mosher, M. Gorbounov, J. Holowczak, I. Fedchenia, J. Khalil, F. Sun, X. Tang, R. Brown, B. Laube and L. Pryor, Advancement of Systems Designs and Key Engineering Technologies for Materials Based Hydrogen Storage, Annual Merit Review, Crystal City, Virginia, May 11, 2011.

References

1. B.A. van Hassel, D. Mosher, J.M. Pasini, M. Gorbounov, J. Holowczak, X. Tang, R. Brown, B. Laube and L. Pryor, Engineering Improvement of $NaAlH_4$ System, AIChE Topical Conference: Hydrogen Production and Storage: Hydrogen Storage System Engineering and Applications, November 7–12, 2010, Salt Lake City, UT, USA, to be published in the Int. J. Hydrogen Energy.

2. Bruce J. Hardy and Donald L. Anton, Hierarchical methodology for modeling hydrogen storage systems. Part I: Scoping models, International Journal of Hydrogen Energy 34 (2009), pp. 2269-2277.

3. Bruce J. Hardy and Donald L. Anton, Hierarchical methodology for modeling hydrogen storage systems. Part II: Detailed models, International Journal of Hydrogen Energy 34 (2009), pp. 2992-3004.

4. José Miguel Pasini, Bart A. van Hassel, Daniel A. Mosher and Michael J. Veenstra, System modeling methodology and analyses for materials-based hydrogen storage, AIChE Topical Conference: Hydrogen Production and Storage: Hydrogen Storage System Engineering and Applications, November 7–12, 2010, Salt Lake City, UT, USA, to be published in the Int. J. Hydrogen Energy.

5. Information Report on the Development of a Hydrogen Quality Guideline for Fuel Cell Vehicles, SAE International Surface Vehicle Information Report, J2719 APR2008, Revised 2008-04.

IV.D.8 Optimization of Heat Exchangers and System Simulation of On-Board Hydrogen Storage System Designs

Sudarshan Kumar (Primary Contact),
Mei Cai, Greg Garabedian, V. Senthil Kumar,
Jerome P. Ortmann, and Martin Sulic
General Motors R&D Center (GM)
30500 Mound Road
Warren, MI 48090
Phone: (586) 986-1614
E-mail: Sudarshan.Kumar@gm.com

DOE Managers
HQ: Ned Stetson
Phone: (202) 586-9995
E-mail: Ned.Stetson@ee.doe.gov
GO: Jesse Adams
Phone: (720) 356-1421
E-mail: Jesse.Adams@go.doe.gov

Contract Number: DE-FC36-09GO19003

Project Start Date: March 1, 2009
Project End Date: January 31, 2014

Fiscal Year (FY) 2011 Objectives

Main objectives of this project are:

- To develop system simulation models and detailed transport models for on-board hydrogen storage systems using metal hydride and adsorbent materials, and to determine system compliance with the DOE technical targets.
- To develop storage media structures with optimized engineering properties for use in storage systems.
- To design and build an experimental vessel for validation of cryoadsorption models.

Technical Barriers

This project addresses the following technical barriers from the Hydrogen Storage section of the Fuel Cell Technologies Program Multi-Year Research, Development, and Demonstration Plan (MYPP):

- (A) System weight and volume
- (C) Efficiency
- (E) Charging/Discharging Rates
- (J) Thermal Management

Approach

As part of the Hydrogen Storage Engineering Center of Excellence (HSECoE) team, the GM team is building system models and detailed transport models for on-board hydrogen storage systems using metal hydrides and adsorbent materials. Detailed transport models have been developed for the metal hydride and adsorbent systems with a focus on optimization of heat exchanger design with the objective of minimizing the heat exchanger mass. We are also working on storage media structuring and enhancement studies for the metal hydride and adsorbent materials. Since the hydrogen storage materials are generally characterized by low density and low thermal conductivity, we are conducting experiments to form pellets and add thermal conductivity enhancers to the storage material, and to improve cycling stability and durability of the metal hydride and adsorbent materials. An additional area of focus has been on designing and building a cryoadsorption vessel for validation of cryoadsorption models.

FY 2011 Accomplishments

- Developed two system simulation models for sodium alanate employing different heat exchanger designs and integrated in the framework model.
- Developed and integrated a system simulation model for high-pressure metal hydrides ($Ti_{1.1}CrMn$).
- Optimized three different heat exchanger designs for the metal hydride systems, and identified the design for minimum heat exchanger weight.
- For adsorbent materials, determined optimum pellet size for fast refueling.
- Pelletization and thermal conductivity enhancement of metal hydride and adsorbent materials.



Results

System Models for Metal Hydride Systems: Three system simulation models have been integrated into a modeling framework developed by the Center for evaluation and comparison on a common basis. For sodium alanate, two system models were developed and integrated – one with a shell and tube heat exchanger with cooling tubes and fins, and second with a helical coil heat exchanger. The third system model is for a high-pressure metal hydride system that contains $Ti_{1.1}CrMn$ and is based on a shell and tube heat exchanger with cooling tubes and fins. The helical coil heat exchanger system for sodium alanate contains multiple beds that were sized to optimize heat

transfer between the alanate bed and the fluid flowing through the helical coil tube. Both systems were run within the framework to determine the sizing adjustments needed to deliver 5.6 kg of useable hydrogen to the fuel cell. Simulations were then run to test the performance of the storage systems for four drive cycles that feature various driving patterns and operating conditions: standard driving, aggressive driving, cold start, and hot start.

A hydrogen mass balance for a simulation of the standard driving cycle with the sodium alanate/helical coil system is presented in Table 1. For comparison, a mass balance for a dual bed sodium alanate system with parallel cooling tubes and fins for heat transfer is also included. Table 2 contains the mass balance for the aggressive driving cycle simulation. These results show that the helical coil heat exchanger design is a better design and is able

TABLE 1. Hydrogen Mass Balance for the Standard Driving Cycle

	H_2 Delivered to the Fuel Cell	H_2 to Heater	H_2 in Bed
Helical Coil	78.4%	20.5%	1.1%
Dual Bed	73.2%	20.8%	6.0%

TABLE 2. Hydrogen Mass Balance for the Aggressive Driving Cycle

	H_2 Delivered to the Fuel Cell	H_2 to Heater	H_2 in Bed
Helical Coil	75.4%	19.0%	5.6%
Dual Bed	58.2%	15.2%	26.0%

to use most of the hydrogen in the bed for both the normal and the aggressive driving cycles. In the Optimization Study detailed in the following, we present results showing that the helical coil design has much lower mass than the base design. For the $Ti_{1.1}CrMn$ storage system, nearly all of the stored hydrogen is delivered to the fuel cell since it does not require a catalytic heater for desorption. While the $Ti_{1.1}CrMn$ system has good cold start capability, it has the disadvantage of having a low H_2 absorption capacity of approximately 2%. Detailed results are presented in references [1,2].

Optimization of Heat Exchanger Designs: Refueling of metal hydride based hydrogen storage systems is a highly exothermic process. Because of the need for fast refueling rates, thermal management of the storage system is very important. Good heat exchanger design is crucial for a metal hydride-based hydrogen storage system in order to maximize gravimetric and volumetric storage densities of the bed and meet system performance requirements. We have analyzed various heat exchanger designs for sodium alanate-based hydrogen storage systems and systematically optimized the design configurations of these heat exchangers. Optimization is performed by employing an automated COMSOL-MATLAB interface tool to conduct parametric sweeps of the geometry to optimize the heat exchanger design.

Three different heat exchanger designs are analyzed for sodium alanate-based hydrogen storage systems. The three designs are shown in Figure 1. COMSOL modeling is employed to optimize each design to yield maximum gravimetric capacity with the constraint that the local temperature of the bed should not rise above a pre-specified temperature. Optimized designs for each heat exchanger type have been compared. The helical coil heat exchanger is found to be the most compact and efficient heat exchanger design. The detailed results are presented in references [3,4].

Two-Dimensional (2-D) Analysis of Non-isothermal Adsorption in Cylindrical Pellets: For ease of handling and enhanced volumetric capacity, adsorbent powders are often

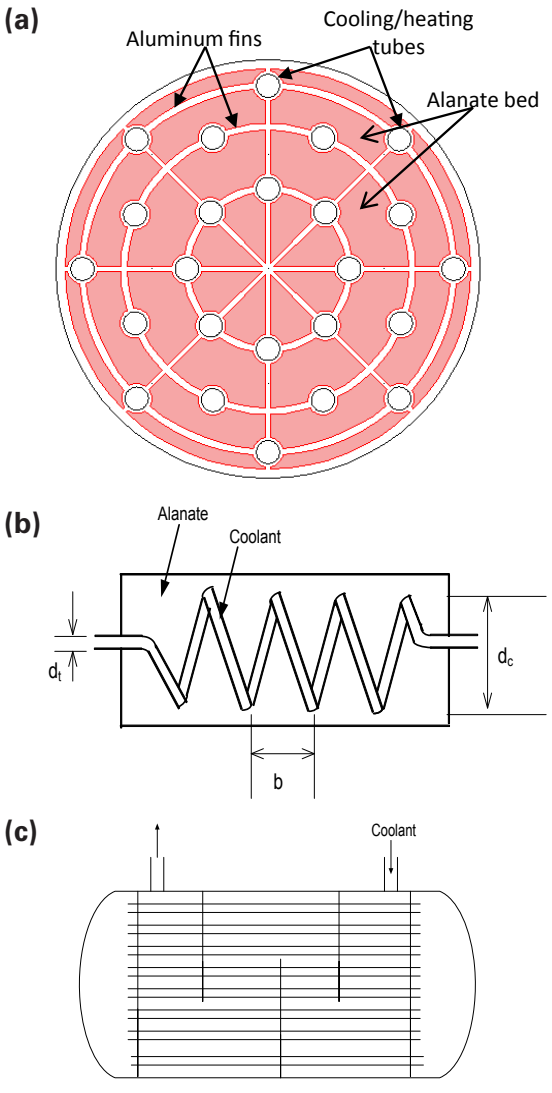


FIGURE 1. (a) Shell and Tube Heat Exchanger with Alanate in Shell; (b) Helical Coil Heat Exchanger; (c) Shell and Tube Heat Exchanger with Alanate in Tubes

compacted into pellets which can be packed in a random or structured fashion in a bed. In either case, one needs to study the intra pellet transport phenomena to arrive at a desired pellet size and aspect ratio. For a random packed bed, often short cylindrical pellets with height identical to diameter are used, since they pack uniformly like spheres.

In the first phase of this study we have analyzed the intra-pellet transport phenomena for short cylindrical pellets at three different sizes, 3 mm, 12 mm and 48 mm. Larger pellets have higher diffusional and thermal resistances, leading to slower adsorption of hydrogen. The aim of this part of the study is to ascertain a typical range of short cylindrical pellet diameters which could be considered for a random packed bed, wherein the intra-pellet transport gradients do not impede achieving short refueling times. A synopsis of these results is discussed below. We are continuing work on the analysis of hockey-puck shaped large pellets which have short heights but large diameters. Such pellets are used in structured packed beds for achieving higher volumetric capacities than a random packed bed.

Model equations were solved to determine the temperature, pressure, and adsorbate concentration fields in short cylindrical pellets. The pressure equilibration occurs quite rapidly, while temperature equilibration is relatively slower. Our analysis shows that simultaneous cooling and adsorption is the rate limiting process. By performing a volume integration of the 2-D total hydrogen content field within the pellet we computed the transient volumetric capacity of the pellet at three different pellet sizes: 3 mm, 12 mm and 48 mm. These results are shown in Figures 2 and 3. The 3 mm pellet reaches its saturation capacity by about 4 seconds, while the 12 mm and 48 mm pellets saturate by about 60 and 600 seconds, respectively. As pellet size increases, a pellet takes longer time to equilibrate with the bulk gas, due to higher diffusional and thermal resistances resulting in a reduced transient volumetric capacity of the pellet. Using very small size pellets increases the bed pressure drop while very large size pellets have poor transient utilization, leading to longer refueling times. This work on single pellet modeling and analysis will help us

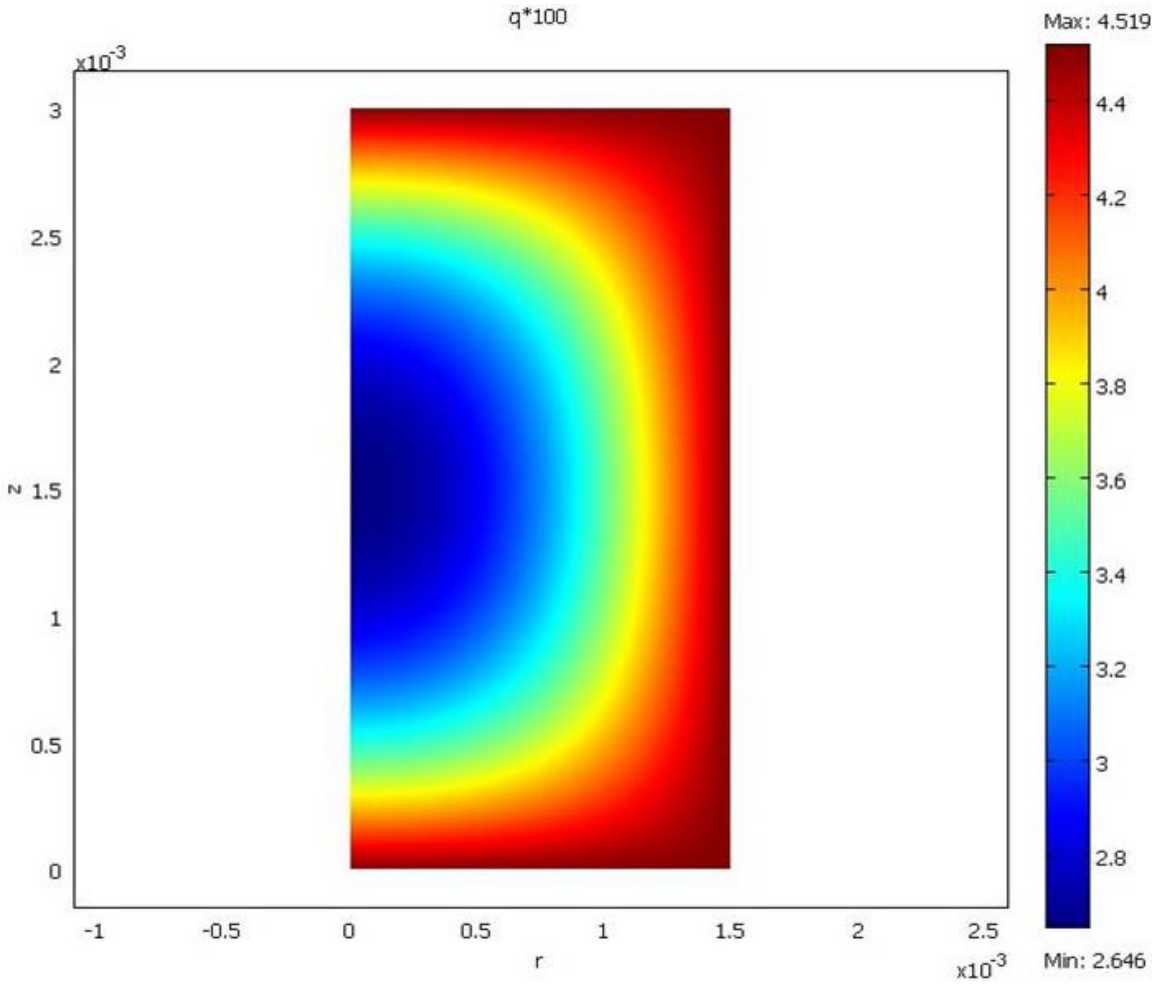


FIGURE 2. Adsorbate Concentration Field in a 3 mm Short Cylindrical Pellet at t = 1 s

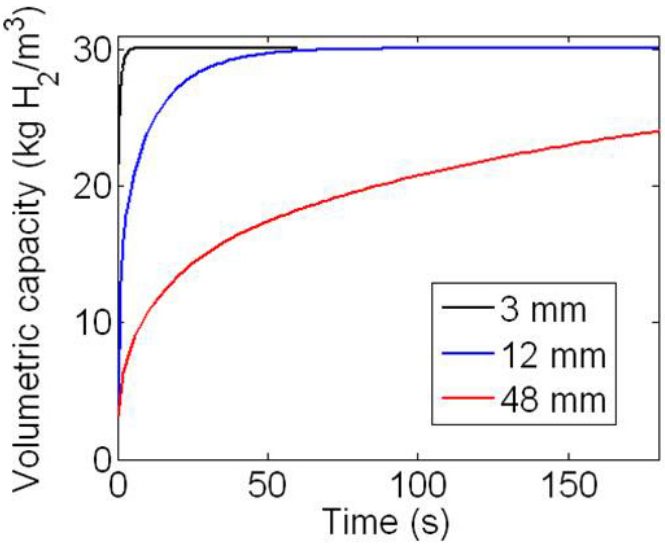


FIGURE 3. Transient Volumetric Capacity for Three Different Pellet Sizes

identify an appropriate range of pellet sizes for conventional packed bed design.

Pelletization of Sodium Alanate and AX-21 Powder: Both the metal hydrides and adsorbent materials for hydrogen storage have low densities and low thermal conductivities. Therefore, it is necessary to find ways to pelletize these materials to increase both the density and thermal conductivity without adversely affecting the hydrogen uptake capacity and kinetics. Experiments conducted in our laboratory show that the high thermal conductivity of pelletized titanium doped sodium alanate ($NaH + Al + TiCl_3$) dramatically degrades (up to 80%) within the first 10 cycles due to extensive pellet expansion. Upon further hydrogen cycling, pellets continue to expand leading to complete failure of structural integrity. To counter thermal conductivity degradation two approaches were explored; incorporation of high thermal conductivity additives (expanded natural graphite and graphite flakes) into the alanate before pelletization and mechanical confinement of pellets during cycling. Both forms of graphite additive exhibited similar loss in thermal conductivity over the first 10 cycles. While pellets with graphite additives have a slightly higher thermal conductivity at each cycle compared to pellets without additives, the overall degradation effect of cycling is similar and not favorable.

While the addition of graphite to sodium alanate pellets lessens the decrease in thermal conductivity over 10 cycles compared to pellets without graphite, pellet expansion (previously reported) is not mitigated and has an overwhelming adverse effect on thermal conductivity. Confinement of sodium alanate pellets by mechanical means showed slowed degradation of thermal conductivity over first 10 cycles, compared to unconfined pellets run in parallel, confined pellets had twice the thermal conductivity after 10 cycles (2.57 and 4.80 W/mK, respectively). After 50 cycles, confined pellets had a thermal conductivity of 3.72 W/mK. Unconfined pellets could not be measured after 10 cycles due to expansion. Various methods of confinement have been explored, all showing similar degradation control. Sodium alanate pellets were also observed to fuse to one another during cycling. Fusion of a pellet stack can minimize surface area contact resistance and allow for improved heat transfer between neighboring pellet bodies. The confined fused pellets show a degradation of thermal conductivity.

The increased volumetric capacity of activated carbon through pelletization requires the addition of a binder. Current procedures employ extensive elevated temperature work-up resulting in lengthy processing time per pellet. To expedite pelletization, we are focusing on room temperature binders. The binder is combined with AX-21 resulting in a fibrous network which holds the activated carbon together. The fiber network cold flows under high pressures allowing the AX-21 mixture to be pelletized rapidly under room temperature conditions. The pellet density is improved by a factor of 1.5-1.8 (0.45-0.55 g/cm^3, powder = 0.3 g/cm^3) but the surface area decreases by 20% compared to the powder alone (2,400 and 3,000 m^2/g, respectively). These pellets show gravimetric capacity similar to that of the powder at 77 K but the volumetric capacity is substantially improved through pelletization compared to the powder. Work on identifying the best room temperature binder and pellet properties is continuing.

Future Direction

- Extend the modeling work to short cylindrical pellets that can be used for structured packing of the bed for high volumetric capacity to determine optimum pellet size.
- Optimize binders for pelletizing activated carbon with respect to engineering properties of interest for hydrogen storage.
- Design and build a cryoadsorption vessel for validating the flow-through cooling concept for recharging.
- Conduct experiments to validate the cryoadsorption models for charging and discharging of adsorption based storage beds.
- With the HSECoE team, determine the material properties for metal hydrides that are necessary to meet DOE 2015 hydrogen storage system goals.

FY 2011 Publications/Presentations

1. S. Kumar et al. (2011) Optimization of heat exchangers and system simulation of on-board storage system designs, presented at the 2011 DOE Hydrogen Program Annual Merit Review Meeting, Washington, D.C.

2. M. Raju, J.P. Ortmann, and S. Kumar (2010) System simulation model for high-pressure metal hydride hydrogen storage systems, Int. J. Hydrogen Energy, 35, 8742-8754.

3. M. Raju M. and S. Kumar S. (2011) System Simulation Modeling and Heat Transfer in Sodium Alanate based Hydrogen Storage Systems. Int J Hydrogen Energy,36*; 1578-1591*.

4. M. Sulic, M. Cai, and S. Kumar (2010): Sodium alanate as a practical automotive on-board solid-state hydrogen storage medium, presented at the Int. Symp. on Metal-Hydride systems, Moscow, July 2010.

5. M. Raju and S. Kumar (2010a) Modeling of a Helical Coil Heat Exchanger for Sodium Alanate based On-board Hydrogen Storage System, presented at the *COMSOL 2010 Conference, Boston, MA*.

6. M. Raju and S. Kumar (2010b) Optimization of Metal Hydride based Hydrogen Storage Bed Designs, presented at the *2010 AIChE Annual Meeting, Salt Lake City, UT.*

7. S. Kumar S., M. Raju and V. Senthil Kumar (2010) System Simulation Models for On-Board Hydrogen Storage Systems, presented at the *2010 AIChE Annual Meeting, Salt Lake City, UT.*

References

1. M. Raju, J.P. Ortmann, and S. Kumar (2010) System simulation model for high-pressure metal hydride hydrogen storage systems, Int. J. Hydrogen Energy, 35, 8742-8754.

2. S. Kumar et al. (2011) Optimization of heat exchangers and system simulation of on-board storage system designs, presented at the 2011 DOE Hydrogen Program Annual Merit Review Meeting, Washington, D.C.

3. M. Raju and S. Kumar (2010a) Modeling of a Helical Coil Heat Exchanger for Sodium Alanate based On-board Hydrogen Storage System, presented at the COMSOL 2010 Conference, Boston, MA.

4. M. Raju and S. Kumar (2010b) Optimization of Metal Hydride based Hydrogen Storage Bed Designs, presented at the 2010 AIChE Annual Meeting, Salt Lake City, UT.

IV.D.9 Ford/BASF-SE/UM Activities in Support of the Hydrogen Storage Engineering Center of Excellence

Andrea Sudik (Primary Contact, Ford), Michael Veenstra (Ford), Donald Siegel (UM), Justin Purewal (UM), Dongan Liu (UM), Stefan Maurer (BASF-SE), Ulrich Müller (BASF-SE), Jun Yang (Ford)
Ford Motor Company
2101 Village Road, RIC Rm. 1519
Dearborn, MI 48121
Phone: (313) 390-1376
E-mail: asudik@ford.com

DOE Managers
HQ: Ned Stetson
Phone: (202) 586-9995
E-mail: Ned.Stetson@ee.doe.gov
GO: Jesse Adams
Phone: (720) 356-1421
E-mail: Jesse.Adams@go.doe.gov

Contract Number: DE-FC36-GO19002

Subcontractors:
- University of Michigan (UM), Ann Arbor, MI
- BASF-SE, Ludwigshafen, Germany

Project Start Date: February 1, 2009
Project End Date: January 31, 2014

Fiscal Year (FY) 2011 Objectives

This project addresses three of the key technical obstacles associated with the development of a viable hydrogen storage system for automotive applications:

- (Task 1) Create accurate system models that account for realistic interactions between the fuel system and the vehicle powerplant.
- (Task 2) Develop robust cost projections for various hydrogen storage system configurations.
- (Task 3) Assess and optimize the effective engineering properties of framework-based hydrogen storage media (such as metal-organic frameworks, MOFs).

Technical Barriers

This project addresses the following technical barriers from the Hydrogen Storage section of the Fuel Cell Technologies Program Multi-Year Research, Development and Demonstration Plan:

(A) System Weight and Volume
(B) System Cost
(C) Efficiency
(D) Durability/Operability
(E) Charging/Discharging Rates
(H) Balance of Plant (BOP)
(J) Thermal Management

Technical Targets

The outcomes of this project affect vehicle and system level models, cost analysis, and materials property assessment/optimization. Insights gained from these studies are applied towards the engineering of hydrogen storage systems that meet the following DOE 2010 and ultimately 2015 hydrogen storage targets shown in Table 1.

TABLE. DOE Hydrogen Storage Targets

Storage Parameter	Units	2010	2015
System Gravimetric Capacity	kg·H_2/kg	0.045	0.055
System Volumetric Capacity	kg·H_2/L	0.028	0.040
Storage System Cost	\$/kWh$_{net}$	To Be Determined	To Be Determined
System Fill Time (for 5 kg H_2)	min	4.2	3.3
Minimum Full Flow Rate	(g/s)/kW	0.02	0.02
Min/Max Delivery Temperature	°C	-40/85	-40/85
Min. Delivery Pressure (Fuel cell)	atm	4	3

FY 2011 Accomplishments

Below is a list of accomplishments by task:

- Task 1. System Modeling
  - Evaluated and constructed baseline fuel cell model to support the interaction with the vehicle and hydrogen storage system model.
  - Completed classification of the 2010 and 2015 DOE hydrogen storage targets for optimization and tradeoff analysis amongst the storage system concepts.
  - Developed a common set of drive-cycles for vehicle simulation performance evaluations.

- Task 2. Cost Analysis
  - Supported the manufacturing and cost analysis technology team in the evaluation of the initial cost assessments for the hydrogen storage systems.
  - Established initial phase of cost analysis through the development of a component cost matrix.
  - Assisted in the approach of using the component library to decompose the key system elements to evaluate the cost drivers and establishing cost sensitivity items for future trade-offs.
- Task 3. Assessment/Optimization of Framework-Based Storage Media
  - Prepared a set of variable-density *neat* MOF-5 compacts ranging from 0.3 to 0.8 g/cm^3 which have the potential to realize significant volumetric capacity improvement as compared to the powder (ρ=0.13 g/cm^3).
  - Characterized key physical and mechanical properties of MOF-5 compacts including crush strength, Brunauer-Emmett-Teller (BET) surface area, and total pore volume for comparison with known sorbent data (e.g. for AX-21, polyether ether ether ketone [PEEK], MOF-177).
  - Determined excess and estimated total gravimetric and volumetric capacities for MOF-5 compacts and realized a 4× improvement in excess volumetric capacity for 0.5 g/cm^3 compact with only a small decrease (~15%) in excess gravimetric capacity (as compared to powder MOF-5).
  - Evaluated principle thermal property data (i.e. thermal diffusivity, heat capacity, and thermal conductivity) for *neat* MOF-5 compacts (e.g. k at 25ºC for 0.35 g/cm^3 is 0.072 W/mK).
  - Prepared a series of variable-density MOF-5 compacts containing expanded natural graphite (ENG; 1, 5, and 10 wt% additions) as a thermal conductivity aid.
  - Evaluated preliminary thermal conductivity and surface area characteristics for ENG-containing MOF-5 compacts, revealing a 5× improvement in thermal conductivity (e.g. 0.56 W/mK for 0.5 g/cm^3 MOF-5 compact w/ 10 wt% ENG as compared to <0.1 W/mK for neat compact).
  - Designed, fabricated hardware, and completed experiment of first-time in situ characterization (via neutron imaging) of hydrogen dynamics in a cryogenic storage vessel on MOF-5 pellets.



Introduction

Widespread adoption of hydrogen as a vehicular fuel depends critically on the development of low-cost, on-board hydrogen storage technologies capable of achieving high energy densities and fast kinetics for hydrogen uptake and release. As present-day technologies -- which rely on physical storage methods such as pressurization or liquefaction -- are unlikely to attain established DOE targets, interest in materials-based approaches for storing hydrogen have garnered increasing attention. To hasten development of these 'hydride' materials, the DOE has established three Centers of Excellence for materials-based hydrogen storage research as part of a "Grand Challenge" to the scientific community. While the Centers of Excellence have made substantial progress in developing new storage materials, significant challenges associated with the engineering of the storage system around a candidate storage material remain largely unresolved.

Approach

As a partner in the Hydrogen Storage Engineering Center of Excellence, Ford-UM-BASF is conducting a multi-faceted research project that addresses three of the key engineering challenges associated with the development of materials-based hydrogen storage systems.

Systems Modeling (Task 1): Drawing on our extensive expertise in the engineering of fuel cell (FC) and H_2 internal combustion engine (H_2-ICE) vehicles, we are evaluating and developing system engineering technical elements with a focus on hydrogen storage system operating parameters. This effort will result in a set of dynamic operating parameters and a high-level system model describing the interaction of the fuel storage system with the FC (or H_2-ICE) power plant.

Cost Analysis (Task 2): We are leveraging the unique capabilities of the "Ford/Massachusetts Institute of Technology cost model" to develop and perform hydrogen storage manufacturing cost analyses for various candidate system configurations and operating strategies. This analysis facilitates a technology roadmap for potential cost reductions and manufacturing optimization, while providing important feedback to Go/No-Go decisions on prototype design and construction.

Sorbent Media Assessment and Optimization (Task 3): We are evaluating and optimizing the "effective engineering properties" of an important class of sorbent materials (MOFs) and other framework-like materials in order to devise improved packing and processing strategies for their use in a systems context. Various mechanical processing routes are being examined (ranging from powders to pelletization to extrusion) in an effort to simultaneously maximize packing density, heat and mass transfer, and hydrogen uptake characteristics.

This work is expected to impact the broader goals for the DOE and FreedomCAR, leading to a significant advance in the engineering of materials-based hydrogen storage systems, refinement in our understanding of the performance targets of hydride materials, and ultimately, the development of commercially viable hydrogen storage systems.

Results

Following is a description of our technical results for each task and how these results relate to achieving the DOE targets.

Task 1. System Modeling

The Integrated Power Plant/Storage System Modeling Technology Area during the past year focused on the framework elements that were needed to establish simulation modeling parameters for a consistent assessment of the storage systems in support of the phase 1 milestone review. Within this year, the modeling framework was established and fully utilized to assess the multiple storage systems in a consistent manner. Further details in the powerplant models were refined such as the fuel cell stack efficiency and the associated parasitics. The fuel cell stack was sized for 80 kW net operating power at 80ºC temperature. In the refinement of the model, the fuel cell system efficiency was evaluated and adjusted to be consistent with the DOE fuel cell system targets for efficiency at rated power (50%) and quarter power (60%) as shown in Figure 1.

The fuel cell model includes the essential elements to interface between the vehicle and the hydrogen storage model blocks. These elements include: the polarization curve to translate requested vehicle power to current and hydrogen flow request, parasitic power from the compressor, and stack temperature to provide the waste heat stream. Each of these elements were integrated and evaluated during this year. The polarization curve transfer functions were compared against the latest results from the general computational (GC) tool. The assessment concluded that an additional effect for temperature would be added to the Hydrogen Storage Engineering Center of Excellence (HSECoE) modeling framework while the GC tool effects to temperature appeared higher due to sensitivity of the future catalyst assumptions. The other activities in the modeling area included confirmation of the maximum flow condition and definition of success criteria for following the flow demand trace within the modeling simulation.

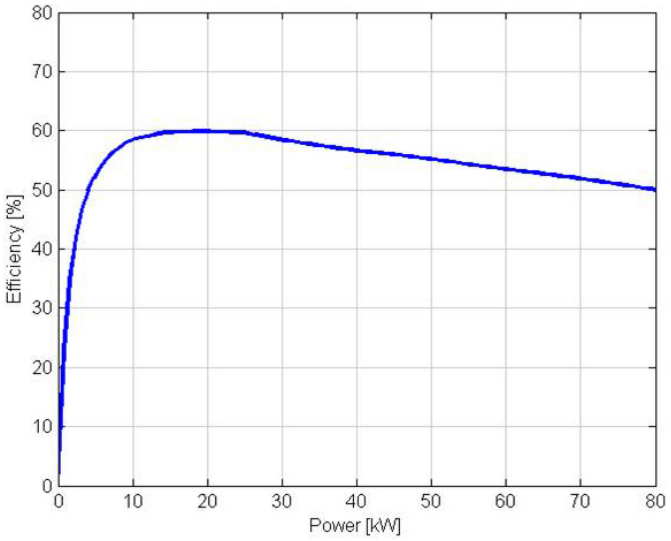


FIGURE 1. Fuel Cell System Efficiency in the HSECoE Universal Framework Model

In this year, a key accomplishment was the establishment of the modeling structure for the baseline vehicle assumptions and drive cycle test cases. In the evaluation of useable hydrogen and other performance attributes, the system architects and storage system modelers had various simulation approaches and assumptions. In order to have a consistent approach, a baseline vehicle and test matrix was developed to establish the storage capacity assessment along with the functional confirmation at the boundary conditions such as high flow, cold cycle, and hot cycle. The initial vehicle proposal was based on the compact vehicle based on a global view of vehicle platforms but was revised to mid-size assumptions to maintain consistency with prior analysis such as those assumed in the Argonne National Laboratory Powertrain Systems Analysis Toolkit model. The emphasis in developing these simulation assumptions was to have consistency and references for the rationale inside of developing unique baseline parameters for the center. The simulation test cases were formulated based on specific needs expected usages to demonstrate a certain performance target. The test case 1 was developed for the basic fuel economy evaluation and confirmation of the usable capacity of the storage systems, which was standardized at 5.6 kg (for consistency with previous studies). The test case 1 utilizes the Environmental Protection Agency (EPA) fuel economy (FE) Urban Dynamometer Driving Schedule (UDDS) and Highway Fuel Economy Test (HWFET) drive cycles and then adjusts them to the post-2008 five-cycle EPA fuel economies from a prior regression correlation in the simulated vehicle fuel economy estimation. The test case 2 consisted of the US06 that simulates aggressive driving and includes the high flow conditions for evaluating the minimum full flow target. The test case 3 is a cold test case with a lower temperature than the EPA cold test to align with the -20ºC start-up criteria within the target requirements. The Federal Test Procedure (FTP)-75 was selected for the cold test case since the cycle has low power demand and has idle periods within the drive cycle which would be worst case for systems depending on waste heat or other usage parameters to increase their operating temperatures. The test case 4 is a hot test case based on the drive cycle and consistent with the temperature utilized in the EPA hot condition testing. The final test case 5 was established for the dormancy test case and was based on a month static storage time period at the high EPA temperature. The resulting test cycle matrix is shown in Table 1.

In addition, the HSECoE requested the original equipment manufacturers (OEMs) to assist in the classification of the DOE hydrogen storage targets. The classification of DOE targets was needed for guiding the upcoming phase 1 milestone (i.e. 4 at 100% and remaining at

TABLE 1. HSECoE Simulation and Evaluation Drive Cycle Matrix

Case	Test Schedule	Cycles	Description	Test Temp (°F)	Distance per cycle (miles)	Duration per cycle (minutes)	Top Speed (mph)	Average Speed (mph)	Max. Acc. (mph /sec)	Stops	Idle	Avg. H2 Flow (g/s)*	Peak H2 Flow (g/s)*	Expected Usage
1	**Ambient Drive Cycle** - Repeat the EPA FE cycles from full to empty and adjust for 5 cycle post-2008	UDDS	Low speeds in stop-and-go urban traffic	75 (24 C)	7.5	22.8	56.7	19.6	3.3	17	19%	0.09	0.69	1. Establish baseline fuel economy (adjust for the 5 cycle based on the average from the cycles) 2. Establish vehicle attributes 3. Utilize for storage sizing
		HWFET	Free-flow traffic at highway speeds	75 (24 C)	10.26	12.75	60	48.3	3.2	0	0%	0.15	0.56	
2	**Aggressive Drive Cycle** - Repeat from full to empty	US06	Higher speeds; harder acceleration & braking	75 (24 C)	8	9.9	80	48.4	8.46	4	7%	0.20	1.60	Confirm fast transient response capability – adjust if system does not perform function
3	**Cold Drive Cycle** - Repeat from full to empty	FTP-75 (cold)	FTP-75 at colder ambient temperature	-4 (-20 C)	11.04	31.2	56	21.1	3.3	23	18%	0.07	0.66	1. Cold start criteria 2. Confirm cold ambient capability – adjust if system does not perform function
4	**Hot Drive Cycle** - Repeat from full to empty	SC03	AC use under hot ambient conditions	95 (35 C)	3.6	9.9	54.8	21.2	5.1	5	19%	0.09	0.97	Confirm hot ambient capability - adjust if system does not perform function
5	**Dormancy Test**	n/a	Static test to evaluate the stability of the storage system	95 (35 C)	0	31 days	0	0	0	100%	100%			Confirm loss of useable H2 target

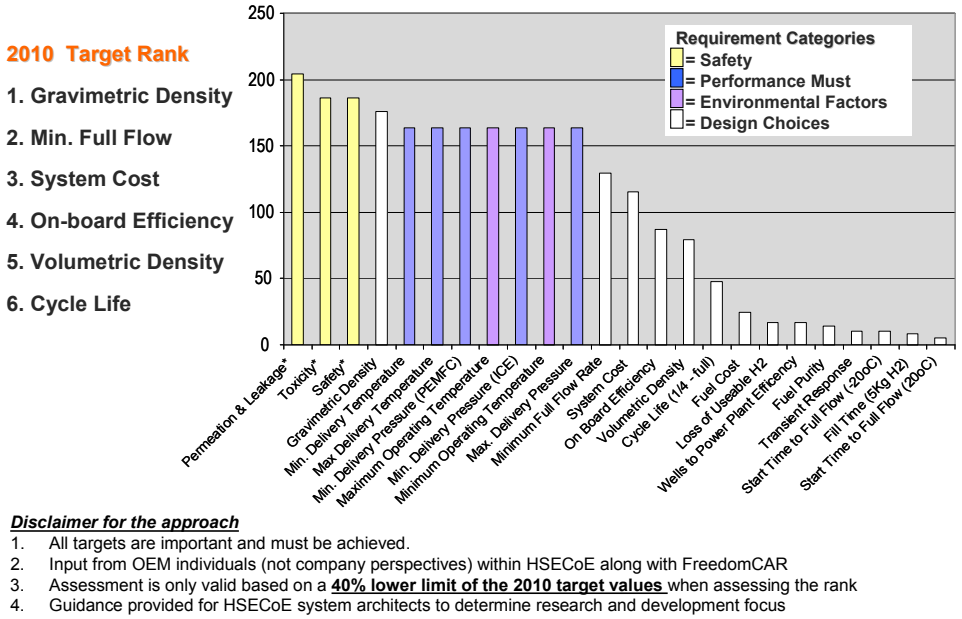
*Based on NREL simulation with mid-size vehicle, 5.6 kg usable H2, 80 kW fuel cell with a 20 kW battery

40% criteria) and for providing trade-off recommendations to the system architects. The Ford team took the leadership role to brainstorm methods and organize the classification approach. After consideration, the decision was to use a quality function deployment (QFD) method since this tool provides an organized structure to assessing the targets using OEM system engineering disciplines. The system engineering approach uses a cascade from the customer musts/wants to the system requirements/targets. The QFD identifies the priorities of the customer attributes and then ranks the relationships of the system targets to the customer attributes. The cause-effect relationships used a 1 (low effect) to 9 (high effect) scale by evaluating the change in the vehicle attribute based on a 40% reduced target. The priority of the customer attributes utilized the analytic hierarchy process which a series of pairwise comparison judgments to express the relative strength or impact of the element compared to another.

The results of this classification process produced the ranking of the 2010 targets as shown in Figure 2. As indicated by the color codes, the OEM team classified the targets as safety, performance musts (required for basic function), environmental factors (not actual targets), and design choices. The targets classified as design choices were viewed as the attributes that should be utilized by the system architects to emphasize the development of the higher ranked items. The lower ranked design choice targets are still important but could be deemphasized in the system design (at a 40% lower limit). It is important to recognize the analysis was conducted based on the DOE phase 1 milestone criteria that allowed a hydrogen storage system to meet a 40% target level. Therefore, this ranking approach is only valid to a 40% lower limit of the existing DOE target. When considering this assumption, certain targets were relatively immune to a 40% setting of the value. The process was repeated for the 2015 targets at a 50% lower limit and the top five target priorities remained the same with only minor changes in the absolute classification levels.

Task 2. Cost Analysis

The Manufacturing and Cost Analysis Technology Team during the past year established the HSECoE component library foundation to provide the cost evaluation and initial assessment of overall system weight and volume attributes. The HSECoE component library was populated to provide the system architects with the elements needed for the system assessments to support phase 1 milestone review. The system architects utilized the library for the system references for the milestone to ensure the common assumptions are being used throughout the HSECoE. Alignment of the library and the structure of cost evaluation analysis were completed during this year. The component library progressed through various reviews and industry



Disclaimer for the approach

1. All targets are important and must be achieved.
2. Input from OEM individuals (not company perspectives) within HSECoE along with FreedomCAR
3. Assessment is only valid based on a **40% lower limit of the 2010 target values** when assessing the rank
4. Guidance provided for HSECoE system architects to determine research and development focus

FIGURE 2. HSECoE Hydrogen Storage Target Classification Pareto Assessment

sources. The effort in developing the library was led by the Pacific Northwest National Laboratory along with input from Ford and other HSECoE partners to ensure the required data for the phase 1 milestone was available. The benchmarking and comparison of other cost models were conducted during this year and will continue as the cost approach advances from catalog components to enhanced manufacturing assessments of key components.

Task 3. Sorbent Media Assessment and Optimization

During the previous year (FY 2010), the HSECoE collaboratively selected MOF-5 as the initial framework material of interest. Therefore during last year a complete set of its fundamental and engineering materials properties were assessed and the primary properties for *powder* MOF-5 deduced including thermal properties (e.g., thermal conductivity, heat capacity), bulk properties (e.g., density, surface area, particle size, pore volume), and isotherm properties. These engineering properties were submitted and distributed to the HSECoE to aid in the creation of preliminary system models for *powder* MOF-5.

Based on preliminary performance modeling data, two principle materials property deficiencies were identified for the *powder* MOF-5 system: 1) low volumetric capacity and 2) poor thermal conductivity. This year's focus aimed at addressing these gaps through both materials compaction and the incorporation of thermal conductivity additives. A series of six *neat* MOF-5 pellets were initially prepared with varying densities from 0.31 to 0.79 g/cm^3. For reference, the loose powder and single crystal densities for MOF-5 are 0.13 and 0.61 g/cm^3, respectively. The goal of MOF-5 compaction is to sufficiently compress the powder to eliminate interparticle voids without compressing the internal (micropores) pores of the MOF structure (i.e. not going beyond the single crystal density). Unlike many other sorbents (e.g. AX-21 or PEEK), addition of a binder is not necessary to form stable MOF-5 compacts, as cohesion within the pellet is high. MOF-5 compacts were fabricated using a manual arbor press with pressing pressures ranging from approximately 30 MPa up to 100 MPa to construct pellets with densities of 0.31 to 0.79 g/cm^3, respectively.

Select physical properties, in particular, phase characterization, BET surface area, and total pore volume of variable density MOF-5 pellets were determined. The phase characterization of each compact was analyzed by powder X-ray diffraction (XRD) to investigate to what extent the original crystal structure of MOF-5 was maintained (i.e. qualitatively evaluate any increase in amorphous content). Based on the XRD data, it was evident that as the pellet density is increases, the intensity of MOF-5 diffraction peaks decreases along with a concomitant increase in the amorphous content (i.e. low angle diffuse scattering). This behavior becomes more pronounced as density is increased from 0.51 g/cm^3 to 0.65 g/cm^3 (i.e. beyond the single crystal density). Thus this data confirms that to simultaneously improve the volumetric efficiency while preserving the MOF-5 structure, it is necessary to use densities slightly below the MOF-5 single crystal density of 0.61 g/cm^3.

Mechanical strength is also an important consideration in determining optimum compact density. To evaluate the mechanical properties of pelletized MOF-5, radial crush strengths of several sets of MOF-5 pellets were determined. These data reveal that compacts with a density of 0.31 g/cm^3 show almost no resistance to compressive loads applied along their radius. However, tablets with larger densities

have greatly improved crush strength. For 0.41 g/cm^3 pellets, the average crush strength was 24 N. This increases to 71 N and 106 N for pellets having densities of 0.51 g/cm^3 and 0.60 g/cm^3, respectively.

The BET surface areas and total pore volumes of the variable density MOF-5 compacts were also determined (Figure 3). These data indicate that as one initially begins to compress MOF-5 from a loose powder density of 0.13 g/cm^3 to 0.3 g/cm^3, the BET surface area and total pore volume remain roughly constant at approximately 2,700 m^2/g and 1.4 cm^3/g, respectively. Beyond 0.3 g/cm^3, the BET surface area and total pore volume decrease linearly with increasing density. The linear decrease in surface area with increasing density is an effect also observed for activated carbon (AX-21). Since the storage of hydrogen in sorbents such as MOFs and activated carbons relies on physisorption of hydrogen onto the surfaces of the host sorbent (i.e. MOF), the hydrogen capacity typically scales with surface area. Based on Figure 3, going to a MOF-5 density of 0.51 g/cm^3 results in a 20% decrease in BET surface area (and total pore volume). One must evaluate the hydrogen storage uptake to determine if the reduction in surface area results in a corresponding 20% reduction in hydrogen capacity.

The excess hydrogen adsorption isotherms for MOF-5 powder and compacts are shown in Figure 4 along with fits to the empirical data (Figure 4, symbols) using the modified D-A model (Figure 4, lines). Similar to the surface area results above, the maximum gravimetric uptake is unchanged in the 0.31 g/cm^3 pellet relative to the powder. However, a 15% or 41% decrease in gravimetric uptake is observed for the 0.51 g/cm^3 or 0.79 g/cm^3 samples; these reductions are comparable to the respective 20% and 50% loss in surface area. This suggests that some of the surface area lost upon compression was not active in uptake of hydrogen. The maximum volumetric excess adsorption is increased by a factor of 2.5 for the 0.31 g/cm^3 sample relative to the powder. The increase is a factor of 3.7 for the 0.79 g/cm^3 sample.

The total amount of hydrogen storage at 77 K by MOF-5 compacts is defined as the excess adsorption plus the gas phase H_2 within the void space of the pellets. Relative to the MOF-5 powder, total storage at 80 bar is increased by 26% in the 0.31 g/cm^3 sample and by 40% in the 0.51 g/cm^3 sample. On the other hand, if desorption occurs isothermally at 77 K by a pressure decrease from 80 bar to 3 bar, then the total hydrogen delivery is increased by 13% in the 0.31 g/cm^3 sample, versus 17% for the 0.51 g/cm^3 sample. The total *materials-based* volumetric capacity for the 0.51 g/cm^3 MOF-5 compact at 80 bar and 77 K is 40 g/L, a 150% improvement as compared to powder (0.13 g/cm^3). (For reference the 2015 DOE *system-based* volumetric capacity target is 40 g/L.[1].)

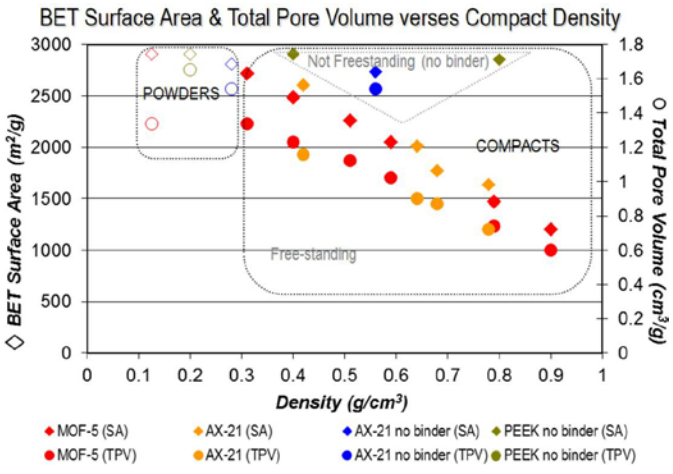


FIGURE 3. BET surface area (◊, primary *y*-axis) and total pore volume (○, secondary *y*-axis) verses compact density for powders (open symbols) of MOF-5 (red), AX-21 with binder (orange), AX-21 without binder (blue) and PEEK without binder (green).

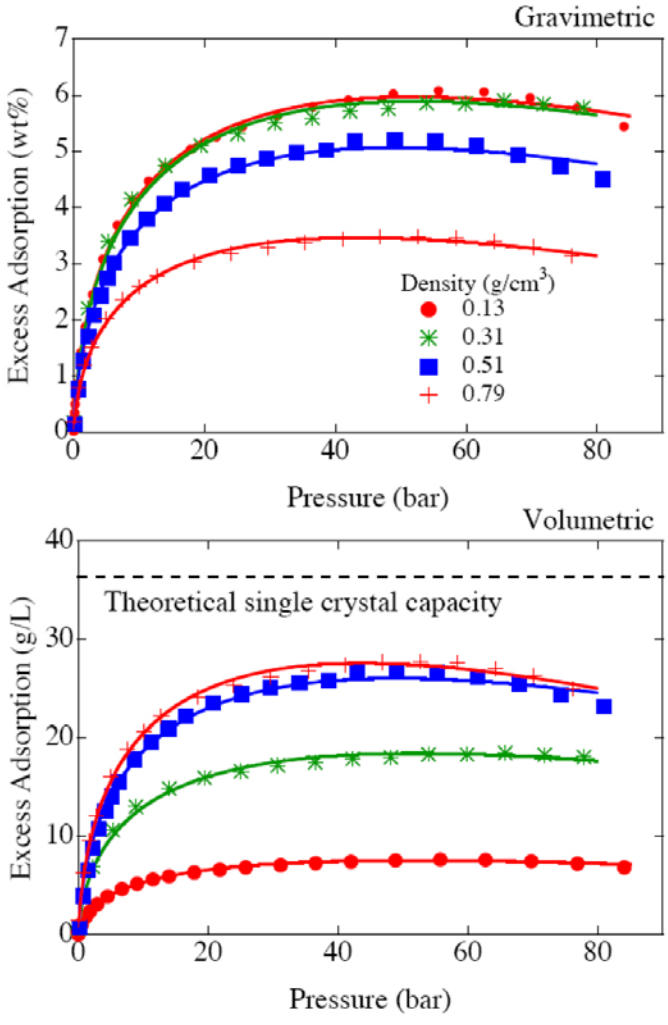


FIGURE 4. Excess hydrogen adsorption at 77 K from 0 to 80 bar by MOF-5 powder (ρ=0.13 g/cm^3) and MOF-5 compacts with ρ=0.31–0.79 g/cm^3. Excess gravimetric adsorption (top) and excess volumetric adsorption (bottom) expressed as a mass fraction (i.e. $m_H/m_{sample} \times 100$). Fits of empirical data (symbols) to the modified D-A model (lines) are shown.

The thermal conductivity of most microporous materials (e.g. MOFs) is expected to be low due to their large pore size (>20 Å in diameter) and high free volume (>90%). For example, the measured thermal conductivity of a single crystal of MOF-5 was previously determined to be 0.3 W/mK between 70 and 300 K [2]. The thermal conductivity (k) for *neat* MOF-5 compacts with densities from 0.35 to 0.69 g/cm^3 were determined over the temperature range of 25 to 65ºC from the measured thermal diffusivity (α), heat capacity (c_p), and density (ρ) using the equation, $k = \alpha \times c_p \times \rho$. Thermal conductivity verses temperature data are shown in Figure 5. Increasing pellet density from 0.35 g/cm^3 to 0.52 g/cm^3 (33% increase) results in only a modest increase in thermal conductivity, from 0.072 to 0.095 W/mK (at 25ºC). We speculate that this small improvement in k arises from a decrease in the amount of inter-particle void space within the pellet volume. Despite this improvement, the neat MOF-5 compact conductivities are all uniformly low and well below the single crystal value of 0.3 W/mK at room temperature. Since hydrogen uptake in sorbents is an exothermic process, low thermal conductivity could restrict the design of efficient MOF-5 based storage systems. In order to achieve targeted refueling times (2015 DOE target is 3.3 min for 5 kg H_2 [1]), and maximize the amount of hydrogen stored, this heat of adsorption must be removed from the storage bed in order to quickly reach the desired operation temperature (e.g. 77 K). Therefore, the identification of methods to augment the thermal conductivity of MOF-5 is desirable; moreover such techniques could be generally applicable to other MOFs as well as the broader class of framework materials (e.g. zeolitic imidizolate frameworks and covalent organic frameworks).

To achieve greater improvements in thermal conductivity, we prepared a series of MOF-5 compacts containing ENG as thermal conductivity enhancer. Analogous to the neat MOF-5 compacts, the MOF-5/ENG composites explored also had densities between 0.35 g/cm^3 and 0.69 g/cm^3 with the ENG mixed at varying mass ratios of 1%, 5% and 10% (by weight). Thermal conductivity verses temperature data are also given in Figure 5. Over the examined temperature range of 25 to 65ºC, there is no systematic temperature dependence, consistent with previous data for MOF-5 [2]. Adding 1 wt% ENG to MOF-5 with compaction up to 0.69 g/cm^3, does not significantly enhance thermal conductivity. However, increasing the ENG content to 5 wt% reveals a 300% enhancement relative to the neat MOF-5 compact of comparable density. For example, at a density of approximately 0.5 g/cm^3, the 5 wt% ENG MOF-5 compact has thermal conductivity of 0.3 W/m·K at 25ºC as compared to the neat MOF-5 compact which has a value of 0.1 W/m·K. Similarly, for a 10 wt% ENG addition, a 600% enhancement is observed. In particular, for the 0.5 g/cm^3 density at 25°C, a thermal conductivity of almost 0.6 W/m·K is observed. Therefore, ENG additions do appear to be effective at increasing the thermal conductivity of MOF-5. Future work (described below) will focus on understanding the impact (tradeoffs) of ENG on other properties such as hydrogen uptake, permeability, crush strength, surface area, etc.

Conclusions and Future Directions

- Task 1. System Modeling
  - Benchmark the system modeling results in comparison to other hydrogen vehicle and storage analysis (i.e. Argonne National Labatory) and identify the areas of differing assumptions or modeling approaches.
  - Enhance the framework and validate the elements of the universal HSECoE Simulink model with the objective of stabilizing the vehicle and fuel cell model blocks within the universal model for the storage optimization analysis.
  - Further refine the fuel cell model to ensure the waste heat and temperature polarization effects are representative of future integration with the hydrogen storage systems and evaluate additional

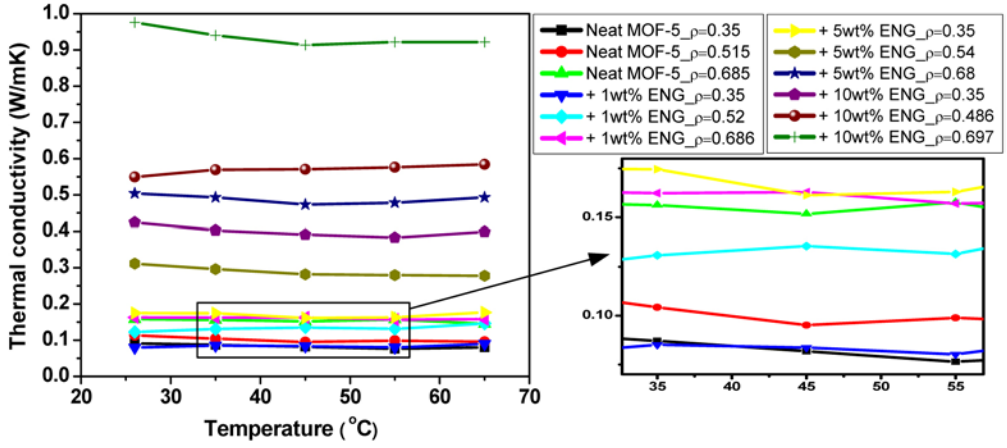


FIGURE 5. Thermal conductivity of pellets of neat MOF-5 and MOF-5/ENG composites with varying densities (from 0.35 to 0.69 g/cm^3) and ENG content (1, 5, or 10 wt%) as a function of temperature (T = 26 to 65°C).

opportunities of vehicle and storage system integration.
  - Assess any needed revisions in the test matrix and modeling assumptions based on the feedback from the phase 1 milestone review.
- Task 2. Cost Analysis
  - Enhance the component library information through the development of the manufacturing model structure of the key components.
  - Evolve the cost and weight estimates in the component from available industry catalog items to projected attributes that are representative of automotive designed systems.
  - Decompose the components for the purpose of detailed system design trade-offs and component optimization in addition to the pursuit of equivalent data sources and sensitivity cost assessments.
  - Develop cost estimating resource tools to be utilized for the manufacturing models with additional cost estimation capability based on an agreed set of manufacturing assumptions of the key cost drivers.
- Task 3. Sorbent Media Assessment and Optimization
  - Validate powder MOF-5 isotherm model parameters at higher pressure (i.e. up to 200 bar), and at temperatures within the anticipated operating window.
  - Continue to assess impact of thermal conductivity aids on other principle hydrogen storage engineering properties (e.g., gravimetric capacity, gas permeability, crush strength, etc.); identify correlation between densification conditions, microstructure, and conductivity.
  - Collaboratively with HSECoE modeling efforts, determine required materials property values which are necessary to yield desired system performance.
  - Establish relationship between density and gas transport; collaboratively with HSECoE modeling teams, determine required value to optimize compact dimensions and shape.
  - Continue to support the experimental validation of sorbent bed and system models through neutron imaging and/or other experimental characterization efforts.

Special Recognitions & Awards

Mike Veenstra received a Special Recognition Award from USCAR for his proactive leadership role as a liaison between the Hydrogen Storage Tech Team and the Hydrogen Storage Engineering Center of Excellence.

FY 2011 Publications/Presentations

1. A. Sudik, Ford/BASF/UM Activities in Support of the Hydrogen Storage Engineering Center of Excellence, Invited Presentation, 2010 American Institute of Chemical Engineers Meeting, Salt Lake City UT, October 2010.

2. J.J. Purewal, Hydrogen Storage by MOF-5 Monoliths and Composites: Materials Processing, Thermal Conductivity, and Neutron Imaging, 2011 Materials Research Society Meeting, San Francisco CA, April 2011.

3. A. Sudik, Hydrogen Storage Materials Research & Development, Invited Presentation, University of California – Los Angeles Materials Science & Engineering Department Symposium, Los Angeles CA, May 2011.

4. A. Sudik, Ford/BASF/UM Activities in Support of the Hydrogen Storage Engineering Center of Excellence, 2011 DOE Hydrogen Program Annual Merit Review Meeting, Arlington, VA, May 2011.

5. J.J. Purewal, D. Liu, J. Yang, A. Sudik, D.J. Siegel, S. Maurer, U. Müller, "Increased volumetric hydrogen uptake of MOF-5 by powder densification," *Int. J. Hydrogen Energy*, **2011**, *In Press.*

6. J.J. Purewal, D. Liu, J. Yang, A. Sudik, D.J. Siegel, S. Maurer, U. Müller, "Increased volumetric hydrogen uptake of MOF-5 by powder densification," American Physical Society 2011 Meeting, March 21-25, Dallas, TX.

7. J.M. Pasini, B. Van Hassel, D. Mosher, and M. Veenstra, "System modeling methodology and analyses for materials-based hydrogen storage," *Int. J. of Hydrogen Energy*, **2011**, submitted for final review.

References

1. http://www1.eere.energy.gov/hydrogenandfuelcells/storage/pdfs/targets_onboard_hydro_storage.pdf.

2. Huang, B.; Ni, Z.; Millward, A.; McGaughey, A.; Uder, C.; Kaviany, M. et al., *Int J Heat Mass Transfer*, **2007**, *50*, 405.

IV.D.10 Microscale Enhancement of Heat and Mass Transfer for Hydrogen Energy Storage

Kevin Drost (Primary Contact), Goran Jovanovic, Vinod Narayanan, Brian Paul, Anna Garrison, Karl F. Schilke, Christopher Loeb, Leif Steigleder, David Haley, Mohammad Ghazvini, Agnieszka Truszkowska
School of Mechanical, Industrial and Manufacturing Engineering
Rogers Hall
Oregon State University (OSU)
Corvallis, OR 97331
Phone: (541) 713-1344
E-mail: Kevin.Drost@oregonstate.edu

DOE Managers
HQ: Ned Stetson
Phone: (202) 586-9995
E-mail: Ned.Stetson@ee.doe.gov
GO: Jesse Adams
Phone: (720) 356-1421
E-mail: Jesse.Adams@go.doe.gov

Contract Number: DE-FC36-08GO19005

Project Start Date: February 1, 2009
Project End Date: January 31, 2014

Fiscal Year (FY) 2011 Objectives

Use microchannel processing techniques to:

- Demonstrate reduction in size and weight.
- Improvement of charge/and discharge rates.
- Reduce size and weight and increase performance of thermal balance-of-plant components.

Technical Barriers

This project addresses the following technical barriers from the Storage section (3.3.4) of the Fuel Cell Technologies Program Multi-Year Research, Development and Demonstration Plan:

(A) System Weight and Volume

(E) Charging/Discharging Rates

(H) Balance of Plant (BOP) Components

Technical Targets

The Phase I technical targets for the Microscale Enhancement of Heat and Mass Transfer for Hydrogen Energy Storage project are:

- Complete identification of the highest value applications of microchannel-based technology.
- Complete experimental investigations and modeling to collect data that will support the Go/No-Go decision to proceed to Phase II.

The Phase I Go/No-Go Criteria associated with these technical goals are:

- Identify and demonstrate, through experiment and simulation, one or more high-priority applications where the application of microchannel technology can make a significant contribution to meeting DOE 2015 performance goals.
- Develop specific performance, weight, and size goals for each application included in the OSU Phase II scope of work.

FY 2011 Accomplishments

Key developments and technical accomplishments for the reporting period are summarized in the following.

- Completed system design of a modular adsorption tank insert that facilitates the use of densified storage media while providing cooling for charging, heating for discharging, and hydrogen distribution (Barriers A and E).
- Initiated experimental investigations to validate key design assumptions used in the design of the modular adsorption tank insert (Barriers A and E).
- Completed system design and production cost estimate for a microchannel combustor/heat exchanger to heat oil using catalytic combustion of discharge hydrogen from storage (Barrier H).
- Completed experimental validation of performance and size estimates used in developing the microchannel combustor/heat exchanger (Barrier H).



Introduction

Hydrogen storage involves coupled heat and mass transfer processes that are significantly impacted the by size, weight, cost, and performance of system components. Micro-technology devices that contain channels of 10-500 microns in characteristic length offer substantial heat and mass transfer enhancements by greatly increasing the surface to volume ratio and by reducing the distance that heat or molecules must traverse. These enhancements

often result in a reduction in the size of energy and chemical systems by a factor of 5-10 over conventional designs, while attaining substantially higher heat and mass transfer efficiency. In cooperation with the OSU Microproducts Breakthrough Institute and groups at the Pacific Northwest National Laboratory, Savannah River National Laboratory, and Los Alamos National Laboratory, we are developing: 1) advanced tank inserts for enhanced and mass transfer during charge and discharge of metal hydride and adsorbent hydrogen storage systems; and 2) microchannel-based thermal balance of plant components such as combustors, heat exchangers, and chemical reactors.

Approach

Our technical approach to meet the Phase I goals involves: 1) OSU will focus on simulation and experimental investigations to identify and prioritize opportunities for applying microscale heat and mass transfer enhancement techniques; and 2) working with other team members, OSU will identify the highest value applications and conduct experimental investigations and modeling to collect data necessary to support the Go/No-Go decision to proceed to Phase II.

For each high-priority component, we plan to use microchannel technology to reduce the relevant barriers to heat and mass transfer. Our approach involves: 1) the optimization of the performance of a single unit cell (i.e., an individual microchannel) and then "number up" using appropriate simulation tools that we then validate by experimental investigation; and 2) develop microlamination methods as a path to "numbering up" by low-cost high-volume manufacturing.

Results

With respect to our Phase I technical targets, we identified two high-value applications of microchannel technology. The first is the development of a modular microchannel tank insert for cooling during charging, heating during discharging, and hydrogen distribution. The tank insert can be used with either metal hydride or cryogenic adsorbing material; however, we have focused on applying the modular tank insert to cryogenic adsorption hydrogen storage. The second application is the development of an integrated microchannel combustor and heat exchanger that can be used for on-board oil heating during discharge of a metal hydride hydrogen storage system. Results relative to these two applications are summarized below.

Microchannel-Based Tank Insert – A tank insert that integrates storage media, microchannel heat exchangers, and microchannel hydrogen distribution plates may provide improved charging of the storage system, rapid startup, and quicker response to changing driving conditions. Progress-to-date on the development of the microchannel-based tank insert includes:

- Cooling Plate Fabrication and Performance Validation – During the reporting period, we completed the assembly and testing of a 5-cm diameter cooling plate that includes two sets of microchannel cooling channels and microchannels for the distribution of hydrogen. The resulting cooling plate is on the order of 1-mm thick. The overall conclusion from these experiments is that the pressure drop through the microchannel heat exchanger and hydrogen distributor plates is reasonably small (15 kPa at a flow rate of 0.15 l/min). Furthermore, the above experiments indicate that the major pressure drop in the cooling subsystem will be located in the coolant feed and in exit lines. These components can be redesigned to further reduce pressure drop.
- Insert Design Development – Figure 1 shows the design of a multi-module tank insert including the headers to distribute cooling fluid. Figure 2 shows

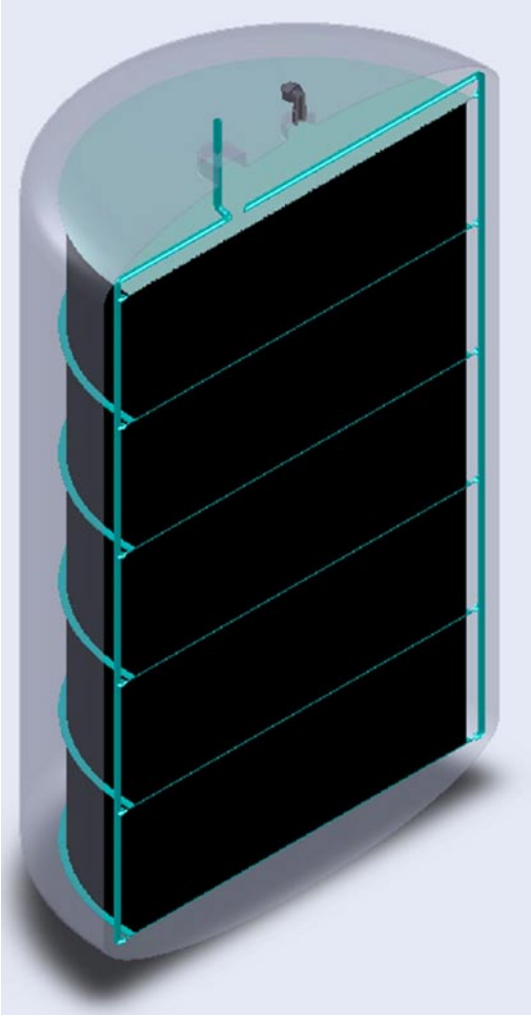


FIGURE 1. Schematic Diagram of Modular Adsorption System including Five Modules and Cooling Fluid Headers

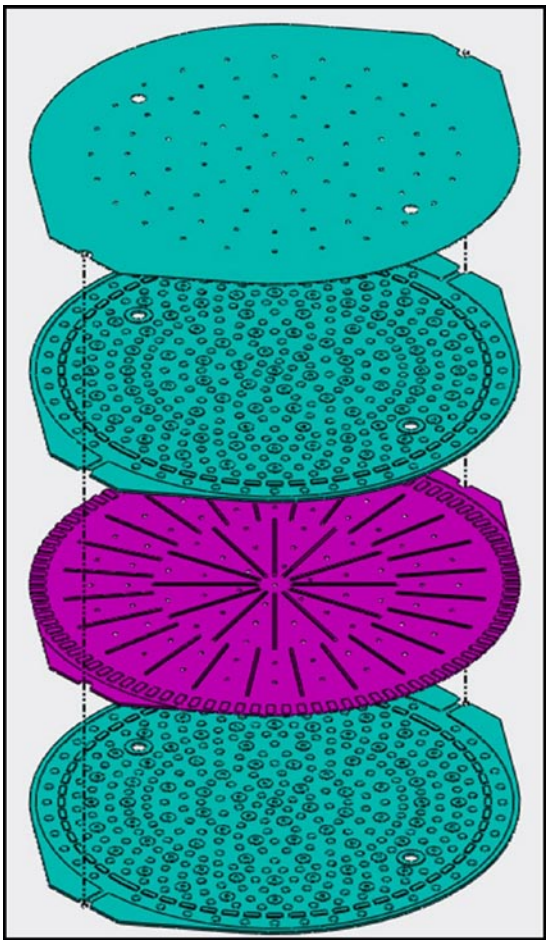


FIGURE 2. Schematic Diagram of Cooling plate including One Hydrogen Distribution Lamina (Purple) and Two Cooling Fluid Lamina (Teal)

the design of one cooling plate with one lamina used for hydrogen distribution and two laminae used for cooling. An individual module will consist of two cooling plates with media located between the cooling plates. Computational fluid dynamics (CFD) modeling was used to predict cooling fluid pressure drop and flow distribution both across one cooling plate as well as for a multi-module system. Overall pressure drop from the cooling fluid system inlet to outlet was predicted to be on the order of 1 bar. CFD modeling showed that flow maldistribution between plates in a single cooling plate was not a problem.

- Insert Fabrication and Weight Analysis – The system design described above was used as the basis for developing a fabrication approach and an estimated system weight. The fabrication strategy is amenable to high-volume production. The weight analysis for a cryo-adsorption hydrogen storage system capable of storing 5.6 kg of hydrogen and being filled in 4 minutes was on the order of 9 kg. This is based on a cooling plate spacing of 5 cm and assumes that the insert if fabricated from aluminum.

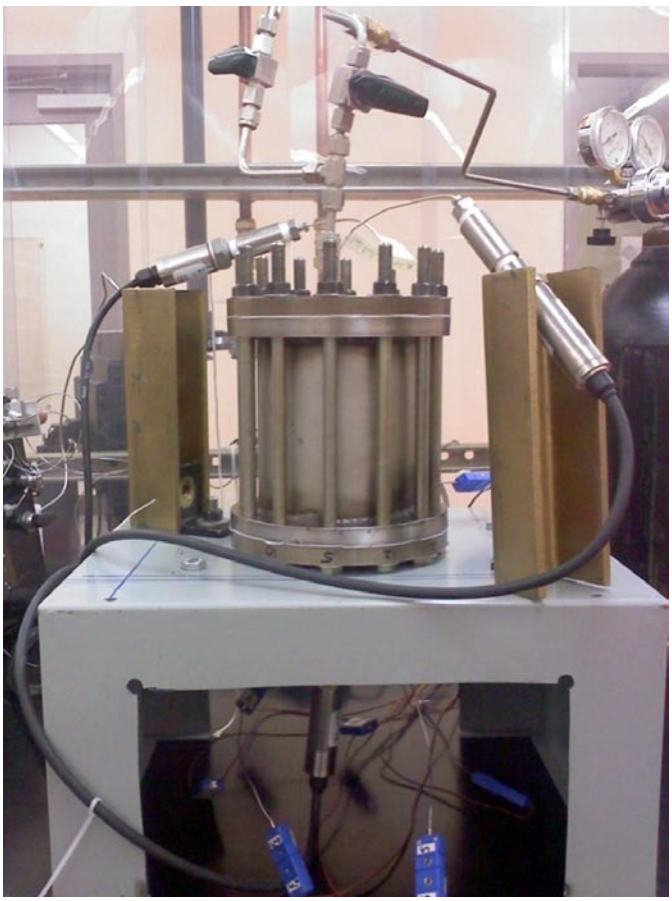


FIGURE 3. Modular Adsorption System Test Apparatus

- Experimental Investigations – We are currently starting up our test apparatus, shown in Figure 3, which will allow the testing of a cooling plate and media. The system is being converted to be able to operate at cryogenic temperatures so that we can test a 5-cm diameter module with liquid nitrogen cooling and hydrogen adsorption. The existing pressure vessel is limited to hydrogen pressures of 50 bars.

Integrated Microscale Combustor/Heat Exchanger (µCHX) – The microscale combustor/heat exchanger (µCHX, Figure 4) will be used to safely and efficiently produce heated oil, which is used to discharge hydrogen from the storage bed. Combining the combustion and heat exchanger systems and the use of microchannels for enhanced heat and mass transfer can drastically reduce the size and weight required for this function, while simultaneously increasing efficiency. A substantial safety benefit of a microscale combustor is that flames cannot be sustained in the sub-millimeter microchannels. Progress-to-date on the development of the µCHX includes:

- µCHX System Design, Weight and Cost Estimate – Previously we used simulation to predict the size, weight, and performance of a single unit cell of the



FIGURE 4. Schematic Diagram of μCHX

µCHX. During the reporting period, we used these results to develop the design of a full-sized µCHX (12 kW to 30 kW heating capacity) including the headers needed to distribute the feed (a mixture of hydrogen and air), combustion products, and oil between a large number of unit cells. The overall system dimensions of a 12 kW µCHX was estimated to be 15.1 cm by 15.6 cm by 4.3 cm with an overall volume of approximately 1 liter. The predicted volume of the µCHX is approximately 10% of the best alternative design. The predicted mass of the µCHX was estimated to be between 1.3 and 3.8 kg with an overall system efficiency of 92% (thermal energy transferred to the oil/chemical energy in the feed stream). Using this design as the basis for a bottom-up cost estimate we predicted a cost for this component of $120 to $200 at an annual production rate of 500,000 units. The production cost assumed that microlamination was used to fabricate the device with chemical etching used for patterning and laser welding used for bonding. Both stainless steel and aluminum were considered for fabrication materials. Simulation suggested that aluminum was a suitable material because material temperatures in the device were well below the temperature limits for aluminum.

- Unit Cell Experimental Validation of µCHX Performance and Weight Estimates – During the reporting period we completed preliminary testing of a single unit cell. The results showed an efficiency of 92%. Our results also showed that 130 to 140 W of thermal energy was being transferred to the oil, which is consistent with our size and weight estimates reported above.

Conclusions and Future Directions

Key conclusions resulting from our research include:

- As shown by the µCHX, when addressing a component that is limited by diffusion (heat or mass transfer), the application of microchannel technology can result in significant reductions in the size and weight of the device. Results also show that the cost of µCHX can be attractive.
- The use of the modular adsorption tank insert allows convenient use of densified adsorption media and is amenable to high volume production.

The future direction of our research on the application of microchannel technology to hydrogen storage includes:

- Complete the demonstration of a 1 kW µCHX demonstrating hindering and overall system performance.
- Complete demonstration of a multi-module 5-cm diameter modular tank insert including heat removal rates, hydrogen distribution, durability, and complete a production cost estimate for the system.

FY 2011 Publications/Presentations

1. Ghazvini, M., and Narayanan, V., "Performance Characterization of a Microscale Integrated Combustor, Recuperator and Heat Exchanger," AJTEC2011-44633, in review, ASME/JSME 2011 8th Thermal Engineering Joint Conference, AJTEC2011, Honolulu, Hawaii.

IV.D.11 Development of Improved Composite Pressure Vessels for Hydrogen Storage

Jon Knudsen (Primary Contact), Norm Newhouse, John Makinson
Lincoln Composites, Inc.
5117 NW 40th Street
Lincoln, NE 68524
Phone: (402) 470-5039
E-mail: jknudsen@lincolncomposites.com

DOE Managers
HQ: Ned Stetson
Phone: (202) 586-9995
E-mail: Ned.Stetson@ee.doe.gov
GO: Jesse Adams
Phone: (720) 356-1421
E-mail: Jesse.Adams@go.doe.gov

Contract Number: DE-FC36-09GO19004

Project Start Date: January 1, 2009
Project End Date: July 31, 2014

Fiscal Year (FY) 2011 Objectives

- To improve the performance characteristics, including weight, volumetric efficiency, and cost, of composite pressure vessels used to contain hydrogen in media such as metal hydrides, chemical hydrides, or adsorbents.
- To evaluate design, materials, or manufacturing process improvements necessary for containing metal hydrides, chemical hydrides, or adsorbents.
- To demonstrate these improvements in prototype systems through fabrication, testing, and evaluation.

Technical Barriers

This project addresses the following technical barriers from the Hydrogen Storage section of the Fuel Cell Technologies Program Multi-Year Research, Development and Demonstration Plan:

(A) System Weight and Volume
(B) System Cost
(G) Materials of Construction

Technical Targets

This project is conducting fundamental studies for the development of improved composite pressure vessels for hydrogen storage. Insights gained from these studies will be applied toward the design and manufacturing of hydrogen storage vessels that meet the DOE 2010 hydrogen storage targets in Table 1.

TABLE 1. Hydrogen Storage Targets

	2010	2015
Gravimetric capacity:	>4.5%	>5.5%
Volumetric capacity:	>0.028 kg H_2/L	>0.040 kg H_2/L
Storage system cost:	TBD	TBD

TBD – to be determined



Introduction

Lincoln Composites is conducting research to meet DOE 2010 and 2015 Hydrogen Storage Goals for a storage system by identifying appropriate materials and design approaches for the composite container. At the same time, continue to maintain durability, operability and safety characteristics that already meet DOE guidelines for 2010 and 2015. There is a continuation of work with Hydrogen Storage Engineering Center of Excellence (HSECoE) partners to identify pressure vessel characteristics and opportunities for performance improvement. Lincoln Composites is working to develop high pressure vessels as are required to enable hybrid tank approaches to meet weight and volume goals and to allow metal hydrides with slow charging kinetics to meet charging goals.

Approach

Lincoln Composites is establishing and documenting a baseline design as a means to compare and evaluate potential improvements in design, materials and process to achieve cylinder performance improvements for weight, volume and cost. Lincoln Composites will then down-select the most promising engineering concepts which will then be evaluated to meet Go/No-Go requirements for moving forward.

The following areas will be researched and documented:

- Evaluation of alternate fiber reinforcement
- Evaluation of boss materials and designs
- Evaluation of resin toughening agents
- Evaluation of alternate liner materials
- Evaluation of damage vs. impact
- Evaluation of stress rupture characteristics
- Evaluation of in situ non-destructive examination (NDE) methods to detect damage

Results

Lincoln Composites has completed the documentation of a baseline design as a means to compare and evaluate potential improvements in design, materials and process to achieve cylinder performance improvements for weight, volume and cost. Baseline characteristics, service conditions and nominal properties, are listed in Table 2.

Lincoln Composites has completed testing on alternate fibers relative to fiber strength and impact tolerance. Baseline fiber was selected as Toray T700. Five alternative carbon fibers were tested as part of the study. Vessels were constructed with each of the five fibers using same parameters on each: mandrel, wind patterns, tooling and processing. Tow count was adjusted, per fiber, to maintain consistent band cross sectional area. Testing was completed on all vessels including burst testing and drop/cycling. (See Table 3 showing a comparison of results of initial testing.) Two of the fibers indicated higher strength than baseline. Four fibers showed a potential lower cost per pound. The testing showed that these new fibers as received and tested did not meet expectations and strength versus cost showed no improvement compared with the baseline. Lincoln Composites worked directly with two of the fiber suppliers, Toho and Grafil, to obtain improved fiber strength. After making improvements to their fibers, additional vessels were fabricated and their fibers were found to match existing baseline fiber in strength during burst testing. A benefit is the fact that having alternate fibers could potentially reduce costs by 10-15% from suppliers. Three fibers now could be used interchangeably in the construction of composite pressure vessels.

Lincoln Composites has completed the testing of an alternative boss material as part of the project. Baseline material is 6061-T6 aluminum. Investigations have been completed to create bosses constructed with aluminum 7075-T73. Properties, of which, are difficult to acquire through entire thickness. Higher strength would allow reduction in boss size and allow aluminum use at high pressures. Proper heat treat is a challenge to get correct strength properties and to avoid embrittlement. Near net shaped bosses were machined from 7075-T6 aluminum with the following

TABLE 2. Service Conditions and Nominal Cylinder Properties

Service Pressure	5,000 psi (344.7 bar)
Gas Settling Temperature	59 °F (15 °C)
Maximum Fill Pressure	6,500 psi (448 bar)
Service Life	20 years
Gas Fill Temperature Limits	-40 to 149 °F (-40 to 65 °C)
Operating Temperature Limits	-40 to 180 °F (-40 to 82 °C)
Proof Test Pressure	7500 psi (517 bar)
Minimum Rupture Pressure	11,700 psi (807 bar)
Cylinder Diameter	21.4 inches (543.4 mm)
Cylinder Length (unpressurized)	63.0 inches (1600 mm)
Cylinder Length at Maximum Fill Pressure	63.34 inches (1609 mm)
Cylinder Empty Weight (excluding hardware)	231 lbs (105 kg)
Cylinder Volume	15,865 in^2 (260 L)
Cylinder Volume at Service Pressure	16,132 in^2 (264.4 L)
Cylinder interior diameter	19.2 inches (488 mm)

TABLE 3. Initial Results of Alternate Fiber Testing

	Performance			Construction	
Fiber	**Virgin Burst (psi)**	**Burst after Drop/ Cycle (psi)**	**% Reduction**	**Tows of Carbon Fiber**	**Band Carbon Cross Section (in^2)**
Toray T700 24K (Baseline)	13,415	-		3	0.00429
Toray T800 24K	16,009	14,599	-9%	5	0.00444
Toho J30743HP 24K	12,249	10,543	-14%	3	0.00433
Grafil TRH50 18K	13,542	12,837	-5%	5	0.00433
Grafil TRH50 60K	12,152	10,193	-16%	2	0.00548
Hexcel AS7 12K	11,721	9,841	-16%	6	0.00414

surface finishes: smooth machining, rough machining, sand blasted and chemical etching. These bosses were then heat treated to a T73 condition. Bosses were sectioned and tensile testing on the specimens has been completed. Testing has confirmed the proper heat treat on the aluminum. Yield strength is 2 times that of 6061-T6 aluminum or 316 SS. Cost of bosses could be same to 1.5 times that of 6061-T6 and 1/5 that of 316 SS. Next step is to incorporate 7075 aluminum into new designs.

Investigations into alternate resin compilation are underway to determine effects on the toughening properties of a full-scale vessel, and would support the reduction in safety factors required for the vessel. First phase was to research and perform testing on alternate hardeners that could be used with our current baseline resin. Several experiments were run with alternate hardeners with an end result that our current hardener performs best. Next step is to use this hardener to begin looking at different resin formulations. One task is to down-select based on screening of viscosity and T_g results. Further testing is planned to determine mechanical and environmental/chemical properties. Upon completion, a down-select activity will determine what resin formulations will be used to produce coupons for impact testing. The last activity will then be to build full-scale vessels with the alternate resin formulations and to perform further testing such as impact. Initial candidates for toughening agents have been selected. This task will be continued as composite coupons and full-scale vessels are built for further testing.

Studies are ongoing with respect to alternate materials to minimize the permeability of gas through the high-density polyethylene (HDPE) liners that Lincoln Composites currently uses. The evaluations of coatings and surface treatments have shown blistering following a hydrogen soak and blow down. Surface treatments have not shown to be effective. The first investigation into Nanoclay additives gave unsuccessful results. The molecular properties of HDPE did not promote dispersion. However, new material found from alternate vendor has shown some improvements, with a reduction of about 40% in permeation. HDPE with titanium dioxide has resulted in a 25% reduction in permeation. Lincoln Composites has also worked with the addition of ethylene vinyl alcohol (EVOH). We encountered problems with layered materials including the ability to weld. We looked at adding as an outside layer to keep the material away from the weld joint, however, have had issues with adhesion of the EVOH to the HDPE. Lincoln Composites is in the process of looking at EVOH that has been modified to increase ductility. The evaluation of nylon as a filler has also been targeted. The cost of nylon, when compared with HDPE, would generate a large cost increase. Liners have been built with the following conditions: HDPE (baseline), HDPE/standard nanoclay, HDPE/development nanoclay, and HDPE/titanium dioxide. These have been wound into short tanks and testing will then move forward on full-scale models. A permeation rate versus cost relative to HDPE is shown in Figure 1. HDPE is the baseline at 1:1. HDPE fillers show a 40% reduction with limited cost increase. Alternate materials show promise of significant permeation reduction while others are prohibitively expensive. Reduction of the liner thickness will increase internal volume, allowing storage of more hydrogen, and will reduce weight. This task will be continued as further means to reduce permeation are investigated.

Lincoln Composites is looking into an improved data base for stress rupture of carbon fiber that may allow for reduced safety factors. This will in turn maintain projected reliability and reduce cost, weight and increase volumetric efficiency with thinner walls. A stress rupture project presented at industry workshop to gain feedback and support was conducted. The project is currently being refined with some collaborators and funding identified. Additional collaboration and funding is being sought, however, this additional funding has not been committed. Stress rupture, fatigue and damage tolerance are all being considered in the study. Fiber stress rupture and cyclic fatigue are directly related to stress ratio and damage tolerance is affected. The reduction in safety factor from 2.25 to 2.00 is planned and studies indicate that high reliability is maintained. Field experience indicates safe operation as long as damage tolerance is addressed. It can be addressed by other designs and testing. The evaluation of damage vs. impact is being considered to characterize safety and ability to remain in service after damage. NDE as a means of monitoring the structural integrity is being considered which will allow for thinner laminates and removal from service before rupture. The benefits of a reduced safety factor include: carbon fiber cost reduction of 10%, potential for increased cylinder volume, and the potential for weight reduction. All factors must be balanced against cost, envelope, and weight of other means of damage

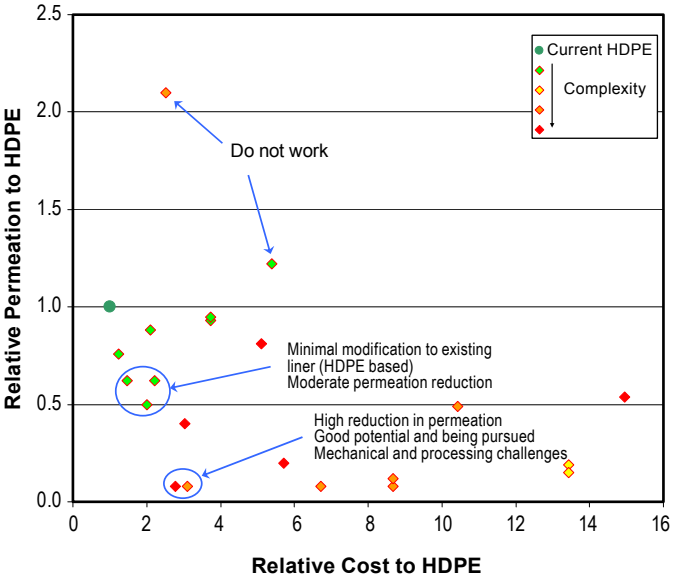


FIGURE 1. Permeation Rate versus Cost Relative to HDPE Liner Material

protection, if necessary. This task is on hold pending location of additional partners and funding.

Conclusions and Future Directions

The studies above have provided progress to meeting DOE goals for hydrogen storage. The full effectiveness of these improvements must be evaluated as part of a full system. However, improvements for the composite vessel itself are as follows:

- Reduced cost and weight from improved boss material.
- Reduced fiber cost by developing alternate fibers of equal strength.
- Reduced cost, potential reduced weight and increase volume, by reducing carbon fiber factor of safety.
- Reduced weight, increased volume, by reducing liner thickness.

For the cylinder itself, these improvements indicate the potential for:

- 11% lower weight
- 4% larger internal volume
- 10% lower cost

Future work for this project will be to continue progress on evaluating potential improvements, particularly as noted above for projects not yet completed. After completion of Phase 1, Lincoln Composites will down-select the most promising engineering concepts and evaluate against DOE 2010 and 2015 Hydrogen Storage Go/No-Go criteria.

Plans are being solidified for the evaluation of liner materials that can withstand high and low temperatures. Current materials in use have an operating temperature range of -40° to +85°C. We plan to look into materials at -200°C on the low end and up to 375°C on the high end. Testing has begun to cycle tanks cold to ambient and hot to ambient followed by a burst test to evaluate our current materials. This was not part of the original scope of the project, but is being requested by team members of the HSECoE. Initial results show cold temperature exposure, to liquid nitrogen and soaking, does not affect the strength. Additional testing will be conducted.

Phase 2 is continuation of container development in support of system requirements. Specific attention will be directed to input from partners in support of concepts selected to go forward with Phase 3 and the fabrication of subscale vessels to support assembly of prototype systems for evaluation.

FY 2011 Publications/Presentations

1. Co-authored paper/presentation, **"Potential Diffusion-Based Failure Modes of Hydrogen Storage Vessels for ON-board Vehicular Use",** Yehia Khalil (UTRC), Norman Newhouse (LC), Kevin Simmons (PNNL), Daniel Dedrick (SNL), at AICHhE 2010 Annual Meeting, Salt Lake City, November 2010.

2. 2011 DOE Hydrogen Program Annual Merit Review, May 11, 2011.

IV.E.1 Quantifying and Addressing the DOE Material Reactivity Requirements with Analysis and Testing of Hydrogen Storage Materials and Systems

Y. (John) F. Khalil
United Technologies Research Center (UTRC)
411 Silver Lane, Mail Stop 129-30
East Hartford, CT 06108
Phone: (860) 610-7307
E-mail: khalilyf@utrc.utc.com

DOE Managers
HQ: Ned Stetson
Phone: (202) 586-9995
E-mail: Ned.Stetson@ee.doe.gov
GO: Katie Randolph
Phone: (720) 356-1759
E-mail: Katie.Randolph@go.doe.gov

Contract Number: DE-FG36-07GO17032

Subcontractor:
Kidde-Fenwal, Combustion Research Center,
Holliston, MA

Project Start Date: June 1, 2007
Project End Date: September 30, 2011

Fiscal Year (FY) 2011 Objectives

Provide improved definition of the DOE Environmental Health and Safety (EH&S) target and its link to material reactivity to guide research of storage materials. Detailed objectives include:

- Develop qualitative and quantitative analysis methods and tools to evaluate risks for materials-based hydrogen storage systems before and after risk mitigation methods.
- Perform dust characterization tests for metal hydride, chemical hydride and adsorbent materials.
- Characterize chemical reactions for material exposures associated with both risk events and mitigation approaches using time resolved X-ray diffraction (XRD), liquid reactivity and other specialized testing.
- Assess the trade-offs between residual risk after mitigation and the system weight and volume as well as reaction rates.

Technical Barriers

This project addresses the following technical barriers from the Hydrogen Storage section of the Fuel Cell Technologies Program Multi-Year Research, Development and Demonstration Plan [1]:

(A) System Weight and Volume

(F) Codes and Standards

Technical Targets

The key technical target of this project is EH&S, having a focus on the safety sub-target with some consideration for toxicity. The technical target for safety is specified generally as "Meets or exceeds applicable standards." For metal hydride, chemical hydride and adsorbent materials and systems, however, no such standards exist today. Furthermore, standards currently under development will be high-level in scope, primarily focused on systems and will not provide adequate guidance for evaluating and selecting viable candidate materials. As part of this effort, trade-offs will be evaluated between residual risks after mitigation and the two technical barriers:

(A) System Weight and Volume

(E) Charging/Discharging Rates

FY 2011 Accomplishments

- Quantitative risk analysis (QRA): developed and quantified fault tree (FT) models for:
  - On-board reversible hydrogen storage system.
  - Solid ammonia borane (AB) off-board regenerable storage system.
  - On-board solid AB thermolysis reactor.
  - Hydrogen permeation/leakage from Type-III and Type-IV storage vessels.
  - Finally, developed a risk reduction worth (RRW) methodology for quantifying the importance of each basic event (BE) in a fault tree system model.
- Qualitative risk analysis (QLRA):
  - Identified critical risks and failure mechanisms of a baseline design of an off-board regenerable alane-based (AlH_3) storage system.
- Risk mitigation:
  - Theoretical studies - performed atomic and thermodynamic modeling of sodium alanate ($NaAlH_4$) oxidation and hydration reactions.
  - Experimental studies - performed the following tests for $NaAlH_4$, $3Mg(NH_2)_2.8LiH$, and NH_3BH_3:
    - Material reactivity in different fluids (water, windshield washing fluid, brine, antifreeze, and engine oil).
    - Fast blowdown (depressurization) which mimics accidental storage vessel breach.

- Dust cloud combustion characterization. Tests also included Maxsorb (AX-21).
- Mechanical impact sensitivity.
- Hot surface contact tests.
- XRD tests for material characterization.



Introduction

Safety is one of the most significant issues affecting consumer acceptance and adoption of hydrogen-fueled vehicles. Through DOE efforts to understand general public opinions, people have indicated that when selecting a fuel supply, safety is the most important factor. The current project, in close coordination with efforts at Savannah River National Laboratory (SRNL) and Sandia National Laboratories (SNL), will provide quantitative insights to the DOE safety target and support the development of future risk-informed hydrogen safety codes and standards (C&S). The results from these collaborative efforts will also have nearer term impact in guiding storage materials research and the development of materials/systems risk mitigation methods.

Approach

The current project has five distinct elements as follows: 1) risk analysis framework (QLRA and QRA), 2) materials reactivity testing, 3) chemical reaction kinetics testing and modeling, 4) risk mitigation methods, and 5) limited scope prototype testing.

Results

QRA

Developed and quantified FT models for: a) on-board reversible hydrogen storage system, b) solid AB off-board regenerable alane-based storage system, c) on-board solid AB thermolysis reactor, and d) hydrogen permeation/

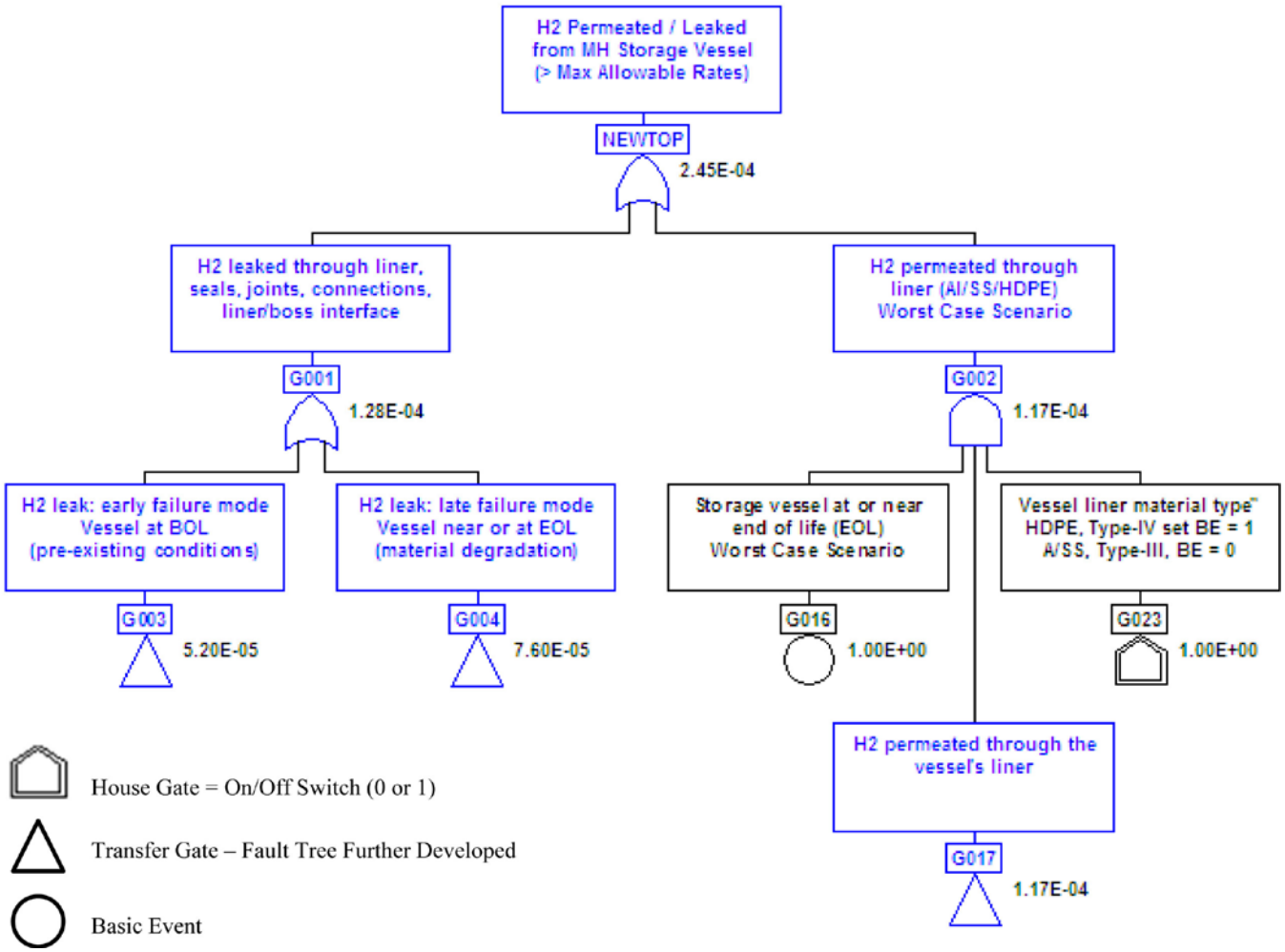


FIGURE 1. Fault Tree Model for Gaseous Hydrogen Permeation/Leakage through Type-III and Type-IV Liners

leakage from Type-III and Type-IV storage vessels. Figure 1 shows the top portion of the FT model for the hydrogen permeation/leakage from the storage vessel. The complete FT model, quantification results, minimal cutsets (i.e., sequences leading to hydrogen permeation or leakage from the storage vessel), and potential failure mechanisms are discussed in detail in reference [2]. The two failure modes for hydrogen leakage through the vessel's seals, joints, connections, liner/boss interfaces include: i) an early failure mode due to pre-existing conditions (Gate G003) in Figure 1 and ii) a late failure mode caused by time-dependent failure mechanisms with the vessel at or near end of life (EOL), Gate G004 in Figure 1. The time-dependent failure mechanisms include cyclic fatigue stresses leading to crack growth and propagation and material aging. Hydrogen permeation through the vessel liner is more likely to be a dominant failure mechanism when the vessel is at or near EOL. As part of the FT modeling and quantification, a RRW methodology has been developed for quantifying the safety importance of each BE in the fault tree model [2].

QLRA

- Developed a baseline design of an off-board regenerable hydrogen storage system using alane (AlH_3) as the solid-state storage medium (Figure 2).
- Performed failure mode and effects analysis (FMEA) for the proposed baseline design.
- Identified the following safety-significant failure mechanisms for this alane-based system:
  - Failure to transport the fresh alane powder through the on-board system.
  - Failure to transport the spent fuel (discharged alane) to the on-board collection tank.
  - Failure of thermal management subsystem of the on-board alane thermolysis reactor.
  - One of the critical hazards of the alane-based off-board regenerable system is related to the accidental exposure of discharged alane powder (spent fuel) to air. Under such postulated condition, the resulting

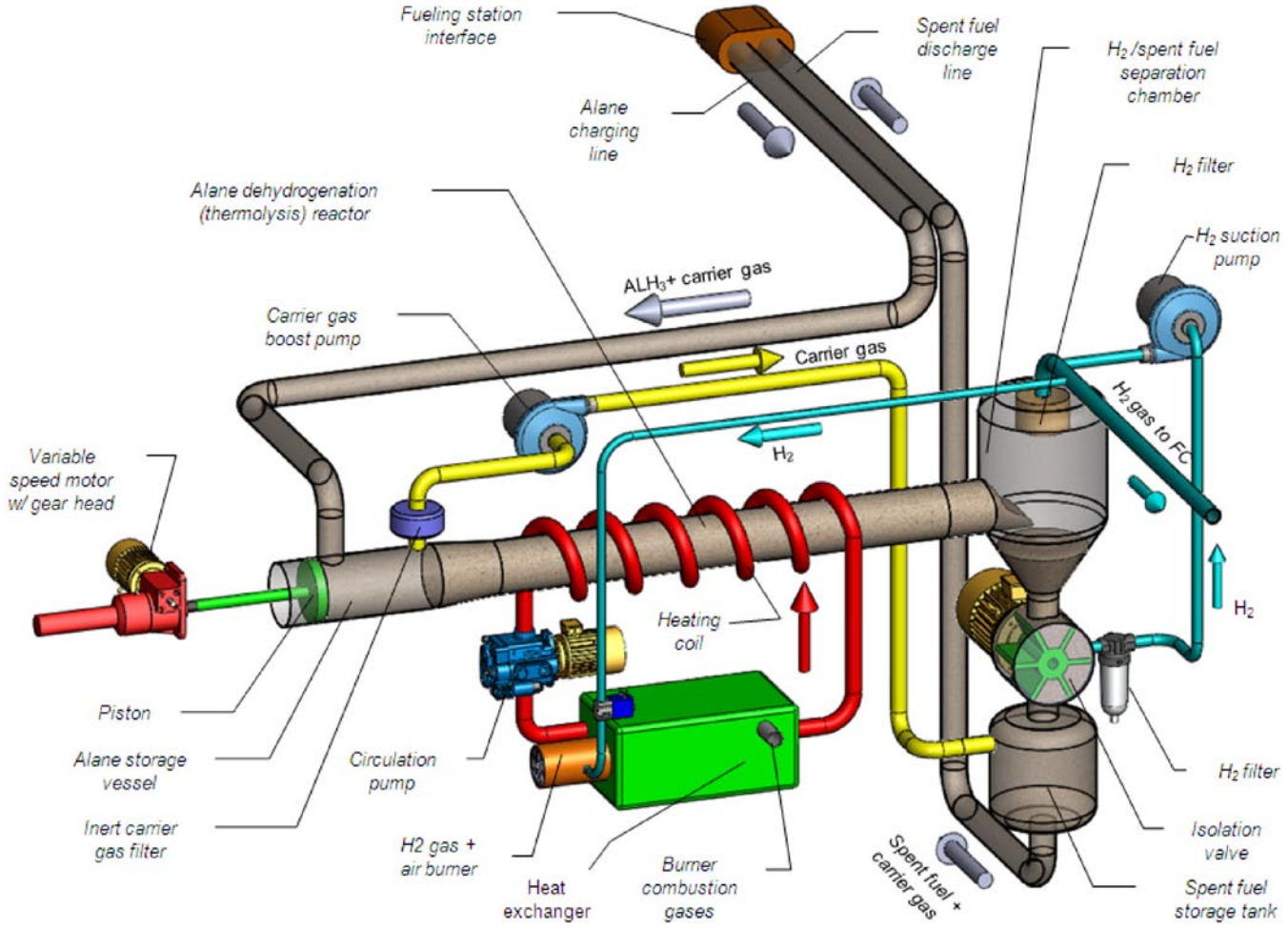


FIGURE 2. UTRC Baseline Design of an Off-Board Regenerable Alane-Based System

dust cloud explosion would be more severe compared to an accidental exposure of charged alane dust to air (Table 1).

Risk Mitigation – Experimental Studies

- Performed a series of scoping tests to evaluate the reactivity of selected complex metal hydrides, $NaAlH_4$ and $3Mg(NH_2)_2.8LiH$, and chemical hydride, NH_3BH_3, under environmental conditions that may exist during a postulated vehicular accident.
  - In immersion tests, loose powder as well as powder compacts (wafers) were immersed in different liquids at room temperature. The liquids selected were water, windshield washing fluid, thermo-oil, engine coolant (antifreeze), engine oil and NaCl solution (brine), respectively. These tests were repeated using powder compacts.
  - In the droplet tests, each of these liquids was dropped on the hydride loose powder and powder compacts (wafers).

The results of these tests demonstrated that powder compaction has a potential for reducing reactivity risks by suppressing the hydride/liquid reaction and, thus, preventing consequential ignition of the evolved reaction gases.

- Performed mechanical impact sensitivity tests (Figure 3) for complex metal hydrides (partially-charged $NaAlH_4$ and charged $3Mg(NH_2)_2.8LiH$) and an as-received chemical hydride (NH_3BH_3). The results of the tests

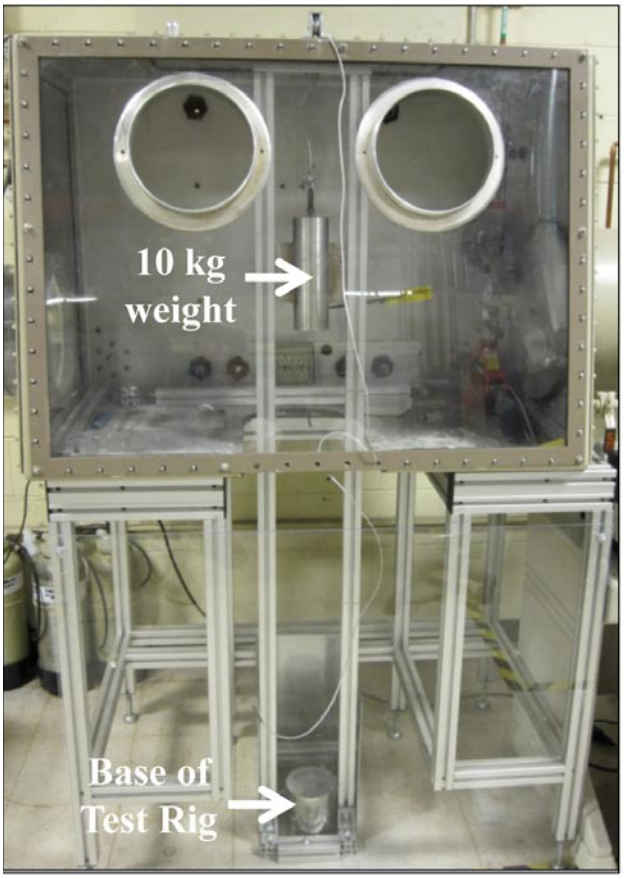


FIGURE 3. UTRC Mechanical Impact Sensitivity Test Rig

TABLE 1. Dust Cloud Combustion Characterizations of Solid-State Hydrogen Storage Materials.

Parameter	Solid-State Hydrogen Storage Materials (Metal Hydrides, Chemical Hydrides, and Adsorbents)							
	Maxsorb (AX-21)	Charged AlH_3	Discharged AlH_3	$2LiBH_4$ + MgH_2	Charged $NaAlH_4$	NH_3BH_3 (as received)	ASTM Reference Material Pittsburgh Seam Coal	H_2 Gas
$(\Delta P)_{MAX}$ Bar-g	8.0	3.7	10.3	9.9	11.9	18.4	7.3	7.9 @ 29 vol% H_2 in air
$(dP/dt)_{max} = R_{MAX}$, bar/s	449	370	4,082	1,225	3,202	2,840	426	5435 @ 29 vol% H_2 in air
K_{ST} bar-m/s	122	101	1,100	333	869	771	116	1,477
MIE, mJ	Range 500-1,000	<10	<10	<9.2	<7	<8.9	110	0.02
MEC, g/m^3	80	30	125-250	30	140	<20	65	4 vol% H_2 in air
T_C, ^0C	760	200	710	230	137.5	n/a	585	n/a
Hazard Class	St-1	St-1	St-3	St-3	St-3	St-3	St-1	
Explosion Severity (ES)	1.16	0.44	13.5	3.9	12.3	16.54	1.0	13.8
Dust Classification	Class-II	Footnote (1)	Class-II	Class-II	Class-II	Class-II	Class-II	n/a

(1) Dust is combustible but not Class-II based in ES criterion alone.
n/a - not applicable; MIE - minimum ignition energy; MEC - minimum explosive concentration

showed that $NaAlH_4$ and $3Mg(NH_2)_2.8LiH$ powder compacts were sensitive to mechanical impact where the test samples ignited on the first impact. The NH_3BH_3 power compact, however, did not ignite during the impact tests.

- Conducted risk mitigation tests to prevent the observed mechanical impact sensitivity of $NaAlH_4$. In these tests, the hydride powder was ball milled for 15 minutes, before compaction, with different flame retardant additives (10 wt% and 20 wt%, respectively) including aluminum oxide (AL_2O_3), aluminum hydroxide ($Al(OH_3)$, magnesium hydroxide ($Mg(OH)_2$), and melamine, respectively. None of these chemical additives was successful in preventing the sensitivity of sodium alanate to mechanical impact. More testing with other chemical additives is in progress.

Risk Mitigation – Atomic and Thermodynamics modeling

The thermodynamic modeling showed that $NaAl(OH)_4$ is the most favorable product to form when 1 mole $NaAlH_4$ reacts with ≥2 moles O_2 or ≥4 moles H_2O in an inert atmosphere. The atomic modeling showed the $NaAl(OH)_4$ product can favorably form a coherent, non-passivating layer on the $NaAlH_4$ surface (Figure 4).

Dust Cloud Combustion Characterization Tests

Table 1 summarizes the results of dust cloud combustion characterization tests for complex metal hydride (charged $NaAlH_4$), chemical hydrides (as received NH_3BH_3, charged/discharged AlH_3), and Maxsorb (AX-21).

Conclusions and Future Work

Conclusions - the work performed this period covered QRA, QLRA, risk mitigation tests, dust cloud characterization tests, and atomic and thermodynamics modeling. The QLRA identified safety significant failure mechanisms of the alane-based off-board regenerable system. The QRA covered FT modeling and quantification of on-board reversible, off-board regenerable systems, and hydrogen permeation/leakage from the storage vessels. The risk mitigation tests evaluated the reactivity of selected complex metal hydrides [$NaAlH_4$ and $3Mg(NH_2)_2.8LiH$] and chemical hydride [NH_3BH_3] (loose powder and powder compacts) under different environmental conditions and postulated scenarios. Finally, performed atomic and thermodynamic modeling of sodium alanate ($NaAlH_4$) oxidation and hydration reactions.

Future work will focus on:

- **Risk Analysis:** 1) complete risk analysis framework (both QLRA and QRA) incorporating results from dust cloud characterization tests, experimental and modeling activities at SNL and SRNL and 2) develop an economic consequence analysis framework for the identified most probable and worst-case scenarios to assess the safety benefits of selected risk mitigation methods.

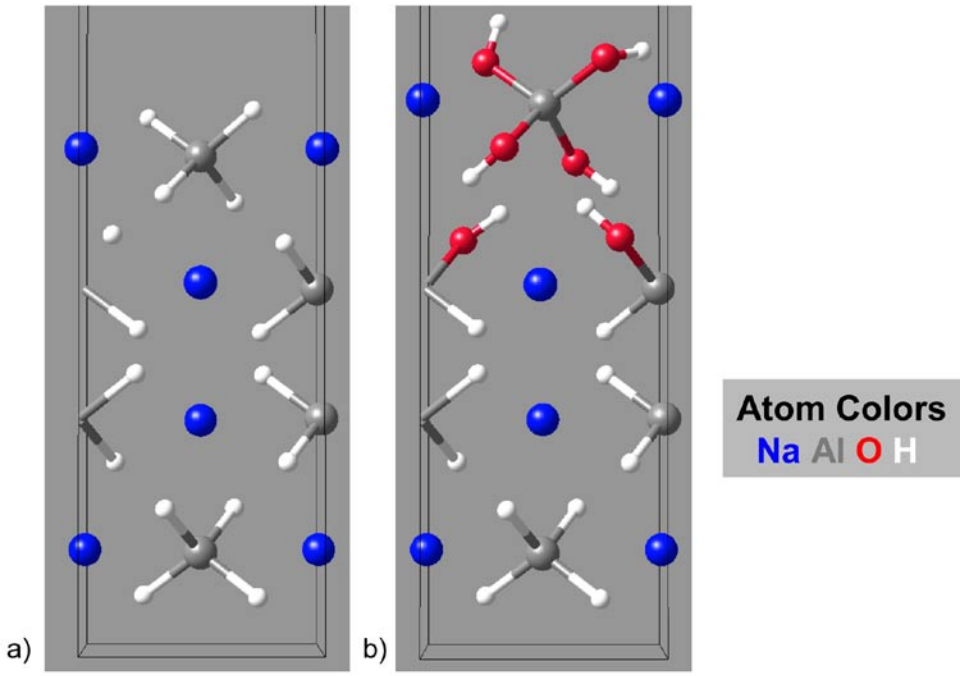


FIGURE 4. Atomic and Thermodynamics Modeling of $NaAlH_4$ Reactions with Air and Water

- **Atomic and Thermodynamic Modeling:** Additional atomic modeling and thermodynamic modeling are underway to identify the mechanisms for $NaAl(OH)_4$ decomposition to the elemental oxide and hydroxide phases under inert and ambient conditions.
- **Risk Mitigation Experimental Studies (including those planned and coordinated with SNL material reactivity project:** 1) evaluate the effectiveness of fire-retardant chemical additives to eliminate the mechanical impact sensitivity of $NaAlH_4$ powder compact and 2) perform the localized flame impingement (external fire) test using UTRC Prototype-2 Type-III storage vessel. Currently, this task is being coordinated with SNL [3].

Special Recognitions & Awards

1. The International Energy Agency, Hydrogen Implementation Agreement (IEA/HIA), Task-31 (Hydrogen Safety) selected Dr. Y. (John) Khalil to lead its Subtask-B on Hydrogen Storage Materials Reactivity, Safety, and Materials Compatibility.

FY 2011 Publications/Presentations

1. Khalil, Y.F. and M. Modarres, "Safety Importance Measures for a Conceptual Baseline Design of an On-Board Reversible Hydrogen Storage System," Proceedings of the First International Conference on Materials for Energy, UTRC/ University of Maryland Joint Paper # 1368, DECHEMA e.V., Karlsruhe, Germany, July 4–8, 2010.

2. Khalil, Y.F., D. Mosher, J. Cortes-Concepcion, C. James, J. Gray and D. Anton, "Adverse Reactivity Effects and Risk Mitigation Methods for Candidate Hydrogen Storage Materials," Proceedings of the First International Conference on Materials for Energy, UTRC/SRNL Joint Paper # 1369, DECHEMA e.V., Karlsruhe, Germany, July 4–8, 2010.

3. Khalil, Y.F. (UTRC), Newhouse, N.L. (Lincoln Composites, Inc.) and Simmons, K.L. (PNNL), "Potential Diffusion-Based Failure Modes of Hydrogen Storage Vessels for On-Board Vehicular Use," invited paper accepted for presentation at the Hydrogen Storage System Engineering and Applications – Risk Reduction Session, AIChE Topical Conference, Salt lake City, UT, November 7–12, 2010.

4. Dedrick, D.E., at al. (SNL) and Khalil, Y.F. (UTRC), "Mitigation Technologies for Hydrogen Storage Systems Based on Reactive Solids," invited paper accepted for presentation at the Hydrogen Storage System Engineering and Applications – Risk Reduction Session, AIChE Topical Conference, Salt lake City, UT, November 7–12, 2010.

5. Khalil, Y.F. and D.E. Dedrick, "Flame Impingement Test Plan for UTRC Prototype-2 Storage Vessel," Joint Presentation, DOE Technical Team Review Meeting, Web-based Conference, November 18, 2010.

6. Khalil, Y.F., "Quantifying & Addressing the DOE Material Reactivity Requirements with Analysis & Testing of Hydrogen Storage Materials & Systems," DOE Quarterly Report 4Q2010, January 30, 2011.

7. Khalil, Y.F., "Quantifying & Addressing the DOE Material Reactivity Requirements with Analysis & Testing of Hydrogen Storage Materials & Systems," DOE Quarterly Report 1Q2011, April 30, 2011.

References

1. Multi-Year Research, Development and Demonstration Plan: Planned Program Activities for 2005-2015, Technical Plan-Storage: http://www1.eere.energy.gov/hydrogenandfuelcells/mypp/pdfs/storage.pdf, updated April 2009.

2. Khalil, Y.F., N.L. Newhouse, K.L. Simmons, and D.E. Dedrick, "Potential Diffusion-based Failure Mechanisms of Hydrogen Storage vessels for On-Board Vehicular r Use," AIChE Topical Conference, Salt lake City, UT, November 7–12, 2010.

3. Khalil, Y.F. and D.E. Dedrick, "Flame Impingement Test Plan for UTRC Prototype-2 Storage Vessel," Joint Presentation, DOE Technical Team Review Meeting, Web-based Conference, November 18, 2011.

IV.E.2 System Level Analysis of Hydrogen Storage Options

Rajesh K. Ahluwalia (Primary Contact), T.Q. Hua, J-K Peng, Romesh Kumar
Argonne National Laboratory
9700 South Cass Avenue
Argonne, IL 60439
Phone: (630) 252-5979
E-mail: walia@anl.gov

DOE Manager
HQ: Grace Ordaz
Phone: (202) 586-8350
E-mail: Grace.Ordaz@ee.doe.gov

Start Date: October 1, 2004
Projected End Date: September 30, 2014

Fiscal Year (FY) 2011 Objectives

The overall objective of this effort is to support DOE with independent system level analyses of various H_2 storage approaches, to help to assess and down-select options, and to determine the feasibility of meeting DOE targets. Specific objectives in FY 2011 included:

- Model various developmental hydrogen storage systems.
- Provide results to Hydrogen Storage Engineering Center of Excellence (HSECoE) for assessment of performance targets and goals.
- Develop models to "reverse-engineer" particular approaches.
- Identify interface issues, opportunities, and data needs for technology development.

Technical Barriers

This project addresses the following technical barriers from the Hydrogen Storage section of the Fuel Cell Technologies Program Multi-Year Research, Development and Demonstration Plan:

(A) System Weight and Volume
(B) System Cost
(C) Efficiency
(E) Charging/Discharging Rates
(J) Thermal Management
(K) System Life Cycle Assessments

Technical Targets

This project is conducting system level analyses to address the DOE 2015 technical targets for on-board hydrogen storage systems:

- System gravimetric capacity: 1.8 kWh/kg
- System volumetric capacity: 1.3 kWh/L
- Minimum H_2 delivery pressure: 5 bar
- Refueling rate: 1.5 kg/min
- Minimum full flow rate of H_2: 0.02 g/s/kW

FY 2011 Accomplishments

- Analyzed the gravimetric and volumetric capacities of Type-3 and Type-4 two-tank compressed hydrogen (cH_2) physical storage systems.
- Updated the on-board and off-board analyses of the activated carbon (AX-21) system with adiabatic liquid hydrogen (LH_2) refueling and cryogenic liner fatigue considerations.
- Conducted the on-board and off-board analyses of the metal-organic framework (MOF-5) system (powder and pellets) with adiabatic LH_2 refueling. Determined the intrinsic capacities, thermodynamics, dormancy, H_2 refueling dynamics, and discharge dynamics.
- Updated system analysis of on-board hydrogen storage systems that use ammonia borane (AB) in ionic liquids (IL) as the hydrogen storage medium.
- Performed off-board analysis of AB regeneration using hydrazine. Identified processes that consume significant amounts of energy in regeneration and provided feedback to stakeholders.
- Revised off-board analysis of alane regeneration using the three-step organometallic approach. Identified processes that consume significant amounts of energy in regeneration and provided feedback to stakeholders.



Introduction

Several different approaches are being pursued to develop on-board hydrogen storage systems with the goal of meeting the DOE targets for light-duty vehicle applications. Each approach has unique characteristics, such as the thermal energy and temperature of charge and discharge, kinetics of the physical and chemical process steps involved, and requirements for the materials and energy interfaces between the storage system and the fuel supply system on the one hand, and the fuel user on the other. Other storage system design and operating parameters influence the projected system costs as well. We are developing models to understand the characteristics of storage systems based on the various approaches, and to evaluate their potential to meet the DOE targets for on-board applications including the off-board targets for energy efficiency.

Approach

Our approach is to develop thermodynamic, kinetic, and engineering models of the various hydrogen storage systems being developed under DOE sponsorship. We then use these models to identify significant component and performance issues, and to assist DOE and its contractors in evaluating alternative system configurations and design and operating parameters. We establish performance criteria that may be used, for example, in developing storage system cost models. We refine and validate the models as data become available from the various developers. We work with the Hydrogen Storage Systems Analysis Working Group to coordinate our research activities with other analysis projects to assure consistency and to avoid duplication. An important aspect of our work is to develop overall systems models that include the interfaces between hydrogen production and delivery, hydrogen storage, and the fuel cell or internal combustion engine hydrogen user.

Results

Physical Storage

We expanded our analysis of cH_2 physical storage to include systems that may use two smaller, equal tanks that are in close communication (equalized pressures) and do not require duplicate controls. There is only a small weight (5-10%) and volume (<3%) increase in going from single-tank to two-tank systems; the penalty would be larger if the two tanks are not in close communication and require duplicate balance-of-plant components.

Hydrogen Storage in Metal-Organic Frameworks (MOF-5)

We conducted an analysis of on-board hydrogen storage in MOF-5 (Basolite Z 100-H) powder (130 $kg.m^{-3}$) and pellets (310-790 $kg.m^{-3}$). Figure 1 shows the principal components of the reference on-board hydrogen storage system with adiabatic refueling, in which the MOF tank is evaporatively cooled during refueling with LH_2. During discharge, the heat of desorption and any temperature swing in the sorbent bed is provided by recirculating the hydrogen through a small ex-tank heat exchanger. The composite pressure vessel consists of T700S carbon fiber (2,550 MPa tensile strength) wound on an Al 6061-T6 alloy liner, and it is thermally insulated with multi-layer vacuum super insulation in a 3-mm-thick Al 6061-T6 alloy vacuum shell. We conducted fatigue analyses to estimate the required liner thickness to meet the target life of 5,500 pressure cycles (Society of Engineers [SAE] J2579 requirement). The thickness of the insulation was determined so as to limit the heat transfer rate from the ambient to 5 W. A geodesic winding algorithm was employed to determine the optimal dome shape for the composite vessel and the carbon fiber thickness required for a 2.35 safety factor (SAE requirement) at the peak storage pressure.

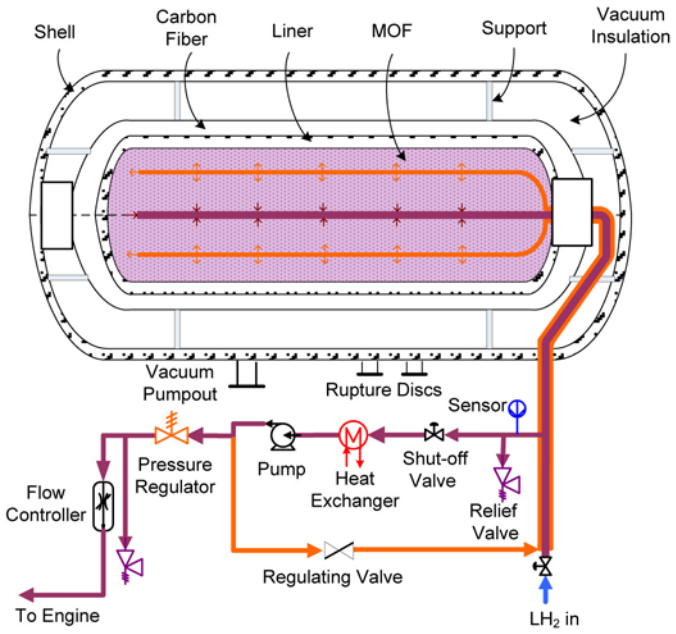


FIGURE 1. On-Board MOF-5 Storage System with LH_2 Refueling

We modeled the MOF-5 powder (130 $kg.m^{-3}$) hydrogen adsorption isotherms by fitting the low-temperature data of Zhou et al. [1] and Sudik et al. [2] to the Dubinin-Astakhov (D-A) equation. We used solution thermodynamics to evaluate the integral enthalpy of adsorption. We modeled the MOF-5 pellets (310-790 $kg.m^{-3}$) hydrogen adsorption isotherms by fitting the data of Sudik et al. [2] to the D-A model. We incorporated the fitted isotherms in our system model to estimate the gravimetric and volumetric capacity for 5.6 kg recoverable H_2 at 5-bar minimum delivery pressure and 1.5-$kg.min^{-1}$ refueling rate. Figure 2 shows the calculated system capacities for powder and pellets. The optimal pressure and temperature for maximum gravimetric capacity are 100-120 bar and ~60 K for powder and 310 $kg.m^{-3}$ pellet bulk density, and ~100 K for 510 $kg.m^{-3}$ pellet bulk density. The gravimetric capacity peaks at 6.6 wt% for powder, 4.8 wt% for 310 $kg.m^{-3}$ pellets, and 3.3 wt% for 510 $kg.m^{-3}$ pellets. The optimal temperature for maximum gravimetric capacity is lower than the temperature at which recoverable excess uptake is at a maximum. The system volumetric capacity increases with pressure for 130-310 $kg.m^{-3}$ bulk density, but does not reach the 40 $g.L^{-1}$ 2015 target. The maximum volumetric capacity for powder is achieved at 150-250 atm, but at those pressures, a higher volumetric capacity can be achieved without using the sorbent. The volumetric capacity for the 510 $kg.m^{-3}$ pellet bulk density decreases with increasing pressures above 100 atm as a result of the lower recoverable excess adsorption. For hydrogen storage in MOF-5 powder (150 atm, 60 K), the containment (liner, carbon fiber, and shell), the storage medium, and the balance-of-plant components account for 44%, 24% and 31%, respectively. The system has a volumetric efficiency of 69%, and 20% of

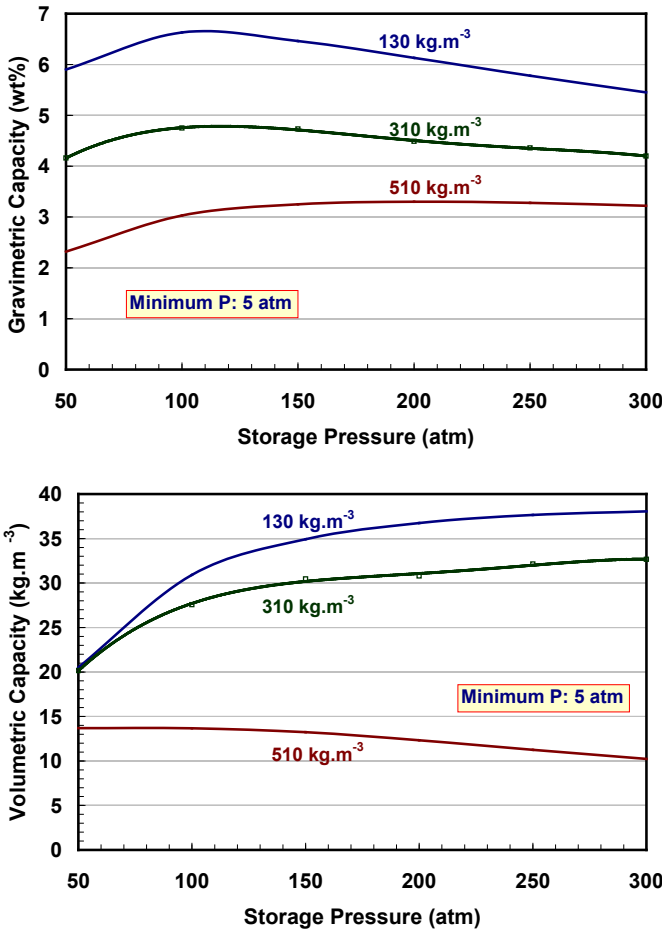


FIGURE 2. Usable Gravimetric and Volumetric Capacities of MOF-5 Powder and Pellets

the system volume is due to the vacuum insulation and the balance-of-plant components.

Analysis of the refueling dynamics showed that the total cooling load is 2, 2.1, and 3.9 MJ (maximum, from completely empty to completely full) for 130, 310 and 510 kg.m^{-3} bulk density, respectively. The heat of hydrogen adsorption accounts for 41-53% of the total cooling load; the thermal mass and the pressure-volume work of compressing the hydrogen in the tank account for the balance of the cooling load. Recoverable adsorption accounts for less than 10% of the 5.6-kg usable H_2 in the system with MOF-5 powder or 310 kg.m^{-3} pellets. For discharge, we estimated that the required bed permeability is 10^{-14} to 10^{-13} m^2 for 1 psi in-bed pressure drop and 20 charge and discharge tubes. The initial measurement [3] is 5.4 x 10^{-13} m^2 for the 360 kg.m^{-3} density pellet. We estimated that the required bed thermal conductivity for 10 U tubes is 0.04–0.05 W.m^{-1}.K^{-1}. The measured conductivity for powder and pellets is 0.088 W.m^{-1}.K^{-1} and ~0.6 W.m^{-1}.K^{-1} for 500 kg.m^{-3} pellets with 10 wt% graphite flakes added to MOF-5.

We determined the dormancy capability of the MOF-5 system as a function of temperature, pressure, and the amount of hydrogen stored at the start of the dormancy period. We estimated the minimum dormancy by analyzing the worst-case scenario, in which a MOF tank is fully charged with H_2 at 150 atm at 60 K, and it is then parked for an extended time. Assuming that the relief valve is set at 25% above the design pressure, H_2 would begin to vent after 6 W.d of cumulative heat transfer (1.2 days at 5 W heat in-leakage rate). In this scenario, the calculated peak H_2 loss rate is 1.9 g.h^{-1}.kg^{-1} for 5 W in-leakage rate. This rate decreases as H_2 vents from the tank. Also, the peak H_2 loss rate decreases to 0.3 g.h^{-1}.kg^{-1} if the tank is initially 25% full, and there is no loss of H_2 if the tank is less than 15% full, or with minimal daily driving.

Chemical Storage

We conducted an on-board analysis for hydrogen storage in a 50:50 (by weight) liquid mixture of AB and an IL, bmimCl (1-butyl-3-methylimidazolium chloride, $C_8H_{15}ClN_2$). This AB solution is a stirrable, viscous liquid at room temperature, with a freezing point below –10°C. However, the solution foams once H_2 is released from the AB in the exothermic process; the foam begins to convert to a white solid after releasing 1 H_2-equiv, with the entire mixture becoming solid after releasing 2 H_2-equiv [4]. Assuming that an alternative IL (or a mixture of ILs) is found such that the solution does not foam or solidify, we developed a conceptual on-board dehydrogenation reactor model using the kinetic data for the AB-bmimCl mixture. The main challenge is to control the peak temperature in this exothermic process, as too high a temperature may lead to undesirable side reactions, as well as issues of solvent stability and AB conversion (complete AB conversion would impede regenerability). The reactor temperatures can be controlled by using a heat transfer coolant, product recycle, or a combination of the two. The reactor model was set up to yield 1.6 g/s of H_2 at 100% conversion (2.35 H_2-equiv) using ethylene glycol as the coolant with a 10°C temperature rise through the reactor. The peak reactor temperature is a function of the solution inlet temperature and the recycle ratio. For a specified conversion, it may not be possible to control the peak temperature adequately by just reducing the inlet temperature.

In our simulations, we varied the coolant flow rate (100°C coolant inlet temperature) to control the reactor outlet temperature. For a fixed reactor outlet temperature (200°C), Figure 3a presents the reactor inlet and peak temperatures as functions of the recycle ratio for 100% conversion, and 100 h^{-1} (square symbols) and 200 h^{-1} (triangle symbols) space velocities (liquid hourly space velocity, LHSV). Figure 3a shows that the reactor inlet temperature decreases with decreasing recycle ratio (R), and drops below 130°C at R = 0.62, at which inlet temperature 100% conversion cannot be achieved. The results in Figure 3a also indicate that the reactor temperatures are insensitive to space velocities over the range of LHSV considered. The reactor outlet temperature has only a

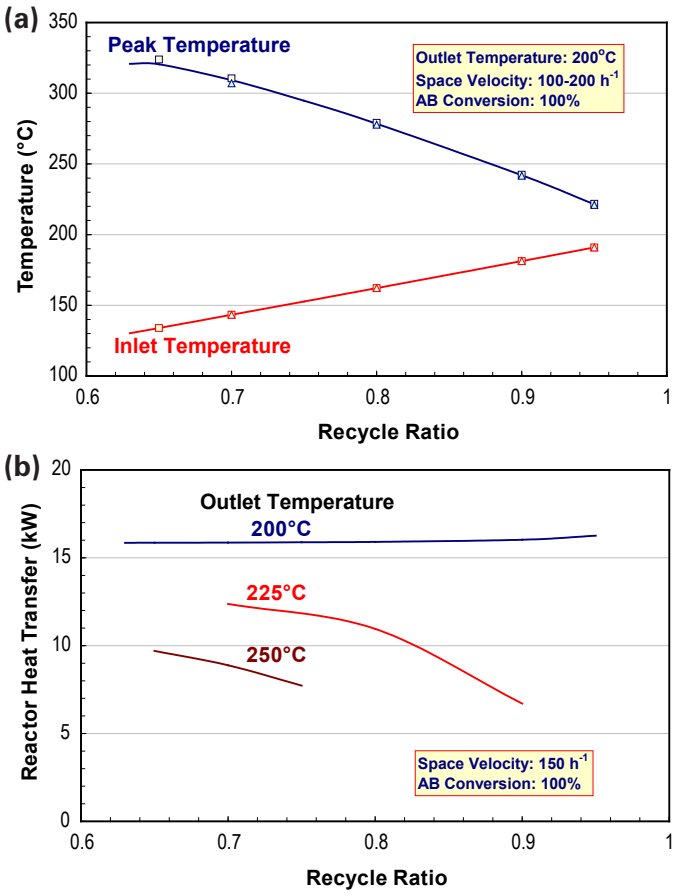


FIGURE 3. Performance of On-Board AB reactor

small effect on the reactor peak and inlet temperatures; the heat transfer, however, is affected by the reactor outlet temperature and the recycle ratio. The reactor heat transfer decreases as the outlet temperature is allowed to rise (see Figure 3b). Finally, we note that whereas high recycle ratios help in limiting the operating temperatures, the inlet flow rate and, therefore, the pumping power increases non-linearly with increasing R.

Our modeling results indicate that the peak rate of H_2 loss from the exothermic decomposition of AB/IL in the storage tank depends on the heat transfer coefficient (assumed 15 $W.m^{-2}.K^{-1}$ for natural convection) in addition to the Avrami kinetics and the ambient temperature. Based on the 75-110°C kinetics data, we estimate that H_2 loss rate from a full tank significantly exceeds the DOE target (0.05 $g.h^{-1}.kg^{-1}$) at >50°C ambient temperature, but is lower than the target at <30°C ambient temperature. The loss rates are proportionally lower with partially full tank. Also, the maximum cumulative loss is limited to 1 H_2-equiv since the kinetics of the second decomposition step that releases H_2 beyond 1 H_2-equiv is slow at low temperatures.

We calculated that the AB/IL system has a gravimetric capacity of 4.9 wt%, which is below the 2015 target, and a volumetric capacity of 49.5 $g.L^{-1}$, which exceeds the 2015 target. The AB/IL solution accounts for 63% of the system weight and 79% of the system volume.

Off-Board Regeneration of Alane

We updated and analyzed two engineering flowsheets for converting spent Al to alane by a three-step method, using information available in the literature as well as recent unpublished experimental data obtained at Brookhaven National Laboratory [5,6]. Figure 4 shows one of the two flowsheets. In the first step, dimethylethylamine reacts with pressurized hydrogen gas and Ti-catalyzed Al in diethyl ether to form dimethylethylamine alane adduct. The second step involves transamination of the adduct by triethylamine to form triethylamine alane adduct which is less stable and can be thermally decomposed in a final step to yield alane. All reagents, except aluminum and hydrogen, are recovered and recycled. In the second flowsheet, trimethylamine replaces dimethylethylamine in the first step to form trimethylamine alane adduct. Most of the process steps in this flowsheet are similar to those in the first flowsheet, with a few exceptions.

We estimated that the well-to-tank (WTT) efficiency of the first flowsheet is 24%, which increases to 42% if low-temperature waste heat is freely available from an external source. The corresponding efficiencies in the second flowsheet are 23 and 37%, respectively. The estimated greenhouse gas emissions in both flowsheet are ~32 kg CO_2-equiv/kg-H_2, which reduce to ~22 kg CO_2-equiv/kg-H_2 if free waste heat is available.

Off-Board Regeneration of AB using Hydrazine

We analyzed the off-board regeneration process for ammonia borane in a single-pot scheme, in which the spent AB is reacted with hydrazine (N_2H_4, limiting reagent) in liquid ammonia [7].

$$BNH_2 + N_2H_4 \rightarrow BH_3NH_3 + N_2$$

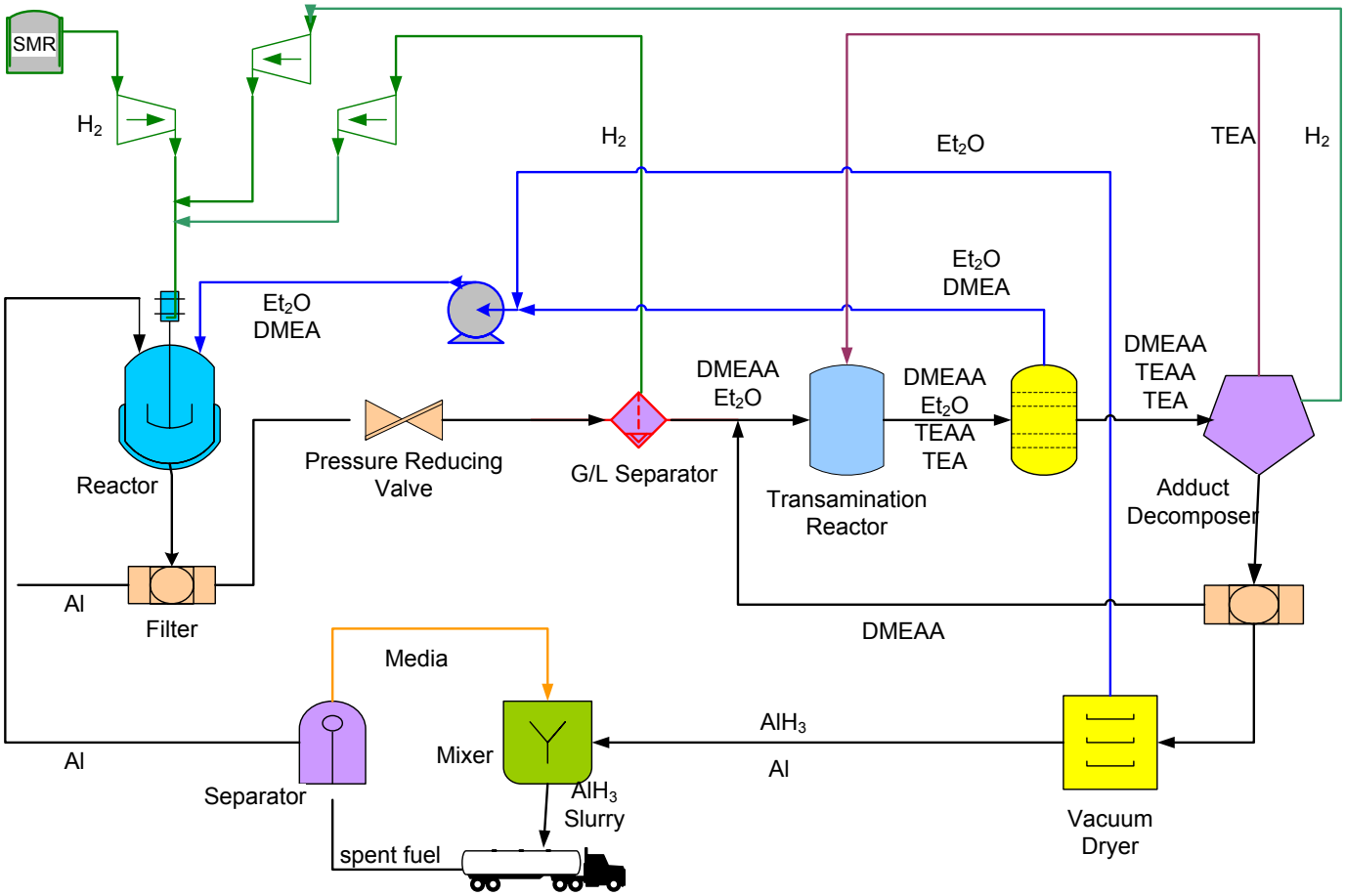
Two flow sheets were constructed to close the cycles by considering the commercial processes (Bayer Ketazine and PCUK) for producing hydrazine. The Bayer Ketazine process requires large amounts of electricity to produce NaOH and Cl_2, which are the feed materials for hydrazine production.

$$2NH_3 + 2NaOH + Cl_2 \rightarrow N_2H_4.H_2O + 2NaCl + H_2O$$

The PCUK process consumes a large amount of steam in making hydrogen peroxide.

$$2NH_3 + H_2O_2 \rightarrow N_2H_4.H_2O + H_2O$$

We estimated that the WTT efficiency for AB regeneration is 12% via the PCUK pathway and 8% via the Bayer Ketazine pathway. We also estimated that the total greenhouse gas emissions are 63 and 101 kg CO_2-equiv/kg-H_2 for the PCUK and Bayer Ketazine pathways, respectively.



DMEAA - dimethlethylamine alane; DMEA - dimethlethylamine; TEAA - triethylamine alane adduct; TEA - triethylamine; SMR - steam methane reformer

FIGURE 4. Process Flowsheet for Regeneration of Alane using Dimethylethylamine

Conclusions and Future Directions

- We project that an on-board MOF-5 system with adiabatic LH_2 refueling and 5.6 kg recoverable H_2 can achieve 6.5 wt% gravimetric capacity and 34.9 $g.L^{-1}$ volumetric capacity at 150 atm. The loss-free time and hydrogen loss rate are functions of the amount of hydrogen stored and the pressure and temperature at the start of the dormancy event.
- Assuming that an alternative IL (or a mixture of ionic liquids) is found such that the AB/IL solution does not foam or solidify upon releasing hydrogen, we calculate that the AB/IL system has a gravimetric capacity of 4.9 wt% and a volumetric capacity of 49.5 $g.L^{-1}$. We estimate that the H_2 loss rate from a full tank significantly exceeds the DOE target (0.05 $g.h^{-1}.kg^{-1}$) at >50°C ambient temperature, but it would meet the target at <30°C ambient temperature.
- We estimate WTT efficiencies of 8-12% for regenerating AB using hydrazine in liquid ammonia in the single pot scheme developed at Los Alamos National Laboratory. We estimate WTT efficiencies of 24-42% for regenerating alane by a three-step organometallic approach using dimethyethylamine or trimethylamine as the primary amine to form an amine alane adduct.
- In FY 2012, we will update our analysis of alane slurry storage with new kinetics data from Brookhaven National Laboratory for micrometer-sized alane.
- In FY 2012, we will analyze hydrogen storage in a generic sorbent system with an arbitrary heat of adsorption, and for the $LiNH_2$:MgH_2 on-board reversible metal hydride system.
- Also in FY 2012, we will further extend our systems analysis work on physical, sorbent, and metal-hydride storage methods.

FY 2011 Publications/Presentations

1. R.K. Ahluwalia, T.Q. Hua, J.K. Peng, S. Lasher, K. McKenney, J. Sinha and M. Gardiner, "Technical Assessment of Cryo-Compressed Hydrogen Storage Systems with Automotive Applications," International Journal of Hydrogen Energy, 35 (2010), 4171-4184.

2. T.Q. Hua, R.K. Ahluwalia, J.K. Peng, M. Kromer, S. Lasher, K. McKenney, K. Law and J. Sinha, "Technical Assessment

of Compressed Hydrogen Storage Systems with Automotive Applications," International Journal of Hydrogen Energy, 36 (2011), 3037-3049.

3. R.K. Ahluwalia, T.Q. Hua and J.K. Peng, "On-Board and Off-Board Performance of Hydrogen Storage Options," Accepted for publication in International Journal of Hydrogen Energy (2011).

4. T.Q. Hua and R.K. Ahluwalia, "Alane Hydrogen Storage for Automotive Fuel Cells – Off-Board Regeneration Processes and Efficiencies," Submitted to International Journal of Hydrogen Energy (2011).

5. R.K. Ahluwalia and T.Q. Hua, "Hydrogen Storage in Ammonia Borane Dissolved in an Ionic Liquid," Submitted to International Journal of Hydrogen Energy (2011).

6. T.Q. Hua, R.K. Ahluwalia, J.K. Peng, M. Kromer, S. Lasher, K. McKenney, K. Law and J. Sinha, "Technical Assessment of Compressed Hydrogen Storage Systems with Automotive Applications," Argonne National Laboratory Report, ANL-10/24, September 2010.

7. R.K. Ahluwalia, T.Q. Hua, J.K. Peng and M. Kromer, "Performance and Cost Analyses of Type 3 and Type 4 Compressed Hydrogen Tanks," Storage System Analysis Working Group, Washington, DC, June 2010.

8. T.Q. Hua and R.K. Ahluwalia, "Process Efficiency for Regeneration of Ammonia Borane," AIChE 2010 Midwest Regional Conference, Illinois Institute of Technology, Chicago, September 2010.

9. R.K. Ahluwalia, T.Q. Hua and J.K. Peng, "On-board and Off-board Performance of Hydrogen Storage Options," AIChE Annual Meeting, Salt Lake City, November 2010.

10. R.K. Ahluwalia, T.Q. Hua and J.K. Peng, "On-board Storage System Analysis," Storage System Analysis Working Group, NREL, Colorado, January 2011.

11. T.Q. Hua, R.K. Ahluwalia and J.K. Peng, "Off-board Storage System Analyses," Storage System Analysis Working Group, NREL, Colorado, January 2011.

12. R.K. Ahluwalia, J.K. Peng and T.Q. Hua, "Cryo-Compressed Hydrogen Storage: Performance and Cost Review," Compressed and Cryo-Compressed Hydrogen Storage Workshop, Arlington, VA, February 2011.

References

1. W. Zhou, H. Wu, M. Hartman and T. Yildirim, "Hydrogen and Methane Adsorption in Metal-Organic Frameworks: A High-Pressure Volumetric Study," J. Phys. Chem. C 2007, 111, 16131-16137.

2. A. Sudik, et al., "Achieving Optimal Hydrogen Storage in MOF-5," 2010 Annual AIChE Meeting, Salt Lake City, UT.

3. A. Sudik, Private Communication 2011.

4. D.W. Himmelberger, L.R. Alden, M.E. Bluhm and L.G. Sneddon, "Ammonia Borane Hydrogen Release in Ionic Liquids," Inorganic Chemistry, 48 (2009), 9883-9889.

5. Lacina D., Wegrzyn J., Reilly J., Celebi Y., Graetz J. Regeneration of aluminum hydride using dimethylethylamine. Energy Environ. Sci. 2010; 3:1099–1105.

6. Lacina D., Reilly J., Celebi Y., Wegrzyn J., Johnson J., Graetz J. Regeneration of aluminum hydride using trimethylamine. J Physical Chemistry C 2011.

7. Nakagawa T., Shrestha R., Davis B., Diyabalanage H., Burrell A., Henson N., Semelsberger T., Stephens F., Gordon J., Ott K., Sutton A. Chemical hydrogen storage R&D at Los Alamos National Laboratory. DOE Hydrogen Program Annual Review, Washington, D.C.; 2010.

IV.E.3 Cost Analyses of Hydrogen Storage Materials and On-Board Systems

Karen Law (Primary Contact), Jeffrey Rosenfeld
TIAX LLC
35 Hartwell Ave.
Lexington, MA 02421
Phone: (408) 517-1580
E-mail: law.karen@TIAXLLC.com

DOE Managers
HQ: Grace Ordaz
Phone: (202) 586-8350
E-mail: Grace.Ordaz@ee.doe.gov
GO: Katie Randolph
Phone: (720) 356-1759
Email: Katie.Randolph@ee.doe.gov

Contract Number: DE-FC36-04GO14283

Start Date: June 2004
Projected End Date: March 2012

Fiscal Year (FY) 2011 Objectives

The overall objective for this project is provide independent analysis to help guide the DOE and developers toward promising research and development (R&D) and commercialization pathways by evaluating the various on-board hydrogen storage technologies on a consistent basis. Specific objectives include:

- Compare different on-board hydrogen storage approaches in terms of lifecycle costs, energy efficiency and environmental impact;
- Identify and compare other performance aspects that could result in barriers to successful commercialization (e.g., on-board system weight and volume);
- Examine the effects of system-level cost and performance trade-offs for different storage approaches; and
- Project performance and cost relative to DOE targets.

Technical Barriers

This project addresses the following technical barriers from the Hydrogen Storage section of the Hydrogen, Fuel Cells and Infrastructure Technologies Program Multi-Year Research, Development, and Demonstration Plan:

(A) System Weight and Volume
(B) System Cost
(K) System Life-Cycle Assessments

Technical Targets

This project evaluates the various on-board hydrogen storage technologies being developed by the DOE Hydrogen Storage Centers of Excellence and independent projects. Insights gained from these evaluations will help guide DOE and developers toward promising hydrogen storage materials and system-level designs and approaches that could meet the DOE targets for storage system cost, specific energy, energy density, fuel cost, and efficiency.

FY 2011 Accomplishments

We have performed preliminary and/or updated assessments for several hydrogen storage systems. For each system assessment, we projected on-board system performance and high-volume (~500,000 units/year) manufactured cost, as well as determined the critical cost drivers and conducted single- and multi-variable sensitivity analyses to bound cost results. We have also completed a preliminary analysis of low-volume compressed single-tank systems. We also reviewed key assumptions and results with developers, DOE, and stakeholders (e.g., material suppliers, national labs, FreedomCAR and Fuel Partnership Tech Teams) and incorporated their feedback into the final results. Finally we compared performance and cost results to other baseline technologies and DOE targets for the on-board storage system. Specific accomplishments include:

- Completed preliminary low-volume (10,000, 30,000, 80,000, 130,000, and 500,000 units/year) on-board system factory cost assessments for 350 and 700 bar compressed single-tank systems. The projected costs for the 350 bar system are $29, $26, $20, $18, and $15/kWh for 10,000, 30,000, 80,000, 130,000, and 500,000 units per year, respectively. The projected costs for the 700 bar system are $36, $33, $25, $22, and $19/kWh for 10,000, 30,000, 80,000, 130,000, and 500,000 units per year, respectively.
- Completed a review of Dow Chemical's ammonia borane (AB) off-board first fill and fuel regeneration cost projections and submitted a final memo to DOE summarizing these results.
- Finalized the liquid carrier hydrogen (LCH_2) storage system cost analysis, submitted a final report to DOE for review, and submitted an executive summary to Argonne National Laboratory (ANL) for inclusion in the combined ANL/TIAX final report. Compared to TIAX's prior analysis, the updated LCH_2 storage system uses an updated catalyst replacement rate, adjusted material and balance-of-plant (BOP) costs, and several additional minor changes. These changes reduced the cost of hydrogen fuel by over 30% from $4.75 to $3.27 and increased the cost of onboard storage by less than 5%, from $15.4 to $15.7/kWh.

- Reviewed and completed analysis for metal organic framework (MOF)-177 and AX-21. We developed a bottom-up cost estimate for MOF-177 and continued to use an older estimate for AX-21. Reviewers felt the approach used for MOF was generally sound, though characterized by high uncertainty. The AX-21 cost estimate is based on information from the literature, and may be high. Rather than revisit the AX-21 cost, we expanded our sensitivity analysis to capture this uncertainty.
- Revised and completed high-volume on-board system factory cost assessments of cryo-compressed and 350 bar and 700 bar compressed tank systems. For the compressed systems, the analysis was extended to include Type 3 and Type 4 tanks and single and dual tank systems. We submitted a revised final report to DOE for review and submitted a revised executive summary to ANL for inclusion in the combined ANL/TIAX final report.
- Supported the Storage Systems Analysis Working Group (SSAWG) evaluation of the well-to-tank (WTT) energy use and greenhouse gas emissions for MOF-177 tanks, cryo-compressed tanks, 350 and 700 bar tanks, and cold gas tanks.



Introduction

DOE is funding the development of a number of hydrogen storage technologies as part of its "Grand Challenge" applied R&D program. This independent analysis project helps guide the DOE and Grand Challenge participants toward promising R&D and commercialization pathways by evaluating the various hydrogen storage technologies on a consistent basis. Using this consistent and complete comparison of various technology options, R&D can be focused and accelerated. Without such an approach, erroneous investment and commercialization decisions could be made, resulting in wasted effort and risk to the development of hydrogen vehicles and a hydrogen infrastructure.

TIAX is conducting system-level evaluations of the on-board storage systems cost and performance for four broad categories of on-board hydrogen storage. The four categories are: reversible on-board (e.g., metal hydrides and alanates), regenerable off-board (e.g., chemical hydrides); and high surface area sorbents (e.g., carbon-based materials), and advanced physical storage (e.g., cryo-compressed hydrogen, liquid hydrogen). Evaluations are based on developers' on-going research, input from DOE and key stakeholders, and in-house expertise.

Approach

This project utilizes an approach that is designed to minimize the risks associated with achieving the project objectives. In coordination with ANL, system-level conceptual designs are developed for each on-board storage system and required fueling infrastructure. We work closely with ANL to develop a bill of materials consistent with their performance assessment. Next, system models and cost models are used to develop preliminary performance and cost results. We utilize in-house activities and product-based cost models to determine high-volume manufactured cost projections for the on-board storage system, and H2A-based discounted cash flow models to estimate hydrogen selling prices based on the required off-board hydrogen infrastructure. Subsequently, these results are vetted with developers and key stakeholders and refined based on their feedback. Coordination with DOE's Hydrogen SSAWG avoids duplication and ensures consistency. This is an on-going and iterative process so that DOE and its contractors can increasingly focus their efforts on the most promising storage technology options.

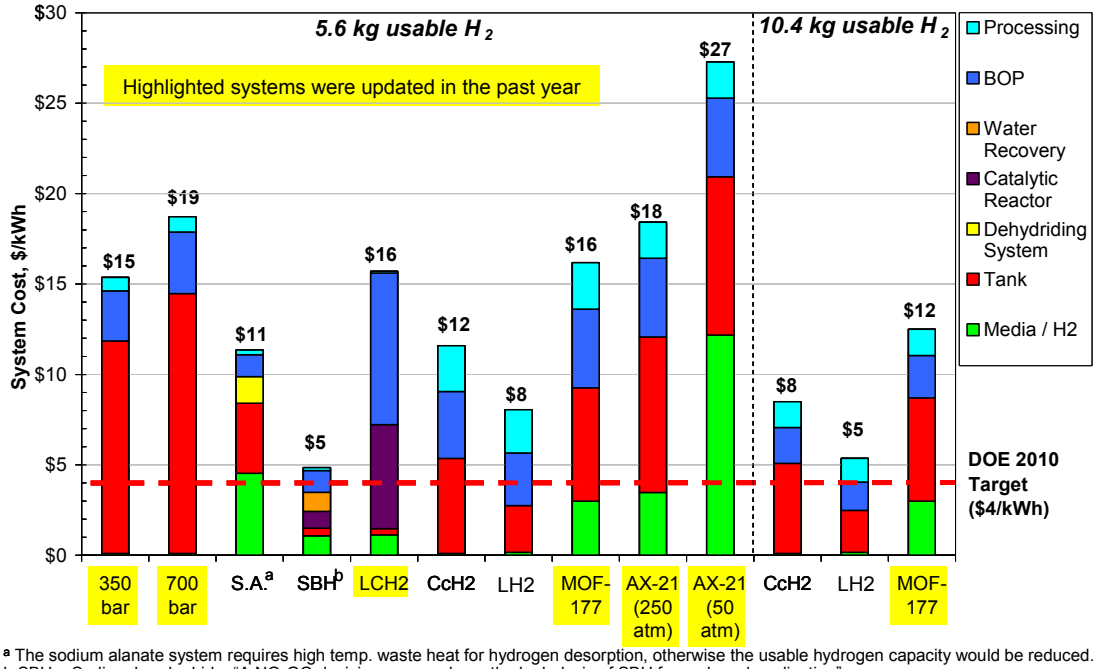
Results

TIAX developed preliminary cost estimates for low-volume manufacturing of 350 and 700 bar compressed storage systems, and updated and completed previous cost estimates for compressed (high-volume one and two tank), cryo-compressed, MOF-177, AX-21, ammonium borane, and LCH_2 storage systems. Each of the storage system cost projections are estimated based on on-board system designs developed by ANL [1]. Figure 1 shows the updated costs for the systems completed in FY 2011. The remaining portion this section discusses the preliminary low-volume manufacturing cost analysis for compressed systems.

Low-volume manufacturing costs were estimated for 10,000, 30,000, 80,000, 130,000, and 500,000 units per year for both 350 and 700 bar systems. The preliminary cost estimate focused mainly on the cost of carbon fiber, differences in manufacturing costs, and BOP costs. The systems modeled are identical to those used for the cost estimate for the 500,000 units per year shown in Figure 1. Figure 2 shows the preliminary costing results for low-volume manufacturing of compressed systems.

The carbon fiber cost for low- and high-volume manufacturing, based on conversations with carbon fiber manufacturers, will stay relatively the same with potentially a small price decrease of $1.5/lb around 80,000 units per year. The projections of carbon fiber cost may go up, independent of volume, due to increases in the costs of carbon fiber precursors. Figure 2 shows that tank material costs, which do not include manufacturing and are primarily carbon fiber costs, remain relatively constant, due to carbon fiber costs remaining relatively constant.

Manufacturing costs were projected assuming a high level of automation, similar to that of high-volume manufacturing. This assumption was made based on the significant amount of manufacturing still required for 10,000 units per year. After recent discussions with tank manufacturers, this assumption will be the main revision for



a The sodium alanate system requires high temp. waste heat for hydrogen desorption, otherwise the usable hydrogen capacity would be reduced.
b SBH = Sodium borohydride, "A NO-GO decision was made on the hydrolysis of SBH for on-board application"

FIGURE 1. Updated Hydrogen Storage System Costs

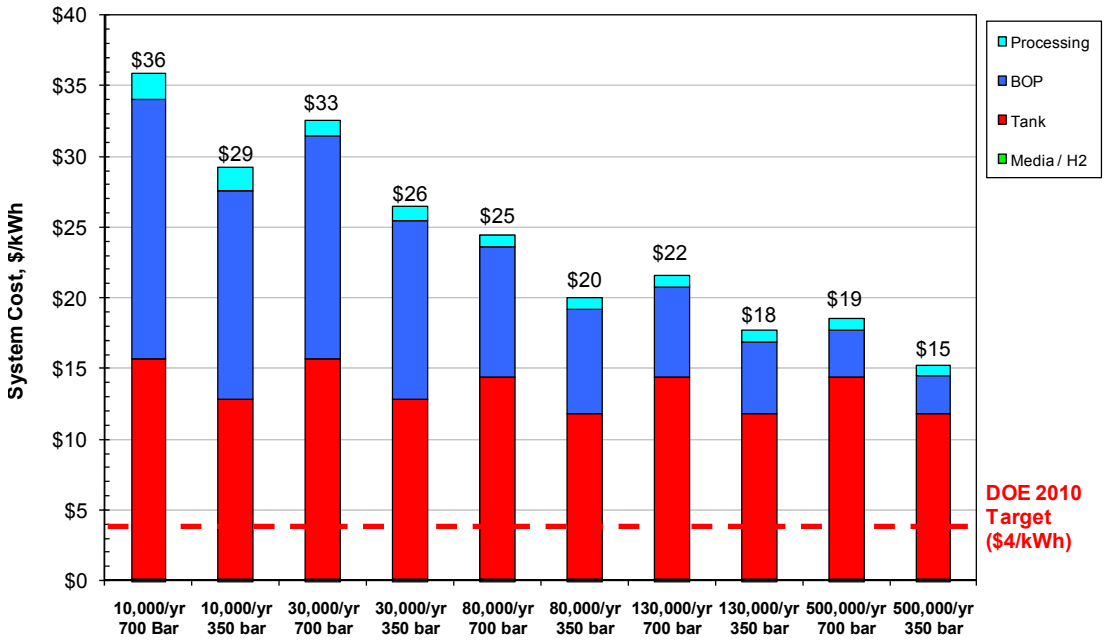


FIGURE 2. Preliminary Low-Volume Manufacturing Results for One-Tank 350 and 700 Bar Compressed Systems

the finalized of cost estimates for low-volume manufacturing. Figure 2 shows that with the assumption of a high level of automation, processing costs are very small compared to tank and BOP costs.

The cost that is most affected by manufacturing volume is the BOP cost. This is a result of components, especially valves, regulators, and sensors, being made at low volumes at the specifications required for high pressure hydrogen. Many of these components need to be individually machined, which is more costly than being forged. The basis of the cost curve for the BOP components is data supplied by a sensor manufacturer and their projected costs for 10,000, 100,000, and 500,000 units per year.

The projected costs for the 350 bar system are $29, $26, $20, $18, and $15/kWh for 10,000, 30,000, 80,000, 130,000, and 500,000 units per year, respectively. The projected costs for the 700 bar system are $36, $33, $25, $22, and $19/kWh for 10,000, 30,000, 80,000, 130,000, and 500,000 units per year, respectively. The BOP components decreased from 50% of the total cost at 10,000 units per year to 17% at 500,000 units per year. The tank increased from 44% of the total cost at 10,000 units per year to 78% at 500,000 units per year.

Conclusions and Future Directions

The cost assessments conducted this year allow direct comparison with prior cost assessments and DOE targets. Our models allow us to identify critical cost components, which enables focused discussion with tank developers and manufacturers.

- None of the systems assessed meet DOE's 2010 cost target of $4/Wh. The cost of the 5.6 kg 350 bar, 700 bar, cryo-compressed, liquid, and MOF-177 storage systems range from 2 to 5 times the cost of the DOE target. Key factors influencing system costs are the carbon fiber material cost, the cost of aluminum, and in the case of the MOF system, the storage media.
- The low-volume compressed systems are 7 and 9 times the 2010 DOE target of $4/kWh, with the cost of BOP components showing the greatest potential for cost reduction.
- The MOF-177 system cost is 3 and 4 times the 2010 DOE target of $4/kWh for the 10.4 and 5.6 kg systems, respectively. Achieving the DOE cost targets will require large reductions in the cost of the storage media and the tank materials (aluminum and carbon fiber).
- The onboard liquid hydrogen system cost is 1.3 and 2 times the 2010 DOE target for the 10.4 and 5.6 kg systems, respectively. While the liquid system has amongst the lowest onboard storage system cost, it has low volumetric efficiency, WTT efficiency, and high fuel costs. These shortcomings are a function of fuel boil off and the high energy requirement associated with liquefaction.
- The cryo-compressed system is 2 and 3 times the 2010 DOE target for the 10.4 and 5.6 kg systems, but meets the 2010 volumetric and gravimetric targets. The base case 350 bar and 700 bar systems are 4 and 5 times higher than the 2010 DOE targets for the 350 bar Type 4 and 700 bar Type 4 systems, respectively, and both systems fall short of the 2010 volumetric capacity targets. Additional analysis of 350 and 700 bar dual tank systems showed minor cost increases of less than 5%; 350 and 700 bar Type 3 systems showed moderate cost increases on the order of 10%. The major cost driver for the compressed system is carbon fiber, while the cryo-compressed system cost is driven by carbon fiber, aluminum liner, and BOP component costs.

The rest of this fiscal year, we plan to continue to work with developers and stakeholders to improve the accuracy of the analyzed on-board and off-board system models and finalize our analysis of storage technology options. Specifically, we plan to:

- Refine the modeling and analysis and complete the report for the low-volume manufacturing of 350 and 700 compressed systems.
- Perform the preliminary and final costing analysis of the MOF-5 system.
- Continue to work with DOE, SSAWG, Centers of Excellence, other analysis projects, developers, Tech Teams and other stakeholders (as necessary) to revise and improve system models.

FY 2011 Publications/Presentations

1. Kromer, M. *et al*. "Review of Cost Assessment for Ammonia Borane 1st Fill and Regeneration Process." TIAX LLC. Memo to Dow Chemical and the Department of Energy. August 25, 2010.

2. Kromer, M. *et al*. "H_2 Storage using Compressed Gas: On-board System and Ownership Cost Update for 350 and 700-bar." TIAX LLC. Final Report to the Department of Energy. August 27, 2010.

3. Kromer, M. *et al*. "H_2 Storage using a Liquid Carrier: Off-board and On-board System Cost Assessments." TIAX LLC. Final Report to the Department of Energy. September 14, 2010.

4. Kromer, M. *et al*. "Project Overview and Status Update." TIAX LLC. Presentation to the Department of Energy. November 9, 2010.

5. Kromer, M. *et al*. "H_2 Storage using Carbon Sorbents: On-board System Cost Assessment." TIAX LLC. Final Report to the Department of Energy. December 13, 2010.

6. Kromer, M. *et al*. "Overview of Approach and FY 2011 Activities." TIAX LLC. Presentation to Hydrogen Storage Systems Analysis Working Group. January 12, 2011.

7. Law, K. *et al*. "Analyses of Compressed Hydrogen On-Board Storage Systems." TIAX LLC. Presentation to Compressed and Cryo-Compressed Hydrogen Storage Workshop. February 14, 2001.

8. Law, K. *et al*. "Updated Hydrogen Storage System Cost Assessments." TIAX LLC. Presentation to DOE Hydrogen Storage Tech Team. April 28, 2011.

9. Law, K. *et al*. "Updated Hydrogen Storage System Cost Assessments." TIAX LLC. Presentation at DOE Annual Hydrogen Merit Review. May 11, 2010.

References

1. Ahluwalia, R.K., Hua, T.Q., Peng, J.K. "System Level Analysis of Hydrogen Storage Options." 2010 DOE Hydrogen Program Review, June 7–11, 2010.

IV.E.4 Analysis of H_2 Storage Needs for Early Market Non-Motive Fuel Cell Applications

Lennie Klebanoff (Primary Contact), Joe Pratt, Terry Johnson, Marco Arienti, Marcina Moreno
Sandia National Laboratories
7011 East Avenue
Livermore, CA 94568
Phone: (925) 294-3471
E-mail: lekleba@sandia.gov

DOE Manager
HQ: Ned Stetson
Phone: (202) 586-9995
E-mail: Ned.Stetson@ee.doe.gov

Project Start Date: September 30, 2010
Project End Date: September 30, 2011

Fiscal Year (FY) 2011 Objectives

- Engage end users in the airport ground support equipment (GSE), portable power, construction equipment, telecom power, and "man-portable" electronics industries to understand what pieces of their non-motive equipment would be good early market introduction points for fuel cells.
- From the engagements above, and with the highest priority equipment identified, determine how the equipment is used and their current requirements for power, duration, gravimetric and volumetric energy densities, as well as the required operating conditions (temperature, etc.).

Technical Barriers

This project addresses the following technical barriers assigned to this project:

(A) System Weight and Volume
(B) Cost
(C) Efficiency

Technical Targets

Data from early markets will allow DOE to determine the technical targets and research and development (R&D) needs for hydrogen storage that would enable the use of fuel cells for early market non-motive applications.

FY 2011 Accomplishments

- Identified highest priority pieces of non-motive equipment in portable power, aviation GSE, construction equipment, cell phone backup power and portable electronics industries.
- Identified how that high priority equipment uses energy, the associated energy densities (gravimetric, volumetric), and what the environmental requirements are (temperature, etc.) for their use.
- Conducted extensive questionnaire surveys of end users and new technology experts about the use of current equipment and therefore the requirements for a new clean technology replacement.
- Held workshop at Sandia-CA, attended by end users of non-motive equipment in the construction industry, telecommunications, entertainment, portable power and aviation industries, as well as the Air Force.



Introduction

Historically the DOE has funded a great deal of work on hydrogen storage. Most of this hydrogen storage R&D has focused on hydrogen storage for light-duty vehicle applications. However, recently DOE has expanded the scope of its fuel cell technology interests to include non-motive early market applications of fuel cells. By non-motive equipment, we mean equipment that is not driven directly by a human being (i.e. does not possess a steering wheel). The equipment is either stationary, or, if portable, it is carried or towed by a person or vehicle. Examples of non-motive equipment included portable power generators, air compressors, airport luggage belt loaders (an example of aviation GSE) and backup power systems for cell phone towers. Additionally, the DOE is interested in how fuel cells might be used as power sources in "man portable" electronic systems, and what the implications are for the hydrogen storage required for using fuel cells for man-portable electronics.

It is highly likely that the hydrogen storage needs for non-motive uses of fuel cells are different than the well-known hydrogen storage needs for light-duty vehicle applications. In order for the DOE to understand the eventual hydrogen storage needs for non-motive fuel cell use, it's important to understand what the highest priority pieces of equipment are in the non-motive equipment realm that would best be suited for conversion to fuel cell power. Additionally, it is vital to fully understand how this non-motive equipment is actually used and what the demands

are on the energy system. Toward that end, the goals of this project are to engage end-users, technical experts and manufacturing experts in various non-motive equipment realms, identify the highest priority pieces of equipment in each one of those realms, and understand in detail how that equipment is used. By understanding how that equipment is used currently, the DOE can better understand where the hydrogen storage performance gaps truly are if hydrogen-fueled fuel cell-based non-motive equipment were to meet or exceed the capabilities of the current equipment.

Approach

To gather this information, we approached end-users, technical experts and mass manufacturers in the following areas: construction equipment, portable power, telecommunications, aviation, and portable electronics. A database of representatives in these markets was generated. Our initial step was to host a workshop at Sandia National Laboratories, Livermore, California on February 8, 2011. The workshop was attended by representatives from the construction equipment, portable power, telecommunications and aviation markets. In aviation, Department of Defense representatives from Travis Air Force Base were also present. During this workshop, the attendees were surveyed with multiple questionnaires to help identify how equipment is used in their respective realms. Also at this workshop, break-out sessions were held to extract the highest priority pieces of equipment in each one of these non-motive early markets, so that specific non-motive pieces of equipment were identified. After the workshop, the results of the surveys were quantified using a Kano-type analysis. In addition, selected representatives of the four areas were contacted again to gain a quantitative understanding, for the highest priority equipment items, of how this non-motive equipment is actually used and what the demands are on the energy system. Furthermore, a quantitative understanding of the operational requirements was gathered.

The portable electronics realm was not covered at the workshop. However this market was engaged after the workshop, using existing contacts in this market provided by the DOE, and also our own research in this area. Similarly, the highest priority portable electronic uses were identified by engaging the man-portable power industry (both end users and manufacturers), and gaining a quantitative understanding of what the needs are for power, duration, frequency of use, and environmental durability if fuel cells were to meet or exceed the capabilities of the current (typically battery-based) portable electronics power systems.

Results

A picture of the attendees for the Sandia-CA workshop held on 2/8/2011 is shown in Figure 1. In all, 22 “end-users” and nine “technology experts” attended the workshop. There were a total of 40 attendees. In the morning the attendees heard fuel cell technology presentations from DOE (Scott McWhorter) and Sandia (Lennie Klebanoff). For the remainder of the morning, the group heard presentations on uses of equipment in construction (Torsten Erbel, Multiquip), entertainment (Russ Saunders, Saunders Electric), telecommunications (Kevin Kenny, Sprint) and in aviation ground support (Roger Hooson, San Francisco International Airport). In the afternoon, break-out sessions were held in the areas of construction equipment, portable power, aviation GSE, and telecom backup power. For each breakout session, we sought to identify the top three highest-priority pieces of equipment to target in each category, and for each one solicit information on the following questions: Who is using it?, How is it being used?, What are the environmental and worksite conditions?, What are the performance requirements?, What is the cost sensitivity?, What works well now, what doesn’t, what could be improved?

From the breakout sessions, the highest priority pieces of equipment were found to be:

Aviation GSE

1. 5–10 kW power generators, the power basis for light towers, light crosses, light ropes, and hand tools. These



FIGURE 1. Workshop Attendees Visiting Sandia-CA on February 8, 2011

were identified as high priority because there are so many of them. These are typically Honda gasoline generators.

2. 90–120 kW portable power based on diesel generators and turbine systems for aircraft electrical support and engine start.
3. Heater carts, run on diesel, 400,000 Btu, 160 hp, used to heat the interiors of aircraft during maintenance. It is important to heat the aircraft during maintenance periods because one cannot allow condensation on the avionics during maintenance.

Some key pieces of learning from the Aviation GSE breakout session were that such equipment is very cost sensitive, the end-users have little desire to pay extra for fuel cell versions. This group also stated that although the fuel cell life cycle savings over diesel equipment carries weight, that argument has a time horizon of only five years or less.

Portable Power

This breakout session identified the following high-priority pieces of equipment:

1. 2–6.5 kW: gasoline generator replacement
2. 60–100 kW: diesel generator replacement
3. 3–5 kW: office trailer generator

Some key learning from this group are that only 2,500 hours of operational life are expected for current small units (~5 kW). In addition, while the capital expense for small generator sets is currently $400-$600/kW, the yearly operating expense can be $700/kW. So the current diesel equipment is very expensive to maintain and operate.

Telecom Backup Power

In this realm, the highest priority item is a 5–30 kW backup power system. Some key learning from this area are that cell phone towers are often placed in very high density areas, making the footprint of a fuel cell-based backup power system very critical.

Construction Equipment

This breakout session identified the following high-priority pieces of equipment:

1. Lighting: Light towers, portable message boards, remote message boards, arrow signs. These are ubiquitous items, currently diesel-powered.
2. Air Compressors: Noisy, much room for improvement of this technology.
3. Scissor Lifts: Want quiet, non-polluting equipment, and more reliable than battery-based.

Some key learning from this breakout session are that construction equipment is very cost sensitive. Lifecycle costs, even project-cycle costs are considered. Furthermore, construction equipment must be very durable. The attendees indicated that because fuel cells "load follow", and only generate power to meet the load demanded, this "smart technology" aspect may be a way for a fuel cell system to gain acceptance faster.

The questionnaires were analyzed using the Kano methodology. An example of how the Kano methodology was used is shown in Figure 2. The question being asked is: "How would you feel if this equipment could be refueled quickly?" In this example, the collection of data points in

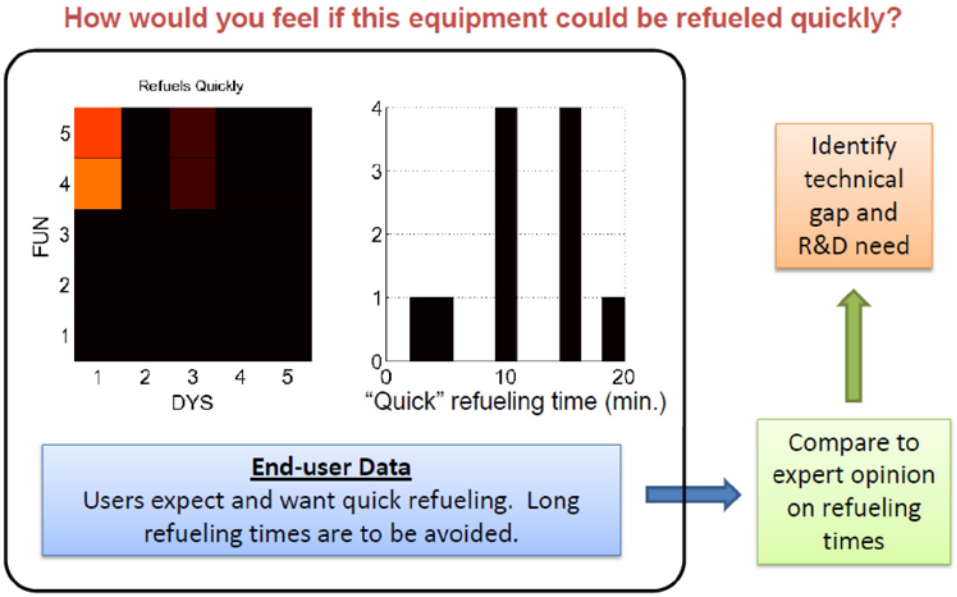


FIGURE 2. Figure Describing an Example Use of Kano Methodology in Extracting Information from Surveys

the upper-left corner of the left-hand figure reveals that end-users not only want quick refueling times, but expect it. That means if refueling times are long, they will be dissatisfied with the equipment. The right-hand figure shows how the end-users define "quick" in terms of number of minutes needed to refuel a tank. Overall, the conclusion is that a hydrogen fuel tank needs to be able to be refueled in about 10–15 minutes or less to gain user acceptance. This data can then be compared to the capability of current hydrogen storage technology to see if improvements in actual refueling times are needed.

Work is ongoing collecting similar market feedback from the portable electronics community.

Conclusions and Future Directions

We have engaged end-users, manufacturers and technology experts in the non-motive equipment realms of construction equipment, portable power, aviation GSE and portable electronics. We have identified high-priority early market non-motive pieces of equipment that would benefit by conversion to fuel cell operation. We have gained a quantitative understanding of the energy requirements for these items, how they are used, and what the environmental requirements are. With this information, the DOE will be able to identify the performance gaps in current hydrogen storage technology that would allow fuel cells to be used in these early market non-motive applications.

Sandia National Laboratories is a multi-program laboratory managed and operated by Sandia Corporation, a wholly owned subsidiary of Lockheed Martin Corporation, for the U.S. Department of Energy's National Nuclear Security Administration under contract DE-AC04-94AL85000.

IV.E.5 Analysis of Storage Needs for Early Motive Fuel Cell Markets

Jennifer Kurtz (Primary Contact), Chris Ainscough, Melanie Caton, Lin Simpson
National Renewable Energy Laboratory
1617 Cole Blvd.
Golden, CO 80401
Phone: (303) 275-4061
E-mail: jennifer.kurtz@nrel.gov

DOE Manager
HQ: Ned Stetson
Phone: (202) 586-9995
E-mail: Ned.Stetson@ee.doe.gov

Subcontractor:
Energetics Inc., Columbia, MD

Project Start Date: October, 2010
Project End Date: September, 2011

Fiscal Year (FY) 2011 Objectives

- Identify needs for onboard energy storage in key early motive markets.
- Target early motive markets such as material handling equipment (MHE), ground support equipment (GSE), public transit, and unmanned vehicles.
- Identify gaps of current hydrogen storage technologies to the onboard energy storage needs.

Technical Barriers

This project addresses the technical barrier of a lack of knowledge of energy storage performance needs for early fuel cell motive markets.

Technical Targets

This project is investigating gaps of current hydrogen storage technologies against the needs of onboard energy storage in early motive markets. Insights gained from this investigation will be used to focus research and development (R&D) efforts in hydrogen storage technologies that can accelerate market adoption.

FY 2011 Accomplishments

- Organized and completed two workshops held in conjunction with the Fuel Cells and Hydrogen Energy Association conference and ProMat2011 expo.
- Summarized top needs for MHE and public transit onboard energy storage based on workshop breakout groups.
- Participated in "Utilizing Hydrogen Power as an Alternative Energy Source" and non-motive stakeholder workshop.
- Implemented Kano Method into questionnaire development and analysis to classify solution-independent customer needs.
- Completed and transmitted electronic questionnaire to key stakeholders and end-users in key early motive markets.
- Collaborated with Sandia National Laboratories (lead for similar activity with non-motive applications) and Pacific Northwest National Laboratory (lead for technology readiness assessment of hydrogen storage technologies).



Introduction

The market adoption of non-motive fuel cell systems can be accelerated by improving storage system technologies. Effective improvements in hydrogen storage systems will result in extended product run times, increased productivity, decreased installation and operating costs, improved delivery methods, improved volumetric capacity, and facilitation of siting and permitting processes. These improvements can be achieved through focused R&D efforts based upon an in-depth understanding of storage requirements in key early markets. As fuel cell systems penetrate these early markets, increased manufacturing volumes, learning-by-doing, and technology advancements will result in cost reductions and performance improvements. Additional market opportunities will open up for fuel cell systems as they become established in key early markets. Early motive fuel cell markets with hydrogen storage can be categorized in three segments:

- **Material Handling and Ground Equipment.** This market includes traditional forklifts and pallet jacks for material handling in warehouses and manufacturing facilities, as well as other ground equipment used in airports, mining operations, and grounds keeping/maintenance operations.
- **Public Transit.** This market includes transit services (urban routes, commuter and para-transit) and shuttle services (airport, campus and large events).
- **Niche Motive Markets.** These markets include applications for unmanned air vehicles, heavy-duty trucks, and other military motive applications.

Approach

NREL is identifying storage R&D needs for fuel cell systems for these early markets by obtaining information

from the broad set of contacts. NREL is leveraging: 1) understanding of early motive market applications through data analysis in NREL's Hydrogen Secure Data Center, 2) expertise in hydrogen storage, and 3) existing industry contacts.

NREL used workshops for gathering and prioritizing hydrogen storage needs, dialog within and across applications, along with conducting interviews with individual companies. NREL is also using an electronic questionnaire designed to categorize the user's needs for onboard energy storage. The questionnaire is based on the Kano Method and identifies important performance metrics and the corresponding quantitative performance levels without specifying a storage technology. Response from the workshops and questionnaires are the basis for the analysis to detail performance gaps of existing hydrogen storage technologies.

Results

The majority of work completed to date has been focused on the information gathering and analysis preparation. Figure 1 is a snap shot of the first two pages of the electronic questionnaire. The questions are asked in positive and negative pairs along with a third question to gather the quantitative data. Topics covered in the questionnaire include run time, refueling, weight, volume, operation lifetime, operation conditions (e.g. temperature, shock and vibration, and environment), safety (procedural controls), cost (e.g. operation, fuel, maintenance, and end of life), preventative maintenance, availability, emissions, reliability, time for maintenance, operator training and expertise, and warranty. To date, 34 people have submitted their responses.

NREL also used workshops held in conjunction with market relevant conference(s) and expo(s) to capitalize on end user attendance. The workshops focused on breakout sessions with two questions:

1. What are the key performance needs for your application?
2. How could advanced onboard energy storage technology improve the performance of your vehicles or operation?

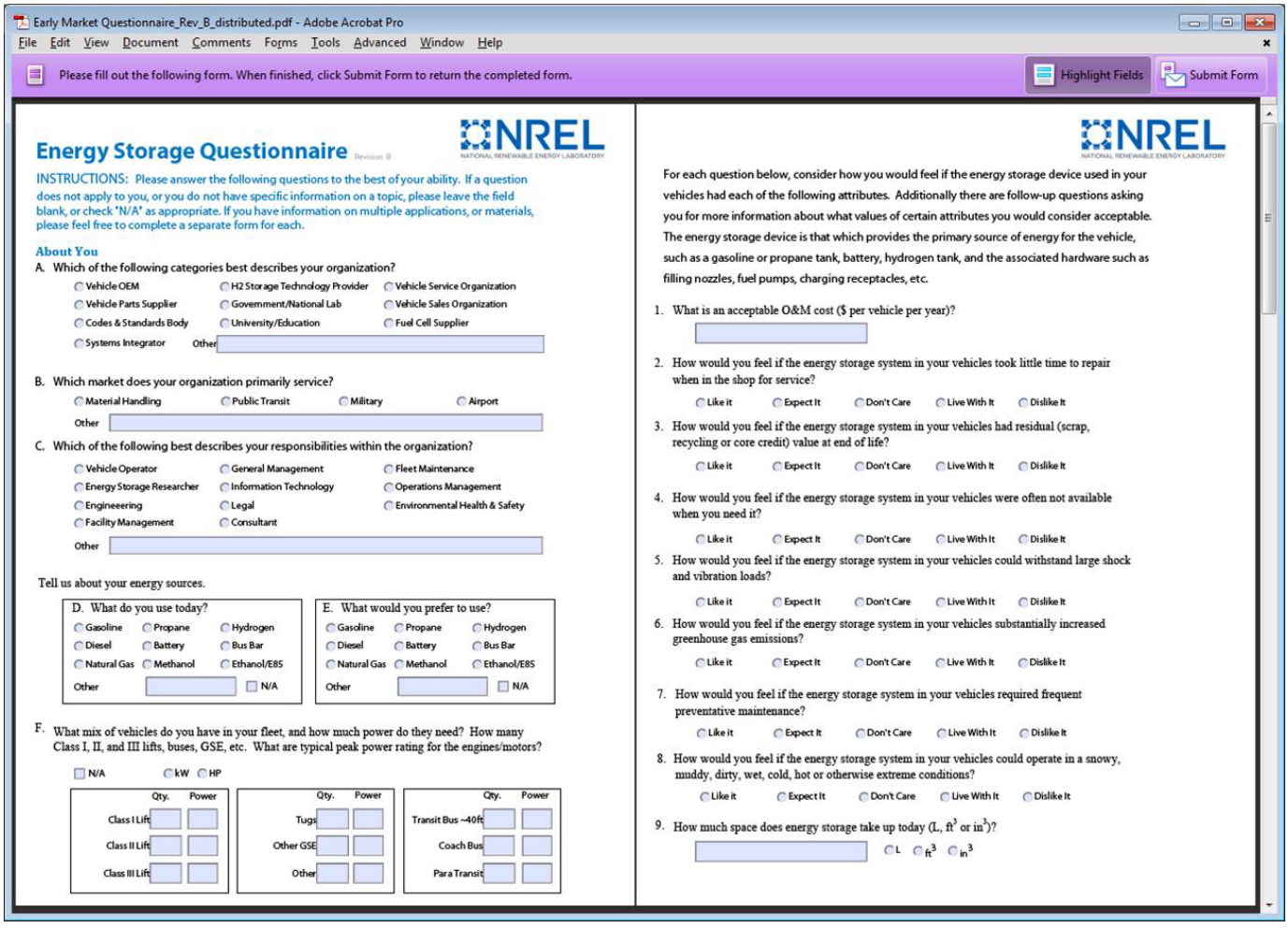


FIGURE 1. Pages 1 and 2 of Electronic Questionnaire

A summary of the top performance needs in MHE as discussed in the workshops are:

- Robust tanks capable of high cycling (fill frequency) over 10 years.
- Certified field support with low maintenance requirements (e.g. 2-3 maintenance hours per 500 operation hours) and cost.
- Onboard storage capacity limits should be about one shift (5 to 8 hours).
- Onboard energy storage should be easy to use with fast and convenient filling.
- Flexible storage designs to fit within existing or custom products.
- Simple, low-cost options to compete with incumbent technologies.

A summary of the top performance needs in public transit as discussed in the workshop are:

- Low cost of storage through consistent tank system designed for low weight.
- Low storage system weight.
- Operation period should match that of the bus (e.g., 12 years/500,000 miles or ~5,000 tank cycles) with a daily operation range of between 200 and 250 miles.

We completed an early set of draft results. Figure 2 includes results for storage capacity, fill rate, operation lifetime, and preventative maintenance. At the time of this figure creation, most of the responses were from the MHE application. (The response analysis in the final report will be broken down by application and the other performance categories.) The four metrics in Figure 2 are all important to the responders and the corresponding bar charts breakdown the expected performance level. For instance, storage capacity is an important metric and most of the responders say that 8-10 hours is the necessary capacity level.

Conclusions and Future Direction

The analysis preparation and workshops have created a foundation for identifying the onboard energy storage needs and the following gap analysis task. So far, the performance needs are application specific and focus around robustness, simplicity, runtime, weight, and cost.

Planned future work includes:

- Continue questionnaire response and information gathering.
- Continue analyzing response and workshop data and summarizing important performance metrics and the corresponding performance levels.

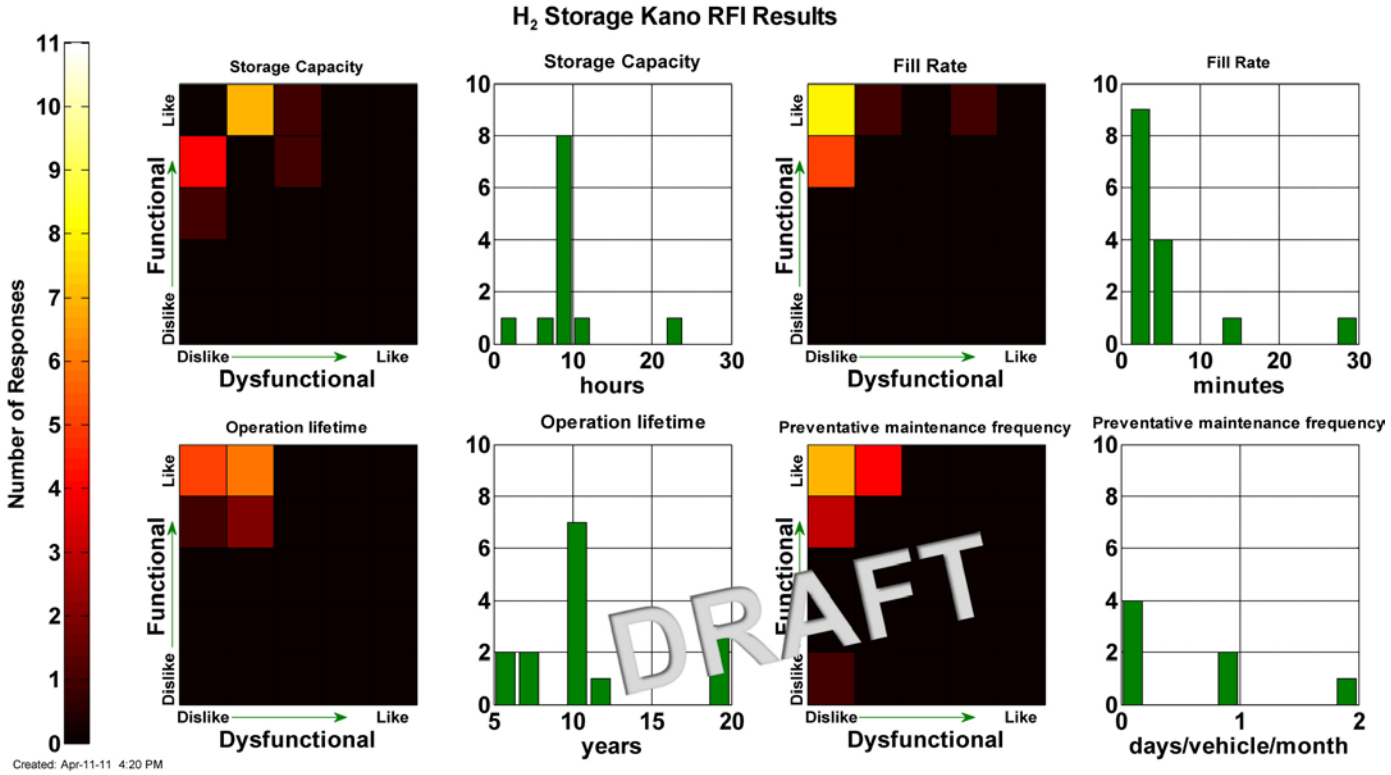


FIGURE 2. Draft Results of Important Performance Metrics using Kano Method

- Summarize capabilities of current hydrogen storage technologies.
- Gap analysis of current hydrogen storage technologies to the early motive fuel cell markets' onboard energy storage needs.
- Complete final report.

FY 2011 Publications/Presentations

1. Kurtz, J.; Ainscough, C.; Simpson, L. "Analysis of Storage Needs for Early Motive Fuel Cell Markets," Presented at DOE's Annual Merit Review, May 13, 2011.

IV.E.6 Standardized Testing Program for Solid-State Hydrogen Storage Technologies

Michael A. Miller (Primary Contact) and
Richard A. Page
Southwest Research Institute® (SwRI)
6220 Culebra Road
San Antonio, TX 78238
Phone: (210) 522-2189; 522-3252
E-mail: mmiller@swri.org; richard.page@swri.org

DOE Managers
HQ: Ned T. Stetson
Phone: (202) 586-9995
E-mail: Ned.Stetson@ee.doe.gov
GO: Jesse Adams
Phone: (720) 356-1421
E-mail: Jesse.Adams@go.doe.gov

Technical Advisor
George Thomas
Phone: (202) 586-8058
E-mail: George.Thomas@hq.doe.gov

Contract Number: DEFC3602AL67619

Subcontractor:
Ovonic Hydrogen Systems LLC, Rochester Hills, MI

Start Date: October 1, 2006
Projected End Date: March 30, 2012

Fiscal Year (FY) 2011 Objectives

Overall

- Support DOE's Hydrogen Storage sub-program by operating an independent, national-level reference laboratory aimed at assessing and validating the performance of novel and emerging solid-state hydrogen storage materials and full-scale systems.
- Conduct measurements using established protocols to derive performance metrics: capacity, kinetics, thermodynamics, and cycle life.
- Support parallel efforts underway within the international community, in Europe and Japan, to assess and validate the performance of related solid-state materials for hydrogen storage.
- Validate the technologies required to achieve the 2015 DOE on-board vehicle hydrogen storage goals.
- Continue new hydrogen storage materials discovery research and development for advanced storage systems.

Current

Analyze hydrogen sorption properties at 77 and 298 K of:

- Polyether ether ether ketone (PEEK)-derived carbon (material provided by the State University of New York, SUNY).
- Microporous carbon (material provided by the National Renewable Energy Laboratory, NREL).
- Porous polymer network (PPN) (material provided by Texas A&M University, TAMU).

Technical Barriers

The technical barriers associated with the operational objectives of the laboratory are:

- Standardization of methods suitable to a wide variety of compositions of matter.
- Development and implementation of "Gold Standard" measurement techniques.

Moreover, this project addresses the following technical barriers from section 3.3.4.2 of the Fuel Cell Technologies Program Multi-Year Research, Development and Demonstration Plan:

- Verification of Material Performance
  (P) Lack of Understanding of Hydrogen Physisorption and Chemisorption
  (A) Reproducibility of Performance
- Verification of System Performance
  (K) System Life-Cycle Assessment
  (Q) Reproducibility of Performance
- (F) Codes and Standards

Technical Targets

This project addresses the fundamental need for establishing a national-level laboratory whose core mission is to study and independently verify the intrinsic sorption characteristics of novel and emerging materials for hydrogen storage, including such activities as they pertain to their use in full-scale storage systems. As a fully qualified laboratory under the purview of the DOE, the laboratory plays a central role in down-selecting materials and systems that emerge from the centers of excellence and outside entities by:

- Providing in-depth analysis and understanding of hydrogen physisorption and chemisorption mechanistic behavior.

- Determining and validating material and system storage capacities.
- Determining material and system kinetics (charging/discharging rates), thermodynamics, and cycle-life durability.
- Contributing to the testing requirements for codes and standards of full-scale systems.
- Providing listing and labeling services for full-scale systems such as fire safety performance.

FY 2011 Accomplishments

- Validated the hydrogen sorption capacity in PEEK-derived carbon at 77 and 298 K using material provided by SUNY. Experimental measurements showed:
  - Maximum excess concentration of 5.5 wt% at 77 K and 49 bar.
  - Absolute volumetric capacity approaching 38 g/L at 77 K and 71 bar.
- Evaluated the hydrogen sorption capacity in microporous carbon at 77 K using material provided by NREL, which showed 4.8 wt% gravimetric excess adsorption at 45 bar and a volumetric capacity of 28.2 g/L at 70 bar.
- Validated the hydrogen sorption capacity in PPN at 77 and 298 K using material provided by TAMU.

✧ ✧ ✧ ✧ ✧

Introduction

Promising classes of materials being developed for reversible on-board hydrogen storage have emerged, thus compelling a rigorous and independent evaluation of their storage capacity, thermodynamics, and kinetics. Occasionally, entirely new chemistries or structural motifs are discovered that yield unexpected properties which must be further studied or validated. Notably, metal organic frameworks (MOFs) [1], destabilized nitrogen-based metal borohydrides [2], and spillover compounds of MOFs and nanoporous carbon materials [3,4] have captured the interest of researchers over the past five years. These examples have resulted in surprisingly favorable storage properties which approach the sought-after material targets for on-board storage (Figure 1).

The laboratory has continued to evaluate important new classes of materials whose validation of hydrogen storage properties is regarded as a high-priority within the solid-state storage community and the DOE. The most recent priorities for the laboratory have concentrated on evaluating hydrogen sorption in PEEK-derived nanoporous carbon and more conventional microporous carbon. A significant amount of experimental and modeling effort was dedicated to the analysis of a PPN based on tetrakis(4-bromophenyl) silane building units [PPN-4(Si)] developed by H-C Zhou's

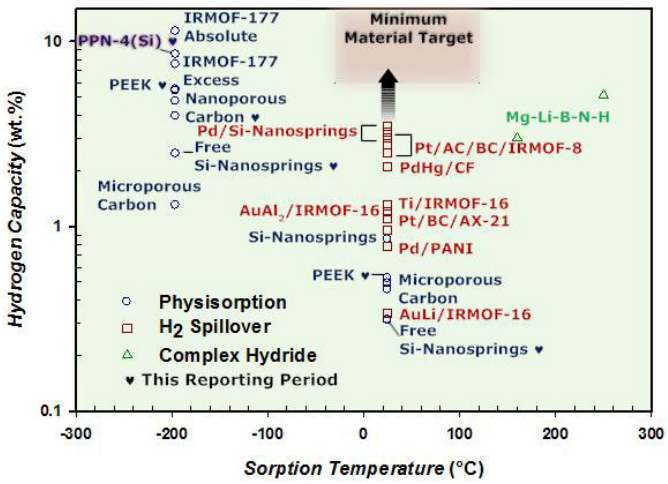


FIGURE 1. Status of material technologies for reversible hydrogen storage via physisorption, spillover, and chemisorption in proximity to DOE material target. New benchmark for excess adsorption is highlighted.

group at TAMU [5]. This material has been shown to exhibit exceptionally-high Brunauer-Emmett-Teller specific surface areas (6,470 m^2/g) with a correspondingly-high gravimetric excess capacity (8.5 wt% at 60 bar) at 77 K: the highest surface area and hydrogen uptake reported to date for a physisorption material.

Approach

Validating the sorption behavior of storage materials and uncovering the mechanisms involved are approached through close collaboration with researchers among the materials centers of excellence (e.g., the Physisorption Center of Excellence), the international community, and SwRI's Internal Research & Development (IR&D) program. The laboratory employs a "best practices" approach based on standard operating procedures-documented analytical methods to critically evaluate novel storage materials of potential impact to the sought-after storage goals. By leveraging SwRI's IR&D program, fundamental aspects of materials research are addressed where critical knowledge or physical matter is presently lacking. This element of the program provides a venue for the discovery of new materials and the elucidation of unknown mechanisms.

Results

PEEK-Derived Carbon

The results of our studies over the past year are highlighted in Table 1. In the case of PEEK-derived carbon (as well as other carbon materials), high-pressure volumetric analysis was encumbered by this material's propensity to absorb helium, thus invalidating the use of a helium calibration for determining the skeletal density of the sample (or free volume of the system). To overcome this

TABLE 1. Overall Summary of Results for Various Classes of Storage Materials under Investigation

Material	Source	Surface Excess Amount (wt% H)		Absolute Volumetric Capacity (g/L) 77 K	MOF-177 Benchmark 77 K	
		298 K	77 K		(wt% H)	(g/L)
CO_2-Activated PEEK-Derived Carbon	Duke University	0.52 @ 80 bar	5.39 @ 55 bar	30 @ 70 bar	7.5 @ 70 bar	47 @ 70 bar
PEEK-Derived Carbon	SUNY	0.31 @ 81 bar	5.50 @ 49 bar	38 @ 71 bar		
Microporous Carbon	NREL	0.49 @ 80 bar	4.75 @ 45 bar	28 @ 70 bar		
Porous Polymer Network [PPN-4(Si)]	TAMU	0.97 @ 92 bar	8.48 @ 60 bar	28 @ 86 bar		

analytical challenge, the high-pressure gravimetric technique was employed to measure the hydrogen isotherm at room temperature. We then assume in the formal definition of the Gibbs excess that the free energy of the adsorbed fluid is equal to the bulk-gas free energy plus a surface potential term, which we equate to the measured Gibbs excess for the gravimetric mass balance, and thus arrive at a simplified local density (SLD) model. When combined with the Bender equation state to accurately calculate hydrogen gas densities and the gas fugacity, the combined expressions for the SLD model were used in a fitting algorithm to derive the hydrogen skeletal density and the pore volume of the sample by treating these characteristic properties as fitting parameters [6].

The corrected hydrogen isotherms at 77 K measured by the volumetric technique are shown in Figure 2. Here the maximum excess concentration for hydrogen uptake was 5.50 wt% at 49 bar. Using the pore volume derived from the SLD model and fitting algorithm, the profile for absolute volumetric capacity was computed. The absolute volumetric capacity for this material approached 38.2 g/L at 71 bar and, while this is a remarkable result, it falls slightly short of the current benchmark of 40 g/L at 70 bar for MOF-177.

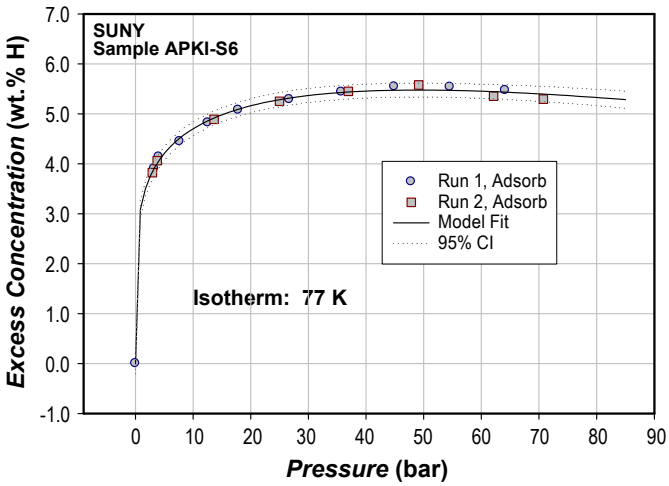


FIGURE 2. Low-temperature (77 K) hydrogen isotherms measured for PEEK-derived nanoporous carbon.

Microporous Carbon

Low-temperature (77 K) hydrogen isotherms were determined using the volumetric technique, again employing the gravimetric technique at room temperature and the SLD model to determine the skeletal density and pore volume of this material. The corrected hydrogen sorption profile, shown in Figure 3, was constructed from four separate analyses due to the long equilibration times associated with each pressure point in the profile. The combined data was fitted to a dose response model in order that the statistical variance of the measurements and the peak excess could be derived. Based on the model fit, a peak uptake for surface excess of 4.75 wt% at 45.3 bar was calculated. The absolute volumetric capacity at 77 K was also determined using the semi-empirically derived pore volume (gravimetric analysis). On this basis, an absolute volumetric capacity of 28 g/L was computed at 69 bar.

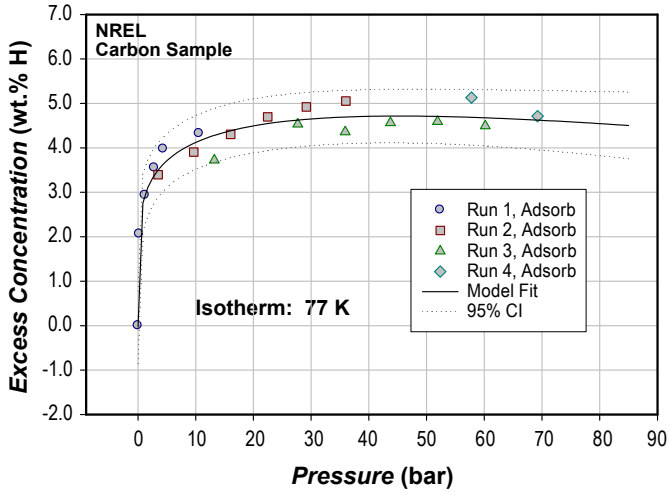


FIGURE 3. Low-temperature (77 K) hydrogen isotherms measured for microporous carbon.

PPN

As in the previous cases for highly active, high surface-area physisorption materials, the analysis of PPN-4(Si) required special attention due to this material's tendency to adsorb helium, thus preventing accurate measurement of the true Gibbs excess concentration and subsequent determination of absolute volumetric capacity. This behavior required that the actual skeletal density be determined using the gravimetric technique. We determined the skeletal density using hydrogen gas and adopted the SLD model as described previously. Additionally, the extremely high specific surface area (6,470 m^2/g) and low bulk density of this material required careful handling methods to prevent fluidization during weighing and sample transfers. These properties further required that the material be mechanically compacted in the sample vessel prior to analysis.

The room temperature gravimetric hydrogen isotherms for the Gibbs excess are compared in Figure 4 with analyses using the volumetric technique at room temperature. The two results are shown to correlate very well after correcting the volumetric measurements for the SLD-derived skeletal density.

The same SLD-derived skeletal density was used to correct low-temperature hydrogen isotherms. After taking into consideration thermal gradient effects, the corrected hydrogen isotherm curves derived from the analyses are represented in Figure 5. In this case, two adsorption and desorption runs (Runs 1 and 2), with thermal-vacuum conditioning between them, were required to construct the composite full-pressure isotherm curves. In order to derive characteristic parameters for the composite data points, a parametric dose-response model was used. The fitted values for the maximum Gibbs-excess concentration at 77 K was 8.4 wt%, which occurred at 60 bar and is higher than our benchmark material, MOF-177 (Table 1).

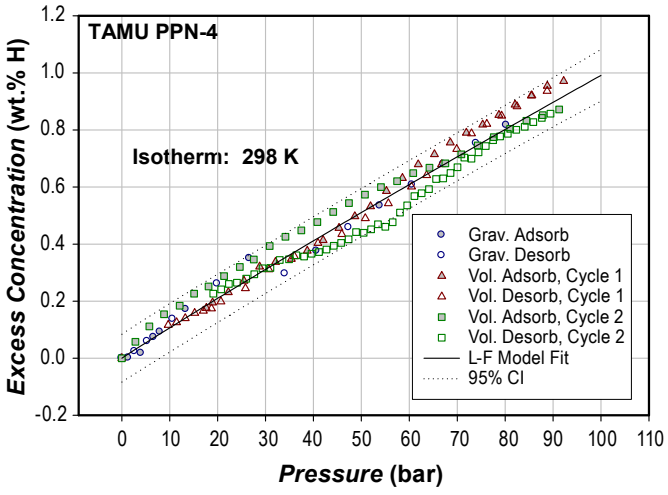


FIGURE 4. Room temperature (298 K) hydrogen isotherms measured for PPN [PPN-4(Si)] using both the volumetric and gravimetric techniques.

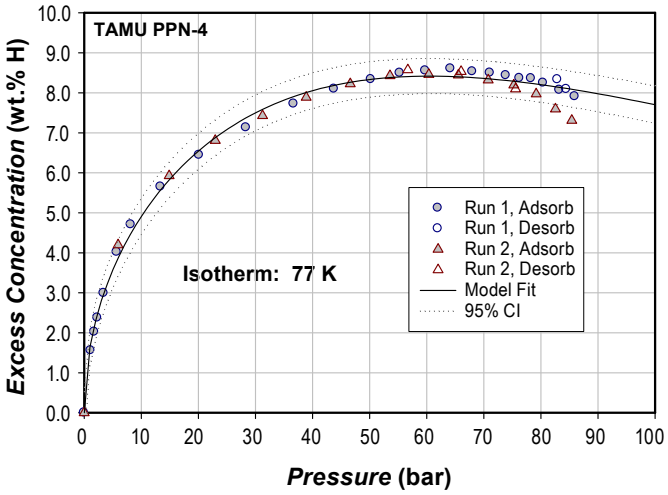


FIGURE 5. Low-temperature (77 K) hydrogen isotherms measured for PPN [PPN-4(Si)] using the volumetric technique.

Additionally, the absolute volumetric capacity was estimated using the SLD-derived skeletal density and adsorbed volume (i.e., pore volume). A value of ~28 g/L absolute volumetric capacity was calculated at 85 bar (77 K). Presently, we have not verified the absolute data theoretically using void-space routines and the kinetic diameter of hydrogen (or helium) since the material is completely amorphous.

Conclusions and Future Directions

In the search for novel forms of active materials for physisorption storage, robust materials have emerged with remarkably high surface areas. Nanoporous carbon derived from PEEK exhibits promising characteristics for hydrogen storage in terms of specific surface area and chemical stability. We found from previous analyses that two forms of such PEEK-derived materials, Duke vs. SUNY, prepared by independent process methods yielded remarkably similar results (Table 1). Additional gains in performance may, however, still be possible as processing methods for the PEEK polymer are further refined.

While the development of new physisorption materials with high surface areas prepared from the pyrolysis of high-melt polymers are promising venues to meeting the much sought-after storage targets, our analyses indicate that engineering the self-assembly of novel classes of non-pyrolytic materials from molecular building units into three-dimensional (amorphous) PPN results in the establishment of a new benchmark in performance for hydrogen excess adsorption: 8.5 wt% at 77 K and 60 bar. An important advantage that PPN structural motifs appear to offer over the existing benchmark, MOF-177, lies in their remarkable thermal and chemical stability, which can be attributed to their entirely covalent bonding network. Indeed, PPNs can be handled in an open-air laboratory environment without

impacting their performance. Studies in the future should examine post-synthetic methods of improving the volumetric capacity of these materials, which currently falls short of the MOF-177 benchmark, by examining what effects high-pressure mechanical compaction (i.e., pelletizing) may have on the gravimetric and volumetric capacity of PPN.

References

1. Furukawa, H.; Miller, M.A.; Yaghi, O.M. *J. Mat. Chem.* **2007**, *17*, 3197-3204.

2. Yang, J.; Studik, A.; Siegel, D.J.; Halliday, D.; Drews, A.; Carter, R.O.; Wolverton, C.; Lewis, G.J.; Sachtler, J.W.A.; Low, J.J.; Faheem, S.A.; Lesch, D.A.; Ozolins, V. *Angew. Chem. Int. Ed.* **2008**, *47*, 882-887.

3. Y.W. Li and R.T. Yang, *J. Am. Chem. Soc.*, **2006**, 128, 8136-8137.

4. Y.W. Li and R.T. Yang, *J. Am. Chem. Soc.*, **2006**, 128, 12410-12411.

5. Yuan, D.; Lu, W.; Zhao, D.; Zhou, H-C *Adv. Mater.* **2011**, DOI: 10.1002/adma.201101759.

6. Puziy, A.M.; Herbst, A.; Poddubnaya, J.G.; and Harting, P., *Langmuir* **2003**, *19*, 314-320.

IV.E.7 Best Practices for Characterizing Engineering Properties of Hydrogen Storage Materials

Karl J. Gross (Primary Contact),
Russell Carrington[1], Steven Barcelo[1],
Abhi Karkamkar[2], Justin Purewal[3], Pierre Dantzer[4],
Shengqian Ma and Hong-Cai Zhou[5], Kevin Ott,
Tony Burrell and Troy Semeslberger[6],
Yevheniy Pivak and Bernard Dam[7],
Dhanesh Chandra[8]

H2 Technology Consulting LLC
8440 Central Ave. Suite 2A
Newark, CA 94560
Phone: (510) 402-4848
E-mail: kgross@h2techconsulting.com

[1]University of California Berkeley
[2]Pacific Northwest National Laboratory
[3]California Institute of Technology
[4]Université Paris-Sud
[5]Texas A&M University
[6]Los Alamos National Laboratory
[7]VU University Amsterdam and the Delft University of Technology
[8]University of Nevada, Reno

DOE Manager
HQ: Ned Stetson
Phone: (202) 586-9995
E-mail: Ned.Stetson@ee.doe.gov

Project Start Date: February 7, 2007
Project End Date: Project continuation and direction determined annually by DOE

Fiscal Year (FY) 2011 Objectives

- To prepare a reference document detailing best practices and limitations in measuring hydrogen storage properties of materials.
- The document will be reviewed by experts in the field.
- The final document will be made available to researchers at all levels in the DOE hydrogen storage program.

Technical Barriers

This project addresses the following technical barriers from the Storage section of the Fuel Cell Technologies Program Multi-Year Research, Development and Demonstration Plan:

(A) System Weight and Volume
(C) Efficiency
(D) Durability/Operability
(E) Charging/Discharging Rates
(J) Thermal Management
(Q) Reproducibility of Performance

Technical Targets

The goal of this project is to prepare a reference document detailing the recommended best practices and limitations in making critical performance measurements on hydrogen storage materials. This reference document will provide a resource to improve the accuracy and efficiency of critical measurements to aid the projects and ultimately the entire program to achieve or exceed the technical storage targets.

In particular this project is focused on the following target related performance measurements:

- Kinetics (Targets: system fill time for 5-kg hydrogen, minimum full-flow rate and start time to full-flow)
- Capacity (Targets: gravimetric and volumetric capacity)
- Thermodynamic Stability (Targets: maximum/minimum delivery pressure of H_2 from tank and impact on capacity and kinetic related targets)
- Cycle-Life Properties (Targets: cycle life and cycle life variation)

FY 2011 Accomplishments

- Modify 2010 Best Practices document with input from the National Renewable Energy Laboratory regarding clarifications of skeletal density and blank sample measurements.
- References collect for Cycle-Life section.
- Thermodynamics section input received and integrated from the Los Alamos National Laboratory.
- Received review of Thermodynamics section from Texas A&M University.
- Contributions to this project from world experts have been received including written materials, examples, presentation or editorial review of draft documents.
- Final Introduction section 100% complete.
- Final Kinetics section 100% complete.
- Final Capacity section 100% complete.
- Final Thermodynamic section in progress 95% complete.
- Final Cycle-Life Properties section in progress 95% complete.
- Draft Thermal Properties section started 15% complete.

- Posted updated Preface, Introduction, Kinetics and Capacity sections to DOE website for world-wide access. Please download the current document from: http://www1.eere.energy.gov/hydrogenandfuelcells/storage/test_analysis.html



Introduction

The Hydrogen Storage goal is the development of hydrogen storage materials that meet or exceed the DOE's targets for the onboard hydrogen storage in a hydrogen-powered vehicle. The growth of research efforts in this field and new approaches to solving storage issues has brought the talents of a wide-range of researchers to bear in solving the grand challenge of hydrogen storage. There is a need to have common metrics and best practices for measuring the practical hydrogen storage properties of new materials that are being developed within the Hydrogen Storage sub-program as well as at an international level. H2 Technology Consulting is tasked with creating a clear and comprehensive resource that will provide detailed knowledge and recommendations for best practices in the measurements of these properties.

Approach

This project is a combined approach of documenting the experience the principal investigator and other experts in the field have with these measurement, incorporating examples from the literature, performing experimental measurements to demonstrate important issues, and finally, condensing key information into a concise reference guide. Each section covers such topics as the overall purpose of the measurements, some basic theory, experimental consideration, methods of measurement, and many details on both material properties and experimental factors that may strongly influence the final results and conclusions. Participation from other experts in the field is being sought out for input, relevant examples, and critical review at all levels.

The current document has been reviewed by many experts from around the world. We greatly appreciate the collaborative efforts of all of the reviewers: Professor Gavin Walker, University of Nottingham, United Kingdom; Dr. Thomas Gennett of the National Renewable Energy Laboratory in Golden, CO; Dr. Gary Sandrock and Dr. George Thomas, consultants to the U.S. Department of Energy; Dr. Michael Miller of Southwest Research Institute in San Antonio, TX; Dr. Anne Dailly and Dr. Frederick Pinkerton of General Motors R&D Center; Dr. Ole Martin Løvvik of the Institute for Energy Technology in Kjeller, Norway; Dr. Eric Poirier of NRC Canadian Neutron Beam Centre Chalk River Laboratories, Canada; Professor Channing Ahn of the California Institute of Technology in Pasadena, CA; Dr. Kevin Ott, Dr. Anthony Burrell, and Dr. Troy Semelsberger of Los Alamos National Laboratory; Professor Richard Chahine, Université du Québec à Trois-Rivières, Canada; Professor Klaus Yvon, University of Geneva, Switzerland; Professor Sam Mao of the University of California Berkeley in Berkeley CA; and Dr. Nobuhiro Kuriyama and Dr. Tetsu Kiyobayashi of the National Institute of Advanced Industrial Science and Technology in Osaka, Japan. In addition, the work has been coordinated and has received important scientific input through our contract monitor Dr. Phil Parilla at the National Renewable Energy Laboratory.

Results

This year the Best Practices document had updates to the capacity measurements based on the need to elucidate measurement issues associated with low density, high surface area materials. In particular, the problems of small sample size and potential calibration errors due to helium adsorption. The need for blank sample measurements to validate accuracy was also addressed. The updated version including a preface, introduction, kinetics and capacity measurement sections is now posted on the DOE website.

This year's work focused in large part on finalizing the Thermodynamics and Cycle-Life measurements sections of the "Best Practices" document. For this work collaborations were established with the following contributing authors: Pierre Dantzer, Université Paris-Sud; Shengqian Ma and Hong-Cai Zhou, Texas A&M University; Kevin Ott, Tony Burrell and Troy Semeslberger, Los Alamos National Laboratory; Yevheniy Pivak and Bernard Dam, VU University Amsterdam and Delft University of Technology; and Dhanesh Chandra of the University of Nevada Reno. A rigorous review of the Thermodynamics section was completed by Professor Gavin Walker of the University of Nottingham. Through these collaborations the document has added perspectives of critical measurement issues from the three main materials research areas: on-board rechargeable hydrides, off-board regenerable hydrides, and hydrogen physisorption storage materials.

The objective of the thermodynamic section of the Best Practices document is to evaluate methodologies for determining equilibrium thermodynamics. In particular, there is a need to shed light on how to separate true equilibrium conditions from kinetic effects. Examples are included below of recent additions incorporated into the thermodynamic measurements section. Figure 1 shows a unique setup for high-throughput measurements of the enthalpy of formation of thin film combinatorial samples using Hydrogenography [1]. This method uses the classic conversion of pressure-composition-temperature isotherms of a reversible hydride to a van't Hoff plot for the determination of the enthalpy and entropy of hydride formation.

Hydrogenography consists of measuring the log of the optical transmission by means of a charge-coupled device

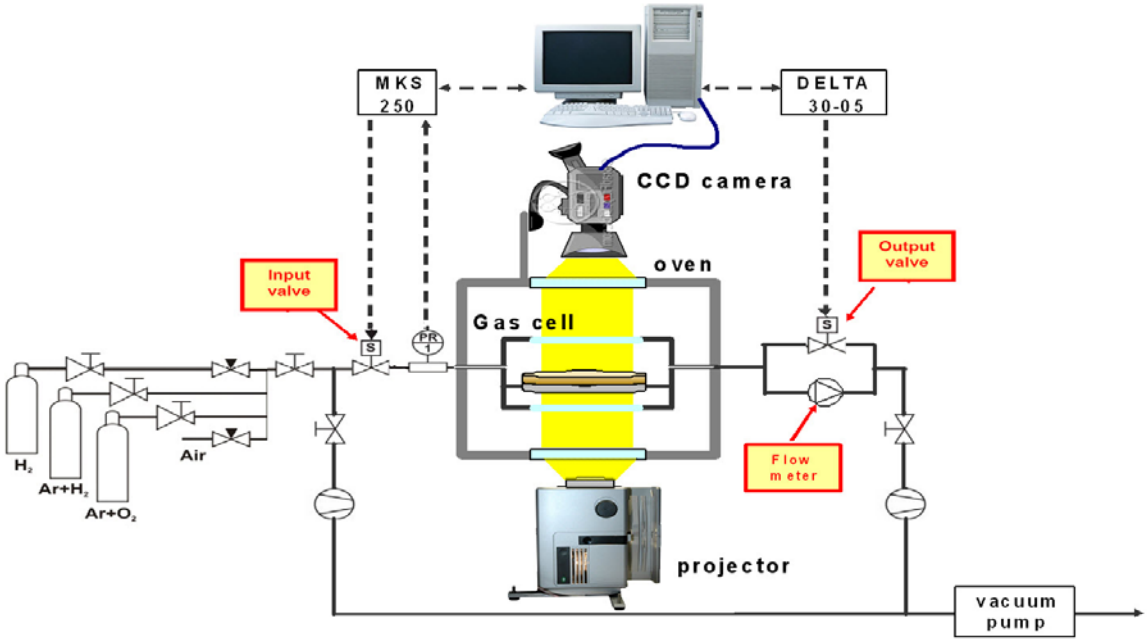


FIGURE 1. Schematic Representation of a Hydrogenography Setup [1]

camera through a thin film sample while increasing or decreasing the hydrogen pressure surrounding the sample. The optical transmission is proportional to the local hydrogen concentration of the material in the two-phase region. A rapid change in optical transmission indicates a hydride formation plateau. Thus, plateau pressures can be measured simultaneously at every point on two-dimensional combinatorial films having composition gradients. Repeating the measurement at several temperatures gives a van't Hoff plot for every point on the film and consequently every material composition. As an example of this, Figure 2 shows the phase diagram (left) and corresponding enthalpy map (right) of the Mg-Ni-Ti ternary system [2].

Cycle-life performance measurements are critical for evaluating the practical use of hydrogen storage materials in applications such as hydrogen-powered vehicles where hundreds to thousands of cycles will be required. An example of the impact on the hydrogen storage performance by making small changes in composition of the intermetallic compound $LaNi_5$ is show below in Figure 3.

The Cycle-Life measurement section covers the advantages and disadvantages of different measurement methods. For example, measurements of the cycle-life performance of hydrogen storage materials can be performed using pressure-temperature cycling or, in some cases, far more quickly by performing a thermal aging process on test

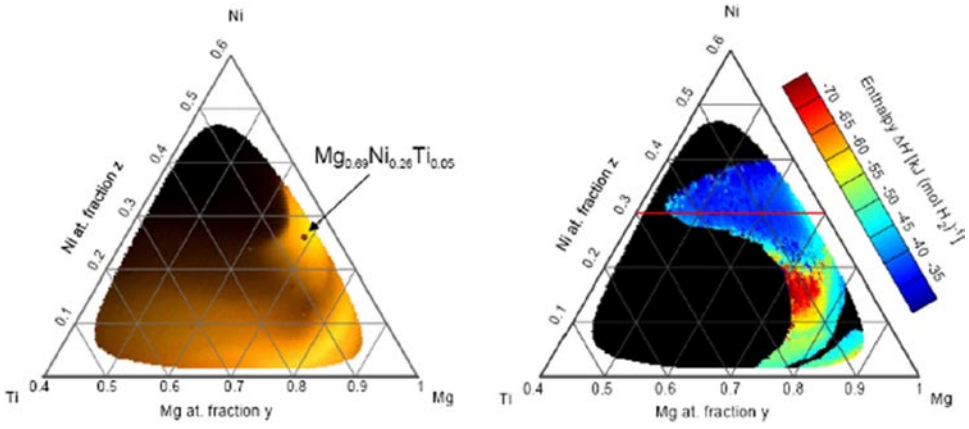


FIGURE 2. Ternary composition diagram (left) showing the final optical transmission state and the enthalpy map (right) of the Mg-Ni-Ti system, estimated using the optically determined hydrogenation plateaus. Black region on the right-hand picture represents chemical compositions that do not have a well defined plateau on the pressure-temperature isotherms [2].

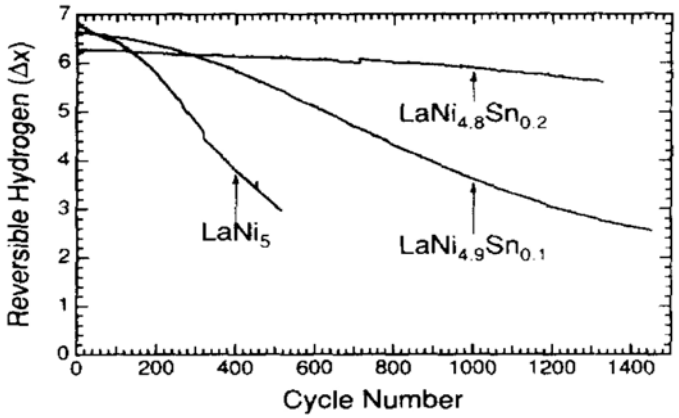


FIGURE 3. Hydrogen concentration changes Δx for $LaNi_{5-y}Sn_yH_x$ obtained from the maximum and minimum pressures for each cycle [3].

samples. In both cases, the measurements can be used to evaluate intrinsic performance degradation by using closed system designs which continuously cycle the same hydrogen gas. A comparison of results for $LaNi_5$ alloys using these two different methods and giving similar results is shown in Figure 4.

Conclusions and Future Directions

In FY 2011 we were able to establish important collaborations and technical assistance from experts in the field. We were able to update the Capacity section in a timely manner. We are currently working on completing the final versions of the Thermodynamic and Cycle-Life measurement sections.

FY 2011 Publications/Presentations

1. Gross, K.J., Carrington, R., Purewal, J., Barcelo, S. Karkamkar, Dantzer, P., Ma, S., Zhou, H.C., Ott, K., Burrell, T., Semeslberger, T., Pivak, Y., Dam, B., and Chandra, D. "Best Practices for Characterizing Hydrogen Storage Properties of Materials", IEA HIA Experts Meeting, April 11–15, 2010 in Death Valley, CA USA.

2. Gross, K.J., Carrington, R., Purewal, J., Barcelo, S. Karkamkar, Dantzer, P., Ma, S., Zhou, H.C., Ott, K., Burrell, T., Semeslberger, T., Pivak, Y., Dam, B., and Chandra, D. "Best Practices for Characterizing Hydrogen Storage Properties of Materials", IEA HIA Experts Meeting, January 16–20, 2011, Fremantle, Australia.

References

1. J.N. Huiberts, R. Griessen, J.H. Rector, R.J. Wijngaarden, J.P. Dekker, D.G. de Groot and N.J. Koeman, Nature 380 (1996) 231.

2. B. Dam, R. Gremaud, C. Broedersz, R. Griessen, Scripta Mater. 56 (2007) 853–858.

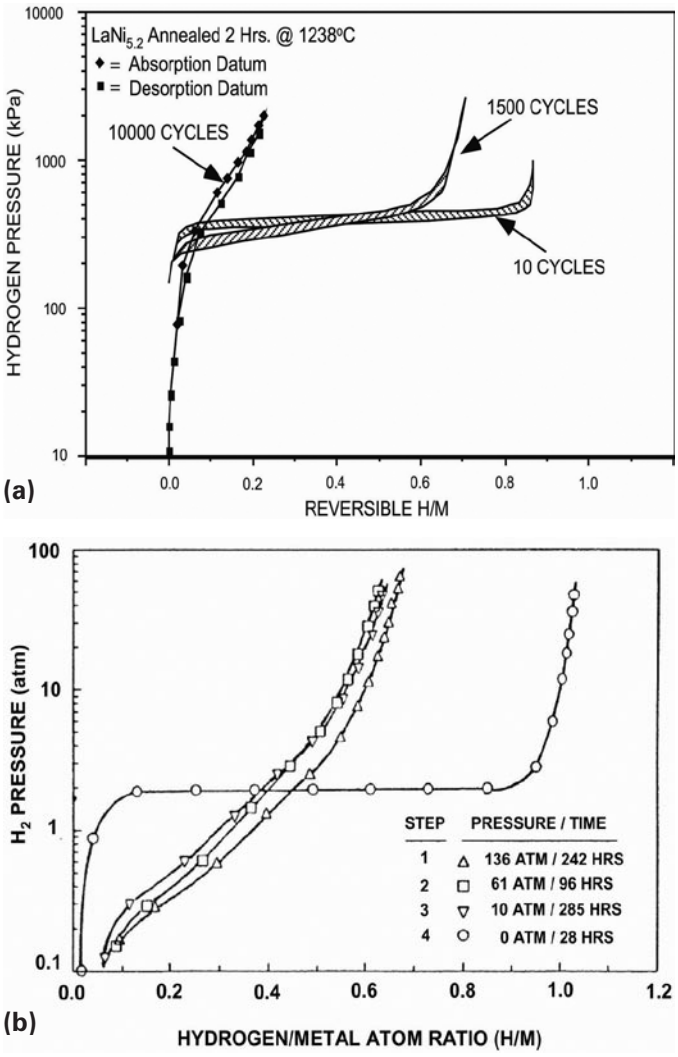


FIGURE 4. a) Isotherm of $LaNi_{5.2}$ taken at 25°C after intrinsic pressure-temperature cycling for: 10 (activation), 1,500, 10,000 cycles, showing severe degradation of this hydride [4]. b) Isotherms of $LaNi_5$ taken at 25°C after subjecting to thermal aging at high and low hydrogen pressures. Note that the isotherm (4) after vacuum aging the sample at 180°C is nearly the same as before aging indicating full reproportionation of the $LaNi_5$ hydride [5].

3. Bowman, R.C., Jr., Luo, C.H., Ahn, C.C., Witham, C.K., and Fultz, B. "The effect of tin on the degradation of LaNi5-ySny metal hydride during thermal cycling". J of Alloys and Comps 217 (1995) 185–192.

4. Chandra, D., "Intermetallics for hydrogen storage", in the book "Solid-state hydrogen storage, Materials and chemistry", edited by Gavin Walker, (2008) Woodhead Publishing Limited, Cambridge England, CRC Press, 327.

5. Sandrock, G.D., et al., "On the disproportionation of the intermetallic hydrides", Zeitschrift Fur Physikalische Chemie Neue Folge, 1989. 164: p. 1285-1290.

IV.E.8 Administration of H-Prize for Hydrogen Storage

Patrick Serfass
Hydrogen Education Foundation (HEF)
1211 Connecticut Avenue, NW, Suite 600
Washington, DC 20036
Phone: (202) 223-5547
E-mail: pserfass@ttcorp.com

DOE Managers
HQ: Ned Stetson
Phone: (202) 596-9995
E-mail: Ned.Stetson@ee.doe.gov
Paul S. Bakke
Phone: (720) 356-1436
E-mail: Paul.Bakke@go.doe.gov

Contract Number: DE-FG36-08GO18159

Subcontractor:
SCRA, Charleston, SC

Project Start Date: September 30, 2008
Project End Date: September 30, 2011

Objectives

- Over a three-year period, design and implement a pilot program for the initial H-Prize award under Section 654 of the Energy Independence and Security Act of 2007 (see the Introduction for a description of H-Prize).
  - If a qualified winner is identified, award $1 million for a significant advancement in hydrogen storage materials for light-duty vehicle applications.
- Create a pilot award process.
- Organize and execute a comprehensive fundraising program to supplement and/or create other awards under Sec. 654.
- Combine the fundraising program with a systematic process that deploys collected funds through fair and open competitions.

Technical Barriers

This project addresses the following technical barriers from section 3.3: Hydrogen Storage of the Fuel Cell Technologies Program Multi-Year Research, Development and Demonstration Plan:

(A) System Weight and Volume
(C) Efficiency
(D) Durability/Operability
(E) Charging/Discharging Rates
(G) Materials of Construction
(J) Thermal Management
(K) System Life-Cycle Assessments
(Q) Reproducibility of Performance
(R) Regeneration Process
(S) By-Product/Spent Material Removal

Technical Targets

H-Prize consists of a series of contests that leverage private funds with core funding provided by the federal government to broaden the base of investment in development of hydrogen technology and advance that technology into the marketplace.

The first H-Prize in this series, for hydrogen storage, was designed to address the challenges that exist in advancing automotive hydrogen storage for fuel cell electric drive vehicles. Its goal was to produce a material that has the potential to be an on-board rechargeable hydrogen storage material. Specifically, the H-Prize required that the storage material have the following characteristics:

- Gravimetric capacity of >7.5 wt% hydrogen (releasable hydrogen):
  - Reversible hydrogen capacity between -40 to +85°C, and between 1.5 to 150 bar hydrogen pressure.
- Volumetric capacity of >70 g/liter (releasable hydrogen):
  - Total volume of hydrogen ab/adsorbed by the solid plus the pressurized hydrogen contained within the pore spaces all divided by the total sample volume including the material's skeletal volume.
- Charging kinetics: greater than or equal to 4×10^{-4} (i.e. 0.0004) grams of hydrogen per gram of material per second:
  - Charging kinetics are to be measured with an inlet hydrogen gas temperature of between -40 to +85 degrees C and an inlet hydrogen pressure of not greater than 150 bar.
- Discharge kinetics: greater than or equal to 2×10^{-5} (i.e. 0.00002) grams of hydrogen per gram of material per second:
  - Discharge kinetics are to be measured at a sample temperature between -40 to + 85°C and with an outlet hydrogen pressure of greater than or equal to 1.5 bar.
- Cycle life of >100 cycles.
- At completion of 100 charge/discharge cycles from less than 5% to greater than 95% of reversible capacity, the sample's reversible capacity must still be greater than or equal to 95% of the gravimetric capacity target (i.e. ≥0.95 times 7.5 wt% or ≥ 7.1 wt%).

Figures 1 and 2 show the relationship between the state of the art for hydrogen storage in 2008 and 2011 compared to the gravimetric and volumetric targets for the hydrogen storage material sought by the first H-Prize.

Accomplishments

Task 1: Contest Rules

- Specific goals and technical targets were established in partnership with DOE staff.
- Feedback was sought from industry and the hydrogen community on technical evaluation criteria for initial H-Prize contest; draft criteria were presented to the Hydrogen and Fuel Cell Technical Advisory Committee (HTAC) in November 2008 and Hydrogen Interagency Working Group in December 2008.
- Set of criteria and basic contest parameters for inclusion in a draft Federal Register Notice was submitted to DOE for review and action in February and March 2009.

Task 2: Announce and Promote Contest

- Preliminary presentations made in November 2008 (to HTAC) and December 2008 (to the Hydrogen Interagency Working Group).
- First announcement was made at National Hydrogen Association Annual Conference in March-April 2009.
- Poster presentation during DOE Annual Merit Review in May 2009.
- Federal Register Notice released on August 26, 2009, announcing the beginning of the outreach campaign.
- HEF press released about contest on September 30, 2009.
- H-Prize website operational at http://hydrogenprize.org.
- Presentation about H-Prize to conference: *Hydrogen Production and Storage* in October 2009.
- Presentation at Resources for the Future in Washington: *The Role of Prizes in Innovation and Entrepreneurship* in December 2009.
- Scores of individual calls and e-mails were sent to people we could identify who were working in or interested in this niche area of hydrogen storage.
- E-mail campaigns were sent out to HEF's 30,000+ person hydrogen and fuel cell mailing list to attract other interest.
- Of 20 registrants, 15 submitted all the materials necessary to participate in the contest.

Task 3: Judging

- In consultation with DOE staff, the panel of judges was developed and their willingness to participate was confirmed.

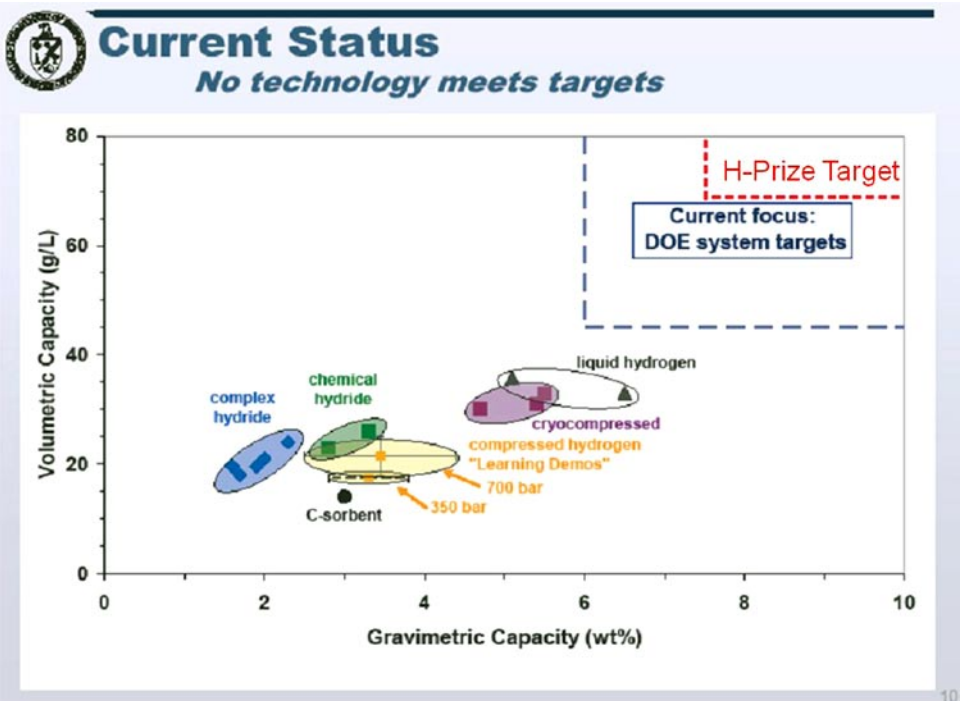


FIGURE 1. H-Prize Targets Relative to the State of Hydrogen Storage Technology as Reported by DOE in 2008 (modified from "Hydrogen Storage," Sunita Satyapal, 2008 Annual Merit Review Proceedings to include H-Prize targets)

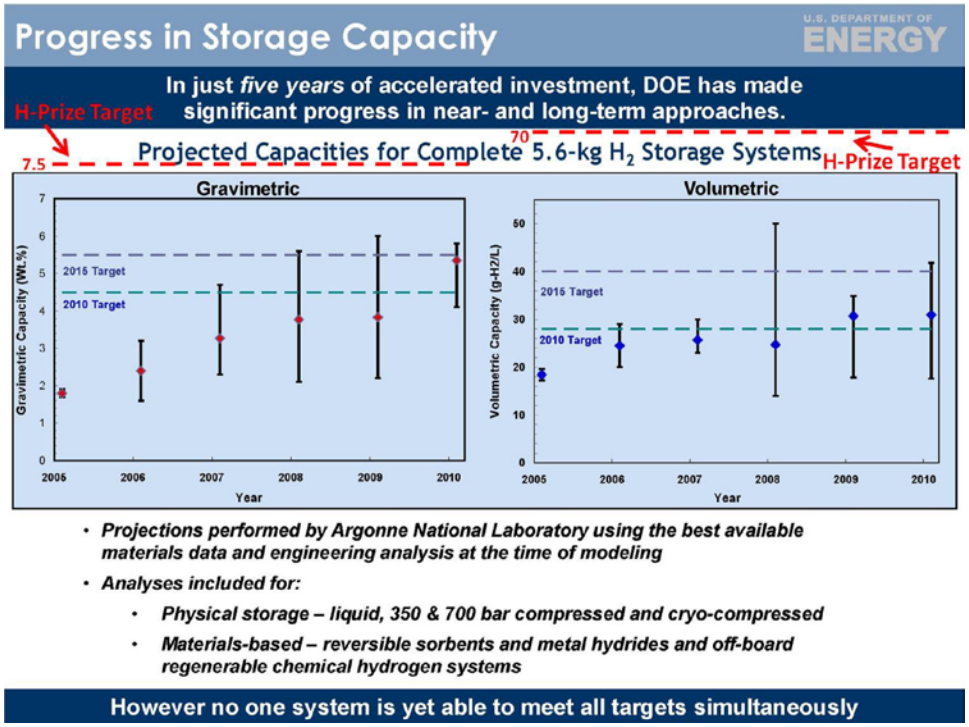


FIGURE 2. H-Prize Targets Relative to the State of Hydrogen Storage Technology as Reported by DOE in 2011 (modified from "Overview of Hydrogen Storage," Ned Stetson, 2011 Annual Merit Review Proceedings to include H-Prize targets)

- In third quarter of 2010, HEF staff and DOE completed Conflict of Interest and Non-Disclosure Agreement forms for panel of H-Prize judges.
- HEF Board of Directors approved slate of recommended judges in third quarter of 2010.
- With the November 15, 2010 deadline for receipt of materials approaching, HEF staff prepared and sent a detailed message to all the eligible H-Prize participants to remind participants of the key upcoming contest deadlines, discuss contest procedures for testing and verification, and encourage the participants to secure their independent testing with adequate time for meeting the November 15th deadline should their storage material qualify.
- Two eligible participant teams, Microbes Unlimited and Zaromb Research Corporation, submitted their testing results. Both submissions were found not to meet the minimum requirements set by the H-Prize and therefore were not sent off to our independent laboratory.
- Zaromb Research Corporation did write a letter disputing the judges' findings. Judge, Bob Bowman, and DOE Staff, Ned Stetson, collaborated on a response to address the issue. They refuted Zaromb Research Corporation's argument.
- No team qualified to advance to the next phase of the Competition.

Task 4: Management

- Kick-off meeting held on October 17, 2008.
- Revised budgets and award contingencies remedied.
- HEF staff met with DOE on March 24, 2010 to discuss next steps and upcoming work items for the H-Prize, such as the judging process, details for how to conduct the required sample testing, and a status update on HEF's administration of the contest. HEF and DOE staff discussed selections for the H-Prize's judging panel.
- Draft conflict of interest and nondisclosure agreements necessary for judging panel were completed.
- Receipt of test results and materials for subsequent independent verification of results deadline was November 15, 2010.

Task 5: Fundraising

- Marketing lists and fliers created in mid-2009 and awaited Federal Register notice authorization.
- Subcontractor SCRA developed and executed the majority of the fundraising plan.
- Outreach completed by physical mail and phone to 226 different foundations identified as having interest in supporting energy-related programs.
  - Received over 130 rejections for funding including 100% of our "top prospects."

  - Successful application to the 2010 Combined Federal Campaign (CFC).
  - Promoted the H-Prize and Hydrogen Education Foundation to CFC offices around the country to encourage donors.
  - Launched an online ad campaign on Govexec.com that targeted visitors interested in activities at the Department of Energy, Green Government, as well as a run of site for visitors in the D.C. area.
  - Received donations from 30 different CFC administrators around the U.S. totaling about $2,300 at the time of writing.
- Utilized a mobile fundraising service to reach a broader audience of givers and allow givers to donate by text message.
- Sent out individual letters to key contacts/ philanthropists, asking for individual donations.



Introduction

The H-Prize was created by an act of Congress as part of the Energy Independence and Security Act of 2007, Section 654, to accelerate the development of hydrogen and fuel cell technologies by offering prizes to motivate and reward outstanding scientific and engineering achievements. H-Prize consists of a series of contests that leverage private funds with core funding provided by the federal government to broaden the base of investment in development of hydrogen and fuel cell technologies and advance that technology into the marketplace.

Approach

HEF staff worked in concert with DOE to develop a contest that supported DOE's program and the legislation enacted by Congress. The first competition was designed to address challenges in hydrogen storage. While developing the Contest, we solicited feedback from industry stakeholders (both individual experts and groups like DOE's HTAC) to create the guidelines and parameters for assessing entries.

In parallel, a vigorous fundraising campaign was launched by HEF and its former subcontractor SCRA to seek non-government financial support for future contests named in the legislation. Over 220 potential sponsors were identified and contacted for possible funding of the contest. In addition, HEF staff applied for and succeeded in participation with the CFC in 2010. HEF has also been accepted into the 2011 CFC.

In addition to the fundraising efforts for future prizes, a marketing campaign was created to promote the first H-Prize competition for on-board hydrogen storage once the theme and guidelines were finalized. After input from various experts and stakeholders, the guidelines were approved by the HEF board of directors and the U.S. Department of Energy and published in the Federal Register in August 2009.

Announcements were made at several industry events, such as the National Hydrogen Association's Annual Conference in Columbia, South Carolina and DOE's Annual Merit Review, through press releases, and individual contact to hydrogen storage experts and groups. Staff developed a contest website, http://www.hydrogenprize.org for communicating the contest to the public and to serve as a tool for administering the competition.

Results

Administration of the H-Prize for Hydrogen Storage:

Applying to compete in the H-Prize for Hydrogen Storage included these basic four steps:

- Register online.
- Submit your application.
- Submit independent testing results showing that your material meets the established criteria.
- Submit a sample of the material for testing by the H-Prize's official laboratory.

For this first completion, a total of 20 organizations registered to participate. Given the niche focus on a specific area of hydrogen storage plus the fact that many of the experts in the hydrogen storage community are funded in part through DOE projects (and therefore were not eligible to compete), this left a very small number of potential applicants. We believe that these 20 registrants represented a majority of the people who could have qualified to compete.

Of the 20 registrants, 15 entities submitted full applications to be considered for the H-Prize and when the deadline passed to submit independent testing results, only two contestants remained. (The 13 organizations who withdrew cited costly independent laboratory work and a lack of resources to complete the required testing.)

The two remaining contestants, Microbes Unlimited and Zaromb Research Corporation, submitted their test results to the HEF and judging panel for review and to determine whether the contestants were qualified for step 4: to submit their hydrogen storage material for testing. The judges determined that the test results from Microbes Unlimited and Zaromb Research Corporation were insufficient for the prize to be awarded based on the parameters identified in the contest. Since both submissions were found not to meet the minimum requirements set by the H-Prize, no materials were requested or tested by the H-Prize laboratory.

Zaromb Research Corporation did write a letter disputing the judges' findings. Chief Judge, Bob Bowman, and DOE's Hydrogen Storage Team Leader for Metal

Hydrides, Ned Stetson, collaborated on a response to address the issue refuting Zaromb Research Corporation's argument. No team advanced to the next phase of the competition and the $1 million prize was not awarded. The contestants were notified, but no public announcement was made.

Looking ahead, significant opportunities exist to administer future prizes differently, and we have options to use the unawarded $1 million prize money in other areas to broaden the base of investment in development of hydrogen and fuel cell technologies.

Fund-Raising for Future H-Prizes:

During the fund-raising period for the H-Prize, over 220 foundations, tens of thousands of individuals and more than 100 companies were contacted to donate funds to support current or future H-Prizes described by the Sec. 654 legislation. Unfortunately, the results of this significant fund-raising effort did not bear the large sum of donations sought: $1-5 million.

From the more than 220 foundations, we received over 130 rejections for funding including 100% of our "top prospects." Since this was one of the primary tactics envisioned for fund raising, once we received rejections from most of our top prospects, we changed our approach and reallocated funding into other areas to try new methods to attract new funding. That shift mostly included utilizing the CFC and raising awareness of HEF's participation in it.

At the time of writing, approximately $2,300 had been collected, entirely from individual donations made through 30 different administrators for the 2010 CFC. Since all but one of the donations were anonymous, we do not know how many donors contributed, but the distribution of the CFC administrators that sent in checks to the HEF seem to indicate that our marketing had good nationwide reach and an unexpected international reach as well. The largest donations were received from the following CFC administrators:

- CFC-Overseas
- National Capital Area CFC
- CFC Portland Oregon
- Southeast Connecticut CFC
- South Hampton Roads (VA) CFC
- Texas Gulf Coast CFC
- Heart of Alabama CFC

We believe the small number of dollars collected can be mostly attributed to a few key things:

- Depressed economy (foundations, corporations and individuals all cited a lack of available resources).
- The subject of the current H-Prize in a very niche area of a technical field did not have the mass/popular appeal to attract funding from entities that would be considered "outside the choir" of the hydrogen and fuel cell industry.
- The technique for reaching out to foundations has changed significantly from the time we competed to administer the H-Prize to the time we started reaching out foundations. More specifically:
  - In the past, one could be successful with a well composed letter, printed materials about the proposed project, follow-up phone calls, etc. (in other words, fund raising remotely).
  - Today, after consulting with foundation fund-raising experts to try to learn if we could change our approach to increase our success with foundations, we learned that hardly anyone raises funds with foundations without first developing an in-person relationship with the foundation's staff. This equates to travel and significant time which the budget of this project was not designed to support.
  - As a result, we decreased our work with our fund-raising subcontractor and added resources to other creative fund-raising methods, including the CFC.

Conclusions and Future Directions

The initial H-Prize contest was not awarded as the two organizations competing for the prize did not meet the criteria for awarding the prize as was determined by the judging panel. In assessing the theme and parameters post-contest, it has become clear that the initial contest was quite limited in scope and the bar set extremely high (see Figures 1 and 2), thus reducing the numbers of prospective contestants. However, if the goal was to reach most of the American organizations who were not receiving DOE funding in hydrogen storage to encourage greater investment among this group, we believe that goal was reached. The number of people who meet these qualifications just happens to be very small.

The staff at the HEF will meet with DOE's H-Prize Manager, Dr. Ned Stetson to discuss lessons learned and new ideas for a new H-Prize since some administration funds remain as well as the $1 million prize money. Prior to this meeting, the HEF will reach out to industry stakeholders to seek input on the challenges they are experiencing today and how the H-Prize may help address those challenges within the context of its objectives as defined above. Initial discussions with colleagues in the hydrogen community have revealed that there is a desire to strengthen relations between hydrogen and fuel cells with the broader renewable energy community including solar, biomass, and wind.

With a fully functional website that is active, marketing capabilities established, and lessons learned from the initial contest, DOE has a significant opportunity to build on these resources to create an even more successful prize in several different categories named in the H-Prize legislation. HEF staff looks forward to discussion what options exist in working with DOE on a second H-Prize in the near future.

IV.F.1 High Strength Carbon Fibers

Felix L. Paulauskas (Primary Contact), Bob Norris (Project Manager), Amit Naskar, Soydan Ozcan, and Ken Yarborough
Oak Ridge National Laboratory (ORNL)
MS 6053
Oak Ridge, TN 37831-6053
Phone: (865) 576-1179
E-mail: ffp@ornl.gov

DOE Manager
HQ: Ned Stetson
Phone: (202) 586-9995
E-mail: Ned.Stetson@ee.doe.gov

Subcontractors:
- Donald G. Baird, James E. McGrath, Jianhua Huang, Myoungbae Lee, Yu Chen, and Ozma Lane; Virginia Polytechnic Institute and State University, Blacksburg, VA
- Fibras Sinteticas de Portugal (FISIPE), SA, Lavradio, Portugal

Project Start Date: November 2006
Project End Date: Project continuation and direction determined annually by DOE

Fiscal Year (FY) 2011 Objectives

- Reduce the manufacturing cost of high-strength carbon fibers by using melt-spun polyacrylonitrile (PAN) precursor technology which has the potential to reduce the production cost by >30%.
- Develop advanced conversion techniques that will significantly reduce the production cost of high-strength carbon fibers suitable for use in compressed hydrogen storage vessels by an additional 20%.

Technical Barriers

High-strength carbon fibers account for approximately 65% of the cost of the high-pressure storage tanks. This project addresses the following technical barriers from the Storage section of the Fuel Cell Technologies Program Multi-Year Research, Development and Demonstration Plan:

(A) System Weight and Volume
(B) System Cost
(D) Durability/Operability
(G) Materials of Construction

High-strength carbon fiber enables the manufacture of durable, lightweight, compressed hydrogen storage vessels for use in high-pressure storage. Unfortunately, current high-strength carbon fiber products are far too expensive to meet DOE goals for storage system costs.

Technical Targets

Working targets are approximate equivalence with Toray T-700 at substantially reduced production costs:

- 700 ksi ultimate tensile strength.
- 33 Msi tensile modulus.
- Production cost reduction of at least 25% versus baseline.

FY 2011 Accomplishments

- Acrylonitrile copolymers were successfully prepared in controlled molecular weight by classical free radical copolymerization. It is has been extended to copolymers with methyl acrylate. The materials have been characterized by melt rheology, fiber spinning, mechanical testing, microscopy and size exclusion chromatography (SEC).
- Demonstrated it is possible to use water as the only plasticizer (instead of water plus organic solvents like acetonitrile) to generate melt-spun PAN fibers as carbon fiber precursors.
- Demonstrated it is possible to melt-spin PAN precursor fibers with the desired denier (10 to 20 microns in diameter) with a one-step spinning/drawing process.



Introduction

The exceptional strength-to-weight ratio of carbon fiber composite tanks makes them prime candidates for use with materials-based, cryogenic, or high-pressure gas for both vehicular and stationary storage applications. Cost is the primary issue with composite tank technology. A critical challenge lies in the cost of the fiber and the manufacture of composite tanks. Current projections of the manufactured cost per unit for high production volumes are about a factor of nine above storage system targets, and it is estimated that about 40-70% of the unit cost is due to the base cost of the carbon fiber (approximately 40% of the fiber cost is due to the precursor and the remainder due to thermal processing). Research and development (R&D) is needed as composite storage technology is most likely to be employed in the near term for transportation applications and will be needed for most materials-based approaches for hydrogen storage.

Currently, composite tanks require high-strength fiber made from carbon-fiber grade PAN precursor. Manufacturing R&D is needed to develop lower cost, high

quality PAN or alternate precursors and reduced energy or faster conversion processes for carbon fiber, such as microwave and/or plasma processing. Developing and implementing advanced fiber processing methods has the potential to reduce cost by 50% as well as provide the technology basis to expand U.S. competitiveness in high-strength fiber manufacturing [1].

This project will leverage previous and ongoing work of the FreedomCAR's program to develop a low-cost, high-strength carbon fiber. At this time, the cost and property targets needed for compressed hydrogen storage are not well understood. Analysis is underway at DOE to determine appropriate targets. Until targets are definitively established, this project will seek to develop carbon fibers with properties equivalent to Toray's T700/24k fiber (24k tow, 700 ksi ultimate tensile strength, 33 Msi tensile modulus), and reduce production costs by at least 25%.

Approach

This project is structured into tasks focused on precursor development and conversion process improvements. Development and demonstration of melt-spinnable PAN is the project's primary precursor option. This requires concurrent activities in both development of melt-stable PAN copolymer and blends as well as the processes necessary to successfully spin the formulations into filamentary tows. Backup options include textile PAN, polyolefins, and incorporation of nanomaterials. Demonstrating and down-selecting a precursor capable of meeting performance targets utilizing conventional conversion processing defines the pathway for the balance-of-project activities. In conversion, critical processability parameters include: (i) highly controlled stretching, especially during pre-treatment and stabilization; (ii) residence time in various conversion modules; (iii) optimal graphitization for maximum strength; (iv) uniform treatment of fibers throughout the tow; and (v) characterization of filaments at various stages of conversion operation. Related ORNL work in advanced processing technologies address these issues, with a focus on increasing line speed in a reduced footprint, with reduced energy consumption. Means to adapt these emerging processes will be developed and evaluated for applicability to meeting requirements of this program area. As the alternative approaches are demonstrated, the energy efficiency and overall economics of the complete system will be evaluated and forecast for production scale up.

Results

Melt processing of PAN is a difficult issue, although Virginia Tech and others have made modest progress over the last decade [2-6]. One of the principal problems is that PAN degrades even without main chain scission or weight loss, and this essentially precludes melt processing. Reactions of the side groups have been discussed in many reports [7-10]. These degradative reactions can take place both in an intra-molecular manner, but also via inter-molecular branching and gelation, which quickly alters the capacity for these materials to be melt fabricated. At 200-220°C, the material can quickly increase in viscosity, thus rendering an intractable material in a very short time. Ideally, one would like to maintain constant viscosity for a required period, and practical considerations suggest that this should be at least 30 minutes or longer.

Random copolymers have been made either by aqueous suspension processes or emulsion systems using polyvinylpyrrolidone for the suspension aid and common organic initiators such as azobisisobutyl nitrile (AIBN) and peroxides. Monomers such as acrylonitrile methyl acrylate, hema, caprolactone and 2-acrylamido-2-methyl-1-propanesulfonic acid were purchased from laboratory supply houses. The suspension reactions were conducted mostly in a Parr rector, which prevents loss of monomer through typical three-neck type apparatus systems. Conversions can be very high; molecular weights were controlled primarily with temperature, initiator concentration, and especially the use and concentration of dodecyl mercaptan as a chain transfer agent. Characterization of the co- and terpolymers utilized spectroscopic methods various rheological measurements.

In some cases, preliminary experiments were done in dimethyl slfoxide, again using AIBN to produce effective random copolymers. Macromonomer grafts were prepared by utilizing hydroxy ethyl methacrylate to initiate caprolactone in the presence of catalytic quantities of stannous octanoate. The resulting methacrylic functionality macromonomer of about 1,000 to 2,000 molecular weight was successfully introduced into the terpolymerization scheme with acrylonitrile and methylacrylate. The rheological behavior was investigated for the copolymers and concurrently for the terpolymers. As shown in Figure 1, there was a noticeable effect of composition on the apparent melt viscosities; 90% or less could produce in many cases a melt processible material, which evidenced little if any degradation over a 30-minute processing period.

A laboratory-pressurized spinning system was developed, which enabled viscosity shear rate behaviors to be generated as a function of temperature and water content. A descriptive plot of viscosity vs. shear rate is provided in Figure 2. The resulting materials could be processed into fibrous materials, which are undergoing continued evaluation. All of the materials described were well characterized by SEC, which has been invaluable in establishing which compositions and molecular weights are indeed melt processible. The work is ongoing and an updated presentation will be given at the meeting.

In FY 2010, the project achieved success in generating a ten-filament mini-tow with AN/VA copolymer. The scanning electron microscope micrographs showed that the void size of the fibers is similar to that of as-spun fibers produced by BASF. The tensile strength of melt spun fibers was about 50 to 70% of industrial precursor fibers which were solution

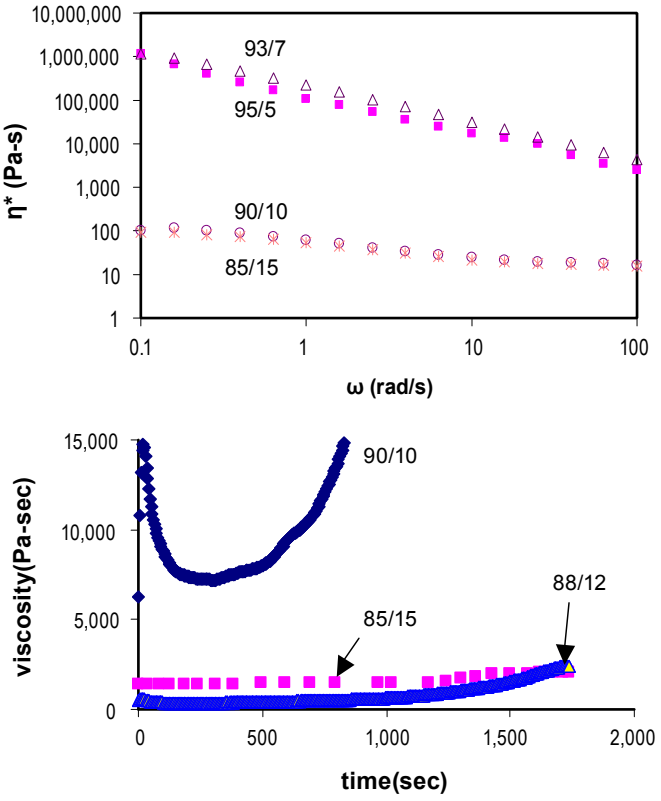
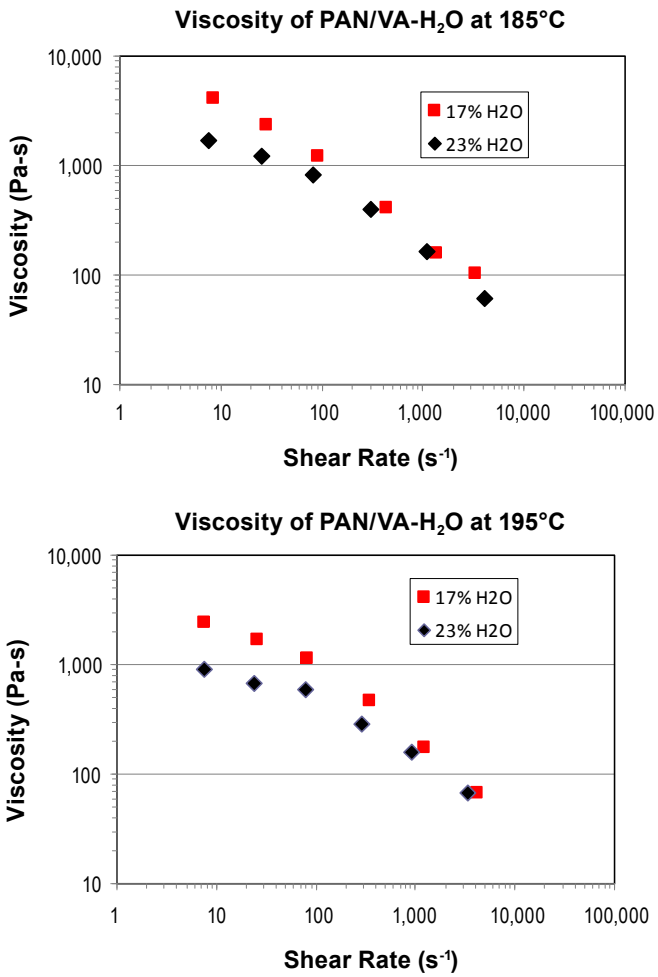


FIGURE 1. Correlation between Melt Viscosity and Copolymer Composition



The viscosity of melt decreases as water content increases.

FIGURE 2. Viscosity of AN Copolymer-H_2O Melt

spun and about four times smaller in diameter. It is expected that with a new spinneret that fibers in the range of 10 µm will be produced with significantly improved strength.

In Table 1, the tensile mechanical properties of VT melt-spun PAN fibers are presented. The properties of industrial precursor fibers are also included in the table/figures for comparison. The strength of VT melt-spun fibers is lower than all industrial precursor fibers, whereas the elongation of VT fibers is similar to that of the industrial fibers, especially Courtaulds and Hexcel fibers. Note that VT fibers are four times larger than all industrial fibers. Because smaller fibers usually have higher strength, the higher strength of melt-spun fibers would be expected when the fiber diameter is reduced to 10 µm or so with the new spinneret.

In FY 2011 efforts were made to design and fabricate a new spinneret (with diameter of 55 microns) and use it to generate a multi-filament (≥10 filaments) precursor tow with AN/VA copolymer (containing 93% AN), targeted at filaments with diameter of 10 to 20 µm and porosity of no more than 1 vol%. Success was achieved in generating melt-spun PAN precursor fibers with diameter of 10 to 20 microns. Effort is now focused on issues associated with

TABLE 1. Mechanical Properties of VT Melt-Spun and Commercial PAN Precursor Fibers*

Name/ Manufacturer	Polymer Composition	Spinning Process	Fiber Diameter (µm)	Peak Stress (KSI)	Strain at Break (%)
VT-1	AN/VA	Melt/H_2O	67.1 (3.1)	37.6 (3.7)	11.89 (1.16)
VT-2	AN/VA	Melt/H_2O	53.8 (4.8)	35.3 (4.0)	10.76 (1.08)
FISIPE-1	AN/VA	Solution	14.15	54.2 (8.5)	15.7 (0.9)
FISIPE-2	AN/VA	Solution	13.7	64.9 (5.5)	14.99 (0.51)
COURTAULDS	AN/MA	Solution	11.7	73.5 (10.5)	11.21 (1.36)
HEXCEL	AN/MA	Solution	12.9	76.6 (5.6)	10.53 (0.76)

* All data were provided by ORNL. Data in parenthesis represent the standard deviation.

generating filaments or a mini-tow with uniform diameter and length greater than 10 ft and preferably up to 100 feet.

A new spinneret with 18 capillaries was designed and built for evaluation. The capillary has a diameter of 55 microns and L/D of 5. It turned out that the spinneret was poorly machined with unacceptable deviation in the capillary diameters. The design was modified and a better qualified company was found to machine the spinneret. As can be seen from Figure 3, the latest spinneret has 19 capillaries with diameter of 55 microns and aspect ratio (L/D) of 2. The spinneret was received on April 19 and appears to be well machined.

PAN fibers produced with the new spinneret are shown in Figure 4. The fibers have a diameter of 10 to 20 microns. The evaluation of the fibers including mechanical property and morphology of the fibers is now underway.

Conclusions and Future Directions

Acrylonitrile copolymers were successfully prepared in controlled molecular weight by classical free radical copolymerization. It is has been extended to copolymers with methyl acrylate. The materials have been characterized by melt rheology, fiber spinning, mechanical testing, microscopy and SEC. Stabilization appears to require 1 or 2 wt% of a novel stabilizer. The stabilization mechanism is unknown, but one speculates a sort of pH control which retards the intra and inter molecular cyclization process. Small amounts of water are observed to be released and a significant increase in Tm has been reported. This suggests that the stabilizer may also serve as a nucleating agent, which could be very important. The utilization of water as a plasticizer has been one of the critical observations

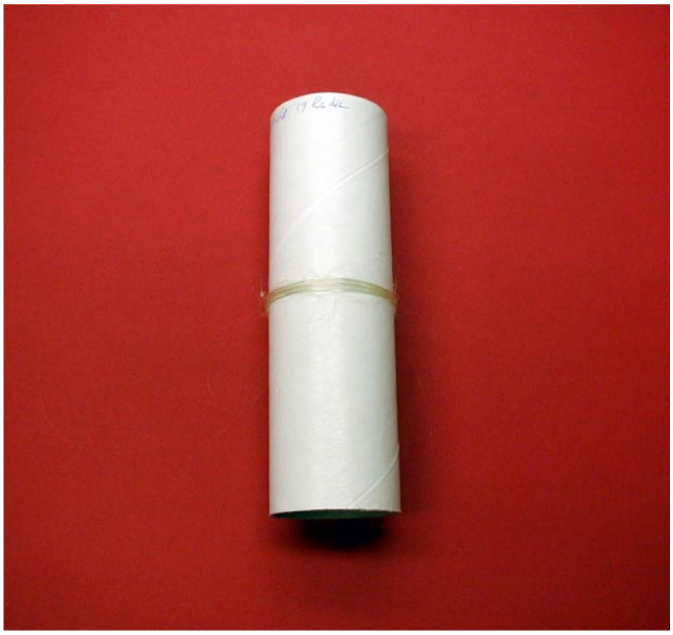


FIGURE 4. Melt-spun PAN/VA fibers using 19-filament die (0.0022" in diameter). The diameter of fibers is about 10 to 20 microns.

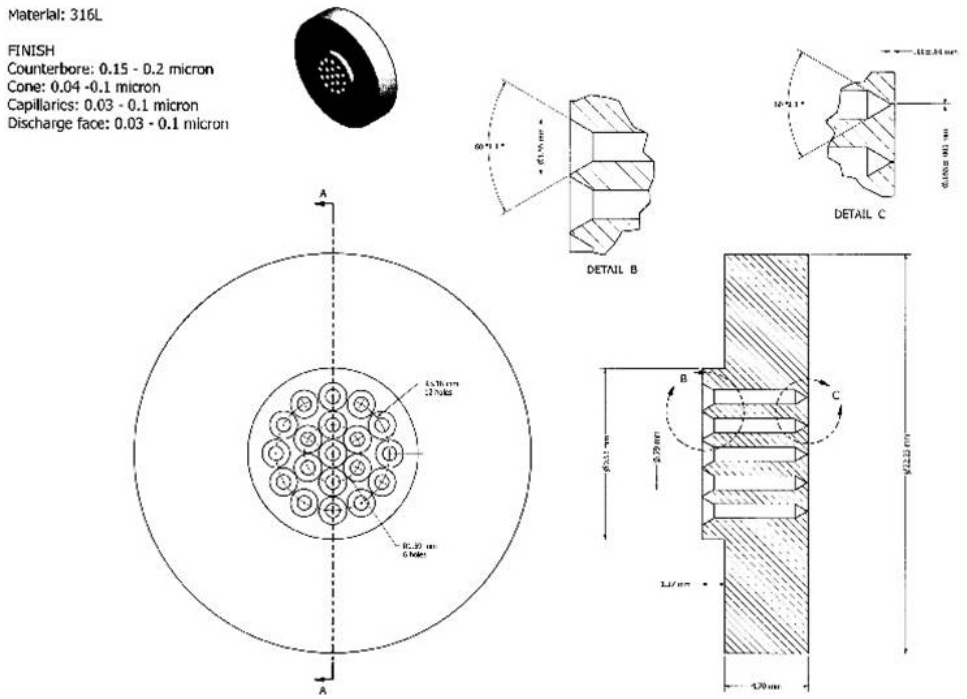


FIGURE 3. Drawing of new spinneret for Instron rheometer fiber spinning system. The spinneret has 19 capillary holes with diameter of 55 microns.

developed thus far that generally permits melt spinning via decreasing the dipole interactions. Controlled (living) radical copolymerization is currently also being explored. This is expected to afford narrower molecular weight distributions and possibly lower branching and chain end unsaturation.

The fiber spinning research so far reveals that:

- It is possible to use water as the only plasticizer (instead of water plus organic solvents like acetonitrile) to generate melt-spun PAN fibers as carbon fiber precursors.
- It is possible to melt-spin PAN precursor fibers with the desired denier (10 to 20 microns in diameter) with a one-step spinning/drawing process.
- In order to generate PAN precursor fibers with desired size and quality, one must have a quality spinneret with small capillary size. However, it was found very difficult to remove the residual PAN polymer from capillaries with diameter of 55 microns or so. Effort is ongoing to overcome this difficulty.
- It was found to be very difficult to remove the residual PAN polymer from the capillaries with diameter of 55 microns. Using solvent to dissolve the polymers at elevated temperature, or using high temperature (~400°C) plus oxygen to burn-off the polymers and then clean the capillaries have been attempted. Unfortunately, none of the methods could clean the capillary completely even after days/weeks of treatment. We are still working on this issue so that we can keep running the fiber spinning experiment with the small capillary diameter spinneret.

Near-term objectives are to:

- Generate a multi-filament (≥10 filaments) precursor tow with AN/VA copolymer (from ORNL with 93% AN), targeted at filaments with diameter of 10 to 20 µm, porosity of no more than 1 vol%, and length of greater than 10 feet.
- Generate a multi-filament (≥10 filaments) precursor tow with AN/MA copolymer (from ORNL, with 95% AN) with desired size and properties.
- Test mechanical property and morphology of PAN/VA and PAN/MA fibers and compare them with that of industrial precursor fibers.
- Consider the design of an extrusion process using an extruder which will allow the generation of a larger quantity of fibers.

ORNL will characterize fiber and conduct conversion trials on precursor filaments generated using its precursor evaluation system. The filaments at various steps of the conversion process will be fully characterized and the data used to commence optimization of precursor chemistry and the filament generation process. We expect to achieve carbon fiber tensile properties of 15 Msi elastic modulus and 150 ksi tensile strength with 1st generation filaments. We are targeting 18 Msi modulus and 200 ksi strength in 2nd generation filaments.

FY 2011 Publications/Presentations

1. Felix L. Paulaukas, "High Strength Carbon Fibers" presentation at 2011 DOE Hydrogen Program and Vehicle Technologies Annual Merit Review and Peer Evaluation Meeting, May 9–12, 2011.

2. Felix L. Paulauskas, "High Strength Carbon Fibers and Status Report", presentation at Hydrogen Storage Tech Team Meeting, June 30, 2011.

References

1. Hydrogen, Fuel Cells and Infrastructure Technologies Program Multi-Year Research, Development and Demonstration Plan Planned program activities for 2005-2015, October 2007 update.

2. Wiles, K.B., V.A. Bhanu, A.J. Pasquale, T.E. Long, and J.E. McGrath, Journal of Polymer Science: Part A: Polymer Chemistry, Vol. 42, 2994-3001 (2004).

3. Bhanu, V.A., P. Rangarajan, K. Wiles, M. Bortner, S. Sankarapandian, D. Godshall, T.E. Glass, A.K. Banthia, J. Yang, G. Wilkes, D. Baird, and J.E. McGrath, Polymer, 43, 4841-4850, (2002).

4. Godshall, D., P. Rangarajan, D.G. Baird, G.L. Wilkes, V.A. Bhanu, and J.E. McGrath, "Polymer 44 (2003), 4221-4228.

5. Rangarajan, P., V.A. Bhanu, D. Godshall, G.L. Wilkes, J.E. McGrath, and D.G. Baird, Polymer 43, 2699-2709 (2002).

6. Bortner, Michael J., Vinayak Bhanu, James E. McGrath, and Donald G. Baird, Journal of Applied Polymer Science, 93(6), 2856-2865 (2004).

7. Peng, Fred M., "Acrylonitrile Polymers," in Mark, Herman F.; Bikales, Norbert M.; Overberger, Charles G.; Menges, Georg; Editors. Encyclopedia of Polymer Science and Engineering, Vol. 1: A to Amorphous Polymers. (1986), 843 pp, pages 426-470, and references therein.

8. Back, Hartwig, C, and Knorr, Raymond S. "Acrylic Fibers," in Mark, Herman F.; Bikales, Norbert M.; Overberger, Charles G.; Menges, Georg; Editors. Encyclopedia of Polymer Science and Engineering, Vol. 1: A to Amorphous Polymers. (1986), 843 pp, pages 334-388, and references therein.

9. Capone, Gary J.; Masson, James C. Fibers, acrylic. Kirk-Othmer Encyclopedia of Chemical Technology (5th Edition) (2005), 11 188-224.

10. Frushour, Bruce G.; Knorr, Raymond S. Acrylic fibers. International Fiber Science and Technology Series (2007), 16(Handbook of Fiber Chemistry (3rd Edition)), 811-973.

IV.F.2 Lifecycle Verification of Polymeric Storage Liners

Barton Smith (Primary Contact) and
Lawrence M. Anovitz
Oak Ridge National Laboratory (ORNL)
P. O. Box 2008
Oak Ridge, TN 37831
Phone: (865) 574-2196
E-mail: smithdb@ornl.gov

DOE Manager
Ned Stetson
Phone: (202) 586-9995
E-mail: Ned.Stetson@ee.doe.gov

Start Date: June 2008
Projected End Date: Project continuation and direction determined annually by DOE

Fiscal Year (FY) 2011 Objectives

Perform durability qualification measurements on specimens of Type IV storage tank liners (polymers) at the nominal working pressure using thermal cycling commensurate with the design lifetime, followed by permeation measurements to determine if the steady-state leakage rate in the tank could potentially exceed the specification for hydrogen fuel cell passenger vehicles.

Technical Barriers

This project addresses the following technical barriers from the Hydrogen Storage section (3.2.4) of the Fuel Cell Technologies Program Multi-Year Research, Development and Demonstration Plan:

(D) Durability/Operability

Technical Targets

This project addresses the following technical targets for on-board hydrogen storage systems research and development [1]:

- Cycle life variation, expressed as percent of mean (min) at percent confidence:
  - FY 2010: 90/90; FY 2015: 99/90
- Environmental Health and Safety:
  - Permeation and leakage: meets or exceeds applicable standards.
  - Loss of usable H_2 (g/h/kg H_2 stored): FY 2010: 0.1; FY 2015: 0.05.

FY 2011 Accomplishments

- Permeation measurements on specimen of Lincoln Composites Type IV high-density polyethylene (HDPE) tank liner show progressive changes in the slope and pre-exponential scaling factor of the permeation curves that occur as the specimen undergoes simulated lifecycle temperature variations.
- Characterization of liner specimen using neutron scattering and electron microscopy (small angle neutron scattering [SANS], ultra small angle neutron scattering [USANS], scanning electron microscopy/back scattered electron mode [SEM/BSE]) show significant structural changes were induced by temperature cycling or hydrogen exposure or both.
- Using permeation coefficient data, the Lincoln Composites HDPE liner in a 350-bar tank can be expected to maintain an H_2 leak rate that meets applicable leakage standards throughout its lifecycle history.



Introduction

Modern high-pressure hydrogen storage tanks use a polymeric liner as a permeation barrier to hydrogen, typically HDPE. Storage tank liners can, however, be stressed by cyclical excursions between temperature extremes, and the cumulative effects of repeated stress could harm the tank's durability. Ultra-high environmental temperatures can promote large hydrogen permeation rates and hydrogen saturation in the liner material. Ultra-low environmental temperatures can severely stress liner materials and possibly induce microcracking. In addition, increasing the pressure of gas in such a tank during filling necessarily raises the temperature of the gas and therefore the enclosing tank. Over the course of many fill cycles during the lifetime of the tank this might affect the permeability characteristics of the liner. Failure modes for the liner's performance based on the interaction of high pressure and extreme temperature cycling might be possible. Hydrogen leakage through a liner microcracked by extreme temperature cycling could accelerate under sustained high temperature and pressure, or hydrogen saturation of the reinforcement layers external to the liner could put backpressure on the liner as the tank pressure decreases during vehicle operation, thereby causing the liner to separate from the reinforcement layers. Minimum temperatures during winter months in northern states may reach -40°C, and maximum temperatures after filling during summer months may reach 125°C. Thus, the purpose of this project is to cycle typical tank liner materials between

these temperature extremes to determine whether such a degradation in properties occurs, and if so, its extent.

Approach

Hydrogen permeation verification measurements for storage tank liner materials are being carried out using ORNL's internally heated high-pressure permeation test vessel (IHPV). The IHPV was previously used in the hydrogen delivery program to measure real-time hydrogen permeation in low-carbon steels and polymer materials *at constant temperatures*. Materials properties such as the temperature- and pressure-dependent hydrogen solubilities, diffusion coefficients and permeation coefficients are extracted from measurements of real-time hydrogen flux through steels and polymers. In the previous project year we modified the IHPV to enable rapid temperature cycling in polymer specimens.

We are using the relevant portion of the test protocol specified in Society of Automotive Engineers standard J2579 [2] to guide our performance of durability test cycling measurements of high-pressure polymeric tank liners. The J2579 test protocol for compressed hydrogen storage systems prescribes long-term thermal cycling at high pressures of hydrogen. The requirement is to subject tank liner specimens to 5,500 thermal cycles over the temperature range -40 to 85°C at hydrogen pressurizations of 43 MPa (6,250 psia) and then 86 MPa (12,500 psia). Testing at 43 and 86 MPa, with cycling between -40 and 85°C, requires an automated temperature control strategy. To replicate the rapid temperature rise in the tank liner during fill cycles (approximately 100°C rise in 3 minutes) we decoupled the cooling and heating control systems in the IHPV. A low-temperature chiller with low-temperature refrigerant circulating to and from a sealed reservoir cools the IHPV's exterior containment vessel to approximately -40°C. A resistive heater situated in the permeation cell is used to ramp the specimen temperature from -30°C to 85°C. A heater controller controls the thermal cycling of the polymer specimen in the cell by applying and removing power to the heater. Process control software that was developed for the temperature-controlled permeation measurements in steels and polymers was modified to provide automated, unattended operation and Internet access so the tests can be remotely monitored and controlled. A complete heating and cooling cycle requires 33.3 minutes, and approximately 127 days are required to perform 5,500 temperature cycles.

The verification measurements occur at regular intervals during the 5,500 temperature cycles. The hydrogen flux is measured at multiple temperatures in the range -30 to 85°C at each interval. The first measurements occur after the completion of 250, 500, 750, 1,000, 1,250 and 1,500 cycles. The remaining measurements occur at 500 cycle intervals until 5,500 temperature cycles have been reached.

Results

We completed permeation measurements on a Lincoln Composites Type IV tank liner specimen (HDPE). The permeation coefficients P have the temperature dependence of an activated process, $P = P_0 \exp(-E_A/kT)$, where the pre-exponential scaling factor P_0 and the activation energy E_A are presumed to be independent of temperature. We performed permeation measurements before cycling and after 250, 500, 750, 1,000, 1,250, 1,500, 2,000, 2,500, 3,000, 3,500 and 4,000 cycles. Semi-log plots of P versus $1/T$ are shown in Figure 1. Lines have been drawn through measurements at 0, 1,000, 2,000, 3,000 and 4,000 cycles to illustrate the systematic changes in E_A and P_0. The decreasing slope and shift in scaling indicates that some physical change occurred in the polymer during cycling, but we did not observe a statistically significant departure from the Arrhenius relationship, which would indicate that microcracking or changes in glass transition temperature had occurred in the polymer. Figures 2a and 2b illustrate the changes in E_A and P_0, respectively. E_A and P_0 each decreased as the specimen was subjected to repeated temperature cycles. The -2.21 J/mole slope for E_A versus number of cycles was approximately five standard deviations from a slope of zero, and the 4.6×10^{-8} mol H_2/cm·s·bar slope for P_0 versus number of cycles was approximately 4 standard deviations from a slope of zero.

Following completion of the temperature cycling we used neutron scattering analysis (SANS and USANS) to look for structural changes on the order 1 nm to 30 μm in

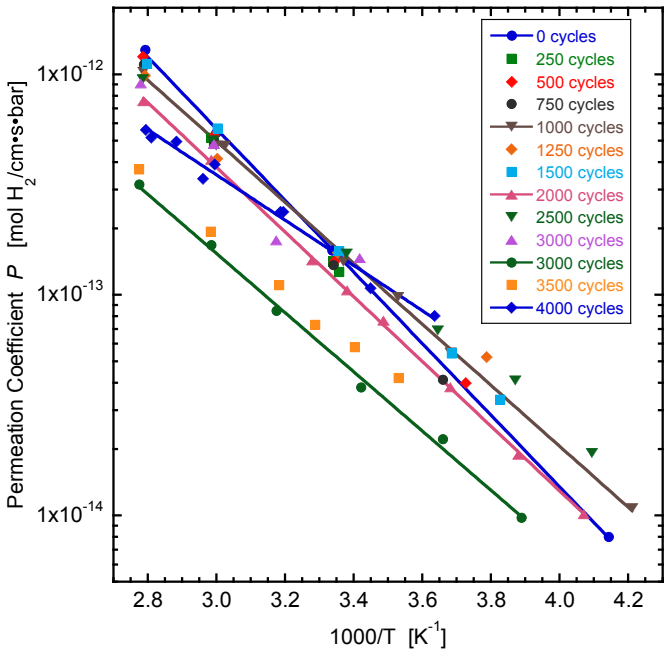


FIGURE 1. Permeation Coefficients P for Hydrogen in Polymer Specimen, Measured at 430 bar

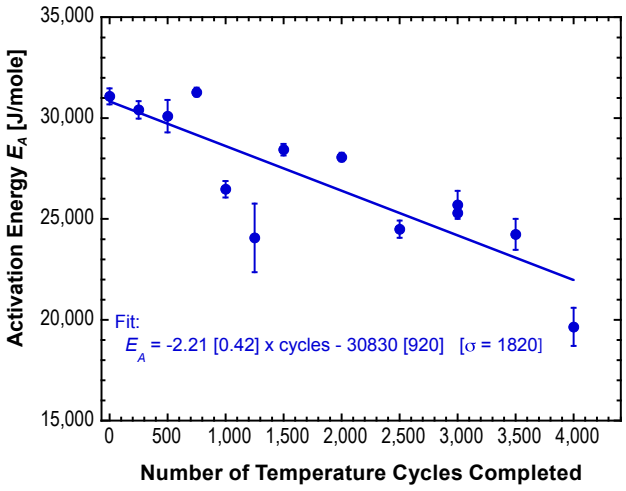


FIGURE 2a. The activation energy E_A of the HDPE specimen decreased through 4,000 temperature cycles, indicating that the polymer experienced small changes in its microstructure.

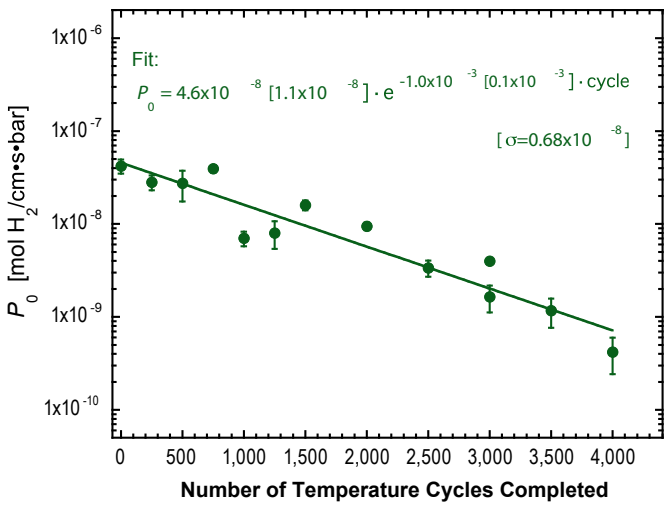


FIGURE 2b. The pre-exponential scaling factor P_0 also decreased through 4,000 temperature cycles, further evidencing small changes in poymer microstructure.

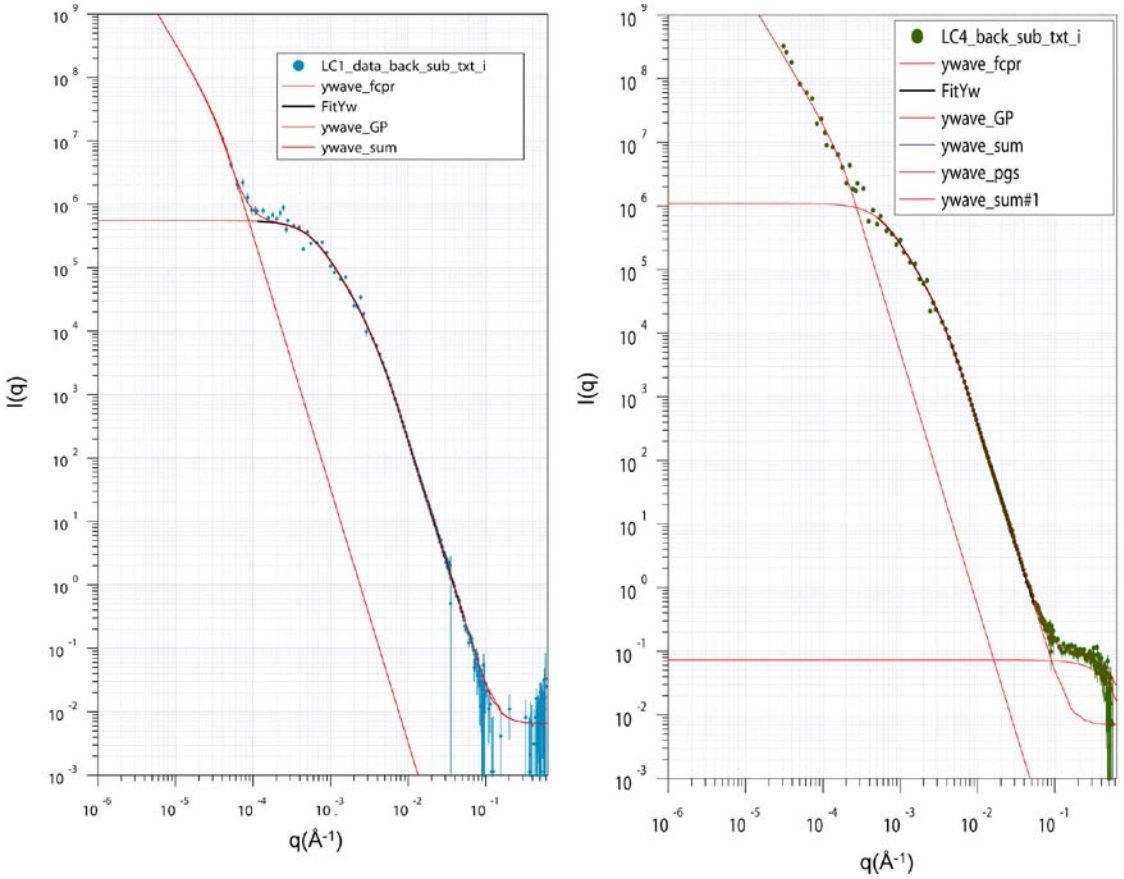


FIGURE 3. Neutron scattering data for Lincoln Composites tank liner specimens, before temperature cycling (left) and after 4,000 temperature cycles (right).

the polymer. We analyzed four HDPE tank liner specimens: 1) before temperature cycling, 2) after a few temperature cycles, 3) after 600 cycles, and 4) after 4,000 cycles. The scattering data for the before-cycling and after-4,000-cycles specimens is shown in Figure 3. The scattering data was analyzed as follows [3]: the low-q section was fit using a

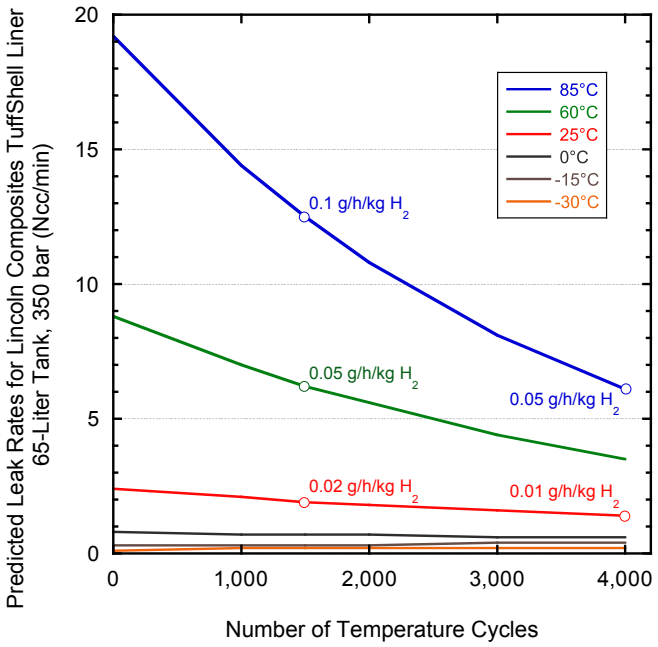


FIGURE 4. Predicted leak rate values for HDPE tank liner as a function of liner temperature and number of temperature cycles.

Guinier-Porod model, the central section was fit using a flexible cylinder with a polydispersed radius model (designed for treatment of polymers, see reference [3]), and the high-q section was fit to a polydispersed (Gaussian) sphere model. In the low-q section, the fit changes slope from -4 (Porod region) to -2 (Guinier region corresponding to plates or laminae). The transition from Porod to Guinier occurs with increasing number of temperature cycles. The presence of low-q scattering in the USANS data indicates the presence of large-scale (>~30 μm) scattering features that change significantly with long-term exposure to hydrogen or increasing number of temperature cycles or both. Similarly, the presence of high-q scattering appears only after temperature cycling.

Conclusions and Future Directions

We used the values of P_0 and E_A obtained from measurements during the temperature cycling to model the behavior of the permeation coefficients P as a function of T and the number of cycles. This modeling shows that at all temperatures the values of the hydrogen permeation coefficients decrease with cycle count, thus implying that the hydrogen leak rate of the tank liner should decrease with the number of temperature cycles.

To obtain a quantitative prediction of the leak rate for an actual tank liner, we used the dimensional specifications for a Lincoln Composites TUFFSHELL® hydrogen fuel tank rated for 350 bar service and with a volumetric capacity of 65.3 liters (water volume). The HDPE tank liner is cylindrical with nearly hemispherical end caps, and the liner wall thickness is about 7 mm. We obtained a family of leak rate curves using the cycle-dependent permeation coefficients in an analytical expression for the tank leak rate. These curves are shown in Figure 4. In this analysis the tank leak rate remains below 75 normal cubic centimeters per minute (Ncc/min) at all temperatures for the duration of 4,000 temperature cycles. Furthermore, for all liner temperatures less than about 60°C, the loss of useable hydrogen remains below 0.05 g/h/kg H_2 for a fully filled tank, i.e., at a 350 bar pressurization.

For the next project year we have crafted a research plan that addresses the findings made in the present year. A second verification test on a fresh tank liner specimen is being carried out at 86 kPa following the same protocol. We will again perform some post-cycling analysis of the specimen to determine the type of structural changes that take place in the polymers. Differential scanning calorimetry measurements, SEM/BSE microscopy, transmission electron microscopy (using microtome sectioning), and perhaps some additional SANS/USANS (neutron scattering) will be used. This analysis will allow us to determine the implications of the structural changes during the lifecycle of the tank liner. Furthermore, we will expand the investigation beyond tests of the existing tank liner materials to future materials, as several tank manufacturers have recently introduced liners made from new less expensive and potentially higher performance (lower permeation) materials. Also under consideration is the need to adequately address the durability of the liner when it is bonded to the tank reinforcement. To this end we are developing a test plan for temperature cycling sectioned specimens from tank structures while they are differentially pressurized with hydrogen (high pressure on the liner side, atmospheric pressure on the outside of the reinforcement). Obtaining a better understanding the adhesion and interaction between the liner and composite matrix layer over the lifetime of the tank would be very valuable for a complete assessment of the lifecycle durability of the Type 4 storage tanks. This measurement will require a significant amount of collaboration with tank manufacturers to obtain their advisement on the testing procedure and their provision of tank sections.

FY 2011 Publications/Presentations

1. 2011 DOE Hydrogen Program Annual Merit Review – Arlington, Virginia – May 9, 2011, poster ST053.

References

1. HFCIT MYRDD Plan, Table 3.3.2, "Technical Targets: On-Board Hydrogen Storage Systems," October 2007.

2. SAE J2579, "Technical Information Report for Fuel Cell and Other Hydrogen Vehicles (January 2009)," Fuel Cell Standards Committee, SAE International.

3. B. Hammouda, The SANS Toolbox, NIST Center for Neutron Research, available at http://tinyurl.com/SANStoolbox

IV.G.1 Purdue Hydrogen Systems Laboratory: Hydrogen Storage*

Jay Gore (Primary Contact), P. Ramachandran, A. Varma, T. Pourpoint, Y. Zheng, R. Kramer, D. Guildenbecher, R. Gejji, P. Gagare, K. Deshpande, S. Basu, T. Voskuilen, A. Al-Kukhun, D. Gao, H.T. Hwang, J. Mullings, E. Ting, L. Pelter
Purdue University
500 Central Drive
West Lafayette, IN 47907
Phone: (765) 496-2829
E-mail: gore@ecn.purdue.edu

DOE Managers
HQ: Grace Ordaz
Phone: (202) 586-8350
E-mail: Grace.Ordaz@ee.doe.gov
GO: Katie Randolph
Phone: (720) 356-1759
E-mail: Katie.Randolph@go.doe.gov

Contract Number: DE-FC36-06GO86050

Subcontractors:
- National Renewable Energy Laboratory, Golden, CO
- University of Wyoming, Laramie, WY

Project Start Date: September 16, 2006
Project End Date: September 30, 2011

*Congressionally directed project

Fiscal Year (FY) 2011 Objectives

- Develop an energy efficient recycling protocol for ammonia-borane (AB) from spent borate.
- Develop AB slurry-based subscale onboard hydrogen storage systems.
- Develop new noncatalytic methods for hydrogen generation from AB and water.

Technical Barriers

This project addresses the following technical barriers from the Storage section of the Fuel Cell Technologies Program Multi-Year Research, Development and Demonstration Plan:

(A) System Weight and Volume
(B) System Cost
(J) Thermal Management
(R) Regeneration Process
(S) By-product/Spent Material Removal

Technical Targets

On-Board Storage	Units	2010/Ultimate	Purdue 2010
System Gravimetric Capacity	H_2 wt%	4.5/7.5	11~14 (material)
Overall efficiency of off-board regeneration	%	>60	In process being optimized

FY 2011 Accomplishments

- AB thermolysis by-product, polyborazylene, was converted to ammonium borate [$NH_4B(OH)_4$], which was subsequently converted to trimethylborate.
- Reduced trimethylborate using diethylsilane with N^1,N^1,N^2,N^2-tetramethylethane-1,2-diamine (TMEDA) to TMEDA-bisborane complex.
- TMEDA-bisborane complex was converted to AB via transamination in 80% yield.
- Reduced ammonium borate to AB using lithium aluminum hydride with ammonium chloride.
- Analyzed gravimetric and volumetric capacities, H_2 release rates, and byproduct removal for liquid, solid and slurry AB-based systems.
- Addressed scientific and engineering issues with reactor capacities from 0.1 to 50 grams.
- Completed system engineering analysis of a baseline AB/ionic liquid slurry H_2 storage system.
- Obtained high H_2 yield (~14 wt%) and rapid kinetics for neat AB thermolysis under effective heat management at near proton exchange membrane fuel cell (PEMFC) operating temperatures (~90°C).
- Quantified ammonia formation in AB dehydrogenation processes and developed effective removal methods.



Introduction

This project allows the creation of a Hydrogen Research Laboratory in a unique partnership between Purdue University's main campus in West Lafayette and the Calumet campus. This laboratory is engaged in basic research in H_2 production and storage and has initiated engineering systems research with goals established as per the DOE Fuel Cell Technologies Program. Hydrogen production research of this project is reported in Purdue Hydrogen Systems Laboratory: Hydrogen Production.

A task of the H_2 storage work has been focused on finding energy efficient ways to recycle the AB thermolysis and hydrolysis by-products to AB. With the advantage of transportability of byproduct obtained from neat thermolysis

of AB and lessons learned with a gram scale neat AB reactor, we focused on the design, build and demonstration of a vehicle scale H_2 storage system. We have demonstrated that, with effective reaction heat management, high H_2 can be obtained from neat AB near PEMFC operating temperatures with rapid kinetics. We also established a physical property database for solvents and five solvents were selected as potential liquid carriers and mechanistic studies of AB dehydrogenation were conducted for each carrier. It has been reported that ammonia is generated during AB dehydrogenation. For use in PEMFCs, ammonia must be removed from the H_2 stream to less than ~10 ppm level. In our work, ammonia formation for AB dehydrogenation processes was quantified and effective methods for its removal were developed. Based on a neat AB thermolysis approach, we developed the concept of a continuous-flow system, and a prototype unit for laboratory evaluation was constructed. In this unit, the AB fuel feeding, reaction and spent fuel removal steps are integrated, and the reactor has provisions for utilization of waste heat from the PEMFC.

Approach

The spent fuel, ammonium borate or poylborazylene will be converted to triacyl- or trialkyl borates, which will provide molecules with weaker B-O bonds. The reduction of trimethyl borate in the presence of TMEDA, followed by the displacement of TMEDA using ammonia will lead to efficient ammonia borane regeneration.

We applied lessons learned on a multi-gram laboratory scale thermolysis batch reactor to design a cartridge based, self-sustained, and well-instrumented reactor system. The system was used to power a H_2 internal combustion engine (HICE) on a club car. The design uses cartridges that are pre-filled with the storage chemical before being loaded onto the vehicle. The reagent cartridges can be recycled off-board. The reactor system has the flexibility to accommodate slurries and other chemical hydrides. We analyzed a full-scale (for a 80 kW fuel cell) system using AB (80 wt%) and BmimCl (20 wt%) as the H_2 storage medium. The system consists of an AB slurry tank, a slurry pump, a slurry rector, a H_2 buffer tank, a recuperator, a gas/liquid separator, a burner, and a heat transfer fluid (HTF) pump. To size these components, we used an in-house one-dimension computational fluid dynamics model to simulate thermo-chemical processes in the reactor and thermo-fluid processes in other components. The simulation was conducted to achieve a steady-state H_2 flow rate of 1.6 g/s. The H_2 buffer tank was sized to meet dynamic (unsteady state) requirements.

The neat AB thermolysis method for H_2 generation was investigated over a wide range of pressure, heating rate, AB density and insulation amount near PEMFC operating temperatures. For effective reaction heat management, some quartz wool was added at the top of the AB sample, which retains heat of exothermic thermolysis reaction while permitting product H_2 to flow. Mechanistic studies (H_2 yield, thermal characteristics, NH_3 formation, etc.) of AB dehydrogenation for selected liquid carriers were conducted and further investigation was carried out to clarify the reaction mechanism using nuclear magnetic resonance, thermogravimetric analysis/differential scanning calorimetry, Fourier transform infrared and X-ray diffraction techniques. After cooling the reactor to room temperature at the end of the experiments, NH_3 was measured by various methods including Drager tubing, mass spectrometry and titration technique. A continuous-flow H_2 generation system was designed, constructed and tested.

Results

We have achieved the conversion of polyborazylene, obtained via the thermolysis of AB, to ammonium tetramethoxyborate [$NH_4B(OMe)_4$] in the presence of methanol, followed by reduction to AB using lithium aluminum hydride and NH_4Cl in 81% yield. In an alternate protocol, ammonium tetramethoxyborate was converted to trimethyl borate in the presence of methanol. The reduction of trimethyl borate in the presence of TMEDA using diethylsilane resulted in the formation of bisamine borane complex in near quantitative yield (90%). The bisamine borane complex could be readily separated by filtration. The displacement of TMEDA from the amine borane complex was readily achieved using liquid ammonia to obtain 80% yield of AB (Figure 1). We have also reported the conversion of ammonium tetrahydroxyborate [$NH_4B(OH)_4$], hydrolysis by-product of AB, to trimethyl borate without the conversion to boric acid. The reduction of trimethyl borate was achieved using either the silane protocol or via reduction to sodium borohydride with NaH and subsequent conversion to AB in the presence of ammonium sulfate (Figure 2). However, our attempted reduction of boron tristriflate and boron tristrifluroacetate using a variety of silanes has not been successful.

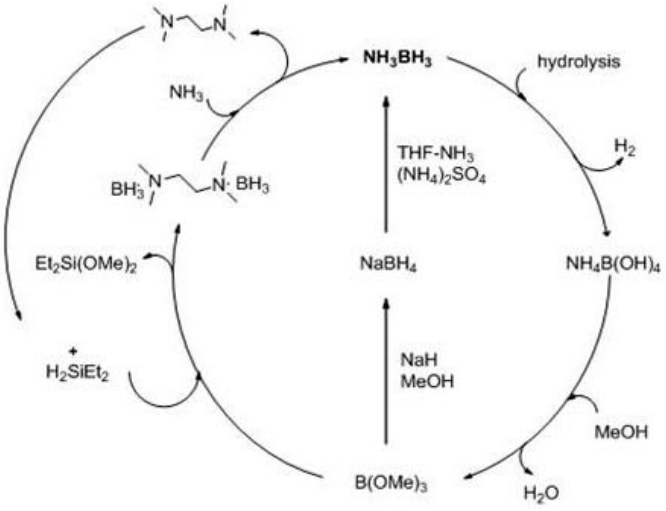


FIGURE 1. AB Hydrolysis Cycle: Recycling of Ammoniumborate

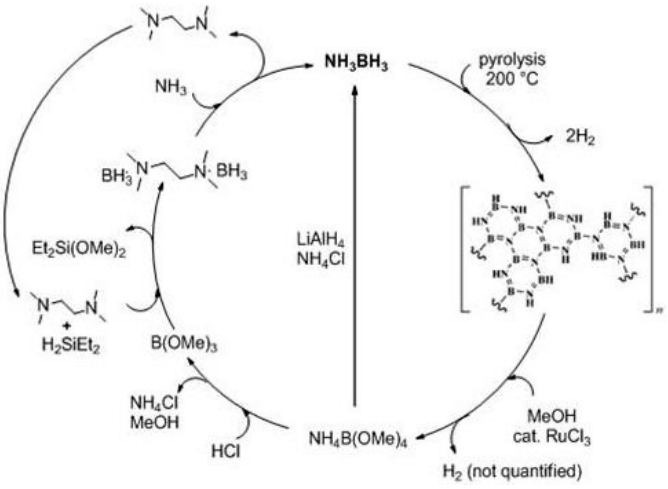


FIGURE 2. AB Themolysis Cycle: Recycling of Polyborazylene

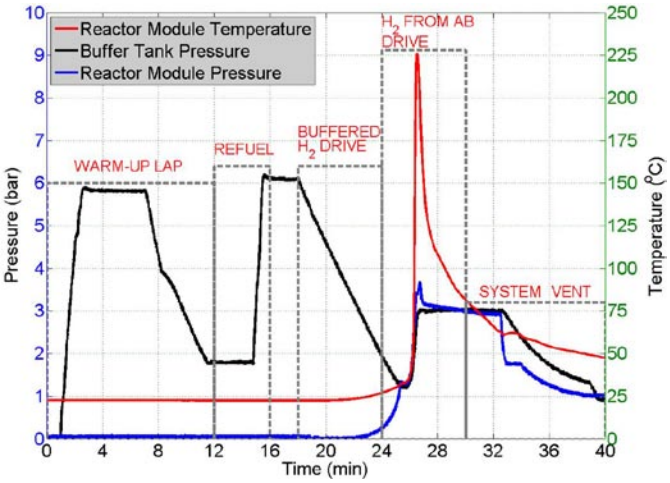


FIGURE 3. Pressure and Temperature Profile in the Club Car Vehicle Demonstration System during System Demonstration using Neat AB pellets

The vehicle-scale system consists of a HICE, four reactor modules, a modified engine exhaust, a buffer tank, and an onboard universal serial bus data acquisition system with a LabVIEW virtual interface for real time monitoring. The modified exhaust line of the HICE diverts using copper spiral tubing the exhaust to the reactor modules. Aluminum honeycomb in contact with the copper spiral further aids heat transfer to the reagent pellets. Figure 3 shows data from a typical experiment with ~50 g of AB pellets loaded in one module. The H_2 buffer tank is first filled to a pressure of ~6 bar from a commercial gas cylinder. Next the HICE is operated on the buffered H_2 and the exhaust is routed away from the reactor modules, allowing for system checks and warm-up. Once proper operation is confirmed, the buffer tank is refilled, and the engine is again operated with the exhaust routed to the first reactor module. The exhaust heat raises the AB temperature until dehydrogenation is achieved.

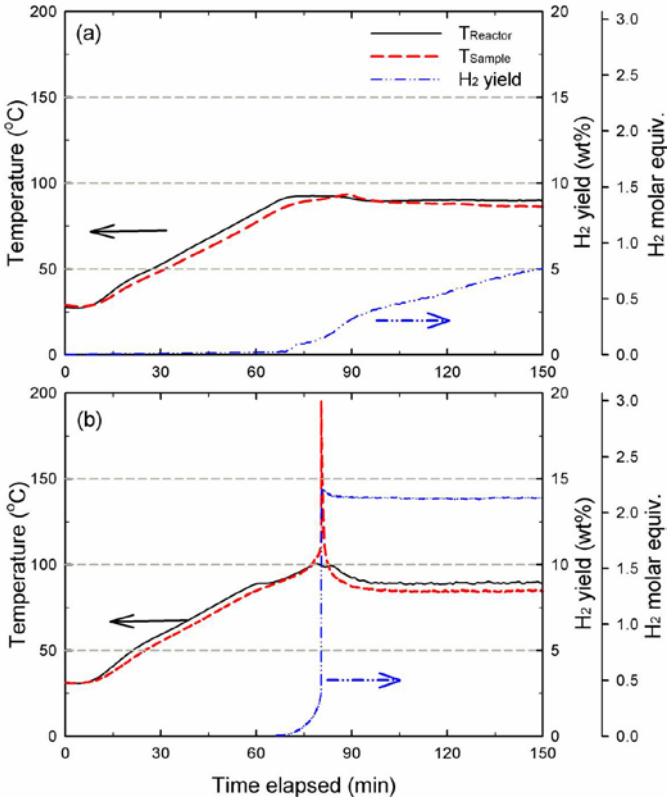


FIGURE 4. H_2 Yield, Temperature Profiles for Neat AB Thermolysis for T_{SP} = 90°C, P_i = 14.7 psia and Heating Rate = 1°C/min (a) without Quartz Wool (b) with Quartz Wool

The reaction leads to a sharp increase in the reactor temperature and increased pressure in the reactor module. The generated H_2 refills the buffer tank and is used to power the HICE. As designed, this process can be repeated with multiple reactor modules, leading to a self-sustained operation. Based on our engineering analysis of a baseline full-scale AB slurry system, a system of 81.2 kg total weight is required to store 5.6 kg usable H_2 or the system gravimetric H_2 storage capacity is 6.9 wt%. Among the total weight, the weight of the AB slurry is 58.5%, the weight of the HTF pump (on-shelf) is 19.7%, the weight of the slurry pump (on-shelf) is 11.7%, and the weight of other components is 10.1%.

We evaluated neat AB thermolysis near PEMFC operating temperature (90°C). For neat AB thermolysis without quartz wool, H_2 gradually evolved with time and only 5 wt% H_2 yield was achieved in 90 min as shown in Figure 4a. On the other hand, under effective heat management, H_2 yield ~14 wt% was achieved and stabilized quickly after sharp heat evolution (Figure 4b). To our knowledge, this value is higher than by any other method using AB at near PEMFC operating temperatures. A key factor is that effective reaction heat management is required to obtain sharp heat evolution, which plays a critical role in providing high H_2 yield. In addition, NH_3 in gaseous product was trace (~1 ppm), much less than that observed in neat AB thermolysis (~400 ppm) without heat

management. The solid products of neat AB thermolysis under heat management were found to be polyborazylene-like species (after 2 H_2 release from AB). At 85°C, similar H_2 yield was obtained from AB in all glycol-type liquid carriers (ethylene glycol, propylene glycol, trimethylene glycol and 1-3-butanediol) and slightly less in dimethyl sulfoxide. However, it was found that all the selected liquid carriers react with AB during dehydrogenation reaction and produce boric acid, which is not preferable from the spent fuel regeneration viewpoint. We demonstrated that NH_3 can be effectively removed by absorption in water, followed by adsorption on impregnated carbon. Our optimization results show that the weight required for the NH_3 removal system can be significantly reduced if water is recycled from the PEMFC. Further, since borazine hydrolyzes readily in water, our proposed method removes ammonia and any volatile borazine present. Based on neat AB thermolysis approach, a continuous-flow H_2 generation system was constructed and tested. Using this system, ~13.5 wt% H_2 yield (~2.1 H_2 molar equivalent) was obtained along with rapid H_2 evolution at 120°C.

Conclusions and Future Directions

We have developed an efficient protocol to prepare AB in large-scale from sodium borohydride and ammonium sulfate. We have developed four protocols to regenerate the spent material; (i) the AB hydrolysis by-product was converted to trimethyl borate and subsequently treated with diethylsilane in the presence of TMEDA to yield TMEDA-Bisborane complex which was converted to AB via transamination using ammonia (ii) the trimethyl borate was reduced to sodium borohydride which upon treatment with ammonium sulfate provided AB, (iii) the AB thermolysis by-product was converted to ammonium tetramethoxyborate and subsequently reduced to AB via silane protocol and (iv) AB was also regenerated form ammonium tetramethoxyborate in the presence of lithium aluminum hydride.

The vehicle-scale reactor system design addresses several engineering concerns with on-board chemical H_2 storage systems. It is compatible with a wide range of H_2 storage chemicals in pure or slurry form and can produce H_2 of sufficient purity for operation with a fuel cell. Future work includes design optimization with a COMSOL-based model, which incorporates reaction kinetics and heat and mass transfer and demonstration with a few other candidate chemicals for comparison. In on-going work we are (1) focusing on the experimental determination of the thermal properties of the ammonia borane pellets used in the vehicle-scale system, and (2) using the thermal property data together with the reaction kinetics data already obtained to improve the fidelity of the numerical model. The AB/BmimCl (80:20) slurry system can meet the 2015 system gravimetric H_2 storage capacity target (5.5 wt%) but can't meet the ultimate target (7.5 wt%). The present on-shelf pumps are too heavy and light HTF and slurry pumps must be developed. In addition, effective spent fuel removal technologies must be developed in the near future.

Under effective reaction heat management, we obtained high H_2 yield (~14 wt%) from neat AB thermolysis at 14.7 psia and T_{SP} 90°C with rapid kinetics, without the use of either catalyst or chemical additives. To our knowledge, this value is higher than by any other method using AB at near PEMFC operating temperatures. We optimized and demonstrated that a sequence of absorption in water and adsorption on impregnated carbon captures ammonia, by-product of AB dehydrogenation, effectively from the product gas stream. Based on neat AB thermolysis, we developed and evaluated a laboratory-scale continuous-flow H_2 generation system. Using this system, ~13.5 wt% H_2 yield was obtained along with rapid H_2 evolution at 120°C. The increase of required reaction temperature, from 90 to 120°C, to rapidly provide high H_2 yield occurs due to heat loss from the reaction zone, and methods to minimize this loss will be investigated in the future.

FY 2011 Publications/Presentations

1. Deshpande, K.A., Voskuilen, T.G., Basu, S., Zheng, Y., Pourpoint, T.L., Gore, J.P., "Design, Construction and Test of a Subscale Ammonia Borane Reactor," *Proceedings of the ASME 2010 International Mechanical Engineering Congress & Exposition IMECE2010*, Nov. 2010, Vancouver, British Columbia, Canada.

2. Basu, S., Zheng, Y., Gore, J.P., "An experimental study of neat and ionic-liquid aided ammonia borane thermolysis," *Journal of Power Sources*, 196: 734-740, 2011.

3. Li, L., Zheng, Y., 2011, "An experimental study of spent fuel transport for onboard hydrogen storage," *Proceedings of the 2011 ASME International Mechanical Engineering Congress and Exposition*, in review.

4. Varma, A., "New Methods to Generate Hydrogen from Boron Compounds and Water for Fuel Cell Applications," *Invited Dept. of Chemical Engineering Seminar*, Columbia University, New York, NY, October 19, 2010.

5. Varma, A., "New Methods to Generate Hydrogen from Boron Compounds and Water for Fuel Cell Applications," *Induction Lecture*, National Academy of Engineering - Mexico, Mexico City, Mexico, November 5, 2010.

6. Hwang, H.T., Al-Kukhun, A., and Varma, A., "Hydrogen Generation From Thermolysis of Neat Ammonia Borane for On-Board Vehicle Applications," *AIChE Annual Meeting*, Salt Lake City, UT, November 8, 2010.

7. Al-Kukhun, A., Hwang, H.T., and Varma, A., "Ammonia Borane Dehydrogenation Always Generates Ammonia, How Much and How to Remove It?," *AIChE Annual Meeting*, Salt Lake City, UT, November 9, 2010.

8. Varma, A., "New Methods to Generate Hydrogen from Boron Compounds and Water for Fuel Cell Applications," *Invited Dept. of Chemical Engineering Seminar*, Georgia Institute of Technology, Atlanta, GA, December 1, 2010.

9. Varma, A., "New Methods to Generate Hydrogen from Boron Compounds and Water for Fuel Cell Applications," *Invited Talk, Tactical Power Sources Summit*, Washington, DC, January 25, 2011.

10. Varma, A., "New Methods to Generate Hydrogen from Boron Compounds and Water for Fuel Cell Applications," *Invited Dept. of Chemical and Biomolecular Engineering Seminar*, Vanderbilt University, Nashville, TN, February 22, 2011.

11. Hwang, H.T., Al-Kukhun, A., and Varma, A., "Hydrogen for Vehicle Applications from Hydrothermolysis of Ammonia Borane: Hydrogen Yield, Thermal Characteristics, and Ammonia Formation," *Industrial & Engineering Chemistry Research*, Vol. 49, pp. 10994-11000, (2010).

12. Diwan, M., Hwang, H., Al-Kukhun, A. and Varma, A., "Hydrogen Generation from Noncatalytic Hydrothermolysis of Ammonia Borane for Vehicle Applications," *AIChE Journal*, Vol. 57, pp. 259-264, (2011).

13. Al-Kukhun, A., Hwang, H.T., and Varma, A., "A Comparison of Ammonia Borane Dehydrogenation Methods for Proton-Exchange-Membrane Fuel Cell Vehicles: Hydrogen Yield and Ammonia Formation and Its Removal," *Industrial & Engineering Chemistry Research* (in press, DOI: 10.1021/ie102157v).

14. Hwang, H.T., Al-Kukhun, A., and Varma, A., "High and Rapid Hydrogen Release from Thermolysis of Ammonia Borane near PEM Fuel Cell Operating Temperatures," (submitted).

IV.G.2 HGMS: Glasses and Nanocomposites for Hydrogen Storage*

Kristina Lipinska-Kalita (Primary Contact), Oliver Hemmers
Harry Reid Center for Environmental Studies
University of Nevada, Las Vegas
4505 Maryland Parkway, Box 454009
Las Vegas, NV 89154-4009
Phones: (702) 895-4450, (702) 895-3742
E-mails: kristina.lipinska@unlv.edu; oliver.hemmers@unlv.edu

DOE Managers
HQ: Grace Ordaz
Phone: (202) 586-8350
E-mail: Grace.Ordaz@ee.doe.gov
GO: Jesse Adams
Phone: (720) 356-1421
E-mail: Jesse.Adams@go.doe.gov

Contract Number: DE-EE0000269

Project Start Date: November 25, 2009
Project End Date: October 31, 2011 - Project delayed by 18 months; new End Date will be determined by DOE.

*Congressionally directed project

Fiscal Year (FY) 2011 Objectives

- To carry out extensive research in fundamental physics and chemistry of glasses and of glass-based nano-crystalline materials.
- To fill gaps in the current understanding of these very complex materials.
- To shed more light on nucleation and crystallization phenomena in glass matrices, which could extend their technological applications.
- The ultimate vision of this project is to develop glass-based materials with structural properties that would make them of interest in H-storage.

Technical Barriers

This project is basic science in nature and involves fundamental research in physics and chemistry of glasses and of glass-based nano-crystalline materials. At this stage it does not address directly any Technical Barriers in hydrogen storage. In particular, hydrogen sorption and desorption tests or possibly kinetic measurements are not part of the project scope. However, the anticipated results could potentially be of interest for the following technical barriers from the Storage section (3.3) of the Fuel Cell Technologies Program Multi-Year Research, Development and Demonstration Plan:

(A) System Weight and Volume
(B) System Cost
(D) Durability/Operability

Technical Targets

This project is conducting studies of fundamental physics and chemistry of glasses and of glass-based nano-crystalline materials. In particular, hydrogen sorption and desorption tests or possibly kinetic measurement are not part of the project scope. However, insights gained from these studies could be applied toward the design and synthesis of new hydrogen storage materials that could potentially be applied towards the following DOE 2011 hydrogen storage technical targets:

- Weight and Volume: 0.045 kg H_2/kg system; 0.028 kg H_2/L system
- Cost: $4/kWh net
- Energy density: 0.9 kWh/L

FY 2011 Accomplishments

- This brand new project required the establishment of two new laboratories: reconstruction/adaptation and purchase of state-of-the-art experimental instrumentation. This process took much longer than anticipated, due to technical issues, and resulted in an 18-month delay in terms of the start of research work.
- The project is composed of several experimental tasks which are sequential and depend on the completion of the new laboratories that is currently in its final phase.
- In the first 18 months of the project (January 2010 – June 2011) focus has been on laboratory space remodel, equipment purchase, installation and testing, hiring of personnel and literature studies.
- Two laboratories were established “from scratch”: the Materials Synthesis Lab combined with Materials at Extreme Environments Lab, as well as the Laser Spectroscopy Lab.
- Materials synthesis and characterization has begun.



Introduction

One of promising concepts for storing hydrogen are micro-containers built of glass and shaped into hollow microspheres. This fundamental research project explores

an extension of this concept where bulk glass materials are proposed to be employed as an inert storage medium. In general, the most desirable materials for hydrogen storage do not interact chemically with hydrogen and possess a high surface area to host substantial amounts of hydrogen. Glasses built of disordered networks with ample void spaces, permeable to hydrogen and glass-derived nanocomposites, hybrids of glass and nanocrystals, appear to be promising candidates for hydrogen storage. Other essential advantages of glasses include simplicity of preparation, flexibility of composition, chemical durability, non-toxicity and mechanical strength, as well as low production costs and environmental friendliness.

For the concept of glass materials to be practically implementable as hydrogen storage media, a considerable amount of fundamental research is still required into bulk glasses and their possible structural modifications. In this respect, this project is at the crossroads of glasses and glass-derived composite materials with structural properties that would make them promising candidates for potential use as hydrogen storage media.

Approach

This project is basic science in nature and it will challenge to extend the concept of using glass-based materials as hydrogen storage media. The focus will be on research of specific glass compositions with emphasis on their fabrication process and characterization using multi-technique experimental approach. The endeavor is to show ways how to tailor the structure of disordered amorphous networks in selected glasses by taking advantage of controlled nucleation and crystallization phenomena and by transforming them into glass-crystal hybrid complex nanocomposites.

Predominantly, this research will fill gaps in the current understanding of a very complex group of materials – glasses – and will shed more light on nucleation phenomena in glasses which will extend the existing variety of their technological applications. A far reaching goal of this project is the successful development of glass-derived composite materials with structural properties that would make them promising candidates for potential use as hydrogen storage media.

Results

The project begun technically only in January 2010 (availability of funds), with the establishment "from scratch" of two new experimental laboratories: Materials Synthesis Lab combined with Materials at Extreme Environments Lab, and the Laser Spectroscopy Lab. The process included reconstruction and adaptation of two lab spaces as well as purchase, installation and testing of state-of-the-art experimental instrumentation. Facility readiness is currently in its final stage, but - due to many technical issues out of this team's control - it resulted in an 18-month delay in terms of the start of research work.

Facility Readiness: Equipment Purchase and Laboratory Setup. This task of the project dealt with lab space reconstruction, which included work on electrical, heating, ventilation and air conditioning, plumbing and fireproofing in order to adapt the lab space to requirements of state-of-the-art new instrumentation. A large portion of the instrumentation had to be selected, negotiated and purchased. This included: a Raman spectrometer, combined with a confocal Raman microscope, a mid-temperature research furnace, optical tables, a multi-wavelength gas laser, a high-temperature research furnace and other minor equipment and lab supplies. After purchase, the instrumentation had to be installed, tested and calibrated in order to be ready for research use. In addition, since the instrumentation includes a spectrometer using a "Class IV" laser radiation source, several layers of physical and safety barriers had to be established to insure safe operation. In order to conform to institution and state and federal requirements Safety Rules, Dos and Don'ts and Use Rules had to be formulated to allow for the laser to be operated.

Experimental Work: Synthesis and Processing of Glass Materials. This task of the project deals with synthesis of the first batch of glass materials. This includes successful fabrication of few silica-based glasses with titanium, tantalum and gallium acting as network formers and/or network modifiers.

Experimental Work: Synthesis of Glass-Based Nanocrystalline Composites. Following the first glass synthesis, this task of the project consisted in successful fabricating of several nanocrystalline composites based on the above mentioned glass batches. This is an important achievement since there are only very few known glass compositions that allow for size-controlled formation of nanocrystals inside a glass matrix.

Conclusions and Future Directions

Technical delays associated with establishment of two new laboratories and purchasing of instrumentation were unavoidable, but difficult to deal with, since they delayed the start of experimental research work in this project.

Future work will involve materials synthesis and characterization:

- Continue synthesis and processing of glass materials.
- Continue synthesis of glass-based nanocrystalline composites.
- Perform micro-structural and nano-structural studies using a multi-technique approach.
- Determine microstructural changes produced in glass networks as a result of nucleation and growth of specific nanocrystalline phases.
- Comprehensive understanding of structure and packing density in the fabricated glasses.

FY 2011 Publications/Presentations

1. Presentation at DOE Annual Merit Review and Peer Evaluation Meeting, May 9–13, 2011, Washington D.C., HGMS: Glasses and Nanocomposites for Hydrogen Storage.

IV.G.3 Hydrogen Storage Materials for Fuel Cell-Powered Vehicles*

Andrew Goudy
Delaware State University
1200 N. Dupont Highway
Dover, DE 19901
Phone: (302) 857-6534
E-mail: agoudy@desu.edu

DOE Managers
HQ: Ned Stetson
Phone: (202) 586-9995
E-mail: Ned.Stetson@ee.doe.gov
GO: Katie Randolph
Phone: (720) 356-1759
E-mail: Katie.Randolph@go.doe.gov

Contract Number: DE-FC36-06GO86046

Start Date: July 1, 2006
Projected End Date: May 30, 2013

* Congressionally directed project

Fiscal Year (FY) 2011 Objectives

The objectives of this project are to:

- Identify complex hydrides that have the potential to meet DOE's goals for storage and demonstrate the optimum temperature and pressure ranges under a variety of conditions. Develop new catalysts and engineering techniques for increasing reaction rates and lowering reaction temperatures.
- Perform kinetic modeling studies and develop methods for improving kinetics and lowering reaction temperatures, thereby reducing refueling time.
- Extend the studies to include other complex hydrides, such as the $LiNH_2/MgH_2$ system, that have greater hydrogen storage potential.
- Extend studies to include carbon materials, metal organic frameworks (MOFs), and possibly other nanostructured and porous materials as potential hydrogen storage materials using hydrogen spillover.
- Design, fabricate and test a hydride-based hydrogen storage system for fuel cell applications in collaboration with our partners at the University of Delaware. Improve the rate at which the hydrogen gas can be charged into a hydride-based hydrogen storage tank, and to improve the hydrogen storage density.

Technical Barriers

This project addresses the following technical barriers taken from the Hydrogen Storage section of the Fuel Cell Technologies Program Multi-Year Research, Development and Demonstration Plan:

(A) System Weight and Volume
(D) Durability/Operability
(E) Charging/Discharging Rates

Technical Targets

This project is conducting fundamental studies of complex borohydride materials and other promising hydrogen storage materials. Insights gained from these studies will be applied toward the design and synthesis of hydrogen storage materials that meet DOE's 2015 goal of 5.5 weight percent hydrogen storage for the system. The following Table summarizes the targets.

TABLE 1. Technical Targets

Storage Parameter	Units	Target
System Gravimetric Capacity: Usable, specific-energy from H_2 (net useful energy/ max system mass)	kWh/kg	1.5
System Volumetric Capacity: Usable energy density from H_2 (net useful energy/max system volume)	kWh/L	1.2
Storage System Cost (and fuel cost)	$/kWh	6

FY 2011 Accomplishments

- The desorption properties for a series of $MgH_2/LiBH_4$ systems of compositions MgH_2-$2LiBH_4$, MgH_2-$4LiBH_4$, and MgH_2-$7LiBH_4$ have been determined. Temperature programmed desorption (TPD) results show that desorption temperatures increase with increasing amounts of $LiBH_4$. Pressure-composition isotherm (PCI) results show that plateau pressures decrease with increasing amounts of $LiBH_4$ and the amount of hydrogen released increases with increasing amounts of MgH_2.
- This work has shown that KH is a very effective catalyst for the desorption of hydrogen from the MgH_2-$2LiNH_2$ system.
- We have determined activation energies for the MgH_2-$2LiNH_2$ system with and without a KH catalyst using Kissinger analysis. Results show that the KH lowers the activation energy.
- The design, fabrication and demonstration of a hydride-based hydrogen storage system for fuel cells is underway. Results show that the heat removal rate can be increased by increasing the effective thermal conductivity by mixing the metal hydride with conductivity-enhanced materials such as aluminum foam or graphite.

Introduction

There has been considerable interest in complex hydrides such as borohydrides and amides because they have been determined to have great potential to meet DOE's goals for hydrogen storage. Current efforts in our research lab are focused on performing hydrogen storage studies on some new destabilized complex hydrides that have been predicted by first principles calculations to be suitable hydrogen storage materials. We will develop methods for the synthesis, characterization, and modeling of these new complex hydrides as well as developing new catalysts and engineering techniques for increasing reaction rates and lowering reaction temperatures. We will also extend these studies to include carbon materials, MOFs and possibly other nanostructured and porous materials as potential hydrogen storage materials. Once a suitable material has been identified for hydrogen storage it will be necessary to design, fabricate and test a hydride-based hydrogen storage system for fuel cell applications. Efforts are currently underway with a partner institution to design a hydrogen storage system and test it using a suitable material. This phase of the research will include using flow, reaction kinetics and thermal modeling, followed by system design, fabrication and performance evaluation.

Approach

To achieve the project objectives, new materials are being developed and characterized using a variety of techniques. Sample preparations prior to analysis were done in an argon-filled glove box (Vacuum Atmosphere Company). The hydrides were made by first ball milling the raw materials in a SPEX 8000 Mixer Miller and then directly combining them with hydrogen in a Sieverts apparatus. X-ray powder diffraction in a Panalytical X'pert Pro MPD Analytical X-Ray Diffractometer was used to confirm the formation of product and to determine phase purity. Thermogravimetric analyses (TGA) and TPD were used to determine the thermal stability and the hydrogen capacity of the mixtures. The TGA analyses were done in a Lab System-Diamond thermo-gravimetric/differential thermal analyzer. This instrument was placed inside of an argon-filled glove box so that samples can be analyzed with virtually no exposure to air and moisture. The TPD analyses were carried out in a PCI unit. The instrument was supplied by Advanced Materials Corporation. Kinetic measurements were done to determine the overall reaction rates.

Results

Previous studies have indicated that the $MgH_2/LiBH_4$ system has the potential to meet DOE's hydrogen storage goals. Therefore the desorption properties of a series of $MgH_2/LiBH_4$ systems were studied to determine how suitable these materials were for hydrogen storage. The systems studied had compositions of MgH_2-$2LiBH_4$, MgH_2-$4LiBH_4$, and MgH_2-$7LiBH_4$. TGA measurements were done on each of the three systems to see if there was any correlation between temperature and composition. The results in Figure 1 show that desorption temperatures increase with increasing amounts of $LiBH_4$. It was also of interest to determine the reversibility of these systems. To accomplish this, pressure-composition-isotherms were constructed for each system at several temperatures. The PCI results shown in Figure 2 demonstrate that plateau pressures decrease with increasing amounts of $LiBH_4$ and the amount of hydrogen released increases with increasing amounts of MgH_2. Kinetics and modeling studies are presently underway to determine the rates of hydrogen release from these materials at constant pressure thermodynamic forces. We have already determined that the rate decreases with increasing amounts of $LiBH_4$. It will

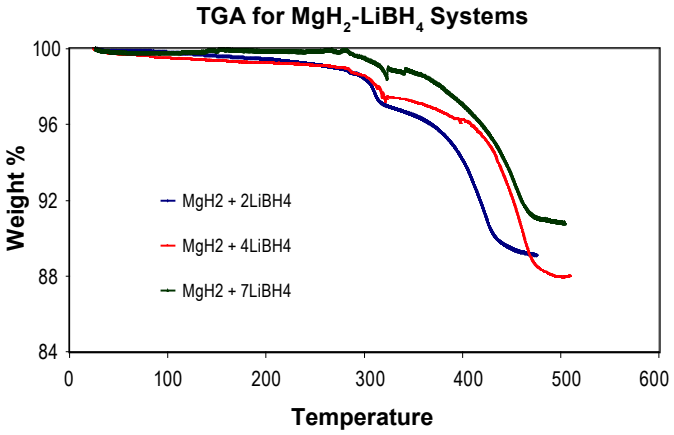


FIGURE 1. Thermal Gravimetric Analyses for Several MgH_2-$LiBH_4$ Systems. Desorption temperatures increase with increasing amounts of $LiBH_4$.

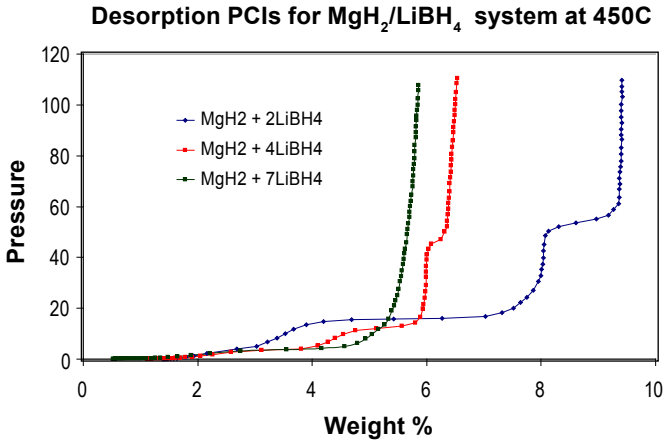


FIGURE 2. Desorption PCIs for $MgH_2/LiBH_4$ System at 450°C. Plateau pressures decrease with increasing amounts of $LiBH_4$ and the amount of hydrogen released increases with increasing amounts of MgH_2.

also be useful to determine if the same or similar processes controls the reaction rates in all three systems.

There have been reports that systems based on $MgH_2/LiNH_2$ may also have the potential to meet DOE's goals for hydrogen storage. Therefore the desorption properties of a $MgH_2/2LiNH_2$ system were determined. PCIs were determined, with and without a KH catalyst, at several temperatures. The results show a well defined plateau region. Van't Hoff plots were used to determine the enthalpies of formation. Kinetics studies were done at constant pressure thermodynamic forces such that the ratio of the plateau pressure to the applied hydrogen pressure was held approximately constant at 10 in all cases. Results shown in Figure 3 indicate that the catalyzed system reacted much faster than the un-catalyzed system. Activation energies were determined by doing differential thermal analyses (DTA). Desorption temperatures were determined at several scan rates. DTA curves showed that the desorption temperatures increase with increasing scan rates. These results were used to construct Kissinger plots. The activation energies for the catalyzed and uncatalyzed systems were 106 and 116 kJ/mol respectively. As expected, the catalyzed system had lower activation energy than the catalyzed one.

Another project is underway entitled "Design, Fabrication and Demonstration of a Hydride-Based Hydrogen Storage System for Fuel Cell Applications". The overall objective is to improve the rate at which the hydrogen gas can be charged into a hydride-based hydrogen storage tank, and to improve the hydrogen storage density. A mathematical model is being used to predict the temperature at selected locations within the storage tank. A series of experiments have been performed to compare the temperature at these locations with the numerically predicted value. Three experiments in Figure 4 were done to compare the temperature in the storage tank to that predicted by a numerical model. The results for experiment agreed to within ±5 degrees. It has been determined that the heat removal rate can be increased by (i) increasing the effective thermal conductivity by mixing the metal hydride with conductivity-enhanced materials such as aluminum foam or graphite, (ii) optimizing the shape of the tank, and (iii) introducing an active cooling environment instead of relying on natural convection. All of this work is being done by our partners at the University of Delaware.

Conclusions and Future Directions

- This work has shown that several destabilized borohydride systems based on $Li(BH_4)_2/MgH_2$ can absorb hydrogen reversibly but the desorption temperatures increase and hydrogen holding capacities decrease as the relative amount of $LiBH_4$ increases. We have also determined that KH is a very effective catalyst for the desorption of hydrogen from the MgH_2-$2LiNH_2$ system.
- In the FY 2011-2012, the following work is planned:
  - Continue the desorption studies on several MgH_2/Amide based destabilized systems using techniques such as ball milling, PCI measurements, XRD, TPD, TGA, kinetics and modeling.
  - Perform kinetics and modeling studies on the $MgH_2/LiBH_4$ systems at constant pressure driving forces in order to establish the rate-controlling process.

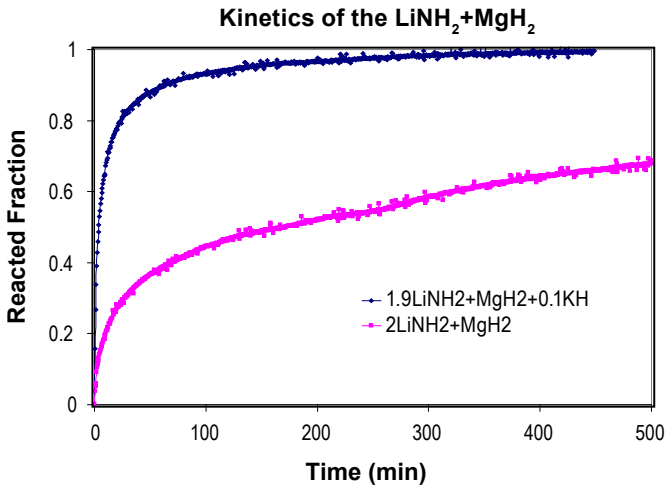


FIGURE 3. Kinetics of the MgH_2-$2LiNH_2$ System. Measurements were done at 210°C and the ratio of the plateau pressure to the applied hydrogen pressure was set at 10. The system containing 3.3 mol% KH catalyst reacts about 10 times faster than the un-catalyzed system. The un-catalyzed system required more than 3,000 min to reach completion.

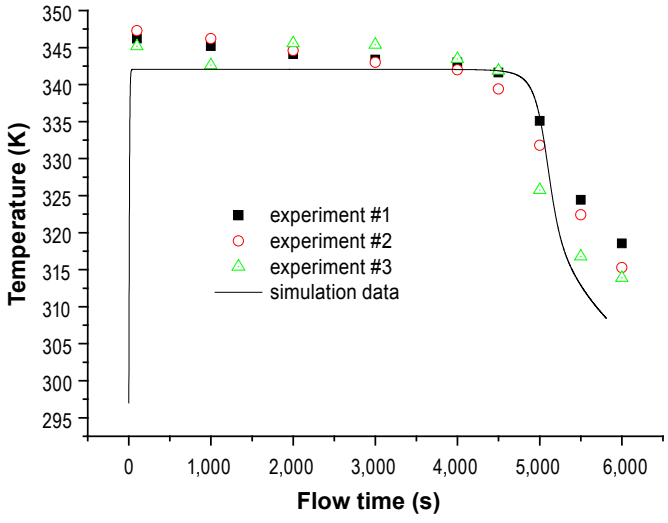


FIGURE 4. A mathematical model was used to predict the temperature at selected locations within the storage tank. Three experiments were done to compare the temperature in the storage tank to that predicted by a numerical model. The results for experiment agreed with the predicted values to within ±5 degrees.

- Use techniques such as residual gas analysis to determine if dehydrogenation is accompanied by the release of other gaseous byproducts.
- Continue with the design, fabrication and demonstration of a hydride-based hydrogen storage system that is on-going with our collaborators at the University of Delaware.

FY 2011 Publications/Presentations

1. Hongwei Yang, Samuel Orefuwa and Andrew Goudy, "Study of Mechanochemical Synthesis in the Formation of the Metal-Organic Framework $Cu_3(BTC)_2$ for Hydrogen Storage", Micropor. Mesopor. Mater., (2011) DOI: 10.1016/j.micromeso.2011.02.003.

2. T. Durojaiye, A. Ibikunle and A.J. Goudy, "Hydrogen Storage in Destabilized Borohydride Materials" Int. J. Hyd. Energy, (2010) DOI: 10.1016/j.ijhydene.2010.08.006

3. S.T. Sabitu, O. Fagbami, A.J. Goudy, "Kinetics and Modeling Study of Magnesium Hydride with Various Additives at Constant Pressure Thermodynamic Driving Forces," J. Alloys Compds, (2010), doi:10.1016/j.jallcom.2010.11.174.

4. Hongwei Yang, Adeola Ibikunle and Andrew J. Goudy, "Effects of Ti-based additives on the hydrogen storage properties of a $LiBH_4/CaH_2$ destabilized system" Advances in Materials Science and Engineering, vol. 2010, Article ID 138642, 7 pages, 2010. doi:10.1155/2010/138642.

5. A.J. Goudy; A. Ibikunle; and T. Durojaiye, "Hydrogen Storage in Destabilized Borohydride Materials", Symposium FB "Materials and Process Innovations in Hydrogen Production and Storage" of the 5th Forum on New Materials of CIMTEC 2010, June 13–18, 2010.

6. S.T. Sabitu, O. Fagbami and A.J. Goudy, "Kinetics and Modeling Study of Magnesium Hydride with Various Additives at Constant Pressure Thermodynamic Driving Forces", International Symposium on Metal-Hydrogen Systems – Fundamentals and Applications, Moscow, Russia, July 19–23, 2010.

7. A. Benson and A.J. Goudy, "Synthesis and Desorption Properties of Mixed Alkali Hexahydride Alanates", Intercollegiate Student Chemists Convention, West Chester, PA, 2011.

V. FUEL CELLS

V.0 Fuel Cells Sub-Program Overview

The Fuel Cells sub-program supports research, development, and demonstration of fuel cell technologies for a variety of stationary, transportation, and portable applications, with a primary focus on reducing cost and improving durability. These efforts include research and development (R&D) of fuel cell stack components, system balance-of-plant (BOP) components, and subsystems, as well as system integration. The sub-program seeks a balanced, comprehensive approach to fuel cells for near-, mid-, and longer-term applications. Existing early markets and near-term markets include portable power, backup power, auxiliary power units, and specialty applications such as material handling equipment. Mid- and longer-term applications with more stringent technical and cost requirements include distributed power generation (e.g., combined heat and power [CHP] for residential and commercial applications) and transportation (e.g., light-duty vehicles and transit buses). The sub-program's portfolio of projects covers a broad range of technologies, including polymer electrolyte membrane fuel cells, direct methanol fuel cells, alkaline fuel cells, and solid oxide fuel cells (SOFCs).

The Fuel Cells sub-program's tasks in the *Fuel Cell Technologies Program Multi-Year Research, Development and Demonstration Plan* are organized around development of components, stacks, sub-systems, and systems; supporting analysis; and testing, technical assessment, and characterization activities. Task areas for fuel cell system and fuel processor sub-system development for stationary power generation applications are included, as are those for early market fuel cell applications, such as portable power, and for the development of innovative concepts for fuel cell systems.

Goal

The sub-program's goal is to advance fuel cell technologies for stationary, portable, and transportation applications to make them competitive in the marketplace in terms of cost, durability, and performance, while ensuring maximum environmental and energy-security benefits.

Objectives[1]

The sub-program's key objectives include:

- By 2015, develop a fuel cell system for portable power (<250 W) with an energy density of 900 Wh/L.
- By 2017, develop a 60% peak-efficient, direct-hydrogen fuel cell power system for transportation, with 5,000-hour durability, that can be mass produced at a cost of $30/kW.
- By 2020, develop distributed generation and micro-CHP fuel cell systems (5 kW) operating on natural gas or liquefied petroleum gas that achieve 45% electrical efficiency and 60,000-hour durability at an equipment cost of $1,500/kW.
- By 2020, develop medium-scale CHP fuel cell systems (100 kW–3 MW) that achieve 50% electrical efficiency, 90% CHP efficiency, and 80,000-hour durability at a cost of $1,500/kW for operation on natural gas and $2,100/kW when configured for operation on biogas.
- By 2020, develop a fuel cell system for auxiliary power units (1–10 kW) with a specific power of 45 W/kg and a power density of 40 W/L at a cost of $1,000/kW.

Fiscal Year (FY) 2011 Technology Status

The need for cost reductions and improvements in durability continue to be the key challenges facing fuel cell technologies. In addition, advances in air, thermal, and water management are necessary for improving fuel cell performance; some stationary applications would benefit from increased fuel flexibility, and, while fuel cells are approaching their targets for power density and specific power, further progress is required to achieve system packaging requirements necessary for commercialization.

One of the most important metrics is the projected high-volume manufacturing cost for automotive fuel cells—the Program tracks this on an annual basis. The 2011 estimate of this cost is $49/kW, which represents

[1] Note: Targets and milestones are under revision; therefore, individual progress reports may reference prior targets.

a 33% decrease since 2008 and an 82% decrease since 2002, as depicted in Figure 1. The 33% decrease in projected cost since 2008 stems in part from a reduction in precious grade metal loading and an increase in cell power density, allowing the design of smaller and less expensive stacks. The 2011 cost analysis estimated the cost of the fuel cell stack to be $22/kW. BOP cost has also been reduced during this time. Major sources of the reduction in BOP cost include reconfiguration of the ejector system based on stakeholder input, redesign of the system controller, and reduction of the radiator size. The reduced radiator size was enabled by improvements in stack components, allowing a higher stack operating temperature.

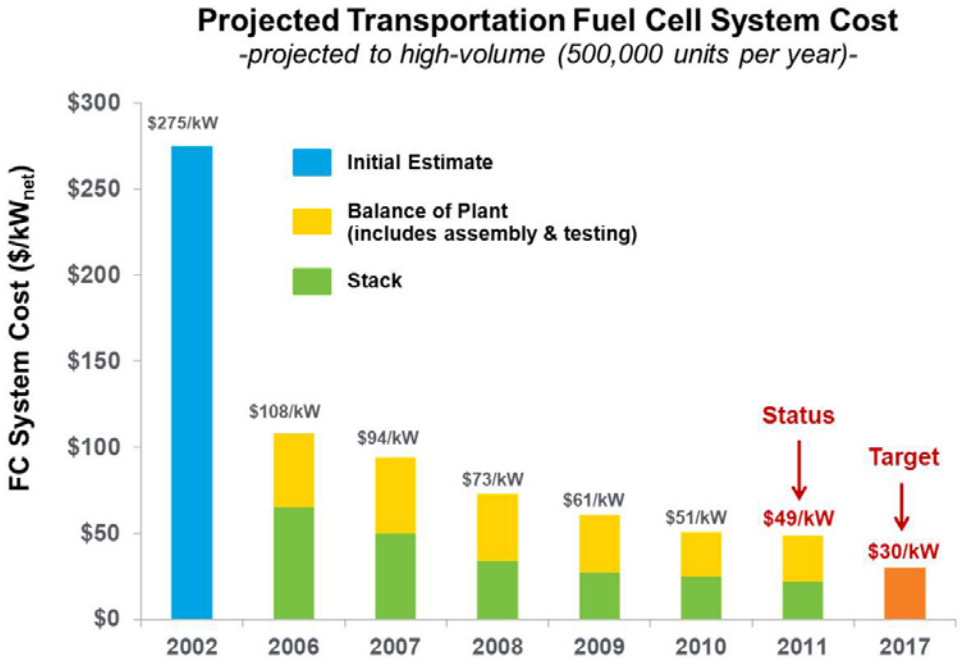


FIGURE 1. Current Modeled Cost of an 80-kW Automotive Fuel Cell System Based on Projection to High-Volume Manufacturing (500,000 units/year)[2]

FY 2011 Accomplishments

In FY 2011, continued progress was made toward meeting 2017 technical and cost targets. Notable technological advances in several component areas have led to significant improvements in performance and durability, with decreased cost. Key advances in FY 2011 include the following:

- **Nano-segregated binary and ternary catalysts demonstrated performance more than 6X that of platinum:** Following on the discovery of the exceptionally high activity of the $Pt_3Ni(111)$ surface for the oxygen reduction reaction, which has specific activity two orders of magnitude higher than that of Pt/C,[3] Argonne National Laboratory (ANL) is working to develop nanosegregated Pt/Ni catalysts that can achieve similar activity in a catalyst suitable for incorporation in fuel cells. Pt/Ni catalysts synthesized thus far at ANL have mass activity six times that of Pt/C (Figure 2), approaching the DOE target activity of 0.44 A/mg. The Pt/Ni catalysts also have better durability than conventional Pt/C. ANL is also developing a variety of ternary catalysts in which an Au core is encapsulated by an FePt shell. These ternary catalysts also exhibit better activity and stability than conventional Pt/C.

[2] DOE Hydrogen and Fuel Cells Program Record #11012, http://hydrogen.energy.gov/pdfs/11012_fuel_cell_system_cost.pdf.
[3] Nenad Markovic et al., "Nanosegregated Cathode Catalysts with Ultra-Low Platinum Loading," 2011 DOE Hydrogen and Fuel Cells Program Annual Merit Review Proceedings, http://www.hydrogen.energy.gov/pdfs/review11/fc008_markovic_2011_o.pdf.

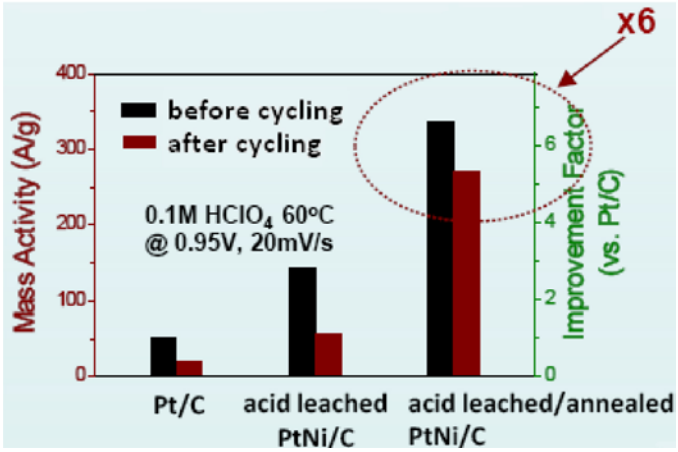


FIGURE 2. Mass Activity of Several Pt-Based Catalysts for the Oxygen Reduction Reaction[4]

- **New cathode and anode catalysts demonstrated durability under startup/shutdown:** Significant progress has been made in addressing degradation that can occur under startup, shutdown, and fuel-starvation conditions. Work led by 3M has resulted in development of new cathode and anode catalysts to increase durability.[5] 3M has incorporated a highly active and highly durable oxygen evolution catalyst on the cathode, based on Ru and Ir. By enhancing oxygen evolution, these catalysts suppress excursions to high voltage, and thus mitigate corrosion of catalysts and supports. In collaboration with 3M, ANL has developed calixarene-modified anodes, on which the oxygen reduction reaction is suppressed without inhibiting hydrogen oxidation. Use of the modified cathode and anode catalysts has enabled successful achievement of 10,000 simulated startup/shutdown cycles with only 2 µg/cm^2 more precious grade metal content, in addition to the 0.15 mg/cm^2 total Pt content (Figure 3).

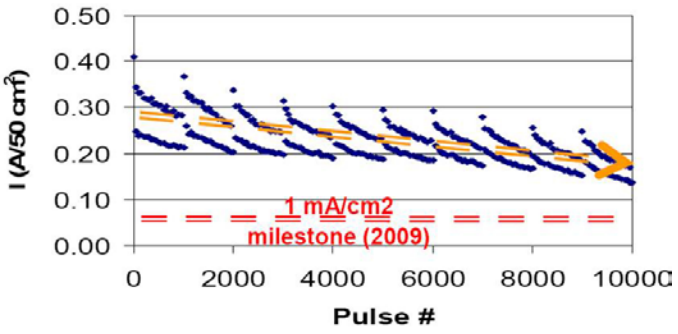


FIGURE 3. Oxygen Evolution Performance Of A Modified Cathode Catalyst – Performance Remains Higher than the Target even after 10,000 Cycles[6]

- **Degradation studies enabled design of more durable electrodes:** Los Alamos National Laboratory has demonstrated the relationship between electrode structure and cell durability.[7] They found that the degree of ordering and agglomeration of perfluorosulfonic acid (PFSA) ionomer during electrode preparation is

[4] Ibid.
[5] Radoslav Atanasoski et al., ""Durable Catalysts for Fuel Cell Protection During Transient Conditions," 2011 DOE Hydrogen and Fuel Cells Program Annual Merit Review Proceedings, http://www.hydrogen.energy.gov/pdfs/review11/fc006_atanasoski_2011_o.pdf.
[6] Ibid.
[7] Rod Borup et al., "Durability Improvements Through Degradation Mechanism Studies," 2011 DOE Hydrogen and Fuel Cells Program Annual Merit Review Proceedings, http://www.hydrogen.energy.gov/pdfs/review11/fc013_borup_2011_o.pdf.

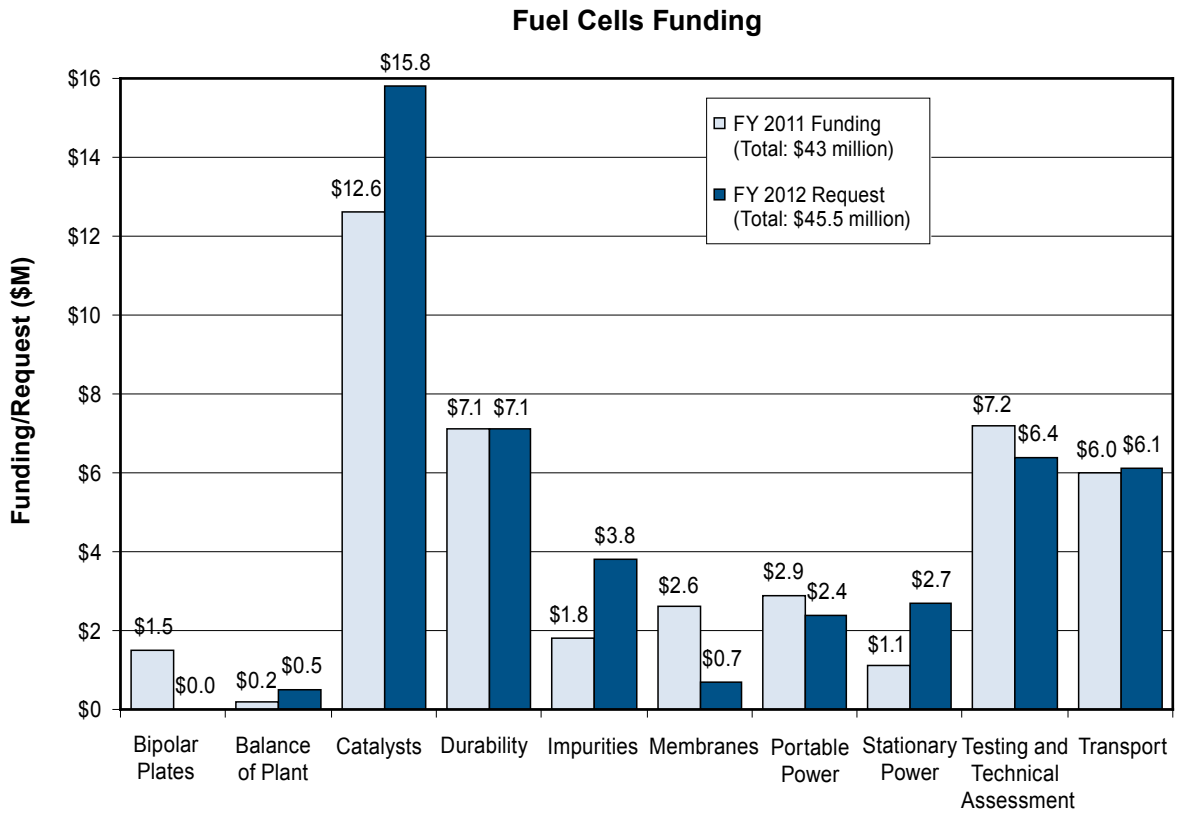
related to the long-term stability, with a higher degree of ordering correlating with lower stability. They also discovered that ionomer aggregation in solution leads to poorer mechanical properties in cast ionomer films, suggesting that the observed electrode stability differences are related to the mechanical properties of the ionomer in the electrode. Electrodes prepared from glycerol-based inks, in which little ionomer agglomeration occurs, demonstrated high stability, with less than 30 mV loss at 0.8 A/cm^2 after 70,000 cycles, exceeding the DOE target of 30,000 cycles. In contrast, electrodes prepared from water/alcohol-based inks, in which ionomer agglomeration occurs, were shown to suffer from severe degradation.

- **Innovative membranes demonstrate high conductivity at low relative humidity:** Progress in development of perfluoroimide acid (PFIA) membranes has enabled 3M to meet most DOE targets for high-temperature membranes, and 3M is close to fulfilling the final target of 0.02 ohm-cm^2 area specific resistance at 120°C and 40 kpA of water vapor.[8] The 3M PFIA ionomer is related to conventional PFSA ionomers, but it incorporates two superacid sites per side chain–an imide acid site in the middle of the chain, and a sulfonic acid site at the end of the chain. This configuration allows use of a lower equivalent weight ionomer with a more highly acidic acid group. The multi-acid side chain approach allows preservation of the perfluorinated backbone crystallinity at lower equivalent weights than with conventional PFSA. This enables higher conductivity under dryer conditions without sacrificing mechanical properties, and it is expected to lead to better performance and durability than conventional PFSAs.
- **Performance and durability of SOFC systems improved:**
  - Reversible SOFCs under development at Versa Power Systems have made significant progress, meeting resistance, degradation, and current density targets.[9]
  - In addition to the increase in SOFC system power density achieved in FY 2010, Acumentrics has demonstrated increased durability, with more than 12,000 hours of operation.[10] Acumentrics also increased system electrical efficiency from 35% to 40%, through enhancements made in reforming technology and generator design. These advances represent a significant step toward production of an SOFC system for widespread commercialization.

Budget

The President's FY 2012 budget request calls for approximately $45.5 million for the Fuel Cells sub-program. The following figure shows the budget breakdown by R&D area for the FY 2011 congressional appropriation of $43 million and the FY 2012 budget request. The sub-program continues to focus on reducing costs and improving durability with an emphasis on fuel cell stack components. The funding profiles for FY 2011 and the FY 2012 request are very similar, with some projects in membranes and bipolar plates ending in FY 2011.

[8] Steven Hamrock et al., "Membranes and MEA's for Dry, Hot Operating Conditions," 2011 DOE Hydrogen and Fuel Cells Program Annual Merit Review Proceedings, http://www.hydrogen.energy.gov/pdfs/review11/fc034_hamrock_2011_o.pdf.
[9] Randy Petri et al., "Advanced Materials for RSOFC Dual Mode Operation with Low Degradation," 2011 DOE Hydrogen and Fuel Cells Program Annual Merit Review Proceedings, http://www.hydrogen.energy.gov/pdfs/review11/fc042_petri_2011_o.pdf.
[10] Norman Bessette et al., "Development of a Low Cost 3-10kW Tubular SOFC Power System," 2011 DOE Hydrogen and Fuel Cells Program Annual Merit Review Proceedings, http://www.hydrogen.energy.gov/pdfs/review11/fc032_bessette_2011_o.pdf.



FY 2012 Plans

In FY 2012, the Fuel Cells sub-program will continue R&D efforts on fuel cells and fuel cell systems for diverse applications, using a variety of technologies (including polymer electrolyte membrane, solid oxide, and alkaline fuel cells) and a range of fuels (including hydrogen, diesel, natural gas, and bio-derived renewable fuels). Support will continue for R&D that addresses critical issues with electrolytes, catalysts, electrodes, and modes of operation. The sub-program will also continue its emphasis on science and engineering at the cell and stack level and on integration and component interactions at the system level. Significant emphasis will be placed on BOP component R&D (such as humidifiers and air compressors) that can lead to lower cost and lower parasitic losses. Ongoing support of modeling will guide component R&D, benchmarking complete systems before they are built and enabling exploration of alternate system components and configurations. Cost analysis efforts have been expanded to include distributed power generation systems (including CHP) and systems for emerging markets for a variety of fuel cell technologies; detailed results of these analyses are expected in FY 2012.

FY 2012 will see the continuation of most existing projects, as well as the initiation of new projects. A fuel cell R&D solicitation closed in FY 2011, and a small number of new R&D projects from the solicitation are expected to begin in FY 2012, subject to appropriations.

Dimitrios Papageorgopoulos
Fuel Cells Team Lead
Fuel Cell Technologies Program
Department of Energy
1000 Independence Ave., SW
Washington, D.C. 20585-0121
Phone: (202) 586-5463
E-mail: Dimitrios.Papageorgopoulos@ee.doe.gov

V.A.1 Analysis of Laboratory Fuel Cell Technology Status – Voltage Degradation

Jennifer Kurtz
National Renewable Energy Laboratory (NREL)
1617 Cole Blvd.
Golden, CO 80401
Phone: (303) 275-4061
E-mail: jennifer.kurtz@nrel.gov

DOE Manager
HQ: Kathi Epping Martin
Phone: (202) 586-7425
E-mail: Kathi.Epping@ee.dog.gov

Project Start Date: July, 2009
Project End Date: Project continuation and direction determined annually by DOE

Fiscal Year (FY) 2011 Objectives

- Benchmark state-of-the-art fuel cell durability.
- Leverage analysis experience from Fuel Cell Vehicle Learning Demonstration project.
- Collaborate with key fuel cell developers on the analysis.

Technical Barriers

This project addresses the following technical barriers from the Fuel Cells section of the Fuel Cell Technologies Program Multi-Year Research, Development and Demonstration Plan:

(A) Durability

Technical Targets

This project is conducting an independent assessment of current laboratory fuel cell stacks and systems durability. The analysis, applied uniformly on all data sets, studies the projected operation time to 10% voltage drop. All results are aggregated to protect proprietary information and reported on by the expected application.

FY 2011 Accomplishments

- Published three composite data products (CDPs) on operation time and projected operation time to 10% voltage drop statistics, projected operation time sensitivity to voltage drop levels, and comparison of automotive lab and field durability projections:
  - Automotive
    - Average projected operation hours to 10% voltage drop ~4,000 hours.
    - Maximum projected operation hours to 10% voltage drop ~12,000 hours.
  - Backup
    - Average projected operation hours to 10% voltage drop ~3,300 hours.
    - Maximum projected operation hours to 10% voltage drop ~7,000 hours.
  - Forklift
    - Average projected operation hours to 10% voltage drop ~13,000 hours.
    - Maximum projected operation hours to 10% voltage drop ~21,000 hours.
  - Stationary
    - Average projected operation hours to 10% voltage drop ~17,000 hours.
    - Maximum projected operation hours to 10% voltage drop ~41,000 hours.
- Analyzed fuel cell stack and system data in four application categories and from eight fuel cell developers.
- All data included many proton exchange membrane (PEM) fuel cells and solid oxide fuel cells (SOFCs) of full active area short stacks and full stacks with systems
- Shared all detailed data analysis results with data providers.



Introduction

The DOE has funded significant research and development activity with universities, national laboratories, and the fuel cell industry to improve market competitiveness of fuel cells. Most of the validation tests to confirm improved fuel cell stack performance and durability (market competitiveness) are completed by the research organizations themselves. Although this allows the tests to be conducted by the developers most familiar with their specific technology, it also presents a number of challenges in sharing progress publicly because test conditions and data analysis take many forms, and data collected during testing are often considered proprietary.

NREL is benchmarking the state-of-the-art fuel cell performance, specifically on durability, through independent assessment of current laboratory data sets. The data processing, analysis, and reporting capitalize on capabilities developed in DOE's Fuel Cell Vehicle Learning Demonstration. Fuel cell stack durability status is reported annually and includes a breakdown of status for different applications. A key component of this project is the collaborative effort with key fuel cell developers to

understand what is being tested in the lab, study analysis results, and expand the included data sets.

Approach

The project involves voluntary submission of data from relevant fuel cell developers. We are contacting the fuel cell developers for multiple fuel cell types to either continue or begin a data sharing collaboration. A continuing effort is to include more data sets, types of fuel cells, and developers.

Raw and processed data are stored in NREL's Hydrogen Secure Data Center. Processing capabilities are developed or modified for new data sets and then included in the analysis processing of NREL's Fleet Analysis Toolkit. The incoming raw data may be new stack test data, or it may be continuation of data that has already been supplied to NREL. After the raw data are processed, the results are analyzed with particular attention to durability and operating conditions. Each individual data set has a set of data figures that are shared with the data provider and used to create the CDPs. CDPs are designed to report on the technology status without revealing proprietary information.

Results

This fuel cell stack durability analysis grew in the number of data sets, applications, fuel cell types, and the details published. Results published in June 2010 were the second update for this analysis effort, and the next analysis update is scheduled for July 2011. In the last published data set, four applications were covered, eight fuel cell developers supplied data (more than one data set in many cases), and the data sets covered PEM and SOFC stack testing. The analyzed data sets are from lab testing of full active area short stacks (e.g, stacks with fewer cells than the expected full power stack) and test systems with full power stacks. The data sets also vary from one to the other in how the stack/system was tested. Data was generated between 2004 and early 2010 from different testing methods that included constant load, transient load, and accelerated testing. The variability in test conditions and test setups create a group of data that can be difficult to compare. Additional breakdown of the data sets is an important aspect of future work and is dependent on the accumulation of more data sets in order to not reveal data supplier contribution to the results or proprietary data.

Fuel cell durability is studied at a design specific current point and measured against a target of 10% voltage drop from beginning of life. The 10% voltage drop metric is used for assessing voltage degradation with a common measurement, but the metric may not be the same as end-of-life criteria and does not address catastrophic failure modes. Figure 1 is an aggregated set of results separated by application and identifies the percentage of short stacks and how many data sets are still operating (at the time of the results) for each application. Each application has the average, maximum, 25th and 75th percentiles values

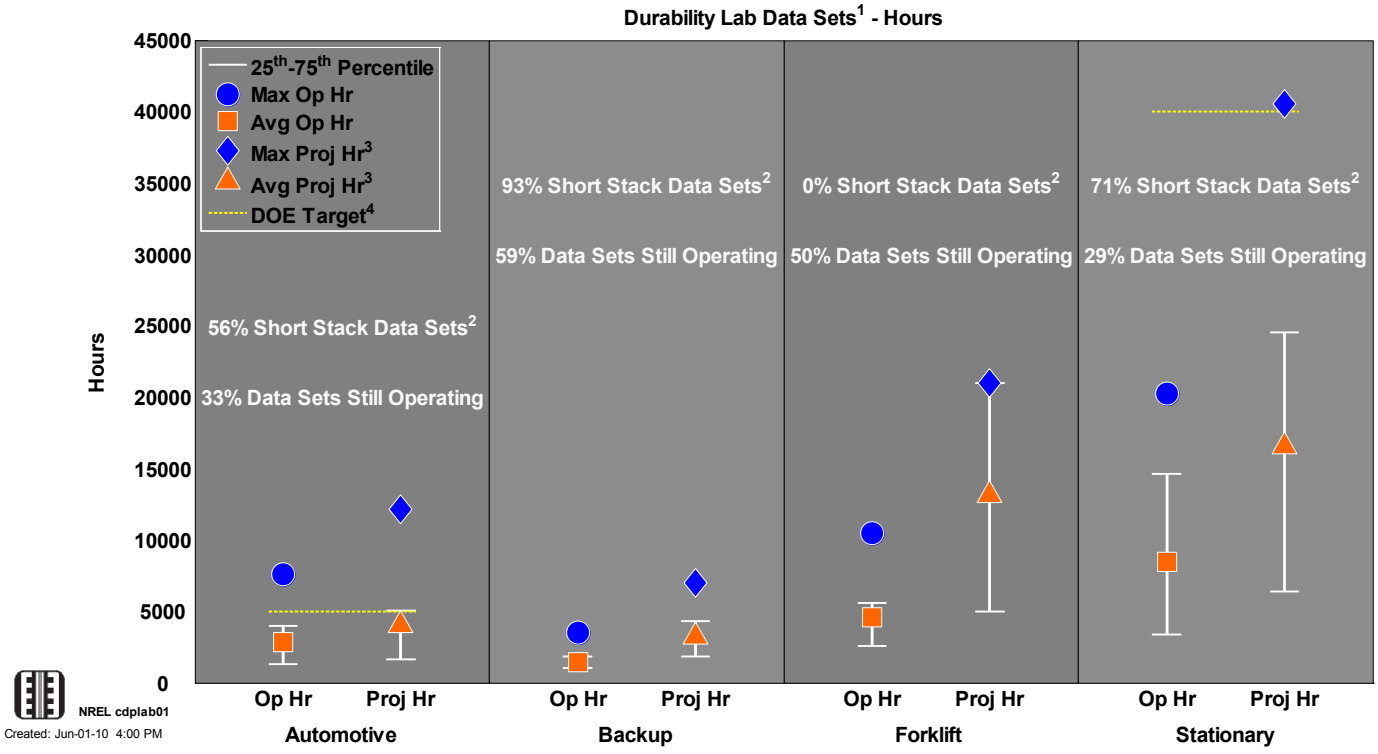


FIGURE 1. Fuel Cell Operation Hours and Projection Hours to 10% Voltage Drop by Application

identified for the operation hours and the projection hours to 10% voltage drop. Table 1 summarizes the average values highlighted in Figure 1.

TABLE 1. Summary of Average Operation Hour and Average Projection Hour to 10% Voltage Drop by Application

Application	Average Operation Hour	~Average Projection Hour to 10% Voltage Drop
Backup	1,424	3,300
Automotive	2,865	4,000
Forklift	4,573	13,000
Stationary	8,438	17,000

The 10% voltage drop level is not necessarily a measurement for end-of-life or even significant reduction in performance. Figure 2 depicts the sensitivity of each application's projected hours to a varying voltage degradation level. Each curve represents the average for each application, but the graph does not imply that all stacks will (or do) operate at these voltage degradation levels. In the analysis, the projection may be limited by the demonstrated operation hours to minimize extrapolations. This limit is why the application average curves flatten out at the higher voltage degradation levels.

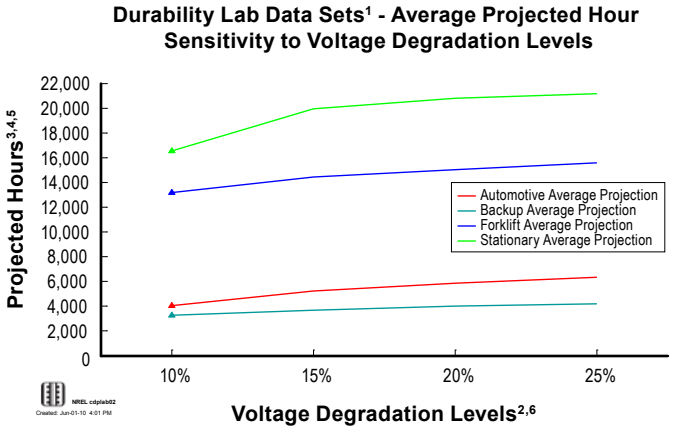


FIGURE 2. Durability Projection Sensitivity to Measured Voltage Degradation Levels

Another avenue for analysis is the comparison of data generated from testing in the lab and real-world operation. Figure 3 is the first phase in this comparison analysis. In addition to this analysis of lab data sets, NREL is also studying the performance of many fuel cell applications in real-world settings. Improvements were demonstrated in the field for Generation 2 fuel cell vehicles as seen in Figure 3. A large improvement is also observed when comparing the

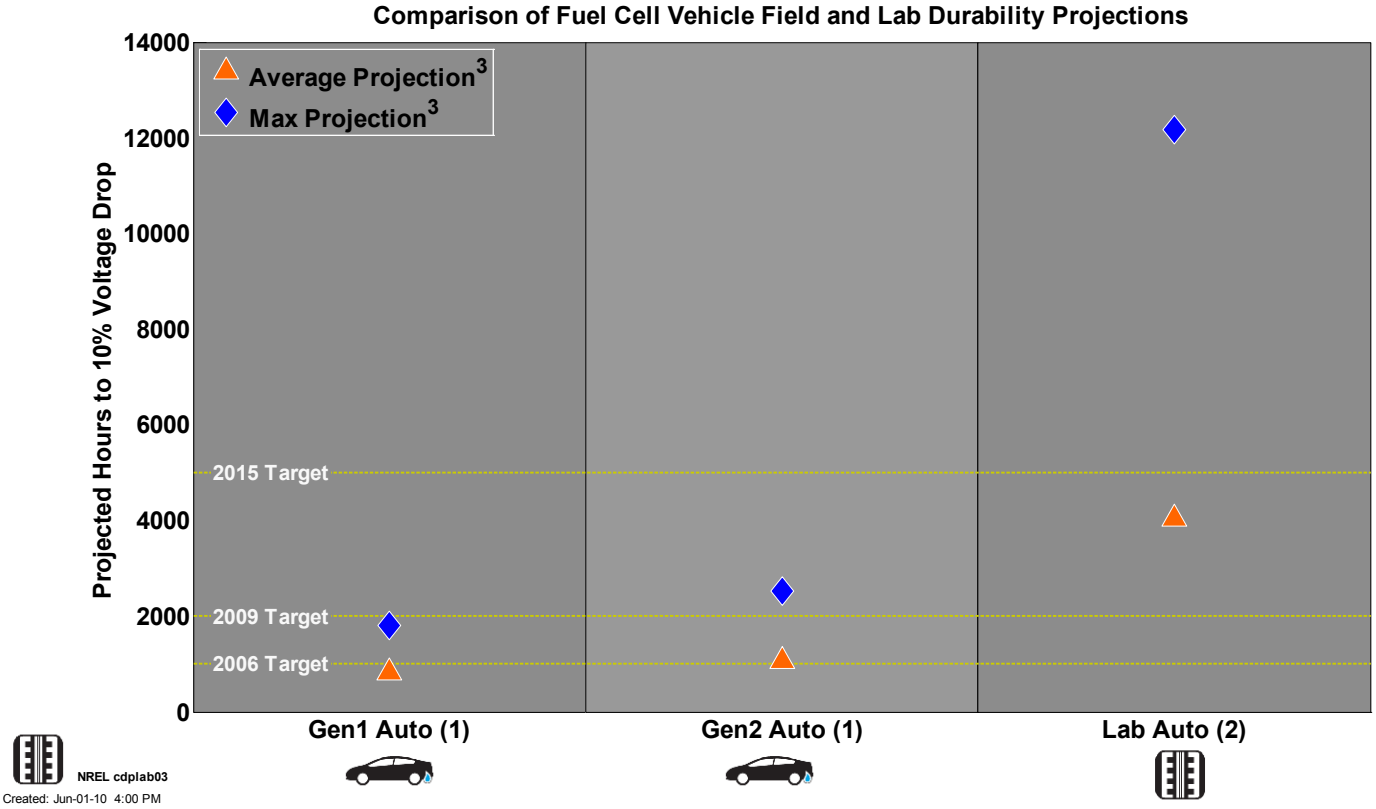


FIGURE 3. Automotive Fuel Cell Durability Projection Comparison between Lab and Field Data

Generation 2 field data with the lab data results. There are a number of potential explanations for the improvements: 1) improvements in technology generation and performance; 2) testing conditions; 3) 56% of the lab data sets are short stacks, and none are integrated into a vehicle; and 4) data providers in the lab category are not all the same as the data providers for the field category.

Conclusions and Future Direction

This analysis effort highlights the positive progress made by the fuel cell developers with the state-of-the-art fuel cell stacks and applies a uniform analysis method to aggregate and report on the results. Results highlight the difference in performance between applications to meet specific market needs as well as the needs for expansion of the results for more details and categories, such as accelerated testing. Data are supplied voluntarily and an important aspect of this project is the collaboration effort to study the data, project durability, and report on the results without revealing proprietary data. Eight fuel cell developers have already supplied data and other fuel cell developers are expected to add data for the next analysis and reporting cycle.

Planned future work is as follows:

- Update analysis results through published CDPs (July 2011).
- Continue collaboration and data sharing with existing data suppliers and other fuel cell developers (on-going).
- Accumulate more data to allow for new and more detailed CDPs (on-going).
- Expand comparison of durability projections between lab data and field data (July 2011).

FY 2011 Publications/Presentations

1. Kurtz, J.; Wipke, K.; Sprik, S. "Fuel Cell Technology Status – Voltage Degradation," presented at DOE's Annual Merit Review May 12, 2011.

2. Kurtz, J.; Wipke, K.; Sprik, S. "Analysis Results of Lab and Field Fuel Cell Durability." presented at 2010 Fuel Cell Seminar October 20, 2011.

V.A.2 Mass-Production Cost Estimation for Automotive Fuel Cell Systems

Brian D. James (Primary Contact), Kevin N. Baum
Directed Technologies, Inc. (DTI)
3601 Wilson Blvd., Suite 650
Arlington, VA 22201
Phone: (703) 243-3383
E-mail: brian_james@directedtechnologies.com

DOE Managers
HQ: Jason Marcinkoski
Phone: (202) 586-7466
E-mail: Jason.Marcinkoski@ee.doe.gov
GO: Greg Kleen
Phone: (720) 356-1672
E-mail: Greg.Kleen@go.doe.gov

Technical Advisor
Bryan Pivovar
Phone: (303) 275-3809
E-mail: bryan.pivovar@nrel.gov

Contract Number: National Renewable Energy Laboratory (NREL) Subcontract No. AGB-0-40628-01 under NREL Prime Contract No. DE-AC36-08GO28308

Project Start Date: July 8, 2010
Project End Date: May 8, 2012

Fiscal Year (FY) 2011 Objectives

- Prepare a written report documenting the results and assumptions used in the 2010 80 kW automotive fuel cell system cost analysis.
- Continue cost analysis of automotive fuel cell systems and update the cost estimates for 2011 technology advances.
- Examine the robustness and technological maturity of the capital equipment projected to be used in fabrication of automotive fuel cell power systems, so as to determine where further research and development is required.
- Determine the optimal operating pressure, air stoichiometry and catalyst loading to achieve minimal system cost.
- Thoroughly examine both currently used and developing quality control (QC) measures for each step of the stack manufacturing process to assess cost impact and high rate production feasibility.
- Explore the trade-off between system efficiency and fuel cost in order to optimize the system for lifecycle cost (LCC).

Technical Barriers

This project addresses the following technical barriers from the Fuel Cells section (3.4.4) of the Fuel Cell Technologies Program Multi-Year Research, Development and Demonstration Plan:

(B) Cost

Technical Targets

This project will provide realistic, defensible fuel cell power systems cost estimates for comparison with the DOE technical targets. Insights gained from these estimates will help to adjust and further validate the DOE targets. Furthermore, our analysis will shed light on the areas in need of the most improvement and thereby provide guidance for future fuel cell research and development efforts.

TABLE 1. DOE Targets/DTI Estimates in $/kW$_{e\ (net)}$ (at 500,000 Systems/Year Manufacturing Rate)

	DOE 2010 Target	DTI 2010 Estimate	DTI 2011 Interim Estimate
Stack Cost	$25	$25	$22
System Cost	$45	$51	$48

Accomplishments

- Document 2010 Cost of Automotive Fuel Cell Systems:
  - Prepared a reference report on the cost of automotive fuel cell systems utilizing 2010 technology.
- Assessment of Capital Equipment and Research and Development (R&D) Needs:
  - Tabulated the major capital equipment needed for the manufacturing of all stack and most major balance-of-plant (BOP) components.
  - Evaluated each process and rated them for both cost assumption risk and process risk.
  - Used this ranking system to identify which components are in need of the most R&D in order to achieve risk reduction.
- Optimization of Operating Conditions to Minimize System Cost:
  - Collaborated with Rajesh Ahluwalia at Argonne National Laboratory (ANL) to develop a simplified five-variable stack polarization curve based on ANL's existing models and 2009 polarization data from 3M.
  - Used this simplified polarization curve to independently vary pressure, catalyst loading, temperature and air stoichiometry to select the

optimal combination of parameters for lowest overall system cost.

- Assessment of Fuel Cell Manufacturing QC Systems:
  - Investigated potential QC systems for each step of the stack production.
  - Determined the optimal QC systems to be used both in the 2010 system and 2015 system.
  - Added the appropriate costs and changed the appropriate process parameters for each QC system.
- LCC Assessment of Automotive Fuel Cell Systems:
  - Collaborated with Rajesh Ahluwalia of ANL to conduct basic LCC analysis to determine the optimal tradeoff between system efficiency and fuel cost.
- Preliminary 2011 Cost Assessment:
  - Integrated the above studies with the 2010 cost estimate to prepare a preliminary 2011 automotive fuel cell system cost assessment.
  - Improved existing conceptual design and component specification of complete fuel cell power systems at two technology levels (2011, and 2015).



Introduction

The project seeks to estimate the material and manufacturing costs of complete 80 kW_{net} direct-hydrogen proton exchange membrane (PEM) fuel cell systems suitable for powering light-duty automobiles. The project examines five annual production rates (1,000, 30,000, 80,000, 130,000, and 500,000 systems per year) and three projected technology levels (2010, 2011, and 2015). The project builds upon work previously conducted by DTI for the DOE under a multi-year effort entitled "Mass-Production Cost Estimation for Automotive Fuel Cell Systems", which focused on annual updates of system cost. Unlike that past effort, the current project is structured as a series of analytic studies, which when taken together, work to strengthen and update the cost analysis to reflect 2011 technology.

Approach

The project consists of a series of semi-independent analyses based on the cost estimation work previously conducted by DTI for 2010 technology automotive fuel cell systems. The approach to each task will be described individually below.

Documentation of the 2010 Cost Estimates: A comprehensive written report was prepared to document the system configuration, designs dimensions, manufacturing and assembly assumptions, and cost results made for the 2010 cost estimates.

Capital Equipment and R&D Needs: Each manufacturing process associated with the stack and some of the BOP components was evaluated both for the cost assumption risk and process risk. Cost assumption risk gauges risk that uncertainty or errors in assumed capital cost or material cost used in the analysis may lead to significant increases in overall system cost. Process risk gauges the risk that uncertainty or errors in defining the manufacturing and assembly process (including process parameters such as cycle times) may lead to an end product that doesn't meet minimum performance standards or otherwise forces system changes that lead to system cost increase. Both risk scales range from 1 to 3. When these ratings are summed, they yield a combined score which may be used to rank the overall risk of that process or component. Components with a combined score of 4 or more are components that warrant R&D attention.

Operating Condition Optimization: In order to represent stack polarization performance within the cost model, ANL exercised their stack performance model over a range of expected operating conditions to create a numerical database of projected polarization curves. A regression analysis was then conducted on the approximately 600 data points to derive a simplified second-order polynomial equation representing 3M's 2009 current density as a function of five independent variables: cell voltage, catalyst loading, pressure, temperature, and air stoichiometry. This enabled the fuel cell cost model to determine system cost for all combination of these variables. Pressure was varied from 1.5 atm to 3 atm. Air stoichiometry was varied from 1.5 to 2.5. Temperature was varied from 75°C to 95°C. Cathode catalyst loading was varied from 0.10 $mgPt/cm^2$ to 0.20 $mgPt/cm^2$. (Anode catalyst loading was held constant at 0.05 $mgPt/cm^2$.) In addition to the manual optimization, a Monte Carlo analysis was conducted using the @Risk plug-in for Excel. Ten thousand iterations of the DTI fuel cell system cost model were run varying the four stack parameters over the ranges previously states. (Cell voltage was held constant at 0.676 V.) The results were then sorted by resulting system cost. The iteration with the lowest system cost was used to identify the optimal stack parameters.

QC: In order to ensure that adequate QC systems were included in the automotive fuel cell system cost estimates, a comprehensive reassessment of stack manufacturing and assembly QC systems was conducted. The reassessment began with the QC systems utilized in the 2010 system cost estimates and combined it with the PEM-focused QC work being conducted at Ballard, BASF, NREL, the National Institute of Standards and Technology, and Precitec Inc.. Competing QC systems from these organizations were conceptually applied to each step of the stack manufacturing process. The systems were extrapolated to high production rates and assessed on the basis of practicality and cost. In some cases, more advanced QC processes, still in the testing phase, were hypothesized for the 2015 system.

LCC: A simplified LCC analysis was conducted to explore the tradeoff between the initial purchase price of the fuel cell power system and the fuel cost over the lifetime of

the vehicle. By assessing this tradeoff, the system efficiency and operating conditions that lead to the lowest overall lifecycle cost may be identified. The methodology employed consists of three main steps: 1) determination of the stack operating parameters (total catalyst loading, temperature, pressure, air stoichiometry) that lead to minimum system cost at stack efficiencies from 48.8% to 57% (which corresponds to cell voltages of 0.6 to 0.7 volts per cell), 2) determine the relationship between system efficiency and vehicle fuel consumption (miles per gallon gasoline equivalent) for a specified set of vehicle assumptions (vehicle mass, frontal area, rolling resistance, drive cycle, etc.) through use of the ANL PSAT model, 3) determine lifecycle system costs by assessing the net present value of vehicle initial cost and annual operating expenses.

Results

- Results for the capital cost tabulation and risk assessment can be found in Table 2. The highest combined risk scores were for the membrane production process and the nano-structured thin filament (NSTF) catalyst coating process with risk scores of 5.5 and 6, respectively. (NSTF risk is high primarily due to lack of demonstrated performance using high rate production techniques.) In the BOP, the only component with a combined risk score above 4 is the membrane humidifier with a score of 6 (also due to lack of demonstration using high rate production techniques).
- Table 3 displays the optimized parameters that lead to lowest system cost as determined via DTI's parametric analysis of the parameters and verified by Monte Carlo analysis. A sequence of four different scenarios is shown in Table 3: the pre-optimization values used in the DTI 2010 cost analysis, the previous case but with minor system adjustments to the assumptions, the previous case with the new simplified polarization equation from ANL, and finally the post-optimization values using the ANL polarization equation. The resulting system cost is observed to decrease from \$51.38/kW_{net} to \$47.81/kW_{net}. In order to achieve such a cost reduction, stack temperature was increased to its upper limit of 95°C, air stoichiometry was reduced to its lower limit of 1.5, stack pressure was increased to the upper limit of 3 atm, and total catalyst loading was increased to 0.186 mgPt/cm^2.
- As shown in Table 4, despite the high capital cost of much of the QC equipment, at the highest production level, the cost impact of the added QC is very low, only \$0.32/kW_{net}. The addition of these systems, however, seeks six-sigma-level quality of the finished products to protect against malfunctions in the manufacturing that would incur costs far exceeding that of the QC equipment.
- The LCC analysis shown in Figure 1 reveals that there is an optimum/minimal lifecycle cost occurring at roughly 44% system efficiency, which translates to 0.61 volts/cell. However, the optimization curve is very flat and shows only a minor cost change (~\$70) over the range of system efficiencies examined (43% to 51%). Decreases in fuel cost due to increased efficiency are almost totally offset by the subsequent increase in power plant purchase price. Sensitivity analysis shows the optimization curve to be surprising flat over all expected parameter ranges.

TABLE 2. Manufacturing Process Risk Assessment

Stack Component Manufacturing			
Step/Component	**Process Risk**	**Cost Assumption Risk**	**Total Score**
Bipolar Plate Stamping	1	1	2
Bipolar Plate Coating	1.67	2	3.67
Membrane Production	2.5	3	5.5
NSTF Coating	3	3	6
Microporous GDL	2	2	4
M & E Hot Pressing	2	2	4
M & E Cutting & Slitting	1	1	2
MEA Frame/Gaskets	2	2	4
Coolant Gaskets (Laser Welding)	2	1	3
End Gaskets (Screen Printing)	2	1	3
End Plates	1	1	2
Current Collectors	1	1	2
Compression Bands	1	2	3
Stack Assembly	1	2	3
Stack Conditioning	2	2	4
BOP Component Manufacturing			
Step/Component	**Process Risk**	**Cost Assumption Risk**	**Total Score**
Membrane Air Humidifier	2	3	5
Belly Pan	1	1	2
Ejectors	2	1	3
Stack Housing	1	1	2
Air Precooler	1	1	2
Demister	1	1	2
CEM	2	2	4

GDL - gas diffusion layer; MEA - membrane electrode assembly; M&E - membrane & electrode; CEM - compressor-expander-motor

Conclusions and Future Directions

Key conclusions from the past year of the project include:

- Membrane fabrication and NSTF catalyst application are the stack components, and the membrane air

TABLE 3. Key Parameters and Cost Results for Different Sets of Parameters

		Base Case (2010 Status)	Base Case w/ Updates	Base Case w/ Updates & ANL Curve Fit	Optimized Case
Annual Production Rate	systems/year	500,000	500,000	500,000	500,000
Stack Efficiency @ Rated Power	%	55%	55%	55%	55%
Cell Voltage @ Rated Power	V/cell	0.676	0.676	0.676	0.676
Oxygen Stoichiometric Ratio		2.5	2.5	2.5	1.5
Peak Stack Operating Pressure	atm	1.69	1.69	1.69	3
Peak Stack Operating Temperature	°C	90	90	90	95
Total Platinum-Group Catalyst Loading	$mgPt/cm^2$	0.15	0.15	0.15	0.186
MEA Areal Power Density @ Rated Pov	mW/cm^2	833	833	732	1,110
Power Density Equation Selected		Standard	Standard	ANL Curve Fit	ANL Curve Fit
System Cost	**$/kW$_{net}$**	**$51.38**	**$51.92**	**$54.72**	**$47.81**

TABLE 4. QC Systems and their Associated Cost Impact

	Total Cost Increase from QC Equipment				
	Technology Level	2011			
	Systems/year	1,000	30,000	80,000	130,000	500,000
QC Cost ($/kW$_{net}$)	Membrane QC	$5.14	$0.17	$0.06	$0.04	$0.01
	NSTF Catalyst Deposition QC	$1.24	$0.04	$0.03	$0.04	$0.03
	MEA QC	$4.76	$0.16	$0.06	$0.04	$0.02
	Bipolar Plates QC	$0.35	$0.03	$0.03	$0.03	$0.03
	MEA Frame Gasket QC	$1.17	$0.19	$0.18	$0.18	$0.18
	GDL QC	$0.61	$0.02	$0.02	$0.02	$0.02
	End Plate QC	$0.21	$0.01	$0.00	$0.00	$0.00
	Laser Welding BPP QC	$0.35	$0.03	$0.03	$0.03	$0.03
	Total ($/kW$_{net}$)	**$13.81**	**$0.66**	**$0.43**	**$0.38**	**$0.32**

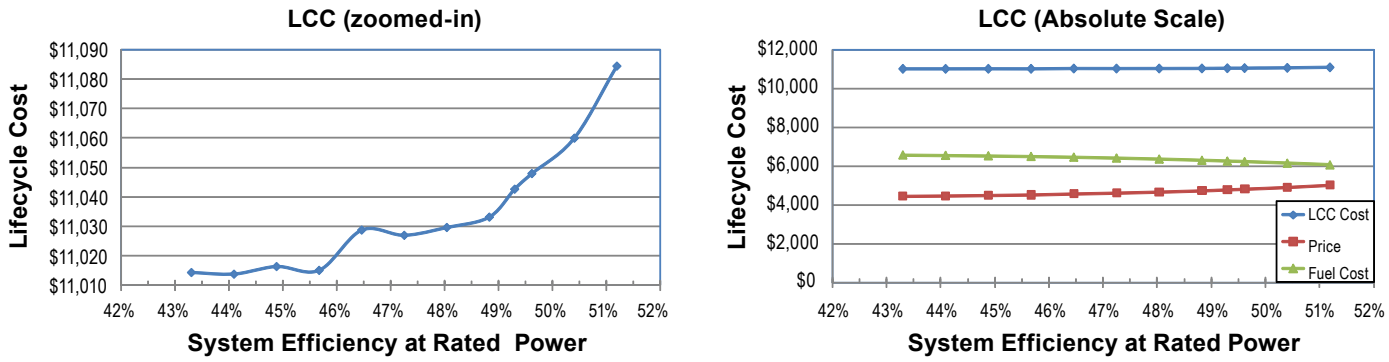


FIGURE 1. Lifecycle Cost Results

humidifier is the BOP component, that carry the highest cost risk. These components have a significant impact on the overall system cost and therefore warrant an R&D focus.

- The system cost is quite sensitive to the oxygen stoichiometric ratio; doubling this value adds roughly $8/kW$_{net.}$ and is a direct consequence of increased compressor size and a larger system gross power.

- Air pressure has a relatively large impact on system cost; the minimum costs at the extremes of the range of validity shift the cost by \$8/kW_{net}. Above this range, the costs are expected to decrease further and bottom out around 4 atm; although performance at pressures greater than 3 atm are outside the range of validity of the ANL polarization curve fits and thus have greater uncertainty.
- Stack temperature has a limited impact on system cost: the system cost difference between 75°C and 95°C peak temperature operation being only \$3/kW.
- The impact of changing the catalyst loading is comparatively minimal. The maximum cost change between systems optimized across this range of loadings is about \$2/kW_{net}.
- With the exception of the catalyst loading, all the parameters leading to the minimum system cost are at one of the limits of their ranges of validity. This suggests that these ranges of validity ought to be examined to see if they can be expanded, so as to lower costs further.
- Increases in discount rate minimize net present value of the fuel costs, thus favoring lower efficiency systems that have lower initial capital investments.
- Conversely, increases in H_2 cost increase the lifecycle fuel costs, favoring higher efficiency. Increasing vehicle lifetime favors higher efficiency systems, since longer lifetime increases the relative impact of fuel cost.
- Finally, power system markup increases favor higher efficiency systems that have a lower power system capital cost, and thus a decreased impact due to a the higher markup.

FY 2011 Publications/Presentations

1. August 18th, 2010 - Detroit, MI: Presentation to Fuel Cell Tech Team.

2. May 12th, 2011 – Washington, DC: Presentation to DOE H_2 Program Review.

3. June 16th, 2011 – Germany: Presentation at 12th Ulm Electrochemical Talks, Presented by DOE (Jason Marcinkoski).

4. "Manufacturing Process Assumptions Used in Fuel Cell System Cost", Journal of Power Sources, doi:10.1016/j.jpowsour.2011.02.035 (Marcinkoski J, James BD, Kalinoski JA, Podolski W, Benjamin T, Kopasz J.).

5. "Performance and Cost of Automotive Fuel Cell Systems with Ultra-Low Platinum Loadings", Journal of Power Sources, doi:10.1016/j.jpowsour.2011.01.059 (Ahluwalia R, Wang X, Kwon J; Rousseau A, Kalinoski JA, James BD, Marcinkoski J.).

6. Automotive fuel cell system cost analysis: Results of task 4.1.1 – 4.1.5. DTI Report to DOE, December 2010.

7. Mass Production Cost Estimation for Direct H2 PEM Fuel Cell Systems for Automotive Applications: 2010 Update, DTI Report to DOE, September 2010.

V.A.3 Drive-Cycle Performance of Automotive Fuel Cell Systems

Rajesh K. Ahluwalia (Primary Contact),
Xiaohua Wang, Romesh Kumar
Argonne National Laboratory
9700 South Cass Avenue
Argonne, IL 60439
Phone: (630) 252-5979
E-mail: walia@anl.gov

DOE Manager
HQ: Nancy Garland
Phone: (202) 586-5673
E-mail: Nancy.Garland@ee.doe.gov

Project Start Date: October 1, 2003
Project End Date: Project continuation and direction determined annually by DOE

Fiscal Year (FY) 2011 Objectives

- Develop a validated model for automotive fuel cell systems, and use it to assess the status of the technology.
- Conduct studies to improve performance and packaging, to reduce cost, and to identify key research and development (R&D) issues.
- Compare and assess alternative configurations and systems for transportation and stationary applications.
- Support DOE/U.S. DRIVE automotive fuel cell development efforts.

Technical Barriers

This project addresses the following technical barriers from the Fuel Cells section of the Fuel Cell Technologies Program Multi-Year Research, Development and Demonstration Plan:

(B) Cost
(C) Performance
(E) System Thermal and Water Management
(F) Air Management
(G) Startup and Shutdown Time and Energy/Transient Operation

Technical Targets

This project is conducting system level analyses to address the following DOE 2015 technical targets for automotive fuel cell power systems operating on direct hydrogen:

- Energy efficiency: 50%-60% (55%-65% for the stack) at 100%-25% of rated power.
- Power density: 650 W/L for system, 2,000 W/L for the stack.
- Specific power: 650 W/kg for system, 2,000 W/kg for the stack.
- Transient response: 1 s from 10% to 90% of rated power.
- Start-up time: 30 s from –20°C and 5 s from +20°C ambient temperature.
- Precious metal content: 0.2 g/kW.

FY 2011 Accomplishments

- Determined the performance of nanostructured thin film catalyst (NSTFC) stacks at low temperatures and on drive cycles.
- Evaluated the dynamic performance of the Honeywell integrated compressor-expander-motor (CEM) module.
- Analyzed the dynamic performance of a parallel ejector-pump hybrid for fuel management.
- Analyzed the dynamic performance of planar and supported liquid membrane humidifiers.
- Analyzed the dynamic performance of microchannel automotive radiators and polymer electrolyte fuel cell (PEFC) stacks during cold start on drive cycles.
- Conducted drive-cycle simulations to determine the fuel economy of hybrid fuel cell vehicles, ownership cost, and optimum fuel cell system (FCS) operating parameters.



Introduction

While different developers are addressing improvements in individual components and subsystems in automotive fuel cell propulsion systems (i.e., cells, stacks, balance-of-plant components), we are using modeling and analysis to address issues of thermal and water management, design-point and part-load operation, and component-, system-, and vehicle-level efficiencies and fuel economies. Such analyses are essential for effective system integration.

Approach

Two sets of models are being developed. The GCtool software is a stand-alone code with capabilities for design, off-design, steady-state, transient, and constrained optimization analyses of FCSs. A companion code, GCtool-ENG, has an alternative set of models with a built-in procedure for translation to the MATLAB®/Simulink® platform commonly used in vehicle simulation codes, such as Autonomie.

Results

In FY 2011, we analyzed the dynamic performance of an 80-kW_e net automotive FCS, shown in Figure 1, and its major components (fuel cell stack, and air, fuel, water and thermal management subsystems) on drive cycle transients [1]. The reference FCS is designed to achieve 45% efficiency at rated power (on the lower heating value basis). The stack operates at 75°C and 1.5-atm inlet pressure, the hydrogen and oxygen utilizations are 50%, and the cell voltage is 622 mV. The dew point temperatures at stack inlet are 61°C for cathode air and 53°C for hydrogen after mixing with the recirculated spent anode gas. Here, the stack temperature refers to the coolant exit temperature, the anode and cathode streams flow in opposite directions (counterflow), and the coolant flows in the same direction as the cathode air (coflow) with a 10°C temperature rise across the stack at rated power.

Figure 1 shows the in-line sensors (thermocouples, pressure transducer, differential pressure transducer, voltmeter, ammeter, and shaft revolutions per minute, rpm) used in our model to control and respond to the dynamic loads. The control model is based on a simple hierarchical logic that does not depend on measuring flow rates. The starting step is to determine the resistive load to vary the cell current, using the measured stack voltage as the guide. The control of the air management system is based on knowing the compressor discharge pressure and the shaft rotating speed (rpm). The model determines the direct current (DC) power to be applied to the motor controller and adjusts the turbine nozzle area as the power demand changes. The fuel management system relies on the measured differential pressure between the cathode and anode inlets to regulate the hydrogen flow rate. The control variable for the water management system is the flow rate of the low-temperature coolant (LTC) to the air pre-cooler using the LTC temperature at the outlet of the traction motor as the measurable temperature. Separate but similar controls are used for the high-temperature coolant (HTC) and LTC circuits of the thermal management system. The control of the HTC circuit depends on the measured HTC temperature at the stack outlet, and the control of the LTC circuit is based on the measured temperature of the LTC at the outlet of the traction motor.

Performance of the Air Management Subsystem

We used experimental data obtained on a full-scale, 100 $g.s^{-1}$ dry air, unit to model Honeywell's CEM with a variable nozzle turbine (VNT) [2-4]. The component maps were incorporated into a model for the compressor,

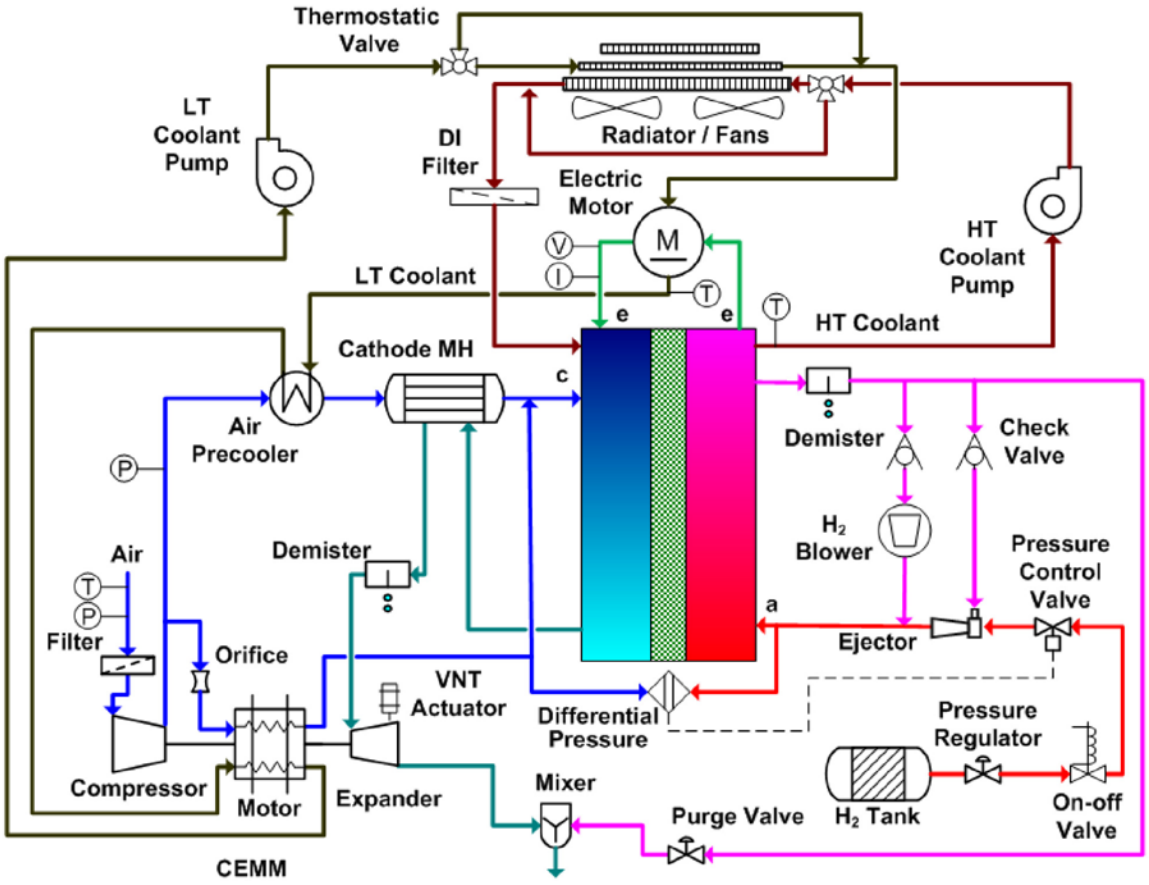
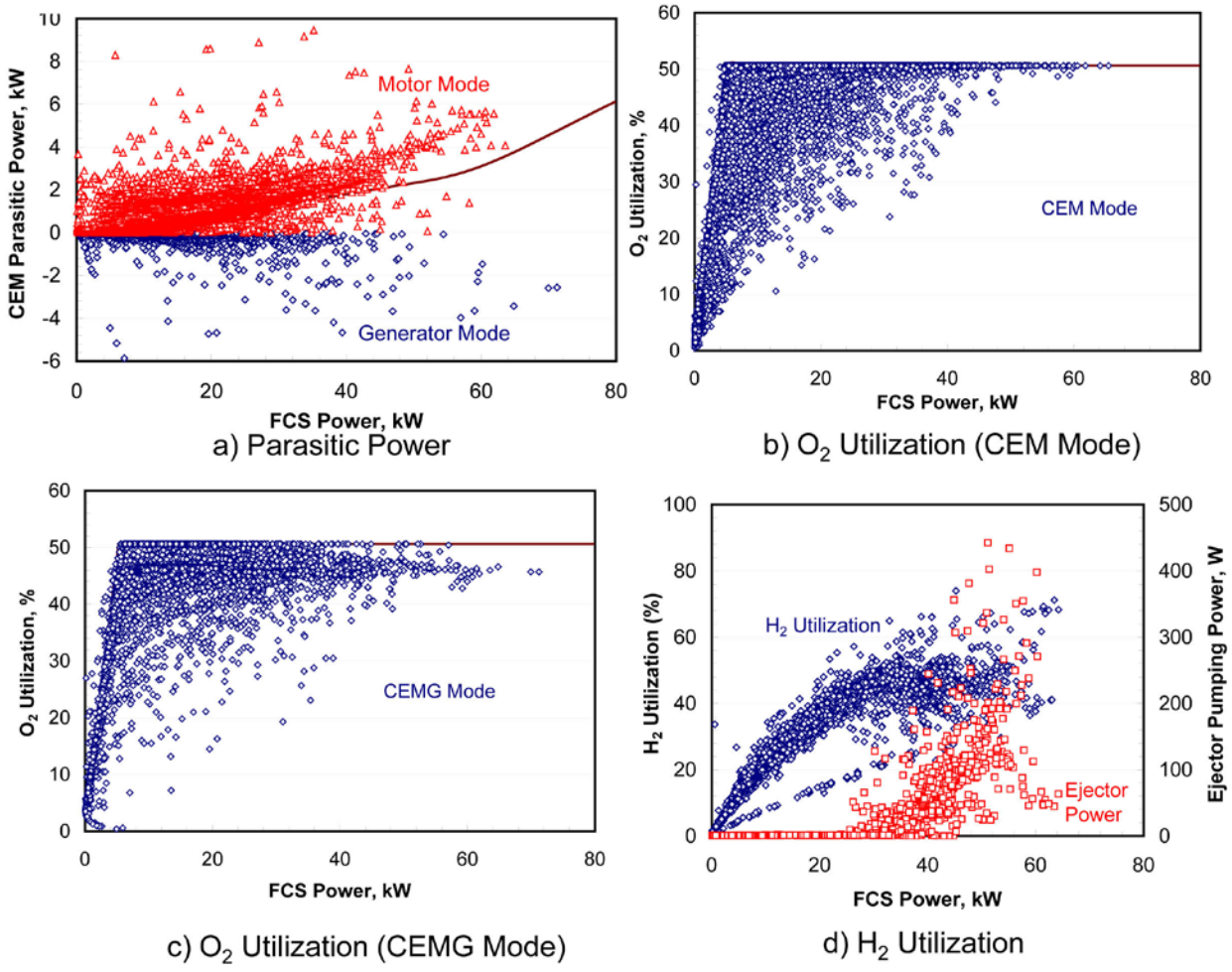


FIGURE 1. Reference FCS with In-line Sensors

expander, and motor that are mounted on a common shaft. The shaft is supported on airfoil bearings, and the motor is powered through a motor controller (DC input). This model was used to analyze the performance of two CEM configurations, one with and one without an expander. The model showed that recovering the compressor bleed air that cools the motor (configuration b with 1-psi pressure drop) reduces the CEM parasitic power by 0.4 to 1.6 kW. Also, an expander reduces the parasitic power by 4 kW if the stack inlet pressure is 2.5 atm (referred to as system S1), and by 1.5 kW if the stack inlet pressure is 1.5 atm (designated as system S2). We found that the CEM turndown (ratio of maximum to minimum flow rate) is a function of the minimum shaft speed (rpm) and may be limited by the compressor surge line. It is desirable to have turndown >10 and a minimum rpm <35,000; otherwise the CEM parasitic power at idle can be >500 W. The minimum shaft speed, if lower than the airfoil bearing lift speed of 36,000 rpm, will affect the durability of the airfoil bearings.

We conducted dynamic simulations to analyze the performance of the CEM (0.25 kg.m^2 moment of inertia) on urban (UDDS) and highway (HWFET) drive cycles [3]. We first developed a map for the optimum shaft speed and nozzle area as a function of the air flow rate (FCS power) at steady state; the map also specified the compressor discharge pressure and the CEM parasitic power at part load. We used the map as the reference to determine the target CEM operating conditions for the dynamic simulations. Given a particular power demand, the nozzle area was adjusted to the target value (assuming that the VNT actuator is fast acting), and the DC power to be applied to the motor controller to reach the target rpm in 100 ms was determined. We assumed that the motor in the CEM could be overloaded to 150% of the design value (6 kW for system S2) for short durations.

The symbols in Figure 2a represent the electric power that must be supplied to the CEM on the UDDS and HWFET drive cycles in the S2 system with an expander and configuration (b). These may be compared with the solid line that represents the power consumed by the CEM at steady state. We see that the power consumed by the CEM during an acceleration transient can be substantially greater than



(symbols: dynamic results; solid line: steady-state simulation)

FIGURE 2. Dynamic Performance of the Air and Fuel Management Subsystems

the power required at steady state because of the extra power needed to increase the shaft speed. Conversely, the power consumed by the CEM during a deceleration transient can be less than the power required at steady-state conditions and may even be zero. Similarly, Figure 2b compares the oxygen utilization on the UDDS and HWFET cycles with the steady-state values represented as solid lines for 50% O_2 utilization and a maximum turndown of 20. We see that the cathode stoichiometric ratio (reciprocal of oxygen utilization) is >2 during deceleration and >>5 at low FCS power.

We also conducted simulations to assess the benefits of operating the motor as a compressor expander motor-generator module (CEMG). Figure 2a shows instances where there is net production of power by the CEMG unit during hard deceleration. However, the instances of higher than steady-state CEMG power requirement are also more frequent, since the shaft speed decreases faster during deceleration and must be increased more rapidly during a subsequent acceleration. Figure 2c indicates that the scattered data points are clustered closer to the steady-state O_2 utilization curve because of faster response to the deceleration transients.

Performance of the Fuel Management Subsystem

We developed a model to analyze the performance of a parallel ejector-pump hybrid in the fuel management system [3]. We considered that the motive gas is pure hydrogen from the compressed gas tank and the suction gas is spent hydrogen from the stack outlet. We assumed that the motive gas is available at a pressure no less than 22 bar (regarded as the empty tank pressure) and that the suction gas is saturated with water vapor (molecular weight of 3-7) at 1-1.15 atm (S2 scenario).

Our dynamic control algorithm for the fuel management system consists of a pressure regulator to lower the pressure of motive hydrogen to 22 bar and a pressure control valve to further lower the pressure at the inlet to the ejector. The hydrogen flow rate is varied by changing the pressure at the throat of the ejector in order to have zero differential pressure across the cathode and anode channels. The maximum hydrogen flow rate is set to 150% of the value at rated power.

Figure 2d summarizes the results from the dynamic simulation of the fuel management system with a single-speed, 40-W blower that is always kept on. The H_2 utilization on the UDDS and HWFET cycles is maintained at about 50% for >30% of the rated FCS power, but it is much less than 50% near idling conditions. With hydrogen feed rate being proportional to the pressure differential between anode and cathode inlets, H_2 utilization can be >60% during rapid deceleration that depressurizes the anode gas channels. Figure 2d also includes the calculated ejector pumping power defined as the flow rate of the entrained gas times the pressure head. We see that the pumping power can approach 400 W, which is equivalent to a 1-kWe reduction in parasitic power (i.e., power that a 40%-efficient blower would need to provide if the system did not include an ejector).

We ran simulations in which the feed hydrogen contains inert impurities at levels of 100-ppm N_2 and 200-ppm He [5]. The simulations include crossover of N_2 from cathode to anode and the crossover of He from anode to cathode. We determined the dynamic buildup of the inerts assuming that 15 standard liters of anode gas (equivalent to 2 times the volume of the anode circuit) are purged by supplying H_2 at the maximum flow rate (150% of the H_2 flow rate at rated power) when the inerts build up to 10 mol%. Our simulations indicate that the purge schedule is largely determined by the crossover of N_2 from cathode air rather than the level of impurities in feed hydrogen.

We determined the purge loss and the interval between purges for constant FCS power and on UDDS and HWFET drive cycles. We found that H_2 purge loss increases as the FCS power decreases; it can exceed 10% of the feed near idling conditions. Also, the purge schedule and loss are proportional to the allowable N_2 concentration in the anode channels. Thus, the interval between purges will be nearly twice as long, and the purge loss will be nearly half as much, if the allowable N_2 concentration is increased from 10% to 20%.

Performance of the Water Management Subsystem

For the membrane humidifier for the cathode inlet air, we developed a transient model to determine the heat and mass transfer between the counterflowing wet and dry streams that are separated by a perfluorosulfonic acid (PFSA) membrane [6]. The model considers water uptake from the wet stream, diffusion through the PFSA membrane, and desorption into the dry stream. The model was validated against experimental data from a full-scale (appropriate for an 80-kW_e automotive FCS), a half-scale, and a sub-scale ($1/10^{th}$) unit assembled as a bundle of Nafion® tubes arranged like a shell and tube heat exchanger [6].

We used the model to analyze the performance of a planar humidifier (20-μm-thick membrane, 3 m^2 active area) sized to raise the dew point temperature of cathode air (S2 configuration) to 61°C by transferring moisture from the spent saturated air leaving the stack at 75°C. The dry air temperature is lowered from 120°C at compressor discharge to 65°C in a pre-cooler.

Figure 3a shows the modeled performance of the humidifier on UDDS and HWFET cycles. The results are shown as a scatter plot of cathode air relative humidity (RH) calculated at the stack (bipolar plate) inlet temperature (nominally 65°C). The triangle symbols designate the results for the initial startup time when the stack and other components are still warming up. The square symbols represent results after the coolant temperature at stack inlet reaches 65°C. A >100% RH in Figure 3a implies that the cathode air is leaving the humidifier at a temperature higher than the bipolar plate temperature at stack inlet. Both

steady-state and dynamic simulations follow the general trend that the RH first increases as the air flow rate (FCS power) is reduced, reaches a peak, and then decreases as the CEM reaches the turndown limit. In the turndown limit, the cathode stoichiometry increases as the FCS power is reduced (see Figure 3a) and at certain points, the RH of air at the stack outlet may drop well below 100%.

Performance of the Thermal Management Subsystem

We analyzed the performance of a cross-flow automotive radiator with 40 plain microchannel fins per inch (0.4 m^2 frontal area, 2.3 m^2 fin area, 500 W blower fan) and evaluated its ability to reject the waste heat from an 80-kW_e S2 system [3,7]. We concluded that the fuel cell powertrains might need to be derated for ambient temperatures higher than 40°C since the fan power doubles for every 5°C increase in ambient temperature. We assessed the prospect of allowing stack temperatures to rise to 95°C under transient conditions (e.g., hill climbing at 55 mph) where high heat rejection may be required for several minutes. We determined that the maximum stack temperature is limited by the system pressure and the dew-point temperature of the cathode air at stack inlet. Also, under these conditions of high load, the CEM motor power may limit the ability to pressurize the cathode air adequately if the CEM does not include an expander.

We ran dynamic simulations of the heat rejection system on UDDS and HWFET cycles using a dynamic control strategy that operates at three levels. First, the flow rate of the stack coolant is varied linearly with the FCS power. Second, the thermostatic valve is completely open so that the coolant bypasses the HTC radiator if the stack outlet temperature is below a minimum set point (70°C). The valve is completely closed to allow all the coolant to flow through the radiator if the coolant temperature is above the design point (75°C). The bypass fraction is linearly varied between 0 and 1 if the coolant temperature is between the two set points. Third, the radiator fan is operated in on-off mode, i.e., the single-speed fan operates only if the coolant temperature at stack inlet exceeds 65°C.

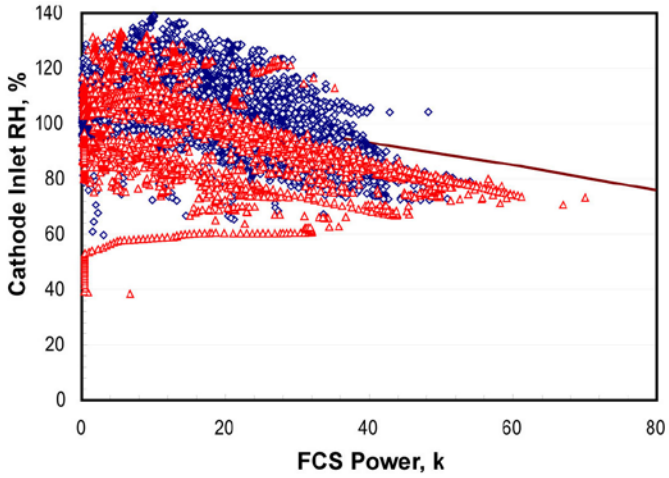
Our results indicate that it takes about 500 s for the polymer electrolyte membrane fuel cell (PEMFC) stack and the stack coolant to reach their design temperatures on the UDDS cycle with cold start from 300 K. After this time, the coolant temperature fluctuates due to variations in vehicle speed (i.e., flow rate of ram air), stack heat load, continuous adjustment of the thermostatic valve, and the blower fan turning on and off.

Stack and System Performance

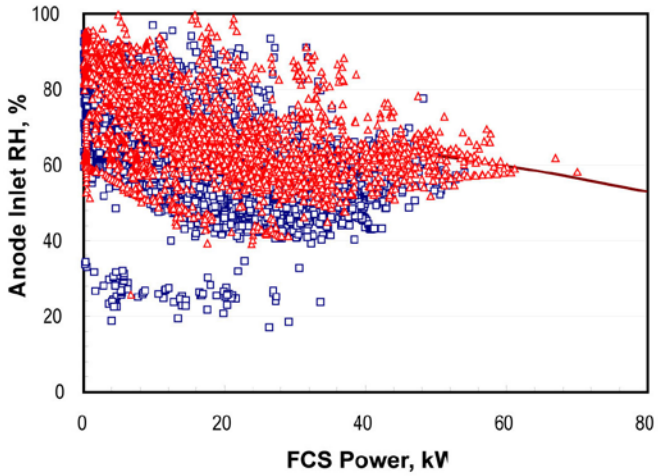
A two-dimensional model [3] was adapted to analyze the performance of a stack with NSTFC-based membrane-electrode assemblies. The NSTFC-specific constants for the model were derived from experimental data with 25-cm^2 active area cells [8].

Figure 4a presents the polarization curves constructed from the results for cold-start simulation on UDDS and HWFET cycles and for steady-state operation (system S2). The operating pressures in these simulations varied with current density (air flow rates) as determined by the CEM module. The scatter in cell voltage for the same current density is due to variations in stack temperature over time, cathode stoichiometry (higher during deceleration), and cathode inlet pressure (function of flow rate and shaft rpm). We have identified the coolant exit temperatures for some of the data points in Figure 4a to indicate the dominating effect of stack temperature on the polarization curves. The results indicated that flooding limits the stack power to ~32 kW_e at 30°C and ~50 kW_e at 45°C.

Figure 3b presents the relative humidity of the anode stream at the inlet to the stack. Since there is no humidifier in the anode circuit, and the feed H_2 is dry, the



a) Inlet Cathode RH



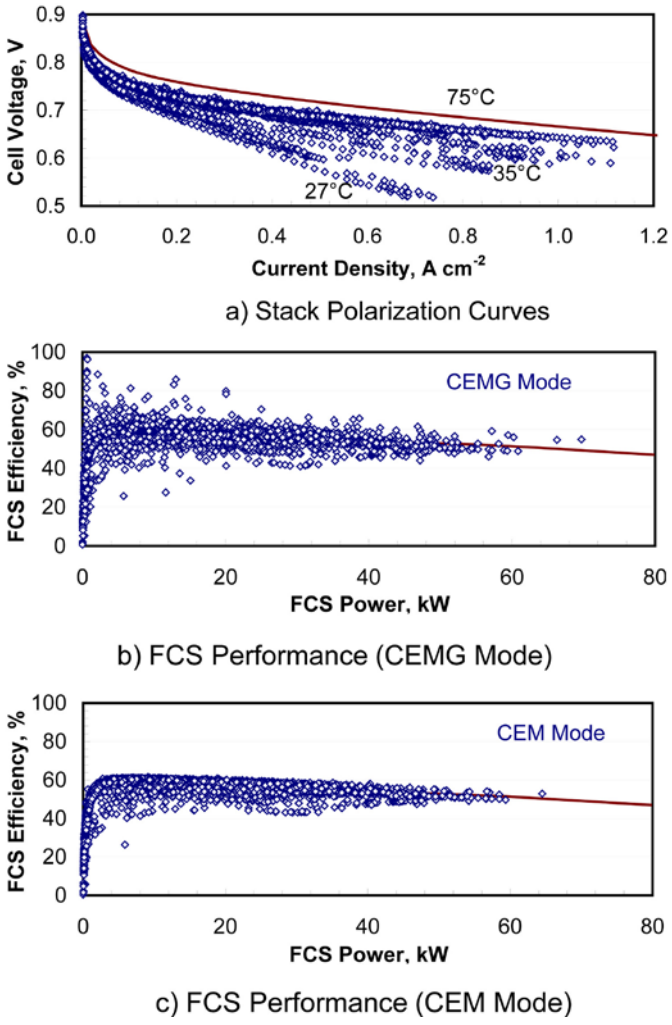
b) Inlet Anode RH

(symbols: dynamic results; solid line: steady-state simulation)

FIGURE 3. Dynamic Performance of the Water Management Subsystem

humidification of the anode stream is entirely due to water transport from the cathode through the membrane and recycle of the spent anode gas. As in Figure 3a, the triangle symbols designate the results for the initial startup time when the stack and other components are still warming up, and the square symbols represent results after the coolant temperature at stack inlet reaches 65°C. The isolated points with very low humidities represent instances of time that the anode is purged to relieve N_2 buildup and the accompanying loss of moisture with the purge gas.

Finally, Figures 4b and 4c summarize the instantaneous FCS efficiency on the UDDS and HWFET drive cycles. We see a larger spread in the efficiencies if the CEM motor is operated as motor/generator. The sporadic high efficiency points in the CEM generator (CEMG) mode are due to power generated by the air management system during rapid deceleration. These are generally followed by sporadic low efficiency points because of the parasitic power consumed in spinning-up of the CEMG shaft to higher speeds.



(symbols: dynamic results; solid line: steady-state simulation)

FIGURE 4. Dynamic Performance of the PEFC Stack and FCS on UDDS and HWFET Cycles

Conclusions and Future Directions

- System performance and stack polarization curves can deviate significantly from the steady-state values, especially during startup from 300 K. The transient FCS efficiency can be much higher than the peak steady-state efficiency during deceleration, or much lower during acceleration and while the stack is below its normal operating temperature of 75°C.
- Operating the CEM motor as motor/generator improves the CEM response during deceleration, although the transient cathode stoichiometry can still be >2 (design point stoichiometry ratio) at low loads and >>2 in the CEM's turndown limit.
- A hybrid blower-ejector arrangement controlled by a differential pressure sensor can maintain H_2 utilization at 50% or lower on the UDDS and HWFET drive cycles. A periodic purge is needed to control the buildup of N_2 in the anode recycle loop due to crossover from cathode air.
- At low loads, the RH can exceed 100% at cathode inlet (60% at design rated power) and reach 80-90% at the anode inlet (50% at design rated power), even without an external anode humidifier.
- In FY 2012, we will investigate the effects of alternative system configurations, rated power efficiency (Pt content) and system operating points on the high-volume manufacturing cost, dynamic drive-cycle performance, and component durability.

FY 2011 Publications/Presentations

1. R.K. Ahluwalia , X. Wang, J. Kwon, A. Rousseau, J. Kalinoski, B. James, and J. Marcinkoski, "Performance and Cost of Automotive Fuel Cell Systems with Ultra-low Platinum Loadings," *J. Power Sources*, 196 (2011), 4619-4630.

2. D. Myers, X.-P. Wang, R. Ahluwalia, X. Wang, M. Smith, and J. Gilbert, "Degradation Mechanisms of Pt-based Oxygen Reduction Reaction Electrocatalysts," 2010 Gordon Research Conference on Fuel Cells, Bryant University, Smithfield, RI, August 1–6, 2010.

3. R.K. Ahluwalia, X. Wang, R. Kumar, J. Kwon, and A. Rousseau, "Fuel Cell Systems with Low-Pt Loading: Cost vs. Performance," Fuel Cell Technical Team Meeting USCAR, Southfield, MI, August 18, 2010.

4. X. Wang and R.K. Ahluwalia, "Water Management in Polymer Electrolyte Fuel Cells," 218th ECS Meeting, Las Vegas, NV, October 10–15, 2010.

5. R.K. Ahluwalia, X. Wang, J. Kwon, A. Rousseau, J. Marcinkoski, and N. Garland, "Performance of Automotive Fuel Cell Systems with Ultra-low Platinum Loadings," 2010 Fuel Cell Seminar & Exposition, San Antonio, TX, October 18–22, 2010.

6. R.K. Ahluwalia , "Fuel Cells for Transportation: Status, Challenges and Prospects," Invited Presentation, Graduate Seminar Series, Department of Mechanical Engineering-Engineering Mechanics, December 2, 2010, Michigan Technological University, Houghton, MI.

References

1. R.K. Ahluwalia, X. Wang, K. Tajiri, and R. Kumar, "Fuel Cell Systems Analysis," 2010 DOE Hydrogen Program Review, Washington DC, June 8–11, 2010.

2. M.K. Gee, "Cost and Performance Enhancement for a PEM Fuel Cell System Turbocompressor," FY 2005 Annual Progress Report, DOE Hydrogen Program, 985, 2005.

3. R.K. Ahluwalia, X. Wang, J. Kwon, A. Rousseau, J. Kalinoski, B. James, and J. Marcinkoski, "Performance and Cost of Automotive Fuel Cell Systems with Ultra-Low Platinum Loadings," *J. Power Sources*, 196, 4619, 2011.

4. R.K. Ahluwalia and X. Wang, "Fuel Cell Systems for Transportation: Status and Trends," *J. Power Sources*, 177, 167, 2008.

5. H. Tomioka, "Prospect of ISO14687-2," ISO/TC192/WG12 Meeting, Vancouver, BC, 2009.

6. X. Wang and R. Ahluwalia, "Water Management in Polymer Electrolyte Fuel Cells," 218th ECS Meeting, Las Vegas, NV, October 2010.

7. Z. Mirza, "Development of Thermal and Water Management System for PEM Fuel Cell," 2010 DOE Hydrogen Program Review, Washington DC, June 8–11, 2010.

8. M.K. Debe, "Advanced Cathode Catalysts and Supports for PEM Fuel Cells," Grant No. DE-FG36-07GO17007, FreedomCAR Technical Team Review, Detroit, MI, March 10, 2010.

V.A.4 Characterization of Fuel Cell Materials

Karren L. More
Oak Ridge National Laboratory (ORNL)
1 Bethel Valley Rd.
Oak Ridge, TN 37831-6064
Phone: (865) 574-7788
E-mail: morekl1@ornl.gov

DOE Manager
HQ: Nancy Garland
Phone: (202) 586-5673
E-mail: Nancy.Garland@ee.doe.gov

Project Start Date: Fiscal Year (FY) 1999
Project End Date: Project continuation and direction determined annually by DOE

FY 2011 Objectives

- Develop new, innovative microanalysis and imaging techniques to characterize fuel cell material constituents before, during, and after electrochemical aging.
- Elucidate membrane electrode assembly (MEA) degradation and/or failure mechanisms by conducting extensive microstructural characterization using advanced electron microscopy techniques. In particular, distinguish individual materials degradation phenomena as a function of aging protocol, including catalysts, supports, ionomer, membrane, microporous layer (MPL), and gas diffusion layer (GDL).
- Develop the critical correlations between MEA microstructure, composition, and architecture, and MEA durability.
- Compare microstructural changes resulting from accelerated stress testing (AST) with microstructures observed after field aging to determine efficacy of ASTs.
- Collaborate with fuel cell component developers and manufacturers, university researchers, and other national laboratories, to evaluate fuel cell material components using electron microscopy and complimentary microstructural and compositional microanalysis techniques.

Technical Barriers

This project addresses the following technical barriers from the Fuel Cells section (3.4.4) of the Fuel Cell Technologies Program Multi-Year Research, Development, and Demonstration Plan:

(A) Durability
(B) Cost
(C) Performance

Technical Targets

Insights gained through extensive microstructure characterization of MEA constituents will be applied toward the design and manufacture of fuel cell materials that meet the following DOE 2015 MEA targets:

- Cost: <$5/kW
- Durability with cycling: 5,000 hours
- Operating temperatures: <120°C
- Total catalyst loading (for both electrodes): 0.2 g/kW (rated)
- Extent of performance degradation over lifetime: 5%

FY 2011 Accomplishments

- Used a combination of analysis techniques and MEA samples to characterize the nature of the recast ionomer (films, pockets, etc.) within electrode structures and to understand the nm-scale phase-separated morphology consistently observed in Nafion® membranes.
- Directly compared degradation phenomena observed in "real world" field-aged proton exchange membrane fuel cell (PEMFC) MEAs with MEAs aged via AST protocols designed to enhance specific degradation mechanisms (e.g., carbon corrosion, catalyst coarsening, etc.).
- Established collaboration with Nissan to evaluate catalysts (in terms of structure, size, and morphology) deposited on a series of carbon supports exhibiting varying degrees of graphitization.
- Initiated fundamental study of Pt deposition on model carbon substrates (graphene) to understand Pt nucleation and growth mechanisms on extended graphitic surfaces.
- Established a new collaboration with General Motors to characterize a complete series of PEM fuel cell MEAs aged to accelerate membrane degradation.
- Optimized analysis parameters for the compositional analysis of catalyst nanoparticles via aberration-corrected scanning transmission electron microscopy (STEM), including elemental mapping.
- Host an international collaborator from Fuel Cell Cubic (FCC), Tokyo, Japan, to characterize new materials for PEM fuel cells. The FCC researcher will work at ORNL for the next year.



Introduction

PEMFCs are being developed for future use as efficient, zero-emission power sources. The performance of PEMFCs degrades during electrochemical aging, and this performance

degradation can be correlated directly with the durability of individual components comprising the MEA, e.g., the electrocatalyst, catalyst support, ionomer, and/or the proton-conducting polymer membrane. Many of the material's microstructural and compositional attributes that contribute to decreased stability of the MEA during long-term electrochemical aging are not yet fully understood and have not directly been correlated with performance as a function of aging protocols. In order to reach DOE's technical targets for MEAs, correlating the individual component materials structure, composition, and interrelationships within the MEA layers with the measured performance as a function of different aging conditions, is critical for applying materials optimization practices to increase fuel cell materials durability for specific applications.

During the course of this project, the Microstructural Characterization Program at ORNL has been focused on forming collaborative relationships with a wide range of industrial PEMFC developers/manufacturers, university researchers, and national laboratories, to utilize advanced microscopy techniques as a means to evaluate as-fabricated and electrochemically aged PEMFC MEAs and, most importantly, to characterize individual PEMFC material components and relate structural and chemical changes of these materials to the performance degradation resulting from particular aging conditions. These studies are used to establish the critical processing-microstructure-performance relationships that can then be reported to the MEA producers (and in many circumstances, the fuel cell community as a whole), which can result in improved stability of the MEA materials, thereby enhancing MEA performance and lifetimes. Understanding the structural and compositional changes to the materials comprising the MEA during electrochemical aging will allow for the implementation of processing changes and critical materials development that are required for optimized PEMFC durability and performance. The techniques developed as part of this "baseline" research project are being applied to other fuel cell systems.

Approach

The microstructural characterization task utilizes advanced electron microscopy analysis techniques to characterize the individual material components comprising PEMFCs, before and after incorporation into an MEA and after electrochemical aging. Our approach is focused on identifying and optimizing novel high-resolution imaging and compositional/chemical analysis techniques, and developing unique specimen preparation methodologies, for the μm-Å-scale characterization of the material constituents of fuel cells (electrocatalyst, catalyst support, ionomer, membrane, etc.). ORNL applies these advanced analytical and imaging techniques for the evaluation of the microstructural and microchemical changes of each material constituent and correlating these observations with fuel cell performance (aging studies are conducted at the collaborator's laboratories). These studies are designed to elucidate the microstructure-related degradation mechanisms contributing to fuel cell performance loss. Most importantly, ORNL is making the techniques and expertise available to fuel cell researchers outside of ORNL via several mechanisms – (1) work for others (proprietary) research, (2) ORNL User Facilities (e.g., Shared Research Equipment User Facility, Center for Nanophase Materials Science), and (3) collaborative non-proprietary research projects via the Microstructural Characterization Project that are in line with ORNL's "baseline" research activities.

Results

Ionomer Characterization

High-resolution microscopy characterization of the recast ionomer "film" distributed within the electrodes of a PEMFC poses numerous challenges, the most critical being the inhomogeneous and non-continuous nature of the ionomer. Typically, the ionomer film is not a uniform-thickness film surrounding the Pt catalysts on carbon black (Pt/CB) supports, but tends to exist in pockets/clumps in localized regions between Pt/CB particles or agglomerates, which have a high number density of Pt nanoparticles. Isolating ionomer regions for high spatial resolution chemical/compositional analysis or imaging is extremely difficult. To study the ionomer phase within an electrode, it was necessary to prepare electrodes with greater amounts of ionomer to create isolated "ionomer-only" regions. Thus, rather than characterizing electrodes with 28-30 wt% ionomer, the samples used for this work contained ~61 wt% ionomer, which resulted in dense electrodes having filled porosity, as shown in Figure 1 where a large pore between Pt/CB regions is completely filled with ionomer. The large ionomer-filled-pore regions (generally >50 μm) were sufficiently large for microanalysis via electron energy loss spectroscopy (EELS) in the transmission electron microscope (TEM)/STEM, and a bulk electrode content high enough for comparing with X-ray photoelectron spectroscopy (XPS) characterization. In addition, these dense electrodes were prepared for TEM/STEM by cryo-microtomy using no epoxy embedding (ensuring that the only polymer present in the sample was the ionomer).

The XPS results acquired from the electrode containing ~61 wt% were also compared with XPS data for a Nafion® 212 membrane. It is important to note that the XPS data were acquired from an electrode that was "chopped up" such that the ionomer inside the electrode (filling pores) was analyzed rather than any ionomer skins present on the bulk electrode surfaces. The primary conclusions from the bulk XPS analyses were (1) the Nafion® 212 membrane exhibited more CF_2-type (PTFE) bonding (the ionomer was depleted in fluorine (CF_2/CF_3=3.8) compared to the membrane (CF_2/CF_3=5.0)) and (2) the -SO_3 (sulfonate) peak shifts to a lower binding energy for the 61 wt% ionomer sample, which is consistent with the sulfonate groups no longer being

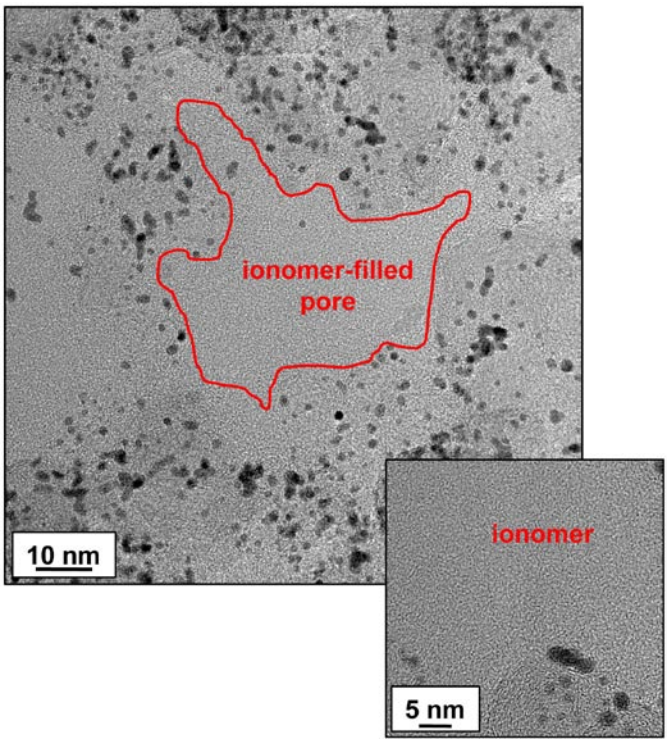


FIGURE 1. To isolate ionomer regions for TEM/STEM/EELS analysis, electrodes were prepared such that the pores were filled with ionomer (61 wt% ionomer mixed with Pt/C decal-electrodes).

influenced by or associated with the $-CF_2$ backbone, i.e., these groups have been removed from the $-CF_2$ backbone or the sulfonate groups are located in a sub-surface position. EELS spectrum images (SI) were acquired in the STEM within the individual ionomer-filled pores surrounded by Pt/CB particles. A typical ionomer pocket used for EELS-SI is shown in the STEM image in Figure 2 together with the derived carbon and sulfur EELS maps. Phase separation within the ionomer is clear – the sulfur (and oxygen – not shown) is associated with the Pt/CB region, whereas the carbon (and fluorine, not shown) is uniformly present within the ionomer filling the pore. Additionally, energy dispersive spectroscopy (EDS) analysis of an MEA (prepared with a "standard" ionomer content of 28 wt%) consistently shows higher sulfur associated with Pt/CB regions. These data are consistent with the XPS data from the ionomer that shows clear "localization or separation" of the sulfonate groups away from the Teflon®-backbone of the Nafion® and the existence of the sulfonates in a sub-surface position. Separation of the hydrophilic sulfonate groups will have the greatest impact on the confinement of water and water uptake within the electrode. In a recent article by Kim and Pivovar [1], PFSA membranes are described as "highly phase-contrasted polymers" due to the extreme hydrophobicity of the CF_2-backbone and mobility of the SO_3-group – phase contrast refers to the extent of separation between the hydrophilic and hydrophobic regions. The ionomer within the electrodes appears to be more phase-contrasted than the membrane and according to [1], this should have the greatest impact on water uptake.

Initiation of Pt Nucleation and Growth Studies Using "Model" Carbon Surfaces

For fuel cell applications, electrocatalysts are currently supported on a variety of carbon black (CB) supports, each exhibiting different degrees of graphitization. These include Ketjen black and Vulcan (high surface area supports) and their heat-treated counterparts, where heat treatments are employed to enhance the graphitic nature of the CB. The high surface area CB support structures are typically textured turbostratic carbon with a particle (domain) size of ~4-5 nm, where the rounded surfaces of the supports are comprised of highly aligned domains that each terminate predominantly with hexagonal carbon (002) planes on the surface. This "mosaic structure" is shown in Figure 3a,

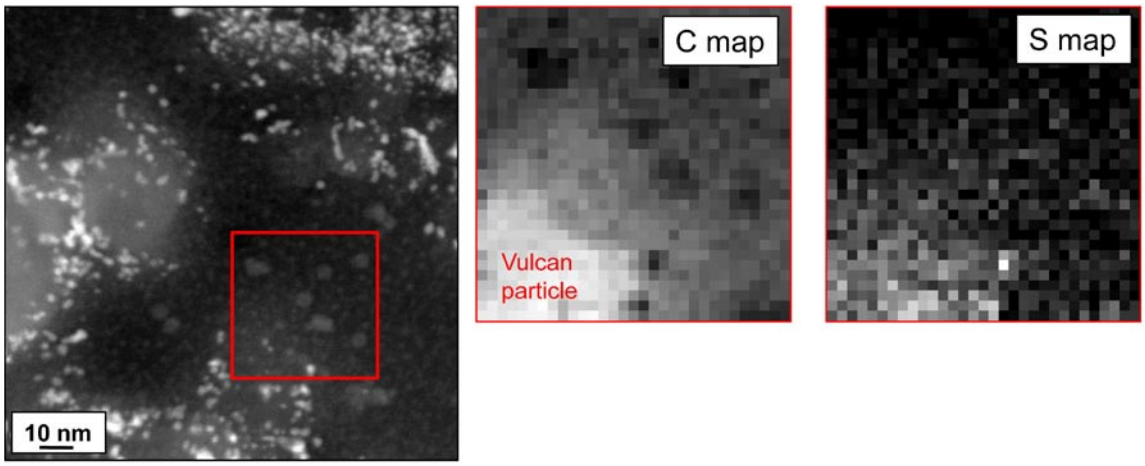


FIGURE 2. EELS spectrum imaging data from 61 wt% ionomer sample. Sulfur was consistently associated with Vulcan Pt/CB regions within the electrode structure.

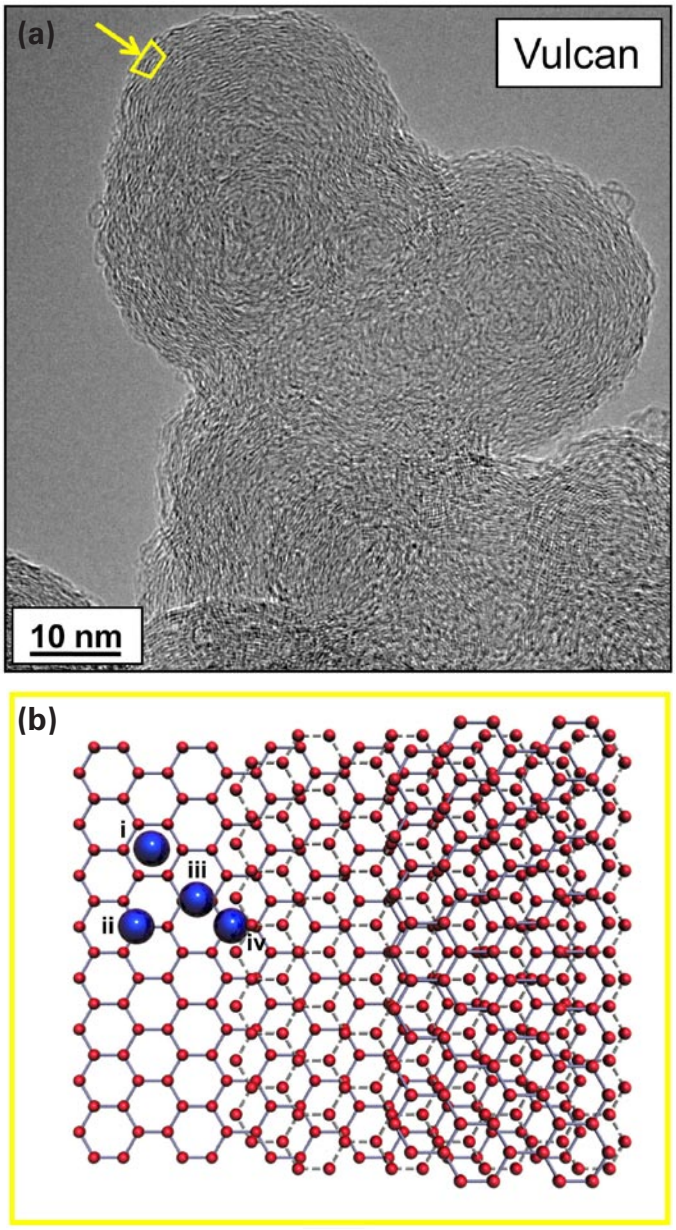


FIGURE 3. (a) Vulcan particle with overlay of typical carbon crystalline domain (yellow). (b) Schematic of (002) graphene surface showing possible Pt atom deposition sites (i) center of 6-atom carbon ring, (ii) top of single carbon atom, (iii) "bridge" site between two carbon atoms, and (iv) step/edge between graphene layers.

where a typical domain is shown by the yellow outline on the TEM image of a Vulcan CB particle. The (002) domain surfaces can be modeled using graphene films, since all nanostructured carbons have "graphene-based" structures, i.e., layered sheets of graphene comprise highly ordered graphite. In this way, sp^2-bonded graphene sheets/films (single- or multi-layered) are being used (in place of CB spheres that are difficult to characterize by TEM/STEM) to identify preferred Pt deposition sites on CB surfaces and to study Pt nucleation and growth mechanisms. These

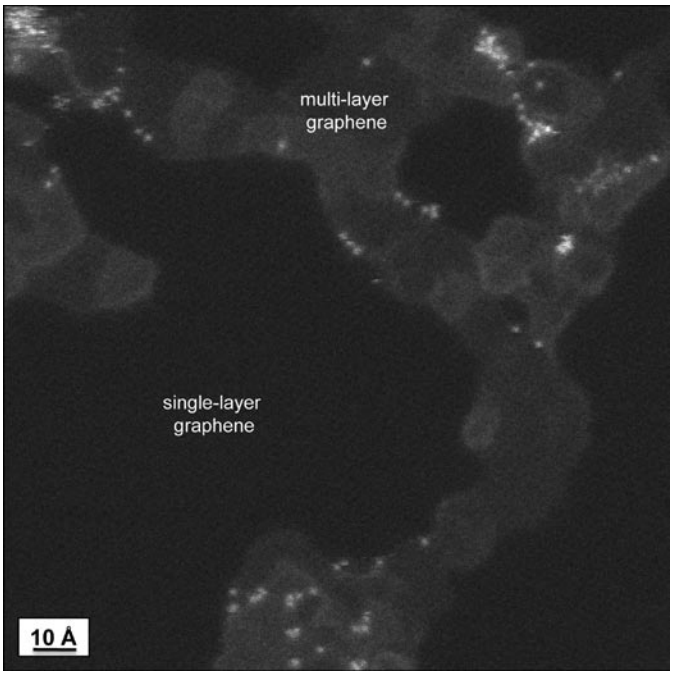


FIGURE 4. Z-contrast STEM image showing the different layers of graphene and individual Pt adatoms (brightly imaging) deposited on surface. Note that all Pt atoms deposit at edge sites and not on sites associated with the sp^2-bonded (002) surfaces.

studies will also be used to identify more stable sites for Pt deposition that can enhance catalyst stability.

Several critical steps have been taken to initiate this fundamental Pt nucleation and growth study in FY 2011. We have identified a source of continuous, multi-layered graphene films supported on the 3 mm Cu grids necessary for the TEM/STEM experiments (source - the Graphene Supermarket). These films are relatively pure/clean and exhibit large areas of single-layer graphene as well as defects – steps/edges, vacancies, etc. – at the regions where graphene sheets overlap. We have also successfully deposited very low levels of Pt (<3 wt%) directly on the 3 mm graphene-coated Cu grids using a $[Pt(NO_3)_2 \cdot (NH_3)_4]$ Pt precursor, such that individual Pt atoms as well as small Pt clusters are deposited, which is the desired loading and dispersion. In this way, we can identify the preferred site for Pt deposition and in the future, the most stable site. Possible sites available on the graphene films for Pt deposition are illustrated in Figure 3b and include (i) the center of the 6-atom carbon ring, (ii) on top of a carbon atom, (iii) the "bridge" site between two carbon atoms, and (iv) the step/edge at the sheets layers. Figure 4 shows a preliminary Z-contrast STEM image of individual Pt atoms (bright spots) distributed on graphene sheets. This preliminary data indicates that Pt atoms prefer to deposit at the edge sites where layers of graphene overlap (from single-layer to double-layer, or double-layer to triple-layer, etc.), and in fact, these are the only sites where Pt atoms were identified on the film surface. This is initial experimental

evidence showing that Pt atoms do not deposit on, nor do clusters nucleate on, the sp^2-bonded surfaces of graphite, but preferentially locate on defects. Additional research is planned to fully explore the adsorption, nucleation, and growth of Pt on carbon (002) surfaces such that carbon structures can be optimized to stabilize Pt electrocatalysts for use in fuel cells, including theoretical modeling (density functional theory calculations), Pt loading studies, introduction of defects in the carbon structure, and heating experiments.

Conclusions and Future Directions

- Complete Pt nucleation and growth study using "model" graphene surfaces, including density functional theory calculations for comparison with experimental results, and in situ heating experiments.
- Correlate microstructural/compositional observations with AST protocols (automotive and stationary), especially related to catalyst coarsening and migration, carbon corrosion, membrane degradation – this is a continuing priority of this research project and has been part of ongoing and proposed "future" research each year.
- Acquire the proper series of durability-tested MEAs to further understand the degradation of polymer electrolytes (membrane and ionomer in electrode) using a combination of characterization techniques – continue ionomer studies initiated in FY 2011.
- Correlate observations of Pt nucleation and growth to long-term stability via in situ liquid electrochemistry experiments.
- Continue to establish collaborations with industries, universities, and national laboratories (including access via ORNL User Facilities) to facilitate "transfer" of unique capabilities.
- Support new DOE projects with microstructural characterization and advanced characterization techniques, which remains the primary focus of this project.

FY 2011 Publications/Presentations

1. K.L. More, K.A. Perry, M. Chi, and K.S. Reeves, "Carbon Support Structural Degradation Observed in PEM Fuel Cell Cathodes," *invited* presentation at 218th Meeting of The Electrochemical Society, Las Vegas, NV, October 12, 2010.

2. K.L. More, R.R. Unocic, K.A. Perry,, and K.S. Reeves, "In-Situ Microscopy of Fuel Cell Nanoparticle Catalyst and Catalyst-Support Degradation," presentation at the 2011 MRS Spring Meeting, San Francisco, CA, April 25–29, 2011.

3. V. Mazumder, M. Chi, K.L. More, and S. Sun, "Synthesis and Characterization of Multimetallic Pd/Au and Pd/Au/FePt Core/Shell Nanoparticles," *Angewandte Chemie International Edition* 49[49] 9368–9372 (2010).

4. V. Mazumder, M.F. Chi, K.L. More, and S.H. Sun, "Core/Shell Pd/FePt Nanoparticles as an Active and Durable Catalyst for the Oxygen Reduction Reaction," *Journal of the American Chemical Society* 132[23] 7848-7849 (2010).

5. L.F Xiong, K.L. More, and T. He, "Syntheses, Characterization, and Catalytic Oxygen Electroreduction Activities of Carbon-Supported PtW Nanoparticle Catalysts," *Journal of Power Sources* 195[9] 2570-2578 (2010).

6. J.A. Xie, F. Xu, D.L. Wood, K.L. More, T.A. Zawodzinski, and W.H. Smith, "Influence of Ionomer content on the Structure and Performance of PEFC Membrane Electrode Assemblies," *Electrochimica Acta* 55[24] 7404-7412 (2010).

7. Z.Y. Liu, J.L. Zhang, P.T. Yu, J.X. Zhang, R. Makharia, K.L. More, and E.A. Stach, "Transmission Electron Microscopy Observation of Corrosion Behaviors of Platinized Carbon Blacks under Thermal and Electrochemical Conditions," *Journal of the Electrochemical Society* 157[6] B906-B913 (2010).

8. Y. Garsany, A. Epshteyn, A.P. Purdy, K.L. More, and K.E. Swider-Lyons, "High-Activity, Durable Oxygen Reduction Electrocatalyst: Nanoscale Composite of Platinum-Tantalum Oxyphosphate on Vulcan Carbon," *Journal of Physical Chemistry Letters* 1[13] 1977-1981 (2010).

9. K. Sasaki, J.X. Wang, H. Naohara, N. Marinkovic, K.L. More, H. Inada, and R.R. Adzic, "Recent Advances in Platinum Monolayer Electrocatalysts for Oxygen Reduction Reaction: Scale-up Synthesis, Structure and Activity of Pt Shells on Pd Cores," *Electrochimica Acta* 55[8] 2645-2652 (2010).

10. C. Wang, D. van der Vliet, K.L. More, N.J. Zaluzec, S. Peng, S. Sun, H. Daimon, G. Wang, J. Greeley, J. Pearson, A.P. Paulikas, G. Karapetrov, D. Strmcnik, N.M. Markovic, and V.R. Stamenkovic, "Multimetallic Au/$FePt_3$ Nanoparticles as Highly Durable Electrocatalysts," *Nano Letters* 11[3] 919-926 (2011).

11. C. Wang, M.F. Chi, G.F. Wang, D. van der Vliet, D.G. Li, K.L. More, H.H. Wang, J.A. Schlueter, N.M. Markovic, V.R. Stamenkovic, "Correlation Between Surface Chemistry and Electrocatalytic Properties of Monodisperse Pt_xNi_{1-x} Nanoparticles," *Advanced Functional Materials* 21[1] 147-152 (2011).

12. G. Wu, K.L. More, and P. Zelenay, "High-Performance Electrocatalysts for Oxygen Reduction Derived from Polyaniline, Iron, and Cobalt," *Science* 332 443-447 (2011).

References

1. Y.S. Kim and B.S. Pivovar, "Moving Beyond Mass-Based Parameters for Conductivity Analysis of Sulfonated Polymers," Annual Review of Chemical and Biomolecular Engineering Vol: 1 J.M. Prausnitz, M.F. Doherty, and M.A. Segalman, eds., pp. 123-148 (2010).

V.A.5 Neutron Imaging Study of the Water Transport in Operating Fuel Cells

Muhammad Arif (Primary Contact),
David L. Jacobson, Daniel S. Hussey
National Institute of Standards and Technology (NIST)
100 Bureau Drive
Gaithersburg, MD 20899
Phone: (301) 975-6303
E-mail: arif@nist.gov

DOE Manager
HQ: Nancy Garland
Phone: (202) 586-5673
E-mail: Nancy.Garland@ee.doe.gov

Contract Number: DE-AI-01-01EE50660

Project Start Date: Fiscal Year (FY) 2001
Project End Date: Project continuation and direction determined annually by DOE

FY 2011 Objectives

- Provide neutron imaging-based research and testing infrastructure to enable the fuel cell industry to design, test, and optimize prototype to commercial-grade fuel cells.
- Provide a secure facility for proprietary research by industry. Make open research data available for beneficial use by the general fuel cell community.
- Continually improve and develop methods and technology to accommodate rapidly changing industry/academia needs.

Technical Barriers

This project addresses the following technical barriers from the Fuel Cells section (3.4) of the Fuel Cell Technologies Program Multi-Year Research, Development and Demonstration Plan:

(A) Durability

(C) Performance

(D) Water Transport within the Stack

Technical Targets

- Unassisted start from low temperature: -40°C.
- Durability with cycling at operating temperature of ≤80°C: 5,000 h.
- System energy density: 650 W/L.
- System specific power: 650 W/kg.
- Energy efficiency: 65% at 25% rated power, 55% at 100% rated power.
- Cost: $35/kW$_e$.
- Start-up time to 50% power: 30 seconds from -20°C, 5 seconds from 20°C.
- Freeze start operation: unassisted start from -40°C.
- Durability with cycling: 5,000 hrs.

FY 2011 Accomplishments

- Developed methods to achieve better than 10 µm spatial resolution:
  - Further improvements to the spatial resolution require new approaches; one method has shown a factor of 25 improvement in spatial resolution.
  - Improvements to the design of this method will be pursued to achieve ~1 µm resolution to enable measurement of water distribution within commercial membrane electrode assemblies (MEAs).
- Carried out studies of water transport in full-scale hardware and 4-cell stacks:
  - Hydrophilic coatings on bipolar plates reduce water retention and time to purge the cell during shutdown.
  - Diffusion media saturation is linked to individual cell failure in stacks.
- High resolution imaging of water transport in thick catalyst layers and impact of water on fuel cell durability:
  - Strategies to overcome flooding will help improve the performance of polyaniline-derived non-precious metal catalysts.
  - Corrosion results in an increased overpotential, which dries out the cell under operation at constant current due to a larger thermal gradient.

✧ ✧ ✧ ✧ ✧

Introduction

At NIST, we maintain the premier fuel cell neutron imaging facility in the world and continually seek to improve its capabilities. This facility provides researchers a powerful and effective tool to visualize and quantify water transport inside operating fuel cells. Imaging the water dynamics of a polymer electrolyte membrane fuel cell (PEMFC) is carried out in real time with the required spatial resolution needed for fuel cells that are being developed today. From these images, with freely available NIST-developed image analysis routines, PEMFC industry personnel and researchers can obtain in situ, non-destructive, quantitative measurements of the water content of an operating PEMFC. Neutron

imaging is the only in situ method for visualizing the water distribution in a "real-world" PEMFC. Unlike X-rays, whose interaction with materials increases with the number density of electrons, neutrons interact via the nuclear force, which varies somewhat randomly across the periodic table, and is isotopically sensitive. For instance, a neutron's interaction with hydrogen is approximately 100 times greater than that with aluminum, and 10 times greater than that with deuterium. It is this sensitivity to hydrogen (and insensitivity to many other materials) that is exploited in neutron imaging studies of water transport in operating fuel cells.

Approach

The typical length scales of interest in a PEMFC are: channels approximately 1 mm wide and 1 mm deep, the diffusion media (DM) are 0.1 mm to 0.3 mm thick, the membrane is 0.01 mm to 0.02 mm thick, and the active area is 2 cm^2 to 500 cm^2. Thus, to nondestructively study in situ the water and hydrogen transport in PEMFCs while in operation we will develop new facilities and improve existing capability for obtaining high spatial and temporal resolution neutron images. Employing the mathematical models of neutron scattering, we will develop a software suite that enables users to obtain quantitative measurements of the water content in an operating PEMFC. Due to the complexity of PEMFCs and the large number of open questions regarding water transport in PEMFCs, we will develop partnerships with industry, academia, and national laboratories to train them in the use of the facility, collaborate with them on research projects, and seek their feedback to pursue future technical breakthroughs.

Results

Visualizing water transport in a fuel cell is a process that occurs on several different length scales. In-plane studies require spatial resolution on the order of 100 µm and this capability has existed from the outset of this project. However, to image water transport in the through-plane of a fuel cell in the DM, membrane, and catalyst layers it has been necessary to improve the image resolution, which currently stands at 10 µm. This resolution is well suited to studies of the DM, but to image the membrane and catalyst layer it is necessary to go well below 10 µm. To do this, new methods must be developed due to fundamental limitations that arise from the physics of neutron capture and detection in the detector that limit the overall resolution to 10 µm. Three different methods have been considered for achieving image spatial resolution better than 10 µm. The first utilizes a technique derived from neutron depth profiling (NDP), the second uses optical magnifying lenses, and the third a scanning set of slits. The NDP technique can possibly achieve a spatial resolution of 100 nm, but the field of view in one dimension is severely restricted to about 10 µm due to the need for charged particles from the neutron capture reaction to escape and be detected. Due to challenges in the fabrication of the detection volume, a proof-of-principle detector has not yet been demonstrated. The second method employing a magnifying lens was used with a charge-coupled device and scintillator, and it also results in unacceptably small fields of view, on the order of 2 mm, and initial results demonstrated spatial resolution of order 15 µm, limited by the scintillator thickness. Finally the slit method requires scanning a slit over the region of interest, which provides high spatial resolution in one direction only, but still makes use of a large field of view. Initial tests demonstrated that a detector with an intrinsic 250 µm resolution, when coupled with a 10 µm slit yielded images with 10 µm spatial resolution, as shown in Figure 1. It is expected that this method can be further developed to achieve near a resolution near 1 µm.

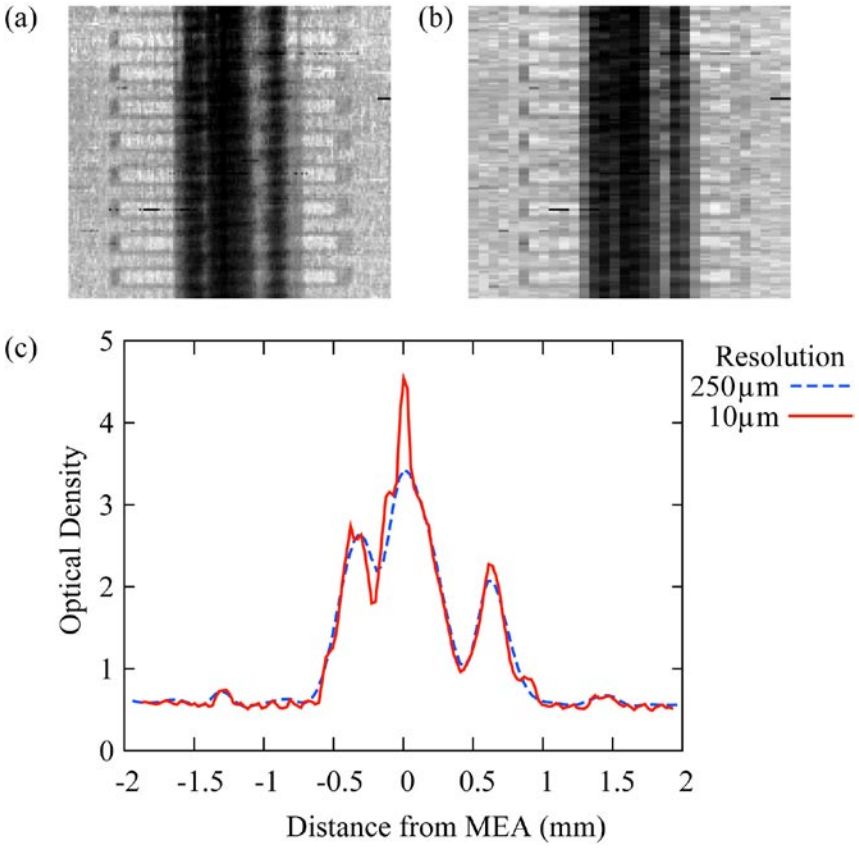


FIGURE 1. Demonstration of improved spatial resolution with a scanning slit. Image of a PEMFC test section is shown with an image spatial resolution of (a) 10 μm (b) 250 μm. (c) Comparison of the through-plane neutron attenuation demonstrating the improvement in resolution.

In collaboration with General Motors, a suite of performance and degradation studies have been carried out on full-scale, commercial hardware. The NIST beam is 26 cm in diameter, which allows nearly the entire full-scale fuel cell to be viewed at once. These full scale images were also captured with a high frame rate (up to 30 Hz) utilizing the amorphous silicon flat panel detector with spatial resolution of 0.25 mm. One output of this work shows the impact of channel surface treatment on water retention (Figure 2). Bipolar plates treated with a hydrophilic coating reduce both the overall water retention during operation and the energy required to purge the active area for in preparation for cold/freeze start. In contrast, hydrophobic treatments increase the amount of water retained by the diffusion media and result in longer times to purge the active area for cold/freeze start. An innovative planar stack was designed to allow radiography studies of stack failure modes. Figure 3 shows the results of using this planar 4-cell stack to study the stability of the stack as a function of anode stoichiometry. This study observed that the cell with the highest DM saturation (Cell 3) is seen to be the first to fail. The other cells (Cells 1, 2 and 4) are seen to have more water in the channels and this channel water diverts gas flow into the DM thus reducing the DM saturation and reducing the electrode flooding. Repeated measurements showed that the cell that failed first varied, but that this cell was always the one that had the highest DM saturation.

Employing the 10 µm spatial resolution micro-channel plate detector, we have collaborated with the Los Alamos fuel cell team in studying flooding in

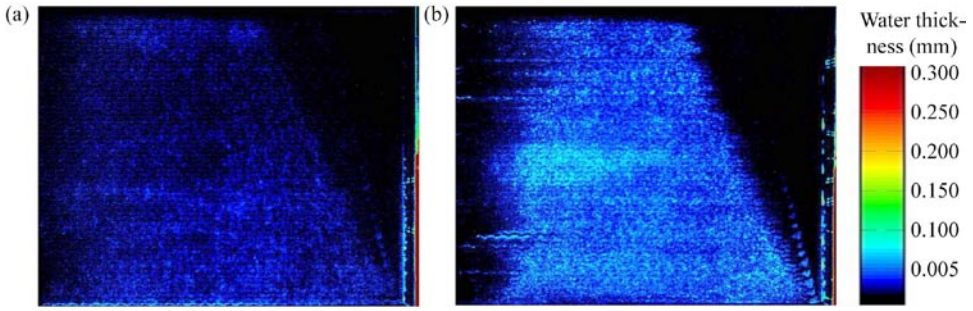


FIGURE 2. Water content of a test section with a (a) hydrophilic bipolar plate (θ_s = 100°) and a (b) hydrophobic bipolar plate (θ_s = 10°). The test section was operated at 0.1 A cm^2, 75°C, and anode (cathode) outlet relative humidity of 121% (108%).

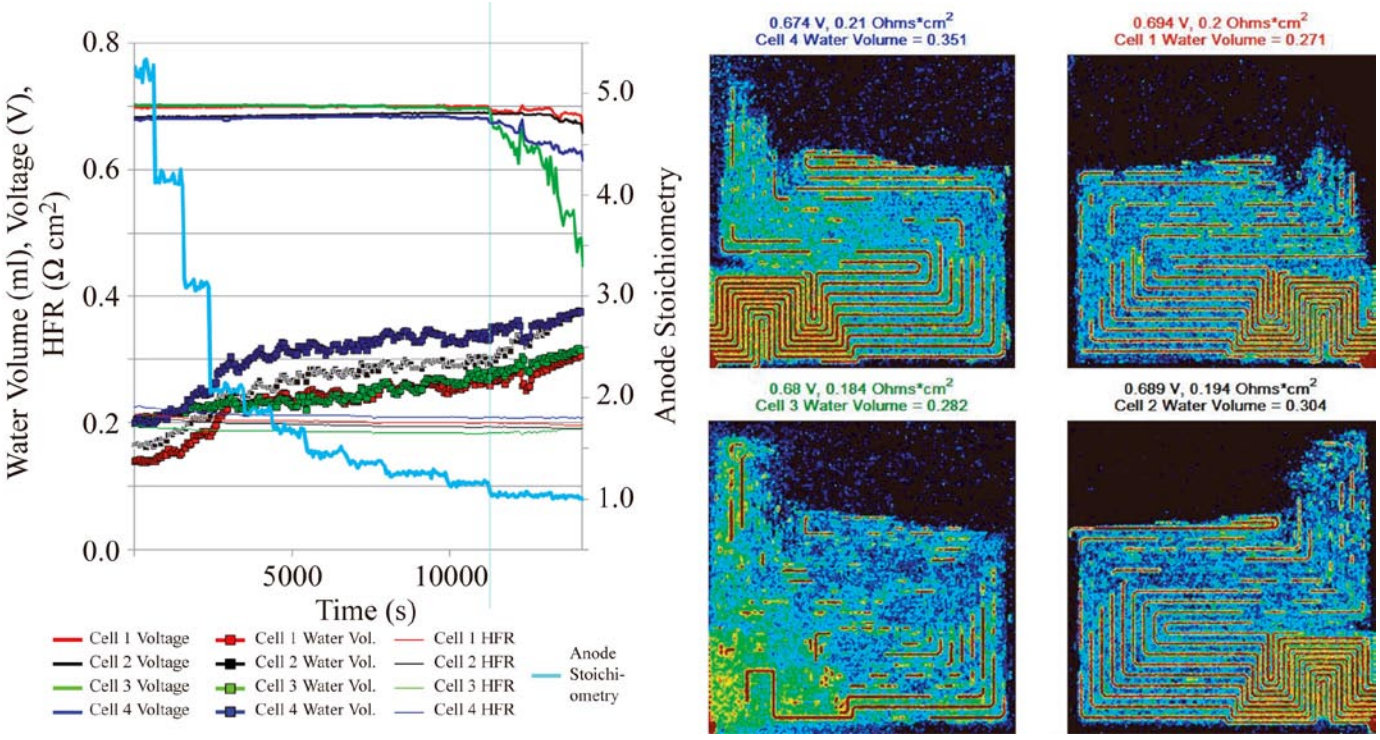


FIGURE 3. Correlation of water content with cell instability in a four-cell stack as a function of anode stoichiometry. The line plot is the voltage, water volume and high frequency resistance at 1 kHz for each cell as a function of the anode stoichiometry. The neutron images are from the point at which the anode stoichiometry drops to about 1, and show that Cell 3, which has the highest gas diffusion layer (GDL) saturation rather than the greatest overall water volume, fails first. The additional water content in Cells 1, 2 and 4 is due to larger channel water content, which diverts flow into the GDL and reduces GDL saturation.

a non-precious group metal (NPGM) oxygen reduction catalyst as well as studying the effects of test two accelerated stress tests (ASTs) on the through-plane water content. In the NPGM study, a polyaniline-derived catalyst was compared to a Pt-based catalyst with a similar thickness. It was seen that the NPGM catalyst retained significantly more water; thus one path to improving this catalysts performance maybe to reduce its hydrophilicity.

The first AST was performed at a constant voltage hold of 1.3 V for 80 min, followed by operation and imaging at a constant current of 0.8 A/cm^2 for 60 min, followed finally by a polarization curve measurement. The goal of this study was to investigate the role of a microporous layer (MPL) on the water transport during degradation. Previous studies have shown that during corrosion the catalyst layer/GDL becomes more hydrophilic, therefore it was expected that water retention due to the increase in hydrophilicity would be a primary contribution to loss of performance during corrosion. Since the corrosion results in a higher overpotential, operation at constant current generates more heat at the membrane. This temperature gradient efficiently transports the water from the catalyst layer to the channel drying out the test section and is a greater effect than the increased hydrophilicity of the corroded catalyst. However, the presence of the MPL improved the test section durability with less water overall in the test section at all points in the AST. The reduced water content due to the catalyst MPL is believed to be the primary factor that leads to less corrosion and better performance.

In the second AST, a test section representing a standard cell from Ballard was cycled under the following conditions: 30 s at 0.6 V, 60 s at 1.4 V, 100% relative humidity, 80°C, 34.5 kPa backpressure, and constant gas flow rates of 1.5 lpm H_2 and 2.5 lpm air. Neutron images, electrochemical impedance spectroscopy (EIS), cyclic voltammatry (CV), and polarization curve measurements were acquired at intermediate cycles to assess the effects of the degradation. The neutron images were taken while operating the cell at a constant voltage of 0.6 V (not constant current as was done in the first AST). The CV data show a loss in electrochemical surface area up to 100 cycles followed by a more gradual loss beyond 100 cycles. The EIS and polarization curve data show only marked performance degradation after 500 cycles. As shown in Figure 4, the neutron images reveal that the water content initially increases during the first 50 AST cycles, but begins to reduce after 100 AST cycles. Additional experiments are planned using the second AST to better elucidate the corrosion mechanism that was observed by the early onset of the reduced water content.

Conclusions and Future Directions

- A range of water transport topics in commercial-sized stacks and small-scale hardware have been studied utilizing neutron imaging:
  - Hydrophilic coating on bipolar plates aids in efficient water removal.
  - Planar stack designs allow for testing and analyzing failure mechanisms in stacks.
  - Catalyst corrosion produces a larger thermal gradient enhancing water removal from the MEA.

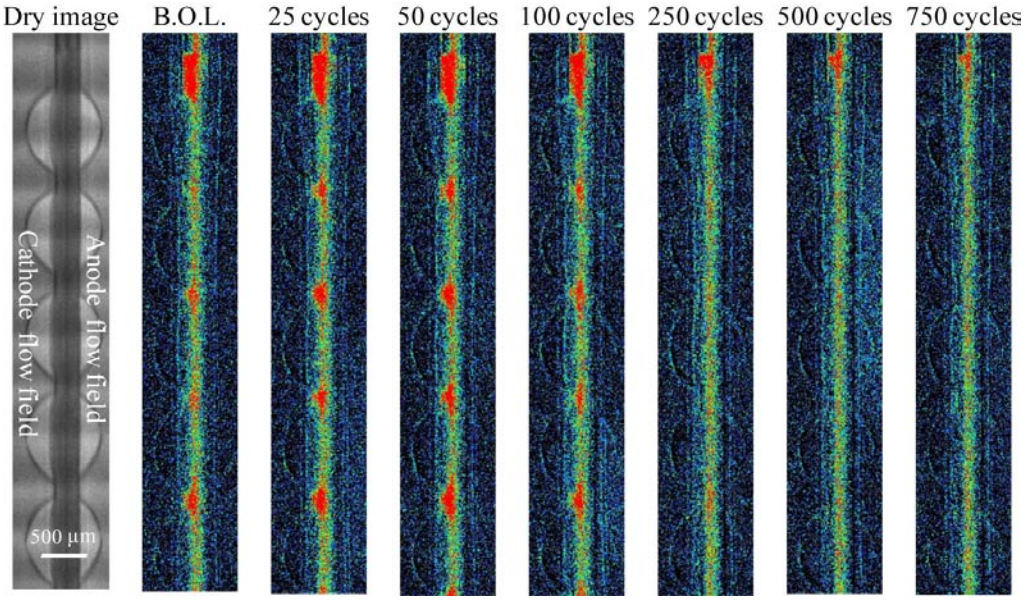


FIGURE 4. Neutron images at intermediary points in the AST cycle from beginning of life (BOL) through 700 cycles. The water content peaks between 25 and 50 cycles. Although the performance after 250 cycles is similar to the BOL, the water content in the cell has already been reduced.

- Future experiments will have enhanced resolution to resolve finer details of membrane and catalyst water profile:
  - Develop new high-resolution techniques to improve the spatial resolution to sub-10 µm with a final goal of 1 µm.
  - Perform experiments to measure and compare with models of water transport through the GDL/MPL/catalyst and membrane with sub-10 µm resolution.
- Expand avenues of fuel cell research allowing larger cells to be imaged with high spatial resolution and even higher temporal resolution:
  - Improve field of view while maintaining spatial resolution to look at larger fuel cells.
  - Provide higher frame rate capabilities up to 100 frames per second in response to user needs.
- Potentially enhance sensitivity of high resolution fuel cell imaging by adding a new cold neutron imaging capability using a new facility to be built for expansion of the NIST Center for Neutron Research.

FY 2011 Publications/Presentations

1. M.C. Hatzell, A. Turhan, S. Kim, D.S. Hussey, D.L. Jacobson, and M.M. Mench, Quantification of Temperature Driven Flow in a Polymer Electrolyte Fuel Cell Using High-Resolution Neutron Radiography, J. Electrochem. Soc. (in press), (2011).

2. Fu R.S. , Preston J.S. , Pasaogullari U., Shiomi T., Miyazaki S., Tabuchi Y., Hussey D.S., Jacobson D.L., Water Transport Across a Polymer Electrolyte Membrane under Thermal Gradients, J. Electrochem. Soc. 158 , B303-B312 (2011).

3. J.S. Preston, R.S. Fu, U. Pasaogullari, D.S. Hussey, D.L. Jacobson. Consideration of the Role of Micro-Porous Layer on Liquid Water Distribution in Polymer Electrolyte Fuel Cells J. Electrochem. Soc. 158 B239 (2011).

4. Jacobson, D.L., Hussey, D.S., Baltic, E., Udovic, T.J., Rush, J.J., Bowman, R.C. Neutron imaging studies of metal-hydride storage beds, International Journal of Hydrogen Energy 35 (23), 12837-12845 (2010).

5. Xuhai Wang, Trung Van Nguyen, Daniel S. Hussey, David L. Jacobson, An Experimental Study of Relative Permeability of Porous Media Used in Proton Exchange Membrane Fuel Cells, J. Electrochem. Soc., Volume 157, Issue 12, pp. B1777-B1782 (2010).

6. Quan, P., Lai, M.-C., Hussey, D.S., Jacobson, D.L., Kumar, A., Hirano, S. Time-Resolved Water Measurement in a PEM Fuel Cell Using High-Resolution Neutron Imaging Technique, J. Fuel Cell Sci. Technol., 2010, 7, 051009.

7. Hussey, D.S., Jacobson, D.L. High resolution neutron radiography analysis of proton exchange membrane fuel cells, Modern Aspects of Electrochemistry, Vol. 49, Pasaogullari, Ugur; Wang, Chao-Yang (Eds.), 2010.

8. D. Spernjak, P.P. Mukherjee, R. Mukundan, J. Davey, D. S. Hussey, D. Jacobson, and R.L. Borup, Measurement of Water Content in Polymer Electrolyte Membranes Using High Resolution Neutron Imaging, ECS Trans. 33 (1), 1451 (2010).

9. J. Mishler, Y. Wang, R. Mukundan, R.L. Borup, D.S. Hussey, and D. Jacobson, In Situ Investigation of Water Distribution in Polymer Electrolyte Fuel Cell Using Neutron Radiography, ECS Trans. 33 (1), 1443 (2010).

10. Y. Gao, T.V. Nguyen, D.S. Hussey, and D. Jacobson, In Situ Imaging of Water Distribution in a Gas Diffusion Layer by Neutron Radiography, ECS Trans. 33 (1), 1435 (2010).

11. D.S. Hussey, E. Baltic, and D. Jacobson, Water Content Measurement of Gas Diffusion Media and Membranes by Neutron Radiography, ECS Trans. 33 (1), 1385 (2010).

12. X. Wang, T.V. Nguyen, D.S. Hussey, and D. Jacobson, Experimental Study of Relative Permeability of Porous Media Used in PEM Fuel Cells, ECS Trans. 33 (1), 1151 (2010).

13. R. Mukundan, J. Davey, J.D. Fairweather, D. Spernjak, J.S. Spendelow, D.S. Hussey, D. Jacobson, P. Wilde, R. Schweiss, and R.L. Borup, Effect of Hydrophilic Treatment of Microporous Layer on Fuel Cell Performance, ECS Trans. 33 (1), 1109 (2010).

14. J.B. Siegel, S. Yesilyurt, and A.G. Stefanopoulou, Reduced Complexity Models for Water Management and Anode Purge Scheduling in DEA Operation of PEMFCs, ECS Trans. 33, 1583 (2010).

15. T. Matsuura, J.B. Siegel, J. Chen, and A.G. Stefanopoulou, "Multiple degradation phenomena in polymer electrolyte fuel cell operation with dead-ended anode", Proceedings of ASME 2011 5th International Conference on Energy Sustainability & 9th Fuel Cell Science, Engineering and Technology Conference, ESFuelCell2011-54344.

16. J. Chen, J.B. Siegel, and A.G. Stefanopoulou, "Nitrogen blanketing and water fording front equilibria in fuel cell dead end anode operation," Submitted to the 2011 American Control Conference, 2011.

17. J.B. Siegel, A.G. Stefanopoulou, and S. Yesilyurt, "Modeling and simulations of PEM-FCs operating with periodically purged dead-ended anode channels," in The 8th International Fuel Cell Science, Engineering and Technology Conference, no. FuelCell2010-33341, (Brooklyn, New York, USA), June 14–16, 2010.

18. J.B. Siegel and A.G. Stefanopoulou, "Parameterization of GDL liquid water front propagation and channel accumulation for anode purge scheduling in fuel cells," in Proc. of the 2010 American Control Conference, 2010.

19. T. Shiomi, R.S. Fu, U. Pasaogullari, Y. Tabuchi, S. Miyazaki, N. Kubo, K. Shinohara, D.S. Hussey, and D.L. Jacobson, Effect of Liquid Water Saturation on Oxygen Transport in Gas Diffusion Layers of Polymer Electrolyte Fuel Cells, ASME Conf. Proc. FUELCELL2010 (2010).

V.A.6 Technical Assistance to Developers

Tommy Rockward (Primary Contact),
Rod Borup (contact person), Eric Brosha,
Jerzy Chilstunoff, John Davey, Fernando Garzon,
Yu Seung Kim, Rangachary Mukundan, Karen Rau,
Mahlon Wilson, and Piotr Zelenay
Los Alamos National Laboratory
PO Box 1663, MS. D429
Los Alamos, NM 87545
Phone: (505) 667-9587 and 667-2823
E-mail: trock@lanl.gov, borup@lanl.gov

DOE Manager
HQ: Nancy Garland
Phone: (202) 586-5673
E-mail: Nancy.Garland@ee.doe.gov

Project Start Date: October 2003
Project End Date: Project direction and continuation determined annually by DOE

Fiscal Year (FY) 2011 Objectives

- Support technically, as directed by DOE, fuel cell component and system developers.
- Assess fuel cell materials and components and give feedback to customers.
- Assist the DOE Durability Working Group with the development of various new material durability testing protocols.
- Provide support to the U.S. Council for Automotive Research (USCAR) and the USCAR/DOE Fuel Cell Technology Team.
- Validate technical findings as directed by DOE.

Technical Barriers

This project can be directed to address any of technical barriers from the Fuel Cells section (3.4.4.2) of the Fuel Cell Technologies Program Multi-Year Research, Development and Demonstration Plan (MYRDDP), however it principally addresses:

(A) Durability
(B) Cost
(C) Performance

Technical Targets

In this particular task, any of the technical targets in Table 3.4.4 of the MYRDDP may be addressed at any given time. Specifically, select tasks that apply to the technical targets in this project are listed below, while their status is listed in the Accomplishments section.

- Provide continued testing insight and advice as directed by the DOE.
- Develop and validate new durability test protocols.
- Offering technical assistance to USCAR and the USCAR/DOE Fuel Cell Technical Team.
- Participating in working groups and review meetings.

Approach

Our approach has consistently focused on collaborative-type interactions as guided by DOE. A large portion of this effort goes unpublished, for proprietary reasons. We have actively participated in the DOE Durability Working Group. Our efforts have been focused on developing durability protocols. More specifically, four protocols are being discussed: rotating disc electrode (RDE)/rotating ring disc electrode (RRDE) measurements of performance and durability of non-precious group metal (PGM) oxygen reduction reaction (ORR) electrocatalysts, ORR electro-catalysts performance and durability measurements in half cell with liquid electrolyte under RDE/RRDE conditions, protocols for evaluating alternative electro-catalyst supports for proton exchange membrane fuel cells, and start/stop protocols for durability life testing. However in this FY, we have continued to provide testing support and actively participated in developing test protocols.

FY 2011 Accomplishments

- Hosted numerous visitors to Los Alamos National Laboratory (LANL).
- Collaborated with multiple industrial, university, or laboratory partners.
- Provided testing to several DOE solicitation winners.
- Participated in the review and development of several durability protocols.
- Hosted LANL-Japanese National Institute of Advanced Industrial Science and Technology-New Energy and Industrial Technology Development Organization Workshop and chaired several sessions (LANL scientists presented, also).

Highlights

Figures 1-5 show some highlights of the technical assistance task for the 2011 FY.

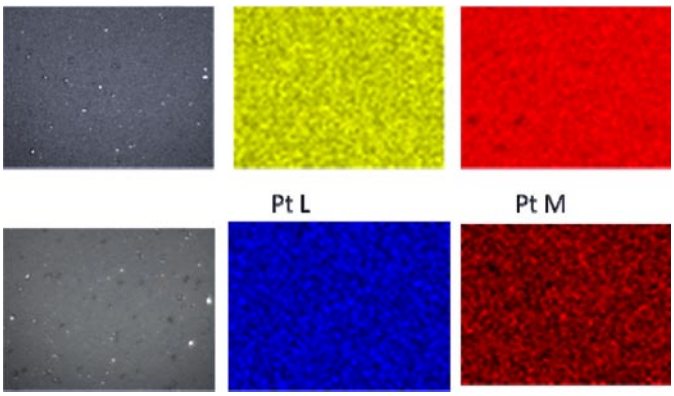


FIGURE 1. Scanning X-ray diffraction of commercial vendor membrane electrode assemblies (MEAs) using two Pt peaks at different energy provides complementary information: L lines show total Pt distribution (both sides of the MEA) and M lines show only one side of MEA.

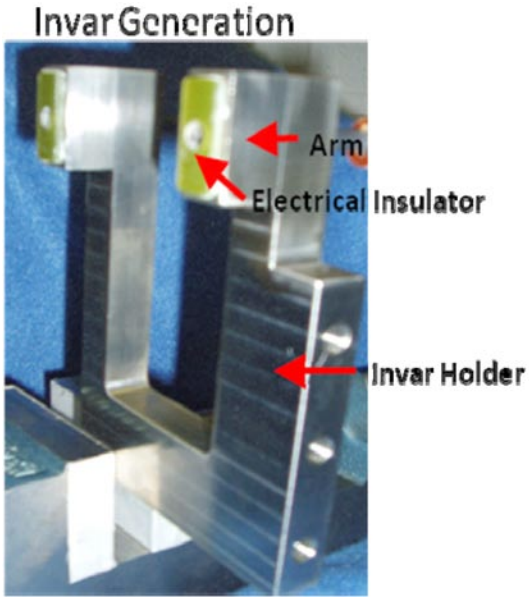
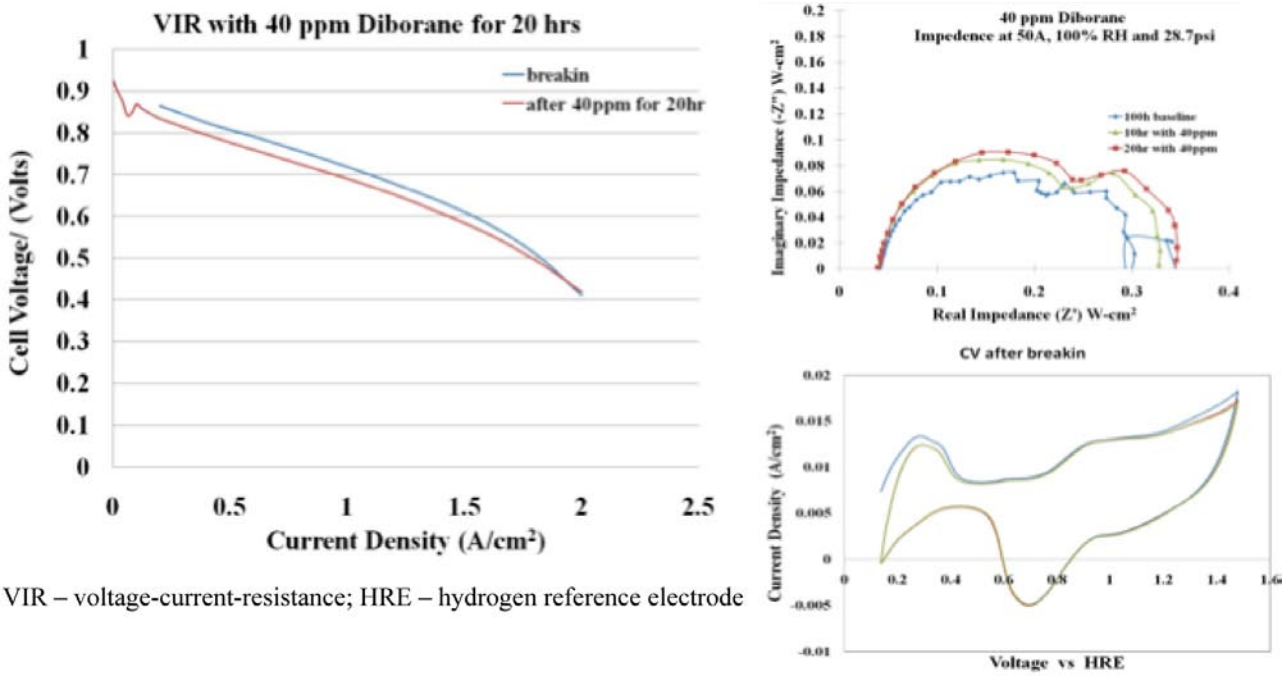
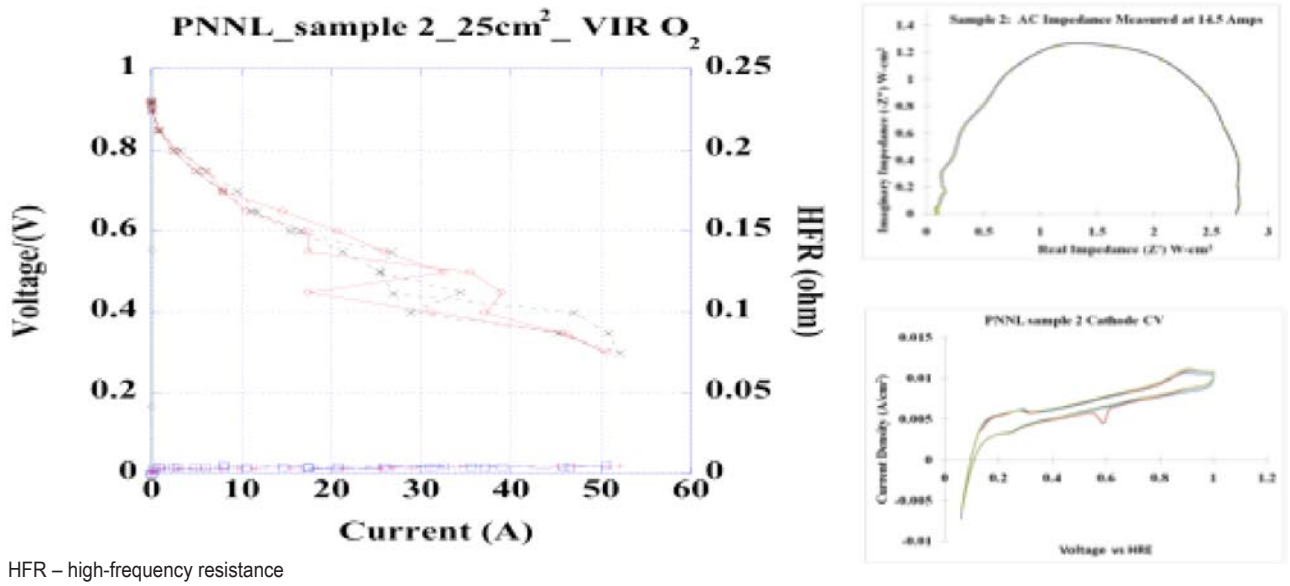


FIGURE 2. LANL designed, built, and provided a new and improved high-resolution fuel cell holder for neutron imaging at the National Institute of Standards and Technology (NIST). The new holder is notable for its uniquely low coefficient of thermal expansion. It has been provided to NIST to make available for all users.



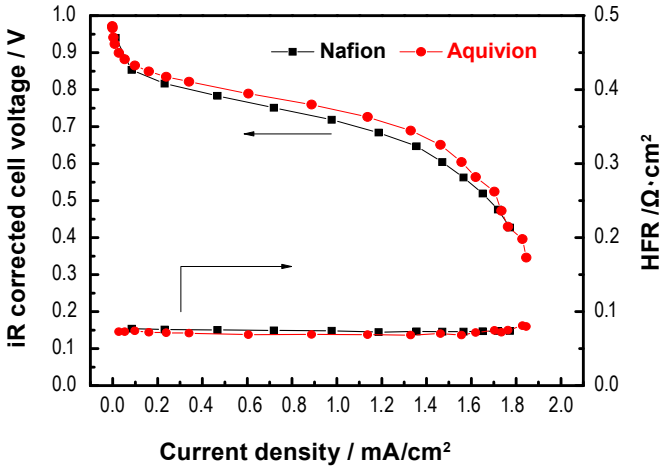
VIR – voltage-current-resistance; HRE – hydrogen reference electrode

FIGURE 3. Examination of the impact of Diborane (being developed as a hydrogen storage material) as an impurity in the anode feedstream of a 50 cm^2 operating fuel cell. Provided voltage-current curves, alternating current impedance results, and cyclic voltammetry as a function of life testing. Shown is performance after exposure to 40 ppm Diborane for 20 hours.



HFR – high-frequency resistance

FIGURE 4. Results shown are from a 25 cm^2 fuel cell tested at 80°C, 100% relative humidity, with 3 stoichiometries at anode and cathode using air (not shown) and oxygen in support of DOE Catalyst Support Project. Alternating current impedance and cyclic voltammetry were also provided.



iR – internal resistance

FIGURE 5. Performance comparison of Nafion® and Aquivion®: Evaluation of short-side chain ionomer (Solvay Solexis).

FY 2011 Publications/Presentations

1. LANL AIST NEDO Workshop, Honolulu Hawaii, August 2010

- Fernando Garzon, Chaired: Durability (Impurities, etc.)
- Christina Johnston, Chaired: Analysis, Characterization, Simulation, Structure Session
- Rod Borup, Chaired: Mass Transportation Session
- Piotr Zelenay, Chaired: Catatlyst Low PGM Session
- Yu Seung Kim, Chaired: Membrane Session
- Rangachary Mukundan, Chaired: Durability Testing (accelerated stress tests, steady-state)

2. Tommy Rockward, Technical Assistance to Developers Update, Fuel Cell Tech Team Update, Detroit MI, December 2010.

3. Tommy Rockward, LANL Program Overview, JARI-DOE Meeting, Washington D.C., February 2011.

V.A.7 Enlarging the Potential Market for Stationary Fuel Cells Through System Design Optimization

Darlene Steward (Primary Contact), Mike Penev, Sam Sprik, Mike Ulsh, Keith Wipke
National Renewable Energy Laboratory (NREL)
1617 Cole Blvd.
Golden, CO 80401
Phone: (303) 275-3837
E-mail: Darlene.Steward@nrel.gov

DOE Manager
HQ: Kathi Epping Martin
Phone: (202) 586-7425
E-mail: Kathi.Epping@ee.doe.gov

Subcontractor:
University of California, Irvine, Irvine, CA (planned)

Project Start Date: January 1, 2011
Project End Date: Project continuation and direction determined annually by DOE

Fiscal Year (FY) 2011 Objectives

- Model fuel cells in realistic combined heat and power (CHP) and combined cooling, heat and power (CCHP) applications to quantify the potential benefits of fuel cell-based distributed power for commercial buildings in the United States
- Identify optimal fuel cell sizes and control strategies based on analysis of the tradeoffs between manufacturing fuel cells that are perfectly matched to every application and fuel cells that are economical to manufacture.

Technical Barriers

This project addresses the following technical barriers from the Fuel Cell section of the Fuel Cell Technologies Program's Multi-Year Research, Development and Demonstration Plan (MYRDDP):

(B) Cost

(C) Performance

Even though the specific performance requirements differ from transportation applications, some of the technical challenges for stationary and other fuel cell systems are the same. For example, the overall cost of these fuel cell power systems must also be competitive with conventional technologies or offer enhanced capabilities. However, stationary and other fuel cell systems have an acceptable price point that is considerably higher than transportation systems.

Technical Targets

The Stationary Fuel Cell Modeling project will provide information about how achieving performance and cost targets for fuel cells in stationary applications could affect the competitiveness of fuel cells in stationary CHP and CCHP applications. The modeling effort will support the fuel cell MYRDDP technical and cost targets by evaluating realistic in situ building energy cost and emissions for CHP fuel cells that meet the targets. The values listed in Table 1, which is an excerpt of selected technical and cost targets for proton exchange membrane (PEM) fuel cell systems, are an example of the types of system characteristics that can be analyzed using the model. The modeling effort will also provide insight into the relative impacts of performance and cost targets on the overall lifecycle cost/benefit of CHP and CCHP installations.

Approach

The model must analyze the tradeoffs between manufacturing fuel cells that are perfectly matched to every application and fuel cells that are economical to manufacture. Therefore, two sub-functions must be optimized together: (1) a function to analyze fuel cells' interactions with various building types and occupancy patterns in various climates, and (2) a function to estimate the cost associated with manufacturing fuel cells of various types and sizes at various production rates. Figure 1 schematically illustrates the interactions between the model functions.

The project is divided into four tasks for 2011.

1. Literature review: Gather information about existing fuel cell and CHP/CCHP models with the goal of identifying useful modeling strategies and identifying potential benchmarks for model validation.
2. Collect building load and other input data: Initially, much of this effort will emphasize identifying data gaps and assessing data quality/needs.
3. Develop graphical user interface proof-of-concept design: Initial emphasis will define the output from the model to meet the overall objective.
4. Demonstrate proof-of-concept tool: The goal of this task is to produce a working model that is capable of providing preliminary results that are reasonably accurate by the end of FY 2011.

TABLE 1. Example Technical Targets for Stationary Fuel Cells That Will Be Evaluated in the Stationary Fuel Cell Model

Excerpted from the 2007 Multi-Year Research, Development and Demonstration Plan Table 3.4.4 Technical Targets: Integrated Stationary PEM Fuel Cell Power Systems (5-250kW) Operating on Reformate and 3.4.5 Technical Targets: Stationary PEM Fuel Cell Stack Systems (5-250 kW) Operating on Reformate				
Characteristic	**Units**	**2003 Status**	**2005 Status**	**2011 Targets**
Electrical Energy Efficiency @ Rated Power	%	30	32	40
CHP Energy Efficiency @ Rated Power	%	70	75	80
Fuel Cell Stack System Cost	$/kWe	N/A	1,500	530
Transient Response Time (from 10% to 90% power)	seconds	<3	<3	<3
Durability @ <10% Rated Power Degradation	hours	15,000	20,000	40,000
Emissions (combined NOx, CO, SOx, hydrocarbon, particulates)	g/1,000 kWh	<8	<8	<1.5

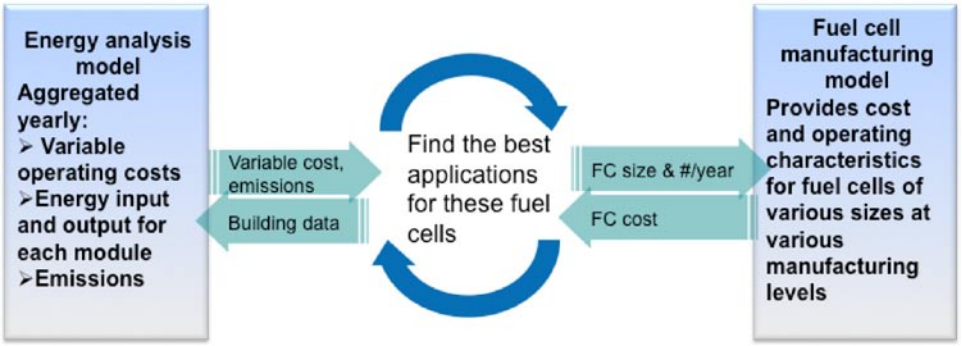


FIGURE 1. Interaction Between Fuel Cell CHP/CCHP Performance Model and Manufacturing Cost Model

FY 2011 Accomplishments

Tasks 1 and 2

- Existing models for benchmarking, partners, and reviewers were identified.
- Attributes for an initial set of buildings, climate, fuel prices, and emissions were collected and entered into an extensible database.
- Attributes of fuel cell manufacturing and performance were collected or estimated for an initial set of fuel cells (proton exchange membrane and solid oxide).

Tasks 3 and 4

- The layout and primary functional screens of the user interface were developed.
- Sub-modules were developed for the initial set of equipment.
- A flexible control strategy was developed.

Future Direction

In FY 2012, NREL will perform the following tasks:

1. Assemble full set of building inventory data and additional fuel cell models.
2. Continue verification and refinement of embedded models and model documentation.
3. Perform initial full-scale optimization analyses.

FY 2012 Planned Milestones

1. Complete draft stationary fuel cell model users guide and model documentation including:
   - Operation of the model including default values and acceptable ranges for input values.
   - Documentation of sources and meta-data for embedded databases and models.
   - Documentation of equations and validation of fuel cell and balance of plant models.
2. Compile detailed plan and prioritized list of proposed additions/enhancements to the model.

Potential Future Model Capabilities

- Interface with building models/or incorporate simple building modeling capability.
- Enhanced environmental analysis capabilities.
- Built-in comparison to other CHP technologies.
- Batteries and/or thermal storage.
- Multi-building/district heating scenarios.
- Hydrogen production for vehicles.

V.A.8 Fuel Cell Testing at the Argonne Fuel Cell Test Facility: A Comparison of U.S. and EU Test Protocols

Ira Bloom (Primary Contact), John Basco, Lee Walker
Argonne National Laboratory (ANL)
9700 South Cass Avenue
Argonne, IL 60439
Phone: (630) 252-4516
E-mail: Ira.Bloom@anl.gov

Collaborators:
G. Tsotridis and T. Malkow
European Commission, Directorate-General Joint Research Center, Institute For Energy
Petten, The Netherlands

DOE Manager
HQ: Nancy Garland
Phone: (202) 586-5673
E-mail: Nancy.Garland@ee.doe.gov

Start Date: 1996
Projected End Date: Project continuation and direction determined annually by DOE

Fiscal Year (FY) 2011 Objectives

- Provide DOE with an independent assessment of the performance of fuel cell systems and components developed under DOE contracts.
- Characterize and benchmark the performance of state-of-the-art commercial fuel cell technology available in the market.

Technical Barriers

This project addresses the following technical barriers from the Fuel Cells section (3.4) of the Fuel Cell Technologies Program Multi-Year Research, Development and Demonstration Plan:

(A) Durability
(C) Performance
(D) Water Transport within the Stack
(G) Start-up and Shut-down Time and Energy/Transient Operation

Contribution to Achievement of DOE Fuel Cells Milestones

This project will contribute to achievement of the following DOE milestones from the Fuel Cells section of the Fuel Cell Technologies Program Multi-Year Research, Development, and Demonstration Plan:

- **Milestone 86**: Evaluate short stack against 2011 targets for operation over the full operating temperature range. (4Q, 2010): We are testing stacks from different developers and documenting their performance according to well-defined test protocols for comparison of the measured performance against DOE targets.
- **Milestone 87**: Test and evaluate fuel cell systems and components such as MEAs, short stacks, bipolar plates, catalysts, membranes, etc., and compare to targets. (1Q, 2011): We are testing fuel cell stacks, balance-of-plant components, and complete systems to document their performance for comparison to DOE targets.
- **Milestone 88**: Test and evaluate fuel cell systems and components such as MEAs, short stacks, bipolar plates, catalysts, membranes, etc., and compare to targets. (4Q, 2015): We are testing fuel cell stacks, balance-of-plant components, and complete systems to document their performance for comparison to DOE targets and to document the improvements made in meeting those targets.

FY 2011 Accomplishments

- Characterized a 10-kW fuel cell stack from NedStack on both the U.S. and European Union (EU) test and aging protocols.
- There was no significant difference between the results obtained with the two different test protocols.



Introduction

This project helps DOE determine and document progress toward achieving its technical targets by providing an independent assessment of evolving fuel cell technology. In addition, in this project we develop standardized fuel cell testing procedures to aid in the evaluation of different stack technologies on a common basis. The procedures and methods used at the Argonne Fuel Cell Test Facility provide a means for easy comparison of the performance and expected life of the technology from different developers. In these procedures, the stack is characterized in terms of initial performance and durability. To further accelerate fuel cell technology developments, these procedures are compared with similar procedures developed by other national and international organizations.

The initial performance establishes a baseline for comparison as the fuel cell ages. The aging process is accelerated to yield a reasonable projection of life at constant power and under driving duty cycles in a reasonable amount of testing time. Periodically during the aging test, the test is interrupted and the stack performance is re-characterized. A life projection is then made by comparing the most recent performance characteristics with those measured earlier.

Approach

We have developed standardized fuel cell and stack test procedures to aid in the evaluation of different stack technologies. These test procedures characterize the stack in terms of initial performance (e.g., power and voltage vs. current, efficiency, hydrogen cross-over), durability, and low-temperature performance. The testing is repeated during and after defined aging under steady-state and potential or load cycling operations to determine performance decay over time.

The test facility is flexible enough to accommodate the unique needs of different fuel cell technologies. Modification and upgrading of the test facility is an ongoing process that is carried out in consultation with fuel cell developers and DOE.

Results

There is interest in the U.S. and in the EU to standardize testing protocols. It is hoped that with standardized protocols, fuel cell development will be accelerated and information exchange will be increased. Under the FCTESTNET framework program, the EU has developed a set of protocols it is proposing as standards. These protocols are being validated under the FCTES^{QA} program in a number of EU laboratories.

As part of our collaboration with FCTES^{QA}, we participated in a round-robin experiment where the results from different test sites are compared using a common fuel cell stack and the FCTES^{QA} test protocols for sequential polarization curves. To complete our work on comparing polarization protocols, we also tested the stack using the DOE protocols. The major differences between the EU and DOE protocols are the sequence of currents used and the portion of the polarization experiment that is reported as the resulting data. Figure 1 shows that the DOE protocol starts at open circuit, and then sequentially increases and decreases the stack current in turn. The FCTESTNET protocol, on the other hand, can start at almost any current setting. In prior work, we used the FCTESTNET example shown Figure 1. Here, the test protocol starts at about 50% of the rated current; the current then increases, decreases, and finally increases again.

For the current work, we used the FCTESTNET protocol shown schematically in Figure 2, which starts

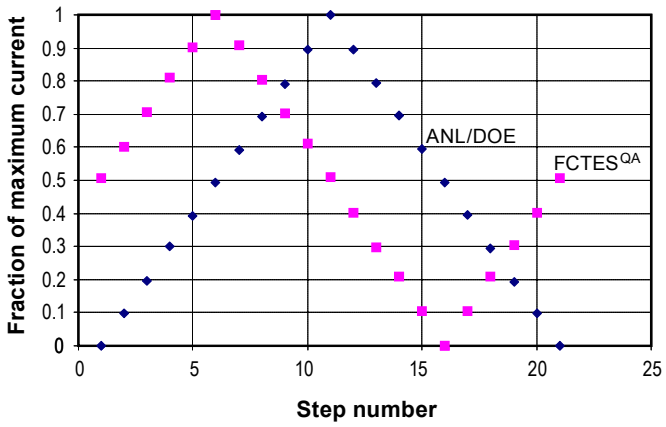


FIGURE 1. Sequence of current levels used in the polarization protocols developed by DOE and by FCTESTNET used in prior work.

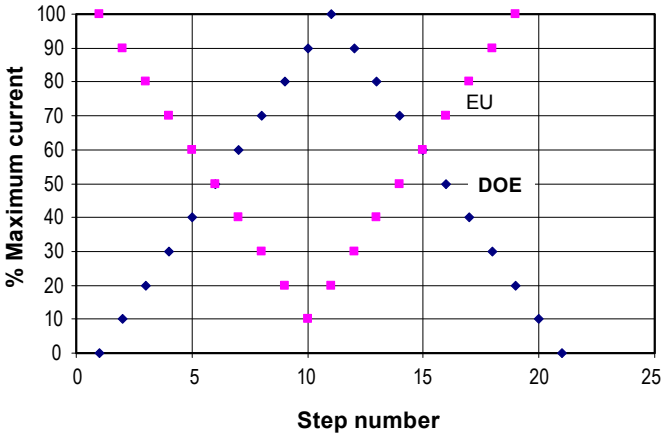


FIGURE 2. Sequence of current levels used in the polarization protocols developed by DOE and by FCTESTNET used in current work.

at 100% of the rated current before decreasing and then increasing. As before, the DOE protocol reports data from both the current-increasing and the current-decreasing sections. For the FCTESTNET protocol, only the results from the current-decreasing portion are reported.

Figure 3 shows the current-decreasing portion of the polarization curves obtained from the 75-cell, 10-kW stack using the two protocols. There was no significant difference between the two curves.

To further characterize the stack as well as the difference between the two protocols, we performed a temperature sensitivity test on the stack. Here, the area-specific resistance (ASR) of the stack was calculated from the polarization results measured at four temperatures, 52.5, 57.5, 62.5 and 67.5°C, and at 1,000 mA/cm^2. These results are summarized in Figure 4.

A linear regression of the data shown in Figure 4 was performed. The regression coefficients, also shown in Figure 4, were greater than 0.95, indicating a strong

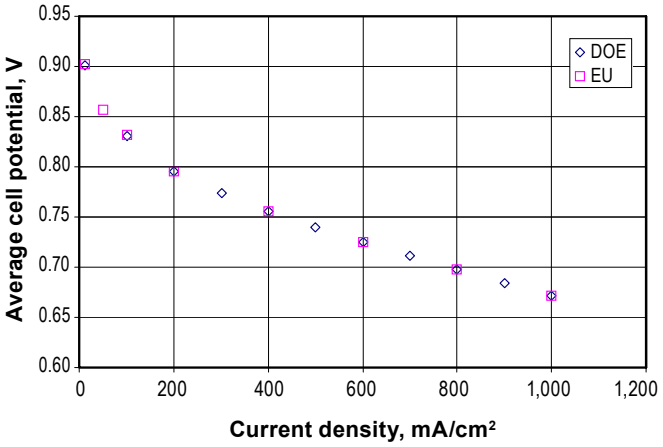


FIGURE 3. Comparison of polarization curves using the current levels and sequence shown in Figure 2. Test conditions: temperature, 62.5°C, air pressure, 0.7 barg; fuel pressure, 0.2 barg; air/fuel stoichiometries, 3/2; inlet gas relative humidity, 85%.

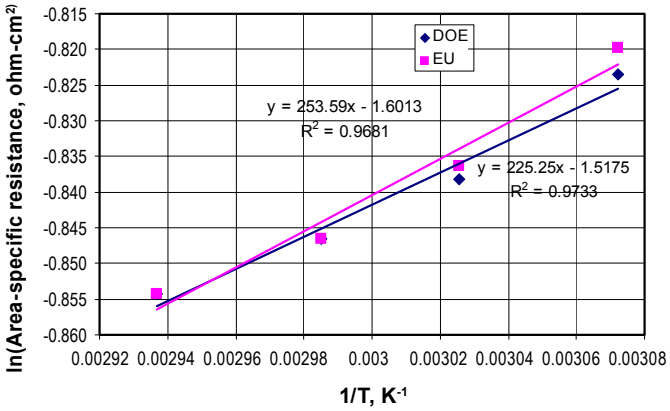


FIGURE 4. Arrhenius plot of stack area-specific resistance measured by both the DOE and EU protocols at 1000 mA/cm^2. The same conditions as described under Figure 3 were used, with the exception of stack temperature.

linear relationship between ln ASR and reciprocal absolute temperature. Thus, the results are consistent with Arrhenius kinetics. Figure 4 also shows that there was a slight difference between the two regression lines, which was due to slight differences (<0.5%) in the calculated values of the ASR.

Finally, we compared our results using the conditions described in Figure 3 with those obtained at JRC's Institute for Energy, as shown in Figure 5. The results showed that, at 1,000 mA/cm^2, there was ~14 mV difference in the average cell potential. It is possible that the slightly higher performance obtained in the testing at ANL versus results obtained at JRC are due to a more precise control of the humidification levels.

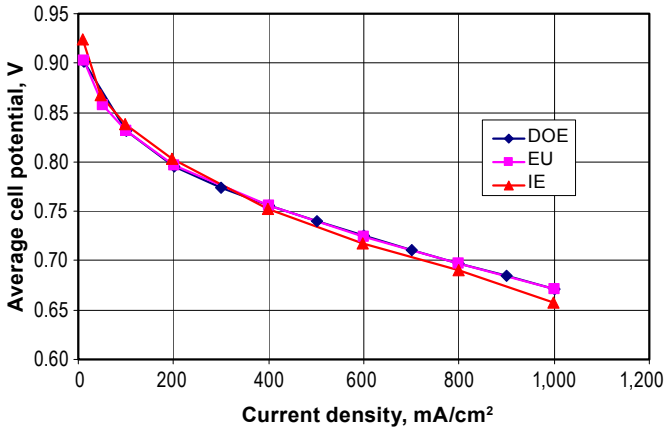


FIGURE 5. Polarization results obtained at ANL and at JRC's Institute for Energy. The curves denoted as DOE and EU were obtained at ANL using the DOE and EU protocols, respectively, under the conditions described under Figure 3. The curve denoted as IE was obtained at JRC's Institute for Energy using the same conditions.

Additional work is needed to evaluate the effects of accelerated aging protocols developed by DOE and FCTESTNET. There may be differences in stress levels under the two testing protocols, which, in turn, may cause differences in aging characteristics. Since we will perform these tests sequentially on the same stack, there may be additional effects in the data, such as path dependency. We will perform the same aging experiments in reverse order to determine if there is path dependency in the results.

Conclusions and Future Directions

- We are collaborating with the EU's FCTESTNET program to compare and validate the fuel cell test protocols being developed by the EU and the DOE. Preliminary results from the testing of a 10-kW stack showed that there was no significant difference between the polarization curves obtained under these two different protocols.
- In future work we will continue to characterize DOE fuel cell contract deliverables, as well as benchmark other fuel cell technologies.
- We will continue to collaborate with other fuel cell testing laboratories, such as the Institute for Energy (Netherlands). Additionally, as part of our work in TC/105/Work Group 11, we will begin to draft a technical specification for single-cell solid oxide fuel cell testing.

FY 2011 Publications

1. "A Comparison of Fuel Cell Test Protocols," I. Bloom, L.K. Walker, J.K. Basco, T. Malkow, G. De Marco and G. Tsotridis, ECS Transactions - 2010 Fuel Cell Seminar & Exposition Vol. 30, "Degradation in PEM Fuel Cells," Feb 2011.

V.B.1 Effect of System Contaminants on PEMFC Performance and Durability

Huyen N. Dinh (Primary Contact), Clay Macomber, Heli Wang, Guido Bender, Kevin O'Neill, Bryan Pivovar,
National Renewable Energy Laboratory (NREL)
1617 Cole Blvd.
Golden, CO 80401-3393
Phone: (303) 275-3605
E-mail: Huyen.Dinh@nrel.gov

DOE Manager
HQ: Kathi Epping Martin
Phone: (202) 586-7425
E-mail: Kathi.Epping@ee.doe.gov

Subcontractors:
- Kelly O'Leary, Balsu Lakshmanan, Rob Reid, General Motors LLC (GM), Honeoye Falls, NY
- John Van Zee and Masato Ohashi, University of South Carolina (USC), Columbia, SC
- Tommy Rockward, Los Alamos National Laboratory (LANL), Los Alamos, NM
- Jean St-Pierre, University of Hawaii, Honolulu, HI
- Ryan Richards and Jason Christ, Colorado School of Mines (CSM), Golden, CO
- Steve Hamrock (in kind subcontractor), 3M, St. Paul, MN

Project Start Date: July 20, 2009
Project End Date: 2013

Fiscal Year (FY) 2011 Objectives

Our overall objective is to decrease the cost associated with system components without compromising function, fuel cell performance, or durability. Our specific project objectives are:

- Identify and quantify system derived contaminants.
- Develop ex situ and in situ test methods to study system components.
- Identify severity of system contaminants and impact of operating conditions.
- Identify poisoning mechanisms and investigate mitigation strategies.
- Develop models/predictive capability.
- Develop material/component catalogs based on system contaminant potential to guide system developers on future material selection.
- Disseminate knowledge gained to the community.

Technical Barriers

This project addresses the following technical barriers from the Fuel Cells section (3.4.4) of the Fuel Cell Technologies Program's Multi-Year Research, Development and Demonstration Plan:

(A) Durability

(B) Cost

Technical Targets

This project focuses on quantifying the impact of system contaminants on fuel cell performance and durability. Insights gained from these studies will be applied toward the development of a catalog of system component materials that help meet the following DOE 2010 targets:

- Cost: $30/kW for transportation, $750/kW for stationary
- Lifetime: 5000 hours for transportation, 40,000 hours for stationary

Accomplishments

- Selected 50 relevant balance-of-plant (BOP) materials based on physical properties, functionality in a fuel cell environment, and cost.
- Established a standard set of experimental protocols for analysis, including leaching, cyclic voltammetry, analytical characterization and in situ fuel cell protocol(s).
- Benchmarked testing protocols and equipment among the different labs.
- Preliminary ex situ screening of 19 polymeric structural plastics.
- Identified leachants via gas chromatography-mass spectroscopy (GC-MS) and selected a few model species for further study.
- Developed a clear long-term project plan with gates and strategies for selecting materials for in-depth fuel cell studies, model species studies, durability testing, and modeling.



Introduction

Cost and durability issues of polymer electrolyte membrane fuel cell (PEMFC) systems have been challenging in the fuel cell industry. The cost of the BOP ($51/kW in 2010 [1]) system has risen in importance with decreasing fuel cell stack cost ($25/kW in 2010 [1] compared to $65/kW in 2006 [2]). Lowering the cost of PEMFC system components requires understanding of the materials used in the system components and the contaminants that are derived from them, which have been shown to affect the performance and

durability of fuel cell systems. Unfortunately, there are many possible contamination sources from system components [3-5]. Currently deployed, high-cost, limited-production systems are using expensive materials for system components. In order to make fuel cell systems commercially competitive, the cost of the BOP components needs to be reduced without sacrificing performance and durability. Fuel cell durability requirements limit the performance loss due to contaminants to at most a few mV over required lifetimes (thousands of hours), which means close to zero impact for system contaminants.

As catalyst loadings decrease and membranes are made thinner (both are current trends in automotive fuel cell research and development), operation of fuel cells becomes even more susceptible to contaminants. In consumer automotive markets, low-cost materials are typically required but lower cost typically implies higher contamination potential. The results of this project will provide the information necessary to help the fuel cell industry make informed decisions regarding cost of specific materials versus the potential contaminant impact on fuel cell performance and durability.

Approach

Our goal is to provide an increased understanding of fuel cell system contaminants and help provide guidance in the implementation, and where necessary, the development of system materials that will help enable fuel cell commercialization. While much attention has been paid to air and fuel contaminants, system contaminants have received very limited attention publicly and very little has been publicly reported [6-9]. Our approach is to perform parametric studies to characterize the effects of system contaminants on fuel cell performance and durability; as well as to identify poisoning mechanisms, recommend mitigation strategies, develop predictive modeling, and disseminate material catalogs that benefit the fuel cell industry in making cost-benefit analyses of system components. We are identifying and quantifying potential contaminants derived from stack/component fabrication materials and quickly screening the impact of the leachants on fuel cell catalyst and membrane via ex situ tests. Model compounds capable of replicating the deleterious impact of system-based contaminants are also being studied. Developing standard test protocols to evaluate materials is important as this approach will allow for broader studies to be performed. Furthermore, information obtained from ex situ methods is being validated with in situ testing.

Our system materials selection is based on properties such as exposed surface area, total mass or volume in a system, fluid contact, function, cost, and performance implications. Current material prioritization and selection to study is based on perceived impact of potential system contaminants (based on GM internal knowledge): structural materials, elastomers for seals and (sub)gaskets, assembly aids (adhesives, lubricants), membrane degradation products, bipolar/end plates, and ions from catalyst alloys. Our project has a strong polymer focus, as much of the system is polymer based. Furthermore, we are studying commercially available, commodity materials. These materials are generally developed for other applications, where common additives/processing aids may not be a concern, but may present problems for fuel cells.

Results

We completed benchmarking of solution conductivity and total organic content (TOC) techniques, using the leachant solutions generated at GM for two polyphthalamide (PPA) structural materials (Dupont Zytel HTN51G35 HSLR® and Zytel HTN52G35 HSL®). As shown in Figure 1, reproducibility among the different labs for these techniques is consistent. Similar benchmarking was carried out at NREL and GM for GC-MS and inductively coupled plasma – optical emission spectroscopy; consistent reproducibility was found.

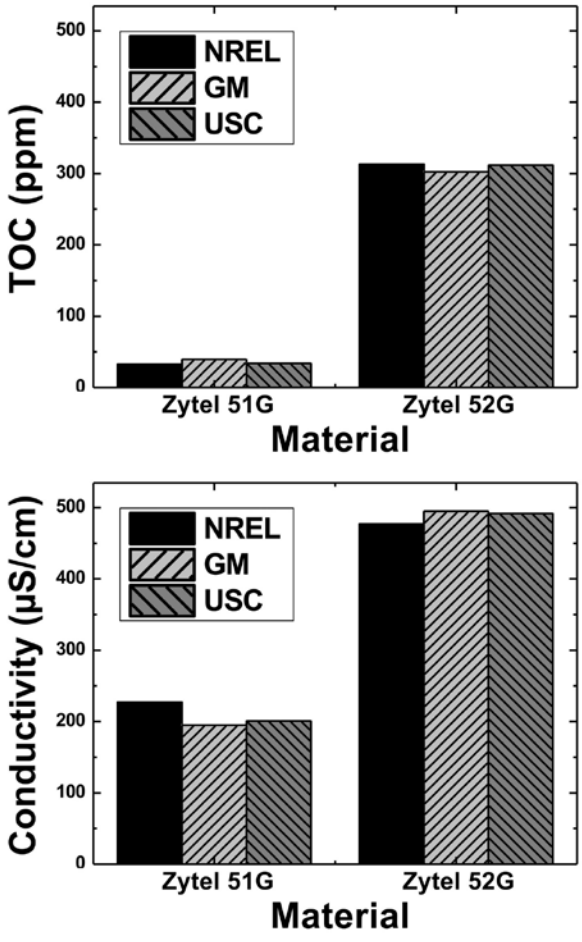


FIGURE 1. The TOC (upper) and solution conductivity (lower) measurements were carried out at NREL, GM, and USC. Reproducibility was consistent among the three labs.

We are screening 19 commercially available structural materials for their potential impact as system contaminants in fuel cell system. They are from the low cost Nylon™ family (polyamide and PPA) and the relatively more expensive polysulfones (PSU), polyphenylenesulfides (PPS) and polyphenylsulfones (PPSU) families. These structural materials underwent leaching protocols (soaked in de-ionized water at 90°C) for six weeks to extract potential contaminants from the parent materials into solution. Figure 2 summarizes the TOC and solution conductivity of these structural materials. As shown, the materials that have high levels of organic leachants do not necessarily have high ionic content. Preferred materials would have low TOC and conductivity values, as highlighted by the circle on the figure.

Initial screening of the leachants after one week of soaking shows that the PPS, PSU and PPSU families are relatively clean materials, with low TOCs and solution conductivities. Also, the liquid GC-MS method did not detect any organic leachants for these materials.

For the polyamide family (PA6, PA6,6, PPA), three common organic species were identified by liquid injection GC-MS: 1,8-diazacyclotetradecane-2,7-dione [DCTDD], caprolactam, and 1,6-hexandiol. The chemical structures of these species are shown in Figure 3. These species will be used as model compounds for further study. It is likely that DCTDD is a Nylon™ decomposition product and/or trapped waste product from the synthetic condensation reaction of adipic acid and hexamethylenediamine. Caprolactam is likely a residual monomer from a ring opening polymerization to synthesize PA6. Knowing the chemistry of the parent polymer and the polymer synthesis, it is understandable where these organic compounds originate from.

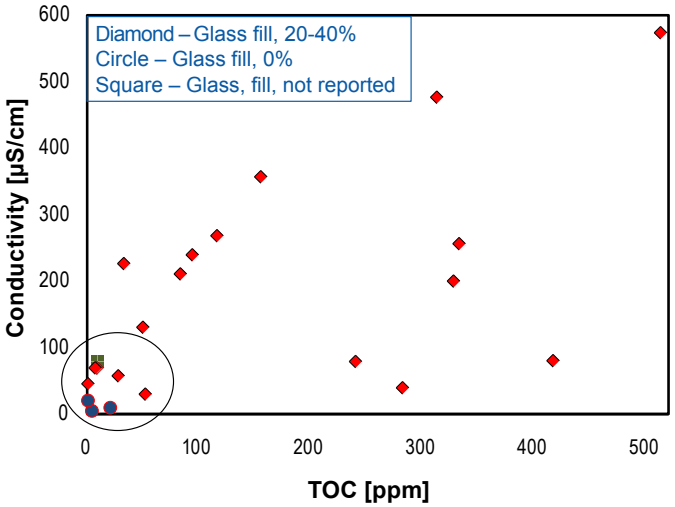


FIGURE 2. Solution conductivity vs. TOC plot for all the structural materials screened to-date. Each point represents a different material tested. Target materials appear at the bottom left corner: low TOC and low solution conductivity.

Conclusions and Future Directions

- We selected a complete set of relevant BOP materials for system contaminant studies based on the level of perceived impact (physical property, function and cost).
- We developed and benchmarked ex situ characterization methods and protocols for screening potential system contaminants.
- We benchmarked fuel cell hardware, test equipment and protocol between the different team members.
- We screened 19 structural materials and identified and quantified the organic and ionic contaminants present.
- We will establish correlations between analytical screening of extract solutions, cyclic voltammatry results, and fuel cell performance loss.
- We will screen the other selected structural materials, assembly aids (adhesives, lubricants), and elastomers for seals and gaskets.
- We will continue to identify and initiate screening of model compounds.
- We will initiate gas-phase durability testing and membrane degradation by-products study.

FY 2011 Publications/Presentations

1. H. Wang, S. Coombs, C. Macomber, K. O'Neill, G. Bender, B. Pivovar, and H.N. Dinh, "Evaluating Polymeric Materials as Potential Sources of PEMFC System Contaminants," ECS Transactions, 33(1) 1617-1625 (2010).

2. H. Cho, M. Jung, J. Navarro, M. Ohashi, and J.W. Van Zee "Aniline as Cationic and Aromatic Contaminants in PEMFC," ECS Transactions, 33(1) 1627-1635 (2010).

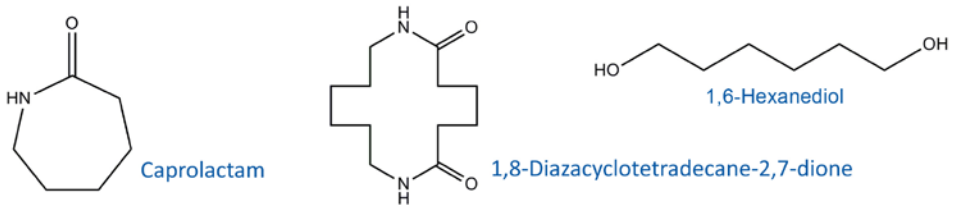


FIGURE 3. Chemical structure of the organic species identified in polyamide family of polymers by liquid GC-MS.

3. C. Macomber, H. Wang, K. O'Neill, S. Coombs, G. Bender, B. Pivovar, and H.N. Dinh, "Characterizing Polymeric Leachants for Potential System Contaminants of Fuel Cells", ECS Transactions, 33(1) 1637-1643 (2010).

4. J. St-Pierre, 'PEMFC contaminant tolerance limit - Foreign cations in ionomers', *Int. J. Hydrogen Energy*, in press, Department of Interior:10.1016/j.ijhydene.2011.01.143.

5. J. St-Pierre, 'PEMFC contamination model: Foreign cation exchange with ionomer protons', *J. Power Sources*, submitted.

6. H. Wang, S. Coombs, C. Macomber, K. O'Neill, G. Bender, B. Pivovar, and H.N. Dinh, "Developing Ex Situ Testing Methods to Evaluate PEMFC System Contaminants," 218th ECS Meeting, Las Vegas, NV, Oct. 2010.

7. H. Cho, M. Jung, J. Navarro, M. Ohashi, and J. W. Van Zee "Aniline as Cationic and Aromatic Contaminants in PEMFC," 218th ECS Meeting, Las Vegas, NV, Oct. 2010.

8. C. Macomber, H. Wang, K. O'Neill, S. Coombs, G. Bender, B. Pivovar, and H.N. Dinh, "Identifying Leachant Contaminants of Fuel Cell System Components and Their Effect on Performance" 218th ECS Meeting, Las Vegas, NV, Oct. 2010.

9. K.A. O'Leary and B. Lakshmanan, "Methodologies for Screening Balance of Plant Materials for Fuel Cell Contamination," 218th ECS Meeting, Las Vegas, NV, Oct. 2010.

10. S. Kocha, Project participation in Durability Working Group Meeting, Las Vegas, NV, Oct. 2010.

11. H.N. Dinh and K. O'Leary, "Effect of System and Air Contaminants on PEMFC Performance and Durability," Fuel Cell Tech Team Meeting, Southfield, MI, Oct . 28, 2010.

12. H.N. Dinh , "Effect of System and Air Contaminants on PEMFC Performance and Durability," DOE Mid-Year Review, Denver, CO, Jan. 19, 2011.

13. J. St-Pierre, 'PEMFC contaminant tolerance limit - Foreign cations in ionomers,' 219th ECS Meeting, Montreal, CA, May 2011.

References

1. B. James, J. Kalinoski, K. Baum,, Mass-production cost estimation for automotive fuel cell system, 2010 U.S. DOE Annual Merit Review and Peer Evaluation Meeting, FC018, Washington, D.C., June 8, 2010.

2. R. Farmer, Presentation on Fuel Cell Technologies: FY2011 Budget Request Briefing, Feb. 12, 2010.

3. D. Gerard, "Powertrain Plastic Materials." SAE Mid Michigan Conference, February 11, 2008.

4. D. Gerard, "Materials and Materials Challenges for Advanced Automotive Technologies being Developed to Reduce Global Petroleum Consumption" (Invited). 2007 Materials Science and Technology, September 16–20, 2007, Detroit, MI.

5. D.A. Masten, A.B. Bosco *Handbook of Fuel Cells* (eds.: W. Vielstich, A. Lamm, H.A. Gasteiger), Wiley (2003): Vol. 4, Chapter *53*, p. 714.

6. Q. Guo, R. Pollard, J. Ruby, T. Bendon, P. Graney and J. Elter, ECS *Trans*. 5(1), 187 (2007).

7. G.A. James, et. al., "Prevention of membrane contamination in electrochemical fuel cells,",US Patent Application US2005089746A.

8. R. Moses, "Materials Effects on Fuel Cell Performance," National Research Council Canada Institute for Fuel Cell Innovation, International Fuel Cell Testing Workshop, September 20–21 (2006).

9. K. O'Leary, B. Lakshmanan, and M. Budinski, "Methodologies for Evaluating Automotive PEM Fuel Cell System Contaminants." 2009 Canada-USA PEM Network Research Workshop, February 16, 2009.

V.B.2 Effects of Impurities on Fuel Cell Performance and Durability

Trent M. Molter
The Connecticut Center for Clean Energy Engineering
The University of Connecticut
44 Weaver Rd. Unit 5233
Storrs, CT 06269
Phone: (860) 486-2898
E-mail: tmolter@engr.uconn.edu

DOE Managers
HQ: Nancy Garland
Phone: (202) 586-5673
E-mail: Nancy.Garland@ee.doe.gov
GO: Reg Tyler
Phone: (720) 356-1805
E-mail: Reginald.Tyler@go.doe.gov

Technical Advisor
Thomas Benjamin
Argonne National Laboratory
Phone: (630) 252-1632
E-mail: Benjamin@anl.gov

Contract Number: DE-FG36-07GO17020

Subcontractors:
- FuelCell Energy, Inc., Danbury, CT
- United Technologies Corporation – Hamilton Sundstrand, Windsor Locks, CT

Project Start Date: March 1, 2007
Project End Date: August 31, 2011

Fiscal Year (FY) 2011 Objectives

- Identify the specific impurities and impurity families and their concentrations present in the fuel stream.
- Develop analytical chemistry protocols and tools to detect the nature and fate of contaminating species within fuel cells.
- Determine through controlled laboratory experimentation and literature study the main drivers for voltage decay.
- Develop impurity analytical models and computer simulations that explain and predict these effects.
- Validate impurity models through single cell experimentation using standardized test protocols.
- Develop and validate novel technologies for mitigating the effects of contamination on fuel cell performance.
- Disseminate results through outreach activities.

Technical Barriers

This project addresses the following technical barriers from the Fuel Cells section (3.4.4) of the Fuel Cell Technologies Program Multi-Year Research, Development and Demonstration Plan:

(A) Durability

Technical Targets

This project is conducting fundamental research into the effects of impurities on fuel cell performance and durability. This activity broadly supports the following technical targets established by DOE:

- By 2010, develop a 60% peak-efficient, durable, direct hydrogen fuel cell power system for transportation at a cost of $45/kW; by 2015, a cost of $30/kW.
- By 2011, develop a distributed generation PEM fuel cell system operating on natural gas or liquefied petroleum gas that achieves 40% electrical efficiency and 40,000 hours durability at $750/kW.

FY 2011 Accomplishments

- Hydrocarbon Testing
  - Completed testing of acetaldehyde and formic acid up to a concentration of 100 ppm showing little effect of acetaldehyde on fuel cell performance but a significant effect of formic acid on fuel cell performance.
  - Developed a better understanding of membrane electrode assembly (MEA) variability and the effects of this factor on impurities testing.
  - Developed analytical procedures for evaluating concentrations of acetaldehyde, formic acid, and formaldehyde in the fuel stream.
  - Developed mixing protocols for injecting specific concentrations of acetaldehyde, formic acid and formaldehyde into the fuel stream.
- Other Impurities
  - Evaluated effects of pertinent cations on the physio-chemical properties of Nafion®.
  - Completed testing of cells with various concentrations of ammonia in the fuel stream.
  - Developed a multi-dimensional model predicting the effects of cationic contaminants on polymer electrolyte fuel cells (PEFCs).
- Mixtures
  - Demonstrated fuel cell tolerance to a hydrogen fuel stream having a composition similar to that of

the International Organization for Standardization (ISO) fuel quality standard.



Introduction

Polymer electrolyte membrane (PEM) fuel cells show significant promise in providing efficient, clean power for stationary and transportation applications. The technology has shown limitations relative to long-term durability goals, particularly with regard to the operational lifetime of MEAs. One of the key causes for this is the introduction of impurities into the fuel stream that impacts the functionality of ion exchange groups within the electrolyte, degrade catalyst activity, and function as diluents causing the cell voltage to degrade.

The initial technical issues being addressed concern the identification of impurity species located in the fuel stream that may have an effect on overall fuel cell performance, and evaluation of these effects against standard test protocols. The U.S. Fuel Cell Council in conjunction with Japanese Automobile Research Institute and others have been developing hydrogen quality standards as well as procedures for contaminant testing of PEM fuel cells. These studies provide the background and basis for the initiation of our research.

Approach

This project is focused on the experimental determination of the effects of key impurities on the performance of PEM fuel cells. Experimental data collected from formalized test protocols will be leveraged to create mathematical models that predict the performance of PEM fuel cells that are exposed to specific contaminant streams. These models will be validated through laboratory experimentation and will be utilized to develop novel technologies for mitigating the effects of contamination on fuel cell performance. Results will be publicly disseminated through papers, conference presentations, and other means.

Results

Hydrocarbon Impurities

Based on input from working groups and industry, our team has focused our efforts on the evaluation of hydrocarbons and halogenated compounds using very specific test protocols developed as part of a multi-laboratory collaborative effort. Our strategy is to evaluate molecules that may be present in a candidate hydrogen fuel stream in order to evaluate the effects of functionality and molecular size (eg. number of carbon atoms).

In support of this, our team has developed techniques to prepare accurate mixtures of impurities in hydrogen and to determine the level of impurities entering the fuel cell through the hydrogen stream. A gas chromatograph has been utilized to characterize both the mixtures entering the fuel cell and those exiting the fuel cell in an effort to assess accumulation and reaction of impurity species within the fuel cell reactor. While previous studies conducted by our group have focused on the evaluation of either gaseous or volatile liquids, recent studies have centered around the development of methods for mixing and analyzing less volatile liquids such as acetaldehyde, formic acid and formaldehyde. Figure 1 shows a saturator apparatus that we have developed to accomplish this task.

Previous testing had been completed using methane, ethane, ethylene, acetaldehyde, and formic acid as the primary fuel stream impurity and later extended to include a mixture of benzene, toluene and CO. Testing has been established as a series of 100-hour test runs using up to 5% of the impurity in the fuel stream with the cell construction as defined in Table 1.

Testing was conducted at 200, 600, 800 and 1,000 mA/cm^2 with standard test conditions defined in Table 2. Conditions were modified as defined to achieve better performance stability during testing.

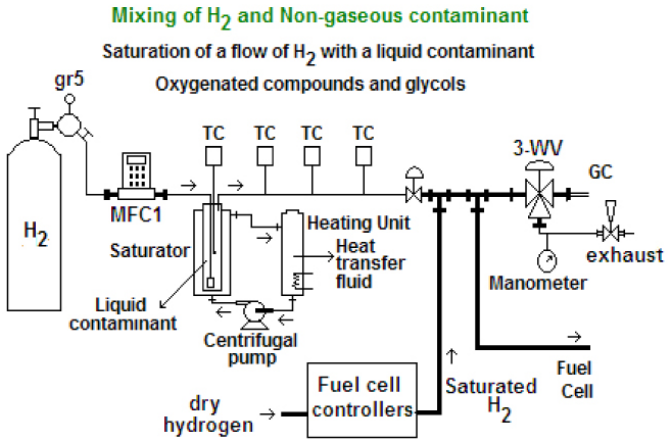


FIGURE 1. Gas Mixing Set-Up for Liquid Hydrocarbons

TABLE 1. Test Cell Definition

Parameter	Early	Intermediate	Recent
Membrane	Nafion®	Nafion® 212	PRIMEA
Loading	0.4/0.2	0.4/0.4	0.1/0.4
MEA OEM	Ion	Ion Power	Gore
GDL	SGL 10	SGL 10 BB	SGL 25
Active Area	25	25	25

OEM - original equipment manufacturer

TABLE 2. Definition of Major Test Parameters

Parameter	Early	Intermediate	Recent
Temperature (°C) (A/Cell/C)	80 / 80 / 80	80 / 80 / 73	80 / 73 / 49
Humidity (%) (A/C)	100 / 100	100 / 75	75 / 25
Stoichiometry (A/C)	1.3 / 2.0	2.0 / 2.0	1.2 / 2.0
Flow Rate (A/C)	Commensurate with current density		
Pressure (psig) (A/C)	25 / 25	25 / 25	7 / 7

A - anode; C - cathode

Ethylene

Testing of the effect of ethylene (C_2H_4) on cell performance was reinvestigated at concentrations of 1% and 5%. These tests were performed to validate previous data obtained with earlier MEAs. No significant effect on cell performance was found during these tests.

Acetaldehyde

Testing of the effect of acetaldehyde (CH_3CHO) on cell performance was investigated at a concentration of 30 ppm. An immediate, but small drop of 20 mV at 800 mA/cm^2 and 50 mV at 1,000 mA/cm^2 was observed with addition of the impurity.

Benzene, Toluene, CO Mixture

The effect of benzene (C_6H_6), toluene (C_7H_8) and CO on fuel cell performance was investigated at an impurity concentration of 10 ppm, 10 ppm and 1 ppm, respectively. Testing showed no significant effect of cell performance during the 100 hour durability test shown in Figure 2.

Hydrogen Pump Studies

NH_3 contamination on PEFCs was investigated with pseudo reversible hydrogen electrodes (pseudo-RHEs). It was found that NH_4^+ can affect the anode causing an increase of the overpotential in a hydrogen pump test. Figure 3 shows the overpotential variations of the anode and the cathode respectively during contamination and recovery. It is seen that 50 ppm NH_3 in H_2 can significantly affect the electrochemical kinetics on the electrodes. The initial drop of the overpotentials is due to the poisoning effect of NH_4^+ on pseudo-RHEs.

Raman Spectroscopy and Gas Chromatograph-Mass Spectroscopy Studies

An investigation of gas diffusion layers (GDLs) revealed minor organic impurities left over from the manufacturing process were still present on the microporous layer of the GDLs. It was found that baking the GDLs would volatize these compounds and clean the surface of organic impurities without damage to the GDLs.

Rotating Disk Electrode

Testing was conducted to further understand the mechanism of formic acid contamination of cell performance. It was found that the concentration of formic acid and presence of hydrogen impacted the oxidation of formic acid as seen in Figure 4. Testing to date has indicated little effect of simple hydrocarbon species on fuel cell performance; however, more complex species do show some performance effects.

Evaluation of Fuel Quality Standards

A model solution of the proposed hydrogen fuel quality ISO standard was evaluated in an operating cell. Results shown in Figure 5 indicate that 100-hour performance was similar to that obtained using pure hydrogen. However, tests run at a contaminant concentration of five times the proposed ISO standard showed significantly higher performance loss over time.

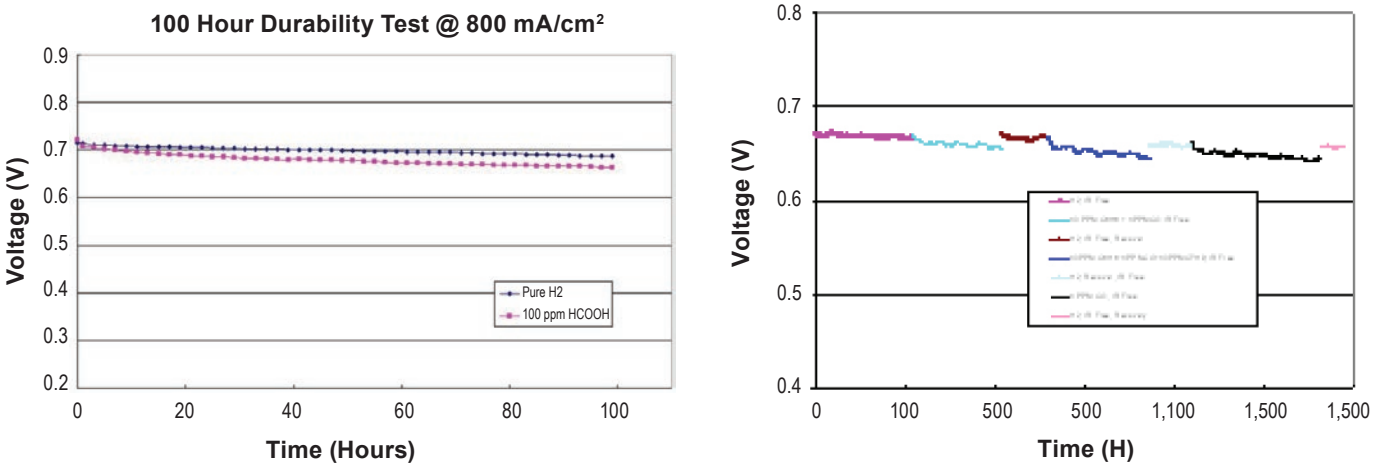


FIGURE 2. Durability Test Using 100 ppm Formic Acid

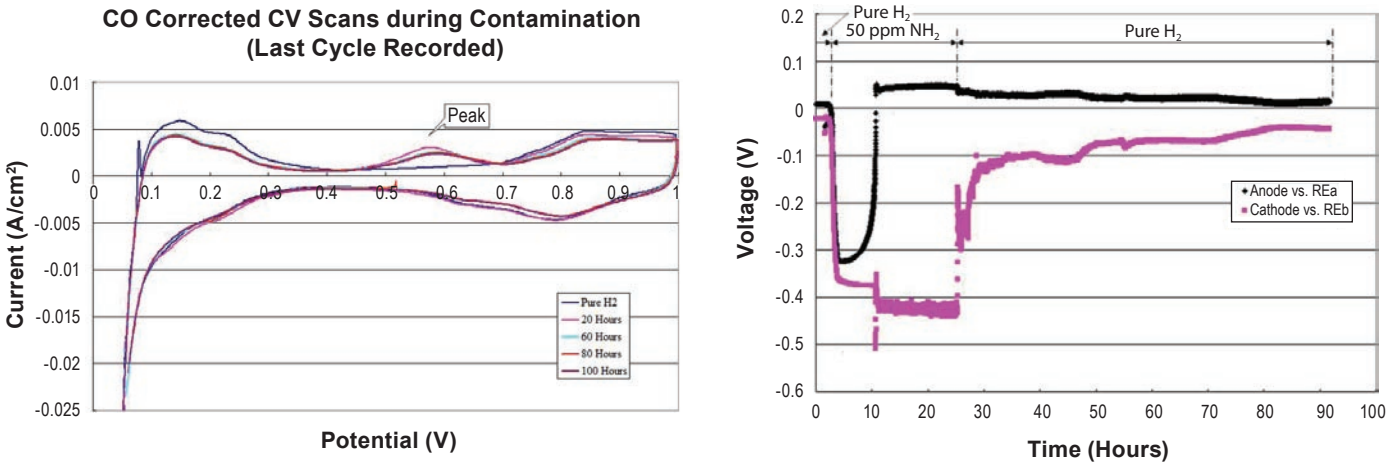


FIGURE 3. The Overpotentials versus RHEs Measured during NH_3 Contamination and Recovery of a 25 cm^2 MEA

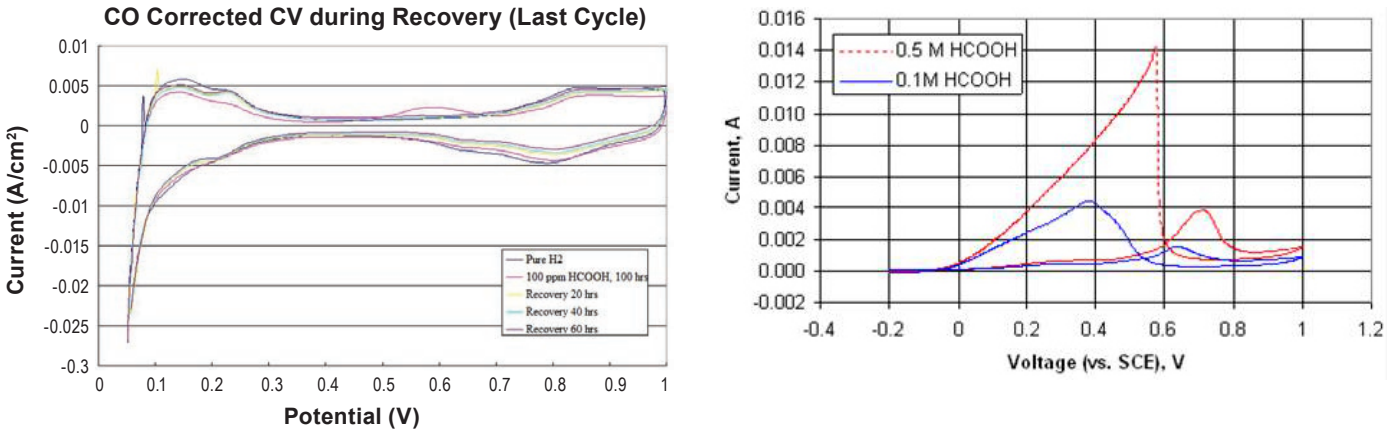


FIGURE 4. Cyclic Voltammetry of 0.1 M and 0.5 M Formic Acid in 0.2 M Sulfuric Acid, No Hydrogen Bubbling

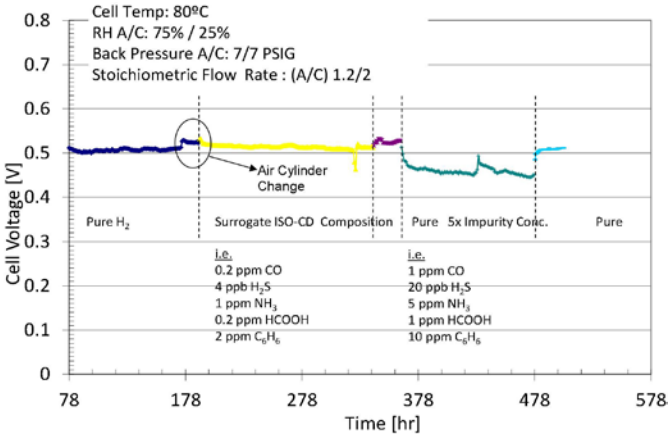


FIGURE 5. Fuel Cell Performance Comparing Pure Hydrogen Feed to Mixtures Emulating the Proposed ISO Fuel Quality Standard, and Contaminant Levels of Five Times the Standard

Conclusions and Future Directions

Conclusions

- Simple hydrocarbons including methane, ethane, ethylene and acetaldehyde do not significantly affect fuel cell performance.
- Formic acid impurities do show an appreciable affect on performance possibly due to adsorption on the electrode surface as well as the formation of reaction byproducts such as CO.
- A multi-component cationic transport model has been created and validated against experimental data.
- Testing with a model hydrogen mixture having chemistry similar to the hydrogen quality standard did not result in significant performance degradation.

Future Directions

- Comprehensive evaluation of formic acid and formaldehyde to support ISO standard development:
  - Continued testing using standard test protocols, MEAs.
  - Target low catalyst loadings (reduction from 0.4 mg/cm^2 to 0.1 mg/cm^2).
  - Develop an understanding of mechanism for performance impact.
  - Modeling of effects/sharing of data.
- Extension to simple halogenated compounds.
- Continued study of effects of cations on membrane properties.
  - Application relevant contamination types/levels.
  - Commercially relevant membranes.
  - Modeling of effects/sharing of data.

FY 2011 Publications/Presentations

1. X. Zhang, H. Galindo, H. Garces, P. Baker, X. Wang, U. Pasaogullari, S. Suib, T. Molter, "Influence of Formic Acid Impurity on Proton Exchange Membrane Fuel Cell Performance", J. of Electrochem. Soc. 157 B409 (2010).

2. Serincan, M.F., Pasaogullari, U., Molter, T., "Modeling the cation transport in an operating polymer electrolyte fuel cell (PEFC)," *Int. J. Hydrogen Energy,* 35(11), 5539 (2010).

V.B.3 The Effect of Airborne Contaminants on Fuel Cell Performance and Durability

Jean St-Pierre (Primary Contact), Yunfeng Zhai, Michael Angelo, Trent Molter, Leonard Bonville, Ugur Pasaogullari, Mark Aindow, William Collins, Silvia Wessel
Hawaii Natural Energy Institute
1680 East-West Road
Honolulu, HI 96822
Phone: (808) 956-3909
E-mail: jsp7@hawaii.edu

DOE Managers
HQ: Nancy Garland
Phone: (202) 586-5673
E-mail: Nancy.Garland@ee.doe.gov
GO: Reginald Tyler
Phone: (720) 356-1805
E-mail: Reginald.Tyler@go.doe.gov

Contract Number: DE-EE0000467

Subcontractors:
- University of Connecticut, Storrs, CT
- UTC Power, South Windsor, CT
- Ballard Power Systems, Burnaby, BC, Canada

Project Start Date: April 1, 2010
Project End Date: March 31, 2014

Fiscal Year (FY) 2011 Objectives

Mitigation of the unknown effects of many airborne contaminants on membrane/electrode assembly materials, adversely impacting system performance and durability:

- Characterize, analyze, understand and prevent the effects of airborne contaminants.
- Disseminate this information in a useful form to industry and other end users.

Technical Barriers

This project addresses the following technical barriers from the Fuel Cells section of the Fuel Cell Technologies Program Multi-Year Research, Development and Demonstration Plan:

(A) Durability

(C) Performance

Technical Targets

The following 2015 transportation technical targets will be addressed by determining contaminant tolerance limits leading to negligible performance losses by extrapolation of tests conducted under high concentrations and using derived mechanistic understanding to increase these tolerance limits with fuel cell mitigation strategies applicable during operation or maintenance cycles.

- Durability: 5,000 h under cycling conditions
- Performance: 60/50 energy efficiency under 25/100% rated power

FY 2011 Accomplishments

- Identified more than 260 airborne contaminants and completed first tier down selection using six qualitative selection criteria including absence of prior data.
- Two quantitative cell performance ranking criteria were devised and the first tier list is currently being prioritized for detailed tests with varied operating conditions.



Introduction

The composition of atmospheric air cannot be controlled and typically includes contaminants. Proton exchange membrane fuel cells operated with ambient air are therefore susceptible to deleterious effects which include decreased cell performance and durability [1]. Numerous air contaminants have not yet been tested in fuel cells and consequently their effects are unknown. This increases the risk of failure for fuel cell systems and thus jeopardizes their introduction into the market. A significant amount of resources is required to characterize the effect of each species on fuel cell performance. Therefore, a method for species down selection is essential to keep the research scope within feasible limits. In this project, airborne contaminants were identified from a variety of sources and down-selected to a manageable yet representative group (first tier). Screening tests were conducted on the first tier contaminants to determine their effects on performance and the ability of the fuel cell to self recover after contaminant exposure. These factors were accounted for with two quantitative cell performance ranking criteria which were used for a second tier down selection. The results of these tests will facilitate the design of mitigation methods.

Approach

Contaminants are separated into three classes (gaseous species, foreign cations and solids) because testing requires different injection strategies and hardware. Key project team organizations are focusing on specific contaminant classes to minimize time consuming benchmarking activities and capabilities duplication. Gaseous species have already been identified and down selected (first tier, Table 1). All

TABLE 1. Down-Selected Gaseous Airborne Contaminants and Some of their Characteristics

Contaminants			Annual maximum concentration (ppm carbon)*			Source	OSHA PEL (ppm)**
Hydrocarbon functionality	Common name	Formula	1 h average	3 h average	24 h average		
N/A	Ozone	O_3	0.197			Chemical manufacture reagent, bleaching agent, disinfectant	400
Alcohol	2-Propanol	$CH_3CH(OH)CH_3$	0.65 μg m^{-3} (indoor max) 0.08 μg m^{-3} (indoor mean)			Cleaning fluid and solvent	No limit
Aldehyde	Acetaldehyde	CH_3CHO	0.022 μg m^{-3} (indoor max) 0.007 μg m^{-3} (indoor mean)			Chemical manufacture precursor	200
Alkene	Propene	C_3H_6	0.625	0.0819	0.102	Polypropylene synthesis precursor and petrochemical feedstock	No limit
Alkyne	Acetylene	C_2H_2	0.117	0.0376	0.0386	Welding fuel and chemical manufacture precursor	No limit
Benzene	Toluene	$C_6H_5CH_3$	0.296	0.0545	1.17	Solvent and industrial feedstock	200
Phenol	2,2-bis(4-hydroxyphenyl) propane	$(HOC_6H_4)_2(CH_3)_2C$			17 pg l^{-1}	Epoxy resin and plastic precursor	0.5
Ketone	Acetone	CH_3COCH_3		0.190	0.2022	Solvent and polymer synthesis precursor	750
Ether	Methyl tert-butyl ether	$(CH_3)_3COCH_3$		0.0017	0.0192	Gasoline additive and solvent	N/A
Ester	Vinyl acetate	$CH_2CHOOCCH_3$			0.102	Polyvinyl alcohol synthesis precursor	10
	Methyl methacrylate	$CH_2CCH_3COOCH_3$			0.00267	Poly(methyl methacrylate) synthesis precursor	100
Nitrogen compound	Acetonitrile	CH_3CN			3.1	Butadiene production solvent	40
Polycyclic aromatic	Naphthalene	$C_{10}H_8$			0.05	Mothball primary ingredient	No limit
Halogen compounds	Dichloromethane	CH_2Cl_2		$8.7x10^{-4}$	0.124	Paint and degreaser solvent	25
	Chlorobenzene	C_6H_5Cl			0.0026	Commodity production intermediate	75
	Bromomethane	CH_3Br			0.0066	Solvent and chemical manufacture precursor	N/A
	Trichlorofluoromethane	CCl_3F			$2.7x10^{-4}$ ***	Former refrigerant	1,000
	1,1-difluoroethane	CH_3CHF_2			$1x10^{-5}$ ***	Refrigerant	N/A
	1,1,1,2-tetrafluoroethane	CH_2FCF_3			$6x10^{-5}$ ***	Refrigerant	N/A

* unless otherwise noted
** OSHA - Occupational Safety and Health Administration
PEL - permissible exposure limit
*** yearly average in atm
N/A - not applicable

selected contaminants will be confirmed by a representative interest group including industry, government and advocacy organizations. Fuel cell performance screening tests will be used to down select contaminants for more detailed studies (second tier) that include variations in key operating conditions (contaminant concentration, current density, temperature, relative humidity). Pressure and stoichiometry are not considered. Pressure represents an alternative to a gaseous concentration change and is not relevant for ionic or solid contaminants. Stoichiometry is irrelevant because the contaminant concentration is approximately constant within the fuel cell based on transport and contamination processes time scales arguments. The project ensures that all contaminant sources are studied. Fuel contaminants were previously studied whereas system contaminants released by

fuel cell materials are currently being investigated in another DOE-funded project.

Results

Species down selection was initially completed on the basis of six criteria (first tier): i) atmospheric presence at a significant level, ii) expectation of reactivity within the fuel cell, iii) absence of recorded data, iv) largest range in chemical functionalities, v) compound toxicity, and vi) suggestions given by project monitors or the fuel cell community. These criteria were sufficient to create a shorter list of 19 contaminants (Table 1) from the larger list of 260+ candidates.

Table 1 shows that most contaminants are organic and are grouped within 12 different chemical functionality classes. Inorganic contaminants are only represented by ozone. All contaminants also originate from large scale industries with production levels exceeding in many cases a million ton per year.

Figures 1 and 2 results show a wide variety of contaminant behaviors. Acetonitrile demonstrates a significant effect but the performance is completely restored after exposure. Other behaviors include: absence of an effect (trichlorofluoromethane), significant effect with an incomplete recovery after exposure (bromomethane), significant effect with a recovery exceeding the initial loss (acetaldehyde). Contamination and recovery time scales also significantly vary within a <1 h to ~20 h range. Such a variety of parameters (performance lost and recovered, time scales) complicates contaminant down selection suggesting the need to develop quantitative criteria consistently applied for selection and minimize qualitatively based decisions.

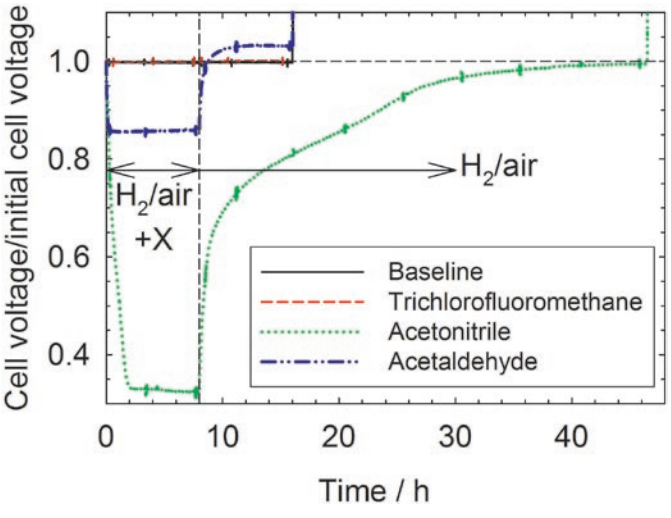


FIGURE 1. Fuel cell response resulting from a temporary contaminant X injection (20 ppm). Gore M715 membrane/electrode assembly, 25 BC SGL Technologies gas diffusion layer, 50 cm^2 active area, 45°C, anode/cathode, H_2/air, 10/10 kPag, 100/50% relative humidity, 2/2 stoichiometry.

Contaminants predominantly behave as illustrated in Figure 3. Upon injection of the contaminant, the cell performance drops until a steady-state is reached after a variable amount of time dependent on operating conditions. After the contamination injection is interrupted, the initial cell performance is partially, fully or supra-recovered. Points a and c correspond to the measured voltage at the time the contaminant is injected and injection is terminated. Points b and d are defined by the intersection of two asymptotes at the beginning and end of the contamination and recovery periods. Two methods were considered for contaminant ranking and rely on these four time/voltage pairs (points a to d). Method 1 relies on the combination of steady-state contamination and irrecoverable performance losses, corresponding time scales and contaminant concentration. Method 2 relies on the combination of the energy lost to contamination and regained during self-recovery:

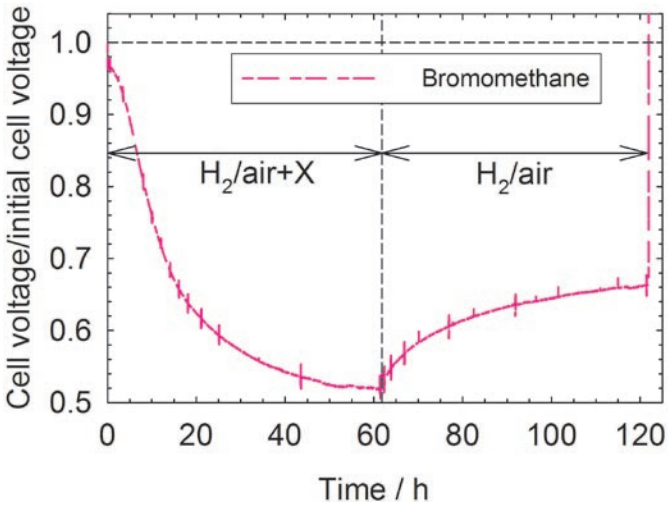


FIGURE 2. Fuel cell response resulting from a temporary contaminant X injection (50 ppm). Gore M715 membrane/electrode assembly, 25 BC SGL Technologies gas diffusion layer, 50 cm^2 active area, 45°C, anode/cathode, H_2/air, 10/10 kPag, 100/50% relative humidity, 2/2 stoichiometry.

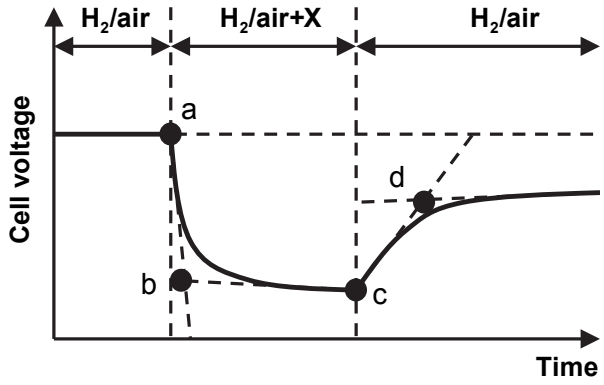


FIGURE 3. Graphical representation of the two methods parameters (points a, b, c and d) used to prioritize tested contaminants. X represents a contaminant.

$$SC_1 = \frac{(V_a - V_b)^2 (V_a - V_d)(t_d - t_c)}{c_{\text{contaminant}} (V_d - V_c)(t_b - t_a)} \quad [1]$$

$$SC_2 = \int_{t_a}^{t_b} (V_a - V)dt \Big/ \int_{t_c}^{t_d} (V - V_c)dt \quad [2]$$

where SC represents a selection criterion (V^2 ppm^{-1} or dimensionless), V_i the cell voltage at point i (V), t_i the time at point i (h), $c_{\text{contaminant}}$ the contaminant concentration in the dry reactant stream (ppm), and V the cell voltage.

Larger SC_1 and SC_2 values generally mean more significant performance losses. Table 2 shows the resulting contaminant rankings. Under wet conditions (100/50% relative humidity), the range in values is larger for SC_1 (more sensitive parameter). Only one of the top four contaminants is the same for SC_1 and SC_2 (bromomethane, italic font). For contaminants that led to a recovery exceeding the initial loss (acetaldehyde, propene), rankings (underlined font) either correspond to low SC_1 values or are scattered over the SC_2 range. Interestingly, SC_2 is not only useful to pinpoint contaminants that have a large negative effect on performance but also others that lead to a recovery exceeding the initial loss (propene). These seemingly beneficial contaminants are a good example of the envisaged use of both selection criteria as a quantitative measure to guide decisions. A strict application of SC_1 would preclude any further interest. However, acetaldehyde and propene unusual behavior may hide some permanent performance benefit.

Conclusions and Future Directions

- Expand tier 1 airborne contaminant list with foreign cations and solids.
- Complete fuel cell contaminant screening tests (tier 1).
- Investigate the cause of the recovery exceeding the contamination performance loss (acetaldehyde, propene).
- Determine which contaminant selection criterion will be used for down selection (tier 2).
- Quantify performance loss for at least four different contaminants under various operating conditions.

FY 2011 Publications/Presentations

1. J. St-Pierre, M. S. Angelo, Y. Zhai, Focusing research by developing performance related selection criteria for PEMFC contaminants, in *Meeting Abstracts*, Electrochemical Society volume 2011-2, The Electrochemical Society, Pennington, NJ,

TABLE 2. Gaseous Airborne Contaminant Rankings

Contaminant *	SC_1 (V^2 ppm^{-1})		SC_2	
	100/50 **	0/0 **	100/50 **	0/0 **
1,1-difluoroethane	*7.23 x 10^{-4}*		0.0259	
1,1,1,2-tetrafluoroethane	2.16 x 10^{-4}		0.0414	
2,2-bis(4-hydroxyphenyl)propane				
Acetaldehyde	−2.35 x 10^{-4}		0.214	
Acetone	−2.86 x 10^{-7}		6.747	
Acetonitrile	*5.78 x 10^{-3}*	9.51 x 10^{-3}	0.0575	0.0410
Acetylene	3.13 x 10^{-6}		*30.623*	
Bromomethane	*4.04 x 10^{-3}*		*7.567*	
Trichlorofluoromethane	No effect		No effect	
Chlorobenzene	*1.57 x 10^{-2}*		0.165	
Dichloromethane	No effect	No effect	No effect	No effect
Iso-propanol	−2.55 x 10^{-7}		*17.796*	
Methyl methacrylate	1.44 x 10^{-5}	1.32 x 10^{-4}	4.863	3.936
Methyl tert-butyl ether	6.69 x 10^{-6}		2.054	
Naphthalene				
Ozone				
Propene	−3.08 x 10^{-5}		*32.063*	
Toluene	5.38 x 10^{-4}		0.349	
Vinyl acetate	−4.42 x 10^{-5}		1.194	

* 20 ppm contaminant concentration with the exception of bromomethane (50 ppm); ** anode/cathode relative humidity (%).

2011, abstract 1035 (forthcoming oral presentation during the 220th Electrochemical Society meeting).

2. J. St-Pierre, K. O'Leary, PEMFC contamination model: Neutral species sorption by ionomer, in *Meeting Abstracts*, Electrochemical Society volume 2011-2, The Electrochemical Society, Pennington, NJ, 2011, abstract 1132 (forthcoming oral presentation during the 220th Electrochemical Society meeting).

3. J. St-Pierre, PEMFC contamination model validation: Foreign cations in ionomers, *Electrochem. Solid-State Lett.*, submitted.

References

1. J. St-Pierre, Air impurities, in *Polymer Electrolyte Fuel Cell Durability*, Edited by F.N. Büchi, M. Inaba, T.J. Schmidt, Springer, 2009, pp. 289-321.

V.B.4 Fundamental Effects of Impurities on Fuel Cell Performance and Durability

James G. Goodwin, Jr. (Primary Contact),
Hector Colon Mercado (SRNL),
Scott Greenway (SRNL), Xunhua Mo,
Kitiya Hongsirikarn, and Jack Zhang
Department of Chemical & Biomolecular Engineering
Clemson University
Clemson, SC 29634-0909
Phone: (864) 650-3807
E-mail: jgoodwi@clemson.edu

DOE Managers
HQ: Nancy Garland
Phone: (202) 586-5673
E-mail: Nancy.Garland@ee.doe.gov
GO: Reg Tyler
Phone: (720) 356-1805
E-mail: Reginald.Tyler@go.doe.gov

Technical Advisor
Walt Podolski
Phone: (630) 252-7558
E-mail: podolski@anl.gov

Contract Number: DE-FG36-07GO17011

Subcontractors:
- Savannah River National Laboratory (SRNL), Aiken, SC
- John Deere, Charlotte, NC

Start Date: February 15, 2007
Projected End Date: September 30, 2011

Fiscal Year (FY) 2011 Objectives

- Investigate the effect of impurities in the hydrogen fuel streams on the operation and durability of fuel cells. These impurities include water, hydrocarbons (including formaldehyde, formic acid), oxygen, inert gases (He, N_2, Ar), CO_2, CO, sulfur-containing gases, ammonia, halogenated compounds and particulates.
- Propose mechanisms for how impurities in the hydrogen fuel stream affect the components of the fuel cell catalyst and polymer membrane.
- Determine strategies to reduce the poisoning effect of these impurities.
- Disseminate findings so that they are available to other members of the DOE Hydrogen Quality team and to FreedomCAR technical teams.

Technical Barriers

This project addresses the following technical barrier from the Fuel Cells section of the Hydrogen, Fuel Cells and Infrastructure Technologies Program Multi-Year Research, Development and Demonstration Plan:

(A) Durability

Technical Targets

This project is addressing fundamental research into effects and mechanisms of impurities on the performance and durability of polymer electrolyte membrane (PEM) fuel cell systems. The activity broadly supports the following technical targets established by DOE:

- Transportation Fuel Cells
  - Durability with cycling: 5,000 h by 2015
- Stationary PEM Fuel Cell Power Systems
  - Durability @ <10% rated power degradation: 40,000 h by 2011

FY 2011 Accomplishments

The following were the significant accomplishments during this project year:

- The degradation of Nafion® by radical products of H_2O_2 formed during fuel cell operation was investigated.
- The effect of Nafion® on Pt/C was studied and the siting of the Nafion® relative to the Pt identified.
- The effect of perchloroethylene on fuel cell and catalyst performance was determined using both PEM fuel cell and fundamental measurements.
- Diborane was established to be a reversible poison for fuel cell performanance.



Introduction

PEM fuel cells show significant potential to enable efficient, clean power for stationary and transportation applications; however, the present-day technology falls short of meeting the necessary product performance and durability requirement standards. An important limitation in the operational life of PEM fuel cells is caused by the presence of hydrogen-feed stream contaminants (e.g., ammonia, carbon monoxide, etc.). These contaminants degrade the functionality of ion exchange groups within the electrolyte, degrade catalyst activity, and result in a degradation of the overall fuel cell efficiency and operational performance.

Approach

This project is a unique combination of phenomenological studies (at Clemson University) and

fuel cell membrane electrode assembly (MEA) durability testing at SRNL, with MEAs tested at SRNL composed of the same/similar materials as being investigated at Clemson. By determining the effect of impurities on the component parts of an MEA as well as overall fuel cell performance, a comprehensive mechanism of poisoning can be proposed which should suggest means to diminish that effect. Development of an integrative model is also being undertaken by Argonne National Laboratory using the fundamental measurement results obtained by Clemson and SRNL. The fuel cell team at SRNL is integrated into the U.S. Fuel Cell Council Joint Hydrogen Quality Task Force, presently engaged to address the International Organization for Standardization Technical Committee 197: Hydrogen Fuel – Product Specification: Proton exchange membrane (PEM) fuel cell application for road vehicles.

Results

During PEM fuel cell operation, formation of H_2O_2 and material corrosion occurs, generating trace amounts of metal cations (i.e., Fe^{2+}, Pt^{2+}) and subsequently initiating the deterioration of cell components and, in particular, PFSA membranes (e.g., Nafion®). In a study at Clemson, a quantitative examination of properties and conductivities of degraded Nafion® membranes at conditions relevant to fuel cell environments (30-100 % relative humidity [RH] and 80°C) was performed. The degradation degree (defined as: loss of ion-exchange capacity, weight, and fluoride content), water uptake, and conductivity of H_2O_2-exposed membranes were found to strongly depend on Fe content and H_2O_2 treatment time (see Figure 1). Fourier transform infrared (FT-IR) analysis revealed that Nafion® degradation preferentially proceeds at the sulfonic end group and at the ether linkage located in the pendant side chain and that the H-bonding of water is weakened after prolonged H_2O_2 exposure.

Results from an investigation at Clemson established a more fundamental understanding of the effect of humidity on CO poisoning of Pt/C at typical fuel cell conditions (80°C, 2 atm). The presence of water vapor decreased the rate of CO adsorption on Pt, but had very little effect on the resulting CO surface coverage on Pt_S (θ_{CO}) at steady-state. The steady-state θ_{CO}'s at 80°C for Pt exposed to H_2 ($P_{H2} = 1$ atm) and a mixture of H_2/H_2O (1 atm H_2, 10%RH) were 0.70 and 0.66 ML, respectively. Furthermore, total strongly-bound surface hydrogen measured after exposure to H_2/H_2O was, surprisingly, the sum of the exchangeable surface hydrogen contributed by each component, even in the presence of CO.

An exploration of the effect and siting (location) of Nafion® on Pt/C as exists in a PEM fuel cell catalyst layer was carried out. Surprisingly, the presence of 30 wt% Nafion® appears to have only a minimal effect on the adsorption capability of either hydrogen or CO on Pt. Experimental and modeling results of cyclopropane hydrogenolysis in an idealized pore suggest that partial blockage of only the pore openings by the Nafion® for the meso-macropores is sufficient to induce diffusion limitations on the reaction. The facts suggest that most of the Pt particles are in the meso-macropores of the C support, whereas Nafion® is present primarily on the external surface of the C where it blocks the micropores but only partially the pore mouths of the meso-macropores.

PCE was chosen as a model compound for chlorinated cleaning and degreasing agents that may be introduced into a fuel cell as contaminants at a fueling station and/or during vehicle maintenance. During this year SRNL completed fuel cell studies using PCE. Figure 2a shows the results of the PCE concentration detected by Fourier transform infrared at different points in the fuel cell. The spectrum of gaseous PCE has three main peaks in the region between 700 and 1,000 cm^{-1}. From this spectrum, the strong peak at 915 cm^{-1} (see insert of Figure 2a) was used to monitor the PCE. Accordingly, a concentration of 164 ppm of PCE was injected at the anode inlet. However, a substantial reduction

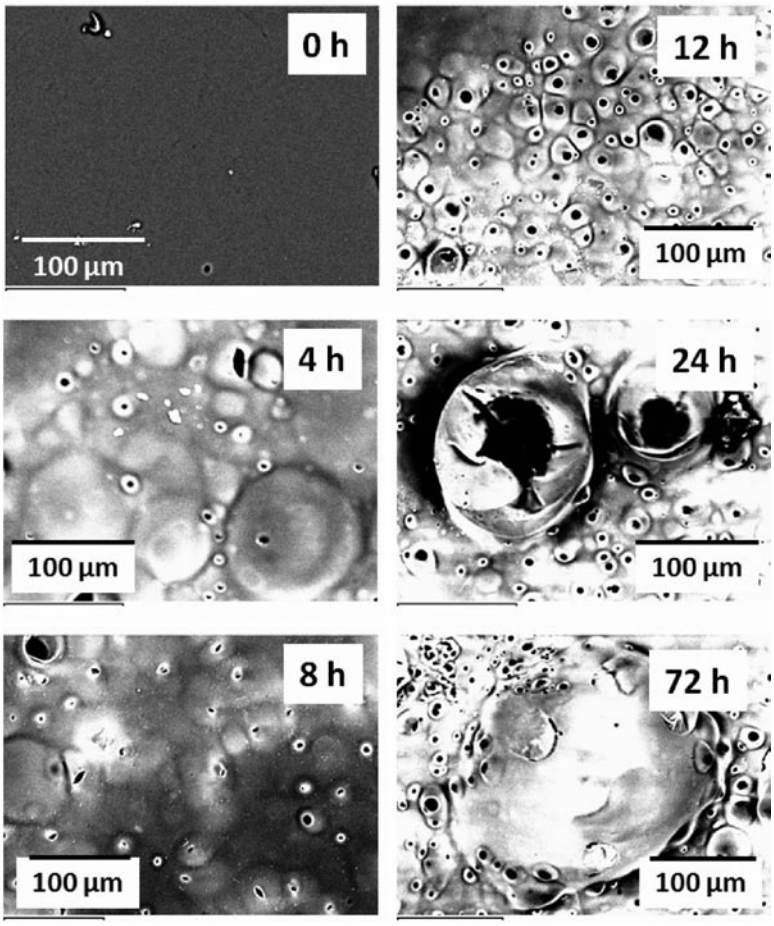


FIGURE 1. Scanning electron microscope images of the surface of a M90 membrane (10% of the H^+ in Nafion replaced by Fe^{2+}) after various times of H_2O_2 treatment.

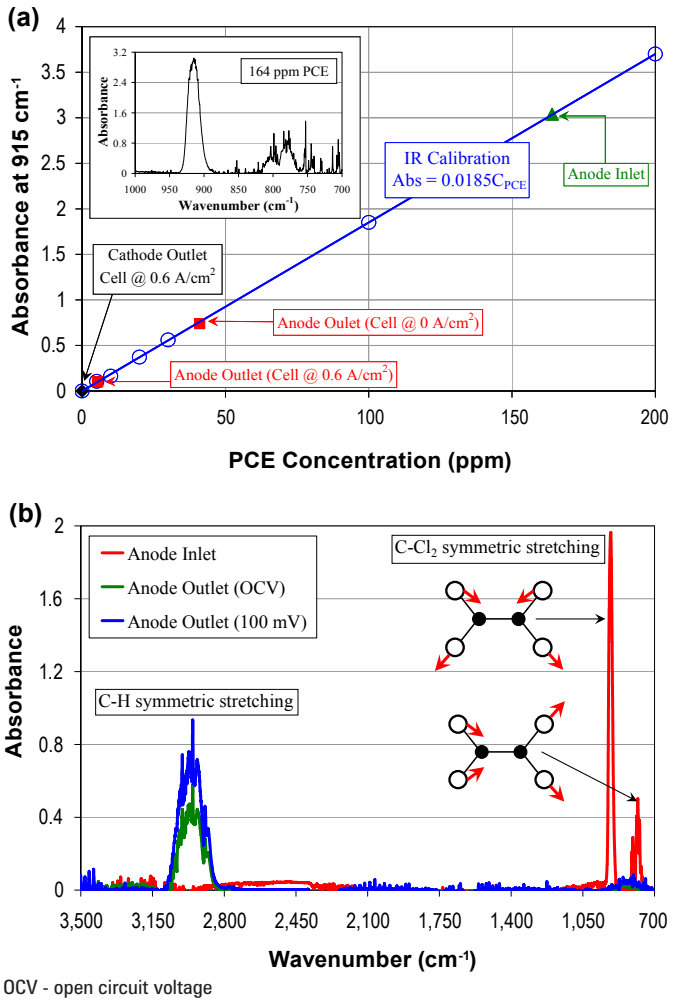


FIGURE 2. (a) FT-IR calibration and concentration detected during fuel cell operation for PCE using the absorbance band at 915 cm^{-1} of the PCE gas phase spectrum (figure insert). (b) FT-IR absorbance spectra of the decomposition products during fuel cell operation with PCE poisoning.

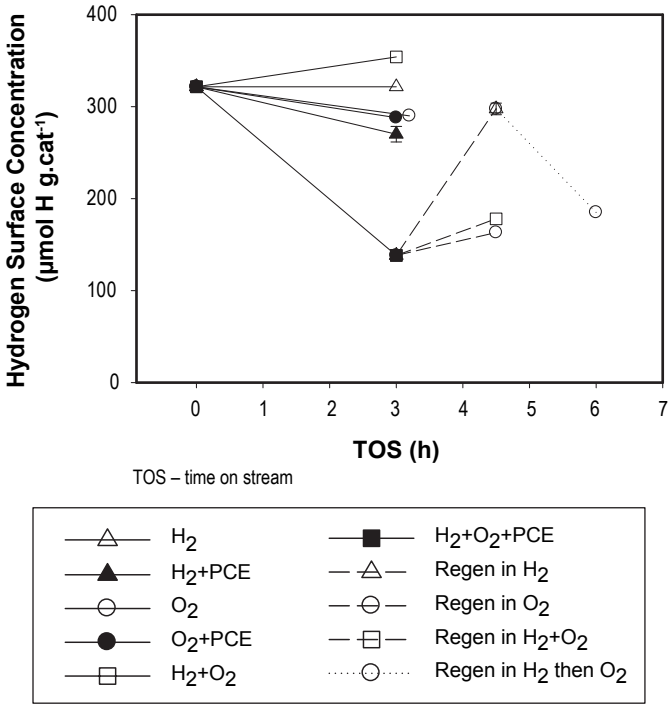


FIGURE 3. Comparison of exposure and poisoning by 150 ppm PCE of Pt/C in different gases (H_2, O_2, and H_2 + O_2) (solid and dotted lines). Effect of different regeneration gases (dashed lines).

to 41 ppm was detected at the anode outlet during open circuit. Moreover, after a current of 0.6 A/cm^2 was applied to the cell, the PCE concentration was further reduced to 5.4 ppm. No PCE was detected at the cathode outlet during any of the tests. Figure 2b shows peak transformation from when the spectra were measured at the inlet of the fuel cell and at the outlet with and without a voltage applied. At the exit after the PCE-containing stream had flowed through the catalyst layer, the C-Cl_2 spectrum disappeared and a carbon-hydrogen symmetric stretching was observed. This result indicates the de-chlorination of PCE.

At Clemson, the poisoning effect of PCE on the activity of a Pt fuel cell catalyst for the adsorption and activation of H_2 was investigated at 60°C and 2 atm using hydrogen surface concentration measurements. In the presence of only H_2, introduction of up to 540 ppm PCE in H_2 to Pt/C resulted in a reduction of available Pt surface atoms (measured by H_2 uptake) by ca. 30% but not enough to shift the H_2-D_2 exchange reaction away from being equilibrium limited. Exposure of Pt/C to PCE in a mixed redox environment (hydrogen+oxygen), similar to that at the cathode of a fuel cell, resulted in a much more significant loss of Pt surface atom availability, suggesting a role of oxygen in PCE decomposition and/or Cl poisoning (see Figure 3). Regeneration of the catalyst activity of poisoned Pt/C showed the highest level of recovery when regeneration was carried out in only H_2, with much less recovery in H_2+O_2 or O_2. The results from this study are in good agreement with those found in the fuel cell study at SRNL.

Diborane (DB) was studied as a model molecule representative of hydrogen storage boron compounds. While no effects were observed on the ionic conductivity and during cyclic voltammetry, a large effect on fuel cell performance was observed as indicated in the potentiostatic curve for a Gore MEA in Figure 4a. There was a drop in performance of about 39% for a concentration of 50 ppm of DB. While the effects seem to be severe, the cell recovers as soon as the DB is removed from the stream. Figure 4b shows the polarization before, during and after recovery from the DB poisoning. The figure indicates that the loss in performance arises mostly from the kinetic limited section (voltage drop in the low current area). However, no indication of catalyst poisoning is observed during cyclic voltammetry. After the DB poisoning is discontinued, the fuel cell performance recovers to approximately 100%.

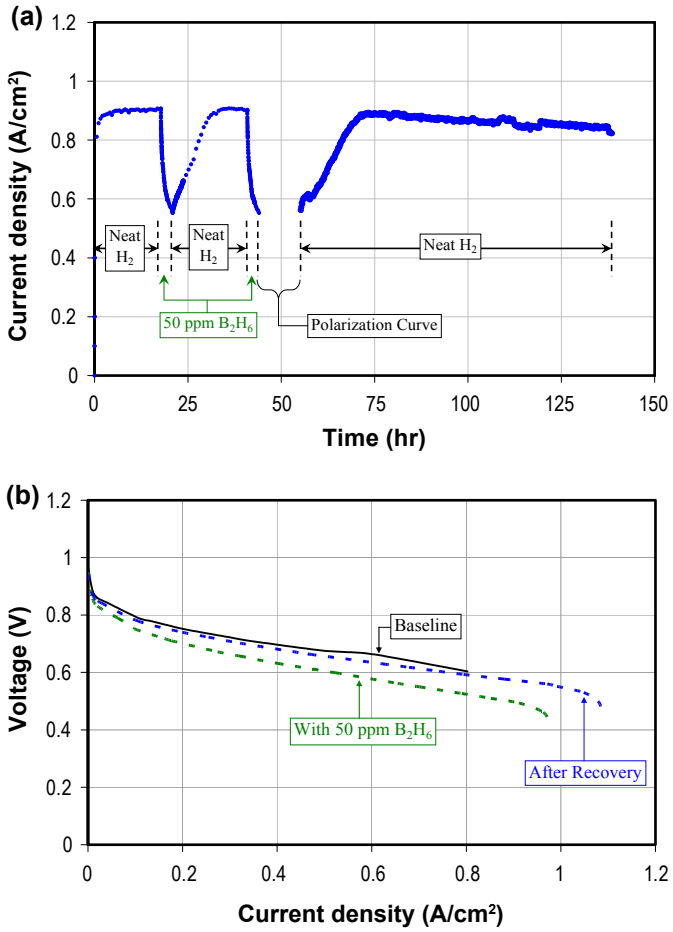


FIGURE 4. (a) Potentiostatic (0.6 V vs. DHE) and (b) polarization scan before, during exposure to 50 ppm of diborane in the hydrogen stream, and after recovery of a fuel cell with a 50 cm^2 Gore MEA having an anode Pt loading of 0.1 mg/cm^2 and operated at 60°C and 50% RH.

Conclusions and Mitigation Strategies

- The presence of trace amounts of Fe_{2+} was found to cause significant-severe degradation of Nafion® by H_2O_2 formed during fuel cell operation, with degradation preferentially proceeding at the sulfonic end group and at the ether linkage located in the pendant side chain of the Nafion®.
- An investigation of Nafion® on Pt/C determined that Nafion® has little/no effect on the Pt catalyst in the catalyst layer, even though it comprises 30 wt% of that layer. Experimental results and modeling suggest that most of the Pt particles are in the meso-macropores of the C support, whereas Nafion® is present primarily on the external surface of the C where it blocks significantly the micropores but only partially blocks the pore mouths of the meso-macropores.
- The presence of water vapor was found to decrease the rate of CO adsorption on Pt, but had very little effect on the resulting CO surface coverage of PtS (qCO) at steady-state (0.66 vs. 0.70 ML in absence of water vapor).
- PEM fuel cell studies of the effects of perchloroethylene (PCE) found that the loss in performance arises from the dechlorination of PCE and affects most likely the cathode electrode.
- Exposure of Pt/C to 150 ppm PCE in a mixed redox environment (hydrogen+oxygen), similar to that at the cathode of a fuel cell, resulted in a much more significant loss of Pt surface atom availability (57% loss) than in hydrogen (15%) or oxygen (11%) alone, suggesting a role of oxygen in PCE poisoning of Pt.
- Regeneration of catalyst activity of PCE poisoned Pt/C showed the highest level of recovery when regeneration used only H_2, with much less recovery in H_2+O_2 or O_2.
- Diborane (B_2H_6, DB), a model impurity from hydrogen storage boron compounds, was found to cause a 39% loss in fuel cell performance. However, full recovery was attainable once diborane was removed from the fuel stream.

Based on the results from this year, the following impurity mitigation strategies can be proposed:

- It is critical to minimize contamination of Nafion® with transition metal ions since they (and especially Fe^{2+}) catalyze the degradation of Nafion® by radical products of H_2O_2 formed during fuel cell operation.
- Higher humidity lessens the degree of degradation of Nafion® conductivity by radical products of H_2O_2.
- Water vapor does not appear to affect CO poisoning of Pt. Therefore, use of higher or lower humidity would appear not to be a factor in improving resistance to CO poisoning.
- Chlorinated compounds should be minimized as contaminants in either the oxygen or hydrogen streams, even though poisoning of the Pt requires the presence of oxygen and takes place apparently at the cathode. Poisoning Cl species can be transported from the anode to the cathode.
- Pt catalysts poisoned by Cl appear to be able to be regenerated by H_2. However, re-exposure of the catalyst to any oxygen even in the absence of PCE in the gas streams results in renewed poisoning of the catalyst.
- DB should be minimized in the hydrogen fuel stream as ppm levels result in significant poisoning of the fuel cell. However, this effect appears to be totally reversible once the DB is removed from the fuel stream.

FY 2011 Publications/Presentations

Publications

1. "Effect of Cations (Na^+, Ca^{2+}, Fe^{3+}) on the Conductivity of a Nafion Membrane," ***Journal of Power Sources*** 195 (2010) 7213-7220 (Kitiya Hongsirikarn, James G. Goodwin, Jr., Scott Greenway, and Stephen Creager).

2. "Effect of Ammonium Ion Distribution on Nafion® Conductivity," ***Journal of Power Sources*** 196 (2011)

644-651(Kitiya Hongsirikarn, Thirapong Napapruekchart, Xunhua Mo, and James G. Goodwin, Jr.).

3. "Effect of H_2O_2 on Nafion® Properties and Conductivity at Fuel Cell Conditions," ***Journal of Power Sources*** 196 (2011) 3060-3072 (Kitiya Hongsirikarn, Xunhua Mo, James G. Goodwin, Jr., and Stephen Creager).

4. "Structure Sensitivity of Cyclopropane Hydrogenolysis on Carbon-Supported Platinum," ***Journal of Catalysis*** 280 (2011) 89-95 (Jack Z. Zhang, Yu-Tung Tsai, Khunya Leng Sangkaewwattana, and James G. Goodwin, Jr.).

5. "The Effect of Low Concentrations of CO on H_2 Adsorption and Activation on Pt/C: Part 2 – in the Presence of H_2O Vapor," ***Journal of Power Sources*** 196 (2011) 6186-6195 (Jack Z. Zhang, Kitiya Hongsirikarn, James G. Goodwin, Jr.).

6. "The effect of Low Concentrations of Tetrachloroethylene on the Performance of PEM Fuel Cells," ***Journal of The Electrochemical Society***, 158 (2011) B698-B702 (M.J. Martínez-Rodríguez, E.B. Fox, W.D. Rhodes, C.S. McWhorter, S.D. Greenway, H. Colón-Mercado).

7. "Effect and Siting of Nafion® in a Pt/C PEM Fuel Cell Catalyst," ***Journal of Power Sources***, in press (2011) (Jack Z. Zhang, Kitiya Hongsirikarn, and James G. Goodwin, Jr.).

8. "The Effect of Low Concentrations of Tetrachloroethylene on H_2 Adsorption and Activation on a Pt Fuel Cell Catalyst," ***Journal of Power Sources***, in preparation (2011) (Jack Z. Zhang, Hector Colon-Mercado, and James G. Goodwin, Jr.).

9. "The Effect of Low Concentrations of Ammonia on the Performance of PEM Fuel Cells," in preparation (2011) (M.J. Martínez-Rodríguez, E.B. Fox, W.D. Rhodes, C.S. McWhorter, S.D. Greenway, H. Colón-Mercado).

Presentations

1. "Prediction of the Conductivity of Nafion® Components in a PEMFC Using an Acid-Catalyzed Reaction", oral presentation, Southeastern Catalysis Society 9th Annual Fall Symposium, Asheville, NC, Sept. 26–27, 2010 (Kitiya Hongsirikarn, Xunhua Mo, Zhiming Liu, and James G. Goodwin, Jr.).

2. "Interaction of Nafion® with Pt in a PEM Fuel Cell Catalyst", oral presentation, Southeastern Catalysis Society 9th Annual Fall Symposium, Asheville, NC, Sept. 26–27, 2010 (Jack Z. Zhang, Kitiya Hongsirikarn, and James G. Goodwin, Jr.).

3. "Fundamental Effects of Impurities on Fuel Cell Performance and Durability," Fuel Cell Tech Team Meeting, Southfield, Michigan, December 9, 2010 (J.G. Goodwin, Jr., Jack Zhang, K. Hongsirikarn, Xunhua Mo, Hector Colon-Mercado, Michael Martinez and Scott Greenway).

4. "Effect of NH_3 and chlorinated hydrocarbons on the performance of PEM Fuel Cells", ACS National Meeting, Anaheim, Ca., March 2011 (M.J. Martínez-Rodríguez, E.B. Fox, C.S. McWhorter, S.D. Greenway, H. Colón-Mercado).

5. "Effects of Impurities on Fuel Cell Performance and Durability," poster presentation, 2011 U.S. DOE Hydrogen Program Annual Merit Review and Peer Evaluation, Washington, DC, May 9, 2011 (James G. Goodwin, Jr., Jack Zhang, Kitiya Hongsirikarn, Hector Colon-Mercado, Scott Greenway, Michael Martinez, and Peter Finamoore).

V.B.5 Effects of Fuel and Air Impurities on PEM Fuel Cell Performance

Fernando H. Garzon (Primary Contact), Tommy Rockward, Rangachary Mukundan, Brian Kienitz, Jerzy Chlistunoff, Eric L. Brosha and Jose-Maria Sansiñena
Los Alamos National Laboratory
MPA-11, MS. D429
Los Alamos, NM 87545
Phone: (505) 667-6643
E-mail: garzon@lanl.gov

DOE Manager
HQ: Nancy Garland
Phone: (202) 586-5673
E-mail: Nancy.Garland@ee.doe.gov

Project Start Date: October, 2007
Project End Date: March, 2011

Fiscal Year (FY) 2011 Objectives

- Investigate effects of impurities on catalysts, membranes and other fuel cell (FC) components.
- Understand the effect of catalyst loadings on impurity tolerance.
- Investigate the impacts of impurities on catalyst durability.
- Develop methods to mitigate negative effects of impurities.
- Develop models of fuel cell-impurity interactions.
- Determine impurity tolerance limits in view of the technical targets for catalyst loading, performance and durability.
- Provide experimental data to hydrogen suppliers for defining fuel specifications.

Technical Barriers

(B) Cost: the cost of fuel cells limits their use:
  – Fuel and air impurity removal systems increase cost, weight and complexity.
  – Higher Pt loading required for maintaining performance, in the presence of impurities, increases cost.

(A) Durability: durability may decrease in the presence of impurities.

(C) Performance: fuel cell performance is degraded by impurity effects.

Technical Targets

The technical targets for catalyst loading are indicated in Table 1. These targets were formulated with the assumption that FC performance will not be degraded by fuel and/or air impurities or contaminates. One of the specific goals of this project is the experimental determination of the limits of impurity tolerance within those technical targets. The results of this project will provide data for defining the FC hydrogen fuel specifications and intake air quality and assess the role of impurities in fuel cell performance degradation.

TABLE 1. Technical Targets: Electrocatalysts for Transportation Applications (Extracted from Table 3.4.12. Technical Plan. April 27, 2007)

Characteristic	Units	2005 Status		Stack Targets	
		Cell	Stack	2010	2015
Platinum group metal (PGM) total content (both electrodes)	g/kW (rated)	0.6	1.1	0.3	0.2
PGM total loading	mg PGM/cm^2 electrode area	0.45	0.8	0.3	0.2

FY 2011 Accomplishments

- Effect of 100 ppb SO_2 in air on 0.1 mg/cm^2 Pt loading cathode fuel cell performance testing completed *(milestone)*.
- Effect of 100 ppb SO_2 in air on 0.2 mg/cm^2 Pt loading cathode fuel cell long term (500 hr) performance testing completed *(milestone)*.
- NO_2 fuel cell poisoning effect was shown to occur via hydrogen reduction of oxides of nitrogen (NO_x) to ammonia.
- Effect of 5 ppm NO_2 in air on 0.2 mg/cm^2 Pt loading cathode fuel cell long term (500 hr) performance testing completed *(milestone)*.
- Iridium oxide solid-state pH sensors were used to determine changes in local proton activity in cation-poisoned, polymer membrane fuel cell electrodes.



Introduction

Fuel cells efficiently convert flows of chemical fuel and oxygen to electrical power. Fuel cell performance may be severely impacted by contaminants or impurities that decrease the electrochemical catalytic rates, interfere with proton transport across the polymer electrolyte, or impede the flow of reactants to/or reaction products away from the

anode or cathode charge transfer interfaces. The impurities may be generated by the fuel synthesis process or be present as ambient air impurities. The platinum metal catalyst surfaces may be deactivated by strongly adsorbing species such as sulfur containing molecules and carbon monoxide. The strongly bound species both block surface sites for catalytic activation and alter the electronic structure of the surface decreasing charge transfer rates. Positively charged contaminant ions often times have much greater chemical affinity to the ion transport sites within the polymer than protons. The foreign cations typically have lower mobilities than protons and reduce ionic conductivity. The presence of impurities may also decrease the operational lifetime of the fuel cell by decreasing performance irreversibly to an unacceptable value or by increasing component failure rate.

Approach

Our approach to understanding impurity interactions with fuel cell components utilizes both experimental and modeling efforts. We carry out fuel cell performance measurements in the presence of known quantities of introduced impurities and then study the impurity interactions with fuel cell components using electrochemical diagnostic methods such as adsorbate stripping voltammetry and alternating current impedance spectroscopy. Sometimes the experiments are performed in neutron imaging systems to visualize the effect of the impurity upon the water content and transport properties of fuel cell components. Post-experimental analysis includes trace level chemical analysis of fuel cell components and effluent water, electron microscopy and X-ray diffraction of the solid materials. We also experimentally determine impurity thermodynamic behavior (ion-exchange, proton and water activity coefficients) and transport properties such as membrane permeability and ionic conductivity.

Theoretical studies include computer models of impurity interactions with anode and cathode electrocatalysis. We also model the effects of foreign cations upon fuel cell performance. The modeling results are validated with experimental measurements such as hydrogen pump experiments and X-ray and electron beam microscopy of impurity distribution.

Results

The most prevalent sulfur containing air species is sulfur dioxide from fossil fuel combustion. The DOE future targets call for a decrease in anode and cathode Pt loading. Last year we evaluated the response of two 50 cm^2 fuel cells: a LANL-prepared Nafion® 212 fuel cell and a commercial fuel cell membrane with an anode/cathode loading: 0.1/0.2 mg Pt/cm^2, to 100 ppb SO_2 in air (2.0 stoichiometry) injection at the cathode inlet past the humidification system (100% saturation). The fuel cell tests were performed at constant current 1 A/cm^2 for 500 hr. The fuel cell operating voltages at constant current decreased rapidly with approximately 200 mV of loss for both cells after sulfur dioxide injection was terminated. This year we evaluated the effect of lowering the cathode loading to 0.1 mg Pt/cm^2. A loss of ~200 mV of fuel cell voltage was also observed for the 1 A/cm^2 constant current experiment. Sulfur dioxide tolerance still remains a key issue in the widespread deployment of fuel cells in areas of poor air quality.

NO_x, from fossil fuel combustion systems, also pose a potential threat to fuel cell performance. High combustion temperatures and pressures promote the reaction of nitrogen with air to form these acid gases. We have studied, by cathode injection, the long term effects of 5 ppm nitrogen dioxide, into an operating fuel cell similar to the one used for the sulfur dioxide experiments. Our experiments last year indicated that NO_2 reduces the fuel cell voltage by ~150 mV but reaches steady-state after about 50 hours of operation. We previously hypothesized that the NO_2 is probably being reduced by hydrogen to ammonium cations; this year we detected, using infrared spectroscopy, the presence of ammonium ions in nitric oxide contaminated fuel cell assemblies.

We have continued the effort to develop iridium oxide-based pH sensors and test their viability as local probes of the effects of cationic impurities in perfluorosulfonic acid polymers on oxygen reduction. Due to the electroneutrality condition, the impurities stoichiometrically replace hydrated protons (H^+_{aq}) in Nafion® and the associated pH changes can be used to monitor local concentrations of the impurities.

The effort has focused on sensors fabricated by the chemical oxidation of pure iridium metal in molten lithium carbonate at 790°C. Such sensors have better mechanical properties than the sensors obtained by the electrochemical deposition of iridium oxide onto metallic substrates and are also less sensitive to interferences from red-ox agents. We tested the sensors using pure and partially neutralized Nafion®, containing 40%, 60%, and 90% of Cs^+. The testing was performed in pure oxygen atmosphere at three temperatures (20, 40 and 60°C) and 100% relative humidity.

As the time necessary to attain equilibrium in the polymer electrolyte was longer than that in liquid electrolytes and the measured potential was frequently unstable for long periods of time, we tentatively assumed that the potential reached its equilibrium value, when its drift did not exceed 1 mV hr^{-1}. The process of equilibration could be accelerated by short time excursions to higher temperatures (60°C), after which the measured potentials were reversible to temperature changes but stable (<1 mV hr^{-1}) at a constant temperature (Figure 1). However, the behavior such as that shown in Figure 1 was observed only for pure and 90% Cs-doped Nafion®. The potentials of Ir/IrO_x sensors comprising pure Nafion® and equilibrated in the above way were found to be sensitive to gaseous ammonia contamination (Figure 2).

The potentials of Ir/IrO_x sensors in Nafion® partially (40% and 60%) doped with Cs^+ exhibited an erratic

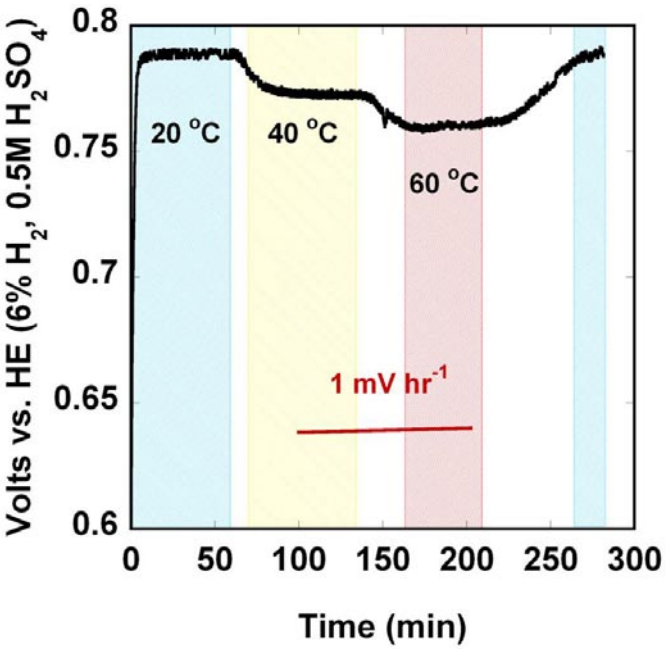


FIGURE 1. Measured potential of a Ir/IrO$_x$ sensor in pure Nafion® at 100% relative humidity and different temperatures. Temperature: 20°C (blue), 40°C (yellow), 60°C (red), variable (no color).

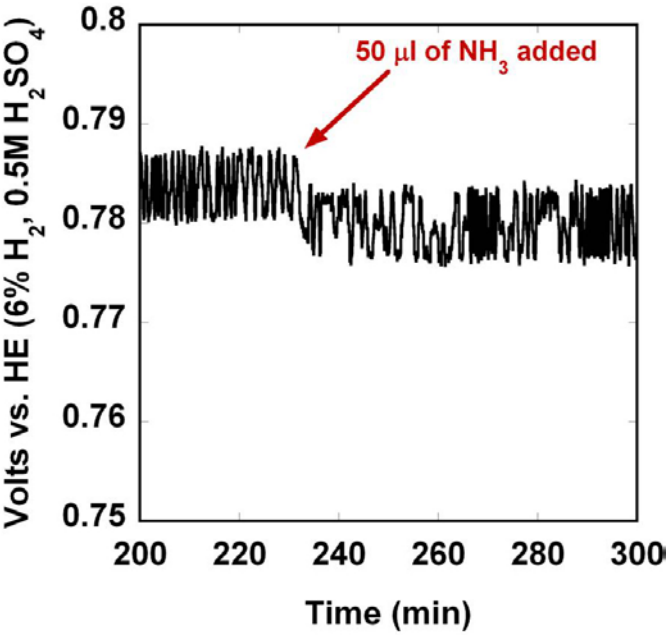


FIGURE 2. Effect of ammonia on the potential of a Ir/IrO$_x$ sensor embedded in pure Nafion®. The experimental chamber had a volume of ~200 cm^3. 50 μl of 25% NH_3 solution was added to ~10 cm^3 of deionized water on the bottom of the chamber. Temperature 20°C, relative humidity 100%.

behavior. No stable potentials could be measured at all selected temperatures. Moreover, temperature increase invariably led to a very quick decrease of the measured potential that significantly exceeded ~1 mV/°C decrease observed for pure (Figure 1) or 90% neutralized Nafion®. The behavior could not be linked to any sensor failure, such as iridium oxide or Nafion® delamination, water condensation, loss of electrical contact, etc., and consequently it is believed to originate from an actual drop in H^+_{aq} concentration (pH increase) at the IrO$_x$/Nafion® boundary. The drop in H^+_{aq} concentration may result from either the interface becoming preferentially occupied by the hydrophobic (backbone) component of Nafion® [1,2] or by Cs-populated ionic component of Nafion® at elevated temperatures. Both options can be linked to temperature induced nanophase transitions in partially doped Nafion®. As the transitions are visible only when Nafion® is nearly half neutralized (40% and 60%) with Cs, the second option seems more likely, i.e., that weaker hydrated Cs^+ rather than H^+_{aq} tend to occupy the interface at elevated temperatures. The conclusion is supported by X-ray radiography, which demonstrates virtually no ion exchange, i.e., persistent phase separation at the boundary between pure Nafion® and Nafion® ~100% neutralized with Cs. Irrespective of the above interpretation of the data, the results indicate that the unfavorable effect of cationic impurities on the oxidation reduction reaction through the lowering of H^+_{aq} concentration and water activity at the fuel cell cathode may be additionally amplified by the unfavorable phase separation phenomena.

Conclusions and Future Directions

Gas phase and cation impurities were demonstrated to decrease fuel cell performance. The mechanisms include: catalyst poisoning, cation ion exchange and a reduction in the local proton concentration near the electroactive cathode interface.

FY 2011 Publications

1. Brosha, E.L.; Rockward, T.; Uribe, F.A.; Garzon, F.H., Measurement of H_2S Crossover Rates in Polymer Fuel Cell Membranes Using an Ion-Probe Technique. Journal Of The Electrochemical Society 2010, 157 (1), B180-B186.

2. Kientiz, B.; Pivovar, B,; Zawodzinski, T.; Garzon, F.H., Cationic Contamination Effects On Polymer Electrolyte Membrane Fuel Cell Performance, accepted for publication, the Journal Of The Electrochemical Society.

3. Lopes, T.; Sansinena, J.-M.; Chlistunoff, J.; Garzon, F. H., Oxygen Reduction Reaction On A Pt/Carbon Fuel Cell Catalyst In The Presence Of Trace Quantities Of Ammonium Ions, submitted to Electrochemica Acta.

V.C.1 Membranes and MEAs for Dry, Hot Operating Conditions

Steven Hamrock
3M Fuel Cell Components Program
3M Center 201-1W-28
St. Paul, MN 55144
Phone: (651) 733-4254
E-mail: sjhamrock@mmm.com

DOE Managers
HQ: Kathi Epping Martin
Phone: (202) 586-7425
E-Mail: Kathi.Epping@ee.doe.gov
GO: David Peterson
Phone: (720) 356-1747
E-mail: David.Peterson@go.doe.gov

Technical Advisor
John P. Kopasz
Phone: (630) 252-7531
E-mail: kopasz@cmt.anl.gov

Contract Number: DE-FG36-07GO17006

Subcontractors:
- Professor David Schiraldi, Case Western Reserve University, Cleveland, OH
- Professor Andrew Herring, Colorado School of Mines, Golden, CO
- Professors Stephen Paddison and Thomas Zawodzinski, University of Tennessee, Knoxville, TN
- Professor Shulamith Schlick, University of Detroit Mercy, Detroit, MI

Project Start Date: April 1, 2007
Project End Date: March 31, 2011

Fiscal Year (FY) 2011 Objectives

- To develop a new proton exchange membrane (PEM) with higher proton conductivity and improved durability under hotter and drier conditions, in order to meet DOE Hydrogen, Fuel Cells and Infrastructure Technologies Multi-Year Research, Development and Demonstration Plan 2010/2015 commercialization targets for automotive fuel cells.
- Test new membrane in fuel cell membrane electrode assemblies.

Technical Barriers

This project addresses the following technical barriers from the Fuel Cells section of the Fuel Cell Technologies Program Multi-Year Research, Development and Demonstration Plan:

(A) Durability
(C) Performance

Technical Targets

TABLE 1. Progress towards Meeting Membrane Technical Targets

All membranes are 15 micron mechanically stabilized 625 EW PFIA or 20 micron unstablized	**Units**	**3M 2011 Status**	**2015 target**
ASR at 120°C (H_2O pp 40-80 kPa)	Ohm cm^2	0.023 (40 kPa) 0.012 (80 kPa)	<0.02
Cond. at 120°C	S/cm	0.087 (25% RH) 0.167 (40% RH)	
ASR at 80°C (H_2O pp 25-45 kPa)	Ohm cm^2	0.017 (25 kPa) 0.006 (44 kPa)	<0.02
Cond. at 80°C	S/cm	0.115 (50% RH) 0.3 (95% RH)	
ASR at 30°C (H_2O pp 4 kPa)	Ohm cm^2	0.02 (3.8 kPa)	<0.03
Cond. at 30°C	S/cm	0.09 (90% RH)	
ASR at -20°C	Ohm cm^2	0.10	<0.2
Cond. at -20°C	S/cm	0.02	
O_2 cross-over	mA/cm^2	≤1.0	<2
H_2 cross-over	mA/cm^2	≤1.8	<2
Durability Mechanical (%RH Cycle) Chemical (OCV)	 Cycles Hours	 >20,000 >2,300	 >20,000 >500

PFIA – perfluoro imide acid; EW – equivalent weight; RH – relative humidity; ASR – area specific resistance; OCV – open circuit voltage

FY 2011 Accomplishments

- We have developed a new PEM for PEM fuel cells. This new membrane comprises a new multi-acid side-chain (MASC) ionomer, stabilizing additives for improved chemical stability and polymer nanofibers for improved mechanical stability.
- In out-of-cell tests this new membrane has shown superior mechanical stability, chemical stability and conductivity compared other available membranes. It has met DOE 2015 targets for conductivity and other physical properties, except for the conductivity under the most aggressive condition, 120°C, 40 kPa H_2O (about 25% RH at 1 atm).
- Membrane electrode assemblies (MEAs) with this new membrane provide increased performance, lower cell resistance and have met all DOE 2015 durability targets (Table 1).



Introduction

Proton exchange membrane fuel cells (PEMFCs) represent a promising power source for a variety of applications. While many breakthroughs have been made over the last few years in the development of PEMFCs, technical and economic barriers for their commercialization still exist. Key areas where improvements are still needed are in expanding the temperature range and lowering the humidification requirements of the stack [1]. Requirements of system size, efficiency, performance, start-up and cooling mean that fuel cells must be able to run robustly and exhibit adequate durability under a wide variety of operating temperatures, including temperatures up to 120°C. They must also be able to do this with little or no external gas humidification (i.e., "dry"), and during start-up, shut-down, or periods of lower stack temperatures, they must run in the presence of, and be stable to, some liquid water in the gas channels. Unfortunately, operation under these hot, dry conditions seriously compromises both the conductivity and durability of the ionomer membrane. The objectives of this collaborative effort are to develop new PEMs for fuel cells capable of providing excellent durability and performance while operating under low humidification conditions and at temperatures ranging from -20°C to 120°C.

Approach

The focus of this project is to develop a new proton exchange membrane which can operate under hotter, drier conditions than the state-of-the-art membranes today. These membranes and MEAs made from them should meet the performance and durability requirements that meet 2010 DOE technical targets for membranes. Activities include:

- Synthesize and test new polymer membranes, including both fluorinated and non-fluorinated polymers as well as composite or hybrid systems, and evaluate their conductivity and chemical and mechanical stability.
- Evaluate new membrane manufacturing methods for increasing membrane mechanical properties and improving MEA lifetime.
- Develop new membrane additives aimed at increasing conductivity and improving membrane stability/durability under these dry conditions.
- Perform both experimental and theoretical studies of factors controlling proton transport and mechanisms of polymer degradation and factors affecting membrane durability in an MEA.
- Focus on materials which can be made using processes which will be scalable to commercial volumes using cost-effective methods that can meet the industry target.

Results

In the course of this four-year project we developed a new PEM with improved proton conductivity, chemical stability and mechanical stability. We incorporated this new membrane into MEAs and evaluated performance and durability. The development of this new membrane involved synthesizing and evaluating new ion-containing polymers, new stabilizing additives and polymer nanofibers for mechanical stabilization. Process development work included developing and/or optimizing methods of making stable dispersions with ionomers and additives as well as coating and post processing nanofiber stabilized membranes. MEA constructions were optimized to allow effective evaluation of the membrane performance and durability in a fuel cell.

In the past we have shown that lower EW ionomers, based on our 3M perfluorinated sulfonic acid (Figure 1, PFSA), provide higher proton conductivity under drier conditions. PFSA membranes with EW under about 700 can meet DOE conductivity targets [2]. Unfortunately, the mechanical integrity of these low EW membranes is poor. The 3M ionomer swells excessively at EWs below about 750 and becomes soluble in boiling water at EWs below about 650-700. At an EW of 700 the tetrafluoroethylene (TFE) segments in the polymer backbone are short, and the crystalinity index, measured by wide angle X-ray scattering is nearly zero. Even lower EW, non-soluble membranes (i.e. 700 EW) swell excessively. Figure 2 shows that membranes prepared from ionomers with EWs above about 750 show a gradual increase in hydration in boiling water with decreasing EW, increasing from about 14 moles of water per sulfonic acid group ($\lambda = 14$) for an EW of 1100, to about 33 waters of hydration per sulfonic acid group ($\lambda = 33$) for an EW of 750. Below this EW water absorption increases dramatically. The 700 EW ionomer has a λ value of >100. Membranes from ionomers with EWs lower than this partially dissolve in boiling water so this test can not be performed [3]. This excessive swelling or membrane solubility is known to lower MEA durability during fuel cell operation [4]. One way to produce polymers with long enough TFE segments in the backbone for crystallization and low enough EW to provide high conductivity is to have more than one protogenic hydrogen on each functional side-chain [5]. Towards this end, we have used the bis sulfonyl imide acid as a protogenic group and linking moiety to prepare several MASC ionomers, some of which are shown in Figure 1. The bis sulfonyl imide acid is highly acidic, in some cases more acidic than a structurally similar sulfonic acid [6]. Fuel cell membranes from polymers containing this functional group have been prepared in the past through the polymerization of imide functional monomers with TFE [7]. We have prepared low EW ionomers starting sulfonyl fluoride polymers which have EWs high enough to provide sufficient backbone crystallinity in the resulting ionomer to control swelling. Swelling data for examples of low EW ionomer prepared by this method are shown in Figure 2. Membrane samples prepared from both the ionomer labeled Ortho Bis Acid and PFIA absorb about 40 waters per acid group, much lower than the 700 EW PFSA. We have prepared samples of the 625 EW PFIA with in-plane linear swelling as low as 20%, similar to what we see for 825 EW

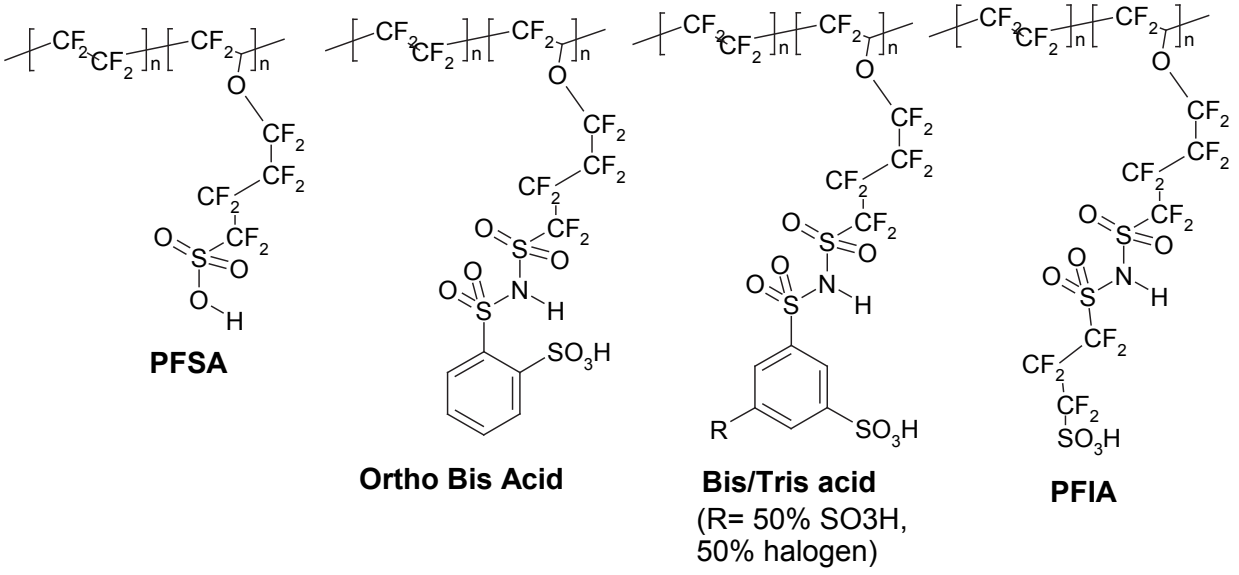


FIGURE 1. Structure of Selected Ionomers Based on the 3M Ionomer Backbone

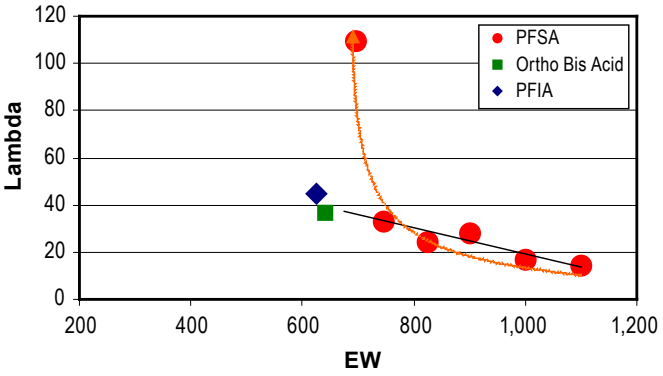
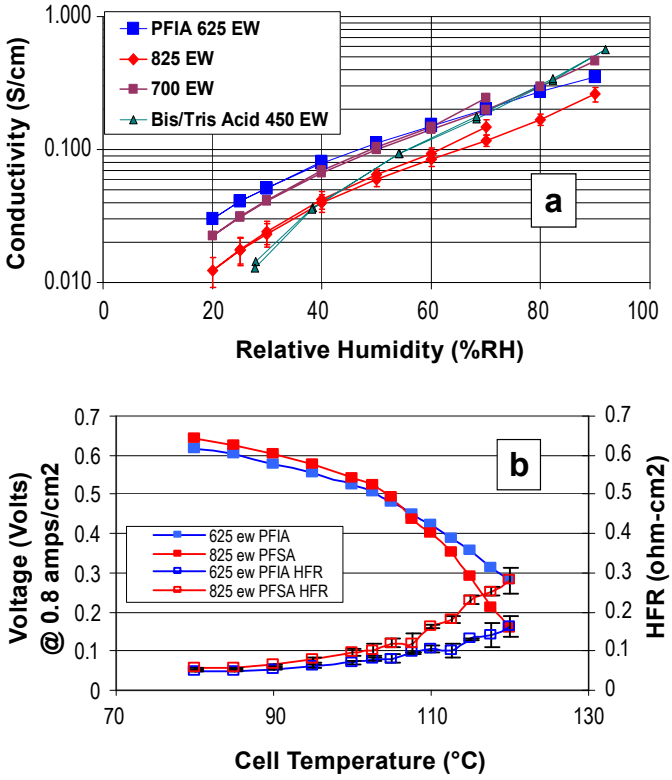


FIGURE 2. Water Absorption in Boiling Water as a Function of EW (Absorption is given as lambda (λ), or the number of water molecules per acid group.)

membranes which have provided up to 18,000 hours in accelerated durability tests in 50 cm^2 MEAs [2].

The ionomer selected for the final evaluation and testing is a 625 EW PFIA ionomer membrane (Figure 3). This membrane is reinforced with polymer nanofibers and also comprised a stabilizing additive package described in previous reports. The durability improvements that this additive package provides, including providing MEAs which lasted up to 18,000 hours in our accelerated durability test, were presented at the 2009 and 2010 Annual Merit Review meetings. A micrograph of the nanofiber reinforced membrane is shown in Figure 4. MEAs prepared from this membrane have also lasted over 2,300 hours in the chemical durability (OCV) test and over 20,000 cycles in the mechanical durability (RH Cycle) test (Table 1) [8]. Based



HFR - high-frequency resistance

FIGURE 3. a) The conductivity at 80°C for selected ionomer membranes. Conductivity was measured using a 4-point, in-plane conductivity cell inside a constant humidity oven. b) The voltage of two 50 cm^2 MEAs with an 825 EW PFSA and a 625 EW PFIA membrane at 0.8 A/cm^2 running on H_2/air at ambient pressure. The cell inlet humidification is held constant with an 80°C dew point and the cell temperature is raised from 80°C to 120°C. This causes the relative humidity to drop from 100% to about 24%.

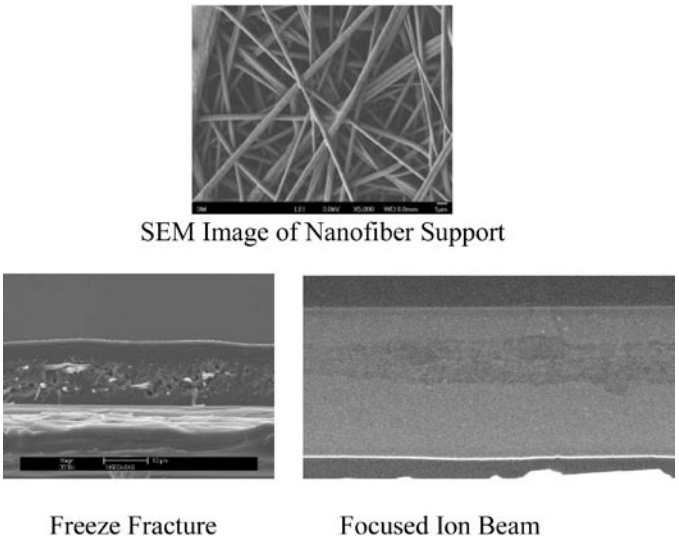


FIGURE 4. Scanning electrode micrographs (SEMs) of the nanofibers and cross-sections showing similar membranes with nanofiber support. Samples were prepared while still on carrier liner (bottom layer in images).

on this and other testing, we down-selected the PFIA as the ionomer which was used in the remainder of this project and focused on further improvements in the chemical and mechanical durability of membranes made from this ionomer to allow them to meet these durability requirements. During the course of this year we have also developed and optimized electrode and MEA construction. We have evaluated different ionomer equivalent weights, ionomer to carbon ratios, catalyst types, gas diffusion layer types, and process variables. Test methods were developed that screened electrodes over a variety of test conditions to optimize performance over the whole range of automotive operating conditions – cool/wet to hot/dry and high current. Results of that work led to gains in performance and a reduction of catalyst loadings 38% over the initial baseline. Gains were also realized in catalyst cycling stability and in the reduction of the overall MEA fluoride release rate. New processing methods and catalyst morphologies provided further gains in both performance and catalyst stability. A summary of performance and durability data collected, including data from the FreedomCAR & Fuel Partnership Fuel Cell Tech Team Cell Component Accelerated Stress Test Protocols for PEM Fuel Cell Membranes, is shown in Table 1 [9].

Conclusions and Future Directions

This project ended March 31, 2011. As stated above, we developed a new ionomer membrane with improved performance and durability. Going forward we intend to build on this new technology to gain further understanding of the factors influencing conductivity and durability in this membranes and develop new materials based on this understanding.

FY 2011 Publications/Presentations

1. Ghassemi, H.; Zawodzinski T.A. jr.; Schiraldi, D.A.; Hamrock S.J. "Perfluoro ionomers with crosslinked structure for fuel cell application" Presented at the 241st ACS National Meeting, March 30, **2011**, Anaheim CA.

2. Hamrock, S.J.; Schaberg, M.S. Abulu, J.E.; Haugen, G.M.; Emery, M.M.; Yandrasits, M.A.; Xiong P.; "New proton exchange membrane development at 3M" Presented at the 241st ACS National Meeting, March 30, **2011**, Anaheim CA.

3. Janarthanan, R.; Haugen, G.M.; Hamrock, S.J.; Herring A.M. "Application of zirconia and ion exchanged heteropolyacid nanocomposite modified PFSA ionomers for proton exchange membrane fuel cells" Presented at the 241st ACS National Meeting, March 30, **2011**, Anaheim CA.

4. Hamrock S.J. "New fluorinated ionomers for proton exchange membrane fuel cells" Presented at the Sustainable Technology through Advanced Interdisciplinary Research Seminar, University of Tennessee, March 21, **2011**, Knoxville, TN.

5. Schiraldi, D.A. "Durability in PEM Polymers" Presented at the Advances in Materials for Proton Exchange Membrane Fuel Cells Systems, February 21, **2011**, Pacific Grove CA.

6. Yandrasits, M.A. "New fluorinated ionomers for proton exchange membranes" Presented at the Advances in Materials for Proton Exchange Membrane Fuel Cells Systems, February 20, **2011**, Pacific Grove CA.

7. Ghassemi, H.; Schiraldi, D.A.; Zawodzinski,T.A.; Hamrock, S.J. "Poly(arylene ether)s with Pendant Perfluoroalkyl Sulfonic Acid Groups as Proton-Exchange Membrane Materials" *Macromolecular Chemistry and Physics, **212(11)**,* 673–678, **2011**.

8. Wu, D.; Paddison, S.J.; Elliott, J.A.; Hamrock, S.J., "Mesoscale Modeling of Hydrated Morphologies of 3M Perfluorosulfonic Acid-Based Fuel Cell Electrolytes" *Langmuir*, ***26(17)***, 14308–14315, **2010**.

9. Schlick, S. "Fragmentation and Stabilization of Proton Exchange Membranes Used in Fuel Cells: Direct ESR and Spin Trapping Methods, Faculty of Chemistry" Jagiellonian University, December 10, **2010**, Krakow, Poland.

10. Schlick, S. "A Dream of Hydrogen. Degradation of Fuel Cell Membranes Using ESR Methods: Ex Situ and In Situ Experiments, Institute of Nuclear Chemistry and Technology" December 8, 2010, Warsaw, Poland.

11. Steven Hamrock, "New Fluorinated Ionomers for Proton Exchange Membrane Fuel Cells, Department of Polymer Science" University of Southern Mississippi, December 1, 2010, Hattiesberg, MS.

12. Schlick, S. "Fuel Cells for Automotive, Stationary and Portable Applications: Challenges and Potential" Solvay Science for Innovation Congress, October 12–14, 2010, Brussels, Belgium.

13. Danilczuk, M.; Perkowski, A.J.; Schlick, S. "Ranking the Stability of Perfluorinated Membranes to Attack by Hydroxyl Radicals" *Macromolecules* **2010**, *43*, 3352-3358.

14. Wu, D.; Paddison, S.J.; Elliott, J.A.; Hamrock, S.J., Mesoscale Modeling of Hydrated Morphologies of 3M Perfluorosulfonic Acid-Based Fuel Cell Electrolytes, *Langmuir,* **2010**, *26 (17),* 14308–14315.

15. Schaberg, M.S.; Abulu, A.E.; Haugen, G.M.; Emery, M.A.; O'Conner, S.J.; Xiong, P.N.; Hamrock, S.J., "New Multi Acid Side-Chain Ionomers for Proton Exchange Membrane Fuel Cells" *ECS Trans.* **2010**, *33 (1),* 627.

16. Maalouf, M.; Bai, Y.; Paddison, S.; Schaberg, M.; Emery, M.; Hamrock, S.; Ghassemi, H.; Zawodzinski, T., "New Ionomeric Membranes for High Temperature Proton Exchange Membrane Fuel Cells: Effects of Different Side Chains' Acidity on Conductivity" Presented at the 218th ECS Meeting, October 10–15, **2010** in Las Vegas, NV.

17. Kumar M.; Paddison S., "Chemical Degradation of the Side Chains of PFSA Membranes: An Ab Initio Study" Presented at the 218th ECS Meeting, October 10–15, **2010** in Las Vegas, NV.

18. Hamrock,S.J.; Schaberg, M.S.; Abulu, A.E.; Haugen, G.M.; Emery, M.A.; O'Conner, S.J.; Xiong, P.N.,New Proton Exchange Membrane Development, Presented at the 218th ECS Meeting, October 10–15, **2010** in Las Vegas, NV.

19. Liu, Y.; Horan, J.L.; Schlichting, G.J.; Hamrock, S.J.; Haugen, G.M.; Herring, A.M., Morphology Study of Perfluorosulfonic Acid Ionomer for PEM Fuel Cell Application, Presented at 218th ECS Meeting, October 10–15, **2010** in Las Vegas, NV.

References

1. S.J. Hamrock and M.A Yandrasits, *Journal of Macromolecular Science, Part C: Polymer Reviews,* 46, 219 (2006).

2. S.J. Hamrock, U.S. Department of Energy Hydrogen Program 2010 Annual Merit Review Proceedings, http://www.hydrogen.energy.gov/pdfs/review10/fc034_hamrock_2010_o_web.pdf.

3. M.A. Yandrasits and S.J. Hamrock in *Fuel Cell Chemistry and Operation,* A.M. Herring, T.A. Zawodzinski Jr., S.J. Hamrock, Editors, p. 15, ACS Symposium Series; American Chemical Society: Washington, DC, (2010).

4. Y.H. Lai, C.K. Mittelsteadt, C.S. Gittleman, and D.A. Dillard, *J. Fuel Cell Sci. Technol.* **6,** 021002 (2009).

5. M.S. Schaberg, A.E. Abulu, G.M. Haugen, M.M. Emery, S.J. O'Conner, P.N. Xiong, S.J. Hamrock, *ECS Trans. 33 (1),* 627 (2010).

6. I.A. Koppel, R.W. Taft, F. Anvia, S.Z. Zhu, L.Q. Hu, K.S. Sung, D.D. DesMarteau, L.M. Yagupolskii, Y.L. Yagupolski, N.V. Ignat'ev, N.V. Kondratenko, A.Y. Volkonskii, V.M. Slasov, R. Notario and P.C. Maria, *J. Am. Chem. Soc.,* **116,** 3047-3057 (1994).

7. S.C. Savett, J.R. Atkins, C.R. Sides, J.L. Harris, B.H. Thomas, S.E. Creager, W.T. Pennington and D.D.J. DesMarteau,. *J. Electrochem. Soc*. 2002, **149,** A1527 (2002).

8. http://www1.eere.energy.gov/hydrogenandfuelcells/pdfs/htmwg_benjamin.pdf.

9. Cell Component Accelerated Stress Test and Polarization Curve Protocols for Polymer Electrolyte Membrane Fuel Cells; http://www.uscar.org/commands/files_download.php?files_id=267.

V.C.2 Dimensionally Stable Membranes (DSMs)

Cortney Mittelsteadt
Giner Electrochemical Systems (GES), LLC
80 Rumford Ave.
Newton, MA 02466
Phone: (781) 529-0529
E-mail: cmittelsteadt@ginerinc.com

DOE Managers
HQ: Donna Ho
Phone: (202) 586-8000
E-mail: Donna.Ho@ee.doe.gov
GO: Gregory Kleen
Phone: (720) 356-1672
E-mail: Greg.Kleen@go.doe.gov

Technical Advisor
Walt Podolski
Phone: (630) 252-7558
E-mail: podolski@anl.gov

Contract Number: Grant DE-FG36-06GO16035

Subcontractor:
State University of New York (SUNY),
Syracuse, NY

Project Start Date: April 3, 2006
Project End Date: November 1, 2011

Fiscal Year (FY) 2011 Objectives

- Demonstrate 20,000 relative humidity (RH) cycles in a 1 mil membrane.
- Manufacture larger, more consistent membranes.
- Manufacture supported membranes that are thinner than 1 mil.
- Utilize lower equivalent weight (EW) ionomers in thin supports.

Technical Barriers

This project addresses the following technical barriers from the Fuel Cells section (3.4.4) of the Fuel Cell Technologies Program Multi-Year Research, Development and Demonstration Plan:

(A) Durability
(B) Cost
(C) Performance

Technical Targets

Progress has been made in achieving the Fuel Cell Technologies Multi-Year Research, Development and Demonstration Program Plan. Table 1 lists the DOE's technical targets and where our research stands to date.

TABLE 1. DOE Technical Targets and GES Status

Characteristic	Unit	2015 Target	GES DSM Status
Inlet water vapor partial pressure	kPa	1.5	20[a]
Oxygen crossover	mA/cm^2	2	1.5[b]
Hydrogen crossover	mA/cm^2	2	1.8[b]
Membrane Conductivity Operating Temperature 20°C -20°C	S/cm	 0.10 0.07 0.01	 0.093[a] 0.083 Not tested
Operating Temperature	°C	≤120	95
Area Resistance	$Ohm*cm^2$	0.02	0.03[c]
Cost	$\$/m^2$	20	~100
Durability with cycling <80°C	cycles	20,000	20,000
Unassisted Start from low temperature	°C	-40	Untested
Thermal cyclability in presence of condensed water		Yes	Yes

[a]95°C with H_2/air at 20 psia balanced pressure. H_2/air stoichiometry 1.1/2.0
[b]Crossover measured for 1 atm of pure H_2 and pure O_2 at 95°C and 50% RH.
[c]For 18 μm two-dimensional laser-drilled (2DSM) material operating at conditions listed above in ([a])

FY 2011 Accomplishments

- Demonstrated 20,000 RH cycles in a 1 mil membrane.
  - Membrane had higher in-plane conductivity than NRE211.
  - Stopped test at 20,000 cycles.
- Manufactured larger membranes.
  - Numerous samples sent to a third party for testing.
- Greatly decreased chemical degradation under open circuit voltage testing.
  - Greater than an order of magnitude reduction.
  - Testing confirmed by a third party for testing.
- Both commercially available polyethersulfone (PES) and ultra-high molecular weight polyethylene (UPE) successfully incorporated as porous supports in 3DSM:
  - Swelling reduction similar to 2DSM.
  - Conductivity penalty of support ~33%.

Introduction

PFSA materials have demonstrated promising high temperature/low RH conductivity, yet are still unsuitable for automotive applications. Increasing acid content and making the membranes thinner are two methods for lowering the resistance of these materials. However, each of these methods adversely affects mechanical durability of the membrane. GES is combining the good conductivity properties of high acid content PFSAs and improve their mechanical properties by making composite materials.

Approach

GES's approach is to use very high acid content PFSA materials and support them with high-strength non-acidic materials. This involves using commercially available PFSA materials as well as generating new PFSA polymers, generating the supports, and finally forming and characterizing the composites.

Results

GES has successfully imbedded high acid content PFSA materials in laser-drilled supports consisting of either polysulfone or polyimide (Kapton). Figure 1 shows the laser-drilled support, as well as the composite DSM. A matrix of support material, pore size, support thickness and EW of PFSA fill has been completed. When the supports are 10% of the total material and have no greater than 60% void space, they nearly eliminate swelling in the x-y direction. This is true regardless of hole size, acid content of the PFSA fill material, or whether polysulfone or polyimide was used as the support. Fuel cell testing has been carried out on a 2-mil (50 micron) DSM membrane consisting of a 1/3-mil (8 micron) polyimide support filled with 700 EW PFSA and the 2DSM far outperforms Nafion® 112 performance.

A sample composite material with low EW PFSA and 10% support material has demonstrated 2-3 times the conductivity of Nafion® 112, the PFSA standard, over the entire range of RH as shown in Figure 2. This conductivity still falls short of the DOE target however, as seen in the figure. Previously it appeared that this approach would not be able to reach the DOE's cost target, however in a separate DOE contract GES has demonstrated a successful method of micro-molding these substrates.

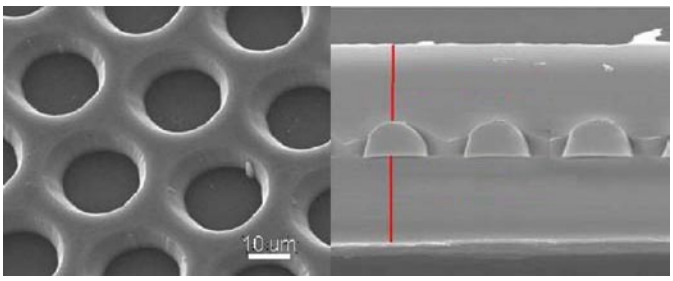


FIGURE 1. Scanning Electron Microscope Images of Laser-Drilled DSM Support (left, top view) and Support Filled with PFSA (right, cross section)

Commercially available porous supports offered an alternative to the cost-prohibitive 2DSM supports: an unforeseen development from the original proposal but very promising as the 3DSMs demonstrated the dimensional stability and improved mechanical properties of the 2DSM. We successfully incorporated both 1100 EW and 830 EW PFSA ionomers into commercially available PES and UPE and tested the membranes under electrolysis conditions. In Figure 3, the electrolysis performance of a 3 mil (75 micron) 3DSM prepared with 830 EW ionomer and UPE support is compared to the 1100 EW electrolysis membrane electrode assembly with comparable thickness. Electrolysis conditions were used as the poor membrane-electrode interface in fuel cell membranes contributes to the overall resistance and thereby decreases fuel cell performance. Electrolyzer testing allows us to test the membranes in an electrochemical cell and determine the performance penalty due to the support, even with a thick membrane. The thinnest PES porous support commercially available is 4 mils (100 micron) thick. We are currently working with Millipore on thinner supports, and they have supplied us with 1- and 2-mil-thick (25 and 50 micron) UPE and 3-mil (75 micron) thick PES.

3DSMs were prepared from low EW ionomer solution and the thin support materials supplied by Millipore. Mechanical durability tests were performed on these 3DSMs at 80°C. In the first RH-cycling test, cast Nafion®, NR211, failed around 4,500 cycles as seen in Figure 4. Two 3DSMs that were sintered to 140°C did not fail in the first 5,000 cycles of the first test. A 3DSM that was sintered to 200°C, which is above the melting temperature of the support, failed around 3,500 cycles. The samples were taken off test at 5,000 cycles because the test stand was needed for another project. A second RH-cycling performance test was initiated this spring to test the mechanical durability of 3DSMs. A 1-mil 3DSM sintered to 140°C successfully completed 20,000 cycles (Figure 4) and was removed form the test stand. The RH-cycling test consists of 2 minutes bone dry, 2 minutes at 95% RH at 80°C. The gas flowrate is 1 SLPM, rather than the 2 SLPM industry standard due to test stand limitations.

To improve performance, we tried to impregnate 3DSM supports with 660 and 700 EW material. Ionomer solution concentrations of 30 wt% or greater are needed to adequately fill the porous supports, but increasing the concentration of an alcohol-based ionomer concentration above 10 wt% causes the solution to become too viscous and collapse the UPE 3DSM support. Aqueous-based solutions are less viscous at higher concentrations, but these solutions are incompatible with the hydrophobic supports. Efforts centered on pretreating the 3DSM supports with a hydrophobic solution prior to casting. 3DSMs were successfully cast with pretreatment and PES supports,

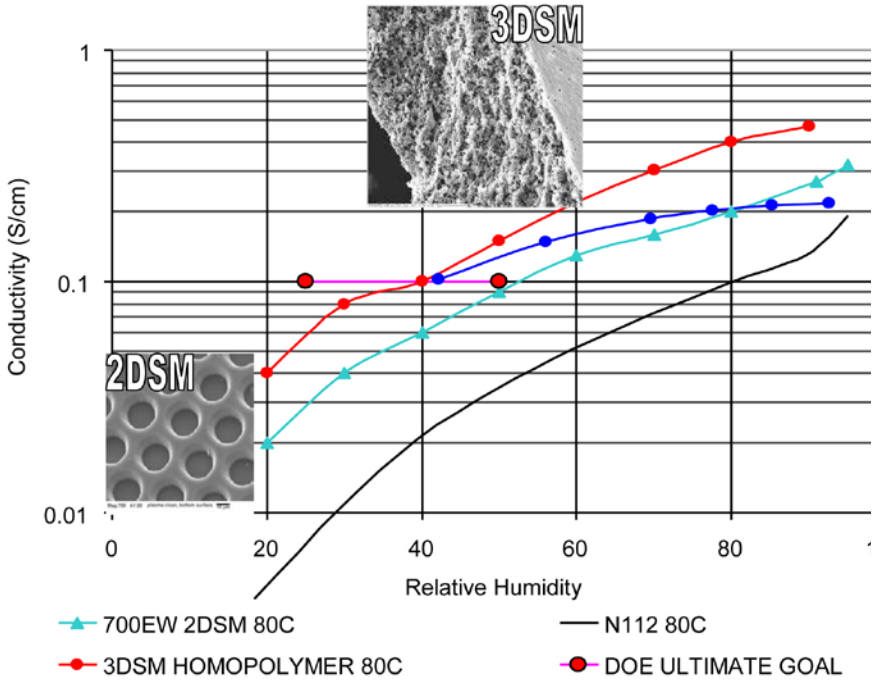


FIGURE 2. Conductivity of 2DSM membrane consisting of 700 EW PFSA in a polyimide support as well as two 3DSMs: one with the SUNY homopolymer at 80°C and a second with highly cross-linked PVEPVE. Insets of the 2DSM and 3DSM membranes are shown.

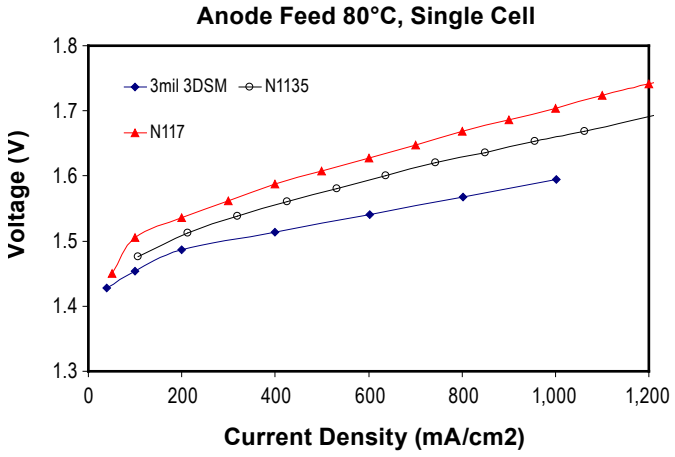


FIGURE 3. Electrolyzer Performance of N1135, N117 and a 3-mil-thick UPE 3DSM Membrane with 820 EW

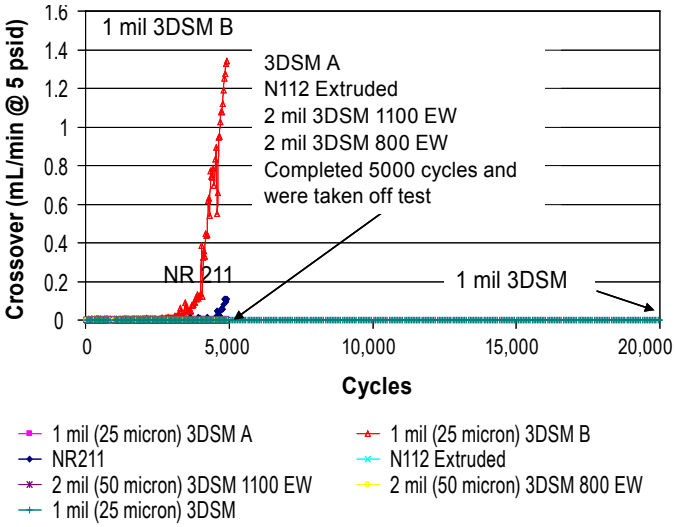


FIGURE 4. RH-Cycling Performance at 80°C for 1- and 2-mil 3DSM and Nafion® Membranes

although the resultant 3DSM was 65 microns thick. Surface oxidation and chlorosulfonation treatment showed dramatic increase in hydrophilicity, but failed to adequately incorporate the 660 and 700EW aqueous dispersions into the supports.

To further increase conductivity PFSAs with even higher acid content are being synthesized at SUNY under the direction of Israel Cabasso. A large number of materials have been synthesized, including the homopolymer of just the active monomer. Improvements in the synthesis of this polymer have led to a film-forming ionomer that can be readily incorporated in GES's 3DSM structures. In the previous years we demonstrated that this material has a conductivity that is approximately twice that of the best 2DSM material to date and approximately five times that of Nafion® 112 over an entire range of RH as seen in Figure 2. Also seen in the figure is that this material comes very close

to meeting the DOE target for conductivity down to 25% RH. Unfortunately this material swelled excessively in water.

Work at SUNY in this past year has centered on reducing this swelling while maintaining the high conductivity at low RH. A highly cross-linked perfluoro (4-methyl-3,6-dioxaoct-7-ene) sulfonyl fluoride (PSEPVE)-based polymer was cast and characterized for conductivity at GES. The conductivity of this polymer was quite high at low levels of RH as seen in Figure 2. Surprisingly the conductivity at higher levels of RH does not increase as quickly as the non-crosslinked materials. We believe that this is due to the lower water contents at higher RH due to the cross-linking. Water sorption isotherms of this material will be conducted to confirm this conclusion.

Conclusions and Future Directions

The DSM with laser-drilled supports has been shown to successfully reduce x-y swelling in high acid content PFSAs over a range of composite dimensions and compositions. Though 2-3 times more conductive than Nafion® 112, it still is short of the DOE's conductivity targets. Work has been done to synthesize PFSAs with even higher acid content, including the homopolymer that contains only the functional monomer. This polymer, when incorporated in the 3DSM has come very close to meeting the DOE targets. This polymer is water soluble however, and eventually leaches out of the 3DSM support. Efforts have begun to cross-link this polymer to make it insoluble and resulted in a polymer with similar low RH performance that is hydrolytically stable. RH cycling of the 2DSM and 3DSM materials has been completed to demonstrate these materials superior mechanical attributes; each of them surpassing 5,000-19,000 cycles, including a 1-mil 830 EW membrane. We are currently focusing on preparing even thinner (~15 µm) 3DSMs for fuel cell testing. Millipore and the Solar Energy Research Center in Florida are assisting in this effort.

FY 2011 Publications/Presentations

1. Mittelsteadt, C.M., VanBlarcom,S. Liu, H., Wie, X., Johnson, F., Cabasso, I. "Dimensionally Stable Membranes" Presentation at Washington, D.C. 2011 U.S. Department of Energy (DOE) Hydrogen and Fuel Cells Program and Vehicle Technologies Program Annual Merit Review and Peer Evaluation Meeting" May 2011, Arlington, VA.

V.C.3 Dimensionally Stable High Performance Membrane (SBIR Phase III)

Cortney Mittelsteadt (Primary Contact),
Avni A. Argun, Castro Laicer, Jason Willey
Giner Electrochemical Systems, LLC (GES)
89 Rumford Avenue
Newton, MA 02466
Phone: (781) 529-0529
E-mail: cmittelsteadt@ginerinc.com

DOE Manager
HQ: Donna Ho
Phone: (202) 586-8000
E-mail: Donna.Ho@ee.doe.gov

Contract Number: DE-EE0004533

Project Start Date: October 1, 2010
Project End Date: September 30, 2013

Fiscal Year (FY) 2011 Objectives

- Develop and characterize membrane electrode assemblies (MEAs) based on the Dimensionally Stable Membrane (DSM) membrane support technology.
- Identify a cost-effective route to fabricate 10-12 µm thick microporous DSM support films with 50% area coverage (pore density) and 10-20 µm diameter holes.
- Qualify the DSM supports by mechanical, freeze/thaw, and wet/dry testing.
- Develop a continuous coating process using molds.
- Investigate alternative molding procedures.
- Go/No-Go Decision: Demonstrate, by the fourth quarter, a scalable method to produce the desired DSM substrates.

Technical Barriers

This project addresses the following technical barriers from the 3.4.4 (Fuel Cells) and 3.5.5 (Manufacturing R&D) sections of the Fuel Cell Technologies Program Multi-Year Research, Development and Demonstration Plan:

(A) Durability
(B) Cost
(C) Performance
(A) High-Volume Membrane Electrode Assembly (MEA) Processes

Technical Targets

Progress has been made in achieving objectives within the Fuel Cell Technologies Multi-Year Research, Development and Demonstration Plan. Table 1 lists the DOE's technical targets and where our research stands to date. There are two other DOE targets for membranes relating to durability, which we have not yet addressed.

TABLE 1. DOE Technical Targets and GES Status

Characteristic	Unit	2015 Target	GES DSM Status
Oxygen Crossover	mA/cm^2	2	1.5[a]
Hydrogen Crossover	mA/cm^2	2	1.8[a]
Membrane Conductivity Operating Temperature 20°C -20°C	S/cm	 0.10 0.07 0.01	 0.093[b] 0.083 Not tested
Operating Temperature	°C	≤120	95
Area Resistance	$Ohm*cm^2$	0.02	0.03[c]
Cost	$\$/m^2$	20	~$100
Durability with Cycling <80°C	cycles	20,000	20,000
Unassisted Start from Low Temperature	°C	-40	Untested
Thermal Cyclability in Presence of Condensed Water		Yes	Yes

[a]Crossover measured for 1 atm of pure H_2 and pure O_2 at 95°C and 50% relative humidity.
[b]For 18 μm DSM operating at 95°C with H_2/air at 20 psi. H_2/air stoichiometry 1.1/2.0.

FY 2011 Accomplishments

- Supplied four laser manufacturing companies with polyimide and polysulfone samples to generate a closely packed (50% area density) microporous DSM support via continuous drilling of pores using direct laser ablation method.
- Established an ultraviolet (UV)-shielded cleanroom to fabricate photo-curable polymers as candidates for DSM supports.
- Collaborated with University of Massachusetts Amherst (UMass), Colorado Photopolymer Solutions, and NanoImprint Lithography Technology to optimize the use of photo-curable polymers for rapid microreplication process.
- Designed a protocol to screen various DSM supports which includes procedures to test acid/alcohol resistance, water uptake, substrate adhesion, and mechanical strength for roll-to-roll fabrication.
- Revisited the phase inversion solvent cast method from Phase II and improved the tensile strength and elastic moduli of cast DSM supports by 3-5 fold.



Introduction

Lowering the equivalent weight (EW) of perfluorinated ionomers is one of the few options available to improve polymer electrolyte membrane conductivity, especially in the low relative humidity (RH) regime. GES believes that an approach utilizing perfluorinated ionomers of low EW is an optimal method to achieve the DOE membrane metrics. GES has developed DSMs (Figure 1) to provide a better support for the conductive ionomer. DSMs are composite membranes that include a highly conductive and high acid content ionomer incorporated into a thin and durable polymer support with well-defined pores. Utilizing high strength engineering polymers, DSMs have completely restrained in-plane swelling. Providing a direct through-plane non-tortuous path minimizes the conductivity penalty due to the support structure. Additionally, when filled with low EW perfluorinated sulfonic acid (PFSA) ionomers, they meet nearly all of the DOE's 2015 durability and performance targets, including those for freeze/thaw cycling and wet/dry cycling operation.

As currently manufactured, DSMs are far too expensive for automotive or even stationary applications. This project is directed toward the commercialization of DSMs for highly reliable fuel cell systems operated under harsh environments. The overall objective of this project is to develop a scaled-up fabrication process geared towards roll-to-roll manufacturing of DSMs.

Approach

A major milestone for the project is to identify a cost-effective route to fabricate 10-12 µm thick microporous DSM support films with 50% area coverage (pore density) and 10-20 µm diameter straight pore holes. Currently, four types of DSM support fabrication techniques have been evaluated based on several criteria including DSM performance, scalability, developmental cost, and final DSM cost. Table 2 shows a brief description of each technique along with their strong and weak points.

Results

Continuous Laser Micromachining. This technique involves the use of a dedicated laser to drill holes through a patterned mask, and it allows for direct, one-step generation of porous films without any intermediate processing steps. Throughout the evaluation of this technique, four laser manufacturing companies have received and tested both polyimide and polysulfone films to generate the hole pattern shown in Figure 1. All four companies have failed to meet the stringent requirements for resolution, speed, and projected cost. As an example, a roll-to-roll continuous laser drilling setup reached a lateral accuracy of ±40µm, much worse than the upper limit of ±3.5 µm to ensure separation of pores. At continuous operation and very high volume, the final cost (excluding the capital equipment) is estimated to reduce to $200/m^2, still an order of magnitude higher than the targeted value of $20/m^2. Based on these results and the high initial and operational costs, the use of continuous laser micromachining is largely eliminated.

TABLE 2. Side-to-Side Comparisons of Various DSM Support Fabrication Techniques

Technique	Description	Pros/Cons
Laser Micromachining	Continuously drilling holes using a dedicated laser	Pro: One step fabrication/materials Con: Slow process and high initial costs
UV Microreplication	UV curing of polymers between a mold and a substrate	Pro: Rapid film formation Con: High material risk
Phase Inversion Solvent Casting	Precipitation of polymers on a mold using a non-solvent	Pro: Ease of processing Con: Waste solvent and film shrinkage
Thermal Perforation	Perforation of polymers using an array of microneedles	Pro: One step fabrication/materials Con: Resolution/ Ragged features

Microreplication of Photo-Curable Polymers. This is a soft lithography approach where ultra-fine (sub-micron) patterns can be generated. It requires the production of a master template, followed by several microreplication processes to obtain the resulting DSM support and eventually the DSM itself after application of the ionomer layer(s). Figure 2 shows an exemplary process flow where a low surface energy mold is applied on a precursor-coated backing layer followed by UV curing to freeze the polymer

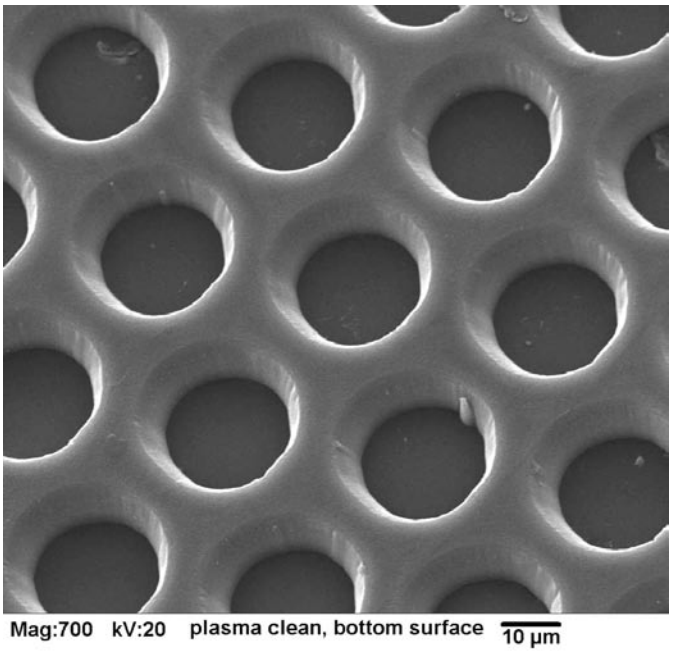


FIGURE 1. Scanning Electron Microscope Photograph of Matrix Support for Low EW PFSA

in place. When the mold is removed, this results in a continuous DSM support with well-defined pores. Due to low material costs and fast processing, this is one of the most promising techniques to meet the target cost of $20/m^2. GES has successfully evaluated a series of photo-curable polymers as DSM support candidates. A UV-shielded cleanroom facility was established to accommodate UV-sensitive material processing. To screen and validate polymers as DSM supports prior to the microfabrication at UMass, commercially available formulations of polyimide, epoxy, thiol-ene, and urethane were cast from their precursors and monomers to desired thickness. Controlled exposure to UV-light yielded films that were tested for water uptake, acid resistance, and dimensional stability at temperatures up to 95°C. Polymers that successfully passed the first stage were then subjected to extensive mechanical testing by immersing the films in hot (80°C) water and determining their static (tensile strength, elongation, modulus) and kinetic (creep under stress) mechanical properties. Photo-curable polymers showed very little water uptake, high dimensional stability, and low creep elongation, all superior to that of the ionomers in water (Nafion®). However, their tensile strength and moduli suffer possibly due to the presence of unreacted monomers.

Phase Inversion Solvent Casting. Phase inversion solvent casting technique, first used during Phase II of this project, aimed to develop a new technology to fabricate DSM supports that are less expensive and easier to scale up compared to the laser micromachining. Poly(dimethyl siloxane) (PDMS) elastomer molds, inverted (pin) pattern of Figure 1, were replicated by GES from a master template fabricated at Harvard University's Center for Nanoscale Systems. In this process, polysulfone was dissolved in a solvent, followed by casting on PDMS to fill the micromold as shown in Figure 3. This assembly was then transferred into a gelation bath filled with non-solvent (e.g. water),

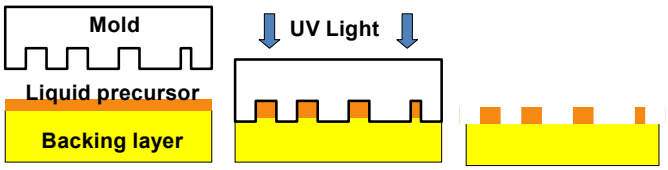


FIGURE 2. Liquid Displacement Method using a Prefabricated Mold followed by UV-Curing to Yield Porous DSM Support

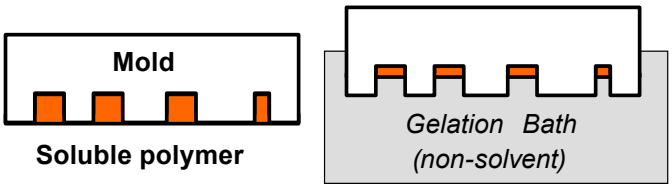


FIGURE 3. Schematic Representation of the Phase Inversion Solvent Casting Process to Precipitate a Polymer in a Non-Solvent

miscible with the initial solvent. This combination yielded the rapid precipitation of the polymer inside the micromold to form a film with well-defined micropores. In Phase II, this approach showed great promise for integration into a fast roll-to-roll process; however, the support prepared by this process is usually not strong enough to withstand further processing and has sponge-like morphology to result in high water uptake. To circumvent this issue, a film has been cast on a PDMS micromold followed by annealing at temperatures above its Tg to show 3-5 fold increase in both eleastic moduli and tensile strength.

Thermal Perforation with Microneedles. If a scalable route can be established for direct perforation of polymers to yield porous support layers, it may prove to be a very attractive technique since the resulting support structure will have identical performance unlike the case for photo-curable and solvent cast films where further material validation is required upon fabrication. To further explore this path, GES has partnered with an acclaimed company in the area of microfabrication to employ embossing (puncturing) of softened thermoplastics using an array of microneedles. Figure 4 shows the preliminary results from a trial run performed for GES where an array of microneedles is used to puncture an 8 µm thick polysulfone (PSU) film. PSU is the ideal material choice for this application due to its low cost, superior mechanical properties and low softening temperature as well as its insignificant dimensional changes in all three axes.

Conclusions and Future Directions

The goal by the end of fourth quarter is to demonstrate a scalable process for cost-effective manufacturing of DSM for fuel cells. In addition to further investigation of feasibility of direct laser machining and mold-based phase inversion cast methods, GES has shown two additional methods that will be capable of performing this goal. The microreplication method requires further validation of mechanical properties of photo-curable polymers, which will be performed in collaboration with UMass. The PSU supports generated by thermal perforation method will be inspected by GES to determine whether the method can produce a material with closely packed micropores to meet the 50% porosity

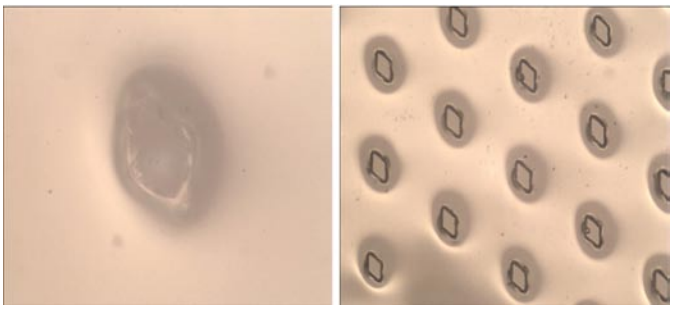


FIGURE 4. Optical Micrographs of a PSU Film Punctured using Microneedles shown at 10X (left) and 40X (right) Magnification

requirement. GES will select the most promising fabrication route and focus on scaling, performance optimization, and cost reduction.

FY 2011 Publications/Presentations

1. Mittelsteadt, C.M. "DE-EE0004533 Giner Electrochemical Systems Q1 Report" Jan. 2011.

2. Mittelsteadt, C.M. "DE-EE0004533 Giner Electrochemical Systems Q2 Report" Apr. 2011.

V.C.4 Poly(p-Phenylene Sulfonic Acids): PEMs with Frozen-In Free Volume

Morton Litt (Primary Contact), Ryszard Wycisk, Kun Si, Casey Check and Daxuan Dong
Case Western Reserve University
10900 Euclid Ave.
Cleveland, OH 44106-7202
Phone: (216) 368-4174
E-mail: mhl2@case.edu

DOE Managers
HQ: Donna Ho
Phone: (202) 586-8000
E-mail: Donna.Ho@ee.doe.gov
GO: Gregory Kleen
Phone: (720) 356-1672
E-mail: Greg.Kleen@go.doe.gov

Technical Advisor
John Kopasz
Phone: (630) 252-7531
E-mail: Kopasz@anl.gov

Contract Number: DE-FC36-06GO16039

Project Start Date: March 1, 2006
Project End Date: June 30, 2012

Fiscal Year (FY) 2011 Objectives

The project objectives are to optimize routes to rigid rod poly (phenylene sulfonic acids) (PPDSA), polymers that retain high conductivity at low humidity, develop methods to make water-insoluble polymers and characterize the materials as proton exchange membranes (PEMs). The requirements are:

- Analyze the Ullman polymerization reaction in order to increase polymer molecular weights and decrease reaction time.
- Increase the polymer sulfonic acid density and water absorption: use phenylene disulfonic acid monomer to make homo- and co-polymers.
- Develop reliable methods for making water-insoluble, dimensionally stable PEMs possibly by grafting non-polar groups on the backbone and crosslinking.
- Synthesize comonomers that can be copolymerized to produce water-insoluble copolymers either directly or in a subsequent step.
- Characterize polymers, copolymers and grafts to understand the relationship between molecular structure, supermolecular organization and PEM properties.
- Submit the most successful materials for intensive testing.

Technical Targets

This project involves the synthesis and characterization of homo- and co-polymer rigid-rod aromatic sulfonic acids and developing methods to make them dimensionally stable.

- Our PEMs have passed the 2005 goals for membrane conductivity and probably reach the 2015 goals.
- Earlier tests of MeOH permeability (<0.04 mA/cm^2 for a 20 μ thick film at 100°C with a 2/1 MeOH/H_2O gas input) imply that the very polar membrane environment should reduce oxygen and hydrogen crossover to values much lower than the target values.
- The starting materials are relatively cheap; there are only two steps from commercial starting materials, fuming sulfuric acid and dibromo benzene (or dibromo biphenyl), to the homopolymer sulfonic acids. Copolymers could raise the cost. (Also, it may be possible to replace dibromo benzene with dichloro benzene, lowering the raw materials cost by a factor of 5.)

Remaining Barriers

- Polymers have low elongation (6-9%) and tear easily.
- Polymer molecular weights are too low. Higher molecular weight should give better mechanical properties.
- Grafting and crosslinking succeeded; good PEMs were made. However, better grafting methods need to be developed.
- Procedures for scaling up polymer production without lowering molecular weight have not yet been developed.
- Crosslinked films swell about 15% in the x and y directions and 30 to 40% in the z direction going from 0 to 98% relative humidity (RH). Can swelling be reduced without decreasing conductivity?

Technical Targets

Progress towards meeting the technical targets for PEMS and membrane electrode assemblies (MEAs) is shown in Table 1.

Fiscal Year 2011 Accomplishments

- PPDSA and copolymers containing the biphenyl group (B2P8) were made in molecular weights high enough that cast films could be handled easily.
- One to 16 mole% biphenyl groups were grafted on the polymers to form biphenyl sulfones.
- Films cast from the grafted polymers were completely crosslinked by heating at 210°C for three hours with no loss of acid over that required to crosslink. Crosslinked

TABLE 1. Progress towards Meeting Technical Targets for PEMs and MEAs; Data for Crosslinked B20P80 gBP 12% (D7).

Characteristics	Units	Target 2015	2010 Status
Maximum Operating Temperature	°C	120	120
Area Specific Resistance at:			
Maximum operating temperature and water partial pressures from 40 to 80 kPa	Ohm cm^2	≤0.02	0.093*
80°C and water partial pressures from 25 to 45 kPa	Ohm cm^2	≤0.02	0.040*
30°C and water partial pressures up to 4 kPa	Ohm cm^2	≤0.03	0.06*
-20°C	Ohm cm^2	≤0.2	N/A
Maximum Oxygen Cross-Over	mA/cm^2	2	N/A
Maximum Hydrogen Cross-Over	mA/cm^2	2	1.9
Minimum Electrical Resistance	Ohm cm^2	1,000	31
Cost	$/$m^2$	≤20	N/A
Durability:			
Mechanical	Cycles w/<10 sccm crossover	≥20,000	N/A
Chemical	hours	>500	N/A

*Sample thickness was ~80 micrometers. A 25 micrometer thick film could meet the requirements. A less heavily grafted film (7% instead of 12%) could meet the requirements at 80 micrometers thick.

polymers were stable for at least two hours at 225°C. Some acid was lost after 2 hours at 250°C.

- Crosslinked films were dimensionally stable, retaining the high conductivity at low RH of the starting graft polymers.
- MEAs prepared from crosslinked films were tested in fuel cells. The best were slightly worse than Nafion211®. This is a very good result for first tests on a completely new class of materials.
- High viscosity copolymers of dibromobenzene disulfonic acid and dibromofluorene disulfonic acid were made. These can be grafted and crosslinked to give dimensionally stable polymers with exceptionally high milliequivalents of acid groups per gram of material (IECs) and high conductivity at low RH (higher than the biphenyl grafted polymers).



Introduction

There are many problems associated with the normal aromatic sulfonic acid PEMs. The better conducting materials swell very much in water. Even with these materials, conductivity drops rapidly as humidity is lowered [1]. Block polymers swell less at high humidity, but conductivity is still poor at low RH [2]. They can be used only at high humidity which limits the fuel cell operating temperature to < 90°C. The materials described in the following were designed to hold water very strongly at low humidity. They could be used effectively at higher temperatures, up to at least 120°C, with little or no added water in the fuel stream since the water generated in the reaction should be sufficient to maintain high conductivity. High temperature operation has the additional advantages that kinetics are faster, lower purity hydrogen can be used and heat can be removed easily.

Approach

Our approach derives from a combination of polymer structure analysis and cost considerations. What type of polymer backbone can have high sulfonic acid content, hold water strongly, and yet have dimensional stability. The analysis suggested that PPDSA, rigid rod liquid crystals that organize with all molecules locally parallel, should be suitable. These structures have small cross-section backbones with projecting sulfonic acid groups. Absorbed water separates the chains. As water is lost at low humidity, the sulfonic acids hit other acid groups or a neighboring polymer backbone. The molecules still have voids that hold water (frozen in free volume): further water loss compresses the molecule, which distorts bond angles and requires high energy. The last few waters are difficult to remove and resorb easily. Water causes the structure to expand perpendicular to the parallel polymer axes. The final structure can be dimensionally stabilized by grafting cross-linking groups on the backbone and subsequently crosslinking them [3] (PPDSA). Grafted groups protrude further from the backbone than the acid groups; this increases the chain (rigid rod) separation and thus can increase the frozen-in free volume [4]). This structural design generates non-collapsible nanopores lined with a high density of sulfonic acid groups that hold water very strongly.

Polymers with grafted non-polar groups, reported last year, lost coherence at high humidity; the film flowed under pressure and disintegrated in water. Crosslinking avoids these problems. Because the molecules are rigid rods, grafted groups react only intermolecularly to cross-link with sulfonic acids on neighboring chains. Thus, a relatively low mole fraction of crosslinkable groups should make such polymers dimensionally stable with little loss of conductivity. This approach has succeeded for these materials.

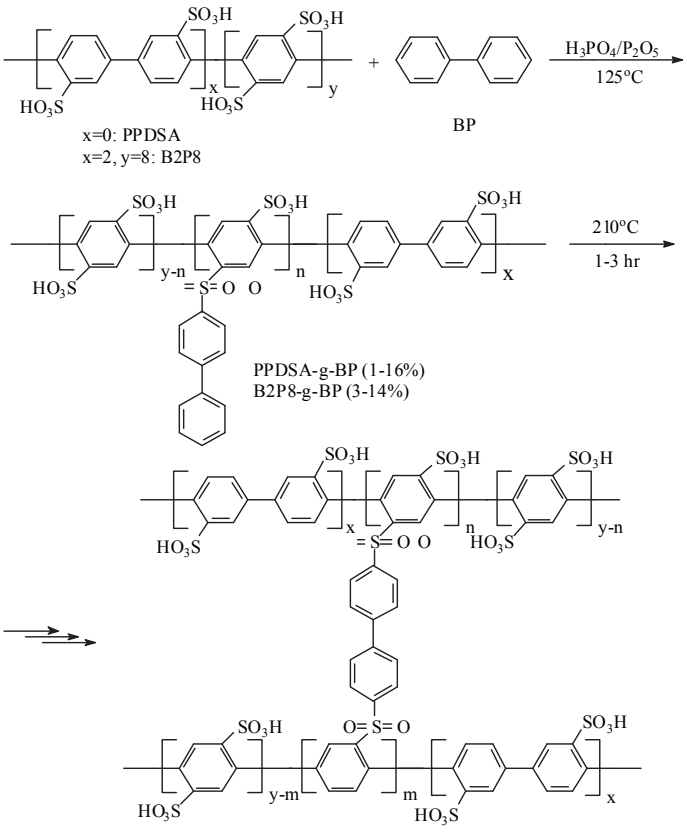
Another approach to generate frozen-in free volume was presented last year. The idea was to make a two-dimensional lattice containing large pores. The molecules should stack to create nano-channels that would contain enough water to give good conductivity along the channels and hold the water even at very low humidity. Cast films with all molecules parallel to the film surface should have very high through conductivity at low RH. The idea was tested and it worked, but as usual, there were complications.

Results

PPDSA and B2P8 Copolymers

Copolymerization: The polymers used for most of this research were PPDSA and a 20/80 copolymer of 1, 4-dibromo phenylene 2, 5-disulfonic acid (DBPDSA) and 4, 4'-dibromobiphenyl 3, 3'-disulfonic acid (DBBPDSA), B2P8. As reported last year, both were made with reasonably high molecular weights. As expected from the discussion above, λ at low RH rose rapidly and stabilized at 2 to 3 waters higher than Nafion117® at higher RHs. This resulted in high conductivity down to very low RHs but with high swelling and poor mechanical properties.

Grafting and Crosslinking: Grafting of alkyl benzene groups on the polymer was abandoned since the resulting grafts had very poor mechanical properties. We have shifted to grafting cross-linkable groups. Biphenyl, the first of many possible cross-linkable structures, was grafted on the polymer backbone to generate dangling biphenyl sulfone groups, Scheme 1. Once one benzene ring reacts, the second benzene ring is deactivated; soluble polymer is isolated. Cast films could be almost completely crosslinked by heating under vacuum at 210°C for at least 1 hour. Studies of heating times and temperatures showed that the polymer was stable for at least two hours at 225°C, but showed some acid loss after 2 hours at 250°C. The 10 and 12 mole% grafts were extensively characterized, though conductivity and water absorption data were obtained for most grafts.



SCHEME 1. Grafting and Crosslinking of PPDSA Polymers and Copolymers

1, 4-Dibromobenzene 2, 5-disulfonic acid was successfully copolymerized with 2, 7-dibromofluorene 3, 5-disulfonic acid in 10/1 and 20/1 mole ratios to give high viscosity copolymers. However, we still have not been able to graft benzyl groups effectively on the fluorene moieties. Each should add two benzyl groups, but as yet we have only reached about 0.5 groups. Films crosslink when heated but they swell too much to be useful.

Properties: Grafted polymer films showed almost the same conductivity and mechanical properties before and after crosslinking. Swelling at a given graft percent was identical up to 50% RH, independent of crosslinking. Crosslinked PEMs (7 to 16 mole% biphenyl graft) swelled 90 to 60% when the RH rose from 0 to 98%. The x and y dimensions increased only 10 to 15% for all crosslinked films. At 98% RH, λ before crosslinking was about 2.5 to 3 higher than after crosslinking, with a corresponding dimensional increase.

Stress/strain measurements were made on many films before and after crosslinking. Elongation at break (22 to 30% RH) varied randomly between 6 and 9%; crosslinked films broke at much higher stress (35 to 45 MPa) than the uncrosslinked films (20 to 25 MPa). Stress concentrators, bubbles or particles in the film or edge defects, probably initiated failure. Lower humidity raised the modulus and break stress but lowered break elongation. Higher humidity drastically lowered the modulus of the uncrosslinked films; they tended to creep at constant force above 3% elongation.

Water absorption from 0 to 98% RH was measured for grafted films before and after crosslinking. Uncrosslinked films had final λs of 12.5 to 14.5; when crosslinked, λ decreased to 8.5 to 12. Differential scanning calorimetry measurements showed that about 9 molecules of water per acid group were strongly bound, much higher than that found for Nafion 117®, and others.

Parallel conductivity was measured at 80°C as a function of RH for many films, both here and at the Florida Solar Energy Center (FSEC). Results agreed within experimental error. Conductivity decreased with higher grafting; however on a log conductivity vs. RH graph, all plots were parallel. Crosslinking did not change conductivity even though it decreased the IEC. Even at the highest grafting levels, low RH conductivity was still very high. Through plane conductivity for a 12 mole% biphenyl grafted and crosslinked B2P8 copolymer, uncorrected for electrode/film resistance, is shown in Figure 1 (measured by Dr. Kevin Cooper, Scribner Associates). The through plane conductivity at 80°C is about that of the parallel conductivity (measured at Case and at Bekktech). Its conductivity at 120°C and 30% RH is 100 mS/cm, close to the DOE 2015 goals. We expect that materials with a lower percentage of grafting will have higher conductivity.

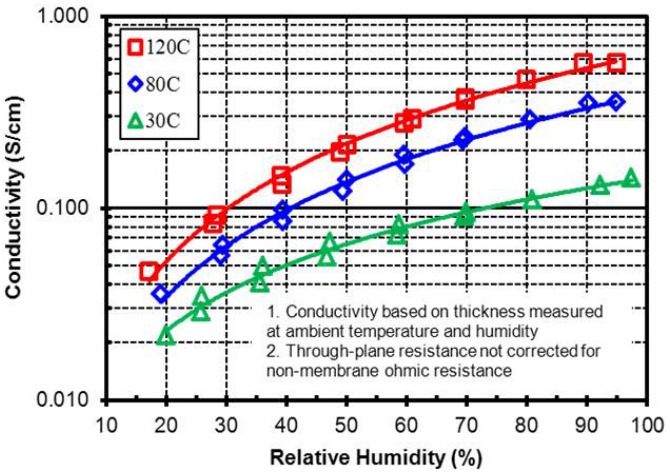


FIGURE 1. Through-Plane Proton Conductivity for B20P80-g-BP12%-210C-3hr (D7) as a function of RH at 30, 80 and 120°C

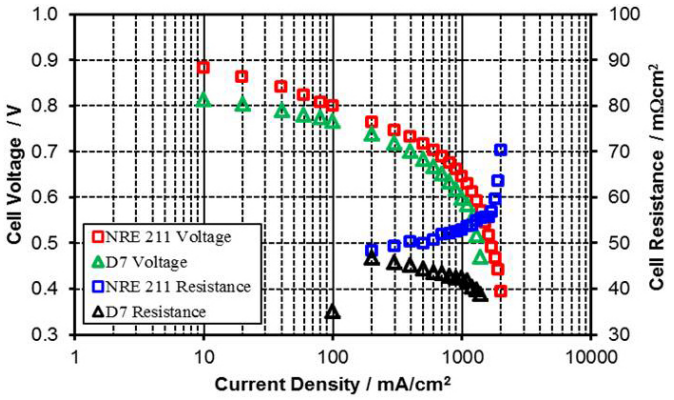


FIGURE 2. Single-Cell Performance of an MEA using B2P8-g-BP12%-210°C-3hr (D7, 80 μ thick) compared to that of Nafion® (NRE211) at 80°C, 100% RH, H_2/air, Ambient Pressure (Work done at FSEC.)

Fuel Cell Testing: Several grafted materials (both as uncrosslinked (D9) and as a final crosslinked film (D7) were sent to the FSEC for testing in MEAs. They tested the film crosslinked at Case Western University (D7) and a second film (D9) cast and crosslinked at FSEC. Both showed high hydrogen leakage, probably from small tears generated in the brittle films during electrode application. Figure 2 shows some results for D7, the best film, a B2P8 copolymer grafted with 12 mole% biphenyl. The hydrogen leakage lowers the voltage at low current densities. Above 100 mA/cm^2, the curves follow each other closely, with the power output for the D7 cell about 95% that of the reference Nafion211® cell over the useful current range. Considering that this was the first fuel cell test on a new material with very different chemical and mechanical properties from the normal PEMs, such good performance is remarkable. We expect that a film without defects should have very low hydrogen and oxygen permeability; the highly polar aqueous phase is a very poor solvent for the non-polar gasses while the organic phase consists of rigid aromatic rings that cannot dissolve the gasses.

A summary of the results for films D7 and D9 compared with that of NRE211, is shown in Table 2. D6, the first entry, is an octyl benzene graft; this could not be crossslinked and disintegrated during testing. The major problem was gas leakage through the membrane that varied widely from one day to the next (probably due to micro tears that opened and closed with changing humidity and history). When gas leakage was accounted for, the membrane performance was about that of DRE211. Since the films had lower resistance, this was unexpected; MEA preparation needs to be improved. However, these are excellent results for a first study.

TABLE 2. First Tests of Case Membranes against NRE211, compared to DOE 2015 Targets

Characteristic	Units	Target 2015	D6[d]	D7[d]	D9[d]	NRE211
Area specific proton resistance[c] at:						
120°C and water partial pressures from 40 to 80 kPa	Ohm-cm^2	≤0.02	N/D	0.093	0.13	0.18
80°C and water partial pressures from 25-45 kPa	Ohm-cm^2	≤0.02	0.076	0.040	0.042	0.05
Maximum hydrogen cross-over [a]	mA/cm^2	2	10.8	1.9	136	0.76
Minimum electrical resistance [b]	Ohm cm^2	1,000	8.4	31	14	2,100
Performance @ 0.8 V (¼ power)	mA/cm^2 mW/cm^2	300 250	N/D N/D	34 27	N/D N/D	151 120
Performance @ rated power	mW/cm^2	1000	N/D	108	N/D	480

[a] Measured in humidified H_2/N_2 at 25°C.
[b] Measured in humidified H_2/N_2 using linear sweep voltammetry curve from 0.4 to 0.6 V at 80°C.
[c] Average cell resistance from current interrupt.
[d] D6 is B2P8-g-16 mole% n-octylbenzene. D7 is B2P8-g BP 12%, cast and crosslinked for 3 hrs at 210°C at Case Western Reserve University. D9 is the same polymer, cast and crosslinked at FSEC.
N/D - not determined

Conclusions and Future Directions

- We have made PEMs with very high conductivity at low RH and have been able to dimensionally stabilize them through crosslinking.
- Some crosslinked membranes were tested as MEAs in single fuel cells and performed well for a first study.
- The major problem for these materials is their low elongation at break, 6 to 9%, which promoted the formation of micro-tears in the MEAs during their preparation. This is mainly the result of their rigid-rod structure. However, elongation will increase with higher molecular weight.
- There has been no study of possible membrane cost. Some procedures used are fine for laboratory preparations but are wasteful. Work will start on lower cost approaches - possible alternate monomers and grafting methods.
- In the coming year, we will concentrate on making higher molecular weight polymers. We are considering two approaches. First, determine the best polymerization conditions. Second, develop comonomers that increase polymer solubility, allowing it to reach higher molecular weight before it precipitates. With these approaches, we should be able to reach high modulus, high elongation PEMs.
- In addition, grafting procedures need to be improved. Grafting is inhomogeneous and expensive. Inhomogeneity reduces crosslinking effectiveness: poorer mechanical properties for a given percent graft. We will work to develop methods to graft homogeneously using minimal amounts of reagents. This should result in PEMs with higher conductivity and lower swelling.
- As better PEMs are made, they will be submitted to the FSEC for extensive testing as MEAs.

FY 2011 Publications/Presentations

1. 10/12/10 ECS, Las Vegas, NV.

2. 10/28/10 FreedomCar Tech Team Review, Southfield, MI .

3. 12/19/10 Pacifichem 2010, Honolulu HI.

4. 5/11/11 DOE Progress Review.

5. Rigid Rod Poly(p-Phenylene Sulfonic Acid) PEMs: High Conductivity at Low Relative Humidity Due to "Frozen-In-Free Volume", Morton Litt, Sergio Granados-Focil, Junwon Kang, Kun Si and Ryszard Wycisk, *Polymer Electrolyte Fuel Cells 10* Editor(s): H. Gasteiger, et al, *Volume 33, Issue 1 - October 10 - October 15, 2010, Las Vegas, NV* pp.695-710 (2010).

References

1. F. Wang, M. Hickner, Y.S. Kim, T.A. Zawodzinski and J.E. McGrath, *J. Membr. Sci.* **2002** *197*, 231.

2. J. McGrath et al, DOE Program review, 6/08 Washington, D.C.

3. S. Granados-Focil, Ph. D. thesis CWRU, 2006; Sergio Granados-Focil. and Morton H. Litt, *ACS Polymeric Materials Science & Engineering Preprints*, **89**, 438 (2003); Sergio Granados-Focil, Thomas Young and Morton H. Litt, ACS *Fuel Chemistry Division Preprints,* **49(2)** 528-529 (2004).

4. Yue Zhang, Ph. D. Thesis, CWRU, 2001; Morton H. Litt, Sergio Granados-Focil; Yue Zhang and Thomas Young, Molecular design of rigid rod polyelectrolytes: Effect of structure on water retention and conductivity. *ACS Fuel Chemistry Division preprints* **49(2)** 594-595 (2004).

V.C.5 NanoCapillary Network Proton Conducting Membranes for High Temperature Hydrogen/Air Fuel Cells

Peter N. Pintauro[1] (Primary Contact) and
Patrick T. Mather[2]

[1]Vanderbilt University
Department of Chemical and Biomolecular Engineering
PMB 351604
2301 Vanderbilt Place
Nashville, TN 37235-1604
Phone: (615) 343-3878
E-mail: peter.pintauro@vanderbilt.edu

[2]Syracuse Biomaterials Institute
Biomedical and Chemical Engineering Department
Syracuse University
Syracuse, NY 13244

DOE Managers
HQ: Kathi Epping Martin
Phone: (202) 586-7425
E-mail: Kathi.Epping@ee.doe.gov
GO: Greg Kleen
Phone: (720) 356-1672
E-mail: Greg.Kleen@go.doe.gov

Contract Number: DE-FG36-06GO16030

Subcontractor:
Eric Fossum, Wright State University, Dayton, OH

Start Date: March 1, 2006
Projected End Date: February 28, 2012

Fiscal Year (FY) 2011 Objectives

- Fabricate a new class of nanofiber-based proton conducting membranes using different sulfonated polymers.
- Characterize the membranes in terms of swelling, proton conductivity, thermal/mechanical stability, and gas permeability.
- Optimize the membrane structure (fiber diameter, mat density, polymer ion-exchange capacity, choice of impregnation polymer, etc.) to achieve the DOE's technical targets for membranes.

Technical Barriers

This project addresses the following technical barriers from the Fuel Cells section of the Fuel Cell Technologies Program Multi-Year Research, Development and Demonstration Plan:

(A) Durability

(B) Cost

(C) Performance

Technical Targets

This project is focused on the fabrication and characterization of a new class of proton conducting membranes for high temperature hydrogen/air fuel cells. The technical targets of this project are listed in Table 1.

TABLE 1. Progress towards Meeting Technical Targets for Membranes

Characteristic	Units	Target 2015	2011 Project Status
Maximum operating temperature	°C	120	
Area specific proton resistance at:			
Maximum operating temp and water partial pressures from 40 to 80 kPa	Ohm cm^2	≤0.02	0.05[a]
80°C and water partial pressures from 25-45 kPa	Ohm cm^2	≤0.02	0.06
30°C and water partial pressures up to 4 kPa	Ohm cm^2	≤0.03	
-20°C	Ohm cm^2	≤0.2	
Maximum oxygen cross-over [a]	mA/cm^2	2	
Maximum hydrogen cross-over [a]	mA/cm^2	2	2
Minimum electrical resistance	ohm cm^2	1,000	
Cost	$\$/m^2$	≤20	27
Durability:			
Mechanical	Cycles w/<10 sccm crossover	≥20,000	12,600
Chemical	hours	>500	842

[a] Proton conductivity at 120°C and 50% relative humidity (RH) – data from Bekktech LLC

FY 2011 Accomplishments

- Fabricated nanofiber composite membranes via a dual fiber electrospinning, where perfluorosulfonic acid (PFSA) proton conducting fibers and uncharged polyphenylsulfone (PPSU) nanofibers are simultaneously electrospun.
- Further developed two methods for processing the dual fiber mat into a functional fuel cell membrane by: (i) allowing the PFSA ionomer fibers to soften and flow without affecting the PPSU mat in order to fill the voids

between PPSU fibers (the nanofiber PPSU becomes a membrane reinforcement mat) and (ii) allowing the PPSU nanofibers to soften and flow to fill all voids while maintaining the structure of the Nafion® mat. Membranes were prepared from method (i) using DuPont's Nafion® and 660 equivalent weight (EW) PFSA from 3M Company and from method (ii) using Nafion® PFSA.

- Nanofiber membranes were characterized in terms of proton conductivity, in-plane, volumetric, and gravimetric water swelling, and mechanical properties.
- Electrospun nanofiber Pt/C fuel cell cathodes were fabricated and tested.



Introduction

Proton exchange membrane (PEM) hydrogen/air fuel cell operation with lightly humidified gases at 120°C would be highly advantageous with regards to heat rejection from a fuel cell stack, compatibility with automotive radiators, tolerance to CO impurities in the hydrogen gas stream, and fast electrode kinetics. For PEM fuel cell operation at temperatures ≤80°C and high RH conditions, PFSA proton conductors (e.g., Nafion®) are the membrane material of choice due to their high conductivity and chemical/mechanical stability. Unfortunately, the conductivity of PFSA membranes drops dramatically at temperatures >100°C under low humidity conditions [1] due to an insufficient number of membrane-phase water molecules for protons to dissociate from sulfonic acid sites, a loss of percolation pathways for proton movement, and structural changes in the polymer which cause membrane pores to collapse.

In order to overcome the limitations of existing membrane materials, a new approach to fuel cell membrane design and fabrication has been developed, where a three-dimensional interconnected network of proton-conducting polymer nanofibers/nanocapillaries is embedded in an inert/impermeable polymer matrix. The nanocapillary network is composed of a high ion-exchange capacity sulfonic acid polymer to ensure high water affinity and a high concentration of protogenic sites. The inert (hydrophobic) polymer matrix controls water swelling of the nanofibers/nanocapillaries and provides overall mechanical strength to the membrane. First-generation membranes [2] were made using sulfonated poly(arylene ether sulfone) with/without sulfonated octaphenyl polyhedral oligomeric silsesquioxanes (sPOSS) to further boost conductivity. Norland Optical Adhesive 63 (NOA63) was employed as the inert embedding polymer. Second-generation membranes were fabricated with nanofibers containing 850 EW PFSA (from 3M Corporation) with/without sPOSS [3]. These films met the DOE's Year 3, 3rd quarter Go/No-Go conductivity target of 100 mS/cm at 120°C and 50% RH. Third-generation films were made using a new dual-fiber electrospinning approach where ionomer and inert polymer are electrospun simultaneously. Advantages of this method over traditional membrane fabrication techniques, e.g., polymer blends or the impregnation of an ionomer in an inert matrix, are: (i) there is no separate polymer impregnation step, (ii) the same dual-fiber mat can be processed into two different membrane morphologies: proton conducting ionomer nanofibers embedded in an uncharged/inert polymer matrix and inert/uncharged polymer nanofibers embedded in (and reinforcing) an ionomer matrix, (iii) there is wide choice of polymers for the ion conduction and inert (uncharged) polymers, (iv) there is intimate mixing of polymer components in the dry state with a polymer component domain size (the fiber diameter) as small as 100 nm, (v) separate polymer components are used for the mechanical and proton-conducting functions of the membrane, and (vi) the domain size and loading of the proton-conducting phase can be easily and independently controlled.

Approach

Membrane Fabrication – Membranes were prepared by a newly developed dual nanofiber electrospinning technique using either 1100 EW Nafion® or 660 EW PFSA from 3M Corporation as the proton conducting material and Radel® R-5500NT polyphenylsulfone (PPSU) from Solvay Advanced Polymers LLC as the inert/uncharged polymer. PFSA materials were electrospun using 0.33-2% poly(ethylene oxide) as a carrier polymer (which was later removed by boiling the final membranes in water). PFSA and PPSU nanofibers were electrospun simultaneously using two separate needle spinnerets. Suitable post-treatment converted the dual-fiber mats into fully dense and defect-free membranes, while maintaining the nanofiber morphology of one polymer component. Membranes were made where: (i) PFSA nanofibers were surrounded by a PPSU matrix (compacted the mat at room temperature and 3,500 psig for a few seconds, exposed the mat to chloroform vapor at 25°C for 16 minutes, and then annealed the membrane for 2 hours at 150°C in vacuum) and (ii) PPSU nanofibers were surrounded by PFSA ionomer (hot pressed the mat at ~15,000 psig and 127°C for 40 seconds and then annealed at 150°C for 2 hours in vacuum). Membranes were evaluated and contrasted in terms of in-plane proton conductivity, in-plane, volumetric, and gravimetric swelling in water, and mechanical properties.

Electrode Fabrication – An electrospinning ink was prepared by mixing Pt/C catalyst powder (40% Pt on carbon black, Alfa Aesar), Nafion® powder, and 450,000 MW poly(acrylic acid) (MW=450,000 g/mol, Aldrich) in an isopropanol/water solvent (2:1 wt ratio). The total polymer and powder content was 13.4 wt%, where the Pt/C:Nafion®:poly(acrylic acid) weight ratio was 75:15:10. The ink was electrospun at 1.5 ml/h with an applied voltage of 7 kV. Nanofibers were collected on a bare rotating drum or on carbon paper (SIGRACET®

GDL 25 BC, Ion Power, Inc) that was fixed to the drum. The drum oscillated horizontally to improve the uniformity of deposited nanofibers. Fuel cell membrane electrode assemblies (MEAs) were prepared with a Nafion® 212 membrane and a decal-processed anode at a loading of 0.40 mg_{Pt}/cm^2. Electrospun cathodes with a Pt-loading of 0.1 mg/cm^2, 0.2 mg/cm^2 and 0.4 mg/cm^2, respectively, were hot-pressed onto anode-coated Nafion® membranes. The resulting MEAs were evaluated in a series of electrochemical and fuel cell tests.

Results

Nanofiber Composite Membranes with 660 EW PFSA – Figure 1 shows proton conductivity as a function of RH for a nanofiber composite membrane (70 vol% 660 EW PFSA + 30 vol% PPSU with an effective ion-exchange capacity of 1.23 mmol/g), as compared to commercial Nafion® 212 and a solution cast film composed of neat 660 EW PFSA. The nanofiber composite film is more conductive than Nafion® 212 due to its higher ion-exchange capacity. The conductivity of the composite is slightly below a neat 660 EW film due to dilution of ionomer by the PPSU reinforcing nanofiber mat. The composite membrane, however, has greatly reduced in-plane volumetric swelling; 5% as compared to 24% for Nafion® 212 and the 84% for the neat 660 EW film (swelling was measured in 23°C water). Thus, the nanofiber composite has more than twice the conductivity of Nafion® 212 over a wide humidity range and 5-times lower in-plane swelling. Low in-plane membrane swelling has been identified as in important property that improves the durability of an MEA during fuel cell operation. Based on the 50% RH conductivity in Figure 1 (at 80°C), the nanofiber composite membrane should have a proton conductivity of 0.090-0.095 S/cm at 120°C (slightly below the DOE target of 0.10 S/cm). The conductivity target can be achieved by decreasing slightly the PPSU content of the composite membrane or by using a slightly lower EW PFSA.

Nanofiber Composite Membranes with Nafion® – Proton conductivity (in 23°C liquid water) as a function of Nafion® volume fraction for the two nanofiber membrane structures (Nafion® with a PPSU nanofiber mat and Nafion® nanofibers surrounded by PPSU) is shown in Figure 2. There are no significant differences in conductivity between the two structures and proton conductivity scaled linearly with Nafion® volume fraction. The two morphologies exhibit the same volumetric and gravimetric water swelling but the in-plane swelling differs (see Figure 3), with the PPSU nanofiber reinforcing mat morphology exhibiting less swelling. The mechanical properties of the two composite membrane morphologies also differ, with the Nafion® nanofiber + PPSU matrix membrane exhibiting a larger Young's modulus (550 MPa) and proportional limit stress (30 MPa) than the inverse structure.

Nanofiber-Based Fuel Cell Cathode – Nanofiber cathode MEAs (where the average electrospun nanofiber diameter was 470 nm) performed very well in a hydrogen/air fuel cell operating at 80°C without back pressure. Exceptionally high fuel cell power densities were achieved at a low Pt loading, e.g. 524 mW/cm^2 at 0.6 V for 0.1 mg_{Pt}/cm^2, as shown in Figure 4. The catalyst mass activity, as measured at 0.9 V in an 80°C H_2/O_2 fuel cell with a pressure of 150 kPa_{abs}, was also exceptionally high at 0.23 A/mg_{Pt}. The accessible electrochemical surface area of the nanofiber cathode was very high (114 m^2/g_{Pt}) and it exhibited improved long-term stability vs. a decal cathode.

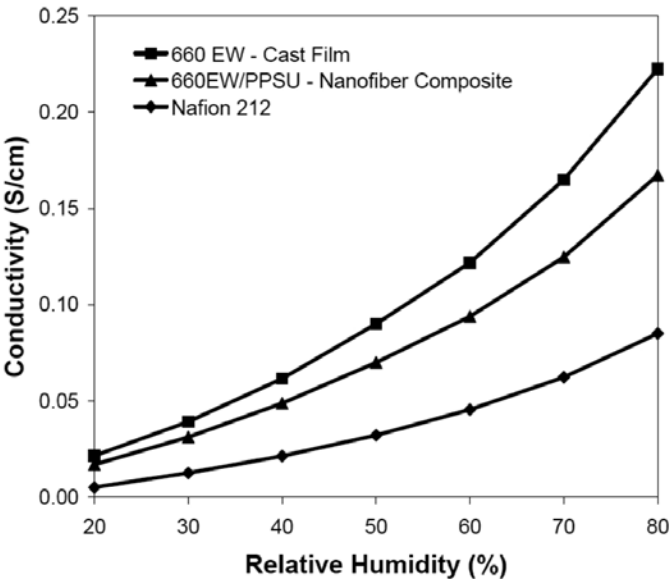


FIGURE 1. Proton conductivity of a nanofiber composite membrane (70 vol% 660 EW PFSA and 30 vol% polyphenylsulfone) at 80oC as a function of RH.

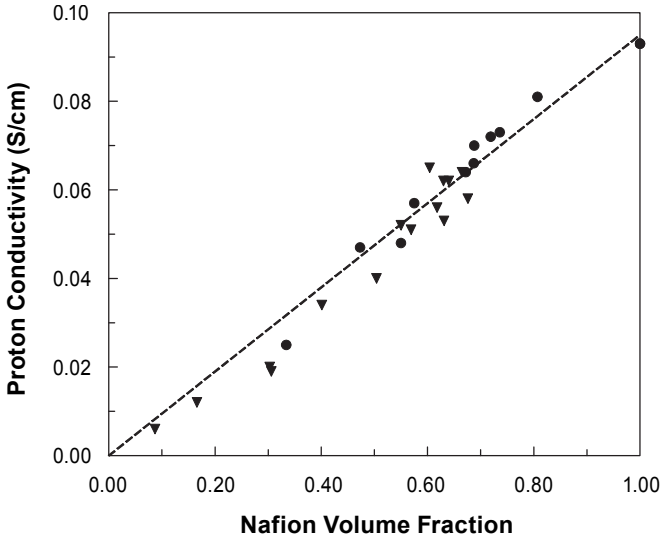


FIGURE 2. Proton conductivity of Nafion®/PPSU composite membranes as a function of Nafion® volume fraction. Conductivity measured in liquid water at room temperature. (▼) Nafion®-fibers/PPSU-matrix, (●) PPSU-fiber/Nafion®-matrix.

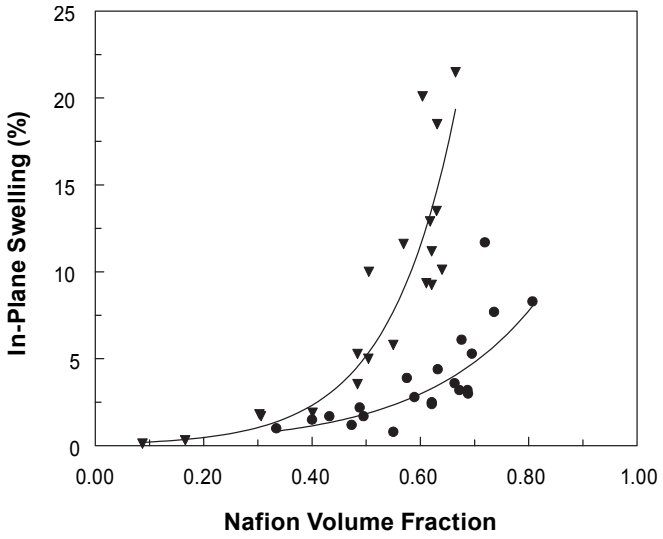


FIGURE 3. In-plane swelling of Nafion®/PPSU composite membranes as a function of Nafion® volume fraction. Swelling was measured in 100°C water. (▼) Nafion®-fibers/PPSU-matrix, (●) PPSU-fiber/Nafion®-matrix.

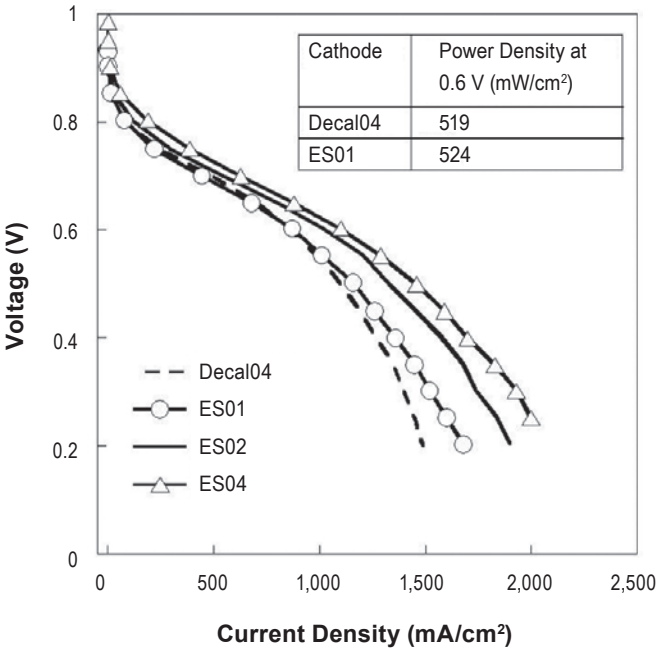


FIGURE 4. H_2/air fuel cell polarization curves at 80°C and ambient pressure with different cathodes, a Nafion® 212 membranes, and a 0.4 mg/cm^2 decal anode. Cathodes: Decal04 = 0.4 mg/cm^2 decal; ES01 = 0.1 mg/cm^2 nanofiber; ES02 = 0.2 mg/cm^2 nanofiber; ES04 = 0.4 mg/cm^2 nanofiber.

The outstanding performance was associated with a more uniform distribution of Pt/C particles and Nafion® binder in the nanofibers, thus allowing for better proton transport and oxygen diffusion to catalyst sites during fuel cell operation.

Conclusions and Future Work

Conclusions

- Two different membrane morphologies were generated from a dual nanofiber (Nafion® + PPSU) electrospun mat: Nafion® with a reinforcing nanofiber mat of PPSU and a nanofiber mat of Nafion® surrounded by PPSU polymer.
- The proton conductivity and volumetric/gravimetric water swelling are identical for the two membrane structures. The in-plane water swelling for membranes with a reinforcing PPSU mat is less than the inverse structure and the mechanical properties (Young's modulus and proportional limit stress) of membranes with a Nafion® nanofiber mat embedded in PPSU are better than films with the inverse structure.
- Dual fiber composite membranes were prepared and evaluated, where a PPSU nanofiber mat was surrounded by 660 EW PFSA (from 3M Corp.). The presence of the PPSU reinforcing mat lowered significantly volumetric and in-plane water swelling, for a membrane with 70 vol% PFSA. The membrane proton conductivity at 80°C and 50% RH was high (0.07 S/cm).
- Fiber composite membranes were estimated to cost \$27/m^2 (\$8/m^2 for sulfonated fluoropolymer and polyphenylsulfone and \$19/m^2 for electrospinning and fiber mat processing).
- An electrospun nanofiber cathode was fabricated, where the fiber composition was 75 wt% Pt/C powder, 15 wt% Nafion®, and 10 wt% poly(acrylic acid). In a H_2/air fuel cell, a nanofiber cathode at 0.1 mg_{Pt}/cm^2 out-performed a 0.4 mg_{Pt}/cm^2 decal cathode.

Future Work

- Continue to prepare and test nanofiber composite membranes with low EW PFSA and polyphenylsulfone using the dual fiber electrospinning approach.
- Prepare and test MEAs with nanofiber network composite membranes containing low EW PFSA.
- Continue to investigate and improve on the performance/properties of electrospun nanofiber fuel cell electrodes.
- Prepare and test a nanofiber MEA (hot-press an electrospun nanofiber anode and cathode onto a nanofiber composite membrane).

Patents

1. P.N. Pintauro and W. Zhang, "Nanofiber Fuel Cell Electrode and Method of Forming Same" U.S. provision patent, filed October 2010.

FY 2011 Publications/Presentations

1. J.B. Ballengee and P.N. Pintauro, "Morphological Control of Electrospun Nafion Nanofiber Mats". *Journal of the Electrochemical Society,* **158**, B568-B572 (2011).

2. "Fabrication of Nanofiber Composite Fuel Cell Membranes via Dual Fiber Electrospinning," Jason Ballengee and Peter N. Pintauro, Extended Abstract #733, 218th Electrochemical Society Meeting, Las Vegas, NV, October 2010.

3. "NanoCapillary Network Proton Conducting Membranes for High Temperature Hydrogen/Air Fuel Cells," Peter Pintauro and Patrick Mather, paper presented by Pintauro at USCAR, Southfield, MI, November 2010.

4. "Nanofiber-Based Membranes for PEM Fuel Cells," Invited Talk, XII International Symposium on Polymer Electrolytes, Padua, Italy, September 2010.

5. "New Membrane Morphologies for Improved Fuel Cell Operation," Chemical Engineering Department Seminar given by Peter Pintauro at University of Tennessee, October 2010.

6. "New Membrane Morphologies for Improved Fuel Cell Operation," Chemical Engineering Department Seminar given by Peter Pintauro at University of Connecticut, November 2010.

7. "New Membrane Morphologies for Improved Fuel Cell Operation," Department Seminar given by Peter Pintauro at Vanderbilt University, Department of Chemistry, November 2010.

References

1. Thampan, T., Malhotra, S., Tang, H., and Datta, R., *J. Electrochem. Soc.* **147**(9), 3242 (2000).

2. Choi, J., Lee, K.M., Wycisk, R., Pintauro, P.N., and Mather, P.T., "Composite Nanofiber Network Membranes for PEM Fuel Cells," in Proton Exchange Membrane Fuel Cells 8, *Electrochem. Soc. Trans.*, **16(2)** 1433 (2008).

3. Choi, J., Lee, K.M., Wycisk, R., Pintauro, P.N., and Mather, P.T., *J. Mater. Chem.* (2010) DOI: 10.1039/C0JM00441C.

V.C.6 Novel Approaches to Immobilized Heteropoly Acid (HPA) Systems for High Temperature, Low Relative Humidity Polymer-Type Membranes

Andrew M. Herring (Primary Contact),
James L. Horan, Mei-Chen Kuo, and Jeri D. Jessop
Colorado School of Mines (CSM)
Department of Chemical Engineering and
Department of Chemistry and Geochemistry
Golden, CO 80401
Phone: (303) 384-2082
E-mail: aherring@mines.edu

DOE Managers
HQ: Kathi Epping Martin
Phone: (202) 586-5673
E-mail: Kathi.Epping@ee.doe.gov
GO: Gregory Kleen
Phone: (720) 356-1672
E-mail: Greg.Kleen@go.doe.gov

Technical Advisor
John Kopaz
Phone: (630) 252-7531
E-mail: Kopasz@anl.gov

Contract Number: DE-FG36-06GO16032

Subcontractors:
Matthew H. Frey and Hui Ren
3M Corporate Research Materials Laboratory, St. Paul, MN

Project Start Date: April 1, 2007
Project End Date: September 30, 2011

Fiscal Year (FY) 2011 Objectives

- To develop a new class of proton exchange membranes using polymers based on heteropoly acid (HPA) functionalized with organic monomers (polyPOMs).
- To understand the mechanism of proton conduction in the polyPOMs and optimize it for proton conduction under low humidity, higher temperature fuel cell operating conditions.

Technical Barriers

This project addresses the following technical barriers from the Fuel Cells section of the Fuel Cell Technologies Program Multi-Year Research, Development and Demonstration Plan:

(A) Durability
(B) Cost
(C) Performance

Technical Targets

The materials have so far only been evaluated in terms of proton conductivity at various temperatures and relative humidity, Table 1.

TABLE 1. Progress towards Meeting Technical Targets for Membranes for Transportation Applications

Target Date met	80°C/100%RH April 2008	30°C/60%RH August 2008	120°C/<50%RH January 2009
H^+ conductivity	300 mS cm^{-1}	126 ms cm^{-1}	>100 ms cm^{-1}

RH – relative humidity

FY 2011 Accomplishments

- Fabricated new HPA-based polymers based on two distinct polymer chemistries which are designed to allow the fabrication of films that will be highly proton conducting, durable, cost-effective and have the required mechanical properties of the proton exchange membrane (PEM) fuel cell membrane.
- Showed that the HPA linkages in one of these systems are robust and will survive 10 hours of boiling water.
- Demonstrated that the new polymers systems are able to show proton conductivities as high as the generation I model system films studied previously.

✧ ✧ ✧ ✧ ✧

Introduction

Currently, fuel cells based on perfluorosulfonic acid (PFSA) PEMs are limited to operating conditions of ≤80°C and very high inlet RHs, because proton conduction in these materials depends strongly on the presence of water. For automotive applications it is desirable to operate the fuel cell at a temperature of ≤120°C and low RH to enable the use of existing radiator technology and to eliminate the parasitic loads and system complications associated with externally humidifying the gas streams. Displacement of internal combustion engines by PEM fuel cells would dramatically facilitate the adoption of the H_2 economy and enable a smooth transition from fossil fuels to H_2 produced solely from renewable resources. Materials suitable for use in automotive PEM fuel cells are being developed that have high proton conductivities, >0.1 S cm^{-1} at 50% RH and operating temperatures of -30 to 120°C, with low area specific resistance, <0.1 Ωcm^{-2}. We anticipate that the use of HPAs will generate membranes with oxidative stabilities higher than observed for any PFSA ionomer to date.

Of all the inorganic proton conductors that have been exploited for fuel cell applications HPAs may have the greatest potential as they not only have high proton conductivities, but they have significant synthetic versatility [1]. In previous work (DE-FC02-0CH11088) we have shown that the HPAs have very high proton conductivities at room temperature and can be operated at ambient conditions in a fuel cell using dry gases [2]. Importantly, we demonstrated that some of the protons in HPA have very impressive rates of proton diffusion at elevated temperatures, >100ºC, under dry conditions. The residual protons in these systems are immobile at elevated temperatures resulting in rather low conductivities. The two key challenges that need to be addressed in practical membranes for fuel cell use, are utilization of all protons under elevated temperature, dry conditions, and immobilization of the water-soluble HPA.

Approach

Our approach is to functionalize HPA with monomers so that they can be fabricated into polymeric materials with the use of a suitable co-monomer. We initially chose to use acrylates as the co-monomers in this project because acrylates represent a polymer system in a kit leaving the synthetic effort to be devoted to making the HPA monomers. This polymer system allowed the chemistry to be easily varied so that the effect of morphology could be studied. In addition as these are free radical polymerizations the materials were obtained easily as films from the polymerization of the cast solutions of co-monomers. We are the first research group to fabricate proton conducting free standing films of these materials, but as they have previously been synthesized as gels [3], we are able to fully disclose our research using this model system. However, the system has certain inherent disadvantages. The acrylate ester linkage is unstable to hydrolysis and the polymers contain readily oxidizable methylene groups. In addition it has been clear the polymers with ≥85 wt% of the HPA are unstable to liquid water.

The team assembled includes inorganic and polymer chemists and chemical and materials engineers from both CSM and 3M. CSM and 3M fabricate the HPA monomers, and the extensive knowledge of polymers at 3M is heavily exploited. The polymer system in this project is not restricted, but the mode of proton conduction is mediated by the HPA. In this year's work we have concentrated on making films with two new polymer chemistries so that we can address the additional criteria, such as cost, durability, and mechanical integrity that are need for a practical proton conducting polymer. We have also used nuclear magnetic resonance (NMR) to measure both the self-diffusion coefficient of water and to quantify the amount of water in the polymer. Comparing the NMR data with the proton conductivity data allows us to understand proton transport in these unique systems. We are correlating proton conductivity with morphology as observed by atomic force microscopy and small angle X-ray scattering (SAXS) to enable us to understand structure proton conductivity relationships.

Results

In the final year of this project we down-selected to two practical polymer systems, both based on perfluorinated backbones. The first is based on trifluorvinyl ether (TFVE) monomers that can be thermally polymerized. In Figure 1 we show the general synthetic route to poly TFVE materials with HPA as the protogenic group. A lacunary HPA is functionalized with TFVE moieties via a silane linkage and is then copolymerized thermally with various bi-functional TFVE co-monomers. The polymerization results in a perflourinated cyclobutane linkage between the co-monomers. As the materials are somewhat brittle we add 10-15 wt% of polyvinylidene fluoride-hexafluoropropylene (PVDF-HFP) so that thin films can be fabricated. The co-monomers consist of biphenyl or phenyl rings bridged by a silane or methylene chains.

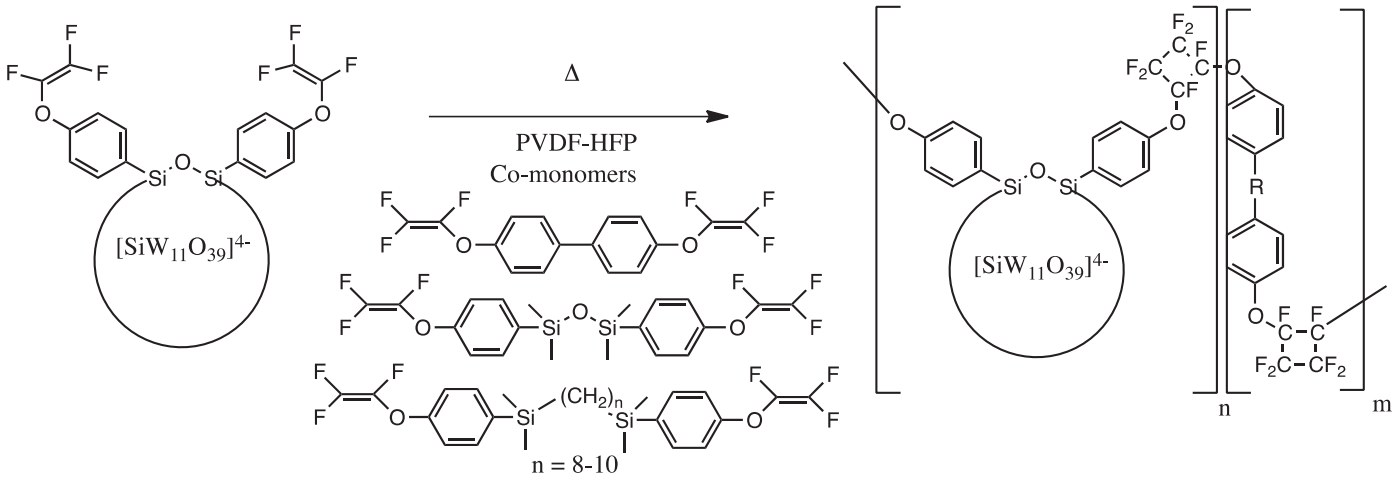


FIGURE 1. General Synthetic Route to Poly Trifluorvinyl Ether (TFVE) Materials with HPA

Pertinent data for these materials is shown in Figure 2. Obviously with four co-monomer and a range of wt% loadings of HPA monomer there is fairly large design space to probe. Our first observation, Figure 2, top left, was that the proton conductivity depended to a large extent on co-monomer chemistry. The homo-polymer, entry 1, even with a very large loading of HPA had negligible conductivity. Materials using the more ridged biphenyl co-monomer and the silicone bridged co-monomer had intermediate conductivity, entries 2 and 3, and the material with the largest conductivity had a long methylene chain incorporated into the polymer backbone. This initial screening pointed us towards further investigation of the co-monomers with methylene chain backbones. Results from this study show a non-linear dependence of proton conductivity with HPA loading, unlike the previously studied acrylate system. In the top right of Figure 2 we show the water uptake and loss during dynamic vapor sorption experiment for an HPA-TFVE polymer co-polymerized with the Si co-monomer. The material shows very little water uptake, but a phase change around 40 wt% water uptake and significant hysteresis on the second wet-up dry-down cycle. In another study involving the C10 methylene co-monomer the phase change is absent but significant water uptake is observed above 90% RH. The SAXS data for both the C10 and the Si bridged co-monomers are shown in the bottom left of Figure 2. Here we see sharp Bragg peaks in the SAXS at low RH indicating that the phase present under drier conditions is crystalline, as the material becomes wetter the Bragg peaks disappear indicating an amorphous phase. It is this amorphous phase that we believe is strongly proton conducting. Finally in the bottom right of Figure 2 we show a comparison of the wt% water uptake between the 825 equivalent weight (EW) 3M ionomer our generation I polyPOM85v acrylate material and an HPA-TFVE material. It should be noted that the water uptake of the HPA proton conductors is much smaller than for the PFSA material and is 10 times lower for the HPA-TFVR polymer than for the PFSA material.

The second polymer investigated was a functionalized Dyneon™ polymer developed at 3M. In Figure 3 we show the general synthetic route to these polymers. First the polymer is dehydrofluorinated and functionalized with bromophenyl ether. The polymer is then phosphonated and hydrolyzed so that a lacunary HPA can be attached. Note that it takes two attachment points to attach one HPA moiety. We believe that HPA only attached to one are not immobilized, and thus, future work will be directed towards double attachment points for all HPA in the film. We discovered that for these materials the method of film

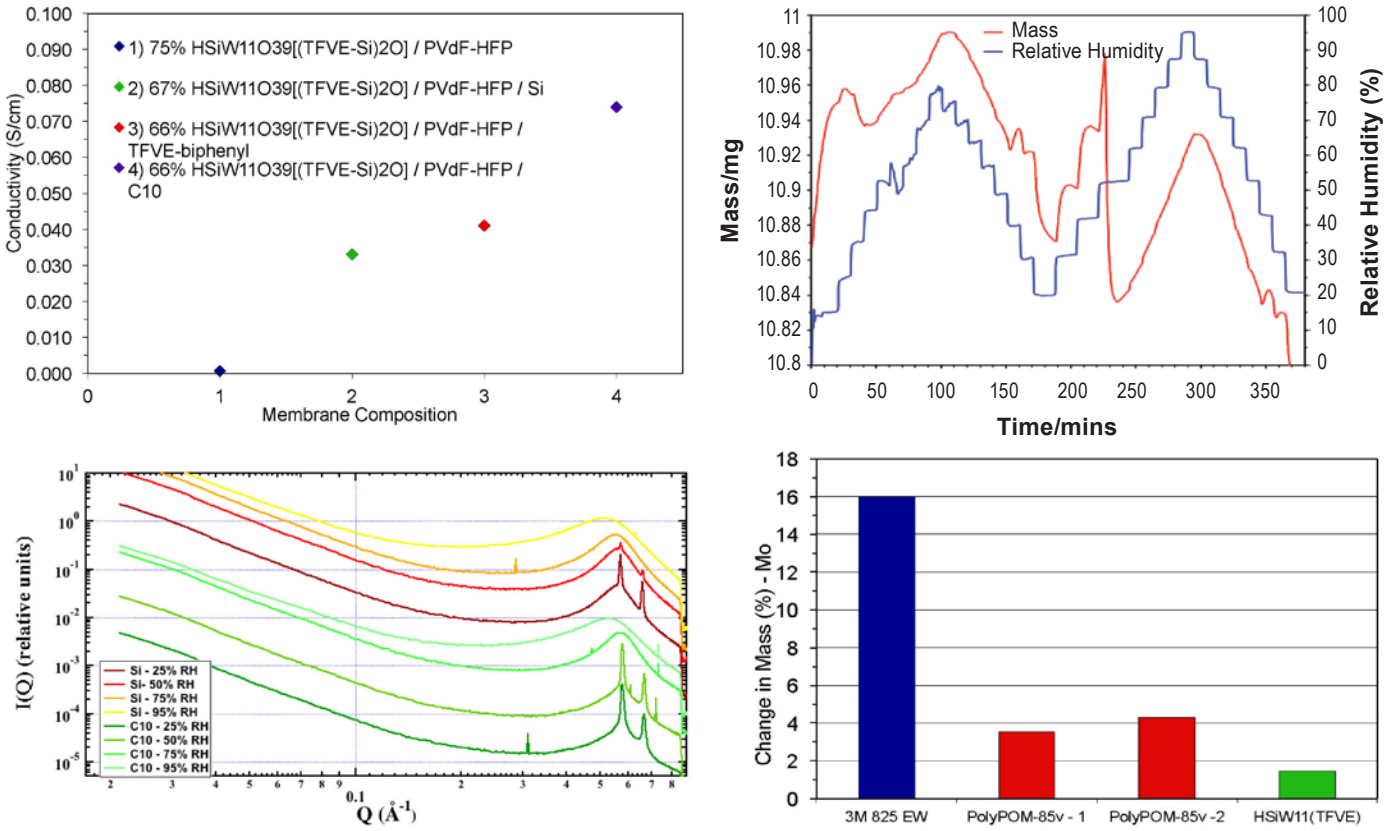


FIGURE 2. Top left, proton conductivity for TFVE polymers with differing co-monmers at 80°C and 80% RH. Top right, dynamic vapor sorption data for a TFVE polymer containing the Si co-monomer. Bottom left, SAXS data for a TFVE polymer with a C10 co-monomer and a Si co-monomer. Bottom right, comparison of wt% water uptake for the 3M 825 EW ionomer, the polyPOM85vinyl acrylate materials and a TFVE polymer with a Si co-monomer.

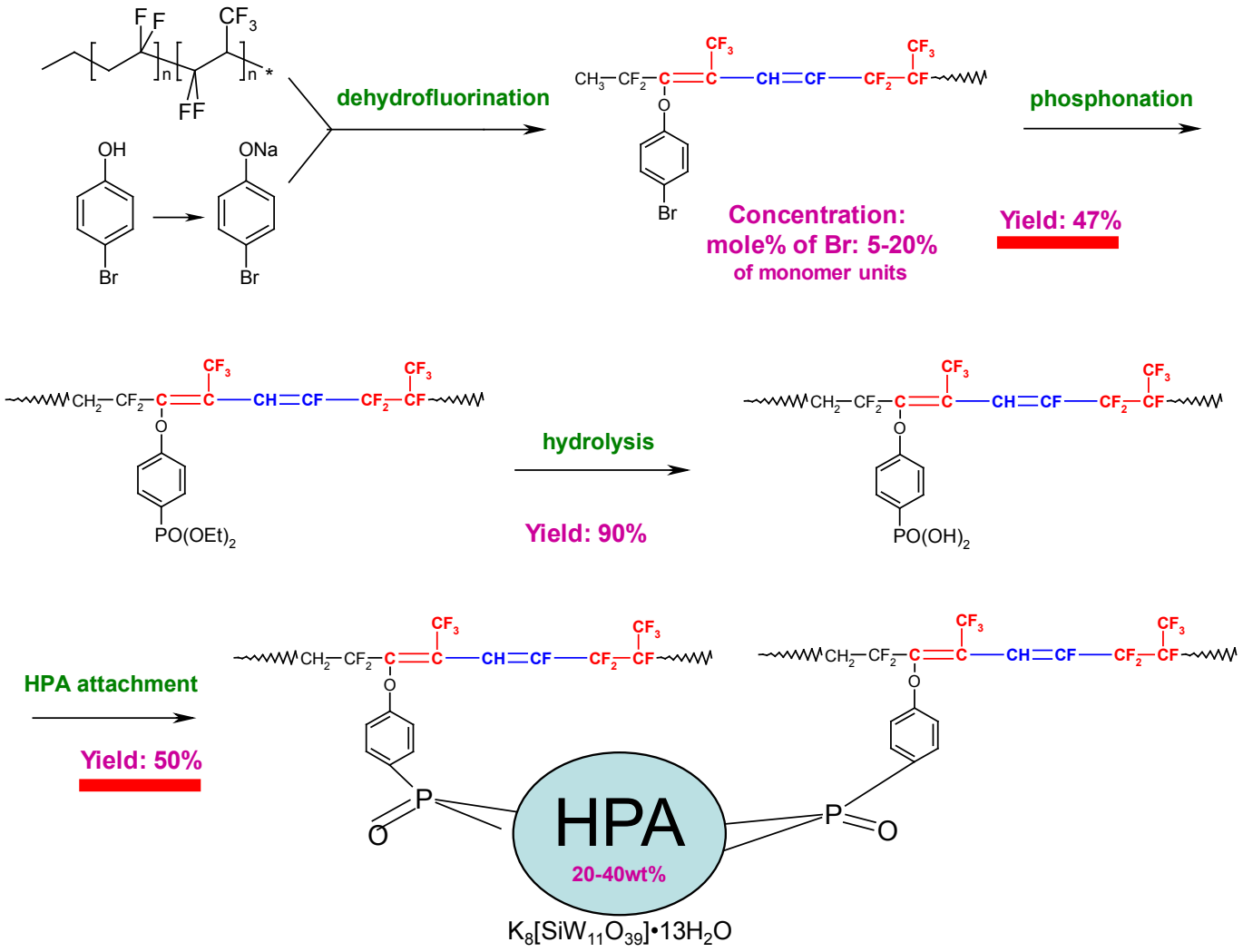


FIGURE 3. General Scheme Showing Functionalization of Dyneon™ Polymer with HPA Moieties

processing is extremely important. In Figure 4, left we show proton conductivity data comparing the HPA functionalized Dyneon™ polymer prepared with differing dissolution times on different liners with the 825EW 3M PFSA ionomer. Interestingly it was the material that was not fully dissolved when cast that gave the best proton conductivity. The material that was fully dissolved reorganized on casting to give dramatically poorer performance. We also compare the stress strain curves for the HPA functionalized Dyneon™ polymer, the 825 EW 3M PFSA ionomer, and our generation I polyPOM85v acrylate polymer. It can be seen that the Dyneon™-based film is much stronger than either the 3M ionomer or the generation I film.

Conclusions and Future Directions

- We have functionalized two different perfluorinated polymer systems with HPA that will ultimately lead to practical polymer systems for fuel cells run under hotter and drier conditions.
- The new polymers have very little water uptake and appear to be stronger than conventional ionomers.
- Although this project is ending, future work will focus on more robust HPA attachment and optimization of the films to meet all DOE targets for membranes.

FY 2011 Publications/Presentations

1. "High Temperature, Low Humidity Operation of Proton Exchange Membrane Fuel Cells" S.J. Hamrock and A.M. Herring, Encyclopedia of Sustainability Science and Technology, R.A. Myers, Ed., Springer, **2012**, in press.

2. "The use of polyoxometallates in fuel cell membranes." S. Sachdeva, J.L. Horan, J.A. Turner, and A.M. Herring,* submitted to "Fuel Cells", A.B. Bocarsley, and D.M.P. Mingos, Eds, Structure and Bonding, Springer, **2011**, *141*, in press.

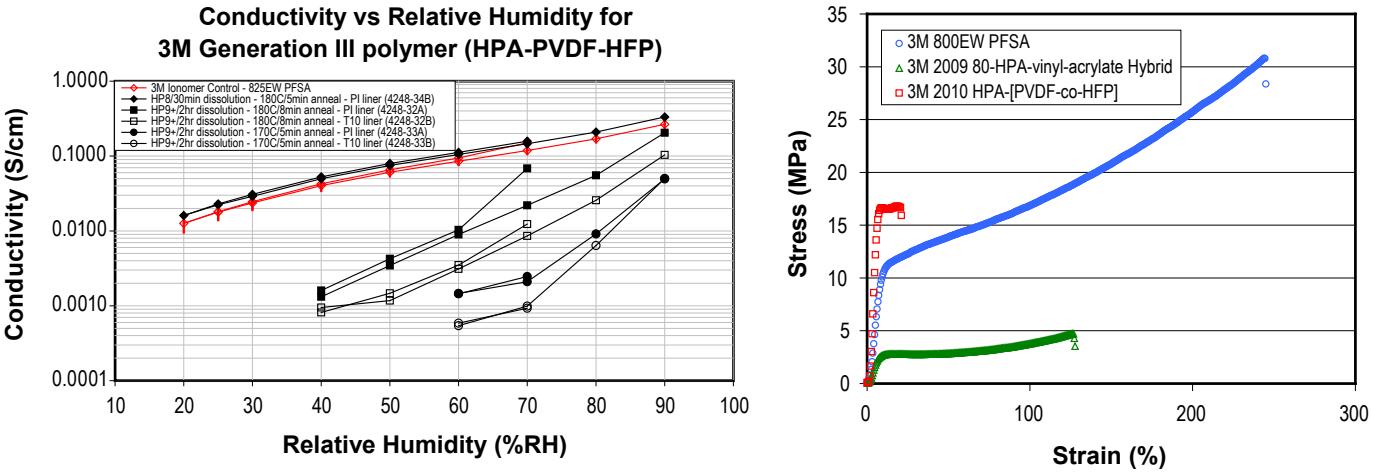


FIGURE 4. Left, conductivity data for the HPA functionalized Dyneon™ polymer and right, stress strain curves comparing the HPA Dyneon™ polymer, the 3M 825 EW PFSA ionomer and our generation I polyPOM85v acrylate polymer.

3. "Novel Hybrid Heteropoly Acid/Polymer Ionomers With Very High Proton Conductivity." J.L. Horan, Mei-Chen Kuo, A.S. Perdue, F. Zhang, Z.C. Ziegler, J.D. Jessop and A.M. Herring, submitted to "Polymer Electrolyte Fuel Cells 10." H. Gasteiger, H. Uchida, V. Ramani, A. Weber, T. Schmidt, T. Fuller, P. Strasser, P. Shirvanian, M. Inaba, M. Edmundson, F. Büchi, D. Jones, C. Lamy, R. Mantz, S. Narayan, R. Darling, T. Zawodzinski, Ed.s, *Electrochemical Society Transactions*, **2010**, *33*, 839.

4. "Understanding the high proton conductivity observed in the polypoms in terms of morphology." J.L. Horan, M.-C. Kuo, S. Sachdeva, H. Ren, A.S. Perdue, S.F. Dec, M.A. Yandrasits, S.J. Hamrock, M.H. Frey, and A.M. Herring. *Prepr. Pap.-Am. Chem. Soc., Div. Fuel Chem.*, **2010**, *51*, 728.

5. "The need for and the challenges of the perfect proton conducting polymer/composite." A.M. Herring, *Polymer Preprints* **2010,** *51*,686.

6. "Understanding the high proton conductivity observed in the polypoms in terms of morphology." J.L. Horan, M.-C. Kuo, S. Sachdeva, H. Ren, A.S. Perdue, S.F. Dec, M.A. Yandrasits, S.J. Hamrock, M.H. Frey, and A.M. Herring, oral presentation, presented at the 239th ACS Meeting, San Francisco, CA, March 2010.

7. "The use of superacidic inorganic moieties for the promotion of proton conductivity." A.M. Herring, G. Schlichting, M.-C. Kuo, J.L. Horan, M.H. Frey, H. Ren, S.J. Hamrock, oral presentation, presented 2010 Spring MRS meeting, San Francisco, CA, April 2010.

8. "Novel Approaches to Immobilized Heteropoly Acid (HPA) Systems for High Temperature, Low Relative Humidity Polymer-Type Membranes." A.M. Herring, and M.N. Frey, oral presentation, to be presented at the at the DOE EERE Fuel Cell annual merit review, Washington, DC, June 2010.

9. "Introduction to Fuel Cells and Hydrogen Energy." A.M. Herring, invited oral presentation, presented at NSF/REMRSEC summer workshop for elementary and middle school students, Golden, CO, July 2010.

10. "The need for and the challenges of the perfect proton conducting polymer/composite." A.M. Herring, invited oral presentation, to be presented at the 240th ACS Meeting, Boston, MA, August 2010.

11. "Hybrid inorganic/polymer ionomers for low RH fuel cell operation." G.J. Schlichting, J.L. Horan, M.-C. Kuo, S.F. Dec, Z.Z., F. Zhang, J. Jessop, S. Nelson, and A.M. Herring, oral presentation, presented at the 240th ACS Meeting, Boston, MA, August 2010.

12. "Novel hybrid super acid/polymer ionomers with very high proton conductivity." A.M. Herring, G.J. Schlichting, J.L. Horan, and M.C. Kuo, oral presentation, presented at ISPE-12, Padova, Italy, August 2010.

13. "Materials issues in polymer electrolyte fuel cells; research towards system compatible materials and more efficient, versatile electrocatalyts." A.M. Herring, invited oral presentation, presented at the Rocky Mountain Section of the Materials Research Society, Boulder, CO, September 2010.

14. "Novel hybrid heteropoly acid/polymer ionomers with very high proton conductivity." A.M. Herring, J.L. Horan, M.-C. Kuo, Z. Ziegler, and J. Jessop, oral presentation, presented at the 218th ECS Meeting, Las Vegas, NV, October 2010.

15. "PolyPOM membranes for hot and dry PEM fuel cell operation." A.M. Herring and M.H. Frey, oral presentation, presented to the DOE Tech team, Detroit, MI, November 2010.

References

1. Herring, A.M., *Polymer Reviews* **2006,** 46, 245 - 296.

2. Malers, J.L.; Sweikart, M.-A.; Horan, J.L.; Turner, J.A.; Herring, A.M., *Journal of Power Sources* **2007,** *172*, 83.

3. Horan, James L.; Genupur, A.; Ren, H.; Sikora, Benjamin J.; Kuo, M.-C.; Meng, F.; Dec, Steven F.; Haugen, Gregory M.; Yandrasits, Michael A.; Hamrock, Steven J.; Frey, Matthew H.; Herring, Andrew M., *ChemSusChem* **2009,** 2, 226-229.

V.C.7 High-Temperature Membrane with Humidification-Independent Cluster Structure

Ludwig Lipp (Primary Contact), Pinakin Patel, Ray Kopp
FuelCell Energy (FCE), Inc.
3 Great Pasture Road
Danbury, CT 06813
Phone: (203) 205-2492
E-mail: llipp@fce.com

DOE Managers
HQ: Donna Ho
Phone: (202) 586-8000
E-mail: Donna.Ho@ee.doe.gov
GO: Greg Kleen
Phone: (720) 356-1672
E-mail: Greg.Kleen@go.doe.gov

Technical Advisor
Thomas Benjamin
Phone: (630) 252-1632
E-mail: benjamin@anl.gov

Contract Number: 36-06GO16033

Start Date: June 1, 2006
Projected End Date: February 29, 2012

Fiscal Year (FY) 2011 Objectives

- Develop humidity-independent, thermally stable, low equivalent weight (EW) composite membranes with controlled ion-cluster morphology, to provide high proton-conductivity at up to 120°C (overall goal: meet DOE 2015 targets).
- Improve mechanical properties to significantly increase the durability and reduce the gas cross-over.
- Reduce the membrane area specific resistance (ASR) to increase cell performance and lower the capital and operating costs.

Technical Barriers

This project addresses the following technical barriers from the Fuel Cells section of the Multi-Year Research, Development and Demonstration Plan [1] of the DOE Fuel Cell Technologies Program:

(A) Durability
(B) Cost
(C) Performance

Technical Targets

This project is developing a multi-component composite (mC^2) membrane to meet the following DOE 2015 technical targets for membranes:

- Membrane Conductivity: At ≤120°C: 0.1 S/cm; at room temperature: 0.07 S/cm; at -20°C: 0.01 S/cm
- Membrane ASR: 0.02 Ωcm^2

FY 2011 Accomplishments

- Conductivity: Met DOE conductivity targets with polymer membrane and composite membrane: target of 0.1 S/cm (achieved >0.1 S/cm).
- ASR: Met DOE membrane ASR target: 0.02 Ωcm^2 (achieved 0.02 Ωcm^2).
- Cross-over: Met DOE hydrogen cross-over target: 2 mA/cm^2 (achieved 0.48 mA/cm^2).
- Polymer Development: Prepared chemically stabilized low EW co-polymer with increased molecular weight (for greater mechanical strength and durability).
- Additive Development: Synthesized zeolite with a mean particle size reduced by >60% (30 nm compared to previously 80 nm) for improved dispersion and greater uniformity of ion-conducting clusters.
- Composite Membrane Fabrication: Integrated lower-cost protonic conductivity enhancer with 80% higher density of mobile protons.
- Membrane Electrode Assembly (MEA) Fabrication:
  - Improved process conditions for lower-EW polymer in collaboration with the University of Central Florida (UCF).
  - Fabricated more than half a dozen MEAs of up to 25 cm^2 active area for characterization testing (UCF).
- MEA Testing: MEA with 5% lower EW, chemically stabilized polymer in the electrodes comprehensively tested by UCF in 11-day cell test (DOE protocol).



Introduction

This project is focused on the development of composite proton exchange membranes (PEMs) that can operate at low relative humidity (RH) and over a wide temperature range (-20 to 120°C). Their main application is in transportation fuel cells. In addition, FCE is considering use of these membranes for co-production of hydrogen from high-temperature fuel cells. The higher operating temperature

imparts improved tolerance to impurities, such as carbon monoxide, thereby increasing the co-production efficiency and simplifying the system.

The goal is to develop a structure in which ion-conducting clusters remain intact at low RH. A major challenge is that current proton conducting polymers cannot sufficiently hold on to water under these conditions. Since the conduction mechanism relies on movement of hydrated species, the conducting path is compromised, resulting in low performance. Membranes that can operate at lower RH at elevated temperatures up to 120°C will reduce the fuel cell system complexity and cost. This project is developing a composite membrane, in which both the ionic conductivity and mechanical properties are enhanced to meet DOE's 2015 goals for transportation fuel cells.

Approach

The approach to address each of the DOE target parameters is summarized in Table 1. The emphasis in the past year has been to integrate a lower-cost protonic conductivity enhancer (di-valent superacid) into the composite membrane.

TABLE 1. Approach for the Composite Membrane

Target Parameter	DOE Target (2015)	Approach
Conductivity at: ≤120°C	0.1 S/cm	Multi-component composite structure, lower EW, additives with highly mobile protons
Conductivity at: Room Temp.	0.07 S/cm	Higher number of functional groups
Conductivity at: -20°C	0.01 S/cm	Stabilized nano-additives
Inlet water vapor partial pressure	<1.5 kPa	Immobilized cluster structure
Hydrogen and oxygen cross-over at 1 atm	2 mA/cm^2	Stronger membrane structure; functionalized additives
Area specific resistance	0.02 Ωcm^2	Improved bonding capability for MEA
Cost	20 $/m^2	Simplified polymer processing
Durability with cycling	5,000 hours	Thermo-mechanically compliant bonds, higher glass transition temp.
Unassisted start from low temp.	-40°C	Stabilized cluster structure design

Results

This year's efforts were focused on improving the performance and durability of the mC^2 membrane. The efforts were centered on improving the following mC^2 components:

- Co-polymer
- Water retention additive
- Protonic conductivity enhancer

The co-polymer provides the basic building block for the membrane. It is an advanced perfluoro sulfonic acid polymer (PFSA) with a short side chain. It has a higher density of functional groups (lower EW) compared to long side chain polymers, such as Nafion®. The lower EW leads to significantly higher proton conductivity. It comes without a reduction in mechanical strength, due to a higher crystallinity of the short side chain PFSA. Grades with higher molecular weight have been synthesized. This leads to greater polymer chain entanglement and therefore better mechanical properties. The higher molecular weight has the added benefit of improving the film forming properties of the polymer dispersion.

The membrane additives are designed to retain water at the low RH conditions and to enhance the composite membrane's proton conductivity by providing an alternate proton conduction path [2]. This path is designed to efficiently transport protons at high temperature as well as subfreezing conditions. Zeolite nanoparticles have been developed to retain water in the membrane. They have a high water uptake capacity without dimensional change, since the water is contained within the three-dimensional tunnel structure. Zeolite synthesis was improved, resulting in a reduction in mean particle size from about 80 nm to about 30 nm. The desired crystalline cuboidal structure of the particles was confirmed by transmission electron microscope (TEM) analysis, as shown in Figure 1. The analysis also confirmed a particle size of predominantly 20-50 nm. The TEM analysis was kindly provided by the Microscopy Group at Oak Ridge National Laboratory. Stability of the zeolite particles was analyzed by dynamic light scattering. Figure 2 shows a mean particle size of 33 nm, measured one year after zeolite synthesis.

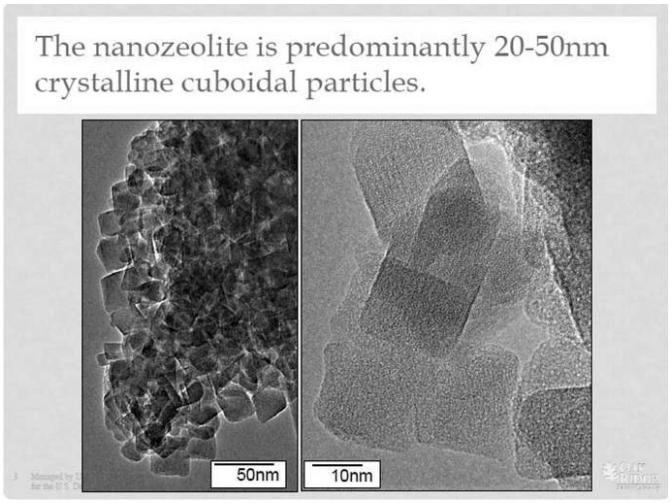


FIGURE 1. Transmission Electron Microscopy of Zeolite Particles used as Water Retention Additive in mC^2

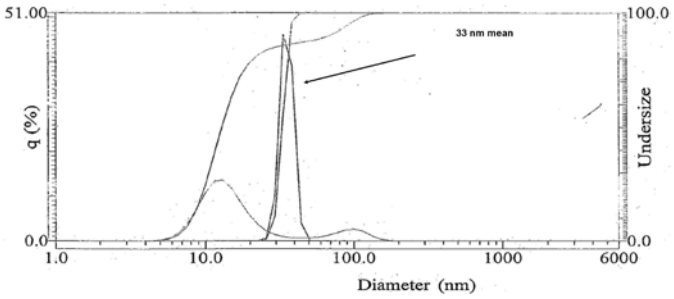


FIGURE 2. Demonstrated Long-Term (1 Year) Zeolite Particle Size Stability

To enhance the proton conductivity of the membrane, a novel superacid, developed in the previous year, was utilized in the mC^2 membrane. It has 80% greater density of highly mobile protons, to increase the transfer rate of protons through the membrane at all operating conditions.

MEA Fabrication and Testing: Membrane samples were supplied to UCF for characterization and MEA fabrication. UCF has been tasked by DOE to fabricate MEAs using membrane samples supplied by FCE, to independently validate their performance. A modified MEA fabrication process was developed, in order to ensure integrity of mC^2 membrane components. Using this process, several MEAs were fabricated by UCF, including B2, B3 and B7. Cell performance results of these MEAs at 120°C and low RH (35%) are shown in Figure 3. MEAs B2 and B3, made with short-side chain ionomer in the electrodes, had higher performance compared to a Nafion® reference MEA at practical current densities (300-1,000 mA/cm^2). As expected, B2 and B3 had significantly lower cell resistance than the Nafion®-based MEA. B7 used a different ionomer in the electrodes. Compared to B2 and B3, it has 5% lower EW and is chemically stabilized. To better understand the performance of B7, a detailed performance analysis was carried out by UCF. It uses a method developed at the University of Connecticut [3] to calculate contributions of activation, membrane, electrode

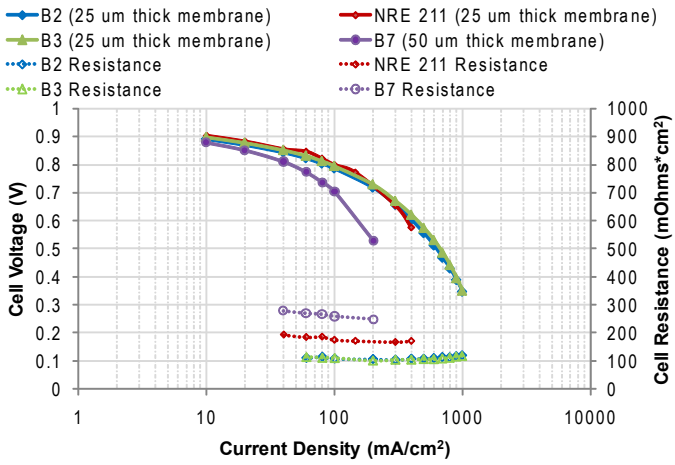


FIGURE 3. Cell Performance at 120°C: B2 and B3 have Lower Cell Resistance than NRE211

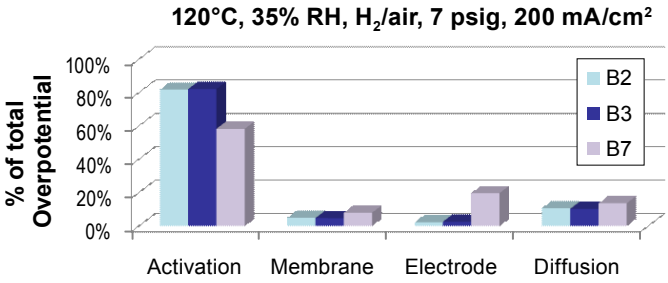


FIGURE 4. Fuel Cell Performance Analysis of Three Different MEAs

and diffusion to the cell's overpotential. Data at 120°C and 35% RH, shown in Figure 4, indicates that B7 has increased electrode and diffusion resistance. This suggests a need to optimize the electrodes when using the lower EW, chemically stabilized ionomer. A study to look at the effect of ionomer content in the electrodes is underway at UCF.

TABLE 2. MEA Test Results Compared to DOE 2015 Targets

Characteristic	Units	Target 2015	B1	B2	B3	B7	NRE 211
Area specific proton resistance[c] at:							
120°C and 70 kPa water partial pressure	Ohm cm^2	≤ 0.02	not determined	0.08	0.08	0.23	0.15
80°C and 38 kPa water partial pressure	Ohm cm^2	≤ 0.02	not determined	0.02	0.02	0.05	0.02
Maximum Hydrogen cross-over [a]	mA / cm^2	2	not determined	1	0.95	0.48	0.76
Minimum electrical resistance [b]	Ohm cm^2	1,000	not determined	1,200	800	500	2100
Performance @ 0.8V (¼ Power)	mA / cm^2 mW / cm^2	300 250	not determined not determined	104 84	177 142	150 120	113 91
Performance @ rated power	mW / cm^2	1,000	not determined	334	567	482	363

* Values are at 80°C unless otherwise noted
[a] Measure in humidified H_2/N_2 at 25°C
[b] Measure in humidified H_2/N_2 using linear sweep voltammetry curve from 0.4 to 0.6 V at 80°C
[c] Determined by subtracting contact resistances from cell current interrupt values

All three MEAs tested by UCF (B2, B3, B7) passed comprehensive 11-day tests at UCF (per DOE-approved protocol). B7, which utilized chemically stabilized polymer, had the lowest hydrogen cross-over at the end of the test with 0.5 mA/cm^2. This is well below the DOE 2015 target of 2 mA/cm^2. UCF post-test analysis showed good integrity of the MEA; no pinholes were detected.

A comparison of the performance of the MEAs to the DOE 2015 targets is shown in Table 2. The parameters that already meet the DOE 2015 targets are highlighted in green. The remaining parameters show good progress towards the DOE targets (highlighted in yellow).

Conclusions and Future Direction

A mC^2 membrane design for high temperature and low RH operation has been implemented to fabricate membranes with enhanced performance at the DOE target conditions (Table 1). Accomplishments include:

- Synthesized water retaining additive (zeolite) with 60% lower particle size (Figure 1).
- Validated long-term particle size stability (Figure 2).
- Demonstrated significantly lower cell resistance of MEAs made with the advanced materials (Figure 3) meeting the DOE ASR target at 80°C (Table 2).
- Met the DOE hydrogen cross-over and electrical resistance targets (Table 2).
- Identified a need for electrode optimization using the improved ionomer (Figure 4).

In the remaining months of the current project we will continue the composite membrane development, with an emphasis on meeting the remaining DOE target parameters (highlighted in yellow in Table 2).

FY 2011 Publications/Presentations

1. L. Lipp, "High Temperature Membrane With Humidification-Independent Cluster Structure", 2011 DOE Hydrogen Program and Vehicle Technologies Program Annual Merit Review and Peer Evaluation Meeting, Washington, D.C., May 9–13, 2011.

References

1. DOE Multi-Year Research, Development and Demonstration Plan, Section 3.4 "Fuel Cells", http://www1.eere.energy.gov/hydrogenandfuelcells/mypp/pdfs/fuel_cells.pdf.

2. L. Lipp, "High Temperature Membrane With Humidification-Independent Cluster Structure", 2008 DOE Hydrogen Program Merit Review and Peer Evaluation Meeting, Arlington, VA, June 11, 2008.

3. M.V. Williams, H.R. Kunz, J.M. Fenton, J. Electrochem. Soc., Vol. 152 (3) A635-A644 (2005).

V.C.8 Corrugated Membrane Fuel Cell Structures

Stephen Grot
Ion Power Incorporated
720 Governor Lea Rd.
New Castle, DE 19720-5501
Phone: (302) 832-9550
E-Mail: s.grot@ion-power.com

DOE Managers
HQ: Donna Ho
Phone: (202) 586-8000
E-mail: Donna.Ho@ee.doe.gov
GO: Reginald Tyler
Phone: (720) 356-1805
E-Mail: Reginald.Tyler@go.doe.gov

Contract Number: DE-EE0000462

Subcontractors:
- Graftech International Holdings Inc., Parma, OH
- General Motors Corporation, Flint, MI

Project Start Date: September 1, 2010
Project End Date: August 31, 2013

Fiscal Year (FY) 2011 Objectives

To pack more membrane active area into a given geometric plate area. Thereby allowing both targets of power density and platinum utilization to be achieved:

- To demonstrate a fuel cell single cell (50 cm^2) with a 2-fold increase in the membrane active area over the geometric area of the cell by corrugating the membrane electrode assembly (MEA) structure.
- Incorporation of an ultra-low Pt-loaded corrugated MEA structure in a 50 cm^2 single cell that achieves the DOE 2015 target of 0.2 gram Pt/kW, while simultaneously reaching the targets of power density:
  - 1 W/cm^2 at full power
  - 0.25 W/cm^2 at ¼ power

Technical Barriers

This project addresses the following technical barriers from the Fuel Cells section of the Fuel Cell Technologies Program Multi-Year Research, Development and Demonstration Plan:

(B) Cost (lower cost metal gas diffusion layer [GDL], lower plate/GDL manufacturing costs)

(C) Performance (high power density with low Pt-loaded MEAs)

TABLE 1. Progress Toward Meeting DOE Fuel Cell Technical Targets

Comparison of Fuel Cells with Different GDLs			
Fuel Cell Data			
Build Date	**3/24/2011**	**4/8/2011**	**4/11/2011**
Build Number	**1720XL100-1No16**	**1720XL100-1No18**	**1732XL100-1No20**
CCM[1] Lot #	**1720**	**1720**	**1732**
Membrane Type	**XL 100**	**XL 100**	**XL 100**
Manufacturer	**Ion Power**	**Ion Power**	**Ion Power**
Membrane + Catalyst Thickness	**2.5 mil (both side catalyst layer)**	**2.8 mil (both side catalyst layer)**	**2.6 mil (both side catalyst layer)**
GDL Anode Side	10BC 1 layer	2x Pt-coated Ti fine screen 1x Pt-coated Ti coarse screen[2]	6 layers Pt-coated Ti fine screen (with 5 welding points)
GDL Cathode Side	10BC 1 layer	2x Pt-coated Ti fine screen 1x Pt-coated Ti coarse screen[2]	10BC 1 layer
Comments of the GDL Packs		The coarse screen is between the fine screen (with 5 welding points)	
Compression Torque Applied to the Fixation Screws	12 inch pounds	11 inch pounds	11 inch pounds

[1]CCM – catalyst-coated membrane
[2]GDL screen packs: The coarse screen is between the fine screen (with 5 welding points)

FY 2011 Accomplishments

Corrugated GDL structure formed with expanded Ti metal screen. Fine 2 mil screen for good diffusion and contact, with course 10 mil thick screen for strength. (See Figures 1 and 2, respectively.)



Introduction

The traditional proton exchange membrane (PEM) fuel cell stack with its bipolar plates, MEAs, seals and end-plates has been the dominant method of construction of multi-kW fuel cells for the past 40 years. Smaller sub-watt and portable applications have explored novel cell design variations such as “jelly roll” concepts but none have been able to achieve the power density of the traditional stacked plate design.

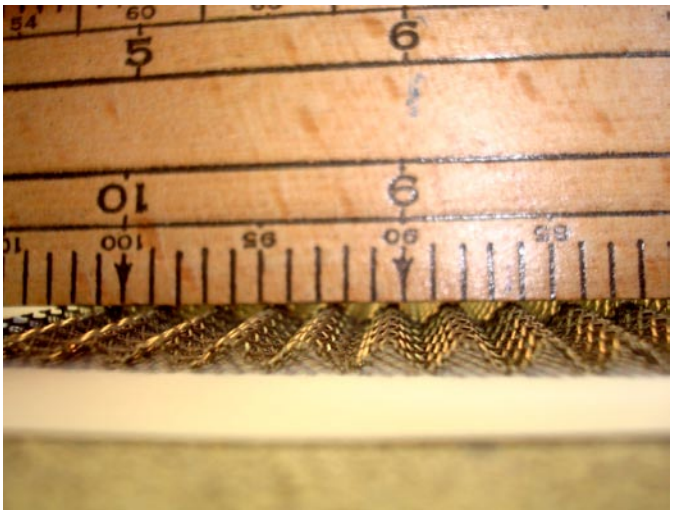


FIGURE 1. Titanium Screen as a Gas Diffusion Layer



FIGURE 2. Corrugated Gas Diffusion Layer Structure

The primary reason for this is the efficient collection of the current and the compact packing of the MEAs.

Approach

At the present time one of the most challenging aspects of traditional PEM fuel cell stacks is the difficulty to achieve the platinum catalyst utilization target of 0.2 g Pt/kWe set forth by DOE [1,2]. Good catalyst utilization can be achieved with state-of-the-art CCMs when ultra-low catalyst loadings (<0.1 mg/cm^2) are used at lower current. Unfortunately when ultra-low loadings are used, the peak power density is lower as compared to conventional loadings [3]. Thus, a larger total active area and a larger bipolar plate are needed, which results in a lower overall stack power density. Therefore, this project aims to realize both the Pt utilization targets as well as the power density targets of the DOE by corrugating the fuel cell membrane electrode structure and thus packing more membrane area into the same geometric plate footprint.

A single cell 50 cm^2 fuel cell test jig (or fixture) will be designed and fabricated such that it will allow testing of both conventional flat MEAs with conventional flow fields and the corrugated single-cell assemblies fabricated. Furthermore, the jig will also allow the hand assembly of each of the individual components. Inserts will be created to generate straight through flow and serpentine flow in both flat and corrugated MEA architectures so that water, thermal and gas flow management issues can be diagnosed.

Results

Results to date show that expanded titanium metal screens can be formed into corrugated structures and incorporated into an operating fuel cell. Electrical resistance of the diffusion material was measured and found to be reduced as a result of the new diffusion material. However, mass transport and water management issues were negatively impacting the results of the tests. These issues are mainly being attributed to gas flow by-passing the corrugated channels, and the large pore size of the GDLs being used. We plan to address these issues by developing more conventional GDLs in the corrugated format that contain the commonly used carbon black/poly-tetrafluoroethylene micro-diffusion layers up against the membrane to form a very fine pore structure interface to the membrane. This is the structure of the current state-of-the-art GDLs that have the proper water-managment and mass-transport requirements for high performance MEAs.

Conclusions and Future Directions

In summary, success has been made in expanded metal screen structures both in cell performance and in structures.

Future work will include: get single cell test fixture working; get corrugated Ti expanded screen GDL attached to Ti plate; demonstrate low contact resistance and good mass transport in flat Ti screen structures; and get mechanical strength modeling effort underway.

FY 2011 Publications/Presentations

1. AMR Presentation May 11, 2011.

References

1. DOE Manufacturing Workshop Web site: www.eere.energy.gov/hydrogenandfuelcells/wkshp_h2_manufacturing.html

2. HFCIT Program “Multi-Year Research, Development and Demonstration Plan”, U.S. DOE Office of Energy Efficiency and Renewable Energy, February 2005. Please see: www.eere.energy.gov/hydrogenandfuelcells/mypp/

3. M.F. Mathias, et al “Two Fuel Cell Cars in Every Garage?” The ECS Interface Fall 2005, pg 24.

V.C.9 Lead Research and Development Activity for DOE's High Temperature, Low Relative Humidity Membrane Program

James Fenton (Primary Contact), Darlene Slattery
Florida Solar Energy Center (FSEC)
1679 Clearlake Road
Cocoa, FL 32927
Phone: (321) 638-1002
E-mail: jfenton@fsec.ucf.edu

DOE Managers
HQ: Kathi Epping Martin
Phone: (202) 586-7425
E-mail: Kathi.Epping@ee.doe.gov
GO: Greg Kleen
Phone: (720) 356-1672
E-mail: Greg.Kleen@go.doe.gov

Technical Advisor
John Kopasz
Phone: (630) 252-7531
E-mail: kopasz@anl.gov

Contract Number: DE-FC36-06GO16028

Subcontractors:
- BekkTech LLC, Loveland, CO
- Scribner Associates, Inc., Southern Pines, NC

Project Start Date: April 1, 2006
Project End Date: September 30, 2011

Fiscal Year (FY) 2011 Objectives

- Fabricate membrane electrode assemblies (MEAs) from team membranes.
- Test team MEAs for fuel cell performance.
- Standardize methodologies for in-plane and through-plane membrane conductivity measurements.
- Provide High Temperature Membrane Working Group (HTMWG) members with standardized tests and methodologies.
- Organize HTMWG bi-annual meetings.

Technical Barriers

This project addresses the following technical barriers from the Fuel Cells section (3.4) of the Fuel Cell Technologies Program Multi-Year Research, Development and Demonstration Plan:

(A) Durability

(C) Performance

Technical Targets

FSEC plays a supporting role to the five teams who are tasked with developing an improved high temperature, low relative humidity membrane for proton exchange membrane fuel cells (PEMFCs). FSEC has developed standardized experimental methodologies to: (1) measure conductivity (in-plane and through-plane); (2) characterize mechanical, mass transport and surface properties of the membranes as working membrane electrode assemblies; and (3) predict durability of the membranes and their membrane electrode assemblies.

This project manufactures, tests and evaluates MEAs for performance and stability. Test results were evaluated against DOEs 2015 membrane targets as shown in Table 1 (A, B and D identify the teams and the numbers are those assigned by FSEC to identify a specific sample).

TABLE 1. Team Membranes Compared to Targets*

Characteristic	Units	Target	D7	B4	A4	NRE211
		2015				
Area specific proton resistance at:						
120°C, water partial pressures from 40 to 80 kPa	Ohm cm^2	≤0.02	0.05	0.08	0.14	0.18
80°C and water partial pressures from 25-45 kPa	Ohm cm^2	≤0.02	0.02	0.02	0.01	0.05
Maximum hydrogen cross-over [a]	mA/cm^2	2	1.9	2.7	0.70	0.76
Minimum electrical resistance [b]	Ohm cm^2	1,000	31	270	813	2100
Performance @ 0.8 V (¼ Power)	mA/cm^2 mW/cm^2	300 250	34 27	255 204	81 65	151 120
Performance @ rated power	mW/cm^2	1,000	108	817	260	480

*Values are at 80°C unless otherwise noted
[a] Measured in humidified H_2/N_2 at 25°C
[b] Measured in humidified H_2/N_2 using linear sweep voltammetry curve from 0.4 to 0.6 V at 80°C

FY 2011 Accomplishments

- Performed conductivity testing on baseline membranes from Giner, Inc. and FuelCell Energy (FCE), and prepared and tested MEAs from these membranes.
- Assisted Case Western Reserve with membrane casting and cross-linking.
- Prepared and tested MEAs from Case Western Reserve University membranes.

- Developed and verified a new method for determining location of crossover in MEAs.
- Established procedures for preparing transmission electron microscopy (TEM) samples and examined samples via TEM.
- Performed stress-strain experiments on several team member samples.
- Completed a study to determine the effect of cell pressure on performance.
- Performed durability test for sample from Giner.
- Collaborated with FCE to optimize ionomer loading in catalyst ink.
- Completed milestone "Define correlation between membrane/MEA degradation rate from accelerated testing and lifetime."



Introduction

Generally, two regimes of PEMFC operation exist: the typical operating temperatures between 60–80°C, and elevated temperatures higher than 100°C. At higher temperatures, heat is more easily rejected from the cell stack, anode catalyst poisoning by CO is less important, water transport is simplified, the kinetics of fuel oxidation will be improved, and gas transport and the efficiency of the cell will be enhanced. However, operation of PEMFCs at high temperature and ambient pressure results in decreased relative humidity, which significantly increases membrane resistance, thus decreasing cell performance. This has driven the need for development of high-temperature membranes and membrane electrode assemblies that could operate at temperatures of up to 120ºC, low relative humidity (RH) and near atmospheric pressure.

The objective of this phase of the project has been to fabricate and test MEAs from fuel cell membrane materials that meet the goals outlined by the DOE in the multi-year plan. Specific goals are: operation at elevated temperatures (up to 120°C), with a demonstrated area specific resistance of <0.02 Ohm cm^2 at 120ºC and 40 kPa inlet water vapor partial pressure to the fuel cell stack (85% RH measured at 80°C).

Approach

The High Temperature, Low Relative Humidity Membrane program includes five teams, each of which is skilled in producing novel membranes expected to meet the goals of the program. Some of these teams are not necessarily skilled in the ability to produce an MEA, or to test the MEAs in a fuel cell. FSEC's objective is to provide the expertise to fabricate MEAs, and assemble cells to test the membranes under fuel cell conditions. FSEC has worked closely with the membrane manufacturers to develop appropriate methods for manufacture of the MEA and to test the MEAs according to a process data base that has been developed at FSEC. This approach involves a detailed logic flow chart that itemizes each step of the manufacture, fuel cell testing and post test analysis of the MEA. Each membrane manufacturer approves the steps of the logic flow chart in advance of the process. Furthermore, FSEC iterates with the teams to optimize the results.

Results

The program began five years ago with 11 teams initially funded to develop high conductivity membranes. After the Go/No-Go decision point, six teams were selected to continue and an additional one was discontinued this year. Over the course of the program, conductivity, stability and performance improved. Many membranes have shown promise. The collaboration between FSEC and the teams guided catalyst-coated membrane (CCM) development, and the program is proving to be an excellent model for future DOE membrane and MEA development projects.

Significant progress toward achieving DOE targets was made over the last five years as shown in Tables 2, 3, and 4 for three of the teams.

TABLE 2. Case Western Membranes Compared to DOE Targets*

Characteristic	Units	Target 2015	D6	D7	D9	NRE211
Membrane thickness	μm		200	63	122	25
Area specific proton resistance at:						
120°C and 70 kPa water partial pressure	Ohm cm^2	≤0.02	N/D	0.05	0.097	0.15
80°C and 38 kPa water partial pressure	Ohm cm^2	≤0.02	0.055	0.02	0.018	0.02
Maximum hydrogen cross-over [a]	mA/cm^2	2	10.8	1.9	136	0.76
Minimum electrical resistance [b]	Ohm cm^2	1,000	8.4	31	14	2100
Performance @ 0.8 V (¼ power)	mA/cm^2 mW/cm^2	300 250	N/D N/D	34 27	N/D N/D	151 120
Performance @ rated power	mW/cm^2	1,000	N/D	108	N/D	480

*Values are at 80°C unless otherwise noted
[a]Measured in humidified H_2/N_2 at 25°C
[b]Measured in humidified H_2/N_2 using linear sweep voltammetry curve from 0.4 to 0.6 V at 80°C
N/D - not determined

In addition to the results for the samples from the teams shown in the tables, samples were received from Colorado School of Mines (CSM) and from Vanderbilt University. Difficulties were encountered with the CSM membranes because stickiness resulting from the Florida humidity made them hard to handle. No successful MEAs were fabricated. Two Vanderbilt membranes were received and MEAs constructed and tested. Data was not analyzed in time for this report.

TABLE 3. Fuel Cell Energy Membranes Compared to DOE Targets*

Characteristic	Units	Target	B2	B3	B4	B5	B7[c]	NRE 211
		2015						
Membrane thickness	μm		29	26	31	36	53	25
Area specific proton resistance at:								
120°C and 70 kPa water partial pressure	Ohm cm^2	≤0.02	0.08	0.08	0.08	0.08	0.23	0.15
80°C and 38 kPa water partial pressure	Ohm cm^2	≤0.02	0.02	0.02	0.02	0.02	0.05	0.02
Maximum Hydrogen cross-over [a]	mA/cm^2	2	1	0.95	2.7	1.8	0.48	0.76
Minimum electrical resistance [b]	Ohm cm^2	1000	1200	800	270	1336	500	2100
Performance @ 0.8 V (¼ Power)	mA/cm^2 mW/cm^2	300 250	104 84	177 142	255 204	209 167	150 120	113 91
Performance @ rated power	mW/cm^2	1000	334	567	817	668	482	363

*Values are at 80°C unless otherwise noted
[a]Measured in humidified H_2/N_2 at 25°C
[b]Measured in humidified H_2/N_2 using linear sweep voltammetry curve from 0.4 to 0.6 V at 80°C
[c]Membrane thickness double that of others in series

TABLE 4. Giner Membranes Compared to DOE Targets*

Characteristic	Units	Target	A1	A2	A3	A4	NRE211
		2015					
Membrane thickness	μm		22	40	28	27	25
Area specific proton resistance at:							
120°C and 70 kPa water partial pressure	Ohm cm^2	≤0.02	0.26	0.24	0.32	0.14	0.15
80°C and 38 kPa water partial pressure	Ohm cm^2	≤0.02	0.05	0.03	0.04	0.01	0.02
Maximum hydrogen cross-over [a]	mA/cm^2	2	0.75	1.6	0.61	0.70	0.76
Minimum electrical resistance [b]	Ohm cm^2	1,000	65	358	1073	813	2100
Performance @ 0.8 V (¼ Power)	mA/cm^2 mW/cm^2	300 250	94 75	222 177	112 89	81 65	151 120
Performance @ rated power	mW/cm^2	1,000	300	708	356	260	480

*Values are at 80°C unless otherwise noted
[a]Measured in humidified H_2/N_2 at 25°C
[b]Measured in humidified H_2/N_2 using linear sweep voltammetry curve from 0.4 to 0.6 V at 80°C

Conclusions and Future Directions

- Eleven teams were initially funded to develop high conductivity membranes.
- Six teams were selected to continue after Go/No-Go, five continuing this year.
- Conductivity, stability and performance improved over course of program.
- Many membranes have shown promise and should be pursued.
- Collaboration between FSEC and teams guided CCM development.
- This project is an excellent model for future DOE membrane development projects.
- Significant progress was made toward developing membrane suitable for fuel cell use.
- In the future, FSEC will continue to work closely with team members, preparing and testing MEAs in fuel cell hardware.
- Additional support will be provided to FCE for electrode optimization.
- FSEC will continue to work closely with Case Western Reserve University to reduce cross-over.
- FSEC is preparing procedures for testing cross-over and electrical resistance that follow DOE guidelines.

FY 2011 Publications/Presentations

1. Brooker, Paul; Bonville, Leonard; Kunz, Harold R.; Slattery, Darlene; Fenton, James. "Effect of Measurement Technique on PEMFC Performance" Presented at the 220th ECS Meeting, Montreal, QC, Canada, May 2011, abstract 199.

2. Rodgers, M.P.; Bonville, L.J.; Kunz, H.R.; Slattery, D.K.; Fenton, J.F., "Defining the Correlation Between Membrane/MEA Degradation Rate from Accelerated Testing and Lifetime", Publication proposal submitted to Chemical Reviews, April, 2011.

V.D.1 Advanced Cathode Catalysts and Supports for PEM Fuel Cells

Mark K. Debe (Primary Contact),
Andrew J. Steinbach, Susan M. Hendricks,
Michael J. Kurkowski, George D. Vernstrom,
Amy E. Hester, Mathew Pejsa, Peter Turner,
Andrew Haug, Paul Kadera, Radoslav T. Atanasoski
Fuel Cell Components Program, 3M Company
3M Center, Building 201-2N-19
St. Paul, MN 55144-1000
Phone: (651) 736-9563
E-mail: mkdebe1@mmm.com

DOE Managers
HQ: Kathi Epping Martin
Phone: (202) 586-7425
E-mail: Kathi.Epping@ee.doe.gov
GO: David Peterson
Phone: (720) 356-1747
E-mail: David.Peterson@go.doe.gov

Technical Advisor
Thomas Benjamin
Phone: (630) 252-1632
E-mail: Benjamin@anl.gov

Contract Number: DE-FG36-07GO17007

Subcontractors and Federally Funded Research and Development Centers:
- Jeff Dahn, David Stevens, Dalhousie University, Halifax, Nova Scotia, Canada
- V. Stamenkovic, Dennis van der Vliet, Nenad Markovic, Argonne National Laboratory (ANL), Argonne, IL
- Charles Hays, Jet Propulsion Laboratory (JPL), Pasadena, CA

Project Start Date: April 1, 2007
Projected End Date: December 31, 2011

Fiscal Year (FY) 2011 Objectives

The objectives of this project are development of a durable, low cost (both precious group metal [PGM] content and manufacturability), high performance cathode electrode (catalyst and support), which is fully integrated into a proton exchange membrane (PEM) electrode assembly (MEA) characterized by:

- total Pt group metal loading per MEA of $\leq$0.25 mg/cm^2,
- short-stack specific power density of $\leq$0.3 g/kW at rated power,
- durability sufficient to operate at >80°C for 2,000 hours, $\leq$80°C for 5,000 hours, with cycling for transportation applications,
- high prospects for 40,000 hours durability under operating conditions for stationary applications, and
- high volume manufacturability.

Technical Barriers

This project addresses the following technical barriers from the Fuel Cells section of the Fuel Cell Technologies Program Multi-Year Research, Development and Demonstration Plan:

(A) Durability
(B) Cost
(C) Performance
(D) Water Transport within the Stack

Technical Targets

This project is focused on improving the performance and durability of the 3M nanostructured thin film (NSTF) roll-good fabricated electrocatalysts and MEAs. Table 1 compares the NSTF current 2nd quarter, calendar year (CY) 2011 status with DOE electrocatalyst targets for 2010/2015 updated from Table 3.4.12 of the DOE Fuel Cell Technologies Program Multi-Year Research, Development and Demonstration Plan to reflect recent accelerated durability test results. The MEAs used for the inverse specific power density values listed in the first row, PGM total content, had PtCoMn catalysts with loadings of 0.05/0.10 mg_{PGM}/cm^2 on the anode and cathode, respectively deposited by 3M's standard P4 process. The short stack results were obtained outside the project but evaluated catalysts and gas diffusion layers (GDLs) developed within the project. The updated accelerated stress test results were obtained with PtCoMn catalysts containing 0.05 mg_{Pt}/cm^2 on the anode and 0.15 mg_{PGM}/cm^2 on the cathode deposited by the new P1 process discussed in the following.

FY 2011 Accomplishments

Water Management for Cool/Wet Operation (Task 5.2)

- Developed key strategy for reducing cathode flooding at cool temperatures by taking product water out the anode, the "water-out-anode" mode.
  - Demonstrated that anode GDL was most critical component for water-out-anode strategy. Significantly improved cool/wet performance at ambient pressure.
  - Developed cathode gradient catalyst hybrid construction that also dramatically helps water management at low temperature as well as high temperature.

TABLE 1. Progress towards Meeting Technical Targets for Electrocatalysts and MEAs for Transportation Applications. Values in blue are new DOE targets this year.

Characteristic	Units	Targets 2015	**Status:** Values for roll-good CCM w/ 0.15mg$_{Pt}$/cm^2 per MEA or as stated
PGM Total Content	g$_{Pt}$/kW$_e$ rated in stack	0.125	**< 0.18 g$_{Pt}$/kW for cell V < 0.67 V** in 50 cm^2 cell at 150kPa inlet. **0.19 g$_{Pt}$/kW, 400 cm^2 GM short stack**
PGM Total Loading	**mg PGM / cm^2 total**	0.125	**0.15 – 0.20, A+C with current PtCoMn alloy**
Mass Activity (150 kPa H_2/O_2 80°C. 100% RH, 1050 sec)	**A/mg-Pt @ 900 mV, 150kPa O_2**	**0.44**	**0.24 A/mg in 50 cm^2 w/ PtCoMn > 0.43 A/mg in 50 cm^2 with SET Pt_3Ni_7**
Specific Activity (150 kPa H_2/O_2 at 80°C, 100% RH)	**μ A/cm^2-Pt @ 900 mV**	**720**	**2,100 for PtCoMn, 0.1 mg$_{Pt}$/cm^2 2,500 for new Pt_3Ni_7, 0.1 mg$_{Pt}$/cm^2**
Durability: 30,000 cycles 0.6 -1.0 V, 50mV/sec,80/80/80°C, 100 kPa,H_2/N_2	**- mV at 0.8 A/cm^2 - % ECSA loss - % Mass activity**	**<30mV <40% <40%**	**- 40 mV loss at 1.5 A/cm^2 - 18% loss ECSA - 48 % loss mass activity**
Durability: 1.2 V for 400 hrs. at 80°C, H_2/N_2, 150 kPa, 100% RH	**- mV at 1.5 A/cm^2 % ECSA loss % Mass activity**	**<30mV <40% <40%**	**- 10 mV loss at 1.5 A/cm^2 -10% loss ECSA -10 % loss mass activity**
Durability: OCV hold for 500 hrs. 250/200 kPa H_2/air, 90°C, 30% RH	**H_2 X-over mA/cm^2 % OCV loss**	**<20 <20%**	**13 ± 4 mA/cm^2 at 500 hrs (5 MEAs) -12 ± 5 % OCV loss in 500 hrs**
Durability under Load Cycling (membrane lifetime test)	**Hours, T ≤ 80°C Hours, T > 80°C**	**5,000 5,000**	**9000 hrs, 3M PEM (20μm, 850 EW w/ stabilizers), 50 cm^2, 80/64/64°C 2000 hrs (OEM short stack,0.1/0.15)**

RH – relative humidity; ECSA – electrochemical surface area ; OEM - original equipment manufacturer; EW - equivalent weight; CCM - catalyst coated membrane; GM - General Motors; OCV - open circuit voltage

New Catalyst Activity and Understanding; Annealing and Process Scale-Up (Task 1.3)

- Extended enhanced catalyst deposition process improvement (P1) from pure Pt to PtCoMn and obtained same dramatic gains in Pt(hkl) grain size and surface smoothing with simpler, more cost-effective coating process.
- Scaled up Surface Energy Treatment (SET) process for roll-to-roll catalyst annealing. Significantly improves oxygen reduction reaction (ORR) activity of some alloys, more than others.
- Demonstrated Pt_3Ni_7 alloy catalyst mass activities in 50 cm^2 cells ranging from 0.35 ± 0.06 A/mg to 0.59 ± 0.08 A/mg at 3M and GM depending on lab, protocol and loading measurement. Gain in ORR activity derived from SET catalyst annealing process.
- Validated Pt_3Ni_7 alloy peak composition in compositional spread rotating disk electrode (RDE) measurements on NSTF whiskers (Dalhousie).
- Obtained first confirmation of Pt_3Ni_7 composition at nm scale of whiskerettes and Pt enrichment of whiskerette tips (JPL).

Catalyst and MEA Durability with Preliminary 2010 "Best of Class MEAs" (Task 2)

- OCV Hold: Demonstrated 12 ± 5% OCV voltage loss after 1,400 hours at 250/200 kPa H_2/air, 90°C, 30%RH, and met cross-over targets.
- 1.2 V hold: Demonstrated 10 mV loss at 1.5 A/cm^2, 10% loss of ECSA and 10% loss of mass activity after 400 hr at 1.2 V at 80°C, 150 kPa, 100% RH.
- 30,000 Cyclic Voltammatry (CV) cycles: Demonstrated 40 mV loss at 1.5 A/cm^2, 18% loss of ECSA, and 48% loss of mass activity under 30,000, 0.6-1.0-0.6 V cycles at 50 mV/sec and 80/80/80°C.
- Demonstrated load cycling lifetimes of 9,000 hours with 2009 "Best of Class" catalyst loadings (0.05/0.10 mg/cm^2) in non-supported 3M PEM with chemical stabilizers.

Membrane-Electrode Integration and CCM Scale Up (Task 5.1)

- Produced 50,000 linear ft combined of NSTF substrate, coated catalyst supports, and CCM for process development, qualification and customer use.

2010 "Best of Class" MEA Down-Selection for Final Stack Testing (Task 5.3)

- Defined and implemented major screening programs for down-selection and integration of all MEA components for 2010 best of class MEA for final stack testing.
- Final short stack testing activities initiated at GM.



Introduction

State-of-the-art PEM fuel cell electrocatalyst technology utilized in today's prototype fuel cell vehicles reveals limitations with respect to general durability and robustness under start-stop cycling, adequate performance with low PGM loadings, and low cost manufacturability. To a large degree, these deficiencies are traceable to properties of the conventional carbon supported dispersed Pt catalysts in use today. The research and development of this contract are focused on overcoming these three most critical barriers for fuel cell MEA automotive deployment by using an alternative catalyst support and deposition method.

Approach

The approach to achieve the above objectives builds on a 14-year DOE/3M funded development of the 3M NSTF catalyst and MEA technology. The NSTF catalyst fundamentally has higher specific activity for oxygen reduction [1-8], removes all durability issues with carbon supports, demonstrates much lower losses due to Pt dissolution and membrane chemical attack [9-12], and has significant high volume all-dry roll-good manufacturing advantages [13].

The scope of work in the previous three-year 1st budget period included extensive work at 3M to increase the NSTF catalyst support film surface area, fabrication and screening of new alloys in 50 cm^2 single cells, and evaluation of multiple deposition parameters to obtain increased catalyst surface area and utilization. Complementary to this work at 3M, collaborative work included high throughput fabrication and characterization of new multi-element Pt alloys (ternaries and quaternaries) with Dalhousie University, fundamental catalyst characterization studies with ANL, and development and evaluation of a pseudo-RDE catalyst evaluation technique with JPL. Research during the fourth year has focused at 3M on: a) continued water management improvements for cool/wet operation via optimization of materials, electrode structure and operating conditions; b) catalyst fabrication process improvements for increased catalyst performance and production efficiency; c) in-depth MEA component screening to down-select final configurations for the final short-stack testing; d) continued accelerated testing to benchmark the NSTF-MEA durability with each generation of MEA components; and e) fabrication of roll-good materials for stack testing by the GM fuel cell laboratory.

Results

The technical accomplishments for the fourth year fall roughly into five areas of research and development corresponding to Project Tasks 1, 2, 5.1, 5.2 and 5.3. We briefly summarize the main results from each of these areas.

Task 1

The NSTF–$Pt_{68}Co_{29}Mn_3$ catalyst has been the workhorse cathode and anode of choice for a number of years. With it we have been able to exceed the previous DOE 2015 target of 0.2 g-Pt/kW in a full size short stack with 0.05 mg/cm^2 of PGM on the anode and 0.1 mg/cm^2 on the cathode [14]. More recent work has focused on improving the NSTF-PtCoMn roll-to-roll process so that the support whiskers and sputter deposited catalyst alloy can be applied simultaneously on the moving substrate web in a single step. This new process, called P1, offers greater simplicity and more cost-effective coating than the standard process called P4. The key is to make sure it does not reduce performance and hopefully improves it. An example of its effectiveness is shown in a series of PtCoMn loadings deposited by the P1 process at 0.054, 0.103, 0.146 and 0.184 mg_{Pt}/cm^2. They were coated in the production equipment and evaluated for structural differences by X-ray diffraction (XRD), scanning electron microscopy (SEM)/transmission electron microscopy (TEM) and fuel cell performance. SEM indicated no substantial differences at 40,000 magnification, but the TEM and XRD results showed significant changes. Figure 1(a) (left) shows that whereas the face-centered cubic (fcc) Pt[hkl] grain sizes by the standard process P4 are essentially independent of loading and 4 to 6 nm in size, the P1process produces grain sizes that increase with loading and are larger, 6 to 12 nm. Consistent with this are the TEM images, Figure 1(a) (right), that show the catalyst coatings on the whiskers are smoother than those obtained by the P4 process, which produces highly oriented whiskerettes growing off the sides of the underlying whisker core, as discussed at length in reference [15]. This can be understood since aspects of the P1 process provide annealing like conditions.

Fuel cell performance of the P1 deposited PtCoMn is also generally the same as with the P4 process, as shown in Figure 1(b). With the conditions shown in the inset of Figure 1(b), in the same 50 cm^2 cell with quad-serpentine flow fields, using the same station and production lots of PEMs and GDLs, the P1 processed anodes and cathodes (0.1 to 0.184 loadings) show very similar performance to each other and to P4 processed 0.10 mg_{Pt}/cm^2 PtCoMn cathode. The galvanodynamic scans with the 0.054 mg/cm^2 cathodes are substantially lower (black open and closed squares) but at least as good if not better than historical results with P4 cathodes at these loadings. More careful inspection of the curves in Figure 1(b), show the P1 process yields about a 10 mV improvement at 0.32 A/cm^2 and 5 mV at 1 A/cm^2 over the P4 process, but very similar performance

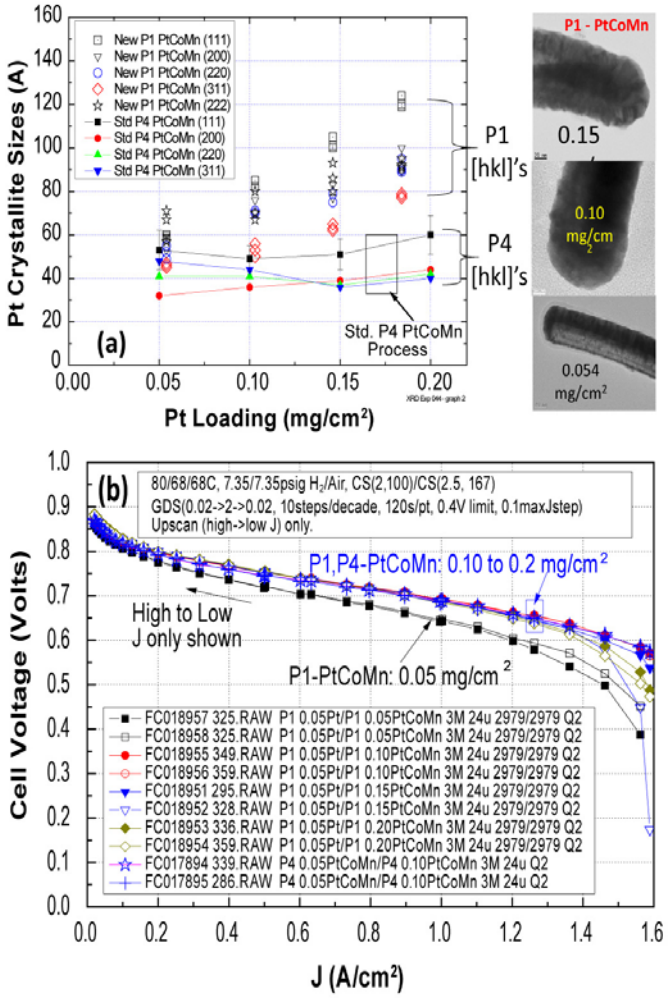


FIGURE 1. (a) Left: PtCoMn fcc[hkl] grain sizes by XRD as a function of Pt loading for catalysts sputter coated by new process P1 versus the standard process P4. Right: TEM images of the PtCoMn coated whiskers using new deposition process P1. At all three loadings the catalyst coating is smoother than by the standard P4 process that produces whiskerettes as discussed in reference [15]. (b) Polarization curves for PtCoMn deposited by the P1 process at ca. 0.05, 0.10, 0.15 and 0.20 mg_{Pt}/cm^2, and the P4 process at 0.10 mg_{Pt}/cm^2, under 80°C cell temperature, 68°C dew points and 150 kPa H_2/air. 3M-24 μm, 850 EW PEM. 3M standard GDLs, all 50 cm^2. Actual Pt loadings of the cathodes are 0.054, 0.103, 0.146 and 0.184 mg_{Pt}/cm^2.

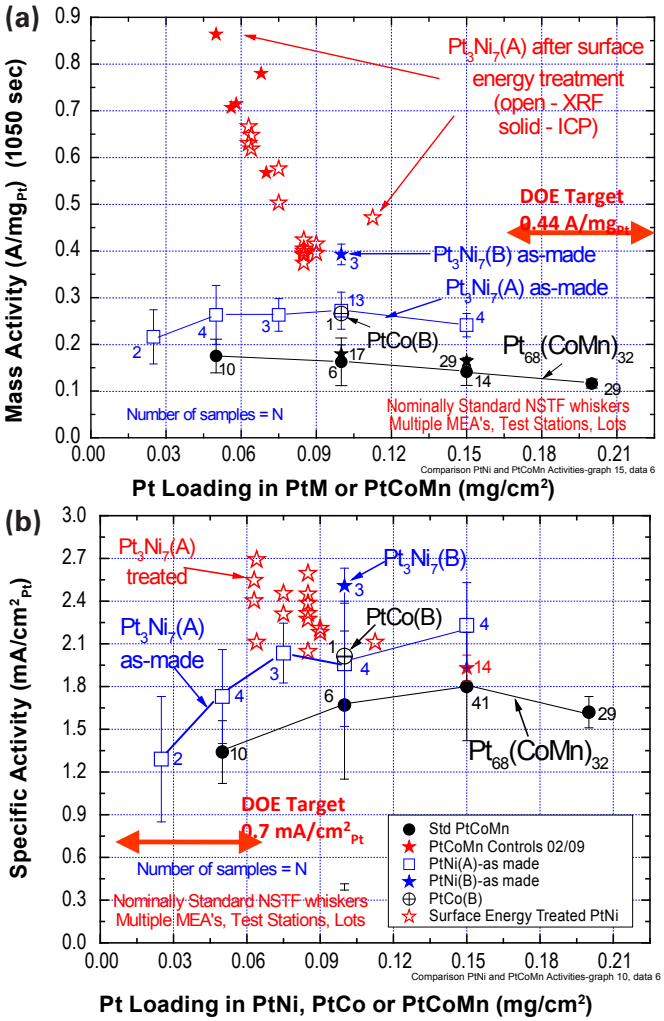


FIGURE 2. Summary of NSTF alloy ORR mass (a) and specific activity (b) as a function of Pt loading, comparing PtCoMn and Pt_3Ni_7 as-made and after surface energy treatment. Pt_3Ni_7 (A) was roll-good production fabricated at 3M. Pt_3Ni_7 (B) was lab coated at Dalhousie University with extremely thin alternating layers compared to (A).

at very low (0.025 A/cm^2) and high (1.5 A/cm^2) currents. Measurements of the absolute and specific activities at 900 mV under 150 kPa H_2/O_2 are very similar for both processes, although the P1 cathodes have slightly higher surface area than the P4 deposited materials. In conclusion, there are slight performance benefits and no penalties for the simpler, faster P1 process for depositing the NSTF alloys.

The recently revised 2015 DOE target of 0.125 g-Pt/kW (down from 0.2 g-Pt/kW for 2015) with a total of 0.125 mg/cm^2 of PGM per cm^2 of MEA will require further work and probably a new NSTF alloy material. This will likely be based on a Pt_xNi_y alloy, such as the unique NSTF- Pt_3Ni_7 introduced in last year's annual report on this project and discussed in detail in reference (16). Figure 2 summarizes the ORR mass (a) and specific activities (b) measured in 50 cm^2 MEAs for both the PtCoMn and as-made PtNi systems. The open squares show the improvement of the as-made Pt_3Ni_7 alloy over the $Pt_{68}Co_{29}Mn_3$ alloy. Much higher activities are possible, however, by post-processing the as-made Pt_3Ni_7 using another process improvement we have been implementing. This process we refer to as a SET process that effectively anneals the as-made NSTF catalyst layers prior to their incorporation into a CCM. This past year it was further scaled up to allow roll-to-roll treatment.

The SET process improves the activities of both the PtCoMn and the PtNi systems, but the latter benefits much

more. SET treated production fabricated Pt_3Ni_7 (type A) cathodes are shown by the stars in Figure 2 and show there is a dramatic improvement of the measured activities over the open squares. The examples in Figure 2 were batch processed and it was necessary to re-measure the loading of the catalysts after the SET treatment in order to get accurate mass activities, as there was some loss of catalyst from the 0.1 mg/cm^2 as-made loadings. This measurement was done by both X-ray fluorescence (XRF) and inductively coupled plasma (ICP) as indicated by the solid and open stars in Figure 2. These values now indicate the promise for significantly exceeding the nominal 2015 DOE electrocatalyst target for mass activity at 900 mV of 0.44 A/mg. To further validate the SET treated Pt_3Ni_7 activities, a multi-sample set of 50 cm^2 MEAs were produced and measured at both 3M and GM using slightly different ORR activity protocols inherent to each lab. The mass loadings were also measured independently by both labs. Table 2 summarizes the results which range from 0.35 to 0.59 A/mg depending on the protocols used and confirm that the activity values are very near the DOE targets.

TABLE 2. Mass activities of surface energy treated Pt_3Ni_7 NSTF alloys measured at 3M and GM using independently measured loadings and ORR activity protocols. 50 cm^2 MEAs. Lab refers to the place of measurement. ORR protocol refers to the source of the protocol.

Loading Measurement Method	Lab/ORR Protocol	Mass Activity (A/mg-Pt) at 900 mV
3M XRF/ICP	3M/3M	0.59 ± 0.08
3M XRF/ICP	GM/3M	0.51 ± 0.06
3M XRF/ICP	GM/GM	0.43 ± 0.06
GM ICP	GM/3M	0.42 ± 0.08
GM ICP	GM/GM	0.35 ± 0.06

Fuel cell performance under H_2/air in the kinetic region with the Pt_3Ni_7 alloy mirrors the gain in mass activity. However a major issue with the current constructs is that the dealloying of the excess Ni into the membrane severely attenuates the high current density performance above about 0.8 A/cm^2, as shown in reference [14]. Proper ex situ dealloying methods are being investigated but ultimately, the structure and composition of the catalyst surface as it actually ends up in the working electrode is what we must make initially to mitigate any complex processing requirements.

Task 2

Any new electrocatalyst alloy must have the requisite durability and stability, so we continuously test our new MEA component compositions and process improvements against the DOE recommended accelerated stress tests. Below are summarized the results of three DOE defined accelerated stress tests (AST) for support, catalyst and MEA durability.

1.2 V Hold: In this test the MEA cathodes are held at 1.2 V vs. the reference hydrogen electrode (RHE) for nominally 400 hours under 150 kPa H_2/N_2 at 80°C. It effectively measures the stability of the catalyst support particle against corrosion. The DOE targets are that ORR activity and surface area will each drop ≤40%, and the performance at 1.5 A/cm^2 will drop less than 30 mV from initial levels. Figure 3(a) shows the series of polarization curves (DOE conditions) measured periodically over a total of 435 hours at 1.2 V, for an MEA having the P1 processed PtCoMn on the anode (0.05 mg/cm^2) and cathode (0.15 mg/cm^2). The MEA used a 3M made 3M-supported membrane with a chemical additive. It is apparent that the test had only a small effect on performance. Surface area loss was 10%, specific activity was unchanged, and the

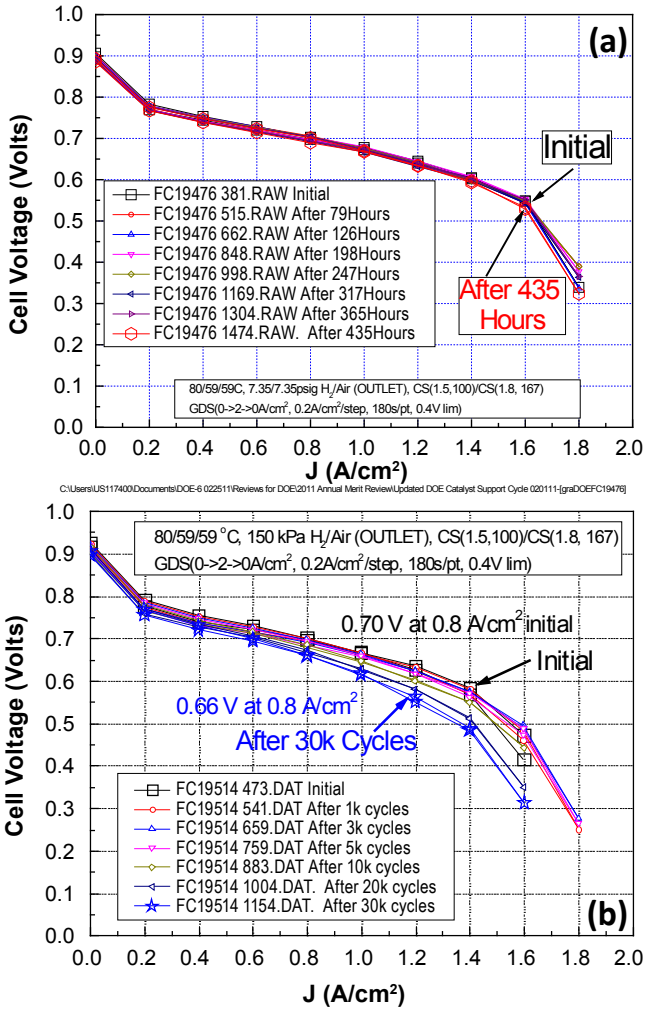


FIGURE 3. (a) Polarization curves versus time during the DOE 1.2 V hold durability test protocol. (b) Polarization curves versus time during the DOE CV cycling durability test protocol, 0.6 - 1.0 - 0.6 V, 50 mV/sec under 100/100 kPa H_2/N_2. Anode /cathode catalysts were all PtCoMn made by the P1 process at 0.05/0.15 mg_{Pt}/cm^2 loadings; 3M-supported PEM with additive; standard 3M GDLs.

performance at 1.5 A/cm^2 dropped only 10 mV, so all targets were met and repeated with a second MEA.

OCV Hold: The objective of this test is assessment of the whole MEA/membrane durability at OCV at 90°C under 30% RH, 250/200 kPa H_2/air. The target is 500 hours with less than 20% loss of OCV. Using similar or the same MEA construction as in the 1.2 V hold test, six MEAs met the 500 hour limit and cross-over targets before stopping the tests. Two MEAs were allowed to go further and have exceeded 1400 hours with ~12% loss of OCV and acceptable H_2 cross-over.

CV Cycling: This AST characterizes the resistance of the catalyst to dissolution, agglomeration or loss of activity due to high voltage cycling. The protocol involves cycling the cathode between 0.6 and 1.0 volts and back again at 50 mV/sec under 100/100 kPa H_2/N_2 at 80°C cell and dew points. The target is to have after 30,000 cycles, less than 40% loss of surface area and ORR activity and a polarization curve loss of less than 30 mV at 0.8 A/cm^2. This test was applied to the same MEA type as used for the previous two ASTs. The surface area loss of 18% met and exceeded the DOE target. The mass activity loss was 48% and therefore did not meet the target of ≤40%. Figure 3(b) shows the polarization curves before and after 30,000 cycles. The loss of cell voltage at 0.8 A/cm^2 was 40 mV, and therefore also did not meet the ≤30 mV loss target. Further results are given in reference [14], but improvements in stability under this test are required.

Task 5

Task 5 embodies all work done under catalyst/membrane integration and scale up, GDL integration and water management, and MEA component down-selection for final stack testing.

Water Management: MEAs utilizing the ultra-thin (<1 μm) 3M NSTFC technology have several demonstrated advantages compared to MEAs comprising conventional, relatively thick (~10 μm) carbon-supported catalyst, as noted in the introduction. However, the low temperature (0-50°C) steady state limiting current density of typical NSTFC MEAs with standard GDLs under usual operating conditions is substantially lower than that of many conventional catalyst MEAs (0.3 v. 1.6 A/cm^2 at 30°C, air cathode). This reduced low temperature performance can be attributed to the NSTFC's much higher water generation rate per unit catalyst volume and to a hydrophilic electrode pore structure that is more susceptible to water condensation. Recent studies have been conducted to better understand water management differences between NSTF and Pt/C electrode MEAs. In one study, the product water effluent rate out the cathode was evaluated at several conditions where NSTF MEAs typically show reduced performance due to flooding. By calculating the fraction of water exiting the cathode in the liquid phase and plotting against the performance loss from 80°C reference performance, reasonably quantitative agreement is observed for both NSTF and Pt/C electrode MEAs. A primary conclusion from this study is that liquid phase product water removal out the cathode is detrimental to performance for both electrode types, but, at a given set of conditions, the total water effluent rate out the cathode is less for Pt/C electrodes than NSTF electrodes. It also stresses that taking water out the anode rather than the cathode is a most desirable strategy if possible.

In light of these results, a logical path forward was based upon the premise of minimizing liquid product water removal out the cathode GDL, which is accomplished by maximizing liquid product water removal out the anode GDL. One such method found to be effective towards this premise is decreasing the total anode pressure to enable both enhanced liquid and vapor phase product water removal out the anode GDL. This concept was introduced in last year's annual report. Decreasing the anode pressure from 200 to 25 kPa resulted in nearly a three-fold gain in the current density at 30°C cell temperature, while the limiting current density increased from 0.4 to over 2 A/cm^2 as the anode pressure was reduced from 150 to 50 kPa at 30°C.

A less system dependent and probably more practical method for improving the low temperature performance of NSTF MEAs is through materials development. This year we have focused on screening the anode GDL backing and microporous layer (MPL) properties. Several different vendor supplied anode GDL backings were evaluated to determine their impact on low temperature response. Figure 4(a) shows results from four tests where the anode GDL backing was varied; all GDLs contained similar hydrophobic treatments and MPLs applied by 3M. Under Test I, the MEAs with GDLs MRC A and Freudenberg A yielded similar performance whereas the MEA with MRC C had lower performance at high current density, due to higher high-frequency resistance (HFR). Under Test II, a pseudo-system startup transient, Freudenberg A GDL provided a short burst of higher performance than MRC A, but the current density dropped to the MRC A level within ~15 s. MRC C, which had lower performance than the other GDLs under Test I, yielded transient current densities which were 50% higher than Freud A and a steady-state current density approximately 3x that of the other two GDLs. Under Test III, MEAs with either MRC A or Freudenberg A GDL had similarly low performances at 30°C. As the cell was heated, the performance with both GDLs improved, with Freudenberg A having better performance at 40°C than MRC A. MRC C, which performed well under Test II, also performed well at low temperatures under Test III. As the cell temperature exceeded 50°C, all three MEAs performed similarly. Under Test IV, MEAs with either Freudenberg A or MRC C performed similarly as the current density was stepped up from 0.02 to 1 A/cm^2 when the cell temperature was 70°C, but at 60°C, Freud A was unable to provide a positive cell voltage at 1 A/cm^2 whereas MRC C only showed a slight loss relative to 70°C. These results show anode GDL properties are the most promising and effective component variable we have identified for solving low temperature

cathode flooding with ultra-thin electrodes. Exactly which properties of the GDL are most critical for this function are still unclear and something we are trying to determine.

We have also explored gradient cathode electrode options that can also provide some benefit, using hybrid combinations of NSTF and thin Pt/C dispersed layers as discussed in last year's annual report. The ratio of benefits to added Pt loading and processing costs are not nearly as favorable as with just anode GDL optimization, and the benefit of selecting the correct anode GDL properties appears larger. This is illustrated in Figure 4(b) which is a larger summary of several GDL responses to the pseudo-system startup transient Test II discussed above, including anode GDLs comprising the MRC C (GDL C in 4(b)) with and without MPLs, the Freudenerg A type and 3M standard GDLs. Also shown in Figure 4(b) is the impact of the gradient or hybrid CCB used on the cathode with either a standard GDL on the anode or Freudenberg A or MRC C on the anode. The top three responses curves in 4(b) are obtained with the MRC C on the anode with or without an MPL and a standard cathode GDL. This combination would seem to be the best solution to the low temperature performance issue with ultra-thin electrodes, but there is still a high temperature issue with the MRC C type due to the HFR that remains to be solved as noted in Figure 4(a) test I.

MEA component down-selection: A primary focus of this project for most of the year has been the screening process for down-selecting the final MEA component sets for the final stack testing. Much of the GDL development work, P1 vs P4 catalyst deposition and SET process work discussed above were all directed at this objective. The MEA component sets investigated in this process included these bulleted items:

- Cathode catalyst: composition, loading, deposition process, post process
- Anode catalyst: composition and deposition process (finalized)
- PEM: thickness, supported vs un-supported, chemical additive levels, etc.
- Anode GDL: Backing layer type, MPL properties
- Cathode GDL: Backing layer type and MPL properties, interfacial coatings

The down-selection process itself involved evaluation of hundreds of MEAs in duplicate covering two dozen or more specific component/process parameter experiments. The results are too extensive to discuss here but more information and some examples can be found in reference [14]. The end result is that for the first short stack test we defined six MEA component configurations with three different membrane options, and three cathode catalyst options. Different GDLs were used for the anodes and cathodes, but only one type of each. The anode catalyst was fixed at NSTF-0.05 mgPt/cm^2 of the P1 processed PtCoMn. These six MEA types were fabricated as roll-goods and used to

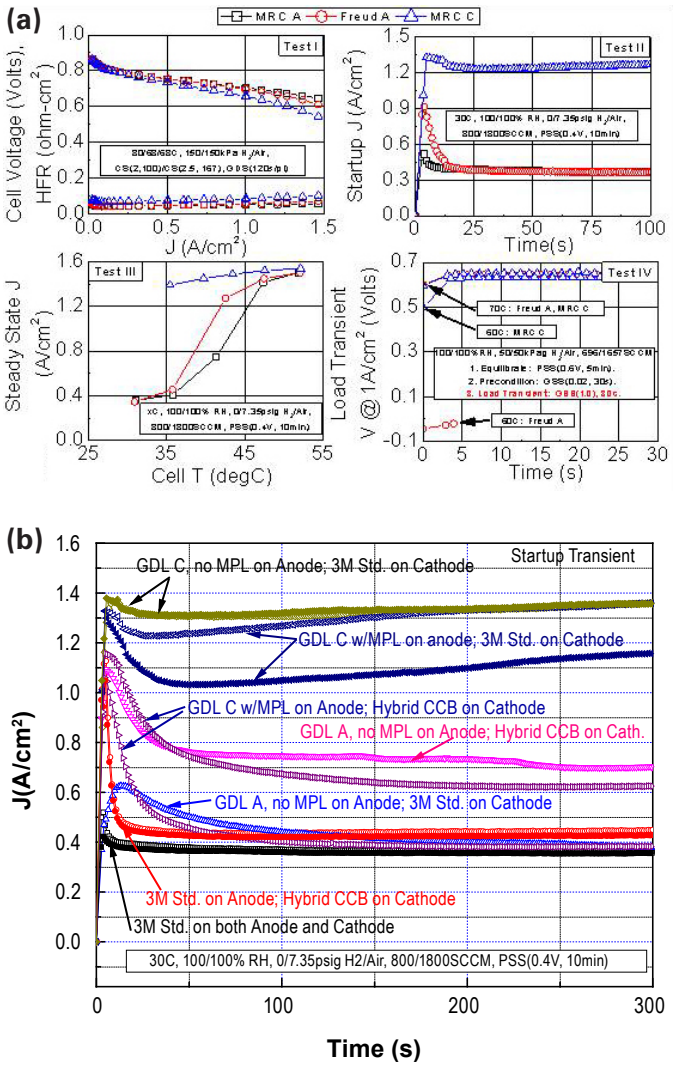


FIGURE 4. (a) Comparison of the 50 cm^2 cell response to four different test protocols sensitive to water management: Test I is steady-state high temperature performance; Test II is a pseudo-system startup transient at 30°C; Test III is steady-state current density at 0.4 V versus temperature; Test IV is a load transient current density step up from 0.02 to 1 A/cm^2 at 60 or 70°C. (b) Comparison of the 50 cm^2 cell response to a start-up transient (OCV to 0.4 V) at 30°C and 100% RH for different anode and cathode GDL combinations. H_2/air pressures are 100/150 kPa. GDL type C performance with or without an MPL is far superior in transient and steady-state operation to the 3M standard GDL.

populate a 29 cell "Rainbow" stack (i.e., term used by stack manufacturers to refer to different MEA configurations used in the stack metaphorically similar to the different colors seen in a rainbow), one "color" for each MEA type, for initial beginning of life operation under various automotive relevant test protocols for beginning of life testing to enable further down-selection for a second stack that will be used for longer durability studies. At the time of this report preparation the first stack is still under test.

Conclusions and Future Directions

Last year we were able to claim that this project had met or exceeded the then currently specified DOE electrocatalyst and MEA performance and durability targets for 2015 using the same MEA component set in 50 cm^2 cell tests. Recent tightening of the DOE 2015 targets for performance (gPt/kW) and durability has reintroduced new challenges that we must demonstrate. Significant improvements in ORR activity with NSTF-PtNi alloys and improved processing methods were demonstrated and further improvements should be possible but may not be reached by the end of this project. Continued advances this past year were made in understanding and improving low temperature water management behavior associated with the ultra-thin NSTF electrodes, particularly by identifying the importance of the anode GDL backing properties. Significant effort focused on screening and down-selecting all MEA component materials and process options for integration into an advanced robust, durable, high performance, roll-good manufactured MEA containing no more than 0.2 mg/cm^2 of PGM total for the final stack testing-deliverable. At this time, the stack testing has been initiated in a rainbow short stack, and performance criteria are being evaluated and compared to past short stacks and single cell results for six different MEA configurations. Specific future work will include:

- Selecting the final one or two MEA configurations for long-term testing in a second stack.
- Fabricating final MEAs sufficient for final stack(s).
- Delivering MEA media for stack integration and executing the testing plan.
- Continuing effort on one or two key issues related to anode GDLs for water management and understanding long term irreversible voltage decay.
- Exploring ex situ dealloying optimization of Pt_3Ni_7 system to achieve high current density (A/cm^2).

FY 2011 Publications/Presentations

1. D.A. Stevens, S. Wang, R.J. Sanderson, G.C. K. Liu, G.D. Vernstrom, R.T. Atanasoski, M.K. Debe and J.R. Dahn, "A combined rotating disk electrode/X-ray diffraction study of Co dissolution from $Pt_{1-x}Co_x$ Alloys," *J. Electrochem. Soc.* **158**(8) B899-B904 (2011).

2. Gary Chih-Kang, D.A. Stevens, J.C. Burns, R.J. Sanderson, G.D. Vernstrom, R.T. Atanasoski, M.K. Debe and J.R. Dahn, "Oxygen reduction activity of dealloyed $Pt_{1-x}Ni_x$ catalysts." *J. Electrochem. Soc.* **158**(8) B919-B26 (2011).

3. D.A. Stevens, R. Mehrotra, R.J. Sanderson, G.D. Vernstrom, R.T. Atanasoski, M.K. Debe and J.R. Dahn, "Dissolution of Ni from high Ni content $Pt_{1-x}Ni_x$ alloys," *J. Electrochem. Soc.* **158**(8) B905-B909 (2011).

4. M.K. Debe, A.J. Steinbach, G.D. Vernstrom, S.M. Hendricks, M.J. Kurkowski, R.T. Atanasoski, P. Kadera, D.A. Stevens, R.J. Sanderson, E. Marvel and J.R. Dahn, "Extraordinary oxygen reduction activity of Pt_3Ni_7," *J. Electrochem. Soc.* **158**(8) B910-B918 (2011), and ECS Trans., **33** 143 (2010).

5. S.K. Deppe, S.M. Hendricks, and E.M. Fischer, "A New Paradigm for PEMFC Ultra-Thin Electrode Water Management at Low Temperatures," *ECS Trans*., **33(1)**, 1179-1188 (2010).

6. A. Steinbach, M. Debe, M. Pejsa, D. Peppin, A. Haug, M. Kurkowski and S. Maier-Hendricks, "Influence of Anode GDL on PEMFC Ultra-thin Electrode Water Management at Low Temperatures," Abstract #781, 220th ECS Meeting, Boston, MA, Oct. 9-14, 2011.

7. M. K. Debe, R. T. Atanasoski and A. J. Steinbach, Invited presentation "Nanostructured Thin Film Electrocatalysts – Current Status and Future Potential," Abstract #805, 220th ECS Meeting, Boston, MA, Oct. 9–14, 2011.

8. Mark K. Debe, Project review at the DOE 2011 Vehicle Technologies and Hydrogen Programs Annual Merit Review, May 10, 2011, Washington, D.C., number FC 001.

9. M.K. Debe, Invited presentation, "Nanostructured Catalyst Developments," 2nd CARISMA Conference, La Grande Motte, France, Sept. 19–22, 2010.

10. Radoslav Atanasoski, Invited presentation, "Fundamental and practical aspects of Nano-structured thin film - NSTF catalysts for PEM fuel cells: Durability under Transient Conditions," 61st ISE – Electrochemical Energy Conversion and Storage, Nice, France, Sept. 2010.

11. D.A. Stevens, Invited presentation, T.D. Hatchard, R.J. Sanderson, R.T. Atanasoski, M.K. Debe and J.R. Dahn, "PEMFC Electrocatalyst Development," Presentation at the 218th ECS meeting, Las Vegas, NV, Oct. 11, 2010.

12. M.K. Debe, A. Steinbach, G. Vernstrom, S. Hendricks, R. Atanasoski, P. Kadera, "Extraordinary ORR activity of Pt_3Ni_7," Presentation at the 218th ECS meeting, Las Vegas, NV, Oct. 12, 2010.

13. Gary Chih-Kang Liu, R.J. Sanderson, D.A. Stevens, G. Vernstrom, R.T. Atanasoski, M.K. Debe and J.R. Dahn, "De-alloying of $Pt_{1-x}M_x$ [M = Ni, Co] $(0 < x < 1)$ catalysts and impact on surface area enhancement, " Presentation at the 218th ECS meeting, Las Vegas, NV, Oct. 12, 2010.

14. Gary Chih-Kang Liu, R. Sanderson, D.A. Stevens, G. Vernstrom, R.T. Atanasoski, M.K. Debe and J.R. Dahn, "RRDE measurements of ORR activity of $Pt_{1-x}Ni_x$ $(0 < x < 1)$ on high surface area NSTF-coated GC disks," Poster paper at the 218th ECS meeting, Las Vegas, NV, Oct.13, 2010.

15. D.A. Stevens, S. Wang, R.J. Sanderson, G.C.K. Liu and J.R. Dahn, G.D. Vernstrom, R.T. Atanasoski and M.K. Debe, "A Combined Rotating Disk Electrode/X-Ray Diffraction study of Co Dissolution from $P_{1-x}Co_x$ alloys," Poster paper at the 218th ECS meeting, Las Vegas, NV, Oct. 13, 2010.

16. A. J. Steinbach, M.K. Debe, J.L. Wong, M.J. Kurkowski, A.T. Haug, D. M. Peppin, S. K. Deppe, S. M. Hendricks and E.M. Fischer, "A New Paradigm for PEMFC Ultra-Thin Electrode Water Management at Low Temperatures," Presentation at the 218th ECS meeting, Las Vegas, NV, Oct. 14, 2010.

17. M.K. Debe, Invited presentation, "NanoStructured Thin Film Catalysts -15 (or is it 28?) Years on an Alternative Path for PEM Fuel Cell Electrocatalysts," Fuel Cell Seminar and Exposition R&D Award presentation, San Antonio, TX, Oct. 19, 2010.

18. M.K. Debe, Invited presentation, "Nanostructured Thin Film Catalysts for PEM Fuel Cells: Status and Path Forward to Meet Performance, Durability and Cost Targets for High Volume Automotive Applications," Workshop on PEM Fuel Cell Catalyst & MEA Preparation and Characterization, HySA Catalysis Competence Center and University of Cape Town, Cape Town, Rondebosch, South Africa, March 28-29, 2011.

19. M.K. Debe, Invited presentation, "NSTF Catalyst Technology for Energy Applications," Northwest University, Potchefstroom, South Africa, March 25, 2011.

20. M.K. Debe, Invited presentation, "A General Introduction to Nano-Structured Thin Film Catalyst (NSTFC) Technology for Hydrogen and Fuel Cell Applications," Council for Scientific and Industrial Research (CSIR), Pretoria, South Africa, March 24, 2011.

References

1. Arman Bonakdarpour, Krystal Stevens, George D. Vernstrom, Radoslav Atanasoski, Alison K. Schmoeckel, Mark K. Debe, and Jeff R. Dahn, "Oxygen Reduction Activity of Pt and Pt-Mn-Co Electrocatalysts Sputtered on Nanostructured Thin Film Support," Electrochimica Acta **53** (2007) 688-694.

2. D. Van der Vliet, D. Strmcnik, C. Wang, R. Atanasoski, M. Debe. N. Markovic and V. Stamenkovic, "Multimetallic Catalysts for Oxygen Reduction Reaction," 216th ECS Meeting, Vienna, Austria, Oct. 4–9, 2009.

3. K.J.J. Mayrhofer, D. Strmcnik, B.B. Blizanac, V. Stamenkovic, M. Arenz, N.M. Markovic, "Measurement of oxygen reduction activities via the rotating disc electrode method: From Pt model surfaces to carbon-supported high surface area catalysts," *Electrochimica Acta* **53** (2008) 3181-3188.

4. Liu, Gary C-K.; Sanderson, R.J.; Vernstrom, G; Stevens, D.A.; Atanasoski, R.T.; Debe, M.K.; Dahn, J.R., "RDE Measurements of ORR Activity of Pt_{1-x} Ir_x ($0<x<0.3$) on High Surface Area NSTF-Coated Glassy Carbon Disks," *J. Electrochem. Soc.* (2010), **157**(2), B207-B214.

5. Gary Chih-Kang, D.A. Stevens, J.C. Burns, R.J. Sanderson, G.D. Vernstrom, R.T. Atanasoski, M.K. Debe and J.R. Dahn, "Oxygen reduction activity of dealloyed $Pt_{1-x}Ni_x$ catalysts." *J. Electrochem. Soc.* **158**(8) B919-B26 (2011).

6. Dennis van der Vliet, Chao Wang, Mark Debe, Radoslav Atanasoski, Nenad M. Markovic and Vojislav R. Stamenkovic, "Platinum-alloy Nanostructured Thin Film Catalysts for the Oxygen Reduction Reaction," submitted to *Electrochimica Acta*.

7. A.K. Schmoeckel, G.D. Vernstrom, A.J. Steinbach, S.M. Hendricks, R.T. Atanasoski and M.K. Debe, "Nanostructured Thin Film Ternary Catalyst Activities for Oxygen Reduction," 2006 Fuel Cell Seminar, Honolulu, Hawaii, Nov. 13–17, 2006.

8. M. Debe, A. Steinbach, G. Vernstrom, S.M. Hendricks, M.J. Kurkowski, R.T. Atanasoski, P. Kadera, D.A. Stevens, R.J. Sanderson, E. Marvel and J.R. Dahn, "Extraordinary oxygen reduction activity of Pt_3Ni_7," *J. Electrochem. Soc.* **158**(8) B910-B918 (2011).

9. Debe, M.K.; Schmoeckel, A.; Hendricks, S.; Vernstrom, G.; Haugen, G.; Atanasoski, R., *ECS Transactions* **1**(1), 51 (2006).

10. Debe, M.K.; Schmoeckel, A.K.; Vernstrom, G.D.; Atanasoski, R., *Journal of Power Sources* **161**, 1002 (2006).

11. Steinbach, A.J.; Noda, K.; Debe, M.K., *ECS Transactions* **3**(1) 835 (2006).

12. Bonakdarpour, A.; Lobel, R.; Atanasoski, R.T.; Vernstrom, G.D.; Schmoeckel, A.K.; Debe, M.K.; Dahn, J.R., *Journal of The Electrochemical Society* **153**, A1835 (2006).

13. M. Debe, A. Hester, G. Vernstrom, A. Steinbach, S. Hendricks, A. Schmoeckel, R. Atanasoski, D. McClure and P. Turner, in proceedings of the 50th Annual Technical Conference of the Society of Vacuum Coaters, Louisville, KY, May 1, 2007.

14. Mark K. Debe, Project review at the DOE 2011 Vehicle Technologies and Hydrogen Programs Annual Merit Review, May 10, 2011, Washington, D.C., number FC 001.

15. Lajos Gancs, Takeshi Kobayashi, Mark K. Debe, Radoslav Atanasoski, and Andrzej Wieckowski, "Crystallographic Characteristics of Nanostructured Thin Film Fuel Cell Electrocatalysts – A HRTEM Study," Chemistry of Materials **20**, 2444-2454 (2008).

16. M.K. Debe, A.J. Steinbach, G.D. Vernstrom, S.M. Hendricks, M.J. Kurkowski, R.T. Atanasoski, P. Kadera, D.A. Stevens, R.J. Sanderson, E. Marvel and J.R. Dahn, "Extraordinary oxygen reduction activity of Pt_3Ni_7," *J. Electrochem. Soc.* **158**(8) B910-B918 (2011), and *ECS Trans*., **33** 143 (2010).

V.D.2 Highly Dispersed Alloy Catalyst for Durability

Vivek S. Murthi (Primary Contact), Elise Izzo, Wu Bi and Lesia Protsailo
UTC Power Corporation (UTCP)
195 Governor's Highway
South Windsor, CT 06042
Phone: (860) 727-2126
E-mail: vivek.srinivasamurthi@utcpower.com

DOE Managers
HQ: Kathi Epping Martin
Phone: (202) 586-7425
E-mail: Kathi.Epping@ee.doe.gov
GO: Reg Tyler
Phone: (720) 356-1805
E-mail: Reginald.Tyler@go.doe.gov

Technical Advisor
Thomas Benjamin
Phone: (630) 252-1632
E-mail: Benjamin@anl.gov

Contract Number: DE-FG36-07GO17019

Subcontractors:
- Johnson Matthey Fuel Cells, Sonning Commons, UK
- Texas A&M University, College Station, TX
- Brookhaven National Laboratory, Upton, NY

Project Start Date: May 1, 2007
Project End Date: October 31, 2011

Fiscal Year (FY) 2011 Objectives

- Develop structurally and compositionally advanced supported alloy catalyst system with loading ≤0.3 mg platinum group metal (PGM)/cm^2.
- Optimize catalyst performance and decay parameters through quantitative models.
- Demonstrate 5,000 cyclic hours below 80°C with less than 40% loss of electrochemical surface area and catalyst mass activity.

Technical Barriers

This project addresses the following technical barriers from the Fuel Cells section (section 3.4.4) of the Fuel Cell Technologies Program Multi-Year Research, Development and Demonstration Plan:

(A) Durability
(B) Cost
(C) Performance

Technical Targets

TABLE 1. DOE 2011 Technical Targets for Electrocatalysts and the Current Status of this Project

Electrocatalyst Targets	Units	Current Status	DOE 2010 Target	DOE 2015 Target
PGM (total content)	g/kW	0.50	0.3	0.2
PGM (total loading)	mg/cm^2	0.40[a]	0.3	0.2
Mass Activity @ 900 mV	A/mg$_{PGM}$ at 900 mV (iR-free)	0.20 (in MEA) 0.30 (in liquid cell)	0.44	0.44
Specific Activity	μA/cm^2 at 900 mV (iR-free)	940 (in MEA) 612 (in liquid cell)	720	720
Cyclic Durability At T ≤80°C At T >80°C	h h	1,450[b,c]	5,000 2,000	5,000 5,000
Electrochemical Area (ECA) Loss	%, percent	30[d]	<40	<40
Cost	$/kW at $51.55/g	~26[e]	5	3
Electrocatalyst Support mV after 400 hours @ 1.2 V	mV	92[f]	<30	<30

[a] Based on current scaled-up 30% Pt$_2$IrCr/C membrane electrode assembly (MEA); anode/cathode loading – 0.1/0.3 mg/cm^2 (PGM).
[b] Under an accelerated vehicle drive cycle protocol in a short stack; 40% mass activity loss under UTCP-defined accelerated single-cell test after 270 hours at 70°C and 120 hours at 80°C.
[c] Short stack durability test is on-going.
[d] Durability data measured after 30,000 cycles under UTC-defined accelerated test protocol.
[e] Five-year average PGM price $51.55/g (Pt = $1,234.33/Troy Oz; Ir = $369.06/troy oz); costs not projected to high volume production.
[f] 40 mV internal resistance (iR)-free O$_2$ performance loss at 1.5 A/cm^2 after 360 hours at 1.2 V.
T - temperature

FY 2011 Accomplishments

- Completed the scale up and MEA optimization of down-selected dispersed catalyst, 30% Pt$_2$IrCr/C for performance in a full-size fuel cell. A mass activity of 0.2 A/mg(PGM) was achieved compared to the previous status of 0.14 A/mg(PGM).
- Completed the durability testing of 30% Pt$_2$IrCr/C in a full-size MEA was completed under an accelerated protocol which showed 400 hrs of stability at 70°C. Currently testing performance and durability of the 30% Pt$_2$IrCr/C in a short stack.
- Durability testing of 30% Pt$_2$IrCr/C in a short stack is in progress under an accelerated vehicle drive cycle

protocol. The stack has accumulated 1,450 hours of uninterrupted operation at 70°C in H_2/air.

- Scaled up a 20% Pt_2IrCr alloy on the down-selected durable carbon, C4, and completed preliminary optimization of MEA for subscale fuel cell performance and stability testing in a porous plate subscale fuel cell under the DOE catalyst support corrosion protocol. A 40 mV iR-free O_2 performance loss at 1.5 A/cm_2 was observed after only 360 hours of potential holds at 1.2 V.
- A No-Go decision was made for core-shell catalysts based on extensive physical characterization and durability studies. Activity and stability of Pt_{ML}/Pd_3Co core-shell catalysts prepared using scalable chemistries were evaluated using both rotating disk electrode (RDE) and subscale fuel cell tests. Higher temperature and more concentrated electrolyte contributes to Pd dissolution and is substantially more damaging than room temperature RDE testing.



Introduction

For the proton exchange membrane fuel cell (PEMFC) technology to become commercially viable, the cost of the components in a fuel cell must be reduced and, more importantly, the durability of the MEA must be improved. This project focuses on two distinct approaches to the DOE 2010 durability and performance targets. The first approach is the development of conventional but high performance highly dispersed Pt alloy catalyst on a carbon support. The second system utilizes a novel "Pt monolayer (ML) core-shell" approach capable of achieving very high Pt mass activities [1-3]. Under this latter concept, the main objectives are to improve the durability of the cathode catalyst by further optimizing the core material selection, shell thickness of the ML, and the particle size of the cores and to develop scalable fabrication methods.

Approach

To achieve the objectives on this project, UTCP has teamed with Brookhaven National Laboratory (BNL), Texas A&M University (TAMU) and Johnson Matthey Fuel Cells (JMFC). The research focus and the role of all partners were reported previously [4]. BNL's role on the project focuses on the development of Pt ML "core-shell" systems on various cores including ideal surfaces such as single crystals. In addition, BNL leads our efforts to understand the effect of electronic properties, crystal structure and particle size on activity and durability of this class of electrocatalysts. TAMU focuses on development of computational atomistic models to study parameters that influence the activity and durability of core shell and dispersed catalyst systems. The overall scope of JMFC activities in the project encompasses development of (i) dispersed Pt alloy catalysts including scale-up on conventional and advanced carbon supports, (ii) novel synthesis methodologies to scale up Pt ML core-shell catalysts, and (iii) MEA optimization and fabrication. Apart from overall project management, UTCP primarily focuses on the development of advanced dispersed Pt-based binary and ternary alloy catalysts. UTCP activities also include electrode modeling for MEA optimization, carbon support corrosion studies, fuel cell testing on single-cell level and fabrication and testing of a 20-cell short stack for verification.

Results

Molecular Modeling

It was previously reported that incorporating Ir into the bimetallic Pt_3M alloy increases the tendency of Pt-skin formation and enhances the stability of the alloy systems [4]. The main topic that was studied this year was calculation of activity and stability of PtIrM ternary alloys based on experimentally found structures including surface segregation trends, Bader charge and D-band center analysis of Pt. Previously, the change in the composition of the Pt, Ir and Co in a 30% Pt_7IrCo_7/C as a function of cycling and the corresponding mass activity from RDE experiments were reported. A substantial loss of Co and Ir within the first 5,000 potential cycles results in a composition equivalent to that of a Pt_3IrCo. The role of Ir and Co on the surface properties of two structures: Pt_8IrCo_3 (that resulted after acid exposure) and $Pt_{11}IrCo_4$ (composition obtained after 5,000 cycles) alloys were studied by density functional theory calculations.

The role of Ir and Co on the surface properties of PtIrCo alloys was studied by a comparative analysis for the Pt_8IrCo_3 and $Pt_{11}IrCo_4$ systems using two different 5-layer distribution structure models as shown in Figure 1. The results show that the most stable structures for Pt_8IrCo_3 are the structures with one layer of Pt skin surface followed by the two-layer Pt skin surfaces. In both cases, the Pt-skin layers are more stable than the un-segregated structure. However, differences among different structures also depend critically on the subsurface composition. For example, the most stable one-layer Pt skin surface has a second layer of Pt_3Co which is slightly more favorable than a PtCo in the second layer. Similar results were obtained for the $Pt_{11}IrCo_4$ system where the most favorable second layer composition is PtCo, followed by Pt_3Co, and the movement of Ir from fourth to the third layer does not affect the results. In summary, for the cycled and acid-treated structures, the single-layer Pt-skin surfaces are the most stable. However, the two-layer Pt-skin surfaces may be formed and are thermodynamically more favorable than the non-segregated structures. Co atoms tend to be in the second and third layers, and Ir atoms tend to be in the core, together with fourth and fifth layer Pt atoms that do not show a trend to segregate towards the top surface.

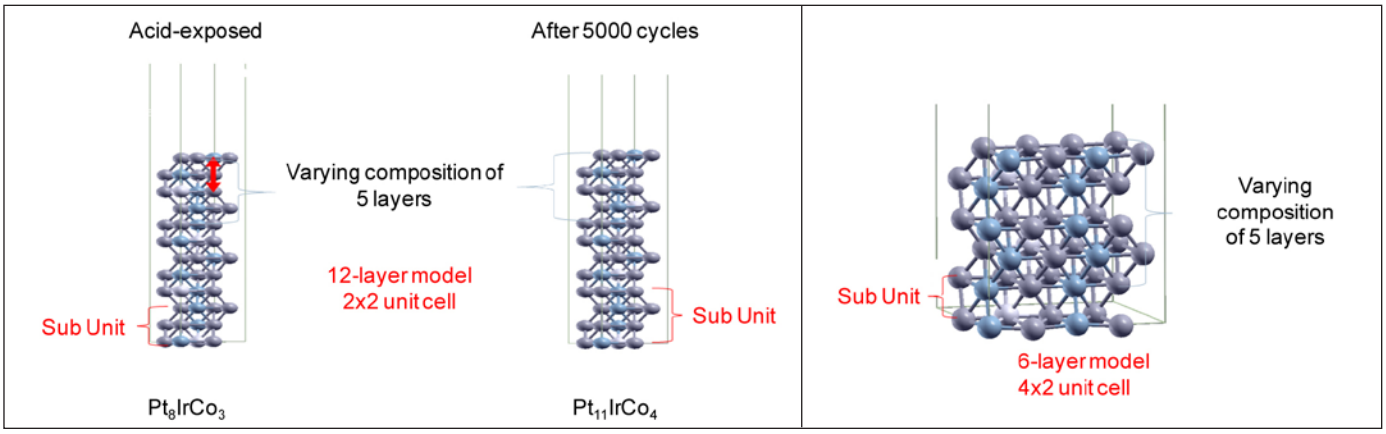


FIGURE 1. (a) 2x2 and (b) 4x2, slab model used to study segregation in Pt_8IrCo_3 and $Pt_{11}IrCo_4$ systems. The first five layers are used to study atomic redistribution after leaching. The optimized lattice constants are 3.853 Å for Pt_8IrCo_3 and 3.851 Å for $Pt_{11}IrCo_4$.

The activity and stability of the 30% Pt_7IrCo_7/C after potential cycling were studied and Table 2 shows the electrochemical stability values for the $Pt_{11}IrCo_4$ (composition after 5,000 cycles) structure in vacuum which shows that the stability of the cycled alloy surface is higher than that of the two-layer skin from Pt_2IrCo and comparable to that of the single-layer skin of Pt_3Co surfaces as shown by their electrochemical potential relative to a Pt (111) surface.

TABLE 2. Electrochemical Stability of Pt Surface Atoms Pt Surface Atoms in Two-Layer Alloy Relative to Clean Pt (111) Surfaces

System	μ_{Pt} (eV)	$\Delta\mu$ (eV)	ΔU (V)
Pt(111)	-6.98	0	0
Pt_3Co (111) Single-layer Pt-skin	-7.22	-0.24	0.12
Pt_2IrCo(111) two-layer Pt-skin	-7.12	-0.14	0.07
$Pt_{11}IrCo_4$(111) two-layer Pt-skin	-7.23	-0.25	0.13

The average charge (based on a Bader charge analysis) of the first four layers of the $Pt_{11}IrCo_4$ indicates a charge transfer from the Co subsurface atoms to the Pt atoms in the second layer and to the Ir atoms in the third layer and that the charge of the surface Pt atoms remains very similar to that on the pure Pt (111) surface suggesting an increased activity of the $Pt_{11}IrCo_4$ surface. Similar results are also obtained from the analysis of the density of states calculations which suggest enhanced reactivity of the surface Pt layer (d-band center shifted in the direction of the Fermi level). Weak adsorption of O and OH intermediates are also observed compared to Pt (111) surfaces which confirms the higher activity of the $Pt_{11}IrCo_4$ alloy surface. Furthermore, the electrochemical stability values for the $Pt_{11}IrCo_4$ structure with 0.25 ML of adsorbed oxygen (Table 3) shows a decrease in surface stability of the cycled alloy surface. However, the stability is still comparable to those on pure Pt (111) surfaces. These findings support the activity and stability of the 30% Pt_7IrCo_7/C observed experimentally [5].

TABLE 3. Electrochemical Stability of Pt Surface Layer Under 0.25 ML of Adsorbed O in Two-Layer Alloy Surface shown in Table 1 Relative to Pure Pt(111) Surfaces

System	μ_{Pt} (eV)	$\Delta\mu$ (eV)	ΔU (V)
Pt(111)	-6.26	0	0
Pt_3Co (111) Single-layer Pt-skin	-6.55	-0.29	0.15
Pt_2IrCo(111) two-layer Pt-skin	-6.32	-0.06	0.03
$Pt_{11}IrCo_4$(111) two-layer Pt-skin	-6.14	0.12	-0.06

Dispersed Pt Alloy Catalyst

Many factors such as structure, particle dispersion, particle size, type of carbon support etc, influence the electro-catalytic activity of Pt and Pt alloy nanoparticles. Previously, within this project, a 30 wt% Pt_2IrCr cathode (0.3 mg_{PGM}/cm^2 loading) showed higher durability in both ECA and mass activity (MA) under potential cycling. This catalyst showed much lower loss (~30% ECA and MA) compared to the standard Gore Pt/C (0.4 mg_{PGM}/cm^2 loading) which showed ~50% loss and was down-selected for further development and scale up into full-size MEAs [4]. In the past year, a significant amount of effort was focused towards development and optimization of the cathode catalyst layer in an MEA with 30% Pt_2IrCr alloy catalyst to improve the catalyst utilization in electrodes keeping low PGM loading and enabling good performance at high current densities. This involved an elaborate investigation to identify key parameters such as catalyst ink formulations and ionomer content, to produce an optimum cathode catalyst layer capable of achieving good fuel cell performance in wide range of current densities.

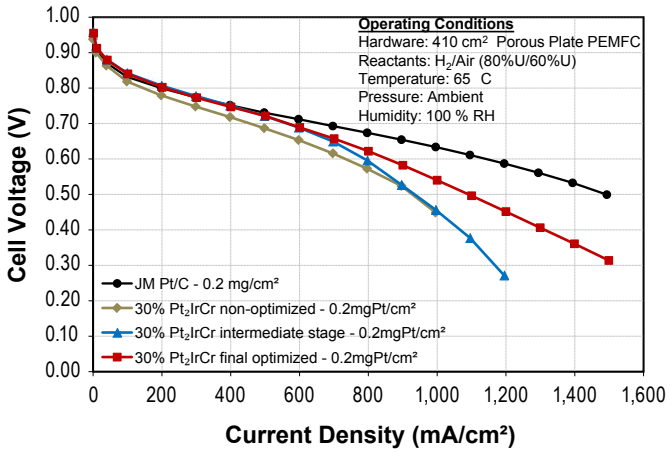


FIGURE 2. Fuel cell polarization curves in H_2/air at 65°C in a water transport plate (WTP) fuel cell at 100% relative humidity (RH) and ambient pressure for an optimized, intermediate stage and un-optimized 30% Pt_2IrCr/C ternary alloy catalyst MEA compared to JMFC Pt/C ($0.2 mg_{Pt}/cm^2$) MEA.

Figure 2 shows the fuel cell performance curves in H_2/air at different stages of the optimization process for the 30% Pt_2IrCr/C MEA in a full size (410 cm^2) WTP fuel cell compared to a baseline JMFC Pt/C MEA. The initial mass activity obtained for the alloy catalyst in the optimized MEA were 0.14 A/mg_{PGM} compared to a MA of 0.19 A/mg PGM observed for the JMFC Pt/C MEA. This low activity is attributed to the low utilization of the catalyst in the MEA as seen by the low ECA of ~30 m^2/g (vs. liquid cell ECA of 45 m^2/g from RDE). However, a clear evidence of improvement for high current density performance on H_2/air in a WTP fuel cell is observed from these catalyst layer optimization steps. Our results show that lower catalyst loading of 0.3 mg_{PGM}/cm^2 in the MEA can achieve high initial performances, although lower than the pure Pt/C. Extensive investigation into MEA fabrication process suggests that specific ink formulations significantly increase either mass transport properties or kinetic performance of alloy catalysts. This increase is attributed to the concentration of the ionomer in the ink formulations which results in the leaching of the Cr atoms from the catalyst surface to different concentrations and concurrently affects the kinetic and high current density performance in an MEA.

Figure 3 shows the (a) MA loss and (b) cell voltage at $0.8A/cm^2$ on H_2/air for the 30% Pt_2IrCr/C and the JMFC Pt/C in a WTP fuel cell under two durability protocols. A higher rate of MA and performance loss is observed for the Pt-alloy compared to the pure Pt at both operating temperatures. This higher rate is attributed to the lower stability of the transition metal in the Pt-alloy which results in the higher rate of MA loss. Additionally, any Cr leaching into the MEA would result in higher iR losses as observed by the cell voltage drop in the high current density region during cycling. Higher MA and cell voltage loss are

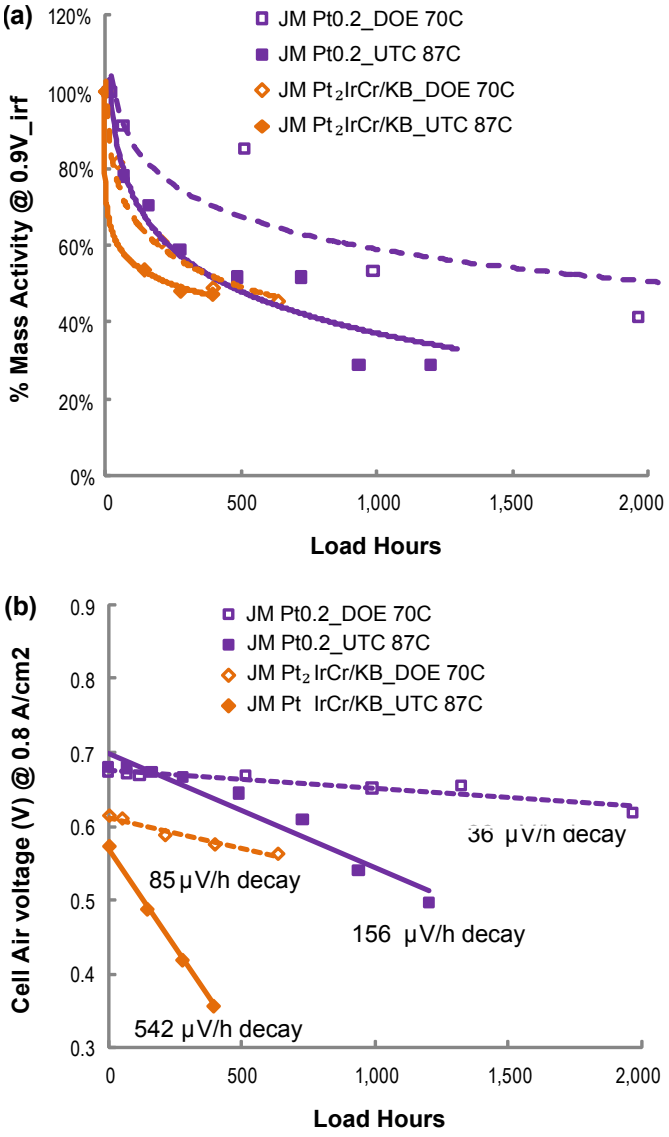


FIGURE 3. (a) Percentage mass activity and (b) cell air voltage at 0.8 A/cm^2 for the optimized 30% Pt_2IrCr/C MEA and JMFC Pt (0.2 mg_{Pt}/cm^2) MEA in a full-size WTP cell under two durability protocols at 70°C and 87°C, respectively.

observed with increase in operating temperature of the fuel cell for both Pt and Pt-alloy. This observation suggests that the rate of degradation of the catalyst is highly dependent on the operating temperature of the fuel cell and the cycling protocol. Due to insufficient data available in the literature on the durability of alloy catalysts under real life conditions, a short stack containing the Pt-alloy was built and its durability under an accelerated vehicle drive cycle protocol will be evaluated.

Durable Carbon Support

The main focus of this task was to explore alternate durable carbon supports capable of withstanding high

voltage spikes relevant for automotive applications. In the past year, a scaled-up batch (200 g) of 20% Pt_2IrCr on the down-selected stable carbon (C4) was prepared by JMFC and optimized for performance in sub-scale size (25 cm^2) WTP cells. The effect of cathode catalyst layer compositions including ionomer equivalent weight and ratio of ionomer to carbon were extensively investigated using subscale fuel cell testing. Figure 4a shows performance curves for a preliminary optimized MEA compared to a commercial Gore 57 Pt/C in subscale size WTP fuel cells operating at 80°C, 100% RH, 0 kPa backpressure. The Pt-alloy/C4 performance at high current operations is still poor mainly due to the low surface area and poor mass transport properties of the carbon support C4. Figure 4b shows the iR-free cell voltages at various current densities (0.1, 1 and 1.5 A/cm^2) for a 0.2 mgPt/cm^2 30% Pt/C4 and 20% Pt_2IrCr/C4 compared to a 30% Pt/C MEA obtained from a 25 cm^2 WTP fuel cell testing at 80°C, 100% RH under H_2/O_2 at zero backpressure. Although the beginning of life performance for the Pt and Pt-alloy supported on C4 low surface area carbon shows lower performance than that of the Pt/C, its performance after the 1.2 V potential hold tests show considerable differences. After the fuel cell corrosion test of a total of 17 potential holds of 24 h each (408 h total) at 1.2 V, the 30% Pt/C4 and 20% Pt_2IrCr/C4 showed 59 mV and 92 mV loss, respectively, at 1.5 A/cm^2 under H_2/O_2. While the alloy on C4 did not meet the 2010 DOE target of less than 30 mV iR-free O_2 performance loss at 1.5 A/cm^2 after 400 h, the voltage loss after 360 h (15 potential holds of 24 h each) at 1.2 V for the alloy catalyst was only 40 mV. The durability of the 20%Pt_2IrCr/C4 under the accelerated potential cycling protocol is currently under investigation.

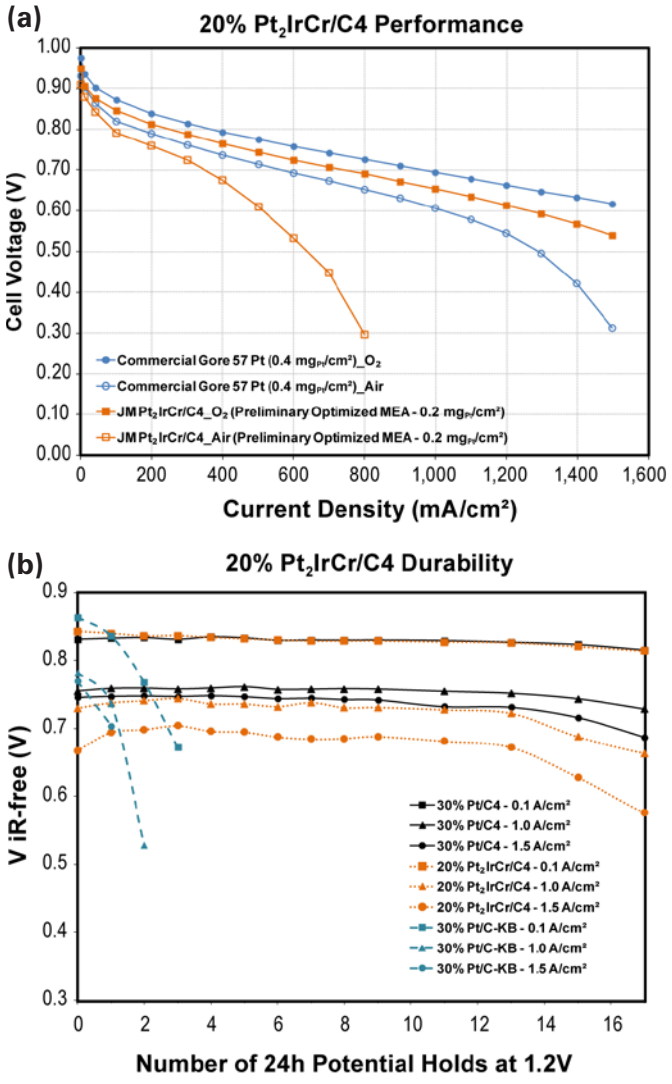


FIGURE 4. (a) Fuel cell performance curves at beginning of life for a 20% Pt_2IrCr/C4 compared to a standard 0.4 mg_{Pt}/cm^2 Gore 57 Pt/C MEA obtained from WTP subscale fuel cell (25 cm^2) testing at 80°C, 100% RH under H_2/air at zero backpressure and (b) H_2/O_2 performance at 0.1, 1 and 1.5 A/cm^2 after 1.2 V potential holds in H_2/N_2 at 80°C, 100% RH in subscale WTP cells for (0.2 mg_{Pt}/cm^2 loading) 30% Pt/C4 and 20% Pt_2IrCr/C4 compared to a 30% Pt/C MEA.

Conclusions and Future Directions

The effects of MEA compositions were studied for the scaled-up 30% Pt_2IrCr/C in full-size WTP fuel cells. A short stack containing the Pt-alloy was built and its durability under an accelerated vehicle drive cycle protocol is currently under investigation. Key barriers to overcome for the incorporation of the 30% Pt_2IrCr in an MEA such as low catalyst utilization in electrodes and the transition metal stability under operating conditions still remain open. A No-Go decision was made for core-shell catalysts due to their poor durability in an MEA under operating fuel cell conditions. The scaled up synthesis of a 20% Pt_2IrCr/C4, the down-selected catalyst on stable carbon, preliminary MEA optimization and corrosion durability testing is complete. However, their performance at high current operations is still poor and is being further investigated.

Future Directions

Our future objective is to demonstrate (i) the durability of the 30% Pt_2IrCr/C in a short stack and (ii) the high current density performance of the 20% Pt_2IrCr/C4 alloy catalyst in a subscale and full-size WTP fuel cell at the conditions relevant for automotive applications. Some of the tasks undertaken to achieve these goals are listed below.

- Continued operation of the 30% Pt_2IrCr/C in a 20-cell short stack under an accelerated vehicle drive cycle protocol.
- Optimization of dispersed alloy catalyst systems on C4 in MEAs is in progress, aiming to approach high current density performance in an operating fuel cell. The higher mass transport losses and poor water management issues are being resolved by tailoring the electrode structure for performance in a WTP fuel cell.
- In the case of the core-shell catalysts, preventing dissolution of the core material from the bulk phase of

nanoparticles remains a major challenge for this class of catalysts, and hence all activities under this task have been terminated and will not be investigated for the rest of the project.

FY 2011 Publications/Presentations

1. Gong, K.; Chen, W.; Sasaki, K.; Su, D.; Vukmirovic, M.B.; Zhou, W.; Izzo, E.L.;Perez-Acosta, C.; Hirunsit, P.; Balbuena, P.B.; Adzic, R. R. "Platinum Monolayer Electrocatalysts: Improving the Activity for the Oxygen Reduction Reaction with Palladium Interlayer on IrCo Alloy Core", J. Electroanal. Chem. **(2010)**, 649, 232.

2. Sarah Ball, "Activity and Stability of Core-shell Electrocatalysts" 2010 Gordon Research Conference in Fuel cells.

3. W. Bi, E. Izzo, V. Murthi, C. Perez-Acosta, J. Lisitano, and L. Protsailo, "Durability of Low Temperature Hydrogen PEM Fuel Cells with Pt and Pt Alloy ORR Catalysts" 218th ECS Meeting - Las Vegas, NV, **(2010).**

References

1. J. Zhang, M.B. Vukmirovic, K. Sasaki, F. Uribe and R.R. Adzic, *J. Serb. Chem. Soc.*, **70**, 513 (2005).

2. M.B. Vukmirovic, J. Zhang, K. Sasaki, A.U. Nilekar, F. Uribe, M. Mavrikakis and R.R. Adzic, *Electrochim. Acta*, **52**, 2257 (2007).

3. M. Shao, K. Sasaki, N.S. Marinkovic, L. Zhang and R.R. Adzic, *Electrochem. Comm.*, **9** 2848, (2007).

4. V.S. Murthi, DOE Hydrogen Program Annual Progress Report (2010).

5. V.S. Murthi, DOE Hydrogen Program Annual Progress Report (2009).

V.D.3 Durable Catalysts for Fuel Cell Protection During Transient Conditions

Radoslav T. Atanasoski (Primary Contact), George D. Vernstrom, Gregory M. Haugen, Theresa M. Watschke, Jess M. Wheldon, Susan M. Hendricks, Ljiljana L. Atanasoska, Amy E. Hester

Fuel Cell Components Program, 3M Company
3M Center, Building 201-2N-05
St. Paul, MN 55144-1000
Phone: (651) 736-9441
E-mail: rtatanasoski@mmm.com

Timothy D. Hatchard, Jessie E. Harlow, Robbie J. Sanderson, David A. Stevens, Connor P. Aiken, Jeff R. Dahn

Dalhousie University, Halifax, Nova Scotia, Canada

David A. Cullen, Karren L. More

Oak Ridge National Laboratory (ORNL), Oak Ridge, TN

Deborah J. Myers, Vojislav R. Stamenkovic, Nenad M. Markovic

Argonne National Laboratory (ANL), Argonne, IL

Sumit Kundu, Wendy Lee

AFCC Automotive Fuel Cell Cooperation,
Burnaby, BC, Canada

DOE Managers

HQ: Kathi Epping Martin
Phone: (202) 586-7425
E-mail: Kathi.Epping@ee.doe.gov

GO: David Peterson
Phone: (720) 356-1747
E-mail: David.Peterson@go.doe.gov

Technical Advisor

Thomas Benjamin
Phone: (630) 252-1632
E-mail: Benjamin@anl.gov

Contract Number: DE-EE0000456

Subcontractors and Federally Funded Research and Development Centers:

- Dalhousie University, Halifax, Nova Scotia, Canada
- Oak Ridge National Laboratory, Oak Ridge, TN

Project Start Date: August 1, 2009
Projected End Date: July 31, 2013

Fiscal Year (FY) 2011 Objectives

- Develop catalysts that will enable proton exchange membrane (PEM) fuel cell systems to weather the damaging conditions in the fuel cell at voltages beyond the thermodynamic stability of water during the transient periods of start-up/shut-down (SU/SD) and fuel starvation.
- Demonstrate that these catalysts will not substantially interfere with the performance of, nor add much, to the cost of the existing catalysts.

Technical Barriers

This project addresses the following technical barriers from the Fuel Cells section of the Fuel Cell Technologies Program Multi-Year Research, Development and Demonstration Plan:

(A) Durability

(G) Start-up and Shut-down Time and Energy/Transient Operation

Technical Targets

While the number of SU/SD cycles for an automotive fuel cell has been estimated to be over 30,000, the number of these events when the cathode electrochemical potential exceeds 1.23 V has been estimated at ~5,000. The number of complete fuel starvation events when a cell experiences a voltage reversal has been estimated at ~200 [1].

In agreement with DOE, the technical targets for the second year of the project have been defined as follows:

- For SU/SD, develop a cathode catalyst that can survive 5,000 excursions (<5 s each) to potentials <1.45 V, with current densities >1 mA/cm^2. Oxygen evolution reaction (OER) catalyst loading to be kept <2 μg/cm^2 of platinum group metals (PGMs)
- For cell reversal, develop anode catalyst that can withstand 200 pulses of -200 mA/cm^2 while maintaining cell voltage <2 V.

FY 2011 Accomplishments

- Both of the technical targets for the second year have been met.
- Generic electrochemical tests for SU/SD and cell reversal were developed and implemented.
- 10,000 SU/SD cycles were achieved with addition of only 2 μg/cm^2 PGM.
- 200 high current densities pulses of -200 mA/cm^2 for cell reversal were achieved with 60 μg/cm^2 of total PGM with cell voltage <1.7 V.
- Platinum dissolution is satisfactorily prevented when the potential is maintained below 1.7 V.
- Advantage of OER-modified Pt/nano-structured thin-film (NSTF) over OER added Pt/C catalyst was clearly established.

- Progress in elucidating the roles of Pt and the added OER catalysts was made.
- Fully characterized coatings with X-ray photoelectron spectroscopy (electron spectroscopy for chemical analysis) show indications of interaction of the OER catalysts with the substrate, potentially favorable from a durability point of view.
- High resolution transmission electron microscopy depicting the nanoparticles of Ir and Ru on NSTF provided insight into the observed fuel cell performance and oxygen reduction reaction (ORR) activity.
- Chemically modified Pt/NSTF anode exhibited very low ORR without inhibiting hydrogen oxidation reaction (HOR).
- Independent original equipment manufacturer testing confirmed the 3M lab results.
- OER catalyst scale-up: large size catalyst-coated membranes were fabricated at the 3M pilot plant.



Introduction

The project addresses a key issue of importance for successful transition of PEM fuel cell technology from the development to pre-commercial phase (2010 - 2015). This issue is the failure of the catalyst and the other thermodynamically unstable membrane electrode assembly (MEA) components during SU/SD and local fuel starvation at the anode, commonly referred to as transient conditions. During these periods, the electrodes can reach potentials up to 1.8 V. One way to minimize the damage from such transient events is to lower the potential seen by the electrodes. At lower positive potentials, increased stability of the catalysts themselves and reduced degradation of the other MEA components is expected.

Approach

This project will try to alleviate the damaging effects during transient conditions from within the fuel cells via improvements to the existing catalyst materials. We are modifying both the anode and the cathode catalysts to favor the oxidation of water over carbon corrosion by maintaining the cathode potential close to the thermodynamic potential for water oxidation. The presence of a highly active OER catalyst on the cathode reduces the overpotential for a given current demand thus reducing the driving force for carbon and platinum dissolution. In addition, inhibition of the ORR on the anode side lowers the ORR current through reduced proton demand which in turn decreases the OER current on the cathode resulting in reduced cathode potential.

Key requirements for both concepts are to implement the added catalyst with negligible inhibition of the fuel cell performance and with minimal increment of PGM.

Results

Task 1. Efficient Oxygen Evolution Reaction Catalysts

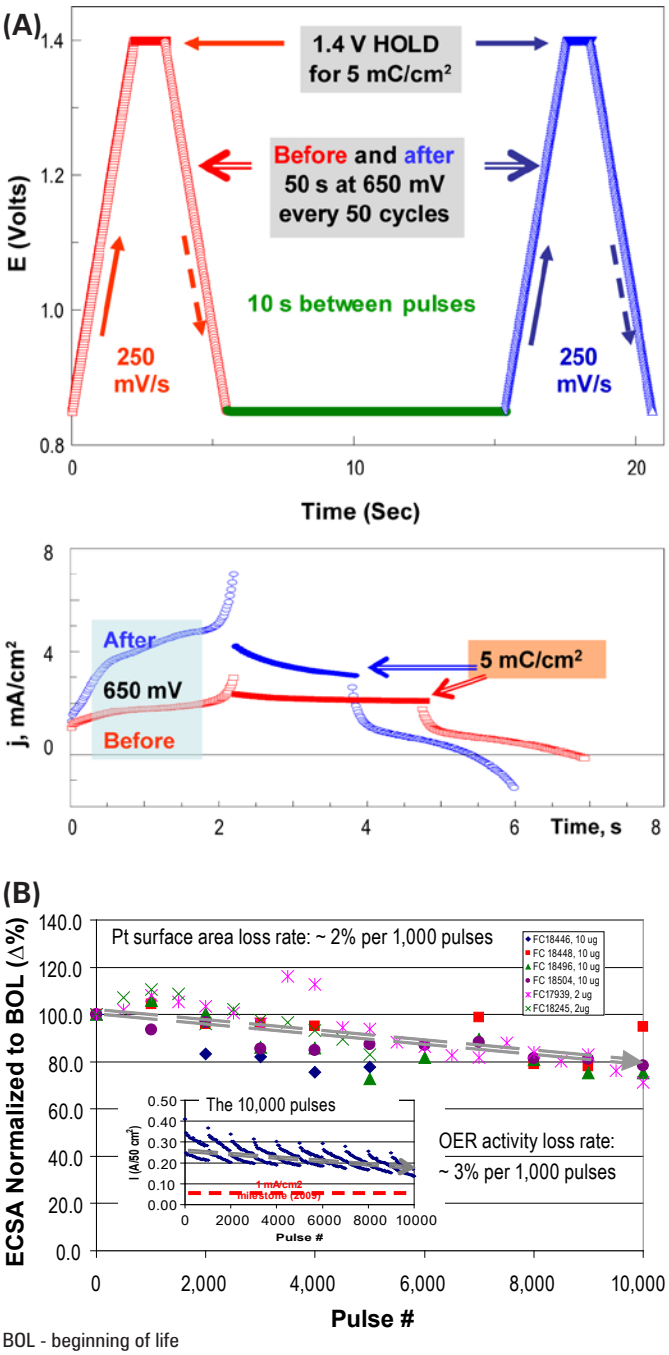
The activity during the second year of the project related to this task and revolved around the model catalyst containing ruthenium and iridium [2]. We have shown that the oxides of ruthenium, known to have the best catalytic properties for OER in aqueous solutions, and iridium, known to be the more stable of the two, exhibit the same properties as tested in an MEA [2,3]. To get the advantage of both Ru and Ir, the OER catalysts tested during this reporting period were nominally 90% Ir and 10% Ru. This composition seemed to exhibit the best stability and to provide enhanced OER activity relative to Ir only. All the catalysts were tested in a 50-cm^2 PEM fuel cell, with the working electrode under nitrogen and the reference/counter under either 1% or 100% hydrogen.

SU/SD Test

The first subtask during the second year of the project was the development of a generic, electrochemical test mimicking the real SU/SD events. The principles of the test were based on:

- The amount of air present in the anode compartment during the startup of the fuel cell stack.
- The equivalent amount of charge required for a substantial portion of the oxygen fraction in the air to be reduced.
- Requirement that the voltage does not go over 1.45 V (project milestone).
- Requirement that the OER current does not fall bellow 1 mA/cm^2 (project milestone).
- Constraint that the time for the required charge to be delivered to is <10 seconds.
- The catalyst should withstand 10,000 high voltage excursions (pulses/cycles).

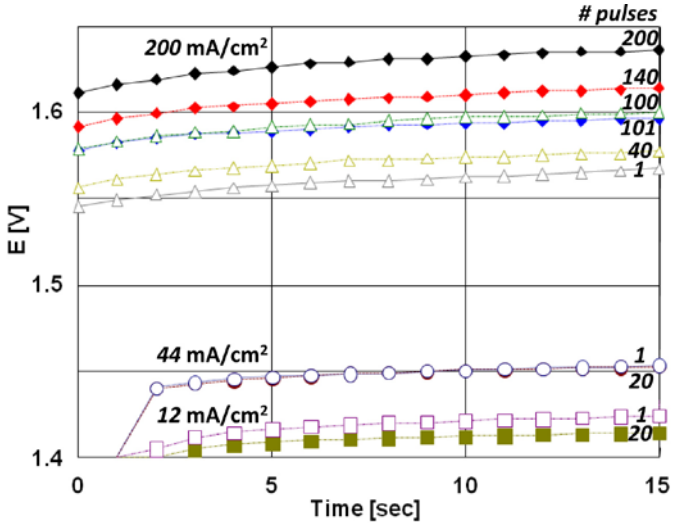
In order to further mimic the real fuel cell operating conditions, after every 50 pulses to 1.45 V, the catalyst was periodically exposed to ~0.7 V. Further, in order to mimic the incoming hydrogen front during the startup, a potential ramp of 250 mV/s from the open-circuit voltage, 0.9 V, was imposed. Schematic presentation of the test protocol along with the actual cell response is presented in Figure 1. There is a difference in the current response depending on whether the potential ramp is imposed immediately after the cell has been exposed to 0.7 V or later on during the consecutive cycles (Figure 1A). This difference is due to the oxidation current going towards formation of the PtOx on freshly reduced catalyst. The OER, however, starts at ~1.3V regardless of the state of the platinum. The change of the Pt surface area was adopted as a metric of the successful protection of the platinum. The electrochemically active surface area (ECSA) was measured after every



BOL - beginning of life

FIGURE 1. (A) Schematic presentation of the electrochemical test protocol (upper) along with the actual cell response (lower). Steps description: 250 mV/s potential sweep up; 1.4 V HOLD to 5 mC/cm^2; 250 mV/s potential sweep down; 10 s at 850 mV; 650 mV every 50 cycles/pulses; ECSA every 1,000 cycles. 50-cm^2 MEA under nitrogen/1% hydrogen, 70°C, fully saturated. *Note*: Current responses during the potential sweep up, mostly reversible, depend dramatically on OER catalyst state. (B) Pt ECSA changes during SU/SD test and OER catalyst activity decay (inset) during 10,000 cycles. Four 0.15 mg Pt/NSTF catalysts with 10 μg/cm^2 and two with 2 μg/cm^2 additional OER catalyst are presented.

1,000 cycles. As presented in Figure 1B, platinum with as little as 2 μg/cm^2 additional OER catalyst was able



Cell Reversal Test Protocol

MEA Conditioning

ECSA

20 pulses* @ 12 mA/cm², 60 s

20 pulses @ 44 mA/cm², 30 s

ECSA

100 pulses⁺ @ 200 mA/cm², 15 s

10 min @ 0V

100 pulses⁺ @ 200 mA/cm², 15 s

ECSA

*square waves pulses followed by 1 mA/cm² for 1 min

⁺2 V upper limit

FIGURE 2. Cell reversal test procedure and the typical outcome; cell voltage responses during first 15 seconds are presented. Note the "reverse" order of the pulse #1 and #20 for 20 mA/cm^2 and 44 mA/cm^2 due to activation of the OER catalyst and between #100 and #101 at 200 mA/cm^2 due to regeneration for 10 minutes at ~0.0 V.

to achieve 10,000 pulses with approximately 2% loss of ECSA/1,000 cycles. At the same time the OER catalyst itself lost 30% of its original activity (see inset in Figure 1B).

Cell Reversal Test

In electrochemical terms, the cell reversal requirements are equivalent to testing the OER activity at high current densities. In Figure 2 the test procedure and the typical outcome is presented. Essentially, the test protocol is based on the fact that during cell reversal the anode is exposed to very positive voltages, 2 V and higher. Usually, such highly damaging conditions do not last for a very long period of time. Consequently, the core of our test consists of 200 pulses at 200 mA/cm^2 followed by 1 minute at potential close to 0 V [1]. As depicted in Figure 2, the potential with every consecutive 200-mA/cm^2 is more positive. However, the presence of a good OER catalyst does keep the

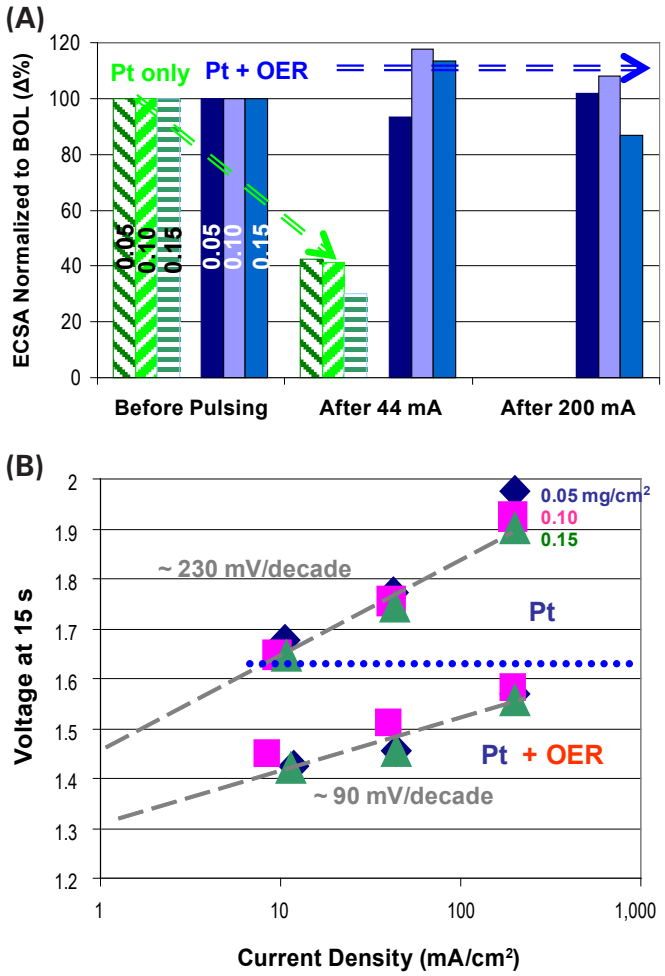


FIGURE 3. The effect of OER catalysts on platinum stability; Pt loading: 0.05, 0.10, and 0.15 mg/cm^2; OER catalyst loading: 10 μg/cm^2. (A) Platinum ECSA loses after 44 mA/cm^2 pulses without (solid blue) and with the OER catalyst (shaded green). (B) Cell voltage dependence on Pt loading. *Note* the Tafel like dependence for both catalysts on Pt loading.

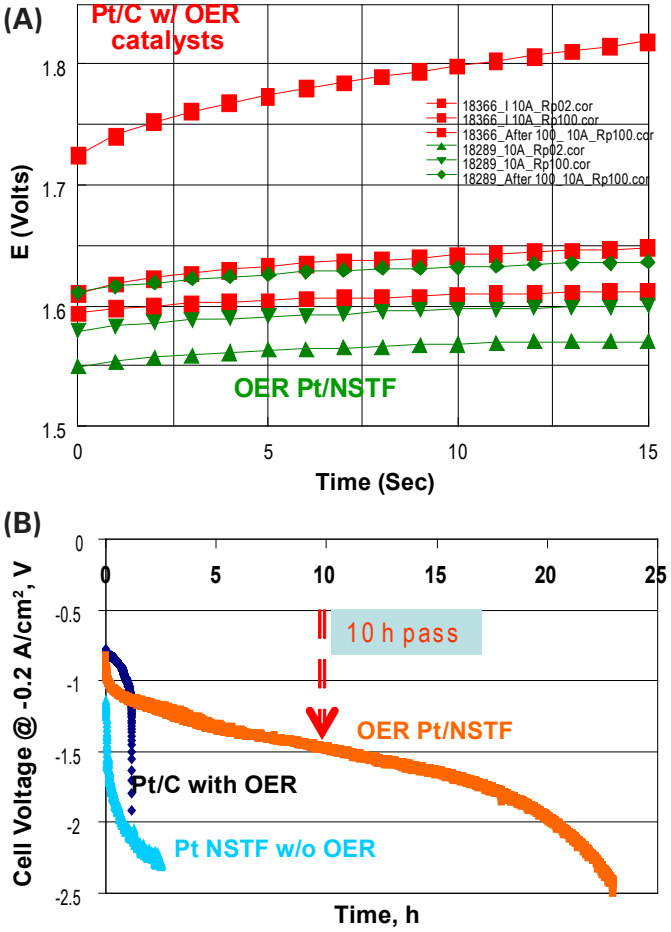


FIGURE 4. Comparison of cell reversal behavior between OER-modified Pt/NSTF substrate and dispersed Pt/C with admixed IrRu catalyst. Same Pt loading; 2X OER catalyst on Pt/C. (A) Cell voltage during 15 seconds pulses at 200 mA/cm^2: Pulse # 2; 100; 200 presented. (B) AFCC cell reversal test under nitrogen/air: Continuous -200 mA/cm^2.

potentials below 1.7 V. In Figure 3 the effect of the presence of the OER catalysts and the effect of the platinum loading are presented. As is clear from the figure, regardless of the loading, platinum without the OER catalyst loses over 50% of the original surface area even after the initial low current densities pulses (Figure 3A). The most obvious reason for this loss is the fact that, at 44 mA/cm^2, the OER on Pt proceeds at potentials almost 0.3 V higher than the same Pt catalyst with addition of the Ir + Ru (Figure 3B).

In Figure 4, a comparison between the cell reversal behavior of OER-modified Pt/NSTF substrate and dispersed Pt/C with admixed IrRu catalyst is presented. In spite of the fact that the dispersed catalyst has twice as much OER catalyst, the performance and therefore the stability of NSTF-based catalyst is far superior (Figure 4A). It is worth pointing out that the Pt ECSA for Pt/C dropped 86% during the test while Pt/NSTF remained practically the same. The superior durability of the Pt/NSTF with OER catalyst was confirmed by an independent testing completed by the stack manufacturer AFCC (Figure 4B). Moreover, the OER-modified Pt/NSTF is the only catalyst that achieved the AFCC required 10 hours "pass" point.

Task 2. Anode Catalysts with Low Oxygen Reduction Reaction Activity

The intent of this work is to find compositions that dramatically reduce the ORR activity of the deposited Pt while still maintaining high HOR activity. Numerous composition spreads were prepared via sputter deposition at Dalhousie University. These spreads included depositions from sputtering targets such as Ti, Ta, ZrO, SiO_2, poly-tetrafluoroethylene (PTFE), etc. over the top of Pt ("overlayer" spreads) and co-depositions from Pt and targets such as Ta, Nb, Ti, Hf, TiO_2, Ag ("intermix" spreads). However, the best success was achieved by our partners at ANL. They successfully deposited calix[4]arene molecules on 3M Pt/NSTF with properties close to ideal to the goal of this task [4].

Conclusions and Future Directions

- The main conclusion is that platinum dissolution can be satisfactorily slowed down when the OER catalyst maintain the electrode potential below 1.7 V.

Future Work

- Modify/simplify test procedure to reflect "real life", taking into account the U.S. DRIVE Tech Team and DOE Durability Work Group inputs.
- Explore further the Ir/Ru/Pt model system space by implementing new Pt + OER catalysts architectures.
- Explore the practicality of sputter-deposited and/or chemically modified anode for low ORR (ANL).
- Understand further the protective domain and the role of the OER catalyst by relying on state-of-the-art instrumental techniques available at the National Labs (ORNL, ANL).
- Work toward reaching the project Go/No-Go targets as proposed according to new DOE performance targets for total PGM loading:
  - 200 cycles of –200 mA/cm^2 for cell reversal with 0.045 mg/cm^2 total PGM on the anode with 1.8 V upper limit.
  - 5,000 startup cycles under the existing protocol with 0.09 mg/cm^2 total PGM on the cathode with Pt ECSA loss of <10%.
  - Reduce ORR current on the anode by a factor of 10.

FY 2011 Publications/Presentations

Papers

1. *Rapid RDE Evaluation of Catalyst Performance and Durability during Transient Conditions: The Pt-Hf Binary System.* T.D. Hatchard, J.E. Harlow, D.A. Stevens, Gary Chi-Kang Liu, R.J. Sanderson, N. van der Bosch, J.R. Dahn, G.M. Haugen, G.D. Vernstrom and R.T. Atanasoski, *Electrochim. Acta (*doi:10.1016/j.electacta.2011.05.059*)*.

2. *Development of Catalysts with Enhanced Tolerance to Fuel Cell Transient Conditions*, D.A. Stevens, R.J. Sanderson, T.D. Hatchard, T.C. Crowtz, J.R. Dahn, G.D. Vernstrom, G.M. Haugen, T. Watschke, L.L. Atanasoska, and R.T. Atanasoski, *ECS Transactions*, 33 (1) 419 (2010).

Invited Presentations

1. R. Atanasoski: "*Durability of Thin Film Catalysts for PEM Fuel Cells*", *Key-Note Lecture*, "Electrochemical Energy Conversion and Storage" symposium , 61st Annual Meeting of the International Society of Electrochemistry, September 2010, Nice, France.

2. R. Atanasoski: *Durable Catalysts for Transient Conditions,*, 6th Annual International Conference, FUEL CELLS DURABILITY & PERFORMANCE 2010*,* Boston, Dec. 09, 2010.

3. R. Atanasoski: *"Role of catalysts durability in PEM Fuel Cells"*, *Key-Note Lecture,* "Role of Catalysis in Fuel Cells" Symposium, 241st Amer. Chem. Soc., Anaheim, CA, 03/29/2011.

Presentations

1. "Development of Catalysts for Enhanced Tolerance to Fuel Cell Transient Conditions" by D. Stevens, G. Vernstrom, R. Sanderson, G. Haugen, T. Hatchard, T. Crowtz, T. Watschke, M. Debe, R. Atanasoski, and J. Dahn, 218th Electrochemical Soc. Meeting, Las Vegas, 2010.

Presentations to DOE

1. "Durable Catalysts for Fuel Cell Protection during Transient Conditions" presented at the FC Tech Team, Detroit, April 27, 2011.

2. "Durable Catalysts for Fuel Cell Protection during Transient Conditions" presented at the DOE 2010 AMR, May 10, 2011, Washington, DC.

3. "Durable Catalysts for Fuel Cell Protection during Transient Conditions" Project Progress Review, presented to DOE, Nov. 08, 2010, St. Paul, Minnesota.

References

1. A. Nelson, Presentation at the *12th Ulm ElectroChemical Talks*, Ulm, Germany, June 15–17, 2010.

2. R.T. Atanasoski, Project review at the DOE 2010 Vehicle Technologies and Hydrogen Programs Annual Merit Review, June 8, 2010, Washington, D.C., FC# 006.

3. R.T. Atanasoski et al., FY 2010 DOE Hydrogen Annual Progress Report Review, V.E.6.

4. B. Genorio, R. Subbaraman, D. Strmcnik, D. Tripkovic, V.R. Stamenkovic, and N.M. Markovic, *Angew. Chem. Int. Ed*. 2011, 50, 5468–5472.

V.D.4 Extended, Continuous Pt Nanostructures in Thick, Dispersed Electrodes

Bryan Pivovar (Primary Contact), Shyam Kocha, Huyen Dinh, Lin Simpson, Chai Engtrakul, Arrelaine Dameron, Tim Olson, KC Neyerlin, Svitlana Pylypenko, Justin Bult, Brian Larsen, Jeremy Leong

National Renewable Energy Laboratory
1617 Cole Blvd.
Golden, CO 80401
Phone: (303) 275-3809
E-mail: Bryan.Pivovar@nrel.gov

DOE Manager
HQ: Kathi Epping-Martin
Phone: (202) 586-7425
E-mail: Kathi.Epping@ee.doe.gov

Subcontractors:
- Karren More (PI), Kelly Perry
  Oak Ridge National Laboratory, Oak Ridge, TN
- Rod Borup (PI)
  Los Alamos National Laboratory, Los Alamos, NM
- Yushan Yan (PI), Shaun Alia
  University of California, Riverside, Riverside, CA
- Robert Geer (PI), John Elter, Jeff Boyer
  State University of New York at Albany, Albany, New York
- Stacey Bent (PI), Han-Bo-Ram Lee
  Stanford University, Stanford, CA
- Tom Zawodzinski (PI)
  University of Tennessee, Knoxville, TN
- Jeremy Meyers (PI)
  University of Texas at Austin, Austin, TX
- Kev Adjemian
  (In-kind) Nissan Technical Center North America, Farmington Hills, MI
- Paolina Atanassova
  (In-kind) Cabot Fuel Cells, Albuquerque, NM
- Fumiaki Ogura
  (In-kind) Tanaka Kikinzoku Kogyo, Hiratsuka, Japan

Project Start Date: July 20, 2009
Project End Date: 2013

Fiscal Year (FY) 2011 Objectives

- Produce novel catalysts based on extended Pt surfaces with increased activity and durability.
- Further increase electrochemically available surface area (ECA) and mass activity of extended surface catalysts.
- Effectively incorporate extended Pt catalysts into more traditional dispersed electrodes for mass transport/water management.
- Demonstrate and validate models for catalysts and electrodes based on extended surfaces.

Technical Barriers

This project addresses the following technical barriers from the Fuel Cells section (3.4.4) of the Fuel Cell Technologies Program's Multi-Year Research, Development and Demonstration Plan:

(A) Durability (of catalysts and membrane electrode assemblies)

(B) Cost (of catalysts and membrane electrode assemblies)

(C) Performance (of catalysts and membrane electrode assemblies)

(D) Start-up and Shut-down Time and Energy/Transient Operation

Technical Targets

This project synthesizes novel extended thin film electrocatalyst structures (ETFECS) and incorporates these catalysts into electrodes with and without carbon for further study. The project has targets outlined in the Multi-Year Research, Development and Demonstration Plan for both electrocatalysts for transportation applications (Table 3.4.12) and membrane electrode assemblies (MEAs) (Table 3.4.13). The specific targets and status of highest relevance are presented in Table 1.

TABLE 1. Technical Targets for Electrocatalysts for Transportation Applications

Characteristic	Units	2010/2015 Targets	Status
Electrochemical Area Loss	%	<40%/<40%	
Mass Activity (150 kPa H_2/O_2 80°C 100% RH)	A/mg-Pt @ 900mV	0.44/0.44	0.33
Specific Activity (150 kPa H_2/O_2 80°C 100% RH)	$\mu A/cm^2$-Pt @ 900 mV	720/720	800-1,300

RH – relative humidity

FY 2011 Accomplishments

- Synthesized novel ETFECS that routinely surpass DOE 2015 target for specific activity.
- Demonstrated ETFECS with ECA as high as 40 m^2/g_{Pt} and mass activities of 330 mA/mg_{Pt} far beyond the surface area of most extended surface catalysts with a mass activity approaching the 2015 DOE target.
- Demonstrated significantly improved durability of ETFECS towards potential cycling in rotating disc electrode (RDE) studies for both the Pt dissolution (0.6-1.0 V) and carbon corrosion region (1.0-1.6 V).

- Incorporated carbon into electrode structures that contain ETFECS while maintaining durability and activity.
- Demonstrated high specific activities of ETFECS in fuel cells.



Introduction

Pt remains a primary limitation for the widespread commercialization of polymer electrolyte fuel cells. To date, approaches looking to replace Pt with a non-platinum-group metal have met with limited success. "Thrifting" of Pt (i.e., ultra-low Pt loadings) seems to be the most likely (near-term) option for meeting cost, performance and durability targets. Typical Pt catalysts for fuel cell applications are small nanoparticles (such as cubooctahedron) that have high surface areas, and therefore significant fractions of Pt atoms are surface accessible. Clearly, having as many Pt atoms on the surface as possible is advantageous. However, catalytic activity and durability of extended surfaces can outweigh the surface area advantages of smaller particles, particularly if these advantages can be maintained at thin wall thickness, as highlighted by the promising work done on nanostructured thin film catalysts based on Pt or Pt alloys at 3M [1] and Pt and Pt alloy nanotubes at UC Riverside [2]. The synthesis of catalysts with high mass activity and the effective implementation of these catalysts in high performance, durable and robust MEAs will help enable fuel cell commercialization on a significant scale.

Approach

Our approach involves synthesizing novel ETFECS using either a nanostructured support material such as carbon nanotubes (CNTs), metal oxide nanoparticles, or perylene red nanowhiskers, or a sacrificial metal template. Pt is deposited on these materials either through vapor deposition (including sputtering and atomic layer deposition [ALD]) or solution deposition (including galvanic displacement). Our goal is to produce nanostructures with thin, continuous films of Pt because similar structures have shown high catalytic activity and durability. The materials synthesized are characterized by several techniques with a strong focus on microscopy and electrochemistry. To date, extended surface catalysts have not been demonstrated in traditional, thick catalyst layers that include Nafion® and have been shown to exhibit good tolerance to a wide range of operating conditions including cold-start. The novel catalysts produced in this project are being implemented in thick, dispersed electrodes to investigate the production of high performance, robust electrodes from these materials. Modeling is being used in support of our catalyst synthesis studies and our electrode studies, extending established models involving wetting of Pt on supports, simulating electrode architecture, and evaluating criteria that impact electrode performance.

Results

In the past year, we added a number of additional substrates to our studies probing supports as extended surface Pt hosts. Included on our list of substrate nanomaterials to date are: carbon nanotubes, inorganic oxides, metals, and perylene red whiskers. Examples of novel templates synthesized this past year are shown in Figure 1.

In the area of Pt deposition, we focused on sputtering, ALD, and spontaneous galvanic displacement (SGD). Sputtering remains an area of interest, as we and 3M [1] have shown it to be a viable technique for depositing thin, continuous Pt layers. We have focused on deposition onto mats and short (>2 µm) vertically aligned CNTs. Transmission electron microscopy close-ups of Pt sputtered CNT mats show a transition between discrete particles and continuous Pt coating. These micrographs suggest that continuous coatings can be obtained at thicknesses of ~2 nm. Unfortunately, our ability to generate these

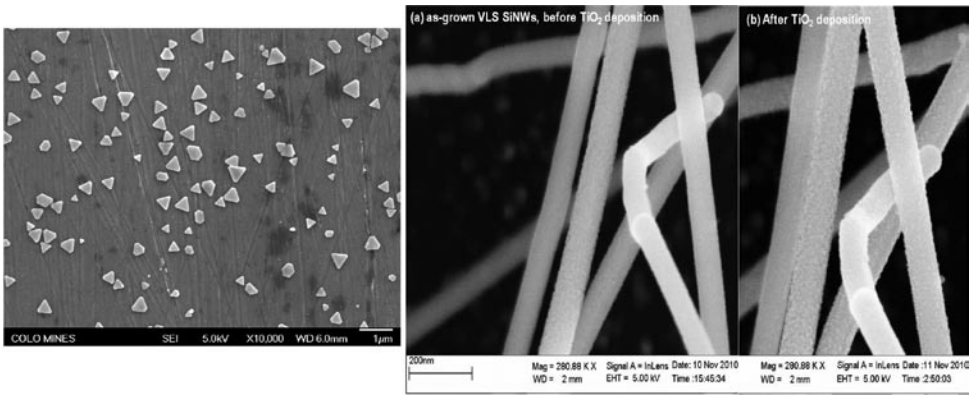


FIGURE 1. Ag nanoplatelets synthesized by solvothermal process (left); SiNWs synthesized by vapor-liquid-solid process (center); after TiO_2 deposition by ALD (right).

materials consistently and in higher yields has been poor. We have continued to investigate ALD for its ability to produce thin continuous Pt films. The most promising results have focused on using TiO_2 as a bonding layer. We found that a minimum thickness of TiO_2 followed by thermal treatment (annealing) results in the conversion of amorphous TiO_2 to anatase. The anatase form showed the fastest and most consistent Pt nucleation rates and is now being explored at ultra-thin (>5 nm) coating thicknesses and on nanostructured substrates. In the area of SGD we used Ag and Cu nanowires and Ag nanoplates as templates for Pt displacement and performed studies that have also included Pd or Au.

Our electrochemical characterization and electrode studies made significant strides in the past year. We established agreement with literature and demonstrated a high degree of reproducibility. We quantified the increases in specific activity from our novel materials and showed reasonably high surface areas (up to 40 m^2/g Pt) in ETFECS. While a few studies with CNTs were performed, our primary focus of electrochemical characterization was on materials synthesized by SGD, because we obtained higher yields and higher performance with these materials. A select portion of our data is highlighted in Figure 2. The three different colors/symbols represent a systematic series of novel materials based on SGD of either Cu or Ag nanowires investigating features including: reactant delivery rate, stoichiometry, temperature, reaction solvent, and post-processing. While we commonly surpass the DOE 2015 target for specific activity (720 µA/cm^2 Pt), highlighted in Figure 3, we have not yet achieved the 2015 target for mass activity. Although extended surface catalysts have typically

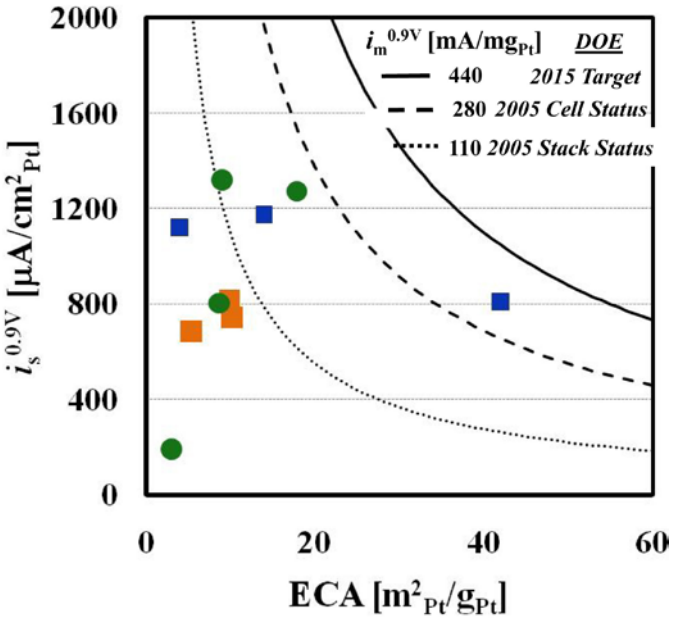


FIGURE 2. Specific activity vs. ECA for SGD ETFECS at NREL. Lines of constant mass activity shown as well.

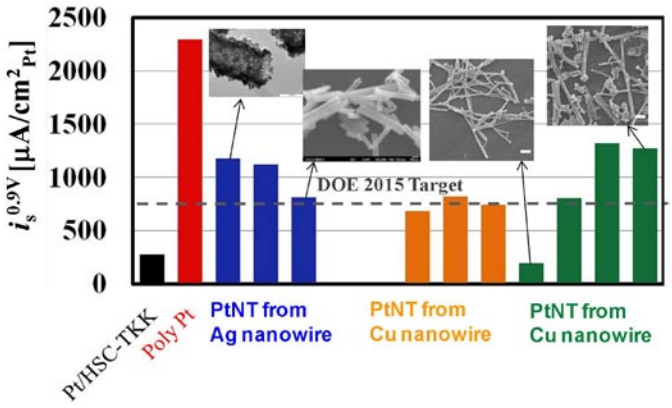


FIGURE 3. Specific activity of ETFECS compared to traditional Pt/C and polycrystalline Pt disc.

been limited to ECAs around 10 m^2/gPt we demonstrated ETFECS with ECA up to ~40 m^2/g Pt. This high ECA material resulted in a novel catalyst with mass activity of 330 µA/gPt, approaching the 440 µA/gPt DOE 2015 target. Continued investigations will seek to further increase both specific activity and ECA.

Beyond the improvements in electrochemical properties determined for the SGD ETFECS already highlighted, we also explored the impact of carbon incorporation on the electrochemical performance of these materials, tested the materials in fuel cells, and investigated the durability of these materials. All of these studies showed the promise of extended surfaces as novel fuel cell catalysts. Highlights from our studies are shown in Figure 4. The specific and mass activities of our ETFECS have essentially no impact on the observed specific and mass activity. Normalized ECAs show that traditional catalysts, as expected, show much poorer durability with potential cycling. Similar results were observed in the Pt dissolution region (0.6-1.0 V) in similar potential cycling studies.

Conclusions and Future Direction

We demonstrated for the first time conformal Pt coatings on CNTs and Pt nanostructures from Cu nanowires. We performed controlled growth of CNTs. We investigated Pt ALD, sputtering, SGD and other solution based routes as Pt deposition techniques. Future work, broken down by topical area, includes:

Templates/Cores:

- Metal oxide substrate development.

Pt Deposition:

- SGD process further optimization focusing on post-processing parameters.
- ALD studies investigating Pt growth on carbon and with reduced thickness/decreased nucleation cycles.

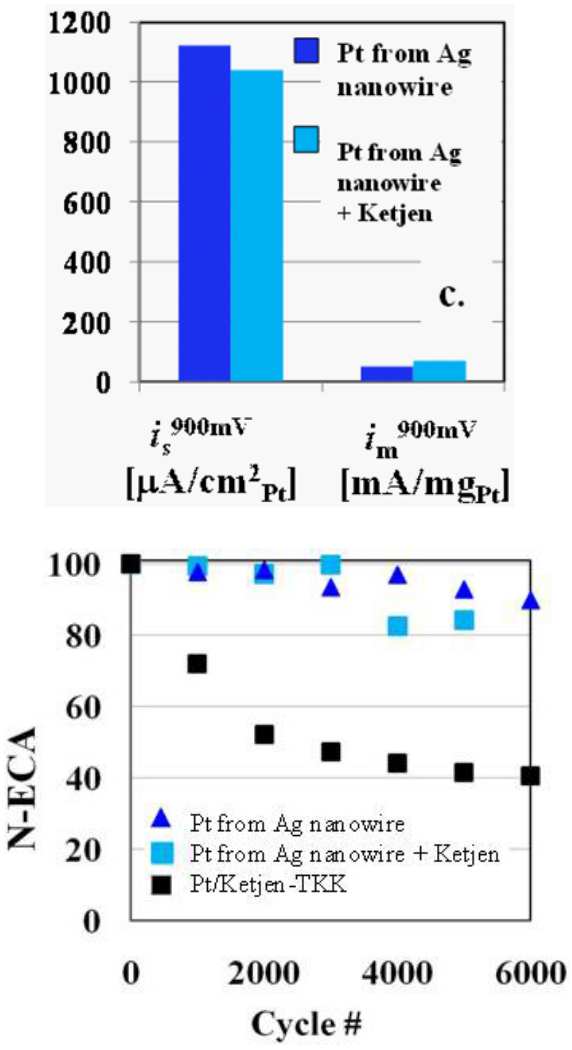


FIGURE 4. Specific and mass activities of ETFECS with and without carbon (top), stability to potential cycling from 1.0-1.6 V (carbon corrosion region), (bottom).

Electrode Studies:

- Electrochemical (RDE) durability screening of ETFECS as a function of initial ECA.
- Incorporation of highest performing catalyst (330 mA/mg_{Pt}) into electrode studies.
- Expanded MEA fabrication and fuel cell testing of ETFECS.

Modeling:

- Advancement of models to electrode structures incorporating model ETFECS – PtNT of 150 nm diameter, 2 micron length.
- Expansion of porous electrode models to ETFECS incorporated electrodes.

FY 2011 Publications/Presentations

1. J. Bult, A. Dameron, S. Pylypenko, C. Engtrakul, C. Bochert, L. Chen, J. Leong, S. Frisco, L. Simpson, H.N. Dinh, B. Pivovar, "Atomic Layer Deposition of Platinum onto Functionalized Aligned MWNT Arrays for Fuel Cell Electrode Application," ECS Trans. 33 (1), 89 (2010).

2. Shyam Kocha, KC Neyerlin, Tim Olson, Bryan Pivovar, "Electrochemical Characterization and Implementation of Extended Surface Pt Catalysts in PEMFCs" 218th ECS Meeting, Las Vegas, NV, Oct. 2010.

3. Brian A Larsen, Svitlana Pylypenko, Tim S. Olson, KC Neyerlin, Bryan S. Pivovar, "Synthesis of Pt-Cu Nanowires by Spontaneous Galvanic Displacement as Novel Catalyst Materials" 218th ECS Meeting, Las Vegas, NV, Oct. 2010.

4. Tim S. Olson, KC Neyerlin, Brian A. Larson, Svitlana Pylypenko, Shyam Kocha, Bryan Pivovar, "Pt-Cu Nanowires for Fuel Cell Catalyst Applications" 218th ECS Meeting, Las Vegas, NV, Oct. 2010.

5. Justin Bult, Arrelaine Dameron, Svitlana Pylypenko, Christopher Bochert, Chaiwat Engtrakul, Limeng Chen, Jeremy Leong, Sarah Frisco, Ryan O'Hayre, Lin Simpson, Huyen Dinh and Bryan Pivovar, "Atomic Layer Deposition of Platinum onto Functionalized Aligned MWNT Arrays for Fuel Cell Application" 218th ECS Meeting, Las Vegas, NV, Oct. 2010.

6. B. Pivovar, "Extended, Continuous Pt Nanostructures in Thick, Dispersed Electrodes", FreedomCAR Fuel Cell Tech Team, March 16, 2011, Southfield, MI.

7. B. Pivovar, "Extended Surface Catalysts", June 2, 2011, LANL, Los Alamos, NM.

8. B. Pivovar, "Extended Surface Catalysts", June 13, 2011, GM, Honeoye Falls, NY.

9. Shyam S. Kocha, K.C. Neyerlin and Bryan Pivovar, "Electrocatalyst Durability in Automotive PEMFCs", PBFC-5, August 2011, Chicago, IL.

10. S. Alia, Y. Zhang, Q. Xu, K. Jensen, C. Contreras and Y. Yan, "Gold Stabilized Platinum and Palladium Nanotubes" AIChE Annual Meeting, Salt Lake City, UT, Nov. 2010.

11. S. Alia, Y. Zhang, Q. Xu, K. Jensen, C. Contreras and Y. Yan, "Copper Templated Platinum Nanotubes as Oxygen Reducing Electrocatalysts" AIChE Annual Meeting, Salt Lake City, UT, Nov. 2010.

12. S. Alia, Y. Zhang, Q. Xu, K. Jensen, C. Contreras and Y. Yan, "Platinum Thin-Coated Palladium Nanotubes for the Oxygen Reduction Reaction" AIChE Annual Meeting, Salt Lake City, UT, Nov. 2010.

13. S.M. Alia, G. Zhang, D. Kisailus, D. Li, S. Gu, K. Jensen, Y. Yan, *Adv. Funct. Mat.* 2010, 20:3742-3746.

References

1. http://www.hydrogen.energy.gov/pdfs/review08/fc_1_debe.pdf.

2. Z. Chen, W. Li, M. Waje, Y. S. Yan, *Angew. Chem. Int. Ed.* 2007, 46:4060-4063.

V.D.5 Nanosegregated Cathode Alloy Catalysts with Ultra-Low Platinum Loading

Nenad M. Markovic (Primary Contact),
Vojislav R. Stamenkovic
Argonne National Laboratory
9700 S. Cass Avenue
Argonne, IL 60439
Phone: (630) 252-5181
E-mail: nmmarkovic@anl.gov

DOE Manager
HQ: Nancy Garland
Phone: (202) 586-5673
E-mail: Nancy.Garland@ee.doe.gov

Subcontractors:
- Karren More, Oak Ridge National Laboratory, Oak Ridge, TN
- Charles Hays, Jet Propulsion Laboratory, Pasadena, CA
- Shuoheng Sun, Brown University, Providence, RI
- Guofeng Wang, University of Pittsburgh, Pittsburgh, PA
- Radoslav Atanasoski, 3M Company, St. Paul, MN

Project Start Date: September, 2009
Project End Date: September, 2013

Fiscal Year (FY) 2011 Objectives

- Fundamental understanding of the oxygen reduction reaction on multimetallic PtM (M = Co, Ni, Fe, Mn, Cr, V, and Ti) and PtM_1N_2 (M_1 =Co or Ni; N_2 = Fe, Mn, Cr, V, and Ti) materials.
- Develop highly-efficient, durable, nanosegregated Pt-skin PtM and PtM_1N_2 catalysts with ultra-low Pt content.
- Develop highly-efficient and durable Au/PtM_3 nanoparticles with ultra-low Pt content.
- Find relationships between activity/stability of well-characterized bulk alloys and real nanoparticles.
- Develop novel chemical and physical methods for synthesis of monodispersed PtM and PtM_1N_2 alloy nanoparticles and thin metal films.
- Resolve electronic/atomic structure and segregation profile of PtM and PtM_1N_2 systems.
- Resolve composition effects of PtM and PtM_1N_2 systems.
- Demonstrate mass activity and stability improvement of PtM and PtM_1N_2 alloy nanoparticles.
- Use computational methods as the basis to form any predictive ability in tailor making binary and ternary systems to have desirable reactivity and durability properties.

Technical Barriers

This project addresses the following technical barriers from the Fuel Cells section (3.4.5) of the Hydrogen, Fuel Cells and Infrastructure Technologies Program Multi-Year Research, Development and Demonstration Plan:

(A) Durability

(B) Cost

(C) Performance

Technical Targets

This project is conducting fundamental studies of the oxygen reduction reaction on Pt-based PtM (M = Ni, Co, Fe, Cr, V, and Ti) binary and PtM_1N_2 (N, M = Fe, Co, and/or Ni) catalysts as well as on Au/Pt_3M ternary nanoparticles. Insights gained from these studies will be applied toward the design and synthesis of highly-efficient, durable, nanosegregated Pt-skin catalysts with ultra-low Pt content that meet or exceed the DOE 2015 targets (Table 1).

TABLE 1. DOE 2015 Targets

Specific activity @ 0.9 ViR-free: 720 mA/cm^2	PGM total content: 0.2 g/kW
Mass activity @ 0.9 V: 0.44 A/mgPt	Total loading: 0.2 mg/cm^2
Catalyst support loss: <30%	Durability w/cycling (80°C): 5,000 hrs

ViR – volt internal resistance; PGM – precious group metal

FY 2011 Accomplishments

- Synthesized wide range of bi/multimetallic nanoparticles with controlled size and composition by colloidal organic solvo-thermal approach.
- Developed vapor deposition/annealing methods to make stable and active Pt thin metal film (1-7 atomic layers) on Pt_3Ni substrate.
- Established relationships between the morphology/thickness of Pt atoms in skeleton structure and stability/activity of the catalysts: Pt film can both effectively protect Ni from dissolution and provide superior catalytic activity (x6 vs. Pt).
- Developed experimental protocol to synthesize PtNi/C nanoparticles with Pt multilayered "skin" (2-3 monolayers, ML) that are mimicking stability/activity of thin metal film systems.
- In a membrane electrode assembly (MEA), for PtNi/C multilayered skin confirmed: (i) three times higher specific amperage (SA ~0.8 mA/cm^2) than benchmark Pt/C catalysts and mass activity of ~0.35 A/mg_{Pt}; (ii) high durability, e.g., after 20,000 cycles activity, surface area loss was only 12% compared to ~40% for Pt/C.
- Performed composition optimization of ternary PtM_1N_2 catalysts.

- Established activity (stability) trends for bimetallic nanoparticles (NPs).
- Demonstrated that ternary alloys could provide additional tunability towards activity and stability.



Introduction

In the quest to make the proton exchange membrane fuel cell (PEMFC) a competitive force, one of the major limitations is to reduce the significant overpotential for the oxygen reduction reaction (ORR) and minimize dissolution of the cathode catalysts. Here, we report progress for FY 2011 in experimental and theoretical studies to addressing the importance of alloying Pt with *3d* elements (M = Ni, Co, Fe etc.) and making a novel tailored nanostructure of Au/Pt_3M in order to form catalytically active materials with so-called nanosegregated profile [1]. We have demonstrated that the nanosegregated surfaces are superior in both: exceptional catalytic activity for the ORR and higher stability of Pt surface atoms.

Approach

To address the challenges that are listed as the DOE targets for the Fuel Cell Technologies Program we rely on our materials-by-design approach [2,3]. This involves four major steps: (i) advanced synthesis of novel nanoscale materials, which enables control of their size, structure and composition; (ii) characterization of atomic and electronic properties by ex situ and in situ surface characterization techniques and theoretical methods; (iii) resolving the surface electronic and crystal structures at atomic/molecular level that govern efficient kinetics of the ORR; and (iv) synthesis/fabrication (scale up) of the highly efficient nanoscale materials, which are guided by the fundamental understanding of structure-function relationships.

Results

From Model Thin Films to Real Pt-Skin PtNi Nanoparticles. The term Pt-skeleton has been coined to describe unique Pt structure that remains on the surface of bi(multi)-metallic alloys after dissolution of non-Pt atoms from the near-surface region in acidic environments [3]. On the other hand, the term Pt-skin has been used to describe another unique formation of Pt surface atoms that is formed after thermal treatment of bimetallic alloys due to tendency of Pt to have complete segregation over Pt_3M systems. In some cases, an oscillatory concentration profile with 100% Pt in the first layer is counterbalanced by depletion of Pt in the second layer, which is followed by enrichment of Pt in the third layer. Alloys with such segregation profile in near surface region we term nanosegregated systems, and they have been found to have superior catalytic properties for the ORR [1]. Particularly, extended Pt_3M electrodes with Pt-skin surfaces are more active for the ORR than the corresponding Pt-skeleton structures [4]. In the previous FY 2010 report, we pointed out that the skeleton-like structure of $Pt_{50}Ni_{50}$/C catalyst, formed by dissolution of the surface/subsurface Ni atoms, has the highest specific (4.0 mA/cm^2) and mass (1.5 A/mg_{Pt}) activities for the ORR compared to the other Pt_xNi_{1-x} NPs. In the mean time, we have revealed that the concentration profile formed after leaching out of *3d* element from Pt_xNi_{1-x} catalysts indicated skeleton type of surface structure, whose thickness depends on the ratio between Pt and Ni [1]. In this report, we summarize the results that are providing both fundamental insights required for efficient transformation of the Pt-skeleton to more active Pt-skin morphology, which we used as guiding principles that have led to the synthesis of an advanced PtNi nanocatalyst with the optimized Pt-skin type of surfaces. In order to evaluate correlation between the thickness of Pt-skeleton overlayer and catalytic properties we used physical vapor deposition method to prepare well characterized Pt-skeleton surfaces over the $Pt_{50}Ni_{50}$ substrate, which was found to be the most active bimetallic catalyst. As depicted in Figure 1, the as-sputtered Pt films consisted of randomly distributed Pt atoms, which simulate the Ni-depleted Pt-skeleton overlayers. Figure 1 also shows that the optimal activity for the ORR (improvement factor 2.5) is observed on the surface covered by ca. 3 MLs of Pt, which is in line with the previous results on polycrystalline Pt_3M bulk alloys with the skeleton type of surfaces. Reduced enhancement was observed for thicker Pt films, e.g., improvement factor of 1.7 for 5 ML of Pt, while the specific activity measured for the 7 ML film was close to that of poly-Pt. In order to transform the Pt-skeleton morphology to more active Pt-skin, we applied a moderate thermal treatment at 400°C, which was previously optimized for bimetallic NPs [5]. Such treatment induced relaxation of low-coordinated Pt surface atoms and formation of energetically favorable adlayer with higher coordination of surface atoms. Electrocatalytic properties and structural characterization of such adlayer revealed the formation of Pt-skin, which was verified by by the suppressed H_{upd} region and substantial positive shift of the Pt-OH_{ad} peak as well as by ~5-times increased in specific activity of the ORR (Figure 1).

The knowledge obtained from the well-defined systems is then used to optimize the catalytic properties of the $Pt_{50}Ni_{50}$ NPs with skeleton type of surfaces mentioned above [FY 2011 Ref. 3]. Further modification of near-surface morphology was obtained by a subsequent annealing of the skeleton-type of NPs at 400°C. This treatment has facilitated relaxation of low-coordinated surface atoms and transition of the particle surface morphology into Pt-skin type. Combined scanning transmission electron microscopy (STEM) and energy dispersive X-ray (EDAX) analyses revealed a concentration profile and the thickness of the Pt overlayer. It has been found that the particle core has

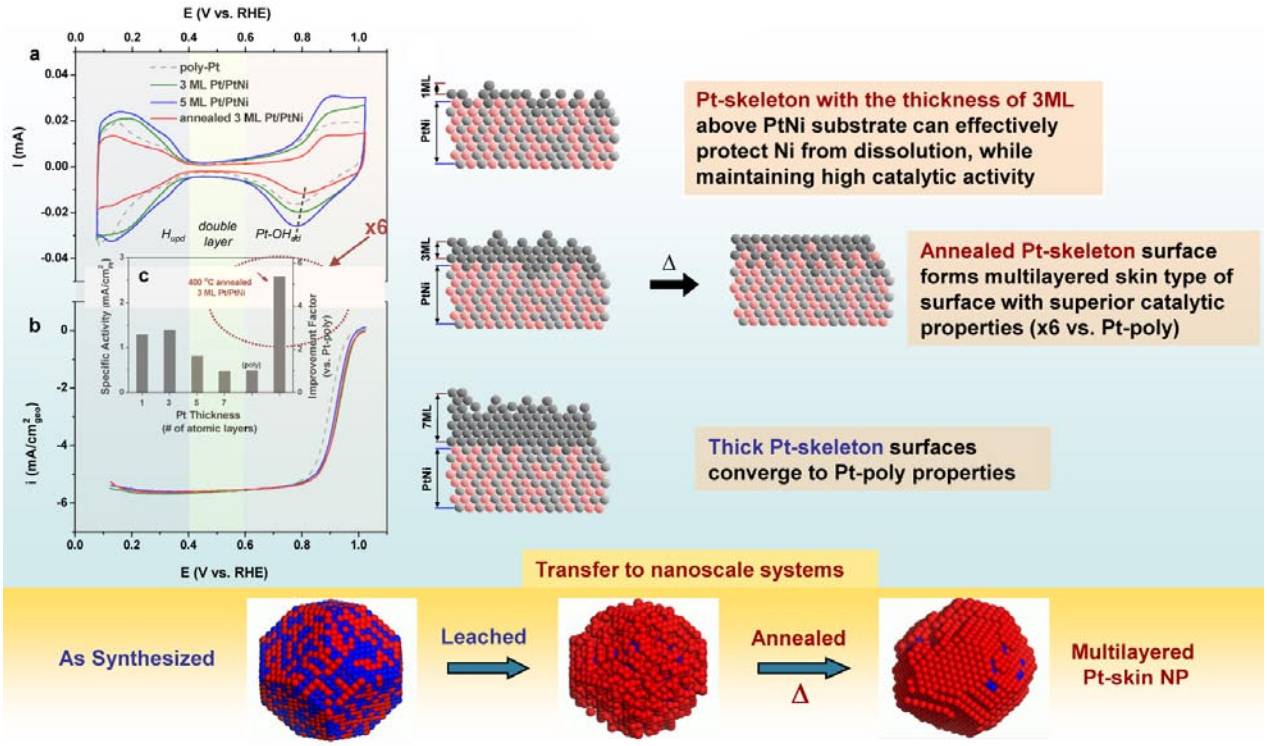


FIGURE 1. Electrochemical studies on the Pt thin films deposited over PtNi substrate by rotating disk electrode (RDE): (a) cyclic voltammograms, (b) polarization curves and (c) summary of specific activities and corresponding improvement factors (vs. polycrystalline Pt surface) for the Pt films of various thicknesses. Cyclic voltammograms were recorded in Ar saturated 0.1 M $HClO_4$ electrolyte with a sweeping rate of 20 mV/s. Polarization curves were recorded in the same electrolyte under O_2 saturation with a sweep rate of 20 mV/s. Specific activities were presented as kinetic currents normalized by electrochemical surface areas obtained from integrated H_{upd}, except that for the annealed 3 ML Pt/PtNi surface it was based on CO_{ad} stripping polarization curve. Schematic representation of surface morphology transformations for PtNi NP.

$Pt_{50}Ni_{50}$composition, while the thickness of the Pt overlayer is about 2-3 ML; schematic representation is depicted in Figure 1. Based on electrochemical characteristics we concluded that these nanoparticles have typical Pt-skin properties, i.e., suppressed H_{upd} region and superior catalytic activity towards the ORR: SA=1 mA/cm^2 at 0.95 V. In addition, PtNi NPs with multilayered skin surfaces are found to have excellent durability after 30,000 cycles between 0.5 to 1.1 V [1].

Finally, catalytic activity and stability of these NPs were tested in an MEA (General Motors R&D facilities). It is found that PtNi/C NPs with Pt multilayer skin surfaces have 3x higher specific activity (0.8 mA/cm^2) than benchmark Pt/C and mass activity of 0.35A/mg_{Pt}. Furthermore, after 20,000 cycles the activity loss was only 12%, while commercially available Pt/C and bimetallic catalysts suffer loss of 30-50%. Therefore, we concluded, that $Pt_{50}Ni_{50}$/C NPs with multilayered Pt skin meet DOE 2015 targets for specific activities and exceed anticipated targets for stability.

Characterization, Activity and Stability of Ternary Systems. Organic colloidal solvo-thermal approach was developed to synthesize Pt_3MN (N,M = Fe, Co, and/or Ni) ternary alloys that potentially could be used as the cathode materials in PEMFC systems. Although many types of catalysts have been synthesized, for our purposes here we present only the results for the most promising ternary catalysts. As summarized in Figure 2, the transmission electron microscope (TEM) image depicts highly uniform particle size of the Pt_3NiCo NPs, with the average particle size of ~6 nm. On the other hand, the analysis of high angle annular dark field (HAADF) and STEM data indicated homogenous distribution of the alloying elements. The X-ray diffraction analysis showed single crystal phase for all NPs, confirming the homogeneous alloy composition. It is obvious, therefore, the solvo-thermal synthesis brings high level of control of the crucial parameters such as homogenous distribution of particle size and composition profiles. We demonstrate further that these types of NPs may possess desirable catalytic activity for the ORR. For example, Figure 3 shows that acid-leached Pt_3CoNi NPs have the highest specific (0.85 mA/cm^2) and mass (0.3 A/mg_{Pt}) activity at 0.95 V. These results strongly suggest that alloying Pt with the 3d elements can provide additional tunability towards the activity of Pt-based alloy catalysts. We anticipate that catalytic activity of the PtMN NPs with skeleton type of

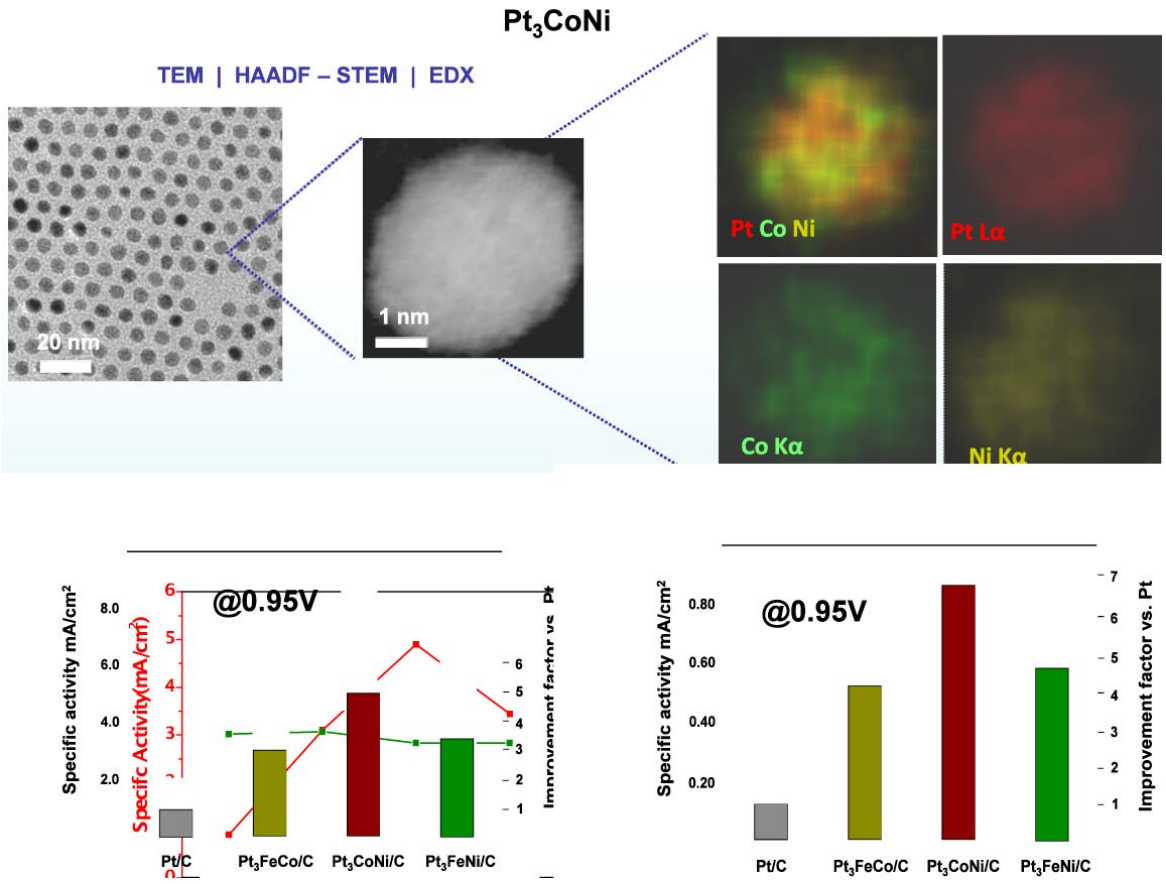


FIGURE 2. TEM, HAADF-STEM, EDAX and electrochemical characterization of Pt_3CoNi ternary alloy nanoparticles. Bar graphs: the summary of specific and mass activities of Pt_3MN NPs measured by rotating disk electrode in 0.1M $HClO_4$ at 0.95 V, 1,600 rpm and 20 mV/s.

surfaces could be further improved by the temperature-induced formation of the Pt-skin morphology.

Shape Controlled Core/Shell Ternary Nanoparticles. In addition to ternary systems mentioned above we develop an approach toward design and synthesis of an advanced three component system with core/shell structure. A ternary catalyst with Au core and bimetallic Pt_3Fe shell is being developed for the ORR. Tailored Au/Pt_3Fe structure has been optimized through the studies of well-defined thin film surfaces and then synthesized by organic solvo-thermal method. The morphology control and preferred composition profile were achieved through epitaxial growth of Pt_3Fe over 7 nm Au seed. Figure 3 depicts the morphology, structure, and size of the Au/Pt_3Fe NPs with the average size of 10 nm. High resolution transmission electron microscopy (HRTEM) images reveal that while both Au NPs and Au/Pt_3Fe NPs possess an icosahedral-like shape, Pt_3Fe particles have a characteristic cubo-octahedral shape. The composition profile of multimetallic particles, established from HAADF-STEM imaging and elemental mapping, signify that the Au seed is surrounded by both Pt and Fe atoms. As shown in Figure 3, these multimetallic Au/Pt_3Fe NPs possess both the high catalytic activity and the superior durability, with mass activity enhancements of more than one order of magnitude over Pt catalysts. Furthermore, TEM images and electrochemical capacitance analysis of cyclic voltammograms acquired before and after durability testing (60,000 cycles in the potential range between 0.6 and 1.1 V in oxygen saturated electrolyte) unambiguously revealed that in contrast to Pt_3Fe/C and Pt/C no significant loss in electrochemically active surface area (360 vs. 340 cm^2/mg_{Pt}) or specific activity (1.5 vs. 1.4 mA/cm^2) before and after cycling was observed for $Au/Pt_3Fe/C$. The increased activity was explained based on electronic effects induced by alloying Pt with Fe, the enhanced durability was achieved by the tailored morphology of icosahedral NPs and unique compositional profile of three alloying components [2]. The reported result for the core-shell type of catalysts has opened new avenues for synthesis of highly active and stable cathode catalysts for the PEMFC applications.

Conclusions and Future Directions

- PtM and PtM_1N_2 NPs cathode catalysts obtained from the organic solvo-thermal synthesis exhibit superior activity and stability than those prepared by the

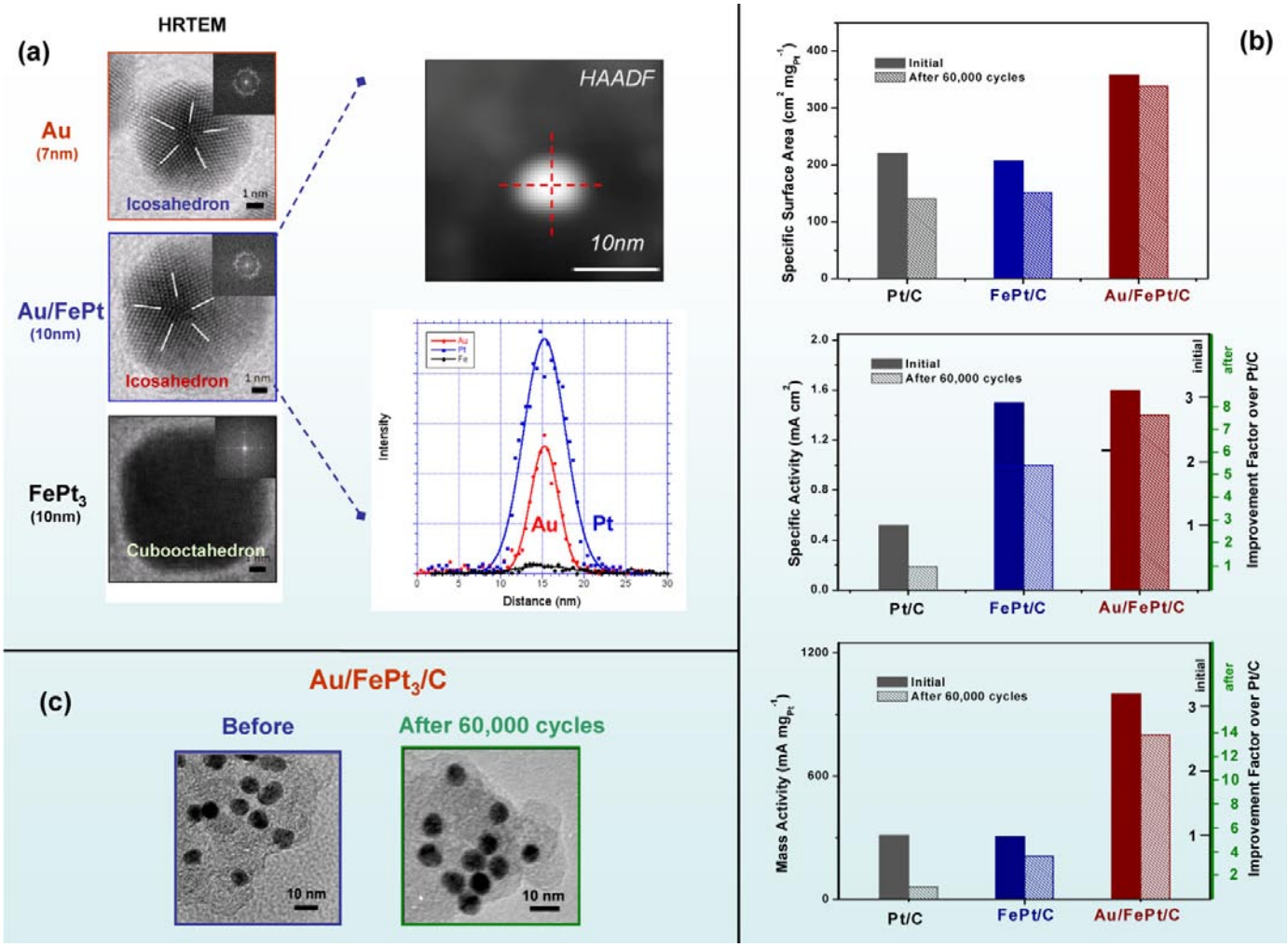


FIGURE 3. Ternary core shell Au/FePt catalyst: (a) HRTEM characterization of Au, Au/FePt and $FePt_3$ nanoparticles. HAADF and energy dispersive X-ray characterization of Au/FePt NP, which confirms core/shell structure. (b) Electrochemical charatcerizaation by RDE at 0.9 V in 0.1M $HClO_4$ for Pt/C, Pt_3Fe and Au/FePt catalysts. (c) Morpphology studies by TEM before and after 60,000 potential cycles in 0.1 M $HClO_4$ between 0.6 to 1.1 V.

conventional methods. The methods of synthesize of PtNi NPs with higly active and stable Pt-skin morphology is developed.

- Significant mass activity and durability improvement are obtained for Pt-skin PtNi/C NPs with multilayered (2-3 atomic layers) Pt skin in both rotating disk electrode configuration and MEA. Advanced theoretical modeling methods are developed for resolving nanosegregated structures.
- Ternary systems possess high activity and stability but understanding the mode of action of two three-dimensional elements added to the Pt host has yet to be addressed.
- In collaboration with industrial partners, further testing in MEA of the most promising multimetallic catalysts is planned as well as scaling up synthesis methods for the larger scale production of the most active catalysts.

FY 2011 Publications/Presentations

1. C. Wang, M. Chi, G. Wang, D. vanderVliet, D. Li, K.L. More, H.Wang, J.A. Schluter, N.M. Markovic, V.R. Stamenkovic, *Relationship between Surface Chemistry and Electrocatalytic Properties of Monodisperse Pt_xNi_{1-x} Nanoparticles,* Advanced Functional Materials, 21(2011)147, Cover Page Article.

2. C. Wang, D.van derVliet, K.L. More, N.J. Zaluzec, S. Peng, S. Sun, H. Daimon, G. Wang, J. Greeley, J. Pearson, A.P. Paulikas, G. Karapetrov, D. Strmcnik, N.M.Markovic, V.R. Stamenkovic, *MultimetallicAu/$FePt_3$ Nanoparticles as Highly Durable Electrocatalysts,* Nano Letters, 11(2011)919-928, Cover PagE Article.

3. C. Wang, M.Chi, D. Li, D. Strmcnik, D. vanderVliet, G. Wang, V.Komanicky, K.-C.Chung, A.P. Paulikas, D. Tripkovic, J. Pearson, K.L. More, N.M. Markovic, V.R. Stamenkovic, *Design and Synthesis of Bimetallic Electrocatalyst with Multilayered Pt-Skin Surfaces,* Journal of American Chemical Society, In press.

5. C. Wang, S. Sun, N. Markovic and V. Stamenkovic, *Epitaxially Conjugated Composite Nanoparticles - Synthesis and Catalytical Applications,* Materials Research Society Spring Meeting, April 2010, San Francisco, CA.

6. C.Wang, D.Strmcnik, D.Tripkovic, K.L.More, N.M.Markovic and V.Stamenkovic, *The Role of Surface Structure and Surface Composition in Electrocatalysis* (Plenary Lecture) International Society of Electrochemistry Regional Meeting, June 2010, Belgrade, Serbia.

7. C.Wang, N.M.Markovic and V.Stamenkovic, *Morphology Controlled Synthesis of Composite Nanoparticles by Rational Designed Conditions,* American Chemical Society Fall Meeting, August 2010, Boston, MA.

8. C. Wang, D. Strmcnik, D.Tripkovic P. Paulikas, D., V. Stamenkovic , N. Markovic, *Understanding the Complexity of Fuel Cell Catalysts,* Gordon Research Conference – Fuel Cells, Smithfield RI, August 1, 2010.

9. D. Strmcnik, R, Subbaraman, D. Tripkovic, V. Stamenkovic and N. M. Markovic, *Electrocatalysis- Learning from the Past to Master the Future,* International NIMS/DOE meeting on fuel cells development, Honolulu, Hawaii, August 2010.

10. C. Wang, N. Markovic and V. Stamenkovic, *PtNi Nanostructure Optimization for Electrocatalytic Reduction of Oxygen,* 2010 Materials Research Society Fall Meeting, November 2010, Boston, MA.

11. M. Chi, C. Wang, N. Markovic, K. More and V. Stamenkovic, *In-Situ Observation of Skin-layer Formation in Pt_3Ni Nanoparticles,* 2010 Materials Research Society Fall Meeting, November 2010, Boston, MA.

12. C. Wang, D. Strmcnik, D. Tripkovic, N. Markovic and V. Stamenkovic, *Advanced Nanoscale Electrocatalysts for Fuel Cells,* 2010 Materials Research Society Fall Meeting, November 2010, Boston, MA.

References

1. V. Stamenkovic, B. Fowler, B.S. Mun, G. Wang, P.N. Ross, C. Lucas, and N.M. Markovic, "Improved Oxygen Reduction Activity on $Pt_3Ni(111)$ via Increased Surface Site Availability", *Science*, **315** (2007) 493-497.

2. N.M. Markovic and P.N. Ross, "Surface Science Studies of Model Fuel Cell Electrocatalysts", *Surface Science Report*, **45** (2002) 121-229.

3. V.Stamenkovic and N.M.Markovic, "Electrocatalysis on Model Metallic and Bimetallic Single Crystal Surfaces, Model Systems in Catalysis: From Single Crystals and Size Selected Clusters", Editor: Robert M. Rioux, Harvard University, USA; Publisher: Elsevier Science, Amsterdam, The Netherlands, *2009*.

4. V. Stamenkovic, B.S. Mun, M. Arenz, K.J.J.Mayrhofer, C. Lucas, G. Wang, P.N. Ross, and N.M. Markovic, " Trends in Electrocatalysis on Extended and Nanoscale Pt-bimetallic Alloy Surfaces ", *Nature Materials.*, **6** (2007) 241-247.

5. C. Wang, D. van der Vliet, K.C. Chang, N.M. Markovic, V.R. Stamenkovic, "Monodisperse Pt_3Co Nanoparticles as Electrocatalyst: the Effect of Particle Size and Pretreatment on Electrocatalytic Reduction of Oxygen", *Phys.Chem.Chem.Phys*., **12**(2010)6933-6939; ***Cover Article***.

6. C. Wang, D. van der Vliet, K.C. Chang, H. You, D. Strmcnik, J.A. Schlueter, N.M. Markovic, V.R. Stamenkovic, "Monodisperse Pt_3Co Nanoparticles as a Catalyst for the Oxygen Reduction Reaction: Size Dependent Activity", *J. Phys. Chem. C.,* **113**(2009)19365.

V.D.6 Contiguous Platinum Monolayer Oxygen Reduction Electrocatalysts on High-Stability Low-Cost Supports

Radoslav Adzic (Primary Contact), Miomir Vukmirovic, Kotaro Sasaki, Jia Wang, Yang Shao-Horn[1], Rachel O'Malley[2]
Brookhaven National Laboratory (BNL), Bldg. 555
Upton, NY 11973-5000
Phone: (631) 344-4522
E-mail: adzic@bnl.gov

DOE Manager
HQ: Nancy Garland
Phone: (202) 586-5673
E-mail: Nancy.Garland@ee.doe.gov

Subcontractors:
[1] Massachusetts Institute of Technology (MIT), Cambridge MA
[2] Johnson Matthey Fuel Cells (JMFC), London, England

Project Start Date: July 1, 2009
Project End Date: September 30, 2013

Fiscal Year (FY) 2011 Objectives

Developing high-performance fuel cell electrocatalysts for the oxygen reduction reaction (ORR) comprising contiguous Pt monolayer (ML) on stable, inexpensive metal or alloy:

- Nanoparticles (NP)
- Nanorods; Nanowires
- Carbon nanotubes (CNT)

Technical Barriers

This project addresses the following technical barriers from the Fuel Cells section of the Fuel Cell Technologies Program Multi-Year Research, Development and Demonstration Plan:

(A) Performance
(B) Cost
(C) Durability

Technical Targets

Progress toward meeting DOE fuel cell electrocatalysts technical targets is shown in Table 1.

FY 2011 Accomplishments

- Demonstrated the stabilization mechanism of core-shell NPs by which a Pt ML shell is being protected by the cores.
- Demonstrated synthesis of hollow Pd NP with hollow-induced lattice contraction enhancing the ORR activity on a Pt ML.
- Demonstrated electrodeposition of Pd nanorods and nanowires on functionalized carbons as a support for high activity and durability of Pt ML catalysts. The performance of a 5 cm^2 MEA shows an excellent activity/stability.
- Demonstrated synthesis of one-dimensional interconnected Pt NPs on amine-functionalized multi-wall carbon nanotubes (MWCNTs).
- Demonstrated synthesis of tetrahedral Pd NPs – an excellent low-Pd content support for a Pt monolayer.
- Developed high performance Pt monolayer on non-noble metal core-noble metal shell NP –Pt/Ir/Ni/C-electrocatalyst. 1 ML Pt and 2MLs Ir around Ni core.
- Fuel cell stability tests of $Pt/Pd_9Au_1/C$ electrocatalysts show no dissolution or loss in activity during 100,000 and 200,000 potential cycles. This electrocatalyst is ready for applications.



TABLE 1. Progress toward Meeting DOE Fuel Cell Electrocatalysts Technical Targets

Characteristic	Units	Target	Target	Achieved
		2010	2015	2010
Platinum Group Metal (PGM) Total Loading	mg PGM/cm^2 electrode area	0.3	0.2	0.11
Mass Activity	A/mg Pt @ 900 $mV_{iR\text{-}free}$	0.44	0.44	2.8 (Pt onPd nanowires)
Specific Activity	$\mu A/cm^2$ @ 900 $mV_{iR\text{-}free}$	720	720	1,100 (Pt on Pd rods)
PGM Mass Activity				0.58 (Pt on hollow Pd)
Durability				No loss in activity in 200,000 cycles Pt/Pd(Au) in fuel cell test

iR-free – internal resistance-free

Introduction

Building on the advances made in the last decade in fuel cell electrocatalysis yielding improved electrocatalysts, and increasing our understanding of the kinetics of the ORR, further developments during the last two years lessened some technological difficulties that used to hamper the automotive applications of fuel cells. The understanding of the properties of Pt ML electrocatalysts, and of a broader class of core-shell electrocatalysts, Pt alloys, dealloying approach, and of complex influence of the NP size and shape on the catalyst's activity made it possible to optimize the properties of certain classes.

Approach

Following our position on the role of OHads on Pt on the ORR from the late eighties, and our recent finding of significant weakening of binding energy of oxygen (BE-O) on the (111) facet compared to the extended surface due to nanoscale induced in-plane lattice contraction, our approach focuses on having surfaces with the high coordination (111) facets. These surfaces are most conducive to the ORR on NPs. In addition, they are less prone to dissolution than low-coordinated edges, defects, and less close-packed facets. Because the ORR rate on Pt is OH-, or O-desorption limited, lowering BE-O enhances the ORR activity. Therefore, smooth, lattice contracted (111) like surface structures are needed to achieve durable high-ORR activity.

Therefore, we synthesized the supporting NPs having predominantly highly coordinated atoms that exist on nanorods, nanowires, smooth NPs, hollow Pd spheres, single crystalline NPs with predominantly (111) facets. We used the electrodeposition to make Pd nanorods on C NPs, Toray paper (5 cm^2), and gas diffusion layer (GDL).

Results

Pt Monolayer on Electrodeposited Pd Nanorods, Nanowires Electrocatalysts

The nanorods and nanowires having smooth surfaces are attractive supports for Pt monolayer. Electrodeposition facilitates a better Pd utilization and a direct formation at the carbon surfaces that provides electrolyte access to a major part of the catalysts' surface and thus its best utilization. Figure 1 shows the polarization curve of 5 cm^2 electrode obtained electrochemically on Toray paper. Total PGM loading is 0.11 mg/cm^2.

Bimetallic IrNi Core Platinum Monolayer Shell Electrocatalysts

To further decrease the PGM content we synthesized the electrocatalyst consisting of a Pt monolayer placed on carbon-supported thermally treated IrNi core–shell NPs.

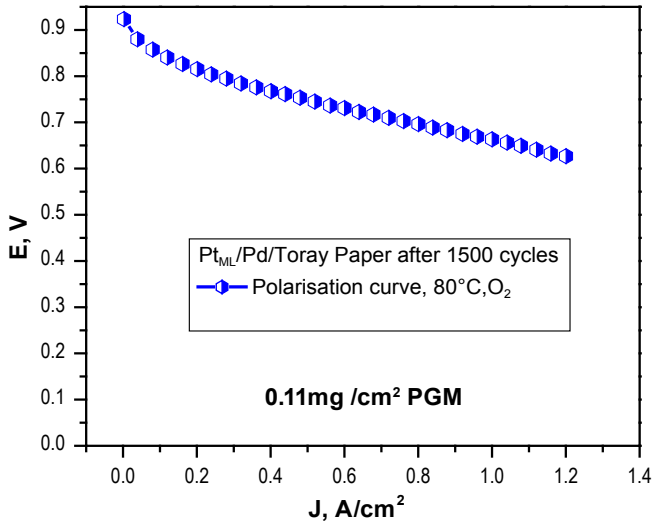


FIGURE 1. Polarization curve for the cell with 5 cm^2 cathode. The catalyst Pt_{ML}/Pd obtained electrochemically on Toray paper. Total PGM loading is 0.11 mg/cm^2.

The Pt mass activity of the Pt_{ML}/IrNi/C electrocatalyst obtained in a scale up synthesis is approximately three times higher than that of the commercial Pt/C electrocatalyst. The electronic and geometrical effects of the IrNi substrate on the Pt monolayer result in its higher catalytic activity that that of Pt NPs. The structure and composition of the core-shell NPs were verified using transmission electron microscopy and in situ X-ray absorption spectroscopy, while potential cycling test was employed to confirm the stability of the electrocatalyst (Figure 2).

Pt Monolayer on Hollow Pd NPs Electrocatalysts

Based on promising results obtained with hollow Pt NPs, we explored possibility to form hollow Pd naoparticle support for a Pt monolayer. It is interesting to see whether hollow can induce a needed lattice contraction in an overlayer. Using Ni NPs as dissolvable template, we produced compact Pd hollow nanospheres. Excellent activity was found after deposition of a Pt monolayer: Pt+Pd+Au mass activity is 0.57 A mg^{-1}; Pt mass activity = 1.62 A mg^{-1}, specific activity = 0.85 $mAcm^{-2}$.

One-Dimensional Interconnected Pt NPs on Amine-Functionalized MWCNTs

MWCNTs were functionalized by amine groups in a Polyol synthesis. Further treatment involved rinsing in 6 M HCl and thermal treatment at 220°C. Excellent specific and mass activities were obtained (Figure 3). PGM mass activity is 1.4 times that of 40% Tanaka Kikinzoku Kogyo, while specific activity is 0.9 mA/cm^2.

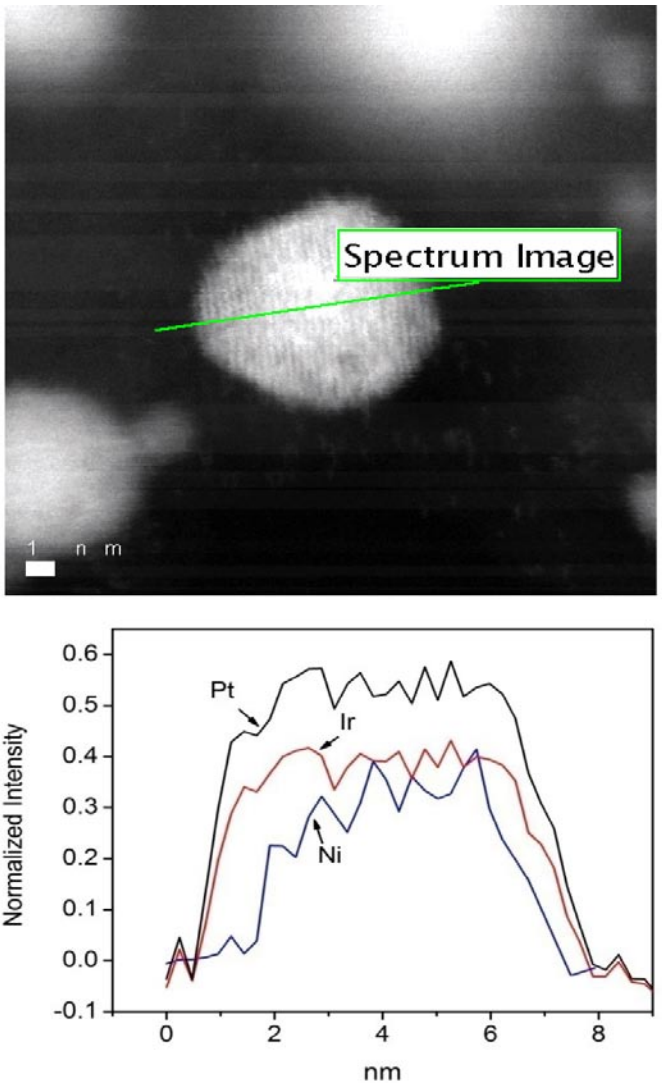


FIGURE 2. Bimetallic Ni-Ir Core Pt ML shell electrocatalysts after 50,000 potential cycles test. Upper panel: High angle annular dark field image of a single NP; Lower panel: Distribution of Pt and IrNi components in a single representative NP from M and L absorption edges. It is clearly shown that the core-shell structure of IrNi NP is maintained even after 50,000 cycles.

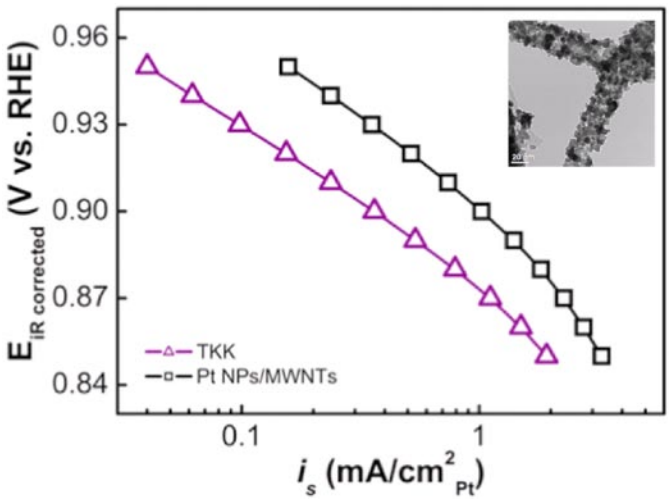


FIGURE 3. Polarization curve for the ORR on Pt interconnected NPs on MWCNTs compared with a commercial Pt/C catalyst. Insert: Scanning transmission electron microscopy image of the segment of CNT with the Pt deposit.

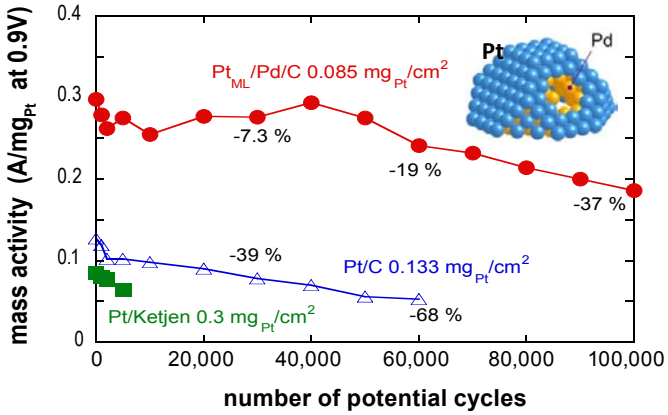


FIGURE 4. Accelerated stability fuel cell tests of the Pt/Pd/C and two commercial Pt/C cathode catalysts given for comparison. Potential cycling from 0.6 and 1.0 V; dwell time 10 sec; square-wave modulation; 80°C.

Fuel Cell Tests of the $Pt_{ML}/Pd/C$ and $Pt_{ML}/Pd_9Au/C$ at Toyota

Several stability tests of Pt/Pd/C and $Pt/Pd_9Au/C$ catalysts involving potential cycling from 0.6 and 1.0 V; dwell time 10 sec; square-wave modulation; 80°C have been performed. High stability of Pt ML and a partial dissolution of Pd in some cases led to the mechanism of stability of core-shell electrocatalysts in which the shell is protected by the core. Pd dissolution precludes dissolution of Pt (cathodic protection effect) and more importantly, the contraction of Pt and Pd lattices, induced by loss of Pd, increases stability and activity of the catalyst – self-healing effect (Figure 4). Negligible loss in activity is observed in 100,000 cycles with Pt/Pd/C catalysts, while with the more stable $Pt/Pd_9Au/C$, no loss is seen. Commercial Pt/C catalysts perish completely within 50,000 cycles. The Pt/Pd/C and $Pt/Pd_9Au/C$ catalysts are ready for applications.

Conclusions and Future Directions

- Smooth surfaces, with highly-coordinated atoms, are suitable to support a Pt ML that yields very active catalysts.
- Pd nanowires were synthesized. Their thickness needs to be reduced and removal of surfactants simplified to obtain an excellent catalyst with a Pt ML.
- Electrodeposited NPs make excellent supports for Pt. Scale up of the cell for electrodeposition of Pd NPs

seems possible to the dimensions required for fuel cell stacks.
- Hollow Pd and Pt NPs are very attractive for further studies.
- Bimetallic IrNi core platinum monolayer shell electrocatalysts are highly promising for scale up syntheses and further reduction of PGM content (one ML of Pt and two MLs of Ir).
- The $Pt/Pd_9Au_1/C$ electrocatalyst is ready for application in fuel cells for electric vehicles.

Future studies will focus on:

- Improve synthesis of Pd nanorods, nanowires, and Pd hollow NPs. (BNL, MIT, JMFC)
- Improve metallization and catalysation of CNTs, oxides, nitrides. (JMFC, MIT, BNL)
- Pd-Nb alloy NPs; start the work on Pd-W NPs and Pd-V. (BNL, MIT)
- Scale up of selected catalysts up to 20 grams. (JMFC, BNL)
- Scale up of electrodeposition on Toray paper and GDL to 50 and 500 cm^2 electrodes.
- MEA fabrication and tests.

Special Recognitions & Awards

1. Radoslav Adzic was named *Inventor of the Year* by Battelle Memorial Institute.

Patent Applications

1. "Hollow nanoparticles as active and durable catalysts and methods for manufacturing the same", Jia X. Wang, Radoslav R. Adzic, provisional application filed on July 14, 2010.

2. BSA 08-33 (2/18/2010) Platinum-Coated Non-Noble Metal-Noble Metal Core-Shell Electrocatalysts.

3. BSA 08-32 (8/26/2010) US2010/0216632 A1 High Stability, Self-Protecting Electrocatalyst Particles.

4. Patent BSA 10-03 entitled "Apparatus and method for the synthesis and treatment of metal monolayer electrocatalyst particles in batch or continuous fashion" BNL docket no. 1004305.034US.

Patents Issued

1. U.S. patent 7,691,780 B2 "Platinum- and Platinum Alloy-coated Palladium and Palladium Alloy Particles and uses thereof" (04/06/2010).

2. U.S. patent 7,704,918 B2 "Synthesis of Metal-Metal Oxide Catalysts and Electrocatalysts Using a metal cation Adsorption/Reduction and Adatom Replacement by More Noble Ones" (04/27/2010).

3. U.S. Patent No. 7,855,021 issued 12_21_2010-Electrocatalysts having Platinum Monolayers on Palladium, Palladium Alloy and Gold Alloy Core-Shell Nanoparticles and Uses Thereof.

FY 2011 Publications/Presentations

1. W-P. Zhou, K. Sasaki, D. Su, Y. Zhu, J.X. Wang, R.R. Adzic, "Structural and Electrocatalytic properties of Large-scale Synthesized Pt Monolayers on Pd_2Co Electrocatalysts for Oxygen Reduction Reaction", *Journal of Physical Chemistry C*, 114(19) (2010) 8950-8957.

2. Core-Protected Platinum Monolayer Shell High-Stability Electrocatalysts for Fuel-Cell Cathodes, Kotaro Sasaki, Hideo Naohara, Yun Cai, Yong Man Choi, Ping Liu, Miomir B. Vukmirovic, Jia X. Wang and Radoslav R. Adzic, Angew. Chem. Int. Ed., 49 (2010) 8602.

3. Platinum Monolayer Electrocatalysts for O2 Reduction: Pt Monolayer on Carbon-Supported PdIr Nanoparticles, Seth L. Knupp, Miomir B. Vukmirovic, Pradeep Haldar, Jeffrey A. Herron, Manos Mavrikakis, and Radoslav R. Adzic, Electrocatal., 1 (2010) 213.

4. Enhancing Oxygen Reduction Reaction Activity via Pd-Au Alloy Sublayer Mediation of Pt Monolayer Electrocatalysts, Yangchuan Xing, Yun Cai, Miomir Vukmirovic, Wei-Ping Zhou, Jia Wang, Radoslav Adzic, Hiroko Karan, J. Phys. Chem. Lett., 1 (2010) 3238.

5. K. Sasaki, J.X. Wang, H. Naohara, M. Marinkovic, K. More, H. Inada, R.R. Adzic, "Recent Advances in Platinum Monolayer Electrocatalysts for Oxygen Reduction Reaction: Scale-up Synthesis, Structure and Activity of Pt Shells on Pd Cores", *Electrichimica Acta*, 55(8) (2010)) 2645-2652.

6. Intermetallics as Support for Pt Monolayer O_2 Reduction Electrocatalysts: Potential for Significantly Improving Properties, Tanushree Ghosh, Miomir B. Vukmirovic, Francis J. DiSalvo, Radoslav R. Adzic, J. Am. Chem. Soc., 132 (2010) 906.

Book Chaper

K. Sasaki, M. B. Vukmirovic, J.X. Wang, R.R. Adzic, "Platinum Monolayer Electrocatalysts: Improving Structure and Activity", *Fuel Cell Science: Theory, Fundamentals, and Bio-Catalysis*, J. Norskov, A. Wieckowski (eds), John Wiley & Sons, Inc. (New York), (2010) p. 215-236.

Presentations

1. R.R. Adzic, Electrocatalysis, Internat. Symp., Kloster Irsee, Germany, August 2010 (key-note lecture).

2. R.R. Adzic, 218th Electrochemical Society Meeting, Las Vegas, NV, October, 2010. (key-note lecture).

3. M.B. Vukmirovic, K. Sasaki, W-P. Zhou, Y. Cai, K. Gong, P. Liu, J.X. Wang, R.R. Adzic, Recent Advances in Developing Platinum Monolayer Electrocatalysts for the O_2 Reduction Reaction, Gordon Conference on Electrodeposition, Colby-Sawyer College in New London, New Hampshire, August 1–6, 2010, Invited Talk.

4. K. Sasaki, H. Naohara, Y. Cai, D. Su and R. Adzic, "Characterization of Platinum Monolayer Electrocatalysts in Long-Term Fuel Cell Cathode Tests", 217th ECS meeting, Vancouver, April 28, 2010.

5. K. Gong, K. Sasaki, M. Vukmirovic and R. Adzic, "In Situ Decomposing Prussian Blue Analogues to Form Multimetallic Aggregations with Various Surface Ensemble for Pt-Monolayer Electrocatalyst", 217th ECS meeting, Vancouver, April 28, 2010.

6. R. Adzic, K. Sasaki, H. Naohara, M. Vukmirovic, J.X. Wang, and Y. Cai, "Advances in Pt Monolayer Electrocatalysts for Oxygen Reduction Reaction and Prospects for Automotive Applications", 218th ECS meeting, Las Vegas, October 13, 2010.

7. A.T. Haug, R.T. Atanasoski, K. Sasaki, Y. Cai, and R. Adzic, "Stability of a Pt-Pd Core-Shell Catalyst: A Comparative Fuel Cell and RDE Study", 218th ECS meeting, Las Vegas, October 13, 2010.

8. K.A. Kuttiyiel, K. Sasaki, and R. Adzic, "Bimetallic Ni-Ir Core Platinum Monolayer Shell Electrocatalysts for the O_2 Reduction Reaction", 218th ECS meeting, Las Vegas, October 12, 2010.

9. Jia X. Wang, Chao Ma, YongMan Choi, Dong Su, Yimei Zhu, Ping Liu, Rui Si, and Radoslav R. Adzic, "Platinum hollow spheres as active and durable nanocatalysts for oxygen reduction in fuel cells", International conference of "Challenges in Inorganic and Material Chemistry", Hong Kong, July 22, 2010.

10. Jia X. Wang, Chao Ma, YongMan Choi, Dong Su, Yimei Zhu, Ping Liu, Rui Si, and Radoslav R. Adzic, "Platinum hollow spheres as active and durable nanocatalysts for oxygen reduction in fuel cells", 218th Electrochemical Society Meeting, Las Vegas, October 12, 2010.

V.D.7 The Science and Engineering of Durable Ultralow PGM Catalysts

Fernando H. Garzon (Primary Contact), Jose-Maria Sansiñena, Mahlon Wilson, Jerzy Chlistunoff, Ivana Matanovic, Neil Henson and Eric L. Brosha

Los Alamos National Laboratory
MPA-11, MS. D429
Los Alamos, NM 87545
Phone: (505) 667-6643
E-mail: garzon@lanl.gov

DOE Manager
HQ: Nancy Garland
Phone: (202) 586-5673
E-mail: Nancy.Garland@ee.doe.gov

Subcontractors:
- Yushan Yan, University of California, Riverside, Riverside, CA
- Abhaya Datye and Elena Beriba-Vera, University of New Mexico, Albuquerque, NM
- Siyu Ye and David Harvey, Ballard Fuel Cells, Burnaby, BC, Canada

Project Start Date: October 2009
Project End Date: October 2014

Fiscal Year (FY) 2011 Objectives

- Development of durable, high mass activity platinum group metal (PGM) cathode catalysts enabling lower cost fuel cells.
- Elucidation of the fundamental relationships between PGM catalyst shape, particle size and activity to help design better catalysts.
- Optimization of the cathode electrode layer to maximize the performance of PGM catalysts improving fuel cell performance and lowering cost.
- Understanding the performance degradation mechanisms of high mass activity cathode catalysts to provide insights to better catalyst design.
- Development and testing of fuel cells using ultra-low loading high activity PGM catalysts – validation of advanced concepts.

Technical Barriers

- PGM catalysts are difficult to synthesize in configurations other than quasi-spherical particles.
- PGM area specific activity may decrease with decreasing particle size.
- Durability may decrease with greater PGM surface area to volume ratios.

Technical Targets

The technical targets for catalyst loading are indicated in Table 1. These targets were formulated with the assumption that fuel cell durability and impurity tolerance would not be impacted by the decreased Pt loadings used in the fuel cells.

TABLE 1. Technical Targets: Electrocatalysts for Transportation Applications (Extracted from Table 3.4.12. Technical Plan. April 27, 2007)

Characteristic	Units	2005 Status		Stack Targets	
		Cell	Stack	2010	2015
PGM total content (both electrodes)	g/kW (rated)	0.6	1.1	0.3	0.2
PGM total loading	mg PGM/cm^2 electrode area	0.45	0.8	0.3	0.2

FY 2011 Accomplishments

- Synthesis, structural, (high resolution transmission electron microscopy [HRTEM] and X-ray diffraction [XRD]) and electrochemical characterization of Pt Pd nanoplates completed.
- Synthesis structural, (HRTEM and XRD) and electrochemical characterization of Pt/ceria/carbons catalysts completed and published.
- Synthesis structural, (HRTEM and XRD) and electrochemical characterization of Pt polypyrrole nanowires completed and published.
- Thermal characterization of Pt/ceria/C catalysts completed and published.
- Theoretical model of Pt-Ni nanoparticles developed and published.
- Theoretical modeling of Pt nanotubes completed.
- Microstructural model of the catalyst electrode layer validated against experimental work.
- Pt nucleation growth study on carbon completed and published.



Introduction

Minimizing the quantity of Pt group metals used in polymer electrolyte membrane fuel cells (PEMFCs) is one of the remaining grand challenges for fuel cell commercialization. Tremendous progress has been achieved over the last two decades in decreasing the Pt loading required for efficient fuel cell performance. Unfortunately, the fluctuations in the price of Pt represent a substantial barrier to the economics of widespread fuel cell use.

Durability and impurity tolerance are also challenges that are tightly coupled to fuel cell Pt electrode loading. Traditional approaches to decreasing the amount of Pt required for good performance include:

- Increasing mass activity by decreasing Pt particle size by supporting on carbon.
- Alloy formulation Pt-Co, Pt-Cr alloys to improve mass activity.
- Increasing Pt utilization by optimization of electronic and ionic contact of the Pt particles.
- Improving conductivity of the electronic and ionic conducting constituents of the membrane electrode assembly.
- Improving reactant to and product mass transport away from the electroactive sites.

Recent novel approaches include the nanoengineering of core shell catalysts and Pt particles of unusual geometries such as nanowires/whiskers.

The success of the aforementioned approaches has been great; however further advances using such approaches have been hampered by a lack of underlining scientific understanding of the catalyst activity, particle growth mechanisms, and optimization strategies for designing composite electrodes.

Approach

Our approach to new PGM catalyst design is multi-tiered. We are designing new low platinum loading catalysts on novel support materials to improve fuel cell performance. Novel PGM shapes; nanoparticles, nanotubes and nanowires are being synthesized in a variety of sizes. We are using contemporary theoretical modeling and advanced computational methods to understand and engineer the new catalysts. We are also modeling and designing appropriate catalyst architectures to maximize the performance of our novel catalysts. Catalyst-support interactions and their effects on durability and mass activity are also investigated. We study and test the performance of the catalysts in electrochemical cells, single cell fuel cells and fuel cell stacks. The new catalysts are be extensively characterized before and after fuel cell operation.

Results

We have improved our theoretical understanding of the Pt-Ni alloy catalyst system, a very promising catalyst system recently demonstrated to meet the DOE technical targets for catalyst activity for oxygen reduction. The structure, reactivity and stability of three different Pt-Ni alloys, PtNi, Pt_3Ni and $PtNi_3$ were studied using periodic density functional theory (DFT) calculations. The influence of the alloying component concentration on the catalytic activity of the platinum surface was studied by calculating equilibrium adsorption potentials for oxygen reduction reaction (ORR) intermediates and by constructing free energy diagrams in the ORR dissociative mechanism network. In addition, the stability of these materials in aqueous environments was investigated in the terms of relative electrochemical dissolution shifts and by determining the most stable state of the surface as a function of pH and potential as represented in Pourbaix diagrams. The (111) surface of all three studied Pt-Ni alloys show improved oxygen reduction activity over Pt(111). The ORR overpotential was calculated to decrease as Pt (0.55 V) > Pt_3Ni (0.24 V) > $PtNi_3$ (0.19 V) > PtNi (0.15 V). Thus, it can be expected that the catalytic activity towards ORR will increase in the order Pt < Pt_3Ni < $PtNi_3$ < PtNi. Around 50% alloying with Ni induced the biggest change in activity. Shifts in the electrochemical dissolution potentials of the studied Pt-Ni alloys relative to platinum were estimated to be -0.27 V for $PtNi_3$, +0.13 V for Pt_3Ni and +0.30 for PtNi. Thus, among all studied materials PtNi is predicted to be the least susceptible to corrosion at similar pH and cell potentials.

The formation of Pt catalysts on active oxide supports may also improve activity and fuel cell durability. Highly crystalline ceria nanoparticles in porous carbon matrices were formed by the simple pyrolysis of cerium-loaded ion-exchange resins. The resulting cerium/carbon composite structures maintain the original bead or powder form of the precursor resins (Figure 1), with an increase in specific surface area. Incorporating Gd or Pr dopants with Ce in the resins provided uniform dispersions and equally small ceria crystallites upon pyrolysis, typically 1–2 nm (Figure 2). Highly active particles were obtained, as demonstrated by air light-off of the ceria/carbon composites as low as 200ºC. The combination of the high pyrolysis temperature (1,000ºC) and the controlled dispersion and stable environment provided by the ion-exchange resin precursors are key to provide highly crystalline and extremely small ceria particles

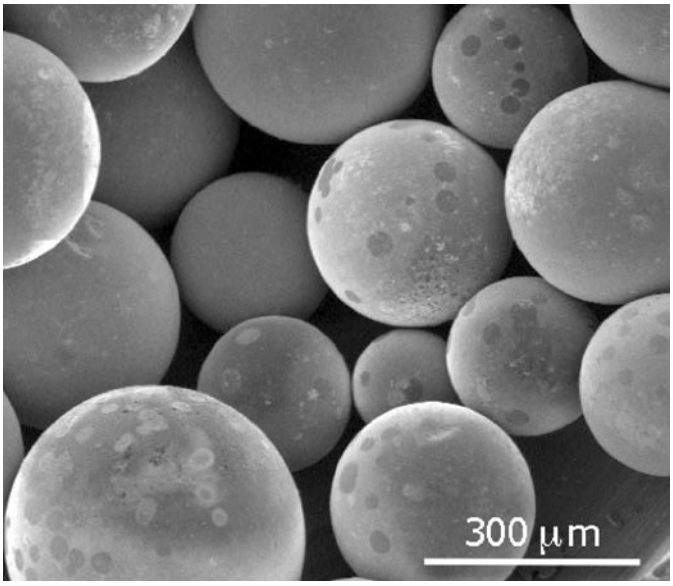


FIGURE 1. Scanning Electron Micrograph of Pyrolyzed IRC748 Beads

in a conductive carbon matrix. Various types of cation-exchange resins are considered and the best results are obtained with highly cross-linked or styrene-divinyl benzene matrices and cation chelating or weak acid functionalities.

One of the outstanding challenges in the wider deployment of PEMFCs is improving the utilization of Pt. While decreasing particle size improves accessibility of the Pt, it also destabilizes the Pt particles and leads to dissolution/re-precipitation and rapid grain growth. A parameter that is as yet poorly characterized is the number of nucleation sites on the carbon support. Increased nucleation site density could provide a valuable approach to improve Pt utilization. We have characterized the nucleation density by determining the number of particles per m^2 using HRTEM and energy dispersive X-ray spectroscopy (EDS). Ranges of metal loadings were explored to investigate their effect on the number of Pt particles on three types of carbon supports. It was concluded that the number of nucleation sites is relatively constant over the Vulcan family of carbon supports, see Table 2. However, activated carbons such as Norit SX-1G show much higher nucleation density.

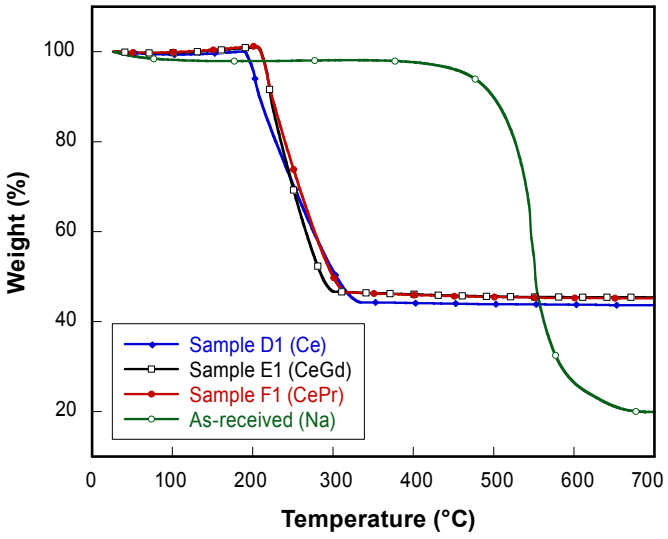


FIGURE 2. Air thermal gravimetric analysis of pyrolyzed IRC748 resins loaded with Ce (D1), Gd-doped Ce (E1), Pr-doped Ce (F1), and as-received Na form.

TABLE 2. Pt number density on Vulcan carbon derived from HRTEM analysis and EDS.

Catalyst	Pt wt%	Number of Pt particles/m^2
Aqueous Impregnation Pt/Vulcan XC72	3.7	1.20E+17
E-TEK 10 wt% Pt/Vulcan XC72R	11.3	1.04E+17
Cabot 20 wt% Pt/Vulcan XC72	29.8	1.01E+17

Conclusions and Future Directions

- Pt/Ceria/catalyst research and development:
  - Improve Pt dispersion and scale up synthesis for fuel cell testing.
  - Calculate optimal MEA geometries.
  - Ionomer incorporation into catalyst layers and MEA optimization.
  - Fuel cell performance and durability testing.
- Pt/Pd nanoplatelet research and development:
  - Decrease nanoplate size by surfactant modification.
  - Scale up syntheis for fuel cell testing.
  - Incorporation into catalyst layers and MEA optimization.
  - Fuel cell performance and durability testing.
- Development of models and theory:
  - DFT model extension to nanoplates and nanowires.
  - Sintering model extension to include dissolution and reprecipation.
  - Microstructural model application to novel catalysts fuel cell validation.

FY 2011 Publications

1. Sansinena, J.-M.; Nelson, M.; Wilson, M.S.; Garzon, F.H., Electrochemical Synthesis of Oxygen Reduction Catalysts Based on Pt Coated Polypyrrole Nanowires Using Starch as Template Molecule. ECS Transactions 2011, 33 (27), 13-19.

2. Berliba-Vera, E.K.; Delariva, A.T.; Atanassov, P.; Datye, A.K.; Garzon, F.H., Nucleation of Platinum on Carbon Blacks. ECS Transactions 2010, 33 (1), 73-82.

3. Wu, G.; Nelson, M.A.; Mack, N.H.; Ma, S.; Sekhar, P.; Garzon, F.H.; Zelenay, P., Titanium dioxide-supported non-precious metal oxygen reduction electrocatalyst. Chemical Communications 2010, 46 (40), 7489-7491.

4. Wilson, M.A.; Garzon, F.H., Synthesis of sub-2nm ceria crystallites in carbon matrixes by simple pyrolysis of ion-exchange resins, accepted for publication, Chemistry of Materials 2011.

5. Matanovic, I.; Henson, N.J.; Garzon; F.H. Theoretical Study of Electrochemical Processes on Pt-Ni Alloys, accepted for publication, Journal of Physical Chemistry C. 2011.

FY 2011 Presentations

1. Sansinena, J.-M.; Nelson, M.; Wilson, M.S.; Garzon, F., Electrochemical Synthesis of Oxygen Reduction Catalysts Based on Pt Coated Polypyrrole Nanowires Using Starch as Template Molecule. ECS Meeting Abstracts 2010, 1002 (6), 356-356.

2. Matanovic, I.; Garzon, F.; Henson, N., Theoretical Study of Electrochemical Processes on Novel Platinum Group Metal Catalysts. ECS Meeting Abstracts 2011, 1101 (41), 1894-1894.

3. Berliba-Vera, E.K.; Delariva, A.; Atanassov, P.; Datye, A.; Garzon, F., Nucleation of Platinum on Carbon Blacks. ECS Meeting Abstracts 2010, 1002 (10), 640-640.

V.D.8 Molecular-Scale, Three-Dimensional Non-Platinum Group Metal Electrodes for Catalysis of Fuel Cell Reactions

John B. Kerr[1] (Primary Contact), Piotr Zelenay[2], Steve Hamrock[3]

[1]Lawrence Berkeley National Laboratory (LBNL)
MS 62R0203, 1 Cyclotron Road
Berkeley, CA 94720
Phone: (510) 486-6279
E-mail: jbkerr@lbl.gov

[2]Los Alamos National Laboratory (LANL)

[3]3M Fuel Cell Components Program

DOE Manager
HQ: Nancy Garland
Phone: (202) 586-5673
E-mail: Nancy.Garland@ee.doe.gov

Collaborators:
- Adam Weber, Rachel Segalman, John Arnold, Jeff Reimer, Martin Head-Gordon, Robert Kostecki (LBNL)
- James Boncella, Yu Sueng Kim, Jerzy Chlistunoff, Neil Henson, (LANL)
- Radoslav Atanasoski (3M)

Project Start Date: August 31, 2009
Project End Date: August 31, 2013

Fiscal Year (FY) 2011 Objectives

1. Demonstrate that non-platinum group metal (non-PGM) catalysts can be used for oxygen reduction reactions (ORRs) in polymer-coated electrode structures based on polyelectrolyte membranes. (Year 1)
2. Incorporate catalysts into polymer binders of composite electrodes for the construction of membrane electrode assemblies (MEAs) to demonstrate that this is an effective matrix for testing of new catalysts. (Year 2)
3. Demonstrate that the three-dimensional structure of polymer-coated electrocatalyst layers can offset slower kinetics of the catalyst centers when compared with two-dimensional platinum or non-platinum catalysts. (Year 3)
4. Demonstrate that significant stability of the matrix is possible. (Year 3)
5. Demonstrate the design, synthesis and scale up of new catalysts capable of performance that is superior to platinum group metals. (Year 4)

Technical Barriers

This project addresses the following technical barriers from the Fuel Cells section (3.4.4) of the Fuel Cell Technologies Program Multi-Year Research, Development and Demonstration Plan:

(C) Performance – more efficient electrodes
(E) System Thermal and Water Management
(B) Cost
(A) Durability

Technical Targets

- Non-Pt catalyst activity per volume of supported catalyst – 300 A/cm^3
- Cost <$3/kW
- Durability >5,000 hours (>120°C)
- Electrochemical area loss <40%
- Electrochemical support loss <30 mV after 100 hrs @ 1.2 V

FY 2011 Accomplishments

- Completed Objective #1 to demonstrate that non-PGM catalysts can be used for oxygen reduction in polymer-coated electrode structures based on polyelectrolyte membranes.
- Completed Objective #2: Non-PGM catalysts have been incorporated into the polymer binders of composite electrodes used in MEAs and have been shown to support high current densities (up to 0.25 A/cm^2).
- Developed modeling procedures for prediction of MEA performance using non-PGM catalyst layers. The model has been validated by comparison of predicted performance with experiment. The model predicts that Objective #3) will be achieved and this remains to be confirmed experimentally in the coming year.
- Use of redox mediators within the catalyst layers has been shown to be an effective method to reduce the overpotential of the ORR and to increase electron conduction within the catalyst layers.
- Demonstrated methods for mechanistic determination that provides intrinsic catalyst activity. Combination of these methods with molecular modeling and targeted catalyst synthesis has been initiated to provide well defined pathways to lower overpotentials and higher turnover frequencies (TOF).
- Initiated chemical analysis of catalysts using ion trap mass spectroscopy combined with separation methods to assess catalyst degradation pathways and to allow determination of catalyst turnover numbers (TONs).



Introduction.

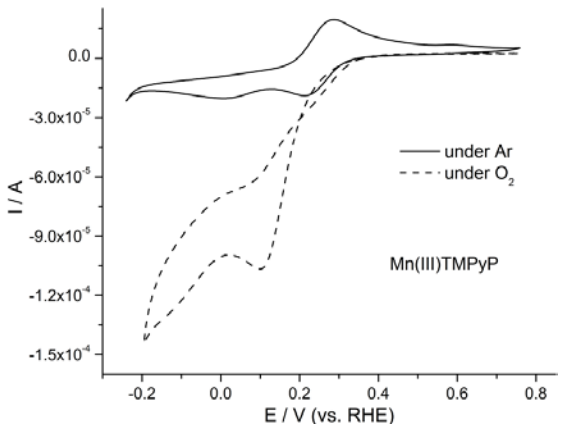
Although polymer electrolyte membrane (PEM) fuel cells are relatively efficient energy conversion devices (~50%), there is considerable interest in improving the performance while reducing the cost. An interesting approach is to develop alternative catalysts that are less expensive and also more efficient. Gasteiger and co-workers [1] have provided a very thorough review of the benchmark activities required for Pt, Pt-alloy and non-Pt catalysts for oxygen reduction and which describes in detail different approaches to catalysis of this important reaction. Methods have been reported to prepare non-PGM catalysts that involve a curious procedure whereby a rather complicated molecule such as a metal porphyrin or a complex such as iron phenanthroline is adsorbed on carbon and then heated to over 800°C to form the catalyst [2-5]. In some cases the carbon support is treated with nitrogenous compounds at high temperature followed by addition of metal ions such as Fe or Co. With these non-platinum catalyst structures it is thought that the density of the non-platinum catalytic sites is insufficient to sustain the desired reaction. With the porphyrin catalysts, for example, their poor solubility results in strong adsorption on to the carbon support and insufficient loading of catalyst as well as possible deactivation of the metal center. The pyrolysis process introduces considerable uncertainty as to the actual identity of the catalytic center. Electrode structures are desired which can allow incorporation of catalytic species of known structure into MEAs, which increase the density of the electrocatalysts in the catalyst layer and which allow the homogeneous activity of the catalyst to be retained.

Approach

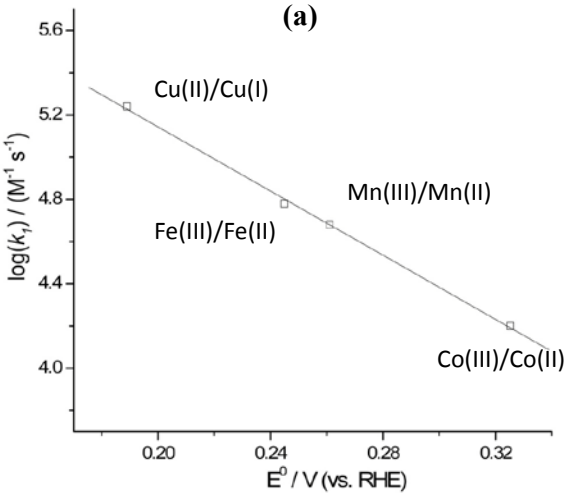
Homogeneous redox catalysis has been the center of considerable academic attention for several decades and a recent review by Saveant [6] provides an extensive overview of the topic and includes methods of tethering catalysts close to the electrode surface. These methods suggest ways to incorporate into fuel cell MEAs electrocatalysts that mimic very efficient enzyme catalyst centers and may lead to better performance at reduced cost. The principles, advantages and drawbacks behind the approach were explained at greater length in the FY 2010 annual report. The most important advantage of the approach is that the catalyst functions essentially as a homogeneous catalyst that can be thoroughly characterized in solution. This makes design and synthesis of the catalysts more straight forward since they can be studied without resort to surface analysis techniques and to the invocation of surface effects that are poorly understood. Thus, catalysts can be designed from first-principles based on well-known chemistry and physics. The structures of the catalytic centers are understood since the catalysts are synthesized and characterized by classical electrochemical and chemical methods in solution thereby avoiding some of the difficulties that have arisen from surface bound catalysts. The catalysts are then incorporated into polymers for coating on electrode surfaces and again the behavior can be characterized by simple electrochemical methods prior to incorporation of the polymer-bound catalysts into composite electrodes for MEAs. This last step is critical for the project and represents the Go/No-Go decision point that allows the flow of more efficient catalysts into the PEM fuel cell platform for practical use. This report outlines the progress that has been made in the last year towards fabrication of the MEAs and the development of methods and procedures that will lead to better catalysts and improved electrode structures.

Results

Figure 1 illustrates the process of catalyst screening and measurement of kinetic parameters in solution that facilitates some degree of mechanistic determination for the ORR reaction. Figure 1(a) shows the voltammetric response of a representative manganese porphyrin complex (Mn(III) tetramethylpyridylporphine [TMPyP]) which is soluble in aqueous trifluoromethanesulfonic acid solution due to the quaternized pyridinium groups. The Mn(III)/Mn(II) redox couple is shown to be mostly reversible under nitrogen (solid line) but clearly shows two reductive processes which indicates the presence of different species in solution. The relative heights of the reduction peaks vary with sweep rate, addition of chloride ion and also the pH. This behavior contrasts with that shown by the Fe(III)TMPyP complex under the same conditions which shows a simple reversible wave. The dotted line in Figure 1(a) shows the effect of the presence of oxygen in the solution and the increase in the reduction current can be attributed to the catalytic reduction of oxygen by the Mn(II)TMPyP complex. Again there is an anomalous “cross-over” of the current on the anodic sweep which indicates that the reaction is not completely straightforward, probably due to the presence of different catalyst species in solution. Nevertheless from measurements such as these it is possible to estimate the rate constants of the catalytic reactions [6]. Figure 1(b) shows the results of such measurements for several different metal TMPyP complexes plotted against the redox potential of the complex. These rate constants are derived assuming the mechanism shown in Figure 1(c) which assumes an outer-sphere electron transfer between the reduced metal complex and oxygen to form superoxide ion. The dependence on potential shown in Figure 1(b) is consistent with this mechanism but the absolute values of the rate constants are much too high given the potential difference between the catalyst and the superoxide redox potentials. A more likely mechanistic scenario is shown in Figure 1(d) which shows the formation of an intermediate adduct of the complex with oxygen which in this case is shown as a dimer as this is consistent with some of the behavior reported in the literature for these catalysts. It should be noted that the rate of reaction of the catalyst with oxygen is potential dependent and this dependence is actually contrary to what is desirable for a good catalyst.



(a)



(b)

(c) Outer-sphere Redox catalysis mechanism (Marcus-Hush)

$$TPyPFe(III) + \ominus e \underset{k_b}{\overset{k_f}{\rightleftharpoons}} TPyPFe(II)$$

$$TPyPFe(II) + O_2 \underset{k_{-1}}{\overset{k_1}{\rightleftharpoons}} TPyPFe(III) + \dot{O}_2^-$$

$$\dot{O}_2^- + H^+ \rightleftharpoons O_2H^\bullet$$

$$TPyPFe(II) + O_2H^\bullet \longrightarrow TPyPFe(III) + O_2H^-$$

(d) Quasi-redox inner-sphere mechanism.

$$2TPyPFe(II) + O_2 \rightleftharpoons TPyPFe(III)\text{-}O_2^{2-}\text{-}Fe(III)TPyP$$

$$TPyPFe(III)\text{-}O_2^{2-}\text{-}Fe(III)TPyP + H^+ \rightleftharpoons TPyPFe(III)\text{-}O_2H^- + TPyPFe(III)$$

$$TPyPFe(III)\text{-}O_2H^- + 2TPyPFe(II) + H^+ \longrightarrow 3\,TPyPFe(III) + 2OH^-$$

FIGURE 1. Electroanalytical screening and characterization of ORR catalysts; (a) voltammetry of Mn(III)TMPyP (0.8mM) in 0.1M HTFSA/water at glassy carbon under argon and in the presence of oxygen, sweep rate 100 mV/s; (b) plot of rate constants for ORR for different metal TMPyP complexes against the redox potential of the catalysts. Kinetic derivation assumes outer-sphere electron transfer mechanism as shown in 1(c); (c) Outer sphere electron transfer mechanism for ORR; (d) postulated quasi-redox inner-sphere mechanism for ORR.

Figure 2(a) shows the voltammetry of the Fe(III)TMPyP catalyst in trifluoromethanesulfonic acid (HTFSA) under argon, in the presence of O_2 and also in the presence of a soluble ferrocene and oxygen. The ferrocene methanol acts as a redox mediator and catalyzes the reduction of oxygen at lower overpotentials. The mechanism whereby this is thought to occur is shown in Figure 2(b). The electron transfer between the ferrocene and the Fe(III)TMPyP catalyst is driven by the rate of the reaction between the reduced catalyst and O_2. The ferrocene also simply acts as an electron mediator to carry the electrons to the catalyst in a polymer layer as is illustrated in Figure 2(c) which schematically shows the FeTMPyP electrostatically bound to Nafion®. Since the catalyst is a 5+ charged cation it is very immobile in the polymer and hence electrons need to be transported to it by some method which the ferrocene fulfills. Figure 2(d) shows how this works in cyclic voltammetry for a Nafion®-coated electrode containing the FeTMPyP catalyst and the ferrocene methanol which is immersed in HTFSA solution. The freshly cast film (blue line) shows strong catalysis of oxygen reduction at the potential that corresponds to the ferrocene methanol. The film was left immersed in the HTFSA solution for two days and the red line shows the resulting behavior for the ORR. The ORR reaction appears to occur at the potential of the FeTMPyP and other non-catalytic couple appears at more positive potentials. This couple appears to correspond to the ester of the ferrocene alcohol which results from reaction with the Nafion® and yields a shift of the potential in the positive direction consistent with the electron withdrawing nature of the ester. The lack of catalysis by the ferrocene ester is consistent with the mechanism shown in Figure 2(b) as the potential difference between the redox potentials of Fe(III)TMPyP and the ferrocene ester is too large for the rate of the oxygen reaction to overcome. Catalysis over this potential range would be possible if the rate of reaction with

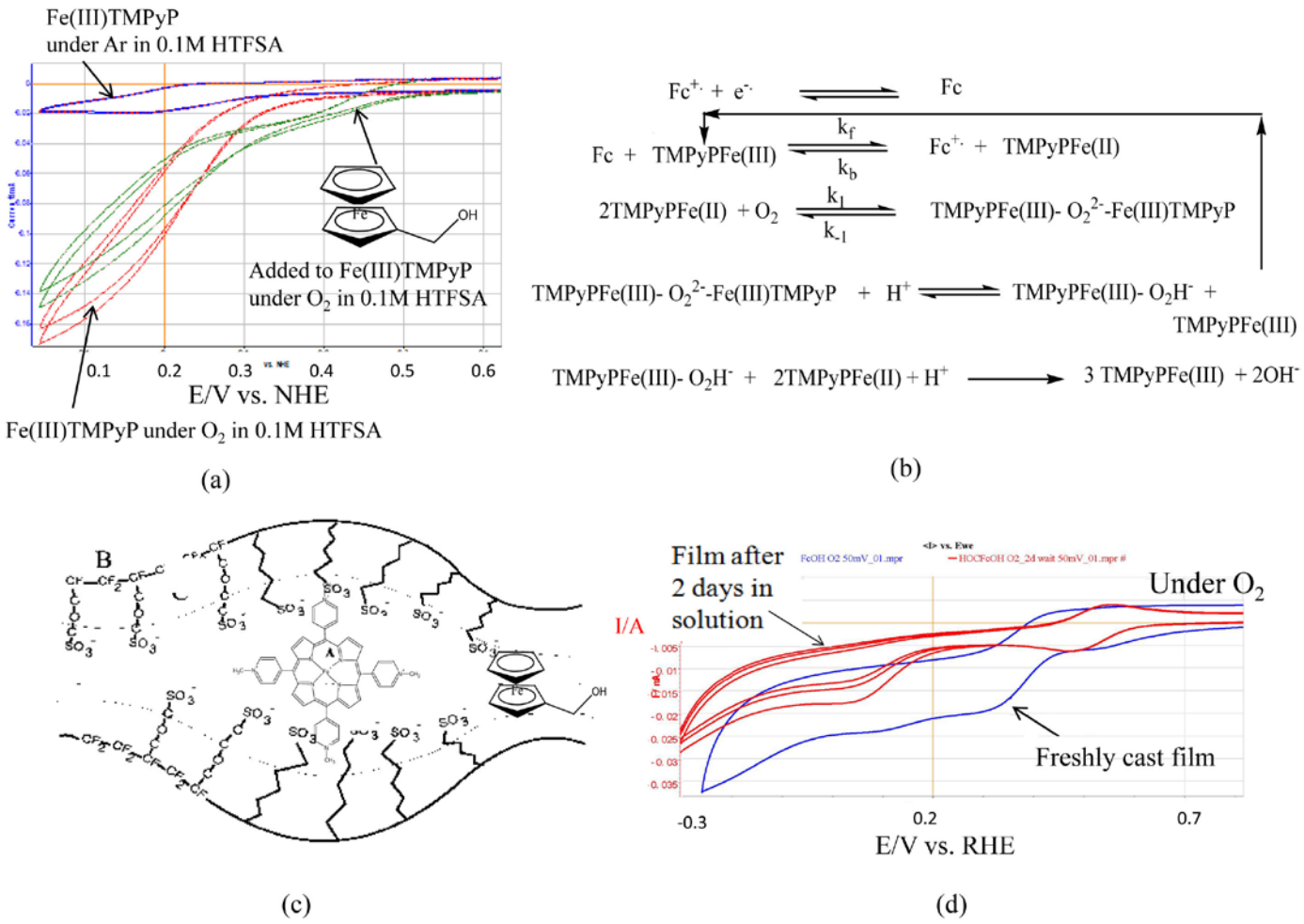


FIGURE 2. (a) Voltammetry of Fe(III)TMPyP in aqueous 0.1M HTFSA at glassy carbon, sweep rate 50 mV/s showing response under argon, in the presence of oxygen and in the presence of oxygen with added ferrocene methanol; (b) mechanism for ORR with addition of ferrocenemethanol to account for ORR at more positive potentials as shown in Figure 1(a); (c) schematic of Fe(III)TMPyP bound to Nafion® polymer layers which also contain ferrocene methanol as an electron mediator; (d) voltammetric response of freshly cast Nafion® film on a glassy carbon electrode containing Fe(III)TMPyP and ferrocene methanol in aqueous 0.1M HTFSA solution saturated with O_2. Blue curve is freshly cast film, red curve is after two days in 0.1M HTFSA solution.

O_2 was much larger, say two orders of magnitude higher. It is important to note also that both catalyst and mediator appear to remain bound in the polymer layer over an extended period which indicates they do not wash out.

The process of transferring these catalysts into the catalyst layer of an MEA is shown in Figure 3. Figure 3(a) shows the catalyst layer consisting of a number of carbon support particles which are coated with the polymer layer containing the catalyst and mediator. The carbon particles connect electronically to the current collector gas diffusion layer. Figure 3(b) shows the dynamics of the charge and mass transport through the polymer layers that have to be accounted for and Figure 3(c) shows the flow of electrons in simplified form. A number of literature measurements for the transport properties of the electrons, protons, oxygen and water have been have been used to try to predict the behavior of the electrode in an MEA and the results of the modeling are shown in Figure 3(d) which are compared with experimental results from the polarization curves of MEAs prepared with catalyst layers containing the Fe(III)TMPyP and ferrocene methanol. The model also makes assumptions regarding the overpotential and the catalytic activity of the catalyst. It can be seen that there is surprisingly close agreement for these early results and the model. Figure 3(e) shows the effect of variation of the formulation of the electrode ink where the catalyst concentration is reduced but the mediator concentration remains the same. However, as a result the concentration of proton carriers also decreases. The MEA performance reflects the lower density of the catalysts as well as the increase in resistance due to fewer proton carriers.

Figure 4(a) shows the best MEA performance to date obtained with the Co(III)TMPyP catalyst, ferrocene methanol mediator and different surface area carbons

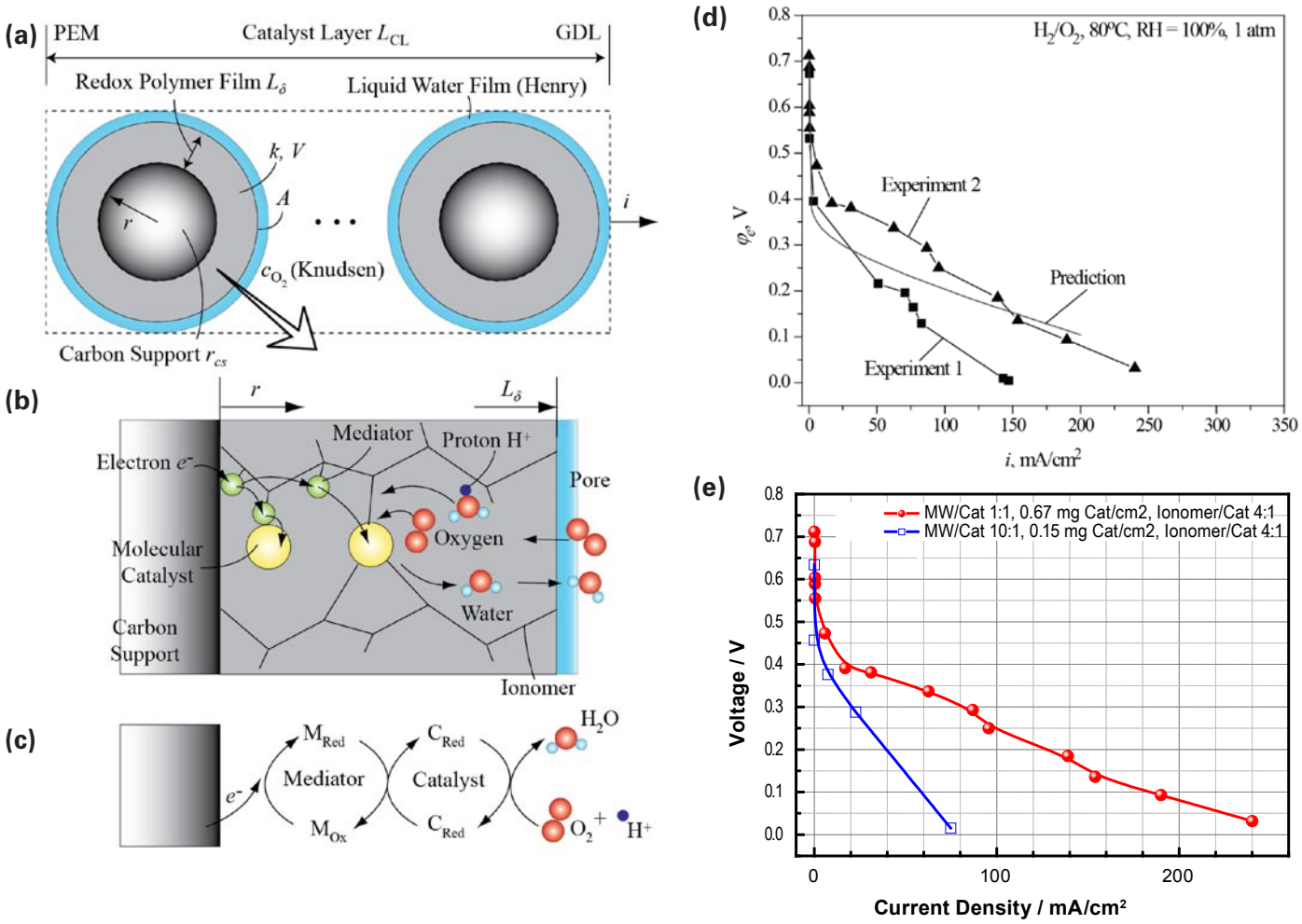


FIGURE 3. Model and experimental results of MEA electrodes containing three-dimensional arrays of Fe(III)TMPyP catalysts and ferrocene methanol mediators; (a) schematic of catalyst layer structure; (b) schematic of polymer film structure and dynamics of transport; (c) simplified diagram of electron transport within the catalyst layer; (d) model prediction compared with experimental results for MEA with Fe(III)TMPyP catalyst and ferrocene methanol mediator; (e) MEA results for lower catalyst density, higher mediator density and lower proton carrier density in catalyst layer.

current collectors. Comparison with control experiments with uncatalyzed carbons show an order of magnitude higher current densities and open-circuit voltage values that are 300 mV higher. It is clear that the concept of the polymer-supported homogenous catalyst actually works and the current densities achieved here correspond to TOF numbers of about 10 per second for the catalysts. The actual loading of catalyst sites estimated for these MEAs is about 100 times less than those reported for pyrrolized MEA systems [7]. However, comparison with commercial platinum electrodes (shown in the inset) demonstrates a long way to go, particularly with respect to voltage. Similar current densities as Pt/C TOF values of around 50/s are required or a higher density of catalyst in the catalyst layer. To achieve a lower overpotential and hence higher cell voltage not only are higher rate catalysts required but catalysts with more positive redox potentials are required.

Figure 4(b) illustrates an approach that involves molecular modeling to determine the structural features that control the catalyst redox potential (nature of the metal center, substituents on the ligands) as well as the rate of reaction with the oxygen. Figure 4(b) shows a model of the Fe(II) TMPyP with a fifth ligand (imidazole) bound to the metal and the oxygen occupying the sixth position. Modeling shows some deformation of the ring geometry occurs. It has also been shown that replacement of the quaternary methyls on the pyridines with protons results in slower reaction with O_2. These results demonstrate the need for a systematic program of modeling, guided synthesis and electrochemical screening to lead the program towards better catalysts. A more empirical approach is shown in Figure 4(c) which shows the electropolymerization of dipyrromethanes which when combined with cobalt ions gives a polymer catalyst layer with interesting catalytic properties as shown in

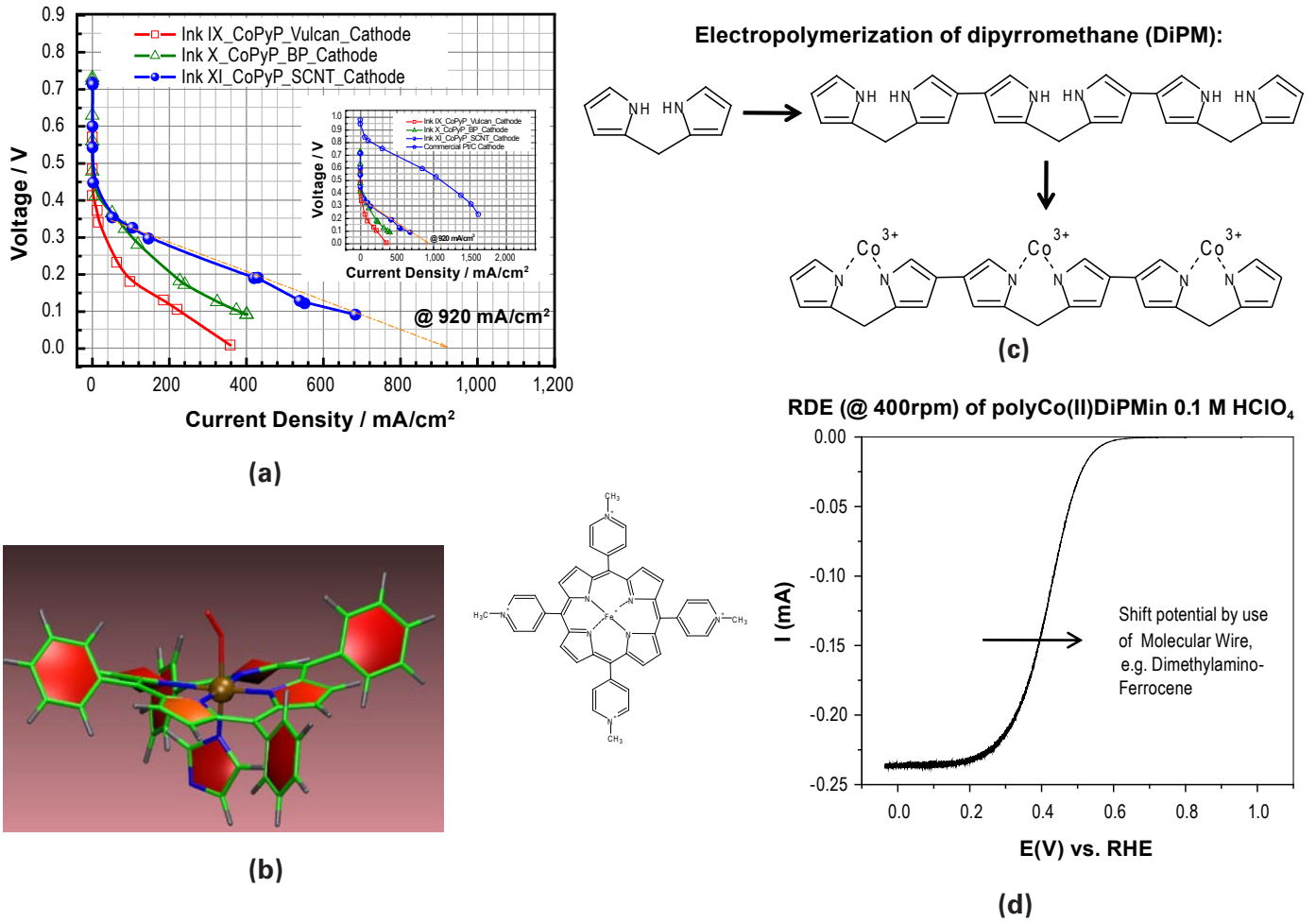


FIGURE 4. (a) Comparison of MEA results from Figure 3(a) with blank carbon with no added catalyst (control). Inset shows comparison with commercial Pt/C electrode under similar conditions; (b) computational model of FeTMPyP complex with imidazole bound as a fifth ligand and O_2 bound to the sixth position; electropolymerization of dipyrromethane and Co^{3+} to form an ORR polymer-catalyst layer; (d) Voltammetric response of catalyst layer formed in 4(c) in the presence of O_2.

Figure 4(d). This approach takes advantage of previously successful combination of catalysts with conducting polymers [7]. Combination with redox mediators and proper construction of catalyst layer structures as illustrated in Figure 3 hold the potential to greatly improve the operating potential of the MEA.

Conclusions and Future Directions

Conclusions

- The results from the MEA experiments reported here represent a proof-of-principle of the concept of polymer-supported three-dimensional catalyst arrays for MEA. The correspondence of the modeling with the experimental results indicates that the correct parameters are being considered.
- The correspondence of the MEA results with the electroanalytical results indicates that a practical method catalyst screening exists that is rapid, inexpensive and relevant to MEA operation. Quantitative electroanalytical results are applicable to MEA operation through the electrode modeling.
- Better catalysts can be obtained through fundamental understanding of the factors that influence redox potential and rate of reaction with oxygen. Molecular modeling can address these problems.

Future Directions

- Optimization of MEA fabrication to improve performance.
- Use of electrochemical techniques including impedance to determine rate limiting phenomena in the MEAs and

correlation with electroanalytical measurements made using conventional cell systems.

- Development of a coordinated molecular modeling/ synthesis/electrochemical screening process that will provide understanding of the catalyst structural features that yield better performance.

FY 2011 Publications/Presentations

1. "Molecular-scale, Three-dimensional Non-Platinum Group Metal Electrodes for Catalysis of Fuel Cell Reactions," John Kerr, DOE Fuel Cell Technologies Program Review Meeting, May 10, 2011, Arlington, VA, presentation FC 11.

2. "Development of Low-Temperature Non-Precious Metal Catalysts for Oxygen Reduction." Lior Elbaz and Piotr Zelenay. 219th Electrochemical Society Meeting , Montreal, Quebec, Canada – May 3rd, 2011.

References

1. Gasteiger, H.A., Kocha, S.S., Sompalli, B. & Wagner, F.T. Activity benchmarks and requirements for Pt, Pt-alloy, and non-Pt oxygen reduction catalysts for PEMFCs. *Applied Catalysis B-Environmental* **56**, 9-35 (2005).

2. Gojkovic, S.L., Gupta, S. & Savinell, R.F. Heat-treated iron(III) tetramethoxyphenyl porphyrin supported on high-area carbon as an electrocatalyst for oxygen reduction - I. Characterization of the electrocatalyst. *Journal of the Electrochemical Society* **145**, 3493-3499 (1998).

3. Gojkovic, S.L., Gupta, S. & Savinell, R.F. Heat-treated iron(III) tetramethoxyphenyl porphyrin chloride supported on high-area carbon as an electrocatalyst for oxygen reduction - Part II. Kinetics of oxygen reduction. *Journal of Electroanalytical Chemistry* **462**, 63-72 (1999).

4. Gouerec, P. & Savy, M. Oxygen reduction electrocatalysis: ageing of pyrolyzed cobalt macrocycles dispersed on an active carbon. *Electrochimica Acta* **44**, 2653-2661 (1999).

5. Sun, G.Q., Wang, J.T. & Savinell, R.F. Iron (III) tetramethoxyphenylporphyrin (FeTMPP) as methanol tolerant electrocatalyst for oxygen reduction in direct methanol fuel cells. *J Appl Electrochem* **28**, 1087-1093 (1998).

6. Saveant, J.M. Molecular catalysis of electrochemical reactions. Mechanistic aspects. *Chemical Reviews* **108**, 2348-2378 (2008).

7. Wu, G., More, K.L., Johnston, C.M. & Zelenay, P. High-Performance Electrocatalysts for Oxygen Reduction Derived from Polyaniline, Iron, and Cobalt. *Science* **332**, 443-447, doi:10.1126/science.1200832 (2011).

V.D.9 Tungsten Oxide and Heteropoly Acid Based System for Ultra-High Activity and Stability of Pt Catalysts in PEM Fuel Cell Cathodes

John Turner (Primary Contact), K. C Neyerlin, Jason Zack, Andrew Herring, Kelly Mason, Mei Kuo, Katherine Hurst, Anne Dillon and Shyam S. Kocha.
National Renewable Energy Laboratory (NREL)
1617 Cole Blvd.
Golden, CO 80401
Phone: (303) 275-4270
E-mail: John.Turner@nrel.gov

DOE Manager
HQ: Kathi Epping Martin
Phone: (202) 586-7425
E-mail: Kathi.Epping@ee.doe.gov

Subcontractors:
- Andrew Herring, Colorado School of Mines (CSM), Golden, CO
- Steve George, University of Colorado-Boulder, Boulder, CO

In-Kind (Industrial) Collaborators:
- 3M, St. Paul, MN
- Nissan Technical Center, North America (NTCNA), Farmington Hills, MI

Project Start Date: July, 2010
Project End Date: September, 2014

Background

One of the critical goals to achieve the automotive commercialization targets is improved durability. Although durability of the fuel cell system has been improved, some of the improvements come with increased system complexity and cost. This project addresses the issue of catalyst support degradation during normal operation and especially under start-stop conditions when the fuel cell cathode experiences high transient potentials approaching 1.6 V. Typical carbon blacks used today corrode easily under these conditions and complex systems operations are being employed to mitigate it at this time. We propose to use corrosion-resistant oxide supports as a solution. In addition to corrosion resistance, this project will attempt to strengthen the support-Pt anchoring and also lower the total Pt loading in the cathode of the catalyst layer.

Fiscal Year (FY) 2011 Objectives

To help DOE address critical shortcomings in catalyst performance and durability by synthesizing novel catalysts based on tungsten oxide and/or heteropolyacid/C supported Pt.

Technical Barriers

This project addresses the following technical barriers from the Fuel Cells section (3.4.4) of the Fuel Cell Technologies Program Multi-Year Research, Development and Demonstration Plan:

(A) Durability (of catalysts and membrane electrode assemblies)

(B) Cost (of catalysts and membrane electrode assemblies)

(C) Performance (of catalysts and membrane electrode assemblies)

(D) Start-up and Shut-down Time and Energy/Transient Operation (Support Corrosion)

Technical Targets

This project synthesizes novel Pt-based electrocatalysts on alternative oxide supports. The project has targets outlined in the Multi-Year Research, Development and Demonstration Plan for both electrocatalysts for transportation applications (Table 3.4.12) and MEAs (Table 3.4.13). An enhancement in electrocatalytic activity by a factor of 4x (from the benchmark Pt/C metrics) and the ability to withstand 30,000 start-up/shut-down cycles and open circuit voltage holds with an electrochemically available surface area (ECA) loss of <30% are included.

FY 2011 Accomplishments

- Prepared different stochiometries of nano-WO_3 for Pt deposition by atomic layer deposition (ALD) and characterized the material using X-ray diffraction and Brunauer-Emmett-Teller. Demonstrated and characterized improved structure Pt/WO_3.
- Evaluated Pt catalyzed support corrosion as a baseline for stability of Pt/WO_3. Evaluated Pt/WO_3 in electrochemical half-cells for ECA and oxygen reduction reaction (ORR) activity. Investigated several alternative methods for the measurement of ECA accurately.
- Completed following milestones:
  - 5.7.0 Demonstrate nano-structured Pt on WO_3, heteropoly acid (HPA), or a combination of the two. (100% completed) 09/2010.
  - 5.7.1 Demonstrate controlled nano-structured Pt placement and loading on WO_3, HPA, or a combination of the two. (100% completed) 12/2010.

- 5.7.2 Obtain cyclic voltammograms (CVs) and mass activity for Pt on WO_3, HPA, or a combination of the two. (100% completed) 2/28/11
- 5.7.3 Prepare high surface area catalyst electrodes based on tungsten oxide and tungsten-based heteropoly acids (HPAs), test electrochemically in half-cells, and compare to the corrosion of typical carbon blacks for proton exchange membrane fuel cells (PEMFCs) up to 1.5 V. (100% completed) 4/2011
- 5.7.4 Obtain CVs and mass activity for Pt on WO_3, HPA or a combination of the two with ECAs greater than 10 m^2/g Pt. (100% completed) 9/2011.



Introduction

Before polymer electrode membrane fuel cells (PEMFCs) can be fully commercialized, improvements in cost and durability must be achieved [1]. Key to the PEMFC operation is the catalysis of the ORR on the cathode. An ideal ORR catalyst efficiently converts O_2, protons, and electrons to water, produces no peroxide byproducts, and is inexpensive and durable. The sluggish kinetics of the ORR on Pt-based electrocatalysts used today requires a high loading of Pt-based catalyst on the cathode with consequent concurrent increased costs. PEMFC cathode catalysts are supported on high surface area carbon blacks that are known to be thermodynamically unstable in the entire fuel cell operating regime. The kinetics of carbon corrosion are slow below 1 V, but catastrophic losses are observed when the cathode sees transient fluctuations in the 1-1.6 V regime (during start-up shut-down phenomena). Under these conditions, Pt nanoparticles are susceptible to agglomeration. Clearly there is a need for an improved corrosion-resistant support that strongly anchors the Pt strongly to the support and synergistically enhances the catalyst system ORR activity [2,3].

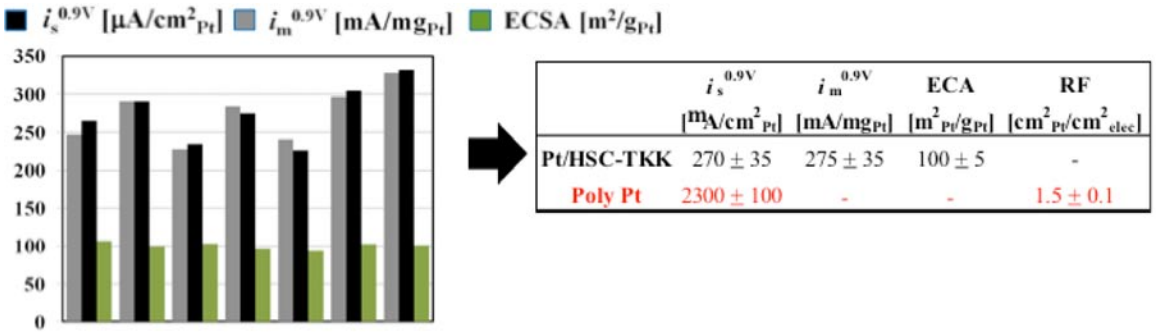
Approach

Our approach is multi-pronged and addresses the catalyst, support, catalyst/support interaction and functionalization of the support. Examination of Pourbaix diagrams reveals that the metals that are fairly stable in acid conditions at the potentials of interest are Ir, Pt and Au, and candidate metal oxides that are thermodynamically stable include Ti, Zr, Nb, Ta and W [2,3]. Various stoichiometries and crystallinities of WO_x nanorods are being grown using hot wire deposition (HWD); wet chemistry is also being pursued to produce different nanostructures of WO_x. These supports are projected to provide the desired higher corrosion resistance at these high transient potentials. Pt nanoparticles are being deposited on WO_x using ALD and wet-chemical methods. Heteropoly acid (HPA) materials being synthesized and characterized at CSM are candidates for co-catalysts because they can be readily synthesized and assembled into nano-ordered ensembles on many electrode materials. The most promising HPA structures are being attached to the WO_x nanoparticles and carbon blacks. Part of the approach is to combine a high surface area carbon electrode with a tungsten oxide and/or HPA that can enable enhanced activity of Pt for the ORR and enhanced stability of the Pt catalyst particles [4,5]. The challenge is to develop i) electrode support materials that are resistant to corrosion in the entire PEMFC operating environment, ii) electrode support materials that strongly anchor the Pt nanoparticles to prevent agglomeration, iii) electrode support and functionalized materials that have sufficient conductivity to provide both electronic and protonic conduction paths, iv) catalyst-support systems that lower peroxide generation, and v) electrode structures that have the optimal electrode structure/porosity/hydrophobicity/hydrophillicity to minimize mass-transport losses. Overall, our approach is to develop a catalyst system that approaches the DOE activity, performance and cost benchmarks.

Results

Commercial Pt/C electrocatalysts were evaluated by rotating disk electrodes (RDEs) and characterized for ECA, specific and mass activity [6-8]. These catalysts were found to meet and even exceed literature benchmarks (Figure 1) validating our measurement and preparation methods. Baseline and newly synthesized materials were also screened for corrosion resistance in electrochemical half-cells. Because standardized protocols for evaluating Pt/alternative supports do not exist, a durability working group sub-team lead by NREL that includes members from Los Alamos National Laboratory, NTCNA and Illinois Institute of Technology are working jointly to develop these protocols. The protocols under development involve potential cycling in the typical automotive regime of 0.6–1.0 V as well as in the start-up/shut-down regime of 1.0–1.6 V. Furthermore, in preparation for testing of selected Pt/alternative support candidates as fuel cell electrodes, baseline Pt/C catalysts were evaluated in subscale fuel cells at NREL and demonstrated to meet and even exceed the DOE benchmarks of ORR electrocatalytic activity (Table 1).

WO_x support materials were prepared by HWD as well as wet chemistry, as shown in Figures 2 and 3 respectively. Pt was deposited onto WO_x supports using ALD but was initially found to have a non-uniform distribution. Using TiO_2 as a proxy support allowed us to monitor in situ the loading of Pt as a function of number of ALD cycles. We were then able to optimize the process and significantly improve Pt nanoparticles dispersed on WO_x (Figure 4). The materials were screened for morphology, surface area, and electrochemical stability by excursions to high potentials. We found them to possess superior stability as compared to carbon blacks. These studies confirmed that WO_x supports are more stable than carbon blacks and Pt/WO_x is more stable than Pt/C (Figure 5).



	$i_s^{0.9V}$ [mA/cm²Pt]	$i_m^{0.9V}$ [mA/mgPt]	ECA [m²Pt/gPt]	RF [cm²Pt/cm²elec]
Pt/HSC-TKK	270 ± 35	275 ± 35	100 ± 5	-
Poly Pt	2300 ± 100	-	-	1.5 ± 0.1

FIGURE 1. Accuracy and Reproducibility of RDE Measurements of ECA and ORR Activity for Baseline Pt/C and Poly-Pt (The x-axis corresponds to the different samples characterized for electrochemical benchmarking.)

TABLE 1. Baseline Pt/C ECA and activity results in RDE and subscale fuel cells tested at NREL and compared to DOE benchmarks.

	Specific Activity (μA/cm²Pt)	Mass Activity (mA/mgPt)
DOE 2015 Target in MEA[1]	**720**	**>440**
DOE 2011 Status	720[3]	240[4]
NREL Pt/C status in MEA[1]	290±10	225±10
NREL Pt/C status in RDE[2]	270±30	270±30

[1]MEAs 900 mV, 50 cm² subscale fuel cells, 15 min/point, 150 kPa (PO_2 = 100 kPa), 80°C, 100% RH, Nafion® membrane.
[2]RDE half-cell - 900 mV, 20 mV/s, 25°C, 0.1 M $HClO_4$
[3]Pt nanostructured catalysts, at 900 mVIR-free
[4]Achieved by 3M

Preliminary Pt/WO_x materials produced by ALD as well as wet chemistry were evaluated in half-cell RDE set-ups for ECA and activity. Two issues arise with electrochemical measurements: In measuring CVs, we find that the WO_x contributes charge to the hydrogen underpotential deposition (UPD) region due to formation of tungstates (Figure 6). This issue can be bypassed by using Cu UPD or CO chemisorption to measure the ECA and has been performed (Figure 7). ECA values are in the range of 10–14 m^2/g. In measuring ORR current-voltage curves, high stoic WO_3 with lower electronic conductivity resulted in lower activity; the impact could be partially mitigated by mixing small amounts of carbon black to the ink formulation (Figure 8). At this time, the highest specific activity measured is comparable to that of conventional Pt/C while the mass activity is lower due to the lower surface area.

Commercial Pt/C (2.5 nm Pt nanoparticles on high surface area carbon) was functionalized with HPA by CSM

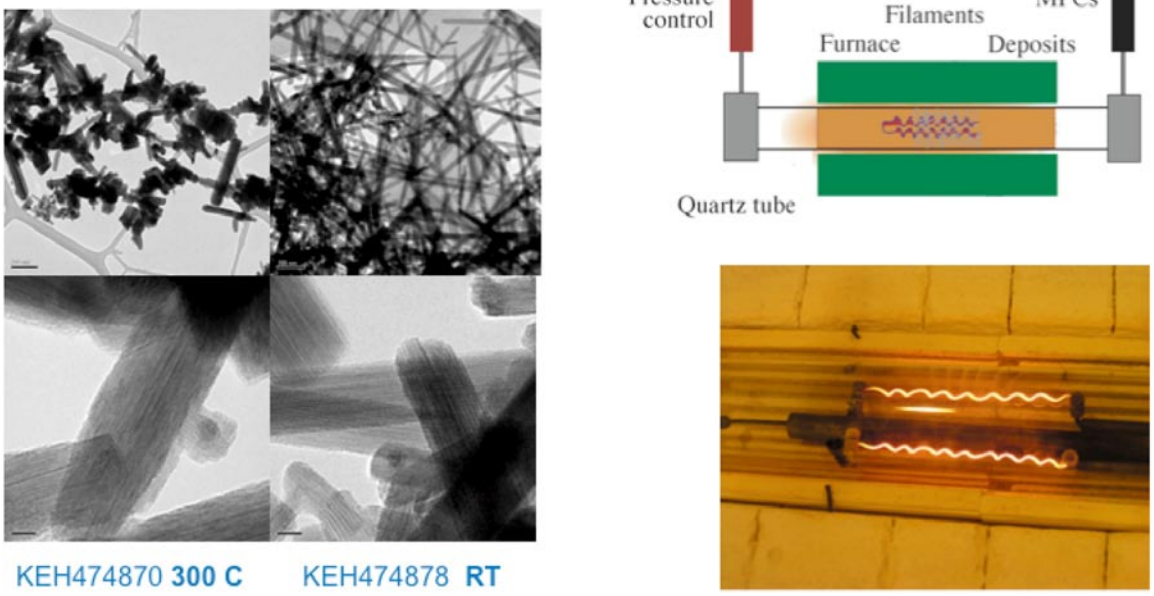


FIGURE 2. Preparation Method of WO_x using HWD and Transmission Electron Microscopy (TEM) Micrographs

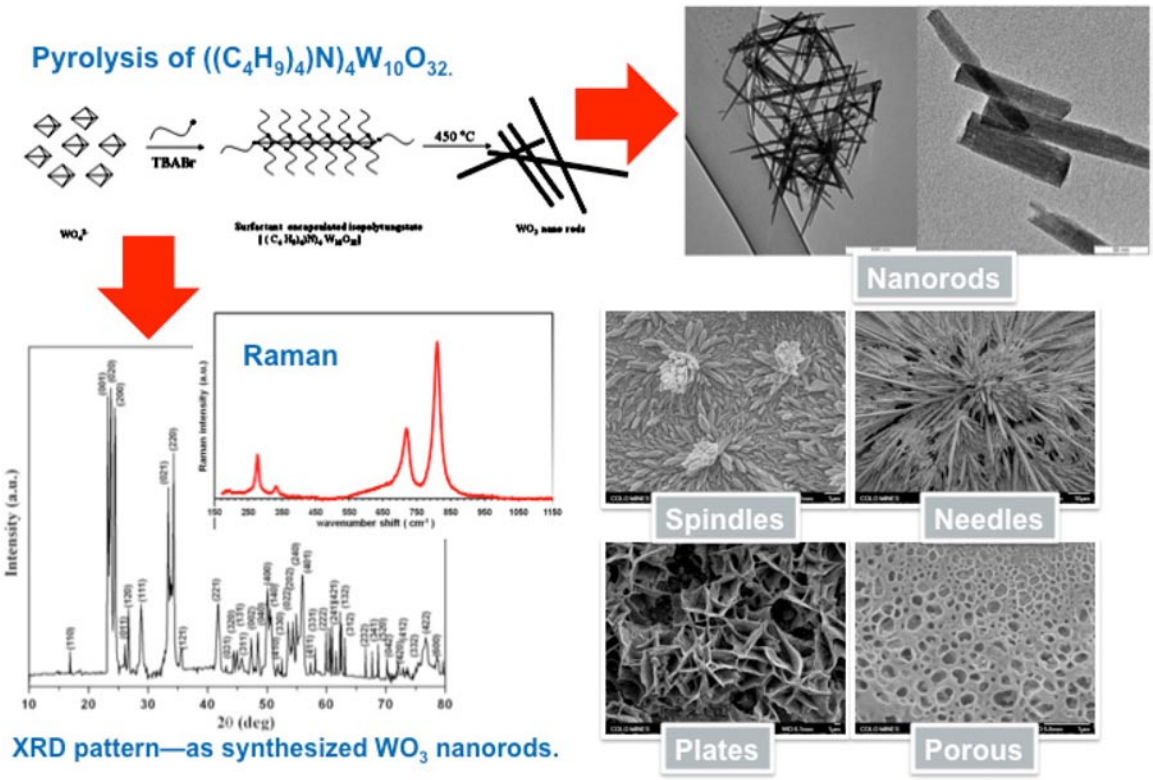


FIGURE 3. Preparation Method of WO_x using Wet Chemistry, TEM Micrographs and Raman Spectra

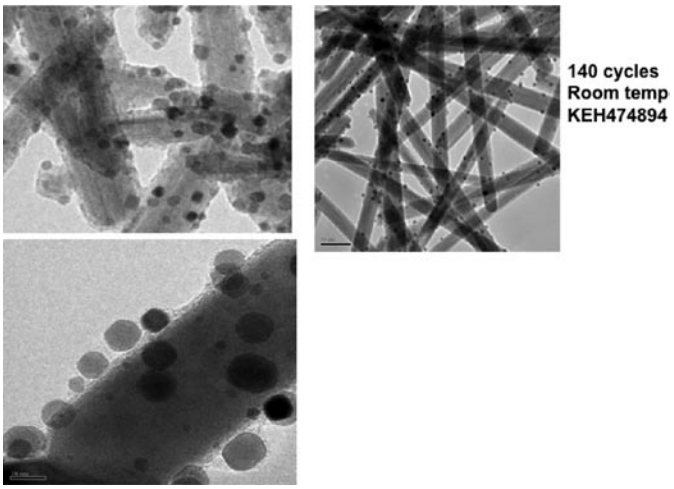


FIGURE 4. TEM Micrographs of Pt/WO_x Grown Using ALD

and the resultant materials tested in RDE for activity and durability. Interesting peaks were found related to the functionalization but no improvement or degradation of ORR activity was observed.

Conclusions and Future Direction

Platinum on WO_x was deposited using ALD producing particle sizes and distribution with good control, albeit with a low surface area of about 10 m^2/g. Electrochemical measurements were conducted to resolve issues of (1) measurement of ECA, (2) the impact of lower electronic conductivity of WO_x on the ORR activity, and (3) significantly improved support corrosion compared to conventional carbon blacks. Future work involves, lowering the particle size thus increasing the ECA and achieving the mass activity of baseline Pt/C while simultaneously demonstrating higher durability using newly developed protocols. The next steps can be outlined as follows:

Tungsten Oxide: Improve the characterization of metal oxide substrate: produce increased quantities.

Pt Deposition: Use ALD and wet-chemistry techniques to deposit smaller and a more uniform distribution of nanoparticles of Pt on the oxide support to increase the ECA.

HPA: Functionalize plain carbon blacks and deposit Pt in a controlled manner on the resultant material. Once the platinum hybrid HPA carbon has been developed CSM will investigate how it can be used to control the morphology of Pt nanoparticles from either Pt black, chemical reduction or electrochemical reduction.

Electrode Studies: Resolve the ECA measurement issues due to contributions from WO_x to the hydrogen UPD. Evaluate the effect of addition of carbon black to the catalyst to enhance electronic conductivity and ORR performance. Develop appropriate protocols for

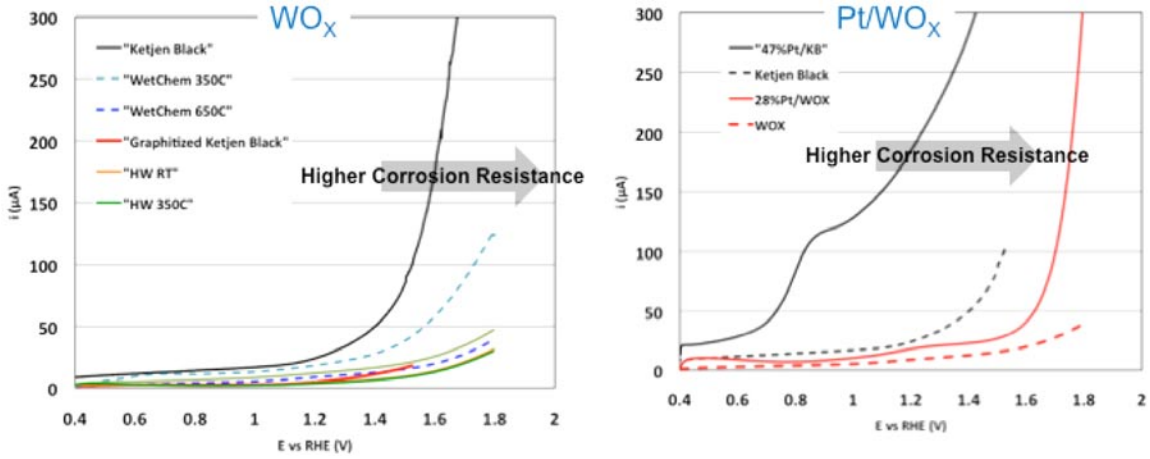


FIGURE 5. Half-Cell Electrochemical Screening Test Showing Onset and Magnitude of Corrosion Currents for Carbon, Pt/C and WO_x and Pt/WO_x

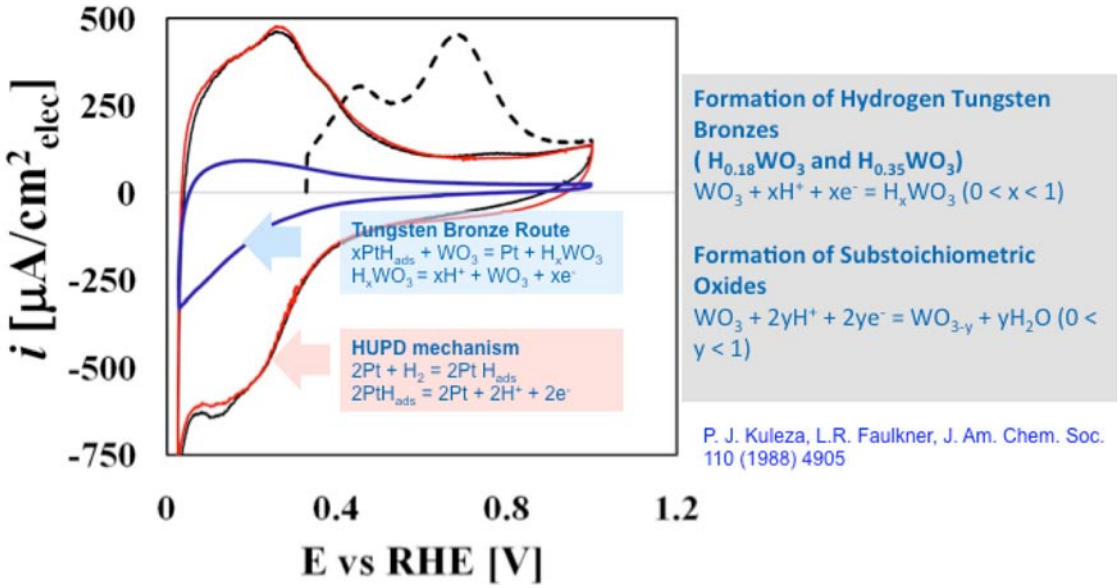


FIGURE 6. CVs showing the impact of contribution from WO_x in the HUPD region. Cu UPD might give a better estimate of ECA since hydrogen UPD region includes charge due to formation of H_xWO_3 as well as spill over effects.

the evaluation of alternative catalyst support durability. Demonstrate electrochemical (RDE) durability of Pt/WO_x as a function of the initial ECA using the developed protocols. Achieve specific and mass activity for Pt/WO_x/HPA that is comparable to and eventually higher than conventional Pt/C.

FY 2011 Publications/Presentations

1. John Turner, "WO_3 and HPA based system for ultra-high activity and stability of Pt catalysts in PEMFC cathodes", 2011 DOE AMR, May 10th, 2011, project FC084, http://www.hydrogen.energy.gov/pdfs/review11/fc084_turner_2011_o.pdf

2. Shyam Kocha, "Protocols for Alternative Supports for PEMFCs", Durability Working Group Meeting, 2011 DOE AMR Meeting, VA (2011).

3. Shyam S. Kocha, K.C. Neyerlin and Bryan Pivovar, "Electrocatalyst Durability in Automotive PEMFCs", PBFC-5, August 1–4, 2011, ANL, Argonne, IL.

4. K.C. Neyerlin, S. Kocha, B. Pivovar and H. Dinh, Cu UPD as a diagnostic technique for the determination of electrochemical surface area of unsupported Pt, Pt/C, Pt/WOx, and PtRu alloys, 242nd ACS National Meeting Denver, CO August 28 – September 1, 2011.

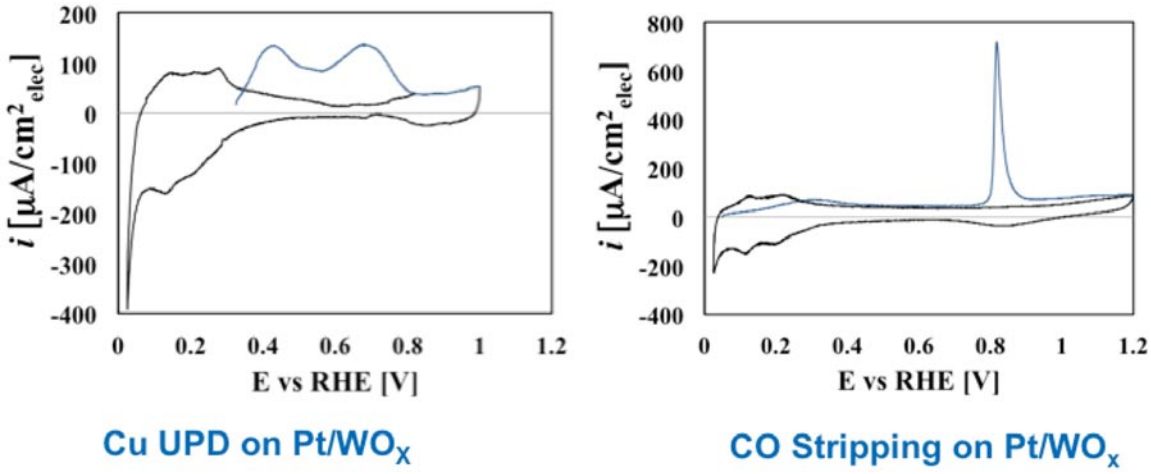


FIGURE 7. Application of Cu UPD and CO stripping to measure ECA. Cu UPD (~14 m^2/g) and CO (~10 m^2/g) stripping on identical Pt/WO_X samples.

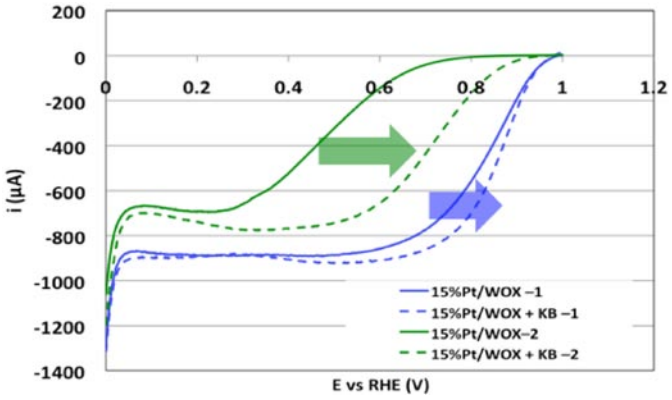


FIGURE 8. Impact of addition of electronically conductive carbon black to Pt/WO_x ORR current-voltage curves. RDE electrode ink modification improves activity and addition of carbon black improves dispersion and electronic conductivity.

5. Supporting platinum on nano-structured metaloxides for proton exchange membrane cathodes. A.M. Herring, M.-C. Kuo, R.J. Stanis, and N. Danforth, Prepr. Pap.-Am. Chem. Soc., Div. Fuel. Chem., 2011, 56, 100.

6. Kelly S. Mason, "Use of Heteropoly Acids and Tungsten Oxides Toward Improved Performance of the PEMFC Cathode Electrocatalyst" 242nd ACS National Meeting, Denver, CO, Aug. 2011.

7. Kelly S. Mason, "Preparation and Characterization of Heteropoly Acid and Tungsten Oxide Modified Pt Electrocatalysts" 220th ECS Meeting, Boston, MA, Oct. 2011. http://ecsmeet2.peerxpress.org/ms_files/ecsmeet2/2011/04/29/00003426/00/3426_0_art_0_lkg4d5.pdf

8. "Supporting platinum on nano-structured metal oxides for proton exchange membrane cathodes." A.M. Herring, M.-C.Kuo, R.J. Stanis, and N. Danforth, oral presentation, presented at the 241st ACS Meeting, Anaheim, CA, March 2011.

9. A.C. Dillon "WO_3 Nanorods for Electrochromic and Fuel Cell Catalyst Applications" SSPC, "Key-Note" SSPC15, Santa Barbara, July, 2010.

10. Katherine Hurst, Virginia Anderson, Robert Tenent, Shyam Kocha, Kenneth Neyerlin, Jason Zack, Steven George, John Turner, and Anne Dillon "Deposition of Pt on tungsten oxide nanoparticles for PEM cathodes" presented at the 241st ACS Meeting, Anaheim, CA, March 2011.

11. Katherine E. Hurst, Virginia R. Anderson, Shyam S. Kocha, Steven M. George, John A. Turner and Anne C. Dillon "Nano-Pt and tungsten oxides as a novel PEM cathode" 242nd ACS National Meeting, Denver, CO, Aug. 2011.

References

1. Mathias, M.F., R. Makharia, H.A. Gasteiger, J.J. Conley, T.J. Fuller, C.J. Gittleman, S.S. Kocha, D.P. Miller, C.K. Mittelsteadt, T. Xie, S.G. Yan and P.T. Yu, "Two Fuel Cell Cars In Every Garage?" INTERFACE 14(3): 24-35 (2005).

2. Swider Lyons, K., M. Teliska, W. Baker, P. Bouwman, J. Pietron, T. Schull, D. Ramaker and W. Dmowski, "Low-Platinum Catalysts for Oxygen Reduction at PEMFC Cathodes," DOE Hydrogen Program Review, Arlington, VA, DOE-EERE (2005).

3. Ioroi, T., Z. Siroma, N. Fujiwara, S.-I. Yamazaki and K. Yasuda, "Sub-stoichiometric titanium oxide-supported platinum electrocatalyst for polymer electrolyte fuel cells," Electrochemistry Communications 7(2), 183-188 (2005).

4. Limoges, B.R., R.J. Stanis, J.A. Turner and A.M. Herring, "Electrocatalyst materials for fuel cells based on the polyoxometalates $[PMo(12n)VnO_4 0](3+n)-$ (n = 0-3)," Electrochim. Acta 50(5), 1169-1179 (2005).

5. Stanis, R.J., M.-C. Kuo, A.J. Rickett, J.A. Turner and A.M. Herring, "Investigation into the activity of HPAs towards the oxygen reduction reaction on PEMFC cathodes," Electrochimica Acta (in press) (2008).

6. Takahashi, I.; Kocha, S.S. J. Power Sources 2010, 195, 6312-6322.

7. Gasteiger, H.A.; Kocha, S.S.; Sompalli, B.; Wagner, F.T. Applied Catalysis B: Environmental 2005, 56, 9-35.

8. Garsany, Y.; Baturina, O.A.; Swider-Lyons, K.E.; Kocha, S.S. Anal. Chem. 2010, 82, 6321-6328.

V.D.10 Synthesis and Characterization of Mixed-Conducting Corrosion Resistant Oxide Supports

Vijay K. Ramani (Primary Contact), Jai Prakash, Chih-Ping Lo, and Mayandi Ramanathan
Illinois Institute of Technology (IIT)
10 W 33rd Street 127 PH
Chicago, IL 60616
Phone: (312) 567-3064
E-mail: ramani@iit.edu

DOE Managers
HQ: Kathi Epping Martin
Phone: (202) 586-7425
E-mail: Kathi.Epping@ee.doe.gov
GO: Katie Randolph
Phone: (720) 356-1759
E-mail: Katie.Randolph@go.doe.gov

Contract Number: DE-EE0000461

Subcontractor:
Nissan Technical Center, North America (NTCNA), Farmington Hills, MI

Project Start Date: September 1, 2010
Project End Date: August 31, 2013

Fiscal Year (FY) 2011 Objectives

- To develop and optimize innovative non-carbon mixed conducting materials that will serve as corrosion resistant, high surface area supports for anode and cathode electrocatalysts; and
- Concomitantly facilitate the lowering of ionomer loading in the electrode (by virtue of surface proton conductivity of the electrocatalyst support), thereby enhancing performance.

Technical Barriers

This project addresses the following technical barriers from the Fuel Cells section of the Fuel Cell Technologies Program Multi-Year Research, Development and Demonstration Plan:

(A) Durability

Technical Targets

This project addresses the following technical targets:

- <40% electrochemical surface area (ECSA) loss in electrocatalysts using the synthesized supports tested per General Motors (GM) protocol.
- <30 mV electrocatalyst support loss in the synthesized supports after 100 hrs at 1.2 mV; tested per GM protocol.

At the time of writing, the first set of samples prepared have undergone durability testing.

FY 2011 Accomplishments

- Demonstrated that the synthesized RuO_2-SiO_2 catalyst supports possess the following properties: a) high Brunauer-Emmett-Teller (BET) surface areas (260 m^2/g), b) excellent electrical conductivity (up to 24 S/cm), and c) improved electrochemical stability. Start-stop stability tests were performed by cycling electrode potential between 0 V to 1.8 V for 1,000 cycles. The results showed no loss in surface area for the RuO_2-SiO_2 catalyst supports, while a 44% drop in surface area was observed in carbon supports tested as a baseline.
- Synthesized functionalized silica supports with several levels of sulfonic acid functionalization. These materials have demonstrated varying degrees of proton conductivity and electrochemical stability.
- Demonstrated fuel cell performance with a platinum catalyst supported on non-carbon catalyst supports synthesized in this study – Pt/RuO_2-SiO_2.



Introduction

While Pt supported on carbon is the most commonly used electrocatalyst for polymer electrolyte fuel cells (PEFCs), the carbon support has limitations with respect to its durability at high temperatures and the excursions to high electrode potentials that arise during start-up and shut-down sequences and during fuel starvation. The issue of carbon-carbon corrosion is a major technical barrier. Carbon corrosion facilitates the agglomeration of Pt particles and dissolution of Pt from the support, which leads to a loss in the ECSA of the electrode [1]. To address this issue, the development of non-carbon mixed-conducting catalyst support materials is explored. Desirable properties of these alternative materials include: (i) high surface area; (ii) high electrical conductivity; and (iii) high electrochemical stability. In addition, it is hypothesized that fuel cell performance can be enhanced by utilizing non-carbon catalyst supports that conduct protons on their surface. The addition of sulfonic acid functionalities on the support surface should permit lowering the ionomer content in the electrode, thereby enhancing gas transport to the catalyst site without compromising on the efficacy of ion transport.

Approach

To achieve the first of two objectives discussed above, two approaches have been employed. The first approach involves the development of a core–shell-like RuO_2-SiO_2 structure that serves as the catalyst support. High surface area silica functionalized with sulfonic acid groups (HSO_3-) was used as core matrix. This matrix was further functionalized with a shell layer of RuO_2 to introduce electronic conductivity; the final material was calcined at temperatures ranging from 100–450°C. The electrochemical stability of RuO_2-SiO_2, Pt/RuO_2-SiO_2, and HSO_3-SiO_2 were measured and compared with that of commercial Pt/C and XC-72R carbon. The electrical and proton conductivities and BET surface areas of materials prepared with different extents of functionalization were also measured.

The second approach involved the synthesis of sulfonic acid functionalized silica with a bimodal pore-structure. The intent of this approach was for RuO_2 to be selectively impregnated in the mesopores of the bimodal structure, while leaving the macropores free for reactant and product transport.

Results

BET Surface Area and Electrical Conductivity

A series of core-shell-like structures of RuO_2-SiO_2, have been synthesized and characterized in terms of electrochemical stability, electrical conductivity, and BET surface area values. The BET surface areas of supports with 0, 9, 33, 50, and 60 mol% of RuO_2 were measured to be 1,100, 470, 420, 260 and 220 m^2/g, respectively. These values show considerable improvement over the values obtained with the co-condensation approach reported in our earlier work [2]. The electrical conductivity of the supports was estimated using a 2-point probe by linear-sweep voltammetry. As shown in Figure 1a, the electronic conductivity was significantly higher for the support materials calcined at 450°C than for those calcined at 100°C. X-ray diffraction (XRD) analysis confirmed that the difference was due to the extent of crystallinity of the material that was enhanced while annealing at higher temperatures. Additionally, the increase in conductivity with RuO_2 loading is very sharp up to a loading of 40%, following which the rate of increase of conductivity is less rapid. This difference in the rate of increase of conductivity with loading is attributed to the amount of RuO_2 particles needed for creating optimal pathways (i.e. percolated network) to conduct electrons. Above 40 mol% of RuO_2, there is a sufficient amount of RuO_2 particles available for electron conductivity. The electrical conductivity of the sample with 33 mol% RuO_2 loading is 3 S/cm, a value that is adequate for fuel cell operation. These results suggest that RuO_2-SiO_2 is indeed a viable high surface area catalyst support with adequate electrical conductivity. Given that the BET surface area is drastically lowered as the amount of RuO_2 in the sample is increased,

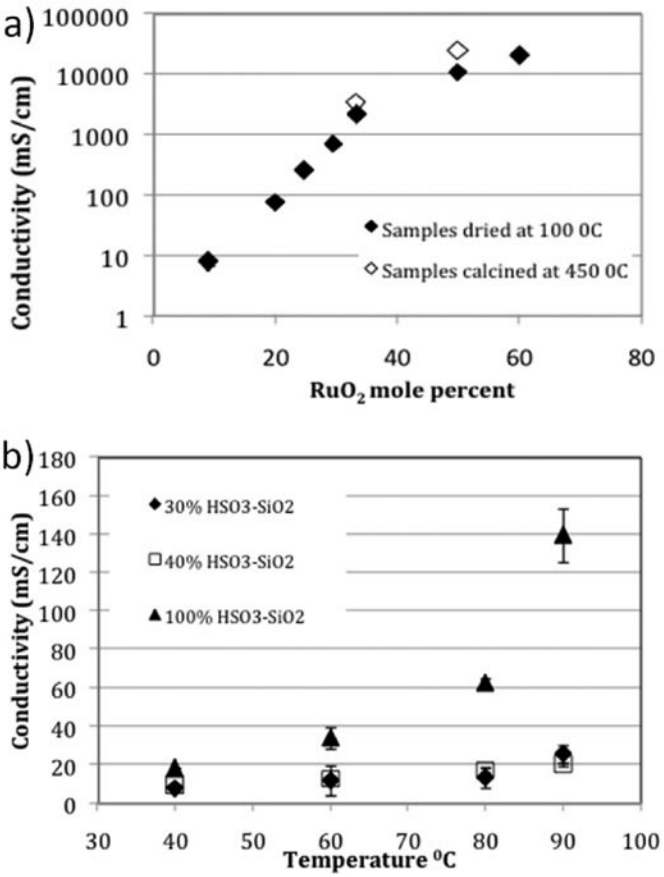


FIGURE 1. (a). Electrical conductivity of RuO_2 functionalized silica. All measurements were obtained at room temperature. (b). Proton conductivity of sulfonic acid functionalized silica at various temperatures. All measurements were obtained at 100% relative humidity (RH).

future research will focus on lowering the RuO_2 content while maintaining or enhancing the electrical conductivity by tuning the distribution of RuO_2 in the silica matrix. To accomplish this task, work has been initiated on the second approach stated above, namely the synthesis of silica with a bimodal pore-structure, wherein the ruthenium oxide can be selectively impregnated in the mesopores, leaving the macropores free for reactant and product transport.

Stability of Catalyst Supports

The stability of the different RuO_2 functionalized silica supports was evaluated by potential cycling using a rotating disk electrode (RDE) setup. The support samples were coated on a glassy carbon (GC) disk electrode and the cycling experiment was carried out in a N_2 saturated 0.1M $HClO_4$ solution. The catalyst support loading was controlled at 200 $\mu g/cm^2$ for all experiments. The supports were cycled between 0 to 1.8 V vs. reference hydrogen electrode (RHE) at a scan rate of 1 V/s for up to 1,000 cycles, and cyclic voltammograms (CVs) were recorded at periodic intervals at a scan rate of 10 mV/s. The CVs recorded were analyzed

to assess the double-layer charge (Q_{DL}) of the supports. This metric was employed as a preliminary estimate of support surface area and stability. The stability data obtained using the RuO_2-SiO_2, HSO_3-SiO_2 and XC-72R carbon samples upon potential cycling are shown in Figure 2. Both RuO_2-SiO_2 supports exhibited excellent stability in contrast to carbon, while still showing Q_{DL} values similar to that of carbon. Carbon showed a 44% drop in Q_{DL} after 1,000 cycles due to loss in surface area, while the RuO_2-SiO_2 supports did not show any loss in Q_{DL}. HSO_3-SiO_2 did not show a change in Q_{DL} during potential cycling, but it had a much lower Q_{DL} compared to carbon. The samples tested here have been shipped to NTCNA for further stability evaluation using prescribed protocols. These tests are underway.

Ion Exchange Capacity (IEC)

The IEC of the silica supports functionalized with varying amounts of sulfonic acid groups was measured by titration. The surface area of the functionalized silica was determined by the BET method. The presence of HSO_3 in these samples was confirmed by IEC measurements, which revealed that the samples had an IEC ranging from 1.7-2.1 meq/g. The IEC did not change substantially with extent of functionalization, but was much higher than the near-zero IEC obtained for unfunctionalized silica samples. The BET surface areas of the 20%, 30%, and 40% functionalized HSO_3-SiO_2 samples were 650, 520, and 450 m^2/g, respectively. The BET surface area decreased as the extent of functionalization was increased; however, the values obtained are in excess of requirements even at high levels of functionalization.

Proton Conductivity

Preliminary proton conductivity measurements were performed at 40, 60, 80 and 90°C at 100% RH for samples with 30, 40 and 100% extents of functionalization (data shown in Figure 1b). Proton conductivity measurements were performed with a two-point conductivity cell using electrochemical impedance spectroscopy. A maximum proton conductivity of 140 mS/cm was obtained for 100% HSO_3-SiO_2, while 30 and 40% HSO_3-SiO_2 had much lower proton conductivities in the range of 7-25 mS/cm. In line with expectations, high levels of functionalization of SiO_2 allowed for more efficient proton conduction. However, the 100% functionalized HSO_3-SiO_2 was not thermally stable and decomposed around 100°C. One approach to solve this issue that is currently being pursued is to employ and functionalize templates with greater thermal stability, such as polyhedral oligomeric silsesquioxanes.

Stability of Catalyst

Platinum was deposited on selected non-carbon supports using conventional deposition methods. The stability of the Pt on RuO_2-SiO_2 supports was again characterized by potential cycling using a RDE. The catalyst loading on the GC disk was controlled to 50 $\mu g/cm^2$ of Pt and 200 $\mu g/cm^2$ of RuO_2-SiO_2 support for all stability experiments. The supports were cycled between 0 to 1.2 V vs. RHE at a scan rate of 1 V/s for up to 10,000 cycles, and CVs were recorded at intermediate points (at 10 mV/s) to determine the ECSA of the Pt.

ECSA was calculated from the difference between the total charge involved in the hydrogen desorption and the double-layer charge using the specific H_{upd} charge of 210 $\mu C/cm^2$. The ECSA values for 20% Pt deposited on RuO_2-SiO_2 and 57% Pt/C are shown in Figure 3. The 20% Pt/RuO_2-SiO_2 exhibited consistently high ECSA (>100 m^2/g_{Pt}) and showed high stability for up to 10,000 cycles. The 57% Pt/C showed deterioration of ECSA under this potential cycling test.

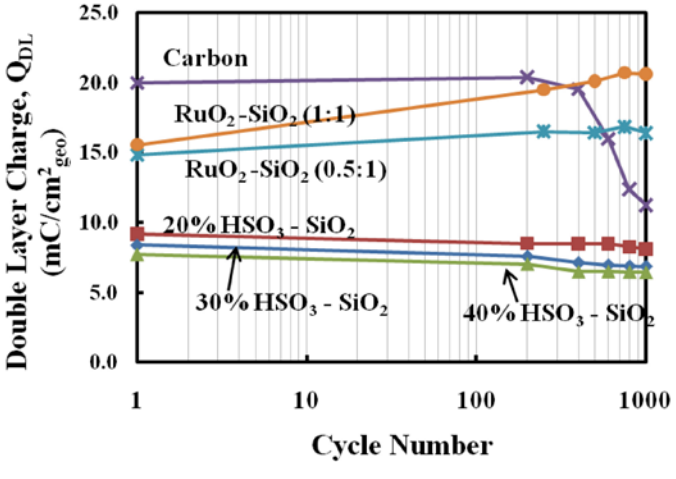


FIGURE 2. Double layer charge obtained from synthesized RuO_2-SiO_2, sulfonic acid functionalized silica, and Vulcan XC-72R carbon during potential cycling between 0 to 1.8 V vs. RHE.

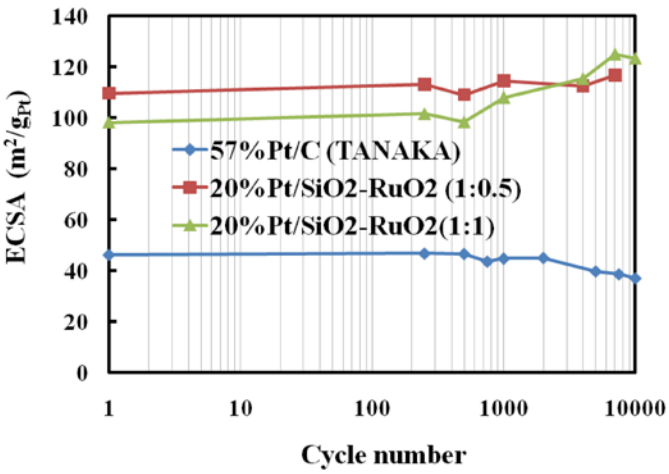


FIGURE 3. ECSA of Pt supported on RuO_2-SiO_2 and Pt/C (57%, TKK) after 10,000 potential cycles between 0 to 1.2 V vs. RHE.

Ex situ benchmarking of various Pt-based catalysts with different carbon supports has been completed at NTCNA. Start-stop cycling and load cycling durability tests have been performed by cycling electrode potential between 1.0 V to 1.5 V (triangular wave form) and between 0.6 V to 1.0 V (rectangular wave form). The results of these tests show that NTCNA has acquired a very good understanding of the interplay between Pt and its support on durability of the catalyst. NTCNA is also performing ex situ benchmarking of various un-catalyzed carbon supports for their durability using the start-stop cycling protocol. These tests are expected to provide a more in-depth understanding of the support material's stability, which will help benchmarking the non-carbon supports being developed under this project. Finally, NTCNA is currently working to evaluate the durability of non-carbon supports developed at IIT using the above protocols. The results obtained at NTCNA will be further described in the forthcoming quarterly report.

Fuel Cell Performance

Preliminary fuel cell performance has been demonstrated with the non-carbon support catalyst. Figure 4 shows the polarization curves of a PEFC employing Pt/RuO_2-SiO_2 at the anode and cathode. The current density at 0.6 V was 750 mA/cm^2, and the maximum power density obtained was 570 mW/cm^2 under H_2/O_2. Further analysis of polarization data is in progress.

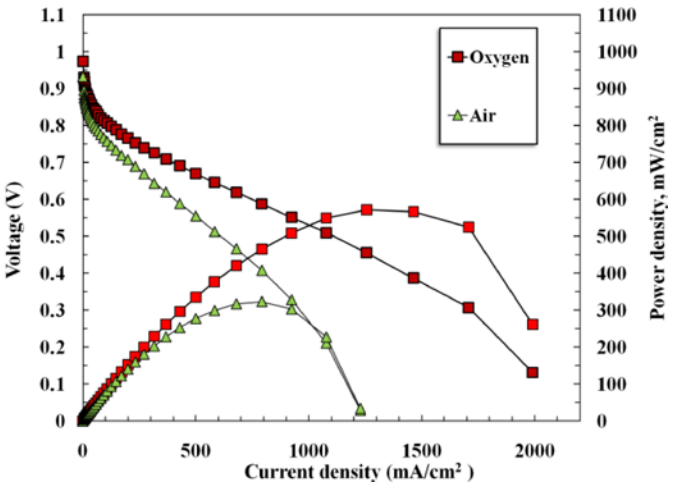


FIGURE 4. Polarization curves obtained from a PEFC membrane electrode assembly prepared using Pt/RuO_2-SiO_2 electrocatalysts at both electrodes. Measurements were conducted at 80°C with 75% RH. Reactant flow rates were set at two times the stoichiometric requirement for both H_2 and O_2/air. Pt loading was controlled at 0.4 mg/cm^2 at the cathode and 0.2 mg/cm^2 at the anode.

Conclusions and Future Directions

- Highly durable RuO_2-SiO_2 catalyst supports with a core–shell-like structure were synthesized with high BET surface areas and electron conductivities.
- Both RuO_2-SiO_2 and Pt/RuO_2-SiO_2 materials exhibited superior electrochemical stability in comparison to carbon catalyst supports under potential cycling tests.
- Several samples of sulfonic acid functionalized silica have been prepared, and they demonstrate excellent proton conductivity.
- Promising preliminary fuel cell performance with H_2/O_2 has been obtained with Pt/RuO_2-SiO_2 electrodes.
- Future efforts will be focused on refining microstructure-property relationships in the ruthenium oxide-silica composite system in terms of extent of functionalization, pore-structure of silica/functionalized silica employed, and platinum loading. Efforts are underway to synthesize a stand-alone mixed conducting support by combining the methods described herein. Work will be performed collaboratively with NTCNA to subject the supports synthesized to a more diverse set of stability testing protocols.

References

1. Landsman, D.A., Luczak, F.J., In Handbook of Fuel Cells Fundamentals, Technology, and Applications; Vielstich, W., Gasteiger, H.A., Lamm, A., Eds.; John Wiley and Sons Ltd.: West Sussex, England, 2003; Vol. 4.

2. Lo, C.-P., Kumar, A., and Ramani, V., ECS Transactions, Vol. 33, PP. 493 – 505, 2010.

V.D.11 Development of Novel Non-PGM Electrocatalysts for Proton Exchange Membrane Fuel Cell Applications

Sanjeev Mukerjee
Department of Chemistry and Chemical Biology
Northeastern University (NEU)
Boston, MA 02115
Phone: (617) 373-2382
Email: S.mukerjee@neu.edu

DOE Managers
HQ: Kathi Epping Martin
Phone: (202) 586 7425
E-mail: Kathi.Epping@ee.doe.gov
GO: Dr. David Peterson
Phone: (720) 356-1747
E-mail: David.Peterson@go.doe.gov

Contract Number: DE-EE0000459

Subcontractors:
- University of New Mexico, Albuquerque, NM (UNM) (Prof. Plamen Atanassov)
- Michigan State University, East Lansing, MI (MSU) (Prof. Scott Barton)
- University of Tennessee, Knoxville, TN (UTK) (Prof. Thomas Zawodzinski)
- Nissan Technical Center, North America (NTCNA), Detroit, MI (Dr. Kev Adjemian)
- BASF fuel cells, Somerset, NJ (BASF) (Dr. Emory De Castro)
- Los Alamos National Laboratory, Los Alamos, NM (LANL) (Dr. Piotr Zelenay)

Project Start Date: August 1, 2010
Project End Date: August 1, 2014

Fiscal Year (FY) 2011 Objectives

The objective of this project is to design non-platinum group (PGM)-based materials and supporting gas transport layer, both in the interfacial reaction layer between the electrode and membrane as well as in the underlying gas diffusion medium, for meeting and exceeding DOE goals for application in solid polymer electrolyte fuel cells. This project is focused on materials development and is assisted by advanced analytical tools, computation, and testing for improving the design via critical understanding of electrocatalysis in these novel structures.

Technical Barriers

This project addresses the following technical barriers from the Fuel Cells section of the Fuel Cell Technologies Program Multi-Year Research, Development and Demonstration Plan:

(B) Cost (reduce precious metal loading of catalysts)

(C) Performance (increase the specific and mass activities of catalysts)

(A) Durability (increase the durability/stability of catalysts with cycling)

Technical Targets

TABLE 1. Progress towards Meeting Technical Targets for Non-PGM Electrocatalysts for Transportation Applications

Characteristic	Units	2015 Target	NEU 2011 status
Specific Activity @ 80°C, 0.1 M $HClO_4$	A/cm^3	150/300	30
Specific Activity @ 80°C, 150 kPa, H_2/O_2, 100% relative humidity (RH)	A/cm^3	150/300	130
Durability at 80°C Cycling: Catalyst Durability	% loss of activity	5	<1
Durability at 80°C Cycling: Carbon Corrosion Durability	% loss of activity	10	<50

FY 2011 Accomplishments

- Current efforts focus on synthesis of non-PGM metals contained in unique liganded environments (mostly using N or O) and its incorporation onto carbon supports for effecting improved oxygen reduction reaction (ORR) performance and stability. Such as those shown by the LANL group.
- Our effort encompasses development of novel bi-dentate and tetra-dentate complexes where tandem electron transfer to oxygen can be facilitated using two or three transition metals with different oxidation states.
- Successful implementation of these strategies has been done at NEU as well as partner institutions which include UTK, UNM and MSU.
- One such rendition of a ligand Fe-based catalyst has also been extensively tested at NTCNA for both fuel cell activity as well as durability. The latter tests involved both catalysts and support stability tests incorporating DOE mandated cycling tests.
- Current status of the non-PGM field puts the volumetric power density at 130 A/cm^3 this however needs to be translated to actual fuel cell performance levels which requires redesign of electrode structures. In addition, excellent durability of the tested catalysts is reported.

Introduction

Polymer electrolyte membrane fuel cells (PEMFCs) are promising candidates as an alternative to traditional energy converters. A primary technical challenge faced in the development of the technology is the sluggish kinetics of the ORR on the cathode. Pt and Pt alloy electrocatalysts remain the choice of electrocatalysts for PEMFCs due to the so called "stability criterion." However, recent reports have shown good activity and stability for alternative non-PGM-based electrocatalysts [1] and Dodelet [2] for the more challenging ORR.

Approach

The objective of this project is to design non-PGM-based materials and supporting gas transport layer, both in the interfacial reaction layer between the electrode and membrane as well as in the underlying gas diffusion medium, for meeting and exceeding DOE goals for application in PEMFCs. This project is focused on materials development and is assisted by advanced analytical tools, computation, and testing for improving the design via critical understanding of electrocatalysis in these novel structures.

Results

UNM explored the effect of support material for the catalyst. It was shown that templating catalysts onto a sacrificial layer of hierarchically structured silica (HSS) or fumed silica allows synthesis of materials with well developed porosity, this cannot be achieved with synthesis methods based on use of carbon black. These HSS materials also offer higher surface areas when compared to catalysts supported on carbon blacks. After etching silica, the cavities left by the vacated silica create an open-framed structure that upon addition of catalysts allows for internal transport of electrolyte and reactant, providing additional surface area for the active sites. Two classes of catalysts were synthesized and characterized: Fe-cyanamide and Fe-4-aminoantipyrine diethanolamine. It was found that heat treatment conditions including ramp rates, durations, and temperatures can have dramatic effects on final catalytic activity, and should be optimized for every combination of Fe and C-N precursors. Furthermore, the density functional theory computations show that nitrogen may play a dual role in non-Pt ORR electrocatalysts: on the one hand it provides a stabilizing coordination environment for transition metals such as cobalt or iron. On the other hand, the ability to stabilize narrow channels due to balancing nitrogen and cobalt content indicates that nitrogen can help stabilize microstructures. The investigated catalysts show significant activity towards oxygen reduction and can be used as inexpensive substitutes for Pt.

The effect of the nitrogen precursor was explored by the team from MSU. Metal-nitrogen-carbon cathode catalysts for the ORR in low temperature fuel cells were synthesized by pyrolysis of iron-acetate, Ketjen black and various nitrogen precursors of varying nitrogen content, including carbon-free nitrogen precursors. In collaboration with UNM a surface analysis was carried out to determine the surface nitrogen content produced by the various precursors. These results were combined with ORR activity results to determine what type of nitrogen precursor produced the best performing catalyst.

In addition, two sample catalysts from MSU that were prepared from melamine and ammonium carbamate precursors were sent to NTCNA Fuel Cell Laboratory for ex situ and in situ characterization.

Understanding the selectivity of the catalyst towards two or four electron pathways is very important for oxygen reduction catalysts. Rotating ring disk electrode (RRDE) experiments were performed for the melamine-based catalyst to verify the formation of peroxide. Peroxide formation was observed to be less than 2% (DOE Target).

Fuel cell testing was carried out and current-voltage (I-V) performance was measured at both atmospheric and 1 bar pressure, 80°C, 100% RH. The high frequency resistance of this MEA was very high due of the amount of ionomer in the catalyst layer and the catalyst layer's thickness. As expected, HFR measured at 1 bar was higher than at atmospheric pressure. These are shown as I-V curves both on a linear and corresponding semi-logarithmic Tafel plots in Figures 1 and 2, respectively. Volumetric activity or volumetric current density is calculated at 0.8 V internal resistance-free voltage and an effective carbon density of 0.4 g/cm^3 was assumed for these calculations. Volumetric current densities of 31 and 131 A/cm^3 were obtained for the melamine-based catalyst MEA without pressure and with

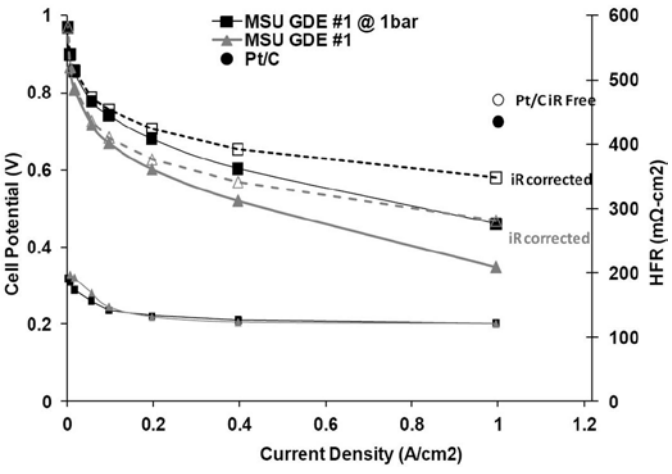


FIGURE 1. I-V performance for Fe-N_x-based catalysts using melamine precursors with (■ and □) and without (▲ and △) back-pressure (100 kPa) conditions under 100% RH, 80°C, and H_2/O_2.

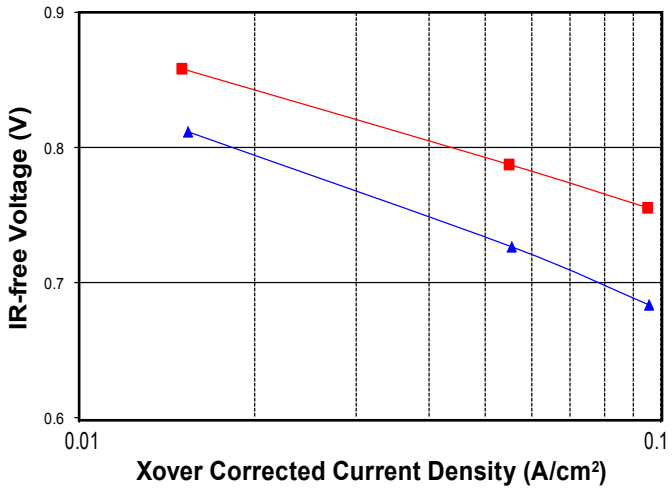


FIGURE 2. Corresponding Tafel Plots for Fe-Nx catalysts prepared using melamine precursors, with (red) and without (blue) back pressure (150 kPa). Plots reflect internal resistance correction and adjustment for hydrogen cross over.

back-pressure of 1 bar, respectively. However, at 80°C under H_2/air with 100% RH or 50% RH, this MEA showed very poor performance.

In situ durability tests were performed on the same MEA (Fe-N_x melamine precursor sample) which was used to evaluate I-V performance (Figures 1 and 2). Two types of in situ durability tests, namely load cycling and start-stop cycling (10,000 cycles) were performed. The first referred to as catalyst durability test (or Pt dissolution protocol in NTCNA parlance) involved square wave potential cycling tests in the range of 0.6 and 1.0 V with 3 s on and 3 s off periods (Figure 3). The same MEA used for support durability tests, here cycling were used in the range of 1.0 and 1.5 V in a triangular profile (Figure 3) referred to as carbon corrosion test. In this case, the open circuit voltage value did change due to the potential cycling resulting in carbon loss.

The I-V performance curves were recorded before and after these durability tests. Catalyst durability cycling showed minimal effect on I-V performance with and without back-pressure. However, carbon corrosion test cycling

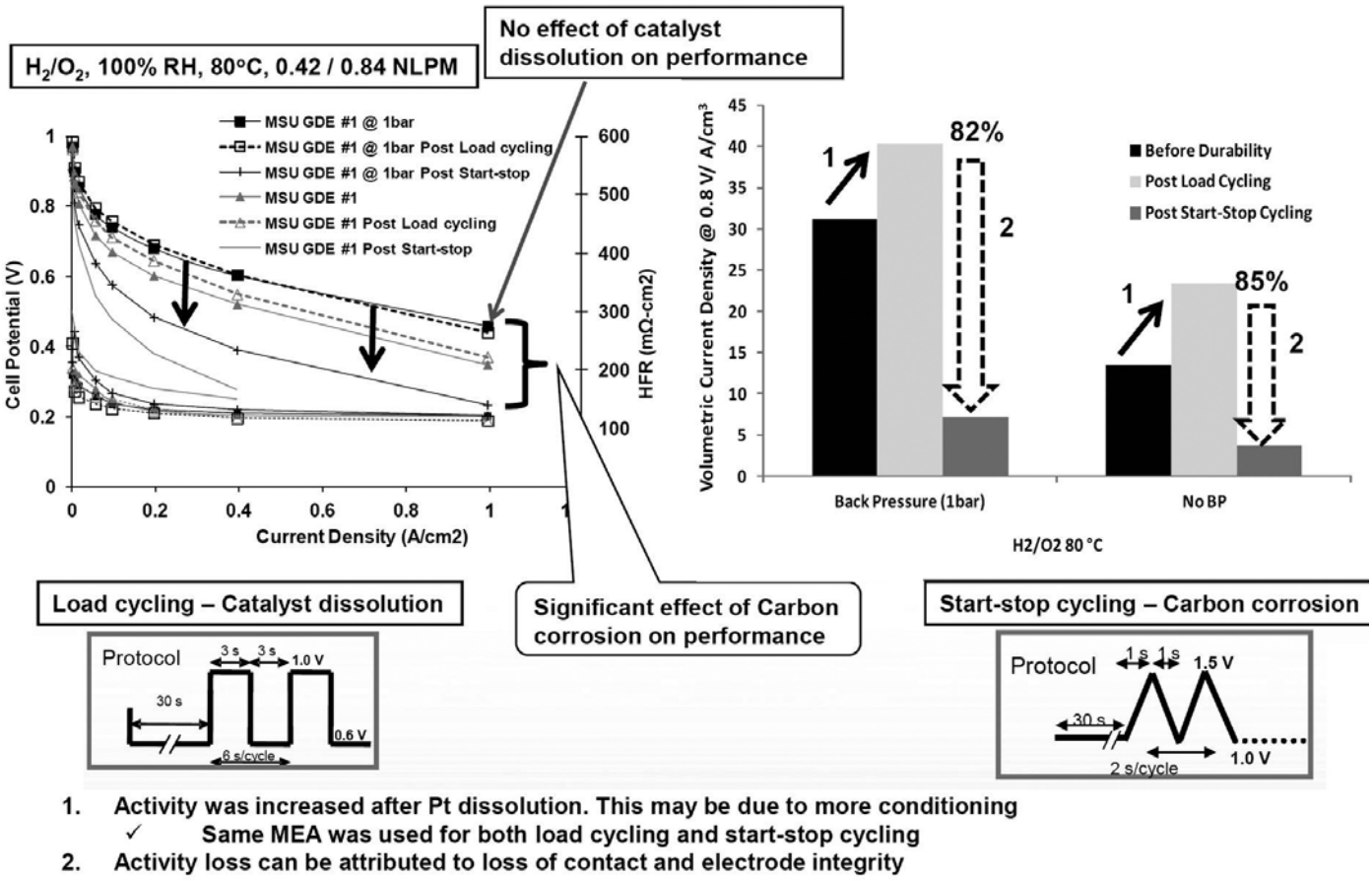


FIGURE 3. Durability tests in single cells (80°C, 100% RH, with and without backpressure, 150 kPa). Two protocols were (a) catalysts durability involving cycling between 0.6 and 1.0 V in a square wave profile with 3 s on and 3 s off periods and (b) carbon corrosion tests between 1.0 and 1.5 V in a triangular profile.

showed significant drop in performance under both pressure conditions. The drop in performance due to start-stop cycling can be attributed to formation of surface oxides on the carbon surface making it hydrophilic in nature. Also, loss in carbon causes a decrease in the electronic conductivity resulting in lower performance which can be observed in the kinetic region.

Conclusions and Future Directions

- A multipronged effort involving several different chemistries is being pursued for the effective development of a non-PGM-based oxygen reduction catalyst.
- Initial results have shown good performance both in RRDE as well as fuel cell test conditions. Performance of 130 A/cm^3 is reported based on projections in a single-cell test conducted at NTCNA. This is close to the 2010 DOE non-PGM target.
- Excellent catalyst durability is reported using NTCNA/DOE cycling protocols, however significant carbon corrosion is measured which needs to be addressed via modifications in pretreatments to carbon blacks, use of grapheme-based materials as well as stable transition metal oxide supports.

FY 2011 Publications/Presentations

1. "Unveiling N-Protonation and Anion-Binding Effects on Fe/N/C-Catalysts for O2 Reduction in PEM Fuel Cells", Herranz, Juan; Jaouen, Frederic; Lefevre, Michel; Kramm, Ulrike; Proietti, Eric; Dodelet, Jean-Pol; Bogdanoff, Peter; Fiechter, Sebastian; Abs-Wurmbach, Irmgard; Bertrand, Patrick; Arruda, Thomas; Mukerjee, Sanjeev, *J. Phys. Chem. C* (In Press).

References

1. Wu, G.; More, K.L.; Johnston, C.M.; Zelenay, P. *Science* **2011**, *332*, 443.

2. Lefevre, M.; Proietti, E.; Jaouen, F.; Dodelet, J.P. *Science* **2009**, *324*, 71.

V.D.12 High-Activity Dealloyed Catalysts

Frederick T. Wagner
General Motors, LLC (GM)
10 Carriage St.
Honeoye Falls, NY 14472
Phone: (585) 624-6726
E-mail: frederick.t.wagner@gm.com

DOE Managers
HQ: Dimitrios Papageorgopoulos
Phone: (202) 586-5463
E-mail: Dimitrios.Papageorgopoulos@ee.doe.gov
GO: Gregory Kleen
Phone: (720) 356-1672
E-mail: Greg.Kleen@go.doe.gov

Contract Number: DE-EE0000458

Subcontractors:
- George Washington University (GWU), Washington, D.C.
- Johnson Matthey Fuel Cells (JMFC), Sonning Common, UK
- Massachusetts Institute of Technology (MIT), Cambridge, MA
- Northeastern University (NEU), Boston, MA
- Technical University Berlin (TUB), Berlin, Germany

Project Start Date: August 1, 2010
Project End Date: May 31, 2013

Objectives

- Prepare, characterize, and test dealloyed catalysts with initial oxygen reduction mass activities exceeding the DOE 2015 target of 0.44 A/mg_{Pt} at 900 mV reversible hydrogen electrode in 50 cm^2 fuel cells.
- Demonstrate, for these materials, loss of no more than 40% of the catalytic (mass) activity after the DOE-specified voltage-cycling test in 50 cm^2 fuel cells.
- Develop and demonstrate, with these catalysts, electrodes giving high current density performance in air adequate to meet the DOE platinum group metal (PGM) loading targets of <0.125 g_{PGM}/kW_{rated} and <0.125 mg_{Pt}/cm^2_{geo}.
- Demonstrate durability of the high current density performance in air in full-active-area fuel cells.
- Determine, at the atomic scale, where alloying-element atoms should reside with respect to the surface of the catalyst particle for simultaneously good activity, durability, and high-current density performance in air.

Technical Barriers

This project addresses the following technical barriers from the Fuel Cells section of the Hydrogen, Fuel Cells and Infrastructure Technologies Program Multi-Year Research, Development and Demonstration Plan:

(A) Durability
(B) Cost
(C) Performance

Technical Targets

TABLE 1. Progress towards Meeting Technical Targets for Electrocatalysts for Transportation Applications

Characteristic	Units	2015 DOE StackTargets	Project 2011 Status (50 cm^2)	
Mass activity	A/mg_{PGM} @ 900 $mV_{i\text{-}free}$	≥0.44	0.58 ($PtCu_3$) 0.37 ($PtCo_3$)	
Loss in catalytic (mass) activity	% lost after 30k cycles 0.6-1.0 V	≤40%	38% ($PtCo_3$) 83% ($PtCu_3$)	
PGM total content	g_{PGM}/kW_{rated}	≤0.125	0.19 @1.5 A/cm^2 in H_2/air	For more highly dealloyed $PtCu_3$
PGM total loading	mg_{PGM}/cm^2_{geo}	≤0.125	0.15	
Specific activity	$\mu A/cm^2_{PGM}$	720	860	

PGM - platinum group metal

Fiscal Year (FY) 2011 Accomplishments

- Demonstrated in 50 cm^2 fuel cells a dealloyed $PtCu_3$ catalyst with initial mass activity of 0.58 A/$mg_{Pt,}$ exceeding the DOE 2015 target of 0.44 A/mg_{Pt}
- Demonstrated in 50 cm^2 fuel cells a dealloyed $PtCo_3$ catalyst with a loss of 38% of its initial mass activity after 30,000 cycles 0.6-1.0 V in H_2/N_2, (slightly) bettering the DOE 2015 target of <40% loss. The initial activity of this $PtCo_3$ catalyst, at 0.37 A/mg_{Pt}, tested slightly below the DOE target for initial activity.
- Developed methods to scale up the production of relevant catalyst precursors from <0.5 g to 100 g.
- Derived similar ~3 monolayer Pt shell/$PtCu_{1.8}$ core structures from transmission electron microscopy (TEM) and extended X-ray absorption fine structure for a dealloyed $PtCu_3$ catalyst.

Introduction

The amount of expensive platinum used in the air electrode of fuel cells must be reduced at least 4-fold to make fuel cells cost-competitive with internal combustion powertrains, requiring a compensating increase in the oxygen reduction activity per gram of Pt used. Pt-alloy catalysts have historically given a ~2-fold increase in activity vs. pure Pt, leaving a 2-fold gap remaining. However, prior to this project the group of project team member Peter Strasser (now at TUB) had found in laboratory experiments that if one started with a large excess of the inexpensive non-noble alloying element and then removed most of that element with an electrochemical voltage-cycling "dealloying" treatment, significantly enhanced activities exceeding the DOE 2015 target of 0.44 A/mg_{Pt} could be achieved [1]. This project seeks to develop and scale up new catalysts that take advantage of this activity gain from dealloying while also achieving the durability and high current density performance needed for production fuel cells.

Approach

Catalyst precursors with the general formulation PtM_3 are being prepared on carbon-black supports, with the choices of M including Cu, Co, Ni, and possibly Fe and V. Electrochemical and chemical processes have been developed to partially dealloy the precursor powders down to a composition of ~Pt_2M. This must be done prior to incorporation of the catalysts into a membrane electrode assembly (MEA) to prevent excessive displacement of hydrogen ions from the ion-exchange sites of the ionomer by M^{x+} ions. This project has scaled up the production of relevant catalyst precursors from a <0.5 g level to the >100 g needed for durability and integration studies. Dealloying methods more suitable to eventual mass production have been developed and are being further optimized.

The catalysts are then tested for oxygen reduction kinetic activity on rotating-disk electrodes (RDEs) and for both activity and durability in 50 cm^2 fuel cells. Advanced TEM and X-ray absorption spectroscopy (XAS) techniques are being applied to fresh and used catalyst samples to determine atomic-scale composition and structure. Iterative cycles of synthesis, testing, and characterization are being used to optimize the dealloyed catalysts. We plan to achieve durability by leaving just the right number of M atoms, and no more, at just the right places in the catalyst particles. At the end of the project, downselected catalysts will be fabricated into full-active-area fuel cell short stacks to test the durability of high current density performance while operating with hydrogen/air.

Results

Figure 1 shows that in 50 cm^2 MEAs in H_2/O_2 fuel cells under standard conditions, GM has obtained initial mass activities of 0.58 A/mg_{Pt} at 900 mV for catalysts prepared from $PtCu_3$/HSC precursors from the Strasser group using a readily manufacturable chemical dealloying process applied to the precursor powder. This value exceeds the DOE target of 0.44 A/mg_{Pt}. A scaleable, though still less convenient, electrochemical dealloying procedure applied to the powder gave 0.32 A/mg_{Pt}. While the initial activity target has been reached with the chemically-dealloyed material, the Strasser group had been able to prepare precursors to highly active dealloyed catalysts only in batches of ≤0.5 g (with thermal annealing being the scale-limiting step), severely limiting the amount of fuel cell testing that could be done. JMFC's initial attempts to scale up (to >80 g) the annealing of $PtCu_3$ precursors under this project led to materials with badly diminished surface areas. After intense study of preparation techniques, including thermal gravimetric analysis, JMFC developed modified preparation procedures at the 100-g scale that can reproduce the physical properties of Strasser's small batches. GM applied its chemical dealloying procedures to this large-batch $PtCu_3$/Ketjen precursor, generating catalysts that show a laboratory RDE activity of 0.52 A/mg_{Pt}, in good agreement with RDE results from the Strasser small batches. However, the first 50 cm^2 MEAs made from the large JMFC batch of $PtCu_3$ have given mass activities of only 0.26 A/mg_{Pt}. While it is unfortunately common to measure lower activities for a catalyst in real fuel cells than in RDE, that had not been the case for the Strasser small batches. The dealloyed JMFC $PtCu_3$ has a higher electrochemical surface area (93 m^2/g_{Pt}) than the Strasser small batch (67 m^2/g_{Pt}), so it may prove useful for JMFC to slightly raise their annealing temperature.

While the dealloyed $PtCu_3$ gave very good initial oxygen reduction reaction activity, Figure 2 shows that it lost 82% of its initial activity after 10,000 potential cycles 0.6-1.0 V

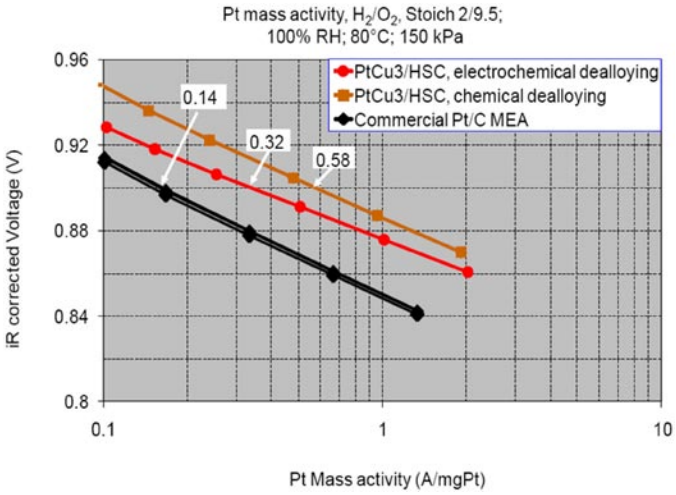


FIGURE 1. Oxygen reduction activity in 50 cm^2 fuel cells (targets at 0.90 V) for Strasser-group $PtCu_3$ precursor dealloyed by chemical or electrochemical methods at GM, plus pure-Pt-catalyzed commercial MEAs for comparison, at the standard conditions shown. X-axis is the current density (A/cm^2_{geo}) divided by the Pt loading (mg_{Pt}/cm^2_{geo}).

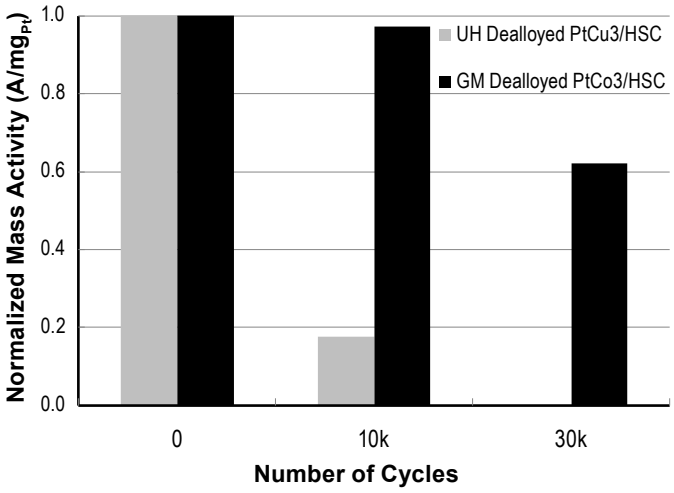


FIGURE 2. Mass activities for dealloyed $PtCu_3$ and dealloyed $PtCo_3$ catalysts, normalized to initial values, after indicated number of potential cycles 0.60-1.00 V in H_2/N_2 50 cm^2 fuel cells. Activities measured in H_2/O_2 under conditions of Figure 1.

in 50 cm^2 H_2/N_2 fuel cells. In contrast, Figure 2 also shows that a GM-prepared dealloyed $PtCo_3$/HSC catalyst lost only 38% of its initial activity after 30,000 cycles, meeting the DOE target of a <40% loss. Since the initial activity of the dealloyed $PtCo_3$, 0.37 A/mg_{Pt}, did not quite meet the initial activity target, we have one catalyst satisfying initial activity ($PtCu_3$) and a different one satisfying durability ($PtCo_3$) targets. Dealloyed PtCo (lower initial Co) has given 0.48 A/mg_{Pt}. under slightly different test conditions.

Through detailed analysis by XAS and several forms of high resolution TEM, we seek to determine which atomic-scale structural and compositional structures confer high activity and which improve durability. With such knowledge in hand, we should be able to prepare catalysts simultaneously satisfying both targets. Our initial XAS and TEM work with dealloyed $PtCu_3$ showed a preponderance of particles with a core of a ~$PtCu_{1.8}$ alloy surrounded by a shell of three monolayers of pure Pt. Preliminary analysis of similar data for dealloyed $PtCo_3$ suggests the presence of thicker Pt shells. Given that the enhanced activity of the surface Pt atoms is believed to arise from lattice-compression [2] and/or direct electronic effects of the non-Pt atoms in the cores, and that these non-Pt atoms are much more susceptible to corrosion, one might expect an increase in shell thickness activity to decrease activity and increase durability, consistent with our preliminary structural observations. However, other parameters being measured (listed below under Conclusions) may exert more direct control than shell thickness. The knowledge gained from the characterization work is guiding our synthetic efforts in an iterative process.

Pre-project work at TUB suggested that dealloyed $PtNi_3$ could be more stable than $PtCo_3$, with at least equivalent activity. TUB and JMFC have developed independent methods to prepare a single-phase (helpful for the production of the uniform catalyst particles needed for definitive experiments) $PtNi_3$ precursor. Initial GM RDE experiments on JMFC small-batch dealloyed $PtNi_3$ have given activities of 0.33 A/mgPt, but no optimization has yet been done on this system.

Excess non-noble metal ions leached from the catalyst can suppress oxygen reduction performance at high current density [3]. We have so far observed a negative correlation between high-current-density performance and the amount of M left in the catalyst after dealloying. We are working to identify just the right number of M atoms, in just the right place in the particle, needed for maximum durable activity, and then to synthesize particles with no excess M.

Conclusions and Future Directions

- A dealloyed catalyst ($PtCu_3$) has met the DOE target for oxygen reduction mass activity.
- A different dealloyed catalyst ($PtCo_3$) has met the DOE target for retention of mass activity after voltage cycling.
- The primary goal for 2011 is to achieve both initial activity and durability targets with the same catalyst, learning from the detailed atomic-scale characterization work.
- Dealloying produces a range of structures featuring pure-Pt shells over M-rich alloy cores.
- The following parameters are being measured, and varied via synthesis, to determine which best correlate with activity and durability: lattice compression in Pt shell, shell thickness, M concentration in core, average Pt d-band vacancy population, and particle size.

FY 2011 Publications/Presentations

1. J. Zhang, Z. Yu, Z. Liu, J. Ziegelbauer, I. Dutta, Y. Liu, R. Srivastava, X. Zhu, P. Strasser and F. Wagner, "An activity and durability study on chemically dealloyed $PtCu_3$/C electrocatalysts for the oxygen reduction reaction in PEM fuel cells", The Electrochemical Society, 1–6 May 2011, Montreal P.Q., manuscript in preparation (mostly pre-project work).

2. J.M. Ziegelbauer, I. Dutta and J. Zhang, "Chemical and Electronic Structure of High-Activity Chemically-Dealloyed PtM-alloy Electrocatalysts", The Electrochemical Society, 1–6 May 2011, Montreal P.Q., manuscript in preparation.

3. Z. Yu, J. Zhang, Z. Liu and F. Wagner, "Activity, Durability, and Structure of a Chemically-Dealloyed Platinum-Cobalt Catalyst for PEM Fuel Cells", North American Catalysis Society, 5–10 June, 2011, manuscript in preparation.

4. F.T. Wagner, "Electrochemistry and the Future of the Automobile", Frederick S. Billig and L. Gordon Croft Lecture at Johns Hopkins University, 28 March 2011 (small section on dealloyed catalysts).

References

1. Koh, S.; Strasser, P., "Electrocatalysis on Bimetallic Surfaces: Modifying Catalytic Reactivity for Oxygen Reduction by Voltammetric Surface Dealloying", J. Am. Chem. Soc., Vol. 129, pp. 12624-12625, 2007.

2. Strasser, P., Koh, S., Anniyev, T., Greeley, J., More, K., Yu, C., Liu, Z., Kaya, S., Nordlund, D., Ogasawara, H., Toney. M.F. and A. Nilsson, "Lattice-strain control of the activity in dealloyed core-shell fuel cell catalysts", Nature Chemistry, Vol. 2, pp. 454-460, 2010.

3. Greszler, T.A., Moylan, T.E. and Gasteiger,H.A., "Modeling the impact of cation contamination in a polymer electrolyte membrane fuel cell", in W. Vielstich, H. Yokokawa and H.A. Gasteiger, eds., "Handbook of Fuel Cells: Fundamentals, Technology and Applications", Vol. 6, Wiley, Chichester, UK, p. 728, 2009.

V.D.13 Development of Ultra-Low Platinum Alloy Cathode Catalysts for PEM Fuel Cells

Branko N. Popov
University of South Carolina (USC)
301Main Street
Columbia, SC 29208
Phone: (803) 777-7314
E-mail: popov@cec.sc.edu

DOE Managers
HQ: Jason Marcinkoski
Phone: (202) 586-7466
E-mail: Jason.Marcinkoski@ee.doe.gov
GO: Reg Tyler
Phone: (720) 356-1805
E-mail: Reginald.Tyler@go.doe.gov

Contract Number: DE-EE0000460

Subcontractors:
- Dr. Inchul Hwang (Co-PI), Dr. Bumwook Roh (Co-PI); Hyundai Motor Company (HMC), S. Korea
- Dr. Hansung Kim (Co-PI); Yonsei University, S. Korea.

Project Start Date: September 1, 2010
Project End Date: May 31, 2014

Fiscal Year (FY) 2011 Objectives

- Develop low cost and durable hybrid cathode catalyst (HCC).
- Develop Pt alloy/activated graphitic carbon (AGC) catalyst.
- Develop corrosion resistant supports.
- Develop facile scale-up catalyst synthesis procedure (at least 100 g).
- Optimize the parameters which control the number of catalytic sites on carbon composite catalyst (CCC).
- Optimize the procedure for the formation of more active Pt alloy catalysts.
- Demonstrate kinetic mass activity in H_2/O_2 fuel cell higher than DOE target of 0.44 A/mg_{PGM} and durability of the mass activity.
- Demonstrate high current performance in H_2/air fuel cell to meet DOE targets.
- Construct short-stack (50 cm^2 up to 10 cells) and evaluate the performance under simulated automotive conditions.

Technical Barriers

This project addresses the following technical barriers from the Fuel Cells section of the Fuel Cell Technologies Program Multi-Year Research, Development and Demonstration Plan:

(A) Durability
(B) Cost
(C) Performance

Technical Targets

The expected outcome of the project is the fabrication of catalysts, fully integrated into a proton exchange membrane electrode assembly (MEA), with the following performance characteristics:

- PGM loading of 0.1 mg/cm^2.
- Mass activity of 0.44 A/mg_{Pt} at 0.9 $V_{iR\text{-}free}$.
- Specific activity of 720 $\mu A/cm^2$ at 0.9 $V_{iR\text{-}free}$.
- Mass activity of at least 0.24 A/mg_{Pt} after 30,000 cycles, DOE protocol (0.6-0.9 V).
- Initial high current density performance of 1.5 A/cm^2 at 0.56 $V_{iR\text{-}free}$ in H_2-air.
- Electrochemical surface area (ECSA) loss less than 40% of initial catalytic activity after 30,000 cycles.
- Short-stack specific power density of 0.1 g/KW at rated power.
- Durability under cycling transportation conditions at ≥80°C for 2,000 hours and at ≤80°C for 5,000 hours.
- High volume production (manufacturability).

TABLE 1. Progress towards Meeting Technical Targets for Electrocatalysts for Automotive Applications

Characteristic	Units	Target 2015	USC 2011 status (25 cm^2 cell)
PGM Total Content	g/kW rated	≤0.125	To be determined
PGM Total Loading	mg PGM/cm^2 electrode area	≤0.125	0.1 (anode)/ 0.1 (cathode)
Loss in Catalytic (mass) Activity	percentage	<40% loss of initial	34%
Current Density Performance in H_2/Air	A/cm^2 at 0.56 $V_{iR\text{-}free}$	1.5 A/cm^2	1.45 (Pt_3M_1/AGC)
Mass Activity	A/mg PGM @ 900 $mV_{iR\text{-}free}$	≥0.44	0.43 (PtM_2/C) 0.42 (Pt/CCC [HCC]) 0.41 (Pt_3M_1/AGC)
Specific Activity	μA/cm^2 @ 900 $mV_{iR\text{-}free}$	720	1135 (Pt_3M_1/AGC)

FY 2011 Accomplishments

- Accomplished onset potential for oxygen reduction on CCC close to 0.9 V and less than 2.5% of peroxide production.
- Accomplished mass activity of 0.43 A/mg_{Pt}, 0.42 A/mg_{Pt} and 0.41 A/mg_{Pt} for PtM_2/C, Pt/CCC (HCC) and Pt_3M/AGC catalysts, respectively.
- Achieved durability of kinetic mass activity of 0.27 A/mg_{Pt} after 30,000 cycles for Pt_3M_1/AGC catalyst in 25 cm^2 cell.
- Accomplished initial high current density of 1.45 A/cm^2 at 0.56 $V_{iR\text{-}free}$ in H_2-air for Pt_3M_1/AGC catalyst.



Introduction

Stable and highly active HCC was developed at USC which shows higher performance than the commercial Pt/C at low loadings (between 0.04 and 0.4 mg/cm^2). The hybrid cathode catalyst is a combination of nitrogen-containing CCC, developed at USC, and platinum for oxygen reduction reaction [1-10]. Yonsei University developed a procedure for the synthesis of leached Pt-alloy catalysts deposited on AGC. Furthermore, Pt dendrites with controlled size have been developed for oxygen reduction reactions (ORR) [11-13]. The dendrites show superior activity for ORR and better selectivity when compared to the commercial Pt/C catalyst. HMC optimizes the design of 50 cm^2 active area bipolar plates and short stack assembly.

Approach

Currently, the main strategies to decrease the platinum loading in cathode electrodes are based on the optimization of electrode structures and implementation of more active Pt alloy catalysts. The new approach used in this work consists of development of a HCC through USC's patented process. The synergetic effect present in HCC results from contribution of the active sites present in CCC which improve the catalyst performance at low potentials, while implementation of Pt or leached Pt-alloy active sites increase the mass activity at high potentials. The goal of our second strategy is the synthesis of Pt-alloy catalysts deposited on AGC. To overcome the drawbacks associated with carbon corrosion under automotive operating conditions, corrosion-resistant catalyst support based on TiO_2 and corrosion-resistant hybrid TiO_2-CCC are under development at USC. HMC optimizes the design of 50 cm^2 active area bipolar plates and short stack assembly.

Results

In this reporting period, Pt/CCC (HCC) and PtM_2/C alloy catalysts were synthesized at USC. Pt and Pt-alloy catalysts deposited on AGC were developed at Yonsei University. HMC optimized the flow-field design of 50 cm^2 active area bipolar plates and short stack assembly. The performance of the catalysts including ECSA, kinetic mass activity, catalyst durability after 30,000 cycles, specific activity and initial high current performance were evaluated using rotating ring disc electrode and in a proton exchange membrane fuel cell (PEMFC).

Figure 1 shows the X-ray diffraction (XRD) of HCC catalyst and the cross-sectional analysis of MEAs utilizing different loadings of HCC catalyst. Shift of the diffraction peaks to higher Bragg angles indicates a decrease in the lattice constant due to alloy formation during the heat treatment. The ECSAs of the HCC catalyst and Pt/C catalyst were calculated to be 102 and 97.2 m^2/g, respectively.

PtM_2/C alloy catalyst was synthesized by depositing a protective layer on the surface of Pt/C to inhibit Pt particle agglomeration during high temperature alloying process. XRD showed slight shift of the diffraction peaks towards higher angle which confirms the lattice contraction even after chemical leaching procedure. With the protecting layer, there is no change of the Pt peak width and intensity suggesting the small change of the Pt particle size after high temperature alloying procedure. The average Pt particle sizes of Pt/C, Pt/C heated at 800°C, and de-alloyed PtM_2/C catalysts are 3, 22.2 and 3.3 nm, respectively. The results show that the Pt particles agglomerated during high temperature heat treatment in the absence of protecting layer. The ECSAs of the 60% Pt/C and 60% PtM_2/C catalysts are calculated to be 56.6 and 40.7 m^2/g, respectively.

Figure 2 compares the mass activities of HCC, PtM_2/C and commercial Pt/C catalysts. The cathode catalyst loadings were maintained at 0.1 mg/cm^2. Nafion® NRE 212 membrane was used for making the MEAs. As shown in Figure 2, the kinetic mass activities of 0.43 A/mg_{Pt} and 0.42 A/mg_{Pt} were estimated for 60% PtM_2/C and 40% HCC catalyst, respectively. The mass activity of 45.9% commercial Pt/C catalyst is 0.154 A/mg_{Pt}.

A new method was developed to functionalize the graphitic carbon through the non-covalent ϖ-ϖ interaction using a bifunctional molecule namely, 1-pyrenecarboxylic acid (1-PCA). The results indicated that this molecule irreversibly adsorbs on the inherently hydrophobic surfaces of carbon nanofibers (PCA-CNFs). The results revealed that the Pt nanoparticles deposited on PCA-CNF are uniformly distributed on the CNFs, with no agglomeration. The average Pt particle size was 2.0 ± 0.2 nm which is smaller than the particle size observed on the raw CNF. The Pt content loaded on 1-PCA treated CNF was 38 wt%, which is much higher than the raw CNF (18 wt%).

To inhibit the agglomeration of Pt particles during the high temperature alloying process, a new impregnation method was developed at Yonsei University to synthesize platinum alloy particles to be uniformly distributed on the support. The Pt-alloy particle size was calculated from the XRD. The normal heat-treatment of commercial

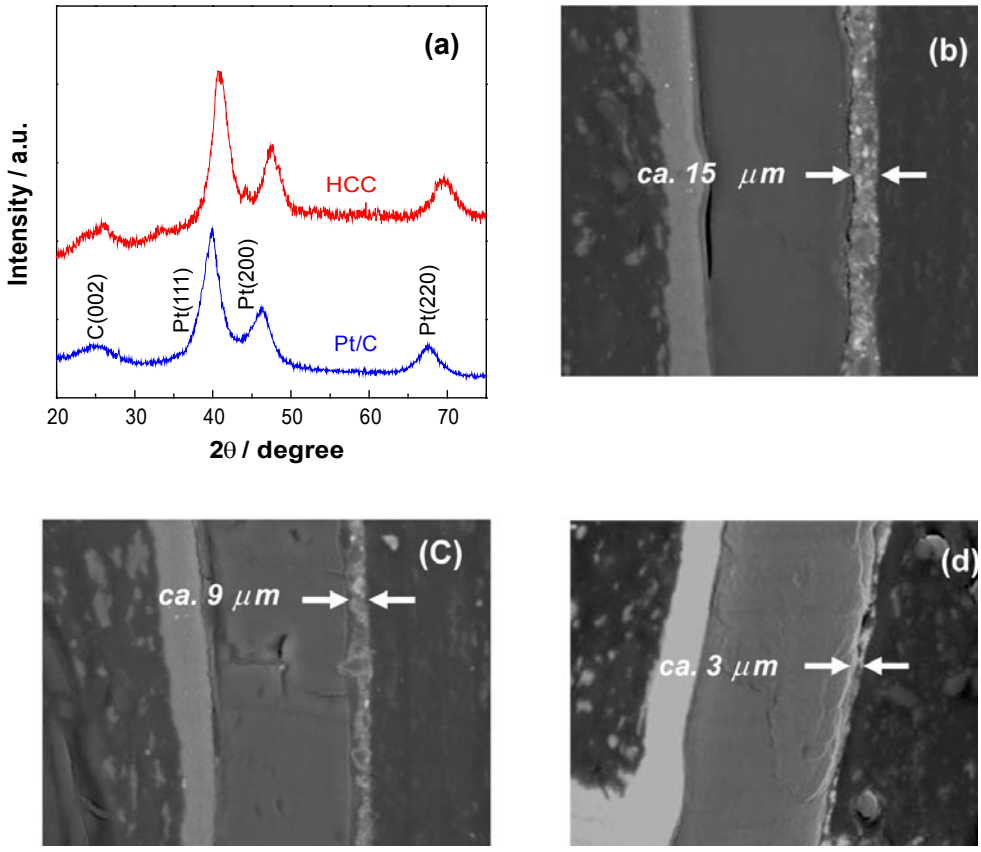


FIGURE 1. (a) XRD of HCC Catalyst — Cross-sectional Images of MEAs Utilizing HCC Catalysts (b) 0.2 mg/cm^2, (c) 0.1 mg/cm^2 and (d) 0.04 mg/cm^2

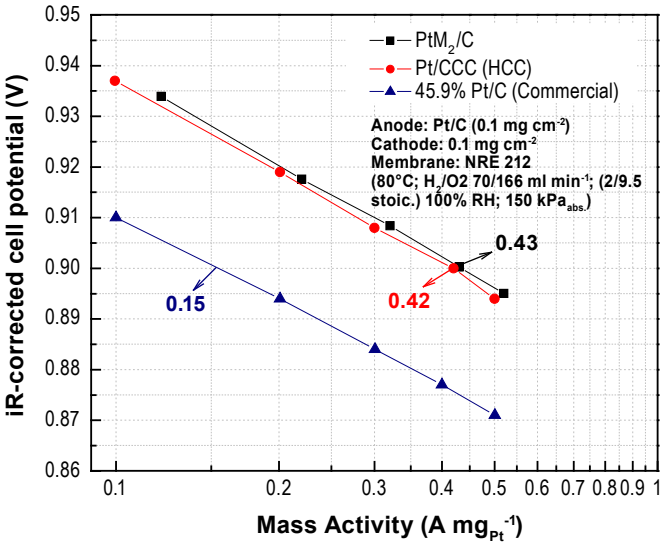


FIGURE 2. Mass Activity Comparison of Pt/CCC (HCC), PtM_2/C and Commercial Pt/C Catalysts

50% Pt_3M_1/C resulted in 10.8 nm particles while the 50% Pt_3M_1/AGC synthesized in this study resulted in 3.4 nm particles. The aggregation of Pt particles was restrained by the protective film used in this study.

The performance of commercial Tanaka Kikinzoku Kogyo K. K. (TKK) 40% Pt/C, 46% Pt/C, and 50% Pt_3M_1/AGC as cathode catalysts was investigated in a PEMFC. The ECSA measured in a three electrode system and fuel cell was used to estimate the catalyst utilization. The utilization ratio for Pt_3M_1/AGC catalyst was estimated to be 88% which is higher than that of TKK 40 wt% Pt/C (76%) and TKK 46 wt% Pt/C (56%). The utilization of 88% observed for the in-house synthesized catalyst is due to better Pt-alloy particle distribution on PCA modified graphitic carbon nanocage which was used as a catalyst support.

To optimize the protecting coating process, Pt_3M_1/AGC catalyst was synthesized with different mass ratio (25, 50 and 60% on a carbon support). XRD was used to determine the alloy particle size. No extra peaks assigned to M_1 or M_1-oxides were identified. The results indicated that a high degree of alloying is present for Pt_3M_1/AGC catalysts. The particle sizes of the Pt_3M_1/AGC catalysts were calculated to be 3.2, 3.4 and 4.1 nm at catalyst loading of 25%, 50% and 60% on the carbon support, respectively.

The performance of the catalysts was estimated from the polarization curves and evaluated based on the mass activity

(A/mg_{PGM} @ 900 $mV_{iR\text{-}free}$) and the specific activity ($\mu A/cm^2$ @ 900 $mV_{iR\text{-}free}$). The specific activity of 50% Pt_3M_1/AGC is 1,023 $\mu A/cm^2$, which is higher than the DOE target (720 $\mu A/cm^2$). The ECSA of the catalyst used to calculate the specific activity was obtained from the MEA.

The durability of 50% Pt_3M_1/AGC catalyst was evaluated using DOE cycling protocol. The active area of the MEA was 25 cm^2. The cathode was cycled under N_2 (relative to the anode under H_2) 30,000 times between 0.6 and 1.0 V at a sweep rate of 50 mV/s. Cell diagnostics of the cathode catalyst such as ECSA, ORR mass activity, and oxygen polarization curves were performed after 3,000, 10,000, 20,000, and 30,000 cycles. The activity of the catalyst was evaluated based on its mass activity. Figure 3 shows the iR-corrected polarization curves under H_2O_2 and 100% relative humidity. The fuel cell operating conditions are given in the graph. The initial mass activity and the mass activity loss after 10,000 and 30,000 cycles are also presented in Figure 3 (inset). The mass activity loss of 50% Pt_3M_1/AGC is 34% which is lower than the DOE target (40% loss). The ECSA loss is only 30% (decreased from 29.5 to 20.8 m^2/g after 30,000 cycles. The DOE target is less than 40%. Comparison of H_2/air fuel cell performance at high current densities of commercial Pt/C and Pt_3M_1/AGC catalyst is shown in Figure 4. Fuel cell operating conditions are shown in the figure.

Conclusions and Future Directions

Accomplishments in the reporting period:

- Achieved onset potential for oxygen reduction close to 0.9 V and less than 2.5% peroxide formation for CCC.

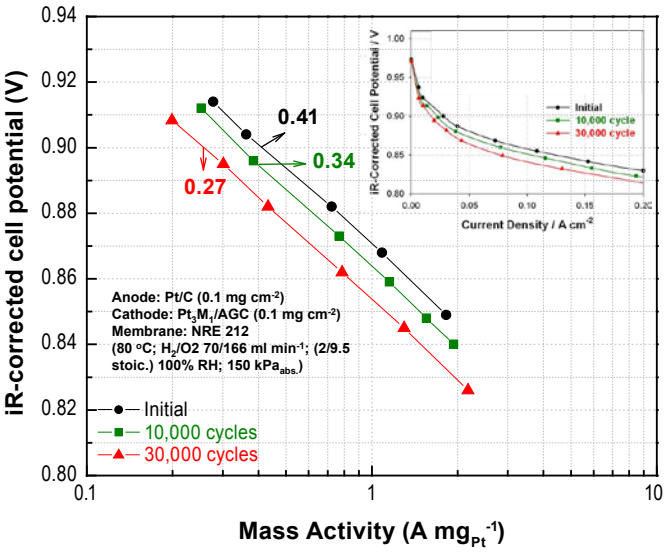


FIGURE 3. Mass Activities of 50% Pt_3M_1/AGC Catalysts as a Function of Number of Cycles (The iR-corrected polarization curves obtained for 50% Pt_3M_1/AGC as function of number of cycles is shown in the inset.)

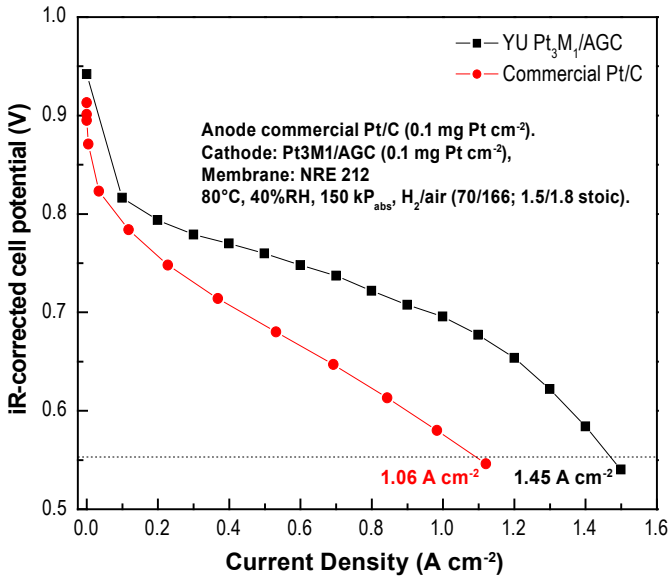


FIGURE 4. Comparison of H_2/Air Fuel Cell Performance of Commercial Pt/C and Pt_3M_1/AGC Catalysts

- The kinetic mass activities of 0.43 A/mg_{Pt}, 0.42 A/mg_{Pt} and 0.41 A/mg_{Pt} were estimated for 60% PtM_2/CCC, 40% HCC catalyst and 50% Pt_3M_1/AGC catalyst, respectively compared with mass activity of 45.9 % commercial Pt/C catalyst is 0.154 A/mg_{Pt}.
- The specific activity of 50% Pt_3M_1/AGC synthesized at Yonsei University is 1,023 $\mu A/cm^2$, which is higher than the DOE target (720 $\mu A/cm^2$).
- The mass activity loss after 30,000 cycles, DOE protocol (0.6-0.9 V) of 50% Pt_3M_1/AGC is 34% is lower than that the DOE target (40% loss).
- The ECSA loss for the same catalyst is only 30% (decreases from 29.5 to 20.8 m^2/g) after 30,000 cycles. The DOE target is less than 40%.

Future anticipated accomplishments are to:

- Achieve ultra-low Pt HCC catalysts for oxygen reduction reaction with mass activity larger than 0.44 A/mg_{Pt} and durability of 0.24 A/mg_{Pt} after DOE suggested potential cycling (0.6 to 1 V) (USC).
- Develop activated high surface area Pt catalyst through synthesis of Pt-alloy catalyst using in-house developed procedures (Yonsei University and USC).
- Accomplish high current density performance and durability in H_2/air fuel cells to meet the DOE targets (USC and Yonsei University).
- Develop support which will increase the catalyst utilization and eliminate the loss of ESCA through: performance optimization of CCC, stable conductive TiO_2 and CCC-TiO_2 hybrid supports developed at USC and modified graphitic carbon developed at Yonsei University. (USC, Yonsei University and HMC)

- Evaluation of MEA and fuel cell stack: To perform accelerated durability tests of MEAs with commercial catalyst to optimize the design of 50 cm^2 active area bipolar plate flow field and short stack assembly (HMC).

Patents Issued

1. Carbon-based composite electrocatalysts for low temperature fuel cells, US 7,629,285, 2009.

2. Composite catalysts supported on modified carbon substrates and methods of making the same, US 7,618,915, 2009.

FY 2011 Publications/Presentations

Publications

1. Liu, Gang, Li, Xuguang, Ganesan, Prabhu, Popov, Branko N, "Studies of oxygen reduction reaction active sites and stability of nitrogen-modified carbon composite catalysts for PEM fuel cells", *Electrochim. Acta*, **55** (2010) 2853-2858.

2. Li, Xuguang, Park, Sehkyu, Popov, Branko N, "Highly stable Pt and PtPd hybrid catalysts supported on a nitrogen-modified carbon composite for fuel cell application", *J. Power Sources*, **195** (2010) 445-452.

3. Xuguang Li, Gang Liu, Branko N. Popov, "Activity and stability of non-precious metal catalysts for oxygen reduction in acid and alkaline electrolytes", *J. Power Sources*, **195** (2010) 6373-6378.

4. B.N. Popov, X. Li and J.W. Lee, "Power source research at USC: Development of advanced electrocatalysts for polymer electrolyte membrane fuel cells", *Int. J. Hyd. Energy*, **36** (2011) 1794-1802.

5. Xuguang Li, Sheng-Yang Huang, Branko Popov, "Development of Low Pt Loading Cathode Catalysts for Polymer Electrolyte Membrane Fuel Cells", *ECS Trans.* 2010, *33*, 239-246.

6. Sheng-Yang Huang, Prabhu Ganesan, Won Suk Jung, Nicholas Cadirov, Branko Popov, "Titania Supported Platinum Catalyst with High Electrocatalytic Activity andStability for Polymer Electrolyte Membrane Fuel Cell", *ECS Trans.* 2010, *33*, 483-491.

7. Sheng-Yang Huang, Prabhu Ganesan, Won Suk Jung, Nicholas Cadirov, Branko Popov, "Development of Supported Bifunctional Oxygen Electrocatalysts with High Performance for Unitized Regenerative Fuel Cell Applications", *ECS Trans.* 2010, *33*, 1979-1987.

Presentations

1. B.N. Popov, Li Xuguang, T. Kawahara, H. Yanagi, "Development of Low Platinum Loading Cathode Catalysts for Polymer Electrolyte Membrane Fuel Cells," 218th ECS Meeting, Las Vegas, Nevada, October 13, 2010. Contributed.

2. B.N. Popov "Recent Advances in Non-Precious Metal Catalyst for Oxygen Reduction Reaction in Fuel Cells," 218th ECS Meeting, Las Vegas, Nevada, October 13, 2010. Contributed.

3. B.N. Popov, S.-Y. Huang, "Titania Supported Platinum Catalyst with High Electrocatalytic Activity and Stability for Polymer Electrolyte Membrane Fuel Cell," 218th ECS Meeting, Las Vegas, Nevada, October 13, 2010. Contributed.

4. B.N. Popov, S.-Y. Huang, "Development of Supported Bifunctional Oxygen Electrocatalysts with High Performance for Unitized Regenerative Fuel Cell Applications,"218th ECS Meeting, Las Vegas, Nevada, October 13, 2010. Contributed.

References

1. N.P. Subramanian, S.P. Kumaraguru, H.R. Colon-Mercado, H. Kim, B.N. Popov, T. Black and D.A. Chen, "Studies on Co-Based Catalysts Supported on Modified Carbon Substrates for PEMFC Cathodes", *J. Power Sources*, **157** (2006) 56-63.

2. R.A. Sidik, A.B. Anderson, N.P. Subramanian, S.P. Kumaraguru and B.N. Popov, "O_2 Reduction on Graphite and Nitrogen-Doped Graphite: Experiment and Theory", *J. Phys. Chem. B*, **110** (2006) 1787-1793.

3. X. Li, H.R. Colon-Mercado, G. Wu, J.-W. Lee, B.N. Popov, "Development of Method for Synthesis of Pt-Co Cathode Catalysts for PEM Fuel Cells," *Electrochem. Solid-State Lett.*, **10** (2007) B201-B205.

4. Nallathambi, Vijayadurga; Lee, Jong-Won; Kumaraguru, Swaminatha P, Wu, Gang; Popov, Branko N, "Development of high performance carbon composite catalyst for oxygen reduction reaction in PEM Proton Exchange Membrane fuel cells", *J Power Sources*, **183** (2008) 34-42.

5. Subramanian, Nalini P, Li, Xuguang, Nallathambi, Vijayadurda, Kumaraguru, Swaminatha P, Colon-Mercado, Hector, Wu, Gang, Lee, Jong-Won, Popov, Branko N, "Nitrogen-modified carbon-based catalysts for oxygen reduction reaction in polymer electrolyte membrane fuel cells", *J Power Sources*, **188** (2009) 38-44.

6. Liu, Gang, Li, Xuguang, Ganesan, Prabhu, Popov, Branko N, Development of non-precious metal oxygen-reduction catalysts for PEM fuel cells based on N-doped, *Appl. Catal. B: Environmental*, **93** (2009) 156-165.

7. Liu, Gang, Li, Xuguang, Ganesan, Prabhu, Popov, Branko N, "Studies of oxygen reduction reaction active sites and stability of nitrogen-modified carbon composite catalysts for PEM fuel cells", *Electrochim. Acta*, **55** (2010) 2853-2858.

8. Li, Xuguang, Park, Sehkyu, Popov, Branko N, "Highly stable Pt and PtPd hybrid catalysts supported on a nitrogen-modified carbon composite for fuel cell application", *J Power Sources*, **195** (2010) 445-452.

9. Xuguang Li, Gang Liu, Branko N. Popov, "Activity and stability of non-precious metal catalysts for oxygen reduction in acid and alkaline electrolytes", *J. Power Sources*, **195** (2010) 6373-6378.

10. B.N. Popov, X. Li and J.W. Lee, "Power source research at USC: Development of advanced electrocatalysts for polymer electrolyte membrane fuel cells", *Int. J. Hyd. Energy*, **36** (2011) 1794-1802.

11. K.H Lim, H-S Oh, H. Kim, Use of a carbon nanocage as a catalyst support in polymer electrolyte membrane fuel cells *Electrochem. Commun*., **11** (2009) 1131-1134.

12. K.H Lim, H-S Oh, S-E Jang, Y-J Ko, H-J Kim, H. Kim, Effect of operating conditions on carbon corrosion in polymer electrolyte membrane fuel cells, *J. Power Sources*, **193** (2009) 575-579.

13. H-S Oh, K.H. Lim, B. Roh, I. Hwang, H. Kim, Corrosion resistance and sintering effect of carbon supports in polymer electrolyte membrane fuel cells, *Electrochim. Acta*, **54** (2009) 6515-6521.

V.D.14 Engineered Nano-Scale Ceramic Supports for PEM Fuel Cells

Eric L. Brosha[1] (Primary Contact),
Karen J. Blackmore[1], Anthony K. Burrell[1],
Lior Elbaz[1], Neil J. Henson[1], Tommy Rockward[1],
Karren More[2], Timothy Ward[3]
[1]Los Alamos National Laboratory (LANL)
MS D429, P.O. Box 1663
Los Alamos, NM 87545
Phone: (505) 665-4008
E-mail: brosha@lanl.gov

DOE Manager
HQ: Nancy Garland
Phone: (202) 586-5673
E-mail: Nancy.Garland@ee.doe.gov

Subcontractors:
[2]Oak Ridge National Laboratory (ORNL), Oak Ridge, TN
[3]University of New Mexico (UNM), Albuquerque, NM

Start Date: September 2009
Project End Date: 2013

Fiscal Year (FY) 2011 Objectives

- Develop a ceramic alternative to carbon material supports for a polymer electrolyte fuel cell cathode.
- Ceramic support replacement for carbon must:
  - Have enhanced resistance to corrosion and Pt coalescence.
  - Preserve positive attributes of carbon such as cost, surface area, and conductivity.
  - Be compatible with present membrane electrode assembly (MEA) architecture and preparation methods.
- Ceramic properties goals:
  - High surface area
  - High Pt utilization
  - Enhanced Pt-support interaction
  - Adequate electronic conductivity
  - Corrosion resistance
  - Synthetic methods amenable to scale up
  - Reasonable synthesis costs

Technical Barriers

This project addresses the following technical barriers from the Fuel Cells section of the Fuel Cell Technologies Program Multi-Year Research, Development and Demonstration Plan:

(A) Durability: Pt sintering, corrosion loss, effects from load-cycling and high potential.

(B) Cost: Better Pt utilization balanced by cost difference of new support vs. carbon.

(C) Performance: Pt sintering, corrosion loss, and loss of electroactive surface area.

Technical Targets

- Precious metal loading (0.2 mg/cm^2)
- Cost (<$3/kW)
- Activity (0.44 A/mg$_{Pt}$ @ 0.9 V$_{iR\text{-}free}$)
- Electrocatalysis support loss (<30 mV after 100 hrs @ 1.2 V)
- Electrochemical surface area loss (<40%) tested per GM protocol (Mathias, M.F., et al., Interface [Electrochemical Society], Fall 2005, p. 24)

FY 2011 Accomplishments

Synthesis of Non-Carbon Support Materials

- "Go" decision made for Mo_2N supports synthesized via polymer assisted deposition (PAD) approach: ahead of schedule.
  - Quarter (Q)8 target moved up to Q5-Q6.
- Evaluation of titania supports prepared by PAD approach ahead of schedule.
  - Q6 targets moved up to Q3-Q4.
- Go/No-Go decision on hexaboride supports: ahead of schedule.
  - No-Go: Q6 decision moved up to Q4.
    - Unable to synthesis using aerosol through plasma (A-T-P) process (Q4).
    - PAD process produced only small amounts of LaB6 (Q6).
- Performance evaluation of Pt/$NbRu_yO_z$ catalysts: ahead of schedule.
  - No-Go: poor activity due to formation of NbOx passivation layer on Pt (Q6).

Testing, Characterization and Evaluation

- Full electrochemical characterization of Mo_2N support and its precursors with and without platinum in organic and aqueous solutions.
- Initial electrochemical characterization of TiO and TiO_2 supports.

Theory and Computation

- Calculations were performed using plane wave periodic density functional theory to create a structural model of gamma Mo_2N: NaCl structure with half of the nitrogen sites vacant creating MoN and Mo-rich surfaces for Pt adhesion.
- The most favorable sites for single Pt atoms and a monolayer was constructed based on these results.
- Nitrogen depleted surface layer on the Mo_2N promotes stronger binding of platinum compared to other defect models and other Mo_xN_y phases.



Introduction

Catalyst support durability is currently a technical barrier for commercialization of proton exchange membrane fuel cells (PEMFCs), especially for transportation applications. Degradation and corrosion of the conventional carbon supports leads to losses in active catalyst surface area and, consequently, reduced performance. As a result, the major aim of this work is to develop support materials that interact strongly with Pt, yet sustain bulk-like catalytic activities with very highly dispersed particles. This latter aspect is key to attaining the 2015 DOE technical targets for platinum group metal (PGM) loadings (0.20 mg/cm^2).

The benefits of the use of carbon-supported catalysts to drastically reduce Pt loadings from the early, conventional Pt-black technology [1–4] are well known. The supported platinum catalyzed membrane approach widely used today for fabrication of MEAs was developed shortly thereafter these early reports [5–7]. Of direct relevance to this present work, are the investigations into Pt particle growth in PEMFCs [8], and subsequent follow-on work showing evidence of Pt particles suspended free of the support within the catalyst layer [9]. Further, durability work has demonstrated the detrimental effects of potential cycling on carbon corrosion [10-14] and the link between electrochemical surface area and particle growth [15].

To avoid the issues with carbon degradation altogether, it has been proposed by numerous fuel cell research groups to replace carbon supports with conductive materials that are ceramic in nature [16, 17, and references therein]. Intrinsically, these many conductive oxides, carbides, and nitrides possess the prerequisite electronic conductivity required, and offer corrosion resistance in PEMFC environments; however, most reports indicate that obtaining sufficient surface area remains a significant barrier to obtaining desirable fuel cell performance. Ceramic materials that exhibit high electrical conductivity and necessary stability under fuel cell conditions must also exhibit high surface area as a necessary adjunct to obtaining high Pt dispersions and Pt utilization targets. Our goal in this work is to identify new synthesis approaches together with materials that will lead to ceramic supports with high surface areas capable of supporting high Pt dispersions. Several strong candidates for use as PEMFC catalyst supports include: transition metal nitrides and sub-stoichiometric titanium oxides, which hither to now have been prepared by other research groups with relatively low surface areas (ca. 1–50 m^2/g typical [16-19]).

This report describes our FY 2011 technical progress related to applying advanced synthetic methods towards the development of new ceramic supports for Pt catalysts for PEMFCs.

Approach

Our approach to preparing ceramic powders with prerequisite properties for use as a PEMFC Pt catalyst support is centered on the application of several novel materials synthesis methods. Initially, in this first year of work, the methods were conducted in parallel to insure the best possible results that ceramic support materials would be available with desirable physical characteristics for platinum disposition and subsequent electrochemical characterization for oxygen reduction activity. Following a down-select process, we are employing a materials synthesis process called PAD that was largely developed at LANL for a variety of applications. This is a solution method for the formation of materials ranging from oxides to nitrides and oxynitrides. In general we have employed this methodology to prepare conformal epitaxial films of metal oxides and nitrides. However, high surface area powder materials can also be obtained using an accelerated heating rate to generate low density, foam-like structures. This projet is presently driving studies into the application of the PAD technique for bulk powder synthesis. The UNM component of the collaborative research project focuses on developing aerosol synthesis methods for high surface area, conductive ceramic supports. Following a No-Go decision made this year (FY 2011) for conductive Nb-RuO_x oxide supports, their goal will be to develop a new approach for nitride and sub-stoichiometric titania as a potential route to the PAD-prepared nitride supports already identified as encouraging non-carbon supports for PEMFCs in this project to date.

Computational methods will be used to complement the experimental effort. Although these techniques provide insight into fundamental processes occurring at the atomic level, our work will focus primarily in two areas, that of aiding the characterization and understanding of experimental data and providing additional direction to the experimental team in the preparation of new support materials with optimized properties. The theory and modeling work will focus on several areas of importance to the development and optimization of new electrode support materials. Initially, computational studies have been carried out to understand the structure and stability of the support materials in the absence of platinum particles. Following this, the parameters may then be used to study the nature of the platinum binding sites on the support and the platinum

adhesion energy, the mobility of platinum on the support and the interplay between the electronic structure of the support and the platinum particle, which is reflected in the calculated density of states. Comparison of these values with bulk platinum can be used as a predictive tool for the optimization of the material.

Results

Molybdenum Nitride

The use of the PAD process has been successful at producing conductive ceramic materials with high surface areas. A milestone for this task has been accelerated such that the Go/No-Go decision in Q8 may be brought forward to early FY 2011. High surface area, conductive foams were successfully synthesized for molybdenum as Mo_2N. The materials are prepared by first creating a water-based solution of the desired metal bound to a polyethyleneimine (PEI) polymer and ethylenediamine tetraacetic acid (EDTA). The solution is concentrated to a thick gel before being heated in a tube furnace to 700 and 950˚C under forming gas. During the heating process, the polymer and the EDTA decomposes to give gaseous products, which aid in foam formation.

During FY 2011, a full electrochemical characterization of the newly synthesized supports was conducted with and without platinum in organic and aqueous solutions in order to study the possible redox reactions of the supports, their possible degradation reactions and electrocatalytic activity for oxygen reduction reaction (ORR). Mo_2N, TiO and TiO_2 show good stability for the length of the experiments conducted in a half cell, and their long-term durability study will be conducted in FY 2012 in a fuel cell.

The electrocatalytic activity of Pt deposited on Mo_2N was studied using electroanalytical techniques such as rotating ring-disk electrode (RRDE) and cyclic voltammetry (CV). Platinum was added (20% wt) to Mo_2N support using an incipient wetness method and deposited on glassy carbon electrode for electrochemical characterization. Figure 1(a) shows the CVs of Pt on Mo_2N and PEI-EDTA supports in deaerated 0.5 M H_2SO_4 solutions. Characteristic Pt redox reactions in acidic medium were observed with both samples including hydrogen adsorption/desorption. The Pt/Mo_2N catalyst has a redox couple at E=0.44V vs. reference hydrogen electrode (RHE) that was not observed with the Pt/PEI-EDTA catalyst and thus is attributed to the Mo_2N support and not the carbon precursor used during its synthesis, this is also supported by the results obtain with the support devoid of platinum. The average electrochemically active surface area calculated from the hydrogen adsorption and desorption peaks of the Pt/Mo_2N catalyst is 120 m^2/g, more than 60% higher than that obtained with a commercial ETEK Pt/C catalysts (74 m^2/g). Figure 1(b) shows the RRDE measurements conducted with the Pt/Mo_2N catalyst. These results show the high ORR activity (expected from Pt-based catalysts), the kinetics and mechanism of the reaction

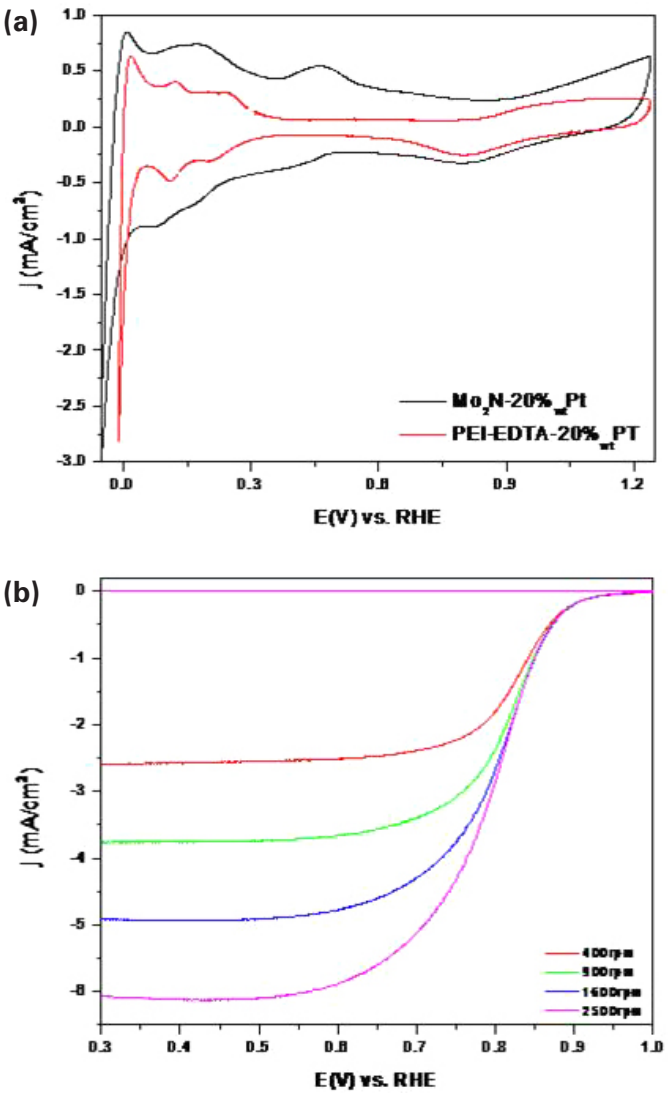


FIGURE 1. (a) CV characterization of 20%$_{wt}$ platinum deposited on Mo_2N sample prepared at 950°C using the PAD process and 20%$_{wt}$ platinum deposited on PEI-EDTA (in deaerated 0.5 M H_2SO_4 at 100 mV/s). (b) RRDE characterization of 20%$_{wt}$ Pt/Mo_2N sample prepared at 950°C using the PAD process (in O_2 saturated 0.5 M H_2SO_4 at100 mV/s).

do not seem to be affected from the Mo_2N support or any interaction it might have with Pt.

Sub-Stoichiometric Titanium Oxides

High surface area, conductive foams were successfully synthesized for titanium as both TiO and TiO_{2-n} using a modified PAD process. As with the molybdenum nitride materials, the titanium oxide ceramics are prepared by first creating a water-based solution of the desired metal bound to a PEI polymer and EDTA. The solution is concentrated to a thick gel before being heated in a tube furnace to 950˚C under forming gas. During the heating process, the polymer and EDTA decomposes to give gaseous products, which aid

in foam formation. In the case of titanium oxide materials, the variation of the flow rate and purge time determine the extent of oxygen reduction. In FY 2011, effort on the titania supports was reduced in order to provide extra resources to study the moly-nitride materials. However, initial electrochemical characterization was carried out on the two samples produced to date. Figure 2 shows the X-ray diffraction (XRD) traces of a PAD-prepared stoichiometric TiO sample (Figure 2(a)) and sample whose XRD trace shows a primary anatase phase (TiO_{2-x}) along with rutile (Figure 2(b)). Both samples are black in appearance and are conductive. The initial Brunauer-Emmett-Teller (BET) surface area measurements performed on the first samples of black titania powders confirm gas accessible surface areas similar to Vulcan XC-72 (e.g. 200–250 m^2/g). These surface areas are significantly higher than commercial, conductive Magnèli phase Ti_4O_7 synthesized through bulk synthesis and reduction (ca. 1-2 m^2/g) or even through hydrogen reduction of nano-crystalline anatase or rutile TiO_2 powders (ca. 25-50 m^2/g) [16,17]. We have started structural characterization of these recently prepared titania supports. Electrochemical characterization was conducted with Pt deposited on TiO and TiO_2 supports. As with the Mo_2N support, the platinum's ORR activity was not affected by the support in comparison to carbon supported Pt.

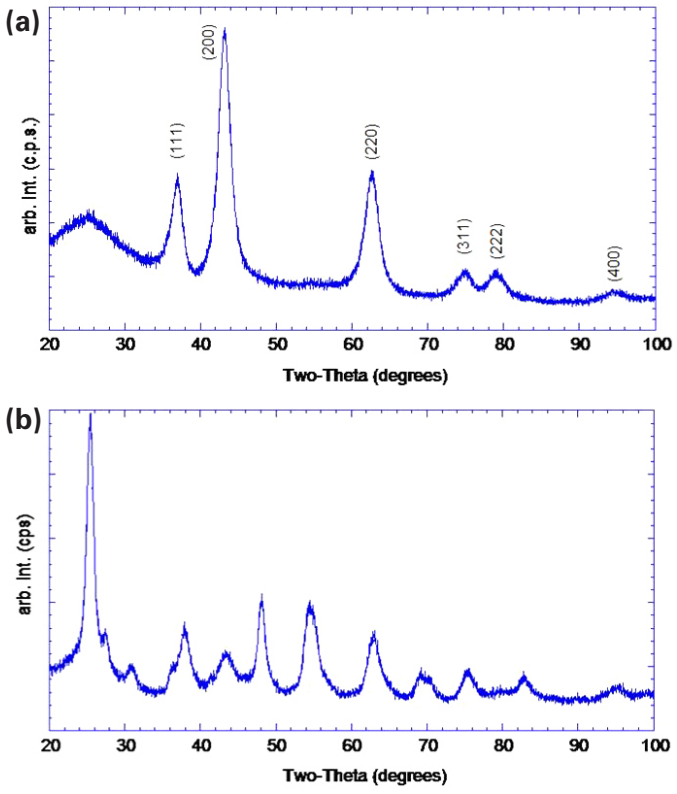


FIGURE 2. (a) XRD trace from 20 to 100° degrees two-theta of a PAD-prepared stoichiometric TiO sample and (b) a sample whose XRD trace shows a primary anatase phase (TiO_{2-x}) along with rutile.

Quantum Chemical Calculations on Catalyst Surface Structure and Activity

In FY 2011, the theory and modeling work was directed to the study of the structure of the interface between the ceramic support and platinum, and the correlation between this and the resulting catalytic activity. The aim of this work is to understand how the support modifies the electronic structure of the platinum to influence the thermodynamics and kinetics of the fundamental steps in the catalytic process. An important target is the computed binding energy of platinum to the surface and relating this to measured catalytic lifetime.

The modeling focused on the dominant γ-Mo_2N phase identified from the characterization of the synthesized samples. The computational strategy was as follows:

1. Construct structural models for Mo_2N phase considering the effect of non-stoichiometry and defect structures.
2. Calculate binding energies for platinum monolayers on surface models.
3. Calculate trends in predicted over-potential for models.

The quantum chemical calculations are based on the plane wave density functional method as implemented in the VASP software. In Q4, we will transition this approach to the study of titanium oxide phases.

The structure of γ-Mo_2N phase is based on the rock salt crystal structure with half the nitrogen sites vacant. There are several models that can be constructed based on this stoichiometry. For example, the highest symmetry model has planes of nitrogen atoms empty as shown in Figure 3(a). This results in the creation of nitrogen-rich and nitrogen-poor surfaces. The binding energies of single platinum atoms on several surface models were calculated. The results for the three sites on a nitrogen-poor γ-Mo_2N surface are shown in Figure 3(b). The results indicate the four-fold coordination site is dominant. Using this result models for a single monolayer of platinum on the ceramic surface were constructed. It is found that the monolayer is bound more strongly to the nitrogen-poor (defective) surface than to the nitrogen-rich (non-defective) surface. This causes a shift in the calculated d-band center for platinum and perturbs the binding energies of intermediates in the oxygen reduction reaction.

UNM Development Work on Conductive Oxide Supports

Mesoporous Nb_2O_5 and $NbRu_yO_z$ (12 wt%) powders were synthesized by aerosol pyrolysis of alcohol solutions of $NbCl_5$, $RuCl_3$ with the addition of pluronic block copolymer P123 as a templating agent. A post acid etch step opened up the internal surface of the as-prepared material yielding a BET surface area as large as 180 m^2/g. Electrical resistance of the compacted powders was assessed and $NbRu_yO_z$ reduced under a 10% H_2/N_2

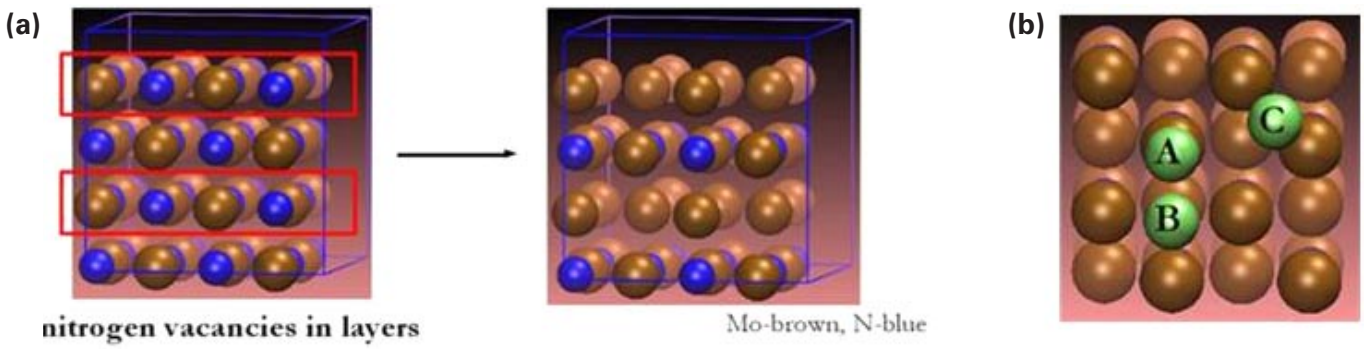


FIGURE 3. (a) Construction of the high symmetry defect model for γ-Mo_2N (b) Calculated binding sites for a single platinum atom on the nitrogen-poor γ-Mo_2N surface (A=on-top, B=bridge, C=four-fold sites)

mixture displayed low resistivity. An optimized synthesis and post-processing scheme was identified producing a black catalyst support. Platinized catalysts were prepared both in situ to the aerosol process and using an incipient wetness approach with the former, direct incorporation of Pt producing better dispersion of Pt nano-particles in the meso-porous support as revealed by transmission electron microscopy (TEM). CV (10 mV/s in 0.1M $HClO_4$) was performed on $NbRu_yO_z$ supported Pt catalysts 30 wt% Pt) and compared to 30 wt% Pt/XC-72 carbon. These results showed low electrochemical activity and after considerable investigation, it was found that the low activity may be attributed to the formation of NbO_x passivation layer over the Pt nano-particles. It was found that controlled thermal treatment (crystallization) reduced the mobility of Nb and improved the electrochemical performance but still resulted in performance well below commercial Pt/C benchmarks. As a result of these findings, a NoGo decision was made and a Go/No-Go milestone was advanced in the project. Given the favorable results to date for the nitride and titantia supports, future work for UNM will focus on aerosol synthesis of high surface area powders without the residual carbon contamination resulting from the PAD process.

Conclusions

- Thermal gravimetric analysis-mass spectrometer (TGA/MS) experiments performed on Mo_2N/C and Pt/Mo_2N/C materials showed carbon residue cannot be removed from ceramic supports by methanization (reducing conditions, 6% H_2) or oxidation (air).
- Carbon is present from PAD process and, unless it can be removed during initial pyrolysis step, will be present if the PAD process is used to form high surface area support powders.
  - Measurements indicate variable amount of residue but typical amounts ca. 40-50 wt% C remaining in titania supports determined by energy dispersive X-ray.
  - Precision TGA (oxidizing conditions) will be used to better estimate quantify of carbon residue in moly-nitride system (assuming stoichiometric gamma phase).
- The effect of carbon residue on durability and fuel cell performance is not yet known.
- Mo_2N-C possesses required surface area and electronic conductivity for fuel cell use.
  - Required stability in acid conditions and under potential cycling.
- 20 wt% Pt/Mo_2N-C (incipient wetness) has comparable activity for ORR as ETEK.
- Pt appears to be associated with Mo_2N and not the residual carbon and this conclusion is supported by:
  - TGA/MS experiments
  - ORNL TEM characterization
  - CV experiments
- Experimental evidence collected to date indicates a stronger Pt-support interaction than with Pt-C catalysts.
- Computational work identified most favorable binding sites for adhesion of Pt atoms, and a monolayer of Pt was constructed based on these results.
  - The structure of the ceramic surface and, in particular, the defect structure appears to be vital to the binding properties of platinum.
  - The modeling results indicated a nitrogen depleted surface layer promotes strong binding of platinum to the support surface.
- Mo_2N-C although not completely understood, is acceptable to move forward to MEA prep and fuel cell testing.

Future Directions

- Scale up amount of PAD-produced Mo_2N, formulate inks, and prepare MEAs for single cell testing.
- Begin fuel cell testing and lifetime-durability observations with Pt/Mo_2N-C system. Optimize inks and MEA fabrication based on Pt/Mo_2N catalysts and prepare single-cell fuel cell for performance and

durability testing. Obtain fuel cell performance data for Pt/Mo_2N catalyst prepared using the PAD approach.

- Resume sub-oxide titania support work with focus on half-cell durability, oxidation resistance (sub-oxides), and stability of carbonaceous PAD residue (TiO_2).
- Develop aerosol precursors and aerosol synthesis method to prepare high surface area (>200 m^2/g) Mo_2N catalyst supports with reduction in residual carbon compared the PAD approach (UNM).
- Calculate the over-potential for the oxygen reduction reaction on a model for platinum supported on molybdenum nitride and compare this value with that for Pt (111).
- Characterization and testing of support materials (on-going through entire project).

FY 2011 Publications/Presentations

1. E. Brosha, K. Blackmore, A. Burrell, and J. Phillips, "Engineered Nano-scale Ceramic Supports for PEM Fuel Cells", 2010 Fuel Cell Seminar and Exposition, October 18–22, 2010, San Antonio, TX.

2. K.J. Blackmore, E. Bauer, L. Elbaz, T.M. McCleskey, and A.K. Burrell, "Engineered Nano-scale Ceramic Supports for PEM Fuel Cells," ECS Transactions for 2010 Fuel Cell Seminar and Exposition, In press summer 2011.

3. K.J. Blackmore, L. Elbaz, E. Bauer, E.L. Brosha, K. More, T.M. McCleskey, and A.K. Burrell, "High Surface Area Nitride Support for Fuel Cell Electrodes," Submitted to J. Electrochem. Soc., In press summer 2011.

4. D.A. Konopka, S. Pylypenko, P. Atanassov, and T.L. Ward, "Synthesis by Spray Pyrolysis of Mesoporous NbRuyOz as Electrocatalyst Supports in Fuel Cells," ACS Applied Materials & Interfaces **2** (1) (2010) 86-95.

5. D. Konopka, B. Kiefer, Y.B. Jiang, T. Ward, and P. Atanassov, "Electrochemical and DFT Analysis of Deactivation of Pt Supported on Niobia," ECS Transactions (2010).

6. D.A. Konopka, B. Kiefer, Y.B. Jiang, T.L. Ward, and P. Atanassov, "Electrochemical Studies and DFT Analysis of Niobia Passivation of the Pt Surface," Submitted to J. Electrochem. Soc. (2010)

7. K. Blackmore, E. Brosha, A. Burrell, L. Elbaz, N. Henson, and K. More, "Alternative Supports for Polymer Electrolyte Fuel Cell Cathodes," 219th Meeting of the Electrochemical Society, Montreal, CA. May 1–6, 2011.

8. K. Blackmore, E. Brosha, A. Burrell, L. Elbaz, N. Henson, and K. More, "Electrochemical study and modeling of Pt-Mo_2N interactions", in preparation.

9. D.A. Konopka, M. Li, K. Artyushkova, N. Marinkovic, K. Sasaki, R. Adzic, T.L. Ward, and P. Atanassov, "Platinum Supported on NbRuyOz as Electrocatalyst for Ethanol Oxidation in Acid and Alkaline Fuel Cells", J. Phys. Chem C **115** (7)3043-3056 (2011).

10. P. Atanassov, D. Konopka, B. Kiefer, Y. Jiang, and T. Ward, "Electrochemical Studies and DFT Analysis of Pt Stability and Surface Passivation on NbRuyOz Support", Journal of The Electrochemical Society, submitted (2011).

References

1. I.D. Raistrick in J.W. Van Zee, R.E. White, K. Kinoshita and H.S. Burney (Eds.), "Proceedings of the Symposium on Diaphragms, Separators, and Ion Exchange Membranes," The Electrochemical Society, (1986) p.172.

2. I.D. Raistrick, 'Electrode Assembly for Use in a Polymer Electrolyte Fuel Cell,' U.S. Patent No. 4,876,115 (1989).

3. E.A. Ticianelli, C.R. Derouin and S. Srinivasan, "Localization of Platinum in Low Catalyst Loading Electrodes to Attain High-power Densities in SPE Fuel Cells," J. Electroanal. Chem. **251** (1988) 275.

4. E.A. Ticianelli, C.R. Derouin, A. Redondo and S. Srinivasan, "Methods to Attain High-Power Densities in Solid-Polymer Electrolyte Fuel-Cells using Low Platinum Loading Electrodes," J. Electrochem. Soc. **135** (1988) 2209.

5. M.S. Wilson, 'Membrane Catalyst Layer for Fuel Cells,' US Patent No. 5,234,777. August 10, 1993.

6. M.S. Wilson and S. Gottesfeld, "High-Performance Catalyzed Membranes of Ultra-Low Pt Loadings for Polymer Electrolyte Fuel-Cells," J. Electrochem. Soc. **139** (1992) L28-30.

7. M.S. Wilson and S. Gottesfeld, "Thin-Film Catalyst Layers for Polymer Electrolyte Fuel-Cell Electrodes," J. Appl. Electrochem. **22** (1992) 1-7.

8. M.S. Wilson, F.H. Garzon, K.E. Sickafus, S Gottesfeld, S., "Modeling and Experimental Diagnostics in Polymer Electrolyte Fuel Cells," J. Electrochem. Soc., **140** (10) (1993) 2872-2877.

9. Karren L. More, 2005 DOE annual report.

10. R. Borup, J.R. Davey, F.H. Garzon, D.L, Wood, and M.A. Inbody, "PEM fuel cell electrocatalyst durability measurements," J. Power Sources **163** (1) 76 (2006).

11. R. Borup, F. H. Garzon, D. L. Wood, J. R. Davey and E. L. Brosha, "PEM Electrode Durability Measurements," Presented at Electrochemical Society, Second International Conference on Polymer Batteries and Fuel Cells, Las Vegas, NV, June 12-17, 2005.

12. Bekkedahl, Timothy A.; Bregoli, Lawrence J.; Breault, Richard D.; Dykeman, Emily A.; Meyers, Jeremey P.; Patterson, Timothy W.; Skiba, Tommy; Vargas, Chris; Yang, Deliang Yi, Jung S., US Patent application 20040081866.

13. F. H. Garzon, J.R. Davey, and R.L. Borup, "Fuel Cell Catalyst Particle Size Growth Characterized by X-ray Scattering Methods," ECS Transactions Vol. 1, iss. 8 (2005) 153-166.

14. R. Borup, J. Davey, D. Wood, F. Garzon, M. Inbody, D. Guidry, 2005 DOE Hydrogen Program Review, May 25, 2005.

15. Garzon F.H., Davey J.R., and Borup, R.L. "Fuel Cell Catalyst Particle Size Growth Characterized by X-Ray Scattering Methods," ECS Meeting Abstracts (2005) Vol. MA 2005-02, p.2223.

16. Antolini, E., and Gonzalez, E.R., "Ceramic materials as supports for low-temperature fuel cell catalysts," Solid State Ionics **180** (2009) p. 746.

17. Y. Shao, J. Liu, Y. Wang, and Y. Lin, "Novel catalyst support materials or PEM fuel cells: current status and future prospects," J. Mat. Chem. **19** (2009) p. 46.

18. T. Ioroi, Z. Siroma, N. Fujiwara, S. Yamazaki, and K. Yasuda, "Sub-stoichiometric titanium oxide-supported platinum electrocatalyst for polymer electrolyte fuel cells," Electrochem. Comm. **7** (2005) p. 183.

19. F. Ettigshausen, A. Weidner, S. Zils, A. Wolz, J. Stuffner, M. Michel, and C. Roth, "Alternative Support Materials for Fuel Cell Catalysts," ECS Trans. **25** (1) (2009) p. 1883.

V.D.15 Development of Alternative and Durable High Performance Cathode Supports for PEM Fuel Cells

Yong Wang (Primary Contact),
Vilayanur. V. Viswanathan, Jun Liu, Yuehe Lin,
Sehkyu Park, Yuyan Shao, Haiyin Wan
Pacific Northwest National Laboratory
902 Battelle Boulevard, PO Box 999
MS K2-12
Richland, WA 99352
Phone: (509) 371-6273
E-mail: yongwang@pnl.gov

DOE Manager
HQ: Nancy Garland
Phone: (202) 586-5673
E-mail: Nancy.Garland@ee.doe.gov

Subcontractors[1]:
- Stephen Campbell, Automotive Fuel Cell Cooperation Corp., Burnaby, BC, Canada
- Sheng Dai, Qing Zhu and Jeseung Lee, Oak Ridge National Laboratory, Oak Ridge, TN
- Jingguang Chen and Irene Hsu, University of Delaware, Newark, DE
- Brian Willis, University of Connecticut, Storrs, CT

Project Start Date: January, 2007
Project End Date: September, 2011[2]

Fiscal Year (FY) 2011 Objectives

Develop new classes of alternative support materials that meet the 2010 DOE performance targets by achieving the following specific objectives:

- Understand structural and compositional requirements of conductive metal oxides (CMO) for improved activity and durability over standard Pt/Vulcan XC-72.
- Demonstrate durability and performance advantages of alternative cathode supports such as carbon nanotubes (CNTs), ordered graphitic mesoporous carbon (OGMC), graphene and graphitized carbon nanotubes (GCNT).
- Demonstrate durability and performance of non-carbon CMO supports such as tin-doped indium oxide (ITO).

Technical Barriers

This project addresses the following technical barriers from Fuel Cells section (3.4) of the Fuel Cell Technologies Program Multi-Year Research for Fuel Cells, Development and Demonstration Plan:

(A) Durability (of Cathode Catalyst Supports)
(C) Performance (of Supported Cathode Catalyst)

Technical Targets

This project is directed at conducting durability and activity studies of Pt on various supports, with the objective of meeting the DOE lifetime criteria.

Membrane electrode assembly (MEA) tests are in progress for lead supports using CMO modification of novel carbon supports, and have shown 3-4X improvement in stability over baseline Vulcan XC-72 carbon supports (Table 1). Rotating disc electrode (RDE) tests have also shown significant improvement in durability over baseline. Optimization of GCNT diameter and CMO content are further expected to improve performance and durability.

TABLE 1. Progress towards Meeting Technical Targets for Electrocatalysts for Transportation Applications

Parameter	Units	2010 Stack Target	PNNL 2011 Status
Accelerated test loss, 200 h @ 1.2 V at 80°C	mV at rated power	< 30	3-4X improvement over baseline for MEA
	% electrochemical surface area (ESA) loss	<40	3-4X improvement for RDE and MEA tests
Durability with cycling at 80°C	Hours	5,000	To be determined

FY 2011 Accomplishments

- Determined optimum GCNT diameter for best performance and durability.
- Used lessons learned from ITO-graphene systems to develop highly stable ITO-modified GCNT with 4X stability of baseline Vulcan carbon support.
- Demonstrated electronic percolation through CMO-modified carbon support[3] and identified need for improving conductivity of non-carbon support by conductivity measurement.
- Improved non-carbon support performance without compromising durability by adding CNT after Pt-CMO synthesis.
- Improved ESA for non-carbon support by tailoring mesoporosity and particle size using hard template synthesis.

[1] Through end of FY 2010
[2] Work will continue through March 2012
[3] Also referred to as hybrid support

- Synthesized non-carbon support using solvothermal annealing method with favorable particle size and crystallinty.



Introduction

Conventional cathode catalyst supports are susceptible to corrosion during high potential excursions, high temperature and under start-stop conditions [1]. Hence, lack of cathode support durability is a major technical barrier with respect to commercialization of fuel cells for transportation [2]. Oxidation of support leads to detachment of Pt from support, while repeated oxidation and reduction of catalyst leads to dissolution and reprecipitation [3]. The dissolution of platinum is accompanied by penetration of Pt into the membrane or gas diffusion layer, while reprecipitation leads to agglomeration of Pt in the catalyst layer. These lead to an overall decrease in ESA along with non-uniform current density distribution, leading to sintering of Pt catalysts caused by localized heating.

In order to overcome these barriers and meet the DOE technical targets for durability and performance, we have developed new classes of alternative and durable cathode supports, based on modifying the carbon surface by conductive metal oxides [4] such as tin-doped ITO, TiO_2 and SnO_2. Alternate supports such as CNT, graphene sheets, OGMC and GCNT were also investigated to take advantage of their superior properties [5-7]. In addition, conductive metal oxides were also used as an alternative to carbon-based supports. The durability and performance have been enhanced due to the following advantages for our cathode supports [8]:

- Thermodynamic stability of Pt-CMO-carbon triple junction, as shown by periodic density functional theory (DFT) calculations, prevents Pt agglomeration.
- Preference of metal oxide nanoparticles to stay at the carbon defect sites lowers carbon corrosion.
- More uniform dispersion of Pt, allowing better performance at equivalent loading.
- Direct contact of Pt with carbon allows use of low cost conductive and non-conductive stable oxides.
- Higher durability of CNT, OGMC and GCNT over Vulcan XC-72 carbon baseline provides potential for an order of magnitude improvement over baseline in durability with metal oxide modification.
- Carbon free metal oxides (ITO) with tailored conductivity and mesoporosity show positive trend in terms of activity and performance.

Approach

New classes of carbon supports modified by CMOs have been developed to improve durability and performance of the cathode catalysts. In order to prevent alloy formation, electrocatalysts were synthesized by the chemical reduction method using ethylene glycol [9]. Durability of various carbon supports such as Vulcan XC-72 carbon, multiwalled CNT (referred to as CNT in this report), GCNT, OGMC and graphene were compared. DFT calculations performed in FY 2010 on Pt-ITO-graphene were leveraged to study benefits of CMO-modified GCNT support. Conductivity studies were performed on hybrid support Nafion® layers to verify electronic percolating through the catalyst layer. Measurements were also done with ITO/Nafion® layers to explore pathways for improvement of performance.

Non-carbon support synthesis was modified to reflect the need for higher conductivity and higher triple phase boundary length. In FY 2010, for CMO supports, a doubling in performance with no loss in stability was obtained using cetyl trimethyl ammonium bromide (CTAB) surfactant assisted CMO synthesis. In FY 2011, in order to improve electronic conductivity and tailor particle crystallinity and mesoporosity, both hard template and solvothermal annealing methods were used to synthesize ITO support.

As described in earlier reports, the durability was investigated ex situ using an internally developed accelerated test protocol, with voltage stepped from 1.4-0.85 V vs. normal hydrogen electrode (NHE). An investigation of the effect of CMO modification of GCNT was conducted. MEA tests were performed on various supports with and without metal oxide modification, with the fuel cell held at 1.2 V at 80ºC, and measurement of ESA, oxygen reduction reaction activity at 0.9 V and polarization curves performed every 20 hours.

Results

DFT calculations in FY 2010 predicted a stable Pt/CMO/graphene interface, with Pt nanoparticles in contact with both CMO and graphene, followed by verification from transmission electron microscope (TEM) images. Durability for CNT supported catalysts was found to be >2X of baseline in FY 2010. In FY 2011, ITO-modified GCNT was found to have 3-4X higher durability than baseline. Optimization of GCNT diameter has also been carried out. With the current ITO synthesis method, 10-20 and 20-30 nm GCNT provided high ESA, with a significant drop for GCNT supported catalyst of >50 nm. The durability was also adversely affected with increasing GCNT diameter, possibly due to poor coverage of GCNT with ITO. ITO synthesis procedure is currently being modified to provide better coverage on GCNT to further improve both the performance and durability.

In FY 2010, significant improvement in ESA for CMO-supported catalysts was obtained using CTAB assisted synthesis that dispersed ITO precursor more uniformly, with a doubling of ESA to 40 m^2/g. Addition of conductive CNT to the synthesized Pt/CNT improved performance without compromising durability, with ESA increasing

to 60 m^2/g. Using hard template synthesis, the ESA was increased further by another 10% from 40 to 45 m^2/g. Tests are ongoing to determine ex situ durability, followed by in situ assessment of performance and durability. Synthesis of mesoporous ITO using solvothermal annealing is currently ongoing to further optimize ITO mesoporosity and conductivity.

The lead cathode catalysts are shown in Figure 1, with Pt/Vulcan XC-72 as the baseline. CTAB assisted synthesis of Pt/ITO showed doubling of ESA to 85% of baseline value, while its durability was 2-3X that of baseline. Addition of electronically percolative CNT after Pt/ITO synthesis improved the ESA to 20% higher than baseline, while durability was still 2-2.5X higher. Modification of GCNT surface with ITO resulted in better distribution of Pt nanoparticles, resulting in 40% increase in ESA and 35% improved durability over non-ITO modified GCNT support. Based on these results, these compositions were selected for in situ MEA testing.

In FY 2011, ITO modification of GCNT was carried out to improve durability and performance. The optimum ITO content was determined to be 30 wt% as shown in Figure 2. This was complemented by conductivity studies on ITO-carbon composite layers in Nafion® that showed that just 30 wt% carbon is sufficient for electronic percolation. Use of this ITO content on GCNT with different diameter showed that activity decreased for >20 nm GCNT, while activity and ESA decreased for >50 nm GCNT (Figure 3). While retention of ESA was the same for all three diameters, the durability in terms of activity retention dropped for GCNT diameter >20 nm. These results show that GCNT support of 10-20 nm was optimum for in situ testing. Efforts are underway to functionalize GCNT to facilitate more uniform ITO deposition and more uniform dispersion of ITO precursor during synthesis. This involved functionalizing with sulfuric and nitric acid to take advantage of the positively charged ITO precursors, and use of polyelectrolytes to enhance ITO precursor dispersion.

MEA tests were conducted on select catalysts, with degradation done by potential hold at 1.2 V at 80°C/7.4 psig/100 % relative humidity, followed by

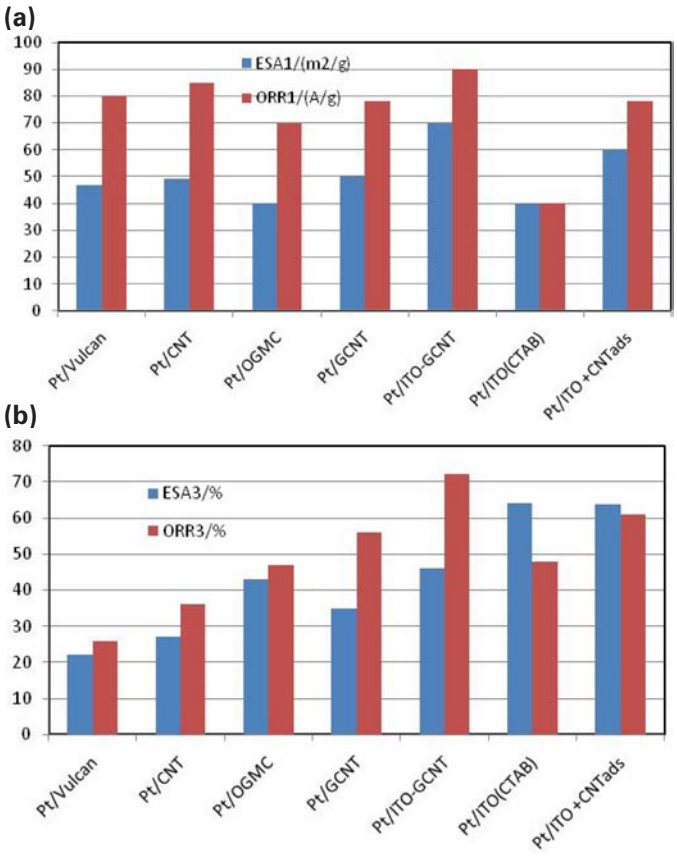


FIGURE 1. ESA (a) and Durability (b) for Lead Cathode Catalysts - RDE Potential Step between 0.85 V (30 sec) to 1.4 V (150 sec) vs. NHE

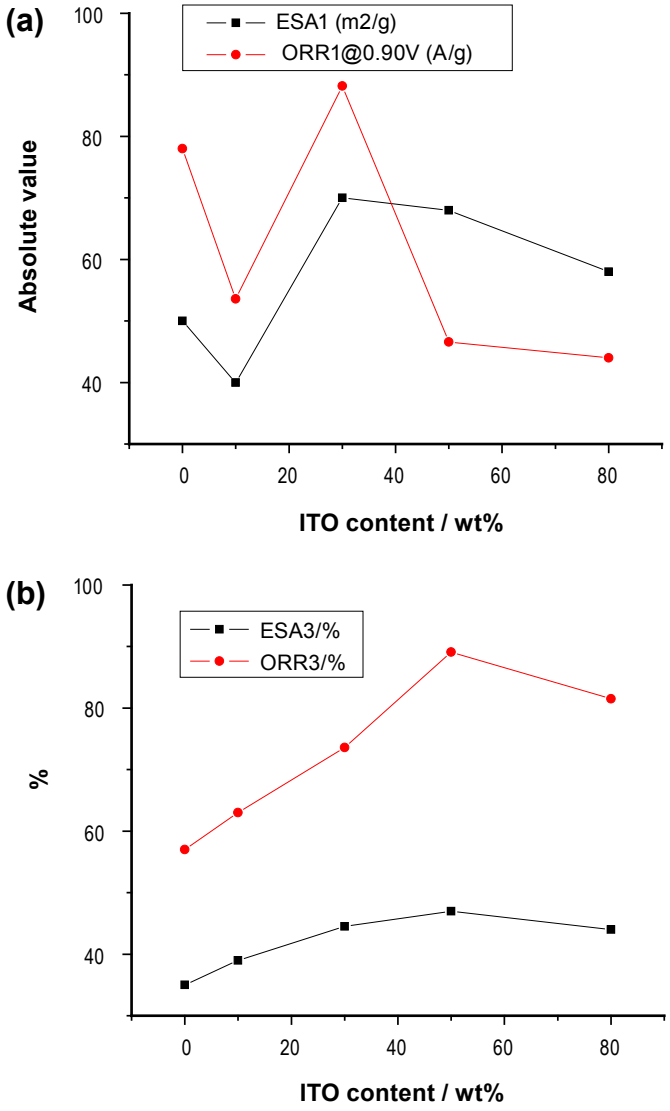


FIGURE 2. Optimization of ITO Content in ITO-GCNT (a) ESA/Activity, (b) Durability

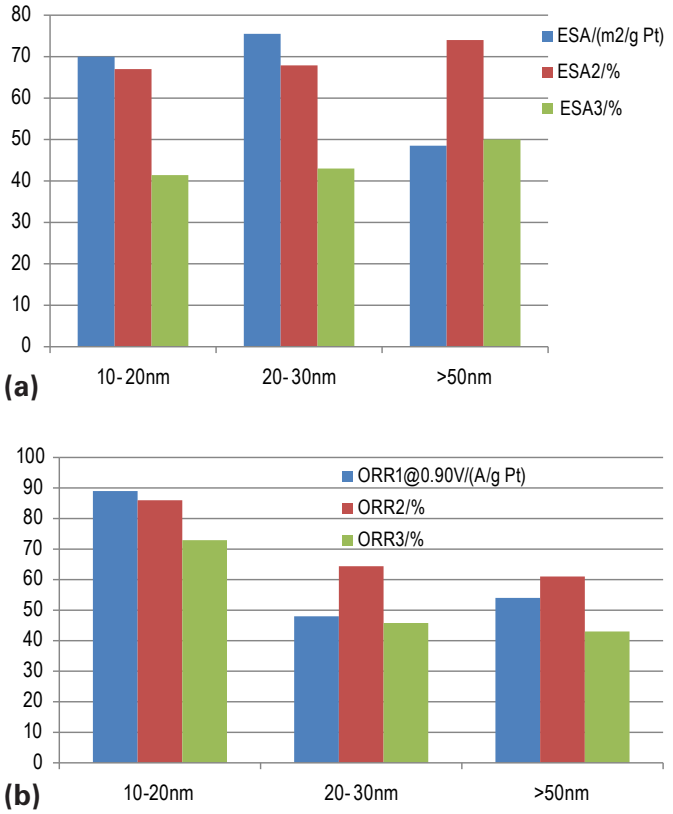


FIGURE 3. Optimization of GCNT Diameter for ITO Modification of GCNT (a) ESA and ESA Retention after 20 and 40 hours (b) Activity and Activity Retention (c) TEM for Optimized Pt/ITO-GCNT for Optimized 10-20 nm dia GCNT

measurement of ESA, activity and polarization curves. In FY 2010, significantly higher durability was achieved for Pt/CNT and slightly higher durability for Pt/OGMC compared to baseline both in terms of ESA degradation.

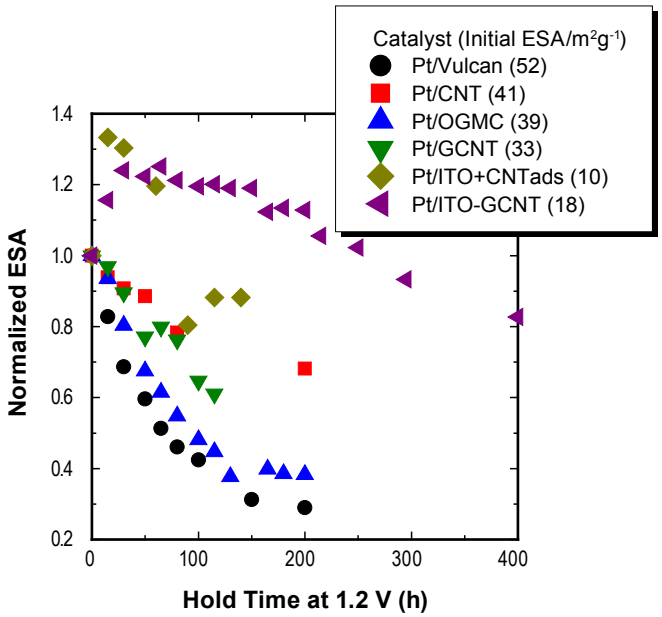


FIGURE 4. MEA Durability Results for Lead Supports (Initial ESA in brackets.)

Figure 4 shows the in situ durability for Pt-supported ITO-modified GCNT, compared with GCNT and baseline supports, with initial ESA provided. While the baseline supported catalyst lost 70% of its ESA in 50 hours and the GCNT supported catalysts lost 40% in 120 hours, Pt/ITO-GCNT lost only 20% of its ESA after 400 hours, thus making it >3-4X more stable than the baseline.

For non-carbon supports, while Pt/ITO was quite stable, its in situ ESA and performance was quite poor (2 m^2/g). Conductivity tests on ITO/Nafion® layer showed an insulating characteristic for this layer. Hence about 20 wt% CNT was added to Pt/ITO in order to increase electron percolation. This resulted in an increase of ESA to 10 m^2/g, with 3X durability of baseline (Figure 4). As seen in Figure 1, the ex situ durability was also 3X that of baseline, while ESA had tripled to 60 m^2/g over Pt/ITO (data for Pt/ITO not shown).

While in situ tests showed better durability than baseline for non-carbon supports, efforts are ongoing to improve activity and ESA. In order to improve the electronic conductivity of ITO while also increasing the triple phase boundary length, solvothermal annealing and hard template synthesis of ITO was carried out to tailor mesoporosity and conductivity. The ESA had increased to 45 m^2/g for ITO synthesized by the hard template method. X-ray diffraction and Brunauer-Emmett-Teller measurements showed that the particle size was around 20 nm, with pore size in the 8-10 nm range. Figure 5 shows TEM images of Pt/ITO synthesized by the above methods. Conductivity measurements on this sample will be carried out prior to in situ testing.

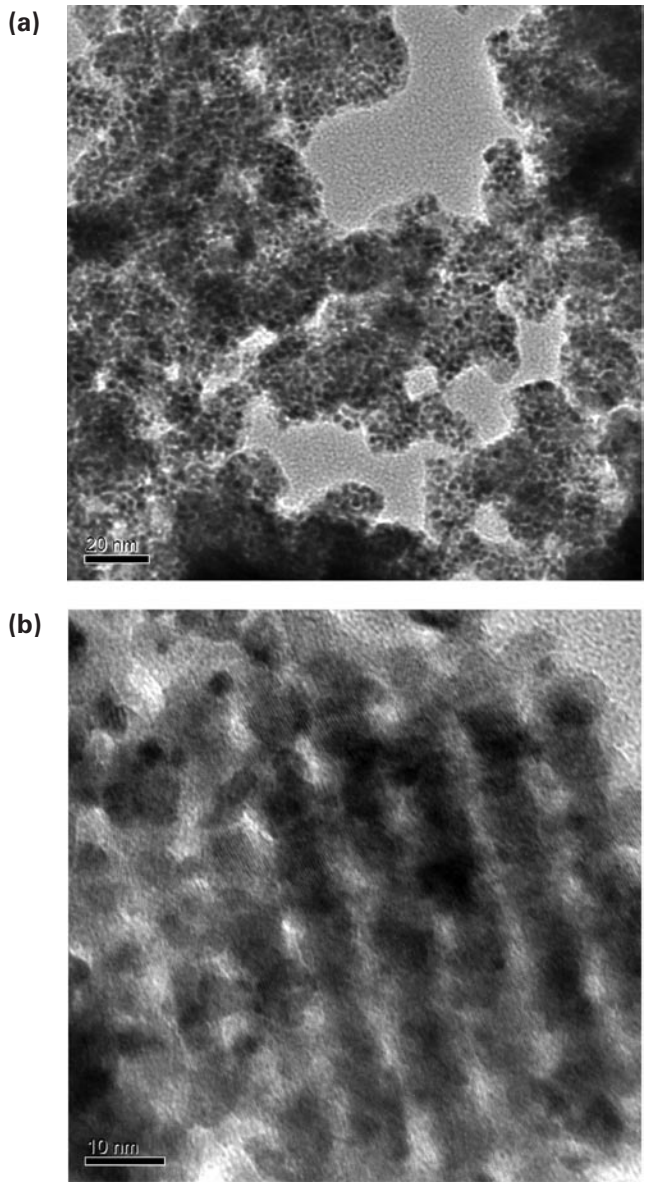


FIGURE 5. Pt/ITO (a) CTAB-Assisted (b) Hard Template Method – Evidence of Mesoporosity for the Hard Template Method

Conclusions and Future Directions

Significant progress has been made in improving supported cathode performance and durability:

- Optimum ITO content in the ITO-GCNT was found to maximize activity and durability.
- Optimum GCNT diameter was determined to maximize performance and durability of ITO-graphene supports.
- Demonstrated >3-4X stability of Pt/ITO-GCNT over baseline Pt/Vulcan carbon.
- Demonstrated 3X durability of Pt/ITO over baseline with improved performance by CNT addition.
- Synthesized non-carbon ITO support with desired mesoporosity and conductivity.

Future work will involve improving the performance of non-carbon CMO supports by incorporating mesoporosity within the supports using hard template and solvothermal annealing approach and improving MEA formulation for these novel supports. ITO deposition on GCNT will be optimized to increase uniformity of coverage by modification of GCNT surface properties and increasing the dispersion of ITO precursors. Electrode architecture optimization will be performed by controlling the Nafion® content, catalyst layer thickness, Pt content, layer porosity and pore size distribution. Accelerated test protocol that increases throughput by 3-6X will also be developed.

FY 2011 Publications/Presentations

1. S. Park, Y. Shao, H. Wan, P.C. Rieke, V.V. Viswanathan, S.A. Towne, L.V. Saraf, J. Liu, Y. Lin, Y. Wang, "Design of graphene sheets-supported Pt catalyst layer in PEM fuel cells", *Electrochem. Commun*. 13 (2011) 258-261.

2. S. Park, Y. Shao, R. Kou, V.V. Viswanathan, S.A. Towne, P.C. Rieke, J. Liu, Y. Lin, Y. Wang, "Polarization Losses under Accelerated Stress Test using Pt Catalyst Supported on Multiwalled Carbon Nanotubes in PEM Fuel Cells", *J. Electrochem. Soc.*158 (3) (2011) B297-B302.

3. Kou R, Y Shao, D Mei, Z Nie, D Wang, CM Wang, VV Viswanathan, SK Park, IA Aksay, Y Lin, Y Wang, and J Liu. 2011. "Stabilization of Electrocatalytic Metal Nanoparticles at Metal-Metal Oxide-Graphene Triple Junction Points." *Journal of the American Chemical Society* 133(8):2541-2547. doi:10.1021/ja107719u.

4. Shao Y, R Kou, D Mei, VV Viswanathan, IA Aksay, Y Lin, Y Wang, and J Liu. 2011. "An experimental and theoretical study of Pt-ITO-graphene electrocatalysts: improved durability and activity at triple junction points." Presented by Yuyan Shao, Yong Wang and Jun Liu at 241st ACS National Meeting & Exposition, Anaheim, CA on March 28, 2011. PNNL-SA-76989.

5. Shao Y, R Kou, D Mei, VV Viswanathan, IA Aksay, J Liu, and Y Wang. 2011. "Pt-ITO-Graphene Electrocatalysts: Stabilization of Pt Nanoparticles at Triple Junction Points" Presented by Yuyan Shao, Yong Wang at 22nd North American Catalysis Society Meeting, Detroit, MI on June 6, 2011. PNNL-SA-77000.

References

1. K.H. Kangasniemi, D.A. Condit, and T.D. Jarvi, "Characterization of Vulcan Electrochemically Oxidized under Simulated PEM Fuel Cell Conditions", *J. Electrochem. Soc.*, **151** (4) E125-E132 (2004).

2. R. Borup *et al.*, "Scientific Aspects of Polymer Electrolyte Fuel Cell Durability and Degradation", *Chem. Rev.* **107** 3904-3951 (2007).

3. Y. Shao, G. Yin, and Y. Gao, "Understanding and Approaches for the Durability Issues of Pt-based Catalysts for PEM Fuel Cell", *J. Power Sources* **171** 558-566 (2007).

4. G. Chen, S.R. Bare, and T.E. Mallouk, "Development of Supported Bifunctional Electrocatalysts for Unitized Regenerative Fuel Cells", *J. Electrochem. Soc.*, **149** (8) A1092-A1099 (2002).

5. Y. Shao, J. Liu, Y. Wang and Y. Lin, "Novel catalyst support materials for PEM fuel cells: current status and future prospects" J. Mat. Chem., **19** 46-59 (2009).

6. R. Kou, Y. Shao et al., Enhanced activity and stability of Pt catalysts on functionalized graphene sheets for electrocatalytic oxygen reduction", **11** 954-957 (2009).

7. S. Park, Y. Shao, H. Wan, P. C. Rieke, V.V. Viswanathan, S.A. Towne, L.V. Saraf, J. Liu, Y. Lin, Y. Wang, "Design of graphene sheets-supported Pt catalyst layer in PEM fuel cells", *Electrochem. Commun*. 13 (2011) 258-261.

8. Kou R, Y Shao, D Mei, Z Nie, D Wang, CM Wang, VV Viswanathan, SK Park, IA Aksay, Y Lin, Y Wang, and J Liu. 2011. "Stabilization of Electrocatalytic Metal Nanoparticles at Metal-Metal Oxide-Graphene Triple Junction Points." *Journal of the American Chemical Society* 133(8):2541-2547. doi:10.1021/ja107719u.

9. W.Z. Li, C.H. Liang, W.J. Zhou et al., Preparation and characterization of multiwalled carbon nanotube-supported platinum for cathode catalysts of direct methanol fuel cells", *J. Phys. Chem. B*, 107 (26) 6292-6299 (2003).

V.E.1 Polymer Electrolyte Fuel Cell Lifetime Limitations: The Role of Electrocatalyst Degradation

Deborah J. Myers (Primary Contact), Xiaoping Wang, Nancy Kariuki, Ram Subbaraman, Rajesh Ahluwalia, and Xiaohua Wang

Argonne National Laboratory
9700 S. Cass Avenue
Lemont, IL 60439
Phone: (630) 252-4261
E-mail: DMyers@anl.gov

DOE Manager
HQ: Nancy Garland
Phone: (202) 586-5673
E-mail: Nancy.Garland@ee.doe.gov

Subcontractors:
- Johnson Matthey Fuel Cells, Sonning Commons, United Kingdom
  Sarah Ball, Jonathan Sharman, Brian Theobald, and Graham Hards
- United Technologies Research Center, East Hartford, CT
  Mallika Gummalla and Zhiwei Yang
- Massachusetts Institute of Technology, Boston, MA
  Yang Shao-Horn
- University of Texas at Austin, Austin, TX
  Paulo Ferreira and Jeremy Meyers
- University of Wisconsin-Madison, Madison, WI
  Dane Morgan

Project Start Date: October 1, 2009
Project End Date: September 30, 2012

Fiscal Year (FY) 2011 Objectives

- Understand the role of cathode electrocatalyst degradation in the long-term loss of polymer electrolyte membrane fuel cell (PEMFC) performance.
- Establish dominant catalyst and electrode degradation mechanisms.
- Identify key properties of catalysts and catalyst supports that influence and determine their degradation rates.
- Quantify the effect of cell operating conditions, load profiles, and type of electrocatalyst on the performance degradation.
- Determine operating conditions and catalyst types/structures that will mitigate performance loss and allow PEMFC systems to achieve the DOE lifetime targets.

Technical Barriers

This project addresses the following technical barriers from the Fuel Cells section of the Fuel Cell Technologies Program Multi-Year Research, Development and Demonstration Plan:

(A) Durability

(B) Cost

(C) Performance

Technical Targets

This project is conducting fundamental studies of platinum-based PEMFC cathode electrocatalyst degradation mechanisms. Insights gained from these studies can be applied toward the definition of operating conditions to extend PEMFC lifetimes and to the development of cathode electrocatalyst materials that meet the following DOE 2015 electrocatalyst durability targets with voltage cycling:

- 5,000 hours (<80°C) and 5,000 hours (>80°C).
- <40% loss of initial catalytic mass activity after 30,000 cycles between 0.6 and 1.0 V.
- <30 mV loss at 0.8 A/cm² after 30,000 cycles between 0.6 and 1.0 V.

FY 2011 Accomplishments

- Completed parametric and particle size studies comparing membrane electrode assembly (MEA) performance degradation for Pt_3Co and Pt cathodes with similar initial particle sizes.
- Determined that voltage cycling from 0.6 to 1.0 V causes Pt particles of <~7 nm to grow to ~9.5 nm, irrespective of initial particle size, with evidence for both dissolution and coalescence growth mechanisms.
- Determined that Pt dissolution increases with decreasing Pt particle size and is correlated with oxide formation.
- Developed Pt cyclic voltammetry and dissolution models and Kinetic Monte Carlo (KMC) model of alloy nanoparticle dissolution for defining the alloy nanoparticle parting limit.



Introduction

One of the primary challenges facing the development of PEMFCs for automotive and stationary power applications is the durability of the fuel cell materials. The observed performance degradation has reversible and irreversible components. The topic of this project is the irreversible degradation of Pt-based cathode catalysts,

because the degradation of this component has the most profound impact on cell performance. The project's primary focus is elucidation of the effects of catalyst and support physicochemical properties and cell operating conditions on the rates and mechanisms of cathode catalyst degradation, with a secondary focus on the impact of catalyst degradation on the transport properties of the cathode. The results of this project will define the operating conditions and catalyst types/structures that will mitigate performance loss and allow PEMFC systems to achieve the DOE lifetime targets.

Approach

The project approach is to perform: (1) systematic cell degradation tests, (2) in situ and ex situ structural characterization of the catalysts, (3) fundamental out-of-cell studies, and (4) theoretical modeling to identify the degradation modes and factors contributing to cathode catalyst degradation. The catalysts studied are benchmark Pt on carbon supports with varying properties, Pt alloys with varying oxophilicity, and three classes of Pt catalysts having the highest reported oxygen reduction activity. Specifically, our approach is to utilize accelerated stress tests of MEAs containing various catalysts and supports and in situ and ex situ dissolution, microscopic, structural, and chemical characterization of these catalysts. To elucidate the effect of particle size, we are systematically varying the particle size of Pt and one Pt alloy (Pt_3Co) on a standard support. To elucidate the effect of catalyst type and catalyst oxophilicity, we are studying four classes of catalysts: Pt, Pt alloys, acid-leached alloys, and core-shell catalysts while either controlling or carefully determining the particle size and particle size distributions. To elucidate support effects, we are studying Pt on carbon supports with varied surface area, pore size, and relative proportions of micro- and mesopores. We are also determining the effects of a catalyst precursor impurity on degradation rates by post-synthesis doping of a Pt/C catalyst with varying levels of a precursor impurity (e.g., Cl^-).

The results of the experimental efforts feed into coupled models at various levels of complexity from atomic-level, *ab initio* oxidation and dissolution calculations, to catalyst degradation models, to cell kinetic and transport models. The modeling effort also defines the experiments necessary to complete the cell model. The project can be categorized into three broad and coupled tasks: (1) MEA studies utilizing accelerated stress test protocols, on-line electrochemical diagnostics, and post-test microscopic and X-ray scattering characterization, (2) mechanistic and physicochemical property studies using aqueous electrochemistry, X-ray spectroscopy/scattering, transmission electron microscopy (TEM), scanning transmission electron microscopy (STEM), in situ TEM, and quartz crystal microbalance measurements, and (3) model development, verification, and implementation. All of these techniques have been demonstrated to provide important and complementary information regarding catalyst degradation mechanisms.

Results

The focus of this year's effort has been on parametric and particle size studies of MEAs with Pt_3Co cathode electrocatalysts, comparison with identical studies of Pt MEAs, electron microprobe (EMPA) and STEM analysis of cycled Pt MEAs, degradation mechanism experiments and modeling of Pt cathode catalysts, and ab initio-based modeling of Pt-Co alloys. Catalysts were prepared containing 40 wt% Pt_3Co nanoparticles with a mean diameter of 5.6 nm on high-surface-area Ketjen black carbon support (Pt_3Co/C). This material was heat treated to form catalysts with mean particle sizes of 8.7 and 14.3 nm. These catalysts were also incorporated into the cathodes of MEAs and subjected to the DOE cycling protocol (0.6 to 1.0 V, 50 mV/s) in the fuel cell environment. Cell diagnostics of cathode catalyst electrochemically active surface area (ECA), oxygen reduction reaction (ORR) mass activity, and air and oxygen polarization curves were performed after 1,000, 3,000, 5,000, and 10,000 voltage cycles. Studies were also performed on the effect of various fuel cell operating parameters (relative humidity [RH], temperature, cycling profile, and upper potential limit) on the degradation of the cathode electrocatalyst performance with MEAs containing the 5.6 nm Pt_3Co/C. The results of the particle size and parametric studies on the Pt_3Co and comparison with the Pt results shown in last year's report are summarized in the following.

- Increasing the upper limit of voltage cycling increases cathode catalyst surface area and mass activity loss.
- Low inlet relative humidity decreases cathode catalyst degradation.
- ECA loss: Depends on catalyst particle size. No statistically meaningful difference was observed between Pt and Pt_3Co MEAs.
- ORR mass activity loss: Depends on catalyst particle size. The mass activity of Pt_3Co is more stable than the mass activity of Pt (Figure 1).
- Initial performance: Pt_3Co-based MEAs showed better beginning of life performance than Pt-based MEAs (~20 mV in H_2/O_2 or ~15 mV in H_2/Air @ 1 A/cm^2).
- Performance degradation: At high currents, the performance loss depends on catalyst particle size, no statistically meaningful difference was observed between Pt and Pt_3Co MEAs (Figure 1).
- The ionic resistance in the electrode is higher for cycled Pt_3Co cells than cycled Pt cells, which offsets the improved mass activity stability of the alloy.

This year's effort in the ex situ characterization tasks included post-cycling EMPA of the Pt_3Co and Pt-containing MEAs and STEM analysis of the Pt-containing MEAs. These MEAs had varying initial Pt particle size (1.9, 3.2, 7.1, and 12.7 nm) and were subjected to the DOE cycling protocol for 10,000 cycles (30,000 for the 7.1 nm particle

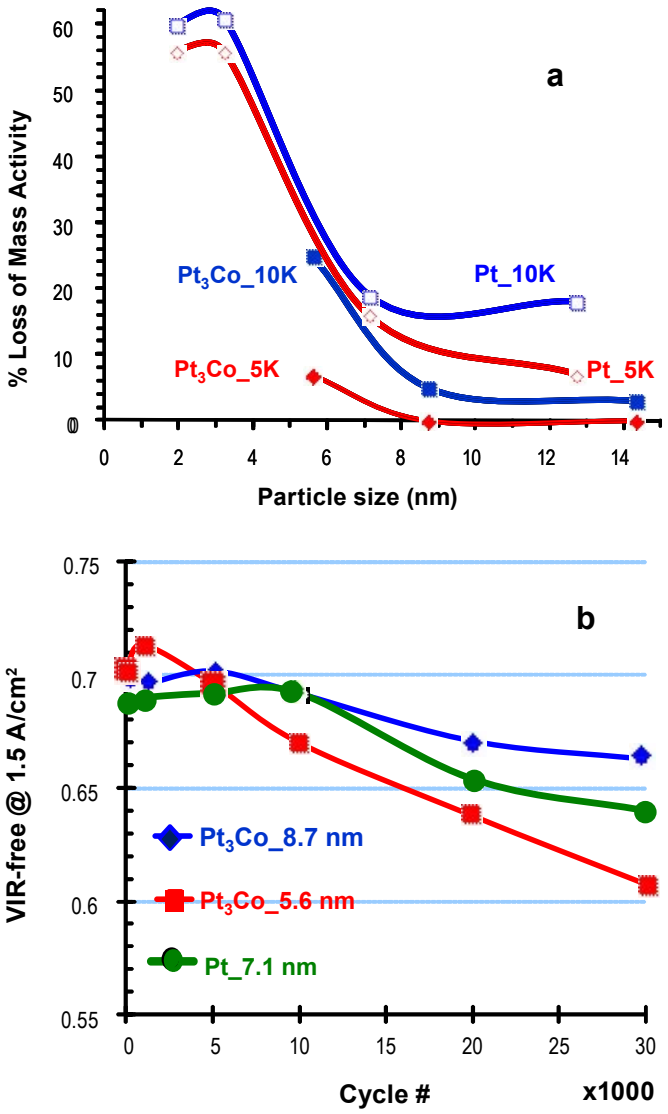


FIGURE 1. (a) Loss of oxygen reduction reaction mass activity after 5,000 (Pt_5K and Pt_3Co_5K) and 10,000 (Pt_10K and Pt_3Co_10K) cycles in an MEA (DOE protocol) as a function of initial mean particle size of Pt and Pt_3Co catalysts and (b) Internal resistance-free cell voltage at 1.5 A/cm^2 on air as a function of cycling in an MEA for Pt_3Co (5.6 and 8.7 nm) and Pt (7.1 nm).

size). MEAs with the 3.2 nm Pt/C cathode catalyst used in the parametric studies mentioned above were also analyzed.

The EMPA results showed that Pt migrated into the membrane for all of the Pt and Pt_3Co MEAs, with the exception of the cells tested at lower relative humidity (30% vs. 100%) and the cell with the largest Pt particle size (12.7 nm). The trends in Pt migration into the membrane observed were the same for Pt and Pt_3Co MEAs, including:

- Lower Pt content in the membranes with larger catalyst particle sizes.
- Lower Pt content in the membrane for low RH cycled cell.
- Higher Pt content in the membrane for high voltage and high temperature cycled cell.

The Pt MEA (7.1 nm) had a higher Pt content in the membrane than the Pt_3Co MEAs (5.6 nm and 8.7 nm) after 30,000 DOE protocol cycles.

TEM analyses of the Pt MEAs after 30,000 DOE protocol cycles showed that the extent of growth in the mean particle size and size distribution depend on position in electrode, that dendrites were formed, indicative of the dissolution/re-precipitation mechanism of particle growth, and that coalesced particle shapes were formed. The quantification of the extent of each of the two particle growth mechanisms (dissolution/re-precipitation and coalescence) is underway. The three smallest particle sizes (1.9, 3.2, and 7.1 nm) evolve to approximately the same average particle size (9.5 nm) after extended potential cycling. The largest particle size (12.7 nm) showed no loss of ECA, but did show particle growth in the region of the electrode closest to the membrane due to formation of a few very large particles.

The ex situ characterization task also included a study of the 3.2 nm Pt/C in an aqueous electrochemical environment (0.1 M $HClO_4$ electrolyte) using anomalous small-angle X-ray scattering (ASAXS). This catalyst was subjected to 900 cycles of two potential cycling protocols: the DOE protocol and 0.4 to 1.05 V square waves (0.4 to 1.05 V, 10 s each potential). The Pt subjected to the DOE cycling protocol only grew by 0.09 nm over 900 cycles, whereas the Pt subjected to the square wave cycling grew by 0.33 nm. Analyses of the change in the particle size distributions for these two sets of data (Figure 2) showed that the mechanism for growth of the mean particle size is similar for the two cycling protocols: loss of particles <3.2 nm and >5 nm, accompanied by an increase in the number of particles in the 3.2-5 nm range, differing only in extent for the two cycling protocols. The largest contributor to surface area loss is loss of particles in the 1.5-3.2 nm diameter range. The majority of the change occurred during the first 100 cycles. Analysis of the ASAXS intensities also shows that there is an overall loss of Pt from the electrodes, with the square wave showing higher loss rates.

In the fundamental out-of-cell studies task, the effect of potential and particle size on the steady-state dissolved concentration of Pt was determined for the Pt/C catalysts (1.9, 3.2, 7.1, and 12.7 nm). This was correlated with the extent of Pt oxide formation, as determined by cyclic voltammetry. These studies, illustrated in Figure 3, showed that the:

- Steady-state dissolved Pt concentration increases with decreasing mean particle size.
- Oxide coverage at constant potentials >0.9 V increases with decreasing particle size.
- Dissolved Pt concentration peaks at an oxide coverage of ~1 O/Pt, decreasing with increasing oxide coverage above a monolayer.

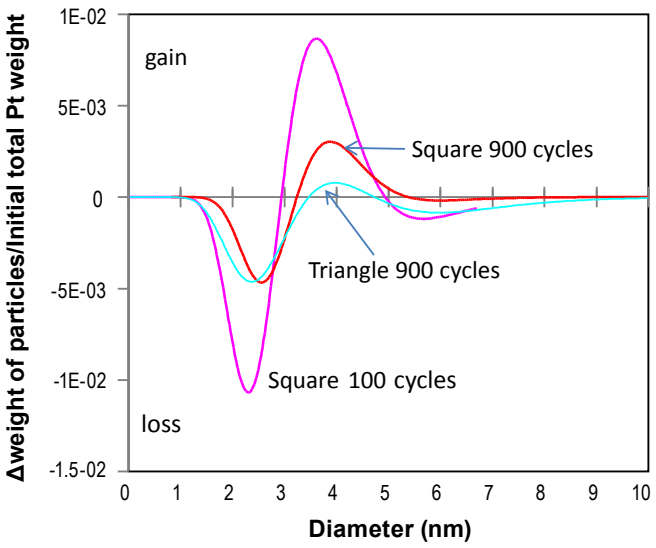


FIGURE 2. Change in the weight of Pt at all particle sizes in the particle size distribution as a result of DOE protocol cycling (0.6 to 1.0 V triangle cycles, 50 mV/s) or square wave cycling (0.4 to 1.05 V, 10 s each potential) in 0.1 M $HClO_4$ electrolyte. The initial mean particle size of the catalyst was 3.2 nm. Weight changes were derived from ASAXS-determined particle size distributions; spherical nanoparticles were assumed to calculate weights.

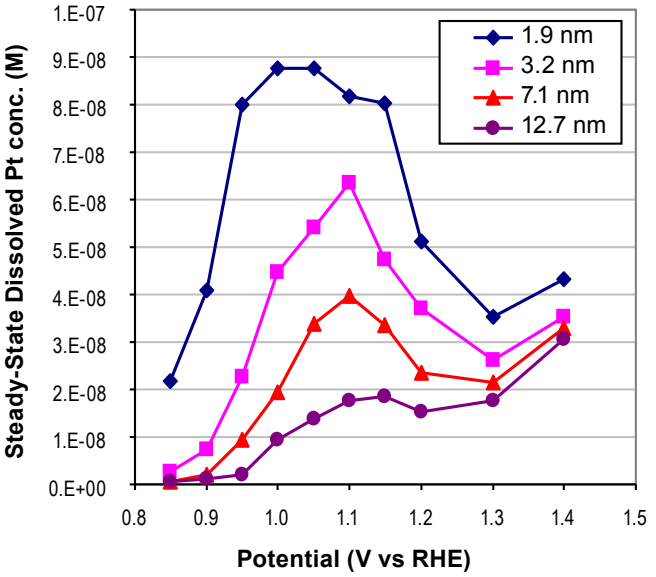


FIGURE 3. Steady-state dissolved Pt concentration in perchloric acid electrolyte as a function of potential for Pt/C of initial mean particle size of 1.9, 3.2, 7.1, and 12.7 nm.

In the theoretical modeling task of the project, a model was developed for Pt cyclic voltammetry and Pt dissolution under steady-state and cycling conditions. A non-ideal solid solution between PtO_x and Pt was assumed where oxide decreases the effective surface activity of Pt. Under steady-state conditions, it was found that: (1) there is a balance between Pt dissolution and protective oxide formation at >0.8 V, (2) the activity of Pt is strongly dependent on oxide coverage, which is strongly dependent on potential at >0.8 V, and (3) the potential dependence of the dissolved Pt concentration is lower than that expected for a two-electron electrochemical reaction due to non-unit activity of Pt caused by formation of oxide. Under cycling conditions, the kinetic constants for Pt dissolution were determined from potentiostatic concentration-time data at 0.9 V and 72-h equilibrium data for other potentials, the kinetic constants for re-deposition from potential cycling data. Conclusions from this work are: (1) at <0.9 V deposition is competitive with dissolution and (2) at >1 V, cycling accelerates Pt dissolution compared to potentiostatic conditions due to incomplete protection of the oxide.

Also in the modeling aspect of the project, the KMC model developed last year for Pt was extended to include Pt alloys and was applied to the evolution of Pt_3Co nanoparticles under fuel cell conditions. An effective bond-energy Hamiltonian was developed from density functional theory fits, which were then implemented in the KMC model of alloy nanoparticle dissolution. The KMC model predicts rapid $Pt_{1-x}Co_x$ nanoparticle de-alloying at $0.25<x<0.5$, which suggests that the concentration limit for retaining some Co in the nanoparticle is less than the 0.55 observed for bulk structures (Figure 4).

Conclusions and Future Directions

The following conclusions can be made from our studies of the degradation of Pt_3Co and Pt/C electrocatalysts:

- Initial fuel cell performance increases with decreasing cathode electrocatalyst mean Pt and Pt_3Co particle size, however degradation of performance with potential cycling increases with decreasing particle size.
- Potential cycling (0.6 to 1.0 V; 50 mV/s) causes Pt catalysts of ≤~7nm initial mean diameter to evolve to mean particle sizes and specific surface areas of 9.5 nm.
- Performance degradation with potential cycling can be attributed to increased rates and extent of ECA loss with decreasing Pt and Pt_3Co particle size, with ECA loss rates being the same for Pt and Pt_3Co. Despite better ORR mass activity stability than Pt, the Pt_3Co MEAs showed approximately the same performance loss with cycling due to decreased cathode proton conductivity (possibly due to Co^{2+} poisoning of proton-conducting sites in electrode).
- Extent of Pt and Pt_3Co nanoparticle cathode electrocatalyst performance loss, caused by loss of ECA, increases with increasing cell temperature, increasing relative humidity, and increasing upper limit of potential cycling; preliminary analyses indicate a correlation of performance loss with extent of Pt dissolution and loss of Pt from the cathode.

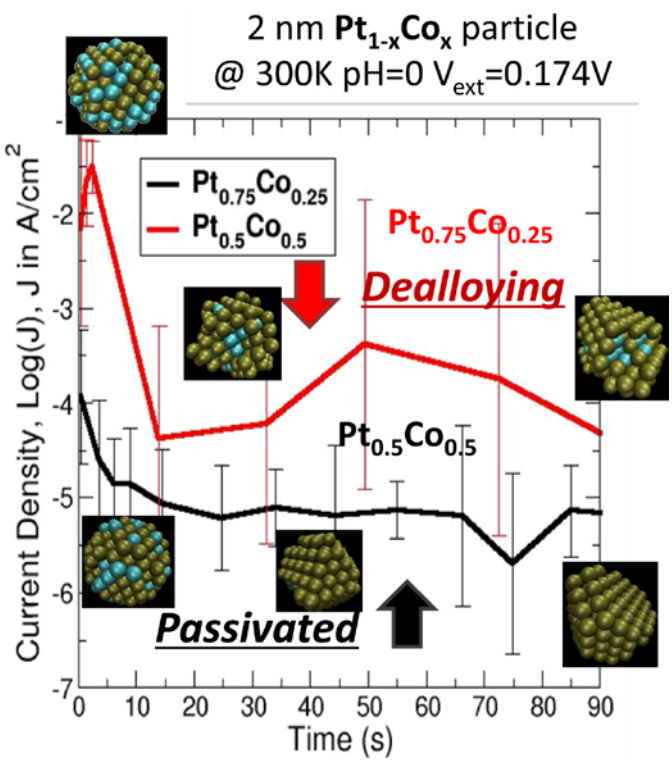


FIGURE 4. Corrosion current density as a function of time for 2 nm $Pt_{0.75}Co_{0.25}$ and $Pt_{0.5}Co_{0.5}$ particles, as derived from Kinetic Monte Carlo calculations. This plot illustrates that $Pt_{0.75}Co_{0.25}$ reaches a stable state, retaining Co in the core, whereas the $Pt_{0.5}Co_{0.5}$ nanoparticle does not passivate before losing all of its Co.

The immediate future direction of the experimental portion of the project is to complete characterization of the Pt_3Co catalysts and cycled MEAs, including acquiring additional data needed for the nanoparticle degradation modeling effort, such as Pt dissolution rates and extent of oxidation as a function of potential. Immediate future work on advanced catalysts will focus on cell fabrication and cycling of MEAs containing Pt_3Sc/C, PtCo/C and $PtCo_3/C$ cathode catalysts.

Near-Term Future Directions

- Characterize Pt dissolution as a function of particle size for Pt_3Co.
- Characterize evolution of Pt_3Co particle size during potential cycling in an MEA using anomalous small-angle X-ray scattering.
- Evaluate the impact of Pt:Co ratio, catalyst leaching, alloying with Sc, alternative carbon support, and impurity doping on degradation.
- Quantify ECA loss due to particle coalescence and Pt dissolution/re-deposition processes by modeling TEM images.
- Complete cyclic voltammetry and dissolution models.

FY 2011 Publications/Presentations

1. "Behavior of Pt and Pt_3Co Nanoparticles in PEM Fuel Cells Observed by High-Resolution TEM, Aberration-Corrected STEM and In-situ TEM", Conference, 17th International Microscopy Congress, Rio de Janeiro, Brazil, September 2010. [Invited]

2. "Atomic Structure and Defect Behavior of Nanoparticles through Aberration-Corrected STEM, High-Resolution TEM and In-situ TEM, Materials Science and Engineering Program", Texas A&M University, College Station, TX, October 2010. [Invited]

3. "Influence of Pt catalyst nanoparticle size on the electrochemical performance of PEM fuel cells", S. Rajasekhara, D.J. Groom, S. Matyas, M. Gummalla, S. Ball, P.J. Ferreira, MRS Spring Meeting, San Francisco, California, April, 2011.

4. "New Understanding of Pt Surface Area Loss in PEMFCs", D. Morgan, E. Holby, and L. Wang, 216th ECS Meeting, Las Vegas, NV, USA Oct. 10-15 (2010). [Invited]

5. "New Approaches to Modeling Fuel Cells: Catalytic Activity and Stability in PEMFC and SOFC", D. Morgan, Drexel University, PA, USA, Nov. 10, 2010. [Invited]

6. "New Approaches to Modeling Fuel Cells: Catalytic Activity and Stability in PEMFC and SOFC", D. Morgan, Columbia University, New York, NY, 2010. [Invited]

V.E.2 Durability Improvements Through Degradation Mechanism Studies

Rod Borup[1] (Primary Contact),
Rangachary Mukundan[1], Yu Seung Kim[1],
Christina Johnston[1], John Davey[1], Roger Lujan[1],
Baeck Choi[1], Zhongfen Ding[1], Cynthia Welch[1],
Andrea Labouriau[1], Bo Li[1], Dusan Spernjak[1],
Joe Fairweather[1], Rex Hjelm[1], Bruce Orler[1],
Nathan Mack[1], Rajesh Ahluwalia[2],
Xiaohua Wang[2], Adam Weber[3], Ahmet Kusoglu[3],
Karren More[4], Mike Brady[4], Sylvia Wessel[5],
Paul Beattie[5], Greg James[5], Daniel Ramrus[5],
Svetlana Loif[5], Warren Williams[5], Steve Grot[6],
Kateryna Artyushkova[7], Plamen Atanassov[7],
Anant Patel[7]

[1]Los Alamos National Laboratory (LANL)
MS D429, P.O. Box 1663
Los Alamos, NM 87545
Phone: (505) 667-2823
E-mail: Borup@lanl.gov

DOE Manager
HQ: Nancy Garland
Phone: (202) 586-5673
E-mail: Nancy.Garland@ee.doe.gov

Subcontractors:
[2] Argonne National Laboratory, Argonne, IL
[3] Lawrence Berkeley National Laboratory, Berkeley, CA
[4] Oak Ridge National Laboratory, Oak Ridge, TN
[5] Ballard Power Systems, Burnaby, BC, Canada
[6] Ion Power, New Castle, DE
[7] University of New Mexico, Albuquerque, NM

Start Date: October 2009
Project End Date: 2013

Fiscal Year (FY) 2011 Objectives

Identify and Quantify Degradation Mechanisms

- Degradation measurements of components and component interfaces.
- Elucidation of component interactions, interfaces, operation leading to degradation.
- Development of advanced in situ and ex situ characterization techniques.
- Quantify the influence of inter-relational operation between different components.
- Identification and delineation of individual component degradation mechanisms.

Understand Electrode Structure Impact - Applied Science Subtask

- Better understand the electrode structural and chemical reasons for differences in durability.
- Understand impact of electrode structure on durability and performance.
- Correlate different electrode structures to fuel cell tests and durability.
- Define different fabrication effects (esp. solvents) on electrode structure.

Develop Models Relating Components and Operation to Fuel Cell Durability

- Individual degradation models of individual fuel cell components.
- Development and dissemination of an integrated comprehensive model of cell degradation.

Methods to Mitigate Degradation of Components

- New components/properties, designs, operating conditions.

Technical Barriers

This project addresses the following technical barriers from the Fuel Cells section of the Fuel Cell Technologies Program Multi-Year Research, Development and Demonstration Plan:

(A) Durability

(B) Cost

Technical Targets

Transportation Durability: 5,000 hours (with cycling)

- Estimated start/stop cycles: 17,000
- Estimated frozen cycles: 1,650
- Estimated load cycles: 1,200,000

Stationary Durability: 40,000 hours

- Survivability: Stationary -35°C to 40°C
- Cost ($25/kW$_e$)

FY 2011 Accomplishments

- Performed all DOE Fuel Cell Tech Team recommended accelerated stress tests (ASTs) on a combination of

materials including ionomers, membranes, catalysts, and catalyst supports.
- Performed neutron imaging determining water profiles to determine effect of carbon corrosion on water management.
- Made durability comparison of electrode layers using Nafion® ionomer and a short-side-chained perfluorinated ionomer.
- Performed small angle neutron scattering determining long-range order effect of electrode solvents on electrode durability for ionomer in proton (H^+) and sodium (Na^+) forms.
- Measured Nafion® crystallinity changes with respect to electrode location.
- Measured component surface species change by X-ray photoelectron spectroscopy.
- Performed characterization of durability in segmented fuel cells.



Introduction

The durability of polymer electrolyte membrane (PEM) fuel cells is a major barrier to the commercialization of these systems for stationary and transportation power applications. Although there has been recent progress in improving durability, further improvements are needed to meet the commercialization targets. Past improvements have largely been made possible because of the fundamental understanding of the underlying degradation mechanisms. By investigating component and cell degradation modes, defining the fundamental degradation mechanisms of components and component interactions, new materials can be designed to improve durability. Various factors have been shown to affect the useful life of PEM fuel cells [1-4]. Other issues arise from component optimization. Operational conditions (such as impurities in either the fuel and oxidant stream), cell environment, temperature (including subfreezing exposure), pressure, current, voltage, etc., or transient versus continuous operation, including start-up and shutdown procedures), represent other factors that can affect cell performance and durability. To achieve a deeper understanding of PEM fuel cell durability and component degradation mechanisms, we have assembled a multi-institutional and multi-disciplinary team with significant experience investigating these phenomena.

Approach

Our approach to understanding durability and degradation mechanisms within fuel cells is structured in three areas: fuel cell testing (life testing, ASTs, ex situ aging), characterization of component properties, and modeling (component aging and integrated degradation modeling). These areas have aspects that can be considered free-standing, but each benefit greatly from work performed in the other areas. The modeling studies tie together what is learned during component characterization and allow better interpretation of the fuel cell studies. This approach and our team give us the greatest chance to increase the understanding of fuel cell degradation and to develop and employ materials that will overcome durability limitations in fuel cell systems. This work is also being coordinated with other funded projects examining durability through a DOE Durability Working Group, and through a US Fuel Cell Council task force on durability.

Results

Correlating Electrode Structure to Durability

In FY 2010, we demonstrated that the solvents used can have a dramatic effect on the performance durability of the fuel cell electrodes, although the electrochemical surface area (ECSA) of the catalyst was unaffected. Electrodes made from water-based catalytic inks show rapid performance degradation, whereas electrodes made from catalytic inks based on glycerol, show virtually no performance loss. Comparing mass activity and ECSA as a function of particle size normally shows a good correlation [1,5,6]. However, with other types of solvent-produced membrane electrode assemblies (MEAs), the correlation can be poor, or even non-existent. To define the effect of different solvents on the electrode structure performance and durability we conducted small angle neutron scattering (SANS) of both different electrode solvents and Nafion® in both H^+ and Na^+ form. The SANS for water/isopropanol is shown in Figure 1a and for glycerol in Figure 1b. A peak at a scattering intensity (Q) of ~ 0.04 indicates that the water/iso-propanol mixture shows more long-ranged order than does the glycerol/Nafion® mixture. Electrode mechanical strength measurements also suggest that glycerol-cast film shows better mechanical properties than water/isopropyl alcohol-cast films, suggesting that aggregation leads to lower mechanical properties and lower electrode durability.

The durability of electrodes formed with Nafion® ionomer was compared to similar electrodes made from Aquivion ionomer, which is ionomer with short-side chains with sulfonic acid. The comparison of the polarization performance during potential cycling ASTs is shown in Figure 2. The MEA using Aquivion ionomer at the cathode showed better stability than the MEA using Nafion® ionomer after 30K potential cycling test. The durability of these electrode structures show a similar disconnect between ECSA and performance for Pt/C reinforced as do electrodes made with the different solvents. Note that a reduction in ionomer content compared with MEAs made with Nafion® allowed for best performance without loss in potential cycling durability.

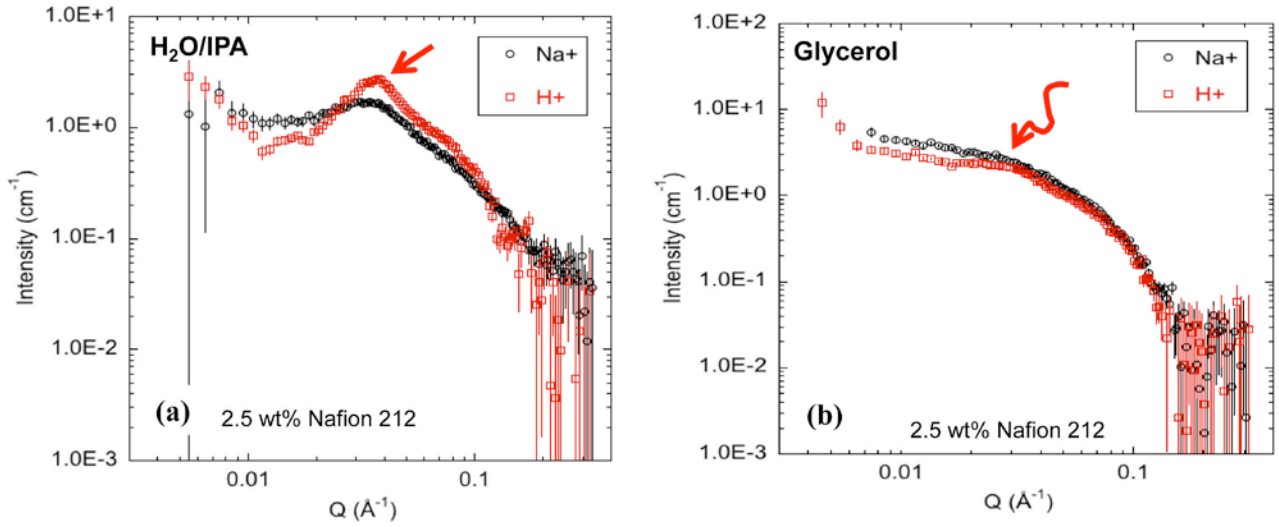


FIGURE 1. SANS of Nafion® dispersions with (a) water and iso-propanol as solvent and (b) glycerol solvent. Arrows identify location of SANS peak.

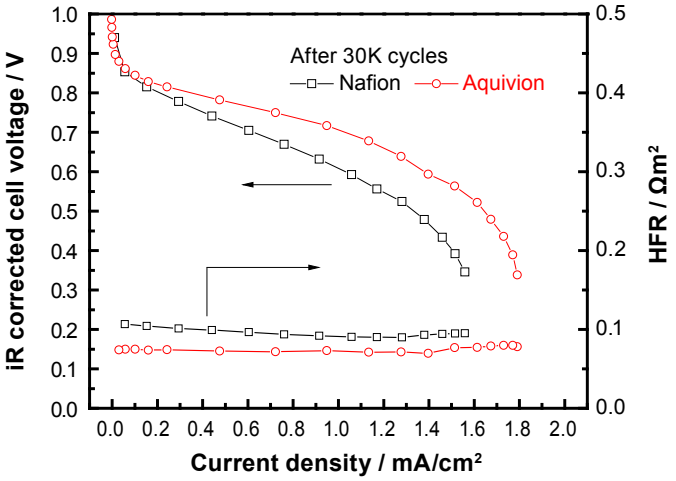


FIGURE 2. Polarization performance after 30,000 potential cycles of Nafion® and Aquivion electrodes. Catalyst, GDLs and membranes all identical.

Membrane Crystallinity Measurements

We previously have noted that the crystallinity of Nafion® during operation changes. To further investigate this phenomenon, we measured the conducted transmission electron microscopy (TEM) of fresh and AST-tested membranes. In fresh MEAs, small F-rich clusters are observed throughout the thickness of the membrane (from cathode to anode), see Figure 3a. Features exhibit some crystalline nature but are not highly crystallized nor have well-defined surfaces. After open-circuit voltage (OCV)-aging, these small F-rich clusters exhibited increased crystallinity on the cathode side without increasing in size (Figure 3b). The changes in Nafion® crystallinity were much more severe on the anode side of the membrane (Figure 3c).

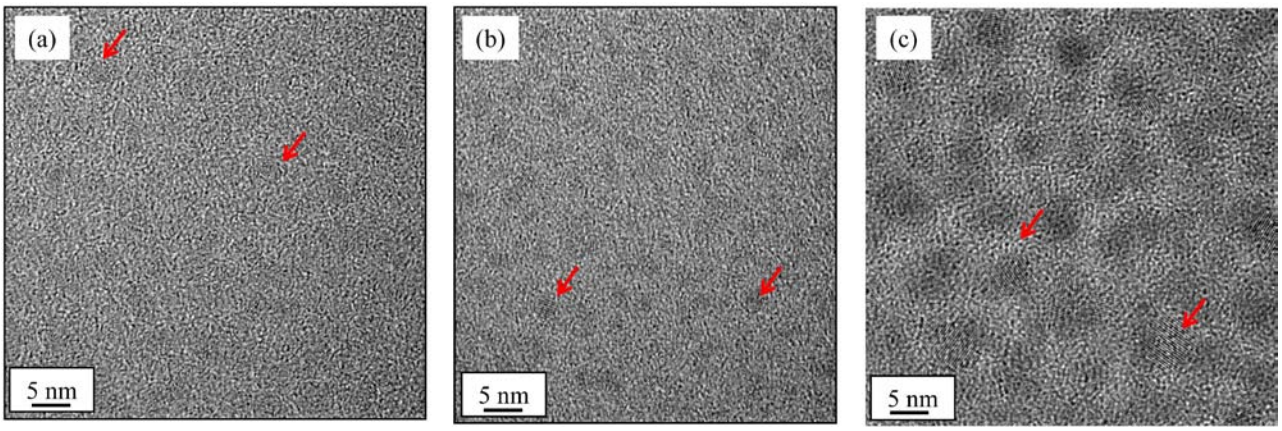


FIGURE 3. TEM of Nafion® membrane (a) fresh MEA membrane next to the cathode, (b) OCV-aged MEA membrane next to cathode and (c) OCV-aged MEA membrane next to anode. Arrows show fluorine-rich crystallites.

Durability Effects of Carbon Corrosion

To measure the effect of carbon corrosion on changes in catalyst and microporous layer hydrophobicity, the interaction of heat generation, and water retention in corroded PEM fuel cells, neutron imaging of water profiles was measured during carbon corrosion ASTs. Because of the importance of water content in determining corrosion rates, simultaneous high-resolution neutron imaging of the cells was used to calculate through-plane water profiles during the AST series. Polarization curves for a cell with 24BC cathode and anode gas diffusion layer (GDL) are shown in Figure 4a, taken after consecutive cathode holds at +1.3 V (vs. H_2 anode). The dramatic performance loss was typical for the highly oxidizing condition, as carbon loss in the cathode reduces catalytic activity and as pore space collapses. EIS at low and high overpotentials confirmed that both kinetic and mass transport resistances increased.

Water profiles at a constant current density of 0.8 A/cm^2 (constant water generation rate) are shown in Figure 4b. The consistent trend was of decreased water retention as the cell was increasingly corroded. Given the lowering of cell potential at constant current due to increasing resistances, we attributed the decreased water content to increasing internal heat generation and increasing transport from the MEA to channels. Surprisingly, we saw no evidence of increasing water holdup in the cathode, despite the tendency of corroded carbon surfaces to become more water-wetting [7]. Increased mass transport resistance during the AST was therefore attributed to collapse of porous pathways, instead of increased blockage by liquid.

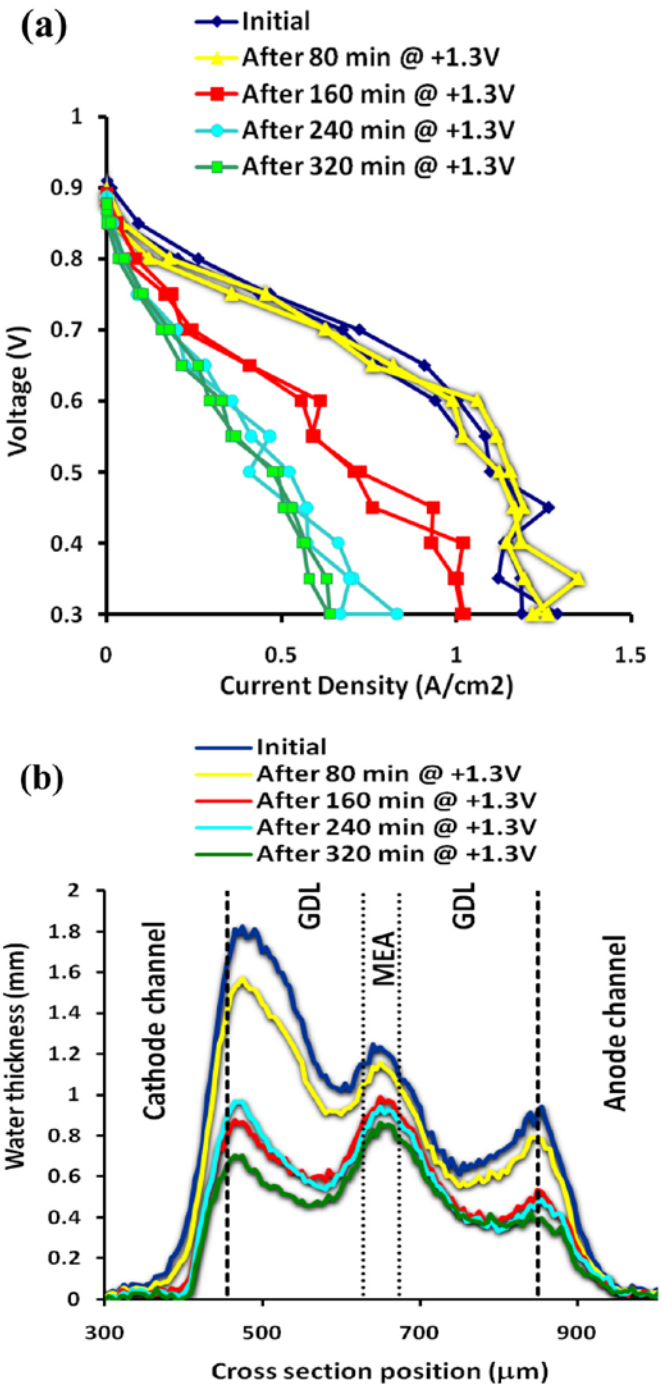


FIGURE 4. (a) Polarization curves for corrosion/imaging cell: 2.5 cm^2, Gore® 510 MEA, SGL® 24BC GDLs; H_2/Air, 80°C, 100% relative humidity (RH). (b) Through-plane water profiles for the above cell at a constant current density of 0.8 A/cm^2, 80°C, 100% RH. Profiles calculated from 20 min. neutron transmission images.

Conclusions

Catalyst and electrode durability remains a primary degradation mode; however the durability of the electrode is also dependent upon the structure of the electrode. The structure of the electrode is dependent on the solvent structure of the electrode, and the ionomer used. The durability of the electrode may be related to ionomer long-range order and the mechanical strength of the electrode. Post-characterization of the membrane shows changes in crystallinity which are dependent upon relative location to the electrodes. Carbon corrosion induces decreased performance and changes in water content.

Future Directions

Identify and Quantify Degradation Mechanisms

Vary MEA materials to better define degradation mechanisms:

- Expand mixed hydrocarbon and perfluorinated sulfonic acid materials for unambiguous chemical analysis.

Evaluate degradation rates with MEA materials; guide integrated model development:

- Material variants include: ionomer, membrane, catalyst, support, electrodes.

- >30 MEA variants, >6 AST tests, >3 fuel cell durability tests.
- Incorporate DOE Durability Working Group protocols into testing shutdown/startup.
- Differential scanning calorimetry (DSC) of ionomer identifying changes in water bonding with age.

Electrode Structure

Identify causes behind ionomer and solvent impact on MEA durability:

- Combine microscopic, porosimetry, helox, O_2, and alternating current impedance information.
- Develop model for the SANS data already obtained from electrodes.

Establish correlation of electrode structure durability to mechanical strength:

- Assess mechanical properties and interface strength of electrode measurements.
- Correlate voltage-current-resistance durability by scratch testing of electrodes by nanoindentation.
- Develop test to be used to screen quality of dispersions intended for electrodes.

Assess short-side-chained ionomers using dispersion approach for potential cycling/OCV durability:

- Expand electrode structure durability testing to include fuel cell life testing.
- Extend study of electrode durability by characterization at various MEA life points.

Component Interactions

Five-cell short stack of ~2,000 hours with previously untested seal materials:

- Analyze product water for contamination over the test time.
- Link contaminant type from stack operation to that determined by leach investigation.
- DSC of aged material samples to see if their respective time to oxidation changes.

Metal bipolar plate evaluation and evaluation of interactions with MEA/GDL composite (graphite) bipolar plate evaluation:

- Surface evaluation improving data consistency to evaluate surface properties.

Correlate GDL properties and cell water profile measurements to surface property changes.

Modeling

Water profile modeling during carbon corrosion comparing overpotential and hydrophobicity changes to water transport. Correlate experimental data with detailed membrane modeling to allow prediction of synergistic effects on membrane degradation. Completion of Pt Dissolution Model and Pt Transport Model:

- Addition of impurity degradation.
- Inclusion of other component durability models into integrated model.

FY 2011 Publications/Presentations

1. *Invited talk,* Johnston, C.M; Kim, Y.S., **Ionomer Structure and Electrode Durability, Advances in Materials for Proton Exchange Membrane Systems**, Asilomar, CA, USA, February 20–23, 2011.

2. *Invited talk,* Johnston, C.M; Kim, Y.S., **Solvent Effects on Nafion Dispersion Morphology and Fuel Cell Electrode Structures**, W.L. Gore & Associates, Inc., Elkton, MD, USA, June 4, 2010.

3. *Oral paper*, Johnston, C.M; Ding, Z.; Choi, B; Kim, Y.S., **Effect of Ionomer on Electrode Performance Durability**, 214th Meeting of the Electrochemical Society, Las Vegas, NV, USA, October 10–15, 2010.

4. *Invited talk,* Borup, R.L., **Degradation Mechanisms and Accelerated Testing in PEM Fuel Cells,** Knowledge Foundation's Fuel Cells Durability & Performance, *December 9–10, 2010, Boston, MA*.

5. *Keynote Invited talk,* Borup, R.L., **PEM Fuel Cell Degradation,** 214th Meeting of the Electrochemical Society, Las Vegas, NV, USA, October 10–15, 2010.

6. Oral Poster, Bo Li, Yu Seung Kim, Rangachary Mukundan, Mahlon S Wilson, Cynthia Welch, James Fenton, and Rodney L. Borup, **Study of Ionomer Degradation within PEMFC Electrode,** 214th Meeting of the Electrochemical Society, Las Vegas, NV, USA, October 10–15, 2010.

7. *Oral paper*, Joseph Fairweather, Bo Li, Dusan Spernak, Rangachary Mukundan, James Fenton, and Rodney Borup, ***In Situ* and *Ex Situ* Characterization of Carbon Corrosion in PEMFCs**, 214th Meeting of the Electrochemical Society, Las Vegas, NV, USA, October 10–15, 2010.

8. *Oral paper*, Karren More, Kelly Perry, Miaofang Chi and Shawn Reeves, **Carbon Support Structural Degradation Observed in PEM Fuel Cell Cathodes**, 214th Meeting of the Electrochemical Society, Las Vegas, NV, USA, October 10–15, 2010.

References

1. Borup, R., J. Meyers, B. Pivovar, et al., *Chemical Reviews*; **107(10)**, 3904 (2007).

2. Chalk S.G.; Miller, J.F. *J. Power Sources* **2006**, *159*, 73.

3. Fowler, M., Mann, R.F.; Amphlett, J.C.; Peppley, B.A.; Roberge, P.R., p. *In Handbook of Fuel Cells, Fundamentals, Technology and Applications, vol. 3, Fuel Cell Technology and Applications, Vielstich, W., Gasteiger, H.A., Lamm A., Eds.; Wiley* **2003**, 663.

4. Wilson, M.S., Garzon, F.H.; Sickafus, K.E., Gottesfeld, S.J. *Electrochem. Soc.* **1993**, *140*, 2872.

5. Mukudan, R., In *2010 Fuel Cell Technologies Merit Review Meeting,* Washington, D.C., 2010.

6. Borup, R. In *2004 Hydrogen and Fuel Cells Merit Review Meeting,* Philadelphia, PA, 2004.

7. Kangasniemi, K.H., D.A. Condit, and T.D. Jarvi. Journal of the Electrochemical Society, 2004. **151**(4): p. E125-E132.

V.E.3 Analysis of Durability of MEAs in Automotive PEMFC Applications

Randal L. Perry
E.I. du Pont de Nemours and Company
Chestnut Run Plaza, 701/209
4417 Lancaster Pike
Wilmington, DE 19805
Phone: (302) 999-6545
E-mail: randal.l.perry@usa.dupont.com

DOE Managers
HQ: Kathi Epping Martin
Phone: (202) 586-7425
E-mail: Kathi.Epping@ee.doe.gov
GO: David Peterson
Phone: (720) 356-1747
E-mail: David.Peterson@go.doe.gov

Technical Advisor
Thomas Benjamin
Phone: (630) 252-1632
E-mail: benjamin@anl.gov

Contract Number: DE-EE0003772

Subcontractors:
- Nissan Technical Center North America, Farmington Hills, MI
- Illinois Institute of Technology, Chicago, Illinois
- 3M, St. Paul, MN

Project Start Date: September 1, 2010
Project End Date: August 31, 2013

Objectives

- Develop and/or confirm accelerated tests designed to separate individual degradation mechanisms. The final tests must ensure that degradation mechanisms seen in membrane electrode assemblies (MEAs) tested in the project match experience from Nissan's previous stack tests.
- Develop an overall degradation model that correlates the stack operating conditions to degradation of the MEA. Data generated using the accelerated tests defined above will be used in the model.
- Develop MEAs with a design lifetime target of 5,000 hours with <7% degradation and that show a clear path towards meeting the DOE 2015 technical targets.

Technical Barriers

This project addresses technical barriers from Section 3.4 – Fuel Cells, of the Fuel Cell Technologies Program Multi-Year Research, Development and Demonstration Plan. The primary technical barrier addressed is:

(A) Durability

There are also some basic requirements in

(C) Performance

but this is a secondary concern, aimed primarily at having performance acceptable to Nissan in order to run the stack test, and to ensure that the durability model is relevant to current materials.

Technical Targets

In order to meet the objectives, a series of milestones were developed that act as technical targets. The last two milestones have Go/No-Go criteria to be met before they are completed. None of the milestones have yet been completed.

- Decide which accelerated tests will be used in addition to DOE specified tests. Tests will be selected based on results of post-mortem analysis. Target date: 5/31/2011.
- Select specific low-equivalent weight membrane for use in stack test. The membrane design must meet accelerated durability targets with results verified in repeated lab testing. Target date: 10/31/2011.
- Define MEA design for stack test. The MEA will be based on durable materials as determined in the lab testing, and must meet minimum performance and durability goals. Target date: 3/31/2012.
- If data generated from the accelerated tests can be shown to discriminate among the various cell components, complete development of durability model. Target date: 8/31/2013.
- If MEA design meets targets, begin stack test to verify lab performance and durability model. Target completion date: 4/20/2013.

Fiscal Year (FY) 2011 Accomplishments

The project was divided into five tasks plus project management, which are more parallel than sequential. The accomplishments are organized by task. Only Task 1 and 2 have been worked on to date. Tasks 3 through 5 are listed for completeness, but no work has begun on these tasks

Task 1.0 Materials Synthesis

- Synthesize short-side chain polymer with desired properties for standard testing.
- Fabricate two standard membrane configurations using semi-commercial equipment.
- Apply semi-commercial coating of anode and cathode decals at desired platinum loading.

- Fabricate catalyst-coated membranes (CCMs) for initial durability tests at DuPont and Nissan.

Task 2.0 Accelerated Aging Tests

- Upgraded test equipment to handle specified DOE tests.
- Began initial accelerated tests at DuPont and Nissan.
- Testing currently in progress includes DOE, Nissan and US Fuel Cell Council accelerated tests.

Task 3.0 Analysis and Modeling

Task 4.0 Stack Testing

Task 5.0 Materials Characterization and Analysis



Introduction

This project deals with the study of the stresses and forces expected in an automotive fuel cell stack operating under real-world driving conditions. For the fuel cell stack, these driving conditions include a wide variety of conditions that stress various components that make up the fuel cell stack. For instance, at high temperature (>80°C) and low relative humidity (RH) conditions, the conductivity of many membranes becomes low, resulting in the failure of fuel cell operation [1]. Moreover, membrane mechanical properties also deteriorate under prolonged humidity cycling, leading to membrane failure [2]. The DOE considers the durability of fuel cell components to be among the major technical barriers for successful implementation of fuel cell systems. The minimum required life expectancy for automotive fuel cell stacks is 5,000 hours.

Incremental improvements will not suffice to bridge the gap between today's technology and the market requirement. This project is focused on both improving the understanding of the mechanisms of component failure, and rapidly incorporating this understanding into component design and thus accelerate the delivery of proton exchange membrane fuel cells (PEMFCs) into the marketplace.

Approach

Degradation mechanisms for all stack components are being studied at varying levels of detail. At a high level, the determination of degradation mechanisms consists of the following tasks:

- Chemical degradation studies of the ionomers, not only in the membrane but also in the catalyst layer.
- Analysis of how chemical degradation impacts water management in the membrane and electrode layers.
- Understanding of the effect of realistic automotive cycling operation on the degradation of MEA components.
- Definition of the mechanisms and conditions that promote MEA degradation not only at a single cell level, but in the environment of an automotive fuel cell stack.
- Fabrication and delivery of an MEA that has improved resistance to degradation for evaluation in a full-scale short stack.

These studies on materials both before and after running the accelerated tests will be used first to compare with Nissan stack results and define the best set of accelerated tests to use in this project. The testing and analyses will then be extended to a range of components, so that a quantitative model of stack degradation can be developed.

Next, the results of degradation mechanism work will be used to develop methods to mitigate some of these mechanisms in order to increase the durability of the membrane electrode assemblies. The improved MEAs will be used in a stack test at Nissan to verify both the model and the improvements in durability.

Results

The start of the testing program has been delayed while confidentiality agreements and subcontracts were being worked out among the parties. The confidential disclosure agreements were signed in June 2011, and materials were then shared so testing could begin. The completion of these agreements also allows the legal work on the actual contracts to begin.

While the agreements were being negotiated, the work focused on defining, fabricating and purchasing the base materials. Because the project is defined for a certain class of short side-chain polymers, the first task in the project involved preparation of materials to be used in the evaluation of the accelerated tests. A short side-chain polymer with the desired range of properties was synthesized in semiworks-scale equipment. Some of this material was converted to dispersion, and several small lots of reinforced membranes were produced on semi-works scale equipment. The team agreed on the importance of testing repeatable materials from processes that could produce semi-commercial quantities of material and be scaled up easily. These membranes use an expanded polytetrafluoroethylene reinforcement, and DuPont's proprietary advanced stabilization system, and were made in nominal thicknesses of 16 and 27 microns. All membranes for the initial phase of the project use the same polymer composition.

The team agreed on using a specific commercially available cathode catalyst. The catalyst consists of 50% Pt on an acetylene carbon black support. A supply of cathode decals based on this ink formulation was produced on the semi-commercial coating line. Both 0.15 and 0.35 mg Pt/cm^2 loadings were produced. This decal supply will be used for the remainder of the accelerated test evaluation work. It is not optimized for either performance or durability, but is

in the right performance and property range for evaluation of testing methods.

The semi-commercial decals were then transferred to N211 and tested under our standard conditioning test to ensure the material quality. These results were compared to CCMs using previous generation materials. These results led us to the conclusion that the electrodes are suitable for the next phase of the work. Once the suitability of the materials was confirmed CCMs were prepared for initial durability tests at DuPont and Nissan.

Test equipment at DuPont was upgraded to handle specified DOE tests, which differed considerably from DuPont's internal testing. Both Nissan and DuPont have begun the accelerated tests of the base materials, but significant test results are not yet available.

Conclusions and Future Directions

Short-Term

- Complete contractual arrangements for all subcontractors and participants.
- Complete automation of DOE Durability Test Protocols.
- Complete analysis of baseline materials.
- Complete first set of accelerated tests and begin post-mortem analyses.
- Make decision on acceleration tests to use in the model development. We anticipate a overall delay of six months due to the timing of the confidentiality agreement and formal contracts.

2011-2012

- Fabricate alternative membranes and CCMs and complete designed experiment to better define effects of material properties on degradation.
- Fabricate durable materials for stack test.

FY 2011 Publications/Presentations

1. 2011 AMR presentation, May 13, 2011.

References

1. A.V. Anantaraman, C.L. Gardner, "Studies on ion-exchange membranes. Part 1. Effect of humidity on the conductivity of Nafion®", *Journal of Electroanalalytical Chemistry*, **1996**, *414*, 115-120.

2. F. Bauer, S. Denneler, M. Willert-Porada, "Influence of temperature and humidity on the mechanical properties of Nafion® 117 polymer electrolyte membrane" *Journal of Polymer Science: Part B*, **2005**, *43*, 786-795.

V.E.4 Development of Micro-Structural Mitigation Strategies for PEM Fuel Cells: Morphological Simulations and Experimental Approaches

Silvia Wessel (Primary Contact), David Harvey
Ballard Power Systems
9000 Glenlyon Parkway
Burnaby, B.C. V5J 5J8
Phone: (604) 453-3668
E-mail: silvia.wessel@ballard.com

DOE Managers
HQ: Kathi Epping Martin
Phone: (202) 586-7425
E-mail: Kathi.Epping@ee.doe.gov
GO: David Peterson
Phone: (720) 356-1747
E-mail: David.Peterson@go.doe.gov

Technical Advisor
John Kopasz
Phone: (630) 252-7531
E-mail: kopasz@anl.gov

Contract Number: DE-EE0000466

Subcontractors:
- Georgia Institute of Technology, Atlanta, GA (S.S. Yang)
- Los Alamos National Laboratory, Los Alamos, NM (R. Borup)
- Michigan Technological University, Houghton, MI (J. Allen)
- Queen's University, Kingston, Ontario (K. Karan, J. Pharoah)
- University of New Mexico, Albuquerque, NM (P. Atanassov)

Project Start Date: January 1, 2010
Project End Date: March 31, 2013

Fiscal Year (FY) 2011 Objectives

- Identify/verify catalyst degradation mechanisms, i.e. Pt dissolution and transport/ plating), carbon-support oxidation/corrosion, ionomeric thinning/conductivity loss, and mechanism coupling/feedback/acceleration.
- Correlate catalyst performance/catalyst structural change as a function of unit cell operational conditions, catalyst layer morphology/composition, and gas diffusion layer (GDL) properties.
- Develop kinetic and material models for catalyst layer aging, i.e. macro-level unit cell model, micro-scale catalyst layer model, and molecular dynamics model of the platinum/carbon/ionomer interface.
- Develop mitigation strategies for catalyst degradation through modification of: operational conditions and component structural morphologies/compositions.

Technical Barriers

This project addresses the following technical barriers of the DOE Fuel Cell Technology Program Multi-year Research, Development, and Demonstration Plan. This plan can be accessed at http://www.eere.energy.gov/hydrogenandfuelcells/mypp/.

(A) Durability

Pt catalyst and Pt catalyst layers degradation:
- Effect of cathode structure and composition
- Effect of operational conditions

(B) Performance
- Effect of cathode catalyst structure and composition

(C) Cost

Technical Targets

This project conducts fundamental studies of Pt/carbon catalyst degradation mechanisms and degradation rates which are correlated with unit cell operational conditions and catalyst layer structure and composition. Furthermore, forward predictive micro and macro models for cathode performance and degradation are being developed. Design curves will be generated, both through model simulations and experimental work, enabling membrane electrode assembly (MEA) designers to optimize performance, durability, and cost towards the 2015 stack targets for fuel cell commercialization [1]:

- Durability: 5,000/40,000 hrs (2015 transportation/2011 stationary application target)
  - Electrocatalyst Support Loss: <30 mV after 100 hrs @ 1.2V
  - Electrochemical Surface Area (ECSA) Loss <40%
- Cost: $15/kW$_e$
  - Precious Group Metal (PGM) total loading: 0.2 mg

FY 2011 Accomplishments

- Validated the one-dimensional (1D), 2-phase MEA model with statistical inputs for material, design, and operational deviations within the 95% variability of the experimental data (baseline MEA).
- Developed a molecular-dynamics-based description of the Pt/C/ionomer system.
- Expanded the micro-structural and 1D-MEA Model for 2-phase flow.
- Quantified Pt/C cathode catalyst layer degradation (performance loss and structural changes) as a function

of carbon catalyst support type, ionomer loading, upper potential voltage cycling in the accelerated stress test (AST), and number of AST cycles.



Introduction

Catalyst/catalyst layer degradation has been identified as a substantial contributor to fuel cell performance degradation and this contribution will most likely increase as MEAs are driven to lower Pt loadings in order to meet the cost targets for full-scale commercialization. Over the past few years significant progress has been made in identifying catalyst degradation mechanisms [2,3] and several key parameters that greatly influence the degradation rates, including electrode potentials, potential cycling, temperature, humidity, and reactant gas composition [2,4-6]. Despite these advancements, many gaps with respect to catalyst layer degradation and an understanding of its driving mechanisms still exist. In particular, acceleration of the mechanisms under different fuel cell conditions, due to different structural compositions, and as a function of the drive to lower Pt loadings remains an area not well understood. In order to close these gaps an understanding of the effect of operating conditions and the layer structure and composition on catalyst layer degradation mechanisms and degradation rates is needed.

The project focus is to develop forward predictive models and to conduct systematic cell degradation studies that enable the quantification of the cathode catalyst layer degradation mechanisms and rates, as well as the coupling between mechanisms for key operational and structural stressors.

Approach

Models will be developed at the molecular, micro-structural, and macro-homogeneous scales that include degradation effects related to platinum dissolution, transport and plating, carbon surface oxidation and corrosion, and ionomer thinning/conductivity loss. The models will provide the ability to study the effects of composition, the morphological design, and the operational window on catalyst degradation via simulated ASTs. The design curves generated in each scale of the modeling work will enable the development of mitigation strategies through trade-off analysis.

Accelerated stress testing coupled with 'state-of-the-art' in situ/ex situ characterization techniques will be used to correlate MEA performance loss with structural changes measured within the Pt cathode, as well as to develop key operational and catalyst/catalyst layer structural degradation design curves. The experimental results will also serve to provide model validation.

Results

Under the modeling tasks, molecular modeling was used to determine the cohesive energy for the Pt clusters and its interaction with H_2O and O_2, carbon and the ionomer. The Microstructural Catalyst Model has been extended to include 2-phase flow in order to simulate the capillary transport inside the catalyst structure. Furthermore, the model has been used to extract effective properties for the low surface area catalysts used in the project, with the results currently implemented in the Macro MEA model. The Macro MEA model was re-scripted in a manner that separated relevant sections of model functionality into self-contained modules enabling the use of statistical inputs based on component to component and operational variability. Shown in Figure 1(a), the model was validated using experimental data generated with different MEAs and test-stands. The model validates within the 95% variability of the experimental data for current densities up to ~1,000 mA/cm^2. Beyond this point the experimental and model data diverge, the discrepancy is believed to be due to the formation of liquid water and its interaction statistically with the MEA structure. To improve the validation, a 2-phase flow module was implemented and a repeat of the validation shows the improved mass transport predictions over the entire polarization range, Figure 1(b), such that the model is fully validated within the 95% variability of the experimental data.

The key operational and structural stressors affecting catalyst layer durability were identified and prioritized based on literature and Ballard data. With a focus on the catalyst layer structure and composition, the impact of catalyst carbon support type, catalyst layer ionomer content, and cathode catalyst layer degradation was investigated using ASTs. In addition, selected designs were also investigated for performance degradation and catalyst layer structural changes as a function of AST upper potential and as a function of AST cycle number. The MEAs were in-house catalyst-coated Nafion® membranes with a anode and cathode loading of 0.1/0.4 mg/cm^2, respectively, and Ballard Material Products' GDLs. The AST standard conditions are: 80°C, 100% relative humidity (RH), air/H_2, square wave cycle from 0.6 V (30 s) to 1.2 V (60 s) for 4,700 cycles. Comprehensive cell diagnostics and characterization were conducted after 50, 700, 1,400, 2,100, and 4,700 cycles and failure analysis was performed at the end of the stress test (4,700 cycles).

The effect of ionomer loading on Pt dissolution/corrosion was investigated for a range of 12 to 50 wt% Nafion® content using a Pt catalyst supported on a low surface area carbon (LSAC). The MEAs were subjected to AST testing (1.2 V upper potential limit, 4,700 cycles). The key findings were:

- ~30% ionomer loading yields optimal beginning of test (BOT) performance in agreement with literature results [7] and internal model predictions.

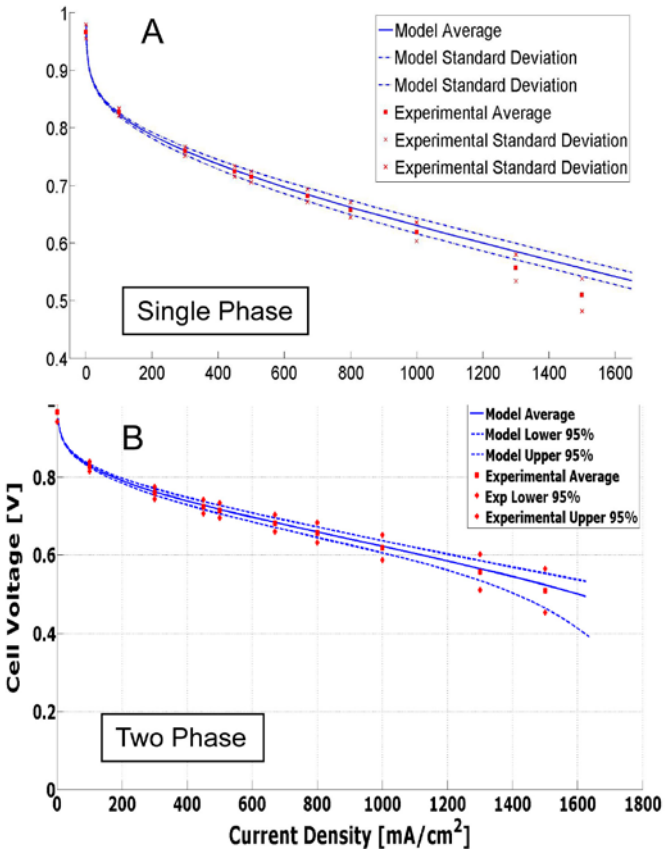


FIGURE 1. 1D MEA Model: Comparison of statistical model predictions with experimental data (a) single phase flow using input parameter uncertainty of 1 standard deviation, (b) 2-phase flow using input parameters confidence level of 95%.

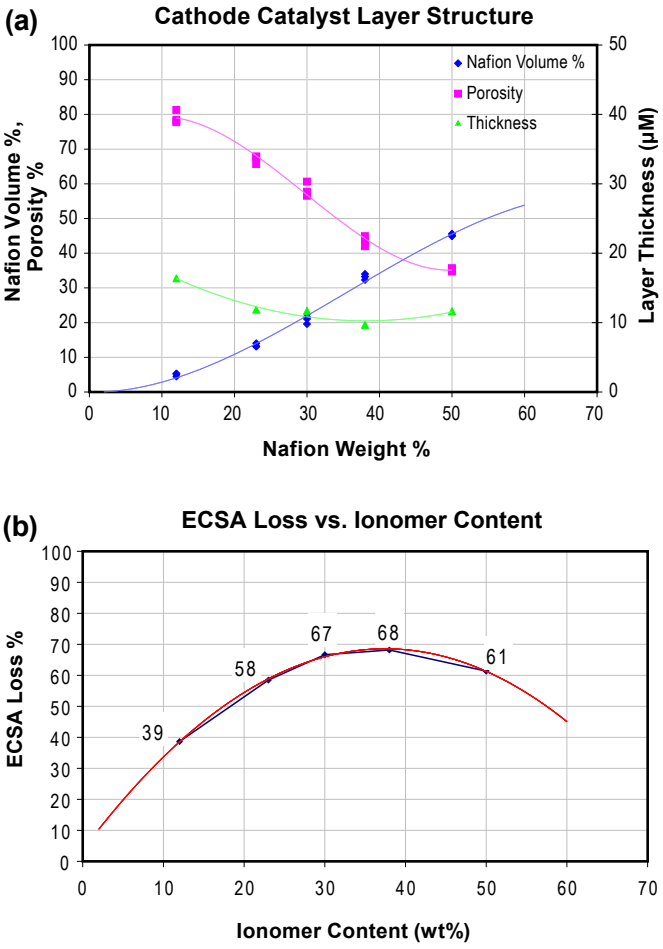


FIGURE 2. Effect of ionomer content in the cathode on (a) catalyst layer structure and (b) cathode ECSA loss after 4,700 AST cycles.

- The ionomer content impacts the BOT catalyst structure: catalyst layer porosity decreases with increasing ionomer loading, Figure 2(a).
- After 4,700 AST cycles end of test (EOT) the highest ECSA loss occurs at an ionomer content of ~30 to 40%, Figure 2(b). The voltage loss is dominated by cathode catalyst layer ionic loss.

The effect of catalyst carbon support type on catalyst performance and degradation was studied using a variety of Pt catalysts supported on different carbons (surface area from <200 m^2/g to 800 m^2/g) at an upper AST potential of 1.0 and 1.2 V. The catalyst powders and carbon support materials were analyzed for surface species, morphology, and particle distribution.

Transmission electron microscope micrographs revealed a carbon aggregate structure with graphitic walls and amorphous center for the LSAC; the mid-range carbon support (MSAC) and Vulcan (V) also exhibit some graphic walls that are in general less uniform. One of the high surface area carbons (HSAC1) showed some graphitic centers throughout the aggregates; while a second one (HSAC2) showed a highly amorphous structure. It was also noticeable that the Pt distribution on the different supports becomes more dispersed with increasing surface area.

In general, Pt catalysts supported on high surface area carbon exhibited higher BOT performance due to higher ECSA; however, the carbon surface structure and surface functionality were found to also have a significant impact on the catalyst layer structure and its resistance to corrosion. The key findings were:

- The BOT performance did not show a clear trend with the carbon support surface area.
- Cycling at 1.0 V upper potential limit (UPL) exhibited similar Pt dissolution and minimal carbon oxidation for all investigated carbons.
- Cycling at 1.2 V UPL showed increased Pt dissolution, Pt agglomeration and Pt in the membrane with increasing carbon surface area due to greater catalyst ECA and Pt dispersion. As expected, greater Pt surface area and distribution enhanced the Pt catalysis of the

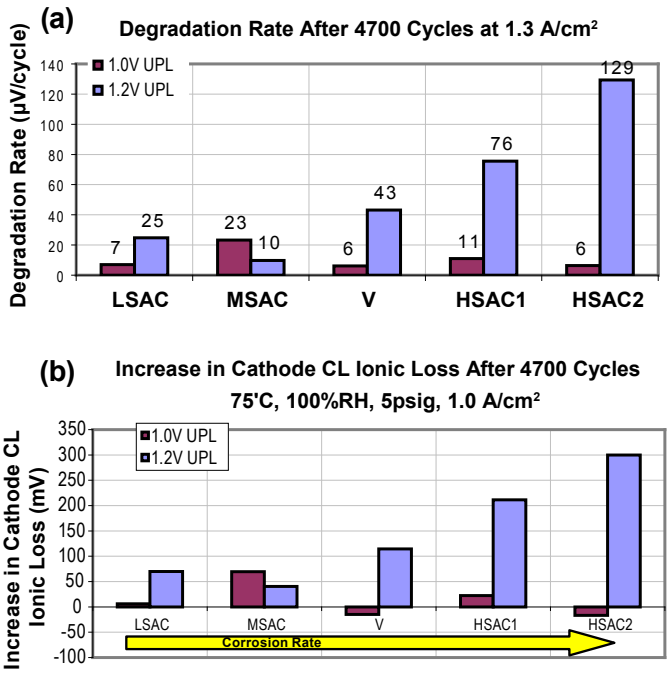


FIGURE 3. (a) Voltage degradation rate and (b) cathode catalyst layer ionic resistance loss after 4,700 AST cycles at an upper potential of 1.0 and 1.2 V for a variety of carbon supports (LSAC - Low, MSAC - Medium, HSAC - High Surface Area Carbon support, V - Vulcan).

carbon support, thus catalyst layer thinning increased with increasing carbon surface area.

- The cathode catalyst layer performance and specifically the ionic resistance were impacted significantly by corrosion, most severely for high surface area carbon supports (Figure 3). The MSAC catalyst was found to be an exception to the trend, likely due to enhanced carbon surface oxidation causing increased cathode catalyst ionic conductivity and consequently higher performance.
- The carbon structure and morphology impacts catalyst layer durability. Pt dissolution (ECSA/kinetic loss) and corrosion (cathode layer ionic/thickness loss) decreased linearly with increasing graphitic content of the carbon support surface.

The effect of upper potential on catalyst layer degradation was studied by subjecting Pt catalysts on MSAC and LSAC supports to AST cycling at upper potentials from 1.0 to 1.4V. The two catalysts exhibit similar platinum dissolution and support corrosion trends with some subtle differences in degradation rates. The LSAC catalyst was found to be slightly more stable at an UPL ≤1.3 V; however, it was notably less stable than the MSAC catalyst at a UPL ≥1.3 V which may be associated with the collapse of the LSAC aggregates due to severe corrosion of the amorphous centers.

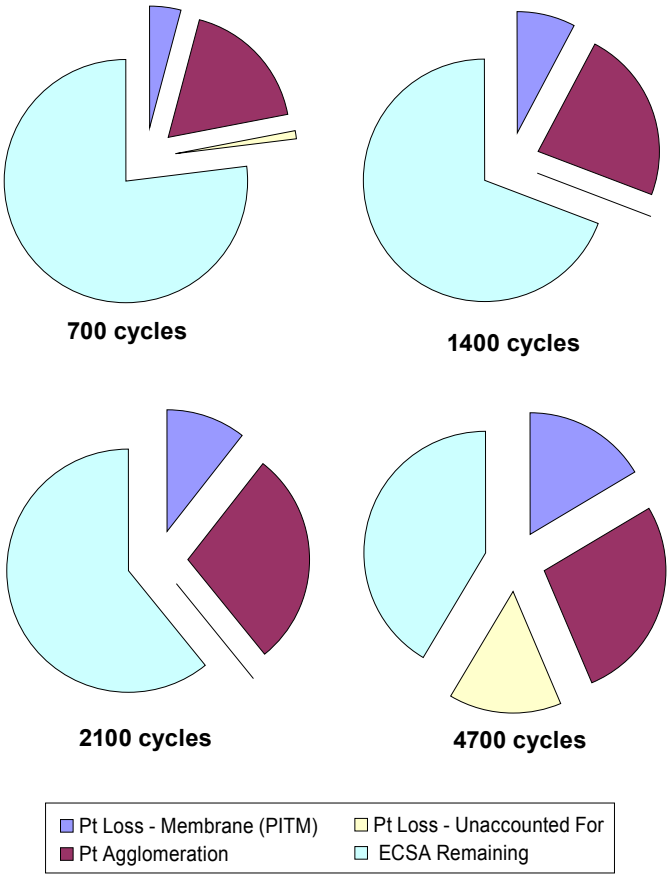


FIGURE 4. Pt loss break-down (Pt agglomeration, Pt in the membrane, and "unaccounted for Pt" at 50, 700, 1,400, 2,100, and 4,700 AST cycles with 1.2 V upper potential.

The impact of AST cycle number on catalyst layer degradation was investigated to quantify changes in degradation mechanisms for the LSAC catalyst with progressive AST cycling. MEAs using the LSAC catalyst were cycled at 1.2 V UPL to different EOT cycle numbers (50, 700, 1,400, 2,100, 4,700 cycles). A significant ECSA loss was observed after only 50 cycles; for <2,100 cycles the kinetic losses were found to dominate (Pt dissolution, agglomeration, Pt in the membrane); while at cycles ≥2,100 the catalyst layer ionic losses became dominant due to the onset of carbon corrosion (catalyst layer thinning). The Pt loss with cycle number with respect to the total initial Pt in the catalyst layer, measured as ECSA, is depicted in the pie chart in Figure 4 as follows: 1) the fraction labeled "ECSA remaining" is still active; 2) the fraction labeled "Pt agglomeration" is ECSA lost due to Pt agglomeration; 3) the fraction labeled "Pt Loss - Membrane (PITM)" is Pt ECSA lost due to dissolved Pt depositing in the membrane; 4) the fraction of initial ECSA lost that can't be accounted for by Pt agglomeration or the Pt found in the membrane is labeled "Pt loss - Unaccounted For" and is presumed to be due to support corrosion and Pt particle detachment from the support.

Conclusions

The interim conclusions are:

- The 1D MEA Model, with 2-phase flow, has been validated within the 95% variability of the experimental data for the entire current density range (up to 1.5 A/cm^2). Additionally, the model has been validated across a range of catalyst compositions and operational conditions.
- The catalyst layer ionomer content affects the catalyst layer structure (porosity). Optimal performance and lowest degradation rate were observed for 30% ionomer content (LSAC catalyst).
- The Pt catalyst carbon support surface area is not the only measure of susceptibility to catalyst support corrosion; the catalyst layer structure and carbon functionality play an important role. The graphitic content of the carbon surface correlates linearly with degradation.
- BOT performance does not show a clear trend with carbon support surface area except for kinetic losses which decrease with increasing surface area. However, catalyst degradation increases with increasing carbon surface area, i.e. higher Pt dissolution (ECSA loss, Pt agglomeration, and Pt in the membrane) and higher corrosion (ionic resistance loss, catalyst layer thickness loss).

Future Directions

- Investigate catalyst degradation rates (Pt dissolution and carbon corrosion) as a function of the Pt/carbon ratio, cathode catalyst loading, and ionomer equivalent weight.
- Correlate degradation with catalyst material properties.
- Model Pt dissolution on the molecular scale.
- Refine two-phase flow implementation and validation for both the micro-structural catalyst and 1D-MEA model (linkage of the two scales).
- Expand the micro catalyst layer and 1D MEA models to transient operation and develop/include degradation mechanisms.
- Integrate electrical contact resistance model with the 1D MEA model.

FY 2011 Publications/Presentations

1. A. Patel, K. Artyushkova, P. Atanassov, A. Young, M. Dutta, Z. Ahmad, V. Colbow, S. Wessel, S. Ye, "Structural and Morphological Properties of Carbon Supports: Effect on Catalyst Degradation", ECS Transactions Volume 33 #1 (2010) Catalysts-Durability.

2. D. Harvey, A. Bellemare-Davis, J.G. Pharoah, K. Karan: Development of a validated statistical Beginning of Life (BOL) Performance Model, Hydrogen and Fuel Cells 2011 Conference, Vancouver, B.C., 15–18 May 2011.

3. D. Harvey, J.G. Pharoah: Development of a full thickness micro structural catalyst model for estimation of effective properties and performance, Hydrogen and Fuel Cells 2011 Conference, Vancouver, B.C., 15–18 May 2011.

4. A. Patel, K. Artyushkova, P. Atanassov, D. Harvey, M. Dutta, V. Colbow, and S. Wessel, "Effect of Graphitic Content on Carbon Supported Catalyst Performance", accepted abstract, 220th ECS Meeting & Electrochemical Energy Summit in Boston, Massachusetts (October 9–14, 2011).

5. S. Knights, R. Bashyam, P. He, M. Lauritzen, C. Startek, V. Colbow, J. Kolodziej, and S. Wessel, "PEMFC MEA and System Design Considerations", accepted abstract, 220th ECS Meeting & Electrochemical Energy Summit in Boston, Massachusetts (October 9–14, 2011).

6. D.B. Harvey, M. Khakbazbaboli, B. Jayasankar, C.C. Chueh, C.A. Bellemare-Davis, J.G. Pharoah, and K. Karan, "Multi-scale Modelling of the PEMFC Catalyst Layer: Coupling Microstructure to Performance", accepted abstract, 220th ECS Meeting & Electrochemical Energy Summit in Boston, Massachusetts (October 9–14, 2011).

References

1. Hydrogen, Fuel Cells & Infrastructure Technologies Program: Multi-Year Research, Development and Demonstration Plan, U.S. Department of Energy, Energy Efficiency and Renewable Energy, October 2007 revision.

2. J. Wu, X.Z. Yuan, J.J. Martin, H. Wang, J. Zhang, J. Shen, S. Wu, W. Merida, A Review of PEM Fuel Cell Durability: Degradation Mechanisms and Mitigation Strategies. Journal of Power Sources 184, 104-119.

3. R. Borup, J.P. Meyers, B. Pivovar, Y.S. Kim, R. Mukundan, N. Garland, D. Myers, M. Wilson, F. Garzon, D. Wood, P. Zelenay, K. More, K. Stroh, T. Zawodinski, J. Boncella, J.E. McGarth, M. Inaba, K. Miyatake, M. Hori, K. Ota, Z. Ogumi, S. Miyata, A. Nishikata, Z. Siroma, Y. Uchimoto, K. Yasuda, K. Kimijima, N. Iwashita, Scientific Aspects of Polymer Electrolyte Fuel Cell Durability and Degradation. Chemical Reviews 2007, 107, 3904-3951.

4. Y. Shao, G. Yin, Y. Gao, Understanding and Approaches for the Durability Issues of Pt-Based Catalysts for PEM Fuel Cell. Journal of Power Sources 2007, 171, 558-566.

5. M.S. Wilson, F. Garzon, K.E. Sickafus, S. Gottesfeld, Surface Area Loss of Supported Platinum in Polymer Electrolyte Fuel Cells. Journal of the Electrochemical Society 1993, 140, 2872-2876.

6. P.J. Ferreira, G.J. Ia O', Y. Shao-Horn, D. Morgan, R. Makharia, S. Kocha, H. Gasteiger, Instability of Pt/C Electrocatalysts Membrane Fuel Cells A Mechanistic Investigation. Journal of the Electrochemical Society 2005, 152, A2256-A2271.

7. E.Passalacqua et al., Electrochimica Acta 46 p.799, (2001).

V.E.5 Durability of Low Platinum Fuel Cells Operating at High Power Density

Scott Blanchet (Primary Contact), Olga Polevaya, May Tan
Nuvera Fuel Cells Inc.
Building 1, 129 Concord Rd.
Billerica, MA 01821
Phone: (617) 245-7667
E-mail: blanchet.s@nuvera.com

DOE Managers
HQ: Kathi Epping-Martin
Phone: (202) 586-7425
E-mail: Kathi.epping@ee.doe.gov
GO: Greg Kleen
Phone: (720) 356-1672
E-mail: Greg.Kleen@go.doe.gov

Technical Advisor
Thomas G. Benjamin
Phone: (630) 252-1632
E-mail: Benjamin@anl.gov

Contract Number: DE-EE0000469

Subcontractors:
- Los Alamos National Laboratory, Los Alamos, NM
- Argonne National Laboratory, Argonne, IL

Project Start Date: September 1, 2009
Project End Date: August 31, 2013

Fiscal Year (FY) 2011 Objectives

- The objective of this project is to study and identify strategies to assure durability of fuel cells designed to meet DOE 2015 cost targets.
- Develop a practical understanding of the degradation mechanisms impacting durability of fuel cells with low platinum loading (≤0.2 mg/cm^2) operating at high power density (≥1.0 W/cm^2).
- Develop approaches for improving the durability of low-loaded, high-power stack designs.

Technical Barriers

This project addresses the following technical barriers from the Fuel Cells section (3.4.4) of the Fuel Cell Technologies Program Multi-Year Research, Development and Demonstration Plan:

(A) Durability

(B) Cost

Technical Targets

TABLE 1. Progress towards Meeting Technical Targets for Transportation Fuel Cell Stacks Operating on Direct Hydrogen for the Transportation Applications

Characteristics	Units	2010/2015 Stack Targets	Nuvera 2010 Status
Cost	$/kWe	25/15	~22 estimated[1]
Durability with Cycling	Hours	5,000	9,000 hrs[2] 2,000 hrs in automotive cycle conditions[3]
Performance at Rated Power	mW/cm^2	1,000	1,100[4] and 1,200[5]

[1] Cost assessment of Nuvera's architecture by Directed Technologies Inc. based on their DOE-sponsored DFMA® (Design for Manufacturing and Assembly) model [1] and comparing the results to an updated "Industry" estimate. 0.55 V/cell @2.0 A/cm^2 was obtained at 0.2 mg/cm^2 platinum loading on Orion stack by Nuvera.
[2] Demonstrated under power profile specific-to-fork truck applications in material handling market at total platinum loading of 0.5 mg/cm^2.
[3] Demonstrated in 360-cm^2 stack by Nuvera in simulated combined city and highway driving cycle at platinum loading of 0.50 mg/cm^2.
[4] Demonstrated in 250-cm^2 Orion stack by Nuvera at platinum loading of 0.2 mg/cm^2.
[5] Demonstrated in 50-cm^2 single cell with open flowfield (SCOF) by Nuvera at platinum loading of 0.2 mg/cm^2.

FY 2011 Accomplishments

- Two program milestones were completed on schedule. The first milestone comprised the development of the durability model framework by Argonne National Laboratory (ANL). The second milestone was achieved with Nuvera delivery of SCOF hardware to Los Alamos National Laboratory (LANL) for characterization and testing under accelerated stress test (AST) conditions and new stress testing representing combined power cycle (NST) protocols.
- The material sets selected for the project in standard 0.45 mg/cm^2 (A) and custom 0.2 mg/cm^2 (B) platinum loadings were delivered by W.L.Gore for various 50 cm^2 single cells including quad-serpentine, SCOF and General Motors/Rensselaer Institute of Technology architectures, as well as for 250- and 360-cm^2 cells for short stack testing. The material development scope of the project is completed.
- SCOF hardware was validated at the range of current densities up to 3 A/cm^2 and demonstrated ohmic, diffusion, and pressure drop benefits over the land-channel cells at Gore and LANL. Catalyst-coated membranes A and B were characterized at the beginning of life (BOL) in Nuvera 50-, 250- and 360-cm^2 cells and LANL 50-cm^2 hardware throughout the range of operating conditions.

- The AST campaign in LANL quad-serpentine cell was completed on all selected membrane electrode assemblies (MEAs) and test protocols. The data analysis concluded that the observed cell voltage decays resulted from the increased activation and mass transport overpotentials in the wide range of operating current densities.
- ANL evaluated platinum dissolution in aqueous media using polycrystalline and dispersed platinum on carbon electrodes, completing the ground work for further development of the platinum stability section of the durability model.
- Durability testing in short stacks continued at Nuvera under NST protocols.



Introduction

Understanding and improving the durability of cost-competitive fuel cell stacks is imperative to successful deployment of the technology. Stacks will need to operate well beyond today's state-of-the-art rated power density with very low platinum loading in order to achieve the cost targets set forth by DOE ($15/kW) and ultimately be competitive with incumbent technologies. Little to no study of durability factors has been carried out in this area of design and operation. The industry today is focusing mostly on reduced platinum loading as it heads for the DOE target point of 0.2 mg/cm^2 platinum and 1.0 W/cm^2 power density. As demonstrated through DOE-sponsored cost modeling, this point falls short of the corresponding $15/kW stack cost target for 2015.

Approach

Nuvera proposes an accelerated cost-reduction path focused on substantially increasing power density to address non-platinum group metals material costs as well as platinum. Understanding the largely unstudied factors affecting stack durability under these high power conditions is the focus of the present project. Of specific interest is the impact of combining low platinum loading with high power density operation, as this offers the best chance of achieving long-term cost targets. The team effort is divided into two activities: modeling and experimentation.

Results

During the past year, two project milestones were completed on schedule. Development of the durability model framework by ANL concluded the first milestone. A durability model is being developed specific to the platinum stability of the selected commercially available material set (cathode 580 and 15-micron membrane M815 by W.L. Gore), independent of the cell architecture. Our modeling approach starts from platinum aqueous kinetics, defining rates for platinum dissolution and re-deposition as well as oxide coverage and continues at the electrode level for platinum ion transport. The model will utilize inputs from catalyst cycle ASTs, BOL properties of the studied material set, and prescribed use cycles to output cathode electrochemical surface area (ECSA), particle size distribution, overpotentials and cell voltage as a function of cycle time and the current density. The second milestone was achieved by delivery of SCOF hardware to LANL for characterization in ASTs and NSTs.

Development efforts were focused on further SCOF validation for performance at elevated current densities and for stability, comparing to the same diagnostics of full format area cells in Nuvera short stacks. Polarization curves of MEAs A and B in SCOF in Figure 1 showed repeatable results in multiple cell assemblies, proving control and uniformity of compression over the active area. Low resistivity and pressure drop of the open flow fields resulted into measurable performance benefits over the quad serpentine cell. High power densities above the DOE target of 1 W/cm^2 were demonstrated in both SCOF and open flowfield short stack tests at 2 A/cm^2, proving the diffusion benefits of open flowfield over the land-channel architecture, tested at Gore and LANL. While the performance of MEA B in land-channel cell was limited below 2 A/cm^2 at low pressure conditions, 1.2 W/cm^2 power density was achieved on the same MEA at 2 A/cm^2 in SCOF.

Over the past year the AST campaign in the quad serpentine cell was completed and currently moved to SCOF. ASTs focused on the electrocatalyst stability under the B1 potential cycle protocol and membrane mechanical stability under the B4 humidity cycle protocol defined by the DOE. In addition, the low platinum cell was subjected to the modified potential cycle test with the lower potential

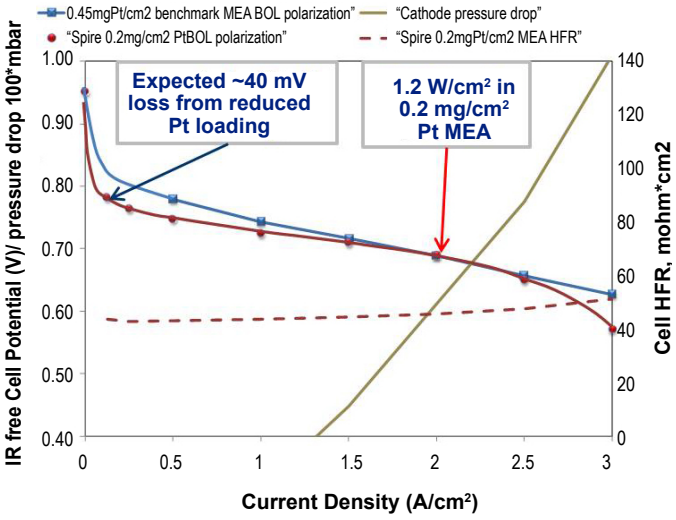


FIGURE 1. Ohmic Resistance-Free Polarization of MEAs A and B in SCOF (Dry cathode, 1.8 bara inlet pressure)

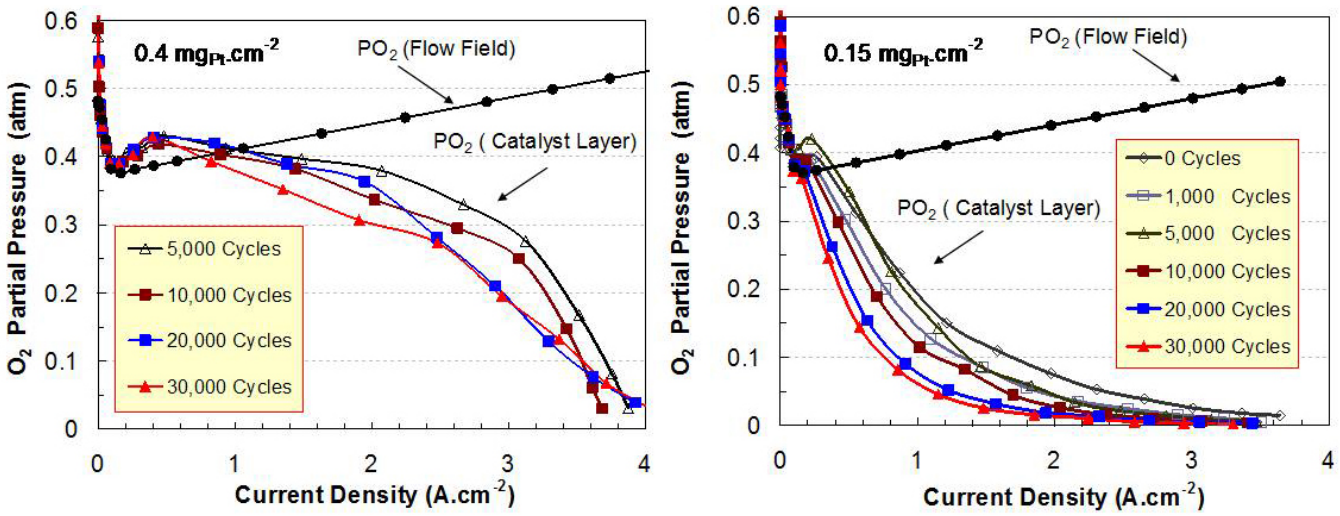


FIGURE 2. Effect of Ageing in B1 AST on the Cathode Oxygen Partial Pressure in MEAs with different Platinum Loading

range of the cycle than in the B1 test. The potentials in the modified cycle protocol correlate with cell voltages achieved in Nuvera large-area cells at 2 A/cm^2, resulting in significant improvement in cathode ECSA stability and less platinum dissolution into the membrane, confirmed by the post-mortem scanning electron microscopy and energy disperse spectroscopy analyses.

AST data, including polarization, ECSA, and impedance diagnostics from all potential cycles obtained in both normal and low-platinum cell tests were analyzed at low and high pressure conditions to determine the effect of ageing on the kinetics of the oxygen reduction reaction (ORR) and on oxygen mass transport. The model based on the electrochemical impedance spectroscopy data at different current densities was set up to distinguish oxygen mass transport coefficients between the cathode catalyst and gas diffusion layers. Observed cell voltage decays were attributed to the increase of activation and mass transport overpotentials in the ASTs and the respective decay of oxygen partial pressure in cathodes in Figure 2.

Durability testing in short stacks continued under the NST3A-2 protocol, representing a combined city and highway driving cycle designed at 2 A/cm^2 rated current density and average cell voltage response shown in Figure 3. In this NST the cathode pressure and flow conditions vary with the current density, following the operating map of the air compressor in the automotive system. Data obtained during 1,000-1,600-hour testing of three stacks were processed using ohmic resistance-corrected, polarization data at low current densities to determine the Tafel slope for the ORR kinetics. Our analysis of ECSA loss from voltage-current (V-I) curves showed consistency with direct measurements by cyclic voltammetry and correlated to the increase of average platinum particle diameter by X-ray diffraction analysis as shown in Figure 4. V-I analysis allowed calculating oxygen partial pressures in the cathodes

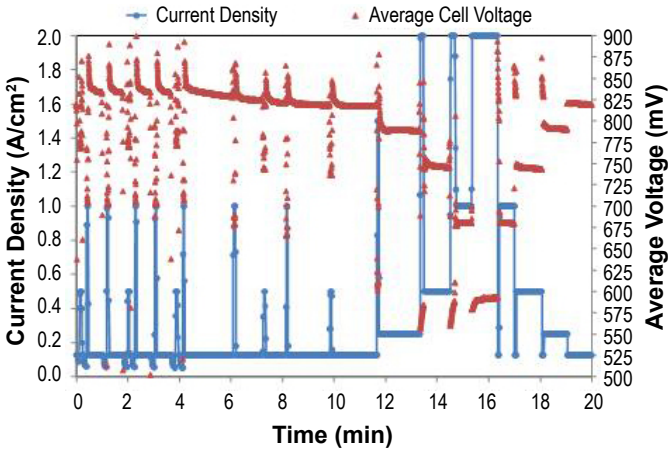


FIGURE 3. Performance of Nuvera Short Stack with MEA A under Simulated Combined City and Highway Drive Load Cycle

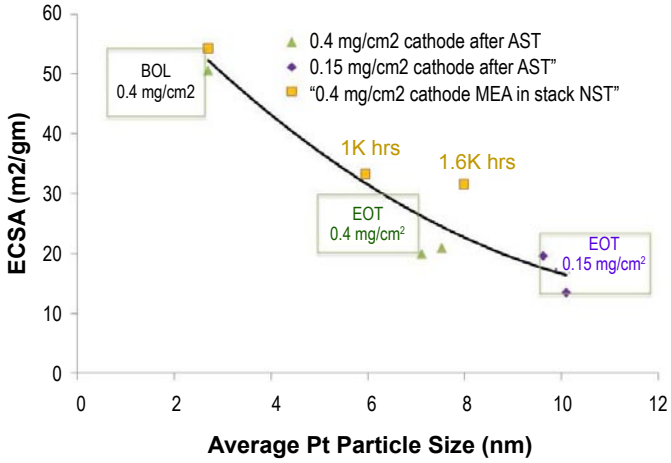


FIGURE 4. Correlation of Cathode ECSA to Average Size of Platinum Particles in ASTs and Stack NSTs

with different loadings at all operating current densities and showed decreasing values from BOL to the end of test.

Conclusions and Future Directions

- Operation at high power densities enabled by the open flowfield architecture and proven at the low platinum loading provided the ground work for accelerated cost-reduction path to the cost targets set by the DOE.
- Two milestones concluded in the reported year served as the basis for experimental and modeling activity started and to be continued in the next year.
- The AST campaign will be moved from serpentine cell to SCOF towards achieving the third project milestone.
- Durability modeling will continue, focused on the platinum stability, and will be synchronized with other durability projects covering different ageing mechanisms with the same partners, extending the current project duration by one year at no cost to the DOE.
- The NST campaign in the large-format cells in short stacks and benchmarking the results between SCOF and large area cells will continue, targeting the Go/No-Go decision.

FY 2011 Publications/Presentations

1. B. Lunt. Advanced single cell test fixture. 6th Annual International Conference on Fuel Cell Durability and Performance 2010, December 5–6, Boston, MA.

2. O. Polevaya, SPIRE Project Review with Freedom Car Technical Team, January 26, 2011, Southfield, MI.

3. S. Arisetty et. al, Effect of platinum loading on catalyst stability under cycling potentials, Abstract accepted to ECS 2011, Boston, MA.

4. F. Gambini et al., Durability of fuel cell under high power density operation, Abstract accepted to ECS 2011, Boston, MA.

5. O. Polevaya, Spire, 2011 DOE Annual Merit Review, Washington, DC, May 11, 2011.

References

1. B. James et al, Mass Production Cost Estimation for Direct H_2 PEM Fuel Cell Systems for Automotive Applications, March 26, 2009.

V.E.6 Improved Accelerated Stress Tests Based on Fuel Cell Vehicle Data

Timothy Patterson (Primary Contact),
V. Srinivasamurthi, W. Bi
UTC Power Corp.
195 Governor's Highway
South Windsor, CT 06074
Phone: (860) 727-2274
E-mail: timothy.patterson@utcpower.com

DOE Managers
HQ: Kathi Epping Martin
Phone: (202) 586-7425
E-mail: Kathi.Epping@ee.doe.gov
GO: David Peterson
Phone: (720) 356-1747
E-mail: David.Peterson@go.doe.gov

Contract Number: DE-EE0000468

Subcontractors:
- United Technologies Research Center, East Hartford, CT
- Los Alamos National Laboratory, Los Alamos, NM
- Oak Ridge National Laboratory, Oak Ridge, TN

Project Start Date: December 1, 2009
Project End Date: November 30, 2011

Fiscal Year (FY) 2011 Objectives

- Correlate real-world operating conditions to cell degradation.
- Correlate existing DOE accelerated stress tests (ASTs) to degradation.
- Assess degradation modes between real-world operating conditions and existing DOE ASTs.
- Recommend modified ASTs that more accurately gauge in situ component behavior.
- Identify life-limiting mechanisms not addressed by current DOE ASTs and recommend new ASTs.

Technical Barriers

- > 5,000 hours stack durability (including cycling and all materials, e.g. membrane, seals).
- < 10% overall performance decay (including start/stop and transient operation).
- Current DOE ASTs not calibrated with real-world degradation.

FY 2011 Accomplishments

- Fleet performance and operating cycle analyses complete.
- Correlation of platinum decay in real-world operation and lab AST complete.
- Lab ASTs for platinum degradation complete.
- Lab ASTs for carbon support corrosion complete.
- Lab ASTs for membrane mechanical degradation complete.
- Lab ASTs for membrane chemical degradation complete.
- Accelerated life test (ALT) complete.



Approach

UTC will lead a top-tier team of industry and national laboratory participants to update and improve DOE's ASTs for hydrogen fuel cells. This in-depth investigation will focus on critical fuel cell components (e.g. membrane electrode assemblies [MEAs]) whose durability represents barriers for widespread commercialization of hydrogen fuel cell technology. UTC has access to MEA materials that have accrued significant load time under real-world conditions in PureMotion® 120 power plants used in transit buses. These materials are referred to as end-of-life (EOL) components in the rest of this document. Advanced characterization techniques are used to evaluate degradation mode progress using these critical cell components extracted from both bus power plants and corresponding materials tested using the DOE ASTs. These techniques will also be applied to samples at beginning of life (BOL) to serve as a baseline. These comparisons will advise the progress of the various failure modes that these critical components are subjected to, such as membrane degradation, catalyst support corrosion, platinum group metal dissolution, and others. Gaps in the existing ASTs to predict the degradation observed in the field in terms of these modes will be outlined. Using these gaps, new ASTs will be recommended and tested to better reflect the degradation modes seen in field operation. Also, BOL components will be degraded in a test vehicle at UTC designed to accelerate the bus field operation.

Results

Task 1 - Fleet Data Analysis

Fleet data analysis has been completed and has been reported previously.

Task 2 - Lab-World Degradation

UTC has facilitated the development of a test vehicle for accelerated evaluation of stack components under

this project. The main motivation for this exercise results from the relatively slow rate of load-hour accrual for buses in the field. Because UTC Power is currently targeting >18,000 hours stack durability for bus fleet applications, a more rapid test vehicle is necessary to increase product maturity on new stack configurations. The test vehicle for accelerated stack component evaluation is termed the ALT. This small power plant has the identical piping and instrumentation configuration as the bus power plant, but operates on a 5-kW short stack. The key operating modes of the bus that have been linked to stack component degradation have been reflected in the protocol. The implementation of the ALT vehicle has been complete. Testing of the unit has been completed. The results are described in the following paragraphs.

Figure 1 shows the UTC bus fleet durability data. The 2006 fleet leader failed after 1,000 hours due to carbon corrosion of the cathode gas diffusion layer (GDL). A carbon corrosion AST was developed to evaluate resistance of cathode GDLs to oxidizing conditions. The protocol for this AST is summarized in Table 1. The acceleration factor for the GDL corrosion based on this test was approximately 10X of the fleet data. Using the AST for carbon corrosion, a new cathode GDL was implemented into the 2008 fleet leader. As shown in Figure 2, the new GDL showed at least a 5X improvement in durability over the 2006 fleet leader GDL at 0.55 V. This enabled the fleet durability to increase from 1,000-1,500 hours to 2,800 hours, at which point the 2008 fleet leader failed due to membrane failure. The failure was caused by mechanical fatigue due to hydration strain cycling at the air inlet. A membrane AST protocol, shown in Table 2, was developed to evaluate membrane resistance to hydration strain cycling. Scanning electron microscope images, shown in Figure 3, of the MEA returned from the field and the MEA tested using the lab AST protocol show that the failure mode was consistent. Figure 4 shows the open circuit voltage (OCV) pressure response with time as a function of temperature, load profile, and membrane type. The MEA in the 2011 fleet leader shows a >16X improvement in lifetime over the 2008 fleet leader MEA in the membrane AST protocol. As shown in

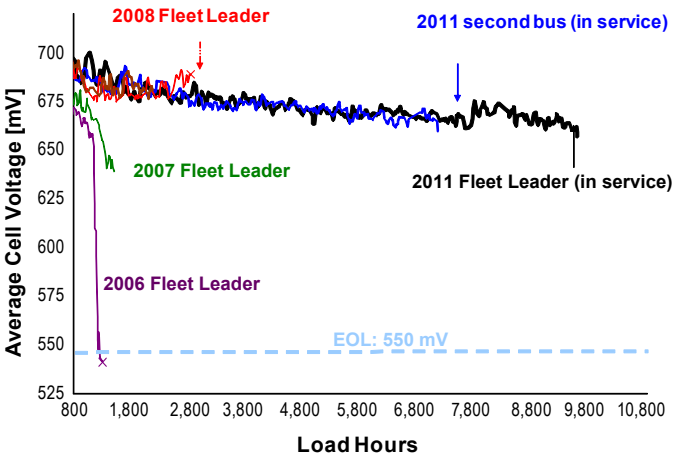


FIGURE 1. UTC Fleet Durability Data

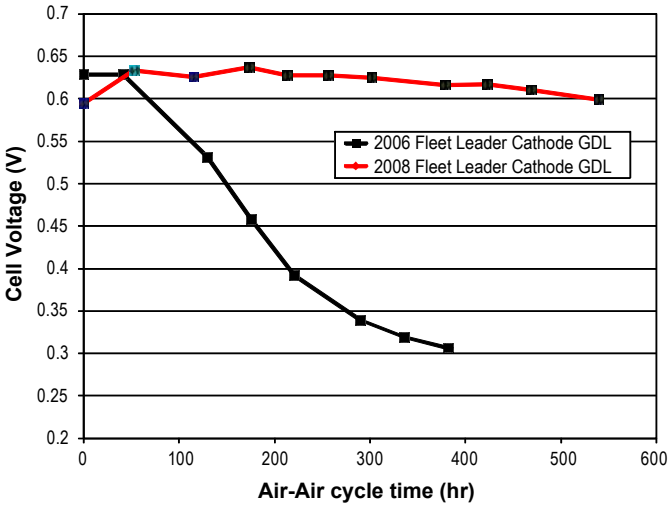


FIGURE 2. Effect of Cathode GDL on Performance Decay in Carbon Corrosion AST

TABLE 1. AST Protocol for Air-Air Cycling Test

Coolant inlet temperature (°C)	**65°C**		
Percent Relative Humidity	**100**		
Cell Current	**0 Amps**		
Reactant flow cycle	**Time**	**Anode Reactant**	**Cathode Reactant**
	5 minutes	H_2	H_2
	5 minutes	N_2	N_2
	1 hour	Air	Air
	5 minutes	N_2	N_2
Applied external resistance	<0.2 mOhm (to avoid potential difference between anode and cathode)		

TABLE 2. AST Protocol for High Temperature Flow/Load Cycling Test

Coolant inlet temperature (°C)	80°C	
Percent Relative Humidity	100	
Anode reactants	Hydrogen, 80% utilization (SR = 1.25)	
Cathode reactants	Air, 60% utilization (SR = 1.66)	
Load cycle	**Time**	**Current density**
	20 sec	10
	15 sec	800 or 1,500 mA/cm^2
OCV Pressure Response	Measure cell voltage difference at open circuit when the anode to cathode cross-pressure is changed from 0 kPa to 15 kPa	

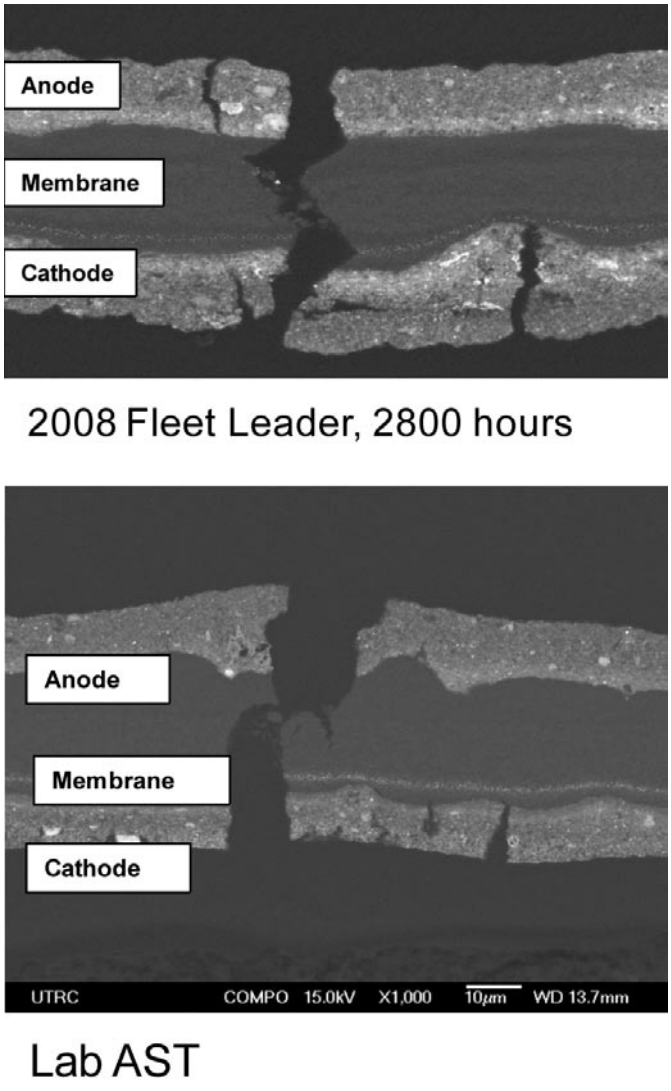


FIGURE 3. Comparison of Microscopy Results for MEAs Run in the Field and in Lab ASTs

Figure 1, implementation of this MEA in the field resulted in an increase in field durability from 2,800 hours to over 9,600 hours, or 3.4 times higher. Based on the acceleration factor measured in the lab AST, the MEA in the 2011 fleet leader is projected to last over 40,000 hours, if mechanical fatigue is still the controlling failure mode.

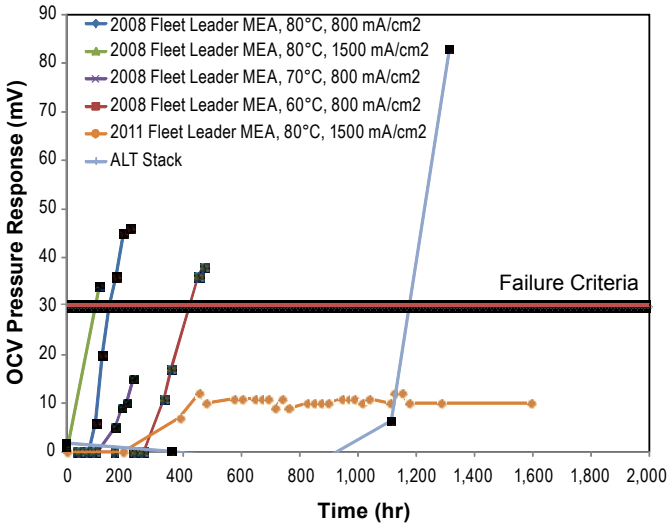


FIGURE 4. Summary of Open Circuit Voltage (OCV) Pressure Response for Single-Cell And Short Stack Membrane AST

The effect of temperature and current density was also investigated. As shown in Figure 4, increasing the temperature from 60°C to 80°C decreased the lifetime by a factor of 4. Increasing the current density from 800 to 1,500 mA/cm^2 decreased the lifetime by about 20%. The ALT rig ran at 70°C, with a load cycling profile that mimics the fleet cycle. The ALT failed at 1,400 hours whereas the single cell, running at the same temperature, failed at 250 hours. The ALT cycle is much faster than the single-cell AST protocol. The membrane stress is lower in the ALT cycle because the rapid cycling does not allow the membrane water content to reach equilibrium. This is also apparent between the single cell run at 60ºC and the field unit, which also runs at 60ºC. The field unit lasted 2,800 hours, or seven times longer than the single cell, which only lasted 400 hours. These results indicate that the load cycle profile is as important to membrane durability, if not more, as the operating temperature. Table 3 summarizes the membrane AST results and membrane lifetime predictions.

TABLE 3. Summary of Membrane AST Data and Membrane Life Predictions

Membrane	Cyclic Protocol	Temperature	Estimated Time to Failure (hr)	Actual Time to Failure (hr)
2008 Fleet leader	Membrane AST	60°C	Not Applicable	425
2008 Fleet leader	Membrane AST	70°C	Not Applicable	~250
2008 Fleet leader	Membrane AST	80°C	Not Applicable	120
2011 Fleet leader	Membrane AST	80°C	Not Applicable	>1,600
2008 Fleet leader	Field (ALT)	70°C	Not Applicable	1,400
2008 Fleet leader	Field	60°C	2,975	2,800
2011 Fleet leader	Field	60°C	45,000	>9,500 (still running)

Conclusions and Future Directions

- Fleet/Real-World: UTC fleet performance and operating cycle analyses have been completed and reported. Teardown analyses of the real-world degraded components have been completed and reported.
- Lab-World: ASTs for platinum group metal decay, carbon support corrosion, membrane mechanical decay, and membrane chemical decay have been completed. Teardown analyses of the lab-world degraded components have been completed and reported.
- ALT: Testing has been completed.
- Next Step: Correlate real-world degradation to lab tested degradation for carbon corrosion of GDLs. Develop ex situ aging method for GDLs to isolate GDL oxidation effects from catalyst layer oxidation effects.

FY 2011 Publications/Presentations

1. "Improved AST's based on FCV data" presentation to Freedom CAR & Fuel Partnership, Fuel Cell Tech Team Review January 13, 2010.

2. "Improved AST's based on FCV data" presentation to DOE Annual Merit Review meeting June 8, 2010.

3. "Improved AST's based on FCV data" presentation to DOE Annual Merit Review meeting May 12, 2011.

4. "GDL Degradation in PEFC", ECS Transactions - Las Vegas, NV Volume 33, Polymer Electrolyte Fuel Cells 10, from the Las Vegas, NV meeting, October 30, 2010.

5. "Use of Mechanical Tests to Predict PEMFC Membrane Durability under Humidity Cycling", Journal of Power Sources, 196 (2011) 3851–3854.

V.E.7 Accelerated Testing Validation

Rangachary Mukundan[1] (Primary Contact), Rod Borup[1], John Davey[1], Roger Lujan[1], Dennis Torraco[1], David Langlois[1], Fernando Garzon[1], W. Yoon[2], Adam Weber[2], Mike Brady[3], Greg James[4], and Steve Grot[5]

[1]Los Alamos National Laboratory
MS D429, P.O. Box 1663
Los Alamos, NM 87545
Phone: (505) 665-8523
E-mail: Mukundan@lanl.gov

DOE Manager
HQ: Nancy Garland
Phone: (202) 586-5673
E-mail: Nancy.Garland@ee.doe.gov

Subcontractors:
[2] Lawrence Berkeley National Laboratory (LBNL), Berkeley, CA
[3] Oak Ridge National Laboratory (ORNL), Oak Ridge, TN
[4] Ballard Power Systems, Burnaby, BC, Canada
[5] Ion Power, New Castle, DE

Project Start Date: October 2009
Project End Date: 2013

Fiscal Year (FY) 2011 Objectives

- Correlation of the component lifetimes measured in an accelerated stress test (AST) to "real-world" behavior of that component.
- Validation of existing component-specific ASTs for electrocatalysts, catalyst supports and membranes (mechanical and chemical degradation).
- Development of new ASTs for gas diffusion layers (GDLs) and bipolar plates.
- Coordinate effort with Fuel Cell Tech Team, Durability Working Group and US Fuel Cell Council (USFCC) Taskforce on Durability.

Technical Barriers

This project addresses the following technical barriers from the Fuel Cells section (3.4) of the Fuel Cell Technologies Program Multi-Year Research, Development and Demonstration Plan:

(A) Durability

(B) Cost

Technical Targets

Cost and durability are the major challenges to fuel cell commercialization. ASTs enable the rapid screening of fuel cell materials and are critical in meeting the long life times required for stationary and automotive environments. Moreover these ASTs can also help predict the lifetime of the various components in "real-world" applications.

Transportation Durability: 5,000 hours (with cycling)

- Estimated start/stop cycles: 17,000
- Estimated frozen cycles: 1,650
- Estimated load cycles: 1,200,000

Stationary Durability: 40,000 hours

- Survivability: Stationary -35°C to 40°C

Cost ($25/kWe)

FY 2011 Accomplishments

- Performed all four DOE Fuel Cell Tech Team recommended ASTs on two different Ballard membrane electrode assemblies (MEAs) that were used in bus stacks.
- Failure analysis of MEAs and correlation between AST and real world data initiated.
- Initial breakdown analysis of two different types of bus stacks completed by Ballard.
- Modeling of voltage loss breakdown completed by LBNL.
- LANL validates the performance of Ion Power MEAs using different Tanaka catalysts and DuPont XL membranes.



Introduction

The durability of polymer electrolyte membrane (PEM) fuel cells is a major barrier to the commercialization of these systems for stationary and transportation power applications [1]. Commercial viability depends on improving the durability of fuel cell components to increase the system reliability and to reduce system lifetime costs by reducing the stack replacement frequency. The need for ASTs can be quickly understood given the target lives for fuel cell systems: 5,000 hours (~7 months) for automotive, and 40,000 hours (~4.6 years) for stationary systems. Thus testing methods that enable more rapid screening of individual components to determine their durability characteristics, such as off-line environmental testing, are needed for evaluating new

component durability in a reasonable turn-around time. This allows proposed improvements in a component to be evaluated rapidly and independently, subsequently allowing rapid advancement in PEM fuel cell durability. These tests are also crucial to developers in order to make sure that they do not sacrifice durability while making improvements in costs (e.g. lower platinum group metal [PGM] loading) and performance (e.g. thinner membrane or a GDL with better water management properties).

DOE has suggested AST protocols for use in evaluating materials, but only for the catalyst layer (electrocatalyst and support), and for the membrane [2,3]. The USFCC has also suggested AST protocols for the same materials [4]. While these protocols have concentrated on the catalyst, catalyst support and membrane materials, to date, no accelerated degradation protocols have been suggested for GDL materials or microporous layers (MPLs), bipolar plates or seals. In spite of recent advances in AST development, a main portion, which is deficient, is the quantitative correlation between the results of a given fuel cell AST, and the degradation rate or life in an operating fuel cell.

Approach

A main desired outcome of this task is the correlation of the component lifetimes measured in an AST to in situ behavior of that component in "real-world" situations. This requires testing of components via ASTs and in operating fuel cells, and delineating the various component contributions to the overall cell degradation. This will primarily be performed by using a simplified one-dimensional model that takes into account the different component contributions like membrane ionic conductivity, cathode catalyst layer kinetic losses and mass transport losses (catalyst layer and GDL) to the overall losses observed in operating cells [5]. This project will then attempt to correlate the performance losses observed due to a particular component in "real-world" situations with the degradation in AST metrics of that component. The correlation between AST and life data, if state-of-the-art materials are used, in essence gives one data point. Thus, for a reasonable correlation to be made, materials with different life spans will be utilized. This relies on the expertise of the suppliers as partners in the proposal. This work is also being coordinated with other funded projects examining durability through a DOE Durability Working Group, and through a USFCC task force on durability.

Results

The DOE Fuel Cell Technical Team recommended ASTs [6] were performed on two different MEA types (viz. P5 and HD6); that were used in buses operated in Hamburg (Germany), and in a bus module operated in the laboratory on an Orange Country Transit Authority cycle, respectively. The results from the potential cycling and high potential hold ASTs are illustrated in Figure 1a and b, respectively.

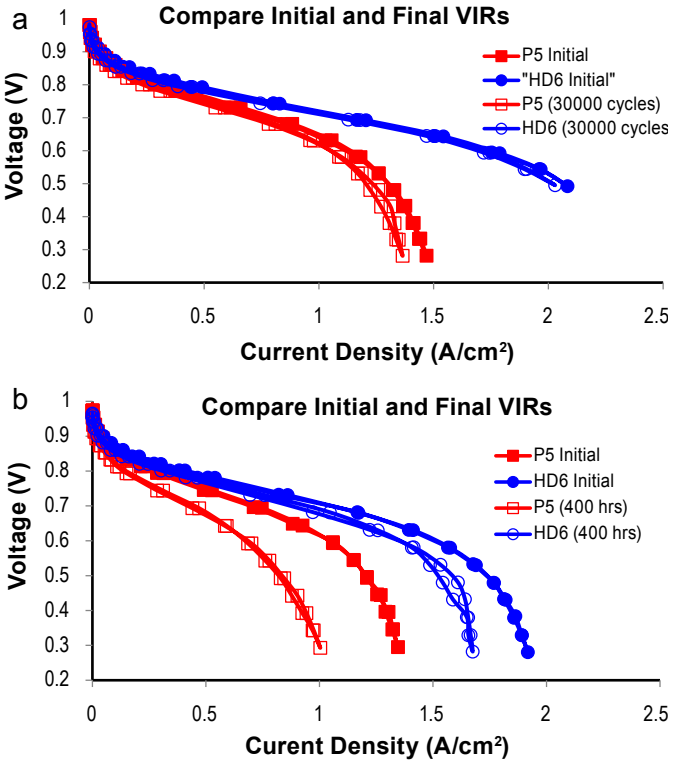


FIGURE 1. Performance of P5 and HD6 MEAs: a) before and after potential cycling and b) before and after high potential hold.

It is seen that the performance of the HD6 (circa 2007) MEA is significantly better than the performance of the P5 (circa 2002) MEA, especially in the mass transport region. Both these MEAs showed excellent durability of the Pt electrocatalyst as illustrated in Figure 1a by little performance loss after 30,000 potential cycles from 0.6 V to 1 V. Both MEAs met all performance targets including electrochemical surface area (ECSA) (<40% loss), mass activity (<40% loss) and voltage loss @ 0.8 A/cm^2 (<30 mV loss). On the other hand, the high potential hold AST resulted in significant degradation due to carbon corrosion especially in the P5 MEA (Figure 1b). While the P5 MEA failed to meet any of the DOE targets, the HD6 MEA met both the ECSA (<40 % loss) and mass activity (<60% loss) targets, but failed to meet the voltage loss (@ 1.5 A/cm^2) target (30 mV loss occurs at 175 hours while the target is 400 hours). This illustrates the fact that carbon corrosion leads to significant mass transport losses in addition to kinetic losses, and the voltage loss target is more relevant than the ECSA and mass activity targets for this particular AST.

The voltage loss breakdown in these cells as a function of ageing time was extracted by using a simple one-dimensional model to fit the polarization curves and impedance response of the single cells. This is illustrated in Figures 2a and b, for the potential cycling AST and high potential hold AST, respectively. During the potential cycling AST (Figure 2a) there is a small (<15 mV) increase in the voltage loss in the kinetic region while the

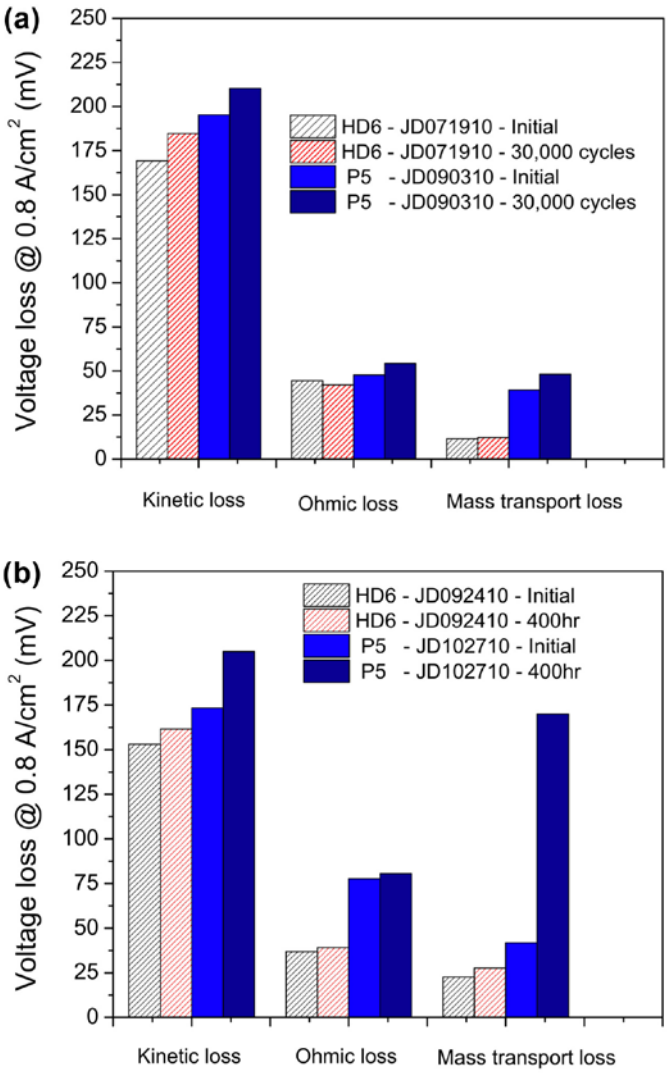


FIGURE 2. Voltage loss breakdown of the P5 and HD6 cells at 0.8 A/cm^2 obtained using a one-dimensional model: a) before and after potential cycling and b) before and after high potential hold.

ohmic and mass transport contributions remain virtually unchanged. This is consistent with the approx. 30% loss in ECSA observed for the two cells. During the 400 hours of high potential hold AST (Figure 2b) there is a much greater increase in both the kinetic (>25 mV loss) and mass transport losses (>125 mV loss) of the P5 cell when compared to the HD6 cell (<20 mV) at a constant current density of 0.8 A/cm^2. This is consistent with the more corrosion-resistant carbon used in the HD6 MEA. Failure analysis of these MEAs has been initiated and the Pt particle sizes and catalyst layer thicknesses will be measured and used to validate these ASTs with real world data from the bus fleets.

The performance of three P5 bus stacks operated in Hamburg (Germany) is illustrated in Figure 3a where all three stacks show a degradation rate of ≈30 μV/cell/hour. This is despite the fact that these stacks were exposed to

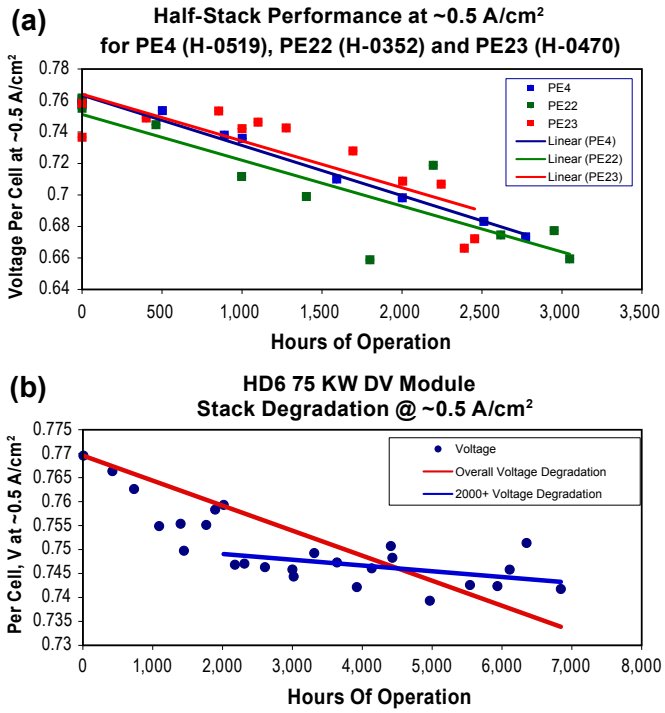


FIGURE 3. Voltage degradation observed in a) three P5 bus stacks operated in the field and b) one HD6 module operated under the Orange Country Transit Authority drive cycle.

different stressors including temperature, relative humidity, voltages and air/air starts. The only tangible difference in the stressors was the lower number of air/air starts (263) in the PE23 stack which was associated with the lowest voltage degradation rate of 26.3 μV/cell/hour. The HD6 stack was operated in a laboratory under drive cycle conditions and showed an average degradation rate of 5.2 μV/cell/hour (Figure 3b). The data quality from this stack is better than the field data and clearly shows two different degradation rates with the 2,000 to 7,000 hour data showing only a degradation rate of 1.2 μV/cell/hour. The failure analysis from these stacks will be utilized to compare the field data with the AST data.

The open circuit voltage and fluorine emission rate in the effluent water during the membrane chemical degradation AST [6] test of the P5 and HD6 MEAs is shown in Figure 4a. Although the P5 MEA was 50 μm thick while the HD6 MEA was only 25 μm thick, the OCV of the P5 MEA degraded slightly faster than that of the HD6 MEA. It is also seen that the P5 MEA has a much larger fluorine emission rate than the HD6 cell, which is consistent with its worse performance in the field. This is illustrated in Figure 4b where the three P5 stacks all failed due to transfer leaks in <3,400 hours while the HD6 showed an increase in transfer leak rates only after 5,500 hours. The results of the AST test and field data will be modeling in the future and will be validated with the failure analysis from both the AST and bus stack MEAs.

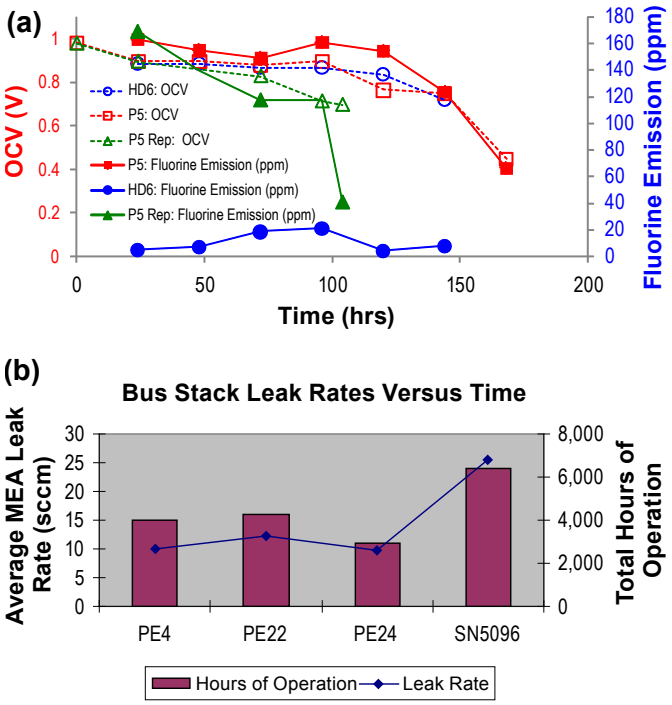


FIGURE 4. a) Fluorine content of the outlet water during an OCV AST test and b) transfer leak rates observed in P5 and HD6 stacks operated in buses.

Conclusions and Future Directions

The results from the P5 and HD6 AST tests are consistent with their performance observed in the field. While the potential cycling AST and relative humidity cycling ASTs showed little difference between the P5 and HD6 samples, the high potential and OCV hold ASTs highlighted the better performance of the HD6 MEAs. This will be correlated with the better performance in the field; both lower voltage degradation rates and delayed membrane transfer leaks. The field data is noisy due to recoverable performance losses and highly varying current demand imposed by the bus drive cycle. Moreover the effect of various stressors including temperature, voltage, relative humidity and air/air cycling complicates interpretation of field data. Failure analysis and voltage loss modeling work have been initiated and are expected to help correlate the AST data with the field data. The following specific work will be carried out in the coming years of this project in order to validate existing ASTs and recommend new ASTs.

AST Testing

- Perform ASTs on materials with differing durability supplied by Ion Power.
- Develop ASTs for ORNL-supplied bipolar plate materials and SGL-supplied GDLs/MPLs.

"Real-World" Testing

- Perform simulated automotive drive cycle testing on selected materials with differing durability.
- Study effect of operating conditions (Stressors) like temperature, pressure and relative humidity on drive cycle testing.

Characterization of Materials

- Ex situ characterization of catalyst particle size distribution, layer thickness, membrane thickness, and GDL hydrophobicity as a function of AST and "real-world" testing.

Correlation of AST to "Real-world" Data

- Statistical correlation of performance degradation with physical properties in both AST and "real-world" data.

FY 2011 Publications/Presentations

1. R.L. Borup and R. Mukundan, PEM Fuel Cell Degradation, ECS Trans. 33 (1), 17 (2010).

2. J.D. Fairweather, B. Li, R. Mukundan, J. Fenton, and R.L. Borup *In Situ* and *Ex Situ* Characterization of Carbon Corrosion in PEMFCs, ECS Trans. 33 (1), 433 (2010).

3. R. Mukundan, G. James, J. Davey, D. Langlois, D. Torraco, W. Yoon, A. Weber, and R. Borup, Accelerated Testing Validation, Abstract accepted, 220th ECS meeting, Boston, MA.

References

1. R. Borup, J. Meyers, B. Pivovar, et al., *Chemical Reviews*; **107(10)**, 3904 (2007).

2. T.G. Benjamin, Abstracts of the International Workshop On Degradation Issues in Fuel Cells, Hersonessos, Crete, Greece, (2007).

3. N.L. Garland, T.G. Benjamin, J.P. Kopasz, *ECS Trans.*, **V. 11 No. 1**, 923 (2007).

4. S. Knight, G. Escobedo, *Meeting Abstracts of 2006 Fuel Cell Seminar*, Honolulu, HI (2006).

5. A.Z. Weber, J. Newman, "Modeling Transport in Polymer-Electrolyte Fuel cells" *Chemical Reviews*, **V. 104**, 4679-4726 (2004).

6. DOE Cell Component AST Protocols for PEM Fuel Cells (Electrocatalysts, Supports, Membranes and MEAs), Revised October 15, 2008.

V.F.1 Water Transport in PEM Fuel Cells: Advanced Modeling, Material Selection, Testing, and Design Optimization

J. Vernon Cole
CFD Research Corporation (CFDRC)
215 Wynn Drive, 5th Fl.
Huntsville, AL 35805
Phone: (256) 726-4852
E-mail: jvc@cfdrc.com

DOE Managers
HQ: Donna Ho
Phone: (202) 586-8000
E-mail: Donna.Ho@ee.doe.gov
GO: David Peterson
Phone: (720) 356-1747
E-mail: David.Peterson@go.doe.gov

Technical Advisor
Walt Podolski
Phone: (630) 252-7558
E-mail: podolski@anl.gov

Contract Number: DE-FG36-07GO17010

Subcontractors:
- Ballard Power Systems, Burnaby, BC, Canada
- BCS Fuel Cells, Bryan, TX
- ESI US R&D, Huntsville, AL
- Techverse, Cary, NC
- SGL Carbon, Meitingen, Germany
- University of Victoria, Victoria, BC, Canada

Project Start Date: June 1, 2007
Project End Date: November 30, 2011

Fiscal Year (FY) 2011 Objectives

- Develop advanced physical models for water transport and generation, and conduct material and cell characterization experiments.
- Improve understanding of the effect of various cell component properties and structure on the gas and water transport in a proton exchange membrane (PEM) fuel cell.
- Encapsulate the developed models in a modeling and analysis tool for cell design and future application.
- Demonstrate improvements in water management in cells and short stacks.

Technical Barriers

This project addresses the following technical barriers from the Fuel Cells section of the Fuel Cell Technologies Program Multi-Year Research, Development and Demonstration Plan:

(A) Durability
(D) Water Transport within Stack
(E) System Thermal and Water Management
(G) Start-up and Shut-down Time and Energy/Transient Operation

Technical Targets

This project addresses fundamental issues in water transport within the fuel cell stack. The resulting understanding will be applied toward the design of stack components and operating strategies that enable meeting the 2015 targets for transportation fuel cell stacks operating on direct hydrogen:

- Stack power density: 2,000 W/L
- Cold start-up time to 50% rated power @ 20°C: 5 secs
- Unassisted start from low temperature: -40°C

FY 2011 Accomplishments

- Predicted design and operating condition sensitivity observed in experimental measurements of wet pressure drop for two-phase flows in channels and gas diffusion layers (GDLs). Applied models to screen channel and cell design for effective water management.
- Integrated membrane water transport models with the computational fluid dynamics (CFD) two-phase cell scale models. Demonstrated improved agreement with measured current density profiles and qualitative agreement with trends in measured liquid water distribution.
- Developed a technique for reproducible, controllable hydrophobic treatment of GDL media that results in less water retention and fewer transport limitations than the treatments applied to commercially available materials.



Introduction

Water management in PEM fuel cells is challenging because of the inherent conflicts between: supplying adequate water to establish and maintain the membrane electrical conductivity, removing the water produced by the electrochemical reactions at the cathode, and uniformly distributing the gaseous reactants at catalyst surfaces near the membrane to effectively utilize these

costly catalysts. As power density of the cells increases, more water will be generated within the same cell volume. Therefore, increasing power density requirements will drive a greater need for design tools incorporating an improved understanding of how liquid water is transported within fuel cells. An additional barrier to widespread use of fuel cells for automotive power is the performance degradation caused when liquid water freezes within the cells. Optimizing water management to influence where the liquid water remains at shutdown is a promising path to improving cold starting capabilities and freeze-thaw reliability.

This project is intended to improve fundamental understanding of water transport within a PEM fuel cell, and capture that knowledge in design tools capable of assisting the industry to meet targets for increased power densities and improved cold-start performance. To achieve these objectives, the project is focused on developing predictive models for water transport in GDL materials, characterizing materials for model inputs and verification, implementing the resulting understanding in engineering design tools, and validating the resulting design tools against fuel cell performance data and in situ diagnostics of water distribution within operating fuel cells.

Approach

To meet the high level objectives of improving the fundamental understanding of water transport in PEMFCs and demonstrating improved performance, the team will integrate experimental characterization with model development and application. The initial focus of the experimental characterization was on measuring relevant physical and transport properties of the GDL materials typically placed between the catalyst and reactant flow channels. Diagnostic and characterization studies have transitioned to water and two-phase (water and air) fluid transport properties of GDL materials and analysis of water transport across material interfaces and in fuel cell channels. The related modeling studies follow a similar progression, with initial emphasis on microscale simulations of single fluid and two-phase transport within GDL materials. The simulations allow us to analyze key effects such as the impact of the microstructure and surface treatment of the solids within porous GDL materials on the two-phase water and gas transport. The knowledge gained from the materials characterization and microscale simulations is being used to develop models suitable for incorporation into an engineering design tool for fuel cell scale analysis of reactant and water transport coupled with power generation. The verification of these models and the resulting design tool will be accomplished by comparing predicted and measured effects of material and operating conditions on cell performance and water distribution within the cell. Applying our models to screen and improve water management strategies, then testing the resulting concepts in prototype fuel cells, will further demonstrate our improved fundamental understanding and validate the resulting design tools.

Results

In this fourth year of research, the emphasis has been on validation of the developed simulation tools and models for fuel cell performance and water transport during operation, application of the modeling tools to evaluate water management and related effects for varying designs and operating conditions, and further development and testing of approaches to improve water management.

The model solution approaches for two-phase flow of liquid water and gases were improved to better address flow across the interfaces between the porous GDLs and the gas channels. CFDRC then simulated two-phase pressure drop experimental studies performed at Ballard, in order to evaluate the current status of the models. This study was intended to gauge the impact of improvements in both the fluid dynamics algorithms, and better understanding of appropriate model setup and property values. The model setup was improved by slightly refining the computational grid, improving the grid node distribution for more uniform computational cell aspect ratios and smoother transitions from fine to coarse regions. Model implementation and solution algorithm improvements for the energy equation could also affect these results, since the Ideal Gas Law was used for gas phase density and the energy equation solution and convergence affect the gas phase density and fluid dynamics. The model was tested against measured pressure drops in the Generation 2 experimental fixture at Ballard, which is more repeatable than the original apparatus due to better sealing. In these experiments, water was injected into a GDL at a constant flow rate mimicking liquid water formation and transport into the channels during cell operation. The air flow rate through the channel was fixed, and pressure drops were measured as a function of time and flow rates. The models predicted the trends in wet pressure drop with operating conditions, Figure 1a, which we were able to capture with earlier models. These models also demonstrated the correct trend for the wet pressure drop response to design variations, particularly changing the channel aspect ratio, Figure 1b, unlike the earlier models.

Ballard has continued to evaluate and apply the simulation tools for a number of cell designs. The numerical stability and accuracy improvements over the last year have enabled an increasing use of computational studies of liquid water effects in non-operational single cells and stacks. The single-channel studies at Ballard demonstrated that the models can accumulate sufficient water in channels to reproduce experimentally observed wet pressure drops. Ballard has also applied the models to two-phase flow in fuel cell stacks, investigating manifold design and flow mal-distribution among as many as 28 parallel channels. The qualitative trends observed in the stack studies are also consistent with experimental observation, particularly the excess air flow required to prevent liquid water from affecting performance. In both the models and experimental stack characterization, it is air stoichiometry and performance in ‘end’ channels that typically suffer

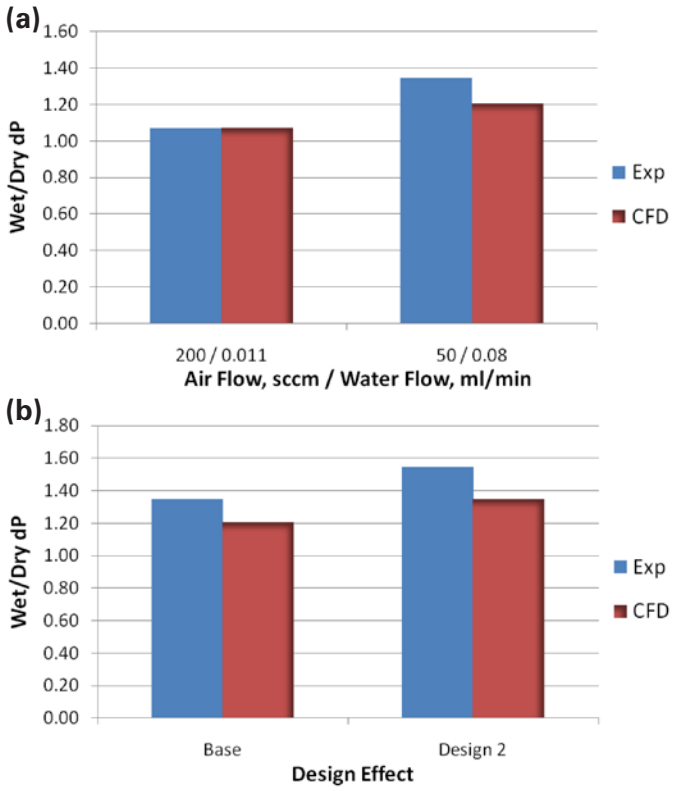


FIGURE 1. Comparison of Predicted and Measured Two-Phase Pressure Drops in Base Channel Design (a) as a Function of Operating Conditions, and (b) at Low Stoichiometry (50/0.08 Flows) Conditions as Function of Channel Design

the greatest reduction in air flow when liquid water in the channels affects performance.

The improvement and evaluation of the two-phase models integrated with electrochemistry, heat transfer, phase change, and water sorption and transport within the membrane has continued. One key model improvement over the past year is improved coupling with the widely used Springer model for transport of water within the membrane [1]. The example experimental data and simulation results presented here are for a three-dimensional model of an operational Ballard MK902 cell, with the simulations including the Springer model. Although this cell has been used previously for model evaluation because of the detailed diagnostic data and past modeling results available for comparison, in this case the experiments were performed at Ballard during the past year. The base operating conditions were cathode stoichiometry 1.8, anode stoichiometry 1.6; relative humidities of the inlet streams cathode 87%, anode 46%; cathode oxidant inlet temperature 65°C, fuel inlet temperature 75°C; and pressure 3 atmospheres in both channels. Model input properties were primarily from historical analysis and fitting at Ballard and CFDRC, with GDL properties updated based on our earlier characterization and a modified capillary pressure function extracted from the measurements of Sole [2]. A residual

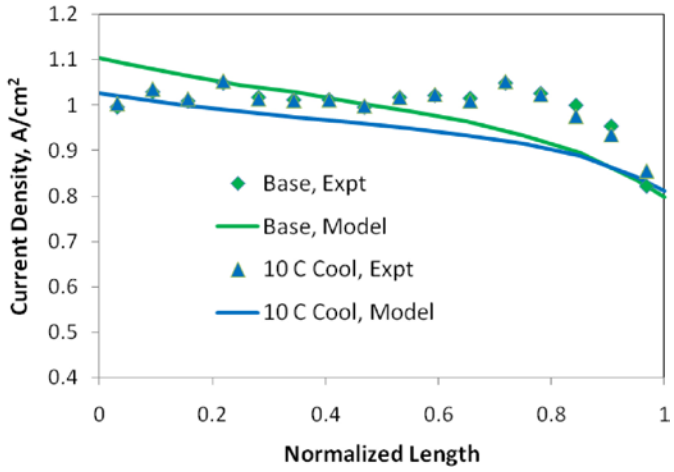


FIGURE 2. Comparison of Predicted and Measured Current Density Profiles for Base and 10°C Cooler Operating Conditions at 1 A/cm^2

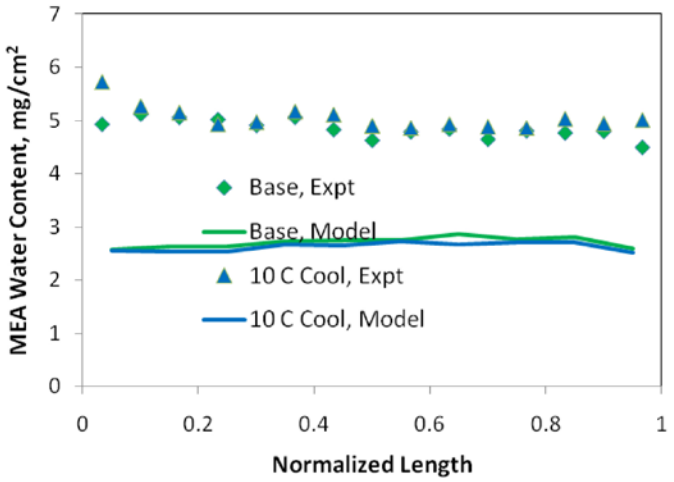


FIGURE 3. Comparison of Predicted and Measured MEA Water Content Profiles for Base and 10°C Cooler Operating Conditions at 1 A/cm^2

saturation of 0.2 was used to obtain the normalized liquid water saturation. Comparison of the predicted and measured current density profiles for the base operating conditions and for 10°C cooler operation, expected to result in additional liquid water, is shown in Figure 2. The experimental data has a large constant current density region along the length of the cell, as opposed to the model results which indicate decreasing current density in the direction of cathode gas flow. The membrane electrode assembly (MEA) water content profiles are more uniform with position in the cell, as shown in Figure 3. Although the prediction is approximately half the measured water mass, the model is capturing the trend of a relatively uniform distribution and little variation of water content between the two operating conditions.

Techverse developed an electrophoresis-based approach for impregnating GDL materials with Teflon®. Various forms

of this treatment are widely used to make the materials hydrophobic, i.e. non-wetting. The samples prepared with the electrophoresis technique consistently have a higher breakthrough pressure than commercially available papers with equivalent Teflon® loading. The materials treated by the developed electrophoresis approach also consistently have a lower residual saturation, indicating a smaller amount of water trapped inside the media. The air permeability of partially saturated samples tends to show greater permeability and less water saturation for a given air flow rate in the Techverse samples. All of these characterization results are consistent with the microscopic imaging analysis, Figure 4, which shows a more uniform Teflon® distribution over the fibers of the GDL in the Techverse samples generated by electrophoresis than in the samples generated by typical commercial production techniques. BCS Fuel Cells prepared fuel cells from the Techverse treated GDLs and measured cell performance. Although the initial tests demonstrated slightly higher electrical contact resistance between the GDL and landings than the control materials, performance improved relative to the control samples as current density was increased. A method for adding a micro-porous layer to the GDLs must be developed to more thoroughly evaluate the Techverse materials, and that process is currently under development.

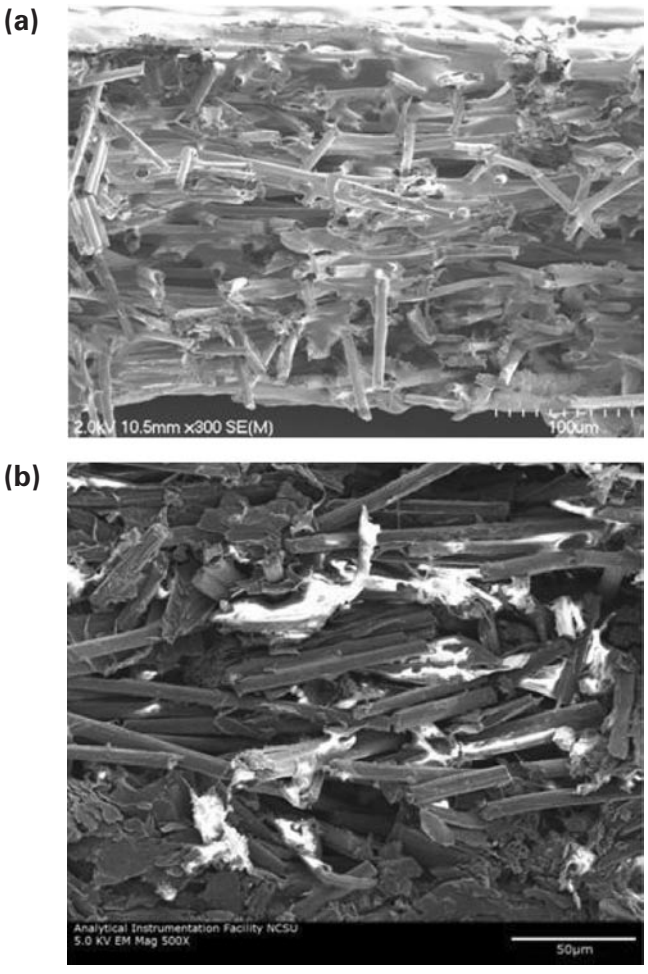


FIGURE 4. Micrographs of (a) Electrophoresis Process Teflonated GDL Material, and (b) Commercially Available Teflonated GDL Material

Conclusions and Future Directions

During the past year, we have demonstrated prediction of liquid water effects for two-phase flows in fuel cell microchannels and begun application to water management issues in cell and stack level component design. A promising materials modification has been developed, increasing the hydrophobicity of GDL materials to reduce water retention and related decreases in cell performance. Specific accomplishments for the past year include:

- Predicted design and operating condition sensitivity observed in experimental measurements of wet pressure drop for two-phase flows in channels and GDLs, applied models to screen channel and cell design for effective water management.
- Integrated membrane water transport models with the CFD two-phase cell scale models, demonstrated improved agreement with measured current density profiles and qualitative agreement with trends in measured liquid water distribution.
- Developed a technique for reproducible, controllable hydrophobic treatment of GDL media that results in less water retention and fewer transport limitations than the treatments applied to commercially available materials.

The key activities planned for the balance of the project are to complete validation of the water transport models based on data gathered during optimization studies, and to make recommendations for water management improvement including operating strategies and GDL materials modifications.

FY 2011 Publications/Presentations

1. S. Mukherjee, A. Gidwani, A. Roy, J. Vernon Cole, K. Jain, C. Bapat, and R. Thoms, "Multiphysics Simulation of Hydrogen PEM Fuel Cell," ECS Trans. 28 (27), pp. 93 – 102 (2010).

2. J. Vernon Cole, "Water Transport in PEM Fuel Cells: Advanced Modeling, Material Selection, Testing, and Design Optimization," Proceedings of the DOE Hydrogen and Fuel Cells Program Annual Merit Review, Crystal City, Virginia, 2011, http://www.hydrogen.energy.gov/pdfs/review11/fc030_cole_2011_o.pdf.

References

1. T.E. Springer, T.A. Zawodzinski, and S. Gottesfeld, *Journal Of The Electrochemical Society* **138**, 2334-2342 (1991).

2. Joshua D. Sole and Michael W Ellis, in *ASME 2008 6th International Conference On Fuel Cell Science, Engineering and Technology*, pp. 829-840, ASME, Denver, CO (2008).

V.F.2 Development and Validation of a Two-Phase, Three-Dimensional Model for PEM Fuel Cells

Ken S. Chen[1] (Primary Contact), Brian Carnes[1], Yun Wang[1a], Chao-Yang Wang[2], Rod Borup[3], Adam Weber[4], Patricia Chong[5], Yuichiro Tabuchi[6]

[1]Sandia National Laboratories (SNL)
Org. 8237, MS 9154, PO Box 969
Livermore, CA 94551-0969
Phone: (925) 294-6818
E-mail: kschen@sandia.gov

DOE Managers:
HQ: Jason Marcinkoski
Phone: (202) 586-7466
E-mail: Jason.Marcinkoski@ee.doe.gov
HQ: Donna Ho
Phone: (202) 586-8000
E-mail: Donna.Ho@ee.doe.gov

Subcontractors:
[1a] University of California, Irvine (UC Irvine), Irvine, CA
[2] The Pennsylvania State University (PSU), University Park, PA
[3] Los Alamos National Laboratory (LANL), Los Alamos, NM
[4] Lawrence Berkeley National Laboratory (LBNL), Berkeley, CA
[5] Ballard Power Systems (Ballard), Burnaby, BC, Canada
[6] Nissan Motor Co. Ltd. (Nissan), Kanagawa, Japan (in-kind or no-fee participant)

Project Start Date: October 2009
Project End Date: September 2012

Objectives

- Develop and validate a two-phase, three-dimensional (3-D) transport model for simulating proton exchange membrane fuel cell (PEMFC) performance under a wide range of operating conditions.
- Apply the validated PEMFC model to improve fundamental understanding of key phenomena involved and to identify performance-limiting processes and develop recommendations for improvements.

Technical Barriers

This project addresses the following technical barriers from the Fuel Cells section of the Fuel Cell Technologies Program Multi-Year Research, Development and Demonstration Plan:

(C) Performance

(D) Water Transport within the Stack

Technical Targets

Since the validated PEMFC model developed in this project can be employed to improve and optimize the design and operation of PEMFCs, insights gained from applying the model will help meet the following technical targets:

- Performance: 650 W/L or 50% energy efficiency for automotive applications; 40% electrical energy efficiency for stationary applications.
- Cost: $30/kW for automotive applications and $750/kW for stationary applications.

Fiscal Year (FY) 2011 Accomplishments

- Developed a 3-D, fully two-phase, single-cell model and completed the Year 2 model-development milestone, "Develop a 3-D, fully two-phase, single-cell PEM fuel cell model".
- Demonstrated the capabilities of the present fully two-phase single-cell model in case studies, including simulating a PEMFC with a complex Chevron flowfield.
- Made significant progress in model validation using polarization and current distribution data obtained by LANL using a *10*x*10* segmented cell.
- Developed and demonstrated a non-isothermal pore-network model for simulating water and thermal transport at the pore level.
- Performed 3-D computational fluid dynamics (CFD) simulation to verify the analytical droplet-detachment model developed previously.
- Carried out simplified calculations to estimate water flux at the gas diffusion layer (GDL)/channel interface.
- Investigated effect of cell segmenting on current-distribution measurements and developed guidelines on how a cell should be segmented to minimize the side effect of cell segmenting.
- Obtained current distribution maps experimentally using LANL's *10*x*10* segmented cell, and completed Year 2 experimental milestone, "Measure*10*x*10* current distribution performance data for model validation for four different operating conditions (relative humidity [RH] =*25%, 50%, 75%, 100%*)".
- "Polarization areas" with upper and lower bounds were obtained experimentally. Simultaneous current and temperature measurements were also obtained using mapping tool.

Introduction

As PEMFC technology matures and enters the stage of commercialization such that the industry strives to achieve desired performance and durability and reduce costs, process design and optimization become increasingly important and indeed critical. Modeling and simulation can provide guidance in PEMFC design and optimization and thus help accelerate the commercialization of PEMFC technology. Despite tremendous research efforts and a large number of models published in the literature (see Chen et al. [1] and references therein), a comprehensive, multi-physics computer model suitable for practical use by PEMFC engineers and designers, particularly in transportation and stationary applications, is still lacking.

The objectives of this project are twofold: 1) to develop and validate a two-phase, 3-D transport model for simulating PEMFC performance under a wide range of operating conditions; and 2) to apply the validated PEMFC model to identify performance-limiting phenomena or processes and develop recommendations for improvements so as to accelerate the commercialization of fuel cell technology. To achieve these two objectives, a multi-institutional and interdisciplinary team with significant experience in modeling PEMFCs and in measuring model-input parameters and model-validation data has been assembled. This team is led by SNL; it includes two other national laboratories (LANL and LBNL), a university (PSU), and two PEMFC manufacturers (Nissan and Ballard). In addition to developing and validating a two-phase, 3-D PEMFC model, we are also coupling the PEMFC model with DAKOTA [2] (a software toolkit for design, optimization, and uncertainty quantification developed by SNL) in order to create a computational capability that can be employed for PEMFC design and optimization. This report documents technical progress made in the project during FY 2011.

Approach

Our approach is both computational and experimental. We first develop a two-phase, 3-D, transport model for simulating PEMFC performance under a wide range of operating conditions by integrating the detailed component sub-models; FLUENT (a commercial CFD code) is employed as the basic computational platform. We then validate our PEMFC model in a staged approach using experimental data available from the literature and those generated by team members. Lastly, we plan to apply the validated PEMFC model to identify performance-limiting phenomena or processes and develop recommendations for improvements. As mentioned previously, we have assembled a team of leading experts in PEMFC modeling as well as in physical, electrochemical and transport property characterization, and cell diagnostics via segmented cell measurements and neutron imaging – this means that our project team is highly qualified and in an excellent position to carry out the project.

Results

Due to space limitation, only sample results are provided here. Figure 1 compares the partially two-phase model (in which flow in the channels is considered as single phase) with the fully two-phase model (in which flow in the channels is treated as two phase) by displaying along-channel contours computed by the two different models. Operating parameters are listed in Table 1, and detailed cell geometry and material (transport and physical) properties are provided in Table 1 of reference [1]. As expected, the partially two-phase model is not capable of capturing the two-phase behavior in the channels but the fully two-phase model does. Near the outlet of the cathode channel, liquid water is seen to be transported first from the channel to the GDL and then to the anode side due to drier anode inlet (note: counter flow is employed in the present work). In addition, the single-phase channel model predicts a dry-wet-dry transition pattern in the GDL-catalyst layer region whereas such wet-dry transition does not appear with the fully two-phase model since it predicts much more water in the channel.

Figure 2 shows liquid-saturation contours at the GFC (gas flow channel)/GDL interface as computed by the fully two-phase model for three anode/cathode inlet RH values: 42.5%, 66.4%, and 91.6%. Operating parameters are listed

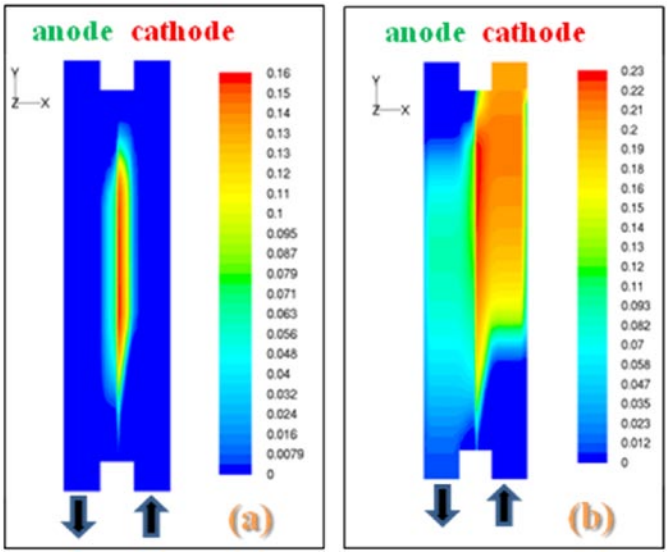


FIGURE 1. Partially two-phase model vs. fully two-phase model – computed liquid saturation contours on the symmetric plane: (a) partially two-phase model; and (b) fully two-phase model.

TABLE 1. Operating Conditions for the Base Case

Current density	0.8 A/cm^2	Anode stoichiometric flow ratio	1.8
Cell temperature	80°C	Cathode stoichiometric flow ratio	2.0
Anode/cathode back pressure	200 kPa	Anode/cathode RH	66.4%

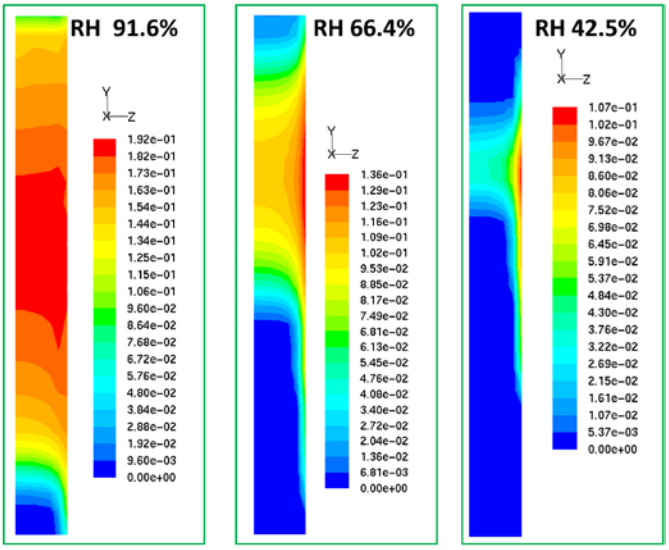


FIGURE 2. Computed liquid-saturation contours at the cathode GFC/GDL interface by the fully two-phase model – effect of inlet RH.

in Table 1. Clearly, more liquid water is accumulated in the cathode gas flow channel (GFC) as anode/cathode inlet RH is raised. Moreover, liquid saturation near the cathode outlet increases with increasing inlet RH, indicating that water transport from cathode to anode decreases.

Figure 3 displays computed liquid-saturation contours at the GFC/GDL interface for two current densities: 0.2 A/cm^2 and 1.5 A/cm^2. Operating parameters are listed in Table 1. It can be seen from Figure 3 that cathode GFC has more liquid water at low current densities than at high current densities – this most likely is due to that sufficiently large drag force is required to remove liquid water from the GFC. Of the four cases (0.1, 0.2, 1.0, and 1.5 A/cm^2) studied, cathode GFC has the most liquid water at current density of 0.2 A/cm^2. Lastly, as current density is reduced, it was found that the wet region in the cathode GFC enlarges gradually in both downstream and upstream, due to the smaller drag force of gas flow.

In Table 2, the current-density distribution computed using the fully two-phase model are compared with that measured using LANL's *10x10* segmented cell. The operating conditions are: 80°C, 50% RH, and 0.4 A/cm^2, and detailed cell geometry and material (transport and physical) properties are provided in Table 1 of reference [1]. From the numbers presented in Table 2, we can conclude that the agreement between computed and measured current density distribution is good with the root-mean-square error being less than 11.3% .

Lastly, a comparison between measured and computed polarization curves is presented in Figure 4, which shows good agreement. Geometric parameters, material (transport and physical) properties, and operating conditions for this study are presented in Table 1 of reference [1]. Further details on this model validation study is provided by Carnes et al. [3].

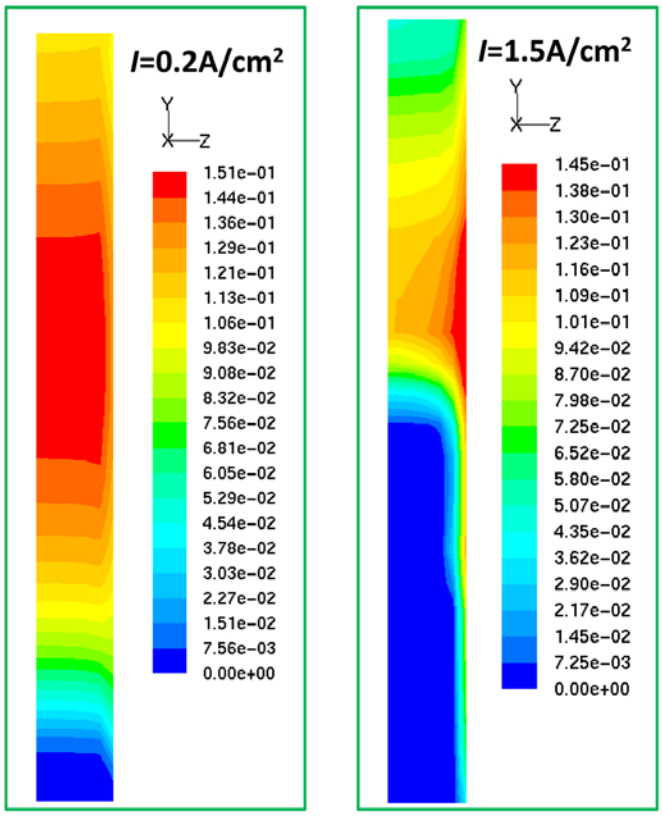


FIGURE 3. Computed liquid-saturation contours at the cathode GFC/GDL interface by the fully two-phase model – effect of current density.

TABLE 2. Computed vs. Measured Current-Density Distribution

(a) Computed current-density distribution

0.31	0.36	0.37	0.37	0.37	0.37	0.38	0.38	0.39	0.34
0.33	0.39	0.39	0.39	0.39	0.39	0.39	0.39	0.39	0.34
0.35	0.41	0.41	0.41	0.40	0.40	0.40	0.39	0.39	0.33
0.33	0.40	0.41	0.41	0.42	0.42	0.42	0.42	0.43	0.36
0.36	0.43	0.43	0.43	0.43	0.43	0.43	0.43	0.42	0.36
0.36	0.44	0.44	0.44	0.43	0.43	0.43	0.43	0.42	0.36
0.34	0.42	0.42	0.43	0.43	0.43	0.44	0.44	0.44	0.37
0.36	0.43	0.43	0.43	0.43	0.43	0.42	0.42	0.42	0.35
0.35	0.42	0.42	0.42	0.42	0.42	0.42	0.41	0.41	0.35
0.31	0.37	0.37	0.38	0.38	0.39	0.39	0.39	0.39	0.34

(b) Measured current-density distribution

0.00	0.43	0.39	0.38	0.38	0.38	0.38	0.37	0.37	0.37
0.36	0.41	0.40	0.41	0.41	0.41	0.41	0.40	0.39	0.39
0.39	0.43	0.44	0.46	0.45	0.46	0.45	0.45	0.42	0.42
0.41	0.46	0.46	0.45	0.48	0.50	0.50	0.48	0.45	0.45
0.41	0.48	0.49	0.47	0.46	0.51	0.53	0.53	0.49	0.48
0.41	0.45	0.47	0.47	0.46	0.49	0.51	0.49	0.48	0.49
0.40	0.43	0.47	0.47	0.48	0.47	0.46	0.46	0.43	0.45
0.37	0.44	0.44	0.46	0.45	0.46	0.45	0.44	0.43	0.44
0.37	0.38	0.40	0.41	0.42	0.44	0.43	0.43	0.45	0.40
0.35	0.36	0.31	0.28	0.38	0.36	0.37	0.38	0.31	0.00

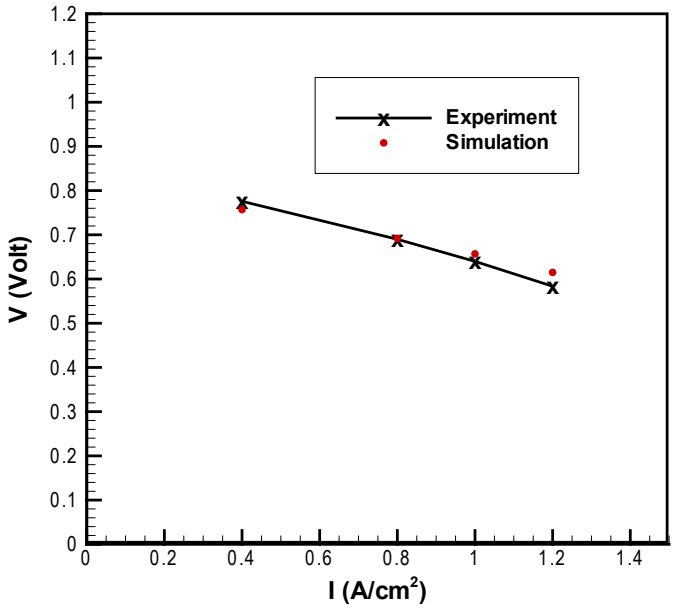


FIGURE 4. Model validation: comparison of measured and computed polarization curves.

Summary and Conclusions

- A 3-D, fully two-phase, single-cell model for simulating PEMFC performance was developed and the milestone of developing a 3-D, fully two-phase, single-cell model was met.
- Significant progress has been made in model validation using polarization and current distribution data obtained by LANL using a *10x10* segmented cell.
- Current distribution maps were obtained experimentally using LANL's *10x10* segmented cell, and the Year 2 experimental milestone, "Measure*10x10* current distribution performance data for model validation for four different operating conditions (RH = *25%, 50%, 75%, 100%*) was met.

Future Directions

- Complete model validation in the single-phase and partially two-phase regimes using LANL current-distribution data from segmented cell experiments, and test data from Ballard and Nissan.
- Complete sub-model and algorithm development, and numerical implementation.
- Develop a 3-D, two-phase, short-stack PEMFC model.
- Obtain water profiles in the through-plane using neutron radiography setup at the National Institute of Standard and Technology (NIST).
- Perform model validation in the fully two-phase regimes using neutron imaging data obtained by LANL at NIST, and test data from Nissan and Ballard.

FY 2011 Publications/Presentations

1. Y. Wang and K.S. Chen, "Elucidating two-phase transport in a polymer electrolyte fuel cell, Part 1: Characterizing flow regimes with a dimensionless group", *Chemical Engineering Science*, **66**, 3557-3567 (2011).

2. Y. Wang, K.S. Chen, J. Mishler, S.C. Cho, X.C. Adroher, "A Review of Polymer Electrolyte Membrane Fuel Cells: Technology, Applications, and Needs on Fundamental Research", *Applied Energy*, **88**, 981-1007 (2011).

3. Y. Ji, G. Luo,a nd C.-Y. Wang, "Pore-level liquid water transport through composite diffusion media of PEMFC", *J. Electrochem. Soc.* **157** (12) B1753–B1761 (2010).

4. Y. Wang and K.S. Chen, "Through-plane water distribution in a polymer electrolyte fuel cell: comparison of numerical prediction with neutron radiography data", *J. Electrochem. Soc.*, **157** (12) B1878-B1886 (2010).

5. Y. Wang and K.S. Chen, "Elucidating through-plane Liquid Water Profile in a Polymer Electrolyte Fuel Cell", in *ECS Transaction*, **33**(1) 1605-1614 (2010).

6. K.S. Chen, B. Carnes, L. Hao, Y. Ji, G. Luo, C.-Y. Wang, and Y. Wang, "Toward the development and validation of a comprehensive PEM fuel cell model," in *ASME Proceedings of ESFuelCell2011*, paper #54693; and also presentation in the 9th Int. Fuel Cell Science, Engineering & Technology Conference, Aug. 7–10, 2011, Washington, DC.

7. B. Carnes, K.S. Chen, L. Hao, G. Luo, Y. Ji, C.-Y. Wang, and D. Spernjak, "Validation and uncertainty quantification of a two-phase, multidimensional PEMFC computer model using high-resolution segmented current collector data," in *ASME Proceedings of ESFuelCell2011*, paper #54746; and also presentation in the 9th Int. Fuel Cell Science, Engineering & Technology Conference, August 7–10, 2011, Washington, D.C.

8. K.S. Chen, "Development and validation of a three-dimensional, two-phase, PEM fuel cell model", presentation at the *2011 DOE Hydrogen Program Annual Merit Review and Peer Evaluation Meeting*, Washington DC, May 9–13, 2011, paper #FC027.

9. K.S. Chen, "Development and Validation of a Two-phase, Three-dimensional Model for PEM Fuel Cells", invited presentation at the 2010 LANL(US)/AIST-NEDO(Japan) Fuel Cell Workshop, Hyatt Regency Waikiki Beach Resort, Honolulu, HI, Aug 9–11, 2010.

Reference

1. K.S. Chen, B. Carnes, L. Hao, Y. Ji, G. Luo, C.-Y. Wang, and Y. Wang, "Toward the development and validation of a comprehensive PEM fuel cell model," in *ASME Proceedings of ESFuelCell2011*, paper #54693 (2011).

2. http://www.cs.sandia.gov/dakota/index.html.

3. B. Carnes, K.S. Chen, L. Hao, G. Luo, Y. Ji, C.-Y. Wang, and D. Spernjak, "Validation and uncertainty quantification of a two-phase, multidimensional PEMFC computer model using high-resolution segmented current collector data," in *ASME Proceedings of ESFuelCell2011*, paper #54746 (2011).

V.F.3 Transport in PEMFC Stacks

Cortney Mittelsteadt (Primary Contact),
John Staser, Hui Xu, Pedro Cortes (GES)
John VanZee, Sirivatch Shimpalee, Visarrn Lilavivat (USC)
James E. McGrath Myoungbae Lee, Nobuo Hara, Kwan-Soo Lee, Chnag Hyun Lee (VT)
Don Conners, Guy Ebbrell (Ballard); Kevin Russel (Tech-Etch)
Giner Electrochemical Systems (GES), LLC
89 Rumford Ave.
Newton, MA 02466
Phone: (781) 529-0529
E-mail: cmittelsteadt@ginerinc.com

DOE Managers
HQ: Donna Ho
Phone: (202) 586-8000
E-mail: Donna.Ho@ee.doe.gov
GO: Gregory Kleen
Phone: (720) 356-1672
E-mail: Greg.Kleen@go.doe.gov

Technical Advisor
John Kopasz
Phone: (630) 252-7531
E-mail: kopasz@anl.gov

Contract Number: DE-EE0000471

Subcontractors:
- Tech-Etch, Plymouth, MA
- Ballard Material Products, Inc., Lowell, MA
- Virginia Polytechnic (VT) Institute and State University, Blacksburg, VA
- University of South Carolina (USC), Columbia, SC

Project Start Date: October 5, 2009
Project End Date: October 4, 2012

Fiscal Year (FY) 2011 Objectives

- Design of fuel cell components targeting specific transport properties:
  - Synthesis of block copolymers.
  - Design of flow fields and gas diffusion layers (GDLs).
- Determination of bulk membrane properties:
  - Water uptake and diffusivity.
  - Gas permeability.
  - Electro-osmotic drag.
- Transient, three-dimensional modeling of fuel cell operation.

Technical Barriers

This project addresses the following technical barriers from the Fuel Cells section of the Fuel Cell Technologies Program Multi-Year Research, Development and Demonstration Plan:

(C) Performance
(D) Water Transport within the Stack
(E) System Thermal and Water Management
(G) Start-up and Shut-down Time and Energy/Transient Operation

Technical Targets

The goals of this project are not to reach specific technical targets put forth by the DOE (i.e., target catalyst loading, target cost per kilowatt). Instead, this project aims to develop fuel cell components (i.e., membranes, GDLs, bipolar plates and flow fields) that possess specific properties (i.e., water transport and conductivity). A computational fluid dynamics model will then be developed to elucidate the effect of certain parameters on these specific properties (i.e., the effect of membrane type and thickness on membrane water transport). Ultimately, the model will be used to determine sensitivity of fuel cell performance to component properties to determine limiting components and guide research.

FY 2011 Accomplishments

- Developed a second system to measure dynamic water uptake and diffusivity of membranes in addition to previously developed static diffusivity apparatus. Water isotherms and diffusivities of various membranes including Nafion® 112, Nafion® 1110 and NRE 212 have been obtained using both systems. We conclusively have shown that membrane interfacial resistance to water transport is negligible.
- Designed segmented cells to quantify fuel cell voltage vs. current at different points along the active area and tested the concept in common 50 cm^2 hardware with negligible change in performance.
- Characterized customized GDLs in terms of scanning electron microscopy (SEM) microstructure and fuel cell performance and correlated them to various pore structure, tortuosity and hydrophobicity.
- Developed the second iteration of fuel cell flow fields with thin metallic sheets to better correlate with automotive cells. Have also developed segmented cells for these plates.
- Modeled the effect of altering polymer electrolyte membrane (PEM) diffusivity to 6x and 1/6x that of PFSA membranes on fuel cell performance and water distribution.

- Synthesized block polysulfone ether polymers-bi phenyl sulfone (BPSH-BPS) multiblock copolymers with higher block lengths and self-assembled nanostructures, which provide designing guidelines for PEMs and will be used for model tests.



Introduction

Many fuel cell component properties that influence water transport and thermal management are not well-understood [1,2]. A better understanding of how water transport and thermal management can be controlled would represent a significant step forward in meeting the DOE's stated 2015 targets. This project aims for a better understanding of water transport and thermal management by tailoring fuel cell components to exhibit specific transport properties. These transport properties will then be modeled, which will enable the prediction of the effect of changing component parameters on transport properties.

Approach

This project seeks to develop fuel cell components possessing specific transport properties. Membranes will be developed to achieve different ratios of water transport and conductivity. Bulk membrane properties (i.e., diffusivity, water uptake, conductivity) will be evaluated and modeled. GDLs and bipolar plates and flow fields will be developed, and also tailored to achieve specific differences in porosity, tortuousity and hydrophobicity. The fuel cell performance will be evaluated using these components. The model will be used to predict the effect changing component parameters (i.e., changing membrane type and thickness, changing flow field configuration) will have on component transport properties and fuel cell performance.

Results

Membrane Synthesis and Nano-Scale Properties

A dynamic water uptake and diffusivity measurement apparatus was developed. This is a further advancement beyond the static water uptake system made in fiscal year 2010. Dynamic water uptake is of interest for it determines rate of water transport in a changing water activity environment. When the relative humidity (RH) changes in the fuel cell, the water content of the membrane changes, and subsequently the membrane must swell or shrink to accommodate this change. There is debate amongst the fuel cell community if this necessary mechanical work (for expanding a membrane to increase water content) slows water transport compared to a static gradient, where water content is not changing across the membrane thickness. For the dynamic system, a small chamber with a membrane strip (2.2 cm × 0.5 cm) is placed in line with an ante-chamber. Both chambers are evacuated. The ante-chamber is then filled with water vapor to a selected RH. A valve between the membrane and ante-chamber is then opened. The two chambers equilibrate immediately, then the pressure begins to drop as the membrane absorbs water. By measuring the kinetics of this pressure drop we can determine the diffusivity of the membrane under those conditions. The pressure in the ante-chamber is then increased and the experiment is repeated to determine diffusivity at the next RH level. Similarly the experiment can be performed for desorption. Finally, by knowing the volume of both chambers, the absolute amount of water absorbed can be determined to obtain the water vapor isotherm.

The diffusion coefficients for NRE 212 at 80°C were measured over a range of membrane water contents by absorption and desorption experiments. These dynamically-measured diffusion coefficients are plotted against the diffusion coefficients measured via steady-state analysis in Figure 1, where the lines on the data points represent the 95% confidence intervals. The diffusion coefficients are nearly identical, regardless of the type of experiment performed (i.e., absorption, desorption or steady-state). The inserted figure shows water uptake isotherms for the Nafion® 1110 and NRE 212 membrane. The solid curve in the figure is the previously-reported water uptake isotherm described by an empirical equation in the reference [3], which is compared with the dotted line obtained by measuring the weight change of the membrane in contact with water vapor. These two isotherms are very nearly identical, indicating that the dynamic uptake experiments are an alternative valid approach to measuring steady-state water uptake.

To determine the current distribution, a current distribution plate made of a thin copper layer attached to a Kapton film was developed as shown in Figure 2. The plate rests between the flow field and the diffusion media and

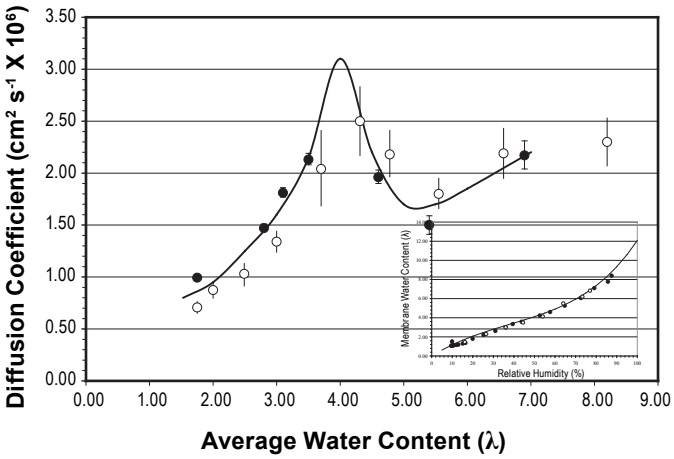


FIGURE 1. Diffusion coefficients measured from (—) steady-state data; (●) dynamic water uptake; (○) dynamic water desorption by Nafion® 212 at 80°C. The inserted figure shows water uptake isotherms for the Nafion® 1110 and NRE 212 membrane.

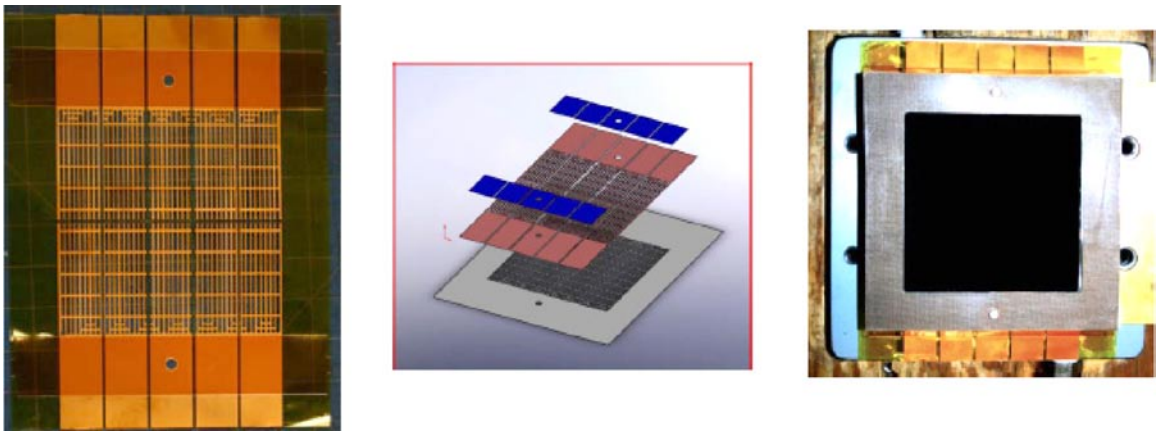


FIGURE 2. A current distribution plate made of Kapton film attached with a thin copper layer. The plate rests between the flow field and the diffusion media and the concept was tested in 50 cm^2 regular fuel cell hardware.

the concept was tested in 50 cm^2 regular fuel cell hardware. The current distribution board adds only 7.5 mOhms-cm^2. The performance discrepancy before and after the current distribution plate addition is negligible. A new flow field with thin metallic sheets was deigned and fabricated since heat transport and fluid cooled plates can have a large impact on the current distribution. This thin plate design with central cooling is being used by automotive manufacturers for fuel cell plates and it is essential to mimic the diffusion media/ flow field interface as closely as possible.

GDLs with various pore structure, tortuosity and hydrophobicity were custom fabricated by BASF and Ballard Materials. The matrix of GDLs is shown Table 1. They were characterized in terms of microstructure, pore size distribution, and fuel cell performance. The fibers constitute the bare substrate when there is no wet proofing. In contrast, materials fill in between fibers in the GDLs with 10% or 40% wet proofing. For the GDLs with 10% and 40% microporous layer (MPL), SEM images reveal a merge between the substrate and the MPL instead of a well defined and a clear boundary. The effect of wet proofing, MPL and porosity on the on the MacMullin Number (ratio of transport resistance with the diffusion media compared to without) was investigated. Increasing the wet proofing decreases the porosity of the substrate layer. Consequently, a higher flow resistance is expected as porosity decreases and tortuosity increases. However, the addition of the MPL decreases the MacMullin number. This effect could be related to the different wet proofing treatments of the substrate and the MPL, which can cause an additional driving force in the liquid through the pores during the experiments. Even when the treated surfaces have the same wet proofing percentage the actual contact angle in each surface could be different.

TABLE 1. Matrix for Customized GDLs

GD	Layers & % Hydrophobicity	Image #	Avg. Porosity
1	Substrate Only (No wet proofing)	a	0.80
2	Substrate Only (10%)	b, d	0.78
3	Substrate (10%) + MPL (10%)	c	0.75
4	Substrate (10%) + MPL (40%)	f	0.74
5	Substrate Only (40%)	c, g	0.69
6	Substrate (40%) + MPL (10%)	h	0.68
7	Substrate (40%) + MPL (40%)	i	0.69

PEM diffusivity in the model was altered to 6x and 1/6x that of PFSA membranes to investigate the effect of diffusivity on performance. Figure 3 shows simulated current density distribution on the MEA surface at three water diffusivities and average current density of 0.6 A/cm^2 with (a) 75% /25% RH and (b) 25%/25% RH (anode/ cathode, co-flow). It is interesting that for both anode humidity conditions, increasing diffusivity gives the most uniformity in current density distribution and 1/6 Dw shows the most non-uniformity in distribution. Also, increasing diffusivity leads to the largest improvement in the dry anode case. This is not surprising as the water needs to diffuse to the anode to counter electro-osmotic drag. The block copolymers being developed are expected to have a very different diffusivity than Nafion®, and will be used to confirm these predictions.

BPSH-BPS multiblock copolymers with higher block lengths and self assembled nanostructures have been synthesized, which provide designing guidelines for PEMs in term of structure, chemistry and phase separation and will be used for model tests. A cluster of multi-block copolymers comprised of hydrophilic telechelic BPS-100 oligomers and 6FPAEB oligomers, both of which vary in molecular weights (i.e., 7k-7k, 14k-14k, 15k-15k, 10k-18k) have been prepared. They clearly demonstrate different nano-phase separated structures based on transmission electron microscope images. Beyond chemistry and block length, thermal history also influences the PEM properties. Figure 4 shows measured conductivities of 6FPAEB-BPSH100 14k-14k at different annealing temperatures as a comparison to Nafion® 212 membrane. It can be seen that annealing at

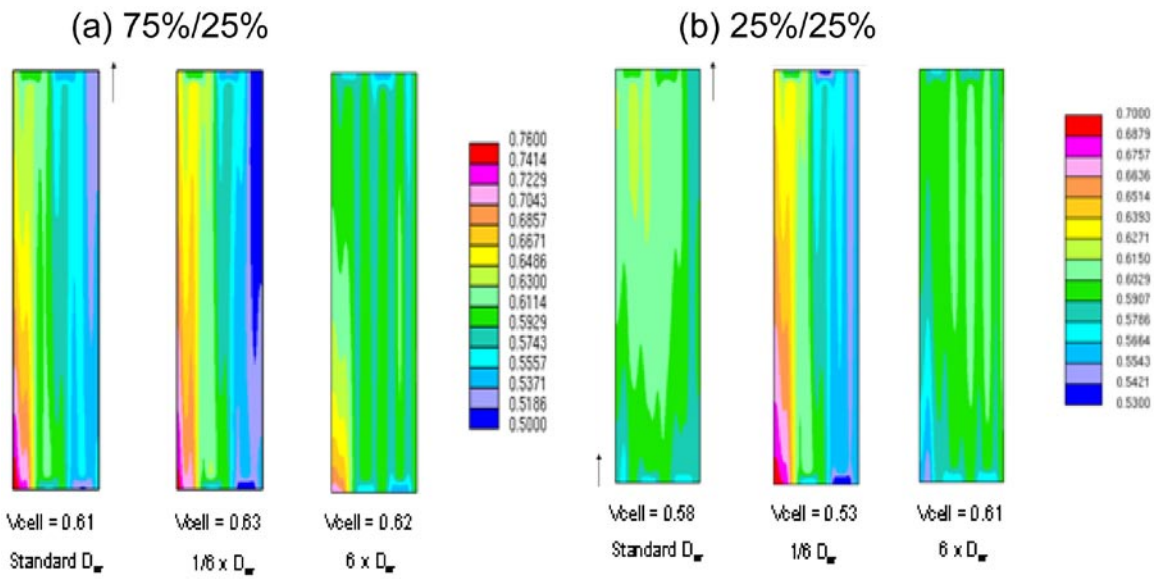


FIGURE 3. Simulated current density distribution on MEA surface at three water diffusivities and average current density of 0.6 A/cm^2: (a) 75%/25% RH and (b) 25%/25%RH, anode/cathode for a co-flow configuration.

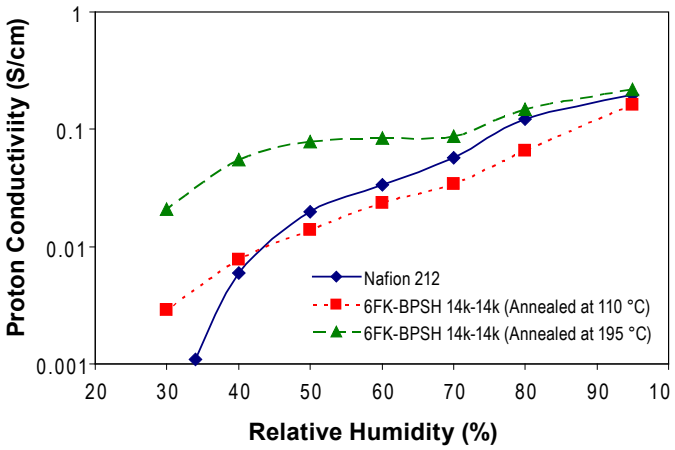


FIGURE 4. Measured conductivities of 6FPAEB-BPSH100 14k-14k at different annealing temperatures as a comparison with Nafion® 212 membrane.

195°C tremendously improves the membrane conductivity in contrast to that at 110°C.

Conclusions and Future Directions

- Many new analytical techniques were developed for characterizing water transport:
  - No interfacial resistance found for Nafion®
  - Static and dynamic diffusivity found to be the same
  - Techniques will be made widely available to the fuel cell research community
- Widely varied PEMs and diffusion media will allow us to model the important parameters of each.
- A base model has been developed and used to describe various performance results with different diffusion media.
- In FY 2012, we plan to: Extend characterizations to alternative materials.
- Extend testing to more realistic automotive platform.
- Down-select alternative polymers and generate larger, consistent materials.
- Confirm model with performance, current distribution and water collection results.
- Use model to determine performance sensitivity to build materials, suggest focus areas.

FY 2011 Publications/Presentations

1. "Transport Studies and Modeling in PEM Fuel Cells," DOE Annual Merit Review, oral FC054, May 9-12, 2011.

2. "Water Transport in Nafion Membranes Advances", in Materials for Proton Exchange Membrane Fuel Cell Systems 2011, Asilomar Conference Grounds, Pacific Grove, CA. February 20–23, 2011.

3. "Poly(arylene ether) Random and Block Copolymer Polyelectrolytes for Fuel Cell and Water Purification Membranes", XII International Symposium on Polymer Electrolytes, Padova, Italy, 29 August – 3 September 2010.

4. "Recent Developments in Linear, Postfluorinated and Terminally Crosslinked Hydrophilic-Hydrophobic Multiblock Copolymer Electrolyte Membranes", Progress in MEA 2010, La Grande Motte, France, 19–22 September 2010.

5. "Through-Mask Electroetching for Fabrication of Metal Bipolar Plate Gas Flow Field Channels" Vol 33 (1), Polymer Electrolyte Fuel Cells 10, The Electrochemical Society pp. 991-1001 (2010).

6. "Characterization of Microporous Layers in Carbon Paper GDL for PEM Fuel Cell", in ECS Transactions Vol. 33 (1), Polymer Electrolyte Fuel Cells 10, The Electrochemical Society, pp. 1133-1141 (2010).

References

1. T.A. Zawodzinski, C. Derouin, S. Radzinski, R.J. Sherman, V.T. Smith, T.E. Springer and S. Gottesfeld, *J. Electrochem. Soc.*, **140**, 1041 (1993).

2. T.V. Nguyen and R.E. White, *J. Electrochem. Soc.*, **140**, 2178 (1993).

3. C.K. Mittelsteadt and H. Liu, "Conductivity, permeability, and ohmic shorting of ionomeric membranes," in *Handbook of Fuel Cells; Fundamentals, Technology and Applications: Vol. 5*, W. Vielstich, H. Yokokawa and H.A. Gasteiger, Eds., John Wiley and Sons, Ltd., Chichester (2009).

V.F.4 Investigation of Micro- and Macro-Scale Transport Processes for Improved Fuel Cell Performance

Jon P. Owejan (Primary Contact), Matthew Mench, Michael Hickner, Satish Kandlikar, Thomas Trabold, Jeffrey Gagliardo, Anusorn Kongkanand, Wenbin Gu, Paul Nicotera
General Motors
10 Carriage Street
Honeoye Falls, NY 14472
Phone: (585) 953-5558
E-mail: jon.owejan@gm.com

DOE Managers
HQ: Donna Ho
Phone: (202) 586-8000
E-mail: Donna.Ho@ee.doe.gov
GO: David Peterson
Phone: (720) 356-1747
E-mail: David.Peterson@go.doe.gov

Technical Advisor
John Kopasz
Phone: (630) 252-7531
E-mail: kopasz@anl.gov

Contract Number: DE-EE0000470

Subcontractors:
- Penn State University, University Park, PA
- University of Tennessee, Knoxville, TN
- Rochester Institute of Technology, Rochester, NY

Project Start Date: June 1, 2010
Project End Date: May 31, 2013

Fiscal Year (FY) 2011 Objectives

- Characterize saturated relationships in state-of-the-art fuel cell materials.
- Obtain a comprehensive down-the-channel validation data set for a baseline and auto-competitive material set.
- Optimize component models to output bulk and interfacial transport resistances.
- Demonstrate integrated transport resistances with a one plus one-dimension (1+1D) fuel cell model solved along a straight gas flow path.
- Identify critical parameters for low-cost material development.

Technical Barriers

This project addresses the following technical barriers from the Fuel Cells section of the Fuel Cell Technologies Program Multi-Year Research, Development and Demonstration Plan:

(B) Cost

(C) Performance

(D) Water Transport within the Stack

Technical Targets

This project supports fundamental studies of fluid, proton and electron transport with focus on saturated operating conditions. Insights gained from these studies are being used to develop modeling tools that capture fundamental transport physics under single and two-phase conditions. This project addresses the expected outcomes from Topic 4a as follows:

- Validated transport model including all component physical and chemical properties:
  - Down-the-channel pseudo-two-dimension (2D) model will be refined and validated with data generated in the project.
- Public dissemination of the model and instructions for exercise of the model:
  - Project website to include all data, statistics, observations, model code and detailed instructions.
- Compilation of the data generated in the course of model development and validation:
  - Reduced data used to guide model physics to be published and described on project website.
- Identification of rate-limiting steps and recommendations for improvements to the plate-to-plate fuel cell package:
  - Model validation with baseline and auto-competitive material sets will provide key performance limiting parameters.

FY 2011 Accomplishments

- Generated distributed down-the-channel current, ohmic resistance, temperature and liquid water validation data for a baseline material set.
- Developed new characterization methods to measure transport relationships as a function of saturation.
- Generated characterization data for bulk and interfacial transport in bulk membrane, thin ionomer films, dispersed catalyst layers, gas diffusion layers and gas delivery channels.
- Developed wet model framework.

- Published validation and characterization data to a project website at: www.pemfcdata.org.



Introduction

The transport physics associated with fuel cell operation is widely debated amongst researchers because comprehensive micro/nano-scale process validation is very difficult. Furthermore, fuel cell operation has a strong interdependence between components making it difficult to separate the key relationships required for predictive models with ex situ methods. Generally, a validated model that predicts operation based on known design parameters for fuel cell hardware and materials is highly desired by developers. Such a model has been proposed by many research groups for dry (less than 100% relative humidity [RH] exhaust) operation with moderate success, however these modelers unanimously assert that their ability to predict wet operation is limited by two-phase component-level understanding of transport processes. Additionally, as two-phase models continue to be refined; benchmarking progress is difficult due to incomplete validation datasets.

In the current work, our team is developing characterization tools for saturated relationships based on the evolution of a dry 1+1D model for accurate wet prediction [1]. To complement this work we are also developing a comprehensive validation dataset based on a wide proton exchange membrane fuel cell (PEMFC) operating space. As data and modeling reach a final form, these are uploaded to a project website at www.pemfcdata.org. All characterization and validation work is conducted with a common material set.

Approach

This project is organized around baseline and next-generation material sets. These materials define parametric bounds for component and integrated down-the-channel modeling efforts. The baseline material set was chosen based on the commercial state of the art that exists today. The next-generation material set consists of transport impacting parametric changes that are in-line with the DOE 2015 targets for reduced cost while improving durability and performance. For characterization and validation experiments, a standard protocol was also developed to enable the team to conduct experiments with the same boundary conditions.

The first phase of this project was experimentally focused on characterization work that is organized by transport domain, comprising thin film ionmers, bulk membranes, porous electrodes, gas diffusion layers and flow distribution channels. More specifically, the key relationships being investigated are outlined as follows:

- Ionomer Characterization
  - Membrane water uptake, water diffusivity and hydraulic permeability.
  - Oxygen and water transport as a function of ionomer layer thickness.
  - Evidence of nanophase/water morphological changes vs. film thickness.
- Diffusion Layer Characterization
  - Microporous layer thermal conductivity and D/D_{eff} as a function of saturation.
  - Catalyst layer liquid water pressure as a function of saturation, pore size, and hydrophobicity.
  - Substrate thermal conductivity (wet and dry) and D/D_{eff} as a function of saturation.
  - Through-plane saturation and wet region boundary as a function of dT and operating temperature.
- Channel Characterization
  - Carbon fiber paper (CFP) to channel interfacial transport resistance as a function of channel saturation.
  - Channel dP as a function of saturation, temperature, flow, and current density.
  - Manifold dP as a function of saturation, temperature, and flow.

These relationships are required to develop component models that output bulk and interfacial transport resistances to the project 1+1D down-the-channel model. In anticipation of this integrated model, a validation data set is being collected in parallel with small scale hardware specifically designed to include automotive stack constraints [2].

Results

Project Website

The project website was made available to the public at www.pemfcdata.org. This information tool is designed for sharing project data and modeling with the broader fuel cell research community to provide a common validation tool that generates dialog about fundamental transport physics in PEMFCs. A navigational map of the current website is given in Figure 1.

This website contains a 'Home' and 'Project' page that describes the funding, participants, news, approach, deliverables, standard materials and testing protocol. The 'Macro' page contains the down-the-channel validation data for the baseline material set and the next-generation material set will be uploaded in the next phase of the project. The 'Micro' page is continuously being updated with characterization data as it becomes available. The list of model parameters is posted to the 'Parameters' page. This list is currently posted for the dry-based model only, which is available on the 'Modeling' page (the wet model is currently being developed and will be posted in the second phase

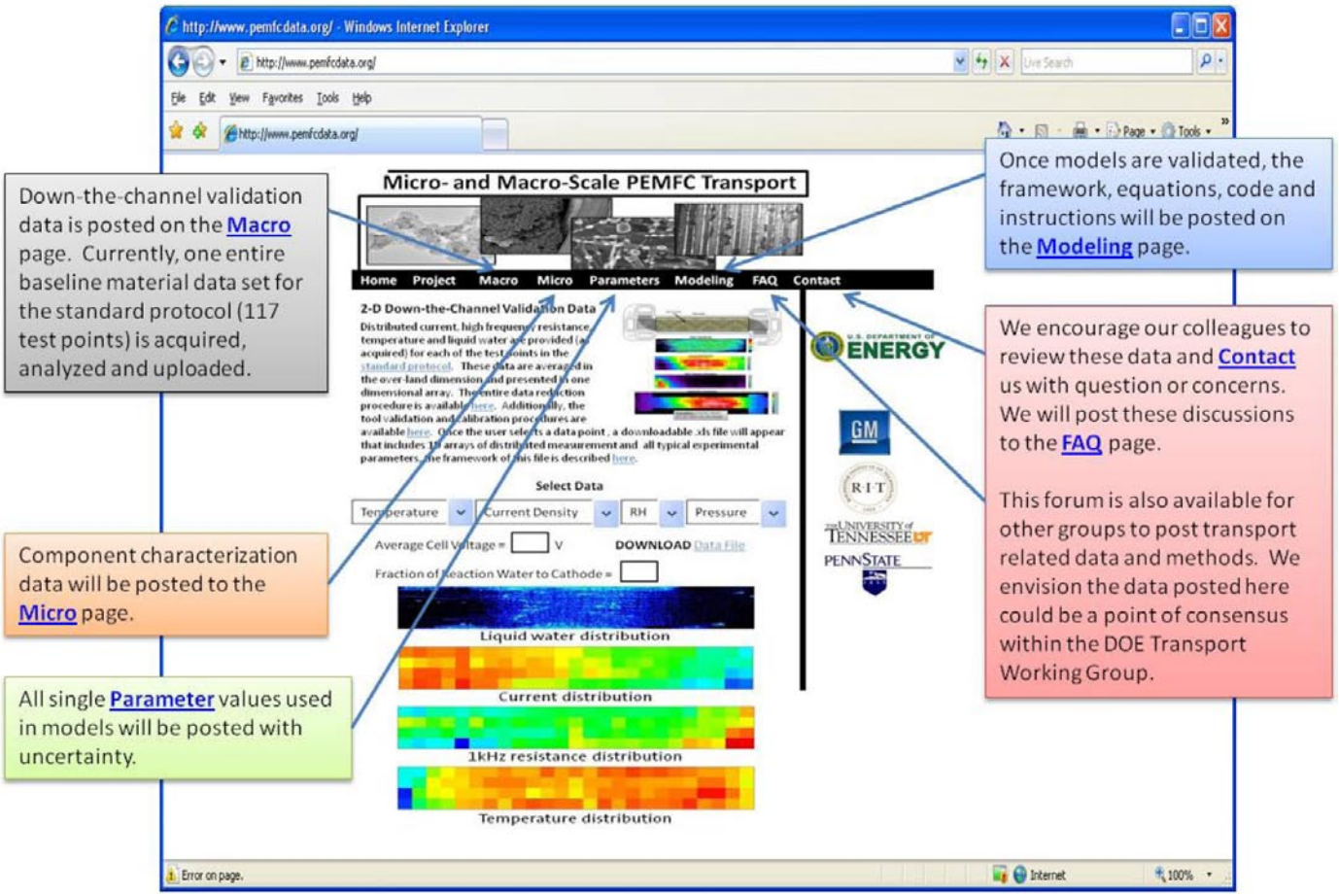


FIGURE 1. Project Website Navigational Map

of the project). Finally, the 'Contact' and 'FAQ' pages are intended to initiate dialog regarding our data and approach.

Baseline Validation Data

Experimental variability was carefully examined prior to collecting the baseline material set data for the 117 point standard protocol. With regard to the controlled test parameters, temperature control with cartridge heaters was found to have the most significant impact on test variation. RH fluctuations within the cell result from temperature variations as heaters cycle, and this impacts all aspects of transport within the cell. Liquid coolant with flow and temperature control was used to mitigate this experimental variability, which was confirmed with our temperature distribution tool by comparing the temperature distributions with and without coolant. This comparison showed a constant temperature profile is achieved with liquid coolant. Moreover, the temperature distribution is more representative of a commercial fuel cell system with coolant, as the temperature gradient should increase toward the coolant outlet side. For this reason, most 50 cm^2 validation experiments will utilize liquid coolant during the course of the project.

The validation data set includes distributed liquid water, current, high frequency resistance and temperature measured across the active area. Additionally, anode vs. cathode water balance based on condensed outlet water was collected for each test point. A tool (shown in Figure 1) was developed to navigate this database such that our team and other interested researchers can select a test point from the standard protocol to download the raw and processed data. Currently the validation dataset is fully populated for the baseline material set.

Transport in Thin Ionomer Films

Ellipsometric, microbalance, and fluorescence measurements on thin Nafion® films have been performed on model surfaces. These characterization techniques on ionomer films with thicknesses between 30 and 600 nm are designed to probe the transport and swelling properties of the thin ionomer films in the catalyst layers. Ellipsometry and microbalance measurements can give us highly accurate measurements of the water content and swelling of these films as a function of RH. The fluorescence measurements shed light on the dynamics of the film, which governs the

water self-diffusion and transport properties. Fluorescence measurements probe the dynamics in the aqueous domains and we have also used grazing incidence small-angle X-ray scattering to probe their structure. Both the water uptake or hydration number (λ) and self-diffusion of water within the film determines its oxygen and proton transport properties as these species move through the aqueous domains of the material. Select microbalance and fluorescence are presented herein to demonstrate the sensitivities being observed in thin films.

Microbalance results shown in Figure 2a indicate that water content for different film thicknesses was similar for Nafion® films on gold thicker than 500 nm [3]. At lower thicknesses, slightly lower water contents were observed, especially at high vapor water activities. The origin of the observed depression in water content is still unclear. Interaction of the ionomer with the Au substrate could constrain the film from swelling, which is essential for water sorption. It is also conceivable that a water impermeable layer (disordering of water channels) at the gas/ionomer interface may contribute to the observation. Fluorescence intensity measurements of 9-([E]-2-carboxy-2-cyanovinyl) julolidine (CCVJ) in thin Nafion® films given in Figure 2b show that the fluorescence response is a function of thickness. Higher I/Io response indicates stiffening of the film upon water uptake which is not observed for the membrane, but has been reported for other thin films [4]. Since the CCVJ fluorescence signal is controlled by the local viscosity or mobility of the sample, it can be used to measure water diffusion in polymers [5]. The I/Io signal will be related to the self-diffusion coefficient of water in the next phase of this work. These measurements indicate different water dynamics in thin and thick films and provide fundamental information on potential differences in proton conductivity and other transport properties as a function of film thickness.

Transport in Diffusion Materials

Several in situ and ex situ measurements are being used to measure transport in the porous components that include the electrode, microporous layer and carbon fiber macroporous substrate. In situ neutron imaging, infrared imaging and acoustic microscopy are being used to map through-plane liquid water distributions within the anode vs. cathode diffusion layers. Ex situ work is focused on thermal conductivity and mass diffusivity as a function of water saturation, and capillary pressure relationships for the baseline diffusion media and catalyst layer are underway. Unique test cells and methodology capable of controlling saturation have been developed to complete this testing.

One characteristic result from the standard protocol has been selected for presentation in this paper and the complete reduced data set has also been made public at the website. Measured with high resolution neutron imaging, Figure 3a shows the effect of anode vs. cathode outlet pressure differentials on water saturation. The operating temperature is 40^{0}C, anode/cathode RH is 95/95% and the current density is 0.8 A/cm^2. It is evident from the plot how the higher pressure on the cathode side shifts the saturation towards the anode and vice versa. These data provide insight into the complex water balance to be modeled. The corresponding voltages have also been recorded in the plot. Polarization curves obtained with fast scans after each operating condition (Figure 3b) demonstrate the effect of the pressure differential on performance. The false color images in Figure 3c show the regions of water accumulation relative to the land/channel geometry for the specific operating conditions. These data also indicate how sensitive anode gas diffusion layer (GDL) saturation is, and this is not typically considered in two-phase models to this point.

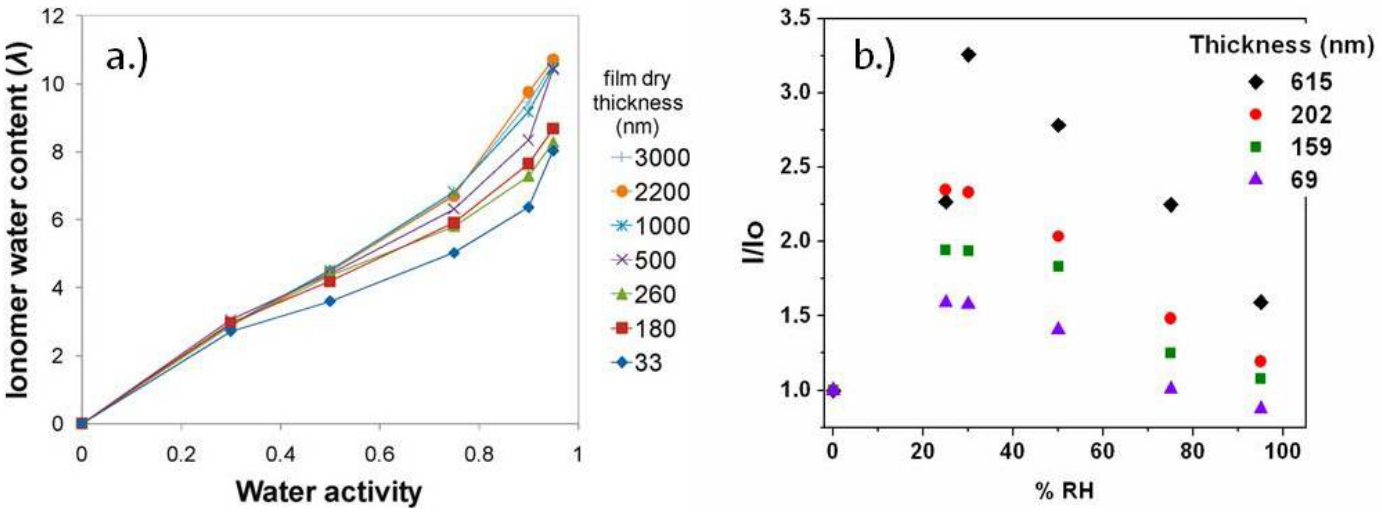


FIGURE 2. Water interaction with varying thicknesses of thin Nafion® films as a function of water activity: a) water uptake at 80°C, b) CCVJ fluorescence response at 25°C.

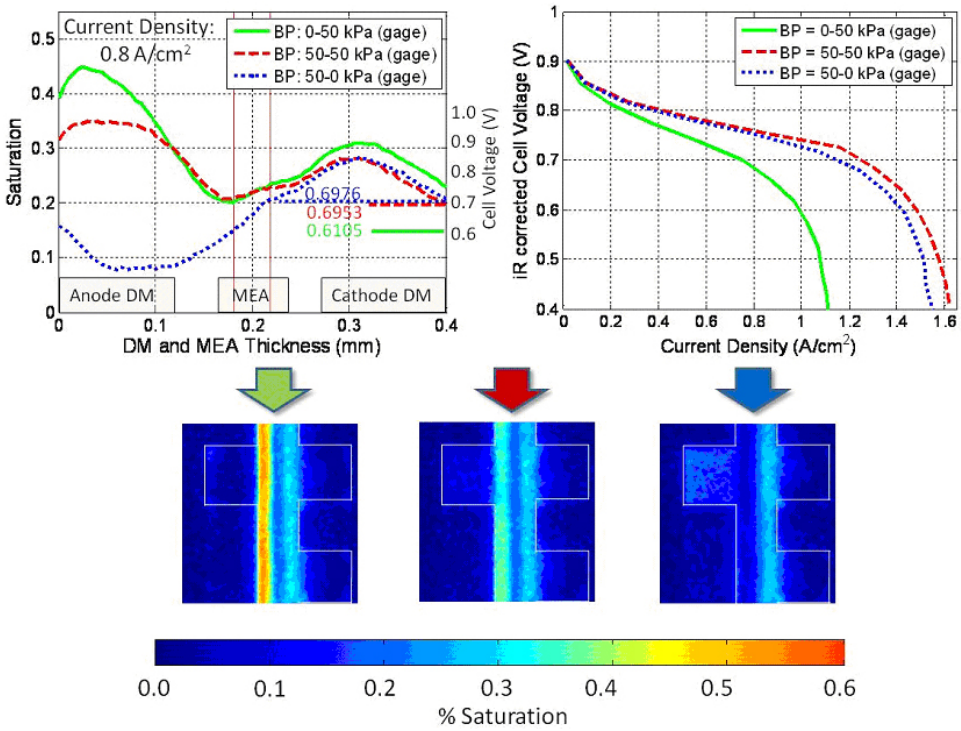


FIGURE 3. Impact of varied outlet pressure: a) GDL water saturation and through-plane, b) polarization curves, c) false color images showing saturation.

Transport in Flow Distributor Channels

Two key components of the down-the-channel model are the relationships between channel water saturation and both CFP to channel interfacial transport resistances, and the channel pressure drop. Therefore, it is critical to establish a well-defined channel water saturation metric. A technique has been developed to quantify the in situ channel water saturation through the combined utilization of high speed videos of the flow field channels during operation and digital image processing [6]. The image processing algorithm automatically detects static and dynamic liquid water, and also characterizes the flow structure of each water object. The water coverage ratio parameter along with channel pressure drop as a function of saturation are providing crucial information pertaining to transport resistance associated with liquid water accumulation in the flow field channels. Sample images showing pre- and post-processed flow field channels and the resulting water detection are shown in Figure 4. In addition to this characterization of water adjacent to the CFP in the active area, experiments are underway to characterize the resistance of liquid water transitioning from the bipolar plate micro-channels in the gas manifolds of a fuel cell stack. Here the combination of low gas shear and contact line pinning has been found to cause water stagnation at the plate edge. This results in additional plate-to-plate flow variations that must be captured in a true two-phase fuel cell model.

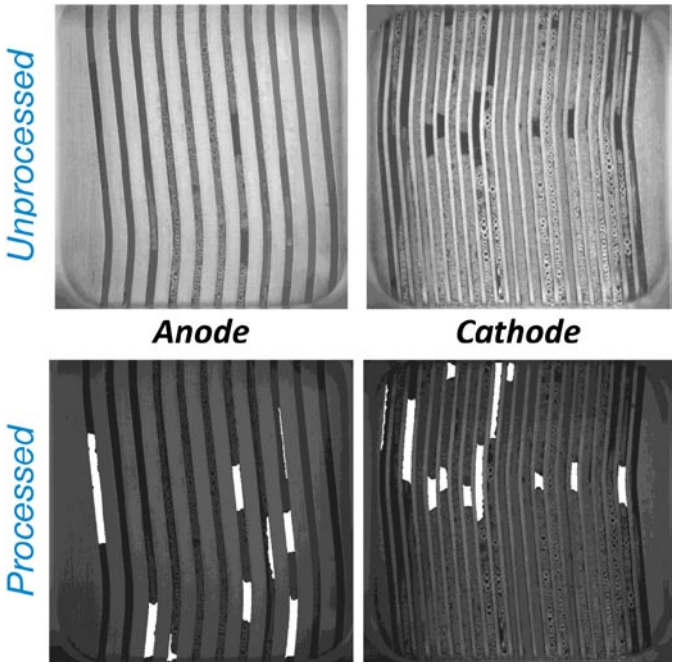


FIGURE 4. Representative unprocessed and processed high speed images of liquid water distribution in both anode and cathode channels. The processed images can provide quantified information of local and overall water coverage ratio.

To optimize the channel design for better water management, the effects of channel surface wettability, cross-sectional geometry and orientation on the two-phase flow in parallel gas channels were investigated. It was found that hydrophilic channels are advantageous over uncoated or slightly hydrophobic channels in terms of uniform water and gas flow distribution and promoting film flow. Stamped metal geometry channels favor film flow when compared to a rectangular geometry. Vertical channel orientation is advantageous over horizontal orientation because it is less prone to slug flow, and facilitates more uniform liquid water distribution and stable operation.

Conclusions and Future Directions

A well organized characterization, modeling and validation framework was developed early in this project. The first phase of execution was largely focused on experimental development with key accomplishments outlined as follows:

- Project is standardized by materials and operating space:
  - Baseline and auto-competitive material sets chosen based on parametric variations that consider degradation and cost vs. performance trade-offs.
- Key relationships required for a wet 1+1D model and characterization methods are defined:
  - Subject matter experts are developing and executing characterization methods to generate physical understanding of fundamental processes.
  - Component models describing processes are being generated and will be used to output bulk and interfacial transport resistances.
  - Modeling framework for 1+1D model is defined.
- Down-the-channel baseline material validation data set complete:
  - Additional repeat experiments being executed to define uncertainty.
- Database on the website for dissemination of data and modeling:
  - Visit www.pemfcdata.org (development will continue throughout the project).

The next phase of this project is focused on refining the component and down-the-channel models in parallel while repeating characterization and validation work for the next-generation material set. This work will support the key deliverable for next year: a validated 1+1D model capable of predicting performance and water balance under saturated conditions with baseline material parameters.

FY 2011 Publications/Presentations

1. J. Gagliardo, J. Fagley, D. Fultz, J. Owejan, "Influence of Through-Plane Thermal Profile on Water Accumulation in Proton Exchange Membrane Fuel Cells" Meeting of the Electochemical Society, Las Vegas, NV. October 2010.

2. Jacob M LaManna, Fengyuan Zhang, Subhadeep Chakraborty, and Matthew M. Mench, Quantification of Through-Plane Liquid Water Gradients and Transport in PEFCs with High Resolution Neutron Imaging. Accepted for Presentation, 2011 ECS Meeting, Montreal Canada.

3. Zijie Lu, Cody Rath, Guangsheng Zhang, Satish G. Kandlikar. Water management studies in PEM fuel cells, part IV: Effects of channel surface wettability, geometry and orientation on the two-phase flow in parallel gas channels, International Journal of Hydrogen Energy (2011).

4. Kongkanand, A., "Interfacial Water Transport Measurements in Nafion Thin Films Using a Quartz-Crystal Microbalance," J. Phys. Chem. C, 115, pp. 11318-11325, (2011).

5. Sergi, J.M., Kandlikar, S.G., "Quantification and Characterization of Water Coverage in PEMFC Gas Channels Using Simultaneous Anode and Cathode Visualization and Image Processing," International Journal of Hydrogen Energy, Accepted Manuscript, 2011.

6. J. Owejan, DOE Annual Merit Review, Arlington VA, May 12, 2011.

References

1. Gu, W., Baker, D.R., Liu, Y., Gasteiger, H.A., "Proton exchange membrane fuel cell (PEMFC) down-the-channel performance model," *Handbook of Fuel Cells* - Volume 5, Prof. Dr. W. Vielstich *et al.* (Eds.), John Wiley & Sons Ltd., (2009).

2. Owejan, J.P., Gagliardo, J.J., Sergi, J.M., Kandlikar, S.G., Trabold, T.A., "Water management studies in PEM fuel cells, Part I: Fuel cell design and in situ water distributions," International Journal of Hydrogen Energy, 34 (8), pp. 3436-3444, (2009).

3. Kongkanand, A., "Interfacial Water Transport Measurements in Nafion Thin Films Using a Quartz-Crystal Microbalance," J. Phys. Chem. C, 115, pp. 11318-11325, (2011).

4. Nolte, A.J.; Treat, N.D.; Cohen, R. E.; Rubner, M.F. Macromolecules, 41, 5793–5798, (2008).

5. Miller, K.E.; Krueger, R.H.; Torkelson, J.M., J. Polym. Sci.: Polym. Phys, 33, 2343-2349, (1995).

6. Sergi, J.M., Kandlikar, S.G., "Quantification and Characterization of Water Coverage in PEMFC Gas Channels Using Simultaneous Anode and Cathode Visualization and Image Processing," International Journal of Hydrogen Energy, Accepted Manuscript, 2011.

V.F.5 Air-Cooled Stack Freeze Tolerance

Dave Hancock
Plug Power Inc.
968 Albany Shaker Rd.
Latham, NY 12110
Phone: (518) 782-7700
E-mail: david_hancock@plugpower.com

DOE Managers
HQ: Donna Ho
Phone: (202) 586-8000
E-mail: Donna.Ho@ee.doe.gov
GO: Reginald Tyler
Phone: (720) 356-1805
E-mail: Reginald.Tyler@go.doe.gov

Technical Advisor
Walt Podolski
Phone: (630) 252-7558
E-mail: podolski@anl.gov

Contract Number: DE-EE0000473

Subcontractor:
Ballard Power Systems, Burnaby, British Columbia, Canada

Project Start Date: June 1, 2009
Project End Date: November 15, 2011

Fiscal Year (FY) 2011 Objectives

- Advance the state of the art in technology for air-cooled proton exchange membrane (PEM) fuel cell stacks and related GenDrive™ material handling application fuel cell systems.
- Demonstrate FCvelocity™ 1020ACS stack durability of 5,000 hours (2.5x nominal durability) through enhanced system operational strategies or utilization of advanced fuel cell stack materials.
- Determine a stack/system concept that is suitable for sub-zero operation down to -30°C.
- Determine a stack/system concept that achieves a total cost that is competitive with incumbent materials handling fuel cell technology solutions.
- Develop, evaluate and trade-off the stack and system to meet materials handling requirements for freeze and cost.
- Develop an understanding around integrating air-cooled stack technology into a dynamic materials handling system.
- Perform life-cycle cost analyses for freeze tolerance strategies.

Technical Barriers

This project addresses the following technical barriers from the Fuel Cells section of the Fuel Cell Technologies Program Multi-Year Research, Development and Demonstration Plan:

(A) Durability (with respect to start-up, freezing and low relative humidity operation)

(B) Cost (with respect to stack and balance of plant [BOP] trade-off)

(C) Performance (with respect to voltage degradation, low relative humidity and sub-zero performance)

Technical Targets

- Stack/system concept that is suitable for sub-zero operation down to -30°C.
- Durability for an air-cooled fuel cell stack ≥5,000 hours operating under material handling conditions including start-stop cycles; a 2x improvement over baseline testing.
- GenDrive™ product cost reduction of 25% or greater using air-cooled stack design over baseline liquid-cooled GenDrive™ product.

FY 2011 Accomplishments

- Conducted screening tests on 27 membrane electrode assembly (MEA) technologies, stack durability tests on five MEA technologies and system compatible testing on three MEA technologies.
- Built a system test bench to test all system interactions, especially the fuel cell and battery, before final packaged design solution was complete. Prior testing was performed on three stack module test benches where the system interactions are managed within an analytical model.
- Completed testing of advanced system operating strategies for the FCvelocity™ 1020ACS air-cooled stack with over 6,000 hours of operation using two advanced operating strategies. These operating strategies focus on reducing cathode catalyst dissolution and corrosion and chemical and mechanical stress on the membrane. System operating strategies provide a 2x extension in durability compared to previous tests.
- Built a prototype system and performed system level high and low ambient temperature testing. Test results demonstrate an air-cooled stack system can operate continuously at both high and low ambient temperature conditions however system improvements are required to optimize performance to ensure long life.

- The project Go/No-Go review was held with the DOE in December 2010. The project cost metric was met and the DOE approved the recommendation to continue the project and advance to Phase 2.



Introduction

Plug Power's objective is to advance the state-of-the-art fork-lift technology by using air-cooled fuel cell stacks and improving related GenDrive™ material handling systems to improve function and reduce cost. This will be accomplished through a collaborative work plan to reduce overall system cost by simplifying the system BOP through the use of an air-cooled stack as well as improve freeze tolerance and mitigate freeze-thaw failure modes through innovative fuel cell system design.

The fuel cell system, derived from Plug Power's commercially available GenDrive™ platforms, is providing battery replacement for equipment in the material handling industry. The fuel cell stacks are Ballard's commercially available FCvelocity™ 9SSL (9SSL) liquid-cooled PEM fuel cell stack and FCvelocity™ 1020ACS air-cooled PEM fuel cell stack. Stack modifications to the FCvelocity™ 1020ACS will be explored through this project. Plug Power will lead design-build-test and design-of-experiment efforts for GenDrive™ systems with support from Ballard Power Systems for the fuel cell stack and stack integration.

Approach

In this project the fuel cell stack, system and fuel cell stack operation will be designed together in order to trade off stack durability and freeze function with overall stack-system cost. Both stack and system level mitigation of freeze failure modes will be explored. The project will develop an understanding of market needs, system requirements, stack-system limitations, historical data, models and small-scale testing to define stack/system operating strategies that achieve required freeze function and durability.

Multiple design, build, test cycles will be employed to increase learning through iteration. Analytical models for durability and freeze will be developed and verified on stacks and system modules. Accelerated testing will be used where possible to reduce testing time. Stacks and systems will be operated under material handling freezer conditions, failure analysis will be performed to understand the root cause of failures, stacks and systems will be designed to mitigate the failure modes, then built and tested. Trade-off analysis will be used to determine the design solutions that are built and tested.

Results

The FCvelocity™ 1020ACS (ACS) stack must first demonstrate performance and durability targets to be considered a viable GenDrive™ product solution. Specifically, the ACS must demonstrate 5,000 hours running a representative load profile including start-stop cycles. The self-humidifying ACS stack is an "open cathode" design where cooling and reactants are supplied by a single fan. This offers system simplicity by eliminating the liquid cooling system, humidifiers, air compressor and on-board water management; providing a significant cost reduction compared to a liquid-cooled, closed cathode stack. As a result the MEA operates very dry, all start-ups are air-air start-ups and, under freeze conditions, the cooling power of the air stream is high making low current density operation difficult. All of these conditions increase the stack degradation and make function under freezing conditions a challenge.

Based on stack/MEA failure modes, two advanced system level operating strategies were developed to mitigate the known failure mechanisms:

- Air-air starts degrade the catalyst and cause voltage degradation.
- Time at open-circuit voltage (OCV) degrades the membrane and causes transfer leaks.
- High currents and stack temperatures stress the membrane.
- Mixed potentials (at start-up and shutdown) degrade the catalyst.

Figure 1 shows stack module bench test results of two system tests for average cell voltage, cumulative number of air-air starts and transfer leak rate versus operating hours; one operating strategy focused on reducing membrane degradation (time at high cell potential) while the other focused on reducing voltage degradation (number of air-air starts). The system strategy to reduce the number of air-air starts demonstrates a lower degradation rate compared to the system strategy that reduces the time at OCV. In the approach to reduce the number of air-air starts, hydrogen is kept on the anode for long periods; the result is more time spent at high cell potentials (or OCV) which has the side effect of increasing the membrane stress. To reduce membrane stress, time at high potentials can be minimized with a possible side effect of increasing the number of air-air starts. A trade-off is required between the two cases because in most cases reducing the number of starts and reducing the time at OCV are linked. The strategy to reduce OCV inherently has more air-air starts and as a result has a higher voltage degradation rate. Less time spent at OCV can increase the time for the MEA to develop a leak because there is less time spent in a state that is damaging to the membrane. Figure 1 also illustrates that although the reduced OCV strategy has the highest voltage degradation rate, it went over 6,000 hours without any indication of a transfer leak. By comparison the reduced starts operating strategy shows signs that a transfer leak was initiated after 5,000 hours due to the time spent at high cell potentials. In this system the end of life criteria is more related to voltage

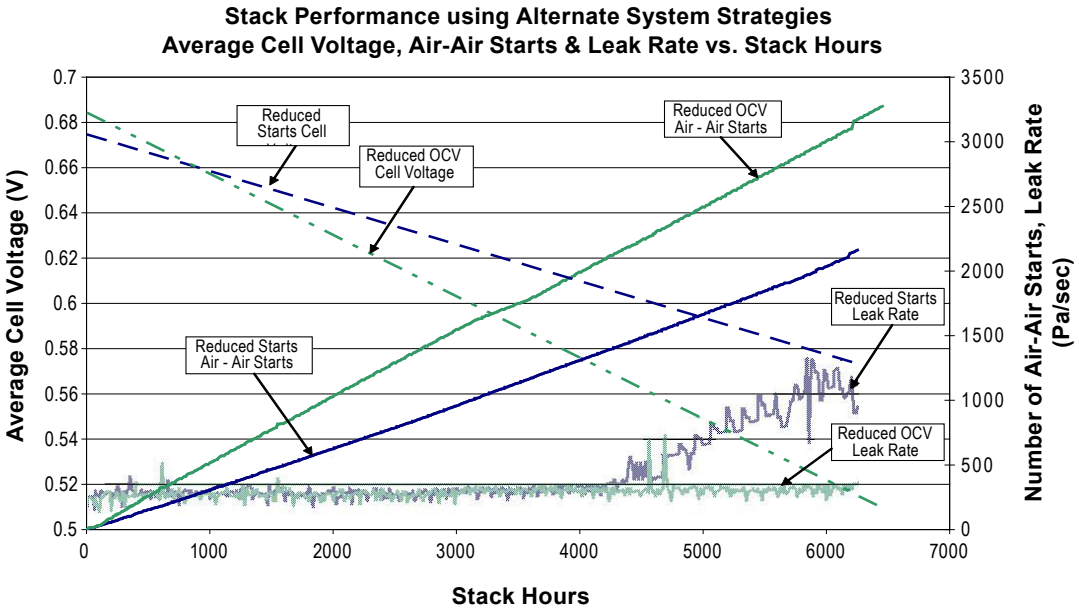


FIGURE 1. Stack Life Test Results

so managing low levels of hydrogen leaks will be accepted in order to extend life.

A prototype system using an air-cooled stack was built and instrumented for purposes of evaluating an air-cooled stack operating at low ambient temperature conditions. All development needed to build a prototype system was undertaken so that a proper system level evaluation could be made. This included activities such as battery hybrid integration, high pressure hydrogen storage integration and controls software development.

Multiple system features for low ambient temperature operation were designed into the prototype system in order to evaluate how each influences performance. A high ambient temperature test was performed first to evaluate any negative effects of system design features intended to allow low ambient temperature operation. The initial high ambient temperature testing indicated excessive pressure drop across the inlet air filter selected for the prototype design. Initially, the stack temperature exceeded the set point even with the fan at maximum speed. Removal of the filter during the test demonstrated the optimal stack temperature could be achieved with the fan operating below 60% capacity. An inlet air filter with lower pressure drop will need to be designed for the next level of tests.

The ambient temperature was then reduced to -30°C while operating a low load profile, reference Figure 2. Although stack temperature is near optimum under freezer conditions, the asymmetry of the air recirculation path produces a non-optimal gradient in stack inlet air temperature (T1, T2 and T3 are different inlet locations). Also discovered during the -30°C testing was ice formation in the air recirculation stream. As the warm exhaust air entered the cold air inlet chamber some of the moisture

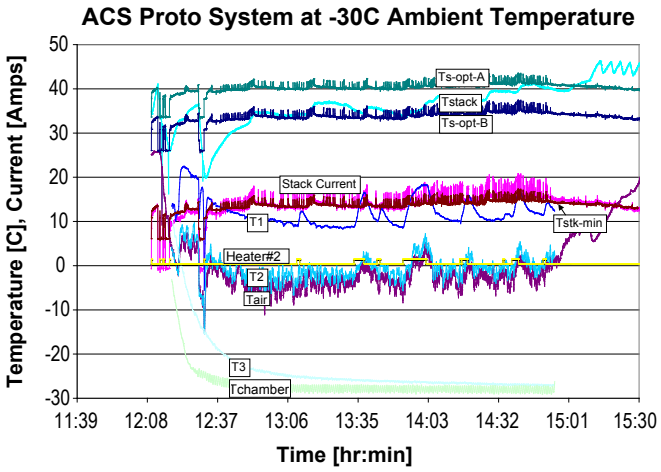


FIGURE 2. Low Ambient Temperature System Test Results

would condense then freeze. Uniform air temperatures across the stack inlet and control of the condensing moisture are critical for sustained -30°C operation. These issues are slated to be addressed during the design mitigation phase of the project.

The project Go/No-Go is based on a cost metric of a product utilizing the air-cooled stack technology. Inherent in developing the product cost is that the air-cooled fuel cell stack solution must meet minimum performance and durability requirements to even be considered for a commercial product. The metric states that a GenDrive™ product cost reduction must be 25% or greater using air-cooled stack design over baseline liquid-cooled GenDrive™ product. A comparison of initial product cost and lifecycle cost is shown in Figure 3. Several product comparisons

are made using the 2009 liquid-cooled (9SSL Technology) GenDrive™ product as the baseline. Cost reductions for the 9SSL in 2010 are primarily from supply chain initiatives. An additional 9SSL cost reduction is projected based on continued supply chain initiatives plus concept system architecture.

The first air-cooled stack comparison is made with Ballard Power System's ACS second generation MEA with 5,000 hour durability. The product cost was estimated using both a top down and bottom up approach; both estimates resulted in very similar (<4% difference) cost estimates. The top down approach started with the existing liquid-cooled product and subtracted and added component differences. The bottom up approach assumed a clean sheet design and cost estimates were applied to each subsystem based on the system process and instrumentation diagram and the actual prototype system. The second air-cooled stack comparison was made with Ballad Power Systems Advanced ACS MEA.

As can be seen, reductions in initial product cost utilizing liquid-cooled technology are starting to level out whereas product cost projections utilizing the air-cooled stack technology indicate a possible step change for the order picker product. All costs are shown normalized to the baseline. A Go/No-Go review was held with the DOE and the project was approved to advance to the next phase of design mitigation to issues uncovered during freeze testing.

One of the major issues uncovered during freeze testing was a non-uniform stack inlet air temperature gradient. Warm exhaust air is re-circulated to the stack inlet and mixed with the cold inlet air to reduce the effects of freezing air on the cathode. Computation fluid dynamics was used extensively to optimize the stack inlet air velocity and temperature gradients in the freezer (-30°C ambient temperature) environment. The initial air recirculation duct work had decent velocity gradients but large temperature gradients at the stack inlet. The air recirculation duct work was then evaluated and re-designed to reduce the air temperature gradients. Figure 4 shows the temperature profile after refinements were made to the air recirculation. The velocity profile is now very uniform; however there is still an area of the stack inlet that has a lower temperature than the rest of the stack. Some additional refinement is still required to reduce the stack inlet air temperature gradient while operating in the freezer.

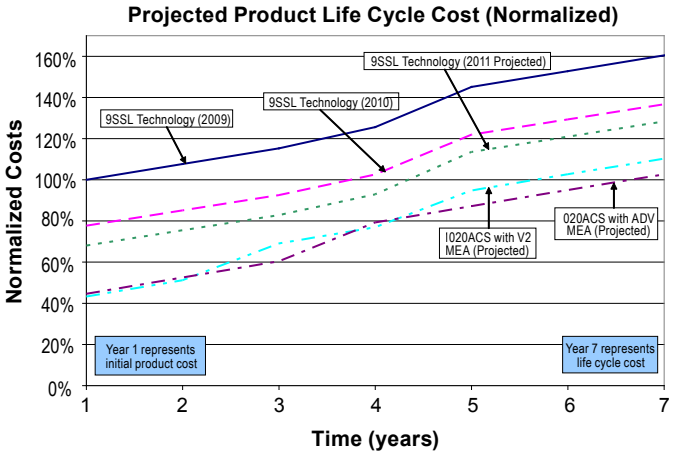


FIGURE 3. Life Cycle Cost Analysis

Conclusions and Future Directions

- Ballard's FCvelocity™ 1020ACS can meet the durability and cost requirements of the order picker GenDrive™ with modified system operating strategies designed to reduce the number of air-air starts.
- With Ballard's FCvelocity™ 1020ACS, the order picker GenDrive™ cost is lower than the liquid-cooled solution even with system strategies to handle freeze condition.
- Complete the design mitigation strategies for issues discovered during the low and high ambient temperature testing.
- Build prototype systems with mitigation strategies.
- Test prototype systems with mitigation strategies at low and high ambient temperatures.

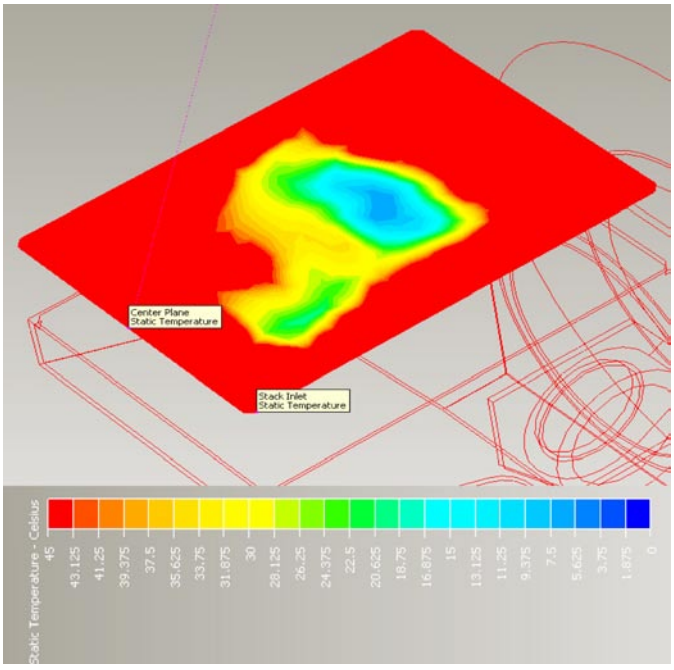


FIGURE 4. Air Temperature Profile at Stack Inlet

V.F.6 Transport Studies Enabling Efficiency Optimization of Cost-Competitive Fuel Cell Stacks

Amedeo Conti (Primary Contact), Robert Dross
Nuvera Fuel Cells, Inc.
129 Concord Road, Building 1
Billerica, MA 01821
Phone: (617) 245-7605
E-mail: aconti@nuvera.com
E-mail: rdross@nuvera.com

DOE Managers
HQ: Kathi Epping Martin
Phone: (202) 586-7425
E-mail: Kathi.Epping@ee.doe.gov
GO: Gregory J. Kleen
Phone: (720) 356-1672
E-mail: Greg.Kleen@go.doe.gov

Technical Advisors
Thomas Benjamin
Phone: (630) 252-1632
E-mail: benjamin@anl.gov
John Kopasz
Phone: (630) 252-7531
E-mail: kopasz@anl.gov

Contract Number: DE-EE0000472

Subcontractors:
- Johnson Matthey Fuel Cell Ltd., London, United Kingdom
- Lawrence Berkeley National Laboratory, Berkeley, CA
- Pennsylvania State University, State College, PA
- University of Tennessee at Knoxville, Knoxville, TN

Project Start Date: September 1, 2009
Project End Date: August 31, 2012

Fiscal Year (FY) 2011 Objectives

- Develop and publish a predictive transport model that enables efficiency maximization at conditions that meet DOE cost targets.
- Demonstrate stable and repeatable high performance on a full-format fuel cell stack, namely 7.5 W/mg-Pt.
- Optimize the efficiency (electric potential at rated current) of a stack technology that meets DOE cost targets.

Technical Barriers

This project addresses the following technical barriers from the Fuel Cells section of the Fuel Cell Technologies Program Multi-Year Research, Development and Demonstration Plan:

(B) Cost

(C) Performance

(E) System Thermal and Water Management

Technical Targets

This project is primarily focused on reducing stack cost and improving efficiency by modeling and optimizing transport properties of the membrane electrode assembly (MEA). Stack cost is reduced through a combination of increased power density and decreased noble metal content. The performance target of 7.5 W/mg-Pt @ 500 mV was selected, based on cost modeling results, as the performance required to achieve the 2015 DOE cost target of $15/kW$_e$. Efficiency (electric potential at rated current) of the stack technology will be optimized with the ultimate goal of approaching the 2015 DOE efficiency targets:

- Stack efficiency @ rated power: 55%
- Stack efficiency @ 25% of rated: 65%

FY 2011 Accomplishments

- A new gradient preserving single-cell fixture capable of high power density operation was delivered to University of Tennessee, Knoxville (UTK)/Penn State University (PSU), and Johnson Matthey Fuel Cells (JM).
- Single-cell testing was conducted on two flowfield architectures, and the results suggest that the performance advantage of open flowfield is the result of improved oxygen diffusion to the cathode reaction sites.
- A two-dimension (2D)+1 mathematical model capable of predicting high current density operation in different architectures was developed and refined, and the accuracy of the model was partially validated with experimental testing.
- MEAs with low Pt loading electrodes, thin membranes, and low equivalent weight (EW) ionomer in the electrodes were developed and optimized for performance at ultra-high current densities.
- The Go/No-Go milestone was satisfied by demonstrating >1 W/cm^2 @ 0.2 mg-Pt/cm^2 on a full-format stack.



Introduction

Hydrogen fuel cells are recognized as one of the most viable solutions for mobility in the 21st century; however, there are technical challenges that must be addressed before the technology can become available for mass production. One of the most demanding aspects is the costs of present-

day fuel cells which are prohibitively high for the majority of envisioned markets. The fuel cell community recognizes two major drivers to an effective cost reduction: (1) decreasing the noble metals content, and (2) increasing the power density in order to reduce the number of cells needed to achieve a specified power level. Nuvera's technology exhibits great promise for increasing power density on account of its proven ability to operate stably at high current densities (>1.5 A/cm^2). However doing so compromises efficiency, increases the heat rejection duty, and is thus more demanding on the cooling system. These competing aspects are being assessed in order to identify the proper trade offs, and ensure the modeling and experimental activities of the AURORA Program respect system-level constraints for automotive applications. This project will develop a predictive transport model to identify and help us reduce losses and increase efficiency for high current density operation.

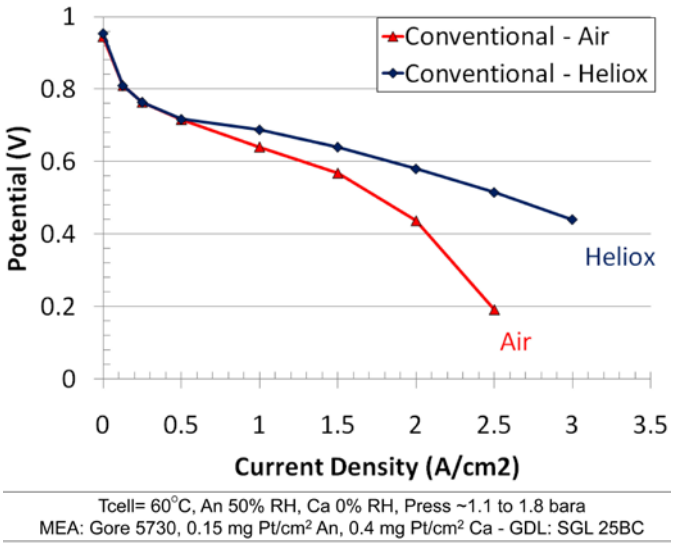
Approach

Nuvera structured the activities in the scope of the project to orbit around a focal point consisting of the fuel cell predictive model. Cost and system analyses were performed in order to define the boundaries of the design space that the model should represent. This analytical work will inform the experimental tests on a new single cell fixture to illuminate the physics and the parameters composing the backbone of the fuel cell model. The predictions generated by the model drive both the process of optimization of the fuel cell operating conditions and the material development. The combined results of these two activities are verified on single cell fixtures as well as on full active area hardware, and the experimental data obtained is used to validate and calibrate the model through multiple iterations.

Results

In FY 2011 Nuvera delivered a new gradient preserving single-cell open flowfield (SCOF) cell to partners UTK/PSU and JM. A new single-cell test station was also received and commissioned to facilitate SCOF testing at Nuvera. A number of test station issues were resolved with hardware upgrades, and the test station is now fully verified, and SCOF testing has begun.

UTK/PSU tested both a conventional land/channel cell and the Nuvera SCOF cell in order to compare the two architectures. The results highlight a significant advantage of the SCOF cell to operate at ultra-high current densities without suffering from diminishing return of power density. As shown in Figures 1 and 2, the conventional land/channel cell exhibits significantly lower performance with air than with heliox while the Nuvera SCOF cell exhibits almost the same performance with both oxidants. The SCOF cell operating with air also exhibited similar performance to the conventional land/channel cell operating with heliox. These results suggest that the performance advantage of the SCOF is the result of improved oxygen diffusion to the cathode reaction sites.



RH - relative humidity; GDL - gas diffusion layer

FIGURE 1. Air vs. Heliox Performance Comparison of Conventional Land/Channel Architecture

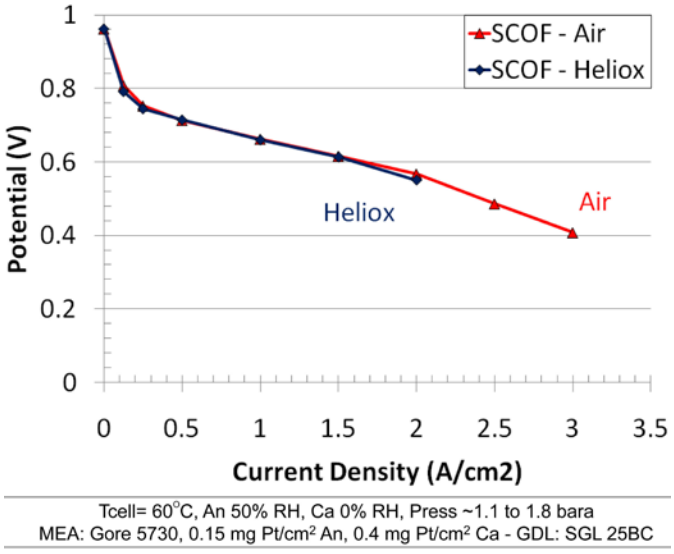


FIGURE 2. Air vs. Heliox Performance Comparison of SCOF Cell With Open Architecture

UTK/PSU also developed and refined a 2D+1 mathematical model capable of predicting high current density operation for different flowfield architectures. The physics and electrochemistry of a previously implemented 2D model was used to create a new 2D+1 "AURORA model" capable of simulating both the conventional land/channel and Nuvera open flowfield architectures. Significant additional physics were added to the model formulation in order to more accurately predict water, gas, and heat transport, and an advanced agglomerate electrode model from Lawrence Berkeley National Laboratory (LBNL) was integrated into the model in order to provide

a more accurate account for cathode kinetic loss. The accuracy of this model has been partially validated with simultaneous in situ experimental testing in terms of performance, high frequency resistance (HFR) and net water drag coefficient. The predictions from the 2D+1 model are compared with experimental results in Figure 3 in terms of performance and HFR with close agreement. Consistent with experimental results, the computational model predicts that the HFR increases with current density, which signifies the onset of the possible membrane dry-out in the ultra-high current density regime. The experimental and modeling investigation found that for the open flow field architecture, gas phase mass transport is not the limiting factor even in the ultra-high current regime.

JM developed low Pt loading MEAs optimized for performance at ultra-high current densities. JM produced and tested a number of MEA design iterations in order to develop an MEA with low Pt loading electrodes, a thin low resistivity membrane, and low EW ionomer in the electrodes. First, a low loading (0.2 mg/cm^2) electrode design was optimized with a thin membrane to achieve a performance improvement of 50 mV @ 2 A/cm^2 over the baseline which had higher Pt loadings (0.5 mg/cm^2) and a thicker membrane. This optimized MEA was produced and delivered to Nuvera for testing. The performance of the MEA was then improved even more by using a low EW ionomer (between 750 and 850) in the electrode. Initial versions of the MEA with low EW ionomer exhibited performance lower than expected as a result of significant electrode flooding. The electrode was then optimized for water management, and the final version was able to achieve a performance improvement of 40 mV @ 2 A/cm^2 in the JM single cell. This new MEA design was also produced and delivered to Nuvera for testing. Development work has started for anode electrodes with very low Pt loading (0.02 mg/cm^2). Initial results show promise at low current densities, however water management has been an issue at high current densities thus far.

Nuvera tested various developmental MEAs from JM on full format automotive stacks. Figure 4 shows performance of two optimized MEA designs, MEA 23 (blue) has a thin membrane with high Pt loadings (0.5 mg/cm^2), and MEA 25 (red) has the same thin membrane with low Pt loadings (0.2 mg/cm^2). As expected, the low Pt loading MEA exhibits lower performance in the low current density Tafel region (30 mV lower @ 0.2 A/cm^2) due to lower electrochemical surface area; however, the ohmic losses of this MEA are lower and the performance approaches that of the high loading MEA at high current density (2 A/cm^2). The high performance demonstrated by the low loading MEA of 0.548 V @ 2 A/cm^2 exceeded the 1 W @ 0.2 mg-Pt/cm^2 target and satisfied the Go/No-Go milestone for the project.

Conclusions and Future Directions

Nuvera has demonstrated high performance (5.57 W/mg-Pt), satisfying the Go/No-Go milestone, and Nuvera will continue evaluating JM development materials with the goal of demonstrating stable and repeatable high power performance of 7.5 W/mg-Pt on a full format fuel cell stack.

JM has achieved significant Pt reduction and performance improvements at high current density and will continue executing the materials development plan investigating reduced loading anode electrodes, graded Pt cathode electrodes, and novel MEA architectures.

UTK/PSU has developed, refined, and partially validated a predictive 2D+1 mathematical model using feedback from simultaneous in situ experimental testing. UTK/PSU will continue tuning and validating the model, in

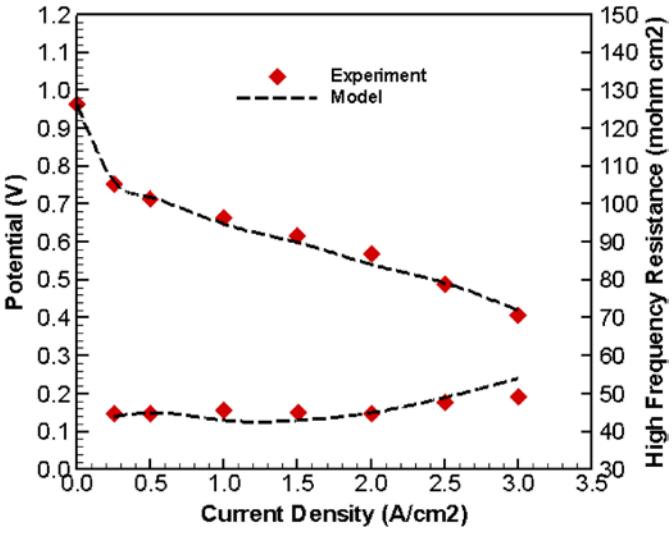


FIGURE 3. Comparison of Voltage and HFR between Experiment and Model

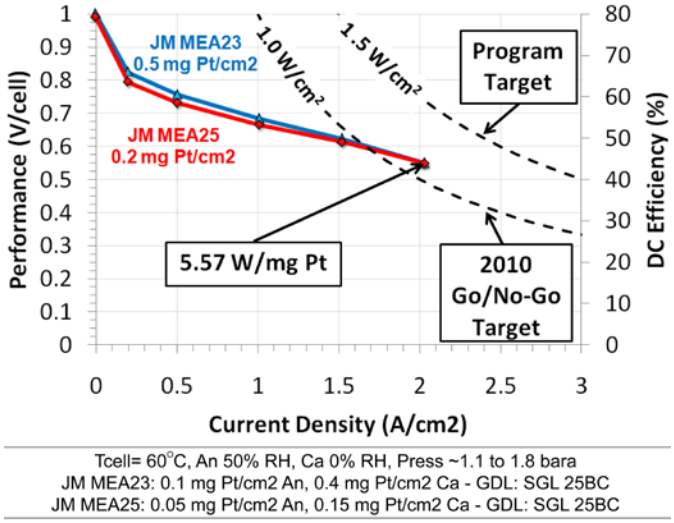


FIGURE 4. Performance Curves of Standard and Low Loading JM MEAs with Thin Membranes

terms of performance, HFR, and net water drag coefficient, with the goal of publishing a fully validated predictive model at the end of the project.

FY 2011 Publications/Presentations

1. May 2011 – Washington, D.C. - 2011 DOE Hydrogen Program Merit Review (FC028).

2. June 2011 – Detroit, MI - FreedomCar Review.

V.F.7 Fuel Cell Fundamentals at Low and Subzero Temperatures

Adam Z. Weber (Primary Contact), John Newman, Clayton Radke
Lawrence Berkeley National Laboratory
1 Cyclotron Rd, MS 70-108B
Berkeley, CA 94720
Phone: (510) 486-6308
E-mail: azweber@lbl.gov

DOE Manager
HQ: Nancy Garland
Phone: (202) 586-5673
E-mail: Nancy.Garland@ee.doe.gov

Subcontractors:
- Los Alamos National Laboratory, Los Alamos, NM
- United Technologies Research Center, East Hartford, CT
- 3M Company, St Paul, MN
- The Pennsylvania State University, State College, PA

Project Start Date: September 21, 2009
Project End Date: September 30, 2013

Fiscal Year (FY) 2011 Objectives

- Fundamentally understand transport phenomena and water and thermal management at low and subzero temperatures.
- Examine water (liquid and ice) management with nano-structured thin-film (NSTF) catalyst layers.
- Enable operational and material optimization strategies to be developed to overcome observed performance bottlenecks.
- Characterize and measure critical transport properties for operation with liquid water.
- Elucidate the associated degradation mechanisms due to subzero operation and enable mitigation strategies to be developed.

Technical Barriers

This project addresses the following technical barriers from the Fuel Cells section of the Fuel Cell Technologies Program Multi-Year Research, Development and Demonstration Plan:

(C) Performance
(A) Durability
(D) Water Transport within the Stack
(E) System Thermal and Water Management
(G) Start-Up and Shut-Down Time and Energy/Transient Operation

Technical Targets

This project is conducting fundamental investigations into fuel cell operation at low and subzero temperatures. The knowledge gained will enable various metrics to be met or exceeded. These include those related to durability, performance, and cost. Specifically,

- Durability
  - 5,000 hr (automotive) and 40,000 hr (stationary).
  - Thermal cycling ability with liquid water.
- Performance
  - Unassisted start from -40°C.
  - Cold start to 50% power in 30 seconds and with 5 MJ or less energy.
  - Efficiency of 65% and 55% for 25% and 100% rated power, respectively.
  - Stack power density of 2 kW/kg.
  - Platinum group metal (PGM) loading of 0.2 g/kW.
- Cost: $15/kW_e$

FY 2011 Accomplishments

- Completed cold-start model and demonstrated that proton limitations may exist during isothermal cold starts as ice lenses build up near the membrane interface.
- Determined impact of membrane thickness, catalyst-layer thickness, and ionomer-to-carbon ratio on isothermal cold-start behavior.
- Developed capabilities and experimental protocols for measuring capillary-pressure–saturation relationships for both gas diffusion layers (GDLs) and microporous layers (MPLs). Demonstrated that this relationship is critical and can be used to explain water transport throughout the material. Also designed a test fixture for measuring water distributions using X-ray tomography.
- Developed rate expression from theory and fit to experimental data showing kinetic freezing phenomena inside GDLs.
- Measured water properties in a traditional catalyst layer including ionomer water uptake and capillary-pressure saturation relationship.

✧ ✧ ✧ ✧ ✧

Introduction

Polymer electrolyte fuel cells experience a range of different operating conditions. As part of that range, they are expected to be able to survive and start at low and subzero temperatures. Under these conditions, there is

a large amount of liquid and perhaps frozen water due to the low vapor pressure of water. Thus, water and thermal management become critical to understanding and eventually optimizing operation at these conditions. Similarly, durability aspects due to freezing and low temperatures are somewhat unknown and need further study in order to identify mechanisms and mitigation strategies. In addition, it is known that thin-film catalyst layers such as the NSTF developed by 3M have issues with large amounts of liquid water due to their thinness. These layers provide routes towards meeting the DOE cost targets due to their high catalytic activities. This project directly focuses on the above aspects with the goal that improved understanding will allow for the DOE targets to be met with regard to cold start, survivability, performance, and cost.

Approach

The overall approach is to use a synergistic combination of cell, stack, and component diagnostic studies with advanced mathematical modeling at various locations (national laboratories, industry, and academia). Ex situ diagnostics will be used to quantify transport properties and to delineate phenomena that are used in the modeling. The multiscale modeling will account for stack position through boundary conditions that are fed to a pseudo three-dimensional or one plus two-dimensional cell model. This model will be used during shutdown to predict the water profile during the subsequent cold start. The model will be validated by comparison of measured in situ cell performance in both stacks and single cells. Durability will be probed by doing cycling and other stress tests as well as taking failed cells from the in situ testing and duplicating their failure ex situ. To understand controlling phenomena and the impact of various layers, a systematic investigation at the component scale will be accomplished. After initial baseline cell assemblies have been tested and explored, various components will be switched to understand the impact of each one on both performance and durability.

Results

When fuel cells operate at low and subzero temperatures, liquid water and water management become more important. Thus, there is a need to study properties of the porous fuel cell layers in the presence of liquid water. As noted last year, the capillary pressure–saturation relationship is critical in understanding the two-phase properties of fuel cell layers. This year, we used this technique to examine the properties of a catalyst layer. For this study, an extra thick (about 30 microns) catalyst layer was made using the tradition ink painting process. This layer was then tested using our capillary pressure apparatus [1], and the results are shown in Figure 1a. As can be seen, the layer is about 60% hydrophilic, which is much different than the results of a GDL, which shows hydrophobic behavior on imbibition and a mixed wettability response. Similarly, we tested the water uptake of these catalyst layers using dynamic vapor sorption

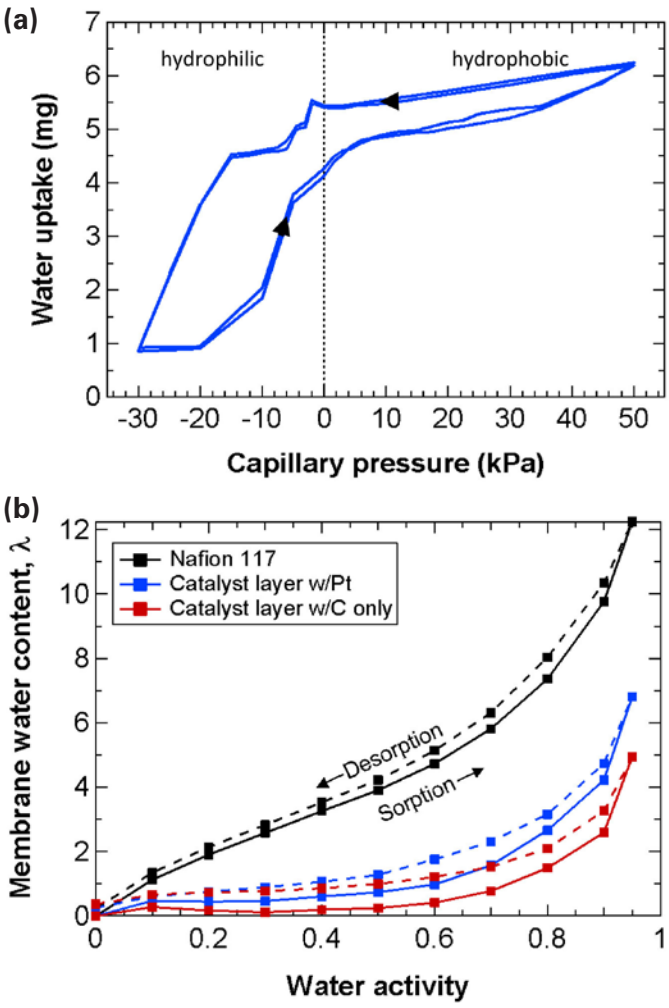


FIGURE 1. (a) Capillary pressure–saturation relationship for a traditional Pt/C catalyst layer. (b) Membrane water content for a Pt/C and C only catalyst layer as a function of humidity (bulk Nafion® is shown as a reference).

apparatus (SMS Instruments). As Figure 1b demonstrates, the water uptake of the ionomer in the catalyst layer is less than that of a bulk ionomer, thereby suggesting a depression of its transport properties as well. Interestingly, samples with Pt/C and not just C show increased water uptake which may be due to the fact that the sulfonic acid sites bind to the Pt (in agreement with results from Oak Ridge National Laboratory), which opens up the membrane morphology to accept more water.

Other diagnostics are aimed at determining what happens when water freezes in the various fuel cell layers. Using nucleation theory and dynamic scanning calorimetry, we were able to develop a rate expression for water freezing inside of a GDL. This expression was used to predict the onset of freezing under different subcoolings as shown in Figure 2. It is interesting to note that ice will not form in GDLs until substantial subcooling has occurred, even over long periods of time. However, that is not to say that freezing will not occur in other components, especially flow fields.

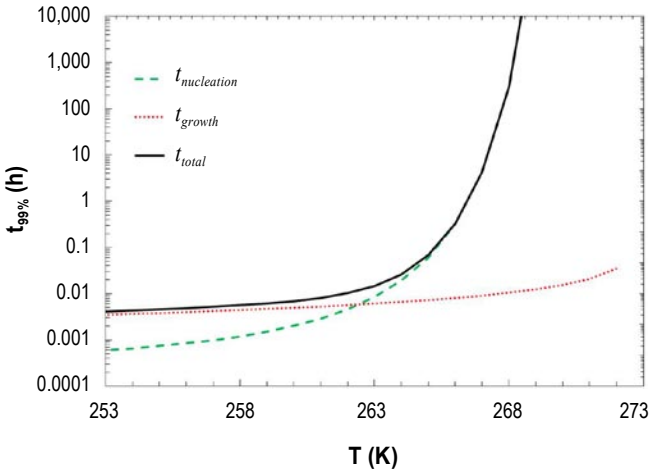


FIGURE 2. Prediction of time to freeze in a GDL as a function of subcooling using experimentally fit and theoretically derived rate expression.

To understand ice formation as a function of MEA properties, isothermal cold-start experiments were undergone. The main variables altered were the catalyst-layer thickness, membrane thickness, and ionomer to carbon ratio. Figure 3a shows the results of changing the membrane thickness, where thicker membranes allow for more water production as long as the temperature is high enough. The reason is that at lower temperatures, there is not a sufficient diffusion flux for water to get into the membrane and saturate it. Figure 3b shows the impact of catalyst-layer thickness, where thinner catalyst layers do not seem to have enough storage capacity to allow for more water generation before failure. This could be critical for NSTF and is something being investigated for next year. Finally, Figure 3c shows the impact of ionomer to carbon ratio. At low values, there is not enough ionomer to provide good proton conductivity and thus the water production before failure is low. However, at high ionomer-to-carbon-ratio contents, the ionomer begins to fill in the pore space of the catalyst layer, thereby limiting oxygen transport and storage capacity of the produced water.

Mathematical modeling was used to understand both isothermal and nonisothermal cold start. The nonisothermal cases demonstrate that starting either at lower voltages or with drier membranes lead to better performance. For isothermal cold start, the simulations demonstrate that the entire pore capacity of the catalyst layer may not be used during the start, especially at high current densities. The reason for this is that an ice front forms and propagates from the membrane interface towards the interface with the GDL as shown in Figure 4. The ice-front propagation is driven by the nonuniform reaction-rate distribution that occurs at high current densities, which is why it is not seen in the case of lower current densities which have a more uniform reaction-rate distribution. The end result of the ice front is that at higher current densities, the cell becomes ohmically limited

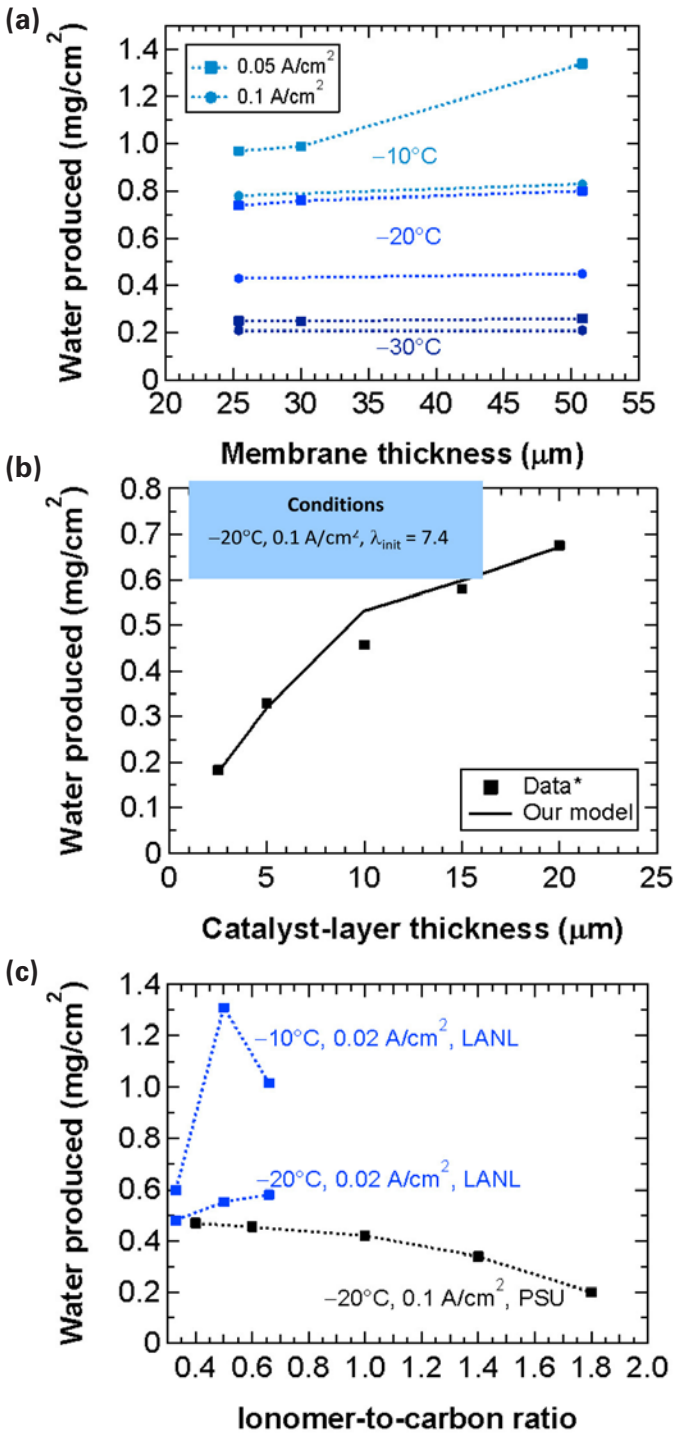


FIGURE 3. Isothermal cold-start data showing water produced before zero volts as a function of (a) membrane thickness, (b) catalyst-layer thickness, and (c) ionomer-to-carbon ratio.

since the protons cannot reach the reaction site as it goes further from the membrane. Thus, the zero cell voltage is not due to a true limiting current and zero oxygen concentration, but due to proton conduction limitations. Understanding these interplays and phenomena will allow for optimum

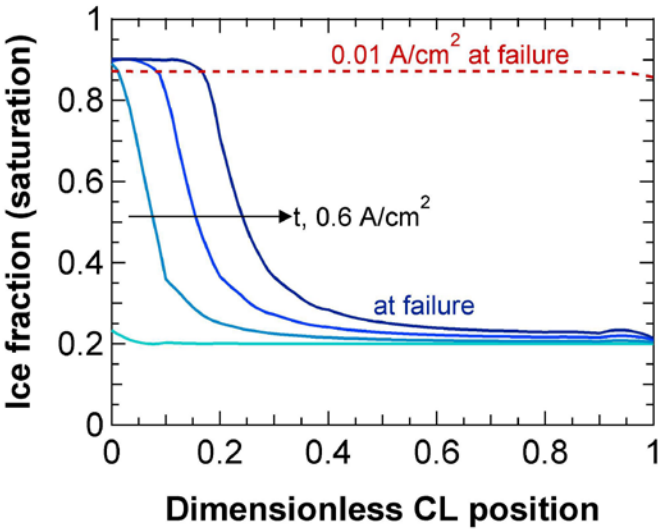


FIGURE 4. Isothermal cold-start simulation results showing ice-fraction profile as a function of time for two current densities.

starting conditions and material properties to be determined such that DOE targets for cold start can be met.

Conclusions and Future Directions

The project focus this year was on exploring liquid and ice formation in traditional catalyst layers and GDLs. The experiments demonstrated the hydrophilicity of the catalyst layer although some hydrophobic character remains; reduced water uptake in catalyst-layer ionomer; the need to subcool GDLs to induce freezing; and that thicker catalyst layers with around 0.4 ionomer-to-carbon ratio provide the best chance to cold start due to their increased water capacity and sufficient ionic conductivity. In addition, the cold-start model was finished, with results helping to explain experimental observations with both isothermal and nonisothermal cold starts including the fact that ohmic and not oxygen mass-transfer limitations can become limiting during cold start at higher current densities. In terms of future work, this can be summarized as:

- Cell Performance
  - Testing of non-baseline assemblies.
  - Isothermal and adiabatic starts including cycling studies for tracking durability.
  - Provide model-validation data.
- Component Characterization
  - Catalyst layers
    - More data on water-related properties.
    - Examine ice generation and form using infrared thermography and X-ray tomography.
  - Diffusion media
    - Capillary pressure – saturation relationships.

      Impact of flowrate, temperature, injection sites (MPL analogs), materials.
    - Measure effective gas-diffusion coefficient as a function of saturation.
- Modeling of Cold Start
  - Examine interplay between water storage and movement for transient and startup.
  - Develop three-dimensional to two-dimensional downscaling correlations.
  - Model the low-anode-pressure and alternative-GDL results that 3M has obtained.
- Stack studies for temperature distribution and performance characterization.
- Understand and increase the operating window with thin-film catalyst layers.

FY 2011 Publications/Presentations

1. T.J. Dursch, C.J. Radke, and A.Z. Weber, 'Crystallization Kinetics of Ice in the Gas-Diffusion Layer of a PEMFC,' Langmuir, submitted (2011).

2. G.-S. Hwang, M. Kaviany, J.T. Gostick, B. Kientiz, A.Z. Weber, M.H. Kim, 'Role of Water States on Water Uptake and Proton Transport in Nafion using Molecular Simulations and Bimodal Network,' Polymer, 52, 5284 (2011).

3. Nobuaki Nonoyama, Shinobu Okazaki, Adam Z. Weber, Yoshihiro Ikogi, and Toshihiko Yoshida, 'Analysis of Oxygen-Transport Diffusion Resistance in Proton-Exchange-Membrane Fuel Cells', J. Electrochem. Soc., 158, B416 (2011).

4. Y. Wang, P.P. Mukherjee, J. Mishler, R. Mukundan, R.L. Borup, 'Cold start of PEFCs', Electro. Acta, 55, 2636 (2010).

5. Thomas J. Dursch, Clayton Radke, and A. Weber, 'Ice Formation in Gas-Diffusion Layers', ECS Transactions, 33 (1), 1143 (2010).

6. Jeff T. Gostick, Haluna Gunterman, Brian Kienitz, JohnxNewman, Alastair MacDowell, and A. Weber, 'Tomographic Imaging of Water Injection and Withdrawal in PEMFC Gas Diffusion Layers', ECS Transactions, 33 (1), 1407 (2010).

7. T.J. Dursch, M.A. Ciontea, C.J. Radke, and A.Z. Weber, 'Isothermal Crystallization Kinetics in the Gas-Diffusion Layer of a Fuel Cell,' 85th Colloid and Surface Science Symposium, Montreal, Canada, June 2011.

8. Ahmet Kusoglu and Adam Z. Weber, 'Dynamic Water Sorption Behavior of PFSA Membranes,' 241st American Chemical Society Meeting, Anaheim, April 2011.

9. B. Kienitz, J. Gostick, A. MacDowell, and A. Weber, 'Investigating Nafion Water Content Using X-ray Radiography,' 218th Meeting of the Electrochemical Society, Las Vegas, October 2010.

10. J.T. Gostick, H. Gunterman, A. MacDowell, J. Newman, and A. Weber, 'Imaging Water Distribution in GDLs Using X-ray

Tomography,' 218th Meeting of the Electrochemical Society, Las Vegas, October 2010.

11. A. Kusoglu, J. Park, and A. Weber, 'Effect of Constraint on the Sorption Behavior of Fuel-Cell Membranes,' 218th Meeting of the Electrochemical Society, Las Vegas, October 2010.

12. H. Gunterman, J. Gostick, J. Newman, and A. Weber, 'Measurement of Air-Water Capillary-Pressure Curves of Microporous Layers,' 218th Meeting of the Electrochemical Society, Las Vegas, October 2010.

V.G.1 Novel Approach to Advanced Direct Methanol Fuel Cell (DMFC) Anode Catalysts

Huyen N. Dinh (Primary Contact),
Thomas Gennett, Bryan Pivovar, David Ginley,
Arrelaine Dameron, Katherine Hurst,
Kevin O'Neill, Steve Christensen, Justin Bult,
Tim Olson, KC Neyerlin, and Sean Culver
National Renewable Energy Laboratory (NREL)
1617 Cole Blvd.
Golden, CO 80401-3393
Phone: (303) 275-3605
E-mail: Huyen.Dinh@nrel.gov

DOE Manager
HQ: Kathi Epping Martin
Phone: (202) 586-7425
E-mail: Kathi.Epping@ee.doe.gov

Subcontractors:
- Ryan O'Hayre, Ryan Richards, Svitlana Pylypenko, Joghee Prabhuram, April Corpuz, Kevin Wood, Colorado School of Mines (CSM), Golden, CO
- Charles Hays, Sri.R. Narayan, Michael Johnson, Jet Propulsion Laboratory (JPL), Pasadena, CA

Project Start Date: July 20, 2009
Project End Date: September 30, 2011

Fiscal Year (FY) 2011 Objectives

Our primary objective is to improve the catalytic activity and durability of PtRu for the methanol oxidation reaction (MOR) via optimized catalyst-support interactions.

- Determine the effect of ion implantation of highly oriented pyrolytic graphite (HOPG) on the catalyst activity and stability of PtRu catalyst nanoparticles deposited by vapor or solution phase processes.
- Determine the effect of doping level and type of dopants (e.g., n or p) on the catalytic activity and durability of the PtRu/HOPG model catalyst system.
- Apply the understanding established from the dopant-engineering approach of the model HOPG planar materials to high surface area carbon supports. The goal is to improve catalyst utilization, activity, and durability for membrane electrode assemblies (MEAs).

Technical Barriers

This project addresses the following technical barriers from the consumer electronics section of the Fuel Cell Technologies Program Multi-Year Research, Development and Demonstration Plan (section 3.4.4):

(A) Durability
(B) Cost
(C) Performance

Technical Targets

This project aims to improve the catalytic activity and durability of PtRu for the MOR via optimized catalyst-support interactions. Insights gained from these studies will be applied toward the development and demonstration of DMFC anode catalyst systems that meet or exceed the following DOE 2010 Consumer Electronics targets:

- Cost: $3/W
- Specific power: 100 W/kg
- Power density: 100 W/L
- Lifetime: 5,000 hours

FY 2011 Accomplishments

- Established the effect of nitrogen dosage and nitrogen functionalities on catalyst durability using the model HOPG system.
- Determined that the dopant type (N_2-, N_2/H_2- CF_4, O_2- and I_2-doped HOPG) affects MOR activity and durability.
- Developed a tool and process for effective ion implantation and sputter deposition processes applicable to high surface area carbon materials.
- Developed and optimized PtRu sputter deposition methods from a single composition PtRu alloy target to produce highly dispersed PtRu nanoparticles of a desired catalyst composition and metal loading on high surface area carbon supports.
- Demonstrated that in-house magnetron sputter deposited PtRu/N-doped Vulcan carbon catalysts are more durable than both the undoped in-house catalysts and commercial PtRu/C catalysts.
- Demonstrated that in-house sputter deposited PtRu/C catalyst outperforms a commercial catalyst in a DMFC.



Introduction

High material cost and insufficient catalytic activity and durability are key barriers to the commercial deployment of DMFCs–the most advanced fuel cell technology for consumer electronics application. DMFCs are attractive for portable commercial and military applications because they offer extremely high theoretical energy density.

To accelerate the commercialization of DMFCs for consumer electronics applications, next generation materials based on leap-frog technology are needed. In DMFCs, the MOR on the anode limits the performance and durability. Breakthroughs in DMFC anode catalysis with respect to performance, cost and durability will help enable and accelerate the commercialization of DMFCs.

Approach

This project focuses on improving the catalytic performance and long-term durability of the anode catalyst for the MOR. Our approach is to modify and optimize catalyst-support interactions in order to substantially increase activity, selectivity, and durability of PtRu catalytic systems. The team systematically investigated the effects of ion-implantation on HOPG, as a model support analogue as demonstrated by a series of recent publications [1-6] on PtRu catalysts. These well-defined systems allow us to assess dopant effects and provide a test-bed for exploring new dopant/catalyst combinations. These undoped and doped, via ion implantation, carbon substrates are decorated with PtRu using both aqueous solution and physical vapor methods. The catalysts are characterized with various techniques such as microscopy, Raman spectroscopy, X-ray diffraction (XRD), X-ray photoelectron spectroscopy (XPS) and electrochemistry to determine the catalyst particle size, dispersion, composition, structure, degree of alloying, MOR activity and electrochemical durability. The catalyst synthesis process and materials are down-selected based on performance and transferred to high surface area carbon studies for further study. The highest performing materials are used in DMFC testing.

Results

We demonstrated that nitrogen implantation on HOPG has a beneficial effect of improved methanol oxidation catalytic activity and durability. XRD results showed no difference in the PtRu composition, structure, or crystallite size for PtRu on N-doped HOPG, Ar-HOPG or undoped HOPG. However, the methanol oxidation activity was higher for PtRu on N-HOPG. Nitrogen doping resulted in an inherent chemical effect and an improved stability as was predicted by theory [2-3].

We also established the role of nitrogen in the durability of PtRu/HOPG catalyst via microscopy and XPS analysis. Figure 1 shows PtRu nanoparticles on N-doped HOPG samples before and after 300 cycles between 0 and 1.1 V vs. Ag/AgCl, at 250 mV/s in 1 M H_2SO_4, for different levels of N-doping. Before cycling, the transmission electron microscope (TEM) images show that PtRu coverage and

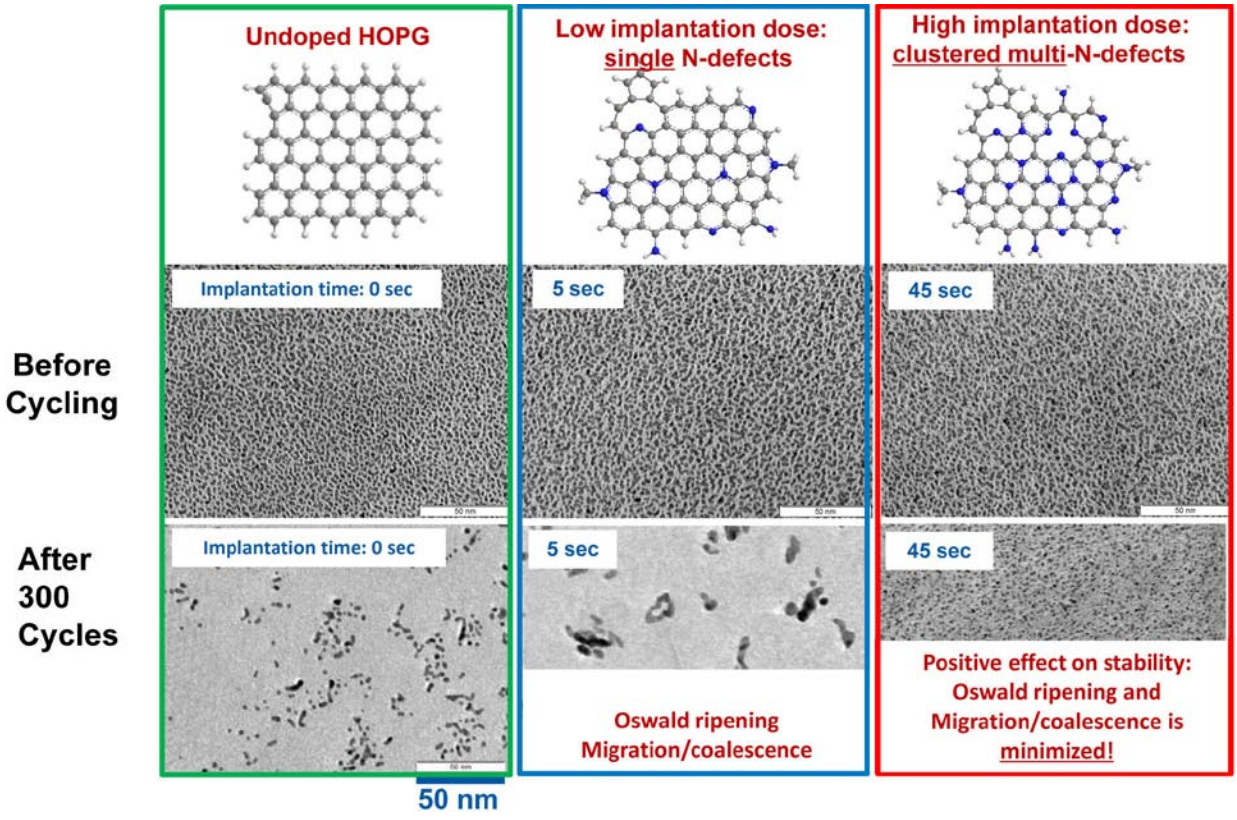


FIGURE 1. TEM images showing the effect of N-dosage on catalyst durability following potential cycling. High N-dosage results in clustered multi-N-defects, which have a positive effect on the stability of PtRu nanoparticles on N-doped HOPG.

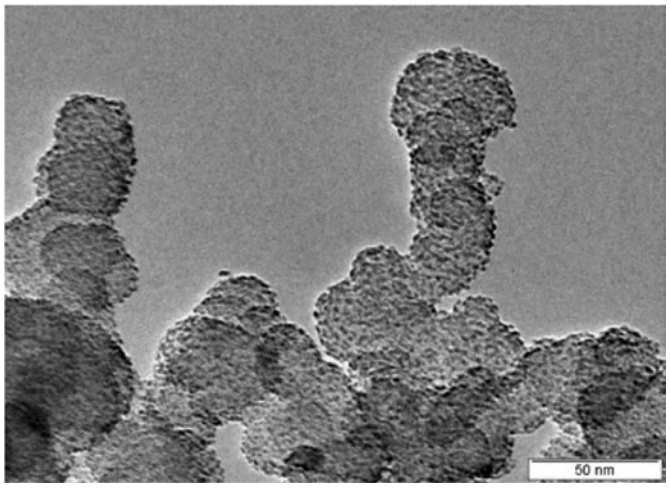


FIGURE 2. Representative TEM sputter-deposited PtRu/Vulcan carbon materials.

composition are independent of the amount of nitrogen present. After cycling to 1.1 V, low implantation dose (5-15 s) resulted in poor stability while high implantation dose (45, 100s) seemed to have greatly increased particle stability. The results indicate that a high amount of N is needed to form clustered multi-N-defects, which appears to minimize coalescence/migration of the PtRu catalyst. Density functional theory (DFT) was used to infer the effect of specific N functionalities on the stability of PtRu. DFT calculations show that N-defects such as pyrrolic and pyridinic N enhances the stability of Pt in PtRu and that pyrrolic N improves the stability of PtRu by stabilizing both Pt and Ru. Hence, a balance between pyrrolic and pyridinic N is needed to stabilize PtRu catalyst.

We established an entirely vapor-phase process for PtRu catalyst material development. By controlling specific, yet interdependent, sputter deposition parameters, we were able to generate high performing and highly dispersed PtRu nanoparticles (Figure 2) of a desired composition, particle size and electroactive surface area on Vulcan carbon support. Table 1 compares the half-cell MOR specific and mass activity of in-house catalysts and a commercial catalyst of a similar metal loading (30 wt%) and PtRu composition (1:1 atomic%). Our in-house sputtered PtRu/C catalysts consistently showed 20%–30% improvement in MOR activity as compared to commercial catalyst of comparable composition. Furthermore, the NREL in-house PtRu on N-doped carbon catalyst proved more durable than the undoped catalyst and commercial catalyst. Further optimization is needed to improve the MOR activity for the in-house N-doped catalysts.

Table 1 compares the electrochemical surface area (ECA), the MOR specific and mass activity, and durability of two in-house and one commercial 30 wt% PtRu/C catalysts. JM5000 is a commercial catalyst purchased from Johnson Matthey. PtRu/N-C is a catalyst that has about 5% N-incorporated in the Vulcan carbon via implantation, followed by sputter deposition of PtRu. The ECA was obtained from CO stripping voltammetry. The MOR activity was measured in a half-cell set up in 1 mol/L methanol + 1 mol/L H_2SO_4. The durability test was done by cycling between 0.23 and 0.80 V vs. reference hydrogen electrode at 20 mV/s in 1 M H_2SO_4. All measurements were carried out at room temperature.

TABLE 1. Half-Cell Catalyst Performance and Durability Comparison

Catalyst	ECA (m^2/g)	Specific Activity @ 0.4 V ($\mu A/cm^2_{metal}$)	Mass Activity @ 0.4 V (A/mg_{metal}) X 10^3	% of ECA after 100x Durability cycles	% of ECA after 5,000x Durability cycles
30 wt% PtRu/C (sputter)	73	33	24	51	10
28 wt% PtRu/N-C (sputter not optimized)	55	30	17	60	40
30 wt% PtRu/C JM5000	69	29	20	48	17

The non-solution process was scaled up to generate a sufficient amount of the best performing in-house catalyst for DMFC testing. Table 2 shows that the in-house sputter 30 wt% PtRu/C outperforms the DMFC commercial catalyst JM5000. MEA preparation method needs to be optimized to improve the DMFC performance further.

Table 2 shows that in-house sputtered PtRu/C catalyst out-performs the commercial JM5000 catalyst of the same catalyst loading (1 mg/cm^2). DMFC testing was carried out at 50°C using a 5 cm^2 MEA, 1 mol/L methanol and humidified air. Anode polarization was carried out using 1 mol/L methanol on the anode and hydrogen on the cathode. ECA was measured using CO stripping voltammetry.

TABLE 2. Catalyst DMFC Performance Comparison

		DMFC Current Density @ 0.4 V			Anode Polarization @ 0.4 V	
Catalyst	PtRu ECA (m^2/g)	(mA/cm^2) Geometric Surface Area	($\mu A/cm^2_{metal}$)	(mA/mg)	($\mu A/cm^2_{metal}$)	(mA/mg)
JM500	55	25	45	25	48	26
Sputtered PtRn/C	41	30	73	30	83	34

Conclusions and Future Direction

- We demonstrated that nitrogen implantation has an inherent beneficial effect on MOR activity and durability and that nitrogen dosage and functionalities play a role on these effects.
- We established an entirely non-solution, scalable process that produced highly dispersed PtRu/C catalyst that outperformed commercial catalysts in both MOR specific and mass activity.
- We demonstrated that PtRu on N-doped Vulcan carbon catalysts are more durable than PtRu on undoped carbon and commercial catalysts.
- We screened several different chemical dopants and determined that dopant level of interaction with carbon matrix affects MOR activity and durability.
- We will continue to optimize catalyst utilization through sputter-implantation parameter control.
- We will evaluate the DMFC performance and durability of PtRu/implanted carbon catalyst materials.
- We will establish catalyst degradation mechanisms, e.g., extent of ruthenium dissolution and catalyst coarsening.
- We will perform soft X-ray and hard X-ray scattering studies in situ during electrochemical analysis to determine the sites for PtRu attachment and study the degradation of PtRu during cycling (at the SLAC National Accelerator Laboratory).

Patents Issued

1. "Advanced Vacuum Deposition of Catalyst Materials," Dameron, T. Olson, H.N. Dinh, D. Ginley, T. Gennett, Preliminary Patent Application, March 2011.

FY 2011 Publications/Presentations

1. Y. Zhou, K.C. Neyerlin, T. Olson, S. Pylypenko, J. Bult, H.N. Dinh, T. Gennett, Z. Shao, R. O'Hayre, *Review paper for Energy & Environmental Science*, 2010, **3**, 1437-1446.

2. S. Pylypenko, A. Queen, K.C. Neyerlin, T. Olson, A. Dameron, K. O'Neill, D. Ginley, B. Gorman, S. Kocha, H.N. Dinh, T. Gennett, and R. O'Hayre, *ECS Transactions,* October 2010.

3. S. Pylypenko, A. Queen, T.S. Olson, A. Dameron, K. O'Neill, K.C. Neyerlin, B. Pivovar, H.N. Dinh, D.S. Ginley, T. Gennett, and R. O'Hayre, *J. Phys. Chem.,* accepted March 2011.

4. S. Pylypenko, A. Queen, T.S. Olson, A. Dameron, K. O'Neill, K.C. Neyerlin, B. Pivovar, H.N. Dinh, D.S. Ginley, T. Gennett, and R. O'Hayre, *J. Phys. Chem.,* accepted April 2011.

5. R. O'Hayre, S. Pylypenko, Y. Zhou, A. Corpuz, R. Richards, T. Holme, K. Neyerlin, T. Olson, A. Dameron, K. O'Neill, K. Hurst, D. Ginley, T. Gennett, and H.N. Dinh, Invited Talk, *Materials Research Society,* 2011 Spring Meeting, San Francisco, CA, April 25–29, 2011.

6. H.N. Dinh, S. Pylypenko, A. Dameron, K.C. Neyerlin, T. Olson, S. Christensen, K. O'Neil, K.E. Hurst, J. Bult, A. Corpuz, S.R. Narayan, A. Karthik, B. Yang, C.C. Hays, M.A. Johnson, R. O'Hayre, B. Pivovar, T. Gennett, Invited talk, *2011 Spring ACS* Meeting in Anaheim, CA, Mar. 27–31, 2011.

7. S.T. Christensen, K.E. Hurst, J.B. Bult, T.S. Olson, A.A. Dameron, D.S. Ginley, H.N. Dinh, T. Gennett, *2011 Spring ACS* Meeting in Anaheim, CA, Mar. 27–31, 2011.

8. K.E. Hurst, T. Gennett, S.T. Christensen, K.J. O'Neill, J.B. Bult, S. Pylypenko, T.S. Olson, A.A. Dameron, D.S. Ginley, R.P. O'Hayre, H.N. Dinh, *2011 Spring ACS* Meeting in Anaheim, CA, Mar. 27–31, 2011.

9. K.E. Hurst, J. Bult, A. Dameron, S. Pylypenko, K. O'Neill, J. Leisch, K.C Neyerlin, T. Olson, R. O'Hayre, H.N. Dinh, T. Gennett, *Pacifichem Meeting*, Honolulu, HI, Dec. 2010.

10. H.N. Dinh, S. Pylypenko, T. Olson, K.C. Neyerlin, K. O'Neill, A. Dameron, J. Leisch, A. Queen, R. O'Hayre, T. Gennett, *Pacifichem Meeting*, Honolulu, HI, Dec. 2010.

11. K.E. Hurst, J. Bult, A. Dameron, S. Christensen, S. Pylypenko, K. O'Neill, T. Olson, R. O'Hayre, H.N. Dinh, T. Gennett, *Fall MRS Meeting,* Boston, MA, Nov. 2010.

12. S. Pylypenko, A. Queen, KC Neyerlin, T. Olson, A. Dameron, K. O'Neill, D. Ginley, B. Gorman, S. Kocha, H.N. Dinh, T. Gennett, and R. O'Hayre, *ECS Meeting*, Las Vegas, NV, Oct. 2010.

13. A.A. Dameron, J.J. Martin, S. Pylypenko, T. Olson, J. Bult, J.L. Leisch, K. O'Neill, R. O'Hayre, H.N. Dinh, D.S. Ginley, and T. Gennett. *ECS Meeting*, Las Vegas, NV, Oct. 2010.

14. K.C. Neyerlin, S. Pylypenko, T. Olson, J. Leisch, K. O'Neill, D. Ginley, R. O'Hayre, B. Pivovar, T. Gennett and H.N. Dinh. *ECS Meeting*, Las Vegas, NV, Oct. 2010.

15. H.N. Dinh, S. Pylypenko, T. Olson; K.C. Neyerlin, A. Dameron, J. Leisch, K.E. Hurst, J. Bult, K. O'Neill, A. Queen, B. Pivovar, R. O'Hayre, T. Gennett. *ECS Meeting*, Las Vegas, NV, Oct. 2010.

16. S. Pylypenko, A. Dameron, T. Olson, K.C Neyerlin, J. Bult, C. Engtrakul, A. Queen, K. O'Neill, T. Gennett, H.N. Dinh, B. Pivovar and R. O'Hayre, *AVS Meeting,* Alburquerque, NM, Oct. 2010.

References

1. Y. Zhou, R. Pasquarelli, J.J. Berry, D. Ginley, R. O'Hayre, *J. Mater. Chem.* 2009, **19**, 7830-7838.

2. Y. Zhou, T. Holme, J. Berry, T.R. Ohno, D. Ginley, R. O'Hayre, *J. Phys. Chem. C*, 2010, **114**, 506-515.

3. T. Holme, Y. Zhou, R. Pasquarelli and R. O'Hayre, *Phys. Chem. Chem. Phys*., 2010, **12**, 9461-9468.

4. Y. Zhou, K.C Neyerlin, T. Olson, S. Pylypenko, J. Bult, H.N. Dinh, T. Gennett, Z. Shao, R. O'Hayre, *Review paper for Energy & Environmental Science*, 2010, **3**, 1437-1446.

5. S. Pylypenko, A. Queen, T.S. Olson, A. Dameron, K. O'Neill, K.C. Neyerlin, B. Pivovar, H.N. Dinh, D.S. Ginley, T. Gennett, and R. O'Hayre, Part I, *J. Phys. Chem*., accepted March 2011.

6. S. Pylypenko, A. Queen, T.S. Olson, A. Dameron, K. O'Neill, K.C. Neyerlin, B. Pivovar, H.N. Dinh, D.S. Ginley, T. Gennett, and R. O'Hayre, Part II, *J. Phys. Chem*., accepted April 2011.

V.G.2 Novel Materials for High Efficiency Direct Methanol Fuel Cells

Chris Roger (Primary Contact), David Mountz, Wensheng He, and Tao Zhang
Arkema Inc.
900 First Ave.
King of Prussia, PA 19406
Phone: (610) 878-6707
E-mail: chris.roger@arkema.com

DOE Managers
HQ: Donna Ho
Phone: (202) 586-8000
E-mail: Donna.Ho@ee.doe.gov
GO: Reginald Tyler
Phone: (720) 356-1805
E-mail: Reginald.Tyler@go.doe.gov

Technical Advisor
John Kopasz
Argonne National Laboratory
Phone: (630) 252-7531
E-mail: kopasz@anl.gov

Contract Number: DE-EE0000474

Subcontractors:
- QuantumSphere Inc. (QSI), Santa Ana, CA
- Illinois Institute of Technology (IIT), Chicago, IL

Project Start Date: July 1, 2010
Project End Date: June 30, 2013

Objectives

- Develop ultra-thin membranes having extremely low methanol crossover, high conductivity, durability, and low cost.
- Develop cathode catalysts that can operate with considerably reduced platinum loading and improved methanol tolerance.
- Produce a membrane electrode assembly (MEA) combining these two innovations that has a performance of at least 150 mW/cm^2 at 0.4 V and a cost of less than $0.80/W for the membrane and cathode catalyst.

Technical Barriers

This project addresses the following technical barriers from the Fuel Cells section of the Fuel Cell Technologies Program Multi-Year Research, Development and Demonstration Plan for portable power devices:

(A) Durability
(B) Cost
(C) Performance

Technical Targets

This project is conducting focused research on next generation membrane and cathode catalyst materials for direct methanol fuel cells. Insights gained from these studies will be applied toward the design of an MEA for portable power applications that meet the DOE 2010 targets:

- Performance: specific power (100 W/kg), power density (100 W/l), and energy density (1,000 Wh/L)
- Cost: $3/W
- Lifetime: 5,000 hours

In translating DOE-published targets, we have defined the following goals for the membrane, cathode catalyst, and MEA performance based on our modeling efforts (Table 1).

TABLE 1. Progress towards Meeting the Project Technical Targets for Portable Power Applications

Characteristic[1]	Units	Industry Benchmark	Project Target	Status
Methanol Permeability	cm^2/s	1-3x10^{-6}	5x10^{-8}	1.5x10^{-7}
Areal Resistance, 70°C	Ωcm^2	0.120 (7 mil PFSA[3])	0.080	0.080
Cathode Catalyst Specific Power (rotating disk electrode, RDE)[2]	mW/mg Platinum Group Metal (PGM)	25	>50	>100
MEA Cathode Catalyst Loading	mg/cm^2 PGM	2.5	2	In progress
MEA Current-Voltage Cell Performance (0.4 V)	mW/cm^2	90	150	120[4]
MEA Lifetime	hours	>3,000	5,000	In progress

[1] Targets based on a methanol concentration of 1M
[2] Conditions at 0.45 V vs. standard hydrogen electrode and 70°C
[3] Perfluorinated sulfonic acid
[4] Measured with commercial gas diffusion electrode (GDE) with 1.5 mg/cm^2 Pt on the cathode and 4.5 mg/cm^2 Pt and Ru on the anode. This is intended to be a reference for MEA development work.

Fiscal Year (FY) 2011 Accomplishments

- Identified 15 high potential membrane candidates with the required areal resistance and a methanol permeation coefficient $\leq 3x10^{-7}$ cm^2/s. One candidate has a permeation coefficient of 1.5x10^{-7} cm^2/s, slightly above the milestone target methanol permeation of 1x10^{-7} cm^2/s.
- Successfully prepared composite membranes with a sulfonated silica additive with no visual indications of large-scale phase separation.

- Demonstrated a power of 120 mW/cm^2 from an MEA with an Arkema membrane and a commercial GDE.
- Successfully synthesized unsupported palladium and palladium-based nanocatalysts having a surface in excess of 90 m^2/g (3-10 nm), both as admixtures and alloys.
- Initiated scale up of Pd catalyst production with an output of 1.2 kg/month at 60% recycling efficiency.
- Achieved a mass activity of 133 mW/mg$_{PGM}$ at 0.45 V for Mn-promoted Pt/C + Pd, which fulfills the target for specific power. This includes an additional 20% reduction in PGM content. Corresponding cost of power is $0.71/W, a 57% catalyst cost savings compared to commercial Pt/C.



Introduction

There is a tremendous need for small, efficient portable power sources. The explosive growth of the lithium-ion batteries market is fueled by the ever-growing demand for portable power used in consumer electronics. For the direct methanol fuel cell industry to emerge as an alternative to batteries, very difficult technical hurdles have to be overcome in terms of drastically reduced methanol cross-over in the membrane and improved anode and cathode catalyst efficiencies.

Approach

Arkema and IIT are developing a new generation of membranes with very low methanol cross-over and high conductivity. The membranes are formed from blends of poly(vinylidene fluoride) (PVDF) with a variety of highly sulfonated polyelectrolytes, technology that was developed in DE-FC36-04GO14051 and DE-FC36-07GO17008. A number of variables can be easily adjusted in the blending process to tailor the membrane properties, such as conductivity and methanol permeation. The key to obtaining the desired properties resides in control of composition, architecture, and morphology of the membrane components. These are controlled on a practical level through polyelectrolyte chemistry, processing, and use of inorganic materials, which are being systematically investigated and correlated with properties.

QSI is developing a new series of cathode catalysts with improved mass activity obtained by suppressing methanol oxidation. The QSI catalyst has demonstrated higher specific activity for oxygen reduction in the presence of methanol compared to commercially used Pt/C. The scope of work in the first year included development of the synthesis and electrochemical characterization of nanoscale Pd-based catalysts, methods to increase catalyst production yield, and basic MEA testing in anticipation of extensive MEA development and testing for the rest of the project.

Results

Membrane Development

Over 100 membrane compositions were fabricated at Arkema with varying polyelectrolyte compositions, PVDF grades, ratios of sulfonated polyelectrolyte to PVDF, and crosslinking agents. Testing for the compositions focused on ex situ conductivity and methanol permeation. Other testing (crystallinity measurements, microscopy, and mechanical testing) was also carried out on a small number of candidates to understand structure-property relationships and morphology. In-cell testing was also done on about 1/3 of the candidates to validate the ex situ property data.

Data from a majority of the samples is shown in Figure 1, along with PFSA and M43 references. The M43 membrane was developed for H_2 fuel cells and is used as a baseline for this project. All of the variables affected performance, but the polyelectrolyte chemistry had the most influence on membrane permselectivity through changes in polarity, equivalent weight, and molecular weight. The polyelectrolyte:PVDF ratio and PVDF grade, which alter equivalent weight and percent crystallinity respectively, also had a significant impact on membrane conductivity and permeation. Fifteen high potential candidates from the group have the required areal resistance and a methanol permeation coefficient $\leq 3\times10^{-7}$ cm^2/s. The most promising of these candidates has a permeation of 1.5×10^{-7} cm^2/s, slightly above the year one milestone target of 1×10^{-7} cm^2/s. Efforts are now focused at refining these high potential candidates to meet the milestone requirements.

The MEA performance of the most promising high potential candidate (Candidate A) and M43 in 3M and 10M

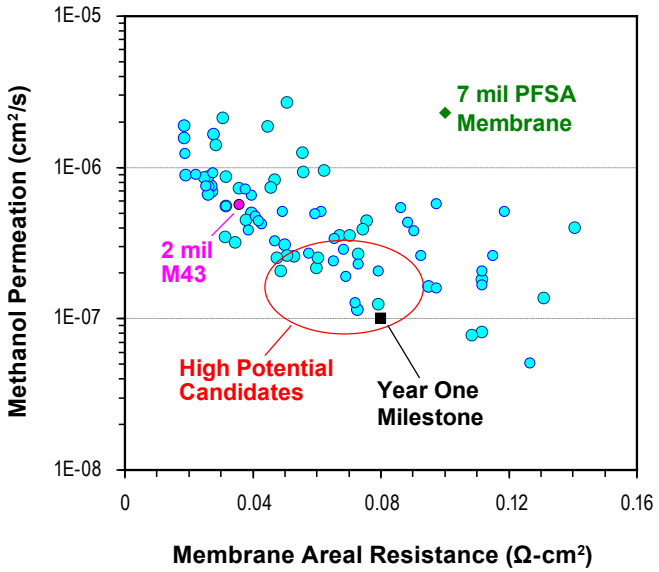


FIGURE 1. Conductivity versus Permeation for the Membrane Compositions Screened at Arkema

methanol is shown in Figure 2. Both materials outperform the PFSA reference at both methanol concentrations. Compared to M43, Candidate A shows slightly higher performance with 10M, and exhibits superior durability due to its mechanical properties. Both Arkema membranes have also demonstrated 120 mW/cm^2 at 0.4 V with 1M methanol using a commercial GDE from Johnson Matthey, which will be used as a baseline in the next stage of the project where QSI's catalyst and Arkema's membrane are incorporated into an MEA.

IIT has been developing novel sulfonated silica materials for use as conductors in the formulation of composite membranes. Addition of inorganic additives to membranes has been shown to lower methanol permeability, but this is usually combined with a reduction in conductivity [1]. This deficiency may be addressed by functionalizing the silica with sulfonic acid groups.

Mesoporous sulfonated silica particles are made by hydrolyzing tetraethyl orthosilicate with HCl and reacting it with (3-mercaptopropyl) trimethoxysilane. The materials were sulfonated over a range of 30-67% (ion exchange capacity = 1.4-2.1 mmol/g). All of them display high conductivity: 100 mS/cm at 60°C and 100% relative humidity.

Thirty percent sulfonated silica was incorporated into an Arkema formulation and cast into composite membranes. The membranes were transparent with no visual indication of particle aggregation. Data from the composites is shown in Table 2. Permeability and conductivity are lowered as the silica is added. Selectivity is more complex, initially decreasing compared to the reference at the lowest silica loading and then increasing with higher silica contents. The composite properties may be improved by using silica with higher sulfonation and this work is in progress.

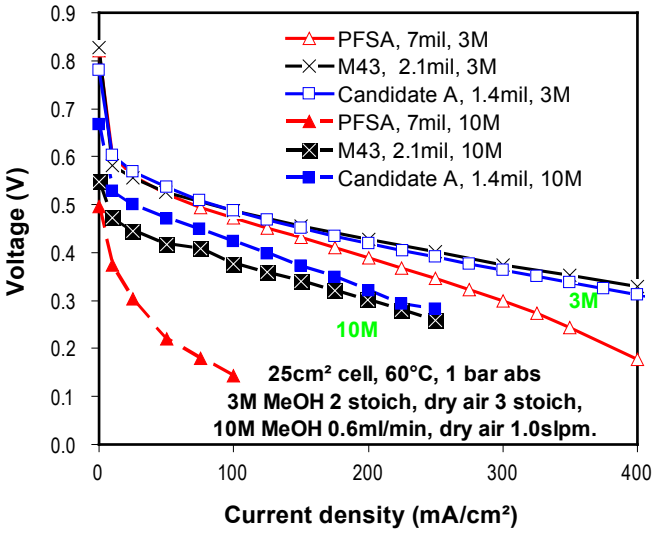


FIGURE 2. Performance of Two Arkema Membranes and a PFSA Benchmark in 3M and 10M Methanol

TABLE 2. Conductivity and Permeation Data for a Membrane Composites Series made with Sulfonated Silica

Membrane + Silica with 30% Sulfonation	Conductivity @ 70°C, mS/cm	Permeability @ Room Temperature, x10^{-7} cm^2/s	Conductivity/ Perm Selectivity
Arkema membrane	125 ± 7	6.7 ± 0.2	19
With 15 wt% silica	75 ± 4	5.7 ± 0.4	13
With 20 wt% silica	49 ± 1	3.4 ± 0.1	14
With 25 wt% silica	58 ± 9	3.2 ± 0.2	18

Catalyst Development

QSI successfully fabricated Pd and Pd-M (M= Ni, Co, Mn, Fe, Cr, Ag, Au, Se) nanocatalysts with high surface area (>90 m^2/g). Catalyst particle sizes are in 3-10 nm range, as illustrated in Figure 3. The oxygen reduction reactivity of Pd-M + Pt/C catalysts (i.e. a mixture) was evaluated using RDE with and without methanol in the electrolyte. The Pd + Pt/C blended catalyst showed doubled mass activity (>100 mW/mg PGM) compared to Pt/C alone in the presence of 0.1M methanol. The resulting PGM costs per watt of various cathode catalysts (assuming cost of $54.00/g for QSI nano-Pd and $128.00/g for 60% Pt/C) are shown in Figure 4. Up to 57% cost savings (M = Mn) is realized when a Pd-M co-catalyst is used with Pt/C.

Conclusions and Future Directions

- Identified 15 high potential membrane candidates with the required areal resistance and a permeation coefficient ≤3x10^{-7} cm^2/s.
- Composite membranes with a sulfonated silica additive were successfully prepared. Higher sulfonation

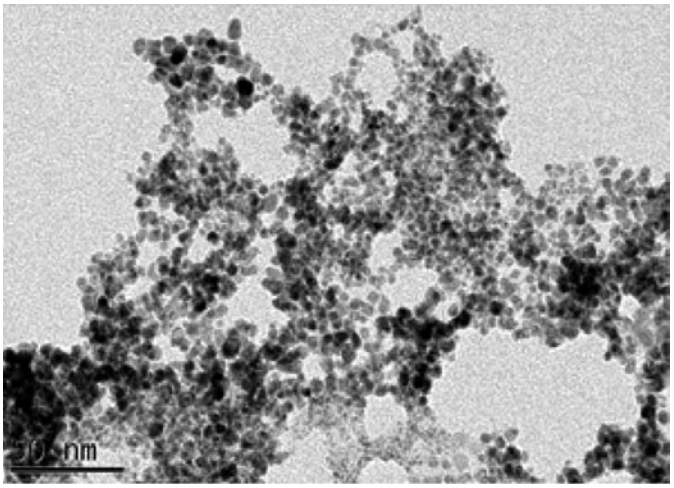


FIGURE 3. Transmission Electron Microscope Image of Pd-Mn Nanocatalysts (The scalebar represents 50 nm.)

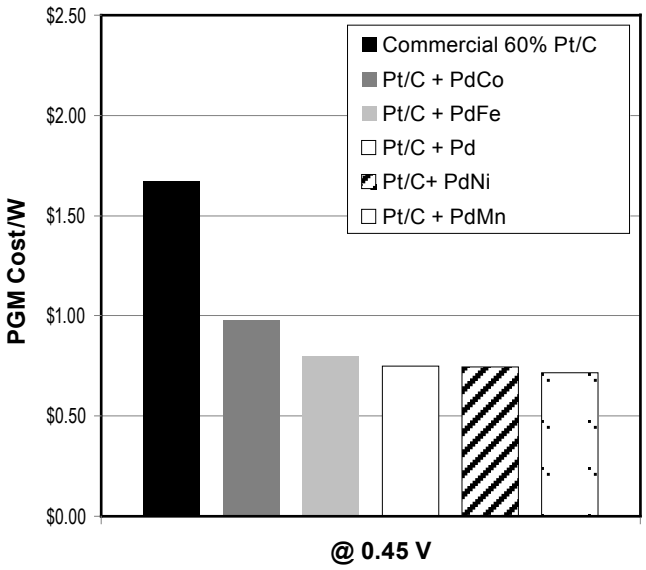


FIGURE 4. Cost of Power at 0.45 V for Cathode Catalyst in the Presence of 0.1M Methanol to Simulate Crossover

levels and better dispersion of the inorganic particles are needed to improve conductivity and decrease permeation, which will be pursued in the future.

- A catalyst containing a mixture of Pt/C + Pd-Mn achieved a mass activity of 133 mW/mg_{PGM} at 0.45 V, which fulfills the target for specific power.
- Down-select membrane and catalyst candidates that meet the year one milestone, refine their properties, and produce target compositions on a pilot-scale for MEA development.
- Initiate MEA development for 50% reduction in PGM content at the cathode to meet the goal of ≤2 mg/cm^2 total PGM loading with the target cell performance.

Patents Issued

1. Goldbach, J.; Mountz, D. "Blend of ionic (co)polymer resins and matrix (co)polymers." U.S. Divisional Patent #7,781,529, Aug 24, 2010.

2. Goldbach, J.; Gaboury, S.; Umpleby, R.; Parvole, J.; Mountz, D. "Blend of ionic (co)polymer resins and matrix (co) polymers." U.S. Divisional Patent #7,815,986, Oct 19, 2010.

FY 2011 Publications/Presentations

1. Poster presentation at the 2010 DOE Hydrogen Program and Vehicle Technologies Program Annual Merit Review and Peer Evaluation Meeting, D. Mountz, W. He, and C. Roger.

References

1. R. Jiang, Kunz, H.R., and Fenton, J.M., Journal of Membrane Science, 272, 116 (2006).

V.G.3 New MEA Materials for Improved Direct Methanol Fuel Cell (DMFC) Performance, Durability, and Cost

James Fletcher (Primary Contact), Philip Cox
University of North Florida (UNF)
1 UNF Drive
Jacksonville, FL 32224
Phone: (904) 620-1844
E-mail: jfletche@UNF.edu

DOE Managers
HQ: Donna Ho
Phone: (202) 586-8000
E-mail: Donna.Ho@ee.doe.gov
GO: Katie Randolph
Phone: (720) 356-1759
E-mail: Katie.Randolph@go.doe.gov

Technical Advisor
Walt Podolski
Phone: (630) 252-7558
E-mail: podolski@anl.gov

Contract Number: DE-EE0000475

Subcontractors:
- University of Florida, Gainesville, FL
- Northeastern University, Boston, MA
- Johnson Matthey Fuel Cells, Swindon, UK

Project Start Date: January 1, 2010
Project End Date: June 30, 2012

Fiscal Year (FY) 2011 Objectives

The primary objective of this project is to optimize the functionality and internal water recovery features of the UNF passive water recovery membrane electrode assembly (MEA) to facilitate overall system simplicity, thereby increasing power and energy density and lowering the cost at the system level to address DOE's fuel cell target goals for consumer electronics applications.

- Optimize the UNF MEA design:
  - Improve durability and reliability
  - Increase power and energy density
  - Lower cost
- Develop commercial production capabilities:
  - Scale up the process to commercial batch operation level:
    - Improve performance and lower reproducibility
    - Lower cost
- Increase catalyst stability and lower loading:
  - Increase the anode catalyst stability
  - Lower MEA cost

Technical Barriers

This project addresses the following technical barriers for consumer based electronic applications of less than 50 W from the Fuel Cells section of the Fuel Cell Technologies Program Multi-Year Research, Development and Demonstration Plan:

(A) Durability
(B) Cost
(C) Performance

Technical Targets

A comparison of the UNF DMFC power supply versus the DOE technical targets for portable fuel cell power supplies is shown in Table 1.

FY 2011 Accomplishments

- Optimized open cathode MEA fabrication processes to provide excellent MEA-to-MEA reproducibility in stack testing.
- Developed MEAs with low on-state degradation <50 µV/h under a range of operating conditions and obtained over 4,000 hours of operation for an eight cell short stack.
- Improved the off-state durability of the MEAs by optimizing the cathode electrode and barrier layer formulation and processing conditions.
- Incorporated system operating conditions to improve MEA off-state durability.
- Scaled up barrier layer coating process from hand production to commercially applicable mixing and coating processes.
- Submitted revised Hydrogen Safety Plan.



Introduction

Typical DMFC systems use bulky condensers and other heat exchangers to recover water at the system level. These system components occupy a large volume and weight within the system design and have a significant impact on the system power and energy density. The UNF passive water recovery MEA (Figure 1) has been designed to incorporate

TABLE 1. Comparison of the status of the UNF 20 W DMFC power supply based on the passive water recovery MEAs optimized in this project versus the DOE technical targets for portable fuel cell power supplies.

Characteristic	Units	UNF 15 W DP3 2008 Status	DOE 2010 Target	UNF Proposed 20W System Design
Specific Power[a]	W / kg	35	100	41.5
Power Density [a]	W / L	48	100	55.6
Energy Density	W-hr / L	250 (1 x 100ml)[b] 396 (1 x 200ml)[b]	1000	193(1 x 100ml) 321 (1 x 200ml) 575 (3 x 200 ml)
	W-hr/kg	155 (1 x 100ml)[b] 247 (1 x 200ml)[b]	N/A	162 (1 x 100 ml) 307 (1 x 200 ml) 638 (3 x 200 ml)
Lifetime [c]	Operating Hours	1,000 hrs in single cell	5,000	2,500 Integrated System
Cost	$ / Watt	11 (est. in volume)	<3	< 10 (est. in volume)

[a] Beginning of life, 30°C, sea level,50% R.H., excluding hybrid battery, power module alone
[b] Normalized from DP3 data from 150 ml cartridge to either 100ml or 200ml for comparison purposes
[c] Lifetime measured to 80% of rated power

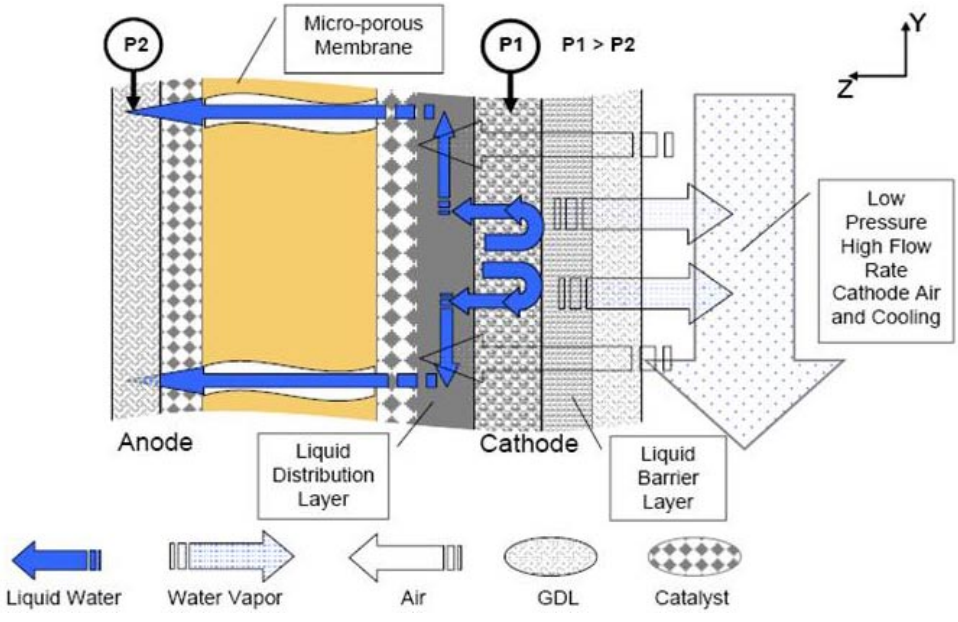


FIGURE 1. Water Transport Characteristics Optimized to Internally Recycle Water to Anode Compartment

novel passive water recycling features within the MEA to provide water recovery and management. This approach enables a significant simplification and miniaturization of the DMFC at the system level and facilitates substantial progress towards the DOE goals for power and energy density in small portable power systems. This progress has been demonstrated in the UNF system design.

Approach

The approach is to optimize the performance of the UNF passive water MEA and transition the technology to commercially viable processes, thereby lowering the cost and increasing the durability of the MEA. The MEA performance will be improved through better anode catalysts

and optimization of the cathode barrier layer water retention capability. By improving the anode catalyst structure to enhance the stability of the ruthenium, the MEA durability will be significantly enhanced. Optimizing the cathode barrier layer parameters will maximize the oxygen content at the cathode catalyst and thus improve the MEA performance.

Scale up of the manufacturing process for the MEA layers is expected to enhance both performance and reliability as well as reduce the overall cost. Optimizing the manufacturing process will move beyond the prototype operation by developing a batch manufacturing process which will improve the MEA-to-MEA reproducibility, increase the durability, and reduce the cost of the overall MEA. The methodology also includes an evaluation of the MEA produced at both the single cell and the system level against system operating conditions required for a small compact DMFC system developed in a related project at UNF.

Results

The UNF baseline passive water recovery MEA design has been successfully transferred to Johnson Matthey. The baseline process for the liquid barrier layer is based on a tedious multilayer, hand painted process to obtain the key water retention properties of water and oxygen diffusion and retention while recycling the liquid water to the cathode. Research during the past year has optimized the formulation and mixing process to enhance the barrier layer reproducibility, as well as improve control of the key barrier layer properties. Johnson Matthey has incorporated dual centrifuge mixing, a commercially applicable, scalable batch mixing processes, to replace the small scale ultrasonic mixing used in the baseline process. The formulation and processing has been further optimized to provide highly reproducible barrier layers leading to excellent MEA-to-MEA reproducibility in short stack testing.

The baseline ink application process requiring layer-by-layer hand painting has been scaled up to a commercially applicable automated coating process. This approach has now introduced rod coating where an excess of the coating is deposited onto the substrate. The wire-wound metering rod, sometimes known as a Meyer Rod, allows the desired quantity of the coating to remain on the substrate. The amount of material deposited is determined by the diameter of the wire used on the rod and the solids loading and viscosity of the coating solution. Using a large diameter wire on the metering rod and optimization of the coating ink characteristics has reduced the number of coatings required, improved reproducibility and reduced production costs. Single layer coatings (Figure 2) with good surface coverage and uniformity have been produced showing comparable baseline performance in MEA testing compared to the multilayer hand painted liquid barrier layers.

MEA durability is a critical factor in system durability. An extensive investigation and optimization of the MEA, liquid barrier layer and catalyst layer production has been

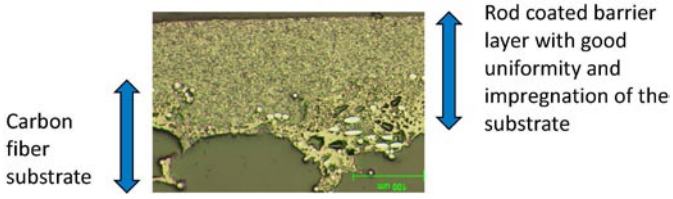


FIGURE 2. Cross-Section of Single Layer Barrier Layer Coating

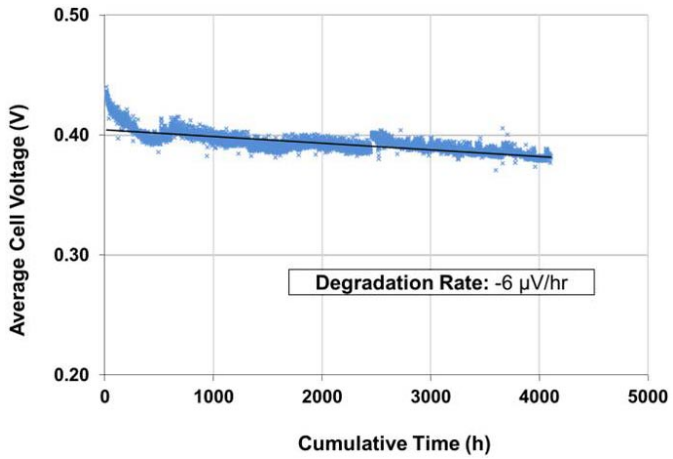


FIGURE 3. Passive water recovery MEAs show excellent durability under continuous operation. Eight cell stack operating at 120 mA/cm^2, 50ºC, and 0.8 M methanol.

conducted in order to remove impurities and optimize the performance and durability both in the on-state as well as the off-state. The current MEA design exhibits excellent durability in continuous operation tests achieving over 4,000 hours of operation in an ongoing test (Figure 3). However, off-state testing has revealed significant degradation. Ex situ analysis of degraded MEAs indicated the presence of an organic impurity in the cathode catalyst structures. Optimization of MEA fabrication methods and improved operating parameters has led to a significant reduction of the quantity and influence of organic impurities. Testing has now shown a substantial reduction in the off-state degradation to acceptable levels for system operation and life.

Anode stability is a particular concern for long-term durability due to the loss of ruthenium from the anode. To address this issue, an ultra-stable ternary anode catalyst has been developed by project partners which incorporates a third metal to both stabilize the ruthenium and enhance the catalyst activity. This new catalyst provides improved durability and a reduction of cost at the system operation level. Project personnel are now in the process of scaling up the production of these catalysts for MEA testing. Additionally, the testing of commercially available catalysts has led to an improved anode catalyst showing significantly improved durability in methanol starvation accelerated testing.

Conclusions and Future Directions

Research conducted during the past year has:

- Successfully scaled up the passive water recovery MEA and improved the MEA-to-MEA reproducibility.
- Produced MEAs with excellent durability with projected life of over 5,000 hours of operation life.
- Identified significant steps in lowering the off-state durability by optimizing both the MEA fabrication and the operational parameters such that the overall MEA durability is in acceptable range for long term operation of the fuel cell system.

Future efforts include:

- Optimization of manufacturing techniques and formulations for the liquid barrier layer to maximize performance and durability.
- Improve MEA performance:
  - Optimization of the cathode structures for water management and power density.
  - Optimize the anode for durability and performance in the passive water recovery MEA.
- Optimization of the fuel cell operational parameters of startup, shut down and operation to maximize MEA performance and durability over the system operating life.
- Continued MEA durability testing to evaluate durability under a range of in-specification and out-of specification conditions.

V.G.4 Advanced Materials and Concepts for Portable Power Fuel Cells

P. Zelenay (Primary Contact), H. Chung, Z. Ding, C.M. Johnston, Y.S. Kim, Q. Li, A. Trendewicz, P. Turner, G. Wu
Materials Physics and Applications Division
Los Alamos National Laboratory
Los Alamos, NM 87545
Phone: (505) 667-0197
E-mail: zelenay@lanl.gov

DOE Manager
HQ: Nancy Garland
Phone: (202) 586-5673
E-mail: Nancy.Garland@ee.doe.gov

Subcontractors:
- R.R. Adzic, M. Li, K. Sasaki, M. Vukmirovic
  Brookhaven National Laboratory, Upton, NY
- Y. Yan, S. Alia
  University of California, Riverside, CA
- J. McGrath, Y. Chen, C. H. Lee, M. Lee
  Virginia Polytechnic Institute and State University, Blacksburg, VA
- N. Permogorov, G. Hards, G. Spikes
  Johnson Matthey Fuel Cells, Swindon, United Kingdom
- V. Graf, C. Böhm, J. Stephens
  SFC Energy, Brunnthal, Germany
- K. More
  Oak Ridge National Laboratory, Oak Ridge, TN
  (no-cost partner)

Project Start Date: September 2010
Project End Date: August 2014

Fiscal Year (FY) 2011 Objectives

The main objective of this project is to:

- Develop advanced materials (catalysts, membranes, electrode structures, membrane electrode assemblies [MEA]) and fuel cell operating concepts capable of fulfilling cost, performance, and durability requirements established by DOE for portable fuel cell systems; assure path to large-scale fabrication of successful materials.

Individual objectives of this research are as follows:

- Synthesize and thoroughly evaluate direct methanol fuel cell (DMFC) anode catalysts with enhanced activity, reduced cost and improved durability.
- Design and implement in fuel cells innovative electrode structures for better activity and durability of portable power systems.
- Develop new hydrocarbon membranes based on (i) multiblock copolymers and (ii) copolymers with cross-linkable end-groups to assure lower MEA cost and enhanced fuel cell performance.
- Develop novel electrocatalysts and evaluate viability of portable power systems based on fuels alternative to methanol: ethanol and dimethyl ether.

Technical Barriers

This project addresses the following technical barriers from the Fuel Cells section (3.4.4) of the Fuel Cell Technologies Multi-Year Research, Development and Demonstration Plan: Planned Program Activities for 2005-2015 [1]:

(A) Durability (catalysts and electrode layers)

(B) Cost (catalysts and MEAs)

(C) Performance (including fuel oxidation kinetics and the impact of fuel crossover on cathode performance)

Technical Targets

Portable fuel cell research in this project focuses on DOE's technical targets specified in Table 3.4.7 (Consumer Electronics) of the Multi-Year Research, Development and Demonstration Plan [1]. Table 3.4.7 defines DOE's Fuel Cell Technologies Program 2010 targets (soon to be modified).

Table 3.4.7 Technical Targets: Consumer Electronics (sub-Watt to 50-Watt)

Characteristic	Units	2005 Status [a, b]	2006	2010
Specific power	W / kg	20	30	100
Power density	W / L	20	30	100
Energy density	Wh / L	300	500	1,000
Cost	$ / W	40 [c]	5	3
Lifetime	hours	>500	1,000	5,000

[a] First year for which status was available.
[b] Unless otherwise noted, status is based on average of available data.
[c] Fuel Cell Seminar Abstracts, 2004, p. 290.

Using DOE's Table 3.4.7 solely as guidance relevant to the portable power system as a whole, we have devised the following specific technical targets for the project:

- System cost target: $3/W
- Performance target: Overall fuel conversion efficiency (η_Σ) of 2.0-2.5 kWh/L
- In the specific case of a DMFC, the above assumption translates into a total fuel conversion efficiency (η_Σ) of 0.42-0.52, corresponding to a 1.620-fold improvement over the state of the art (ca. 1.250 kWh/L). Assuming fuel utilization (η_{fuel}) and balance-of-plant efficiency (η_{BOP}) of 0.96 and 0.90, respectively (efficiency numbers based on information obtained from DMFC systems developers), and using theoretical voltage (V_{th}) of 1.21 V at 25°C, the cell voltage (V_{cell}) targeted in this project can be calculated as:

$$V_{cell} = V_{th} [\eta_\Sigma (\eta_{fuel} \eta_{BOP})^{-1}] = 0.6\text{-}0.7 \text{ V}$$

Thus, the ultimate target of the materials development effort in the DMFC part of this project is to assure an operating single fuel cell voltage of at least 0.6 V. Very similar voltage targets have been calculated for the fuel cells operating on the two other fuels, ethanol (EtOH) and dimethyl ether (DME).

FY 2011 Accomplishments (in the first nine months of the project)

- Activity of "thrifted" PtRu catalyst of methanol (MeOH) oxidation significantly increased, much above that defined by an interim 2011 mass activity target of 200 mA/mg_{Pt}.
- PtRu-nanotube catalysts demonstrated with high specific MeOH oxidation activity.
- Lower MeOH permeability and better DMFC performance than that of Nafion® shown with hexafluoro bisphenol A benzonitrile-biphenyl sulfone (6FPAEB-BPS100) multiblock copolymers.
- $PtRhSnO_2$ electrocatalysts with unprecedented activity for ethanol oxidation designed, synthesized and demonstrated in electrochemical cell.
- Highest ever performance of gas-fed direct dimethyl ether fuel cell (DDMEFC) demonstrated with a $Pt_{50}Ru_{50}$ anode catalyst at 80°C.



Introduction

This multitask, multi-partner project targets advancements to portable fuel cell technology through the development and implementation of novel materials and concepts for (i) enhancing performance, (ii) lowering cost, (iii) minimizing size, and (iv) improving durability of fuel cell power systems for consumer electronics and other mobile and off-grid applications. The primary focus of the materials research in this project is on electrocatalysts for the oxidation of MeOH, EtOH, and DME, on innovative nanostructures for fuel cell electrodes, and on hydrocarbon membranes for lower cost of the MEA and enhanced fuel cell performance (fuel crossover, proton conductivity). In parallel with new materials, this project targets development of various operational and materials-treatment concepts, concentrating among others on improvements to the long-term performance of individual components and the complete MEA.

Approach

The two primary research goals of this project are (i) the development of binary and ternary catalysts for the oxidation of MeOH, EtOH, and DME and (ii) synthesis of hydrocarbon polymers (multiblock copolymers, copolymers with cross-linkable functional groups) for lower cost and better fuel cell performance through reduced fuel crossover and increased protonic conductivity. Better understanding of the key factors impacting the performance of both catalysts and polymers is also pursued through a major characterization effort including X-ray absorption spectroscopy, X-ray photoelectron spectroscopy, nuclear magnetic resonance (NMR), and transmission electron microscopy (TEM).

Development of new catalysts and polymers is closely tied to novel electrode nanostructures tailored to minimize precious metal content, maximize mass activity, and enhance durability. The electrode-structure component of the effort concentrates on two groups of materials: (i) solid-metal nanostructures (e.g., nanowires and nanotubes) and (ii) carbon-based nanostructures acting as metal catalyst supports.

In addition to short-term testing and initial performance assessment, the catalysts, membranes, supports, electrode structures, and membrane-electrode assemblies developed in this project are subject to long-term performance (durability) testing. Performance limiting factors and degradation mechanisms are being identified and, if possible, addressed. Fabrication and scale up of viable catalysts, membranes, and supports is also being tackled through collaboration between partners in this project.

Results

DMFC Catalysts — New methanol oxidation catalysts were developed through "thrifting" of Pt in the binary PtRu catalysts. As shown by the anode polarization data in Figure 1, the "advanced MeOH catalyst" matched the performance of a benchmark HiSPEC® 12100 catalyst used at a much higher loading. The mass activity of 550 mA/mg_{Pt} was reached at 0.35 V (80°C), exceeding by 175% the interim 2011 mass-activity target (200 mA/mg_{Pt} at 0.35 V; orange star in the Figure 1). The anode catalyst research using the "thrifting" approach is on track to reach the project goals of 200 mA/mg_{Pt} at an anode potential of 0.25 V (Figure 1;

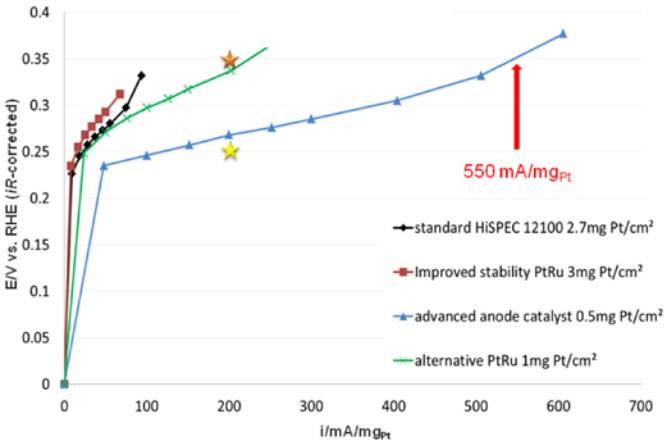


FIGURE 1. DMFC anode polarization plots recorded with three "Pt-thrifted" PtRu catalysts and a benchmark HiSPEC® 12100 PtRu catalyst in 0.5 M MeOH at 80°C.

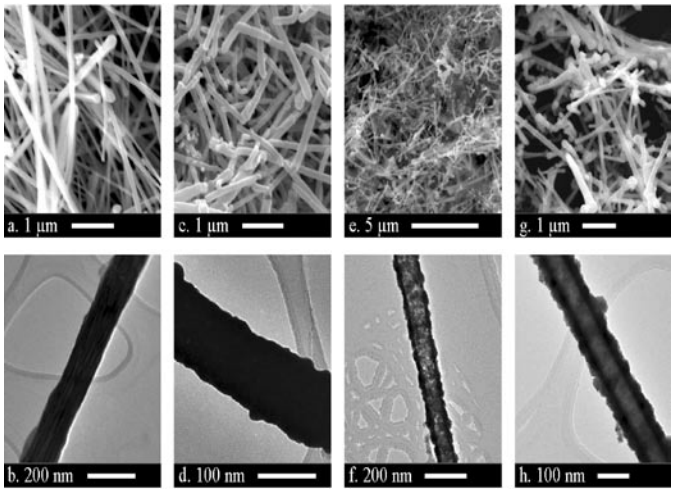


FIGURE 2. Top: SEM images of (a) CuNW; (c) PtNT; (e) $Pt_{80}Ru_{20}$; (g) $Pt_{50}Ru_{50}$. Bottom: TEM images of (b) CuNW; (d) PtNT; (f) $Pt_{80}Ru_{20}$; (h) $Pt_{50}Ru_{50}$.

yellow star) and 150 mA/cm^2 in a DMFC MEA at a voltage of 0.60 V.

In addition to the performance testing, the newly developed DMFC catalysts were subject to stability testing under cyclic voltammetry (CV) conditions. An increase in the Pt-character was observed during the first 200 cycles (0.0-0.85 V, 20 mV/s, 80°C), with virtually no change thereafter. 300 CV cycles resulted in 20-30 mV fuel cell performance loss at 0.50 V, attributable to the anode (based on the anode polarization data).

Innovative Electrode Structures — PtRu nanotube catalysts of MeOH oxidation were obtained using (i) displacement of Ag in an Ag nanowire template to form PtNT, followed by Ru deposition and reduction via a chemical method, followed by annealing to form a PtRu alloy; (ii) displacement of Ag in an Ag nanowire template to form PtNT, followed by electrochemical deposition of Ru; and (iii) simultaneous displacement of Cu in a Cu nanowire template to create PtRuNT, followed by annealing to form a PtRu alloy. Scanning electron microscope (SEM) and TEM images of Cu nanowires and PtRu nanotube catalysts, obtained using the last of the three methods, are shown in Figure 2.

Excellent specific activity for MeOH oxidation was demonstrated with several PtRuNT catalysts, with the onset potential of methanol oxidation of 0.33 V matching the one measured with a state-of-the-art commercial catalyst (HiSPEC® 12100). However, the mass activity of PtRu nanotube catalysts was relatively low.

Multiblock Copolymers for Reduced MeOH Crossover — Partial fluorination of a hydrophobic block was used to enhance proton conductivity via better phase separation and to improve adhesion (intactness) to the Nafion® ionomer used in the electrodes. In turn, benzonitrile was employed to reduce MeOH permeability via complexation reaction with H_2O molecules, and highly-sulfonated hydrophilic block was used to increase proton conductivity. ^{1}H-NMR confirmed the intended chemical structure of the multiblock copolymer. Higher water uptake (undesirable) and proton conductivity (desirable) than in random copolymer were observed with multiblock copolymer. By controlling the block length of multiblock copolymers improved conductivity was achieved while maintaining the level of water uptake similar to that of random copolymers.

Good adhesion of multiblock-copolymer membranes and Nafion®-bonded electrodes was observed during MEA processing and in DMFC testing. MeOH permeability of multiblock-copolymer membranes was found to be three times lower than that of Nafion®, allowing for the use of thinner membranes. As a result, multiblock-copolymer membranes were found to outperform Nafion® 117 in DMFC testing, even at a relatively low MeOH concentration of 0.5 M MeOH (Figure 3). Even larger improvement relative to Nafion® is expected at higher MeOH concentrations.

EtOH Oxidation Catalysts — The effort here focused on the development of ternary catalysts, $PtRhSnO_2$ in particular. The ternary $PtRhSnO_2$ catalyst was found capable of oxidizing EtOH to CO_2 thanks to its multifunctional character. In that catalyst, Pt assists in the abstraction and oxidation of H atoms; SnO_2 serves as a source of OH for the oxidation of strongly bound intermediates; and Rh, placed either on SbO_2 or on Pt itself, aids in C-C bond scission. As a result of such an in-concert action of the three components, the optimized $PtRhSnO_2$ catalysts (Pt:Rh:Sn atomic ratios of 1:1/3:1 and 1:1/2:1) showed unprecedented activity in the oxidation of EtOH to CO_2 (Figure 4). The activity in complete oxidation of EtOH to CO_2 is especially evident at low potentials – a highly desirable property.

Other ternary catalysts were also studied, including $PtIrSnO_2$. The Ir-based ternary catalysts showed significant

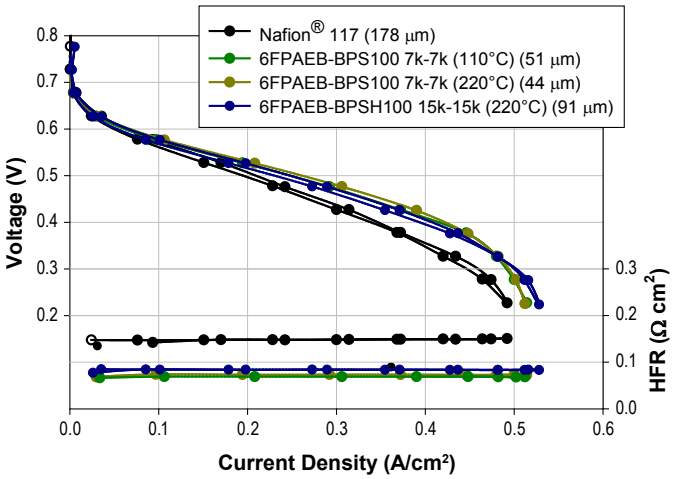


FIGURE 3. DMFC polarization and high-frequency resistance plots of MEAs using Nafion® and 6FPAEB-BPS100 multiblock copolymer membranes at 80°C. Numbers in parenthesis stand for the heat treatment temperature and membrane thickness. Anode: 6 mg/cm^2 $Pt_{50}Ru_{50}$ black, 1.8 mL/min 0.5 M MeOH solution; Cathode: 4 mg/cm^2 Pt black, 20 psig, 500 sccm air.

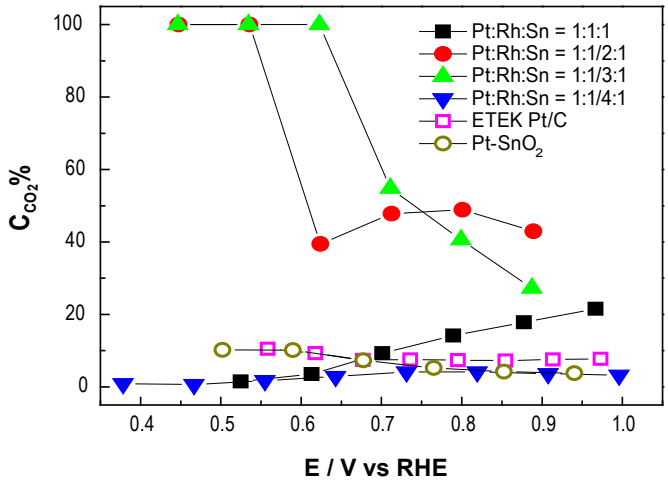


FIGURE 4. Carbon monoxide yields determined from infrared absorption spectra for four ternary $PtRhSnO_2$ catalysts, an Rh-free $PtSnO_2$ catalyst and a Pt/C reference catalyst from E-TEK.

activity in EtOH oxidation to acetic acid (CH_3COOH) but their selectivity for CO_2 formation was much lower than that of the best $PtRhSnO_2$ catalysts. Also studied were catalysts obtained via deposition of a Pt monolayer on gold single crystals, Au(111) in particular, these catalysts revealed promising activity in both EtOH and MeOH oxidation.

DME Fuel Cell Research — In general, DDMEFC exhibits lower performance than DMFC with MEAs optimized for methanol (but not yet for DME). DDMEFC performance was found to strongly depend on pressure but not much on the fuel flow rate (40-200 sccm; 5 cm^2 test cell). A wide range of Pt-to-Ru atomic ratios was screened

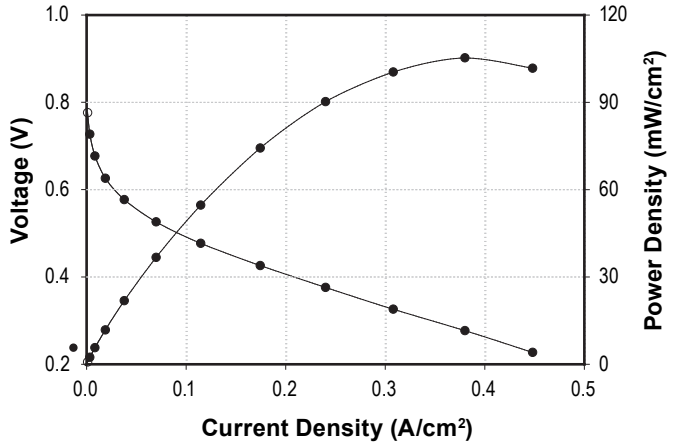


FIGURE 5. DDMEFC polarization and power density plots at 80°C. Anode: 6 mg/cm^2 $Pt_{80}Ru_{20}$ black, 40 sccm DME gas, 30 psig; Cathode: 4 mg/cm^2 Pt black, 20 psig, 500 sccm air; Membrane: Nafion® 117.

for DME anode performance for the first time. Although a $Pt_{50}Ru_{50}$ catalyst exhibited overall the best performance in high and middle voltage ranges, Pt-rich catalysts performed better at low voltages (near peak power), together attesting to a behavior much more complex than that of DMFC anode catalysts.

The above limitations notwithstanding, careful optimization of the anode catalyst and DDMEFC operating conditions allowed the achievement of a specific power density in excess of 100 mW/cm^2 (Figure 5). In spite of using gaseous DME feed, this result represents the best performance ever published for a DDMEFC at 80°C, surpassing that of Im et al. [2].

PtRu anode deactivation was found to occur at high potentials, likely due to the surface oxide formation (more oxophilic and thus less active surface). Fuel crossover experiments revealed much lower DME oxidation current at the cathode than that of MeOH, especially at higher potentials, indicating lower DME crossover and possibly inactivity of the oxidized Pt surface in DME oxidation.

Conclusions

- Selected "thrifted" PtRu catalysts of MeOH oxidation meet and significantly exceed 2011 interim mass activity target for methanol oxidation (200 mA/mg_{Pt}); PtRu nanotube catalysts exhibit promising methanol oxidation activity, however, mass activity needs to be increased by, for example, thinning tube walls.
- Ternary $PtRhSnO_2$ electrocatalysts of EtOH oxidation show unprecedented activity for ethanol oxidation, producing large amounts of CO_2; ternary catalysts with a Rh-to-Pt ratio between 1:3 and 1:2 exhibit the highest activity in EtOH oxidation; an increase in the catalyst particle size may be required for efficient EtOH adsorption and dehydrogenation; Au represents

potentially promising support for EtOH and MeOH oxidation catalysts.

- Multiblock copolymers with improved mechanical properties and high proton conductivity show lower MeOH permeability and better DMFC performance than Nafion®-based membranes.
- Unlike in MeOH oxidation, the optimal PtRu catalyst composition varies depending on the operating voltage of the DME fuel cell (anode potential); DME crossover is less than that of MeOH under typical testing conditions; a DDMEFC operating with a $Pt_{50}Ru_{50}$ anode catalyst has shown the highest performance reported to date at 80°C.

Future Directions

- MeOH Oxidation Catalysis: Perform comprehensive activity and stability study of advanced MeOH oxidation catalysts versus HiSPEC® 12100 as a benchmark; complete evaluation of PtSnX catalysts for upcoming Go/Go-No decision on PtSn catalysts in FY 2012; evaluate the degree of Ru crossover resulting from advanced MeOH oxidation catalysts.
- Innovative Membranes and Electrode Structures: Determine durability of multiblock copolymers in an operating fuel cell; reduce polymer water uptake; improve dimension control and eliminate oxidation of CuNW (before galvanic displacement); significantly reduce wall thickness of PtRu nanotubes to at least double the catalyst surface area.
- EtOH Oxidation Catalysis: Increase the size of PtRh nanoparticles to enhance the size of Pt ensembles in $PtRhSnO_2$ catalyst and thus facilitate adsorption and dehydrogenation of the EtOH molecule; scale up the synthesis of a selected ternary catalyst to 2 g per batch for MEA testing; evaluate Au clusters and/or supported Au-monolayers as catalyst supports; complete differential electrochemical mass spectroscopy instrument set up.
- DME Research: Determine the effect of anode catalyst composition on Ru crossover and cathode performance (relevant to both DDMEFC and DMFC); complete half-cell DME studies with PtRu catalysts; assess DDMEFC feasibility versus DMFC following full optimization of the DME anode (Go/No-Go decision on DME research in FY 2012).

References

1. Multi-Year Research, Development and Demonstration Plan: Planned Program Activities for 2005-2015, Fuel Cell Technologies Program, 2007. http://www1.eere.energy.gov/hydrogenandfuelcells/mypp/pdfs/fuel_cells.pdf

2. J.-Y. Im, B.-S. Kim, H.-G. Choi, S.M. Cho, *J. Power Sources*, 179, 301-304 (2008).

FY 2011 Publications

1. "The Effect of Ruthenium Crossover in Polymer Electrolyte Fuel Cells Operating with Platinum-Ruthenium Anode;" A. Trendewicz, M.Sc. Thesis (P. Zelenay, Co-advisor), University of Iceland, Reykjavik, Iceland and The School of Renewable Energy Science, Akureyri, Iceland; January 2011.

2. "Ethanol electrooxidation on the ternary Pt-Rh-SnO_2/C electrocatalysts with varied Pt:Rh:Sn ratios;" M. Li, A. Kowal, K. Sasaki, N.S. Marinkovic, D. Su, E. Korach, P. Liu, R.R. Adzic, *Electrochim. Acta*, **55**, 4331 (2010).

3. "Molecular Design Aspect of Sulfonated Polymers for Direct Methanol Fuel Cells;" D.S. Kim, M. Guiver, B.S. Pivovar, and Y.S. Kim, *ECS Trans.*, **33**, 711-717 (2010).

FY 2011 Presentations

1. National Renewable Energy Laboratory, Golden, Colorado, March 29, 2011. Title: "Ruthenium Crossover in Polymer Electrolyte Fuel Cells;" P. He, T.T.H. Cheng, R. Bashyam, A.P. Young, S. Knights, Y.S. Kim, and P. Zelenay.

2. 4th Santa Fe Workshop on Materials and Energy Conversion, Catalysts for Ethanol Oxidation and Electro-oxidation, Santa Fe, New Mexico, November 4–6, 2010. Title: "Catalyst Crossover in Polymer Electrolyte Fuel Cells;" P. He, T.T.H. Cheng, R. Bashyam, A.P. Young, S. Knights, Y.S. Kim, and P. Zelenay.

V.H.1 Low-Cost PEM Fuel Cell Metal Bipolar Plates

Conghua "CH" Wang
TreadStone Technologies, Inc.
201 Washington Rd.
Princeton, NJ 08543
Phone: (609) 734-3071
E-mail: cwang@TreadStone-Technologies.com

DOE Managers
HQ: Jason Marcinkoski
Phone: (202) 586-7466
E-mail: Jason.Marcinkoski@ee.doe.gov
GO: David Peterson
Phone: (720) 356-1747
E-mail: David.Peterson@go.doe.gov

Technical Advisor
Thomas Benjamin
Phone: (630) 252-1632
E-mail: benjamin@anl.gov

Contract Number: 09EE0000463

Subcontractors:
- Gas Technology Institute, Des Plaines, IL
- The State University of New York, Stony Brook, Stony Brook, NY
- IBIS Associations, Inc., Waltham, MA
- Ford Motor Company, Dearborn, MI

Project Start Date: September 1, 2009
Project End Date: August 31, 2011

Fiscal Year (FY) 2011 Objectives

- Reduce or eliminate the small amount of gold used in TreadStone's current corrosion resistant metal plate technology for polymer electrolyte membrane (PEM) fuel cell applications.
- Develop the low-cost metal bipolar plates using commercially available low-cost carbon steel or aluminum as the substrate materials.
- Optimize the fabrication process for large scale manufacture.
- Demonstrate TreadStone's low-cost metal plate technology in the applications of portable, stationary and automobile fuel cell systems.

Technical Barriers

This project addresses the following technical barriers from the Fuel Cells section of the Fuel Cell Technologies Program Multi-Year Research, Development and Demonstration Plan:

(A) Durability

(B) Cost

(C) Performance

Technical Targets

The focus of this project is to further develop TreadStone's proprietary corrosion resistant metal plate technology reducing the metal plate cost to <$3/kW, while still meeting the performance requirements. There are a number of performance requirements for PEM fuel cell bipolar plates. The most challenging requirements for metal bipolar plates are summarized in Table 1. The status of TreadStone's low-cost metal plates is summarized in the table as well.

TABLE 1. TreadStone's Metal Plate Status and DOEs Targets

Parameter	Unit	TreadStone 2010 Status	DOE Targets	
			2010	2015
Plate Cost [a]	$/kW	$3.82	5	3
Plate Weight [b]	kg/kW	<0.4	<0.4	<0.4
Corrosion Anode [c]	$\mu A/cm^2$	not available	<1	<1
Corrosion Cathode [d]	$\mu A/cm^2$	<0.01	<1	<1
Resistance [e]	Ohm cm^2	<0.01	<0.02	<0.02

[a] Based on 50% utilization of active area on the whole plate surface, stainless steel (SS) foil cost at historical average of $2/lb, 1 W/$cm^2$ power density and projected 500,000 stacks per year production.
[b] Based on the 0.1 mm thick SS foil.
[c] pH 3, 0.1 ppm hydrofluorhydric acid (HF), 80°C, peak active current $<1X10^{-6}$ A/cm^2 (potentiodynamic test at 0.1 mV/s, -0.4 V to +0.6 V (Ag/ AgCl)) de-aerated with Ar purge.
[c] pH 3, 0.1 ppm HF, 80°C, passive current $<5X10^{-8}$ A/cm^2 (potentiostatic test at +0.6 V (Ag/AgCl)) for at least 24 hours, aerated solution.
[d] Includes contact resistance (on as-received and after potentiostatic experiment) measured.

FY 2011 Accomplishments

- Completed the low-cost, gold free conductive vias development. Demonstrated the processing technologies for carbon nanotubes and conductive carbides as the conductive vias. The corrosion current of metal plates with these vias are below 1 $\mu A/cm^2$ in pH 3 H_2SO_4 + 0.1 ppm HF solution under 0.8 V normal hydrogen electrode (NHE) at 80°C.
- Completed the large fabrication-scale cost analysis of metal plates using the gold-free vias technologies.
- Developed the processing technology and the identified the coating materials for aluminum substrate for PEM fuel cell applications.
- Demonstrated the current gold dots metal plates in portable and stationary applications, operating at ambient pressure conditions, with a small (30 cm^2 active

area of each cell) 200 W and a large (267 cm^2 active area each cell) 1 kW stack, respectively.

- Demonstrated 1,000 hours stable operation of the gold dots metal plate in a 300 cm^2 active area, 10-cell, 2.5 kW short stack under durability testing cycle (including the Federal Test Procedure [FTP] cycle along with others) to mimic the automobile real world driving conditions at Ford Motor Company.

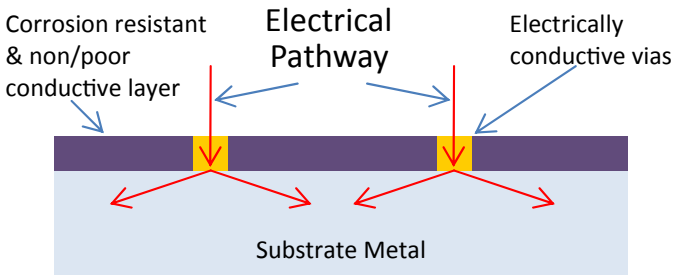


FIGURE 1. Schematic Drawing of TreadStone's Corrosion Resistant Metal Plate Design

Introduction

It has been reported that using metal bipolar separate plates can reduce the PEM fuel cell stack weight and volume by 40-50%, comparing with current graphite-based bipolar plates [1]. The major barrier to use metal bipolar plates in PEM fuel cells is the severe corrosion condition during stack operation. Most metals do not have adequate corrosion resistance in a PEM fuel cell environment, which results in rapid performance degradation due to the formation of the electrically resistive surface oxide scale, and potential contamination of the membrane electrode assembly by the dissolved ions from the metal plates. Various corrosion protection techniques have been investigated to prevent the metal plate corrosion in PEM fuel cell environments [2-7]. Some of these technologies have developed corrosion-resistant metal plates that can meet the performance requirements. However, it is still a challenge to have the metal bipolar plate that can meet both the performance and cost requirements. The focus of TreadStone's project is to develop corrosion resistant metal bipolar plates at the low-cost to meet DOE's 2015 targets.

Approach

Most research on metal bipolar plates has been focused on covering the whole plate surface with an electronically conductive and corrosion-resistant material to protect the metal from corrosion and maintain the electrical conductance of the metal. The challenge of this approach is that there is only a limited number of low-cost materials that can meet electrical conductivity and corrosion resistance requirements for PEM fuel cell applications. In addition, the processing required to apply these materials on metal substrate is either difficult or at high cost.

TreadStone takes a different approach to develop metal bipolar plates for PEM fuel cell applications. It was found that it is unnecessary to have the whole surface electrically conductive to ensure the low contact resistance (interfacial contact resistance < 10 $m\Omega.cm^2$) between bipolar plates and the gas diffusion layer (GDL). TreadStone's approach is based on this principle, as shown in Figure 1.

The majority of the metal surface area is covered with the low-cost corrosion-resistant but non- (or poor) conductive material (purple layer in Figure 1). A corrosion resistant and highly electrically conductive material (such as Au) forms the paths for electron transport, in the form of small conductive vias (yellow bars) penetrating through the non-conductive layer. Electrons generated from the anode reaction will flow through the GDL to the conductive vias (illustrated as red arrows) passing through the metal plate to the other side for the cathode reaction on the cathode of the adjacent cell. The conductive vias, having a dimension as small as several micrometers, are distributed on the metal surface. The average distance between the conductive vias is 20-70 μms. The dense distribution of conductive vias ensures a uniform current distribution between the GDL and metal bipolar plates.

TreadStone's approach is unique because it uses only a small portion (<1-2%) of the plate surface for electrical contact. It was found that more than 500,000 via/in^2 cover the metal plate surface as the electrical contact point of metal plate with GDL, when small (<5 μm) conductive vias are used. It is because of the high amount of the contact points that enable the low contact resistance of metal plates.

Results

TreadStone's current metal bipolar plate uses a small amount of gold as the electrical contacting material in the form of conductive vias, and SS as the substrate material. In this project, we plan to develop a lower cost material to reduce the gold usage, or replace gold as the contact material. We have finished the process development to use a palladium/gold composite as the contact materials. We also developed the process to use carbon nanotubes and conductive carbides as the conduct material. All of the approaches have met the performance requirements. Figure 2 shows the scanning electron microscope (SEM) picture of the chromium carbide particles that are bonded on the SS surface using chromium-nickel alloy.

The large-scale fabrication cost analysis of the metal plates using alternative conductive vias was conducted based on a post-forming coating process. The assumptions of the cost analysis are based on 50% utilization of active area on the whole plate surface, stainless steel foil cost at historical average of $2/lb, 1 W/$cm^2$ power density and projected 500,000 stacks per year production. The fabrication flow

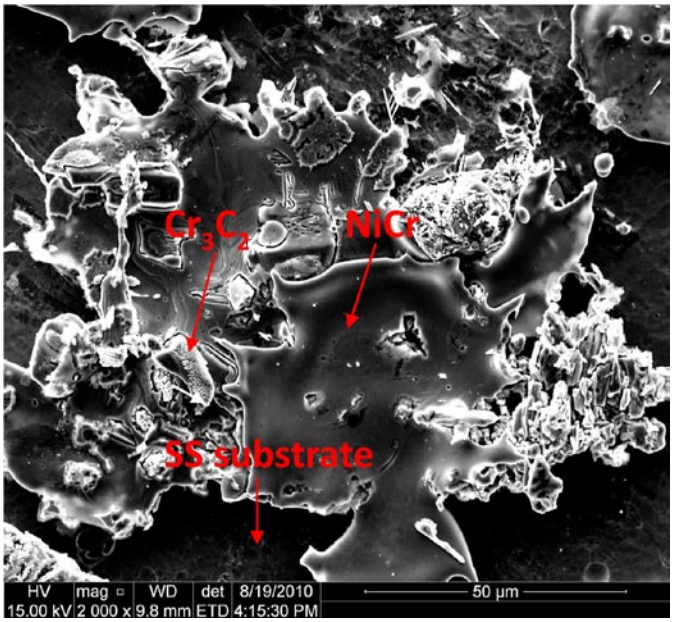


FIGURE 2. SEM Picture of Chromium Carbide Particles Bonded on SS Substrate

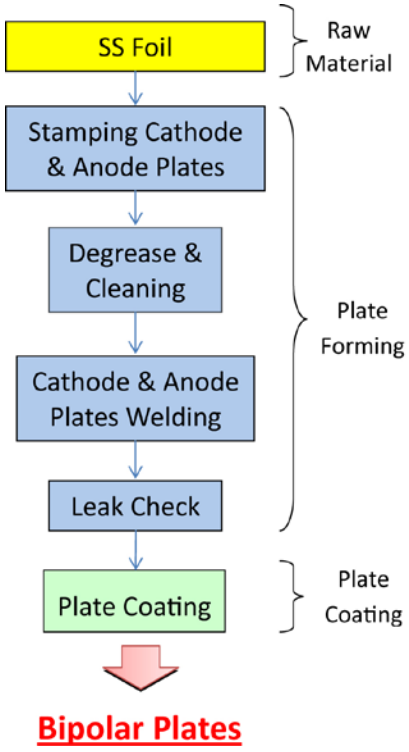


FIGURE 3. Fabrication Flow Diagram for Cost Analysis

diagram is shown in Figure 3. It includes the raw material (SS foil), bipolar plate forming step, and coating step. The cost of each portion is listed in Table 2.

TABLE 2. TreadStone Metal Plate Large-Scale Fabrication Cost Components

Process Step	316 SS foil	Forming	Coating		
			Pd/Au	C-tube	Carbides
Cost[1]	$0.75	$0.48	$0.31	$0.79	$0.30

[1] The cost is $/plate, based on 400 cm^2 active area on each plate.

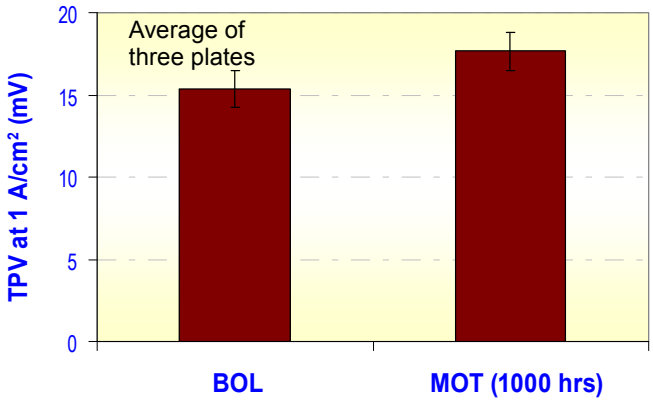


FIGURE 4. Comparison of the TPV Drop of TreadStone's Metal Plates before and after the 1,000 hr Stack Durability Test under Dynamic Loading Conditions at Ford

Table 2 shows that metal plate coating cost using TreadStone's technology can be as low as $0.30/plate, which is a minor part of the bipolar plate cost. SS substrate material cost is the major cost item that accounts of ~50% of the total plate cost, even using the commercial available lower cost 304 SS foil. The metal forming (including laser welding and leak checking) cost is very high as well. Therefore, using lower cost substrate materials, such as carbon steel or aluminum substrate is very useful to reduce the bipolar plates cost. Alternative, low-cost forming process is also important for the low-cost bipolar plate production.

The stacks using TreadStone's metal plates have been designed, and optimized for portable, stationary and automobile applications. The portable power stack has 30 cm^2 active area on each cell. The peak power is 200 W. The stationary stack has 263 cm^2 active area on each cell. The peak power is 1 kW. The initial performance of these two stacks has been characterized. The long-term durability tests of the stacks are underway.

A 10-cell, 2.5 kW short stack for automobile application has also been assembled and tested at Ford Motor Company. The stack has 300 cm^2 active area on each cell, and operates under high pressure. The stack is being tested for utilizing durability cycle (which includes the FTP cycle along with others) mimicking "real-world" driving conditions. After finishing 1,000 hours of stable operation, the stack was disassembled for inspection of all components. There was no sign of corrosion of the metal plates after the 1,000-hour test. The comparison of the through-plate voltage drop

(TPV, under 1 A/cm^2) before beginning of life (BOL) and after the middle of test (MOT) for the 1,000 hours durability test is compared in Figure 4. The TPVs meet the DOE's requirement (<20 mV), although there is small increase (from 15 mV to 18 mV) after the test.

Conclusions and Future Directions

TreadStone's unique corrosion-resistant metal bipolar plates have demonstrated stable operation for PEM fuel cell applications in portable, stationary and automobile applications. The processes can reduce the metal plate coating cost to as low as $0.30/plate. Further development will be focused on:

- Scale up of the lower cost conductive vias processing technique for the large-scale production.
- Demonstration of the low-cost carbon steel and aluminum plates based bipolar plates.
- Demonstration of the long-term operation stability of the TreadStone's low-cost metal plates in PEM fuel cell applications.

Publications

1. L. Zhang, J. Finch, G. Gontarz and C. Wang, "Development of Low Cost PEMFC Metal Bipolar Plates" presented at 218th Meeting of Electrochemical Society, Oct. 2010, Las Vegas, NV.

References

1. A.S. Woodman, E.B. Anderson, K.D. Jayne, and M.C. Kimble, AESF SUR/FIN '99 Proceedings, 6/21-24, 1999.

2. M.P. Brady, B. Yang, H. Wang, J.A. Tuner, K.L.More, M. Wilson, and F. Garzon, JOM, 2006, 58, 50.

3. H. Wang, M.P. Brady, K.L. More, H.M. Meyer and J.A. Turner, J. Power Sources, 2004, 138, 75.

4. Y. Wang, D.O. Northwood, Int. J. Hydrogen Energy 2007, 32, 895.

5. C.Y. Chung, S.K. Chen, P.J. Chiu, M.H. Chang, T.T. Hung, T.H. Ko, J. Power Sources 2008, 176, 276.

6. M.A.L. Garcia, M.A. Smith, J. Power Sources 2006, 158, 397.

7. D.G. Nam, H.C. Lee, J. Power Sources 2007, 170, 268.

8. R. Tian, J. Sun, L. Wang, Int. J. Hydrogen Energy 2006, 31, 1874.

V.H.2 Metallic Bipolar Plates with Composite Coatings

Jennifer Mawdsley (Primary Contact),
J. David Carter, Suhas Niyogi, Xiaoping Wang
Argonne National Laboratory
9700 S. Cass Ave.
Argonne, IL 60439
Phone: (630) 252-4608
E-mail: mawdsley@anl.gov

DOE Manager
HQ: Nancy Garland
Phone: (202) 586-5673
E-mail: Nancy.Garland@ee.doe.gov

Subcontractors:
- Rasit Koc, Southern Illinois University Carbondale, Carbondale, IL
- Chinbay Fan, Gas Technology Institute, Des Plaines, IL
- George Osterhout, Orion Industries, Chicago, IL

Project Start Date: August 1, 2009
Project End Date: September 30, 2011

Fiscal Year (FY) 2011 Objectives

- Develop a fluoropolymer-inorganic filler composite coating that is electrically conductive and provides a physical barrier to corrosive species within the fuel cell.
- Apply the composite coating to aluminum alloy substrates using an established high-volume manufacturing process.
- Measure the corrosion resistance at 80°C and area specific resistance of the composite coated aluminum plates.
- Apply the composite coating to stamped and welded bipolar plates, and then conduct a single cell, 2,000-hour test.
- Conduct an analysis to determine the anticipated cost of manufacturing the plates at high volume.

Technical Barriers

This project addresses the following technical barriers from the Fuel Cells section of the Fuel Cell Technologies Program Multi-Year Research, Development and Demonstration Plan:

(A) Durability
(B) Cost
(C) Performance

Technical Targets

The goal of this work is to develop an aluminum-based bipolar plate that meets all of the DOE technical targets for bipolar plates shown in Table 1. This goal will be met by applying a composite coating that is both electrically conductive and corrosion resistant to the aluminum plate, using an established high-volume manufacturing process.

TABLE 1. Project Progress Toward Meeting DOE Technical Targets for Bipolar Plates [1]

Characteristic	Units	2015 Target	Project 2011 Status
Cost	$/kW	3	TBD
Weight	kg/kW	<0.4	0.35
H_2 Permeation Flux	$cm^3\ sec^{-1}\ cm^{-2}$ @ 80°C, 3 atm	$<2 \times 10^6$	$<2 \times 10^6$
Corrosion	$\mu A/cm^2$	<1	<1 (cathodic) 11 (anodic)
Electrical Conductivity	S/cm	>100	37
Area Specific Resistance[a]	Ohm-cm^2	0.02	0.58
Flexural Strength	MPa	>25	TBD
Flexibility	% deflection at midspan	3 to 5	TBD

[a] Tentative revised target
TBD – to be determined

FY 2011 Accomplishments

- Nano-size titanium carbide (TiC) powder has been synthesized using a low-cost process that is scalable.
- A patent application has been filed for the low-cost CaB_6 powder synthesis procedure.
- TiC was identified as the most acid resistant of the cermet powders tested for acid stability and electrochemical stability at 80°C and room temperature in sulfuric acid solutions.
- Substituting nano-size TiC for half of the flake graphite filler in the composite coatings was found to significantly reduce area specific resistances of the coated aluminum samples.
- The composite coated aluminum plates meet the DOE target for electrochemical corrosion resistance under cathodic conditions at 80°C.
- Composite-coated, stamped aluminum plates were made using wet spraying, a high volume manufacturing process.

- A composite-coated, stamped aluminum plate tested in a single-membrane electrode assembly (MEA), two-bipolar plate cell test showed improved performance over untreated aluminum.



Introduction

Aluminum bipolar plates offer a potential weight reduction over stainless steel, while still having the desired mechanical properties that a metal offers. Furthermore, untreated aluminum can meet all of the DOE bipolar plate targets except for corrosion resistance. To overcome this one weakness, the project team has been applying a composite coating consisting of a matrix of an acid-resistant fluoropolymer and a filler material that is electrically conductive and acid-resistant. Metal carbides, metal borides, metal silicides, and carbon-based materials, such as graphite, carbon black, and carbon fibers, were identified as candidate filler materials based on reported electrical conductivity and acid resistance properties [2]. In the first year of the project, we found that metal borides were not stable under simulated fuel cell conditions, so in the second year, TiC and titanium disilicide ($TiSi_2$) were evaluated. The composite-coated aluminum bipolar plates have been being fabricated using techniques, such as stamping, welding, and spraying, that are currently used for high-volume manufacturing of many consumer goods. In the second year of the project, we have focused on meeting the corrosion and electrical properties targets.

Approach

The titanium carbide powder currently available commercially is expensive and not available in sub-micrometer sizes. So, titanium carbide was made at Southern Illinois University (SIU) using a low-cost process that produces nano-size particles [3]. Acid stability tests at 80°C and electrochemical stability tests in sulfuric acid were conducted to determine if TiC and $TiSi_2$ are durable enough for use in proton exchange membrane (PEM) fuel cells. Argonne has worked on identifying the formulation of fluoropolymer and filler that can provide the desired electrical conductivity in a composite coating. We have sprayed fluoropolymer (ethylene-tetrafluoroethylene, EFTE, or polychlorotrifluoroethylene, PCTFE) mixed with TiC, graphite, and/or carbon black onto non-conductive substrates, and we have measured the surface conductivity/resistivity of these samples. We have varied the ratio of graphite to TiC, the type of fluoropolymer, and the ratio of filler to fluoropolymer to increase the electrical conductivity of the coatings. We have conducted electrochemical corrosion studies of the coated aluminum samples at 80°C using the conditions specified by the DOE. Finally, initial tests were conducted of stamped, welded, and coated aluminum plates in a single cell test.

Results

Of the metal carbides, TiC was chosen because it has the desired combination of reported electrical conductivity, density, and corrosion resistance [2]. Low-cost processes were used to synthesize nano-size TiC powder at SIU. These processes allowed for tuning the electrical properties of the powder. Inexpensive TiO_2 and propylene precursors were used in the 2-step synthesis procedure, which used processing temperatures of up to 1,500°C. Powder X-ray diffraction results showed only the desired titanium carbide phase. Analysis by scanning electron microscope (SEM) showed that particle sizes were, on average, <200 nm in diameter, Figure 1, and that the particles formed an interconnected network.

The environment inside a PEM fuel cell is acidic due to the presence of the Nafion® membrane and the Nafion® ionomer in the electrodes, combined with the humidity [4]. Acid stability tests were conducted on the synthesized TiC, graphite (Superior Graphite), and $TiSi_2$ at 80°C in 3.5% H_2 in helium for 30 days. The sulfuric acid solution used in the tests was 0.001M H_2SO_4 (pH=3) with 0.1 ppm NaF. The results of the tests are shown in Table 2. The values shown in the "% Sample Remaining" column were calculated from the measured change in the weight of the samples.

Electrochemical corrosion experiments using the thin-film rotating disk-electrode technique were also conducted on the TiC and $TiSi_2$ powders to corroborate the findings of the acid stability tests. Powders of TiC (SIU) and $TiSi_2$ (Aldrich, ball milled) were made into an ink by mixing them

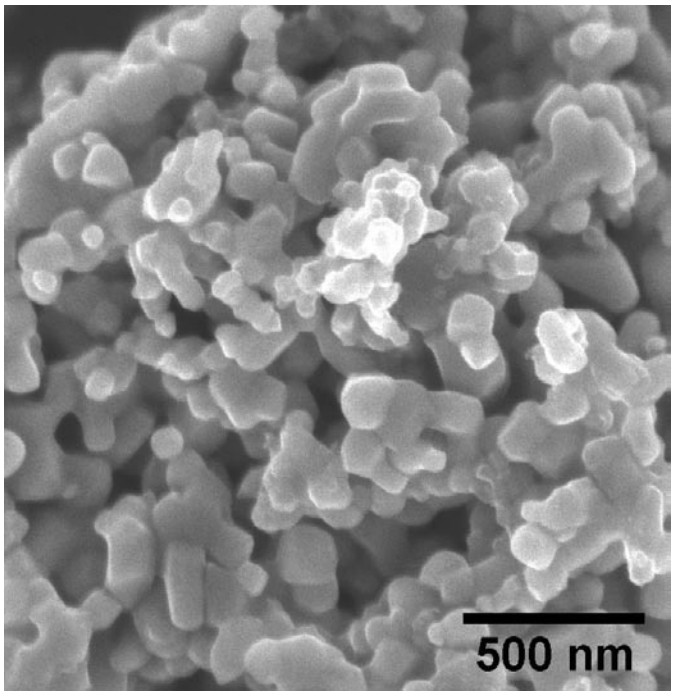


FIGURE 1. SEM Images of Nano-Size TiC Powder Synthesized by a Low-Cost Process at SIU

TABLE 2. Results of the Sulfuric Acid Stability Experiments at 80°C in 3.5% Hydrogen

Sample	% Sample Remaining	Extra Phases in XRD	Ion Concen. (mol/L)
TiC	109%	none	Ti: n.d.*
$TiSi_2$ (with TiSi & Si impurities)	132%	Ti_3O_5, TiO_2	Ti: n.d.* Si: $5.6x10^{-3}$
Graphite	94 %	none	n.a.

*The detection limit is $1.3x10^{-6}$ mol Ti/L
n.a. – not analyzed; n.d. – not determined

with Nafion® and an organic solvent. The volume ratio of the powder to dry Nafion® was 50:50. A thin film of the mixture was applied to a rotating disk electrode (RDE) and electrochemically tested at room temperature in both O_2-saturated and O_2-free (Ar-purged) 0.1 M H_2SO_4. The loading of powder on the RDE was 155 μg/cm^2. Potential holds at several potentials and potential scans relevant to the bipolar plate application were run. The results are shown in Table 3. The $TiSi_2$ sample performed the best with no redox features observed in the cyclic voltammetry (CV) tests. The TiC was acceptable, but a small oxidation peak at 0.56 V occurred when cathodic scan went to a potential less than 0.4 V. Since these tests were performed at room temperature there are some differences from the acid stability experiments. Based the results from the two types of stability tests, TiC was chosen as the best candidate, along with graphite and carbon black, for the filler phase in the composite coatings.

TABLE 3. Results of RDE Electrochemical Stability Experiments

Sample	Corrosion Current (A/cm^2)			Observations
	0.84 V in Ar	0.84 V in O_2	0.14 V in Ar	
TiC (SIU)	6.24×10^{-6}	1.34×10^{-5}	7.06×10^{-6}	A small oxidation peak at 0.56 V occurred when cathodic scan went to a potential less than 0.4 V.
TiC (Aldrich, milled)	4.92×10^{-5}	2.87×10^{-5}	2.27×10^{-5}	Same features as for unmilled SIU TiC
$TiSi_2$ (Aldrich, milled)	5.65×10^{-6}	5.70×10^{-6}	4.75×10^{-6}	No obvious redox features

Surface electrical conductivity/sheet resistance were measured using the Van der Pauw technique [5] and a four-point probe (Jandel) on the composite coatings deposited on non-conductive ceramic substrates. Through-sample area specific resistivity (ASR) measurements [6,7] were conducted at an applied pressure of 200 psi on aluminum-based samples that were coated on both sides. Slurries were made by ball milling the desired amounts of filler (graphite, nano-size TiC, and/or carbon black) and fluoropolymer (PCTFE or ETFE) with solvents. The slurries were then sprayed onto either aluminum or ceramic substrates and sintered at 240 to 300°C for 2 to 4 h. Selected ASR and sheet resistance results are shown in Table 4. The measured electrical conductivities of the composites were significantly lower than the published bulk conductivities of the fillers possibly because the fluoropolymer may act to separate the filler particles as it flows between the particles during sintering. The coatings that have lower ASR tend to also have higher surface resistance. This may be due to the even distribution of the fillers into the bulk of the coating versus segregating onto the surface.

TABLE 4. Selected Results of Surface and Through-Plane Electrical Conductivity Measurements of Composite Coated Samples

Coating Composition		ASR (Ω-cm²)	Sheet Resistance (Ω)
Vol % Fluoropolymer	Vol% Filler(s)		
40% PCTFE	60% Graphite	0.68	4.2
40% PCTFE	40% Graphite, 20% Carbon black	0.97	3.3
40% PCTFE	30% TiC, 30% Graphite	0.27	8.4
50% PCTFE	25% TiC, 25% Graphite	0.11	25
50% PCTFE	50% Graphite	3.3	5.0
50% ETFE	25% TiC, 25% Graphite	0.58	27
50% ETFE	50% Graphite	2.7	20
40% ETFE	60% Graphite	0.75	2.8

Corrosion resistance of coated aluminum samples was measured using electrochemical methods [7] to evaluate the ability of the coatings to provide a physical barrier between the aluminum substrate and the corrosive media in a fuel cell. In these experiments, conducted at 80°C, the electrolyte was 0.001M sulfuric acid (pH= 3) with 0.1 ppm NaF. For cathodic corrosion tests, air was bubbled continuously through the acid solution and a potential of 0.6 V vs. Ag/AgCl (0.8 V vs. normal hydrogen electrode, NHE) was applied for 24 h. For anodic corrosion tests, argon was continuously bubbled through the acid solution and a potential of -0.4 V vs. Ag/AgCl (-0.2 V vs. NHE) was applied for 24 h. The results for aluminum plates with a coating of 25 vol% TiC/25% graphite/50 vol% EFTE applied by spraying at Orion Industries are shown in Figure 2. The corrosion current densities for the cathodic tests were below the DOE corrosion target, however, the anodic corrosion current densities were higher than the DOE target.

A total of 75 uncoated aluminum bipolar plates with flow fields have been stamped with a 60 cm^2 active area. The design is based on the GTI patented trapezoidal flow field structure for PEM fuel cells with very low pressure drop. The hydrogen permeability of the formed plates was tested and the results did not show any detectable hydrogen pass-through at 50 psig (3.4 atm), meeting the DOE target. In addition, the cell design was proven during fuel cell testing, and it showed that the stacks can be well sealed against fuel, oxidant, and cooling water leaks. In order to improve electrical conductivity through the samples GTI has

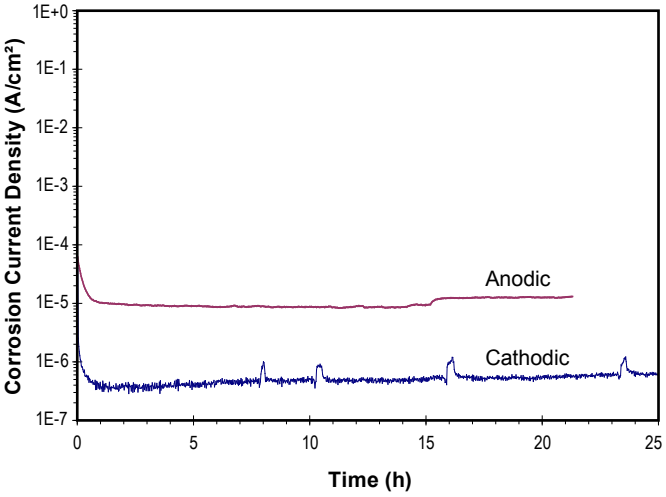


FIGURE 2. Electrochemical Corrosion Test Results for 25% TiC/25% Graphite/50% ETFE on Aluminum Panels Produced by Orion

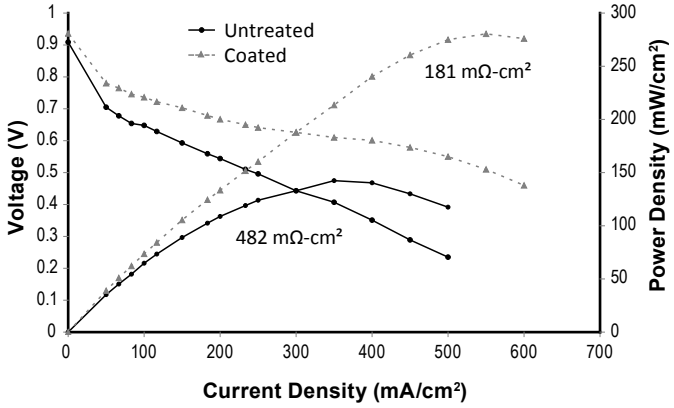


FIGURE 3. Performance Curves for 92% Graphite Coating on Aluminum and Uncoated Aluminum in a Single MEA–Two Bipolar Plate Cell

developed surface treatments that deposit a small amount of metal on the surface of the aluminum before the coating is applied. Two of these treated and coated stamped aluminum plates have been tested in a single-MEA, two-bipolar plate cell at 50°C using a Gore MEA fed with hydrogen and air. The results are shown in Figure 3 and compared to the results obtained with untreated aluminum bipolar plates. The treated and coated aluminum bipolar plates performed better compared to the untreated aluminum bipolar plates. This is because the uncoated aluminum plates had formed a resistive oxide layer on the surface, whereas it was removed and prevented from forming on the treated and coated bipolar plates. Figure 4 shows a photograph of the stamped and coated aluminum plates.

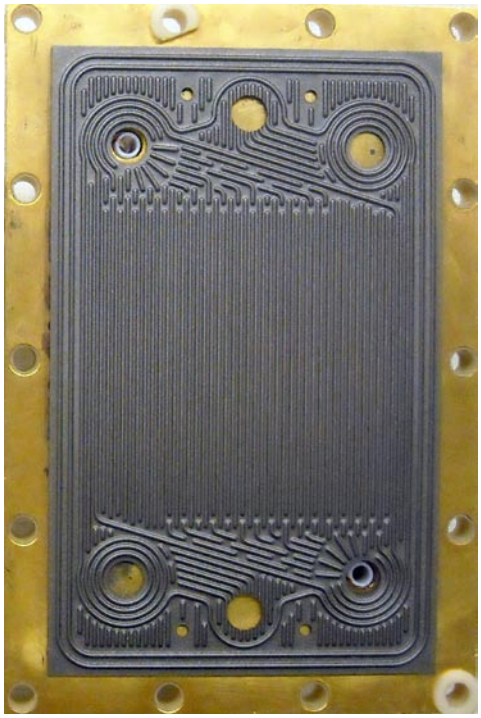


FIGURE 4. Picture of Stamped and Coated Aluminum Bipolar Plate Prior to the Single Cell Test

Conclusions and Future Directions

- Composites made with a combination of flake graphite and nano-size titanium carbide as the filler have the highest electrical conductivities.
- These coatings provide adequate corrosion protection under cathodic conditions.
- Coatings from Orion will be made thinner and with a higher fraction of conductive filler to improve electrical properties.
- Aluminum surface treatments will be evaluated for improved conductivity and corrosion resistance.
- A different fluoropolymer will be evaluated for its potential to improve anodic corrosion resistance.
- A manufacturing cost analysis will be conducted.

FY 2011 Publications/Presentations

1. Jennifer Mawdsley, J. David Carter, Suhas Niyogi, Xiaoping Wang, John Vaughey, and Rasit Koc, "Aluminum bipolar plates with composite coatings for proton exchange membrane fuel cells", to be presented at the American Chemical Society Fall 2011 National Meeting and Exposition, Denver, CO, Aug. 28 – Sept. 1, 2011.

2. A.Akkoyunlu, R. Koc, J. Mawdsley and J.D. Carter, "Synthesis of Submicron-size CaB_6 Powders Using Various Boron Sources", accepted for publication in *Ceramic Engineering and Science Proceedings*.

3. N. Siddiqui, R. Koc, J. Mawdsley and J.D. Carter, "Synthesis of Sub-micron/Nano-sized CaB_6 from Carbon Coated Precursors", accepted for publication in *Ceramic Engineering and Science Proceedings*.

4. R. Duddukuri, R. Koc, J. Mawdsley and J.D. Carter, "Synthesis of Nano-size TiB_2 Powders Using Carbon Coated Precursors", accepted for publication in *Ceramic Engineering and Science Proceedings*.

5. S. Stariha, S. Niyogi, T.K. Honaker-Schroeder, J.D. Carter, and J.R. Mawdsley, "Hydrophilic Surface Treatments for Graphite-Fluoropolymer Composite Coatings on Metallic Bipolar Plates," (Poster) 241st American Chemical Society (ACS) Meeting and Exposition, Anaheim, CA, March 27–31, 2011.

6. N. Siddiqui, R. Koc, J. Mawdsley, and J.D. Carter, "Synthesis of Nano-Size CaB_6 Powders Using Carbon-Coated Precursors," 35th International Conference and Exposition on Advanced Ceramics and Composites (ICACC'11), Daytona Beach, FL, Jan. 23–28, 2011.

7. A. Akkoyunlu, R. Koc, J. Mawdsley, and J. D. Carter, "Synthesis of Nano-Size CaB_6 Powders Using Various Boron Sources," 35th International Conference and Exposition on Advanced Ceramics and Composites (ICACC'11), Daytona Beach, FL, Jan. 23–28, 2011.

8. R. Dudukuri, R. Koc, J. Mawdsley, and J.D. Carter, "Synthesis of Nano-Size TiB_2 Powders Using Carbon-Coated Precursors," 35th International Conference and Exposition on Advanced Ceramics and Composites (ICACC'11), Daytona Beach, FL, Jan. 23–28, 2011.

9. Jennifer Mawdsley, J. David Carter, Suhas Niyogi, Xiaoping Wang, Rasit Koc, Chinbay Fan, and George Osterhout, "Composite-Coated Aluminum Bipolar Plates for PEM Fuel Cells," (Poster) 5th International Conference on Polymer Batteries and Fuel Cells (PBFC-5), Argonne, IL, Aug. 1–5, 2011.

References

1. *Fuel Cell Technologies Program Multi-Year Research, Development and Demonstration Plan*. 2007, U.S. Department of Energy, Fuel Cell Technologies Program: Washington, DC.

2. Samsonov, G.V. and I.M. Vinitskii, *Handbook of Refractory Compounds*. 1980, New York, NY: IFI/Plenum.

3. Koc, R. and J.S. Folmer, *Carbothermal synthesis of titatium carbide using ultrafine titania powders.* Journal of Materials Science, 1997. **32**(12): p. 3101-3111.

4. Knigge, D., et al. *Electrochemical Corrosion Testing and In-Stack Aging of Metallic Bipolar Plates for PEM Fuel Cells*. in *16th World Hydrogen Energy Conference*. 2006.

5. Van der Pauw, L.J., *A Method of Measuring Specific Resistivity and Hall Effect of Discs of Arbitrary Shape.* Philips Research Reports, 1958. **13**: p. 1.

6. *Electrical conductivity testing protocol: Through-plane electrical conductivty testing protocol for composite materials*. 2004, U.S. Fuel Cell Council: Washington, DC.

7. Wang, H.L., M.A. Sweikart, and J.A. Turner, *Stainless steel as bipolar plate material for polymer electrolyte membrane fuel cells.* Journal of Power Sources, 2003. **115**(2): p. 243-251.

V.I.1 Resonance-Stabilized Anion Exchange Polymer Electrolytes

Yu Seung Kim (Primary Contact), Dae-Sik Kim, Andrea Labouriau, Hoon Jung, Piotr Zelenay
Los Alamos National Laboratory (LANL)
Los Alamos, NM 87545
Phone: (505) 667-5782
E-mail: yskim@lanl.gov

DOE Manager
HQ: Nancy Garland
Phone: (202) 586-5673
E-mail: Nancy.Garland@ee.doe.gov

Subcontractors:
- Michael Hibbs, Cy Fujimoto, Sandia National Laboratories, Albuquerque, NM
- Charles C. Hays, Daniel Konopka, Michael A. Johnson, Adam Kosor, Povan Bahrami, Michael Errico, Jet Propulsion Laboratory, Pasadena, CA

Project Start Date: October 1, 2009
Project End Date: September 30, 2011

Fiscal Year (FY) 2011 Objectives

- Synthesize highly conductive and stable anion exchange membranes.
- Prepare highly gas permeable perfluorinated ionomers for electrode layers.
- Develop non-precious metal catalysts for oxygen reduction reactions.
- Demonstrate single-cell performance of alkaline membrane fuel cells.
- Perform an extended term alkaline fuel cell test under steady state conditions.

Technical Barriers

This project addresses the following technical barriers from the Fuel Cells section (3.4.4) of the Fuel Cell Technologies Program Multi-Year Research, Development and Demonstration Plan:

(A) Durability
(B) Cost
(C) Performance

Technical Targets

This project is conducting fundamental aspects of anion exchange membrane fuel cell (AMFCs) for practical use in intermediate (10-50 kW) power applications. Insights gained from these studies will be applied toward the next stage of development of AMFC systems. Since there were no technical targets for AMFCs in the current DOE Fuel Cell Technologies Program, we have proposed the technical targets based on state-of-the-art alkaline fuel cells/materials in the original proposal (2008). Key technical targets, and FY 2011 and 2012 statuses are shown in Table 1.

FY 2011 Accomplishments

- Synthesized highly conductive (0.1 S/cm), chemically stable (>700 h) and mechanically robust poly(phenylene) (PP)-based anion exchange membranes.
- Prepared stable hydrocarbon and perfluorinated-based guanidinium functionalized ionomers having electron donating spacer.
- Measured the oxygen reduction reaction (ORR) kinetics of non-Pt catalysts (Ag, Ni, Pd, and carbon) with KOH and guanidinium electrolytes.
- Demonstrated H_2/O_2 and H_2/air alkaline membrane fuel cell performance at various operating conditions and under steady-state extended term operating conditions.



Introduction

Current quaternary ammonium-tethered anion exchange polymer electrolytes do not show enough stability under alkaline conditions due to the chemical degradation under highly pH conditions. Furthermore, ionomer used in electrode layers has limited gas permeability that

TABLE 1. Technical Targets and FY 2011 and 2012 Status for the Project

Characteristics	2011 Target	2008 state of the art	LANL 2010 status[a]	LANL 2011 Status[b]
Ion conductivity (mS/cm)	50 (80°C)	27 (20°C)	80 (80°C)	100 (80°C)
Stability (h, at <10% σ loss 1 M NaOH)	500 h	>48 h 1 M KOH at (60°C)	380 h (0.5 M NaOH at 80°C)	700 h (at 60°C, 4 M NaOH)
Maximum power density (mW/cm^2 at 80°C)[c]	200 (H_2/air)	196 (H_2/O_2)	NA	300 (H_2/air)
Fuel cell durability[d]	500 h	NA	NA	300 h

[a] as of June 30; [b] as of June 7; [c] platinum-based catalysts; [d] under steady-state conditions; NA: not available

significantly reduces cell performance [1]. In FY 2010, we demonstrated successful synthesis of stable guanidinium functionalized poly(arylene ether)s and initiated synthesis of perfluorinated ionomers for the catalyst layers. In FY 2011, continuing efforts to develop new anion exchange polymer electrolytes and electro-catalysts have been made in order to demonstrate the performance and stability of AMFCs.

Approach

Our approach to achieve high performance AMFCs is to develop new materials which have improved properties and minimal interference between them when the materials are used in membrane electrode assemblies (MEAs). Sandia National Laboratories investigated the properties of PP-based anion exchange membranes for practical use in AMFCs. LANL continued to develop the guanidinium functionalized ionomers for the catalyst layer, which have electron donating stabilizers which may provide good cation stability under high pH conditions. The Jet Propulsion Laboratory (JPL) and LANL investigated the catalytic activity of various catalysts in guanidinium solution in order to screen the best class of catalysts for alkaline membrane fuel cell systems. Extensive efforts on fabrication of AMFC MEAs and fuel cell testing were performed at LANL in order to demonstrate good AMFC performance. The ultimate goal for these approaches is to realize good AMFC performance by integration of these materials into an MEA.

Results

Anion Exchange Polymer Electrolytes

Mechanical properties for both poly(ether sulfone) (PES)- and PP-based anion exchange membranes were investigated as a function of exposure to high pH conditions in order to gain some insight into the practicality of using these polymers in AMFCs (Figure 1). The PES membranes showed a surprising diminishment of both elongation (strain) and strength (stress) after just 30 minutes in 0.5 M NaOH at 80°C. These effects become more pronounced with increases in both NaOH concentration and temperature, indicating that they are due to degradation of the polymer backbone and not simply the exchange of bromide anions (in the control) for hydroxide anions. This indicates that PES-based polymers lack the chemical stability required for them to be used in AMFCs, an important result given that several recently reported anion exchange membranes and ionomers are based on similar PESs [2,3]. By contrast, the results for the PP-based membranes do not show a continual weakening of the mechanical properties with successive exposures to NaOH. An initial exposure to 0.5 M NaOH at 80°C for 1 hour does result in an elongation decrease of about 40% and a strength decrease of about 10%, but after conversion back to bromide ion form, the curve looks very similar to the control. A second NaOH treatment does not diminish the mechanical properties any more than the first treatment. Thus the shifting of the curves in Figure 1b is indicative of membrane property changes that are due to the identity of the anion present and not due to polymer degradation.

LANL continues to develop guanidinium functionalized ionomers for the catalyst layer. Guaninidinium functionalized ionomers were synthesized via activated fluorinophenyl-amine reaction [4], followed by the methylation with dimethyl sulfate. The activated fluorine-amine reaction gives precise control of cation functionality without the deleterious side-reactions and allows the direct connection of guanidinium into stable phenyl rings. For perfluorinated ionomer, fluoroaniline or six-membered imides were used as electron donating spacers which reacted with perfluorinated carboxylic acid (equivalent

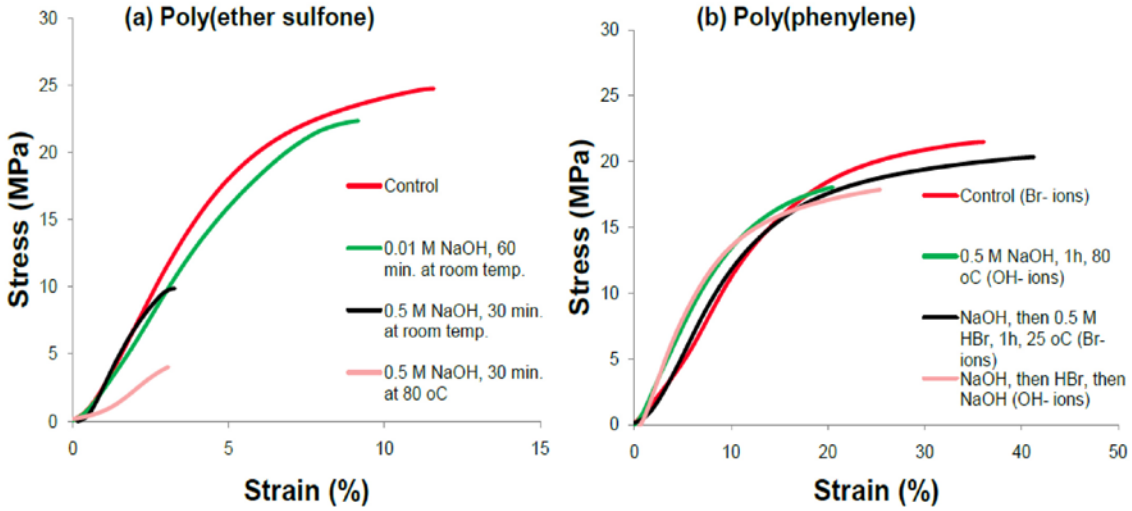


FIGURE 1. Mechanical test results at 50°C and 50% relative humidity for (a) PES-based anion exchange membranes and (b) PP-based anion exchange membranes.

weight=1100). The chemical stability of the ionomer with the electron donating spacers was much improved compared FY 2010 ionomer as it showed less than 10% degradation after soaking the membranes in NaOH solution at 80°C for 100 h. The solubility of the ionomer is good in aprotic solvents such as N-methylpyrrolidone, dimethyl acetamide and high alcohols such as glycerol.

Electro-Catalysts

JPL investigated the reaction kinetics of various electro-catalysts with KOH and guanidinium electrolytes. These experiments were conducted on Pt and Pd surfaces. The Pt surface exhibits H_2O redox processes in 0.1 M tetramethyl guanidine $(TMG)_{(aq)}$ similar to those in KOH/NaOH electrolytes, and remains highly active for oxygen reduction. Electrochemical tests performed via rotating disk electrode (RDE) measurements on elemental Pt electrodes show that Pt exhibits the major electrochemical reactions: hydrogen evolution reaction (HER), hydrogen oxidation reaction (HOR), hydrogen adsorption and the ORR in 0.1 M TMG and 0.1 M KOH. Surface reconstruction and activity in KOH mirror that of Pt in acids, and in 0.1 M TMG, only (110) crystal plane is active after cycling to 1.1 V (vs. reversible hydrogen electrode, RHE). Electrochemical tests performed via RDE on elemental Pd electrodes show that Pd exhibits HER, H_{upd}, and ORR in 0.1 M TMG and 0.1 M KOH. The ORR current density (at 0.9 V RHE) for Pd surfaces in alkaline electrolytes exceeds that for Pt surfaces in acid solutions, as shown in Figure 2. Thus, Pd or Pd-based alloys are very attractive for use as the cathode in AMFCs. RDE tests on Pd are ongoing to examine potential dependence of surface reconstruction in KOH and TMG electrolytes. To date, in 0.1 M TMG, only (110) crystal plane is active after cycling to 1.1 V (vs. RHE). Our temporal tests have shown that the TMG electrolyte shows remarkable stability after two months, with some signs of increasing resistivity such as the positive potential shift of the H-desorption peak. TMG and its byproducts can adsorb onto the Pt surface below ~0.8 V, obscuring the transition between typical kinetic and mass-limiting regions during oxygen reduction. This effect is especially pronounced at low rpm (low oxygen concentrations). Though the nature of TMG adsorption onto a polarized Pt electrode needs to be better understood, this study shows that free TMG can be used to support electro-catalytic activity on Pt, in place of NaOH or KOH salts. Because AMFCs require frequent replenishment of metal cation electrolyte to avoid precipitation of bicarbonates, the use of TMG electrolyte could still improve such systems despite its slow degradation. Particularly if it serves to better stabilize functional groups within the membrane, itself.

LANL developed nitrogen-doped carbon-based catalysts. The N-doped carbon-based catalysts showed promising ORR activities ca. half-wave potentials reached up to 0.95 V (vs. RHE) which is superior to the ORR activities of Pt/C catalysts in alkaline media (Figure 3). The durability of the N-doped carbon-based catalysts was measured during potential cycling (0.6-1.0 V vs. RHE) in O_2-saturated electrolytes. The ORR activities were enhanced after 1 k cycles and stabilized after 5 k cycles. The N-doped carbon based catalysts showed good ORR kinetics in guanidinium electrolytes. The onset potential (vs. RHE) of N-doped catalyst (0.2 mg/cm^2) in guanidinium 0.1 M aqueous solution is 1.03 V which is same with the Pt/C catalyst (60 μg/cm^2) in NaOH and higher than Pt/C in $HClO_4$.

Fuel Cell Performance

While MEA performance using newly developed catalysts is in progress, AMFC performance using a PP-based membrane, guanidinium functionalized ionomer

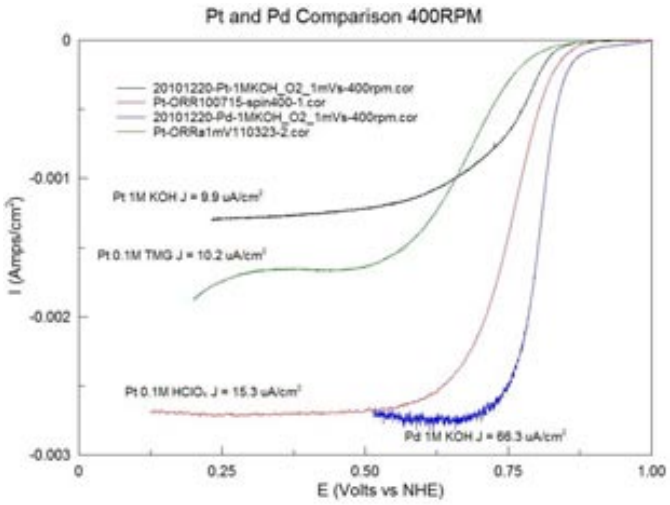


FIGURE 2. Oxygen reduction reaction curves for Pt and Pd surfaces in 0.1 M TMG and 0.1 M KOH electrolytes.

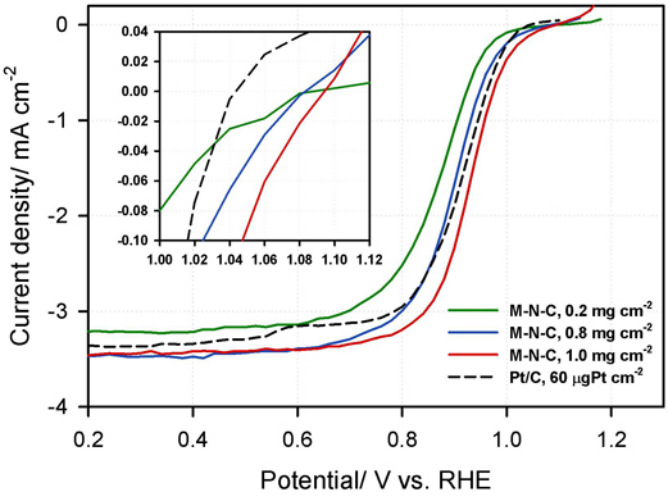


FIGURE 3. ORR activity of M-N-C catalysts in NaOH solution; RDE experimental conditions: 0.1 M NaOH; 900 rpm, room temperature; steady state potential (OCP, 120 s, 20 mV steps, 25 s/step)

and Pt black catalyst was measured under various conditions. The electrode composition and humidification were optimized. Degrees of anode flooding and cathode dehydration strongly depend on membrane and ionomer type and fuel cell operating conditions. After the optimization process, maximum power density of 500 and 300 mW/cm^2 was achieved for the MEAs at 80°C and under H_2/O_2 and H_2/air conditions, respectively (Figure 4). Much inferior performance was obtained when tetraalkyl ammonium functionalized poly(phenylene) polymers were used as electrode ionomer (e.g. maximum power density of 200 mW/cm^2 under H_2/O_2 condition). Guanidinium functionalized ionomer also showed promising durability during a 300 h AMFC operation at 60°C and constant voltage of 0.3 V. Tafel-slope of internal resistance-free polarization curves before and after lifetime test changed from 62.4 to 69.6 mV/decade (24 μV/dec h), indicating that minimal ionomer degradation occurred during the lifetime test while more than six times faster degradation rate was observed for tetraalkylammonium functionalized ionomer.

Conclusions and Future Directions

- Newly synthesized PP-based anion exchange membranes exhibited excellent chemical stability after immersion in 0.5 M NaOH solution. Stable guanidinium functionalized perfluorinated ionomers with electron donating spacer were prepared in liquid dispersion.
- Catalytic activities of Pt, Pd and N-doped carbon-based electro-catalysts showed excellent ORR kinetics in KOH and guanidinium solution. The N-doped carbon-based catalysts showed unprecedented activity (ca. half-wave potentials reached up to 0.95 V [vs. RHE]) in alkaline conditions.

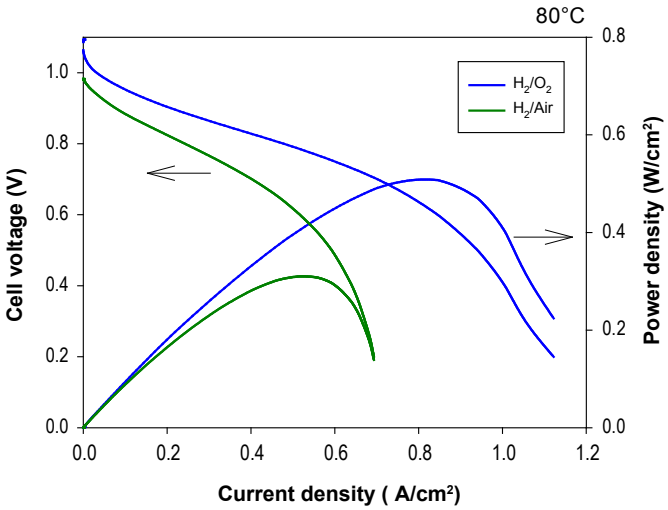


FIGURE 4. H_2/O_2 and H_2/air AMFC performance at T_{cell} = 80°C under fully hydrated conditions

- The maximum power density of alkaline membrane fuel cells under H_2/O_2 and H_2/air conditions reached to 500 and 300 mW/cm^2 which exceeded the project target performance. The preliminary extended term life test indicated that only minimal degradation of ionomer (24 μV/dec h) occurred during steady-state AMFC operation.
- AMFC performance tests using non-precious metal catalysts are yet to be assessed. Longer term test up to 800 h is under investigation.

Patents Issued

1. Solid State Alkaline Fuel Cells, DOE S-121,575 Patent pending (2011).

2. Anion Exchange Polymer Electrolytes, DOE S-121589 Patent pending (2011).

3. Fuel Cell Catalysts, DOE S-121083 Patent pending (2010).

FY 2011 Publications/Presentations

1. D.S. Kim, A. Labouriau, M.D. Guiver, Y.S. Kim, Guanidinium Functionalized Anion Exchange Polymer Electrolytes via Activated Fluorophenyl-Amine Reaction, Chemistry of Materials, 2011, 23, 3795.

2. M. Hibbs, C.H. Fujimoto, T. Lambert, D.S. Kim, Y.S. Kim, Poly(phenylene)-based anion exchange membranes for alkaline fuel cells, NAMS meeting, Las Vegas, June (2011).

3. M. Hibbs, C.H. Fujimoto, T. Lambert, D.S. Kim, Y.S. Kim, Poly(phenylene)-based anion exchange membranes and ionomers for alkaline fuel cells, ACS national meeting, Denver, August (2011).

4. D. Konopka, M.A. Johnson, M. Errico, P. Bahrami,and C.C. Hays, ECS 220 Meting, Boston, MA October (2011).

5. D. Konopka, M.A. Johnson, M. Errico, P. Bahrami, and C.C. Hays, Oxidation and oxygen reduction on polycrystalline platinum in aqueous tetramethylguanidine alkaline electrolyte, (Manuscript to be submitted to Electrochemical and Solid-State Letters).

References

1. D.S. Kim, C. Welch, R. Hjelm, M. Guiver, Y.S. Kim, "Polymers in MEA" in Comprehensive Polymer Science Vol 10, Polymers for Sustainable Environment and Energy, Ed. James McGrath and Michael Hickner, Elsevier, 2011.

2. S. Gu, R. Cai, T. Luo, Z. Chen, M. Sun, Y. Liu, G. He, Y. Yan, "A soluble and highly conductive ionomer for high-performance hydroxide exchange membrane fuel cells", Angew. Chem. Int. Ed., 2009, 48, 1.

3. J. Wang, S. Li, S. Zhang, "Novel hydroxide-conduncting polyelectrolyte composed of an poly(arylene ether sulfone) containing pendant quaternary guanidinium groups for alkaline fuel cell applications" Macromolecules 2010, 43, 3890.

4. Kim, D.S.; Robertson, G.P.; Guiver, M.D. "Comb-shaped poly(arylene ether sulfone)s as proton exchange membranes" Macromolecules, 2008, 41, 2126.

V.I.2 Advanced Materials for RSOFC Dual Operation with Low Degradation

Eric Tang, Tony Wood, Sofiane Benhaddad, Casey Brown, Hongpeng He, Ben Nuttall, Mark Richards, Randy Petri (Primary Contact)
Versa Power Systems Inc.
8392 S Continental Divide Rd. Ste. 101
Littleton, CO 80127
Phone: (303) 226-0762
E-mail: randy.petri@versa-power.com

DOE Managers
HQ: Kathi Epping Martin
Phone: (202) 586-7425
E-mail: Kathi.epping@ee.doe.gov
GO: David Peterson
Phone: (720) 356-1747
E-mail: David.Peterson@go.doe.gov

Contract Number: DE-EE0000464

Project Start Date: October 1, 2009
Project End Date: September 30, 2011

Fiscal Year (FY) 2011 Objectives

The objective of project is to advance reversible solid oxide fuel cells (RSOFCs) cell stack technology in the areas of endurance and performance.

Technical Barriers

This project addresses the following technical barriers from the Hydrogen Production section of the Fuel Cell Technologies Program Multi-Year Research, Development and Demonstration Plan [1]:

(G) Capital Cost
(H) System Efficiency
(I) Grid Electricity Emissions (for distributed power)
(J) Renewable Electricity Generation Integration (for central power)

Technical Targets

Technical targets will be achieved through RSOFC materials development and reversible stack design. The project objectives are to meet the following performance and endurance targets in a kW-class RSOFC stack demonstration:

- RSOFC dual mode operation of 1,500 hours with more than ten SOFC/solid oxide electrolysis cell (SOEC) transitions.
- Operating current density of more than 300 mA/cm^2 in both SOFC and SOEC modes.
- Overall decay rate of less than 4% per 1,000 hours of operation.

Meeting those performance and endurance technical targets will be the key RSOFC cell stack technology development step towards meeting DOE's Technical Targets for Distributed Water Electrolysis Hydrogen Production by an RSOFC system.

FY 2011 Accomplishments

- Developed 12 candidate cell material systems, of which five systems exceeded both performance (area specific resistance [ASR] <0.3 Ω-cm^2) and endurance (degradation rate less than 4% per 1,000 hours) targets in both fuel cell and electrolysis modes.
- Validated cell material systems through electrolysis/fuel cell cyclic operation. Over 100 daily cycles were demonstrated over 2,500 hours. The degradation rate is less than 1% per 1,000 hours.
- Completed stack design and component down select, conducted a kW-class RSOFC stack development test for over 5,000 hours.



Introduction

RSOFCs are energy conversion devices. They are capable of operating in both power generation mode (SOFC) and electrolysis modes (SOEC). RSOFCs can integrate renewable production of electricity and hydrogen when power generation and steam electrolysis are coupled in an "energy storage system" that can turn intermittent solar and wind energy into "firm power," or can enable intermittent power to aide in the selective arbitrage between peak power rates and power company resource deployment and turndowns. In order to address the technical and cost barriers, DOE funded a number of research projects over the past ten years [2]. Although significant progress was made in those projects, further development is required, especially in the areas of RSOFC performance and endurance. In this project, Versa Power Systems (VPS) is addressing performance and endurance issues for RSOFC cell and stack.

Approach

VPS has identified four task areas in an effort to improve the performance and endurance of RSOFC systems: degradation mechanism study, cell material development,

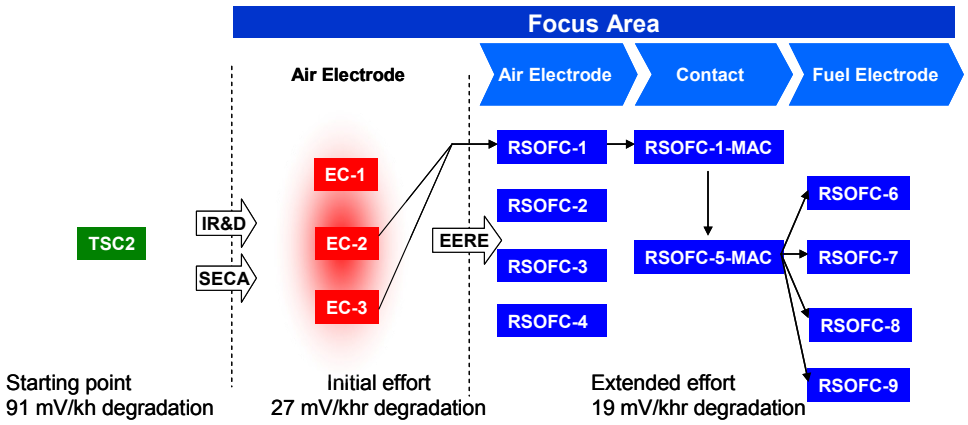


FIGURE 1. RSOFC Cell Development Path at VPS

interconnect material development, and stack design and demonstration. A stage-gate project management process is employed with a quantitative Go/No-Go decision point. The scope of the work has been carried out by:

- Building on VPS' strong SOFC cell and stack baseline, and leveraging cell and stack advancements from the DOE Solid State Energy Conversion Alliance program.
- Carrying out parallel materials development activities and integrating them with cell production technology development.
- Conducting RSOFC stack and process designs to address durability, performance, and cost in both fuel cell and electrolysis operating modes.

Results

The development path for RSOFC cell technology at Versa Power Systems can be summarized in Figure 1. Twelve material systems have been developed in the project.

Table 1 summarizes the RSOFC cell technology at the project Go/No-Go decision point. The best cell material system–RSOFC-7–demonstrated 223 and 224 mΩ-cm^2 ASR values in electrolysis and fuel cell modes, respectively, at 750°C compared with the target of less than 300 mΩ-cm^2. The degradation rate of the RSOFC-7 in steady-state electrolysis mode was 1.5% per 1,000 hours compared with a target of less than 4% per 1,000 hours for over 1,000 hours.

RSOFC cell material systems have been further developed in fuel cell/electrolysis cyclic operation. A cyclic test profile was designed and implemented to simulate an integrated reversible SOFC/solar power system. The test runs a 24 hour cycle with 10.5 hours in electrolysis, 12.5 hours in fuel cell operation, and the balance for transitions. Figure 2 depicts the cell voltage against time over 105 simulated day-night cycles of electrolysis and fuel cell operation. The performance decay, calculated from fuel cell mode, was 0.21 mV/cycle (0.89% per 1,000 hours) over 105 days (or cycles, representing over 2,500 hours).

A number of RSOFC stacks were built and tested in parallel for cell and interconnect materials development. A kW-class stack test (Figure 3) demonstrated over 5,000 hours of stable electrolysis operation with a split between constant current and constant voltage operation. This kW-class stack design and RSOFC-7 cell materials system have been chosen for the end-of-the-project stack metric test. The performance decay, calculated from fuel cell

TABLE 1. Summary of RSOFC Performance and Endurance Status at Project Go/No-Go Decision Point

	Target	Status
Performance (area specific resistance in both SOFC and SOEC operating modes)	<0.3 Ω-cm^2	0.223 Ω-cm^2 in SOFC 0.224 Ω-cm^2 in SOFC
Degradation (Overall decay rate)	<4% per 1000 hours of operation	~1.5% per 1,000 hours of operation
Operating Duration	>1,000 hours	1,005 hours (as of Oct. 29, 2010)
Operating Current Density	>300 mA/cm^2	500 mA/cm^2

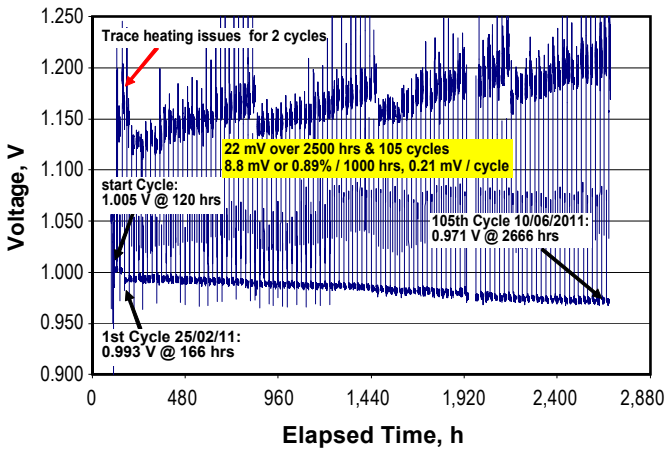


FIGURE 2. Fuel Cell and Electrolysis Cyclic Testing of a RSOFC-7 Cell

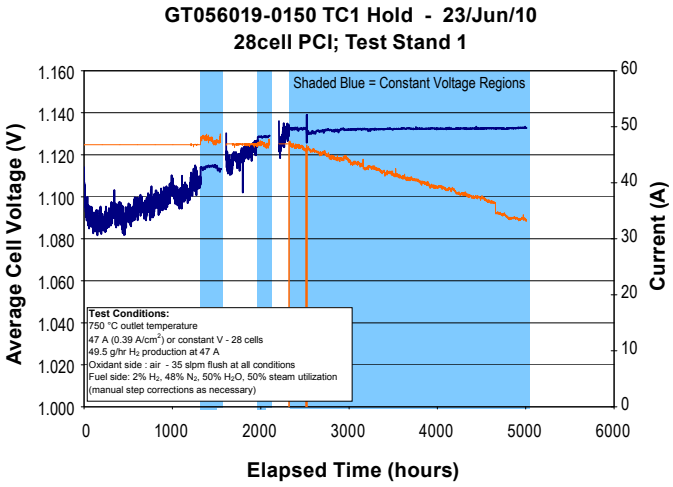


FIGURE 3. GT056019-0150 kW-Class Stack Electrolysis Tests in Both Constant Current and Constant Voltage (shaded blue) Conditions

mode, was 0.21 mV/cycle (0.89% per 1,000 hours) over 105 days (or cycles, representing over 2,500 hours). The test is on-going and will be updated as testing continues.

Conclusions and Future Directions

In the coming year, the project team will continue on the current development path. This work includes:

- Continuation of the RSOFC cell and stack development and testing.
- Completing the end-of-the-project kW-class RSOFC stack metric test.

FY 2011 Publications/Presentations

1. An oral presentation for this effort was made at the 2011 DOE Hydrogen and Vehicle Technologies Programs Annual Merit Review and Peer Evaluation Meeting.

References

1. DOE EERE Multi-Year Research, Development and Demonstration Plan, Page 3.1-7 (2007).

2. J. Guan et al., High Performance Flexible Reversible Solid Oxide Fuel Cell, Final Technical Report, DOE DE-FC36-04GO14351.

V.J.1 Materials and Modules for Low-Cost, High-Performance Fuel Cell Humidifiers

William B. Johnson
W.L. Gore and Associates, Inc.
201 Airport Road
P.O. Box 1488
Elkton, MD 21922-1488
Phone: (410) 506-7567; Fax: (410) 506-7633
E-mail: wjohnson@wlgore.com

DOE Managers
HQ: Jason Marcinkoski
Phone: (202) 586-7466
E-mail: Jason.Marcinkoski@ee.doe.gov
GO: Jesse Adams
Phone: (720) 356-1421
E-mail: Jesse.Adams@go.doe.gov

Contract Number: DEEE0000465

Subcontractor:
dPoint Technologies, Inc.
Vancouver, British Columbia, Canada

Start Date: April 1, 2010
Projected End Date: September 30, 2012

Fiscal Year (FY) 2011 Objectives

- Demonstrate a durable, high-performance water transport membrane.
- Build and test a compact, low-cost, membrane-based module utilizing that membrane for use in an automotive stationary and/or portable fuel cell water transport exchangers.
- Model and show high-volume costs associated with membrane and module.

Technical Barriers

This project addresses the following technical barriers from section 3.3, Fuel Cells, of the Fuel Cell Technologies Program Multi-Year Research, Development and Demonstration Plan in Task 7, "Develop balance of plant components":

(B) Cost

(E) System Thermal and Water Management

(A) Durability and (C) Performance: by allowing the fuel cell to operate in less harsh, more humid environments they will perform better and be more durable.

FY 2011 Accomplishments

- Humidifier operating conditions for stationary, automotive and portable fuel cells have been established using input from manufacturers and other stakeholders.
- A range of humidifier membrane materials have been prepared and characterized.
- Permeance, air permeability and membrane durability testing for a range of humidifier membranes has been performed. One class of Gore prepared membranes has been identified as particularly promising.
- A room temperature static water vapor transport test protocol has been developed for rapid permeance testing and/or quality control of humidifier membranes.
- Humidifier cost modeling for the most promising candidate has been completed. The model shows acceptable high volume production costs for the most promising class of Gore prepared membranes.
- Initial module modeling and prototyping indicate that the composite Gore humidifier membrane will allow automotive module performance, size and durability targets to be met.



Introduction

Today it is essential to humidify the gases supplied to the fuel cell inlets for automotive and many stationary fuel cell stack designs. In this work, we are providing a new, inexpensive, composite membrane capable of very high water vapor transport and low air cross-over. The composite structure has been designed to allow lower total cost while still meeting automotive and stationary humidifier water transport and durability targets.

Because the transport rates of these new materials are so high, current planar membrane humidifier designs are not capable of fully utilizing the high rates. Therefore, the project is using an innovative, low-cost humidifier module with customized channel geometries that can take advantage of the high water transport rates. By having a materials development effort integrated with a humidifier module-system design and build program, we will be able to effectively exploit the improved material properties in an actual device.

Approach

Perfluorosulfonic acid (PFSA) membranes fulfill most of the requirements for the water transport media at the heart of the planar membrane water exchanger. They fall short

primarily on cost, and secondarily on durability, especially when they are made thin to increase performance and lower cost. W.L. Gore and Associates, Inc. (Gore) has developed a composite water vapor transport membrane that has overcome both of these limitations. The basic composite structure consists of a very thin ionomer layer sandwiched between two microporous polymer layers. The ionomer layer provides the active water transport and provides an impermeable layer to prevent gas cross-over. The water transport rate can be engineered to be very high either through the use of a material that has very high inherent water transport rates (e.g., PFSA polymers), or by making it extremely thin (e.g., <5 µm). The microporous layer provides three critical features: first it protects the thin ionomer layer from mechanical damage during handling; second, it confers strength to the thin layer allowing it to be more durable during use; and third, it offers a strong, protective support layer for placement of a macroporous gas diffusion layer.

Our subcontractor, dPoint Technologies, has developed an innovative pleated planar membrane humidifier that is able to achieve automotive manufacturer water transport and pressure drop requirements. The pleated design utilizes existing low-cost, high-volume pleating equipment that is used to manufacture air filters for automotive and heating, ventilation and air conditioning applications. The pleated humidifier is a proven technology that dPoint has been developing in cooperation with several major automotive manufacturers. Further improvement in humidifier size, cost and performance is possible through the use of the Gore membrane and optimizing the flow field channel design to take full advantage of this new membrane.

Results

A range of composite membranes have been produced by Gore, including ionomers coated on microporous membranes, shown schematically in cross-section in Figure 1a, and "sandwich" structures shown schematically in Figure 1b. The ability to prepare very thin layers of an ionomer allows very high permeances to be achieved with these materials. For example, using an ~5 micron PFSA layer (Figures 1c and 1d) in a sandwich structure, described as GORE™ M311.05, permeances of close to two times the next best alternative (Figure 2), i.e., a 25 micron homogeneous PFSA membrane, are achieved. A high-volume cost model for this class of composite membranes has also been completed, and it shows that these materials can be produced for ½ to ⅓ the cost of the next best alternative homogeneous membranes [4].

Initial studies of the durability of the sandwich composite microstructures, e.g., M311, show virtually no performance degradation with time at 65ºC (Figure 3), a temperature consistent with stationary and/or backup power systems. Studies at 80ºC and above, where most automotive systems operate, are underway. Initial results at these higher temperatures indicate there may be some limited reduction in performance after long times, but the magnitude of the loss will be manageable through appropriate module design and sizing.

The design and prototyping of humidifier modules by dPoint Technologies is well underway. Using a finite element model, the module flow field and other design parameters have been optimized (Figures 4a and 4b). Several subscale modules, (Figure 4c), have been built

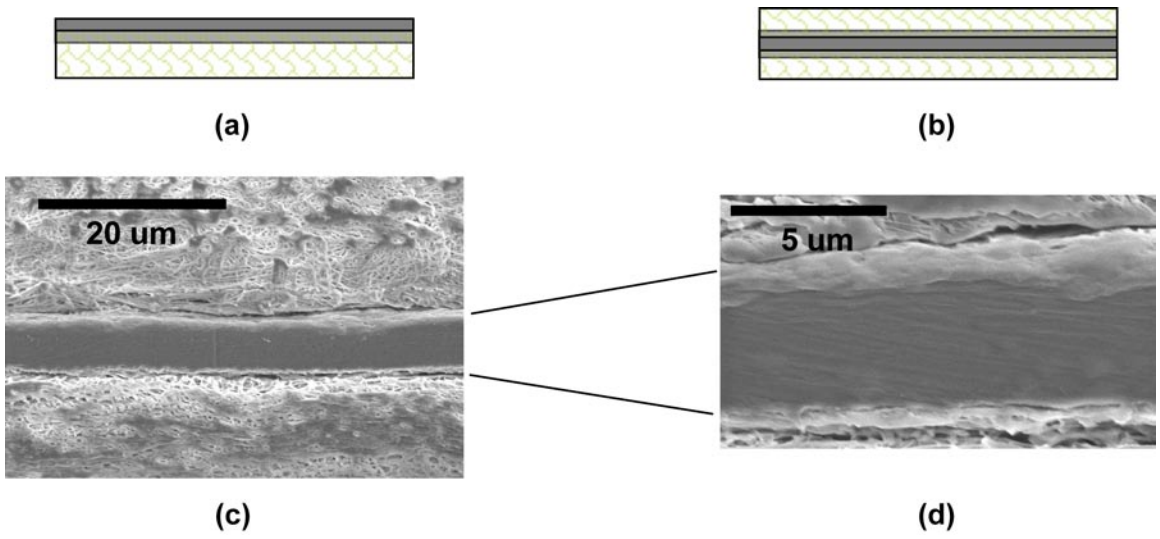


FIGURE 1. A range of composite membranes have been produced including ionomers coated on microporous membranes, shown schematically in cross-section in (a), and "sandwich" structures shown schematically in (b). One example of a "sandwich" composite structure is shown in a cross-sectional micrograph in (c). A higher magnification micrograph in (d) shows the ionomer layer is ~5 microns thick.

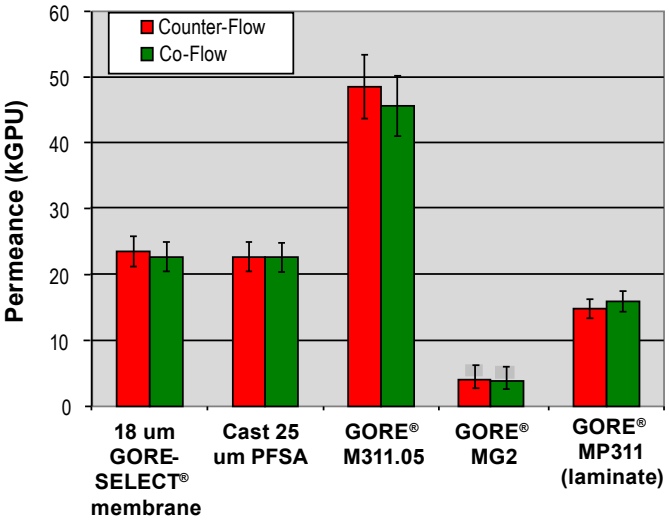


FIGURE 2. The permeance of a wide range of potential humidifier membrane materials has been measured using a dynamic permeance cell [1-3]. The results indicate the sandwich structures using PFSA ionomers, illustrated here by GORE™ M311.05, have permeances much higher than other potential alternatives. GORE™ MG2 is a hydrocarbon ionomer coated on a microporous substrate, while MP311 is an inexpensive hydrocarbon ionomer in a similar sandwich structure to M311.05.

using the designs identified by the modeling. The initial results from these subscale modules indicate that the high permeance Gore composite materials will allow modules to be built that have the requisite size and water transport characteristics required in demanding fuel cell automotive humidifier module applications.

Conclusions and Future Directions

- Water transport rates through GORE™ humidification membranes can be very high, especially for the fluorinated ionomer-based materials.
- A range of alternate materials have been prepared and water permeance and air-impermeability has been measured. Sandwich structures using thin PFSA layers offer the best combination of performance, durability and cost.
- A high-volume cost model has demonstrated that automotive cost targets can be met using the most promising Gore composite membranes.
- Initial module modeling and subscale prototypes show that using the high-performance Gore composite humidifier membrane will enable an automotive

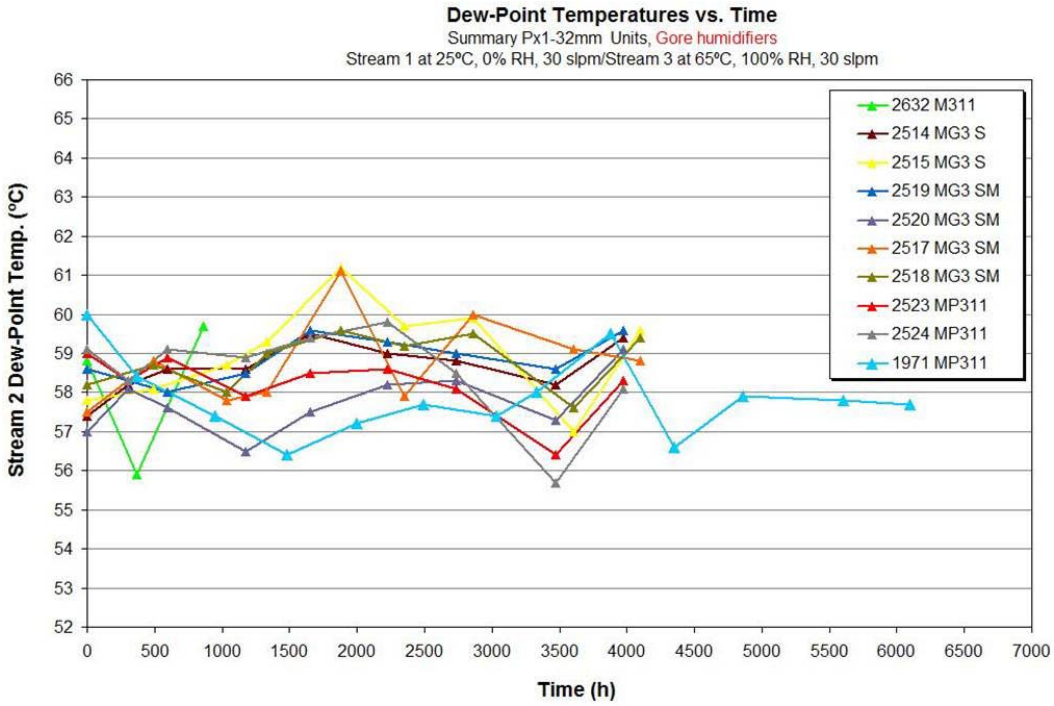


FIGURE 3. The performance of the composite humidifier membranes made in this program do not degrade with time under the conditions shown in this figure, where the stream 2 dew point temperature is the dew point of the dry outlet.

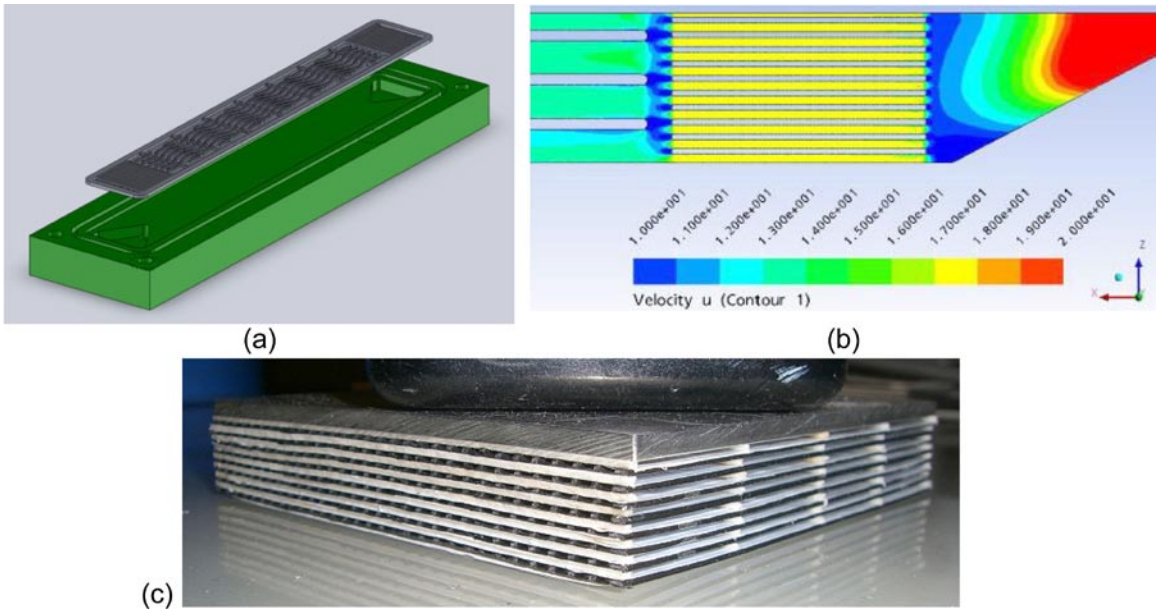


FIGURE 4. Using a finite element model of potential flow field geometries (a), the velocity contours, (b), have been used to optimize the module design. Several subscale modules, (c), have been built using several designs. The initial results indicate that the high permeance Gore composite materials will allow modules to be built that have the requisite size and water transport characteristics.

humidifier module that meets the demanding cost, durability and performance fuel cell automotive targets.

- In the final year of the project, the durability testing will be completed, the most promising membrane candidate and backer combination will be identified and scaled up, the best module design will be identified through further subscale tests, and a full-scale module will be built for DOE testing.

References

1. Yamakawa, Keiichi; Johnson, Wiliam B.; Murthy, Mahesh; Berta, Thomas; "Composite Membrane and Moisture Adjustment Module Using Same", U.S. Patent Publication 2009/0324929 A1, 12/31/2009.

2. Gibson, Phillip W., "Effect of temperature on water vapor transport through polymer membrane laminates", Polymer Testing, 19(6), 673-691(2000).

3. Majsztrik, Paul; Bocarsly, Andrew; Benziger, Jay; "Water Permeation through Nafion Membranes: The Role of Water Activity", The Journal of Physical Chemistry B,112(51), 16280-16289.(2008).

4. William. B. Johnson, "Materials and Modules for Low-Cost, High Performance Fuel Cell Humidifiers", DOE Annual Review, Crystal City, VA, May 12, 2011, Oral Presentation fc067, available from www.doe.gov.

FY 2011 Publications/Presentations

1. Materials and Modules for Low-Cost, High Performance Fuel Cell Humidifiers, DOE Annual Review, May 12, 2011, Oral Presentation fc067.

2. Materials and Modules for Low-Cost, High Performance Fuel Cell Humidifiers, Freedom Car Technical Team Review, November 10, 2010.

V.J.2 Development of Thermal and Water Management System for PEM Fuel Cell

Zia Mirza
Honeywell Aerospace
2525 W. 190th Street
Torrance, CA 90504
Phone: (310) 512-3374
E-mail: zia.mirza@honeywell.com

DOE Managers
HQ: Jason Marcincoski
Phone: (202) 586-7466
E-mail: Jason.Marcincoski@ee.doe.gov
GO: Reginald Tyler
Phone: (720) 356-1805
E-mail: Reginald.Tyler@go.doe.gov

Technical Advisor
Rajesh Ahluwalia
Phone: (630) 252-5979
E-mail: walia@anl.gov

Contract Number: DE-FC36-03GO13109

Project Start Date: December, 2002
Project End Date: December 30, 2011

Fiscal Year (FY) 2011 Objectives

- Develop an advanced heat exchanger (radiator) that can efficiently reject heat with a relatively small difference between fuel cell stack operating temperature and ambient air temperature.
- Test humidification systems to meet fuel cell inlet air humidity requirements. The moisture from the fuel cell outlet air is transferred to inlet air, thus eliminating the need for an outside water source.
- Reliability testing of select humidification system for 5,000 cycles.

Technical Barriers

This project addresses the following technical barriers from the Fuel Cells section of the Fuel Cell Technologies Multi-year Research, Development and Demonstration Plan:

(E) System Thermal and Water Management

Technical Targets

TABLE 1. Technical Targets for Proton Exchange Membrane (PEM) Fuel Cell Thermal and Water Management System

Characteristics	Units	Target	Honeywell Status
Humidity of PEM cell stack inlet air	**% at 80°C**	**>60**	**50%**
Cooling requirements with 85°C coolant temperature and flow rate of 2.5 kg/sec, with frontal area not to exceed 0.32 sq meter	kW	50	50
Radiator cost (by TIAX LLC) without markup	$	58	50
Reliability of radiator	hrs	5,000	Under test
Total parasitic power (air fan + cooling pump)	kW	<2.4	To be determined

FY 2011 Accomplishments

- Thermal management portion of the project was successfully completed and the final test report for the thermal management was submitted to DOE in December 2009. The full-scale radiator performance test data was provided to Argonne National Laboratory for their fuel cell system model.
- Water Management
  - Full-scale and sub-scale membrane humidier system was successfully tested. The water transfer efficiency was lower than the required 60%.
  - The enthalpy wheel-based humidification system and planer membrane-based humidity device testing is successfully completed; the test data is presented here.



Introduction

Balance-of-plant (BOP) components of a PEM fuel cell automotive system represents a significant portion of total cost based on the 2008 study by TIAX LLC, Cambridge, MA.

The objectives of this thermal and water management project are twofold:

- Develop an advanced cooling system to meet the fuel cell cooling requirements. The heat generated by the fuel cell stack is a low-quality heat (lower temperature) heat that needs to be dissipated to the ambient air. To minimize size, weight, and cost of the radiator, advanced fin configurations were evaluated.

- Evaluate air humidification systems which can meet the fuel cell stack inlet air humidity requirements. Four humidification devices were successfully tested, three based on membranes and the fourth based on a rotating enthalpy wheel. The lab-scale units, one membrane module and enthalpy wheel, have been successfully tested by the suppliers.

Approach

To develop a high-performance radiator for a fuel cell automobile, various advanced surfaces were evaluated including foam; advanced, offset, and slit louver fins; and microchannel with various fin densities. A value function was developed to evaluate and compare the cost of various fin geometry radiators. The value function based on the cooling system weight, performance, parasitic power, and initial cost. Two fin geometries -- 18 fins per inch (fpi) louver and 40 fpi microchannel -- were down-selected. The full-scale radiators were built and tested. The results were presented in annual progress report as well as final test report submitted in 2009.

A full and half-scale Nafion® membrane module, full-scale planar membrane module with Gore memebrane and enthalpy wheel was designed, built and was tested to validate the performance. A test stand was designed and built, to test the humidification devices similating the 80 kW fuel cell stack operating conditions. The test results for the first two systems were presented in previous reports. And the results for the last two systems (enthalpy wheel and planar modules) are presented in this report.

Results

The test results for the enthalpy wheel are pesented in Figures 1 and 2. One of the variables unique to the enthalpy wheel is its rotational speed. The water transfer efficency at three flow rates was measured as a function of rotational speed. In Figure 1 the water transfer ratio of humidty outlet stream (primary out) and inlet stream (secondary in) is plotted against the enthalpy wheel rotational speed. As expected the transfer efficiency improved with higher speed. The enthalpy wheel water transfer rate reaches over 70% above 30 revolutions per minute (RPM) at high flow rate. The water balance (in Figure 2) during high flow rate tests was under 10% which is exceptionally good, however at low flow rate and low speed the water balance was poor which may be attributed to measurement error. The water transfer rate for the enthalpy wheel was the best among all the four devices tested and it met the goal of 60% required for the PEM fuel cell.

Planar membrane water transfer and balance test data are presented in Figures 3 and 4, respectively. The water transfer rate varied from 20-37% with decreasing efficiency at high humidity levels. The water balance test results show the opposite trend where the water balance improved with high inlet humidity. The average water balance error during entire water humidity range was about 15% which is not unreasonable considering the limitations of humidity measurements devices used for high flow rate and humidity levels. Due to instrumentation and test stand limitations,

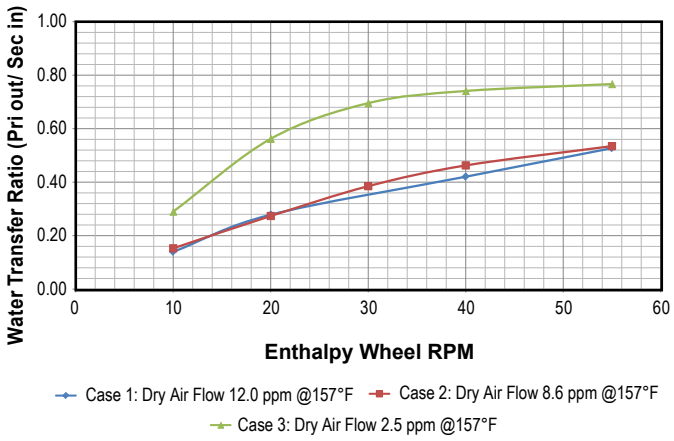


FIGURE 1. Enthalpy Wheel Water Transfer Rate vs. Rotational Speed

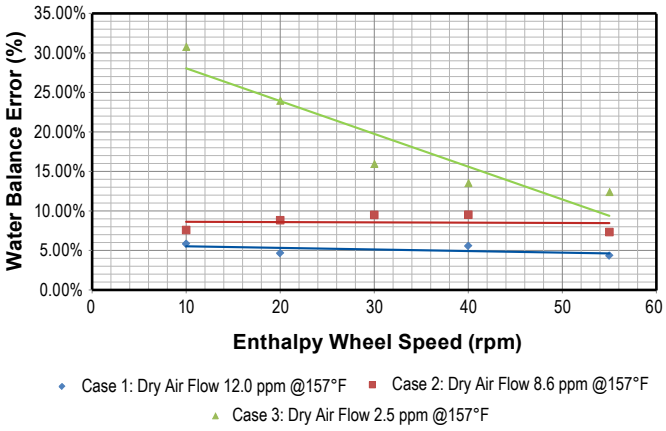


FIGURE 2. Enthalpy Wheel Water Balance Errors vs. Rotational Speed

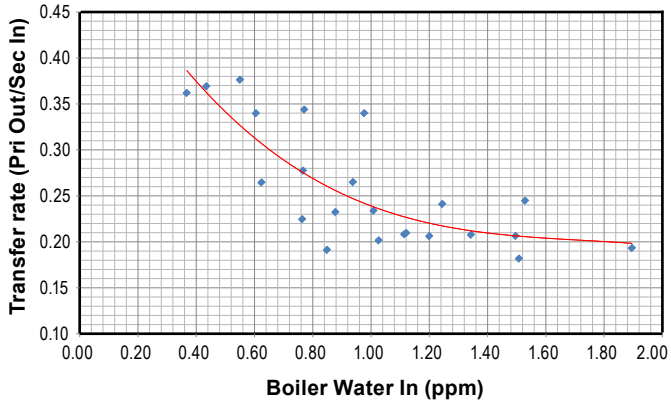


FIGURE 3. Planar Membrane Module Water Transfer Rate vs. Total Water in

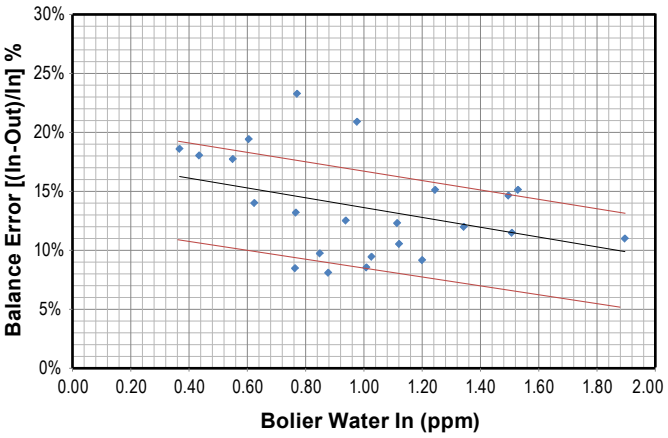


FIGURE 4. Planar Membrane Module Water Balance vs. Total Water in

the humidity of the humidifier inlet stream was limited to about 80 percent. The data scatter cannot be explained; each test point was taken when the system reached the steady-state condition.

Conclusions and Future Directions

All three different types of humidification systems were successfully tested. The enthalpy wheel showed the best water transfer efficeincy out of three different types of humidification system tested. The system has a motor for rotation of the wheel and requires seals to isolate the two flow streams.

The last remaining task for this 9-year project is to test a select himidificaiton system for 5,000 cycles reliability testing. Each cycle will consist of step changing the inlet humidity from high to low level and back to high level. The test stand has been modified and the testing has started.

FY 2011 Publications/Presentations

1. 2011 DOE Hydrogen Program and Vehicle Technologies Program; Annual Merit Review and Peer Evaluation Meeting – Washington, DC – May 9, 2011. Poster Presentation FC#039.

V.J.3 Large Scale Testing, Demonstration and Commercialization of Nanoparticle-Based Fuel Cell Coolant

Satish Mohapatra (Primary Contact) and Patrick McMullen
Dynalene, Inc.
5250 W. Coplay Rd.
Whitehall, PA 18052
Phone: (610) 262-9686
E-mail: satishm@dynalene.com

DOE Manager
HQ: Kathi Epping Martin
Phone: (202) 586-5463
E-mail: Kathi.Epping@ee.doe.gov

Contract Number: EE00004532

Subcontractors:
- University of Tennessee, Knoxville, TN
- Protonex Inc., Southborough, MA

Project Start Date: October 1, 2010
Project End Date: September 30, 2013

Fiscal Year (FY) 2011 Objectives

The overall objective of this Phase III Small Business Innovation Research project is to demonstrate the 5,000 hr durability of the nanoparticle-based coolant fluid developed in Phase I and II, and perform further research into how durability is affected and how to improve it. The specific objectives are:

- Validate 5,000 hr durability of the coolant fluid by developing long-term test plans in-house as well as in subcontractor locations.
- Study the effect of nanoparticle properties on its durability under severe conditions such as thermal cycling, high electric field and presence of contaminants.
- Determine the efficiency of corrosion inhibitors in long-term tests under severe conditions.
- Increase the nanoparticle surface charge to >500 μeq/g for both cationic and anionic particles.
- Perform testing of the coolant samples by fuel cell companies and begin commercialization.

Technical Barriers

This project addresses the following technical barriers from the Fuel Cells section (3.4.4) of the Fuel Cell Technologies Program Multi-Year Research, Development and Demonstration Plan:

(A) Durability
(B) Cost

Technical Targets

Dynalene's fuel cell coolant (Dynalene FC) is expected to help the fuel cell industry achieve their durability and cost targets to some degree. First of all, the coolant itself is being designed to have a life of 5,000 hrs. It is also expected to have excellent compatibility with the system materials and inhibit corrosion in the coolant loop. This will help in extending the durability of the fuel cell system components such as the pump, the radiator, valves, seals/gaskets and any other components coming in contact with the coolant. The coolant is also designed to work at -40°C, which will assist both transportation and stationary fuel cells to quickly warm up during cold starts.

The cost target for the coolant (in plant-scale production) is about $10/gallon, which is very close to the retail price of current automotive coolants. This coolant will also eliminate the de-ionizing filter and other hardware associated with it (i.e. fittings, valves). It is also being designed to work with cheaper, lighter and thermally efficient components such as aluminum radiators (instead of stainless steel) and brass heat exchangers.

FY 2011 Accomplishments

This project was originally awarded on a conditional basis until all the financial audits by the DOE were complete. The project started to gain momentum when the final contract was signed in March 2011. The following are the accomplishments:

- Design of the fuel cell system to test Dynalene coolant at the University of Tennessee (UT) facility is complete and parts are ordered.
- Dynalene completed negotiations with Protonex who is building a fuel cell system to supply to Dynalene. Protonex also will test the final coolant (after optimization) for >5,000 hours in one of its systems.
- Dynalene has performed preliminary glassware corrosion tests and has demonstrated the effectiveness of inhibitors towards aluminum and brass.



Introduction

This project addresses the goals of the Fuel Cell Technologies Program of the DOE to have a better

thermal management system for fuel cells. Proper thermal management is crucial to the reliable and safe operation of fuel cells. A coolant with excellent thermo-physical properties, non-toxicity, and low electrical conductivity is desired for this application.

An ideal coolant must be durable for >5,000 hr of operation, and therefore, the coolant must be tested for such duration. Electrical conductivity of the coolant should be less than 10 μS/cm throughout the testing period and the coolant must be compatible with all the materials (metals, plastics, rubbers and composites) at the highest operating temperature. Current automotive coolants do not satisfy the electrical conductivity criteria due to the presence of ionic corrosion inhibitors in them. Water/glycol solutions without inhibitors can have low starting electrical conductivity, but it can increase rapidly due to corrosion of metal components leading to build-up of ions in the coolant. Fuel cell developers are using water or water/glycol mixtures with a de-ionizing filter in the coolant loop. The filter needs to be replaced frequently to maintain the low electrical conductivity of the coolant. This method significantly increases the operating cost and also adds extra weight/volume to the system.

Dynalene Inc. has developed and patented a fuel cell coolant with the help of DOE Small Business Innovation Research Phase I and Phase II funding (Project # DE-FG02-04ER83884). This technology has been patented in the United States, Canada and Europe. The technical feasibility of this coolant was demonstrated in short-term tests using a dynamic re-circulating loop. The nanoparticles used in the coolant were optimized for size and surface charge density.

Approach

In this Phase III project, Dynalene's plan is to validate the durability of the coolant fluid by developing long-term test plans in-house as well as in subcontractor locations. Nanoparticle-based coolant will be subjected to severe conditions such as thermal cycling, high electric field and presence of contaminants. Efficiency of the non-ionic corrosion inhibitors in long-term tests will be evaluated using electrochemical and glassware corrosion tests. Further research will be dedicated to increase the surface charge density of the nanoparticles. Lastly, samples will be sent to fuel cell companies (including subcontractors) for long-term testing and Dynalene's business development team will start the commercialization effort.

Results

A representative fuel cell coolant and heat rejection system was designed by UT researchers to accurately simulate the environmental, material, and operational conditions experienced in full-sized fuel cell systems. The ultimate goal is to enable Dynalene to more rapidly develop next generation coolants for fuel cell systems and provide potential customers with application specific independent validation of the benefits of the Dynalene coolant product. Additionally, fundamental understanding of the key controlling parameters that result in ionic impurity contamination within typical coolant subsystems will be determined.

The testing facility designed by UT researchers will emulate the conditions of coolant in an operating fuel cell. Figure 1 shows a schematic of the test system as designed along with the chosen components. Since the project contract was only recently made official, the design of the test rig is complete, and parts will be ordered as soon as the final internal paperwork is completed shortly. The experimental test system will include an operating fuel cell with fully functional coolant flow plate designs, coolant pump, and interchangeable lengths of chosen materials that will be in contact with the coolant. Since the fuel cell will not be a full size stack, an appropriate heat load will be applied to the flow entering the fuel cell to simulate fuel cell stack operating temperature. The system is designed so that different material exposures can be easily implemented by changing component piping materials and lengths. A real fuel cell system radiator will be obtained from industrial suppliers, and has been arranged through Dynalene. Species extraction as shown will enable ex situ measurement of the fluid contents and a variety of important diagnostics to be taken to reveal the key controlling parameters in the degradation of coolant performance. Diagnostics will monitor the coolant system pressure drop, electrical

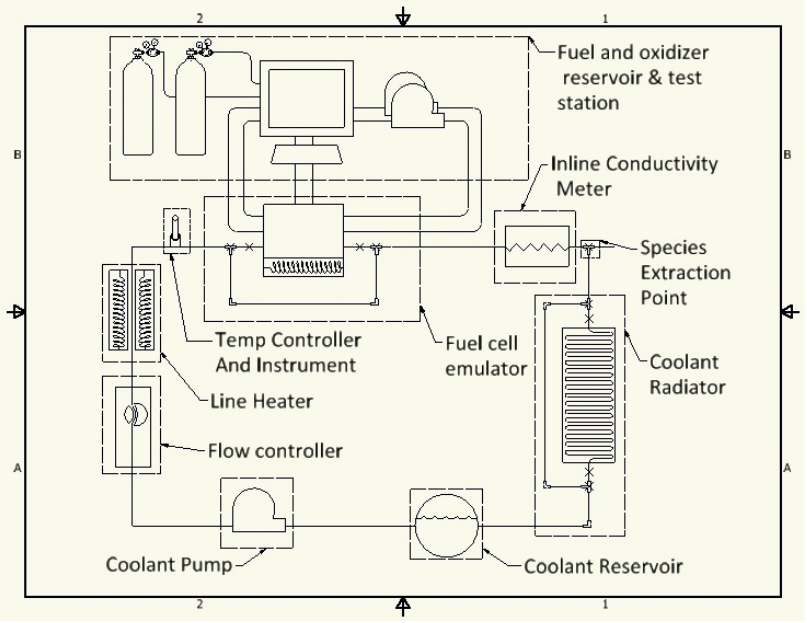


FIGURE 1. Schematic Diagram of the Fuel Cell Coolant Test System at UT

conductivity, flow rate, and heat capacity of the coolant as a function of operating conditions including temperature, coolant flow, and electrical load. A coolant bleed off valve will be installed to allow ex situ evaluation of the type and quantity of contaminants entering the coolant as a function of operating parameters. Both metal and graphite bipolar plate designs with material and coatings purchased from known suppliers and used in operating systems will be integrated into the test system, which will help identify the source of corrosion components. Ex situ surface examination by energy dispersive X-ray spectroscopy, scanning electron microscopy, and other spectroscopic methods will be used to visualize and reveal the composition of local ionic impurities. When complete, this test bed will be validated using different coolant fluids doped with controlled levels of conductive impurities, and the diagnostic systems will be evaluated and calibrated before regular testing.

Dynalene has conducted preliminary corrosion tests using aluminum and brass coupons. These metal coupons were tested in de-ionized water, ethylene glycol/water, propylene glycol/water and Dynalene's fuel cell coolant, Dynalene FC. The tests were conducted in glass jars at 80°C. Figure 2 shows the pictures of these coupons after 350 hours and 700 hours of exposure to the fluid. When they are compared to the control (untested coupons), it is clearly evident that the Dynalene FC fluid has the least corrosive effect towards the metal coupons. It is due to the presence of the non-ionic corrosion inhibitors.

Protonex Inc. has provided Dynalene with a scope of work on how they will test the coolant samples in their fuel cell system. Protonex also will provide a fuel cell system to Dynalene (to be installed at Dynalene's facility) for several long-term tests including 5,000-hr tests. The details of the project and the costs are already worked out. A photograph of the system is shown in Figure 3.

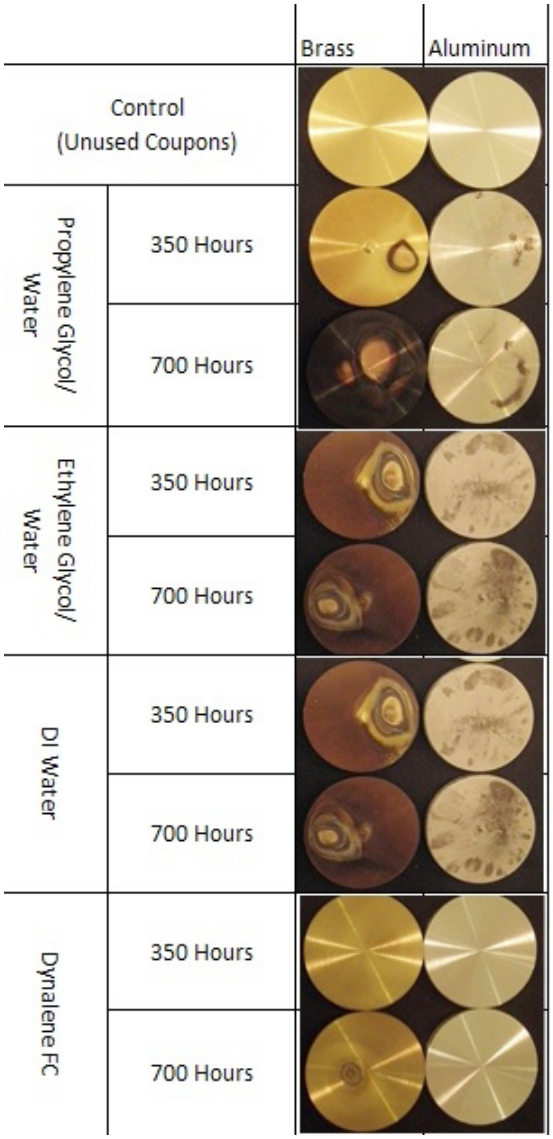


FIGURE 2. Aluminum and Brass Corrosion Testing in Various Coolant Fluids

Conclusions and Future Directions

A fuel cell coolant test system has been designed by the UT team that will study the effect of thermal cycling, electric field and the presence of contaminants. Dynalene is preparing various samples of the coolant and performing corrosion and compatibility testing. Preliminary results showed that the corrosive effect of the coolant towards aluminum and brass is much lower than de-ionized water, propylene glycol/water, and ethylene glycol/water. A fuel cell system is being built by Protonex that will be used at Dynalene's facility for 2,000 and 5,000 hr tests.

UT is in the process of ordering all the parts for its test system. Assembly of the system should take place in the next few weeks and should be finished in August. Dynalene will supply three different variations of the coolant for testing. Dynalene will also continue the corrosion and compatibility testing with different system materials. At the same time, samples will be sent to fuel cell developers for

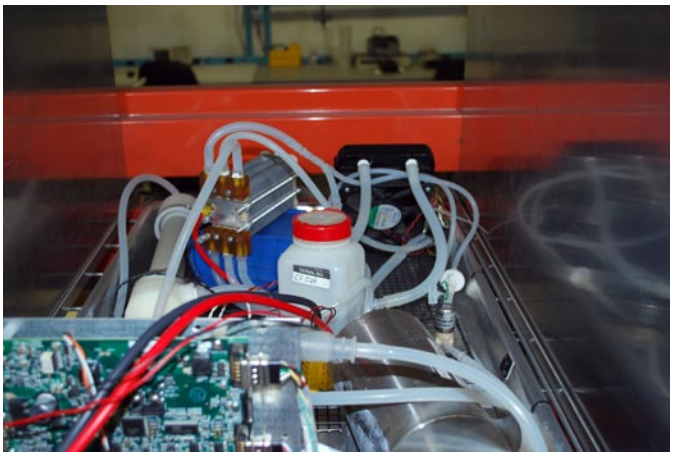


FIGURE 3. System Photograph

testing in their systems. Feedback from time to time will help Dynalene researchers to optimize the coolant further.

FY 2011 Presentations

1. McMullen, P, Mock, J and S. Mohapatra, "Fuel Cell Coolant Optimization and Scale-up", Poster presented at the Annual DOE Hydrogen Program Review Meeting, May 2011, Washington, D.C.

V.K.1 Development of a Low-Cost 3-10 kW Tubular SOFC Power System

Norman Bessette
Acumentrics Corporation
20 Southwest Park
Westwood, MA 02090
Phone: (781) 461-8251
E-mail: nbessette@acumentrics.com

DOE Managers
HQ: Dimitrios Papageorgopoulos
Phone: (202) 586-5463
E-mail: Dimitrios.Papageorgopoulos@ee.doe.gov
GO: Reginald Tyler
Phone: (720) 356-1805
E-mail: Reginald.Tyler@go.doe.gov

Contract Number: DE-FC36-03NT41838

Project Start Date: April 1, 2008
Project End Date: September 30, 2012

Fiscal Year (FY) 2011 Objectives

The goal of the project is to develop a low-cost 3-10 kW solid oxide fuel cell (SOFC) power generator capable of meeting multiple market applications. This is accomplished by:

- Improving cell power and stability.
- Cost reduction of cell manufacturing.
- Increase stack and system efficiency.
- Prototype testing to meet system efficiency and stability goals.
- Integration to remote and micro-combined heat and power (mCHP) platforms to allow short and longer term market penetrations.

Technical Barriers

This project addresses the following technical barriers from the Fuel Cells section of the Fuel Cell Technologies Program Multi-Year Research, Development and Demonstration Plan:

(A) Durability
(B) Cost
(C) Performance

Technical Targets

This project is directed toward achieving the stationary generation goals of the DOE fuel cell power systems (Table 1). This project will work on cost reduction of the desired product while also demonstrating required life and efficiency targets through multi-level testing.

TABLE 1. Progress towards Meeting Technical Targets for Stationary Fuel Cell Power Generators

Characteristic	Units	2011 Goal	2011 Status
Electrical Efficiency	%	40	40
Combined Heat and Power Efficiency	%	80	85
Durability @<10% rated power degradation	hours	40,000	12,000
Start-up Time	minutes	<30	<20
Transient Response (from 10-90%)	seconds	<3	<10
Cost	$/kWe	750	729 (estimate on volume)

FY 2011 Accomplishments

- Improved electrical efficiency of stationary units from 35% to 40%.
- Improved durability to over 7,000 hrs demonstrated to over 12,000 hrs demonstrated.
- Increased operating current density and power per cell by 67% while maintaining performance stability.
- Developed a cell manufacturing process capable of cutting high temperature firing times in half with improved yield and cell cost.



Introduction

Achieving combined heat and power goals of over 40% net electrical efficiency and over 85% total energy efficiency are goals of the DOE and present administration to reduce our dependence on foreign energy and reduce the emission of greenhouse gases. SOFCs, with their ability to use the present U.S. fuel infrastructure and high grade waste heat are ideal candidates for this challenge. To date, the limitation on making this goal a reality has been the reliability and cost of such systems.

This project is designed to address these limitations and bring this promising technology to the market place. This is being achieved by working on all aspects of the SOFC power generator including: (1) improving cell power and stability, (2) cost reducing cell manufacture, (3) increasing stack and system efficiency, (4) prototype system testing, (5) and integration into a mCHP platform. This phase of the project

will make a major drive toward the DOE's goals set forth for 2012 stationary power generators.

Approach

To achieve the project objectives, the approach has been to perfect the individual system pieces followed by optimizing their integration through:

- **Cell Technology:** Improving power and stability of the cell building block.
- **Cell Manufacturing:** Improving processing yield and productivity while decreasing material consumption.
- **Stack Technology:** Refining stack assembly and improve heat removal and integrity while cost reducing individual component costs.
- **System Performance:** Developing simplified controls and balance-of-plant components to allow for a reliable, highly efficient unit.

Results

In the past years review, substantial power per tube as well as the significant reduction in operating temperature were demonstrated. It was then stated that the focus of 2010 would then need to revolve around assuring that these increased power per tube figures did not result in any deleterious effects on life expectancy and that they did not interfere with the overall continual goal of cost reduction. Likewise, it was stated that the increased cell power would be further utilized with a number of new generator designs and reforming technology to result in increased overall efficiency meeting the DOE's multi-year goals. All of these goals were met in the research performed under this project in 2010.

Figure 1 shows through testing for nearly 4,000 hrs that an increase in cell current density and cell power did not result in an increased rate of performance decay. The figures shows that for approximately 500 hrs of the initial test the current density was held at 150 mA/cm^2 and was subsequently increased to 400 mA/cm^2 for an additional 3,000 hrs. Over this initial period at the pre-2010 operating conditions the voltage decay was limited to -18 mV/1,000 hrs. When the current density was increased, the two cells tested resulted in a decay of -14 and -19 mV/1,000 hrs which is statistically the same under both operating conditions.

Longer term data was also collected to demonstrate the ability to meet DOE's multi-year goal of 40,000 hr stack life. Figure 2 shows the data for one field unit operational for nearly 1.5 yrs. This unit is a full system located outside operating on residential line natural gas including any necessary clean-up and sulfur removal. In previous year reporting it was shown to have 4,500 hrs of operation and Figure 2 shows the stability for 10,000 hrs. This unit is presently at just over 12,000 hrs and continues to operate stably demonstrating over 25% achievement of the DOE goal. This unit will continue to operate and be monitored for stability.

In additions to gains in cell power enhancements were made into reforming technology and generator design to yield efficiency improvements. Figure 3 demonstrates both the power and efficiency gains resulting from these improvements. A fuel cell stack of the pre-2010 vintage was operated under its standard conditions resulting in ~500 W power output at 35-35% electrical efficiency (power/lower heating value of natural gas). The improved cell technology integrated with improved reforming technology resulted in slightly over 1,000 W power output at 42-43% efficiency.

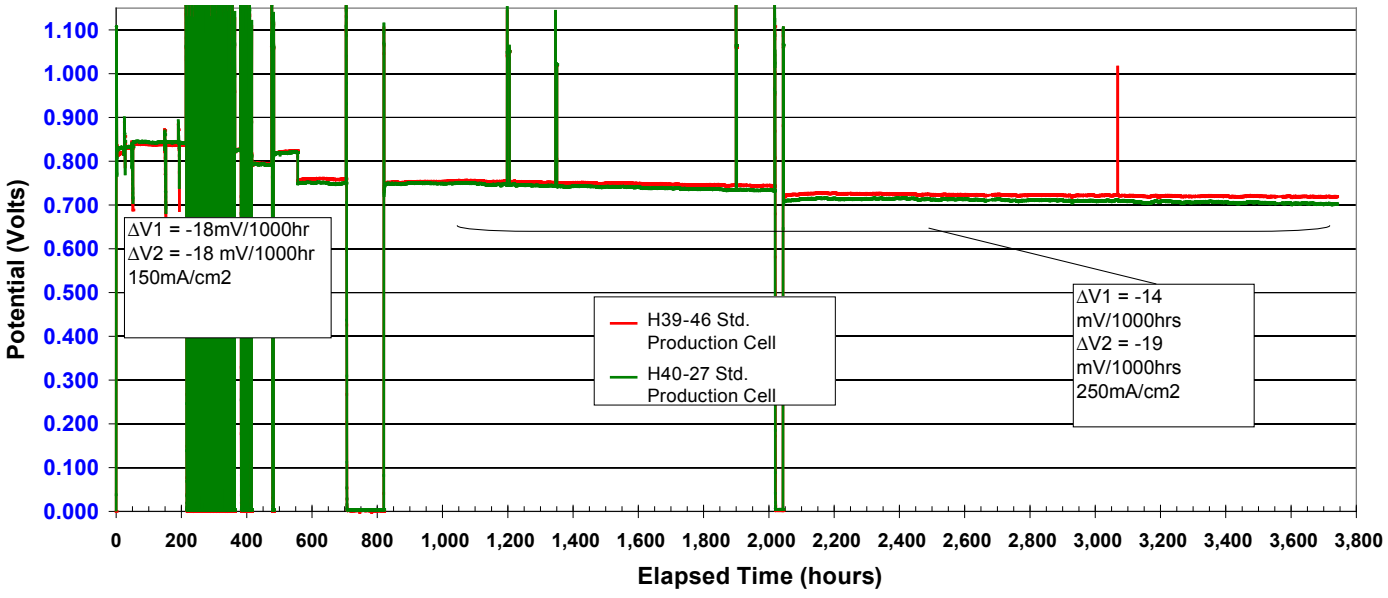
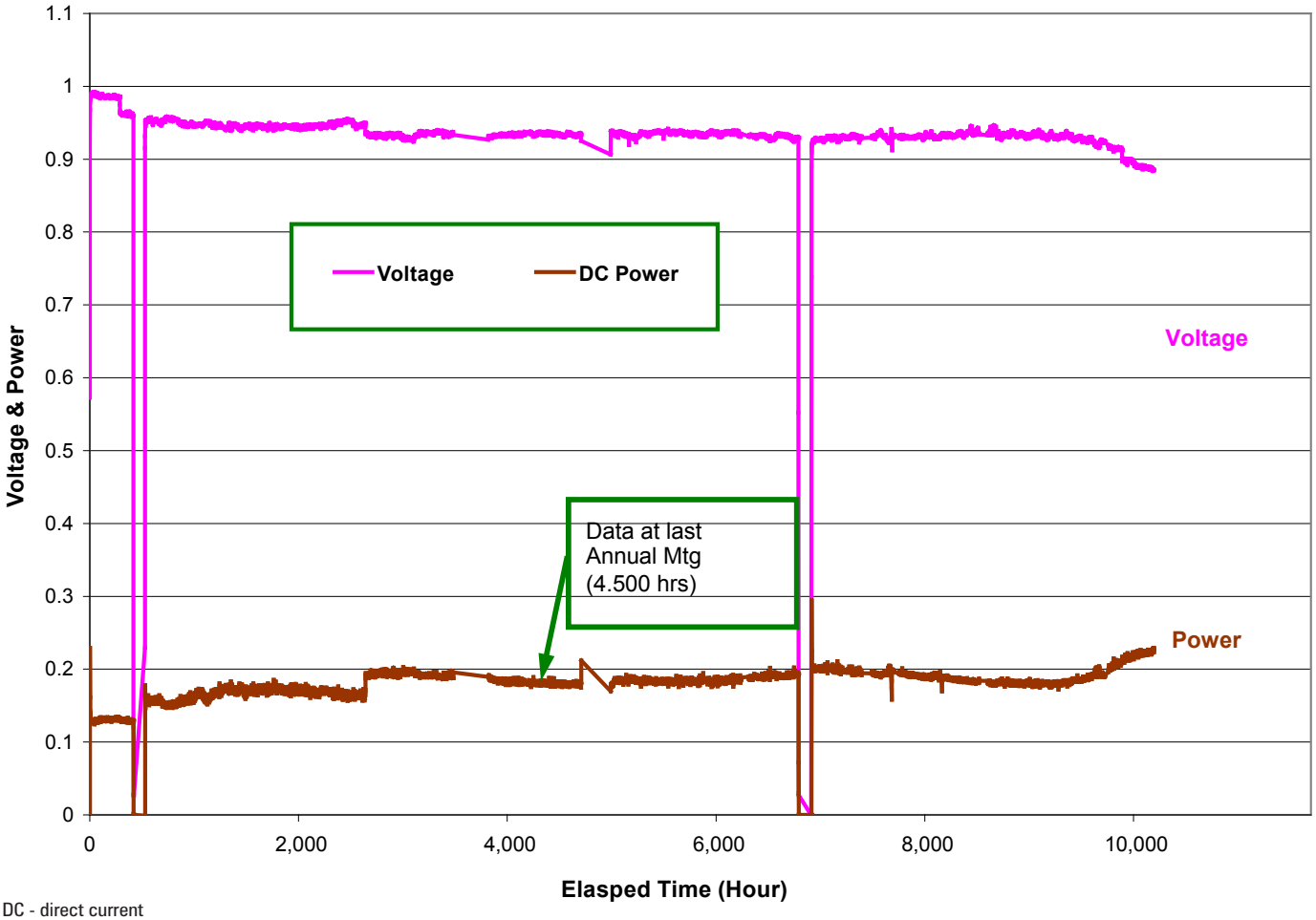


FIGURE 1. Cell Stability at Increased Power per Cell



DC - direct current

FIGURE 2. Long-Term Durability Testing

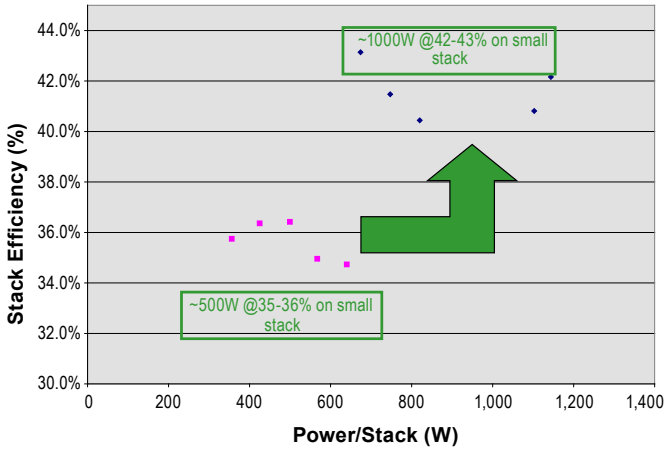


FIGURE 3. Power and Efficiency Enhancements

This doubling of power and seven efficiency point gains result in a lower cost unit since less cells are required for a given power output and allows Acumentrics' units to achieve over 40% efficiency meeting DOE's long-term goals.

In addition to cell power and stability enhancements, there have been a number of improvements in cost reduction. The fuel cell tube remains the major component to cost and the focus of significant cost reduction activities. Present technology has required that the anode be pre-sintered or "bisque" fired followed by an electrolyte application and subsequent high temperature firing. During the past year research focused on combining these two steps to allow for a co-sintering of the layers. This advancement results in significant cost reduction and productivity enhancements through reduction in capital required. Figure 4 shows the firing sequence of the two step process in addition to the single-step process. The original two-step process required over 85 hours of kiln firing while the single step reduces that to less than 50 hrs. This not only saves on capital equipment but saves on labor cost considering the removal of an unload and re-load step. Reducing handling also reduces loss from breakage further increasing yield and reducing cost. This process is presently being implemented into production.

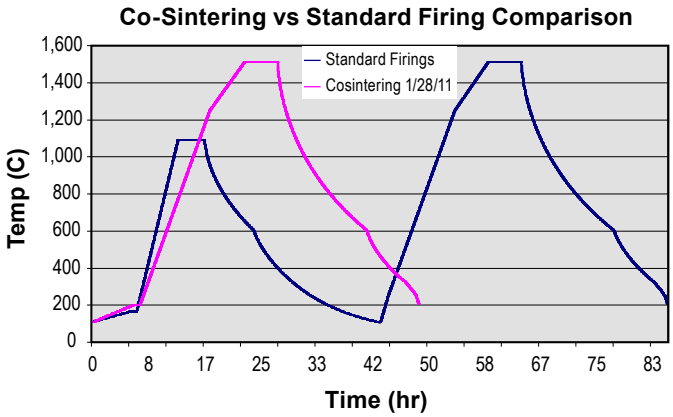


FIGURE 4. Electrolyte Co-Sintering Kiln Firing Cycles

Conclusions and Future Directions

Significant strides have been made in achieving the goals set forth for stationary fuel cell generators under the DOE multi-year plan:

- Improved electrical efficiency of stationary units from 35% to 40%.
- Improved durability to over 12,000 hrs demonstrated.
- Increased operating current density and power per cell by 67% while maintaining performance stability.
- Developed a cell manufacturing process capable of cutting high temperature firing times in half with improved yield and cell cost.

Moving forward, further testing to achieve all of the DOE multi-year goals will be performed as well as cost reduction of the cell and all major sub-systems. Work will continue on market introduction of the technology into remote markets for short term introduction as well as mCHP for longer term market penetration.

FY 2011 Publications/Presentations

1. 2010 Fuel Cell Seminar, "Progress in Acumentrics' Fuel Cell Program", San Antonio, TX, October, 2010.

2. 2011 DOE Hydrogen Program Review. Washington, D.C., May 12, 2011.

V.K.2 Development and Demonstration of a New-Generation High Efficiency 10 kW Stationary Fuel Cell System

Dr. Durai Swamy (Primary Contact),
Diane Aagesen
Intelligent Energy (IE)
2955 Redondo Ave.
Long Beach, CA 90806
Phone: (562) 304-7688
Email: durai.swamy@intelligent-energy.com

DOE Managers
HQ: Kathi Epping Martin
Phone: (202) 586-7425
E-mail: Kathi.Epping@ee.doe.gov
GO: David Peterson
Phone: (720) 356-1747
E-mail: David.Peterson@go.doe.gov

Contract Number: DE-FG36-07GO17013

Project Start Date: July 28, 2007
Project End Date: June 30, 2012

Fiscal Year (FY) 2011 Objectives

- To identify core technology improvements, methodologies and engineered solutions to overcome challenges facing the development of fuel cells (FCs) for use in combined heat and power (CHP) applications.
- To design an integrated system based on the most promising down-selected fuel cell and fuel processor building blocks.
- To build and test a prototype unit in a laboratory setting and collect 300 hours of operating data.
- To optimize, redesign and retrofit a pressure swing adsorption (PSA) unit using lessons learned from prototype to develop a field demonstrator.
- Conduct a six month demonstration in an International Partnership for the Hydrogen Economy country.

Technical Barriers

This project addresses the following technical barriers from the Fuel Cells section of the Fuel Cell Technologies Program Multi-Year Research, Development and Demonstration Plan:

(A) Durability
(B) Cost
(C) Performance

Technical Targets

Work under the project is aimed at developing novel fuel processing, polymer electrolyte membrane (PEM) fuel cell technologies and integration strategies in order to make progress toward achieving DOE targets for stationary PEM fuel cell power systems for year 2011. These targets and project progress are shown in Table 1.

TABLE 1. DOE Targets vs. Project Achievements

Metric	2010 Project Status	2011 Project Achievement	2011 DOE Target[1]
Electrical efficiency at rated power	32.6%-prototype	To be determined-demonstration unit testing underway	40%
CHP energy efficiency	60.8%-prototype	To be determined -demonstration unit testing underway	80%
Operating lifetime	832 hours on hydrogen generator	3,425 hours on hydrogen generator[2]	40,000 hours

[1]Complete DOE Table 3.4.4 found at http://www1.eere.energy.gov/hydrogenandfuelcells/mypp/pdfs/fuel_cells.pdf
[2]Accumulated on prototype, new retrofit hydrogen generator integrated into demonstration CHP unit now under test through February 2012.

Other challenges being addressed under the project are:

- Reduced startup time by improved thermal management design.
- Reduced size by improved subassembly integration and packaging.

FY 2011 Accomplishments

- Conformité Européenne ("European Conformity") compliant design of demonstration unit resulting in:
  - 30% size reduction.
  - Grid tie enabled using commercial solar photovoltaic inverter.
  - Integrated feed gas compressor, water system and gas quality monitoring.
  - On-board safety and emissions management.
  - System health monitor with remote data acquisition and analysis for predictive maintenance.
  - Twin stack fuel cell system developed for CHP application to improve system efficiency.
  - Modeled combined heat and power efficiency increased to 78%.[1]

[1] Expected performance based on model of updated system developed during retrofit redesign and new optimization approach: actual validation testing planned for Q4 FY 2011 - Q2 FY 2012 thus is noted as to be determined in Table 1.

  - Modeled natural gas-to-electrical efficiency of 37%.[2]
- Construction of field demonstration unit.
- Prove-out of the feasibility of adsorption enhanced reforming (AER) as a potential lower cost fuel processor option (eliminates expensive alloys and PSA required by steam methane reformer [SMR] technology).

Table 2 shows run-time hours of the prototype between those reported last year versus additional time logged since then (for FY 2011). The mode of particular importance is that for pure hydrogen production; the increase in hours logged by more than 70% without loss of mechanical integrity and/or notable deterioration in fuel conversion is indicative of a fundamentally sound reformer design.

TABLE 2. Accumulated Hours on Prototype

Mode	Hours-FY 2010	Hours-FY 2011
Hot-Idle[1]	2,164	3,425
Pure Hydrogen Production	832	1432
Power Production	396	733

[1] Reformer combustor hot (700°C) only without synthesis gas or power production occurring.



Introduction

The development of highly efficient and cost-effective clean energy solutions is not without challenge. Hydrogen fuel cell technologies are expected to become a significant player in reducing our dependence on imported fossil fuels and curb the further accumulation of greenhouse gases and criteria pollutants.

This project is focused on the design, fabrication and field demonstration of a stationary CHP system that will provide multi-dwelling residential and light commercial end-users with on-site generated electrical and heating needs. The proposed technology addresses DOE targets by using PEM fuel cell stacks as they have been proven to achieve high efficiency, greater durability and lower costs than competing fuel cell technologies.

Approach

The approach to achieving this project's 40% electrical efficiency target is incremental and based on (1) optimization of the SMR+FC architecture and (2) the development of an 80% or greater thermally efficient AER hydrogen generator that can "plug-and-play" into the same SMR+FC hydrogen feed interface. The SMR+FC optimization relies on allowing slightly less than 100% hydrogen to enter the FC (99% H_2, balance methane [inert to the FC]) which has a negligible impact on the FC performance, but allows for increased hydrogen recovery from the processor whereby its thermal efficiency can be boosted from 70% up to as much as 73%. Process simulations indicate that this method when combined with the benefits of a twin-stack FC configuration can increase the overall CHP system electrical efficiency from its current status of 32.6% (achieved on prototype last year) to approximately 37% (demonstration unit now under test).

An AER hydrogen generator produces a feed stream similar to what the optimized SMR+FC system would receive but operates at 500°C versus 900°C. This means less external energy is needed for AER making it more thermally efficient than SMR. Predictive models developed for us by Sandia National Laboratories during Year 1 of the project indicate that an efficiency of up to 85% can be achieved with the AER compared to only 70%-73% which is the maximum one can obtain with SMR. The product of the AER hydrogen generator and the fuel cell efficiencies, less 12% (assumed value) for the parasitic power requirements to run the CHP system ([0.85 x 0.55] -0.12), would result in a total system electrical efficiency of approximately 41%. Furthermore, with AER, carbon dioxide removal and reforming occur simultaneously thereby eliminating the need to have an additional purification step (such as a PSA) ultimately leading to lower cost and smaller system. Our work on AER culminated in Year 2 as further development and funding is required to mature the technology to the point of a "plug-and-play" swap of SMR.

At the beginning of this last year of the project, a twin-stack FC configuration was chosen for integration into the CHP demonstrator. Since each of the two stacks can run at a lower output and be combined to produce 10 kW, the efficiency of each stack will be at its maximum point thereby synergistically operating together to achieve an improvement of efficiency from 53% (single stack) to 59%. The result of using two stacks together in terms of total performance can be seen in Figure 1 of the Results section.

Results

Over the course of FY 2011, our project team focused on (1) twin-stack fuel cell system development and testing, (2) stack testing to evaluate the effect on efficiency when feeding 99% hydrogen (balance methane) vs. 100% hydrogen, and (3) a retrofit design and repackaging to accommodate a shorter PSA for the purpose of optimization through relaxing the hydrogen purity requirement all while achieving a system size reduction.

As was determined experimentally (Figure 1) at the 10 kW nominal load to which the CHP system has been designed, a twin-stack configuration performs notably better than a single stack when considered as a total system. The efficiency of a single stack reaches its maximum at approximately 5 kW, while having twin stacks it is possible to run each at this mid-range load and achieve a combined efficiency of 59% vs. 53%.

[2] See footnote 1: prototype achieved 32.6% electrical efficiency-increase to 37% predicted by model of updated system.

According to our latest model that forms the design basis of the retrofitted demonstrator, this approach alone adds 1%-2% to the overall CHP system electrical efficiency. Thermal management of the reformer and the reduction of parasitic power demands from the balance of plant also contribute to improving efficiency over the prototype developed in FY 2009-10.

In conclusion, using a twin-stack configuration can increase system efficiency up to 59%:

- The higher voltage output of two stacks enables grid-tie via a commercially available photovoltaic inverters without a boost converter.
- May extend life and ultimately decrease costs as each stack operates at a lower nominal load.
- Air blower output is shared across stacks thus reducing its back pressure and parasitic power draw.

To better understand the potential impact on efficiency running our PEM stacks with less than 100% pure hydrogen in support of our SMR+FC optimization approach, our Research and Technology Group made rig modifications required to run mixes of hydrogen (99%) and methane (1%). Tests were run on a 20-cell evaporatively cooled stack with hydrogen to air stoichiometry of 2:1.

Stack testing was performed over 15 hours during which period our team determined that the mean cell voltage was not adversely impacted by using the mix. Figure 2 depicts a baseline and overlay of cell voltages for pure hydrogen and the mix, respectively.

The work also confirmed that operating the FC with the mix requires more frequent anode purging than when using pure hydrogen in order to maintain the same cell voltage: at 100 A the purge frequency would need to be increased to 5 seconds compared to 6.4 seconds. It should be noted that this hydrogen does not necessarily have to be lost because when the FC is integrated into a CHP unit, the stream is blended into the same fuel that goes to the reformer. As the demonstration unit now under test has been designed to Conformité Européenne directives whereby it must comply with strict combustible emissions limits, it does indeed recycle this hydrogen.

In parallel to developing the twin-stack fuel cell system and conducting bench tests with 99% hydrogen, our mechanical and process design teams spent a great part

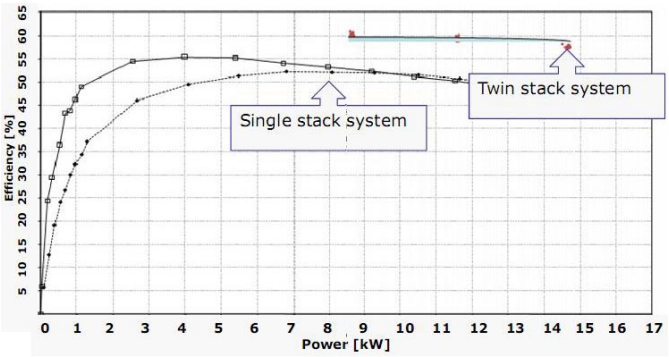


FIGURE 1. Twin-Stack System Efficiency vs. Single Stack Configuration

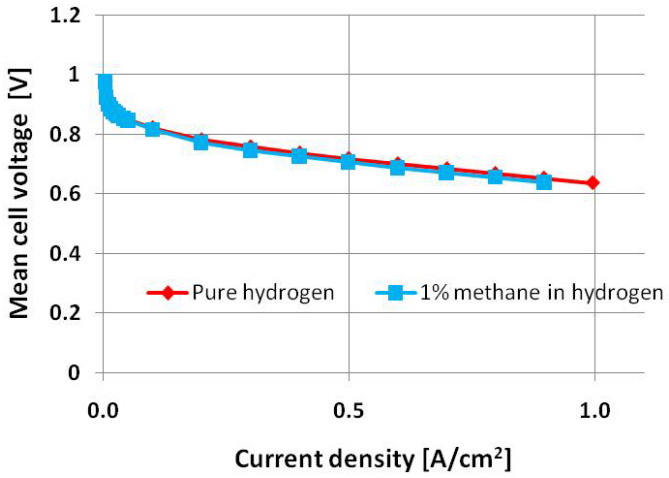


FIGURE 2. Mean Cell Voltage with 99% H_2 Feed vs. 100% H_2 Feed

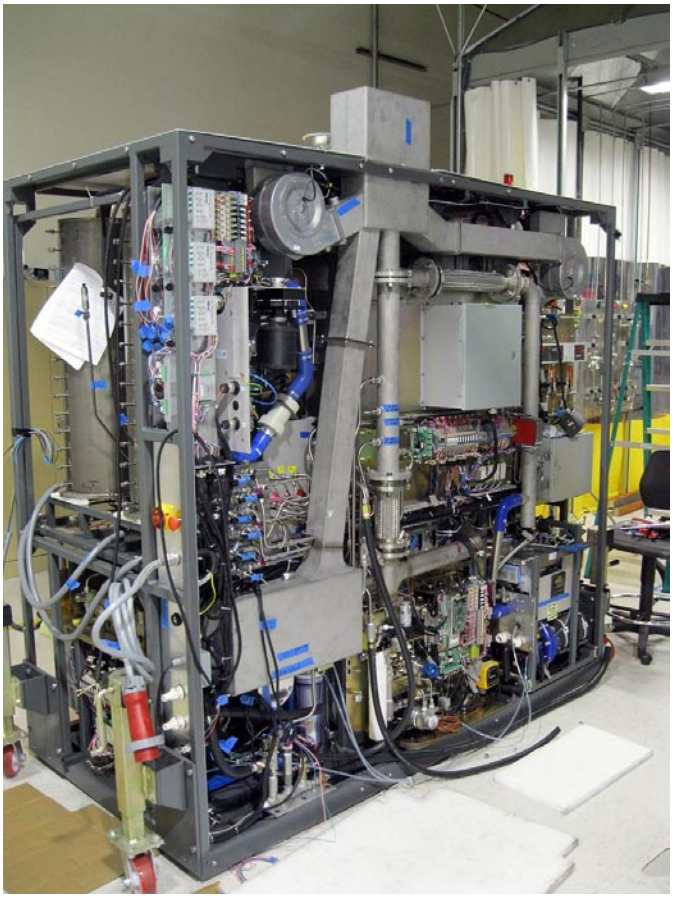


FIGURE 3. Retrofit Demonstration Unit



FIGURE 4. Packaged Demonstration Unit

of this last year evolving the CHP system "from project to product." The demonstration unit shown in Figure 3 and Figure 4, was subjected to IE's normal four stage-gated design review process which facilitated being able to reduce the number of subsystems from 23 (on prototype) down to just nine. Key component suppliers were also engaged early on to provide a purpose built PSA that is 1.5' shorter than the previous generation, and a natural gas compressor suitable for integration within the main frame by being less than one third in size compared to its equivalent standard model.

The field unit of course must meet all safety and environmental regulations as mandated by the European Union, and as such has been implemented with an emissions monitoring and redundant, hard-wired safety shut down subsystem that constantly watches over the main system controller and software. The unit was also designed for ease of installation requiring that the site connections comprise nothing more than city water and gas, drain, heating water inlet and outlet, network connection, and flue. Components that will demand periodic maintenance while under field trial are located in areas of the machine that provide quick and easy access (e.g. water filters, sulfur adsorbent, etc.).



FIGURE 5. Greenwatt Way Demonstration Site

While on site, the system will show real-time status and performance data on a local user interface while also being streamed back to IE headquarters. Startup and shutdowns will normally occur based on those commands the unit receives from the site's own energy management system.

In addition to designing and building the demonstration unit this last year, the planned site received National Environmental Protection Act (NEPA) determination as required by the project and federal law. A six-month field trial will take place 40 miles southwest of London, England at a multi-residential housing development called Greenwatt Way. This site is owned by Scottish and Southern Energy with whom IE has formed a joint venture and will serve to showcase green technologies and provide housing for up to eight families. A conceptual layout of the site can be seen in Figure 5.

Conclusions and Future Directions

- 2010 - Demonstration site receives NEPA determination.
- 2011 - Conformité Européenne compliant field demonstrator designed and built:
  - Approximately 30% smaller than prototype.
  - Projected system electrical efficiency increased to 37%.
  - Added functionality.
- 2011 - Testing of fuel cell stacks with 99% hydrogen showing no adverse impact:
  - Allows for the evaluation of system level trade-off between FCS and H_2 generator to maximize performance.
- 2012 – Six-month field demonstration and project closure:
  - Logan Energy to provide installation and system maintenance support.
  - System health monitor will relay real-time data back to the IE Knowledge Center.
  - Energy store will showcase ground-source heat pump, biomass boiler, photovoltaic and CHP system.

Patent Pending

1. K. Duraiswamy, A. Chellappa; Hydrogen Generation Utilizing Integrated CO_2 Removal With Steam Reforming, WO/2011/075490.

FY 2011 Publications/Presentations

1. K. Duraiswamy, A. Chellappa, G. Smith, Y. Liu, M. Li. "Development of High Efficiency Hydrogen Generators for Fuel Cell based Distributed Power Generation", Intl. J. Hydrogen Energy, 35(17), 2010, p 8962-8969.

2. M. Li and K. Duraiswamy. Process integration of adsorption enhanced reforming for use in conjunction with fuel cell. In The 21st International Symposium on Chemical Reaction Engineering, Philadelphia, PA, 2010.

3. Mingheng Li and Kandaswamy DuraiSwamy, Development of a High-Efficiency Hydrogen Generator Based On Adsorption Enhanced Pulsing Feed Reforming, presented at the AIChE Annual meeting, Salt Lake City, Nov 2010.

4. K. Durai Swamy, Diane Aagesen, Chris Jackson "Development and Demonstration of a New Generation High Efficiency 10kW Stationary PEM Fuel Cell System", U.S. DOE Annual Merit Review Proceedings, Arlington, VA. May 9, 2011.

V.K.3 Research & Development for Off-Road Fuel Cell Applications

Michael T. Hicks
IdaTech, LLC
63065 NE 18th Street
Bend, OR 97701
Phone: (541) 322-1040
E-mail: mhicks@idatech.com

DOE Managers
HQ: Kathi Epping-Martin
Phone: (202) 586-7425
E-mail: Kathi.Epping@ee.doe.gov
GO: David Peterson
Phone: (720) 356-1747
E-mail: David.Peterson@go.doe.gov

Technical Advisor
Walt Podolski
Phone: (630) 252-7558
E-mail: podolski@anl.gov

Contract Number: DE-FC36-04G014303

Subcontractors:
- The Toro Company, Bloomington, MN
- University of California, Davis, CA (UC Davis)

Project Start Date: August, 2007
Project End Date: March, 2012

Fiscal Year (FY) 2011 Objectives

- Build test stand for evaluation of commercial air filters for off-road applications.
- Evaluate air-filtration technologies for off-road applications.

Technical Barriers

This project addresses the following technical barriers from the Fuel Cells section (3.4.4) of the Fuel Cell Technologies Program Multi-Year Research, Development and Demonstration Plan:

(A) Durability

FY 2011 Accomplishments

- Gathered information on the air contaminants that may have an effect on fuel cell operation.
- Built exterior test facility to house air filtration test stand.

✧ ✧ ✧ ✧ ✧

Introduction

Air filters are a critical part of a fuel cell system. They remove harmful contaminants from the oxidant stream before they reach and damage the fuel cell stack. However, filter suppliers routinely characterize air filters according to standard test procedures that are not suitable for fuel cell systems. These test methods evaluate contaminants at ppm levels when ppb levels are more representative; they only test one contaminant at a time when multiple contaminants exist in ambient air; and they do not evaluate the impact of ambient air conditions (temperature and humidity) on air filter performance. These shortcomings make it impossible to extrapolate the results from the standard test conditions to fuel cell test conditions. As a result, IdaTech proposes to evaluate air filters under "real life" conditions.

Approach

- Determine reasonable air contaminant levels.
- Perform ex situ testing of air filters to evaluate breakthrough and filter capacitance at different contaminant levels, gas flow rates, temperatures and relative humidity.
- Utilize statistical design of experiments to plan and analyze experimental data.

Results

The outdoor test shelter (Figure 1) for the test equipment was built. All electrical wiring is complete. All large items (compressor, chiller, etc.) are installed in the test shelter. Construction of the frames and mounts to house the filter housing, mass flow controllers, and sampling valve



FIGURE 1. Constructed Outdoor Test Shelter at UC Davis

manifold are complete. A National Electrical Manufacturers Association enclosure for the electrical equipment, instrumentation and gas analyzers has been prepared for equipment installation. Air heaters have been assembled and are ready for installation. Conduit has been installed to connect the test shelter to the control room.

Conclusions and Future Directions

- Complete the installation of all test equipment and plumbing in the outdoor shelter.
- Start shaken with estimated completion of August 1 with testing commencing shortly thereafter.

V.K.4 Power Generation from an Integrated Biomass Reformer and Solid Oxide Fuel Cell

Patricia Irving (Primary Contact), Quentin Ming
InnovaTek, Inc.
3100 George Washington Way, Suite 108
Richland, WA 99354
Phone: (509) 375-1093
E-mail: irving@innovatek.com; ming@innovatek.com

DOE Manager
HQ: Kathi Epping Martin
Phone: (202) 586-7425
E-mail: Kathi.Epping@ee.doe.gov

Contract Number: DE-EE0004535

Subcontractor:
Energy Technology Services, Glastonbury, CT

Project Start Date: October 1, 2010
Project End Date: September 30, 2013

Fiscal Year (FY) 2011 Objectives

- Establish the requirements and design for an integrated fuel cell and fuel processor that will meet the technical and operational needs for distributed energy production.
- Develop and integrate key system components – including the fuel cell stack, fuel processor, water management, thermal management, burner, air handling, control system and software.
- Demonstrate that component and mechanical design for the proposed energy system proves the technical and commercial potential of the technology for energy production, emissions, and process economics.
- Develop and demonstrate a 5-10 kW power plant with at least 40% efficiency that is located in the Tri-City Research District Innovation Zone Renewable Energy Demonstration Park.

Technical Barriers

This project addresses the following technical barriers from the Fuel Cells section of the Fuel Cell Technologies Program Multi-Year Research, Development and Demonstration Plan:

(A) Durability
(B) Cost
(C) Performance
(E) System Thermal and Water Management

Technical Targets

InnovaTek's research plan addresses several DOE technical targets for stationary applications for fuel processors. Progress in meeting DOE's technical targets is provided in Table 1. DOE has also established technical targets for integrated stationary proton exchange membrane (PEM) fuel cell power systems operating on natural gas or liquefied petroleum gas (LPG) [1]. Although the InnovaTek system includes a solid oxide fuel cell (SOFC) rather than a PEM fuel cell and reforms bio-oil rather than natural gas, our research plan is addressing the same characteristics for energy efficiency and cost, Table 2.

TABLE 1. Progress toward Meeting Technical Targets for Stationary Fuel Processors for Stationary Applications

Characteristic	Units	2011 Target	InnovaTek 2011 Status
Cost	$/kW$_e$	220	1,160[a]
Cold start-up time to rated power @ -20°C ambient	minutes	<30	<30
Transient response time (for 10% to 90% power)	minutes	<1	<1
Durability[b]	hours	40,000	To be determined
Survivability (min and max ambient temp)	°C	-25 +40	To be determined

[a] Includes projected cost advantage of high-volume production (30,000 units per year). Does not include integrated auxiliaries, battery and power regulator for unassisted start.
[b] Time between catalyst and major component replacement.

TABLE 2. Progress toward Meeting Technical Targets for Integrated Stationary Fuel Cell Power Systems Operating on Reformate[a]

Characteristic	Units	2011 Target[c]	InnovaTek 2011 Status[d]
Electrical Energy Efficiency[b] @ rated power	%	40	40
Cost	$/kW$_e$	750	3,500

[a] Includes fuel processor, stack, and all ancillaries.
[b] Ratio of direct current output energy to the lower heating value (LHV) of the input fuel average value of rated power over life of power plant; theoretical calculation.
[c] For a PEM fuel cell system using natural gas or LPG as fuel.
[d] For an SOFC system using bio-oil as fuel.

FY 2011 Accomplishments

- A design requirements document was established that specifies system subcomponents that meet required safety, codes and standards for a fuel cell distributed energy system.

- An optimum process configuration was selected for the production of electricity from pyrolysis oil based on the integrated results of four process models developed by InnovaTek – bio-oil reforming model, SOFC model, anode off gas combustor model, and heat exchanger models.
- A complete mass and energy balance was conducted for the integrated system's 26 different process streams. The results indicate that the system has a theoretical total electrical efficiency of about 40%. This result will be confirmed during testing.
- A prototype system design was completed that will reduce costs through improved thermal management, lower materials cost, and reduced catalyst loading.



Introduction

Alternative energy sources must be sought to meet energy demand for our growing economy and to improve energy security while reducing environmental impacts. Power generation from biomass, along with solar energy, wind energy, nuclear energy, geothermal energy, and others will inevitably be the ingredients of our future energy mix [2]. In addition to facilitating the use of a renewable fuel source, cost and durability are among the most significant challenges to achieving clean, reliable, cost-effective fuel cell systems. Therefore this project is focusing on lowering the cost and increasing the durability of a fuel cell distributed renewable energy system, while also assuring that its performance meets or exceeds that of competing technologies. Work was performed to develop proprietary steam reforming technology that will make it possible to use bio-oil with an SOFC. A highly efficient integrated system design with an SOFC was developed that reduces the loss of heat through an effective thermal design and the use of micro-channel heat exchangers. Modeling and simulations were completed to produce designs for prototype components and to analyze process flow for alternative system configurations. Design alternatives were compared and an integrated system design was completed during this period.

Approach

The technological approach utilizes a steam reforming reactor to convert bio-oil derived from bio waste to hydrogen-rich reformate which fuels an integrated SOFC for power generation. The project will evolve through three developmental stages. Meeting targets for system performance, cost, and durability will be emphasized at each stage.

1. Optimization of SOFC and fuel processor integration – is completed using process simulation and analysis to optimize system design and produce a complete mass and energy balance for individual components of the system. Process flow as well as piping and instrumentation diagrams are prepared to analyze possible system configurations using Mathcad and FEMLAB models to simulate the process flow paths in the system.
2. Design for manufacturing and field operation – requires continued modeling and analysis such as failure mode effects analysis and several iterations of component builds and tests to compare design options. The dimensions, geometries and flow patterns defined from optimization modeling work completed in stage 1 are translated into three-dimensional computer-aided design (CAD) images and drawings.
3. System demonstration and validation for commercial applications – takes place after down-selection of the final design. Several complete systems will be built to meet the required codes and standards for demonstration at a field site to gain performance data necessary to validate the design and operation of the system. Type tests (requirements validation) and routine tests will be performed before and during the demonstration, and system durability will be assessed.

Results

Design Requirements

The functional and safety requirements for a distributed energy application were identified for a 5 kW fuel cell power plant, including hydrogen production capacity, output power and conditioning requirements, parasitic power use, minimum system efficiency, physical size, feed input and requirements, and lifetime. Criteria were determined for:

- Site establishment
- Enclosure and external surfaces
- Power system design requirements
  - Identify all reasonably foreseeable hazards throughout the anticipated equipment lifetime.
  - Estimate the risk of all hazards from a combination of their probability of occurrence and their foreseeable severity.
  - Eliminate or reduce all hazards as far as practical.
  - Use components that are listed or certified by a nationally recognized testing laboratory.
- Marking
- Technical documents

Process Configuration and Modeling

Important system processes were evaluated to determine materials and energy balances, product yields, and equipment size. The steps in process analysis were: 1) mathematical specification of the process, 2) detailed analysis to obtain mathematical models describing the process, and 3) synthesis and presentation of results to

ensure full understanding of the process. In this task, we used process simulation tools to analyze the system configuration and to develop an optimal system design with detailed mass and energy balance. The mass and energy balance information and component simulations were used for the design of the reactor and heat exchangers. For example our microchannel heat exchanger analyses indicate that our proprietary designs meet the criteria for high heat transfer density with low pressure drop (Figure 1). The appropriate management of thermal systems determines the overall system efficiency; therefore, special attention was placed on the thermal and water management in the system, the two most technically challenging aspects of system integration. Mass and energy balance calculations for the system were used to determine system input requirements and to estimate product output and exhaust rate and composition. This information allowed us to calculate a system electrical efficiency of about 40% based on LHV of fuel input.

Prototype System Design

Manufacturability and integrated product development concepts were used to achieve cost and performance targets for a pre-commercial fuel cell energy system. Various design concept alternatives were considered early in the process. The alternatives were evaluated against design for manufacturing objectives to help reduce both capital equipment costs and maintenance cost while increasing lifetime and robustness. CAD/computer-aided engineering was used to aid in cost effectively developing and analyzing design alternatives. Finite element analysis and other design analysis tools were used to assess the ability of the design to meet functional requirements prior to manufacture as well as assess a part's or product's robustness. Solids modeling helped to visualize the individual part; understand part relationships, orientation and clearances during assembly; detect errors and assembly difficulties; and design the integrated system enclosure (Figure 2).

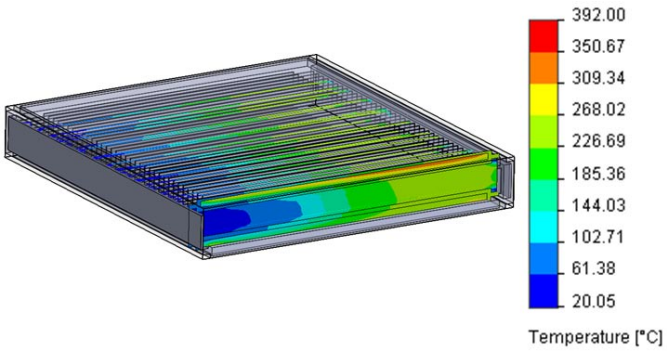


FIGURE 1. Micro channel heat exchanger component simulation — temperature profile through water channel. Results verified that pressure drop across channels meets design criteria; the design results in high heat transfer density; heat transfer meets design criteria.



FIGURE 2. Solid Model of InnovaGen Fuel Cell Distributed Energy 5 kW Power Plant System

Conclusions and Future Directions

- Modeling and analyses indicate that a 5 kW fuel cell distributed energy system that is fueled with renewable, non-food bio-oil is possible through integration of InnovaTek's steam reforming technology and a SOFC.
- On the basis of careful systems modeling and component integration using CAD and thermal systems design with micro-channel heat exchangers, we calculate an overall system electrical efficiency of 40% is possible.
- Prototype construction is underway and testing will verify modeling and simulation results. These results will be used to optimize the design for field-ready systems to be constructed and demonstrated in the City of Richland Renewable Energy Park where they will be tied to the electric utility grid.
- Fabrication and demonstration results will be used to determine whether system cost, performance, and durability targets for a commercially viable system can be met.

Patents Issued

1. Received Notice of Allowance for Canadian Patent Application No. 2,593,413 entitled "Hydrocarbon Fuel Reforming Catalyst and Use Thereof".

FY 2011 Publications/Presentations

1. A presentation regarding the project was made by Patricia Irving at DOE Headquarters to DOE staff having oversight or interest in the project and to other Phase III awardees on March 30, 2011.

References

1. Hydrogen, Fuel Cells and Infrastructure Technologies Program Multi-Year Research, Development and Demonstration Plan, U.S. Department of Energy, 2007. http://www.eere.energy.gov/hydrogenandfuelcells/mypp/

2. Duane B. Myers, Gregory D. Ariff, Reed C. Kuhn, and Brian D. James; Hydrogen from Renewable energy sources: Pathway to 10 quads for transportation uses in 2030 to 2050. Hydrogen, Fuel Cells, and Infrastructure Technologies, 2003 DOE Hydrogen, Fuel Cells, and Infrastructure Technologies Progress Report.

V.L.1 Development of Kilowatt-Scale Coal Fuel Cell Technology*

Steven S.C. Chuang (Primary Contact),
Felipe Guzman, Tritti Siengchum,
Azadeh Rismanchian, and Jelvehnaz Mirzababaei
The University of Akron
302 Buchtel Common
Akron, OH 44310-3906
Phone: (330) 972-6993
E-mail: schuang@uakron.edu

DOE Managers
HQ: Dimitrios Papageorgopoulos
Phone: (202) 586-5463
E-mail: Dimitrios.Papageoropoulos@ee.doe.gov
GO: Reg Tyler
Phone: (720) 356-1805
E-mail: Reginald.Tyler@go.doe.gov

Contract Number: DE-FC36-08GO0881114

Project Start Date: June 1, 2008
Project End Date: May 31, 2012

*Congressionally directed project

Fiscal Year (FY) 2011 Objectives

Develop a kilowatt-scale coal-based solid oxide fuel cell (SOFC) technology. The outcome of this research effort will form the technological basis for developing a megawatt-scale coal-based SOFC technology. Objectives for 2011 included the following:

- Investigate the effect of the type of solid carbon fuel on the ability to generate electric power in the coal-based SOFC.
- Determine the effect of the concentration of CO_2 on the performance of the coal-based SOFC.
- Develop anode materials that exhibit resistance to deactivation due to exposure to sulfur-containing species.

Technical Barriers

This project addresses the following technical barriers from the Fuel Cells section of the Fuel Cell Technologies Multi-Year Research, Development and Demonstration Plan:

(A) Durability
(B) Cost
(C) Performance

Technical Targets

This project will develop a technological basis for the scale up of power generation capability of a kW SOFC to megawatt scale. A current density of 100 mA/cm^2 at 0.4 V was the initial target for demonstration of a coal-based SOFC.

FY 2011 Accomplishments

FY 2011 research focused on achieving the following milestones:

- Studied the generation of electric power in the coal-based SOFC using two types of solid carbon fuels: biomass-based coconut coke and bituminous Ohio #5 coke.
- Demonstrated that exposure to CO_2 streams increases the performance of Ni-based anode SOFCs during electrochemical oxidation of carbon.
- Synthesized a Cu-Ni/YSZ (yttria-stabilized zirconia) anode catalyst that exhibits higher resistance to deactivation due to SO_2 exposure, as compared to conventional Ni/YSZ anodes.



Introduction

Coal-based SOFCs produce electricity by direct utilization of solid carbon in coal. The use of solid carbon as fuel constitutes a highly desirable technology because of its high energy density (20 kW h/L) compared to methane (0.011 kW h/L), hydrogen (0.003 kW h/L) and diesel (9.8 kW h/L) at standard conditions (i.e., 1 atm and 273 K) [1]. Direct conversion of the chemical energy of carbon to electricity could reduce the complexities associated with fuel processing, facilitating the utilization of abundant carbon resources, and mitigating emission of pollutants (i.e., NOx species). Coal-based SOFCs with all solid-state components offer significant advantages over molten hydroxide and molten carbonate coal-based fuel cells including (i) ease of stack assembly, and (ii) avoiding electrolyte degradation/corrosion [2]. The performance of the coal-based fuel cell is limited by the extent of contact between the solid carbon and the anode electrode, where the electrochemical oxidation reaction takes place. As a result, development of a highly active coal-based SOFC requires developing anode catalysts that exhibit high activity towards electrochemical oxidation of carbon in coal, and resistance to poisoning due to contaminants such as sulfur. The main objectives of this project are (i) improving the anode catalyst activity and durability, (ii) developing and refining the coal-based SOFC fabrication techniques, and (iii) testing a small-scale coal SOFC system. Successful development of this novel coal fuel cell technology will significantly enhance the energy security of the U.S. and improve the market penetration of fuel cells.

Approach

An experimental campaign was designed and implemented to (i) fabricate anode supported SOFCs comprising a Ni/yttria-stablized zirconia (YSZ) anode, YSZ electrolyte, and YSZ/lanthanum strontium manganese oxide (LSM) cathode, and (ii) evaluate the voltage–current polarization plots (i.e., V-I curves) of the SOFCs at 750°C and 1 atm during testing in H_2, CH_4, CO_2, SO_2, and two types of solid carbon fuel (biomass-based coconut coke and bituminous Ohio #5 coke). Ohio #5 coke was produced by pyrolysis of Ohio #5 coal samples, as described in previous work [3]. The effect of the type of solid carbon fuel was studied by testing the fuel cell in batch mode with 10 g of each fuel, recording the fuel cell steady-state power output at a constant load. The SOFC performance was correlated with the structure and chemical composition of the carbon fuel, which was characterized by diffuse reflectance infrared fourier transformed spectroscopy (DRIFT) and X-ray fluorescence (XRF). The effect of CO_2 streams on the SOFC performance was studied by recording the steady-state V-I polarization plots in H_2 and Ohio # 5 coke, and analyzing the composition of gases at the exhaust of the cell. The Ni/YSZ anode electrodes were modified by addition of copper in order to investigate the resistance to deactivation by sulfur poisoning. Cu-Ni/YSZ anode fuel cells were prepared by depositing a layer of copper (Cu^0) on the surface of reduced Ni/YSZ cells, according to the electroless deposition method. The resistance of the Cu-Ni/YSZ anode to sulfur species was investigated by exposing a Cu-Ni/YSZ fuel cell to a H_2/He and CH_4/He streams containing SO_2 (1.0 vol%.), operating the cells at a constant load. The fuel cells used in these studies were characterized by XRF, scanning electron microscopy (SEM), and electrochemical impedance spectroscopy (EIS).

Results

The generation of electric power in the coal-based SOFC was investigated using two types of solid carbon: biomass-based coconut coke and bituminous Ohio #5 coke produced by pyrolysis of Ohio #5 coal. Figure 1 shows direct use of biomass-based coconut coke in the SOFC produced a power density of 125 mW/cm^2 continuously at 750°C, while the power density with Ohio #5 coke fuel decreased from 50 to 2 mW/cm^2 after 15 h of testing. The decreased power density was attributed to low activity of Ohio #5 coke, which contains less functional groups and alkali metals as compared to biomass-based coconut coke. Figure 2 shows the DRIFT spectra of Ohio #5 coke and coconut coke, confirming the stronger characteristic infrared (IR) absorptions of saturated (2,927 cm^{-1}) and aromatic C-H bands (3,045 cm^{-1}), aromatic C=C band (1,607 cm^{-1}), and oxygenates present on the surface of coconut coke. The less intensive characteristic IR absorption of Ohio #5 coke was attributed to the removal of surface functional groups during pyrolysis of Ohio #5 coal. Pyrolysis of coal

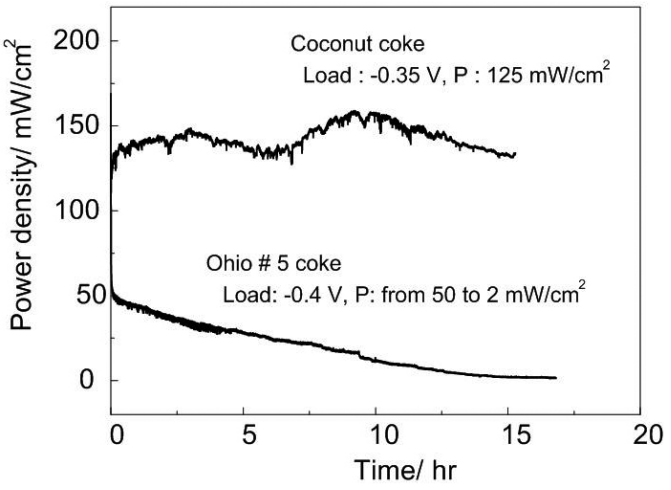


FIGURE 1. Fuel cell power output as a function of time recorded during operation in 10 g of biomass-based coconut coke and bituminous Ohio # 5 coke.

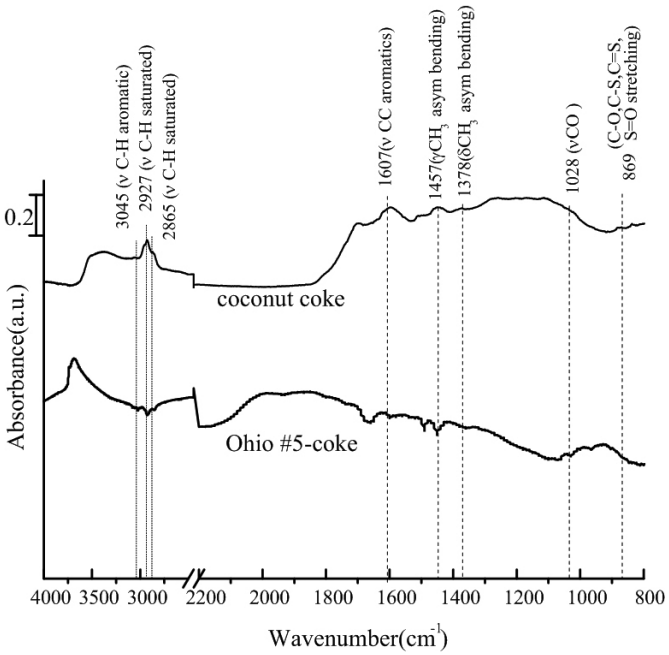


FIGURE 2. DRIFT spectra of Ohio #5 coke and biomass-based coconut coke.

caused the loss of surface functionality and heterogeneity through dehydrogenation, dealkylation, and oxidation reactions. XRF elemental analysis of Ohio #5 coke and coconut coke revealed the higher content of K in coconut coke with respect to Ohio #5 coke. The alkaline metals, e.g. Li, Na, and K, have been reported to catalyze gasification of carbon [4]. Thus, the solid carbon containing alkaline metals would be expected to be more active in gas-phase reactions than the carbon without catalysts. The high fuel cell performance observed during testing in coconut coke suggests that alkaline metals catalyzed the carbon

gasification to produce CO, which can be further undergo electrochemical oxidation by reacting with O^{2-} on the anode surface increasing power density. In contrast, the Ohio #5 coke lacked sufficient gasification activity, resulting in low rate of electrochemical oxidation.

Research studies conducted during FY 2011 provided experimental evidence of the improvement in the performance of Ni-based anode fuel cells in the presence of CO_2 streams. Figure 3 shows the voltage vs. current characteristics of a Ni/YSZ anode supported fuel cell at 750°C in 10 g of low–ash carbon and a He/CO_2 stream containing different concentrations of CO_2 (25-100 vol% CO_2). Increasing the CO_2 concentration from 25 to 75 vol% caused an improvement in the fuel cell performance of nearly 71%, which corresponded to maximum power density of 69 mW/cm^2. The improvement on the fuel cell performance in the presence of higher CO_2 concentrations could result from electrochemical oxidation of CO produced by gasification reactions of the low–ash carbon and CO_2 (i.e., Boudouard reaction, $C + CO_2 \rightarrow 2CO$). The extent of the low–ash carbon gasification reactions, and their impact on the fuel cell energy efficiency will be further investigated in future studies.

Testing experiments demonstrated that Cu-Ni/YSZ anodes prepared by the electroless deposition of Cu onto Ni/YSZ anodes possess high electrochemical oxidation activity and resistance to deactivation by sulfur containing species. Figure 4 shows a plot of current density as a function of time for a Cu-Ni/YSZ and a Ni/YSZ anode fuel cell exposed to a CH_4/He stream (100 sccm, 50 vol% CH_4) before and after addition of 1vol% SO_2. The Cu-Ni/YSZ anode fuel cell produced a current density output of 0.45 A/cm^2 in CH_4/He. Addition of 1 vol% SO_2 resulted in a gradual decrease in the current density output until reaching 0.39 A/cm^2 (13% decay) after 15 min of operation. Further exposure to SO_2 did not cause noticeable changes

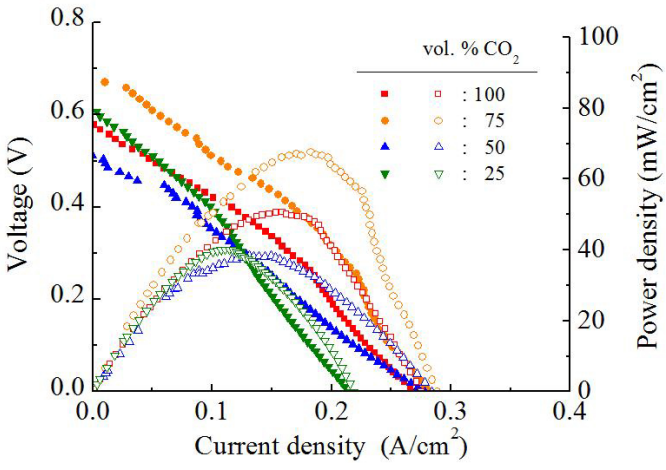


FIGURE 3. Voltage vs. current (closed symbols) and power vs. current (open symbols) characterisitcs of a Ni anode supported fuel cell at 750°C in 10 g of low–ash carbon and a He/CO_2.

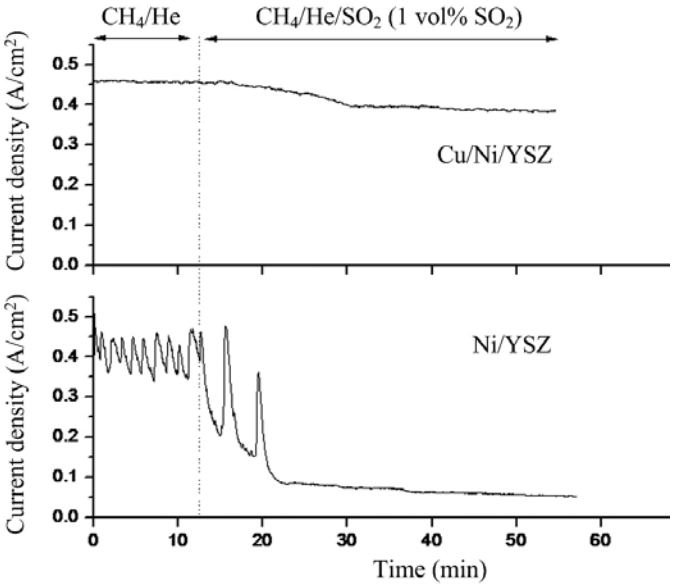


FIGURE 4. Current density as a function of time for a Cu-Ni/YSZ and a Ni/YSZ anode fuel cell exposed to a CH_4/He stream (100 sccm, 50 vol% CH_4) before and after addition of 1 vol% SO_2.

in current density output, manifesting the resistance of the Cu-Ni/YSZ anode to deactivation by sulfur poisoning. Exposure of the Ni/YSZ anode fuel cell to the CH_4/He stream produced a fluctuating current density output with an average close to 0.4 A/cm^2. The variation in the current density output could result from rapid formation of carbon deposits on the Ni/YSZ anode (i.e., coking). Addition of 1vol% SO_2 resulted in a rapid decay in the fuel cell current density output, reaching 0.04A/cm^2 (90% decay) after 8 min. XRD and XRF analysis of the Ni/YSZ fuel cells after the testing experiments (data not shown) revealed exposure to SO_2 resulted in formation of Ni_3S_2 on the anode surface. Formation of Ni_3S_2 on the Ni/YSZ anode fuel cell could reduce the number of sites available for reaction, resulting in significant losses in the fuel cell current density output. Unlike the Ni/YSZ anode, XRF and XRD spectra of the Cu-Ni/YSZ did not reveal the presence of sulfur-containing species. The absence of sulfur species could result from higher dissociation energy of sulfur species on Cu-Ni surfaces, as described in previous studies [5].

Conclusions and Future Directions

Studies conducted during fiscal year 2011 documented the effects of the chemical composition of solid carbon on the performance of the coal-based SOFC. Addition of CO_2 to Ni-based anode SOFCs was found to increase the gasification of carbon producing CO, which in turn can be electrochemically oxidized increasing the fuel cell power output. Electroless deposition of Cu onto Ni/YSZ anodes was found to improve the fuel cell resistance to sulfur containing species such as SO_2.

Future studies will focus on:

- Refining the composition, structure, and thickness of the anode catalyst to obtain higher current densities and improved resistance to deactivation.
- Evaluating the long-term anode and cathode catalyst durability.
- Improving a coal injection and fly-ash removal systems for continuous operation for the coal-based SOFC in solid carbon fuels.

FY 2011 Publications/Presentations

1. Guzman, F., Singh, R., Chuang, SSC., *Energy & Fuels*. **2011**, 25, 2179.

References

1. Zecevic, S.; Patton, E.M.; Parhami, P., *Carbon* **2004**, 42, (10), 1983.

2. Nabae, Y.; Pointon, K.D.; Irvine, J.T.S., *J. Electrochem. Soc.* **2009**, 156, (6), B716.

3. Singh, R.; Guzman, F.; Khatri, R.; Chuang, S.S.C., *Energy & Fuels.* **2010**, 24, (2), 1176.

4. Li, C.; Shi, Y.; Cai, N., J. *Power Sources* **2010**, 195, (15), 4660.

5. Galea, N.M.; Knapp, D.; Ziegler, T., *J. Catal.* **2007**, 247, (1), 20.

V.L.2 Alternate Fuel Cell Membranes for Energy Independence*

Robson F. Storey (Primary Contact),
Daniel A. Savin, Derek L. Patton
The University of Southern Mississippi
118 College Drive #5050
Hattiesburg, MS 39406
Phone: (601) 266 6298
E-mail: Robson.Storey@usm.edu;
laura.fosselman@usm.edu

DOE Managers
HQ: Dimitrios Papageorgopoulos
Phone: (202) 586-5463
E-mail: Dimitrios.Papageorgopoulos@ee.doe.gov
GO: David Peterson
Phone: (720) 356-1747
E-mail: David.Peterson@go.doe.gov

Contract Number: DE-FG36-08GO88106

Project Start Date: August 1, 2009
Project End Date: August 31, 2011

*Congressionally directed project

Fiscal Year (FY) 2011 Objectives

Molecular-morphological tailoring and evaluation of novel, low-cost hydrocarbon fuel cell membranes with high-temperature performance and long-term chemical/mechanical durability. This effort supports the Hydrogen Program stated in the Multi-Year Program Plan by developing high-temperature, low relative humidity (RH), high proton conductive membranes for use in polymer electrolyte membrane (PEM) fuel cells – focus is on alternative materials with performance up to 120°C at low RH.

- Synthesis of aromatic hydrocarbon polymers. Organic structure tailoring includes variation of linking moieties between aromatic groups, ion exchange density/distribution, molecular weight and block vs. random copolymers (Storey, Patton, Savin).
- Fundamental information regarding microstructure and physical properties and correlation using advanced characterization tools (Mauritz, Savin).
- Having identified superior materials and optimized membrane electrode assembly (MEA) processing, the nature/mechanisms of coupled chemical and mechanical degradation and morphological alteration investigated during accelerated ex situ degradation and PEM fuel cell testing (Mauritz).
- Mechanical/chemical/thermal stability of the membranes will be increased over a broad temperature-humidity range. MEAs fabricated from synthesized ionomers and tested for fuel cell performance and durability.
- Utilize synthesized proton-conducting block copolymers to produce films that exhibit nanophase-separated morphologies based on block composition; determine the relationship between proton conductivity and membrane morphology.

Technical Barriers

This project addresses the following technical barriers from the Fuel Cells section of the Fuel Cell Technologies Program Multi-Year Research, Development and Demonstration Plan:

(B) Cost
(C) Performance

Technical Targets

- Synthesize bisphenolic comonomers for poly(arylene-ether-sulfone) (PAES) that contain an ion-exchange moiety on a perfluoroalkyl chain tether. Polymerize new comonomers and study membrane conductivity, accelerated degradation, and fuel cell in situ properties. Reproduce known sulfonated poly(arylene-ether-sulfone) (sPAES) benchmark polymers and subject to identical testing. Compare our materials to performance standards established by the DOE.
- Investigate influence of annealing on macromolecular structure, chain dynamics and morphology.
- Knowledge of chemical and mechanical degradation mechanisms and their inter-relationship in membranes.

FY 2011 Accomplishments

- Verified polymer coupling via solution self-assembly (dynamic light scattering, DLS) and have begun to observe nanophase-separated morphologies in polymer films via atomic force microscopy (AFM) and transmission electron microscopy (TEM).
- Explored new coupling chemistries for reactions between perfluorinated polymers and other proton-conducting polymers, utilizing different functionalities to improve coupling efficiency and stability of linkage.



Introduction

The basic theme of the synthetic effort is the synthesis of aromatic hydrocarbon polymers of the poly(arylene ether sulfone) (PSf) or poly(arylene ether ketone) type, containing ion exchange groups tethered to the backbone via perfluorinated alkylene linkages. The implementation

of the 1-H-1,2,3-triazole into a PSf is an approach to create a proton exchange membrane that can operate at high temperatures and low humidity. Triazoles are amphiprotic charge carriers, e.g., moieties capable of serving both as proton donors and proton acceptors, so water is no longer necessary as a proton transport medium. Also, the fuel cell can operate at higher temperatures increasing the efficiency of the electrodes.

Traditionally, polymers have been blended for many years to create hybrid properties in a bulk material. Mixing polymers that are chemically/physically incompatible usually results in large, inconsistent phase segregation of each polymer within the bulk material. However, covalent linking of these incompatible polymers to create "diblock copolymers" results in materials with uniform microphase behavior (morphology) and the associated morphologies as a function of block composition ϕ_A and segregation strength χN for bulk coil-coil block copolymers. In our work, our intention was produce block copolymers containing a proton-conducting block and a perfluorinated propylene oxide (PFPO) polymer; the PFPO block is highly incompatible (strongly segregating) with the proton-conducting block leading to well-defined morphologies based on established criteria. By varying the composition of each respective block in the copolymer, we seek to produce a myriad of well-defined morphologies with long-range order (creating proton-conducting channels) and develop a relationship between membrane morphology and proton conductivity. Phase behavior of block copolymers will be mapped vs. block composition using TEM, AFM and small angle X-ray scattering (SAXS). Synthesized materials will be characterized for proton conductivity and mechanical/chemical/thermal stability over broad temperature and RH ranges using a variety of spectroscopic, dielectric, microscopic and viscoelastic methods and evaluated for fuel cell performance.

Approach

In the past year, new structural variations were examined with the aim of providing improved morphological connectivity of ion exchange groups within the bulk membrane material. These approaches included synthesis of hydrophilic/hydrophobic multi-block copolymers, new ion-containing comonomers with a longer tether length, and new hydrophobic comonomers.

A 1-H-1,2,3-triazole tethered PSf has the potential to eliminate a lot of issues associated with the current PEM material. The 1-H-1,2,3-triazole can be achieved through a copper-catalyzed 1,3-dipolar cycloaddition of an alkyne with azidomethyl pivalate to give the terminal N-protected triazole. Further synthesis can afford a 4-bromophenol functionalized triazole followed by a C-H activation and Suzuki-Miyaura reaction onto the PSf backbone.

For block copolymer synthesis, our interests lie in determining factors that affect bulk morphology, water content, and ion exchange capacity in block copolymers composed of PFPO and a proton-conducting block. We synthesize a variety of polymers with varying composition to map the phase behavior of PFPO-based/proton-conducting block copolymers. Successful synthesis of block copolymers will be confirmed by NMR and DLS. Solutions of the synthesized block copolymers will then be cast and annealed to make films, whereby the films will be characterized in terms of morphology by AFM, TEM, and SAXS. Lastly, we will determine ion exchange capacity and water uptake.

Results

PAES multi-block copolymers were prepared from hydrophilic and hydrophobic prepolymers. Prepolymers were synthesized by reaction of the new ion-containing comonomer, N,N-diisopropylethylammonium 2,2-*bis*(p-hydroxyphenyl)pentafluoropropanesulfonate (HPPS) (see Figure 1), with bis-(4-fluorophenyl) sulfone (FPS), and biphenol (BP) with FPS, respectively. Prepolymers and multi-block copolymers were prepared at 180°C in N,N-dimethylacetamide in the presence of K_2CO_3. The prepolymers were reacted overnight; the multi-block copolymers were reacted only 80 min to minimize transetherification. ^{19}F NMR provided molecular weight of hydrophilic prepolymers bearing aryl fluoride end groups. Gel permeation chromatography was used to characterize the multi-block copolymers. Copolymer block lengths were determined by quantifying ^{13}C NMR peak areas of quaternary carbon atoms adjacent to sulfur in FPS moieties. Hydrophilic and hydrophobic block lengths were in the range 9.4-23.4 and 4.4-11.8 repeating units, respectively. AFM

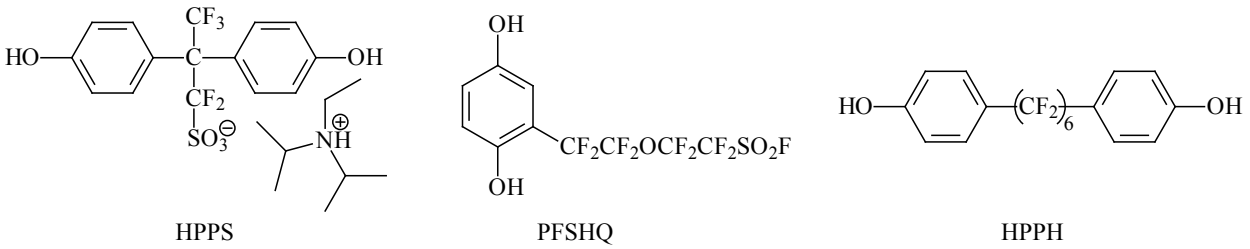


FIGURE 1. Three New Monomers for Ion-Containing PAES

showed phase separation for all block lengths. Conductivity at 80°C and 100% RH ranged from 6.2–34.3 mS/cm, with the best value obtained for hydrophilic/hydrophobic block lengths of 13.3/6.0.

Performance of HPPS-containing PAES were disappointing, and it was hypothesized that the tether element was too short. Thus, a new ion-containing bisphenolic monomer incorporating a longer tether, 2-(5-fluorosulfonyl-3-oxaoctafluoropentyl)-1,4-dihydroxybenzene (PFSHQ) (see Figure 1), was synthesized in two steps from 1,4-dimethoxybenzene and the tether element, 5-iodooctafluoro-3-oxapentanesulfonyl fluoride. Purified yield for the first step was low (12%); purified yield of the second step was 64%. The structure of the monomer (potassium sulfonate form) was proven by NMR and mass spectrometries. Gram quantities of the new monomer were produced, and used in an attempted synthesis of a new poly(arylene ether sulfone) polymer; however, a crosslinked product resulted.

Synthesis of a new hydrophobic monomer, 1,6-di(4-hydroxyl)phenylperfluorohexane (HPPH) (see Figure 1), was accomplished using a copper coupling reaction between 2 eq of 4-iodophenol and 1 eq of 1,6-diiodoperfluorohexane. The yield was 56%, the structure was confirmed by NMR spectroscopy. Copolymerization of HPPH with 3,3′-disulfonate-4,4′-difluorodiphenylsulfone in the presence of K_2CO_3, however, resulting only in homopolymerization of HPPH to yield an insoluble polymer (assumed to be crosslinked). The failure of both PFSHQ and HPPH in nucleophilic aromatic substitution polymerization is apparently due to attachment of a CF_2 moiety directly to the aromatic ring. In contrast, HPPS polymerizes in a very predictable fashion.

The synthesis of triazole-functionalized polymers followed Figure 2. The rigidity of the PSf backbone limits the mobility of the mobility of the triazoles and decreases its charge transfer capabilities even at a concentration of triazoles of one per repeat unit. The stiffness of the backbone also limits the ability of the material to undergo phase separation to create channels for the protons to travel through.

Initially, our work establishing efficient coupling strategies of acid chloride-functional PFPO with hydroxyl-functional poly(styrene) was centered around direct coupling of the two blocks. The challenges here were to determine proper solvent/solvent mixtures, reaction temperatures, concentrations, etc., to effectively produce block copolymers. The DLS results confirm (1) successful polystyrene (PS)-b-PFPO (SF) copolymer formation and (2) aggregate size in methanol after sulfonation of the PS blocks thereby forming sulfonated-PS-b-PFPO (sSF) block copolymers. Figure 3 presents an AFM phase image for SF 5-4 (~55 wt% polystrene). This image suggests cylindrical formation with domain sizes of approximately 10 nm. The aggregate size in tetrahydrofuran illustrates efficient synthesis of SF block copolymers; however, after sulfonation,the aggregate sizes are extremely small. This suggests that scission is possibly occurring between PS and PFPO which seems to be a likely occurrence since the two blocks are connected by an ester linkage (susceptible to hydrolysis).

Further work has persisted on (1) modifying the functionality of PFPO-COOH to facilitate efficient coupling with proton-conducting blocks (i.e. PAES) and (2) attempted coupling reactions of modified PFPO with hydroxyl-terminated PAES to yield stable, robust linkages. PFPO chain end modification was performed by reacting PFPO-COOH with diamino halide compounds to form benzimidazole groups. We attempted nucleophilic aromatic substitution coupling with hydroxyl-terminated PAES. Encouragingly, we were able to make a homogenous solution in hexafluoroisopropanol, and the reaction was allowed to react for 1 day at 120 °C. We are currently performing light scattering and NMR experiments to confirm to product of the reaction, and we note that the reaction yielded a product with a color (reddish) different from the two reactants.

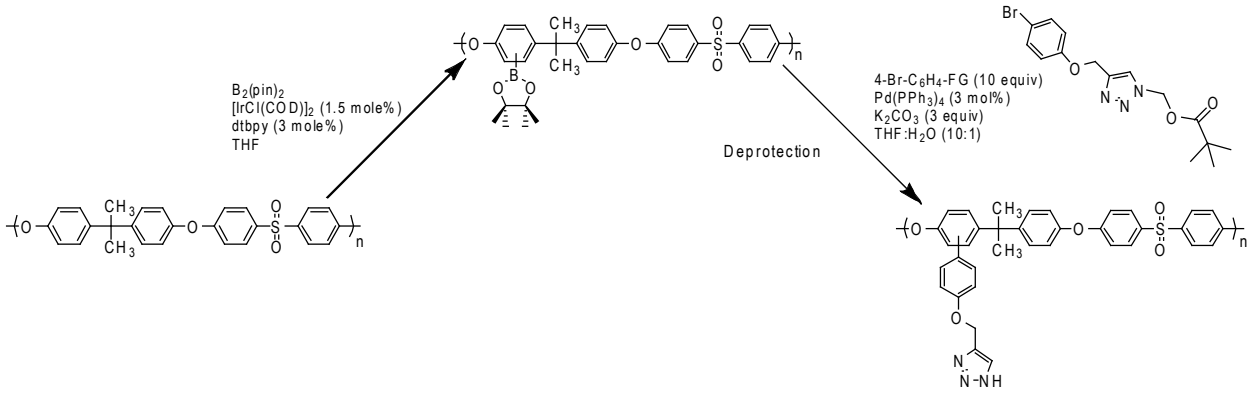


FIGURE 2. Functionalization of Aromatic Rings of Polysulfone through C-H Activation and Suzuki-Miyaura Reaction followed by Deprotection under Basic Conditions

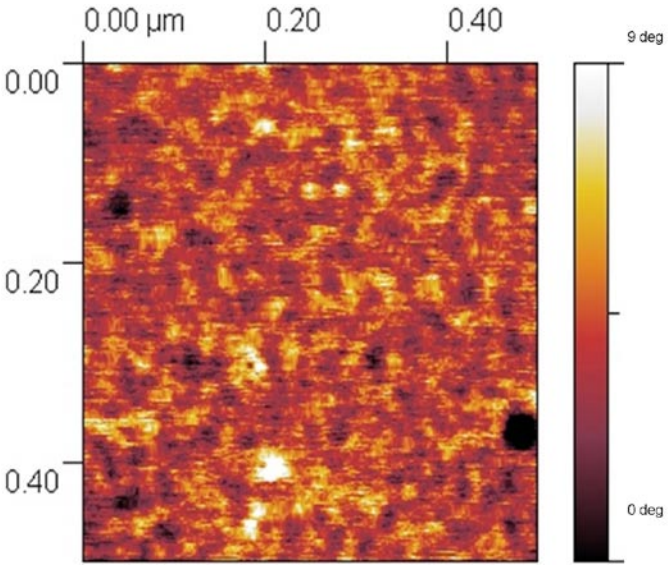


FIGURE 3. AFM Phase Image of a 50 mg/mL $PFPO_{4K}$-PS_{5K} Spin-Cast from a solution of 80% Trifluorotoluene and 20% Methoxynonafluorobutane

Mechanically robust membranes were prepared by blending the triazole-PSf and phosphonic acid PSf. However, preliminary conductivity measurements show the films exhibit low conductivity at 120°C. Triazole-PSf membrane films were also doped with phosphoric acid to improve their conductivity at high temperatures. However, conductivities at 120°C for the films were very low at over the range of RH. The reason for low conductivity is thought to be the –NH groups of the triazole tether is not accessible to H_3PO_4 or phosphonic acid groups. Efforts are now in progress to prepare and test PSf backbone with higher concentrations of tethered triazole (Figure 4).

Conclusions and Future Directions

- The single tethered triazoles are limited due to the rigidity of the PSf backbone.
- A higher concentration of triazoles will allow for better phase separation to occur and can be achieved by growing triazole based monomers from a chloromethalated PSf backbone via atom transfer radical polymerization.
- Produce films of synthesized block copolymers and study the nanophase-separated behavior (due to the coupling producing triblock copolymers, we can exploit the block composition to produce even more morphologies than we see with diblock copolymers).
- Coupling of PFPO-bzimF with hydroxyl-functional PAES that has a higher degree of sulfonation (higher hydrophilicity and introduction of proton conductivity).

FY 2011 Publications/Presentations

Publications

1. Li, H.; Jackson, A.B.; Kirk, N.J.; Mauritz, K.A.; Storey, R.F. "Poly(arylene ether sulfone) Statistical Copolymers Bearing Perfluoroalkylsulfonic Acid Moieties" *Macromolecules* **2011**, *44*(4), 694–702.

2. Li, H.; Kirk, N.J.; Mauritz, K.A.; Storey, R.F. "Poly(arylene ether sulfone) Multi-Block Copolymers Bearing Perfluoroalkylsulfonic Acid Groups" *Polymer*, **2011**, DOI: 10.1016/j.polymer.2011.05.057.

3. Nalawade, A.; Hassan, M.K.; Mauritz, K.A.; Litt, M.H. *ACS Preprints, Div. Fuel Chem.* **2010**, *55 (2)*, 243. "Broadband Dielectric Spectroscopy Studies of Instrument - in situ Annealed Poly (2,5- benzimidazole) Membrane Materials."

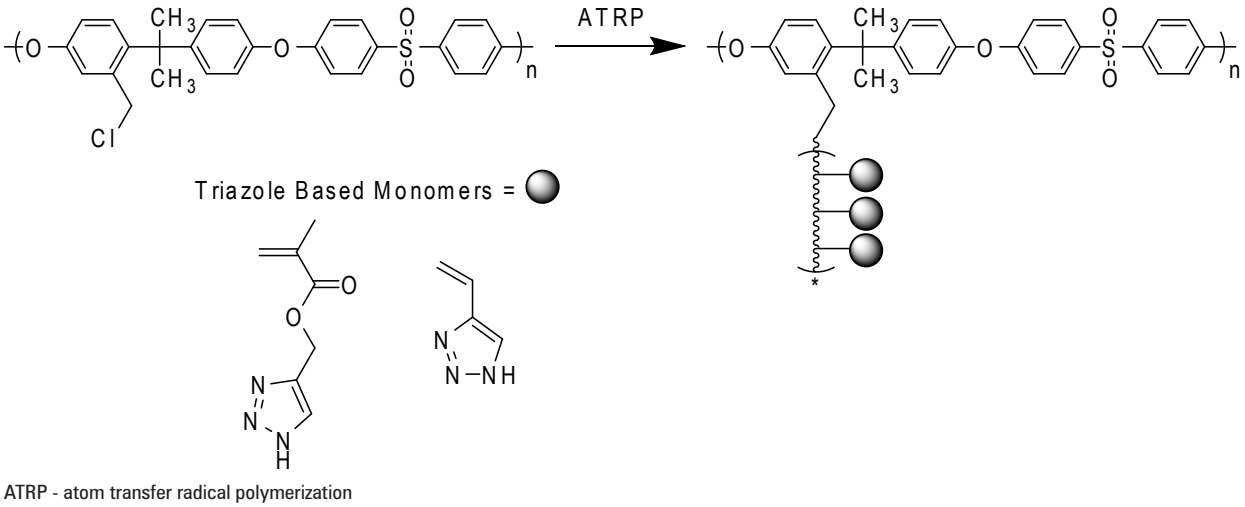


FIGURE 4. Polymerization of Triazole-Based Vinyl Monomers off of a Chloromethalated PSf Backbone via Atom Transfer Radical Polymerization

4. Nalawade, A.; Hassan, M.K.; Jarrett, W.A.; Mauritz, K.A.; Litt, M.H. "Broadband Dielectric Spectroscopy Studies of Glassy State Relaxations in Annealed Poly (2,5-benzimidazole)", **Accepted**, *Polymer International.*

5. Analysis of Macromolecular and Proton Motions in Fuel Cell Membranes using Dielectric Spectroscopy. Mohammad K. Hassan, Amol Nalawade, and Kenneth A. Mauritz, Polymer Preprints **2011**, ACS Preprint Website.

6. Mauritz, K.A.; Nalawade, A.; Hassan, M.K. "Proton Exchange Membranes for H_2 Fuel Cells Applications"; Submitted to the book "Sol-Gel Processing for Conventional and Alternative Energy"; Klein, L.C. et al., Editor, Springer, 2011.

Presentations

1. Amol Nalawade, "Broadband Dielectric Spectroscopy Studies of Instrument - in situ Annealed Poly (2,5- benzimidazole) Membrane Materials", Oral talk, 240th ACS National Meeting: Fuel Chem. Division, August 22–26, 2010, Boston, Massachusetts.

2. Amol Nalawade, "Analysis of Macromolecular and Proton Motions in Fuel Cell Membranes using Dielectric Spectroscopy", Poster, 241th ACS National Meeting: Polymer Chemistry Division, March 27–31, 2011, Anaheim, California.

V.L.3 Extended Durability Testing of an External Fuel Processor for SOFCs*

Mark Perna (Primary Contact), Anant Upadhyayula
Rolls-Royce Fuel Cell Systems (US) Inc.
6065 Strip Avenue NW
North Canton, OH 44720
Phone: (330) 491-4830
E-mail: Mark.Perna@RRFCS.com

DOE Managers
HQ: Dimitrios Papageorgopoulos
Phone: (202) 586-5463
E-mail: Dimitrios.Papageorgopoulos@ee.doe.gov
GO: Jesse Adams
Phone: (720) 356-1421
E-mail: Jesse.Adams@go.doe.gov

Contract Number: DE-FG36-08GO88113

Project Start Date: August 1, 2008
Project End Date: June 30, 2012

*Congressionally directed project

Fiscal Year (FY) 2011 Objectives

The main goal of this project is to perform extended durability testing of the external fuel processor (EFP) for a one megawatt (MWe) solid oxide fuel cell (SOFC) power plant concept being developed by Rolls-Royce Fuel Cell Systems (US) Inc. (RRFCS). The specific objectives are to:

- Conduct long-term tests in relevant environments for the three EFP subsystems that support operation of a 1-MWe SOFC power plant. The subsystems include:
  - Synthesis-gas subsystem
  - Start-gas subsystem
  - Desulfurizer subsystem
- Determine long-term performance of key components such as catalysts, sorbents, heat exchangers, control valves, reactors, piping, and insulation.
- Evaluate the impact of ambient temperatures (hot and cold environment) on performance and component reliability.
- Determine system response for transient operation.

Technical Barriers

This project addresses the following technical barriers from the Fuel Cells section of the Fuel Cell Technologies Program Multi-Year Research, Development and Demonstration Plan:

(A) Durability
(C) Performance
(G) Start-Up and Shut-Down Time and Energy/Transient Operation

These barriers will be addressed as they relate to the three external fuel processor subsystems.

Technical Targets

This project addresses milestone 59 in the Fuel Cells section of the Fuel Cell Technologies Program Multi-Year Research, Development and Demonstration (RD&D) Plan. Milestone 59 is to "evaluate fuel processing subsystem performance for distributed generation against system targets for 2011." These targets will be addressed as they relate to durability, performance (gas quality) and transient response of the EFP subsystems. Table 1 shows the technical targets for the project.

TABLE 1. Technical Targets

Characteristic	Units	2005 Status	DOE 2011 Targets	RRFCS 2011 Targets
Cold start-up time to full load @ -20°C ambient	**minutes**	**< 90**	**< 30**	**60**
Transient response (10 to 90% load) Load rate of change	**Minutes (% per min)**	**< 5 (16)**	**1 (80)**	**2 (40)**
Durability	**hours**	**20,000**	**40,000**	**8,000**
Survivability (min and max ambient temperature)	**°C °C**	**-25 +40**	**-35 +40**	**-40 +40**
Sulfur content in product stream	**ppbv (dry)**	**< 10**	**< 4**	**< 100**

FY 2011 Accomplishments

- Prepared samples from the post-test inspection of synthesis gas subsystem for analysis.
- Completed commissioning of the desulfurizer subsystem.
- Completed 4,649 hours of the 8,000-hr desulfurizer subsystem durability test.
- Commissioned mechanical and electrical hardware for the start-gas subsystem.
- Started commissioning of the control system software for the start-gas subsystem.



Introduction

RRFCS is developing a 1-MWe SOFC power plant for stationary power application. An integral part of the SOFC power plant is the EFP. It uses pipeline natural gas and compressed air to generate all the gas streams required by the SOFC power plant for start-up/shut-down (non-flammable reducing gas referred to as start gas), low-load operation (synthesis gas) and normal operation (desulfurized natural gas). Thus it eliminates the need for on-site storage of high-pressure, bottled gases such as nitrogen and hydrogen.

Approach

The approach for this project is to conduct durability tests in relevant environments using full-scale components for the EFP of a 1-MWe SOFC power plant. The components were designed and built as part of another project and made available for the durability testing. An outdoor test facility was constructed as part of a third project so that the EFP could be tested under hot- and cold-weather conditions that would be expected for a 1-MWe SOFC power plant operating in northeast Ohio. Figure 1 shows a photograph of the EFP desulfurizer subsystem under test in February 2011 in the outdoor test facility.

The durability testing includes:

- Synthesis-gas subsystem testing for multiple start-ups and 1,000 hours of operation in a heated, indoor enclosure. This subsystem is used only during low-load operation of the SOFC to balance the thermal input and is required to operate for only a few hundred hours per year. Therefore the 1,000-hour test will simulate a 5-year service life.
- Start-gas subsystem testing for multiple start-ups and 1,000 hours of operation in an outdoor (hot and cold) environment. This subsystem is used only during start-up and shut-down of the SOFC and is required to operate for only a few hundred hours per year. Therefore the 1,000-hour test will simulate a 5-year service life.



FIGURE 1. Desulfurizer Subsystem Being Tested in the Outdoor Test Facility (-23°C)

- Desulfurizer subsystem testing for 8,000 hours in an outdoor (hot and cold) environment. This subsystem operates whenever the SOFC is making power therefore it is expected to operate for much longer periods compared to the other two subsystems. The 8,000-hour test represents the time period between yearly maintenance intervals.

After completing the durability tests, post-test analyses of the hardware will be performed. Subsystem components (catalysts, sorbents, piping, reactors, insulation, valves, heaters, heat exchangers, nitrogen membrane, etc.) will be inspected for deposits, signs of wear, damage, corrosion, and erosion. Physical and chemical analyses will be performed on components as required.

The durability tests will demonstrate that the EFP subsystems are ready for a full-scale SOFC system demonstration.

Results for 2011

Synthesis-Gas Subsystem

The synthesis-gas subsystem was disassembled after completion of the 1,000-hour durability test. The catalyst was removed from the reactor and samples were submitted for chemical and physical analyses. Small samples of the subsystem's metal components were prepared for chemical and physical analyses to quantify metal loss and corrosion. Results from these analyses had not been received by the time of this report.

Desulfurizer Subsystem

The desulfurizer subsystem was the second of the three subsystems to be tested. It generates pressurized, desulfurized natural gas (DNG) from high-pressure pipeline natural gas. The RRFCS target for maximum allowable sulfur level in the DNG is 100 parts per billion (ppb) on a volume basis.

The software packages for the desulfurizer subsystem's control and safety systems were commissioned and verified for automatic operation. This enables unattended operation to support long-term (8,000-hr) durability testing. The desulfurizer subsystem is being operated in the outdoor test facility to determine the impact of ambient temperature on start-up and system operation. The testing also determined the transient response to load changes and subsystem durability.

The desulfurizer subsystem uses a natural gas burner to provide warm gas (300°C) to heat up the sorbent beds for start-up. The heat-up from 20°C required about 12 hours. This time increased to 27 hours when the heat-up was performed at -23°C, the coldest temperature recorded through the winter season at the outdoor test facility in North Canton, Ohio. The heat-up time at the very cold condition was longer than desired. The procedure for desulfurizer subsystem heat-up is being modified to reduce the time required to heat up from very cold conditions.

Once the sorbent was at temperature, it was maintained in a standby state using electric heaters. When in the standby state, gas flows were initiated for start up of the desulfurizer subsystem. Start-ups were performed at ambient temperatures ranging from -23 to 30°C. The start-up time required to begin producing DNG typically ranged from 56 to 74 minutes for these temperatures. These results were considered acceptable by RRFCS.

The transient response for the desulfurizer subsystem was tested over a load change from 10% to 40% of the design DNG flow rate. The upper range used for the load change was limited by the natural gas compressor and not the desulfurizer subsystem. The time required by the desulfurizer subsystem for the load change was 25 seconds. This gives a load rate of change of 72% per minute. This exceeded the RRFCS target of 40% per minute. The plots

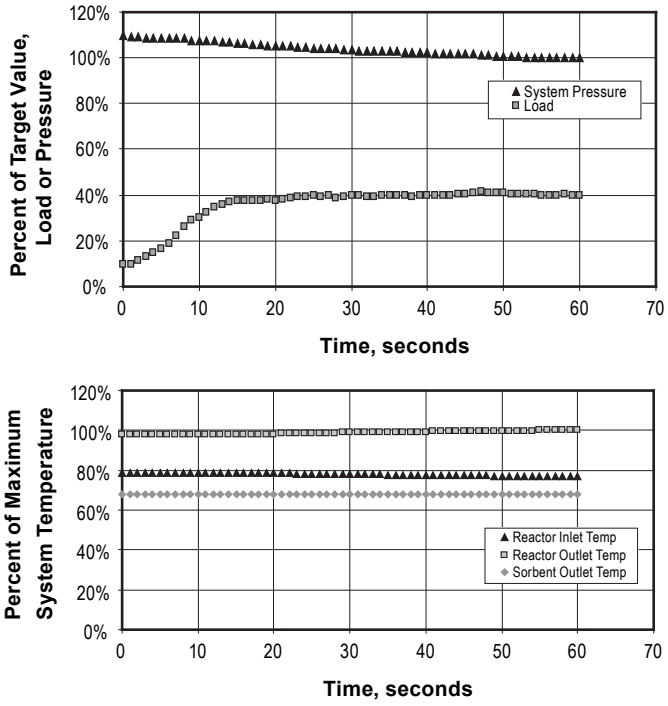


FIGURE 2. Desulfurizer Subsystem's Transient Response to Load Change

in Figure 2 show the load change as a function of time along with the response of the system pressure and temperatures. The pressure declined slightly at the higher load while the temperatures remain fairly constant. All the process variables showed a well controlled response to the rapid change in load.

The desulfurizer subsystem has been operating over the past eight months. It had logged a total of 4,649 hours on stream by the beginning of June 2011. The subsystem has maintained the sulfur level in the DNG to less than 10 ppb (the lower detection limit of the on-line sulfur analyzer) for the vast majority of the durability test period. This was lower than the RRFCS target of 100 ppb. The subsystem has successfully endured four trips due to auxiliary system failures (natural gas compressor, flare stack, and site power) and also has undergone two planned shutdowns to remove test-coupon samples. The plot in Figure 3 shows the sulfur level and the total hydrocarbons in the DNG leaving the desulfurizer subsystem. A small fraction of the hydrocarbons in the natural gas feed are converted into carbon dioxide and water to provide the heat required to support the desulfurization process.

The desulfurizer subsystem continues to operate and is expected to achieve the 8,000-hour durability target by mid-November (2011).

Start-Gas Subsystem

The mechanical and electrical commissioning for the start-gas subsystem has been completed. The operation of

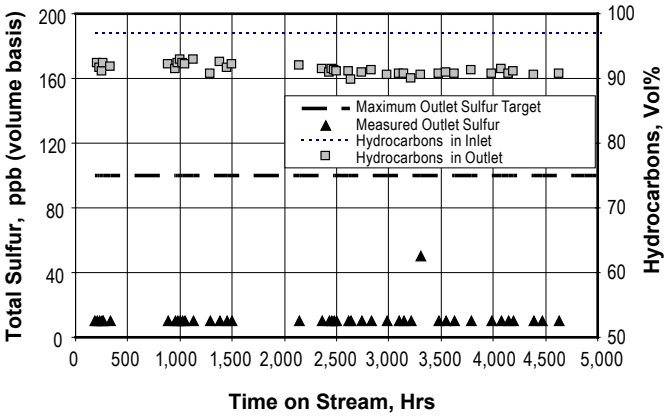


FIGURE 3. Sulfur Level and Total Hydrocarbons in Desulfurized Natural Gas

all control and safety system hardware was verified. Work continues on commissioning the control system software to allow automatic operation. Automatic operation of the start-gas subsystem had not been achieved by the time of this report. However, the subsystem was successfully started and operated at the full load condition in the manual mode of operation.

Conclusions

The desulfurizer subsystem durability testing has logged 4,649 hours of the planned 8,000- hour test. It is working well with test results showing that performance is meeting or exceeding RRFCS requirements:

- Transient response (load rate of change) was 72% per minute.
- Sulfur level was less than 10 ppb.
- Start-up times ranged from 56 minutes to 74 minutes for ambient temperatures ranging from -23 to 30°C.

The start-gas subsystem is ready for final commissioning activities. Once they are completed, durability testing will begin.

Future Directions

2011

- Complete commissioning of control system software for the start-gas subsystem (fourth quarter 2011).
- Complete the 8,000-hour desulfurizer subsystem durability test (fourth quarter 2011).

2012

- Begin durability testing of start-subsystem (first quarter 2012).
- Reduce heat-up time at cold conditions for desulfurizer subsystem (first quarter 2012).
- Complete durability testing of start-gas subsystem (second quarter 2012).
- Complete inspections of start-gas and desulfurizer subsystems (second quarter 2012).
- Issue final report for project (second quarter 2012).

FY 2011 Publications/Presentations

1. Presentation at 2011 Hydrogen Program Annual Merit Review and Peer Evaluation Meeting in Arlington, Virginia by A. Upadhyayula on May 20, 2011.

2. Presentation at Fuel Cell Seminar & Exposition 2010 in San Antonio, Texas by M. Perna on October 20, 2010.

V.L.4 Hydrogen Fuel Cell Development in Columbia (SC)*

Ken Reifsnider (Primary Contact), F. Chen, B. Popov, J. Van Zee, W. Chao, C. Xue
University of South Carolina
300 Main Street
Columbia, SC 29208
Phone: (803) 777-0084
E-mail: Reifsnider@cec.sc.edu

DOE Managers
HQ: Dimitrios Papageorgopoulos
Phone: (202) 586-5463
E-mail: Dimitrios.Papageorgopoulos@ee.doe.gov
GO: Reg Tyler
Phone: (720) 356-1805
E-mail: Reginald.Tyler@go.doe.gov

Contract Number: DE-FG36-08GO88116

Project Start Date: July 31, 2008
Project End Date: July 31, 2011

*Congressionally directed project

Fiscal Year (FY) 2011 Objectives

- Development of metal-free oxygen reduction catalysts to reduce cost, facilitate manufacturing, and enhance durability of fuel cells (Barriers A-C; Task 2-electrodes)
- Development of redox stable mixed ionic and electronic conductors for bi-electrode supported cell (BSC) symmetrical solid oxide fuel cell (SOFC) designs, to reduce cost by simplifying manufacturing, enhance durability, and greatly reduce sensitivity to thermal cycling (Barriers A-C,G; Tasks 8-portable power, 11-innovative fuel cells, 10-long term failure mechanisms)
- Development of durable, low cost seals for polymer electrolyte membrane (PEM) stacks, through the establishment of laboratory characterization methodologies that relate to cell/stack performance (Barriers A, C; Task 6-seals)
- Development of understandings and methodologies to establish hydrogen quality as it relates to PEM cell applications for transportation needs (Barriers B,C,G; Tasks 9-models for impurities, 8-portable operation)
- Development of a first principles multiphysics durability models based on interpretations of electrochemical impedance spectroscopy (EIS) data that link the multiphysics processes, the microstructure, and the material states, with cell impedance responses and global performance, mechanistically, as a foundation for engineering durability during design and manufacture of fuel cells (Barriers A-G; Tasks 9-models, 10-long term failure mechanisms, 11-innovative fuel cell design and manufacture)

Technical Barriers

This project addresses the following technical barriers from the Fuel Cells section of the Hydrogen, Fuel Cells and Infrastructure Technologies Program Multi-Year Research, Development and Demonstration Plan:

(A) Cost
(B) Durability
(C) Performance
(D) Water Transport within the Stack
(E) System Thermal and Water Management
(F) Air Management
(G) Start-up and Shut-down Time and Energy/Transient Operation

Technical Targets

Carbon-based catalysts: To develop non-precious-metal catalysts for PEM fuel cells with high selectivity and durability which perform as well as conventional Pt catalysts with a cost of at least 50% less than the target of 0.2 g (Pt loading)/peak kW.

SOFC materials: Develop SOFC electrode materials that enable direct operation on hydrocarbon fuels.

Low-cost seals: Determine PEM seals materials that have no appreciable weight loss or leachants over a 60-week test period.

Hydrogen contamination: Establish the rate and mechanism of NH_3 transport in PEM cells over a 60-week period; identify the species of sulfur contamination on Pt catalysts in the presence of various gas species, e.g., H_2O and O_2.

Multiphysics-based durability modeling: Use impedance spectroscopy to identify specific material state change driven degradation mechanisms during SOFC operation.

FY 2011 Accomplishments

- Metal-free oxygen reduction catalysts have been developed to reduce cost, facilitate manufacturing, and enhance durability of PEM fuel cells.
- Redox stable mixed ionic and electronic conductors for BSC symmetrical (and other) SOFC designs have been developed (completed 2010).
- The development of durable, low cost seals for PEM stacks, through the establishment of laboratory characterization methodologies that relate to cell/stack performance.
- Understandings and methodologies have been developed to enable the establishment of hydrogen

quality as it relates to PEM cell applications for transportation needs (completed 2010).
- First principles multiphysics durability models based on interpretations of EIS data have been developed that form a foundation for engineering durability during design and manufacture of BSC SOFC fuel cell designs (completed 2010).



Introduction

The activities of the present project are contributing to the goals and objectives of the Fuel Cell element of the Hydrogen, Fuel Cells and Infrastructure Technologies Program of the Department of Energy through five sub-projects. Three of these sub-projects have focused on PEM cells, addressing the creation of carbon-based metal-free catalysts, the development of durable seals, and an effort to understand contaminant adsorption/reaction/transport/performance relationships at low contaminant levels in PEM cells. Two sub-projects addressed barriers in SOFCs: an effort to create a new symmetrical and direct hydrocarbon fuel SOFC designs with greatly increased durability, efficiency, and ease of manufacturing; and an effort to create a multiphysics engineering durability model based on EIS interpretations that associate the micro-details of how a fuel cell is made and their history of (individual) use with specific prognosis for long term performance, resulting in attendant reductions in design, manufacturing, and maintenance costs and increases in reliability and durability.

Approach

- Work on a previous DOE project, DE-FC36-03GO13108, was leveraged to create new carbon-based, metal-free catalysts for oxygen reduction.
- Develop new materials and material designs to create a high performance SOFC that can directly operate on hydrocarbon fuels with high power density.
- Recent advances at the University of South Carolina in controlled hydration and temperature characterization of polymer-based materials were used to establish a methodology for characterization of materials in seals in PEM stacks, and to develop a fundamental understanding how the degradation mechanisms of polymeric materials affects the performance and life of gasket/seals in PEM fuel cells.
- On-going work with the National Renewable Energy Laboratory, Argonne National Laboratory, Savannah River National Laboratory, and Los Alamos National Laboratory formed a foundation for the work on developing an understanding of the contaminant adsorption/reaction/transport/performance relationships at low contaminant levels in PEM cells. The study provided equilibrium and rate constants suitable for use in new and existing models, and in computer codes at Argonne National Laboratory.
- Conceptual foundations laid by research supported by the National Science Foundation, the Air Force Office of Scientific Research and several industries including United Technologies Fuel Cells were expanded to create a multiphysics engineering durability model based on electrochemical impedance spectroscopy interpretations that associate the micro-details of how SOFC fuel cells are made and their history of individual use with long term performance, to achieve reductions in design, manufacturing and operating costs.

Results

Only one example of salient results is presented in the limited space available here. Other results appear in the quarterly reports.

Project 1. Development of Carbon Composite Electro Catalyst for the Oxygen Reduction Reaction (ORR) – Dr. Branko Popov

Objectives

- Synthesize carbon-based metal-free catalysts and carbon composite catalysts for ORR.
- Optimize catalytic active reaction sites as a function of carbon support, surface oxygen groups, nitrogen content, surface modifiers, pyrolysis temperature and porosity.

Technical Barriers

This project addresses the following technical barriers from the Fuel Cells section of the Hydrogen, Fuel Cells and Infrastructure Technologies Program Multi-Year Research, Development and Demonstration Plan:

(A) Cost
(B) Durability
(C) Performance

Technical Targets

- Non-Pt catalyst activity per volume of supported catalyst >130 A cm^{-3} (stack) at 0.8 internal resistance (iR_{free}).
- Cost: at least 50% less than a target of 0.2 g (Pt loading)/peak kW.

- Durability: >2,000 h operation with less than 10% power degradation.

Accomplishments

- The non-precious metal catalysts (NPMCs) with the exceptional activity and stability for oxygen reduction in alkaline electrolyte are developed by introducing N-based active sites.
- The pyridinic-N and graphitic-N are believed to play important roles in the active sites of NPMCs.
- The NPMCs shows comparable performance with Pt/C in alkaline fuel cells with the open circuit potential of 0.97 V and maximum power density of 177 mW cm^{-2}.

✧ ✧ ✧ ✧ ✧

Introduction

Pt and Pt-based alloy catalysts are widely used in PEM fuel cells because of their high catalytic activity and selectivity as well as high corrosion resistance. In the last few years, several transition metal compounds such as macrocycle-based metal porphyrin system, chevrel phase-type compounds and other transition metal chalcogenides have been proposed as selective catalysts for ORR. However, significant increase in activity and stability of the catalyst is still essential for PEM fuel cell applications. The goal of this project is to develop highly active and stable carbon-based metal-free catalysts and carbon composite catalysts with strong Lewis basicity (π electron delocalization) to facilitate ORR.

We have systematically studied the activity and stability, as well as the nature of active sites of NPMCs for the ORR. In this work, the NPMC with high activity and stability in alkaline electrolyte was developed. The fuel cell performance of the catalyst was studied using an anion exchange membrane fuel cell.

Approach

The approach used to synthesize the catalyst includes the following steps: (i) the modification of a porous carbon black support; (ii) the deposition of Co-N or Co-Fe-N chelate complex on the support; (iii) the first high-temperature pyrolysis; (iv) the chemical post-treatment (acid leaching); and (v) the second high-temperature pyrolysis.

Results

Figure 1a shows polarization curves for oxygen reduction of NPMC heat-treated at 900°C (NPMC-900 or CoFeN/C-HLH) before and after potential cycling in 0.1 M KOH. The cycling was performed in N_2-saturated 0.1 M KOH with a scan rate of 10 mV s^{-1} between 0.8-1.2 V vs. the reference hydrogen electrode. The polarization curves

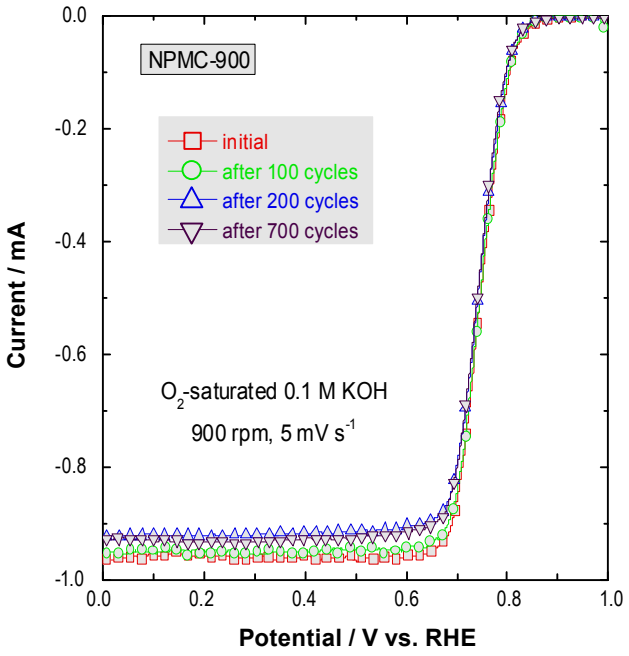


FIGURE 1A. Polarization curves for the oxygen reduction reaction in O_2-saturated 0.1 M KOH of NPMC heat-treated at 900°C before and after the potential cycling stability test; scan rate: 5 mV s^{-1}; rotation rate: 900 rpm.

were measured before and after 100, 200, and 700 cycles, respectively. It is evident that the NPMC-900 catalyst does not show any performance degradation during 700 cycles indicating that the catalyst is very stable in alkaline solution.

Figure 1b shows the X-ray photoelectron spectroscopy (XPS) spectra of N_{1s} for the NPMC-900 before and after the potential cycling stability test in 0.1 M KOH. The peaks of N_{1s} at 398.6 ± 0.3 eV, 401.3 ± 0.3 eV, and 403.3 ± 0.3 eV can be attributed to the pyridinic-N, graphitic-N, and pyridine-N-oxide, respectively. The pyridinic-N and graphitic-N are believed to be active catalytic sites for oxygen reduction. As shown in Figure 1b, the profile of the N_{1s} spectra of NPMC-900 is still similar to that of fresh catalyst indicating high stability of NPMC for oxygen reduction in alkaline electrolytes.

The kinetic parameters for oxygen reduction reaction on CoFeN/C subject to heat-treatment, leaching, and re-heat-treatment (CoFeN/C-HLH) and Pt/C catalysts including the ring currents, the numbers of electron exchanged and polarization curves were obtained using a rotating ring disc electrode (RRDE) system in O_2-saturated 0.1 M KOH. Figure 2 summarizes the RRDE results. The data of carbon black are also presented for comparison. The ring currents were measured on a Pt ring electrode held at 1.2 V for CoFeN/C-HLH and Pt/C catalysts. It is evident that the ring currents for CoFeN/C-HLH and Pt/C are comparable. In contrast, the ring current for carbon is much higher. The number of electrons exchanged in the redox reaction for CoFeN/C-HLH and Pt/C is 3.9-4.0 at high potentials.

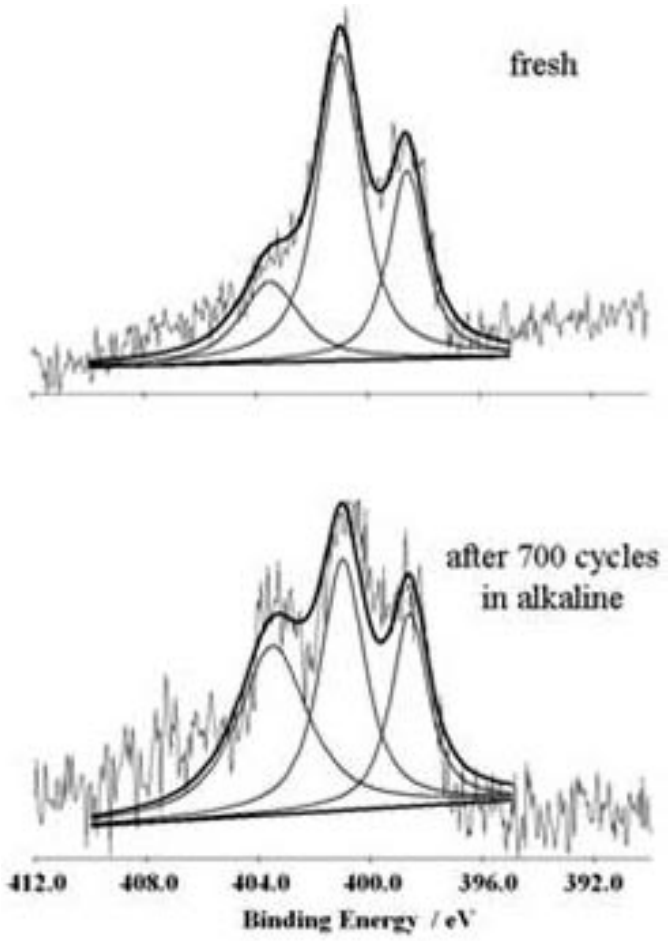


FIGURE 1B. XPS spectra of N1s obtained for: (a) fresh NPMC and for catalyst cycled 700 cycles in 0.1 M KOH.

The results indicate that both CoFeN/C-HLH and Pt/C catalysts catalyze the ORR mainly via a four-electron pathway in alkaline electrolyte. For carbon black alone, a lower selectivity with number of electrons exchanged in the range of 3.3-3.6 was observed at high potentials. The catalytic performance of CoFeN/C-HLH is comparable with Pt/C for oxygen reduction in alkaline electrolytes.

Figure 3 shows the preliminary performance of a H_2-O_2 anion exchange membrane fuel cell. The operation temperature is 50°C. The Pt loading at anode is 0.4 mg cm^{-2}, whereas the catalyst loadings at cathode are 4 mg cm^{-2} for CoFeN/C-HLH and 0.4 mg_{Pt} cm^{-2} for Pt/C. Anode and cathode gases are humidified at 50°C. The flow rates of H_2 and O_2 are 200 and 400 mL min^{-1}. The open circuit potentials are 0.97 and 1.04 V for CoFeN/C-HLH and Pt/C, respectively. The maximum power densities are 177 and 196 mW cm^{-2} for CoFeN/C-HLH and Pt/C, respectively. At high potential, the performance of CoFeN/C-HLH is slightly lower than Pt/C. At intermediate potential, they show very similar performance. The lower performance of

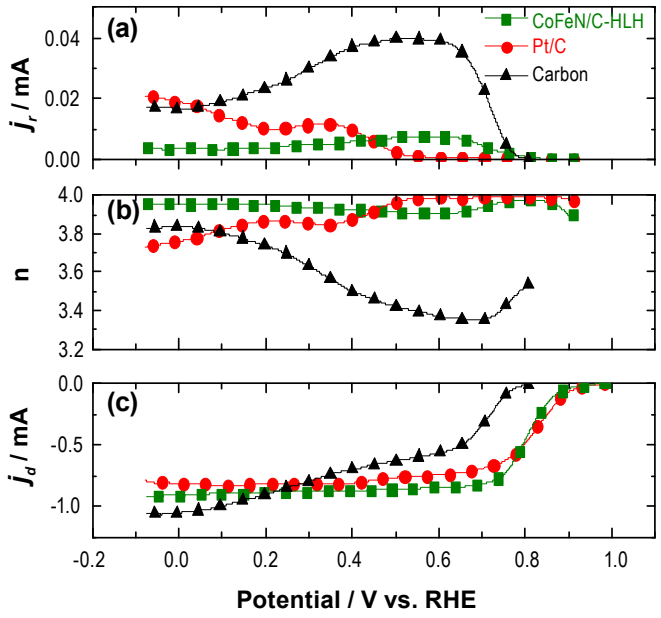


FIGURE 2. Comparison of CoFeN/C-HLH and Pt/C catalysts for the oxygen reduction reaction in O_2-saturated 0.1 M KOH. Scan rate: 5 mV s^{-1}; rotation rate: 900 rpm. (a) ring currents; (b) the number of electron exchanged during oxygen reduction; (c) polarization curves.

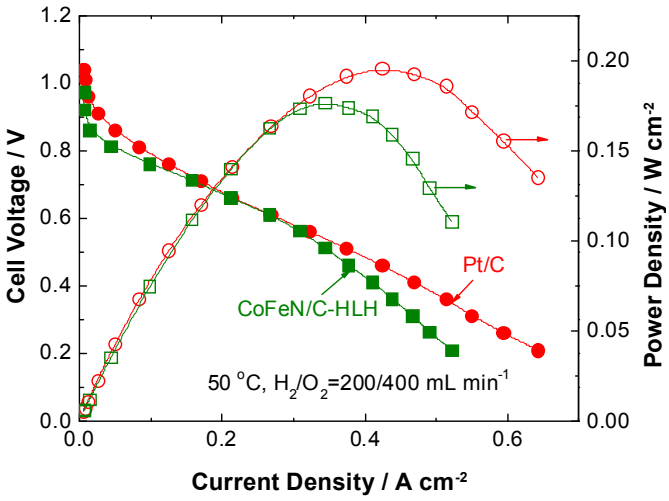


FIGURE 3. Preliminary performance of a H_2-O_2 anion exchange membrane fuel cell. The operation temperature is 50°C. The Pt loading at anode is 0.4 mg cm^{-2}, whereas the catalyst loadings at cathode are 4 mg cm^{-2} for CoFeN/C-HLH and 0.4 mg_{Pt} cm^{-2} for Pt/C. Anode and cathode gases are humidified at 50°C. The flow rates of H_2 and O_2 are 200 and 400 mL min^{-1}.

CoFeN/C-HLH over Pt/C at low potential may be attributed to higher mass-transfer resistance of the former resulting from higher catalyst loading and thus higher thickness of catalyst layer.

Conclusions and Future Directions

- NPMCs for oxygen reduction in alkaline electrolyte are developed by heating metal-nitrogen containing chelates followed by chemical post-treatment.
- The pyridinic-N and graphitic-N supported on graphitized carbon are active sites for oxygen reduction with high stability in alkaline electrolytes.
- The NPMCs exhibits comparable performance with Pt/C in anion exchange membrane fuel cells with the open circuit potential of 0.97 V and maximum power density of 177 mW cm^{-2}.

Future work includes the following tasks:

- Hydrogen Quality - Extract rate constants from experimental data for the case of a contaminant that desorbs from the catalyst surface; establish correlations between experimental data and model that will allow predictions of the effect of contaminant concentration and electrode potential.
- Carbon Composite Catalyst – Confirm protocol for preparation of mesoporous carbon support; improve integrity of the carbon composite catalyst layer in the membrane electrode assembly (MEA); reduce MEA resistance by decreasing the catalyst layer thickness and by increasing the specific gravity and activity of the catalyst.
- Hydrocarbon-Fueled SOFC - Evaluate solid oxide fuel cell performance using hierarchically porous electrode and $LaGaO_3$- as well as SFM-based ceramic anode.
- Gaskets and Seals - Design new compression set tests to include various compression strains and more realistic heating/cooling cycles to fuel cell operation; develop a life prediction model; and compare the performance of several off-the-shelf seal materials in the fuel cell environment.
- Durability Modeling in SOFC - Complete button cell test system and EIS test protocols; complete conductivity model of bi-supported cell electrode configuration.

Special Recognitions & Awards/Patents Issued

1. Prof. Ken Reifsnider, PI of this effort, is Director of the DoE Energy Frontiers Research Center on Heterogeneous Functional Materials, the "HeteroFoaM Center."

2. The Crystal Flame Innovation Award in Research from FuelCell South was presented to Dr. Popov's research group for research work in the field of non-precious catalyst development and preparation thin film assemblies with nano-structured catalysts and the development of the pulse deposition technique for preparation of membrane electrode assemblies.

FY 2011 Publications/Presentations

1. Chih-Wei Lin, Chi-Hui Chien, Jinzhu Tan, Yuh J. Chao, and J.W. Van Zee , "Chemical Degradation of Five Elastomeric Seal Materials in a Simulated and an Accelerated PEM Fuel Cell Environment," Journal of Power Source, 196(4), 2011, 1955-1966.

2. Cui,Tong, Lin, C-W., Chien,C.H., Chao, Y.J., Van Zee, J.W., " Service Life Estimation of Liquid Silicone Rubber Seals in Polymer Electrolyte Membrane Fuel Cell Environment," Journal of Power Source, 196 (2011) 1216-1221.

3. B.N. Popov, X. Li, G. Liu, Int. J. Hydrogen Energy 36 (2011) 1794-1802.

V.L.5 Fuel Cell Balance of Plant Reliability Testbed*

Susan Shearer (Primary Contact), Rob Shutler
Stark State College of Technology
6200 Frank Ave.
Canton, OH 44720
Phone: (330) 494-6170 x 4680
E-mail: shearer@starkstate.edu

DOE Managers
HQ: Kathi Epping Martin
Phone: (202) 586-7425
E-mail: Kathi.Epping@ee.doe.gov
GO: Greg Kleen
Phone: (720) 356-1672
E-mail: Greg.Kleen@go.doe.gov

Technical Advisor
Kristian Whitehouse
Phone: (720) 356-1363
E-mail: kristian.whitehouse@go.doe.gov

Contract Number: DE-FG36-08GO88111

Subcontractor:
Lockheed Martin-IDT, Akron, OH

Project Start Date: August 1, 2008
Project End Date: July 31, 2011

*Congressionally directed project

Fiscal Year (FY) 2011 Objectives

There are two primary objectives of this project:

- To establish a testing project resulting in a reliability database for candidate proton exchange membrane (PEM) fuel cell balance-of-plant (BOP) components.
- To enhance the education of the technical workforce trained in PEM fuel cell system technology.

Technical Barriers

This project addresses the following technical barriers from the Fuel Cells section of the Fuel Cell Technologies Program Multi-Year Research, Development and Demonstration Plan:

(A) Durability

This project also addresses the following technical barrier from the Education section of the Fuel Cell Technologies Program Multi-Year Research, Development and Demonstration Plan:

(D) Lack of Educated Trainers and Training Opportunities

Technical Targets

Reliability of the fuel cell system BOP components is a critical factor that needs to be addressed prior to fuel cells becoming fully commercialized. Failure or performance degradation of BOP components has been identified as a life-limiting factor in fuel cell systems [1]. The goal of this project will be to develop a series of test beds that will test system components such as pumps, valves, sensors, fittings, etc., under operating conditions anticipated in real PEM fuel cell systems. Results will be made generally available to begin removing reliability as a roadblock to the growth of the PEM fuel cell industry.

Stark State College students participating in the project, in conjunction with their coursework, will gain technical knowledge and training in the handling and maintenance of hydrogen, fuel cells and system components as well as component failure modes and mechanisms. This fuel cell work force development program will result in students trained in PEM fuel cell system technology.

TABLE 1. Progress towards Meeting Technical Targets for BOP Components for Transportation Applications

Characteristic	Units	2010/2015 Stack Targets	2011 Project Status
Durability with cycling at operating T ≤80°C	Hours	5,000	To be determined

FY 2011 Accomplishments

- Students are being trained on the construction, programming and operation of the life cycle test beds.
- Commercial off-the-shelf test components have been identified based on functionality, cost and size.
- Candidate sensors have been purchased, integrated and tested in the test beds.
- Testing protocols have been designed for each component.
- Students have:
  - Fabricated third testbed.
  - Fabricated and tested housing and electrical design for sensors.
  - Implemented I^2C protocol.
  - Incorporated Hydrogen Safety Plan protocol in testbed operation.



Introduction

One of the major challenges that must be addressed by the fuel cell industry prior to commercialization is the reliability of the components of a system. To this end Stark State College of Technology and Lockheed Martin have teamed to address this critical factor.

Approach

Stark State College of Technology and Lockheed Martin have developed a series of test beds that test fuel cell system components such as pumps, tubing types, sensors, valves etc., operating under conditions anticipated in real PEM fuel cell systems. The test beds operate under various conditions continuously. Parts that continue operating demonstrate lifetime for potential fuel cell systems. Parts that have failed are removed and examined to learn the cause of the failure. Feedback will allow manufacturers to improve the products for future use in PEM fuel cells. Results will allow for a path towards removing reliability as a roadblock to the growth of the PEM fuel cell industry. A total of three test beds have been developed for this project; two at Stark State College of Technology and one at Lock Martin. In each case students in the engineering technology will monitor the test beds as part of their education program.

Results

A fuel cell system consists of a fuel cell and its supporting BOP – the pumps, valves, sensors, fittings, piping, etc. needed to turn a fuel cell into a useful power plant. Components in this complex system can have long-term exposure to hydrogen, air (oxygen), high purity water, heat and other chemicals. The BOP reliability test beds will be a simplified design, simulating the conditions of an operating fuel cell. The first two test beds are designed to replicate humidified hydrogen exposure in the PEM fuel cell at ≤80°C. These test beds are a hydraulic loop simulation of the fuel cell system to test the piping, connectors, sensors, valves, pumps, etc., without the fuel cell. Testing will be done to simulate the flow rates, temperature and pressure of operation, initially under a humidified nitrogen system with eventual operation under reactant conditions. This exposure would simulate the anode flow areas just before the fuel cell entrance and conditions in the hydrogen re-circulation loop. The humidified hydrogen would be circulated using a hydrogen blower such as the Parker Hannifin Model 55™ Univane rotary compressor [2].

Figure 1 shows the test bed process flow diagram. The test bed design can be viewed as two "separate" pieces. The upper flow diagram designated "Life Cycle Test" is the loop that will circulate humidified hydrogen. This loop will be

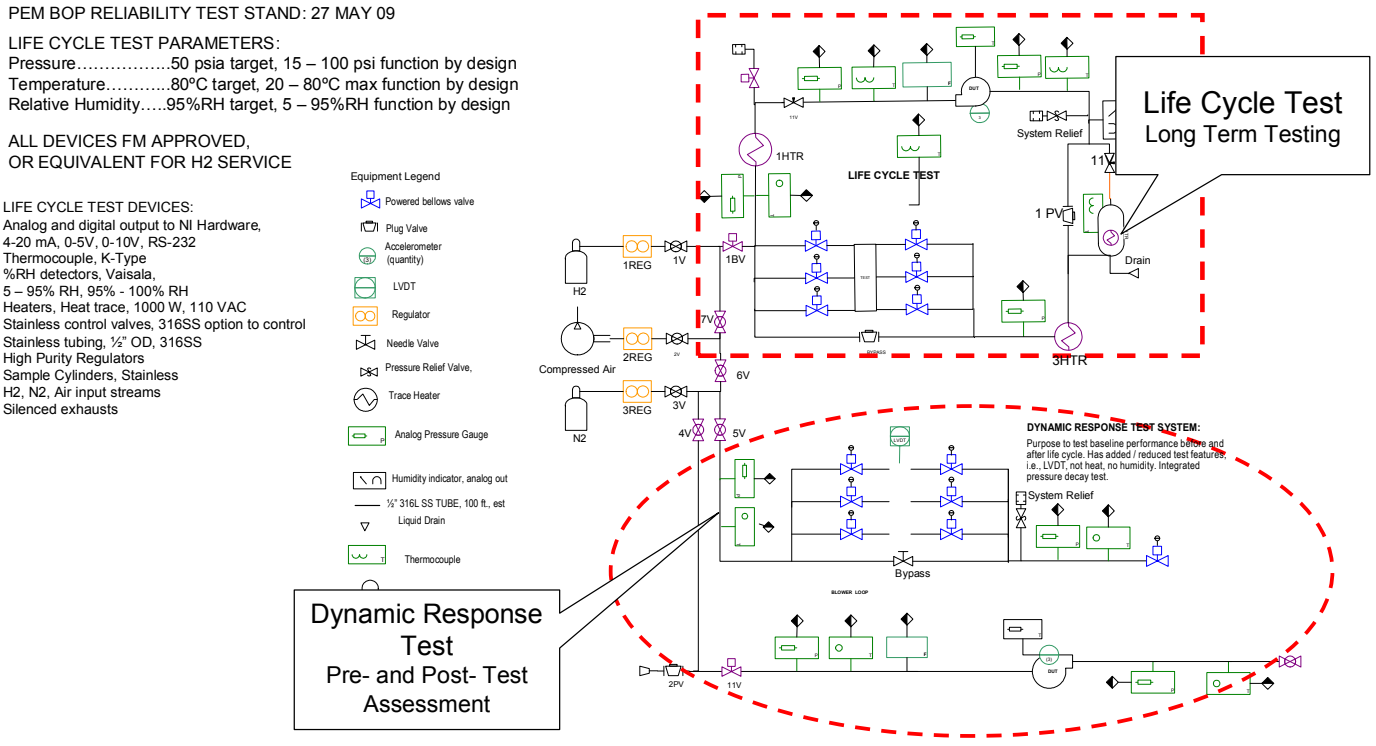


FIGURE 1. Fuel Cell BOP Reliability Test Bed Design

pre-tested with nitrogen for leaks before hydrogen usage. Operating conditions will be 50 psi static, 80°C, 70-95% relative humidity and 6-7 SCFM flow rate in the closed-loop system. The lower loop is designated for dry nitrogen or air only. The lower loop consists of the blower platform and the dynamic response test system. This section is for the pre- and post-test validations in our reliability testing, pump performance mapping, and pressure decay (leak) testing of the components.

A LabVIEW-based data acquisition program has been written for each test stand to log critical experimental parameters. Pressure, temperature and humidity sensors are currently under test. The testing protocol consisted of comparison of devices under test with traceable probes. The device then underwent testing to verify accuracy, measuring range and short term stability before longer term testing. Figures 2 and 3 show example evaluation testing for candidate pressure transducers. The system transducers

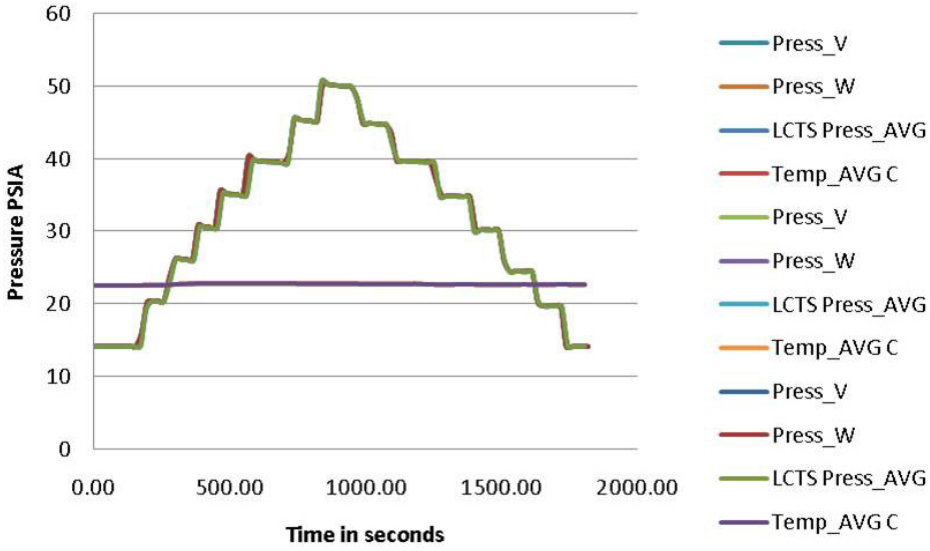


FIGURE 2. Testing Performance of Pressure Sensors

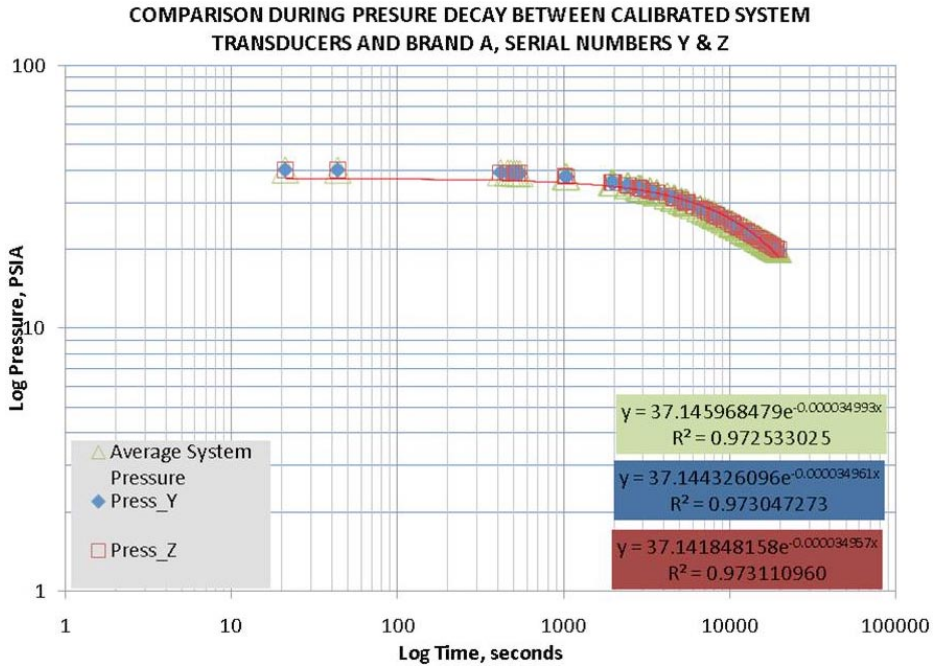


FIGURE 3. Pressure Decay Comparison

are traceable to the National Institute of Standards and Technology using a HEISE PTE-1 Calibrator with 0-200 psig pressure module to 0.02% accuracy.

A trade study of pressure sensing elements led to a product decision matrix of low-cost pressure transducers from large original equipment manufacturers. Of the transducers specified and evaluated thus far, two failures, one soft and one hard failure, have occurred under time conditions less than the PEM BOP and manufacturer's ratings. Sensors that have qualified continue to be tested on the Life Cycle testbed, exposed to high temperatures and humidity.

Low-cost, lightweight precision temperature sensors, typically procured in high quantities, required repackaging in a form that would impose negligible impedance on performance. These sensors were built-in with a high performance epoxy encapsulant of very high thermal conductivity and very low electrical conductivity. Evaluation of the temperature sensors and several encapsulation designs are continuing on the Life Cycle testbed. Integrated humidity and temperature sensors, in compact, lightweight form are also under test. These sensors utilize the I^2C protocol for allowing upward of 100 sensors to be connected serially to a single data bus, eliminating the need for multiple controller cards. Special housings were also designed for these sensors and fabricated. Humidity/temperature sensors are currently being evaluated in the Life Cycle testbed.

Student training has been ongoing for the operation of the testbed. The training has continued for participating students to have a greater depth of understanding in LabVIEW programming and exposure to a broader range of software programming techniques to implementation of the I^2C protocol. Training has included embedded controller information for LabVIEW programming and compiling to make a stand-alone program for data acquisition, control and analysis of the data, implementation of testing protocol, as well as compliance with the Hydrogen Safety Plan protocol.

Conclusions and Future Directions

- Further characterization of lower cost sensors over a wider range of test conditions.
- Further refinement of sensor housing and electronics for lower price sensors.
- Investigation of electrical actuated valves including modifications for improving flow, lowering power consumed and decreasing size and weight [3].
- Permeation testing of different tubing materials.
- The future is being planned with students being trained on the construction, programming and operation of the life cycle test beds.
- A one year extension no cost extension has been requested.

FY 2011 Publications/Presentations

1. *Fuel Cell Balance of Plant Reliability Testbed*, Vern Sproat and Rob Shutler, Poster session at DOE Hydrogen Program Annual Merit Review, Washington, D.C., May 2011.

References

1. *Automotive Fuel Cell R&D Needs*, Craig Gittleman, David Masten, and Scott Jorgensen, DOE Fuel Cell Pre-Solicitation Workshop March 16, 2010.

2. *Cost Analyses of Fuel Cell Stack/Systems*, J. Sinha, S. Lasher, and Y. Yang, DOE Hydrogen Program Annual Report, V.A.3.

3. *Balance of Plant Needs and Integration of Stack Components for Stationary Power and CHP Applications*, Chris Ainscough, DOE Fuel Cell Pre-Solicitation Workshop - March 16, 2010.

V.L.6 Biomass Fuel Cell Systems*

Neal Sullivan (Primary Contact), Robert Braun, Anthony Dean, Robert Kee, Ryan O'Hayre, Tyrone Vincent
Colorado School of Mines
1500 Illinois Street
Golden, CO 80401
Phone: (303) 273-3656
E-mail: nsulliva@mines.edu

DOE Managers
HQ: Kathi Epping Martin
Phone: (202) 586-7425
E-mail: Kathi.Epping@ee.doe.gov
GO: Reginald Tyler
Phone: (720) 356-1805
E-mail: Reginald.Tyler@go.doe.gov

Contract Number: DE-EE0000260

Project Start Date: October 1, 2009
Project End Date: September 30, 2012

*Congressionally directed project

Fiscal Year (FY) 2011 Objectives

- Develop solid oxide fuel cell (SOFC) materials and architectures for robust operation on renewable/biomass fuel streams.
- Identify optimal fuel-processing strategies for renewable fuels, specifically biogas derived from anaerobic digesters commonly utilized for sludge remediation at wastewater treatment facilities.
- Employ system modeling to optimize SOFC system configurations.
- Extend model-predictive control strategies to integrate system hardware for improved load following and dynamic response.

Technical Barriers

- Durability: Broaden SOFC operating windows under hydrocarbon and bio-derived fuel streams.
- Balance-of-plant costs: Integrate fuel reforming and heat recuperation hardware into a single low-cost ceramic micro-channel reactive heat exchanger.
- Performance: Increase efficiency and decrease costs through system optimization and balance-of-plant component development and integration.
- Transient operation: Develop model-predictive control algorithms for use in dynamic control.

This project addresses the following technical barriers from the Fuel Cells section of the Fuel Cell Technologies Program Multi-Year Research, Development and Demonstration Plan:

(A) Durability

(C) Performance

(G) Start-up and Shut-down Time and Energy/Transient Operation

Technical Targets

In this project, we conduct a range of studies to improve the durability, efficiency, and transient operation of SOFC systems. Fuel streams for these systems include anaerobic digester-derived biogas. Insights gained from these studies will be applied toward the design and synthesis of SOFC materials and systems to meet the DOE 2015 Technical Target for durability (35,000 hours), start-up time (15-30 minutes), and cycle capability (250 cycles).

FY 2011 Accomplishments

- Demonstrated over 16 days of continuous SOFC power generation on unreformed simulated biogas (65% CH_4 + 35% CO_2).
- Established biogas fuel processing strategies and operating windows for upstream conversion of biogas into syngas.
- Quantified performance of SOFCs under biogas reformate fuel streams, and established performance comparisons under hydrogen fuel streams.
- Developed hybrid computational fluid dynamics (CFD)-chemical kinetics model to examine design tradeoffs in ceramic microchannel fuel reformer/heat exchanger.
- Utilized computation models to examine thermal, chemical, and electrochemical fields within tubular SOFC stack.
- Developed rapid, lower-order dynamic models to map response of slower, high-order physical models for use in dynamic system control of fuel-reformer hardware.



Introduction

The objective of this project is to advance the current state of technology of SOFC systems to improve performance when operating on biomass-derived fuel streams. The target fuel stream is "biogas" (~65% CH_4/35% CO_2) generated by the anaerobic digesters that are widely used for treatment of sludge in

municipal wastewater treatment facilities. In this project, we are developing new SOFC materials and architectures to improve the robustness of systems operating under biogas. Additionally, modeling and experimentation is being conducted to examine performance tradeoffs across numerous fuel-processing strategies for this fuel. Fuel-reforming processes are being integrated with exhaust gas recuperation processes through development of a single low-cost ceramic microchannel reactive heat exchanger, created in collaboration with industrial partner CoorsTek, Inc. System-level models are being used to predict SOFC system efficiencies under biogas fuels utilizing the fuel-reforming microchannel-reactor integration strategies under development. Model-predictive control strategies are being developed and applied to improving the dynamic response of the fuel-reformer hardware.

Approach

The Colorado School of Mines (CSM) has assembled a strong and diverse team of scientists and researchers with broad skill sets applicable to fuel cell development. Coordinated through the Colorado Fuel Cell Center, this team examines both the fundamental underpinnings and the key technical problems facing SOFC operation under biomass-derived fuel streams. We develop new SOFC materials and architectures to address the technical challenges and operating windows associated with SOFC operation on biomass-derived fuels. Through development of low-cost ceramic microchannel reactive heat exchangers with industrial partner CoorsTek, Inc., we create system-integration strategies to combine balance-of-plant processes into single hardware units, increasing system simplicity and decreasing cost. A range of computational models are developed to examine the physical processes underway during SOFC and fuel-reformer operation. Model-predictive control strategies are created and applied to fuel-reforming hardware in an effort to improve the dynamic response of SOFC systems.

Results

SOFC Materials and Architectures: Barrier Layers for Improved Robustness

Fuel cell reliability and performance can be greatly improved through development of new materials and architectures that promote robust SOFC operation on renewable and hydrocarbon fuels. In this task, we are currently developing new SOFC anode architectures utilizing anode "barrier layers" that mitigate carbon-deposit formation, seeking to optimize the structure of the cell for maximum efficiency and reliability. A conceptual drawing of a tubular SOFC with an inert barrier layer is shown in Figure 1a. The barrier layer reduces the transport of electrochemically produced steam out of the anode support. This increases the concentration of steam within the

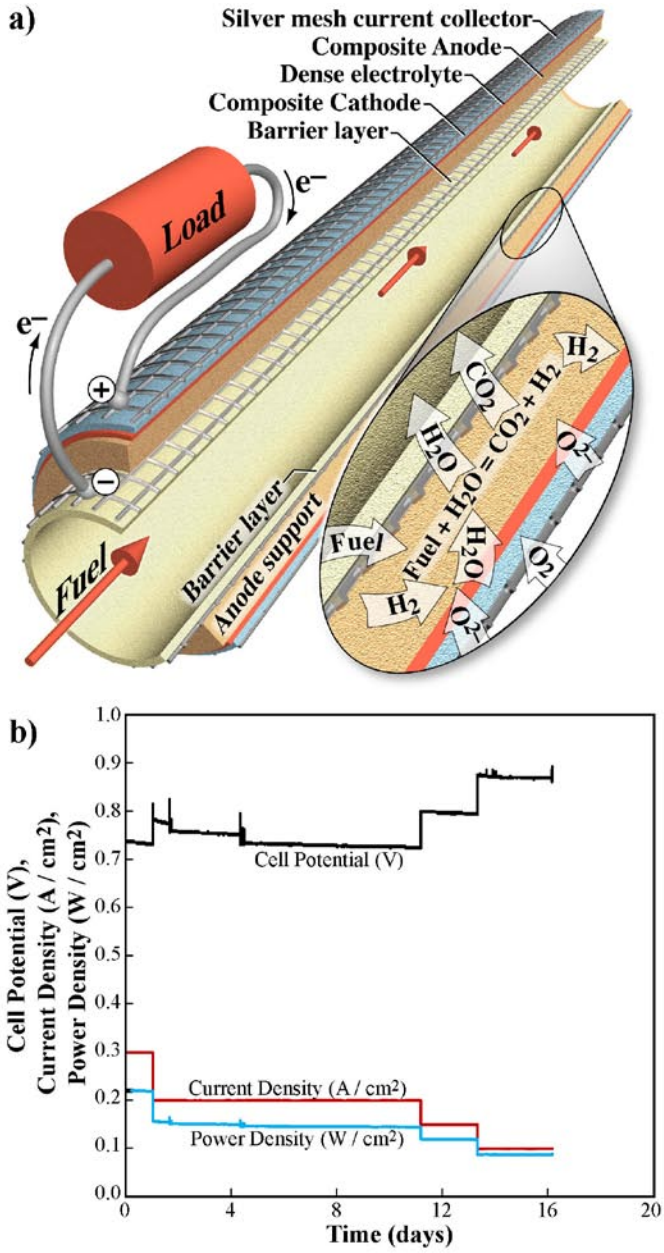


FIGURE 1. a) Illustration of a tubular SOFC employing an anode barrier layer with inset depicting internal-reforming processes; b) extended operation of barrier-layer equipped tubular SOFC under direct biogas fuel. Step changes represent changes in load applied to the cell.

support, promoting methane internal-reforming reactions over solid-carbon-forming reactions, preventing carbon deposition and cell deactivation.

During the previous year, we successfully integrated a barrier layer into a tubular CoorsTek SOFC, and continuously operated this assembly under a simulated humidified biogas fuel stream (63% CH_4 + 34% CO_2 + 3% H_2O). Biogas is a byproduct of anaerobic-digestion processes widely utilized in landfills and wastewater-treatment facilities for sludge remediation. Some cleaning

of biogas is generally required to remove siloxanes and sulfur-containing species upstream of biogas-fueled power generators. In this project, biogas is synthesized from near-pure compressed-gas cylinders to simulate the cleaned biogas fuel composition. The barrier-layer equipped SOFC continuously converted the chemical energy in the simulated biogas into electricity for over 16 days with negligible performance degradation as shown in Figure 1b. No biogas fuel reforming upstream of the SOFC was conducted. The barrier layer was fabricated in the Colorado Fuel Cell Center by slip-casting of lanthanum-doped strontium titanate ($Sr_{0.8}La_{0.2}TiO_3$). The CoorsTek SOFC utilizes fairly conventional materials, including a yttria-stabilized zirconia (YSZ) electrolyte, nickel-YSZ anode, and strontium-doped lanthanum manganate cathode. Testing was conducted at 850°C under very low fuel utilization in order to present a "worst-case" scenario for carbon-deposit formation. Steady operation was observed at each current density. This result presents the first long-term operation of a barrier-layer-equipped tubular SOFC under simulated biogas fuel, and the first multi-day performance of an SOFC on unreformed simulated biogas fuel.

Biomass-Derived Fuel Processing

In this task, we examine fuel-reforming strategies to convert biogas into syngas for subsequent electrochemical conversion in SOFCs. Upstream reforming of biogas prior to introduction into the SOFC stack presents a nearer-term solution to SOFC operation on biogas in comparison to barrier-layer architectures. The goal is to develop flexible, efficient fuel-processing strategies for the robust use of biogas fuels in SOFCs. The effort includes computational model development of biogas fuel reforming, experimental validation, and electrochemical performance measurements of biogas-reformate-fueled SOFCs. As part of this task, we examine the relationship between SOFC performance and biogas fuel-reforming approach, contrasting results of steam reforming with catalytic partial oxidation (CPOX) using air, and CPOX using oxygen. While CPOX with oxygen may at first seem impractical, many wastewater treatment facilities utilize cryogenically stored pure oxygen to decrease energy usage during waste-aeration processes. Such an oxygen source could potentially be utilized by a co-located SOFC electric generator.

During the previous year, a series of numerical and physical experiments were conducted to quantify biogas-reformate composition across a number of reforming approaches and operating conditions. Both modeling and experimentation focused on use of a rhodium-based catalyst on a porous alumina foam support. The operating conditions probed included reforming temperature, steam-to-carbon ratio, oxygen-to-carbon ratio, and space velocity. Computational modeling was first conducted to identify optimal biogas-reforming conditions over a wide operational space. These numerical results were then analyzed, and then experimentally validated for select conditions with high methane-conversion levels.

The high CO_2 content of biogas can result in surprising reformate compositions. Through dry-reforming reactions ($CH_4 + CO_2 \rightarrow 2\ CO + 2\ H_2$), the biogas-borne CO_2 is reduced to CO. Higher reforming temperatures are required to drive this endothermic reaction. Within the SOFC anode, carbon monoxide is further internally reformed through the water-gas shift reaction ($CO + H_2O \rightarrow CO_2 + H_2$). Thus the CO generated from CO_2 during dry reforming directly leads to additional H_2 formation within the cell. This additional H_2 is in-turn electrochemically oxidized, resulting in additional electricity generation. Because of internal reforming, it is important to consider the CO content of the reformate as a fuel in the SOFC. Generating reforming conditions that maximize conversion of biogas-borne CO_2 to CO is critical to realizing peak efficiency. Increased dry reforming decreases the parasitic thermal requirements for addition of steam or air oxidizers to reform the biogas into syngas.

Our experimental and modeling efforts found that while steam reforming generates the highest H_2 mole fraction in the reformate (~54%), the combined H_2 + CO mole fraction reaches only 78%. In contrast, biogas reforming via CPOX with O_2 results in a combined H_2 + CO mole fraction of nearly 86%, and 10% higher utilization of the biogas chemical potential. This potential benefit comes with the added simplicity of the CPOX system design, as catalytic partial oxidation is a far more elegant reforming approach in comparison to that of steam reforming. Such results may prove valuable to engineers and scientists that design biogas-fueled SOFC systems.

After establishing the desired reforming conditions and reformate compositions for each of the three different approaches, SOFC electrochemical performance under the different reformate compositions was measured. Using the experimental results from the simulated-biogas reforming experiments, biogas reformate was synthesized and supplied to a tubular SOFC operating at 800°C in the Colorado Fuel Cell Center. An important aspect to the performance testing was ensuring that each test resulted in the same utilization of the supplied fuel (70%), and that each cell was operated at the same electric potential (0.65 V). Performance on reformate was compared to that under hydrogen fuel, with results shown in Figure 2.

Not surprisingly, the highest performance was observed under hydrogen-fuel conditions. Power density under reformate generated via CPOX using O_2 is 0.145 W/cm^2, only 3% lower than that of the pure-hydrogen condition (~0.15 W / cm^2). In contrast, cell performance under reformate generated by steam reforming and CPOX with air is approximately ~0.124 W/cm^2, nearly 20% lower than the hydrogen condition. These electrochemical-performance differences can have significant impacts on the size, footprint, and cost of biogas-fueled SOFC systems.

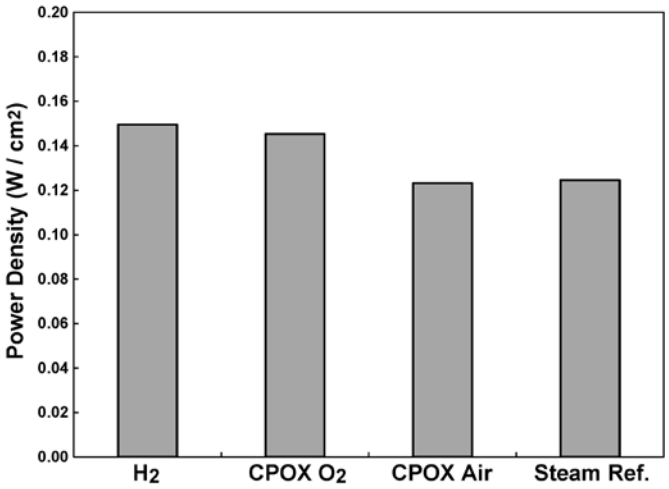


FIGURE 2. SOFC electrochemical performance at 0.65 V and 70% utilization under hydrogen and biogas-reformate fuel streams.

Ceramic Microchannel Reactors

Building on the biogas-reforming results, we are now configuring our ceramic microchannel reactor technology for biogas reforming. An illustration of this reactor is shown in Figure 3a and 3b. The reactor is fabricated by industrial partner CoorsTek, Inc. using low-cost ceramic materials (Al_2O_3) that are joined in a single high-temperature sintering process. This greatly reduces the materials and fabrication costs of the heat-exchanger device, with significant potential for decreasing SOFC balance-of-plant expenses. These microchannel reactors offer great advantages over conventional shell-and-tube reactors through improved heat transfer and thermal regulation of reforming processes. Exothermic reforming processes can cause hot spots in conventional reactors that reduce the efficiency and effectiveness of the reforming process. Similarly, supplying heat for endothermic-reforming processes can pose significant parasitic losses in SOFC systems. In microchannel reactors, the hot and cold streams are tightly integrated, so that thermal regulation, reforming activity, and reformate selectivity are maximized.

We are developing deposition processes of catalyst materials within the microchannel reactor. Sealing and manifolding of the microchannel reactors is also an area of development, with manifolding design and testing ongoing. An important aspect to our microchannel-reactor effort is the development and application of high-fidelity computational models to guide reactor design and operation. ANSYS-Fluent CFD models are being modified to incorporate elementary chemical kinetic mechanisms for high-fidelity modeling of fuel reforming within the microchannel reactor. Such incorporation of elementary chemistry into CFD models is quite challenging; CSM is working directly with ANSYS-Fluent developers on this effort.

Characteristic methane-steam-reforming results from the hybrid CFD-kinetics model are shown in Figure 3c and 3d.

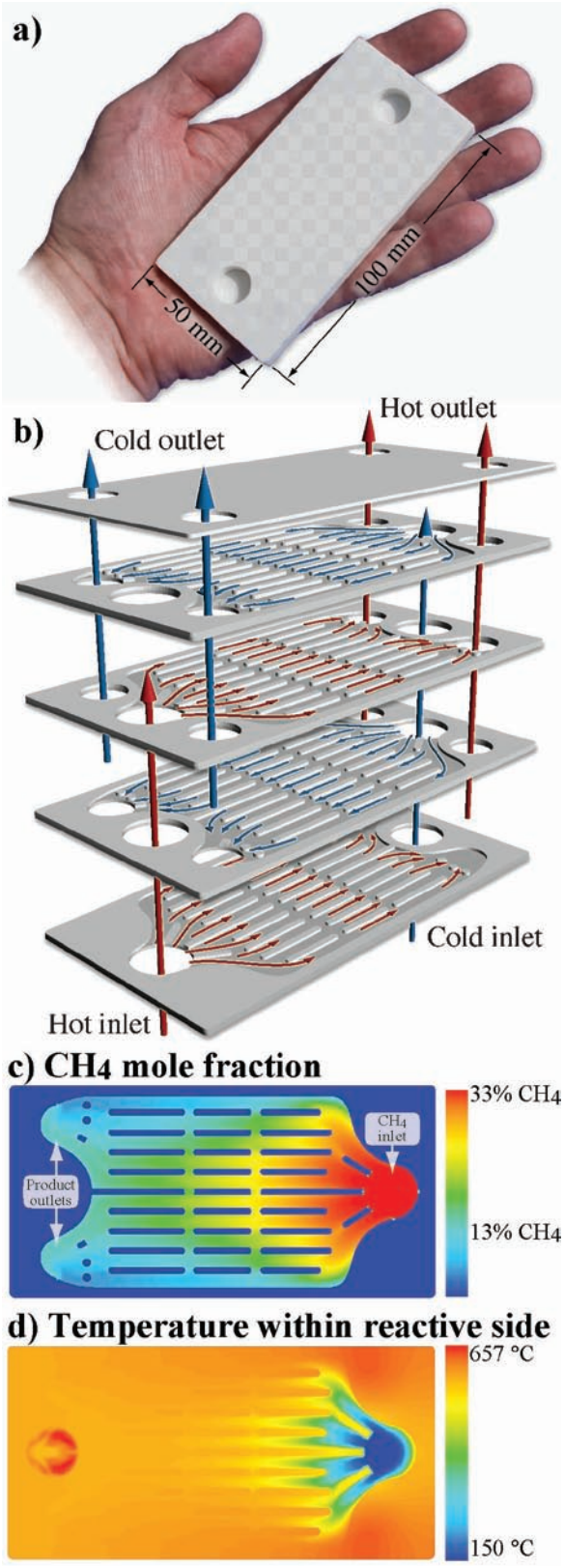


FIGURE 3. a) Image and b) exploded illustration of ceramic microchannel reactor; c) results from hybrid CFD-chemical kinetics model predicting methane mole fraction and d) temperature fields over the catalytically active layer of the microchannel reactor.

The catalytically active layers are fed with a methane–steam mixture at a ratio of 1 CH_4 : 2 H_2O flowing from the inlets at the right to the outlets at the left at a flow rate of 4 SLPM and temperature of 150°C. The model catalyst is rhodium, which has exceptional methane-steam-reforming activity and resistance to carbon-deposit formation. The heterogeneous reforming chemistry takes place on the walls of the catalytically active layers within the microchannel reactor. The non-reactive backing channels are fed with air flowing at 60 SLPM and an inlet temperature of 800°C. The hybrid model solves the complete three-dimensional flow field, and the conjugate heat transfer between the two inlet gas streams and the solid ceramic reactor body. These operating conditions result in 51% conversion of methane. The methane-steam inlet gas is heated from 150°C to reforming temperature within the first bank of microchannels, with reactions taking place primarily in the first and second banks of channels. Flow uniformity is reasonable, though some improvements seem possible. Peak temperatures within the reactive side reach approximately 600°C, a bit lower than desired for optimal steam reforming. This temperature could be increased through higher flow rates of the air supplied to the non-reactive backing channels, or higher inlet temperatures of either the air or the reactive methane-steam mixture.

This result demonstrates the application of a powerful research and development tool in which three-dimensional computational fluid dynamics and heat transfer are coupled to high-fidelity elementary chemical kinetics. Over the remainder of the project, we will utilize this tool to define operating windows for biogas reforming that result in high methane conversion and high selectivity to hydrogen and carbon monoxide.

System-Level Modeling

The complex component geometries of the SOFC hot zone and the chemical and electrochemical reactions within are coupled with heat transfer and three-dimensional fluid flow to simulate hot zone thermal energy management of representative SOFC geometries. A central feature of this task is to accurately capture the three-dimensional transport phenomena within the hot zone and derive representative reduced-order models. In this task, these reduced-order models are directed towards use in system process design and parameter specification. The domain of the CFD model includes the entire cathode and stack endplates along with the majority of the recuperator, fuel/air preheat flow, and system insulation. The hot zone is modeled after the 600-W tubular SOFC stack developed by industrial partner Protonex Technology Corporation.

A characteristic result is shown in Figure 4. It is increasingly clear that the outer tubes located near the periphery act as radiation shields, keeping inner-radii tube groups warmer. Local species concentration fields identify of critical O_2-depletion zones. These results and modeling tools can be utilized by stack developers to improve stack design, performance, and efficiency.

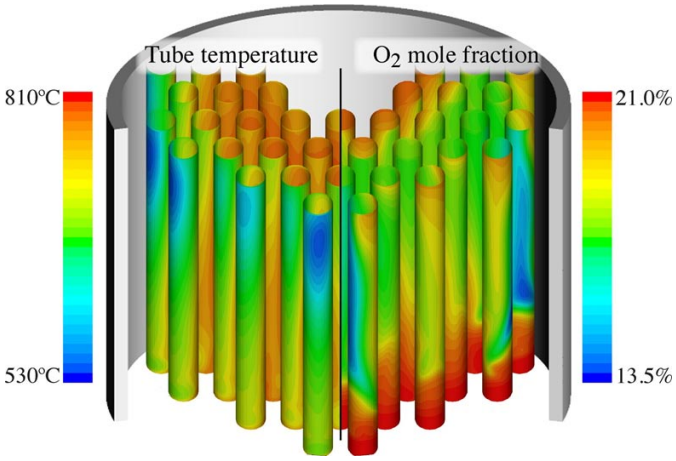


FIGURE 4. Model Predictions of Thermal and Oxygen-Concentration Fields across 600-W Tubular Stack

Model-Predictive Control

Dynamic control efforts have focused on the effects of balance-of-plant components on performance and control. The balance-of-plant components of the stack include the fuel reformer, air and fuel blowers, heat exchanger, and tail-gas-combustion burner. A complete SOFC system is highly connected via the temperatures and mass compositions that flow through each of these components. As such, model-based dynamic control must incorporate the dynamics of all balance-of-plant components within safe operating limits. For example, the reformer outlet gas composition must be controlled in order to prevent carbon deposition within the stack. At the same time, carbon deposition is dependent upon the stack operating temperature and power level, which drives the operation of the reformer. Additionally, limits on reformer catalyst temperature need to be maintained while ensuring the mass flow and fuel composition provided to the stack are sufficient for the desired current output. The stack air temperature must also be high enough to prevent stack excessive stack cooling. It is for these reasons, that a system-wide control-oriented dynamic model is needed.

Current work has provided a system-wide model consisting of the fuel reformer, tubular SOFC stack, and heat exchanger. Improvements over existing system-wide models include the use of component models that allow for composition estimation throughout the system. Although increasing the required model complexity, composition is highly coupled with both performance of the system and robustness to real-world inputs. A characteristic result of this model is shown in Figure 5, which shows that even small changes on the inlet fuel composition to the fuel reformer has impacts on the stack performance.

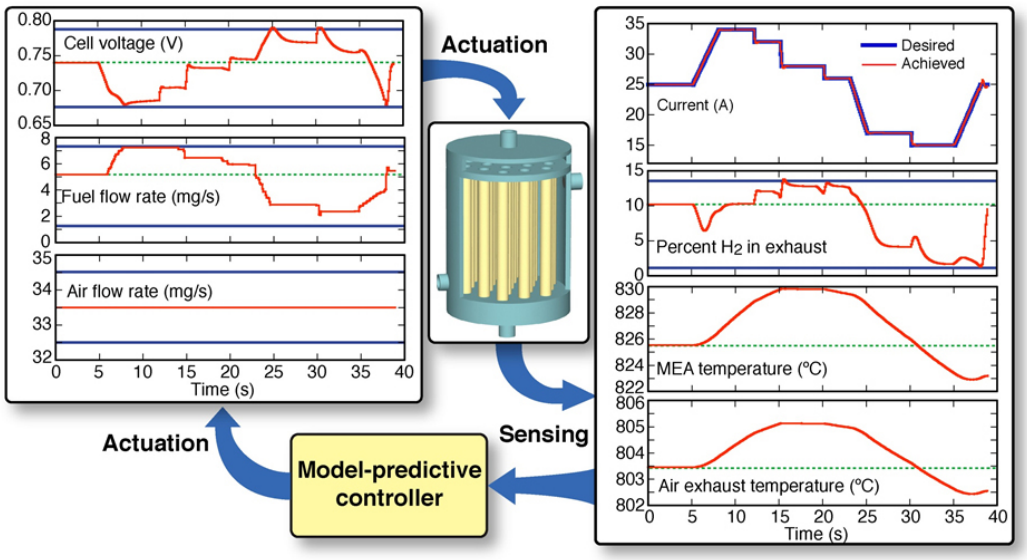


FIGURE 5. Dynamic Response Predictions from Model-Predictive Control Algorithms

Future Directions

Biomass-Derived Fuel Processing

- Explore operating windows for reforming of biogas within ceramic microchannel reactor.
- Extend hybrid CFD/chemical-kinetics modeling to examine effects of fuel-processing strategies on heat-exchanger effectiveness and fuel-reformate composition and quality.

System Modeling

- Quantify efficiency of SOFC operation on biogas under the different reforming conditions that may be utilized.
- Examine benefits of integrated unit processes enabled by utilization of the ceramic microchannel reactor.

System Control

- Implement explicit form for Model Predictive Control for use in biogas-reforming system.
- Extend model-predictive control strategy to reactive heat exchanger.

FY 2011 Publications/Presentations

1. R.J. Kee, B.B. Almand, J.M. Blasi, B.L. Rosen, M. Hartmann, N.P. Sullivan, H. Zhu, A.R. Manerbino, S. Menzer, W.G. Coors, J.L. Martin, "The design, fabrication, and evaluation of a ceramic counter-flow microchannel heat exchanger," *Applied Thermal Engineering* (in press, 2011).

2. A.E. Richards, N.P. Sullivan, R.J. Kee, and H. Zhu, "Internal reforming chemistry in novel SOFC anodes and architectures," *European Fuel Cell Forum*, Lucerne, Switzerland, June 28 – July 2, 2010.

3. S. Babiniec, N.P. Sullivan, A.E. Richards, and N. Faino, "Multi-phase tubular perovskite-based anodes for use in hydrocarbon-fueled solid-oxide fuel cells," *European Fuel Cell Forum*, Lucerne, Switzerland, June 28 – July 2, 2010.

4. D. Storjohann, and N.P. Sullivan, "Barrier-layer structures to mitigate carbon formation in tubular bio-fueled solid oxide fuel cells," *European Fuel Cell Forum*, Lucerne, Switzerland, June 28 – July 2, 2010.

5. A. Colclasure, B. Sanandaji, T. Vincent, R.J. Kee, "Modeling and control of tubular solid-oxide fuel cell systems. I: Physical models and linear model reduction" *Journal of Power Sources* 196:196-207 (2011).

6. B. Sanandaji, A. Colclasure, T. Vincent, R.J. Kee, "Modeling and control of tubular solid-oxide fuel cell systems: II. Nonlinear model reduction and model predictive control" *Journal of Power Sources*, 196:208-217 (2011).

7. K.J. Kattke and R.J. Braun, "Implementing thermal management modeling into SOFC system-level design," *ASME Journal of Fuel Cell Science, Engineering and Technology* (in press 2010).

8. K.J. Kattke, R.J. Braun, A. Coclasure, and G. Goldin, "High-fidelity stack and system modeling for tubular SOFC system design and thermal management," submitted to *Journal of Power Sources* (2010).

9. K.J. Kattke and R.J. Braun, "Implementing thermal management modeling into SOFC system-level design," Proceedings of the ASME 2010 Eighth International Fuel Cell Science, Engineering and Technology Conference, New York, NY, June 2010.

10. A.A. Shoaibi, A.M. Dean, "Kinetic analysis of C4 alkane and alkene pyrolysis: Implications for SOFC operation" *Journal of Fuel Cell Science and Technology* 7 (2010).

V.L.7 Fuel Cell Coolant Optimization and Scale Up*

Satish Mohapatra (Primary Contact), P. McMullen and J. Mock
Dynalene Inc.
5250 W. Coplay Rd.
Whitehall, PA 18052
Phone: (610) 262-9686
E-mail: satishm@dynalene.com

DOE Managers
HQ: Kathi Epping Martin
Phone: (202) 586-7425
E-mail: Kathi.Epping@ee.doe.gov
GO: David Peterson
Phone: (720) 356-1747
E-mail: David.Peterson@go.doe.gov

Contract Number: 09EE0000278

Subcontractor:
Lehigh University, Bethlehem, PA

Project Start Date: September 1, 2009
Project End Date: August 31, 2011

*Congressionally directed project

Fiscal Year (FY) 2011 Objectives

The overall objective of this project is to optimize and scale up the process to make Dynalene FC fuel cell coolant with a great deal of reproducibility. Following are some specific objectives that would help to reach the overall goal of the project:

- Demonstrate the production of one key ingredient of the coolant (a nanoparticle) in 10 L, 20 L and 100 L batches in a pilot-scale operation and study the effect of various process parameters on the size and charge density of the particles.
- Produce the nanoparticles necessary for the fuel cell coolant, Dynalene FC, in a very consistent manner (i.e., particle size, charge density and yield).
- Optimize the filtration process for the nanoparticles to minimize the cleaning time for different scales of operation.

Technical Barriers

This project addresses the following technical barriers from the Fuel Cells section (3.4.4) of the Fuel Cell Technologies Program Multi-Year Research, Development and Demonstration Plan:

(B) Durability
(C) Cost

Technical Targets

Dynalene FC is expected to help the fuel cell industry achieve their durability and cost targets to some degree. First of all, the coolant itself is being designed to have a life of 5,000 hrs. It is also expected to have excellent compatibility with the system materials and inhibit corrosion in the coolant loop. This will help in extending the durability of the fuel cell system components such as the pump, the radiator, valves, seals/gaskets and any other components coming in contact with the coolant. The coolant is also designed to work at -40°C, which will assist both transportation and stationary fuel cells to quickly warm up during cold starts.

The cost target for the coolant (in plant-scale production) is about $10/gallon, which is very close to the retail price of current automotive coolants. This coolant will also eliminate the deionizing filter and other hardware associated with it (i.e. fittings, valves). It is also being designed to work with cheaper, lighter and thermally efficient components such as aluminum radiators (instead of stainless steel) and brass heat exchangers.

Accomplishments

Dynalene FC has been demonstrated by field testing to maintain a very low electrical conductivity and stay stable over several years. This was possible due to the addition of a nanoparticle into the coolant. This project addresses the optimization and scale up of this nanoparticle ingredient. The main accomplishments in this project so far are the design and set up of 10 L, 20 L and 100 L reactor vessels, and optimization of the production of nanoparticles in the 10 L scale. Optimization in the 100 L scale is continuing now and it is expected to be finished by the project end date (August 31, 2011). Other accomplishments include the development and optimization of the filtration process for the nanoparticles and quality control procedures.



Introduction

This project addresses the goals of the Fuel Cell Technologies Program of the DOE to have a better thermal management system for fuel cells. Proper thermal management is crucial to the reliable and safe operation of fuel cells. A coolant with excellent thermophysical properties, non-toxicity, and low electrical conductivity is desired for this application.

Dynalene Inc. has developed and patented a fuel cell coolant with the help of DOE Small Business Innovation Research Phase I and Phase II funding (Project # DE-FG02-

04ER83884). However, this coolant can only be produced in lab scale (500 ml to 2 L) due to problems in optimization and scale up of a nanoparticle ingredient. This project will optimize the nanoparticle production process in 10 L, 20 L and 100 L reactors, optimize the filtration process, and develop a high throughput production method for the final coolant formulation.

Approach

Before this project, Dynalene researchers were producing the nanoparticles ingredients used in the fuel cell coolant in 100 ml, 500 ml and 2 L reactors. At 100 ml scale, the nanoparticles were produced using magnetic stirring and the heating was provided by a constant temperature bath. At the 500 ml scale, the stirring mechanism was changed to a mechanical stirrer with impellers, while the heating mechanism was still through a constant temperature bath. At the 2 L scale, the stirring was through a mechanical stirrer whereas the heating was accomplished by pumping hot water through the jacket of the reactor. In this project (for 10 L and 100 L reactors), mechanical mixers with multiple impellers and heating systems using the jacket of the reactor will be used. Mixing/stirring mechanism as well as the heating method impacts the particle size, charge density and the yield of the reaction. Therefore, an understanding of the influence of these parameters is very essential to obtain the nanoparticles with reproducible properties. Dynalene and Lehigh University have partnered to develop the scale up criteria needed to go from a 2 L scale to a 10 or 20 or 100 L scale. The two types of emulsion polymerization methods used in this project to make the nanoparticles are batch and shot-growth methods.

Results

The batch style polymerization recipe at the 10 L scale did not produce the desired results (in terms of particle size and charge density). This method was abandoned in favor of optimizing the shot growth procedure which showed promise in the 2 L scale.

Shot growth polymerization is when a large portion of the reaction components are added to the reactor at the beginning of the reaction, the reaction is initiated, and the reaction is allowed to progress to 80 to 90% completion before a “shot” of co-monomers is added quickly to the reactor. This approach gives an added level of control to the reaction because the ratio of co-monomers in the shot has a large effect on the final particles.

The shot growth method has benefits over the batch method. The first is the large number of variables that can be altered to achieve the desired result. The following is a list of those parameters:

- Ratio of co-monomers
- Concentration of co-monomers
- Timing of shot
- Speed of shot
- Use of dip tube for shot addition
- Pre-emulsion of shot components

The shot growth method also has the benefit of a much higher solids concentration than the batch method. This higher concentration gives a much more efficient and cost-effective synthesis due to the increase in yield over the batch recipe. The optimum co-monomer concentrations and their ratio were determined at the 2 L scale and were left constant for the 10 L experiments. Experiments were also carried out to determine the correct timing of the shot, which was found to be between 2.5 and 3.0 hours after initiation of the reaction. All subsequent experiments were run with this timing.

Impeller position and the stirring speed were optimized next. Several reactions were run with the multi-impeller set-up in combination with the slower stirring speed. The scanning electron microscope (SEM) picture (Figure 1) showed a uniform, consistent particle size in the 200-250 nm range. Surface charge density was also within the expected range of 500-1,000 µeq/g (Table 1).

Optimization of cationic nanoparticle synthesis at 10 L scale was completed and the initial testing with the 100 L reactor begun. The testing started with dyed oil and water in which the oil represents the styrene. It is necessary to decrease the stirring speed when scaling up because the tip speed on the larger impellers is much greater at the same rotational speed. Too much shear creates unwanted

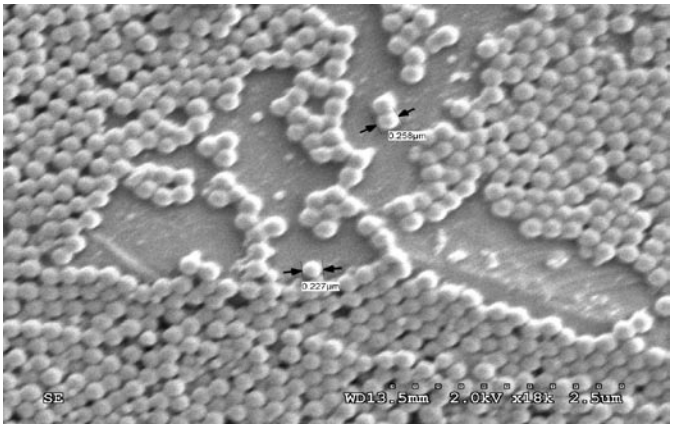


FIGURE 1. SEM Picture of the Cationic Particles Produced in 10 L Scale

TABLE 1. 10 L Scale Cationic Particle Experiments with Optimized Parameters

Experiment	Reaction type	Particle Size (nm)	Surface Charge Density (µeq/g)
JWM-0002-07	10 L shot growth	230	500-1,000
JWM-0002-10	10 L shot growth	225	500-1,000
JWM-0002-12	10 L shot growth	230	500-1,000
JWM-0002-14	10 L shot growth	235	500-1,000

results in the final latex, mostly coagulum and non-uniform particle distribution. The impellers were initially set up with geometric similarity to the final placement at the 10 L scale.

Testing was conducted at room temperature first to determine the minimum mixing speed to mix efficiently without high shear. It was not possible to achieve complete mixing at a speed low enough to eliminate vortexing at the initial reaction volume. It was necessary to either add another impeller or reduce the volume in the reactor to increase mixing efficiency. It was determined to decrease the reaction volume to better fit the reactor with the current number of impellers. The impeller spacing was altered to work with the decreased reaction volume.

Testing was resumed at room temperature with the new impeller placement and decreased volume concentration. It was possible with the new set-up to achieve complete mixing without the formation of a vortex. Photographs of the dyed oil/water mixing study can be seen in Figure 2.

Testing of the heating system also was carried out in conjunction with the mixing study. This testing included measuring the efficiency of the heating system while studying the effect of temperature on mixing efficiency. It was discovered at this time that the current heating system configuration was not able to heat the full volume of the 100 L reactor to the reaction temperature. A larger pump was installed in the heating system to increase the flow rate of the heating water through the reactor jacket. Testing was resumed and the reactor achieved the reaction temperature within two hours.

The impeller configuration and stirring speed were optimized at the 100 L scale with dyed oil and water at the initial reaction volume. Further testing is currently being done to optimize the stirring conditions with the addition of the shot to the reactor.

Conclusions and Future Directions

Dynalene has set up all the reactors for the nanoparticle production. After some preliminary testing, the 10 L reactor was used for the synthesis of the nanoparticles. The scale up criteria developed in collaboration with Lehigh University was verified. It was determined that a shot-growth approach was better suited than a batch synthesis. Shot addition time and the process as well as the speed of the stirrer were optimized to obtain the right size and surface charge of the particles. Nanoparticle synthesis in the 10 L scale was repeated several times and the particle size

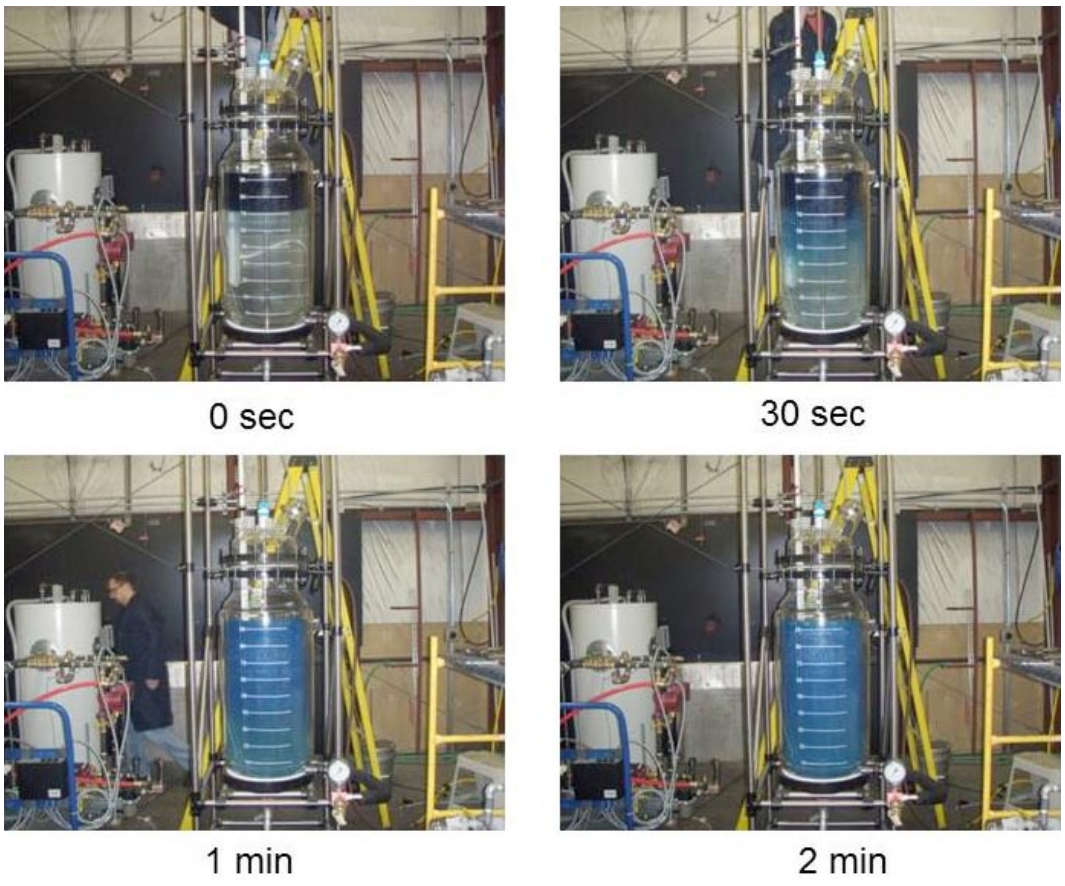


FIGURE 2. Oil/Water Study to Determine Mixing Parameters in the 100 L Glass Reactor

as well as the surface charge density was reproduced, thus making it a viable process for future commercial production. An oil/water study was conducted in the 100 L scale to optimize the stirrer position and the speed. In the future, nanoparticle synthesis will be performed at this scale, and filtration will be performed in 5 L scale to produce clean nanoparticles for subsequent production and testing of the fuel cell coolant.

FY 2011 Publications/Presentations

1. McMullen, P, Mock, J and S. Mohapatra, "Fuel Cell Coolant Optimization and Scale-up", Poster presented at the Annual DOE Hydrogen Program Review Meeting, May 2011, Washington, D.C.

V.L.8 21st Century Renewable Fuels, Energy, and Materials Initiative*

K.J. Berry (Primary Contact), Susanta K. Das (co-PI), Abhijit Sarkar, Claire Hartmann-Thompson, C.H. Schilling, Steven E. Keinath, Jianfang Chai, James P. Godschalx, Salma Rahman, Li Sun, Edmund J. Stark and Dave Namenye

Center for Fuel Cell Systems and Powertrain Integrations
Kettering University
1700 University Avenue
Flint, MI 48504
Phone: (810) 762-7833
E-mail: jberry@kettering.edu, sdas@kettering.edu

DOE Managers

HQ: Dimitrios Papageorgopoulos
Phone: (202) 586-3388
E-mail: Dimitrios.Papageorgopoulos@ee.doe.gov

GO: James Alkire
Phone: (720) 356-1426
E-mail: James.Alkire@go.doe.gov

Contract Number: DE-EE0003109

Project Start Date: July 1, 2010
Project End Date: June 30, 2012

*Congressionally directed project

Fiscal Year (FY) 2011 Objectives

- Research, develop and fabricate an improved high-temperature proton exchange membrane (PEM) fuel cell membrane capable of low-temperature starts (<100°C) with enhanced performance.
- Research, develop and fabricate a 5 kWe novel catalytic flat plate steam reforming process for extracting hydrogen from multi-fuels and integrate with high-temperature PEM fuel cell systems.
- Research and develop improved oxygen permeable membranes for high power density lithium air battery with simple control systems and reduced cost.
- Research and develop a novel high energy yield agriculture bio-crop (Miscanthus) suitable for reformate fuel/alternative fuel with minimum impact on human food chain.
- Extend math and science alternative energy educator program to include bio-energy and power.

Technical Barriers

This project addresses the following technical barriers from the Fuel Cells section of the Fuel Cell Technologies Program Multi-Year Research, Development and Demonstration Plan:

(A) Durability
(B) Cost
(C) Performance

Technical Targets

This project is conducting fundamental studies to develop a new class of high-temperature PEM fuel cell materials capable of conducting protons at elevated temperature (180°C), multi-fuel reformer system, high power density lithium-air battery, and high energy yield bio-crop cost analysis and production model. If successful, insights gained from these studies will be applied toward the design and manufacturing of advanced membrane materials, lithium-air battery and multi-fuel reforming system that meet the following DOE 2015 targets:

- Cost: $20/m^2 for high-temperature PEM membrane.
- Improved membrane conductivity and durability.
- Cost-effective multi-fuel reformer system.
- High power density lithium-air battery with simple control systems at a reduced cost.
- High energy yield agriculture bio-crop cost analysis and production model.

FY 2011 Accomplishments

- Polybenzimidazole (PBI)-polyamide (PA) membrane with good mechanical integrity has been successfully fabricated and a reproducible fabrication method has been developed where molecular mass was a function of the mechanical stirrer torque. Fabricated PBI-PA membranes with high molecular mass and good mechanical integrity. Sulfonic acid polyhedral oligomeric silsesquioxane (POSS) nanoadditive (S-POSS) was already prepared on the 100-g scale. Phosphonic acid POSS (P-POSS) nanoadditive was also prepared on the 2-g scale.
- The developed high-temperature PBI-PA-based PEM membrane is capable of meeting proton conducting membrane materials requirement at a cost of 60% below the DOE targets for 2015. Fabrication of a membrane electrode assembly (MEA) (Pt/C-membrane-Pt/C) is currently underway subject to exact real-world fuel cell operating conditions.
- Optimized design of a multi-fuel catalytic flat plate steam reformer with combustion and reforming catalyst separated by solid flat plate boundary is completed based on a computational fluid dynamics (CFD) model simulation results. Based on the optimized design, a first generation fuel reformer prototype has been fabricated. Currently we are testing the multi-fuel reformer prototype to generate data to benchmark the performance.

- Fabricated numerous button cell lithium-air battery prototypes to evaluate performance of various components. Characterized various battery properties including charge-discharge cycle testing, open-circuit voltage (OCV), and total charge-discharge capacity. Characterized electrolyte conductivity and electrode polarization resistance for improved performance of lithium-air battery. Fabricated an oxygen permeable membrane for lithium-air battery cathode with an oxygen permeability of 10^4 to $4x10^3$ barrer and a moisture permeability of 1 to 5 barrer.
- Two primary methods have been demonstrated at scale for the production of ethanol from cellulosic biomass crops, Miscanthus giganteus (MG) as a feedstock for ethanol: (i) giganteus hydrolysis and fermentation; and (ii) gasification and microbial reaction. The main output of this task will be a comprehensive cost- and energy-balance for the production of MG and its conversion to ethanol by each of these methods. A spreadsheet model has been developed that enables the practitioner/bio-crop producer to evaluate the role of key agronomic factors on MG production costs and net energy balance relative to those of alternative energy crops.
- Learning objectives for the alternative energy educator program (workshop) are being developed. The development of the instructional design document including instructional strategy methodologies has begun. The identification and/or development of learning activities that will engage the participants in the learning process are also in process.



Introduction

Low-temperature PEM fuel cells operate at 80°C and requires nearly pure (99.9999%) hydrogen [1]. However, the lack of a hydrogen refueling infrastructure has been a significant barrier for commercialization, especially for large volume markets such as commercial transport, military silent watch, residential homes, telecommunications, and waste fuel processing to power applications [1]. To leverage the significant commercial potential of this immerging technology globally, the solution has always been considered as on-board fuel processing (or fuel reforming) for hydrogen extraction from locally available logistics fuels such as propane, diesel, JP8 fuel (for military), natural gas, methanol, ethanol, synthetic, and bio-renewable fuels [1]. However, the challenge has been the development of an on-board hydrogen fuel reforming "system" that is cost effective, compact, and commercially viable. Since the production of pure hydrogen required additional equipments and cost for fuel reforming, low-temperature PEM fuel cells are not a viable option for use with logistic fuels for large scale global fuel cell markets [1]. As such the primary technical and commercial challenge is the development of a cost-effective fuel cell electric power generation system capable of using locally available logistics fuels and applicable for small- and large-scale applications worldwide. Traditionally, the approach has been to focus on the development of fuel reforming technology for low-temperature PEM fuel cells, including the removal of fuel impurities [1]. Unfortunately, this approach results in excessive fuel reformer cost, larger reformer size and high complexity. Conversely, our solution is to focus on the development of a more robust "PEM fuel cell combined with fuel reforming system" that is more tolerant of fuel impurities which reduces not only the fuel reformer cost, complexity, and size, but also increases the overall system efficiency. Since a high-temperature PEM fuel cell operates at 160-180°C, it allows the use of non-pure hydrogen (2% CO mixed with hydrogen stream) as a fuel [2] while maintaining the cost and expanding the application flexibility benefits comparable to low-temperature PEM fuel cells. The expected outcomes include: 1) more efficient use of thermal energy or by-product heat as a combined heat and power application resulting in high system efficiency; 2) reduction of balance-of-plant (BOP) components for cooling, water management and purification resulting in reduced maintenance and simpler operations and controls; 3) when using reformed fuels rather than pure hydrogen, the result is increased tolerance to carbon monoxide (CO) which reduce the equipment and capital cost necessary to remove fuel impurities; and 4) will move this emerging technology closer to meeting DOE's 2015 power density target of 100 W/L for fuel cells and reformed fuels.

In this project, using Michigan Molecular Institute's (MMI's) patented [3] nanoadditives-based high-temperature PBI-PPA membranes those are known to be thermally stable up to 200°C with superior proton conductivity, we plan to test the performance of a 25 cm^2 active area high temperature PEM fuel cell with up to 5% CO mixed reformate directly pumped from the reformer to the cell. At Kettering, we designed and built the multi-fuel reformer based on a rigorous CFD model simulation to use locally available logistic fuels/bio-fuels. Bio-fuels are planned to be extracted from a high energy yield agriculture bio-crop, MG, which is suitable for bio-fuel extraction without any impact on human food chain. For fuel cell energy storage purpose, we are developing and fabricating lithium-air battery with superior charge-discharge capacity. Finally, we intend to extend math and science alternative energy educator program to include the research results in bio-energy and power generation topics.

Approach

- Use patented novel polymer synthesis technology to prepare a high-temperature proton exchange polymeric media that has been designed primarily to have high proton exchange capability at elevated temperature.
- Using CFD model results, design and fabricate a 5 kWe novel catalytic flat plate steam reforming system for extracting hydrogen from multi-fuels and integrate with high-temperature PEM fuel cell systems.

- Develop improved oxygen permeable polymer membranes for high power density lithium air battery and use it to design simple control systems at reduced cost.
- Develop and research of novel high energy yield agriculture bio-crop (Miscanthus) suitable for reformate fuel/alternative fuel with minimum impact on human food chain.

Results

In the past year, the main focus has been on S-POSS and P-POSS nanoadditive synthesis, and development of a method for synthesizing high molecular mass PBI in PPA, and casting mechanically robust membranes from the same PBI-PPA reaction solution. The S-POSS synthesis has been completed on a 100-g scale (one-step process, Figure 1a) and the P-POSS synthesis has been completed on a 2-g scale (three-step process, Figure 1b, in which the first two steps have been scaled up to 10-50 g). In order to achieve maximum molecular mass, and therefore the best film integrity upon casting for the PBI syntheses in PPA, it was determined that a precise 1:1 monomer ratio was of paramount importance, we found that 4% solids in PPA was optimum, and minor deviations in either direction caused a significant decrease in molecular mass (see Table 1). A digitally controlled stirrer was used and the torque (related to viscosity and molecular mass) was monitored during the reaction. After 24 hours at 205°C, a plateau torque value of 40 in-oz was measured. Regarding reaction vessels, plain wall resin kettles performed better than indented wall resin kettles (in which reagents were trapped in the indents). Films were cast by pouring the hot PPA mixture onto a substrate and spreading it using a doctor blade. Final membrane thickness can be controlled by adjusting the doctor blade setting (where the size of the gap determines the film thickness). Granite and glass substrates were evaluated and granite was selected because it had a flatter surface to ensure uniform film thickness, and appeared resistant to temperature and acid exposure. The membrane thickness in the final MEA should be able to be controlled by varying the time, temperature, and pressure during the MEA pressing process.

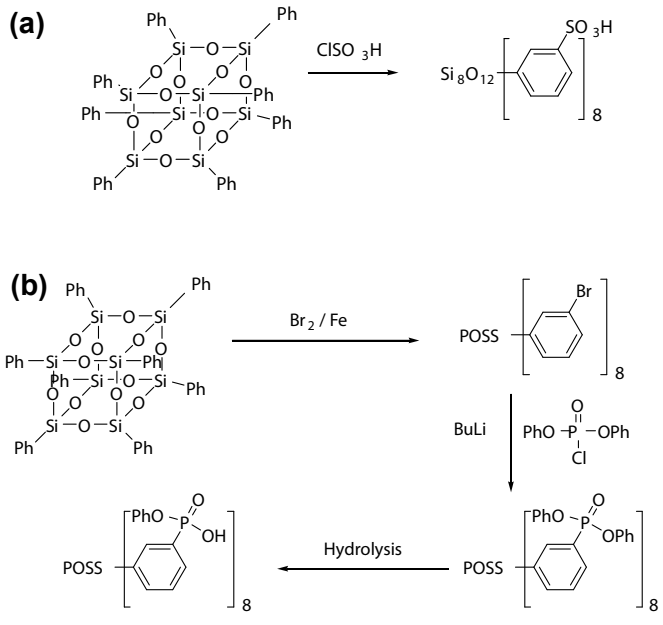


FIGURE 1. (a) Production of S-POSS Nanoadditive (b) Production of P-POSS Nanoadditive

TABLE 1. *m*-PBI Inherent Viscosity as a Function Of Reaction Conditions

Reference	Time (hrs)	Temperature (°C)	% Solids in PPA	Inherent viscosity (dL/g)
805-13	168	205	6.52	1.597
805-18	96	205	6.18	0.866
815-1	24	205	3.75	1.585
815-4	72	205	4.00	2.419
815-9	48	205	4.00	2.247
815-12	48	205	3.99	1.779

During the past year, by taking into account the effect of channel length, inlet gas velocity and catalyst layer thickness for flat plate reformer system we optimized the multi-fuel reformer system with water-gas shift (WGS) reaction in order to build a flat plate reformer prototype for real world testing. Figure 2a represents the production of dry H_2 with WGS reaction and optimized reformer geometry for methane reforming. The reformer geometry is optimized based on the optimized channel height, inlet velocity and catalyst layer thickness. From Figure 2a we see that the production of dry hydrogen only went up by 2% (mole fraction of H_2 from 0.76 to 0.78) with the WGS reaction. It is due to the fact that no methane is available in the WGS zone to produce H_2. Figure 2b represents the production of dry CO with the WGS reaction and optimized reformer geometry. From Figure 2b we see that the amount of dry CO was reduced by more than 50% (mole fraction of CO went down from 0.158 to 0.072 on dry basis) with WGS reaction. Therefore, it is advantageous to include WGS reaction with the optimized fuel reformer geometry especially in order to get low CO-rich reformate H_2. We already built a flat plate fuel reformer based on this optimized simulation study and the real world testing is underway to evaluate the effect of different parametric conditions.

For the lithium-air battery, in the past year, the main focus has been on fluorinated hyperbranched polymer (HBP) synthesis for oxygen permeable membrane fabrication, cathode development, solid electrolyte development, cell fabrication, and cell characterization. The fluorinated HBP was synthesized using MMI's patented bimolecular non-linear polymerization technology and used

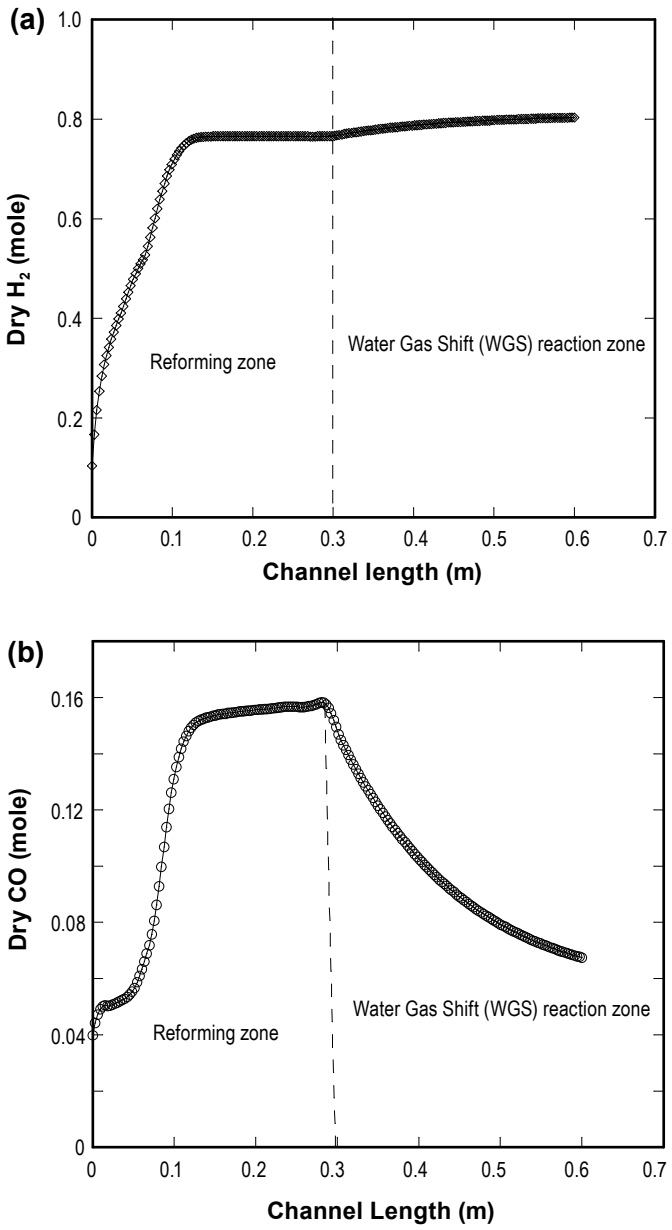


FIGURE 2. (a) Production of Dry H_2 with WGS and Optimized Reformer Geometry (b) Production of Dry CO with WGS and Optimized Reformer Geometry

in the oxygen selective membrane fabrication. A commercial porous PTFE/polypropylene (PP) support coated with the fluorinated HBP has been prepared. The evaluation for oxygen and moisture permeability is currently being carried out. Air cathodes for the lithium-air battery were based on nickel foam (current collector), carbon (electrical conductor), lithium aluminum germanium phosphate (LAGP)-based ion conductor, and PTFE (binder). The LAGP/C ratio was varied from 75/25 to 25/75 in order to obtain the best cell capacity and performance. A cobalt catalyst was explored which was found to enhance the cell capacity. The use of a solid ceramic electrolyte greatly improves safety and durability of the cells, but requires the cells to operate at elevated temperature for best performance. In addition, the rigid ceramic electrolyte can suppress dendrite formation from the lithium anode during the charging process. A literature process was replicated as a starting point to develop an optimum battery. A three-layer electrolyte comprising a LAGP ceramic center sandwiched between two polymer electrolytes was used. A polymer electrolyte was used as a protective layer to prevent the direct contact of Li metal with the ceramic disc. In addition, the polymer layers also improve the contact between the electrolyte and both the anode and cathode. Several kinds of polyethylene oxide (PEO)-based polymer electrolyte layers were prepared. PC(Li_2O), PC(BN), and PC(SN) discs were obtained by ball mill mixing followed by pressing at elevated temperature. The three layer PC(BN)/LAGP/PC(Li_2O) electrolyte was obtained by lamination of the three layers at elevated temperature. The conductivities of these solid electrolytes were measured and shown in Figure 3a. Solid button cells were fabricated utilizing the Ni/C/LAGP/PTFE based cathode, the PC(Li_2O)/LAGP/PC(BN) solid electrolyte, and a lithium metal anode. The cells were tested under dry air using a 0.1 mA discharge current. The OCV of the cells were above 3.1 V, however, the cells did not show any discharge capacity at room temperature. When the cells were tested at elevated temperature (60-80°C) they did show some discharge capability even in the absence of any catalyst in the cathode. The cell capacity increased with an increase of the amount of carbon in the cathode. In addition, as expected, the specific cell capacity was greatly enhanced with the addition of a Co_3O_4 catalyst to the cathode (1,160 mAh/g C). Although the cells showed some promising properties, the maximum discharge current allowed was small. The internal resistance of the cells was very high at room temperature (>2,000 ohm) and decreased with an increase of temperature. However, the same or even higher internal resistance with a single layer polymer electrolyte compared to that of a three layer electrolyte suggests that interfaces, not the electrolyte itself, are the main factors for the high internal resistance and thus a low discharge current. A cell with a liquid electrolyte wetted interface between the solid electrolyte and the Li anode showed significantly improved cell capacity as shown in Figure 3b. To improve on the small discharge current, alternative polymer and gel type electrolytes are being explored. HBP materials based on organosilane and polyethylene glycol (PEG) are under development. Siloxanes are nonvolatile, nonflammable, highly resistant to oxidation, nontoxic, have a low T_g, and are environmentally benign. PEG is effective in solvating lithium salts and thus is lithium ion conducting. To further improve on the electrolyte, polar molecules are attached to the HBP periphery. For example, the reaction of tetrakis(dimethylsiloxy)silane with diacrylated PEG was carried out in toluene in the presence of platinum catalyst. A portion of the Si-H end groups (50-90%) are converted into polar groups such as cyclic carbonate, which can increase solvation and ion pair separation ability of the HBP.

(a)

Temp (°C)	Conductivity (10^{-4} S/cm)				
	LAGP	PC(Li O)	PC(BN)	PC(SN)	PC(BN)/LAGP/PC(Li O) laminate
24	3.18	1.78	0.54	5.03	
35	4.90	4.92	1.08	7.53	
40	5.64	7.11	2.18	10.4	2.57
50	7.49	14.1	3.83	14.8	5.50
60	9.36	23.8	6.60	20.3	8.51
70	11.6	35.6	12.0	26.1	13.5
80	13.7	54.4	18.3		20.5
90	15.6	71.2			29.2
100	18.0	84.2			

(b)

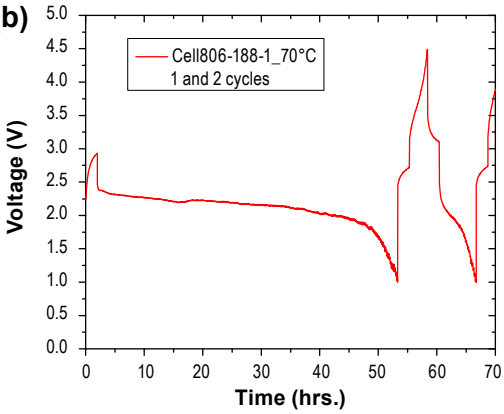


FIGURE 3. (a) Data of conductivity of the solid electrolyte components and three layer stacks. (b) The first two cycles (charge-discharge) of lithium-air battery prototype cell tested at 70°C.

In addition, it was expected that fast molecular motion of the hyperbranched side chains would contribute to fast ionic transport.

For high energy-yield bio-fuel agriculture crop MG production, during the past year, we developed a spreadsheet model for predicting the costs of production of MG relative to other energy crops (eg. switchgrass). Results of these studies are drawn together with the purpose of providing the U.S. Department of Energy with a convenient and flexible method of calculating production costs relative to alternative energy crops. The method is based on a standard, cost-accounting approach reported in earlier studies on MG production by Khanna et al. [4]. Using discount methodology [4], that analysis accounts for the outputs generated and the inputs required (cash flow) over the lifespan of the crop. The main result is a calculation of net present value, which is the total margin over the crop lifetime, converted into equivalent value in today's money. With that method, a breakeven price is calculated as the price in current dollars needed to offset all production costs over the lifetime of the crop discounted to current prices divided by the discounted value of successive crop yields:

$$\text{Breakeven price} = \frac{\sum_{i=0}^{imax} C_i/(1+r)^i}{\sum_{i=0}^{imax} \phi_i/(1+r)^i} \quad (1)$$

In this expression, i_{max} is the crop lifetime in years, ϕ_i is the yield per hectare in year i, r is the discount rate, and C_i is the cost of production per hectare in year i. Currently, we are performing detailed sample calculations to guide the user in building a spreadsheet model. Costs of production are split between one-time establishment costs in year one, and annual maintenance and harvesting operations in each subsequent year. Costs of production are further split among the primary unit operations of rhizome propagation, crop establishment, cultivation, harvesting, baling and storage, and delivery to a bio-energy plant.

Conclusions and Future Directions

From FY 2010 to the current date has resulted in a great knowledge expansion regarding manufacturing processes of new high-temperature PEM materials, lithium-air battery development and fabrication process, and multi-fuel reformer prototype development. We now understood the manufacturing process of new materials and the performance validation protocols in quantitative terms at least at the laboratory-based manufacturing stage. We have a good understanding of the polymer chemistry, thermodynamics and electro-kinetics. This information is critical to develop new high-temperature membrane materials for fuel cell applications where chemical treatment, polymer casting, and performance evaluations are of the utmost importance. Although the DOE deliverables of our project to date have been achieved, this year we intend to submit final project report after finishing the following attributes:

- Having developed a reliable method of membrane fabrication, PBI-PPA membranes carrying S-POSS or P-POSS at appropriate loadings will be prepared, compared with PBI-PA control membranes, and characterized for in-plane proton conductivity, tensile strength and elongation to break, phosphoric acid content (via titration), and morphology and domain structure. The best method of making MEAs to specifications suitable for utilization in fuel cell stacks will be developed. MEAs will be evaluated in stacks and also used to make through-plane conductivity measurements.
- Evaluate the multi-fuel reformer performance for different parametric conditions and further refinement of multi-fuel reformer will be performed if needed.
- Further refinements to the cathode formulation, electrolyte composition, solid electrolyte fabrication, and/or button cell fabrication will be made and the resultant batteries will be tested to insure that a reproducible system is obtained. Lithium-air batteries

will then be fabricated incorporating the fluorinated HBP-based membranes and tested under varying relative humidity conditions to determine how effective the membranes are towards enabling oxygen permeation while retarding moisture permeation. Prototype battery fabrication will require switching to a pouch type battery with non-ceramic electrolytes to achieve the desired voltage and power output.

- Develop a detailed cost- and energy-balance for miscanthus production.

References

1. Larminie J. and Dicks A., *Fuel cell systems explained*, John Willey & Sons, New York (2000).

2. Susanta K. Das, Antonio R. and K. J. Berry, Experimental Evaluation of CO Poisoning on the Performance of a High Temperature PEM Fuel Cell Stack, Journal of Power Sources, Vol. 193, p. 691-698 (2009).

3. Improved Fuel Cell Proton Exchange Membranes, Nowak, R.; Hartmann-Thompson, C.; Bruza, K.; Thomas, L., Meier, D. (Michigan Molecular Institute, USA), WO 2008127645 A1 (2008).

4. Khanna, M., Dhungana, B., and Clifton-Brown, J., "Costs of producing Miscanthus and switchgrass for bioenergy in Illinois," *Biomass and Bioenergy,* Vol. 32, p. 482-493 (2008).

V.L.9 Improving Reliability and Durability of Efficient and Clean Energy Systems*

Prabhakar Singh
Center for Clean Energy Engineering
University of Connecticut (UCONN)
44 Weaver Road, Unit 5233
Storrs, CT 06268-5233
Phone: (860) 486-8379
E-mail: singh@engr.uconn.edu

DOE Managers
HQ: Dimitrios Papageorgopoulos
Phone: (202) 586-5463
E-mail: Dimitrios.Papageorgopoulos@ee.doe.gov
GO: Reginald Tyler
Phone: (720) 356-1805
E-mail: Reginald.Tyler@go.doe.gov

Technical Advisor
Thomas Benjamin
Phone: (720) 356-1805
E-mail: benjamin@anl.gov

Contract Number: DE-EE00003226

Project Start Date: August 1, 2010
Project End Date: July 31, 2012

*Congressionally directed project

Fiscal Year (FY) 2011 Objectives

- Develop an understanding of the degradation processes in advanced electrochemical energy conversion systems.
  - Advance fuel cell-based power generation systems architecture, including renewable hybridized energy conversion and storage.
  - Develop novel cell and stack structural and functional materials and validate their performance under the nominal and transient operational conditions for the evaluation of long-term bulk, interfacial and surface stability.
  - Gain fundamental understanding of chemical, mechanical, electrochemical and electrical processes related to:
    - Utilization of fuels ranging from bio-derived fuels to liquid petroleum to hydrogen.
    - The role of fuel impurities on degradation and processes for removal from feedstock.
    - Surface and interface phenomena related to surface adsorption, interfacial compound formation, and electron/ion generation and transport.
    - Electrodics and electrochemistry.
    - Novel membranes, heterogeneous catalyst materials and structures will be developed and subsequently validated.
- Develop collaborative research projects with industries to improve the performance stability and long-term reliability of advanced fuel cells and other power generations systems.

Technical Barriers

This project addresses the following technical barriers from the Fuel Cells section of the Fuel Cell Technologies Program Multi-Year Research, Development and Demonstration Plan:

(A) Durability
(B) Cost
(C) Performance

Technical Targets

The projects address technical aspects of stationary fuel cells and stationary fuel processors. DOE 2011 targets are as follows:

- Stationary proton exchange membrane fuel cell stack systems (5-250 kW) operating on reformate:
  - Cost: $530/kWe
  - Durability: 40,000 hours
- Stationary fuel processors (equivalent to 5-250 kW) to generate hydrogen-containing fuel gas:
  - Cost: $220 /kWe
  - Durability: 40,000 hours
  - H_2S content in product stream: <4 ppbv (dry)

FY 2011 Accomplishments

- The Center for Clean Energy Engineering has successfully developed 10 (year one) new industrially sponsored research, development and engineering projects in the field of clean and sustainable energy.
- These collaborative projects have leveraged DOE funds with industrial financial support to accelerate the development of advanced materials, cell and stack components, catalysts and fuel cleanup, and balance-of-plant sub-systems.
- The industrial projects support DOE through the development of reliable and cost-effective advanced clean and efficient fuel cell power generation systems.



Introduction

The overall scope of the energy systems and technology research and development initiative, at the UCONN Center for Clean Energy Engineering, will focus on the development and validation of the mechanistic understanding and subsequent creation of novel cost-effective materials to mitigate degradation processes. Through a unique collaborative program with industry we will solve technology gaps through joint industry/university projects. These relationships will accelerate the development and deployment of clean and efficient multi-fuel power generations systems.

The scope of the research projects will include identification and prioritization of the technology gaps and research needs along with the development of enabling technologies that meet the overall stack and balance-of-plant improvements from a durability, cost and performance perspective. Specifically, the performance stability and reliability of the power generation systems will be improved through the implementation of advanced materials and fabrication processes. Technical areas of interest, to be addressed by the industry/university collaborations will include: a) performance, stability and reliability of fuel cell systems, b) fuels, fuel processing and catalysis, c) advanced functional and structural materials, processes and systems, d) hydrogen storage and power management and e) renewable energy and resources.

Approach

The approach used for this project was to develop collaborative industry/university research projects aimed specifically at accelerating the development and deployment of clean and efficient multi-fuel power generation systems. Through a competitive process faculty developed relationships with industry that provided additional amounts of cash and in-kind support thus leveraging funding available through this project. By requiring a financial commitment from industry this methodology ensured that technology problems of commercialization relevance would be addressed.

During the first year industry collaborations have been executed with UTC Power, FuelCell Energy, UTC Research Center, nzymSys, NanoCell Systems, APSI, Oasys Water and W.R. Grace & Company. The project topics have addressed issues ranging from performance stability and reliability of fuel cell systems to fuels, fuel processing and catalysis and finally including advanced functional and structural materials, processes and systems.

Results

Modeling Resin Flow in Phosphoric Acid Fuel Cells (PAFCs) Gas Diffusion Layers (GDLs) – Project PI: Prof. Rajeswari Kasi, Industry Partner – UTC Power

UTC Power (UTCP) is interested in attaining stable graphitized GDLs that are used in PAFCs. GDLs coated with catalyst (also called electrodes) are used to facilitate electrochemical reactions in PAFCs manufactured by UTCP. Resin flow into carbon fiber substrates blocks the open pore structure of the fibers impacting mass flow of various components to the catalyst layer. Furthermore, attaining stable GDLs is important to (1) increase the lifetime of GDLs, (2) efficiency of the power plant and (3) in lowering the cost of stationary and backup power. Thus in keeping with energy efficiency and renewable energy effort of DOE, the stability of GDLs is important for fuel cells to provide a clean, reliable, low-maintenance option for critical energy needs. So, UTCP is interested in generally understanding the morphology of these GDLs and overall resin distribution.

To address this issue, we have used optical imaging tools to qualitatively investigate the morphology of the carbon scaffold at every step of production of the GDLs. This allows us to establish where the carbonized resin is present in the final substrate. UTCP has supplied us with proprietary materials made via proprietary processing conditions. Using imaging as a tool, we have been able to identify two samples that show relatively uniform carbonized resin distribution as compared to other test variants. Our imaging studies (both surface and cross-sectional) have supplemented UTCP to understand the resin distribution and its impact on GDL morphology. In closing, this collaboration between UCONN and UTCP has resulted in improved understanding of morphology and material properties for GDLs in PAFCs, in keeping with the efforts of DOE. Furthermore, the knowledge gained from this study will be useful to implement in other examples of supported catalysts where optimal distribution of catalytic sites is essential for best catalytic performance.

Evaluation of Enzyme-Based Sulfur Removal Technology for Gas Cleanup – Project PI: Prof. Ashish Mhadshwar, Industrial Partner – nzymSys

A system designed for the enzymatic desulfurization of biogas has been tested at the lab scale. We have investigated the effect of several operational parameters such as enzyme concentration, biogas flow rate and enzyme boost on process performance. To date, our results show H_2S removal rates up to 100% without adverse effect on the methane and carbon dioxide concentration of the biogas. Long-term studies performed at high enzyme concentration (20 wt%) demonstrated formation of elemental sulfur, which could be recovered as a valuable product. As expected, the enzyme performance upon H_2S removal decreases when biogas retention time in the liquid enzyme is reduced. The H_2S breakthrough occurs at earlier times for higher biogas flow rates with a very steep change in concentration. Furthermore, fast enzyme saturation results upon increasing the gas flow rate. This could be overcome with enzyme replenishment, which indicates that this process could be potentially operated continuously for consistent removal of H_2S. This simple, reliable, non-conventional technology has various advantages to become one of the most efficient and economical desulfurization technologies and it could

be considered for larger scale applications. Future work will concentrate on evaluate the effect of reactor scale up and effect on mixing (stirring and packing material) on enzymatic desulfurization of biogas.

Waste to Energy: Biogas Cleanup (Desulfurization) for Energy Generation – Project PI: Prof. Steven Suib, Industry Partner – FuelCell Energy

This project involves the generation of getters (or adsorbents) and catalysts to react with sulfur species in feeds that would be used for fuel cells. The sulfur contaminants include hydrogen sulfide as well as various carbon sulfide materials. The major accomplishment of this work is that new adsorbents and catalyst materials have been made and are being tested for degradation of sulfur contaminants. Various materials have been prepared that are different from commercial desulfurization materials.

Testing of these systems with desulfurization studies clearly show that differences are observed for the various adsorbent materials. Breakthrough curves of various sulfur-containing species have been measured in this case of 0% relative humidity. In addition, studies have been done at various levels of relative humidity. Our results suggest that we have made materials that are more active than commercially available getters and adsorbents. Characterization studies are being done in order to optimize the performance of these materials.

Mechanistic Understanding of Matrix Stability in Molten Carbonate Fuel Cells – Project PI: Prof. Prabhakar Singh, Industry Partner – FuelCell Energy

Short-term and long-term electrically tested electrolyte matrix samples, obtained from our industrial partner FuelCell Energy, have been examined for morphological and structural changes to understand the coarsening and particle growth behavior. As received samples were examined at the matrix – anode and matrix – cathode interfaces. Samples were subsequently washed in glacial acetic acid-acetic anhydride mixture to dissolve and remove the electrolyte. Obtained samples were further analyzed for the morphology of $LiAlO_2$ matrix material. It was observed that the matrix materials show different growth pattern in the anodic and the cathodic environments.

Two matrix samples tested for 240 and 6,984 hours were evaluated using X-ray diffraction, scanning electron microscopy (SEM), and Brunauer-Emmett-Teller techniques. As expected, the matrix samples containing electrolyte showed fully dense matrix structure (with localized porosity on the cathode side). The electrolyte was found susceptible to moisture as evidenced by localized overgrowth of hydrated crystals (Figure 1). Figure 2 shows the fractured cross-section of the matrix on the anode (AD-Side) and cathode (CD-side) tested for 240 h. The matrix morphology shows the presence of reinforcing fibers and core-shell structure. Very little change in the particle growth pattern is noted due to shorter exposure.

Figure 3 shows the cross-section of the electrolyte matrix electrically tested for 6,984 h. The matrix showed the features related to enforcement and core shell structure as observed earlier. Unlike the short-term tested sample, however, the long-term exposed sample showed growth in the particle size.

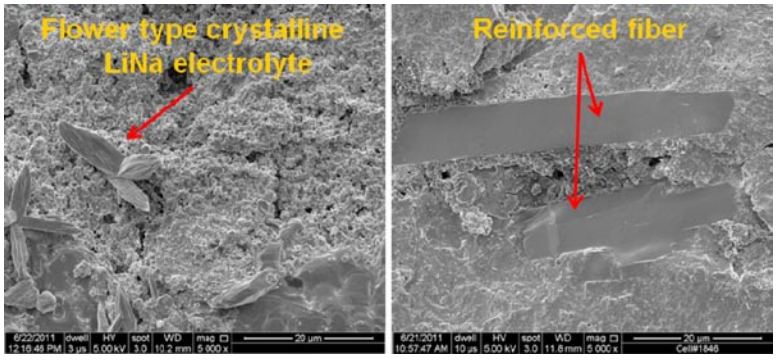


FIGURE 1. Field emission scanning electron microscope (FESEM) images of fracture cross-section of tested matrix. Flower type localized growth of Li-Na electrolyte and reinforced fibers in the matrix (right side).

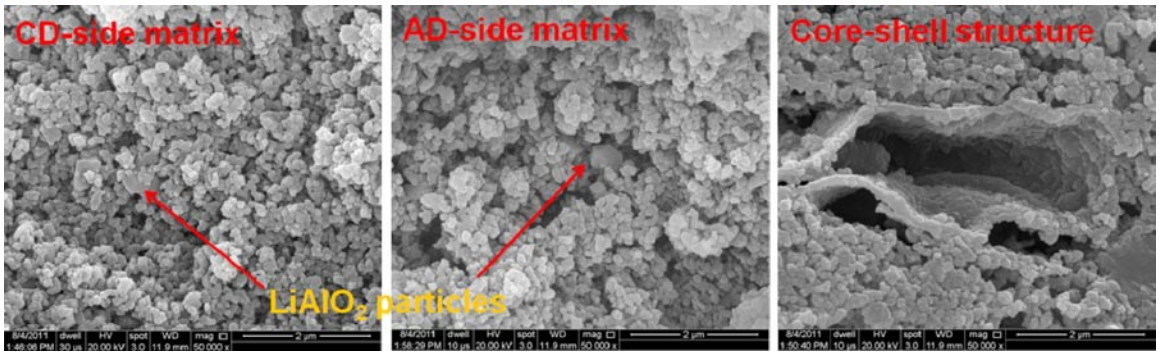


FIGURE 2. FESEM images of fracture cross-section of matrix tested for 240 h. Core shell structure shows the agglomeration of $LiAlO_2$ particles. Anode side matrix shows large crystallites.

It was also observed that the growth of particles in the anode side of the matrix was more pronounced than the particles present near the cathode electrode.

Evaluation of the Performance of Rapidly Quenched Yttria-Stablized Zirconia (YSZ) Electrolytes in a Solid Oxide Fuel Cell (SOFC) and Its Comparison with Conventional SOFC Architecture – Project PI: Prof. Radenka Maric, Industrial Partner – NanoCell Systems

The microstructure and properties of rapidly quenched YSZ was investigated for 8 mol% YSZ (8-YSZ) powder manufactured by plasma sprayed using the solution precursor plasma spray technique, to produce metastable nanostructured powders using a pyrolytic melting or vaporization of an aerosol-solution precursor in a direct current-arc plasma. The preparation was done at the Center for Clean Energy Engineering at University of Connecticut in Storrs, Connecticut.

The material, plasma sprayed powder prepared in one processing step, was characterized for the microstructure of powder, thermal analysis and crystalline material structure at various temperatures and atmospheres. It showed stability of structure and composition in all the ranges of temperature and atmosphere the investigations were conducted. Conductivity tests for the plasma sprayed samples displayed slightly better conductivity than the most used YSZ powder, commercial available on market.

Optimization of Fluid Catalytic Cracking (FCC) Selectivity through Detailed Modeling of Catalyst Evaluation Experiments and the Contributions of Catalyst Components – Project PI: Prof. George Bollas, Industry Partner – W.R. Grace & Co.

An integrated model for Short Contact MicroActivity Testing (SCT-MAT) catalyst testing reactors (fixed bed) has been successfully developed. It couples a hydrodynamic model of a fixed bed reactor and a kinetic network that follows a lumping scheme. Moreover, it allows the comparison of predicted yields of the multicomponent mixture from the reactor with experimental data provided by the industrial partner and acquired through a user interface developed in Microsoft Excel. The algorithm that simulates the fixed bed reactor solves a mathematical model derived from the continuity equation for multicomponent mixtures, using a more general approach than previous studies in the field, taking into account operational peculiarities of the SCT-MAT catalyst testing unit, as employed by the industrial partner. The kinetic network used involves parameters from lumping schemes. These parameters are obtained from an optimization algorithm developed to estimate reaction rates and constants, using the experimental data provided by the industrial partner. Thus, comparison between predicted and experimental yields of the different products of the catalyst testing reactors is available. More sophisticated hydrodynamic models have been developed for the Advanced Catalyst Evaluation (bubbling bed) and the Davison Circulating MicroActivity Riser catalyst testing reactors. Kinetic network models that provide a better insight of the reactions that take place in catalytic cracking reactors are being analyzed. In the near future, the effect of matrix type, zeolite content and diffusion characteristics, such as the crystal size, on the kinetic constants of the lumped kinetic network will be explored. In addition, a user-friendly interface has been developed in Microsoft Excel using visual basic serving two goals: (a) to facilitate the everyday use of the developed process models, and (b) to link the models with the extensive database provided by the industrial partner and ease usage of model during development.

These studies on rector efficiency, lumped reaction kinetics and contributions of catalytic components will enhance productivity in catalyst research and development, will result in optimizing catalyst selectivity, and eventually lead to improving the overall refinery efficiency. Understanding the origins of coke deposits will help reducing the pollution from the FCC regenerator, while at the same time increasing FCC capacity by relaxing its carbon burning constraints. In that notion, this research project will aim to make FCC a cleaner process. Moreover,

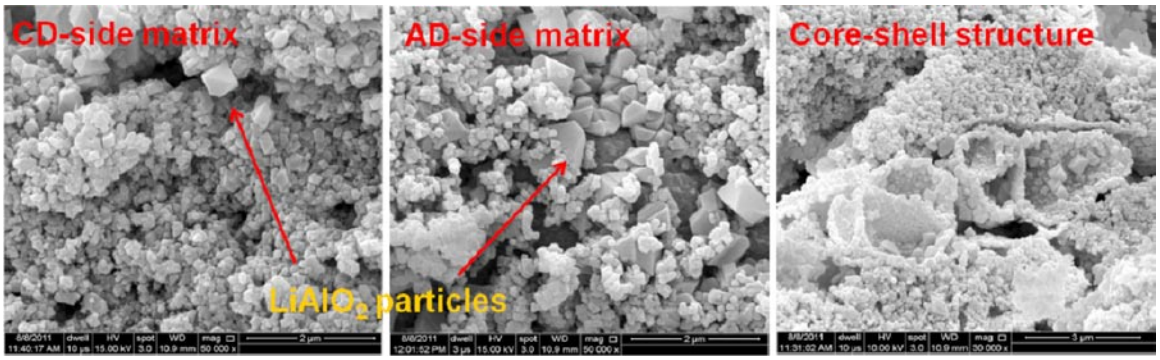


FIGURE 3. FESEM images of fracture cross-section of matrix tested for 6,984 h. $LiAlO_2$ particle coarsening is evident in cathode and anode side matrix. Core-shell structure shows the overgrowth of $LIAlO_2$ particles.

the fundamental knowledge acquired while decoupling reaction kinetics and catalyst deactivation and separation of the effects of zeolite and matrix on catalyst activity and selectivity, can be used to decouple gas and catalyst residence times to optimize biomass gasification and pyrolysis while decreasing secondary reactions.

Stannate-Based Semiconductor Nanocomposites for Solar Energy Utilization – Project PI: Prof. Puxian Gao, Industry Partner – UTC Research Center

First, continuous zinc hydroxystannate (ZHS) cube films have been achieved on both polycrystalline metallic substrates and transparent conductive substrates using hydrothermal synthesis method. As an example, via a fluidic chamber assisted hydrothermal method, continuous ZHS nanocube film have been fabricated on quartz or glass substrates, as shown in Figure 4. The temperature, pressure, and base concentration have been successfully used to control the cube coverage, crystallinity, size and film density.

Second, the structure evolution of ZHS cubes under various ambient annealing conditions has been extensively studied using a combination of structure, morphology and thermal analyses. Various in situ and ex situ microscopy and spectroscopy techniques have been utilized. The temperature windows of various phase transitions have been identified during the thermal decomposition of ZHS. Both temperature and ramping rate are found to be important parameters to control during the thermal processing of ZHS cube films, in order to achieve desired gradient functional composite cube films. The electronic and optical properties evolution in the ZHS cubes have been investigated. Using ZHS micro- or nano-cubes as template and precursor, gradient core-shell stannate-based composite cubes have been achieved after thermal processing. The optical and electronic properties of the gradient structures and corresponding photovoltaic cell performance are under investigation.

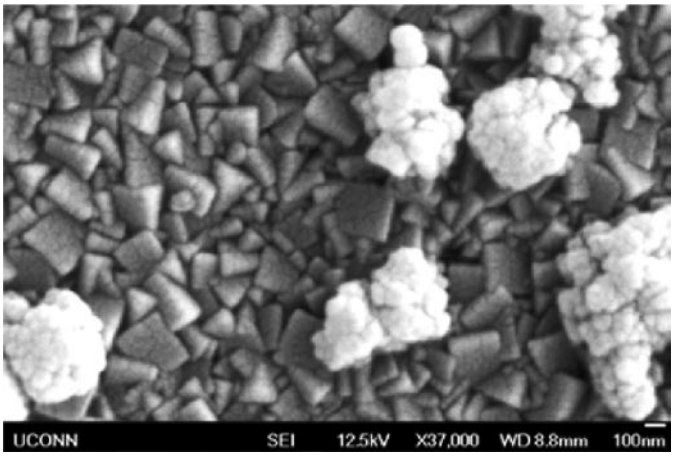


FIGURE 4. An SEM image for ZHS nano-cube films on quartz substrate synthesized by fluidic chamber assisted hydrothermal method.

Fuel Cell Electrode Microstructure: Nanoscale Stability and Efficiency – Project PI: Prof. Bryan Huey, Industrial Partner – UTC Power

Main results focus on two key aspects of fuel cell electrode microstructures.

First, atomic force microscopy (AFM) reveals profound differences in the catalytic nanoparticles in their raw state (Figure 5) and as a floc (upon Teflon® coating, Figure 6). The particle size is larger, Teflon® is occasionally drawn into fibers by the manufacturing process, and the <50 nm particles common in the raw material increases to >100 nm following Teflon® coating.

Second, upon phosphoric acid (PA) loading of the electrode, the Teflon® is occasionally found to separate from the underlying catalyst particles. This is clearly observed

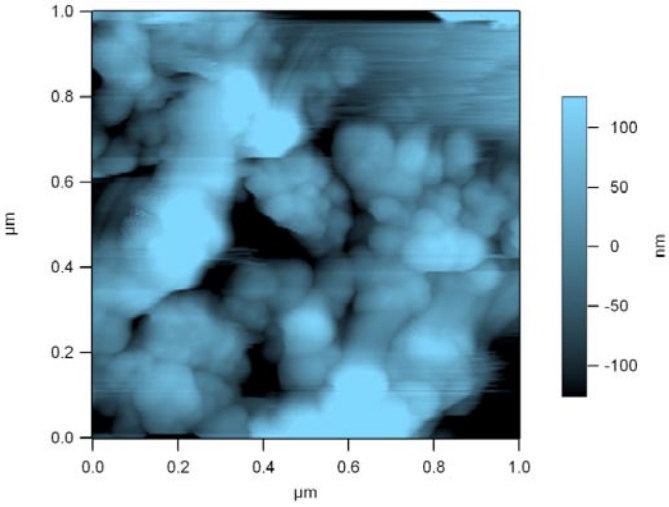


FIGURE 5. Pure Catalyst (10-100 nm particles)

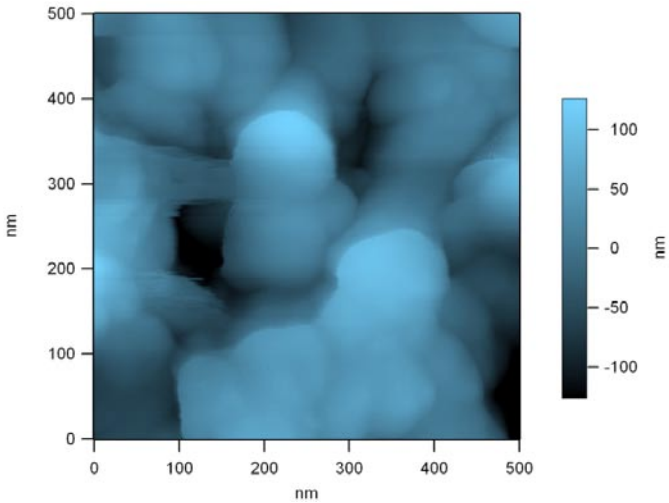


FIGURE 6. Teflon® Floc (>100 nm particles)

by AFM, both in topographic images where the Teflon® appears to have delaminated from the catalyst, as well as in simultaneous AFM phase contrast which reveals the local mechanical compliance. Notably, Teflon®/catalyst separation was only observed following PA loading, but never before PA exposure. It is unclear whether the PA loading procedure, or the simple act of Teflon® swelling upon PA exposure, causes such rupture.

Waste Heat Recovery using the Ammonia-Carbon Dioxide Osmotic Heat Engine – Project PI: Prof. Jeff McCutcheon, Industrial Partner – Oasys Water

Salinity gradient power technologies are quickly coming to the forefront of alternative approaches for producing electricity. One such technology being developed by Oasys Water is the Osmotic Heat Engine, a modified version of an engine cycle that uses a liquid phase intermediate to transfer energy to a turbine. Our work has been primarily focused on developing new membranes for this process. Our approach has two tasks.

First, we have developed a unique benchtop system for testing membranes under pertinent conditions in the osmotic heat engine. These systems are generally unavailable, and our system has shown that it can measure the power generating capacity of membranes (in watts/m^2). The system has yielded positive results using a commercial membrane designed for *forward osmosis*, a sister technology to osmotic power. Figure 7 shows power densities approaching 4 watts/m^2 using 1M NaCl salt solutions. This is near the industry target (4 watts/m^2) and this is the first time this commercial membrane has been successfully tested under this condition.

The second task has been to develop new membrane technology for pressure retarded osmosis (PRO) specifically.

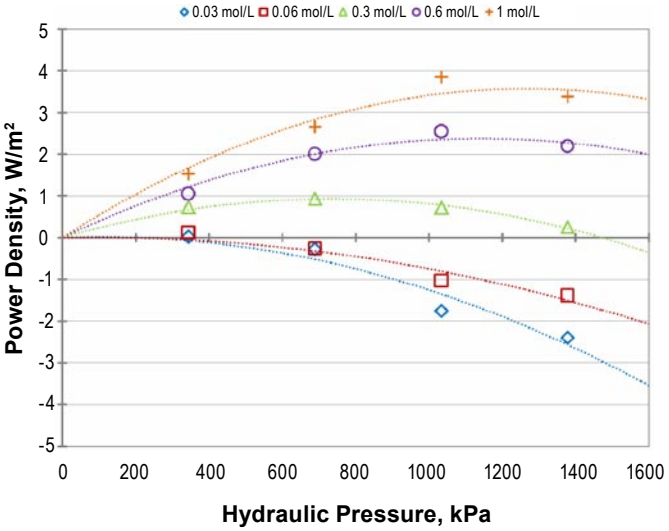


FIGURE 7. Power densities of commercial forward osmosis membrane using different salt concentrations over a range of hydraulic pressures.

We have found a way to modify current generation reverse osmosis (RO) membranes (which can operate under PRO conditions, but in the past have been very poor performers). We have modified RO membranes with polydopamine, a hydrophilic bio-inspired polymer to enhance osmotic flux. Our modifications have resulted in 8-12X increase in osmotic fluxes (Figure 8). Our next tasks will be to optimize this modification technique and test power density with the PRO system.

Fuel Reforming Catalysts for Efficient Energy Usage – Project PI: Prof. Steven Suib, Industry Partner – APSI

The major accomplishment of this project is that a new method has been discovered that allows formation of a fuel reforming catalyst with much less catalyst. This decreases cost and increases efficiency of the reforming of fuel. This method has been submitted as a patent application. The ability of this next generation catalyst to activate the reforming of hydrocarbons is under investigation and looks promising. This method involves the use of thin metal foils of various compositions that are immersed in solutions of precursors of other metals to produce metal alloy catalysts.

Characterization of these materials has involved surface composition, bulk composition, structure, electronic, and morphological properties. Various methods like atomic absorption, inductively coupled plasma, energy dispersive X-ray analysis, SEM, scanning Auger microscopy, X-ray powder diffraction, surface area, and pore size distribution methods are being used. Catalytic testing of the catalyst is being done with various fuels. Characterization of reactants,

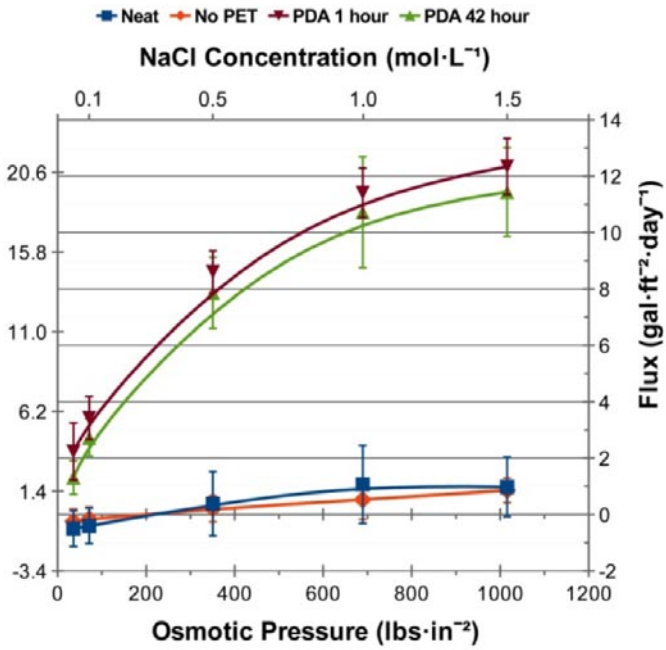


FIGURE 8. Osmotic fluxes of native and modified off the shelf reverse osmosis membrane from Dow Water and Process Solutions.

products and intermediates is done using gas chromatography, liquid chromatography, mass spectrometry, and temperature programmed desorption studies.

Conclusions and Future Directions

The 10 first-year projects are still ongoing and will continue through the balance of this calendar year. As appropriate, this list may be expanded to include a small number of additional relevant projects that address the technology gaps and barriers described. Future directions may include:

- Advanced functional and structural materials research and development will continue to address long-term surface, interface and bulk instabilities at engineered systems level. Research will continue in areas related to solid-liquid-gas interactions as they relate to surface corrosion, electrochemical poisoning, agglomeration and coarsening of porous aggregates, and catalytic degradation.
- UCONN and its partners will continue to develop advanced fuel cleanup and processing technologies to enable multi-fuel capabilities of advanced fuel cell systems. Cost-effective technologies for the removal of contaminants from gas phase will be developed and validated.
- Developed technologies will be transferred to industries to accelerate the development and deployment of advanced fuel cell systems.
- Research findings will be presented and published in technical meetings and peer reviewed journals. Intellectual property will be disclosed through invention disclosures and review by the university's center for science and technology commercialization.

Patents Issued

1. Invention Disclosure filed for efforts associated with program on the Evaluation of Enzyme-Based Sulfur Removal Technology For Gas Clean up with nzymSys as the industrial partner.

2. P.X. Gao, and C.H. Liu, Method of making gradient composite nanostructures through thermal engineering, UConn Invention Disclosure, in preparation, Fall 2011.

FY 2011 Publications/Presentations

1. P.X. Gao, P. Shimpi, W.J. Cai, H.Y. Gao, D.L. Jian, G. Wrobel, Hierarchical Composite Nanowires for Energy, Environmental and Sensing Applications, *Proceedings of SPIE* Vol. 7940, pp. 79401A1-11, 2011 (invited).

2. P.X. Gao, Hierarchical Composite Nanowires for Energy, Environmental and Sensing Applications, *SPIE Photonics West Conferences*, San Francisco, Jan. 25, 2011 (Invited).

3. P.X. Gao, P. Shimpi, H.Y. Gao, W.J. Cai, and G. Wrobel, Multifunctional Composite Nanostructures for Energy and Environmental Applications, *The 4th International Symposium for Advancement of Chemical Science: Challenges in Renewable Energy*, Boston, July 5-8, 2011.

4. G. Wrobel, M. Piech, S. Dardona, and P.X. Gao, *MS&T 2011 fall meeting*, Oct 16-21, 2011, Columbus, OH. (Accepted, oral presentation).

5. C.H. Liu, G. Wrobel, S. Dardona, M. Piech, and P.X. Gao, *MRS 2011 Fall meeting*, Boston, Nov. 28-Dec. 2, 2011, submitted.

6. K.T. Liao, P. Shimpi, and P.X. Gao, *MRS 2011 Fall meeting*, Boston, Nov. 28-Dec. 2, 2011, submitted.

7. G. Bollas, D Orlicki, and H Ma, FCC selectivity studied in lab-scale units and pilot plants, *ACS Annual Meeting*, August 2010, Boston, MA.

8. G. Bollas, D Orlicki, and H Ma, Some uses and misuses of FCC catalyst testing experimental data *AIChE Annual Meeting*, November 2010, Salt Lake City, UT USA.

9. R. Maric, M. Dragan, and J. Roller, 2011 HiTemp Conference, Sept. 20-22, 2011, Boston.

10. R. Maric, M. Dragan, and J. Roller, 2011 MRS Conference, Nov. 28 – Dec. 2, 2011, Boston.

11. Kailash Patil and Prabhakar Singh, "$LiAlO_2$ solubility measurement in (Li-K) carbonate melt," Materials Science & Technology 2011 Conference & Exhibition, October 16–20, 2011 Columbus, Ohio.

Proposals Developed Leveraging Results of this Program

1. Small Business Innovation Research proposal submitted to Department of Defense on "Biogas purification for fuel cells".

2. P.X. Gao (PI), M. Piech (coPI), and S. Dardona (coPI), Thermally engineered graded composite nanostructures for solar energy harvesting, National Science Foundation GOALI proposal, in preparation, Fall 2011.

V.L.10 Solid Oxide Fuel Cell Systems Print Verification Line (PVL) Pilot Line*

Susan Shearer
Stark State College
6200 Frank Ave. NW
North Canton, OH 44720
Phone: (330) 494-6170 ext. 4680
E-mail: sshearer@starkstate.edu

Greg Rush
Rolls-Royce Fuel Cell Systems (US) Inc., North Canton, OH

DOE Managers
HQ: Dimitrios Papageorgopoulos
Phone: (202) 586-5463
E-mail: Dimitrios.Papageorgopoulos@ee.doe.gov
GO: Jesse Adams
Phone: (720) 356-1421
E-mail: Jesse.Adams@go.doe.gov

Contract Number: DE-EE0003229

Subcontractor:
Rolls-Royce Fuel Cell Systems (US) Inc. (RRFCS)
North Canton, OH

Project Start Date: March 1, 2010
Project End Date: June 30, 2011

*Congressionally directed project

Objectives

- Complete the electrical/mechanical build of the RRFCS fuel cell Stack Block Test System (SBTS)
- Perform mechanical commissioning tests to assure SBTS readiness prior to fuel cell stack block install.

Technical Barriers

This project addresses the following technical barriers for the Fuel Cells section of the Fuel Cell Technologies Program Multi-Year Research, Development and Demonstration Plan:

(A) Durability
(C) Performance

Technical Targets

This project completes the mechanical and electrical build of a test apparatus (referred to as SBTS) that will allow RRFCS to test at fuel cell stack product size, full operating temperature and pressure, and with fuel cell inlet anode gas pre-processed from pipeline natural gas. Testing will prove the mechanical functionality of the SBTS prior to install of a fuel cell stack for electrical testing.

FY 2011 Accomplishments

- Demonstrated SBTS mechanical performance over the required range of RRFCS fuel cell operating temperature, pressure and anode/cathode gas compositions.
- About 200 hrs of operating time at temperature with long-term operation planned in 2011 as part of the DOE Solid State Energy Conversion Alliance (SECA) program.
- Control and safety system hardware/software demonstrated up to powered stack operation.



Introduction

This project supported the mechanical/electrical build completion and mechanical commissioning of the SBTS located at the Stark State College (SSC) Fuel Cell Prototyping Center in North Canton, OH. As a result, SBTS is ready to support installation and powered operation of a RRFCS solid oxide fuel cell (SOFC) stack block in the second quarter of 2011. The SBTS will be used to evaluate the performance, reliability and durability of developmental fuel cell stacks at powers of about 20 kW. Fuel cell tubes that compose the SOFC stack are manufactured on the RRFCS PVL. The PVL is a fully automated production line for printing anode and cathode electrodes on fuel cell substrates, with the resulting assembly passed to a furnace for material sintering.

Approach

This project leverages earlier investments by the Ohio Department of Development (ODOD Grant TECH 08-053) through Ohio's Third Frontier and the Department of Energy (DOE Award No. DE-FE0000303, SECA), under which the SBTS mechanical build was completed. The subject work completed the mechanical/electrical build and completed the mechanical commissioning that included controls and safety system software checkout.

Results

Task 1 – Controls Software

Control functions were manually exercised to cover stack heat-up from room temperature to 900°C for stack reduction, transition from the stack reduction temperature to a lower temperature for stack electrical loading and stack cool down to ambient temperature. Startup burner control was established. The catalytic partial oxidation (CPOX) reactor light-off was proven with proper anode fuel gas composition provided to the stack. Operator actions were implemented into the automatic control system for SOFC

stack heat-up from ambient to about 750°C following startup burner light-off. Control functions associated with stack electrical operation (e.g., stack reduction and stack electrical loading) will be developed with existing manual control capabilities and then transferred into the automatic controls software as part of electrical commissioning under the 2011 SECA program.

In parallel with controls software development, the independent safety system software was exercised in response to trip signals with the SBTS responding properly during the emergency shutdown control sequence.

The user interface (HMI) to the control system was proven and enhanced as the various mechanical commissioning tests were completed under this contract. The HMI provides a satisfactory interface for SBTS operation and support for the future electrical commissioning tests.

Task 2 – Facility Electrical and Controls Wiring

All wiring tasks were completed in January 2011 with the installation of the high voltage (~1,100 V direct current) SOFC stack bus bar wires to the load controllers. Operational checks of the eight load controllers and calibration of associated current and voltage transducers were completed including communications to the control system and HMI. All instrumentation associated with SBTS was operated during mechanical commissioning except those associated with the electrical stack operation. The two items associated with cleaning of the oxygen supply tubing and cooling water connection to the load controllers were completed.

Task 3 – Commissioning

Stage 1 commissioning scope included the following:

- Hardware and Configuration. Verification of electrical continuity, component operation and instrument continuity through the control programmable logic controller and HMI. Verification of data storage to disk for each instrument.
- Instrument Calibration. Operation and calibration check of each flow meter.
- Facility and Safety System. Verify operability of natural gas; compressed air; and steam boiler delivery systems, system flare, exhaust pressure control system, and facility safety system/alarms. Exercise the CPOX reactor to demonstrate its functional performance and operating procedure.

System operation. Operation of the entire SBTS as a system from ambient temperature startup to hot stack operation at a condition ready for electrical power loading (Stage 2 commissioning performed in 2011 under the DOE SECA program). Demonstrate normal control system shutdown and safety system emergency shutdown. Perform control loop tuning to achieve acceptable response and stability during normal operation and expected transients.

All of the planned Stage 1 commissioning tasks described by the previous bulleted items were completed by the middle of November, 2010. Progress was interrupted at the end of June due to damage of the high temperature insulation. Following its replacement, Stage 1 commissioning resumed and demonstrated the capability of SBTS to achieve the highest stack operating temperature of 900°C. During the interim period while the insulation was being replaced, the SBTS was able to operate for CPOX reactor control setup as well as establish the stack back pressure automatic control. Operation and automatic control of the startup burner was demonstrated. Functional performance and operation of the CPOX reactor was demonstrated with fuel delivered to the stack, albeit not electrically active for the Stage 1 program testing. All operations of the SBTS were demonstrated as needed to heat the stack from room temperature to 900°C for stack reduction and subsequent return to a lower stack temperature as required for stack electrical loading. Electrical stack tests will be accomplished outside of this project and part of the 2011 DOE SECA program.

Normal shutdown and safety/emergency shutdown response of the SBTS was demonstrated.

Controls operation was discussed in Task 1. During Task 3 commissioning, control loops were tuned to achieve acceptable response during SBTS operation.

For reference, Figures 1 and 2 show the completed SBTS test vessel and its installation for the Stage 1 project test.

Task 4 – Post-Operation Inspection

Following Task 3 test completion, inspection of the stack and hot zone components was made. In general, the internals were found to be in good condition and suitable

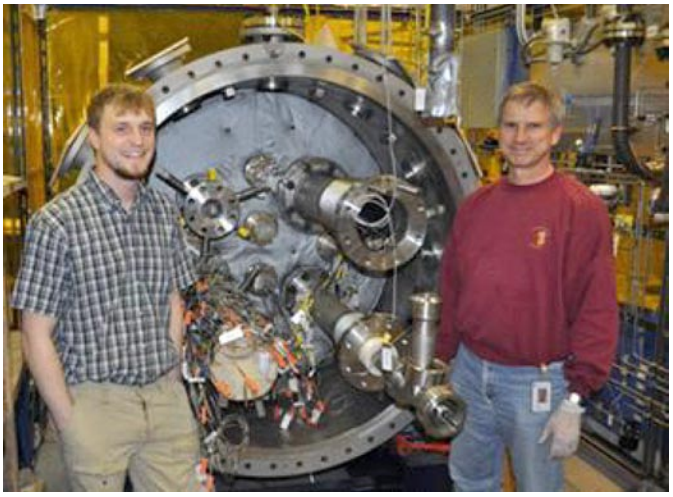


FIGURE 1. SBTS Vessel Assembly Prior to Install of the Outer Vessel Head

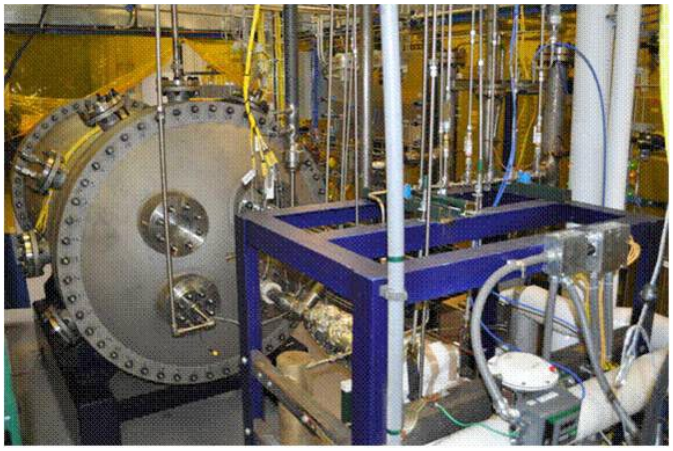


FIGURE 2. SBTS Ready for Commissioning Test

for use in the next test series subsequent to this contract. Carbon was observed in the burner inlet fuel line from CO use and will not be used in subsequent tests.

Conclusions and Future Directions

- Completion of the mechanical commissioning test proved the readiness of SBTS for install of a fuel cell stack and electrical commissioning test. Such testing is planned to begin in April of 2011.
- Control of the major SBTS subsystems was exercised and proven.
- The control and safety system software were exercised and shown ready for electrical commissioning test.
- The SBTS will be used in 2011 by RRFCS to obtain further performance and durability data for the RRFCS solid oxide fuel cell stack block which is the repeat unit for power generation at 1-MW scale.

FY 2011 Publications/Presentations

1. 2011 DOE Hydrogen and Fuel Cells Program and Vehicle Technologies Program Annual Merit Review and Peer Evaluation Meeting, Poster, May, 2011.

© 2011 Rolls-Royce Fuel Cell Systems (US) Inc. This material is based upon work supported by the U.S. Department of Energy under Award Number DE-EE0003229 and pursuant to 10 CFR Part 600.325 Appendix A(c)(1), Rights in Data - General (OCT 2003), Rolls-Royce Fuel Cell Systems (US) Inc. has granted to the Government, and others acting on its behalf, a paid-up nonexclusive, irrevocable, worldwide license to reproduce, prepare derivative works, distribute copies to the public, and perform publicly and display publicly, by or on behalf of the Government, for all such data.

VI. MANUFACTURING R&D

VI.0 Manufacturing R&D Sub-Program Overview

The Manufacturing R&D sub-program supports research and development needed to reduce the cost of manufacturing hydrogen and fuel cell systems and components. The manufacturing research and development (R&D) effort will enable the mass production of components (in parallel with technology development) and will foster a strong domestic supplier base. Activities will address the challenges of moving today's laboratory-produced technologies to high-volume, pre-commercial manufacturing to drive down the cost of hydrogen and fuel cell systems. This sub-program focuses on the manufacture of components and systems that will be needed in the early stages of commercialization. Research investments are focused on reducing the cost of components currently used (or planned for use) in existing technologies, as well as reducing the cycle times of the processes being developed. Progress toward goals is measured in terms of reductions in the cost of producing fuel cells, increased manufacturing processing rates, and growth of manufacturing capacity.

In Fiscal Year (FY) 2011, manufacturing projects continued in the following areas: novel electrode deposition processes for membrane electrode assembly (MEA) fabrication, high-volume fuel cell leak-test processes, novel assembly processes for low cost MEAs, gas diffusion layer cost reductions, flow field plate manufacturing variability and its impact on performance, and fabrication technologies for high-pressure composite storage tanks.

Goal

Research and develop innovative technologies and processes that reduce the cost of manufacturing fuel cells and related systems–providing critical support to industry and helping to spur the growth of a strong domestic supplier base.

Objectives[1]

Currently, the sub-program is focused on technologies and processes for manufacturing polymer electrolyte membrane (PEM) fuel cells and tanks for high-pressure hydrogen storage.

Key objectives for fuel cell manufacturing include:

- By 2012, develop continuous in-line measurement for MEA fabrication.
- By 2013, reduce the cost of manufacturing MEAs by 25%, relative to 2008 baseline of \$63/kW_e (at 1,000 units/year).
- By 2015, reduce the cost of PEM fuel cell stack assembly and testing by 50%, relative to the 2008 baseline of \$0.84/kW_e (at 1,000 units/year).
- By 2017, develop improved fabrication and assembly processes for polymer electrolyte membranes that will enable an automotive fuel cell system cost of \$30/kW (projected to high-volume).

Cost targets for hydrogen storage tanks are currently being re-evaluated.

FY 2011 Technology Status

Presently, fuel cell systems are fabricated in small quantities. The cost of 5-kW, low-temperature PEM fuel cell systems for stationary applications is projected to be ~\$3,100/kW_{net} at a volume of 1,000 systems per year.[2] There were almost 2,000 stationary fuel cell systems shipped by North American manufacturers in 2010.[3] For automotive applications using today's technology, the cost of an 80-kW PEM fuel cell system is projected to be \$49/kW for high-volume manufacturing (500,000 systems/year) and about \$220/kW at manufacturing

[1] Note: Targets and milestones are under revision; therefore, individual progress reports may reference prior targets.
[2] James, B. D., et al., "Low Temperature PEM Stationary Fuel Cell System Cost Analysis: Preliminary Results", NREL Subcontract Report, Subcontract number AGB-0-40628-01, May 2011.
[3] *2010 Fuel Cell Technologies Market Report*, U.S. Department of Energy, June 2011. www1.eere.energy.gov/hydrogenandfuelcells/pdfs/2010_market_report.pdf.

volumes of 1,000 systems/year.[4] The projected high-volume cost includes labor, materials, and related expenditures, but does not account for manufacturing R&D investment.

FY 2011 Accomplishments

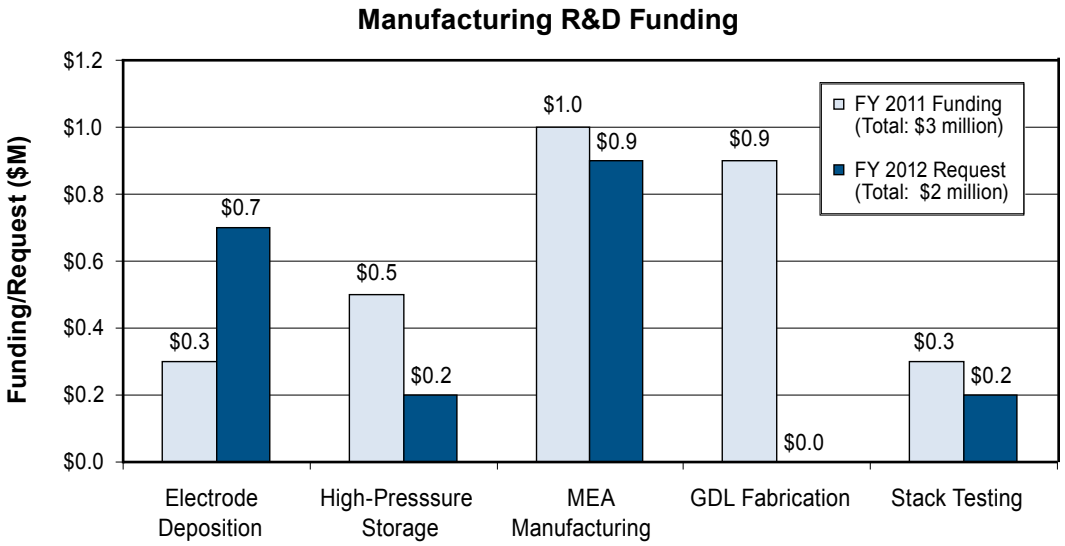
FY 2011 saw a number of advancements in the manufacture of fuel cells and storage systems, including:

- **Gas Diffusion Layer (GDL) Fabrication:** Ballard improved thickness and basis-weight uniformity of GDLs by adding mass flow meters to the "Many-at-a-Time" coating equipment, resulting in GDL cost reduction of over 60% since 2008, while increasing manufacturing capacity nearly four-fold.
- **Electrode Deposition:** W.L. Gore reduced membrane thickness, eliminated membrane backers, reduced scrap with better coating process, and eliminated finishing operations such as electrode and membrane edge trim. Gore previously demonstrated, using their cost model, that a new three-layer MEA process has the potential to reduce MEA cost by 25%.
- **High-Pressure Storage:** Quantum saved 17.4 kg of composite from the baseline (all fiber wound) vessel (23% savings).
- **MEA Manufacturing:** BASF reduced ink preparation time and the number of coating applications by >50%, and improved fuel cell performance by 20 mV over the baseline of 0.67 V at 0.2 A/cm^2. BASF also demonstrated a microporous layer on a production coater with full-width cloth.
- **Component and Stack Measurement:** The National Renewable Energy Laboratory demonstrated the ability to detect defects ≥6.25 mm^2 (e.g., pinholes, electrical shorts, and electrode thickness variations) and catalyst loading variations ≥10% (at nominal 0.45 mg Pt/cm^2) in MEAs using their internal resistance/direct current diagnostic.
- **Bipolar Plate Flow Field Uniformity:** Using their non-contact sensor apparatus for vertical and lateral measurement of flow field dimensions, the National Institute for Science and Technology showed that there was very little accuracy degradation as the scan rate was increased from 30 mm/s to 500 mm/s– allowing high-speed, fully-automated inspection.
- **Hydrogen and Fuel Cells Manufacturing R&D Workshop:** In August 2011, the National Renewable Energy Laboratory and DOE hosted a workshop to identify strategies and R&D needs for lowering the cost of manufacturing hydrogen production, delivery, and storage systems and fuel cell systems and components. The input from the workshop will be used to identify key barriers and needs for future Program activities as well as funding opportunities.

Budget

The President's FY 2012 budget request for the Fuel Cell Technologies Program includes $2 million for Manufacturing R&D. The FY 2011 appropriation for Manufacturing R&D was $3 million.

[4] James, B.D., et al., "Manufacturing Cost Analysis of Fuel Cell Systems," 2011DOE Hydrogen and Fuel Cells Program Annual Merit Review Proceedings, May 2011, www.hydrogen.energy.gov/pdfs/review11/fc018_james_2011_o.pdf, May 2011.



FY 2012 Plans

In FY 2012, activities in the Manufacturing R&D sub-program will: scale up production of low-cost MEAs; update the cost model of hydrogen pressure vessels to include the consideration of lower-performance carbon fiber; demonstrate a 2x reduction in the cost of MEAs by reducing labor involved in ink preparation and reducing the number of coating applications; and further develop the National Renewable Energy Laboratory's continuous in-line measurement of MEA fabrication.

Participants at the Hydrogen/Fuel Cell Manufacturing Workshop suggested a number of follow-on activities for DOE, including:

1. Hosting a meeting of manufacturers to initiate efforts to:
   - Establish a consensus on standard specifications for hydrogen and fuel cell systems and components.
   - Facilitate leveraging the buying power of multiple customers to reduce costs.
   - Facilitate development and expansion of the supply chain.
2. As an output of the first meeting, defining sub-groups to discuss and make plans to address (if possible) individual issues. Each sub-group can involve different supply chain vendors as necessary for their tasks/ issues.
3. Hosting a meeting in which the sub-groups report back to the full working group for prioritization, decisions, etc.

Nancy Garland
Manufacturing R&D Team Lead (Acting)
Fuel Cell Technologies Program
Department of Energy
1000 Independence Ave., SW
Washington, D.C. 20585-0121
Phone: (202) 586-5673
E-mail: Nancy.Garland@ee.doe.gov

VI.1 Fuel Cell Membrane Electrode Assembly Manufacturing R&D

Michael Ulsh (Primary Contact), Guido Bender, Niccolo Aieta, Huyen Dinh
National Renewable Energy Laboratory (NREL)
1617 Cole Blvd.
Golden, CO 80401
Phone: (303) 275-3842
E-mail: michael.ulsh@nrel.gov

DOE Manager
HQ: Nancy Garland
Phone: (202) 586-5673
E-mail: Nancy.Garland@ee.doe.gov

Partners:
- Lawrence Berkeley National Laboratory (LBNL), Berkeley, CA
- Colorado School of Mines, Golden, CO
- University of Hawaii, Hawaii Natural Energy Institute, Honolulu, HI
- Rensselaer Polytechnic Institute, Troy, NY
- 3M, St. Paul, MN
- Arkema Inc., King of Prussia, PA
- Ballard Material Products, Lowell, MA
- BASF Fuel Cells, Somerset, NJ
- General Motors, Honeoye Falls, NY
- Johnson Matthey Fuel Cells, Sonning Common, Reading, U.K.
- Proton OnSite, Wallingford, CT
- W.L. Gore and Associates, Elkton, MD
- National Institute of Standards and Technology, Gaithersburg, MD

Project Start Date: July 16, 2007
Project End Date: Project continuation and direction determined annually by DOE

Fiscal Year (FY) 2011 Objectives

NREL and its collaborators are developing capabilities and acquiring knowledge for in-line quality control during manufacturing of polymer electrolyte membrane (PEM) fuel cells. We are focusing on membrane electrode assembly (MEA) components (membranes, coated electrodes, and gas diffusion media) in the transition to high-volume manufacturing methods. Our main tasks are to:

- Evaluate and develop in-line diagnostics for MEA component quality control and validate diagnostics in-line.
- Investigate the effects of MEA component manufacturing defects on MEA performance and durability to understand the required performance of diagnostic systems and contribute to the basis of knowledge available to functionally determine manufacturing tolerances for these materials.
- Use established models to predict the effects of local variations in MEA component properties, and integrate modeling of the operational and design characteristics of diagnostic techniques into the design and configuration of in-line measurement systems.

These objectives have strong support from our industry partners. Our specific development activities have been and will continue to be fully informed by direct input from industry. As new technologies emerge and as the needs of the industry change, the directions of this project will be adjusted. Additionally, in support of DOE's expanded scope, we have initiated activities to understand quality control needs for high-temperature fuel cell production and assess relevant inspection technologies.

Technical Barriers

This project addresses the following technical barriers, from the Manufacturing section (3.5) of the Hydrogen, Fuel Cells and Infrastructure Technologies Program's Multi-Year Research, Development and Demonstration Plan:

(A) Lack of High-Volume Membrane Electrode Assembly (MEA) Processes

(F) Low Levels of Quality Control and Inflexible Processes.

Contribution to Achievement of DOE Manufacturing Milestones

This project contributes to the achievement of the following DOE milestones, from the Manufacturing section (3.5) of the Hydrogen, Fuel Cells and Infrastructure Technologies Program Multi-Year Research, Development and Demonstration Plan:

- **Milestone 1**: Develop prototype sensors for quality control of MEA manufacturing (4Q, 2011).
- **Milestone 2**: Develop continuous in-line measurement for MEA fabrication (4Q, 2012).
- **Milestone 3**: Demonstrate sensors in pilot-scale applications for manufacturing MEAs (4Q, 2013).
- **Milestone 4**: Establish models to predict the effect of manufacturing variations on MEA performance (4Q, 2013).

FY 2011 Accomplishments

NREL accomplished the following in FY 2011:

- Developed continuous process prototype test-beds to enable initial validation of diagnostic techniques with moving substrates (simulating in-line measurement).

- Demonstrated the operation of our infrared diagnostic system with direct current excitation (IR/DC) with moving gas diffusion media (GDM) and catalyst-coated membrane (CCM) sheet materials.
- Integrated LBNL modeling of the operational and design characteristics of the IR/DC technique into the design process for the in-line configuration of the diagnostic system.
- Developed a second infrared-based technique using reactive gas excitation to measure the spatial uniformity of electrodes on porous substrates, i.e., gas diffusion electrodes.
- Demonstrated the operation of our optical reflectometer diagnostic for areal membrane thickness imaging and defect identification with moving membrane sheet materials.
- Performed studies on the effects of MEA component defects, using single and segmented cells, including electrode thin spots, voids, and mud-cracks, and GDM polytetrafluoroethylene (PTFE) uniformity.
- Installed and commissioned a segmented cell system, using a 3M-developed design with 121 segments, to enable spatially resolved studies of the effects of as-manufactured defects in MEA components.
- Demonstrated the feasibility of using our optical diagnostic platform to make measurements of tape-cast solid oxide fuel cell layer uniformity.
- Continued collaboration with our industry partners, including three of DOE's competitively awarded manufacturing research and development (R&D) projects, in accordance with our project charter.
- Developed industry relationships and gained an understanding of quality control needs for the manufacture of high temperature cells.



Introduction

In FY 2005-2007, NREL provided technical support to DOE in developing a new key program activity: manufacturing R&D for hydrogen and fuel cell technologies. This work included a workshop on manufacturing R&D, which gathered inputs on technical challenges and barriers from the fuel cell industry, and subsequent development of a roadmap for manufacturing R&D. In late FY 2007, NREL initiated a project to assist the fuel cell industry in addressing these barriers, initially focusing on in-line quality control of MEA components. The project is utilizing the unique and well-established capabilities of NREL's National Center for Photovoltaics for developing and transferring diagnostic and process technology to the manufacturing industry.

Defects in MEA components differ in type and extent depending on the fabrication process used. The effects of these defects also differ, depending on their size, location in the cell relative to the reactant flow-field, cell operating conditions, and which component contains the defect. Understanding the effects of these different kinds of defects is necessary to be able to specify and/or develop diagnostic systems with the accuracy and data acquisition/processing rates required for the speed and size scales of high-volume continuous manufacturing methods. Furthermore, predictive capabilities for manufacturers are critical to assist in the development of transfer functions and to enable assessment of the effects of material and process changes.

Approach

NREL and its partners are addressing the DOE manufacturing milestones listed above by evaluating, developing, and validating (in-line) diagnostics that will support the use of high-volume manufacturing processes for the production of MEAs and MEA component materials. Prioritization of this work is based on inputs from our industry partners on their critical manufacturing quality control needs. We are focusing on diagnostic capabilities not addressed by commercially available in-line systems, in particular evaluating methods to make areal rather than point measurements such that discrete defects can be identified. Given that specification of the required accuracy and precision of a diagnostic device to measure or identify material property variability or defects requires information about how this variability affects the functionality of the MEA, we are developing test methodologies to study the effects of size and/or extent of each important type of variability or defect. These results will additionally assist our industry partners in validating manufacturing tolerances for these materials, ultimately reducing scrap rates and cost, and improving supply chain efficiency. Finally, predictive models are being used at LBNL to understand the operational and design characteristics of diagnostic techniques by simulating the behavior of MEA components in different excitation modes. These results are being fed back to our design effort in configuring the diagnostics for in-line implementation. MEA models are also being utilized to understand the in-situ behavior of defect MEAs to guide and further elucidate experiments.

Results

Significant progress was made in moving our two diagnostic platforms, optical- and infrared-based, closer to in-line implementation. Benchtop prototype systems were designed and fabricated at NREL to enable validation of the operation and data acquisition of these techniques with a moving (as opposed to stationary) measurement target, a critical step in proving the viability of these techniques for in-line measurement. Using these systems, we successfully demonstrated the operation of the IR/DC and optical reflectometer diagnostics using GDM, CCM, and membrane sheet materials from our industry partners. Figure 1 shows the benchtop roller system used to validate

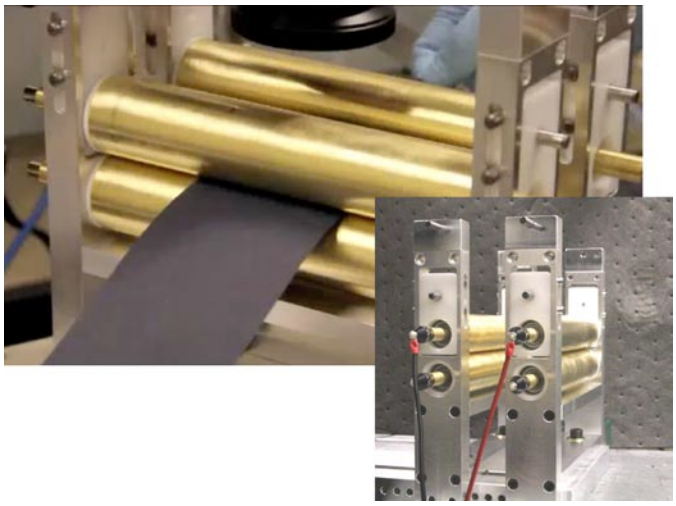


FIGURE 1. Benchtop Roller System (Inset: side view showing sliding electrical connectors.)

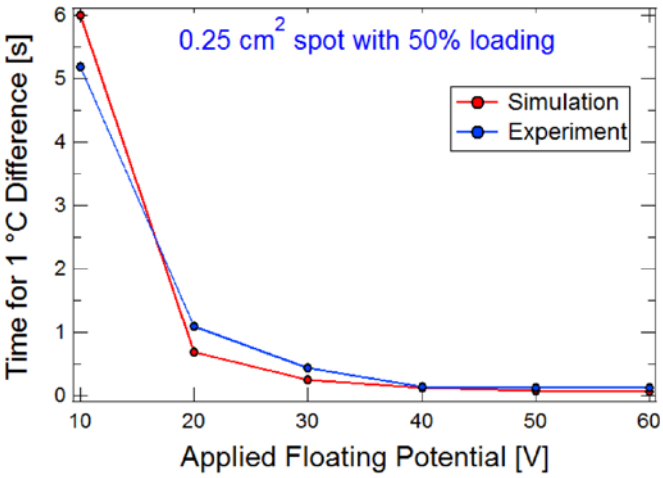


FIGURE 3. Comparison of modeling and experimental results indicating the response time for a given detection criteria and electrode defect size as a function of the DC excitation magnitude.

the IR/DC technique. Figure 2 shows an example from that validation, in this case scratch defects in a GDM sheet, and the resulting thermal response to those defects while the sheet was moving through the system. Studies were also performed to assess the response time and sensitivity, and to ensure that the technique would not damage the material during measurement. Models were developed by LBNL to assess the behavior of MEA materials during the DC excitation, enabling a full characterization of the operational space for the process, in terms of defect size and loading, detection criteria, response time, and magnitude of excitation. Figure 3 shows modeling and experimental results that indicate the response time for a given detection criteria and defect size as a function of the excitation magnitude. These simulations have fed back to the design specifications for an in-line system. We also performed in situ studies, using single and segmented cells, to determine the effect on initial performance of MEA component defects, including electrode thin spots, voids, and mud-cracks, and GDM PTFE loading.

Continuing our efforts to expand the applicability of our optical reflectometer platform, we evaluated techniques to deconvolute membrane thickness from a composite measurement of a membrane still on its casting liner. This would enable the quality measurement farther forward in the manufacturing process, maximizing value. Depending on the difference in optical properties between the membrane and liner, the technique appears to be feasible. Software development to automate this calculation is ongoing. We also demonstrated the feasibility of using this diagnostic to measure the uniformity of tape-cast solid oxide fuel cell layers.

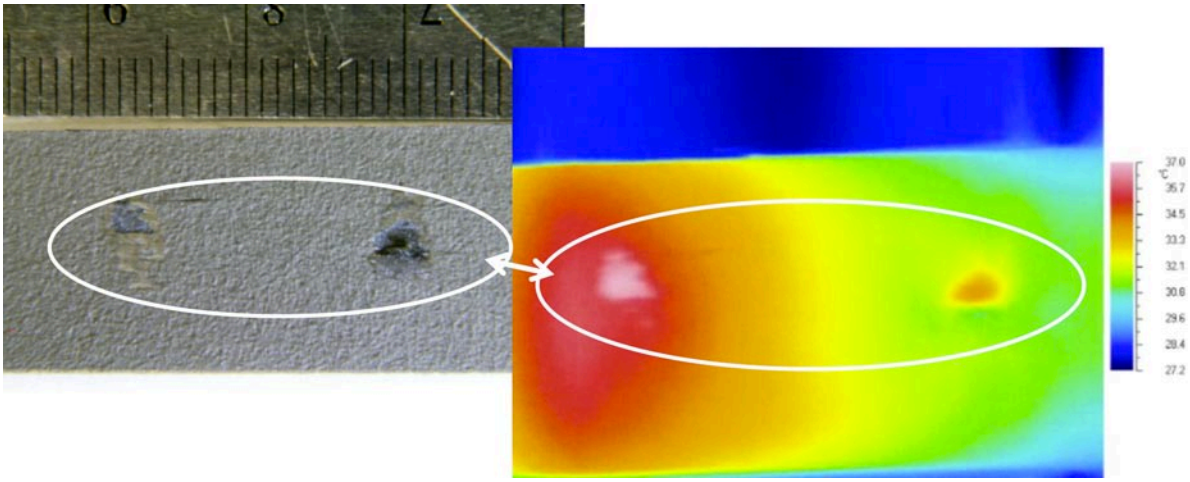


FIGURE 2. GDM sheet material with scratches and associated thermal response to those scratches, using the IR/DC technique on the benchtop roller system. The velocity of the sheet motion was approximately 10 feet per minute.

Future Directions

- Demonstrate the IR/DC and optical reflectometry diagnostics on our research web-line.
- Continue to use predictive modeling and single and segmented cell test methods to feed requirement and configuration information back to diagnostic development, device design, and detection algorithm assessment.
- Study how as-manufactured defects affect the performance of MEAs over time using standard or modified accelerated stress tests.
- Continue to work with our industry partners to ensure the relevance of our studies to their evolving needs and directions, including ongoing prioritization of diagnostic development needs.

FY 2011 Publications and Presentations

1. "IR Thermography for Quality Assessment of PEMFC Components," Aieta, Perdue, Ulsh; Advances in Materials for Proton Exchange Membrane Fuel Cell Systems, Asilomar, Pacific Grove, CA; February, 2011.

2. "New Technique for Rapid, Spatially Resolved, Detection of Pt in PEMFC Electrodes," Aieta, Bender, Perdue, Penev, Ulsh; 218th ECS Meeting, Las Vegas, NV; October, 2010.

3. "Formation and Detection of Catalyst Layer Cracks in PEMFCs," Perdue, Herring, Aieta, Dinh, Bender, Ulsh; 218th ECS Meeting, Las Vegas, NV; October, 2010.

4. "2010 Manufacturing Readiness Assessment Update to the 2008 Report for Fuel Cell Stacks and Systems for the Backup Power and Material Handling Equipment Markets," D. Wheeler and M. Ulsh, *submitted to DOE and under review*, December, 2010.

5. "A study of the adoption of automation and continuous processes in manufacturing of stationary and CHP fuel cell applications," M. Ulsh, D. Wheeler, P. Protopappas, *submitted to DOE and under review*, July, 2010.

6. "Fuel Cell MEA Manufacturing R&D," DOE Fuel Cell Technologies Program Annual Merit Review, May, 2011, Washington, DC.

VI.2 Reduction in Fabrication Costs of Gas Diffusion Layers

Jason Morgan
Ballard Material Products (BMP)
2 Industrial Ave.
Lowell, MA 01851
Phone: (978) 452-8961 x5213
Email: Jason.Morgan@Ballard.com

DOE Managers
HQ: Nancy Garland
Phone: (202) 586-5673
E-mail: Nancy.Garland@ee.doe.gov
GO: Jesse Adams
Phone: (720) 356-1421
E-mail: Jesse.Adams@go.doe.gov

Contract Number: DE-FG36-08GO18051/A000

Subcontractors:
- The Pennsylvania State University, University Park, PA
- Ballard Power Systems (BPS), Burnaby, BC

Project Start Date: October 1, 2008
Project End Date: August 31, 2011

Fiscal Year (FY) 2011 Objectives

- Reduce the fabrication costs of gas diffusion layer (GDL) products by:
  - Reducing the number of process steps.
  - Replacing batch processes with continuous processes.
  - Utilizing in-line measurement tools to reduce costly ex situ testing.
- Develop and implement new, high volume GDL process technologies.
- Produce high-performance, low-cost GDLs at sufficient volumes for near-term fuel cell markets.
- Research, develop, and implement new in-line process control and measurement tools consistent with high volume manufacturing.
- Advance the understanding of the relationship between process parameters, ex situ GDL properties and fuel cell performance to maximize production of high-performance, low-cost GDLs for near-term markets.

Technical Barriers

This project addresses the following technical barriers from the Manufacturing R&D section of the Fuel Cell Technologies Program Multi-Year Research, Development and Demonstration Plan:

(A) Lack of High-Volume Membrane Electrode Assembly Processes

(F) Low Levels of Quality Control and Inflexible Processes

Contribution to Achievement of Manufacturing R&D Milestones

This project will contribute to achievement of the following DOE milestones from the Manufacturing R&D section of the Fuel Cell Technologies Program Multi-Year Research, Development and Demonstration Plan:

- Milestone 1: Develop prototype sensors for quality control of MEA manufacturing. (4Q, 2011)
- Milestone 2: Develop continuous in-line measurement for MEA fabrication. (4Q, 2012)
- Milestone 3: Demonstrate sensors in pilot scale applications for manufacturing MEAs. (4Q, 2013)
- Milestone 4: Establish models to predict the effect of manufacturing variations on MEA performance. (4Q, 2013)

FY 2011 Accomplishments

- Reduced GDL costs by 55% from $36/kW to $16/kW from FY 2008 to FY 2010 by:
  - Increasing the manufactured width from 40 cm to 80 cm wide.
  - Implementing process control tools to improve product uniformity, reducing the amount of ex situ testing, improving product yields and minimizing scrap rates.
  - Installing new equipment enabling the production of rolls over 800 m in length.
  - Developing empirical models to predict and control critical GDL properties early in the manufacturing process, thereby improving manufacturing efficiency.
- Manufactured multiple batches of various types of microporous layer (MPL) inks (10^{+} gallons per batch) using a 2” continuous mixer.
  - Purchased a rheometer to measure the visco-elastic properties of these various MPL inks:
    - Developed test methods to characterize our inks.
    - Collected data on both our standard and continuous inks.
    - Began to determine relationships between continuous mixing parameters and key fluid properties.

  - Established mixing procedures to reduce the amount of agglomerations formed during the continuous mixing process.
  - Successfully developed a process to filter and de-gas the continuous MPL inks.
- Manufactured rolls of GDL material combining the many-at-a-time (MAAT) coating process with continuously made inks:
  - Produced multiple rolls (~80 m) of both anode and cathode material within production specifications with minimal defects.
  - Verified fuel cell performance in both a single-cell and a 10-cell short-stack.
  - Optimized dryer profile utilizing non-contact infrared thermocouples throughout the oven and dew point sensors to prevent premature drying of top layer.
  - Due to modifications to the MPL ink formulations, the coating head slot heights were altered to eliminate coating defects and improve basis weight uniformity.
  - Improved GDL uniformity by installing mass flow meters for each MPL ink and continuously monitoring basis weight with an in-line basis weight tool.
- Identified, purchased and installed new process control tools for multilayer coating, in-line mixing and heat treatment processes:
  - Mass flow meters (in-line mixing/MAAT coating).
  - In-line basis weight tool.
  - In-line viscometers.
  - Non-contact thermocouples for MAAT drying conditions.
  - Non-contact thermocouples for heat treatment process (high temperature).
- Developed a method to relate continuous on-line Raman scanning, to slow off-line area Raman scanning in an effort to:
  - Investigate a link between poly-tetrafluoroethylene (PTFE) distribution throughout the GDL and GDL drying conditions.
  - Demonstrate that on-line Raman scanning will detect the differences at required speeds for an on-line manufacturing tool.
  - Determine if differences in PTFE distribution throughout the GDL have an impact on critical ex situ properties of GDL and/or in situ fuel cell performance.
- Examined each step of the manufacturing process and determined relationships between specific process parameters and critical GDL properties.
  - Developed empirical models to predict and control critical GDL properties early in the manufacturing process.
  - Implemented methods to adjust the manufacturing process to center GDL properties within production specifications to ensure proper functionality.
- Improved manufacturing capacity 4-fold from FY 2008 to FY 2010.
  - Additional capacity increases are expected to reach ~9-fold with the full implementation of continuous mixing and multilayer coating technologies demonstrated in this project (requires additional capital investment to complete).



Introduction

This project addresses the Manufacturing R&D sub-program's goal of research, development and demonstration of technologies and processes that reduce the manufacturing cost of proton exchange membrane fuel cell systems. Specifically, this project reduces the fabrication costs of high-performance GDL products, while also increasing manufacturing capacity and improving product uniformity. The end result of this project is the production of low-cost, high-performance GDLs for near-term fuel cell markets, such as back-up power or materials handling. A conceptual design of a Greenfield manufacturing plant that is capable of meeting the 2015 GDL target price of $4/kW at specified volumes will also be developed.

Approach

The largest barrier to the commercialization of fuel cell products is cost. The cost of the GDL was evaluated at the end of 2008 and found to be $36/kW, almost 10 times the DOE cost target for 2015. A breakdown of this cost revealed that the majority of the fabrication cost of GDLs was due to manufacturing labor, specifically for ink mixing, coating and quality control.

It was believed that much of that cost could be removed by reducing the number of process steps, replacing slow batch processes with faster continuous processes, and utilizing modern on-line tools to improve product quality and reduce the amount of ex situ testing. In addition to these process modifications, it was also critical to determine the relationships between manufacturing parameters and critical GDL properties. From this understanding, empirical models will improve production controls, ensure product performance, and aid in the development of next generation GDLs that can meet the needs of state-of-the-art membranes and catalysts. Although the costs cannot be reduced to the DOE program target through this project alone, Ballard will use the knowledge gained in this project to design a Greenfield facility that is capable of producing

GDLs at or below $4/kW which should help meet the DOE stack target cost of $30/kW in 2015 at appropriate manufacturing volumes.

Results

Throughout this project, BMP has been able to reduce the fabrication costs of GDLs by 55% from $36/kW to $16/kW, as shown in Figure 1. This has been accomplished by increasing the manufactured width of the GDL from 40 cm to 80 cm, installing new web-handling equipment to allow for processing of rolls in excess of 800 m long, implementing better process controls, and incorporating an empirical process model which has resulted in improved process yields and reduced scrap rates. As a result of these efforts, the plant capacity has been increased 4-fold, as shown in Figure 2, which allows for production of low-cost, high-performance GDLs at volumes suitable for near-term markets.

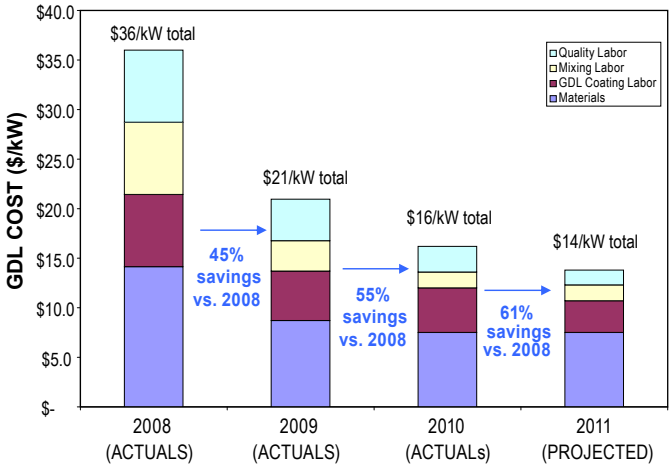


FIGURE 1. GDL Cost Reduction Data

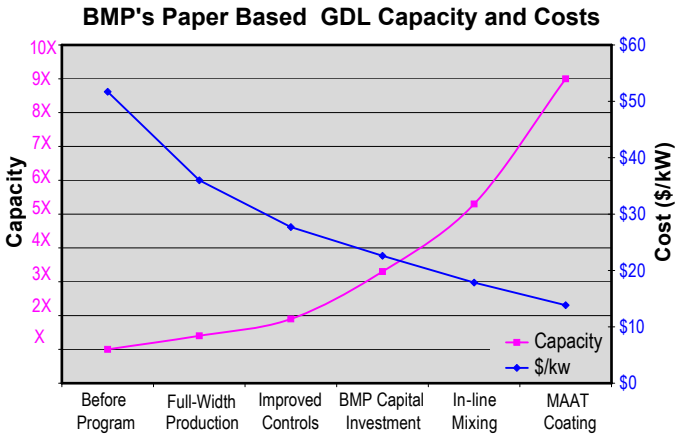


FIGURE 2. Impact of Various Program Milestones on Manufacturing Capacity and GDL Cost

Ballard has also demonstrated methods for future cost reductions based on the implementation of MAAT coating and continuous mixing. Multiple short rolls (~80 m) of anode and cathode GDL designs have been manufactured to date, demonstrating that GDLs manufactured with this new technology are similar to standard baseline materials [1]. Ex situ validation of GDLs made with these methods is shown in Figure 3, while in situ validations are still being completed and will be available in the next quarterly report. This validation work is different than previously reported work because it combines both MAAT coating and continuous mixing technologies together for the ultimate low-cost GDL design. Additional capital investments will be required by Ballard to fully integrate these new technologies into the GDL manufacturing process, but this work is critical in demonstrating their viability for GDL production.

In addition to the cost reduction work, Ballard has determined relationships between critical GDL properties and fuel cell durability and performance. Additionally, BMP has examined every step in their manufacturing process to find relationships between manufacturing process variables and these critical GDL properties [1]. These relationships have led to the development of empirical models, which allow BMP to predict and control critical GDL properties early in the manufacturing process. This understanding also allows BMP to make adjustments during the manufacturing process to meet specific customer targets, allowing for a more stable, consistent product, that improves yield rates and cell performance. This knowledge will also allow for the development of enhanced GDL designs that are tailored for a specific application (e.g. air-cooled vs. liquid-cooled) and should help in manufacturing GDLs with tight specifications.

The Pennsylvania State University, under the direction of Dr. Michael Hickner, is working with BMP to develop an in-line method for measuring the chemical homogeneity of the GDL. This work has led to the discovery of a potential link between PTFE distribution and GDL drying conditions,

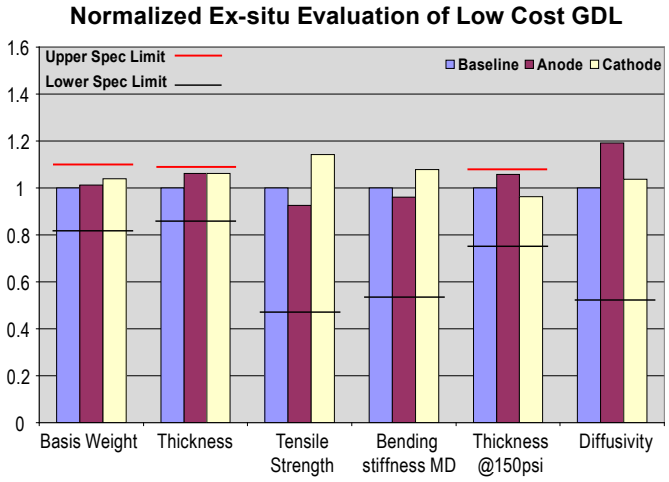
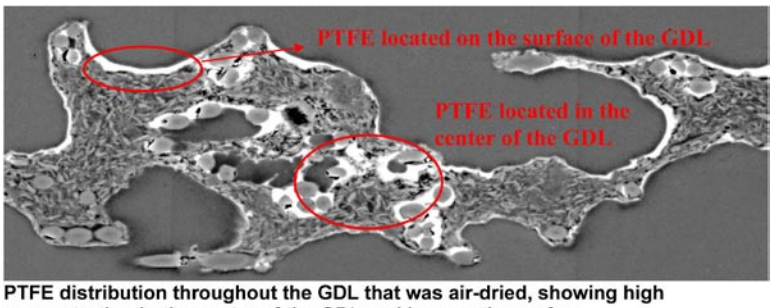
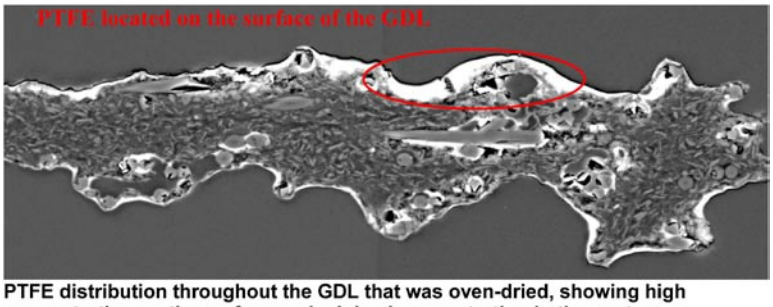


FIGURE 3. Ex Situ Evaluation of Low-Cost Anode and Cathode GDL Materials



PTFE distribution throughout the GDL that was air-dried, showing high concentration in the center of the GDL and less on the surface



PTFE distribution throughout the GDL that was oven-dried, showing high concentration on the surface and minimal concentration in the center

FIGURE 4. Impact of Drying Conditions on PTFE Distribution throughout the GDL

as shown in Figure 4. Dr. Hickner's team has demonstrated that on-line Raman scanning can detect differences in the PTFE distribution at speeds high enough to be used as an on-line manufacturing tool. In an effort to further this understanding, BMP has manufactured a variety of GDL designs with different PTFE loadings that were exposed to various drying profiles. Dr. Hickner's team is now working on determining if differences in PTFE distribution throughout the GDL are seen in these samples, while BMP and BPS are working to determine if there is a significant impact on critical ex situ properties of GDL and/or in situ fuel cell performance. This work will be valuable to the fuel cell community as a whole, by either providing a method to determine the PTFE distribution throughout the GDL with an on-line tool or demonstrating that variations in the PTFE distribution do not impact critical GDL properties or fuel cell performance.

Conclusions and Future Directions

BMP was able to reduce the fabrication costs of GDLs by 55%, while increasing manufacturing capacity 4-fold and improving product quality throughout this project. Multilayer coating and in-line mixing technologies have been successfully combined and ex situ testing showed that both anode and cathode materials were within production specification, while in situ testing (both single cell and short stack testing) is underway to validate fuel cell performance. These technologies will lead to further cost reductions (~65% from FY 2008) and capacity increases (~4-fold from FY 2008) with appropriate capital investments by Ballard to bring them on-line. In addition, Ballard has been able to determine relationships between critical GDL properties and fuel cell performance/durability. BMP has determined relationships between various manufacturing parameters and these critical GDL properties, which will allow for more uniform GDL production, improved GDL design and increased production yields. This work is beneficial for production of high-performance, low-cost GDLs for near-term fuel cell markets, as well as the development of new GDLs to meet the needs of state-of-the-art membranes and catalysts.

The Pennsylvania State University, under the direction of Dr. Michael Hickner, has determined a method to measure PTFE distribution in the GDL using Raman Scanning at rates fast enough to be considered for use as an on-line tool. They are currently examining a variety of GDL designs with different PTFE loadings made with different drying profiles to determine if there are differences in PTFE distribution. This work, combined with ex situ GDL measurements and in situ cell performance data gathered by Ballard, is important to understand how variations in the PTFE distribution throughout the GDL influence fuel cell performance, if at all.

In the final months of this project the activities include:

- Production of commercial length rolls of both anode and cathode GDL designs using both continuously made inks and MAAT coating.
- Validation of these low-cost GDL materials utilizing ex situ validation as well as single-cell, short-stack and full-stack testing.
- Determination of manufacturing capability with these new process technologies with a goal of achieving 6 sigma standards.
- Completion of the design of a Greenfield facility capable of producing GDLs that meet the DOE 2015 target at specified volumes.
- Determination of the impact of PTFE distribution on both ex situ GDL properties and in situ fuel cell performance, as well as development of a measurement process that could be used as an on-line process control tool for GDL manufacturing.
- Pennsylvania State University will complete their work on Raman scanning and deliver a measurement procedure that is capable of being converted to an on-line process control tool with the appropriate capital investment.

Special Recognitions & Awards

1. 2011 DOE Hydrogen and Fuel Cell Program R&D Award.

FY 2011 Publications/Presentations

1. Mendoza A.J., Hickner M.A., Morgan J., Rutter K., and Legzdins C., "Raman Spectroscopic Mapping of the Carbon and PTFE Distribution in Gas Diffusion Layers", Fuel Cells, No. 2, 248-254, 2011.

2. DOE Hydrogen Program and Vehicle Technologies Program Annual Merit Review and Peer Evaluation Meeting, Washington, DC, May 12, 2011.

References

1. Morgan, J, "Reduction of Fabrication Costs of Gas Diffusion Layers", DOE Hydrogen Program and Vehicle Technologies Program Annual Merit Review and Peer Evaluation Meeting, Washington, DC, May 12, 2011.

Acknowledgements

I would like to acknowledge the technical leadership and contributions of Don Connors, Dan Nelson & Kathryn Rutter at Ballard Material Products, as well as Dr. Michael Hickner & Alfonso Mendoza at Pennsylvania State University and our colleagues at Ballard Power Systems in Burnaby, B.C.

VI.3 Modular, High-Volume Fuel Cell Leak-Test Suite and Process

Ru Chen (Primary Contact), Hugh McCabe, Ian Kaye
UltraCell Corporation
399 Lindbergh Avenue
Livermore, CA 94551
Phone: (925) 455-9400
E-mail: rchen@ultracellpower.com

DOE Managers
HQ: Nancy Garland
Phone: (202) 586-5673
E-mail: Nancy.Garland@ee.doe.gov
GO: Jesse Adams
Phone: (720) 356-1421
E-mail: Jesse.Adams@go.doe.gov

Contract Number: DE-FG36-08GO18054

Subcontractors:
- Pacific Northwest National Laboratory, Richland, WA
- Cincinnati Test Systems, Cleves, OH

Project Start Date: September 1, 2008
Project End Date: June 14, 2011

Fiscal Year (FY) 2011 Objectives

- Design a modular, high-volume fuel cell leak-test suite.
- Performance leak tests in-line during assembly and break-in steps.
- Demonstrate improved fuel cell stack yield rate.
- Reduce labor time.
- Reduce fuel cell stack manufacturing cost.

Technical Barriers

This project addresses the following technical barriers from the Manufacturing section (3.5.5) of the Fuel Cell Technologies Program Multi-Year Research, Development and Demonstration Plan:

(F) Low Levels of Quality Control and Inflexible Processes

Contribution to Achievement of DOE Manufacturing Milestones

This project will contribute to achievement of the following DOE milestones from the Fuel Cells section of the Fuel Cell Technologies Program Multi-Year Research, Development and Demonstration Plan:

- **Milestone 9:** Select stack assembly processes to be developed. (4Q, 2010)
- **Milestone 10:** Develop automated pilot scale stack assembly processes. (4Q, 2012)
- **Milestone 12:** Demonstrate pilot scale processed for assembling stacks. (4Q, 2013)

FY 2011 Accomplishments

- Tested and evaluate leak-test suite prototype.
- Achieved five part per hour leak test rate on the prototype.
- Demonstrated that the stack test labor time is reduced dramatically.
- Demonstrated that the stack leak failure is reduced significantly.
- Demonstrated that the prototype can accurately detect leaks in stacks.
- Demonstrated that the prototype does not cause any new failure modes in fuel cell stacks and systems.



Introduction

There are three fluid circuits in a fuel cell stack. Any fluid leakage between these circuits or to the external atmosphere leads to reduced individual cell or stack performance and results in a failure during stack testing. Fuel cell stacks are typically hand assembled and tested, and it is very time-consuming. Furthermore, the leak-test equipment is often composed of expensive analytical devices, with extensive and excessive capabilities, that are not well suited to rapid testing of stack assemblies in medium- or high-volume manufacturing environments. High labor content and expensive test equipment limit the amount of online leak checks during the assembly process, leading to high scrap rates and low yields.

The development of a modular, high-volume fuel cell leak-test suite and process is proposed to address these challenges by reducing labor content; providing more robust, high confidence automated testing; and increasing the speed and throughput at which manufacturing is performed. Each leak test component will be highly specialized to its specific task and optimized for high throughput, thereby allowing for dramatic cost savings. A variety of methods will be employed to test for leaks between the fuel cell fluidic paths and the environment during the entire process from build to break-in to final test. The test suite will enable manufacturers to select modular test components as needed.

Approach

Six leak-test methods were proposed in the project. These tests include crossover current, current interrupt, voltage decay, pressure decay, flexo-tiltometer test, and fuel cell sensor for coolant leak. These methods will be investigated, and some will be selected to implement in the leak-test suite. These tests will automatically perform in-line during fuel cell stack manufacturing. The leak-test methods not only check the overall leakage, but also identify the location of leak and accelerate the diagnostics and remediation of fuel cell stacks.

Phase I of the project focuses on the analysis of current manufacturing processes, stack failure modes, and leak-test processes. A verity of leak-test methods will be surveyed, and recommendations for the leak-test suite will be made. Leak-test suite prototype will be designed, fabricated, and evaluated. A leak-test suite with 50 stacks per hour capability will be designed. Phase II will focus on pilot production line modification, leak-test suite fabrication, integration, and verification. A limited production test run will be carried out to validate the 50 stacks per hour operation.

Results

Twenty-three fuel cell stacks were built and tested on the leak-test suite prototype. There were 12 cells in each stack. The Celtec-P 1000 high temperature membrane electrode assembly with 18 cm^2 active area was used. Pressure decay (PD), crossover current (CC), and open-circuit voltage (OCV) decay were used to detect leak in stacks. The results are shown in Table 1. This demonstrated that 95% of leaks can be detected by the prototype. The leak test times are shown in Table 2. The average leak test time is 590 seconds, and the leak test rate is 6 parts per hour, which exceeds the Phase I milestone: 5 parts per hour.

TABLE 1. Leak Test Results

	YES	NO
PD correctly confirms CC or OCV results	19	4
CC correctly detects failure on retest	15	0
OCV correctly detects failure on retest	15	0
CC/OCV correctly detects swap or replacement	24	0

TABLE 2. Leak Test Time

Leak Test Process	Test Time (sec)
Pressure decay	227
Crossover current	253
OCV decay	60
Flexo-tiltometer	50
Total	**590**

Five stacks were built and tested on the leak-test suite prototype. These stacks passed leak, break-in, and performance tests. Then they were subjected to 30-day life test with one start/stop per day. The stack life test results are shown in Figure 1. All stacks completed life test and meet exit criteria. One cell in stack 084618-02 failed due to the fuel starvation, and was replaced at ~400 hr. However, this type of failure is occasionally observed in production stacks, so the failure should not be attributed to the prototype. Overall, the stack life test demonstrates that leak-test suite prototype does not cause new failure modes in stack.

Three stacks were built and tested on the leak-test suite prototype. These stacks passed leak, break-in, and performance tests. Then they were integrated into fuel cell systems. The system tests include static/dynamic load, cartridge run, -5°C performance, 50°C performance, emission, surface temperature, and polarization curve. System 26 and 50 passed all tests. System 45 passed all tests except emission and polarization curve test (Table 3). During diagnostics, a stainless steel tube on fuel processor broke off. This indicated there was a bad welding in the fuel line. This might cause fuel leak and result in fuel starvation in fuel cell. Later, an air compressor was found to have a manufacturing defect that caused an air leak. The failures

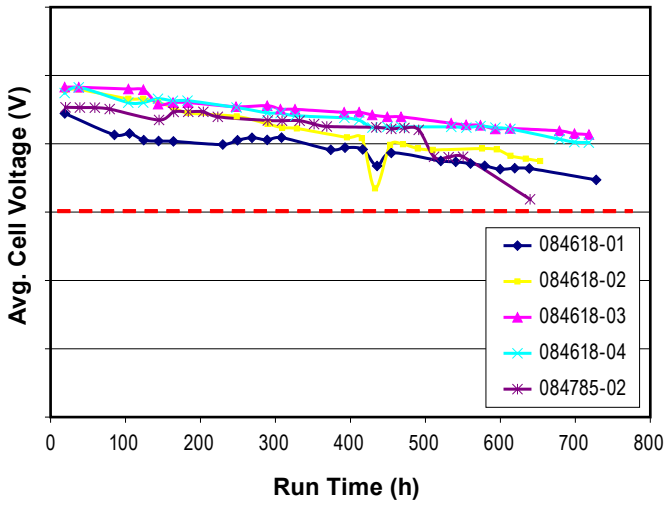


FIGURE 1. Fuel Cell Stack 30-Day Life Test

TABLE 3. System Test Results

System Tests	25E1LC0026	25ENDY0050	25E1LC0045
Static/Dynamic Load	Pass	Pass	Pass
Cartridge Run	Pass	Pass	Pass
-5C Performance	Pass	Pass	Pass
50C Performance	Pass	Pass	Pass
Emission	Pass	Pass	Fail
Surface Temperature	Pass	Pass	Pass
Polarization Curve	Pass	Pass	Fail

in the system test are due to the balance of plant component failure and not related to the fuel cell stack. The system validation test demonstrates the leak test suite prototype does not cause new failure modes in the fuel cell stack.

Conclusions and Future Directions

The conclusions include the following:

- The fuel cell stack leak-test suite prototype was tested and evaluated. The prototype achieved five part per hour leak test rate. The prototype is fully automated, significantly reducing the stack test labor time.
- The validation test demonstrated that the prototype can accurately detect leaks in stacks. The leak test processes do not cause any new failure modes in fuel cell stack and system.

FY 2011 Publications/Presentations

1. Chen, R. et al., "Modular, High-Volume Fuel Cell Leak-Test Suite and Process", presentation at the 2010 Hydrogen Program and Vehicle Technologies Program Annual Merit Review and Peer Evaluation Meeting, Washington, D.C., May 9–13, 2011.

VI.4 Manufacturing of Low-Cost, Durable Membrane Electrode Assemblies Engineered for Rapid Conditioning

F. Colin Busby
W.L. Gore & Associates, Inc. (Gore)
Gore Electrochemical Technologies Team
201 Airport Road
Elkton, MD 21921
Phone: (410) 392-3200
E-mail: CBusby@WLGore.com

DOE Managers
HQ: Nancy Garland
Phone: (202) 586-5673
E-mail: Nancy.Garland@ee.doe.gov
GO: Jesse Adams
Phone: (720) 356-1421
E-mail: Jesse.Adams@go.doe.gov

Contract Number: DE-FC36-086018052

Subcontractors:
- UTC Power, South Windsor, CT
- University of Delaware, Newark, DE
- University of Tennessee, Knoxville, TN

Project Start Date: October 1, 2008
Project End Date: June 30, 2013

Fiscal Year (FY) 2011 Objectives

The overall objective of this project is to develop a unique, high-volume manufacturing processes that will produce low-cost, durable, high-power density 5-layer (5-L) membrane electrode assemblies (MEAs) that minimize stack conditioning:

- Manufacturing process scalable to fuel cell industry MEA volumes of at least 500k systems/year.
- Manufacturing process consistent with achieving \$15/kW$_e$ DOE 2015 transportation stack cost target.
- The product made in the manufacturing process should be at least as durable as the MEA made in the current process for relevant automotive duty cycling test protocols.
- The product developed using the new process must demonstrate power density greater or equal to that of the MEA made by the current process for relevant automotive operating conditions.
- Product form is designed to be compatible with high-volume stack assembly processes: 3-layer (3-L) MEA roll-good (anode electrode + membrane + cathode electrode) with separate rolls of gas diffusion media (GDM).
- The stack break-in time should be reduced to 4 hours or less.

Phase 2 Objectives:

- Low-Cost MEA Research and Development (R&D)
  - New 3-L MEA Process Exploration
    - Investigate equipment configuration for low-cost MEA production.
    - Investigate raw material formulations.
    - Map out process windows for each layer of the MEA.
  - Mechanical Modeling of Reinforced 3-L MEA
    - Use model to optimize membrane reinforcement for 5,000+ hour durability and maximum performance.
    - Develop a deeper understanding of MEA failure mechanisms.
  - 5-L Heat and Water Management Modeling
    - Optimization of GDM thermal, thickness, and transport properties to enhance the performance of thin, reinforced membranes and unique properties of direct-coated electrodes using a validated model.
  - Optimization
    - Execute designed experiments which fully utilize University of Delaware (UD) and University of Tennessee, Knoxville (UTK) modeling results to improve the new MEA process and achieve the highest possible performance and durability.
  - MEA Conditioning
  - Evaluate potential for new process to achieve DOE cost targets prior to process scale up (Go/No-Go decision).
- Scale-Up and Process Qualification
- Stack Validation

Technical Barriers

This project addresses the following technical barriers from the Manufacturing section of the Fuel Cell Technologies Program Multi-Year Research, Development and Demonstration Plan:

(A) Lack of High-Volume Membrane Electrode Assembly (MEA) Processes

(D) Manual Stack Assembly

Contribution to Achievement of DOE Manufacturing Milestones

This project will contribute to achievement of the following DOE milestones from the Manufacturing section of the Fuel Cell Technologies Program Multi-Year Research, Development and Demonstration Plan:

3.5 Manufacturing R&D/ Fuel Cells/ Task 1: Membrane and MEA

4. Establish models to predict the effect of manufacturing variations on MEA performance. (4Q, 2013)

3.4 Fuel Cells/ Task 3: Membrane Electrode Assemblies Meeting All Targets

38. Evaluate progress toward 2015 targets. (4Q, 2012)

FY 2011 Accomplishments

- Direct Coating Process Development
  - The primary path for the new 3-L MEA process has succeeded in incorporating the previously modeled process improvements which indicated potential for a 25% reduction in high-volume 3-L MEA cost.
  - Lab-scale development of the new 3-L MEA process is nearing completion:
    - Primary and alternative paths have been determined.
    - Current density of un-optimized direct-coated electrodes is equivalent to or better than current commercial electrodes over a robust range of automotive operating conditions.
- Gore has demonstrated mechanical durability of a 12 micron expanded polytetrafluoroethylene (ePTFE) reinforced membrane. In previous testing, GORE™ MEAs exceeded 2,000 hours of accelerated mechanical durability testing, which has been equated to achieving 9,000 hours of membrane durability in an 80°C automotive duty cycle. This exceeds the DOE 2015 membrane durability target of 5,000 hours. Gore's 12 micron ePTFE reinforced membrane technology has been successfully incorporated into the lab-scale new 3-L MEA process.
- A quasi-static elastic/plastic layered structure MEA mechanical model has been modified to include visco-elastic/plastic behavior. Mechanical property experiments which are required to calculate model input parameters are 95% complete. The final model will be used to predict reinforced MEA mechanical lifetime for a variety of temperature and relative humidity cycling scenarios. The model will also be used to explore different reinforcement strategies and optimize mechanical durability of the MEA structure targeted by the new low-cost process.
- 5-Layer Heat & Water Management Model development at UTK is complete and the experimental test progress is on track to enable efficient optimization of GDM for the new 3-L MEA.



Introduction

Over the past 20 years, great technical progress has been made in the area of improving power density and durability of fuel cell stacks, so much so that most of the requisite technical targets are now within reach. Yet, three major technical challenges remain. First and foremost is meeting the cost targets. The second challenge is producing components that are amenable for use in a high-speed, automotive assembly line. One impediment to this latter goal is that stack components must currently go through a long and tedious conditioning procedure before they produce optimal power. This so-called "break-in" can take many hours, and can involve quite complex voltage, temperature and/or pressure steps. These break-in procedures must be simplified and the time required reduced, if fuel cells are to become a viable power source. The third challenge is to achieve the durability targets in real-world operation. This project addresses all three challenges: cost, break-in time, and durability for the key component of fuel cell stacks: MEAs.

Approach

- The overall objective of this project is to develop unique, high-volume manufacturing processes for low-cost, durable, high-power density 3-L MEAs that require little or no stack conditioning. In order to reduce MEA and stack costs, a new process will be engineered to reduce the cost of intermediate backer materials, reduce the number and cost of coating passes, improve safety and reduce process cost by minimizing solvent use, and reduce required conditioning time and costs. MEA mechanical durability will be studied and optimized using a combination of ex situ mechanical property testing, non-linear mechanical model optimization, and in situ accelerated mechanical durability testing. Fuel cell heat and water management will be modeled to optimize electrode and GDM thermal, geometric, and transport properties and interactions. Unique enabling technologies that will be employed in new process development include:
  - Direct coating which will be used to form at least one membrane–electrode interface.
  - Gore's advanced ePTFE membrane reinforcement and advanced perfluorosulfonic acid ionomers which enable durable high-performance MEAs.
  - Advanced fuel cell testing and diagnostics.

Results

Low-Cost MEA Process Development

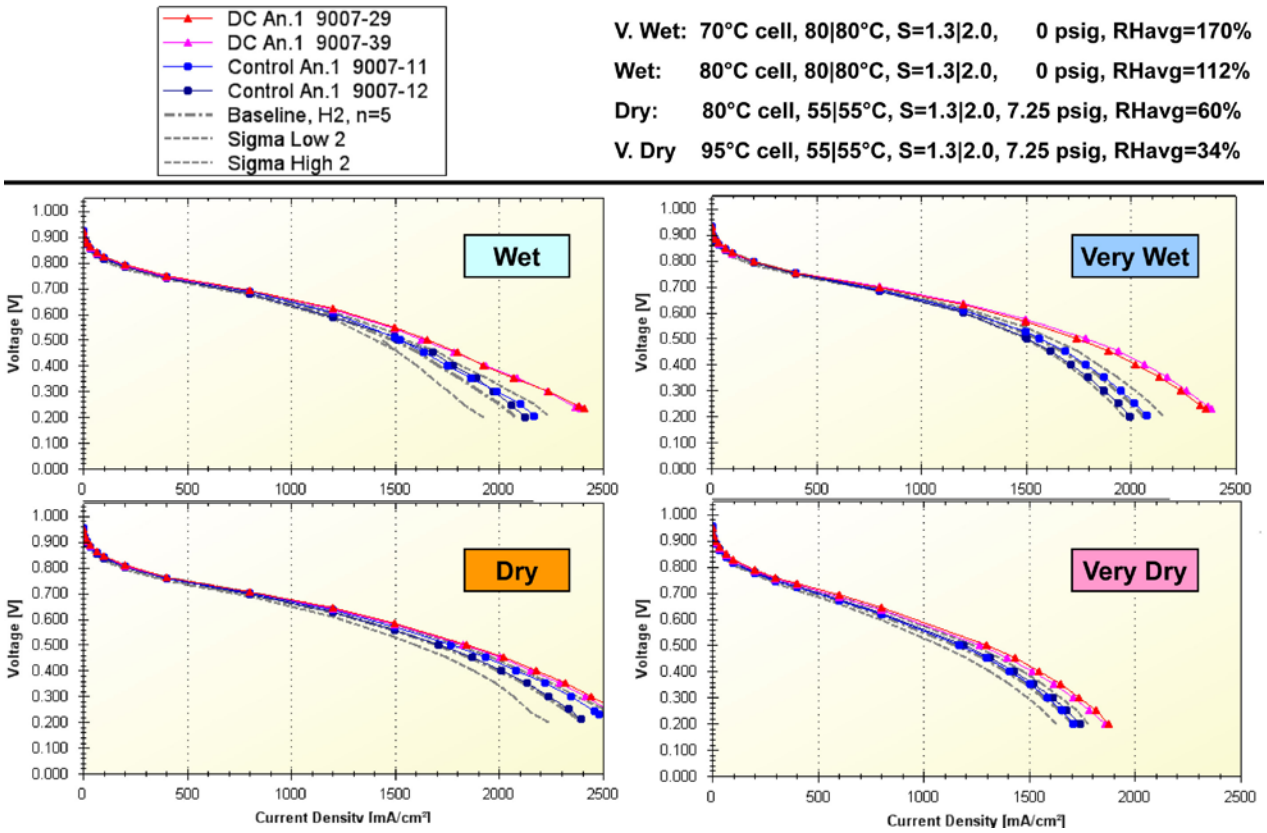
The primary path has changed during the past year and process development for the current primary path is progressing rapidly.

- Previous Primary Path
  - Process step 1: Direct coat cathode electrode on a carrier-film-supported reinforced membrane.
  - Process step 2: Remove carrier film and direct coat anode electrode on 2-layer intermediate.
- Current Primary Path
  - Process step 1: Coat bottom electrode on low-cost, non-porous backer.
  - Process step 2: Direct coat reinforced membrane on top of the bottom electrode.
  - Process step 3: Direct coat top-side electrode on top of the reinforced membrane.

The alternate path is to directly coat the anode electrode onto a backer-supported reinforced half-membrane to make an anode-side 1.5-layer intermediate rolled-good. The cathode electrode is then directly coated onto a backer-supported reinforced half-membrane in a similar process. In the final step, the backers are removed from the anode-side and cathode-side 1.5-layers intermediates and the webs are laminated together to form the 3-L product.

Electrodes made using lab-scale versions of the current primary path process equipment have demonstrated performance equivalent to or better than the current commercial electrodes across a broad range of operating conditions. This is a substantial improvement over the previous primary path which produced electrodes that were equivalent, at best, to the current commercial electrodes. Figures 1 and 2 show performance of direct coated electrodes paired with opposing control electrodes in a range of operating conditions which can be used to assess the viability of an MEA for different applications (automotive, stationary, portable, etc.), or for dynamic operation within a single application.

Coating research during the past year focused on developing the new primary path process and understanding the interactions between cathode ink formulation and low-cost backer for the current primary path, in which the cathode is the first layer to be coated in the 3-L MEA. Future experiments will combine direct-coated anodes and direct-coated cathodes and test the durability of direct-coated electrodes.



RHavg = average relative humidity

FIGURE 1. Direct Coated Anode Performance (PL = Platinum loading in mg/cm^2)

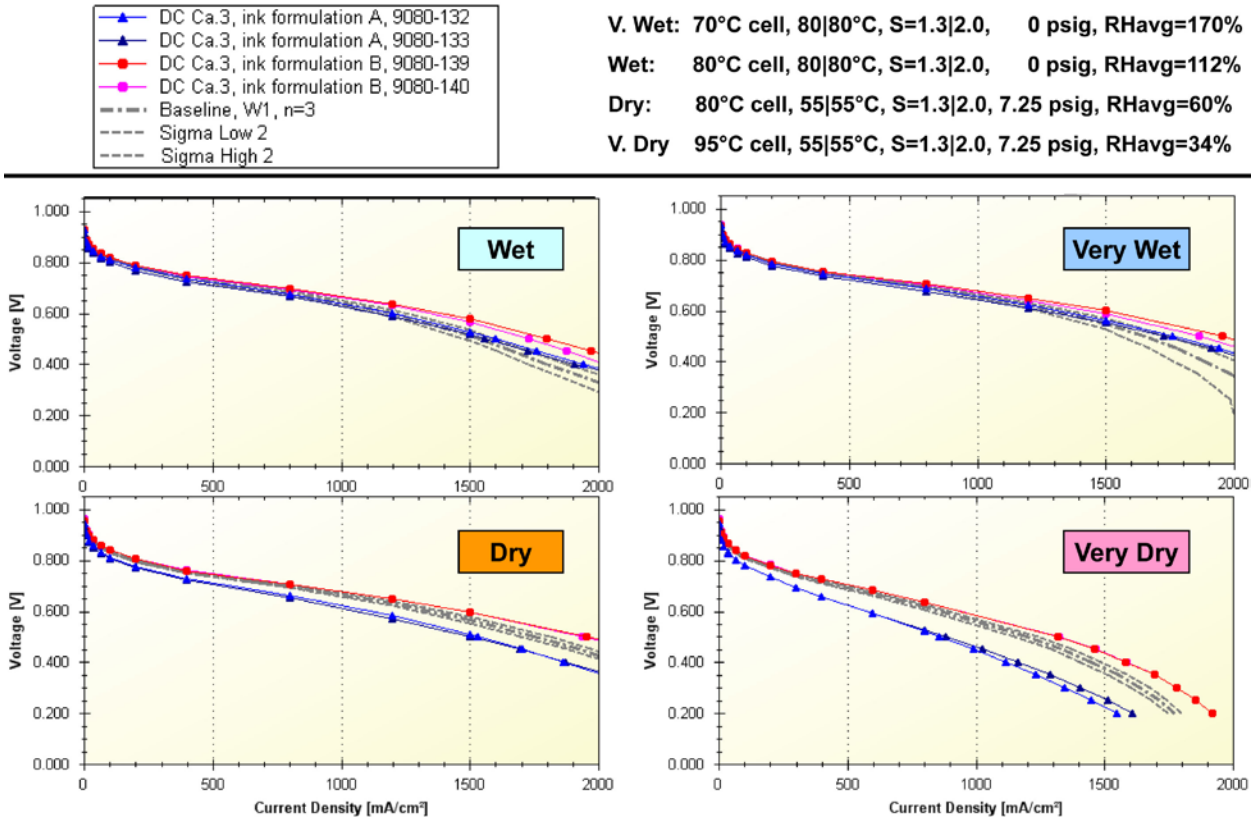


FIGURE 2. Direct Coated Cathode Performance (PL = Platinum loading in mg/cm^2)

Mechanically Durable 12 μm Reinforced Membrane

Gore has successfully incorporated a mechanically durable 12 µm reinforced membrane into the current primary path process. The 12 µm membrane construction has also demonstrated high performance due to reduced resistance and increased waster back-diffusion (see Figure 3). In previous testing, GORE™ MEAs exceeded 2,000 hours of accelerated mechanical durability testing, which has been equated to achieving 9,000 hours of membrane durability in an 80°C automotive duty cycle. This exceeds the DOE 2015 membrane durability target of 5,000 hours. The accelerated mechanical durability testing protocol is summarized below:

Tcell (°C)	Pressure (kPa)	Flow (Anode/Cathode, cc/min)
80	270	500 N_2/1,000 N2

- Cycle between dry feed gas and humidified feed gas
- (sparger bottle temp = 94°C)
- Dry feed gas hold time: 15 seconds
- Humidified feed gas hold time: 5 seconds
- For further protocol information, see: W. Liu, M. Crum [1]

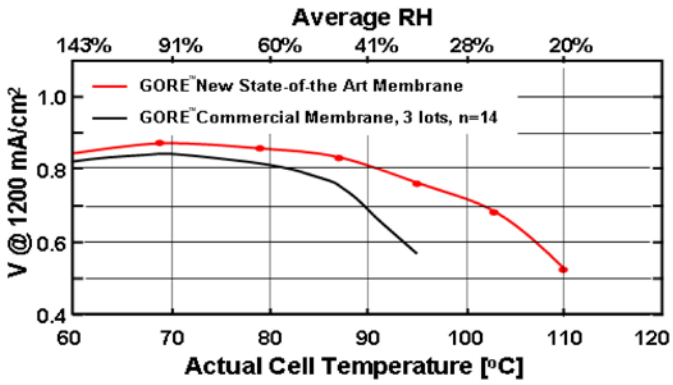


FIGURE 3. Performance of Thin, Mechanically Durable Reinforced Membrane

Mechanical Modeling of Reinforced 3-L MEA (UD)

A quasi-static elastic/plastic layered structure MEA mechanical model has been modified to include visco-elastic/plastic behavior. Mechanical property experiments which are required to calculate model input parameters are 95% complete.

Nafion® 211 membrane is used for the model membrane and the temperature, relative humidity, and time dependant

properties are calculated from the ongoing experimental results. The viscous properties are modeled using a 2-layer viscoplastic constitutive model. This material model consists of an elastoplastic "arm" that is in parallel with an elastoviscous "arm." The elastoplastic arm consists of an elastic spring (stiffness K_p) and a plastic component (yield stress, σ_y and hardening H'). Yielding according to the Mises criterion is used here. The elastoviscous arm has two elements, one spring (stiffness K_v) and one dashpot (using a time hardening law $\dot{\varepsilon}_v = A\sigma_v^n$). Thus, the instantaneous elastic stiffness of the material is the sum of the elastic elements, $K_p + K_v$. In summary, the parameters that are required for this model are K_p, σ_y, H', K_v, A and n. These properties are determined from the experimental results. Figure 4 shows the modeled membrane stress as a function of membrane water fraction for two cycling scenarios using preliminary experimental data.

Tensile testing was conducted for a range of displacement rates to investigate the influence of this parameter on the mechanical response. The rates were selected so that the full visco-elastic-plastic constitutive equations can be determined. The relationships obtained from the MEA testing are "composite properties," combining the properties of the membrane with the electrodes. The constitutive equations for the electrodes will be obtained via reverse analysis. The experimental results have shown that the mechanical response of Nafion® 211 membrane and the MEA is dependent on temperature and humidity as well as displacement rate. Results also indicate that lower temperature, lower humidity or faster displacement rate result in a larger stress for a given strain.

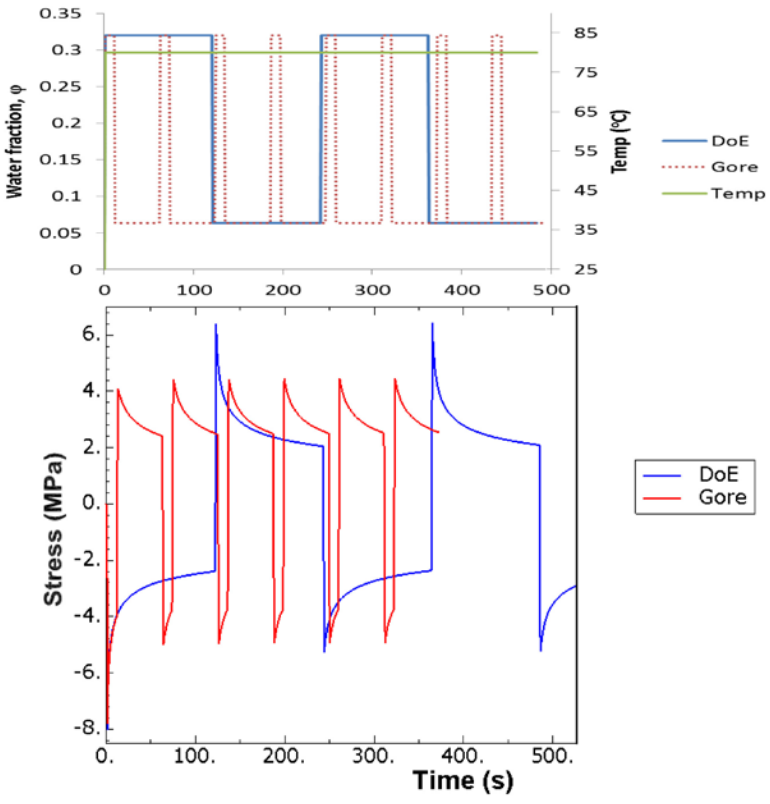


FIGURE 4. Modeled Membrane Stress as a Function of Membrane Water Fraction for Two Cycling Scenarios

5-L Heat and Water Management Modeling (UTK)

Membrane electrode assemblies and diffusion media materials were selected and experimental testing was initiated. Computationally, an initial first round of two-dimensional single-phase computational model simulation was completed to simulate the impact of diffusion media and membrane thickness and thermal properties. This analysis has enabled some understanding of the consequences of the various micro/macro diffusion media designs. The thermal properties of the diffusion media and micro-porous layer were shown to be critical to facilitate proper water management and are critical engineering parameters. Later, computational simulations were upgraded to include multi-phase flow.

Conclusions and Future Directions

The combination of Gore's advanced materials, expertise in MEA manufacturing, and fuel cell testing with the mechanical modeling experience of University of Delaware and the heat and water management experience of University of Tennessee enables a robust approach to development of a new low-cost MEA manufacturing process.

- Electrodes made using lab-scale versions of the current primary path process equipment have demonstrated performance equivalent to or better than the current commercial electrodes across a broad range of operating conditions. Future work will focus on combining direct coated anodes and cathodes as well as accelerated stress testing to ensure that durability of the new, direct-coated MEAs is equivalent to or better than the current commercial control MEA.
- Fuel cell heat and water management modeling will be used to efficiently optimize electrode and GDM thermal, geometric, and transport properties and interactions. Direct coated electrodes will be paired with the most appropriate GDM materials identified in this study. In this way, GDM will enable maximum performance and durability of the low cost 3-L MEA.
- A quasi-static elastic/plastic layered structure MEA mechanical model has been modified to include visco-elastic/plastic behavior.

Mechanical property experiments which are required to calculate model input parameters are 95% complete. When data collection is complete, the model will be validated with MEA accelerated durability testing. The final model will then be used to predict reinforced MEA lifetime for a variety of temperature and relative humidity cycling scenarios. The model will also be used to explore different reinforcement strategies and optimize mechanical durability of the MEA structure targeted by the new low-cost process.

FY 2011 Publications/Presentations

1. 2011 Hydrogen Program Annual Merit Review: mn004_busby_2011_o.pdf.

References

1. W. Liu and M. Crum. ECS Transactions 3, 531-540 (2007).

Nafion® is a registered trademark of E. I. DuPont de Nemours & Company

GORE and designs are trademarks of W. L. Gore & Associates, Inc.

VI.5 Adaptive Process Controls and Ultrasonics for High-Temperature PEM MEA Manufacture

Daniel F. Walczyk (Primary Contact),
Stephen J. Rock
Center for Automation Technologies and Systems
Rensselaer Polytechnic Institute
Suite CII 8011
110 8th Street
Troy, NY 12180-3590
Phone: (518) 276-2397
E-mail: walczd@rpi.edu

DOE Managers
HQ: Nancy Garland
Phone: (202) 586-5673
E-mail: Nancy.Garland@ee.doe.gov
GO: Jesse Adams
Phone: (720) 356-1421
E-mail: Jesse.Adams@do.doe.gov

Contract Number: DE-FG36-08GO18053/A000

Subcontractor:
Arizona State University, Tempe, AZ

Project Start Date: September 1, 2008
Project End Date: June 30, 2012

Fiscal Year (FY) 2011 Objectives

The high level objective of the proposed work is to enable cost-effective, high-volume manufacture of high- (160-180°C) and low-temperature (<100°C) proton exchange membrane fuel cell (PEMFC) membrane electrode assemblies (MEAs) by:

- Achieving greater uniformity and performance of high-temperature MEAs through the application of adaptive process control (APC) combined with effective in situ property sensing to the MEA pressing process.
- Greatly reducing MEA pressing cycle time through the development of novel, robust ultrasonic bonding processes.

Technical Barriers

This project addresses the following Manufacturing R&D technical barriers in the Manufacturing R&D section (3.5.5) of the Fuel Cell Technologies Program Multi-Year Research, Development and Demonstration Plan:

(A) Lack of High-Volume Membrane Electrode Assembly (MEA) Processes

(F) Low Levels of Quality Control and Inflexible Processes

Contribution to Achievement of DOE Manufacturing Milestones

This project will contribute to achievement of the following DOE milestones from the Manufacturing R&D section (3.5.7) of the Fuel Cell Technologies Program Multi-Year Research, Development and Demonstration Plan:

- **Milestone 2**: Develop continuous in-line measurement for MEA fabrication. (4Q, 2012)
- **Milestone 3**: Demonstrate sensors in pilot scale applications for manufacturing MEAs. (4Q, 2013)
- **Milestone 4**: Establish models to predict the effect of manufacturing variations on MEA performance. (4Q, 2013)

FY 2011 Accomplishments

- Added APC capability to Rensselaer's MEA thermal bonding station.
- Designed, built, and tested temperature-controlled stack hardware, servo press, and fuel cell test stand that can handle one MEA and short stacks of 5 and 10 high-temperature MEAs (50 cm^2 active area) bonded using thermal pressing and APC or ultrasonics.
- Designed, built and tested thermal and ultrasonic bonding tools, component assembly and laser cutting fixtures, and single cell test hardware for thermal pressing, ultrasonic bonding, and characterization of larger scale high-temperature MEAs (140 cm^2).
- Found that heat treatment (to boil off excess water), low pressing pressure, low anvil support backer stiffness, and high booster amplitude were optimal process parameters for ultrasonic bonding of high-temperature MEAs.
- Created a vibration model coupled with thermal finite element analysis (FEA) model to accurately predict transient temperatures through MEA thickness during ultrasonic bonding.
- Found that current heat treatment time can be reduced as much as 50% without adversely affecting performance, membrane thickness and acid concentration in the MEA.
- Designed, built, and tested thermal and ultrasonic bonding tools, component assembly and laser-cutting fixtures, and single cell test hardware for low-temperature (Nafion®) MEAs (10 cm^2 active area).
- Found that MEAs sealed ultrasonically with optimized process parameters exhibit excellent stability (no cell voltage degradation and minimal cell internal resistance change) under extreme start/stop operating conditions over a period of 200 hours.

- New cost model predictions between Phase I and Phase II based on actual experimental data include lower cost reductions for implementing APC (29% vs. 38%) but higher reductions for implementing ultrasonics (90% vs. 84%).



Introduction

To realize the tremendous potential that fuel cell technology has to improve the world's environment and reduce our dependence on fossil fuels, it is essential that high volume, high quality manufacturing technologies are developed in parallel with the materials and designs for MEAs, stacks, and the other stack components, which is currently not the case. There are currently three main barriers to the development of high volume fuel cell manufacturing. First, the current practice involving extensive testing and burn-in of components and stacks will not allow the industry to achieve the necessary cost targets and throughput for stacks, components, and systems. Second, for the current process used to press low-temperature (e.g. Nafion®) MEAs used in both PEMFCs and direct methanol fuel cells, it is common to thermally press for as long as 1½-5 minutes. Even the pressing process for high-temperature (polybenzimidizole, or PBI) MEAs, while much shorter than for Nafion®-based MEAs at about one minute, is still too long for high volume manufacture. Third is the variability of MEA performance. The component materials, including gas diffusion layer or gas diffusion electrode (GDE), membranes or catalyst-coated membrane, and gasketing materials all exhibit variations in key properties such as thickness, porosity, catalyst loading, and water or acid content and concentration. Yet, it is common practice to employ a fixed combination of pressing process parameter values (time, temperature and pressure), regardless of these variations. As a result, MEAs exhibit variations in physical and performance related properties.

The research being conducted in this project will help reduce all three of these barriers by reducing the unit process cycle time for MEA pressing by the use of ultrasonic sealing, and by minimizing the variability in performance of MEAs produced using adaptive process control. This will in turn help lead to the reduction or elimination of the practice of burn-in testing of fuel cell stacks. All of these benefits will contribute to a reduction in manufacturing costs for MEAs.

Approach

The current state of practice in MEA manufacturing calls for the application of fixed pressing process parameters (time, temperature, and pressure), even though there are significant variations in incoming material properties of the membrane and electrodes including thickness, mechanical properties, and acid/water content. MEA manufacturers need to better understand the relationships among those incoming material properties, the manufacturing process parameters, the resulting MEA physical and electrochemical properties, and the eventual electrical performance of the MEA in a stack.

We plan to address the problems associated with different methods of pressing high-temperature MEAs, specifically PBI with phosphoric acid as the electrolyte, by applying APC techniques and ultrasonics, and pressing low-temperature MEAs, specifically Nafion®-based, by applying ultrasonics. Through extensive experimentation and testing, we will develop analytical and empirical models of the relationships among incoming component material properties, the manufacturing process parameters, the resulting MEA properties, and the performance of the MEA in a stack. With the knowledge gained and new hardware designs, we will then attempt to identify one or more key properties (e.g., alternating current [AC] impedance, electrochemical capacitance) of the MEA that can be measured in situ during the thermal or ultrasonic pressing process, and then correlate these properties to the eventual physical and electrochemical performance of the MEA in a stack. If we are successful in identifying such an in situ measurement(s), adaptive control algorithms along with integrated process parameter and MEA performance sensing capabilities will be developed to allow us to vary the thermal and ultrasonic pressing process parameters in real time in order to achieve optimal uniformity of MEA performance.

We anticipate that the APC and processing techniques being investigated can be applied equally well, with certain modifications, to the pressing of both high-temperature and low-temperature MEAs, although the focus of this work to date has been on the former because of our extensive experience with these materials and the enhanced performance they offer (e.g., high operating temperature, no water management issues, high CO and H_2S tolerance). Our research is not application specific as the results may be applied to a broad range of fuel cell applications.

Results

APC: The application of APC to the experimental manufacturing of high-temperature PEMFCs has been an on-going effort. Experiments have been conducted to determine the best sensing method to correlate real-time electrical characteristics to eventual performance for MEAs made by thermal pressing. Using in situ alternating current (AC) impedance measurements, we are able to determine when the electrochemical cell has been formed by observing the drastic change in reactance. Our experimentation points to this change, specifically when the impedance reaches a minimum, as being the indicator of the completion of the manufacturing process.

In our current work, we apply the instrumentation method to our manufacturing process and complete the cycle when the impedance (sensed with a 1 kHz milliohmmeter) becomes a minimum. In preliminary tests,

we have found that the cycle time is reduced significantly. Our continuing experimentation will determine how much of an improvement will be made to the uniformity of performance of the cells produced using this method.

MEA Performance Evaluation Via Stack Testing: High-temperature MEAs (with 50 cm^2 active area) produced using APC and ultrasonics will be tested in single cell test fixtures and the performance of the MEAs will be compared to those tested during the Phase I experimentation. MEAs will also be tested in short stacks of 5 and 10 cells to determine cell to cell performance variations (e.g., voltage, temperature). Uniformity of MEAs produced by thermal pressing with APC and by ultrasonics will be compared to those produced by thermal pressing alone.



FIGURE 1. Fuel cell stack for testing 50 cm^2 MEAs produced using thermal pressing, thermal pressing with APC, and ultrasonics.

We have completed the design and fabrication of the stack that will be used for this investigation, as shown in Figure 1. It is be highly instrumented so that we will be able to identify individual cell performance (impedance, voltage, temperature) and also stack performance.

A serious experimental issue that was identified and corrected involved leaching of phosphoric acid into the porous graphite bipolar plates during testing. The solution was to procure POCO graphite plates that are first machined and then subjected to a post surface sintering process to completely seal surfaces.

The current experimental schedule will test single baseline MEAs (i.e. made by thermal pressing only), then a 5-cell stack, and finally a 10-cell stack test to validate the hardware. After stack performance is validated, the performance of thermally bonded MEAs with APC and ultrasonic MEAs will be tested in stacks.

Large-Scale MEA Testing: Tooling for thermal and ultrasonically bonding large scale MEAs has been designed, built and tested. The ultrasonic and thermal press tooling including registration fixtures is shown in Figures 2a and 2b, respectively. An MEA with 140 cm^2 active area was specially designed for this task, because the size is similar to those used in automotive applications and it was the maximum size that could be accommodated by ultrasonic horns commercially available from Branson Ultrasonics Corporation, a project collaborator. Laser cutting fixtures and a carrier frames were also designed and built. MEAs have already been fabricated using thermal and ultrasonic bonding. Performance testing of thermally and ultrasonically bonded large-scale MEAs are on-going.

Ultrasonic Bonding Process Optimization and Process Modeling: Optimal process parameters were determined for ultrasonic bonding of high temperature MEAs. Since heat treatment (i.e. boiling off excess water using an oven) was identified as the most significant process parameter in a previous designed experiment and statistical analysis (Phase I), all membranes were heat treated while the other process parameters – membrane thickness, anvil support backer stiffness, sealing pressure, and energy flux - were

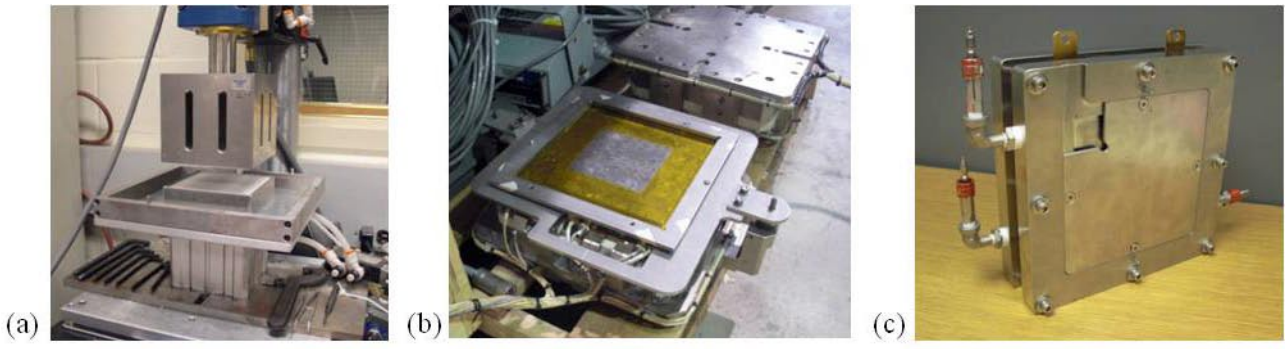


FIGURE 2. (a) Ultrasonic tooling, (b) thermal press tooling and (c) single-cell test fixture for large-scale MEAs (140 cm^2)

systematically varied in a two-level, full-factorial (2^4) experimental design with two replicates. Testing including creating a pole curve and measuring cell resistance after a 16-hour incubation period required for the hydrolysis and vaporization reactions to reach equilibrium. Specifically, current density at two voltages (0.4 and 0.6 V) and cell resistance were measured as output variables. In addition to heat treatment, process conditions for making optimal performing MEAs included low pressing pressure, low anvil support backer stiffness, and high booster amplitude based on analysis of variance. A comparison of polarization curves between the manufacturer's baseline thermally pressed MEA and an MEA fabricated with optimal ultrasonic process parameters is shown in Figure 3.

The MEA ultrasonic bonding process is being modeled using a combination of vibration and FEA theory. The vibrational model – masses coupled in series with a spring and spring/damper in parallel for each of the three layers (GDE, membrane, GDE) – currently contains six degrees of freedom. Model input is a high frequency (20 kHz) and low amplitude (20 μm) vibrational signal along with a constant preload (pressing pressure) from the ultrasonic horn. Because of the extreme ratio of the model spring stiffness to the model mass, the natural frequencies are very high. This necessitates the use of a stiff computational solver. Currently, the model is still being refined to balance model accuracy with computational time. Heat dissipated by the dampers in real time is used in a COMSOL FEA transient thermal analysis with internal heat generation at each of the MEA material interfaces (GDE/membrane × 2). Because of the symmetry of the model and the fact that the heating is assumed to be uniform, the COMSOL model is now two-dimensional, rather than three-dimensional. A one-dimensional model was found not to give as clear of a visualization of the heating process.

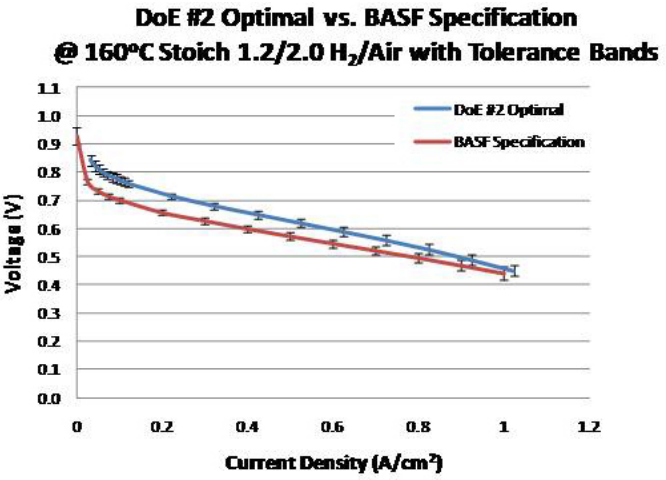


FIGURE 3. Polarization curve of optimal ultrasonically bonded MEA with superior performance as compared to the BASF specification.

Using experimentally derived stiffness and damping values for each layer of the MEA (no fudge factors), the model closely matches thermocouple temperatures measured through the MEA thickness during ultrasonic bonding.

Heat Treatment Optimization: A 2-factor, 3-level, 2-replicate design of experiment was designed for the MEAs with oven temperature and soak time as the variables. Single cell evaluation of the heat-treated MEAs was performed after an 18-hour burn-in period at 200 mA/cm^2 followed by polarization curve measurements at 160°C. The single cell performance of the heat-treated, ultrasonically sealed MEAs was measured along with membrane thickness and acid concentration. Statistical analysis showed that the middle and low temperature and their corresponding heat treatment duration were all significant. More importantly, heat treatment duration beyond the lowest level (15 min) provided no performance benefit.

Ultrasonic Bonding of Low Temperature MEAs: Low-temperature MEAs with 10 cm^2 active area have been successfully sealed using a 20 kHz ultrasonic machine and by thermal pressing. With ultrasonic bonding, the MEA is built carefully by hand, ensuring alignment between the two electrodes, on a piece of Kapton. A second layer of Kapton is placed on top of the assembly to protect the ultrasonic horn, and it is placed on a smooth anvil in the ultrasonic sealer. The ultrasonic welding setup is shown in Figure 4a. Finally, registration holes for alignment in the single cell test hardeware are laser-cut into the oversized Nafion® membrane. An ultrasonically welded MEA is shown in Figure 4b.

Testing of the low-temperature MEAs is planned so that those that are ultrasonically bonded can be compared to thermally pressed baseline MEAs. The bonding process on the ultrasonic setup will be optimized by varying the sealing pressure and energy flux and evaluating the performance. Various techniques and "recipes" to produce thermally pressed MEAs will be explored to maximize the baseline performance.

Durability Testing of Ultrasonically Bonded MEAs: Accelerated durability testing of the high-temperature MEAs (50 cm^2) was performed using test protocols designed to simulate real life operating conditions. The accelerated durability testing protocols involved fuel cell startup/shutdown, load cycling and thermal cycling processes performed over 200 hours. MEAs sealed ultrasonically with optimized process parameters exhibited excellent stability, i.e. no cell voltage degradation and minimal cell internal resistance change, during the 200-hour tests. The authors believe that the ultrasonic sealing technique combined with accelerated durability testing will be vital to the development of high volume fuel cell manufacturing

Conclusions and Future Directions

We are encouraged by the performance of ultrasonically bonded high temperature MEA performance made using

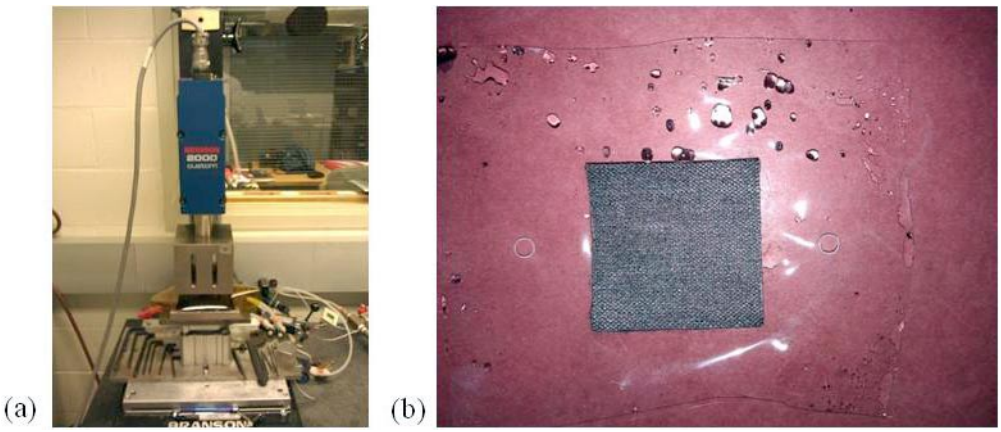


FIGURE 4. (a) Ultrasonic setup used to bond low-temperature MEAs and (b) resulting MEA after laser cutting alignment holes.

optimized process parameters based on single-cell testing after standard incubation and accelerated durability testing. Performance to date has been at least equal to baseline data provided by the manufacturer for thermally bonded MEAs. APC offers a way to minimize cycle time and improve the consistency of thermally pressed MEAs, although cycle times will still be at least an order of magnitude longer than for ultrasonic bonding. Likewise, cost model predictions based on actual experimental data include a 29% reduction by implementing APC and 90% by implementing ultrasonics. The entire research team is prepared to test the performance of 50 cm^2 high temperature MEAs made by standard thermal pressing, APC, and ultrasonic bonding in short stacks and monitor individual cell characteristics. We are also prepared to test and compare larger scale (140 cm^2) high temperature MEAs made using the same three bonding methods. Finally, the team is prepared to compare the performance of small (10 cm^2) low-temperature MEAs made by thermal pressing and ultrasonic bonding. Major activities planned for the remainder of Phase II include:

- Showing how MEAs made by thermal pressing with APC and ultrasonic bonding perform in short stacks compared to those made by conventional thermal pressing.
- Showing how the ultrasonic bonding process scales by comparing the performance of larger scale MEAs (ultrasonically and thermally bonded) to that of standard size MEAs.
- Continue refining the ultrasonic bonding models, validate with experimental data, and demonstrate how such a model would be used for process design and optimization.
- Showing how ultrasonic bonding works for low-temperature MEAs and identifying significant process parameters.

Patents Issued

1. Snelson, T., Puffer, R., Pyzza, J., Walczyk, D. and Krishnan, L., "Method for the production of an electrochemical cell," *U.S. and International Patents Pending*, 2011.

FY 2011 Publications/Presentations

1. Guglielmo, D., Snelson, T. and Walczyk, D., "Modeling Ultrasonic Sealing of Membrane Electrode Assemblies for High-Temperature PEM Fuel Cells," *Proceedings of the ASME 9th Fuel Cell Science, Engineering and Technology Conference*, Washington, DC, Aug. 7–10, 2011, Paper # ESFuelCell2011-54427.

2. Pyzza, J., W. Sisson, W. and Puffer, R., "Manufacturing Implementation of Ultrasonic Sealing of Membrane electrode assemblies for high temperature PEM fuel cells" *Proceedings of the ASME 9th Fuel Cell Science, Engineering and Technology Conference*, Washington, DC, Aug. 7–10, 2011, Paper # ESFuelCell2011-54441.

3. Pyzza, J., "Implementation of Ultrasonic Welders in Automated High Temperature PEM Fuel Cell Membrane Electrode Assembly Manufacturing," *M.S. Thesis*, Department of Mechanical, Aerospace & Nuclear Engineering, Rensselaer Polytechnic Institute, Troy, NY, 2011.

4. Snelson, T., "Ultrasonic Sealing of PEM Fuel Cell Membrane Electrode Assemblies," Ph.D. Thesis, Department of Mechanical, Aerospace & Nuclear Engineering, Rensselaer Polytechnic Institute, Troy, NY, 2011.

5. Puffer, R. and Walczyk, D., "Adaptive Process Controls and Ultrasonics for High Temperature PEM MEA Manufacture," *Fuel Cell Tech Team Meeting (USCAR)*, Southfield, MI, March 16, 2011.

6. Krishnan, L., Snelson, T., Walczyk, D. and Puffer, R., "Effect of Heat Treatment Process Parameters on Polybenzimidazole-based Membrane Electrode Assemblies," *Journal of Fuel Cell Science and Technology* (in review).

7. Krishnan, L., Snelson, T., Walczyk, D. and Puffer, R., "Durability Studies of Ultrasonically Sealed Membrane Electrode Assemblies for High Temperature PEMFCs," *Journal of Fuel Cell Science and Technology* (in review).

8. Snelson, T., Pyzza, J., Krishnan, L., Walczyk, D. and Puffer, R., "Ultrasonic Sealing of Membrane Electrode Assemblies for High-Temperature PEM Fuel Cells," *Journal of Fuel Cell Science and Technology* (in review).

VI.6 Cause-and-Effect: Flow Field Plate Manufacturing Variability and its Impact on Performance

Eric Stanfield
National Institute of Standards and Technology (NIST)
100 Bureau Drive, MS 8211
Gaithersburg, MD 20899-8211
Phone: (301) 975-4882
E-mail: eric.stanfield@nist.gov

DOE Managers
HQ: Nancy Garland
Phone: (202) 586-5673
E-mail: Nancy.Garland@ee.doe.gov
GO: Jesse Adams
Phone: (720) 356-1421
E-mail: Jesse.Adams@go.doe.gov

Contract Number: DE-EE0001047

Subcontractor:
Los Alamos National Laboratory (LANL), Los Alamos, NM

Project Start Date: October 1, 2007 Revised Interagency Agreement (October 1, 2009)
Project End Date: October 1, 2009 Revised Interagency Agreement (October 1, 2011)

Fiscal Year (FY) 2011 Objectives

Develop a pre-competitive knowledge base of engineering data relating fuel cell performance variation to bipolar plate manufacturing process parameters and dimensional variability.

Technical Barriers

This project addresses the following technical barriers from the Manufacturing R&D section of the Fuel Cell Technologies Program Multi-Year Research, Development and Demonstration Plan:

(B) Lack of High-Speed Bipolar Plate Manufacturing Processes

(F) Low Levels of Quality Control and Inflexible Processes

Contribution to Achievement of DOE Manufacturing R&D Milestones

This project will contribute to achievement of the following DOE milestones from the Manufacturing R&D section of the Fuel Cell Technologies Program Multi-Year Research, Development and Demonstration Plan:

- **Milestone 13**: Complete development of standards for metrology of PEM fuel cells. (4Q, 2010)

FY 2011 Accomplishments

- Implemented performance testing protocol improvements to better highlight performance issues (1/2011).
- Quantified baseline repeatability of performance testing as a metric for determining what differences are statistically significant (1/2011).
- Completed initial round of performance testing on all experimental cathode plates at 25 psig back pressure which showed some significant performance differences (2/2011).
- Expanded protocol to include testing at ambient back pressure (as a result of a 2010 Annual Merit Review meeting reviewer comment) using the two worst performing experimental plates #3 and #7 (3/2011):
  - This testing showed that the performance differences still existed, regardless of back pressure.
  - The best performing experimental cathode plate #5 was to be tested under this extended protocol but broke during assembly (fabrication of replacement in process).



Introduction

Based on a workshop organized by the Center of Automobile Research and NIST in December 2004; industry bipolar plate manufacturers identified a need for engineering data that relates geometric bipolar plate tolerances to fuel cell performance. This need is in response to pressure from fuel cell designers to produce lower cost plates, as such, plate manufacturers are being forced to consider potential quality related trade-offs to achieve desired cost targets. To justify these trade-offs, manufacturers are questioning the relevance of stated tolerances on dimensional features of bipolar plates; they expressed a desire for published engineering data relating performance and dimensional quality of the plates that can be used as reference when making these decisions. In response to the identified need, this project was conceived in 2004 and partially funded through the NIST Advanced Technology Program (ATP) Intramural Competition for a period of three years (FY 2005-FY 2007). The ATP funding was also intended to aid NIST with the development and validation of a single-cell testing laboratory. In 2008, funding was provided through DOE in an attempt to bring this project to a successful completion by the end of FY 2008.

To date, the reference single-cell design has been selected, the fabrication and dimensional verification of all experimental plates has been completed according to a statistically based design-of-experiments. All that remains to be completed is the repeatability testing to verify the initial performance test results, the fabrication, dimensional verification, and performance testing of replacement cathode plate #5C at the various back pressures, and the analysis of the performance testing along with the derivation of conclusions based on the full-factorial design of experiments.

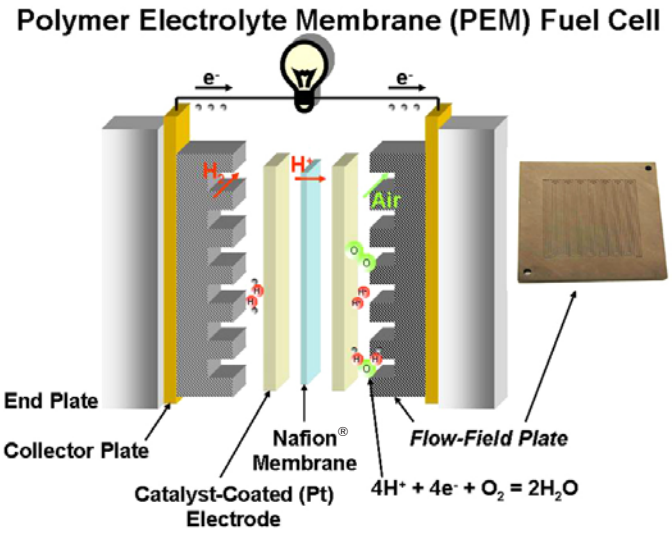


FIGURE 1. Concept - Reference Single-Cell and NIST Fabricated Cathode Flow Field Plates

Approach

Using a statistically based design-of-experiments (Figure 1), fabricate experimental "cathode" side flow field plates with various well defined combinations of flow field channel dimensional variations (Figure 2); then through single-cell fuel cell performance testing using a well defined protocol, quantify the performance effects, if any, and correlate these results into required dimensional fabrication tolerance levels.

Results

The initial performance testing last year, as reported, revealed some very necessary modifications to the protocol.

	2^{4-1} Fractional Factorial Design with replicated center point (k=4,n=10)							
	Sidewall Straightness	Sidewall Straightness	Bottom Straightness	Sidewall Taper				
	Amplitude	Phase	Amplitude			Sequence		Drawing
Part	*X1*	*X2*	*X3*	*X4*	*Machining*	*Measuring*	*Perf. Testing*	*Cross-Section*
9	0(25µm)	0(90)	0(25µm)	0(5)	1	1	1	
3	-1(0)	+1(180)	-1(0)	+1(10)	2	2	2	
2	+1(50µm)	-1(0)	-1(0)	+1(10)	3	3	3	
4	+1(50µm)	+1(180)	-1(0)	-1(0)	4	4	4	
8	+1(50µm)	+1(180)	+1(50µm)	+1(10)	5	5	5	
5	-1(0)	-1(0)	+1(50µm)	+1(10)	6	6	6	
7	-1(0)	+1(180)	+1(50µm)	-1(0)	7	7	7	
10	0(25µm)	0(90)	0(25µm)	0(5)	8	8	8	
6	+1(50µm)	-1(0)	+1(50µm)	-1(0)	9	9	9	
1	-1(0)	-1(0)	-1(0)	-1(0)	10	10	10	

FIGURE 2. Design of Experiment 2^{4-1} Fractional Factorial Design…4 Parameters, 2 Levels, and Replicate Center Point

The most significant was that the same catalyst coated membrane (CCM) could not be reused from plate-to-plate thus a new CCM had to be used. To increase the likelihood of acceptable repeatability, we ensured that all the CCMs came from the same batch. As any particular level of repeatability cannot be assumed, we then performed multiple voltage-current (V-I) curves using the same plate configuration with a different CCM. The results as shown in Figure 3 demonstrate repeatability commensurate with previous high-level single cell testing round robins where multiple labs tested the same single cell assembly, thus we concluded we have attained the desired benchmark repeatability.

Two more recent modifications were identified to better highlight the impact of the intentional dimensional variabilities on performance in the mass transport region. To promote the onset of mass transport we: (1) reduced the anode and cathode platinum loadings from 0.2/0.4 mg/cm^2 respectively to 0.1/0.2 mg/cm^2 and (2) increased the cathode utilization from 50% to 71%. These modifications proved effective, thus we completed the initial V-I curves for all 10 experimental cathode plates as shown in Figure 4. These data were collected applying 25 psig backpressure at the outlets as originally defined in our protocol.

After receiving the reviewers' comments from the 2010 DOE Annual Merit Review meeting in June 2010 we added some additional testing to address a specific reviewer's concern that the backpressure chosen was not within realistic operating conditions. To address this concern, we selected cathode plates #3C, #5C, and #7C which represent the best and worst performers for repeated testing at an intermediate backpressure and ambient. The results for plates #3C and #7C are shown in Figure 5. Unfortunately plate #5C, the best performer, broke during assembly due to a misalignment of one of the sealing gaskets.

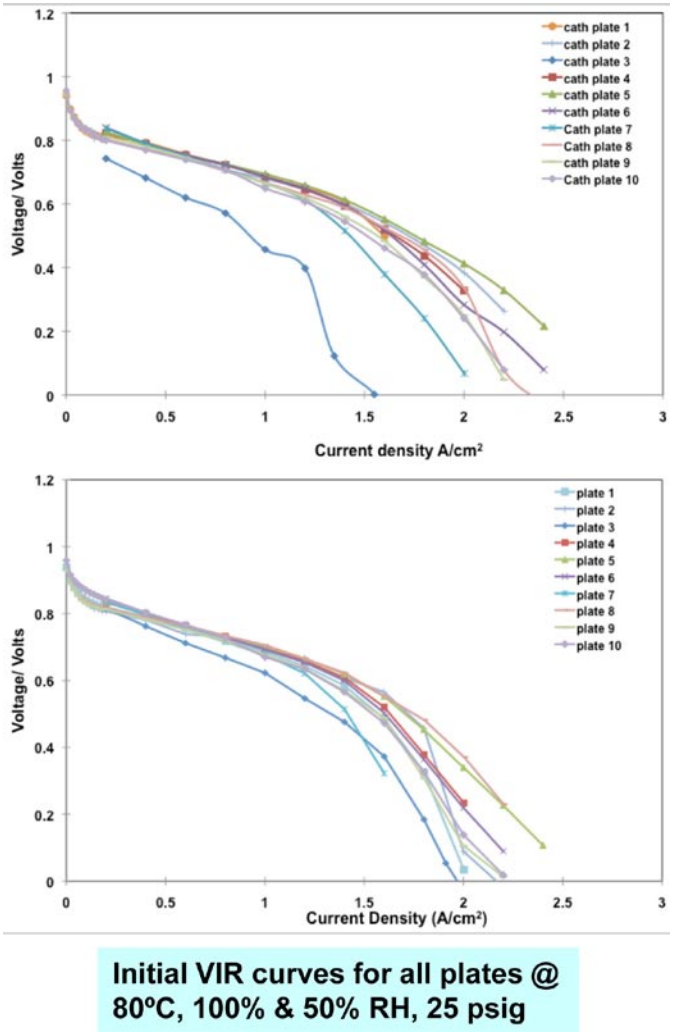


FIGURE 4. Initial Polarization Data for All 10 Experimental Cathode Plates

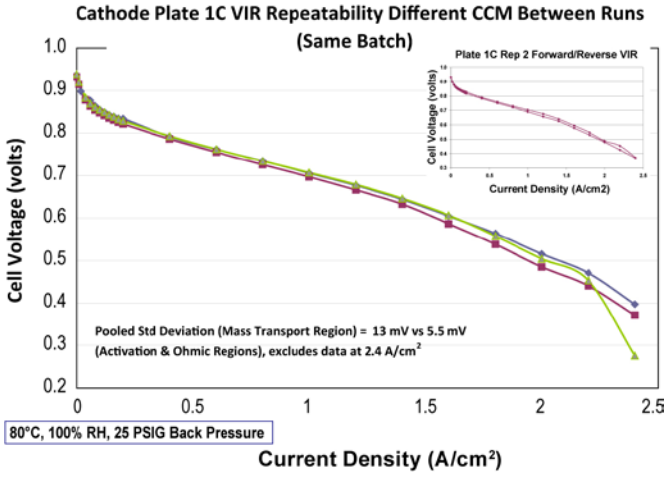


FIGURE 3. Polarization Curve Repeatability with CCM Change-Out between Runs

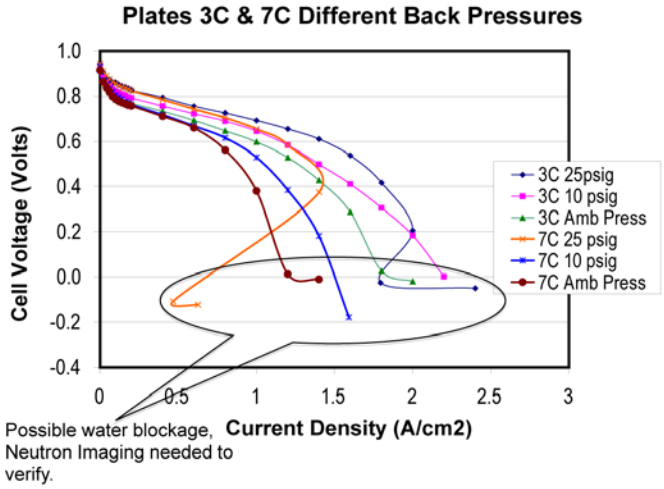


FIGURE 5. Polarization Testing of Select Plates at Different Back Pressures

As expected the polarization curves shifted lower with lower back pressures, however the plate-to-plate performance differences remained. A replacement for plate #5C is currently being fabricated.

Conclusions

- Protocol revisions were carefully derived and meticulously verified, thus the repeatability objectives were achieved and were better than expected.
- To this point testing shows that the intentional dimensional variability at the magnitudes chosen does affect the performance significantly.
- Additional testing, to this point, clearly demonstrates that these performance differences exist regardless of the outlet back pressure.

Future Direction

Project Deliverables

- NIST will fabricate and dimensionally verify a replacement experimental cathode plate #5C.
- Using the replacement #5C plate, LANL will repeat the initial polarization curve at 25 psig backpressure to ensure the results correlate with those of the original plate and complete the polarization curves at the intermediate and ambient backpressures.
- With the assistance of the NIST Statistical Engineering Division, correlate the polarization curve results with the design-of-experiments to elucidate which parameters or combination of parameters have the biggest impact on performance.
- Publish results.

Optional Deliverables (contingent on funding availability through either NIST or DOE)

The addition of the optional deliverables is to dispel the hypothesis that the water management issues are due to the serpentine flow field design or more specifically water being trapped in the turns rather than due to the dimensional perturbations. This concern was raised during a voluntary presentation we gave to the FreedomCAR Technical Team in March of 2011. All experimental plates use the same flow field design and perturbations do not exist in the turns therefore it is believed that repeatable performance differences are due to the perturbations.

- NIST will fabricate and dimensionally verify a subset of the experimental cathode flow field designs into a metallic flow field plate compatible with the LANL 50 cm^2 single cell designed for neutron imaging.
- LANL will perform the polarization protocol at the NIST Neutron Center for Neutron Imaging in order to identify where exactly within the flow field the mass transport issues are occurring.

Suggested Future Work

- Repeat experiments using a parallel flow field design in a metallic plate using the more critical parameters identified in this study along with other parameters, such as, surface finish not previously tested.

Disclaimer

Certain commercial equipment, instruments, or materials are identified in this paper in order to specify the experimental procedure adequately. Such identification is not intended to imply recommendation or endorsement by the National Institute of Standards and Technology, nor is it intended to imply that the materials or equipment identified are necessarily the best available for the purpose.

Acknowledgements

The work detailed in this report would not have been possible without the contributions of the following, all are NIST personnel and guest researchers unless otherwise noted: Tommy Rockward (LANL), Ted Doiron, David Bergman, Martin Misakian, Alkan Donmez, Manny Hahn, Brian Pries

FY 2011 Publications/Presentations

1. E. Stanfield and M. Stocker, "Metrology for Fuel Cell Manufacturing," DOE Annual Merit Review Proceedings, MN006, May 12, 2011, http://www.hydrogen.energy.gov/pdfs/review11/mn006_stanfield_2011_o.pdf

2. E.Stanfield, M. Stocker, and B. Muralikrishnan, "Metrology for Fuel Cell Manufacturing," Invited Presentation Given to the FreedomCAR Tech Team, USCAR, Southfield, MI, March 16, 2011.

3. E. Stanfield, "Cause-and-Effect: Flow Field Plate Manufacturing Variability and its Impact on Performance," FY 2010 Annual Progress Report, DOE Hydrogen and Fuel Cells Program, February 2011, http://www.hydrogen.energy.gov/pdfs/progress10/vi_6_stanfield.pdf

VI.7 High Speed, Low Cost Fabrication of Gas Diffusion Electrodes for Membrane Electrode Assemblies

Emory S. De Castro
BASF Fuel Cell, Inc.
39 Veronica Avenue
Somerset, NJ 08873
Phone: (732) 545-5100 ext 4114
E-mail: Emory.DeCastro@BASF.com

DOE Managers
HQ: Nancy Garland
Phone: (202) 586-5673
E-mail: Nancy.Garland@ee.doe.gov
GO: Jesse Adams
Phone: (720) 356-1421
E-mail: Jesse.Adams@go.doe.gov

Contract Number: DE-EE0000384

Subcontractor:
Dr. Vladimir Gurau
Case Western Reserve University, Cleveland, OH

Project Start Date: July 1, 2009
Project End Date: June 30, 2012

Fiscal Year (FY) 2011 Objectives

- Reduce cost in fabricating gas diffusion electrodes (GDEs) through the introduction of high speed coating technology, with a focus on materials used for the high temperature membrane electrode assemblies (MEAs) that are used in combined heat and power (CHP) generation.
- Relate manufacturing variations to actual fuel cell performance in order to establish a cost-effective product specification.
- Develop advanced quality control methods to guide realization of these two objectives.

Technical Barriers

This project addresses the following technical barriers from the Manufacturing R&D section of the Fuel Cell Technologies Program Multi-Year Research, Development and Demonstration Plan (Section 3.5):

(A) Lack of High Volume Membrane Electrode Assembly (MEA) Processes

(F) Low Levels of Quality Control and Inflexible Processes.

This project will contribute to achievement of the following DOE milestones from the Manufacturing R&D section of the Fuel Cell Technologies Program Multi-Year Research, Development and Demonstration Plan (Section 3.5.7):

- Develop continuous in-line measurement for MEA fabrication. (4Q, 2012)
- Establish models to predict the effect of manufacturing variations on MEA performance. (4Q, 2013)

This project addresses coating speed and uniformity of GDEs, a critical component for MEA fabrication. One sub-task is to develop a continuous X-ray fluorescence analyzer that directly measures catalyst deposition level and distribution on rolled goods, ultimately guiding improvements in through-put and uniformity. This sub-task directly contributes to the fourth quarter 2012 goal for in-line measurement. Another sub-task is to develop models that predict the effect of manufacturing variations in catalyst distribution and porosity in GDEs, and relate these variations as six-sigma limits for a component specification. The establishment of a model that predicts MEA performance based on manufacturing variations in GDEs contributes to improving the quality of the component as well as achieving the fourth quarter 2013 DOE milestone above.

FY 2011 Accomplishments

- Reduced labor cost to manufacture GDE by 50%.
- Improved cathode catalyst utilization by ~25% through 20 mV gain in performance.
- Met key milestone of doubling throughput for GDE at production scale.
- Coated carbon cloth GDEs at >2X width – timing is ahead of milestone plan.
- Demonstrated pilot-scale fabrication of GDEs on a lower cost non-woven web.



Introduction

The basis of this project is to create GDEs at a far lower cost than those currently available. GDEs are critical components of membrane electrode assemblies and represent the highest cost subcomponent of the MEA. Cost reduction will be accomplished through development of a higher throughput coating process, modeling the impact of defects due to the higher speed process, and overcoming these limitations and providing a six-sigma manufacturing specification that relates performance to defects. The main focus of the effort is creating next-generation inks through

advanced additives and processing methodologies. As part of our approach, we will also develop on-line quality control methods such as determination of platinum concentration and distribution during the coating process. The on-line mapping of platinum will guide the ink development process and provide feedback on uniformity.

For this reporting period we significantly advanced our understanding of the inherent limitations of suspensions of carbon black or carbon black catalysts mixed with a hydrophobic binder. The use of a hydrophobic binder is critical to create GDEs for high temperature MEAs. Through this project's understanding we developed improved inks that can be made more concentrated and thus reduce the number of applications needed per pass. These new inks also used substantially less time to prepare, and afforded greater utilization of the catalyst once in the MEA, improving performance. We also began to apply the ink development sequence to lower non-woven carbon paper cost.

Approach

GDEs are comprised of a gas diffusion layer coated with catalyst. The gas diffusion layer is simply carbon cloth or a non-woven carbon that has been coated with carbon black and serves as a current collector for the catalyst. For both the carbon black and catalyst, a hydrophobic binder is added to achieve critical porosity and hydrophobicity in the final structure. Of the carbon black, catalyst, or hydrophobic binder none are highly soluble in aqueous solutions. Aqueous solutions must be used as solvents since the use of organic solvents with a highly active catalyst is too dangerous in a production environment. Also, the hydrophobic binder is shear-sensitive, meaning it becomes less stable when pumped or subjected to shear forces in the coating applicator. Thus, the challenge in this project is overcoming the inherent physical limitations in these materials through advanced formulations and processing.

Our approach to solving this challenge begins with identifying key quality GDE metrics that relate directly to ink performance, develop an understanding of the forces behind ink stability, and introduce solution measurement methods that relate ink performance to the quality metrics. With more stable ink formulations, we anticipate being able to coat longer and wider webs at higher speeds. If an ink can be made more concentrated and remain stable we can use less application passes and save cost. The ink development process is supplemented by two other activities that ultimately lead to lower cost GDEs. We will develop a model that will predict the impact of manufacturing variations on MEA performance, and use this model to determine the level of coating quality needed to maintain consistent current and voltage. Also, we will create on-line instruments to lead development of more precise coating processes.

In this period, we combined next generation stabilizing additives with high energy dispersion techniques to greatly improve the inks, and scaled these through to the production coater.

Results

Microporous Layer

One significant problem was posed by the hydrophobic carbon used in the microporous layer (MPL). When benchmark inks and additives are used, this ink became less viscous as the shear rate increases. This shear-thinning behavior indicates strong particle-particle interactions and is shown as the trace labeled "baseline, low solids" in Figure 1. The shear-thinning becomes worse when we increased the solid content of the ink – desirable to reduce number of coating passes (see trace "baseline, high solids"). High shear-thinning indicates instability for the formulation as well as higher potential for non-uniformity under the shear forces of the applicator. By using a combination of additives and a high energy preparation method, we were able to create inks for the MPL that are Newtonian, that is, shear insensitive over a wide range. See the Figure 1 trace labeled "improved, highest solids." Note the solid content of this ink enabled >55% reduction in number of application passes needed, as well as a 50% reduction in time to prepare the ink. We scaled this MPL ink formulation to the production coater and demonstrated full width coating ahead of plan.

Cathode Electrode Layer

Last year we reported improvements in the cathode catalyst ink formulation that decreased the number of coating defects due to agglomeration and held potential to reduce the number of application passes by 30% when using our pilot-scale coater. We have now identified an

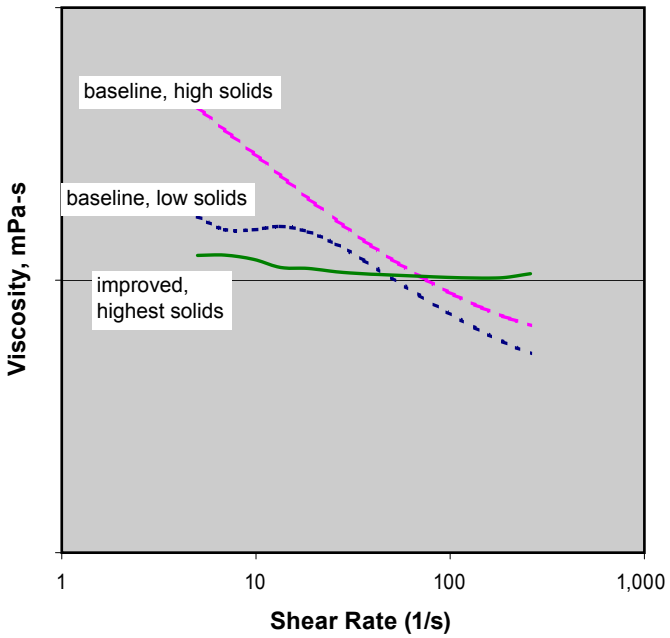


FIGURE 1. Viscosity vs. shear rate for three different ink formulations: baseline (low solids), baseline (high solids), and improved (highest solids).

improved additive system (several additives that work in concert) that not only stabilize higher concentrations of inks, but completely eliminated a labor-intensive step in ink making. We have scaled this improvement to our production scale coater as well as demonstrated a savings of >60% in labor hours for ink making and decrease in number of coating passes by 40%. Furthermore, these inks have shown a remarkable improvement in cathode performance as evidenced in Figure 2. We attribute the ~20 mV gain over baseline to an increase in platinum utilization through enhanced uniformity by 25%.

Anode Electrode Layer

A key difference between the anode and cathode electrodes is the catalyst. The cathode employs an alloy to facilitate oxygen reduction. Since the MEAs being developed under this project operate between 160°–180°C, they are highly tolerant to carbon monoxide (CO) and operate well at 1%-2% CO using only a pure platinum catalyst. Throughout this project we have adhered to the ink additive selection rules that are summarized as follows: select compounds that stabilize the ink components, leave no or minimal residue in the MPL or electrode layers, and do not disturb the intended porosity and hydrophobicity profiles. The anode catalyst is sufficiently different than the cathode that not only was a modified suite of additives employed, but extensive efforts were needed to develop a removal sequence to both minimize residues and preserve optimal hydrophobicity in the electrode layer. We were successful in developing an anode ink that also eliminated the labor-intensive step of the cathode, and also reduced ink preparation labor by 50% and decreased the time for coating passes by 40%. This ink has been scaled through to the full production coating machine.

Conversion of Lower Cost Substrates

A second major focus of this project is to develop lower cost substrates into GDEs. Non-woven carbon fiber materials ("carbon paper") are believed to be ~30% lower in cost compared to the carbon cloth at higher volumes. The porosity, hydrophobicity, and absorption properties of the carbon papers are totally different than carbon cloth, and we had to develop an entirely new class of inks for the MPL, anode electrode layer, and cathode electrode layer. Although in the pilot-scale with limited coating lengths, we have established good progress. Figure 3 shows our status with a MPL plus cathode catalyst layer compared to the benchmark carbon cloth performance in hydrogen/air at 160°C. The inks developed for the carbon paper have been able to preserve the higher solid content of the carbon cloth inks and reduced number of application passes.

Conclusions and Future Directions

Through last year's foundation in understanding principle mechanisms behind ink destabilization and additive selection, we have been able to significantly improve the coatings of MPLs, anode catalyst layers, and cathode catalyst layers. While the objective of this project is to decrease cost by increasing throughput, we have also improved the overall process by decreasing the labor content for ink preparation by ~50%. We have scaled these new formulations to a full-

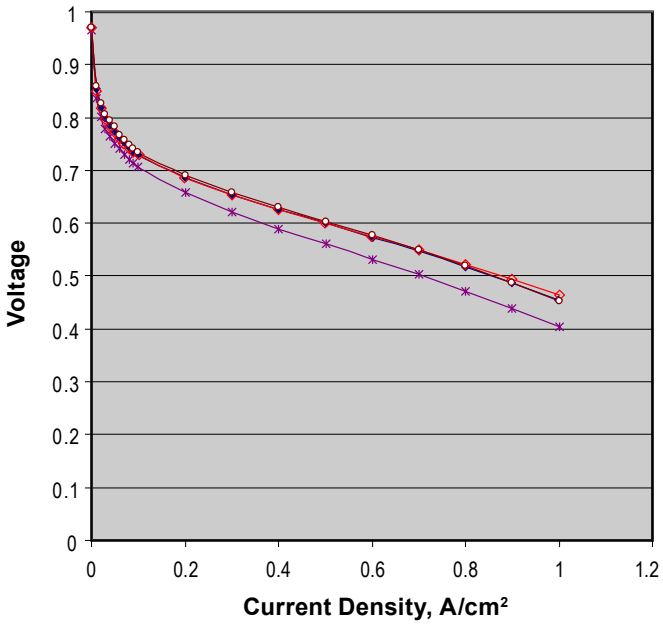


FIGURE 2. Voltage vs. current plot of baseline high temperature MEA vs. same with improved cathode catalyst layer at pilot and production coating scales. 160°C, H_2/air, 1.2/2, ambient pressure.

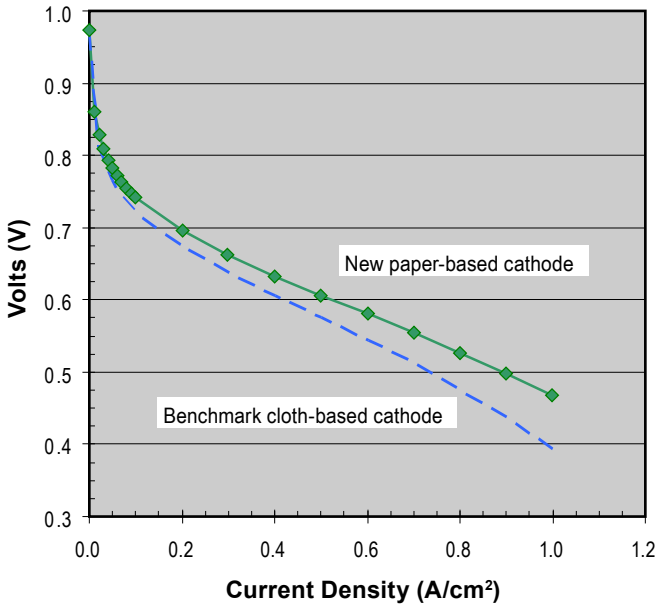


FIGURE 3. Voltage vs. current plot of baseline high temperature MEA vs. same made with carbon paper substrate at pilot coating scales. 160°C, H_2/air, 1.2/2, ambient pressure.

scale production coater, and achieved our key milestone of doubling throughput. A fringe benefit of the more uniform structures created by this approach is an improvement in performance by ~20 mV, inferring an increase in catalyst utilization by around 25%. Pilot-scale results on low cost non-woven substrates are encouraging and show a path for further decease of costs. Advances in this project are being transitioned to our current production techniques with a direct immediate impact on component cost.

Upcoming Focus

1. Develop full-width carbon cloth coating to gain another 2X throughput factor.
2. Qualify current formulations on full-width, full length production coating trials.
3. Develop formulations for non-woven carbon paper for a further reduction in cost: demonstrate on production coater.

FY 2011 Publications/Presentations

1. "Celtec®-P high temperature MEAs making a difference in power applications," F-Cell, September 2010, Stuttgart, Germany, Emory S. De Castro (Invited Speaker).

VI.8 MEA Manufacturing R&D Using Drop-On-Demand Technology

Peter C. Rieke (Primary Contact) and
Silas A. Towne
Pacific Northwest National Laboratory
P.O. Box 999
Richland, WA 99354
Phone: (509) 375-2833
E-mail: peter.rieke@pnnl.gov

DOE Manager
HQ: Nancy Garland
Phone: (202) 586-5673
E-mail: Nancy.Garland@ee.doe.gov

Project Start Date: June 1, 2010
Project End Date: Project continuation and direction determined annually by DOE

Fiscal Year (FY) 2011 Objectives

- Evaluate membrane electrode assembly (MEA) fabrication process and compare catalyst printing and coating process.
- Critically evaluate inkjet or "drop-on-demand" printing technology to meet the criteria specified in the above objective.

Technical Barriers

This project addresses the following technical barriers from the Manufacturing R&D section (3.5.5) of the Fuel Cell Technologies Program Multi-Year Research, Development and Demonstration Plan:

(A) Lack of High-Volume Membrane Electrode Assembly (MEA) Processes

(F) Low Levels of Quality Control and Inflexible Processes

Contribution to Achievement of DOE Manufacturing R&D Milestones

This project will contribute to achievement of the following DOE milestones from the Manufacturing R&D section of the Fuel Cell Technologies Program Multi-Year Research, Development and Demonstration Plan:

- Develop fabrication and assembly processes for polymer electrolyte membrane automotive fuel cell that meets cost of $30/kW. (4Q, 2015)

FY 2011 Accomplishments

- Technical analysis of printing coating fabrication process completed and report to DOE in final draft.
- Developed printhead control algorithms suitable for printing of thin films.
- Thin film printing station constructed and has undergone initial testing and calibration. Will be brought on line soon.
- Demonstrated that MEAs prepared by inkjet fabrication have comparable performance to commercially available MEAs. Needs optimization.



Introduction

One of the primary DOE goals for use of proton exchange membrane fuel cells (PEMFCs) as power plants in transportation includes the reduction of manufacturing costs to below $30/kW. Today's low-volume, actual cost is greater than $1,000/kW and the high-volume manufacturing cost, based upon current manufacturing process, is extrapolated to be less than $300/kW [1-3]. New manufacturing processes are needed and must be able to:

- Adapt to the transition from low-volume specialty to the high-volume automotive markets,
- Rapidly incorporate advances in PEMFC technology, and
- Accommodate both small and large production runs.

Approach

Digital fabrication, in combination with unique catalyst-layer ink formulations, will eliminate or simplify many of the currently necessary, but slow and cumbersome, pre- and post-deposition processing steps. In earlier work [4] we have shown that for the digital fabrication process that:

- No hot-press/lamination is needed to ensure catalyst layer adhesion to the membrane,
- Wastage of membrane and catalyst materials are minimized,
- Catalyst utilization can be enhanced with XY and Z gradations in composition,
- The hydrogen form of the membrane can be directly used and no chemical transformation to the sodium form is needed, and
- Digital fabrication is highly adaptable in an evolving technology scenario.

It is the goal of the project to understand fully the implications of digital fabrication on processing, design prototype digital fabrication facilities to test production methods, provide a basis for quantitative cost comparison with current fabrication technology, integrate the fabrication with the rest of PEMFC stack assembly and develop

design criteria for a pilot plant manufacturing line based upon digital fabrication. The project digital-fabrication approach will lead to a higher quality product with improved performance, fabricated by a simpler and more cost-effective production process. Digital fabrication will be an agile and versatile means of production, and will provide a viable route to meeting DOE production targets for PEMFC-based power plants.

Results

Analysis of Catalyst Layer Printing and Coating Technologies

A review of the advantages and disadvantages of printing and coating technologies in the fabrication of catalyst coated membranes was conducted [5-7]. This included direct contact methods such as offset and flexographic printing, ink spreading systems such as the myriad forms of roll coating, doctor blading and slot die coating and Gravure printing. Noncontact methods include aerosol and airless spraying as well as piezoelectric and thermal inkjet processes were also considered.

Process deposition speed is not the only requirement to be considered in the manufacturing process and may be of minor importance especially for an emerging industry. The criteria for evaluation of the catalyst coating process were 1) ink development complexity, 2) suitability to long, medium and short production runs, 3) coating speed and adaptability, 4) ability "patch" coat, 5) ability to grade catalyst layer composition, and 6) coating thickness and variability.

In comparison of the various techniques slot die, Gravure and inkjet printing provide the best characteristics for at least some scalability in comparison to the other techniques discussed:

- Each of these three methods conserves expensive catalyst and membrane material.
- Each has highly variable speeds although slot die coating quality has a stronger dependence on speed.
- Inkjet coating is easier to integrate into a process line whereas slot die and Gravure process will constrain if not dominate the process line design.
- Slot die coating cannot be used to grade coatings.
- Slot die coating provides a relatively thick single pass coating.
- Gravure printing is not well suited to lab scale and small job scale production.
- A combination of digital and continuous inkjet printing provides scalability from the lab- to automotive-scale.

Requirements of Thin Film Inkjet Printing

Inkjet printing technology is focused at printing words or images for which surface reflectivity is the most important physical criteria. Further continuous films are not required and half toning and dithering are used to achieve color and gray scale but often leave distinct significant portions of the substrate without an ink deposit. The properties are not compatible with thin film structures that must have uniform or graded but continuous structure over many centimeters. Further a printed layer of a given composition may have to interface with an under or over lying layer of different composition.

To address this issue we developed a unique print algorithm that was implemented for the 2x25 printhead pattern of a HP-26 print cartridge. The algorithm ensures that:

- All jets are used evenly to prevent clogging,
- No single pixel is printed more than once,
- The jet patterns are "woven" to prevent vertical and horizontal banding,
- The algorithm can be adapted to a particular printhead jet pattern, and
- Successive prints can be offset slightly to ensure uniformity.

A printer was fabricated to allow testing of printing parameters in future work – see the following. The printer was based upon two HP-26 inkjet cartridges and is capable of depositing up to four inks although only one ink systems have been tested to date. The system uses a Microchip PIC24J256GB110 microprocessor to control XYZ table movements and individual jet firing and communication with a universal serial bus (USB) storage device. MATLAB was used to implement the algorithm discussed above, and convolute the print pattern with an image pattern. The file output from this is stored on the USB device in a simple form ready for microprocessor implementation. Figure 1 shows an approximately 10 μm thick film of yittria-stabilized zirconia (YSZ) printed with this experimental printer. YSZ suspensions were used for initial testing as the suspensions are very stable and the average particle size is two orders of magnitude smaller than the jet orifice size.

We previously had worked closely with Hewlett-Packard and used their experimental print facilities for initial work. However we did not have permission to sufficiently modify those instruments to allow close control of humidity and substrate temperature. The new printer, although less sophisticated, will allow better examination of the printing process.

Printhead Reliability

Printheads after many thousands (if not millions) of firing cycles are subject to clogging by the presence of minute quantities of large particles. We conducted two tests using identical printheads with 20 and 28 μm diameter jets. The 20 μm jets failed due to clogging after only a few hundred cycles while the 28 μm jets did not fail during

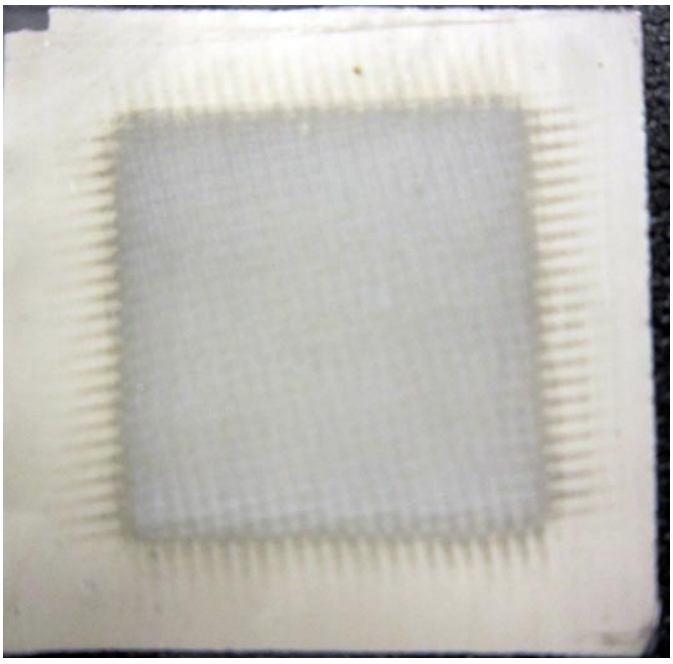


FIGURE 1. Photograph of an Approximately 10 μm Thick YSZ Film

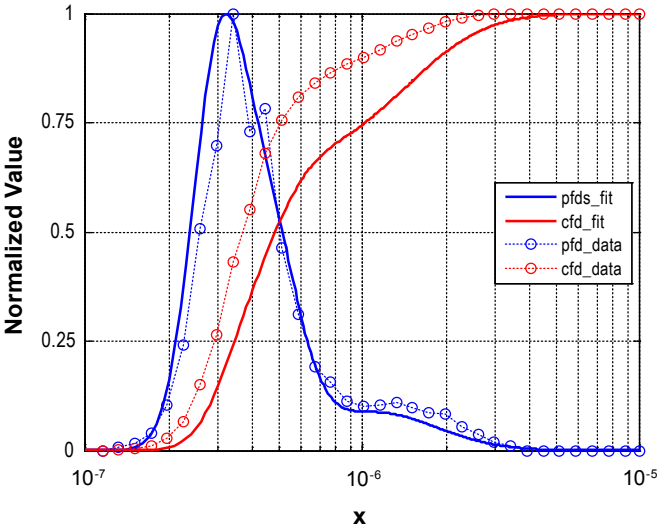


FIGURE 2. Normalized Particle Size Distribution and Log Normal Fits of Catalyst Inks

experimental use. Figure 2 shows the normalized particle size distribution of our catalyst inks as well as the log normal fits to these data. Note the presence of a large shoulder at about 1.5 μm off the main peak at about 0.3 μm. These peaks are much smaller than the 20 and 28 μm jet diameters yet the 20 μm jets clogged while the 28 μm jets did not clog. The log normal fit to the data was used to estimate the distribution of very large particles in a suspension that could not in reality be detected by particle size analysis. As shown in Figure 3, the probability of clogging after 1,000 fires is

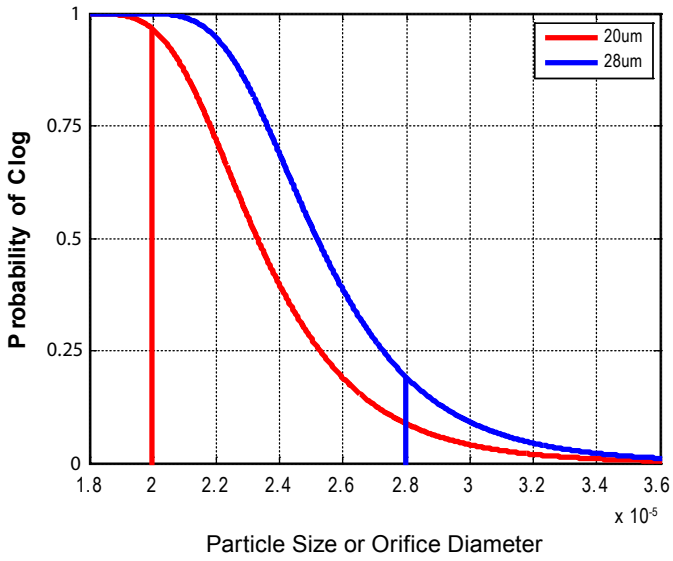


FIGURE 3. Probability of Clogging after 1,000 Fires for 20 μm and 28 μm Jet Orifices

98% for a 20 μm jet while that for a 28% jet is only 25%. By eliminating the large shoulder through appropriate filtering, the probability of clogging can be substantially reduced but this work demonstrates the need to carefully consider ink stability and to prevent particle aggregation before use.

Comparison of Commercial and Inkjet Printed Electrodes

To realistically compare catalyst coated membranes fabricated by different processes we adapted standard performance tests into a series of 15 electrochemical tests that allowed comparison of performance under a wide variety of conditions including back pressure up to 15 psig, O_2 vs. air, different cathode and anode relative humidities and stoichiometries. Shown in Figure 4 are current-voltage curves, taken with air at the cathode and at 0 and 15 psig backpressure, for a digitally fabricated MEA and one purchased from Ion Power. Both had 0.2 mg/cm^2 of platinum. The Ion Power electrode was distinctly better but not so much better that the difference can be attributed to the fabrication method. It may well be that difference in electrode composition may be more important. We note that, with O_2 at the cathode, the inkjet fabricated electrodes outperformed the Ion Power electrodes.

Conclusions

- Technical analysis of printing and coating processes completed and report in final draft.
- Defined algorithms suitable for printing of thin films.
- Thin film printing station constructed and has undergone initial testing and calibration. Will be brought on line soon.

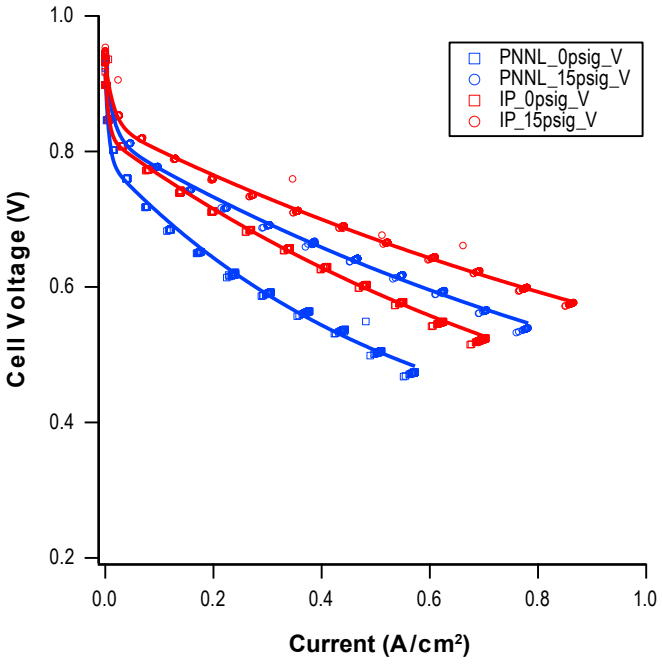


FIGURE 4. Comparison of in-house digitally fabricated MEAs with commercially produced MEAs. Results shown are for air at the cathode and at 0 and 15 PSIG backpressure.

- Demonstrated that MEAs prepared by inkjet fabrication have comparable performance to commercially available MEAs. Needs optimization.

Future Directions

- Develop catalyst-compatible inks that prevent particle aggregation and jet clogging.
- Optimize ink composition (ionomer, carbon, catalyst ratio).
- Determine optimal printing conditions - relative humidity, substrate temperature.
- Quantify relationship of substrate wettability to thin film uniformity.
- Determine maximum single pass thickness.
- Quantify development needs for continuous inkjet fabrication.

FY 2011 Publications/Presentations

1. "Approaches to Manufacturing of MEAs for PEM fuel Cells", Peter C. Rieke, Silas A. Towne, Report to DOE. In final draft.

2. "MEA Manufacturing R&D Using Drop-on-Demand Technology", Peter C. Rieke, Silas A. Towne, DOE Hydrogen Program Annual Merit Review, Washington, DC, May 2011.

References

1. Fuel Cell Market Report, 2009, U.S. Dept of Energy, Office of Energy Efficiency and Renewable Energy.

2. Hydrogen, Fuel Cells & Infrastructure Technologies Program Multi-Year Research, Development and Demonstration Plan, 2009.

3. E.J. Carlson, P. Kopf, J. Sinha, S. Sriramulu, Y. Yang, Cost Analysis of PEM Fuel Cell Subcontract Report, NREL/SR-560-39104 2005.

4. Peter C. Rieke, Silas A. Towne, DOE Hydrogen Program Review, May 20, 2009.

5. Flexographic Technical Association, Flexography:principles and practices, 2000.

6. A.A. Tracton, Coatings Technology Handbook, CRC, 2006.

7. Kipphan, Helmut, Handbook of print media: technologies and production methods. Springer, 2001.

VI.9 Development of Advanced Manufacturing Technologies for Low Cost Hydrogen Storage Vessels

Mark Leavitt
Quantum Fuel Systems Technologies Worldwide, Inc.
25242 Arctic Ocean Drive
Lake Forest, CA 92630
Phone: (949) 399-4584
E-mail: mleavitt@qtww.com

DOE Managers
HQ: Nancy Garland
Phone: (202) 586-5673
E-mail: Nancy.Garland@ee.doe.gov
GO: Jesse Adams
Phone: (720) 356-1421
E-mail: Jesse.Adams@go.doe.gov

Contract Number: DE-FG36-08GO18055

Subcontractors:
- Boeing Research and Technology, Seattle, WA
- Lawrence Livermore National Laboratory (LLNL), Livermore, CA
- Pacific Northwest National Laboratory (PNNL), Richland, WA

Project Start Date: September 26, 2008
Project End Date: March 31, 2012

Fiscal Year (FY) 2011 Objectives

Develop new methods for manufacturing Type IV pressure vessels for hydrogen storage with the objective of lowering the overall product cost by:

- Optimizing composite usage through combining traditional filament winding (FW) and advanced fiber placement (AFP) techniques.
- Exploring the usage of alternative fibers on the outer layers of the FW process.
- Building economic and analytical models capable of evaluating FW and AFP processes including manufacturing process variables and their impact on vessel mass savings, material cost savings, processing time, manufacturing energy consumption, labor and structural benefits.
- Studying polymer material degradation under high-pressure hydrogen environment.

Technical Barriers

The project addresses the following technical barriers from the Manufacturing R&D section (3.5) of the Fuel Cell Technologies Program Multi-Year Research, Development and Demonstration Plan:

(G) High-Cost Carbon Fiber

(H) Lack of Carbon Fiber Fabrication Techniques for Conformable Tanks

Contribution to Achievement of DOE Manufacturing R&D Milestones

This project will contribute to achieving Milestone 24 from the Manufacturing R&D section of the Fuel Cell Technologies Program Multi-Year Research, Development and Demonstration Plan:

- Develop fabrication and assembly processes for high-pressure hydrogen storage technologies that can achieve a cost of $2/kWh. (4Q, 2015)

FY 2011 Accomplishments

- Passed burst test with Vessel 7 and reduced 22.9% of carbon fiber from baseline vessel.
- Completed cost model for hybrid process according to the latest vessel design.
- Characterized polymer materials in high-pressure hydrogen environment.
- Completed the design, build, and integration of the next-generation AFP head.
- Down-selected a lower-cost and lower-strength carbon fiber suitable for vessel outer layers.



Introduction

The goal of this project is to develop an innovative manufacturing process for Type IV high-pressure hydrogen storage vessels, with the intent to significantly lower costs. Part of the development is to integrate the features of high precision AFP and commercial FW.

In this project period, a vessel was designed that passed the burst test successfully. Boeing's improvements included re-machining the foam mandrels to resolve the wrinkling issues due to poor fit-up between the end caps and the liner, refining the AFP processes, and developing a new AFP head to reduce downtime and increase productivity for processing of pressure vessels. Energy and cost targets were improved significantly in the cost model developed by PNNL after the success of Vessel 7. PNNL also characterized polymer materials in high-pressure hydrogen environments.

Approach

The hybrid vessel designs were based on finite element analysis results to optimize strain distribution and achieve uniform displacement in the domes of the vessel.

Results

Vessel Designs

Vessel 3: At the time of writing the 2010 annual report, Vessel 3 was in the process of being manufactured. It achieved a burst pressure of 21,658 psi, which is lower than the requirement of current CSA America Hydrogen Gas Vehicle (HGV) standard of 22,843 psi. However, it was an improvement over Vessel 2 by almost 3,000 psi. (See Table 1 for test result summary.) Since the burst pressure was 95% of the standard's minimum burst requirement, the plan was to lower the peak strain of design 3 by 7%.

Vessel 4: The peak strain location of Vessel 4 was relocated to the cylinder section by adding localized hoops at the transitions between AFP and FW. The outer layers of FW composite were reordered to have a hoop as the outer layer (vs. helical). This was done to keep tension in the last helical circuit and reduce voids. Vessel 4 reached a burst pressure of 21,719 psi, below the design requirements (Table 1) and slightly lower than the burst value for Vessel 3, even though strains were reduced by 7% as planned. In post test analysis a 1" X 2" block was cut from the aft end and inspected under a microscope. The inspection showed that the second group of AFP layers had waviness on top of the FW surface, but the first AFP did not show any sign of waviness. It was concluded that the waviness of the second AFP layer was due to the non-uniform surface of the FW base layers that they were built on. When a layer of fiber is wavy, it does not carry the portion of the load that those layers are designed for.

Vessel 5: Vessel 5 was essentially completely redesigned while keeping certain key design characteristics of Vessel 1 (passed burst test) and applying the lessons learned from previous vessels: 1) use single AFP to avoid fiber waviness and streamline manufacturing process, 2) maintain or reduce strain values of Vessel 1, and 3) manufacture AFP end caps on rigid foam tool. The design was much improved from that of Vessel 1 in terms of fiber usage, stress distribution, and strain values. It achieved a burst pressure of 20,500 psi, which was lower than Vessel 4 but had a fiber reduction of 10.6 kg from Vessel 4 (Table 1).

Earlier installation of the AFP end caps (Figure 1) on Vessels 3 and 4 revealed that they did not adequately fit the contour of the liner. The caps required significant manipulation to align them onto the dome, ultimately resulting in wrinkled tows and lower strength. Therefore, the foam mandrels were re-machined to a new and more accurate surface according to the liner contour data defined and measured by a laser tracking system. The newly cut surfaces also included higher-fidelity features for the boss

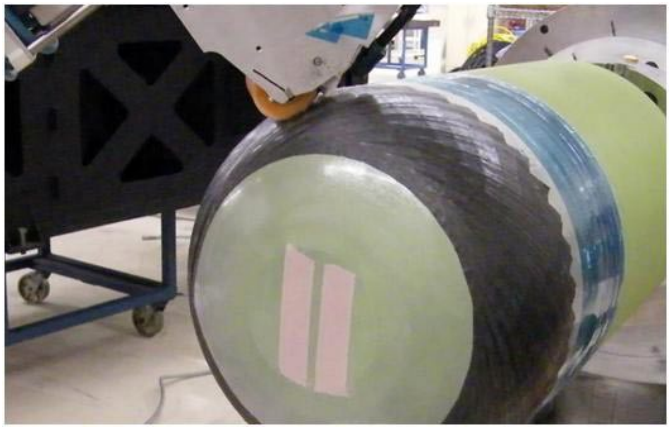


FIGURE 1. Fiber Placement of the End Cap (Older Generation Head)

TABLE 1. Vessel Test Result Summary

Vessel #	Weight (kg)	% Wt. Down from Baseline	Burst Pressure (psi)	% Under Std.[1]	Burst Area
0 (Baseline)	76.0	-	-	-	-
1	64.9	14.61	23,771	-	Mid Cylinder
2	N/A	-	18,666	18.29	Aft
3	67.11	11.70	21,658	5.19	Aft
4	65.04	14.42	21,719	4.92	Aft
5	54.44	29.37	20,500	10.26	Aft
6	Built identically to Vessel 5 for analysis only				
7	58.63	22.86	22,925	-	Mid Cylinder
8	57.29[2]	24.62	-[3]	-	-

[1] Current HGV standard burst pressure requirement is 22,843 psi.
[2] Continuous winding and additional squeegeeing contribute to even lower weight.
[3] Cycle test ended after 13,500 cycles, thus no burst test afterward.

detail; further reducing wrinkling in the key polar regions. The better fit of the AFP end caps to the liner successfully eliminated wrinkling at each end of Vessel 5.

Vessel 6: Due to the inconsistencies seen in burst performance vs. fiber strains, Vessel 6 was built identically to Vessel 5 for destructive analyses. Half of the forward and aft ends of the vessel were sent to Boeing. At Boeing, computed tomography-scanning and photo-microscopy were performed to quantify porosity and resin rich areas within the structure, along with FW fiber waviness. At Quantum, after polishing the remaining ends, excessive voids were found in the aft end due to bridging (Figure 2). Bridging was caused by incorrect assumption of the "necking factor" value used in the design input file. Necking factor is defined as the ratio of fiber bandwidth at the polar opening vs. bandwidth in the cylinder section.



FIGURE 2. Voids are Shown in the Sectioned Aft Dome of Vessel 6



FIGURE 3. Vessel 7 Burst Test Result Showing Rupture in Mid Cylinder

Vessel 7: It was believed that the bridging issue was causing separation and reduction of load translation between the FW layers, which led to Vessel 5 failure. After entering the new necking factor, the models on both fwd and aft ends showed multiple opportunities to reduce bridging in the design. The excessive bridging locations were resolved by adjusting the fiber angles and polar openings. The total weight savings on Vessel 7 was 17.37 kg or 22.9% from the baseline (all FW) vessel (Table 1). Vessel 7 passed the burst test at 22,925 psi. The burst location was in the mid cylinder as designed (Figure 3).

Vessel 8: Vessel 8 was built identically to Vessel 7 for cycle test, but it developed a leak after 13,500 cycles, 1,500 cycles short of the requirement. Root cause of the leak will be determined in Phase III.

New Six-Tow Quarter Inch AFP Head Development

Boeing has built a prototype tow-placed head designed specifically for processing of pressure vessels. The ¼-inch, 6-tow machine has improved infrared heating capabilities and a more compact size enabled by the use of stainless steel (vs. aluminum). Boeing's new head is able to apply fiber ½-inch closer to the polar boss. This enables a more-efficient, lower-weight pressure vessel design. Boeing has incorporated the ability to cut each individual tow, as well as a reverse-style cutter, allowing for higher speed cutting on the fly. Overall, Boeing has decreased downtime and increased productivity by improving the ease of operation and maintenance. The entire head opens up with only one tool allowing the operator to quickly clear jams. This increases the production of pressure vessels and reduces touch labor.

The head has been integrated onto a robotic cell, which will utilize a rail and a KUKA KR240 long arm system to provide more control and flexibility during lay-up. The system will allow the optimal placement of the robot base to minimize wasted motion and be capable of fiber placing a vessel with one tooling setup. An important characteristics of this cell is the significantly lower cost of the overall system compared to what is available in the industry.

Cost Model

Meeting the burst requirement with Vessel 7 showed that the AFP end caps can be successfully made in a parallel manufacturing line. This allows optimization of machine usage. Parallel AFP and FW processing lines reduce the vessel manufacturing time from 8.2 hr to 4.3 hr. This reduces the required number of FW cells by 48% and the number of AFP cells by 52% (for 500,000 units/year). This equals a $30 per vessel savings in manufacturing cost. The reduced composite weight of Vessel 7 increased the specific energy from 1.5 to 1.78 kWhr/kgH_2 and reduced the vessel cost from $23.45 to $20.80/kW-hr.

Polymer Materials Characterization

PNNL has quantified the impact of high-pressure hydrogen environments on the mechanical properties of high density poly-ethylene (HDPE). Over 100 tensile specimens (ASTM D638 type 3) were tested after exposure to 4,000 psi H_2 to quantify the impact of H_2 concentration on the mechanical properties of polymers. Samples were soaked in the high pressure H_2 for at least 7 days per batch to ensure full H_2 saturation based on simple diffusion limited rate calculations.

Preliminary analysis of the standard HDPE H_2 exposed data shows reproducible trends. First, there is a nearly 20% decrease in elastic modulus that recovers as hydrogen diffuses from the material with time. Second, a nearly 10% decrease is seen in the tensile strength with a corresponding increase in ultimate strain (these are the peak values before the material necks), these also recover with time and escape of hydrogen from the HDPE. Recovery time scales were measured to be on the order of 1 day. Tests were also performed on a lower crystallinity material – low density poly-ethylene (LDPE). LDPE exposed to the same high pressure H_2 conditions demonstrates markedly different

behavior, with strong evidence of internal blistering and non-recoverable changes to the material. It appears that higher crystallinity and cross-linking densities are beneficial for reduced permeation and material durability under H_2 exposure.

Assessment of Alternate Composite Resins

Nonlinear stress analysis of the vessel composite layup was performed to estimate the increase in burst pressure that may be achieved by transitioning to a particle-reinforced resin with higher strength and stiffness. The ABAQUS finite element code was enhanced to include the Eshelby-Mori-Tanaka Approach for NonLinear Analysis model, which is a nonlinear composites material model that incorporates progressive damage and lamina failure criteria. The model with the standard epoxy closely predicted the actual burst pressure from testing, and the model with high performance filled epoxy predicted a 12% increase in burst pressure with the same composite lay-up.

Conclusions and Future Directions

- The hybrid manufacturing method is able to produce pressure vessels that achieve the required burst pressure and save carbon fiber (22.9% in Vessel 7) at the same time.
- Equipment and factory costs for hybrid process are small relative to fiber cost reduction.
- Absorption of H_2 by HDPE reduces the material's modulus and yield strength, but is reversible.
- Design vessel with lower-cost and lower-strength fiber to replace T700S for vessel outer layers.
- Perform testing on latest vessel design according to the latest automotive standards.
- Shake down improved AFP head design hardware for production.
- Update cost model.

FY 2011 Publications/Presentations

1. Development of Advanced Manufacturing Technologies for Low Cost Hydrogen Storage Vessels, Annual Merit Review, Department of Energy, May 9–13, 2011, Washington, D.C.

VI.10 Non-Contact Sensor Evaluation for Bipolar Plate Manufacturing Process Control and Smart Assembly of Fuel Cell Stacks

Eric Stanfield
National Institute of Standards and Technology (NIST)
100 Bureau Drive, MS 8211
Gaithersburg, MD 20899-8211
Phone: (301) 975-4882
E-mail: eric.stanfield@nist.gov

DOE Managers
HQ: Nancy Garland
Phone: (202) 586-5673
E-mail: Nancy.Garland@ee.doe.gov
GO: Jesse Adams
Phone: (720) 356-1421
E-mail: Jesse.Adams@go.doe.gov

Contract Number: DE-EE0001047

Subcontractor:
Los Alamos National Laboratory, Los Alamos, NM

Project Start Date: October 1, 2007 Revised Interagency Agreement (October 1, 2009)
Project End Date: October 1, 2009 Revised Interagency Agreement (October 1, 2011)

Fiscal Year (FY) 2011 Objectives

- Identify and evaluate the capability and uncertainty of commercially available non-contact, high-speed scanning technologies for applicability to bipolar plate manufacturing process control.
- Using capabilities identified in the first objective, demonstrate smart assembly concept (new under revised interagency agreement).

Technical Barriers

This project addresses the following technical barriers from the Manufacturing R&D section of the Fuel Cell Technologies Program Multi-Year Research, Development and Demonstration Plan:

(B) Lack of High-Speed Bipolar Plate Manufacturing Processes

(F) Low Levels of Quality Control and Inflexible Processes

Contribution to Achievement of DOE Manufacturing R&D Milestones

This project will contribute to achievement of the following DOE milestones from the Manufacturing R&D section of the Fuel Cell Technologies Program Multi-Year Research, Development and Demonstration Plan:

- **Milestone 7**: Develop manufacturing [quality control measurement] processes for graphite resin, natural flake graphite, and metal plates. (4Q, 2010)
- **Milestone 12**: Demonstrate pilot scale processes for assembling stacks. (4Q, 2013)
- **Milestone 13**: Complete development of standards for metrology of PEM fuel cells. (4Q, 2010)

FY 2011 Accomplishments

- Completed the design, fabrication and testing of a dedicated fuel cell metrology station using Aerotech translation stages (stages procured in August 2010) and Keyence laser spot triangulation probes.
- There are several interesting features to note in this design:
  - We integrated two laser spot triangulation probes that are titled in opposing directions. The use of two tilted probes allows collection of data from the side walls of the channels; a single probe looking straight down cannot acquire any side wall information.
  - The data from the laser triangulation probes is synchronized with the position from the translation stage and therefore velocity fluctuations are no longer a concern.
  - The stage has a maximum travel speed of 2,000 mm/sec. We have evaluated channel depth and height on fuel cell plates from speeds of 30 mm/sec to 500 mm/sec without noticing any significant degradation in accuracies at higher speeds.
- Performed numerous tests on the fuel cell station using calibrated gage blocks. The details are recorded in our project update submitted on January 21st, 2011 [1] and in a paper currently under review.
- Measured channel width and height on carbon bipolar plates using this non-contact system. Width and height results were within ±2 µm of the values obtained using a contact coordinate measuring machine (CMM).
- Performed detailed uncertainty budgets for channel width and height for carbon bipolar plates which showed expanded uncertainty of 6 µm (k=2) for width and 3.8 µm (k=2) for height. The details are recorded in [2].
- Completed design of fixtures required to perform thickness measurements on fuel cell plates (one probe looking down on the plate while the second probe is positioned below the plate looking up). Thickness

and parallelism measurements on plates are critical for 'smart assembly'.



Introduction

The objective of this project is to enable cost reduction in the manufacture of fuel cell plates by providing a rapid non-contact measurement system that can be used for in-line process control. Manufacturers currently either visually inspect plates or use machine vision systems for verifying tolerances. Such methods do not provide the sub-10 µm accuracy that manufacturers are targeting. In this context, we have studied available non-contact sensors in the market for their suitability to be used for fuel cell plate metrology. From our studies, we have short listed laser spot triangulation probes as one of the promising candidates for further exploration. We have since incorporated these probes in a unique two-probe system to develop a rapid yet high accuracy non-contact system that manufacturers can adopt towards process control and metrology. We plan on further extending our design to perform thickness measurements using opposed probe configuration that will enable 'smart assembly'. The concept of "smart assembly" is that if plate parallelism is measured and tagged to each plate, then assembly can be done in an automated fashion where plates are configured ideally to minimize the overall stack parallelism. This will allow lower tolerances on individual plate parallelism.

Approach

We studied numerous sensors to assess their suitability as a rapid non-contact dimensional measurement tool for bipolar fuel cell plates. We selected laser spot triangulation probes for further investigation because they offered large range (±5 mm) and micrometer level resolution. Our approach then is to build a dedicated fuel cell metrology station with Aerotech translation stages and laser triangulation probes as the non-contact probe of choice. We then intend to test the performance of our system using calibrated gage blocks and subsequently measure numerous bipolar fuel cell plates that have also been previously measured with a contact CMM. Such measurements will enable us to place bounds on errors; a detailed uncertainty budget will also be created to understand dominant error sources. Finally, we also plan on performing thickness and parallelism measurements using two laser triangulation probes (one probe looking down on the plate while the second probe is positioned below the plate looking up). Tagging each plate with thickness and parallelism data will enable the selection of those plates that reduce the combined total parallelism of the stack, a process we describe as 'smart assembly'.

Results

During the last year, we have made significant progress in developing and testing our non-contact fuel cell metrology station. We describe major results next.

Characterizing Triangulation Probe Errors

Our investigations on laser triangulation probes revealed numerous error sources that impact dimensional measurements. Many of these are error sources have been described in the literature before [3]; our studies have attempted to place bounds on errors for linear dimensional measurements and also serve to caution users that laser triangulation probes are not plug-and-play devices as they are often described to be in manufacturer's literature. Despite their limitations, we believe these probes are superior to other non-contact options available currently, if carefully employed.

Our experiments studied the following factors: repeatability and noise levels, linearity errors, influence of material/optical properties on height and width measurements, effect of spot size on width measurements, side wall reflections, secondary reflections, and measurements at grazing angle. Figure 1 shows the linearity error over the 10 mm range of the probe for a ceramic and graphite test object. The manufacturer's specification of ±5 µm is only valid for the ceramic case; it is clear from Figure 1 that it does not hold for the graphite case. While these and other such results are summarized in [1] and also in a paper currently under review, we highlight one particular source of error that has significant implications for fuel cell plate measurements under our dual-probe design (discussed next), namely, the influence of part material and optical properties on dimensional measurements. It is well known that triangulation probe suffers from volumetric scattering and surface penetration. We have used ceramic gage blocks and demonstrated experimentally that width and height errors of the order of 10 µm are possible when material/optical properties are not identical for the different

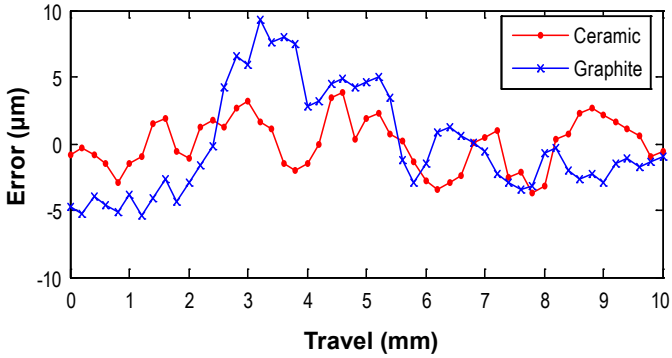


FIGURE 1. Linearity Error when the Probe's Laser is Incident at 25° with the Surface

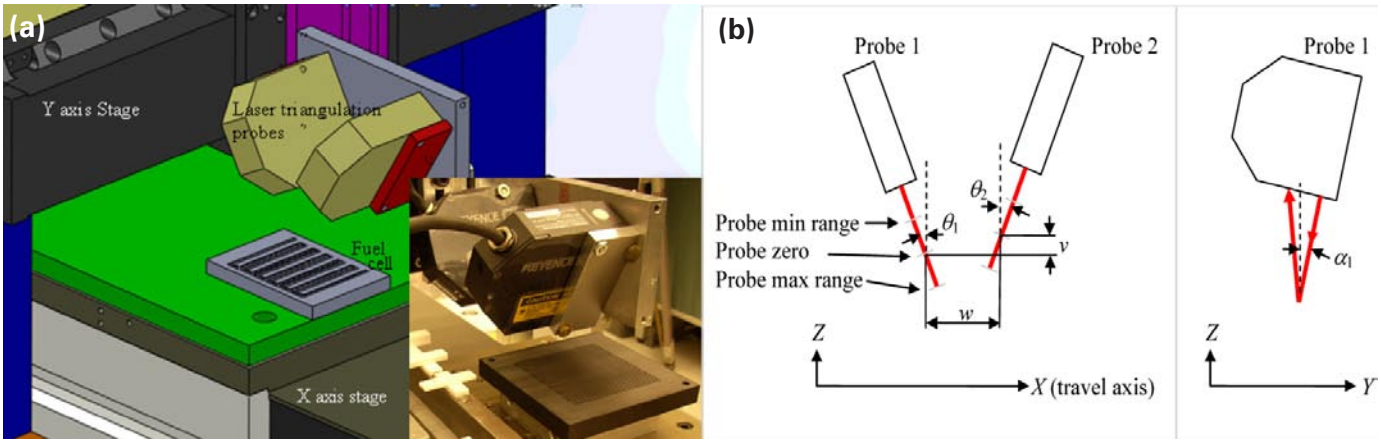


FIGURE 2. (a) The fuel cell metrology station showing two laser triangulation probes, each tilted in opposing directions to obtain side wall information. (b) Six system parameters to be determined by calibration.

surfaces that comprise a height or width feature, although these surfaces may appear to be visually similar. This implies that care must be taken in calibrating the dual-probe system with an artifact made of identical material as the part.

The Dual-Probe Fuel Cell Metrology Station

One unique aspect of our fuel cell station design is that we have incorporated two laser triangulation probes that are titled in opposing directions as Figure 2(a) shows. The purpose of having two tilted probes is to be able to acquire channel side wall information, which a single probe looking straight down cannot accomplish. But having two probes necessities the determination of six system parameters (tilt angles and offsets) shown in Figure 2(b); we have developed a calibration procedure for this purpose and have described it in detail in [2]. Determining these system parameters accurately is essential in superimposing the data from the two probes into a common frame of reference.

While it may appear that the tilt angle θ of the probes can be determined by measuring a calibrated height block, we show in [2] that such measurements are corrupted by misalignment angle α and are therefore not very accurate. We further demonstrate that vertical profile measurements (measurements on the vertical face of a gage block) can yield much higher accuracies because the misalignment angle α can be separated out. The mathematics and uncertainty in such calculations are described in [2].

Bipolar Plate Measurements and Uncertainty

We have compared measurement results on fuel cell plates from our non-contact system against a contact CMM. Our results for channel height and width on a graphite bipolar plate agree to within ±2 µm as Figure 3 shows. The expanded uncertainties on height and width for the contact CMM are 0.5 µm and 1.7 µm. We have developed detailed

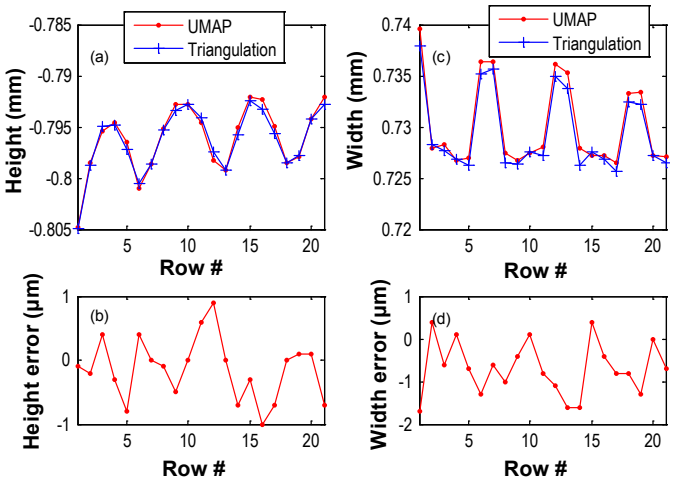


FIGURE 3. (a) Measured height of each row using both the ultrasonic micro and accurate probe (UMAP) and the dual-probe laser triangulation system (b) Height error for each row (c) Measured width of each row using both the UMAP and the dual-probe laser triangulation system (b) Width error for each row.

uncertainty budgets for the graphite bipolar plate channel height and width measurements; they are described in [2]. We estimate expanded uncertainty of 6 µm (k=2) for width and 3.8 µm (k=2) for height using our non-contact system on the graphite part. Major contributors to the uncertainty are the probe linearity errors and pitch motion of the stage.

Speed Tests

We performed width measurements at different speeds on an etched plate. The results from 30 mm/sec to 500 mm/sec are shown in Figure 4. There is no significant degradation in accuracy at 500 mm/sec in comparison to that at 30 mm/sec as Figure 4 shows. We have also verified the same for height measurements; those data are not shown here.

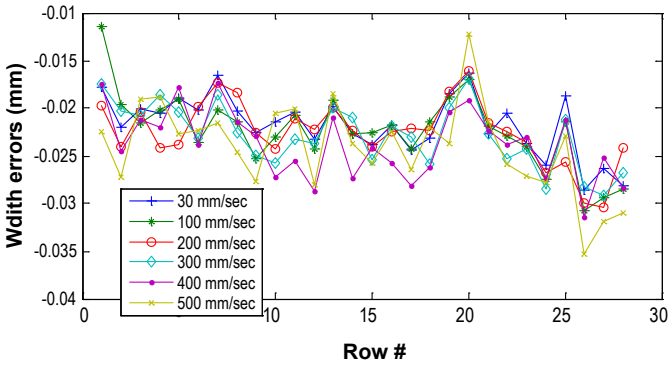


FIGURE 4. Width Errors at Different Speeds as a Function of Row # for an Etched Plate

Conclusions

To date, we have designed, built, and tested a dedicated dual-probe fuel cell station system for dimensional inspection of fuel cell plates. The two probes are oriented in a novel configuration that increases the accuracy of lateral dimensions and simultaneously provides the ability to capture side wall information for form evaluation. With this design we performed numerous experiments to study the different error sources (such as edge effects, linearity errors, spot sizes, etc.) in laser triangulation probes and their impact on dimensional measurements. With a thorough understanding of the error sources the limitations of these probes can be overcome making their application suitable for fuel cell metrology. Following careful evaluation of the sensor errors and approaches to minimizing them we made comparison measurements of channel height and width using sample fuel cell plates fabricated by common methods that were previously measured using a micro-feature CMM. With a high quality fuel cell flow field plate we demonstrated agreement with reference measurements to within ±2 µm. From our error source investigation and intercomparison measurements we developed a detailed uncertainty for both height and width measurements. We then furthered our capability study to evaluate accuracy as a function of scan speed, finding that there was no noticeable degradation of accuracy up to 500 mm/s.

Future Directions

The final phase of this project involves developing a configuration that provides the capability to measure variation in plate thickness. The opposing probe design modification has been developed and the additional mounting fixtures are being fabricated. Upon completion of the new probe fixturing components we will began demonstrating the capability of the system to measure variation in thickness along the development of a detailed measurement uncertainty. From these data we intend to show that parallelism from variation-in-thickness can be derived and used for the concept of "smart assembly."

Disclaimer

Certain commercial equipment, instruments, or materials are identified in this paper in order to specify the experimental procedure adequately. Such identification is not intended to imply recommendation or endorsement by the National Institute of Standards and Technology, nor is it intended to imply that the materials or equipment identified are necessarily the best available for the purpose.

Acknowledgements

The work detailed in this report would not have been possible without the contributions of the following, all are NIST personnel and guest researchers unless otherwise noted: Bala Muralkrishnan, Wei Ren, Dennis Everett, Ted Doiron, Patrick Egan, Heather McCrabb (Faraday Technology), CH Wang (TreadStone Technologies), and SGL Carbon.

FY 2011 Publications/Presentations

1. Eric Stanfield, Non-Contact Sensor Evaluation for Bipolar Plate Manufacturing Process Control and Smart Assembly of Fuel Cell Stacks, Project Update, January 21, 2011.

2. B. Muralikrishnan, W. Ren, D. Everett, E. Stanfield, T. Doiron, Dimensional Metrology of Bipolar Fuel Cell Plates Using Laser Spot Triangulation Probes, Measurement Science and Technology, 22(7), July 2011.

3. E. Stanfield, "Non-Contact Sensor Evaluation for Bipolar Plate Manufacturing Process Control," FY 2010 Annual Progress Report, DOE Hydrogen and Fuel Cells Program, February 2011 http://www.hydrogen.energy.gov/pdfs/progress10/vi_7_stanfield.pdf

References

1. Eric Stanfield, Non-Contact Sensor Evaluation for Bipolar Plate Manufacturing Process Control and Smart Assembly of Fuel Cell Stacks, Project Update, January 21, 2011.

2. B. Muralikrishnan, W. Ren, D. Everett, E. Stanfield, T. Doiron, Dimensional Metrology of Bipolar Fuel Cell Plates Using Laser Spot Triangulation Probes, Measurement Science and Technology, 22(7), July 2011.

3. A. Garces, D. Huser-Teuchert, T, Pfeifer, P Scharsich, F. Torres-Leza, E Trapet, Performance test procedures for optical coordinate measuring probes, Final project report, part 1, July 1993, European Communities Brussels, Contract No. 3319/1/0/159/89/8-BGR-D (30).

VI.11 Optical Scatterfield Metrology for Online Catalyst Coating Inspection of PEM (Fuel Cell) Soft Goods

Eric Stanfield
National Institute of Standards and Technology (NIST)
100 Bureau Drive, MS 8211
Gaithersburg, MD 20899-8211
Phone: (301) 975-4882
E-mail: eric.stanfield@nist.gov

DOE Managers
HQ: Nancy Garland
Phone: (202) 586-5673
E-mail: Nancy.Garland@ee.doe.gov
GO: Jesse Adams
Phone: (720) 356-1421
E-mail: Jesse.Adams@go.doe.gov

Contract Number: DE-EE0001047

Subcontractor:
Los Alamos National Laboratory, Los Alamos, NM

Project Start Date: October 1, 2007 Revised Interagency Agreement (October 1, 2009)
Project End Date: October 1, 2009 Revised Interagency Agreement (October 1, 2011)

Fiscal Year (FY) 2011 Objective

Evaluate the suitability of optical scatterfield metrology (OSM) as a viable measurement tool for in situ manufacturing process control of dual-side simultaneous catalyst coating of membranes.

Technical Barriers

This project addresses the following technical barriers from the Manufacturing R&D section of the Fuel Cell Technologies Program Multi-Year Research, Development and Demonstration Plan:

(F) Low Levels of Quality Control and Inflexible Processes

Contribution to Achievement of DOE Manufacturing Milestones

This project will contribute to achievement of the following DOE milestones from the Manufacturing R&D section of the Fuel Cell Technologies Program Multi-Year Research, Development and Demonstration Plan:

- **Milestone 1.** Develop prototype sensors for quality control of MEA manufacturing. (4Q, 2011)
- **Milestone 2.** Develop continuous in-line measurement for MEA fabrication. (4Q, 2012)
- **Milestone 13.** Complete development of standards for metrology of PEM fuel cells. (4Q, 2010)

FY 2011 Accomplishments

- Demonstrated 0.03 to 0.05 mg/cm^2 sensitivity to loading differences using 3M pure Pt catalyst nano-structured thin-film (NSTF) samples that included four different loadings ranging from 0.05 mg/cm^2 to 0.20 mg/cm^2 (September 2010).
- Investigated transmission properties of the thin NSTF samples and eliminated interference from the substrate (sample holder) material reflection (October 2010).
- Using sample reversal along with atomic force microscopy (AFM), we discovered that the cause of a repeatable asymmetrical reflectivity response for the 0.20 mg/cm^2 pure Pt NSTF CCM was due to a large physical macroscopic sample asymmetry (November 2010).
- Demonstrated 0.03 to 0.04 mg/cm^2 sensitivity to loading differences using W.L. Gore & Associates Pt on carbon catalyst-coated membrane (CCM) (A510/M710.18/C510) samples that included four different loadings ranging from 0.10 mg/cm^2 to 0.40 mg/cm^2 (December 2010).
- Procured and took delivery of a spectroscopic ellipsometer which enables measurements of material optical properties n and k that are critical to the modeling effort (February 2011).
- Using the new ellipsometer, began spectroscopic measurements of constituent materials supplied by 3M that comprise their NSTF CCM and attempted bulk material measurements (using effective medium approximation) of the current Gore samples (March 2011).
- Continued refinement of our simulation models for both the 3M NSTF and the W.L. Gore & Associates Pt on carbon CCM (optical constants remain only limitation to having a useful working model) (March 2011).



Introduction

Industry has identified the need for high-speed, in situ process control measurement techniques for controlling the quantity of the platinum in the catalyst layer and for the rapid identification of critical defects. Online

X-ray fluorescence (XRF) is the current in situ technique for controlling the various parameters of interest, most commonly catalyst loading; however this technique provides the total through sample platinum loading thus must be implemented prior to the transfer of the anode and cathode catalyst layer to the membrane in the production of a CCM. The ideal solution would provide in-line process control of the finished product (CCM) by way of dual-side simultaneous but independent measurement of catalyst loading. The solution would eliminate concerns related to platinum lost and not accounted for during the decal transfer step and it would ultimately enable real-time loading process control when dual-side direct catalyst layer application becomes the standard approach.

The Mechanical Metrology Division within the Physical Measurement Laboratory has years of expertise with a technology identified as OSM [1], specifically its development as a process control tool for the semiconductor industry. This technique is a combination of the best attributes of traditional bright-field optical microscopy and scatterometry. This technique focuses on the complex optical signatures of subwavelength size features, where the response can be optimized by varying the illumination angle, varying the illumination source wavelength, and application of various image analysis algorithms. The overall objective of this project is to demonstrate the applicability of the OSM technique to this application with the hope that it will provide proton exchange membrane (PEM) CCM manufacturers with an automated high-throughput approach for process control inspection of Pt loading with sensitivity equal to or better than that currently provided by XRF and simultaneous identification/quantification of other parameters of interest, such as critical defects. Model-based simulations will be developed concurrently as they are critical to the study and optimization of this technique for this application and will ultimately give manufacturers insight that will enable them to tune their measurement equipment to the parameter(s) of interest as design changes are made.

Approach

The initial focus, driven by industry input, is to demonstrate that the OSM tool is sensitive to differences in catalyst loading. To reach this Go/No-Go point this project has relied heavily on support from CCM manufacturers, specifically in the supply of samples by which sensitivity studies could be performed. CCM manufacturers were also helpful in establishing a benchmark catalyst loading sensitivity of 0.01 mg/cm^2 which is equivalent to that of the online XRF tool currently used. At this juncture, we now know that the tool is indeed sensitive to changes in catalyst loading at the benchmark level based on a sample set of 3M Pt alloy NSTF-type CCMs. With sensitivity successfully demonstrated, the remainder of the project is dedicated to developing accurate analytical models for each type of CCM tested then to use these models for simulations aimed at understanding and optimizing the tool's sensitivity to catalyst loading based on variation of the adjustable parameters of the tool and to further extend the study of the applicability of the tool to other critical catalyst layer parameters identified by the manufacturers. In the development of these models, we will again rely heavily on CCM manufacturers to supply specialized samples so that we can experimentally obtain optical constants for the constituent materials which are critical to ensuring accuracy. Lastly, to claim that a thorough investigation has been performed we aim to demonstrate the tool's capabilities on many of the common types of CCMs being manufactured, these include 3M's NSTF CCM with Pt and Pt alloy catalysts and the different conventional Pt on carbon-based CCMs made by several manufacturers.

Results

At the beginning of 2011, we determined that the Pt loading sensitivity was 0.03 to 0.05 mg/cm^2 for the 3M NSTF pure Pt CCM samples with loadings of 0.05, 0.10, 0.15, and 0.20 mg/cm^2 (Figure 1).

However, the reflectivity signature versus illumination angle for the 0.20 mg/cm^2, not shown in Figure 1, appeared non-symmetrical in comparison to the other three samples. Additionally, these pure Pt samples did not appear as opaque as the pure Pt alloy samples did thus we became concerned about transmission of the light through the sample and the effect of the reflection from the substrate or sample holder material. Both findings could be contributing to the

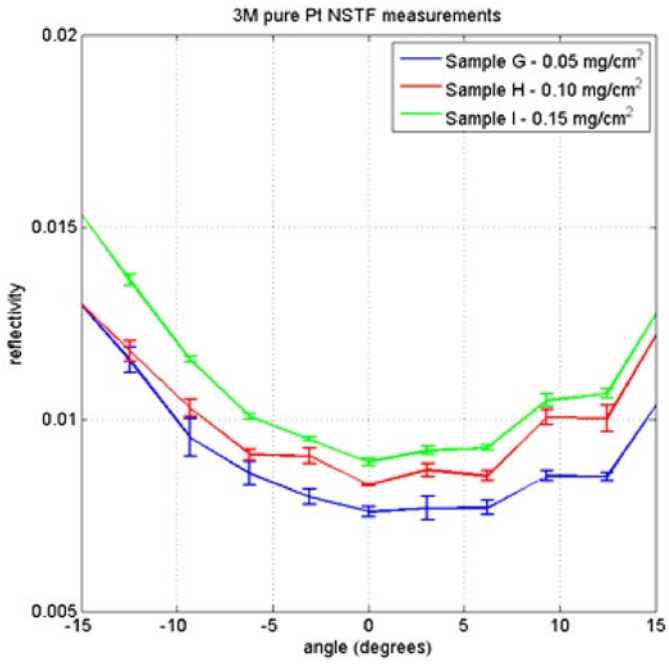


FIGURE 1. 3M NSTF pure Pt sample loading data. The separation between the curves relative to the error bars is a measure of the sensitivity.

increased variability as indicated in the calculated sensitivity level, which is short of the 0.01 mg/cm^2 target.

In order to determine if the asymmetry was associated with the optical tool or the sample, we performed a physical reversal of the sample. From this data seen in Figure 2, the asymmentry for the suspicious sample rotated with the reorientation of the sample but similar measurements using one of the other three samples did not change thus this was determined to be sample effect. To further understand the cause of the asymmetry our investigation focused on the sample. With the aid of an AFM we measured the profile of the samples macroscopic structure and compared the results from similar measurements performed on the other samples to find that there is a larger than normal asymmetry of the unique macrostructure geometry. The asymmetry is unimportant to the performance of the fuel cell, thus we were advised to find a way to make the measurement insensitive to this effect. This remains an ongoing effort. With regards to the transmission concern, experiments were performed where the intensity of the illumination source was significantly increased and where we changed the reflectivity characteristics of the substrate by introducing light absorbing material, both caused unexpected changes in the signature profile however the sensitivity and offsets between the samples remained. This too remains a work in progress and it is our hope that accurate simulation models will give us greater insight into these two effects.

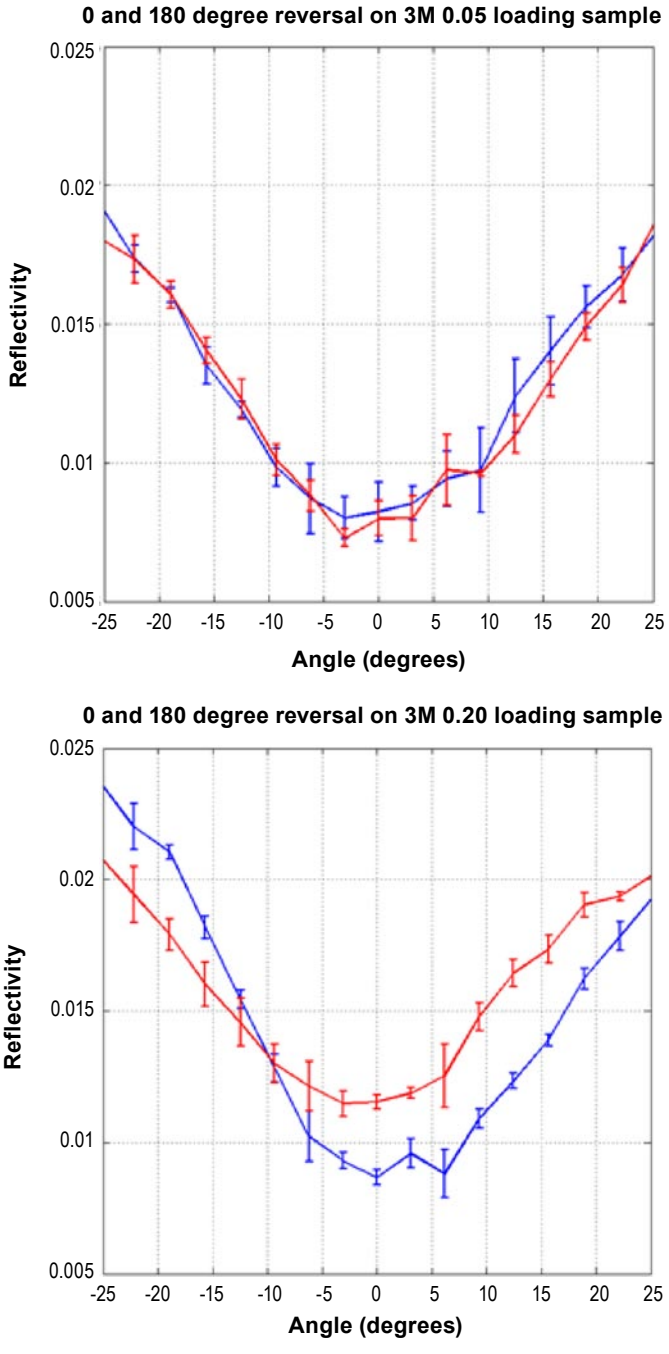


FIGURE 2. The plot on the top is the 0 and 180 degree reversal data for the 0.05 mg/cm^2 sample. The plot on the botttom is the 0 and 180 degree reversal data for the 0.20 mg/cm^2 sample, which displays the asymmetric behavior.

With sensitivity demonstrated on both catalyst compositions using the 3M NSTF samples, we investigated the applicability of the tool to catalyst loading sensitivity using W.L. Gore & Associates conventional Pt on carbon CCM samples of 0.10, 0.20, 0.30, and 0.40 mg/cm^2 loadings (A510/M710.18/C510). We performed experiments varying the angle of illumination and wavelength on two different tools. For the angle resolved measurements, sensitivity was demonstrated on the order of 0.03 to 0.04 mg/cm^2. Excellent static repeatability (multiple measurement scans same location) was shown for the wavelength resolved measurements. Performing wavelength resolved measurements at five locations on multiple days revealed variations in loading from one location to the next (on the scale of several millimeters apart), which makes the overall repeatability worse. However, this is not a limitation of the technique, it is a sample issue. This static repeatability and localized variation data are shown in Figure 3.

An integral part of the OSM technique is electromagnetic scattering simulation of the samples being measured. Simulation provides a flexible and efficient method to evaluate the various parameters that have an effect on the actual physical measurement. Accurate simulation requires accurate inputs to the models, such as target dimensions, layer thicknesses, surface roughness, materials optical properties (complex index of refraction), etc. NIST procured and took delivery of a spectroscopic ellipsometer which enables measurements of material optical properties (n and k) that are critical to the modeling effort (February 2011). Using this new ellipsometer, NIST began spectroscopic measurements of constituent materials supplied by 3M that make up their NSTF CCM and attempted bulk material measurements of the current Gore samples (March 2011) as shown in Figure 4. In performing these measurements, it became apparent that surface roughness was limiting our ability to measure the n and k of the materials and began using an effective medium approximation for evaluating the materials optical

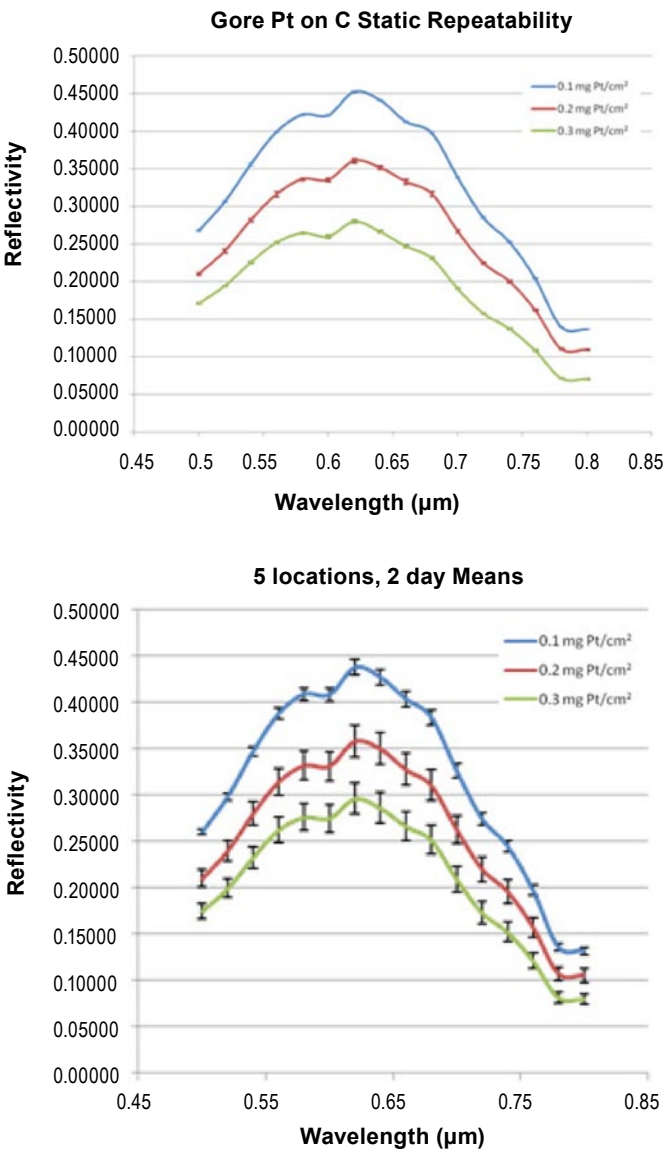


FIGURE 3. The plot on the top shows static repeatability data, looking at one location on each loading sample numerous times. The plot on the bottom is localized variation data, looking at five different locations on each loading sample over multiple days.

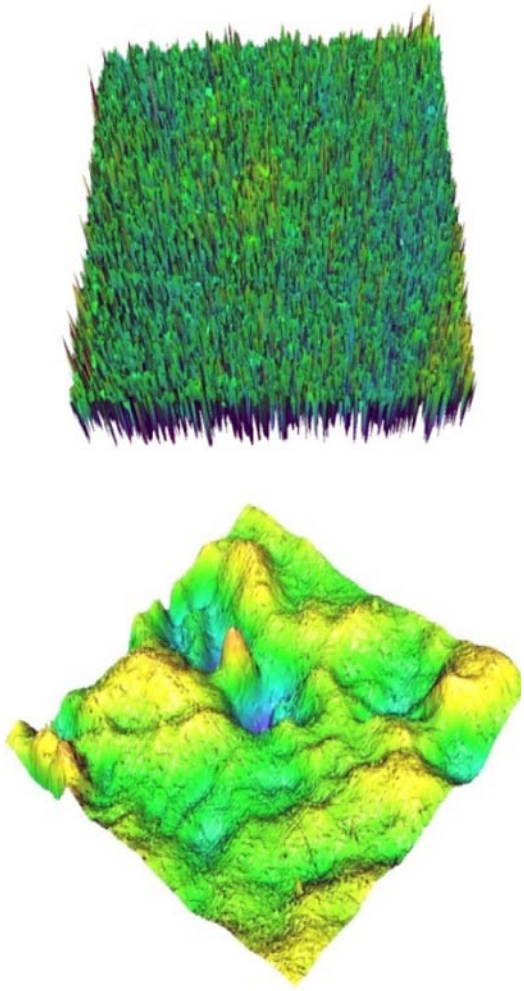


FIGURE 4. The plot on the top is a measure of the surface roughness of the Gore PEM layer. The plot on the bottom is a measure of the surface roughness of the 3M PEM layer.

properties. We continued refinement of our simulation models for both the 3M NSTF and the W.L. Gore & Associates Pt on carbon (optical constants remain only limitation to having a useful working model) (March 2011).

Conclusions

The work presented for this project, to date, undeniably shows that OSM has sensitivity to catalyst loading regardless if the loading is pure Pt or a Pt alloy. The ability to achieve sensitivity levels equivalent to the 0.01 mg/cm^2 benchmark has been shown for the sample types investigated. From the conventional Pt on C catalyst CCM samples we clearly see that this sensitivity level is achievable, however local variations in catalyst loading increase the uncertainty of assigning a definitive loading figure to a sample. Also from the work to date we see that this technique is clearly sensitive to other variables whether they are other sample specific parameters (i.e., macro geometry) or external (i.e., through sample transmission/background interference). These issues alone solidify the need for determination of material optical properties in support of the development of accurate models, which has eluded us to this point. Furthermore, optical property determination is not a simple task and in itself requires a significant effort. Support from major manufactures has been excellent but sensitivity regarding intellectual property rights always impacts the rate of progress. At this juncture, we clearly have all the elements in place to make commendable strides towards true optimization of the OSM tool for this specific application. It is our belief that manufacturers like 3M and W.L. Gore & Associates see the potential for this measurement technique thus are eagerly

awaiting completion of the development work and subsequent availability of a commercialized product.

Future Directions

Our focus for the remainder of this project will be acquiring much needed material optical constants using our new spectroscopic ellipsometer and with these constants we intend to refine our models to a level that predictive simulations can be performed to study sensitivity to different variables ultimately leading us to an optimized tool configuration that may be unique to the samples of interest. An accurate model will be achieved when predictions can be made using the model and those predictions verified experimentally. Concurrently, we hope to explore the sensitivity of the technique to different defects identified by the manufacturers as being critical through the measurement of samples with know defects and investigated further through simulation efforts.

Disclaimer

Certain commercial equipment, instruments, or materials are identified in this paper in order to specify the experimental procedure adequately. Such identification is not intended to imply recommendation or endorsement by the National Institute of Standards and Technology, nor is it intended to imply that the materials or equipment identified are necessarily the best available for the purpose.

Acknowledgements

The work detailed in this report would not have been possible without the contributions of the following, all are NIST personnel and guest researchers unless otherwise noted: Mark Debe (3M), Judy Rudolf and Collin Busby (W.L. Gore), Mike Ulsh (National Renewable Energy Laboratory, NREL), Guido Bender (NREL), Michael Stocker, Richard Silver, Andras Vladar, John Kramar, Bin Ming, Brad Damazo, Bryan Barnes, Richard Quintanilha, Hui Zhou, Yeung-Joon Sohn, Francois Goasmat, Jing Qin.

FY 2011 Publications/Presentations

1. E. Stanfield and M. Stocker, "Metrology for Fuel Cell Manufacturing," DOE Annual Merit Review Proceedings, MN006, May 12, 2011, http://www.hydrogen.energy.gov/pdfs/review11/mn006_stanfield_2011_o.pdf.

2. E.Stanfield, M. Stocker, and B. Muralikrishnan, "Metrology for Fuel Cell Manufacturing," Invited Presentation Given to the FreedomCAR Tech Team, USCAR, Southfield, MI, March 16, 2011.

3. E. Stanfield, "Optical Scatterfield Metrology for Online Catalyst Coating Inspection of PEM Soft Goods," FY 2010 Annual Progress Report, DOE Hydrogen and Fuel Cells Program, February 2011, http://www.hydrogen.energy.gov/pdfs/progress10/vi_8_stanfield.pdf

References

1. R.M. Silver, B.M. Barnes, R. Attota, J. Jun, M. Stocker, E. Marx, and H. Patrick, "Scatterfield Microscopy for Extended Limits of Image-Based Optical Metrology," Applied Optics, Vol. 46, No. 20 (2004).

VII. TECHNOLOGY VALIDATION

VII.0 Technology Validation Sub-Program Overview

Introduction

The Technology Validation sub-program demonstrates, tests, and validates hydrogen and fuel cell technologies and uses the results to provide feedback to the Program's research and development activities. The Technology Validation sub-program has been focused on conducting learning demonstrations that emphasize co-development and integration of hydrogen infrastructure with hydrogen fuel cell–powered vehicles to permit industry to assess progress toward technology readiness. As the vehicle and infrastructure demonstrations are coming to a close, the sub-program is increasing its focus on other areas, such as combined hydrogen, heat, and power (tri-generation or CHHP) as well as stationary power applications.

Goal

Validate–under real-world operating conditions–the status, relative to Program targets, of hydrogen and fuel cell technologies that will be used in both the initial market entry and early market periods of fuel cells for transportation and stationary power generation.

Objectives[1]

- **2014:** Validate a stationary fuel cell system that co-produces hydrogen and electricity at 40% efficiency, with 40,000-hour durability.
- **2019:** Validate fuel cell electric vehicles (FCEVs) achieving 5,000-hour durability (service life of vehicle) and a 300-mile driving range between fueling.

Fiscal Year (FY) 2011 Technology Status

National Learning Demonstration

In 2011, the National Learning Demonstration–a government-industry cost-shared project initiated in 2004 with four automobile and energy company teams–continued to provide data for evaluating the technology status with respect to fuel cell durability, driving range, and power park demonstrations. Six years of the seven-year project are complete. A total of 155 vehicles have been deployed through the first quarter of FY 2011, with 23 currently in operation. Thus far, more than 3 million miles have been traveled by the FCEVs in the project and 140,000 kg of hydrogen has been either produced or dispensed, with some of this hydrogen being used in vehicles outside the Learning Demonstration. New durability results will be available in autumn 2011; however, 2010 durability results indicate fuel cell durability exceeded 2,500 hours. Fuel cell vehicles have met or exceeded the 250-mile driving-range goal and fuel cell system efficiency data at 25% net power is 53–59%, which is close to the DOE target of 60%. Figure 1 shows all of the major key performance metrics that have been reported in the National Hydrogen Learning Demonstration.

- **General Motors (GM) Hydrogen Vehicle and Infrastructure Demonstration and Validation:** GM has deployed 60 vehicles, demonstrating two generations of GM's proprietary fuel cell technology. GM continues to operate and maintain 10 baseline Phase 2 FCEVs through 2011 or until failure. In 2010, GM inserted ten additional Phase 2 FCEVs equipped with technology developed during the initial part of Phase 2 to extend learnings (Figure 2). GM has also established retail and retail-like hydrogen stations for public fueling: Six fueling stations are in operation across the Eastern and Western regions, with various types of hydrogen generation and delivery––such as delivered compressed gas and on-site electrolysis. Two stations are infrared capable and able to fast fill more than three vehicles back-to-back. Hydrogen quality testing has been completed, and stations have been tested at 700 bar.
- **Mercedes-Benz North America:** Over the course of the project, the Mercedes Team has deployed 30 Gen-1 vehicles into customer hands for real-world operations in various climatic regions of the United States. The Mercedes Team has transitioned FCEV activities from research and development to mainstream

[1] Note: Targets and milestones are under revision; therefore, individual progress reports may reference prior targets.

commercial activities, and they have now begun customer operations of production-level Gen-2 vehicles. (The first Gen-2 FCEVs were delivered to external customers in December of 2010.) B-Class F-CELL vehicles have been incorporated into Mercedes' standard business processes within departments such as Warranty, Customer Assistance, Parts & Distribution, as well as Roadside Assistance and Sales.

Learning Demonstration Key Performance Metrics Summary

Vehicle Performance Metrics	Gen 1 Vehicle	Gen 2 Vehicle	2009 Target
Fuel Cell Stack Durability			**2,000 hours**
Max Team Projected Hours to 10% Voltage Degradation	**1,807 hours**	**2,521 hours**	
Average Fuel Cell Durability Projection	821 hours	1,062 hours	
Max Hours of Operation by a Single FC Stack to Date	2,375 hours	1,261 hours	
Driving Range	**103-190 miles**	**196-254 miles**	**250 miles**
Fuel Economy (Window Sticker)	42 – 57 mi/kg	43 – 58 mi/kg	no target
Fuel Cell Efficiency at ¼ Power	51 - 58%	53 - 59%	60%
Fuel Cell Efficiency at Full Power	30 - 54%	42 - 53%	50%

Infrastructure Performance Metrics			2009 Target
H_2 Cost at Station (early market)*	On-site natural gas reformation **$7.70 - $10.30**	On-site Electrolysis **$10.00 - $12.90**	**$3/gge**
Average H_2 Fueling Rate	0.77 kg/min		1.0 kg/min

*Outside of this project, DOE independent panels concluded at 500 replicate stations/year:
Distributed natural gas reformation at 1500 kg/day: **$2.75-$3.50/kg** (2006)
Distributed electrolysis at 1500kg/day: **$4.90-$5.70** (2009)

FIGURE 1. Summary of Key Performance Metrics for the Learning Demonstration

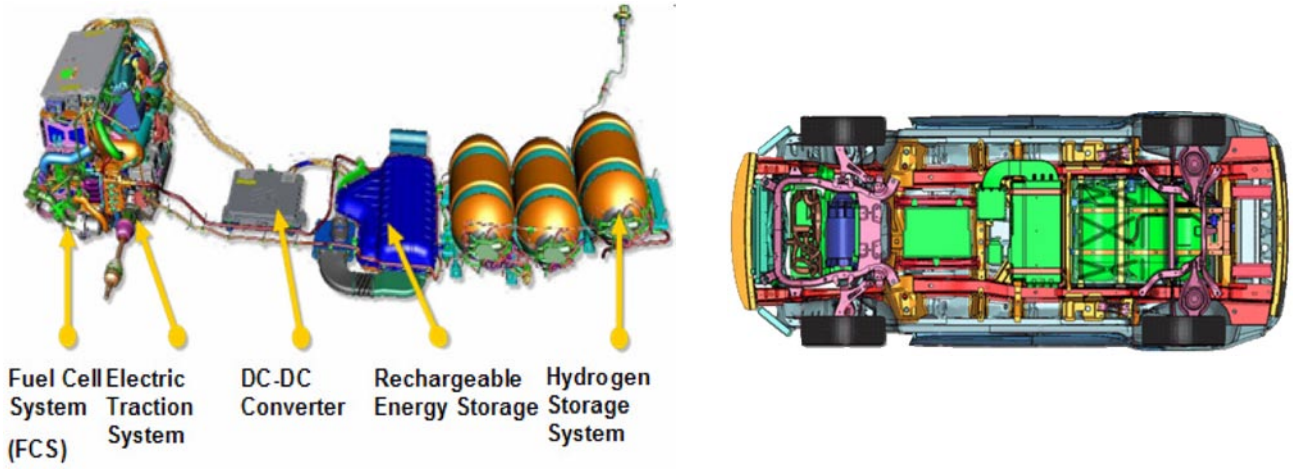


FIGURE 2. Gen-2 Chevrolet Fuel Cell Electric Vehicle with Technology Insertion

FY 2011 Accomplishments

National Learning Demonstration

The National Renewable Energy Laboratory (NREL) verified that Gen-2 learning demonstration vehicles maintained high fuel cell efficiency (53-59%). GM has concluded that FCEVs fully meet all functional needs for day-to-day customer use, FCEVs are fully functional in sub-freezing and cold weather conditions, and GM FCEVs exhibited very fast cold-start/drive-away times under sub-freezing temperatures. Mercedes-Benz demonstrated that A-Class F-CELLs exceed the 2,000-hour stack durability target. Initial test results show Gen-2 fuel cell stacks will most likely meet the 2015 DOE target of 5,000-hour durability. Engineers validated the 250-mile range and cold-start capability down to -17°C while reaching 50% of maximum power within 30 seconds (Figure 3). Hydrogen Infrastructure has been demonstrated to be customer-friendly in daily use by individual and fleet vehicle operators in a "retail-like" self-service mode.



FIGURE 3. Mercedes Engineers Validated Cold-Start Capability Down to -17°C while Reaching 50% of Maximum Power within 30 Seconds

Fuel Cell Bus Evaluation

By the end of April 2011, NREL had documented a total of 1.5 million miles of operation for three fuel cell bus (FCB) systems, with each operating in excess of 6,000 hours with no major repairs. One of these systems has logged more than 9,000 hours of service (Figure 4). Based on in-service fuel economies of 5 to 7 miles per kilogram of hydrogen, hybrid FCBs can achieve a range between 250 and 350 miles per fill, with no loss in cargo and passenger space (however, the added weight of the hydrogen storage system limits the number of standing passengers allowed on the bus). Fuel cell buses compared to baseline buses at three locations showed a fuel economy improvement ranging from 48% to 123% over diesel and compressed natural gas (CNG) baseline buses, respectively. Transit routes are unique for each location, so the duty cycles varied between the locations.



FIGURE 4. In FY 2011, NREL completed their first report on a next-generation fuel cell bus. The bus, which is in service at SunLine Transit Agency in Thousand Palms, California, is a New Flyer 40-foot bus with a Bluways hybrid system, Ballard fuel cells, and lithium-ion batteries. The bus has accumulated more than 9,000 miles and 818 hours on the fuel cell, with an average fuel economy of 5.75 miles per kg. This is nearly two times higher than the fuel economy for the baseline CNG buses.

California Hydrogen Infrastructure Project

In early 2011, construction was completed on the world's first fueling station supplied by a hydrogen pipeline (Figure 5), which was partially funded through a prior year congressionally directed project. This project aims to demonstrate a low-cost, reliable supply of hydrogen. The station, which is located in Torrance, California, close to an existing Air Products hydrogen pipeline, was developed by Shell Hydrogen. A 4-kg/hr compressor skid has been installed, along with storage for 100 kg of hydrogen at 7,777 psig and



FIGURE 5. The Dispenser Area at Shell's Torrance, California, Fueling Station, which is Supplied by an Air Products Pipeline



FIGURE 6. HF-150 Mobile Refueler at the District Office of the U.S. Forest Service in Placerville, California

20 kg of hydrogen at 15,000 psig. This station dispenses hydrogen according to SAE International technical information report J2601, and it includes the first example of hydrogen purification technology for production of an ultra-pure hydrogen stream from an industrial-grade pipeline supply. Two dual dispensers for both 350- and 700-bar hydrogen have been installed, and four vehicles can be filled simultaneously. Based on a 50% compressor on-stream factor, the station will have the capacity to dispense 48 kg/day, enough to refuel approximately 12 cars per day. When starting with full storage, six cars can be filled in succession. Vehicle test fills were completed in March 2011.

In December 2010, Air Products completed a nine-month deployment of an HF-150 mobile refueler at the district office of the U.S. Forest Service in Placerville, California (Figure 6). The Air Products HF-150 maintains about 150 kg of gaseous hydrogen at 6,600 psig. It can dispense approximately 80 to 90 kg before needing to be refilled. It is ideal for small fleet fueling and offers the advantage of being an automated, highly reliable, cost-effective fueling system that can be easily installed.

Energy Station at Fountain Valley[2]

The Hydrogen Energy Station was installed at the Orange County Sanitation District (OCSD) in Fountain Valley, California, and became fully operational in FY 2011 as the world's first fuel cell energy station that produces electric power and hydrogen from wastewater treatment gas (Figure 7).

- The first co-production of hydrogen (using natural gas) at the Hydrogen Energy Station in OCSD took place in October 2010.
- Over 1,000 hours of operation in power and (power + hydrogen) modes has been completed during the performance period. The hydrogen produced has met all quality standards.
- The unit achieved nominal 54% efficiency (power + hydrogen) when operating in hydrogen co-production mode.
- In February 2011, the first hydrogen from the Hydrogen Energy Station at OCSD was sent to the hydrogen fueling station. Initial test fills of fuel cell vehicles at the hydrogen fueling station were completed in March 2011.
- In May 2011, operation on biogas from the wastewater treatment facility began.

[2] This station is based on a technology that co-produces power, heat, and hydrogen. This type of system is referred to as a CHHP (combined heat, power, and hydrogen or tri-generation) system. The station uses a high-temperature fuel cell to co-generates electricity, heat, and hydrogen. The fuel cell can use a diversity of hydrogen-rich fuels, including digester gas, natural gas, landfill gas, and syngas. This technology is expected to provide a source of cost-competitive hydrogen, which can be renewable when digester gas or landfill gas is used as the feedstock.

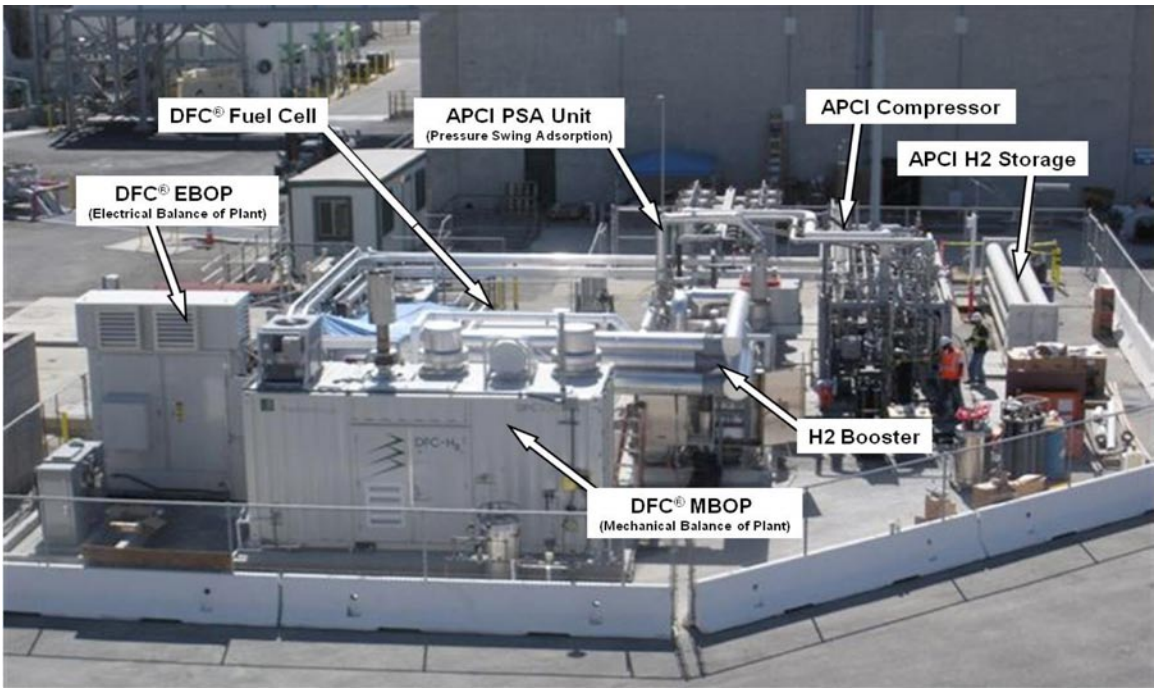
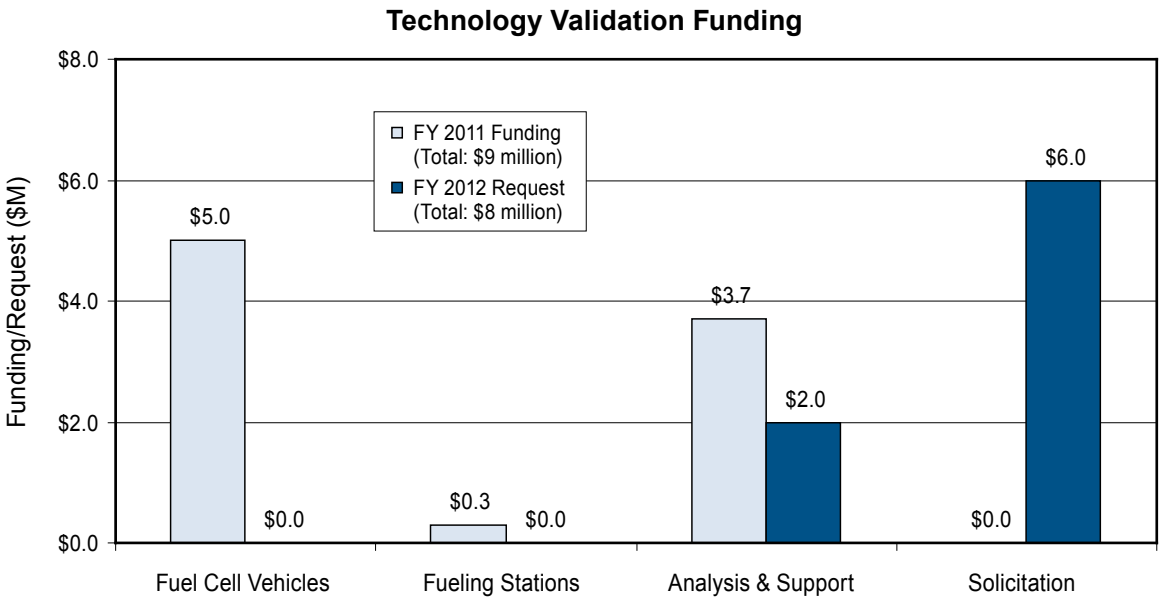


FIGURE 7. Energy Station at Fountain Valley, California (dispensing area not shown)

Budget

The funding portfolio for Technology Validation addresses the need to validate integrated hydrogen and fuel cell technologies for transportation and electric power generation in a systems context, under real-world operating conditions. In FY 2011, $9 million in funding was appropriated for the Technology Validation sub-program. The President's FY 2012 request includes $8 million for Technology Validation activities.



FY 2012 Plans

A set of composite data products (CDPs) based on data collected through June 2011 ("Fall 2011 CDPs") will be created for publication and reporting in November 2011. In the first quarter of FY 2012 the final two National Learning Demonstration projects (GM and Mercedes-Benz North America) will conclude and final reports will be prepared.

The Technology Validation sub-program will continue to collaborate with the Department of Transportation to validate fuel cell and hydrogen technologies in transit bus demonstrations conducted by the Federal Transit Administration. Efforts will also continue to harmonize data collection with other FCB demonstrations worldwide. Future FCB projects will include:

- Collecting, analyzing, and reporting on performance data for next-generation hydrogen-fueled vehicles in California, including AC Transit, SunLine, the City of Burbank, and additional sites as funding allows.
- Investigating the reliability and durability of FCBs as a part of ongoing evaluations; these efforts complement the DOE light-duty FCEV demonstrations
- Coordinating with Federal Transit Administration to ensure harmonized data-collection efforts for the National Fuel Cell Bus Program

The Integrated Hydrogen Energy Station will continue to be operated on anaerobic digester gas from the wastewater treatment facility. Data will be provided to DOE for the first six months of operation under a three-year program sponsored by the California Air Resources Board and the South Coast Air Quality Management District.

The Technology Validation sub-program is planning a funding opportunity announcement for FY 2012, subject to appropriations. Potential areas of interest may include: medium-scale (50- to 500-kW) CHHP production; medium-scale (50- to 500-kW) hydrogen and power production; on-site hydrogen generation for back-up power and specialty applications (e.g. material handling); fuel cell-powered ground support equipment for ports, terminals, and distribution hubs; and polymer electrolyte membrane fuel cells for stationary power. Final topics will consider input from the request for information that was issued to the stakeholder community and the public in FY 2011.

John Garbak
Technology Validation Team Lead
Fuel Cell Technologies Program
Department of Energy
1000 Independence Ave., SW
Washington, D.C. 20585-0121
Phone: (202) 586-1723
E-mail: John.Garbak@ee.doe.gov

VII.1 Controlled Hydrogen Fleet and Infrastructure Analysis

Keith Wipke (Primary Contact), Sam Sprik, Jennifer Kurtz, Todd Ramsden, Chris Ainscough, Genevieve Saur
National Renewable Energy Laboratory (NREL)
1617 Cole Blvd.
Golden, CO 80401
Phone: (303) 275-4451
E-mail: keith.wipke@nrel.gov

DOE Manager
HQ: John Garbak
Phone: (202) 586-1723
E-mail: John.Garbak@hq.doe.gov

Start Date: October 2003
Projected End Date: Project continuation and direction determined annually by DOE

Objectives

- By 2008, validate that hydrogen vehicles have a greater than 250-mile range without impacting passenger or cargo compartments.
- By 2009, validate 2,000-hour fuel cell durability in vehicles and hydrogen infrastructure that results in a hydrogen production cost of less than $3.00/gallon gasoline equivalent (gge) (untaxed) delivered and safe and convenient fueling by drivers (with training).
- Help DOE demonstrate the use of fuel cell electric vehicles (FCEVs) and hydrogen infrastructure under real-world conditions, using multiple sites, varying climates, and a variety of hydrogen sources.
- Analyze detailed fuel cell and hydrogen data from vehicles and infrastructure to obtain maximum value for DOE and industry from this "learning demonstration."
- Identify the current status of the technology and its evolution over the project duration.
- Provide feedback and recommendations to DOE to promote hydrogen and fuel cell research and development (R&D) activities and assess technical progress.
- Publish results for key stakeholder use and investment decisions by generating composite data products (CDPs) for public dissemination.

Technical Barriers

This project addresses the following technical barriers from the Technology Validation section (3.6.4) of the Fuel Cell Technologies Program Multi-Year Research, Development, and Demonstration Plan:

(A) Lack of Fuel Cell Vehicle Performance and Durability Data

(B) Hydrogen Storage

(C) Lack of Hydrogen Refueling Infrastructure Performance and Availability Data

(D) Maintenance and Training Facilities

(E) Codes and Standards

(H) Hydrogen from Renewable Resources

(I) Hydrogen and Electricity Co-Production

Contribution to Achieving DOE Technology Validation Milestones

Throughout this project, researchers are gathering data and providing technical analysis that contributes to achieving the following DOE technology validation milestones from the Fuel Cell Technologies Program Multi-Year Research, Development, and Demonstration Plan:

- *Milestone 2: Demonstrate FCEVs that achieve 50% higher fuel economy than gasoline vehicles (Quarter [Q]3, Fiscal Year [FY] 2005).* This milestone was achieved.
- *Milestone 3: Decision for purchase of additional vehicles based on projected vehicle performance and durability and hydrogen cost criteria (Q4, FY 2006).* This milestone was achieved.
- *Milestone 4: Operate fuel cell vehicle fleets to determine if 1,000 hour fuel cell durability, using fuel cell degradation data, was achieved by industry (Q4, FY 2006).* This milestone was achieved.
- *Milestone 5: Validate vehicle refueling time of 5 minutes or less for a 5 kg tank [1kg/min] (Q4, FY 2006).* At the time of the milestone, we had analyzed more than 2,000 vehicle fueling events and had calculated an average rate of 0.69 kg/min and median rate of 0.72 kg/min, with 18% of the events exceeding the 1 kg/min target. Updates 3.5 years later, data from more than 25,000 fueling events showed improved results with an average rate of 0.77 kg/min with 23% of fueling events exceeding 1 kg/min. This milestone was achieved.
- *Milestone 7: Validate refueling time of 5 minutes or less for 5 kg of hydrogen (1 kg/min) at 5,000 psi through the use of advanced communication technology (Q4, FY 2007).* Currently, the data show that communication fills can fuel at a higher rate (up to 1.8 kg/min) and have an average fill rate 30% higher than non-communication fills (0.86 kg/min versus 0.66 kg/min). This milestone was achieved.
- *Milestone 8: Fuel cell vehicles demonstrate the ability to achieve a 250-mile range without impacting passenger cargo compartment (Q4, FY 2008).* This milestone

was achieved in 2008 using data from the Learning Demonstration results, with demonstrated range of 196–254 miles. In June 2009, an on-road driving range evaluation was performed in collaboration with Toyota and Savannah River National Laboratory. The results indicated a 431-mile on-road range was possible in southern California using Toyota's FCHV-adv fuel cell vehicle [1]. This milestone was achieved.

- *Milestone 10: Validate FCEVs 2,000-hour fuel cell durability using fuel cell degradation data (Q4, FY 2009)*. On-road fuel cell voltage data from second-generation fuel cell systems were analyzed and published in the Fall 2009 CDP results. Results indicate that the highest projected team average to 10% voltage degradation for second-generation systems was 2,521 hours, with a four-team average of 1,020 hours. The Spring 2010 results only slightly increased the average (to 1,062 hours) and the highest team remained the same at 2,521 hours. This milestone was achieved.
- *Milestone 12: Validate cold start capability at -20 C (2Q, 2011)*. This milestone was achieved and published in the Fall 2008 CDPs, demonstrating freeze starts from between -9 and -20 degrees C and documenting both time to drive away and time to maximum fuel cell power.
- *Milestone 23: Total of 10 stations constructed with advanced sensor systems and operating procedures (Q1, FY 2008)*. This milestone was achieved.
- *Milestone 24: Validate a hydrogen cost of $3.00/gge (based on volume production) (Q4, FY 2009)*. Cost estimates from the Learning Demonstration energy company partners were used as input to an H2A analysis to project the hydrogen cost for 1,500 kg/day early market fueling stations. Results indicate that on-site natural gas reformation would lead to a range of $8-$10/kg and on-site electrolysis would lead to $10-$13/kg hydrogen cost. Although these results do not meet the $3/gge cost target, two external independent panels concluded that distributed natural gas reformation could lead to $2.75-$3.50/kg [2] and distributed electrolysis could lead to $4.90-$5.70 [3]. This milestone was achieved outside the Learning Demonstration project.

Accomplishments

- Received and processed data quarterly from a total of 460,000 individual vehicle trips, amounting to more than 107 gigabyte (GB) of on-road data, since project inception.
- Created and published a total of 85 CDPs, with the Spring 2011 CDP results including five new CDPs since last year and updates to 18 previously published CDPs. The results emphasized the changes observed in the last 12 months, and included data from two Learning Demo manufacturers plus the Air Products' California Hydrogen Infrastructure Project.
- Documented and archived each quarter's analysis results in the Fleet Analysis Toolkit (FAT) graphical user interface. Executed NREL FAT to produce detailed data results and CDPs in parallel for convenient industry and internal review.
- Presented project results publicly at the Fuel Cell Seminar, EVS-25, the Fuel Cell and Hydrogen Energy Association conference, the Japanese Fuel Cell Demonstration Project conference, and the 2011 DOE Fuel Cell Technologies Program Merit Review meeting.
- Maintained NREL's Web page at http://www.nrel.gov/hydrogen/cdp_topic.html to allow direct public access to the latest CDPs organized by topic, date, and CDP number.
- Provided presentations of results to key stakeholders, including two FreedomCAR and Fuel technical teams (storage and fuel cells).
- Continued to leverage key NREL analysis tools and capabilities to enable results to be quickly generated from fuel cell forklifts and other early market fuel cell applications. This year we also began performing some new analyses on FCEVs that were developed originally for fuel cell forklifts.



Introduction

The primary goal of this project is to validate vehicle/infrastructure systems using hydrogen as a transportation fuel for light-duty vehicles. This means validating the use of FCEVs and hydrogen fueling infrastructure under real-world conditions using multiple sites, varying climates, and a variety of sources for hydrogen. Specific targets for 2009 were hydrogen vehicles with a range greater than 250 miles, 2,000-hour fuel cell durability, and $3.00/gge hydrogen production cost (based on modeling for volume production). We are identifying the current status of the technology and tracking its evolution over the project duration, particularly between the first- and second-generation fuel cell vehicles, and further improvements to the second-generation vehicles demonstrated in the final two years. NREL's role in this project is to provide maximum value for DOE and industry from the data produced by this "learning demonstration." We seek to understand the progress toward the technical targets, and provide information to help move the Fuel Cell Technologies (FCT) R&D activities more quickly toward cost-effective, reliable hydrogen FCEVs and supporting hydrogen fueling infrastructure.

Approach

Our approach to accomplishing the project's objectives has been structured around a highly collaborative relationship with each industry team including Chevron/Hyundai-Kia, Daimler/BP, Ford/BP, General Motors/Shell,

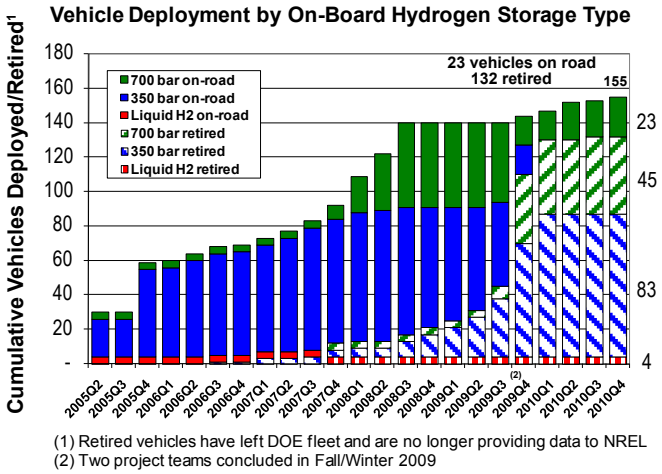
and Air Products (through the DOE California Hydrogen Infrastructure Project). We are receiving raw technical data from the hydrogen vehicles and from the fueling infrastructure that enable us to perform unique and valuable analyses across all teams. Our primary objectives are to feed the current technical challenges and opportunities back into the DOE FCT R&D Program and assess the current status and progress toward targets.

To protect the commercial value of these data for each company, we established the Hydrogen Secure Data Center at NREL to house the data and perform our analysis. To ensure value is fed back to the hydrogen community, we publish CDPs twice a year at technical conferences to report on the progress of the technology and the project, focusing on the most significant results. Additional CDPs are being conceived as additional trends and results of interest are identified, and as we receive requests from DOE, industry, and the codes and standards community. We also provide our detailed analytical results (not public) to each individual company's data to maximize the industry benefit of NREL's analysis work and to obtain feedback on our methodologies.

Results

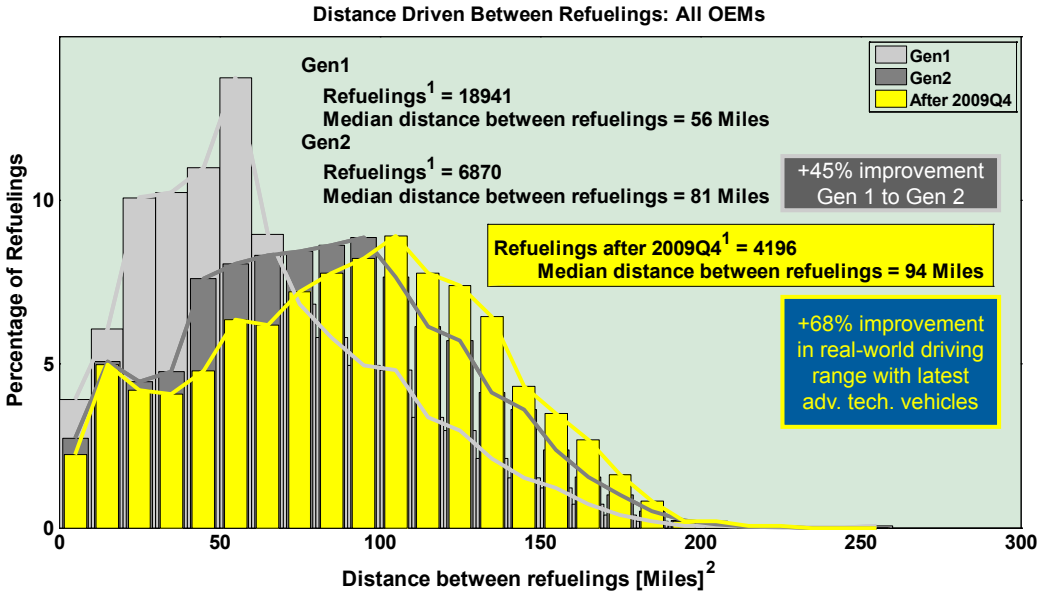
The results in FY 2011 came from analyzing an additional year of data (January–December 2010), creating five new and 18 updated CDPs, and presenting these results at several technical conferences. This brings the total number of CDPs published to 85. To accomplish this, we continued to improve and revise our in-house analysis tool, FAT. In 2007 NREL launched a Web page at http://www.nrel.gov/hydrogen/cdp_topic.html to provide stakeholders and the public with direct access to the results. Some results have also been presented publicly at conferences in the last year as two distinct sets of results (labeled "Fall 2010" and "Spring 2011"). All 85 of the results are now available on the Web site, so this report will include only a few highlights from the last year.

- Status of Vehicle Deployment: Figure 1 shows the cumulative number of vehicles that have been deployed by quarter and hydrogen storage system type since project inception. A total of 155 vehicles were deployed through December 2010; 132 are retired from the project and 23 are still on the road. Before the conclusion of the project about 40 vehicles should be on the road providing data to NREL with about 170 vehicles deployed since project inception.
- Real-World Vehicle Driving Range: In FY 2008, the driving range of the project's FCEVs was evaluated based on fuel economy from dynamometer testing and on-board hydrogen storage amounts and compared to the 250-mile target. Additional on-road data were obtained from second- and first-generation vehicles in 2009, as well as improved second-generation vehicles in 2010. This enabled us to evaluate the distribution of real-world driving ranges of all the vehicles in the project. The data show (Figure 2) a 45% improvement in the median real-world driving range of second-generation vehicles (81 miles) compared to first-generation (56 miles), based on distances driven between more than 25,000 fueling events. In 2010, with continued operation of some second-generation vehicles and the introduction of some improved performance second-generation vehicles, we have seen an increase in the median distance traveled between fuelings to 94 miles. This reflects a 68% improvement in real-world driving range with the latest advanced technology vehicles compared to the first-generation vehicles first introduced in 2005. As previously discussed, all the vehicles are capable of two to three times greater range than this when pushed to their full capabilities with sufficient fueling infrastructure, but the median distance traveled between fuelings is one way to measure the improvement in the vehicles' capability as well as the way in which they are actually being driven. We believe the reason for the increase in median driving distance between fuelings is due to slight improvements in the vehicle capabilities (better efficiency) and in more widespread infrastructure, which enables the vehicle storage tanks to be drawn down closer to empty because drivers are confident they can obtain fuel close by.
- Fuel Cell Durability: The Spring 2010 results indicated that the highest average projected team time to 10% voltage degradation for second-generation systems was 2,521 hours, with a multi-team average projection of 1,062 hours. Therefore, the 2,000-hour target for durability was achieved. Since that time, two automotive teams concluded their participation in the project and additional data were acquired on some second-generation vehicles. Improved second-generation vehicles were also introduced to the project. Only two companies now provide durability data, and some vehicles have limited hours on the road, so we will create new durability CDPs in Fall 2011 when



(1) Retired vehicles have left DOE fleet and are no longer providing data to NREL
(2) Two project teams concluded in Fall/Winter 2009

FIGURE 1. Cumulative Vehicles Deployed by Quarter and by Storage Type



1. Some refueling events are not detected/reported due to data noise or incompleteness.
2. Distance driven between refuelings is indicative of driver behavior and does not represent the full range of the vehicle.

FIGURE 2. Real-World Improvement in Driving Range Between Gen 1, Gen 2, and Latest Advanced Technology Learning Demonstration Vehicles

additional data are available to provide robust analysis and identity protection for all the companies.

- Vehicle Fueling Rates: Because of the change in makeup of the automotive and energy teams for the final two years of the project, we separated out the fueling rates for the five years up through 2009 Q4 from the fueling rates for the year after 2009 Q4 (Figure 3). We found that in the first five years of the project, from more than 25,000 fueling events, the average fill rate was 0.77 kg/min with 23% of the events exceeding DOE's target of 1 kg/min, representing a 5 kg fill in 5 minutes. Over the last year, from a limited set of 2,766 fills,

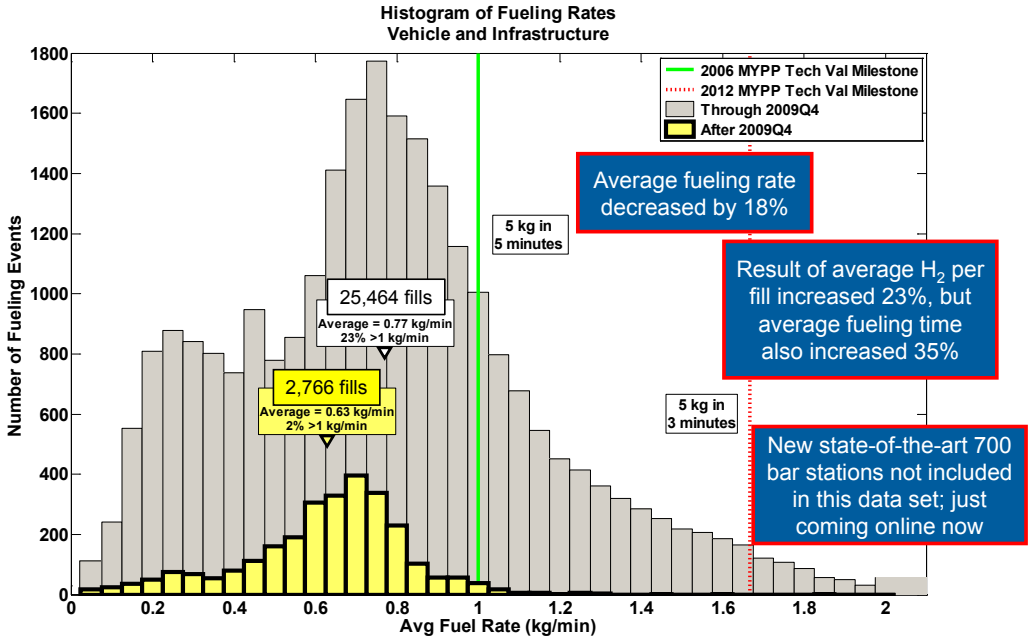


FIGURE 3. Fueling Rate Trends are Monitored as Industry Moves to 700 bar Pressure as Standard

we have observed an average fill rate of 0.63 kg/min with just 2% of the fills exceeding the 1 kg/min target. Several factors explain this 18% drop in fueling rate. The average hydrogen dispensed per fill increased by 23%, but the average fueling time increased by 35%. The root cause is that the hydrogen community is migrating toward 700 bar pressure fueling as the new standard, but the state-of-the-art stations that can achieve a fast and complete fill at this pressure with precooling are just now coming online, and data from those stations were not available through December 2010. Additionally, some 350 bar stations and vehicles that demonstrated fast-fill times have been decommissioned. So this reduction in reported fill rate should be a temporary phenomenon until the new 700 bar station data are included in the dataset later this year. With the new data and analysis results, NREL will be able to document the significant progress that has been made relative to 700 bar infrastructure.

- Hydrogen Fueling Infrastructure Usage Patterns: The final technical result to highlight is the usage patterns of the hydrogen fueling stations within the project over the last year. Figure 4 shows the percentage of hydrogen dispensed by day of the week (bars with left-axis labels) along with the average amount of hydrogen dispensed by day for each of the six stations included in this dataset (curves with right-axis labels). The data show that weekday fueling is still more common than weekend fueling, which had been shown in a previous CDP from the first five years of the project. The graph also shows that two stations have relatively high average throughput (8-14 kg/day); the other four are only lightly used, dispensing 3 kg/day or less on average. This type of result will be useful as we go forward to be able to track the throughput of each station individually and by specific geographic region to better coordinate and advise stakeholders on optimal future vehicle deployments and new station placement.

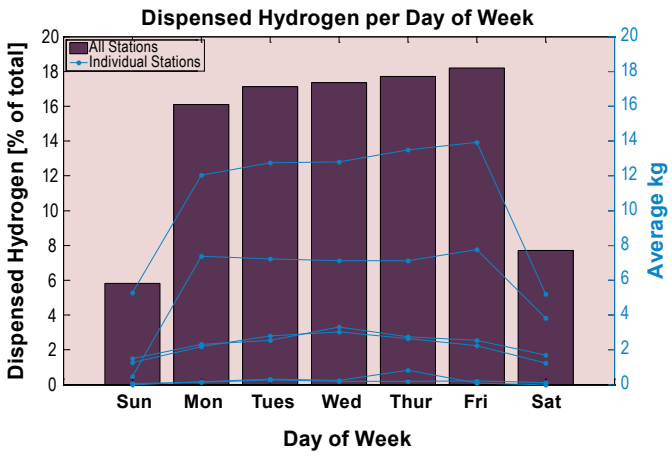


FIGURE 4. New Infrastructure CDP Provides Insight into Specific Fueling Usage Patterns

Conclusions and Future Direction

- Completed the first six years of the seven-year project with 155 vehicles deployed in fleet operation, 24 project fueling stations demonstrated, and no major safety barriers encountered.
- Analyzed data from 460,000 individual vehicle trips covering >3 million miles traveled and 140,000 kg hydrogen produced or dispensed.
- Verified that high fuel cell system efficiency was maintained from Gen 1 to Gen 2 systems, with Gen 2 efficiency at quarter-power of 53%–59%, close to the 60% DOE target.
- Published 85 CDPs to date and made them directly accessible to the public from an NREL website.
- We will create new and update CDPs based on data collected through June 2011 (Fall 2011 CDPs) and present results for publication at the 2011 Fuel Cell Seminar.
- NREL will support DOE's September 2011 milestone to document operation of advanced technology fuel cell vehicles with up to 600 hours of operation.
- We will support original equipment manufacturers, energy companies, and state organizations in California in coordinating early infrastructure plans.
- We will gather and analyze data from a relatively large (100 kg/day on-site production) hydrogen station in Burbank, California, along with many new stations that are being opened in California in 2011 (for example, the Torrance pipeline station and the Fountain Valley tri-generation station).
- NREL will continue to identify opportunities to feed findings from the project back into the Vehicle Technologies and FCT programs and industry R&D activities to maintain the project as a "learning demonstration."
- We will continue to gather data from FCEVs and hydrogen stations through the end of calendar year 2011, when the auto manufacturer Learning Demonstration projects conclude, and publish one final set of results in Spring 2012.
- As the last deliverable from this project, we will write a final comprehensive summary report for publication.
- We will continue to identify and exploit new opportunities to document fuel cell vehicle and hydrogen progress publicly beyond the end of this project.

FY 2011 Publications/Presentations

1. Wipke, K., Sprik, S., Kurtz, T., Ramsden, T., Ainscough, C., Saur, G., "Controlled Hydrogen Fleet and Infrastructure Analysis," 2011 U.S. DOE Hydrogen Program and Vehicle Technologies Program Annual Merit Review and Peer Evaluation Meeting, Washington, D.C, May 2011. (presentation)

2. Wipke, K., presentation of Learning Demonstration results to FreedomCAR and Fuels Hydrogen Storage Tech Team, April 2011. (presentation)

3. Wipke, K., Sprik, S., Kurtz, J., Ramsden, T., "National FCEV Learning Demonstration Report: Spring 2011 – All Composite Data Products with Updates through March 29, 2011," Golden, CO: National Renewable Energy Laboratory, published April 2011. (presentation)

4. Wipke, K., Sprik, S., Kurtz, J., Ramsden, T., Ainscough, C., Saur, G., "Status of U.S. FCEV and Infrastructure Learning Demonstration Project," Japan Hydrogen Fuel Cell (JHFC) Demonstration Project, March 2011. (presentation)

5. Wipke, K., Sprik, S., Kurtz, J., Ramsden, T., Ainscough, C., Saur, G., "Next Steps for the FCEV Learning Demonstration Project," Fuel Cell & Hydrogen Energy Conference (FCHEA), Washington, DC, February, 2011. (presentation)

6. Wipke, K., Sprik, S., Kurtz, J., Ramsden, T., Garbak, J., "Entering a New Stage of Learning from the U.S. Fuel Cell Electric Vehicle Demonstration Project," prepared for the 25th International Battery, Hybrid and Fuel Cell Electric Vehicle Symposium (EVS-25), Shenzhen, China, November 2010. (paper and presentation)

7. Kurtz, J., Wipke, K., Eudy, L., Sprik, S., Ramsden, T., "Fuel Cell Technology Demonstrations and Data Analysis," draft submitted to editors of CRC book entitled Hydrogen Energy and Vehicle Systems, November, 2010. (book chapter)

8. Wipke, K., Sprik, S., Kurtz, J., Ramsden, T., 2010 Annual Progress Report for NREL's "Controlled Hydrogen Fleet and Infrastructure Analysis Project," Section VIII.1, November 2010. (paper)

9. Wipke, K., Sprik, S., Kurtz, J., Ramsden, T., "U.S. Fuel Cell Electric Vehicle Demonstration Project 2010 Status Update," presented at the 2010 Fuel Cell Seminar and Exposition, San Antonio, TX, October 2010. (presentation)

10. Wipke, K., Sprik, S., Kurtz, J., Ramsden, T., "Fall 2010 Composite Data Products for the Controlled Hydrogen Fleet and Infrastructure Demonstration and Validation Project," Golden, CO: National Renewable Energy Laboratory, published September 2010. (presentation)

11. Wipke, K., Sprik, S., Kurtz, J., Ramsden, T., "Learning Demonstration Interim Progress Report – July 2010," NREL/TP-560-49129, September 2010. (paper)

12. Wipke, K., Sprik, S., Kurtz, J., Ramsden, T., Garbak, J., "DOE's National Fuel Cell Vehicle Learning Demonstration Project – NREL's Data Analysis Results," Electric and Hybrid Vehicles, Power Sources, Models, Sustainability, Infrastructure and the Market, Chapter 12, ISBN 978-0-444-53565-8, NREL/CH-560-47111, Elsevier B.V., August 2010. (paper)

References

1. Wipke, K., Anton, D., Sprik, S., "Evaluation of Range Estimates for Toyota FCHV-adv Under Open Road Driving Conditions," prepared under SRNS CRADA number CR-04-003, August 2009.

2. Fletcher, J., Callaghan, V., "Evaluation Cost of Distributed Production of Hydrogen from Natural Gas – Independent Review," NREL/BK-150-40382, October 2006.

3. Genovese, J., Harg, K., Paster, M., Turner, J., "Current (2009) State-of-the-Art Hydrogen Production Cost Estimate Using Water Electrolysis – Independent Review," NREL/BK-6A1-46676, September 2009.

VII.2 Hydrogen Vehicle and Infrastructure Demonstration and Validation

Gary P. Stottler
General Motors (GM)
10 Carriage Street
Honeoye Falls, NY 14472
Phone: (585) 624-6709
E-mail: gary.stottler@gm.com

DOE Managers
HQ: John Garbak
Phone: (202) 586-1723
E-mail: John.Garbak@ee.doe.gov
GO: Doug Hooker
Phone: (720) 356-1578
E-mail: Doug.Hooker@go.doe.gov

Contract Number: DE-FC36-04GO14284, A018

Project Start Date: October 1, 2004
Project End Date: September 30, 2011

Objectives

GM and energy partner Shell Hydrogen, LLC, will deploy a system of hydrogen fuel cell electric vehicles (FCEVs) integrated with a hydrogen refueling infrastructure to operate under real world conditions. With this deployment GM and Shell Hydrogen will:

- Demonstrate progressive generations of fuel cell system technology.
- Demonstrate multiple approaches to H_2 generation and delivery for vehicle refueling.
- Collect and report operating data.

Technical Barriers

This project addresses the following technical barriers from the Technology Validation section (3.6.4) of the Hydrogen, Fuel Cells and Infrastructure Technologies Program Multi-Year Research, Development and Demonstration Plan:

(A) Lack of Fuel Cell Electric Vehicle Performance and Durability Data

(C) Lack of Hydrogen Fueling Infrastructure Performance and Availability Data

(D) Maintenance and Training Facilities

(E) Codes and Standards

Contribution to Achievement of DOE Technology Validation Milestones

This project contributes to the achievement of the DOE Technology Validation milestones listed below from the Technology Validation section of the Hydrogen, Fuel Cells and Infrastructure Technologies Program Multi-Year Research, Development and Demonstration Plan:

- **Milestone 2**: Demonstrate FCEVs that achieve 50% higher fuel economy than gasoline vehicles. (3Q, 2005)
- **Milestone 4**: Operate fuel cell vehicle fleets to determine if 1,000-hour fuel cell durability, using fuel cell degradation data, was achieved by industry. (4Q, 2006)
- **Milestone 22**: Six stations and two maintenance facilities constructed with advanced sensor systems and operating procedures. (4Q, 2006)

Accomplishments Through Fiscal Year (FY) 2011

GM has accomplished the following project milestones:

- Deployed 60 vehicles demonstrating two generations of GM's proprietary fuel cell technology in various terrains, driving conditions, and climates (see Figure 1).
- Constructed and utilized first-class maintenance and training facilities located in Ardsley, NY; Ft. Belvoir, VA; and Burbank, CA with a satellite hub located in Lake Forest, CA.
- Established retail and retail-like hydrogen stations for public fueling:
  - Six fueling stations in operation spreading across the Eastern and Western regions.
  - Different types of hydrogen generation/delivery options are demonstrated such as delivered compressed gas and on-site electrolysis.
  - Two stations are infrared-capable and able to fast-fill 3+ vehicles back-to-back.
  - Hydrogen quality testing has been completed in both Eastern and Western regions, among the first stations in the U.S. to be tested at 700 bar.
- Shell Hydrogen opened new stations in the New York City metropolitan area at the John F. Kennedy (JFK) airport and in Bronx during 2009. They also commissioned a station in Culver City, California (Los Angeles [LA]). These stations utilize hydrogen compressed gas delivered by truck and dispense hydrogen at 700 bar utilizing equipment supplied by several companies.
- Gathered comprehensive feedback on all elements of customer experience and vehicle performance to guide future FCEV and infrastructure development.

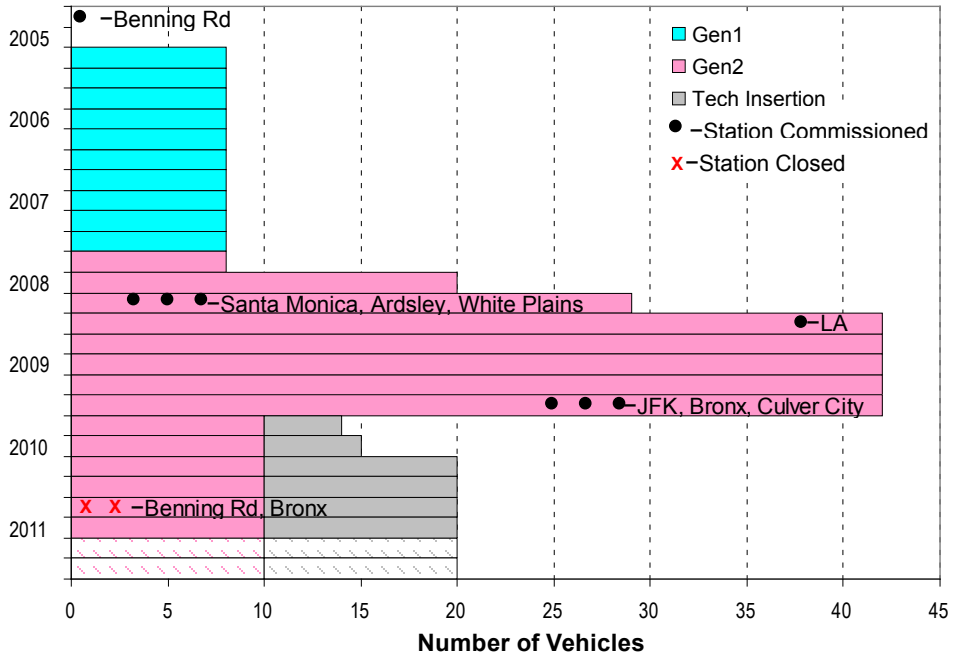


FIGURE 1. GM FCEV and Refueling Station Implementation

- Collected vehicle and station data using automated logbook entry and automated wireless data transfer from vehicles to a data server.
- Conducted and verified extensive cold weather performance testing; additionally, vehicles were deployed in the northeast United States through several winters and performed as customers expected (see Figure 2).
- GM continues to operate and maintain 10 baseline Phase 2 FCEVs through 2011 or until failure.
- Ten additional Phase 2 FCEVs equipped with technology developed during the initial part of Phase 2 were added in 2010 in order to extend learnings. These "Technology Insertion" vehicles were deployed and are accumulating miles (see Figure 3).
- Three fuel cell systems were instrumented with the same hardware as the Technology Insertion vehicles and are running accelerated durability tests on test stands.



Introduction

Over the six-year period to date, the project has made significant progress in support of the long-term goals of DOE's Technical Validation sub-program. GM has deployed eight Phase 1 FCEVs and 42 of its commercially developed Phase 2 FCEVs and has maintained them through the use of two primary maintenance and training hubs and two additional satellite locations.

For the rest of the project, GM will continue to operate and maintain 10 baseline Phase 2 FCEVs. These baseline Phase 2 FCEVs will continue to operate through 2011 or until failure. The purpose is to demonstrate long stack durability with extended vehicle operating hours (see Figure 4). In addition, 10 new Phase 2 FCEVs were equipped with the most recent materials and controls technology in order to demonstrate the progress made in the project to date. These "Technology Insertion" vehicles are currently deployed and are accumulating miles and generating data for submission to DOE according to the National Renewable Energy Laboratory (NREL) Data Reporting Templates.

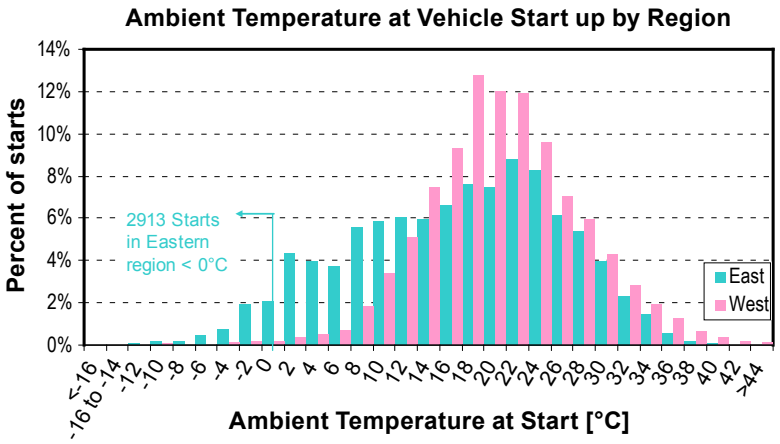
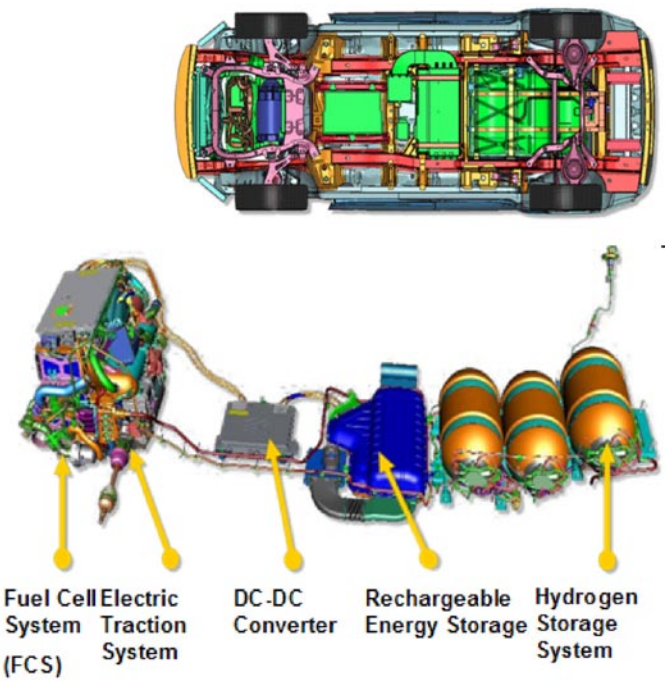


FIGURE 2. 2,913 Vehicle Starts at Ambient Temperatures <0°C



DC - direct current

FIGURE 3. Gen2 Chevrolet FCEV with Technology Insertion

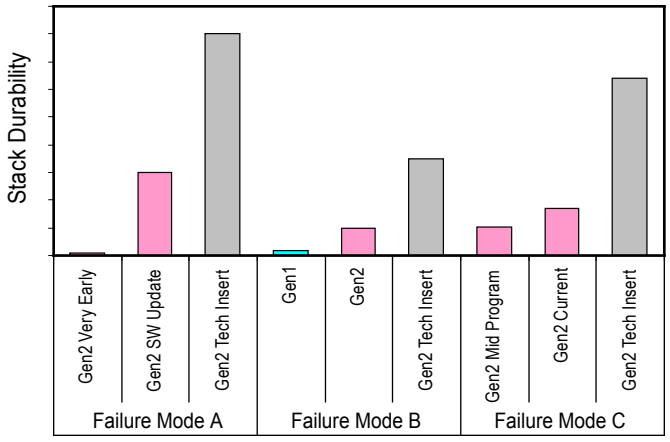


FIGURE 4. Stack Durability Projections: Stack Durability Improves as Successive Iterations Mitigate Failures

Approach

- Demonstrate FCEVs:
  - Deploy FCEVs in various terrains, driving conditions, and climates including cold weather.
  - Demonstrate two generations of fuel cell technology.
- Insert technology with recent advances to test Phase 2 learnings.
- Establish retail-like hydrogen stations for public fueling:
  - Install and operate total of six fueling stations on east and west coasts.
  - Explore hydrogen generation/delivery options such as electrolysis.
- Set up maintenance and service operations in support of FCEVs:
  - Train personnel in maintenance, fueling, technical support, and safety.
- Generate and report data required under the project:
  - Capture vehicle on-road and dynamometer test data.
  - Capture hydrogen infrastructure production/fueling data.
- Evaluate vehicle performance against targets:
  - Vehicle range, stack durability, cold weather performance.
- Focus on accumulating durability hours:
  - More intensive operation of vehicle fleet.
  - Work with commercial customers.
  - Fuel cell system accelerated durability testing.

Results

Phase 2 FCEVs were launched in the fourth quarter of 2007 in the Eastern and Western regions. All 42 Phase 2 vehicles were deployed by the end of the third quarter of 2008. Thirty-two vehicles completed their deployment at the end of the third quarter of 2009, and 10 baseline Phase 2 vehicles will continue to report data thru the third quarter of 2011 or until failure in order to support stack durability estimates. All 10 Technology Insertion vehicles were deployed by the end of the second quarter of 2010. Twenty project vehicles are now over three years old with 40-50 thousand miles.

Beginning-of-life chassis dynamometer testing was conducted for Phase 2 Chevrolet Equinox FCEVs, which included cold weather tests. Dynamometer testing was completed on one Phase 2 vehicle in September 2009 and one "Technology Insertion" vehicle in June 2010. Another round of dynamometer testing was completed in December 2010 on one Technology Insertion vehicle so the results can be compared to previous testing.

Shell Hydrogen is no longer participating in the project but GM will continue to utilize the Shell stations at JFK, Culver City, West LA, Torrance and the new opening of Newport Beach, CA in 2011. GM will continue to submit refueling data for the Ardsley, NY station, Los Angeles Airport station, and the Culver City station according to the DOE data templates. In addition, the FCEVs may refuel at any of the non-project refueling stations including Honeoye Falls, Rochester Institute of Technology, Monroe County, Fort Belvoir, White Plains, Santa Monica Blvd, Camp Pendleton, University of California, Irvine, and Shell, Torrance.

GM is also anticipating the opening of numerous hydrogen stations in California over the next 18 months, which are supported by Air Resources Board and Energy Commission grants. In total, 18 new and upgraded stations, a majority which will be located in the LA metropolitan area, will be able to support the FCEV fleet.

The hydrogen orientation program for emergency first responders continues to be delivered on request in cities where GM's DOE vehicles operate. To date over 1,500 people trained have been trained and new training sessions continue to be requested on a regular basis.

NextEnergy Center chaired task groups made up of a consortium of industry experts on hydrogen to provide feedback on the National Fire Protection Agency (NFPA) hydrogen codes. Task Groups completed their review of the latest NFPA revision. NextEnergy Center has successfully transferred hydrogen permitting database tools to new website. They coordinated with DOE and its partners to transfer the databases' layout and functionality to DOE ownership, for public benefit. NextEnergy has concluded their participation in the project as of the fourth quarter of 2009.

Three fuel cell systems began running accelerated durability testing in November 2010 and will continue to operate through 2011. In order to accelerate the learnings on the most recent technology stack design, these systems were instrumented with the same hardware as the Technology Insertion vehicles and are running accelerated durability cycles on test stands. These fuel cell systems operate under a stressful, accelerated protocol in order to capture early learnings.

Conclusions and Future Directions

- FCEVs fully meet all functional needs for day-to-day use by individual customers.
- FCEVs are fully functional in sub-freezing cold weather conditions. GM FCEVs exhibited very fast cold-start/driveaway times under sub-freezing temperatures.
- Hydrogen Infrastructure has been demonstrated to be customer friendly in daily use by individual/retail and fleet vehicle operators in a "retail-like" self-service mode.
- Fuel cell stack durability rapidly increased and is expected to meet or exceed the DOE target of 2,000 hours during the completion of the demonstration project.
- GM is taking a significant step by introducing elements of our next generation fuel cell stack and system into a small group of Equinox FCEVs for continued Gen2 operation/demonstration during 2010 and 2011. GM believes that the learnings from the project so far have helped enable materials and operating controls within the fuel cell system that will clearly demonstrate the ability of the Gen2 vehicles to meet and exceed the project stack durability goal of 2,000 hours.
- Furthermore, GM looks forward to a continued relationship and collaboration with NREL in the areas of fuel cell stack and FCEV data analysis methods. GM believes that this work is helping establish a strong foundation for future work throughout the fuel cell industry to develop universally accepted metrics for assessing the performance of fuel cells and FCEV.
- GM will continue to provide data for baseline and Technology Insertion vehicles that are deployed and operating until the end of the project in the fourth quarter of 2011.
- GM will continue to provide lab data from accelerated durability testing to enhance understanding of fuel cell durability until the end of the project in the fourth quarter of 2011.
- GM negotiated its first agreements to purchase fuel "by the kilogram." GM continues to launch new relationships with hydrogen station partners outside original project stations:
  - Rochester Institute of Technology
  - Town of Hempstead, NY
  - SunHydro, Wallingford, CT

FY 2011 Publications/Presentations

1. On May 9, 2011, GM participated and presented at the 2011 U.S. DOE HYDROGEN and FUEL CELLS PROGRAM and VEHICLE TECHNOLOGIES PROGRAM ANNUAL MERIT REVIEW and PEER EVALUATION MEETING.

2. An onsite review meeting with NREL, DOE, and GM personnel is planned for July 2011.

VII.3 Hydrogen to the Highways – Controlled Hydrogen Fleet and Infrastructure Demonstration and Validation Project

Ronald Grasman
Mercedes-Benz Research & Development North America, Inc.
850 Hansen Way
Palo Alto, CA 94304
Phone: (248) 633-4541
Email: ronald.grasman@daimler.com

DOE Managers
HQ: John Garbak
Phone: (202) 586-1723
E-mail: John.Garbak@ee.doe.gov
GO: Doug Hooker
Phone: (720) 356-1578
E-mail: Doug.Hooker@go.doe.gov

Contract Number: DE-FC36-04GO14285

Subrecipients:
- Daimler, Stuttgart, Germany
- Mercedes-Benz USA LLC (MBUSA), Montvale, NJ
- DTE Energy, Detroit, MI
- NextEnergy, Detroit, MI

Start Date: December 22, 2004
Projected End Date: September 30, 2011

Fiscal Year (FY) 2011 Objectives

- Record, collect and report data from fuel cell vehicles and the hydrogen fueling operations to validate DOE targets (Table 1).
- Demonstrate the safe installation of hydrogen fueling stations and fuel cell service facilities as well as the safe operation of all fuel cell vehicles (FCVs).
- Continuously update safety manuals and provide training.
- Participate in various working groups to ensure continuous progress towards establishing codes and standards essential for FCV commercialization.
- Raise public awareness of hydrogen technology and demonstration projects.

TABLE 1. Targets

Performance Measure	2009	2015
Fuel Cell Stack Durability	2000 hours	5000 hours
Vehicle Range	250+ miles	300+ miles
Hydrogen Cost at Station	$3/gge	$2-3/gge

gge – gasoline gallon equivalent

Technical Barriers

This project addresses the following technical barriers from the Technology Validation secion (3.6.4) of the Hydrogen, Fuel Cells and Infrastructure Technologies Program Multi-Year Research, Development and Demonstration Plan:

(A) Lack of Fuel Cell Vehicle Performance and Durability Data
(B) Hydrogen Storage
(C) Lack of Hydrogen Refueling Infrastructure Performance and Availability Data
(D) Maintenance and Training Facilities
(E) Codes and Standards
(H) Hydrogen from Renewable Resources

Contribution to Achievement of DOE Technology Validation Milestones

This project will contribute to achievement of the following DOE Technology Validation milestones from the Technology Validation section of the Hydrogen, Fuel Cells and Infrastructure Technologies Program Multi-Year Research, Development and Demonstration Plan:

- **Milestone 7**: Validate vehicle refueling time of 5 minutes or less for a 5kg of hydrogen (1kg/min) at 5,000 psi through the use of advanced communication technology (4Q2007).
- **Milestone 8**: Demonstrate the ability to achieve 250 mile range without impacting passenger cargo compartment (4Q2008).
- **Milestone 10**: Validate FCV's 2,000 hour fuel cell durability using fuel cell degradation data (4Q2009).
- **Milestone 12**: Validate cold start capability at -20C (2Q2011).

FY 2011 Accomplishments

- Submitted over 110 compact disks (CDs) of data to demonstrate that fuel cell vehicles are on track to be commercially viable by 2015.
- Successfully completed seven years of external operations of Gen I vehicles (five years past the original target date).
- Maintained smooth operations of the DTE hydrogen station.
- Transitioned FCV activities from research and development (R&D) to mainstream commercial efforts.

- Began customer operations of production-level Gen II vehicles.
- Participated in various working groups to ensure continuous progress with regards to codes and standards.
- Worked with California Energy Commission (CEC), Air Resources Board (ARB) and other original equipment manufacturers (OEMs) to prepare fueling infrastructure.



Introduction

The primary goal of this project is to validate fuel cell technologies for infrastructure, transportation as well as assess technology/commercial readiness for the market. The Mercedes Team, together with its partners, have been testing the technology by operating and fueling hydrogen FCVs under real world conditions in varying climate, terrain and driving conditions. Vehicle infrastructure data has been collected to monitor the progress toward the hydrogen vehicle and infrastructure performance targets of $2.00-3.00/gge hydrogen production cost and 2,000-hour fuel cell durability. Furthermore, progress has been made to validate cold start capability at -20°C. Finally, to prepare the public for a hydrogen economy, outreach activities have been designed to promote awareness and acceptance of hydrogen technology.

Approach

To achieve the project goals, the Mercedes Team deployed 30 Gen I vehicles into customer hands for real-world operations in various climatic regions of the United States. The Team is also providing data from Gen II vehicles under the similar operations as Gen I vehicles to compare technology maturity during project duration. All vehicles have been equipped with a data acquisition system that automatically collects statistically relevant data for submission to National Renewable Energy Laboratory (NREL), which monitors the progress of the FCVs against the DOE technology validation milestones. The energy partners have installed an infrastructure to provide hydrogen to the Mercedes Team's FCVs and to evaluate the technologies which have the potential to achieve the DOE hydrogen cost targets.

To raise public awareness of hydrogen technology and demonstration projects, the Mercedes Team aligned its communication activities with the goals of the DOE. In addition, project safety was maintained through continued inter-team communication, vehicle and infrastructure training, employee and customer education, and emergency responders training.

Results

Gen I and Gen II FCVs

Although Gen I FCVs were designed for a 2-year operation, A-Class F-CELLs have outperformed engineering expectations as the vehicles have been in full operation for over seven consecutive years. Since the inception of this demonstration project, the Mercedes Team submitted over 110 CDs of Gen I Raw Data to NREL and demonstrated that A-Class F-CELLs exceed the 2,000-hour stack durability target. Through the course of 2010, the Mercedes Team gradually transitioned the vehicle activities from Gen I A-Class to Gen II B-Class FCVs.

The engineering team performed extensive vehicle durability and performance test prior to launching the Gen II B-Class FCVs. First, Gen II vehicles were tested in temperatures ranging from -30°C (Sweden) to 50°C (Death Valley). Furthermore, engineers validated the 250-mile range and cold-start capability down to -17°C while reaching 50% of maximum power within 30 seconds (see Figure 1). Initial test results show Gen II fuel cell stack will most likely meet the 2015 DOE target of 5,000 hours durability.

Prior to deploying Gen II vehicles into customer hands, the Mercedes Team transitioned FCV activities from R&D to mainstream commercial activities. B-Class F-CELL vehicles were incorporated into Mercedes' standard business processes within departments such as warranty, customer assistance, parts and distribution as well as roadside assistance and sales (see Figure 2). Unfortunately, due to limitation of fueling infrastructure, the Mercedes Team had to hand-select Gen II FCV customers to ensure that these individuals were in close proximity to the few hydrogen fueling stations functioning in Southern California. Once the customers were chosen, the customer acquisition process became the responsibility of the dealership. Customers were then required to undergo the same documentation review and qualification processes as typically expected.



FIGURE 1. Cold Weather Testing of Gen II Vehicles



FIGURE 2. Transitioning FCV Efforts from R&D to Commercial Activities



FIGURE 3. Deployment of Gen II Vehicles to External Customer (Vance van Petten)

The first Gen II FCVs were delivered to external customers in December of 2010 (see Figure 3). Customers have fuelled and driven B-Class F-CELL vehicles in a variety of regions providing a complete range of climate and traffic conditions from congested city driving to open road highways to rural roads. All Gen II vehicles have been equipped with data acquisition and reporting capability, allowing the Mercedes Team to generate substantial vehicle raw data for submission to NREL.

World Drive

Setting out from Stuttgart in Germany, three B-Class F-CELLs have undertaken a 125-day circumnavigation of the world (see Figure 4). Traveling across four continents and through 14 countries, the three vehicles have confirmed technical maturity of fuel cell technology, as well as the suitability for everyday use of the vehicles. On February 25th, the F-CELL World Drive embarked on the second leg of its tour when three B-Class F-CELL set out from Fort Lauderdale on the East Coast of the United States across eight cities including New Orleans, Miami, San Antonio, Phoenix, Los Angeles, Sacramento, Salem and Seattle. Vehicle raw data generated from the 19,000-mile World Drive has been collected and will be submitted to NREL for analysis.

Codes and Standards

Much progress was made with respect to codes and standards. First of all, a decision was reached with respects to the 70 MPa fueling connector geometry. This subject was reason for intense discussions in working group titled International Organization for Standardization (ISO) 17268, “Gaseous Hydrogen Land Vehicle Refuelling Connection Devices”, which decided to keep the nozzle and receptacle design primarily used in Europe and United States. The same design was selected for Society of Automotive Engineers (SAE) J2600, “Compressed Hydrogen Surface



FIGURE 4. World Drive Tour in San Francisco, California

Vehicle Fueling Connection Devices”. Consequently, the ISO and SAE teams were able to finalize and harmonize these documents.

J2719, “Information Report on the Development of Hydrogen Quality Guideline for Fuel Cell Vehicles” was recently finalized and is currently up for ballot. After the first version of J2601, “Fueling Protocols for Gaseous Hydrogen Surface Vehicles”, was published in 2010 and became the foundation for many hydrogen refueling protocol discussions, the SAE interface group began working on Version 2 of J2601, which has been expanded to include bus, home and fork lift refueling.

NextEnergy

Serving as voting member and Committee Chair of National Fire Protection Association (NFPA) 2, NextEnergy continued to work on the standard intended to streamline as well as clarify the infrastructure design

and permitting process. During the course of the year, the Team released the first public version of NFPA 2 and is in the process of expanding the document for a 2014 revision cycle. Furthermore, NextEnergy hosted an annual Hydrogen Codes and Standards Conference, which attracted first responders, local officials, hydrogen industry experts, and national code development organizations that provided updates on the latest developments of national and international hydrogen codes and standards. NextEnergy continued to host DOE's Permitting Guide for Hydrogen Technologies and Specifications on its website at www.nextenergy.org.

Outreach and Media

Mercedes-Benz FCVs were on display at several car shows over the course of 2010. The year began with a presence at the Detroit Auto Show where the B-Class F-CELL was part of a green vehicle ride-n-drive. At the Washington Auto Show in Washington, D.C. in February, the F-CELL was incorporated into the MBUSA exhibit. The vehicle was then displayed at the show in New York after being introduced on a nationally broadcast morning talk show. Over the summer of 2010, the F-CELL was also displayed at the Aspen Ideas Festival in Colorado and the U.S. Tennis Open in New York, both of which MBUSA officially sponsors.

At the Detroit Auto Show in January of 2011, one FCV was wrapped with F-CELL World Drive decals and displayed during the press conference when the world tour was announced. The Fuel Cell and Hydrogen Energy Association Conference and Exposition took place in Washington, D.C. in February. Mercedes-Benz was present with a vehicle display which emphasized the lease program in California and the World Drive which had just commenced in Europe.

Fueling Stations and Co-Production Facilities

DTE Hydrogen Technology Park

Since the electrolyzer and dispenser were replaced, the site equipment has run its best for cold weather operations. The electrolyzer ran without any problems and system testing was conducted for all safety circuits. DTE Energy has had a number of tours of the DTE Energy Hydrogen Technology Park both from industry, educational institutions and the general public. Under the auspices of the Department of International Visitor Leadership Program, visitors from Romania, Kosovo and Estonia toured the Technology Park to understand how non-governmental sectors foster innovative and efficient public-private relationship as well as promote community development and corporate citizenship (see Figure 5).



FIGURE 5. Tour of the DTE Energy Hydrogen Technology Park

Preparing for Fueling Infrastructure

As FCVs transition from a demonstration phase to commercialization, the development of well-established hydrogen fueling station network is critical and, as a result, the Mercedes Team has been actively collaborating with other OEMs, government officials and energy partners to build a hydrogen fueling infrastructure:

- Supported ARB/CEC by recommending station specifications, site locations and supplier qualification guidelines.
- Worked with the California Fuel Cell Partnership to develop an action plan detailing strategy for deploying hydrogen fueling stations and FCVs.
- Collaborated with other OEMs to determine and coordinate locations of future fueling stations.

The number of stations is increasing. However, the number of present operational and public stations is the limiting factor for customer selection. The Mercedes Team strongly supports a joint approach of automotive OEMs, energy companies and government agencies such as DOE to overcome the fueling limitation by 2015, the year anticipated for the beginning of commercialization.

Conclusions and Future Directions

Conclusions

- Maintained smooth operations of the DTE station.
- Worked with CEC/ARB and other OEMs to prepare fueling infrastructure.
- Finalized Gen I operations and deployed Gen II F-CELLs to external customers.
- Transitioned FCV activities from R&D to mainstream commercial efforts.

- Participated in various working groups to ensure continuous progress with regards to codes and standards.
- Continued data collection, analysis and reporting.

Future Work

- Maintain and finalize smooth operation of Gen II FCVs.
- Submit final report.
- Continue the development and transition to commercialization of hydrogen FCVs.

FY 2011 Presentations

1. Becker, S. "Technology Demonstration with F-CELL Vehicles," Zero Emission Conference 2010, November 2010.

2. Becker, S. "Emission-Free Mobility with Fuel Cell Vehicles," HyNor Conference 2010, November 2010.

3. Froeschle, P. "Lessons Learned in German FC/Hydrogen Initiative," New York State Fuel Cell and Hydrogen Infrastructure Planning Summit NYSERDA, December 2010.

4. Froeschle, P. "Current FCV Program Plans for Commercialization," New York State Fuel Cell and Hydrogen Infrastructure Planning Summit NYSERDA, December 2010.

5. Froeschle, P. "H2 Mobility – An Initiative to Build a Hydrogen Infrastructure," Fuel Cell & Hydrogen Energy Conference and Expo, February 2011.

6. Froeschle, P., Wolfsteiner, M. "Daimler's Global Fuel Cell Vehicle Demonstration Program with the Mercedes-Benz B-Class F-CELL," Fuel Cell & Hydrogen Energy Conference and Expo, February 2011.

7. Grasman, R. "Emission-Free Mobility with Fuel Cell and Battery Electric Vehicles," North European Renewable Energy Convention, September 2010.

8. Grasman, R. "Our Roadmap to Emission-Free Mobility," North European Renewable Energy Convention, September 2010.

9. Grasman, R. "Daimler Fuel Cell & Electric Drive Strategy," H2Expo, June 2011.

10. Kaehler, B. "H2-Mobility – An Initiative to Build a Hydrogen Infrastructure," 8th Symposium Hybrid- And Electric-Vehicles, February 2011.

11. Mohrdieck, C. "Mobility with Hydrogen and Fuel Cells – One Step Closer to Commercialization" Fuel Cell & Hydrogen Energy Conference and Expo, February 2011.

12. Mohrdieck, C., Hinsenkamp, G. "Requirements for Components of an Advanced Fuel Cell Power train System for Mobile Applications," Fuel Cell & Hydrogen Energy Conference and Expo, February 2011.

13. Wind, J. "The Electrification of the Automobile – Fuel Cell Electric Vehicles and Battery Electric Vehicles", F-Cell Symposium, September 2010.

14. Wolfsteiner, M. "On the Road to Sustainable and Emission-Free Mobility," First Bavarian Electro mobility Days, November 2010.

VII.4 Validation of an Integrated Hydrogen Energy Station

Edward C. Heydorn
Air Products and Chemicals, Inc. (APCI)
7201 Hamilton Blvd.
Allentown, PA 18195
Phone: (610) 481-7099
E-mail: heydorec@airproducts.com

DOE Managers
HQ: John Garbak
Phone: (202) 586-1723
E-mail: John.Garbak@ee.doe.gov
GO: Jim Alkire
Phone: (720) 356-1426
E-mail: James.Alkire@go.doe.gov

Contract Number: DE-FC36-01GO11087

Subcontractor:
FuelCell Energy, Danbury, CT

Project Start Date: September 30, 2001
Project End Date: March 31, 2011

Fiscal Year (FY) 2011 Objectives

Demonstrate the technical and economic viability of a hydrogen energy station using a high-temperature fuel cell designed to produce power and hydrogen.

- Complete a technical assessment and economic analysis on the use of high-temperature fuel cells, including solid oxide and molten carbonate, for the co-production of power and hydrogen (energy park concept).
- Build on the experience gained at the Las Vegas H2 Energy Station and compare/contrast the two approaches for co-production.
- Determine the applicability of co-production from a high-temperature fuel cell for the existing merchant hydrogen market and for the emerging hydrogen economy.
- Demonstrate the concept at a suitable site with demand for both hydrogen and electricity.
- Maintain safety as the top priority in the system design and operation.
- Obtain adequate operational data to provide the basis for future commercial activities, including hydrogen fueling stations.

Technical Barriers

This project addresses the following technical barriers from the Technology Validation section (3.5.4) of the Fuel Cell Technologies Program Multi-Year Research, Development and Demonstration Plan:

(C) Hydrogen Refueling Infrastructure
(I) Hydrogen and Electricity Co-production

Contribution to Achievement of DOE Technology Validation Milestones

This project will contribute to achievement of the following DOE Technology Validation milestones from the Technology Validation section of the Fuel Cell Technologies Program Multi-Year Research, Development and Demonstration Plan:

- **Milestone 37**: Demonstrate prototype energy station for 6 months; projected durability >20,000 hours; electrical energy efficiency >40%; availability >0.80. (4Q, 2008)
- **Milestone 38**: Validate prototype energy station for 12 months; projected durability >40,000 hours; electrical energy efficiency >40%; availability >0.85. (1Q, 2014)

FY 2011 Accomplishments

- In July 2010, the Hydrogen Energy Station was shipped from FuelCell Energy's facility in Danbury, CT, to Orange County Sanitation District (OCSD) in Fountain Valley, CA. System installation and tie-ins were completed in August, and first low-load power production from the high-temperature fuel cell unit took place on 13 September 2010. On 20 September 2010, the fuel cell operated for the first time at full load (300 kW) on natural gas feedstock.
- The first coproduction of hydrogen from the Hydrogen Energy Station took place on 20 October 2010.
- Over 1,000 hours of operation in power and (power + hydrogen) modes was completed during the performance period. Hydrogen quality met all performance standards.
- Achieved nominal 54% (power + hydrogen) efficiency of the unit when operating in hydrogen co-production mode.
- On 25 February 2011, the first hydrogen from the Hydrogen Energy Station was sent to the hydrogen fueling station. Initial test fills of fuel cell vehicles at the hydrogen fueling station were completed on 08–10 March 2011.
- The DOE Cooperative Agreement was extended to 30 September 2011.



Introduction

One of the immediate challenges in the development of hydrogen as a transportation fuel is finding the optimal means to roll out a hydrogen-fueling infrastructure

concurrent with the deployment of hydrogen vehicles. The low-volume hydrogen requirements in the early years of fuel cell vehicle deployment make the economic viability of stand-alone, distributed hydrogen generators challenging. A potential solution to this "stranded asset" problem is the use of hydrogen energy stations that produce electricity in addition to hydrogen. To validate this hypothesis, a four-phase project is being undertaken to design, fabricate and demonstrate a high-temperature fuel cell co-production concept. The basis of the demonstration will be a FuelCell Energy DFC®-300 Molten Carbonate Fuel Cell modified to allow for the recovery and purification of hydrogen from the fuel cell anode exhaust using an Air Products-designed hydrogen purification system.

The DFC® technology is based on internal reforming of hydrocarbon fuels inside the fuel cell, integrating the synergistic benefits of the endothermic reforming reaction with the exothermic fuel cell reaction. The internal reforming of methane is driven by the heat generated in the fuel cell and simultaneously provides efficient cooling of the stack, which is needed for continuous operation. The steam produced in the anode reaction helps to drive the reforming reaction forward. The hydrogen produced in the reforming reaction is used directly in the anode reaction, which further enhances the reforming reaction. Overall, the synergistic reformer-fuel cell integration leads to high (~50%) electrical efficiency.

The baseline DFC® power plant (electricity only) is designed to operate at 75% fuel utilization in the stack. The remaining 25% of fuel from the anode presents a unique opportunity for low-cost hydrogen, if it can be efficiently recovered from the dilute anode effluent gases. The recovery and purification of hydrogen from the anode presents several challenges:

- The anode off-gas is a low-pressure, high-temperature gas stream that contains ~10% hydrogen by volume.
- The anode exhaust stream must be heat integrated with the fuel cell to ensure high overall system efficiency.
- The parasitic power used for purification must be optimized with the hydrogen recovery and capital cost to enable an economically viable solution.

Approach

A hydrogen energy station that uses a high-temperature fuel cell to co-produce electricity and hydrogen will be evaluated and demonstrated in a four-phase project. In Phase 1, Air Products completed a feasibility study on the technical and economic potential of high-temperature fuel cells for distributed hydrogen and power generation. As part of the Phase 1 analysis, three different high-temperature fuel cells were evaluated to determine the technology most suitable for a near-term demonstration. FuelCell Energy's DFC®-300 technology was selected for concept development. In Phase 2, a process design and cost estimate were completed for the hydrogen energy station that integrates the high-temperature fuel cell with a pressure swing adsorber (PSA) system selected and designed by Air Products. Economics were developed based on actual equipment, fabrication, and installation quotes as well as new operating cost estimates. High-level risks were identified and addressed by critical component testing. In Phase 3, a detailed design for the co-production system was initiated. The system was fabricated and shop tested. Prior to shipping to the field, the entire system was installed at FuelCell Energy's facility in Danbury, CT for complete system check-out and validation. In Phase 4, the system will be operated on municipal waste water derived biogas at OCSD, Fountain Valley, California, under a 3-year program with the California Air Resources Board, with co-funding by the South Coast Air Resources Board. DOE will receive six months of data from the initial operating phase to validate the system versus DOE and economic performance targets.

Results

Figure 1 shows the process flow diagram for the Hydrogen Energy Station. Methane (in this case, from natural gas) is internally reformed at the fuel cell anode to hydrogen and carbon dioxide. The fuel cell operates near 600°C and uses molten carbonate electrolyte as the charge carrier. Heated air is combined with the waste gas from the hydrogen purification system and oxidized. These resultant waste gases are fed to the cathode. The fuel cell cathode converts waste gas carbon dioxide to the carbonate charge carrier to complete the fuel cell circuit. The fuel cell stack generates a direct current voltage, which is then converted to alternating current (AC) by an inverter in the electrical balance of plant. The system produces 480 VAC, 60 Hz, and a nominal 300 kW without hydrogen co-production. Excess carbon dioxide and water leave the cathode as exhaust, and heat can be recovered from these exhaust gases.

About 70 to 80% of the hydrogen is converted to power, and some hydrogen remains available for recovery. The anode exhaust gas is cooled and sent to a water-gas shift catalytic reactor to convert most of the carbon monoxide present in the stream to hydrogen and carbon dioxide. After an additional cooling step, this gas stream is then compressed and sent to the PSA system. The PSA uses adsorbents to remove carbon monoxide, carbon dioxide, and water to produce a high-purity hydrogen stream. The waste gas from the PSA is catalytically oxidized and returned to the cathode. The PSA system can also be placed in stand-by mode to stop hydrogen production and allow for maximum power production by the DFC® system, thereby improving the system efficiency and economics.

In late 2008, the Hydrogen Energy Station was installed at FuelCell Energy's facilities in Danbury, CT for a system check-out and validation of performance on natural gas and simulated digester gas. This testing had several key objectives, including the demonstration of variable production of both electricity and hydrogen, optimization of the process control system and overall controls philosophy, and testing and development (if needed) of systems that respond to

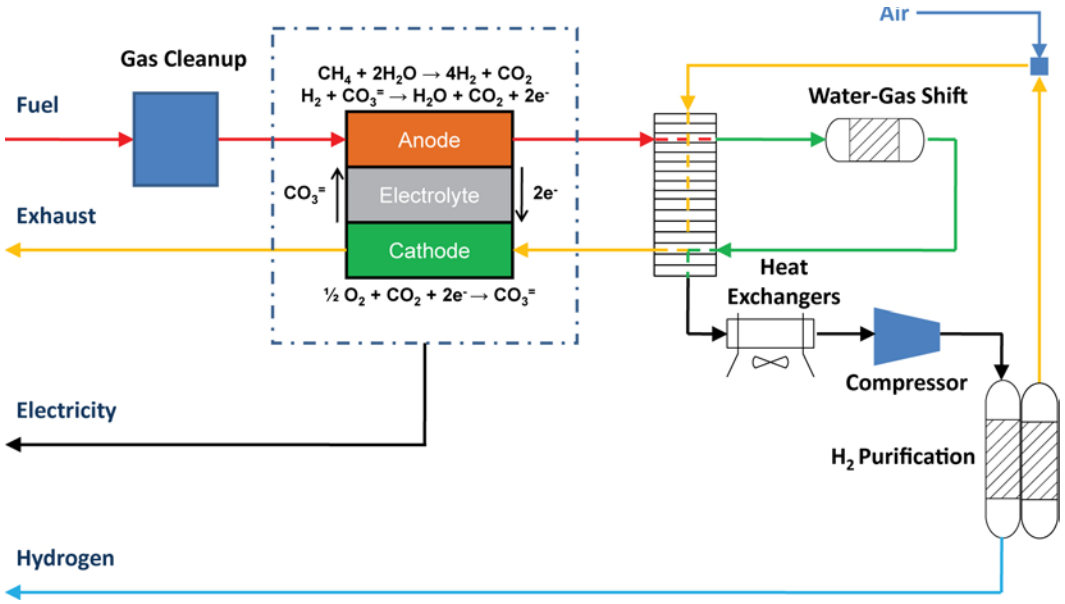


FIGURE 1. Hydrogen Energy Station Process Flow Diagram

upset conditions. The operation and control of the system, including automated integration and de-integration of the PSA from the balance of plant, was excellent.

In June 2010, the Hydrogen Energy Station was disassembled and prepared for shipment from Danbury, CT to the Orange County Sanitation District wastewater treatment plant in Fountain Valley, CA. The system was delivered in early July, and installation and tie-in work was completed in August 2010. A photograph of the installation at OCSD is provided in Figure 2. Following commissioning activities, the DFC®-300 was brought online on 13 September 2010, and full-load operation on natural gas was achieved on 20 September 2010.

The hydrogen purification system was then commissioned, and initial co-production of hydrogen from the Hydrogen Energy Station on natural gas at OCSD

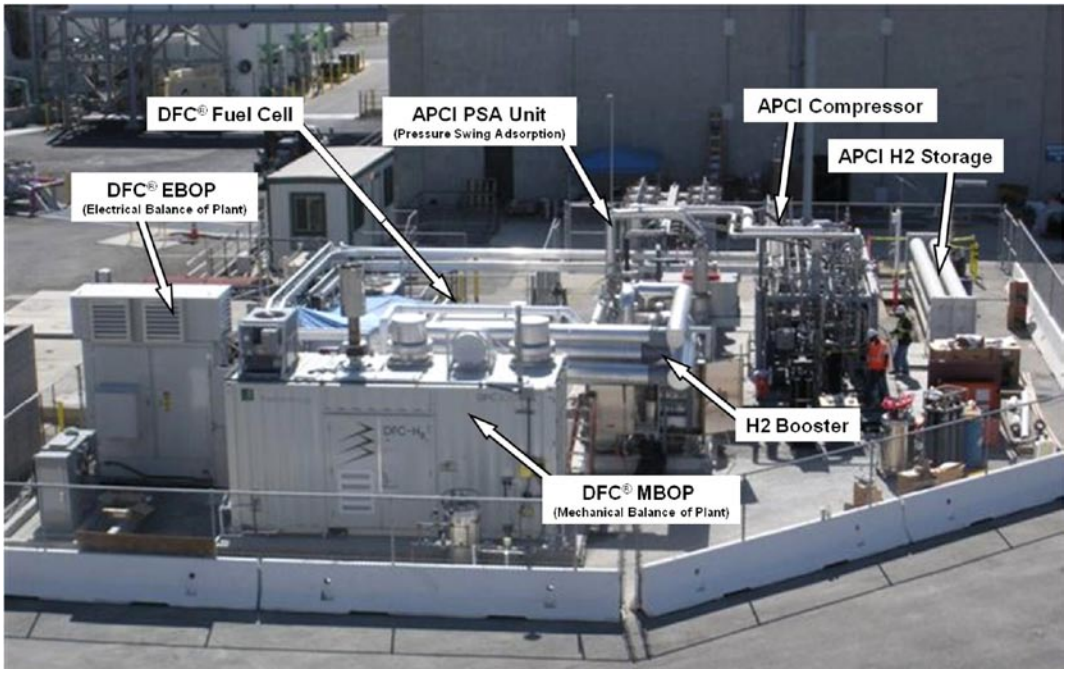


FIGURE 2. Hydrogen Energy Station Installation at Orange County Sanitation District

occurred on 20 October 2010. A heat and material balance was performed during this initial operating period, and a (power + hydrogen) efficiency of 54.5% was calculated. A summary of the heat and mass balance is provided in Figure 3.

Following this initial operating performance, power quality issues associated with the local grid within the wastewater treatment plant were identified. The power conditioning unit/inverter associated with the fuel cell showed unusual behavior in its ability to connect with the local grid, and changes were required to match the highly inductive power factor (0.6 to 0.8) and larger voltage sags (5-10%). On 14 December 2010, a module within the inverter was damaged by an electrical fault. Repairs and determination of the root cause were completed by FuelCell Energy and their supplier of the inverter, and the fuel cell was restarted in February 2011. Hydrogen co-production was then brought online, and the first hydrogen from the Hydrogen Energy Station was sent to the hydrogen fueling station; the fueling station (sized at 100 kilograms per day) and a gas cleanup skid to remove contaminant species such as sulfur from the anaerobic digester gas supply are being installed under a second DOE project (Cooperative Agreement No. DE-FC36-05GO85026). Initial test fills of fuel cell vehicles at the hydrogen fueling station were successfully completed on 8-10 March 2011.

Conclusions and Future Direction

- The Hydrogen Energy Station was shipped to OCSD and brought online. Initial performance in power and (power + hydrogen) modes was excellent. Issues with site power quality led to an electrical fault within the inverter of the fuel cell; repairs were completed, and operation resumed in February 2011.
- Operation on anaerobic digester gas from the wastewater treatment facility is expected to begin in May 2011 following installation of the gas cleanup skid that will remove trace contaminant species from the biogas. Data will be provided to DOE for the first six months of operation under a 3-year program sponsored by the California Air Resources Board and South Coast Air Quality Management District.

FY 2011 Publications/Presentations

1. Presentation at the DOE Annual Merit Review Meeting, Washington, D.C., May 2011.

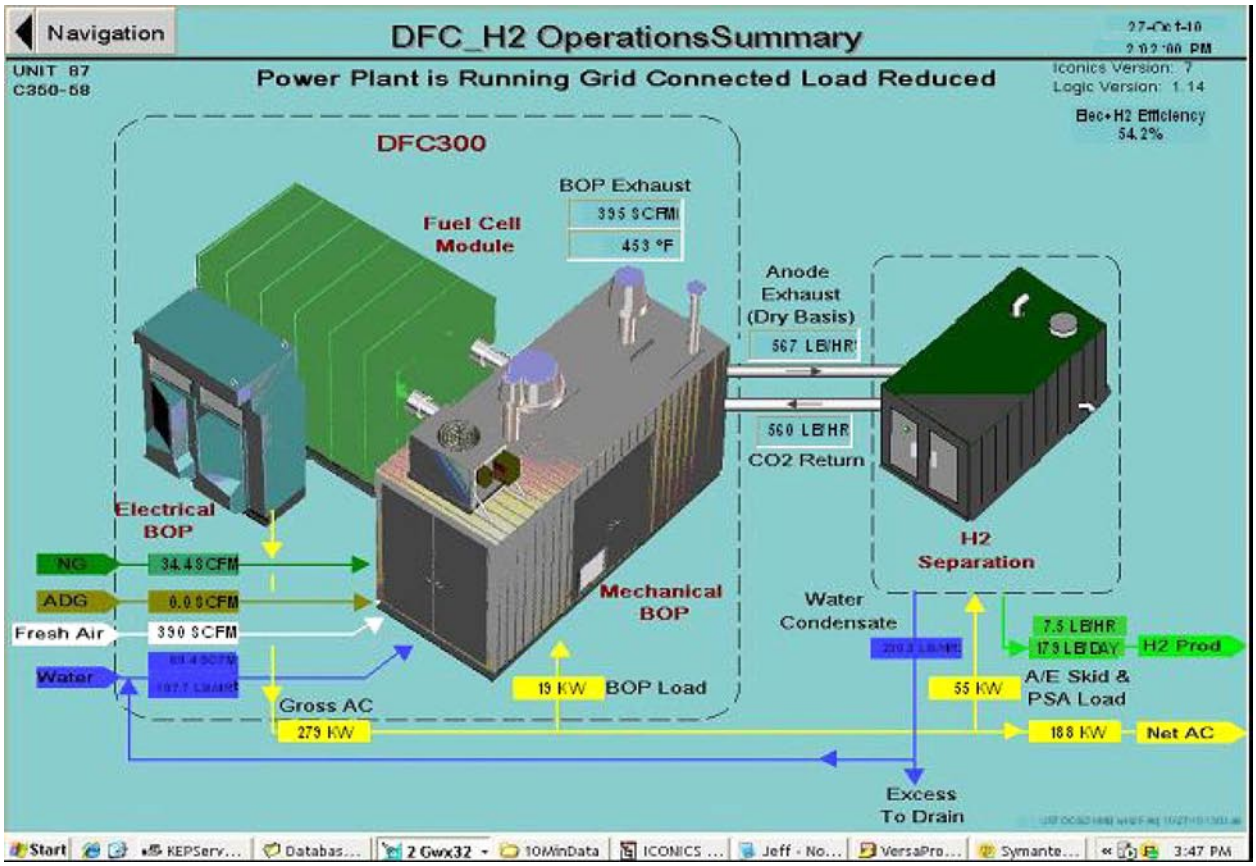


FIGURE 3. Hydrogen Energy Station Performance (October 2010)

VII.5 Technology Validation: Fuel Cell Bus Evaluations

Leslie Eudy
National Renewable Energy Laboratory (NREL)
1617 Cole Blvd.
Golden, CO 80401
Phone: (303) 275-4412
E-mail: leslie.eudy@nrel.gov

DOE Manager
HQ: John Garbak
Phone: (202) 586-1723
E-mail: John.Garbak@ee.doe.gov

Subcontractor:
Kevin Chandler, Battelle, Columbus, OH

Start Date: March 2001
Projected End Date: Projected continuation and direction determined annually by DOE

Fiscal Year (FY) 2011 Objectives

- Determine the status of fuel cell bus (FCB) technologies in transit applications by evaluating them in real-world service.
- Coordinate with the Department of Transportation's Federal Transit Administration (FTA) on the data collection for the National Fuel Cell Bus Program and with international work groups to harmonize data-collection methods and enable the comparison of a wider set of vehicles.

Technical Barriers

This project addresses the following technical barriers from the Technology Validation section of the Fuel Cell Technologies Program Multi-Year Research, Development, and Demonstration Plan:

(A) Lack of Fuel Cell Vehicle Performance and Durability Data

(C) Lack of H_2 Fueling Infrastructure Performance snd Availability Data

(D) Maintenance and Training Facilities

Technical Targets

Milestone 18: Validate fuel cell durability of 3,500 hours, 300+ mile range and fuel cell stack power density of 1.5 kW/L. (4Qtr 2012) By the end of April 2011, NREL had documented three FCB fuel cell systems with operation in excess of 6,000 hours with no major repairs. One of these systems has logged more than 9,000 hours in service. Based on in-service fuel economies between 5 and 7 miles per kilogram, hybrid FCBs can achieve a range between 250 and 350 miles per fill. This efficiency depends on duty-cycle. There are no major issues with lost cargo/passenger space on FCBs because the tanks are typically mounted on the roof; however, the added weight of the system limits the number of standing passengers allowed on the buses.

FY 2011 Accomplishments

- Published final reports on current-generation performance and operational data on five full-size hybrid FCBs in revenue service in the United States.
- Published first report on next-generation FCB in service in Palm Springs, CA.
- Began data collection on next-generation fuel cell system in revenue service at two additional transit agencies.



Introduction

Transit agencies continue to aid the FCB industry in developing and optimizing advanced transportation technologies. These in-service demonstration programs are necessary to validate the performance of the current generation of fuel cell systems and to determine issues that require resolution. Using fuel cells in a transit application can help accelerate the learning curve for the technology because of the high mileage accumulation in short periods of time. During the last year, major progress was made in improving fuel cell durability; however, more work is needed to improve reliability, increase durability to meet the needs of transit agencies, lower capital and operating costs, and transition the maintenance to transit staff.

Approach

NREL uses a standard evaluation protocol to provide:

- Comprehensive, unbiased evaluation results of advanced technology vehicle development and operations.
- Evaluations of hydrogen infrastructure development and operation.
- Descriptions of facility modifications required for the safe operation of FCBs.
- Detailed results on fuel cell systems for buses and the requisite hydrogen infrastructure to complement the light-duty demonstrations and further DOE goals.

The evaluation protocol includes two levels of data: operation and maintenance data on the bus and

infrastructure, and more detailed data on the fuel cell, system, and components. The first set of data is considered non-sensitive and is obtained mainly from the transit fleet. The analysis, which consists of economic, technical, and safety factors, focuses on performance and use, including progress over time and experience with vehicle systems and supporting infrastructure.

The detailed data are collected with cooperation from the bus/fuel cell system manufacturers and are considered highly sensitive. Results include aggregate data products that protect each manufacturer's specific data. To date, NREL has collected this type of data from two fuel cell manufacturers. Aggregate results will be published if and when enough data are available to protect each company's identity and source data.

Results

During FY 2011, NREL completed data collection and analysis on current-generation FCB demonstrations at three transit agencies in the United States: SunLine Transit Agency in Thousand Palms, California; Connecticut Transit (CTTRANSIT) in Hartford, Connecticut; and AC Transit in Oakland, California. The first two of these evaluations were funded by DOE, and the third evaluation was covered by funding from FTA. Under DOE funding, NREL also began collecting data on next-generation FCBs at three agencies: City of Burbank, California; AC Transit; and SunLine. NREL published results from the current-generation FCBs. A summary of selected results is included in this report, followed by an overview and early results of the next-generation FCBs being evaluated.

The current-generation FCBs in service at AC Transit, CTTRANSIT, and SunLine were all of the same basic design: Van Hool 40-ft buses with ISE Corp. hybrid-electric drives and UTC Power fuel cell power systems. As reported in the previous annual report, the manufacturer partners used the early performance data to validate the systems and further develop the product and components. Beginning in November 2007, UTC Power replaced the fuel cell power systems in each of the five buses with newer versions that were developed incorporating many of the lessons learned from the previous operation of these FCBs. NREL collected operational and performance data on these FCBs and conventional baseline buses at each agency. Table 1 provides a summary of results from the operation at each agency after the new fuel cells were installed. Data from the baseline buses are included in the table. Note that the data from the buses at AC Transit ended in September 2010. These three buses were retired during that year; however, two of the fuel cell power systems were transferred into the bodies of the next generation buses and continue to accumulate hours.

Figure 1 shows the fuel economy of the buses at each location in miles per diesel gallon equivalent. (Note that the baseline buses at SunLine are compressed natural gas [CNG] buses – SunLine does not operate diesel buses.) The FCBs at the three locations showed fuel economy improvement ranging from 48% to 133% when compared to diesel and CNG baseline buses. This figure also illustrates the variability of the results from fleet to fleet. The results are affected by several factors, including duty-cycle characteristics (average number of stops, average speed, and idle time). Also, the diesel buses at AC Transit do not have air conditioning, but the fuel cell buses do. The CTTRANSIT diesel buses operate at twice the average speed of the FCB operating on the Star Shuttle Route, which causes significantly lower fuel economy for the FCB compared to the fuel economies at the other two agencies.

One measure of reliability for the transit industry is miles between roadcall (MBRC). A roadcall is the failure of an in-service bus that causes the bus to be replaced on route

TABLE 1. Summary Data Results for Early Generation FCBs

	AC Transit		CTTRANSIT		SunLine	
Vehicle data	FCB	Diesel	FCB	Diesel	FCB	CNG
Number of buses	3	6	1	3	1	5
Data period	Nov 07 - Sep 10	Jan - Dec 07	Jan 08 - Jan 11	Aug 07 - Oct 09	Apr 08 - Jan 11	Nov 08 - Jan 11
Number of months	~34	12	37	27	34	15
Total fleet miles	194,288	266,337	46,558	259,547	67,553	636,954
Average miles per month	2,136	3,699	1,258	3,204	1,987	4,718
Total FC hours	19,802	--	7,187	--	9,448	--
Fuel economy (mi/kg)	5.93	--	4.83	--	7.15	3.11
Fuel economy (mi/diesel eq. gal)	6.70	4.20	5.46	3.68	8.08	3.47
Average speed (mph)	9.8	not available	6.5	not available	13.0	not available
Availability	66%	85%	62%	85%	70%	92%

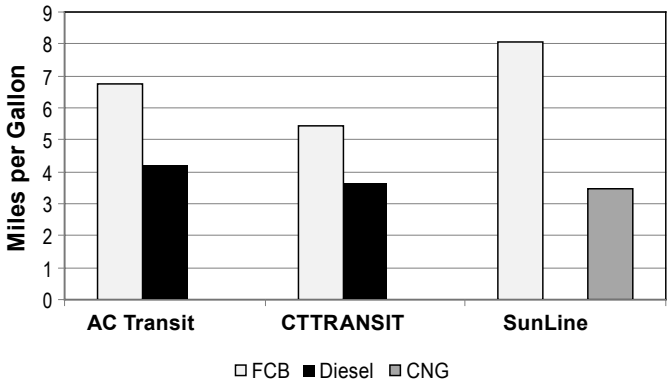


FIGURE 1. Fuel Economy Comparison by Fleet (Diesel Equivalent)

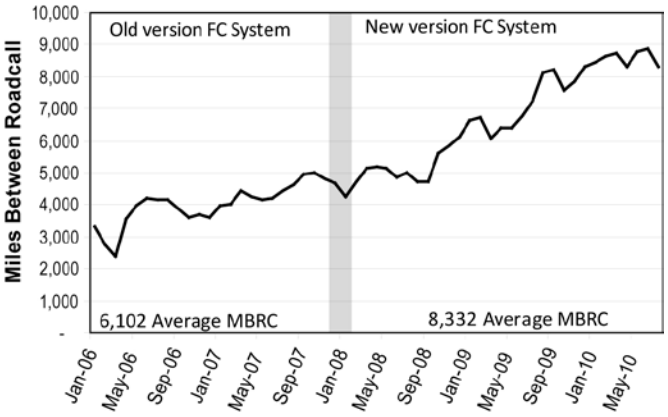


FIGURE 2. Miles between Roadcall for the Fuel Cell Propulsion System (12-Month Rolling Average)

or causes a significant delay in schedule. NREL typically reports MBRC for the entire bus and for the propulsion system separately to show the reliability of the FCBs. Over time, these FCBs have been shown to have propulsion system MBRCs that are much lower than MBRCs for the baseline buses. This is not necessarily due to the fuel cell power system, but instead has mostly been because of traction battery issues. To illustrate the improvement in reliability of the fuel cell power system in the buses, Figure 2 tracks the combined fuel cell system MBRC since the buses went into service. The shading in the middle of the chart marks the time during which all five FCBs had the newer version fuel cell systems installed. In the 2010 annual report, NREL reported this upward trend for the average fuel cell system MBRC. The trend has continued to show improvement; increasing from 21% to 37% with the newer version system. The two leading fuel cell systems have accumulated significant hours without any major repairs (one is over 9,000 hours and a second is over 8,000 hours).

NREL began collecting data on several next-generation FCBs during the year. Figure 3 shows the newest fuel cell bus in service at SunLine. This bus is a New Flyer 40-ft. bus with a Bluways hybrid system, Ballard fuel cells, and lithium ion batteries. NREL completed its first report on this bus in service at SunLine. As of November 2010, the bus had accumulated more than 9,000 miles and 818 hours on the fuel cell with an average fuel economy of 5.75 miles per kg. This is nearly two times higher than the fuel economy for the baseline CNG buses.

NREL began collecting data on other next generation fuel cell buses at the following transit agencies:

- City of Burbank – one battery dominant, plug-in hybrid FCB developed by Proterra using Hydrogenics fuel cells and lithium titanate batteries.
- AC Transit – 12 next-generation Van Hool FCBs with a hybrid system integrated by Van Hool and UTC Power fuel cell power system.
- Additional sites funded by the FTA include four buses at CTTRANSIT and a bus in service in Columbia, SC.



FIGURE 3. SunLine's Newest Fuel Cell Bus

Conclusions and Future Direction

First-generation fuel cell propulsion systems in buses have continued to show progress in fuel economy and longer durability. Changes incorporated into the design based on early lessons learned have resulted in fuel cells that are nearing a target of 10,000 hours. While this is encouraging, there are still challenges to overcome before fuel cell buses can match the current standard of diesel bus performance. These include:

- Lowering costs of purchasing, operating, and maintaining buses and infrastructure.
- Increasing durability/reliability of the fuel cell systems and other components to match transit needs.
- Transferring all maintenance to transit personnel.

Future work by NREL includes:

- Collecting, analyzing, and reporting on performance data for next-generation hydrogen-fueled vehicles in service at the following sites:

  - Bay Area FCB Demonstration led by AC Transit
  - SunLine
  - City of Burbank
  - Additional sites as funding allows
- Investigating reliability, durability, and life cycle of FCBs as a part of ongoing evaluations; these efforts complement the DOE light-duty fuel cell electric vehicle demonstrations.
- Coordinating with FTA to ensure harmonized data-collection efforts for the National Fuel Cell Bus Program.
- Coordinating with national and international FCB demonstration sites.

FY 2011 Publications/Presentations

1. L. Eudy. (2010). *Fuel Cell Bus Takes a Starring Role in BurbankBus Fleet.* Fact Sheet: NREL/TP-560-47893. National Renewable Energy Laboratory, Golden, CO, May.

2. K. Chandler, L. Eudy. (2010). *National Fuel Cell Bus Program: Accelerated Testing Evaluation Report # 2 and Appendices.* NREL/TP-560-48106-1 & 48106-2. Federal Transit Administration, Washington, DC, June.

3. L. Eudy, (2010). *Technology Validation: Fuel Cell Bus Evaluations.* Poster Presentation at the DOE Hydrogen Program Annual Merit Review, Arlington, VA, June.

4. L. Eudy. (2010). *Bay Area Transit Agencies Propel Fuel Cell Buses Toward Commercialization.* Fact Sheet: NREL/TP-560-48115. National Renewable Energy Laboratory, Golden, CO, July.

5. L. Eudy, K. Chandler. (2010). *Fuel Cell Bus Evaluation: Joint Evaluation Plan for the Dept. of Energy and Federal Transit Admin. and Appendices*. NREL/TP-560-49342-1 & 49342-2. National Renewable Energy Laboratory, Golden, CO, November.

6. L. Eudy, K. Chandler, C. Gikakis. (2010). *Fuel Cell Buses in U.S. Transit Fleets: Current Status 2010*. NREL/TP-560-49379. National Renewable Energy Laboratory, Golden, CO, November.

7. L. Eudy. (2011). *SunLine Leads the Way in Demonstrating Hydrogen-Fueled Bus Technologies.* Brochure: NREL/TP-5600-49673. National Renewable Energy Laboratory, Golden, CO, January.

8. L. Eudy. (2011). *Fuel Cell Electric Buses Demonstrate Early Market Progress*. Presentation at the Fuel Cell & Hydrogen Energy Conference, Washington, DC, February.

9. L. Eudy, K. Chandler. (2011). *SunLine Transit Agency Advanced Technology Fuel Cell Bus Evaluation: First Results Report.* NREL/TP-5600-50500. National Renewable Energy Laboratory, Golden, CO, March.

VII.6 California Hydrogen Infrastructure Project

Edward C. Heydorn
Air Products and Chemicals, Inc.
7201 Hamilton Boulevard
Allentown, PA 18195
Phone: (610) 481-7099
E-mail: heydorec@airproducts.com

DOE Managers
HQ: John Garbak
Phone: (202) 586-1723
E-mail: John.Garbak@ee.doe.gov
GO: Jim Alkire
Phone: (720) 356-1426
E-mail: James.Alkire@go.doe.gov

Contract Number: DE-FC36-05GO85026

Working Partners/Subcontractors:
- University of California, Irvine (UCI), Irvine, CA
- National Fuel Cell Research Center (NFCRC), Irvine, CA

Project Start Date: August 1, 2005
Project End Date: December 31, 2011

Fiscal Year (FY) 2011 Objectives

Demonstrate a cost-effective infrastructure model in California for possible nationwide implementation:

- Design, construct and operate seven hydrogen fueling stations.
- Collect and report infrastructure data.
- Document permitting requirements and experiences.
- Validate expected performance, cost, reliability, maintenance, and environmental impacts.

Implement a variety of new technologies with the objective of lowering costs of delivered H_2:

- New Delivery Concept (NDC).
- High pressure/high purity clean up equipment.

Technical Barriers

This project addresses the following technical barriers from the Technology Validation section (3.6.4) of the Fuel Cell Technologies Program Multi-Year Research, Development and Demonstration Plan:

(C) Hydrogen Refueling Infrastructure

Contribution to Achievement of DOE Technology Validation Milestones

This project will contribute to achievement of the following DOE Technology Validation milestones from the Technology Validation section of the Fuel Cell Technologies Program Multi-Year Research, Development and Demonstration Plan:

- **Milestone 23**: Total of 10 stations constructed with advanced sensor systems and operating procedures. (1Q, 2008).

FY 2011 Accomplishments

- Completed construction of, and vehicle test fills, at the hydrogen pipeline fueling station (350 and 700 bar dispensing) in Torrance, CA.
- Completed 9-month deployment of 350 bar mobile station (HF-150) in Placerville, CA.
- Completed construction of and began initial vehicle test fills at the hydrogen pipeline fueling station (350 and 700 bar dispensing) in Fountain Valley, CA.



Introduction

Air Products and Chemicals, Inc. is leading a comprehensive, multiyear project to demonstrate a hydrogen infrastructure in California. The specific primary objective of the project is to demonstrate a model of a "real-world" retail hydrogen infrastructure and acquire sufficient data within the project to assess the feasibility of achieving the nation's hydrogen infrastructure goals. The project will help to advance hydrogen station technology, including the vehicle-to-station fueling interface, through consumer experiences and feedback. By encompassing a variety of fuel cell vehicles, customer profiles and fueling experiences, this project is obtaining a complete portrait of *real market needs*. The project is also opening its stations to other qualified vehicle providers at the appropriate time to promote widespread use and gain even broader public understanding of a hydrogen infrastructure. The project is engaging major energy companies to provide a fueling experience similar to traditional gasoline station sites to foster public acceptance of hydrogen.

Approach

Work over the course of the project was focused in multiple areas. With respect to the equipment needed, technical design specifications were written, reviewed, and finalized. Both safety and operational considerations were

a part of this review. After finalizing individual equipment designs, complete station designs were started including process flow diagrams and systems safety reviews. Material quotes were obtained, and in some cases, depending on the project status and the lead time, equipment was placed on order and fabrication was started. Consideration was given for expected vehicle usage and station capacity, standard features needed, and the ability to upgrade the station at a later date.

In parallel with work on the equipment, discussions were started with various vehicle manufacturers to identify vehicle demand (short- and long-term needs). Discussions included identifying potential areas most suited for hydrogen fueling stations, with focus on safe, convenient, fast-fills. These potential areas were then compared and overlaid with suitable sites from various energy companies and other potential station operators. Work continues to match vehicle needs with suitable fueling station locations. Once a specific site has been identified, the necessary agreements can be completed with the station operator and expected station users. Detailed work can begin on the site drawings, permits, safety procedures and training needs. Once stations are brought online, infrastructure data will be collected and reported to DOE using Air Products' eRAM system. Feedback from station operators will be incorporated to improve the station user's fueling experience.

Results

The first of the hydrogen fueling stations within the California Hydrogen Infrastructure Project continued operation at the NFCRC at UCI. The capability for fueling vehicles with gaseous hydrogen at 350 bar, involving the installation of a 1,500 gallon horizontal liquid hydrogen tank, 2 kg/hr compressor skid, storage for 50 kg of hydrogen, and a dual dispenser for both 350 and 700 bar hydrogen was brought onstream in August of 2006. The 700 bar system, including the installation of a booster compressor, was commissioned in February of 2007. Based on a 50% compressor on-stream factor, the station has the capacity to dispense 24 kg/day or approximately six cars per day. The station continues to see high usage, with daily throughput often reaching 50 kg/day. A proposal by Air Products to expand the station to 100 kg/day capacity was selected for support by the California Energy Commission. A photograph of the dispensing system is provided in Figure 1.

The world's first fueling station supplied by a hydrogen pipeline completed construction in early 2011 to demonstrate a low-cost, reliable supply of hydrogen. A site in the Torrance, CA area in proximity to an existing Air Products hydrogen pipeline was developed by Shell Hydrogen. A 4 kg/hr compressor skid and a total of 100 kg of 7,777 psig storage and 20 kg of 15,000 psig storage have been provided. This station dispenses hydrogen according to SAE TIR-J2601. Hydrogen purification technology has been deployed for the first time in this application to demonstrate the production of an ultra-pure hydrogen stream from the



Photo by Lorin Humphries

FIGURE 1. UCI 350/700 Bar Hydrogen Fueling Station

industrial-grade pipeline supply. Two dual dispensers for both 350 and 700 bar hydrogen have been installed, and four vehicles can be filled simultaneously. Based on a 50% compressor on-stream factor, the station will have the capacity to dispense 48 kg/day or approximately 12 cars per day. When starting with full storage, six cars can be filled in succession. A photograph of the completed dispenser area is provided in Figure 2. Vehicle test fills were completed in March 2011, and a station opening ceremony was planned for May 2011.

The HF-150 (shown in Figure 3) is ideal for small fleet fueling and offers the advantages of being a highly reliable, cost-effective, and automated fueling system that can be easily installed. The HF-150 maintains about 150 kg of gaseous hydrogen at 6,600 psig. It can dispense approximately 80 to 90 kg before needing to be refilled. In December 2010, Air Products completed a 9-month deployment of an HF-150 mobile fueler at the District Office of the U.S. Forest Service in Placerville, CA.

Air Products was selected under California Air Resources Board Solicitation 06-618, "Establish Demonstration Hydrogen Refueling Stations," to install a renewable-based hydrogen fueling station and cleanup system for anaerobic digester gas at Orange County Sanitation District in Fountain Valley, CA. Under this project, hydrogen will be produced utilizing the Hydrogen Energy Station concept being developed under a second DOE project (Cooperative Agreement No. DE-FC36-01GO11087). The statement of work for this project was modified to include the procurement and installation of a



FIGURE 2. Torrance, CA Hydrogen Pipeline Fueling Station



FIGURE 3. Air Products HF-150 Hydrogen Fueler – Placerville, CA

hydrogen fueling station (sized at 100 kilograms per day) and of a gas cleanup skid to remove contaminant species such as sulfur from the anaerobic digester gas that will be fed to the Hydrogen Energy Station. The fueling station includes compression, storage, and dispensing of hydrogen at 350 and 700 bar according to SAE TIR-J2601. Construction of the fueling station was completed in November 2010, and hydrogen produced from natural gas by the Hydrogen Energy Station was sent to the storage tubes in the fueling



FIGURE 4. Fountain Valley Renewable Hydrogen Station

station on 25 February 2011. Initial test fills of vehicles were performed in March 2011. A photograph of the fueling station area, with the dispenser in the foreground and the balance of fueling station equipment in the background, is provided in Figure 4. Delivery of the clean-up system for the anaerobic digester gas is expected in May 2011, after which production of renewable hydrogen for use in the fueling station is expected to begin in June 2011.

Conclusions and Future Directions

Planned future work includes:

- UCI Fueling Station – continue operation of both 350 and 700 bar systems.
- Torrance Pipeline Fueling Station – continue operation of both 350 and 700 bar systems.
- Fountain Valley Renewable Station – begin operation of (1) clean-up system for anaerobic digester gas and (2) 350 and 700 bar systems.
- Infrastructure Data Acquisition, Analysis and Delivery – report data to DOE.

FY 2011 Publications/Presentations

1. A presentation regarding the overall project status was given at the DOE Annual Merit Review Meeting (May 2011).

VII.7 Hawaii Hydrogen Power Park

Richard (Rick) E. Rocheleau (Primary Contact), Mitch Ewan
Hawaii Natural Energy Institute (HNEI)
University of Hawaii at Manoa
1680 East-West Road, POST 109
Honolulu, HI 96822
Phone: (808) 956-8346
E-mail: rochelea@hawaii.edu

DOE Manager
HQ: John Garbak
Phone: (202) 586-1723
E-mail: John.Garbak@ee.doe.gov

Contract Number: DE-FC51-02R021399 A008

Project Start Date: June 29, 2009 (Final Agreement with State of Hawaii)
Project End Date: September 30, 2012

Fiscal Year (FY) 2011 Objectives

Island of Hawaii (Big Island)

- Install hydrogen dispensing infrastructure at Hawaii Volcanoes National Park (HAVO) on the Big Island of Hawaii (hydrogen provided under a separate program: "Hydrogen Energy Systems as a Grid Management Tool").
- Support the operations of the National Park Service (NPS) hydrogen plug-in hybrid electric vehicle (PHEV) shuttle buses through September 2012.
- Conduct engineering and economic analysis of HAVO bus operations on different routes, grades, elevations and climatic conditions.
- Validate fuel cell system performance in harsh environments including high SO_2 concentrations.
- Attract new partners and applications for the Big Island hydrogen infrastructure.
- Conduct outreach to local authorities and the general public regarding hydrogen infrastructure.

Oahu

- Support operations of the General Motors (GM) Equinox Fuel Cell Vehicle (FCV) Hawaii demonstration program in partnership with the Office of Naval Research.
- Install a Powertech hydrogen production, storage, and dispensing system at Marine Corps Base Hawaii (MCB Hawaii);
- Procure and operate a lightweight hydrogen delivery trailer to support fueling requirements; and
- Conduct engineering and economic analysis of GM FCV fueling operations.

Technical Barriers

This project addresses the following technical barriers from the indicated sections of the April 2009 edition of the Fuel Cell Technologies Program Multi-Year Research, Development and Demonstration Plan:

Technology Validation, Section 3.6.4

(A) Lack of Fuel Cell Vehicle Performance and Durability Data

(C) Lack of Hydrogen Refueling Infrastructure Performance and Availability Data

(H) Hydrogen from Renewable Resources

Hydrogen Safety, Section 3.8.4

(H) Lack of Hydrogen Knowledge by Authorities Having Jurisdiction

Technical Targets

This project will contribute to the following DOE milestones from sections of the Multi-Year Research, Development and Demonstration Plan:

Technology Validation section 3.6.6 Milestones

- **Milestone 34**: Complete power park demonstrations and make recommendations for business case economics. (2Q, 2008) Our HAVO system will utilize electrolytic hydrogen produced at a nearby geothermal plant and delivered by tube trailer from the geothermal plant to HAVO. The geothermal hydrogen production plant is funded by a DOE/Naval Research Laboratory (NRL) project (not part of Power Park) and the Power Park is leveraging this investment. Our MCB Hawaii system will support the early deployment of a small fleet of GM Equinox FCVs. Data will be collected to evaluate cost and technical performance of the MCB Hawaii and HAVO systems.

FY 2011 Accomplishments

- Signed an implementation agreement with the State of Hawaii (DOE funds via State Energy Office) contracting HNEI as the project "Implementing Partner" on behalf of the State of Hawaii.
- Secured State of Hawaii $1.2 million cost share funds via Kolohala Holdings LLP.

- Completed a hydrogen fueling station specification.
- Obtained Kilauea Military Camp (KMC) approval and support as the site of the fueling station.
- Completed background noise survey at the KMC site.
- Assisted HAVO to develop a noise specification for the fueling station.
- Assisted HAVO to secure bus funding from NPS ($1 million) and from the State of Hawaii ($600,000).
- Re-scoped the project to support the GM Hawaii Equinox FCV rollout at MCB Hawaii.
- Completed factory acceptance of the Powertech system and demonstrated compatibility with GM Equinox FCVs.
- Developing several memorandums of agreement among project partners:
  - HAVO
  - KMC
  - MCB Hawaii
- Initiated actions to relocate the Powertech integrated hydrogen production and dispensing system to MCB Hawaii on Oahu.
- National Environmental Protection Act (NEPA) approval for the HAVO site.
- NEPA approval for the MCB Hawaii site.
- Obtained funding and initiated actions to upgrade the Powertech station to 700 bar fast-fill to support GM Equinox FCVs.
- Developed the infrastructure specifications for MCB Hawaii.
- Selected the contractor to install infrastructure at MCB Hawaii.
- Secured an additional $600,000 in state funding for the MCB Hawaii infrastructure.
- Purchased the hydrogen delivery tube trailer for use on Oahu.



Introduction

The Hawaii Hydrogen Power Park (Power Park) was established to support the DOE Technology Validation sub-program. The Power Park is funded by the DOE through the Hawaii Department of Business, Economic Development and Tourism's Strategic Industries Division, in its role as the Hawaii State Energy Office, with the University of Hawaii's Hawaii Natural Energy Institute as the implementing partner, with the objective to conduct engineering and economic validation of pre-commercial hydrogen technologies. Power Park is supporting the testing and validation of hydrogen fueling system technologies on the Big Island of Hawaii and Oahu, including production utilizing renewable energy, compression, storage, delivery, and dispensing to hydrogen vehicles. In parallel, the HAVO is planning to acquire, initially, two battery-dominant fuel cell PHEV shuttle buses. The source of HAVO funds is from the Department of Transportation though the NPS Alternative Transportation in the Parks and Public Lands Program. It is intended to support HAVO's hydrogen fueling requirements with the infrastructure developed in the Power Park. In 2011 the scope of the project was expanded to include support for the GM Equinox FCV demonstration on Oahu. The fueling station originally planned for HAVO is being reallocated to the MCB Hawaii on Oahu. A fueling dispenser will be installed at HAVO and supplied with hydrogen produced at the Puna Geothermal Ventures (PGV) geothermal plant under a separate award and delivered by lightweight hydrogen delivery trailers to HAVO.

Approach

Due to the expanded scope of the project, activities are now being conducted on the Big Island of Hawaii and on Oahu. The approach is to install hydrogen fueling stations at each of the sites and conduct fueling operations to support small fleets of fuel cell vehicles. On the Big Island a compressor fueling dispenser will be installed at the KMC facility located at HAVO to support two PHEV battery-dominant fuel cell shuttle buses that will be used to shuttle visitors around the park. The hydrogen will be supplied via tube trailers from the PGV geothermal site. This leverages a non-related DOE/NRL project that is utilizing electrolyzers as a potential grid load management system while producing hydrogen that can be used for transportation.

On Oahu the project will install a fully integrated hydrogen production, storage, and dispensing system at MCB Hawaii. The station will be used to support the operation of a small fleet of GM Equinox FCVs. Initially dispensing hydrogen at 350 bar, the station will be upgraded to 700 bar utilizing Office of Naval Research funding.

Results

Legal and Insurance

This project relies on the installation of major hydrogen systems and infrastructure to enable the demonstration of a variety of technologies in an integrated system and a real-world environment. The installation of infrastructure in the private community requires interfacing with local authorities having jurisdiction and covers a variety of subject areas relating primarily to safety in form of permitting and related codes and standards, fire fighting and first responders training, and, as we have experienced in this project, legal issues involving risk management, liability, indemnification and insurance coverage. Multiple partners add to the complexity of developing legal agreements and we have experienced a significant educational requirement to ensure a high level of comfort with these projects among all the parties. While significant progress in working through these issues has been made, it is incremental and time-consuming,

and introduces delays to the project schedule. HNEI has identified this as a systemic issue and raised it with the DOE. Apparently many hydrogen projects have reported similar experiences. HNEI has proposed that DOE work on developing a systemic solution that includes working with the insurance industry. Initial meetings have been held and follow-on meetings have been planned. In the meantime, HNEI continues to draft appropriate agreements that address indemnification and liability concerns.

Program Development

Due to changed circumstances, it was decided that the best use of project resources would be to leverage a new separately-funded project entitled Hydrogen Energy Systems as a Grid Management Tool that will produce hydrogen at the PGV geothermal plant. The new plan will deliver hydrogen from PGV to HAVO using lightweight composite hydrogen delivery trailers towed by a light-duty truck. Fueling operations will be accomplished by a compressor-fill hydrogen dispenser connected to the hydrogen tube trailer. These changes make use of lower cost electricity and provide a clear linkage to producing hydrogen from a renewable energy source. The original Powertech fueling station will be deployed to the MCB Hawaii on Oahu to support the deployment of a fleet of GM Equinox FCVs. This 350 bar station will be upgraded to provide a 700 bar fast-fill capability using funds provided by the Office of Naval Research. This change resulted in the requirement to apply for approvals from the DOE and the State of Hawaii, amend project documentation, and submit new NEPA forms.

Technical

During this reporting period HNEI conducted a successful factory acceptance trial of a turnkey Powertech hydrogen production and dispensing system at Powertech in Vancouver. The factory acceptance trial was supported by GM which deployed an Equinox FCV to prove compatibility of the FCV with the fueling station. Several fueling and de-fueling operations were conducted to ensure proper communications between the fueling station and the vehicle's onboard monitoring and control system. The design of the MCB Hawaii supporting site improvement infrastructure was completed, and a request for quotes was issued for the "turn-key" installation of the site improvements. Further technical progress will be accomplished after all legal agreements are in place.

Conclusions and Future Directions

Oahu

- Execute remaining memorandums of agreement with project partners.
- Complete the MCB Hawaii infrastructure site improvements.
- Install the Powertech system at MCB Hawaii.
- Upgrade the Powertech system to 700 bar fast-fill.

Island of Hawaii (Big Island)

- Install a hydrogen 350 bar dispensing system at HAVO.
- Deliver geothermal hydrogen to HAVO with tube trailer.
- Support HAVO bus operations.
- Collect and analyze fueling station and vehicle data.
- Seek opportunities for expansion of fleets and/or additional hydrogen infrastructure.

FY 2011 Publications/Presentations

1. R. Rocheleau and M. Ewan, "The Hawaii Hydrogen Power Park," US DOE Annual Merit Review, Washington, DC, May 2011.

VII.8 Florida Hydrogen Initiative (FHI)*

David L. Block, Director Emeritus
Florida Solar Energy Center (FSEC)
University of Central Florida
1679 Clearlake Road
Cocoa, FL 32922
Phone: (321) 638-1001
E-mail: block@fsec.ucf.edu

DOE Managers
HQ: John Garbak
Phone: (202) 586-1723
E-mail: John.Garbak@ee.doe.gov
GO: Greg Kleen
Phone: (720) 356-1672
E-mail: Greg.Kleen@go.doe.gov

Contract Number: DE-FC36-04GO14225

Subcontractors:
- EnerFuels, Inc., West Palm Beach, FL
- Florida Solar Energy Center, Cocoa, FL
- SRT Group, Inc., Miami, FL
- University of Florida, Gainesville, FL
- Florida State University, Tallahassee, FL
- Bing Energy, Inc., Tallahassee, FL
- Florida Institute of Technology, Melbourne, FL
- University of South Florida, Tampa, FL

Project Start Date: October 1, 2004
Project End Date: June 30, 2012

*Congressionally directed project

Fiscal Year (FY) 2011 Objectives

Develop Florida's hydrogen and fuel cell infrastructure and to assist the U. S. Department of Energy in its hydrogen and fuel cell programs and goals by:

- Developing hydrogen and fuel cell infrastructure.
- Creating partnerships for applied technology demonstration projects.
- Sponsoring research and development in the production, storage and use of hydrogen and in the use and application of fuel cells.
- Facilitating technology transfers between the public and private sectors to create, build and strengthen high-growth potential, high technology companies.
- Developing industry support or potential for widespread applications.
- Developing unique hydrogen/fuel cell university-level education programs.

Technical Barriers

This project addresses technical barriers from the Technology Validation section of the Fuel Cell Technologies Program Multi-Year Research, Development and Demonstration Plan as follows:

(A) Lack of Fuel Cell Vehicle Performance Data and Durability Data

(B) Hydrogen Storage

(C) Lack of Hydrogen Refueling Infrastructure and Availability Data

(H) Hydrogen from Renewable Resources

(I) Hydrogen and Electricity Co-Production

Contribution to Achievement of DOE Technology Validation Milestones

This project will contribute to achievement of the DOE Technology Validation milestones 6, 11, and 24 from the Fuel Cell Technologies Program Multi-Year Research, Development and Demonstration Plan.

- Validate on-board cryo-compressed storage system on a technology development vehicle achieving 1.5 kWh/kg and 1.0 kWh/L. (2Q, 2007)
- Decision to proceed with Phase 2 of the learning demonstration. (2Q, 2010)
- Validate a hydrogen cost of $3.00/gge (based on volume production). (4Q, 2009)

Accomplishments

- Project has solicited proposals to conduct work.
- Project composed of 12 projects with three projects completed.
- Presently have nine active projects – one old project with new demo site, three new projects started on April 1, 2010, and five new projects started on December 1, 2010.



Introduction and Approach

The FHI is a hydrogen and fuel cell program funded for the purpose of developing a hydrogen and fuel cell infrastructure. The FHI program has operated by funding individual projects which conduct the research, development and demonstration activities. Each of the individual projects are approved by DOE before work can begin. Following the change in operation and management of FHI, the project

management began the process of allocating the remaining funds (~$2.5 million) to new projects and finishing and/or completing old projects. At the present time, there are nine active projects with four in fuel cells, three in hydrogen and two in hydrogen and fuel cells.

Individual Project Descriptions

With the above background, the nine active projects are briefly described in the following sections.

Task 2. Hydrogen Technology Rest Area – Michael Fuchs, EnerFuel, Inc.

The project objectives are to design, construct, and demonstrate a 10 kW_{net} polymer electrolyte membrane fuel cell (PEMFC) stationary power plant operating on methanol, to achieve an electrical energy efficiency of 32% and to demonstrate transient response time <3 ms. The yearly accomplishments successfully incorporated the existing inverter and fuel cell systems into the design of the charging station, completed system testing at EnerFuel prior to delivery to Florida Atlantic University. Final activities are to operate the charging station for a period of three months, determine overall electrical efficiency, document system transient response to load changes, and determine overall performance and effectiveness of charging station.

Task 7. Chemochromic Hydrogen Leak Detectors for Safety Monitoring – Dr. N. Mohajeri and Dr. N. Muradov, FSEC

The objective of this project is to develop and demonstrate a cost-effective, high specific chemochromic (visual) hydrogen leak detector for safety monitoring at any facility engaged in handling and use of hydrogen. The work will lead to two classes of chemochromic hydrogen sensors, an irreversible one and a reversible one. The yearly activities have evaluated the performance (sensitivity) of the sensors at different hydrogen concentrations in air (from 1 to 100 vol%) and found no interference with other reducing gases (CO, NH_3, CH_4, H_2S).

For the irreversible sensors, the results are several new chemochromic pigments that have been synthesized and tested. Three new formulations show faster kinetics with the response time for PK-2-31NM49 chemochromic sensor being 80% faster than first generation irreversible pigment. For the reversible sensors, the results are 20 novel Mo-, W-, V-based chemochromic formulations that have been synthesized and tested and the effect of the co-catalyst/activator on the rate of coloration in presence of hydrogen has been determined.

Task 8. Development of High Efficiency Low Cost Electrocatalysts for Hydrogen Production and PEM Fuel Cell Applications – Dr. C. Huang and Dr. M Rodgers, FSEC

The objectives of this project are to develop nanosized and high efficiency electrocatalysts based on alloys and metal-metal oxides composites. The new catalysts will be evaluated for their activity toward H_2 evolution via water electrolysis as well as oxygen reduction reaction for PEMFC applications. The relevance of this project is that Pt metal catalysts are the most effective PEMFC catalysts, but their use is impeded by costs, efficiency, and life span for oxygen reduction reaction. Approaches to overcome these limitations involve reducing Pt loading while maintaining high performance of catalysts. The methods of increasing Pt activity include optimization of the size and shape of the Pt particles, alloying Pt with other metals, and depositing catalyst particles only where the electrocatalytic reaction takes place.

In PEMFC applications, for Pt in a catalyst layer to be active, it must be deposited at the "three phase reaction zone." This can be done by sputtering deposition or pulse electrodeposition. The approach of catalyst preparation is to electrodeposit catalyst particles on three phase zones by coating a carbon microporous and Nafion® layer on carbon paper. A rotating disk electrode (RDE) technique is used to carry out pulse electrodeposition. The results indicate that Pt catalyst prepared by the pulse electroplating technique show higher activities than that of a commercial catalyst. The prepared catalysts can also be used for H_2 production via water electrolysis with higher efficiency. The future work is to synthesize alloy-based electrocatalysts and to perform catalyst characterization.

Task 9. Understanding Mechanical and Chemical Durability of Fuel Cell Membrane Electrode Assemblies – Dr. D. Slattery, FSEC

The objective of this project is to increase the knowledge base of the degradation mechanisms for membranes used in PEMFCs. The yearly results are that fluoride emission of 1100 equivalent weight perfluorinated sulfonic acid membranes can be reduced by the addition of cerium oxide to the membrane, the formulation of the ceria changes its efficacy, the improvements in durability are dependent on the ceria concentration, and improved cell durability can be achieved by using Pt-Co/C rather than Pt/C results and the addition of phosphotungstic acid to the electrode sublayer reduced membrane degradation.

The planned future work is to continue analysis of cerium oxide to determine the source of improvements, to conduct accelerated durability tests and compare the results to the Fenton tests, to determine the amount and location of Pt in the membrane by electron microscopy tests, to determine by cell testing the effect of heteropoly acid on platinum migration to identify performance losses and then optimize the sublayer electrode to reduce these losses.

Task 10. Production of Low-Cost Hydrogen from Biowaste (HyBrTec™) – Mr. R. Parker, SRT Group, Inc.

The objective of this project is to conduct research and development on biowaste reactor (called HyBrTec™) that

does not have the problems associated with conventional biowaste-to-fuel processing using an anaerobic digester. This new reactor will reduce the cost and improve energy efficiency. The project approach is to produce hydrogen bromide (HBr) from wet-cellulosic waste (co-produces carbon dioxide and thermal energy) and then use electrolysis to dissociate hydrogen bromide ($E^o = 0.555$ V) producing recyclable bromine and hydrogen (endothermic), and follow with combustion in order to react hydrogen with the more energetic oxygen ($E^o = 0.1229$ V), affording a theoretical process efficiency of 100%.

The project is in its initial stages of development and the accomplishments to date are that the reactor/electrolysis vessel is designed, the preliminary bromination experiments at <200°C are favorable, and assembly of a bench-top 500 ml prototype reactor/electrolysis vessel has begun. The future work is to conduct the high temperature HBr electrolysis, integrate bromination/electrolysis to determine optimum temperature and pressure, perform analysis of by-products and conduct preliminary economic analysis.

Task 11. Development of a Low-Cost and High-Efficiency 500 W Portable PEMFC System – Drs. J. Zheng, R. Liang, and W. Zhu, Florida State University, Mr. H. Chen, Bing Energy, Inc.

The project research objectives are to demonstrate new catalyst structures comprised of high conducting buckpaper and Pt catalyst nanoparticle coated at or near the surface of buckpaper and to demonstrate efficiency, durability improvement, and cost reduction using carbon nanotube buckpaper-based electrodes.

The technical approach is to use carbon nanotubes that are suspended on buckpaper, to use electrodeposition of Pt, and to characterize the catalysts by cyclic voltammetry of a PEMFC using the buckpaper. The results have developed an innovative fuel cells assembly, taken images of two-layered Pt/buckpaper and determined cell performance. Current results have been achieved by Florida State University/Bing Energy, Inc. for electrocatalyst and membrane electrode assemblies. These results show the meeting of some DOE goals with the future expectation of meeting all DOE goals.

Task 12. Hydrogen and Fuel Cell Technology Academic Program - Mary Helen McCay, PhD, PE, Kurt Winkelmann, PhD, Florida Institute of Technology, Melbourne Florida

This project has the objective to develop a hydrogen and fuel cell technology (HFCT) academic program at the Florida Institute of Technology (FIT) in Melbourne, FL. The resulting program will allow students to follow hydrogen technology from introduction to long-term applications, obtain a basic understanding, redirect their current technology focus as a means for new career options, measure students' gains in knowledge of hydrogen as an energy source and satisfy the need for hydrogen technology graduates. The approaches to accomplish the program goals are to establish a Masters Degree area of specialization, develop modules for existing undergraduate courses, support senior design and capstone projects and prepare hydrogen-themed general chemistry lab experiments.

The FIT HFCT program began on December 1, 2011 and is in its initial stages of development. The technical accomplishments and progress are the hydrogen knowledge and opinion surveys have been administered to mechanical and aerospace engineering and chemistry students, graduate courses and modules are under development, and hydrogen-themed general chemistry lab experiments are designed to improve students' views about chemistry and their knowledge about hydrogen as an alternative energy source. The anticipated results are a strong curriculum on hydrogen and fuel cell technology that will assist undergraduate students in furthering their understanding of hydrogen and fuel cell technology, to offer graduate students a career path into renewable energy and prepare students for entry into research and other positions related to hydrogen technology.

Task 13. Design and Development of an Advanced Hydrogen Storage System using Novel Materials – Drs. E. Stefanakos, D. Goswami, and A. Kumar, University of South Florida

The project objectives are to design and develop novel conducting polymeric nanomaterials for on-board hydrogen storage with a system gravimetric capacity of 5.5 wt% or greater and with complete reversible hydrogen storage characteristics at moderate temperature (<100°C).

The proposed approach is to perform the synthesis of polyanitine (PANI), a solid state hydrogen storage material, and to modify the synthesis parameters for optimized storage capabilities. The major challenge is to develop polymer nanostructures that can store hydrogen at room temperature, and be reversible for many cycles. The preliminary work has used PANI nanostructures for H_2 storage and studies the morphological effects of H_2 cycling on PANI nanofibers that are electrospun. This work shows the PANI nanostructures combine physisoption and chemisorption, reversible storage of >3 wt% is possible at room temperature, and reversible storage of <10 wt%, is possible at 100°C.

Task 14. Advanced HiFoil™ Bipolar Plates – Mr. J. Braun, EnerFuel, Inc.

The project objectives are to address cost and durability barriers for high temperature proton exchange membrane fuel cells (HTPEMFC) by providing a low cost, easy to form, corrosion-resistant laminate bipolar plate having high thermal conductivity and improved mechanical strength/crack resistance. The existing commercial bipolar plate technology includes machined expanded graphite composite plates and gold-coated stainless steel plates – all costly. The new EnerFuel patent-pending laminate technology has shown excellent performance and corrosion resistance. A HTPEMFC stack was tested for 1,000 hours with no failure, and thermal cycled from room temperature to 200°C over 10,000 times with no failure.

The expected results are demonstration and characterization of advanced fuel cell materials that combine the strength of metal with the corrosion résistance of graphite, for use as a bipolar plate in HTPEMFCs operating at 200°C.

Conclusions and Future Directions

FHI has completed three projects and continues work on nine projects. All project budget funds are committed and the projects are scheduled for completion in 2012.

Publications/Presentations

1. Rodgers, M., Bonville, L., & Slattery, D. (2011, March). "Evaluation of the durability of polymer electrolyte membrane fuel cells containing Pt/C and Pt-Co/C Catalysts under accelerated testing." Paper presented at the Annual Joint Symposium & Exhibition of the Florida Chapter of the AVS Science and Technology Society, Orlando, FL.

VII.9 Sustainable Hydrogen Fueling Station, California State University, Los Angeles*

David Blekhman
California State University, Los Angeles
Los Angeles, CA 90032
Phone: (323) 343-4569
E-mail: blekhman@calstatela.edu

DOE Managers
HQ: John Garbak
Phone: (202) 586-1723
E-mail: John.Garbak@ee.doe.gov
GO: Gregory Kleen
Phone: (720) 356-1672
E-mail: Greg.Kleen@go.doe.gov

Contract Number: DE-EE0000443

Subcontractor:
General Physics Corp., Elkridge, MD

Project Start Date: January 1, 2009
Project End Date: 2012

*Congressionally directed project

Fiscal Year (FY) 2011 Objectives

- Procure core equipment for the CSULA hydrogen station.
- Install/integrate the core equipment.

Technical Barriers

This project addresses the following technical barriers from the Technology Validation section of the Fuel Cell Technologies Program Multi-Year Research, Development and Demonstration Plan:

(C) Lack of Hydrogen Refueling Infrastructure Performance and Availability Data

(D) Maintenance and Training Facilities

(E) Codes and Standards

Contribution to Achievement of DOE Technology Validation Milestones

This project will contribute to achievement of the following DOE milestones from the Technology Validation section of the Fuel Cell Technologies Program Multi-Year Research, Development and Demonstration Plan:

- **Milestone 26.** Validate refueling site stationary storage technology provided by the delivery team. (4Q, 2012)
- **Milestone 28.** Validate the cost of compression, storage and dispensing at refueling stations and stationary power facilities to be <$.80/gge of hydrogen. (4Q, 2013)

FY 2011 Accomplishments

- Identified, procured, and installed station electrolyzer: HySTAT-A 1000D-30-10. **(M26)**
- Identified, procured, and installed 350 bar compressor: PDC-4-1000-6500. **(M26, M28)**
- Identified, procured, and installed two 700 bar compressors: Hydro-Pac C12-60-10500LX. **(M26, M28)**
- Identified, procured, and installed three 350 bar storage tanks: CPI-20 kg. **(M26, M28)**



Introduction

The College of Engineering, Computer Science, & Technology at California State University, Los Angeles (CSULA) as part of its energy curriculum is building a sustainable hydrogen station to teach and demonstrate the production and application of hydrogen as the next generation of fully renewable fuel for transportation. The funding is applied for the acquisition of the core hydrogen station equipment: electrolyzer, compressors and hydrogen storage.

Approach

The CSULA hydrogen station will deploy the latest technologies with the capacity to produce 60/kg/day, sufficient to fuel 15 vehicles or a bus and five more vehicles. The station will be utilizing a Hydrogenics electrolyzer, first and second stage compressors capable of fast filling at 10,000 psi (700 bar), 60 kg of hydrogen storage, water purification and equipment cooling system. The station will be grid-tied and powered by 100% renewables.

The station will also be used as an applied research facility for equipment testing and verification, testing of fuel purity and dispensing accuracy. Another primary function of the station is to introduce hydrogen as a safe transportation fuel through public education and local partnerships.

Results

The equipment under this funding is purchased through General Physics. The equipment integration and station design is through Weaver Construction. The team consisting

of representatives from CSULA, Weaver and General Physics have bi-weekly meetings to regularly discuss the construction progress.

The grant provided funding for acquisition of the core hydrogen station equipment: electrolyzer, compressors and hydrogen storage. The compressors and storage arrived in November 2010, see Figure 1. The electrolyzer and other units were moved onsite on their foundations in January 2011, see Figure 2. After the payments for the equipment from DOE and non-federal funding cost share, the project will be essentially complete, see Figure 3.



FIGURE 1. CSULA Hydrogen Fueling Facility, Compressors and Storage, January 2011



FIGURE 2. CSULA Hydrogen Fueling Facility, Electrolyzer Delivery, January 2011



FIGURE 3. CSULA Hydrogen Fueling Facility, Current Status, June 2011

Conclusions and Future Directions

This year work concentrated on procuring and integrating the core equipment for the CSULA Hydrogen station. This task was completed in January 2011. The construction has continued and the expected station commissioning is in the August-September 2011. Future research into station/vehicle performance is planned.

VIII. SAFETY, CODES & STANDARDS

VIII.0 Safety, Codes & Standards Sub-Program Overview

The Safety, Codes & Standards sub-program supports research and development (R&D) that provides critical information needed to define requirements and close gaps in codes and standards and safety to enable the widespread commercialization and safe deployment of hydrogen and fuel cell technologies. In Fiscal Year (FY) 2011, the sub-program focused on continuing to identify measures to reduce the risk and mitigate the consequences of potential incidents that could hinder the commercialization of these technologies.

The sub-program promotes collaboration among government, industry, codes and standards development organizations (CDOs and SDOs), universities, and national laboratories in an effort to harmonize regulations, codes, and standards (RCS) both internationally and domestically. Communication and collaboration among codes and standards stakeholders is emphasized in order to maximize the impact of the sub-program's efforts and activities in international RCS. The sub-program is leading a round-robin testing effort by the Regulations, Codes and Standards Working Group of the International Partnership for Hydrogen and Fuel Cells in the Economy (IPHE), which aims to harmonize high-pressure tank testing protocols required for tank certification. Additionally, DOE continues to work with the Department of Transportation to support its role as the U.S. representative to the United Nations ECE-WP29/GRPE to develop a global technical regulation for hydrogen-fueled vehicles.

The sub-program supports the development and implementation of best practices and procedures to ensure safety in the operation, handling, and use of hydrogen and fuel cell technologies for Program-funded projects. To achieve this goal, the sub-program utilizes the expertise of the Hydrogen Safety Panel, which evaluates the safety plans and practices of Program-funded projects. The Safety Panel provides recommendations on the safe conduct of project work as well as lessons learned and best practices that can be of broad benefit to the Program.

In addition, extensive external stakeholder input–from the fire-protection community, academia, automobile manufacturers, and the energy, insurance, and aerospace sectors–is used to create and enhance safety knowledge tools for emergency responders and authorities having jurisdiction. The sub-program has renewed its emphasis on ensuring the continual availability of safety knowledge tools, distributed via an array of media outlets to reach the largest number of safety personnel possible.

Goals

The sub-program's key goals are to provide the validated scientific and technical basis required for the development of codes and standards, to promulgate safety practices and procedures to allow for the safe deployment of hydrogen and fuel cell technologies, and to ensure that best safety practices underlie all research, technology development, and market deployment activities supported by the Hydrogen and Fuel Cells Program.

Objectives

The sub-program's key objectives are to:

- By 2015, enable development and promulgation of codes and standards essential for widespread market entry of hydrogen and fuel cell technologies, and by 2020, enable the completion and harmonization of all essential domestic and international RCS. These objectives will be achieved through:
  - Conducting R&D efforts to provide data needed to define requirements in developing codes and standards.
  - Developing and validating test measurement protocols and methods to support and facilitate international harmonization of codes and standards.
  - Coordinating with international stakeholders.
- On an ongoing basis, develop and implement practices and procedures for the safe conduct of all projects funded by the Hydrogen and Fuel Cells Program.
- On an ongoing basis, ensure that safety-related information resources and lessons learned are widely available to first responders, authorities having jurisdiction, and other key stakeholders.

FY 2011 Status

The sub-program continues to support R&D to provide the technical basis for codes and standards development with projects in a wide range of areas, including fuel specification, separation distances, materials and components compatibility, and hydrogen sensor technologies. Utilizing the results from these R&D activities, the sub-program continues to actively participate in discussions with SDOs such as the National Fire Protection Association (NFPA), International Code Council, SAE International, Canadian Standards Association (CSA), and International Organization for Standardization (ISO) to promote domestic and international collaboration and harmonization of RCS. Figure 1 gives an overview of the timeline of codes and standards development work:

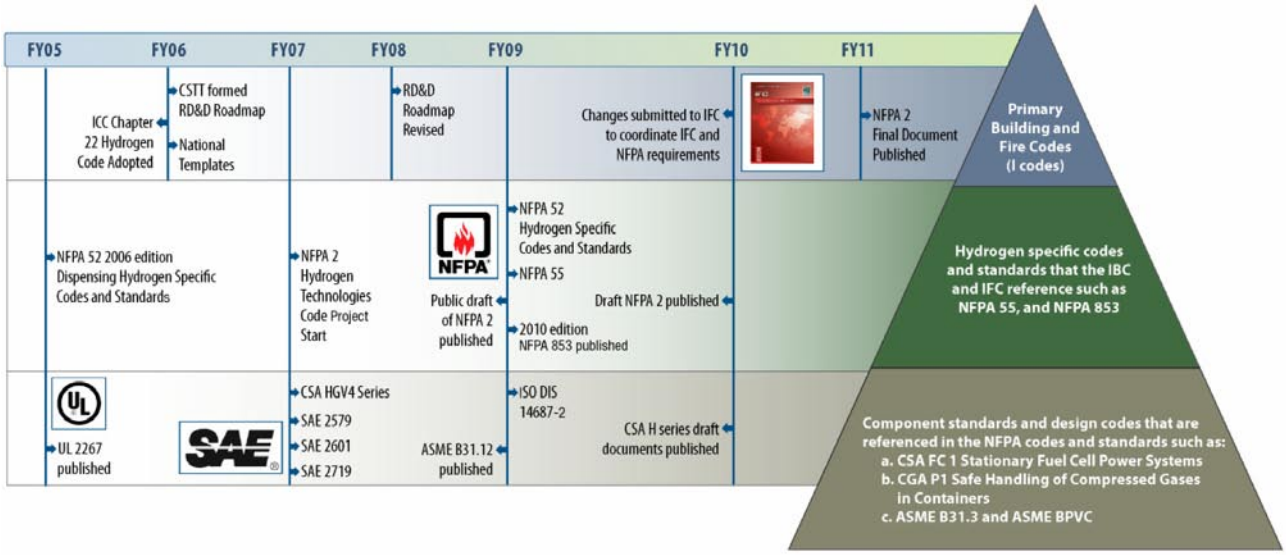


FIGURE 1. Overview of Codes and Standards Development Work

The following websites provide additional, up-to-date information relevant to the status of the sub-program's activities:

Technical Reference for Hydrogen Compatibility of Materials
http://www.ca.sandia.gov/matlsTechRef/

Hydrogen Incident Reporting and Lessons Learned Database
http://www.h2incidents.org/

Hydrogen Bibliographic Database
http://www.hydrogen.energy.gov/biblio_database.html

Hydrogen Safety Best Practices Manual
http://www.h2bestpractices.org/

Hydrogen Safety Training for Researchers
https://www-training.llnl.gov/training/hc/HS5094DOEW/index.html#

Permitting Hydrogen Facilities Compendium
http://www.hydrogen.energy.gov/permitting/

Introduction to Hydrogen for Code Officials
http://www.hydrogen.energy.gov/training/code_official_training/

Hydrogen Safety for First Responders
http://www.hydrogen.energy.gov/firstresponders.html

FY 2011 Accomplishments

Hydrogen Sensors

- Completed testing of laboratory and pre-commercial sensor prototypes, including comparison of mixed potential and impedance modality in laboratory prototypes; completed fabrication of multiple pre-commercial sensor prototype devices for testing (National Renewable Energy Laboratory [NREL]).
- Performed an assessment of hydrogen sensors and their related targets, through a Sensor Workshop, which enabled the Program to update sensor performance targets set in 2007. (Workshop attendees included representatives from industry, national laboratories, and sensor manufacturers; the workshop minutes contain updated sensor performance targets based on the comprehensive input provided by the attendees.)
- Completed round-robin testing on hydrogen sensors, in coordination with the European Commission's Joint Research Center. (Data derived from this testing, including performance, sensitivity, and reversibility was presented at the 2011 International Conference on Hydrogen Safety and validates the test approaches and methodologies.)

Fuel Quality

- Quantified the impact of fuel contaminants–for example, completed multiple tests on proton exchange membrane fuel cells under various conditions using calibrated quantities of NH_3, CO, and H_2S.
- Hydrogen fuel quality standard SAE J2719 was published. Developed and validated ASTM International techniques for measuring key constituents in the fuel.

Indoor Fueling

- Validated a model of unintended hydrogen releases and delayed ignition deflagration during indoor refueling of hydrogen-powered lift trucks. The validated model is being used in the development of requirements in NFPA 2, including specification of room volume and ventilation requirements (Sandia National Laboratories [SNL]).

Coordination of Codes and Standards Development, Domestic and International

- Harmonized and compared risk-informed approaches for the specification of separation distances in NFPA2 2011 edition codes and initiated an effort to harmonize NFPA codes with ISO 20100 codes.
- Developed procedures for performance-based pressure testing of storage vessels with gaseous hydrogen to be included in CSA HPIT1, SAE J2579, and the Global Technical Regulations Phase I (SNL).
- Held a forum on high-pressure hydrogen tanks in Beijing to identify key gaps in high-pressure vessel testing and qualification.
- Launched a new International Energy Agency (IEA) task on hydrogen safety (SNL, in partnership with Natural Resources Canada). The work plan has been approved and the initial meeting was held in Germany in April 2011. This new task (IEA Hydrogen Implementing Agreement Task 31) is a collaboration of experts from more than 12 countries.

Hydrogen Effects in Materials

- Hosted the Hydrogen Compatible Materials Workshop at SNL. Workshop participants included more than 40 international experts from industry, universities, and research laboratories. Results have been published in proceedings, which describe the prioritized research pathways for overcoming the science, engineering, and codes and standards barriers related to hydrogen compatibility with various materials. High-priority research pathways include crack initiation and crack propagation in materials in a hydrogen environment.
- Validated procedures for testing low-alloy steel materials and tanks used in lift trucks. It was found that engineering predictions of cycle-life for low-alloy pressure vessels have been lower than the actual results shown by full-scale performance testing (SNL).

- Published four additional chapters on plain carbon ferritic steels and nickel alloys in the *Hydrogen Compatibility of Materials Technical Reference*, focused on the assessment of materials compatibility for component designs and test methodologies.

Hydrogen Safety Panel

- The Hydrogen Safety Panel reviewed 60 safety plans for projects within the Program's R&D portfolio and American Recovery and Reinvestment Act-funded fuel cell deployments. Panel teams conducted safety review site visits for four Program-funded projects and participated in a 30% design review of the new Energy Systems Integration Facility at NREL (Pacific Northwest National Laboratory).
- Six project safety evaluation reports were issued. Overall results for these safety evaluations indicate that over 90% of report recommendations have been voluntarily completed or are well in progress.
- New content was added to the *Hydrogen Safety Best Practices Manual* for the following topics: hydrogen properties focusing on combustion and liquid hydrogen expansion; the indoor refueling of hydrogen fuel cell–powered forklifts; and chemical hydrogen storage. A new section, "So You Want to Know Something about Hydrogen," was created as a resource for students, technicians, and young engineers less familiar with hydrogen.
- The Hydrogen Incident Reporting and Lessons Learned Database added 56 new records from national laboratories, universities, and private-sector firms in the U.S. and other countries.

First Responders

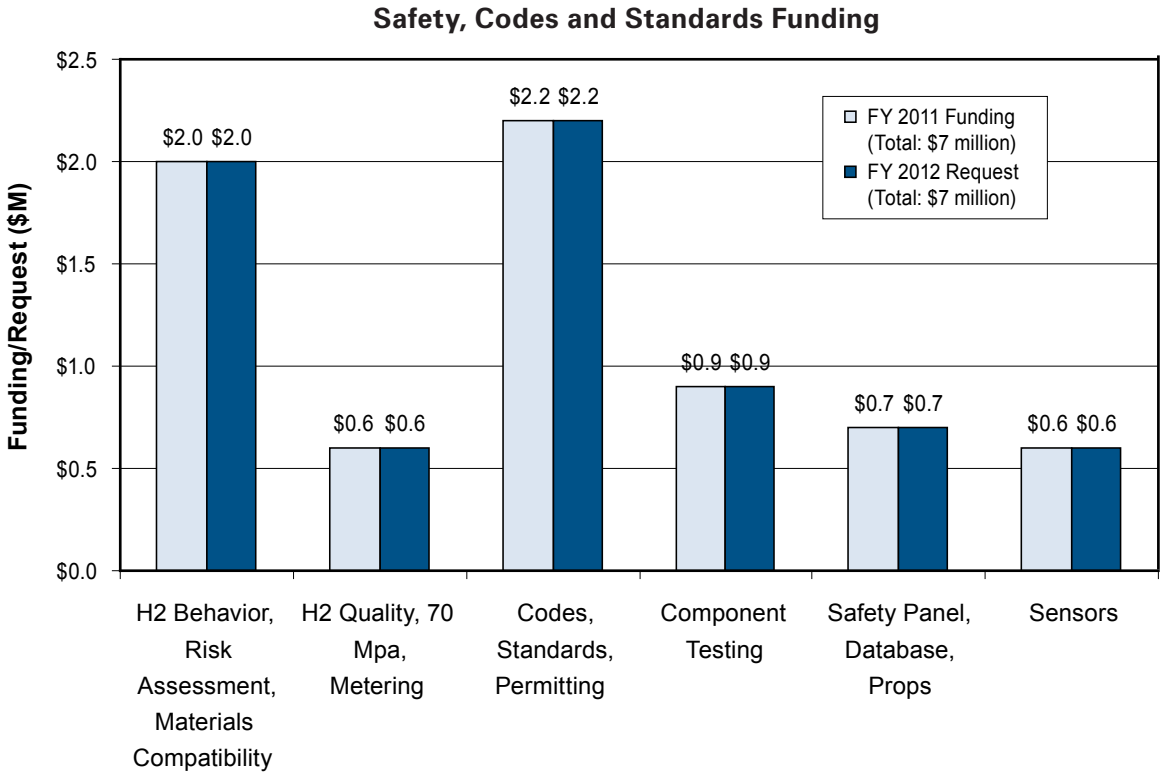
- The operations-level, prop-based course, Hydrogen Emergency Response Training for First Responders, was conducted at the Department of Defense's Defense Logistics Agency (DLA) near Tracy, California, where hydrogen fuel cell–powered forklifts are being used. Six one-day classes were conducted over a two-week period at the DLA's San Joaquin sites. To-date, approximately 350 first responders from 18 states have completed this course.

Education and Outreach

- Conducted Codes and Standards workshop in Anaheim, California, in collaboration with the Southern California Fire Protection Officers Association and the California Fuel Cell Partnership. Attendees included fire service members from at least seven key jurisdictions in the Los Angeles metropolitan area.

Budget

The sub-program received an appropriation of $7.0 M in FY 2011. This allowed for sustained progress in key R&D and codes and standards development work. The President's FY 2012 budget request includes $7.0 M for safety, codes and standards, which will ensure continuity in key R&D and focus areas as shown in the following figure.



FY 2012 Plans

The Safety, Codes & Standards sub-program will continue to work with codes and standards organizations to identify and address needs for the development of new hydrogen-specific codes and standards. To address these challenges, the sub-program will continue to support its rigorous technical R&D program.

In FY 2012 and beyond, the sub-program will continue to focus on critical safety R&D, such as assessment of materials compatibility for component designs, high-pressure tank cycle testing, and promoting a quantitative risk assessment approach to ensure the development of technically sound codes and standards. The sub-program will continue to promote the domestic and international harmonization of RCS by working with the appropriate domestic and international organizations such as NFPA, International Code Council, SAE International, CSA, and the ISO. The sub-program will continue to participate in the IPHE's Regulations, Codes and Standards Working Group and the IEA's Hydrogen Implementing Agreement, both of which have been engaged in hydrogen safety work.

Antonio Ruiz
Safety, Codes & Standards Team Lead
Fuel Cell Technologies Program
Department of Energy
1000 Independence Ave., SW
Washington, D.C. 20585-0121
Phone: (202) 586-0729
E-mail: Antonio.Ruiz@ee.doe.gov

VIII.1 Hydrogen Safety, Codes and Standards R&D – Release Behavior

Daniel Dedrick (Primary Contact), William Houf, Jeffrey LaChance, Greg Evans, William Winters, Isaac Ekoto, Adam Ruggles, and Jay Keller
Sandia National Laboratories
P.O. Box 969
Livermore, CA 94551-0969
Phone: (925) 294-1552
E-mail: dededri@sandia.gov

DOE Manager
HQ: Antonio Ruiz
Phone: (202) 586-0729
E-mail: Antonio.Ruiz@ee.doe.gov

Start Date: Fiscal Year (FY) 2002
End Date: Project continuation and direction determined annually by DOE

FY 2011 Objectives

(1) Scenario Analysis, Risk Assessments for Safety
- Develop a scientific basis and the associated technical data for modifying or developing new codes and standards for the commercial use of hydrogen.
- Develop benchmark experiments and a defensible analysis strategy for risk assessment of hydrogen systems.
- Develop and apply risk-informed decision-making tools in the codes and standards development process.

(2) Hazards Mitigation Technologies for Hydrogen Applications
- Determine the effectiveness of ventilation, active sensing, and similar engineered safety features.

(3) Codes and Standards Advocacy
- Provide technical management and support for the Safety, Codes and Standards sub-program element.
- Participate in the hydrogen codes and standards development/change process.

Technical Barriers

This project addresses technical barriers from the Codes and Standards section of the Fuel Cell Technologies 2007 Multi-Year Research Plan:

(F) Limited DOE Role in the Development of International Standards

(I) Conflicts Between Domestic and International Standards

(N) Insufficient Technical Data to Revise Standards

(P) Large Footprint Requirements for Hydrogen Fueling Stations

(Q) Parking and Other Access Restrictions

Contribution to Achievement of DOE Codes and Standards Milestones

This project will contribute to achievement of the following DOE milestones from the Codes and Standards section of the Fuel Cell Technologies Program Multi-Year Research, Development and Demonstration Plan:

- **Milestone 21**: Completion of necessary codes and standards needed for the early commercialization and market entry of hydrogen energy technologies. (4Q, 2012)
- **Milestone 8**: Complete investigation of safe refueling protocols for high pressure systems. (1Q, 2012)
- **Milestone 9**: Complete risk mitigation analysis for advanced transportation infrastructure systems. (1Q, 2015)
- **Milestone 12**: Complete research needed to fill data gaps on hydrogen properties and behaviors. (2Q, 2010)

FY 2011 Accomplishments

- Improved hydrogen jet release and ignition understanding with high-fidelity data.
- Measured dispersion statistics and ignition probability boundaries for a high source pressure release with a choked exit flow and compared measurements to predicted values.
- Acquired and analyzed hydrogen release data into vehicle compartments in support of a new Global Technical Regulation in support of a performance-based test methodology for hydrogen powered vehicles.
- Key validation experiments of H_2 releases and delayed ignition deflagration have been performed for indoor hydrogen forklift trucks.
- A consequence model for indoor releases from hydrogen forklift trucks has been developed and validated with experimental data.
- The Sandia turbulent entrainment model for cold hydrogen jets has been validated against high-momentum jet data (from Forschungszentrum Karlsruhe tests) and used in a liquid hydrogen separation distance study for National Fire Protection Association (NFPA) 2.



Introduction

The purpose of this project is to enable risk-informed development of codes and standards for hydrogen fuel cell technology that is based on a traceable, scientific foundation. Our scenario analysis and risk assessment efforts focus on defining scenarios for the unintended release of hydrogen and quantifying the consequences through scientific experimentation and modeling. Quantitative risk assessment (QRA) is used to identify risk drivers and risk mitigation strategies for the commercial use of hydrogen. We combine our validated models with QRA to support risk-informed decision-making in the code development process.

Approach

We develop an understanding of combustion behavior and thermal effects from the unintended releases of hydrogen in the built environment. We consider ignition characteristics, partially confined spaces such as hydrogen forklift trucks in warehouses, and liquid hydrogen handling. Technical information is disseminated through a variety of public channels and is used by codes and standards developers writing for the International Code Council and NFPA. International partnerships for vetting technical data and analysis methods occur through activities such as International Energy Agency Task 31 on Hydrogen Safety. Efforts in FY 2011 have focused on developing the basis for regulations and codes and standards development in the area of hydrogen releases in enclosures, ignition mechanisms, and liquefied hydrogen release behavior.

Results

Fundamental Ignition Phenomena of Unintended Hydrogen Releases

Ignition boundaries for turbulent natural gas jets have previously been found to correlate well with the flammability factor (FF), or the integration of the probability density function (PDF) between the fuel flammability limits. Although the FF does not predict flame light-up probability, it nonetheless allows modelers to determine the likelihood that an ignition kernel will form within a jet region when an ignition source is present. To verify the FF concept applies to hydrogen releases, light-up boundary, ignition probability, and concentration statistics for turbulent hydrogen jets were quantified at Sandia during FY 2008 through a combination of laser spark ignition and planar laser Raleigh scatter (PLRS) imaging. These measurements were also performed for methane jets, and it was found that the methane jet maximum axial and radial extents of the light-up boundaries were roughly a third lower. It should be noted, however, that smaller jet exit diameters and Reynolds number used for the Sandia study may have impacted the light-up flow features. An additional discrepancy, however, was that the centerline measured FF did not agree well with the measured laser spark ignition probability in the jet far field. Thus, it was concluded that the experimental methodology needed to be refined.

New ignition probability and jet light-up boundary measurements were performed in FY 2011 with the following experimental modifications: (1) the sample size was doubled; (2) a longer stabilization time was between sparks was used; (3) the number of thermocouples used to detect ignition was increased from 3 to 10; and (4) air conditioner vents and wind tunnel outlets were blocked to minimize air current disruptions. With these improvements, the new ignition probability measurements had much better agreement with the previously recorded methane and methane jet FF values, as can be seen in Figure 1. Nonetheless, methane and hydrogen light up boundaries, were essentially unchanged from the previous literature measurements; thus it was concluded the differences in flame light-up boundary were primarily driven by flow characteristics. Future measurements will quantify the jet flow features during ignition to support the engineering model development of sustained light-up phenomena.

Modeling of High Source Pressure Releases

Self-similar behavior for turbulent, subsonic heterogeneous jets exists for a broad range of gases, including hydrogen, which allows jet behavior to easily be modeled using canonical analytic expressions. However, for releases from storage pressures above the critical ratio (~1.9 for hydrogen), the exit flow chokes and underexpanded jets form, which are characterized by complex shock structure and nonuniform velocity distributions. A Mach disk at the end of the shock structure serves as the supersonic/subsonic boundary and is used as the effective source for the subsonic dispersion models; it

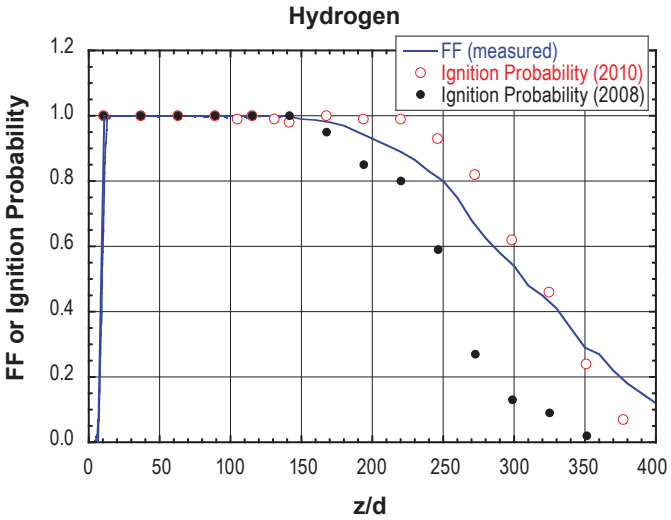


FIGURE 1. Original and Repeated Centerline Profile FF and Laser Spark Ignition Probability Measurements

is generally several factors wider than the jet exit diameter. Although source models that predict effective Mach disk diameter size and jet exit thermodynamic variables have been developed, limited validation data is available for choked hydrogen releases.

In FY 2011, the equation-of-state in these models was updated (Able-Noble) to better account for hydrogen compressibility. A new high-pressure stagnation chamber was integrated into Sandia's Turbulent Combustion Laboratory, and was used to acquire validation data from a choked hydrogen jet with a 10:1 pressure ratio and 1.5 mm nozzle diameter. The maximum measured centerline light-up distance was 367 mm downstream from the nozzle exit. Downstream concentration statistics were collected using PLRS imaging, while jet exit shock structure was imaged with schlieren photography. Measured (black) and modeled (red) FF contours from the concentration measurements are shown in Figure 2. Close agreement is achieved between the two methods, which indicate the self-similar jet behavior is preserved in the subsonic portion of the jet release. Computed effective source diameters, which are linearly proportional to ignitable boundary maximum extents, are tabulated for each model on the right. Although no model prediction was within 10% of the SNL experimental value, simpler models that neglect momentum and energy conservation performed the best while more complicated models that accounted for entropy change across the Mach disk performed the worst. More work is needed to determine why, but this is likely at least partially due to poorly predicted entrainment within the jet near field around the Mach disk. These data will ultimately be used to extend and validate the predictive capabilities of the ignition and flame light-up models and will form an important QRA input that ultimately impacts codes and standards separation distance decisions in NFPA 2, NFPA 55, and International Energy Agency 19.

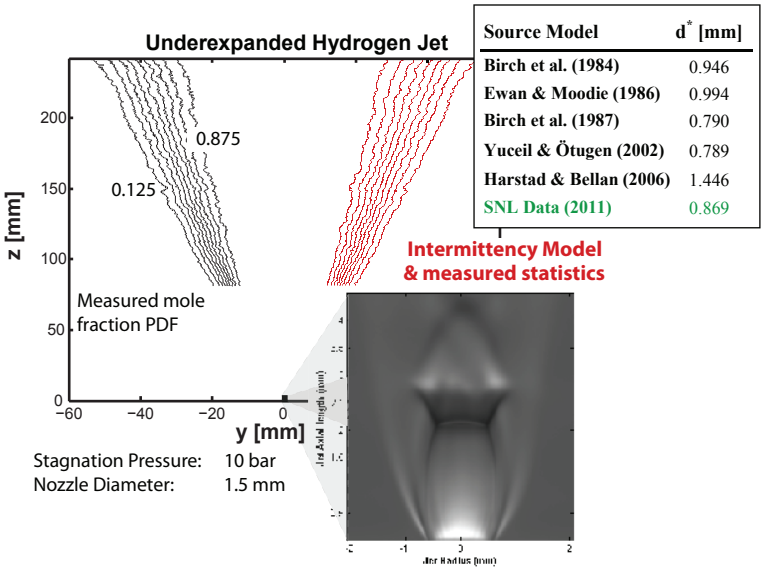


FIGURE 2. Flammability factor maps for the choked hydrogen jet ($p_0/p = 10$, $d = 1.5$ mm), with black contours generated from direct PDF integration, while red contours were generated from concentration statistics and an applied intermittency model. A schlieren image of jet exit shock structure is shown at the bottom, while tabulated predictions (black) and measurements (green) of the effective source diameter are shown to the right.

Performance-Based Hydrogen Leakage Testing in Passenger Vehicle Compartments

International regulatory representatives have proposed the performance-based test methodology for hydrogen fuel cell vehicle fuel system integrity certification in a new global technical regulation (GTR). For this testing methodology, automotive original equipment manufacturers (OEMs) self certify each vehicle. To ensure compliance, government regulators periodically inspect the system performance of randomly selected vehicles during barrier/rollover crash tests. Since a single failure for any safety criteria may result in a model line recall, OEMs are strongly incentivized to maintain vehicle safety compliance; however, OEMs have the flexibility to decide the design approach that best achieves the prescribed safety level. The GTR proposal specifies that the test is failed if within 1 hour post-crash, hydrogen leakage rates exceed 118 liters/min or flammable mixtures develop within the passenger cabin or trunk. An analysis of the capabilities necessary to detect the second failure mode was performed through exploratory in-vehicle leakage tests at SRI International's Corral Hallow Experimental Site. Hydrogen concentrations were primarily derived from oxygen depletion sensors, and were compared to directly measured concentrations from co-located hydrogen sensors (location details are shown in Figure 3a). Close agreement between the two sensor technologies was observed as shown in Figure 3b. Since oxygen depletion measurements have the additional advantage that nonflammable gases can be used, helium was investigated as a surrogate due to its similar diffusion and jet spreading characteristics. Good agreement in overall dispersion trends for both gases highlights the flexibility of the indirect sensor method. While hydrogen mixture fractions strongly depended on release characteristics (e.g., rate, location, type), results of an analytic examination indicate that pinhole leaks from moderate source pressures likely would produce unacceptably high in-vehicle hydrogen concentrations. The optimum sensor location for leak detection was determined to be high above the release point. Accordingly, sensor placement for crash tests involving vehicle rollovers must account for the final vehicle orientation. Test results provided quantifiable support for the U.S. National Highway Traffic Safety Administration proposal for a multinational performance-based hydrogen leakage test standard at a GTR meeting held September 8, 2010 in San Francisco, CA.

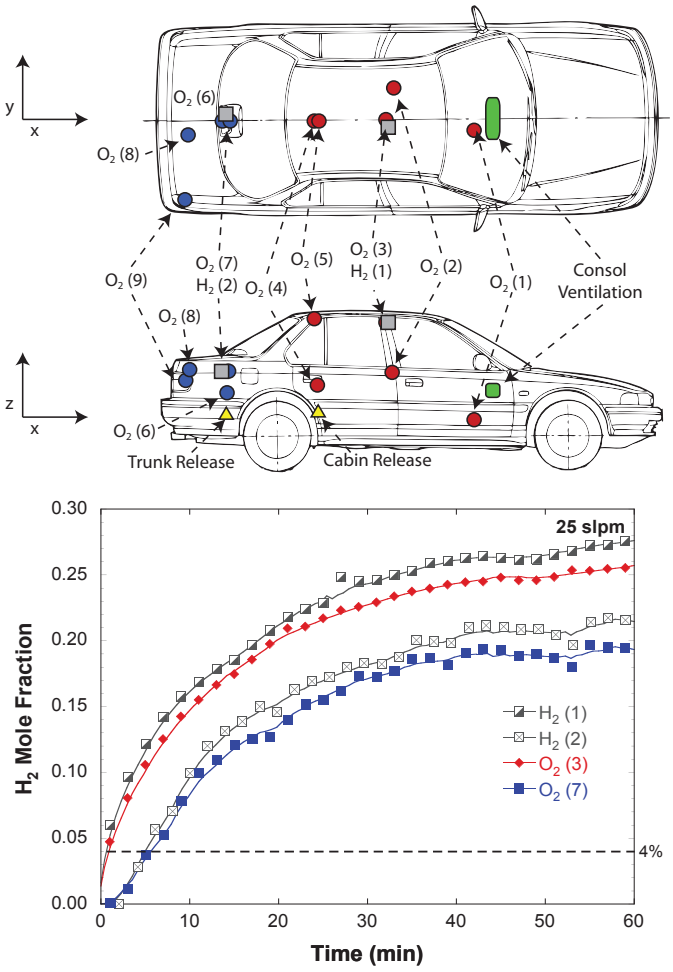


FIGURE 3. Schematic of trunk O_2 (blue), passenger cabin O_2 (red), and H_2 sensors (grey), along with ventilation (green) and release (yellow) points within the simulated fuel cell vehicle. Data shows a comparison of volumetric concentration measurements from co-located H_2 and O_2 sensors in the trunk and passenger cabin for the baseline condition.

Unintended Releases of Hydrogen in Partially Enclosed Spaces

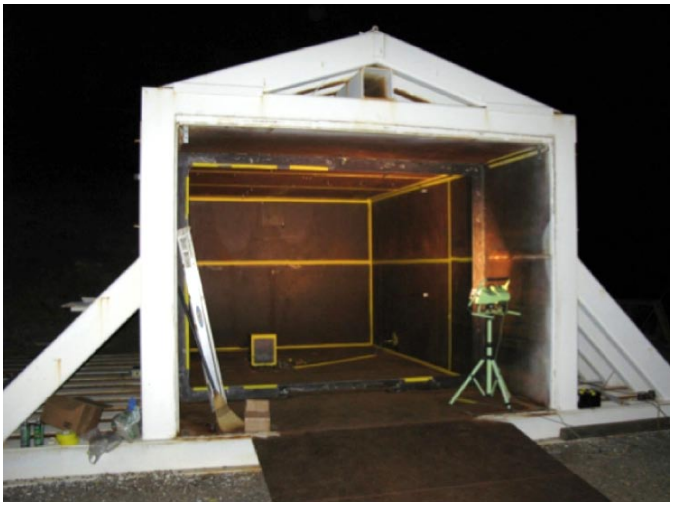
Sandia has been working with OEMs to develop scientific understanding that will form the basis for risk-informed safety codes and standards for safe operation of indoor hydrogen fuel cell forklift vehicles. A combined modeling and experimental approach has been used to develop an experimentally validated model for dispersion and ignition of unintended releases from hydrogen forklift vehicles in warehouses. As part of this work the validated forklift warehouse release model has been used to study the effect of leak size, ignition delay time, ventilation, and warehouse volume on the associated consequences. Results of this modeling study are being used in a risk analysis to develop new risk-informed indoor refueling codes and standards.

The indoor hydrogen release experiments were designed based on OEM forklift specifications and leak size, and the gaseous hydrogen indoor dispensing code in NFPA 2 and 52. The warehouse sizing, ventilation, and amount of vehicle onboard hydrogen were based on the parameters outlined in the NFPA codes. The experiments were performed in a subscale warehouse test facility (Figure 4) at the SRI Corral Hollow Experiment Site to provide data for model validation. The SRI subscale warehouse has a volume and height approximately 1/2.8 that of a full-scale 1,000 m^3 warehouse with a 7.62 m ceiling. The release diameter for the experiments was designed so that the mass flowrate matched the scaled mass flow rate versus scaled tank blow-down curve for a full-scale forklift release. Measurements were made of the hydrogen concentration, flame speed, and ignition delay overpressure in the scaled warehouse. As part of the work a dispersion model and deflagration model of the subscale warehouse and forklift geometry were developed. These models were used prior to the tests to estimate the placement of concentration and pressure sensors in the subscale warehouse and to determine the amount of expected overpressure from ignition of the hydrogen release. Pretest ignition deflagration simulations of the test geometry indicated that the maximum ignition overpressure would be approximately 30 kPa (0.3 barg) if the warehouse was completely (100%) sealed and the effects of wall heat transfer were neglected. Based on these simulations a wooden pressure relief panel was designed and placed in the doorway of the steel front wall of the scaled warehouse prior to the beginning of the deflagration testing.

Figure 4 shows comparisons of the predicted ignition overpressure from the simulations with data from the experiment for a pressure sensor in the center of the warehouse side wall nearest the forklift. Results are shown for simulations with and without heat transfer to the walls and also for the cases where the warehouse is completely sealed (100%) or the measured leakage area (36.7 cm^2) is incorporated into the model. The results with the measured air leakage rate and heat transfer to the walls are found to be in good agreement the experimental data. Figure 4 also shows that incorporating natural ventilation in the warehouse reduces the peak deflagration overpressure from approximately 25 kPa to 5 kPa.

The results of the modeling and experiments demonstrate that pressure relief panels or passive natural ventilation can be used as an effective means to mitigate deflagration overpressure arising from ignition of the released hydrogen. Simulation results also indicate that increasing the warehouse volume beyond the requirements currently specified also reduces the overpressure. Both simulations and experiments show that forced ventilation has little effect on the hydrogen concentration and deflagration overpressure in the early stages of the release.

Results of the modeling and experiments were presented to the DOE Technical Team, the Hydrogen Industrial Panel on Codes and Standards, and at the Annual Fuel Cell and Hydrogen Energy Conference. Based on feedback from these presentations a new indoor refueling task group was formed



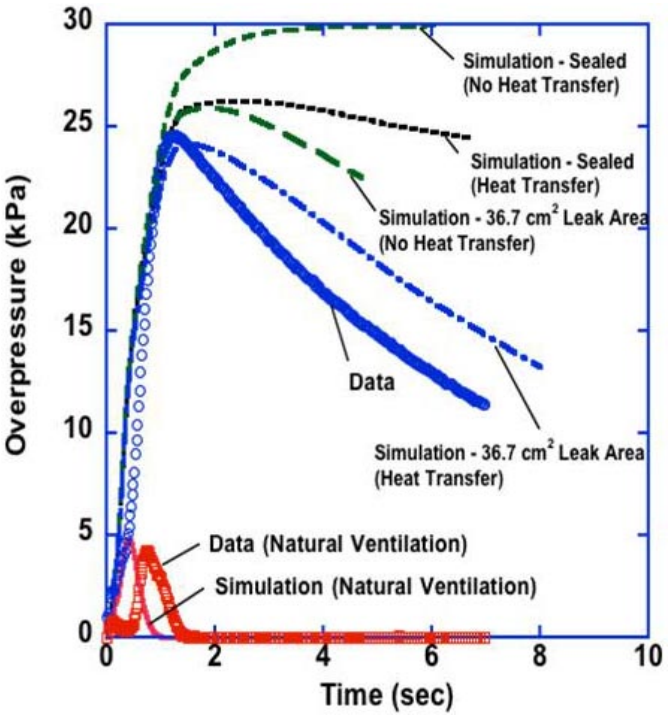


FIGURE 4. Comparison of Measured Ignition Overpressure in the SRI International Subscale Warehouse Facility with Results from FUEGO/FLACS Model Simulations

within NFPA 2 to utilize the experimental data and validated model in a science-based risk-informed process to develop new indoor refueling codes and standards for NFPA 2.

Conclusions and Future Directions

This project provides key understanding to enable the deployment of early market hydrogen systems. In FY 2011:

- We performed consequence analysis of indoor refueling and operation of hydrogen powered industrial trucks.
- Incorporated data from existing demonstration and projects into the QRA of hydrogen technologies.
- Improved the existing predictive model of ignition in turbulent flames to include sustained flame light-up probability.
- We improved the understanding of high-source pressure hydrogen releases in support of improved NFPA 2 separation distances from compressed gas applications.
- We developed an understanding of high-momentum low-temperature hydrogen plume behavior and supported NFPA 2 separation distance activities on liquid hydrogen.
- Performed risk analysis of advanced storage materials in support of NFPA 2 activities.

This project will continue to enable hydrogen and fuel cell technology deployment through developing the defensible technical basis for codes and standards. We will perform work to:

- Complete risk analysis of indoor refueling and work with codes and standards development organizations to provide technical data for science-based risk-informed indoor refueling codes and standards
- Perform study to identify potential mitigation features associated with hydrogen refueling stations and indoor refueling efforts.

FY 2011 Publications/Presentations

1. Houf, W.G., Evans, G.H., Ekoto, I., Merilo, E., and Groethe, M., "Hydrogen Releases and Ignition from Fuel-Cell Forklift Vehicles in Enclosed Spaces," 2011 Annual Fuel Cell and Hydrogen Energy Conference, Washington, D.C. Area, February 13–16, 2011.

2. Houf, W.G., and Winters, W.S., "Results from an Analytical Investigation of High Pressure Liquid Hydrogen Releases," 2011 Annual Fuel Cell and Hydrogen Energy Conference, Washington, D.C. Area, February 13–16, 2011.

3. Ekoto, I.W., Dedrick, D.E., Merilo, E., and Groethe, M., "Performance-Based Testing for Hydrogen Leakage into Passenger Vehicle Compartments," 2011 Annual Fuel Cell and Hydrogen Energy Conference, Washington, D.C. Area, February 13–16, 2011.

4. Ekoto, I.W., Merilo, E. and Groethe, M., "Hydrogen Releases and Ignition from Fuel-Cell Forklift Vehicles in Enclosed Spaces," HIPOC Meeting, Washington, D.C., February 17, 2011.

5. Houf, W.G., Evans, G., Ekoto, I., "Consequence Analysis for Unintended Hydrogen Releases within Enclosed Spaces," Combustion Research Facility News, March, 2011.

6. Houf, W.G., Evans, G., Ekoto, I., LaChance, J., Dedrick, D., Keller, J. "Hydrogen Release Behavior in Enclosures," NFPA 52 Meeting, Las Vegas, NV, Sept. 16, 2010.

7. Houf, W.G., Evans, G., James, S.C. "Unintended Hydrogen Releases in Tunnels," NFPA 52 Meeting, Las Vegas, NV, Sept. 16, 2010.

8. Houf, W.G., Evans, G., Ekoto, I., Ruggles, A., Zhang, J., LaChance, J., Dedrick D., Keller, J., "Update on Sandia Hydrogen Releases Program," IEA Task 31 Meeting, Istituto Superiore Antincendi (ISA), Rome, Italy, Oct. 4–6, 2010.

9. Houf, W. and LaChance, J., "Risk-Informed Separation Distances for Hydrogen Gas Storage Facilities," 5th Annual Hydrogen Codes and Standards Conference, NextEnergy Center, Detroit, MI, Sept. 21, 2010.

10. Houf, W.G., Evans, G.H., Ekoto, I., Merilo, E. and Groethe, M., "Hydrogen Releases and Ignition from Fuel-Cell Forklift Vehicles in Enclosed Spaces," 4th International Conference on Hydrogen Safety, San Francisco, CA, Sept. 12–14, 2011.

11. Houf, W.G. and Winters, W.S., "Simulation of High Pressure Liquid Hydrogen Releases," 4th International Conference on Hydrogen Safety, San Francisco, CA, Sept. 12–14, 2011.

12. Ekoto, I.W., Merilo, E.G., Houf, W.G., Evans, G.H., Groethe, M.A., "Hydrogen Fuel-Cell Forklift Vehicle Releases in Enclosed Spaces," 4th International Conference on Hydrogen Safety, San Francisco, CA, Sept. 12–14, 2011.

13. Merilo, E., Groethe, M., Adamo, R., Schefer, R., Houf, W., Dedrick, D., "Self-Ignition of Hydrogen Jet Fires by Electrification of Entrained Particulates," 4th International Conference on Hydrogen Safety, San Francisco, CA, Sept. 12–14, 2011.

14. Ruggles, A.J., and Ekoto, I.W., "Ignitability and Mixing of Underexpanded Hydrogen Jets," 4th International Conference on Hydrogen Safety, San Francisco, CA, Sept. 12–14, 2011.

15. Winters, W. and Houf, W., "Simulation of Small-Scale Releases from Liquid Hydrogen Storage Systems," Int. Jour. of Hydrogen Energy, Vol. 36, Issue 6, pp. 3913-3921, March, 2011.

16. Schefer, R., Merilo, E., Groethe, M., Houf, W., "Experimental Investigation of Hydrogen Jet Fire Mitigation by Barrier Walls," Int. Jour. of Hydrogen Energy, Vol. 36, Issue 3, pp. 2530-2537, Feb., 2011.

17. Houf, W. Evans, G., Schefer, R., Merilo, E., Groethe, M., "A Study of Barrier Walls for Mitigation of Unintended Releases of Hydrogen," Int. Jour. of Hydrogen Energy, Vol. 36, Issue 3, pp. 2520-2529, Feb., 2011.

18. Brennen, S., Bengaouer, A., Carcassi, M., Cerchiara, G., Evans, G., Friedrich, A.,Gentilhomme, O., Houf, W., Kotchourko, A., Kotchourko, N., Kudriakov, S., Molkov, V., Papanikolaou, E., Pitre, C., Royle, M., Schefer, R., Stern, G., Venetsanos, A., Veser, A., et al., "Hydrogen and Fuel Cell Stationary Applications: Key Findings of Modelling and Experimental Work in the HYPER Project," Int. Jour. of Hydrogen Energy, Vol. 36, Issue 3, pp. 2711-2720, Feb. 2011.

19. LaChance, J., Phillips, J., Houf, W., "Risk Associated with the Use of Barriers in Hydrogen Refueling Stations," National Hydrogen Association Hydrogen and Fuel Cell Safety Report, June 20, 2010.

20. Houf, W., Evans, G., Merilo, E., Groethe, M., "Evaluation of Barrier Walls for Mitigation of Unintended Releases of Hydrogen," Int. Jour. of Hydrogen Energy, Vol. 35, Issue 10, pp. 4758-4775, May 2010.

Sandia National Laboratories is a multi-program laboratory managed and operated by Sandia Corporation, a wholly owned subsidiary of Lockheed Martin Corporation, for the U.S. Department of Energy's National Nuclear Security Administration under contract DE-AC04-94AL85000.

VIII.2 Risk-Informed Safety Requirements for H2 Codes and Standards Development

Daniel Dedrick (Primary Contact), Jeffrey LaChance, William Houf, and Jay Keller
Sandia National Laboratories
P.O. Box 969
Livermore, CA 94551-0969
Phone: (925) 294-1552
E-mail: dededri@sandia.gov

DOE Manager
HQ: Antonio Ruiz
Phone: (202) 586-0729
E-mail: Antonio.Ruiz@ee.doe.gov

Start Date: Fiscal Year (FY) 2002
End Date: Project continuation and direction determined annually by DOE

FY 2011 Objectives

(1) Scenario Analysis, Risk Assessments for Safety
- Develop a scientific basis and the associated technical data for modifying or developing new codes and standards for the commercial use of hydrogen.
- Develop benchmark experiments and a defensible analysis strategy for risk assessment of hydrogen systems.
- Develop and apply risk-informed decision-making tools in the codes and standards development process.

(2) Hazards Mitigation Technologies for Hydrogen Applications
- Determine the effectiveness of ventilation, active sensing, and similar engineered safety features.

(3) Codes and Standards Advocacy
- Provide technical management and support for the Safety, Codes and Standards sub-program element.
- Participate in the hydrogen codes and standards development/change process.

Technical Barriers

This project addresses technical barriers from the Codes and Standards section of the Fuel Cell Technologies 2007 Multi-Year Research Plan:

(F) Limited DOE Role in the Development of International Standards

(I) Conflicts Between Domestic and International Standards

(N) Insufficient Technical Data to Revise Standards

(P) Large Footprint Requirements for Hydrogen Fueling Stations

(Q) Parking and Other Access Restrictions

Contribution to Achievement of DOE Codes and Standards Milestones

This project will contribute to achievement of the following DOE milestones from the Codes and Standards section of the Fuel Cell Technologies Program Multi-Year Research, Development and Demonstration Plan:

- **Milestone 21:** Completion of necessary codes and standards needed for the early commercialization and market entry of hydrogen energy technologies. (4Q, 2012)
- **Milestone 9:** Complete risk mitigation analysis for advanced transportation infrastructure systems. (1Q, 2015)

FY 2011 Accomplishments

- Expanded use and acceptance of quantitative risk assessment (QRA) to establish risk-informed codes and standards requirements.
- Harmonization of National Fire Protection Association (NFPA) and International Organization for Standardization (ISO) use of risk in establishing gaseous hydrogen facility separation distances.
- Evaluation of risk-reduction potential of accident mitigation features.



Introduction

The purpose of this project is to enable risk-informed development of codes and standards for hydrogen fuel cell technology that is based on a traceable, scientific foundation. Our scenario analysis and risk assessment efforts focus on defining scenarios for the unintended release of hydrogen and quantifying the consequences through scientific experimentation and modeling. Quantitative risk assessment is used to identify risk drivers and risk mitigation strategies for the commercial use of hydrogen. We combine our validated models with QRA to support risk-informed decision-making in the code development process.

Approach

Risk-informed code development enables commercialization of and fuel cell and hydrogen technologies by identifying code requirements that will reduce the associated risk to socially acceptable levels. Our risk activities include QRAs of hydrogen facilities, development of risk management strategies, and global harmonization of performance-based standards. Efforts in FY 2011 have focused on (A) harmonization of the NFPA and ISO risk-informed approaches for establishing separation distances; and (B) risk prevention and mitigation feature analysis. The hazards involved with unintended releases of hydrogen may be mitigated through early detection technologies or suppressed through thermal management techniques and engineered responses. As a result of the analysis of accident prevention and mitigation features, we will be able to inform credit tables that will be assembled for separation distances and other requirements in hydrogen codes.

Results

Harmonization of NFPA and ISO Separation Distances

The development of a set of safety codes and standards for hydrogen facilities is necessary to ensure they are designed and operated safely. To help ensure that a hydrogen facility meets an acceptable level of risk, code and standard development organizations (SDOs) are utilizing risk-informed concepts in developing hydrogen codes and standards. Two SDOs, the NFPA and the ISO have been developing standards for gaseous hydrogen facilities that specify the facilities have certain safety features, use equipment made of material suitable for a hydrogen environment, and have specified separation distances. Under DOE funding, Sandia National Laboratories (SNL) has been supporting efforts by both of these SDOs to develop the separation distances included in their perspective standards. Important goals in these efforts are to use a defensible, science-based approach to establish these requirements and to the extent possible, harmonize the requirements. International harmonization of regulations, codes and standards is critical for enabling global market penetration of hydrogen and fuel cell technologies.

Efforts to harmonize the ISO and NFPA approaches for establishing separation distances have generally been successful as both used essentially the same risk approach for evaluating separation distances developed by SNL [1]. Similarly, the SNL consequence models and the hydrogen leak data generated by SNL [1] have also been generally adopted for use in the ISO separation distance evaluation. However, there are some important differences in the ISO and NFPA analyzes that make it difficult to compare the resulting separation distances. These differences include the scope of the application (i.e., bulk storage versus fueling station), the differences in the separation distance table format used in the specific standards (pressure ranges and exposures), the risk criteria used in the risk analysis, the utilization of component leak data in the risk assessment, and the importance placed on the risk results. Additional efforts occurred this year to understand the impact of differences in the data used in the two analyses and the effect on the resulting separation distances.

A major difference between the NFPA and ISO analyses was due to the component leak frequencies used in the analysis. The difference in the leak frequencies is related to the binning of the data used by SNL for generating hydrogen-specific leak frequency estimates using Bayesian analysis. A cursory analysis of the generic data by the ISO TC 197 [2] separation distance task leader was utilized in a non-rigorous statistical approach to generate the leak frequencies used in the ISO QRA. The ISO data analysis only utilized a subset of the available generic data, did not include any hydrogen-specific data, and did not evaluate the leak frequencies using a justifiable statistical approach. Instead, the limited review of the generic data was utilized to generate arbitrary, idealized linear (on a log–log plot) versions of leak frequency distributions generated by SNL. More importantly, the ISO leak frequencies were essentially shifted an order of magnitude based on the argument that some of the generic data was mis-binned and that a different binning scheme should be utilized.

In an effort to more rigorously evaluate the impact of the data binning performed by ISO and the resulting leak frequencies, SNL performed sensitivity studies in which both the generic and hydrogen specific data were rebinned, where appropriate, into the binning categories utilized in the ISO QRA. The rebinned data was then utilized in a Bayesian analysis to generate estimates of hydrogen component leak frequencies. The results for valves are highlighted in Figure 1.

A review of the generic leak frequencies for valves indicated that some of the data had been conservatively binned in the initial Bayesian analysis performed by SNL. The actual leak size represented in this data is uncertain. However, some of the data was rebinned into lower leak sizes, especially the data points identified by the ISO working group. In particular, many of the data points initially binned as ruptures (30% to 100% leaks) were rebinned into smaller leak categories. However, several data points remained as 100% leaks. A Bayesian analysis was performed using this revised data. As illustrated in Figure 1, the resulting hydrogen mean leak frequency curve has lower frequencies than those reported in Reference 1. However, the frequencies are not substantially less (less than a factor of 2 different) which does not justify, for example, using the 100% leak size frequency as representative of leaks in the 10% to 100% range (this is a non-conservative value for that range of leaks). In contrast, it would be conservative to utilize the leak frequency for 10% leaks to represent the leaks in that range. A more realistic result would occur if the original leak size bins from reference [1] were utilized

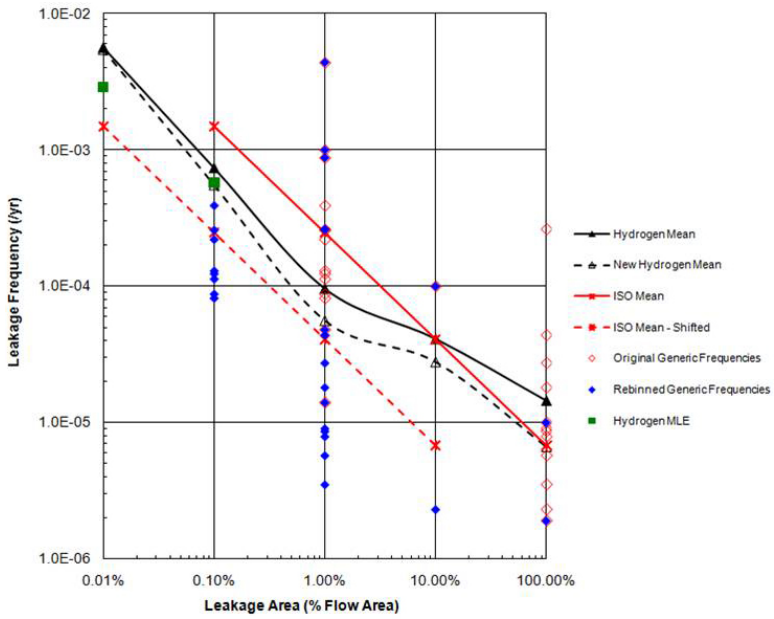


FIGURE 1. Results of Bayesian Analysis with Valve Data Rebinned

(i.e., leaks between 30% to 100% of the flow area are better represented by the leak frequency estimate for a 100% leak).

The results of the rebinning of data and Bayesian analysis for compressors resulted in similar results as for valves. The effect of the rebinning of the data for joints and hoses was negligible. Based on this more rigorous evaluation, the rebinning of selected generic data performed by the ISO working group does not provide an adequate basis for shifting the SNL-generated hydrogen leak frequencies reported in reference [1].

The ignition probabilities used in the QRA were also different in the NFPA and ISO QRAs. The NFPA QRA utilized ignition probabilities that changed with leak size and whether the ignition occurred immediately or was delayed. The NFPA ignition probabilities are provided in Table 1. The ISO risk model included a single ignition probability of 0.04 that was independent of leak size or ignition time. Although the selected ISO ignition probability was conservative over a range of leak sizes, as indicated below, its use skews the actual risk profile and the resulting selection of the separation distances.

TABLE 1. Hydrogen Ignition Probabilities used in NFPA QRA

Hydrogen Release Rate (kg/s)	Immediate Ignition Probability	Delayed Ignition Probability
<0.125	0.008	0.004
0.125–6.25	0.053	0.027
>6.25	0.23	0.12

To examine the significance of these differences in data, the impact of using the same component leak frequencies and hydrogen ignition probabilities used in the NFPA QRA on the ISO risk results and associated separation distances was evaluated. The results are shown in Figure 2 for four ISO-specified systems that have varying number of components most susceptible to developing leaks. As indicated in Figure 2, the resulting risk profiles are very different than from the ISO QRA and result in generally higher risk estimates for a person standing at a specified distance. Although the risk is higher for most of the systems/modules, the risk is acceptable over a range of separation distances. For example, the highest risk level is associated with the complex gas system (C). Using the ISO risk criteria of 1E-5/yr and 4E-6/yr, the associated separation distances are approximately 5 m and 9 m, respectively. The risk estimate for both of these distances using the NFPA data is 2E-5/yr. However, for the very simple gas system (VS), the ISO risk estimate is nearly identical to that predicted using the NFPA data.

Accident Prevention and Mitigation Feature Evaluation

A concept being pursued in the NFPA hydrogen standard development is to take credit for prevention and mitigation features as a means to reduce separation distances. The reduction in the separation distance could be expressed as a reduction factor that represents the ratio of the separation distance without any mitigation feature to the separation distance with a mitigation feature credited. QRA has been performed, using the hydrogen

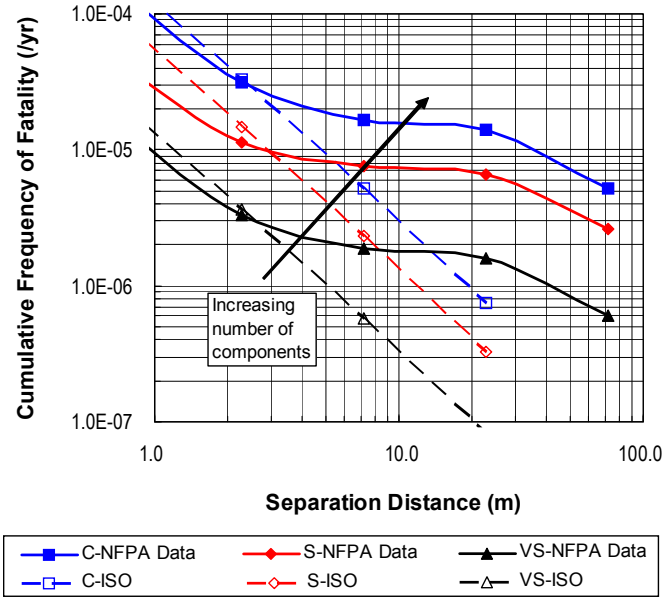


FIGURE 2. Results of Requantification of ISO QRA using NFPA Leak Frequency and Ignition Probabilities

system configurations and associated risk model used to establish the NFPA separation distances, for the following mitigation features taken individually (the risk reduction of combinations of these features has currently not been performed):

- Automatic leak detection and isolation
- Use of flow limiting orifices
- Use of barriers
- Reduction in number of components

The risk reduction potential and impact on separation distances associated with barriers was reported in 2010. The risk reduction potential of the other features was evaluated using the hydrogen system configurations and associated risk model used to establish the NFPA separation distances [1]. Preliminary results are summarized in the following.

Three different forms of detection and isolation are considered possible in a hydrogen bulk storage system:

- External flame and/or hydrogen detectors which can actuate one or more isolation valves.
- Internal process measurement (e.g., high flow or low pressure) that actuate one or more isolation valves.
- Excess flow valve that closes when flow exceeds a set amount.

These three different forms of detection and isolation may not be viable in specific hydrogen system applications. Furthermore, the set point for detection may be variable for each method. Rather than evaluate each method specifically, a generic risk assessment was performed where it is assumed that each detection system would detect leaks equal to or greater than 1% of the flow area in the largest pipe connected to the bulk storage system and isolate a portion of the bulk storage system. The probability of successful detection and isolation is assumed to be 0.9. Sensitivity calculations were performed for the case where the detection systems are only capable of measuring leaks equal to or greater than 10% of the flow area. Sensitivity calculation for the detection/system reliability was not performed as a 0.9 reliability appears to be sufficient to reduce the risk from hydrogen leaks.

The risk reduction potential for a detection/isolation system is dependent upon the location of the isolation valve. The closer the isolation valve is to the bulk storage system the better is the risk reduction potential. Figure 3 shows the results with isolation at the three different locations in a bulk storage system operating at 20.7 MPa. The reduction in separation distances range from a factor of 2 (7 m, corresponds to 0.75% leak) for isolation at the stanchion outlet to 2.8 (5 m, corresponds to 0.38% leak) for isolation at the tube trailer manifold, to 7 (2 m, corresponds to 0.06% leak) if isolation is on the tube trailer cylinders. Note that a large risk reduction is possible if the isolation valve can be placed on each tube trailer cylinder since this location would mitigate almost all leaks in the system. Reducing the

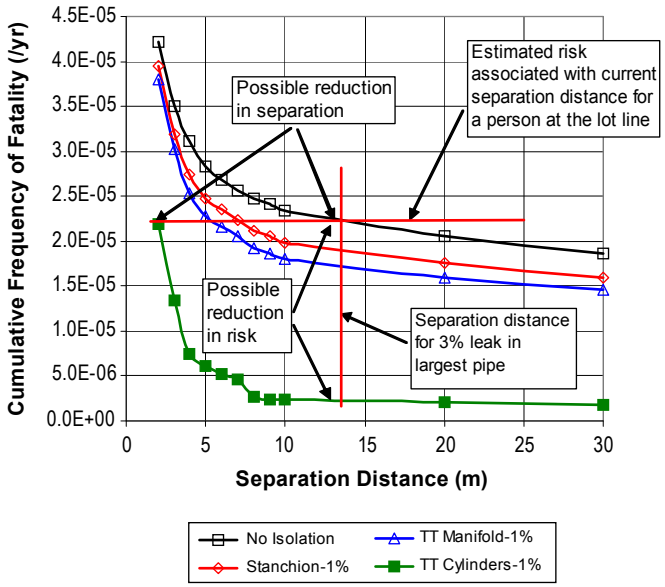


FIGURE 3. 20.7 MPa System Risk Results, Isolation at Different Locations (leaks equal to or greater than 1% of the flow area detected)

detection capability such that only leaks equal to or greater than 10% of the system flow area results in smaller risk and separation distance reductions.

Flow limiting orifices can also be used to limit the size of a leak and thus reduce the required separation distance. Similar to isolation systems, the location of the flow limiting orifice is important with regard to reducing risk and separation distances. For example, a flow orifice located in the tube trailer manifold in the 20.7 MPa bulk storage system modeled in the NFPA QRA would limit the flow rate from all leaks occurring downstream of the orifice. Using a flow orifice that is equivalent to 1% of the flow area would reduce the separation distance from 14 m (no orifice) to 6 m (a reduction factor of 2.33) if the same fatality risk is maintained. If the flow restriction can only be limited to 10% of the flow area, the separation distance reduces to 9 m (a reduction factor of 1.56). Locating a flow orifice at locations downstream of the tube trailer manifold would result in lower separation distance reduction factors.

The dominant risk contributors that were identified in the NFPA QRA [1] include leakage from valves, joints, and compressors. Limiting the number of these components in a hydrogen system would reduce the potential for hydrogen leakage and thus reduce the associated risk. To illustrate how this might impact risk and separation distances, 110 MPa systems with different number of risk-significant components was evaluated. All the system components were assumed to be at the same pressure and have an internal diameter of 8 mm. The results are shown in Figure 4 when a risk guideline of 2E-5/yr is used to select separation distances.

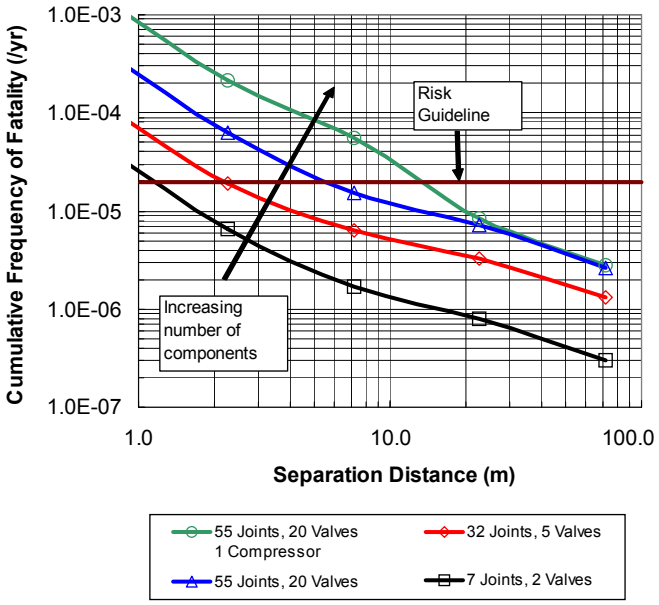


FIGURE 4. Risk Reduction Associated with Reducing the Number of High-Risk Components (110 MPa system with 8 mm inside diameter components)

References

1. LaChance, J., Houf, W., Middleton, B., Fluer, L., "Analysis to Support Development of Risk-Informed Separation Distances for Hydrogen Codes and Standards," Sandia Report SAND2009-0874, March 2009.

2. ISO/CD 20100, "Gaseous hydrogen – Fuelling stations," International Organization for Standardization, August 12, 2008.

Sandia National Laboratories is a multi-program laboratory managed and operated by Sandia Corporation, a wholly owned subsidiary of Lockheed Martin Corporation, for the U.S. Department of Energy's National Nuclear Security Administration under contract DE-AC04-94AL85000.

VIII.3 Component Standard Research and Development

Robert Burgess (Primary Contact), William Buttner, Matthew Post, Carl Rivkin, Chad Blake
National Renewable Energy Laboratory (NREL)
1617 Cole Blvd.
Golden, CO 80401
Phone: (303) 275-3823
E-mail: robert.burgess@nrel.gov

DOE Manager
Antonio Ruiz
Phone: (202) 586-0729
E-mail: Antonio.Ruiz@ee.doe.gov

Subcontractor:
Society of Automotive Engineers (SAE), Troy, MI

Project Start Date: FY 2008
Project End Date: Project continuation and direction determined annually by DOE.

Fiscal Year (FY) 2011 Objectives

- Support development of new codes and standards required for commercialization of hydrogen technologies.
- Create code language that is based on the latest scientific knowledge by providing analytical, technical and contractual support.
- Participate directly on codes and standards committees to identify technology gaps, then work to define research and development needs required to close those gaps.
- Conduct laboratory testing to provide a basis for improved code language.
- Collaborate with industry, university and government researchers to develop improved analytical and experimental capabilities.

Technical Barriers

This project addresses the following technical barriers from the Hydrogen Codes and Standards section (3.7.4) of the Fuel Cell Technologies Program's Multi-Year Research, Development and Demonstration Plan:

(A) Limited Government Influence on Model Codes
(B) Competition among SDOs and CDOs
(C) Limited State Funds for New Codes
(F) Limited DOE Role in the Development of International Standards
(G) Inadequate Representation at International Forums
(H) International Competitiveness
(I) Conflicts between Domestic and International Standards
(J) Lack of National Consensus on Codes and Standards
(K) Lack of Sustained Domestic Industry Support at International Technical Committees
(N) Insufficient Technical Data to Revise Standards

Contribution to Achievement of DOE Safety, Codes & Standards Milestones

This project contributes to achievement of the following DOE milestones from the Hydrogen Codes and Standards section of the Fuel Cell Technologies Program's Multi-Year Research, Development and Demonstration Plan:

- **Milestone 21**: Completion of necessary codes and standards needed for the early commercialization and market entry of hydrogen energy technologies. (4Q, 2012)

FY 2011 Accomplishments

- Completed sensor test laboratory objective, round I and II of the NREL/Joint Research Centre (JRC) round robin inter-laboratory comparison, completed under a formal Memorandum of Understanding with the JRC laboratory (a European Commission funded laboratory). Round robin test result comparison provided validation of test methods.
- Hydrogen safety sensor market characterization composite data study is approximately 50% complete.
- Collaborative partnerships were established to develop four new hydrogen safety sensor technologies. These technologies are being developed by both public and private organizations. Testing of each of these sensor technologies was completed as part of NREL's sensor evaluation process.
- NREL/DOE field deployment study was completed in support of hydrogen safety sensor installation in an NREL facility. This study included testing sensors being evaluated by NREL's Environmental Health and Safety organization. NREL hosted a hydrogen safety sensor workshop, June 2011 to bring together key industry representatives. Results included defining gaps and setting research and development needs for sensor commercialization.
- Conducted hydrogen pressure relief device (HPRD) contract testing in support of HPRD1 component standards development. Test results were used to modify test protocols defined in the draft standard.



Introduction

Development of codes and standards has been identified in the DOE multi-year program plan as a key area needing support for the commercialization and growth of hydrogen technologies. NREL is providing research and development (R&D) support to these codes and standards organizations through validation testing, analytical modeling, and product commercialization efforts. NREL has been tasked with these responsibilities as defined in the DOE multi-year program plan.

Approach

NREL is participating on relevant codes and standards committees to help identify gaps and define R&D needs to close those gaps. Working at the committee level allows us to quickly identify areas that need R&D support and to work directly with the technical experts in planning a path forward. This process is instrumental in avoiding delays and setbacks in the development of new codes and standards and in the revision of existing codes and standards. By providing support from a national lab we are able to help establish codes and standards language with solid technical basis.

Hydrogen safety sensors are a key component for the safe commercialization of hydrogen technologies. NREL is tasked with being a national resource for testing sensors designed to meet the needs of this growing market. By developing standard test methods and measuring sensor performance of a wide range of sensors of different designs and from a many different manufacturers, NREL is characterizing sensor performance and identifying gaps relative to DOE performance targets. With this information we work closely with sensor manufacturers so that they can better understand the performance of their sensor relative to the needs of hydrogen stationary applications. This work is directed toward sensor R&D, such that sensor manufacturers, utilizing the resources of a national lab, can expedite their product development life cycle. In addition, the sensor market expertise gained by NREL will be used to support commercialization through development of representative codes and standards for safety sensor certification. Commercialization support includes collaboration with key stakeholders as well as direct participation on the relevant codes and standards committees.

Results

NREL has been working toward identifying gaps and supporting R&D efforts for developing new and improved hydrogen codes and standards. Results reported here are for efforts specifically directed at component level standards. Results are organized in the following three sections; Hydrogen Safety Sensors, Canadian Standards Association (CSA) HPRD1 and Codes and Standards Support.

Hydrogen Safety Sensors

DOE published performance targets for hydrogen safety sensors in the multi-year program plan. NREL has tested more than 40 commercially available sensors and near-term developmental sensors from six sensor categories. This test data is being compiled in a generic format as a resource for end users. This format will allow for publishing a characterization study of the sensor market, while keeping individual results proprietary. NREL is approximately 50% complete with compilation of this composite data product.

NREL completed validation testing of the sensor test apparatus that was built in FY 2010. Validation testing consisted of systems level testing to characterize the repeatability and reproducibility of the apparatus, showing capabilities surpassing requirements in certification standards. Capabilities were further validated through round robin testing completed with the JRC Institute for Energy laboratory in Petten, Netherlands.

NREL is currently working directly with more than 20 sensor developers to support commercialization as their products move from prototype designs to full-scale production. This effort is directed at providing independent evaluation and testing of sensor platforms. This work has been completed in conjunction with other DOE supported projects in developing new technologies that have shown promise in meeting the identified DOE sensor targets.

CSA HPRD1

Pressure relief devices have been identified as a key safety component on hydrogen storage systems. Inadvertent opening can result in a failure mode where there is a release of the entire contents of the storage vessel. CSA component standard HPRD1 is in draft format. This standard defines performance-based certification tests designed to show end-of-life reliability. NREL and CSA worked together to define validation testing required for hydrogen service suitability testing as part of the CSA HPRD1 draft standard. Defined testing includes pneumatic cycle testing in hydrogen on three valves of three different designs, three surrogate designs and post-test metallurgical examination. Test results identified leakage issues at -40°C low temperature test conditions. Further evaluation of the test methods identified thermal transients that were more severe than the valves would see in actual low temperature service. This information was reviewed by the HPRD1 technical committee, concluding that a revised set of test conditions are required to more accurately depict worst case low temperature operation. Revised test definitions now include low temperature soak conditions. Testing was repeated successfully validating the revised test procedures. HPRD validation testing has been completed based on a revised test scope to both validate the revised test protocol and to stay within the budgetary limits first determined within this subcontract test program. A final report is being written for completion within FY 2011.

Codes and Standards Support

Through direct participation on the hydrogen components codes and standards committees, NREL has identified R&D gaps, including further HPRD testing, localized fire testing, tank level stress rupture testing and radio-frequency identification fill protocol validation. NREL has developed statements of work required to close these gaps and finalize these components requirements.

Conclusions and Future Direction

NREL made significant contributions in supporting commercialization of hydrogen sensor technologies. This includes collaborative work with domestic and international partners. NREL hosted a hydrogen sensor workshop in June 2011to identify R&D gaps to help define future sensor test laboratory direction. We completed validation testing in support of HPRD1 component standards and continue to work closely with codes and standards development organizations to close gaps and promulgate codes and standards that are based on the latest technical knowledge.

In addition to continuing to support component level codes and standards development, NREL will undertake a number of initiatives including:

- Identifying gaps to hydrogen technology commercialization.
- Providing national laboratory support needed to provide a sound basis for component level codes and standards content.
- Working directly with sensor manufacturers in order to reach performance targets defined in the DOE multi-year program plan.
- Executing sensor laboratory testing over a wider range of environmental conditions and finalizing long-term exposure and response time testing methodologies.
- Leveraging our efforts with national and international collaborations to provide a path toward commercialization of hydrogen components that are designed to meet the latest safety standards.

FY 2011 Publications/Presentations

1. "An Overview of Hydrogen Safety Sensors and Requirements," Buttner et al., 3rd International Conference on Hydrogen Safety (ICHS), September 2009 (publication in International Journal of Hydrogen Energy, 2010 special issue).

2. "Indoor Hydrogen Fueling Safety Codes and Standards," Rivkin, C. and Buttner, W.J., Proceedings of the National Hydrogen Association Conference and Expo, Long Beach, CA, May 3–6, 2010.

3. "Round Robin Testing of Commercial Hydrogen Sensor Performance – Observations and Results," Buttner, W.; Burgess, R.; Rivkin, C.; Post, M.; Boon-Brett, L.; Black, G.; Harskamp, F.;. Moretto, P.; Proceedings of the National Hydrogen Association Conference and Expo, Long Beach, CA, May 3–6, 2010.

4. "Round Robin Testing of Commercial Hydrogen Sensor Performance – Observations and Results,".Post, M., NHA Conference and Expo, May 2010.

5. "Hydrogen Sensor Performance – Calibration and Maintenance Issues," Buttner, W.; Post, M.; Burgess, R.; Rivkin, C.; Telcordia Fire Forum Denver, CO September 2, 2010.

6. "U.S. DOE Hydrogen Component and System Qualification Workshop Summary," Sandia National Laboratory, Livermore , CA, November 4, 2010.

7. "SAE J2579 Validation Testing Program Powertech: Final Report," McDougall, M., NREL Report No. SR-5600-49867, Dec 2010.

8. "Hydrogen Safety Sensor Testing and Deployment--The NREL Sensor Laboratory," Buttner, W. J.; Burgess, R.; Post, M.; Rivkin, C.; to be published in the Proceedings of the Fuel Cell and Hydrogen Energy Association Conference, February 13–16, 2011, National Harbor, MD.

9. "Validation Testing in Support of Hydrogen Codes and Standards Development," Burgess, R.; McDougall, M.; Newhouse, N.; Buttner, W.; Rivkin, C.; Post, M.; International Conference on Hydrogen Safety (ICHS), Sep 2011.

10. "Matrix Effects on Hydrogen Safety Sensors," Buttner, W.J.; Burgess, R.; Rivkin, C.;. Post, M.; Boon-Brett, L.; Black, G.; Harskamp, F.; Moretto, P.; International Conference on Hydrogen Safety (ICHS), San Francisco, September, 2011.

VIII.4 Hydrogen Materials and Components Compatibility

Daniel Dedrick (Primary Contact), Brian Somerday, Chris San Marchi
Sandia National Laboratories
P.O. Box 969
Livermore, CA 94551-0969
Phone: (925) 294-1552
E-mail: dededri@sandia.gov

DOE Manager
HQ: Antonio Ruiz
Phone: (202) 586-0729
E-mail: Antonio.Ruiz@ee.doe.gov

Start Date: Fiscal Year (FY) 2003
End Date: Project continuation and direction determined annually by DOE

FY 2011 Objectives

(1) Populate Technical Reference on Hydrogen Compatibility of Materials
  - Summarize data from published technical documents in a Web-based resource.
  - Update published Technical Reference chapters to reflect new data from Sandia materials testing activities.

(2) Develop and Validate Materials and Components Test Methods
  - Enable technology deployment by generating critical material-property data for structural materials in hydrogen gas, emphasizing commercial materials tested in high-pressure hydrogen.
  - Optimize efficiency and reliability of standardized test procedures for generating design data for structural materials in high-pressure hydrogen gas.

(4) Provide Science-Basis for Codes and Standards Development
  - Perform testing and analysis to provide the technical basis for codes and standards.
  - Provide leadership in the hydrogen codes and standards development/change process.

Technical Barriers

This project addresses technical barriers from the Hydrogen Codes and Standards section of the Fuel Cell Technologies 2007 Multi-Year Research Plan:

(F) Limited DOE Role in the Development of International Standards

(I) Conflicts between Domestic and International Standards

(N) Insufficient Technical Data to Revise Standards

Contribution to Achievement of DOE Codes and Standards Milestones

This project will contribute to achievement of the following DOE milestones from the Codes and Standards section of the Fuel Cell Technologies Program Multi-Year Research, Development and Demonstration Plan:

- **Milestone 21:** Completion of necessary codes and standards needed for the early commercialization and market entry of hydrogen energy technologies (4Q, 2012). This project enables the development and implementation of codes and standards by providing expertise and data on hydrogen compatibility of structural materials.
- **Milestone 25:** Draft regulation for comprehensive hydrogen fuel cell vehicle requirements as a GTR approved (UN Global Technical Regulation). (4Q, 2010)

FY 2011 Accomplishments

- Organized and convened Hydrogen Compatible Materials Workshop in November, 2010.
- Exercised leadership roles in developing standards (Society of Automotive Engineers [SAE] J2579 and Canadian Standards Association [CSA] Compressed Hydrogen Materials Compatibility [CHMC]1) for qualifying hydrogen compatibility of materials and components.
- Conducted materials testing designed to improve fatigue life methods in SAE J2579 and CSA CHMC1 standards.



Introduction

A major barrier to the deployment of hydrogen technologies is the lack of validated safety codes and standards. The purpose of this project is to provide the technical basis for assessing the safety of hydrogen-based systems with the accumulation of knowledge feeding into the development or modification of relevant codes and standards. The materials compatibility effort focuses on developing optimized materials qualification methodologies and assembling a resource entitled the Technical Reference on Hydrogen Compatibility of Materials. This effort is driven by the need for a materials guide, as identified in the Multi-Year Research, Development and Demonstration Plan (Table 3.7.5). The content of the Technical Reference

is assembled through the process of vetting, consolidating, and documenting materials data from journal articles and institutional reports. Gaps in the database content uncovered during the process of composing the Technical Reference are addressed through a materials testing activity. Results from this materials testing illuminate the pathways to optimize materials qualification methods, enabling efficient, high quality testing to support rapid technology deployment.

Approach

The focus of the Hydrogen Materials and Components Compatibility project is to optimize materials characterization methodologies, generate critical hydrogen compatibility data for materials to enable technology deployment, and compose the Technical Reference on Hydrogen Compatibility of Materials. Two activities proceed in parallel: generating new data and understanding through materials testing, and identifying and summarizing existing data from technical documents. The high-priority structural materials featured in these activities are low-alloy and carbon steels, austenitic stainless steels, and aluminum alloys. The materials testing activity emphasizes high hydrogen gas pressures (>100 MPa), fatigue crack initiation and propagation test methods, and technology-critical material fabrication (e.g. welds) and service variables (e.g., temperature). The data from materials testing are rigorously reviewed to identify pathways to improve the test methods and to ensure the data are suitable for implementation in structural design.

As part of codes and standards advocacy, Sandia personnel provide leadership in the codes and standards development process through direct participation in organizations such as the American Society of Mechanical Engineers, CSA, and SAE. This participation ensures that the standards development organizations have the most current technical information on structural materials compatibility. Sandia personnel provide leadership in the development of both component design standards as well as materials testing standards.

Results

Sandia led a Hydrogen Compatible Materials Workshop on November 3, 2010. The goal of the workshop was to coordinate and plan international research and development (R&D) to harmonize characterization and design methodologies for hydrogen-compatible materials and components. The output from the workshop was a summary document that would guide international R&D and code development road mapping. The workshop format consisted of several overview presentations followed by a working meeting involving 35 leading experts from research labs, government, industry, and standards development organizations. The presentations were designed to provide the context for identifying gaps in technology research and development as well as standards development for structural materials in hydrogen containment.

In the documented results of the workshop, several high-priority gaps were identified in the areas of technology development, code development, and research. For example:

- High-strength, low-cost materials for long-life hydrogen service.
- Measurements of mechanical properties of structural metals in high-pressure hydrogen gas, in particular fatigue properties.
- Influence of welds on hydrogen compatibility of structures.
- Publicly available database for properties of structural materials in hydrogen gas.

The Sandia team has leadership roles in developing sections of the SAE J2579 (“Technical Information Report for Fuel Systems in Fuel Cell and Other Hydrogen Vehicles”) and the CSA CHMC1 standards that are pertinent to qualifying structural metals for hydrogen containment. Currently, the potential for hydrogen effects on fatigue cracking of structural metals is not adequately addressed in the SAE J2579. The containment vessel is qualified for severe pressure-cycle service using hydraulic testing only. Sandia has provided the technical basis for the following safety qualification philosophy applied to the containment vessel:

- Certain structural metals exhibit minimal effects of hydrogen on fracture properties. For these structural metals, hydraulic testing is sufficient for qualifying the containment vessel for severe pressure cycling. Currently, two structural metals are in this category: 6061 aluminum and 316 stainless steel with greater than 12% nickel. Other structural metals can be included in this category provided the materials are subjected to four tests and meet the specified acceptance criterion for each test. The four tests (described in a new Appendix C.15) are the slow strain rate tensile test, two fatigue life tests, and the fatigue crack growth test, in which each test is conducted in hydrogen gas.
- Structural metals that do not meet the materials testing acceptance criteria in Appendix C.15 can still be selected for containment vessel components. In this case, the containment vessel must be subjected to both the hydraulic pressure cycling test and an additional severe pressure cycling test using hydrogen gas. The protocol for conducting this durability performance test using hydrogen gas has been included in the new Appendix C.14.

The SAE J2579 effort has involved coordination with international experts from the U.S., Japanese, and European automakers. The sections on qualifying structural metals for hydrogen containment are expected to also form the

foundation for addressing hydrogen compatibility of metal components in the Global Technical Regulation (GTR).

The Sandia team has a leadership role in the new CSA Technical Advisory Group (TAG) for the CHMC1 standard. The content of this standard focuses on reliable test methods for structural materials in hydrogen gas. This standard was motivated by the lack of specific methods for qualifying structural metals for hydrogen service in component standards, such as the CSA standards for fuel cell vehicle components. Component standards that do not contain specific guidance for qualifying structural metals in hydrogen service can reference the CHMC1 standard. The CHMC1 document is scheduled for review by CSA in August 2011.

The fatigue life materials test is considered to be particularly relevant for many hydrogen containment components on fuel cell vehicles. For example, this test has been included in both the CSA CHMC1 and SAE J2579 standards. Fatigue life tests that employ smooth or notched specimens are intended to evaluate the effect of hydrogen on fatigue crack initiation. The output from fatigue life testing is an "S-N curve" for the material, which is a locus of points representing the number of cycles to failure (N) for a constant stress amplitude (S) applied to the test specimen. One of the principal objectives of the fatigue life testing in this Materials Compatibility task is to evaluate whether fatigue crack initiation dominates the number of cycles to failure. For this objective, it must be recognized that the number of cycles to failure (N) consists of the number of cycles for crack initiation (N_i) plus the number of cycles for crack propagation (N_p). Since tests on smooth or notched specimens are intended to evaluate the effect of hydrogen on crack initiation, the ratio of N_i/N should be nearly equal to 1. The first series of tests in this task were intended to establish the N_i/N ratio for a notched specimen geometry that is proposed for the CSA CHMC1 and SAE J2579 standards.

The S-N curve was measured for cylindrical, circumferentially notched specimens fabricated from the austenitic stainless steel 21Cr-6Ni-9Mn (21-6-9). Specimens from hydrogen-charged (200 wppm H) and non-charged 21-6-9 were tested at constant stress amplitudes, and the number of cycles to failure, N, were recorded for each test. The tests were conducted at a load ratio, R (ratio of minimum stress to maximum stress), equal to 0.1 and a load-cycle frequency of 1 Hz. In addition, each specimen was instrumented with an extensometer and the direct-current potential difference system to detect crack initiation. Results showing the number of cycles for crack initiation, N_i, and the number of cycles to failure, N, for both hydrogen-charged and non-charged specimens are summarized in Figure 1.

Two results are notable in Figure 1. First, hydrogen does not have a significant effect on the fatigue life of the 21-6-9 stainless steel. Second, the number of cycles for crack initiation, N_i, is approximately 50% of the total number of cycles to failure. The second observation

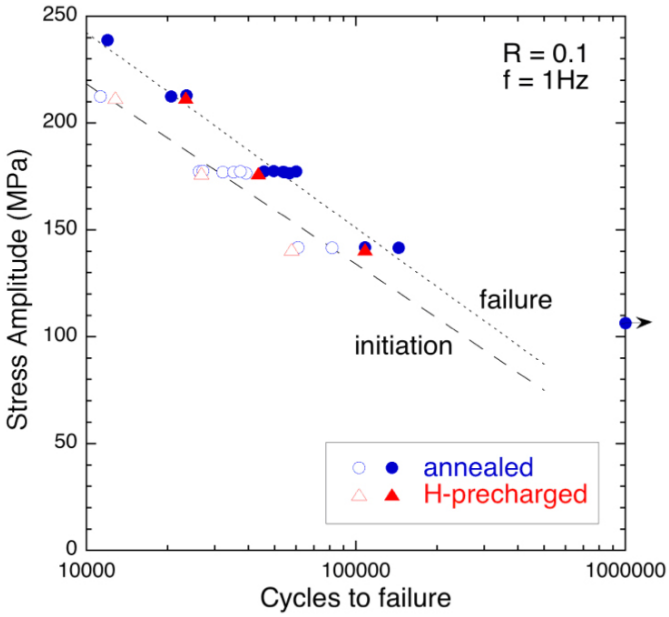


FIGURE 1. Stress amplitude (S) vs. number of cycles for crack initiation (N_i) and total number of cycles to failure (N) for hydrogen-charged and non-charged 21-6-9 stainless steel.

indicates that the number of cycles to failure measured from the circumferentially notched specimen does not adequately approximate the number of cycles for crack initiation. This insight may influence the specimen geometry that is specified in the CSA CHMC1 and SAE J2579 standards.

Hydrogen containment component stakeholders have expressed interest in aluminum alloys due to their compatibility with hydrogen gas and low cost relative to stainless steels. Consequently, Sandia has included modern, high-performance aluminum alloys in its materials testing activity. Although aluminum alloys are generally considered to be resistant to hydrogen-assisted fracture in dry hydrogen gas, some questions remain about applying reliable test methods. Sandia has conducted some preliminary fatigue crack growth testing on 7475-T7351 aluminum in 103 MPa hydrogen gas. Testing duration was greater than 60 hours, and the cyclic plastic deformation associated with fatigue testing was intended to promote the exposure of "fresh" (non-oxidized) metal surface to hydrogen gas. However, even in this testing condition, the results in Figure 2 show essentially no difference between the test in hydrogen gas and a test performed in laboratory air. These initial results support the notion that aluminum alloys have superior hydrogen compatibility among common structural metals.

Conclusions and Future Directions

In FY 2011:

- Hydrogen Compatible Materials Workshop identified important technology gaps:

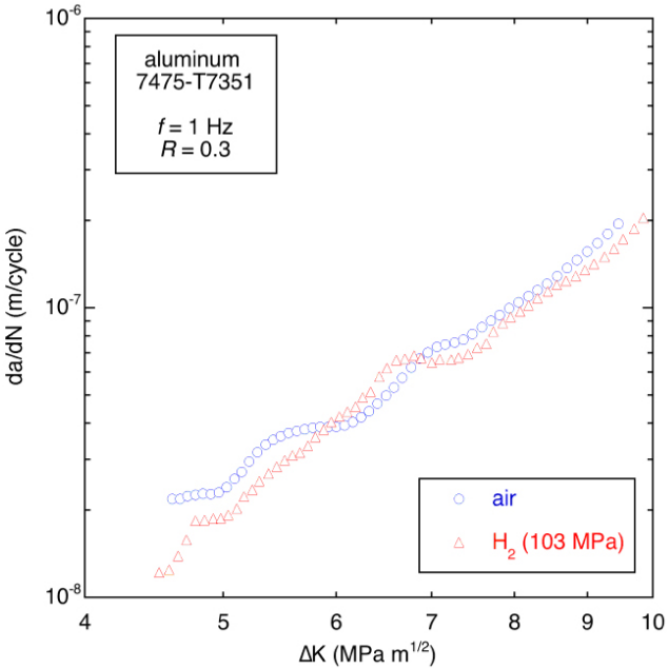


FIGURE 2. Fatigue crack growth rate (da/dN) vs. stress-intensity factor range (ΔK) relationships for 7475-T7351 aluminum in 103 MPa hydrogen gas and air.

  - Workshop output guides R&D prioritization.
- Methods developed for qualifying hydrogen compatibility of materials and components in two standards: SAE J2579 and CSA CHMC1.
- Materials testing motivated by standards development:
  - Improving fatigue life testing methods impacts SAE J2579 and CSA CHMC1.

Future Work:

- Establish optimum methods for measuring fatigue properties of steels in high-pressure hydrogen for inclusion in standards.
- Measure hydrogen-affected properties of representative stainless steel welds in gas distribution manifolds.
- Complete first draft of CSA CHMC1 standard.
- Procure pressure vessel with variable-temperature feature for new fatigue testing capability.

FY 2011 Publications/Presentations

1. (invited) "Addressing Hydrogen Embrittlement in the Fuel Cell Vehicle Standard SAE J2579", B. Somerday, International Hydrogen Energy Development Forum 2011, Fukuoka, Japan, Feb. 2011.

2. (invited) "Improving the Fatigue Resistance of Ferritic Steels in Hydrogen Gas", B. Somerday, I^{2}CNER Kick-off Symposium, Fukuoka, Japan, Feb. 2011.

3. "Hydrogen Effects on Materials for CNG / H_2 Blends", B. Somerday, D. Farese, and J. Keller, International Hydrogen Fuel and Pressure Vessel Forum 2010, Beijing, China, Sept. 2010.

4. "Fracture and Fatigue Tolerant Steel Pressure Vessels for Gaseous Hydrogen", K. Nibur, C. San Marchi, and B. Somerday, Proceedings of the ASME 2010 Pressure Vessels & Piping Division / K-PVP Conference (PVP2010), July 18–22, 2010, Bellevue, Washington, USA.

5. "Austenitic Stainless Steels", C. San Marchi, in *Gaseous Hydrogen Embrittlement of Materials in Energy Technologies*, R. Gangloff and B. Somerday, Eds., Woodhead Publishing, Cambridge, UK, 2011, in press.

6. "Mechanical Test Methods for Gaseous Hydrogen Embrittlement ", K. Nibur and B. Somerday, in *Gaseous Hydrogen Embrittlement of Materials in Energy Technologies*, R. Gangloff and B. Somerday, Eds., Woodhead Publishing, Cambridge, UK, 2011, in press.

Sandia National Laboratories is a multi-program laboratory managed and operated by Sandia Corporation, a wholly owned subsidiary of Lockheed Martin Corporation, for the U.S. Department of Energy's National Nuclear Security Administration under contract DE-AC04-94AL85000.

VIII.5 Component Testing for Industrial Trucks and Early Market Applications

Daniel Dedrick (Primary Contact), Brian Somerday, Chris San Marchi
Sandia National Laboratories
P.O. Box 969
Livermore, CA 94551-0969
Phone: (925) 294-1552
E-mail: dededri@sandia.gov

DOE Manager
HQ: Antonio Ruiz
Phone: (202) 586-0729
E-mail:Antonio.Ruiz@ee.doe.gov

Start Date: Fiscal Year (FY) 2010
End Date: Project continuation determined annually by DOE

FY 2011 Objectives

(1) Provide technical basis for the development of standards defining the use of steel (type 1) storage pressure vessels for gaseous hydrogen:
  - Compare fracture mechanics based design approach for fatigue assessment of pressure vessels for gaseous hydrogen to full-scale performance tests.
  - Generate performance test methods and data for fatigue assessment of full-scale pressure vessels with gaseous hydrogen.

(2) Codes and standards advocacy:
  - Participate in the standards development activities for gaseous hydrogen storage in pressure vessels, in particular Canadian Standards Association (CSA) and Society of Automotive Engineers (SAE) activities.

Technical Barriers

This project addresses technical barriers from the Codes and Standards section of the Fuel Cell Technologies 2007 Multi-Year Research Plan:

(F) Limited DOE Role in the Development of International Standards

(I) Conflicts between Domestic and International Standards

(N) Insufficient Technical Data to Revise Standards

Contribution to Achievement of DOE Codes and Standards Milestones

This project will contribute to achievement of the following DOE milestones from the Codes and Standards section of the Fuel Cell Technologies Program Multi-Year Research, Development and Demonstration Plan:

- **Milestone 21:** Completion of necessary codes and standards needed for the early commercialization and market entry of hydrogen energy technologies (4Q, 2012). This project enables the development and implementation of codes and standards by providing expertise and data on hydrogen compatibility of hydrogen pressure vessels.
- **Milestone 25:** Draft regulation for comprehensive hydrogen fuel cell vehicle requirements as a GTR approved (UN Global Technical Regulation). (4Q, 2010)

FY 2011 Accomplishments

- Built infrastructure for accelerated pressure cycling of hydrogen storage tanks.
- Fatigue crack growth testing of low-alloy steels extracted for pressure vessels shows engineering predictions to be conservative relative to performance testing of pressure vessels.
- Pressure cycling of two pressure vessel designs (T1 and T2 respectively):
  - T1 design: >47,000 cycles (and continuing three tanks as of July 2011).
  - T2 design: >26,000 cycles (and continuing one tank as of July 2011).
- Pressure cycling pressure vessels with engineered defects to quantify effects of existing flaws:
  - Four failures observed (stable through-wall cracks).
  - Greater number of cycles to failure than predictions.
- Procedures for pressure testing with gaseous hydrogen are being included in CSA Hydrogen Powered Industrial Truck (HPIT)1 and SAE J2579 working documents for performance testing.



Introduction

Fatigue cracks can nucleate and grow in metals subjected to cyclic stress. The increment of crack growth per load cycle (da/dN) is a function of the driving force for fatigue cracking, which is called the applied stress intensity factor range (ΔK). Under conditions of stable fatigue crack growth, a simple empirical relationship can be used to describe fatigue crack growth in terms of the driving force: $da/dN = C(\Delta K)^m$, where C and m are experimentally determined constants.

Fatigue crack growth of a pressure vessel subjected to pressure cycling is enabled by the presence of manufacturing defects in the steel and accelerated by exposure to gaseous hydrogen. The latter characteristic is often referred to as "hydrogen embrittlement" and depends on the partial pressure of the gaseous hydrogen and the kinetics of hydrogen uptake into the steel. Consequently, the fatigue crack growth relationship is affected by variables such as hydrogen pressure, pressure-cycle frequency, pressure-time relationship (wave form), and temperature.

Although steel pressure vessels may be vulnerable to fatigue crack growth aided by hydrogen embrittlement, the industrial gas companies have used such pressure vessels for hydrogen transport and storage for decades. Typically, these pressure vessels are subjected to less than one pressure cycle per day (and in many cases less than one cycle per month), thus fatigue crack growth is generally not a concern. Pressure vessels for hydrogen storage in new applications such as those for lift trucks are anticipated to experience up to six pressure cycles per day, approaching an order of magnitude greater than the duty cycle of typical transportable industry gas pressure vessels.

Since the duty cycle for lift truck pressure vessels is outside the window of current experience, a methodology for determining the cycle life must be established. A deterministic engineering analysis for quantifying the progression of fatigue cracks is provided in the American Society of Mechanical Engineers (ASME) Boiler and Pressure Vessel Code (Section VIII, Division 3, Article KD-4) and extended to the specific case of high-pressure gaseous hydrogen in Article KD-10. This framework provides a method for conservatively estimating the fatigue cycle life of pressure vessels based on assessment of existing flaws in the pressure vessel. An alternate method has been proposed based on the measured performance of manufactured pressure vessels subjected to pressure cycling coupled with statistical assessment of the quality of the pressure vessels and desired cycle life. These two methods have been referred to as engineering analysis method and performance evaluation method respectively.

Approach

During this project, pressure vessels are being pressure cycled with gaseous hydrogen; the pressure vessels are identical to those in service for fuel cell forklift applications with gaseous hydrogen, with the exception that defects are engineered in some pressure vessels. The engineered defects were designed to simulate manufacturing flaws in the pressure vessels. Engineering analysis methods are being employed to compare the engineering analysis predictions with experimental results from the performance evaluation of full-scale pressure vessels. These efforts have required collaborations with fuel cell system integrators and pressure vessel manufacturers to obtain as-manufactured pressure vessels and produce pressure vessels with engineered defects for cycle testing, as well as develop a testing plan that reflects relevant engineering conditions, including pressure vessel designs, manufacturing flaws, and pressurization schedules. Additionally, direct participation in standards development activities has been a cornerstone of this effort, in particular with the technical advisory group for CSA's HPIT1 and the subgroup drafting the language for the pressure vessel appendix in SAE J2579.

Results

Materials Testing

Sandia National Labs measured the rate of fatigue crack growth for three heats of 4130 steels in high-pressure gaseous hydrogen; testing coupons were extracted from pressure vessels supplied by the industrial partners (each heat of material came from a different vendor). Details of these experiments are given in reference [1]. The measured fatigue crack growth rates are shown in Figure 1, showing that all three materials performed nominally the same in gaseous hydrogen. ASME Boiler and Pressure Vessel Code (VIII-3) Article KD-10 requires the testing of three heats of a given steel to demonstrate that the effects of hydrogen are not sensitive to variations in the material's microstructure or processing history. These measured fatigue crack growth rates are used to predict cycle life using engineering analysis methodologies that quantify crack growth through the vessel wall from manufacturing flaws in the pressure vessel.

Full-Scale Tank Testing

A system was designed and constructed to pressure cycle up to 10 full-scale tanks in parallel at a rate of approximately 250 discrete pressure cycles per day (approximately 5-minute pressure cycle time). The pressure vessels are cycled between 3.4 and 43.8 MPa, with an approximately 2-minute pressure ramp rate, 2-minute hold time at maximum pressure, 30-second depressurization rate,

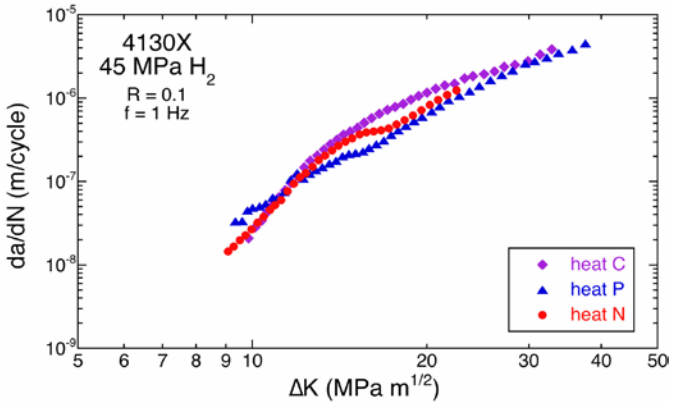


FIGURE 1. Fatigue Crack Growth Rates for three Heats of 4130X Steels (taken from reference [2])

and 30-second hold at minimum pressure. Details of the system, experimental procedures, and additional explanation of results are given in reference [2]. At the time of writing, pressure vessels have cycled for as many as 47,000 cycles without failure, although not all pressure vessels have experienced this number of cycles. Pressure vessels with engineered defects have been subjected to fewer cycles and four vessels have failed after as few as 8,000 cycles. Figure 2 shows the number of cycles that many of the pressure vessels have experienced as a function of the initial defect size for those pressure vessels with engineered defects. Also shown in this figure are the estimates of the cycle life assuming the engineered defects began propagating after the first pressure cycle. Clearly, these estimates underestimate the cycle life. Generally, there are two components to fatigue life, crack initiation and crack propagation. The engineering predictions are based on crack propagation only, since there is no broadly accepted way to account for crack initiation.

Leak-before-burst was observed for each of the four pressure vessel failures. This is an important observation because larger safety factors are generally applied when burst is a probable failure mode. Additionally, postmortem analysis suggests that the engineered defects form cracks that propagate with a semicircular profile (Figure 3), although as the crack depth reaches the full thickness of the vessel the shape again changes (Figure 4). This is also an important observation if shown to be generally true. Cracks with larger aspect ratios (such as the aspect ratio of the engineered defects) propagate at higher rates because the driving force is greater for a “long” crack compared to a “short” crack of the same depth.

These results are currently being discussed in the technical advisory committee for CSA HPIT1. The testing procedures are also being considered in SAE J2579.

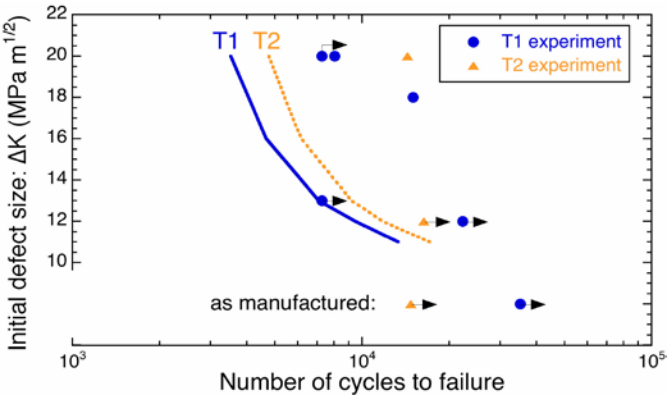


FIGURE 2. The number of cycles to failure in the cycled pressure vessels are given by symbols; arrows indicate that the pressure vessel is still cycling at the time of writing. The curves represent the estiamted cycles to propgate the initial defect to a through-wall crack (taken from reference [2]).

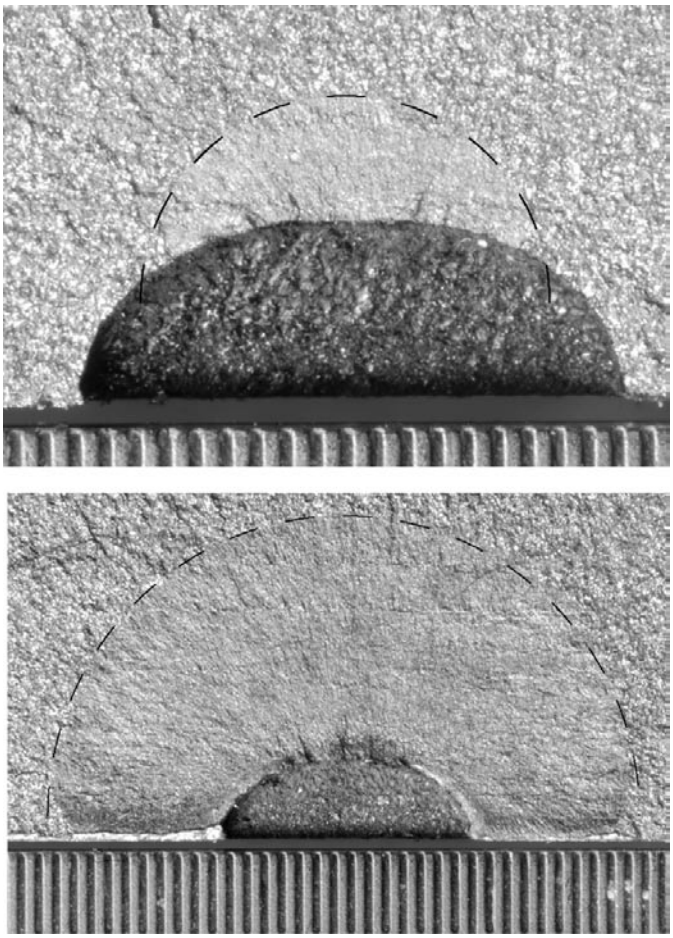


FIGURE 3. Crack extension from engineering defects that did not extend through the thickness of the pressure vessel have a semicircular profile.

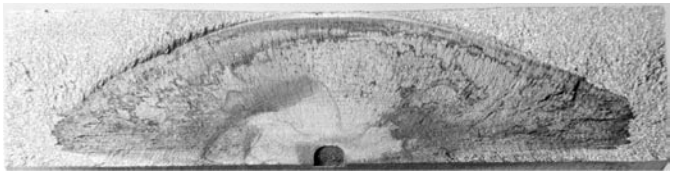


FIGURE 4. Through-wall cracks associated with the engineering defects do not have a semicircular crack profile.

Conclusions and Future Directions

- Commercial pressure vessels being used for hydrogen storage on forklifts have been subjected to more than 47,000 pressure cycles with gaseous hydrogen (between pressure of 3.4 and 43.8 MPa):
  - Primary aim of the remainder of project is to cycle tanks until they fail or reach 50,000 cycles.
- Fatigue crack growth assessment of engineered defects in these pressure vessels using engineering analysis appears to be conservative:

  - Post-mortem analysis is being used to refine predictions and interpret failure process.
- Code language based on the test methods developed in this study are being drafted as part of CSA HPIT1 and SAE J2579 for performance based tests:
  - Results are being shared with committees as they are generated.
- Leak-before-burst was observed in all failures.

References and FY 2011 Publications/ Presentations

1. "Fracture and Fatigue Tolerant Steel Pressure Vessels for Gaseous Hydrogen", K. Nibur, C. San Marchi, and B. Somerday, *Proceedings of the ASME 2010 Pressure Vessels & Piping Division / K-PVP Conference*, Bellevue, Washington, July 18–22, 2010.

2. "Pressure Cycling of Type 1 Pressure Vessels with Gaseous Hydrogen", C. San Marchi, D.E. Dedrick, P. Van Blarigan, B.P. Somerday, K.A. Nibur, 4th International Conference on Hydrogen Safety (ICHS4), 12–14 September 2011, San Francisco CA.

Sandia National Laboratories is a multi-program laboratory managed and operated by Sandia Corporation, a wholly owned subsidiary of Lockheed Martin Corporation, for the U.S. Department of Energy's National Nuclear Security Administration under contract DE-AC04-94AL85000.

VIII.6 National Codes and Standards Coordination

Carl Rivkin, (Primary Contact), Chad Blake, Robert Burgess, William Buttner, and Matthew Post
National Renewable Energy Laboratory (NREL)
1617 Cole Boulevard
Golden, CO 80401
Phone: (303) 275-3839
E-mail: carl.rivkin@nrel.gov

DOE Manager
HQ: Antonio Ruiz
Phone: (202) 586-0729
E-mail: Antonio.Ruiz@ee.doe.gov

Subcontractors:
- Bethlehem Hydrogen, Emmaus, PA
- CSA Standards, Cleveland, OH
- FP2 Fire Protection Engineering, Golden, CO
- GWS Solutions, Tolland, CT
- Kelvin Hecht, Avon, CT
- MorEvents, Englewood, CO
- SAE International (SAE), Warrendale, PA
- Sloane Solutions, Oxford, MI
- Steele Consulting, Cypress, CA

Project Start Date: 1995
Project End Date: Project continuation and direction determined annually by DOE

Fiscal Year (FY) 2011 Objectives

- Facilitate the safe deployment of hydrogen and fuel cell technologies.
- Identify the codes and standards required to deploy hydrogen and fuel cell technologies. Identify the research and validation testing required to support the development of the needed codes and standards.
- Advance safety, code development, and market transformation through collaboration with appropriate stakeholders.

Technical Barriers

This project addresses the following technical barriers from the Safety, Codes and Standards section (3.7) of the Fuel Cell Technologies Program Multi-Year Research, Development and Demonstration Plan:

(A) Limited Government Influence on Model Codes
(B) Competition among SDOs and CDOs
(C) Limited State Funds for New Codes
(D) Large Number of Local Government Jurisdictions.
(E) Lack of Consistency in Training of Officials
(F) Limited DOE Role in the Development of International Standards
(G) Inadequate Representation at International Forums
(H) International Competitiveness
(I) Conflicts between Domestic and International Standards
(J) Lack of National Consensus on Codes and Standards
(K) Lack of Sustained Domestic Industry Support at International Technical Committees
(L) Competition in Sales of Published Standards
(M) Insufficient Technical Data to Revise Standards
(N) Affordable Insurance is Not Available
(O) Large Footprint Requirements for Hydrogen Refueling Stations
(P) Parking and Other Access Restrictions

Technical Targets

Table 1 shows the NREL support for achieving DOE technical targets, specifically supporting the development of the codes and standards required to deploy hydrogen and fuel cell technologies. This technical target is described on pages 3.7-1 and 2 of the Codes and Standards – Technical Plan.

FY 2011 Accomplishments

NREL accomplished the following in support of section 3.7 of the DOE Fuel Cell Technologies Program Multi-Year Research, Development and Demonstration Plan:

- NREL supported the development of National Fire Protection Association (NFPA) 2 Hydrogen Technologies Code that was published as a final document January 2011. NREL staff acted as a principal member of the NFPA Hydrogen Technology Technical Committee and acted as task group leader with the planning task group.
- Sensor Workshop: NREL conducted a Sensor Workshop in June 2011. The purpose of the workshop was to review the performance benchmarks set at the 2007 DOE Sensor Workshop and refine them based on defining performance criteria for specific applications. These applications include indoor hydrogen fueling, hydrogen storage, and residential fuel cells and fuel dispensing.
- Component testing: Initiated test work on compressed natural gas (CNG) nozzle failures. The purpose of this project is to determine the root cause for CNG nozzle failures that took place approximately 10 years ago. The concern is that the same failure mechanism may be an issue with hydrogen fueling operations. Test results should be available by the end of FY 2011.

TABLE 1. Progress toward Meeting Technical Targets for Safety Codes and Standards

DOE Accomplishments in Support of the Development of Regulations, Codes and Standards for the Deployment of Hydrogen and Fuel Cell Technologies			
Regulation, Code, or Standard	**NREL Support**	**Status**	**Time Saved Producing Document (resulting from DOE support)**
1. Global Technical Regulation for Fuel Cell Vehicles	Tank testing data, SAE standard that provided basis for document, expert technical support from Dr. Sloane and Glenn Scheffler	Phase 1 work complete in 2011	5 years
2. NFPA 2 Hydrogen Technologies Code	Extensive technical analysis to develop risk informed requirements for siting hydrogen storage systems. Extensive logistical support including support committee chair and consultant producing draft code document	Final document promulgated 2011	3 years
3. International Fire Code (IFC) Section 2209 Hydrogen Motor-Fuel Dispensing and Generation Facilities	Supported Hydrogen Ad Hoc Working Group that wrote section 2209	Final document promulgated 2003	6 years
4. SAE J2579 Technical Information Report (TIR) for Fuel Systems in Fuel Cell and Other Hydrogen Vehicles	Performed validation testing through subcontractor Provided logistical support for SAE Fuel Cell Technical Committee	TIR published 2009	3 years
5. SAE J2601 Fueling Protocols for Light Duty Gaseous Hydrogen Surface Vehicles	Performed validation testing for fueling algorithm in standard. Provided logistical support for SAE Fuel Cell Technical Committee	Standard published 2010	3 years
6. International Organization for Standardization (ISO) 14687 Hydrogen fuel – Product specification – Part 2: Proton exchange membrane fuel cell applications for road vehicles, SAE J2719 – Development of a Hydrogen Quality Guideline for Fuel Cell Vehicles	Extensive test data, logistical support, and coordination of ISO/SAE standard development activities	Both documents will likely be issued as final in 2011	5 years
7. CSA Standards H series of component standards for hydrogen dispensing operations and onboard vehicle safety	Extensive logistical support as well as validation testing of the high-pressure relief device standard	Documents published as drafts to be issued as final documents in 2011 and 2012 for hydrogen gaseous vehicle 4.3	6 years
8. American Society of Mechanical Engineers B31.12 Hydrogen Piping and Pipelines	Provided test data and logistical support	Final document 2008	3 years
9. Compressed Gas Association Hydrogen Documents including G-5 through G5-8	Provided logistical support	Documents issued 2004 through 2007	3 years

- Fuel quality specification: NREL continued to support the promulgation of ASTM standards that require contaminant testing to show compliance with the ISO standard through funding the production of calibration gases required to verify the ASTM test methods. Additionally, NREL supported the work of Michael Steele, Chairman of the SAE Fuel Cells Technical Committee, who has produced an Information Report on the development of a hydrogen quality guideline for fuel cell vehicles.
- Codes and standards coordination: NREL continued to support the coordination of codes and standards development through software that identified the standards development organizations (SDOs) and dode development organizations (CDOs) involved in hydrogen and fuel cell technologies codes and standards development. NREL has updated this software to include current project information.
- Subcontract Management: NREL assumed responsibility for several additional subcontracts. NREL staff developed new statements of work for these subcontracts that reflect DOE priorities and budget constraints.

Introduction

It is essential to develop and promulgate codes and standards in order to provide for the safe use of hydrogen and fuel cell technologies. With the help of key stakeholders, the DOE Fuel Cell Technologies (FCT) Program and NREL are coordinating a collaborative national effort to prepare, review, and promulgate codes and standards for all hydrogen and fuel cell technologies.

Approach

The FCT program recognizes that domestic and international codes and standards must be established to enable the timely commercialization and safe use of hydrogen and fuel cell technologies. The lack of codes and standards applicable to hydrogen and fuel cell technologies is an institutional barrier to deploying these technologies. It is in the national interest to eliminate this potential barrier. As such, the sub-program works with domestic and international SDOs to facilitate the development of performance-based and prescriptive codes and standards. These standards are then referenced by building and other codes to expedite regulatory approval of hydrogen and fuel cell technologies. This approach ensures that United States (U.S.) consumers can purchase products that are safe and reliable, regardless of their country of origin, and that U.S. companies can compete internationally by having coordinated consistent requirements.

Results

The Safety, Codes and Standards work is divided into three major areas:

1. Codes and Standards Coordination
2. Codes and Standards Research
3. Codes and Standards Training and Outreach

This report addresses the National Template.

Codes and Standards Coordination

Figure 1, Hierarchy of Codes and Standards Implementation, shows both the hierarchy for enforcing codes and standards and some of the progress made in promulgating the codes and standards required to implement hydrogen and fuel cell technologies. Figure 2 shows the front page of the coordinating software NREL has developed to track codes and standards development activities.

In FY 2011 substantial progress was made in this implementation effort. NFPA 2 Hydrogen Technologies Code was published as a final document in January 2011. NREL will be working on coordinating the requirements of NFPA 2 with the hydrogen requirements in the IFC through a proposal to reference NFPA 2 in the 2015 edition of the IFC. NREL supported the development of NFPA 2 in several ways, including:

- Participated as a principal member of the technical committee.
- Funded subcontractors actively participating in the development of the document such as FP2 Fire Protection Engineering.
- Hosted Report on Comment meeting.

Another important part of codes and standards is the development of hydrogen fueling station component and system standards being performed by CSA Standards. These H-4 series of documents consists of nine component standards and one system standard that addresses hydrogen dispensing. An NREL staff member participated as a member of the CSA technical committee drafting these documents.

NREL supports the Fuel Cell and Hydrogen Energy Codes and Standards Coordinating Committee by coordinating and directing monthly meetings where SDOs,

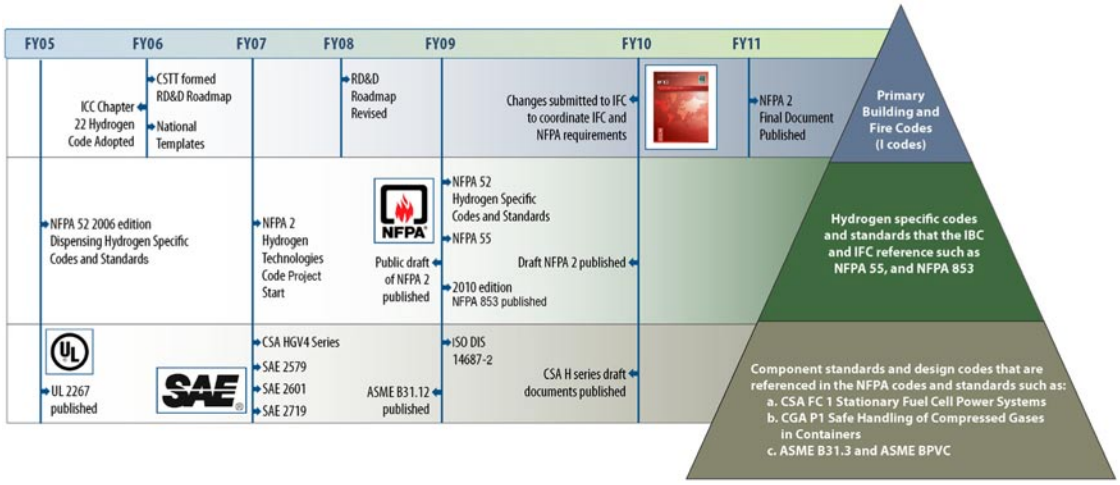


FIGURE 1. Hierarchy of Codes and Standards Implementation

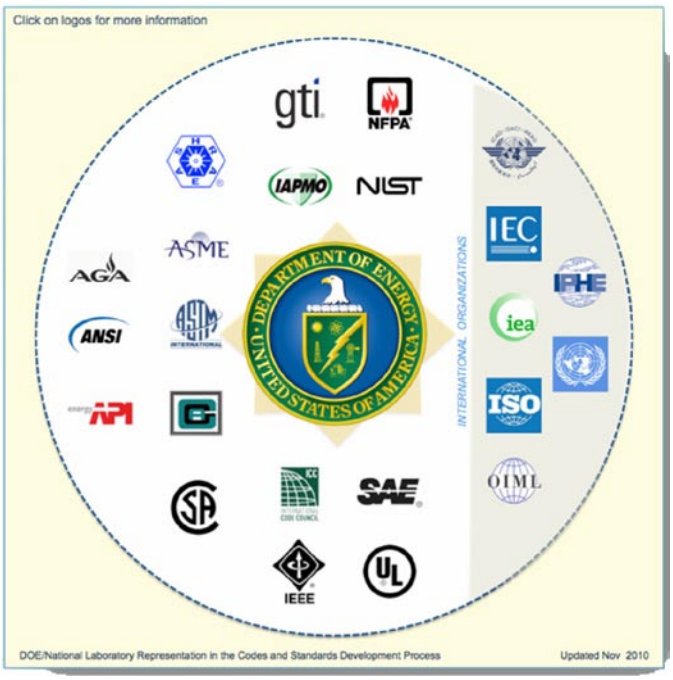


FIGURE 2. NREL Codes and Standards Coordinating Software

DOE laboratories, industry representatives, DOE and other interested parties are given topical information on codes and standards development activities.

NREL also supports the Hydrogen Industry Panel on Codes that has as its primary objective the coordination of hydrogen safety requirements in the IFC and other key International Code Council codes such as the International Building Code and the NFPA hydrogen safety requirements that reside primarily in NFPA 2.

NREL supports both the development of fuel quality standards through acquiring test data and coordinating the activities of the ISO Technical Committee 197 and the SAE Fuel Cell Technical Committee. These efforts resulted in the promulgation of SAE J2719.

Conclusions and Future Direction

NREL will continue to support the development of codes and standards by:

- Working with DOE to implement a plan for identifying and supporting the development of the codes and standards required to deploy hydrogen and fuel cell technologies with a particular emphasis on road vehicles by the year 2020 (the 2020 Deployment Plan).
- Continuing research and development at the NREL Sensor Laboratory to support the development of sensors required to deploy hydrogen and fuel cell technologies.
- Managing subcontracts required to support the 2020 Deployment Plan.
- Performing outreach work to distribute information on hydrogen and fuel cell technologies to code officials, project developers, and other interested parties.
- Coordinating domestic codes and standards and international standards to ensure consistent requirements.

FY 2011 Publications/Presentations

1. Rivkin, C., "Hydrogen Fuel Cell Vehicle Regulations, Codes, and Standards," 2011 (Draft Chapter in Hydrogen Technologies Book).

VIII.7 Codes and Standards Outreach for Emerging Fuel Cell Technologies

Carl Rivkin, (Primary Contact), Chad Blake, Robert Burgess, William Buttner, and Matthew Post
National Renewable Energy Laboratory (NREL)
1617 Cole Boulevard
Golden, CO 80401
Phone: (303) 275-3839
E-mail: carl.rivkin@nrel.gov

DOE Manager
HQ: Antonio Ruiz
Phone: (202) 586-0729
E-mail: Antonio.Ruiz@ee.doe.gov

Subcontractor:
MorEvents, Englewood, CO

Project Start Date: 1995
Project End Date: Project continuation and direction determined annually by DOE

Fiscal Year (FY) 2011 Objectives

- Facilitate the safe deployment of hydrogen and fuel cell technologies.
- Provide information on hydrogen and fuel cell technologies codes and standards to code officials, project developers, and other interested parties.
- Present workshops on hydrogen and fuel cell technologies codes and standards to code officials, project developers, and other interested parties in geographic areas where these technologies are being deployed.
- Develop tools to streamline the permitting process for fuel cell and hydrogen technology projects.
- Perform site visits to fuel cell and hydrogen technology project sites to obtain safety, codes and standards information for publication in technical reports.
- Present safety, codes and standards information on DOE websites and through webinars.

Technical Barriers

This project addresses the following technical barriers from the Safety, Codes and Standards section (3.7) of the Fuel Cells Technologies Program Multi-Year Research, Development and Demonstration Plan:

(A) Limited Government Influence on Model Codes
(B) Competition among SDOs and CDOs
(C) Limited State Funds for New Codes
(D) Large Number of Local Government Jurisdictions.
(E) Lack of Consistency in Training of Officials
(F) Limited DOE Role in the Development of International Standards
(G) Inadequate Representation at International Forums
(H) International Competitiveness
(I) Conflicts between Domestic and International Standards
(J) Lack of National Consensus on Codes and Standards
(K) Lack of Sustained Domestic Industry Support at International Technical Committees
(L) Competition in Sales of Published Standards
(M) Insufficient Technical Data to Revise Standards
(N) Affordable Insurance is Not Available
(O) Large Footprint Requirements for Hydrogen Refueling Stations
(P) Parking and Other Access

Technical Targets

Table 1 shows the NREL support for achieving DOE technical targets, specifically supporting the development of the codes and standards required to deploy hydrogen and fuel cell technologies. This technical target is described on pages 3.7-1 and 2 of the Codes and Standards – Technical Plan.

TABLE 1. Progress towards Meeting Technical Targets for Safety Codes and Standards

DOE/NREL Accomplishments in Support of the Development of Regulations, Codes and Standards for the Deployment of Hydrogen and Fuel Cell Technologies Outreach Activities		
Activity	Primary Impacted Groups	Progress Towards Meeting DOE Targets
Safety Codes and Standards Workshops	Code officials, project developers, and other interested parties	Workshops make information available to expedite process for developing and permitting fuel cell and hydrogen technology projects
Sensor Workshop	Sensor developers, project managers	Improve performance of sensors to increase project safety
Updating codes and standards citations on DOE websites	Code officials, project developers, and other interested parties	Web information make information available to expedite process for developing and permitting fuel cell and hydrogen technology projects
Permitting template for hydrogen dispensing stations	Code officials and project developers	Standardized permitting will streamline permitting for fuel cell and hydrogen technology projects
Hydrogen dispensing station site visit and technical report	Project developers	Improve fuel cell and hydrogen codes and standards by identifying safety issues that can be addressed by codes and standards modifications

Accomplishments

NREL accomplished the following in support of section 3.7 of the DOE Fuel Cell Technologies Program Multi-Year Research, Development and Demonstration Plan:

- Sensor Workshop: NREL conducted a Sensor Workshop in June 2011. The purpose of the workshop was to review the performance benchmarks set at the 2007 DOE Sensor Workshop and refine them based on defining performance criteria for specific applications. These applications include indoor hydrogen fueling, hydrogen storage, and residential fuel cells and fuel dispensing.
- Web Updates: NREL updated the codes and standards citations on the DOE website. Additionally, NREL streamlined the website by removing redundant material.
- Codes and Standards Workshops: NREL conducted a Codes and Standards Workshop on April 19, 2011 in collaboration with the California Fuel Cell Partnership and the Southern California Fire Protection Officers Association. Attendees at this workshop included fire service representatives from several of the key jurisdictions in the Los Angeles metropolitan area.
- Permit Template for Hydrogen Dispensing Stations: NREL developed a permitting template for hydrogen dispensing stations that contains the basic codes and standards requirements used across the United States (U.S.) jurisdictions can modify this template to create a standard permit for hydrogen dispensing stations.
- Hydrogen Dispensing Station Site Visit: NREL performed a site visit to a hydrogen dispensing station to evaluate code compliance and safety issues. The results of the visit will be documented in a NREL Technical Report.



Introduction

It is essential to develop and promulgate codes and standards in order to provide for the safe use of hydrogen and fuel cell technologies. With the help of key stakeholders, the DOE Fuel Cell Technologies Program and NREL are coordinating a collaborative national effort to prepare, review, and promulgate codes and standards for all hydrogen and fuel cell technologies. To complement this codes and standards development effort, NREL is conducting outreach activities to inform code officials, project developers, and other interested parties of these codes and standards requirements.

Approach

Domestic and international codes and standards must be established to enable the timely commercialization and safe use of hydrogen and fuel cell technologies. The lack of codes and standards applicable to hydrogen and fuel cell technologies is an institutional barrier to deploying these technologies. It is in the national interest to eliminate this potential barrier. As such, the sub-program works with domestic and international standards development organizations to facilitate the development of performance-based and prescriptive codes and standards. These standards are then referenced by building and other codes to expedite regulatory approval of hydrogen and fuel cell technologies. This approach ensures that U.S. consumers can purchase products that are safe and reliable, regardless of their country of origin, and that U.S. companies can compete internationally by having coordinated consistent requirements.

Results

The Safety Codes and Standards work is divided into three major areas:

1. Codes and Standards Coordination
2. Codes and Standards Research
3. Codes and Standards Training and Outreach

This report addresses the Outreach activities

Codes and Standards Outreach

In FY 2011 NREL continued outreach work in both in-person workshops and Web activities. The workshops and other outreach activities consisted of the following:

- Codes and Standards Workshop presented on April 19, 2011 in collaboration with the California Fuel Cell Partnership and the Southern California Fire Protection Officers Association.
- Sensor Workshop held June 8, 2011 in Rosemont, IL. This workshop was well attended and achieved the objective of collecting information to revise the performance criteria for safety sensors.
- Incident Workshop to be held September 2011.
- Codes and standards citations were updated for DOE website.
- Codes and standards permit template for hydrogen fueling stations completed.

Figure 1 shows the invitation for the April 2011 workshop. The invitation describes the material that was covered and workshop partners.

Conclusions and Future Direction

NREL will continue to support the development of codes and standards by:

- Working with DOE to implement a plan for identifying and supporting the development of the codes and

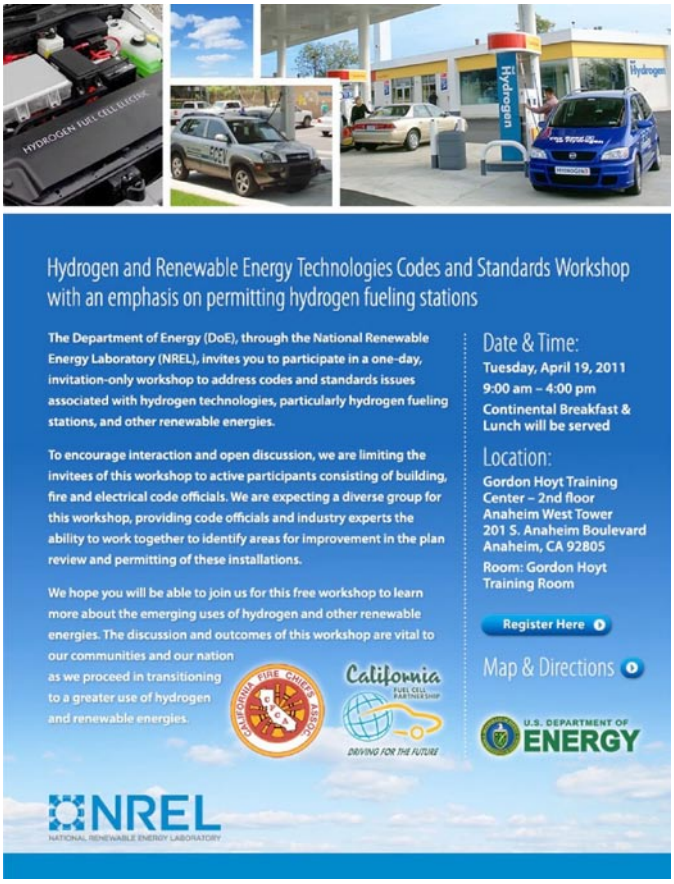


FIGURE 1. NREL Codes and Standards Workshop Invitation Anaheim, CA

standards required to deploy hydrogen and fuel cell technologies by the year 2020 (the 2020 Deployment Plan).

- Managing subcontracts required to support the 2020 Deployment Plan and outreach activities.
- Performing outreach work to distribute information on hydrogen and fuel cell technologies to code officials, project developers, and other interested parties.
- Collecting information from outreach activities to help identify gaps in codes and standards and research and testing projects that could fill these gaps.
- Performing site visits at fuel cell and hydrogen technology project sites to collect information to assist in the code development process and project permitting process.

FY 2011 Publications/Presentations

1. Codes and Standards Workshop, April 19, 2011, Anaheim, CA.
2. Sensor Workshop, June 8, 2011, Rosemont, IL.

VIII.8 Leak Detection and H_2 Sensor Development for Hydrogen Applications

Eric L. Brosha (Primary Contact)[1],
Fernando H. Garzon[1],
Robert S. Glass (Primary Contact)[2],
Rangachary Mukundan[1], Catherine G. Padro[1],
Praveen K. Sekhar[1], and Leta Woo[2]

[1]Los Alamos National Laboratory (LANL)
MS D429, P.O Box 1663
Los Alamos, NM 87545
Phone: (505) 665-4008
E-mail: brosha@lanl.gov

[2]Lawrence Livermore National Laboratory (LLNL)

DOE Manager
HQ: Antonio Ruiz
Phone: (202) 586-0729
E-mail: Antonio.Ruiz@ee.doe.gov

Project Start Date: Fiscal Year (FY) 2008
Project End Date: FY 2012

FY 2011 Objectives

- Develop a low-cost, low-power, durable, and reliable hydrogen safety sensor for vehicle and infrastructure applications.
- Demonstrate working technology through application of commercial and reproducible manufacturing methods and rigorous life testing results guided by materials selection, sensor design, and electrochemical research and development investigation.
- Recommend sensor technologies and instrumentation approaches for engineering design.
- Disseminate packaged prototypes to DOE laboratories and commercial parties interested in testing and fielding advanced commercial prototypes while transferring technology to industry.

Multi-Year Program Plan Technical Barriers from the Hydrogen Safety section (3.8) of the Fuel Cell Technologies Program

(D) Liability Issues: Potential liability issues and lack of insurability affecting the commercialization of hydrogen technologies: need for reliable H2 safety sensor.

(A) Variation in Standard Practice of H_2 Safety Assessments: The requirement to calibrate and commercialize safety sensors.

(G) Expense of Data Collection and Maintenance

Technical Targets

- Sensitivity: 1 vol % in air.
- Accuracy: 0.04-4% ± 1%.
- Response Time: <1 min at 1% and <1 sec at 4%; recovery <1 min.
- Temperature: -40°C to 60°C.
- Durability: Five years without calibration.
- Cross-Sensitivity: Minimal interference to humidity, H_2S, CH_4, CO, and volatile organic compounds.

FY 2011 Accomplishments

- Completed testing of FY 2009 and FY 2010 laboratory and pre-commercial prototypes for long-term evaluation (>3,000 hrs, LLNL and 4,000 hrs, LANL including temperature cycling) including comparison of mixed potential and impedance modality in laboratory prototypes: down-select to mixed potential.
- For laboratory prototypes, evaluated impregnated composite electrodes for better long-term stability and demonstrated stability and reproducibility to over 3,000 hrs in laboratory testing.
- Designed more advanced sensor substrates incorporating on-board temperature control and completed initial calibration procedures for pre-commercial prototypes.
- Effective packaging scheme adopted for pre-commercial prototypes.
- Partnered with BJR Sensors and co-developed an algorithm using a novel approach to eliminate the cross interference affecting existing technologies.
- Fabrication of multiple pre-commercial prototype devices for National Renewable Laboratory (NREL) testing; six devices prepared with high level of reproducibility.
- First round of devices shipped to NREL for testing; devices returned and durability studied.
- Positive NREL feedback already used to improve sensor platforms and to prepare for Round 2 NREL testing – focus on electronics.
- Calculated an estimate of sensor element cost for large scale up in production.
- Designed and constructed prototype sensor electronics (impedance buffer and controlled heater circuit) in preparation of Round 2 NREL testing.



Introduction

Recent developments in the search for renewable energy coupled with the advancements in fuel cell vehicles (FCVs) have augmented the demand for hydrogen safety sensors [1]. There are several sensor technologies that have been developed to detect hydrogen, including deployed systems to detect leaks in manned space systems and hydrogen safety sensors for laboratory and industrial usage. Among the several sensing methods electrochemical devices [2-8] that utilize high temperature-based ceramic electrolytes are largely unaffected by changes in humidity and are more resilient to electrode or electrolyte poisoning. The desired sensing technique should meet a detection threshold of 1% (10,000 ppm) H_2 and response time of ≤1 sec [9] targets for infrastructure and vehicular. Further, a review of electrochemical hydrogen sensors by Korotcenkov et.al [10] and the report by Glass et.al [11] suggest the need for inexpensive, low power, and compact sensors with long-term stability, minimal cross-sensitivity, and fast response. As part of the Hydrogen Codes and Standards sub-program, LANL and LLNL are working together to develop and test inexpensive, zirconia-based, electrochemical (mixed potential) sensors for H_2 detection in air. Previous work conducted at LLNL showed [8] that indium tin oxide (ITO) electrodes produced a stable mixed potential response in the presence of up to 5% of H_2 in air with no response to CO_2 or water vapor. The sensor also showed desirable characteristics with respect to response time and resistance to aging, and degradation due to thermal cycling.

In this investigation, the development and testing of an electrochemical H_2 sensor prototype based on 'ITO/ yttria-stabilized zirconia (YSZ)/Pt' configuration is detailed. The device fabricated on an alumina substrate integrates a resistive Pt heater to achieve precise control of operating temperature while minimizing heterogeneous catalysis. Targeting fuel cell-powered automotive applications, the safety sensor was subjected to interference studies, temperature cycling, operating temperature variations, and long-term testing over 4,000 hrs. The sensor responded in real time to varying concentrations of H_2 (1,000 to 20,000 ppm). Among the interference gases tested such as nitric oxide (NO), nitrogen dioxide (NO_2), ammonia (NH_3), carbon monoxide (CO), and propylene (C_3H_6), the sensor showed cross-sensitivity to C_3H_6. Analyzing the overall device performance over 4,000 hrs of testing for 5,000 ppm of H_2, (a) the sensitivity varied between 0.135 to 0.17 V with a minimum low of 0.12 V, (b) the baseline signal ranged from 0 to 0.04 V, and (c) the response rise time fluctuated between 3 to 47 s.

The salient features of the H_2 sensor prototype developed by LANL are (a) the low power consumption, (b) compactness to fit into critical areas of application, (c) simple operation, (d) fast response, (e) a direct voltage read-out circumventing the need for any additional conditioning circuitry, and (f) conducive to commercialization.

Approach

The sensor design approaches from LANL and LLNL were used to develop devices with superior performance.

LANL Design: Controlled Electrode/Electrolyte/Gas Interface

At LANL, electrochemical potentiometric modality is utilized for designing the sensors. Mixed potential sensors are a class of electrochemical devices that develop an open-circuit electromotive force due to the difference in the kinetics of the redox reactions of various gaseous species at each electrode/electrolyte/gas interface, referred to as the triple phase boundary [12]. Therefore these sensors have been considered for the sensing of various reducible or oxidizable gas species in the presence of oxygen. Based on this principle, a unique sensor design was developed. The uniqueness of LANL sensors [13] derives from minimizing heterogeneous catalysis (detrimental to sensor response) by avoiding gas diffusion through a catalytically active material and minimizing diffusion path to the 3-phase interface (electrode/electrolyte/gas referred to as tripe phase boundary). Unlike the conventional design of these devices that use a dense solid electrolyte and porous thin film electrodes (similar to the current state-of-the-art zirconia-based sensors and fuel cells), the LANL design uses dense (either metal wires, oxide pellets or thin film) electrodes and porous electrolytes (bulk or thin film). Such a sensor design facilitates a stable and reproducible device response, since dense electrode morphologies are easy to reproduce and are significantly more stable than the conventional porous morphologies. Moreover, these sensors develop higher mixed potentials since the gas diffusion is through the less catalytically active electrolyte than the electrode. Further, the choice of electrodes is primarily based on their O_2 reduction kinetics. Sensors fabricated at LANL will typically involve one electrode with fast (Pt) and another with slow (Au or $LaCrO_3$) O_2 reduction kinetics aimed to improve the sensitivity.

LLNL Design

In the LLNL design, a new impedance-based measurement technique, originally developed for electrochemical oxides of nitrogen (NO_x) sensors, was shown to generate more stable sensor responses and may be able to offer a way to compensate for cross-sensitivity effects. The technique is based on the measurement of parameters related to the complex impedance of the sensor in the frequency range of 1 Hz to 10 kHz. Measurements are typically made at a single frequency selected to maximize the desired sensitivity, although measurements performed at additional frequencies have been shown to be useful for correcting the response to interfering gases. LLNL has also found in the NO_x sensor studies that it may be possible to use a wider variety of electrodes for the sensor in

impedance-based sensing. Additional possible advantages included better tolerance to mechanical defects (such as delamination) and better longer-term stability.

Results

Commercial Platform Packaging and Preparation of Multiple Devices

In order to facilitate the transfer of sensors to testing partners, a ceramic packaging was devised. A two-piece packaging made from a commercial machinable ceramic material. The sensor element was supported from its heater and sense wires using four metal posts that protruded from the case such that long lead wires could easily be soldered to the device. A ceramic cap with a 0.5" stainless-steel mesh was then affixed to the lower packaging using a ceramic adhesive. Figure 1 shows the completed, 1" diameter, packaged H_2 sensor. The packaging is insulating and at normal sensor operating temperature, the safety sensor may be handled comfortably without personal protective equipment.

A new method of characterizing hydrogen sensor response was developed to test sensor response in a non-flow, safety sensor mode. Figure 2 illustrates the approach adopted in preparation to transferring sensors to NREL for independent testing and validation. The sensors were placed into a 1.7 ft^3 plexiglas enclosure with dry or humidified air entering through a 0.25" pass-through. The enclosure was fitted with several 0.25" pass-through holes for venting. When commended to do so, H_2 was added to the air stream such that resulting hydrogen concentration was 2%. Figure 2 also shows the sensor response and the actual hydrogen concentration present immediately in front of the packaged sensor.

A total of six packaged H_2 sensors were prepared (four with ITO working electrode and two with lanthanum manganese oxide working electrodes) for parallel testing at LANL, LLNL, and NREL.

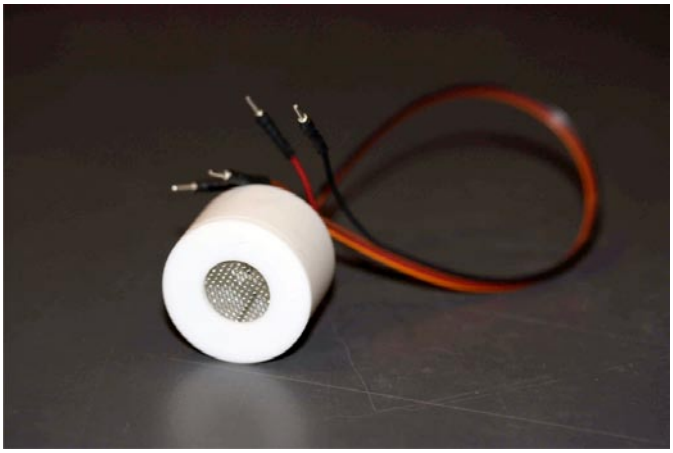


FIGURE 1. Photograph of a Packaged LANL/LLNL Mixed-Potential, Electrochemical H_2 Safety Sensor

Transfer of Packaged, Pre-Commercial H_2 Safety Sensors to NREL for Testing

Two packaged, pre-commercial H_2 safety sensors were shipped in October 2010 to NREL for testing and validation (Figure 3). Earlier, a mock-up of the packaging without sensor element was shipped to NREL to insure that test ports on the NREL apparatus would accept the LANL/LLNL sensors without complications. Testing commenced in January of 2011 and one of the heater leads of one of the packaged sensors broke during transport. That sensor was quickly replaced with a back up unit. The sensor's response to H_2, relative humidity influence, barometric pressure, and changes in ambient temperature were subsequently

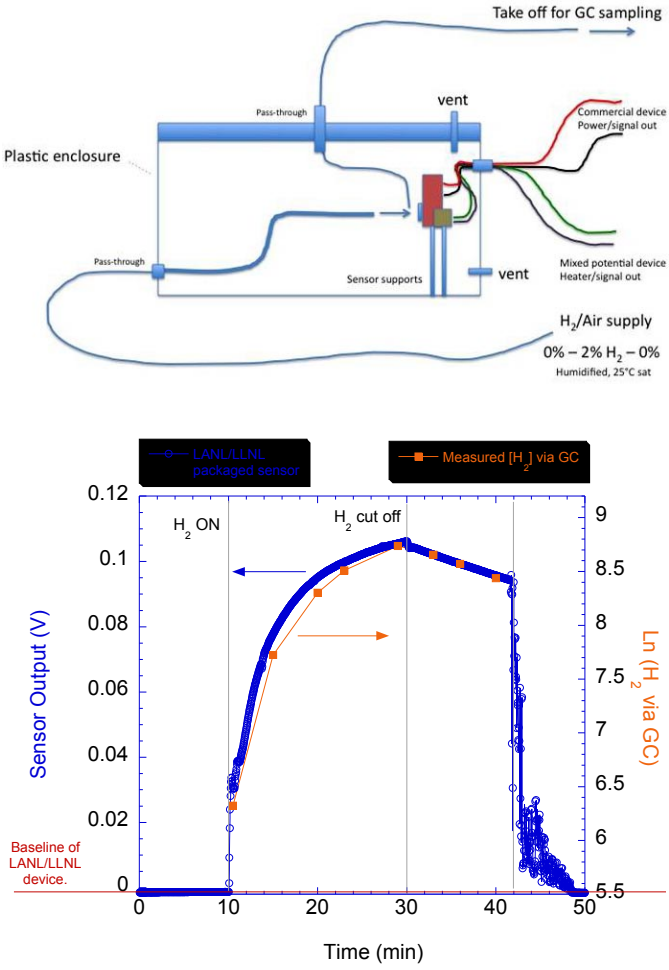


FIGURE 2. (top) A schematic of a test 1.7 cubic ft test enclosure cable of testing a pre-commercial, electrochemical-based LANL/LLNL H_2 sensor simultaneously with other technologies while extractive gas chromatograph measures actual hydrogen concentrations. (bottom) The response of a packaged, pre-commercial LANL/LLNL sensor while simulating a leak of hydrogen (2% H_2/air mix) into the enclosure.

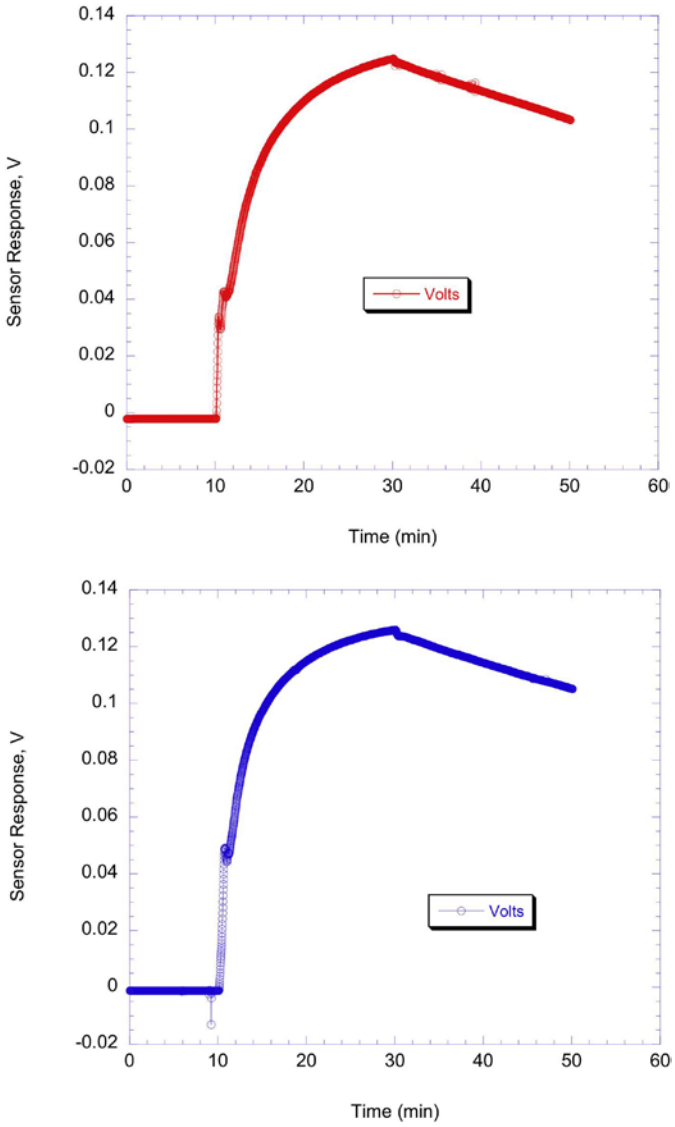


FIGURE 3. Comparison of the response of two packaged LANL/LLNL H_2 sensors to identical experiment profiles. Due to slight differences in positioning of the sensor element within the packaging and possible differences in heater resistance, the applied heater currents differed slightly (5 V/0.64 A top and 5 V/0.65 A bottom).

measured. The behavior or both sensors were similar as was predicted based on results shown in Figure 2. The sensors' response were insensitive to changes in relative humidity and the H_2 response to changes in ambient temperature of the testing chamber were as predicted (these devices did not have active temperature control). This latter result will be corrected once active temperature control is available using resistive thermal device (RTD) embedded in the sensor platform. However, there was a large non-zero baseline voltage not previously seen in these devices. This anomalous baseline voltage in air (no hydrogen) has never been seen at sensor testing at LANL or LLNL and may be attributed to impedance mismatches with the data acquisition system or

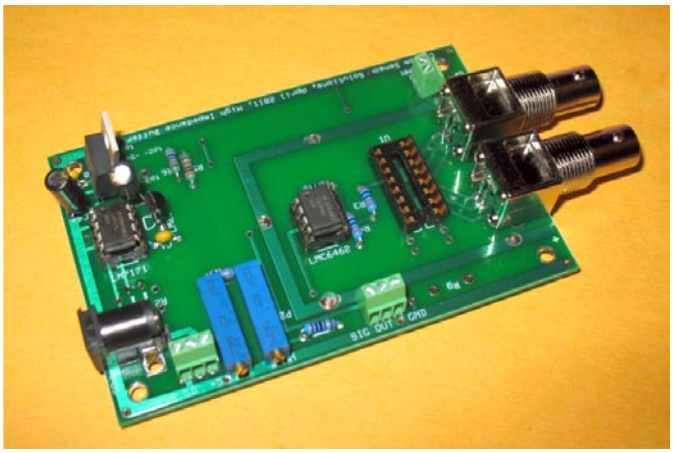


FIGURE 4. Custom-designed sensor impedance buffer circuit to isolate electrochemical sensor from external electrical influences. Photograph provided by Custom Sensor Solutions, Inc.

stray currents or voltages in some component of the NREL system since both sensors did not exhibit this behavior upon return to LANL after NREL testing. Based on these experimental results, a new high impedance/buffer circuit was designed to isolate the sensors from external influences. In addition, a circuit was designed to use the RTD output to control sensor operating temperature thus eliminating sensor response to changes in ambient testing temperature in the next round of testing at NREL.

Sensor Electronics: Circuit Design/Prototyping

Figure 4 shows an actual photograph of the completed high impedance buffer board. As of this report, multiple boards have been received from Custom Sensor Solutions, Inc. and compatible shielding and cables are being selected prior to testing and optimization. New, packaged sensors will be prepared and tested using this circuitry. Once the baseline response is well characterized on sensor test stations at LANL and LLNL (with and without impedance buffer to understand what effect – if any – the circuit has on sensor response), sensors and electronics will be transferred to NREL for the next round of testing/validation.

Conclusions

- All FY 2011 milestones on target to be completed this year.
- Improved electrode materials with potentially better performance were investigated where dense electronically conducting oxide (lanthanum strontium manganite) counter electrode showed better long-term stability.
- An alternate impedancemetric sensing modality was explored to evaluate improvements in long-term performance and stability.
- A viable H_2 safety sensor technology has been developed on a pre-commercial sensor platform that continues to

improve. A pre-commercial H_2 sensor prototype was fabricated on an alumina substrate with ITO and Pt electrodes and YSZ electrolyte with an integrated Pt heater to achieve precise operating temperature and minimize heterogeneous catalysis.

- A sensor platform cost analysis was performed by commercialization partner (scale up of existing pre-commercial platform to production of 100K and 500K units) and sensor cost estimated to be in the $6 to $9 range in line with a modern automotive lambda sensor.
- Multiple sensors were prepared and packaged that exhibited excellent response and device-to-device reproducibility.
- Sensors were prepared and transferred to NREL for independent testing and validation. Valuable feedback was obtained and used to design sensor isolation/impedance matching electronics and for sensor heater control.
- Device technology advanced from naked sensor to near-commercial state.
- Novel attributes of mixed electrochemical, mixed-potential sensor exploited in conjunction with novel pulse discharge technology as a method to reject influence from interference gases.

Future Directions

- Fabricate new sensors on platform with embedded temperature feedback sensor (RTD).
- Improve pre-commercial sensors and packaging using results from NREL testing.
- Work with NREL partners to develop testing protocols for mixed potential type, electrochemical gas sensors.
- Work with NREL to test prototype electronics (circuit and board design validation) for mixed potential type, electrochemical gas sensors:
  - Fabricate electronics to protect sensors from external influences, leakage currents, etc.
  - Impedance matching and signal amplification, baseline adjustment, etc.
  - Design and test constant resistance feedback circuit for temperature control.
- Utilize on-board RTD and incorporate active temperature control for next round of NREL testing.
- Provide new sensors and electronics to NREL for Round 2 testing.

Collaboration and Coordination with Other Institutions

- Los Alamos National Laboratory
- Lawrence Livermore National Laboratory
- National Renewable Energy Laboratory
- ESL ElectroScience, Inc.
- BJR Sensors, LLC.
- Custom Sensor Solutions, Inc.

Publications and Presentation

1. P.K.Sekhar, E.L.Brosha, R. Mukundan, T.L. Williamson, M.A. Nelson and F.H. Garzon, "Development and Testing of a Hydrogen Safety Sensor Prototype", *Sensors and Actuators B: Chemical* **148**, 469 (2010).

2. P.K. Sekhar, E.L. Brosha, R. Mukundan, B. Farber, P. Shuk, and F.H. Garzon, "Investigation of a New Conditioning Method for Improved Performance of non-Nernstian Sensors", *Electrochemical Society (ECS) Transactions* **28** (20), 1 (2010).

3. P.K. Sekhar, E.L. Brosha, R. Mukundan, B. Farber, and F.H. Garzon, "Statistical Investigation of a Novel Signal Conditioning Circuit for Reliable Detection of Exhaust Gas Components", *ECS Transactions* **33** (8), 101 (2010).

4. E.L. Brosha, P.K. Sekhar, R. Mukundan, T.L. Williamson, F.H. Garzon, L.Y. Woo, and R.S. Glass, "Development of Sensors and Sensing Technology for Hydrogen Fuel Cell Vehicle Applications", *ECS Transactions***26** (1) 475 (2010).

5. P.K. Sekhar, E.L.Brosha, R. Mukundan, and F.H. Garzon, "Packaging and Testing of an Electrochemical Hydrogen Safety Sensor Prototype", 219th ECS Meeting, May 1–5, Montreal, QC, Canada, 2011.

6. L.Y. Woo, R.S. Glass, E.L. Brosha, P.K. Sekhar, R. Mukundan, and F.H. Garzon, "Tin-doped Indium Oxide/Yttria-Stabilized Zirconia Composite Electrode Prepared by Impregnation for Electrochemical Hydrogen Sensors", Materials Research Society Spring Meeting, Apr 25–29, San Francisco, 2011.

7. P.K. Sekhar, E.L. Brosha, R. Mukundan, and F.H. Garzon, "Development of a Reliable, Miniaturized Hydrogen Safety Sensor Prototype", Fuel Cell Seminar and Exposition, Oct 18–22, 2010.

8. P.K.Sekhar, E.L Brosha, R. Mukundan, B.Farber, and F. H. Garzon, "Statistical Investigation of a Novel Signal Conditioning Circuit for Reliable Detection of Exhaust Gas Components", 218th ECS Meeting in Las Vegas, NV, Oct 10–15, 2010.

References

1. L. Boon-Brett, J. Bousek, G. Black, P. Moretto, P. Castello, T. Hübert, and U. Banach, Identifying performance gaps in hydrogen safety sensor technology for automotive and stationary applications, International Journal of Hydrogen Energy, 35 (2010), 373-384.

2. H. Iwahara, H. Uchida, K. Ogaki and H. Nagato, Nernstian Hydrogen Sensor Using $BaCeO_3$-Based, Proton-Conducting Ceramics Operative at 200-900°C, Journal of The Electrochemical Society, 138 (1991), 295-299.

3. Y. Tan and T.C. Tan, Characteristics and Modeling of a Solid State Hydrogen Sensor, The Journal of Electrochemical Society, 141 (1994), 461-466.

4. Z. Samec, F. Opekar, and G.J.E.F. Crijns, Solid-state Hydrogen Sensor Based on a Solid-Polymer Electrolyte, Electroanalysis, 7 (1995), 1054-1058.

5. Y-C. Liu, B-J. Hwang, and I.J. Tzeng, Solid-State Amperometric Hydrogen Sensor Using Pt/C/Nafion Composite Electrodes Prepared by a Hot-Pressed Method, Journal of The Electrochemical Society, 149 (2002), H173-H178.

6. L.B. Kriksunov, and D.D. Macdonald, Amperometric hydrogen sensor for high-temperature water, Sensors and Actuators B, 32 (1996), 57-60.

7. G. Lu, N. Miura, and N. Yamazoe, High-temperature hydrogen sensor based on stabilized zirconia and a metal oxide electrode, Sensors and Actuators B, 35-36 (1996), 130-135.

8. L.P. Martin and R.S. Glass, Hydrogen Sensor Based on Yttria-Stabilized Zirconia Electrolyte and Tin-Doped Indium Oxide Electrode, Journal of The Electrochemical Society, 152 (2005), H43-H47.

9. R.S. Glass, J. Milliken, K. Howden, R. Sullivan (Eds.), Sensor Needs and Requirements for Proton-Exchange Membrane Fuel Cell Systems and Direct-Injection Engines, 2000, pp. 7–15. DOE, UCRL-ID-137767.

10. G.Korotcenkov, S.D.Han and J.R.Stetter, Review of Electrochemical Hydrogen Sensors, Chemical Review, 109 (2009), 1402-1433.

11. L.P. Martin and R.S. Glass, Electrochemical Sensors for PEMFC Vehicles, presented at The 2004 DOE Hydrogen, Fuel Cells, and Infrastructure Technologies Program Review, Philadelphia, PA (May 27, 2004).

12. F.H. Garzon, R. Mukundan, and E.L. Brosha, Solid state mixed potential gas sensors: theory, experiments and challenges, Solid State Ionics, 136-137 (2000), 633-638.

13. P.K. Sekhar, E.L. Brosha, R.Mukundan, M.A. Nelson and F.H. Garzon, Application of Commercial Automotive Sensor Manufacturing Methods for NO_x/NH_3 Mixed Potential Sensors for Emission Control, ECS Transactions. 19 (2009), 45-49.

VIII.9 Hydrogen Fuel Quality Research and Development

Tommy Rockward (Primary Contact), Eric Brosha, Fernando Garzon, Rangachary Mukundan, Calita Quesada, Karen Rau, and Catherine Padro (Project Leader)
Los Alamos National Laboratory (LANL)
PO Box 1663, MS. D429
Los Alamos, NM 87545
Phone: (505) 667-9587 and 667-5539
E-mail: trock@lanl.gov; Padro@lanl.gov

DOE Manager
HQ: Antonio Ruiz
Phone: (202) 586-5673
E-mail: Antonio.Ruiz@ee.doe.gov

Project Start Date: October 2006
Project End Date: Project direction and continuation determined annually by DOE

Fiscal Year (FY) 2011 Objectives

- Provide data and analysis to the international effort to determine the levels of non-hydrogen constituents in support of the development of an international standard for H_2 fuel quality.
- Test the critical constituents (NH_3, CO, and H_2S).
- Isolated and combined at various conditions.
- Present data and have open discussions at International Organization for Standardization (ISO) TC197/Working Group 12 Meetings.
- Solicit guidance from leading industrial experts.

Technical Barriers

This project is directed to ameliorate many of the technical barriers from the Codes and Standards section (3.7) of the Fuel Cell Technologies Program Multi-Year Research, Development and Demonstration Plan, however it is focused on the following primary barriers:

(I) Conflicts between Domestic and International Standards

(N) Insufficient Technical Data to Revise Standards

Technical Targets

Technical targets in Table 3.4.4 of the Fuel Cell Technologies Program Multi-Year Research, Development and Demonstration Plan are addressed in this project. Specifically, select tasks that apply to the technical targets in this project are listed in the following, while their status is listed in the Accomplishments section.

- Provide testing results from Common membrane electrode assembly (MEA) in the presence of critical constituents.
- Measure the fuel cell tolerance to carbon monoxide using Common MEAs.
- Identify MEA manufacturer to provide Common MEA DOE 2015 target loadings.
- Perform baseline test with lower anode loading MEAs.
- Participation in domestic and international working groups and review meetings.



Approach

We approached our 2011 technical targets by conducting multiple fuel cell tests mimicking conditions that a fuel cell may be subjected to in vehicular applications. Initially, we employed 'Common MEAs' to perform these tests with 0.1 and 0.4 mg Pt/cm^2 loadings on the anode and cathode, respectively. Although, theses loadings are not identical to the DOE targets (0.05 and 0.15 mg Pt/cm^2), the results provide a means for comparing different testers and facilities. These results were presented and discussed at several forums throughout the year. In addition, commercial suppliers of the DOE 2015 technical target loadings were being identified and, the preliminary testing steps were put in place to qualify their materials.

FY 2011 Accomplishments

- Completed multiple tests under various conditions using calibrated quantities of the critical constituents.
- Measured CO tolerance level of Common MEA.
- Interacted with multiple industrial, university, or laboratory partners, as well as international collaborators.
- Identified Ion Power as the Common MEA supplier for DOE 2015 platinum loadings.
- Performed initial baseline tests to qualify lower loaded MEAs.

Results and Discussions

The development of international hydrogen fuel specifications has been discussed for several years. In particular, the focus has been on determining the acceptable level of non-hydrogen constituents. LANL researchers have continued fuel cell testing at the agreed upon contaminant levels using a Common MEA loaded at 0.1 and 0.4 mg Pt/cm^2 under various operating conditions. Although the loadings mentioned are slightly higher than DOE

targets, the results are useful. Previous tests results with contaminant mixtures showed that the fuel cell performance losses were due to hydrogen sulfide (H_2S), ammonia (NH_3), and carbon monoxide (CO). These are referred to as 'critical constituents'. Our fuel cell test results include investigating the critical constituents both isolated and combined.

H_2S has a strong affinity for platinum surfaces and blocks the dissociative chemisorption of hydrogen on the electrode surface. This platinum-sulfur interaction inhibits the hydrogen electrooxidation process, which consequently reduces fuel cell performance. In separate experiments, we exposed the anode of operating fuel cells to both 4 and 8 ppb for 50 hours each. The fuel cells operated in constant current mode (1 A/cm^2) at 80°C, 100% relative humidity (RH) and 25 psig backpressure. We performed polarization experiments before and after sulfide exposure. After 50 hours of exposure, the fuel cell did not show performance loss in the presence of 4 ppb, however the performance is progressively depressed when the concentration of H_2S was increased. This effect is demonstrated in Figure 1. As expected, we did not observe any change in the alternating current (AC) high frequency resistance. However, in the low frequency charge transfer region, the semi-circle grew as the H_2S concentration increased. This implies the sulfur coverage on the platinum surface also increased with concentration. Cyclic voltammetry (CV) also confirmed this finding. Also, in the mass transport region, we observed unexpected losses for 4 PPB H_2S. This result is being further investigated.

In order to study the effect of CO concentration upon fuel cell performance, we exposed a fuel cell with an anode loading of either 0.05 or 0.1 mg Pt/cm^2 to several different concentrations at 80°C. We kept the dosage in each experiment constant (20 ppm-hr CO) by varying both concentration and exposure times. CVs were used to clean the platinum surface after CO exposure following each experiment. The CVs were performed, with ultra-high purity (UHP) N_2 flowing through the anode and UHP H_2 flowing through the cathode after pre-purging the cathode for 20 minutes with UHP N_2. The scan rate was 20 mV/s and the applied voltage ranged between 0.06 V and 1.1 V for 4 cycles. The cleaning procedure allowed us to use the same cell in subsequent experiments. Figure 2 shows the experimental results for a Pt loading of 0.1 mg Pt/cm^2 for the differing concentrations of CO. We also measured the voltage loss for each test and plotted it as a function of CO concentration. This allowed us to extrapolate the point at which the voltage loss approaches zero; the concentration under these tested conditions, that the fuel cell is tolerant to CO. Figure 2 highlights these results. Similar experiments were performed at 60°C and 45°C.

Ammonia is yet another important impurity constituent deemed critical in this effort. It typically reacts with proton in the ionomer forming ammonium cations and affects the ionomer throughout the MEA by lowering its conductivity. Figure 3 illustrates the impact of a variety of ammonia concentrations and RH. Tests were carried out at 50 A

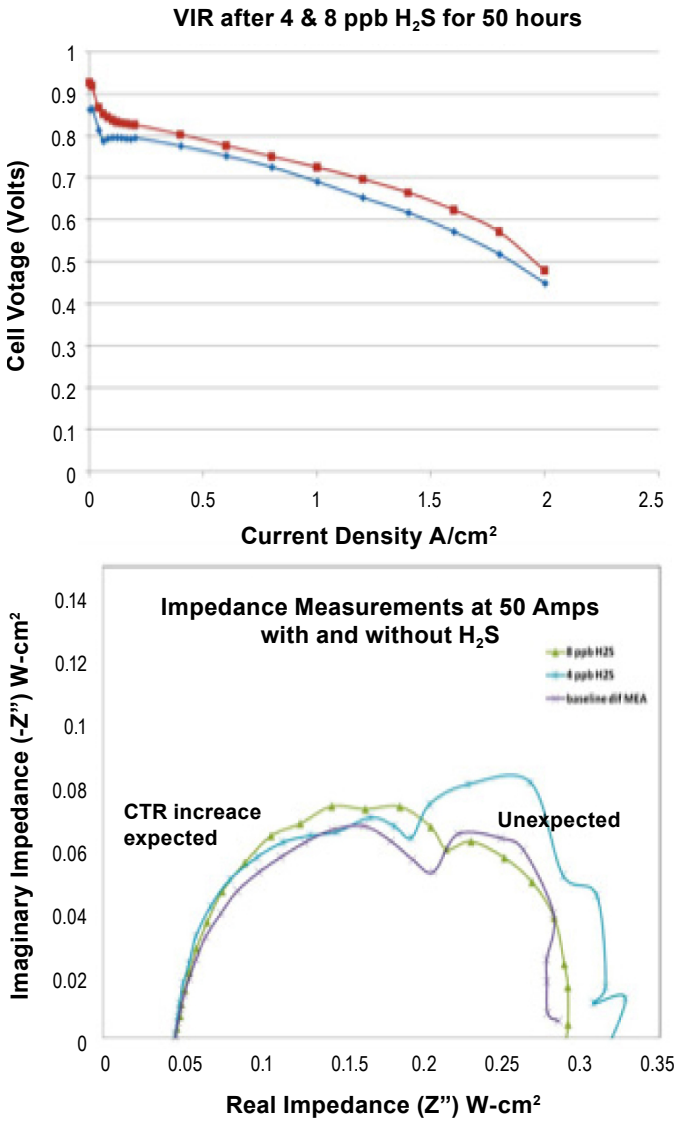


FIGURE 1. Voltage-current-resistance tests and AC Impedance measured using the Common MEA after being exposed to 4 and 8 ppb of hydrogen sulfide for 50 hours.

(constant current mode) using 25 psig backpressure. We used three different concentrations: 100, 200, and 500 ppb. The RH ranged from 25 to 100%. The entire data set is not included in this report, but the findings indicate that the performance decreases as the concentration of ammonia is increased. Because ammonia is water soluble, as the RH increased for identical concentrations, the performance losses decreased from 24 mV at 25% RH to 8 mV at 50% RH (see Figure 3).

The previously mentioned results were obtained from Common MEAs with Pt loading greater than the DOE targets. This year, we identified Ion Power as a commercial supplier to provide MEAs at DOE targeted loadings. We ran preliminary test to investigate the durability of the new materials. Figure 4 shows VIR tests competed 150 hours

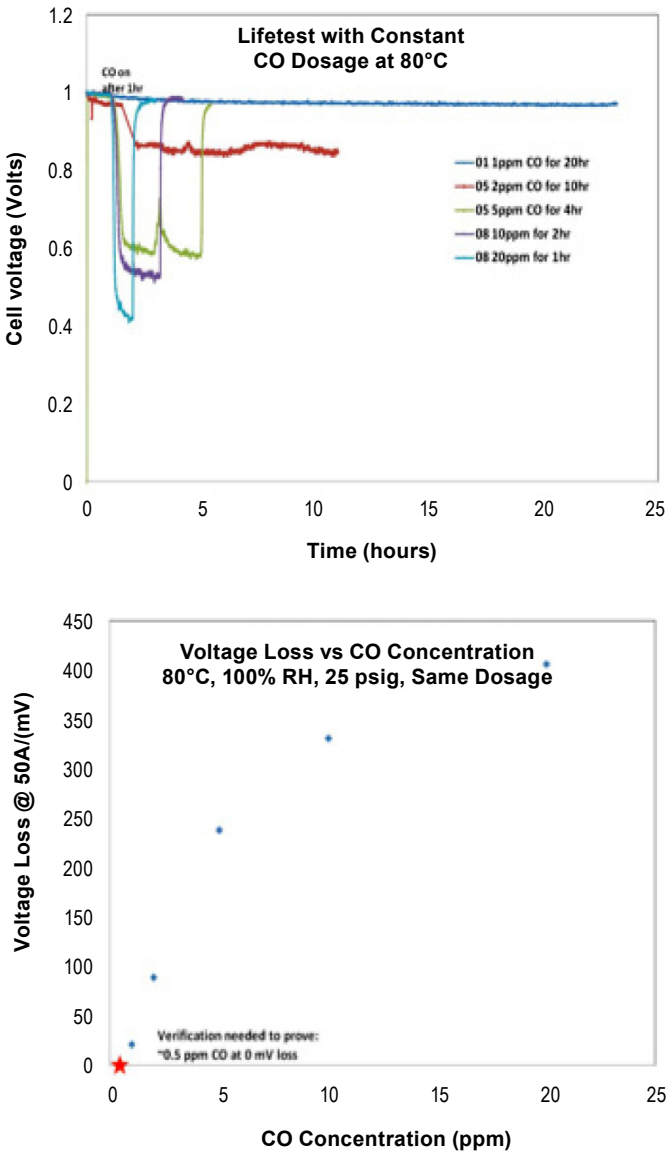


FIGURE 2. Results show the impact of CO on an operating fuel cell using identical doses. The adjacent graph allows the CO tolerance level to be extrapolated.

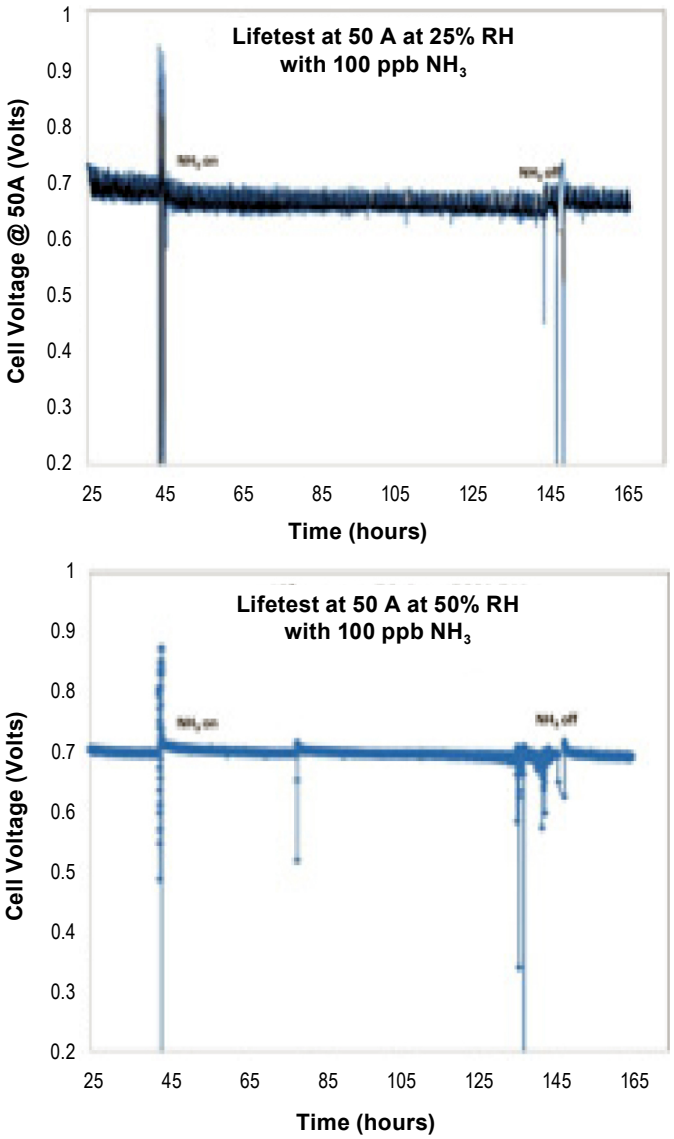


FIGURE 3. Cell voltage monitored before, during and after 100 ppb ammonia exposure at two different RHs for a fuel cell operating at 1 A/cm^2.

apart. The performance improved during that period. This indicates the MEA was fully broken in at 150 hours. However, more importantly, this result demonstrated membrane durability. We also performed other preliminary tests such as AC impedance (shown in Figure 4 on the right) and CV.

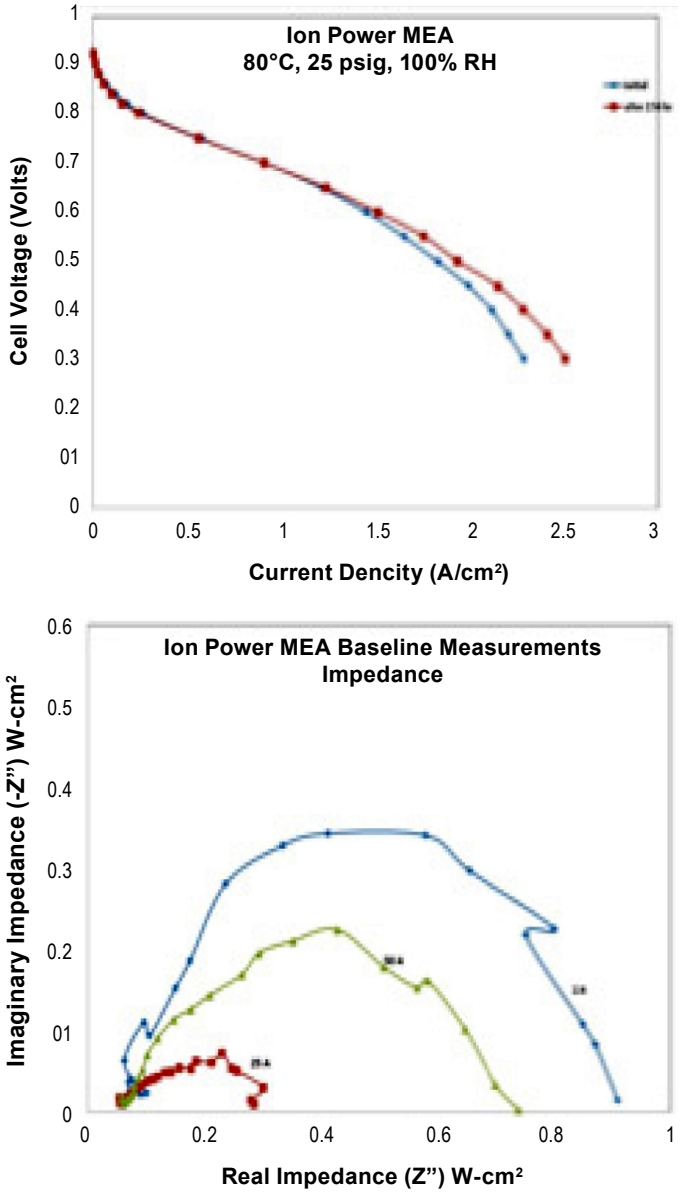


FIGURE 4. Initial tests results of Ion Power MEA (i.e. low loading) to probe durability concerns/issues.

VIII.10 Hydrogen Safety Panel

Steven C. Weiner
Pacific Northwest National Laboratory (PNNL)
901 D Street SW, Suite 900
Washington, DC 20024-2115
Phone: (202) 646-7870
E-mail: sc.weiner@pnnl.gov

DOE Manager
HQ: Antonio Ruiz
Phone: (202) 586-0729
E-mail: Antonio.Ruiz@ee.doe.gov

Subcontractors:
- Addison Bain, NASA (ret), Melbourne, FL
- David J. Farese, Air Products and Chemicals, Inc., Allentown, PA
- William C. Fort, Shell Global Solutions (ret), Houston, TX
- Don Frikken, Becht Engineering, St. Louis, MO
- Richard A. Kallman, City of Santa Fe Springs, CA
- Michael Pero, Hydrogen Safety, LLC, Newington, CT
- Glenn W. Scheffler, GWS Solutions of Tolland, LLC, Tolland, CT
- Andrew J. Sherman, Powdermet Inc., Euclid, OH
- Ian Sutherland, General Motors, Warren, MI
- Edward G. Skolnik, Energetics, Inc. Columbia, MD
- Robert G. Zalosh, Firexplo, Worcester, MA

Project Start Date: 2004
Project End Date: Project continuation and direction determined annually in consultation with DOE

Fiscal Year (FY) 2011 Objectives

- Provide expertise and recommendations to DOE and assist with identifying safety-related technical data gaps, best practices and lessons learned.
- Help DOE integrate safety planning into funded projects to ensure that all projects address and incorporate hydrogen and related safety practices.

Technical Barriers

This project addresses the following technical barriers from the Hydrogen Safety section (3.8) of the Fuel Cell Technologies (FCT) Program Multi-Year Research, Development and Demonstration Plan:

(A) Limited Historical Database
(B) Proprietary Data
(C) Validity of Historical Data
(D) Liability Issues
(E) Variation in Standard Practice of Safety Assessments for Components and Energy Systems
(F) Safety is Not Always Treated as a Continuous Process
(G) Expense of Data Collection and Maintenance
(H) Lack of Hydrogen Knowledge by Authorities Having Jurisdiction
(I) Lack of Hydrogen Training Facilities for Emergency Responders

Contribution to Achievement of DOE Hydrogen Safety Milestones

This project contributes to achievement of the following DOE milestones from the Hydrogen Safety section of the Fuel Cell Technologies Program Multi-Year Research, Development and Demonstration Plan:

- **Milestone 8**: Complete investigation of safe refueling protocols for high pressure systems. (1Q, 2012)
- **Milestone 20**: Update peer-reviewed Best Practices Handbook. (4Q, 2008/ongoing)

Related milestones in Task 3 (Failure Modes), Task 5 (Safety of DOE R&D Projects), Task 6 (Hydrogen Safety and Incidents), Task 7 (Best Practices Handbook) and Task 8 (Hydrogen Safety Props) of the above reference have all been achieved with support from the Hydrogen Safety Panel.

FY 2011 Accomplishments

- Conducted Hydrogen Safety Panel meeting in Washington, D.C., April 7-8, 2010; planned Hydrogen Safety Panel meeting (September 11, 2011) in conjunction with the International Conference on Hydrogen Safety, San Francisco, CA.
- Reviewed 60 safety plans since July 1, 2010 for projects in fuel cell research and development (R&D) and American Recovery and Reinvestment Act (ARRA)-funded fuel cell deployments.
- Conducted safety review site visits for four FCT-funded projects; completed and submitted six safety evaluation reports; conducted three follow-up teleconferences for previously issued safety evaluation reports and submitted interview reports; published two issues of *H2 Safety Snapshot* (http://www1.eere.energy.gov/hydrogenandfuelcells/codes/snapshot.html).
- Provided technical guidance, source material and review for the Hydrogen Incident Reporting and Lessons Learned database (www.h2incidents.org) and Hydrogen Safety Best Practices (www.h2bestpractices.org).

Introduction

Safety is an essential element for realizing the "hydrogen economy" – safe operation in all of its aspects from hydrogen production through storage, distribution and use; from research, development and demonstration to commercialization. As such, safety is given paramount importance in all facets of the research, development, demonstration and deployment work of the DOE FCT Program Office.

Recognizing the nature of the DOE program and the importance of safety planning, the Hydrogen Safety Panel was formed in December 2003 to bring a broad cross-section of expertise from the industrial, government and academic sectors to help ensure the success of the program as a whole. The experience of the Panel resides in industrial hydrogen production and supply, hydrogen R&D and applications, process safety and engineering, materials technology, industrial liability and facility insurance, risk analysis, accident investigation and fire protection. The Panel provides expertise and recommendations on safety-related issues and technical data gaps, reviews individual DOE-supported projects and their safety plans and explores ways to bring best practices and lessons learned to broadly benefit the DOE program.

Approach

The Panel strives to raise safety consciousness most directly at the project level. Safety should be driven at the project level by organizational policies and procedures, safety culture and priority. Project safety plans are reviewed in order to encourage thorough and continuous attention to safety aspects of the specific work being conducted. Panel-conducted safety reviews focus on engagement, learning, knowledge-sharing and active discussion of safety practices and lessons learned, rather than as audits or regulatory exercises. Through this approach, DOE and the Hydrogen Safety Panel are trying to achieve safe operation, handling and use of hydrogen and hydrogen systems for all DOE projects.

Results

The Hydrogen Safety Panel was formed in FY 2004 and the first meeting was held in Washington, D.C., December 11-12, 2003. The 15th Panel meeting was held in Washington, D.C., April 7-8, 2011 and included two topical themes: (1) "incident owners" discussed what was learned from specific hydrogen safety events; (2) Panel work on ARRA-funded fuel cell deployment projects, including materials handling applications, was reviewed. Planning is in progress for the 16th meeting to be held in San Francisco, CA, September 11, 2011, in conjunction with the International Conference on Hydrogen Safety.

Current Panel membership is noted in Table 1.

TABLE 1. Hydrogen Safety Panel

Richard A. Kallman, Chair	City of Santa Fe Springs, CA
Steven C. Weiner, Program Manager and Panel Coordinator	PNNL
Addison Bain	NASA (ret)
David J. Farese	Air Products and Chemicals, Inc.
William C. Fort	Shell Global Solutions (ret)
Don Frikken	Becht Engineering
Miguel J. Maes	NASA White Sands Test Facility
Michael Pero	Hydrogen Safety, LLC
Glenn W. Scheffler	GWS Solutions of Tolland, LLC
Andrew J. Sherman	Powdermet Inc.
Ian Sutherland	General Motors
Robert G. Zalosh	Firexplo
Nicholas F. Barilo, Technical Support	PNNL
Edward G. Skolnik, Technical Support	Energetics, Inc.

The Panel conducted safety reviews for projects as noted in Table 2 since the last reporting (safety reviews have been conducted for 45 projects since March 2004). Final reports issued to DOE with recommendations are also noted [1-6]. At the National Renewable Energy Laboratory's invitation, a Panel team participated (September 21, 2010) in a 30% design review of a new facility, the Energy Systems Integration Facility.

In FY 2010, the Panel first established a follow-up protocol to interview project teams in order to identify actions, findings and conclusions regarding safety review recommendations as one means for measuring the value of this work. Action on report recommendations represents a rich source of safety knowledge that can have broader benefits to others. Table 2 indentifies the follow-up interviews that were conducted since the last reporting [7-9] and Table 3 summarizes the conclusions for all follow-up interviews conducted to date.

The Panel concluded that all interviewees have improved the safety aspects of the work they are conducting. Overall, over 90% of the recommendations – 90 in number – have been implemented in some manner or are in progress for the 11 follow-up interviews conducted. The Panel has concluded that the mechanism used by the Panel for seamless discussion and knowledge sharing at the project level has helped augment the prime responsibility of any organization to ensure the safe conduct of work [10].

The Hydrogen Safety Panel contributes to PNNL's ongoing work in updating and adding new technical content to two safety knowledge tools, the Hydrogen Safety

TABLE 2. Project Safety Reviews and Reports Since July 1, 2010

Program Area	Project Title	Contractor
Storage	*#A Joint Theory and Experimental Project in the High-Throughput Synthesis and Testing of Porous Covalent-Organic Framework and Zeolitic Imidazolate Framework Materials for On-Board Vehicular Hydrogen Storage [1,8]	University of California, Los Angeles
Storage	*#Development of Improved Composite Pressure Vessels for Hydrogen Storage [2,9]	Lincoln Composites, Lincoln, NE
Storage	Design of Novel Multi-Component Metal Hydride-Based Mixtures for Hydrogen Storage [3]	Northwestern University, Evanston, IL
Storage	New Carbon-Based Materials with Increased Heats of Adsorption for Hydrogen Storage [4]	Northwestern University, Evanston, IL
ARRA	H-E-B Grocery Total Power Solution for Fuel Cell-Powered Material Handling Equipment [5]	Nuvera Fuel Cells/H-E-B, San Antonio, TX
ARRA	Fuel Cell-Powered Lift Truck Fleet Deployment [6]	Sysco Food Services, Houston, TX
Production and Delivery	#Water-Gas Shift Reaction via a Single-Stage Low-Temperature Membrane Reactor [7]	MPTI, Pittsburgh, PA

* Safety evaluation report for previously conducted site visit
# Follow-up interview and report

Best Practices website (www.h2bestpractices.org) and the Hydrogen Incident Reporting and Lessons Learned database (www.h2incidents.org). For example, the Panel supported work on best practices to add new content on hydrogen properties, chemical hydrogen storage and indoor refueling of hydrogen-powered fuel cell forklifts. Panel members also assisted in reviewing technical content for the following postings in the Lessons Learned Corner of the above mentioned safety event database:

- The Importance of Purging Hydrogen Piping and Equipment
- Hydrogen Use in Anaerobic Chambers
- Adequate Ventilation of Battery Charging Facilities
- Learning from Burst Disk Failures

With Panel members serving as technical contributors and reviewers, two issues of the topical newsletter, *H2 Safety Snapshot*, were published:

- Handling Compressed Hydrogen Gas Cylinders [11]
- Identifying Safety Vulnerabilities [12]

Leadership has been provided to the International Energy Agency Hydrogen Implementing Agreement Task 31 (Hydrogen Safety) for the work under Subtask D, Knowledge Analysis, Dissemination and Use. The recently completed work under Task 19 (Hydrogen Safety) helped facilitate collaboration between member countries on the incident lessons learned and best practices databases [13].

Conclusions and Future Directions

Being conscious of the need to use safe practices is a necessary first step for the conduct of all work. The work and approaches taken by the Panel will continue to focus on how safety knowledge, best practices and lessons learned can be brought to bear on the safe conduct of project work.

The Panel will undertake a number of initiatives in FY 2012 including:

- Safety plan reviews, safety review site visits and a final report for ARRA fuel cell deployment projects in specialty vehicle, auxiliary and back-up power, portable and combined heat and power applications.
- Follow-up teleconferences with all project teams for which safety review site visit reports have been issued in order to identify actions taken, findings, conclusions and other learnings.

TABLE 3. Categorizing Actions Taken on Report Recommendations - 11 Interviews

Category	Recommendations Implemented	Partial or In Progress	No Action	Total Recommendations
Safety Vulnerability/ Mitigation Analysis	15	4	5	24
System/Facility Design Modifications	7	5	1	13
Equipment/Hardware Installation and Operations and Maintenance	10	6	0	16
Safety Documentation	7	7	0	14
Training	1	3	0	4
Housekeeping	9	6	0	15
Emergency Response	7	3	2	12
Total	**56**	**34**	**8**	**98**

- Technical support for work on future issues of *H2 Safety Snapshot* and PNNL's hydrogen safety knowledge databases.
- Additional topics for study consistent with the Hydrogen Safety Panel's charter to identify safety-related data and knowledge gaps.

The 17th and 18th meetings of the Hydrogen Safety Panel are planned for April 2012 and September 2012, respectively.

FY 2011 Publications/Presentations

1. Weiner, S.C., Fassbender, L.L. and K.A. Quick, "Using Hydrogen Safety Best Practices and Learning from Safety Events," PNNL-SA-70148, International Journal of Hydrogen Energy, Volume 36, Issue 3, February 2011, pp. 2729-2735.

2. Weiner, S.C. and Fassbender L.L., "Lessons Learned from Safety Events," PNNL-SA-78868, International Conference on Hydrogen Safety, San Francisco, CA, September 12–14, 2011 (manuscript accepted June 1, 2011).

3. Weiner, S.C., Fassbender, L.L., Blake, C., Aceves, S., Somerday, B.P. and Ruiz, A., "Web-based Resources Enhance Hydrogen Safety Knowledge," PNNL-SA-79693, HYPOTHESIS IX, San José, Costa Rica, December 12–15, 2011 (abstract accepted June 24, 2011).

References

1. Barilo, N.F., R.A. Kallman, E.G. Skolnik and S.C. Weiner, "Safety Evaluation Report: A Joint Theory and Experimental Project in the High-Throughput Synthesis and Testing of Porous COF and ZIF Materials for On-Board Vehicular Hydrogen Storage, University of California, Los Angeles," PNNL-19900, October 19, 2010.

2. Fort, W.C., R.A. Kallman, M.J. Maes, E.G. Skolnik and S.C. Weiner, "Safety Evaluation Report: Development of Improved Composite Pressure Vessels for Hydrogen Storage, Lincoln Composites, Lincoln, NE," PNNL-20082, December 28, 2010.

3. Bain, A., N.F. Barilo, A.J. Sherman, E.G. Skolnik and S.C. Weiner, "Safety Evaluation Report: Design of Novel Multi-Component Metal Hydride-Based Mixtures for Hydrogen Storage, Northwestern University, Evanston, IL," PNNL-20280, March 28, 2011.

4. Bain, A., A.J. Sherman, E.G. Skolnik and S.C. Weiner, "Safety Evaluation Report: New Carbon-Based Materials with Increased Heats of Adsorption for Hydrogen Storage, Northwestern University, Evanston, IL," PNNL-20406, May 17, 2011.

5. Fort, W.C., G.W. Scheffler, E.G. Skolnik and S.C. Weiner, "Safety Evaluation Report: H-E-B Grocery Total Power Solution for Fuel Cell-Powered Material Handling Equipment, H-E-B, San Antonio, TX," PNNL-20480, June 14, 2011.

6. Fort, W.C., G.W. Scheffler, E.G. Skolnik and S.C. Weiner, "Safety Evaluation Report: Fuel Cell-Powered Lift Truck Fleet Deployment, Sysco Food Services of Houston, Inc., Houston, TX," PNNL-20504, June 27, 2011.

7. Skolnik, E.G., Safety Evaluation Follow-up Report for "Water-Gas Shift Reaction via a Single-Stage Low-Temperature Membrane Reactor, Media and Process Technology, Inc., Pittsburgh and Schenley, PA," August 6, 2010.

8. Skolnik, E.G., Safety Evaluation Follow-up Report for "Safety Evaluation Report: A Joint Theory and Experimental Project in the High-Throughput Synthesis and Testing of Porous COF and ZIF Materials for On-Board Vehicular Hydrogen Storage, University of California, Los Angeles," May 16, 2011.

9. Skolnik, E.G., Safety Evaluation Follow-up Report for "Safety Evaluation Report: Development of Improved Composite Pressure Vessels for Hydrogen Storage, Lincoln Composites, Lincoln, NE," May 16, 2011.

10. Weiner, S.C., R.A. Kallman and E.G. Skolnik, "Speaking of Safety: Learning from Safety Reviews," PNNL-SA-71062, 18th World Hydrogen Energy Conference, Essen, Germany, May 18, 2010.

11. Barilo, N.F. and Fassbender, L.L., "Handling Compressed Hydrogen Gas Cylinders," *H2 Safety Snapshot*, Volume 2, Issue 1, PNNL-SA-75299, November 2010.

12. Barilo, N.F. and Fassbender, L.L., "Identifying Safety Vulnerabilities," *H2 Safety Snapshot*, Volume 2, Issue 2, PNNL-SA-77099, July 2011.

13. Weiner, S.C. and Blake, C.W., "Safety Knowledge Tools Enhanced by International Collaboration," A White Paper of the International Energy Agency Hydrogen Implementing Agreement Task 19 – Hydrogen Safety, PNNL-19901, October 18, 2010.

VIII.11 Hydrogen Safety Knowledge Tools

Linda Fassbender
Pacific Northwest National Laboratory (PNNL)
P.O. Box 999
Richland, WA 99352
Phone: (509) 372-4351
E-mail: Linda.Fassbender@pnnl.gov

DOE Manager
HQ: Antonio Ruiz
Phone: (202) 586-0729
E-mail: Antonio.Ruiz@ee.doe.gov

Project Start Date: March 2003
Project End Date: Project continuation and direction determined annually by DOE

Fiscal Year (FY) 2011 Objectives

- Hydrogen Safety Best Practices - Capture the vast knowledge base of hydrogen experience and make it publicly available. The best practices online manual is a "living" document that provides guidance for ensuring safety in DOE hydrogen projects, while serving as a model for all hydrogen projects and applications.
- Hydrogen Incident Reporting and Lessons Learned - Collect information and share lessons learned from hydrogen incidents and near-misses, with the goal of preventing similar safety events from occurring in the future.

Technical Barriers

This project addresses the following technical barriers from the Hydrogen Safety section of the Fuel Cell Technologies (FCT) Program Multi-Year Research, Development and Demonstration Plan:

(A) Limited Historical Database

(B) Proprietary Data

Contribution to Achievement of DOE Safety, Codes & Standards Milestones

This project has already met the following DOE milestones from the Hydrogen Safety section of the FCT Program Multi-Year Research, Development and Demonstration Plan:

- **Milestone 18**: Publish safety bibliography and incident databases (3Q, 2006).
- **Milestone 19**: Publish a Best Practices Handbook (1Q, 2008).
- **Milestone 20**: Update peer-reviewed Best Practices Handbook (4Q, 2008).

FY 2011 Accomplishments

Hydrogen Safety Best Practices

- Added a new section on Hydrogen Properties, which is focused on combustion and liquid hydrogen expansion.
- Added a new section for students, technicians, and young engineers less familiar with hydrogen called "So You Want to Know Something about Hydrogen."
- Added a new section on Indoor Refueling of Hydrogen-Powered Forklifts with assistance from a team of industry experts.
- Added a new section on Chemical Hydrogen Storage.
- Added more photos to enhance the website appearance.

Hydrogen Incident Reporting and Lessons Learned

- Added 56 new safety event records from national laboratories, universities, and private-sector firms in the U.S. and other countries since the 2010 Annual Merit Review (AMR), for a total of 195 records currently in the database.
- Created quarterly postings of the Lessons Learned Corner to analyze and present hydrogen safety themes illustrated with database content.



Introduction

PNNL has developed and continues to improve two software tools to support the Hydrogen Safety, Codes and Standards sub-program. This report covers the Hydrogen Safety Best Practices online manual (http://www.H2BestPractices.org) and the Hydrogen Incident Reporting and Lessons Learned database (http://www.H2Incidents.org). The National Research Council's second report on the FreedomCAR and Fuel Partnership states that "The creation of a database on incidents involving hydrogen will be useful in promoting safety" [1]. The report also states that "The committee encourages DOE to continue to develop, publish, and update the best practices document."

Approach

Hydrogen Safety Best Practices - There are many references and resources that deal with the safe use of hydrogen, and our intent is to organize and compile relevant information in an easy-to-use Web-based manual without

duplicating existing resources. PNNL teams with the Hydrogen Safety Panel, other national laboratory staff, and other subject matter experts to compile hydrogen-specific best practices from a variety of references. Links to Web-based resources and files are provided on the website.

Hydrogen Incident Reporting and Lessons Learned - The purpose of "H2Incidents.org" is to facilitate open sharing of lessons learned from hydrogen safety events to help avoid similar incidents in the future. Our approach includes encouraging DOE-funded project teams and others to voluntarily submit incidents and near-misses and to provide specific lessons learned. We continue to pursue the addition of new records by actively seeking news reports on hydrogen incidents and searching existing databases and other sources for hydrogen-related safety event records. We contact private-sector companies who experience hydrogen-related safety events to solicit their permission to publish such records. We continue to maintain a mechanism for online submission of records. Specific safety event records are linked to Best Practices online manual content to emphasize safe practices for working with hydrogen and avoiding future incidents. Expert review of all safety events and lessons learned is provided by PNNL subject matter experts and the Hydrogen Safety Panel.

Results

Hydrogen Safety Best Practices – Existing content was supplemented with four new sections, and we added a number of photos to enhance the website appearance. A new section on Hydrogen Properties was added, which is focused on combustion and liquid hydrogen expansion. This section was developed collaboratively with members of the Hydrogen Safety Panel and the National Aeronautics and Space Administration White Sands Test Facility.

To serve the needs of students, technicians, and young engineers less familiar with hydrogen, a new section was added called "So You Want to Know Something about Hydrogen." The new section discusses properties and behavior, applications, and systems and controls, and a subsection on Hydrogen Hazards covers leaks, flames, and explosions. The Hydrogen Hazards section is not intended to dissuade anyone from working with hydrogen, but to make them aware that constant vigilance is necessary when working with or around hydrogen. In fact, hydrogen is just as safe as gasoline or any other commonly used fuel, it's just different. If you understand the differences, you will understand how to work safely with hydrogen.

Another new section on Indoor Refueling of Hydrogen-Powered Forklifts was developed with a team of subject matter experts from Air Products and Chemicals, Nuvera Fuel Cells, the National Renewable Energy Laboratory, and PNNL. This section covers design considerations, piping safeguards, leak mitigation, vehicle safety features, operations, and training.

A new section on Chemical Hydrogen Storage complements the existing material on Metal Hydride Storage and Handling. The term "chemical hydrogen storage" is used to describe storage technologies in which hydrogen is released and then later restored through chemical reactions. Many of the compounds that are being investigated for chemical hydrogen storage have never been synthesized, so material safety data sheets do not exist. Chemical hydrides present special hazards, including toxic byproducts, water and air reactivity, pyrophoricity, potential for runaway reactions with gas formation, and room-temperature gas emissions and instabilities.

Hydrogen Incident Reporting and Lessons Learned - We added 56 new incident records since the 2010 AMR. These records came from national laboratories, universities, and private-sector firms in the U.S. and other countries. We currently have 195 records in the database, with at least 30 more in progress. Most incident alerts were obtained from DOE or Google Alerts for hydrogen and fuel cell vehicles. Significant time was spent interacting with incident "owners" to encourage them to submit records of incidents and near-misses. We also posted quarterly installments of the Lessons Learned Corner to analyze hydrogen safety themes illustrated by database content.

We incorporated bar graphs to characterize the database contents in terms of settings, equipment, damage/injuries, probable causes, and contributing factors. The visual display makes it clear that the content is dominated by laboratory incidents (almost as many incidents as the next four highest settings combined).

Last year, we created a Lessons Learned Corner (LLC) to analyze the database content. We publish the LLC quarterly based on a specific theme that is illustrated with safety event records in the database. Themes covered to date include:

- Management of Change
- Working with Reactive Metal-Hydrides
- The Importance of Purging Hydrogen Piping and Equipment
- Hydrogen Use in Anaerobic Chambers
- Adequate Ventilation of Battery Charging Facilities
- Learning from Burst Disk Failures.

As an example, the basic theme of the LLC on The Importance of Purging Hydrogen Piping and Equipment is that all personnel should be trained on proper procedures for taking hydrogen systems offline and bringing them back online. Hydrogen Safety Panel members utilized their significant industrial experience to assist us in extracting clear lessons learned about purging systems. When getting ready for maintenance, you should always be conservative and assume that hydrogen is present and use a properly vented inert gas subsystem for purging. Likewise, when bringing a hydrogen system back online, you should always

assume that air is present and reduce oxygen levels below 1% before putting the system back online. Three very diverse incidents that were caused by improper purging are highlighted in the LLC – one from a power plant setting, one from a hydrogen production facility, and one that occurred in a laboratory. In each incident, standard operating procedures related to system purging were ignored or altered, without thorough consideration of the potential consequences. Hydrogen was ignited in all three incidents, and serious explosions could have occurred if larger volumes of hydrogen had been in use.

Conclusions and Future Directions

Hydrogen Safety Best Practices - Our future work includes improving existing website content as well as drafting new content. Ideas for new content come from the Hydrogen Safety Panel, other national laboratories, technical reviewers at the DOE AMR, and actual website users. We are planning a brainstorming session with the Hydrogen Safety Panel to identify any gaps in website content that should be addressed.

PNNL continues to monitor website usage and respond to user feedback. Users have submitted many requests for additional information and guidance through the website's comment submittal feature. We routinely seek guidance from one or more Hydrogen Safety Panel members in crafting our responses to these requests. Website utility is enhanced by continuing to link the content to safety event records in the Hydrogen Incident Reporting and Lessons Learned database and by adding photos, graphics, and videos to complement the text.

Hydrogen Incident Reporting and Lessons Learned - Our future work will focus on increasing the number of records in the database, in part through identifying additional sources of hydrogen safety event data and lessons learned. A significant part of our effort involves working with the national laboratories, universities, and private-sector firms that experience hydrogen incidents and/or near-misses to help them communicate what happened, what the probable causes and contributing factors were, and most importantly, what lessons were learned by their organizations that could benefit others if they were freely shared. We will continue to monitor website usage and respond to user feedback.

We will also continue to encourage all DOE-funded projects, universities, private-sector organizations, and others to voluntarily submit records of their hydrogen incidents and near-misses. Success requires that people use the database and submit information without fear of negative consequences from reporting and publicizing safety events. We will continue to maintain confidentiality for the organizations that voluntarily submit safety event records.

FY 2011 Publications/Presentations

1. Weiner, S.C., Fassbender, L.L., Blake, C., Aceves, S., Somerday, B.P. and Ruiz, A., "Web-based Resources Enhance Hydrogen Safety Knowledge," PNNL-SA-79693, HYPOTHESIS IX, San José, Costa Rica, December 12–15, 2011 (abstract accepted June 24, 2011).

2. Weiner, S.C. and Fassbender, L.L. "Lessons Learned from Safety Events," PNNL-SA-76793, International Conference on Hydrogen Safety, San Francisco, CA, September 12–14, 2011 (manuscript accepted June 1, 2011).

3. Barilo, N.F. and Fassbender, L.L. "Identifying Safety Vulnerabilities," *H2 Safety Snapshot*, Volume 2, Issue 2, PNNL-SA-77099, March 2011.

4. Weiner, S.C., Fassbender, L.L. and Quick, K.A. "Using Hydrogen Safety Best Practices and Learning from Safety Events," PNNL-SA-70148, International Journal of Hydrogen Energy, Volume 36, Issue 3, February 2011, pp. 2729-2735.

5. Fassbender, L.L. "Hydrogen Safety Knowledge Tools," PNNL-SA-77093, Hydrogen and Fuel Cell Safety, Fuel Cell and Hydrogen Energy Association, January 2011. http://www.hydrogenandfuelcellsafety.info/2011/jan/index.asp.

6. Barilo, N.F. and Fassbender, L.L. "Handling Compressed Hydrogen Gas Cylinders," *H2 Safety Snapshot*, Volume 2, Issue 1, PNNL-SA-75299, November 2010.

References

1. National Research Council, 2008, Review of the Research Program of the FreedomCAR and Fuel Partnership, Second Report, The National Academies Press, Washington, D.C.

VIII.12 Hydrogen Emergency Response Training for First Responders

Monte R. Elmore
Pacific Northwest National Laboratory (PNNL)
902 Battelle Blvd.
Richland, WA 99352
Phone: (509) 372-6158
E-mail: monte.elmore@pnnl.gov

DOE Manager
HQ: Antonio Ruiz
Phone: (202) 586-0729
E-mail: Antonio.Ruiz@ee.doe.gov

Subcontractors:
- Jennifer Hamilton, California Fuel Cell Partnership (CaFCP), Sacramento, CA
- Hanford Fire Department, Richland, WA
- Hazardous Materials Management and Emergency Response (HAMMER) Training and Eduction Center, Richland, WA

Project Start Date: October 2004
Project End Date: Project continuation and direction determined annually in consultations with DOE

Fiscal Year (FY) 2011 Objectives

- Support the successful demonstration and deployment of hydrogen and fuel cell technologies by providing technically accurate hydrogen safety and emergency response information to first responders.
- Provide a one-day first responder training course, "Hydrogen Emergency Response Training for First Responders," that integrates the use of DOE's mobile hydrogen fuel cell vehicle (FCV) prop.
- Continue to support the Web-based awareness-level course, "Introduction to Hydrogen Safety for First Responders." www.hydrogen.energy.gov/firstresponders
- Disseminate first responder hydrogen safety educational materials at appropriate fire fighter conferences to raise awareness.

Technical Barriers

This project addresses the following technical barriers from both the Hydrogen Safety (SAF) and Education (ED) sections (3.8 and 3.9, respectively) of the Fuel Cell Technologies Program Multi-Year Research, Development and Demonstration Plan:

(A) Lack of Readily Available, Objective, and Technically Accurate Information (ED)

(C) Disconnect Between Hydrogen Information and Dissemination Networks (ED)

(D) Lack of Educated Trainers and Training Opportunities (ED)

(H) Lack of Hydrogen Knowledge by Authorities Having Jurisdiction (SAF)

(I) Lack of Hydrogen Training Facilities for Emergency Responders (SAF)

Contribution to Achievement of DOE Hydrogen Safety/ Education Milestones

This project will contribute to achievement of the following DOE milestones from the Hydrogen Safety and Education sections of the Fuel Cell Technologies Program Multi-Year Research, Development and Demonstration Plan:

- Milestone 6 (ED): Update "prop-course" for first responders. (4Q, 2011)
- Milestone 7 (ED): Update "Awareness-Level" information package for first responders. (4Q, 2012)
- Milestone 9 (ED): Update "prop-course" for first responders. (4Q, 2014)
- Milestone 10 (ED): Update "Awareness-Level" information package for first responders. (4Q, 2015).

In addition, the following milestones were met in previous years:

- Milestone 1 (ED): Develop "Awareness-Level" information package for first responders. (4Q, 2006)
- Milestone 3 (ED): Develop "prop-course" using hands-on training devices for first responders. (4Q, 2008)
- Milestone 4 (ED): Update "Awareness-Level" information package for first responders. (4Q, 2009).
- Milestone 21 (SAF): Conduct first hydrogen safety class (non-prop) offered at HAMMER. (3Q, 2005)
- Milestone 22 (SAF): Complete first life-size prop for hands-on training of emergency responders. (1Q, 2008).

FY 2011 Accomplishments

Prop-Based Course: This operations-level course was presented at several fire training centers throughout California in the past year. Three consecutive one-day training classes were held at each of the following locations:

- Rio Hondo College Fire Academy, Santa Fe Springs, CA (Aug 2010)
- Orange County Fire Authority, Irvine, CA (Aug 2010)
- Sunnyvale Dept. of Public Safety, Sunnyvale, CA (Sept 2010)

- San Joaquin Defense Logistics Agency (DLA), Tracy Site (June 2011)
- San Joaquin DLA, Sharpe Site (June 2011).

The last two noted DLA sites are military depots expecting installations of hydrogen fueling stations and hydrogen fuel cell-powered forklifts later this year. Therefore, the course material was updated this year to include additional information on the growing use of hydrogen fuel cell-powered industrial lift trucks (forklifts), and related emergency response information. Approximately 350 first responders from the above sites received this training. Extremely positive feedback from each of the sites continues to reinforce the value of this course to first responder organizations.

In October 2010, PNNL hosted a visit by the FreedomCAR directors and USCAR representatives. During their visit, attendees were given a demonstration of how the FCV prop is used for first responder training.

The Fire Department News Network produced a video of portions of the operations-level course during delivery of the course at Orange County Fire Authority in August 2010. The video was first aired on their website (www.fdnntv.com) in November 2010.

Awareness-Level Course: Our website still averages ~300 unique visits per month from almost every state and some foreign countries. The course is registered on the TRAIN (TrainingFinder Realtime Affiliate Network) website for broader dissemination to first responders. TRAIN is a central repository for public health training courses. Almost 30,000 TRAIN users identify themselves as emergency responders.

Outreach: Compact disks of the awareness-level course were distributed through the DOE Energy Efficiency and Renewable Energy Information Center. PNNL and HAMMER hosted a booth at a first responder conference (Fire Rescue International 2010) in Chicago, IL, August 2010.



Introduction

Safety in all aspects of a future hydrogen infrastructure is a top priority, and safety concerns influence all DOE hydrogen and fuel cell projects. Despite the most concerted effort, however, no energy system can be made 100% risk-free. Therefore, for any fuel and energy system, a suitably trained emergency response force is an essential component of a viable infrastructure. The Fuel Cell Technologies Program has identified training of emergency response personnel as a high priority, not only because these personnel need to understand how to respond to a hydrogen incident, but also because firefighters and other emergency responders are influential in their communities and can be a positive force in the introduction of hydrogen and fuel cells into local markets.

This project employs the Occupational Safety and Health Administration and National Fire Protection Association frameworks for hazardous materials emergency response training to provide a tiered hydrogen safety education program for emergency responders. The effort started with development and distribution of the awareness-level Web-based course in FY 2006-2007. A more advanced course and materials to facilitate education were developed in FY 2008-2009, complementing the design, construction, and operation of a fuel cell vehicle prop (developed under PNNL's Hydrogen Safety project). The overall first-responder education program will continue to be updated. In addition, PNNL has implemented outreach efforts to key stakeholder groups to facilitate delivery of the training to a broad audience.

Approach

PNNL works with subject matter experts in hydrogen safety and first responder training to develop hydrogen safety course materials. Draft materials undergo considerable review and revision before being released. The PNNL team works with DOE to make stakeholder groups aware of training opportunities and to provide "live" training when appropriate. The Web-based awareness-level course is available "online" or on compact disks and provides the student with a basic understanding of hydrogen properties, uses, and appropriate emergency response actions. The prop-based course, a more advanced operations-level course, was initially presented at the HAMMER training facility in Richland, WA. Subsequently, the mobile prop has enabled the course to be delivered at several offsite fire training centers (in California during 2010-11) in order to reach larger audiences in areas where hydrogen and fuel cell technologies are being deployed.

Results

Prop-Based Course: The focus of the curriculum is on teaching first responders what is the same and what is different about hydrogen and FCVs as compared to conventional fuels and vehicles. Course evaluation forms are distributed and feedback obtained at each class to help us improve the course content and delivery. Based on feedback from all the class sessions held this past year (August 2010, September 2010, and June 2011), we conclude that following the training, first responders are more familiar with the properties and behavior of hydrogen, and are prepared to operate in a safe and effective manner if a hydrogen incident should occur in their jurisdiction.

The FCV prop has been integrated into the "Hydrogen Emergency Response Training for First Responders" course. The prop (shown in Figure 1) demonstrates potential conditions that could be encountered during the control



FIGURE 1. A Team of Fire Fighters Rescues a "Victim" from the Live-Fire Hydrogen FCV Prop

and suppression of a FCV fire. The photo shows a team of firefighters training to respond to a motor vehicle accident, in this case a multi-vehicle accident involving a hydrogen FCV and a conventional vehicle.

Conclusions and Future Directions

The introductory Web-based course has been quite successful, based on the usage recorded and feedback received. The course is fulfilling a need expressed by the first responder community to receive more information about hydrogen and fuel cells so they will be prepared in the rare event of a hydrogen incident. The in-depth prop-based course builds on that success and is very useful in giving first responders a hands-on experience with simulated FCV incidents that integrates well with classroom training. PNNL will continue to update both courses as needed to reflect current applications and markets for hydrogen and fuel cells.

There is an identified need for the prop course curriculum to achieve a better balance between the vehicles and stationary facilities modules, through the development of some type of prop for stationary applications of fuel cells. An interactive video training tool of virtual hydrogen incident scenarios and responses to simulate both outdoor fueling of passenger FCVs and indoor fueling of hydrogen forklifts could address that need. We propose to develop a virtual model by first demonstrating the concept with a simplified model, and subsequently adding additional features and capabilities.

The prop course will be offered at additional first responder training facilities in California in FY 2012. As additional hydrogen fueling stations are commissioned and more FCVs appear on the road, more first responder organizations are inquiring about this training. As with the previous training classes, the prop will be transported to California in its trailer and left at each site for about a week. Multiple classes will be offered at each site. In future years, the prop will be transported to other locations across the country for use in delivery of this course at training centers in areas that have emerging deployments of hydrogen and fuel cell technologies. PNNL will also work with DOE and other stakeholders to determine what, if any, additional types of educational courses and materials are warranted, and to develop and implement plans to provide education to specific groups.

FY 2011 Publications/Presentations

1. Fassbender, L.L., "Hydrogen Safety Training for First Responders," PNNL-SA-76870, Fuel Cell and Hydrogen Energy Association, January 2011. www.hydrogenandfuelcellsafety.info/2011/jan/firstResponders.asp

2. Elmore, M.R. "Hydrogen Emergency Response Training for First Responders." PNNL-SA-78366, DOE Annual Merit Review and Peer Evaluation Meeting, Washington, D.C., May 11, 2011.

3. Elmore, M.R., Fassbender, L.L., Hamilton, J.J., and Weiner, S.C. "Hydrogen Emergency Response Training for First Responders," PNNL-SA-79009, International Conference on Hydrogen Safety, San Francisco, CA, September 12–14, 2011.

VIII.13 Hydrogen Safety Training for Researchers and Technical Personnel

Salvador M. Aceves (Primary Contact),
Francisco Espinosa-Loza, Guillaume Petitpas,
Timothy O. Ross, Vernon Switzer
Lawrence Livermore National Laboratory (LLNL)
7000 East Avenue, L-792
Livermore CA 94550
Phone: (925) 422 0864
E-mail: saceves@llnl.gov

DOE Manager
HQ: Antonio Ruiz
Phone: (202) 586-0729
E-mail: Antonio.Ruiz@ee.doe.gov

Project Start Date: October 2008
Project End Date: Project continuation and direction determined annually by DOE

Fiscal Year (FY) 2011 Objectives

- Prepare safety training materials for researchers running H_2 laboratory experiments.
- Prepare advanced safety training materials for personnel in charge of hydrogen systems.

Technical Barriers

This project addresses the following technical barriers from the Hydrogen Safety section (3.8) of the Fuel Cell Technologies Program Multi-Year Research, Development and Demonstration Plan:

(H) Lack of Hydrogen Knowledge by Authorities Having Jurisdiction

(I) Lack of Hydrogen Training Facilities

Contribution to Achievement of DOE Hydrogen Safety, Codes & Standards Milestones

This project will contribute to achievement of the following DOE milestones from the Hydrogen Safety section of the Fuel Cell Technologies Program Multi-Year Research, Development and Demonstration Plan:

- **Milestone 17**: Identify user needs for basic safety information

FY 2011 Accomplishments

- Released a final version of the Web-based "Hydrogen Safety Class for Researchers."
- Acquired Web domain www.h2labsafety.org for intuitive, easy to remember access.
- Registered 100+ Web class completions.
- Procured materials and equipment for hands-on class.
- Completed lesson plan for hands-on class.



Introduction

LLNL has been conducting hydrogen research for more than 50 years, starting with national security applications and continuing with energy research. For many of these years, LLNL was designated as the pressure safety training facility for the whole DOE complex and other government institutions such as the National Aeronautics and Space Administration. Many technicians and researchers visited LLNL to receive training on many aspects of pressure safety, including hydrogen technology, cryogenics, leak detection, and vacuum technology.

The national security hydrogen and high-pressure research conducted at LLNL demanded unique testing facilities, and these were built with funding from DOE National Nuclear Security Administration. These facilities include a high pressure laboratory equipped with four hydrogen-compatible test cells, each rated for 80,000 psi, and 4 pounds of trinitrotoluene (TNT) equivalent stored energy. LLNL also has a high explosive test facility (Site 300) for experiments with many pounds of TNT equivalent and many kg H_2. Experiments at Site 300 are typically conducted in outdoor firing tables and monitored from the safety of a bunker. The remote location of this facility protects employees and property from any hazard.

These unique facilities and the expertise necessary to operate them are now being made available for hydrogen energy research through the development of training materials that may contribute to safe operation within the many institutions working on hydrogen technology.

Approach

We are pursuing a two-pronged approach to hydrogen safety training:

- Researchers conducting laboratory experiments can benefit from basic training on hydrogen and pressure safety. This Web-based training can be completed in ~4 hours.
- Technical personnel in charge of setting up experimental equipment require comprehensive hands-on training on all aspects of hydrogen systems. This extensive training is planned for three full days.

Results

The Web-based hydrogen safety class (www.h2labsafety.org) was publicly released in September of 2010. Since then we have registered over 100 completions from universities, government institutions, and private companies from five countries (USA, Canada, United Kingdom, Japan, and Mexico). Before public release, class materials were thoroughly reviewed by a panel of safety experts through two rounds of peer review, focusing on the technical aspects as well as on the teaching aspects of the class. Further improvement is always possible, however, and we therefore invite readers to take the class and submit comments to the authors that may improve the learning experience, update the class information, and/or report bugs or malfunctions. Class authors can be contacted by e-mail at any time during the course, by clicking on the "help" button in the top menu (or use author's e-mail address listed above).

In addition to the Web-based fundamentals class, we are developing a hands-on hydrogen safety class for pressure operators. This comprehensive training includes basic hydrogen safety, regulators, relief devices, leak detection, and flash arrestors, followed by hands-on assembly and test of a hydrogen pressure system and a final evaluation. Training can be conducted during a three-day session at LLNL, or at remote institutions if appropriate facilities (classroom, compressed gas supply, and pressure testing laboratory) exist.

The hands-on training class starts with a full day of classroom instruction covering essential topics of pressure system assembly and operation (Table 1). Classroom instruction focuses on identifying hazards, safety precautions, personal protective equipment, and pressurized hydrogen system components and their function. This class greatly expands the descriptions from the Web-based hydrogen safety class, going into detailed operational information about every component in pressure systems, describing their inner functionality, applicability, and recommended use. Teaching is aided by segmented components that reveal their inner operational details (Figure 1). At the end of classroom instruction, students will be able to identify (i) the main hydrogen pressure system components, (ii) pressure and hydrogen based hazards, (iii) the types of personal protective equipment that are used for pressurized hydrogen systems, and (iv) the pressurized hydrogen system component categories and their functions. In the final activity of the day, students are tested on the class materials.

Days two and three will be spent in the laboratory for practical application of the classroom information from day one. On day two, students will be handed a safety document and instructed to assemble the pressure system described therein (Figure 2). Students will have to select, inspect and install pressure components, bend tube, install pipe and compression fittings, and assemble the entire system.

On day three this system will be leak checked with a mass spectrometer helium leak detector with a leak rate of no more than 1.0×10^{-5} atm-cc/sec helium. The pressure system will then be connected to the data acquisition system and pressure tested remotely at 150% of the maximum allowable working pressure. The last leak test will be conducted using liquid leak detection fluid at the system's maximum operating pressure. Finally, the students will operate the system to reach a desired pressure.

TABLE 1. Hands-On Safety Class Structure

	Modules
Day 1	**Classroom Teaching**
	1. Definitions 2. Hazards 3. Personal Protective Equipment 4. Gas Cylinders 5. Gas Cylinder Manifold 6. Pressure Reducing Regulators 7. Gauges/Pressure Transducers 8. Regulator Safety Manifold 9. Relief Devices 10. Valves 11. Fittings 12. Tubing and Piping 13. Flash Arrestors 14. Quiz
Day 2	**Pressure system assembly**
	Given a system schematic and description, select components, inspect and install, cut and bend tube, apply various fittings, and assemble full system
Day 3	**System leak test and operation**
	Leak test using a mass spectrometer leak detector; setup data acquisition; conduct remote pressure test; leak test at maximum operating pressure using leak detection fluid; operate system to reach a desired pressure

During the two days of laboratory work, students will be tested as they build and test the system. On day two, tests will focus on correct system assembly (select appropriate components, inspect them, install them in the right place, bend tubing correctly, install plumbing at the correct place, and install pipe and compression fittings). On day three, students will be tested during leak checks and necessary system rebuilds to meet the leak test criterion. At the end of day three, based on the successful completion and testing of the assembled panel, students will be awarded a Certificate of Completion for "LLNL Hands-On Hydrogen Safety Training".

The hands-on class is still under development. Two working benches and instructional materials including segmented pressure components (regulators, valves, gauges, Figure 1) have been prepared as teaching materials to best instruct component function. Classroom instruction materials are being prepared.

Conclusions and Future Directions

LLNL is contributing to safe hydrogen operations by developing instructional materials for researchers and technical operators:

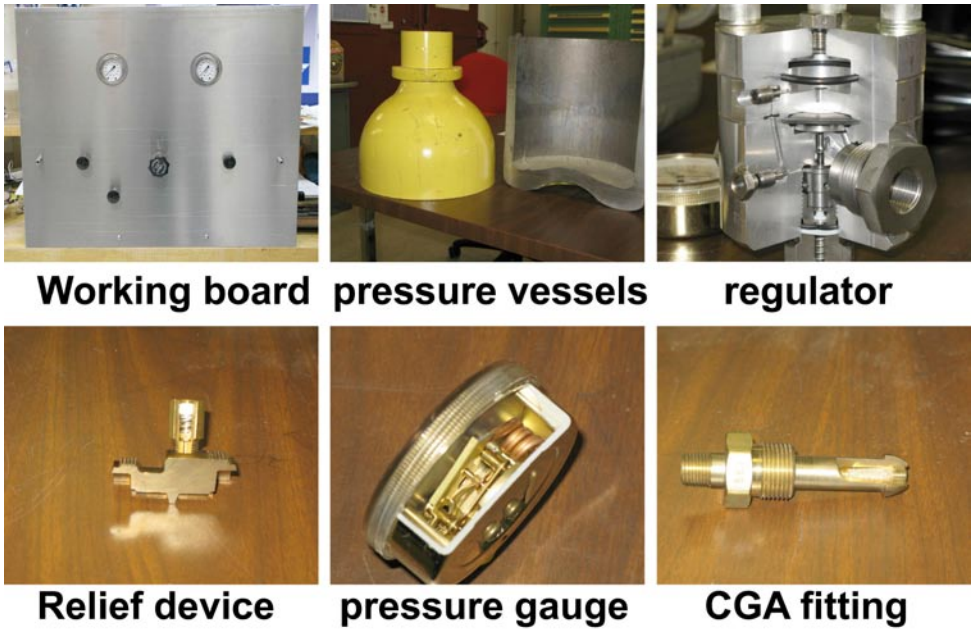


FIGURE 1. Working board and different pressure components segmented to illustrate internal structure and operability.

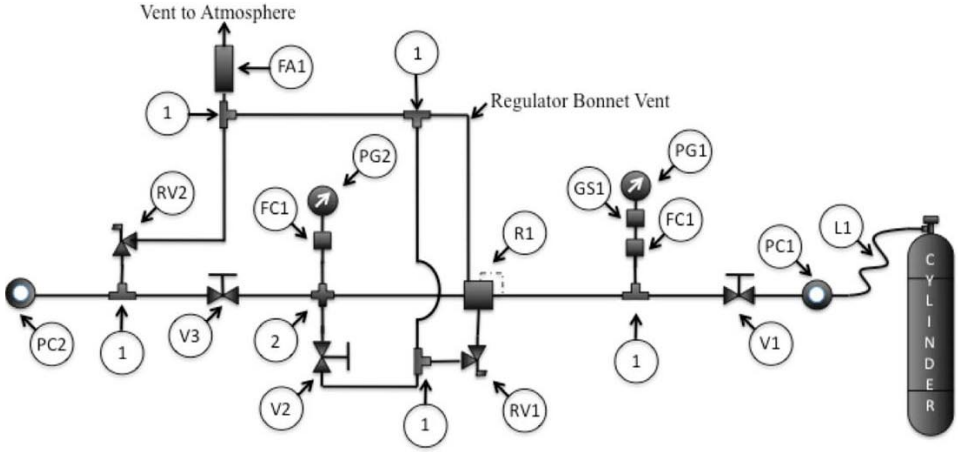


FIGURE 2. Piping and instrumentation diagram for the pressure system to be assembled during the hands-on hydrogen safety class.

- *Laboratory researchers* can obtain basic hydrogen safety information from a 4-hour Web-based class (free online access at http://www.h2labsafety.org/) addressing hydrogen fundamentals: properties, pressure and cryogenic safety, emergency response and codes and standards.
- *Technical operators* in charge of building and testing experimental hydrogen equipment require more in-depth information than provided by the Web-based class. We are therefore preparing a 3-day hands-on safety class that presents detailed information for installation, testing, and operation of hydrogen pressurized systems. The hands-on class includes a full day of classroom instruction followed by two days of laboratory work where students assemble, test and operate a pressure system based on a schematic and component description.

We strongly encourage participation of the members of the hydrogen community to improve the technical and educational aspects of the class by providing feedback and comments.

FY 2011 Publications/Presentations

1. Aceves, S.M., Espinosa-Loza, F., Petitpas, G., Ross, T.O, and Switzer, V.A., "Hydrogen Safety Training for Researchers and

Technical Personnel," Accepted for Publication, International Conference on Hydrogen Safety, San Francisco, CA, 2011.

2. Petitpas, G., Aceves, S.M., "Modeling of Sudden Hydrogen Expansion from Cryogenic Pressure Vessel Failure," Accepted for Publication, International Conference on Hydrogen Safety, San Francisco, CA, 2011.

VIII.14 Hydrogen Leak Detection System Development

R.A. Lieberman (Primary Contact), M. Beshay
Intelligent Optical Systems (IOS), Inc.
2520 W. 237th St.
Torrance, CA 90505
Phone: (310) 530-7130
E-mail: rlieberman@intopsys.com

DOE Managers
HQ: Mr. Antonio Ruiz
Phone: (202) 586-0729
E-mail: Antonio.Ruiz@ee.doe.gov
GO: Katie Randolph
Phone: (720) 356-1759
E-mail: Katie.Randolph@go.doe.gov

Contract Number: DE-FG36-08G088098

Project Start Date: June 1, 2008
Project End Date: November 30, 2011

Overall Objectives

- Integrate hydrogen indicator chemistry into a complete optoelectronics package with well-defined sensing characteristics and a known end-use market.
- Develop signal processing and user interface software/firmware to assure sensor meets appropriate standards for commercial acceptance.

Fiscal Year (FY) 2011 Objectives

- Select and finalize hydrogen sensor components and outline scalable cost analysis.
- Finalize sensor data processing algorithms with minimum false alarms.
- Fabricate, test, and validate performance of 14 fully packaged prototypes.
- Deploy prototypes at four different field test sites.
- Collect and analyze real-time test data under various deployment conditions.
- Reach end-users through field demonstrations and field trails.

Technical Barriers

This project addresses the following technical barriers from several sections of the Fuel Cell Technologies Program Multi-Year Research, Development and Demonstration Plan (MYRDDP):

- **Delivery: Barrier I.** Hydrogen Leakage and Sensors (MYRDDP page 3.2-20: "Low cost hydrogen leak detector sensors are needed")
- **Storage: Barrier H.** Balance of Plant (BOP) Components (MYRDDP page 3.3-14: "Light-weight, cost-effective… components are needed…These include… sensors")
- **Manufacturing R&D: Barrier F.** Low Levels of Quality Control and Inflexible Processes (MYRDDP page 3.5-11: "Leak detectors… are needed for assembly of fuel cell power plants.")
- **Technology Validation: Barrier C.** Lack of Hydrogen Refueling Infrastructure Performance and Availability Data (MYRDDP page 3.6-8: "…the challenge of providing safe systems including low-cost, durable sensors [is an] early market penetration barrier")

This project will contribute to the achievement of the following DOE milestones from the Hydrogen Safety/Leak Detection Technology section of the Fuel Cell Technologies Program Multi-Year Research, Development and Demonstration Plan:

- MYRDDP Milestone: Develop sensors meeting technical targets. (4Q, 2012)
- MYRDDP Milestone: Develop leak detection devices for pipeline systems. (4Q, 2015)

FY 2011 Accomplishments

The hydrogen safety sensor being developed in this project has advanced from the applied research stage (DOE technology readiness level, TRL, 3) to the engineering prototype (TRL 6) stage. Initial work focused on exploring a family of colorimetric hydrogen sensor formulations and physical embodiments for different venues and markets. These included porous glass "optrodes," polymer integrated optic chip sensors, and hydrogen-sensitive optical fibers many meters in length (Figure 1). Economic and regulatory considerations led to the selection of an optrode-based handheld/wall-mounted format for the engineering prototypes. Key accomplishments during the past year include:

- Hydrogen safety sensor prototype refined/ruggedized.
- Optrodes have high sensitivity and rapid hydrogen response.
- Sensor repeatability/reversibility validated in third-party (National Renewable Energy Laboratory, NREL) tests.
- Hydrogen alarm algorithm developed and validated in field tests.
- Potential for high-accuracy concentration measurement demonstrated.

Introduction

Assuring safety is critically important to fostering commercial acceptance of hydrogen energy technologies, and to sustaining the use of hydrogen as a green energy source. A key to maintaining safety in hydrogen vehicles and installations is the ability to detect and warn of potentially hazardous conditions.

The overarching goal of this project is to create a reliable, cost-effective, alarm that warns of hydrogen leaks before they reach flammable concentrations. In the course of meeting this goal, we have demonstrated a proprietary hydrogen indicator chemistry that can be deployed in variety of optical formats, suitable for applications ranging from wide-area monitoring to point detection. Under DOE guidance, we have integrated a miniaturized indicator-bearing optical transducer with optoelectronic hardware and advanced signal processing software into a compact "smoke-detector-style" unit that will meet DOE- and customer-specified goals for sensitivity, response time, and reliability. This safety sensor will find use in many environments, including fuel cell-powered industrial vehicles, stationary power units, hydrogen generation and refueling stations, and storage locations.

Approach

- The hydrogen alarm sensor uses an optoelectronic platform (Figure 2) to monitor a porous glass sensor element ("optrode") hosting a colorimetric indicator. Upon hydrogen exposure, the optrode changes color, and the sensor unit uses the resulting optical signal to calculate hydrogen concentration. A second porous glass element, not containing the hydrogen indicator, gives the sensor an "internal reference" that minimizes environmentally induced false alarms (Figure 1).
- IOS' hydrogen sensor approach is unique in many aspects. First, each sensor unit uses an intrinsically safe low-power sensing element that functions without the heat required by many electronic hydrogen sensors. The unit employs another porous glass element, not containing the hydrogen indicator, gives the sensor an "internal reference" to minimize environmentally induced false alarms. Second, the unit has a faster response time and higher sensitivity levels, over a wider range of environmental conditions (i.e., temperature and humidity), than most of its counterparts. The sensor module can also be cabled to a readout unit for remote monitoring applications.

Results

In preparation for construction and delivery of 14 hydrogen sensor alarms for field testing, several elements

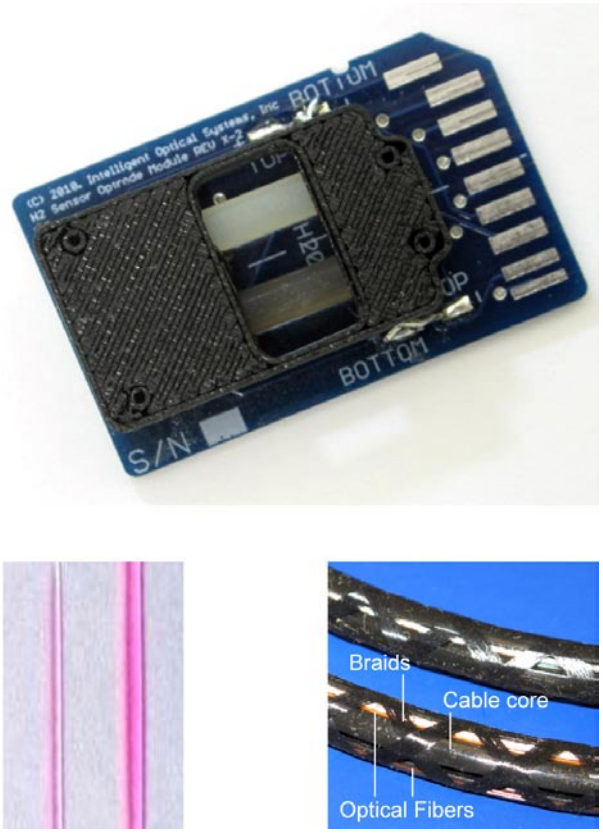


FIGURE 1. Optical Hydrogen Sensor Formats Top: optrodes in prototype mount; Bottom Left: integrated optic polymer waveguides; Bottom Right: extended-length sensor cable.



FIGURE 2. Compact Hydrogen Safety Sensor Unit

of the second-generation compact sensor were upgraded. Most notably, "noise" and "drift" in optical signals has been significantly reduced by redesigning the quick-connect optrode holder (Figure 1, top) to improve optical coupling between sensor elements and optoelectronic components. Changes in printed wiring board design were also implemented to simplify construction and address issues uncovered during testing of earlier versions. The result is a fully finalized physical and electronic design. All components have been procured, and construction of the field-test prototype units has begun. We project a mass-produced unit sale price of $100-$400, depending on features.

Sensor element materials and processing have also been finalized; a fabrication procedure has been selected that reproducibly generates optrodes of uniformly high quality. These transducers can respond to hydrogen at very low concentrations (Figure 3, top), and have been used to implement a high-speed alarm algorithm (Figure 3, bottom). Alarm response times are shown in Table 1. For all hydrogen concentrations at or above 10% of the lower flammability limit, (4% H_2 in air), the hydrogen leak detector sounds an alarm in less than 5 seconds.

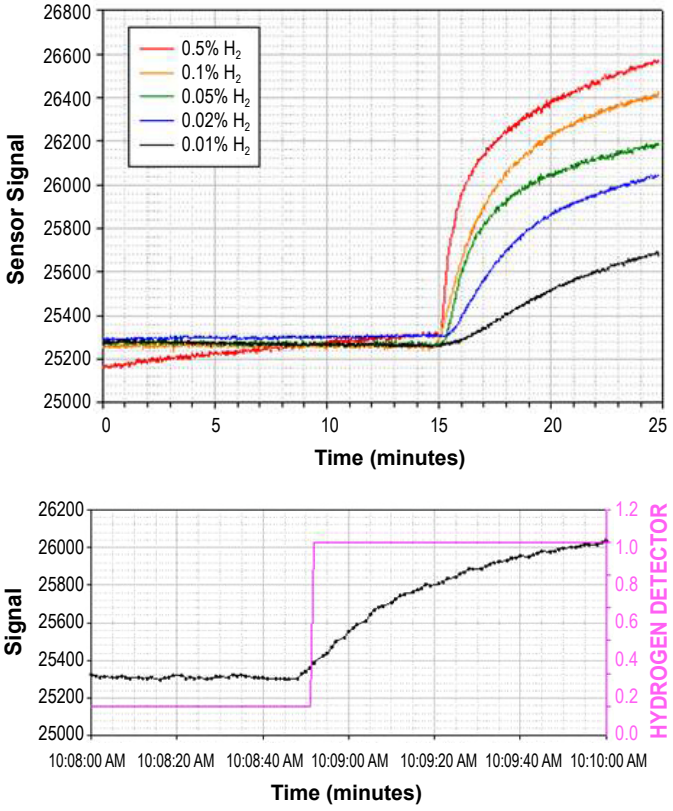


FIGURE 3. Rapid Response and High Sensitivity Top: response to low concentrations of hydrogen (0.01% H_2 = 0.25% of lower flammability limit; 0.5% H_2 = 12.5% lower flammability limit); Bottom: alarm algorithm (red line) triggers rapidly as optrode responds (black line) to 0.4% H_2 (10% lower flammability limit).

TABLE 1. Hydrogen Alarm Response Times

H_2 (%)	Detection Time (s)*
4.0	3
2.0	3
1.0	3
0.5	3
0.1	10
0.05	10
0.02	30
0.01	120

Determinations of sensor response and alarm algorithm function carried out at IOS have been independently verified in third-party tests carried out at NREL. Measurements of optrode signal sensitivity (Figure 4), repeatability, and reversibility (lack of hysteresis), have produced identical results to within the precision of the measurement apparatus. Multiple exposures to hydrogen release at NREL also showed the robustness of the rapid-response alarm algorithm (Figure 5). Preliminary tests of sensor response to simulated real-world leaks were carried out during a controlled release of hydrogen into a building at Sandia National Laboratories' Livermore facility. Optrode response closely tracked the hydrogen concentration in the building (Figure 6), verifying the feasibility of using optrodes not only for the development of safety alarms, but in high-accuracy hydrogen concentration sensors as well.

Conclusions and Future Directions

The prototype hydrogen leak alarm design is complete, and incorporates several upgrades based on results from IOS, NREL, and Sandia National Laboratories tests of earlier test units. Preliminary verification of the alarm

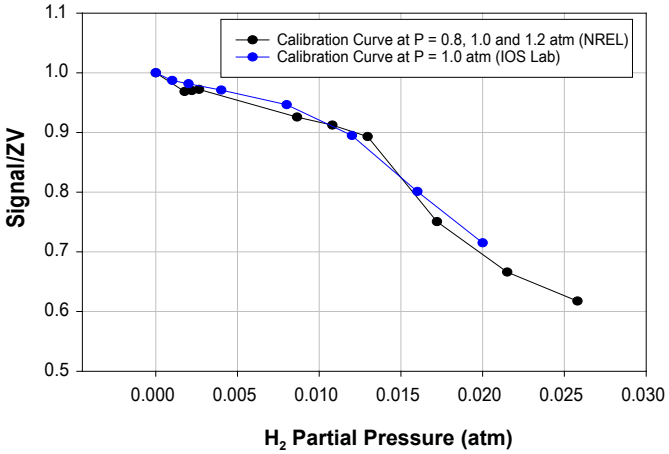


FIGURE 4. Optrode Response Validation Blue – Data taken at NREL; Black – Data taken at IOS.

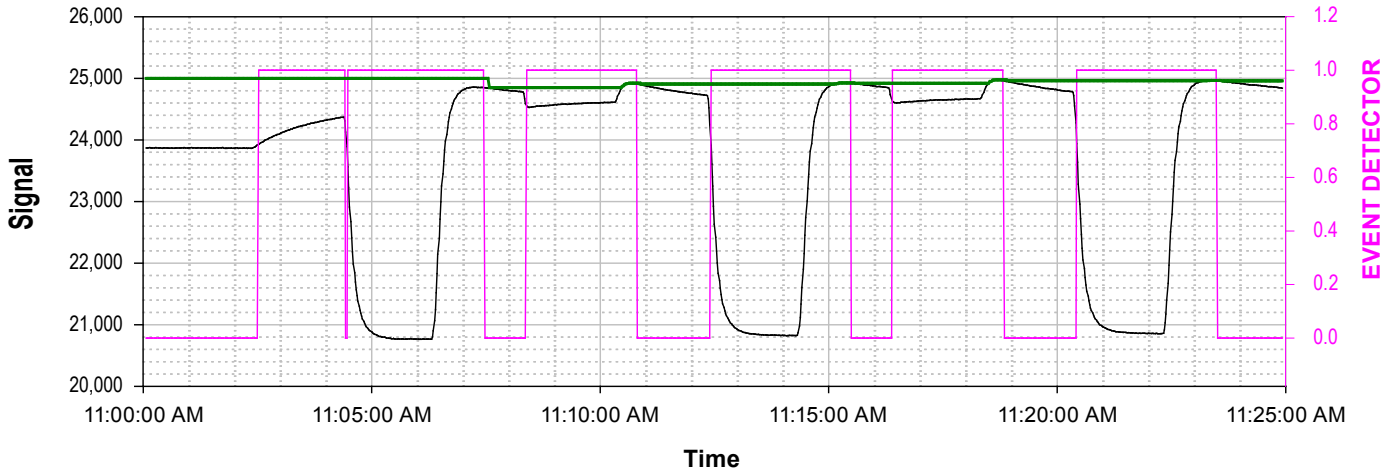


FIGURE 5. Hydrogen Alarm Algorithm Validation Black: optrode response; Red: alarm algorithm signal. Trigger point set at 2% H_2 (50% lower flammability limit, NREL data).

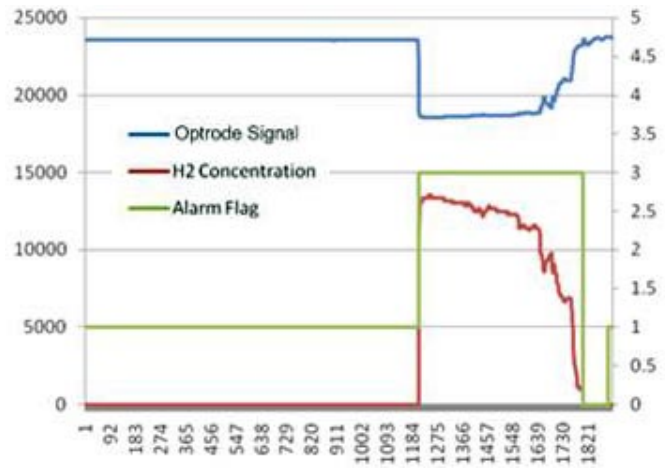


FIGURE 6. Building Release Trial at Sandia National Laboratories

algorithm has confirmed rapid response to all hydrogen concentrations of interest for safety monitoring. Remaining work in the project, which will advance the hydrogen detection leak system to TRL 7 includes:

- Development and installation of upgraded signal processing software.
- Assembly and delivery of 14 prototypes for field testing at DOE–selected sites.
- Extended temperature- and humidity-range testing of detector performance.
- Post-test upgrade of signal processing algorithms and final delivery of prototypes.

Patents Issued

1. "Sensor for Detection of Gas Such as Hydrogen and Method of Fabrication," U.S. Patent No. 7,897,057, issued March 1, 2011.

FY 2011 Publications/Presentations

1. "Intrinsically safe oxygen and hydrogen optical leak detector," M. Beshay, S. Garon, D. Ruiz, L. U. Kempen, Proc. SPIE Vol. 8026: Photonic Applications for Aerospace, Transportation, and Harsh Environment II, Alex A. Kazemi; Bernard Kress; Eric Y. Chan; Nabeel A. Riza; Lothar U. Kempen, Editors, 802605; 2011.

2. "Miniaturized real-time monitor for fuel cell leak applications," M. Beshay, J. G. Chandra Sekhar, J. Delgado Alonso, C. Boehr, R. A. Lieberman, Proc. SPIE Vol. 8026: Photonic Applications for Aerospace, Transportation, and Harsh Environment II, Alex A. Kazemi; Bernard Kress; Eric Y. Chan; Nabeel A. Riza; Lothar U. Kempen, Editors, 802606; 2011.

VIII.15 International Energy Agency Hydrogen Implementing Agreement Task 19 Hydrogen Safety

William Hoagland
Element One, Inc.
7253 Siena Way
Boulder, CO 80301
Phone: (720) 222-3214
E-mail: whoagland@elem1.com

DOE Manager
HQ: Antonio Ruiz
Phone: (202) 586-0729
E-mail: Antonio.Ruiz@ee.doe.gov

Sandia National Laboratories Manager
J.O. Keller
Phone: (925) 294-3316
E-mail: jokelle@sandia.gov

Contract Number: Sandia National Laboratories P.O. 970632

Project Start Date: October 12, 2004
Project End Date: October 31, 2010

Fiscal Year (FY) 2011 Objectives

The goal of the Hydrogen Safety Task is to survey and analyze effective risk management techniques, testing methodologies, test data, contribute to development of fundamental knowledge on hydrogen related to hydrogen safety and develop targeted information products that will facilitate the accelerated adoption of hydrogen systems.

The specific objectives of this task are to:

- Survey risk assessment methodologies based on case studies provided by collaborative partners.
- Survey available test data, develop recommendations on modeling and testing methodologies, and share future test plans around which collaborative testing programs can be conducted thus avoiding duplication of work among collaborative partners.
- Collect information on the effects of component or system failures of hydrogen systems.
- Use the results obtained to develop targeted information packages for selected hydrogen energy stakeholder groups.

Technical Barriers

This project addresses the following technical barriers from the Hydrogen Safety section (3.8) of the Fuel Cell Technologies Program Multi-Year Research, Development and Demonstration Plan:

(A) Limited Historical Database
(B) Proprietary Data
(C) Validity of Historical Data
(D) Liability Issues
(E) Variation in Standard Practice of Safety Assessments for Components and Energy Systems
(F) Safety is not Always Treated as a Continuous Process
(G) Expense of Data Collection and Maintenance
(H) Lack of Hydrogen Knowledge by Authorities Having Jurisdiction

Contribution to Achievement of DOE Hydrogen Safety Milestones

This project will contribute to achievement of the following DOE milestones from the Hydrogen Safety section of the Fuel Cell Technologies Program Multi-Year Research, Development and Demonstration Plan:

- **Milestone 2**: Develop sensors meeting technical targets. (4Q, 2012)
- **Milestone 7**: Complete risk mitigation analysis for baseline transportation infrastructure systems. (1Q, 2012)
- **Milestone 8**: Complete investigation of safe refueling protocols for high pressure systems. (1Q, 2012)
- **Milestone 9**: Complete risk mitigation analysis fir advances transportation infrastructure system.s (1Q, 2012)
- **Milestone 12**: Complete research needed to fill data gaps on hydrogen properties and behaviors. (2Q, 2010)

FY 2011 Accomplishments

In 2010, the task continued to compare experimental data with risk analysis methods to validate the models and further close the knowledge gaps identified in earlier work. The subtask also completed the development of the Hydrogen Technical Experimental Database (HyTEx). Starting in late 2009, the populating of the data base with data from participating countries was begun. Technical progress on the development of risk informed approval criteria for hydrogen projects to provide a solid basis for risk informed codes and standards was completed.

- Established a list of relevant engineering models that had been used to evaluate the safety of hydrogen systems, categorized them, and performed a comparative analysis with actual testing data.

- Several dispersion models were further developed in 2009 by extending their capabilities to include surface and transient effects (November 2009).
- Developed a more detailed thermal radiation model.
- Completed development of HyTEx.
- Task participants presented many papers at technical conferences on subjects that dealt with the collaborative work.
- The International Energy Agency (IEA) Hydrogen Implementing Agreement co-organized the September 2009 Third International Conference on Hydrogen Safety and Task 19 members presented more than 10 technical papers.



Introduction

Acceptability of new systems is traditionally measured against regulations, industry and company practices and the judgment of design and maintenance engineers, however contemporary practice also incorporates systematic methods to balance risk measurement and risk criteria with costs. Management decisions are increasingly relying on quantitative risk assessment (QRA) for managing the attainment of acceptable levels of safety, reliability and environmental protection in the most effective manner. QRA is being applied more frequently to individual projects and may be requested by regulators to assist in making acceptance and permitting decisions. This task was approved by the executive committee of the IEA Hydrogen Implementing Agreement (HIA) in October 2004. The Task is currently comprised of 11 participating countries.

Approach

This task, aimed at reducing the barriers to widespread adoption of hydrogen energy systems, is being accomplished within three subtasks:

Subtask A. Risk Management - To survey QRA methodologies and compare assessments of hydrogen systems with conventional fuels to develop recommendations for modeling and testing methodologies around which collaborative testing programs can be conducted. Subtask A Risk Management is concentrating on the following four activities:

- Develop uniform risk acceptance criteria and establish link with risk-informed codes and standards.
- Develop a list of appropriate engineering models and modeling tools. Develop simple but realistic physical effects models for all typical accident phenomena (i.e., jet fires, vapor cloud explosions, flash fires, boiling liquid expanding vapor explosions, pool fires, etc.) for education and training, design evaluation and simplified quantitative risk analysis purposes.
- Develop a methodology for consistent site risk assessment based on the HyQRA approach.
- Release updates to all published products: Risk assessment methodology survey, knowledge gaps white paper and Review and comparison of risk assessment studies.

Subtask B. Testing and Experimental Program - To conduct a collaborative testing program to evaluate the effects of equipment or system failures under a range of real life scenarios, environments and mitigation measures. This subtask will summarize and ultimately coordinate and guide the experimental programs being conducted within the 11 countries participating in the task. The approach is to identify such testing programs, the facilities being used, and to coordinate the activities to fill in the data and knowledge gaps for the development of risk informed codes and standards. Subtask B focuses on both testing and experimental data, i.e., testing data as collected by checking the performance of applications and equipment and experimental data as collected by experiments with hydrogen release, ignition, fire, explosions and preventive and protective measures.

Subtask C. Information Dissemination - To disseminate results of the task through targeted information packages for stakeholders. An important aspect of information dissemination is to ensure that the review and vetting of all work products for Task 19 are consistent with the requirements and procedures for producing, approving and distributing various types of IEA reports and other information products. A protocol has been adopted by Task 19 partners and is being applied appropriately for Task 19 work. It is expected that several of these Subtask C products will be updated and enhanced over the course of the period covering Task 19 through October, 2010.

Results

The IEA HIA Task 19 on Hydrogen Safety was approved in FY 2004 and the first task definition meeting was held in Washington, D.C. in June 2004. The Task 19 participants conducted their 11th and 12th meetings in FY 2011. FY 2011 task participation is comprised of experts as noted in Table 1.

The active work on Task 19 ended very early in FY 2010. A draft Final Technical Management Report was submitted to the IEA HIA Secretariat in May 2011. The HIA Secretariat is in the process of changing the format and enhancing the content of these reports and as a result the final report is waiting that information and will revise the report to comply as soon as it is available.

In 2010, the task continued to compare experimental data with risk analysis methods to validate the models and further close the knowledge gaps identified in earlier work. The subtask also completed the development of the HyTEx. Starting in late 2009, the populating of the data base with

TABLE 1. Task 19 Participants Attending the Karlsruhe Meeting

Name	Company/Institute	Country Represented
Hoagland, Bill	ELEMENT ONE	Operating Agent
Benard, Pierre	UQTR	Canada
Weiner, Steven C.	PNNL	USA
Tchouvelev, Andrei V.	AVT	Canada
Bernard-Michel, Gilles	CEA	France
Khalil, John	UTRC	USA
Venetsanos, Alex	NCSRD	Greece
Miyashita, Sam	ENAA	Japan
Koos, Ham	TNO	The Netherlands
Prankul, Middha,	GexCon	Norway
Kotchourko, Alexei	KIT – Campus Nord	Germany
Molkov, Vladimir	UU	UK
Bouet, Rémy	INERIS	France
Kessler, Armin	Fraunhofer ICT	Germany
Vagsaether, Knut	TELEMARK U.C:	Norway
Hoskin, Aaron	NRCan	Canada
Houf, Bill	Sandia	USA
Jordan, Thomas	KIT-Campus Nord	Germany
Carcassi, Marco	UNIPI	Italy
Buttner, Bill	NREL	USA
Ruban, Sidonie	AIR LIQUIDE	France
Baraldi, Daniele	JRC	EC

data from participating countries was begun. Technical progress on the development of risk informed approval criteria for hydrogen projects to provide a solid basis for risk informed codes and standards was completed.

Risk Management

Prior to 2010, the task had established a list of relevant engineering models that had been used to evaluate the safety of hydrogen systems and categorized them. In past year, they were compared to each other to assess their limitations and validity. Part of this effort was achieved through comparing the engineering models to actual testing data. Several dispersion models were further developed in 2009-2010 by extending their capabilities to include surface and transient effects. A more detailed thermal radiation model was also developed that would account for crosswinds.

A risk assessment methodologies survey was completed for existing risk assessment methodologies to identify their key elements, approaches, methodologies, methods of analysis, key results and recommendations, and post-study developments. Keeping this information in one document was useful to the ongoing evaluation to ascertain their differences and applicability. The survey also identified interesting findings when each was reviewed and compared. This gave insights to allow the identification of knowledge gaps. It was intended that this document be continually updates and new information was identified. This survey was followed by a comparative analysis of the available risk assessment studies.

A knowledge gaps report which was started at the beginning of the Task 19 was updated and wil continue to be updated in the new Task 31. The goal of this activity was to focus research and development resources on critical topics for which there was insufficient information to complete a detailed QRA new commercial systems. Improved safety comes from understanding the outcomes and probabilities of undesirable events that may occur with new technologies, and by mitigating any unacceptable risks posed by these new technologies. In this regard, while a lot is known about hydrogen combustion and its safe handling, it is important to realize that hazards with new hydrogen technologies that are unrecognized or not completely understood are difficult to mitigate. As a result, before appropriate mitigations can be developed, the underlying risks must be identified, quantified, and be well understood. In a white paper, the IEA Task 19 hydrogen experts tried to identify knowledge gaps and barriers for selected applications and to indicate how they can be overcome.

Testing and Experimental Program

An inventory of existing testing and experimental data is in progress and the participants have started sharing information during and beyond the Task 19 into Task 31 which was approved in October 2010. Ongoing work and future activities will start with a search by the partners for available data existing in their respective countries and around the world. In order to secure a continuing refinement of the survey, the data and/or references will be stored in HyTEx. The Subtask B databases HyTEx, Hydrogen Projects and Hydrogen Testing and Experimental Facilities will be used as a source of information for any missing data in relation to the knowledge gaps as defined by and resulting from the Subtask A activities. If data is not available this could give rise to recommendations on new testing and experimental programs. Several technical knowledge gaps were identified in Subtask A and described in the white paper 'Knowledge Gaps in Hydrogen Safety'. Currently identified knowledge gaps are: spontaneous ignition, protective barriers and consequence modeling.

Development of Targeted Information Packages for Stakeholder Groups

The targeting of information packages for selected hydrogen energy stakeholder groups is central to the work and objectives of Task 19, currently focused on risk assessment methodologies and studies, testing and experimental programs, safety training and knowledge resources and hydrogen facility siting. Information packages

can take a variety of forms: IEA publications, publicly available web-based tools, databases and documents for use by Task 19 partners.

Conclusions and Future Directions

The current task ended in October 2010 and a new task on hydrogen safety was approved to continue to build on the very effective collaboration of this six-year effort. A kick-off meeting for the new task was held in Karlsruhe, Germany in April 2011. It is anticipated that one of the major outcomes of this ongoing work will a technical and credible basis for the development of risk informed codes and standards that will not be unnecessarily restrictive. This will eliminate a major barrier to the widespread commercial adoption of hydrogen energy systems. Future work will support this goal by improving hydrogen risk assessment methodologies and quantitative risk analysis and closing knowledge gaps with regard to consequences of hydrogen related accidents and incidents, the effects of mitigation methods, and failure probabilities of system components.

FY 2011 Publications/Presentations

1. International Energy Agency Hydrogen Implementing Agreement Task 19, Hydrogen Safety Final Technical Management Report (Draft), June 4, 2011.

VIII.16 MEMS Hydrogen Sensor for Leak Detection

Barton Smith (Primary Contact) and
Scott R. Hunter
Oak Ridge National Laboratory
P. O. Box 2008
Oak Ridge, TN 37831
Phone: (865) 574-2196
E-mail: smithdb@ornl.gov

DOE Manager
HQ: Antonio Ruiz
Phone: (202) 586-0729
E-mail: Antonio.Ruiz@ee.doe.gov

Start Date: August 2007
Projected End Date: Project continuation and direction determined annually by DOE

Fiscal Year (FY) 2011 Objectives

- Develop sensing technology that achieves DOE research and development (R&D) targets for hydrogen safety sensors.
- Characterization of response time, recovery time, sensitivity and accuracy within the operating temperature range.
- Demonstrate sensor performance and compliance with safety goals.
- Establish partnership to develop pre-commercial sensor prototype.

Technical Barriers

The project addresses the following technical barriers from the Hydrogen Safety section (§3.8.4) of the Fuel Cell Technologies Program Multi-Year Research, Development and Demonstration Plan (October 2007):

(D) Liability Issues

(E) Variation in Standard Practice of Safety Assessments for Components and Energy Systems

Technical Targets

The long-term project objective is to achieve commercialization and regulatory acceptance of fiber-reinforced polymer pipeline technology for hydrogen transmission and distribution. Accordingly, the project tasks address the challenges associated with meeting the DOE hydrogen delivery performance and cost targets for 2017:

- Measurement Range: 0.1%-10%
- Operating Temperature: -30 to 80°C
- Response Time: less than one second
- Accuracy: 5% of full scale
- Gas Environment: ambient air, 10%-98% relative humidity range
- Lifetime: 10 years
- Resistant to Interferents (e.g., hydrocarbons)

Accomplishments

(The project did not receive funding in FY 2011.)

- Winner of a 2011 R&D 100 Award, for "Hydrogen Safety Sensor Based on Nanostructured Palladium." Our hydrogen sensor was recognized by R&D Magazine as one of the top 100 technologically significant products that was introduced into the marketplace over the past year. Our entry was one of three inventions recognized in the Safety and Security technology category.



Introduction

Utilization of hydrogen as a transportation fuel requires comprehensive safety management during its storage, handling and use. Although safety-by-design and passive mitigation systems are the preferred methods for safety management, it is vitally important to develop technologies that can detect hydrogen releases and alert to system failures. The DOE Fuel Cell Technologies Program's Hydrogen Safety sub-program recognizes the need to develop and commercialize hydrogen sensors that provide the appropriate response time and the sensitivity and accuracy necessary for use in safety applications, thereby reducing risk and helping to establish public confidence in the hydrogen infrastructure.

This project addresses the above needs by developing, proving and commercializing a hydrogen detection device based on nanostructured thin film palladium microcantilever arrays. This hydrogen sensor has been shown to provide major performance improvements over existing and other recently developed sensors. The overall objective is to develop sensor technology that achieves DOE R&D targets for hydrogen safety sensors at lower cost and with the potential for wide-area hydrogen gas detection.

Approach

Microcantilever-based chemical sensors were first seriously explored as a trace gas sensing technology in 1990s with the first reported use of Pd-coated microcantilevers for sensing H_2 occurring in 2000. Adsorption of a gas onto a thin film surface can cause large changes in stress

and consequent bending of a thin cantilever structure. This bending response can be sensitively detected using piezoresistive, capacitive and optical techniques such that sub part-per-billion sensitivities are achievable. Microcantilever-based chemical sensors have been shown to have high sensitivity, wide dynamic range and fast response times. Optically read microcantilever sensors are particularly advantageous in the presence of combustible or explosive gases and vapors (e.g. H_2) due the possibility of vapor ignition when using heated or electrically operated sensors. Other advantages of this sensing technique include very low power consumption, and their potential use in distributed wide area sensor networks allowing multiple low cost chemical sensors to be located at storage or processing facilities (e.g. in the H_2 fuel economy) or on H_2-powered or transportation vehicles.

One of the most challenging aspects of detecting and quantifying the amount of a low concentration gas or vapor in the environment is the effect of potential interferents on the gas sensor response. Interferents can lead to false positive responses or suppressed responses to the gas being detected. One approach to overcoming this problem is the use of a multiplexed sensor array, with each sensor having a distinct sensitivity response to the gas or vapor of interest and any potential interferents. A much simpler approach is to use a single sensor, or small array of sensors, to sense a single gas species, as the computational processing of the array responses is much less intensive than for the multiplexed sensor array. The single sensor mode of operation is feasible if a coating can be found that responds primarily to the gas species of interest with minimal response to any potential interferents. Palladium has previously been used as a sensing medium in a number of sensor technologies due to its strong and reasonably unique response to H_2. The possibility of using Pd-coated microcantilever sensors to detect H_2 leaks has been examined in several previous studies. The issue with most previous thin-film Pd studies, and all of the previous microcantilever-based work, is that the sensor response and recovery times are far longer than acceptable for most applications; response times for these microcantilever-based H_2 sensor studies varied from a few minutes to as long as 1 hour. The long response and recovery times are attributed to the long diffusion time for elemental hydrogen to diffuse into and out of the palladium film to form palladium hydride.

Our approach is to use a new nanostructured Pd/Ag alloy that we developed specifically for the hydrogen sensing application. Microcantilever sensors coated with this alloy have fast, near ideal response characteristics when monitoring low concentration H_2 gas. In particular, the response and recovery times measured with these sensors are far shorter (<10 s) than those reported in all previous microcantilever-based H_2 sensor studies. The development work performed to optimize the performance of our sensor consisted of efforts to increase the sensitivity and dynamic range, to minimize the response and recovery times, to improve its resistance to interferents, and to increase its accuracy, repeatability and lifetime. We are presently working on the development of a prototype that can be performance-evaluated by third parties and adapting the sensor system for use in wide-area sensing.

Results

We conducted sensitivity and performance measurements of the Pd-Ag functionalized, optically read microcantilever using a benchtop setup consisting of the microcantilever in a gas flow cell, an optical readout system, a flow control valve and sample loop, and a LabVIEW®-based data acquisition system. The threshold and dynamic range test results revealed a lower-limit-detection of 0.01% (100 ppm) H_2 in argon, with three orders of magnitude dynamic range. Response and recovery times for 4% H_2 in argon were <3 s and <10 s, respectively. Over an eight-month period the sensor accuracy and repeatability remained constant within ±2%, indicating that the projected operational lifetime of this early version of the sensor could be as long as several years. Measurements of sensor specificity to common impurities and carrier gases (CO_2, CH_4, H_2O, N_2, He, CO) showed that in all cases, the responses from the interferents were an order of magnitude or more smaller than that observed for H_2 at similar concentrations. This degree of discrimination against interfering species will be adequate in all but the most demanding applications.

As illustrated in Table 1, in laboratory tests completed to date, we demonstrated that our microcantilever-based H_2 sensors meet all but the most stringent requirements for automotive sensing applications.

Conclusions and Future Directions

We have demonstrated that Pd-Ag functionalized, optically read microcantilever H_2 sensors have nearly ideal attributes required for distributed low-cost sensing of hydrogen leaks in many applications. These include high sensitivity, wide dynamic range, adequate response and recovery times and repeatable response. These sensors have been operating in a laboratory environment for more than a year without noticeable changes in sensitivity, specificity and response and recovery times. Work is also progressing on the development of low-cost portable detector prototypes that can be used to validate the expected performance of this potentially lower cost, better performing sensing technique. To this end, we have developed and done preliminary performance studies on two generations of portable instrumentation with encouraging results. We plan to report on these studies at a later date.

In the next project year we plan to:

- Fabricate a field portable instrument that can be evaluated at the National Renewable Energy Laboratory (NREL) Safety Sensor Testing Laboratory:

TABLE 1. ORNL microcantilever-based H_2 sensor meets all requirements for stationary and automotive applications and possibly exceeds performance of other recent sensors.

	Performance Requirement*	ORNL Measured Performance	Competitor #1 (IOS)	Competitor #2 (LANL)
Sensitivity Range	< 0.1% to > 4%	0.01 – 10%	0.2 – 10%	0.1% - 2%
Survivability Limit	100%	Linear response to 100% H_2	unknown	unknown
Response Time	Automotive: < 3 sec Stationary: < 30 sec	1-3 sec	> 5 sec	3 – 8 sec; figures show much longer response times
Recovery Time	Automotive: < 3 sec Stationary: < 30 sec	3-10 sec	> 5 sec	3 – 8 sec; figures show much longer recovery times
Temperature Range	Automotive: -40^{0}C to +125^{0}C Stationary: -20^{0}C to +50^{0}C	Yes	Yes	Yes
Pressure Range	Automotive: 62-107 kPa Stationary: 80-110 kPa	Yes	Yes	Yes
Ambient Relative Humidity Range	Automotive: 0 – 95% Stationary: 20 – 80%	0-100% - little response to changes in humidity	significant response to changes in humidity	unknown
Interferent Resistance	No false positive responses	Excellent	poor – H_2S, CO, CH_4	unknown
Power Consumption	< 1 Watt	0.2-0.5 Watt	0.5 watt	5-10 watt
Operating Temperature	Room temperature	room temperature	room temperature	535^{0}C
Lifetime	Automotive: 6,000 hr Stationary: > 5 years	Demonstrated > 12 months	unknown	2000 hours; Response times much longer at longer times
Accuracy and Repeatability	Automotive: 5-10% Stationary: 10%	> +/- 5%	> +/- 5%	+/- 10%

*See L. Boon-Brett et al., "Identifying performance gaps in hydrogen safety sensor technology for automotive and stationary applications," *Int. J. Hydrogen Energy*, **35**, 373-384 (2010).

  - The goal of the testing is to demonstrate that the sensor can meet all safety goals, including a projected longevity of 10 years. The suite of tests at NREL involves evaluation of the following parameters: short-term repeatability, linearity/ dynamic range, sensitivity to H_2 mixtures in air, atmospheric pressure sensitivity, sensitivity to temperature and relative humidity, long-term stability, response and recovery kinetics, and sensitivity to interferents.
  - We expect that the testing at NREL will be done with the technical and financial assistance of a commercialization partner.
- Complete technology transfer activities with an industrial partner:
  - Our commercialization plan will begin with an exploration of the market potential of our sensor technology, assessing factors such as the size of the potential market for our hydrogen sensor, the life-cycle cost target, the necessary performance characteristics, and future sales trends for hydrogen sensors.
  - Following the market assessment we will perform a technology readiness level assessment to determine the amount of effort that will be required to get the technology to the desired end product. A primary role of the industrial partner will be to evaluate the various risks involved in getting the sensor to market such as business model performance, marketing cost analysis, and execution risks.

FY 2011 Publications/Presentations

1. "Rapid response microsensor for hydrogen detection using nanostructured palladium films," S.R. Hunter, J.R. Patton, M.J. Sepaniak, P.G. Datskos and D.B. Smith, Sensors & Actuators: A Physical 163 (2010), 464-470.

References

1. L. Boon-Brett et al., "Identifying performance gaps in hydrogen safety sensor technology for automotive and stationary applications," Int. J. Hydrogen Energy, 35, 373-384 (2010).

Special Recognitions

1. Selected as one of the winners of the 2011 R&D 100 Awards, for "Hydrogen Safety Sensor Based on Nanostructured Palladium." See R&D Magazine announcement at http://www.rdmag.com/Awards/RD-100-Awards/2011/06/R-D-100-2011-Winners-Overview.

IX. EDUCATION

IX.0 Education Sub-Program Overview

The Education sub-program supports and facilitates hydrogen and fuel cell demonstration, deployment, and early market introduction by providing technically accurate and objective information to key target audiences that can help transform the market (see Table 1).

TABLE 1. Key Target Audiences for the Education Sub-Program

Target Audience	Rationale
Code Officials	Code officials must be familiar with hydrogen to facilitate the permitting process and local project approval.
First Responders	Firefighters, as well as law enforcement and emergency medical personnel, must know how to handle potential incidents; their understanding can also facilitate local project approval.
Local Communities/ General Public	Local communities will be more likely to welcome hydrogen and fuel cell projects if they are familiar with hydrogen.
Potential End-Users	Potential early adopters need information about commercially available hydrogen and fuel cell products and the opportunities for incorporating the technologies into their operations.
State and Local Government Representatives	A broad understanding of hydrogen encourages favorable decision-making regarding opportunities for near-term deployment and lays the foundation for long-term change.
Middle School and High School Teachers and Students	Teachers need technically accurate information and usable classroom activities to educate the next generation of potential researchers, engineers, policy-makers, and end-users about the technologies.
University Faculty and Students	Graduates are needed for research and development in government, industry, and academia.

The Education sub-program develops and disseminates information resources and conducts training. It strives to communicate a balanced message to help target audiences become familiar with hydrogen and fuel cell technologies and how they fit in the portfolio of renewable energy and energy-efficiency options. To aid with market introduction, the sub-program helps target audiences develop an accurate understanding of hydrogen safety, recognize opportunities for deployment in near-term markets, and understand the role of early markets in facilitating the use of hydrogen and fuel cells.

Goals

Educate key audiences about hydrogen and fuel cell technologies to facilitate near-term demonstrations and commercialization in early markets and longer-term widespread commercialization and market acceptance.

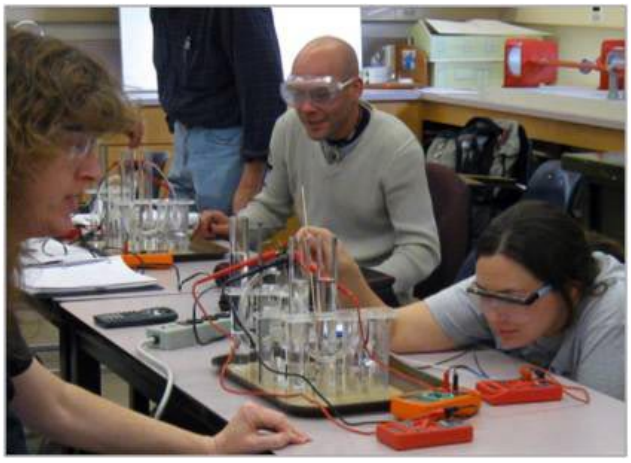
Objectives

The Education sub-program is closely coordinated with the Program's activities in technology demonstration and validation; safety, codes and standards; and early market deployment and associated market transformation activities. It is also coordinated with state- and regional-based hydrogen and fuel cell outreach programs. These integrated efforts form a comprehensive strategy to transform success in demonstrating and deploying technologies into success in the broader marketplace. Specific objectives for the Education sub-program include the following:

- Increase the acceptance and inclusion of hydrogen and fuel cell technologies as a part of a clean energy portfolio in federal, state, and local government investments, as well as private sector investments.

- Reduce the "soft costs" associated with the deployment and early adoption of hydrogen and fuel cell technologies in multiple applications (e.g., insurance, permitting, uniform codes and standards) through education, outreach, and training of "second generation" clean energy professionals.
- Increase general knowledge and awareness of the benefits of the use of hydrogen and fuel cell technologies in multiple applications among key target audiences.
- Increase awareness of the broad range of applications for fuel cells and hydrogen–beyond light-duty vehicles and buses.

Fiscal Year (FY) 2011 Status



The Education sub-program continued to support state and regional outreach efforts by providing consistent messages, readily available information resources, and other activities, as appropriate. The sub-program's seven outreach projects are focused on states with an active hydrogen and fuel cell presence, and they are working to develop case studies, best practices, and technical assistance resources to help decision-makers identify and assess opportunities for future deployment. In the area of academics, the sub-program also continued to support university, high-school, and middle-school education, including dissemination of lesson plans, curricula, and laboratory materials. Continuing its work with first responders, the sub-program conducted several sessions of a hands-on "prop course" for firefighters and continues to maintain the Web-based "Introduction to Hydrogen Safety for First Responders," which is registered on the Training-finder Real-time Affiliate Network website, a central repository for health training courses, with 30,000 members. The sub-program also continued to work closely with the Safety, Codes and Standards sub-program, expanding the code and permitting official e-learning package with indoor fueling information and developed permitting case studies, in support of increasing early market deployments.

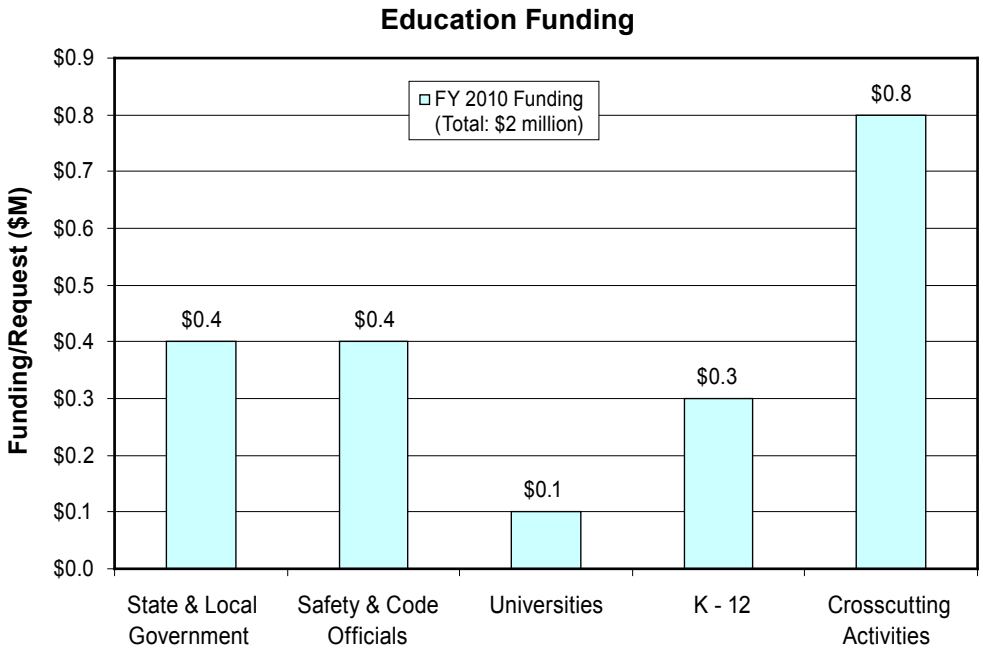
FY 2011 Accomplishments

- In coordination with the Systems Analysis sub-program, developed a model to analyze the economic impacts of early market deployment of fuel cells in primary power, backup-power, and material-handling applications. The user-friendly spreadsheet tool is used to calculate the impacts of the production, installation, and utilization of hydrogen and fuel cells on a regional or national level. Early versions of the model were demonstrated to stakeholders and industry representatives to obtain feedback on desired functionality, granularity, and outputs.
- Completed deployment and outreach activities with two Caterpillar electric trucks, each powered by a Hydrogenics Fuel Cell Power Pack. Continued to educate stakeholders on the benefits of fuel cell and hydrogen technologies in material handling applications including facility management, operators, maintenance personnel, safety groups, first responders, authorities having jurisdiction, and technical/community colleges. Continued demonstration of fuel cell and hydrogen technology for lift trucks in real-world applications at large prominent companies.
- Continued to promote and deploy the "H2 Educate" middle-school learning module–reaching a total of more than 8,800 teachers in 35 states since the project was launched. Preliminary survey results indicate that over 90 percent of survey participants felt that the resources have made it possible to teach hydrogen more often and in more detail and that the materials increased student knowledge and understanding of hydrogen.

- Developed network of key stakeholders in the Northeast region–in order to leverage regional efforts through increased collaboration–including Northeast Energy & Commerce Association, Clean Energy States Alliance, Massachusetts Hydrogen Coalition, Hydrogen Energy Center, and New Energy New York.
- Identified target locations for fuel cell deployment in the Northeast service area based on deployment criteria including energy intensive commercial building types identified by the Environmental Protection Agency's Commercial Building Energy Consumption Survey and mapped out locations using ArcGIS software.
- Developed a Web-based virtual Regional Resource Center that provides online information, models, and other tools to assist local, state, and regional planners in the Northeast to quantify the costs and benefits of hydrogen and fuel cell technology at potential sites. Models address environmental value, energy management, renewable hydrogen generation, distributed technology comparisons, and cost/economics of stationary fuel cells.
- Continued to facilitate the Hydrogen Student Design Contest. In 2011, the contest challenged teams to plan and design a residential hydrogen fueling system. Fifty-four university teams registered from 19 countries, including seven of the top 20 engineering schools in the world.
- Developed videos to be aired on TV and posted online to YouTube and other sites, including the development of two segments for Motorweek entitled "Hydrogen and Fuel Cells Emerging Markets" and "Vehicles and Infrastructure Update."
- Produced report and briefing paper on hydrogen production and storage for distribution to state policymakers and others. Developed case studies on early markets for hydrogen and fuel cell technologies including: fuel cell lift trucks, combined heat and power, and telecommunications backup power.
- Organized, publicized, hosted, and facilitated five webinars on hydrogen and fuel cell topics of interest to state policymakers, local leaders, and end users. For the last two webinars, more than 300 people registered, including many state policymakers. The sub-program also held three webinars to provide information to stakeholders throughout South Carolina and developed a first-responders webinar workshop.
- Continued to reach influential audiences including state policymakers, financial institutions, business leaders, end users, and others by giving presentations and distributing fuel cell literature and briefing papers at multiple conferences and meetings. Conferences attended in FY 2011 included the Clean Energy States Alliance Fall 2010 Members Meeting, the National Conference of State Legislatures Fall Forum, the Building Energy Conference, the Fuel Cells Finance and Investment Summit, the Ohio Fuel Cell Symposium, and the Northeast Commerce and Energy Association.
- Increased offering of university certificates and minors at universities including a "Graduate Certificate in Hybrid and Electric Vehicles" from Michigan Tech and a hydrogen and fuel cell technology concentration as an option in the engineering program at the University of North Carolina at Charlotte.
- Developed modules to introduce hydrogen and fuel cell technologies to students taking core chemical, mechanical, and electrical engineering courses.
- Facilitated creation of two fuel cell development intern positions at Protonex Technology Corporation for summer 2011; filled these positions with two Humboldt State University engineering students who had previously participated in H2E3 curriculum. Placed summer interns at the National Renewable Energy Laboratory, Oak Ridge National Laboratory, and the National Center for Hydrogen Technology.
- Published the two-week high school curriculum titled "Investigating Alternative Energy: Hydrogen & Fuel Cells." Held a two-day workshop for teacher professional development in February 2011. Materials were disseminated via 13 presentations to secondary science educators and hydrogen and fuel cell professionals.

Budget

The Education sub-program's FY 2011 budget and FY 2012 request are zero. New projects that were competitively awarded in FY 2004 and FY 2008 were fully funded in FY 2010. Most projects are scheduled to be completed in FY 2011. Given budget constraints and the need for including hydrogen and fuel cells within the broader Energy Efficiency and Renewable Energy portfolio, education and outreach activities will be coordinated with other DOE-wide efforts. Target audiences have been prioritized according to their near-term relevance and the effect on the use of hydrogen and fuel cell technologies today.



FY 2012 Plans

In FY 2012, the Education sub-program will complete expenditures of prior-year appropriations in relevant areas and focus on facilitating the introduction of hydrogen and fuel cell technologies into early markets. Future efforts will coordinate with other DOE-wide efforts to leverage recent project successes through the development of educational materials and webinars to highlight the benefits of hydrogen and fuel cell technologies.

Gregory J. Kleen
Education Team Lead (Acting)
Fuel Cell Technologies Program
Department of Energy Golden Field Office
1617 Cole Blvd.
Golden, CO 80401
Phone: (720) 356-1672
E-mail: Gregory.Kleen@go.doe.gov

IX.1 Employment Impacts of Early Markets for Hydrogen and Fuel Cell Technologies

Marianne Mintz
Argonne National Laboratory
9700 S. Cass Ave.
Argonne, IL 60439
Phone: (630) 252-5627
E-mail: mmintz@anl.gov

DOE Managers
HQ: Fred Joseck
Phone: (202) 586-7932
E-mail: Fred.Joseck@ee.doe.gov
GO: Greg Kleen
Phone: (720) 356-1672
E-mail: Greg.Kleen@go.doe.gov

Project Start Date: October 2010
Project End Date: September 2012

Partner:
RCF Economic and Financial Consulting, Inc., Chicago, IL

Fiscal Year (FY) 2011 Objectives

- Facilitate early market deployment of fuel cells in prime power, backup power and material handling applications by developing a user-friendly tool to calculate economic impacts.
- Calculate gross direct and indirect economic impacts of fuel cell expenditures by state, geographic region, and the nation as a whole.
- Calculate net national changes in jobs and economic output.
- Meet stakeholder needs for identifying industry sectors benefiting most from fuel cell production and deployment.
- Explore impact of different fuel cell production and deployment options on state, regional and national employment, earnings and economic output.

Technical Barriers

This project directly addresses the following technical barriers from the Education section of the Fuel Cell Technologies (FCT) Program Multi-Year Research, Development and Demonstration Plan:

(A) Lack of Readily Available, Objective, and Technically Accurate Information

(E) Regional Differences

(F) Difficulty of Measuring Success

Technical Targets

The project is developing and using a computer model to estimate the impact of deploying stationary fuel cells in early markets. Insights from the model will assist FCT and its stakeholders in estimating employment and other economic impacts from DOE technology development and in identifying fuel cell markets and industrial sectors that are most likely to generate jobs and economic activity.

FY 2011 Accomplishments

- Reviewed existing fuel cell market studies, impact assessment tools and assumptions in the 2008 Report to Congress.
- Identified viable near-term markets and technologies in the stationary power and specialty vehicle sectors.
- Characterized the supply chain (in terms of the dollar purchases from individual industrial sectors per fuel cell kW) for low temperature polymer electrolyte membrane (PEM) fuel cells; developed initial supply chain characterizations for phosphoric acid fuel cell (PAFC) and molten carbonate fuel cell (MCFC) technologies.
- Completed major portions of a spreadsheet model capable of projecting regional or national employment benefits of fuel cell deployment, including:
  - Design and implementation of input and output screens and user interface.
  - Design and implementation of state and regional interfaces.
  - Development of manufacturing cost algorithms incorporating economies of scale, learning-by-doing and technology advancement functions.
- Conducted a series of meetings/webinars with stakeholders including:
  - Connecticut Center for Advanced Technology
  - South Carolina Hydrogen and Fuel Cell Alliance
  - California Fuel Cell Partnership
  - California Stationary Fuel Cell Collaborative
  - Virginia Clean Cities
  - Clean Energy States Alliance
- Demonstrated early versions of the model to stakeholders and industry representatives to obtain feedback on desired functionality, granularity, and outputs.



Introduction

Section 1820 of the Energy Policy Act of 2005 (Public Law 109-58) directed DOE to assess the impact of a large-scale transition to hydrogen on U.S. employment. In response to that directive, RCF Economic and Financial Consulting, Inc., Argonne National Laboratory, and other partners undertook an in-depth analysis of the economic impacts of hydrogen deployment in the transportation sector. That study relied on input-output analysis to estimate net employment changes at the national level and produced a final report which was submitted to Congress in July 2008. But the study did not address the possibility that stationary fuel cells might be the initial wide-scale fuel cell application, with vehicle applications occurring later. Neither did it develop a model to permit the examination of alternative fuel cell deployment scenarios and their employment impacts. Now, however, it is increasingly important to estimate net and gross employment impacts associated with various scenarios of fuel cell early market development. Developing that modeling capability is the focus of this study.

Results

In FY 2011, Argonne National Laboratory and RCF Economic and Financial Consulting began work on the design and implementation of a spreadsheet tool to calculate the economic impact of fuel cell production, installation, and utilization in early markets (i.e., 2015–2020) at the state, regional and national level. Known as the Job and Output Benefits of Stationary Fuel Cells the tool is designed as a user-friendly, spreadsheet-based application. Figure 1 shows the various geographies incorporated into it. Note that the regions are groups of states that correspond to the nine U.S. census regions.

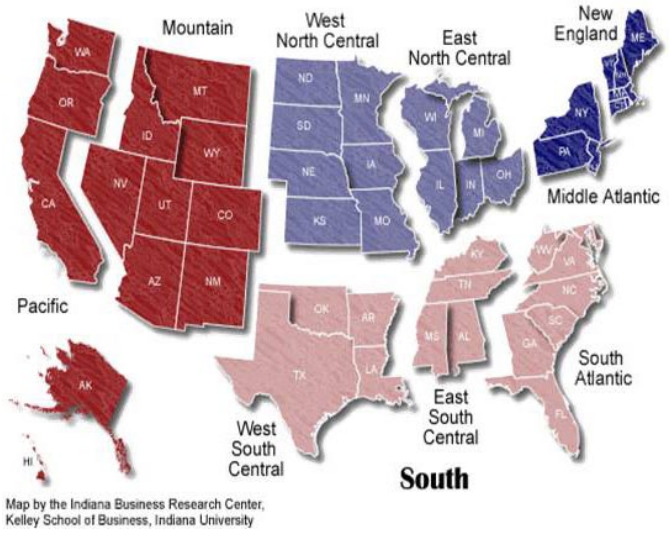


FIGURE 1. U.S. Census Regions

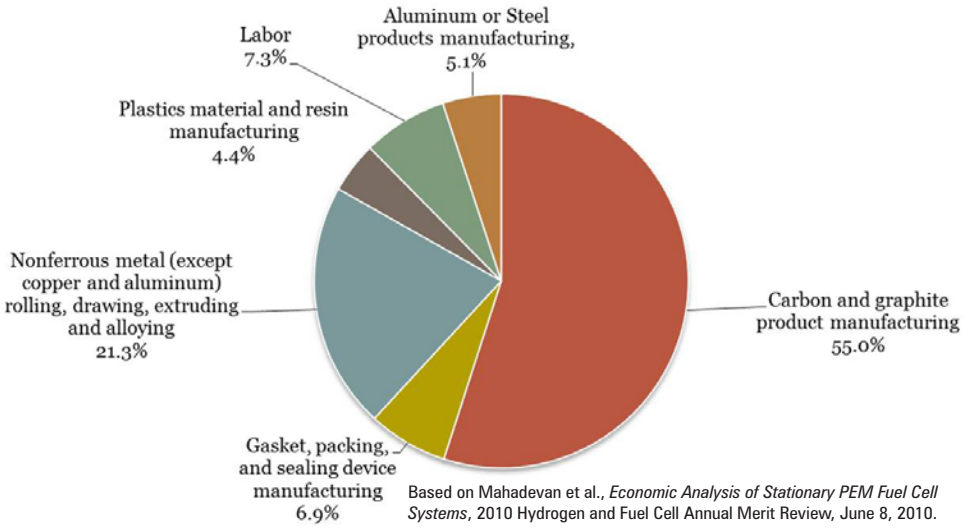
For each of these 60 geographies – 50 states, nine census regions and the nation as a whole – Job and Output Benefits of Stationary Fuel Cells estimates the effect of fuel cell deployment. It does so by adjusting the dollar flows among 440 existing economic sectors. Supply chains for PEM fuel cell, PAFC and MCFC technologies are used to modify those flows to represent purchases by and sales from a nascent fuel cell industrial sector. Figures 2 and 3 illustrate supply chains for the manufacture of PEM fuel cell stacks and balance of plant (BOP). Similar supply chains were developed for MCFC and PAFC stacks and BOP. Note that the underlying dollar flow among existing sectors are based on the Regional Input-Output Modeling System (RIMS) input-output model.

In addition to selecting a geographic area or region of interest and a fuel cell type, users must also select an application (material handling, backup power or prime power) and a market (e.g., Class 1-2 or Class 3 forklifts, cell phone towers or emergency responders) as well as such other variables as fuel cell size, current and future in-region production volumes, imports and exports, and analysis time. These variables define both the overall scenario and anticipated changes in fuel cell manufacturing cost. The manufacturing cost module incorporates the combined effects of manufacturing scale, learning and technology development, based on recent work by Greene et al. (Status and Outlook for the U.S. Non-Automotive Fuel Cell Industry: Impacts of Government Policies and Assessment of Future Opportunities, ORNL/TM-2011/101, May 2011.)

Figure 3 illustrates a representative scenario for deploying roughly 2,000 domestically produced forklifts per year plus a much smaller number of imported units in the out years. Note that indirect employment associated with fuel cell manufacturing, installation and fueling/operation and maintenance (O&M) exceeds direct employment for those categories in all years. Also, since employment in fuel cell installation and fueling/O&M depends on the stock of fuel cells in operation, it grows faster than employment in fuel cell manufacturing which tracks new sales.

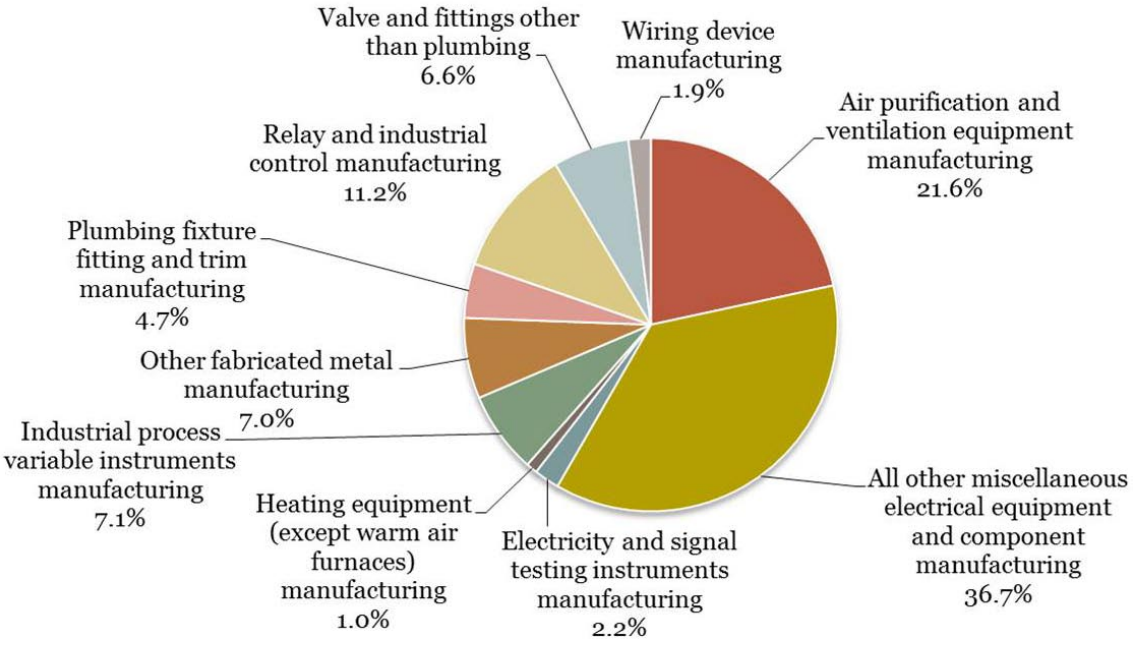
Conclusions and Future Directions

FY 2011 work focused on developing a prototype spreadsheet model to estimate gross state, regional and national economic and employment impacts from the manufacture, installation fueling and operation of fuel cells in distributed prime power, backup power and material handling (e.g. forklift) applications. That work included a review of technology and manufacturing progress; model design and development; discussions with industry and subject matter experts to characterize fuel cell costs and supply chains; the formation of a stakeholder panel to provide input on model design, functionality, data sources and validation; and meetings/presentations to stakeholder groups. FY 2012 work will build on that



Based on Mahadevan et al., *Economic Analysis of Stationary PEM Fuel Cell Systems*, 2010 Hydrogen and Fuel Cell Annual Merit Review, June 8, 2010.

FIGURE 2. Supply Chain for PEM Fuel Cell Stack



Based on Mahadevan et al., *Economic Analysis of Stationary PEM Fuel Cell Systems*, 2010 Hydrogen and Fuel Cell Annual Merit Review, June 8, 2010.

FIGURE 3. Supply Chain for PEM Fuel Cell Balance of Plant

effort, incorporating stakeholder recommendations for enhancements to the functionality and scope of the model, as well as review and beta testing of the tool, and application of it to estimate the employment impacts of projects funded under the American Recovery and Reinvestment Act.

Model enhancements include adding solid oxide fuel cell and high temperature PEM options for prime power, distributed hydrogen production as an option for forklift fueling, the capability of modeling site-specific installations, and the ability to estimate employment impacts of DOE's hydrogen and fuel cell research and development funding.

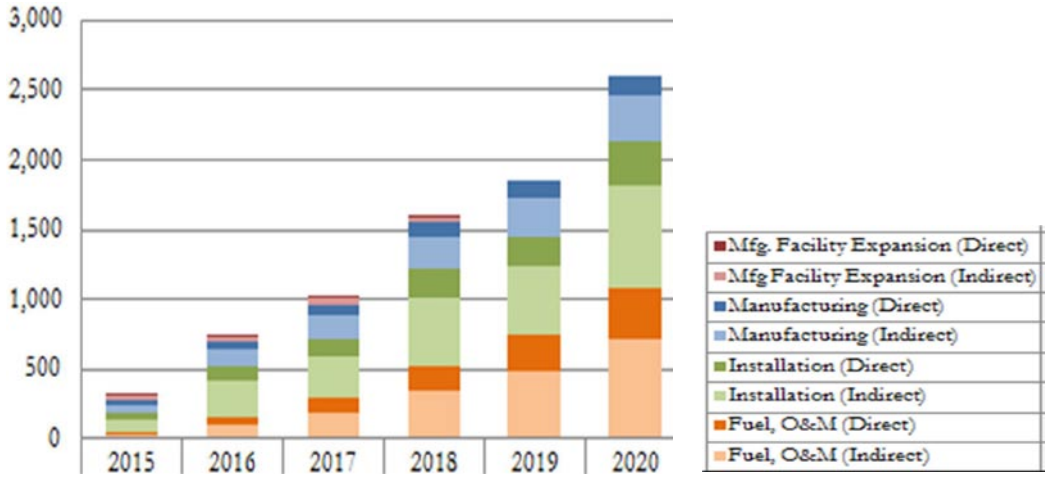


FIGURE 4. Illustrative Example of Gross Jobs Created for a National PEM Fuel Cell Forklift Deployment Scenario

IX.2 State and Local Government Partnership

Joel M. Rinebold
Connecticut Center for Advanced Technology, Inc. (CCAT)
222 Pitkin Street, Suite 101
East Hartford, CT 06108
Phone: (860) 291-8832
E-mail: Jrinebold@ccat.us

DOE Manager
GO: Greg Kleen
Phone: (720) 356-1672
E-mail: Greg.Kleen@go.doe.gov

Contract Number: DE-FC36-08GO18116 / 003

Project Start Date: September 1, 2008
Project End Date: August 30, 2011

Fiscal Year (FY) 2011 Objectives

- Foster strong relationships among federal, state, and local government officials, industry, and appropriate stakeholders.
- Serve as a conduit between the DOE and state and local government decision makers.
- Provide technically accurate and objective information to government decision-makers and identified stakeholders to improve/enhance decision making.
- Increase the knowledge base and improve awareness regarding hydrogen and fuel cells.
- Provide support for hydrogen and fuel cells in early market applications, consistent with DOE's market transformation efforts.

Technical Barriers

This project addresses the following technical barriers from the Education section of the 2009 Fuel Cell Technologies Program Multi-Year Research, Development and Demonstration Plan:

(A) Lack of Readily Available, Objective, and Technically Accurate Information

(C) Disconnect Between Hydrogen Information and Dissemination Networks

Contributed to Achievement of Education Milestones

This project will contribute to the achievement of the following DOE milestones from the Hydrogen Education section of the 2009 Fuel Cell Technologies Program Multi-Year Research, Development and Demonstration Plan:

- **Milestone 17:** Hold "Hydrogen 101" seminars (4Q, 2008 through 4Q, 2012).
- **Milestone 30:** Evaluate knowledge and opinion of hydrogen technology of key target audit audiences and progress toward meeting objectives. (4Q, 2012).

Related milestones in Task 3 (Educate State and Local Government Representatives) and Task 7 (Assess Knowledge and Opinions of Hydrogen Technologies) of the above reference have both been achieved with support from the State and Local Government Partnership.

FY 2011 Accomplishments

- Identified key stakeholders in Connecticut such as legislators, state agencies (utility, environment, energy, transportation, etc.), mayors, first selectmen, public works officials, council of governments and completed a pre and post-project survey to assess knowledge.
- Expanded database to include key stakeholders in the "Northeast Region" while strengthening existing relationships with state stakeholders, and regional partners, including Northeast Energy & Commerce Association, Clean Energy States Alliance, Massachusetts Hydrogen Coalition, Hydrogen Energy Center, and New Energy New York.
- Undertook economic modeling through the use of an IMPLAN economic model to assess the economic impact of the hydrogen and fuel cell industry in terms of its direct, indirect, and induced economic effects, in all eight states.
- Identified target locations for fuel cell deployment in the service area based on deployment criteria including energy intensive commercial building types identified by Environmental Protection Agency's (EPA's) Commercial Building Energy Consumption Survey (CBECS) and mapped out locations using ArcGIS software.
- Developed a web-based virtual Regional Resource Center (RRC) that provides online information, models and other tools to assist local, state and regional planners quantify the costs and benefits of hydrogen and fuel cell technology at potential sites. Models address environmental value, energy management, renewable hydrogen generation, distributed technology comparisons, and cost/economics of stationary fuel cells.
- Developed a comprehensible plan with the Connecticut Department of Transportation for hydrogen fueling infrastructure and vehicles for Connecticut.
- Organized a regional briefing for Northeast stakeholders held on July 22, 2010 in Westborough, Massachusetts.
- Presented at regional planning agencies/regional councils of government; the Green Energy & Building Expo and Connecticut Power and Energy Society

Meeting; exhibited at the Connecticut Conference of Municipalities Conference; and participated on bi-monthly State and Regional Initiative calls.

- Presented at events such as the Fuel Cell and Hydrogen Energy Association Annual Conference, the Northeast Sustainable Energy Association Annual Conference "Building Energy 11", and the 2010 Fuel Cell Seminar and Exposition.
- Developed and held the Fuel Cells for Municipalities Workshop on September 22, 2009 in Glastonbury, Connecticut and a legislative briefing/forum for state policy makers on January 22, 2010 in East Hartford, Connecticut.
- Provided technical and economic information to municipal decision makers including hydrogen and fuel cell benefits and project analysis.
- Participated on the NEPOOL ISO Planning Advisory Committee to identify regional energy issues, problems and solutions; and in a webinar organized by the Clean Energy States Alliance that addressed hydrogen and fuel cell technology and the development of guidance document "Roadmaps" to enhance support for the industry and facilitate deployment.
- Developed two hydrogen and fuel cell educational videos titled "Hydrogen and Fuel Cell Technology, Connecticut Hydrogen Fuel Cell Coalition" and "Hydrogen and Fuel Cell Technology, a World of Opportunity."



Introduction

This project assists with the building of partnerships between the DOE, states and municipalities. CCAT has developed a structure with an approach that provides an opportunity for federal, regional, state, and local involvement to encourage and promote the use of hydrogen and fuel cell technology. The structure includes leadership by the DOE; the establishment of collaborative meetings, workshops, and briefings to provide information to municipal and state decision makers; the provision of resources for potential developers to assess opportunity for deployment; support for state stakeholder groups to implement initiatives in support of state and federal policies; identification and assessment of economic benefits of the hydrogen and fuel cell industry and implementation of strategies to facilitate the deployment of hydrogen and fuel cell systems in the state.

The structure also includes a virtual RRC developed by CCAT that provides online information, models, and other tools to assist decision makers and end users to quantify the costs and benefits of hydrogen and fuel cell technology at potential sites. The RRC provides tools for implementation to assist local and state planners and decision-makers in identifying potential opportunities for the deployment of hydrogen and fuel cell technologies. The models available through the RRC are used to assess environmental value, energy management, renewable energy, cost and economics, and comparisons of competing technologies. CCAT is also developing guidance documents or Hydrogen/Fuel Cell "Roadmaps" for the New England States, New York, and New Jersey.

Approach

CCAT's approach has been to develop resources for hydrogen and fuel cell deployment to aid in the education of state and local decision makers. These resources include online information, models, and tools for potential users to analyze the costs and benefits of hydrogen and fuel cell technology. Coordination and cooperation is sought by both local and state decision-makers in order to introduce hydrogen and fuel cell technology in early market applications. The project uses local "bottom-up" decisions guided by state/regional "top-down" assistance to help reduce conflict, improve state/regional and municipal relations, and provide better solutions to community-based energy problems. Because of the high risk and high capital cost of implementing new technologies, CCAT also coordinates with local, state, and regional decision makers to identify innovative funding and procurement mechanisms, such as group purchases and corporate tax credits, to encourage market growth, reduce costs, and increase public acceptance.

Results

CCAT has developed and refined resources to analyze potential sites for hydrogen and fuel cell deployment throughout the region. These models make available information for non-technical and technical audiences, including state and local decision makers and potential end users and will be an integral component of education and outreach efforts. The RRC models are described in Table 1.

Economic Impact

A study was conducted to examine the economic impact for each state of the Northeast Region. The economic impact was defined as the direct output, employment, and labor income associated with the 25 hydrogen and fuel cell original equipment manufacturers located in CT, MA, and NY, as well as the region-wide multiplier effects supported by the purchases of businesses and workers related to the industry (Figure 1).

Awareness

CCAT has also completed an assessment of the level of knowledge and opinions of hydrogen and fuel cell technologies of local and state stakeholders to determine the effectiveness of the project implementation. As shown in Figure 2, the results of the awareness survey suggest that there

TABLE 1. RRC Models and Descriptions

Model Type	Description
Environmental	Assesses the environmental benefits of hydrogen and fuel cell applications compared with other conventional technologies. The model can be used to assess potential emissions reductions, including greenhouse gases, using hydrogen and fuel cell technology.
Economic/Cost	Assesses potential yearly heating and electricity cost savings when using a commercially available fuel cell for baseload power. The model allows users to assess the economic viability of a fuel cell system.
Energy Management	Assesses the efficiency benefits of stationary fuel cell applications. The model can be used to assess the potential energy savings using a fuel cell to replace conventional electricity generating technologies.
Distributed Technology Comparison	Allows a user to compare fuel cells with other distributed energy technologies including microturbines, combustion turbines, reciprocating engines, photovoltaic systems, and wind turbines, based on certain criteria such as installation cost, efficiency, emissions, heat rate, etc.
Hydrogen Generation From Renewable Technology	Assesses wind, photovoltaic and hydroelectric power generation technologies to identify hydrogen production capacities and average cost per kilogram of generated hydrogen from these renewable technologies.

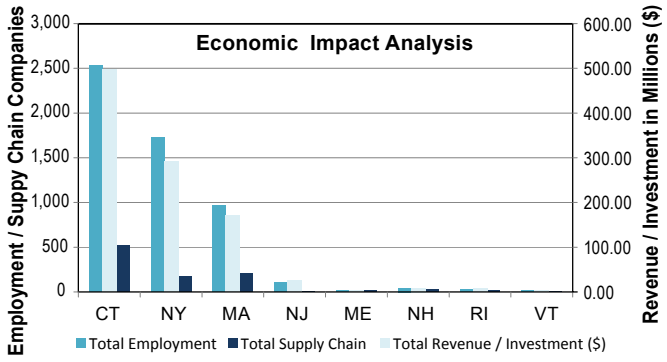


FIGURE 1. Economic Analysis Results

was an increase in level of knowledge regarding hydrogen and fuel cell technology, its application, costs, and benefits.

Conclusions and Future Directions

This partnership effort has successfully identified a process with stakeholder participants, created models and tools that will allow potential adapters to assess opportunities for deployment of hydrogen and fuel cell technologies in early market applications, and has been expanded to replicate the stakeholder process and tools to develop guideline "Roadmap" documents in each of the New England States, New York, and New Jersey. The process models and tools and guideline documents have been

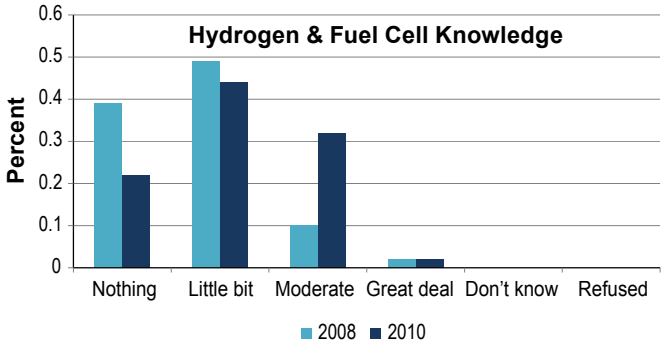


FIGURE 2. Level of Awarene

created to facilitate the education of decision makers and end users and to provide the ability to analyze potential sites for hydrogen and fuel cell technologies.

Next steps: CCAT will continue to build upon existing relationships and partnerships while creating new opportunities. Identified target locations for fuel cell deployment in the service areas based on energy intensive commercial building types identified by EPA's CBECS will be mapped by locations using ArcGIS software and included within the individual state guidance documents. In addition, CCAT will facilitate the dissemination of information to municipal decision makers and stakeholders, and keep state officials abreast of activities to deploy hydrogen and fuel cell technologies through the use of collaborative meetings and briefings to achieve state goals including energy reliability, security, efficiency, emissions and economic development. CCAT will also provide the information on financial and investment opportunities to encourage market growth, reduce costs, and increase public acceptance.

CCAT will continue its education and outreach efforts on the regional scale and continue to support the development of state roadmaps. These roadmaps should serve to effectively encourage and support the successful development and deployment of hydrogen and fuel cell projects in the New England, New York, and New Jersey regions.

Special Recognitions

2011 Annual Merit Review Awards

On May 11, 2011, DOE recognized CCAT for work on the advancement of fuel cell and hydrogen technologies for Connecticut and the Northeast. The award highlighted CCAT's collaborative educational outreach efforts that span the Northeast with groups such as the Northeast Energy Commerce Association and the Northeast Sustainable Energy Association, the analysis of job growth and economic development impacts attributable to the fuel cell industry and its supply chain, and the development of models to help potential fuel cell customers evaluate the life-cycle costs and benefits of deploying fuel cells.

FY 2011 Publications/Presentations

1. Rinebold, J.M, "State Hydrogen/Fuel Cell Roadmap Development", presentation at 2010 Fuel Cell Seminar and Exposition, October 21, 2010.

2. Rinebold, J.M., "State Supply Chain and Cluster Development", presentation at Clean Energy State Alliance, October 28, 2010.

3. Rinebold, J.M., "Connecticut Hydrogen Fuel Cell Industry Status and Direction 2010 and 2011"; December 2010.

4. Rinebold, J.M., "Economic Development through the Northeast Electrochemical Energy Storage Cluster", presentation at the Fuel Cell and Hydrogen Energy Association Annual Expo, Washington, D.C., February 14, 2011.

5. Rinebold, J.M., "Fuel Cells and Storage: The Path Forward", presentation at the 2011 Northeast Sustainable Energy Association Annual Conference "Building Energy 11", Boston, MA, March 10, 2011.

6. Gabe, Todd, Ph.D., "Economic Impact of the Northeastern Hydrogen and Fuel Cell Industry (DOE State and Local Government Partnership Project)", Version 1.0; April 2011.

7. Rinebold, J.M., "State and Local Government Partnership", presentation at the 2011 DOE Annual Merit Review and Peer Evaluation Meeting, Washington, D.C., May 10, 2011.

IX.3 Hydrogen Education State Partnership Program

Warren Leon
Clean Energy States Alliance (CESA)
50 State Street, Suite 1
Montpelier, VT 05602
Phone: (978) 317-4559
E-mail: wleon@cleanegroup.org

DOE Manager
GO: Greg Kleen
Phone: (720) 356-1672
E-mail: Greg.Kleen@go.doe.gov

Contract Number: DE-FC3608GO18111 A000

Subcontractors:
- National Conference of State Legislatures, Denver, CO
- Dr. Timothy Lipman, University of California, Berkeley, Berkeley, CA

Project Start Date: September 1, 2008
Project End Date: August 31, 2011

Fiscal Year (FY) 2011 Objectives

- Identify state hydrogen project best practices and policies.
- Develop strategies and information to overcome many state policymakers' resistance to providing support for fuel cells.
- Provide information and technical assistance to state policymakers and state renewable energy programs to foster effective fuel cell programs.
- Promote strategic opportunities for states and DOE to advance fuel cell deployment through partnerships, collaboration, and targeted activities.

Technical Barriers

This project addresses the following technical barriers from the Education section (3.9.5) of the 2009 Fuel Cell Technologies Program Multi-Year Research, Development and Demonstration Plan:

(A) Lack of Readily Available, Objective, and Technically Accurate Information

(B) Mixed Messages

(C) Disconnect between Hydrogen Information and Dissemination Networks

Contribution to Achievement of DOE Education Milestones

This project contributes to achievement of the following DOE milestones from the Education section of the 2009 Fuel Cell Technologies Program Multi-Year Research, Development and Demonstration Plan:

- **Milestone 17** in Task 3: Educate State and Local Government Representatives. (recurring annually, including 2011)
- **Milestone 19 in Task 4**: Educate Potential End-Users. (4Q, 2011)
- **Milestone 14 in Task 2**: Educate Local Communities. (recurring annually, including 2011)
- **Milestone 30 in Task 7**: Assess Knowledge and Opinions of Hydrogen Technologies. (4Q, 2012)

Accomplishments

- Produced report and briefing paper about hydrogen production and storage for distribution to state policymakers and others.
- Organized, publicized, hosted, and facilitated five webinars on hydrogen and fuel cell topics of interest to state policymakers, local leaders, and end users. For the last two webinars, more than 300 people registered, including many state policymakers. All webinar presentations and recordings are posted on the CESA website.
- Informed state legislators through joint activities with the National Conference of State Legislatures (NCSL), including a webinar, a presentation at the NCSL Fall Forum, and a *NCSL LegisBrief,* an *NCSL WebBrief.*
- Encouraged cooperation and collaboration among DOE state education grantees by organizing, hosting, and facilitating six monthly calls focused on information exchange and strategy discussions.
- Reached influential audiences–state policymakers, financial institutions, business leaders, end users, and others–by giving presentations and distributing several of CESA's fuel cell briefing papers at conferences and meetings, including the CESA Fall 2010 Members Meeting, the NCSL Fall Forum, the Building Energy Conference, Fuel Cells Finance and Investment Summit, Ohio Fuel Cell Symposium, and the Northeast Commerce and Energy Association.



Introduction

Over the past two decades, the states have played a crucial role in advancing various clean energy technologies by implementing supportive policies and providing financial incentives. The states have the potential to do much to speed fuel cell commercialization. However, relatively few states are currently targeting fuel cell installation or

deployment with incentives or support programs. This hesitance to support fuel cells stems, in part, from reductions in available state funding for clean energy, but can also be attributed to the opinion that other energy technologies will provide a larger return on investment.

This project seeks to encourage states to consider taking steps to advance fuel cells, particularly stationary applications. It does this by providing state policymakers with accurate, convenient, easily digestible information and by directly addressing specific fuel cell-related issues that are of most concern to state policymakers. CESA is an ideal organization to lead this project, because the members have an in-depth understanding of the perspective of state clean energy agencies and other state energy policymakers, and have had considerable success facilitating state collaboration

Approach

The foundation for CESA's work on this project is a solid understanding of the perspectives and needs of state policymakers. For that reason, we maintain ongoing contact with key state policymakers–both from states that are providing financial support for fuel cells and from those that are not–through interviews, informal group discussions, and monitoring of relevant developments at the state level. From this intelligence gathering, we have identified the specific reasons why state policymakers have not been taking more aggressive action to promote fuel cells. We have then crafted messages and materials designed to encourage action. Those messages are delivered through well-attended webinars, widely circulated briefing papers, conference presentations, a webpage (www.cleanenergystates.org/projects/hydrogen-and-fuel-cells) a project listserv, and other means. We emphasize case studies of model projects and the identification of targeted actions that can appeal to state policymakers.

We also make sure that our work is well coordinated with the work of other DOE state-related fuel cell grantees, by facilitating monthly conference calls and maintaining regular one-on-one contact with those grantees.

Results

Early in this project, we identified hydrogen production and storage as an important topic on which state policymakers needed education. Because many of them were unfamiliar with current fuel cell technology and current uses of hydrogen, they had concerns about hydrogen safety and whether there would be an adequate supply of hydrogen if stationary fuel cells start to be used more widely. To directly address those two concerns, we produced and disseminated a briefing paper and a more detailed report on the topic of hydrogen production and storage. The longer report was written by Timothy Lipman, researcher and lecturer at the University of California, Berkeley and Director of the U.S. Department of Energy Pacific Region Clean Energy Application Center. The briefing paper, which is designed to provide policymakers with the most essential information in a user-friendly format, draws on the longer report. We also hosted a webinar during which Dr. Lipman discussed his findings.

Because states have limited funding for supporting fuel cells and agency staff members have limited band-width to devote to fuel cells, we believe it makes sense for them to focus on those few market niches and audiences where near-term progress can be easiest and most likely. We identified supermarkets as one such niche, because several supermarket chains were already experimenting with fuel cells with the help of state support and because some supermarkets have an energy load profile that enables them to efficiently use both the electricity and heat produced by fuel cells. Moreover, this is a market dominated by large chains which have the ability to become repeat fuel cell customers if they are satisfied with their first installations. We used a webinar, attended by approximately 250 people, to encourage the consideration of fuel cells for supermarkets.

Although only a few states currently allow natural gas-fueled fuel cells to qualify for their renewable portfolio standards (RPSs), our research suggests that other states could be open to making such fuel cells eligible for inclusion. Concerns about local economic development and baseload power, as well as the limitations that the Interstate Commerce Clause of the Constitution places on RPSs, could make natural gas fuel cells appealing to states. We therefore organized a webinar on the topic, attended by 263 people, and various policymakers responded favorably to the presentations. The coincidental announcement by officials in Delaware that they would try to expand their RPS to include fuel cells gave additional attention to this topic.

We believe that we have played a valuable role over the past year by encouraging and facilitating greater cooperation and collaboration among DOE's state-related fuel cell grantees. Starting in December 2010, we organized monthly conference calls that have gone beyond the sharing of updates and announcements to discussions about strategy-related topics, such as key messages, target audiences, and model practices. We have maintained regular contact with many of the grantees and have tried to help their efforts by providing them with information about state policies and promoting their publications and events to our mailing list. As an example, we recently helped Virginia Clean Cities organize a webinar about fuel cells and first responders and are hosting that webinar, because Virginia Clean Cities does not have the platform or resources to do so.

Our other outreach activities–including presentations at conferences, the distribution of materials, and website updates–have all served the purpose of educating state policymakers, local leaders, and end users about fuel cells.

Conclusions and Future Directions

The grant from DOE for this project ends on August 31, 2011. But, before then, we will carry out several activities that will extend the reach and impact of the project. We will:

- Produce a briefing paper on fuel cells for supermarkets, including case studies of several supermarket projects. This briefing paper will build upon the webinar on the same topic and place the most essential information into a user-friendly form.
- Send out a printed packet of all five of CESA's briefing papers to a mailing list of several hundred state energy officials plus key state legislators. We believe that they will find this packet to be convenient and useful, and delivering hard copies will increase the likelihood that they will read the material.
- Hold a webinar on the topic of new financing approaches for fuel cells, including leasing and power purchase agreements. We believe that the increasing use of these financing models can make support for fuel cells more appealing to state policymakers.
- Hold a discussion with relevant state policymakers and others (e.g., representatives of Pacific Northwest National Laboratory) on the topic of performance monitoring of fuel cells. This discussion will enable them to share information on their individual performance monitoring approaches and to consider how they can cooperate on joint efforts.
- Continue ongoing activities, including disseminating information through the CESA fuel cell website and listserv and hosting monthly calls of DOE grantees.

Our efforts over the past year have significantly increased our understanding of state policymakers' views and needs related to fuel cells. We then identified and carried out focused activities that are helping to move state fuel cell efforts forward. CESA is well placed to encourage states to undertake further concrete market transformation actions related to stationary fuel cells, especially in regard to fuel cell financing, RPSs, supermarkets, and performance monitoring. However, additional funding would be required to allow us to devote significant attention to those topics after August.

FY 2011 Publications/Presentations

1. Presentation: Presenter at "Hydrogen & Fuel Cell Activities Regional Briefing," Northeast Energy and Commerce Association, Westborough, MA. (July 22, 2010).

2. Publication: "Hydrogen Fuel Cells: On-Site Energy Generation," *NCSL LegisBrief* (August-September 2010). Available at www.ncsl.org/default.aspx?tabid=21094.

3. Webinar Presentations: "Hydrogen Fuel Cells: Technology and State Policy" (September 28, 2010). Available at www.cleanenergystates.org/projects/hydrogen-and-fuel-cells/hydrogen-and-fuel-cell-resource-library/?start=10.

4. Publication: "California Energy Commission: PIER/Advanced Energy Recovery System," *State Leadership in Clean Energy Award* (October 2010). Available at www.cleanenergystates.org/assets/Uploads/Resources-post-8-16/cesa-awardCECPIER.pdf.

5. Presentations: Workshop on "Fuel Cells and State Policy," at Fall 2010 CESA Members Meeting, Washington, D.C. (October 28, 2010).

6. Presentation: "Fuel Cells and the States," at NCSL Fall Forum, Phoenix, AZ (December 10, 2010).

7. Webinar Presentation: "DOE Hydrogen and Fuel Cell Programs," (December 14, 2010). Available at www.cleanenergystates.org/projects/hydrogen-and-fuel-cells/hydrogen-and-fuel-cell-resource-library/resource/doe-hydrogen-and-fuel-cell-overview-presentation-by-sunita-satyapal.

8. Webinar Presentation: "Hydrogen Production and Storage" (February 2, 2011). Available at www.cleanenergystates.org/projects/hydrogen-and-fuel-cells/hydrogen-and-fuel-cell-resource-library/resource/webinar-hydrogen-production-and-storage-for-fuel-cells.

9. Publication: "Fuel Cells–Clean and Reliable Energy," *NCSL WebBrief* (March 2011). Available at www.ncsl.org/default.aspx?tabid=22352.

10. Webinar Presentation: "Fuel Cells for Supermarkets" (April 4, 2011). Available at www.cleanenergystates.org/projects/hydrogen-and-fuel-cells/hydrogen-and-fuel-cell-resource-library/resource/webinar-recording-fuel-cells-for-supermarkets-wmv.

11. Publication: Timothy Lipman, *An Overview of Hydrogen Production and Storage Systems with Renewable Hydrogen Case Studies* (May 2011). Available at www.cleanenergystates.org/projects/hydrogen-and-fuel-cells/hydrogen-and-fuel-cell-resource-library/resource/an-overview-of-hydrogen-production-and-storage-systems-with-renewable-hydrogen-case-studies.

12. Presentations: Several at Stationary Fuel Cell Finance and Investment Summit, San Diego, CA (May 3–5, 2011).

13. Presentation: "Hydrogen Education State Partnership Program," DOE Annual Merit Review, Crystal City, VA (May 20, 2011).

14. Publication: Charles Kubert and Warren Leon, *Hydrogen Production and Storage* (June 2011). Available at www.cleanenergystates.org/projects/hydrogen-and-fuel-cells/hydrogen-and-fuel-cell-resource-library/resource/hydrogen-production-and-energy-storage.

15. Webinar Presentations: "Fuel Cells and Renewable Portfolio Standards" (June 9, 2011). Available at www.cleanenergystates.org/projects/hydrogen-and-fuel-cells/hydrogen-and-fuel-cell-resource-library/resource/webinar-presentations-fuel-cells-and-renewable-portfolio-standards.

IX.4 Development of Hydrogen Education Programs for Government Officials

Shannon Baxter-Clemmons (Primary Contact), Chris Daetwyler
South Carolina Hydrogen and Fuel Cell Alliance (SCHFCA)
Post Office Box 12302
Columbia, SC 29211
Phone: (803) 727-2897
E-mail: baxterclemmons@schydrogen.org

DOE Manager
GO: Greg Kleen
Phone: (720) 356-1672
E-mail: Greg.Kleen@go.doe.gov

Contract Number: DE-FG36-08GO18113

Subcontractor:
Scott Greenway, Greenway Energy, Aiken, SC

Project Start Date: October 1, 2008
Project End Date: July 31, 2011

Fiscal Year (FY) 2011 Objectives

- Synthesize objective and technically accurate information that will be made available to a wide audience through the Internet, a national meeting, and training sessions.
- Design and develop educational programs that will clarify the benefits and challenges of developing a hydrogen infrastructure and avoid over-selling hydrogen technologies.
- Leverage relationships with project team organizations in South Carolina to distribute hydrogen education materials to government and code officials.
- Train a group of hydrogen educators at the project team institutions (the South Carolina [SC] Energy Office, the state fire marshal's office, the SCHFCA and Greenway Energy) who will be resources to the target audiences.

Technical Barriers

This project addresses the following technical barriers from the Education section (3.9.5) of the 2009 Fuel Cell Technologies Program Multi-Year Research, Development and Demonstration Plan:

(A) Lack of Readily Available, Objective, and Technically Accurate Information
(B) Mixed Messages
(C) Disconnect Between Hydrogen Information and Dissemination Networks
(D) Lack of Educated Trainers and Training Opportunities
(E) Regional Differences
(F) Difficulty of Measuring Success

Contribution to Achievement of DOE Education Milestones

This project will contribute to achievement of the following DOE milestones from the Education (3.9) section of the 2009 Fuel Cell Technologies Program Multi-Year Research, Development and Demonstration Plan:

- **Milestone 11**: Develop set of introductory materials suitable for a non-technical audience. (4Q, 2006)
- **Milestone 13**: Develop materials for community seminars. (4Q, 2008)
- **Milestone 14**: Hold community seminars to introduce local residents to hydrogen. (4Q, 2008 through 4Q, 2012)
- **Milestone 17**: Hold "Hydrogen 101" seminars. (4Q, 2008 through 4Q, 2012)
- **Milestone 29**: Evaluate knowledge and opinion of hydrogen technology of key target audiences and progress toward meeting objectives. (4Q, 2009)

FY 2011 Accomplishments

- In person presentations to over 30 groups of targeted South Carolina decision makers.
- Held three webinars to provide information to stakeholders throughout South Carolina.
- Reached 1,744 targeted additional state and local government officials and decision makers.
- Webinar presentations can be viewed through a SlideShare channel.
- Videos of educational information on hydrogen are available on the SCHFCA YouTube channel.
- Developed case studies on early markets for hydrogen and fuel cell technologies including: fuel cell lift trucks, combined heat and power, and telecommunications backup power.
- Presentations to groups including the National Congressional Candidates, Gubernatorial Candidates, State House and Senate Candidates, Head of the South Carolina Department of Commerce, Agency heads at the South Carolina Department of Health and Environmental Control.
- Hydrogen 101 materials were utilized in wider public education efforts that reached additional non-decision makers.
- Educational efforts with South Carolina House and Senate members to demonstrate the effect of state level incentives for fuel cells and renewable technologies on creating viable markets.

Introduction

Hydrogen and fuel cell technologies are moving out of the laboratory and into economically competitive niche markets such as cell phone tower backup power and forklift operations. As hydrogen technologies become competitive in these early markets, communities will need to be educated about the opportunities afforded by hydrogen technologies and about safety concerns associated with them. The Hydrogen 101 program led by the SCHFCA seeks to raise awareness about hydrogen and fuel cells to community leaders within SC and the southeast.

SC is among a small, but growing, number of states that have a hydrogen implementation strategy and is on the leading edge of fuel cell research and adoption. The state has been recognized as one of the top five leaders in hydrogen and fuel cells, but a significant lack of information on hydrogen still exists among state and local leaders. In order to maximize the resources existing in the state and surrounding region, it is imperative that an effective outreach and education program be conducted so that the decision to accept hydrogen technologies in the local community is informed and wise.

Approach

The project team is composed of SC-based hydrogen experts with connections to technically accurate information; and, civic organizations and associations with the communications networks and events with our target audience already established. The entire team works together to identify specific messaging that the local audience and sub audiences are interested in. Based on the feedback we gather from the civic organizations and other community opinion leaders, education materials and demonstrations are developed.

The marketing of the program is conducted through the existing websites, e-mail distribution lists and communication networks. The distribution of the material is primarily conducted at events associated with each of the civic associations partnering on the project, however, several stand-alone events and webinars are planned.

Results

Building on the educational successes that assisted in the passage of the South Carolina Hydrogen Permitting Act, SCHFCA has focused its attention on renewing relationships with decision makers in FY 2011 and reaching out to new candidates to in state and national political offices. These efforts have been focused on discussing the success of hydrogen and fuel cell technologies in early markets and methods to increase adoption of hydrogen technologies within the state and region.

In 2011 the Hydrogen 101 program expanded its audience to include business leaders and economic development officials based on input gathered from stakeholders. The focus of interactions with decision makers has focused on emphasizing the business case for fuel cells in early markets. This education focuses on helping them understand where fuel cells can provide a value proposition for their organizations. The program performed outreach to these groups through presentations and small or individual meetings. Presentation materials were updated and expanded depending on the audience and brochures were printed to summarize key messages.

The SCHFCA Hydrogen 101 program far exceeded its goals of 3 webinars and 30 in-person presentations. The number of direct stakeholders reached was 1,744 and the wider educational efforts that leveraged Hydrogen 101 materials reached over 2 million people. In addition to the education of leadership groups, the SCHFCA contacted candidates for political offices who will be filling vacated offices in 2011 and has continued discussions with newly elected leaders. The educational efforts focused on helping them understand how the hydrogen and fuel cell industry is growing the state economy, creating high paying jobs, and saving businesses money.

Groups have been overwhelmingly supportive of hydrogen and fuel cell technologies as a result of the presentations and view the technologies as having the potential to foster economic development within the state. Work has been started to collaborate with other states including Tennessee, North Carolina, and Florida. These collaborations will help educate regional leaders about opportunities for a hydrogen technologies in their state and the potential to grow an interconnected regional hydrogen infrastructure.

Conclusions and Future Directions

The SCHFCA Hydrogen 101 program has met all of its goals and its efforts are having an impact on the wider support of hydrogen. Education about the effect of state level incentives on the market for fuel cell and other renewable technologies has started to show how states can grow their hydrogen infrastructure. In 2012, educational efforts will focus on presenting the value proposition for fuel cell systems to stakeholders and working to develop a more regional approach to hydrogen and fuel cell industry growth. The project will use a mixture of webinars, in-person presentations, and electronically available resources to train decision makers.

IX.5 VA-MD-DC Hydrogen Education for Decision Makers

Chelsea Jenkins
Virginia Clean Cities (VCC)
860 Greenbrier Circle, Ste 404
Chesapeake, VA 23320
Phone: (757) 256-8528
E-mail: cjenkins@hrccc.org

DOE Manager
GO: Greg Kleen
Phone: (720) 356-1672
E-mail: Greg.Kleen@go.doe.gov

Contract Number: DE-FG36-08GO18115

Subcontractors:
- Catherine E. Grégoire Padró, Los Alamos National Laboratory, Los Alamos, NM
- Greg Jackson and Peter B. Sunderland, University of Maryland (UM), College Park, MD
- Christopher Bachmann, James Madison University (JMU), Harrisonburg, VA

Project Start Date: September 1, 2008
Project End Date: September 30, 2011

Fiscal Year (FY) 2011 Objectives

The goal of this three-year project is to increase the targeted audience's understanding of hydrogen and fuel cells, including early market applications, and to provide specific examples of actions that state and local government leaders can take to support the development and use of hydrogen and fuel cell technology leading to better understanding of community benefits. The main objectives of the two-year project are to:

- Conduct a dozen workshops by technical experts and professional educators.
- Produce video resources for public television, seminar use, DOE, and the general public.
- Use hardware demonstrations when possible and provide real-world examples of technology.
- Produce electronic "magazine" articles on hydrogen and fuel cell technology demonstrations and other instructional project deliverables.

Technical Barriers

This project addresses the following technical barriers from the Education section (3.9) of the 2009 Fuel Cell Technologies Program Multi-Year Research, Development and Demonstration Plan:

(A) Lack of Readily Available, Objective, and Technically Accurate Information
(B) Mixed Messages
(C) Disconnect between Hydrogen Information and Dissemination Networks
(D) Lack of Educated Trainers and Training Opportunities
(F) Difficulty in Measuring Success

Contribution to Achievement of DOE Education Milestones

This project will contribute to achievement of the following DOE milestones from the Education Technical Plan (3.9) section of the 2009 Fuel Cell Technologies Program Multi-Year Research, Development and Demonstration Plan:

- **Milestone 17**: Hold "Hydrogen 101" seminars. (4Q 2008 through 4Q, 2011)

FY 2011 Accomplishments

The following has been accomplished during FY 2011:

- Maintained key partnerships with over 30 different public and private organizations in Virginia, Washington, D.C., and Maryland to promote program and message.
- Conducted four "Hydrogen 101" seminars in Virginia, Washington D.C., and Maryland.
- Aired Motorweek "Hydrogen and Fuel Cells Emerging Markets" video and developed Y3 "Vehicles and Infrastructure Update" video.
- Developed and updated website and social media tools (Facebook, YouTube, Twitter).
- Held ride-n-drives of Equinox Fuel Cell Electric at three events.
- Published quarterly newsletters.
- Developed first responders webinar workshop.
- Implemented surveys at two workshops.
- Completed fuel cell scooter demo with James Madison University Alternative Fuel Vehicle Lab and showcased at two events.



Introduction

In order to change the way we use energy and to increase the deployment of hydrogen and fuel cell technologies, decision makers will need to make informed

public policy decisions and continue to support research and development as well as deployment activities. This project aims to raise awareness of hydrogen and fuel cell technologies, provide examples of what state and local government can do, and show how decision makers can support the development and use of hydrogen and fuel cell technologies.

The objectives of this project are to provide hydrogen and fuel cell technology learning opportunities through seminars, multi-media, and video resources, and to provide technical support and demonstrations to local and state government and decision makers. These activities will help leaders become familiar with hydrogen and how it fits into the portfolio of near-term and long-term energy choices, develop an accurate understanding of hydrogen safety, recognize opportunities, and understand their part in facilitating use of hydrogen and fuel cell technologies.

Approach

Our primary approach is to host in-person and webcast seminars for our target market. Messaging ties to the hydrogen knowledge survey, on which the subprogram objectives and targets are based. Under DOE guidance, existing Education sub-program resources and new contributions by team members are considered. Educational content focuses primarily on a basic understanding of hydrogen properties and the energy security and environmental benefits of hydrogen and fuel cell technologies, but also focuses on more technical subjects related to fuel cells and other modes of hydrogen energy conversion. Special consideration has been given to "following the technology" and resources also concentrate on areas where hydrogen and fuel cells are publicly visible through demonstration projects or early niche market commercialization efforts, such as hydrogen fuel cell forklift program at the Defense Distribution Depot Susquehanna, Pennsylvania, and fuel cell installations at Gills Onions and Sierra Nevada Brewery in California.

The key to state and local government representative education is a broad understanding of how hydrogen supports decision-making on current opportunities and how to lay the foundation for long-term change. Additionally, providing real-world examples and demonstrations has been a key component of each seminar.

Results

The major achievements over the last year include hosting four successful, and highly received events completing a shooting schedule and beginning production of a third seven-minute video for seminar use and broadcasting on PBS and Discovery HD Theatre developing webinar curriculum and developing, completing, and showcasing a university student senior thesis deployment project.

Seminar Results

The curriculum prepared and presented by Dr.'s Chris Bachmann, Dr. Peter Sunderland, and Dr. Greg Jackson at workshops in Harrisonburg, Virginia, and College Park, Maryland included:

- Overview of the current energy system
- What is hydrogen and what is a fuel cell?
- Hydrogen production, storage, distribution, and use
- Environmental, energy and economic implications of fuel cells and hydrogen
- Safety, codes and standards
- The future of hydrogen and fuel cells

Ride and drive events were held along with a screening of the "Emerging Markets" MotorWeek video. The JMU event also featured presentations by Hampton Roads Hydrogen, Marz Industries, and the JMU AFV demo team. Also, at both of these seminars, a post-workshop survey was distributed to assess the usefulness of each workshop component. The results of these surveys are provided in Table 1. Two additional events were held in conjunction with the presentation of senior thesis projects at James Madison University and as part of a general Fleet Innovation Seminar held at the Fairfax County government center in Fairfax, Virginia. The JMU event featured a "Hydrogen 101" presentation and a presentation highlighting the development and features of the Alternative Fuel Vehicle Lab scooter. Dr. Greg Jackson contributed a "Hydrogen 101" presentation at VCC's Fleet Innovation Seminar in addition to a Fuel Cell Equinox Ride and Drive.

TABLE 1. Survey Results for Participants at 2/25 JMU and 3/11 UM Workshops (58 Total Attendees)

i. Overview and Introduction to Hydrogen & Fuel Cells		
Very Useful	Useful	Not Useful
58%	42%	0%
ii. Our Current Energy System and the Potential of Hydrogen		
Very Useful	Useful	Not Useful
67%	29%	4%
iii. Hydrogen Production, Storage, Distribution, and Use		
Very Useful	Useful	Not Useful
54%	46%	0%
iv. Environmental, Energy, and Economic Implication of Hydrogen		
Very Useful	Useful	Not Useful
67%	33%	0%
v. MotorWeek Video		
Very Useful	Useful	Not Useful
33%	63%	4%
vi. Ride-N-Drive		

TABLE 1. Survey Results for Participants at 2/25 JMU and 3/11 UM Workshops (58 Total Attendees) (Continued)

Very Useful	Useful	Not Useful
42%	54%	4%
vii. Overall Event		
Very Useful	Useful	Not Useful
67%	33%	0%
Why did you attend today's seminar?		
• To contribute and learn. • To learn more about the state of the science of creating environmentally friendly hydrogen. • To see what the current status of hydrogen power is. • Get more information about hydrogen, it's use, and applications. • Interested in hydrogen production technologies. • To become informed. • To see student presentations. • Learn more about advancements in development of hydrogen as an energy source. • Learn about fuel cells and stations in VA. • Knowledge of alternative energy source. • Interest in and concern about our energy policy as it affects our economy and investments. • General interest in renewable energy options. • Learn about hazards and safety involving fuel cells. • We are considering alternate fuel vehicles. • Improve knowledge of hydrogen characteristics, use, and safety issues. • Support Clean Cities mission and interested in fuel cells. • Learn more about current state of fuel cell technology, especially as it relates to transportation, including current Administration support and potential involvement of state agencies.		
What was the most interesting part of today's seminar?		
• Multiple sources of info. • Discussion of stationary applications. • Vehicles running on hydrogen using combustion engines. • Discussion of variety of applications. • Emerging applications. • Who is using fuel cells. • How long fuel cells have been in use as fuel/energy provider. • Production and storage info. • Stationary applications. • Characteristics of hydrogen and impact on fire safety. • General operation and components of fuel cell systems.		
What did we NOT cover today that you desired? How can we improve?		
• Small hydrogen generator systems using solar power. • Have flyer with local, regional, and national avenues with grant funding/assistance with trying to implement hydrogen facilities within government. • More on economics, where are we going and how fast? • More technical information regarding cutting edge research.		
Other comments?		
• Dr. Bachmann did a great job. • Excellence coverage and balance of topics. • Schedule event for fire fighters and fire safety personnel.		

MotorWeek "Emerging Markets" Video

Virginia Clean Cities and the DOE worked with MotorWeek to produce and air a video entitled "Emerging Markets." In addition to footage of many fuel cell electric vehicles and early market applications at the 2010 National Hydrogen Association conference, footage also included interviews with leaders of hydrogen and fuel cell focused organizations and industry leaders who have implemented fuel cells. The video is approximatley seven minutes and includes an overview of hydrogen and fuel cell applications that are in use presently.

MotorWeek "Vehicles and Infrastructure Update" Video

This video will highlight progress made in fuel cell electric vehicle design and use, as well as advances in infrastructure towards the planned release. Footage will include video of several vehicles and General Motor's newest fuel cell engine, along with video of various fueling installations.

Conclusions and Future Directions

The seminars that have been held to date have been very well received and the participants' knowledge of hydrogen and fuel cell technology has increased as indicated by the surveys. At least two more events/outreach projects targeted at decision makers will be carried out in the remainder of the project period. This project will end in September 2011.

Future Project Outputs

- Complete outreach efforts including First Responders Webinar.
- Complete production and airing of third MotorWeek video focusing on vehicles.

Planning and Improvements

After surveying several targeted individuals, it was confirmed that travel restrictions and time constraints have affected our ability to attract participants at in-person workshops. It is our hope that events such as the upcoming first responders webinar and other targeted outreach activities will address this issue.

Key Issues

The project's main issue is that current participants and the target audience in general are being assigned extra demands and do not have time to take part in the seminars and webinars.

FY 2011 Publications/Presentations

1. Greg Jackson PowerPoint for 3/11 and 3/23 seminars.

2. Peter Sunderland PowerPoint for 3/11 seminar.
3. Chris Bachmann PowerPoint for 2/25 seminar.
4. PowerPoint for 6/11Annual Merit Review oral presentation.
5. Student presentations of hydrogen demo thesis project.
6. MotorWeek “Emerging Markets” video.

All presentations available at http://www.hrccc.org/cleaner-transportation-options/hydrogen/hydrogen-seminars/

IX.6 H2L3: Hydrogen Learning for Local Leaders

Patrick Serfass
Technology Transition Corporation
1211 Connecticut Ave., NW Suite 600
Washington, D.C. 20036
Phone: (202) 457-0868
E-mail: pserfass@ttcorp.com

DOE Manager
GO: Greg Kleen
Phone: (720) 356-1672
E-mail: Greg.Kleen@go.doe.gov

Contract Number: GO18114

Subcontractors:
- Public Technology Institute (PTI), Washington, D.C.
- Schatz Energy Research Center, Humboldt State University, Arcata, CA

Project Start Date: October 2008
Project End Date: August 2011

Fiscal Year (FY) 2011 Objectives

- Create presentation materials tailored to effectively communicate with state and local government leaders. Relate hydrogen to their interests and spheres of responsibility.
- Establish pathways for working with national associations of state and local officials as a route for disseminating information about hydrogen. Set pattern for on-going information flow.
- Launch learning sessions by conducting initial workshops for local and state officials at national gatherings. Achieve nationwide reach.
- Provide market analysis around the fuel cell infrastructure. The report produced will establish an improved understanding of the current state of production, distribution, storage, and the use of hydrogen, which is a critical fuel for the fuel cell industry.

Technical Barriers

This project addresses the following technical barriers from the Education section of the 2009 Fuel Cell Technologies Program Multi-Year Research, Development and Demonstration Plan:

(A) Lack of Readily Available, Objective, and Technically Accurate Information

(B) Mixed Messages

(C) Disconnect Between Hydrogen Information and Dissemination Networks

(D) Lack of Educated Trainers and Training Opportunities

Contribution to Achievement of DOE Education Milestones

The H2L3 project will directly address the following milestones of the Education sub-program:

- **17**: Hold "Hydrogen 101" seminars. (4Q, 2008 through 4Q, 2012)
- **18**: Develop end-user workshop materials for use at events. (4Q, 2009)
- **30**: Evaluate knowledge and opinion of hydrogen technology of key target audiences and progress toward meeting objectives. (4Q, 2012)

The H2L3 project directly contributes to achieving these milestones by conducting education workshops with hundreds of local and state officials from across the country and by training motivated local officials to replicate the workshops in their own communities. By fostering and using the H2L3 team's existing network of national associations of local and state government officials, the reach and the credibility of the outreach will be substantially and uniquely strengthened. This network will continue to support the goals of the DOE beyond the three-year life of this project by establishing institutional relationships that will enable on-going and expanding opportunities for hydrogen and fuel cells outreach through the national associations representing local and state officials.

FY 2011 Accomplishments

- Core Curriculum
  - Comprehensive, basic presentation developed to communicate with state and local officials.
  - Curriculum trimmed or modified for specific audiences as needed.
- Advisory Committee of Local and State Officials
  - Established an advisory committee comprised of Public Technology Institute members (local) and National Association of State Energy Officials members (state) to review the curriculum and provide input.
- Peer Presenters
  - Identified four different peer presenters who have been or will be utilized to help spread the information in the curriculum to other local leaders.
- Hydrogen 101 Workshops
  - Held three workshops at annual national meetings of the Public Technology Institute and National Association of State Energy Officials.

  - Reached over 100 local leaders who have been individually identified, 700+ counted and several thousand reached so far (radio and online) with educational materials.
- U.S. Market Report: Hydrogen and Fuel Cells
  - Completed research covering 57 different sectors of the hydrogen and fuel cell industries.
  - Peer reviewed, endorsed by the National Hydrogen Association (NHA), published www.hydrogenassociation.org/marketreport.
  - Over 70,000 downloads of the report so far.
  - Data and charts used by DOE in annual reports and presentations.
- Hydrogen Learning for Local Leaders Breakfast at NHA Conference with the California Fuel Cell Partnership
  - Informal networking breakfast targeted to southern California local leaders.
  - Used an unconventional, non-presentation-based approach by mingling experts with local leaders to create intimate conversations.
  - Very successful. Allowed questions to emerge organically and multiple future opportunities.
- Hydrogen Business Solutions Forum at the NHA Conference
  - Peer-to-peer series of presentations presented by current users of fuel cells for current and potential users of fuel cells.
  - www.hydrogenconference.org/h2fcForum.asp
- 2010 Hydrogen Student Design Contest
  - Challenged teams of university students from around the world to plan and design the basic elements of a hydrogen community in Santa Monica, CA.
  - Thirty-tow teams registered, 12 submitted designs from four countries: United States, Canada, Bangladesh, Ukraine.
  - Three winning teams presented designs at NHA Hydrogen Conference and Expo in Long Beach, California; Grand Prize: Missouri University of Science and Technology; Honorable Mentions: University of Waterloo and the National University of Kyiv (Ukraine).
  - Grand-prize winning team presented at the World Hydrogen Energy Conference in Essen, Germany.
- 2011 Hydrogen Student Design Contest
  - Challenged teams of university students from around the world to plan and design a residential hydrogen fueling system.
  - Fifty-four registered universities (a new record) from 19 countries, including seven of the top 20 engineering schools in the world.
  - Grand Prize: University of Waterloo (5-time winner); Honorable Mentions: Imperial College London, University of California, Riverside.
  - Eighty-nine percent of survey respondents say they would participate in the contest again; other 11% would consider, depending on theme.



Introduction

Increasing education about hydrogen and fuel cells is key to enable widespread commercialization. This project began with the goal of educating local leaders. As the project progressed, tactics broadened to include additional paths to local leaders and new audiences to provide educational and information tools that increase knowledge about hydrogen and fuel cells.

Approach

Activities include Hydrogen 101 in-person presentations, webinars, the creation of a market report that features industry data not published before, the creation of a business solution forum for existing and potential hydrogen customers, and a student contest to engage university students to design a hydrogen community in southern California.

Going forward, the approach will include a series of webinars. The electronic format should allow us to reach more local leaders with reduced cost to allow the remaining resources to be stretched further

Results

Following is a summary of select results:

Partnered with the Public Technology Institute and the National Association of State Energy Officials to provide Hydrogen 101 presentations. Local leaders have been engaged from the following areas:

- Cincinnati Health Department
- City of Boston Environment Department
- City of Carlsbad, California
- City of Cincinnati, Ohio
- City of Culver, California
- City of Dayton, Ohio
- City of Des Moines, Iowa
- City of Fort Wayne, Indiana
- City of Fort Worth, Texas
- City of North Kingstown, Rhode Island
- City of Orlando, Florida
- City of Phoenix, Arizona

- City of San Diego, California
- City of Santa Monica, California
- City of South Sioux City, Nevada
- City of Wilmington, North Carolina
- City of Winston-Salem, North Carolina
- Washington, D.C.
- Fairfax County Dept. of Vehicle Services, Virginia
- Los Angeles County, California
- Regional Governmental Services of California
- San Diego County, California

Feedback from attendees Hydrogen 101:

- "Very understandable."
- "For the first time, I understood what hydrogen is."
- "This was really good."
- "Really informative."
- "Showing the number of fueling stations made it real. I thought hydrogen was more of an impossibility before."

The U.S. Market Report: Hydrogen and Fuel Cells includes 57 different research areas. The full report and eight-point brief (see Figure 1) can be viewed and downloaded from: http://ttcorp.com/2011/pdf/marketReport.pdf. The report has become the most popular download on the NHA Web site and has been downloaded over 70,000 times to date.

Accolades for the U.S. Market Report: Hydrogen and Fuel Cells

- It's outstanding and will be a very useful resource for the community. NHA should be proud to put our logo on your work..... Thanks for the chance to review this impressive document. –Ken Schultz, Operations Director, Energy Group, General Atomics.
- Lot of great data. I had no idea that there are so many renewable projects. –Sandy Thomas, former President, H2Gen Innovations.
- A really good report. I think the front sections will make a great reference tool on the hydrogen industry generally and I already learned a few things!-Lisa Calaghan Jerram, Fuel Cell Today.
- This is an excellent report. I think it is very useful.- Dr. Finis H. Southworth, Chief Technology Officer, AREVA NP Inc.
- I am working on a hydrogen study for the University of Colorado and the Reliability and Sustainability Energy Institute (RASEI). Your US Market report on Hydrogen is great.
- Excellent reports - some of the most salient data & information out there, and very well presented.–From Randy Cole, CEO at Renewable Opportunities, Inc, via LinkedIn.

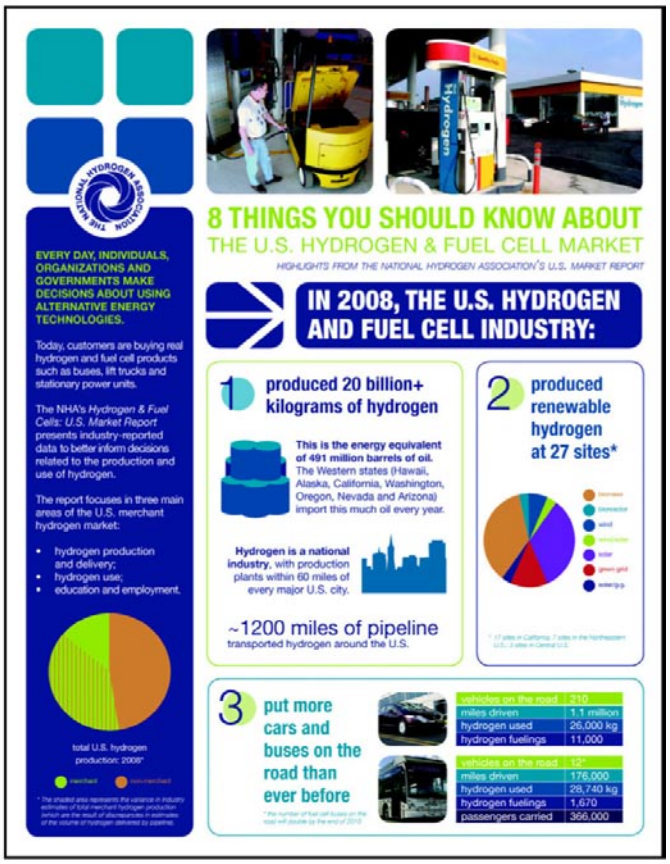


FIGURE 1. The 8-point brief of the U.S. Market Report: Hydrogen and Fuel Cells http://www.ttcorp.com/marketReport/brief.pdf

- Love the 8-point brief. Succinct and direct. Thanks for drawing our attention to it. - Tom Sperrey, Chief Executive Officer (CEO), UPS Systems plc, via LinkedIn.
- The brief version is my kind of report! The full version looks very useful; many thanks for sharing the link. - Graham Cooley, CEO at ITM Power Plc, via LinkedIn.
- Very well done and very much needed! -Bay Elliott, EVP, Partner, Executive Recruiter, The Farwell Group, via LinkedIn.
- Is it possible to obtain a copy of your report in a non-pdf format? I would like to utilize some of the graphs and figures regarding H2 Energy in an internal slide presentation. If not the whole study, specifically pages 26-37. –from an industrial gas supplier (obviously a significant compliment if they're happy using this information internally).
- These are very nice reports. I circulated them within Proton. –Mark Schiller, Vice President of Business Development, Proton Energy Systems.
- You and your team did an excellent job. Congratulations! - Patricia Irving, Ph.D., President & CEO, InnovaTek, Inc.
- This looks really, really nice. Thank you. I've stared teaching the graduate course at Wayne State University

in alternative energy, and I plan to share this report with my class, as well as working it into my thinking about price and market position. Thank you again, and good luck with your work. - Robert Buxbaum, President, REB Research & Consulting.

The 2010 Hydrogen Student Design Contest challenged teams of university students from around the world to plan and design the basic elements of a hydrogen community in Santa Monica, California. They were asked to design one scalable hydrogen fueling station; identify renewable hydrogen sources in the community; and identify customers for early market hydrogen applications.

University teams from the United States, Canada, Bangladesh, and the Ukraine submitted contest entries. These entries were evaluated across ten different categories by a team of judges from government and industry.

The team from Missouri University of Science and Technology was declared the Grand Prize winner (see team photo, Figure 2). Teams from the University of Waterloo and the National University of Kyiv received Honorable Mention awards. Winning designs can be viewed at www.HydrogenContest.org.

The 2011 Hydrogen Student Design Contest challenged teams of university students from around the world students to plan and design a residential hydrogen fueling system. As a part of their entry, teams developed a technical design; conducted an economic analysis; and developed business, marketing, and public education plans for their systems.

University teams from 19 countries and seven of the top 20 engineering schools in the world competed. These entries were evaluated across ten different categories by a team of judges from government and industry.

The team from the University of Waterloo was declared the Grand Prize winner. This Grand Prize marks the fifth award for the University of Waterloo in the six-year history of the Contest (see team photo, Figure 3). Contest newcomers Imperial College London and University of California, Riverside were awarded honorable mentions. The 2011 Contest was sponsored by the U.S. Department of Energy, Praxair, Honda, and Proton Energy Systems. Winning designs can be viewed at www.HydrogenContest.org.



FIGURE 2. The Hydrogen Student Design Contest's 2009-10 grand-prize winning team: Missouri University of Science and Technology, http://www.hydrogencontest.org/.

Conclusions and Future Directions

The feedback we have received about this project has been overwhelmingly positive. Where improvements have been suggested, adjustments have been made to improve the experience for any audience. Going forward, we recommend continuation of the Hydrogen 101 presentations using a webinar format, an expansion of the Market Report to include the next year's data to show trends (reinforced by at least one reviewer at the Annual Merit Review) and future Hydrogen Student Design Contests.

FY 2011 Publications/Presentations

1. NCSL short Hydrogen Overview for states, October 2010, http://www.ncsl.org/?tabid=21289.

2. Three papers on the topic "Hydrogen Student Design Contest 2011: Residential Refueling Station," presented at Fuel Cell and Hydrogen Energy 2011, February 2011, http://hydrogencontest.org/previous.asp.

3. Seven papers on the topic "Hydrogen Student Design Contest 2011: Residential Refueling Station," published on the Hydrogen Contest website, February 2011, http://hydrogencontest.org/previous.asp.

4. "Local Leaders Create Fuel Cell Success Stories: Spotlight on Leading Local Companies" webinar held May 17, 2011, http://ttcorp.com/2011/webinars.asp.

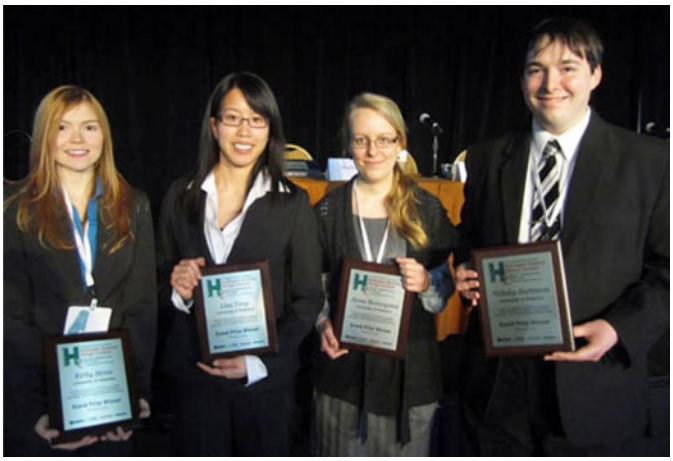


FIGURE 3. Five-time award winner presents Grand Prize design to industry professionals at Fuel Cell and Hydrogen Energy 2011 conference The Grand Prize winning team from the University of Waterloo at the 2011 Fuel Cell and Hydrogen Energy Conference in Washington, D.C., http://www.hydrogencontest.org/.

5. "The Top 5 Fuel Cell States: Why Local Policies Mean Green Growth" webinar held June 21, 2011, http://ttcorp.com/2011/webinars.asp.

6. "Where the Jobs Are: Hydrogen Fuel Cells in Your Area" webinar held July 19, 2011, http://ttcorp.com/2011/webinars.asp.

7. "Go Local: Maximizing Your Local Renewable Resources With Fuel Cells" webinar held August 16, 2011, http://ttcorp.com/2011/webinars.asp.

IX.7 Raising H_2 and Fuel Cell Awareness in Ohio

Patrick Valente
Ohio Fuel Cell Coalition
737 Bolivar Road, Suite 1000
Cleveland, OH 44115
Phone: (216) 363-6890
E-mail: Pat.valente@fuelcellcorridor.com

DOE Manager
GO: Greg Kleen
Phone: (720) 356-1672
E-mail: Greg.Kleen@go.doe.gov

Contract Number: DE-FC36-08GO18117

Subcontractor:
Edison Material Technology Center, Dayton, OH

Project Start Date: March 2009
Project End Date: June 30, 2012

Fiscal Year (FY) 2011 Objectives

- Increase understanding of hydrogen and fuel cell technologies among state and local governments by 10% compared to 2004 baseline.
- Increase knowledge of hydrogen and fuel cell technologies among key target populations (state and local governments) by 20 percent compared to 2004 baseline.

Technical Barriers

This project addresses the following technical barriers from the Education section of the Fuel Cell Technologies Program Multiyear Research Development and Demonstration Plan:

(A) Lack of Readily Available, Objective and Technical Accurate Information
(B) Mixed Messages
(C) Disconnect Between Hydrogen Information and Dissemination Networks
(D) Lack of Educated Trainers and Training Opportunities
(E) Regional Differences
(F) Difficulty of Measuring Success

Contribution to Achievement of DOE Education Milestones

This project will contribute to the following DOE Milestones from the Education section of the Fuel Cell Technologies Program Multiyear Research Development and Demonstration Plan.

- **Milestone 11**: Develop set of introductory materials suitable for a non-technical audience (3Q, 2009)
- **Milestone 13**: Develop material for community seminars (ongoing)
- **Milestone 16**: Develop database of state activities (ongoing)
- **Milestone 17**: Hold "Hydrogen 101" seminars (3Q, 2009 through 2Q, 2012)

FY 2011 Accomplishments

- July 13, 2010 – Ohio Fuel Cell Coalition Board Meeting - Dublin, Ohio – 45 people
- July 14, 2010 – China Export Commission - Toledo, Ohio - 15 people
- July 22, 2010 – Cleveland, Ohio – 40 people
- August 7, 2010 – Akron, Ohio – 25 people
- August 26, 2010 – Columbus, Ohio – 100 people
- September 16, 2010 – Canton, Ohio – 25 people
- September 30, 2010 – Dublin, Entrepreneur Center Presentation - Dublin, Ohio – 50 people
- October 18- 21, 2010 – Annual Fuel Cell Seminar - San Antonio, Texas – 25 people
- October 26, 2010 – Youngstown, Ohio – 35 people
- November 2, 2010 – Presentation at First Energy - Eastlake, Ohio – 50 people
- November 23, 2010 – Regional Economic Development Forum - Mansfield, Ohio – 35 people
- December 2, 2010 – Kent, Ohio – 20 people
- December 20, 2010 – IAB Board Meeting - Canton, Ohio – 10 people
- January 7, 2011 – Cincinnati, Ohio – 10 people
- January 25, 2011 – Ohio Fuel Cell Coalition Board Meeting - Logan, Ohio – 20 people
- February 15, 2011 – Ohio Fuel Cell Members Forum - Washington, DC – 20 people
- March 1, 2011 – Dayton, Ohio – 20 people
- March 23, 2011 – Kent City Leadership - Kent, Ohio – 20 people
- April 18 & 19, 2011 – North Canton, Ohio – Ohio Fuel Cell Symposium – 210 people
- April 26, 2011 – Wayne County Chamber - Orville, Ohio – 10 people
- May 21, 2011 – Ohio Society of Professional Engineers - Cleveland, Ohio – 50 people
- June 7, 2011 – Regional Leadership Forum - Lima, Ohio – 50 people
- June 8, 2011 – Northwest Ohio Leadership Forum - Perrysburg, Ohio – 30 people

The Ohio Fuel Cell Coalition was tasked with raising the awareness and understanding of Fuel Cells and the Hydrogen economy. In 2010 through 2011 the Ohio Fuel Cell Coalition held 23 community leaders forums. An annual community leader's forum was held in conjunction with the 2011 Ohio Fuel Cell Symposium. On April 18 and 19 over 210 people gathered at the Kent State Stark Campus for the 2011 Ohio Fuel Cell Symposium, the theme this year was Economic Opportunities Through the Fuel Cell Supply Chain. The symposium presented by the Ohio Fuel Cell Coalition began with two USDOE Community Leaders forum where participants had an opportunity to learn about Fuel Cells and the Hydrogen Economy. On Day 2 of the symposium the audience heard from a series of fuel cell integrators and fuel cell leaders, on the importance of the supply chain in fuel cell development. In the morning of the first day we heard from Mark Fleiner of Rolls-Royce Fuel Cell Systems and John O'Donnell, President of Stark State College of Technology discussed the emerging fuel cell clusters in North Canton, Ohio. A panel discussion was held in the afternoon with Steve Sinsabaugh, Lockheed Martin; Tim Lowe, Vice President of Sales of Energy Technologies and Vince Contini from Battelle who discussed Ohio's strength in the fuel cell genset arena. This event allowed the Coalition to educate over 210 individuals on fuel cells and the hydrogen economy which exceeded our expectations.



Approach

The approach we used and will be using for all the Community Leaders Forums will be presentations by the Ohio Fuel Cell Coalition in conjunction with regional leaders. The presentations will be followed by question and answers periods followed up by informal discussions on fuel cells and the hydrogen economy.

Results

In summary, the Community Leader Forums have been very successful in the last year with over 915 people being drawn to them. As always we followed up the forums with a survey and the survey results were very positive in that the participants had a significant increase in knowledge and awareness of fuel cells and the hydrogen economy.

Conclusions and Future Directions

We have received additional input on the Community Leaders Forums and we continued to add input to future events. The following Community Leader Forums will be held in the next three months:

- Cincinnati, Ohio
- Toledo, Ohio
- Athens, Ohio
- Cleveland, Ohio
- Akron, Ohio

IX.8 Dedicated to the Continued Education, Training and Demonstration of PEM Fuel Cell-Powered Lift Trucks in Real World Applications

Thomas Dever
Carolina Tractor & Equipment Co., Inc.
DBA Carolina Cat – LiftOne Division
5509 David Cox Rd.
Charlotte, NC 28269
Phone: (704) 597-7866, extension 4431
E-mail: tdever@liftone.net

DOE Manager
GO: Jim Alkire
Phone: (720) 356-1426
E-mail: James.Alkire@go.doe.gov

Contract Number: DE-FC36-08GO18105

Subcontractor:
Hydrogenics, Mississauga, Ontario, Canada

Project Start Date: September 1, 2008
Project End Date: August 31, 2011

Fiscal Year (FY) 2011 Objectives

Through both segments of the project: 1) Education and 2) Deployment, the objective has been focused on increasing hydrogen awareness through:

- Continued education of an ever-broadening group of stakeholders to the benefits of fuel cell and hydrogen technologies in material handling applications to include: facility management, operators, maintenance personnel, safety groups, first responders, authorities having jurisdiction, technical/community colleges.
- Demonstration of fuel cell and hydrogen technology through the continuing demonstration schedule of two hydrogen fuel cell-powered lift trucks in real-world applications at large prominent companies.
- Demonstration of these fuel cell-powered trucks at high profile public events.
- Assisting in the further commercialization of fuel cell and hydrogen technology by establishing a series of cost value propositions to interested companies.

Technical Barriers

This project addresses the following technical barriers from the Education section (3.9.5) of the 2009 Fuel Cell Technologies Program Multi-Year Research, Development and Demonstration Plan:

(B) Mixed Messages for Education
  – Product Performance
  – Infrastructure/Cost Justification
  – Difficulty in Measuring Success

Contribution to Achievement of DOE Education Milestones

This project has and will continue to contribute to achievement of the following DOE milestones from the Education section of the Fuel Cell Technologies Multi-Year Research, Development and Demonstration Plan:

- **Milestone 1**: Developed "Awareness- Level" information for first responders (3Q, 2010). This work continued during the LiftOne Program's 6th and final fuel cell-powered lift truck deployment at AGI in Forest City, NC - through the active participation of the local Forest City Fire Department at the H2 Orientation/ Safety Training sessions.
- **Milestone 14**: Hold Community Seminars to introduce local segments of those communities to hydrogen (3Q, 2010, 4Q 2009, 1Q 2010). Handled through participation and "Live" fuel cell-powered lift truck demonstrations at regional business events such as the "Green Is Good For Business Expo" - Columbia, SC (9/14/2010); Odyssey Week Events in Columbia, SC (10/11/2010), and Charlotte, NC (10/14/2010) (Figure 1).
- **Milestone 18**: Develop end-user workshop materials for use at events (3Q-2010 through 2Q-2011). The LiftOne hydrogen fuel cell-powered lift trucks continued to be shown at sessions conducted with selected end-users at their facilities as well as at the LiftOne branch locations.



FIGURE 1. LiftOne Demonstrating Fuel Cell-Powered Lift Truck at the Odyssey Day Event at Central Piedmont Community College, Charlotte, NC on October 15, 2010

Updated cost justification information has been shared with key company personnel at the sessions.

FY 2011 Accomplishments

- Within the past 12 months, LiftOne successfully completed the project's 6th and final deployment of two CAT® electric trucks, each powered by a Hydrogenics Fuel Cell Power Pack. The performance was very good, with all data compiled and sent to the National Renewable Energy Laboratory for analysis and comparison to similar fuel cell projects.
- These LiftOne deployments have allowed important end-users operating large lift truck fleets to test the benefits associated with hydrogen fuel cell power, while experiencing hands-on refueling. Their involvement has enhanced those opportunities present for acquisition and eventual conversion to hydrogen fuel at some point in the future.
- LiftOne's continued participation at strategic regional Clean Energy/Green Expo events again provided a large cross section of the business and local community with an introduction to H_2 power and included live demonstrations of the fuel cell-powered lift truck. These events held in Charlotte (NC), as well as Greenville and Columbia (SC), were attended by well over 1,000 people and increased overall hydrogen awareness levels.
- With the valuable experience gained over the course of the lift truck deployments, LiftOne's Hydrogen Education Program Director Tom Dever has participated as a presenter as well as provided material handling expertise at several notable hydrogen events, and has been referenced in several national fuel cell publications.



Introduction

The materials handling industry, a $12 billion global market representing approximately 750,000 lift trucks sold each year, has proven to be a significant near-term market for proton exchange membrane (PEM) fuel cell adoption in a mobility application. This is due to the lack of emissions and the increased productivity the technology provides vs. that of using lead-acid batteries or fossil fuels (liquefied petroleum gas, gasoline, diesel) for lift trucks and other material-handling units. As a leading dealership in the Carolinas and Virginia, LiftOne first demonstrated PEM fuel cells in 2007, and was able to gain early field trial experience, while recognizing the acute need for overall hydrogen education.

To assist in facilitating the integration of hydrogen fuel cells into real-world material handling application, LiftOne developed a Hydrogen Education and Awareness Presentation for lift truck users. These sessions have been conducted at each of the LiftOne branches on a rotational basis. Additional sessions have been tailored for presentations at selected technical colleges, professional organization meetings, industrial shows and to large companies with actual live demos at their facilities. These Hydrogen Awareness Classes began in early 2009, and will continue through August of 2011. The Deployment Segment of the LiftOne project, where the two fuel cell-powered lift trucks are put into real-world applications at six strategically selected major companies' facilities for one-month long trials, have provided an excellent method for demonstrating the viability of fuel cell power. The deployments began in May of 2009 and concluded in August of 2010.

Approach

Recognizing the need to help increase hydrogen awareness among material handling users, LiftOne's approach for Hydrogen Education has been focused on the identification of key target audiences. This strategy has been employed for both the Education and Deployment segments. For the Education segment, the seminar content has been designed for the layman's introduction to hydrogen and included in the 4- to 5-hour long sessions are a thorough review of hydrogen uses, its properties, infrastructure review as well as acquisition cost models and a live demonstration. The target audience for the Education Segment includes representatives from companies operating medium to large electric material handling fleets, with a secondary audience being those operating fossil fuel powered fleets. Smaller fleet operators also have participated.

For the LiftOne Deployment Segment, high profile companies with sizable fleets and multiple locations were selected for the trial sites, in order to gain the best opportunities with potential for effective regional exposure. For each site, presentations and proposals for the trials were made, detailing the equipment, fueler location/regulations, on-site monitoring arrangements and data gathering. At the conclusion of each deployment, comprehensive review meetings are held, in which all performance data presented, feedback from operators reviewed, and a cost justification evaluations presented with full proposals for fuel cell and infrastructure acquisition for more involved "pilot" type projects.

Results

Over the past year, LiftOne has seen positive results in both the Education and Deployment segments associated with the project. Sessions have been conducted at the LiftOne branches, at customer locations, at community colleges and at the regional "Green"-type business expos attended. LiftOne has included the live demonstration of the working fuel cell-powered lift truck, an essential element necessary to satisfy the interest present and maximize awareness.

The Deployment Segment of the project generally yielded very good results. The deployments were conducted at: 1) Stanley Tools, 2) a distribution center (name withheld

by request), 3) Bausch & Lomb, 4) BMW, 5) Electrolux and 6) AGI - In Store, which was conducted this past year (Table 1). There were decent run times, truck performance, power, and ease of refueling (Figure 2). All sites were able to experience fuel cell power, with well over 200 employees at each site made aware of the hydrogen power. As was mentioned at this time last year - LiftOne's participation at the BMW trial (Site # 4), alongside other fuel cell manufacturers (Plug Power and Nuvera), solidly contributed to that trial's overall success and BMW's eventual large-scale fuel cell acquisition in 2010.

TABLE 1. Site # 6 – LiftOne Fuel Cell Deployment Summary

LiftOne Site # 6 - AGI - In Store: 25 days
* Truck 0264 / Cell # 17 ran 190 hrs
* Truck 0265 / Cell # 18 ran 229 hrs
* 86 kg of H2 used / 62 fills / 53.75 tanks
* 4.7 minutes average fuel time
* 7.8 hrs avg run time per tank (1.6kg)
Notes: water pump, purge valve
Straight forks - sideshifter application
Good trial - 2 technical issues fixed.
Decent hours run. Good time per tank.

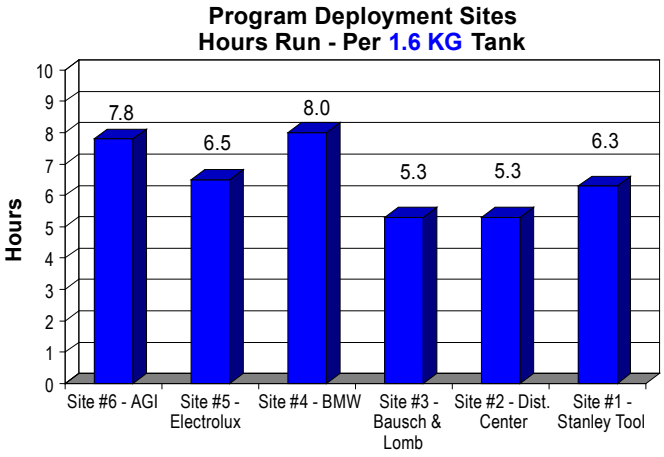


FIGURE 2. LiftOne – Average Hours Run per Tank for all Six Deployment Sites

Conclusions and Future Directions

For the third and final year of the LiftOne Hydrogen Education Program, the following conclusions have been determined:

- A wide variety of users have learned about hydrogen, and seen the fuel cells powering lift trucks in real-world applications. LiftOne's project addressed this critical "first step".
- There still remains a large degree of intrigue, but the adoption of fuel cells by major corporations has greatly increased H_2 awareness through the accompanying positive publicity.
- While viable in many large applications, the fuel cell power option is still not economically justified for lift truck fleets of less than 30-35 units at this point in time.
- There is a need for more viable competition in the fuel cell manufacturer arena in order for the necessary price efficiencies, broadened product improvements and size offerings.
- Infrastructure cost remains the major concern for companies considering fuel cell adoption. It has been the single largest obstacle to overcome during proposals.

Future plans for year three of the project involve:

- The LiftOne Hydrogen Education sessions with the live demo will continue at company sites through the remainder of the project term (August 31, 2011).
- LiftOne has considered trying to complete one additional deployment with another supplier's fuel cells prior to the project's completion. Time constraints may not allow for this to take place.

FY 2011 Publications/Presentations

1. Tom Dever, Hydrogen Education Program Director – LiftOne, Presenter: "Dedicated To The Continued Education, Training and Demonstration of PEM Fuel Cell Powered Lift Trucks In Material Handling Applications", Fuel Cell & Hydrogen Energy Conference, Washington, D.C., February 14, 2011.

IX.9 Hydrogen and Fuel Cell Education at California State University, Los Angeles

David Blekhman (Primary Contact), Trinh Pham, Chivey Wu
California State University, Los Angeles (CSULA)
5151 State University Drive
Los Angeles, CA 90032
Phone: (343) 323-4569
E-mail: blekhman@calstatela.edu

DOE Manager
GO: Greg Kleen
Phone: (720) 356-1672
E-mail: Greg.Kleen@go.doe.gov

Contract Number: DE-FG36-08GO18106

Project Start Date: October 15, 2008
Project End Date: June 30, 2011

Fiscal Year (FY) 2011 Objectives

California State University, Los Angeles, has partnered with the DOE in addressing the workforce preparation and public education needs of the fuel cell industry and the U.S. economy through a comprehensive set of curriculum development and training activities:

- Developing and offering several courses in fuel cell technologies, hydrogen and alternative fuels production, alternative and renewable energy technologies as means of zero emissions hydrogen economy, and sustainable environment.
- Establishing a zero emissions proton exchange membrane (PEM) fuel cell and hydrogen laboratory supporting curriculum and graduate students' teaching and research experiences.
- Providing engaging capstone projects for multi-disciplinary teams of senior undergraduate students.
- Fostering partnerships with automotive manufacturers and energy providers.

Technical Barriers

This project addresses the following technical barriers from the Education section (3.9.5) of the 2009 Fuel Cell Technologies Program Multi-Year Research, Development and Demonstration Plan:

(A) Lack of Readily Available, Objective, and Technically Accurate Information
(B) Mixed Messages
(D) Lack of Educated Trainers and Training Opportunities

Contribution to Achievement of DOE Education Milestones

This project will contribute to achievement of the following DOE milestones from the Education section of the 2009 Fuel Cell Technologies Program Multi-Year Research, Development and Demonstration Plan:

- Milestone 11: Develop set of introductory materials suitable for a non-technical audience. (4Q, 2006)
- Milestone 21: Launch new university hydrogen education program. (4Q, 2009)
- Milestone 27: Launch high school teacher professional development. (4Q, 2008 through 3Q, 2011)

FY 2011 Accomplishments

- In the 2010-2011 academic year, we continued to offer course modules and hydrogen and fuel cell technology (HFCT) dedicated courses; TECH 470-Electric and Hybrid Vehicles (enrollment 10 technology, eight mechanical); TECH 250-The Impact of Technology on the Individual and Society (detailed in the next section). Milestone 21 (**M:21**).
- TECH 250-The Impact of Technology on the Individual and Society course is a general education required course, which contains one week module on fuel cells and hydrogen economy. It is open to all majors in the university and is selected to deliver our message to the university-wide student body. Multi-section course enrollment exceeded 200 students. **M:21.**
- CSULA students built a fuel cell vehicle and participated in 2011 Shell-Eco competition, Houston, TX. CSULA built fuel cell vehicle Hydrogen Super Eagle was on display at AltCar Expo, Santa Monica 2010, October 2010, Los Angeles Auto Show, in November 2010 and the Metropolitan Water District of Southern California Sustainable Expo, May 2011. The vehicle participated in filming the Mercedes-Benz F-Cell World Drive video EcoTrek 7 (at 3rd minute): http://www.youtube.com/watch?v=qDPhJsMUBR4. **M:21,** Milestone 11 (**M:11**).
- CSULA students participated in 2010 and 2011 Hydrogen Design Contests organized by the National Hydrogen Association. **M:21.**
- CSULA has been selected for EcoCAR 2 *Plugging into the Future* competition 2011-2014. **M:21, M:11.**
- The College of Engineering, Computer Science and Technology (ECST) is completing the 10 kW solar photovoltaic installation. The system consists of 56 Sharp and 23 Solec modules and three SMA inverters. The funds were provided by Southern California Edison, ECST and this funding. **M:21.**
- There has been an appreciable number of public outreach and educational activities through which fuel cell and hydrogen technologies and the new curriculum

at CSULA were promoted. CSULA participated in numerous meetings and discussions of future projects and collaborations with fuel cell vehicle manufacturers, federal and state government officials. Significant collaboration has been developed with California Fuel Cell Partnership. **M:11.**

- CSULA is completing the construction of a hydrogen station with 60 kg/day generation capacity. That will enable further development of educational program and research into hydrogen technologies. **M:21.**
- Multidisciplinary team of CSULA faculty, including Dr. Blekhman, received National Science Foundation (NSF) funding to establish Center for Energy and Sustainability. The same group has secured American Recovery and Reinvestment Act funding to renovate laboratory spaces including the Zero Emissions Fuel Cell and Hydrogen Laboratory (ZEFC). Dr. Blekhman has been awarded NSF Major Research Instrumentation funding to conduct research into hydrogen purity. These will contribute to the longevity of the research program. **M:21.**



Introduction

Our interest in developing hydrogen and fuel cell education stems from the recognition of the urgent need for workforce development and public education in the entire spectrum of alternative and renewable energy technologies (ARET). ECST is taking steps to graduate more students fluent in ARET as well as to raise campus and state-wide awareness of green technologies. This includes the ongoing construction of a hydrogen fueling station on campus. The comprehensive nature of the university, its strategic location in the hydrogen and fuel cell abundant industrial region and a historically minority-serving charter has made CSULA an ideal candidate to carry out the tasks listed in the objectives.

Approach

Design of a comprehensive engineering and technology curriculum addressing fuel cells and hydrogen technologies is the foundation for our contribution toward green workforce training. This is accomplished through a mix of new courses or special modules in existing courses to introduce the concepts of fuel cell technologies, hydrogen and alternative fuels, alternative and renewable energy technologies as means of zero emissions hydrogen economy, and sustainable environment. ECST has established the ZEFC to support curriculum, undergraduate and graduate students' teaching and research experiences. Further, enrichment of student experiences is accomplished through projects and fostering partnerships with automotive manufacturers and industry.

Community education and public outreach goals are met through a series of on campus and off-campus public events and demonstrations.

Results

The initial grant period was extended by nine months which allowed supporting students that led team efforts in creating a fuel cell vehicle and participating in 2011 Hydrogen Design Contests organized by the National Hydrogen Association. The contest was to design a home hydrogen refueling facility. The twelve-student team included two students from East Los Angeles College. CSULA took 7th place among 17 teams that submitted and 54 registered, third place among the U.S. teams.

An ECST team of six students built a fuel cell vehicle. The team participated in 2011 Shell-Eco competition, Houston, TX. The fuel cell vehicle called Hydrogen Super Eagle was also on display at AltCar Expo, Santa Monica 2010, October 2010, Los Angeles Auto Show, November 2010 and the Metropolitan Water District of Southern California Sustainable Expo, May 2011. The vehicle participated in filming the Mercedes-Benz F-Cell World Drive, see Figure 1. The multi-episode documentary is called Eco Trek and is available on YouTube. CSULA is featured in EcoTrek 7 (at third minute): http://www.youtube.com/watch?v=qDPhJsMUBR4.

Two courses with integrated fuel cell/hydrogen modules were offered: TECH 470-Electric and Hybrid Vehicles and TECH 250-The Impact of Technology on the Individual and Society. The latter had multiple sessions throughout the year.

CSULA has actively pursued public outreach and educational activities through which the DOE-sponsored Fuel Cell and Hydrogen curriculum at CSULA was promoted. During the fall of 2010, ECST hosted a Boeing open house for middle and high-school students. More than

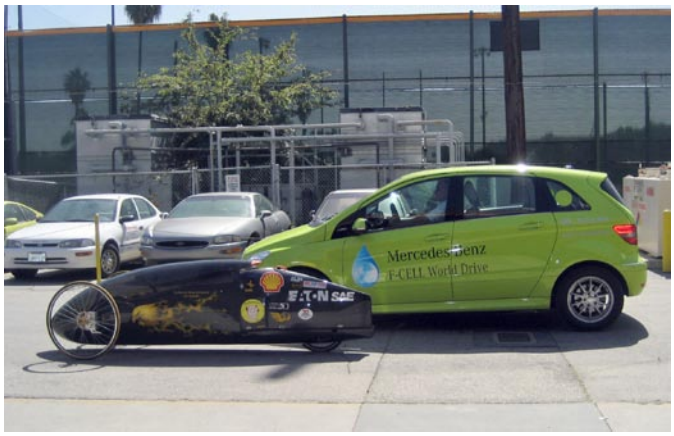


FIGURE 1. CSULA-Built Fuel Cell Vehicle Driving along Mercedes-Benz F-Cell World Drive Car

a hundred of them toured the ZEFC. There were multiple additional events with K12 students being introduced to fuel cells, see Figure 2.

CSULA is nearing the completion of a $4.5 M hydrogen station on campus, see Figure 3. It will deploy the latest technologies with the capacity of 60 kg/day, sufficient to fuel 15+ vehicles or a bus and five more vehicles. The station is utilizing a Hydrogenics electrolyzer, first and second stage compressors capable of fast-filling at 5,000 psi and 10,000 psi, and 60 kg of hydrogen storage. The station will be grid-tied and powered by 100% renewable power.

Dr. Blekhman attended the 2011 Annual Merit Review and 2011 NHA conference both in Washington, D.C., and the 2011 ASEE conference in Vancouver, BC.

Conclusions and Future Directions

CSULA has been very successful in meeting the objectives proposed in the grant. In this extended period of funding, the team has continued to offer courses with modules addressing fuel cell and hydrogen technologies. The work in ZEFC laboratory progressed with the solar installation that will be powering the lab electrolyzer and the rest of the engineering building. Students continued to be challenged through industry and competition projects far beyond those proposed initially.

CSULA is well poised to continue fuel cell and hydrogen educational and research efforts beyond current funding, which provided the foundation for many other activities. Among future activities are operating the hydrogen station, participating in EcoCAR 2 competition and operating a high-quality gas chromatograph-mass spectroscopy for testing hydrogen purity in Southern California. We will also continue our educational program, outreach and collaborations with the industry.



FIGURE 2. Marengo Elementary School Science Night; a Fuel Cell Display is Demonstrated, in January 2011



FIGURE 3. CSULA Hydrogen Station Construction on June 22, 2011

IX.10 Hydrogen Energy in Engineering Education (H_2E^3)

Richard A. Engel (Primary Contact),
Peter A. Lehman
Schatz Energy Research Center
Humboldt State University Sponsored Programs Foundation
1 Harpst St.
Humboldt State University (HSU)
Arcata, CA 95521
Phone: (707) 826-4345
E-mail: rae7001@humboldt.edu

DOE Manager
GO: Gregory Kleen
Phone: (720) 356-1672
E-mail: Greg.Kleen@go.doe.gov

Contract Number: DE-FG36-08GO18107

Subcontractor:
University of California, Berkeley (UCB), Berkeley, CA

Project Start Date: September 15, 2008
Project End Date: September 15, 2011

Objectives

The Hydrogen Energy in Engineering Education (H_2E^3) project is designed to increase awareness of and hands-on experience with hydrogen and fuel cell technology among engineering students in California's public universities. H_2E^3's objectives are:

- To deliver effective, hands-on hydrogen energy and fuel cell learning experiences to a large number of engineering students at multiple campuses in the California State University (CSU) and University of California (UC).
- To provide follow-on internship opportunities for students at fuel cell companies.
- To develop commercializable hydrogen teaching tools including a basic fuel cell test station and a fuel cell/electrolyzer experiment kit suitable for use in university engineering laboratory classes.

Technical Barriers

This project addresses the following technical barriers from the Education section (3.9.5) of the 2009 Fuel Cell Technologies Program Multi-Year Research, Development and Demonstration Plan:

(D) Lack of Educated Trainers and Training Opportunities. Only a small number of universities in California offer hydrogen and fuel cell-specific learning opportunities for undergraduate engineering students. Even at these campuses, the number of engineering faculty with direct experience using fuel cells remains small, and fuel cell course content is underdeveloped.

(E) Regional Differences. California has the advantages of being home to many hydrogen and fuel cell developers and on the leading edge of hydrogen energy infrastructure development. These features call for a special hydrogen energy education effort in California universities that makes use of these existing resources available in close proximity to many campuses.

Contribution to Achievement of DOE Education Milestones

This project has contributed to achievement of the following DOE milestone from the Education section of the Fuel Cell Technologies Program Multi-Year Research, Development and Demonstration Plan:

- **Milestone 21**: Launch new university hydrogen education program (4Q, 2009).

The project supports attainment of the above milestone by creating curriculum, teaching tools, and industry-based learning opportunities that can be replicated by other universities working with industry partners. By the same token, the project also supports completion of Task 5 in the Multi-Year Research, Development and Demonstration Plan: "Facilitate Development and Expansion of College and University Hydrogen Technology Education Offerings," specifically the subtask described as "Work with university partners to develop and expand hydrogen technology course offerings and facilitate networking among schools with similar programs."

Fiscal Year (FY) 2011 Accomplishments

- Continued expansion of H_2E^3 curriculum adoption at host universities HSU and UCB, including activities for three additional courses:
  - Transport phenomena (ENGR 416) at HSU, in which students used a fuel cell test station to perform a heat balance on an operating fuel cell stack.
  - Renewable energy power systems (ENGR 475) at HSU, in which students evaluated fuel cell stack performance under different temperature and air stoichiometry conditions.
  - A hydrogen safety seminar at UCB, in which graduate engineering students visited UCB's new hydrogen fueling station and attended a safety presentation alongside local emergency responders.

- Visited and/or supplied sample experiment kits to faculty at seven California universities:
  - California State University, Los Angeles
  - San Francisco State University
  - Sonoma State University
  - University of California, Santa Cruz
  - Berkeley Center for Green Chemistry
  - University of California, Riverside
  - California State University, San Bernardino
- Successfully recruited faculty from three universities to adopt curriculum:
  - San Francisco State University
  - Sonoma State University
  - University of California, Riverside
- Fabricated 24 additional hydrogen experiment kits for placement at newly recruited campuses.
- Developed the project website (hydrogencurriculum.org) to include curriculum downloads, equipment user manuals, streaming videos, project news, and recommended readings.
- Planned, filmed, edited, and posted online (hydrogencurriculum.org) nine instructional videos explaining how to use the H_2E^3 laboratory equipment.
- Facilitated creation of two fuel cell development intern positions at Protonex Technology Corporation for summer 2011; filled these positions with two HSU engineering students who had previously participated in H_2E^3 curriculum.
- Performed monitoring and evaluation of classroom and lab activities.



Introduction

A recurring theme in the hydrogen energy field is the unmet need for a new generation of graduating engineers trained specifically in hydrogen and fuel cell energy technologies. The purpose of our project is to help meet this need, specifically in the context of the California State University and University of California systems. Together these universities grant over 7,000 engineering degrees each year.

The three-year project, branded as "Hydrogen Energy in Engineering Education" (H_2E^3) is being led by the Schatz Energy Research Center, a unit of the Humboldt State University Sponsored Programs Foundation. Our principal partner on the project is the UCB, represented by their Institute of Transportation Studies. The project also includes fuel cell industry partner Protonex Technology Corporation, which is providing internships for students who have participated in the curriculum.

Approach

Adding hydrogen curriculum to existing undergraduate engineering programs is not a trivial task. Engineering departments and the organization that accredits them require students to meet numerous stringent requirements in order to graduate. There is little slack in a typical undergraduate engineering course plan to add new curriculum. In order to add hydrogen education to existing engineering programs, we need to find creative ways to fold it into courses and help instructors meet their existing course objectives.

We have worked closely with engineering faculty as part of this project to develop lesson plans that can be substituted for segments of existing courses, including introductory engineering, introductory and advanced thermodynamics, renewable energy power systems, transport phenomena, and in courses on the general topic of energy and society. We have also developed laboratory hardware that students use to perform hands-on experiments that reinforce key points covered in the lecture material. The partners on this effort bring years of relevant experience in teaching about hydrogen energy and developing fuel cell technology.

Results

During the first two years of the project, the focus was primarily on development of curriculum and the related lab equipment. In the third year, we are focused on marketing and distributing the curriculum to other universities and creating follow-on internships for participating students.

Curriculum Development and Deployment. At HSU and UCB, we continued use of the curriculum in courses where it was introduced in year two. We also brought the curriculum into several new courses at these and other campuses. Table 1 details progress to date in incorporating curriculum in various courses.

While the project was originally designed to reach undergraduate engineering students, we have found the curriculum has broader appeal. For example, the curriculum is being used at Sonoma State University with students in a non-engineering energy management and design program. The curriculum is also being evaluated for use in training high school science teachers at California State University, San Bernardino. Reviewers at the 2011 Annual Merit Review meeting also suggested that the curriculum should be adapted for use with high school students.

Equipment Deployment. Using $15,000 in supplemental funding from DOE, we produced an additional 30 hydrogen experiment kits for distribution to newly participating campuses. We have placed most of these kits at the campuses that have joined the project during year three. Most of the kits are being used to perform lab activities developed by Schatz Energy Research Center. However, one UCB chemistry professor assigned her students to work in teams to analyze performance of the

TABLE 1. California Campuses and Courses where H_2E^3 Curriculum has Been Used to Date

Campus	Fall 2009	Spring 2010	Fall 2010	Spring 2011
Humboldt State	• Intro to Engineering (Engr) • Intro to Thermo	• Intro to Engr • Intro to Thermo • Advanced Thermo	• Intro to Engr • Intro to Thermo • Statistical Analysis • Renewable Energy • Energy for non-Engrs	• Intro to Engr • Intro to Thermo • Statistical Analysis • Transport Phenomena
UC Berkeley	• Energy and Society	• Intro to Engineering	• Energy and Society	• General and Quantitative Chem. Analysis • Hydrogen Safety
Sonoma State				• Energy Forum
San Francisco State				• Engineering Experimentation
UC Riverside				• Green Engineering

kits and recommend improvements. The students presented their work in a May 2011 poster session (see Figure 1).

Curriculum Marketing. Our project Web page (hydrogencurriculum.org) is aimed principally at faculty and features downloadable presentations, streaming videos produced in-house on using the equipment (see Figure 2), handouts for lab activities for a variety of courses, and a recommended readings list. Project staff visited faculty at four campuses (see Figure 3), bringing them sample kits and curriculum. Additional kits were shipped to interested faculty at other campuses.

Monitoring and Evaluation. We continued to use pre- and post-activity assessments of student learning at HSU in all courses where the curriculum was used. In addition, faculty at University of California, Riverside and Sonoma State University agreed to provide pre- and post-activity assessments and written feedback on use of the lectures and labs in their courses. This process has been helpful



FIGURE 2. Still from one of the H_2E^3 lab equipment instructional videos produced and posted online.

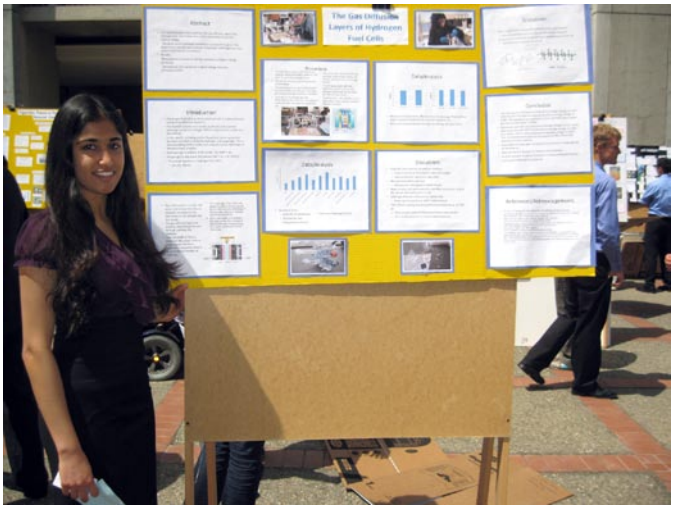


FIGURE 1. UC Berkeley chemistry student Nisha Mair displays her team's poster explaining their efforts to measure and improve performance of the H_2E^3 hydrogen experiment kits.



FIGURE 3. San Francisco State University engineering faculty evaluate H_2E^3 hydrogen experiment kit.

in making iterative improvements to the curriculum and equipment (see Figure 4).

Fuel Cell Industry Internships. Due to the economic downturn, we experienced difficulty during years two and three in placing interns with fuel cell companies as had been originally envisioned. In the second quarter of 2011, we determined that we could reallocate a portion of our project budget to cost share with companies on intern stipends. Using this funding mechanism, we successfully placed two HSU students at Protonex Technology Corporation, where they are currently working on proton exchange membrane and solid oxide fuel cell projects.

Conclusions and Future Directions

As this three-year project nears its September 2011 conclusion, it has been a success on many fronts, reaching well over a thousand students at five campuses. Student and instructor responses to the curriculum and equipment have been very positive. The strategy of using fuel cells and hydrogen energy concepts to meet the teaching objectives of existing engineering courses has been well-received by faculty.

In order to bring the funded project to completion we will:

- Continue to facilitate and evaluate the ongoing student internships.
- Produce two additional instructional videos, a virtual tour of the hydrogen fueling station at HSU and assembly of a PEM fuel cell stack.
- Continue to refine and extend the Web page.
- Determine who will be given continuing stewardship of the lab equipment.

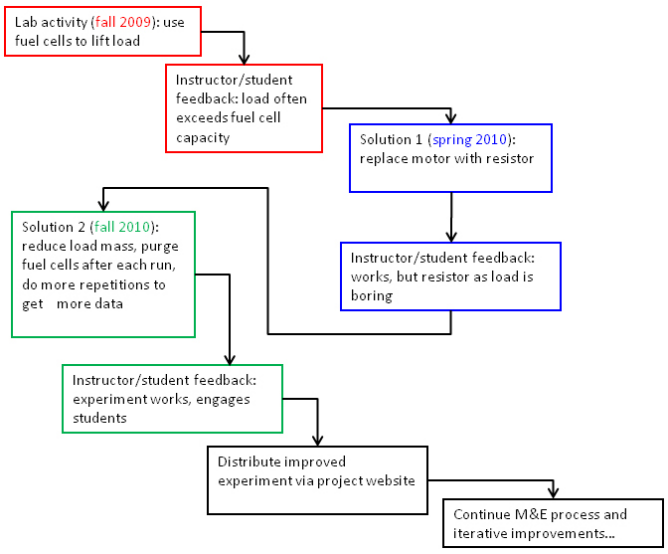


FIGURE 4. Example of iterative improvements to curriculum using monitoring and evaluation process.

Beyond the current funding, we hope to:

- Maintain and build on our established collaborations with other campuses in California.
- Identify universities outside California interested in adopting the curriculum.
- Seek manufacturing partners to commercialize the kits and/or test stations, scaling them up for mass production.
- Seek an opportunity to adapt the curriculum for high school use, as recommended by reviewers at the 2011 Annual Merit Review meeting.

FY 2011 Publications/Presentations

1. Materials for Probability and Statistics Course

- Pre-lab lecture presentation: "The HSU Hydrogen Fueling Station"
- Assignment handout: "Performance of the Electrolyzer at the HSU Hydrogen Fueling Station"

2. Materials for Test Station Lab for Renewable Energy Power Systems Course

- Lecture Presentations: "Hydrogen and Fuel Cells" and "Using the Fuel Cell Test Station"
- Assignment handout: "Performance and Design of PEM Fuel Cell Stacks"

3. Materials for Test Station Lab for Transport Phenomena

- Assignment handout: "Fuel Cell Heat Balance Lab"

4. Materials for Energy Forum senior/graduate level course

- Lecture presentations: "Hydrogen, Electrolyzers, and Fuel Cells" and "Fuel Cell and Electrolyzer Lab Activity"

5. Materials for Graduate Level Hydrogen Safety Seminar

- Lecture presentations: "The Promise of Hydrogen" and "First Responder Training for UC Berkeley Richmond Field Station Hydrogen Fueling Station"

6. "Tools for Teaching About Hydrogen and Fuel Cells." Two-page flyer distributed to University of California and California State University faculty to publicize the H_2E^3 curriculum.

7. Instructional videos:

- H_2E^3 - Using and Caring for the H2E3 Fuel Cell/ Electrolyzer Kits. http://youtube/I6i3Z_WLyjM
- H_2E^3 - Introduction to Engineering Fuel Cell and Electrolyzer Lab. http://youtu.be/Rx_lcFp-mzs
- H_2E^3 - Introductory Thermodynamics Lab I and Lab II. http://youtu.be/7BKxYyKH2eU
- H_2E^3 - Fuel Cell Test Station Software Overview. http://youtu.be/IFooNsV8eqs
- H_2E^3 - Fuel Cell Test Station Orientation and Care. http://youtu.be/3xDSjetWob4
- H_2E^3 - Fuel Cell Test Station Startup and Shutdown Part I. http://youtu.be/GoywLP40e1I

- H_2E^3 - Fuel Cell Test Station Startup and Shutdown Part II. http://youtu.be/1mOfgnxqs-w
- H_2E^3 - Fuel Cell Test Station Startup and Shutdown Part III. http://youtu.be/Vm_uxl1222o
- H_2E^3 - Fuel Cell Test Station Startup and Shutdown Part IV. http://youtu.be/IvxjrIgMzzU

8. Spanish language publications:

- "Juego para Experimentos con Hidrógeno: Celda de Combustible y Electrolizador. Guía para docentes para uso en cursos introductorios en ingeniería y termodinámica" (translation/adaptation of "Hydrogen Fuel Cell / Electrolyzer Kit Instructor Guide for Use in Introductory Engineering and Introductory Thermodynamics Courses" from H_2E^3 curriculum collection).
- "Actividad: Diseño de Celda de Combustible" (translation/adaptation of "Fuel Cell System Design Activity" originally created as part of the DOE-funded HyTEC high school hydrogen curriculum development project).

9. Petroske, Jarad. "Positive Energy: The Schatz Energy Research Center is Building a Renewable Future Today." *Humboldt Magazine*. Spring 2011. http://magazine.humboldt.edu/magazine_pdf/humboldtMagazine_spring11.pdf

10. Presentation for May 2011 Merit Review and Peer Evaluation Meeting.

IX.11 Hydrogen Education Curriculum Path at Michigan Technological University

Jason M. Keith (Primary Contact), Dan Crowl, Dave Caspary, Jeff Naber, Jeff Allen, Abhijit Mukherjee, Dennis Meng, John Lukowski, Barry Solomon, Jay Meldrum
Michigan Technological University
1400 Townsend Dr.
Houghton, MI 49931
Phone: (906) 487-2106
E-mail: jmkeith@mtu.edu

DOE Manager
GO: Gregory Kleen
Phone: (720) 356-1672
E-mail: Greg.Kleen@go.doe.gov

Contract Number: DE-FG36-08GO18108

Project Start Date: September 1, 2008
Project End Date: July 31, 2011

Fiscal Year (FY) 2011 Objectives

The objectives of this project are to educate university students on the advantages, disadvantages, challenges, and opportunities of hydrogen and hydrogen fuel cells within the United States energy economy. In particular, this project will:

- Develop and/or refine courses in hydrogen technology.
- Develop curriculum programs in hydrogen technology.
- Develop modules for core and elective engineering courses.
- Develop modules to supplement commonly used chemical engineering texts.
- Meet all Department of Energy project management and reporting requirements.

Technical Barriers

This project addresses the following technical barriers from Education section (3.9) of the Fuel Cell Technologies Program Multi-Year Research, Development and Demonstration Plan:

(A) Lack of Readily Available, Objective, and Technically Accurate Information

(B) Mixed Messages

(C) Disconnect between Information and Dissemination Networks

Contribution to Achievement of DOE Education Milestones

This project will contribute to achievement of the following DOE milestones from the Education section (3.9) of the Fuel Cell Technologies Program Multi-Year Research, Development and Demonstration Plan:

- **Milestone 21:** Launch new university hydrogen education program. (4Q, 2009)

FY 2011 Accomplishments

The major accomplishments of this project to date are listed as follows:

- We have developed and taught one lecture and one laboratory course in hydrogen energy and two courses in fuel cells.
- Over 40 modules have been developed to introduce students in core chemical engineering courses to hydrogen and fuel cell technology; similar efforts have been accomplished for core mechanical engineering (20 modules) and electrical engineering (6 modules) courses.
- 90 example problems have been created as supplementary material to be used in the sophomore level introductory chemical engineering course.
- Over 70 example problems have been created as supplementary material to be used in the junior level courses in fluid mechanics, heat transfer, and mass transfer fundamentals and their associated unit operations.
- Over the entire project, fifteen oral presentations have been given and seven conference proceedings have been published, with six oral presentations and two conference proceedings during the past year.

Introduction

There is a strong need for a transformative curriculum to train the next generation of engineers who will help design, construct, and operate fuel cell vehicles and the associated hydrogen fueling infrastructure. In this project, we build upon the project-based, hands-on learning that has been a cornerstone of engineering education at Michigan Technological University (MTU). This teaching and learning style is supported by the engineering education literature which indicates that students learn by doing, particularly through team-based interactive projects with a real-world flavor.

This project has resulted in the formation of an "Interdisciplinary Minor in Hydrogen Technology" at MTU. We focus on student centered design projects, and add additional technical material through elective courses, modules for core courses, and textbook supplements. As a final note, aggressive dissemination of the project results will occur through presentations at the annual meetings of several professional societies.

Approach

The ultimate goal for the hydrogen education program should be to establish an educational infrastructure and database of hydrogen and fuel cell related educational materials, particularly projects and problem sets. The efforts of this project support this mission.

At MTU, we have embraced the concept of hands-on learning as the cornerstone of a newly approved "Interdisciplinary Minor in Hydrogen Technology." Students that obtain this minor are also required to take newly developed elective courses in fuel cells and hydrogen technology. Focusing on a subset of graduates who choose these options is not enough. In order to reach a wider audience at MTU, modules are being developed for the core curricula in chemical engineering, mechanical engineering, and electrical engineering. Each module stands alone and can be assigned to students as an in-class problem, a homework assignment, or a project. The modules use the fundamental concepts taught within the core course and apply them to hydrogen generation, distribution, storage, or use within a fuel cell. Thus, students are able to see the applications of the fundamentals from their courses. Finally, we are creating supplements to two of the most popular chemical engineering textbooks as another way to introduce hydrogen technology and fuel cells to university students.

The core course modules are to be tested throughout the nation. The results of this curriculum project and testing results are to be disseminated through professional societies in chemical engineering, mechanical engineering, electrical engineering, and engineering education. Course materials, modules, and textbook supplements will be available for use by engineering educators worldwide.

Results

Results for Task 1.0, Develop and/or Refine Courses in Hydrogen Technology:

- To date, we have created two new courses, "Fundamentals of Hydrogen as an Energy Carrier" to be taught in fall semesters and "Hydrogen Measurements Laboratory" to be taught in spring semesters. We also modified two fuel cell courses. The hydrogen as an energy carrier course and both fuel cell courses were taught during the most recent academic year and were well received by students.

Results for Task 2.0, Develop Curriculum Programs in Hydrogen Technology:

- The "Interdisciplinary Minor in Hydrogen Technology" was approved by the university effective April 2009.
- The "Graduate Certificate in Hybrid and Electric Vehicles" was approved by the university effective May 2010.
- During the 2010-2011 academic year, there were several group projects in the "Alternative Fuels Group" Enterprise. This enterprise consisted of undergraduate students in chemical, mechanical, and electrical engineering, as well as materials science and engineering. Students were in their sophomore, junior, or senior year of study. By participating in the group projects, students earned credit towards their degree and (if desired) towards the new minor mentioned above. Student projects included:
  - Design of methanol production facility for use in direct methanol fuel cell (DMFC) applications (Figures 1 and 2) and analysis of DMFC membrane materials.
  - Integration of Bloom Box solid oxide fuel cells (SOFCs) into the Michigan Technological University electrical grid.

Results for Task 3.0, Develop Modules for Core and Elective Engineering Courses:

- The third task of this project is to develop modules for core courses in chemical, mechanical, and electrical engineering courses. Up to this point, we have developed over 40 chemical engineering modules, 20 mechanical engineering modules, and six electrical engineering modules. It is noted that the modules are available online at: http://www.chem.mtu.edu/~jmkeith/fuel_cell_curriculum/. Plans have been made to test these modules in the classroom at the following institutions: MTU, University of Michigan, Bucknell University, Illinois Institute of Technology, Michigan State University, Mississippi State University, Tennessee Technological University, University of Kentucky, Rowan University, San Jose State University, Oklahoma State University, University of Wyoming, and the University of Texas at Austin. Student feedback at these other institutions has been very positive.

Results for Task 4.0, Develop Modules to Supplement Commonly Used Chemical Engineering Texts:

- We have developed a set of 90 examples to supplement the textbook *Elementary Principles of Chemical Processes* authored by R. M. Felder and R. W. Rousseau and published by Wiley. The problems are organized in "workbook" format where there are blank spaces for students to insert numbers in order to carry out the solutions. It is noted that this textbook is used in the very first chemical engineering undergraduate course

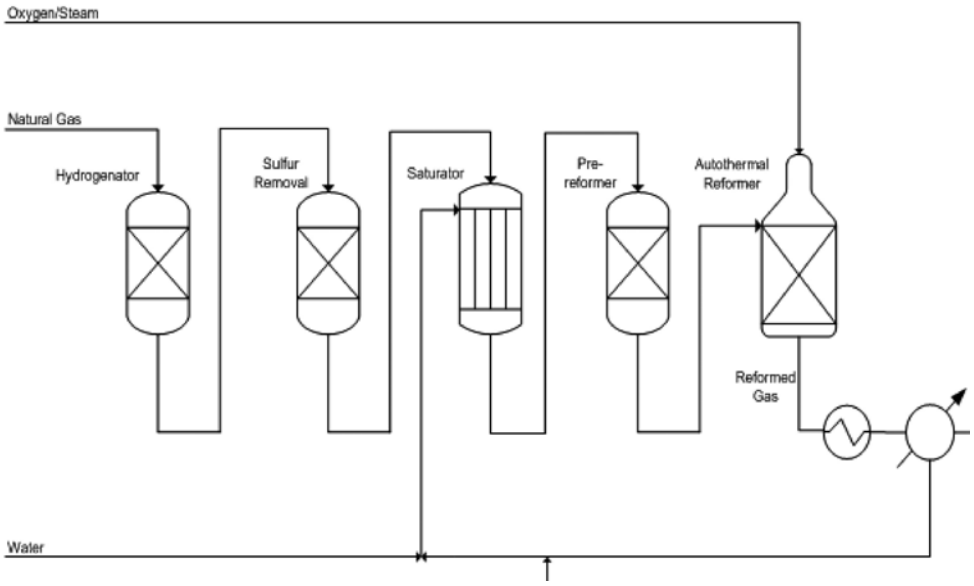


FIGURE 1. Process Diagram for Hydrogen Production via Steam Reforming

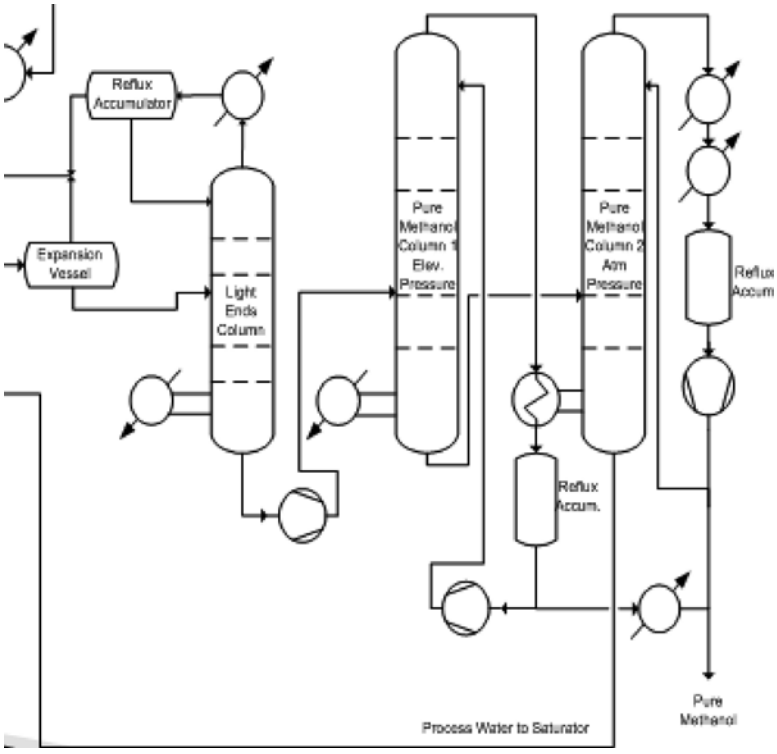


FIGURE 2. Process Diagram for Methanol Purification

at most universities in the nation. The main emphasis of the course is on engineering problem solving for chemical engineers. Students learn best by solving a large number of problems. This supplement is intended to meet the student's needs while teaching them about hydrogen technology and fuel cells.

- We have developed a set of over 70 examples to supplement the textbook *Transport Processes and Separation Process Principles* authored by C.J. Geankoplis and published by Prentice Hall. These problems follow the same format as those described above, and can be used to integrate fuel cell and hydrogen production concepts into fluid mechanics, heat transfer, and mass transfer topics and their associated unit operations.

Results for Task 5.0, Project Management and Reporting:

- To date, 10 quarterly reports (out of 12) have been submitted. In addition, a Powerpoint presentation was prepared and an oral presentation was given at the Annual Merit Review.

Conclusions and Future Directions

The most significant result of this project to date is the approval of a new minor at MTU with title "Interdisciplinary Minor in Hydrogen Technology." The groundwork is in place to teach new courses in hydrogen and fuel cell technology and to introduce these concepts in the core chemical engineering curriculum at MTU.

This project is nearing a close. The remaining modules (Task 3) and reports (Task 5) will be completed by the end of the project.

FY 2011 Publications/Presentations

1. Oral Presentation: J.M. Keith, D.Crowl, D. Caspary, J. Allen, D. Meng, A. Mukherjee, J. Naber, J. Lukowski, J. Meldrum, and B. Solomon, "Hydrogen Curriculum Path at Michigan Technological University," 2011 DOE Hydrogen Program Annual Merit Review, Arlington, VA.

2. Web Publication: J.M. Keith, "The Short Term Hydrogen Economy: Fueling Fuel Cells from Natural Gas," Knovel Engineering Cases, 2010.

3. Oral Presentation: J.M. Keith, D. Crowl, D. Caspary, J. Allen, D. Meng, A. Mukherjee, J. Naber, J. Lukowski, J. Meldrum, and B. Solomon, "An Interdisciplinary Minor in Hydrogen Technology at Michigan Technological University," 2010 AIChE Annual Meeting, Salt Lake City, UT.

4. Oral Presentation: J.M. Keith, T.F. Edger, G.P. Towler, H.S. Fogler, D. Crowl, D. Allen, "Energy Modules for the ChE Curriculum," 2010 AIChE Annual Meeting, Salt Lake City, UT.

5. Oral Presentation: D. Lopez Gaxiola and J.M. Keith, "Hydrogen and Fuel Cell Workbook for Material and Energy Balances," 2010 AIChE Annual Meeting, Salt Lake City, UT.

6. Oral Presentation and Conference Proceeding: J.M. Keith, D. Lopez Gaxiola, D. Crowl, D. Caspary, D. Meng, J. Naber, J. Allen, A. Mukherjee, J. Lukowski, B. Solomon, J. Meldrum, and T. Edgar, "Development and Assessment of Energy Modules in the Chemical Engineering Curriculum," 2011 ASEE Annual Meeting, Vancouver, BC, Canada.

7. Oral Presentation and Conference Proceeding: A. Minerick, J.M. Keith, F. Morrison, M. Tafur, A. Gencoglu, "Connecting Mass and Energy Balances to the Continuum Scale with COMSOL DEMoS," 2011 ASEE Annual Meeting, Vancouver, BC, Canada.

IX.12 Hydrogen and Fuel Cell Technology Education Program (HFCT)

David L. Block
University of Central Florida/Florida Solar Energy Center
1679 Clearlake Road
Cocoa, FL 32922
Phone: (321) 638-1001
E-mail: block@fsec.ucf.edu

Ahmed Sleiti (Co-PI)
University of North Carolina at Charlotte, NC

DOE Manager
GO: Greg Kleen
Phone: (720) 356-1672
E-mail: greg.kleen@go.doe.gov

Contract Number: DE-FG36-08GO18109

Subcontractor:
University of North Carolina at Charlotte, NC

Project Start Date: August 1, 2008
Project End Date: September 30, 2011

Fiscal Year (FY) 2011 Objectives

- Develop and implement an accredited engineering technology baccalaureate program in hydrogen and fuel cell technologies (HFCT) at the University of North Carolina at Charlotte (UNCC).
- Prepare students to work as hydrogen and fuel cell technology professionals in government, industry, and academia.
- Prepare program graduates with a mastery of the knowledge, techniques, skills and modern tools related to hydrogen and fuel cell technologies.
- Prepare program graduates with the ability to apply current knowledge and to adapt to emerging applications in the area of hydrogen and fuel cell technologies.
- Disseminate program information and HFCT activities to community colleges, high schools, industrial partners, governmental agencies, other universities, and the public.

Technical Barriers

This project addresses the following technical barriers from the Education section (3.9.5) of the 2009 Fuel Cell Technologies Program Multi-Year Research, Development and Demonstration Plan:

(A) Lack of readily available, objective, and technically accurate information

(F) Mixed messages

Contribution to Achievement of DOE Education Milestones

This project will contribute to achievement of the following DOE milestones from the 2009 Fuel Cell Technologies Program Multi-Year Research, Development and Demonstration Plan:

- Milestone 21 – Facilitate development and expansion of college and university hydrogen technology education offerings.

FY 2011 Accomplishments

The HFCT project was successful and accomplished all its goals and objectives as follows:

- All hydrogen and fuel cell courses have been developed and offered at UNCC.
- All laboratories were equipped and experiments were developed and offered.
- A HFCT program concentration was implemented as an option in the UNCC engineering programs.
- Industry collaborations are established.
- The program continues as part of national HFCT educational work, is positioned for continuation, and future activities are planned.

The website for HFCT is part of the UNCC engineering programs as follows: http://et.uncc.edu/about-us/facilities-a-labs/178.html. The UNCC website is http://www.uncc.edu/.



Introduction and Approach

The objective of the Hydrogen and Fuel Cell Technology education program is to develop and deliver an accredited baccalaureate level HFCT educational program at the UNCC. This objective has been successfully accomplished by developing HFCT courses and associated laboratories, teaching the new courses and labs and integrating the HFCT option into the UNCC mechanical engineering technology and mechanical engineering programs. The program has also established ongoing collaborations with the UNCC energy related centers. The HFCT courses have been offered successfully and student enrollments are good. HFCT results have been disseminated and published and the program has cooperative efforts with industries representatives. The HFCT program has addressed DOE goals by supplying readily available, objective and technically accurate information that is available to students, industry and the public. In addition, the program has supplied

educated trainers and training opportunities for the next generation workforce needed for research, development, and demonstration activities in government, industry, and academia.

The UNCC is an urban university that has a student body of 24,700 and offers 92 bachelors, 59 masters, and 18 doctoral programs. The HFCT courses are part of the UNCC College of Engineering. The engineering college has 4,000 students with 950 students in the Mechanical Engineering Department and 850 students in the Engineering Technology Department.

Results

The HFCT project was comprised of the completion of five project tasks and the results of the project activities can be presented as two major areas – course and laboratory development and offerings and program recruitment, promotions and collaborations.

I. Course and Laboratory Development and Offerings

Over the project period, the primary activity has been the development and offering of the HFCT courses and accompanying laboratories. This process has taken three years with the courses first being developed and then offered each year over the timeframe. The 11 courses that were developed and offered are presented in Table 1.

These courses are described as follows.

1. **Applied Energy Systems – ETM 4220.** The Applied Energy Systems course is an introduction course to topics of energy, work and thermal systems and processes. The course presents fundamentals of thermodynamics, electricity and nuclear technologies and the process of obtaining electricity from solar, wind, biomass and geothermal energy sources. The course also includes the efficiency of the different energy sources and effects on the environment. A one semester-long group project is assigned to students.
2. **Analysis of Renewable Energy – ETGR 3000-01 & ETME 4250.** The Renewable Energy course is an upper level course that looks at analysis of renewable energy systems. Topics include well-to-wheels analysis, lifecycle energy and emissions and total cost. Students learn skill sets, methodologies and tools needed to analyze various technologies on a consistent basis for a given application.
3. **Combined Hydrogen Production & Storage with Labs – ETGR 3000-02, MEGR 3090-020 & ETME 4260.** The Combined Hydrogen Production & Storage with Labs course presents basic concepts and principles of hydrogen technologies to include properties, usage, safety and a fundamental understanding of hydrogen storage and production technologies. The three laboratories are:
4. **Laboratory 1: Hydrogen and Fuel Cell Experiment.** Purpose: To calculate well-to-wheel values.
5. **Laboratory 2: Hydrogen as an Energy Carrier.** Purpose: To calculate power output from photovoltaics input to electrolyzer and the power outputs from fuel cell. Find photovoltaics max current and max power point locations on a voltage-current (V-I) curve.
6. **Laboratory 3: Methanol Fuel Cell.** Purpose: To draw V-I curve, interpret characteristic curve, enter operating voltage and current of the motor in V-I characteristic curve, draw power-current diagram, and calculate motor's power consumption and enter the values in power vs. current diagram.

TABLE 1. HFCT Courses and Course Offerings

Course	Prefix	Credit Hours	Offered	Future Offering
Applied Energy Systems	ETM 4220	4	Spring 2009	
Analysis of Renewable Energy Systems	ETGR 3000-01 and ETME 4250	3	Spring 2010	Spring 2011
Combined Hydrogen Production & Storage with Labs	ETGR 3000-02, MEGR 3090-020 and ETME 4260	3	Summer 2010	Summer 2012
Lab 1: Hydrogen and Fuel Cell Experiment	Part of ETGR 3000	-	Summer 2010	Summer 2012
Lab 2: Hydrogen as a Energy Carrier	Part of ETGR 3000	-	Summer 2010	Summer 2012
Lab 3: Methanol Fuel Cell	Part of ETGR 3000	-	Summer 2010	Summer 2012
Fuel Cell Tech 1	ETGR 3000-M01 MEGR 3090-M03 and ETME 4270	3	Fall 2010	Fall 2011
Lab 1: Assembly MEA FC	Part of ETGR 3000	-	Fall 2010	Fall 2011
Lab 2: Fuel Cell Performance Testing	Part of ETGR 3000	-	Fall 2010	Fall 2011
Lab 3: FC Performance as function of temp. & humidity	Part of ETGR 3000	-	Fall 2010	Fall 2011
Senior Design Course	MEGR 3255-001 ETGR 4100-EC1	4	Spring 2010, Fall 2010, Spring 2011.	Fall 2011

7. **Fuel Cell Tech I with Labs– ETGR 3000-M01 & MEGR 3090-M03 & ETME 4270.** The Fuel Cell Tech I with Labs course presents basic concepts and principles of fuel cell technologies to include chemistry, thermodynamics, electrochemistry, cell components, operating conditions and fuel cell systems. The three laboratories are:
8. **Laboratory 1: Assembling a 3-layer Membrane Electrode Assembly (MEA) Fuel Cell.** Purpose: To learn and practice the assembly of a proton exchange membrane (PEM) fuel cell.
9. **Laboratory 2: Fuel Cell Performance Testing.** Purpose: To acquire understanding and experience in employing electrochemical test methods to determine the performance characteristics of a hydrogen PEM fuel cell, to become acquainted with the concepts of fuel cell reactant consumption rates and utilization and the associated calculations and to evaluate the performance of PEM fuel cell as a function of O_2 concentration and stoichiometry with an emphasis on their effects on electrode kinematics, mass transport limitations and cell resistance.
10. **Laboratory 3: Performance of a hydrogen PEM fuel cell as a function of temperature and humidity.** Purpose: To implement basic experimental and analysis techniques that demonstrates and characterizes the performance of a hydrogen PEM fuel cell as a function of temperature and reactant gas humidity levels.
11. **Senior Design Course – MEGR 3255-001 & ETGR 4100-EC1.** The Senior Design course is a two semester for four hours "capstone" or final year experience intended to integrate a students' academic training with real-world engineering projects and community partners.

II. Promoting the Program through Advertisement, Recruiting Students and Outreach Plans

The objectives of this task are to recruit students, to promote the HFCT program and to disseminate information on the program and its activities in order to form collaborations with industrial partners, governmental agencies and other universities. Details follow.

Recruit Students: In an effort to recruit as many students as possible, the team has hosted seminars and visited community colleges and high schools. These efforts have concentrated on community colleges that currently have technology programs with potential to transfer students directly into the HFCT option of the Bachelor of Science in Engineering Technology program.

Program Promotion and Collaborations: Closely tied with recruiting students is the promotion of the HFCT program with various organizations and groups in order to receive external recognition and support. Industry collaborations are also closely tied with these promotion efforts. Industry, national laboratories and technical organizations were visited under this sub task.

Conclusions and Future Directions

The HFCT education project has successfully developed courses and associated laboratories, taught the new courses and labs and integrated the HFCT option into the accredited mechanical engineering technology and mechanical engineering programs at the UNCC. The HFCT courses have been offered successfully and student enrollments are good.

Future plans include the continued offering and evaluation of the developed courses and labs at UNCC, continued project promotion and collaborations with industry, university and other organizations, the development of web-based HFCT courses, the extension to a Master of Science program and the development of a research component.

FY 2011 Publications/Presentations

1. Sleiti, A. (2011, February). Hydrogen and Fuel Cell Education for Engineering and Engineering Technology Disciplines, 2011 Conference for Industry and Education Collaboration (CIEC*), San Antonio, TX.

2. Blekhman, D., Keith, J., **Sleiti, A.**, Cashman, E., Lehman, P., Engel, R., Mann, M., & Salehfar, H. (2010). National Hydrogen and Fuel Cell Education Program Part I: Curriculum, ASEE Annual Conference & Exposition, Louisville, KY.

3. Blekhman, D., Keith, J., **Sleiti, A.**, Cashman, E., Lehman, P., Engel, R., Mann, M., & Salehfar, H. (2010). National Hydrogen and Fuel Cell Education Program Part II: Laboratory Practicum, ASEE Annual Conference & Exposition, Louisville, KY.

IX.13 Development of a Renewable Hydrogen Production and Fuel Cell Education Program

Michael Mann (Primary Contact), Hossein Salehfar
University of North Dakota (UND)
241 Centennial Drive, Stop 7101
Grand Forks, ND 58202-7101
Phone: (701) 777-3852
E-mail: mikemann@mail.und.edu

DOE Manager
GO: Greg Kleen
Phone: (720) 356-1672
E-mail: Greg.Kleen@go.doe.gov

Contract Number: DE-FG36-08GO18110

Project Start Date: August 30, 2008
Project End Date: September 1, 2011

Fiscal Year (FY) 2011 Objectives

The objective of this project is to develop a comprehensive university level education program that will:

- Provide exposure to the basics of hydrogen-based technologies to a large number of students. This exposure will provide a level of training that will allow students to converse and work with other scientists and engineers in this field. It will also serve to spark a level of interest in a subset of students who will then continue with more advanced coursework and/or research.
- Provide a "mid-level" training to a moderate level of students. More detailed and directed education will provide students with the ability to work to support industry and government development of hydrogen technologies. This level of training would be sufficient to work in the industry, but not be a leader in research and development.
- Provide detailed training to a smaller subset of students with a strong interest and propensity to make significant contributions to the technology development. These individuals will have extensive hands-on experience through internships that will allow them to play a major role in industry, government, and academia.

For the purposes of this grant, the terms hydrogen-based technologies, hydrogen energy and hydrogen education are used broadly to include the production, transport, storage, and utilization of hydrogen. This includes both electrolysis and fuel cell applications.

Technical Barriers

This project addresses the following technical barriers from the Education Section (3.9) of the 2009 Fuel Cell Technologies Program Multi-Year Research, Development and Demonstration Plan:

(A) Lack of Readily Available, Objective, and Technically Accurate Information

(B) Mixed Messages

(C) Disconnect Between Hydrogen Information and Dissemination Networks

(D) Lack of Educated Trainers and Training Opportunities

Contribution to Achievement of DOE Education Milestones

This project will contribute to achievement of the following DOE milestones from the Education Section of the 2009 Fuel Cell Technologies Program Multi-Year Research, Development and Demonstration Plan:

- **Milestone 21**: Launch new university hydrogen education program. (4Q, 2009)

FY 2011 Accomplishments

There were seven tasks in this project. Major accomplishments include:

- Task 1 – Case Study Development: Case studies were developed and implemented into the undergraduate curriculum. The most successful of these case studies were presented for publication in the National Science Foundation (NSF) National Center for Case Study Teaching in Science.
- Task 2 – Development of New Courses: A new course, Hydrogen Production and Storage was developed. The content of our Renewable Energy Systems course was modified to highlight fuel cells and electrolysis and Fuels Technology was modified to highlight hydrogen production technologies. All courses were taught simultaneously to undergraduate, graduate and distance students
- Task 3 – Laboratory Experiments in Hydrogen: Experiments were developed for undergraduate chemical and electrical engineering laboratory classes. The experiments are accomplished using three sets of equipment – a single-cell electrolzer/fuel cell combination, a 40-watt fuel cell system, and a 600 watt fuel cell system. A set of experiments was designed to demonstration fuel cell membrane design, construction and testing.

- Task 4 – MS/PhD Teaching Experience: Doctoral (PhD) and Masters of Science (MS) students developed laboratory experiments, provided input for case studies, and participated in summer outreach programs for undergraduate students.
- Task 5 – Summer Internship: The project helped place summer interns at the National Renewable Energy Laboratory (NREL), Oak Ridge National Laboratory, and the DOE National Center for Hydrogen Technology.
- Task 6 – Hydrogen Seminary Series: Students were exposed to various aspects of hydrogen technology through a series of seminars that were offered each semester. Students were provided with the opportunity to attend the annual UND Energy & Environmental Research Center Hydrogen Summit.
- Task 7 – Develop Modules for PowerOn!: PowerOn provides hands on demonstrations for students in grades 4-9. A special topics class engaged students in the development and presentation of these modules.



Introduction

The basic concept of the project is to introduce hydrogen education to a broad distribution of students through the use of structured case studies and experiments that are built into the students required coursework. This guarantees that all undergraduate students in the program will be exposed to the technologies. This level of exposure should generate interest in a subset of these students who would then be interested in taking full semester courses related to hydrogen technologies. This will provide a significant cohort of students that will have a good understanding of the basics making them candidates for entry level jobs in hydrogen-related industries. A smaller subset of these students showing strong interest and aptitude will participate in directed research and internships to produce bachelor of science, MS, and PhD graduates that will play a major role in the future development of the hydrogen technology. UND's distance education experience will be used to reach a large and widely dispersed group of students.

Approach

UND is taking advantage of existing infrastructure and programs to provide a comprehensive renewable hydrogen production and fuel cell education program. This program is comprehensive from the standpoint of the level and number of students that will be involved in the program. It is designed to provide multi-discipline formal training to both undergraduate and graduate level engineers and scientists. This will be accomplished by developing case studies that will be implemented into classes through all four years of the undergraduate curriculum. These case studies will be broadly disseminated though the National Center for Case Studies in Science Teaching website making them available to any school in the United States. Two new classes will be generated that will be offered as technical electives at the undergraduate and graduate level. In addition to our on-campus students, the undergraduate class will also be offered though our Distance Education Degree Program (DEDP) to provide access to hundreds of off-campus students across the country and other nations. UND's DEDP program is the nation's only ABET EAC accredited undergraduate engineering program. Several new hydrogen-related student experiments will be added to our undergraduate laboratory sequence to provide hands-on experience for our students. Additional hands-on experience will be available to selected students through summer intern programs to be established with NREL and Proton Energy Systems (designer and manufacturer of proton exchange membrane [PEM] hydrogen production systems). UND will develop a hydrogen seminar, brining in experts in the field from NREL and Proton to present to UND students. Internships and research opportunities are also available for students at UND Energy & Environmental Research Center.

This program is designed to provide an introduction of hydrogen energy to a large number of students, both on and off the UND campus through the case studies and student laboratories. It will provide more detailed training on the topic to a smaller, but still significant group of students through new courses added to our curriculum and offered through our distance program. In-depth training will be provided to a select group of undergraduate and graduate students through in-house research and internships. We feel this approach will provide high quality students with the exposure of hydrogen energy required to support research, development, and demonstration activities in the government, industry and academia sectors.

Results

A variety of case studies were developed for the undergraduate curriculum, designed to fit into specific courses with the intent of reinforcing fundamental concepts using hydrogen production and/or utilization examples. While these were found to provide a good introduction to hydrogen, there was some difficulty incorporating these into core courses. While most faculty like new problems for application in their courses, they have limited time within the semester schedule to add significant content. They found it difficult to implement a case study that required a whole class period. A better approach was found to be utilizing the problem-based learning concept implemented in the Michigan Tech program, where shorter directed-problems were developed.

Case studies were found to be successful in survey courses where faculty are looking to expose students to examples of how technology can meet the needs of today's society. These courses are good places to introduce "non-technical" aspects of engineering to students, such as political and social constraints in making engineering

decisions. The most successful case studies were presented for publication in NSF National Center for Case Study Teaching in Science.

A new course, Hydrogen Production and Storage was developed and added to the curriculum. In addition, the content of our Renewable Energy Systems course was modified to highlight fuel cells and electrolysis and our Fuels Technology course was modified to highlight gasification and other hydrogen production technologies. These courses were effective in stimulating interest in hydrogen related technologies. An indication of this interest is the number of students choosing hydrogen related projects for their senior design. All courses were taught simultaneously to undergraduate, graduate and distance students to help maximize exposure.

An existing Hydro-Geniuses laboratory experimental setup consisting of a solar cell, a single-cell PEM electrolyzer, two single-cell PEM fuel cells, and a small resistive load is used by students to generate the current-voltage characteristic curves of the fuel cell and the electrolyzer and analyzed system efficiencies. The two fuel cells were operated both in series and in parallel. Two new series of laboratory experiments have been developed and implemented into the undergraduate curriculum using new experimental setups purchased from Heliocentris though the support of the DOE Hydrogen Education Program. The HP 600 includes a 600 watt water-cooled PEM fuel cell stack, a direct current (DC)/DC and DC/alternating current (AC) converter, metal hydride storage kit, electric load, and an integrated control system. The off-grid instructor includes a 40-watt fuel cell with integrated microprocessor, electronic load, metal hydride storage, and the constructor kit. A Masters student developed the set of laboratories that were implemented into the undergraduate curriculum.

To help improve the depth of knowledge and skills of our MS and PhD candidates, a variety of teaching experience opportunities were provided. PhD and MS students developed the laboratory experiments for implementation in the undergraduate labs. This provided the opportunity to test the equipment and determine which of its capabilities could be best utilized to demonstrate the fundamentals of hydrogen based energy. These students also provided input for case studies and participated in the summer outreach programs for undergraduate students.

One of the goals of this program was to provide internship opportunities for students that received training through a combination of their laboratory experience and the hydrogen related classes. This training was expected to add value to the student, making it easier for them to obtain internships. Students were placed in summer internships at NREL, Oak Ridge National Laboratory, and the DOE National Center for Hydrogen Technology.

Students were exposed to various aspects of hydrogen technology through a series of seminars that were offered each semester. Students were also provided with the opportunity to attend the annual UND Energy & Environmental Research Center Hydrogen Summit.

PowerOn is an outreach activity that provides hands on demonstrations for students primarily in the grades 4-9. The demonstrations and the infrastructure to support PowerOn are provided from other non-project funds. A special topics class engaged students in the development and presentation of these modules. Having students develop these modules on a “for credit basis” rather than for pay allowed projects to be developed without any monetary contributions from the project. Presentation of the PowerOn demonstrations allows students to gain practice in presenting engineering related concepts to the general public. While the general audience in middle school, experience has been that kids of all ages have a strong interest. The program also indirectly educates parents, as they often accompany their children in these public events.

Conclusions and Future Directions

Over 200 students were directly impacted by program.

- Over 150 chemical and electrical engineering undergraduate students were exposed to various aspects of hydrogen through in-class case studies and laboratory experiments.
- Twenty-seven students were involved in senior design projects related to hydrogen.
- Three hydrogen related courses were developed and taught, with enrollment of 73 students.
- Twenty-one undergraduate students were involved with PowerOn to develop modules to demonstrate hydrogen and other renewable energy technologies. Demonstrations were made to over 1,000 youth.
- Two PhD and two MS students were trained through the development of instructional material for this program. Nine interns were placed working in hydrogen related fields.
- Two undergraduates were placed at the DOE National Hydrogen Center and one at NREL. Two PhD graduates were placed with Nissan in their fuel cell division in Detroit.
- Results of this work have been presented at the 2010 annual American Society for Engineering Education meeting in addition to the DOE annual merit review meetings.

The final activities of this project will be to publish selected case studies and to publish a paper that summarizes the lessons learned during this program.

Special Recognitions

The paper, “National Hydrogen and Fuel Cell Education Program Part I: Curriculum” received the Best Paper Award at the ASEE Annual Conference and Exposition.

FY 2011 Publications/Presentations

1. Development of a Renewable Hydrogen Production and Fuel Cell Education Program presented at the 2009, 2010 and 2011 U.S. DOE Hydrogen Program and Vehicle Technologies Program Annual Merit Review and Peer Evaluation Meetings.

2. Blekhman, D., J. Keith, A. Sleiti, E. Cashman, P. Lehman, R. Engel, M. Mann, and H. Salehfar, 2010, "National Hydrogen and Fuel Cell Education Program Part I: Curriculum," ASEE Annual Conference & Exposition, Louisville, KY.

3. Blekhman, D., J. Keith, A. Sleiti, E. Cashman, P. Lehman, R. Engel, M. Mann, and H. Salehfar, 2010, "National Hydrogen and Fuel Cell Education Program Part II: Laboratory Practicum," ASEE Annual Conference & Exposition, Louisville, KY.

4. Goldade, J., T. Haagenson, H. Salehfar, and M. Mann, 2010, "Design of A Laboratory Experiment to Measure Fuel Cell Stack Efficiency and Load Response," ASEE Annual Conference & Exposition, Louisville, KY.

IX.14 H_2 Educate! Hydrogen Education for Middle Schools

Mary Spruill
The National Energy Education Development (NEED) Project
8408 Kao Circle
Manassas, VA 20110
Phone: (703) 257-1117
E-mail: mspruill@need.org

DOE Manager
GO: Reg Tyler
Phone: (720) 356-1805
E-mail: Reginald.Tyler@go.doe.gov

Contract Number: DE-FG36-04GO14278

Subcontractors:
- Sentech, Inc., Bethesda, MD
- Los Alamos National Laboratory, Los Alamos, NM

Project Start Date: August 1, 2004
Project End Date: October 31, 2011

Fiscal Year (FY) 2011 Objectives

- Collaborate to develop, design, and deliver a first-class, comprehensive middle school hydrogen education program that includes: training, classroom materials, technical and best-practices exchange, and evaluation.
- Design a program to link hydrogen science and technology and the concept of a hydrogen economy to the classroom.
- Educate the 4-12th grade audience about hydrogen and fuel cell technologies to facilitate market acceptance and understanding.

Technical Barriers

This project addresses the following barriers from the Education chapter of the 2009 Fuel Cell Technologies Multi-Year Program Plan:

(A) **Lack of Readily Available, Objective, and Technically Accurate Information**

As awareness of hydrogen increases with increased media activity and inclusion in many state and local energy plans, there continues to be a lack of information that is readily available, accurate, and objective. Many hydrogen advocacy groups have produced educational information that in some areas would be considered more public relations information than education. This project addresses the need for educational materials that are available, objective, and accurate. Based on NEED's core principle of delivery of objective energy information, the H_2 Educate materials are reviewed by subject matter experts, are made readily available via the Web, are delivered to educators at workshops, and are compared and contrasted with other hydrogen materials on a regular basis. This project's materials will continue to adapt as the need for additional and more robust materials becomes apparent.

(B) **Mixed Messages**

This project was created and continues with the intent to provide cornerstone materials that address misconceptions, provide clarity of information, and link to accurate and available information when necessary and possible. The hydrogen community continues to have disparate views on certain subjects and the key messaging to use. NEED, with review from DOE, national labs, and subject matter experts, works to provide this project with common, clear language and messaging that students, teachers, and their families find useful and appropriate for age and knowledge level. NEED works to mitigate the misinformation from the diverse messages and provide a concise message for the intended audience.

(C) **Disconnect between Hydrogen Information and Dissemination Networks**

NEED has capitalized on this disconnect and continues to work with various groups and organizations to become a stronger dissemination network – using local energy and education networks to deliver training and information about hydrogen to the intended audience. NEED – acting as a dissemination network – provides a conduit for valuable and accurate hydrogen information for the 4th–12th grade community. In addition, NEED has created its own information and dissemination network of 4th–12th grade educators and the education community to deliver quality hydrogen education materials and training.

(D) **Lack of Educated Trainers and Training Opportunities**

This project addresses the lack of educated trainers by providing professional development opportunities for teachers and energy professionals. These training opportunities provide participants with general background, foundation knowledge, and expansion information for more technically advanced audiences. NEED trains a network of trainers to deliver the information in local communities as well.

(E) **Regional Differences**

This project is adapted – in training methods and messaging – for local and regional differences – including proximity to hydrogen use and production. NEED's programming is locally based, with local needs – both economic and educational – considered as programs are created. Regional differences in attitudes are addressed and discussed in training programs. In

addition, regional access to hydrogen infrastructure is part of the program. Should hydrogen fueling stations, vehicles or fuel cells be nearby, the infrastructure is included in the programming.

(F) **Difficulty in Measuring Success**

The project is measuring knowledge gain among its target audience and finding good results. Educational programs often have longer term impacts that are not easily measurable in the course of a month or year. True attitude change takes a longer period of time than information gain. In all cases, educators report a minimum of a 40% knowledge increase in hydrogen knowledge upon completion of the H_2 Educate workshop. NEED is in the process of analyzing the results from a survey conducted of all educators who have participated in professional development since the beginning of the program to provide additional results for review.

Contribution to Achievement of DOE Education Milestones

This project contributes to achievement of the following DOE education milestones from the Education section of the 2009 Fuel Cell Technologies Program Multi-Year Research, Development and Demonstration Plan – Task Six: Facilitate Development and Expansion Hydrogen Technology Education for Middle and High Schools

- **Milestone 6.22**: Develop curriculum for middle schools (2Q, 2006)
- **Milestone 6.23**: Hold teacher workshops. (2Q, 2007 – 1Q, FY2012)
- **Milestone 6.24 and 25**: Revise curriculum materials (2008 and 2011)
- **Milestone 6.26 and 27**: Materials developed are in use in high schools and training is also provided to high school educators.

FY 2011 Accomplishments

- In 50% of the time estimated, the team created the middle school H_2 Educate learning module. In spite of resource constraints, the project is 100% complete with its revised scope and now is in replication and outreach to more communities. The project is scalable and can be deployed incrementally with additional resources.
- The effort has garnered additional support from a variety of partners – state energy offices, Clean Cities organizations, utilities, energy companies and others.
- Over 8,800 teachers trained.
- Training programs completed in 35 states with additional training in 2011 with extension of DOE funding.
- On average, pre-workshop survey scores were 5 out of 15 correct on the survey of hydrogen knowledge. After completing the workshop the average score was 13 out of 15 correct demonstrating a significant improvement in hydrogen knowledge as the result of the workshops.
- Preliminary survey results indicate that over 90 percent of survey participants felt that the resources made it possible to teach hydrogen more often and in more detail and that the materials increased student knowledge and understanding of hydrogen.



Introduction

In 2004, NEED and DOE launched the H_2 Educate Program for middle school and high school educators. The program included extensive curriculum development, hands-on kits for classrooms and teacher training. Using partner support from state energy offices, private industry, and trade associations, NEED extended the reach of the program to reach more teachers than originally planned.

Approach

The NEED Project brings its 30+ year history in energy education, curriculum development, teacher training, and networking efforts to H_2 Educate for middle school curriculum development, teacher training, and the expansion of hydrogen understanding and knowledge in classrooms throughout the country. NEED, with SENTECH, Inc. of Bethesda, Maryland as a key partner, launched a bold effort to exceed the DOE's expectations for a hydrogen education program in 2004 and have exceeded development calendar and outreach targets.

H_2 Educate and the activities undertaken as part of this project are the result of a collaborative effort among teachers, students, advisors, technical specialists, federal employees and professional educators. This effort brings together resources from NEED and its national partners and the DOE, to capitalize on success, resources, networking opportunities, and curriculum development and delivery capabilities. Key elements of this program are NEED's national network, a strong relationship with the National Association of State Energy Officials, and an annual budget capable of doubling the resources provided by this cooperative agreement. Making up this network are a conservatively estimated 65,000 classrooms touched by NEED materials and training each year.

Results

Results of the project continue to show success with pre-training survey results showing a 5 out of 15 correct successful response and a post-training survey result showing a 13 out of 15 correct successful response.

Workshop outreach expanded from six training programs and several hundred teachers trained in the first year of the program with over 8,800 teachers trained by 2011. NEED works to deliver the H_2 Educate curriculum

throughout the network of NEED schools and the schools they reach with educational outreach.

- Curriculum materials are available live on the NEED and DOE websites. Website statistics indicated substantial download activity. For example, hydrogen information has been added to the EIA Kid's Page www.eia.doe.gov/kids and statistics indicate 350,000 users per month.
- Addition of hydrogen information and activities to the Energy Information Association Kid's Page www.eia.doe.gov/kids (350,000 users per month).
- H_2 Educate materials have been included in NEED's curriculum redesign to provide a fresh, graphic look to the materials.
- Students and teachers show knowledge gain and deeper understanding of hydrogen knowledge.
- On post-workshop surveys, teachers indicate feeling prepared to teach the materials in their classrooms.
- Preliminary results from a survey of all educators that have participated in the program indicate that over 90 percent of educators had implroved hydrogen knowledge and were more aware of hydrogen technology after the unit.

Conclusions and Future Directions

H_2 Educate programs this year continued to expand the reach of the program to middle schools throughout the country. Additional outreach via state energy offices has allowed additional programs to be delivered outside of the programs within the DOE funding for this program. NEED continues to provide hydrogen materials through the National Energy Conference for Educators, the National Science Teachers Association annual conference and a number of state science conferences throughout the country.

The Virginia Department of Mines, Minerals and Energy and the Virginia General Assembly appropriated funding to provide teacher workshops and curriculum kits and materials to schools in Virginia in execution of the Virginia Hydrogen Roundtable recommendations.

Future Directions

- An H_2 Educate session will be hosted at NEED's National Energy Conferences for Educators in July 2011.
- H_2 Educate materials will be presented at 650 local teacher workshops.
- Work with other hydrogen partners to maximize reach of programs and materials – i.e. working with infrastructure grantees to provide educational resources.
- Continue incorporation of materials and programming into NEED's existing training initiatives.
- Annually update materials with new data and provide major changes to educational community.
- The addition of H_2 Educate website for materials, links and additional information.

Deliver maximum number of hands-on resources to classrooms leveraging resources to do so. Expand partnerships with infrastructure grant recipients to provide outreach and education programming to additional communities.

IX.15 Hydrogen Technology and Energy Curriculum (HyTEC)

Barbara Nagle
University of California, Berkeley
Lawrence Hall of Science #5200
1 Centennial Drive
Berkeley, CA 94720-5200
Phone: (510) 642-8718
E-mail: bnagle@berkeley.edu

DOE Manager
GO: Reg Tyler
Phone: (720) 356-1805
E-mail: Reginald.Tyler@go.doe.gov

Contract Number: DE-FG36-04-GO14277

Subcontractor:
Schatz Energy Research Center, Humboldt State University, Arcata, CA

Project Start Date: September 1, 2004
Project End Date: February 28, 2012

Fiscal Year (FY) 2011 Objectives

- Develop, field test, revise, publish, and complete a two-week curriculum module on hydrogen and fuel cells for high school students.
- Develop and implement a professional development plan for teachers who will use the materials.
- Develop a model for collaboration among school districts, informal science centers, university scientists, local transportation agencies, and other leaders in the field.
- Disseminate the materials to a broad national audience.
- Evaluate the quality and effectiveness of the curriculum materials and professional development strategies.

Technical Barriers

This project addresses the following technical barriers from the Education section (3.9.5) of the Fuel Cell Technologies Program Multi-Year Research, Development and Demonstration Plan:

(A) Lack of Readily Available, Objective, and Technically Accurate Information

(C) Disconnect Between Hydrogen Information and Dissemination Networks

(D) Lack of Educated Trainers and Training Opportunities

(E) Regional Differences

Contribution to Achievement of DOE Education Milestones

This project will contribute to achievement of the following DOE milestones from the Education section of the Fuel Cell Technologies Program Multi-Year Research, Development and Demonstration Plan:

- **Milestone 26**: Develop modules for high schools. (4Q, 2007)
- **Milestone 27**: Launch high school teacher professional development. (4Q, 2008 through 3Q, 2011)

FY 2011 Accomplishments

- Publication of the two-week high school curriculum that was the major goal of this project. The curriculum is titled "Investigating Alternative Energy: Hydrogen & Fuel Cells."
- Production of the kit that accompanies the module by LAB-AIDS, Inc.
- Redesign of the website that supports the curriculum.
- A two-day workshop for teacher professional development was held in February 2011.
- The materials were disseminated via 13 presentations to secondary science educators and hydrogen and fuel cell professionals and by display at the publisher's booth at many of these conferences.

✧ ✧ ✧ ✧ ✧

Introduction

This project is producing a curriculum module about hydrogen and fuel cells for high school students. A group of experienced science curriculum developers, teacher professional developers, leaders in the field of hydrogen and fuel cell technology and its application to transportation, and publishers of instructional materials are collaborating to develop and produce this curriculum as a commercial educational module. The module is intended to fit into high school courses such as physical science, chemistry, environmental science, and physics. In order to ensure that it can be used in these courses, the module addresses topics teachers usually teach and correlates to the National Science Education Standards and/or state and local standards. This project is also developing professional development workshops to prepare teachers to teach the curriculum and develop teacher leaders. Project evaluation focuses on evaluating the classroom usability of the curriculum module, students' progress toward the intended learning goals, and the effectiveness of the professional development workshops. The past years' work focused on completing, publishing,

and disseminating the curriculum module along with an equipment kit and support materials such as a digital video disk (DVD) and website.

Approach

The curriculum materials are developed and revised through a close collaboration between curriculum developers at the Lawrence Hall of Science (LHS), scientists and engineers at the Schatz Energy Research Center (SERC), experienced teacher associates, local and national field test teachers, and LAB-AIDS, Inc., an established publisher of kit-based science curriculum materials. The materials are developed by LHS with input from SERC, and classroom-tested by the developers, then by expert teachers, and finally by a broader group of teachers from local and national sites.

The module uses an issue-oriented approach to teaching concepts related to chemistry and energy topics. This approach teaches about hydrogen and fuel cells in the context of energy issues and current and future options for powering vehicles. This approach also demonstrates to students both the relevance of their science education to their lives and the role of scientists and engineers in conducting research and development to solve practical problems.

Teachers who field-test the curriculum receive two to three days of professional development prior to using the curriculum and have access to additional support as needed during the field test. The professional development workshops prepare the teachers with content background and hands-on experience for teaching the curriculum and for providing thorough feedback on the curriculum. In addition, these early professional development workshops for field-test teachers help to identify teacher leaders who will assist with dissemination and implementation of the published curriculum.

Dissemination is conducted by presentations and displays of the materials at science teacher education conferences and through the extensive networks of both LHS and LAB-AIDS, Inc.

Results

The curriculum module addresses Education technical barrier A (Lack of Readily Available, Objective, and Technically Accurate Information) by providing information about hydrogen and fuel cells in a curriculum format that is usable by teachers and students in typical classrooms. The development of the curriculum was led by the Science Education for Public Understanding Program (SEPUP), a curriculum development group that produces issue-oriented science materials that avoid advocacy. Prior to the work that took place in the past year, the module was developed through four rounds of classroom testing and revision to ensure that it works well in a wide variety of high school settings, thus addressing barrier E (Regional Differences). At each stage of development, scientists and engineers at SERC reviewed the module for scientific and technical accuracy. Work during the past year focused on collaborating with the publisher, LAB-AIDS, Inc., and the editorial and design studio they hired to prepare the materials for publication. This involved reviewing all edits and page layouts through several iterations, and reviewing the final art that was prepared to our specifications. It also involved photo research and acquisition.

The module includes a two-week sequence of six activities that teach students about hydrogen and fuel cells. The module cover is shown in Figure 1. This cover features a photograph of the student laboratory equipment, screen shots of a simulation from the website that accompanies the curriculum, and a photograph of a hydrogen fuel cell bus provided by AC Transit. The print materials are accompanied by a kit, which includes the materials featured on the cover along with additional materials required for the laboratory and modeling activities in the curriculum module. A website provides additional material used in the module, including 1) videos of hydrogen fuel cell applications, 2) interactive computer simulations of the hydrogen fuel

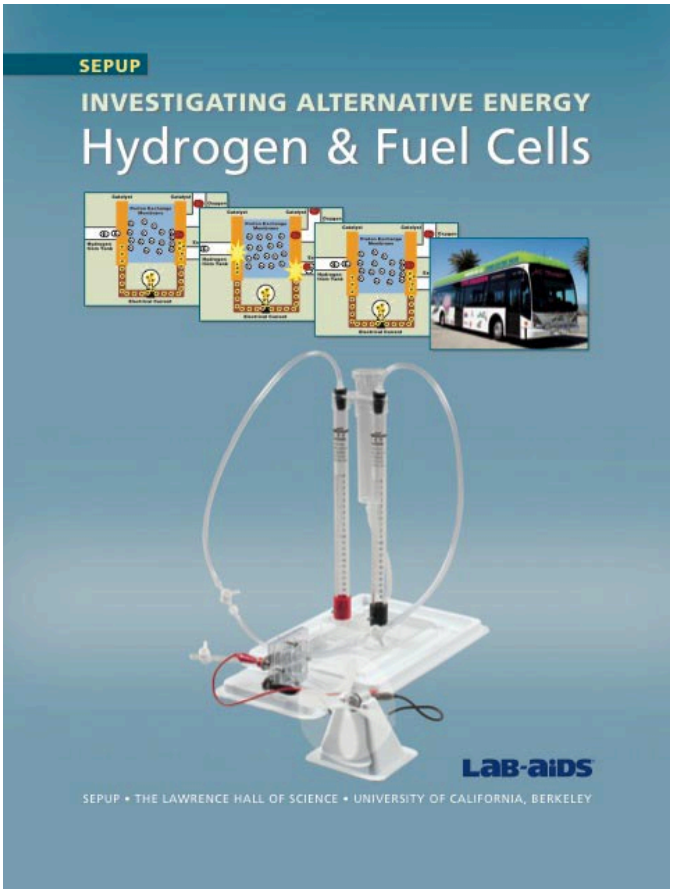


FIGURE 1. Cover of the Module – Investigating Alternative Energy: Hydrogen & Fuel Cells

cell reaction and the production of hydrogen in an alkaline electrolyzer, and 3) resources for the module's culminating activity. The video and simulations are also included on a DVD that is provided with the module, so teachers who have problems accessing the internet in their classrooms can use the DVD when teaching. The website also offers additional information about hydrogen and fuel cells for teachers, students, and the public. A pilot evaluation of student learning conducted with data collected from a sample of students during the module field-test yielded significant and educationally meaningful learning gains.

The professional development work addresses Education technical barriers C (Disconnect Between Hydrogen Information and Dissemination Networks) and D (Lack of Educated Trainers and Training Opportunities) by building on the dissemination networks of the LHS and partners and preparing teachers who will be able to provide professional development in their regions. Teachers receive professional development in the unit content, teaching approaches, science of hydrogen and fuel cells, and fuel cell applications. During the past year, one two-day professional development conference was held in Berkeley and attended by 13 teachers from Connecticut, northern and southern California, Ohio, South Carolina, and Texas. In an evaluation of the workshop, teachers gave very high ratings to all aspects of the workshop. Out of a possible high score of 5 points, teachers' average ratings were 4.73 for the curriculum, 5 for the activity presentations, and 4.85 in comparison with other professional development they have attended. Each participating teacher received a complete module and two sets of the classroom equipment.

Presentations at science teacher conferences reached over 220 teachers during the past year. These presentations targeted national and regional conferences plus conferences in states with significant fuel cell research and development and states known for good attendance at their science teacher conferences (see Figure 2). In these one to two-hour presentations, teachers were introduced to the module and information about fuel cells in the U.S. and their state,

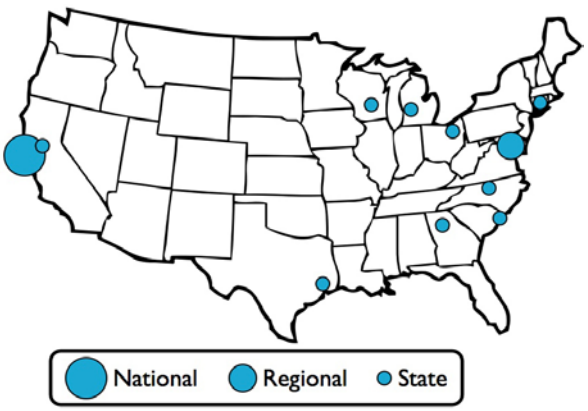


FIGURE 2. Locations of 2010–2011 Conference Presentations



FIGURE 3. Workshop at the National Science Teachers Association Convention, San Francisco, March 2011

and conducted an activity on the fuel cell reaction that they were then given to take back to their classrooms and try out. Figure 3 shows teachers at the National Science Teacher's Association Convention conducting part of Activity 4: Modeling the Fuel Cell Reaction.

Conclusions and Future Directions

Conclusions:

- The complete curriculum module and kit are now commercially available. They have been extensively tested by high school teachers working in a variety of science subject areas (chemistry, physics, physical science, integrated science, and advanced placement environmental science), in diverse settings, and with diverse student populations.
- A professional development workshop prepared 13 teachers to implement the module in their classrooms.
- Thirteen presentations at national, state, and regional teacher workshops reached over 220 teachers. Reactions to these workshops were positive.
- Evaluations of the curriculum and teacher professional development were highly positive.

Future work will focus on:

- Preparing additional teacher support materials for the project website, including video of how to use and care for the kit equipment.
- Collaborating with the publisher and other partners to disseminate the curriculum, develop teacher leaders, and support new users of the program.

FY 2011 Publications/Presentations

Publication

1. SEPUP. (2011). Investigating Alternative Energy: Hydrogen & Fuel Cells. The Lawrence Hall of Science, University of California, Berkeley. Published by Lab-Aids, Inc. Ronkonkoma, NY.

Presentations

1. Keller, C. "Alternative Energy for Transportation: Hydrogen and Fuel Cells." California Science Education Conference. October 22, 2010. Sacramento, CA.

2. Nagle, B. & Percoski, T. "Alternative Energy for Transportation: Hydrogen and Fuel Cells." Connecticut Science Education Conference. October 30, 2010. Hamden, Connecticut.

3. Nagle, B. "Alternative Energy for Transportation: Hydrogen and Fuel Cells." South Carolina Science Council (SC^2). November 4, 2010. Myrtle Beach, South Carolina.

4. Howarth, J. "Alternative Energy for Transportation: Hydrogen and Fuel Cells." North Carolina Science Teachers Association Professional Development Institute. November 11, 2010. Greensboro, North Carolina.

5. Lenz, L. "Teach Chemistry with Hydrogen Fuel Cells." NSTA Area Conference. November 11, 2010. Baltimore, Maryland.

6. Nagle, B. "Teach Chemistry with Hydrogen and Fuel Cells." Conference for the Advancement of Science Teaching (CAST) 2010. November 12, 2010. Houston, Texas.

7. Lenz, L. "Alternative Energy for Transportation Hydrogen Fuel Cells." Science Education Council of Ohio (SECO). February 12, 2011. Akron, Ohio.

8. Lenz, L. "Alternative Energy for Transportation: Hydrogen and Fuel Cells." Georgia Science Teacher's Association. February 18, 2011. Atlanta, Georgia.

9. Howarth, J. "Alternative Energy for Transportation: Hydrogen and Fuel Cells." Michigan Science Teachers Association. February 26, 2011. Grand Rapids, Michigan.

10. Zoellick, J. SEPUP Pathway Session: "Alternative Energy and Transportation: Hydrogen Fuel Cell and Other Bus Technologies." National Science Teachers Association. March 10, 2011. San Francisco, California.

11. Keller, C. "Teaching About Hydrogen Fuel Cells." National Science Teachers Association. March 12, 2011. San Francisco, California.

12. Willcox, M. "Alternative Energy for Transportation: The Chemistry of Hydrogen Fuel Cells." Wisconsin Society of Science Teachers Conference. March 18, 2011. Wisconsin Dells, Wisconsin.

13. Nagle, B., "HyTEC," FG36-04-GO14277, DOE Hydrogen Program and Vehicle Technologies Program Review, Arlington, VA, May 10, 2011. (http://www.hydrogen.energy.gov/annual_review11_edu.html)

14. Keller, C., and Nagle, B. "Hydrogen Technology and Energy Curriculum (HyTEC)." Workshop presented at the Chabot Space & Science Center's Climate Change Teacher Institute. June 27, 2011.

X. MARKET TRANSFORMATION

X.0 Market Transformation Activities

Introduction

The Market Transformation sub-program is conducting activities to help promote and implement commercial and pre-commercial hydrogen and fuel cell systems in real-world operating environments and to provide feedback to research programs, U.S. industry manufacturers, and potential technology users. One of the sub-program's goals is to achieve sufficient manufacturing volumes in emerging commercial applications that will enable cost reductions through economies of scale, which will help address the current high cost of fuel cells (currently the capital and installation costs of fuel cells are from five to six times higher than incumbent technologies[1]). These early market deployments will also address other market acceptance factors, resulting in further expansion of market opportunities.

Current key objectives of the Market Transformation sub-program are to build on past successes in material handling equipment, such as lift trucks, and emergency backup power applications that were part of the Recovery Act, by exploring potential and emerging applications for market viability. Fiscal Year (FY) 2011 activities were primarily focused on initiating 10 diverse projects, using FY 2010 appropriations. These projects are highly leveraged, with an average of more than half of the projects' funds being provided by DOE's partners. Partners providing resources to these projects have shown a high level of interest in exploring these applications and markets, and this level of industry interest is very promising for the potential growth of the domestic fuel cell industry.

Goals

Market Transformation activities provide financial and technical assistance for the use of hydrogen and fuel cell systems in early market applications, with the key goals of achieving sales volumes that will enable cost reductions through economies of scale, supporting the development of a domestic industry, and providing feedback to testing programs, manufacturers, and potential technology users.

Objectives[2]

- Advance the knowledge and expertise regarding the use of fuel cells for waste-to-energy systems, shipboard auxiliary power units (APUs), and aviation applications through targeted testing and evaluation efforts in coordination with the Technology Validation sub-program and in partnership with Department of Defense (DOD) and civilian agencies such as the Department of Agriculture and the Federal Aviation Administration by evaluating design requirements for aircraft APUs by 2012, shipboard APUs by 2013, and waste-to-energy fuel cells by 2014.
- By 2013, establish baseline energy efficiency and reliability performance metrics for commercially available emergency backup power, material handling, and light commercial/residential power fuel cell systems and provide feedback to component suppliers regarding cost reduction opportunities.
- By 2014, test emerging approaches to grid management using renewable hydrogen storage and fuel cell systems, in coordination with the DOE Office of Electricity Delivery and Energy Reliability.
- By 2015, develop and launch energy efficiency and reliability certification programs for fuel cells.
- By 2016, Identify lessons learned from existing policies and regulations and promote the development of effective and applicable incentives for hydrogen and fuel cell technologies.
- By 2020, enable capital equipment cost of fuel cell-powered lift trucks and emergency backup power systems to be on a par with conventional technologies.

FY 2011 Status

Fuel cells have been enjoying growing success in key early markets, particularly in material handling (e.g., forklift) and backup power applications. The Program's early market deployment efforts–including Market Transformation funding and Recovery Act funding–have successfully catalyzed a significant level of market

[1] *Catalog of CHP Technologies*, U.S. Environmental Protection Agency, December 2008, www.epa.gov/chp/basic/catalog.html.
[2] Note: Targets and milestones are under revision; therefore, individual progress reports may reference prior targets.

activity in these areas, which has been accompanied by substantial reductions in the price of fuel cells. The sub-program is actively pursuing additional opportunities for effective stimulation of market activity. Ongoing activities and additional areas of interest include the following:

- **Backup Power:** A joint effort has been initiated by DOD's U.S. Army Corps of Engineers and the Program to install 18 emergency backup power fuel cell systems at eight DOD locations. Data will be collected and analyzed during a five-year period of operation.
- **Hydrogen Bus Deployment:** The Program is continuing to support the deployment of hydrogen-powered internal combustion engine buses produced by Ford Motor Company. The buses are being used at national laboratories and federal facilities, for special events, campus tours, new employee orientations, and as part of shuttle bus fleets.
- **Combined Heat and Power (CHP) Feasibility Studies:** Eleven technical, site-specific feasibility studies have been completed. The resulting reports, which assess the installation and operation of distributed power or CHP fuel cells at DOE locations, have been provided to U.S. fuel cell manufacturers; discussions about specific siting and financing options are underway at several sites, including Los Alamos National Laboratory and the National Renewable Energy Laboratory.
- **Material Handling Equipment (MHE):** As a complement to the hydrogen fuel cell forklift deployments currently underway, the sub-program is investigating the use of direct methanol fuel cell (DMFC) technologies. DMFC MHE will provide the same operational benefits as hydrogen-powered fuel cell MHE, with significant additional benefits from the use of a liquid fuel, including reduced infrastructure costs, high energy density, and low overall fueling costs. Other activities involving hydrogen-fueled lift trucks are ongoing, including collaboration with the Defense Logistics Agency (DLA). The DLA's Eastern Distribution Center now has 55 fuel cell-powered lift trucks. Recent deployments of fuel cell-powered stand-up lift trucks have completed the portfolio of MHE classes that have been retrofitted, which could lead to the complete elimination of battery infrastructure at DOD sites that fully convert to fuel cell power for their MHE needs.
- **Mobile Lighting:** The sub-program is exploring the potential for expanded use of fuel cells for mobile lighting, which is commonly used for road maintenance, general construction, and large outdoor events. Unlike conventional diesel-based systems, fuel cells offer the benefits of nearly silent operation, with no harmful exhaust emissions. Working with manufacturers of fuel cells and mobile lighting equipment, the Program has supported the design, construction, and testing of fuel cell power mobile lighting prototypes (Sandia National Laboratories). Demonstration and testing was conducted at a Boeing Manufacturing Plant, NASA Kennedy Space Center, Caltrans, Paramount Pictures/Saunders Electric, and the San Francisco International Airport.
- **Market Analysis and Deployment Tools:** The sub-program continues to pursue opportunities for collaboration through the DOE-DOD memorandum of understanding, including two projects that have analyzed the technical feasibility of using fuel cells for auxiliary power onboard commercial passenger airliners, addressing both low-temperature polymer electrolyte membrane (PEM) fuel cells (Sandia National Laboratories), and high-temperature ceramic-type fuel cells (Pacific Northwest National Laboratory).
- **Micro CHP:** To document market viability of fuel cells for small facilities, the sub-program is working with fuel cell manufacturers and their partners to demonstrate CHP systems at several light commercial facilities. Baseline technical performance models have been established, the most competitive projects have been selected, and a final contract has been issued with ClearEdge Power to provide up to 38 fuel cells at up to 10 locations. A key objective of this work is to obtain performance data on these systems over the course of several years.
- **Green Communities:** The sub-program is working to help communities incorporate hydrogen and fuel cell technologies into their existing energy efficiency, sustainable energy, and greenhouse gas reduction plans. A decision-matrix tool has been developed and has been used to identify five community types as having high potential benefits for deployment of hydrogen and fuel cells. Actual communities will be selected through the Sources Sought and Request for Proposal processes. The sub-programs efforts in this area also include identifying opportunities for education and outreach to increase the public's awareness of hydrogen and fuel cell technologies.
- **Big Island of Hawaii Hydrogen Energy Storage Project:** In partnership with the Naval Research Laboratory and the University of Hawaii's Hawaii Natural Energy Institute, the sub-program is supporting

the demonstrattion of using a hydrogen energy storage system as a grid management tool. While hydrogen produced from the system could be used for a variety of value-added products, the initial phase of the project will use the hydrogen to fuel two Ford E-450 shuttle buses operated by the County of Hawaii Mass Transportation Agency.

- **South Carolina Landfill Gas Purification Project:** The sub-program is demonstrating the business case and technical viability of using landfill gas (LFG) as a source of renewable hydrogen production, using BMW's assembly plant in South Carolina as the host site. Should such a scale-up operation prove viable, it would represent a first-of-its-kind LFG-to-hydrogen production project in the nation, and it would serve as a model for future adoption of renewable biogas as a feedstock for hydrogen production.

FY 2011 Accomplishments

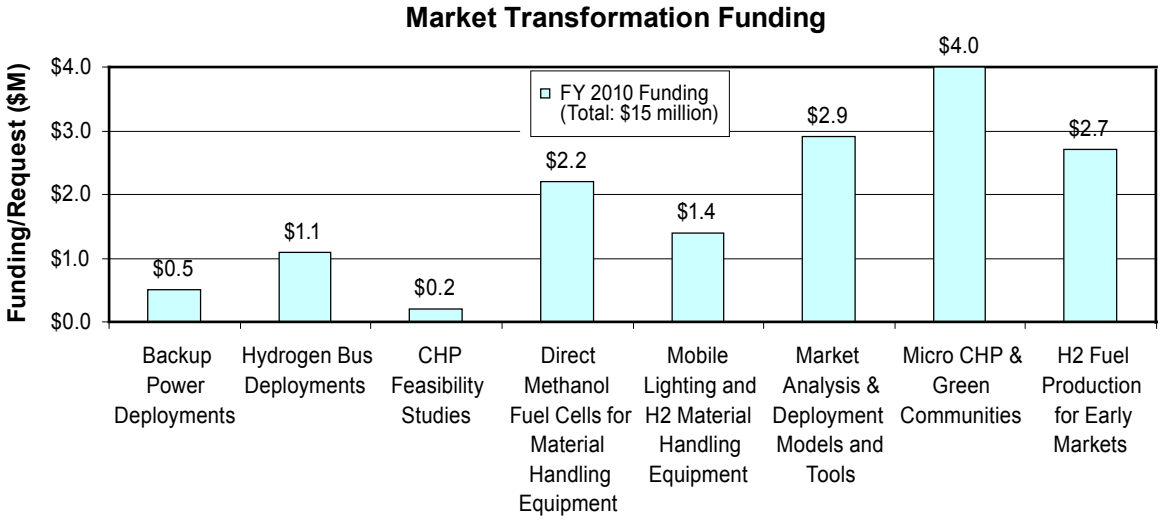
In FY 2011, the sub-program developed deployment tools and business cases for various fuel cell applications, conducted public outreach activities, and analyzed and tested potential new early markets in mobile lighting, DMFC-powered lift trucks, and auxiliary power. The following are some of the key milestones the sub-program achieved in FY 2011:

- Created a federal fuel cell user's forum for backup power fuel cells deployed at Army, Navy, NASA, and national laboratory sites.
- Completed design of a fuel cell mobile lighting system that combines high-pressure (5,000 psi) hydrogen storage, efficient plasma lighting, and a 5-kW PEM fuel cell; built five fuel cell mobile lights that are being field tested at industry and government installations; and expanded public awareness of the technology by using fuel cell mobile lighting at the 2011 Golden Globe Awards and 2011 Grammy Awards.
- Completed deployment and outreach activities for 22 hydrogen-powered buses at federal facilities and national laboratories. The buses were shown to thousands of attendees at several events such as the "Taste of Colorado" in Golden, Colorado; the Innovation for Green Advanced Transportation Excellence's National Energy Systems Technology Incubator opening in Livermore, California; the Southwest Region Fleet Transportation Regional Managers Conference in Camp Pendleton, California; "Expanding Your Horizons in Math and Science" in San Ramon, California; and at multiple Earth Day Celebrations in California, Hawaii, and South Carolina.
- Developed a decision matrix tool that highlights the most promising community types for hydrogen and fuel cell system deployment projects; and used this tool to rank 56 community types, with the top five identified as "high-potential" deployment sites for hydrogen and fuel cell systems.
- Published a business case for a utility with renewable resources, in which excess or "spilled" wind power is used to produce hydrogen via electrolysis for later use in fuel cell power generation; and updated utility energy storage model to include purchase of curtailed wind energy. A key conclusion is that hydrogen produced from un-dispatchable renewable power can be used for grid management and high-value products, such as transportation fuel.
- Developed overall system requirements, specifications, and a conceptual system design for a hydrogen energy storage system to be used as a grid management tool.
- Built, tested, and delivered 75 DMFCs to customer warehouse sites for use and testing in class-III material handling equipment.
- Completed a feasibility study of a LFG-to-hydrogen project. A key finding is that LFG-to-hydrogen production needs to be at a rate of more than 500 kg/day to be competitive with vendor-supplied hydrogen.
- For aircraft auxiliary power applications, analyzed the electrical system using a PEM fuel cell on a direct current bus that will reduce power conversion losses and reduce in-flight jet fuel consumption; obtained extensive information from Boeing on the 787 electrical system, including generation and distribution systems, load profiles, and fuel consumption. A key finding was that for some hotel power loads–such as galley and peak-power needs–the use of a PEM fuel cell APU could save up to 30% of the jet fuel these loads would normally consume (which would result in a reduction of 20,000 metric tons of CO_2 emissions annually, for a fleet of 1,000 airplanes).[3]

[3] Pratt, J. W., et al., "Proton Exchange Membrane Fuel Cells for Electrical Power Generation On-Board Commercial Airplanes," Sandia National Laboratories, May 2011, http://www1.eere.energy.gov/hydrogenandfuelcells/pdfs/pem_onboard_airplane.pdf.

Budget

No funding was requested for Market Transformation in FY 2011 or FY 2012. With the market successes that have been achieved by fuel cells in lift trucks and backup power applications as a result of FY 2009 and Recovery Act funding, the focus of FY 2010 funds was on new applications, such as micro CHP and mobile lighting applications.



FY 2012 Plans

In FY 2012, the sub-program will continue to document lessons learned associated with previously funded projects, including the strategies developed for market entry and for risk management with respect to safety, environmental, and siting requirements. Planning for business case analysis and case studies will be initiated. Collection and evaluation of data from these projects will provide the basis for verifying the business cases for various early market fuel cell systems, as well as providing an assessment of the performance of these integrated systems. Data will be made publicly available so that more customers will become aware of the benefits of integrated hydrogen and fuel cell systems. In addition, a near-term priority will be to continue collaborating with other federal agencies–in accordance with existing interagency cooperative agreements such as the DOE-DOD memorandum of understanding–to increase the use of fuel cells in market-ready applications and to increase awareness of the benefits of these deployments.

Pete Devlin
Market Transformation and Interagency Coordination Manager
Fuel Cell Technologies Program
Department of Energy
1000 Independence Ave., SW
Washington, D.C. 20585-0121
Phone: (202) 586-4905
E-mail: Peter.Devlin@ee.doe.gov

X.1 Fuel Cell Mobile Lighting

Lennie Klebanoff
Sandia National Laboratories
7011 East Avenue
Livermore, CA 94568
Phone: (925) 294-3471
E-mail: lekleba@sandia.gov

DOE Manager
HQ: Pete Devlin
Phone: (202) 586-4905
E-mail: Peter.Devlin@ee.doe.gov

Project Start Date: March 15, 2010
Project End Date: September 30, 2011

Fiscal Year (FY) 2011 Objectives

- Design a fuel cell mobile lighting system to replace current diesel-based systems.
- Organize a project development team that includes new technology holders, mass manufacturing partners and end users.
- Build five fuel cell mobile lights, field test with deployment partners.
- Design a commercial system, produce a commercially available product.
- Deploy the technology in high-profile events to increase public awareness of hydrogen fuel cell technology.

Technical Barriers

This project addresses the following technical barriers assigned to this project:

(A) System Weight and Volume
(B) Cost
(C) Efficiency

Technical Targets

- Promote exposure of public to H_2/fuel cells (trade shows, high profile events).
- Promote use of H_2/fuel cells in aviation (use at San Francisco International Airport [SFO], in Boeing manufacturing plant).
- Promote use of H_2/fuel cells in entertainment (use at Paramount Pictures, award shows).
- Promote use of H_2/fuel cells in construction (use with California Department of Transportation [Caltrans]).
- Promote use of H_2/fuel cells in high technology (use at National Aeronautics and Space Administration (NASA) Kennedy Space Center).

FY 2011 Accomplishments

- Designed a fuel cell mobile lighting system combining high pressure (5,000 psi) hydrogen storage, efficient plasma lighting and a 5 kW proton exchange membrane (PEM) fuel cell.
- Designed a hybrid fuel cell mobile light incorporating both high pressure (5,000 psi) hydrogen tankeage and a interstitial metal hydride tank.
- Organized a project development team that includes new technology holders, mass manufacturing and end users. The project team includes Multiquip Inc., Stray Light Optical Technology, SFO, Ovonic Hydrogen Systems, Altergy Systems, Golden State Energy, Caltrans, the California Fuel Cell Partnership (CaFCP), Lumenworks, Boeing, Luxim, and Saunders Electric.
- Built five fuel cell mobile lights, being field tested at Boeing Manufacturing Plant, NASA Kennedy Space Center, Caltrans, Paramount Pictures/Saunders Electric and at SFO.
- Promoted exposure of public to H_2/fuel cells (use of system at 2010 Oscars, 2011 Golden Globes, 2011 Grammy Awards and the 2011 Screen Actors Guild Award Show).
- Achieved a fuel cell mobile light that will run for 66 hours, with a greater than 73% reduction in greenhouse gas emissions (GHG) emissions compared to current technology. System is significantly quieter than current diesel technology
- Designed a commercial fuel cell mobile light system, now commercially available by Multiquip Inc. as the H_2LT system.



Introduction

The vast majority of mobile light-to-medium construction equipment is based on combustion of diesel fuel. Equipment examples include diesel-fueled mobile lighting towers, portable power generators, mobile water pumps and concrete-masonry equipment. Such equipment is commonly used for road maintenance, general construction and other industrial applications. As diesel-based systems, the current equipment technology suffers from well-known problems including release of toxic air contaminants and particles into the air (threatening human health), and also emission of CO_2 and other GHG

(contributing to global climate change). These diesel systems are also comparatively inefficient in their use of energy, as well as distractingly loud, which is a safety issue for those using them. The goal of this project has been to replace diesel-powered mobile lighting systems with clean, energy efficient new technology based on fuel cell power. Our goals in this project are not to perform a demonstration, but rather design, build, test and commercialize a fuel cell-based mobile lighting system that customers can buy to start reducing GHG and other criteria pollutants.

Approach

After an initial design of the fuel cell mobile light, we put together a development team comprised of new technology holders, mass manufacturing and end users. The project team includes the new technology holders Altergy Systems (PEM fuel cells), Luxim, Lumenworks and Stray Light Optical Technologies (plasma lighting), hydrogen systems storage and integration (Sandia) and metal hydride hydrogen storage (Ovonic Hydrogen Systems). The mass manufacturing partners are Multiquip Inc. (the largest manufacturer of rental construction equipment), Altergy Systems (mass manufacturer of PEM fuel cells) and Luxim, Stray Light Optical Technologies and Lumenworks (manufacturers and designers of plasma light technology). End users include the SFO, Caltrans, Boeing and Saunders Electric Inc. Golden State Energy made critical contributions to the development of the project team, and the CaFCP has been an important advisor on hydrogen refueling stations/technology, and on the current codes and standards associated with hydrogen fueling. Special thanks go to Paramount and NASA Kennedy Space Center who will also be deploying the technology.

Our work has been focused on designing, building, and deploying a fuel cell mobile light system to replace existing diesel-powered lighting towers commonly seen along highways in road maintenance work. After deploying the mobile light, the fuel cell technology is being proliferated into a newly created Multiquip Inc. fuel-cell-based product line called EarthSmart™.

Results

The first result was the design of a near-commercial "Beta" unit that improved the operating characteristics beyond the "Alpha" system that was built prior to DOE funding of the project. The Beta unit utilizes four commercially available 5,000 psi composite hydrogen tanks, along with eight plasma light fixtures (from Luxim, Stray Light Optical Technologies and Lumenworks). The 5 kW PEM fuel cell (Altergy) was incorporated, along with full "near-commercial" integration of the electronics for the fuel cell and lighting controls. The Beta system was designed by Sandia, Multiquip, Altergy and Stray Light Optical Technologies, with the system integrated by Multiquip in its Boise, Idaho manufacturing facility. It is worth noting that Multiquip had no prior manufacturing experience with high-pressure gas, fuel cells or hydrogen systems in general. Early on, a training class in high-pressure systems design, hydrogen safety, and hydrogen and fuel cell technology took place at Altergy Systems on November 14, 2010. Attendees included Multiquip manufacturing management and staff, along with other project partners.

Sandia felt that it was important for the project partners (especially Multiquip) to have some experience with metal hydride hydrogen storage technology. As a result, Sandia designed a hybrid fuel cell mobile light system that combines high-pressure storage with one metal hydride tank (from Ovonic). The design incorporates and accommodates thermal management issues that arise with metal hydride technology, namely heat needing to be supplied to the metal hydride material from fuel cell waste heat, and heat needing to be removed from the material when the metal hydride material is recharged with hydrogen. Construction of a hybrid unit will be complete by Sandia and Multiquip in August of 2011.

The first construction activity was an upgrade of the Alpha system that had been built prior to DOE funding. The upgrade of the system included a more commercial looking cabinet, and the introduction of weatherproof lighting housings. This upgrading allowed the Alpha system to be a field-deployable unit from which early learning could be gathered. The Alpha system was deployed at the NASA Kennedy Space Center in support of the last two shuttle launches. A picture of the Alpha system at the Kennedy Space Center is shown in Figure 1. Eventually the Alpha system at the NASA Kennedy Space Center will be replaced by a Beta system which has twice the endurance of the Alpha system, and more commercial integration of the fuel cell and lighting controls.

Endurance data on the Alpha system was collected by Sandia at its Livermore, California facility. Monitoring the power consumed by the lighting, hydrogen pressure, and the system endurance, results indicated that a commercial fuel cell mobile light using plasma light technology could last 66 hours on a single fueling. This is somewhat longer than the typically 50-hour duration of diesel-based systems. Using the test data, a PEM fuel cell efficiency of 47% was observed.

The first Beta fuel cell mobile light system was used to introduce the H_2 fuel cell mobile light to the power generation community at PowerGen 2010 in Orlando, Florida on December 13, 2010. The response was excellent from the power generation community particularly with regard to its quiet operation, and ability to be used indoors. The Beta system was also shown to the realm of construction equipment at the World of Concrete Show in Las Vegas, Nevada on January 17, 2011. At this show, the Beta fuel cell mobile light, now termed H_2LT (hydrogen light tower) as an official Multiquip product, received the prestigious 2011 Most Innovative Product Award, World of Concrete Editors Choice Award for General Tools and Equipment. A picture of the Beta unit from the World of Concrete Show is shown in Figure 2.



(Photo courtesy of Lennie Klebanoff Productions)

FIGURE 1. Deployment of Alpha Fuel Cell Mobile Light at the NASA Kennedy Space Center, 4/21/2011, Cape Canaveral Florida



(Photo Courtesy of Lennie Klebanoff Productions)

FIGURE 2. The Beta Fuel Cell Mobile Light at the World of Concrete Show, January 17, 2011, Las Vegas, Nevada

The second Beta unit was constructed and delivered to Caltrans on April 19, 2011. Caltrans, using its own internal resources, is having the H_2LT tested in a comprehensive series of tests conducted by the University of California, Davis (UC Davis) Advanced Highway Maintenance and Construction Technology Research Center. The California Highway Patrol is also participating in this characterization project. The UC Davis team is characterizing the performance of the H_2LT with regard to lighting efficacy (illumination uniformity, glare, and visibility), emissions (compared with diesel system), refueling efficacy (refueling time, ease of operation, costs) and design robustness (engineering analysis of performance, other testing). Caltrans will use its Beta system in its road construction work, graffiti removal work, as well as at a snow-chain checkpoint in the Sierra Mountains of Northern California to test its use in cold weather.

Boeing received its Beta unit in late July of 2011. The unit will be used at Boeing's Paine Field operations, as well as inside its aircraft manufacturing facility in Everett, Washington. The Paine Field operations will allow the unit to be tested against rain, sleet, and cold foggy conditions which are present at that location in the winter months. Similarly, the Hybrid Unit which will be deployed at SFO will be severely tested against the rain, wind, and fog present at that facility which often leads to very early rusting of equipment in use on the airfield. The Beta system which will be eventually deployed at the NASA Kennedy Space Center will be exposed to extreme heat, humidity and salty air at the Cape Canaveral Florida location. Finally, testing of the fuel cell mobile light with Saunders Electric and Paramount Pictures will assess its usefulness in the entertainment industry. In particular use of the unit for remote Paramount film shoots will allow Multiquip to assess the sound conditioning which is really required for the unit. Up until this point, units have not been sound conditioned in any way, yet the response from potential customers has been that the naturally quiet fuel cell technology is already remarkably better than noise from diesel-based systems. The project may attempt to sound condition a unit to see just how low the noise can be brought on the H_2LT technology.

The Alpha version of the fuel cell mobile light was used at the 2010 Academy Awards on March 7, 2010, at the invitation of Saunders Electric Inc. who provides all the portable power for the Oscars. For this event, the unit was used in the construction of the red carpet by construction



(Photo courtesy of the Academy of Motion Picture Arts and Sciences)

FIGURE 3. Use of the Alpha Fuel Cell Mobile Light at the 2010 Academy Awards, Red Carpet Construction, 3/6/2010



(Photo courtesy of Ron Roy Productions)

FIGURE 4. Use of the Alpha Fuel Cell Mobile Light at the 2011 Golden Globe Awards, Red Carpet Construction, January 16, 2011

crews of the Academy of Motion Picture Arts and Sciences, and used the day of the event to provide lighting and power at a security entrance to the red carpet. A picture from the Academy Awards red carpet preparations is shown in Figure 3. The upgraded Alpha was also used at the 2011 Golden Globe awards in Los Angeles California on January 16, 2011 for the red carpet construction, as shown in Figure 4. Saunders Electric also deployed the technology at the 2011 Screen Actors Guild Award show on January 30, 2011, and at the 2011 Grammy Awards on February 13, 2011.

Conclusions and Future Directions

The fuel cell mobile light project has allowed the design, construction, deployment and commercialization of the first fuel cell technology used in the construction equipment realm. The response from the construction, entertainment and power community has been excellent, with recognition of the project from a number of sources and use of the technology in a number of high-profile events. The H_2LT system is the first product in a newly formed EarthSmart™ product line from Multiquip Inc. Future directions for could involve the construction of fuel cell versions of other construction equipment, for example portable power generators, and air compressors used in construction.

Special Recognitions

1. 2011 DOE Hydrogen and Fuel Cells Program R&D Award, "In recognition of outstanding contributions to Fuel Cell Market Transformation Activities," for Fuel Cell Mobile Light Project, presented to Lennie Klebanoff, Sandia National Laboratories, May 11, 2011.

2. U.S. Congress Certificate of Special Recognition, 2011 Dream Makers and Risk Takers Award Winner, presented to Lennie Klebanoff and Terry Johnson (Sandia) "in recognition of outstanding and invaluable service to the community," for Fuel Cell Mobile Light Project, issued by John Garamendi, Member of U.S. Congress, March 29, 2011.

3. 2011 Dreamers and Risk Takers Technology Award, Livermore CA Chamber of Commerce, presented to Lennie Klebanoff and Terry Johnson (Sandia) for Fuel Cell Mobile Light Project, March 29 2011.

4. 2011 Most Innovative Product Award, World of Concrete Editors Choice Award for General Tools and Equipment, Fuel Cell Mobile Light (H_2LT), presented to Multiquip Inc.

5. 2010 Federal Laboratory Consortium Award "Mid-Continent Region" for "Notable Technological Achievement", Sandia National Laboratories, Fuel Cell Mobile Light Project, September 2010, presented to Lennie Klebanoff.

Sandia National Laboratories is a multi-program laboratory managed and operated by Sandia Corporation, a wholly owned subsidiary of Lockheed Martin Corporation, for the U.S. Department of Energy's National Nuclear Security Administration under contract DE-AC04-94AL85000.

X.2 Economic Analysis of Large-Scale Hydrogen Storage for Renewable Utility Applications

Susan Schoenung
Longitude 122 West, Inc.
885 Oak Grove Avenue, Suite 304
Menlo Park, CA 94025
Phone: (650) 329-0845
E-mail: susan.schoenung@sbcglobal.net

DOE Managers
HQ: Pete Devlin
Phone: (202) 586-4905
E-mail: Peter.Devlin@ee.doe.gov
SNL: Jay Keller
Phone: (925) 294-3316
E-mail: jokelle@sandia.gov

Contract Number: SNL 1024882

Project Start Date: May 2010
Project End Date: November 2011

Fiscal Year (FY) 2011 Objectives

- Model bulk hydrogen storage integrated with intermittent renewable energy production of hydrogen via electrolysis for utility applications.
- Determine cost-effective scale and design characteristics.
- Explore potential attractive business models.

Barriers

This project addresses the following barriers assigned to this project:

- Non-technical barriers to commercialization of hydrogen and fuel cells.
- Ensure continued technology utilization growth for domestically produced hydrogen and fuel cell systems.
- Enable greater penetration of clean renewable energy production while addressing the market for large-scale storage of hydrogen and hydrogen technologies.

FY 2011 Accomplishments

- Updated utility energy storage model to include purchase of curtailed wind energy.
- Updated costs for fuel cell and hydrogen systems and other storage technologies and compared. Other technologies are pumped hydro storage, compressed air energy storage, advanced lead-acid batteries, sodium sulfur batteries and flow batteries.
- Performed sensitivity analyses, primarily around the operating times and economic factors.
- Established a utility with renewables business case, in which excess, or "spilled" wind power is used to produce hydrogen via electrolysis. Large-scale storage stores the hydrogen for later use in fuel cell power generation. The excess power is used at no cost. In discussions with a number of utilities and grid operators, the case of excess wind for a period up to six hours was established for analysis.
- Made benefit/cost estimates based on the present value of costs and benefits, where benefit values are recently published in the utility energy storage literature.



Introduction

Previous work by this author [1,2] and others [3] has explored the potential use by the electric utility industry of hydrogen produced and stored in bulk. These studies show promise in some applications, especially where large scale is demanded and particularly in conjunction with intermittent energy resources such as wind.

The use of hydrogen will compete with other energy storage technologies, including modular systems, such as batteries, and other large-scale systems such as compressed air energy storage and pumped hydro storage. The major weakness in the hydrogen system is the relative inefficiency of energy conversion through the electrolysis and fuel cell subsystems. The major advantage is low storage cost and high volumetric energy density. The use of "spilled wind" presents an opportunity to install large scale hydrogen storage.

Approach

The approach to this work proceeds along the following steps:

- Assume a design concept in which energy storage is connected to an electric grid that includes power generation from wind. The storage system is charged from the grid and discharged back to the grid.
- Calculate the capital cost of the energy storage systems, dependent on the size of the storage system, i.e., the number of hours of stored energy for full power discharge. Cost assumptions for the hydrogen system components and other storage technologies are shown in Tables 1 and 2 [4,5].

TABLE 1. Cost and Efficiencies of Hydrogen Technologies in this Study

	Current Efficiency	Target Efficiency	Current Cost - Mid	Target Cost - Low
Electrolyzer	73.5%	75%	340 $/kW	125 $/kW
Gas Storage	Not Applicable	Not Applicable	15 $/kWh	2.5 $/kWh
Underground Storage	Not Applicable	Not Applicable	0.3 $/kWh	0.3 $/kWh
Fuel Cell	55%	58%	500 $/kW	100 $/kW

TABLE 2. Cost and Performance Assumptions for Energy Storage Technologies

Technology	Power Subsystem Cost $/kW	Energy Storage Subsystem Cost $/kWh	Round-Trip Efficiency %	Cycles
Advanced Lead-Acid Batteries (2,000 cycle life)	400	330	80	2,000
Sodium/Sulfur Batteries	350	350	75	3,000
Flow Batteries	400	400	70	3,000
Compressed Air Energy Storage	700	5	N/A (70)	25,000
Pumped Hydro	1,200	75	85	25,000

- Calculate the annual life cycle cost, including the costs of operations and maintenance, charging electricity, replacement costs, and capital charge.
- Convert to present value for comparison with benefits estimates from published literature.

Results

Results include comparison of annualized costs for energy storage technologies in "load-leveling" mode. This required an update of the energy storage cost model and the cost estimates for hydrogen systems and other technologies. The economic model was then modified for the "spilled wind" application. Figure 1 shows the comparison of hydrogen at medium and low hydrogen cost estimates with other technologies for the spilled wind case. If spilled wind is available free of charge for six hours each day (or night), the hydrogen approach is competitive with other technologies, even compressed air energy storage (CAES).

The present value of costs is compared with the present value of benefits estimated for electric utility value propositions. Figure 2 shows the present value (PV) of costs for load-leveling and spilled wind cases for medium and low-cost hydrogen systems on a $/kW basis, compared with the present value of benefits based on a study published by Sandia National Laboratories (SNL) for the DOE Energy Storage Systems program [5]. These results show a positive benefit/cost ratio if capacity credits are added to time-shift benefits.

Figure 3 shows the same comparison on a $/kWh basis, where benefits have been estimated by the Electric Power

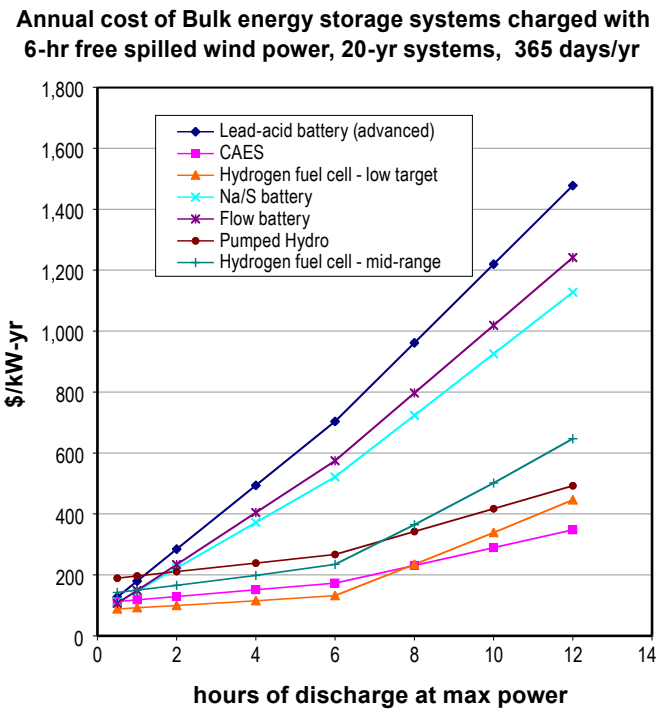


FIGURE 1. Annualized Cost of Energy Storage Systems for Spilled Wind Case

Research Institute (EPRI) [6]. In this case, the energy capacity credit is very large, so that even the medium cost system has a positive benefit/cost ratio. This represents an attractive opportunity for bulk hydrogen storage with wind.

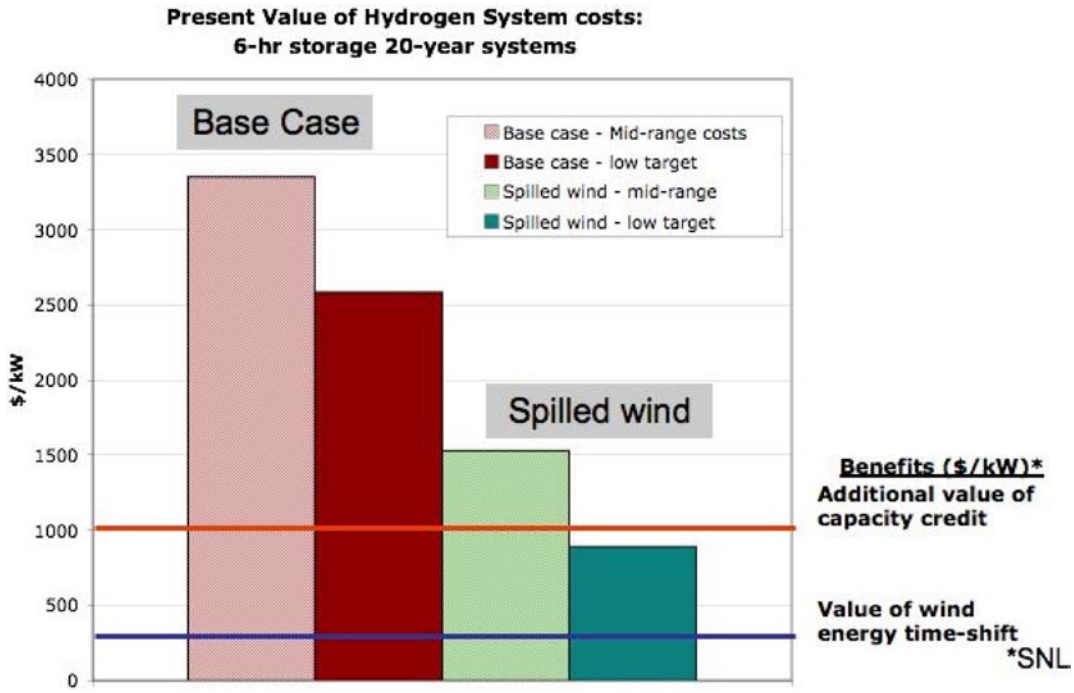


FIGURE 2. Present Value of Costs and Benefits on a $/kW Basis

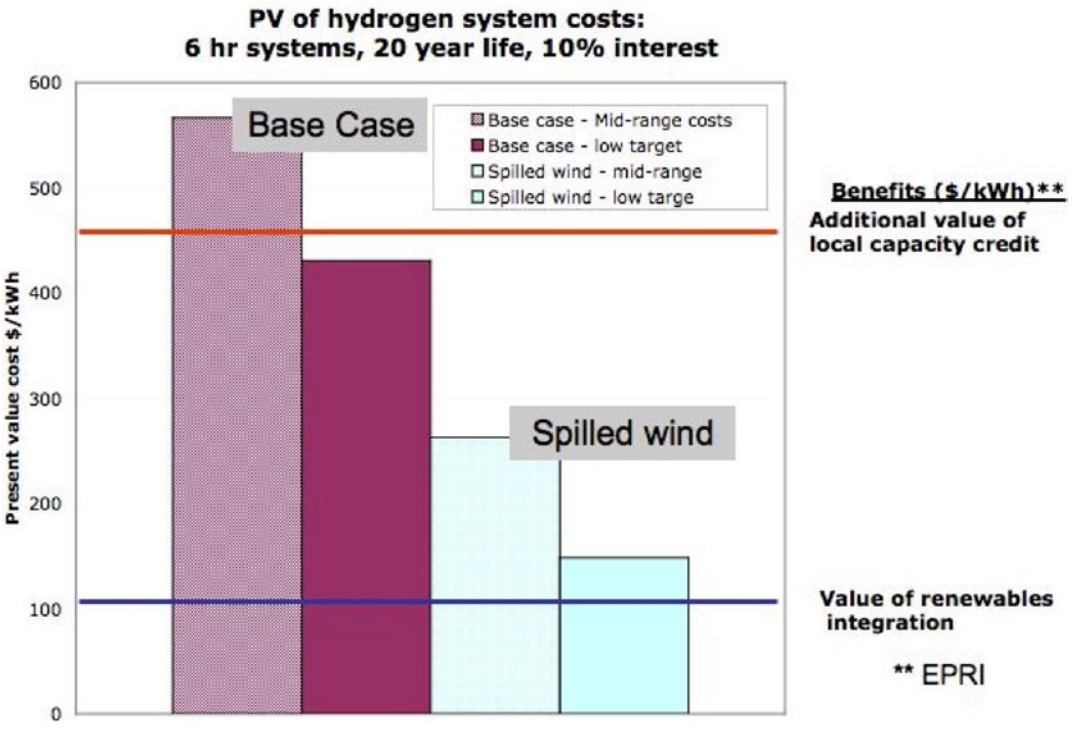


FIGURE 3. Present Value of Costs and Benefits on a $/kWh Basis

Conclusions and Future Directions

Some conclusions from this study include the following:

- Hydrogen energy storage is an ideal match for renewables of all scales, especially large-scale wind, and particularly when excess wind is available off-peak.
- Hydrogen with renewables is effective for reducing greenhouse gases from power generation.
- Underground storage offers opportunities to store hydrogen because it can provide high capacity at cost competitive rates.
- Market opportunities for bulk hydrogen storage need development.

Recommendations for further work include:

- Add scaling considerations to utility business model, considering the spectrum of value propositions, both at much large scale of storage, and smaller scale of storage.
- Add location considerations to cost and benefit analysis.
- Build third-party (non-utility) opportunities into business model.
- Continue discussions and deliberations with commercial interests, market potential.

FY 2011 Publications/Presentations

1. Eyer, Jim and Schoenung, Susan, "A comprehensive survey of utility-related storage: value propositions and technology," Electric Utility Consultants, Inc., *Electricity Storage: Business and Policy Drivers Conference*, 24–25 January 2011, Houston, TX.

2. Schoenung, Susan, "Economic Analysis of Large-Scale Hydrogen Storage for Renewable Utility Applications," *International Colloquium on Environmentally Preferred Advanced Generation*, sponsored by the National Fuel Cell Research Center, 8–10 February, 2011, Costa Mesa, CA.

3. Schoenung, Susan, "Economic Analysis of Large-Scale Hydrogen Storage for Renewable Utility Applications," *International Conference on Sustainable Energy Storage*, 22–24 February, 2011, Belfast, UK.

4. Schoenung, Susan, "Energy Storage – Emerging technology for climate change mitigation," a lecture at Stanford University, Department of Mechanical Engineering, March 2011.

5. Schoenung, S.M. *Economic Analysis of Large-Scale Hydrogen Storage for Renewable Utility Applications*. SAND2011-4845.

References

1. Schoenung, S.M. and Hassenzahl, W.V. *Long- vs. Short-term Energy Storage Technologies Analysis: A Life-Cycle Cost Study*. SAND2003-2783. 2003.

2. Schoenung, Susan and Eyer, James. *Benefit/Cost Framework for Evaluating Modular Energy Storage*. SAND2008-0978. 2008.

3. Steward, D. et al, *Lifecycle cost analysis of hydrogen versus other technologies for electrical energy storage*. NREL/TP-560-46719. 2009.

4. Schoenung, S.M., Energy Storage Systems Cost Update, SAND2011-2730, 2011.

5. Schoenung, S.M., *Economic Analysis of Large-Scale Hydrogen Storage for Renewable Utility Applications*. SAND2011-4845.

6. Eyer, J. and Cory, G., *Energy Storage for the Electricity Grid: Benefits and Market Potential Assessment Guide.*" SAND2010-0815. 2010.

7. *Electricity Energy Storage Technology Options: A White Paper Primer on Applications, Costs and Benefits.* EPRI. 12-23-2010.

X.3 Hydrogen Energy Systems as a Grid Management Tool

Richard (Rick) E. Rocheleau, Mitch Ewan
Hawaii Natural Energy Institute (HNEI)
University of Hawaii at Manoa
1680 East-West Road, POST 109
Honolulu, HI 96822
Phone: (808) 956-8346
E-mail: rochelea@hawaii.edu

DOE Manager
HQ: Pete Devlin
Phone: (202) 586-4905
E-mail: Peter.Devlin@ee.doe.gov

Naval Research Laboratory Technical Representative
Karen Swider-Lyons
Phone: (202) 404-3314
E-mail: karen.lyons@nrl.navy.mil

Project Start Date: September 30, 2010
Project End Date: September 29, 2012

Fiscal Year (FY) 2011 Objectives

- Demonstrate dynamic operation of electrolyzers as a grid management tool to mitigate the impacts of intermittent renewable energy on the grid.
- Characterize performance/durability of commercially available electrolyzers under dynamic load conditions.
- Provide hydrogen to fuel two Ford E-450 internal combustion engine shuttle buses for local community bus service operated by the County of Hawaii Mass Transit Agency.
- Conduct performance/cost analysis to identify benefits of integrated systems including grid services and off-grid revenue streams.

Technical Barriers

This project addresses the following technical barriers from the indicated sections of the April 2009 edition of the Fuel Cell Technologies Program Multi-Year Research, Development and Demonstration Plan:

Hydrogen Production, Section 3.1.4

(I) Grid Electricity Emissions

(J) Renewable Energy Generation Integration

(Q) Testing and Analysis

Technology Validation, Section 3.6.4

(H) Hydrogen from Renewable Resources

Hydrogen Safety, Section 3.8.4

(H) Lack of Hydrogen Knowledge by Authorities Having Jurisdiction

FY 2011 Accomplishments

- Developed overall system requirements and specification.
- Developed conceptual system design.
- Progressed legal agreements among project participants, including resolution of liability, indemnification, and insurance issues and requirements.
- Applied for additional funding from the State of Hawaii to augment DOE funding.
- Prepared and issued a request for proposal for the supply of the hydrogen system.
- Conducted a bidders' conference in Washington, D.C.
- Bids received and evaluated.
- Hydrogen system supplier selected.
- Initiated site design with infrastructure contractor.



Introduction

While solar and wind resources offer a major opportunity for supplying energy for electricity production and delivery systems, their variability and intermittency can raise significant interconnection challenges. At very high penetration levels, grid-operational issues caused by these renewable sources are a challenge and can lead to curtailment of the renewable resource, adding additional cost to the electricity supplied by these renewable resources. Hydrogen production through electrolysis may provide the means to mitigate curtailment and grid management costs by serving as a controllable load that varies in response to frequency signals from the grid. Such dynamic operation of the hydrogen production can provide the power producer or systems operator with increased options for coordinating system loads. The renewable hydrogen product can also create new revenue streams for the power producers through the sale of hydrogen products to customers outside of the electricity delivery system. Accordingly, hydrogen energy storage at a utility-scale offers the potential for increasing the levels of variable renewable energy that can be harnessed by the power producers or systems operators.

Approach

HNEI is using a four-step process to evaluate options to evolve the energy systems:

1. Develop and validate rigorous analytic models for electricity and transportation.
2. Develop and model scenarios for the deployment of new energy systems including additional renewables.
3. Identify and analyze mitigating technologies (demand side management, storage, Smart Grid, advanced controls, forecasting, future gen) including hydrogen production to address systems integration (grid stability) and institutional issues.
4. Conduct testing and evaluation to validate potential solutions to facilitate utility acceptance.

Under separate DOE and industry-funded efforts, HNEI has been conducting energy roadmapping and technology validation to identify economically viable technologies to transform island energy infrastructures. HNEI's subcontractor, General Electric (GE), developed two models of the Big Island grid utilizing GE's proprietary modeling technology. Transient performance was modeled using the GE Power Systems Load Flow software model:

- Full network model incorporating generator governors and automated generation control.
- Transient stability simulation looking at challenging times with fluctuating renewables to check transient stabilities.
- Long-term dynamic simulation.

A production cost model was developed using the GE Multi Area Production Simulation software model:

- Representation of dispatch and unit commitment rules.
- Hour-by-hour simulation of grid operations for a full year, taking into account ramp rates and dispatch rules; for example, minimum percentage load for baseload units.
- Model outputs include cumulative fuel usage, emissions, and variable cost.

Frequency variability due to wind fluctuation of the Big Island grid was used as the initial test of the model. The Big Island grid has the following characteristics:

- 100 to 200 MW with early evening peak
- 30 MW wind
- 30 MW unregulated geothermal
- Significant and growing photovoltaics

To explore the potential of the hydrogen energy storage opportunity, this project will evaluate the value proposition of using utility-scale electrolyzers to both regulate the grid and use excess electricity from renewables to make hydrogen for various products. In this initial phase of the project, an electrolyzer will be installed at the Puna Geothermal Ventures (PGV) geothermal plant on the Big Island. The electrolyzer will be operated in a dynamic mode designed to validate its ability to be ramped up and down to provide frequency regulation. Data will be collected to analyze the ability of the electrolyzer to ramp up and down, and to determine its durability and performance under these dynamic operating conditions. The hydrogen produced by the system will be used to fuel two hydrogen-fueled buses to be operated by the County of Hawaii bus company.

Future Directions

- The project is underway but equipment and infrastructure need to be installed and operated before any results can be evaluated.
- Future work involves the procurement, installation, and operation of the following:
  - Installing hydrogen production systems and infrastructure at the PGV geothermal site.
  - Installing hydrogen dispensing systems and infrastructure at the County of Hawaii Mass Transit Agency bus depot site in Hilo.
  - Procuring and operating two Ford E-450 shuttle buses.
  - Operating the electrolyzer and hydrogen systems at the PGV and County of Hawaii Mass Transit Agency sites.
  - Collecting and analyzing system performance data.
  - Preparing performance reports and sharing it with project sponsors and industry.
- If results show positive results, apply for a phase 2 follow-on project that increases the size of the electrolyzers.

FY 2011 Publications/Presentations

1. R. Rocheleau and M. Ewan, "*Hydrogen Energy Systems as a Grid Management Tool,*" *US DOE Annual Merit Review*, Washington, DC. May 2011.

2. R. Rocheleau, "Hawaii Hydrogen Energy Storage Project," Electric Storage Association 21st Annual Meeting, San Jose, CA, June 6–9, 2011.

X.4 Fuel Cell Combined Heat and Power Industrial Demonstration

Michael W. Rinker (Primary Contact),
Whitney G. Colella, Ryan J. Timme
Pacific Northwest National Laboratory (PNNL)
902 Battelle Blvd.
Richland, WA 99352
Phone: (509) 375-6623
E-mail: Mike.Rinker@pnnl.gov

DOE Manager
HQ: Pete Devlin
Phone: (202) 586-9995
E-mail: Peter.Devlin@ee.doe.gov

Contract Number: DE-AC05-76RL01830

Project Start Date: May, 2010
Project End Date: September, 2013

Fiscal Year (FY) 2011 Objectives

The overall objective of this project is:

- To demonstrate combined heat and power fuel cell (CHPFC) systems in small commercial facilities.
- Assess the system performance of the demonstration systems.
- Document market viability of this class of fuel cells for small commercial facilities.

This objective is being accomplished by working with commercial fuel cell manufacturers and their partners to manufacture and install CHPFC systems for application and demonstration at several small industrial facilities.

Technical Barriers

This project aims to address technical and economic issues preventing the full commercialization of fuel cell systems (FCSs). This includes:

- Lack of long-term validated performance data for 5 kilowatt electric (kWe) to 100 kWe FCS
- Energy performance
- Durability
- Reliability
- Installation, operations, and maintenance costs

FY 2011 Accomplishments

We established baseline technical performance models, down-selected the most competitive projects and issued a final contract with ClearEdge Power to provide up to 38 fuel cells at up to 10 partner locations centered primarily in California and Oregon.

- The PNNL team conducted site visits and telephone calls with many FCS manufacturers to gain insight from manufacturers prior to generating the request for proposal (RFP).
- We established an open dialog with manufacturers regarding overall requirements for the RFP through the Fuel Cell and Hydrogen Energy Association.
- PNNL finalized Technical Requirements and Evaluation Criteria documents in which the technical proposal was worth 60 percent of the points, and the cost proposal was worth 40 percent of the points.
- The RFP was released in December, and proposals were due in early February.
- We established models of FCS cost and technical performance which was part of the technical proposal submittal.
- Decision to negotiate award ClearEdge Power from Portland, Oregon in March.
- PNNL and ClearEdge signed a contract in late May, 2011.



Introduction

Research and development progress has paved the way for fuel cells to enter the commercial market in applications including stationary power generation and propulsion for vehicles. Accelerating fuel cell use in these key early markets will create jobs in an industry that needs high volume purchases to ramp up production, decrease costs, support commercialization, and enable a domestic supplier base. Early markets will also greatly expand the growth of green jobs with new opportunities associated with manufacturing fuel cells and related hydrogen technologies, fuel cell maintenance and support systems, and hydrogen production, delivery, and storage. In addition, the success of these early markets will help the fuel cell industry overcome a number of non-technical barriers that also face the broader marketplace, including the lack of practical user operating experience, the lack of user confidence, and the inherent resistance to new technologies.

As stated above, the objective of this project is to demonstrate CHPFC systems in small commercial facilities and assess their performance to help determine and document market viability. This information is important for the DOE, the fuel cell community, and most importantly for small commercial facilities that have power and heat requirements for their operations. PNNL is working with commercial fuel cell manufacturers and their partners to

manufacture and install CHPFC systems for application and demonstration at several small industrial facilities. It is also our objective to work with the fuel cell manufacturers and industrial partners to obtain performance data on these systems over the course of several years. The information that is gathered, analyzed, and documented during these demonstrations will be used to benefit and bolster the domestic supply base, increase user confidence, compete in the market place in terms of value provided, and provide favorable reduced lifecycle cost, energy, and emission savings compared to incumbent technologies (e.g., lead acid batteries, combustion engines, or power/heat generators) without tax incentives and with a reasonable chance of approaching parity through short-term technology or mass production improvements. In addition, it is expected that we will gather and analyze "real-world" data from units "in the customer's hands" to validate performance, durability and reliability; installation, operations, and maintenance costs; and identify remaining barriers to widespread commercialization.

Approach

Our approach to the deployment of CHPFCS at small industrial locations was based upon the notion that the manufacturers of fuel cells know their customers and would propose deployments at locations that would meet the requirements set forth by PNNL. In addition, our approach is to have PNNL monitor and analyze the performance data resulting in the development.

First, we established a baseline model input for cost and technical performance of the fuel cell systems in order to have a common basis in which to evaluation the systems that will eventually be deployed. Several key data packages were included in the input that was categorized into three areas:

- Engineering performance of the installed systems.
- Financial performance of the FCSs including FCS cost, and the breakdown of cost elements.
- Environmental performance of each deployment including feedstock energy source, greenhouse gas emissions, other pollutants, and end-of-life plans (recycle).

Next we set out to acquire the fuel cell systems for demonstration. The acquisition process was conducted through an open competition in which both U.S. and foreign companies were solicited for proposals. While foreign competition was encouraged, all of the deployments were required to occur in the U.S. We required that the manufactures and the end-user demonstration sites would team together for this acquisition. As such, the industrial team would serve as the integrator for each demonstration. Also, as part of the procurement process, we required a minimum 50% cost share from the fuel cell manufacturer and end-user team for each deployment.

After the fuel cell manufacturers and their industrial partners were selected, the fuel cells would be deployed at each of the end-user industrial sites. At that point, we will initiate the continuous monitoring key parameters of the systems. Key parameters that we are planning on remotely monitoring include:

- Instantaneous and cumulative power generation.
- Grid voltage at the inverter.
- Power that is utilized by the facility as well as power that is exported to the grid.
- Internal cabinet temperatures.
- Heating and cooling temperatures of water as well as the flow rates.
- Heat exchanger cooling fan speeds.
- Exhaust temperature.
- Fuel inlet flow rate and cumulative fuel use.
- Heat generation rate and cumulative heat generated.
- Cumulative system time on load.
- System availability.

The last step in our approach is to analyze and document the performance data collected over at least a two-year period of each fuel cell system deployed. These analyses will include recommendations on the technical performance, economic performance, and the environmental performance. Based upon this information, a case will be presented on the viability of this class of fuel cells for light industrial applications.

Results

At this early point in the project, a contract has been signed with ClearEdge Power in Hillsboro, Oregon to manufacture and deploy fuel cells in Southern California, Northern California, and Oregon. The process of fielding these systems is occurring during the third and fourth quarter of FY 2011, and when the systems are commissioned, data collection and analysis will be initiated. At the time of this report, there are no technical results of real time monitoring available, nor has any analysis been conducted.

Publications/Presentations

1. Colella, WG, RJ Timme. "Thermodynamic and Chemical Engineering Models of Combined Cooling, Heating, and Electric Power (CCHP) Fuel Cell Systems (FCSs) using Absorption Chillers." American Society of Mechanical Engineers (ASME) Journal of Fuel Cell Science and Technology, expected 2011.

2. Colella, WG, RJ Timme., "Chemical Engineering Models of Combined Cooling, Heating, and Electric Power (CCHP) Fuel Cell Systems (FCSs): Part B – Electric Chillers." ASME Journal of Fuel Cell Science and Technology, expected 2011.

3. Colella, WG, RJ Timme, J Brouwer, NS Sammes. "Fuel Cell Efficiency can Exceed 50% at Peak Power." Journal of Power

Sources, 2011, in print, manuscript can be seen at http://dx.doi.org/10.1016/j.jpowsour.2011.02.061.

4. Colella, WG, SH Schneider, DM Kammen, A Jhunjhunwala, N Teo. 2010. "Optimizing the Design and Deployment of Stationary Combined Heat And Power (CHP) Fuel Cell Systems (FCS) for Minimum Costs and Emissions – Model Design (Part I of II)." ASME Journal of Fuel Cell Science and Technology 8(2), DOI:10.1115/1.4001756. Available online at http://tinyurl.com/4l3bwto.

5. Colella, WG, SH Schneider, DM Kammen, A Jhunjhunwala, N Teo. 2010. "Optimizing the Design and Deployment of Stationary Combined Heat And Power (CHP) Fuel Cell Systems (FCS) for Minimum Costs and Emissions – Model Results (Part II of II)." ASME Journal of Fuel Cell Science and Technology 8(2), DOI:10.1115/1.4001757. Available online at http://tinyurl.com/4akey74.

Oral Conference Presentations

1. Colella WG, R Timme, M Rinker. 2011. "Fuel Cells for Commercial Buildings." European Fuel Cell Forum, Lucerne, Switzerland, July 1st, 2011.

2. Colella, WG, R Timme, M Rinker. 2011. "Deployment and Independent Monitoring of Stationary Combined Heat and Power (CHP) Fuel Cell Systems (FCSs) in Light Commercial Buildings." ASME 9th Fuel Cell Science, Engineering, and Technology Conference, Washington D.C., Aug. 7th-10th, 2011.

3. Colella, WG, R Timme, M Rinker. 2011. "Independent Testing of Micro-Combined Heat and Power (CHP) Fuel Cell Systems (FCSs)." ASME 2011 Energy Sustainability Conference, Washington D.C., Aug. 7th-10th, 2011.

4. Colella, WG, R Timme, M Rinker. 2011. "Fuel Cell Combined Heat and Power Industrial Demonstration." U.S. DOE Hydrogen and Fuel Cells Program and Vehicle Technologies Program Annual Merit Review and Peer Evaluation Meeting, May 10th, 2011.

Invited Presentations

1. Colella, WG., Timme, R., Rinker, M., Independent Monitoring and Analysis of Stationary Combined Heat and Power (CHP) Fuel Cell Systems (FCSs) Deployed in Light Commercial Buildings, École Polytechnique Fédérale de Lausanne (EPFL) Seminar, EPFL, Laboratoire d'énergétique industrielle, Lausanne, Switzerland, June 27th, 2011.

2. Colella, WG., Timme, R., Rinker, M., Deployment of Micro-Cogeneration Fuel Cell Systems (FCSs) in Commercial Buildings, E4Tech Seminar, E4Tech, Lausanne, Switzerland, July 4th, 2011.

3. Colella, WG, M Rinker, J Holladay, C Baker, Carl. 2010. Combined Heat and Power (CHP) and Combined Cooling Heating and Electric Power (CCHP) Fuel Cell Systems (FCSs) for Light Commercial Applications. ClearEdge Inc., Portland, OR, Nov. 23rd, 2010.

4. Colella, WG, M Rinker, J Holladay, C Baker. 2010. Fuel Cells for Commercial Buildings. Webinar-linked presentation between Pacific Northwest National Laboratory, Richland, WA and the Fuel Cell and Hydrogen Energy Association Power Generation Working Group, Nov. 16th, 2010.

X.5 Green Communities

John Lewis
National Renewable Energy Laboratory (NREL)
1617 Cole Blvd.
Golden, CO 80401
Phone: (303) 275-3021
E-mail: John.Lewis@nrel.gov

DOE Manager
HQ: Pete Devlin
Phone: (202) 586-4905
E-mail: Peter.Devlin@ee.doe.gov

Project Start Date: July 30, 2010
Project End Date: Project continuation and direction determined annually by DOE

Fiscal Year (FY) 2011 Objectives

NREL is fostering the integration of hydrogen and fuel cell technologies into communities to support the goals of energy efficiency, conservation, sustainability, renewable energy and reduced greenhouse gas (GHG) emissions. Our main tasks are to:

- Develop methods and techniques for identifying and evaluating candidate communities for suitable hydrogen and fuel cell technology projects.
- Assist communities in deploying and using hydrogen and fuel cell technologies in innovative integration projects with existing energy efficiency, conversation and renewable energy investments.
- Collect and report performance data, as well as lessons learned, on the hydrogen and fuel cell systems deployed into communities.
- Develop case studies that enable the replication of successful deployments to other similar communities.
- Develop and pursue community education and outreach opportunities for hydrogen and fuel cell systems.
- Build relationships with communities embracing hydrogen and fuel cell technologies. These relations will allow NREL to identify emerging community opportunities for the deployment of hydrogen and fuel cell systems in conjunction with renewable energy and energy efficiency projects.

Technical Barriers

This project addresses the following technical barriers relevant to the published sections of the Fuel Cell Technologies Program Multi-Year Research, Development and Demonstration Plan:

(A) Hydrogen from Renewable Resources
(B) Hydrogen and Electricity Co-Production
(C) Expanding Market Opportunities
(D) Technology Validation
(E) Education and Outreach

Technical Targets

The Market Transformation Activity does not develop new component technologies or sub-system configurations and, therefore, does not have technology targets. Instead, this subprogram assists in deploying technology systems developed within the other program elements.

FY 2011 Accomplishments

NREL has accomplished the following:

- Developed a decision matrix tool that highlights the most promising community types for hydrogen and fuel cell system deployment projects.
- Ranked 56 community types, using the decision matrix tool developed in this project, against a set of ranking criteria developed by DOE and NREL.
- Executed a Sources Sought effort that resulted in receiving responses from communities proposing to integrate hydrogen and fuel cell systems into their communities.
- Executed a request for proposals (RFP) effort that resulted in receiving formal proposals for community projects that integrate hydrogen and fuel cell systems with existing energy efficiency and renewable energy investments.



Introduction

NREL and DOE are supporting community usage of fuel cell and hydrogen technologies as part of an overall energy efficiency, conservation and renewable energy portfolio. This support includes assisting communities that have existing energy efficiency plans, GHG reduction plans, sustainable energy plans and the like in place to incorporate hydrogen and fuel cell technologies as another option to achieve energy savings and GHG reduction goals. This support also includes identifying opportunities for education and outreach to increase the public's awareness of hydrogen and fuel cell technologies.

Green communities can be thought of as residential, mixed-use, light commercial, municipal or state sites, as examples, that have made a documented commitment to mitigating their environmental impact (reducing their carbon footprint, increasing their energy efficiency,

decreasing their resource consumption rate, and installing renewable energy). This effort will help communities accomplish innovative projects that integrate hydrogen and fuel cell technologies with other complementary energy efficiency, conservation and renewable energy investments. DOE's Energy Efficiency and Conservation Block Grant (EECBG) Program included $3.2 billion in 2009 Recovery Act federal funds to deploy the least expensive, cleanest, and most reliable energy technologies available–energy efficiency and conservation–across the country. The goals of this investment were to: reduce fossil fuel emissions; reduce the total energy use of the eligible entities; improve energy efficiency in the transportation, building and other appropriate sectors; and create and retain jobs. This project complements this example investment and seeks to leverage the energy efficiency, conservation and renewable energy investments already made (by the EECBG program and others) in communities by identifying communities and potential projects for integrating hydrogen and fuel cell technologies into a community's existing energy efficiency and conservation plan. Integrating hydrogen and fuel cell technologies with energy efficiency, conservation and renewable energy technologies will contribute energy savings and environmental benefits to the community.

Approach

NREL applied the decision matrix tool developed in this project to assess the technical, environmental, economic and social benefits of integrating hydrogen and fuel cell systems into a community. NREL used a systems level approach to understand the project value to the community, as well as the potential for enabling the use of renewable energy. NREL used the following criteria in identifying and selecting candidate communities and deployment projects: innovation of project concept (40%), technical approach (35%) and ability to execute the project (25%).

Results

In order to assess the ability of the candidate community to successfully integrate hydrogen and fuel cell systems into its existing infrastructure, the decision matrix tool evaluates the community in 18 ranking criteria grouped into four categories. The four categories are: 1) technical considerations, 2) market potential, 3) project financials, and 4) opportunities for public outreach and learning. Critical elements for a successful community deployment of a hydrogen or fuel cell system include:

- Community adoption of plans and strategies for GHG reduction, energy efficiency, conservation, clean energy and renewable energy.
- Ability to articulate a hydrogen or fuel cell project that leverages and integrates the existing energy efficiency, conservation and renewable energy investments in the community.
- Ability to describe the value and benefit of a project to the community.
- Knowledge of and connections with the proposed hydrogen and fuel cell technology.
- Ability to conduct high profile public outreach and education activities that increase the public's awareness of hydrogen and fuel cell technologies.

Based on this initial analysis, five community types were identified as high potential deployment sites for hydrogen and fuel cell systems. The community types cited here are example profiles. Once subcontracts are executed with the actual communities identified through the Sources Sought and RFP processes, NREL will collect and analyze the resulting deployment data to build case studies and validate the predictive nature of the decision matrix tool.

Community 1: An off-grid community has just completed extensive energy efficiency, time of use and conservation studies followed by an implementation program that has resulted in a 40% reduction in energy consumption by the community. Now the community has adopted a plan to generate 80% of its remaining energy needs from clean energy sources. The analysis conducted to baseline the community's energy usage profile has also identified opportunities for leveraging clean energy sources available in the community. The analysis indicates that biogas from an anaerobic digester located in the community could be used to used to operate a fuel cell system that generates electrical power and high quality heat needed by the community. The low quality heat and exhaust gas (rich in carbon dioxide and moisture) from the fuel cell system could also be integrated with a community greenhouse used to produce fresh vegetables for this off-grid community throughout the year. The value of this project to the community is measured in terms of contributing to the community's clean energy plan, reducing GHG emissions and increasing local food production with a decreased carbon footprint.

Community 2: A technology campus has an environmental mandate to improve energy efficiency and reduce GHG emissions by 50%. Retrofitting the existing buildings with energy saving measures has resulted in a 30% reduction in energy consumption; however, more improvements are still required to satisfy the mandate. Additionally, this environmental mandate must be balanced with the business mission of the community, which requires continuous, reliable, high quality power. A proposed fuel cell system could provide continuous back-up power to critical business operations and protect this community from power grid failures that would result in economic losses. Additionally, analysis shows that the fuel cell system would contribute to satisfying the community's base electrical load requirements during normal power grid operation with improved energy efficiency and decreased GHG emissions relative to the grid supplied power. The value of this project to the community is measured in terms of increased

power security for the community's business mission, and contributing to the community's mandate for improved energy efficiency and reduced GHG emissions.

Community 3: A group of mixed-use buildings in an urban setting has banded together to form a community and implemented a district heating and cooling network based on an advanced hydronic loop system. This community has reduced their overall thermal energy requirements by 30% and reduced GHG emissions by 20% relative to their previous levels by implementing this technology. However, the community still has thermal and electrical energy needs that are not being met by on-site generators, and the community's sustainable energy plan calls for installing on-site generators that operate with greater energy efficiency and lower GHG emissions than power delivered via the grid from a coal-fired power plant. Analysis (supported in part by a DOE technical assistance program) indicates that a fuel cell cogeneration plant could provide sufficient electric power and heat to meet the community's requirements. The value of this project to the community is measured in terms of achieving energy efficiency and GHG emission goals adopted in the community's sustainable energy plan.

Community 4: A municipality has defined a plan for becoming a zero net energy community. The municipality has already leveraged federal funds and private foundation grants to greatly reduce community needs for vehicles, thermal and electrical energy. Renewable energy investments in the municipality are not capable of reliably meeting all of the community's energy requirements during peak consumption periods, even with the reduced demands resulting from the existing energy efficiency and conservation investments. The municipality has analyzed its energy consumption profile and identified a system capable of integrating with the existing renewable energy generators to produce hydrogen from renewable sources for use as an energy storage media. The community's plan for achieving net zero energy status includes the acquisition of a fleet of fuel cell-powered buses in the near future. In order to accommodate this future hydrogen demand, the system will be sized to produce sufficient hydrogen to fuel these buses. The value of this project to the community is measured in terms of achieving its goal of becoming a zero net energy community and reducing GHG/air emissions.

Community 5: A community with excess renewable energy production is forced to curtail production when the grid is saturated. Installation of an electrolyzer in the community would allow them to store and sell excess renewable energy production in the form of renewably produced hydrogen. The electrolyzer would generate a new revenue stream for the community by selling the excess hydrogen as fuel to a distribution warehouse located in the community with a fleet of fuel cell-powered material handling equipment. The value proposition for the community is justified by more fully utilizing existing renewable energy investments to shorten the financial payback period on these investments, and increasing revenue for the community. The use of renewable hydrogen by a local employer increases public awareness of hydrogen and fuel cell technologies, as well as providing a unique and valuable marketing tool for a business located within the community.

Analyzing the responses to the Sources Sought notice revealed the trends shown graphically in Figures 1 and 2. Figure 1 shows that slightly less than half (45%) of the responses were submitted by teams led by traditional communities (e.g. cities, municipalities, counties). Interestingly, this indicates some community awareness of hydrogen and fuel cell systems, and a willingness by community members to take ownership of these systems in their communities. The remaining responses (55%) were led by non-community entities. These non-community led responses were typically championed by commercial entities motivated by the opportunity for the sale of commercial product.

Figure 2 shows the breakdown of technology types proposed in the Sources Sought responses. Some of the responses incorporated multiple technologies, so each of the proposed technologies was accounted for separately in this analysis. The most common type of proposed technology in the Sources Sought responses was a stationary fuel cell for

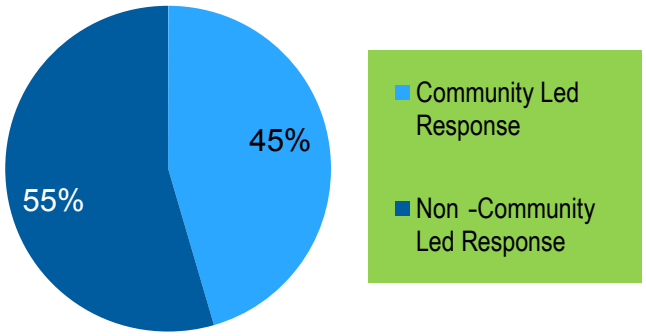


FIGURE 1. Of the Sources Sought responses received, 45% were community led responses while 55% were non-community led responses.

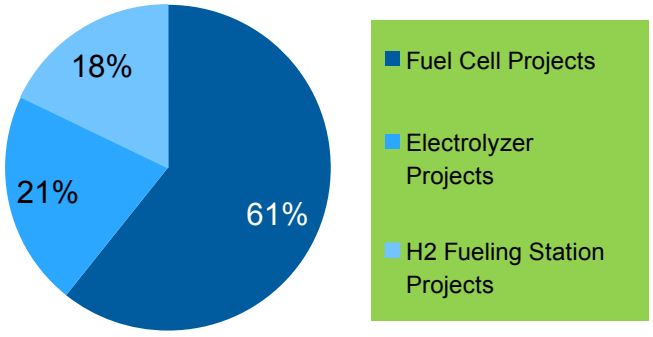


FIGURE 2. The breakdown of technology types proposed in the Sources Sought responses. Fuel cell projects were identified in 61% of the responses, followed by electrolyzer projects in 21% of the responses and hydrogen fueling station projects in 18% of the responses.

generation of electricity and heat, which was identified in 61% of the responses. The second most common proposed technology was an electrolyzer for splitting water into hydrogen and oxygen gases, typically utilizing electricity from a renewable energy source such as wind or solar. The third most common technology found in the Sources Sought responses was a hydrogen fueling station for dispensing hydrogen for transportation applications.

Future Direction

- Complete subcontract negotiations which will result in NREL awarding subcontracts to communities to assist them in achieving innovative integrations of hydrogen and fuel cell systems.
- Monitor the awarded subcontracts.
- Analyze operational data collected by the subcontracted communities. This analysis will include hydrogen and fuel cell system performance data, and will quantify how the project helped the community in progressing towards its sustainability and conservation goals.
- Build case studies from the successful deployment projects that will serve as precedence for similar communities to execute their own hydrogen and fuel cell projects.

FY 2011 Publications/Presentations

1. "A Methodology for Identifying and Modeling Candidate Communities for Distributed and Community Hydrogen," John Lewis, International Energy Agency – Hydrogen Implementation Agreement Task 29 Meeting, February 2011, Istanbul, Turkey.

2. "Hydrogen and Fuel Cell Systems for Agricultural Applications and Rural Communities," John Lewis, USDA Natural Resources Conservation Service Meeting, March, 2011, Denver, CO.

3. "Green Communities: A Methodology," John Lewis, 2011 Alliance for Sustainable Colorado Meeting, April, 2011, Denver, CO.

4. "Green Communities," John Lewis, 2011 Hydrogen and Fuel Cells and Vehicle Technologies Programs Annual Merit Review and Peer Evaluation Meeting, May, 2011, Washington, D.C.

5. "Green Communities: A Methodology," John Lewis, 2011 Colorado Renewable Energy Conference, June, 2011, Ft. Collins, CO.

X.6 Direct Methanol Fuel Cell Material Handling Equipment Demonstration

Todd Ramsden
National Renewable Energy Laboratory
1617 Cole Blvd.
Golden, CO 80401
Phone: (303) 275-3704
E-mail: Todd.Ramsden@nrel.gov

DOE Manager
HQ: Peter Devlin
Phone: (202) 586-4905
E-mail: Peter.Devlin@ee.doe.gov

Subcontractor:
Oorja Protonics, Inc., Fremont, CA

Project Start Date: June 1, 2010
Project End Date: December 30, 2012

Fiscal Year (FY) 2011 Objectives

- Deploy and test fuel cell-powered material handling equipment (MHE) using renewable liquid fuels (in particular, methanol).
- Compile operational data of direct methanol fuel cells (DMFCs) and validate their performance under real-world operating conditions.
- Provide an independent technology assessment that focuses on DMFC system performance, operation, and safety.
- Evaluate the business case and market viability of using DMFC technologies in material handling applications.
- In the longer term, help transform the market for the use of fuel cells in material handling applications.

Barriers

This project addresses non-technical issues that prevent full commercialization of fuel cells.

Technical Targets

No specific technical targets have been set.

FY 2011 Accomplishments

- Seventy-five DMFC systems were built, tested, and delivered to customer warehouse sites for real-world use and testing in Class III MHE (as of June 2011).
- DMFC systems underwent initial, beginning of life testing that will be used to provide a performance benchmark for the DMFC systems.
- Initial testing shows that DMFC systems used in Class III pallet jacks achieve 14 hours of operation on a single methanol fueling, compared to an average of less than 7 hours of autonomy for traditional battery-powered lifts.



Introduction

The National Renewable Energy Laboratory (NREL) and the U.S. Department of Energy (DOE) are interested in supporting the development of early market applications for fuel cell technologies. A study by Battelle Memorial Institute, "Identification and Characterization of Near-term Direct Hydrogen Proton Exchange Membrane Fuel Cell Markets," showed that fuel cells have the potential to power material handling equipment (also known generically as forklifts) at a lower overall cost than lead-acid batteries for certain types of operations [1]. Battery-powered forklifts typically use lead-acid batteries that can only provide enough power for one 8-hour shift. Multi-shift operations, therefore, generally require additional battery packs and battery change-outs, which reduces productivity and increases costs of operation.

DOE is currently demonstrating the potential benefits for hydrogen-fueled polymer electrolyte membrane (PEM) fuel cell-powered forklifts compared to 100% battery-powered forklifts. As a supplement to the hydrogen-fueled PEM fuel cell-powered forklift deployment testing, NREL is investigating the use of DMFC technologies in material handling applications. DMFCs, which use a liquid methanol fuel, hold promise to deliver many of the same operational benefits of hydrogen-powered fuel cell MHE, including long run times, short fueling times, and increased productivity. Liquid alcohol fuels such as methanol offer reduced infrastructure costs, high energy density, and low overall fueling costs. (See Table 1 for an overview of the benefits of using DMFCs in material handling applications.)

TABLE 1. Benefits of DMFC Power for MHE Compared to Batteries

Expected DMFC Benefits Over Battery MHE	
Longer run times between fueling/charging	Estimated 12-14 hours of autonomy on one fill.
Increased battery and lift reliability	Maintaining state-of-charge and eliminating deep discharge of batteries should extend battery life.
Increased productivity	Reduced need for fills (versus charging) and reduced time for fills (versus charging).
Lower greenhouse gas emissions	Compared to charging batteries using a typical electricity grid mix.
Low-cost infrastructure	Liquid alcohol fuels such as methanol offer low storage and dispensing costs.
Low cost of ownership	Productivity, reliability, and battery life gains expected to enable lower overall cost.

Approach

NREL has partnered with Oorja Protonics on a two-year project to demonstrate and evaluate DMFCs to provide power for MHE in four commercial wholesale distribution centers. In total, 75 DMFC-powered Class III pallet jacks have been deployed in warehouses operated by Unified Grocers, Testa Produce, and Earp Distribution. DMFC lifts are being operated two shifts per day for 15 months, with 5,000 total operational hours expected on each unit. The demonstration includes the use of renewable, bio-derived methanol to characterize the impact on DMFC systems of using renewable methanol fuel.

As part of the project, Oorja built, tested, and deployed pallet jacks using its OorjaPac Model 3 DMFC power pack, which delivers an output power of approximately 1.5 kW and includes a 12-liter methanol storage tank expected to provide 12-14 hours of autonomy between fuelings. Methanol fuel is being dispensed to the DMFC MHE using the OorjaRig methanol dispenser, which is designed to meet all relevant fire and safety codes for indoor methanol dispensing. Oorja is collecting data on both the DMFC systems and the supporting methanol fueling infrastructure. NREL is compiling and analyzing these data and is providing a third-party assessment on the performance of DMFCs used in material handling applications.

Results

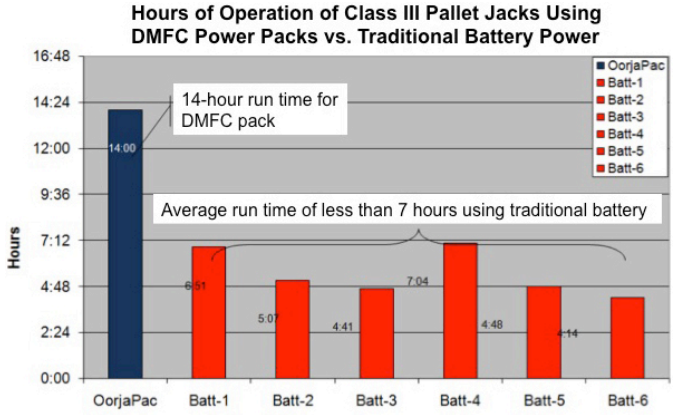
Until recently, the primary target use for DMFCs has been for portable power applications, particularly micropower applications. In FY 2011, NREL investigated companies developing DMFC systems that produced output power above 1 kW and were capable of powering Class III MHE. Based on this, NREL released a competitive request for proposals to demonstrate DMFCs to power MHE in commercial warehouse operations. In early 2011, NREL awarded a subcontract to Oorja Protonics to build, test, and deploy 75 DMFC-powered Class III pallet jacks in four commercial food warehousing and distribution centers.

The OorjaPac Model 3 DMFC power packs that are used in this deployment project act in concert with traditional MHE battery systems. Unlike traditional battery systems that have limited run time and require frequent battery changes and charging from the electricity grid, the OorjaPac DMFC system acts as an onboard battery charger, maintaining the battery pack state-of-charge and eliminating electric grid-based battery charging. Figure 1 shows the OorjaPac DMFC system, on its own (left), and integrated with a Class III pallet jack and its battery (right). Initial testing of these DMFC systems show that the OorjaPac needs to be fueled with methanol (with fills expected to take 1-2 minutes) after 14 hours of operation, compared to average run times of less than seven hours for traditional battery systems (see Figure 2). Initial testing using data loggers on operating pallet jacks showed the OorjaPac DMFC system maintained



Photo courtesy of Oorja Protonics

FIGURE 1. The OorjaPac Model 3 DMFC System



Run times come from a SSI data logger installed on a 24V pallet jack

FIGURE 2. Run Time for DMFC Class III MHE Compared to Battery-Powered MHE

a more consistent state-of-charge on the battery packs and avoided deep discharges of the batteries.

The specific configuration of the OorjaPac DMFC system was built to meet customer performance needs. To accomplish this, Oorja performed testing using data loggers of MHE at all four customer sites under this deployment project to benchmark the necessary performance. This information was used to determine the specific fuel cell count in the OorjaPac as well as the hybridization algorithms needed to provide sufficient performance and run times to meet customer needs. Based on this benchmark testing, Oorja built DMFC systems for use at all four demonstration sites. Prototype systems were tested on target customer Class III pallet jacks to ensure proper electrical and mechanical linkage, as well as proper safety, ergonomics, and counterbalance.

Individual DMFC systems underwent performance, reliability, and emissions testing. Beginning of life performance testing of the OorjaPac DMFC systems showed a maximum power output of 1.65 kW. Emissions testing at the anode and cathode sides of the DMFC pack showed overall carbon dioxide emissions to be well below OSHA limits of 200 ppm. Vibration table testing showed minimal impact on system performance from vibration.

Environmental testing showed that operation in higher temperature environments tended to lower overall system efficiency because of higher parasitic power requirements needed to maintain thermal balance. Improved system controls were developed to avoid any freezing of system components during lower temperature use.

Conclusions and Future Direction

- Seventy-five OorjaPac DMFC systems were built, tested, and delivered to customer warehouse sites for real-world use and testing (as of June 2011).
- DMFC systems underwent beginning of life testing that will be used to provide a performance benchmark for the systems.
- Data from these DMFC systems based on real-world use in providing power to Class III pallet jacks are being collected by Oorja and compiled by NREL.

In the next year, NREL will use real-world operating data to characterize the performance of DMFC systems used in material handing applications, including characterization of:

- Site Operations – hours of DMFC forklift use, amount of methanol dispensed, number of fueling events.
- Infrastructure Performance – average fueling time, average fueling rate, number of safety incidences, maintenance required.
- DMFC Performance – hours of operation between fuelings, hours of operation per gallon of methanol, average battery life, battery state-of-charge.

The analysis of real world data will be used to develop a total cost of ownership estimate of DMFC systems, including any productivity improvements, for comparison to battery MHE.

FY 2011 Publications/Presentations

1. Todd Ramsden, "Direct Methanol Fuel Cell Material Handling Equipment Demonstration," DOE Fuel Cell Technologies Program Annual Merit Review, May 10, 2011.

References

1. K. Mahadevan, et al., "Identification and Characterization of Near-Term Direct Hydrogen Proton Exchange Membrane Fuel Cell Markets," Battelle. April 2007.

X.7 Landfill Gas-to-Hydrogen

Shannon Baxter-Clemmons (Primary Contact), Russ Keller[1]
South Carolina Hydrogen Fuel Cell Alliance
PO Box 12302
Columbia, SC 29211
Phone: (803) 727-2897
E-mail: baxterclemmons@schydrogen.org; russ.keller@ati.org

DOE Managers
HQ: Pete Devlin
Phone: (202) 586-4905
E-mail: Peter.Devlin@ee.doe.gov
GO: Greg Kleen
Phone: (720) 356-1672
E-mail: Greg.Kleen@go.doe.gov

Contract Number: DE-FG36-08GO18113

Subcontractors:
- [1]Advanced Technology International, Charleston, SC
- Ameresco, Inc., Framingham, MA
- Gas Technology Institute, Des Plains, IL

Project Start Date: June 17, 2011
Project End Date: October 31, 2011

Fiscal Year (FY) 2011 Objectives

- Validate that a financially viable business case exists for a full-scale deployment of commercially available equipment capable of taking landfill gas (LFG) to hydrogen under the specific BMW operating environment.
- Validate that commercially available clean-up and reformation equipment can convert BMW's LFG to hydrogen at purity levels consistent with fuel cell industry standards.
- Conduct a side-by-side operational verification of fuel cell material handling equipment (MHE) performance and durability between a test group operating on LFG-supplied hydrogen and a control group operating on delivered hydrogen supplied by an industrial gas provider.

Technical Barriers

This project addresses the following technical barriers:

- Integration of individually-proven technologies into an unproven "end-to-end" solution.
- Unknown impact of long-term fuel cell performance when operating on LFG-derived hydrogen.

Technical Targets

- Months 1-3: Financial/business case feasibility.
- Months 4-10: Technical feasibility of producing fuel cell-quality hydrogen from LFG source.
- Months 11-17: Validate impact of LFG-derived hydrogen on fuel cell durability and compare it with fuel cell performance using hydrogen supplied by an industrial gas provider.



Approach

With the support of federal, state and private sponsors and stakeholders, the project will be conducted in three distinct phases:

- First, the project team would determine whether a viable business case exists that would permit recovering methane from the existing LFG source, converting it to hydrogen at large scale through an optimized capital equipment investment, and providing that hydrogen via a long term fee-for-services to the host site as the fueling source for its entire fleet of MHE.
- Should such a business case exist, the project next would validate the technical feasibility of taking the existing LFG stream that already has been filtered, dried and pre-treated sufficiently for use in gas turbine electrical generator sets, further cleaning and purifying it to remove the remaining trace contaminants, and then recovering the hydrogen using commercially available steam-methane reformer technology.
- As the final phase of this project, the hydrogen produced from the purified LFG source would be compressed, stored, and distributed to a single site within the host site manufacturing facility to permit a "side-by-side" performance evaluation using actual fuel cell-powered MHE. Hydrogen already available on-site from the contracted industrial gas provider would fuel the "control group" of MHE pieces; hydrogen produced from the pilot-scale LFG-to-hydrogen project would fuel the "test group" of MHE pieces. The performance evaluation would gather data for a period of six months from the control and test group fuel cells, and draw conclusions regarding the impact, if any, of the LFG source of hydrogen on fuel cell durability and maintenance requirements.

FY 2011 Accomplishments

Feasibility study (phase 1) began on June 17, 2011. Expected completion date is September 2011.

Future Directions

- "Go/No-Go" decision for proceeding with subsequent phases of the project will be made upon completion of the feasibility study. Based upon information already available to the project team, the likelihood of a finding of financial feasibility is high.
- Once financial feasibility has been confirmed, the project team will begin the technical feasibility portion of the project at pilot-scale (notionally 15 kilograms per day of hydrogen production).

FY 2011 Publications/Presentations

1. Presented project overview at Annual Merit Review (poster session) on May 10, 2011.

X.8 Incorporation of Two Ford H_2 ICE Buses into the Shuttle Bus Fleet

Bob Glass
Lawrence Livermore National Laboratory (LLNL)
7000 East Avenue
Livermore, CA 94550
Phone: (925) 423-7140
E-mail: glass3@llnl.gov

Lennie Klebanoff
Sandia National Laboratories (SNL)
7011 East Avenue
Livermore, CA 94568
Phone: (925) 294-3471
E-mail: lekleba@sandia.gov

DOE Manager
HQ: Pete Devlin
Phone: (202) 586-4905
E-mail: Peter.Devlin@ee.doe.gov

Project Start Date: July 1, 2010
Project End Date: September 30, 2011

Fiscal Year (FY) 2011 Objectives

- To promote the early market adoption of hydrogen technology.
- To displace diesel-fueled taxi vehicles at LLNL and SNL.
- To help promote public education on the benefits of hydrogen and fuel cell technology.

Technical Barriers

This project addresses the following technical barriers assigned to this project:

(A) Non-technical issues preventing full commercialization of hydrogen and fuel cell systems.
(B) Hydrogen storage.
(C) Lack of hydrogen refueling infrastructure performance and availability data.
(D) Maintenance and training facilities.

Technical Targets

- Promote the use of hydrogen technology to the public.
- Reduce diesel use at the LLNL and SNL sites.
- Gain extensive experience using H_2 buses by driving daily with high mileage use.

FY 2011 Accomplishments

- Worked with LLNL Operations and Business Offices/ Facilities and Infrastructure Directorate and its Sandia counterparts to permit mobile H_2 refueling station at LLNL and H_2 bus use at the LLNL/SNL facilities.
- Collaborated with Air Products and Chemicals to bring mobile H_2 refueler to LLNL.
- Instituted refueling training and H_2 bus operation for drivers.
- Worked through insurance issues associated with on-site refueling and public ridership.
- Instituted H_2 shuttle bus service for LLNL and SNL and have executed several community outreach activities.
- Established means to monitor ridership, refueling, and vehicle operations.



Introduction

As part of the "Walk the Talk" initiative within DOE, whereby the use of hydrogen technology in the DOE complex is increased, DOE has asked LLNL and SNL to establish and manage a hydrogen bus (taxi service) project servicing SNL and LLNL in Livermore, California. Ford has made available a number of hydrogen buses (internal combustion engine [ICE], with high pressure storage of hydrogen) that seat 12 people, plus driver (or 7 plus one wheelchair and driver), have a range of 150 miles, and on-board storage of 30 kg of hydrogen at 5,000 psi. These vehicles achieve near-zero regulated emissions (below Super Ultra Low Emission Vehicle regulation for oxides of nitrogen) and no CO_2 emissions. In the past year, SNL and LLNL have partnered to lease two buses (one year lease) for the demonstration project. The buses have been serving the local LLNL/SNL staff community. They directly replaced two diesel buses that were in use, thereby achieving reductions in diesel emissions at the two sites.

The purpose of this project is to demonstrate hydrogen technologies and educate the community. As part of the community outreach goals, we have engaged the broader Tri-Valley area (cities of Livermore, Dublin, Pleasanton, San Ramon) and others on event support using the H_2 buses. We have also initiated educational activities with nearby Las Positas College. We also plan to coordinate with the Livermore community public transportation companies to enhance operations.

Approach

Our approach to this project was as follows. Prior to receiving the buses, extensive discussions were carried

out with LLNL and SNL facilities management, and with the LLNL Site Manager for the Nuclear National Security Administration to secure "buy-in" for the project. With the project receiving strong acceptance and support, we leased the H_2 buses from the Ford Motor Company, followed by an initial certification of them in collaboration with Ford maintenance staff. During this certification phase, we designed appealing "wraps" for the bus to bring attention to their H_2 technology (Figure 1). There are no hydrogen stations currently operating in the Tri-Valley area, so we had to establish a mobile refueling station at the LLNL site using an Air Products Mobile Refueler, shown in Figure 2.

With reliable fueling established, the buses were integrated into the LLNL/Sandia taxi service, replacing two buses that were operated on diesel fuel. Thus, use of the H_2 buses led to a decrease in diesel fuel use at the two laboratories. Furthermore, the H_2 buses were used for educating the local public on the benefits of hydrogen and fuel cell technology. We managed frequent maintenance problems that arose with the buses, these problems being unrelated to the hydrogen technology (except for the need to replace a sensor, with the failure being detected with on-board diagnostics), and many involved traditional bus mechanical systems.



FIGURE 1. Final Design of "Wrap" for Bus



FIGURE 2. Air Products Mobile Refueler Servicing the Two H_2 Buses

Results

In November of 2010, the two H_2 buses were integrated into the LLNL/SNL fleet. The buses travel all over the LLNL and SNL sites, as well as to the local commuter train station, picking up LLNL and SNL employees and transporting them to our campuses. The typical ridership per shuttle bus is ~80-100 passengers/day with each H_2 bus traveling ~80-100 miles each day. The H_2 buses are "topped off" with hydrogen each day with ~13 kg of hydrogen. We have put on 8,757 miles on the buses in approximately six months of operation (up to June 30, 2011). The average number of miles driven by each bus is 730 miles per month. With regard to a fuel comparison, the average number of gallons of diesel used on our previous buses is 168 gallons per month (per bus), so that is our savings. It is our understanding that this level of use is among the highest for DOE facilities using such buses.

Both buses found extensive use in a number of community outreach activities. Two of these are described in a little more detail here. The first community event was a joint SNL/LLNL Celebration of Hydrogen Technology in downtown Livermore on February 22, 2011. This event was organized by the project and LLNL and SNL protocol and public relations personnel. Approximately 70 members of the public, media, local dignitaries and LLNL and SNL management and staff were on hand to see the two H_2 buses, along with the H_2 Fuel Cell Mobile Light, the cryo-compressed hydrogen vehicle from LLNL, and a number of posters on hydrogen research and development being conducted at the labs. Speakers included:

1. Ron Cochrane, Executive Officer from LLNL and Bob Carling, Director of the Transportation Energy Center from SNL.
2. John Garbak, DOE Technology Development Manager
3. John Marchand, Vice Mayor, City of Livermore
4. Alice Williams, Nuclear National Security Administration Site Manager

KPIX television (San Francisco) broadcast video from the celebration on their evening news, and press from two local newspapers attended as well. Representation from Congressmen Garamendi's and McNerney's offices and California State Assembly member Joan Buchanan were also in attendance. A picture from the event is shown in Figure 3. The public were given rides on the buses, and had a chance to talk with LLNL and SNL staff scientists about the hydrogen technology depicted in the posters.

In another community outreach event one of the H_2 buses was on display at the Expanding Your Horizons conference on Saturday February 26, 2011 at the Diablo Valley Community College, San Ramon campus, with rides given to attendees. The Expanding Your Horizons conference serves to:



FIGURE 3. Celebration of Hydrogen Technology in Downtown Livermore, February 22, 2011



FIGURE 4. Students attending the the Expanding Your Horizons conference on Saturday February 26, 2011 at the Diablo Valley Community College, San Ramon campus, on-board the H_2 Bus.

- Increase the interest of young women in math and science through positive hands-on experience (over 300 present).
- Foster awareness in math- and science-related careers.
- Provide young women with opportunities to meet and interact with positive role models who are active in math- and science-related careers.

A picture of Expanding Your Horizons attendees in the H_2 bus is shown in Figure 4.

Other outreach events include the John Muir Birthday-Earth Day Celebration in Martinez, California on April 16, 2011. This event provided a shuttle service from the parking area to the event main gate. Over 1,000 people attended this event. In addition, lectures were given on hydrogen technology (fuel cells, hydrogen storage, H_2 bus, H_2 mobile light) to an environmental science class at Las Positas Community College in Livermore on April 12, 2011. One of the buses was also used at the SNL "Take Your Sons and Daughters to Work Day" on April 28, 2011. The buses were on display at the Bay Area American Chemical Society meeting in Oakland, California on April 30, 2011. The buses were also highlighted at the LLNL internal safety fair on June 22, 2011. Finally, the buses were on display at the opening of the Innovation for the Green Advanced Transportation Center in Livermore which is located near the laboratories on June 30, 2011. The opening was attended by 300 people, including Congressman John Garamendi. At all of these events we handed out brochures that explain the DOE Hydrogen Market Transformation sub-program and information about the buses. We were on hand to answer questions about the buses.

Conclusions and Future Directions

Two Ford H_2 buses were successfully integrated in the LLNL/SNL taxi fleet, and have been extensively used for transporting laboratory staff within the LLNL/SNL campuses, and also to a local commuter rail stop. To our knowledge, the LLNL/SNL buses have received the most use (highest number of miles driven, greatest number of refuelings) of any H_2 bus effort in the DOE program. Use is ongoing at this time. Future activities associated with the H_2 buses, until the end of FY 2011, include:

- Monitoring shuttle bus mileage, ridership, and vehicle operation.
- Maintaining the vehicles in collaboration with Ford.
- Conduct community outreach events.
- Curriculum development with Las Positas College and high school demonstrations.
- Annual Community Festivals/Antique Automobile Shows/farmers markets.

X.9 PEM Fuel Cell Systems for Commercial Airplane Systems Power

Lennie Klebanoff (Primary Contact), Joseph W. Pratt, Karina Munoz-Ramos, Abbas A. Akhil, Dita B. Curgus, and Benjamin L. Schenkman
Sandia National Laboratories
PO Box 969, MS-9161
Livermore, CA 94551-0969
Phone: (925) 294-3471
E-mail: lekleba@sandia.gov

DOE Manager
HQ: Pete Devlin
Phone: (202) 586-4905
E-mail: Peter.Devlin@ee.doe.gov

Project Start Date: July 1, 2010
Project End Date: March 31, 2011

Fiscal Year (FY) 2011 Objectives

- Determine feasibility of implementing a proton exchange membrane (PEM) fuel cell on-board a commercial airplane.
- Quantify the performance benefit (or penalty) of such a fuel cell system.
- Understand the impact of the fuel cell on the existing electrical distribution system.

Technical Barriers

This project addresses the following technical barriers:

(A) System Weight and Volume
(B) Cost
(C) Efficiency

Technical Targets

Our project determines the PEM fuel cell applications and configurations that have the lowest volume and mass, and the configurations that lead to the highest energy efficiencies for aircraft use. Cost is addressed indirectly: the results of this project may make it easier for airplane companies to incorporate fuel cells into their designs, thus increasing the quantities of fuel cells manufactured and leading to lower per-unit costs.

FY 2011 Accomplishments

- Feasibility: Found that it is technically feasible to install and operate a PEM fuel cell system on-board a commercial airplane.
- Performance Impact: Found that, in some scenarios, using an on-board PEM fuel cell system could decrease the amount of jet fuel needed to generate electricity by over 30%. The amount of CO_2 that could be avoided by a fleet of PEM fuel cell-equipped airplanes could be over 20,000 metric tons per year (assuming renewable hydrogen is used to power the fuel cell). However, this benefit is not reachable using current fuel cell and hydrogen storage technology but rather requires DOE-target (2015) technology for both hydrogen storage and PEM fuel cells.
- Electrical System: Discovered that the addition of a fuel cell system does not adversely affect the existing electrical system, and in fact can provide a faster transient response that current aircraft generators that operate off of engine shaft power.



Introduction

Fuel cells have become increasingly important as alternative sources of power, offering the potential for drastic reduction in emissions in particulate matter (PM), nitrogen oxides (NO_x), and CO_2. In addition, they offer exceptionally quiet operation, highly efficient use of the fuel energy, and a high energy storage density compared to batteries. For a number of years, the manufacturers of commercial aircraft, most notably Boeing and Airbus, have realized that fuel cells may offer advantages for commercial aircraft operation. Apart from the emissions reductions and thermal efficiency referenced above, they can constitute distributed power systems, enabling locating the power near the point of use and also reducing the power draw from the engines.

The real question is if fuel cells offer operational advantages over traditional power in systems that are used routinely in flight, for example galley power, in-flight entertainment, and to provide additional power to the aircraft electrical grid when "peaker" power is needed. This interest in the use of fuel cells is timely, as the electrical needs on-board aircraft are going up considerably. Systems that were formerly hydraulic in operation are now being converted to electric operation [1]. For the new Boeing 787, the aircraft-wide electrical generation capacity is 1.5 MW – almost an order of magnitude larger than previous designs. This study, then, is an initial investigation of the use of PEM fuel cells on-board commercial aircraft. We seek to understand how to physically deploy a fuel cell on an aircraft, the impact of system volume and weight on the airplane, and the impact on jet fuel consumption, both in relation to fuel currently devoted to electricity generation, and the overall fuel needed by the airplane to fly a given mission.

Approach

To accomplish this analysis, two basic airplane designs were considered: one airplane without a fuel cell (the base airplane), and one airplane designed to perform the same mission as the first airplane, only carrying a fuel cell and associated hardware to fulfill a specific electrical need. The difference in the performance of these two airplanes is made quantitative by calculating the fuel required to fly the mission in the two cases, which requires understanding the influence of weight, volume, and thermal issues on the airplane drag. Calculating the required fuel also allows us to assess fuel use as it directly relates to power generation on the airplane. The key point here is that we assess not only the benefit of the fuel cell on generating electricity, but also the penalty the fuel cell system places on the airplane's performance due to its added weight and possibly drag issues that arise from handling fuel cell thermal issues. Combining these two is necessary to determine the overall effect of the fuel cell system.

We performed the analysis by designing and examining several system options using realistic assumptions about performance and size of the various components. After assessment of the available state of the art in commercially available PEM fuel cells, the Hydrogenics HyPM 12 PEM fuel cell was chosen as a unit representative of the industry. For hydrogen storage, several options were considered: 350 bar compressed gas, 700 bar compressed gas, metal hydrides, and liquid hydrogen storage, in both conventional cryogenic storage and "cryo-compressed" storage. For storing hydrogen for the PEM aviation fuel cell, we selected 350 bar compressed gas tank technology due to its combination of high specific energy and current availability. Other equipment such as heat exchangers, blowers, and pumps were all selected based on commercially available units with the specifications appropriate for the system. For the electrical components, a ±270 volt direct current distribution system provided the lowest system weight, although the increase in weight due to a 230 volt alternating current system was less than 50 kg (110 lb). Both of these options provide the advantage of direct interface with the existing electrical system on the 787.

Results

After consideration of factors such as safety, available space, maintenance, and wiring and tubing/piping lengths, we chose to locate the fuel cell system in the airplane's fairing area (where the wings join the fuselage), although locating the system in the tail cone would not change the results by much. Locating the fuel cell system next to the load it serves could save up to 150 kg (331 lb) of mass and provide some redundancy benefits, but this was avoided because of the concern with occupying space that is currently used for other purposes.

The amount and method of recovering the heat rejected from the fuel cell (waste heat recovery) was found to be a critical factor in determining the performance benefit of the fuel cell system. To this end, eleven different waste heat recovery options were examined thermodynamically. We found that a system that uses the heat from the fuel cell to pre-heat the jet fuel carried by the airplane will provide the largest overall performance benefit. This method of heat recovery is already used in commercial airplanes within the engine compartment, where the lubrication oil is cooled by jet fuel, and it is more ubiquitous in military aircraft where the fuel is used to cool many of the military airplane's systems.

We considered the integration of the fuel cell system with the airplane's electrical system, for it is necessary to ensure that the addition of the fuel cell system does not disrupt the electrical system or cause instabilities. Through dynamic simulation we found that the fuel cell system performed satisfactorily whether connected to the airplane's system or as a stand-alone system. In fact, our results indicate that the integration of the fuel cell system with the existing electrical system may provide a faster response to load changes than the current configuration.

Conclusions and Future Directions

In the end, we found that while adding a fuel cell system using today's technology for the PEM fuel cell and hydrogen storage is technically feasible, it will not give the airplane a performance benefit no matter which configuration was chosen (although there may be other benefits that make it worthwhile from the airplane manufacturer's or airline's point of view). However, when we repeated the analysis using DOE-target technology for the PEM fuel cell and hydrogen storage, we found that the fuel cell system would provide a performance benefit to the airplane (i.e., it can save the airplane some fuel), depending on the way it is configured. This analysis also showed that the DOE-target technology fuel cell system could generate electricity using over 30% less fuel than the current airplane, even considering the penalties due to the fuel cell system's weight and drag (Figure 1). If a fleet of 1,000 airplanes were equipped with such systems, it could save over 20,000 metric tons of CO_2 annually (Figure 2).

This project is complete. It is recommended that subsequent work on this topic focus on detailed design and testing of an actual aviation PEM fuel cell system, including both mechanical and electrical aspects.

FY 2011 Publications/Presentations

1. J.W. Pratt, L.E. Klebanoff, K. Munoz-Ramos, A.A. Akhil, D.B. Curgus, and B.L. Schenkman, "Proton Exchange Membrane Fuel Cells for Electrical Power Generation On-Board Commercial Airplanes," Sandia Report SAND2011-3119, May 2011.

2. Lennie Klebanoff, Joe Pratt, Karina Munoz-Ramos, Abbas Akhil, Dita Curgus, and Ben Schenkman, "PEM Fuel Cell Systems for Commercial Airplane Systems Power," presented

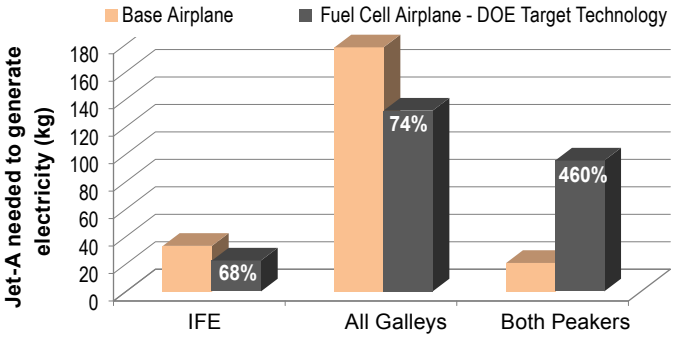


FIGURE 1. The amount of fuel required by the Base Airplane and the Fuel Cell Airplane to generate electricity and heat for each of three different loads: the in-flight entertainment (IFE), all galleys, and both peakers. IFE is a 20 kW load; All Galleys refers to a fuel cell providing power for three on-board galleys with a total power consumption of 120 kW, and Both Peakers refers to providing power for a short duration in times of peak power demand at 150 kW. The Base Airplane uses the main engine generator with a fuel-to-electricity efficiency of 34%, while the Fuel Cell Airplane assumes a PEM fuel cell system cooled by the airplane's jet fuel, and consists of DOE target technology for the PEM fuel cell and hydrogen storage.

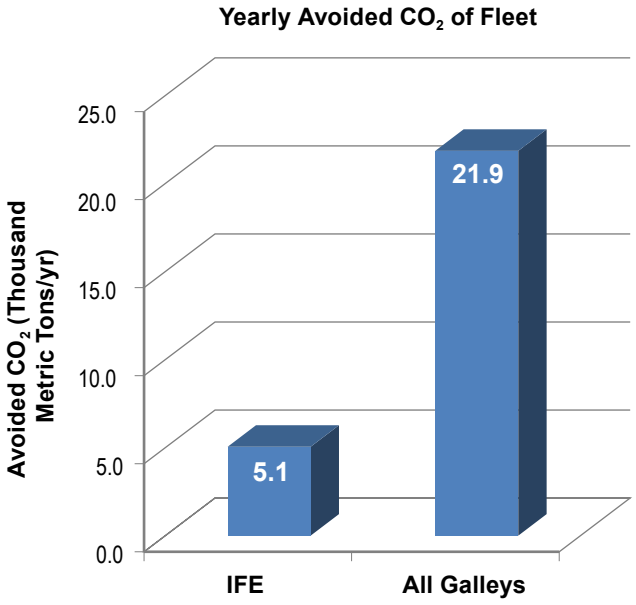


FIGURE 2. Yearly avoided CO_2 emissions for a fleet of 1,000 fuel cell-carrying airplanes operating 750 hrs/yr for each of two different loads: the IFE and All Galleys. The fuel cell system is fuel cooled and assumes renewable hydrogen, as compared to the Base Airplane generating electricity via the main engines at 34% efficiency.

at 2011 DOE Hydrogen and Fuel Cells Program and Vehicle Technologies Program Annual Merit Review and Peer Evaluation Meeting May 9-13, 2011, Arlington, Virginia.

References

1. Sinnett, M. (2007). "787 No-Bleed Systems: Saving Fuel and Enhancing Operational Efficiencies." Aero Quarterly, 6-11.

X.10 Assessment of Solid Oxide Fuel Cell Power System for Greener Commercial Aircraft

Larry Chick (Primary Contact), Greg Whyatt
Pacific Northwest National Laboratory (PNNL)
P.O. Box 999
Richland, WA 99352
Phone: (509) 375-2145
E-mail: larry.chick@pnl.gov

DOE Manager
HQ: Peter Devlin
Phone: (202) 586-4905
E-mail: Peter.Devlin@ee.doe.gov

Project Start Date: July 19, 2010
Project End Date: September 30, 2011

Fiscal Year (FY) 2011 Objectives

- Examine electrical power generation for commercial aircraft using solid oxide fuel (SOFC) technology.
- Determine amount of weight reduction required to make SOFC power systems net fuel efficient on aircraft.

Technical Barriers

Identify and quantify barriers to deployment of fuel cell power systems on commercial aircraft.

FY 2011 Accomplishments

- Obtained extensive information from Boeing on the 787 electrical system, including generation and distribution systems, load profiles and fuel consumption.
- Conceived electrical system using an SOFC on a direct current (DC) bus that will save ~100 kW in power conversion losses and almost 270 kg in conversion equipment.
- Modeled a matrix of SOFC power systems to determine anticipated fuel efficiencies. Most promising system uses steam reforming, anode recycle and compressor/expander.
- Determined breakeven weight change vs. flight distance for various SOFC system efficiencies: a system with 70% conversion efficiency can add up to 4,600 kg and still break even on fuel consumed.
- Generated estimates of system weights (not yet complete) for SOFC system with steam reformer, anode recycle and compressor/expander.



Introduction

This study examines electrical power generation for commercial aircraft using SOFC technology. The focus of this study is "more-electric" airplanes with the Boeing 787 used as a case study. More-electric airplanes minimize extraction of bleed air from the engine compressor stages and instead run electrical generators driven by the engines to satisfy loads. More-electric airplanes have higher electrical generation rates and thus stand to show greater benefit from an increase in the efficiency of electrical generation.

SOFC technology can generate electrical power at higher efficiency than is achieved by using power from the main engine shaft to run a generator. Hence, unlike the existing auxiliary power unit (APU), which is turned off once the main engines are started, a fuel cell power unit would operate throughout the flight to maximize fuel savings. Fuel cell power units are expected to be somewhat heavier than turbine APUs resulting in a heavier aircraft. For an SOFC power unit to be feasible, the fuel savings for electrical generation must exceed the increase in fuel consumption due to weight.

Approach

System flowsheets were analyzed to estimate weight and efficiency. Mass and energy balance was modeled using ChemCAD software coupled with a PNNL stack performance model of a planar anode-supported SOFC. The stack performance model is calibrated to actual data for a promising new materials set that yields about 75% higher power density than previous cells. Based on input values for pressure, inlet temperature, flow rates, compositions, and cell voltage, the SOFC model predicts the power density achieved. All systems modeled were assumed to operate using desulfurized jet fuel that is loaded into a dedicated tank. Approaches to the flowsheet included auto-thermal reforming, steam reforming and anode recycle steam reforming. All systems included a compressor/expander to compress air drawn in from the atmosphere and then expand the exhaust gases to recover work. System pressures were examined at 0.835 atm (cruise cabin pressure), 3 atm and 8 atm. Operating cell voltages of 0.70, 0.75, 0.80 and 0.85 V were analyzed.

A revised 787 electrical distribution system was considered to take advantage of the SOFC power being generated as DC rather than alternating current (AC) power. An estimate of the electrical power required was developed based on an understanding of the Boeing 787 loads. The impact of the addition of the SOFC APU weight on main engine fuel consumption was determined using a PianoX (http://www.lissys.demon.co.uk/index2.html)

model of the 787-8. Flight profiles for trips of 1,000, 3,000, 5,000 and 7,000 nautical miles were calculated for a range of payloads. The PianoX model was allowed to select appropriate parameters for each flight such as rate of climb, initial cruise altitude, rate of descent, etc., and provided fuel consumption data as a function of payload. A breakeven weight for the APU was calculated by determining the point at which the fuel saved during the flight due to the efficiency of the SOFC would be offset by the increase in main engine fuel consumption required to carry the additional APU weight. Estimates of APU weight were compared to the breakeven weight.

Results

Key factors in the comparison of SOFC power system weights to break even values include:

Modification of Power Distribution - For the SOFC-based electrical system, the aircraft distribution system was modified so that the SOFC directly produces the +/-270 VDC power used for major loads. The existing 230 VAC loads are moved to +/-270 VDC bus and 80% efficient DC/DC and DC/AC power conversions are used to provide power to 115 VAC and 28 VDC loads. This approach reduces the conversion losses, reducing the required gross power generation from 918 kW to 821 kW. The weight saved in power conversion equipment is estimated to be 268 kg.

Elimination of Turbine APU - It is expected that the SOFC power system would be divided into multiple independent units to provide redundancy. In this configuration, the turbine APU could be eliminated, saving 245 kg. The ram air turbine was assumed to still be present. Engine generators cannot be eliminated since they double as starters for the main engines.

SOFC System Configuration - The extent of fuel savings depends on the flowsheet for the SOFC system. Key system features include the air compression/expansion, the fuel cell itself and the approach to reforming the fuel.

Air Compression - In all cases, ram air is compressed to SOFC pressure in a compressor (80% efficient) and exhaust gases expanded through a turbine (85% efficient) to ambient to recover mechanical energy. Weight and performance of the compressor/expander was based on a Williams WR2 jet engine. Adjustments were made to scale the estimated weight based on the air flow and compression ratio required for each flowsheet. Shaft power is balanced by either using electrical power as input or generating AC power and converting it to +/-270 VDC. Cabin air is not used as input to the compressor to avoid concern over upsetting normal cabin venting.

Fuel Cell - The fuel cell is based on a Delphi Gen 4 stack with a new material set which is capable of higher power density than the more established materials currently used. The new materials set has been tested in small button cells, but has not yet been scaled up. The weight of the stack was taken to be 62 kg for a 100-cell stack. This weight represents the current weight of a 100-cell Gen 4 stack design minus a relatively heavy base plate and frame (33.5 kg). It is believed that a much lighter weight solution to the base plate and frame can be developed. The power density in the stack is a function of anode gas composition, fuel utilization, excess air, operating pressure and voltage. Stack electrical conversion efficiency is purely a function of stack voltage.

Reforming Approach - Autothermal reforming, single anode pass steam reforming and anode recycle steam reforming flowsheets were modeled. Figure 1 shows the logical layout of the anode recycle flowsheet. Figure 2 shows that the anode recycle steam reforming provided significantly higher system efficiency than other approaches. In this approach all steam required for reforming is generated on the SOFC anode and waste heat from the fuel cell is used to drive the enothermic steam reforming reaction. Net power from the compressor-expander provided only a small contribution (3.2% to 4.7% at 3 atm) to total net power output. Since the SOFC offers higher efficiency than a turbine, efficiency is improved with more power from the SOFC and less from the turbine as long as electrical power is not required as input to drive the compressor. Also, the decision to configure the system to directly generate DC power penalizes the turbine for losses in AC/DC conversion.

Weight Estimates - The system was assumed to be placed in a titanium vessel designed for a safety factor of 1.5 on yield stress. The heat exchangers, anode blower and

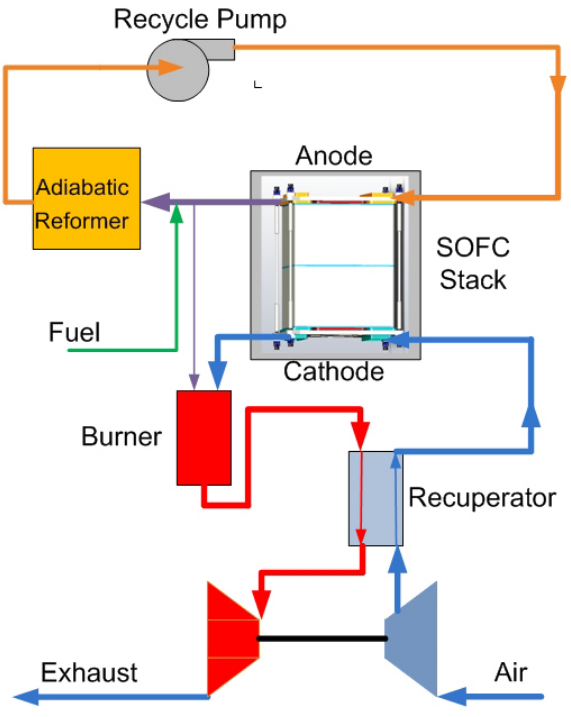


FIGURE 1. Logical Flowchart for Anode Recycle Steam Reforming Flowsheet

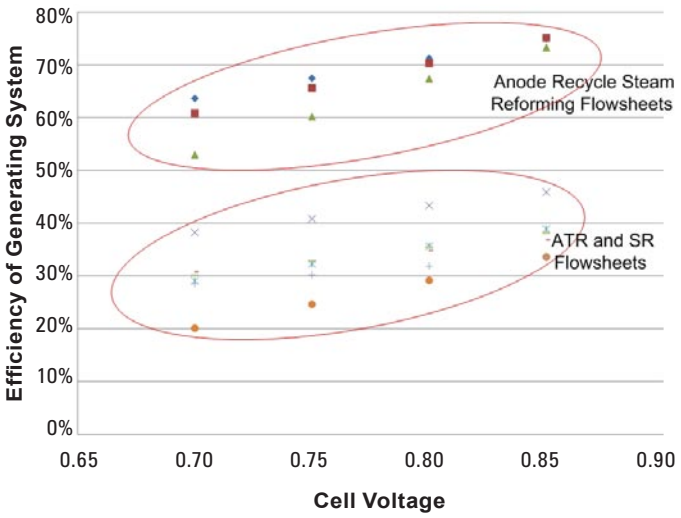


FIGURE 2. Efficiency as a Function of Cell Voltage Flowsheet Configuration

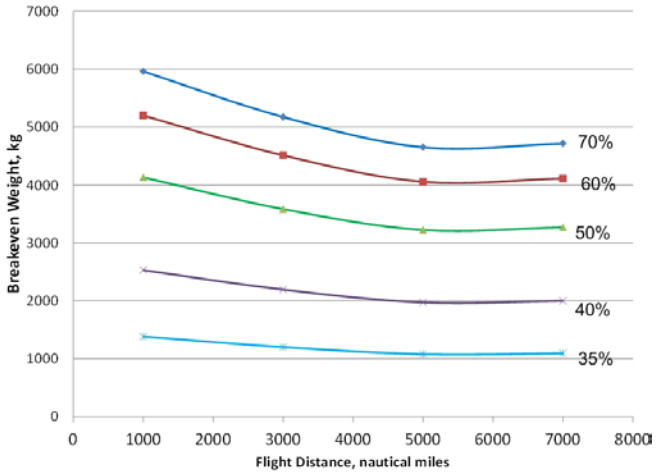


FIGURE 3. Breakeven Weights as a Function of Efficiency

reformer were scaled based on an existing SOFC power system operating at 6.3 kW. Stacks were estimated at 62 kg/100 cells. Current weight estimates do not account for the insulation, connecting pipes, support structure, instrumentation and controls. Table 1 shows a summary of the estimated net efficiency and weight for analyzed anode recycle cases. Highlighted cells indicate the most attractive regions for operation.

TABLE 1. Net Efficiency and Weight Added by SOFC Power Unit (kg)

Pressure	SOFC Cell Voltage			
	0.85	0.80	0.75	0.70
0.8 atm	75%	71%	68%	64%
	8,956	5,264	4,392	4,163
3.0 atm	75%	70%	66%	61%
	4,828	3,901	3,729	3,825
8.0 atm	73%	67%	60%	53%
	3,709	3,510	3,726	4,135

Breakeven Weights - The breakeven weight as a function of power unit efficiency is shown in Figure 3. The breakeven weight indicates the SOFC power unit weight at which the aircraft fuel consumption would be the same as the current engine generators due to weight added. The highest breakeven weights occur for shorter flights. This occurs because the electrical generation is assumed constant but aircraft velocity during climb and descent is lower causing more fuel to be saved per mile compared to the higher velocity cruise phase. Figure 4 shows that current weight estimates are below breakeven weights indicating a potential to save fuel compared to engine generators. However, current weight estimates do not yet include insulation, connecting ducting and tubing and support structure which will possibly impact on the fuel savings.

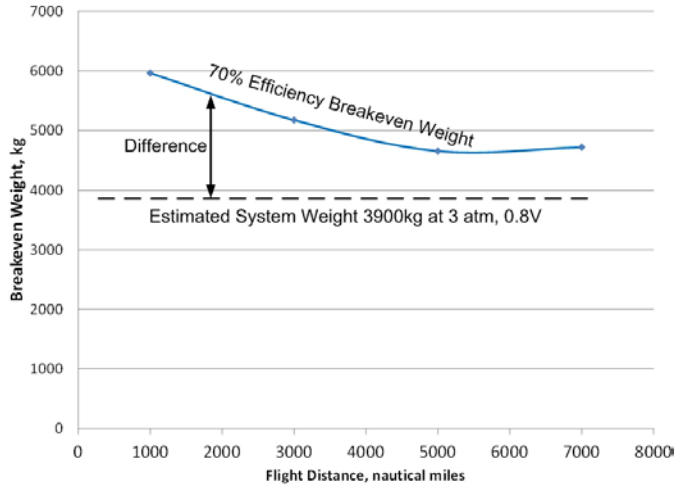


FIGURE 4. Comparison of Breakeven Weight to Estimated System Weight (3 atm, 0.8 V/cell)

Conclusions and Future Directions

- Existing SOFC technology is potentially capable of saving fuel during flight.
- Measurements of SOFC performance at high pressure will be made to support predictions of performance at high pressure.
- Additional modeling in the region of best performance will be conducted.
- A conceptual design will be developed to improve estimates of system weight.

FY 2011 Publications/Presentations

1. Chick, LA., May 2010, "*Assessment of Solid Oxide Fuel Cell Power System for Greener Commercial Aircraft.*"

XI. SYSTEMS ANALYSIS

XI.0 Systems Analysis Sub-Program Overview

Systems Analysis supports decision-making by providing a greater understanding of technology gaps, opportunities and risks, the contribution of individual technology components to the overall system (i.e., from fuel production to utilization), and the interaction of the components within the system. Analysis is also conducted to assess issues that cut across all the various aspects of hydrogen and fuel cell technologies–for example, examining how hydrogen and fuel cells can be integrated with the electrical sector and with other renewable fuels. Particular emphasis is given to assessing stationary fuel cell applications, the impact of fuel quality on fuel cell performance, and potential options for hydrogen infrastructure.

The Systems Analysis sub-program made several significant contributions to the Program during Fiscal Year (FY) 2011. The sub-program developed the hydrogen threshold cost, which represents the cost at which hydrogen fuel cell electric vehicles (FCEVs) are projected to become competitive on a cost per mile basis with the competing fuel-and-vehicle combination–gasoline in hybrid-electric vehicles (HEVs). This cost was determined to be $2–$4/gasoline gallon equivalent (gge, untaxed). Analytical tools, including HyDRA and the Macro-System Model, were updated and peer reviewed to support the analytical process. Infrastructure and early market analyses were conducted to better understand the supply and demand issues involved. A cost model was developed to evaluate the cost of removing impurities from the resource streams for hydrogen production. In addition, a study was initiated to evaluate the impact of biogas impurities on fuel cell performance and durability. The Greenhouse gases, Regulated Emissions, and Energy use in Transportation (GREET) model was modified to enable greenhouse gas emissions to be evaluated on a well-to-wheels basis for hydrogen energy storage from renewable electricity generation.

Goal

Provide system-level analysis to support the development of hydrogen and fuel cell technologies by: evaluating technologies and pathways, including resource and infrastructure issues; guiding the selection of RD&D projects; and estimating the potential value of RD&D efforts.

Objectives

- By 2011, enhance the Macro-System Model by including stationary electrical generation and infrastructure for long-term applications analysis.
- By 2011, complete a study comparing combined-heat-and-power (CHP) fuel cell systems with other CHP technologies.
- By 2012, evaluate the use of hydrogen for energy storage and as an energy carrier to supplement the energy and electrical infrastructure.
- By 2012, evaluate fueling station costs for early FCEV penetration to determine the cost of different hydrogen fueling pathways for low and moderate demand rates.
- By 2014, complete environmental studies needed for technology readiness of FCEVs–including analyses of potential greenhouse gas and criteria pollutant emissions reductions from the penetration of FCEVs in the light-duty vehicle fleet.
- By 2015, analyze the ultimate potential for hydrogen, stationary fuel cells, and FCEVs. (This analysis will address necessary resources, hydrogen production, transportation infrastructure, performance of stationary fuel cells and FCEVs, and the system effects resulting from the growth of hydrogen's market shares in the various sectors of the economy.)
- By 2018, complete analysis of Program performance, the cost status of various technologies, and the potential for use of fuel cells for a portfolio of commercial applications.
- On an ongoing basis, provide milestone-based analyses–including risk analysis, independent reviews, financial evaluations and environmental analysis–to support the Program's needs as new fuel cell applications achieve technology readiness.
- On an ongoing basis, periodically update life-cycle analyses of the energy use, petroleum use, and greenhouse gas and criteria pollutant emissions for various fuel cell applications and hydrogen production pathways. (These updates will include technological advances or changes in the underlying parameters.)

FY 2011 Status

Analysis conducted in FY 2011 included: updating the Hydrogen Threshold Cost; working with the DOE Vehicle Technologies Program to examine the life-cycle costs of various vehicle platforms including FCEVs; and identifying early markets for fuel cells and opportunities to reduce cost through various mechanisms, such as tax credits and other legislation. The Systems Analysis sub-program has transitioned from activities focused on key model development to the application of the developed models for completing critical analyses. The sub-program's initial strategy has been effective in enabling the completion of a portfolio of analytical projects; several of these are discussed in the following section, "FY 2011 Accomplishments."

FY 2011 Accomplishments

Development and Maintenance of Models

- The Macro-System Model, a dynamic engineering transition model, was updated to enable evaluation of the impacts of stationary fuel cells on electricity distribution. The Macro-System Model is used to simulate of the performance, cost, and the potential for reducing emissions and petroleum use by hydrogen and fuel cell technologies. The model uses a distributed architecture to link existing and emerging models for system components. Stationary fuel cell analysis capabilities were made possible by adding the National Renewable Energy Laboratory's (NREL's) Fuel Cell Power Model to the Macro-System Model.

Studies and Analysis

Market Analysis

- Oak Ridge National Laboratory analyzed the status and outlook for the U.S. non-automotive fuel cell industry by examining the impacts of government policies and funding. They found that fuel cell manufacturers have been able to achieve large cost reductions of ~50% over the last two to five years, as shown in Figure 1; and, they found that government funding and incentives have been key elements in enabling these cost reductions. They also found that continuation or enhancement of current policies, such as the investment tax credit and government procurement, combined with progress by industry will be necessary to establish a viable domestic fuel cell industry.
- Pike Research completed global and domestic analyses and studies of the fuel cell markets for material handling equipment, stationary power, and portable power. The studies identified increased growth for fuel cells in the domestic and international markets, as shown in Figure 2. In particular, the U.S. market grew more than 50% from 2008 to 2010 in terms of megawatts of fuel cell systems shipped.

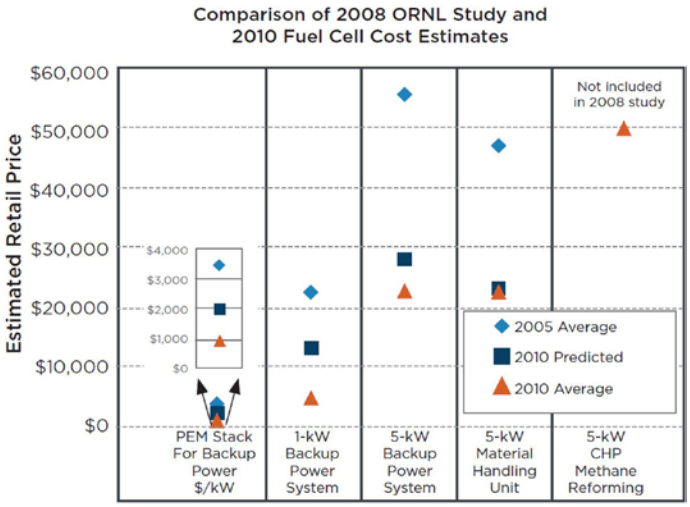


FIGURE 1. Cost Reductions in Early Market Fuel Cells. A 2008 study[1] by Oak Ridge National Laboratory assessed the average cost (in 2005) of fuel cells for early markets and then predicted what these costs would be in 2010, based on a model that included economies of scale and technology progress. An updated 2011 study[2] by the same group has estimated the average 2010 cost, which was shown to be equal to or even lower than the predictions. 2005 and 2010 averages based on estimates supplied by original equipment manufacturers. Predicted 2010 costs assumed total government procurements of 2,175 units per year, across all market segments. These predictions also assumed a progress ratio of 0.9 and scale elasticity of -0.2.

[1] David Greene and K.G. Duleep, "Bootstrapping a Sustainable North American PEM Fuel Cell Industry: Could a Federal Acquisition Program Make a Difference?" Oak Ridge National Laboratory, October 2008, http://cta.ornl.gov/cta/Publications/Reports/ORNL_TM_2008_183.pdf.

[2] David Greene, et al., "Status and Outlook for the U.S. Non-automotive Fuel Cell Industry: Impacts of Government Policies and Assessment of Future Opportunities," Oak Ridge National Laboratory, May 2011, http://cta.ornl.gov/cta/Publications/Reports/ORNL_TM2011_101_FINAL.pdf.

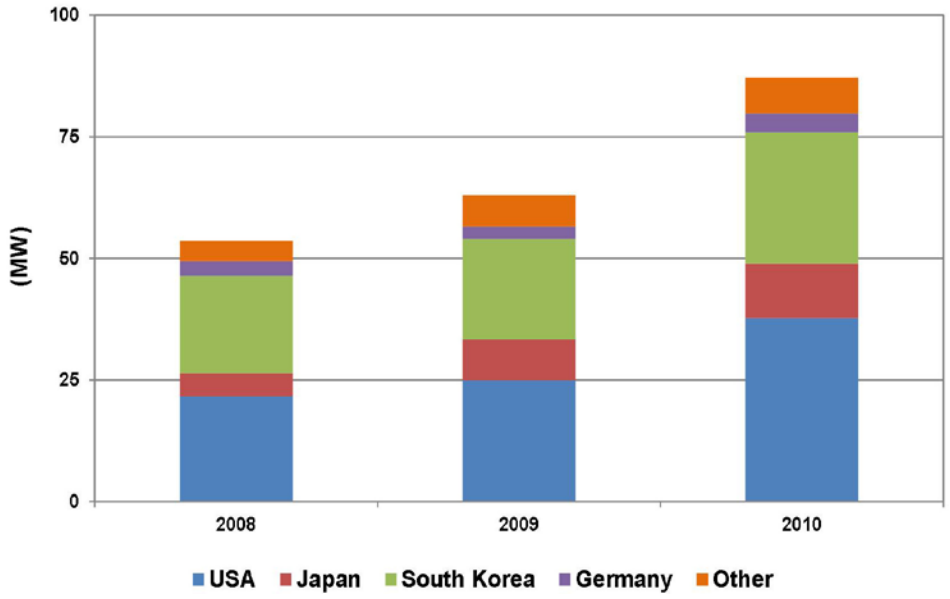


FIGURE 2. Megawatts of Fuel Cells Shipped.[3] Fuel cell shipments, in terms of megawatts, continue to increase (~36% in 2010). U.S. shipments grew by more than 50% in 2010.

Infrastructure Analysis

- Infrastructure analysis conducted by NREL with the Scenario Evaluation and Regionalization Analysis model and Sandia National Laboratories revealed that synergies between fuel cells for stationary power generation and transportation could be realized in the early phases of market adoption of hydrogen for FCEVs. Widespread deployment of stationary fuel cell systems that co-produce power, heat, and hydrogen ("combined-heat-hydrogen-and-power" or CHHP systems) could reduce the problem of hydrogen availability in the early stages of transition to FCEVs. Model results indicate that the production of hydrogen from CHHP could result in smaller stations with higher capital utilization and lower hydrogen cost. Hydrogen produced this way could supplement hydrogen supplied from distributed natural gas–based steam methane reforming, particularly for the early years of FCEV penetration, when hydrogen demand and station sizes will be small. The analysis shows that hydrogen costs from CHHP units drop from $7–$9/gge in the early years when demand is low to $5–$7/gge in the later years when demand is higher.
- NREL examined cost reduction opportunities for components of hydrogen infrastructure by conducting a workshop on February 16–17, 2011, with a diverse group of stakeholders and through infrastructure cost assessment with a cost calculator of early market fueling stations. Stakeholders identified potential cost reductions of 50% through standardization and modular approaches of station design. They found that station costs could be reduced by an additional 20–30% by adopting a uniform permitting process. The results of the stakeholder input from the workshop and cost calculator will be published by the end of 2011.

Environmental Analysis

- Argonne National Laboratory analyzed the impact of feedstock quality on stationary fuel cell performance; identified contaminate removal solutions for sulfur, halogen and silica compounds; and estimated the costs associated with meeting the required feedstock quality specifications. The feedstocks primarily assessed included natural gas and biogas (from landfills and anaerobic digestion of wastewater). The key impurity analysis shows sulfur, siloxanes (organo-silica compounds), and halides are detrimental to the fuel cell

[3] *2010 Fuel Cell Technologies Market Report*, U.S. Department of Energy, June 2011, http://www1.eere.energy.gov/hydrogenandfuelcells/pdfs/2010_market_report.pdf.

anode. The level of impurities was found to vary among feedstocks. For example, halogens were found to be higher in landfill gas, while siloxane compounds are typically higher in biogas produced from wastewater treatment, as shown in Figure 3. Ammonia, CO, and hydrocarbons are less damaging for higher temperature fuel cells such as solid oxide and molten carbonate fuel cells. The costs of contaminate removal will be determined for different removal schemes.

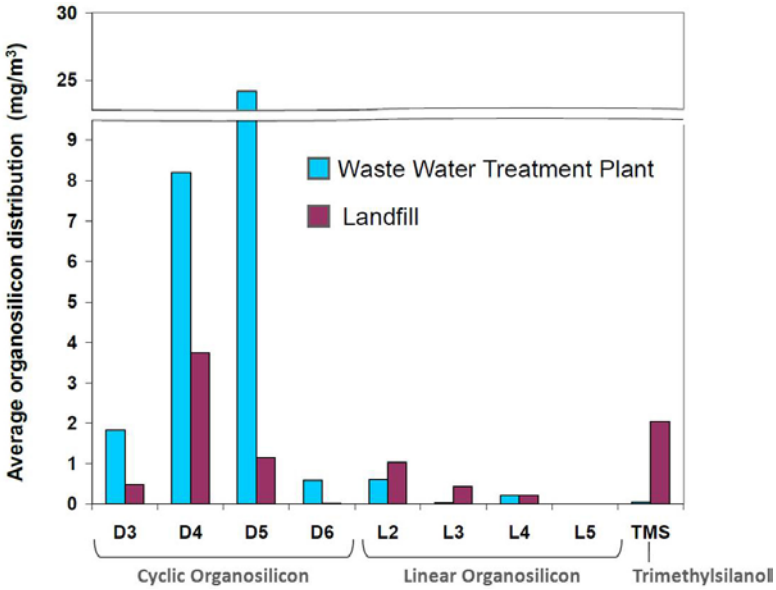


FIGURE 3. Impurities in Biogas Streams[4]

Energy Storage Analysis

- NREL analyzed the potential of utilizing renewable electricity generation from various wind farm locations combined with hydrogen production and storage systems to provide renewable hydrogen for energy storage and vehicle applications. Results of the analysis exhibit the delivered cost of electricity from the capture of curtailed wind-generated electricity would range from $0.13-$0.29/kWh on a levelized basis, depending on the location of the wind farm. The equipment cost, including the electrolyzer cost, was found to be one of the key drivers for the electricity cost delivered from hydrogen energy storage systems.

Programmatic Analysis

- A cost threshold for hydrogen was developed to assist DOE in focusing and prioritizing research and development (R&D) options. The cost threshold represents the cost of hydrogen at which FCEVs are projected to become competitive on a cost per mile basis with the competing fuel/vehicle combination–gasoline in HEVs. Its calculation includes projected vehicle fuel economies for HEVs and FCEVs, projected costs of gasoline, and projected incremental costs of FCEVs on a per-mile basis. Due to the uncertainty in all the parameters, both single-value and stochastic sensitivities were performed. The resulting hydrogen threshold cost is in the range of $2–$4/gge (in 2007 dollars). A graphical representation of the hydrogen threshold cost is shown in Figure 4.
- Pacific Northwest National Laboratory analyzed the commercial benefits of the DOE Fuel Cell Technologies (FCT) Program by tracking the commercial products, technologies, and patents developed from FCT R&D funding. The results show that more than 300 patents had been awarded and 30 products had been commercialized by 2011 as a result of research funded by FCT in the areas of fuel cells and hydrogen storage, production, and delivery (see Figure 5). These findings have been highlighted in the 2011 *Pathways to Commercial Success*[5] report.

[4] D. Papadias, et al., "Fuel Quality Effects on Stationary Fuel Cell Systems," 2011 DOE Hydrogen and Fuel Cells Program Annual Merit Review Proceedings, May 2011, http://hydrogen.energy.gov/pdfs/review11/an010_ahmed_2011_o.pdf.

[5] *Pathways to Commercial Success: Technologies and Products Supported by The Fuel Cell Technologies Program*, Pacific Northwest National Laboratory, September 2011, http://www1.eere.energy.gov/hydrogenandfuelcells/pdfs/pathways_2011.pdf.

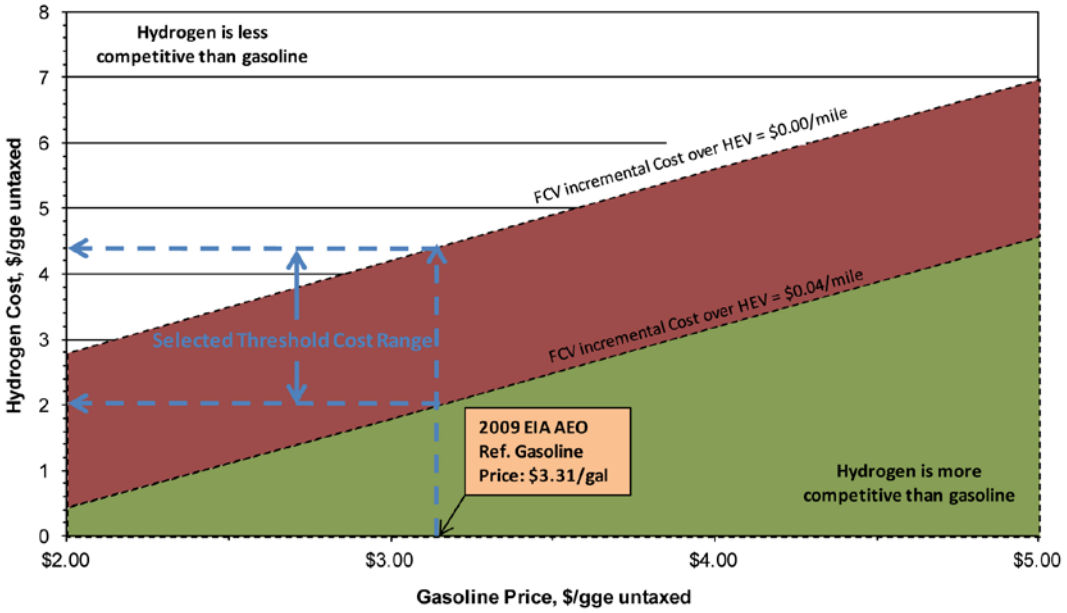
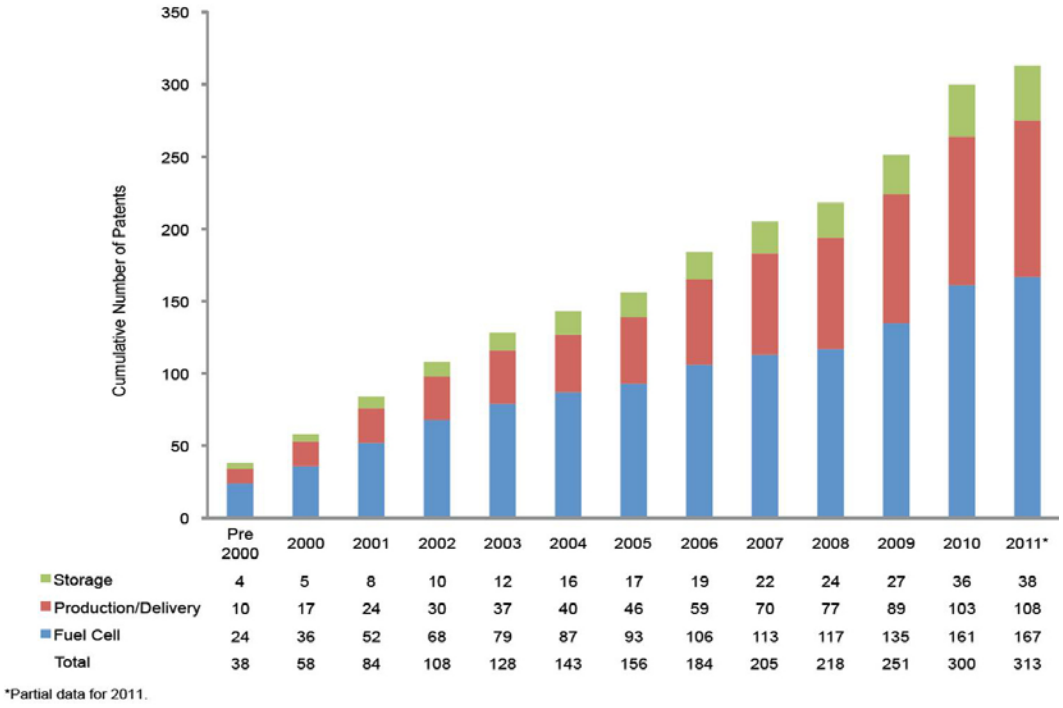


FIGURE 4. Effect of Gasoline Price on Hydrogen Threshold Cost



	Pre 2000	2000	2001	2002	2003	2004	2005	2006	2007	2008	2009	2010	2011*
Storage	4	5	8	10	12	16	17	19	22	24	27	36	38
Production/Delivery	10	17	24	30	37	40	46	59	70	77	89	103	108
Fuel Cell	24	36	52	68	79	87	93	106	113	117	135	161	167
Total	38	58	84	108	128	143	156	184	205	218	251	300	313

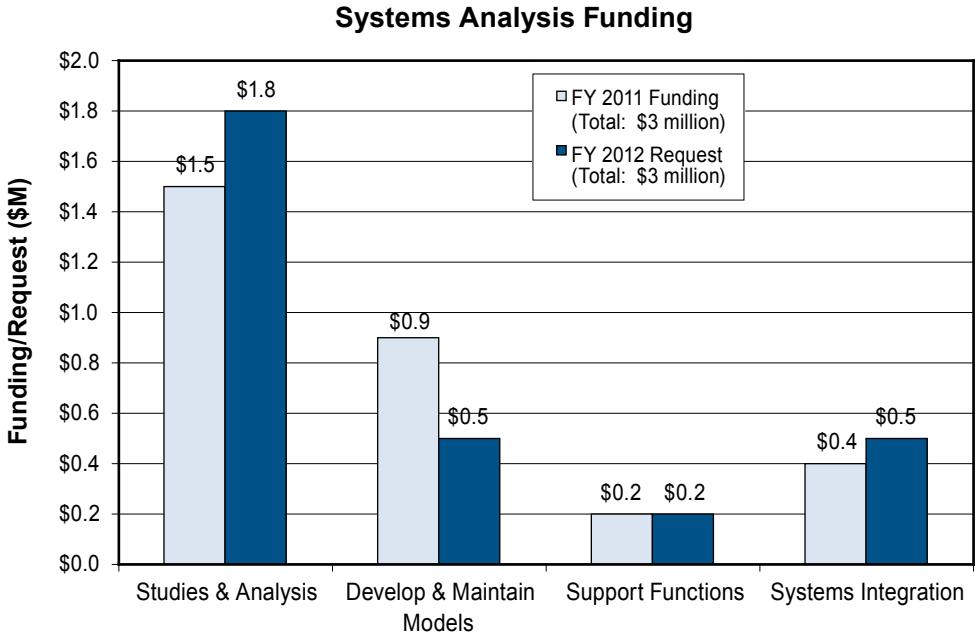
*Partial data for 2011.

FIGURE 5. Cumulative Number of Patents Awarded as a Result of FCT Program Funding

Budget

The FY 2011 appropriation included $3 million for Systems Analysis, and the FY 2012 request is $3 million. The budget for Systems Analysis is consistent with the goals and objectives of the sub-program and allows the Program to assess fuel cell applications for energy storage, stationary power generation, specialty

applications, and light-duty transportation. The FY 2012 budget request includes funding for early fuel cell and hydrogen market and infrastructure analysis, as well as fuel quality evaluation, environmental analysis, overall program analysis, modeling, and systems integration.



FY 2012 Plans

In FY 2012, Systems Analysis will focus on conducting analyses to determine technology gaps for: fuel cell systems and infrastructure for different applications, and the use of fuel cells for energy storage and transmission. Analyses will include: assessing the tradeoffs and regional impacts of fuel cells with other alternative fuels; light-duty vehicle life-cycle costs for multiple platforms; socio-economic impacts of job creation based on fuel cell and hydrogen manufacturing, and the synergies of linking stationary fuel cell power generation with the electrical sector. New opportunities for using fuel cells for energy storage and integration with existing energy supply networks such as natural gas transmission will also be explored.

Fred Joseck
Systems Analysis Team Lead
Fuel Cell Technologies Program
Department of Energy
1000 Independence Ave., SW
Washington, D.C. 20585-0121
Phone: (202) 586-7932
E-mail: Fred.Joseck@ee.doe.gov

XI.1 Non-Automotive Fuel Cells: Market Assessment and Analysis of Impacts of Policies

David L. Greene
Oak Ridge National Laboratory (ORNL)
NTRC, MS 6472
Knoxville, TN 37932
Phone: (865) 946-1310
E-mail: dlgreene@ornl.gov

DOE Manager
HQ: Fredrick Joseck
Phone: (202) 586-7932
E-mail: Fred.Joseck@ee.doe.gov

Subcontractors:
- The University of Tennessee, Knoxville, TN
- ICF, International, Washington, D.C.
- Fuel Cell Today, Royston, UK

Project Start Date: October 1, 2007
Project End Date: Project continuation and direction determined annually by DOE

Fiscal Year (FY) 2011 Objectives

- Analyze the status and prospects of the fuel cell industry and impacts of policies.
- Simulate market transformation to hydrogen fuel cell vehicles in the United States.
- Conduct systems analysis of fuel cell technologies.

Technical Barriers

This project addresses the following technical barriers from section 4.5 of the Fuel Cell Technologies Program Multi-Year Research, Development and Demonstration Plan:

(A) Future Market Behavior

Understanding the behavior and drivers of the fuel and vehicle markets is necessary to determine the long-term applications. Another major issue is the hydrogen supply, vehicle supply, and the demand for vehicles and hydrogen are all dependent and linked. To analyze various hydrogen fuel and vehicle scenarios, models need to be developed to understand these issues and their interactions.

(D) Suite of Models and Tools

The program currently has a group of models to use for analysis; however, the models are not sufficient to answer all analytical needs. A macro-system model is necessary to address the overarching hydrogen infrastructure as a system. Improvement of component models is necessary to make them more useable and consistent.

(E) Unplanned Studies and Analysis

Every year, many analysis questions are raised that require analysis outside and, in some cases, instead of the plans made for that year. Many analysis questions need responses in brief periods of time particularly when they are driven by external requests or needs. A flexible capability to provide those results is necessary.

Contribution to Achievement of DOE Systems Analysis Milestones

This project will contribute to achievement of the following DOE milestones from the Systems Analysis section of the Fuel Cell Technologies Program Multi-Year Research, Development and Demonstration Plan:

Provide system-level analysis products to support hydrogen infrastructure development and technology readiness by evaluating technologies and pathways, guiding the selection of research, development and demonstration (RD&D) projects, and estimating the potential value of RD&D efforts:

- By 2015, analyze the ultimate potential for hydrogen and fuel cell vehicles. The analysis will address necessary resources, hydrogen production, transportation infrastructure, vehicle performance, and interactions between a hydrogen economic sector and other sectors.
- Provide milestone-based analysis, including risk analysis, independent reviews, financial evaluations and environmental analysis, to support the program's needs prior to technology readiness.
- **Milestone 26**: Annual model update and validation. (4Q, 2008; 4Q, 2009; 4Q, 2010; 4Q, 2011; 4Q, 2012; 4Q, 2013; 4Q, 2014; 4Q, 2015)
- **Milestone 39**: Annual update of Analysis Portfolio. (4Q, 2007; 4Q, 2008; 4Q, 2009; 4Q, 2010; 4Q, 2011; 4Q, 2012; 4Q, 2013; 4Q, 2014; 4Q, 2015)

FY 2011 Accomplishments

- Completed analysis of the status and outlook for the U.S. non-automotive fuel cell industry and quantified impacts of government policies on costs and production volumes.
- Completed analyses and assessments of markets, benefits and barriers to fuel cell deployment.

- Completed comparative lifecycle assessment of greenhouse gas emissions for fuel cell and internal combustion engine technologies.



Introduction

Hydrogen fuels cells for both automotive and non-automotive applications are novel technologies with potentially enormous social benefits in terms of reduced environmental impacts, energy security and sustainability of global energy resources. To be successful, hydrogen fuel cell technologies must further reduce costs and improve durability while at the same time overcoming the "lock-in" of established technologies, such as the petroleum-fueled internal combustion engine. Because the chief benefits of these technologies are public goods (i.e., environmental quality, national security) public policy will play a key role in the market transformation that must take place if hydrogen and fuel cells are to be successful.

Models for analyzing the transition to hydrogen and fuel cells are essential to understanding how such a market transformation could occur, over what time frame, and the roles of government, industry and consumers in the transition. Analytical tools are needed to understand the technological and economical prerequisites for a successful transition, as well as its costs and benefits. This project assists the Department of Energy by developing integrated models for simulating and analyzing the market transformation to hydrogen and fuel cells and conducting special analyses to develop new information about critical aspects of that phenomenon.

Approach

ORNL developed the HyTrans model to simulate the transition of light-duty vehicle transportation to hydrogen and to analyze scenarios and policies to achieve such a transformation. HyTrans is a non-linear dynamic optimization model that integrates the supply of hydrogen fuel, fuel cell vehicle manufacturing, and consumer demand. It simulates market barriers such as the "chicken or egg" problem (lack of hydrogen fuel and lack of hydrogen-powered vehicles), lack of diversity of vehicle choices during the early market transition, learning-by-doing and scale economies. HyTrans has been used to construct comprehensive scenarios of the transformation of the light-duty vehicle market and to measure the costs and benefits of such a transition.

ORNL has also conducted assessments of the status of fuel cells for non-automotive applications. These assessments included in-depth interviews with foreign and domestic fuel cell manufacturers and observation of their manufacturing facilities, data collection and construction of a model for simulating the evolution of fuel cell markets over time, including competition with established technologies. The markets addressed include combined heat and power (CHP), uninterruptible and backup power, and materials handling.

Results

The most significant accomplishment of FY 2011 was the completion of an analysis of the status and prospect for the U.S. non-automotive fuel cell industry and the impacts of government policies. The non-automotive fuel cell industry, worldwide, has made impressive progress since a previous assessment in 2007 [1]. Still, the global industry is dependent on public policies and is likely to be for several years.

- Non-automotive fuel cell manufacturers are making progress in a limited number of markets: for proton exchange membrane (PEM) fuel cells, back-up and uninterruptible power (especially for telecommunications), material handling equipment (forklifts), micro-CHP; for larger phosphoric acid and molten carbonate fuel cells, CHP and grid-independent stationary power.
- All manufacturers have achieved large cost reductions of 50% or more over the past 2-5 years. Nonetheless, all manufacturers believe that costs must be further reduced by 40% to 50% in order to compete successfully in the marketplace without government support.
- In the current market, government incentives are essential to sustaining the U.S. fuel cell industry. This is likely to remain the case for the next five years. Given continued or enhanced incentives fuel cell manufacturers might achieve sufficient cost reductions to continue without government support sometime between 2015 and 2020.
- Most manufacturers believe that future cost reductions will come primarily though economies of scale and cost reductions in the supply chain, with technological advances playing a somewhat smaller role than in the past. Estimated scale elasticities (the percent reduction in cost for a 1% increase in annual production) are typically in the range of -0.2 to -0.3, implying that doubling output would reduce costs by 20% to 30%.
- Substantial improvements in the durability of fuel cells have also been achieved. PEM fuel cell stacks in backup power applications today are expected to operate under real-world conditions for 5,000 to 10,000 hour lifetimes. ENEFARM[1] systems have been operating for 20,000 hours in Japanese homes and are guaranteed for 40,000-hour lifetimes. Large-scale (>300 kW) fuel cells for CHP and stationary power already exceed 40,000 hours before requiring replacement. Still, manufacturers believe that durability must and can be further improved.
- Almost all of the manufacturers interviewed were operating well below their existing production capacity

[1] ENEFARM is the brand name of Japan's residential PEM fuel cell CHP product.

and all had the capability to expand capacity by 50% to 300% within one year.

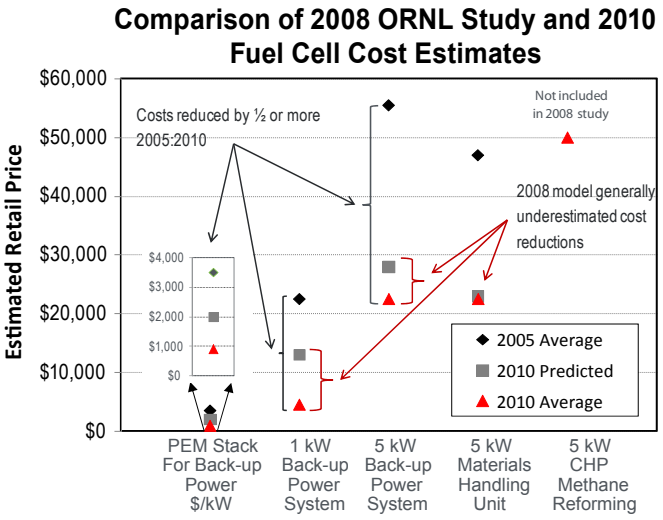
- Today, fuel cell manufacturers are dependent on government incentives or government procurements for viability. Without policies such as the investment tax credit, California's Self-Generation Incentive Program, research and development funding and government procurements, most companies' sales would be drastically reduced.
- For U.S. manufacturers, the key domestic markets are in California and the northeast states. South Korea is an important overseas market today, with sizable potential markets in the European Union. In the backup power area, manufacturers believe that developing countries represent large potential markets.
- For fuel cell CHP and micro-CHP manufacturers, both purchase incentives and high electricity prices (or feed-in tariffs) are essential to creating a viable market.
- For PEM fuel cells in back-up power and material handling, the cost and availability of hydrogen is a significant impediment to commercial success. While the American Recovery and Reinvestment Act of 2009 (ARRA) and other programs have provided important incentives for purchasing fuel cells, the problem of hydrogen availability for non-automotive applications has not yet been adequately addressed.

The 2008 report [1] estimated current costs for PEM fuel cell stacks and products and projected costs to 2010 based on assumed production levels, scale elasticities of approximately -0.2 and progress ratios of 0.95 for stack suppliers and 0.91 for manufacturers. These estimates, together with cost data gathered in the course of this study are shown in Figure 1. In every case, manufacturers have equaled or exceeded the manufacturing costs projected by the 2008 study. Large cost reductions have been achieved over the period 2005-2010:

- PEM stack costs have come down from roughly $4,000/kW to $1,000/kW.
- The cost of 1 kW backup power units have also been reduced by a factor of 4.
- The cost of 5 kW backup power units is down from about $55,000 to $22,000.
- The cost of 5 kW forklift systems has declined from $48,000 to about $22,000.

Similar cost reductions have been achieved by large, high-temperature fuel cell manufacturers. Fuel Cell Energy, for example, has reported cost reductions of a factor of five for its molten carbonate fuel cell product over the period 1996 to 2008 [2]. Foreign manufacturers whose governments have also supported fuel cell research, development and deployment have achieved similar cost reductions.

The model of the domestic fuel cell industry constructed for this study estimated that existing programs have



2005 and 2010 averagesbased on estimates supplied by manufacturers 2010 predicted assumed government procurements of 2,175 units per year, total for all market segments. Predictions assumed a progress ratio of 0.9 and scale elasticity of -0.2.

FIGURE 1. Comparison of 2008 ORNL Study and 2010 Fuel Cell Cost Estimates

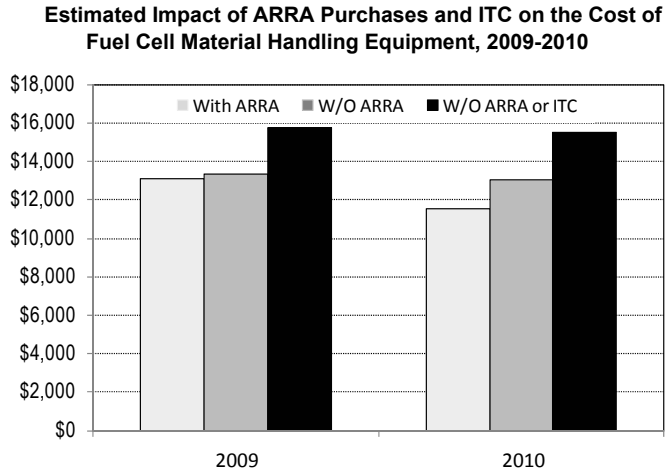
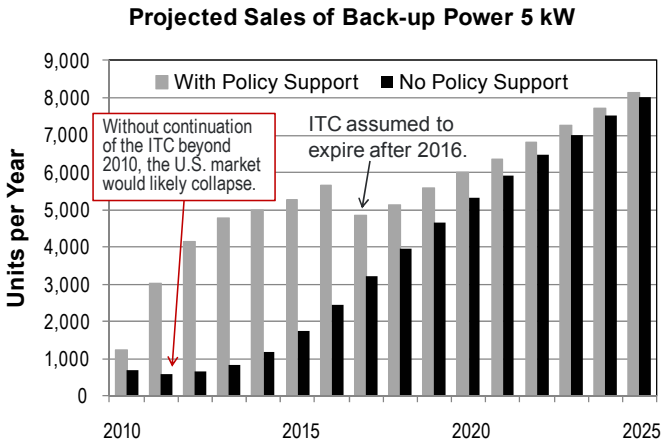


FIGURE 2. Estimated Impact of ARRA Purchases and Investment Tax Credit (ITC) on the Cost of Fuel Cell Material Handling Equipment in 2009 and 2010

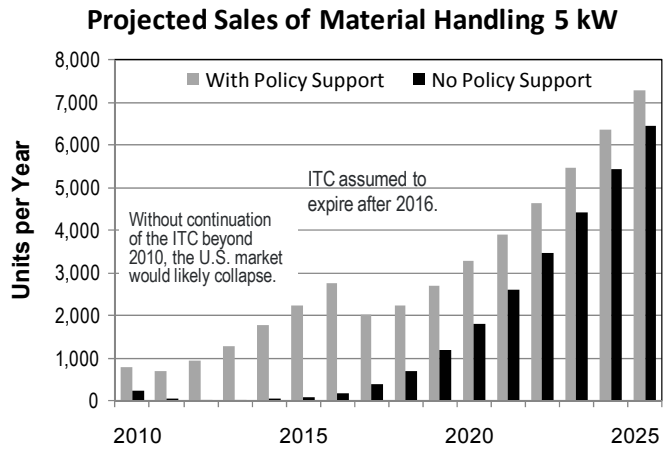
important beneficial impacts on the industry, without which the industry might not become sustainable. The ARRA has contributed to reducing costs of fuel cell manufacturers in the material handling and backup power segments (Figure 2). Without either the ARRA or the investment tax credit, it is estimated that the cost of fuel cell material handling systems would be about $4,000 higher than the actual costs in 2010. Continuation of the investment tax credit through 2016 appears to be essential to sustaining a domestic fuel cell industry and could lead to a viable industry before 2020. The model's estimates suggest that continuing current policies could lead to growing markets in all three applications (Figures 3-4).

However, production volumes, especially for material handling equipment but also for micro-CHP and large-scale CHP may not be sufficient to sustain manufacturers over the next 1-4 years. Enhanced incentives for fuel cell purchases should therefore be considered to increase the industry's chances for successful transition to viability. The most promising policy for all types of fuel cells appears to be conversion of the investment tax credit now capped at 30% of capital cost to an uncapped $3,000/kW tax credit. Feed-in tariffs are an especially attractive policy for large and small CHP.



Only ARRA purchases have been excluded from the "No Policy" case. Other government procurements prior to 2011 are included inboth cases. Progress ratioof 0.9 and scale elasticity of -0.2. Number of manufacturers is assumed to be 3. Government and private purchases for demonstrations are 100 units/yr. in the policy case.

FIGURE 3. Projected Sales of 5 kW Backup Power Units With and Without Current Policies



Only ARRA purchases have been excluded from the "No Policy" case. Other government procurements prior to 2011 are included inboth cases. Progress ratio of 0.9, scale elasticity of -0.2. Government and private procurements of 100 units/yr. for demonstrations continue in the policy case.

FIGURE 4. Projected Sales of 5 kW Material Handling Units With and Without Current Policies

Conclusions and Future Directions

The non-automotive fuel cell industry study documents the substantial progress domestic and foreign fuel cell manufacturers have made in reducing costs and improving performance over the past three years as well as the beneficial impacts of government policies. Still, the industry faces substantial barriers to market success, including further reducing costs via scale economies, learning by experience and for material handling applications, increasing the availability of moderately priced hydrogen.

Research in FY 2012 will focus on developing new scenarios of the potential transition to hydrogen, incorporating what has been learned about technologies and markets since the 2007 study. In particular, new scenarios will be developed to analyze the potential for hydrogen fuel cell, battery electric and grid-connected hybrid vehicles to compete in different market segments. In addition, the potential for maximum use of renewable energy in hydrogen and electricity production may be a focus. The HyTrans model will be used in these analyses but, in collaboration with the National Renewable Energy Laboratory (NREL), ORNL will explore the potential to combine ORNL's MA3T model with NREL's Scenario Evaluation, Regionalization and Analysis model to simulate the transitions at a much higher level of geographic detail and market segmentation.

FY 2011 Publications/Presentations

1. Greene, D.L., K.G. Duleep and G. Upreti, 2011. *Status and Outlook for the U.S. Non-Automotive Fuel Cell Industry: Impacts of Government Policies and Assessment of Future Opportunities*, ORNL/TM-2011/101, Oak Ridge National Laboratory, Oak Ridge, TN, May.

2. Greene, D.L., 2011. "Non-automotive Fuel Cells: Market Assessment and Analysis of Impacts of Policies", presented at the 2011 Hydrogen Program and Vehicle Technologies Program Annual Merit Review, Arlington, Virginia, June 10, 2011.

3. Greene, D.L., 2011. "National Security and Alternative Fuels: Observations on a Transportation Energy Transition", presentation to the Military Advisory Board of the Center for Naval Analysis, Alexandria, Virginia, March 8, 2011.

3. Greene, D.L., 2010. "Transportation's Energy Efficiency: What's Needed Today and by 2050", ACEEE: 30 Years of Energizing Efficiency, Washington, D.C., December 7, 2010.

4. Greene, D.L., 2010. "Transportation's Energy Challenges", Appalachian State University, Boone, NC, November 1, 2010.

5. Das, S., 2011. "Reducing GHG Emissions in the Transportation Sector", *Energy for Sustainable Development*, May, 2011.

6. Das, S., forthcoming, "Status of Advanced Light-Duty Transportation Technologies in the U.S.", submitted for publication in the Energy Policy journal, June'11.

References

1. Greene, D.L. and K.G. Duleep, 2008. *Bootsrapping a Sustainable North American PEM Fuel Cell Industry: Could a Federal Acquisition Program Make a Difference?*, ORNL/TM-2008/183, Oak Ridge National Laboratory, Oak Ridge, Tennessee, October.

2. Adamson, K., 2008. "2008 Large Stationary Survey", Fuel Cell Today, www.fuelcelltoday.com, August.

XI.2 Hydrogen Infrastructure Market Readiness Analysis

Marc Melaina
National Renewable Energy Laboratory
1617 Cole Blvd.
Golden, CO 80401
Phone: (303) 275-3836
E-mail: marc.melaina@nrel.gov

DOE Manager
HQ: Fred Joseck
Phone: (202) 586-7932
E-mail: Fred.Joseck@hq.doe.gov

Subcontractors:
- IDC Energy Insights, Framingham, MA
- Energetics, Columbia, MD

Project Start Date: October 2010
Project End Date: September 2011

Fiscal Year (FY) 2011 Objectives

- Collect stakeholder input on key issues pertaining to hydrogen infrastructure market readiness, with a focus on cost reduction opportunities.
- Identify quantitative and qualitative cost reduction opportunities associated with economies of scale, volume production, learning, standardization, streamlining station design and permitting processes, technology research and development, and other any other relevant factors.
- Communicate cost reduction opportunity findings in a cohesive final report.

Technical Barriers

This project addresses the following technical barriers from the Systems Analysis section of the Fuel Cell Technologies Program Multi-Year Research, Development and Demonstration Plan:

(A) Future Market Behavior

(C) Inconsistent Data, Assumptions, and Guidelines

(B) Stove-Piped, Siloed Analytical Capability

Contribution to Achievement of DOE Systems Analysis Milestones

This project will contribute to achieving the following DOE milestone from the System Analysis and System Integration sections of the Fuel Cell Technologies Program Multi-Year Research, Development and Demonstration Plan:

- Milestone 8 (System Analysis): Complete analysis and studies of resource/feedstock, production/delivery, and existing infrastructure for technology readiness. (4Q, 2014)

Accomplishments

- Convened a 1.5-day Market Readiness Workshop with more than 60 expert participants to discuss and prioritize technology market readiness and cost reduction opportunities.
- Collected feedback from panel discussions and breakout groups during the Market Readiness Workshop.
- Designed and distributed an Excel-based cost calculator that calculates the cost of hydrogen based on stakeholder responses to detailed cost questions about four general types of hydrogen stations: state-of-the-art, early commercial, larger stations, and more stations.
- Participated in meetings and supported the analysis process associated with the infrastructure rollout planning being undertaken by the California Fuel Cell Partnership (CaFCP).
- Integrated findings and feedback from all project activities into a final report.
- Initiated discussions about follow-up activities to better understand subtopics associated with hydrogen infrastructure market readiness.



Introduction

The cost of hydrogen infrastructure components required to support early markets for hydrogen fuel cell electric vehicles (FCEVs) is a significant barrier because of high investment risks and technology uncertainty. Past studies of the hydrogen transition have highlighted the importance of competitive early infrastructure costs to market transformation [1,2]. Cost and performance of infrastructure technologies have improved in recent years, especially with growth in emerging markets such as forklifts and telecommunications. An update on current status is necessary to inform the investment community and to improve the realism of scenario transition models.

Approach

This project examines cost reduction opportunities for hydrogen stations through three distinct activities: 1) conducting an expert workshop to discuss and prioritize opportunities, 2) distributing a cost calculator that enables stakeholders to provide quantitative feedback, and

3) coordinating with efforts at the CaFCP to integrate recent developments. These activities are summarized in the following.

The Hydrogen Infrastructure Market Readiness Workshop was held on February 16–17, 2011 in conjunction with the annual Fuel Cell and Hydrogen Energy Association conference. More than 60 attendees participated in two panel sessions during the afternoon of February 16; group discussions and breakout sessions were held all day on February 17. Each breakout group, with assistance from Energetics facilitators, used a voting system to prioritize opportunities. The mix of breakout group participants was predetermined to include diverse stakeholder perspectives in each group (see Figure 1). Breakout groups focused on the following key questions:

- What are the biggest opportunities to reduce the costs of hydrogen fueling stations over the next 2–5 years?
- What can we do to achieve the high-priority cost reduction opportunities?
- Who needs to do what when? What kind of help is needed? Is information sharing or coordination needed?

The Hydrogen Station Cost Calculator was distributed to a select group of experts to collect feedback on costs for stations designed to support early FCEV markets, as well as stations supporting expanding markets. The calculator was designed to enable experts to provide multiple levels of detail on cost and performance, and provides direct feedback on the implied cost of hydrogen ($/kg) using the Hydrogen Analysis (H2A) discounted cash flow financial framework [3]. A Beta version of the calculator was distributed for review, and revisions were made based on suggestions for improvement before the final version was distributed. IDC Energy Insights distributed the calculator through a clean room mechanism, ensuring the anonymity of all responses and delivering only aggregate results to NREL staff. The third project activity, coordination with the CaFCP, has occurred by attending planning meetings and providing California-specific infrastructure cost estimates based on NREL cost models.

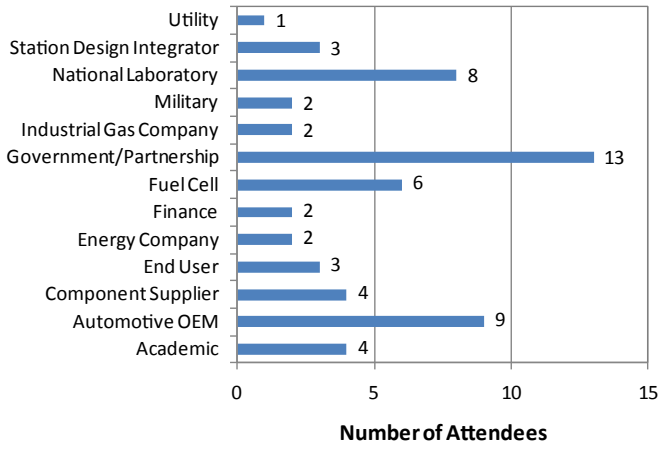


FIGURE 1. Distribution of Workshop Attendees by Stakeholder Group

Results

To date, complete results are available from the first activity only; feedback from the calculator is still being collected and the CaFCP is still being engaged. Figure 2 shows aggregate results of the Market Readiness Workshop cost reduction opportunity prioritization process; the number of opportunities in each category is shown on the vertical axis, and the number of points received though the prioritization process is indicated on the horizontal axis. Color coding indicates categories of a similar type. Two points were allocated to each opportunity identified during the panel sessions, and one point for each opportunity raised in the breakout groups. Additional points were added based on the voting process, with each breakout group attendee allocating three points in two prioritization sessions. With the choice of categorization shown in Figure 2, streamlining the station permitting process is a high-priority cost reduction opportunity. Other types of categorization, especially around station design (green boxes), would highlight other priorities. Examples of specific hydrogen station cost reduction opportunities are:

System Station Costs (Design, Performance Requirements)

- Eliminate station design/installation requirements with ultraconservative requirements.
- Increase the number of station components and equipment that have achieved third-party certification for use in hydrogen service.
- Target processes and components that cause station reliability problems (O-rings, infrared nozzles, etc.).
- Encourage modular station designs that harmonize requirements for small, medium, and large stations, and enable modular station expansion.
- Provide awards for networks of stations using the same (or a similar) design, rather than one-off projects.
- Harmonize and standardize dispensing equipment specifications.
- Increase the number of suppliers of hydrogen station components and systems.

Component Level Costs

- Reduce capital equipment costs, especially for high-pressure equipment.
- Reduce hydrogen storage costs (e.g., enable use of 14,000 psi storage; composite tanks).
- Reduce compressor capital, and operations and maintenance costs.

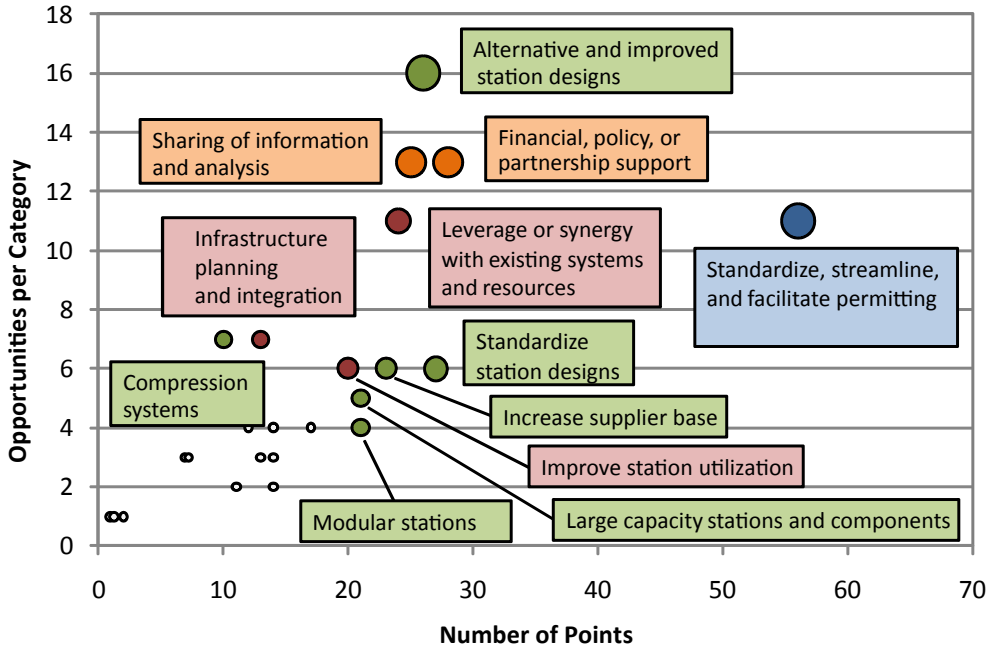


FIGURE 2. Summary of cost reduction opportunities collected from workshop breakout groups (vertical axis) and points allocated through voting process (horizontal axis).

Reduce Dispensing Costs

- Reduce planning and permitting costs (siting, cost of compliance).
- Institute a "type approval" approach for hydrogen stations to simplify and streamline the permitting process.
- Develop a model or models for a streamlined, uniform permitting process (written for permitting officials).
- Develop targeted, "plain language" information products and forums to educate fire marshals, permitting officials, municipal officials, the public, and the insurance industry about hydrogen stations.

Economies of Scale and Learning by Doing

- Modular approaches and standardized manufacturing can lead to as much as 50% cost reduction.
- More uniform permitting processes could reduce station costs by 20%–30%.
- Cut equipment operations and maintenance costs by 75% by using validated components.

Collaborative Actions

- Detailed station deployment plan – include automotive original equipment manufacturers, focused markets, potentially contractual, with a 5–10 year outlook.
- Early market hydrogen users group – webinar series, conferences, briefings to be posted on website, codes and standards database, Annual Merit Review meeting-like exchange of information across industries.

Research and Development

- Design modular expansion stations.
- Design a targeted DOE program on large-scale compression.

Conclusions and Future Directions

NREL researchers have identified numerous diverse opportunities to further reduce the cost of hydrogen stations that are designed to serve early FCEV markets. These opportunities must be pursued through a variety of means, including technical design, codes and standards, and policy mechanisms. Station design and streamlining the permitting process appear to be two general categories that include multiple high-priority cost reduction opportunities. This project ends in FY 2011, but plans are to provide improved characterizations of distinct cost reduction opportunities through follow-up stakeholder workshops. All results and feedback will be compiled in a final report.

Special Recognitions

1. 2011 Department of Energy Hydrogen and Fuel Cells Program R&D Award, Dr. Marc Melaina, National Renewable Energy Laboratory, Infrastructure Analysis and Program Model Development.

References

1. Greene, D.L., P.N. Leiby, et al. (2008). Analysis of the Transition to Hydrogen Fuel Cell Vehicles & the Potential Hydrogen Energy Infrastructure Requirements. Oak Ridge National Laboratory. Report number: ORNL/TM-2008/30. Available online: http://www.hydrogen.energy.gov/analysis_repository/project.cfm/PID=223

2. NAS (2004). The Hydrogen Economy: Opportunities, Costs, Barriers, and R&D Needs. National Academy of Sciences / National Research Council, National Academies Press, Washington, D.C.

3. The Department of Energy Hydrogen Analysis (H2A) Cost models are available online: http://www.hydrogen.energy.gov/h2a_analysis.html

XI.3 Infrastructure Analysis of Early Market Transition of Fuel Cell Vehicles

Brian Bush (Primary Contact), Marc Melaina, Olga Sozinova, Karen Webster
National Renewable Energy Laboratory
1617 Cole Boulevard, Mail Stop RSF300
Golden, CO 80401
Phone: (303) 384-7472
E-mail: brian.bush@nrel.gov

DOE Manager
HQ: Fred Joseck
Phone: (202) 586-7932
E-mail: Fred.Joseck@ee.doe.gov

Subcontractor:
Jon Svede, Allegiance Consulting, Denver, CO

Project Start Date: May 1, 2005
Project End Date: Project continuation and direction determined annually by DOE

Fiscal Year (FY) 2011 Objectives

The Scenario Evaluation, Regionalization and Analysis (SERA) model is a geospatially and temporally oriented analysis model that determines the optimal production and delivery scenarios for hydrogen, given resource availability and technology cost. The objectives of the most recent phase of the project are:

- Interoperability
  - Add functions to SERA to work with new HyDRA (Hydrogen Demand and Resource Analysis) [1] tool features.
  - Import detailed H2A (hydrogen analysis) [2,3] cost models into SERA.
- Infrastructure Integration
  - Develop cost submodels representing a variety of alternative infrastructure development pathways.
- Scenario Analysis
  - Hydrogen production from biogas.
  - Niches for combined heat, hydrogen, and power (CHHP).
  - Minimizing delivery cost of renewable hydrogen.
  - Implications of stakeholder behavior and consumer preferences.
  - Price points between competing technologies.

Technical Barriers

This project addresses the following technical barriers from the Systems Analysis section (4.5) of the Fuel Cell Technologies Program Multi-Year Research, Development and Demonstration Plan:

(B) Stove-piped/Siloed Analytical Capability
(D) Suite of Models and Tools
(E) Unplanned Studies and Analysis

Contribution to Achievement of DOE Systems Analysis Milestones

This project is contributing to achievement of the following DOE milestones from the Systems Analysis section of the Fuel Cell Technologies Program Multi-Year Research, Development and Demonstration Plan:

- **Milestone 3.** Begin a coordinated study of market transformation analysis with H2A and Delivery models.
- **Milestone 5.** Complete analysis and studies of resource/feedstock, production/delivery and existing infrastructure for various hydrogen scenarios.
- **Milestone 24.** Complete the linear optimization model (HyDS) to analyze the optimum production facilities and infrastructure for hydrogen demand scenarios.
- **Milestone 26.** Annual model update and validation.

FY 2011 Accomplishments

- Enhanced cost model:
  - Addition of biogas, CHHP, and wind cost models for hydrogen production.
  - Addition of rail and composite-tank truck delivery pathways.
  - New, advanced method for rapidly incorporating updates to H2A cost models into SERA.
- Added new submodels:
  - Vehicle choice
  - Vehicle stock
- Conducted first-of-kind studies:
  - Hydrogen production from biogas.
  - Niches for CHHP.
  - Minimizing delivery cost of renewable hydrogen.
  - Implications of stakeholder behavior and consumer preferences.
- Achieved significant enhancements in SERA usability:
  - Cleaner user interface.
  - Streamlined data storage mechanisms.



Introduction

The SERA model fills a unique and important niche in the temporal and geospatial analysis of hydrogen infrastructure build-out for production and delivery. It nicely complements other hydrogen analysis tools and is well suited to contribute to scenario analysis involving the temporally specific geospatial deployment of hydrogen production and transmission infrastructure. Its key capabilities are (i) an optimization of the physical build-out of hydrogen infrastructure; (ii) the unified treatment of production, transmission, and distribution; (iii) the ease with which new technologies can be added to an analysis; (iv) the consistent physical and economic computations; (v) the ability to estimate costs and cash flows; (vi) the spatial and temporal resolution of hydrogen infrastructure networks; (vii) regional specificity; and (viii) the allowance for exogenously specified urban hydrogen demands. Its internal architecture is flexible, and it is compatible with geographic information systems (GIS) and the H2A models [2,3]. SERA is designed to answer questions such as: Which pathways will provide least-cost hydrogen for a specified demand? What network economies can be achieved by linking production facilities to multiple demand centers? How will particular technologies compete with one another?

Approach

In order to answer such questions, SERA supports analyses aimed at identifying optimal infrastructure to meet specified annual urban hydrogen demands, perhaps coupled to other multiple objectives and constraints. Cash flows are computed, detailed by infrastructure component, city, and region, and these provide insights into components of hydrogen costs, which are determined by year, volume, and locality. Four methods of long distance hydrogen transport are considered: pipeline, gaseous truck, liquid truck, and railroad. The major use of SERA is for studying potential turning points in infrastructure choice via sensitivity analysis on infrastructure, feedstock, and fuel cost inputs in the context of the complex transient and transitional interactions between increasing hydrogen demand and hydrogen infrastructure construction. With carefully constructed input data sets, SERA can also weigh tradeoffs between investments in various infrastructure types, given policy constraints (e.g., greenhouse gas). Figure 1 shows the interrelationship between the input data for SERA and the algorithms applied to them in order to compute the delivered cost of hydrogen. The infrastructure networks are optimized using a simulated-annealing algorithm that explores the large set of potential build-out plans that meet the input requirements for hydrogen delivery at cities over time. The hydrogen transport computations are based on graph-theoretic algorithms for determining optimal flows in networks. The cash flow computations rely on standard discounting approaches. Figure 2 shows sample SERA output in the form of an optimized hydrogen infrastructure network.

Results

We finalized a study that examines the relative cost-effectiveness of supplying hydrogen refueling stations via CHHP or on-site steam methane reforming (SMR) for a large urban area, under three fuel cell electric vehicle (FCEV) penetration scenarios. The major conclusions of this work are: (i) CHHP-based hydrogen production for use in nearby hydrogen refueling stations typically only has cost advantages over on-site SMR hydrogen production at some of those refueling stations, particularly for the early years of FCEV penetration scenarios where hydrogen demand and station sizes are initially small; (ii) variations in SMR or CHHP facility and energy-input costs can dramatically affect the overall cost of hydrogen, but they do not affect the mix of CHHP and SMR deployment as strongly; and (iii) for these scenarios and this study region, hydrogen costs typically drop from slightly above $6/kilogram (kg) in early years to below $5/kg in later years.

Furthermore, we finalized a study of the SERA biogas capability. This involved (i) provisionally incorporating the

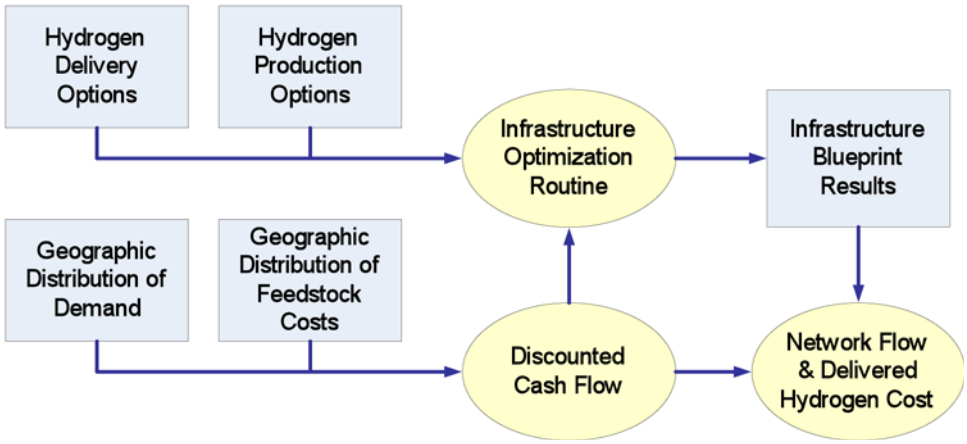


FIGURE 1. SERA Input and Output Data and Algorithms

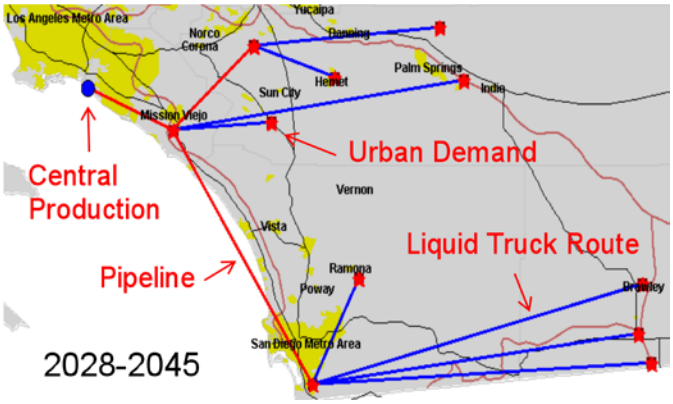


FIGURE 2. Illustrative Hydrogen Infrastructure Network Output from SERA

latest NREL biogas systems characterization into SERA, (ii) performing an illustrative analysis of infrastructure build-out highlighting the significance of biogas pathways, and (iii) developing insights for future in-depth studies involving biogas pathways. SERA uses cost estimates from the H2A biomethane systems model in conjunction with those from the H2A production model to evaluate the delivered cost of biogas-originated hydrogen. In the sample analysis that we performed (on a test case of Midwestern cities), the optimal choice of infrastructure often hinges upon the difference between biogas and natural gas prices: when the biogas price, plus the processing cost to biomethane, is less than the natural gas price, the biogas pathways have lower costs. In general, the most competitive biogas scenario is when a single large biogas plant supplies a dozen or more (typically small) on-site SMR plants.

We also explored three diverse avenues for the production of hydrogen from renewable resources in the context of substantial adoption of fuel cell vehicles and the large scale use of renewable for electricity production: (i) the production of hydrogen from wind-generated electricity that would have been curtailed by electric power grid congestion, (ii) the production of hydrogen directly from wind resources without the co-production of electricity, and (iii) co-production with a balance between electricity transmission and electrolysis. In this context, we varied the technological characteristics of the hydrogen production in considering current, future, and "breakthrough" situations. We found total delivered costs in the $4-$10/kg range (see Figure 3), along with a diverse use of infrastructure that highlights the niches where particular delivery pathways are most cost effective. The use of curtailed wind energy can lower the delivered cost of hydrogen dramatically, although sufficient curtailed resource is not available to allow wind-produced hydrogen to supply the majority of hydrogen in high penetration FCEV scenarios.

We completed the development of vehicle-choice and vehicle-stock capabilities for SERA. The objectives of this effort were to (i) incorporate the latest version of the Automotive Deployment Option Projection Tool (ADOPT) [4] vehicle choice model into SERA, (ii) verify that output from the SERA vehicle choice model matches that from ADOPT, (iii) integrate the new vehicle choice model with a existing vehicle stock model that tracks the ageing and energy use of vehicles, and (iv) develop insights for future studies involving vehicle choice and stock. This allows us to generate regional market shares for new vehicles over time. The new vehicle choice model can handle any user-defined set of vehicle makes and models, any user-defined set of vehicle types (e.g., internal combustion engines, FCEVs, electric vehicles), and any user-defined set of geographic regions (e.g., zip codes, counties, states, census regions, national). It aggregates the user-defined geographic regions into larger regions, generates annual market shares, estimates splits between fuel types, and provides output suitable for input into the SERA vehicle stock model. Furthermore, it supports the future inclusion of alternative algorithms for vehicle choice if those are deemed necessary for an analysis study. The current version of the SERA vehicle choice model exactly reproduces the output of the ADOPT model. The output of the SERA vehicle choice and stock models is used as input for SERA-based infrastructure optimization studies.

Finally, we made major progress automating the computations of hydrogen costs based on the H2A models, which are encoded as Excel spreadsheets. This capability is

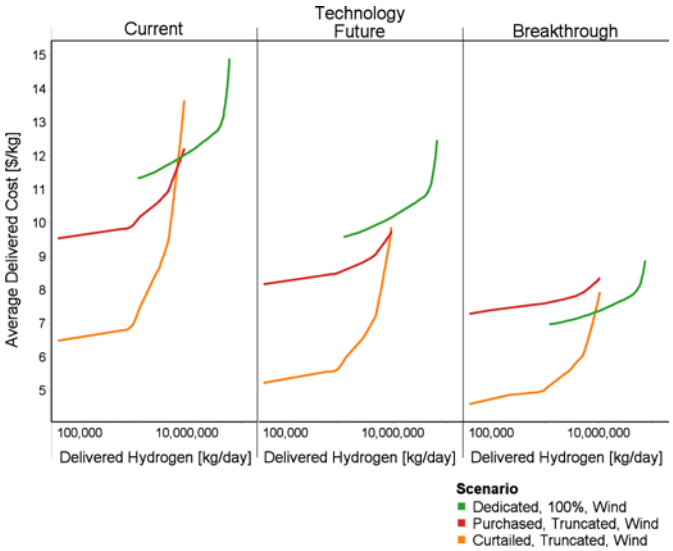


FIGURE 3. Effective-cost curves for wind-hydrogen scenarios. The "dedicated" cases are when the whole wind resource is used for hydrogen production; the "purchased" cases are when the curtailed wind resource is supplemented with additional electricity purchased from the wind farm; and the "curtailed" cases are when only the curtailed wind energy is used for electrolysis. The "current" and "future" technology cases roughly correspond to estimated 2010 and 2030 costs; the "breakthrough" technology case assumes costs substantially lower than the "future" case.

invaluable in keeping the cost inputs to SERA completely in synchronization with the latest H2A production and components models.

Conclusions and Future Direction

In summary, SERA is an effective, integrated, cross-cutting model for optimization-analysis studies of hydrogen infrastructure build-out compatible with the H2A models. It searches for optimal combinations of hydrogen production and transmission infrastructure to meet time-varying demand in urban areas over a region.

The SERA software is now essentially complete, but continued use of the tool in scenario studies requires regular updating of H2A and other cost inputs, software modifications to take advantage of new HyDRA features, and minor usability enhancements in response to analysts' requests. SERA will be applied to more complex deployment scenarios such as (i) identifying regional niches for production technologies and delivery infrastructure and (ii) assessing the influence of feedback from computed delivered costs of hydrogen to consumer and stakeholder decisions. We also plan collaborative exchange of data and scenarios assumptions with other models for the conduct of integrated multi-fuel studies, particularly when they involve scenarios with opportunities for addressing cost barriers in early years of FCEV transition.

FY 2011 Publications/Presentations

1. M. Melaina, *Optimal Production, Transport, and Delivery Infrastructure for Hydrogen Production from Renewable Resources*, Fuel Cell & Hydrogen Energy Conference, 13–16 February 2011. (conference presentation)

2. B. Bush, A. Jalalzadeh, M. Melaina, G. Saur, *SERA Biogas Capability Preview*, 30 June 2010. (management report)

3. B. Bush, A. Jalalzadeh, M. Melaina, G. Saur, *SERA Biogas Capability*, 31 July 2010. (management report)

4. B. Bush, M. Melaina, M. Penev, O. Sozinova, D. Steward, *CHHP Case Study and Cost Curves*, 27 September 2010. (management report)

5. B. Bush, M. Melaina, M. Penev, O. Sozinova, D. Steward, J. Svede, *Scenario Evaluation & Regionalization Analysis (SERA) Final Report for 2010*, 27 September 2010. (management report)

6. B. Bush, M. Melaina, K. Webster, A. Brooker, *SERA Vehicle Choice Capability*, 31 December 2010. (management report)

References

1. National Renewable Energy Laboratory. HyDRA Model. https://rpm.nrel.gov/node/9. Accessed 30 Apr 2009.

2. "H2A Production Models and Case Studies." Version 2.1.2. *DOE H2A Production Analysis.* http://www.hydrogen.energy.gov/h2a_production.html. Accessed 17 Jan 2009.

3. "H2A Delivery Scenario Model." Version 2.0. *DOE H2A Delivery Analysis.* http://www.hydrogen.energy.gov/h2a_delivery.html. Accessed 17 Jan 2009.

4. National Renewable Energy Laboratory. Automotive Deployment Option Projection Tool (ADOPT). 2010.

XI.4 Analysis of the Effects of Developing New Energy Infrastructures

David Reichmuth
Sandia National Laboratories
P.O. Box 969
Livermore, CA 94551-0969
Phone: (925) 294-3393
E-mail: dreichm@sandia.gov

DOE Manager
HQ: Fred Joseck
Phone: (202) 586-7932
E-mail: Fred.Joseck@ee.doe.gov

Subcontractor:
Andy Lutz, Alamo, CA

Project Start Date: December 1, 2007
Project End Date: September 30, 2012

Fiscal Year (FY) 2011 Objectives

- Develop models of interdependent energy infrastructure systems.
- Analyze the impacts of widespread deployment of a hydrogen fueling infrastructure and hydrogen fuel cell vehicle fleet.
- Analyze the impacts of stationary fuel cell systems for distributed power.

Technical Barriers

This project addresses the following technical barriers from the Systems Analysis section of the Fuel Cell Technologies Program Multi-Year Research, Development and Demonstration Plan:

(A) Future Market Behavior
(B) Stove-Piped/Siloed Analytical Capability
(E) Unplanned Studies and Analysis

Contribution to Achievement of DOE Systems Analysis Milestones

This project will contribute to achievement of the following DOE milestones from the Systems Analysis section of the Fuel Cell Technologies Program Multi-Year Research, Development and Demonstration Plan:

- **Milestone 5**: Complete analysis and studies of resource/feedstock, production/delivery and existing infrastructure for various hydrogen scenarios. (4Q, 2010)
- **Milestone 7**: Analysis of the hydrogen infrastructure and technical target progress for the hydrogen fuel and vehicles. (2Q, 2011)
- **Milestone 8**: Complete analysis and studies of resource/feedstock, production/delivery and existing infrastructure for technology readiness. (4Q, 2014)

Accomplishments

- Sandia National Laboratories developed a dynamic tool for analyzing the potential impact of an emergent hydrogen fuel infrastructure on the existing energy infrastructures.
- Developed models of the behavior of natural gas, refined petroleum, hydrogen, and electricity generation cost for eight geographic regions in the U.S.
- Incorporated a light-duty vehicle adoption model for hydrogen fuel cell (HFCV), plug-in hybrid electric (PHEV), battery electric (BEV) and a new generation of conventional vehicles that meet the 2016 Corporate Average Fuel Economy regulation [1]. Added market segmentation to assign alternative vehicles to three vehicle classes: small cars, large cars, and trucks.
- Quantified the impact of large-scale HFCV adoption on key metrics such as petroleum use and carbon emissions and analyzed the relative benefits of BEV and HFCV. Our analysis shows that HFCVs could enable nearly 10-fold larger savings in petroleum use, as compared to BEVs.
- Examined impact of combined power and hydrogen production from stationary fuel cells on early HFCV market.



Introduction

This systems analysis task is designed to examine the impact of emerging hydrogen infrastructure and fuel cell vehicles on key metrics, such as petroleum use and carbon emissions. To make a meaningful assessment of the benefits of fuel cell technologies, potential competing technologies must be included in the analysis. For this reason, we include multiple hydrogen and electricity production pathways and a range of vehicle sizes and powertrain combinations. It is also important to consider the time scale for technology development and deployment. Therefore our analysis includes time-dependent data for the deployment of potential fuel production and delivery pathways along with the evolution of the light-duty vehicle fleet.

Sandia National Laboratories (SNL) developed a system dynamics (SD) model for studying the competition of

HFCVs, PHEVs, BEVs, and advanced gasoline vehicles and the resulting impact on energy infrastructures. In addition, our model includes the possible adoption of stationary fuel cell systems for distributed power and hydrogen fuel production. To demonstrate the utility of the SD approach, in FY 2009 and 2010 SNL analyzed the likely impact on the California markets for gasoline, natural gas, and electricity. This state was selected because it is home to one or more "lighthouse" cities for early hydrogen adoption, and because of the interdependencies between electricity and natural gas infrastructures (a significant fraction of electricity generation is derived from natural gas boilers and gas turbines). Our current work expands on the analysis to the national scale, with a regionally differentiated model that can examine geographic differences in vehicle fleet composition and transportation energy sources.

Approach

We use an SD model to simulate the future vehicle fleet composition [2]. The model is comprised of three main submodules: energy sources, fuels, and vehicles. The vehicle portion of the model calculates the changing composition of the vehicle fleet, in part due to the cost of fuel calculated by the fuel submodule. The cost of the fuels changes in response to changing demand from the vehicle model, with both positive and negative feedback elements. Positive feedbacks include factors such as decreasing cost of hydrogen delivery with increasing infrastructure utilization, while negative feedback elements include competition and exhaustion of primary energy sources. We consider multiple pathways to generate hydrogen and electricity, and the model uses a cost-based choice function to allocate new production capacity. For hydrogen production, we currently model natural gas distributed steam-methane reforming and centralized electrolysis from wind power.

The SD model chooses future vehicle sales by applying a multinominal logit choice model based on the amortized purchase cost, penalty factors (e.g. for low vehicle range) and the annual fuel cost [3]. This choice function allocates sales among the various combinations of vehicle powertrains and sizes included in the model. The cost of fuels and the purchase cost of the vehicles change over time, which causes the distribution of powertrain choice to evolve over time. A summary of vehicle efficiency assumptions is shown in Table 1. The model allows for analysis of the sensitivity to input assumptions by using multiple model runs with variation of input parameters, using Latin hypercube sampling of the input space.

Results

The projected evolution of the light-duty vehicle (LDV) fleet over time is shown in Figure 1. Our baseline case assumes moderate growth in the vehicle fleet, at a net rate of 0.9%, equal to the estimate for overall U.S. population growth [4]. The overall growth rate is a result of an annual vehicle sales rate of 6.9% per year and a scrap rate of 5.8% per year. The baseline case also assumes that the price of crude oil starts at $90/barrel and increases (in constant dollars) $3/barrel per year. In this baseline case, alternative fuel vehicles (AFVs) make up approximately 50% of the LDV fleet by 2050. The dominant AFV in 2050 is the HFCV, with nearly 100 million vehicles in service. The PHEV40 and BEV vehicles' market penetration is lower in large part due to unavailability of larger-sized vehicles, while PHEV10

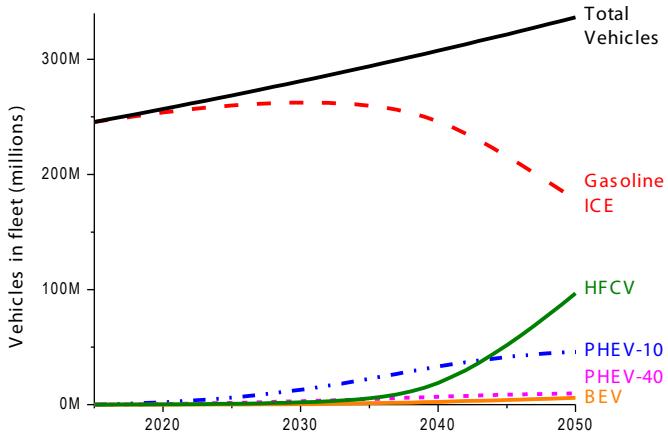


FIGURE 1. LDVs in the U.S. by powertrain for the baseline case. By 2050, approximately 50% of the vehicles in the fleet are AFVs.

TABLE 1. Analysis Assumptions for Vehicle Fuel Efficiency in 2010, 2016, and 2035

MPGe in 2010/2016/2035	Gasoline ICE	HFCV	PHEV10 Gas (77%) Elect (23%)	PHEV40 Gas (37%) Elect (63%)	BEV
Small Car	36/42/45	69/71/76	41/45/56 (gas) 84/102/136	30/34/47 (gas) 94/110/148	99/110/148
Large Car	18/30/39	69/71/76	35/39/47 72/87/116	25/29/40 80/94/126	N/A
Truck	18/30/39	69/71/76	20/23/28 42/51/68	N/A	N/A

MPGe – miles per gallon equivalent; ICE – internal combustion engine; N/A – not applicable

vehicles enter into the fleet in significant numbers due to their lower purchase price. The vehicle sales for the baseline case are shown in Figure 2. PHEVs initially make up most of the AFV sales, however HFCV sales greatly increase, starting in 2035. By 2050, HFCV sales make up over half of all new LDV sales. The shape and timing of the HFCV sales curve is consistent with prior studies by Greene *et al* [5]. It is important to note that the sales of HFCV are highly dependent on the assumption of rising petroleum prices. If crude oil prices remain constant at $90/barrel, our results show little (<5%) penetration of AFVs (data not shown).

The impact of the significant AFV sales in the baseline case is shown in Figure 3. Both LDV carbon emissions and gasoline consumption show significant decreases (42% and 56%, respectively) relative to the start of the simulation, despite the fact that the total number of vehicles rises 37% over the 35-year simulation run. By 2050, LDV gasoline consumption has dropped to less than 60 billion gallons per year. This level of emissions and petroleum reductions is enabled by AFVs, however predicted improvements to conventional gasoline vehicles are responsible for a large portion of the savings. Gasoline vehicle improvements alone would result in 25% reductions in both gasoline use and carbon emissions in 2050 (relative to 2015).

In the baseline case, we assume all AFV powertrains (PHEV10, PHEV40, BEV, and HFCV) are available. However, AFV technologies require substantial infrastructure investment and research and development progress, and it is possible that not all AFV powertrains will reach large-scale commercial viability. We examine the effects of powertrain unavailability in Figure 4 and Table 2. These data show the effect of not having BEVs, HFCVs or both on key metrics. As shown in Figure 4, the reduction in carbon emissions due to HFCV availability is over 5-fold greater than the reduction due to BEV. In Table 2, the impact of powertrain availability on LDV gasoline consumption is shown and the HFCVs show almost an order of magnitude greater reduction.

Conclusions and Future Directions

Under our baseline case of moderate oil price increases, our analysis predicts 50% hydrogen fuel cell and electric vehicles by 2050. The large-scale market penetration of HFCVs would allow significant greenhouse gas emission and gasoline use reductions, with over 50% decrease in gasoline use in 2050 (relative to 2015 levels). Increasing oil prices

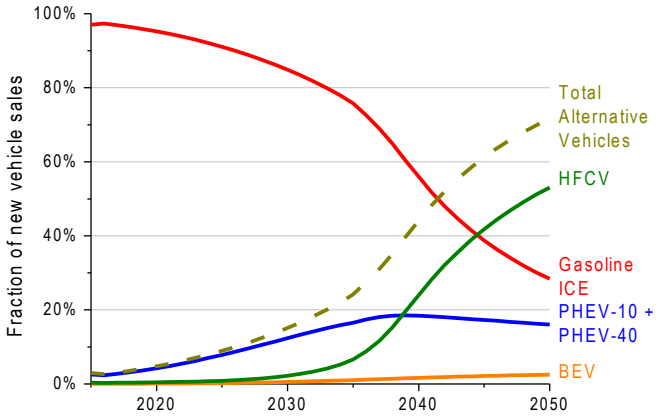


FIGURE 2. Fraction of LDV sales by powertrain for the baseline case. PHEVs are the dominant AFV at the start of the simulation, however HFCV sales rise quickly starting in 2035.

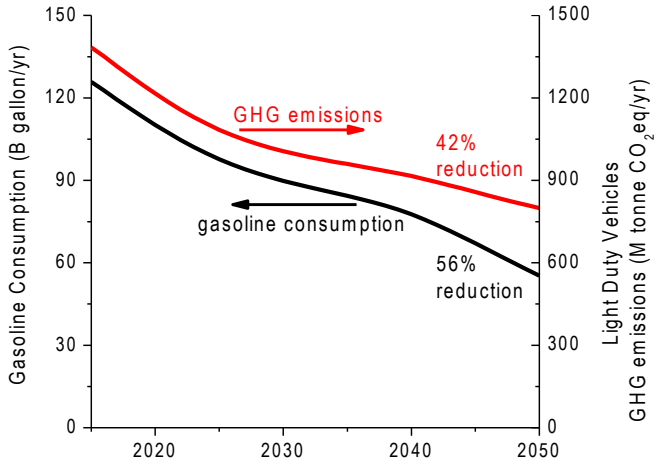


FIGURE 3. Gasoline consumption and carbon emissions from the LDV fleet in the baseline case. Reductions shown are relative to the values in 2015.

TABLE 2. Annual LDV Gasoline Consumption under Different Assumptions for Gasoline Price Projections (Constant Dollars) and Vehicle Powertrain Availability

Oil Price, 2015→2050	ICE+PHEV	ICE+PHEV+BEV	ICE+PHEV+HFCV	ICE+PHEV+HFCV+BEV
$90/bbl, no increase	92.7 B gal/yr	92.6 B gal/yr	91.4 B gal/yr	91.3 B gal/yr
$90/bbl → $195/bbl	84.5 B gal/yr	82.6 B gal/yr	56.2 B gal/yr	55.3 B gal/yr
$90/bbl → $265/bbl	79.6 B gal/yr	75.6 B gal/yr	40.5 B gal/yr	39.2B gal/yr

bbl - barrel

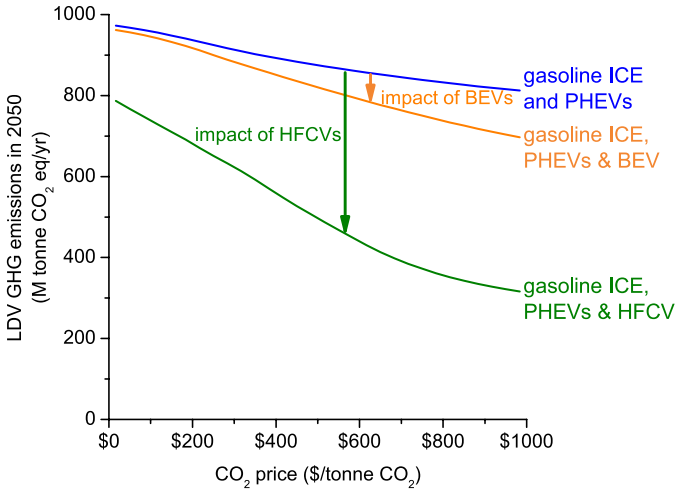


FIGURE 4. Carbon emissions as a function of carbon price in cases with different powertrain availability. The highest emissions are for the scenario in which only gasoline ICE and PHEVs are available (no HFCVs or BEVs). The middle line shows the emissions with gasoline ICE, PHEV and BEV vehicles (no HFCVs), and shows moderate reductions in carbon emissions due to BEV availability. The lowest line corresponds to the scenario with gasoline ICE, PHEV and HFCV vehicles (no BEVs). The impact of HFCV availability is much greater than BEV availability.

(and/or policies that give a price to carbon) are needed for significant numbers of HFCVs (or AFVs) to penetrate the LDV fleet. Our analysis predicts HFCVs will have much larger effect than BEVs on both gasoline consumption and LDV carbon emissions.

The model described in this report analyzes a subset of possible hydrogen production pathways, limiting our ability to model hydrogen infrastructure development and also limiting analysis of carbon-neutral transportation options. Future work will include more energy sources and production processes, with an emphasis on low-carbon hydrogen production options, so that infrastructure requirements and potential limiting factors for hydrogen fuel cell technologies will be better understood.

Acknowledgements

We acknowledge helpful discussions and assistance from the SNL "Transportation Energy Pathways" Laboratory Directed Research and Development team, led by Dawn Manley and Todd West. Sandia National Laboratories is a multi-program laboratory managed and operated by Sandia Corporation, a wholly owned subsidiary of Lockheed Martin Corporation, for the U.S. Department of Energy's National Nuclear Security Administration under contract DE-AC04-94AL85000.

FY 2011 Publications/Presentations

1. Annual Merit Review, Washington, D.C., May 2011.

2. D.S. Reichmuth and J.O. Keller, "Impact of Hydrogen Resource and Vehicles on U.S. Greenhouse Gas Emissions and Petroleum Use," 9th Fuel Cell Science, Engineering, and Technology Conference, Washington, D.C., August 2011.

References

1. Light-Duty Vehicle Greenhouse Gas Emission Standards and Corporate Average Fuel Economy Standards; Final Rule. In Envionmental Protection Agency, Department of Transportation,, Ed. Federal Register: 2010; Vol. 40 CFR 85,86,600 49 CFR 531,533,536,537.

2. Lutz, A. and Reichmuth, D., "Analysis of Energy Infrastructures and Potential Impacts from an Emergent Hydrogen Fueling Infrastructure", DOE Hydrogen Program FY 2009 Annual Progress Report.

3. Struben, J. and Sterman, J., "Transition challenges for alternative fuel vehicle and transportation systems." *Environment and Planning B*. 35, 1070-1097. (2008)

4. Population Division, U.S. Census Bureau,*Projections of the Population and Components of Change for the United States: 2010 to 2050*; 2008.

5. Greene, D., Leiby, P., James, B., Perez, J., Melendez, M., Milbrandt, A., Unnasch, S., Hooks, M., "Analysis of the Transition to Hydrogen Fuel Cell Vehicles and the Potential Hydrogen Energy Infrastructure Requirements", ORNL/TM-2008/30, March 2008.

XI.5 Cost and GHG Implications of Hydrogen for Energy Storage

Darlene Steward (Primary Contact),
Genevieve Saur
National Renewable Energy Laboratory
1617 Cole Blvd.
Golden, CO 80401
Phone: (303) 275-3837
E-mail: Darlene.Steward@nrel.gov

DOE Manager
HQ: Fred Joseck
Phone: (202) 586-7932
E-mail: Fred.Joseck@ee.doe.gov

Project Start Date: October 2008
Project End Date: Project continuation and direction determined annually by DOE

Objective

Use analysis of scenarios for renewable electricity generation coupled with hydrogen systems to find opportunities for cost savings and other benefits of hydrogen energy storage and renewable hydrogen for vehicles.

Technical Barriers

This project addresses the following technical barriers from the Systems Analysis section (4.5) of the Fuel Cell Technologies Program Multi-Year Research, Development and Demonstration Plan:

(B) Stove-Piped/Siloed Analytical Capability

(D) Suite of Models and Tools

(E) Unplanned Studies and Analysis

Technical Targets

The update of the H2A models directly supports the following milestones from the Systems Analysis function from FY 2004 through FY 2016.

Milestone 26	Annual model update and validation. (4Q, 2008; 4Q, 2009; 4Q, 2010; 4Q, 2011; 4Q, 2012; 4Q, 2013; 4Q, 2014; 4Q, 2015)
Milestone 39	Annual update of Analysis Portfolio. (4Q, 2007; 4Q, 2008; 4Q, 2009; 4Q, 2010; 4Q, 2011; 4Q, 2012; 4Q, 2013; 4Q, 2014; 4Q, 2015

FY 2011 Accomplishments

- Four case study (theoretical) wind farms were identified using the NREL Western Wind Dataset (http://www.nrel.gov/wind/integrationdatasets/western/methodology.html).
- Cost estimates were developed for wind turbines, transmission lines, storage cavern development, electrolyzers, fuel cells and auxiliary equipment based on literature values.
- Two primary scenarios were developed and analyzed for the four wind farms.
  - Load leveling of the wind farm electrical output using hydrogen for electricity storage.
  - Hydrogen production via electrolysis used as dispatchable load for times of high wind output.
- The NREL Fuel Cell Power Model (http://www.hydrogen.energy.gov/ fc_power_analysis.html), which combines hourly energy analysis of various generators and loads with the H2A discounted cash flow analysis tool, was used to calculate the levelized cost of all output energy (electricity and/or hydrogen) from the wind farms and storage systems.



Introduction

In FY 2008, NREL began investigating the use of hydrogen as an energy storage mechanism for electric utilities. In this application, various system configurations were modeled for producing hydrogen from renewable energy via electrolysis and storing it. The stored hydrogen can later be converted back to electricity using fuel cells to meet peak electricity demand. In subsequent analyses, NREL evaluated the costs of competing energy storage technologies (batteries, compressed air energy storage, and pumped hydro), additional fuel cell types, and investigated the potential dual benefit of producing excess hydrogen for the vehicle market (see reference [1]). This work builds on previous studies and incorporates more realistic analysis of the impacts of variable wind farm output. Four theoretical wind farms of various sizes and proximity to demand centers are analyzed for two primary scenarios: (1) hydrogen for energy storage; and (2) hydrogen production for transportation using otherwise curtailed wind-generated electricity.

Approach

Four theoretical wind farms were identified using the Western Wind Dataset. Groups of 10, 3-MW turbines were aggregated to the desired total wind farm size and the 10-minute power output data from the dataset was averaged to 1-hour data to create one hourly dataset for each wind farm (see Table 1 and Figure 1).

TABLE 1. Four Theoretical Wind Farms Used in the Energy Analysis

Location	Size (Nameplate Capacity MW)	Capacity Factor	Dedicated Transmission Line Distance (miles)
North Portal, ND	1050	42%	1,000
Wyoming	1620	41%	300
Oklahoma	330	37%	300
Palmdale, CA	450	39%	50

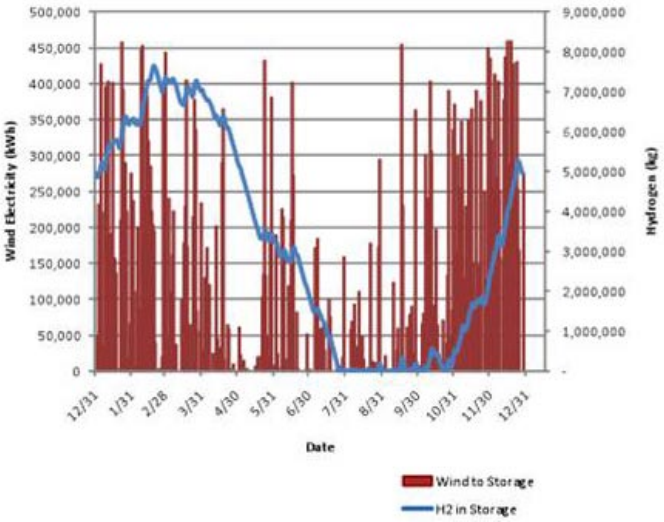


FIGURE 1. Curtailed Electricity and Hydrogen Storage use for the North Dakota Wind Farm

The Fuel Cell Power model calculates the levelized, profited cost of energy output from the system being analyzed. A "base case," in which there is no storage system or hydrogen production, was analyzed for each wind farm. The amount of electricity curtailed is determined by the capacity of the dedicated transmission line for the wind farm. In this analysis the transmission line capacity was varied from 100% to 55% of the nameplate capacity rating of the wind farm, resulting in curtailment of 0% to ~25%. The amount curtailed at each transmission line size varied depending on the specific wind profile for that site. The base case provided a baseline cost of delivered electricity for the wind farm, taking into account the unrealized value of the curtailed electricity. Additional costs to install the storage system or electrolyzer are offset by the additional revenue from capturing some value of the curtailed wind. Thus, the primary cost metric for the analyses answers the question of whether the revenue from the storage system or hydrogen fully offsets the cost of installing additional equipment.

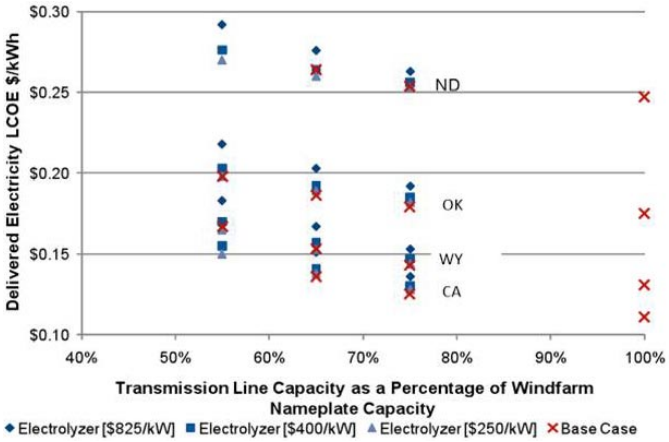


FIGURE 2. Levelized Cost of Delivered Electricity for the Four Wind Farms at Various Transmission Line Capacities

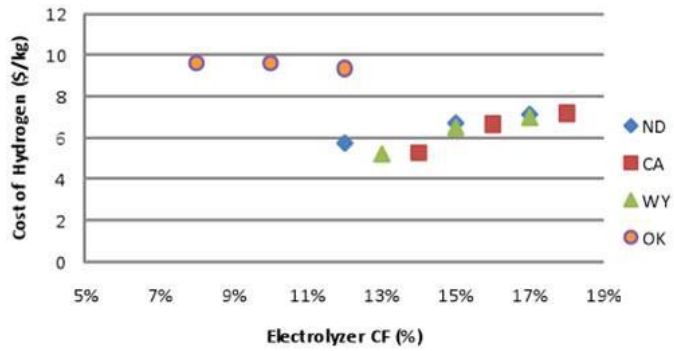


FIGURE 3. Economic Analysis for use of Otherwise Curtailed Wind for Hydrogen Production

Results

Figure 2 presents the results of adding a hydrogen energy storage system to each wind farm. The base case for each wind farm, in which some electricity is curtailed, is indicated by the red "X"s. The blue symbols show the delivered cost of electricity for the same wind farms where hydrogen energy storage has been added. In all cases, the electrolyzer has been sized to capture all the wind-generated electricity that would otherwise have been curtailed. The results indicate that the electrolyzer cost must be less than $400/kW in most cases to make the energy storage system pay for itself.

Results of the analysis using electrolysis as a dispatchable load to produce hydrogen for the transportation sector are shown in Figure 3. The electrolyzer use was increased by diverting more of the wind farm output to the electrolyzer. Electricity in excess of what would have been curtailed must be "purchased" for electrolysis. The analysis results indicate that diverting more electricity to the electrolyzer increases the electrolyzer capacity factor and

increases the cost of the hydrogen produced for all but the Oklahoma wind farm. At the Oklahoma wind farm, the very low equipment use causes the capital cost of the electrolyzer to be the primary cost driver. In this case, increasing use, even with higher input electricity cost, reduces the resulting hydrogen cost. In all other cases, increasing the cost of electricity increases the hydrogen cost, even with better equipment use.

Conclusions and Future Directions

Increasing power generation from intermittent renewable resources will require new strategies for balancing generation and demand, including energy storage and dispatchable demand, both of which are addressed by the two hydrogen systems studied in this work. If hydrogen can play a role in addressing these needs, hydrogen will be more likely to gain a foothold as a viable alternative vehicle fuel. Two potential benefits are:

- The availability of renewable resources dedicated to hydrogen production will be limited in the near term, as these resources are being developed for electricity generation. Therefore, hydrogen must be integrated into the electricity system in such a way that it provides a service or use for excess power in addition to its value as a vehicle fuel. The strategies being analyzed in this work accomplish that objective.
- The high cost of alkaline electrolysis is primarily due to labor-intensive manufacturing methods and low production volumes. Using electrolysis to produce hydrogen, either for electricity storage or for vehicles, could increase demand to the point that more automated manufacturing methods could be used and costs would be dramatically decreased.

The analyses indicate that equipment costs, including electrolyzer costs analyzed here, must be reduced for hydrogen to be an economical alternative for energy storage or production of vehicle fuel from otherwise curtailed wind-generated electricity. However, no additional credit was taken for the various potential services that could be provided by hydrogen production, nor was any attempt made to take advantage of arbitrage opportunities.

Future work will focus on developing similar analyses for solar installations and quantifying greenhouse gas emissions and carbon tax implications, especially in comparison to compressed air energy storage.

References

1. Steward, D.; Saur, G.; Penev, M.; Ramsden, T. Lifecycle Cost Analysis of Hydrogen Versus Other Technologies for Electrical Energy Storage, NREL TP-560-46719, 2009. http://www.nrel.gov/docs/fy10osti/46719.pdf.

XI.6 Emissions Analysis of Electricity Storage with Hydrogen

Amgad Elgowainy
Argonne National Laboratory
ESD362/E361
9700 South Cass Avenue
Argonne, IL 60439
Phone: (630) 252-3074
E-mail: aelgowainy@anl.gov

DOE Manager
HQ: Fred Joseck
Phone: (202) 586-7932
E-mail: Fred.Joseck@ee.doe.gov

Project Start Date: October 2010
Project End Date: October 2012

Fiscal Year (FY) 2011 Objectives

Conduct life-cycle analysis of hydrogen as energy storage for integration of large renewable generation sources into the electric grid.

Technical Barriers

This project addresses the following technical barriers from the Systems Analysis section (4.5) of the Fuel Cell Technologies Program Multi-Year Research, Development and Demonstration Plan:

(C) Inconsistent Data, Assumptions and Guidelines

(D) Suite of Models and Tools

(E) Unplanned Studies and Analysis

Contribution to Achievement of DOE Systems Analysis Milestones

This project contributes to achievement of the following DOE milestone from the Systems Analysis section of the Fuel Cell Technologies Program Multi-Year Research, Development and Demonstration Plan:

- **Milestone 11**: Complete environmental analysis of the technology environmental impacts for the hydrogen scenarios and technology readiness. (2Q 2015)

FY 2011 Accomplishments

- Conducted fuel cycle analysis of hydrogen storage and alternative energy storage options in various utility regions.



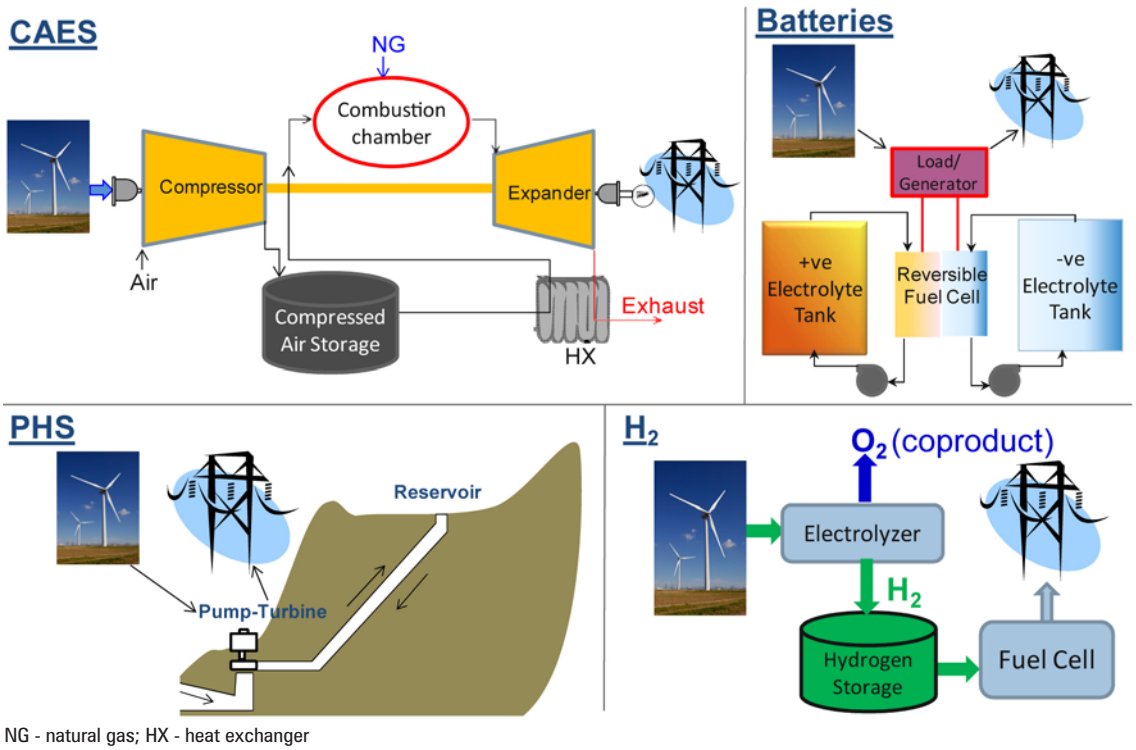
Introduction

The U.S. has wind resources to potentially produce large amounts of electricity each year. The U.S. also has significant resources of solar power, particularly in the southwestern regions of the country. These renewable sources of power are inherently intermittent and the supply of power from them cannot be controlled to match precisely the diurnal and regional demand. These renewable sources are typically curtailed when their supply becomes a large share of overall power supply, and they are supplemented with other fossil sources when their supply is less than the demand. Such intermittency imposes severe limitations on the potential large-scale utilization of renewable sources and the economics of their operation. Hydrogen has been proposed and examined in the U.S. and Europe as a potential energy storage medium to mitigate the intermittency of these renewable sources and to increase their utilization, especially with the expected large growth of these renewable sources to meet the renewable portfolio standards targets in the electric sector across the U.S. With hydrogen as a storage medium, when the incremental supply of renewable power exceeds the incremental demand, the excess power can be used to produce hydrogen for storage for later withdrawal during periods of peak power demand. Thus, hydrogen storage provides a buffer to match the supply and demand of electric power, and it could provide a significant reduction in energy use and greenhouse gas (GHG) emissions by reducing or eliminating the dependence on fossil sources that would otherwise serve the non-base (peak) load.

Argonne National Laboratory (ANL) examined the potential fuel cycle energy and emissions benefits of integrating hydrogen storage with renewable power generation. ANL also examined the fuel cycle energy use and emissions associated with alternative energy storage systems, including pumped hydro storage (PHS), compressed air energy storage (CAES), and vanadium-redox batteries (VRB). Figure 1 depicts these alternative energy storage systems for integration with grid electricity. The following sections present our approach to the above mentioned analysis, as well as the important stages, results, and key issues associated with the hydrogen use in energy storage applications.

Approach

The fuel-cycle analysis of energy storage systems depends mainly on the round-trip efficiency of each alternative storage system. The round-trip efficiency is defined as the amount of electricity produced by the energy storage system per unit electric energy input to the storage system. Table 1 lists the round-trip efficiency for the different energy storage systems considered in this analysis.



NG - natural gas; HX - heat exchanger

FIGURE 1. Alternative Energy Storage Systems

TABLE 1. Round-Trip Efficiency of Alternative Energy Storage Systems

Energy Storage System	Round-Trip Efficiency
Hydrogen	34%
Pumped hydro storage (PHS)	74%
Compressed air energy storage (CAES)	71%
Batteries	74%

This analysis assumes that the electricity produced from the energy storage system displaces the non-base load electricity (as provided in the eGrid database of the Environmental Protection Agency) for the different utility regions. The displacement of non-base load electricity provides an improved estimate over the displacement of fossil-based electricity generation when calculating the emission reduction benefits of clean energy projects. The electricity generation displaced by the electricity produced by the energy storage system are tracked upstream to their primary fuel sources for energy use and emissions calculations. The impact of "oxygen" as a co-product of hydrogen production via electrolysis is also included in this analysis.

Results

The fuel-cycle GHG emissions benefits per kWh of electricity produced by the energy storage systems are shown in Figure 2 for the states of California, Texas, New York, and

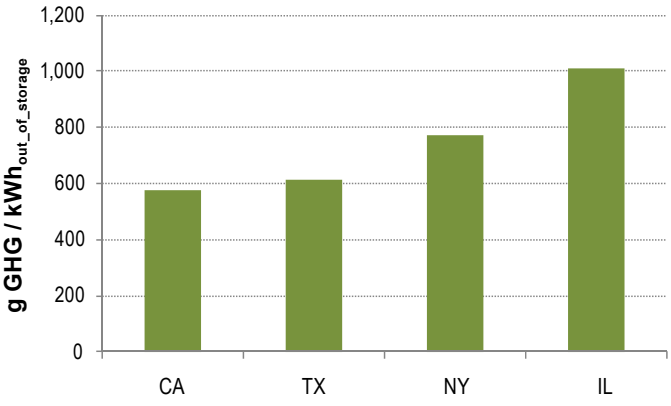


FIGURE 2. Fuel Cycle GHG Emissions Benefits of Energy Storage Systems in Different Regions (per kWh out of storage)

Illinois. Figure 2 reflects the GHG emissions saved in these regions by displacing the non-base load electricity generation units with energy produced from the storage of renewable electricity. Figure 3 shows the additional GHG savings due to the co-production of oxygen (O_2) via electrolysis using the hydrogen energy storage system. The byproduct oxygen is a high value product with high purity (>99%) that is widely used in medical facilities, steel production, semiconductor production, wastewater treatment plants, etc. Significant amounts of oxygen are coproduced (8 kg_{O2} for each kg_{H2}) which can displace oxygen conventionally produced in

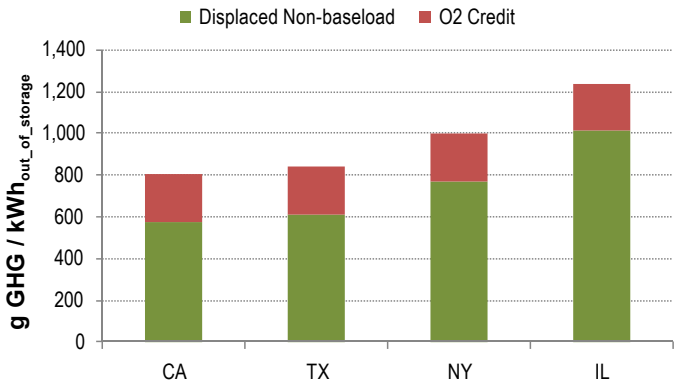


FIGURE 3. Fuel Cycle GHG Emissions Benefits of Hydrogen Energy Storage System in Different Regions (per kWh out of storage)

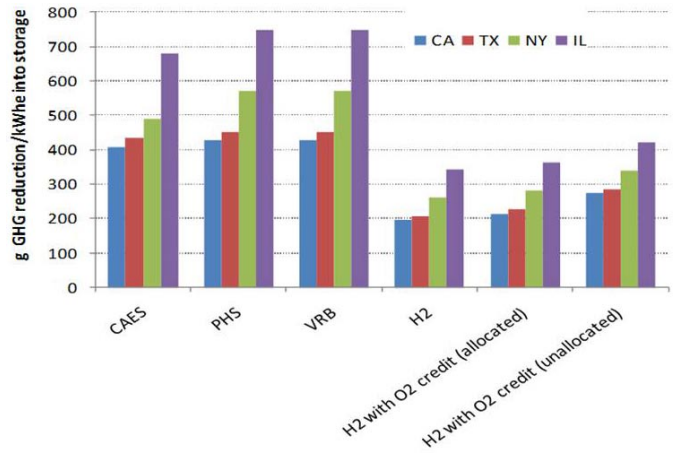


FIGURE 4. Fuel Cycle GHG Emissions Benefits of Alternative Energy Storage Systems in Different Regions (per kWh into storage)

air separation units where 0.7 kWh of electricity is used to produce 1 kg of O_2 (only 0.165 kWh/kg_{O2} if allocating electricity use by mass with N_2). Figure 4 shows the GHG emissions benefits of the alternative energy storage systems in different regions per kWh into storage. The impact of the round-trip efficiency of the alternative energy storage systems is apparent in Figure 4, with greater GHG benefits for the storage systems associated with higher round-trip efficiency. The O_2 byproduct credit associated with the hydrogen storage system partially compensates for its low round-trip efficiency and improves its competitiveness with the other alternative storage systems.

Conclusions and Future Directions

Conclusions:

Using hydrogen for storage of electricity from renewable sources provides potential for significant reduction of GHG emissions by displacing electricity generation units that serve the non-base load in different utility regions. Energy storage systems achieve greater GHG emissions reduction when displacing more carbon intensive generation. However, the GHG emissions benefits of employing hydrogen energy storage systems are less than those associated with the alternative storage systems using CAES, PHS and batteries due to the low round-trip efficiency of the hydrogen pathway. The round-trip efficiency is crucial for life-cycle analysis of energy storage systems. Higher potential for GHG emissions reduction can be realized as the round-trip efficiency increases. The O_2 byproduct credit associated with hydrogen storage system improves its competitiveness with alternative storage systems. The emissions benefits of alternative energy storage systems should be evaluated in conjunction with other economical and technological aspects unique to each technology option.

Future Directions:

Expand the system boundary to include the energy and emissions associated with the construction of the storage facilities in the life-cycle analysis of alternative energy storage systems.

XI.7 NEMS-H2: Hydrogen's Role in Climate Mitigation and Oil Dependence Reduction

Frances Wood and Niko Kydes
OnLocation, Inc.
Energy Systems Consulting
501 Church Street, Suite 300
Vienna, VA 22180

Thomas Jenkin and Marc Melaina (Primary Contact)
National Renewable Energy Laboratory (NREL)
1617 Cole Blvd.
Golden, CO 80401
Phone: (303) 275-3836
E-mail: marc.melaina@nrel.gov

DOE Manager
HQ: Fred Joseck
Phone: (202) 586-7932
E-mail: Fred.Joseck@hq.doe.gov

Subcontractor
OnLocation, Inc., Vienna, VA

Project Start Date: July, 2008
Project End Date: August, 2011

Fiscal Year (FY) 2011 Objectives

- Provide a comprehensive, market-based context for analyzing hydrogen scenarios.
- Use an economic framework with competition among vehicle and hydrogen production technologies.
- Analyze the impact of alternative technology outcomes (hydrogen production, fuel cell vehicles, etc.).
- Analyze the potential role and cost of policies to accelerate adoption of fuel cell electric vehicles (FCEVs).
- Demonstrate the potential contribution of FCEVs to meeting national goals of reducing greenhouse gas (GHG) emissions and oil imports.

Technical Barriers

This project addresses the following technical barriers from the Systems Analysis section of the Fuel Cell Technologies Program Multi-Year Research, Development and Demonstration Plan:

(A) Future Market Behavior

(B) Stove-Piped, Siloed Analytical Capability

Contribution to Achievement of DOE Systems Analysis Milestones

This project will contribute to achievement of the following DOE milestones from the System Analysis and System Integration sections of the Fuel Cell Technologies Program Multi-Year Research, Development and Demonstration Plan:

- Milestone 8 (System Analysis) – Complete analysis and studies of resource/feedstock, production/delivery and existing infrastructure for technology readiness (4Q, 2014).

FY 2011 Accomplishments

- Estimated the future responsiveness of market success with hydrogen FCEVs to various degrees of research and development (R&D) success.
- Estimated the rate of growth in adoption of hydrogen FCEVs in response to hydrogen retail station size and availability as well as responsiveness to station subsidies.
- Examined variations in future reliance on different production technologies in response to R&D and carbon policies, including allocation of biomass resources between electricity production (for the grid), biomass to liquids, cellulosic ethanol, and hydrogen production.
- Examined the effectiveness of a range of vehicle subsidy types, levels and FCEV prices.
- Developed 19 distinct scenarios (six reference cases, eight sensitivity cases and five policy cases) achieving a range of reductions in GHG emissions (up to 72%) and variations in oil imports (from a 12% increase to a 14% reduction) by 2050 compared to a 2005 base year for light-duty vehicles.



Introduction

The National Energy Modeling System (NEMS) is used by the DOE and the Energy Information Administration (EIA) to provide an integrated economic analysis of the future U.S. energy system under a variety of scenarios [1]. We developed the NEMS-H2 model as a modification of the existing NEMS model specifically to better address the potential role of hydrogen within the context of the U.S. energy system. As an integrated energy model, NEMS-H2 can capture interactions among various fuels as hydrogen production creates demand for different feedstocks, such as natural gas or coal, and at the same time displaces

traditional vehicle fuel use (primarily petroleum, but potentially biofuels as well). In this study we analyze a variety of scenarios to illustrate how hydrogen-powered FCEVs might provide oil and greenhouse gas emission reductions and identify other impacts on the energy system. These scenarios address the following questions:

1) What is the relative influence of different policy options in terms of penetration of hydrogen vehicles and associated benefits, and how does this depend on technological advances?
2) What are the carbon emissions and oil import reduction implications of reduced fuel demand and fuel switching as a result of technological advances in different types of hydrogen production and vehicle technologies?

Approach

The Office of Energy Efficiency and Renewable Energy (EERE) uses NEMS to estimate the benefits of its portfolio of R&D and deployment programs and to perform various types of policy analyses. Although well suited for representing most of the EERE programs, the original version of NEMS had limited hydrogen analysis capability. Hydrogen technologies were represented within NEMS on the demand side with natural gas fuel cells for stationary combined heat and power and with gasoline and hydrogen fuel cells in light-duty vehicles. The only representation of hydrogen supply is natural gas reforming used to meet the internal requirements of petroleum refineries and a simple assumption regarding natural gas consumption for hydrogen fuel cell light duty-vehicles. Therefore, one of the primary motivations for the original NEMS-H2 development was to add a representation of hydrogen pathways to NEMS to enhance its ability to estimate the benefits of the Fuel Cell Technologies Program.

The development of NEMS-H2 followed a multi-phased approach with additional features added incrementally. At this stage, the model contains the basic elements laid out in the design report, but not all of the features originally envisioned for the eventual production version have been implemented. The model has also been extended to 2050, which was essential for analysis in that the potential emergence of hydrogen as a significant source of energy supply is not anticipated until near the end of the standard NEMS time horizon of 2030 or 2035. For more detail on NEMS, see EIA's extensive NEMS documentation [1].

The major addition to the original NEMS model is a new conversion module called the Hydrogen Market Model (HMM), which takes as input from the other NEMS sub-models the prices for various fuels and the demand for hydrogen. The HMM then provides outputs of the delivered price of hydrogen for each region and market along with demand for feedstocks used in hydrogen production. Similar to the other conversion models within NEMS for the electricity and refinery sectors, HMM is formulated as a linear programming problem, although much smaller in size.

NEMS-H2 is also modified to include more detailed geographic representation of demand, with the following explicit market segmentations: large cities (population greater than 1 million), small cities (population between 50,000 and 1,000,000), and rural markets outside city areas (populations <50,000). With these market segments captured in each of the nine census regions used in NEMS, the NEMS-H2 model includes relatively detailed spatial representations of hydrogen pathways, including 12 production methods (eight central types, one city gate, and three distributed), multiple delivery pathways, and two retail station capacities (300 and 1,500 kg per day). Pathway costs are based upon H2A Production models from NREL, and delivery costs are based upon a set of iterative runs of Argonne National Laboratory's H2A Delivery Scenario Analysis Model (HDSAM). Though dynamic and more geographically explicit delivery costs have been developed using NREL's Scenario Evaluation and Regionalization Assessment model, the present version of NEMS-H2 relies upon delivery costs from HDSAM.

Results

Given that NEMS-H2 models the entire U.S. energy economy, a wide range of results have been collected through the development of 19 distinct scenarios. Some of the highlights are summarized in the following.

- In the carbon reference case, where significant carbon policies are adopted across the economy, FCEVs achieve 10 percent light-duty vehicle (LDV) market share by 2030 and approach 70 percent by 2050 if all R&D goals are met. In the 50% R&D success case, market share is very small before 2045 and just over 20 percent by 2050. Figure 1 indicates the on-road LDV stock associated with meeting R&D goals in the carbon reference case.

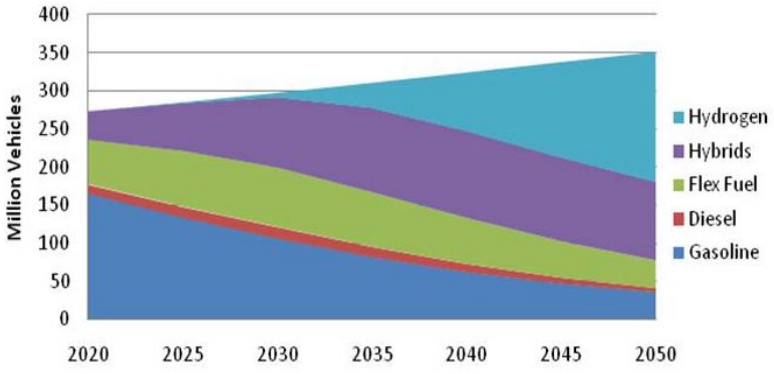


FIGURE 1. Light-Duty Vehicle Stock in the Carbon Policy Reference Case with FCEV R&D Success

- Introducing smaller stations results in greater station availability, accelerating consumer adoption (which is otherwise dampened by a lack of stations). Figure 2 indicates the influence of including small stations (300 kg/day) in NEMS-H2 in the carbon reference case, as opposed to only including large stations (1,500 kg/day).
- Sources of hydrogen are highly sensitive to carbon policy. With no carbon policy, onsite steam methane reforming and central coal gasification without sequestration are the dominant least-cost pathways, while strong carbon policy shifts production to central biomass with sequestration and coal with sequestration.

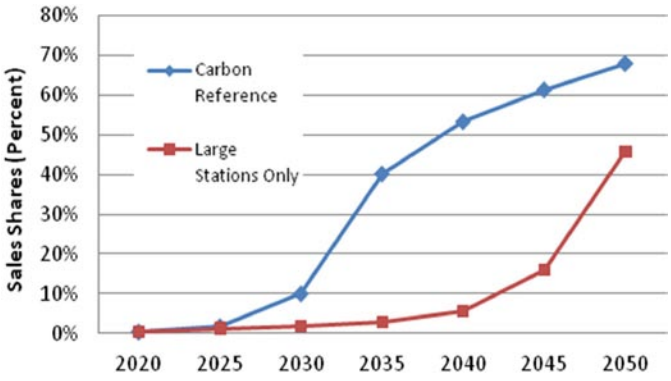


FIGURE 2. Influence of Including Smaller Stations in the Carbon Reference Case

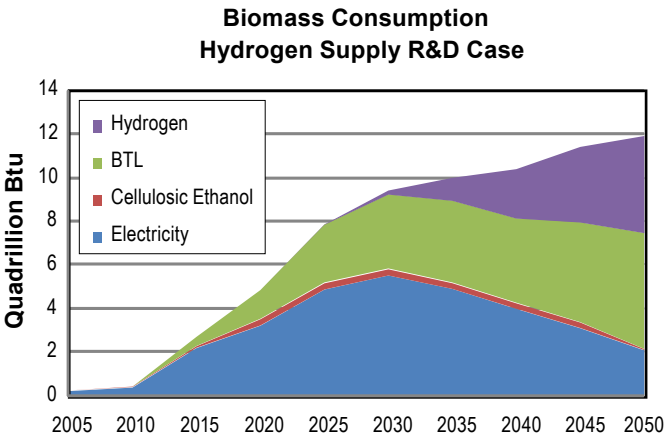


FIGURE 3. Biomass Supply and Products in the Production R&D Success Scenario

- Vehicle subsidies can be relatively effective (ranging from \$7–\$70/ton CO_2 reduced), but their effectiveness is highly dependent upon successful R&D.
- Significant use of biomass in hydrogen production could be realized if production and delivery R&D goals are met. Figure 3 shows the trend for growing biomass use in electricity, shifting toward liquid fuels around 2020, and then to hydrogen after 2030.

Conclusions and Future Directions

Our analysis has estimated the potential role of hydrogen FCEVs in the U.S. energy system using a modified version of the NEMS. The new model, NEMS-H2, estimates market share adoption and reductions in greenhouse gas emissions and petroleum consumption as a result of adopting FCEVs in the light-duty vehicle sector. We developed 19 distinct scenarios to examine important market dynamics, sector and technology interactions, R&D effects and policy strategies. Among these various scenarios, GHG emissions were reduced across a range of 16–72 percent by 2050 relative to 2005, while petroleum consumption increased in cases where FCEVs were not successful and was reduced by as much as 18 percent where they were successful. Other notable results include the importance of smaller stations in stimulating market growth, the sensitivity of hydrogen production sources to carbon policy, and the dependence of vehicle subsidy effectiveness on continued R&D progress.

FY 2011 Publications/Presentations

1. Hydrogen's Role in Climate Mitigation and Oil Dependence Reduction, 2011. F. Wood, N. Kydes, M. Melaina, T. Jenkin. National Renewable Energy Laboratory, technical report (forthcoming).

References

1. This version of NEMS-H2 is compatible with NEMS used for the Annual Energy Outlook 2008 (Energy Information Administration, "Annual Energy Outlook 2008 with Projections to 2030," DOE/EIA-0383(2008), June 2008). Documentation can be found on the EIA web site: http://tonto.eia.doe.gov/reports/filterD.cfm?other=Documentation

XI.8 GREET Model Development and Life-Cycle Analysis Applications

Michael Wang (Primary Contact),
Amgad Elgowainy, and Jeongwoo Han
Argonne National Laboratory
ESD362/E337
9700 South Cass Avenue
Argonne, IL 60439
Phone: (630) 252-2819
E-mail: mqwang@anl.gov

DOE Manager
HQ: Fred Joseck
Phone: (202) 586-7932
E-mail: Fred.Joseck@ee.doe.gov

Project Start Date: October 2002
Project End Date: Project continuation is determined annually in consultation with DOE

Objectives

- Conduct fuel-cycle analysis of early market applications of fuel cell (FC) systems (to help development of hydrogen production and FC technologies).
- Evaluate environmental benefits of renewable hydrogen production pathways.
- Conduct well-to-wheels (WTW) analysis of hydrogen fuel cell vehicles (FCVs) with various hydrogen production pathways.
- Conduct vehicle-cycle analysis of hydrogen FCVs.
- Provide life-cycle results for DOE's Fuel Cell Technologies (FCT) Program activities such as the Multi-Year Research, Development, and Demonstration Plan.
- Engage in discussions and dissemination of energy and environmental benefits of FC systems and applications.

Technical Barriers

This project addresses the following technical barriers from section 4.5 of the Fuel Cell Technologies Program Multi-Year Research, Development and Demonstration Plan:

(C) Inconsistent Data, Assumptions, and Guidelines

(D) Suite of Models and Tools

(E) Unplanned studies and analysis

Contribution to Achievement of DOE Systems Analysis Milestones

This project contributes to achievement of the following DOE milestone from the Systems Analysis section of the Fuel Cell Technologies Program Multi-Year Research, Development and Demonstration Plan:

- Milestone 11: Complete environmental analysis of the technology environmental impacts for the hydrogen scenarios and technology readiness. (2Q 2015)

Accomplishments

- Expanded the fuel-cycle analysis of renewable feedstock options for hydrogen production to include renewable natural gas (RNG) from landfill gas (LFG) and anaerobic digestion (AD) of animal waste.
- Conducted energy use and greenhouse gas (GHG) emissions analysis of FC systems for combined heat and power (CHP) and combined heat, hydrogen, and power (CHHP) generation using conventional natural gas (NG) and RNG.
- Evaluated the WTW energy and emissions benefits of FCVs powered by hydrogen from RNG.
- Conducted vehicle-cycle analysis of FCVs relative to conventional gasoline internal combustion engine (ICE) vehicles and gasoline hybrid electric vehicles (HEVs).
- Supported the collaborative effort of DOE's FCT Program and Vehicle Technologies Program (VTP) in updating DOE's WTW record for alternative fuel/vehicle systems, including FCVs and plug-in hybrid electric vehicles (PHEVs) [1].

✧ ✧ ✧ ✧ ✧

Introduction

The stages included in life-cycle analysis (LCA) are raw material acquisition, transportation and processing and product manufacturing, distribution, use and disposal or recycling. LCA of a fuel is called fuel-cycle analysis, while LCA of a vehicle is called vehicle-cycle analysis. A fuel cycle is also known as a WTW cycle when the fuel is used in transportation applications (vehicles). Combining WTW results with the vehicle-cycle energy use and emissions facilitates the comparison of alternative fuel/vehicle systems on a common (life-cycle) basis. Argonne examined fuel-cycle energy use and emissions associated with the use of RNG in stationary fuel cell applications. Argonne also conducted WTW analysis of hydrogen FCVs, including alternative feedstock sources for hydrogen production. To complete the LCA of hydrogen FCVs, Argonne evaluated the vehicle-cycle energy use and emissions associated with manufacturing FCVs and compared them to those of the manufacturing of gasoline ICEVs and HEVs.

Recovered methane (CH_4) gas from landfills or from AD originates from a renewable resource and is thus considered renewable energy. Because it is chemically identical to fossil natural gas yet produces far fewer GHG emissions,

this RNG can power stationary fuel cells to produce heat and power with the option of co-producing hydrogen while providing significant GHG emissions benefits. According to Environmental Protection Agency, over 190 million metric tonnes (MMT) of CO_2-equivalent (CO_2e) emissions came from landfills, animal manure and wastewater treatment facilities in 2009, while another 98 MMT and 16 MMT were avoided by landfill gas-to-energy and manure biogas recovery projects, respectively [2,3]. By avoiding the release of methane and instead recovering and using it in stationary applications or to produce transportation fuels, large reductions in GHG emissions can be realized relative to petroleum gasoline. In the CHHP application, the excess hydrogen may be stored and used for the refueling of fuel cells powering material handling equipment (i.e., forklifts) or for the generation of supplemental electricity to satisfy the electric load during peak demand periods. The availability of a hydrogen co-product can also overcome one of the barriers to introducing hydrogen FCVs to some early FCV market places by facilitating a distributed source of hydrogen while effectively employing the primary energy source and the initial capital investment of the fuel cell to serve a facility's demand for electric and heat energy. In a mature FCV market, renewable hydrogen can be produced via steam methane reforming (SMR) of RNG to satisfy the demand for the hydrogen fuel in that market. This is especially important in places such as California where regulations require 33% of the hydrogen produced for use as fuel to come from renewable sources [4].

Approach

This study examines the fuel cycle of landfill gas and animal waste conversion to RNG, and the subsequent conversion of RNG to hydrogen fuel for FCVs. To assess the environmental benefits of RNG, we account for energy use and emissions in the reference case (or base case) and for those associated with the recovery and conversion of the renewable feed to RNG. Since the reference case consumes energy and generates emissions (in the absence of conversion to RNG), the net emissions associated with producing RNG are calculated by subtracting the reference case emissions from those emitted in the conversion process to RNG. The conversion processes of landfill gas and animal waste to RNG are described in details elsewhere [5,6].

The energy use and emissions associated with the use of RNG in stationary fuel cells for CHP and CHHP generation, and the slate of the co-products depend mainly on the efficiency of the integrated internal reformer. The individual conversion efficiencies to produce electricity, heat and hydrogen are extracted from the H2A power model developed by the National Renewable Energy Laboratory. We use the displacement approach to compare the generation of electricity and hydrogen among the different feedstock sources, and to calculate credits for the byproduct heat. The system boundary for this approach includes the fuel cell system and assumes full utilization of byproduct heat. The energy use and emissions for this approach are evaluated per one million Btu of net electricity and hydrogen generation. The credit of byproduct heat is calculated from the displacement of equivalent amount of heat from a typical standalone heating system. The displaced heat is assumed to be produced from a NG-fired heater with 90% efficiency. Hydrogen produced from RNG for FCV applications assumes 72% efficiency for the SMR conversion process. The WTW results of the alternative fuels and vehicle systems in this report are presented in per-mile basis as well as per-kg of hydrogen equivalent basis.

Results

The fuel-cycle GHG emissions for molten carbon fuel cell (MCFC) CHP and CHHP systems are shown in Figure 1. Employing RNG in CHP and CHHP fuel cell applications achieve 78-79% GHG emissions reduction relative to conventional NG-powered fuel cells. This large reduction in GHG emissions incorporates the impact of a 2% methane leakage rate assumed for the processing of RNG. Without accounting for such leakage, the reduction in GHG emissions for RNG pathways would be 96% relative to fuel cells powered with conventional NG. The GHG emissions credit due to the displacement of conventional heat with the byproduct heat is implied in Figure 1 for each of the investigated feedstock sources.

Figure 2 shows the WTW GHG emissions of various hydrogen production pathways, including the hydrogen use in FCVs. While hydrogen produced from renewable wind power sources for use in FCVs provides the largest reduction in GHG emissions (92%) relative to gasoline ICE vehicles, hydrogen produced from RNG provides the next largest reduction in GHG emissions (85%) relative to gasoline ICE vehicles. The corresponding reduction in GHG emissions for biomass, coal with carbon capture and sequestration (w/CCS), coal without carbon capture and sequestration (w/o CCS), coke oven gas, and conventional natural gas feedstock sources are 81%, 76%, 8%, 71%, and 45%, respectively. The conversion of gasoline consumption in an ICE vehicle to per-kg of hydrogen equivalent in Figure 2 employs an energy equivalency ratio (EER)[1] of 2.3 as adopted from California Air Resources Board's Low Carbon Fuel Standard [7]. The WTW GHG emissions per mile for the alternative feedstock sources for hydrogen production and use in FCVs are presented in Figure 3. The GHG emissions for hydrogen FCVs occur entirely in the well-to-pump (WTP) activities of hydrogen production, compression, and transportation, while the majority of GHG emissions for the baseline gasoline ICE vehicle occur in the pump-to-wheels (PTW) stage (i.e., during vehicle operation). To compare FCVs with baseline gasoline ICE vehicles on a life-cycle basis, we evaluated the vehicle cycle energy use and emissions associated with manufacturing FCVs and compared it to the manufacturing of gasoline ICEVs and

[1] EER = miles per unit energy of hydrogen used in a FCV/miles per unit energy of gasoline used in an ICEV.

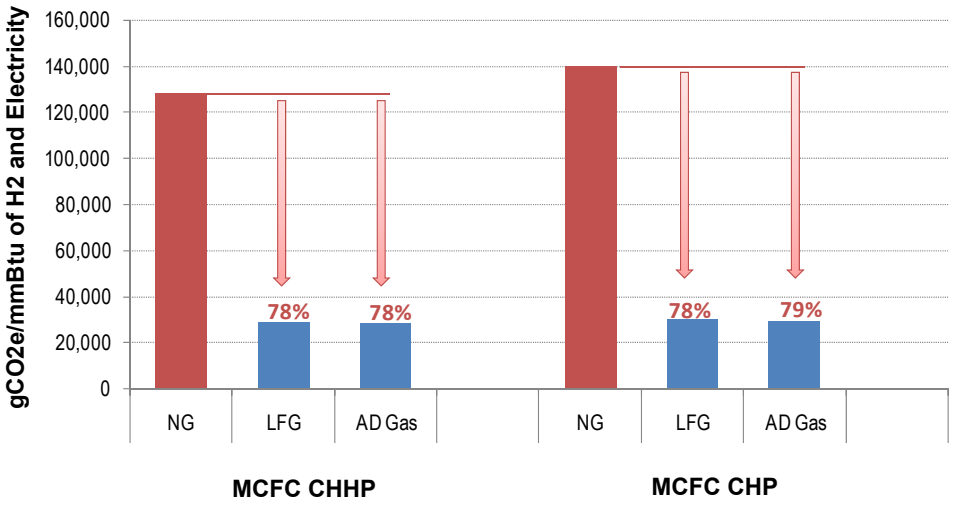


FIGURE 1. Fuel Cycle GHG Emissions from Conventional and Renewable Natural Gas Use in Stationary Fuel Cell Applications

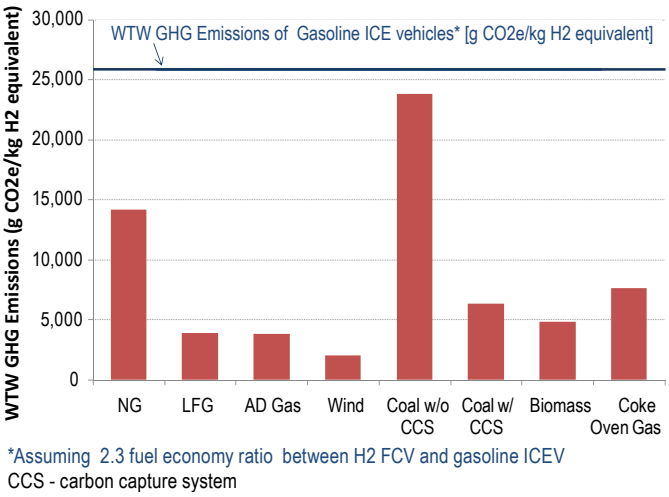


FIGURE 2. WTW GHG Emissions from Alternative Feedstock Sources for Hydrogen Production and Use in FCV Applications (per-kg H2 equivalent)

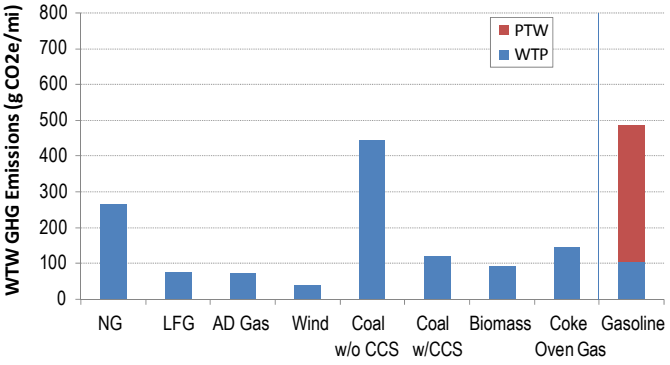


FIGURE 3. WTW GHG Emissions from Alternative Feedstock Sources for Hydrogen Production and Use in FCV Applications (per mile)

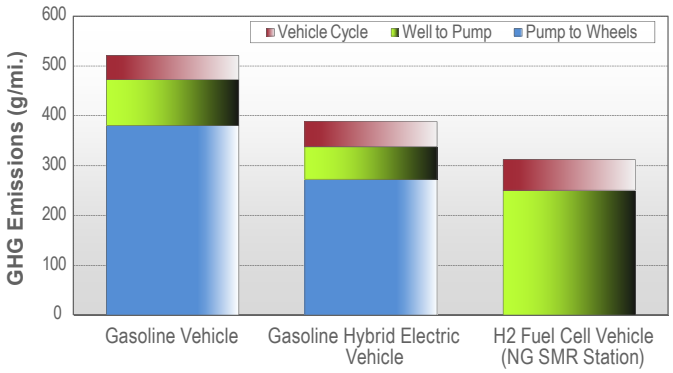


FIGURE 4. Comparison of Vehicle Cycle GHG Emissions of Hydrogen FCVs with Gasoline ICEVs and HEVs

HEVs. Figure 4 shows that while GHG emissions associated with the manufacturing of hydrogen FCVs are larger compared to gasoline ICEVs, the combined fuel cycle and vehicle cycle GHG emissions for FCVs (using hydrogen from SMR of natural gas) are 40% lower than gasoline ICEVs.

Conclusions

Hydrogen produced from RNG sources can achieve significant reductions in GHG emissions:

- CHHP and CHP FC systems powered by RNG achieve 78-79% GHG reduction relative to those powered by conventional NG.
- FCVs with hydrogen produced from RNG achieve WTW GHG reduction by:
  - 73% relative to FCVs with hydrogen produced from conventional NG.
  - 85% relative to gasoline ICEVs.

- On a vehicle-cycle basis, manufacturing FCVs require more energy and generate more GHG emissions compared to gasoline ICEVs, but FCVs reduce energy and emissions on a life-cycle basis (i.e., combined vehicle and fuel cycles).

Future Work

- Examine alternative feedstock sources for renewable hydrogen production such as waste water treatment plants.

FY 2011 Publications/Presentations

1. Nguyen, T. and Ward, J., 2010, "Well-to-Wheels Greenhouse Gas Emissions and Petroleum Use for Mid-Size Light-Duty Vehicles," Record # 10001, Offices of Vehicle Technologies & Fuel Cell Technologies, October 25.

2. Han, J., M. Mintz, M. Wang, 2011, "Life Cycle Analysis of Renewable Hydrogen from Waste", AIChE 2011 Spring Meeting, Chicago, IL, March 14–17.

3. Mintz, M., J. Han, M. Wang, C. Saricks, 2010, "Well-to-Wheels analysis of landfill gas-based pathways and their addition to the GREET model", ANL/ESD/10-3, Argonne National Laboratory, Argonne, IL.

4. Elgowainy, A, and Wang, M., 2011, "Well-To-Wheel Analysis of Sustainable Vehicle Fuels," Robert A. Meyers (ed.), Encyclopedia of Sustainability Science and Technology, DOI 10.1007/978-1-4419-0851-3.

5. Han, J., M. Mintz, M. Wang, 2011, "Life Cycle Analysis of Renewable Hydrogen from Waste", AIChE 2011 Spring Meeting, Chicago, IL, March 14-17.

6. Mintz, M., J. Han, M. Wang, C. Saricks, 2010, "Well-to-Wheels analysis of landfill gas-based pathways and their addition to the GREET model", ANL/ESD/10-3, Argonne National Laboratory, Argonne, IL.

References

1. Nguyen, T. and Ward, J., 2010, "Well-to-Wheels Greenhouse Gas Emissions and Petroleum Use for Mid-Size Light-Duty Vehicles," Record # 10001, Offices of Vehicle Technologies & Fuel Cell Technologies, October 25.

2. U.S. EPA, 2011b. AgSTAR Program. http://www.epa.gov/agstar/. Accessed on July 1st, 2011.

3. U.S. EPA, 2011c. Landfill Methane Outreach Program. http://www.epa.gov/lmop/index.html. Accessed on July 1st, 2011.

4. California Senate Bill 1505: Environmental Performance Standards for Hydrogen Fuel.

5. Han, J., M. Mintz, M. Wang, 2011, "Life Cycle Analysis of Renewable Hydrogen from Waste", AIChE 2011 Spring Meeting, Chicago, IL, March 14-17.

6. Mintz, M., J. Han, M. Wang, C. Saricks, 2010, "Well-to-Wheels analysis of landfill gas-based pathways and their addition to the GREET model", ANL/ESD/10-3, Argonne National Laboratory, Argonne, IL.

7. California Air Resources Board (CARB), 2009, "Proposed Regulation to Implement the Low Carbon Fuel Standard," Volume I, Staff report: Initial Statement of Reasons. Sacramento, California.

XI.9 Macro-System Model

Mark F. Ruth* (Primary Contact),
Michael E. Goldsby†, Timothy J. Sa†,
Victor Diakov*

*National Renewable Energy Laboratory
1617 Cole Blvd.
Golden, CO 80401
Phone: (303) 817-6160
E-mail: Mark.Ruth@nrel.gov

† Sandia National Laboratories
7011 East Ave.
Livermore, CA 94550
Phone: (925) 294-3207
E-mail: megolds@sandia.gov and tjsa@sandia.gov

DOE Manager
HQ: Fred Joseck
Phone: (202) 586-7932
E-mail: Fred.Joseck@ee.doe.gov

Subcontractors:
- Directed Technologies, Inc., Arlington, VA
- SRA International, Inc., Fairfax, VA

Project Start Date: February 2005
Project End Date: Project continuation and direction determined annually by DOE

Fiscal Year (FY) 2011 Objectives

- Develop a macro-system model (MSM):
  - aimed at performing rapid cross-cutting analysis
  - utilizing and linking other models
  - improving consistency between models
- Support decisions regarding programmatic investments through analyses and sensitivity runs.
- Support estimates of program outputs and outcomes.

Technical Barriers

This project addresses the following technical barriers from the Systems Analysis section (4.0) of the Fuel Cell Technologies Program Multi-Year Research, Development and Demonstration Plan:

(A) Future Market Behavior
(B) Stove-Piped/Siloed Analytical Capability
(C) Inconsistent Data, Assumptions and Guidelines
(D) Suite of Models and Tools

Contribution to Achievement of DOE Systems Analysis Milestones

This project will contribute to achievement of the following DOE milestones from the System Analysis section of the Fuel Cell Technologies Program Multi-Year Research, Development and Demonstration Plan:

- **Milestone 5**: Complete analysis and studies of resource/feedstock, production/delivery and existing infrastructure for various hydrogen scenarios. (4Q, 2009)
- **Milestone 27**: Complete the 2nd version of the Macro-System Model to include the analytical capabilities to evaluate the electrical infrastructure. (2Q, 2011)

FY 2011 Accomplishments

- Completed Version 1.3 of the MSM and used it for programmatic analysis.
- Created, and (later) updated the MSM User Guide (version 1.3.2).
- Linked H2A Production cases with the Hydrogen Delivery Scenario Analysis Model (HDSAM), the Greenhouse Gases, Regulated Emissions, and Energy Use in Transportation (GREET) Model, and physical property information from the Hydrogen Analysis Resource Center (HyARC) and validated the use of those models and the results generated using them.
- Enhanced the Web-based user interface so that many members of the analysis community can use the MSM.
- Added stochastic (Monte Carlo) capabilities to the MSM.
- Upgraded the MSM to the latest versions of H2A Production (V.2.1.1-3), HDSAM (V 2.2) and GREET (V 1.8d.1).
- Linked with geospatial model HyDRA to add the spatial dimension to the MSM.
- Linked MSM with the temporal pathway evolution assessment tool HyPro.
- Linked the MSM with vehicle cycle analysis model GREET 2.7.
- Linked the Fuel Cell Power Model (FC Power) in the MSM framework.



Introduction

At the DOE Fuel Cell Technologies Program's behest, we are developing an MSM to analyze cross-cutting issues because no existing model sufficiently simulates the entire system, including feedstock, conversion, infrastructure, and vehicles, with the necessary level of technical detail. In

addition, development of the MSM exposes inconsistencies in methodologies and assumptions between different component models so that they can be identified and corrected when necessary.

Version 1.0 of the MSM has been developed and is available to the hydrogen analysis community. It links H2A Production, HDSAM, GREET, and physical property information from HyARC to estimate the economics, primary energy source requirements, and emissions of multiple hydrogen production/delivery pathways. A Web-based user interface has been developed so that many users have access to the MSM; stochastic capabilities have been added to it to provide uncertainty ranges around the results. The MSM has been used for several analyses to compare pathways and to understand the effects of varying parameters on pathway results.

Approach

The MSM is being developed as a tool that links existing models across multiple platforms. This approach was chosen because the task of building a single monolithic model incorporating all of the relevant information in the existing models would have been overwhelming because the necessary expertise to do so was spread among half a dozen DOE laboratories and a dozen or more universities and private contractors. Linking models allows model users that depend on data from component models to continue using their models while retrieving data from component models in a less labor-intensive manner. In addition, it provides a common platform for data exchange necessary to update integrated models when the component models have been updated.

The MSM is being built on a framework inspired by an example of the federated object model (FOM). FOMs also link together models and are exemplified by the Department of Defense high level architecture (HLA) [1]. The general MSM framework provides a common interlingua that is extensible (accommodates new models with a minimum of difficulty), distributable (can be used by multiple people in different areas of the country), and scalable (to large numbers of participating models). Version 1.0 of the MSM uses Ruby and Ruby interfaces to Microsoft Excel and other platforms to collect, transfer, and calculate data.

Results

Levelized hydrogen costs, primary energy requirements, and emissions have been estimated for multiple pathways using H2A V2.1 [2], HDSAM V2.2 [3], and GREET V1.8d.1 [4]. Within the MSM, hydrogen production and other costs [5] are connected with associated emissions, which is one of the advantages that the MSM provides by linking together different models. Figure 1 shows the levelized hydrogen fuel cost per mile and the well-to-wheels (WTW) greenhouse gas (GHG) emissions for each of the seven pathways assessed

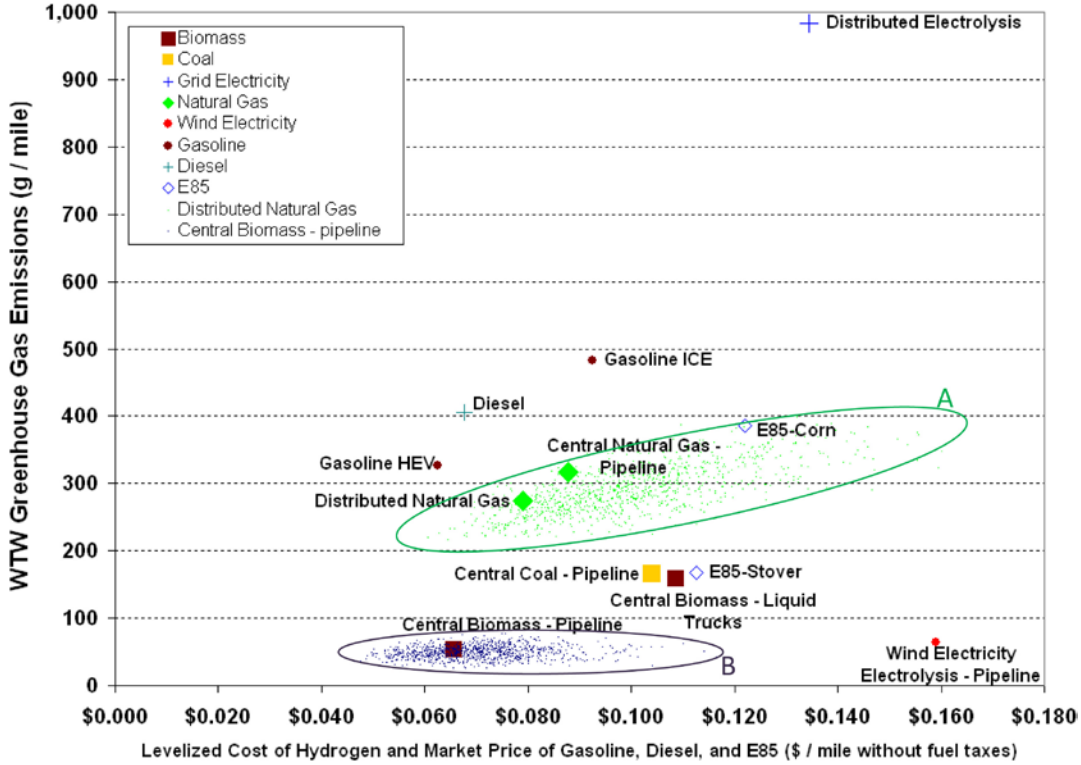


FIGURE 1. Pathways Levelized Costs and GHG Emissions

based on U.S. average fuel costs and fuel cycle energy requirements. For comparison, it also shows the projected 2009 market price per mile (in 2005 dollars) and GHG emissions for gasoline-, diesel-, and E85-fueled vehicles. The levelized fuel cost was put onto a per-mile basis. The projected fuel cost per mile for most of the hydrogen pathways (based on projected, mature fuel cell electric vehicle [FCEV] markets) is similar to that for gasoline in a traditional vehicle and corn ethanol as E85 fuel in a flexible-fuel internal combustion engine (ICE) vehicle. The fuel costs per mile for gasoline in a hybrid electric vehicle (HEV) and diesel in a conventional diesel ICE vehicle are lower.

The dotted green cloud in the figure (surrounded by oval A) represents the stochastic analysis results obtained based on input distributions for the forecourt SMR production option [6]. The dispersion of the data points well surpasses the differences between the central (with pipeline delivery) and distributed SMR production options. This relates to both the per-mile cost of hydrogen and the WTW GHG emissions. Similarly, the blue cloud surrounded by oval B shows the stochastic analysis result for the central biomass case. For the latter, as seen in the figure, the data point distribution is less significant when compared with the differences incurred by switching from pipeline to liquid truck delivery.

As key MSM inputs are sometimes region-specific, it is important to add the geospatial dimension into the range of the MSM features. Bilateral links with the online geospatial tool HyDRA [7] have been developed that allow the MSM user to easily apply regional electricity and natural gas (NG) feedstock data as MSM inputs and, conversely, update the HyDRA database and maps with the latest MSM version outputs.

Naturally, the user can specify input data as needed (it is not required that the inputs are region specific). As an example, Figure 2 shows the results obtained from NREL's FC Power model for a range of electricity grid mixes (ranked along the x-axis based on the level of upstream GHG emissions, the dotted line shows the average U.S. electricity generation mix upstream emissions level). Depending on the region-specific electricity generation mix, the combined heat, hydrogen, and power fuel cell generation can alleviate or aggravate the level of GHG emissions.

As a part of the ongoing enhancement of the user interface, detailed MSM outputs have been made available to the users via the Web. When combined with detailed MSM inputs access (developed earlier, in FY 2010), it makes the remote, Web-generated MSM runs almost as transparent as if the user has the MSM running on their own computer.

The transition to high-market-penetration levels for hydrogen fuel cell vehicles will likely involve several hydrogen production/delivery/dispensing pathways. To facilitate this analysis and to involve the temporal dimension, the temporal pathway evolution assessment tool HyPro [8] was developed in previous years by Directed Technologies, Inc. It is a computational model that simulates industries decisions regarding construction of new hydrogen production facilities, delivery infrastructure, and dispensing given perfect foresight of hydrogen demand. It is linked to the MSM so HyPro inputs are now updated automatically. A wide range of analysis possibilities of infrastructure evolution are now available using the MSM.

One analysis is the potential effect of a constant GHG tax on the cost-optimal succession of hydrogen production/delivery/dispensing pathways. The results of that analysis are presented in Figure 3 where the three graphs show results over a 40-year buildout scenario resulting in over 5,000,000-kg of hydrogen produced daily during the final

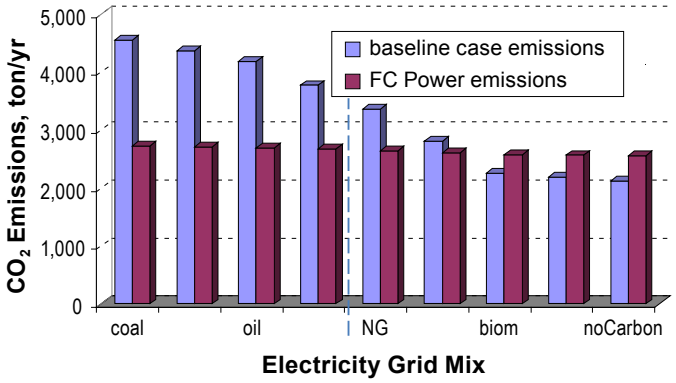


FIGURE 2. Fuel Cell Combined Heat, Hydrogen and Power Generation: Associated Emissions

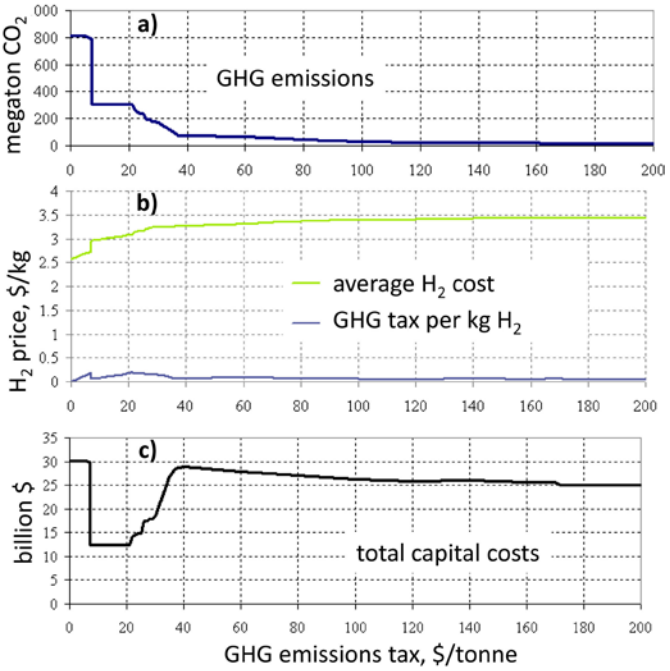


FIGURE 3. GHG Emissions Tax Effect on the Overall Emissions Level (a), Produced H_2 Costs (b) and Capital Costs (c) for a Mega-City with 12 Million Population

year. The x-axis for all graphs is a GHG emissions tax that ranges from $0/metric tonne to $200/metric tonne. Note that the GHG tax is held constant over each buildout scenario. Graph a shows the cumulative GHG emissions over the buildout scenario; graph b shows the average levelized hydrogen cost over the 40 years and the portion of that cost that pays for the GHG tax; graph c shows the cumulative capital investment for infrastructure over the scenario.

When the GHG tax is set to zero, forecourt SMR stations are built initially and those are replaced with central coal gasifiers without CCS and with pipeline delivery of hydrogen once the levelized cost of gasifier/pipeline hydrogen is less than the forecourt SMR cost. When the tax rate is between $7/tonne and $20/tonne, distributed SMR production option becomes more economical than central coal gasification throughout the 40-year buildout scenario so no coal facilities are selected. That choice results in a large decrease in GHG emissions (graph a) because SMR is less carbon intensive than coal gasification and a large decrease in capital costs (graph c) because SMR is less capital intensive. On the other hand, it causes an increase in average levelized cost because large coal facilities have a lower levelized cost than distributed SMR facilities. If the GHG emissions tax is between $20/tonne and $40/tonne, distributed SMR is replaced by coal gasification with CCS. At levels above $40/tonne biomass gasification is the dominant technology. Notably, the largest effect (in terms of overall GHG emissions reduction) is achieved at relatively low tax levels. The penalty (in terms of H_2 cost increase) is significant (up to $1/kg) but not prohibitively high. Only a small fraction of the cost increase is paid as GHG tax (the GHG tax curve on chart b) with most of the cost increase due to technology selection. Finally, higher GHG tax tends to decrease total capital costs of building the H_2 infrastructure.

Conclusions and Future Directions

- By linking production/delivery/dispensing models, the MSM is a tool for rapid cross-cutting comparative analysis of various production/delivery pathways.
- The U.S. region-specific data are readily available as MSM inputs via live MSM/HyDRA links.
- As a result of linking HyPro with the MSM, pathway evolution is examined in a manner consistent with latest versions of H2A and HDSAM.

Future Directions

- Further analyze production, delivery and distribution options, compare pathways to identify strengths of each.
- Analyze hydrogen buildout scenarios.
- Identify potential effects of not meeting targets and ensuing trade-offs.

FY 2011 Publications/Presentations

1. Ruth, M., Diakov, V., Goldsby, M., Sa, T. (2010) Macro-System Model: a Federated Object Model for Cross-Cutting Analysis of Hydrogen Production, Delivery, Consumption and Associated Emissions. In Infraday Conference, 2010.

2. James, B., Diakov, V., Ruth, M., Spisak, A., Perez, J. (2011). Hydrogen Pathway Evolution Analysis within HyPro-MSM modeling Framework. In Fuel Cell and Hydrogen Energy Conference, 2011.

3. Diakov, V., Ruth, M., Goldsby, M., Sa, T. (2011) Macro-System Model for Hydrogen Energy Systems Analysis in Transportation. Accepted for the International Mechanical Engineering Conference and Exhibit, 2011.

References

1. Judith S. Dahmann, Richard Fujimoto, and Richard M. Weatherly. "The Department of Defense high level architecture." In Winter Simulation Conference, pages 142–149, 1997.

2. Steward, D., Ramsden, T., and Zuboy, J. (2008, September). *H2A Production Model, Version 2 User Guide*. Golden, CO: National Renewable Energy Laboratory.

3. Mintz, M., Elgowainy, A., and Gillette, J. (2008, September). *H2A Delivery Scenario Analysis Model Version 2.0* (HDSAM 2.0) User's Manual*. Argonne, IL: Argonne National Laboratory.

4. Argonne National Laboratory. (2009, May). *How Does GREET Work?* Retrieved from http://www.transportation.anl.gov/modeling_simulation/GREET/index.html.

5. Ruth, M., Laffen, M., and Timbario, T.A. (2009, September). Hydrogen Pathways: Cost, Well-to-Wheels Energy Use, and Emissions for the Current Technology Status of Seven Hydrogen Production, Delivery, and Distribution Scenarios. Golden, CO: National Renewable Energy Laboratory.

6. Duffy, M., Melaina, M., Penev, M., and Ruth, M. Management Report NREL/MP-150-43250, May 2008. Risk Analysis for Hydrogen, Fuel Cells and Infrastructure Program: Predecisional Report.

7. HyDRA: http://rpm.nrel.gov/.

8. James, B., Schmidt, P., and Perez, J. (2008, December). HyPro: A Financial Tool for Simulating Hydrogen Infrastructure Development (U.S. DOE Contract # DE-FG36-05G01519 Final Report).

XI.10 HyDRA: Hydrogen Demand and Resource Analysis Tool

Daniel Getman (Primary Contact), Johanna Levene, Witt Sparks
National Renewable Energy Laboratory (NREL)
1617 Cole Blvd.
Golden, CO 80401
Phone: (303) 275-4677
E-mail: dan.getman@nrel.gov

DOE Manager
HQ: Fred Joseck
Phone: (202) 586-7932
E-mail: Fred.Joseck@hq.doe.gov

Subcontractor:
Alumni Consulting, Greenwood Village, CO

Project Start Date: October 1, 2006

Project End Date: Project continuation and direction determined annually by DOE

Fiscal Year (FY) 2011 Objectives

- Develop a Web-based Geographic Information System (GIS) tool to allow analysts, decision makers, and general users to view, download, and analyze hydrogen demand, resource, and infrastructure data spatially and dynamically.
- Provide a repository for hydrogen spatial data inputs and model results.
- Display and aggregate the results of spatial analyses.
- Support interoperability between HyDRA and similar applications in other domains of energy infrastructure research.
- Expand visualization and querying of temporal and multivariate datasets.
- Extend data acquisition and ingestion capabilities.
- Enhance analysis capabilities within HyDRA.

Technical Barriers

This project addresses the following technical barriers from the Systems Analysis section of the Fuel Cell Technologies Program Multi-Year Research, Development and Demonstration Plan:

(A) Stove-Piped/Siloed Analytical Capability

(B) Inconsistent Data, Assumptions, and Guidelines

(C) Suite of Models and Tools

Contribution to Achievement of DOE Systems Analysis Milestones

This project will contribute to achievement of the following DOE milestones from the System Analysis and System Integration sections of the Fuel Cell Technologies Program Multi-Year Research, Development and Demonstration Plan:

- Milestone 8 (System Analysis): Complete analysis and studies of resource/feedstock, production/delivery and existing infrastructure for technology readiness. (4Q, 2014)
- Milestone 27 (System Analysis): Complete the 2nd version of the Macro-System Model (MSM) to include the analytical capabilities to evaluate the electrical infrastructure. (2Q, 2011)
- Milestone 15 (System Integration): MSM analysis test cases. (4Q, 2006; 3Q, 2009; 4Q, 2010)

FY 2011 Accomplishments

- Interoperability has been established with other models and applications, including the Scenario Evaluation and Regionalization Analysis (SERA) model.
  - HyDRA data is now available as Web Mapping Service and Web Feature Service which can be used by any external application capable of interacting with these standards-based services.
- Attribute querying capability has been added to HyDRA.
- Basic charting of datasets in HyDRA will be completed within FY 2011.
- Interaction with the BioenergyKDF project.
  - HyDRA and the BioenergyKDF are now interoperable and capable of actively sharing data.
- The OpenEI project will leverage data to be used by HyDRA, with plans to ingest a variety of datasets to be used within HyDRA. These services should be available in FY 2012.
- Increased the number of spatial data layers related to hydrogen resource, infrastructure, and demand to over 100 layers. These datasets are comprised of background data, model input data, and results from spatial analysis and modeling activities.
- A diverse group of 257 users from 62 countries have accessed the HyDRA application in FY 2011, including university (University of Chicago, Sonoma State University, University of California, Davis), industry (Air Products and Chemicals, Inc., Apple, Matheson Tri-gas), and government agency stakeholders (Office of the Secretary of Defense, DOE)

Introduction

The HyDRA tool was developed to conduct dynamic geographic analysis of hydrogen processes in a Web-based environment. This capability is important as resource conversion, demand, and infrastructure components vary regionally for different hydrogen production, delivery, storage and retail dispensing systems. HyDRA provides a repository for storing spatial data used by hydrogen analyses and tools, and allows analysis results from multiple domains of research to be explored and compared from within a single interface.

Approach

The HyDRA tool is a state-of-the-art, Web 2.0 application that has the look, feel, and functionality of a traditional client-based GIS application. It provides the capability to view hydrogen data and how they vary across the United States on a regional basis. HyDRA provides analysis results in the form of maps that can be queried to access the numbers behind the visualization. It is available at http://maps.nrel.gov. Users can view spatial hydrogen data and interact with the maps to create custom analyses. Data can be downloaded from the application and used in other analyses. To ensure HyDRA's usability, NREL recently redesigned it from its original code base to provide an easier to use, more intuitive interface. Users will be able to create their own spatial datasets and upload them into the HyDRA application to create a completely customizable and dynamic analysis tool.

The capability to explore and query spatial data layers is a core capability of the HyDRA application. There are currently more than 100 datasets available in the system including resource cost and availability, hydrogen production potential, hydrogen production cost, resource consumption, hydrogen demand, infrastructure, and results from integration with other hydrogen models. The ability to access externally hosted datasets, and also to run the MSM from within HyDRA, will provide access to a significant number of datasets and analysis results. Additionally, dynamic data acquisition services will provide up to date versions of data that change over time.

Results

The major HyDRA efforts that have been accomplished this year involve interoperability, data querying, and visualization. HyDRA is now capable of full interoperability with other standards-based geospatial data systems and is sharing datasets with the BioenergyKDF. This capability will also allow HyDRA to share data with SERA, MSM, and any other modeling, analysis, or data exploration application that can use standards-based data (Figures 1 and 2).

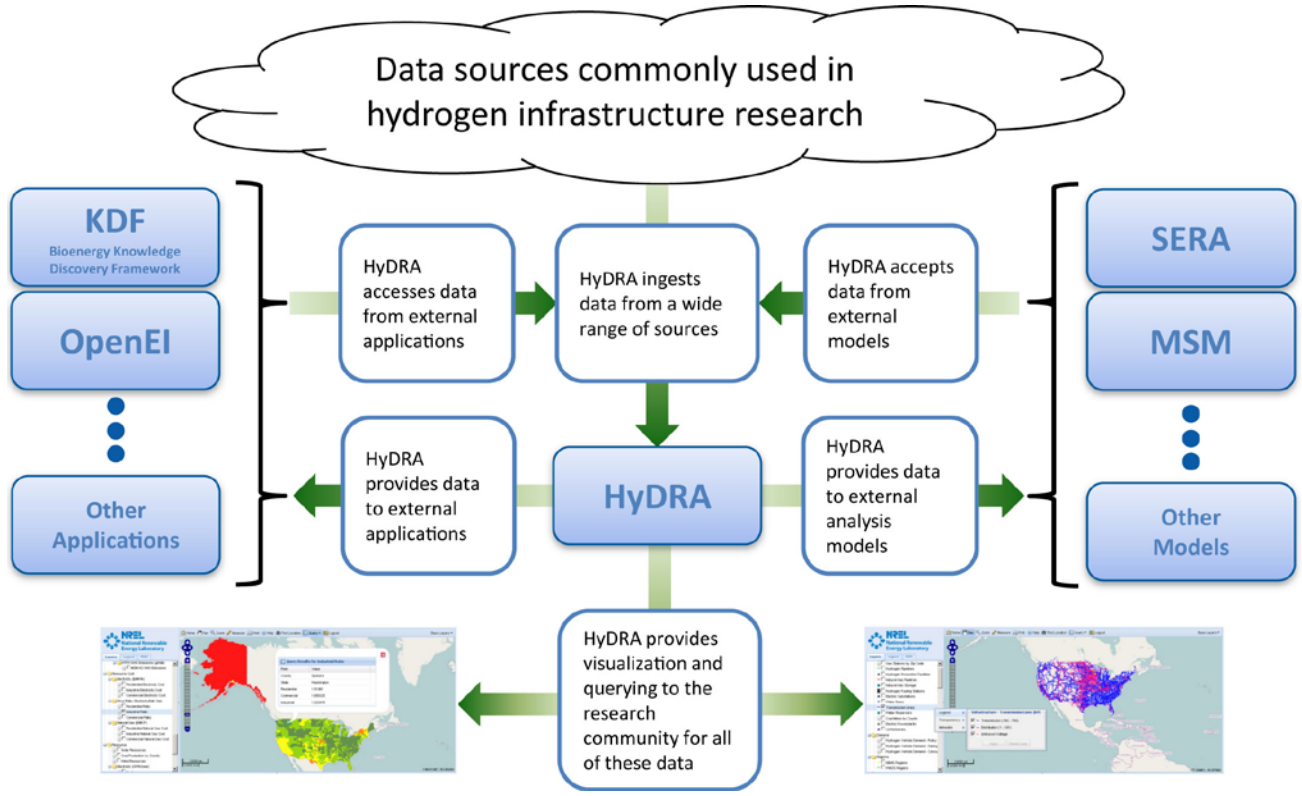


FIGURE 1. Interoperability Between HyDRA and Other DOE-Funded Applications And Modeling Efforts

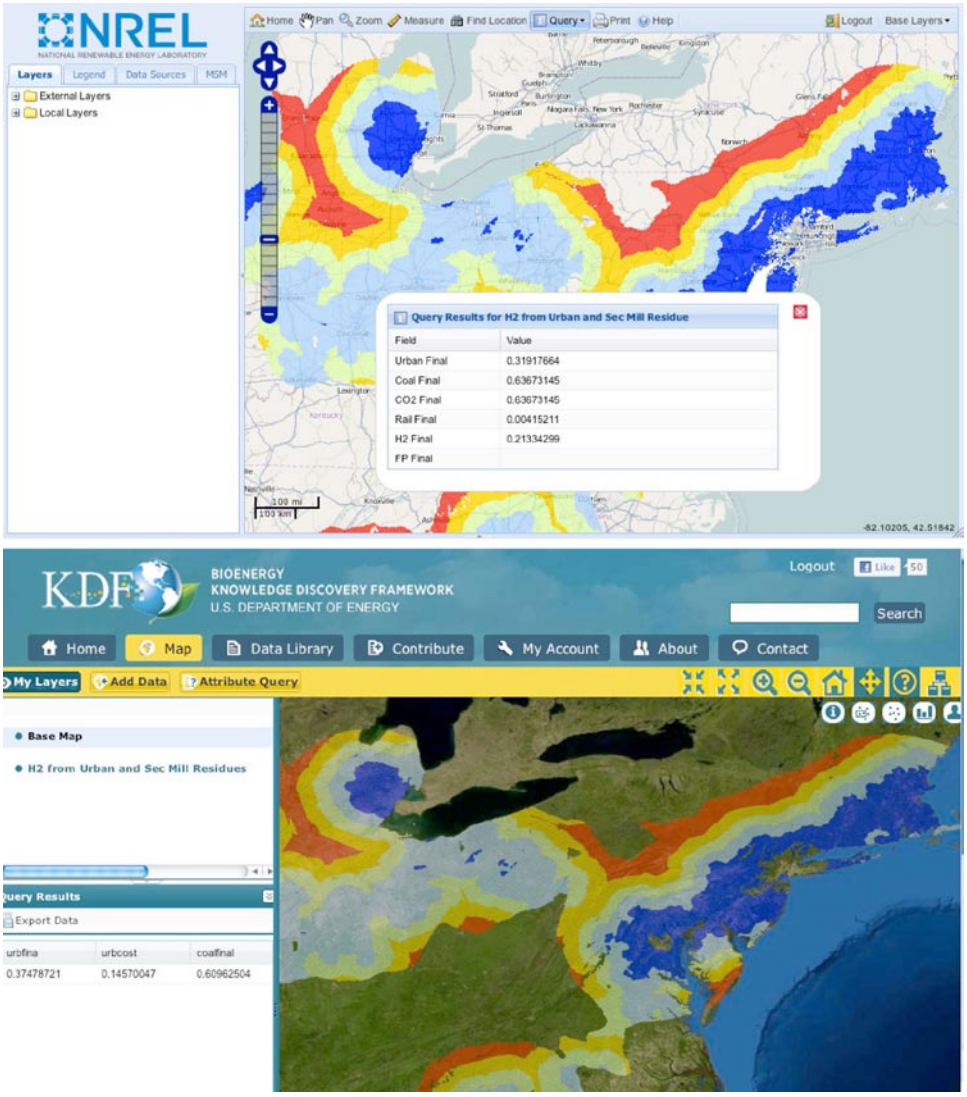


FIGURE 2. Data Stored in HyDRA and Accessed in both HyDRA and the BioenergyKDF

An advanced attribute querying capability has been implemented in HyDRA. For any layer within HyDRA the user can select multiple attributes to build a complex query and then run that query in the interface to select features that meet specific parameters. This capability will allow users to ask complicated questions about data within the HyDRA application and to explore research results in a more sophisticated manner than was previously possible (Figure 3).

In an effort to provide users with another path to visualize research data within HyDRA, a first level charting capability is being implemented in FY 2011. For any layer within the HyDRA application, users can specify up to four attributes to chart from the dataset. In combination with the spatial display and new querying capabilities, this elevates the potential to use HyDRA for analysis and provides information tailored to more specific decision making activities for users (Figure 4).

Additionally, several new datasets have been ingested into HyDRA and are available for use with the new attribute query, for use in external applications, and will be available for charting by the end of FY 2011.

Conclusions and Future Directions

HyDRA provides a single point of access to spatial data related to hydrogen systems. Improvements to the user interface and functionality provide a more intuitive user experience and improved analysis capabilities. Additionally, the enhanced interoperability of HyDRA simplifies the direct use of this data in analysis and modeling activities, and places HyDRA at the center of many other applications and research efforts. In the future HyDRA will focus on the following areas:

- HyDRA as a collaboration tool:

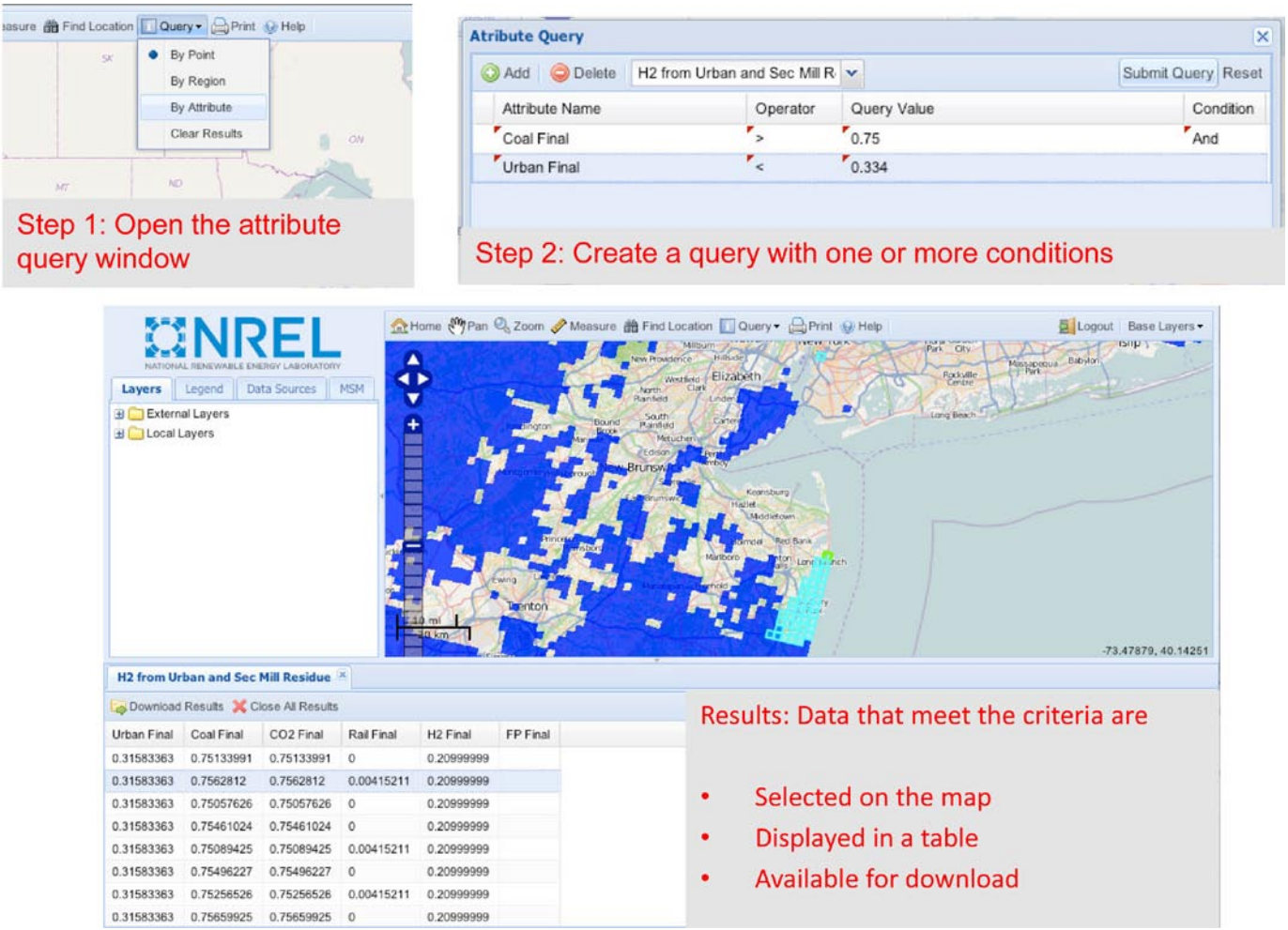


FIGURE 3. Attribute Query Example in HyDRA

- HyDRA will be used as a means of communicating spatial and temporal results from a number of future scenario studies, including wind-to-hydrogen analyses, California and other early market growth case studies, and nationwide hydrogen infrastructure rollout scenarios.
- Coordination with OpenEI will result in the development a process for automatically updating some datasets in the HyDRA application on a regular basis.
- Continue to integrate with other hydrogen models and analyses to develop new data input layers and to display model results using both manual and dynamic data integration.
- Allow for simple hydrogen system cost calculations through the HyDRA interface, relying upon H2A model result and assumptions.
- Formalize data interoperability relationships and data exchanges between other spatial data analysis and visualization applications in other domains of research.

- Completion of the advanced visualization tool:
  - The visualization tool that was cut this FY will be further developed in FY 2012 and focused mainly on exploring the results of NREL hydrogen systems analyses. In its final version, this visualization tool will open within HyDRA and be used to explore data from a wide range of sources, including runs of the MSM and SERA models.
- OpenCarto:
  - Develop complex querying capability, including enhanced spatial queries, to analyze temporal and multivariate datasets.
  - Collaboration with multiple projects that use OpenCarto to improve this framework and to enhance its capabilities in FY 2012 to support new geospatial technologies including advanced visualization and querying.
  - More interaction through the user interface to support communication about data availability and quality.

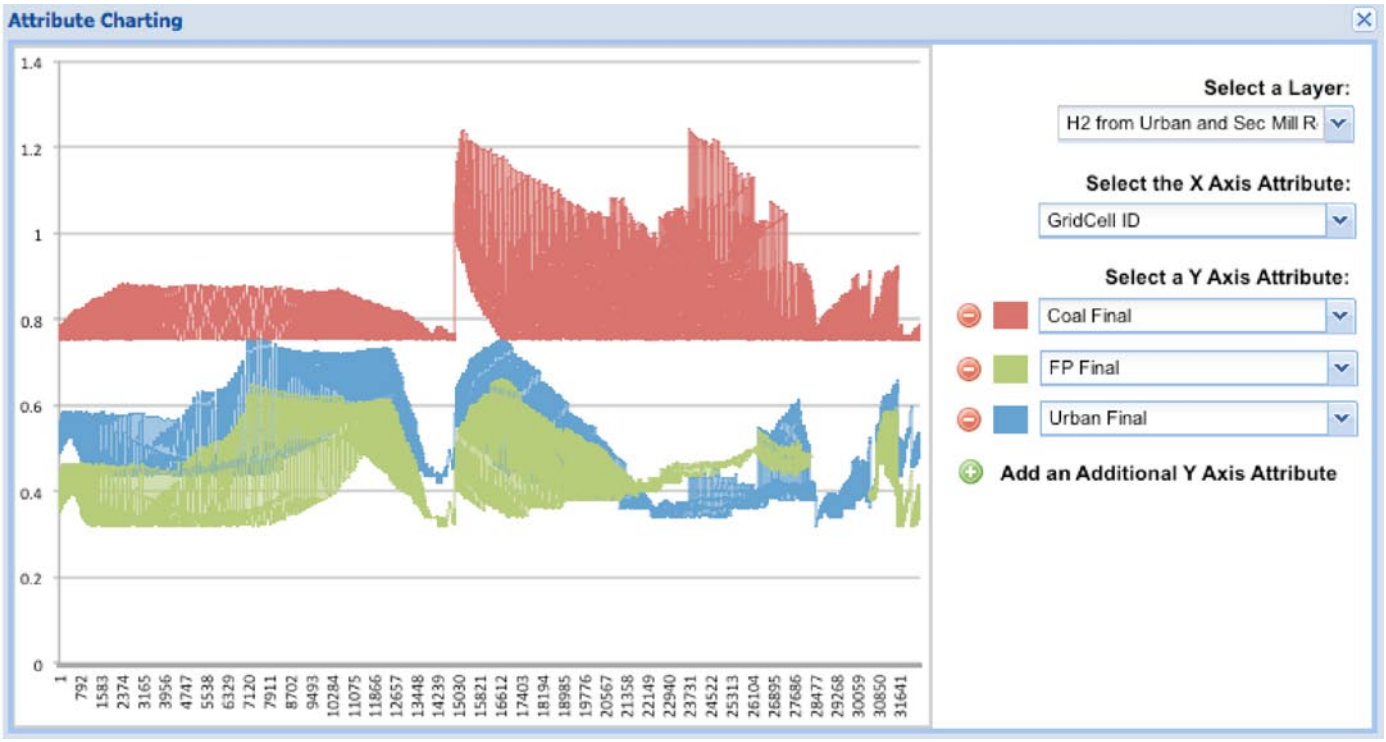


FIGURE 4. A Schematic of Layer Charting in HyDRA

- Long-term project support and data updates.
- Allow users to customize map classification and dynamically manipulate charting variables.
- Provide an interface to dynamically create, print, and export images of maps and charts.
- Continue to develop the capability to generate dynamic layers in the HyDRA application from user and model generated data.
- Develop and deploy basic analysis functions such as graphing, changing underlying assumptions, and buffering.

FY 2011 Publications/Presentations

1. Getman, D., Levene, J. "Developments in the Hydrogen Demand and Resource Assessment (HyDRA) Model: Improvements in Data Interoperability, Availability, and Querying". Hydrogen Annual Merit Review, 10 May 2011. (Poster Presentation)

2. Levene, J., Getman, D. "Recent Developments in the Hydrogen Demand and Resource Assessment (HyDRA) Model". Hydrogen Annual Merit Review, 8 June 2010. (Poster Presentation)

3. B. Bush, D. Getman, D. Hettinger, J. Levene, M. Melaina. "Interoperability between SERA and HyDRA". National Renewable Energy Laboratory, 31 March 2010. (Internal management report)

XI.11 Energy Informatics: Support for Decision Makers through Energy, Carbon and Water Analysis

A.J. Simon (Primary Contact), Clara Smith and Rich Belles
Lawrence Livermore National Laboratory (LLNL)
7000 East Ave., L-103
Livermore, CA 94551
Phone: (925) 422-9862
E-mail: simon19@llnl.gov

DOE Manager
HQ: Fred Joseck
Phone: (202) 586-7932
E-mail: Fred.Joseck@ee.doe.gov

Project Start Date: October 1, 2007
Project End Date: Project continuation and direction determined annually by DOE

Fiscal Year (FY) 2011 Objectives

- Depict energy use at the state and international level.
- Depict water use at the state level.
- Depict carbon emissions at the state level.
- Increase the fidelity of conceptual energy depictions in the residential and transportation sectors.

Technical Barriers

This project addresses the following technical barriers from the Systems Analysis section of the Fuel Cell Technologies Program Multi-Year Research, Development and Demonstration Plan:

(A) Future Market Behavior

(D) Feedstock Issues

(E) Unplanned Analyses

Contribution to Achievement Systems Analysis Milestones

This project will contribute to achievement of the following DOE milestones from the Systems Analysis section of the Fuel Cell Technologies Program Multi-Year Research, Development and Demonstration Plan:

- **Milestone 1:** Complete evaluation of the factors (geographic, resource availability, existing infrastructure) that most impact hydrogen fuel and vehicles. (3Q, 2005)
- **Milestone 5:** Complete analysis and studies of resource/feedstock, production/delivery and existing infrastructure for various hydrogen scenarios. (4Q, 2009)
- **Milestone 11:** Complete environmental analysis of the technology environmental impacts for the hydrogen scenarios and technology readiness. (2Q 2015)

FY 2011 Accomplishments

- Produced an "atlas" of 51 state-level energy flowcharts (50 states plus Washington, D.C.) using automated analysis of the Energy Information Administration's (EIA) State Energy Data System (SEDS).
- Published an "atlas" of 51 state-level carbon flowcharts (50 states plus Washington, D.C.) by combining expert analysis of EIA's Greenhouse Gas reports with automated analysis of SEDS.
- Created an "atlas" of 52 state-level water flowcharts (50 states plus Puerto Rico and the Virgin Islands) using automated analysis of Unites States Geological Survey (USGS) water use and disposition data.
- Compiled an "atlas" of 136 national-level foreign country energy flowcharts using automated analysis of International Energy Agency data.



Introduction

Energy informatics is the combination of expert knowledge of the energy system with data-science tools and information technology. The products of an informatics program are methodologies, tools, visualizations and reports that enable analysts and decision makers to better understand the energy system at multiple scales.

The Fuel Cell Technologies Program has enabled stakeholders to visualize critical commodity flows at geographic scales relevant to decision-makers. These commodities include energy, carbon and water. Adoption of hydrogen fuel may alter the structure of the energy system, shift or reduce the emissions of carbon dioxide, and place new demands on water infrastructure. In previous years, LLNL has analyzed the quantitative impacts of hydrogen's potential impacts on local water systems. This year, through a campaign of energy informatics, we have provided qualitative (structural visualizations) and quantitative (energy statistics) descriptions of energy, carbon and water systems at multiple scales.

Approach

The energy flowcharts (EFCs) (http://flowcharts.llnl.gov) have long been recognized for their importance in visualizing energy and material flows in a way that highlights

resources, carriers, transformations and services. But, like a map of the interstate system, the published EFCs provide only a high-level view of the country's energy infrastructure. The usefulness of this top-down view is limited by the level of detail that can be conveyed in a single image.

In order to provide a more detailed view of energy, carbon and water systems to state-level and international-level decision-makers, we have applied software tools developed here at LLNL to produce visually informative graphics from analytical reductions of publicly available statistical data sets.

Results

Although example charts are included in this report, the reader is encouraged to download each of the "atlases" of flowcharts from http://flowcharts.llnl.gov.

Flowcharts were produced depicting energy at the state level. This collection includes all 50 U.S. states as well as the District of Columbia, for a total of 51 charts. As an example, Figure 1 shows the energy use in the state of California. Because this report does not permit full-page figures, the reader is encouraged to download the entire "atlas" of state-level flowcharts from http://flowcharts.llnl.gov. The report, entitled "Estimated State-Level Energy Flows in 2008," explains how the 30 megabyte SEDS data archive [1] is compressed to ~40 critical energy indicators for each state. In these figures, stakeholders at the state level can view their consumption of various energy resources, and visually compare the energy intensity of various economic sectors within their states. These charts also include information on net electricity imports/exports across state lines. There are significant differences between states. For example, it is well known that Texas is one of the states with the highest overall energy use, but the flowchart depicts that much of this energy is consumed by industry. It is also easy to see Hawaii's dependence on petroleum.

Flowcharts were produced depicting carbon emissions at the state level. This collection includes all 50 U.S. states as well as the District of Columbia, for a total of 51 charts. As an example, Figure 2 shows the carbon emissions in the state of California. Because this report does not permit full-page figures, the reader is encouraged to download the entire "atlas" of state-level flowcharts from http://flowcharts.llnl.gov. The report, entitled "Estimated Carbon Emissions in 2008: United States" explains how the 30 megabyte SEDS data archive [1] is compressed to ~40 critical energy indicators for each state and combined with EIA's greenhouse gas emissions data [2,3] to determine CO_2 flows. In these figures, stakeholders at the state level can view their CO_2 emissions, and visually compare the carbon intensity of various energy-related activities within their states. For example, from these charts, it is clear that California's CO_2 emissions are dominated by transportation, whereas Wyoming's and West Virginia's emissions are dominated by coal-fired electricity. A quick glance at the energy flowcharts for these two states shows that they are also major electricity exporters.

Flowcharts were produced depicting water use at the state level. This collection includes all 50 U.S. states as well

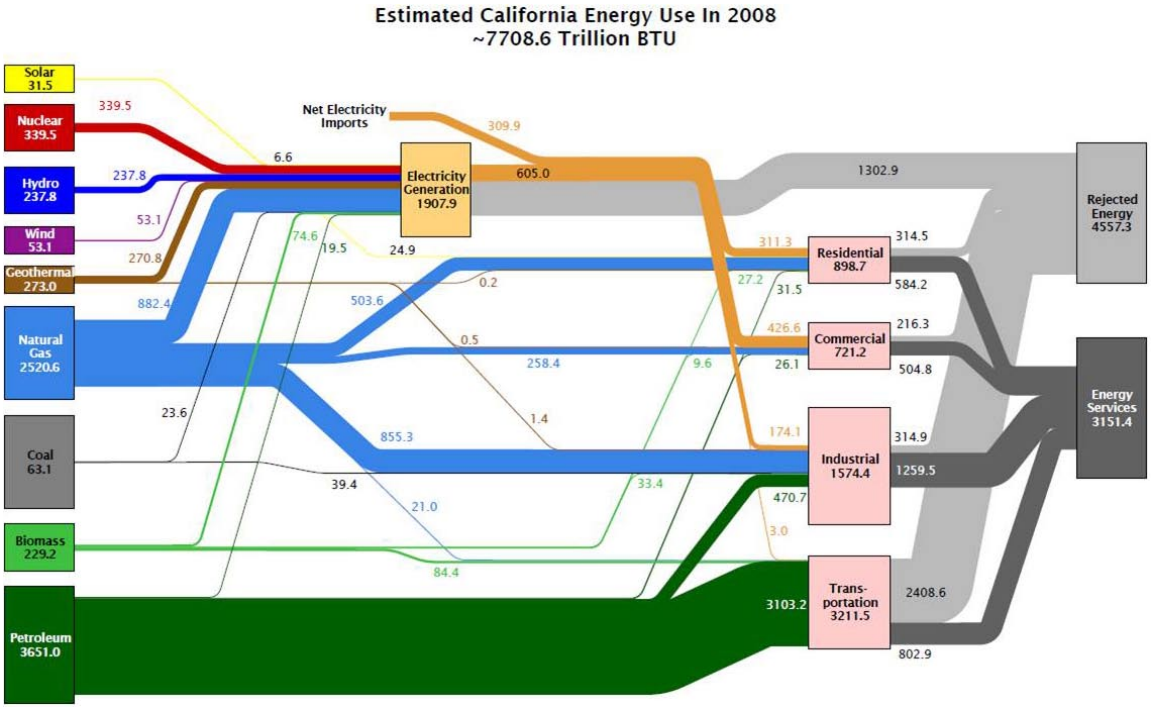


FIGURE 1. California Energy Flow in 2008

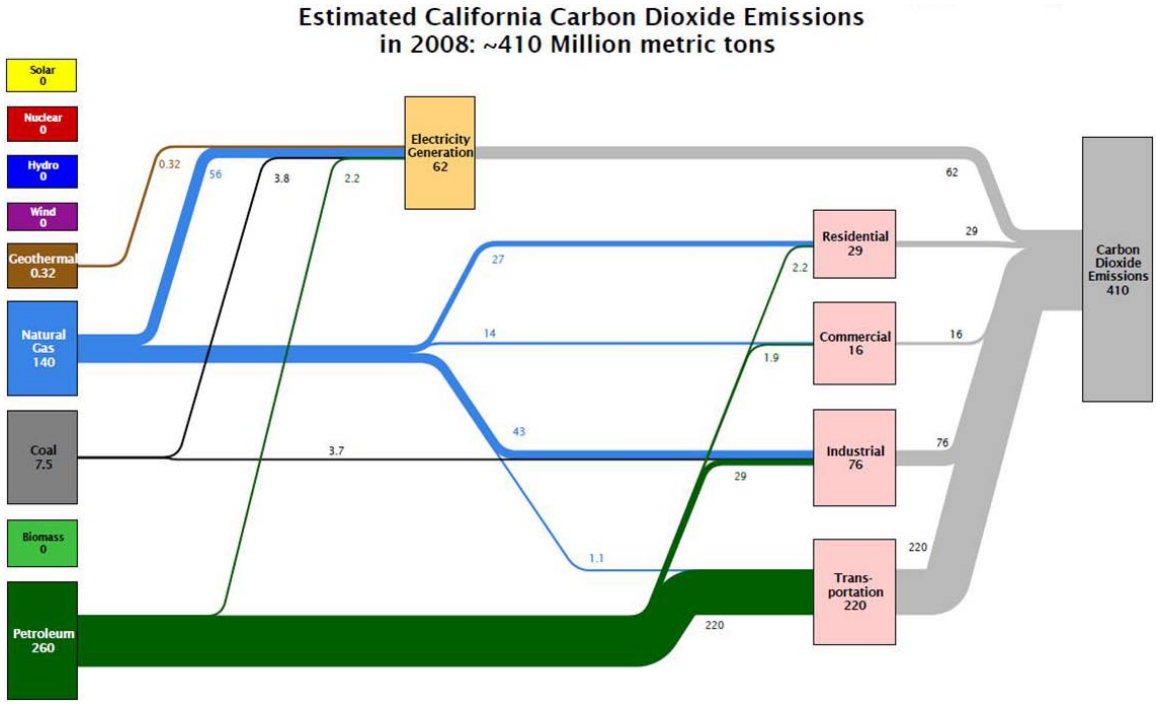


FIGURE 2. California Carbon Emissions in 2008

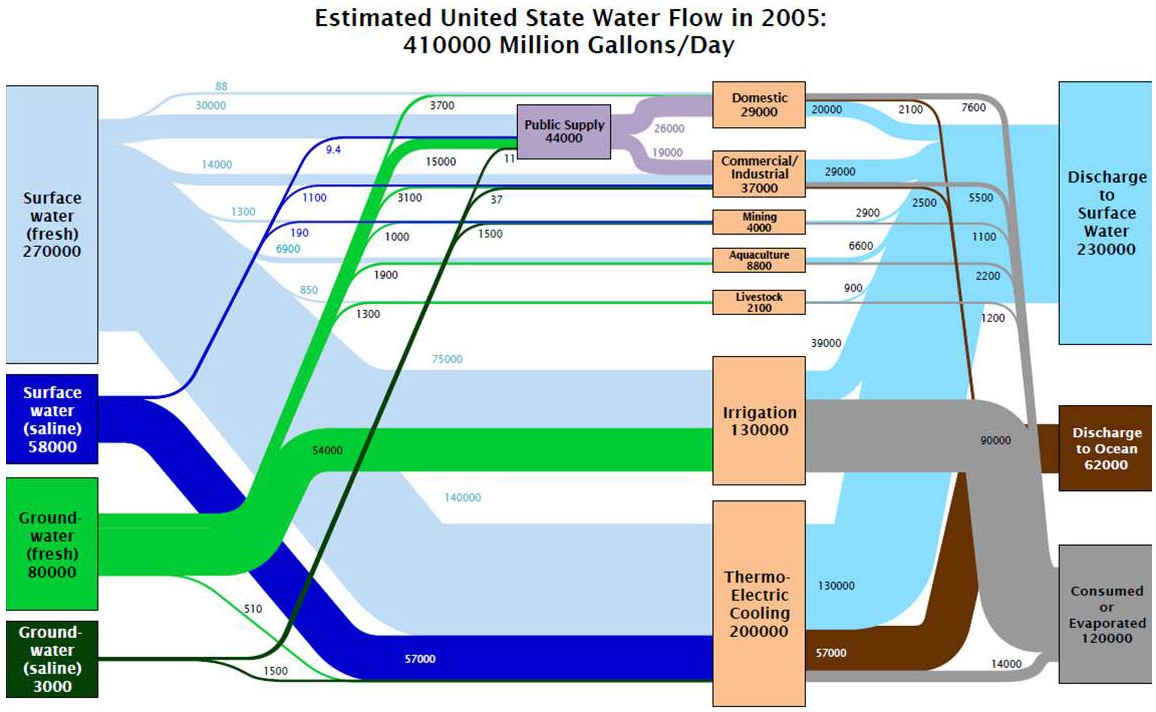


FIGURE 3. U.S. Water Flow in 2005

as the Puerto Rico and the Virgin Islands.. It also includes a composite national-level water flowchart for a total of fifty-three. As an example, Figure 3 shows the national-level water flowchart. Because this report does not permit full-page figures, the reader is encouraged to download the entire "atlas" of state-level flowcharts from http://flowcharts.llnl.gov. The report, entitled "Estimated Water Flows in 2005: United States" describes how the ~300,000 county-level water statistics compiled by the USGS [4] are reduced to ~40 critical water indicators for each state. These

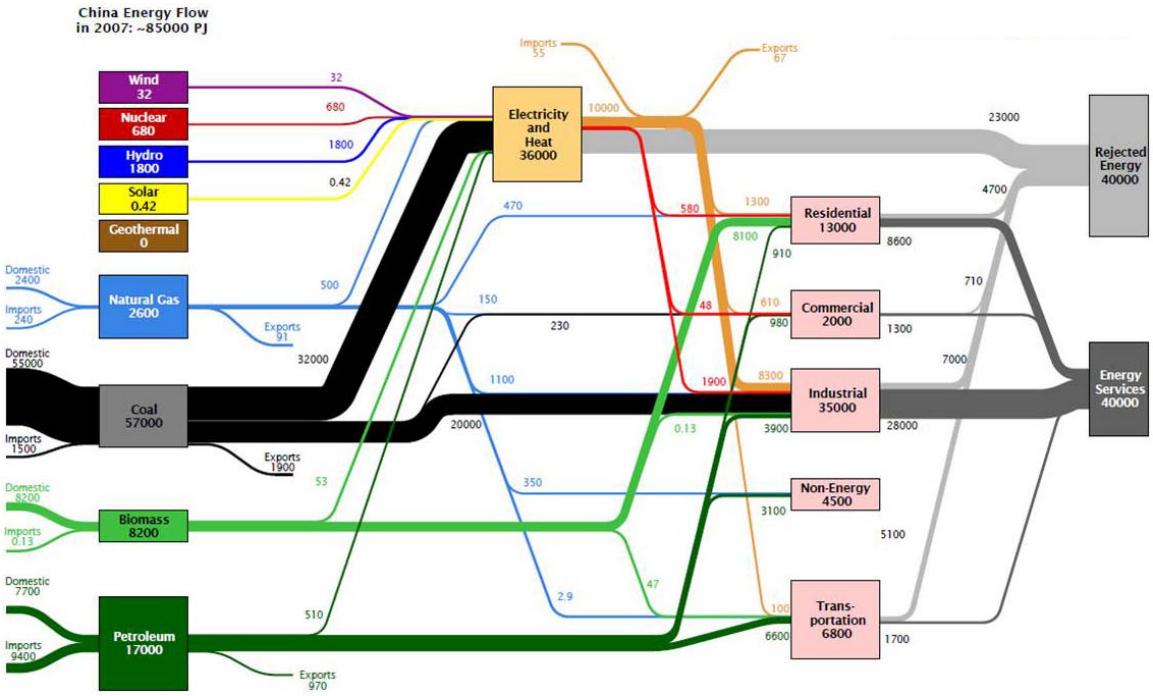


FIGURE 4. China Energy Use in 2007

figures allow a broad variety of stakeholders, including government, industrial, agricultural and environmental professionals, to quantitatively describe the structure of the water procurement, use and disposal systems. Of particular interest is the difference between western states and eastern states: managed water use in states such as Montana, New Mexico, Colorado and California tends to be dominated by irrigation, with power plant cooling as the only other water consumer at that magnitude. In the east, managed irrigation is significantly smaller due to more abundant rainfall.

One-hundred, thirty-six national-level energy flowcharts were produced depicting energy resources, use and disposition in foreign countries. This collection also includes a global-level aggregate energy flowchart for world energy use. As an example, Figure 4 shows the national-level energy flowchart for China. Because this report does not permit full-page figures, the reader is encouraged to download the entire "atlas" of state-level flowcharts from http://flowcharts.llnl.gov. The report, entitled "2007 Estimated International Energy Flows" describes how international energy data [5] are reduced from ~5,000 data points for each country to ~60 critical energy indicators. These figures enable visualizations of energy use patterns beyond the borders of the U.S., thereby giving stakeholders a quantitative and structural view of alternative energy infrastructures. Despite major differences between developed, transitional and developing economies, the resources, transformations and uses of energy as depicted are sufficient to capture all of the statistics. One major outlier is South Africa, whose coal liquefaction industry is large enough to warrant a separate transformation step.

Conclusions and Future Directions

Flowcharts, or "Sankey Diagrams" provide quantitative and qualitative information about flows of vital commodities within a defined geographical area or economic sector. As a result of this project, LLNL has produced flowcharts the three material flows most critical to the transformation of the energy economy.

- Decision makers now have access to a visual representation of state-level energy and carbon flows. Because environmental and technology regulations are often enforced at the state-level, these charts will empower the stakeholders closest to policy to better understand their energy use and environmental impact.
- Decision makers now have access to a visual representation of state-level water flows. Water is a fundamentally local commodity; water is used in such great quantity that the engineering of meaningful long-distance water conveyance is costly and therefore the rare exception. A quantitative and qualitative visual description of water supply, use and disposition at the state-level enables policy decisions at a geographic-scale comparable to that of many hydrologic basins.
- Decision makers now have access to a visual representation of national-level energy flows for most of the world's nations. Clearer intuition regarding foreign countries' energy use will enhance economic and security policymaking, as well as provide examples of alternative energy use patterns.

- Future directions of this research include visualizations of the details of energy use within the residential, transportation and industrial sectors. While we have demonstrated that flowcharts can be used to enable decision makers at finer geographic scales, we also intend to "zoom in" to finer structural details of the energy system.

FY 2011 Publications/Presentations

1. Simon, A.J. and Belles, R.D. "Estimated State-Level Energy Flows in 2008". LLNL-MI-410527. Available online at: https://flowcharts.llnl.gov/content/energy/energy_archive/energy_flow_2008/2008StateEnergy.pdf.

2. Smith, C.A., Simon, A.J. and Belles, R.D. "Estimated Carbon Dioxide Emissions in 2008: United States." LLNL-TR-480261. Available online at: https://flowcharts.llnl.gov/content/carbon/carbon_emissions_2008/2008StateCarbon.pdf.

3. Smith, C.A, Simon, A.J., and Belles, R.D. "Estimated Water Flows in 2005: Unites States." LLNL-TR-475772. Available online at: https://flowcharts.llnl.gov/content/water/water_flow_archive/2005USStateWater.pdf.

4. Smith, C.A., Simon, A.J. and Belles, R.D. "2007 Estimated International Energy Flows." LLNL-TR-473098. Available online at: https://flowcharts.llnl.gov/content/international/2007EnergyInternational.pdf.

5. Simon, A.J. and Smith, C.A. "Energy Informatics: Support for Decision Makers through Energy, Carbon and Water Analysis" Presented at DOE Hydrogen and Vehicle Technologies Annual Merit Review, Arlington, VA, May 10, 2011.

References

1. Energy Information Administration. State Energy Data System, 2008. Available online at: http://www.eia.doe.gov/states/_seds.html. DOE/EIA-0214(2008) June 2010.

2. Energy Information Administration. Annual Energy Review 2009. Available at: http://www.eia.gov/aer. DOE/EIA-0384(2009) August, 2010.

3. Energy Information Administration. U.S. Electric Power Industry Estimated Emissions by State. Available at: http://www.eia.doe.gov/cneaf/electricity/epa/emission_state.xls DOE/EIA-767, EIA-906, EIA-920, and EIA-923. Revised January 4, 2011.

4. Kenny, J.F., Barber, N.L., Hutson, S.S., Linsey, K.S., Lovelace, J.K., and Maupin, M.A., 2009, Estimated use of water in the United States in 2005. Available at: http://pubs.usgs.gov/circ/1344/ U.S. Geological Survey Circular 1344. Released October, 2009.

5. International Energy Agency. Extended World Energy Balances 2007. Available by subscription at http://data.iea.org August, 2010.

XI.12 Fuel Quality Effects on Stationary Fuel Cell Systems

Shabbir Ahmed (Primary Contact),
Dennis Papadias, Romesh Kumar
Argonne National Laboratory
9700 South Cass Avenue
Argonne, IL 60439
Phone: (630) 252-4553
E-mail: ahmeds@anl.gov

DOE Manager
HQ: Fred Joseck
Phone: (202) 586-7932
E-mail: Fred.Joseck@ee.doe.gov

Project Start Date: October 1, 2006
Project End Date: Project continuation and direction determined annually by DOE

Fiscal Year (FY) 2011 Objectives

- Study the effects of impurities on fuel cell systems for stationary applications.
- Correlate the cost of electricity to impurity concentrations in the fuel feedstock.

Technical Barriers

This project addresses the following technical barriers from the Systems Analysis section of the Fuel Cell Technologies Program Multi-Year Research, Development and Demonstration Plan:

(B) Stove-piped/Siloed Analytical Capability

(D) Suite of Models and Tools

Contribution to Achievement of DOE Systems Analysis Milestones

This project will contribute to achieving the following DOE Systems Analysis milestones from the Systems Analysis section of the Fuel Cell Technologies Program Multi-Year Research, Development, and Demonstration Plan:

- **Milestone 8**: Complete analysis and studies of resource/feedstock, production/delivery and existing infrastructure for technology readiness (4Q, 2014). The study described here analyzes the quality of resources/feedstocks, their conversion to reformate, and subsequent purification to meet the tolerance levels of the fuel cell stacks in stationary fuel cell systems. The analysis results in estimates of the differential cost of hydrogen attributable to gas clean-up.

FY 2011 Accomplishments

- A database, started in the last FY, to document the impurities encountered in stationary fuel cell systems by reviewing the literature and other public domain information has been extended to include halocarbons, volatile organic compounds (VOCs), and organosilicon compounds.
- The tolerance limits of various types of fuel cells to fuel impurities have been documented.
- A model of a stationary fuel cell-based combined heat and power system has been developed to estimate the effect of impurity levels on the cost of hydrogen:
  - Fueled by anaerobic digester gas cleaned through available technologies.
  - Power generated with a molten carbonate fuel cell.



Introduction

Fuel cell systems are being deployed in stationary applications for the generation of electricity, heat, and hydrogen. These systems use a variety of fuel cell types, ranging from the low temperature polymer electrolyte fuel cell (PEFC) to the high temperature solid oxide fuel cell (SOFC). Depending on the application and location, these systems are being designed to operate on reformate or syngas produced from various fuels that include natural gas, biogas, coal gas, etc. All of these fuels contain species that can potentially damage or pose a hazard for the fuel cell anode or other unit operations and processes that precede the fuel cell. These effects include loss in performance or durability, and attenuating these effects requires additional components to reduce, if not eliminate, the impurity concentrations to tolerable levels. These impurity management options increase the complexity of the fuel cell system, and they add to the capital and operating costs (regeneration, replacement and disposal of spent material, maintenance, etc.).

This project reviews the public domain information available on the impurities encountered in stationary fuel cell systems and their effects on fuel cells. A database has been set up which classifies the impurities, especially in renewable fuels such as landfill gas and anaerobic digester gas. It documents the deleterious effect on fuel cells and the maximum allowable concentrations of select impurities suggested by manufacturers and researchers. A generic model of a stationary fuel cell-based power plant is being developed; it includes a gas processing unit followed by a fuel cell system. The model is being used to conduct an economic analysis to estimate the effect of impurities (according to the class of materials, such as siloxanes) on

the cost of electricity. The model identifies the key relevant design and process parameters, and their effects on the capital and operating costs, as a function of the impurity content in the fuel feedstock.

Approach

The project evaluated the fuel feedstocks used in the stationary fuel cell power plants and identified the impurities and their concentrations that are typically present. The effect of these impurities on the fuel cell stack and suggested tolerance limits have been documented. The literature review helped identify the impurity removal strategies that are available and their effectiveness, such as capacity, cost, etc. A system model has been set up to consolidate the information and correlate the interactions and demands on the system. The key impurity removal steps are being modeled to enable predictions of impurity breakthrough, component sizing, and utility needs. The energy needs and process efficiency results from the model will be entered into the H2A model to calculate the cost of electric power. Sensitivity analyses will be conducted to correlate the concentrations of key impurities in the feedstock to the cost of electric power.

Results

Biogas from a waste digester contains 50-60% methane, with the balance of the biogas being mostly carbon dioxide, and is a viable fuel for fuel cell systems. It also contains trace contaminants some of which are produced by biological digestion while others are volatilized from the waste stream being digested. The contaminant matrix can be rather complex, containing many species that can be harmful to the fuel cell. The nature and amounts of such contaminants depend on the type and age of the waste, temperature, pressure, etc.

In general, while many contaminant species are present in biogas, three classes of impurities are of particular concern for its use in fuel cell systems.

- Reduced sulfur compounds are common in all biogas sources. The primary reduced sulfur compound of concern is hydrogen sulfide (H_2S), which may be present in biogas at concentrations up to several thousand parts per million by volume. While H_2S represents the bulk of sulfur in the biogas, organic sulfur, such as mercaptans and dimethylsulfide, is also present although typically in much lower concentrations (~1 ppm or less).
- Siloxanes emanating from personal hygiene products are generally present in landfill gas and wastewater treatment plant sludge digester gas in concentrations of 10 ppmv or less. Siloxanes (**sil**icon, **ox**ygen, alk**ane**) are organo-silicon compounds with the formula R_2SiO, where R is H or a hydrocarbon group. Siloxanes can be cyclic (e.g., hexamethylcyclotrisiloxane [D3], etc.) or linear (e.g, hexamethyldisiloxane [L2], etc.). Out of all the hundreds of different siloxanes in use, the most commonly occurring ones in landfill and biogases are L2-L5 and D3-D6 [1]. Siloxanes are converted to solid silica in flames. The solid silica may accumulate on surfaces inside power generation equipment and it can prematurely deactivate the catalytic surfaces in reformers and fuel cells.
- VOCs include alkanes, alcohols, aromatics and halogenated species. Of primary concern are halogens that can deactivate the catalytic surfaces in reformers and react with the electrolytes in fuel cells. Halogens from landfill gas generally originate from discarded refrigerants, plastic foams, etc. Many compounds are stable and slowly evaporate to maintain significant levels of halogens for many years. The concentrations of halogenated species from waste water treatment plants (WWTP) are typically below 1 ppm, while landfill gas may contain halogenated species up to about 40 ppm.

The requirements for gas cleaning will vary, depending on the type of biogas, impurity concentrations in the biogas and the tolerance limits to the impurities of the specific fuel cell system. A single gas purification step is seldom sufficient to clean the biogas; rather, a combination of methods is used to ensure a fuel quality that matches the tolerance limits for the fuel cell system. Reviewing the literature that includes case studies for fuel cell systems operating both on landfill gas and digester gas [2-5], it was found that the general gas cleaning strategies involve several steps, which can be broken down to a) primary clean-up of bulk impurities (e.g., H_2S with iron oxide) and b) gas polishing (i.e. adsorption) of trace contaminants of concern before the gas is delivered to the fuel cell system.

A generic model of a stationary fuel cell-based power plant has been developed to determine the overall electrical efficiency and costs of clean-up and maintenance, as a function of the biogas impurity matrix. A schematic of the fuel cell power plant is shown in Figure 1. A base case system considers a fuel cell system operated on digester gas from a waste water treatment plant. Major sections of the system include the gas processing system, fuel processor/fuel cell stack, and thermal management system. First the bulk impurity H_2S is removed using an appropriate sorbent, such as iron oxide media or impregnated activated carbon. The gas is further cooled to condense the water as moisture can significantly reduce the adsorption capacity in subsequent clean-up steps. The gas can even be deeply cooled to below -20°C to condense some of the siloxanes and heavier VOCs.

The dry gas is further passed to the secondary polishing equipment that can contain a series of adsorbents and removes organic sulfur, siloxanes, and halogens. The cleaned gas enters the fuel cell system where it is converted to electricity and usable heat. The heat generated by the electrochemical reaction is removed to an external heat rejection system, where it is recovered for use by the sewage treatment plant, in particular, to meet the energy needs for

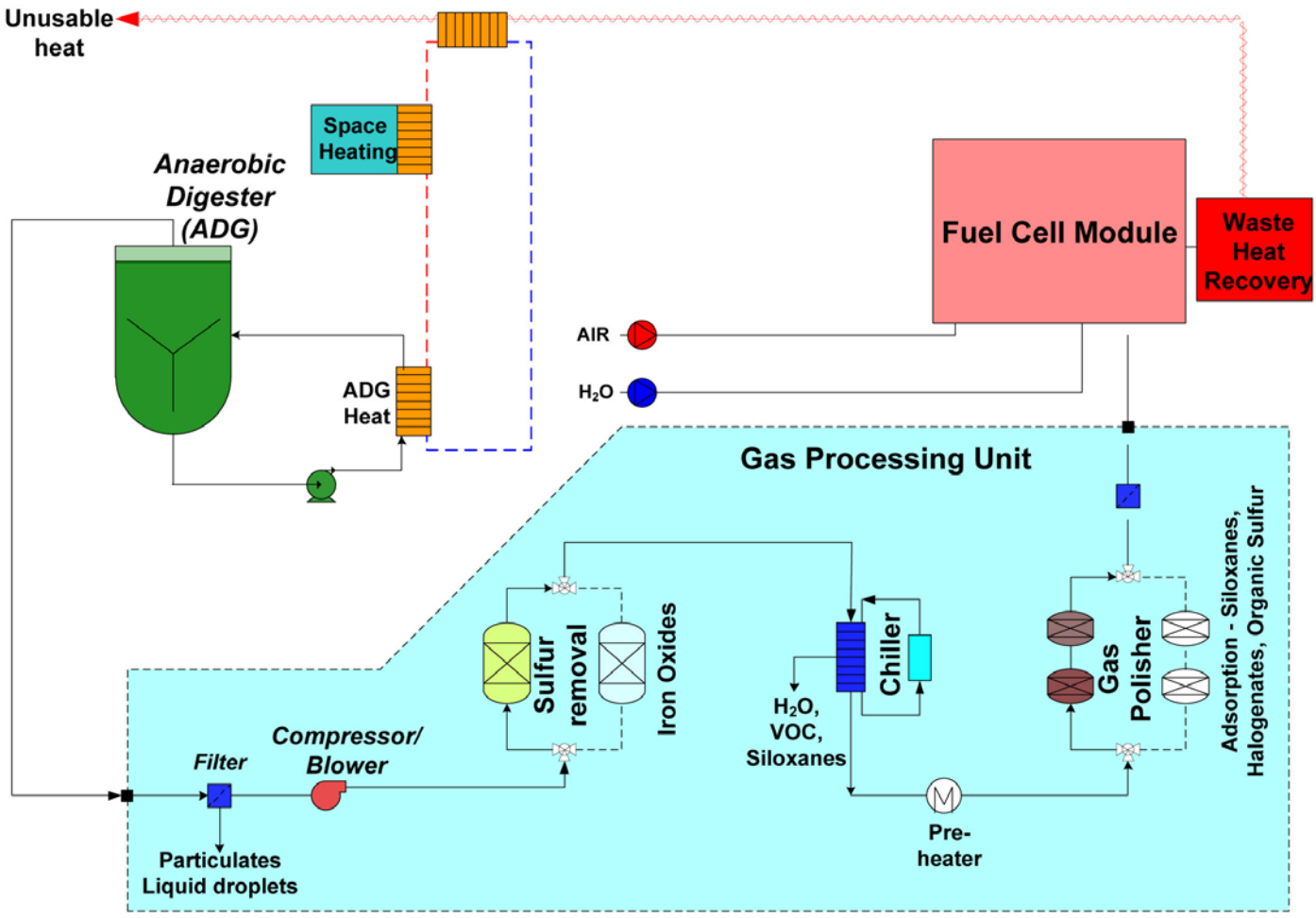


FIGURE 1. A Base Case Fuel Cell System Operating on Anaerobic Digester Gas

the anaerobic digestion process and, possibly, for other uses, e.g., space heating.

The overall process model has been set up initially for a molten carbonate fuel cell, and various component models are being developed to determine the utilization of the adsorbents (and, ultimately, the replacement costs) as function of impurity concentrations in the raw gas. For example, Figure 2 shows the adsorption capacity of activated carbon on some select trace impurities typically found in digester gas from WWTPs. The lines are modeled adsorption isotherms on pure organic components as a function of concentration (partial pressure) [6-7], and have been calibrated with available experimental data on activated carbon [8]. The shaded region in the graph is a range of concentration limits on a) the lower impurity tolerance limits for a fuel cell, and b) the typical maximum concentrations of individual trace impurities entering the gas polisher. Unsupported activated carbon has a rather low adsorption capacity for hydrogen sulfide, and so H_2S must be removed prior to the gas polisher. Some species, such as chlorobenzene and aromatics (e.g., toluene), show very high adsorption affinities for carbon, even at low

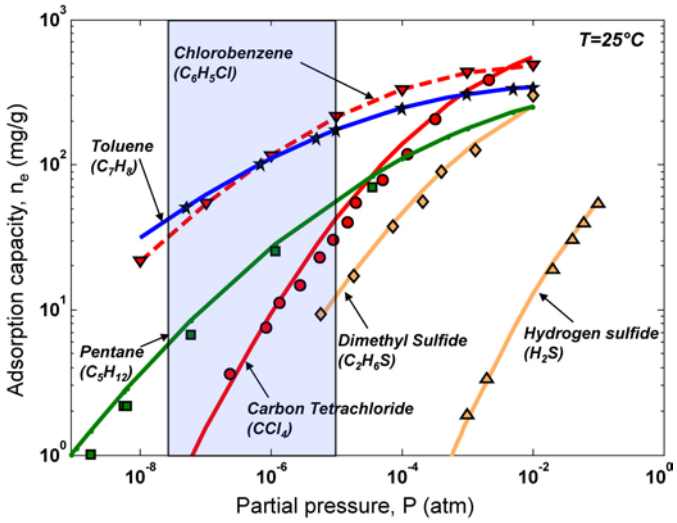


FIGURE 2. Adsorption isotherms on activated carbon (BPL) on some of the most frequent encountered trace impurities in digester gas. Solid lines are modeled pure component isotherms and symbols corresponding experimental data from the literature.

concentrations. Aromatics at ppm levels will not pose any hazard to the fuel cell system as such, but they will compete with available adsorption space and reduce the adsorption capacity for halogens and siloxanes – species of concern for the durability of the fuel cell system.

Conclusions and Future Directions

- Data available on biogas sources with respect to trace contaminant matrix and clean-up options and performance has been collected into a database. This information, along with the effects and removal of the various species that have significant deleterious effects on fuel cell performance or lifetimes, is categorized in classes of impurities, biogas source, and unit operations of the systems.
- Impurities of particular concern for the fuel cell system are sulfur, siloxanes, and halogens, which vary in concentration and speciation, depending on the biogas source of interest. Higher hydrocarbons, aromatics, and alcohols are also present in the biogas. While their concentrations may not be of direct threat to the fuel cell, they can greatly reduce the capacity of the various adsorbents to remove siloxanes and halides.
- A base case system has been set up for economic analysis and initially considers a molten carbonate fuel cell system operating on digester gas from waste water treatment plants. A generic model of a stationary fuel cell-based power plant has been developed, including component models of typical gas processing units, to determine the utilization of various adsorbents as a function of the biogas impurity type and concentration matrix.
- Cost data are being gathered for the various components in the power plant to complete the cost analysis for the base-case system. Further work will determine costs for different fuel cells, bio-gas sources, and clean-up technologies. Trade-off analyses between cost of clean-up versus degradation and power loss of fuel cell system are also important to determine life-cycle costs. Ultimately, these models and results will need to be validated with data from operating plants.

FY 2011 Publications/Presentations

1. "Fuel Quality in Fuel Cell Systems," Presented at the 2011 DOE Hydrogen Program and Vehicle Technologies Program Annual Merit Review and Peer Evaluation Meeting, Arlington VA, May 9–13, 2010.

References

1. McBean, E. A., (2008). *Siloxanes in biogases from landfills and wastewater digesters,* Canadian Journal of Civil Engineering **35**, 431-436.

2. City of Klemath Falls – Spring Street Sewage System (2010). Biogas Energy Management Study, Final Submittal.

3. Steinfeld, G. and Sanderson, R. (1998). Landfill Gas Cleanup for Carbonate Fuel Cell Power Generation. NREL/SR-570-26037.

4. King County Fuel Cell Demonstration Project – Final Report (2009). Prepared for the U.S. Environmental Agency.

5. Spiegel, R.J. and Preston, J.L. (2003). *Technical Assessment of Fuel Cell Operation on Landfill Gas at the Groton, CT, Landfill*. Energy, 28, 397-409.

6. Wood, G.O. (2001). *Affinity Coefficients of the Polanyi/Dubinin Adsorption Isotherm Equations. A Review with Compilations and Correlations*. Carbon, 39, 343-356.

7. Ye, X., Qi, N., Ding, Y. and LeVan M.D. (2003). *Prediction of Adsorption Equilibrium using a Modified D-R Equation: Pure Organic Compounds on BPL Carbon*. Carbon, 41, 681-686.

8. Himeno, S. and Urano, K. (2006). *Determination and Correlation of Binary Gas Adsorption Equilibria of VOCs*. Journal of Environmental Engineering, March, 301-308.

XII. AMERICAN RECOVERY AND REINVESTMENT ACT ACTIVITIES

XII.0 American Recovery and Reinvestment Act Activities

In April 2009, the Department of Energy (DOE) announced the investment of $41.6 million in American Recovery and Reinvestment Act (ARRA or Recovery Act) funding for fuel cell technologies. These investments were made to accelerate the commercialization and deployment of fuel cells and to spur the growth of a robust fuel cell manufacturing industry in the United States, with accompanying jobs in fuel cell manufacturing, installation, maintenance, and support services. Twelve grants were awarded to develop and deploy a variety of fuel cell technologies, including polymer electrolyte membrane, solid oxide, and direct-methanol fuel cells in auxiliary power, backup power, combined heat and power, lift truck, and portable-power applications. The cost share provided by the project teams is about $54 million, more than 56% of the total cost of the projects.

The ARRA fuel cell projects are addressing the objectives stated above as well as the overall ARRA goals of creating new jobs and saving existing ones, spurring economic activity, and investing in long-term economic growth. Significant progress toward these goals has been made, including the deployment of more than 830 fuel cells by the end of FY 2011, out of the total planned deployment of up to 1,000 fuel cells. These deployments have required project teams to address key challenges, including siting and permitting, fueling infrastructure, and fuel cell lifetime and reliability. These deployments have also attracted significant attention, with media events taking place at three of the ARRA deployment sites.

All ARRA project teams submit quarterly reports, which are available to the public through the Recovery.gov website. These reports include technology and deployment status as well as data on jobs created and funds spent. Collection and analysis of operational data from the fuel cell deployments are being performed by the National Renewable Energy Laboratory's (NREL's) Hydrogen Secure Data Center (HSDC) to assess the performance and commercial readiness of the fuel cell technologies. Data are aggregated across multiple systems, sites, and teams, and are made available on a quarterly basis through Composite Data Products (CDPs), published on NREL's website. Eleven presentations containing all CDPs have been published thus far, with the latest CDPs including performance, reliability, maintenance, and safety data for material handling equipment and backup power.

The Hydrogen Safety Panel has made four deployment site visits and has reviewed each project's safety plan. In addition, Sandia National Laboratories (funded through the Safety, Codes & Standards sub-program) has obtained two types of high-pressure hydrogen tanks for testing, from two ARRA project fuel cell partner companies and from tank manufacturers. Tank testing and analysis, which began at Sandia National Laboratories in FY 2010[1], are being done to facilitate market entry for fuel cell–powered lift trucks. This effort continues to address fatigue crack initiation and growth in steel tanks used in high-cycle applications. Testing thus far has shown the engineering predictions to be conservative relative to the performance of the pressure vessels—i.e., the number of cycles to failure has been higher than predicted. The procedures for pressure testing with gaseous hydrogen are being included in Canadian Standards Association HPIT1 and SAE International J2579 working documents for performance testing.

ARRA Project Summaries

Auxiliary Power

Delphi Automotive (Troy, Michigan and Rochester, New York): Delphi is developing a 3- to 5-kW solid oxide fuel cell (SOFC) auxiliary power unit (APU) for heavy-duty commercial Class-8 trucks at their laboratory in Rochester, New York. Delphi will test and demonstrate the diesel APU in a high visibility fleet vehicle that will provide power for vehicle hotel loads and other vehicle needs under real-world operating conditions. There will also be a series of in-house tests, including on-vehicle testing, to validate the "road worthiness" of the diesel APU prior to installation on the demonstration truck. Delphi will provide a comprehensive system specification and—with original equipment manufacturer partner PACCAR—will define commercial requirements. System development efforts will improve Delphi's current-generation SOFC technology by increasing net output power and fuel processing efficiency, decreasing heat loss and parasitic power loss, and establishing diesel fuel compatibility. The primary focus will be accelerating the development

[1] "Component Testing for Industrial Trucks and Early Market Applications," Daniel Dedrick et al., this volume.

and acceptance of the APU by the Class-8 heavy-duty truck market. Partners include Electricore Inc., PACCAR Inc., and TDA Research Inc.

Backup Power

ReliOn Inc. (Spokane, Washington): ReliOn is deploying backup-power fuel cell systems at approximately 190 telecommunications and utility network sites operated by AT&T and Pacific Gas & Electric (PG&E). These deployments span nine states, and they include the deployment of a refillable stationary hydrogen storage module and accompanying refueling logistics platform for AT&T sites. This effort will add reliability to communications networks where no backup power was previously available. ReliOn will provide DOE with data on installation, fueling logistics, and operations for fuel cells in voice and data communications networks in mountain, desert, and urban locations. Partners include Air Products & Chemicals Inc., AT&T, and PG&E.

Sprint Nextel Inc. (Reston, Virginia): Sprint Nextel is planning to demonstrate the technical and economic viability of deploying 1- to 10-kW polymer electrolyte membrane (PEM) hydrogen fuel cells with 72 hours of on-site fuel storage (using a new Medium Pressure Hydrogen Storage Solution with on-site refueling) to provide backup power for critical code division multiple access cell sites on the Sprint Wireless network. Over 200 new hydrogen fuel cell systems will be deployed at sites in California, Connecticut, New Jersey, and New York. Partners include Air Products & Chemicals Inc., Altergy Systems, Black & Veatch Corporation, Burns & McDonnell Engineering Co. Inc., Ericsson Services Inc., and ReliOn Inc.

Plug Power Inc. (Latham, New York): This project will demonstrate the market viability of low-temperature, 6-kW PEM GenCore® fuel cells fueled by liquid petroleum gas (LPG) to provide clean and reliable primary power and emergency backup power (72 hours or more). Plug Power will install and operate 20 fuel cell systems at Fort Irwin in Barstow, California, and Warner Robins Air Force Base in Warner Robins, Georgia. These units will run continuously on LPG, providing power to the grid and will switch to emergency backup power during a grid failure. A small battery pack will be used to accommodate spikes in power demand. Partners include IdaTech, the U.S. Army Corps of Engineers' Construction Engineering Research Laboratory, Warner Robins Air Force Base, and Fort Irwin.

Combined Heat and Power (CHP)

Plug Power Inc. (Latham, New York): Plug Power is evaluating the performance of up to 12 high-temperature, natural gas-fueled, 5-kW micro-CHP fuel cell units (GenSys Blue®). The objective of the project is to validate the durability of the fuel cell system and verify its commercial readiness. Six units will undergo an internal Plug Power test regime to estimate failure rates, and up to six units will be installed and tested in real-world residential and light commercial end-user locations in California. Partners include Sempra Energy and the National Fuel Cell Research Center at the University of California, Irvine.

Fuel Cell-Powered Lift Trucks

FedEx Freight East (Harrison, Arkansas): FedEx is deploying 35 fuel cell systems as battery replacements for a complete fleet of electric lift trucks at FedEx's service center in Springfield, Missouri. Success at this service center may lead to further fleet conversions at some or all of FedEx's other 470 service centers. Partners include Air Products & Chemicals Inc. and Plug Power Inc.

GENCO (Pittsburgh, Pennsylvania): GENCO is deploying 357 fuel cell systems as battery replacements for fleets of electric lift trucks at five existing distribution centers (Coca-Cola in Charlotte, North Carolina; Kimberly Clark in Graniteville, South Carolina; Sysco Foods in Philadelphia, Pennsylvania; Wegmans in Pottsville, Pennsylvania; and Whole Foods in Landover, Maryland). Success at these distribution centers may lead to further fleet conversions at some or all of GENCO's other 109 distribution centers. Partners include Air Products & Chemicals Inc., Linde North America, and Plug Power Inc.

Nuvera Fuel Cells (Billerica, Massachusetts): Nuvera is deploying 14 fuel cell forklifts in H-E-B Grocery Company's distribution facility in San Antonio, Texas. Fuel will be supplied by Nuvera's natural gas reformer and its storage and dispensing system. Partners include H-E-B Grocery Co.

Sysco Houston (West Houston, Texas): Sysco is deploying 98 fuel cell systems as battery replacements for a fleet of lift trucks at Sysco's new distribution center in Houston, Texas, opened in March 2010. This

installation is the first-ever greenfield installation without prior battery infrastructure for a pallet truck fleet. Success at this distribution center may lead to further fleet conversions at some or all of Sysco's other 169 distribution centers. Partners include Air Products & Chemicals Inc. and Plug Power Inc.

Portable Power

Jadoo Power (Folsom, California): Jadoo is developing portable, propane-fueled SOFC generators and an electro-mechanical propane fuel interface as a potential replacement for traditional gas/diesel generators and lead-acid batteries. Two portable fuel cell generators will be deployed in this project. One of them will be used in a demonstration with police and fire first-responders in the City of Folsom, California, to power equipment in emergency and off-grid situations; both units will then be used to power media production equipment at automobile racing events at multiple locations throughout the United States. Partners include Delphi Inc., NASCAR Media Group, and the City of Folsom, California.

MTI MicroFuel Cells (Albany, New York): MTI is demonstrating a 1-watt consumer electronics power pack. The project is focused on improving reliability to meet the standards required by the electronics market and includes testing of individual components, subsystems, and complete direct methanol fuel cell (DMFC) systems. MTI is also developing manufacturing processes to improve product yields and reduce overall costs.

University of North Florida (Jacksonville, Florida): The University of North Florida is continuing work on a portable power system for use in mobile computing, further integrating and miniaturizing the components and analyzing failure modes to increase durability. The power system would be a DMFC that meets their initial commercial entry requirements for power density, energy density, and lifetime. The University will also conduct a design-for-manufacturability-and-assembly review to ensure that the systems meet their cost targets for commercialization. Partners include the University of Florida, Gainesville.

Data Collection & Analysis

National Renewable Energy Laboratory (Golden, Colorado): NREL is analyzing operational data (operation, maintenance, and safety) from the ARRA fuel cell deployments to better understand and highlight the business case for fuel cell technologies. Data collected by the project partners will be stored, processed, and analyzed in NREL's HSDC. Reports on the technology status will be generated on a quarterly basis, while technical CDPs will be published every six months.

FY 2011 Status and Accomplishments

As of the end of September 2011, more than 460 fuel cell lift trucks and more than 370 fuel cell backup-power systems for cellular communications towers and stationary backup-power systems had been deployed, and over 80% of the ARRA project funds had been spent by the projects. A total of 46 direct jobs have been created or retained as a result of these ARRA projects. Supply chain and other indirect jobs are not included– if it is assumed that at least three indirect jobs are created for each direct job, this would indicate that over 180 total jobs were created or retained as a result of these ARRA projects. NREL's HSDC has established data reporting protocols with each of the project teams. CDPs and detailed data products showing progress to date have been prepared. The CDPs are available on the NREL HSDC website, http://www.nrel.gov/hydrogen/proj_fc_market_demo.html. The Fuel Cell Technologies Program's ARRA projects were also included in a recent assessment of the impacts of government policy on the fuel cell industry.[2]

Auxiliary Power

Delphi Automotive Systems has initiated the system and subsystem vibration analysis and has completed over 20% of their planned thermal cycle testing on their A-Level SOFC APU. They have also conducted initial road testing, driving >3,000 miles with the unit mounted on a Peterbilt Class 8 truck. A new stack with improved system efficiency and new endothermic reformer with improved heat transfer and lower cost have been integrated into the B-Level, next-generation system. Over the next year Delphi will begin monitoring the SOFC APU performance in an on-road, real-world demonstration.

[2] *Status and Outlook for the U.S. Non-Automotive Fuel Cell Industry: Impacts of Government Policies and Assessment of Future Opportunities*, David Greene et al., May 2011, http://www-cta.ornl.gov/cta/Publications/Reports/ORNL_TM2011_101_FINAL.pdf.

Backup Power

ReliOn Inc. has completed the site qualification stage for the entire project. As of the end of June 2011, they have installed and commissioned over 270 fuel cells at 118 sites (109 for AT&T and nine for PG&E). Fourteen additional AT&T sites are undergoing construction, and nine more are pending. In 2011 ReliOn will construct and commission all remaining sites, and they will continue to obtain and report operational data to NREL's HSDC.

Sprint Nextel has completed over 580 site surveys at potential deployment sites for their fuel cell backup-power systems. They have installed and commissioned 32 new PEM backup-power fuel cells as of June 2011, with an additional 190 planned over the next year.

Plug Power has installed 10 GenCore® fuel cells at the Warner Robins Air Logistics Center, at Warner Robins Air Force Base. The units are providing backup power for lighting within the building. Plug Power also plans to install 10 additional fuel cells at an engineering building at Fort Irwin in Barstow, California, in FY 2012.

Combined Heat and Power

Plug Power is continuing durability tests on its six internal GenSys Blue® micro-CHP test systems, which were commissioned in January 2010. Since then, they have logged over 30,000 hours of stack operation, averaging over 30% electrical efficiency and over 85% thermal efficiency. In May and June 2011, three systems were installed at the National Fuel Cell Research Center at the University of California, Irvine, for real-world testing in a light commercial environment. The National Fuel Cell Research Center has also continued its dynamic modeling work of the GenSys Blue® system. Over the next year, Plug Power will install fuel cell systems in at least one Sempra Energy customer site in California. A customer site has already been recommended for the first installation.

Fuel Cell-Powered Lift Trucks

FedEx Freight East deployed 35 Class-1 fuel cell-powered lift trucks in June 2010, at their 53,000 square-foot distribution center in Springfield, Missouri. Due to the favorable operational results, they purchased an additional five fuel cell lift trucks, *without any additional DOE funding*. As of April 2011, the lift trucks have accumulated over 28,000 hours of operation and used 13,500 kilograms of hydrogen. FedEx has already seen 30–60% more operating hours in between repairs for fuel cell lift trucks than for propane-powered internal combustion engine lift trucks. Over the next year they will continue to monitor the performance of their fuel cell lift truck fleet, and they plan to work with Plug Power on resolving issues related to cold-weather operation.

GENCO has deployed over 270 GenDrive® fuel cells in lift trucks across five distribution facilities as of May 2011. The lift trucks at Wegmans in Pottsville, Pennsylvania, Whole Foods in Landover, Maryland, and Kimberly Clark in Graniteville, South Carolina, are fully deployed and operational. Some of the power units at the Wegmans site have already accumulated over 5,000 hours of operation. Coca-Cola and Sysco Philadelphia have initiated deployments of fuel cell lift trucks, and over the next year, GENCO will deploy the remaining fuel cells to Coca-Cola and Sysco Philadelphia.

Nuvera Fuel Cells installed 14 PowerEdge™ fuel cells in lift trucks and installed their PowerTap™ hydrogen infrastructure technology at the H-E-B Grocery Co. distribution center in San Antonio, Texas. As of May 2011, Nuvera's on-site reformer had generated 5,570 kilograms of hydrogen and had maintained 100% hydrogen availability at the pumps. Their lift trucks have accumulated nearly 22,900 hours of operation and have demonstrated a 10% productivity gain over battery-powered lift trucks. Based on the success of this deployment site, H-E-B plans to purchase 28 additional PowerEdge™ fuel cell units, requiring two additional PowerTap™ systems–*with no additional DOE funding*.

Sysco Houston has deployed 98 hydrogen fuel cell-powered Class-3 pallet trucks and Class-2 forklifts at their 585,000 square-foot food distribution facility in Houston, Texas. As of February 2011, the lift trucks had accumulated over 300,000 hours of operation and used 17,620 kilograms of hydrogen (from 31,000 fueling events). While Sysco Houston is currently not experiencing any difference in cost between charging batteries and fueling with hydrogen, they are saving nearly $100,000 annually in fewer man-hours spent refueling

lift trucks compared with swapping batteries. Based in part on the success of this deployment site, Sysco Corporate is planning to replace about 1,000 batteries with 500 or more fuel cells at seven sites over the next 24 months–*with no additional DOE funding.*

Portable Power

Jadoo Power has completed a detailed analysis of the power needs of NASCAR's cameras. Desulfurizer hardware from Delphi has been fully tested, and the reformer testing is near completion. Jadoo's propane fuel interface has been developed and is ready for system integration testing. They have also created preliminary designs for the overall system packaging. Over the next year, Jadoo plans to deploy the systems for the field trial and begin to collect data on the units.

MTI MicroFuel Cells has demonstrated high performance, high fuel efficiency, and low degradation for a one-watt DMFC charger for consumer electronics. They have achieved or exceeded all their technical metrics for the project. MTI sent out 75 complete systems to be tested in real-world environments by individuals, original equipment manufacturers, and government and military personnel. Overall feedback from the field tests has been very positive, and MTI plans to use the data gathered to guide future product development.

The University of North Florida has nearly completed component and subsystem testing for the DMFC portable power system. As of June 2011, three brassboards have been tested, with over 500 hours of operation on each system at multiple locations. The design for the packaged system is complete, with the subassemblies in the manufacturing and assembly phase. The University will assemble multiple packaged systems and test them extensively to evaluate performance, robustness, and durability.

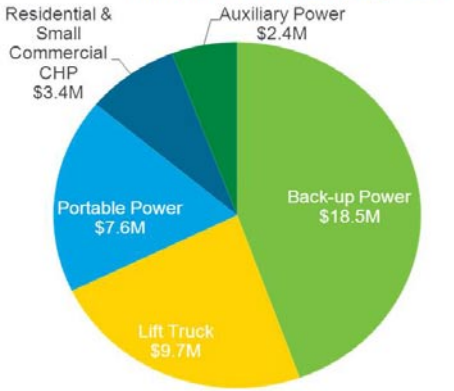
Data Collection & Analysis

NREL has published six deployment-focused CDPs and three cycles of technical CDPs–composed of 42 CDPs for material handling equipment and 10 CDPs for backup power. In addition, they have provided hundreds of detailed data results to the individual projects. NREL has created a website to host these published results and presentations. Over the next year, they plan to continue collecting and analyzing ARRA deployment data and publishing the results on their website.

Budget

FROM the LABORATORY to DEPLOYMENT:

DOE funding has supported R&D by all of the fuel cell suppliers involved in these projects.



Approximately $54 million in cost-share funding from industry participants—for a total of about $96 million.

COMPANY	AWARD	APPLICATION
Delphi Automotive	$2.4 M	Auxiliary Power
FedEx Freight East	$1.3 M	Lift Truck
GENCO	$6.1 M	Lift Truck
Jadoo Power	$2.2 M	Portable
MTI MicroFuel Cells	$3.0 M	Portable
Nuvera Fuel Cells	$1.1 M	Lift Truck
Plug Power, Inc. (1)	$3.4 M	CHP
Plug Power, Inc. (2)	$2.7 M	Back-up Power
Univ. of N. Florida	$2.4 M	Portable
ReliOn, Inc.	$8.5 M	Back-up Power
Sprint Nextel	$7.3 M	Back-up Power
Sysco of Houston	$1.2 M	Lift Truck

FY 2012 Plans

Continued data collection on performance and productivity at the various deployment sites is a priority for FY 2012. In FY 2012, deployment of over 250 additional fuel cell systems for backup power, combined heat and power, and lift truck applications is planned. Five projects are expected to end in early FY 2012. All projects will conclude by the end of FY 2013.

Finally, in FY 2012, DOE will continue to document the lessons learned associated with the ARRA projects, including strategies developed for market entry and management of risks relating to safety, environmental, and siting requirements. Energy Efficiency and Renewable Energy will initiate an evaluation in FY 2012, focused on early-stage "market change" impacts (for the period of 2010 through the end of 2012), of the Recovery Act fuel cell deployments.

Sara Dillich
Lead for the Fuel Cell Technologies Program's ARRA Activities and
Supervisor, Research & Development
Fuel Cell Technologies Program
Department of Energy
1000 Independence Ave., SW
Washington, D.C. 20585-0121
Phone: (202) 586-7925
E-mail: Sara.Dillich@ee.doe.gov

XII.1 Commercialization of 1 Watt Consumer Electronics Power Pack

Charles Carlstrom
MTI Micro Fuel Cells
431 New Karner Road
Albany, NY 12205
Phone: (518) 533-2226
E-mail: ccarlstrom@mechtech.com

DOE Managers
HQ: Donna Lee Ho
Phone: (202) 586-8000
E-mail: Donna.Ho@ee.doe.gov
GO: Reginald Tyler
Phone: (720) 356-1805
E-mail: Reginald.Tyler@go.doe.gov

Contract Number: EE0000477

Project Start Date: January 8, 2009
Project End Date: March 31, 2011

Objectives

Demonstrate and field test a commercially viable 1 Watt direct methanol fuel cell (DMFC) charger for consumer electronic devices:

- Design for low-cost, high-volume manufacturing processes and ease of assembly.
- Demonstrate performance across temperature and humidity range of consumer electronic devices.
- Deploy 75 units into the field to obtain real world usage feedback.

Relevance to the American Recovery and Reinvestment Act (ARRA) goals of saving and creating jobs:

- Project funding created/retained 11 full-time equivalent jobs in Albany, NY.
- The DOE funds enabled MTI to obtain private investment.

Relevance to the U.S. DOE Fuel Cell Technologies (FCT) ARRA goals of accelerating the commercialization and deployment of fuel cells:

- Components have been redesigned for low-cost, high-volume manufacturing.
- Seventy-five fuel cell systems have been deployed during field test.

Technical Barriers

Progress against the barriers listed below is discussed in the following sections.

- Cost and manufacturability
- Performance and degradation
- Market acceptance

Accomplishments

- Deployed 75 fuel cell systems into the field for real world evaluation.
- Reduced cost and improved manufacturability and assembly.
- Demonstrated high performance, high fuel efficiency, and low degradation.
- Demonstrated system temperature and humidity latitude (0-40°C, 0-90% relative humidity).
- Achieved or exceeded all technical metrics.



Introduction

The objective of this project is to demonstrate and field test a commercially viable 1 Watt DMFC charger for consumer electronic devices. The fuel cell system and replaceable methanol cartridge will meet all requirements for commercialization. The system will achieve targets of cost, performance, and design reliability at a level compatible to the standards and requirements of the consumer electronics market.

Approach

The project's environmental and safety plans had been developed and submitted during 2009. The project has been organized into three phases.

The tasks in phase 1 include component cost reduction, redesign for manufacturability, performance and reliability testing, and system integration. Phase 2 tasks include tool fabrication, debugging, and tooled component prove-out in working systems. Phase 3 tasks include demonstrating the DMFC charger's functionality in the hands of real users while also providing feedback for potential design improvements. This field test is the first time a significant number of MTI units (shown in Figure 1) are put into the field to test usability and functionality. The objective of the field test is to generate user feedback on product viability as well as identify potential product improvements.

Results

A major focus of this project was to reduce the cost of MTI's DMFC-powered charger to attain a competitively priced product when in production. To achieve a low cost system many of the components had to be redesigned so that they could be produced using low-cost, high-volume, manufacturing processes. The system also had to be redesigned for ease of assembly to increase build yield and reduce the amount of labor content needed. In addition, the assembly process had to be simplified so that technicians and assemblers could perform the assembly rather than engineers and scientists.

During phase 1 of this project many parts and process steps were completely eliminated or were significantly simplified. In one instance a complete subassembly, with all associated cost and reliability issues, was eliminated. At the completion of phase 1 almost all components were redesigned for reduced cost and high volume manufacturing. The following are examples of component redesigns implemented to reduce cost and make the components capable of being manufactured using common, low-cost, high-volume manufacturing processes:

- Plastic components previously machined were designed to be injection moldable.
- Sheet metal components previously machined were redesigned to be stamped.
- Many adhesives and small bridge plates were completely eliminated by integrating their function in other interfacing components.

During phase 2 of the project, tools were fabricated and parts were produced for evaluation of the design intent product. This required several iterations of part, tool and process changes until the parts produced off of the tooling met the design requirements. Comprehensive subsystem level testing was carried out to quantify the impact the redesigned subsystems had on durability and performance. There was also a significant amount of system integration work done to bring the new lower cost subsystems together. Testing at the system level was used to verify that the system is capable of operating well during transients such as start-up and shut-down and at all specified temperatures, humidity, and orientations.

During phase 3 of the project 75 user evaluation kits were sent out which contained the contents shown in Figure 2. The kit included a mobion handheld generator, two cartridges filled with methanol, quick start guides, and a cable that had interchangeable tips enabling use with all of the common connections for handheld electronic devices. Although only two cartridges were sent with the units there were more available upon request.

The fuel cell systems were deployed to the groups specified in the statement of work including individual users,



FIGURE 1. MTI Mobion DMFC Charger



FIGURE 2. Contents of Box Field Trial Participant Received

original equipment manufacturers (OEMs), various military groups and government agencies. The allocation of the units is shown in Figure 3.

Feedback from the field test has been very positive overall. Below are some verbatim comments from the participants within the larger groups that have participated in the field trial:

- *"Just finished off my first cartridge today. I charged my (iPhone) phone approx 10x from ~25% to 100% battery before it needed replacement" – OEM*
- *"We were impressed with the form factor and with the chemical conversion technology. It repeatedly charged our iPhones in a timeframe similar to that from a standard electrical outlet." - OEM*
- *"The device works excellently and has not provided many inconsistencies. Mostly, not being able to have the fuel cell in an enclosed space (i.e., laptop bag) while it is generating power was an inconvenience though not a major problem." – Individual user*
- *"Alternative energy on the battlefield is evolving into one of the most salient issues of the day. We believe that despite initial concerns, Mobion should continue advancement of this unique technology to potentially meet some of the existing and future tactical energy requirements." - Military*

An online post-test survey was used to capture user feedback. Figure 4 shows results from one of the questions on the survey that captured the attributes users liked.

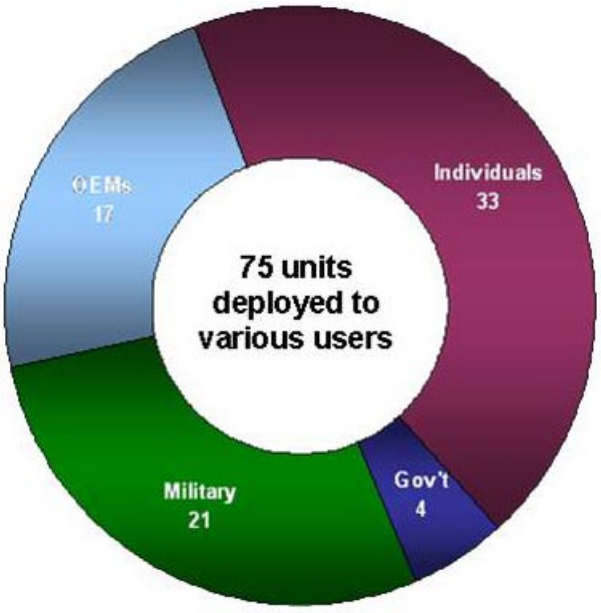


FIGURE 3. Allocation of the 75 Units Deployed for Field Trial

This field trial accomplished the objective of obtaining real world usage feedback and identifying areas of product

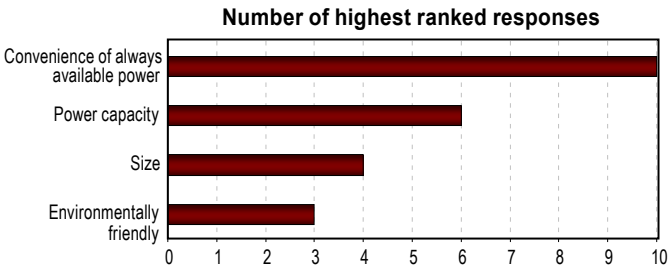


FIGURE 4. Results from Feedback Form - What Users Liked

improvement. Valuable feedback was coming in just days after the initial units were being shipped. For example, there was a compatibility issue the fuel cell had when connected to one of the newer smart phones. The issue was quickly resolved and did not reappear throughout the duration of the trail. This issue exemplifies the enormous value the field trial added to the product development process. There are some issues, such as the one described, that will not show up in the lab and that will only be uncovered when units are deployed into the field in significant numbers. The user interface was another area that benefited greatly from this user field test. The user interface functioned well but was confusing to some users because it had two buttons. The feedback on the user interface from this field trial led to the development of a new single switch user interface and other features to make the device more intuitive.

A secondary benefit of the filed trial was that it enabled the participant and the organizations they represent to become aware of the commercial readiness of this product. In general, the participants that have evaluated fuel cell offerings from other companies in the past were most impressed with the Mobion charger during the field trial. Sending units for evaluation gave credibility to the product claims, specifications, and commercial readiness. Several business relationships initiated or strengthened by the field trial will further impact the commercialization of this product and technology in the coming months.

Conclusions and Future Directions

- High power density and high fuel efficiency has been achieved simultaneously.
- Low stack degradation rate exceeding product requirements has been demonstrated.
- Performance of system at temperature and humidity latitude (0-40°C, 0-90% relative humidity) has been demonstrated.
- Seventy-five unit field test has been completed:
  - Seventy-five units built, tested, and shipped
  - Product improvements identified

Although this project is complete several product improvements have been identified that will continue to guide our product development in the coming months.

FY 2011 Publications/Presentations

1. Carlstrom, C, 2011, "Commercialization of 1 Watt Consumer Electronics Power Pack ," DOE Annual Merit Review, Arlington, Virginia, USA.

2. Prueitt, J., 2010, "Portable Fuel Cell Panel," Clean Energy Conference, Boston, MA.

XII.2 Jadoo Power Fuel Cell Demonstration

Ken Vaughn
Jadoo Power Systems, Inc.
181 Blue Ravine Rd.
Folsom, CA 95630
Phone: (916) 673-3417
E-mail: kvaughn@jadoopower.com

DOE Managers
HQ: Ned Stetson
Phone: (202) 586-9995
E-mail: Ned.Stetson@ee.doe.gov
GO: Greg Kleen
Phone: (720) 356-1672
E-mail: Greg.Kleen@go.doe.gov

Contract Number: DE-EE0000479

Subcontractor:
Delphi Automotive, Rochester, NY

Project Start Date: January 1, 2010
Projected End Date: September 9, 2012

Objectives

- The development of two portable electrical generators in the 1,000 watt range utilizing solid oxide fuel cells (SOFCs) as the power element and liquefied petroleum gas (LPG) as the fuel.
- The development and demonstration of a proof-of-concept electromechanical LPG fuel interface that provides a user-friendly capability for managing LPG fuel.
- The deployment and use of the fuel cell portable generators to power lighting and video production equipment over the course of several months at multiple National Association for Stock Car Auto Racing (NASCAR) automobile racing events.
- The deployment and use of the fuel cell portable generators by first responders (police, fire) of the City of Folsom, California to power equipment in emergency and/or off-grid situations.
- Capturing data with regard to the systems' ability to meet DOE technical targets and evaluating the ease of use and potential barriers to further adoption of the systems.

Relevance to the American Recovery and Reinvestment Act (ARRA) of 2009 Goals

This project will create or save existing jobs and spur economic activity in California and New York. This project will demonstrate the efficacy of fuel cell generators in multiple applications that have near-term potential for commercialization and development of the fuel cell market.

Technical Barriers

- Reducing stack and balance of system to size allowing portability.
- Reliability of SOFC system under rough field conditions.
- User factors related to start-up times and refueling.
- Effectiveness/complexity of processing LPG to remove sulfur.
- Potential constraints on type or source of LPG.

Technical Targets and Milestones

- Develop LPG desufurizer - reduce the level of sulfur in LPG to less than 10 ppb for eight continuous hours.
- Develop SOFC portable generator - produce 1 kW using LPG for eight continuous hours.
- Operation of generator at minimum 30% efficiency for minimum of 2,000 cumulative hours.
- Develop a user-friendly electromechanical LPG fuel interface — indicate the amount of LPG within ± 10% of the actual amount for the entire range from full to empty.
- Test two SOFC generator units at several NASCAR racing events as replacements for gasoline powered generators.
- Test SOFC generators in first responder applications with Folsom Police and Fire Departments.
- Analyze technical performance and human factors issues to evaluate readiness of the technology to move into commercialization phase.

Accomplishments

- Detailed analysis of NASCAR camera equipment power needs completed including baseline load evaluation and logistics evaluation.
- Focus group with City of Folsom, City of Sacramento, Office of Emergency Services, CalFire and Federal Emergency Management Agency has been conducted.
- Requirements definition completed.
- Desulfurization development and testing completed.
- Reformer development near completion.
- Mechanical packaging design and system testing underway.
- LPG fuel interface ready for system integration testing.

Introduction

Deploying a commercial power system into a portable space is a challenge for fuel cell applications. Moving a fuel cell power system from the laboratory to consumers' hands requires a complete systems or solution approach. A portable application requires consideration for real world conditions; requiring a wide array of control and power electronics to handle load following, startup/shutdown, safety considerations and system security. A level of ruggedness to handle frequent shocks from deployment and shipping is necessary as well as a convenient and safe fuel system interface. Jadoo has identified several specific applications related to outdoor sporting events and emergency response that are ideally suited to the technical characteristics of fuel cells and which would gain significant benefit from a fuel cell generator that could replace existing gasoline or diesel powered generators. This project entails the development of a portable fuel cell generator utilizing LPG fuel that can address the targeted applications.

Approach

Portable generators are to be developed by leveraging parallel work by Delphi Automotive related to use of a SOFC in a trucking auxiliary power unit (APU) application. Delphi SOFC technology will be modified and packaged for portable application with alternating current power capability. Delphi is modifying a reformer from its diesel APU to allow the use of LPG. Delphi is also developing a desulfurizer to allow use of commonly available consumer grade LPG as fuel source. Jadoo Power is developing an electromechanical fuel interface by leveraging prior learning from the development of an interface between proton exchange membrane fuel cells and metal hydride canisters for use by non-technical personnel.

Results

The requirements of the NASCAR application have been characterized. The general areas addressed include electrical power requirements, runtime requirements, and portability and mechanical requirements. One key application that has been targeted for application of the fuel cell generators is providing power to television cameras. These consist of fixed camera locations (with and without special effects modules) that are operated by camera people and remote camera locations with robotic mechanisms that are operated by a remotely located camera person. The power levels of the typical locations are shown in Table 1.

The desulfurizer subsystem has been selected, qualified and tested. A continuous performance test of the LPG desulfurizer for 40 hours has been conducted using a high sulfur content LPG source. The analysis data showed all sulfur species in the desulfurized LPG was generally below detection limits. Hence with an estimated dilution factor of 5~8, total sulfur level in the corresponding reformate would be expected to be <10 ppb.

TABLE 1. Television Camera Power Requirements Summary

CAMERA TYPE	NOMINAL POWER	PEAK POWER
Fixed camera without special effects module	150 Watts	170 Watts
Fixed camera with special effects module	200 Watts	220 Watts
Robotically assisted Remote camera	100 Watts	175 Watts

The reformer subsystem development and testing have been completed. Bench testing and characterization has demonstrated performance levels are at or near design targets.

Preliminary designs have been completed for the overall system packaging utilizing a "pit-box" form factor as shown in Figure 1. This form factor was selected as it is consistent with other equipment utilized by NASCAR and is compatible with the transportation requirements.

The LPG fuel interface prototype has been designed, fabricated and assembled (see Figure 2) and is ready for system integration testing.

Conclusions and Future Directions

The key technical risk elements of this development have been successfully addressed in bench testing and subsystem level implementations. The form factor will be larger than anticipated but will still be suitable for many application identified for the field trials.

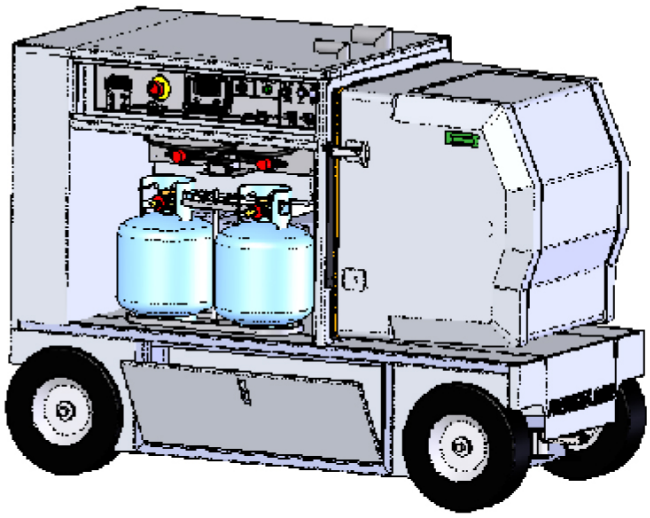


FIGURE 1. Mechanical Chassis Model

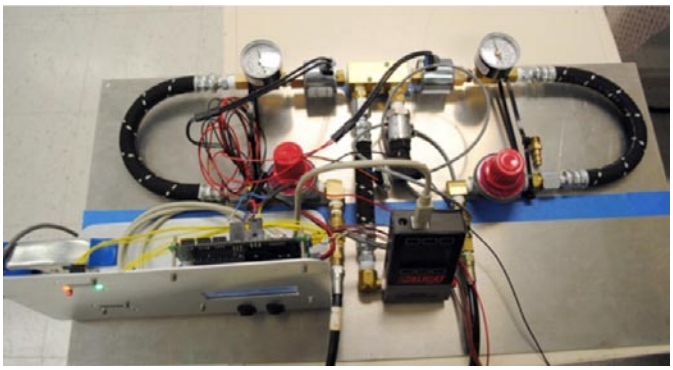


FIGURE 2. LPG Fuel Interface

The key remaining steps related to the program are as follows:

- Test the LPG interface to demonstrate measurement accuracy of +/- 10%.
- Fabricate the mechanical chassis.
- Integrate the subsystems together on the mechanical chassis.
- Perform system level testing and validation.
- Deploy the systems in the field trial with NASCAR.
- Deploy the systems in the field trial with the City of Folsom, CA.
- Gather the field trial data and prepare the final reports.

XII.3 Advanced Direct Methanol Fuel Cell for Mobile Computing

James Fletcher (Primary Contact), Joseph Campbell
University of North Florida (UNF)
1 UNF Drive
Jacksonville, FL 32224
Phone: (904) 620-1844
E-mail: JFletche@unf.edu

DOE Managers
HQ: Ned Stetson
Phone: (202) 586-9995
E-mail: Ned.Stetson@ee.doe.gov
GO: Katie Randolph
Phone: (720) 356-1759
E-mail: Katie.Randolph@go.doe.gov

Contract Number: DE-EE0000476

Subcontractor:
University of Florida, Gainesville, FL

Project Start Date: January 1, 2010
Project End Date: December 31, 2011

Objectives

- The project objective is to develop a direct methanol fuel cell (DMFC) power supply for mobile computing using the novel passive water recycling technology acquired by UNF from PolyFuel, Inc., which enables significant simplification of DMFC systems.
- The objective of the 2011 effort is to build on the objectives completed in 2010 in order to finalize the system design, build and test the packaged 20 W power supply. To date, the system components have been selected and integrated into a brassboard (unpackaged system) for in situ testing. Based on the feedback provided by brassboard and component testing, the final design has undergone minor design revisions. The packaged system is currently in the manufacturing and assembly phase, once the system assembly has been completed, control strategies will be applied and optimized for the packaged system.

Relevance to the American Recovery and Reinvestment Act (ARRA) of 2009 Goals

This project will contribute to the relevance of DOE's objectives for ARRA projects in general and the DMFC projects in particular.

- Create direct and supporting jobs nationwide as the UNF fuel cell technology becomes commercially available.
- Reduce the necessity and use of the power grid as fuel cells power increasing numbers of portable electronic devices, thereby creating more "green" jobs.
- Create more business activity in the fuel cell supply industry.
- Expand the user base of new alternative power technologies.
- Increase the level of competition among producers of alternative energy technologies.

Technical Barriers

This project addresses the following technical barriers for advanced DMFCs outlined by the DOE.

- Specific power
- Energy density
- Operating lifetime
- Manufacturing Cost
- Balance-of-plant components

Technical Targets and Milestones

TABLE 1. UNF Progress toward Meeting Technical Targets for Advanced Direct Methanol Fuel Cell for Mobile Computing

Characteristic	Units	UNF 15 W DP3 2008 Status	DOE 2010 Target	UNF Proposed 20 W System Design
Specific Power[a]	W/kg	35	100	54
Power Density[a]	W/L	48	100	63
Energy Density	W-hr/L	250 (1 x 100 ml)[b] 396 (1 x 200 ml)[b]	1,000	198 (1 x 100 ml) 313 (1 x 200 ml) 507 (3 x 200 ml)
	W-hr/kg	155 (1 x 100 ml)[b] 247 (1 x 200 ml)[b]	N/A	180 (1 x 100 ml) 302 (1 x 200 ml) 532 (3 x 200 ml)
Lifetime[c]	Operating Hours	1,000 hrs in single cell	5,000	2,500 Integrated System
Cost	$/Watt	11 (est. in volume)	<3	<10 (est. in volume)

[a] Beginning of life, 30°C, sea level,50% relative humidity (RH), excluding hybrid battery, power module alone.
[b] Normalized from Design Prototype 3 (DP3) data from 150 ml cartridge to either 100 ml or 200 ml for comparison purposes.
[c] Lifetime measured to 80% of rated power.

Accomplishments

- Submission of revised Hydrogen Safety Plan.
- Baseline testing of components and subsystems complete.

- Integration of subsystems/components into brassboard (unpackaged system).
- Completion of three separate brassboards with hundreds of hours of operation at multiple locations.
- Control strategy optimization from brassboard operation.
- Preliminary design review held for packaged Design Prototype 4 (DP4) system.
- Packaged system components currently in manufacturing and assembly phase.
- Passed Go/No-Go milestone review in January 2011.



Introduction

The project objective is to develop a DMFC power supply for mobile computing using the UNF novel passive water recycling technology which enables significant simplification of DMFC systems. The objective of the 2011 effort to date is to perform system engineering and extensive brassboard (unpackaged) testing to move towards the 2010 technical targets. The remainder of the project will focus on optimizing the performance of the packaged system.

Approach

This project is focused on balance of plant (pumps, blowers, sensors, etc.) development and overall system integration. These components will be rigorously tested individually, as subsystems, and ultimately at the system level. Initially, existing components will be evaluated for durability and failure modes, and the results will be used to further define component requirements. Once available, the design prototype components will be evaluated for durability and robustness. Subsystems will be integrated for testing, first onto a brassboard enabling detailed instrumentation of the system and verification of sub-system design, and then into an integrated package with auxiliary instrumentation. Control system development will optimize the key operational protocols for start-up, rest/rejuvenation, and shut-down to optimize operating lifetime and minimize both operational and storage degradation rates. In addition, this effort is highly integrated with the UNF-led Topic 5A: New MEA Materials for Improved DMFC Performance, Durability, and Cost project (DOE funded) which focuses on optimizing the passive water recovery membrane electrode assembly (MEA).

UNF submitted a Hydrogen Safety Plan for initial review on June 30, 2010. Based on very helpful comments received on from a DOE reviewer received on December 13, 2010, a revised plan was submitted to DOE on February 28, 2011.

Results

In order to progress towards the DOE 2010 technical targets for advanced DMFCs for mobile computing, it is imperative that each component in the system be tested for both optimal efficiency and robustness. Therefore, an extensive test plan was executed for each component/subsystem with the DP4 system.

The cathode blower subsystem was optimized using two separate methods. First, performance of numerous fans was tested against the component requirements in order to select the optimal cathode fan for the design condition. As shown in Figure 1, the ADDA AD4505HX-K90 offers the lowest parasitic power compared to the other fans that were tested. The ADDA fan has since undergone over 2,000 hours of durability testing while still meeting the design requirements.

The second series of tests that were conducted with the cathode blower subsystem examined flow optimization. This testing revealed the optimal cathode flow channel depth/configuration as well as the sensitivity of spacing between the fan and fuel cell stack inlet.

The recirculation pump used to flow the anode solution through the stack and support components (reservoir tank, gas liquid separator, etc.) was extensively tested. Numerous pumps were selected for testing based on the design requirements. Extensive testing showed that the KNF5 is significantly more efficient than other similar pumps relative

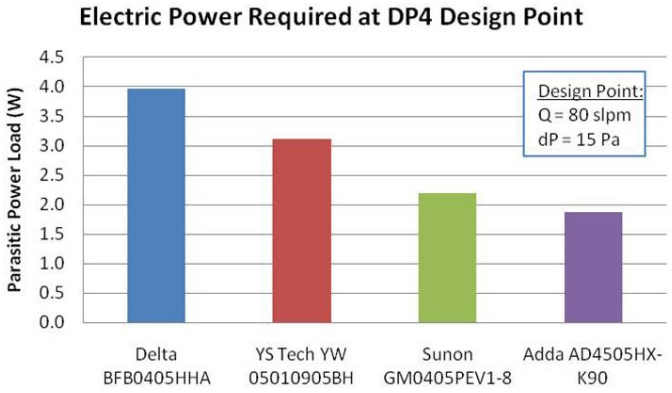


FIGURE 1. Comparison of Candidate Cathode Fan Performance

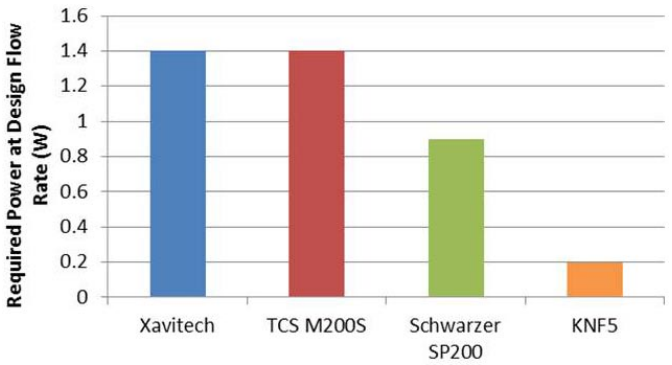


FIGURE 2. Comparison of Candidate Recirculation Pump Performance

to size, weight and hydraulic performance (Figure 2), thus resulting in the best system power and energy density.

The methanol injection pump that was selected for use in the DP4 is one of the few pumps that were able to meet the design requirements. Although the Microbase MBP2115BD has been able to provide hundreds of hours of operation during harsh environmental conditions, testing has revealed inconsistencies in the performance from pump to pump. Currently, testing is underway to determine if there is a significant variation in pump performance due to manufacturing.

The FC-10 methanol sensor was selected as the primary candidate for system integration. Extensive testing was conducted in order to determine any sensitivities to drift or thermal effects. It was determined that the FC-10 has a high sensitivity to temperature fluctuations. In addition, the sensor is not optimized for the application due to size, weight and cost. Therefore other methanol sensing technologies are under active investigation from manufacturers Spreeta and Japan Radio Corporation.

The gas liquid separator has undergone multiple revisions and tests to better understand the behavior of extruded Teflon® and the effect of its performance relative to temperature, pressure and ambient conditions. As a result, a significant reduction in the amount of water loss through the gas liquid separator has been achieved compared to the previous generation gas liquid separator.

The near completion of component and subsystem testing allowed for the design and assembly of the DP4 brassboard (Figure 3). To date, three brassboards have been assembled and tested with over 500 hours of operation on each system at multiple locations. The brassboards have allowed for components and subsystems to be tested in an in situ environment. Hundreds of hours of in situ testing highlighted design revisions and modifications in order to improve overall system reliability and robustness. The brassboard has also enabled accelerated evolution of software code revisions due to its accessibility and ease of use. Furthermore, the control strategies along with the startup and shutdown algorithms have been greatly improved in order to better handle dynamic conditions and different system configurations.

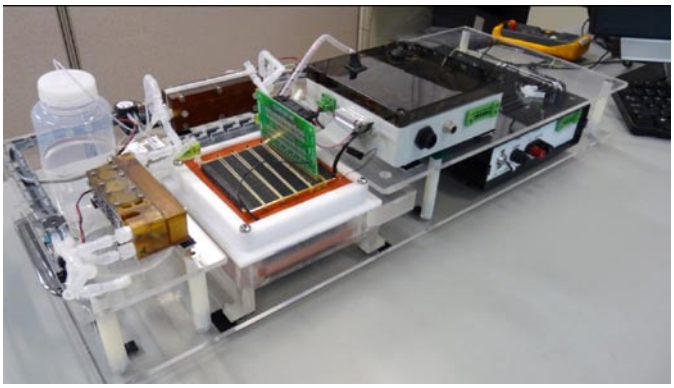


FIGURE 3. DP4 Brassboard (Unpackaged) System

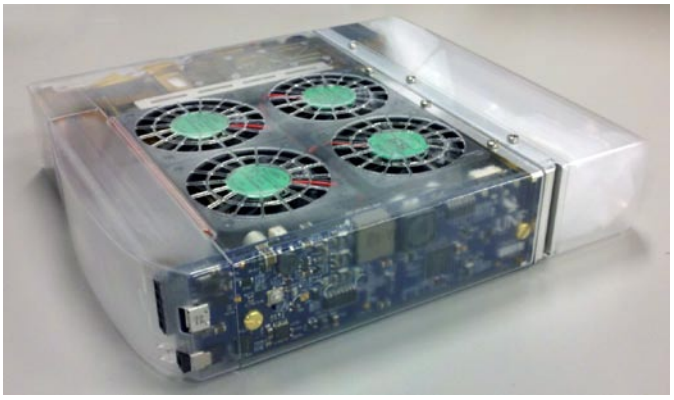


FIGURE 4. Packaged 20 W DP4 Fuel Cell Power Supply

The DP4 packaged system (Figure 4) concept design review was held at the beginning of 2011. Since then, the system has undergone minor design revisions due to the feedback provided from brassboard and component testing. The system is now in the final design stage and integrated prototypes are in the manufacturing and assembly phase. In addition to the completion of the mechanical design, the control board design has been completed and has been sent out for manufacturing. The first packaged system was presented at the Annual Merit Review meeting presentation in May of 2011 and is now in the testing phase.

Conclusions and Future Directions

- System components were tested to establish a benchmark to determine the system requirements.
- The best components were selected to meet the design requirements of the system and were subjected to durability and robustness testing.
- Each component was incorporated into its respective subsystem assembly and integrated into the brassboard system.
- In situ testing provided by brassboard operation allowed for component and control strategy optimization.
- Packaged system design is complete and subassemblies are in the manufacturing and assembly phase.
- Assemble multiple packaged systems for testing.
- Complete development of advanced control strategies with packaged system.
- Test the system extensively to evaluate performance, robustness, and durability.

FY 2011 Publications/Presentations

1. Advanced Direct Methanol Fuel Cell for Mobile Computing (AMR Presentation 05/12/11).

XII.4 Solid Oxide Fuel Cell Diesel Auxiliary Power Unit Demonstration

Andrew Rosenblatt (Primary Contact), Jim Banna, Dan Hennessy
Delphi Automotive Systems, LLC
300 University Drive
m/c 480-300-385
Auburn Hills, MI 48326
Phone: (248) 732-0656
E-Mail: Andrew.rosenblatt@delphi.com

DOE Managers
HQ: Dimitrios Papageorgopoulos
Phone: (202) 586-5463
E-Mail: Dimitrios.Papageorgopoulos@ee.doe.gov
GO: David Peterson
Phone: (720) 356-1747
E-Mail: David.Peterson@go.doe.gov

Contract Number: DE-EE0000478

Subcontractors:
- Electricore, Inc., Valencia, CA
- PACCAR, Inc., Bellevue, WA
- TDA Research, Inc., Wheat Ridge, CO

Project Start Date: August 1, 2011
Project End Date: January 31, 2012

Objectives

- Design, develop, and demonstrate a 3-5 kW solid oxide fuel cell (SOFC) auxiliary power unit (APU) for heavy-duty commercial Class 8 Trucks (Figure 1).
- Utilize Delphi's next generation SOFC system as the core power plant and prove the viability of the market opportunity for a 3-5 kW diesel SOFC APU system.
- Test and demonstrate the diesel SOFC APU system in a high visibility fleet customer vehicle application that will support hotel loads and other real world operating conditions.

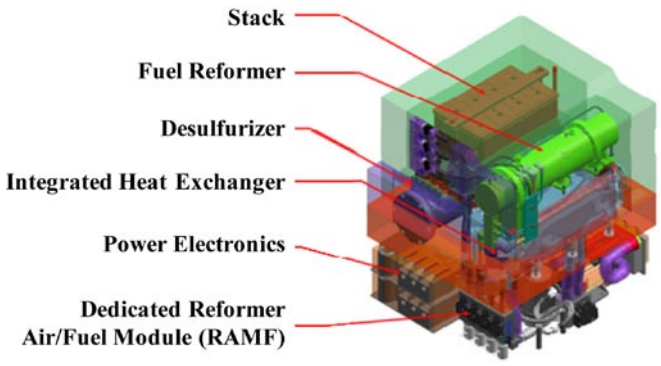


FIGURE 1. Delphi Solid Oxide Fuel Cell Auxiliary Power Unit (A-Level Prototype) Schematic

Relevance to the American Recovery and Reinvestment Act (ARRA) of 2009 Goals

- During this phase of the project, a total of 21 jobs were created/maintained:
  - Delphi 18 jobs
  - Electricore 1 job
  - PACCAR 1 job
  - TDA 1 job
- As a result of this project, Delphi will be able to install its SOFC APU on a high visibility fleet truck. This will provide Delphi, and its fleet customer, with real world use experience as well as the associated fuel consumption and emission data. This demonstration should increase the overall awareness of SOFC APUs and provide positive momentum in preparing to commercialize this product.

Technical Barriers

- As a result of the successful execution of this project, Delphi will have addressed:
  - System vibration robustness
  - Overall system packaging
  - System weight
  - System cost
  - System manufacturability
  - System durability/reliability
- During a recent SOFC APU system test, we discovered an issue with the desulfurizer during repeated thermal cycles. This issue needs to be resolved before the unit could begin fleet testing.

Technical Targets and Milestones

- Build next generation prototype (B-Level) SOFC APU for installation on fleet customer truck during the fourth quarter of 2011. Begin on-road, real-world application demonstration.
- Provide 3-5 kW of power during idle periods allowing for reduced fuel consumption and harmful emissions.
- Specific power ≥15 w/kg.
- Power density ≥10 w/l.
- Net system efficiency ≥35%.
- ≥2,000 hours of operation.

Accomplishments

- A-Level SOFC APU mounted on Peterbilt Class 8 truck and driven >3,000 miles (Figure 2):
  - SOFC APU air inlet was modified based upon data from road-test.
- A-Level SOFC APU completed >50 thermal cycles of 250 planned.
- System and Subsystem vibration analysis initiated:
  - System tested to the equivalent of 17,000 highway miles on a vibration table.
  - Stack tested to the equivalent of 3.5-million miles on a vibration table.
- Integrated next generation stack into B-Level build. Addresses improved system efficiency and packaging barriers listed above.
- Integrated a sorbent bed for removal of hydrogen sulfide (H_2S) from the reformate. Abovementioned issue needs to be addressed:
  - Able to remove H_2S to <0.010 ppm.
- Enhanced the heat exchanger subsystems using a common footprint for each. Provides a more robust and cost-effective design.
- Launched the next generation endothermic reformer. Provides improved heat transfer and an improved cost due to reduced manufacturing complexity.



Introduction

Delphi's SOFC power system, installed on heavy-duty commercial trucks as an APU, addresses the growing concerns about emissions, fuel consumption, and noise. In the United States today, there are more than one million long-haul heavy-duty commercial trucks with sleeper cabs on the road. When drivers stop for their mandatory rest periods or loading/unloading, they often leave their engines idling in order to heat/cool their sleeping areas and operate other vehicle systems. This idling practice is costly to the driver, the fleet owner, and harmful to the environment. The Environmental Protection Agency's SmartWay Transport Partnership estimates that each year, long duration idling of truck engines consumes approximately 960-million gallons of diesel fuel and emits 11 million tons of carbon dioxide, 180,000 tons of nitrogen oxide, and 5,000 tons of particulate matter into the air. In addition to the consumed fuel and emissions, idling trucks create elevated noise levels. The SOFC APU has the potential to decrease idling fuel consumption by up to 85%, reduce exhaust emissions below federal regulation emission standards, and decrease radiated noise levels to less than 60 dBA when compared to the truck's main engine.



FIGURE 2. Delphi Solid Oxide Fuel Cell Auxiliary Power Unit (A-Level Prototype) Installed on PACCAR Truck

As a result of the on-road demonstration under this project, Delphi will be able to present user profile data from its fleet customer. This data will reinforce the lab-generated data showing that use of a SOFC APU as an anti-idling solution will provide drivers and fleets with reduced fuel consumption as well as reduced emissions and noise. This demonstration should increase the overall awareness of SOFC APUs and provide positive momentum in preparing to commercialize this product.

Approach

Under this project, Delphi is pursuing a 3-phased approach to conduct its research. During Phase 1, Delphi, working with its truck manufacturer partner PACCAR, will establish the applications specifications and commercial requirements for a SOFC APU. Phase 2 work will focus on design verification and system testing (bench-top and on-vehicle). Phase 3 will include the demonstration of the SOFC APU on a heavy-duty Class 8 vehicle. The data collected during this phase will be analyzed and reported will respect to fuel consumption, emissions, and noise.

All Delphi facilities involved with this project are required to meet Delphi's stringent safety requirements which are aligned with the Safety Planning Guidance documentation specified by DOE.

Results

During this report period, Delphi has completed several of the tasks necessary to provide a road-ready SOFC APU to our fleet customer.

- Completed requirements document.
- Completed SOFC APU B-Level system design release.
- Completed SOFC APU system integration.
- Completed in-house subcomponent and system testing.
- Started SOFC APU system build. Scheduled to be delivered and installed on fleet customer truck during the third quarter of 2011.

Specific subcomponent and system development achievements are described in the Accomplishment section above.

Conclusions and Future Directions

Delphi continues to make significant progress towards introducing a production-intent SOFC APU for use by heavy-duty truck manufacturers, fleets, and drivers. This leading edge technology will provide users with the ability to run their hotel electrical loads during idling without the need to run their main truck engine or a diesel generator. As a result of using a SOFC APU, they will see reduced fuel consumption, reduced harmful emissions, and reduced noise.

Under this specific project, Delphi will next complete assembly and deliver its B-Level prototype SOFC APU to its fleet customer. After vehicle installation and fleet/driver user training, the unit will be deployed in a real-world application. During this demonstration period, Delphi will be able to monitor the SOFC APU performance real time through a dedicated telematic connection.

Patents Issued

1. Patent Filing Number 12/964806; Filing Date 10 Dec 2010.

FY 2011 Publications/Presentations

1. Jan 2011 21st Century Truck Partnership and National Academy Sciences Review Committee Presentation: "Solid Oxide Fuel Cell Development at Delphi", Rick Kerr.

2. May 2011 DOE Hydrogen Program Peer Review Presentation: "Solid Oxide Fuel Cell Diesel Auxiliary Power Unit Demonstration," Dan Hennessy.

XII.5 Demonstrating Economic and Operational Viability of 72-Hour Hydrogen PEM Fuel Cell Systems to Support Emergency Communications on the Sprint Nextel Network

Kevin Kenny (Primary Investigator)
Sprint Nextel
12000 Sunrise Valley Drive
MS: VARESQ0401-E4064
Reston, VA 20191
Phone: (703) 592-8272
E-mail: kevin.p.kenny@sprint.com

Deployment Project Manager
Jeremy Gore
Ericsson Services, Inc.
Phone: (678) 520-9986
E-mail: jeremy.gore@ericsson.com

DOE Managers
HQ: Sara Dillich
Phone: (202) 586-7925
E-mail: sara.dillich@ee.doe.gov
GO: James Alkire
Phone: (720) 356-1426
E-mail: james.alkire@go.doe.gov

Contract Number: EE-0000486

Subcontractors:
- Air Products & Chemicals, Inc., Allentown, PA (Fuel Project Partner)
- Altergy Systems, Folsum, CA (PEM Fuel Cell Project Partner)
- Black & Veatch Corporation, Overland Park, KS (A&E Project Partner)
- Burns & McDonnell Engineering Co., Inc., Kansas City, MO (A&E Project Partner)
- Ericsson Services, Inc., Overland Park, KS (Deployment Management Project Partner)
- ReliOn, Inc., Spokane, WA (PEM Fuel Cell/ A&E Project Partner)

Project Start Date: March 18, 2010
Project End Date: December 31, 2012

Objectives

- Eliminate barriers to siting and permitting 72-hours of hydrogen fuel storage
- Eliminate barriers to re-fueling sites at the required level of performance
- Collect and analyze data sample to evaluate economic and operational metrics

Relevance to the American Recovery and Reinvestment Act (ARRA) of 2009 Goals

Sprint, through this deployment effort, seeks to:

- Support the creation of new jobs.
- Maintain existing jobs.
- Bring proton exchange membrane (PEM) technology into the market which will foster job training opportunities.
  - Installation
  - Service
  - Repair

Relevance to the DOE-Fuel Cell Technologies' ARRA Project Goals

Through the successful deployment of this technology, it is expected that the following goals shall be achieved:

- Demonstrate the operational acceptance and financial viability of using PEM technology to support critical emergency power requirements:
  - Telecommunications.
  - Health care/life support systems.
  - Critical government operations.
- Expanded user community offers many positive market opportunities:
  - Increased demand prompts greater production volume – lowers unit cost.
  - Cross industry adoption spurs "services" growth (construction, maintenance, ancillary support) as more units are deployed – lower costs due to competition.
  - Fueling infrastructure is "pulled" into the market by true demand rather than being "pushed" into the market to support speculative potential.

Technical Barriers

Major barriers being addressed under our project are summarized as follows:

- Higher costs: initial capital cost, as well as operating expenditure (increased site lease costs to support code mandated hydrogen setbacks) than incumbent technology (diesel generator).

- Siting and permitting: due to variations in the applicable code requirements and versions recognized by the authorities having jurisdiction (AHJ), each market launch requires time with the local officials (building, fire) to help them understand the referenced codes and how Sprint interprets/complies with code requirements.
- Fueling infrastructure: this project deploys a new model for stationary hydrogen fuel cells, relying upon an on-site refillable medium pressure storage solution rather than the low pressure hydrogen cylinder exchange model. Our project partner, Air Products, has invested in a small fleet of transport vehicles to deliver bulk compressed hydrogen to small, geographically diverse, remote cell sites.

Technical Targets and Milestones

The following performance targets and associated milestones have been set for this project.

- Install 260 additional PEM fuel cells for backup power by end of December, 2012.
  - California – 100 units
  - Connecticut – 30 units
  - New Jersey – 65 units
  - New York – 65 units
- Retrofit a total of 70 existing Low Pressure Hydrogen Storage Systems with the new Medium Pressure On-Site Refillable Hydrogen Storage Solution in the following states:
  - California
  - Louisiana
  - Texas

Accomplishments

- Completed the required documentation for National Environmental Policy Act (NEPA) clearance and received the requested comprehensive Categorical Exclusion on May 12, 2011.
- Thus far, our team has conducted site surveys at 583 candidate sites to support new PEM deployments at 260 locations.
- A total of 283 of the 583 candidates were removed from consideration for a variety of reasons during Phase 1 (site survey, entitlement review).
  - Space constraints within the cell site compound (real estate and setbacks).
  - Access restrictions for hydrogen fueling vehicle.
- An additional 37 candidates “fell out” during Phase 2 (site acquisition) due to:
  - Cost.
  - Zoning issues.
- Commissioned the first new unit on 05/11/2011 in Alloway, NJ. As of 06/30/2011, a total of 32 new PEM fuel cells have been commissioned into service.
- Expect to have 194 new PEM fuel cells commissioned by the end 2011.



Introduction

The relevance of this project to the goals of ARRA of 2009 is threefold. First, Sprint seeks to support the creation of new jobs, as well as maintain existing jobs, to successfully complete this deployment effort. Second, Sprint intends to spur economic activity through the positive impact to various industries and service providers at all levels of the supply chain. And finally, Sprint is confident that this investment in PEM hydrogen fuel cells, to provide emergency power to our critical wireless network facilities, will truly benefit our nation’s long-term economic growth.

Approach

After reviewing the Code Division Multiple Access (CDMA) Network Site Inventory, a master candidate site list was created based upon the restoration priority of the facility, and whether or not the site was equipped with a fixed generator. Sprint focused on specific markets to exploit the site’s proximity to the hydrogen distribution facility (within 200 miles), as well as to concentrate on market clusters to minimize site acquisition, siting/permitting, installation, commissioning, and training expenditures. In addition, this cluster approach helps to minimize costs associated with the maintenance of a PEM spare parts inventory. Finally, this concentration permits a consistent presentation to the local building officials, which in turn helps to clarify applicable code (Uniform Building Code, National Fire Protection Association, etc.) interpretations. In theory, all of these efforts should help to facilitate a rapid, safe, and successful deployment in the market.

Our Hydrogen Safety Plan (HSP) was submitted to DOE on 07/13/2010. On 01/18/2011, feedback from the Safety Panel team at DOE was received. Additional work is required on the HSP to ensure that the issues identified by DOE are satisfactorily addressed prior to resubmission. In reality, modifications to the HSP were put on the “back burner” as our efforts to demonstrate progress on new PEM deployments required our team’s full time and attention – now targeting delivery of the revised HSP to DOE by end of calendar year 2011.

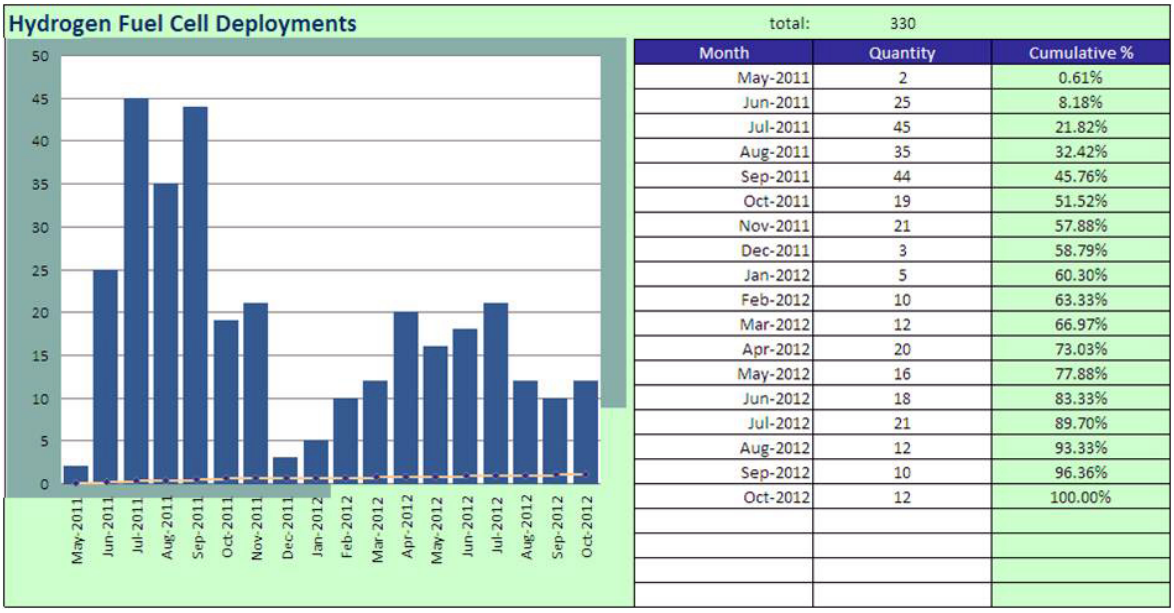
A NEPA comprehensive Categorical Exclusion was secured on May 12, 2011.

Results

At long last, Sprint has successfully commissioned the first of many PEM fuel cells equipped with the Medium Pressure, Refillable On-Site, Hydrogen Storage Solution. Since the initial installation under this DOE/ARRA funded project on May 11, 2011, a total of 32 systems have been brought into service (as of 06/30/11). These installations, coupled with our original stand-alone deployment effort (243 systems in the 2005–2007 timeframe), provide a grand total of 275 PEM fuel cells providing backup power for critical cell site locations on the Sprint Network. When the planned 260 new and 70 retrofits (fuel storage converted from low pressure tanks to the medium pressure refillable solution) are completed, we will have more than doubled the number of sites in our Network with emergency power provided by PEM fuel cells. Figure 1 provides the deployment schedule for this project.

To date, a total of 583 sites have been evaluated to determine if the cell site location is suitable for new PEM deployment or, if equipped with a PEM today, can it support the use of the new hydrogen fuel storage solution. Figure 2 provides a summary of the various reasons so many sites are dropped from consideration following the completion of Phase 1 activities.

Once the candidate site makes it through Phase 1, sites can be dropped from consideration during Phase 2. Figure 3 provides a summary of the various reasons a site



Month	Quantity	Cumulative %
May-2011	2	0.61%
Jun-2011	25	8.18%
Jul-2011	45	21.82%
Aug-2011	35	32.42%
Sep-2011	44	45.76%
Oct-2011	19	51.52%
Nov-2011	21	57.88%
Dec-2011	3	58.79%
Jan-2012	5	60.30%
Feb-2012	10	63.33%
Mar-2012	12	66.97%
Apr-2012	20	73.03%
May-2012	16	77.88%
Jun-2012	18	83.33%
Jul-2012	21	89.70%
Aug-2012	12	93.33%
Sep-2012	10	96.36%
Oct-2012	12	100.00%

FIGURE 1. EE0000486 Deployment Schedule

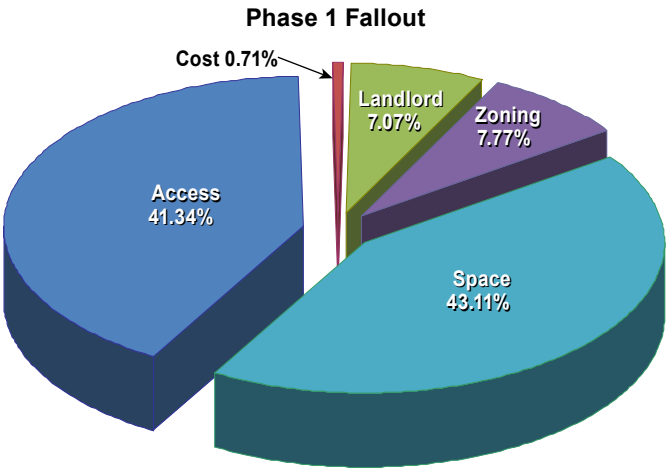


FIGURE 2. Phase 1 (Site Survey/Entitlement Review) Fallout Summary

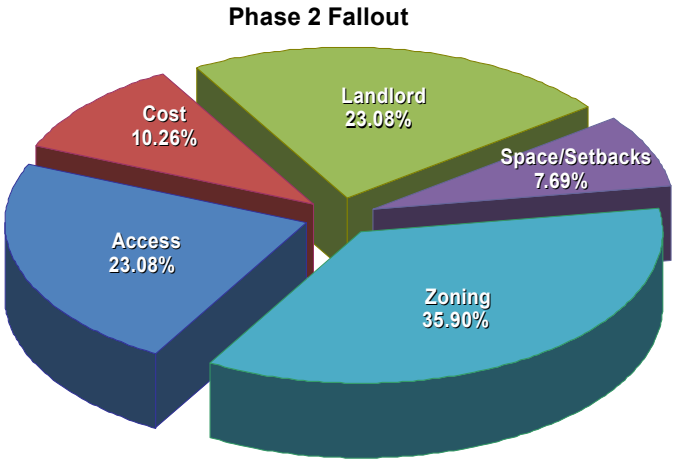


FIGURE 3. Phase 2 (Site Acquisition/Zoning) Fallout Summary

can be dropped at this stage of deployment. Interestingly, it appears that the education of property owners (landlords, tower aggregators), municipal officials, and/or the zoning board might permit more sites to remain in consideration.

Conclusions and Future Directions

We recognized going into this project that the fallout rate for candidate sites would be in the 40% range due to the limited amount of space available in the cell site compound. Limited real estate, in the case of PEM deployment, can be a double edged sword. There may be physical space to permit the placement of the equipment on-site, however, code mandated setback distances may or may not be able to be supported at the facility. Without uniform AHJ recognized hydrogen/fire codes, it appears that PEM deployment will continue to require more time/effort/money to deploy versus the incumbent diesel generator solution.

XII.6 PEM Fuel Cell Systems Providing Backup Power to Commercial Cellular Towers and an Electric Utility Communications Network

Mike Maxwell (Primary Contact), Mark Cohen
ReliOn Inc.
15913 E. Euclid Ave.
Spokane Valley, WA 99216
Phone: (509) 228-6612
E-mail: mmaxwell@relion-inc.com

DOE Managers
HQ: Ned Stetson
Phone: (202) 586-9995
E-mail: Ned.Stetson@ee.doe.gov
GO: James Alkire
Phone: (720) 356-1426
E-mail: James.Alkire@go.doe.gov

Contract Number: DE-EE0000487

Subcontractors:
- Fortune Wireless, Indianapolis, IN
- Betacom, Inc., Pompano Beach, FL
- United Commercial Real Estate Services, Inc., Lake Mary, FL
- Peek Site-Com, Inc., Auburn, CA
- Jeffrey Rome and Associates, Newport Beach, CA
- Vertical Horizons Contracting, Lincoln, NE
- Telecom, Tower and Power, LLC, Romulus, MI
- Front Range Wireless, Centennial, CO
- Air Products and Chemicals, Inc. (APCI), Allentown, PA

Project Start Date: August 1, 2009
Project End Date: December 31, 2011

Objectives

- Install 189 fuel cell cabinets (385 fuel cell systems total) with 72-hour capacity as back-up power equipment for communications sites in use by Pacific Gas & Electric (PG&E), a California utility, and as critical emergency reserve power for cell sites operated by AT&T.
- Demonstrate that fuel cells are a reliable source of clean back-up power for key communications facilities.
- Transform the market within PG&E and AT&T by moving beyond limited demonstration sites to wider deployments

Relevance to the goals of the American Recovery and Reinvestment Act (ARRA) of 2009, and to the goals of U.S. DOE Fuel Cell Technologies' (FCT) ARRA project for accelerating the commercialization and deployment of fuel cells and fuel cell manufacturing, installation, maintenance, and support services.

This project will contribute to achievement of the DOE's objectives for ARRA projects in general, and the FCT projects in particular:

- Create direct and indirect jobs in seven regions across the continental United States, throughout the supply chain.
- Train and deploy installers of fuel cell systems.
- Increase the number of commercially available fuel cell systems.
- Generate volume for fuel cell supply chain.
- Create and deploy new refillable hydrogen storage for stationary hydrogen fuel cells.
- Create and deploy new hydrogen delivery model for stationary hydrogen fuel cells.
- Expand practical user operating experiences.
- Validate performance.

Technical Barriers (Market Transformation Barriers)

This project addresses the barriers to market transformation for stationary backup fuel cell equipment:

- Site Selection: myriad considerations in site selection factor into the adoption of fuel cells for backup equipment.
- Permitting: multiple stakeholders, including authorities having jurisdiction, fire officials, building officials, and landlords, all have varying perspectives and reference a variety of non-harmonized standards for permitting.
- Fueling infrastructure: this project deploys a new model for stationary hydrogen fuel cells, relying on a refillable storage module, in place of the historically used cylinder exchange model. This requires the development of a fueling infrastructure that can deliver bulk compressed hydrogen to small, geographically diverse, remote sites.

Technical Targets and Milestones

- Survey candidate sites to identify 189 sites for installation.
- Secure all permitting, site acquisition, lease amendments, etc. to proceed with installations.
- Manufacture, ship, install, and commission 189 stationary fuel cell sites (385 systems).
- Collect data on operation, fuel service, and maintenance.

Accomplishments

- Reviewed database records of an additional 82 candidate AT&T sites for a total of 736 to down-select sites based on the feasibility of fuel cell installation and on-site refueling accessibility.

- Performed physical site surveys at an additional 60 candidate AT&T sites for a total of 520 to further down-select sites based on the feasibility of fuel cell installation and refueling accessibility.
- Generated and delivered 65 unique quotes for additional services needed to support the 180 AT&T sites to be constructed and 132 replacement quotes for site acquisition and installation services corresponding to replacement sites for 66 previously cancelled sites.
- Processed an additional 178 unique purchase orders (for a total of 487) from AT&T Procurement for site acquisition (SAC) services, fuel cell installation services, and supplemental shelter direct air cooling equipment and installation services.
- Initiated the SAC process (leasing, zoning/planning, permits, etc.) on an additional 64 AT&T sites for a total of 252 sites.
- Completed the SAC process for an additional 116 AT&T sites for a total of 132 sites.
- Fabricated, integrated, and delivered fuel cell equipment (48 cabinets = 120 systems) for an additional 48 AT&T sites for a total of 180 sites, and hydrogen storage modules (HSMs) for an additional 111 AT&T sites for a total of 180 sites.
- Constructed and commissioned an additional 101 sites (227 systems) for a total of 109 sites (244 systems) and provided hand-off to AT&T.
- Generated an additional unique scope of work for one replacement PG&E site used to replace a site that was unable to be successfully acquired by PG&E's real estate group.
- Constructed and commissioned all nine PG&E sites (9 systems) and provided hand-off to customer.



Introduction

Market transformation is best achieved by reaching a critical mass in the market that significantly raises awareness and direct experience of the value proposition. With the assistance of this project, ReliOn is installing 385 fuel cell systems (within 189 cabinets) into the telecommunications and utility networks at AT&T and PG&E for backup power, across nine states, combined with the deployment of a refillable stationary HSM unit and the accompanying refueling logistics platform for 180 AT&T sites. These are real-world, tangible changes to the market resulting in the use of hydrogen based systems to harden critical communications networks.

Approach

ReliOn's approach begins with the basic research needed to identify viable candidate sites and then narrow down the list in order to focus efforts on the most viable and critical sites that can be installed and refueled successfully, ensuring that these assets will remain viable for decades. This work is primarily performed by ReliOn personnel. The next task is to secure rights to perform the construction through the use of SAC vendors who structure the leasing and permitting packages to prepare the sites for construction. ReliOn utilizes third parties who are skilled in this profession and will remain part of the program until all SAC activities have been completed.

As a site clears the SAC process, it is then constructed (typically within one month) and brought on-line as a fully functional back-up power system. Installation construction is performed only after the SAC vendor has secured the installation and operating rights for each site. ReliOn utilizes third parties to perform installation construction, yet retains the roles of project management and supervision. ReliOn partnered with an established hydrogen provider, APCI an industry expert in hydrogen storage and delivery for the development and production of the HSM. Once the sites are installed, fueled and operational, they are monitored remotely for data collection. ReliOn personnel collect and report fuel cell operational data to the DOE/National Renewable Energy Laboratory (NREL). The use of both ReliOn and third party resources maximizes the effectiveness of the project, creates or retains jobs across a breadth of companies and regions, and delivers the maximum amount of infrastructure for the given financial investment.

Results

To date, ReliOn has completed the site qualification stage for the entire project. This has allowed for the successful initiation of SAC activities on all target sites, plus a few reserve sites as contingencies for sites that may fail to complete the SAC process due to unforeseen circumstances. Since project inception, 66 AT&T sites and one PG&E site have been cancelled and successfully replaced. SAC has been completed on a total of 132 AT&T sites to date with 54 presently undergoing the SAC process. ReliOn has installed 253 fuel cell systems at 118 sites to date (244 systems at 109 sites for AT&T and nine systems at nine sites for PG&E) with 14 more AT&T sites (34 systems) presently in the construction phase and nine more sites (21 systems) pending construction. This ongoing process of SAC approval and site construction has resulted in the continuous need for labor and has secured multiple jobs. PG&E performed the SAC of their nine sites using their internal real estate and legal department resources, and all PG&E construction is now complete.

Figure 1 shows an AT&T site located in Michigan which has just completed the initial fill of the HSM during the commissioning process. The fill was performed using the newly developed single-axle 'straight truck.' This vehicle makes the fueling of certain remote sites feasible and more efficient due to its reduced size, improved mobility, and higher service pressure in comparison to legacy tube trailers pulled by semi-tractors.



FIGURE 1. Completed AT&T Site in MI Showing 'Straight Truck'



FIGURE 2. Fueling of HSM at Completed AT&T Site in CO

Figure 2 shows a close up of an AT&T site located in Colorado undergoing the initial fill of the HSM during the commissioning process. The leftmost cabinet is the fuel cell equipment enclosure with an adjacent six-cylinder hydrogen storage cabinet. The larger cabinet to the right with the doors open and red cylinders in view is the HSM. The HSM is connected to the system in parallel with the six-cylinder hydrogen storage cabinet, and contains the majority of the fuel capacity.

This project deploys fuel cell systems within eight states as shown in Figure 3, though it promotes jobs and supports business in other states which are the home bases of various subcontractors. AT&T presently has systems operating in all eight states. As a California utility, all of PG&E's systems are located within California and they are all presently operational.

As discussed earlier, the SAC activity is a primary task that must be completed before fuel cell system installation construction can commence. Each site's respective SAC activity concludes with an official "notice to proceed" package which is the trigger for the call out of fuel cell equipment from the warehouse for delivery to the site and delivery of the work release package for the installation contractor(s). ReliOn discovered during the past year that the original schedule for the completion of SAC was too optimistic and that the SAC process in general takes twice as long as originally expected. These SAC delays have resulted in the inability to start and complete the construction of sites per the original deployment schedule milestones. Figure 4 shows the project schedule for the completion of AT&T site construction. Note the adjustment made to the schedule goals at the end of the first quarter of 2011. This course correction was put in place to readjust the schedule to conform to the reality of the situation created by the delays in the SAC process. A no-cost contract extension was requested by ReliOn and received from the DOE, extending the contract to December 31, 2011.

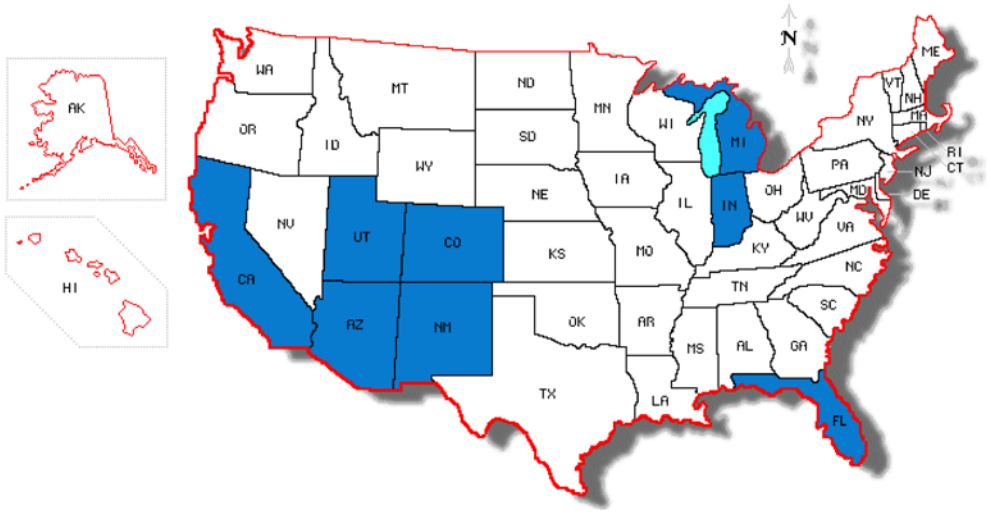


FIGURE 3. States Benefiting from the AT&T/PG&E Regional Fuel Cells

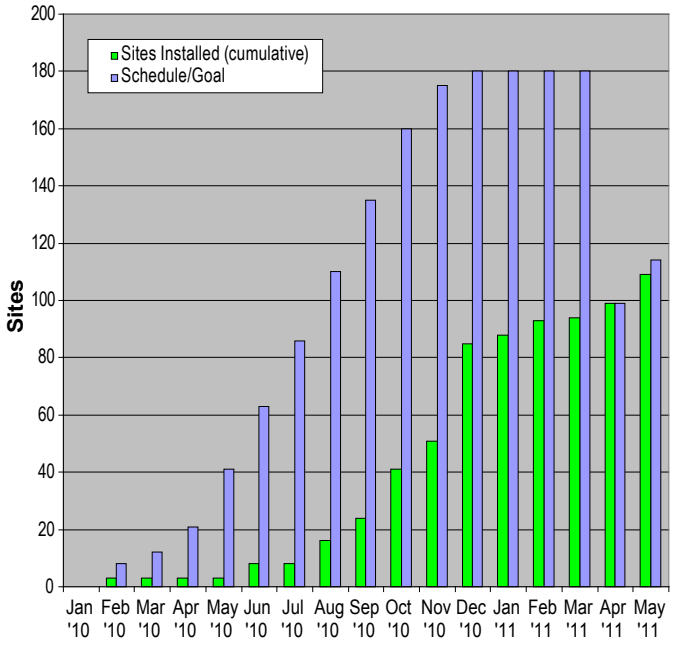


FIGURE 4. SAC Initiation Progress Through 6/1/2011 for 180 AT&T Sites

Conclusions and Future Directions

During the past year of effort, ReliOn learned that the drop out rate of sites undergoing SAC was higher than expected. One in three sites has been cancelled due to circumstances beyond ReliOn's control, resulting in a cycle of additional replacement site reviews, physical site surveys, quote and purchase order modifications, and re-submittal of sites into the SAC process. This additional activity has added cost and stretched ReliOn resources dedicated to the project. It was also discovered that the SAC process takes longer on average than originally estimated by subcontractors. Where two months was originally considered an adequate gestation period for the process, it was discovered that six months is a more typical average time to acquire the site.

Tasks planned for the remainder of the project through the end of 2011 include:

- Complete the SAC process for all remaining sites within the project:
  - This activity includes working with the local authorities having jurisdiction to educate them on hydrogen safety, fuel cells, and codes & standards to resolve any questions/issues that arise during SAC.
- Construct all remaining sites and commission the equipment for hand-off to the customer/end-user.
- Obtain and report operational data to fulfill the DOE/NREL data reporting requirement.
- Continue to generate and provide all DOE reports per the required schedule.

FY 2011 Publications/Presentations

1. Blanchard, J. "A Roadmap for Tier 1 Telecom Carrier Fuel Cell Installation", OSP Expo, San Antonio, Texas, October 13, 2010. (Oral Presentation)

XII.7 Analysis Results for ARRA Projects: Enabling Fuel Cell Market Transformation

Jennifer Kurtz (Primary Contact), Keith Wipke, Sam Sprik, Todd Ramsden, Genevieve Saur, and Chris Ainscough
National Renewable Energy Laboratory (NREL)
1617 Cole Blvd.
Golden, CO 80401
Phone: (303) 275-4061
E-mail: jennifer.kurtz@nrel.gov

DOE Manager
HQ: Sara Dillich
Phone: (202) 586-7925
E-mail: Sara.Dillich@ee.doe.gov

Subcontractor
Pacific Northwest National Laboratory, Richland, WA

Project Start Date: August, 2009
Project End Date: Project continuation and direction determined annually by DOE

Objectives

- Independent technology assessment in real-world operation conditions focusing on fuel cell system and hydrogen infrastructure.
- Leverage data processing and analysis capabilities developed under the Fuel Cell Vehicle Learning Demonstration.
- Support market growth through reporting on technology status to key stakeholders and analyses relevant to the markets' value proposition.
- Study fuel cell systems operating in material handling equipment (MHE), backup power, portable power, and stationary power applications; includes up to 1,000 deployed fuel cell systems.

Technical Barriers

This project addresses the technical barrier of commercialization of fuel cells in key early markets and the associated performance capabilities and benefits.

Technical Targets

- Deployment of up to 1,000 fuel cell systems: By December 2010, 557 systems were delivered and 483 of those systems were in operation.

Accomplishments

- Expanded the NREL Fleet Analysis Toolkit (NRELFAT) to include MHE, backup power, and stationary power data processing, analysis, and reporting.
- Published three deployment focused Composite Data Products (CDPs), updated on a quarterly basis.
- Published two cycles of technical focused CDPs (42 CDPs for MHE and 10 CDPs for backup power data) and hundreds of detailed data results were shared with individual data providers, updated bi-annually. Key performance results include operation time, fill time, maintenance, reliability, safety, usage patterns, and durability.
- Created a website and maintained it for all published results and presentations.



Introduction

The DOE has designated more than $40 million in American Recovery and Reinvestment Act (ARRA) funds for the deployment of up to 1,000 fuel cell systems. This investment is enabling fuel cell market transformation through development of fuel cell technology, manufacturing, and operation in strategic markets where fuel cells can compete with conventional technologies. The strategic markets include MHE, backup power, stationary power, and portable power, where the majority of the deployed systems are in the MHE and backup power markets. NREL is analyzing operational data from these key deployments to better understand and highlight the business case for fuel cell technologies and report on the technology status.

Approach

Data (operation, maintenance, and safety) are collected on site by the project partners for the fuel cell system(s) and infrastructure. NREL receives the data quarterly and stores, processes, and analyzes the data in NREL's Hydrogen Secure Data Center (HSDC). The HSDC is an off-network room with access for a small set of approved users. An internal analysis of all available data is completed quarterly and a set of technical CDPs are published every six months. The CDPs are aggregated data across multiple systems, sites, and teams in order to protect proprietary data and summarize the performance of hundreds of fuel cell systems and thousands of data records. A review cycle is completed before the publication of CDPs. The review cycle includes Detailed Data Products (DDPs) of individual system and site performance results provided to the individual data provider. DDPs also identify the individual contribution

to CDPs. NRELFAT is an internally created tool for data processing and analysis structured for flexibility, growth, and applications. Analyses are created for general performance studies as well as application or technology specific studies.

Results

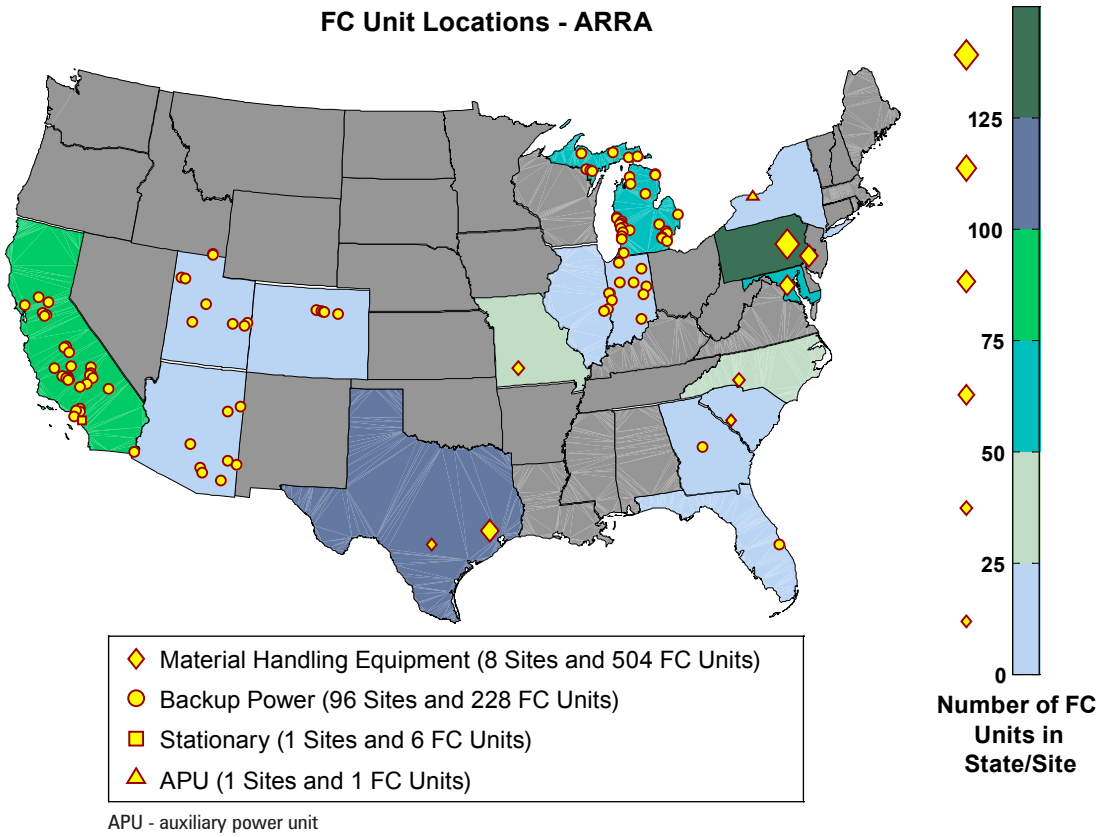
NREL created NRELFAT to efficiently process and analyze large amounts of data for the study of performance at the system, fleet, application, and across applications levels. Because the analysis results are created with multiple purposes and expected audiences, the set of results is varied and comprehensive of many aspects of the hydrogen and fuel cell deployments.

One result topic is where the systems are deployed and what some of the site specifications are. Each marker on the map in Figure 1 identifies the application, system(s) location, and deployment size at that site. There are 96 backup power sites (with more sites to be determined in the next few months), but most have only one to three systems installed at the site. There are eight MHE sites, but some of these sites have around 100 systems operating. Fuel cell systems are deployed in many regions of the United States, expanding the user base familiar with hydrogen and fuel cell technologies.

In the set of results published in the spring of 2011, 308 MHE systems were analyzed and had accumulated 307,433 operation hours in less than one year. Each site has a different system and operational conditions for the fuel cell MHEs. Figure 2 highlights the variation in average daily fuel cell system operation hours by fleet. (A fleet is a collection of same class MHEs and a site may have multiple fleets.) The range of average daily operation hours is between two and eight hours.

Refuel time is a critical performance metric for the operation of fuel cell MHEs and benefit over competing technologies. Figure 3 depicts the fueling rate for 38,795 hydrogen fills with an average of 0.33 kg/min. The inset graph highlights that all of the sites averaged very similar fill rates. The average fill time was just under two minutes per fill.

The backup power deployments have a very different operating metric than the fuel cell MHE sites. In certain locations a backup system may not operate because of a grid outage for many months. Figure 4 depicts the number of attempted and successful starts by calendar month as well as conditioning starts. A conditioning start is an automated operation for regular system checks and hydration after long periods of no operation (typically a month). Conditioning starts account for 59% of the start attempts and 408 out of 409 starts were successful.



APU - auxiliary power unit

FIGURE 1. Fuel Cell (FC) System Locations by Application and Deployment Size

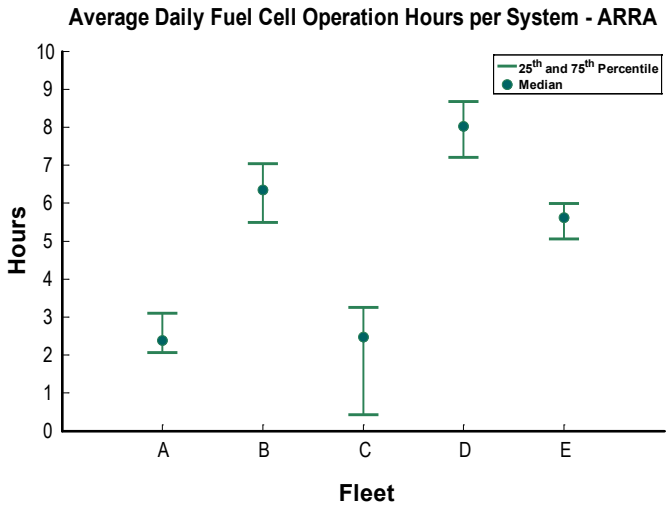


FIGURE 2. Average Daily Fuel Cell System Operation Hours by Fleet

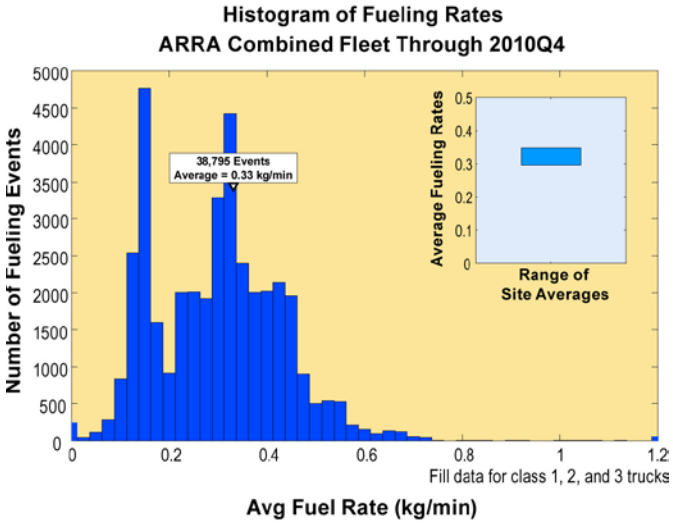


FIGURE 3. MHE Histogram of Fueling Rates and Range of Site Average Fueling Rates

Conclusions and Future Direction

This project has seen rapid deployment of hundreds of fuel cell systems in markets where the technology is ready to compete with incumbent technologies. Many aspects of the deployment and operation are analyzed and reported on via the CDPs. The CDPs have highlighted the magnitude of operation in operation hours (over 307,600 hours combined) and hydrogen fills (over 38,800 combined). These systems are demonstrated the capability to meet end user demands while learning lessons to integrate into future products and the operations are proving to be safe.

Planned future work includes:

- Quarterly publication of deployment focused CDPs.

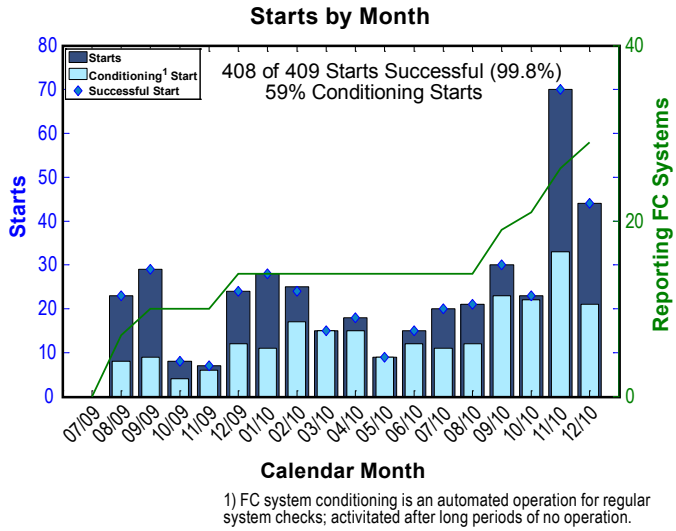


FIGURE 4. Count of Backup Power Attempted and Successful Starts by Month

- Bi-annual publication of technical focused CDPs and DDPs.
- Technical monitoring and coordination of hydrogen safety panel reviews and site visits.
- Quarterly analysis of operation, maintenance, and safety data for fuel cell systems and hydrogen infrastructure.
- Collaboration with key stakeholders to identify valuable analyses for technology status updates and metrics important to the value proposition.

FY 2011 Publications/Presentations

1. Kurtz, J.; Wipke, K.; Sprik, S.; Ramsden, T.; Saur, G.; Ainscough, C. "Analysis Results of ARRA Fuel Cell Early Market Projects." Presented at Hydrogen + Fuel Cells 2011 conference May 17, 2011.

2. Kurtz, J.; Wipke, K.; Sprik, S.; Ramsden, T.; Saur, G.; Ainscough, C. "Analysis Results for ARRA Projects: Enabling Fuel Cell Market Transformation." Presented at DOE's Annual Merit Review February 16, 2011.

3. Kurtz, J.; Wipke, K.; Sprik, S.; Ramsden, T.; Saur, G.; Ainscough, C. "Early Fuel Cell Market Deployments: ARRA and Combined - May 2011." Published May 10, 2011.

4. Kurtz, J.; Wipke, K.; Sprik, S.; Ramsden, T.; Saur, G.; Ainscough, C. "ARRA Fuel Cell Deployments: Operation Data Overview." Presented at Hydrogen Safety Panel Meeting February 16, 2011.

5. Kurtz, J.; Wipke, K.; Sprik, S.; Ramsden, T.; Saur, G.; Ainscough, C. "Spring 2011 Composite Data Products - ARRA Material Handling Equipment." Published April 6, 2011.

6. Kurtz, J.; Wipke, K.; Sprik, S.; Ramsden, T.; Saur, G.; Ainscough, C. "Spring 2011 Composite Data Products - Backup Power." Published March 29, 2011.

7. Kurtz, J.; Wipke, K.; Sprik, S.; Ramsden, T.; Saur, G.; Ainscough, C. "Analysis Results for ARRA Fuel Cell Deployments." Presented at Fuel Cell and Hydrogen Energy Association February 16, 2011.

8. Kurtz, J.; Wipke, K.; Sprik, S.; Ramsden, T.; Saur, G.; Ainscough, C. "Early Fuel Cell Market Deployments: ARRA and Combined - February 2011." Published February 10, 2011.

9. Kurtz, J.; Wipke, K.; Sprik, S.; Ramsden, T.; Saur, G.; Ainscough, C. "Early Fuel Cell Market Deployments: ARRA and Combined - November 2010." Published November 30, 2011.

10. Kurtz, J.; Wipke, K.; Sprik, S.; Ramsden, T. "ARRA Fuel Cell Deployment and Operation." Presented at 2010 Fuel Cell Seminar October 20, 2011.

XII.8 H-E-B Grocery Total Power Solution for Fuel Cell-Powered Material Handling Equipment

Gus Block (Primary Contact), Nathanial Schomp
Nuvera Fuel Cells
129 Concord Road
Billerica, MA 01821
Phone: (617) 245-7553
E-mail: gblock@nuvera.com

DOE Managers
HQ: Dimitrios Papageorgopoulos
Phone: (202) 586-5463
E-mail: Dimitrios.Papageorgopoulos@ee.doe.gov
GO: Greg Kleen
Phone: (720) 356-1672
E-mail: Greg.kleen@go.doe.gov

Contract Number: DE-EE0000489

Subcontractors:
- Airgas Southwest, San Antonio, TX
- Airgas Merchant Gases, Bozrah, CT
- Parkway Systems, San Antonio, TX

Project Start Date: September 1, 2009
Project End Date: August 30, 2011

Objectives

Validate DOE market transformation activities by demonstrating:

- Fuel cell-powered forklifts operating in a high-usage, highly transient mobility application.
- An on-site natural gas-based hydrogen generation and refueling station as a precursor to future distributed automotive fuel cell refilling stations.

Relevance to the American Recovery and Reinvestment Act (ARRA) of 2009 Goals:

- Stimulate use of emerging technologies – additional investment by H-E-B is anticipated, without ARRA funding.
- Develop jobs and job skills (manufacturing, product development, repair and maintenance) in clean energy growth industries.
- Develop product and performance improvements to make fuel cells and hydrogen refueling equipment commercially viable.

Technical Barriers Addressed

- Reliability of technology (fuel cell systems and hydrogen generation, storage, and compression equipment) used in a highly demanding materials handling application and environment.
- Durability of fuel cell systems and hydrogen generation, storage, and compression equipment.
- Quantification of costs associated with operation and maintenance of all equipment.
- Proper safety planning and safe operation of all equipment.
- Safe hydrogen use indoors, in high-throughput, high-density distribution center.
- Obtaining necessary permitting for motive fuel cell power units and hydrogen generation and refueling equipment, requiring collaboration of authorities having jurisdiction (AHJs), the industrial truck fleet manager, the environmental health and safety (EHS) coordinator, and the industrial truck equipment provider.
- Obtaining insurance coverage for the use of all equipment.
- Availability of hydrogen generated on-site from a steam methane reformer.

Technical Targets and Milestones

- Install 14 proton exchange membrane (PEM) fuel cells in Class II forklift trucks and operate for two years in produce and dry goods grocery distribution centers.
- Generate hydrogen on-site from natural gas to support forklift truck fleet and maintain 100% availability of hydrogen at the pump through combination of hydrogen generator and hydrogen tube trailer backup.

Accomplishments

- Built a permanent PowerTap hydrogen refueling station and introduced 14 PowerEdge systems into 24/7 service at a grocery distribution center owned and operated by a nationally recognized industry leader.
- Generated 11,002 kg of hydrogen on site through July 2011.
- Maintained >99% hydrogen availability at the pump for forklift refueling.
- Logged 21,899 operating hours on 14 PowerEdge fuel cell power units through July 2011.
- Demonstrated 10% productivity gain associated with fuel cells vs. lead acid batteries.

- Redesigned the next generation PowerEdge system for greater performance and reliability.
- Obtained field data that has been fundamental in next-generation PowerEdge fuel cell system and PowerTap hydrogen refueling equipment designs.
- Provided extensive data on PowerTap and PowerEdge performance to the National Renewable Energy Laboratory.



Introduction

H. E. Butt Grocery Company, Inc. (H-E-B) is a privately-held supermarket chain with 310 stores throughout Texas and northern Mexico. The company agreed to convert a portion of its lift truck fleet to fuel cell power to verify the value proposition and environmental benefits associated with the technology. H-E-B management believes that fuel cell forklifts can help alleviate several issues in its distribution centers, including truck operator downtime associated with battery changing, truck and battery maintenance costs, and reduction of grid electricity usage. It is also interested in other uses of hydrogen produced on site in the future, such as for auxiliary power units used in tractor-trailers in its fleet.

Currently, the H-E-B distribution center operates a total of approximately 300 Class II reach trucks and 700 Class III pallet jacks over two work shifts, for a total of 20 hours per day. There are three temperature zones in the facility, ranging from dry goods at ambient temperature, to refrigerated goods at 34°F (1°C), to freezer goods at -13°F (-25°C). The PowerEdge units provided are powering Class II fork lift trucks that were designed for use with 1,000 Ah lead acid batteries, and are capable of operation in both the ambient and refrigerated goods temperature zones of the San Antonio facility. Data collected from this initial installation will enable H-E-B to make economic decisions on expanding the fleet of PowerEdge and PowerTap units in the company.

Approach

In order to verify compatibility of the PowerEdge fuel cell power units with H-E-B's forklift fleet, information was gathered regarding truck make and model and usage profile within H-E-B's grocery and produce distribution centers. Power monitoring of the trucks was undertaken in order to confirm that the duty cycle was achievable with the PowerEdge product, and to determine the number of units that could be supported by a PowerTap system producing 50 kg/day of hydrogen. We determined that 14 PowerEdge systems could be supported by the PowerTap production capacity, which is how that number of forklifts was chosen for repowering.

A site-specific installation plan was prepared that detailed where all hydrogen generation, compression, storage, and dispensing equipment would be placed. As the site plan was being developed, the PowerTap and PowerEdge equipment was manufactured and delivered to the H-E-B facility, where it was installed in accordance with required codes and standards. Upon final sign-off from both the local AHJ and the insurance carrier, the forklift fleet was deployed for operation in the grocery and perishable sections of the distribution center alongside forklifts operating with standard lead-acid batteries. Side-by-side operation allows H-E-B to assess the value associated with the PowerEdge and PowerTap products compared with conventional battery technology.

Results

As presented in Table 1 below, the build of all 14 PowerEdge systems and the PowerTap hydrogen refueling equipment was complete as of October 30, 2009. In parallel, Nuvera application engineers, working with H-E-B facility engineers, created site-specific service and installation plans. Nuvera and H-E-B's EHS coordinator also developed a comprehensive safety plan, which was reviewed by a DOE-appointed safety panel over the last 6 months.

TABLE 1. Work Breakdown Schedule

Task #	Project Milestones	Milestone Completion Date			
		Original Planned	Revised Planned	Actual	Percent Complete
1	Build	10/30/09		10/30/09	100%
2	Site Plan	10/30/09		10/30/09	100%
3	Deployment	11/30/09	2/28/10	2/28/10	100%
	Go/No-Go: 2 PowerEdges Productivity Trial; certify passing of FAT; permitting and approvals	11/30/09	12/30/09	12/30/09	100%
4	Confirm Value Proposition	5/31/11	5/31/11		100%
5	Final Testing	8/31/11	8/31/11		0%
6	Project Management & Reporting	8/31/11	8/31/11		96%

FAT – factory acceptance test

A total of 60 H-E-B forklift operators received hydrogen and fuel cell training. Based on the agreed site plan, Nuvera identified and provided basic training to two local fuel cell service personnel, who work for an H-E-B wholly-owned subsidiary, Parkway Systems. The role of the Parkway service provider is to keep the PowerEdge systems operational by providing a fast response to diagnosing system faults and repairing the units. This type

of service includes scheduled preventive maintenance, basic troubleshooting, and the repair or replacement of non-safety critical items. Nuvera's Customer Care group provides spare parts, training, data analysis, and more complex field support, including troubleshooting and repairs of safety-critical items (high pressure, high voltage). Nuvera also trained and qualified three Airgas personnel (two from Airgas Southwest, the local service provider, and one from Airgas Bozrah, responsible for 24-hour hydrogen system monitoring) for Tier 1 service of the PowerTap hydrogen generator and the PowerTap hydrogen station (compression, storage, dispensing).

During this process, all relevant codes and standards were identified, and working with the AHJ and the H-E-B insurance carrier, all permits were obtained for site construction, installation, and operation.

The deployment process began upon establishing the final site plan and was completed on February 28, 2010.

H-E-B Grocery Total Power Solution for Fuel Cell-Powered Material Handling Equipment

In May 2010, H-E-B conducted an analysis to determine whether any productivity benefits were realized in association with the fuel cell forklift conversion. H-E-B concluded that the fleet was 10% more productive than it was running on lead acid batteries, a combination of the elimination of the battery changing task and the improved performance of the trucks. The equipment maintenance supervisor also noted a marked decrease in motor controller failures on lift trucks running on fuel cells, a consequence of the elimination of voltage sag associated with batteries. As part of the project conclusion, H-E-B is quantifying the value proposition benefits.

PowerEdge Fuel Cell Systems

Over the first three months of operation, H-E-B reported an increase in productivity of 10% for the PowerEdge systems compared to forklifts running on batteries.

As part of the ongoing program, Nuvera provides data to the National Renewable Energy Laboratory using jointly-agreed data templates. Information collected during the course of daily operations includes the following:

- Power pack fault code indication
- Service notifications
- Operating status
- Fuel cell run time
- Fuel cell power
- Total kWh energy produced
- Total kWh energy consumed

The full fleet of 14 fuel cell-powered trucks was operational until July 2010, when hot weather combined with several other factors caused reliability of the systems to suffer and to negatively impact operations. Since these issues were disruptive to H-E-B's operations, Nuvera scaled back the number of units in service. We identified the root causes of the problems and determined the required corrective actions. The solutions were implemented on four operational PowerEdge fuel cell units in early October, 2010. The solutions were validated, and Nuvera implemented them on the remaining 10 PowerEdge units and introduced them back into service in December 2010.

PowerTap Hydrogen Generation and Refueling Systems

Figure 1 shows the amount of hydrogen provided at the site from the PowerTap system and from the back-up tube trailer. The percent of hydrogen supplied by PowerTap is also indicated. Note that reduced usage from July through November reflects reduced fuel cell fleet size.

Conclusions and Future Directions

- Our next generation PowerEdge system design will address performance and reliability issues that have surfaced in this demanding application. Specifically, our new product for the reach truck application will:
  - Replace the 'ultrabattery' with a lithium ion battery, which our analysis indicates will improve battery life to be on par with the remainder of the system (>20,000 hours).
  - Incorporate an 'auto-on' feature to turn the PowerEdge unit on in the event that the truck is being used but the operator has neglected to also start the fuel cell system.
  - Incorporate a fuel cell stack with approximately twice the power rating at end of life (10 kW) as the current system.
  - Incorporate more robust power circuits.
  - Improve controls to extend stack life.
- Similarly, the next generation PowerTap design will incorporate improvements required for satisfactory operation in a demanding materials handling application, including the following:
  - A solution to avoid water pump damage associated with superheated steam.
  - A controls upgrade to avoid reformate compressor wear.
  - A higher capacity desulfurizing system to avoid sulfur breakthrough.
- H-E-B has determined that fuel cells are their preferred motive power source for reach trucks. They have already set aside the budget required for expanding the fleet by purchasing 28 additional PowerEdge units, pending a demonstration of acceptable performance of our next generation higher power system. The increased fleet size will required the addition of two PowerTap systems.

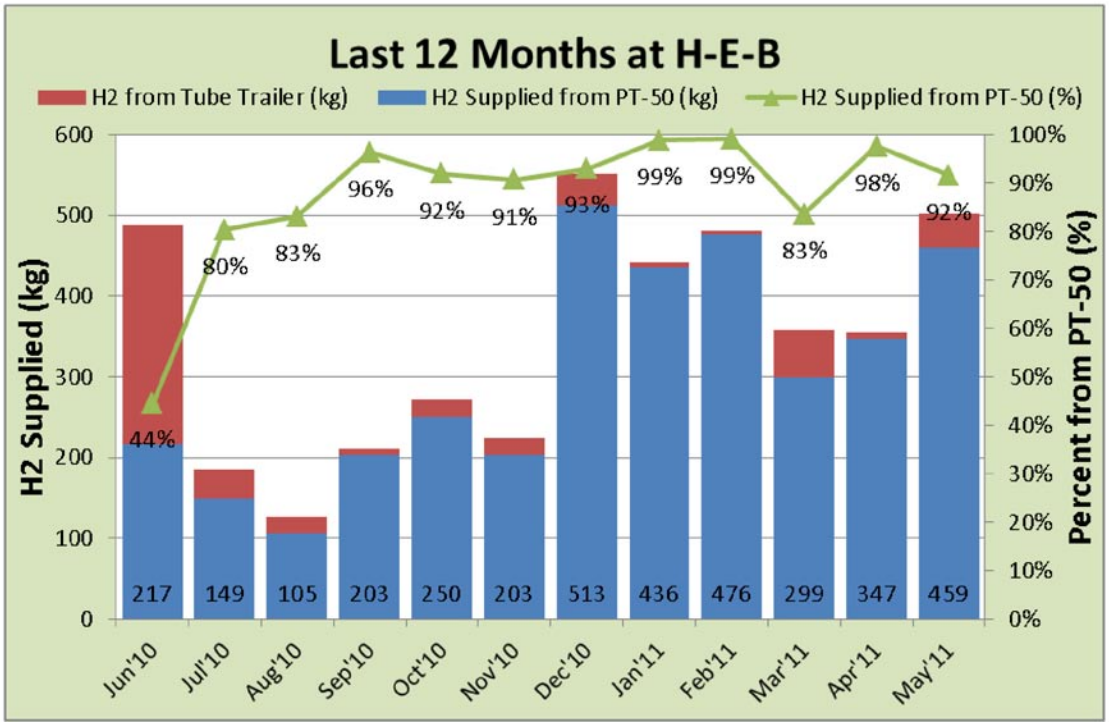


FIGURE 1. PowerTap PT-50 Usage and Reliability at H-E-B, June 2010 through May 2011

FY 2011 Publications/Presentations

1. Gus Block, *H-E-B Grocery Total Power SolutionTM for Fuel Cell Powered Material Handling Equipment,* 2011 U.S. Department of Energy Hydrogen Program and Vehicle Technologies Program Annual Merit Review and Peer Evaluation Meeting, Washington, D.C., May 13, 2011.

XII.9 Fuel Cell-Powered Lift Truck FedEx Freight Fleet Deployment

Jonathan King
FedEx Freight
2200 Forward Drive
Harrison, AR 72601
Phone: (870) 391-4149 ext. 2022
E-mail: jonathan.king@fedex.com

DOE Managers:
HQ: Dimitrios Papageorgopoulos
Phone: (202) 586-5463
E-mail: dimitrios.papageorgopoulos@ee.doe.gov
GO: David Peterson
Phone: (720) 356-1747
E-mail: david.peterson@go.doe.gov

Contract Number: DE-EE0000482

Subcontractors:
- Plug Power Inc., Latham, NY
- Air Products and Chemicals, Inc., Allentown, PA

Project Start Date: October 1, 2009
Project End Date: September 30, 2013

Objectives

The objectives of this project are to:

- Convert an entire fleet of 35 class-1 electric lift trucks to hydrogen fuel cells at the FedEx Freight facility in Springfield, MO.
- Demonstrate the safe and reliable operation of hydrogen-fueled material handling equipment (MHE).
- Demonstrate the economic benefits of conversion to hydrogen fuel cell-powered MHE.
- Demonstrate operator acceptance of hydrogen fuel cell-powered MHE.
- Provide a cost-effective and reliable hydrogen fuel supply.
- Spur further lift truck fleet conversions to hydrogen fuel cells.
- Establish a proving ground for hydrogen fuel cell-powered MHE.

Relevance to the American Recovery and Reinvestment Act (ARRA) of 2009 Goals

This project advances the goals of the ARRA of 2009 to create new jobs, save existing jobs, and spur economic activity and investment in long-term economic growth by:

- Creating jobs at Plug Power to design, build and commission the fuel cell power units.
- Creating jobs at Air Products to design, install and commission hydrogen storage and fueling equipment.
- Creating jobs at Air Products to deliver hydrogen to the FedEx Freight Springfield, MO facility.
- Training FedEx Freight lift truck operators in hydrogen safety, fueling procedures and fuel cell operation.
- Training FedEx Freight lift truck maintenance personnel to service fuel cells.
- Improving the overall economic efficiency of material handling operations.

This project advances the DOE Fuel Cell Technologies' ARRA project goals of accelerating the commercialization and deployment of fuel cells and fuel cell manufacturing, installation, maintenance, and support services by demonstrating:

- Safe and reliable operation of hydrogen storage and fueling equipment and fuel delivery.
- Reliable and efficient operation of hydrogen fuel cells.
- Economic and environmental advantages of fuel cells over batteries.
- Practical operation and maintenance of fuel cells.

Technical Barriers

This project addresses the following technical barriers to the use of fuel cell powered lift trucks:

- Repair frequency of hydrogen fuel cells.
- Cold weather operation of hydrogen fuel cells.
- Cold weather operation of hydrogen storage and fueling equipment.

Technical Targets and Milestones

The technical targets and milestones of this project include:

- Installing hydrogen storage and fueling equipment by May 2010.
- Developing a hydrogen safety plan by May 2010.
- Commissioning 35 class-1 power units by December 2009.
- Completing startup and training by June 2010.
- Starting operation and evaluation by July 2010.

Accomplishments

The accomplishments of this project include:

- Commissioning 35 GenDrive class-1 power units by December 2009.

- Commissioning hydrogen storage and fueling equipment by June 2010.
- Completing all fueling, operation and maintenance training by June 2010.
- Purchasing and commissioning an additional five GenDrive class-1 power units in December 2010 (without DOE funding).
- Determining that problems with air-actuated valves during cold-weather operation of the hydrogen storage and fueling system were caused by excessive moisture in the air supply.
- Modifying lift trucks to prevent drive-offs that damaged the hydrogen fueling hose.
- Logging over 48,000 hours of fuel cell operation by the end of July.
- Purchasing 18,300 kilograms of hydrogen by the end of July.
- Monitoring operating costs and reliability of 40 GenDrive power units (ongoing).
- Demonstrating 30-60% more operating hours per repair for fuel cells compared to propane lift trucks between July 2010 and February 2011.



Introduction

The purpose of this project is to demonstrate that hydrogen fuel cells are a safe and economical alternative to batteries for powering electric lift trucks. The primary barriers to widespread use of hydrogen fuel cells for material handling equipment are concerns about the safety of hydrogen storage and fueling equipment, operating costs for fuel and maintenance, and the long-term reliability of fuel cells.

Approach

This project evaluates the safety and economics of using hydrogen fuel cells to power a fleet of 35 class-1 electric lift trucks at the FedEx Freight facility in Springfield, MO. FedEx Freight supplies the lift trucks, Plug Power supplies the GenDrive fuel cell power units and Air Products supplies the hydrogen fuel and the hydrogen storage and fueling equipment. The fuel cell equipment is maintained by FedEx Freight personnel with assistance from Plug Power and Air Products personnel when necessary. Plug Power and Air Products also assisted FedEx Freight in developing a comprehensive hydrogen safety plan.

Previous FedEx Freight field trials with a limited number of GenDrive power units demonstrated productivity gains and improved performance compared to battery-powered lift trucks. The lift truck fleet conversion in Springfield is expected to demonstrate improved operational efficiencies and help the environment by reducing greenhouse gas emissions and the use of toxic battery materials. A successful demonstration of these advantages at the Springfield facility could lead to additional fleet conversions at other FedEx Freight facilities.

The Hydrogen Safety plan has been completed and reviewed. The changes to the safety plan are in the process of being made.

The National Environmental Policy Act forms were submitted to the DOE. There are no outstanding National Environmental Policy Act requirements. The project was granted a categorical exclusion determination prior to the project commencing.

Results

To date, this project has successfully demonstrated the safe and economical operation of 40 GenDrive class-1 power units and associated hydrogen storage and fueling equipment. The power units have accumulated over 48,000 hours of operation and consumed 18,300 kilograms of hydrogen.

A few problems occurred during cold-weather operation. Problems with air-actuated valves in the hydrogen storage and fueling system were caused by excessive moisture in the air supply. Problems with the power units were resolved by adding thermal insulation to sensitive components.

Fueling hoses were damaged on two occasions when lift trucks were driven away from the fueling station while the fueling hoses were still attached to the lift truck. The lift trucks were subsequently modified to prevent them being driven while the fueling hoses were attached.

FedEx Freight found that the fuel cell-powered lift trucks at the Springfield facility had 63% more hours of operation per repair (115.2 hours/repair) compared to similar propane-powered lift trucks at the South Dallas facility (70.5 hours/repair) and 30% more hours of operation per repair compared to propane lift trucks at all FedEx Freight facilities (88.3 hour/repair).

Figure 1 shows a breakdown of the types of fuel cell repairs. Instrumentation and control (35%), cooling (16%), hydrogen (13%), and humidification (11%) systems accounted for 75% of all repairs. Figure 2 shows that 74% of all repairs required less than two hours of labor. Figure 3 shows that 35% of all fuel cell repairs to date have occurred during the first 100 hours of operation.

Based on the favorable operational results with the initial 35 power units, FedEx Freight purchased an additional five power units in December 2010 without DOE funding.

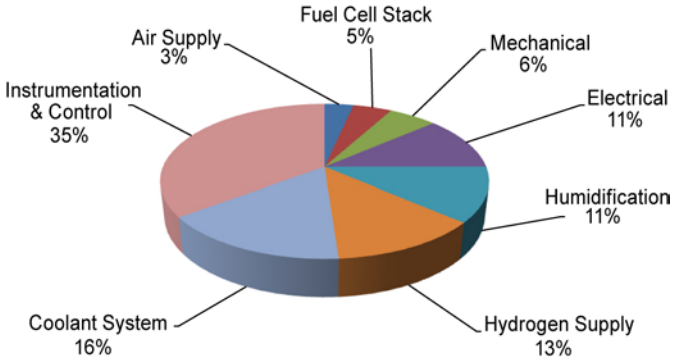


FIGURE 1. Types of Fuel Cell Repairs

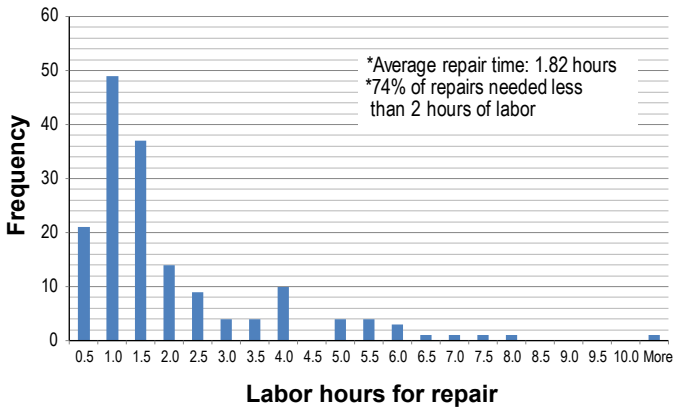


FIGURE 2. Labor Hours for Fuel Cell Repairs

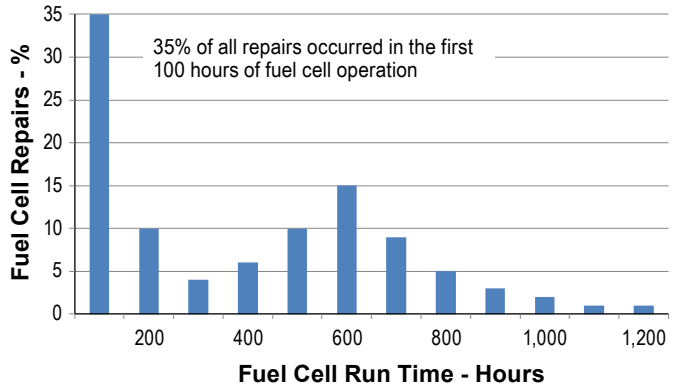


FIGURE 3. Fuel Cell Repair Frequency vs. Run Time

Conclusions and Future Directions

Based on our operational experience to date, hydrogen fuel cells appear to be a safe and economical alternative to batteries for electric lift trucks. We will continue to monitor the long-term costs and reliability of hydrogen fuel cells by:

- Providing ongoing operational and maintenance support for the GenDrive power units and the hydrogen storage and fueling equipment.
- Collecting data from the power units to evaluate performance, operability and safety.
- Collecting data from the hydrogen storage and fueling equipment to evaluate performance, operability and safety.
- Resolving cold-weather operation problems with air-actuated valves in the hydrogen storage and fueling equipment.
- Working with Plug Power to resolve cold-weather operation problems with fuel cells.

FY 2011 Publications/Presentations

1. Held an official ribbon-cutting ceremony in October 2010 to inaugurate the hydrogen fuel cell project at the FedEx Freight service center in Springfield, MO.

2. Delivered an American Recovery and Reinvestment Act merit review presentation in Washington, DC in May 2011.

3. Contributed a synopsis of project progress to the DOE's *Energy Empowers* blog.

XII.10 Fuel Cell-Powered Lift Truck Sysco Houston Fleet Deployment

Scott Kliever
Sysco Houston
10710 Greens Crossing Boulevard
Houston, TX 77038
Phone: (713) 679-5574
E-mail: kliever.scott@hou.sysco.com

DOE Managers
HQ: Dimitrios Papageorgopoulos
Phone: (202) 586-5463
E-mail: Dimitrios.Papageorgopoulos@ee.doe.gov
GO: David Peterson
Phone: (720) 356-1747
E-mail: David.Peterson@go.doe.gov

Contract Number: DE-EE0000485

Subcontractors:
- Plug Power Inc., Latham, NY
- Air Products and Chemicals, Inc., Allentown, PA
- Big-D Construction, Salt Lake City, UT

Project Start Date: October 1, 2009
Project End Date: September 30, 2013

Objectives

The objectives of this project are to:

- Convert a fleet of 79 class-3 electric lift trucks to hydrogen fuel cells at the Sysco Houston facility (including seven temporary rental units and 25 sub-zero temperature units).
- Demonstrate the safe and reliable operation of hydrogen-fueled material handling equipment (MHE).
- Demonstrate the economic benefits of conversion to hydrogen fuel cell-powered MHE.
- Demonstrate operator acceptance of hydrogen fuel cell-powered MHE.
- Demonstrate the operation of hydrogen fuel cells in sub-zero temperatures.
- Provide a cost-effective and reliable hydrogen fuel supply.
- Spur further lift truck fleet conversions to hydrogen fuel cells.
- Establish a proving ground for hydrogen fuel cell-powered MHE.

Relevance to the American Recovery and Reinvestment Act (ARRA) of 2009 Goals

This project advances the goals of the American Recovery and Reinvestment Act (ARRA) of 2009 to create new jobs, save existing jobs, and spur economic activity and investment in long-term economic growth by:

- Creating jobs at Plug Power to design, build and commission the fuel cell power units.
- Creating jobs at Air Products and Big-D Construction to design, install and commission hydrogen storage and fueling equipment.
- Creating jobs at Air Products to deliver hydrogen to the Sysco Houston facility.
- Training Sysco Houston lift truck operators in hydrogen safety, fueling procedures and fuel cell operation.
- Training Sysco Houston lift truck maintenance personnel to service fuel cells.
- Improving the overall economic efficiency of material handling operations.

This project advances the DOE-Fuel Cell Technologies' ARRA project goals of accelerating the commercialization and deployment of fuel cells and fuel cell manufacturing, installation, maintenance, and support services by demonstrating:

- Safe and reliable operation of hydrogen storage and fueling equipment and fuel delivery.
- Reliable and efficient operation of hydrogen fuel cells.
- Economic and environmental advantages of fuel cells over batteries.
- Practical operation and maintenance of fuel cells.

Technical Barriers

This project addresses the following technical barriers to the use of fuel cell-powered lift trucks:

- Safe and reliable hydrogen use in a high-throughput distribution center.
- Fuel cell use in sub-zero temperatures.
- Fuel cell lifetime and reliability.

Technical Targets and Milestones

The technical targets and milestones of this project include:

- Installing hydrogen storage and fueling equipment by December 2009.
- Developing a hydrogen safety plan by May 2010.

- Commissioning 79 class-3 power units by February 2010.
- Completing startup and training by February 2010.
- Starting operation and evaluation by March 2010.

Accomplishments

The accomplishments of this project include:

- Commissioning hydrogen storage and fueling equipment by December 2009.
- Commissioning 79 GenDrive class-3 power units by February 2010.
- Completing all fueling, operation and maintenance training by February 2010.
- Training over 100 Sysco personnel in the safe use and fueling of hydrogen fuel cells.
- Commissioning 26 GenDrive class-2 power units by April 2010 (these power units are not included in the scope of this project).
- Logging 12 months and over 300,000 hours of fuel cell operation by February 2011.
- Completing 31,000 fueling operations, consuming 38,760 pounds (17,618 kilograms) of hydrogen by February 2011.
- Demonstrating the successful operation of 25 class-3 power units in sub-zero temperatures.
- Monitoring operating costs and reliability of all GenDrive power units (ongoing).



Introduction

The purpose of this project is to demonstrate that hydrogen fuel cells are a safe and economical alternative to batteries for powering electric pallet jacks and lift trucks. The primary barriers to widespread use of hydrogen fuel cells for MHE are concerns about the safety of hydrogen storage and fueling equipment, operating costs for fuel and maintenance, and the long-term reliability of fuel cells.

Approach

This project will evaluate the safety and economics of using hydrogen fuel cells to power a fleet of 26 class-2 and 79 class-3 electric lift trucks at the Sysco Houston facility. Sysco Houston will supply the lift trucks, Plug Power will supply the GenDrive fuel cell power units, Air Products and Big-D Construction will supply the hydrogen storage and fueling equipment, and Air Products will supply the hydrogen fuel. The equipment will be maintained by Sysco Houston personnel with assistance from Plug Power and Air Products personnel when necessary. Plug Power and Air Products will also assist Sysco Houston in developing a comprehensive hydrogen safety plan.

Sysco Houston and Plug Power will monitor the operation and maintenance of the power units and the hydrogen storage and fueling equipment over the duration of the project. This information will be reported to the DOE and National Renewable Energy Laboratory quarterly and summarized annually.

Results

This project has successfully demonstrated the safe and economical operation of 26 class-2 and 72 class-3 power units and associated hydrogen storage and fueling equipment. The class-2 power units were not included in the funding for this project. Seven of the original 79 power units were rentals and have been returned to Plug Power. Twenty-five of the class-3 power units were modified to operate in sub-zero temperatures.

The fuel cell power units accumulated over 300,000 hours of operation and consumed 13,500 kilograms of hydrogen by February 2011. The current cost of hydrogen fuel is approximately the same as the cost of electricity to charge lead-acid batteries but Sysco is saving nearly $100,000 per year in fewer man-hours spent refueling fuel cells compared to swapping batteries. The lift truck operators also appreciate the improved performance of fuel cells compared to lead-acid batteries.

Sysco and Plug Power have been monitoring the type and frequency of fuel cell repairs. Figure 1 shows the distribution of repairs by class and Figure 2 shows the mean time between repairs (MTBR) distribution by class. To date, no conclusions have been drawn to explain the differences in repair statistics between the class-2 and class-3 power units. However, Sysco has changed the way they maintain pallet jack and lift truck power sources from reactive maintenance with lead-acid batteries to preventative maintenance with the hydrogen fuel cells.

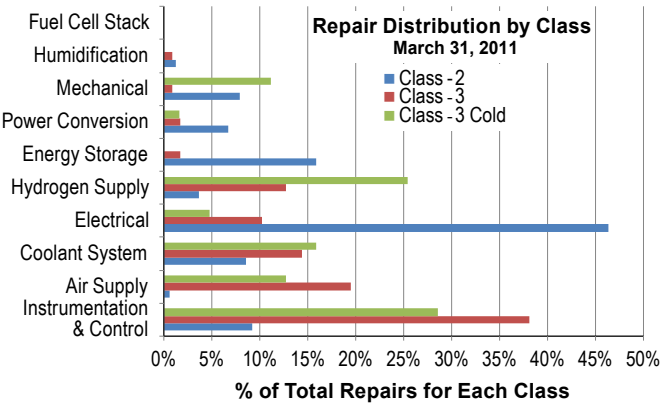


FIGURE 1. Repair Distribution by Class

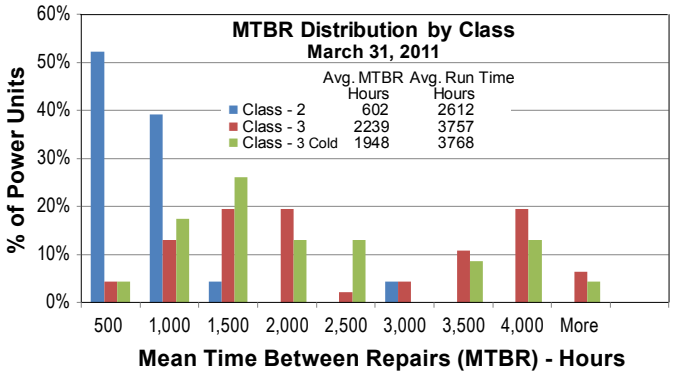


FIGURE 2. MTBR Distribution by Class

Conclusions and Future Directions

Based on the proven reliability and safety of current hydrogen fuel cell operations at Sysco Houston, Sysco's future directions include:

- Ongoing operational and maintenance support for power units and hydrogen storage and fueling equipment.
- Ongoing data collection from power units and hydrogen storage and fueling equipment.
- Planning to replace approximately 1,000 lead-acid batteries with 500+ fuel cells at seven additional sites over the next 24 months.
- Committed to fuel cell fleet conversions at Philadelphia, San Antonio, Long Island and Northeast Redistribution Center facilities.
- Considering additional fuel cell fleet conversions for Los Angeles, San Francisco, and Boston facilities.
- Supporting the conversion to fuel cells to help reduce the overall costs of fuel cell power units and hydrogen fuel.
- Helping other Sysco facilities develop hydrogen safety plans.

FY 2011 Publications/Presentations

1. Sysco hosted several open houses to showcase the fuel-cell-powered lift truck fleet, which subsequently became the subject of various local news articles and television news stories.

2. Scott Kliever delivered a presentation at the 2010 Fuel Cell Seminar and Exposition in San Antonio, TX, October 18–20, 2010.

3. Sysco and Plug Power prepared a case study of the Sysco Houston distribution center.

4. Scott Kliever was interviewed for the April 2011 cover story in *Materials Handling & Logistics* magazine titled *Making Sense of Power Sources*.

5. Scott Kliever delivered an American Recovery and Reinvestment Act merit review presentation in Washington, D.C. in May 2011.

6. Scott Kliever delivered a presentation at the Hydrogen + Fuel Cells 2011: International Conference and Exhibition, May 15–18, 2011, in Vancouver, BC, Canada.

XII.11 GENCO Fuel Cell-Powered Lift Truck Fleet Deployment

Jim Klingler
GENCO Infrastructure Solutions
100 Papercraft Park
Pittsburgh, PA 15238
Phone: (412) 820-3718
E-mail: klinglej@genco.com

DOE Managers
HQ: Sara Dillich
Phone: (202) 586-7925
E-mail: Sara.Dillich@ee.doe.gov
GO: James Alkire
Phone: (720) 356-1426
E-mail: James.Alkire@go.doe.gov

Contract Number: DE-EE0000483

Subcontractors:
- Plug Power Inc., Latham, NY
- Air Products, Allentown, PA
- Linde North America, Murray Hill, NJ

Project Start Date: October 1, 2009
Project End Date: September 30, 2013

Objectives

The objectives of this project are to:

- Convert 357 electric-drive fork lift trucks from batteries to fuel cell power units in five large distribution centers and manufacturing facilities.
- Demonstrate the safe and reliable operation of hydrogen-fueled material handling equipment (MHE).
- Demonstrate the economic benefits of conversion to hydrogen fuel cell-powered MHE.
- Demonstrate operator acceptance of hydrogen fuel cell-powered MHE.
- Provide a cost-effective and reliable hydrogen fuel supply.
- Spur further lift truck fleet conversions to hydrogen fuel cells.
- Establish a proving ground for hydrogen fuel cell-powered MHE.

Relevance to the American Recovery and Reinvestment Act (ARRA) of 2009 Goals

This project advances the goals of the American Recovery and Reinvestment Act (ARRA) of 2009 to create new jobs, save existing jobs, and spur economic activity and investment in long-term economic growth by:

- Creating jobs at Plug Power to design, build and commission the fuel cell power units.
- Creating jobs at Air Products and Linde to design, install and commission hydrogen storage and fueling equipment.
- Creating jobs at Air Products and Linde to deliver hydrogen to GENCO facilities.
- Training lift truck operators in hydrogen safety, fueling procedures and fuel cell operation.
- Training lift truck maintenance personnel to service fuel cells.
- Improving the overall economic efficiency of material handling operations.

This project advances the DOE Fuel Cell Technologies' ARRA project goals of accelerating the commercialization and deployment of fuel cells and fuel cell manufacturing, installation, maintenance, and support services by demonstrating:

- Safe and reliable operation of hydrogen storage and fueling equipment and fuel delivery.
- Reliable and efficient operation of hydrogen fuel cells.
- Economic and environmental advantages of fuel cells over batteries.
- Practical operation and maintenance of fuel cells.

Technical Barriers

This project addresses the following technical barriers to the use of fuel cell-powered lift trucks:

- Represents a change in technology, which is often met with reluctance.
- Uncertain power unit reliability due to lack of widespread performance data.
- Safety and expense of hydrogen and fueling equipment.
- Difficulty in obtaining permits and approvals for hydrogen fueling stations.

Technical Targets and Milestones

The class and number of power units and the hydrogen supplier for each GENCO location are shown in Table 1.

The status of project milestones for deploying fuel cell power units and hydrogen storage and fueling equipment are shown in Table 2.

TABLE 1. Power Unit Distribution and Hydrogen Suppliers

Power Unit	Wegmans Pottsville PA	Whole Foods Landover MD	Coca-Cola Charlotte NC	Sysco Philadelphia PA	Kimberly-Clark Graniteville SC	Total
Class-1	0	45	40	0	25	**110**
Class-2	36	14	0	25	0	**75**
Class-3	100	2	0	70	0	**172**
Total	**136**	**61**	**40**	**95**	**25**	**357**
Hydrogen Supplier	Air Products	Linde	Linde	Air Products	Air Products	

TABLE 2. Project Milestones (June 2011)

Milestone	Wegmans	Whole Foods	Coca-Cola	Sysco Philadelphia	Kimberly-Clark
Hydrogen storage and fueling equipment commissioned	Completed Jan 2010	Completed Jan 2011	Completed May 2011	Completed Apr 2011	Completed Dec 2010
Power units commissioned	49 of 136 completed Jan 2010, balance by Dec 2010	Completed Sep 2010	Completed Jan 2011	36 of 95 completed Mar 2011, balance by Apr 2012	Completed Dec 2010
Facility operational	Started Jan 2010	Started Jan 2011	Started May 2011	Started May 2011	Started Dec 2010
Project completed	Sep 2013	Sep 2013	Sep 2013	Sep 2013	Sep 2013

Accomplishments

The accomplishments of this project include:

- Commissioning hydrogen storage and fueling equipment at all sites (see Table 2 for completion dates).
- Commissioning power units at all sites (see Table 2 for completion dates).
- Completing fueling, operation and maintenance training at all sites.
- Operating power units at all sites (see Table 2 for starting dates).
- Some power units at Wegmans have accumulated over 5,000 hours of operation.



Introduction

The purpose of this project is to demonstrate that hydrogen fuel cells are a safe and economical alternative to lead-acid batteries for powering electric-drive lift trucks. The primary barriers to widespread use of hydrogen fuel cells for material handling equipment are concerns about the safety of hydrogen storage and fueling equipment, operating costs for fuel and maintenance, and the long-term reliability of fuel cells.

Approach

This project will evaluate the safety and economics of using hydrogen fuel cells to power over 350 lift trucks at five GENCO facilities. GENCO will supply the lift trucks, Plug Power will supply the GenDrive fuel cell power units, Air Products and Linde will supply the hydrogen storage and fueling equipment and the hydrogen fuel. The equipment will be maintained by GENCO personnel with assistance from Plug Power, Air Products and Linde personnel when necessary.

GENCO and the subcontractors will monitor the operation and maintenance of the power units and the hydrogen storage and fueling equipment over the duration of the project. This information will be reported to the DOE and National Renewable Energy Laboratory quarterly and summarized annually.

Results

This project has successfully demonstrated the safe and economical operation of 300 class 1, 2 and 3 fuel cell power units and associated hydrogen storage and fueling equipment at five GENCO facilities. An additional 57 power units will be added at the Sysco Philadelphia facility by April 2012.

Some of the fuel cell power units at the Wegmans facility have accumulated over 5,000 hours of operation. GENCO and Plug Power have been monitoring the type and

frequency of repairs on these power units. Figure 1 shows the repair frequency of these power units and Figure 2 shows the types of power unit repairs.

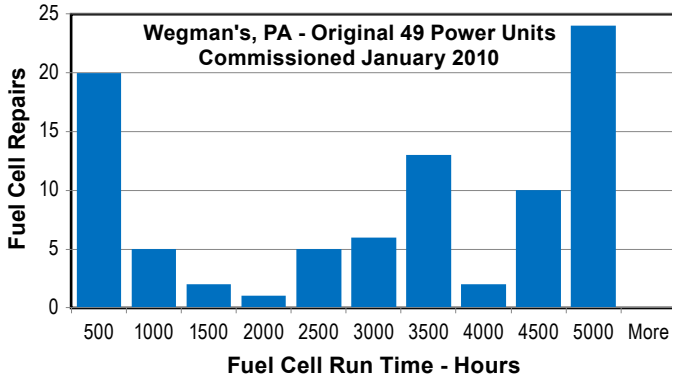


FIGURE 1. Fuel Cell Repair Frequency

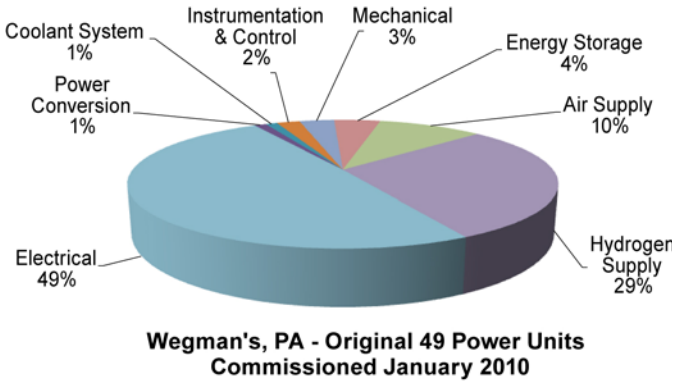


FIGURE 2. Types of Fuel Cell Repairs

Conclusions and Future Directions

Based on the proven reliability and safety of current hydrogen fuel cell operations at GENCO facilities to date, future directions include:

- Ongoing operational and maintenance support for power units and hydrogen storage and fueling equipment.
- Ongoing data collection from power units and hydrogen storage and fueling equipment.
- Helping to reduce the overall costs of fuel cell power units and hydrogen fuel by supporting the conversion to fuel cells at other locations.

Fiscal Year 2011 Publications/Presentations

1. Key federal and state government officials, leaders in sustainable energy solutions and executives from Kimberly-Clark, GENCO ATC, Plug Power and Air Products attended a ribbon-cutting ceremony and technology demonstration at the Kimberly-Clark site on February 11, 2011.

2. GENCO delivered an American Recovery and Reinvestment Act merit review presentation in Washington, DC in May 2011.

XII.12 Highly Efficient, 5 kW CHP Fuel Cells Demonstrating Durability and Economic Value in Residential and Light Commercial Applications

Donald Rohr
Plug Power, Inc.
968 Albany Shaker Road
Latham, NY 12110
Phone: (518) 738-0343
E-mail: Don_Rohr@plugpower.com

DOE Managers
HQ: Jason Marcinkoski
Phone: (202) 586-7566
E-mail: Jason.Marcinkoski@ee.doe.gov
GO: Reg Tyler
Phone: (720) 356-1805
E-mail: Reginald.Tyler@go.doe.gov

Contract Number: DE-EE0000480

Subcontractor:
University of California, Irvine (UCI), Irvine, CA

Project Start Date: October 1, 2009
Project End Date: September 30, 2012

Fiscal Year (FY) 2011 Objectives

- Demonstrate the durability and economic value of GenSys Blue.
- Verify its technology and commercial readiness for the marketplace.

Relevance to American Recovery and Reinvestment Act of 2009 and DOE Fuel Cell Technologies Goals

- The project deploys GenSys Blue, natural-gas fueled, micro-combined heat and power (µCHP) fuel cell units that provide economic savings and environmental benefits for residential and light commercial users.
- The project maintains five U.S., high-tech jobs in New York State and provides work for U.S. suppliers and field service contractors.

Technical Barriers

- **Durability**: Push system durability to commercially viable levels. Critical subsystems and components include stack, burner, reformer, pumps, air delivery module, and controls/software.
- **Cost**: Drive cost down through design simplification, low-cost manufacturing and supply chain.
- **Performance**: Improve system performance and efficiency so the device's value is observed by the customer.

FY 2011 Accomplishments

- Home site assessments were performed in California.
- Three systems shipped to UCI and infrastructure installed at UCI for site preparation.
- Stack life in Latham systems went from an average of 1,500 hours to 3,800 hours.



Introduction

The high-temperature proton exchange membrane (PEM) fuel cell system is the culmination of a nine-year technology development effort that has produced numerous technical innovations. Plug Power began exploring the application and feasibility of high-temperature PEM technology in 1999 with the creation of an "Alpha" system to demonstrate technical feasibility. It was quickly evident that the high-quality heat produced and the resulting system simplification would make this a preferred technology for µCHP applications–one that held the promise of a commercial, grid-connected, stationary fuel cell product that provided a cost benefit to the end user. Indeed, high-temperature PEM technology offers a unique value proposition over low-temperature PEM systems in applications where heat utilization is required. In a low-temperature system, the quality of the heat supplied may be insufficient to meet consumer needs and comfort requirements, so peak heaters or supplemental boilers may be required. The higher operating temperature of the polybenzimidazole (PBI) membrane technology allows the fuel cell to produce heat for applications that demand higher temperatures required to obtain desirable heat transfer rates without additional equipment.

GenSys Blue is a pre-commercial, 5 kW, natural gas-fueled product that is technically ready to be demonstrated in real-world residential and light commercial installations. The key risks for this technology lie in supply chain readiness and stack material supply. Further refinements in the areas of PBI technology, stacks, advanced controls, and fuel reforming will be made as Plug Power continues to understand technology development needs and product development requirements for this fuel cell system.

Approach

Plug Power is executing a demonstration project that will test multiple units of its high-temperature PEM fuel cell system in residential and light commercial µCHP applications in New York and California. The specific objective of the proposed demonstration project is to understand the durability of GenSys Blue, and thereby verify its path to technology and commercial readiness for the marketplace. In the proposed demonstration project, Plug Power, in partnership with the National Fuel Cell Research Center (NFCRC) at UCI, and Sempra, will execute two major tasks:

- **Task 1**: Internal durability/reliability fleet testing. Six GenSys Blue units will be built and will undergo an internal test regimen consisting of typical residential load profiles to estimate failure rates.
- **Task 2**: External customer testing. Four GenSys Blue units will be installed and tested in real-world residential and light commercial end-user locations in California. (Note: this task was to originally install six systems, but after discussions with DOE was reduced to four)

Results

Plug Power's employees are supporting this effort maintaining an internal and external reliability fleet of GenSys Blue natural gas power systems. Researchers at the NFCRC at UCI are also providing resources to test and understand this system. Commercial suppliers are delivering stack, reformer and balance-of-plant components.

The NFCRC at UCI continued its dynamic modeling efforts of the GenSys Blue system this year. The team has had very good success in modeling the individual subsystems and reactors. Modeling the complete system, however, has proven to be a very difficult task due to the numerical stiffness of the problem. These numerical difficulties arise because this system contains many thermal, energy, and material interconnections. Those interconnections cause the numerical problem to become large and its solution to become slow and unwieldy. The team is exploring methods to help speed up a solution.

Sempra Energy and members of the Plug Power team have begun to finalize the list of sites for the California fleet and have begun preliminary planning and design. The sites are evaluated based on ease of installation, match between customer load profile and system capability, ability to service a given customer site, flexibility of customer in the case of system outage, and anticipated value to the customer.

The team continued long-term reliability testing on the internal fleet installed in Plug Power labs (Figure 1). Table 1 shows that since commissioning in January 2010 the fleet has logged over 30,000 hours of stack operation producing over 50 MWhrs of electricity and 417 MWhrs of heat; averaging over 30% electrical efficiency and over 85% thermal efficiency. During this time the overall, uncorrected, CHP product availability of the fleet was 73%. This compares to 85% from last quarter and is the result of non-operating systems due to the discontinuity in stack material supply. The corrected CHP availability remains at approximately 91%.

In addition, three systems were installed in the NFCRC at UCI. A significant amount of infrastructure work was required to prepare the installation. The installation of heat rejection systems, wiring, piping, and exhaust ducts was completed recently. Plug Power completed two stacks in May 2011 and installed them in the systems in June 2011. The three units at UCI are now running; two systems are in CHP mode and one system is in heat-only operation until a stack is available for installation.

In the past year, the team has seen improvements in stack life. Plug Power has implemented some key advances in stack materials and assembly to more than double stack life. Stack life went from an average of 1,500 hours to 3,800 hours. One stack sample ran in system operation



FIGURE 1. Reliability Testing Fleet Plug Power (left) and UCI (right)

TABLE 1. GenSys Blue Reliability Fleet Statistics

HT GenSys Reliability Fleet Stats Through 4/18/2011 0:00								
System S/N	Commissioned Date	System Runtime (Hours)	Current Stack Runtime	Burner Runtime	Electrical kWh	Thermal kWh	Startup Reliability	CHP Operational A(t)
EpsilonPlus8	1/8/2010 14:50	7823	6058	6665	15247	71909	0.67	0.97
EpsilonPlus9	1/11/2010 15:14	4381	3802	5701	7349	60768	0.72	0.51
EpsilonPlus10	4/9/2010 8:55	1777	1777	4744	2520	60265	0.83	0.74
Foxtrot2	1/8/2010 14:59	7325	5256	6251	12769	90359	0.68	0.76
Foxtrot3	3/2/2010 10:47	5011	3098	6517	6679	74977	0.60	0.74
Foxtrot4	6/11/2010 14:45	3212	3212	5851	5948	59111	0.68	0.67
Totals	-	29530	23203	35729	50511	417389	-	-
Average	-	4922	3867	5955	8419	69565	0.70	0.73

for an excess of 6,000 hours. These improvements have been attributed to plate and membrane electrode assembly advances.

Figure 2 shows the breakdown in failure types within the Latham, NY fleet. Although stack life receives a lot of attention because of the cost, we have seen a higher frequency of nuisance failures in the thermal management module (TMM), air delivery module (ADM), and controls module (CM). These reliability issues are correctable and less costly than stack replacement but still need to be addressed in order to move toward commercial readiness.

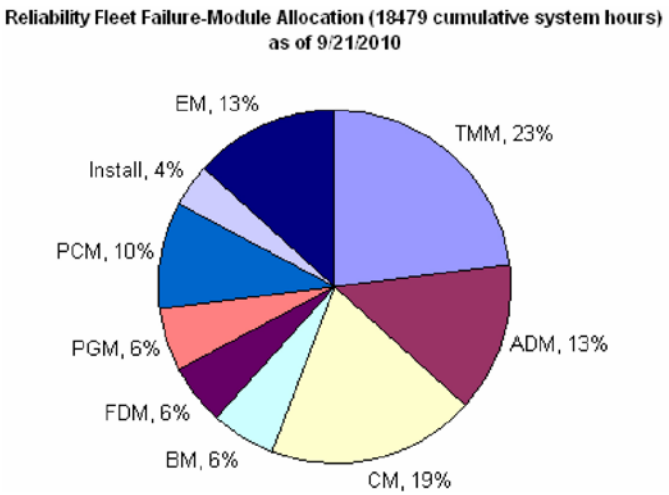


FIGURE 2. Fleet Failure Mode Allocation

Conclusions and Future Directions

The internal reliability fleet has continued to generate data during this past year. The California systems are just coming online and will help us understand the California requirements better. Availability of stack materials remains to be a pacing item and we continue to try to improve the external supply chain and internal manufacturing methods.

Continued progress will help us achieve the following milestones:

- Completion of the full system model by NFCRC.
- Ship and install remaining systems in California.
- Maintain the reliability fleet, capturing requirements from the California market.
- 2nd Go/No-Go decision.
- Perform economic analysis.

XII.13 Accelerating Acceptance of Fuel Cell Backup Power Systems

Donald F. Rohr
Plug Power, Inc.
968 Albany Shaker Road
Latham, NY 12110
Phone: (518) 738-0343
E-mail: Don_Rohr@plugpower.com

DOE Managers
HQ: Jason Marcinkoski
Phone: (202) 586-7466
E-mail: Jason.Marcinkoski @ee.doe.gov
GO: Reg Tyler
Phone: (720) 356-1805
E-mail: Reginald.Tyler@go.doe.gov

Contract Number: DE-EE0000488

Project Start Date: June 1, 2009
Project End Date: December 31, 2012

Objectives

- Increase distributed power generation.
- Improve reliability and efficiency of mission critical backup power.
- Decrease fossil fuel dependencies for power generation.

Relevance to American Recovery and Reinvestment Act of 2009 and DOE Fuel Cell Technology Goals

- Demonstrate market viability and increase pull of hydrogen and fuel cell systems within our government customers/partners.
- Deploy 20 GenSys hybrid, hydrogen start/liquefied petroleum gas (LPG) or natural gas units that provide economically viable backup power in excess of 72 hours.
- Maintain seven United States (U.S.), high-tech jobs in New York State and provide work for U.S. suppliers and field service contractors.

Accomplishments

- The Robins Air Force Base, Georgia has been developed through detailed engineering and is currently under construction.
- As of June 2011 several engineering and environmental buildings were assessed and considered to be in need of backup power at Ft. Irwin, California.



Introduction

Since 2001, Plug Power has installed more than 800 fuel cell systems worldwide. Plug Power's prime power systems have produced approximately 6.5 million kilowatt hours of electricity and have accumulated more than 2.5 million operating hours. Intermittent or backup power products have been deployed with telecommunications carriers, government and utility customers in North and South America, Europe, the United Kingdom, Japan and South Africa. The low-temperature GenSys fuel cell system provides remote, off-grid and primary power where grid power is unreliable or nonexistent. Built reliable and designed rugged, low-temperature GenSys delivers continuous or backup power through even the most extreme conditions (-5°C to 40°C, altitudes up to 1,000 m, and remote locations). Coupled with high-efficiency ratings (25%-30% depending on the operating point), low-temperature GenSys reduces operating costs making it an economical solution for prime power requirements. Field trials at telecommunication and industrial sites in India, U.S., Asia, and Europe have demonstrated the advantages of fuel cells–lower maintenance, fuel costs and emissions, as well as longer life–compared with traditional internal combustion engines.

Approach

This project will leverage technology from Plug Power's Gensys product line to create a reliable power source that starts fast and runs as long as fuel is available. The project tasks and status are shown below.

Cost Analysis and Commercialization Study	100% complete
Site Planning and Applications Engineering	50% complete
Site Specific Engineering Development	30% complete
System Builds and Factory Testing	90% complete
Field Deployment Go/No-Go	Post-installation
Fleet Operation and Managed Services	Not started
Project Closeout	Not started
Program Management	45% complete

For the past year Plug Power has collaborated with partners Army Construction Engineering Research Laboratory and Warner Robins Air Force Base to demonstrate technical viability and increase market pull of hydrogen fuel cell systems. To date, 45 percent of the project has been completed and barriers are actively being addressed, including: cost, system reliability and market volume.

Results

Approximately four of Plug Power's employees are supporting this effort to deploy 20 GenSys LPG-run units. Commercial suppliers are delivering stack, reformer and balance-of-plant components. In addition, Plug Power licensed this technology to IdaTech and Plug Power has proposed the use of IdaTech as a subcontractor for this project. Plans have been developed with IdaTech to provide resources for service, data analysis, and reliability assessment.

As of March 2011 Plug Power developed a detailed site plan for Robins Air Force Base in Warner Robins, Georgia. The Warner Robins Air Logistic Center is the proposed building site and the units will be backing up key lighting circuits in the building. The site plan includes power interconnect strategy, operational layout, and site construction plans. A contractor was identified in the second quarter of 2011 and was hired to install infrastructure for the 10 systems. Work has progressed quickly and the site will be ready for systems in July 2011. In parallel, Plug Power has been performing pre-commissioning tests on 10 systems to ensure acceptable quality and performance standards are met. Eight of the systems have completed pre-commissioning tests and the remaining two should be ready in time for installation in July.



FIGURE 1. Progress at Robbins Air Force Base: (Left) Final Cement Poured for Systems Pad, (Right) Conduit and Interconnection Wiring



FIGURE 2. Backup Power for Engineering Building and Telecom Center will be Proposed: (Left) Engineering Building, (Right) Telecommunication Room.

XIII. SMALL BUSINESS INNOVATION RESEARCH (SBIR) HYDROGEN PROGRAM NEW PROJECTS AWARDED IN FY 2011

XIII.0 Small Business Innovation Research (SBIR) Hydrogen Program New Projects Awarded in FY 2011

The Small Business Innovation Research (SBIR) program provides small businesses with opportunities to participate in DOE research activities by exploring new and innovative approaches to achieve research and development (R&D) objectives. The funds set aside for SBIR projects are used to support an annual competition for Phase I awards of up to $100,000 each for about nine months to explore the feasibility of innovative concepts. Phase II is the principal research or R&D effort, and these awards are up to $750,000 over a two-year period. Small Business Technology Transfer (STTR) projects include substantial (at least 30%) cooperative research collaboration between the small business and a non-profit research institution.

Table 1 lists the SBIR projects awarded in FY 2011 related to the Hydrogen and Fuel Cells Program. On this and the following page are brief descriptions of each.

TABLE 1. FY 2011 SBIR Projects Related to the Hydrogen and Fuel Cells Program

	Title	Company	City, State
XIII.1	Ultra-Lightweight High Pressure Hydrogen Fuel Tanks Reinforced with Carbon Nanotubes (Phase I Project)	Applied Nanotech, Inc.	Austin, TX
XIII.2	Alternative Fiber Evaluation and Optimization of Filament Winding Processing (Phase I Project)	Quantum Fuel Systems Technologies Worldwide, Inc.	Irvine, CA
XIII.3	New High Performance Water Vapor Membranes to Improve Fuel Cell Balance of Plant Efficiency and Lower Costs (Phase I Project)	Tetramer Technologies, LLC	Pendleton, SC
XIII.4	Fuel Cell Range Extender for Battery-Powered Airport Ground Support Equipment (Phase I Project)	Innovatek, Inc.	Richland, WA

PHASE I PROJECTS

XIII.1 Ultra-Lightweight High Pressure Hydrogen Fuel Tanks Reinforced with Carbon Nanotubes

Applied Nanotech, Inc.
3006 Longhorn Blvd.
Austin, TX 78758

One effective way to lower the weight, thus decreasing the carbon fiber usage and lowering the cost, of a carbon fiber reinforced plastic (CFRP) tank is to improve the mechanical properties of the CFRP composite resin matrix using nano-reinforcement. This project will reduce the cost of the carbon fiber by 30-40% by reducing the weight of the CFRP composite by 30-40% reinforced with carbon nanotubes used in the structure of the high-pressure hydrogen fuel tank, while maintaining or improving the performance of the tank at the regular weight while the fuel efficiency is significantly improved.

XIII.2 Alternative Fiber Evaluation and Optimization of Filament Winding Processing

Quantum Fuel Systems Technologies Worldwide, Inc.
17872 Cartwright Road
Irvine, CA 92614-6217

In an effort to improve emissions, reduce the carbon footprint and decrease the dependency on oil, this project will investigate alternative methods to lower the cost of hydrogen storage vessels.

XIII.3 New High Performance Water Vapor Membranes to Improve Fuel Cell Balance of Plant Efficiency and Lower Costs

Tetramer Technologies, LLC
657 South Mechanic Street
Pendleton, SC 29670-1808

This project will reduce the U.S. dependence on foreign oil and reduce hydrocarbon emissions, by lowering the cost of fuel cell technology for both stationary and transportation applications.

XIII.4 Fuel Cell Range Extender for Battery-Powered Airport Ground Support Equipment

Innovatek, Inc.
3100 George Washington Way, Suite 108
Richland, WA 99354-1663

InnovaTek will develop a fuel cell power system that operates on bio-jet fuel to facilitate the replacement of fossil fuels with renewable fuels for airport ground service equipment thereby improving environmental conditions at airports and their locals as well as improving energy security and sustainability for airport operations.

XIV. Acronyms, Abbreviations and Definitions

α-AlH_3	Alpha polymorph of aluminum hydride
~	Approximately
@	At
°C	Degrees Celsius
°F	Degrees Fahrenheit
Δ	Change, delta
ΔG	Gibbs free energy of reaction
ΔH	Enthalpy of reaction, Enthalpy of hydrogenation
$\Delta H°_f$	standard heat of formation
ΔK	Stress intensity factor
ΔP	Pressure drop, pressure change
$\approx$	Equals approximately
$>$	Greater than
$\geq$	Greater than or equal to
$<$	Less than
$\leq$	Less than or equal to
µCHX	Microscale combustor/heat exchanger
µc-Si	Microcrystalline silicon
µm	Micrometer(s), micron(s)
η	Viscosity
#	Number
Ω	Ohm(s)
Ω/cm^2	Ohm(s) per square centimeter
Ω-cm^2	Ohm-square centimeter
%	Percent
®	Registered trademark
$	United States dollars
^{11}B-NMR	Boron 11 Nuclear Magnetic Resonance
^{19}FNMR	^{19}Fluorine nuclear magnetic resonance
1-D, 1D	One-dimensional
1Q	First quarter of the fiscal year
2-D, 2D	Two-dimensional
2Q	Second quarter of the fiscal year
3-D, 3D	Three-dimensional
3Q	Third quarter of the fiscal year
4Q	Fourth quarter of the fiscal year
6FPAEB-BPS100	Hexafluoro bisphenol A benzonitrile-biphenyl sulfone
A	Ampere, amps
Å	Angstrom
AAO	Anodic aluminum oxide
AB	Ammonia-borane, NH_3BH_3
AC	Activated carbon
AC	Alternating current
ACF	Activated carbon fibers
A/cm^2	Amps per square centimeter
ACN	Acetonitrile
ACNT	Aligned carbon nanotube
AD	Anaerobic digestion
ADG	Anaerobic digester gas
ADM	Air delivery module
ADOPT	Automotive Deployment Option Projection Tool
A&E	Architecture and engineering
AEO	Annual Energy Outlook
AER	Absorption-enhanced reforming, all-electric range
AFM	Atomic force microscopy; anti-ferromagnetic
AFP	Automated fiber placement
AFV	Alternative fuel vehicle
Ag	Silver
AGC	Activated graphitic carbon
AgCl	Silver chloride
AGM	Absorbed glass mat
A-h	Amp-hour
AHJ	Authorities having jurisdiction
AIBN	Azobisisobutyl nitrile
AISI	American Iron & Steel Institute
Al	Aluminum
Al*	Aluminum particles catalyzed with titanium
Al_2O_3	Aluminum oxide
Al-AB	Aluminum-ammonia-borane
$AlCl_3$	Aluminum chloride
ALD	Atomic layer deposition
AlH_3	Aluminum hydride; alane
ALS	Advanced Light Source at Lawrence Berkeley National Laboratory
ALT	Accelerated life test
AM 1.5	Air Mass 1.5 solar illumination
AMBH	Ammine metal borohydride
AMFC	Anion exchange membrane fuel cell
AMR	Annual Merit Review
AMRL	Active magnetic regenerative liquefier
AMRR	Active magnetic regenerative refrigerator
ANL	Argonne National Laboratory
APC	Adaptive process control

APR	Aqueous-phase reforming
APU	Auxiliary power unit
Ar	Argon
ARB	Air Resources Board
ARET	Alternative and renewable energy technologies
ARRA	American Recovery and Reinvestment Act
As	Arsenic
ASAXS	Anomalous small-angle X-ray scattering
a-Si	Amorphous silicon
a-SiC	Amorphous silicon carbide
a-SiGe	Amorphous silicon germanium
a-SiN	Amorphous silicon nitride
ASME	American Society of Mechanical Engineers
ASPEN	Modeling software, computer code for process analysis
ASR	Area-specific resistance
AST	Accelerated stress test
ASTM	ASTM International, originally known as the American Society for Testing and Materials
AT	Ammonia triborane
at%	Atomic percent
ATG	Adenine,Thymine,Guanine, the 3 base combinations that indicate the first translatable amino acid on the DNA molecule
atm	Atmosphere
A-T-P	Aerosol through plasma
ATP	Adenosine triphosphate; Advanced Technology Program
ATPase	Adenosine triphosphatase
ATR	Autothermal reformer; autothermal reforming, attenuated total reflection
ATR-FTIR	Attenuated total reflectance Fourier transform infrared
ATRP	Atom transfer radical polymerization
a.u.	Arbitrary units
Au	Gold
Avg	Average
AZO	Aluminum zinc oxide
^{11}B-NMR	Boron 11 Nuclear Magnetic Resonance
B	Boron
B_2O_3	Boron oxide; diboron trioxide
Ba	Barium
barg	Bar gauge
BBC	4,4',4''-(benzene-1,3,5-triyl-tris(benzene-4,1-diyl))tribenzoate
BCC	Body-centered cubic
BCM	Battery-charging mode
BCN	Boron carbon nitride
Be	Beryllium
BE	Basic event
BET	Brunauer-Emmett-Teller surface area analysis method
BEV	Battery electric vehicle
BFZ1	$BaFe_{0.90}Zr_{0.10}O_3$
B-G	Boron doped graphitic material
B-H	Boron/hydrogen bond
B-H, BH	Borohydride
BH_4	Borohydride
Bi	Bismuth
BM	Ball-milled, ball mill
bmimCl	1-butyl-3-methyl-imidazolium chloride
BN	Boron-nitrogen
BNH	Boron-nitrogen-hydrogen
BNHx	Dehydrogenated ammonia-borane
BNL	Brookhaven National Laboratory
BOL	Beginning of life
BOM	Bill of materials
BOP, BoP	Balance of plant
BOT	Beginning of test
BPDC	Biphenyl-4,4'-dicarboxylate
BPS	Bi Phenyl Sulfone
BPSH	Block polysulfone ether polymers
BPV	Boiler and Pressure Vessel
Br	Bromine
Br_2	Diatomic bromine
BSC	Bi-electrode supported cell
BTE	4,4',4''-(benzene-1,3,5-triyltris(ethyne-2,1-diyl))tribenzoate
BTTCD	Octa-carboxylate ligand
BTU, Btu	British thermal unit(s)
C	Carbon
C	Couloumb
C_2H_4	Ethylene
C_2H_6	Ethane
C_3H_8	Propane
Ca	Calcium
CA	Carbon aerogel
CAD	Computer-aided design
CAE	Computer-assisted engineering
CAES	Compressed air energy storage
CaFCP	California Fuel Cell Partnership
CAFE	Corporate Average Fuel Economy

CaI	*Clostridium acetobutylicum* hydrogenase
CaO	Calcium oxide
CARB	California Air Resources Board
CaS	Calcium sulfide
CB	Conduction band
CBM	Conduction band minimum
CBN	Carbon-boron-nitrogen
CBS	Casa Bonita strain, complete basis set
cc	Cubic centimeter(s)
CC	Crossover current
CCC	Carbon composite catalyst
CCD	Charge-coupled device
CCD	Catalytic cracking deposition
cc/g cat/hr	Cubic centimeter(s) per gram catalyst per hour
CcH2	Cryo-compressed hydrogen
CCM	Catalyst-coated membrane; coordinate measuring machine
Cc/min, ccm	Cubic centimeters per minute
ccp	Cubic close-packing
CCP	Combined cooling and power
CCS	Carbon capture and storage
CCVJ	9-([E]-2-carboxy-2-cyanovinyl)julolidine
Cd	Cadmium
CD	Compact disk, charge depleting, cathode dewpoint
CDC	Carbide-derived carbon
cDNA	Complementary DNA
CDO	Code development organization
CDP	Composite data product
CdS	Cadmium sulfide
Ce	Cerium
CE	Cluster Expansion
CEA	Commissariat à l'Energie Atomique
CEC	California Energy Commission
CEM	Compressor/expander motor
CEMG	Compressor expander motor-generator module
CEMM	Compressor-expander motor module
CeO_2	Ceric oxide
CEPCI	Chemical Engineering's Plant Cost Index
CF	Carbon fiber, carbon foam
CFD	Computational fluid dynamics
cfm	Cubic feet per minute
CFP	Carbon fiber paper
CFRP	Carbon fiber reinforced plastic
CGH2	Compressed gaseous hydrogen
CGO	Cerium gadolinium oxide, Gd-doped CeO_2
CGS	Copper gallium diselenide, $CuGaSe_2$
CGSe	Copper gallium diselenide
$CGSe_2$	Copper gallium diselenide
CH	Hydrogenated graphene
cH_2	Compressed hydrogen gas
CH_4	Methane
CHARM	Cost-effective High-efficiency Advanced Reforming Module
CHHP	Combined heat, hydrogen, and power
Chl	Chlorophyll
CHMC	Compressed Hydrogen Materials Compatibility
CHP	Combined heat and power
CHPFC	Combined heat and power fuel cell
CHS	Chemical hydrogen storage
CHSCoE	Chemical Hydrogen Storage Center of Excellence
CIGSe	Copper indium gallium diselenide
$CIGSe_2$	Copper indium gallium diselenide
CIS	CuInSe (alloy of copper, indium, and selenium)
Cl	Chlorine
CL	Catalyst layer
cm	Centimeter
CM	Controls module
cm^2	Square centimeter
CMM	Coordinate measuring machine
CMO	Conductive metal oxides
CMR	Composite membrane reactor
CMWNT	Carbon multi-walled nanotube
CN	Carbon-nitrogen
CNF	Carbon nano-fiber
CNG	Compressed natural gas
CNO	Cesium niobate
CNP	Combinatorial nanoparticle
CNT	Carbon nanotube
Co	Cobalt
CO	Carbon monoxide
CO_2	Carbon dioxide
CoE	Center of Excellence
COE	Cost of electricity
COF	Covalent-organic framework
COF_2	Carbonyl fluoride
COPV	Composite overwrapped pressure vessel
COS	Carbon oxysulfide; carbonyl sulfide
c_p	Specific heat

CpI	*Clostridium pasteurianum* [FeFe]- hydrogenase
CPO, CPOX	Catalytic partial oxidation
CPV	Composite pressure vessel
Cr	Chromium
CR	Compression ratio
CRADA	Cooperative Research and Development Agreement
Cs	Cesium
CS	Ceramic support
C&S	Codes and standards
CSA	Canadian Standards Association
CSA	Cell stack assembly
CSTT	Codes and Standards Tech Team
CSU	California State University
CTAB	Cetyl trimethyl ammonium bromide
CTE	Coefficient of thermal expansion
CTTRANSIT	Connecticut Transit
Cu	Copper
CU	University of Colorado
Cu_2O	Cuprous oxide
cu in.	Cubic inch
CuO	Cupric oxide, copper(II) oxide
cu.yd.	Cubic yard(s)
CV	Cyclic voltammatry; cyclic voltammogram
CVD	Chemical vapor deposition
CVM	Cell voltage monitor
CWRU	Case Western Reserve University
CY	Calendar year
CZO	Ceria-zirconia
d	Day(s)
D_2	Deuterium
D-A	Dubinin-Astakhov
DB	Diborane (B_2H_6)
dB(A)	Decibel(s) A scale
DBBPDSA	4, 4'-dibromobiphenyl 3, 3'-dislufonic acid, monomer
DBPDSA	1, 4-dibromo phenylene 2, 5-disulfonic acid
DC	Direct current
DCHX	Direct contact heat exchanger
DCTDD	1,8-diazacyclotetradecane-2,7-dione
DDGS	Distiller's dried grains
DDMEFC	Direct dimethyl ether fuel cell
DDP	Detailed Data Products
d_{DR}	Dubini-Radushkevich average micropore diameter
DDR	A zeolite structure code
DEDP	Distance Education Degree Program
Deg	Degree
DEGDBE	Diethylene glycol dibutyl ether
ΔB_a	The difference in magnetic induction at high and low applied magnetic fields
ΔG	Gibbs free energy of reaction
ΔH	Enthalpy of reaction, Enthalpy of hydrogenation
ΔH°_f	standard heat of formation
ΔK	Stress intensity factor
ΔP	Pressure drop, pressure change
DFC	Direct fuel cell
DFM	Design for manufacturing
DFMA®	Design for Manufacturing and Assembly
DFT	Density functional theory
DI	Deionized, de-ionized water
DLA	Defense Logistics Agency
DLC	Diamondlike carbon
dL/g	Deciliters per gram
DLS	Dynamic light scattering
DM	Diffusion media
DMC	Diffusion Monte Carlo, direct manufactured cost
DME	Dimethyl ether, dimethoxyethane
DMEA	Dimethlethylamine
DMEAA	Dimethlethylamine alane
DMF	n, n-di-methyl formamide
DMFC	Direct methanol fuel cell
DNA	Deoxyribonucleic acid
DNG	Desulfurized natural gas
DOD	Depth of discharge
DOD	U.S. Department of Defense
DOE	U.S. Department of Energy
DOT	Department of Transportation
DOT/NHTSA	Department of Transportation/National Highway Traffic Safety Administration
DP	Dew point
DP4	Design Prototype 4
DRIFTs	Diffuse reflectance infrared Fourier transform spectroscopy
DSC	Differential scanning calorimetry; dynamic scanning calorimetry
DSM™	Dimensionally stable membrane
DTA	Differential thermal analysis
DVD	Digital video disk
e^-	Electron
E	Activation energy, kJ/mol
E85	85%-15% blend of ethanol with gasoline

Ea	Activation energy
E_{ad}	Hydrogen adsorption heat
EC	Electrochemical capacitance
ECA	Electro-catalytic additive
ECA	Electrochemical area
ECA	Estimated surface area
ECSA	Electrochemically active surface area, Electrochemical surface area
ECST	College of Engineering, Computer Science and Technology
EDA	Ethylene diamine
EDAX	Manufacturer of energy dispersive X-ray hardware and software
EDS	Energy dispersive X-ray spectroscopy, energy dispersive spectrum
EDTA	Ethylenediamine tetraacetic acid
EDX	Energy dispersive X-ray
EECBG	Energy Efficiency and Conservation Block Grant
EELS	Electron energy loss spectroscopy
EER	Miles per unit energy of hydrogen used in a FCV/miles per unit energy of gasoline used in an ICEV
EERE	U.S. DOE Office of Energy Efficiency and Renewable Energy
EFC	Energy flow chart
EFP	External fuel processor
EFTE	Ethylene-tetrafluoroethylene
EHC	Electrochemical hydrogen compressor
EHS	Environmental Health and Safety
EIA	Energy Information Administration of the U.S. Department of Energy
EIS	Electrochemical impedance spectroscopy
EISA	Evaporation induced self assembly
e.g.	*Exempli gratia*: for example
ELAT®	Registered Trademark of De Nora North America, Inc., covers GDLs and GDEs
EMF	Electromagnetic field
EMPA	Electron microprobe
EMTEC	Edison Materials Technology Center
ENG	Expanded natural graphite
eNMR	Electrochemical nuclear magnetic resonance
EOL	End of life
EOT	End of test
EPA	U.S. Environmental Protection Agency
EPRI	Electric Power Research Institute
ePTFE	Expanded polytetrafluoroethylene
ERW	Electric resistance weld
ES	Energy storage
ESA	Electrochemically active surface area
et al.	*Et Alii*: and others
etc.	*Et cetera*: and so on
E-TEK	Division of De Nora North America, Inc.
ETFE	Ethylene-tetrafluoroethylene
ETFECS	Extended thin film electrocatalyst structures
EtOH	Ethanol
eV	Electron volt
EVOH	Ethylene vinyl alcohol
EW	Enthalpy wheel
EW	Equivalent weight
EWH	Enthalpy wheel humidifier
EXAFS	Extended X-ray absorption fine structure analysis
F	Fluorine
F	Faraday constant, the amount of electric charge in one mole of electrons (96,485.3383 coulomb/mole)
F^-	Fluorine ion
FA	Furfyl alcohol
FAT	Fleet Analysis Toolkit; factory acceptance test
FC	Fuel cell
FCB	Fuel cell bus
FCC	Face-centered cubic; Fuel Cell Catalyst
FCE	FuelCell Energy
F-Cell	Daimler Fuel Cell vehicle
FCEV	Fuel cell electric vehicle
FCFP	FreedomCAR and Fuel Partnership
FCHEA	Fuel Cell Hydrogen Energy Association
FCPP	Fuel cell power plant
FCS	Fuel cell system
FCT	Fuel Cell Technologies
$FCTES^{QA}$	Fuel Cell Testing, Safety and Quality Assurance (an international effort to harmonize fuel cell testing procedures)
FCTESTNET	Fuel Cell Testing and Standardization Network
FCTT	Fuel Cell Technical Team
FCV	Fuel cell vehicle
Fd	Ferredoxin
Fe	Iron
Fe_2O_3	Ferric oxide
FEA	Finite element analysis
FEM	Finite element model
FEP	Fluorinated ethylene propylene; Teflon®
FESEM	Field emission scanning electron microscope

FF	Flammability factor
FFT	Fast fourier transform
FHI	Florida Hydrogen Initiative
FHWA	Federal Highway Administration
FIB	Focused ion beam
FIT	Florida Institute of Technology
FLUENT	Computer code for computational fluid dynamics
FMEA	Failure modes and effects analysis
FOM	Federated object model
FOM	Figure of merit
fpi	Fins per inch
fpm	Feet per minute
FPS	Bis(4-fluorophenyl)sulfone, Fuel processing system
FRP	Fiber-reinforced composite piping; fiber-reinforced polymer
FRR	Fluoride release rate
FSEC	Florida Solar Energy Center
F-SPEEK	Fluorosulfonic acid of polyetheretherketone
FSW	Friction stir welding
ft	Feet
FT	Fault tree
ft^2	Square feet
ft^3	Cubic feet
FTA	Federal Transit Administration
FT-IR, FTIR	Fourier transform infrared
FTIR-ATR	Fourier transform infrared attenuated total reflection
FTO	Fluorine-doped tin oxide
FTP, FTP-75	Federal Test Procedure
FW	Formula weight
FW	Filament winding
FY	Fiscal year
g	Gram; acceleration of gravity
G	Graphite
Ga	Gallium
GaAs	Gallium arsenic
gal	Gallon
GaP	Gallium phosphide
GB	Gigabyte
GC	Gas chromatograph; general computational
GC	Glassy, or vitreous carbon; a pure carbon that is amorphous (non- crystalline)
g/cc	Grams per cubic centimeter
GCLP	Grand-canonical linear programming
GCMC	Grand Canonical Monte Carlo
GC-MS	Gas chromatograph-mass spectroscopy
GCNT	Graphitized carbon nanotubes
GCtool	Software package developed at ANL for analysis of fuel cells and other power systems
Gd	Gadolinium
GDC	Gadolinium-doped ceria
GDE	Gas diffusion electrode
GDL	Gas diffusion layer
GDM	Gas diffusion media
Ge	Germanium
Gen I	First generation
GES	Giner Electrochemical Systems, LLC
GF	Glass fiber
GFC	Gas flow channel
GGA	Generalized gradient approximation
GGE, gge	Gasoline gallon equivalent
GH_2	Gaseous hydrogen
GHG	Greenhouse gas
GHSV	Gas hourly space velocity
GIS	Geographic information system
GJ	Gigajoule(s)
g/kW	Gram(s) per kilowatt
GLACD	Glancing angle co-deposition
GLAD	Glancing angle deposition
GLY	Glycerol
Glyme	Dimethoxyethane
gm	Gram(s)
GM	General Motors
gm/day	Gram(s) per day
g/min	Gram(s) per minute
GNF	Graphite nanofiber
GPa	Gigapascal(s)
GREET	Greenhouse gases, Regulated Emissions and Energy use in Transportation model
g/s	Grams per second
GSE	Ground support equipment
GTI	Gas Technology Institute
GTR	Global Technical Regulations
GUI	Graphical user interface
GWe	Gigawatt(s) electric
h	Hour(s)
H	Hydrogen
H+	Proton
H^-	Hydride
H_2	Diatomic hydrogen
H2A	Hydrogen Analysis project sponsored by DOE

H2-ICE, H_2 ICE	Hydrogen internal combustion engine
H_2O	Water
H_2O_2	Hydrogen peroxide
H2QWG	DOE Hydrogen Quality Working Group
H_2S	Hydrogen sulfide
H_2SO_4	Sulfuric acid
H_3PO_4	Phosphoric acid
HAADF	High-angle annular dark-field
HAADF-STEM	High angle annular dark field scanning transmission electron microscopy
HAMMER	Hazardous Materials Management and Emergency Response
HAVO	Hawaii Volcanoes National Park
HAZ	Heat affected zone
HAZID	Hazard Identification Analysis
HAZOP	Hazards and Operational Safety Analysis, hazards and operability analysis
HBP	Hyperbranched polymer
HBr	Hydrogen bromide
HCC	Hybrid cathode catalyst
HCl, HCL	Hydrochloric acid, Hydrogen chloride
$HClO_4$	Perchloric acid
HCN	Hydrogen coordination number
hcp	Hexagonal close-packing
HDPE	High-density polyethylene
HDSAM	Hydrogen Delivery Scenario Analysis Model
He	Helium
HE	Hydrogen embrittlement
H-E-B	H-E-B Grocery Company, Inc.
HEPA	High efficiency particulate air filter
HER	Hydrogen evolution reaction
HEV	Hybrid electric vehicle
HEX	Heat exchanger
Hf	Hafnium
HF	Hydrogen Fueler
HF	Hydrofluorhydric acid, hydrogen fluoride, Hartree Fock
HFB	Hexafluorobenzene
HFC	Hydrogen fuel cell
HFCIT	Hydrogen, Fuel Cells and Infrastructure Technologies Program
HFCT	Hydrogen and fuel cell technology
HFCV	Hydrogen fuel cell vehicle
HFI	Hydrogen Fuel Initiative
HFP	Hexafluoropropylene
HFR	High-frequency resistance
HFV	Hydrogen-fueled vehicle
HHV	Higher heating value
HI	Hydrogen iodide, hydriodic acid
HIA	Hydrogen-induced amorphization, Hydrogen Implementing Agreement
HICE	Hydrogen internal combuation engine
HIx	Blend of hydrogen iodide, iodine, and water
HLA	High level architecture
HMC	Hyundai Motor Company
HMM	Hydrogen Market Model
HNEI	Hawaii Natural Energy Institute
HNO_3	Nitric acid
HOPG	Highly-ordered pyrolytic graphite
HOR	Hydrogen oxidation reaction
hp	Horsepower
HP	High-pressure
HPA	Heteropoly acid
HPIT	Hydrogen Powered Industrial Truck
HPLC	High performance liquid chromatography
HPPH	1,6-di(4-hydroxyl)phenylperfluorohexane
HPPS	*N,N*-diisopropylethylammonium 2,2-bis(*p*-hydroxyphenyl) pentafluoropropanesulfonate
HPR	Hydrogen production rate
HPRD	Hydrogen pressure relief device
hr	Hour(s)
HRA	Home refueling appliance
HRT	Hydraulic retention times
HRTEM	High-resolution transmission electron microscopy
HSC	Database name derived from the letters for enthalpy, entropy and heat capacity
HSCoE	Hydrogen Sorption Center of Excellence
HSDC	Hydrogen Secure Data Center
HSE	High surface area electrode
HSECoE	Hydrogen Storage Engineering Center of Excellence
HSM	Hydrogen storage module
HSMCoE	Hydrogen Storage Material Center of Excellence
HSO_4	Bisulfate anion
HSP	Hydrogen safety plan
HSS	Hierarchically structured silica
HSSIM	Hydrogen Storage SIMulator
HSU	Humboldt State University
HTAC	Hydrogen and Fuel Cell Technical Advisory Committee
HTC	High temperature coolant
HTE	High-temperature electrolysis

HTF	Heat transfer fluid, Hydrogen test fixture
HTFSA	Trifluomethylsulfonic acid
HTM	High-temperature membrane
HTM	Hydrogen transport membrane
HTMWG	High Temperature Membrane Working Group
HTWGS	High-temperature water-gas shift
HVAC	Heating, ventilation and cooling
HWD	Hot wire deposition
HWFET	Highway Fuel Economy Test
HX	Heat exchanger
HyDRA	Hydrogen Demand and Resource Analysis
HYPER	HYdrogen PERmitting
HyPro, HYPRO	Analysis tool
HyS	Hybrid sulfur
HYSYS®	Process simulation software by Aspentech, computer code for flowsheet analysis
HyTEC	Hydrogen Technology and Energy Curriculum
HyTEx	Hydrogen Technical Experimental (database)
HyTRANS	DOE's market simulation model for the transition to hydrogen vehicles
Hz	Hertz
HZM	Hot zone module
i	Current density (mA/cm^2)
I	Current
I_2	Diatomic iodine
IC	Internal combustion
ICC	International Code Council
ICE	Internal combustion engine
ICEV	Internal combustion engine vehicle
ICP	Inductively coupled plasma
ICPME	Institut de Chimie et des Matériaux
ICP-MS	Inductively coupled plasma mass spectrometry
ICR	Interfacial contact resistance
ID	Inside diameter
i.e.	*id est*: that is
IEA	International Energy Agency
IEA-HIA	International Energy Agency Hydrogen Implementing Agreement
IEC	Ion exchange capacity; milliequivalents of acid groups per gram of material
IFC	International Fire Code
IFE	In-flight entertainment
IGCC	Integrated gasification combined cycle
IGCC-CMR	Integrated gasification combined cycle-catalytic membrane reactor
IGCC-MR	Integrated gasification combined cycle-membrane reactor
IGCC-PBR	Integrated gasification combined cycle-paladium-based reactor
IGT	Institute of Gas Technology
IHPV	Internally heated high-pressure vessel
IL	Illinois
IL	Ionic liquid
ILS	Integrated laboratory scale, Instrument landing systems
IML	Inner mold line
In	Indium
In., in	Inch
in^2	Square inch
INER	Institute of Nuclear Energy Research
InP	Indium phosphorus
INS	Inelastic neutron scattering
IOS	Intelligent Optical Systems, Inc.
IP	Induction period
IP	Intellectual property
IPA	Isopthalate
IPA	Isopropyl alcohol
IPCC	Intergovernmental Panel on Climate Change
IPES	Inverse photoemission spectroscopy
IPHE	International Partnership for the Hydrogen Economy
IR	Infrared
iR	Internal resistance; voltage loss due to resistance
Ir	Iridium
IR/DC	Infrared diagnostic system with direct current excitation
IRMOF	Isoreticular metal organic framework
IrO_x	Iridium oxide
ISO	International Organization for Standardization
ISS	Ion scattering spectroscopy
ITM	Ion transport membrane
ITO	Indium tin oxide
ITP	Indium tin phosphate
IV	Current-voltage
J	Current
J	Hydrogen flux through the membrane, $ml/[cm^2\text{-}min]$
J	Joule(s)
JFK	John F. Kennedy (airport)

JM	Johnson Matthey
JMFC	Johnson-Matthey Fuel Cells, Inc.
JPL	Jet Propulsion Laboratory
JRC	Joint Research Centre
J-V	Current density-voltage
K	Sievert's constant, ml/[cm2-min-atm½]
K	Kelvin, absolute temperature
K	Potassium
kÅ	1000 angstroms
kA/m^2	Kilo-ampere(s) per square meter
kb	Kilo-base pair, a unit of measurement used in genetics equal to 1,000 nucleotides
KBr	Potassium bromide
kcal	Kilocalorie(s)
kcal/mol	Kilocalorie(s) per mole
KeV	Kilo electron volt(s)
kg	Kilogram(s)
kg/d	Kilogram(s) per day
kg/hr	Kilogram(s) per hour
kg/m^3	Kilogram(s) per cubic meter
KH	Potassium hydride
kHz	Kilohertz
K_{IH}	Fracture toughness measured in hydrogen gas
kJ	Kilojoule(s)
K_{JIC}	Fracture toughness
kJ/mol	Kilojoule(s) per mole
km	Kilometer(s)
KMC	Kinetic Monte Carlo, Kilauea Military Camp, Kia Motors Corporation
KOH	Potassium hydroxide
kPa	Kilopascal(s)
kph	Kilometer(s) per hour
Kth, K_{th}	Fracture toughness threshold
K_{TH}	Hydrogen-assisted crack growth threshold
kW	Kilowatt(s)
kW_e	Kilowatt(s) electric
kWh	Kilowatt-hour(s)
kWh/kg	Kilowatt-hour(s) per kilogram
kWh/L	Kilowatt-hour(s) per liter
kW/kg	Kilowatt(s) per kilogram
kWt	Kilowatt(s) thermal
L, l	Liter(s)
La	Lanthanum
LAGP	Lithium aluminum germanium phosphate
λ	Lambda, hydration number
LAMH	Lithium amide and magnesium hydride
LANL	Los Alamos National Laboratory
LAO	Lanthanum-modified alumina
LAX	Los Angeles International Airport
lb	Pound(s)
LBM	Lattice Boltzmann method
lbmol	Pound-mole(s)
LBNL	Lawrence Berkeley National Laboratory
LC	Liquid carrier
LCA	Life cycle assessment; life-cycle analysis
LCC	Life cycle cost
LCC	$La_{0.7}Ca_{0.3}CrO_{3-\delta}$
LCH_2	Hydrogenated liquid carrier; compressed hydrogen produced from liquid hydrogen
LCH_2	Liquid to compressed hydrogen
LC-MS	Liquid chromatography-mass spectroscopy
L/D	Length to diameter ratio
LDPE	Low density poly-ethylene
LDV	Light-duty vehicle
LED	Light emitting diode
LEF	linear electron transfer
LEL	Lower explosion limit
LFG	Landfill gas
LFL	Lower flammability limit
L/h, l/h	Liter(s) per hour
LH2, LH_2	Liquid hydrogen
LHC	Light-harvesting chlorophyll
LHS	Lawrence Hall of Science
LHSV	Liquid hourly space velocity, h^{-1}
LHV	Lower heating value
Li	Lithium
Li_3N	Lithium nitride
Li-AB	Lithium amidoborane, Li-NH_2-BH_3
$LiBH_4$	Lithium borohydride
LIBS	Laser-induced breakdown spectroscopy
LiH	Lithium hydride
LIM	Liquid injection molding, liquid injection moldable
LLC	Limited Liability Company
LLC	Lessons Learned Corner
LLNL	Lawrence Livermore National Laboratory
LMWO	Lanthanum molybdenum tungsten oxide (*e.g.*, $La_2Mo_{1.8}W_{0.2}O_{9-x}$)
L/min, l/min	Liter(s) per minute
LN_2	Liquid nitrogen
LNG	Liquefied natural gas
LOD	Limit of detection
LP	Lattice parameter

LPG	Liquefied petroleum gas
LPM	Liters per minute
LPR	Liquid-phase reforming
LQ*	Dehydrogenated liquid carrier
LQ*H2	Hydrogenated liquid carrier
LRS	Laser raman spectroscopy
LSAC	Low surface area carbon
LSC	Lanthanum strontium cobalt oxide, (La, Sr) CoO_3, strontium-doped lanthanum cobaltite, $La_{0.8}Sr_{0.2}CoO_{3+\delta}$
LSCF	Lanthanum strontium cobalt iron oxide, (La, Sr)(Co, Fe)O_3
LSCM	Lanthanum strontium chromium manganese oxide, (La, Sr)(Cr, Mn)O_3
LSCr	Lanthanum strontium chromium oxide, (La, Sr)CrO_3
LSL	Lower specification limit
LSM	Lanthanum strontium manganese
LSMO	Lanthanum strontium manganese oxide, (La, Sr)MnO_3, strontium-doped lanthanum manganite, $La_{0.8}Sr_{0.2}MnO_{3+\delta}$
LST	Lanthanum strontium titanium oxide, (La, Sr)TiO_3
LSV	Lanthanum strontium vanadate, Linear sweep voltammetry
LT	Low-temperature
LTC	Low temperature coolant
m	Meter(s)
M	Mole, molar
M	Million
m^2	Square meter(s)
m^2/g	Square meter(s) per gram
m^2/s	Square meter(s) per second
m^3	Cubic meter(s)
MA	Mass activity; methyl acrylate
MAAT	Many-at-a-time
μA	Micro ampere(s)
mA	MilliAmps (s)
MA	Mass activity
M-AB	Metal ammonia-borane
MAB, M-AB	Metal amidoboranes
$\mu A/cm^2$	Micro ampere(s) per square centimeter
mA/cm^2	Milliamp(s) per square centimeter
MAS	Magic angle spinning
MAS ^{11}B-NMR	Magic angle spinning boron-11 nuclear magnetic resonance spectroscopy
MAS-NMR	Magic angle spinning nuclear magnetic resonance
MASC	Multi-acid side-chain
MB	Megabyte
MBE	Molecular beam epitaxy
MBL	Modified boundary layer
MBMS	Molecular beam mass spectrometry
MBRC	Miles between roadcall
MC	Monte Carlo
MC	Microchannel
MC	Methyl cellulose
mC^2	Multi-component composite (membrane)
MCB	Marine Corps Base
$mC\text{-}cm^{-2}$	MilliCouloumb(s) per square centimeter
MCFC	Molten carbonate fuel cell
mCHP	Micro-combined heat and power
μc-Si	Microcrystalline silicon
MDE	Mid-duty electric
MDES	Methyl-diethoxy silane
MEA	Membrane electrode assembly
MeAB	Methylamine borane
MEC	Microbial electrolysis cell, Minimum explosive concentration
MeCN	Acetonitrile
MeOH	Methanol
MEP	Minimum energy pathway
meq	Milliequivalents
meq/g	Milliequivalents/gram
MeV	Mega electron volt
MFI	A zeolite structure code
Mg	Megagram(s)
μg	Microgram(s)
mg	Milligram(s)
MG	Miscanthus giganteus
$MgCl_2$	Magnesium chloride
mg/cm^2	Milligram(s) per square centimeter
MgH_2	Magnesium hydride
MgO	Magnesium oxide
$Mg(OH)_2$	Magnesium hydroxide
MH, M-H	Metal hydride
MHC	Metal hydride-based compressor
MHCoE	Metal Hydride Center of Excellence
MHE	Material handling equipment
MHz	Megahertz
mi	Mile(s)
μCHP	Micro-combined heat and power
μCHX	Microscale combustor/heat exchanger
MIE	Minimum ignition energy
MIEC	Mixed ionic and electronic conduction

mi/kg	Mile(s) per kilogram
mil	Millimeter(s)
min	Minute(s)
MIT	Massachusetts Institute of Technology
MiTi®	Mohawk Innovative Technologies Inc.
MJ	Megajoule(s)
mL, ml	Milliliter(s)
ML	Monolayer
MLCT	Metal-to-ligand charge-transfer
MLI	Multi-layer vacuum insulation
μm	Micrometer(s); micron(s)
μM	Micromolar
mM	Millimolar
mm	Millimeter(s)
MMBtu	Million British thermal units
MMOF	Microporous metal-organic framework
mmol	Millimole(s)
μmol	Micromole(s)
MMT	Million metric tonnes
Mn	Manganese
Mn_2O_3	Manganese oxide
M-N-H	Amide/imide
MnO	Manganese oxide
mΩ	Milli-ohm(s)
MΩ	Mega-ohm(s)
$m\Omega/cm^2$	Milli-ohm(s) per square centimeter
$\mu\Omega\text{-}cm^2$	Micro-ohm(s) - square centimeter
Mo	Molybdenum
MOF	Metal-organic framework
mol	Mole(s)
mol%	Mole percent
mol/min	Mole(s) per minute
MOR	Methanol oxidation reaction
MPa	Megapascal (s)
MPG, mpg	Mile(s) per gallon
MPGGE	Miles per gasoline gallon equivalent
mph	Mile(s) per hour
MPL	Microporous layer
mpy	Mils per year
MR	Membrane reactor
MRI	Magnetic resonance imaging
MRL	Manufacturing readiness level
ms	Millisecond(s)
MS	Mass spectroscopy, mass spectrometry
MSAC	Mid-range carbon support
mS/cm	Milli-Siemen(s) per centimeter
MSR	Metal-steam reforming
MSR	Membrane steam reformer
MTBF	Mean time between failure
MTBR	Mean time between repairs
mtorr	Millitorr
μV	Micro volt(s)
mV	Millivolt(s)
MV	Methyl viologen
mW	Milliwatt(s)
MW	Megawatt(s)
MW	Molecular weight
mW/cm^2	Milliwatt(s) per square centimeter
MWCNT	Multiple-wall carbon nanotube
MWe	Megawatt(s) electric
MWh	Megawatt-hour(s)
MWNT	Multi-wall carbon nanotube
MWOE	Midwest Optoelectronics, LLC
MWth	Megawatt(s) thermal
MYPP	Multi-Year Program Plan (the HFCIT Program's Multi-Year Research, Development and Demonstration Plan), Multi-year product plan
MYRDD, MYRD&DP	Multi-Year Research, Development and Demonstration Plan
N	Normal (e.g., 1N H_3PO_4 is 1 normal solution of phosphoric acid)
N	Nitrogen atom
N	Newton (unit of force)
N112	Nafion® 1100 equivalent weight, 2 millimeter thick membrane
N_2	Diatomic nitrogen
N_2O	Nitrous oxide
Na	Sodium
NA	North American
Na_2S	Sodium sulfide
Na_3AlH_6	Trisodium hexahydroaluminate
$NaAlH_4$	Sodium aluminum hydride; sodium tetrahydroaluminate; sodium alanate
$NaBH_4$	Sodium borohydride
$NaBO_2$	Sodium metaborate
NaCl	Sodium chloride
Nafion®	Registered Trademark of E.I. DuPont de Nemours
NaH	Sodium hydride
NA NG	North American natural gas
NaOH	Sodium hydroxide
NAS	National Academy of Sciences

NASA	National Aeronautics and Space Administration
NASCAR	National Association for Stock Car Auto Racing
Nb	Niobium
N/cm^2	Newton(s) per square centimeter
NCCC	National Carbon Capture Center
NCSL	National Conference of State Legislators
ND	Not determined at this time
NDA	Non-disclosure agreement
NDC	New delivery concept, Naphthalene-2,6-dicarboxylate
NDE	Non-destructive examination
NDP	Neutron depth profiling
NDTE	Non-destructive testing and evaluation
NEB	Nudged elastic band
NEED	National Energy Education Development Project
NE ISO	New England Independent System Operator
NEMS	National Energy Modeling System
NEPA	National Environmental Policy Act
NETL	National Energy Technology Laboratory
NFC	Near-frictionless coating
NFCRC	National Fuel Cell Research Center
NFM	Nanoporous framework material
NFPA	National Fire Protection Association
ng	Nanogram
NG	Natural gas
NGV	Natural gas vehicle
NH_3	Ammonia
NHE	Normal hydrogen electrode
NHI	Nuclear Hydrogen Initiative
Ni	Nickel
NiMH	Nickel metal hydride
NIR	Near infra-red
NIST	National Institute of Standards and Technology
NL	Normal liter(s)
nm	Nanometer(s)
NM	Noble metal
Nm^3	Normal cubic meter(s)
NMHC	Non-methane hydrocarbons
nmol	Nanomole(s)
NMR	Nuclear magnetic resonance
NMSU	New Mexico State University
NMT	New Mexico Tech
NNA	Non-North American
NNA NG	Non-North American natural gas
NNIF	NIST neutron imaging facility
NMOC	Non-methane organic carbons
NO_2	Nitric oxide
NOx, NO_x	Oxides of nitrogen
NP	Nanoparticle
NPC	Nanoporous carbon; normalized photocurrent
NPD	Neutron powder diffraction
NPGM	Non-precious metal group
NPMC	Non-precious metal catalyst
NFPA	National Fire Protection Association
NPM	Non-precious metal
NPS	National Park Service
NPT	Normal pressure and temperature
NPV	Net present value
NR	Nanorod
NREL	National Renewable Energy Laboratory
NRELFAT	NREL Fleet Analysis Toolkit
NSF	National Science Foundation
NST	New stress test
NSTF	Nano-structured thin-film
NT	Nanotube
NTCNA	Nissan Technical Center, North America
NVS	Neutron vibrational spectroscopy
NY ISO	New York Independent System Operator
Ω	Ohm(s)
Ωcm^2	Ohm(s) - square centimeter
O	Oxygen
O_2	Diatomic oxygen
O/C	Oxygen-to-carbon ratio
OCP	Open circuit potential
OCV	Open-circuit voltage
o.d.,OD	Outer diameter
OEM	Original equipment manufacturer
OER	Oxygen evolution reaction
OGMC	Ordered graphitic mesoporous carbon
OH^-	Hydroxyl radical
O&M	Operation and maintenance
OMC	Ordered mesoporous carbon
OML	Outer mold line
ORNL	Oak Ridge National Laboratory
ORNL-HTML	Oak Ridge National Laboratory High Temperature Materials Laboratory
ORR	Oxygen reduction reaction
OSC	Oxygen storage capability

OSM	Oregon Steel Mills, Optical scatterfield microscopy
OSU	Ohio State University
OTM	Oxygen transport membrane
P	Phosphorus
P	Pressure
Pa	Pascal(s)
PA	Phenylacetylene, Polyamide
PAA	Poly(acrylic acid)
PAD	Polymer assisted deposition
PAES	Poly(arylene-ether-sulfone)
PAF	Porous aromatic framework
PAFC	Phosphoric acid fuel cell
PAN	Peroxyacetyl nitrate, polyacrylonitrile
PANI	Polyaniline
PAS	Photoactive semiconductor
Pb	Lead
PB	Polyborazylene
PbA	Lead acid
PBI	Polybenzimidazole
PbO	Lead oxide
PC	Polycarbonate
PC	Personal computer
PCA	Pyrenecarboxylic acid
PCE	Perchloroethylene
PCI	Pressure-composition isotherm
PCL	Polycaprolactone
PCM	Power control module
PCR	Polymerase chain reaction
PCT, P-C-T	Pressure-concentration-temperature
PCTFE	Polychlorotrifluoroethylene
Pd	Palladium
PD	Pressure decay
PdAg	Palladium-silver alloy
Pd-CR	Palladium-based chemical resistor
PdCu, Pd-Cu	Palladium-copper alloy
PdCuTM	Palladium copper transition metal
PDF	Probability density function
PDMS	Polydimethylsiloxane
PDU	Process development unit
PEEK	Polyether ether ether ketone
PEFC	Polymer electrolyte fuel cell
PEFC	Proton exchange fuel cell
PEG	Polyethylene glycol
PEGS	Prototype electrostatic ground state
PEI	Polyetherimide, polyethylene imine
PEKK	Poly (ether ketone ketone)
PEM	Proton exchange membrane, Polymer electrolyte membrane
PEMFC	Polymer electrolyte membrane fuel cell
PEMFC	Proton exchange membrane fuel cell
PEO	Poly(ethylene oxide)
PES	Polyethersulfone
PET	Polyethylene teraphthalate
PFA	Polyfurfuryl alcohol
PFD	Process flow diagram
PFIA	Perfluoro imide acid
PFPO	Perfluorinated propylene oxide
PFSA	Perfluorinated sulfonic acid, perfluorosulfonic acid, poly(fluorosulfonic acid)
PFSHQ	2-(5-fluorosulfonyl-3-oxaoctafluoropentyl)-1,4-dihydroxy-benzene
PGE	Platinum group element
PG&E	Pacific Gas and Electric Company
PGM	Precious group metal, Platinum group metal
PGV	Puna Geothermal Ventures
pH	Power of the hydronium ion
p-H_2	Para-hydrogen
PHEV	Plug-in hybrid vehicle
PHS	Pumped hydro storage
PI	Principal investigator
PI	Polyimide
P&ID	Piping and instrumentation diagram, process and instrumentation diagram
PIL, pIL	Protic ionic liquid
PIM, pIM	Protic ionic membrane
pK_a	Acid dissociation constant
PLC	Programmable logic controller
PLRS	Planar laser Raleigh scatter
PM	Particulate matter
PNNL	Pacific Northwest National Laboratory
pO_2	Oxygen partial pressure
POC	Proof of concept
POF	Polymeric-organic frameworks; Porous organic framework
POP	Porous organic polymers
POSS	Polyhedral oligomeric silsesquioxane
POX	Partial oxidation
PP	Polyphosphazene, polypropylene, poly(phenylene)
PPA	polyphosphoric acid; polyphthalamide
ppb	Part(s) per billion
ppbv	Part(s) per billion by volume

PPDSA	Poly (p-phenylene disulfonic acid)
PPI	Pore(s) per inch
ppm, PPM	Part(s) per million
ppmv	Part(s) per million by volume
ppmw	Part(s) per million by weight
PPN	Porous polymer network
PPOR	Metalloporphyrin porous organic polymer
P-POSS	Phosphonic acid polyhedral oligomeric silsesquioxane
PPS	Polyphenylene sulfide
PPSA	Poly (p-phenylene sulfonic acid)
PPSA	Partial pressure swing adsorption
PPSU	Polyphenylsulfone
PRD	Pressure relief device
PRO	Pressure retarded osmosis
PSA	Pressure swing adsorption, adsorber
PSAT	Powertrain Systems Analysis Toolkit, a vehicle simulation software package developed at Argonne National Laboratory
PSD	Particle size distribution, pore size distribution
PSEPVE	Perfluoro (4-methyl-3,6-dioxaoct-7-ene) sulfonyl fluoride
PSf	Poly(arylene ether sulfone)
psi, PSI	Pound(s) per square inch
PSI	Photosystem I
psia	Pound(s) per square inch absolute
psid	Pound(s) per square inch differential
psig, PSIG	Pound(s) per square inch gauge
PSII	Photosystem II
PSM	Protic salt membrane
PSOFC	Planar solid oxide fuel cell
PSS	Porous stainless steel, potentiostatic scan
PSU	Polysulfone
PSU	Pennsylvania State University
Pt	Platinum
P-T	Pressure-temperature
Pt_3Co	Platinum-cobalt alloy
Pt_3Fe	Platinum-iron alloy
Pt_3Ni	Platinum-nickel alloy
PTA	Phosphotungstic acid
Pt/C	Platinum/carbon
PTFE	Teflon® – poly-tetrafluoroethylene
Pt-FePO	Platinum iron phosphate
PtO	Platinum oxide
PtO_2	Platinum dioxide
PtRu	Platinum ruthenium
PTW	Pump-to-wheels
PV	Photovoltaic; present value
PVA	Polyvinyl alcohol
PVC	Polyvinyl chloride
PVD	Physical vapor deposition
PVDC	Poly-vinylidene chloride
PVDF	Polyvinylidene fluoride
PVL	Print verification line
PVP	Polyvinylpyrrolidone
PVPP	Polyvinyl pyridinium phosphate
PVT, P-V-T	Pressure-Volume-Temperature
PXRD	Powder X-ray diffraction
Q	Neutron momentum transfer
Q1, Q2, Q3, Q4	Quarters of the fiscal year
QC	Quality control
QCM	Quartz crystal microbalance
QE	Quantum efficiency
QENS	Quasielastic neutron scattering
QFD	Quality function deployment
QLRA	Qualitative risk analysis
QMC	Quantum Monte Carlo
QNS	Quasielastic neutron scattering
QRA	Quantitative risk assessment
R	Universal or ideal gas constant, 8.314472 $J \cdot K^{-1} \cdot mol^{-1}$
RAMAN	A spectroscopic technique
R&D	Research and development
RD&D, R,D&D	Research, development & demonstration
RDE	Rotating disk electrode
Re	Rhenium
Rf	Generic fluoroalkyl group
RF, rf	Radio frequency
RF	Roughness factor
RFP	Request for proposals
RGA	Residual gas analyzer (analysis)
Rh	Rhodium
RH	Relative humidity
RHE	Reference hydrogen electrode; reversible hydrogen electrode
RNA	Ribo nucleic acid
RNG	Renewable natural gas
RO	Reverse osmosis
ROM	Rough order of magnitude
RPC	Ruthenium-polypridyl complex
RPI	Rensselaer Polytechnic Institute

rpm	Revolution(s) per minute
RPS	Renewable portfolio standard
RRC	Regional resource center
RRDE	Rotating ring disc electrode
RRW	Risk reduction worth
RSA	Random sequential adsorption
RSOFC	Reversible solid oxide fuel cell
RT	Room temperature
RTD	Resistive thermal device
Ru	Ruthenium
s	Second(s)
S	Siemen(s)
S	Sulfur
SA	Specific amperage
SA	Sulfur-ammonia thermochemical water-splitting cycle
SAC	Site acquisition
SAE	SAE International, originally known as the Society of Automotive Engineers
SAFC	Solid acid fuel cell
SAH	Sodium aluminum hydride
SAM	Scanning Auger microscopy
SANS	Small angle neutron scattering
SAXS	Small angle X-ray scattering
S_{BET}	BET specific surface area
SBIR	Small Business Innovation Research
SBTS	Stack Block Test System
SBU	Secondary building unit
Sc	Scandium
S/C	Steam to carbon ratio
sccm, SCCM	Standard cubic centimeter(s) per minute
SCE	Saturated calomel electrode
SCF, scf	Standard cubic feet, supercritical fluid
scfd	Standard cubic feet per day
SCFH, scfh	Standard cubic feet per hour
SCFM	Standard cubic feet per minute
S/cm	Siemen(s) per centimeter
SCOF	Single cell with open flowfield
SC-PC	Supercritical pulverized coal
SCR	Selective catalytic reduction
SCS	Solution combustion synthesis
SCT-MAT	Short Circuit MicroActivity Testing
SD	Standard deviation, System dynamics
SDO	Standards development organization
Se	Selenium
sec	Second(s)
SEC	Size exclusion chromatography
SECA	Solid State Energy Conversion Alliance
SEDS	State Energy Data System
SEM	Scanning electron microscopy, scanning electron microscope
SEM	Secondary electron microscopy
SEPUP	Science Education for Public Understanding Program
SERA	Scenario Evaluation, Regionalization and Analysis
SET	Surface Energy Treatment
SF	Polystyrene-b-PFPO
SF_6	Sulfur hexafluoride
SFA	Sulfonic acid
SFO	San Francisco International Airport
SGD	Spontaneous galvanic displacement, system gravimetric density
SHE	Standard hydrogen electrode
Si	Silicon
S-I	Sulfur-iodine
SI	Sulfur-iodine cycle; spectrum image
Si^3N^4	Silicon nitride
SiC	Silicon carbide
SiCN	Silicon carbonitride
SIMS	Secondary ion emission spectroscopy
SiO_2	Silicon dioxide
SIU	Southern Illinois University
sL	Standard liter (0°C, 1 atm)
SLD	Simplified local density
slpm, slm, sL/min	Standard liter(s) per minute
SMR	Steam methane reformer; steam methane reforming
Sn	Tin
SNL	Sandia National Laboratories
SNR	Signal-to-noise ratio
SNTT	Spiral notch torsion test
SLAC	Stanford Linear Accelerator Center
SLPH	Standard liter(s) per hour
SLPM	Standars liter(s) per minute
SLT	Strontium-doped lanthanum titanate
SnO	Tin oxide
SnO_2	Tin oxide
SO_2	Sulfur dioxide
SO_3	Sulfur trioxide
SOC	State-of-charge
SOEC	Solid oxide electrolysis cell; solid oxide electrolyzer cell
SOFC	Solid oxide fuel cell

SOFEC	Solid oxide fuel-assisted electrolysis cell
SOx	Oxides of sulfur
sPAES	Sulfonated poly(arylene ether sulfone)
SPEEK	Sulfonated poly(ether ether ketone)
SPEK	Sulfonated poly-etherketone-ketone
SPEKK	Sulfonated polyether(ether ketone ketone)
SPEX	Type of milling machine
SPM	Scanning probe microscope
sPOSS	sulfonated octaphenyl polyhedral oligomeric silsesquioxanes
sq. in.	Square inch(es)
Sr	Strontium
SR	Steam reformer; steam reforming
SR-M	Steam reformer membrane
SRNL	Savannah River National Laboratory
SrO	Strontium oxide
$SrTiO_3$	Strontium titanate, the proton conducting material
SS	Stainless steel
SSA	Specific surface area
SSAWG	Storage System Analysis Working Group
SSR	Solid-state reaction
SSWAG	Storage System Working Analysis Group
STCH	Solar Thermochemical Hydrogen
STEM	Scanning transmission electron microscopy
STEM	Science, technology, engineering, and mathematics
STH	Solar-to-hydrogen
STM	Scanning tunneling microscopy
STMBMS	Simultaneous thermogravimetric modulated beam mass spectrometer
STP	Standard temperature and pressure
STS	Scanning tunneling spectroscopy
STTP	Shared Technology Transfer Project
STTR	Small Business Technology Transfer
SU/SD	Start-up and shut-down
SV	Space velocity
SVD	System volumetric density
SWCNT	Single-walled carbon nanotube
SWNH	Single-walled nanohorn
SWNT	Single-wall nanotube
SwRI®	Southwest Research Institute
S_y	Yield strength
SYT	Yttrium-doped strontium titanate
T	Temperature
T, t	Ton, tonne
T	Tesla (unit of magnetic induction)
t	Time
T_{1bar}	Temperature at which equilibrium pressure of hydrogen is 1 bar for a hydrogen exchange reaction
Ta	Tantalum
TAG	Technical Advisory Group
TBAB	Tetra-n-butylammonium bromide
$TBA_2B_{12}H_{12}$	Tetra-*n*-butylammonium dodecahydrododecaborate
TBABh	Tetra-n-butylammonium borohydride
TBA-PF_6	Tetra-*n*-butylammonium hexafluorophosphate
TBD	To be determined
TC	Thermocouple
TC	Transparent conducting
TCCR	Transparent, conducting and corrosion resistant
TCD	Thermal conductivity detector
TCO	Transparent conductive oxide
Te	Tellurium
te	Metric ton or tonne (1,000 kg)
TEA	Triethylamine
TEAA	Triethylamine alane adduct
TEDA	Triethylenediamine
TEM	Transmission electron microscopy
TEOA	Triethanolamine
TEOM	Tapered element oscillating microbalance
tf	Thin film
TFE	Tetrafluoroethylene
TF-RDE:	Thin film rotating disk electrode
tf-Si	Thin-film silicon
TFVE	Trifluorovinyl ether
TGA	Thermal gravimetric analysis; thermogravimetric analysis; thermogravimetric analyzer
TGA-DSC	Thermo-gravimetric analysis-differential scanning calorimetry
TGA-MS	Thermogravimetric analysis-mass spectrometer
THF	Tetrahydrofuran
Ti	Titanium
$TiCl_3$	Titanium trichloride
TiF_3	Titanium trifluoride
TiH_2	Titanium hydride
Ti-IRMOF-16	Titanium (Ti) intercalated IRMOF-16
TIO	Technology improvement opportunities
TiO_2	Titanium dioxide (anatase)
TKK	Tanaka Kikinzoku Kogyo K. K.

Tla	Truncated light-harvesting chlorophyll antenna
tla1	Mutant of the Tla1 gene (GenBank Assession No. AF534570)
tlaR	Mutant of unknown gene with a truncated light-harvesting chlorophyll antenna
tlaX	Mutant of unknown gene with a truncated light-harvesting chlorophyll antenna
TM	Transition metal
TMA	Thermal mechanical analyzer
TMB	Trimethylborate
TMEDA	Tetramethylethane-1,2-diamine; N^1,N^1,N^2,N^2-tetramethylethane-1,2-diamine
TMF	The Molecular Foundry
TMG	Tetramethyl guanidine
TMM	Thermal management module
TMPyP	Tetramethylpyridylporphine
TNT	Trinitrotoluene
TOC	Total organic content
TOF	Turnover frequency
TON	Turnover number
TPA	Tripropylamine, Temperature-programmed adsorption
TPB	Triple phase boundary
TPD	Tonne(s) per day
TPD	Thermally programmed desorption; Temperature-programmed desorption
TPO	Temperature-programmed oxidation
TPR	Temperature-programmed reduction
TPV	Through plate voltage
TR	Traditional reactor
TRAIN	TrainingFinder Realtime Affiliate Network
TRL	Technology readiness level
tr. oz.	Troy ounce
TSA	Temperature swing adsorption
TV	Test vehilce
UC	University of California
UCB	University of California, Berkeley
UCF	University of Central Florida
UCI	University of California, Irvine
UCLA	University of California, Los Angeles
UCONN	University of Connecticut
UCSB	University of California, Santa Barbara
UDDS	Urban Dynamometer Driving Schedule
UEL	Upper explosive limit
UFL	Upper flammability limit
UH	University of Hawaii
UHP	Ultra-high purity
UHV	Ultra-high vacuum
UIUC	University of Illinois, Urbana-Champaign
UL	Underwriters Laboratory
ULSD	Ultra-low sulfur diesel
um	Micrometer(s)
UMC	Unsaturated metal centers
UNCC	University of North Carolina at Charlotte
UNLV	University of Nevada, Las Vegas
UNLVRF	UNLV Research Foundation
UNM	University of New Mexico
UNR	University of Nevada, Reno
UPD	Underpotentially deposited
UPE	Ultra-high molecular weight polyethylene
UPL	Upper potential limit
UPS	Ultraviolet photoelectron spectroscopy
U.S.	United States
US06	Environmental Protection Agency vehicle driving cycle
USA	United States of America
USANS	Ultra small angle neutron scattering
USB	Universal serial bus
USC	University of South Carolina
USC	University of Southern California
USCAR	United States Council for Automotive Research, U.S. Cooperative Automotive Research
USFCC	United States Fuel Cell Council
USGS	Unites States Geological Survey
USM	University of Southern Mississippi
UT	University of Tennessee
UTC	University of Tennessee, Chattanooga
UTCP	UTC Power
UTRC	United Technologies Research Center
UV	Ultraviolet
UV-vis	Ultraviolet-visual
V	Vanadium
V	Volt
VA	Vinyl acetate
VAC	Volts alternating current
VACNTs	Vertically aligned carbon nanotubes
VANTA	Vertically aligned nanotube arrays
VASP	Vienna ab initio simulation package
VB	Valence band
VBM	Valence band minimum
VBM	Valence band maximum
VC	Vanadium carbide
VC	Vulcan carbon

VDC	Volts direct current
VDF	Vinylidene fluoride
VDOS	Vibrational density of states
vdW	van der Waals
VI	Venter Institute
V-I	Voltage – current
VIR	Voltage-current-resistance
V_{mp}	Micropore volume
VMT	Vehicle miles travelled
VNT	Variable nozzle turbine
VOC	Volatile organic compound
VOC	Voltage open circuit
vol	Volume
vol%	Volume percent
V_{pore}	Total pore volume
VRB	Vanadium-redox battery
W	Tungsten
W	Watt(s)
WAXD	Wide-angle x-ray diffraction
WAXS	Wide angle X-ray scattering
WC	Tungsten carbon, tungsten carbide
W/cm^2	Watt(s) per square centimeter
W_e	Watt(s) electric
WECC	Western Electric Coordinating Council
WGS	Water-gas shift
WGSR	Water-gas shift reactor
WGSMR	Water-gas shift membrane reactor
Wh	Watt-hour(s)
$W(H_2)$	Gravimetric hydrogen storage capacity
W-h/kg	Watt-hour(s) per kilogram
W-h/L, Wh/liter, Wh/L	Watt-hour(s) per liter
WHSV	Weight hourly space velocity
Wind2H2	Wind to hydrogen demonstration project
W/kg	Watt(s) per kilogram
W/L, W/l	Watt(s) per liter
W/m-K, W/m.K, W/mK	Watt(s) per meter-Kelvin (unit of thermal conductivity)
WO_3	Tungsten trioxide
Wppm	Weight part(s) per million
wt	Weight
Wt	Watt(s) thermal
wt%, wt.%	Weight percent (percent by weight)
WTP	Well-to-pump
WTP	Water transport plate
WTT	Well-to-tank
WTW	Well-to-wheels
w/v	Weight by volume
WWTP	Waste water treatment plants
XAFS	X-ray absorption fine structure
XANES	X-ray absorption near-edge spectroscopy
XAS	X-ray absorption spectroscopy
XC72	High-surface-area carbon support made by Cabot
XES	X-ray emission spectroscopy
XPS	X-ray photoelectron spectroscopy, X-ray photon spectroscopy, X-ray photoemission spectroscopy, X-ray photoluminescence spectroscopy
XRD	X-ray diffraction
XRF	X-ray fluorescence
Y	Yttrium
yr, YR	Year
YSZ	Yttria-stablized zirconia
ZEV	Zero emission vehicle
ZHS	Zinc hydroxystannate
ZIF	Zeolitic imidazolate framework
Zn	Zinc
ZnO	Zinc oxide
Zr	Zirconium
ZrO_2	Zirconium dioxide
ZrSPP	Zirconium phosphate sulfophenylphosphonate
ZVI	Zerovalent iron

XV. Primary Contacts Index

A

Aceves, Salvador III.14, VIII.13
Adams, Michael. II.K.3
Adams, Thad III.6
Adzic, Radoslav. V.D.6
Ahluwalia, Rajesh IV.E.2, V.A.3
Ahmed, Shabbir. XI.12
Allen, Philip. II.K.16
Allendorf, Mark. IV.A.8
Anton, Don IV.A.1, IV.D.1
Arif, Muhammad. V.A.5
Armstrong, Neal II.K.17
Atanasoski, Radoslav V.D.3
Ayers, Katherine II.E.2

B

Balachandran, Balu II.A.3
Baldwin, Don III.7
Barclay, John III.17
Baxter-Clemmons, Shannon IX.4, X.7
Berry, Joel. V.L.8
Bessette, Norman V.K.1
Billo, Richard. II.J.3
Blanchet, Scott V.E.5
Blekhman, David VII.9, IX.9
Block, David VII.8, IX.12
Block, Gus XII.8
Bloom, Ira V.A.8
Borup, Rod. V.E.2
Brewer, Karen II.K.11
Brosha, Eric V.D.14, VIII.8
Burgess, Robert VIII.3
Busby, Colin. VI.4
Bush, Brian XI.3

C

Cabasso, Israel. IV.C.8
Carlstrom, Chuck XII.1
Chen, Ken V.F.2
Chen, Ru. VI.3
Chick, Larry. X.10
Chuang, Steven V.L.1
Cole, Vernon V.F.1
Conti, Amedeo. V.F.6
Czernik, Stefan II.A.2

D

Dalton, Luke II.J.2
Damle, Ashok II.C.3
Davis, Benjamin IV.B.2
De Castro, Emory VI.7
Debe, Mark V.D.1
Dedrick, Daniel. VIII.1, VIII.2, VIII.4, VIII.5
Dever, Tom. IX.8
Di Bella, Frank III.8
Dinh, Huyen V.B.1, V.G.1
Drost, Kevin IV.D.10
Dunn, Paul. II.E.3
Dutton, Les II.K.13

E

Eisman, Glenn. II.E.5
Elgowainy, Amgad XI.6
Elmore, Monte. VIII.12
Emerson, Sean. II.B.1, II.D.3
Engel, Richard. IX.10
Eudy, Leslie VII.5
Evenson, Carl II.D.2

F

Fassbender, Linda VIII.11
Fenske, George III.16
Fenton, James V.C.9
Fletcher, Jim. V.G.3, XII.3
Fujita, Etsuko II.K.15

G

Garzon, Fernando. V.B.5, V.D.7
Gennett, Thomas. IV.C.7
Getman, Dan. XI.10
Ghirardi, Maria. II.H.1, II.K.5, II.K.8
Glass, Bob X.8
Golbeck, John II.K.19
Goodwin, James V.B.4
Gore, Jay. II.H.5, IV.G.1
Goudy, Andrew IV.G.3
Graetz, Jason IV.A.6
Grasman, Ron VII.3
Greene, David XI.1
Gross, Karl. IV.E.7
Grot, Stephen V.C.8
Gupta, Arunava. II.K.14

H
Hamdan, Monjid II.E.1
Hamrock, Steven. V.C.1
Hancock, Dave V.F.5
Harrison, Kevin. II.E.4
Harwood, Caroline II.K.2
Herring, Andrew V.C.6
Heshmat, Hooshang III.9
Heske, Clemens II.G.4
Heydorn, Ed. VII.4, VII.6
Hicks, Mike V.K.3
Hoagland, William VIII.15
Hoefelmeyer, James. II.G.9
Holladay, Jamie IV.D.6

I
Irving, Patricia. V.K.4

J
James, Brian. V.A.2
Jaramillo, Thomas. II.G.1
Jenkins, Chelsea IX.5
Jensen, Craig IV.A.3
Johnson, Will. V.J.1

K
Keith, Jason IX.11
Keller, Jay III.1
Kenny, Kevin XII.5
Kerr, John. V.D.8
Khalil, John IV.E.1
Kim, Yu Seung. V.I.1
King, David II.A.1
King, John XII.9
Klebanoff, Lennie IV.E.4, X.1, X.9
Kliever, Scott XII.10
Klingler, Jim. XII.11
Knudsen, Jon IV.D.11
Krumholz, Lee II.K.6
Kumar, Darsh IV.D.8
Kurtz, Jennifer. IV.E.5, V.A.1, XII.7

L
Law, Karen. IV.E.3
Leavitt, Mark. VI.9
Leigh, John. II.K.4
Leon, Warren. IX.3
Lewis, John X.5
Lewis, Michelle II.F.2
Lewis, Nathan II.K.20
Lieberman, Robert VIII.14
Lin, Jerry Y.S. II.C.1
Lipinska-Kalita, Kristina IV.G.2
Lipp, Ludwig III.10, V.C.7
Litt, Morton V.C.4
Liu, D.J. IV.C.5
Liu, Paul. II.C.2
Liu, Shih-Yuan. IV.B.1
Lueking, Angela IV.C.6

M
Ma, Yi Hua (Ed) II.D.4
Madan, Arun II.G.5
Maness, Pin-Ching II.H.2
Mann, Michael IX.13
Markovic, Nenad. V.D.5
Mawdsley, Jennifer V.H.2
Maxwell, Mike. XII.6
Mazumder, Malay II.G.7
Melaina, Marc XI.2, XI.7
Melis, Tasios. II.H.4
Miller, Michael IV.E.6
Mintz, Marianne III.2, IX.1
Mirza, Zia V.J.2
Misra, Mano II.G.8
Mittelsteadt, Cortney V.C.2, V.C.3, V.F.3
Mohapatra, Satish. V.J.3, V.L.7
Molter, Trent V.B.2
More, Karren V.A.4
Morgan, Jason VI.2
Motyka, Ted IV.D.5
Mukerjee, Sanjeev. V.D.11
Mukundan, Rangachary. V.E.7
Murthi, Vivek V.D.2
Myers, Deborah. V.E.1

N
Nagle, Barbara. IX.15
Norman, Timothy II.J.1
Nozik, Art II.K.21

O
Ogitsu, Tadashi II.G.3
Owejan, Jon V.F.4

P
Parfenov, Alexander II.J.4
Parkinson, Bruce. II.K.18

Patterson, Timothy V.E.6
Paulauskas, Felix. IV.F.1
Perna, Mark V.L.3
Perry, Randy V.E.3
Petri, Randy V.I.2
Pfeifer, Peter IV.C.3
Pintauro, Peter. V.C.5
Pivovar, Bryan V.D.4
Popov, Branko V.D.13
Prezhdo, Oleg II.K.9

R

Ramani, Vijay V.D.10
Ramsden, Todd X.6
Reichmuth, Dave. XI.4
Reifsnider, Kenneth V.L.4
Reiter, Joseph IV.D.4
Rieke, Peter VI.8
Rinebold, Joel IX.2
Rinker, Mike X.4
Rivkin, Carl VIII.6, VIII.7
Roberts, Mike II.B.2
Robertson, Ian. IV.A.5
Rocheleau, Richard. VII.7, X.3
Rockward, Tommy V.A.6, VIII.9
Roger, Chris V.G.2
Rohr, Donald XII.12, XII.13
Rosenblatt, Andrew XII.4
Ruth, Mark. XI.9

S

Saur, Genevieve. II.E.6
Schoenung, Susan X.2
Schwartz, Joseph. II.D.1, III.11
Selloni, Annabella. II.K.10
Semelsberger, Troy IV.D.3
Serfass, Patrick IV.E.8, IX.6
Shearer, Susan. V.L.5, V.L.10
Siegel, Nathan II.F.3
Simon, A.J. XI.11
Singh, Prabhakar V.L.9
Smith, Barton III.13, IV.F.2, VIII.16
Smith, Robert II.G.10
Snurr, Randy IV.C.4
Sofronis, Petros III.12
Sozinova, Olga III.4
Spruill, Mary IX.14
Stanfield, Eric VI.6, VI.10, VI.11
Steward, Darlene. II.I.1, V.A.7, XI.5
Storey, Robson. V.L.2
Stottler, Gary VII.2
St-Pierre, Jean V.B.3
Subramanian, Ravi II.G.11
Sudik, Andrea IV.D.9
Sullivan, Neal V.L.6
Swamy, Durai V.K.2
Swartz, Jim. II.K.1

T

Taylor, Robin II.F.1
Thornton, Matthew. IV.D.2
Turner, John II.G.2, II.G.12, V.D.9

U

Udovic, Terry IV.A.9
Ulsh, Michael. VI.1

V

Valente, Pat IX.7
van Hassel, Bart IV.D.7
Vaughn, Ken XII.2

W

Wagner, Fred V.D.12
Walczyk, Dan VI.5
Wall, Judy. II.K.7
Wang, Conghua V.H.1
Wang, Michael. XI.8
Wang, Yong V.D.15
Weber, Adam V.F.7
Weimer, Al II.F.4
Weiner, Steven. VIII.10
Weisberg, Andrew. III.5
Wessel, Silvia V.E.4
Weyman, Phil II.H.3
Wind, Rikard II.G.13
Wipke, Keith VII.1
Wolverton, Christopher IV.A.2

X

Xu, Liwei II.G.6

Y

Yaghi, Omar. IV.C.2, IV.C.9

Z

Zelenay, Piotr V.G.4

Zhang, Jin. II.K.12
Zhang, Wei. III.3, III.15
Zhao, J.-C. IV.A.4
Zhou, Joe IV.C.1
Zidan, Ragaiy. IV.A.7

XVI. Hydrogen and Fuel Cells Program Contacts

Sunita Satyapal, Program Manager
DOE Hydrogen and Fuel Cells Program
Fuel Cell Technologies Program
DOE Office of Energy Efficiency and Renewable Energy
Phone: (202) 586-2336
E-mail: Sunita.Satyapal@ee.doe.gov

Rick Farmer, Deputy Program Manager
Fuel Cell Technologies Program
DOE Office of Energy Efficiency and Renewable Energy
Phone: (202) 586-1623
E-mail: Richard.Farmer@ee.doe.gov

John Vetrano
Materials Sciences and Engineering Division
Basic Energy Sciences Program
DOE Office of Science
Phone: (301) 903-5976
E-mail: John.Vetrano@science.doe.gov

Guido B. Dehoratiis
Division of Advanced Energy Systems
DOE Office of Fossil Energy
Phone: (202) 586-2795
E-mail: Guido.B.Dehoratiis@hq.doe.gov

Carl Sink
Office of Gas Cooled Reactor Technologies
DOE Office of Nuclear Energy
Phone: (301) 903-5131
E-Mail: Carl.Sink@nuclear.energy.gov

Hydrogen Production and Delivery

Sara Dillich, Acting Hydrogen Production and Delivery Team Leader
Fuel Cell Technologies Program
DOE Office of Energy Efficiency and Renewable Energy
Phone: (202) 586-7925
E-mail: Sara.Dillich@ee.doe.gov

Hydrogen Storage

Ned Stetson, Hydrogen Storage Team Leader
Fuel Cell Technologies Program
DOE Office of Energy Efficiency and Renewable Energy
Phone: (202) 586-9995
E-mail: Ned.Stetson@ee.doe.gov

Fuel Cells

Dimitrios Papageorgopoulos, Fuel Cells Team Leader
Fuel Cell Technologies Program
DOE Office of Energy Efficiency and Renewable Energy
Phone: (202) 586-5463
E-mail: Dimitrios.Papageorgopoulos@ee.doe.gov

Manufacturing R&D

Nancy Garland, Acting Manufacturing R&D Team Leader
Fuel Cell Technologies Program
DOE Office of Energy Efficiency and Renewable Energy
Phone: (202) 586-5673
E-mail: Nancy.Garland@ee.doe.gov

Technology Validation

John Garbak, Technology Validation Team Leader
Fuel Cell Technologies Program
DOE Office of Energy Efficiency and Renewable Energy
Phone: (202) 586-1723
E-mail: John.Garbak@ee.doe.gov

Safety, Codes & Standards

Antonio Ruiz, Safety, Codes and Standards Team Leader
Fuel Cell Technologies Program
DOE Office of Energy Efficiency and Renewable Energy
Phone: (202) 586-0729
E-mail: Antonio.Ruiz@ee.doe.gov

Education

Gregory J. Kleen, Acting Education Team Leader
Fuel Cell Technologies Program
Department of Energy Golden Field Office
Phone: (720) 356-1672
E-mail: Gregory.Kleen@go.doe.gov

Market Transformation

Pete Devlin, Market Transformation Manager
Fuel Cell Technologies Program
DOE Office of Energy Efficiency and Renewable Energy
Phone: (202) 586-4905
E-mail: Peter.Devlin@ee.doe.gov

Systems Analysis

Fred Joseck, Systems Analysis Team Leader
Fuel Cell Technologies Program
DOE Office of Energy Efficiency and Renewable Energy
Phone: (202) 586-7932
E-mail: Fred.Joseck@ee.doe.gov

American Recovery and Reinvestment Act (ARRA) Activities

Sara Dillich, Lead for Fuel Cell Technologies ARRA Activities
and Supervisor for Research & Development
Fuel Cell Technologies Program
DOE Office of Energy Efficiency and Renewable Energy
Phone: (202) 586-7925
E-mail: Sara.Dillich@ee.doe.gov

XVII. Project Listings by State

Alabama

II.K.14 University of Alabama, Tuscaloosa: Protein-Templated Synthesis and Assembly of Nanostructuctures for Hydrogen Production 267

V.F.1 CFD Research Corporation: Water Transport in PEM Fuel Cells: Advanced Modeling, Material Selection, Testing, and Design Optimization 814

V.F.1 ESI US R&D: Water Transport in PEM Fuel Cells: Advanced Modeling, Material Selection, Testing, and Design Optimization 814

Arizona

II.C.1 Arizona State University: Zeolite Membrane Reactor for Water-Gas Shift Reaction for Hydrogen Production 46

II.K.17 University of Arizona: Formation and Characterization of Semiconductor Nanorod/Oxide Nanoparticle Hybrid Materials: Toward Vectoral Electron Transport in Hybrid Materials. 275

VI.5 Arizona State University: Adaptive Process Controls and Ultrasonics for High-Temperature PEM MEA Manufacture 977

Arkansas

II.G.7 University of Arkansas, Little Rock: PEC-Based Hydrogen Production with Self-Cleaning Solar Concentrator. 154

XII.9 FedEx Freight: Fuel Cell-Powered Lift Truck FedEx Freight Fleet Deployment 1316

California

II.C.2 University of Southern California: Development of Hydrogen Selective Membranes/Modules as Reactors/Separators for Distributed Hydrogen Production 53

II.F.1 Science Applications International Corporation: Solar High-Temperature Water Splitting Cycle with Quantum Boost 102

II.F.1 Thermochemical Engineering Solutions: Solar High-Temperature Water Splitting Cycle with Quantum Boost 102

II.F.1 University of California, San Diego: Solar High-Temperature Water Splitting Cycle with Quantum Boost 102

II.F.3 Sandia National Laboratories: Solar Hydrogen Production with a Metal Oxide-Based Thermochemical Cycle 112

II.F.3 Jenike and Johanson: Solar Hydrogen Production with a Metal Oxide-Based Thermochemical Cycle 112

II.G.1 Stanford University: Nano-Architectures for 3rd Generation PEC Devices: A Study of MoS_2, Fundamental Investigations and Applied Research. 123

II.G.1 Board of Trustees of the Leland Stanford Junior University: Nano-Architectures for 3rd Generation PEC Devices: A Study of MoS_2, Fundamental Investigations and Applied Research 123

II.G.2 Stanford University: Semiconductor Materials for Photoelectrolysis 129

II.H.3 J. Craig Venter Institute: Hydrogen from Water in a Novel Recombinant Oxygen-Tolerant Cyanobacterial System 195

II.H.4 University of California, Berkeley: Maximizing Light Utilization Efficiency and Hydrogen Production in Microalgal Cultures 200

II.J.4 Physical Optics Corporation: Photochemical System for Hydrogen Generation. 225

II.K.1 Stanford University: SISGR: Using *In vitro* Maturation and Cell-free Evolution to Understand [Fe-Fe]hydrogenase Activation and Active Site Constraints 228

II.K.12 University of California, Santa Cruz: Hydrogen Generation Using Integrated Photovoltaic and Photoelectrochemical Cells 260

California (Continued)

II.K.20 California Institute of Technology: Fundamental Optical, Electrical, and Photoelectrochemical Properties of Catalyst-Bound Silicon Microwire Array Photocathodes for Sunlight-Driven Hydrogen Production . . . 283

III.1 Sandia National Laboratories: Hydrogen Embrittlement of Structural Steels . . . 299

III.5 Lawrence Livermore National Laboratory: Demonstration of Full-Scale Glass Fiber Composite Pressure Vessels for Inexpensive Delivery of Cold Hydrogen . . . 316

III.5 Spencer Composites Corporation: Demonstration of Full-Scale Glass Fiber Composite Pressure Vessels for Inexpensive Delivery of Cold Hydrogen . . . 316

III.8 HyGen Industries: Development of a Centrifugal Hydrogen Pipeline Gas Compressor . . . 331

III.14 Lawrence Livermore National Laboratory: Thermodynamic Modeling of Rapid Low Loss Cryogenic Hydrogen Refueling . . . 358

III.14 Linde LLC: Thermodynamic Modeling of Rapid Low Loss Cryogenic Hydrogen Refueling . . . 358

IV.A.8 Sandia National Laboratories: Tunable Thermodynamics and Kinetics for Hydrogen Storage: Nanoparticle Synthesis Using Ordered Polymer Templates . . . 416

IV.A.8 Lawrence Livermore National Laboratory: Tunable Thermodynamics and Kinetics for Hydrogen Storage: Nanoparticle Synthesis Using Ordered Polymer Templates . . . 416

IV.C.2 University of California, Los Angeles: A Joint Theory and Experimental Project in the Synthesis and Testing of Porous COFs/ZIFs for On-Board Vehicular Hydrogen Storage . . . 439

IV.C.7 H2 Technology Consulting LLC: Weak Chemisorption Validation . . . 464

IV.C.9 University of California, Los Angeles: Hydrogen Storage in Metal-Organic Frameworks . . . 474

IV.D.1 Jet Propulsion Laboratory: Hydrogen Storage Engineering Center of Excellence . . . 479

IV.D.1 California Institute of Technology: Hydrogen Storage Engineering Center of Excellence . . . 479

IV.D.4 Jet Propulsion Laboratory: Key Technologies, Thermal Management, and Prototype Testing for Advanced Solid-State Hydrogen Storage Systems . . . 494

IV.D.4 California Institute of Technology: Key Technologies, Thermal Management, and Prototype Testing for Advanced Solid-State Hydrogen Storage Systems . . . 494

IV.E.4 Sandia National Laboratories: Analysis of H_2 Storage Needs for Early Market Non-Motive Fuel Cell Applications . . . 554

IV.E.7 H2 Technology Consulting LLC: Best Practices for Characterizing Engineering Properties of Hydrogen Storage Materials . . . 567

V.D.1 Jet Propulsion Laboratory: Advanced Cathode Catalysts and Supports for PEM Fuel Cells . . . 699

V.D.4 University of California, Riverside: Extended, Continuous Pt Nanostructures in Thick, Dispersed Electrodes . . . 719

V.D.4 Stanford University: Extended, Continuous Pt Nanostructures in Thick, Dispersed Electrodes . . . 719

V.D.5 Jet Propulsion Laboratory: Nanosegregated Cathode Catalysts with Ultra-Low Platinum Loading . . . 723

V.D.7 University of California, Riverside: The Science and Engineering of Durable Ultralow PGM Catalysts . . . 734

V.D.8 Lawrence Berkeley National Laboratory: Molecular-Scale, Three-Dimensional Non-Platinum Group Metal Electrodes for Catalysis of Fuel Cell Reactions . . . 738

V.E.2 Lawrence Berkeley National Laboratory: Durability Improvements Through Degradation Mechanism Studies . . . 788

V.E.7 Lawrence Berkeley National Laboratory: Accelerated Testing Validation . . . 810

V.F.2 Sandia National Laboratories: Development and Validation of a Two-Phase, Three-Dimensional Model for PEM Fuel Cells . . . 818

V.F.2 Lawrence Berkeley National Laboratory: Development and Validation of a Two-Phase, Three-Dimensional Model for PEM Fuel Cells . . . 818

V.F.2 University of California, Irvine: Development and Validation of a Two-Phase, Three-Dimensional Model for PEM Fuel Cells . . . 818

V.F.6 Lawrence Berkeley National Laboratory: Transport Studies Enabling Efficiency Optimization of Cost-Competitive Fuel Cell Stacks . . . 837

California (Continued)

V.F.7 Lawrence Berkeley National Laboratory: Fuel Cell Fundamentals at Low and Subzero Temperatures 841
V.G.1 Jet Propulsion Laboratory: Novel Approach to Advanced Direct Methanol Fuel Cell (DMFC) Anode Catalysts 846
V.G.2 QuantumSphere Inc.: Novel Materials for High Efficiency Direct Methanol Fuel Cells 850
V.G.4 University of California, Riverside: Advanced Materials and Concepts for Portable Power Fuel Cells 858
V.I.1 Jet Propulsion Laboratory: Resonance-Stabilized Anion Exchange Polymer Electrolytes 872
V.J.2 Honeywell Aerospace: Development of Thermal and Water Management System for PEM Fuel Cell 883
V.K.2 Intelligent Energy: Development and Demonstration of a New Generation High Efficiency 10 kW Stationary PEM Fuel Cell System 894
V.K.3 University of California, Davis: Research & Development for Off-Road Fuel Cell Applications 899
VI.3 UltraCell Corporation: Modular, High-Volume Fuel Cell Leak-Test Suite and Process 968
VI.9 Quantum Fuel Systems Technologies Worldwide, Inc.: Development of Advanced Manufacturing Technologies for Low Cost Hydrogen Storage Vessels 995
VI.9 Lawrence Livermore National Laboratory: Development of Advanced Manufacturing Technologies for Low Cost Hydrogen Storage Vessels 995
VII.3 Mercedes-Benz Research & Development North America, Inc.: Hydrogen to the Highways – Controlled Hydrogen Fleet and Infrastructure Demonstration and Validation Project 1027
VII.6 University of California, Irvine: California Hydrogen Infrastructure Project 1040
VII.9 California State University, Los Angeles: Sustainable Hydrogen Fueling Station, California State University, Los Angeles 1050
VIII.1 Sandia National Laboratories: Hydrogen Safety, Codes and Standards R&D – Release Behavior 1061
VIII.2 Sandia National Laboratories: Risk-Informed Safety Requirements for H2 Codes and Standards Development 1067
VIII.4 Sandia National Laboratories: Hydrogen Materials and Components Compatibility 1075
VIII.5 Sandia National Laboratories: Component Testing for Industrial Trucks and Early Market Applications 1079
VIII.6 Steele Consulting: National Codes and Standards Coordination 1083
VIII.10 City of Santa Fe Springs: Hydrogen Safety Panel 1100
VIII.12 California Fuel Cell Partnership: Hydrogen Emergency Response Training for First Responders 1107
VIII.13 Lawrence Livermore National Laboratory: Hydrogen Safety Training for Researchers and Technical Personnel 1110
VIII.14 Intelligent Optical Systems, Inc.: Hydrogen Leak Detection System Development 1114
IX.3 University of California, Berkeley: Hydrogen Education State Partnership Program 1139
IX.6 Humboldt State University: H2L3: Hydrogen Learning for Local Leaders 1148
IX.9 California State University, Los Angeles: Hydrogen and Fuel Cell Education at California State University, Los Angeles 1158
IX.10 Humboldt State University Sponsored Programs Foundation: Hydrogen Energy in Engineering Education (H_2E^3) 1161
IX.10 University of California, Berkeley: Hydrogen Energy in Engineering Education (H_2E^3) 1161
IX.15 University of California, Berkeley: Hydrogen Technology and Energy Curriculum (HyTEC) 1180
IX.15 Humboldt State University: Hydrogen Technology and Energy Curriculum (HyTEC) 1180
X.1 Sandia National Laboratories: Fuel Cell Mobile Lighting 1191
X.2 Longitude 122 West, Inc.: Economic Analysis of Bulk Hydrogen Storage for Renewable Utility Applications 1196
X.6 Oorja Protonics, Inc.: Direct Methanol Fuel Cell Material Handling Equipment Demonstration 1209
X.8 Lawrence Livermore National Laboratory: Incorporation of Two Ford H_2 ICE Buses into the Shuttle Bus Fleet 1214
X.9 Sandia National Laboratories: PEM Fuel Cell Systems for Commercial Airplane Systems Power 1217

California (Continued)

XI.4 Sandia National Laboratories: Analysis of the Effects of Developing New Energy Infrastructures 1244
XI.4 Andy Lutz: Analysis of the Effects of Developing New Energy Infrastructures 1244
XI.11 Lawrence Livermore National Laboratory: Energy Informatics: Support for Decision Makers through Energy, Carbon and Water Analysis 1270
XII.2 Jadoo Power, Inc.: Jadoo Power Fuel Cell Demonstration 1291
XII.4 Electricore, Inc.: Solid Oxide Fuel Cell Diesel Auxiliary Power Unit Demonstration 1297
XII.5 Altergy Systems, Folsum: Demonstrating Economic and Operational Viability of 72-Hour Hydrogen PEM Fuel Cell Systems to Support Emergency Communications on the Sprint Nextel Network 1300
XII.6 Peek Site-Com, Inc.: PEM Fuel Cell Systems Providing Backup Power to Commercial Cellular Towers and an Electric Utility Communications Network 1304
XII.6 Jeffrey Rome and Associates: PEM Fuel Cell Systems Providing Backup Power to Commercial Cellular Towers and an Electric Utility Communications Network 1304
XII.12 University of California, Irvine: Highly Efficient, 5 kW CHP Fuel Cells Demonstrating Durability and Economic Value in Residential and Light Commercial Applications. 1325

Colorado

II.A.2 National Renewable Energy Laboratory: Distributed Bio-Oil Reforming 29
II.C.3 Colorado School of Mines: High Performance Palladium-Based Membrane for Hydrogen Separation and Purification 58
II.D.1 Colorado School of Mines: Advanced Hydrogen Transport Membranes for Coal Gasification 62
II.D.3 United Technologies Research Center: Advanced Palladium Membrane Scale Up for Hydrogen Separation. 69
II.E.4 National Renewable Energy Laboratory: Renewable Electrolysis Integrated System Development and Testing 92
II.E.4 Spectrum Automation Controls: Renewable Electrolysis Integrated System Development and Testing. 92
II.E.6 National Renewable Energy Laboratory: Hour-by-Hour Cost Modeling of Optimized Central Wind-Based Water Electrolysis Production 98
II.F.3 University of Colorado: Solar Hydrogen Production with a Metal Oxide-Based Thermochemical Cycle 112
II.F.4 University of Colorado: Solar-Thermal ALD Ferrite-Based Water Splitting Cycle 118
II.G.2 National Renewable Energy Laboratory: Semiconductor Materials for Photoelectrolysis 129
II.G.3 Lawrence Livermore National Laboratory: Characterization and Optimization of Photoelectrode Surfaces for Solar-to-Chemical Fuel Conversion. 134
II.G.5 MVSystems, Incorporated: Photoelectrochemical Hydrogen Production 146
II.G.6 National Renewable Energy Laboratory: Critical Research for Cost-Effective Photoelectrochemical Production of Hydrogen 150
II.G.8 National Renewable Energy Laboratory: Photoelectrochemical Hydrogen Generation from Water Using $TiSi_2$–TiO_2 Nanotube Core-Shell Structure 160
II.G.12 National Renewable Energy Laboratory: Photoelectrochemical Materials: Theory and Modeling. 176
II.G.13 Synkera Technologies Inc.: Nanotube Array Photoelectrochemical Hydrogen Production 181
II.H.1 National Renewable Energy Laboratory: Biological Systems for Hydrogen Photoproduction. 185
II.H.2 National Renewable Energy Laboratory: Fermentation and Electrohydrogenic Approaches to Hydrogen Production 190
II.H.5 National Renewable Energy Laboratory: Purdue Hydrogen Systems Laboratory: Hydrogen Production 203
II.I.1 National Renewable Energy Laboratory: H2A Production Model Updates 207
II.K.5 National Renewable Energy Laboratory: Structural, Functional, and Integration Studies of Solar-Driven, Bio-Hybrid, H_2-Producing Systems 240

Colorado (Continued)

II.K.8 National Renewable Energy Laboratory: Regulation of H_2 and CO_2 Metabolism: Factors Involved in Partitioning of Photosynthetic Reductant in Green Algae . . . 248

II.K.21 National Renewable Energy Laboratory: New Directions for Efficient Solar Water Splitting Based on Two Photosystems and Singlet Fission Chromophores . . . 286

III.4 National Renewable Energy Laboratory: Hydrogen Delivery Analysis . . . 312

IV.C.7 National Renewable Energy Laboratory: Weak Chemisorption Validation . . . 464

IV.D.1 National Renewable Energy Laboratory: Hydrogen Storage Engineering Center of Excellence . . . 479

IV.D.2 National Renewable Energy Laboratory: System Design, Analysis, Modeling, and Media Engineering Properties for Hydrogen Energy Storage . . . 486

IV.E.5 National Renewable Energy Laboratory: Analysis of Storage Needs for Early Motive Fuel Cell Markets . . . 558

IV.G.1 National Renewable Energy Laboratory: Purdue Hydrogen Systems Laboratory: Hydrogen Storage . . . 585

V.A.1 National Renewable Energy Laboratory: Analysis of Laboratory Fuel Cell Technology Status – Voltage Degradation . . . 605

V.A.7 National Renewable Energy Laboratory: Enlarging the Potential Market for Stationary Fuel Cells Through System Design Optimization . . . 634

V.B.1 National Renewable Energy Laboratory: Effect of System Contaminants on PEMFC Performance and Durability . . . 640

V.B.1 Colorado School of Mines: Effect of System Contaminants on PEMFC Performance and Durability . . . 640

V.C.1 Colorado School of Mines: Membranes and MEAs for Dry, Hot Operating Conditions . . . 662

V.C.6 Colorado School of Mines: Novel Approaches to Immobilized Heteropoly Acid (HPA) Systems for High Temperature, Low Relative Humidity Polymer-Type Membranes . . . 685

V.C.9 BekkTech LLC: Lead Research and Development Activity for DOE's High Temperature, Low Relative Humidity Membrane Program . . . 696

V.D.4 National Renewable Energy Laboratory: Extended, Continuous Pt Nanostructures in Thick, Dispersed Electrodes . . . 719

V.D.9 National Renewable Energy Laboratory: Tungsten Oxide and Heteropoly Acid Based System for Ultra-High Activity and Stability of Pt Catalysts in PEM Fuel Cell Cathodes . . . 745

V.D.9 Colorado School of Mines: Tungsten Oxide and Heteropoly Acid Based System for Ultra-High Activity and Stability of Pt Catalysts in PEM Fuel Cell Cathodes . . . 745

V.D.9 University of Colorado: Tungsten Oxide and Heteropoly Acid Based System for Ultra-High Activity and Stability of Pt Catalysts in PEM Fuel Cell Cathodes . . . 745

V.G.1 National Renewable Energy Laboratory: Novel Approach to Advanced Direct Methanol Fuel Cell (DMFC) Anode Catalysts . . . 846

V.G.1 Colorado School of Mines: Novel Approach to Advanced Direct Methanol Fuel Cell (DMFC) Anode Catalysts . . . 846

V.I.2 Versa Power Systems: Advanced Materials for RSOFC Dual Mode Operation with Low Degradation . . . 876

V.L.6 Colorado School of Mines: Biomass Fuel Cell Systems . . . 927

VI.1 National Renewable Energy Laboratory: Fuel Cell Membrane Electrode Assembly Manufacturing R&D . . . 959

VII.1 National Renewable Energy Laboratory: Controlled Hydrogen Fleet and Infrastructure Analysis . . . 1017

VII.5 National Renewable Energy Laboratory: Technology Validation: Fuel Cell Bus Evaluations . . . 1036

VIII.3 National Renewable Energy Laboratory: Component Standard Research and Development . . . 1072

VIII.6 National Renewable Energy Laboratory: National Codes and Standards Coordination . . . 1083

VIII.6 FP2 Fire Protection Engineering: National Codes and Standards Coordination . . . 1083

VIII.6 MorEvents: National Codes and Standards Coordination . . . 1083

VIII.7 National Renewable Energy Laboratory: Codes and Standards Outreach for Emerging Fuel Cell Technologies . . . 1087

VIII.7 MorEvents: Codes and Standards Outreach for Emerging Fuel Cell Technologies . . . 1087

Colorado (Continued)

IX.3 National Conference of State Legislatures: Hydrogen Education State Partnership Program 1139
X.5 National Renewable Energy Laboratory: Green Communities 1205
X.6 National Renewable Energy Laboratory: Direct Methanol Fuel Cell Material Handling Equipment Demonstration 1209
XI.2 National Renewable Energy Laboratory: Hydrogen Infrastructure Market Readiness Analysis. 1236
XI.3 National Renewable Energy Laboratory: Infrastructure Analysis of Early Market Transition of Fuel Cell Vehicles. 1240
XI.3 Allegiance Consulting: Infrastructure Analysis of Early Market Transition of Fuel Cell Vehicles 1240
XI.5 National Renewable Energy Laboratory: Cost and GHG Implications of Hydrogen for Energy Storage. 1248
XI.7 National Renewable Energy Laboratory: NEMS-H2: Hydrogen's Role in Climate Mitigation and Oil Dependence Reduction. 1254
XI.9 National Renewable Energy Laboratory: Macro-System Model 1261
XI.10 National Renewable Energy Laboratory: HyDRA: Hydrogen Demand and Resource Analysis Tool 1265
XI.10 Alumni Consulting: HyDRA: Hydrogen Demand and Resource Analysis Tool. 1265
XII.4 TDA Research, Inc.: Solid Oxide Fuel Cell Diesel Auxiliary Power Unit Demonstration 1297
XII.6 Front Range Wireless: PEM Fuel Cell Systems Providing Backup Power to Commercial Cellular Towers and an Electric Utility Communications Network. 1304
XII.7 National Renewable Energy Laboratory: Analysis Results for ARRA Projects: Enabling Fuel Cell Market Transformation. 1308

Connecticut

II.B.1 United Technologies Research Center: A Novel Slurry-Based Biomass Reforming Process 37
II.D.4 Worcester Polytechnic Institute: Composite Pd and Alloy Porous Stainless Steel Membranes for Hydrogen Production and Process Intensification. 73
II.E.2 Proton Energy Systems: High Performance, Low Cost Hydrogen Generation from Renewable Energy 83
II.E.3 Avalence, LLC: High-Capacity, High Pressure Electrolysis System with Renewable Power Sources. 87
II.J.2 Proton Energy Systems: Hydrogen by Wire - Home Fueling System. 215
III.10 FuelCell Energy, Inc.: Electrochemical Hydrogen Compressor 342
III.10 Sustainable Innovations, LLC: Electrochemical Hydrogen Compressor 342
IV.D.1 United Technologies Research Center: Hydrogen Storage Engineering Center of Excellence 479
IV.D.7 United Technologies Research Center: Advancement of Systems Designs and Key Engineering Technologies for Materials-Based Hydrogen Storage 511
IV.E.1 United Technologies Research Center: Quantifying and Addressing the DOE Material Reactivity Requirements with Analysis and Testing of Hydrogen Storage Materials and Systems 538
V.B.2 University of Connecticut: The Effects of Impurities on Fuel Cell Performance and Durability. 644
V.B.2 FuelCell Energy, Inc.: The Effects of Impurities on Fuel Cell Performance and Durability. 644
V.B.2 United Technologies Corporation – Hamilton Sundstrand: The Effects of Impurities on Fuel Cell Performance and Durability. 644
V.B.3 University of Connecticut: The Effect of Airborne Contaminants on Fuel Cell Performance and Durability 649
V.B.3 UTC Power: The Effect of Airborne Contaminants on Fuel Cell Performance and Durability 649
V.C.7 FuelCell Energy, Inc.: High-Temperature Membrane with Humidification-Independent Cluster Structure. 690
V.D.2 UTC Power: Highly Dispersed Alloy Catalyst for Durability. 708
V.D.15 University of Connecticut: Development of Alternative and Durable High Performance Cathode Supports for PEM Fuel Cells 777
V.E.1 United Technologies Research Center: Polymer Electrolyte Fuel Cell Lifetime Limitations: The Role of Electrocatalyst Degradation 783

Connecticut (Continued)

V.E.6 UTC Power: Improved Accelerated Stress Tests Based on Fuel Cell Vehicle Data 806
V.E.6 United Technologies Research Center: Improved Accelerated Stress Tests Based on Fuel Cell Vehicle Data 806
V.F.7 United Technologies Research Center: Fuel Cell Fundamentals at Low and Subzero Temperatures 841
V.K.4 Energy Technology Services: Power Generation from an Integrated Biomass Reformer and Solid Oxide Fuel Cell. 901
V.L.9 University of Connecticut Global Fuel Cell Center: Improving Reliability and Durability of Efficient and Clean Energy Systems 943
VI.4 UTC Power: Manufacturing of Low-Cost, Durable Membrane Electrode Assemblies Engineered for Rapid Conditioning 971
VII.4 FuelCell Energy, Inc.: Validation of an Integrated Hydrogen Energy Station 1032
VIII.6 Kelvin Hecht: National Codes and Standards Coordination 1083
VIII.6 GWS Solutions of Tolland, LLC: National Codes and Standards Coordination 1083
VIII.10 Hydrogen Safety, LLC: Hydrogen Safety Panel 1100
VIII.10 GWS Solutions of Tolland, LLC: Hydrogen Safety Panel 1100
IX.2 Connecticut Center for Advanced Technology, Inc.: State and Local Government Partnership 1135
XII.8 Airgas Merchant Gases: H-E-B Grocery Total Power Solution for Fuel Cell-Powered Material Handling Equipment 1312

Delaware

IV.G.3 Delaware State University: Hydrogen Storage Materials for Fuel Cell-Powered Vehicles 593
V.C.8 Ion Power Inc.: Corrugated Membrane Fuel Cell Structures 694
V.D.15 University of Delaware: Development of Alternative and Durable High Performance Cathode Supports for PEM Fuel Cells 777
V.E.2 Ion Power Inc.: Durability Improvements Through Degradation Mechanism Studies 788
V.E.3 E.I. du Pont de Nemours and Company: Analysis of Durability of MEAs in Automotive PEMFC Applications 794
V.E.7 Ion Power Inc.: Accelerated Testing Validation 810
VI.4 University of Delaware: Manufacturing of Low-Cost, Durable Membrane Electrode Assemblies Engineered for Rapid Conditioning 971

Florida

V.C.9 University of Central Florida: Lead Research and Development Activity for DOE's High Temperature, Low Relative Humidity Membrane Program 696
V.G.3 University of North Florida: New MEA Materials for Improved Direct Methanol Fuel Cell (DMFC) Performance, Durability, and Cost 854
V.G.3 University of Florida: New MEA Materials for Improved Direct Methanol Fuel Cell (DMFC) Performance, Durability, and Cost 854
VII.8 University of Central Florida: Florida Hydrogen Initiative (FHI) 1046
VII.8 EnerFuels, Inc.: Florida Hydrogen Initiative (FHI) 1046
VII.8 Florida Solar Energy Center: Florida Hydrogen Initiative (FHI). 1046
VII.8 SRT Group, Inc.: Florida Hydrogen Initiative (FHI) 1046
VII.8 University of Florida: Florida Hydrogen Initiative (FHI) 1046
VII.8 Florida State University: Florida Hydrogen Initiative (FHI) 1046
VII.8 Bing Energy, Inc.: Florida Hydrogen Initiative (FHI) 1046
VII.8 Florida Institute of Technology: Florida Hydrogen Initiative (FHI) 1046
VII.8 University of South Florida: Florida Hydrogen Initiative (FHI) 1046
VIII.10 Addison Bain: Hydrogen Safety Panel 1100

Florida (Continued)

IX.12 University of Central Florida: Hydrogen and Fuel Cell Technology Education Program (HFCT) 1170
XII.3 University of North Florida: Advanced Direct Methanol Fuel Cell for Mobile Computing 1294
XII.3 University of Florida: Advanced Direct Methanol Fuel Cell for Mobile Computing 1294
XII.6 Betacom, Inc.: PEM Fuel Cell Systems Providing Backup Power to Commercial Cellular Towers and an Electric Utility Communications Network 1304
XII.6 United Commercial Real Estate Services, Inc.: PEM Fuel Cell Systems Providing Backup Power to Commercial Cellular Towers and an Electric Utility Communications Network 1304

Georgia

II.K.3 University of Georgia: Fundamental Studies of Recombinant Hydrogenases 234
III.6 Savannah River National Laboratory: Fiber Reinforced Composite Pipeline 322
IV.A.1 Savannah River National Laboratory: Amide and Combined Amide/Borohydride Investigations..... 383
IV.A.7 Savannah River National Laboratory: Electrochemical Reversible Formation of Alane 413
IV.D.1 Savannah River National Laboratory: Hydrogen Storage Engineering Center of Excellence 479
IV.D.5 Savannah River National Laboratory: SRNL Technical Work Scope for the Hydrogen Storage Engineering Center of Excellence: Design and Testing of Metal Hydride and Adsorbent Systems 498
V.E.4 Georgia Institute of Technology: Development of Micro-Structural Mitigation Strategies for PEM Fuel Cells: Morphological Simulations and Experimental Approaches 797

Hawaii

II.G.5 University of Hawaii at Manoa: Photoelectrochemical Hydrogen Production.....146
IV.A.3 University of Hawaii: Fundamental Studies of Advanced High-Capacity, Reversible Metal Hydrides.....393
IV.C.7 University of Hawaii: Weak Chemisorption Validation 464
V.B.1 University of Hawaii: Effect of System Contaminants on PEMFC Performance and Durability..... 640
V.B.3 Hawaii Natural Energy Institute: The Effect of Airborne Contaminants on Fuel Cell Performance and Durability..... 649
VII.7 Hawaii Natural Energy Institute: Hawaii Hydrogen Power Park 1043
X.3 Hawaii Natural Energy Institute: Hydrogen Energy Systems as a Grid Management Tool 1200

Illinois

II.A.3 Argonne National Laboratory: Distributed Reforming of Renewable Liquids Using Oxygen Transport Membranes (OTMs) 33
II.B.2 Gas Technology Institute: One Step Biomass Gas Reforming-Shift Separation Membrane Reactor 42
II.F.2 Argonne National Laboratory: Membrane/Electrolyzer Development in the Cu-Cl Thermochemical Cycle 108
III.2 Argonne National Laboratory: Hydrogen Delivery Infrastructure Analysis 303
III.12 University of Illinois at Urbana-Champaign: A Combined Materials Science/Mechanics Approach to the Study of Hydrogen Embrittlement of Pipeline Steels 349
III.16 Argonne National Laboratory: Hydrogen Pipeline Compressors 367
IV.A.2 Northwestern University: Efficient Discovery of Novel Multicomponent Mixtures for Hydrogen Storage: A Combined Computational/Experimental Approach..... 388
IV.A.5 University of Illinois at Urbana-Champaign: Reversible Hydrogen Storage Materials - Structure, Chemistry, and Electronic Structure..... 403
IV.C.4 Northwestern University: New Carbon-Based Porous Materials with Increased Heats of Adsorption for Hydrogen Storage..... 450
IV.C.5 Argonne National Laboratory: Hydrogen Storage through Nanostructured Porous Organic Polymers (POPs) 455
IV.C.5 University of Chicago: Hydrogen Storage through Nanostructured Porous Organic Polymers (POPs).... 455
IV.E.2 Argonne National Laboratory: System Level Analysis of Hydrogen Storage Options 544

Illinois (Continued)

V.A.3 Argonne National Laboratory: Drive-Cycle Performance of Automotive Fuel Cell Systems 614

V.A.8 Argonne National Laboratory: Fuel Cell Testing at the Argonne Fuel Cell Test Facility: A Comparison of U.S. and EU Test Protocols. 637

V.D.1 Argonne National Laboratory: Advanced Cathode Catalysts and Supports for PEM Fuel Cells. 699

V.D.5 Argonne National Laboratory: Nanosegregated Cathode Catalysts with Ultra-Low Platinum Loading 723

V.D.10 Illinois Institute of Technology: Synthesis and Characterization of Mixed-Conducting Corrosion Resistant Oxide Supports 752

V.E.1 Argonne National Laboratory: Polymer Electrolyte Fuel Cell Lifetime Limitations: The Role of Electrocatalyst Degradation. 783

V.E.2 Argonne National Laboratory: Durability Improvements Through Degradation Mechanism Studies 788

V.E.3 Illinois Institute of Technology: Analysis of Durability of MEAs in Automotive PEMFC Applications 794

V.E.5 Argonne National Laboratory: Durability of Low Platinum Fuel Cells Operating at High Power Density 802

V.G.2 Illinois Institute of Technology: Novel Materials for High Efficiency Direct Methanol Fuel Cells 850

V.H.1 Gas Technology Institute: Low-Cost PEM Fuel Cell Metal Bipolar Plates 863

V.H.2 Argonne National Laboratory: Metallic Bipolar Plates with Composite Coatings 867

V.H.2 Southern Illinois University, Carbondale: Metallic Bipolar Plates with Composite Coatings 867

V.H.2 Gas Technology Institute: Metallic Bipolar Plates with Composite Coatings 867

V.H.2 Orion Industries: Metallic Bipolar Plates with Composite Coatings. 867

IX.1 Argonne National Laboratory: Employment Impacts of Early Markets for Hydrogen and Fuel Cell Technologies 1131

IX.1 RCF Economic and Financial Consulting, Inc.: Employment Impacts of Early Markets for Hydrogen and Fuel Cell Technologies 1131

X.7 Gas Technology Institute: Landfill Gas-to-Hydrogen 1212

XI.6 Argonne National Laboratory: Emissions Analysis of Electricity Storage with Hydrogen. 1251

XI.8 Argonne National Laboratory: GREET Model Development and Life-Cycle Analysis Applications 1257

XI.12 Argonne National Laboratory: Fuel Quality Effects on Stationary Fuel Cell Systems 1275

Indiana

II.H.5 Purdue University: Purdue Hydrogen Systems Laboratory: Hydrogen Production. 203

IV.G.1 Purdue University: Purdue Hydrogen Systems Laboratory: Hydrogen Storage 585

XII.6 Fortune Wireless: PEM Fuel Cell Systems Providing Backup Power to Commercial Cellular Towers and an Electric Utility Communications Network 1304

Kansas

XII.5 Black & Veatch Corporation: Demonstrating Economic and Operational Viability of 72-Hour Hydrogen PEM Fuel Cell Systems to Support Emergency Communications on the Sprint Nextel Network 1300

XII.5 Ericsson Services, Inc.: Demonstrating Economic and Operational Viability of 72-Hour Hydrogen PEM Fuel Cell Systems to Support Emergency Communications on the Sprint Nextel Network 1300

Maryland

II.H.1 Johns Hopkins University: Biological Systems for Hydrogen Photoproduction. 185

IV.A.9 National Institute of Standards and Technology: Neutron Characterization in Support of the DOE Hydrogen Storage Sub-Program 420

IV.E.5 Energetics, Inc.: Analysis of Storage Needs for Early Motive Fuel Cell Markets. 558

Maryland (Continued)

V.A.5 National Institute of Standards and Technology: Neutron Imaging Study of the Water Transport in Operating Fuel Cells . . . 626

V.J.1 W. L. Gore & Associates, Inc.: Materials and Modules for Low-Cost, High-Performance Fuel Cell Humidifiers . . . 879

VI.4 W. L. Gore & Associates, Inc.: Manufacturing of Low-Cost, Durable Membrane Electrode Assemblies Engineered for Rapid Conditioning . . . 971

VI.6 National Institute of Standards and Technology: Cause-and-Effect: Flow Field Plate Manufacturing Variability and its Impact on Performance . . . 983

VI.10 National Institute of Standards and Technology: Non-Contact Sensor Evaluation for Bipolar Plate Manufacturing Process Control and Smart Assembly of Fuel Cell Stacks . . . 999

VI.11 National Institute of Standards and Technology: Optical Scatterfield Metrology for Online Catalyst Coating Inspection of PEM (Fuel Cell) Soft Goods . . . 1003

VII.9 General Physics Corporation: Sustainable Hydrogen Fueling Station, California State University, Los Angeles . . . 1050

VIII.10 Energetics, Inc.: Hydrogen Safety Panel . . . 1100

IX.5 University of Maryland: VA-MD-DC Hydrogen Education for Decision Makers . . . 1144

IX.14 Sentech, Inc.: H_2 Educate! Hydrogen Education for Middle Schools . . . 1177

XI.2 Energetics, Inc.: Hydrogen Infrastructure Market Readiness Analysis . . . 1236

Massachusetts

II.E.1 Giner Electrochemical Systems, LLC: PEM Electrolyzer Incorporating an Advanced Low-Cost Membrane . . . 79

II.J.1 Giner Electrochemical Systems, LLC: Unitized Design for Home Refueling Appliance for Hydrogen Generation to 5,000 psi . . . 211

III.8 Concepts NREC: Development of a Centrifugal Hydrogen Pipeline Gas Compressor . . . 331

IV.A.8 Massachusetts Institute of Technology: Tunable Thermodynamics and Kinetics for Hydrogen Storage: Nanoparticle Synthesis Using Ordered Polymer Templates . . . 416

IV.C.8 PoroGen, LLC: Nanostructured Activated Carbon for Hydrogen Storage . . . 470

IV.E.1 Kidde-Fenwal: Quantifying and Addressing the DOE Material Reactivity Requirements with Analysis and Testing of Hydrogen Storage Materials and Systems . . . 538

IV.E.3 TIAX, LLC: Cost Analyses of Hydrogen Storage Materials and On-Board Systems . . . 550

V.C.2 Giner Electrochemical Systems, LLC: Dimensionally Stable Membranes (DSMs) . . . 667

V.C.3 Giner Electrochemical Systems, LLC: Dimensionally Stable High Performance Membrane (SBIR Phase III) . . . 671

V.D.6 Massachusetts Institute of Technology: Contiguous Platinum Monolayer Oxygen Reduction Electrocatalysts on High-Stability Low-Cost Supports . . . 729

V.D.11 Northeastern University: Development of Novel Non-PGM Electrocatalysts for Proton Exchange Membrane Fuel Cell Applications . . . 756

V.D.12 Massachusetts Institute of Technology: High-Activity Dealloyed Catalysts . . . 760

V.D.12 Northeastern University: High-Activity Dealloyed Catalysts . . . 760

V.E.1 Massachusetts Institute of Technology: Polymer Electrolyte Fuel Cell Lifetime Limitations: The Role of Electrocatalyst Degradation . . . 783

V.E.5 Nuvera Fuel Cells, Inc.: Durability of Low Platinum Fuel Cells Operating at High Power Density . . . 802

V.F.3 Giner Electrochemical Systems, LLC: Transport in PEMFC Stacks . . . 822

V.F.3 Tech-Etch: Transport in PEMFC Stacks . . . 822

V.F.3 Ballard Material Products, Inc.: Transport in PEMFC Stacks . . . 822

V.F.6 Nuvera Fuel Cells, Inc.: Transport Studies Enabling Efficiency Optimization of Cost-Competitive Fuel Cell Stacks . . . 837

Massachusetts (Continued)

V.G.3 Northeastern University: New MEA Materials for Improved Direct Methanol Fuel Cell (DMFC) Performance, Durability, and Cost 854

V.J.3 Protonex Inc.: Large Scale Testing, Demonstration and Commercialization of the Nanoparticle-Based Fuel Cell Coolant 886

V.K.1 Acumentrics Corporation: Development of a Low-Cost 3-10 kW Tubular SOFC Power System. 890

VI.2 Ballard Material Products, Inc.: Reduction in Fabrication Costs of Gas Diffusion Layers 963

VIII.10 Firexplo: Hydrogen Safety Panel 1100

X.7 Ameresco, Inc.: Landfill Gas-to-Hydrogen. 1212

XI.2 IDC Energy Insights: Hydrogen Infrastructure Market Readiness Analysis 1236

XII.8 Nuvera Fuel Cells, Inc.: H-E-B Grocery Total Power Solution for Fuel Cell-Powered Material Handling Equipment 1312

Michigan

III.3 Victor Li Independent Consultant: Vessel Design and Fabrication Technology for Stationary High-Pressure Hydrogen Storage. 307

IV.D.1 General Motors Company: Hydrogen Storage Engineering Center of Excellence. 479

IV.D.1 Ford Motor Company: Hydrogen Storage Engineering Center of Excellence 479

IV.D.1 University of Michigan: Hydrogen Storage Engineering Center of Excellence 479

IV.D.8 General Motors Company: Optimization of Heat Exchangers and System Simulation of On-Board Storage Systems Designs 517

IV.D.9 Ford Motor Company: Ford/BASF-SE/UM Activities in Support of the Hydrogen Storage Engineering Center of Excellence 522

IV.D.9 University of Michigan: Ford/BASF-SE/UM Activities in Support of the Hydrogen Storage Engineering Center of Excellence 522

IV.E.6 Ovonic Hydrogen Systems LLC: Standardized Testing Program for Solid-State Hydrogen Storage Technologies 562

V.B.1 General Motors Company: Effect of System Contaminants on PEMFC Performance and Durability 640

V.C.1 University of Detroit Mercy: Membranes and MEAs for Dry, Hot Operating Conditions 662

V.C.8 General Motors Company: Corrugated Membrane Fuel Cell Structures 694

V.D.10 Nissan Technical Center: Synthesis and Characterization of Mixed-Conducting Corrosion Resistant Oxide Supports 752

V.D.11 Michigan State University: Development of Novel Non-PGM Electrocatalysts for Proton Exchange Membrane Fuel Cell Applications 756

V.D.11 Nissan Technical Center: Development of Novel Non-PGM Electrocatalysts for Proton Exchange Membrane Fuel Cell Applications 756

V.D.12 General Motors Company: High-Activity Dealloyed Catalysts 760

V.E.3 Nissan Technical Center: Analysis of Durability of MEAs in Automotive PEMFC Applications 794

V.E.4 Michigan Technological University: Development of Micro-Structural Mitigation Strategies for PEM Fuel Cells: Morphological Simulations and Experimental Approaches. 797

V.F.4 General Motors Company: Investigation of Micro- and Macro-Scale Transport Processes for Improved Fuel Cell Performance 827

V.H.1 Ford Motor Company: Low-Cost PEM Fuel Cell Metal Bipolar Plates. 863

V.L.8 Kettering University: 21st Century Renewable Fuels, Energy, and Materials Initiative 937

VII.2 General Motors Company: Hydrogen Vehicle and Infrastructure Demonstration and Validation 1023

VII.3 DTE Energy: Hydrogen to the Highways – Controlled Hydrogen Fleet and Infrastructure Demonstration and Validation Project 1027

VII.3 NextEnergy: Hydrogen to the Highways – Controlled Hydrogen Fleet and Infrastructure Demonstration and Validation Project 1027

VIII.3 SAE International: Component Standard Research and Development. 1072

Michigan (Continued)

VIII.6 Sloane Solutions: National Codes and Standards Coordination 1083
VIII.10 General Motors Company: Hydrogen Safety Panel 1100
IX.11 Michigan Technological University: Hydrogen Education Curriculum Path at Michigan Technological University 1166
XII.4 Delphi Automotive Systems, LLC: Solid Oxide Fuel Cell Diesel Auxiliary Power Unit Demonstration 1297
XII.6 Telecom, Tower and Power, LLC: PEM Fuel Cell Systems Providing Backup Power to Commercial Cellular Towers and an Electric Utility Communications Network 1304

Minnesota

II.A.2 University of Minnesota: Distributed Bio-Oil Reforming 29
II.D.1 T3 Scientific: Advanced Hydrogen Transport Membranes for Coal Gasification 62
II.E.2 Entegris, Inc.: High Performance, Low Cost Hydrogen Generation from Renewable Energy 83
V.B.1 3M Company: Effect of System Contaminants on PEMFC Performance and Durability 640
V.C.1 3M Company: Membranes and MEAs for Dry, Hot Operating Conditions 662
V.C.6 3M Company: Novel Approaches to Immobilized Heteropoly Acid (HPA) Systems for High Temperature, Low Relative Humidity Polymer-Type Membranes 685
V.D.1 3M Company: Advanced Cathode Catalysts and Supports for PEM Fuel Cells 699
V.D.3 3M Company: Durable Catalysts for Fuel Cell Protection During Transient Conditions 714
V.D.5 3M Company: Nanosegregated Cathode Catalysts with Ultra-Low Platinum Loading 723
V.E.3 3M Company: Analysis of Durability of MEAs in Automotive PEMFC Applications 794
V.F.7 3M Company: Fuel Cell Fundamentals at Low and Subzero Temperatures 841
V.K.3 The Toro Company: Research & Development for Off-Road Fuel Cell Applications 899

Mississippi

V.L.2 University of Southern Mississippi: Alternative Fuel Cell Membranes for Energy Independence 909

Missouri

II.K.7 University of Missouri: Genetics and Molecular Biology of Hydrogen Metabolism in Sulfate-reducing Bacteria 245
IV.A.8 University of Missouri, St. Louis: Tunable Thermodynamics and Kinetics for Hydrogen Storage: Nanoparticle Synthesis Using Ordered Polymer Templates 416
IV.C.3 University of Missouri: Multiply Surface-Functionalized Nanoporous Carbon for Vehicular Hydrogen Storage 444
IV.C.3 Midwest Research Institute: Multiply Surface-Functionalized Nanoporous Carbon for Vehicular Hydrogen Storage 444
VIII.10 Becht Engineering: Hydrogen Safety Panel 1100
XII.5 Burns & McDonnell Engineering Co., Inc.: Demonstrating Economic and Operational Viability of 72-Hour Hydrogen PEM Fuel Cell Systems to Support Emergency Communications on the Sprint Nextel Network 1300

Nebraska

II.G.10 University of Nebraska, Omaha: Novel Photocatalytic Metal Oxides 170
III.7 Lincoln Composites, Inc.: Development of High Pressure Hydrogen Storage Tank for Storage and Gaseous Truck Delivery 326
IV.D.1 Lincoln Composites, Inc.: Hydrogen Storage Engineering Center of Excellence 479
IV.D.11 Lincoln Composites, Inc.: Development of Improved Composite Pressure Vessels for Hydrogen Storage 534
XII.6 Vertical Horizons Contracting: PEM Fuel Cell Systems Providing Backup Power to Commercial Cellular Towers and an Electric Utility Communications Network 1304

Nevada

II.G.2 University of Nevada, Las Vegas: Semiconductor Materials for Photoelectrolysis 129
II.G.4 University of Nevada, Las Vegas: Characterization of Materials for Photoelectrochemical (PEC) Hydrogen Production 140
II.G.8 University of Nevada, Reno: Photoelectrochemical Hydrogen Generation from Water Using $TiSi_2$–TiO_2 Nanotube Core-Shell Structure 160
II.G.11 University of Nevada, Reno: Solar Thermal Hydrogen Production 173
IV.G.2 University of Nevada, Las Vegas: HGMS: Glasses and Nanocomposites for Hydrogen Storage 590

New Jersey

II.K.10 Princeton University: Theoretical Research Program on Bio-inspired Inorganic Hydrogen Generating Catalysts and Electrodes. 253
IV.C.6 Rutgers University: Hydrogen Trapping through Designer Hydrogen Spillover Molecules with Reversible Temperature and Pressure-Induced Switching 459
V.D.11 BASF Fuel Cell: Development of Novel Non-PGM Electrocatalysts for Proton Exchange Membrane Fuel Cell Applications 756
V.H.1 TreadStone Technologies, Inc.: Low-Cost PEM Fuel Cell Metal Bipolar Plates. 863
VI.7 BASF Fuel Cell: High Speed, Low Cost Fabrication of Gas Diffusion Electrodes for Membrane Electrode Assemblies. 987
XII.11 Linde North America: GENCO Fuel Cell-Powered Lift Truck Fleet Deployment. 1322

New Mexico

IV.B.2 Los Alamos National Laboratory: Fluid Phase Chemical Hydrogen Storage Materials 429
IV.C.7 University of New Mexico: Weak Chemisorption Validation. 464
IV.D.1 Los Alamos National Laboratory: Hydrogen Storage Engineering Center of Excellence. 479
IV.D.3 Los Alamos National Laboratory: Chemical Hydride Rate Modeling, Validation, and System Demonstration 491
V.A.6 Los Alamos National Laboratory: Technical Assistance to Developers 631
V.B.1 Los Alamos National Laboratory: Effect of System Contaminants on PEMFC Performance and Durability 640
V.B.5 Los Alamos National Laboratory: Effects of Fuel and Air Impurities on PEM Fuel Cell Performance 659
V.D.4 Los Alamos National Laboratory: Extended, Continuous Pt Nanostructures in Thick, Dispersed Electrodes 719
V.D.7 Los Alamos National Laboratory: The Science and Engineering of Durable Ultralow PGM Catalysts 734
V.D.7 University of New Mexico: The Science and Engineering of Durable Ultralow PGM Catalysts 734
V.D.11 University of New Mexico: Development of Novel Non-PGM Electrocatalysts for Proton Exchange Membrane Fuel Cell Applications 756
V.D.11 Los Alamos National Laboratory: Development of Novel Non-PGM Electrocatalysts for Proton Exchange Membrane Fuel Cell Applications 756
V.D.14 Los Alamos National Laboratory: Engineered Nano-Scale Ceramic Supports for PEM Fuel Cells 770
V.D.14 University of New Mexico: Engineered Nano-Scale Ceramic Supports for PEM Fuel Cells 770
V.E.2 Los Alamos National Laboratory: Durability Improvements Through Degradation Mechanism Studies . . . 788
V.E.2 University of New Mexico: Durability Improvements Through Degradation Mechanism Studies 788
V.E.4 Los Alamos National Laboratory: Development of Micro-Structural Mitigation Strategies for PEM Fuel Cells: Morphological Simulations and Experimental Approaches 797
V.E.4 University of New Mexico: Development of Micro-Structural Mitigation Strategies for PEM Fuel Cells: Morphological Simulations and Experimental Approaches. 797
V.E.5 Los Alamos National Laboratory: Durability of Low Platinum Fuel Cells Operating at High Power Density. 802

New Mexico (Continued)

V.E.6 Los Alamos National Laboratory: Improved Accelerated Stress Tests Based on Fuel Cell Vehicle Data . . . 806
V.E.7 Los Alamos National Laboratory: Accelerated Testing Validation . . . 810
V.F.2 Los Alamos National Laboratory: Development and Validation of a Two-Phase, Three-Dimensional Model for PEM Fuel Cells . . . 818
V.F.7 Los Alamos National Laboratory: Fuel Cell Fundamentals at Low and Subzero Temperatures . . . 841
V.G.4 Los Alamos National Laboratory: Advanced Materials and Concepts for Portable Power Fuel Cells . . . 858
V.I.1 Los Alamos National Laboratory: Resonance-Stabilized Anion Exchange Polymer Electrolytes. . . . 872
V.I.1 Sandia National Laboratories: Resonance-Stabilized Anion Exchange Polymer Electrolytes. . . . 872
VI.6 Los Alamos National Laboratory: Cause-and-Effect: Flow Field Plate Manufacturing Variability and its Impact on Performance . . . 983
VI.10 Los Alamos National Laboratory: Non-Contact Sensor Evaluation for Bipolar Plate Manufacturing Process Control and Smart Assembly of Fuel Cell Stacks . . . 999
VI.11 Los Alamos National Laboratory: Optical Scatterfield Metrology for Online Catalyst Coating Inspection of PEM (Fuel Cell) Soft Goods . . . 1003
VIII.8 Los Alamos National Laboratory: Leak Detection and H_2 Sensor Development for Hydrogen Applications . . . 1090
VIII.9 Los Alamos National Laboratory: Hydrogen Fuel Quality Research and Development. . . . 1096
IX.5 Los Alamos National Laboratory: VA-MD-DC Hydrogen Education for Decision Makers . . . 1144
IX.14 Los Alamos National Laboratory: H_2 Educate! Hydrogen Education for Middle Schools . . . 1177

New York

II.C.3 Pall Corporation: High Performance Palladium-Based Membrane for Hydrogen Separation and Purification . . . 58
II.D.1 Praxair, Inc.: Advanced Hydrogen Transport Membranes for Coal Gasification . . . 62
II.E.5 H2Pump, LLC: Process Intensification of Hydrogen Unit Operations Using an Electrochemical Device. . . . 95
II.E.5 Plug Power, Inc.: Process Intensification of Hydrogen Unit Operations Using an Electrochemical Device. . . . 95
II.F.1 Electrosynthesis Co. Inc.: Solar High-Temperature Water Splitting Cycle with Quantum Boost . . . 102
II.K.9 University of Rochester: Excited State Dynamics in Semiconductor Quantum Dots . . . 250
II.K.15 Brookhaven National Laboratory: Catalyzed Water Oxidation by Solar Irradiation of Band-Gap-Narrowed Semiconductors . . . 270
II.K.16 Stony Brook University: Quantum theory of Semiconductor-Photo-Catalysis and Solar Water Splitting . . . 273
III.8 Praxair, Inc.: Development of a Centrifugal Hydrogen Pipeline Gas Compressor . . . 331
III.9 Mohawk Innovative Technologies, Inc.: Oil-Free Centrifugal Hydrogen Compression Technology Demonstration . . . 338
III.11 Praxair, Inc.: Advanced Hydrogen Liquefaction Process . . . 345
IV.A.6 Brookhaven National Laboratory: Aluminum Hydride . . . 409
IV.C.8 State University of New York, Syracuse: Nanostructured Activated Carbon for Hydrogen Storage. . . . 470
V.C.2 State University of New York, Syracuse: Dimensionally Stable Membranes (DSMs) . . . 667
V.D.2 Brookhaven National Laboratory: Highly Dispersed Alloy Catalyst for Durability . . . 708
V.D.4 State University of New York, Albany: Extended, Continuous Pt Nanostructures in Thick, Dispersed Electrodes . . . 719
V.D.6 Brookhaven National Laboratory: Contiguous Platinum Monolayer Oxygen Reduction Electrocatalysts on High-Stability Low-Cost Supports. . . . 729
V.F.4 Rochester Institute of Technology: Investigation of Micro- and Macro-Scale Transport Processes for Improved Fuel Cell Performance . . . 827

New York (Continued)

V.F.5 Plug Power Inc.: Air-Cooled Stack Freeze Tolerance 833
V.G.4 Brookhaven National Laboratory: Advanced Materials and Concepts for Portable Power Fuel Cells 858
V.H.1 State University of New York, Stony Brook: Low-Cost PEM Fuel Cell Metal Bipolar Plates. 863
VI.5 Rensselaer Polytechnic Institute: Adaptive Process Controls and Ultrasonics for High-Temperature PEM MEA Manufacture. 977
XII.1 MTI Micro Fuel Cells Inc.: Commercialization of 1 Watt Consumer Electronics Power Pack 1287
XII.2 Delphi Automotive Systems, LLC: Jadoo Power Fuel Cell Demonstration. 1291
XII.9 Plug Power Inc.: Fuel Cell-Powered Lift Truck FedEx Freight Fleet Deployment 1316
XII.10 Plug Power Inc.: Fuel Cell-Powered Lift Truck Sysco Houston Fleet Deployment 1319
XII.11 Plug Power Inc.: GENCO Fuel Cell-Powered Lift Truck Fleet Deployment. 1322
XII.12 Plug Power Inc.: Highly Efficient, 5 kW CHP Fuel Cells Demonstrating Durability and Economic Value in Residential and Light Commercial Applications 1325
XII.13 Plug Power Inc.: Accelerating Acceptance of Fuel Cell Backup Power Systems 1328

North Carolina

II.H.1 North Carolina State University: Biological Systems for Hydrogen Photoproduction 185
V.C.9 Scribner Associates, Inc.: Lead Research and Development Activity for DOE's High Temperature, Low Relative Humidity Membrane Program 696
V.F.1 Techverse: Water Transport in PEM Fuel Cells: Advanced Modeling, Material Selection, Testing, and Design Optimization 814
IX.8 Carolina Tractor & Equipment Co. Inc.: Dedicated to The Continued Education, Training and Demonstration of PEM Fuel Cell-Powered Lift Trucks In Real-World Applications 1155
IX.12 University of North Carolina at Charlotte: Hydrogen and Fuel Cell Technology Education Program (HFCT) 1170

North Dakota

II.B.1 University of North Dakota: A Novel Slurry-Based Biomass Reforming Process 37
II.D.3 University of North Dakota: Advanced Palladium Membrane Scale Up for Hydrogen Separation 69
IX.13 University of North Dakota: Development of a Renewable Hydrogen Production and Fuel Cell Education Program 1173

Ohio

II.C.1 University of Cincinnati: Zeolite Membrane Reactor for Water-Gas Shift Reaction for Hydrogen Production 46
II.C.1 Ohio State University: Zeolite Membrane Reactor for Water-Gas Shift Reaction for Hydrogen Production 46
II.D.4 Adsorption Research, Inc.: Composite Pd and Alloy Porous Stainless Steel Membranes for Hydrogen Production and Process Intensification 73
II.G.6 Midwest Optoelectronics, LLC: Critical Research for Cost-Effective Photoelectrochemical Production of Hydrogen 150
II.G.6 Xunlight Corporation: Critical Research for Cost-Effective Photoelectrochemical Production of Hydrogen 150
II.G.6 University of Toledo: Critical Research for Cost-Effective Photoelectrochemical Production of Hydrogen 150
IV.A.4 Ohio State University: Lightweight Metal Hydrides for Hydrogen Storage 398
V.C.1 Case Western Reserve University: Membranes and MEAs for Dry, Hot Operating Conditions 662
V.C.4 Case Western Reserve University: Poly(p-Phenylene Sulfonic Acids): PEMs with Frozen-In Free Volume 675

Ohio (Continued)

V.C.5 Wright State University: NanoCapillary Network Proton Conducting Membranes for High Temperature Hydrogen/Air Fuel Cells . . . 680
V.C.8 Graftech International Holdings Inc.: Corrugated Membrane Fuel Cell Structures . . . 694
V.L.1 University of Akron: Development of Kilowatt-Scale Coal Fuel Cell Technology . . . 905
V.L.3 Rolls Royce Fuel Cell Systems Inc.: Extended Durability Testing of an External Fuel Processor for SOFCs . . . 914
V.L.5 Stark State College of Technology: Fuel Cell Balance of Plant Reliability Testbed . . . 923
V.L.5 Lockheed Martin-IDT: Fuel Cell Balance of Plant Reliability Testbed . . . 923
V.L.10 Stark State College of Technology: Solid Oxide Fuel Cell Systems Print Verification Line (PVL) Pilot Line . . . 950
V.L.10 Rolls Royce Fuel Cell Systems Inc.: Solid Oxide Fuel Cell Systems Print Verification Line (PVL) Pilot Line . . . 950
VI.3 Cincinnati Test Systems: Modular, High-Volume Fuel Cell Leak-Test Suite and Process . . . 968
VI.7 Case Western Reserve University: High Speed, Low Cost Fabrication of Gas Diffusion Electrodes for Membrane Electrode Assemblies . . . 987
VII.5 Battelle: Technology Validation: Fuel Cell Bus Evaluations . . . 1036
VIII.6 CSA Standards: National Codes and Standards Coordination . . . 1083
VIII.10 Powdermet Inc.: Hydrogen Safety Panel . . . 1100
IX.7 Ohio Fuel Cell Coalition: Raising H_2 and Fuel Cell Awareness in Ohio . . . 1153
IX.7 Edison Material Technology Center: Raising H_2 and Fuel Cell Awareness in Ohio . . . 1153

Oklahoma

II.K.6 University of Oklahoma: Genes Needed For H_2 Production by Sulfate Reducing Bacteria . . . 242

Oregon

II.B.2 ATI Wah Chang: One Step Biomass Gas Reforming-Shift Separation Membrane Reactor . . . 42
IV.B.1 University of Oregon: Hydrogen Storage by Novel CBN Heterocycle Materials . . . 425
IV.D.1 Oregon State University: Hydrogen Storage Engineering Center of Excellence . . . 479
IV.D.10 Oregon State University: Microscale Enhancement of Heat and Mass Transfer for Hydrogen Energy Storage . . . 530
V.K.3 IdaTech, LLC: Research & Development for Off-Road Fuel Cell Applications . . . 899

Pennsylvania

II.B.2 National Energy Technology Laboratory: One Step Biomass Gas Reforming-Shift Separation Membrane Reactor . . . 42
II.B.2 Schott North America: One Step Biomass Gas Reforming-Shift Separation Membrane Reactor . . . 42
II.C.2 Media and Process Technology Inc.: Development of Hydrogen Selective Membranes/Modules as Reactors/Separators for Distributed Hydrogen Production . . . 53
II.D.2 Eltron Research & Development Inc.: Scale Up of Hydrogen Transport Membranes for IGCC and FutureGen Plants . . . 66
II.D.3 Power & Energy, Inc.: Advanced Palladium Membrane Scale Up for Hydrogen Separation . . . 69
II.E.2 Pennsylvania State University: High Performance, Low Cost Hydrogen Generation from Renewable Energy . . . 83
II.H.2 Pennsylvania State University: Fermentation and Electrohydrogenic Approaches to Hydrogen Production . . . 190
II.K.13 University of Pennsylvania: Modular Designed Protein Constructions for Solar Generated H_2 from Water . . . 264
II.K.19 Pennsylvania State University: A Hybrid Biological-Organic Half-Cell for Generating Dihydrogen . . . 281

Pennsylvania (Continued)

IV.C.6 Pennsylvania State University: Hydrogen Trapping through Designer Hydrogen Spillover Molecules with Reversible Temperature and Pressure-Induced Switching. 459

V.D.5 University of Pittsburgh: Nanosegregated Cathode Catalysts with Ultra-Low Platinum Loading 723

V.F.2 Pennsylvania State University: Development and Validation of a Two-Phase, Three-Dimensional Model for PEM Fuel Cells 818

V.F.4 Pennsylvania State University: Investigation of Micro- and Macro-Scale Transport Processes for Improved Fuel Cell Performance 827

V.F.6 Pennsylvania State University: Transport Studies Enabling Efficiency Optimization of Cost-Competitive Fuel Cell Stacks. 837

V.F.7 Pennsylvania State University: Fuel Cell Fundamentals at Low and Subzero Temperatures 841

V.G.2 Arkema Inc.: Novel Materials for High Efficiency Direct Methanol Fuel Cells 850

V.J.3 Dynalene Inc.: Large Scale Testing, Demonstration and Commercialization of the Nanoparticle-Based Fuel Cell Coolant 886

V.L.7 Dynalene Inc.: Fuel Cell Coolant Optimization and Scale Up. 933

V.L.7 Lehigh University: Fuel Cell Coolant Optimization and Scale Up 933

VI.2 Pennsylvania State University: Reduction in Fabrication Costs of Gas Diffusion Layers 963

VII.4 Air Products and Chemicals, Inc.: Validation of an Integrated Hydrogen Energy Station 1032

VII.6 Air Products and Chemicals, Inc.: California Hydrogen Infrastructure Project 1040

VIII.6 SAE International: National Codes and Standards Coordination. 1083

VIII.6 Bethlehem Hydrogen: National Codes and Standards Coordination 1083

VIII.10 Air Products and Chemicals, Inc.: Hydrogen Safety Panel. 1100

XII.5 Air Products and Chemicals, Inc.: Demonstrating Economic and Operational Viability of 72-Hour Hydrogen PEM Fuel Cell Systems to Support Emergency Communications on the Sprint Nextel Network 1300

XII.6 Air Products and Chemicals, Inc.: PEM Fuel Cell Systems Providing Backup Power to Commercial Cellular Towers and an Electric Utility Communications Network 1304

XII.9 Air Products and Chemicals, Inc.: Fuel Cell-Powered Lift Truck FedEx Freight Fleet Deployment. 1316

XII.10 Air Products and Chemicals, Inc.: Fuel Cell-Powered Lift Truck Sysco Houston Fleet Deployment 1319

XII.11 GENCO Infrastructure Solutions: GENCO Fuel Cell-Powered Lift Truck Fleet Deployment 1322

XII.11 Air Products and Chemicals, Inc.: GENCO Fuel Cell-Powered Lift Truck Fleet Deployment. 1322

Rhode Island

V.D.5 Brown University: Nanosegregated Cathode Catalysts with Ultra-Low Platinum Loading. 723

South Carolina

II.E.5 PBI Performance Products, Inc.: Process Intensification of Hydrogen Unit Operations Using an Electrochemical Device 95

IV.E.8 SCRA: Administration of H-Prize for Hydrogen Storage 571

V.B.1 University of South Carolina: Effect of System Contaminants on PEMFC Performance and Durability. . . 640

V.B.4 Clemson University: Effects of Impurities on Fuel Cell Performance and Durability. 654

V.B.4 Savannah River National Laboratory: Effects of Impurities on Fuel Cell Performance and Durability. . . . 654

V.B.4 John Deere: Effects of Impurities on Fuel Cell Performance and Durability 654

V.D.13 University of South Carolina: Development of Ultra-Low Platinum Alloy Cathode Catalyst for PEM Fuel Cells. 764

V.F.3 University of South Carolina: Transport in PEMFC Stacks 822

V.L.4 University of South Carolina: Hydrogen Fuel Cell Development in Columbia (SC) 918

IX.4 South Carolina Hydrogen and Fuel Cell Alliance: Development of Hydrogen Education Programs for Government Officials 1142

South Carolina (Continued)

IX.4 Greenway Energy: Development of Hydrogen Education Programs for Government Officials. 1142
X.7 South Carolina Hydrogen and Fuel Cell Alliance: Landfill Gas-to-Hydrogen. 1212
X.7 Advanced Technology International: Landfill Gas-to-Hydrogen. 1212

South Dakota

II.G.9 University of South Dakota: USD Catalysis Group for Alternative Energy 164
II.G.9 South Dakota School of Mines and Technology: USD Catalysis Group for Alternative Energy 164

Tennessee

II.C.3 Oak Ridge National Laboratory: High Performance Palladium-Based Membrane for Hydrogen Separation and Purification 58
II.D.2 Eastman Chemical Compnay: Scale Up of Hydrogen Transport Membranes for IGCC and FutureGen Plants. 66
II.E.2 Oak Ridge National Laboratory: High Performance, Low Cost Hydrogen Generation from Renewable Energy 83
III.3 Oak Ridge National Laboratory: Vessel Design and Fabrication Technology for Stationary High-Pressure Hydrogen Storage. 307
III.13 Oak Ridge National Laboratory: Composite Technology for Hydrogen Pipelines. 354
III.15 Oak Ridge National Laboratory: Integrity of Steel Welds in High-Pressure Hydrogen Environment 362
IV.F.1 Oak Ridge National Laboratory: High Strength Carbon Fibers 576
IV.F.2 Oak Ridge National Laboratory: Lifecycle Verification of Polymeric Storage Liners. 581
V.A.4 Oak Ridge National Laboratory: Characterization of Fuel Cell Materials 621
V.C.1 University of Tennessee: Membranes and MEAs for Dry, Hot Operating Conditions. 662
V.C.5 Vanderbilt University: NanoCapillary Network Proton Conducting Membranes for High Temperature Hydrogen/Air Fuel Cells 680
V.D.3 Oak Ridge National Laboratory: Durable Catalysts for Fuel Cell Protection During Transient Conditions. 714
V.D.4 Oak Ridge National Laboratory: Extended, Continuous Pt Nanostructures in Thick, Dispersed Electrodes. 719
V.D.4 University of Tennessee: Extended, Continuous Pt Nanostructures in Thick, Dispersed Electrodes 719
V.D.5 Oak Ridge National Laboratory: Nanosegregated Cathode Catalysts with Ultra-Low Platinum Loading. 723
V.D.11 University of Tennessee: Development of Novel Non-PGM Electrocatalysts for Proton Exchange Membrane Fuel Cell Applications 756
V.D.14 Oak Ridge National Laboratory: Engineered Nano-Scale Ceramic Supports for PEM Fuel Cells 770
V.D.15 Oak Ridge National Laboratory: Development of Alternative and Durable High Performance Cathode Supports for PEM Fuel Cells. 777
V.E.2 Oak Ridge National Laboratory: Durability Improvements Through Degradation Mechanism Studies 788
V.E.6 Oak Ridge National Laboratory: Improved Accelerated Stress Tests Based on Fuel Cell Vehicle Data 806
V.E.7 Oak Ridge National Laboratory: Accelerated Testing Validation 810
V.F.4 University of Tennessee: Investigation of Micro- and Macro-Scale Transport Processes for Improved Fuel Cell Performance 827
V.F.6 University of Tennessee: Transport Studies Enabling Efficiency Optimization of Cost-Competitive Fuel Cell Stacks 837
V.G.4 Oak Ridge National Laboratory: Advanced Materials and Concepts for Portable Power Fuel Cells 858
V.J.3 University of Tennessee, Knoxville: Large Scale Testing, Demonstration and Commercialization of the Nanoparticle-Based Fuel Cell Coolant. 886
VI.4 University of Tennessee: Manufacturing of Low-Cost, Durable Membrane Electrode Assemblies Engineered for Rapid Conditioning. 971

Tennessee (Continued)

VIII.16 Oak Ridge National Laboratory: MEMS Hydrogen Sensor for Leak Detection 1122

XI.1 Oak Ridge National Laboratory: Non-Automotive Fuel Cells: Market Assessment and Analysis of Impacts of Policies 1231

XI.1 University of Tennessee: Non-Automotive Fuel Cells: Market Assessment and Analysis of Impacts of Policies 1231

Texas

II.J.3 University of Texas at Arlington: Value-Added Hydrogen Generation with CO_2 Conversion 218

III.8 Texas A&M University: Development of a Centrifugal Hydrogen Pipeline Gas Compressor. 331

IV.C.1 Texas A&M University: A Biomimetic Approach to Metal-Organic Frameworks with High H_2 Uptake 432

IV.E.6 Southwest Research Institute®: Standardized Testing Program for Solid-State Hydrogen Storage Technologies 562

V.D.2 Texas A&M University: Highly Dispersed Alloy Catalyst for Durability 708

V.D.4 University of Texas at Austin: Extended, Continuous Pt Nanostructures in Thick, Dispersed Electrodes 719

V.E.1 University of Texas at Austin: Polymer Electrolyte Fuel Cell Lifetime Limitations: The Role of Electrocatalyst Degradation 783

V.F.1 BCS Fuel Cells: Water Transport in PEM Fuel Cells: Advanced Modeling, Material Selection, Testing, and Design Optimization 814

VIII.10 William C. Fort: Hydrogen Safety Panel 1100

XII.8 Airgas Southwest: H-E-B Grocery Total Power Solution for Fuel Cell-Powered Material Handling Equipment 1312

XII.8 Parkway Systems: H-E-B Grocery Total Power Solution for Fuel Cell-Powered Material Handling Equipment 1312

XII.10 Sysco of Houston: Fuel Cell-Powered Lift Truck Sysco Houston Fleet Deployment. 1319

Utah

II.E.3 HyPerComp Engineering, Inc.: High-Capacity, High Pressure Electrolysis System with Renewable Power Sources 87

III.3 MegaStir Technologies: Vessel Design and Fabrication Technology for Stationary High-Pressure Hydrogen Storage. 307

XII.10 Big-D Construction: Fuel Cell-Powered Lift Truck Sysco Houston Fleet Deployment. 1319

Vermont

IX.3 Clean Energy States Alliance: Hydrogen Education State Partnership Program 1139

Virginia

II.A.3 Directed Technologies, Inc.: Distributed Reforming of Renewable Liquids Using Oxygen Transport Membranes (OTMs). 33

II.E.1 Virginia Polytechnic Institute and State University: PEM Electrolyzer Incorporating an Advanced Low-Cost Membrane 79

II.I.1 Directed Technologies, Inc.: H2A Production Model Updates. 207

II.K.11 Virginia Polytechnic Institute and State University: Photoinitiated Electron Collection in Mixed-Metal Supramolecular Complexes: Development of Photocatalysts for Hydrogen Production 257

IV.F.1 Virginia Polytechnic Institute and State University: High Strength Carbon Fibers 576

V.A.2 Directed Technologies, Inc.: Mass-Production Cost Estimation for Automotive Fuel Cell Systems 609

V.F.3 Virginia Polytechnic Institute and State University: Transport in PEMFC Stacks 822

V.G.4 Virginia Polytechnic Institute and State University: Advanced Materials and Concepts for Portable Power Fuel Cells 858

Virginia (Continued)

IX.5 Commonwealth of Virginia: VA-MD-DC Hydrogen Education for Decision Makers 1144

IX.5 James Madison University: VA-MD-DC Hydrogen Education for Decision Makers 1144

IX.14 National Energy Education Development Project: H_2 Educate! Hydrogen Education for Middle Schools 1177

XI.7 OnLocation, Inc.: NEMS-H2: Hydrogen's Role in Climate Mitigation and Oil Dependence Reduction 1254

XI.9 Directed Technologies, Inc.: Macro-System Model 1261

XI.9 SRA International, Inc.: Macro-System Model 1261

XII.5 Sprint Nextel: Demonstrating Economic and Operational Viability of 72-Hour Hydrogen PEM Fuel Cell Systems to Support Emergency Communications on the Sprint Nextel Network 1300

Washington

II.A.1 Pacific Northwest National Laboratory: Biomass-Derived Liquids Distributed (Aqueous Phase) Reforming 25

II.A.1 Washington State University: Biomass-Derived Liquids Distributed (Aqueous Phase) Reforming 25

II.K.2 University of Washington: Phototrophic metabolism of organic compounds generates excess reducing power that can be redirected to produce H_2 as a biofuel 232

II.K.4 University of Washington: Prospects for Hydrogen Production from Formate by *Methanococcus maripaludis* 237

III.3 Global Engineering and Technology: Vessel Design and Fabrication Technology for Stationary High-Pressure Hydrogen Storage 307

III.17 Prometheus Energy: Active Magnetic Regenerative Liquefier 371

IV.D.1 Pacific Northwest National Laboratory: Hydrogen Storage Engineering Center of Excellence 479

IV.D.6 Pacific Northwest National Laboratory: Systems Engineering of Chemical Hydride, Pressure Vessel, and Balance of Plant for On-Board Hydrogen Storage 503

V.D.15 Pacific Northwest National Laboratory: Development of Alternative and Durable High Performance Cathode Supports for PEM Fuel Cells 777

V.H.1 IBIS Associations, Inc.: Low-Cost PEM Fuel Cell Metal Bipolar Plates 863

V.K.4 InnovaTek, Inc.: Power Generation from an Integrated Biomass Reformer and Solid Oxide Fuel Cell 901

VI.3 Pacific Northwest National Laboratory: Modular, High-Volume Fuel Cell Leak-Test Suite and Process 968

VI.8 Pacific Northwest National Laboratory: MEA Manufacturing R&D Using Drop-On-Demand Technology 991

VI.9 Boeing Research and Technology: Development of Advanced Manufacturing Technologies for Low Cost Hydrogen Storage Vessels 995

VI.9 Pacific Northwest National Laboratory: Development of Advanced Manufacturing Technologies for Low Cost Hydrogen Storage Vessels 995

VIII.10 Pacific Northwest National Laboratory: Hydrogen Safety Panel 1100

VIII.11 Pacific Northwest National Laboratory: Hydrogen Safety Knowledge Tools 1104

VIII.12 Pacific Northwest National Laboratory: Hydrogen Emergency Response Training for First Responders 1107

VIII.12 Hanford Fire Department: Hydrogen Emergency Response Training for First Responders 1107

VIII.12 Hazardous Materials Management and Emergency Response Training and Eduction Center: Hydrogen Emergency Response Training for First Responders 1107

VIII.15 Sandia National Laboratories: International Energy Agency Hydrogen Implementing Agreement Task 19 Hydrogen Safety 1118

X.4 Pacific Northwest National Laboratory: Fuel Cell Combined Heat and Power Industrial Demonstration 1202

X.10 Pacific Northwest National Laboratory: Assessment of Solid Oxide Fuel Cell Power System for Greener Commercial Aircraft 1220

Washington (Continued)

XII.4 PACCAR, Inc.: Solid Oxide Fuel Cell Diesel Auxiliary Power Unit Demonstration 1297
XII.5 ReliOn, Inc.: Demonstrating Economic and Operational Viability of 72-Hour Hydrogen PEM Fuel Cell Systems to Support Emergency Communications on the Sprint Nextel Network. 1300
XII.6 ReliOn, Inc.: PEM Fuel Cell Systems Providing Backup Power to Commercial Cellular Towers and an Electric Utility Communications Network 1304
XII.7 Pacific Northwest National Laboratory: Analysis Results for ARRA Projects: Enabling Fuel Cell Market Transformation 1308

Washington, D.C.

IV.E.8 Hydrogen Education Foundation: Administration of H-Prize for Hydrogen Storage 571
V.D.12 George Washington University: High-Activity Dealloyed Catalysts 760
IX.6 Technology Transition Corporation: H2L3: Hydrogen Learning for Local Leaders 1148
IX.6 Public Technology Institute: H2L3: Hydrogen Learning for Local Leaders 1148
XI.1 ICF, International: Non-Automotive Fuel Cells: Market Assessment and Analysis of Impacts of Policies 1231

Wisconsin

V.E.1 University of Wisconsin, Madison: Polymer Electrolyte Fuel Cell Lifetime Limitations: The Role of Electrocatalyst Degradation. 783

Wyoming

II.H.5 University of Wyoming: Purdue Hydrogen Systems Laboratory: Hydrogen Production 203
II.K.18 University of Wyoming: Combinatorial methods for the Improvement of Semiconductor Metal Oxide Photoelectrodes 279
IV.G.1 University of Wyoming: Purdue Hydrogen Systems Laboratory: Hydrogen Storage. 585

Foreign Countries

Canada

IV.D.1 Université du Québec à Trois-Rivières: Hydrogen Storage Engineering Center of Excellence 479
IV.D.5 Université du Québec à Trois-Rivières: SRNL Technical Work Scope for the Hydrogen Storage Engineering Center of Excellence: Design and Testing of Metal Hydride and Adsorbent Systems 498
V.B.3 Ballard Power Systems: The Effect of Airborne Contaminants on Fuel Cell Performance and Durability 649
V.D.1 Dalhousie University: Advanced Cathode Catalysts and Supports for PEM Fuel Cells 699
V.D.3 Dalhousie University: Durable Catalysts for Fuel Cell Protection During Transient Conditions 714
V.D.7 Ballard Fuel Cells: The Science and Engineering of Durable Ultralow PGM Catalysts 734
V.D.15 Automotive Fuel Cell Cooperation Corp.: Development of Alternative and Durable High Performance Cathode Supports for PEM Fuel Cells 777
V.E.2 Ballard Power Systems: Durability Improvements Through Degradation Mechanism Studies 788
V.E.4 Ballard Power Systems: Development of Micro-Structural Mitigation Strategies for PEM Fuel Cells: Morphological Simulations and Experimental Approaches 797
V.E.4 Queen's University: Development of Micro-Structural Mitigation Strategies for PEM Fuel Cells: Morphological Simulations and Experimental Approaches 797
V.E.7 Ballard Power Systems: Accelerated Testing Validation 810
V.F.1 Ballard Power Systems: Water Transport in PEM Fuel Cells: Advanced Modeling, Material Selection, Testing, and Design Optimization 814
V.F.1 University of Victoria: Water Transport in PEM Fuel Cells: Advanced Modeling, Material Selection, Testing, and Design Optimization 814

Canada (Continued)

V.F.2 Ballard Power Systems: Development and Validation of a Two-Phase, Three-Dimensional Model for PEM Fuel Cells 818
V.F.5 Ballard Power Systems: Air-Cooled Stack Freeze Tolerance 833
V.J.1 dPoint Technologies, Inc.: Materials and Modules for Low-Cost, High-Performance Fuel Cell Humidifiers 879
VI.2 Ballard Power Systems: Reduction in Fabrication Costs of Gas Diffusion Layers 963
IX.8 Hydrogenics: Dedicated to The Continued Education, Training and Demonstration of PEM Fuel Cell-Powered Lift Trucks In Real-World Applications 1155

France

IV.C.7 Institut de Chimie et des Matériaux: Weak Chemisorption Validation 464

Germany

IV.C.7 Max Planck Institute: Weak Chemisorption Validation 464
IV.D.1 BASF GmbH: Hydrogen Storage Engineering Center of Excellence 479
IV.D.9 BASF-SE: Ford/BASF-SE/UM Activities in Support of the Hydrogen Storage Engineering Center of Excellence 522
V.D.12 Technical University Berlin: High-Activity Dealloyed Catalysts 760
V.F.1 SGL Carbon: Water Transport in PEM Fuel Cells: Advanced Modeling, Material Selection, Testing, and Design Optimization 814
V.G.4 SFC Energy: Advanced Materials and Concepts for Portable Power Fuel Cells 858
VII.3 Daimler: Hydrogen to the Highways – Controlled Hydrogen Fleet and Infrastructure Demonstration and Validation Project 1027
VII.3 Mercedes-Benz USA LLC: Hydrogen to the Highways – Controlled Hydrogen Fleet and Infrastructure Demonstration and Validation Project 1027

Japan

III.9 Mitsubishi Compressor Company: Oil-Free Centrifugal Hydrogen Compression Technology Demonstration 338

Portugal

IV.F.1 Fibras Sinteticas de Portugal, SA: High Strength Carbon Fibers 576

Russia

II.H.1 Institute of Basic Biological Problems: Biological Systems for Hydrogen Photoproduction 185

South Korea

V.D.13 Hyundai Motor Company: Development of Ultra-Low Platinum Alloy Cathode Catalyst for PEM Fuel Cells 764
V.D.13 Yonsei University: Development of Ultra-Low Platinum Alloy Cathode Catalyst for PEM Fuel Cells 764

United Kingdom

II.E.1 Parker Hannifin Ltd domnick hunter Division: PEM Electrolyzer Incorporating an Advanced Low-Cost Membrane 79
V.D.2 Johnson Matthey Fuel Cells: Highly Dispersed Alloy Catalyst for Durability 708
V.D.6 Johnson Matthey Fuel Cells: Contiguous Platinum Monolayer Oxygen Reduction Electrocatalysts on High-Stability Low-Cost Supports 729
V.D.12 Johnson Matthey Fuel Cells: High-Activity Dealloyed Catalysts 760
V.E.1 Johnson Matthey Fuel Cells: Polymer Electrolyte Fuel Cell Lifetime Limitations: The Role of Electrocatalyst Degradation 783

United Kingdom (Continued)

V.F.6 Johnson Matthey Fuel Cells: Transport Studies Enabling Efficiency Optimization of Cost-Competitive Fuel Cell Stacks. 837
V.G.3 Johnson Matthey Fuel Cells: New MEA Materials for Improved Direct Methanol Fuel Cell (DMFC) Performance, Durability, and Cost 854
V.G.4 Johnson Matthey Fuel Cells: Advanced Materials and Concepts for Portable Power Fuel Cells 858
XI.1 Fuel Cell Today: Non-Automotive Fuel Cells: Market Assessment and Analysis of Impacts of Policies . . . 1231

XVIII. Project Listings by Organization

3M Company

V.B.1 Effect of System Contaminants on PEMFC Performance and Durability 640
V.C.1 Membranes and MEAs for Dry, Hot Operating Conditions 662
V.C.6 Novel Approaches to Immobilized Heteropoly Acid (HPA) Systems for High Temperature, Low Relative Humidity Polymer-Type Membranes 685
V.D.1 Advanced Cathode Catalysts and Supports for PEM Fuel Cells 699
V.D.3 Durable Catalysts for Fuel Cell Protection During Transient Conditions. 714
V.D.5 Nanosegregated Cathode Catalysts with Ultra-Low Platinum Loading 723
V.E.3 Analysis of Durability of MEAs in Automotive PEMFC Applications 794
V.F.7 Fuel Cell Fundamentals at Low and Subzero Temperatures. 841

Acumentrics Corporation

V.K.1 Development of a Low-Cost 3-10 kW Tubular SOFC Power System 890

Addison Bain

VIII.10 Hydrogen Safety Panel 1100

Adsorption Research, Inc.

II.D.4 Composite Pd and Alloy Porous Stainless Steel Membranes for Hydrogen Production and Process Intensification. 73

Advanced Technology International

X.7 Landfill Gas-to-Hydrogen. 1212

Air Products and Chemicals, Inc.

VII.4 Validation of an Integrated Hydrogen Energy Station 1032
VII.6 California Hydrogen Infrastructure Project 1040
VIII.10 Hydrogen Safety Panel 1100
XII.5 Demonstrating Economic and Operational Viability of 72-Hour Hydrogen PEM Fuel Cell Systems to Support Emergency Communications on the Sprint Nextel Network 1300
XII.6 PEM Fuel Cell Systems Providing Backup Power to Commercial Cellular Towers and an Electric Utility Communications Network 1304
XII.9 Fuel Cell-Powered Lift Truck FedEx Freight Fleet Deployment 1316
XII.10 Fuel Cell-Powered Lift Truck Sysco Houston Fleet Deployment. 1319
XII.11 GENCO Fuel Cell-Powered Lift Truck Fleet Deployment 1322

Airgas Merchant Gases

XII.8 H-E-B Grocery Total Power Solution for Fuel Cell-Powered Material Handling Equipment. 1312

Airgas Southwest

XII.8 H-E-B Grocery Total Power Solution for Fuel Cell-Powered Material Handling Equipment. 1312

Allegiance Consulting

XI.3 Infrastructure Analysis of Early Market Transition of Fuel Cell Vehicles 1240

Altergy Systems, Folsum

XII.5 Demonstrating Economic and Operational Viability of 72-Hour Hydrogen PEM Fuel Cell Systems to Support Emergency Communications on the Sprint Nextel Network 1300

Alumni Consulting
XI.10 HyDRA: Hydrogen Demand and Resource Analysis Tool 1265

Ameresco, Inc.
X.7 Landfill Gas-to-Hydrogen. 1212

Andy Lutz
XI.4 Analysis of the Effects of Developing New Energy Infrastructures. 1244

Argonne National Laboratory
II.A.3 Distributed Reforming of Renewable Liquids Using Oxygen Transport Membranes (OTMs) 33
II.F.2 Membrane/Electrolyzer Development in the Cu-Cl Thermochemical Cycle 108
III.2 Hydrogen Delivery Infrastructure Analysis 303
III.16 Hydrogen Pipeline Compressors 367
IV.C.5 Hydrogen Storage through Nanostructured Porous Organic Polymers (POPs). 455
IV.E.2 System Level Analysis of Hydrogen Storage Options 544
V.A.3 Drive-Cycle Performance of Automotive Fuel Cell Systems. 614
V.A.8 Fuel Cell Testing at the Argonne Fuel Cell Test Facility: A Comparison of U.S. and EU Test Protocols . . . 637
V.D.1 Advanced Cathode Catalysts and Supports for PEM Fuel Cells 699
V.D.5 Nanosegregated Cathode Catalysts with Ultra-Low Platinum Loading 723
V.E.1 Polymer Electrolyte Fuel Cell Lifetime Limitations: The Role of Electrocatalyst Degradation 783
V.E.2 Durability Improvements Through Degradation Mechanism Studies. 788
V.E.5 Durability of Low Platinum Fuel Cells Operating at High Power Density 802
V.H.2 Metallic Bipolar Plates with Composite Coatings 867
IX.1 Employment Impacts of Early Markets for Hydrogen and Fuel Cell Technologies 1131
XI.6 Emissions Analysis of Electricity Storage with Hydrogen 1251
XI.8 GREET Model Development and Life-Cycle Analysis Applications 1257
XI.12 Fuel Quality Effects on Stationary Fuel Cell Systems 1275

Arizona State University
II.C.1 Zeolite Membrane Reactor for Water-Gas Shift Reaction for Hydrogen Production 46
VI.5 Adaptive Process Controls and Ultrasonics for High-Temperature PEM MEA Manufacture 977

Arkema Inc.
V.G.2 Novel Materials for High Efficiency Direct Methanol Fuel Cells. 850

ATI Wah Chang
II.B.2 One Step Biomass Gas Reforming-Shift Separation Membrane Reactor 42

Automotive Fuel Cell Cooperation Corp.
V.D.15 Development of Alternative and Durable High Performance Cathode Supports for PEM Fuel Cells. 777

Avalence, LLC
II.E.3 High-Capacity, High Pressure Electrolysis System with Renewable Power Sources. 87

Ballard Fuel Cells
V.D.7 The Science and Engineering of Durable Ultralow PGM Catalysts. 734

Ballard Material Products, Inc.
V.F.3 Transport in PEMFC Stacks. 822

Ballard Material Products, Inc. (Continued)
VI.2 Reduction in Fabrication Costs of Gas Diffusion Layers 963

Ballard Power Systems
V.B.3 The Effect of Airborne Contaminants on Fuel Cell Performance and Durability 649
V.E.2 Durability Improvements Through Degradation Mechanism Studies 788
V.E.4 Development of Micro-Structural Mitigation Strategies for PEM Fuel Cells: Morphological Simulations and Experimental Approaches 797
V.E.7 Accelerated Testing Validation 810
V.F.1 Water Transport in PEM Fuel Cells: Advanced Modeling, Material Selection, Testing, and Design Optimization 814
V.F.2 Development and Validation of a Two-Phase, Three-Dimensional Model for PEM Fuel Cells 818
V.F.5 Air-Cooled Stack Freeze Tolerance 833
VI.2 Reduction in Fabrication Costs of Gas Diffusion Layers 963

BASF Fuel Cell
V.D.11 Development of Novel Non-PGM Electrocatalysts for Proton Exchange Membrane Fuel Cell Applications 756
VI.7 High Speed, Low Cost Fabrication of Gas Diffusion Electrodes for Membrane Electrode Assemblies 987

BASF GmbH
IV.D.1 Hydrogen Storage Engineering Center of Excellence 479

BASF-SE
IV.D.9 Ford/BASF-SE/UM Activities in Support of the Hydrogen Storage Engineering Center of Excellence. 522

Battelle
VII.5 Technology Validation: Fuel Cell Bus Evaluations 1036

BCS Fuel Cells
V.F.1 Water Transport in PEM Fuel Cells: Advanced Modeling, Material Selection, Testing, and Design Optimization 814

Becht Engineering
VIII.10 Hydrogen Safety Panel 1100

BekkTech LLC
V.C.9 Lead Research and Development Activity for DOE's High Temperature, Low Relative Humidity Membrane Program 696

Betacom, Inc.
XII.6 PEM Fuel Cell Systems Providing Backup Power to Commercial Cellular Towers and an Electric Utility Communications Network 1304

Bethlehem Hydrogen
VIII.6 National Codes and Standards Coordination. 1083

Big-D Construction
XII.10 Fuel Cell-Powered Lift Truck Sysco Houston Fleet Deployment. 1319

Bing Energy, Inc.
VII.8 Florida Hydrogen Initiative (FHI) 1046

Black & Veatch Corporation

XII.5 Demonstrating Economic and Operational Viability of 72-Hour Hydrogen PEM Fuel Cell Systems to Support Emergency Communications on the Sprint Nextel Network 1300

Board of Trustees of the Leland Stanford Junior University

II.G.1 Nano-Architectures for 3rd Generation PEC Devices: A Study of MoS_2, Fundamental Investigations and Applied Research. 123

Boeing Research and Technology

VI.9 Development of Advanced Manufacturing Technologies for Low Cost Hydrogen Storage Vessels. 995

Brookhaven National Laboratory

II.K.15 Catalyzed Water Oxidation by Solar Irradiation of Band-Gap-Narrowed Semiconductors. 270

IV.A.6 Aluminum Hydride 409

V.D.2 Highly Dispersed Alloy Catalyst for Durability 708

V.D.6 Contiguous Platinum Monolayer Oxygen Reduction Electrocatalysts on High-Stability Low-Cost Supports 729

V.G.4 Advanced Materials and Concepts for Portable Power Fuel Cells. 858

Brown University

V.D.5 Nanosegregated Cathode Catalysts with Ultra-Low Platinum Loading 723

Burns & McDonnell Engineering Co., Inc.

XII.5 Demonstrating Economic and Operational Viability of 72-Hour Hydrogen PEM Fuel Cell Systems to Support Emergency Communications on the Sprint Nextel Network 1300

California Fuel Cell Partnership

VIII.12 Hydrogen Emergency Response Training for First Responders 1107

California Institute of Technology

II.K.20 Fundamental Optical, Electrical, and Photoelectrochemical Properties of Catalyst-Bound Silicon Microwire Array Photocathodes for Sunlight-Driven Hydrogen Production 283

IV.D.1 Hydrogen Storage Engineering Center of Excellence 479

IV.D.4 Key Technologies, Thermal Management, and Prototype Testing for Advanced Solid-State Hydrogen Storage Systems 494

California State University, Los Angeles

VII.9 Sustainable Hydrogen Fueling Station, California State University, Los Angeles 1050

IX.9 Hydrogen and Fuel Cell Education at California State University, Los Angeles 1158

Carolina Tractor & Equipment Co. Inc.

IX.8 Dedicated to The Continued Education, Training and Demonstration of PEM Fuel Cell-Powered Lift Trucks In Real-World Applications 1155

Case Western Reserve University

V.C.1 Membranes and MEAs for Dry, Hot Operating Conditions 662

V.C.4 Poly(p-Phenylene Sulfonic Acids): PEMs with Frozen-In Free Volume 675

VI.7 High Speed, Low Cost Fabrication of Gas Diffusion Electrodes for Membrane Electrode Assemblies 987

CFD Research Corporation

V.F.1 Water Transport in PEM Fuel Cells: Advanced Modeling, Material Selection, Testing, and Design Optimization 814

Cincinnati Test Systems
VI.3 Modular, High-Volume Fuel Cell Leak-Test Suite and Process 968

City of Santa Fe Springs
VIII.10 Hydrogen Safety Panel 1100

Clean Energy States Alliance
IX.3 Hydrogen Education State Partnership Program. 1139

Clemson University
V.B.4 Effects of Impurities on Fuel Cell Performance and Durability. 654

Colorado School of Mines
II.C.3 High Performance Palladium-Based Membrane for Hydrogen Separation and Purification. 58
II.D.1 Advanced Hydrogen Transport Membranes for Coal Gasification 62
V.B.1 Effect of System Contaminants on PEMFC Performance and Durability 640
V.C.1 Membranes and MEAs for Dry, Hot Operating Conditions. 662
V.C.6 Novel Approaches to Immobilized Heteropoly Acid (HPA) Systems for High Temperature, Low Relative Humidity Polymer-Type Membranes 685
V.D.9 Tungsten Oxide and Heteropoly Acid Based System for Ultra-High Activity and Stability of Pt Catalysts in PEM Fuel Cell Cathodes 745
V.G.1 Novel Approach to Advanced Direct Methanol Fuel Cell (DMFC) Anode Catalysts 846
V.L.6 Biomass Fuel Cell Systems 927

Commonwealth of Virginia
IX.5 VA-MD-DC Hydrogen Education for Decision Makers 1144

Concepts NREC
III.8 Development of a Centrifugal Hydrogen Pipeline Gas Compressor 331

Connecticut Center for Advanced Technology, Inc.
IX.2 State and Local Government Partnership 1135

CSA Standards
VIII.6 National Codes and Standards Coordination. 1083

Daimler
VII.3 Hydrogen to the Highways – Controlled Hydrogen Fleet and Infrastructure Demonstration and Validation Project. 1027

Dalhousie University
V.D.1 Advanced Cathode Catalysts and Supports for PEM Fuel Cells 699
V.D.3 Durable Catalysts for Fuel Cell Protection During Transient Conditions. 714

Delaware State University
IV.G.3 Hydrogen Storage Materials for Fuel Cell-Powered Vehicles. 593

Delphi Automotive Systems, LLC
XII.2 Jadoo Power Fuel Cell Demonstration 1291
XII.4 Solid Oxide Fuel Cell Diesel Auxiliary Power Unit Demonstration 1297

Directed Technologies, Inc.
II.A.3 Distributed Reforming of Renewable Liquids Using Oxygen Transport Membranes (OTMs) 33
II.I.1 H2A Production Model Updates 207
V.A.2 Mass-Production Cost Estimation for Automotive Fuel Cell Systems. 609
XI.9 Macro-System Model. 1261

dPoint Technologies, Inc.
V.J.1 Materials and Modules for Low-Cost, High-Performance Fuel Cell Humidifiers 879

DTE Energy
VII.3 Hydrogen to the Highways – Controlled Hydrogen Fleet and Infrastructure Demonstration and Validation Project. 1027

Dynalene Inc.
V.J.3 Large Scale Testing, Demonstration and Commercialization of the Nanoparticle-Based Fuel Cell Coolant 886
V.L.7 Fuel Cell Coolant Optimization and Scale Up 933

E. I. du Pont de Nemours and Company
V.E.3 Analysis of Durability of MEAs in Automotive PEMFC Applications 794

Eastman Chemical Compnay
II.D.2 Scale Up of Hydrogen Transport Membranes for IGCC and FutureGen Plants 66

Edison Material Technology Center
IX.7 Raising H_2 and Fuel Cell Awareness in Ohio 1153

Electricore, Inc.
XII.4 Solid Oxide Fuel Cell Diesel Auxiliary Power Unit Demonstration 1297

Electrosynthesis Co. Inc.
II.F.1 Solar High-Temperature Water Splitting Cycle with Quantum Boost. 102

Eltron Research & Development Inc.
II.D.2 Scale Up of Hydrogen Transport Membranes for IGCC and FutureGen Plants 66

EnerFuels, Inc.
VII.8 Florida Hydrogen Initiative (FHI) 1046

Energetics, Inc.
IV.E.5 Analysis of Storage Needs for Early Motive Fuel Cell Markets 558
VIII.10 Hydrogen Safety Panel 1100
XI.2 Hydrogen Infrastructure Market Readiness Analysis 1236

Energy Technology Services
V.K.4 Power Generation from an Integrated Biomass Reformer and Solid Oxide Fuel Cell. 901

Entegris, Inc.
II.E.2 High Performance, Low Cost Hydrogen Generation from Renewable Energy 83

Ericsson Services, Inc.

XII.5 Demonstrating Economic and Operational Viability of 72-Hour Hydrogen PEM Fuel Cell Systems to Support Emergency Communications on the Sprint Nextel Network 1300

ESI US R&D

V.F.1 Water Transport in PEM Fuel Cells: Advanced Modeling, Material Selection, Testing, and Design Optimization 814

FedEx Freight

XII.9 Fuel Cell-Powered Lift Truck FedEx Freight Fleet Deployment 1316

Fibras Sinteticas de Portugal, SA

IV.F.1 High Strength Carbon Fibers 576

Firexplo

VIII.10 Hydrogen Safety Panel 1100

Florida Institute of Technology

VII.8 Florida Hydrogen Initiative (FHI) 1046

Florida Solar Energy Center

VII.8 Florida Hydrogen Initiative (FHI) 1046

Florida State University

VII.8 Florida Hydrogen Initiative (FHI) 1046

Ford Motor Company

IV.D.1 Hydrogen Storage Engineering Center of Excellence 479

IV.D.9 Ford/BASF-SE/UM Activities in Support of the Hydrogen Storage Engineering Center of Excellence 522

V.H.1 Low-Cost PEM Fuel Cell Metal Bipolar Plates. 863

Fortune Wireless

XII.6 PEM Fuel Cell Systems Providing Backup Power to Commercial Cellular Towers and an Electric Utility Communications Network 1304

FP2 Fire Protection Engineering

VIII.6 National Codes and Standards Coordination. 1083

Front Range Wireless

XII.6 PEM Fuel Cell Systems Providing Backup Power to Commercial Cellular Towers and an Electric Utility Communications Network 1304

Fuel Cell Today

XI.1 Non-Automotive Fuel Cells: Market Assessment and Analysis of Impacts of Policies 1231

FuelCell Energy, Inc.

III.10 Electrochemical Hydrogen Compressor 342

V.B.2 The Effects of Impurities on Fuel Cell Performance and Durability 644

V.C.7 High-Temperature Membrane with Humidification-Independent Cluster Structure 690

VII.4 Validation of an Integrated Hydrogen Energy Station 1032

Gas Technology Institute
II.B.2 One Step Biomass Gas Reforming-Shift Separation Membrane Reactor 42
V.H.1 Low-Cost PEM Fuel Cell Metal Bipolar Plates. 863
V.H.2 Metallic Bipolar Plates with Composite Coatings 867
X.7 Landfill Gas-to-Hydrogen. 1212

GENCO Infrastructure Solutions
XII.11 GENCO Fuel Cell-Powered Lift Truck Fleet Deployment 1322

General Motors Company
IV.D.1 Hydrogen Storage Engineering Center of Excellence 479
IV.D.8 Optimization of Heat Exchangers and System Simulation of On-Board Storage Systems Designs. 517
V.B.1 Effect of System Contaminants on PEMFC Performance and Durability 640
V.C.8 Corrugated Membrane Fuel Cell Structures. 694
V.D.12 High-Activity Dealloyed Catalysts. 760
V.F.4 Investigation of Micro- and Macro-Scale Transport Processes for Improved Fuel Cell Performance. 827
VII.2 Hydrogen Vehicle and Infrastructure Demonstration and Validation 1023
VIII.10 Hydrogen Safety Panel 1100

General Physics Corporation
VII.9 Sustainable Hydrogen Fueling Station, California State University, Los Angeles 1050

George Washington University
V.D.12 High-Activity Dealloyed Catalysts. 760

Georgia Institute of Technology
V.E.4 Development of Micro-Structural Mitigation Strategies for PEM Fuel Cells: Morphological Simulations and Experimental Approaches 797

Giner Electrochemical Systems, LLC
II.E.1 PEM Electrolyzer Incorporating an Advanced Low-Cost Membrane. 79
II.J.1 Unitized Design for Home Refueling Appliance for Hydrogen Generation to 5,000 psi. 211
V.C.2 Dimensionally Stable Membranes (DSMs) 667
V.C.3 Dimensionally Stable High Performance Membrane (SBIR Phase III). 671
V.F.3 Transport in PEMFC Stacks 822

Global Engineering and Technology
III.3 Vessel Design and Fabrication Technology for Stationary High-Pressure Hydrogen Storage 307

Graftech International Holdings Inc.
V.C.8 Corrugated Membrane Fuel Cell Structures. 694

Greenway Energy
IX.4 Development of Hydrogen Education Programs for Government Officials 1142

GWS Solutions of Tolland, LLC
VIII.6 National Codes and Standards Coordination. 1083
VIII.10 Hydrogen Safety Panel 1100

H2 Technology Consulting LLC
IV.C.7 Weak Chemisorption Validation 464

H2 Technology Consulting LLC (Continued)
IV.E.7 Best Practices for Characterizing Engineering Properties of Hydrogen Storage Materials 567

H2Pump, LLC
II.E.5 Process Intensification of Hydrogen Unit Operations Using an Electrochemical Device. 95

Hanford Fire Department
VIII.12 Hydrogen Emergency Response Training for First Responders 1107

Hawaii Natural Energy Institute
V.B.3 The Effect of Airborne Contaminants on Fuel Cell Performance and Durability 649
VII.7 Hawaii Hydrogen Power Park 1043
X.3 Hydrogen Energy Systems as a Grid Management Tool 1200

Hazardous Materials Management and Emergency Response Training and Eduction Center
VIII.12 Hydrogen Emergency Response Training for First Responders 1107

Honeywell Aerospace
V.J.2 Development of Thermal and Water Management System for PEM Fuel Cell 883

Humboldt State University
IX.6 H2L3: Hydrogen Learning for Local Leaders 1148
IX.15 Hydrogen Technology and Energy Curriculum (HyTEC) 1180

Humboldt State University Sponsored Programs Foundation
IX.10 Hydrogen Energy in Engineering Education (H_2E_3) 1161

Hydrogen Education Foundation
IV.E.8 Administration of H-Prize for Hydrogen Storage 571

Hydrogen Safety, LLC
VIII.10 Hydrogen Safety Panel 1100

Hydrogenics
IX.8 Dedicated to The Continued Education, Training and Demonstration of PEM Fuel Cell-Powered Lift Trucks In Real-World Applications 1155

HyGen Industries
III.8 Development of a Centrifugal Hydrogen Pipeline Gas Compressor 331

HyPerComp Engineering, Inc.
II.E.3 High-Capacity, High Pressure Electrolysis System with Renewable Power Sources. 87

Hyundai Motor Company
V.D.13 Development of Ultra-Low Platinum Alloy Cathode Catalyst for PEM Fuel Cells 764

IBIS Associations, Inc.
V.H.1 Low-Cost PEM Fuel Cell Metal Bipolar Plates. 863

ICF, International
XI.1 Non-Automotive Fuel Cells: Market Assessment and Analysis of Impacts of Policies 1231

IdaTech, LLC
V.K.3 Research & Development for Off-Road Fuel Cell Applications 899

IDC Energy Insights
XI.2 Hydrogen Infrastructure Market Readiness Analysis 1236

Illinois Institute of Technology
V.D.10 Synthesis and Characterization of Mixed-Conducting Corrosion Resistant Oxide Supports 752
V.E.3 Analysis of Durability of MEAs in Automotive PEMFC Applications 794
V.G.2 Novel Materials for High Efficiency Direct Methanol Fuel Cells. 850

InnovaTek, Inc.
V.K.4 Power Generation from an Integrated Biomass Reformer and Solid Oxide Fuel Cell. 901

Institut de Chimie et des Matériaux
IV.C.7 Weak Chemisorption Validation 464

Institute of Basic Biological Problems
II.H.1 Biological Systems for Hydrogen Photoproduction 185

Intelligent Energy
V.K.2 Development and Demonstration of a New Generation High Efficiency 10 kW Stationary PEM Fuel Cell System. 894

Intelligent Optical Systems, Inc.
VIII.14 Hydrogen Leak Detection System Development 1114

Ion Power Inc.
V.C.8 Corrugated Membrane Fuel Cell Structures. 694
V.E.2 Durability Improvements Through Degradation Mechanism Studies. 788
V.E.7 Accelerated Testing Validation. 810

J. Craig Venter Institute
II.H.3 Hydrogen from Water in a Novel Recombinant Oxygen-Tolerant Cyanobacterial System. 195

Jadoo Power, Inc.
XII.2 Jadoo Power Fuel Cell Demonstration 1291

James Madison University
IX.5 VA-MD-DC Hydrogen Education for Decision Makers 1144

Jeffrey Rome and Associates
XII.6 PEM Fuel Cell Systems Providing Backup Power to Commercial Cellular Towers and an Electric Utility Communications Network 1304

Jenike and Johanson
II.F.3 Solar Hydrogen Production with a Metal Oxide-Based Thermochemical Cycle 112

Jet Propulsion Laboratory
IV.D.1 Hydrogen Storage Engineering Center of Excellence 479
IV.D.4 Key Technologies, Thermal Management, and Prototype Testing for Advanced Solid-State Hydrogen Storage Systems 494

Jet Propulsion Laboratory (Continued)
V.D.1 Advanced Cathode Catalysts and Supports for PEM Fuel Cells . . . 699
V.D.5 Nanosegregated Cathode Catalysts with Ultra-Low Platinum Loading . . . 723
V.G.1 Novel Approach to Advanced Direct Methanol Fuel Cell (DMFC) Anode Catalysts . . . 846
V.I.1 Resonance-Stabilized Anion Exchange Polymer Electrolytes . . . 872

John Deere
V.B.4 Effects of Impurities on Fuel Cell Performance and Durability . . . 654

Johns Hopkins University
II.H.1 Biological Systems for Hydrogen Photoproduction . . . 185

Johnson Matthey Fuel Cells
V.D.2 Highly Dispersed Alloy Catalyst for Durability . . . 708
V.D.6 Contiguous Platinum Monolayer Oxygen Reduction Electrocatalysts on High-Stability Low-Cost Supports . . . 729
V.D.12 High-Activity Dealloyed Catalysts . . . 760
V.E.1 Polymer Electrolyte Fuel Cell Lifetime Limitations: The Role of Electrocatalyst Degradation . . . 783
V.F.6 Transport Studies Enabling Efficiency Optimization of Cost-Competitive Fuel Cell Stacks . . . 837
V.G.3 New MEA Materials for Improved Direct Methanol Fuel Cell (DMFC) Performance, Durability, and Cost . . . 854
V.G.4 Advanced Materials and Concepts for Portable Power Fuel Cells . . . 858

Kelvin Hecht
VIII.6 National Codes and Standards Coordination . . . 1083

Kettering University
V.L.8 21st Century Renewable Fuels, Energy, and Materials Initiative . . . 937

Kidde-Fenwal
IV.E.1 Quantifying and Addressing the DOE Material Reactivity Requirements with Analysis and Testing of Hydrogen Storage Materials and Systems . . . 538

Lawrence Berkeley National Laboratory
V.D.8 Molecular-Scale, Three-Dimensional Non-Platinum Group Metal Electrodes for Catalysis of Fuel Cell Reactions . . . 738
V.E.2 Durability Improvements Through Degradation Mechanism Studies . . . 788
V.E.7 Accelerated Testing Validation . . . 810
V.F.2 Development and Validation of a Two-Phase, Three-Dimensional Model for PEM Fuel Cells . . . 818
V.F.6 Transport Studies Enabling Efficiency Optimization of Cost-Competitive Fuel Cell Stacks . . . 837
V.F.7 Fuel Cell Fundamentals at Low and Subzero Temperatures . . . 841

Lawrence Livermore National Laboratory
II.G.3 Characterization and Optimization of Photoelectrode Surfaces for Solar-to-Chemical Fuel Conversion . . . 134
III.5 Demonstration of Full-Scale Glass Fiber Composite Pressure Vessels for Inexpensive Delivery of Cold Hydrogen . . . 316
III.14 Thermodynamic Modeling of Rapid Low Loss Cryogenic Hydrogen Refueling . . . 358
IV.A.8 Tunable Thermodynamics and Kinetics for Hydrogen Storage: Nanoparticle Synthesis Using Ordered Polymer Templates . . . 416
VI.9 Development of Advanced Manufacturing Technologies for Low Cost Hydrogen Storage Vessels . . . 995

Lawrence Livermore National Laboratory (Continued)
VIII.13 Hydrogen Safety Training for Researchers and Technical Personnel 1110
X.8 Incorporation of Two Ford H_2 ICE Buses into the Shuttle Bus Fleet 1214
XI.11 Energy Informatics: Support for Decision Makers through Energy, Carbon and Water Analysis 1270

Lehigh University
V.L.7 Fuel Cell Coolant Optimization and Scale Up 933

Lincoln Composites, Inc.
III.7 Development of High Pressure Hydrogen Storage Tank for Storage and Gaseous Truck Delivery 326
IV.D.1 Hydrogen Storage Engineering Center of Excellence 479
IV.D.11 Development of Improved Composite Pressure Vessels for Hydrogen Storage 534

Linde LLC
III.14 Thermodynamic Modeling of Rapid Low Loss Cryogenic Hydrogen Refueling 358

Linde North America
XII.11 GENCO Fuel Cell-Powered Lift Truck Fleet Deployment 1322

Lockheed Martin-IDT
V.L.5 Fuel Cell Balance of Plant Reliability Testbed 923

Longitude 122 West, Inc.
X.2 Economic Analysis of Bulk Hydrogen Storage for Renewable Utility Applications 1196

Los Alamos National Laboratory
IV.B.2 Fluid Phase Chemical Hydrogen Storage Materials 429
IV.D.1 Hydrogen Storage Engineering Center of Excellence 479
IV.D.3 Chemical Hydride Rate Modeling, Validation, and System Demonstration 491
V.A.6 Technical Assistance to Developers 631
V.B.1 Effect of System Contaminants on PEMFC Performance and Durability 640
V.B.5 Effects of Fuel and Air Impurities on PEM Fuel Cell Performance 659
V.D.4 Extended, Continuous Pt Nanostructures in Thick, Dispersed Electrodes 719
V.D.7 The Science and Engineering of Durable Ultralow PGM Catalysts 734
V.D.11 Development of Novel Non-PGM Electrocatalysts for Proton Exchange Membrane Fuel Cell Applications 756
V.D.14 Engineered Nano-Scale Ceramic Supports for PEM Fuel Cells 770
V.E.2 Durability Improvements Through Degradation Mechanism Studies 788
V.E.4 Development of Micro-Structural Mitigation Strategies for PEM Fuel Cells: Morphological Simulations and Experimental Approaches 797
V.E.5 Durability of Low Platinum Fuel Cells Operating at High Power Density 802
V.E.6 Improved Accelerated Stress Tests Based on Fuel Cell Vehicle Data 806
V.E.7 Accelerated Testing Validation 810
V.F.2 Development and Validation of a Two-Phase, Three-Dimensional Model for PEM Fuel Cells 818
V.F.7 Fuel Cell Fundamentals at Low and Subzero Temperatures 841
V.G.4 Advanced Materials and Concepts for Portable Power Fuel Cells 858
V.I.1 Resonance-Stabilized Anion Exchange Polymer Electrolytes 872
VI.6 Cause-and-Effect: Flow Field Plate Manufacturing Variability and its Impact on Performance 983
VI.10 Non-Contact Sensor Evaluation for Bipolar Plate Manufacturing Process Control and Smart Assembly of Fuel Cell Stacks 999

Los Alamos National Laboratory (Continued)

VI.11 Optical Scatterfield Metrology for Online Catalyst Coating Inspection of PEM (Fuel Cell) Soft Goods 1003

VIII.8 Leak Detection and H_2 Sensor Development for Hydrogen Applications 1090

VIII.9 Hydrogen Fuel Quality Research and Development 1096

IX.5 VA-MD-DC Hydrogen Education for Decision Makers 1144

IX.14 H_2 Educate! Hydrogen Education for Middle Schools 1177

Massachusetts Institute of Technology

IV.A.8 Tunable Thermodynamics and Kinetics for Hydrogen Storage: Nanoparticle Synthesis Using Ordered Polymer Templates 416

V.D.6 Contiguous Platinum Monolayer Oxygen Reduction Electrocatalysts on High-Stability Low-Cost Supports 729

V.D.12 High-Activity Dealloyed Catalysts 760

V.E.1 Polymer Electrolyte Fuel Cell Lifetime Limitations: The Role of Electrocatalyst Degradation 783

Max Planck Institute

IV.C.7 Weak Chemisorption Validation 464

Media and Process Technology Inc.

II.C.2 Development of Hydrogen Selective Membranes/Modules as Reactors/Separators for Distributed Hydrogen Production 53

MegaStir Technologies

III.3 Vessel Design and Fabrication Technology for Stationary High-Pressure Hydrogen Storage 307

Mercedes-Benz Research & Development North America, Inc.

VII.3 Hydrogen to the Highways – Controlled Hydrogen Fleet and Infrastructure Demonstration and Validation Project 1027

Mercedes-Benz USA LLC

VII.3 Hydrogen to the Highways – Controlled Hydrogen Fleet and Infrastructure Demonstration and Validation Project 1027

Michigan State University

V.D.11 Development of Novel Non-PGM Electrocatalysts for Proton Exchange Membrane Fuel Cell Applications 756

Michigan Technological University

V.E.4 Development of Micro-Structural Mitigation Strategies for PEM Fuel Cells: Morphological Simulations and Experimental Approaches 797

IX.11 Hydrogen Education Curriculum Path at Michigan Technological University 1166

Midwest Optoelectronics, LLC

II.G.6 Critical Research for Cost-Effective Photoelectrochemical Production of Hydrogen 150

Midwest Research Institute

IV.C.3 Multiply Surface-Functionalized Nanoporous Carbon for Vehicular Hydrogen Storage 444

Mitsubishi Compressor Company

III.9 Oil-Free Centrifugal Hydrogen Compression Technology Demonstration 338

Mohawk Innovative Technologies, Inc.
III.9 Oil-Free Centrifugal Hydrogen Compression Technology Demonstration 338

MorEvents
VIII.6 National Codes and Standards Coordination. 1083
VIII.7 Codes and Standards Outreach for Emerging Fuel Cell Technologies 1087

MTI Micro Fuel Cells Inc.
XII.1 Commercialization of 1 Watt Consumer Electronics Power Pack 1287

MVSystems, Incorporated
II.G.5 Photoelectrochemical Hydrogen Production 146

National Conference of State Legislatures
IX.3 Hydrogen Education State Partnership Program. 1139

National Energy Education Development Project
IX.14 H_2 Educate! Hydrogen Education for Middle Schools 1177

National Energy Technology Laboratory
II.B.2 One Step Biomass Gas Reforming-Shift Separation Membrane Reactor 42

National Institute of Standards and Technology
IV.A.9 Neutron Characterization in Support of the DOE Hydrogen Storage Sub-Program. 420
V.A.5 Neutron Imaging Study of the Water Transport in Operating Fuel Cells 626
VI.6 Cause-and-Effect: Flow Field Plate Manufacturing Variability and its Impact on Performance 983
VI.10 Non-Contact Sensor Evaluation for Bipolar Plate Manufacturing Process Control and Smart Assembly of Fuel Cell Stacks 999
VI.11 Optical Scatterfield Metrology for Online Catalyst Coating Inspection of PEM (Fuel Cell) Soft Goods 1003

National Renewable Energy Laboratory
II.A.2 Distributed Bio-Oil Reforming. 29
II.E.4 Renewable Electrolysis Integrated System Development and Testing 92
II.E.6 Hour-by-Hour Cost Modeling of Optimized Central Wind-Based Water Electrolysis Production 98
II.G.2 Semiconductor Materials for Photoelectrolysis 129
II.G.6 Critical Research for Cost-Effective Photoelectrochemical Production of Hydrogen 150
II.G.8 Photoelectrochemical Hydrogen Generation from Water Using $TiSi_2$–TiO_2 Nanotube Core-Shell Structure 160
II.G.12 Photoelectrochemical Materials: Theory and Modeling 176
II.H.1 Biological Systems for Hydrogen Photoproduction 185
II.H.2 Fermentation and Electrohydrogenic Approaches to Hydrogen Production 190
II.H.5 Purdue Hydrogen Systems Laboratory: Hydrogen Production 203
II.I.1 H2A Production Model Updates 207
II.K.5 Structural, Functional, and Integration Studies of Solar-Driven, Bio-Hybrid, H_2-Producing Systems. 240
II.K.8 Regulation of H_2 and CO_2 Metabolism: Factors Involved in Partitioning of Photosynthetic Reductant in Green Algae. 248
II.K.21 New Directions for Efficient Solar Water Splitting Based on Two Photosystems and Singlet Fission Chromophores. 286
III.4 Hydrogen Delivery Analysis 312

National Renewable Energy Laboratory (Continued)

IV.C.7 Weak Chemisorption Validation . . . 464
IV.D.1 Hydrogen Storage Engineering Center of Excellence . . . 479
IV.D.2 System Design, Analysis, Modeling, and Media Engineering Properties for Hydrogen Energy Storage . . . 486
IV.E.5 Analysis of Storage Needs for Early Motive Fuel Cell Markets . . . 558
IV.G.1 Purdue Hydrogen Systems Laboratory: Hydrogen Storage . . . 585
V.A.1 Analysis of Laboratory Fuel Cell Technology Status – Voltage Degradation . . . 605
V.A.7 Enlarging the Potential Market for Stationary Fuel Cells Through System Design Optimization . . . 634
V.B.1 Effect of System Contaminants on PEMFC Performance and Durability . . . 640
V.D.4 Extended, Continuous Pt Nanostructures in Thick, Dispersed Electrodes . . . 719
V.D.9 Tungsten Oxide and Heteropoly Acid Based System for Ultra-High Activity and Stability of Pt Catalysts in PEM Fuel Cell Cathodes . . . 745
V.G.1 Novel Approach to Advanced Direct Methanol Fuel Cell (DMFC) Anode Catalysts . . . 846
VI.1 Fuel Cell Membrane Electrode Assembly Manufacturing R&D . . . 959
VII.1 Controlled Hydrogen Fleet and Infrastructure Analysis . . . 1017
VII.5 Technology Validation: Fuel Cell Bus Evaluations . . . 1036
VIII.3 Component Standard Research and Development . . . 1072
VIII.6 National Codes and Standards Coordination . . . 1083
VIII.7 Codes and Standards Outreach for Emerging Fuel Cell Technologies . . . 1087
X.5 Green Communities . . . 1205
X.6 Direct Methanol Fuel Cell Material Handling Equipment Demonstration . . . 1209
XI.2 Hydrogen Infrastructure Market Readiness Analysis . . . 1236
XI.3 Infrastructure Analysis of Early Market Transition of Fuel Cell Vehicles . . . 1240
XI.5 Cost and GHG Implications of Hydrogen for Energy Storage . . . 1248
XI.7 NEMS-H2: Hydrogen's Role in Climate Mitigation and Oil Dependence Reduction . . . 1254
XI.9 Macro-System Model . . . 1261
XI.10 HyDRA: Hydrogen Demand and Resource Analysis Tool . . . 1265
XII.7 Analysis Results for ARRA Projects: Enabling Fuel Cell Market Transformation . . . 1308

NextEnergy

VII.3 Hydrogen to the Highways – Controlled Hydrogen Fleet and Infrastructure Demonstration and Validation Project . . . 1027

Nissan Technical Center

V.D.10 Synthesis and Characterization of Mixed-Conducting Corrosion Resistant Oxide Supports . . . 752
V.D.11 Development of Novel Non-PGM Electrocatalysts for Proton Exchange Membrane Fuel Cell Applications . . . 756
V.E.3 Analysis of Durability of MEAs in Automotive PEMFC Applications . . . 794

North Carolina State University

II.H.1 Biological Systems for Hydrogen Photoproduction . . . 185

Northeastern University

V.D.11 Development of Novel Non-PGM Electrocatalysts for Proton Exchange Membrane Fuel Cell Applications . . . 756
V.D.12 High-Activity Dealloyed Catalysts . . . 760
V.G.3 New MEA Materials for Improved Direct Methanol Fuel Cell (DMFC) Performance, Durability, and Cost . . . 854

Northwestern University

IV.A.2 Efficient Discovery of Novel Multicomponent Mixtures for Hydrogen Storage: A Combined Computational/Experimental Approach 388

IV.C.4 New Carbon-Based Porous Materials with Increased Heats of Adsorption for Hydrogen Storage 450

Nuvera Fuel Cells, Inc.

V.E.5 Durability of Low Platinum Fuel Cells Operating at High Power Density 802

V.F.6 Transport Studies Enabling Efficiency Optimization of Cost-Competitive Fuel Cell Stacks 837

XII.8 H-E-B Grocery Total Power Solution for Fuel Cell-Powered Material Handling Equipment 1312

Oak Ridge National Laboratory

II.C.3 High Performance Palladium-Based Membrane for Hydrogen Separation and Purification 58

II.E.2 High Performance, Low Cost Hydrogen Generation from Renewable Energy 83

III.3 Vessel Design and Fabrication Technology for Stationary High-Pressure Hydrogen Storage 307

III.13 Composite Technology for Hydrogen Pipelines 354

III.15 Integrity of Steel Welds in High-Pressure Hydrogen Environment 362

IV.F.1 High Strength Carbon Fibers 576

IV.F.2 Lifecycle Verification of Polymeric Storage Liners 581

V.A.4 Characterization of Fuel Cell Materials 621

V.D.3 Durable Catalysts for Fuel Cell Protection During Transient Conditions 714

V.D.4 Extended, Continuous Pt Nanostructures in Thick, Dispersed Electrodes 719

V.D.5 Nanosegregated Cathode Catalysts with Ultra-Low Platinum Loading 723

V.D.14 Engineered Nano-Scale Ceramic Supports for PEM Fuel Cells 770

V.D.15 Development of Alternative and Durable High Performance Cathode Supports for PEM Fuel Cells 777

V.E.2 Durability Improvements Through Degradation Mechanism Studies 788

V.E.6 Improved Accelerated Stress Tests Based on Fuel Cell Vehicle Data 806

V.E.7 Accelerated Testing Validation 810

V.G.4 Advanced Materials and Concepts for Portable Power Fuel Cells 858

VIII.16 MEMS Hydrogen Sensor for Leak Detection 1122

XI.1 Non-Automotive Fuel Cells: Market Assessment and Analysis of Impacts of Policies 1231

Ohio Fuel Cell Coalition

IX.7 Raising H_2 and Fuel Cell Awareness in Ohio 1153

Ohio State University

II.C.1 Zeolite Membrane Reactor for Water-Gas Shift Reaction for Hydrogen Production 46

IV.A.4 Lightweight Metal Hydrides for Hydrogen Storage 398

OnLocation, Inc.

XI.7 NEMS-H2: Hydrogen's Role in Climate Mitigation and Oil Dependence Reduction 1254

Oorja Protonics, Inc.

X.6 Direct Methanol Fuel Cell Material Handling Equipment Demonstration 1209

Oregon State University

IV.D.1 Hydrogen Storage Engineering Center of Excellence 479

IV.D.10 Microscale Enhancement of Heat and Mass Transfer for Hydrogen Energy Storage 530

Orion Industries
V.H.2 Metallic Bipolar Plates with Composite Coatings 867

Ovonic Hydrogen Systems LLC
IV.E.6 Standardized Testing Program for Solid-State Hydrogen Storage Technologies 562

PACCAR, Inc.
XII.4 Solid Oxide Fuel Cell Diesel Auxiliary Power Unit Demonstration 1297

Pacific Northwest National Laboratory
II.A.1 Biomass-Derived Liquids Distributed (Aqueous Phase) Reforming 25
IV.D.1 Hydrogen Storage Engineering Center of Excellence 479
IV.D.6 Systems Engineering of Chemical Hydride, Pressure Vessel, and Balance of Plant for On-Board Hydrogen Storage. 503
V.D.15 Development of Alternative and Durable High Performance Cathode Supports for PEM Fuel Cells. 777
VI.3 Modular, High-Volume Fuel Cell Leak-Test Suite and Process 968
VI.8 MEA Manufacturing R&D Using Drop-On-Demand Technology 991
VI.9 Development of Advanced Manufacturing Technologies for Low Cost Hydrogen Storage Vessels. 995
VIII.10 Hydrogen Safety Panel 1100
VIII.11 Hydrogen Safety Knowledge Tools 1104
VIII.12 Hydrogen Emergency Response Training for First Responders 1107
X.4 Fuel Cell Combined Heat and Power Industrial Demonstration 1202
X.10 Assessment of Solid Oxide Fuel Cell Power System for Greener Commercial Aircraft 1220
XII.7 Analysis Results for ARRA Projects: Enabling Fuel Cell Market Transformation. 1308

Pall Corporation
II.C.3 High Performance Palladium-Based Membrane for Hydrogen Separation and Purification. 58

Parker Hannifin Ltd domnick hunter Division
II.E.1 PEM Electrolyzer Incorporating an Advanced Low-Cost Membrane. 79

Parkway Systems
XII.8 H-E-B Grocery Total Power Solution for Fuel Cell-Powered Material Handling Equipment. 1312

PBI Performance Products, Inc.
II.E.5 Process Intensification of Hydrogen Unit Operations Using an Electrochemical Device. 95

Peek Site-Com, Inc.
XII.6 PEM Fuel Cell Systems Providing Backup Power to Commercial Cellular Towers and an Electric Utility Communications Network 1304

Pennsylvania State University
II.E.2 High Performance, Low Cost Hydrogen Generation from Renewable Energy 83
II.H.2 Fermentation and Electrohydrogenic Approaches to Hydrogen Production 190
II.K.19 A Hybrid Biological-Organic Half-Cell for Generating Dihydrogen 281
IV.C.6 Hydrogen Trapping through Designer Hydrogen Spillover Molecules with Reversible Temperature and Pressure-Induced Switching 459
V.F.2 Development and Validation of a Two-Phase, Three-Dimensional Model for PEM Fuel Cells 818
V.F.4 Investigation of Micro- and Macro-Scale Transport Processes for Improved Fuel Cell Performance. 827
V.F.6 Transport Studies Enabling Efficiency Optimization of Cost-Competitive Fuel Cell Stacks 837

Pennsylvania State University (Continued)
V.F.7 Fuel Cell Fundamentals at Low and Subzero Temperatures. 841
VI.2 Reduction in Fabrication Costs of Gas Diffusion Layers 963

Physical Optics Corporation
II.J.4 Photochemical System for Hydrogen Generation 225

Plug Power Inc.
II.E.5 Process Intensification of Hydrogen Unit Operations Using an Electrochemical Device. 95
V.F.5 Air-Cooled Stack Freeze Tolerance 833
XII.9 Fuel Cell-Powered Lift Truck FedEx Freight Fleet Deployment 1316
XII.10 Fuel Cell-Powered Lift Truck Sysco Houston Fleet Deployment. 1319
XII.11 GENCO Fuel Cell-Powered Lift Truck Fleet Deployment 1322
XII.12 Highly Efficient, 5 kW CHP Fuel Cells Demonstrating Durability and Economic Value in Residential and Light Commercial Applications 1325
XII.13 Accelerating Acceptance of Fuel Cell Backup Power Systems. 1328

PoroGen, LLC
IV.C.8 Nanostructured Activated Carbon for Hydrogen Storage. 470

Powdermet Inc.
VIII.10 Hydrogen Safety Panel 1100

Power & Energy, Inc.
II.D.3 Advanced Palladium Membrane Scale Up for Hydrogen Separation 69

Praxair, Inc.
II.D.1 Advanced Hydrogen Transport Membranes for Coal Gasification 62
III.8 Development of a Centrifugal Hydrogen Pipeline Gas Compressor 331
III.11 Advanced Hydrogen Liquefaction Process. 345

Princeton University
II.K.10 Theoretical Research Program on Bio-inspired Inorganic Hydrogen Generating Catalysts and Electrodes 253

Prometheus Energy
III.17 Active Magnetic Regenerative Liquefier 371

Proton Energy Systems
II.E.2 High Performance, Low Cost Hydrogen Generation from Renewable Energy 83
II.J.2 Hydrogen by Wire - Home Fueling System. 215

Protonex Inc.
V.J.3 Large Scale Testing, Demonstration and Commercialization of the Nanoparticle-Based Fuel Cell Coolant 886

Public Technology Institute
IX.6 H2L3: Hydrogen Learning for Local Leaders 1148

Purdue University
II.H.5 Purdue Hydrogen Systems Laboratory: Hydrogen Production 203
IV.G.1 Purdue Hydrogen Systems Laboratory: Hydrogen Storage. 585

Quantum Fuel Systems Technologies Worldwide, Inc.

VI.9 Development of Advanced Manufacturing Technologies for Low Cost Hydrogen Storage Vessels. 995

QuantumSphere Inc.

V.G.2 Novel Materials for High Efficiency Direct Methanol Fuel Cells. 850

Queen's University

V.E.4 Development of Micro-Structural Mitigation Strategies for PEM Fuel Cells: Morphological Simulations and Experimental Approaches 797

RCF Economic and Financial Consulting, Inc.

IX.1 Employment Impacts of Early Markets for Hydrogen and Fuel Cell Technologies 1131

ReliOn, Inc.

XII.5 Demonstrating Economic and Operational Viability of 72-Hour Hydrogen PEM Fuel Cell Systems to Support Emergency Communications on the Sprint Nextel Network 1300

XII.6 PEM Fuel Cell Systems Providing Backup Power to Commercial Cellular Towers and an Electric Utility Communications Network 1304

Rensselaer Polytechnic Institute

VI.5 Adaptive Process Controls and Ultrasonics for High-Temperature PEM MEA Manufacture 977

Rochester Institute of Technology

V.F.4 Investigation of Micro- and Macro-Scale Transport Processes for Improved Fuel Cell Performance. 827

Rolls Royce Fuel Cell Systems Inc.

V.L.3 Extended Durability Testing of an External Fuel Processor for SOFCs 914

V.L.10 Solid Oxide Fuel Cell Systems Print Verification Line (PVL) Pilot Line 950

Rutgers University

IV.C.6 Hydrogen Trapping through Designer Hydrogen Spillover Molecules with Reversible Temperature and Pressure-Induced Switching. 459

SAE International

VIII.3 Component Standard Research and Development 1072

VIII.6 National Codes and Standards Coordination. 1083

Sandia National Laboratories

II.F.3 Solar Hydrogen Production with a Metal Oxide-Based Thermochemical Cycle 112

III.1 Hydrogen Embrittlement of Structural Steels 299

IV.A.8 Tunable Thermodynamics and Kinetics for Hydrogen Storage: Nanoparticle Synthesis Using Ordered Polymer Templates 416

IV.E.4 Analysis of H_2 Storage Needs for Early Market Non-Motive Fuel Cell Applications 554

V.F.2 Development and Validation of a Two-Phase, Three-Dimensional Model for PEM Fuel Cells 818

V.I.1 Resonance-Stabilized Anion Exchange Polymer Electrolytes 872

VIII.1 Hydrogen Safety, Codes and Standards R&D – Release Behavior 1061

VIII.2 Risk-Informed Safety Requirements for H2 Codes and Standards Development 1067

VIII.4 Hydrogen Materials and Components Compatibility 1075

VIII.5 Component Testing for Industrial Trucks and Early Market Applications 1079

VIII.15 International Energy Agency Hydrogen Implementing Agreement Task 19 Hydrogen Safety. 1118

X.1 Fuel Cell Mobile Lighting 1191

Sandia National Laboratories (Continued)
X.9 PEM Fuel Cell Systems for Commercial Airplane Systems Power. 1217
XI.4 Analysis of the Effects of Developing New Energy Infrastructures. 1244

Savannah River National Laboratory
III.6 Fiber Reinforced Composite Pipeline 322
IV.A.1 Amide and Combined Amide/Borohydride Investigations. 383
IV.A.7 Electrochemical Reversible Formation of Alane 413
IV.D.1 Hydrogen Storage Engineering Center of Excellence 479
IV.D.5 SRNL Technical Work Scope for the Hydrogen Storage Engineering Center of Excellence: Design and Testing of Metal Hydride and Adsorbent Systems. 498
V.B.4 Effects of Impurities on Fuel Cell Performance and Durability. 654

Schott North America
II.B.2 One Step Biomass Gas Reforming-Shift Separation Membrane Reactor 42

Science Applications International Corporation
II.F.1 Solar High-Temperature Water Splitting Cycle with Quantum Boost. 102

SCRA
IV.E.8 Administration of H-Prize for Hydrogen Storage 571

Scribner Associates, Inc.
V.C.9 Lead Research and Development Activity for DOE's High Temperature, Low Relative Humidity Membrane Program 696

Sentech, Inc.
IX.14 H_2 Educate! Hydrogen Education for Middle Schools 1177

SFC Energy
V.G.4 Advanced Materials and Concepts for Portable Power Fuel Cells. 858

SGL Carbon
V.F.1 Water Transport in PEM Fuel Cells: Advanced Modeling, Material Selection, Testing, and Design Optimization 814

Sloane Solutions
VIII.6 National Codes and Standards Coordination. 1083

South Carolina Hydrogen and Fuel Cell Alliance
IX.4 Development of Hydrogen Education Programs for Government Officials 1142
X.7 Landfill Gas-to-Hydrogen. 1212

South Dakota School of Mines and Technology
II.G.9 USD Catalysis Group for Alternative Energy 164

Southern Illinois University, Carbondale
V.H.2 Metallic Bipolar Plates with Composite Coatings 867

Southwest Research Institute®
IV.E.6 Standardized Testing Program for Solid-State Hydrogen Storage Technologies 562

Spectrum Automation Controls
II.E.4 Renewable Electrolysis Integrated System Development and Testing 92

Spencer Composites Corporation
III.5 Demonstration of Full-Scale Glass Fiber Composite Pressure Vessels for Inexpensive Delivery of Cold Hydrogen 316

Sprint Nextel
XII.5 Demonstrating Economic and Operational Viability of 72-Hour Hydrogen PEM Fuel Cell Systems to Support Emergency Communications on the Sprint Nextel Network 1300

SRA International, Inc.
XI.9 Macro-System Model 1261

SRT Group, Inc.
VII.8 Florida Hydrogen Initiative (FHI) 1046

Stanford University
II.G.1 Nano-Architectures for 3rd Generation PEC Devices: A Study of MoS_2, Fundamental Investigations and Applied Research 123
II.G.2 Semiconductor Materials for Photoelectrolysis 129
II.K.1 SISGR: Using *In vitro* Maturation and Cell-free Evolution to Understand [Fe-Fe]hydrogenase Activation and Active Site Constraints 228
V.D.4 Extended, Continuous Pt Nanostructures in Thick, Dispersed Electrodes 719

Stark State College of Technology
V.L.5 Fuel Cell Balance of Plant Reliability Testbed 923
V.L.10 Solid Oxide Fuel Cell Systems Print Verification Line (PVL) Pilot Line 950

State University of New York, Albany
V.D.4 Extended, Continuous Pt Nanostructures in Thick, Dispersed Electrodes 719

State University of New York, Stony Brook
V.H.1 Low-Cost PEM Fuel Cell Metal Bipolar Plates 863

State University of New York, Syracuse
IV.C.8 Nanostructured Activated Carbon for Hydrogen Storage 470
V.C.2 Dimensionally Stable Membranes (DSMs) 667

Steele Consulting
VIII.6 National Codes and Standards Coordination 1083

Stony Brook University
II.K.16 Quantum theory of Semiconductor-Photo-Catalysis and Solar Water Splitting 273

Sustainable Innovations, LLC
III.10 Electrochemical Hydrogen Compressor 342

Synkera Technologies Inc.
II.G.13 Nanotube Array Photoelectrochemical Hydrogen Production 181

Sysco of Houston
XII.10 Fuel Cell-Powered Lift Truck Sysco Houston Fleet Deployment 1319

T3 Scientific
II.D.1 Advanced Hydrogen Transport Membranes for Coal Gasification 62

TDA Research, Inc.
XII.4 Solid Oxide Fuel Cell Diesel Auxiliary Power Unit Demonstration 1297

Tech-Etch
V.F.3 Transport in PEMFC Stacks 822

Technical University Berlin
V.D.12 High-Activity Dealloyed Catalysts 760

Technology Transition Corporation
IX.6 H2L3: Hydrogen Learning for Local Leaders 1148

Techverse
V.F.1 Water Transport in PEM Fuel Cells: Advanced Modeling, Material Selection, Testing, and Design Optimization 814

Telecom, Tower and Power, LLC
XII.6 PEM Fuel Cell Systems Providing Backup Power to Commercial Cellular Towers and an Electric Utility Communications Network 1304

Texas A&M University
III.8 Development of a Centrifugal Hydrogen Pipeline Gas Compressor 331
IV.C.1 A Biomimetic Approach to Metal-Organic Frameworks with High H_2 Uptake 432
V.D.2 Highly Dispersed Alloy Catalyst for Durability 708

The Toro Company
V.K.3 Research & Development for Off-Road Fuel Cell Applications 899

Thermochemical Engineering Solutions
II.F.1 Solar High-Temperature Water Splitting Cycle with Quantum Boost 102

TIAX, LLC
IV.E.3 Cost Analyses of Hydrogen Storage Materials and On-Board Systems 550

TreadStone Technologies, Inc.
V.H.1 Low-Cost PEM Fuel Cell Metal Bipolar Plates 863

UltraCell Corporation
VI.3 Modular, High-Volume Fuel Cell Leak-Test Suite and Process 968

United Commercial Real Estate Services, Inc.
XII.6 PEM Fuel Cell Systems Providing Backup Power to Commercial Cellular Towers and an Electric Utility Communications Network 1304

United Technologies Corporation – Hamilton Sundstrand
V.B.2 The Effects of Impurities on Fuel Cell Performance and Durability 644

United Technologies Research Center

II.B.1 A Novel Slurry-Based Biomass Reforming Process 37
II.D.3 Advanced Palladium Membrane Scale Up for Hydrogen Separation 69
IV.D.1 Hydrogen Storage Engineering Center of Excellence 479
IV.D.7 Advancement of Systems Designs and Key Engineering Technologies for Materials-Based Hydrogen Storage.....511
IV.E.1 Quantifying and Addressing the DOE Material Reactivity Requirements with Analysis and Testing of Hydrogen Storage Materials and Systems 538
V.E.1 Polymer Electrolyte Fuel Cell Lifetime Limitations: The Role of Electrocatalyst Degradation.....783
V.E.6 Improved Accelerated Stress Tests Based on Fuel Cell Vehicle Data 806
V.F.7 Fuel Cell Fundamentals at Low and Subzero Temperatures.....841

Université du Québec à Trois-Rivières

IV.D.1 Hydrogen Storage Engineering Center of Excellence 479
IV.D.5 SRNL Technical Work Scope for the Hydrogen Storage Engineering Center of Excellence: Design and Testing of Metal Hydride and Adsorbent Systems.....498

University of Akron

V.L.1 Development of Kilowatt-Scale Coal Fuel Cell Technology 905

University of Alabama, Tuscaloosa

II.K.14 Protein-Templated Synthesis and Assembly of Nanostructuctures for Hydrogen Production 267

University of Arizona

II.K.17 Formation and Characterization of Semiconductor Nanorod/Oxide Nanoparticle Hybrid Materials: Toward Vectoral Electron Transport in Hybrid Materials 275

University of Arkansas, Little Rock

II.G.7 PEC-Based Hydrogen Production with Self-Cleaning Solar Concentrator 154

University of California, Berkeley

II.H.4 Maximizing Light Utilization Efficiency and Hydrogen Production in Microalgal Cultures..... 200
IX.3 Hydrogen Education State Partnership Program.....1139
IX.10 Hydrogen Energy in Engineering Education (H_2E^3) 1161
IX.15 Hydrogen Technology and Energy Curriculum (HyTEC) 1180

University of California, Davis

V.K.3 Research & Development for Off-Road Fuel Cell Applications..... 899

University of California, Irvine

V.F.2 Development and Validation of a Two-Phase, Three-Dimensional Model for PEM Fuel Cells 818
VII.6 California Hydrogen Infrastructure Project..... 1040
XII.12 Highly Efficient, 5 kW CHP Fuel Cells Demonstrating Durability and Economic Value in Residential and Light Commercial Applications 1325

University of California, Los Angeles

IV.C.2 A Joint Theory and Experimental Project in the Synthesis and Testing of Porous COFs/ZIFs for On-Board Vehicular Hydrogen Storage 439
IV.C.9 Hydrogen Storage in Metal-Organic Frameworks.....474

University of California, Riverside
V.D.4 Extended, Continuous Pt Nanostructures in Thick, Dispersed Electrodes 719
V.D.7 The Science and Engineering of Durable Ultralow PGM Catalysts. 734
V.G.4 Advanced Materials and Concepts for Portable Power Fuel Cells 858

University of California, San Diego
II.F.1 Solar High-Temperature Water Splitting Cycle with Quantum Boost. 102

University of California, Santa Cruz
II.K.12 Hydrogen Generation Using Integrated Photovoltaic and Photoelectrochemical Cells 260

University of Central Florida
V.C.9 Lead Research and Development Activity for DOE's High Temperature, Low Relative Humidity Membrane Program 696
VII.8 Florida Hydrogen Initiative (FHI) 1046
IX.12 Hydrogen and Fuel Cell Technology Education Program (HFCT) 1170

University of Chicago
IV.C.5 Hydrogen Storage through Nanostructured Porous Organic Polymers (POPs). 455

University of Cincinnati
II.C.1 Zeolite Membrane Reactor for Water-Gas Shift Reaction for Hydrogen Production 46

University of Colorado
II.F.3 Solar Hydrogen Production with a Metal Oxide-Based Thermochemical Cycle 112
II.F.4 Solar-Thermal ALD Ferrite-Based Water Splitting Cycle. 118
V.D.9 Tungsten Oxide and Heteropoly Acid Based System for Ultra-High Activity and Stability of Pt Catalysts in PEM Fuel Cell Cathodes. 745

University of Connecticut
V.B.2 The Effects of Impurities on Fuel Cell Performance and Durability 644
V.B.3 The Effect of Airborne Contaminants on Fuel Cell Performance and Durability 649
V.D.15 Development of Alternative and Durable High Performance Cathode Supports for PEM Fuel Cells. 777

University of Connecticut Global Fuel Cell Center
V.L.9 Improving Reliability and Durability of Effi cient and Clean Energy Systems. 943

University of Delaware
V.D.15 Development of Alternative and Durable High Performance Cathode Supports for PEM Fuel Cells. 777
VI.4 Manufacturing of Low-Cost, Durable Membrane Electrode Assemblies Engineered for Rapid Conditioning. 971

University of Detroit Mercy
V.C.1 Membranes and MEAs for Dry, Hot Operating Conditions 662

University of Florida
V.G.3 New MEA Materials for Improved Direct Methanol Fuel Cell (DMFC) Performance, Durability, and Cost 854
VII.8 Florida Hydrogen Initiative (FHI) 1046
XII.3 Advanced Direct Methanol Fuel Cell for Mobile Computing. 1294

University of Georgia
II.K.3 Fundamental Studies of Recombinant Hydrogenases 234

University of Hawaii
IV.A.3 Fundamental Studies of Advanced High-Capacity, Reversible Metal Hydrides. 393
IV.C.7 Weak Chemisorption Validation 464
V.B.1 Effect of System Contaminants on PEMFC Performance and Durability 640

University of Hawaii at Manoa
II.G.5 Photoelectrochemical Hydrogen Production 146

University of Illinois at Urbana-Champaign
III.12 A Combined Materials Science/Mechanics Approach to the Study of Hydrogen Embrittlement of Pipeline Steels 349
IV.A.5 Reversible Hydrogen Storage Materials - Structure, Chemistry, and Electronic Structure 403

University of Maryland
IX.5 VA-MD-DC Hydrogen Education for Decision Makers 1144

University of Michigan
IV.D.1 Hydrogen Storage Engineering Center of Excellence 479
IV.D.9 Ford/BASF-SE/UM Activities in Support of the Hydrogen Storage Engineering Center of Excellence. 522

University of Minnesota
II.A.2 Distributed Bio-Oil Reforming. 29

University of Missouri
II.K.7 Genetics and Molecular Biology of Hydrogen Metabolism in Sulfate-reducing Bacteria. 245
IV.C.3 Multiply Surface-Functionalized Nanoporous Carbon for Vehicular Hydrogen Storage 444

University of Missouri, St. Louis
IV.A.8 Tunable Thermodynamics and Kinetics for Hydrogen Storage: Nanoparticle Synthesis Using Ordered Polymer Templates 416

University of Nebraska, Omaha
II.G.10 Novel Photocatalytic Metal Oxides 170

University of Nevada, Las Vegas
II.G.2 Semiconductor Materials for Photoelectrolysis 129
II.G.4 Characterization of Materials for Photoelectrochemical (PEC) Hydrogen Production 140
IV.G.2 HGMS: Glasses and Nanocomposites for Hydrogen Storage. 590

University of Nevada, Reno
II.G.8 Photoelectrochemical Hydrogen Generation from Water Using $TiSi_2$–TiO_2 Nanotube Core-Shell Structure 160
II.G.11 Solar Thermal Hydrogen Production 173

University of New Mexico
IV.C.7 Weak Chemisorption Validation 464
V.D.7 The Science and Engineering of Durable Ultralow PGM Catalysts. 734
V.D.11 Development of Novel Non-PGM Electrocatalysts for Proton Exchange Membrane Fuel Cell Applications 756

University of New Mexico (Continued)
V.D.14 Engineered Nano-Scale Ceramic Supports for PEM Fuel Cells 770
V.E.2 Durability Improvements Through Degradation Mechanism Studies 788
V.E.4 Development of Micro-Structural Mitigation Strategies for PEM Fuel Cells: Morphological Simulations and Experimental Approaches 797

University of North Carolina at Charlotte
IX.12 Hydrogen and Fuel Cell Technology Education Program (HFCT) 1170

University of North Dakota
II.B.1 A Novel Slurry-Based Biomass Reforming Process 37
II.D.3 Advanced Palladium Membrane Scale Up for Hydrogen Separation 69
IX.13 Development of a Renewable Hydrogen Production and Fuel Cell Education Program 1173

University of North Florida
V.G.3 New MEA Materials for Improved Direct Methanol Fuel Cell (DMFC) Performance, Durability, and Cost 854
XII.3 Advanced Direct Methanol Fuel Cell for Mobile Computing 1294

University of Oklahoma
II.K.6 Genes Needed For H_2 Production by Sulfate Reducing Bacteria 242

University of Oregon
IV.B.1 Hydrogen Storage by Novel CBN Heterocycle Materials 425

University of Pennsylvania
II.K.13 Modular Designed Protein Constructions for Solar Generated H_2 from Water 264

University of Pittsburgh
V.D.5 Nanosegregated Cathode Catalysts with Ultra-Low Platinum Loading 723

University of Rochester
II.K.9 Excited State Dynamics in Semiconductor Quantum Dots 250

University of South Carolina
V.B.1 Effect of System Contaminants on PEMFC Performance and Durability 640
V.D.13 Development of Ultra-Low Platinum Alloy Cathode Catalyst for PEM Fuel Cells 764
V.F.3 Transport in PEMFC Stacks 822
V.L.4 Hydrogen Fuel Cell Development in Columbia (SC) 918

University of South Dakota
II.G.9 USD Catalysis Group for Alternative Energy 164

University of South Florida
VII.8 Florida Hydrogen Initiative (FHI) 1046

University of Southern California
II.C.2 Development of Hydrogen Selective Membranes/Modules as Reactors/Separators for Distributed Hydrogen Production 53

University of Southern Mississippi
V.L.2 Alternative Fuel Cell Membranes for Energy Independence 909

University of Tennessee

V.C.1 Membranes and MEAs for Dry, Hot Operating Conditions 662
V.D.4 Extended, Continuous Pt Nanostructures in Thick, Dispersed Electrodes 719
V.D.11 Development of Novel Non-PGM Electrocatalysts for Proton Exchange Membrane Fuel Cell Applications 756
V.F.4 Investigation of Micro- and Macro-Scale Transport Processes for Improved Fuel Cell Performance. 827
V.F.6 Transport Studies Enabling Efficiency Optimization of Cost-Competitive Fuel Cell Stacks 837
VI.4 Manufacturing of Low-Cost, Durable Membrane Electrode Assemblies Engineered for Rapid Conditioning. 971
XI.1 Non-Automotive Fuel Cells: Market Assessment and Analysis of Impacts of Policies 1231

University of Tennessee, Knoxville

V.J.3 Large Scale Testing, Demonstration and Commercialization of the Nanoparticle-Based Fuel Cell Coolant 886

University of Texas at Arlington

II.J.3 Value-Added Hydrogen Generation with CO_2 Conversion. 218

University of Texas at Austin

V.D.4 Extended, Continuous Pt Nanostructures in Thick, Dispersed Electrodes 719
V.E.1 Polymer Electrolyte Fuel Cell Lifetime Limitations: The Role of Electrocatalyst Degradation 783

University of Toledo

II.G.6 Critical Research for Cost-Effective Photoelectrochemical Production of Hydrogen 150

University of Victoria

V.F.1 Water Transport in PEM Fuel Cells: Advanced Modeling, Material Selection, Testing, and Design Optimization 814

University of Washington

II.K.2 Phototrophic metabolism of organic compounds generates excess reducing power that can be redirected to produce H_2 as a biofuel 232
II.K.4 Prospects for Hydrogen Production from Formate by *Methanococcus maripaludis*. 237

University of Wisconsin, Madison

V.E.1 Polymer Electrolyte Fuel Cell Lifetime Limitations: The Role of Electrocatalyst Degradation 783

University of Wyoming

II.H.5 Purdue Hydrogen Systems Laboratory: Hydrogen Production 203
II.K.18 Combinatorial methods for the Improvement of Semiconductor Metal Oxide Photoelectrodes 279
IV.G.1 Purdue Hydrogen Systems Laboratory: Hydrogen Storage. 585

UTC Power

V.B.3 The Effect of Airborne Contaminants on Fuel Cell Performance and Durability 649
V.D.2 Highly Dispersed Alloy Catalyst for Durability 708
V.E.6 Improved Accelerated Stress Tests Based on Fuel Cell Vehicle Data 806
VI.4 Manufacturing of Low-Cost, Durable Membrane Electrode Assemblies Engineered for Rapid Conditioning. 971

Vanderbilt University

V.C.5 NanoCapillary Network Proton Conducting Membranes for High Temperature Hydrogen/Air Fuel Cells. 680

Versa Power Systems
V.I.2 Advanced Materials for RSOFC Dual Mode Operation with Low Degradation 876

Vertical Horizons Contracting
XII.6 PEM Fuel Cell Systems Providing Backup Power to Commercial Cellular Towers and an Electric Utility Communications Network 1304

Victor Li Independent Consultant
III.3 Vessel Design and Fabrication Technology for Stationary High-Pressure Hydrogen Storage 307

Virginia Polytechnic Institute and State University
II.E.1 PEM Electrolyzer Incorporating an Advanced Low-Cost Membrane. 79
II.K.11 Photoinitiated Electron Collection in Mixed-Metal Supramolecular Complexes: Development of Photocatalysts for Hydrogen Production 257
IV.F.1 High Strength Carbon Fibers 576
V.F.3 Transport in PEMFC Stacks. 822
V.G.4 Advanced Materials and Concepts for Portable Power Fuel Cells. 858

W.L. Gore & Associates, Inc.
V.J.1 Materials and Modules for Low-Cost, High-Performance Fuel Cell Humidifiers 879
VI.4 Manufacturing of Low-Cost, Durable Membrane Electrode Assemblies Engineered for Rapid Conditioning. 971

Washington State University
II.A.1 Biomass-Derived Liquids Distributed (Aqueous Phase) Reforming 25

William C. Fort
VIII.10 Hydrogen Safety Panel 1100

Worcester Polytechnic Institute
II.D.4 Composite Pd and Alloy Porous Stainless Steel Membranes for Hydrogen Production and Process Intensification 73

Wright State University
V.C.5 NanoCapillary Network Proton Conducting Membranes for High Temperature Hydrogen/Air Fuel Cells. 680

Xunlight Corporation
II.G.6 Critical Research for Cost-Effective Photoelectrochemical Production of Hydrogen. 150

Yonsei University
V.D.13 Development of Ultra-Low Platinum Alloy Cathode Catalyst for PEM Fuel Cells 764



U.S. DEPARTMENT OF
ENERGY

www.hydrogen.energy.gov